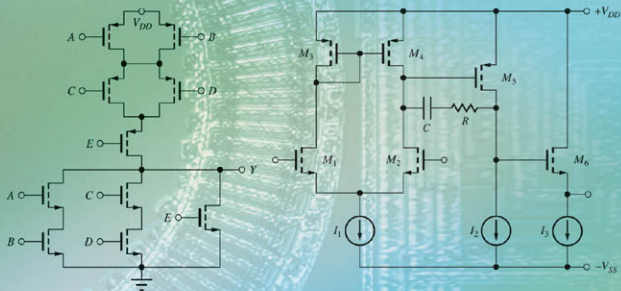
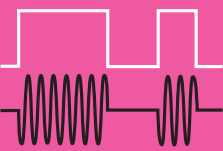


FOURTH EDITION

# MICROELECTRONIC Circuit Design



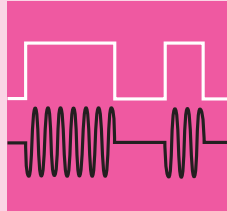
RICHARD C. JAEGER | TRAVIS N. BLALOCK



# MICROELECTRONIC CIRCUIT DESIGN

*This page intentionally left blank*

FOURTH EDITION



# MICROELECTRONIC CIRCUIT DESIGN

RICHARD C. JAEGER  
*Auburn University*

TRAVIS N. BLALOCK  
*University of Virginia*



## MICROELECTRONIC CIRCUIT DESIGN, FOURTH EDITION

Published by McGraw-Hill, a business unit of The McGraw-Hill Companies, Inc., 1221 Avenue of the Americas, New York, NY 10020. Copyright © 2011 by The McGraw-Hill Companies, Inc. All rights reserved. Previous editions © 2008, 2004, and 1997. No part of this publication may be reproduced or distributed in any form or by any means, or stored in a database or retrieval system, without the prior written consent of The McGraw-Hill Companies, Inc., including, but not limited to, in any network or other electronic storage or transmission, or broadcast for distance learning.

Some ancillaries, including electronic and print components, may not be available to customers outside the United States.

 This book is printed on recycled, acid-free paper containing 10% postconsumer waste.

1 2 3 4 5 6 7 8 9 0 WDQ/WDQ 1 0 9 8 7 6 5 4 3 2 1 0

ISBN 978-0-07-338045-2  
MHID 0-07-338045-8

Vice President & Editor-in-Chief: *Marty Lange*  
Vice President, EDP / Central Publishing Services: *Kimberly Meriwether-David*  
Global Publisher: *Raghothaman Srinivasan*  
Director of Development: *Kristine Tibbets*  
Developmental Editor: *Darlene M. Schueler*  
Senior Sponsoring Editor: *Peter E. Massar*  
Senior Marketing Manager: *Curt Reynolds*  
Senior Project Manager: *Jane Mohr*  
Senior Production Supervisor: *Kara Kudronowicz*  
Senior Media Project Manager: *Sandra M. Schnee*  
Design Coordinator: *Brenda A. Rolwes*  
Cover Designer: *Studio Montage, St. Louis, Missouri*  
Senior Photo Research Coordinator: *John C. Leland*  
Photo Research: *LouAnn K. Wilson*  
Compositor: *MPS Limited, A Macmillan Company*  
Typeface: *10/12 Times Roman*  
Printer: *Worldcolor*

All credits appearing on page or at the end of the book are considered to be an extension of the copyright page.

### Library of Congress Cataloging-in-Publication Data

Jaeger, Richard C.

Microelectronic circuit design / Richard C. Jaeger, Travis N. Blalock. — 4th ed.

p. cm.

ISBN 978-0-07-338045-2

1. Integrated circuits—Design and construction. 2. Semiconductors—Design and construction. 3. Electronic circuit design. I. Blalock, Travis N. II. Title.

TK7874.J333 2010

621.3815—dc22

2009049847

**TO**

**To Joan, my loving wife and partner**

**—Richard C. Jaeger**

**In memory of my father, Professor Theron Vaughn Blalock, an inspiration to me and to the countless students whom he mentored both in electronic design and in life.**

**—Travis N. Blalock**

# BRIEF CONTENTS

Preface xx

## PART ONE

### SOLID STATE ELECTRONICS AND DEVICES

- 1 Introduction to Electronics 3
- 2 Solid-State Electronics 42
- 3 Solid-State Diodes and Diode Circuits 74
- 4 Field-Effect Transistors 145
- 5 Bipolar Junction Transistors 217

## PART TWO

### DIGITAL ELECTRONICS

- 6 Introduction to Digital Electronics 287
- 7 Complementary MOS (CMOS) Logic Design 367
- 8 MOS Memory and Storage Circuits 416
- 9 Bipolar Logic Circuits 460

## PART THREE

### ANALOG ELECTRONICS

- 10 Analog Systems and Ideal Operational Amplifiers 529
- 11 Nonideal Operational Amplifiers and Feedback  
Amplifier Stability 600

- 12 Operational Amplifier Applications 697
- 13 Small-Signal Modeling and Linear Amplification 786
- 14 Single-Transistor Amplifiers 857
- 15 Differential Amplifiers and Operational Amplifier  
Design 968
- 16 Analog Integrated Circuit Design Techniques 1046
- 17 Amplifier Frequency Response 1128
- 18 Transistor Feedback Amplifiers and Oscillators 1228

## APPENDICES

- A Standard Discrete Component Values 1300
- B Solid-State Device Models and SPICE Simulation  
Parameters 1303
- C Two-Port Review 1310

Index 1313

# CONTENTS

Preface xx

## PART ONE SOLID STATE ELECTRONIC AND DEVICES 1

### CHAPTER 1 INTRODUCTION TO ELECTRONICS 3

- 1.1 A Brief History of Electronics:  
From Vacuum Tubes to Giga-Scale  
Integration 5
- 1.2 Classification of Electronic Signals 8
  - 1.2.1 Digital Signals 9
  - 1.2.2 Analog Signals 9
  - 1.2.3 A/D and D/A Converters—Bridging  
the Analog and Digital  
Domains 10
- 1.3 Notational Conventions 12
- 1.4 Problem-Solving Approach 13
- 1.5 Important Concepts from Circuit Theory 15
  - 1.5.1 Voltage and Current Division 15
  - 1.5.2 Thévenin and Norton Circuit  
Representations 16
- 1.6 Frequency Spectrum of Electronic  
Signals 21
- 1.7 Amplifiers 22
  - 1.7.1 Ideal Operational Amplifiers 23
  - 1.7.2 Amplifier Frequency Response 25
- 1.8 Element Variations in Circuit Design 26
  - 1.8.1 Mathematical Modeling of  
Tolerances 26
  - 1.8.2 Worst-Case Analysis 27
  - 1.8.3 Monte Carlo Analysis 29
  - 1.8.4 Temperature Coefficients 32
- 1.9 Numeric Precision 34
  - Summary 34
  - Key Terms 35
  - References 36
  - Additional Reading 36
  - Problems 37

### CHAPTER 2 SOLID-STATE ELECTRONICS 42

- 2.1 Solid-State Electronic Materials 44
- 2.2 Covalent Bond Model 45
- 2.3 Drift Currents and Mobility in  
Semiconductors 48
  - 2.3.1 Drift Currents 48
  - 2.3.2 Mobility 49
  - 2.3.3 Velocity Saturation 49
- 2.4 Resistivity of Intrinsic Silicon 50
- 2.5 Impurities in Semiconductors 51
  - 2.5.1 Donor Impurities in Silicon 52
  - 2.5.2 Acceptor Impurities in Silicon 52
- 2.6 Electron and Hole Concentrations in Doped  
Semiconductors 52
  - 2.6.1 *n*-Type Material ( $N_D > N_A$ ) 53
  - 2.6.2 *p*-Type Material ( $N_A > N_D$ ) 54
- 2.7 Mobility and Resistivity in Doped  
Semiconductors 55
- 2.8 Diffusion Currents 59
- 2.9 Total Current 60
- 2.10 Energy Band Model 61
  - 2.10.1 Electron–Hole Pair Generation in an  
Intrinsic Semiconductor 61
  - 2.10.2 Energy Band Model for a Doped  
Semiconductor 62
  - 2.10.3 Compensated Semiconductors 62
- 2.11 Overview of Integrated Circuit  
Fabrication 64
  - Summary 67
  - Key Terms 68
  - Reference 69
  - Additional Reading 69
  - Important Equations 69
  - Problems 70

### CHAPTER 3 SOLID-STATE DIODES AND DIODE CIRCUITS 74

- 3.1 The *pn* Junction Diode 75
  - 3.1.1 *pn* Junction Electrostatics 75
  - 3.1.2 Internal Diode Currents 79

3.2	The $i$ - $v$ Characteristics of the Diode 80	3.14	Full-Wave Rectifier Circuits 123
3.3	The Diode Equation: A Mathematical Model for the Diode 82	3.14.1	Full-Wave Rectifier with Negative Output Voltage 124
3.4	Diode Characteristics Under Reverse, Zero, and Forward Bias 85	3.15	Full-Wave Bridge Rectification 125
3.4.1	Reverse Bias 85	3.16	Rectifier Comparison and Design Tradeoffs 125
3.4.2	Zero Bias 85	3.17	Dynamic Switching Behavior of the Diode 129
3.4.3	Forward Bias 86	3.18	Photo Diodes, Solar Cells, and Light-Emitting Diodes 130
3.5	Diode Temperature Coefficient 89	3.18.1	Photo Diodes and Photodetectors 130
3.6	Diodes Under Reverse Bias 89	3.18.2	Power Generation from Solar Cells 131
3.6.1	Saturation Current in Real Diodes 90	3.18.3	Light-Emitting Diodes (LEDs) 132
3.6.2	Reverse Breakdown 91	<i>Summary</i>	133
3.6.3	Diode Model for the Breakdown Region 92	<i>Key Terms</i>	134
3.7	<i>pn</i> Junction Capacitance 92	<i>Reference</i>	135
3.7.1	Reverse Bias 92	<i>Additional Reading</i>	135
3.7.2	Forward Bias 93	<i>Problems</i>	135
3.8	Schottky Barrier Diode 93		
3.9	Diode SPICE Model and Layout 94		
3.10	Diode Circuit Analysis 96		
3.10.1	Load-Line Analysis 96	<b>CHAPTER 4</b>	
3.10.2	Analysis Using the Mathematical Model for the Diode 98	<b>FIELD-EFFECT TRANSISTORS</b> 145	
3.10.3	The Ideal Diode Model 102	4.1	Characteristics of the MOS Capacitor 146
3.10.4	Constant Voltage Drop Model 104	4.1.1	Accumulation Region 147
3.10.5	Model Comparison and Discussion 105	4.1.2	Depletion Region 148
3.11	Multiple-Diode Circuits 106	4.1.3	Inversion Region 148
3.12	Analysis of Diodes Operating in the Breakdown Region 109	4.2	The NMOS Transistor 148
3.12.1	Load-Line Analysis 109	4.2.1	Qualitative $i$ - $v$ Behavior of the NMOS Transistor 149
3.12.2	Analysis with the Piecewise Linear Model 109	4.2.2	Triode Region Characteristics of the NMOS Transistor 150
3.12.3	Voltage Regulation 110	4.2.3	On Resistance 153
3.12.4	Analysis Including Zener Resistance 111	4.2.4	Saturation of the $i$ - $v$ Characteristics 154
3.12.5	Line and Load Regulation 112	4.2.5	Mathematical Model in the Saturation (Pinch-Off) Region 155
3.13	Half-Wave Rectifier Circuits 113	4.2.6	Transconductance 157
3.13.1	Half-Wave Rectifier with Resistor Load 113	4.2.7	Channel-Length Modulation 157
3.13.2	Rectifier Filter Capacitor 114	4.2.8	Transfer Characteristics and Depletion-Mode MOSFETs 158
3.13.3	Half-Wave Rectifier with $RC$ Load 115	4.2.9	Body Effect or Substrate Sensitivity 159
3.13.4	Ripple Voltage and Conduction Interval 116	4.3	PMOS Transistors 161
3.13.5	Diode Current 118	4.4	MOSFET Circuit Symbols 163
3.13.6	Surge Current 120	4.5	Capacitances in MOS Transistors 165
3.13.7	Peak-Inverse-Voltage (PIV) Rating 120	4.5.1	NMOS Transistor Capacitances in the Triode Region 165
3.13.8	Diode Power Dissipation 120	4.5.2	Capacitances in the Saturation Region 166
3.13.9	Half-Wave Rectifier with Negative Output Voltage 121	4.5.3	Capacitances in Cutoff 166
		4.6	MOSFET Modeling in SPICE 167

4.7	MOS Transistor Scaling 169	5.3	The <i>pnp</i> Transistor 225
4.7.1	Drain Current 169	5.4	Equivalent Circuit Representations for the Transport Models 227
4.7.2	Gate Capacitance 169	5.5	The <i>i-v</i> Characteristics of the Bipolar Transistor 228
4.7.3	Circuit and Power Densities 170	5.5.1	Output Characteristics 228
4.7.4	Power-Delay Product 170	5.5.2	Transfer Characteristics 229
4.7.5	Cutoff Frequency 171	5.6	The Operating Regions of the Bipolar Transistor 230
4.7.6	High Field Limitations 171	5.7	Transport Model Simplifications 231
4.7.7	Subthreshold Conduction 172	5.7.1	Simplified Model for the Cutoff Region 231
4.8	MOS Transistor Fabrication and Layout Design Rules 172	5.7.2	Model Simplifications for the Forward-Active Region 233
4.8.1	Minimum Feature Size and Alignment Tolerance 173	5.7.3	Diodes in Bipolar Integrated Circuits 239
4.8.2	MOS Transistor Layout 173	5.7.4	Simplified Model for the Reverse-Active Region 240
4.9	Biasing the NMOS Field-Effect Transistor 176	5.7.5	Modeling Operation in the Saturation Region 242
4.9.1	Why Do We Need Bias? 176	5.8	Nonideal Behavior of the Bipolar Transistor 245
4.9.2	Constant Gate-Source Voltage Bias 178	5.8.1	Junction Breakdown Voltages 246
4.9.3	Load Line Analysis for the Q-Point 181	5.8.2	Minority-Carrier Transport in the Base Region 246
4.9.4	Four-Resistor Biasing 182	5.8.3	Base Transit Time 247
4.10	Biasing the PMOS Field-Effect Transistor 188	5.8.4	Diffusion Capacitance 249
4.11	The Junction Field-Effect Transistor (JFET) 190	5.8.5	Frequency Dependence of the Common-Emitter Current Gain 250
4.11.1	The JFET with Bias Applied 191	5.8.6	The Early Effect and Early Voltage 250
4.11.2	JFET Channel with Drain-Source Bias 191	5.8.7	Modeling the Early Effect 251
4.11.3	<i>n</i> -Channel JFET <i>i-v</i> Characteristics 193	5.8.8	Origin of the Early Effect 251
4.11.4	The <i>p</i> -Channel JFET 195	5.9	Transconductance 252
4.11.5	Circuit Symbols and JFET Model Summary 195	5.10	Bipolar Technology and SPICE Model 253
4.11.6	JFET Capacitances 196	5.10.1	Qualitative Description 253
4.12	JFET Modeling in SPICE 197	5.10.2	SPICE Model Equations 254
4.13	Biassing the JFET and Depletion-Mode MOSFET 198	5.10.3	High-Performance Bipolar Transistors 255
	<i>Summary</i> 200	5.11	Practical Bias Circuits for the BJT 256
	<i>Key Terms</i> 202	5.11.1	Four-Resistor Bias Network 258
	<i>References</i> 203	5.11.2	Design Objectives for the Four-Resistor Bias Network 260
	<i>Problems</i> 204	5.11.3	Iterative Analysis of the Four-Resistor Bias Circuit 266
<b>CHAPTER 5</b>			
<b>BIPOLAR JUNCTION TRANSISTORS 217</b>			
5.1	Physical Structure of the Bipolar Transistor 218	5.12	Tolerances in Bias Circuits 266
5.2	The Transport Model for the <i>npn</i> Transistor 219	5.12.1	Worst-Case Analysis 267
5.2.1	Forward Characteristics 220	5.12.2	Monte Carlo Analysis 269
5.2.2	Reverse Characteristics 222		<i>Summary</i> 272
5.2.3	The Complete Transport Model Equations for Arbitrary Bias Conditions 223		<i>Key Terms</i> 274
			<i>References</i> 274
			<i>Problems</i> 275

## PART TWO

# DIGITAL ELECTRONICS 285

### CHAPTER 6

#### INTRODUCTION TO DIGITAL ELECTRONICS 287

- 6.1 Ideal Logic Gates 289
- 6.2 Logic Level Definitions and Noise Margins 289
  - 6.2.1 Logic Voltage Levels 291
  - 6.2.2 Noise Margins 291
  - 6.2.3 Logic Gate Design Goals 292
- 6.3 Dynamic Response of Logic Gates 293
  - 6.3.1 Rise Time and Fall Time 293
  - 6.3.2 Propagation Delay 294
  - 6.3.3 Power-Delay Product 294
- 6.4 Review of Boolean Algebra 295
- 6.5 NMOS Logic Design 297
  - 6.5.1 NMOS Inverter with Resistive Load 298
  - 6.5.2 Design of the  $W/L$  Ratio of  $M_S$  299
  - 6.5.3 Load Resistor Design 300
  - 6.5.4 Load-Line Visualization 300
  - 6.5.5 On-Resistance of the Switching Device 302
  - 6.5.6 Noise Margin Analysis 303
  - 6.5.7 Calculation of  $V_{IL}$  and  $V_{OH}$  303
  - 6.5.8 Calculation of  $V_{IH}$  and  $V_{OL}$  304
  - 6.5.9 Load Resistor Problems 305
- 6.6 Transistor Alternatives to the Load Resistor 306
  - 6.6.1 The NMOS Saturated Load Inverter 307
  - 6.6.2 NMOS Inverter with a Linear Load Device 315
  - 6.6.3 NMOS Inverter with a Depletion-Mode Load 316
  - 6.6.4 Static Design of the Pseudo NMOS Inverter 319
- 6.7 NMOS Inverter Summary and Comparison 323
- 6.8 NMOS NAND and NOR Gates 324
  - 6.8.1 NOR Gates 325
  - 6.8.2 NAND Gates 326
  - 6.8.3 NOR and NAND Gate Layouts in NMOS Depletion-Mode Technology 327
- 6.9 Complex NMOS Logic Design 328
- 6.10 Power Dissipation 333
  - 6.10.1 Static Power Dissipation 333
  - 6.10.2 Dynamic Power Dissipation 334
  - 6.10.3 Power Scaling in MOS Logic Gates 335
- 6.11 Dynamic Behavior of MOS Logic Gates 337

- 6.11.1 Capacitances in Logic Circuits 337
- 6.11.2 Dynamic Response of the NMOS Inverter with a Resistive Load 338
- 6.11.3 Pseudo NMOS Inverter 343
- 6.11.4 A Final Comparison of NMOS Inverter Delays 344
- 6.11.5 Scaling Based Upon Reference Circuit Simulation 346
- 6.11.6 Ring Oscillator Measurement of Intrinsic Gate Delay 346
- 6.11.7 Unloaded Inverter Delay 347
- 6.12 PMOS Logic 349
  - 6.12.1 PMOS Inverters 349
  - 6.12.2 NOR and NAND Gates 352
  - Summary* 352
  - Key Terms* 354
  - References* 355
  - Additional Reading* 355
  - Problems* 355

### CHAPTER 7

#### COMPLEMENTARY MOS (CMOS) LOGIC DESIGN 367

- 7.1 CMOS Inverter Technology 368
  - 7.1.1 CMOS Inverter Layout 370
- 7.2 Static Characteristics of the CMOS Inverter 370
  - 7.2.1 CMOS Voltage Transfer Characteristics 371
  - 7.2.2 Noise Margins for the CMOS Inverter 373
- 7.3 Dynamic Behavior of the CMOS Inverter 375
  - 7.3.1 Propagation Delay Estimate 375
  - 7.3.2 Rise and Fall Times 377
  - 7.3.3 Performance Scaling 377
  - 7.3.4 Delay of Cascaded Inverters 379
- 7.4 Power Dissipation and Power Delay Product in CMOS 380
  - 7.4.1 Static Power Dissipation 380
  - 7.4.2 Dynamic Power Dissipation 381
  - 7.4.3 Power-Delay Product 382
- 7.5 CMOS NOR and NAND Gates 384
  - 7.5.1 CMOS NOR Gate 384
  - 7.5.2 CMOS NAND Gates 387
- 7.6 Design of Complex Gates in CMOS 388
- 7.7 Minimum Size Gate Design and Performance 393
- 7.8 Dynamic Domino CMOS Logic 395
- 7.9 Cascade Buffers 397
  - 7.9.1 Cascade Buffer Delay Model 397
  - 7.9.2 Optimum Number of Stages 398
- 7.10 The CMOS Transmission Gate 400
- 7.11 CMOS Latchup 401

*Summary* 404  
*Key Terms* 405  
*References* 406  
*Problems* 406

## CHAPTER 8

### MOS MEMORY AND STORAGE CIRCUITS 416

- 8.1 Random Access Memory 417
  - 8.1.1 Random Access Memory (RAM) Architecture 417
  - 8.1.2 A 256-Mb Memory Chip 418
- 8.2 Static Memory Cells 419
  - 8.2.1 Memory Cell Isolation and Access—The 6-T Cell 422
  - 8.2.2 The Read Operation 422
  - 8.2.3 Writing Data into the 6-T Cell 426
- 8.3 Dynamic Memory Cells 428
  - 8.3.1 The One-Transistor Cell 430
  - 8.3.2 Data Storage in the 1-T Cell 430
  - 8.3.3 Reading Data from the 1-T Cell 431
  - 8.3.4 The Four-Transistor Cell 433
- 8.4 Sense Amplifiers 434
  - 8.4.1 A Sense Amplifier for the 6-T Cell 434
  - 8.4.2 A Sense Amplifier for the 1-T Cell 436
  - 8.4.3 The Boosted Wordline Circuit 438
  - 8.4.4 Clocked CMOS Sense Amplifiers 438
- 8.5 Address Decoders 440
  - 8.5.1 NOR Decoder 440
  - 8.5.2 NAND Decoder 440
  - 8.5.3 Decoders in Domino CMOS Logic 443
  - 8.5.4 Pass-Transistor Column Decoder 443
- 8.6 Read-Only Memory (ROM) 444
- 8.7 Flip-Flops 447
  - 8.7.1 RS Flip-Flop 449
  - 8.7.2 The D-Latch Using Transmission Gates 450
  - 8.7.3 A Master-Slave D Flip-Flop 450
  - Summary* 451
  - Key Terms* 452
  - References* 452
  - Problems* 453

## CHAPTER 9

### BIPOLAR LOGIC CIRCUITS 460

- 9.1 The Current Switch (Emitter-Coupled Pair) 461
  - 9.1.1 Mathematical Model for Static Behavior of the Current Switch 462

- 9.1.2 Current Switch Analysis for  $v_I > V_{REF}$  463
- 9.1.3 Current Switch Analysis for  $v_I < V_{REF}$  464
- 9.2 The Emitter-Coupled Logic (ECL) Gate 464
  - 9.2.1 ECL Gate with  $v_I = V_H$  465
  - 9.2.2 ECL Gate with  $v_I = V_L$  466
  - 9.2.3 Input Current of the ECL Gate 466
  - 9.2.4 ECL Summary 466
- 9.3 Noise Margin Analysis for the ECL Gate 467
  - 9.3.1  $V_{IL}, V_{OH}, V_{IH}$ , and  $V_{OL}$  467
  - 9.3.2 Noise Margins 468
- 9.4 Current Source Implementation 469
- 9.5 The ECL OR-NOR Gate 471
- 9.6 The Emitter Follower 473
  - 9.6.1 Emitter Follower with a Load Resistor 474
- 9.7 “Emitter Dotting” or “Wired-OR” Logic 476
  - 9.7.1 Parallel Connection of Emitter-Follower Outputs 477
  - 9.7.2 The Wired-OR Logic Function 477
- 9.8 ECL Power-Delay Characteristics 477
  - 9.8.1 Power Dissipation 477
  - 9.8.2 Gate Delay 479
  - 9.8.3 Power-Delay Product 480
- 9.9 Current Mode Logic 481
  - 9.9.1 CML Logic Gates 481
  - 9.9.2 CML Logic Levels 482
  - 9.9.3  $V_{EE}$  Supply Voltage 482
  - 9.9.4 Higher-Level CML 483
  - 9.9.5 CML Power Reduction 484
  - 9.9.6 NMOS CML 485
- 9.10 The Saturating Bipolar Inverter 487
  - 9.10.1 Static Inverter Characteristics 488
  - 9.10.2 Saturation Voltage of the Bipolar Transistor 488
  - 9.10.3 Load-Line Visualization 491
  - 9.10.4 Switching Characteristics of the Saturated BJT 491
- 9.11 A Transistor-Transistor Logic (TTL) Prototype 494
  - 9.11.1 TTL Inverter for  $v_I = V_L$  494
  - 9.11.2 TTL Inverter for  $v_I = V_H$  495
  - 9.11.3 Power in the Prototype TTL Gate 496
  - 9.11.4  $V_{IH}, V_{IL}$ , and Noise Margins for the TTL Prototype 496
  - 9.11.5 Prototype Inverter Summary 498
  - 9.11.6 Fanout Limitations of the TTL Prototype 498
- 9.12 The Standard 7400 Series TTL Inverter 500
  - 9.12.1 Analysis for  $v_I = V_L$  500
  - 9.12.2 Analysis for  $v_I = V_H$  501

9.12.3	Power Consumption 503	10.9	Analysis of Circuits Containing Ideal Operational Amplifiers 552
9.12.4	TTL Propagation Delay and Power-Delay Product 503	10.9.1	The Inverting Amplifier 553
9.12.5	TTL Voltage Transfer Characteristic and Noise Margins 503	10.9.2	The Transresistance Amplifier—A Current-to-Voltage Converter 556
9.12.6	Fanout Limitations of Standard TTL 504	10.9.3	The Noninverting Amplifier 558
9.13	Logic Functions in TTL 504	10.9.4	The Unity-Gain Buffer, or Voltage Follower 561
9.13.1	Multi-Emitter Input Transistors 505	10.9.5	The Summing Amplifier 563
9.13.2	TTL NAND Gates 505	10.9.6	The Difference Amplifier 565
9.13.3	Input Clamping Diodes 506	10.10	Frequency-Dependent Feedback 568
9.14	Schottky-Clamped TTL 506	10.10.1	Bode Plots 568
9.15	Comparison of the Power-Delay Products of ECL and TTL 508	10.10.2	The Low-Pass Amplifier 568
9.16	BiCMOS Logic 508	10.10.3	The High-Pass Amplifier 572
9.16.1	BiCMOS Buffers 509	10.10.4	Band-Pass Amplifiers 575
9.16.2	BiNMOS Inverters 511	10.10.5	An Active Low-Pass Filter 578
9.16.3	BiCMOS Logic Gates 513	10.10.6	An Active High-Pass Filter 581
	<i>Summary</i> 513	10.10.7	The Integrator 582
	<i>Key Terms</i> 515	10.10.8	The Differentiator 586
	<i>References</i> 515		<i>Summary</i> 586
	<i>Additional Reading</i> 515		<i>Key Terms</i> 588
	<i>Problems</i> 516		<i>References</i> 588
			<i>Additional Reading</i> 589
			<i>Problems</i> 589

## PART THREE ANALOG ELECTRONICS 527

<b>CHAPTER 10</b>	
<b>ANALOG SYSTEMS AND IDEAL OPERATIONAL AMPLIFIERS 529</b>	
10.1	An Example of an Analog Electronic System 530
10.2	Amplification 531
10.2.1	Voltage Gain 532
10.2.2	Current Gain 533
10.2.3	Power Gain 533
10.2.4	The Decibel Scale 534
10.3	Two-Port Models for Amplifiers 537
10.3.1	The $g$ -parameters 537
10.4	Mismatched Source and Load Resistances 541
10.5	Introduction to Operational Amplifiers 544
10.5.1	The Differential Amplifier 544
10.5.2	Differential Amplifier Voltage Transfer Characteristic 545
10.5.3	Voltage Gain 545
10.6	Distortion in Amplifiers 548
10.7	Differential Amplifier Model 549
10.8	Ideal Differential and Operational Amplifiers 551
10.8.1	Assumptions for Ideal Operational Amplifier Analysis 551

## CHAPTER 11 NONIDEAL OPERATIONAL AMPLIFIERS AND FEEDBACK AMPLIFIER STABILITY 600

11.1	Classic Feedback Systems 601
11.1.1	Closed-Loop Gain Analysis 602
11.1.2	Gain Error 602
11.2	Analysis of Circuits Containing Nonideal Operational Amplifiers 603
11.2.1	Finite Open-Loop Gain 603
11.2.2	Nonzero Output Resistance 606
11.2.3	Finite Input Resistance 610
11.2.4	Summary of Nonideal Inverting and Noninverting Amplifiers 614
11.3	Series and Shunt Feedback Circuits 615
11.3.1	Feedback Amplifier Categories 615
11.3.2	Voltage Amplifiers—Series-Shunt Feedback 616
11.3.3	Transimpedance Amplifiers—Shunt-Shunt Feedback 616
11.3.4	Current Amplifiers—Shunt-Series Feedback 616
11.3.5	Transconductance Amplifiers—Series-Series Feedback 616
11.4	Unified Approach to Feedback Amplifier Gain Calculation 616

11.4.1	Closed-Loop Gain Analysis 617	11.12.5	An Alternate Interpretation of CMRR 657
11.4.2	Resistance Calculation Using Blackman's Theorem 617	11.12.6	Power Supply Rejection Ratio 657
11.5	Series-Shunt Feedback—Voltage Amplifiers 617	11.13	Frequency Response and Bandwidth of Operational Amplifiers 659
11.5.1	Closed-Loop Gain Calculation 618	11.13.1	Frequency Response of the Noninverting Amplifier 661
11.5.2	Input Resistance Calculation 618	11.13.2	Inverting Amplifier Frequency Response 664
11.5.3	Output Resistance Calculation 619	11.13.3	Using Feedback to Control Frequency Response 666
11.5.4	Series-Shunt Feedback Amplifier Summary 620	11.13.4	Large-Signal Limitations—Slew Rate and Full-Power Bandwidth 668
11.6	Shunt-Shunt Feedback—Transresistance Amplifiers 624	11.13.5	Macro Model for Operational Amplifier Frequency Response 669
11.6.1	Closed-Loop Gain Calculation 625	11.13.6	Complete Op Amp Macro Models in SPICE 670
11.6.2	Input Resistance Calculation 625	11.13.7	Examples of Commercial General-Purpose Operational Amplifiers 670
11.6.3	Output Resistance Calculation 625	11.14	Stability of Feedback Amplifiers 671
11.6.4	Shunt-Shunt Feedback Amplifier Summary 626	11.14.1	The Nyquist Plot 671
11.7	Series-Series Feedback—Transconductance Amplifiers 629	11.14.2	First-Order Systems 672
11.7.1	Closed-Loop Gain Calculation 630	11.14.3	Second-Order Systems and Phase Margin 673
11.7.2	Input Resistance Calculation 630	11.14.4	Step Response and Phase Margin 674
11.7.3	Output Resistance Calculation 631	11.14.5	Third-Order Systems and Gain Margin 677
11.7.4	Series-Series Feedback Amplifier Summary 631	11.14.6	Determining Stability from the Bode Plot 678
11.8	Shunt-Series Feedback—Current Amplifiers 633		<i>Summary</i> 682
11.8.1	Closed-Loop Gain Calculation 634		<i>Key Terms</i> 684
11.8.2	Input Resistance Calculation 635		<i>References</i> 684
11.8.3	Output Resistance Calculation 635		<i>Problems</i> 685
11.8.4	Series-Series Feedback Amplifier Summary 635		
11.9	Finding the Loop Gain Using Successive Voltage and Current Injection 638		
11.9.1	Simplifications 641		
11.10	Distortion Reduction Through the Use of Feedback 641		
11.11	DC Error Sources and Output Range Limitations 642		
11.11.1	Input-Offset Voltage 643	12.1	Cascaded Amplifiers 698
11.11.2	Offset-Voltage Adjustment 644	12.1.1	Two-Port Representations 698
11.11.3	Input-Bias and Offset Currents 645	12.1.2	Amplifier Terminology Review 700
11.11.4	Output Voltage and Current Limits 647	12.1.3	Frequency Response of Cascaded Amplifiers 703
11.12	Common-Mode Rejection and Input Resistance 650	12.2	The Instrumentation Amplifier 711
11.12.1	Finite Common-Mode Rejection Ratio 650	12.3	Active Filters 714
11.12.2	Why Is CMRR Important? 651	12.3.1	Low-Pass Filter 714
11.12.3	Voltage-Follower Gain Error Due to CMRR 654	12.3.2	A High-Pass Filter with Gain 718
11.12.4	Common-Mode Input Resistance 656	12.3.3	Band-Pass Filter 720
		12.3.4	The Tow-Thomas Biquad 722
		12.3.5	Sensitivity 726
		12.3.6	Magnitude and Frequency Scaling 727

## CHAPTER 12 OPERATIONAL AMPLIFIER APPLICATIONS 697

12.1	Cascaded Amplifiers 698
12.1.1	Two-Port Representations 698
12.1.2	Amplifier Terminology Review 700
12.1.3	Frequency Response of Cascaded Amplifiers 703
12.2	The Instrumentation Amplifier 711
12.3	Active Filters 714
12.3.1	Low-Pass Filter 714
12.3.2	A High-Pass Filter with Gain 718
12.3.3	Band-Pass Filter 720
12.3.4	The Tow-Thomas Biquad 722
12.3.5	Sensitivity 726
12.3.6	Magnitude and Frequency Scaling 727

12.4	Switched-Capacitor Circuits 728	13.5	Small-Signal Models for Bipolar Junction Transistors 799
12.4.1	A Switched-Capacitor Integrator 728	13.5.1	The Hybrid-Pi Model 801
12.4.2	Noninverting SC Integrator 730	13.5.2	Graphical Interpretation of the Transconductance 802
12.4.3	Switched-Capacitor Filters 732	13.5.3	Small-Signal Current Gain 802
12.5	Digital-to-Analog Conversion 733	13.5.4	The Intrinsic Voltage Gain of the BJT 803
12.5.1	D/A Converter Fundamentals 733	13.5.5	Equivalent Forms of the Small-Signal Model 804
12.5.2	D/A Converter Errors 734	13.5.6	Simplified Hybrid Pi Model 805
12.5.3	Digital-to-Analog Converter Circuits 737	13.5.7	Definition of a Small Signal for the Bipolar Transistor 805
12.6	Analog-to-Digital Conversion 740	13.5.8	Small-Signal Model for the <i>pnp</i> Transistor 807
12.6.1	A/D Converter Fundamentals 741	13.5.9	ac Analysis Versus Transient Analysis in SPICE 807
12.6.2	Analog-to-Digital Converter Errors 742	13.6	The Common-Emitter (C-E) Amplifier 808
12.6.3	Basic A/D Conversion Techniques 743	13.6.1	Terminal Voltage Gain 809
12.7	Oscillators 754	13.6.2	Input Resistance 809
12.7.1	The Barkhausen Criteria for Oscillation 754	13.6.3	Signal Source Voltage Gain 810
12.7.2	Oscillators Employing Frequency-Selective RC Networks 755	13.7	Important Limits and Model Simplifications 810
12.8	Nonlinear Circuit Applications 760	13.7.1	A Design Guide for the Common-Emitter Amplifier 810
12.8.1	A Precision Half-Wave Rectifier 760	13.7.2	Upper Bound on the Common-Emitter Gain 812
12.8.2	Nonsaturating Precision-Rectifier Circuit 761	13.7.3	Small-Signal Limit for the Common-emitter Amplifier 812
12.9	Circuits Using Positive Feedback 763	13.8	Small-Signal Models for Field-Effect Transistors 815
12.9.1	The Comparator and Schmitt Trigger 763	13.8.1	Small-Signal Model for the MOSFET 815
12.9.2	The Astable Multivibrator 765	13.8.2	Intrinsic Voltage Gain of the MOSFET 817
12.9.3	The Monostable Multivibrator or One Shot 766	13.8.3	Definition of Small-Signal Operation for the MOSFET 817
	<i>Summary</i> 770	13.8.4	Body Effect in the Four-Terminal MOSFET 818
	<i>Key Terms</i> 772	13.8.5	Small-Signal Model for the PMOS Transistor 819
	<i>Additional Reading</i> 773	13.8.6	Small-Signal Model for the Junction Field-Effect Transistor 820
	<i>Problems</i> 773	13.9	Summary and Comparison of the Small-Signal Models of the BJT and FET 821
<b>CHAPTER 13</b>			
<b>SMALL-SIGNAL MODELING AND LINEAR AMPLIFICATION 786</b>			
13.1	The Transistor as an Amplifier 787	13.10	The Common-Source Amplifier 824
13.1.1	The BJT Amplifier 788	13.10.1	Common-Source Terminal Voltage Gain 825
13.1.2	The MOSFET Amplifier 789	13.10.2	Signal Source Voltage Gain for the Common-Source Amplifier 825
13.2	Coupling and Bypass Capacitors 790	13.10.3	A Design Guide for the Common-Source Amplifier 826
13.3	Circuit Analysis Using dc and ac Equivalent Circuits 792	13.10.4	Small-Signal Limit for the Common-Source Amplifier 827
13.3.1	Menu for dc and ac Analysis 792		
13.4	Introduction to Small-Signal Modeling 796		
13.4.1	Graphical Interpretation of the Small-Signal Behavior of the Diode 796		
13.4.2	Small-Signal Modeling of the Diode 797		

13.10.5 Input Resistances of the Common-Emitter and Common-Source Amplifiers 829 13.10.6 Common-Emitter and Common-Source Output Resistances 832 13.10.7 Comparison of the Three Amplifier Resistances 838  13.11 Common-Emitter and Common-Source Amplifier Summary 838 13.11.1 Guidelines for Neglecting the Transistor Output Resistance 839  13.12 Amplifier Power and Signal Range 839 13.12.1 Power Dissipation 839 13.12.2 Signal Range 840 <i>Summary</i> 843 <i>Key Terms</i> 844 <i>Problems</i> 845	14.3 Follower Circuits—Common-Collector and Common-Drain Amplifiers 886 14.3.1 Terminal Voltage Gain 886 14.3.2 Input Resistance 887 14.3.3 Signal Source Voltage Gain 888 14.3.4 Follower Signal Range 888 14.3.5 Follower Output Resistance 889 14.3.6 Current Gain 890 14.3.7 C-C/C-D Amplifier Summary 890  14.4 Noninverting Amplifiers—Common-Base and Common-Gate Circuits 894 14.4.1 Terminal Voltage Gain and Input Resistance 895 14.4.2 Signal Source Voltage Gain 896 14.4.3 Input Signal Range 897 14.4.4 Resistance at the Collector and Drain Terminals 897 14.4.5 Current Gain 898 14.4.6 Overall Input and Output Resistances for the Noninverting Amplifiers 899 14.4.7 C-B/C-G Amplifier Summary 902  14.5 Amplifier Prototype Review and Comparison 903 14.5.1 The BJT Amplifiers 903 14.5.2 The FET Amplifiers 905  14.6 Common-Source Amplifiers Using MOS Inverters 907 14.6.1 Voltage Gain Estimate 908 14.6.2 Detailed Analysis 909 14.6.3 Alternative Loads 910 14.6.4 Input and Output Resistances 911  14.7 Coupling and Bypass Capacitor Design 914 14.7.1 Common-Emitter and Common-Source Amplifiers 914 14.7.2 Common-Collector and Common-Drain Amplifiers 919 14.7.3 Common-Base and Common-Gate Amplifiers 921 14.7.4 Setting Lower Cutoff Frequency $f_L$ 924  14.8 Amplifier Design Examples 925 14.8.1 Monte Carlo Evaluation of the Common-Base Amplifier Design 934  14.9 Multistage ac-Coupled Amplifiers 939 14.9.1 A Three-Stage ac-Coupled Amplifier 939 14.9.2 Voltage Gain 941 14.9.3 Input Resistance 943 14.9.4 Signal Source Voltage Gain 943 14.9.5 Output Resistance 943 14.9.6 Current and Power Gain 944
--	--

## CHAPTER 14

### SINGLE-TRANSISTOR AMPLIFIERS 857

14.1 Amplifier Classification 858 14.1.1 Signal Injection and Extraction—The BJT 858 14.1.2 Signal Injection and Extraction—The FET 859 14.1.3 Common-Emitter (C-E) and Common-Source (C-S) Amplifiers 860 14.1.4 Common-Collector (C-C) and Common-Drain (C-D) Topologies 861 14.1.5 Common-Base (C-B) and Common-Gate (C-G) Amplifiers 863 14.1.6 Small-Signal Model Review 864  14.2 Inverting Amplifiers—Common-Emitter and Common-Source Circuits 864 14.2.1 The Common-Emitter (C-E) Amplifier 864 14.2.2 Common-Emitter Example Comparison 877 14.2.3 The Common-Source Amplifier 877 14.2.4 Small-Signal Limit for the Common-Source Amplifier 880 14.2.5 Common-Emitter and Common-Source Amplifier Characteristics 884 14.2.6 C-E/C-S Amplifier Summary 885 14.2.7 Equivalent Transistor Representation of the Generalized C-E/C-S Transistor 885
--

14.9.7	Input Signal Range 945	
14.9.8	Estimating the Lower Cutoff Frequency of the Multistage Amplifier 948	
<i>Summary</i>	950	
<i>Key Terms</i>	951	
<i>Additional Reading</i>	952	
<i>Problems</i>	952	
<b>CHAPTER 15</b>		
<b>DIFFERENTIAL AMPLIFIERS AND OPERATIONAL AMPLIFIER DESIGN</b>		968
15.1	Differential Amplifiers 969	
15.1.1	Bipolar and MOS Differential Amplifiers 969	
15.1.2	dc Analysis of the Bipolar Differential Amplifier 970	
15.1.3	Transfer Characteristic for the Bipolar Differential Amplifier 972	
15.1.4	ac Analysis of the Bipolar Differential Amplifier 973	
15.1.5	Differential-Mode Gain and Input and Output Resistances 974	
15.1.6	Common-Mode Gain and Input Resistance 976	
15.1.7	Common-Mode Rejection Ratio (CMRR) 978	
15.1.8	Analysis Using Differential- and Common-Mode Half-Circuits 979	
15.1.9	Biasing with Electronic Current Sources 982	
15.1.10	Modeling the Electronic Current Source in SPICE 983	
15.1.11	dc Analysis of the MOSFET Differential Amplifier 983	
15.1.12	Differential-Mode Input Signals 985	
15.1.13	Small-Signal Transfer Characteristic for the MOS Differential Amplifier 986	
15.1.14	Common-Mode Input Signals 986	
15.1.15	Two-Port Model for Differential Pairs 987	
15.2	Evolution to Basic Operational Amplifiers 991	
15.2.1	A Two-Stage Prototype for an Operational Amplifier 992	
15.2.2	Improving the Op Amp Voltage Gain 997	
15.2.3	Output Resistance Reduction 998	
15.2.4	A CMOS Operational Amplifier Prototype 1002	
15.2.5	BiCMOS Amplifiers 1004	
15.2.6	All Transistor Implementations 1004	
15.3	Output Stages 1006	
15.3.1	The Source Follower—A Class-A Output Stage 1006	
15.3.2	Efficiency of Class-A Amplifiers 1007	
15.3.3	Class-B Push-Pull Output Stage 1008	
15.3.4	Class-AB Amplifiers 1010	
15.3.5	Class-AB Output Stages for Operational Amplifiers 1011	
15.3.6	Short-Circuit Protection 1011	
15.3.7	Transformer Coupling 1013	
15.4	Electronic Current Sources 1016	
15.4.1	Single-Transistor Current Sources 1017	
15.4.2	Figure of Merit for Current Sources 1017	
15.4.3	Higher Output Resistance Sources 1018	
15.4.4	Current Source Design Examples 1018	
	<i>Summary</i> 1027	
	<i>Key Terms</i> 1028	
	<i>References</i> 1029	
	<i>Additional Reading</i> 1029	
	<i>Problems</i> 1029	
<b>CHAPTER 16</b>		
<b>ANALOG INTEGRATED CIRCUIT DESIGN TECHNIQUES</b>		1046
16.1	Circuit Element Matching 1047	
16.2	Current Mirrors 1049	
16.2.1	dc Analysis of the MOS Transistor Current Mirror 1049	
16.2.2	Changing the MOS Mirror Ratio 1051	
16.2.3	dc Analysis of the Bipolar Transistor Current Mirror 1052	
16.2.4	Altering the BJT Current Mirror Ratio 1054	
16.2.5	Multiple Current Sources 1055	
16.2.6	Buffered Current Mirror 1056	
16.2.7	Output Resistance of the Current Mirrors 1057	
16.2.8	Two-Port Model for the Current Mirror 1058	
16.2.9	The Widlar Current Source 1060	
16.2.10	The MOS Version of the Widlar Source 1063	

16.3	High-Output-Resistance Current Mirrors 1063
16.3.1	The Wilson Current Sources 1064
16.3.2	Output Resistance of the Wilson Source 1065
16.3.3	Cascode Current Sources 1066
16.3.4	Output Resistance of the Cascode Sources 1067
16.3.5	Regulated Cascode Current Source 1068
16.3.6	Current Mirror Summary 1069
16.4	Reference Current Generation 1072
16.5	Supply-Independent Biasing 1073
16.5.1	A $V_{BE}$ -Based Reference 1073
16.5.2	The Widlar Source 1073
16.5.3	Power-Supply-Independent Bias Cell 1074
16.5.4	A Supply-Independent MOS Reference Cell 1075
16.6	The Bandgap Reference 1077
16.7	The Current Mirror As an Active Load 1081
16.7.1	CMOS Differential Amplifier with Active Load 1081
16.7.2	Bipolar Differential Amplifier with Active Load 1088
16.8	Active Loads in Operational Amplifiers 1092
16.8.1	CMOS Op Amp Voltage Gain 1092
16.8.2	dc Design Considerations 1093
16.8.3	Bipolar Operational Amplifiers 1095
16.8.4	Input Stage Breakdown 1096
16.9	The $\mu$ A741 Operational Amplifier 1097
16.9.1	Overall Circuit Operation 1097
16.9.2	Bias Circuitry 1098
16.9.3	dc Analysis of the 741 Input Stage 1099
16.9.4	ac Analysis of the 741 Input Stage 1102
16.9.5	Voltage Gain of the Complete Amplifier 1103
16.9.6	The 741 Output Stage 1107
16.9.7	Output Resistance 1109
16.9.8	Short Circuit Protection 1109
16.9.9	Summary of the $\mu$ A741 Operational Amplifier Characteristics 1109
16.10	The Gilbert Analog Multiplier 1110
	<i>Summary</i> 1112
	<i>Key Terms</i> 1113
	<i>References</i> 1114
	<i>Problems</i> 1114

## CHAPTER 17

### AMPLIFIER FREQUENCY RESPONSE 1128

17.1	Amplifier Frequency Response 1129
17.1.1	Low-Frequency Response 1130
17.1.2	Estimating $\omega_L$ in the Absence of a Dominant Pole 1130
17.1.3	High-Frequency Response 1133
17.1.4	Estimating $\omega_H$ in the Absence of a Dominant Pole 1133
17.2	Direct Determination of the Low-Frequency Poles and Zeros—The Common-Source Amplifier 1134
17.3	Estimation of $\omega_L$ Using the Short-Circuit Time-Constant Method 1139
17.3.1	Estimate of $\omega_L$ for the Common-Emitter Amplifier 1140
17.3.2	Estimate of $\omega_L$ for the Common-Source Amplifier 1144
17.3.3	Estimate of $\omega_L$ for the Common-Base Amplifier 1145
17.3.4	Estimate of $\omega_L$ for the Common-Gate Amplifier 1146
17.3.5	Estimate of $\omega_L$ for the Common-Collector Amplifier 1147
17.3.6	Estimate of $\omega_L$ for the Common-Drain Amplifier 1147
17.4	Transistor Models at High Frequencies 1148
17.4.1	Frequency-Dependent Hybrid-Pi Model for the Bipolar Transistor 1148
17.4.2	Modeling $C_\pi$ and $C_\mu$ in SPICE 1149
17.4.3	Unity-Gain Frequency $f_T$ 1149
17.4.4	High-Frequency Model for the FET 1152
17.4.5	Modeling $C_{GS}$ and $C_{GD}$ in SPICE 1153
17.4.6	Channel Length Dependence of $f_T$ 1153
17.4.7	Limitations of the High-Frequency Models 1155
17.5	Base Resistance in the Hybrid-Pi Model 1155
17.5.1	Effect of Base Resistance on Midband Amplifiers 1156
17.6	High-Frequency Common-Emitter and Common-Source Amplifier Analysis 1158
17.6.1	The Miller Effect 1159
17.6.2	Common-Emitter and Common-Source Amplifier High-Frequency Response 1160
17.6.3	Direct Analysis of the Common-Emitter Transfer Characteristic 1162

17.6.4	Poles of the Common-Emitter Amplifier 1163	<i>Summary</i> 1213 <i>Key Terms</i> 1215 <i>Reference</i> 1215 <i>Problems</i> 1215
17.6.5	Dominant Pole for the Common-Source Amplifier 1166	
17.6.6	Estimation of $\omega_H$ Using the Open-Circuit Time-Constant Method 1167	
17.6.7	Common-Source Amplifier with Source Degeneration Resistance 1170	
17.6.8	Poles of the Common-Emitter with Emitter Degeneration Resistance 1172	
17.7	Common-Base and Common-Gate Amplifier High-Frequency Response 1174	
17.8	Common-Collector and Common-Drain Amplifier High-Frequency Response 1177	
17.9	Single-Stage Amplifier High-Frequency Response Summary 1179	
	17.9.1 Amplifier Gain-Bandwidth Limitations 1180	
17.10	Frequency Response of Multistage Amplifiers 1181	
	17.10.1 Differential Amplifier 1181	
	17.10.2 The Common-Collector/Common-Base Cascade 1182	
	17.10.3 High-Frequency Response of the Cascode Amplifier 1184	
	17.10.4 Cutoff Frequency for the Current Mirror 1185	
	17.10.5 Three-Stage Amplifier Example 1187	
17.11	Introduction to Radio Frequency Circuits 1193	
	17.11.1 Radio Frequency Amplifiers 1194	
	17.11.2 The Shunt-Peaked Amplifier 1194	
	17.11.3 Single-Tuned Amplifier 1197	
	17.11.4 Use of a Tapped Inductor—The Auto Transformer 1199	
	17.11.5 Multiple Tuned Circuits—Synchronous and Stagger Tuning 1201	
	17.11.6 Common-Source Amplifier with Inductive Degeneration 1202	
17.12	Mixers and Balanced Modulators 1205	
	17.12.1 Introduction to Mixer Operation 1205	
	17.12.2 A Single-Balanced Mixer 1206	
	17.12.3 The Differential Pair as a Single-Balanced Mixer 1207	
	17.12.4 A Double-Balanced Mixer 1208	
	17.12.5 The Gilbert Multiplier as a Double-Balanced Mixer/Modulator 1210	
		CHAPTER 18
		<b>TRANSISTOR FEEDBACK AMPLIFIERS AND OSCILLATORS 1228</b>
18.1	Basic Feedback System Review 1229	
	18.1.1 Closed-Loop Gain 1229	
	18.1.2 Closed-Loop Impedances 1230	
	18.1.3 Feedback Effects 1230	
18.2	Feedback Amplifier Analysis at Midband 1232	
18.3	Feedback Amplifier Circuit Examples 1234	
	18.3.1 Series-Shunt Feedback—Voltage Amplifiers 1234	
	18.3.2 Differential Input Series-Shunt Voltage Amplifier 1239	
	18.3.3 Shunt-Shunt Feedback—Transresistance Amplifiers 1242	
	18.3.4 Series-Series Feedback—Transconductance Amplifiers 1248	
	18.3.5 Shunt-Series Feedback—Current Amplifiers 1251	
18.4	Review of Feedback Amplifier Stability 1254	
	18.4.1 Closed-Loop Response of the Uncompensated Amplifier 1254	
	18.4.2 Phase Margin 1256	
	18.4.3 Higher-Order Effects 1259	
	18.4.4 Response of the Compensated Amplifier 1260	
	18.4.5 Small-Signal Limitations 1262	
18.5	Single-Pole Operational Amplifier Compensation 1262	
	18.5.1 Three-Stage Op Amp Analysis 1263	
	18.5.2 Transmission Zeros in FET Op Amps 1265	
	18.5.3 Bipolar Amplifier Compensation 1266	
	18.5.4 Slew Rate of the Operational Amplifier 1266	
	18.5.5 Relationships Between Slew Rate and Gain-Bandwidth Product 1268	
18.6	High-Frequency Oscillators 1277	
	18.6.1 The Colpitts Oscillator 1278	
	18.6.2 The Hartley Oscillator 1279	
	18.6.3 Amplitude Stabilization in LC Oscillators 1280	
	18.6.4 Negative Resistance in Oscillators 1280	

18.6.5 Negative  $G_M$  Oscillator 1281  
18.6.6 Crystal Oscillators 1283  
*Summary* 1287  
*Key Terms* 1289  
*References* 1289  
*Problems* 1289

## APPENDICES

A Standard Discrete Component Values 1300  
B Solid-State Device Models and SPICE  
    Simulation Parameters 1303  
C Two-Port Review 1310

Index 1313

# PREFACE

Through study of this text, the reader will develop a comprehensive understanding of the basic techniques of modern electronic circuit design, analog and digital, discrete and integrated. Even though most readers may not ultimately be engaged in the design of integrated circuits (ICs) themselves, a thorough understanding of the internal circuit structure of ICs is prerequisite to avoiding many pitfalls that prevent the effective and reliable application of integrated circuits in system design.

Digital electronics has evolved to be an extremely important area of circuit design, but it is included almost as an afterthought in many introductory electronics texts. We present a more balanced coverage of analog and digital circuits. The writing integrates the authors' extensive industrial backgrounds in precision analog and digital design with their many years of experience in the classroom. A broad spectrum of topics is included, and material can easily be selected to satisfy either a two-semester or three-quarter sequence in electronics.

## IN THIS EDITION

This edition continues to update the material to achieve improved readability and accessibility to the student. In addition to general material updates, a number of specific changes have been included in Parts I and II, Solid-State Electronics and Devices and Digital Electronics, respectively. A new closed-form solution to four-resistor MOSFET biasing is introduced as well as an improved iterative strategy for diode Q-point analysis. JFET devices are important in analog design and have been reintroduced at the end of Chapter 4. Simulation-based logic gate scaling is introduced in the MOS logic chapters, and an enhanced discussion of noise margin is included as a new Electronics-in-Action (EIA) feature. Current-mode logic (CML) is heavily used in high performance SiGe ICs, and a CML section is added to the Bipolar Logic chapter.

This revision contains major reorganization and revision of the analog portion (Part III) of the text. The introductory amplifier material (old Chapter 10) is now introduced

in a "just-in-time" basis in the three op-amp chapters. Specific sections have been added with qualitative descriptions of the operation of basic op-amp circuits and each transistor amplifier configuration as well as the transistors themselves.

Feedback analysis using two-ports has been eliminated from Chapter 18 in favor of a consistent loop-gain analysis approach to all feedback configurations that begins in the op-amp chapters. The important successive voltage and current injection technique for finding loop-gain is now included in Chapter 11, and Blackman's theorem is utilized to find input and output resistances of closed-loop amplifiers. SPICE examples have been modified to utilize three- and five-terminal built-in op-amp models.

Chapter 10, Analog Systems and Ideal Operational Amplifiers, provides an introduction to amplifiers and covers the basic ideal op-amp circuits.

Chapter 11, Characteristics and Limitations of Operational Amplifiers, covers the limitations of nonideal op amps including frequency response and stability and the four classic feedback circuits including series-shunt, shunt-shunt, shunt-series and series-series feedback amplifiers.

Chapter 12, Operational Amplifier Applications, collects together all the op-amp applications including multi-stage amplifiers, filters, A/D and D/A converters, sinusoidal oscillators, and multivibrators.

Redundant material in transistor amplifier chapters 13 and 14 has been merged or eliminated wherever possible. Other additions to the analog material include discussion of relations between MOS logic inverters and common-source amplifiers, distortion reduction through feedback, the relationship between step response and phase margin, NMOS differential amplifiers with NMOS load transistors, the regulated cascode current source, and the Gilbert multiplier.

Because of the renaissance and pervasive use of RF circuits, the introductory section on RF amplifiers, now in Chapter 17, has been expanded to include shunt-peaked and tuned amplifiers, and the use of inductive degeneration in common-source amplifiers. New material on mixers includes passive, active, single- and double-balanced mixers and the widely used Gilbert mixer.

Chapter 18, Transistor Feedback Amplifiers and Oscillators, presents examples of transistor feedback amplifiers and transistor oscillator implementations. The transistor oscillator section has been expanded to include a discussion of negative resistance in oscillators and the negative  $G_m$  oscillator cell.

Several other important enhancements include:

- SPICE support on the web now includes examples in NI Multisim™ Software in addition to PSpice®.
- At least 35 percent revised or new problems.
- New PowerPoint® slides are available from McGraw-Hill.
- A group of tested design problems are also available.

The Structured Problem Solving Approach continues to be utilized throughout the examples. We continue to expand the popular Electronics-in-Action Features with the addition of Diode Rectifier as an AM Demodulator; High Performance CMOS Technologies; A Second Look at Noise Margins (graphical flip-flop approach); Offset Voltage, Bias Current and CMRR Measurement; Sample-and-Hold Circuits; Voltage Regulator with Series Pass Transistor; Noise Factor, Noise Figure and Minimum Detectable Signal; Series-Parallel and Parallel-Series Network Transformations; and Passive Diode Ring Mixer.

Chapter Openers enhance the readers understanding of historical developments in electronics. Design notes highlight important ideas that the circuit designer should remember. The World Wide Web is viewed as an integral extension of the text, and a wide range of supporting materials and resource links are maintained and updated on the McGraw-Hill website ([www.mhhe.com/jaeger](http://www.mhhe.com/jaeger)).

Features of the book are outlined below.

The Structured Problem-Solving Approach is used throughout the examples.

Electronics-in-Action features in each chapter.

Chapter openers highlighting developments in the field of electronics.

Design Notes and emphasis on practical circuit design.

Broad use of SPICE throughout the text and examples.

Integrated treatment of device modeling in SPICE.

Numerous Exercises, Examples, and Design Examples.

Large number of new problems.

Integrated web materials.

Continuously updated web resources and links.

Placing the digital portion of the book first is also beneficial to students outside of electrical engineering, particularly computer engineering or computer science majors, who may only take the first course in a sequence of electronics courses.

The material in Part II deals primarily with the internal design of logic gates and storage elements. A comprehensive discussion of NMOS and CMOS logic design is presented in Chapters 6 and 7, and a discussion of memory cells and peripheral circuits appears in Chapter 8. Chapter 9 on bipolar logic design includes discussion of ECL, CML and TTL. However, the material on bipolar logic has been reduced in deference to the import of MOS technology. This text does not include any substantial design at the logic block level, a topic that is fully covered in digital design courses.

Parts I and II of the text deal only with the large-signal characteristics of the transistors. This allows readers to become comfortable with device behavior and  $i-v$  characteristics before they have to grasp the concept of splitting circuits into different pieces (and possibly different topologies) to perform dc and ac small-signal analyses. (The concept of a small-signal is formally introduced in Part III, Chapter 13.)

Although the treatment of digital circuits is more extensive than most texts, more than 50 percent of the material in the book, Part III, still deals with traditional analog circuits. The analog section begins in Chapter 10 with a discussion of amplifier concepts and classic ideal op-amp circuits. Chapter 11 presents a detailed discussion of non-ideal op amps, and Chapter 12 presents a range of op-amp applications. Chapter 13 presents a comprehensive development of the small-signal models for the diode, BJT, and FET. The hybrid-pi model and pi-models for the BJT and FET are used throughout.

Chapter 14 provides in-depth discussion of single-stage amplifier design and multistage ac coupled amplifiers. Coupling and bypass capacitor design is also covered in Chapter 14. Chapter 15 discusses dc coupled multistage amplifiers and introduces prototypical op amp circuits. Chapter 16 continues with techniques that are important in IC design and studies the classic 741 operational amplifier.

Chapter 17 develops the high-frequency models for the transistors and presents a detailed discussion of analysis of high-frequency circuit behavior. The final chapter presents examples of transistor feedback amplifiers. Discussion of feedback amplifier stability and oscillators conclude the text.

## DESIGN

Design remains a difficult issue in educating engineers. The use of the well-defined problem-solving methodology presented in this text can significantly enhance the students' ability to understand issues related to design. The design examples assist in building an understanding of the design process.

Part II launches directly into the issues associated with the design of NMOS and CMOS logic gates. The effects of device and passive-element tolerances are discussed throughout the text. In today's world, low-power, low-voltage design, often supplied from batteries, is playing an increasingly important role. Logic design examples have moved away from 5 V to lower power supply levels. The use of the computer, including MATLAB®, spreadsheets, or standard high-level languages to explore design options is a thread that continues throughout the text.

Methods for making design estimates and decisions are stressed throughout the analog portion of the text. Expressions for amplifier behavior are simplified beyond the standard hybrid-pi model expressions whenever appropriate. For example, the expression for the voltage gain of an amplifier in most texts is simply written as  $|A_v| = g_m R_L$ , which tends to hide the power supply voltage as the fundamental design variable. Rewriting this expression in approximate form as  $g_m R_L \cong 10V_{CC}$  for the BJT, or  $g_m R_L \cong V_{DD}$  for the FET, explicitly displays the dependence of amplifier design on the choice of power supply voltage and provides a simple first-order design estimate for the voltage gain of the common-emitter and common-source amplifiers. The gain advantage of the BJT stage is also clear. These approximation techniques and methods for performance estimation are included as often as possible. Comparisons and design tradeoffs between the properties of BJTs and FETs are included throughout Part III.

Worst-case and Monte-Carlo analysis techniques are introduced at the end of the first chapter. These are not topics traditionally included in undergraduate courses. However, the ability to design circuits in the face of wide component tolerances and variations is a key component of electronic circuit design, and the design of circuits using standard components and tolerance assignment are discussed in examples and included in many problems.

## PROBLEMS AND INSTRUCTOR SUPPORT

Specific design problems, computer problems, and SPICE problems are included at the end of each chapter. Design problems are indicated by , computer problems are indicated by , and SPICE problems are indicated by .

dicated by , and SPICE problems are indicated by . The problems are keyed to the topics in the text with the more difficult or time-consuming problems indicated by \* and \*\*. An Instructor's Manual containing solutions to all the problems is available from the authors. In addition, the graphs and figures are available as PowerPoint files and can be retrieved from the website. Instructor notes are available as PowerPoint slides.

## ELECTRONIC TEXTBOOK OPTION

This text is offered through CourseSmart for both instructors and students. CourseSmart is an online resource where students can purchase the complete text online at almost half the cost of a traditional text. Purchasing the eTextbook allows students to take advantage of CourseSmart's web tools for learning, which include full text search, notes and highlighting, and email tools for sharing notes between classmates. To learn more about CourseSmart options, contact your sales representative or visit [www.CourseSmart.com](http://www.CourseSmart.com).

## COSMOS

Complete Online Solutions Manual Organization System (COSMOS). Professors can benefit from McGraw-Hill's COSMOS electronic solutions manual. COSMOS enables instructors to generate a limitless supply of problem material for assignment, as well as transfer and integrate their own problems into the software. For additional information, contact your McGraw-Hill sales representative.

## COMPUTER USAGE AND SPICE

The computer is used as a tool throughout the text. The authors firmly believe that this means more than just the use of the SPICE circuit analysis program. In today's computing environment, it is often appropriate to use the computer to explore a complex design space rather than to try to reduce a complicated set of equations to some manageable analytic form. Examples of the process of setting up equations for iterative evaluation by computer through the use of spreadsheets, MATLAB, and/or standard high-level language programs are illustrated in several places in the text. MATLAB is also used for Nyquist and Bode plot generation and is very useful for Monte Carlo analysis.

On the other hand, SPICE is used throughout the text. Results from SPICE simulation are included throughout and numerous SPICE problems are to be found in the problem sets. Wherever helpful, a SPICE analysis is used with most examples. This edition also emphasizes the differences and utility of the dc, ac, transient, and transfer function analysis modes in SPICE. A discussion of SPICE

device modeling is included following the introduction to each semiconductor device, and typical SPICE model parameters are presented with the models.

## ACKNOWLEDGMENTS

We want to thank the large number of people who have had an impact on the material in this text and on its preparation. Our students have helped immensely in polishing the manuscript and have managed to survive the many revisions of the manuscript. Our department heads, J. D. Irwin of Auburn University and L. R. Harriott of the University of Virginia, have always been highly supportive of faculty efforts to develop improved texts.

We want to thank all the reviewers and survey respondents including

Vijay K. Arora  
*Wilkes University*  
Kurt Behpour  
*California Polytechnic State University,  
San Luis Obispo*  
David A. Borkholder  
*Rochester Institute of Technology*  
Dmitri Donetski  
*Stony Brook University*  
Ethan Farquhar  
*The University of Tennessee,  
Knoxville*  
Melinda Holtzman  
*Portland State University*

Anthony Johnson  
*The University of Toledo*  
Marian K. Kazimierczuk  
*Wright State University*  
G. Roientan Lahiji  
*Professor, Iran University  
of Science and  
Technology*  
Adjunct Professor,  
*University of Michigan*  
Stanislaw F. Legowski  
*University of Wyoming*  
Milica Markovic  
*California State University  
Sacramento*

James E. Morris  
*Portland State University*  
Maryam Moussavi  
*California State University  
Long Beach*

Kenneth V. Noren  
*University of Idaho*  
John Ortiz  
*University of Texas at San Antonio*

We are also thankful for inspiration from the classic text *Applied Electronics* by J. F. Pierce and T. J. Paulus. Professor Blalock learned electronics from Professor Pierce many years ago and still appreciates many of the analytical techniques employed in their long out-of-print text.

We would like to thank Gabriel Chindris of Technical University of Cluj-Napoca in Romania for his assistance in creating the simulations for the NI Multisim™ examples.

Finally, we want to thank the team at McGraw-Hill including Raghethaman Srinivasan, Global Publisher; Darlene Schueler, Developmental Editor; Curt Reynolds, Senior Marketing Manager; Jane Mohr, Senior Project Manager; Brenda Rolwes, Design Coordinator; John Leland and LouAnn Wilson, Photo Research Coordinators; Kara Kudronowicz, Senior Production Supervisor; Sandy Schnee, Senior Media Project Manager; and Dheeraj Chahal, Full Service Project Manager, MPS Limited.

In developing this text, we have attempted to integrate our industrial backgrounds in precision analog and digital design with many years of experience in the classroom. We hope we have at least succeeded to some extent. Constructive suggestions and comments will be appreciated.

*Richard C. Jaeger  
Auburn University*

*Travis N. Blalock  
University of Virginia*

# CHAPTER-BY-CHAPTER SUMMARY

## PART I—SOLID-STATE ELECTRONICS AND DEVICES

**Chapter 1** provides a historical perspective on the field of electronics beginning with vacuum tubes and advancing to giga-scale integration and its impact on the global economy. Chapter 1 also provides a classification of electronic signals and a review of some important tools from network analysis, including a review of the ideal operational amplifier. Because developing a good problem-solving methodology is of such import to an engineer's career, the comprehensive Structured Problem Solving Approach is used to help the students develop their problem solving skills. The structured approach is discussed in detail in the first chapter and used in all the subsequent examples in the text. Component tolerances and variations play an extremely important role in practical circuit design, and Chapter 1 closes with introductions to tolerances, temperature coefficients, worst-case design, and Monte Carlo analysis.

**Chapter 2** deviates from the recent norm and discusses semiconductor materials including the covalent-bond and energy-band models of semiconductors. The chapter includes material on intrinsic carrier density, electron and hole populations, *n*- and *p*-type material, and impurity doping. Mobility, resistivity, and carrier transport by both drift and diffusion are included as topics. Velocity saturation is discussed, and an introductory discussion of microelectronic fabrication has been merged with Chapter 2.

**Chapter 3** introduces the structure and *i-v* characteristics of solid-state diodes. Discussions of Schottky diodes, variable capacitance diodes, photo-diodes, solar cells, and LEDs are also included. This chapter introduces the concepts of device modeling and the use of different levels of modeling to achieve various approximations to reality. The SPICE model for the diode is discussed. The concepts of bias, operating point, and load-line are all introduced, and iterative mathematical solutions are also used to find the operating point with MATLAB and spreadsheets. Diode applications in rectifiers are discussed in detail and a

discussion of the dynamic switching characteristics of diodes is also presented.

**Chapter 4** discusses MOS and junction field-effect transistors, starting with a qualitative description of the MOS capacitor. Models are developed for the FET *i-v* characteristics, and a complete discussion of the regions of operation of the device is presented. Body effect is included. MOS transistor performance limits including scaling, cut-off frequency, and subthreshold conduction are discussed as well as basic  $\Delta$ -based layout methods. Biasing circuits and load-line analysis are presented. The FET SPICE models and model parameters are discussed in Chapter 4.

**Chapter 5** introduces the bipolar junction transistor and presents a heuristic development of the Transport (simplified Gummel-Poon) model of the BJT based upon superposition. The various regions of operation are discussed in detail. Common-emitter and common-base current gains are defined, and base transit-time, diffusion capacitance and cutoff frequency are all discussed. Bipolar technology and physical structure are introduced. The four-resistor bias circuit is discussed in detail. The SPICE model for the BJT and the SPICE model parameters are discussed in Chapter 5.

## PART II—DIGITAL ELECTRONICS

**Chapter 6** begins with a compact introduction to digital electronics. Terminology discussed includes logic levels, noise margins, rise-and-fall times, propagation delay, fan out, fan in, and power-delay product. A short review of Boolean algebra is included. The introduction to MOS logic design is now merged with Chapter 6 and follows the historical evolution of NMOS logic gates focusing on the design of saturated-load, and depletion-load circuit families. The impact of body effect on MOS logic circuit design is discussed in detail. The concept of reference inverter scaling is developed and employed to affect the design of other inverters, NAND gates, NOR gates, and complex logic functions throughout Chapters 6 and 7. Capacitances in MOS

circuits are discussed, and methods for estimating the propagation delay and power-delay product of NMOS logic are presented. Details of several of the propagation delay analyses are moved to the MCD website, and the delay equation results for the various families have been collapsed into a much more compact form. The pseudo NMOS logic gate is discussed and provides a bridge to CMOS logic in Chapter 7.

CMOS represents today's most important integrated circuit technology, and **Chapter 7** provides an in-depth look at the design of CMOS logic gates including inverters, NAND and NOR gates, and complex logic gates. The CMOS designs are based on simple scaling of a reference inverter design. Noise margin and latchup are discussed as well as a comparison of the power-delay products of various MOS logic families. Dynamic logic circuits and cascade buffer design are discussed in Chapter 7. A discussion of BiCMOS logic circuitry has been added to Chapter 9 after bipolar logic is introduced.

**Chapter 8** ventures into the design of memory and storage circuits, including the six-transistor, four-transistor, and one-transistor memory cells. Basic sense-amplifier circuits are introduced as well as the peripheral address and decoding circuits needed in memory designs. ROMs and flip-flop circuitry are included in Chapter 8.

**Chapter 9** discusses bipolar logic circuits including emitter-coupled logic and transistor-transistor logic. The use of the differential pair as a current switch and the large-signal properties of the emitter follower are introduced. An introduction to CML, widely used in SiGe design, follows the ECL discussion. Operation of the BJT as a saturated switch is included and followed by a discussion of low voltage and standard TTL. An introduction to BiCMOS logic now concludes the chapter on bipolar logic.

## PART III – ANALOG ELECTRONICS

**Chapter 10** provides a succinct introduction to analog electronics. The concepts of voltage gain, current gain, power gain, and distortion are developed and have been merged on a “just-in-time” basis with the discussion of the classic ideal operational amplifier circuits that include the inverting, noninverting, summing, and difference amplifiers and the integrator and differentiator. Much care has been taken to be consistent in the use of the notation that defines these quantities as well as in the use of dc, ac, and total signal notation throughout the book. Bode plots are reviewed and amplifiers are classified by frequency response. MATLAB is utilized as a tool for producing Bode plots. SPICE simulation using built-in SPICE models is introduced.

**Chapter 11** focuses on a comprehensive discussion of the characteristics and limitations of real operational am-

plifiers including the effects of finite gain and input resistance, nonzero output resistance, input offset voltage, input bias and offset currents, output voltage and current limits, finite bandwidth, and common-mode rejection. A consistent loop-gain analysis approach is used to study the four classic feedback configurations, and Blackman’s theorem is utilized to find input and output resistances of closed-loop amplifiers. The important successive voltage and current injection technique for finding loop-gain is now included in Chapter 11. Relationships between the Nyquist and Bode techniques are explicitly discussed. Stability of first-, second- and third-order systems is discussed, and the concepts of phase and gain margin are introduced. Relationships between Nyquist and Bode techniques are explicitly discussed. A section concerning the relationship between phase margin and time domain response has been added. The macro model concept is introduced and the discussion of SPICE simulation of op-amp circuits using various levels of models continues in Chapter 11.

**Chapter 12** covers a wide range of operational amplifier applications that include multistage amplifiers, the instrumentation amplifier, and continuous time and discrete time active filters. Cascade amplifiers are investigated including a discussion of the bandwidth of multistage amplifiers. An introduction to D/A and A/D converters appears in this chapter. The Barkhausen criterion for oscillation are presented and followed by a discussion of op-amp-based sinusoidal oscillators. Nonlinear circuits applications including rectifiers, Schmitt triggers, and multivibrators conclude the material in Chapter 12.

**Chapter 13** begins the general discussion of linear amplification using the BJT and FET as C-E and C-S amplifiers. Biasing for linear operation and the concept of small-signal modeling are both introduced, and small-signal models of the diode, BJT, and FET are all developed. The limits for small-signal operation are all carefully defined. The use of coupling and bypass capacitors and inductors to separate the ac and dc designs is explored. The important  $10V_{CC}$  and  $V_{DD}$  design estimates for the voltage gain of the C-E and C-S amplifiers are introduced, and the role of transistor amplification factor in bounding circuit performance is discussed. The role of Q-point design on power dissipation and signal range is also introduced.

**Chapter 14** proceeds with an in-depth comparison of the characteristics of single-transistor amplifiers, including small-signal amplitude limitations. Appropriate points for signal injection and extraction are identified, and amplifiers are classified as inverting amplifiers (C-E, C-S), noninverting amplifiers (C-B, C-G), and followers (C-C, C-D). The treatment of MOS and bipolar devices is merged from Chapter 14 on, and design tradeoffs between

the use of the BJT and the FET in amplifier circuits is an important thread that is followed through all of Part III. A detailed discussion of the design of coupling and bypass capacitors and the role of these capacitors in controlling the low frequency response of amplifiers appears in this chapter.

**Chapter 15** explores the design of multistage direct coupled amplifiers. An evolutionary approach to multistage op amp design is used. MOS and bipolar differential amplifiers are first introduced. Subsequent addition of a second gain stage and then an output stage convert the differential amplifiers into simple op amps. Class A, B, and AB operation are defined. Electronic current sources are designed and used for biasing of the basic operational amplifiers. Discussion of important FET-BJT design tradeoffs are included wherever appropriate.

**Chapter 16** introduces techniques that are of particular import in integrated circuit design. A variety of current mirror circuits are introduced and applied in bias circuits and as active loads in operational amplifiers. A wealth of circuits and analog design techniques are explored through the detailed analysis of the classic 741 operational amplifier. The bandgap reference and Gilbert analog multiplier are introduced in Chapter 16.

**Chapter 17** discusses the frequency response of analog circuits. The behavior of each of the three categories of single-stage amplifiers (C-E/C-S, C-B/C-G, and C-C/C-D) is discussed in detail, and BJT behavior is contrasted with that of the FET. The frequency response of the transistor is discussed, and the high frequency, small-signal models are developed for both the BJT and FET. Miller multiplication is used to obtain estimates of the lower and upper cutoff frequencies of complex multistage amplifiers. Gain-bandwidth products and gain-bandwidth tradeoffs in design are discussed. Cascode amplifier frequency response, and tuned amplifiers are included in this chapter.

Because of the renaissance and pervasive use of RF circuits, the introductory section on RF amplifiers has been expanded to include shunt-peaked and tuned amplifiers, and the use of inductive degeneration in common-source amplifiers. New material on mixers includes passive and active single- and double-balanced mixers and the widely used Gilbert mixer.

**Chapter 18** presents detailed examples of feedback as applied to transistor amplifier circuits. The loop-gain analysis approach introduced in Chapter 11 is used to find the closed-loop amplifier gain of various amplifiers, and Blackman's theorem is utilized to find input and output resistances of closed-loop amplifiers.

Amplifier stability is also discussed in Chapter 18, and Nyquist diagrams and Bode plots (with MATLAB) are used to explore the phase and gain margin of amplifiers. Basic single-pole op amp compensation is discussed, and the unity gain-bandwidth product is related to amplifier slew rate. Design of op amp compensation to achieve a desired phase margin is discussed. The discussion of transistor oscillator circuits includes the Colpitts, Hartley and negative  $G_m$  configurations. Crystal oscillators are also discussed.

Three Appendices include tables of standard component values (Appendix A), summary of the device models and sample SPICE parameters (Appendix B) and review of two-port networks (Appendix C). Data sheets for representative solid-state devices and operational amplifiers are available via the WWW.

## FLEXIBILITY

The chapters are designed to be used in a variety of different sequences, and there is more than enough material for a two-semester or three-quarter sequence in electronics. One can obviously proceed directly through the book. On the other hand, the material has been written so that the BJT chapter can be used immediately after the diode chapter if so desired (i.e., a 1-2-3-5-4 chapter sequence). At the present time, the order actually used at Auburn University is:

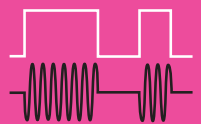
1. Introduction
2. Solid-State Electronics
3. Diodes
4. FETs
5. Digital Logic
6. CMOS Logic
7. Memory
8. The BJT
9. Bipolar Logic
- 10–18. Analog in sequence

The chapters have also been written so that Part II, Digital Electronics, can be skipped, and Part III, Analog Electronics, can be used directly after completion of the coverage of the solid-state devices in Part I. If so desired, many of the quantitative details of the material in Chapter 2 may be skipped. In this case, the sequence would be

1. Introduction
2. Solid-State Electronics
3. Diodes
4. FETs
5. The BJT
- 10–18. Analog in sequence

## PART ONE

# SOLID STATE ELECTRONIC AND DEVICES



CHAPTER 1

INTRODUCTION TO ELECTRONICS 3

CHAPTER 2

SOLID-STATE ELECTRONICS 42

CHAPTER 3

SOLID-STATE DIODES AND DIODE CIRCUITS 74

CHAPTER 4

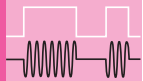
FIELD-EFFECT TRANSISTORS 145

CHAPTER 5

BIPOLAR JUNCTION TRANSISTORS 217

*This page intentionally left blank*

# CHAPTER 1



## INTRODUCTION TO ELECTRONICS

### CHAPTER OUTLINE

- 1.1 A Brief History of Electronics: From Vacuum Tubes to Ultra-Large-Scale Integration 5
- 1.2 Classification of Electronic Signals 8
- 1.3 Notational Conventions 12
- 1.4 Problem-Solving Approach 13
- 1.5 Important Concepts from Circuit Theory 15
- 1.6 Frequency Spectrum of Electronic Signals 21
- 1.7 Amplifiers 22
- 1.8 Element Variations in Circuit Design 26
- 1.9 Numeric Precision 34
- Summary 34
- Key Terms 35
- References 36
- Additional Reading 36
- Problems 37

### CHAPTER GOALS

- Present a brief history of electronics
- Quantify the explosive development of integrated circuit technology
- Discuss initial classification of electronic signals
- Review important notational conventions and concepts from circuit theory
- Introduce methods for including tolerances in circuit analysis
- Present the problem-solving approach used in this text

November 2007 was the 60th anniversary of the 1947 discovery of the bipolar transistor by John Bardeen and Walter Brattain at Bell Laboratories, a seminal event that marked the beginning of the semiconductor age (see Figs. 1.1 and 1.2). The invention of the transistor and the subsequent development of microelectronics have done more to shape the modern era than any other event. The transistor and microelectronics have reshaped how business is transacted, machines are designed, information moves, wars are fought, people interact, and countless other areas of our lives.

This textbook develops the basic operating principles and design techniques governing the behavior of the devices and circuits that form the backbone of much of the infrastructure of our modern world. This knowledge will enable students who aspire to design and create the next



**Figure 1.1** John Bardeen, William Shockley, and Walter Brattain in Brattain's laboratory in 1948.  
*Reprinted with permission of Alacatel-Lucent USA Inc.*



**Figure 1.2** The first germanium bipolar transistor.  
*Lucent Technologies Inc./Bell Labs*

generation of this technological revolution to build a solid foundation for more advanced design courses. In addition, students who expect to work in some other technology area will learn material that will help them understand microelectronics, a technology that will continue to have impact on how their chosen field develops. This understanding will enable them to fully exploit microelectronics in their own technology area. Now let us return to our short history of the transistor.

After the discovery of the transistor, it was but a few months until William Shockley developed a theory that described the operation of the bipolar junction transistor. Only 10 years later, in 1956, Bardeen, Brattain, and Shockley received the Nobel prize in physics for the discovery of the transistor.

In June 1948 Bell Laboratories held a major press conference to announce the discovery. In 1952 Bell Laboratories, operating under legal consent decrees, made licenses for the transistor available for the modest fee of \$25,000 plus future royalty payments. About this time, Gordon Teal, another member of the solid-state group, left Bell Laboratories

to work on the transistor at Geophysical Services, Inc., which subsequently became Texas Instruments (TI). There he made the first silicon transistors, and TI marketed the first all-transistor radio. Another early licensee of the transistor was Tokyo Tsushin Kogyo, which became the Sony Company in 1955. Sony subsequently sold a transistor radio with a marketing strategy based on the idea that everyone could now have a personal radio; thus was launched the consumer market for transistors. A very interesting account of these and other developments can be found in [1, 2] and their references.

**A**ctivity in electronics began more than a century ago with the first radio transmissions in 1895 by Marconi, and these experiments were followed after only a few years by the invention of the first electronic amplifying device, the triode vacuum tube. In this period, electronics—loosely defined as the design and application of electron devices—has had such a significant impact on our lives that we often overlook just how pervasive electronics has really become. One measure of the degree of this impact can be found in the gross domestic product (GDP) of the world. In 2008 the world GDP was approximately U.S. \$71 trillion, and of this total more than 10 percent was directly traceable to electronics. See Table 1.1 [3–5].

We commonly encounter electronics in the form of telephones, radios, televisions, and audio equipment, but electronics can be found even in seemingly mundane appliances such as vacuum cleaners, washing machines, and refrigerators. Wherever one looks in industry, electronics will be found. The corporate world obviously depends heavily on data processing systems to manage its operations. In fact, it is hard to see how the computer industry could have evolved without the use of its own products. In addition, the design process depends ever more heavily on computer-aided design (CAD) systems, and manufacturing relies on electronic systems for process control—in petroleum refining, automobile tire production, food processing, power generation, and so on.

**TABLE 1.1**  
Estimated Worldwide Electronics Market

CATEGORY	SHARE (%)
Data processing hardware	23
Data processing software and services	18
Professional electronics	10
Telecommunications	9
Consumer electronics	9
Active components	9
Passive components	7
Computer integrated manufacturing	5
Instrumentation	5
Office electronics	3
Medical electronics	2

## 1.1 A BRIEF HISTORY OF ELECTRONICS: FROM VACUUM TUBES TO GIGA-SCALE INTEGRATION

Because most of us have grown up with electronic products all around us, we often lose perspective of how far the industry has come in a relatively short time. At the beginning of the twentieth century, there were no commercial electron devices, and transistors were not invented until the late 1940s!<sup>1</sup> Explosive growth was triggered by first the commercial availability of the bipolar transistor in the late 1950s, and then the realization of the integrated circuit (IC) in 1961. Since that time, signal processing using electron devices and electronic technology has become a pervasive force in our lives.

Table 1.2 lists a number of important milestones in the evolution of the field of electronics. The Age of Electronics began in the early 1900s with the invention of the first electronic two-terminal devices, called **diodes**. The **vacuum diode**, or diode **vacuum tube**, was invented by Fleming in 1904; in 1906 Pickard created a diode by forming a point contact to a silicon crystal. (Our study of electron devices begins with the introduction of the solid-state diode in Chapter 3.)

The invention of the three-element vacuum tube known as the **triode** was an extremely important milestone. The addition of a third element to a diode enabled electronic amplification to take place with good isolation between the input and output ports of the device. Silicon-based three-element devices now form the basis of virtually all electronic systems. Fabrication of tubes that could be used reliably in circuits followed the invention of the triode by a few years and enabled rapid circuit innovation. Amplifiers and oscillators were developed that significantly improved radio transmission and reception. Armstrong invented the super heterodyne receiver in 1920 and FM modulation in 1933. Electronics developed rapidly during World War II, with great advances in the field of radio communications and the development of radar. Although first demonstrated in 1930, television did not begin to come into widespread use until the 1950s.

An important event in electronics occurred in 1947, when John Bardeen, Walter Brattain, and William Shockley at Bell Telephone Laboratories invented the **bipolar transistor**.<sup>1</sup> Although field-effect devices had actually been conceived by Lilienfeld in 1925, Heil in 1935, and Shockley in 1952 [2], the technology to produce such devices on a commercial basis did not yet exist. Bipolar devices, however, were rapidly commercialized.

Then in 1958, the nearly simultaneous invention of the **integrated circuit (IC)** by Kilby at Texas Instruments and Noyce and Moore at Fairchild Semiconductor produced a new technology that would profoundly change our lives. The miniaturization achievable through IC technology made available complex electronic functions with high performance at low cost. The attendant characteristics of high reliability, low power, and small physical size and weight were additional important advantages.

In 2000, Jack St. Clair Kilby received a share of the Nobel prize for the invention of the integrated circuit. In the mind of the authors, this was an exceptional event as it represented one of the first awards to an electronic technologist.

Most of us have had some experience with personal computers, and nowhere is the impact of the integrated circuit more evident than in the area of digital electronics. For example, 4-gigabit (Gb) dynamic memory chips, similar to those in Fig. 1.3(c), contain more than 4 billion transistors. Creating this much memory using individual vacuum tubes [depicted in Fig. 1.3(a)] or even discrete transistors [shown in Fig. 1.3(b)] would be an almost inconceivable feat.

### Levels of Integration

The dramatic progress of integrated circuit miniaturization is shown graphically in Figs. 1.4 and 1.5. The complexities of memory chips and microprocessors have grown exponentially with time. In the four decades since 1970, the number of transistors on a microprocessor chip has increased by

<sup>1</sup> The term **transistor** is said to have originated as a contraction of “transfer resistor,” based on the voltage-controlled resistance of the characteristics of the MOS transistor.

**TABLE 1.2**  
**Milestones in Electronics**

YEAR	EVENT
1874	Ferdinand Braun invents the solid-state rectifier.
1884	American Institute of Electrical Engineers (AIEE) formed.
1895	Marconi makes first radio transmissions.
1904	Fleming invents diode vacuum tube—Age of Electronics begins.
1906	Pickard creates solid-state point-contact diode (silicon).
1906	Deforest invents triode vacuum tube (audion).
1910–1911	“Reliable” tubes fabricated.
1912	Institute of Radio Engineers (IRE) founded.
1907–1927	First radio circuits developed from diodes and triodes.
1920	Armstrong invents super heterodyne receiver.
1925	TV demonstrated.
1925	Lilienfeld files patent application on the field-effect device.
1927–1936	Multigrid tubes developed.
1933	Armstrong invents FM modulation.
1935	Heil receives British patent on a field-effect device.
1940	Radar developed during World War II—TV in limited use.
1947	Bardeen, Brattain, and Shockley at Bell Laboratories invent bipolar transistors.
1950	First demonstration of color TV.
1952	Shockley describes the unipolar field-effect transistor.
1952	Commercial production of silicon bipolar transistors begins at Texas Instruments.
1952	Ian Ross and George Dacey demonstrate the junction field-effect transistor.
1956	Bardeen, Brattain, and Shockley receive Nobel prize for invention of bipolar transistors.
1958	Integrated circuit developed simultaneously by Kilby at Texas Instruments and Noyce and Moore at Fairchild Semiconductor.
1961	First commercial digital IC available from Fairchild Semiconductor.
1963	AIEE and IRE merge to become the Institute of Electrical and Electronic Engineers (IEEE)
1967	First semiconductor RAM (64 bits) discussed at the IEEE International Solid-State Circuits Conference (ISSCC).
1968	First commercial IC operational amplifier—the μA709—introduced by Fairchild Semiconductor.
1970	One-transistor dynamic memory cell invented by Dennard at IBM.
1970	Low-loss optical fiber invented.
1971	4004 microprocessor introduced by Intel.
1972	First 8-bit microprocessor—the 8008—introduced by Intel.
1974	First commercial 1-kilobit memory chip developed.
1974	8080 microprocessor introduced.
1978	First 16-bit microprocessor developed.
1984	Megabit memory chip introduced.
1987	Erbium doped, laser-pumped optical fiber amplifiers demonstrated.
1995	Experimental gigabit memory chip presented at the IEEE ISSCC.
2000	Alferov, Kilby, and Kromer share the Nobel prize in physics for optoelectronics, invention of the integrated circuit, and heterostructure devices, respectively.

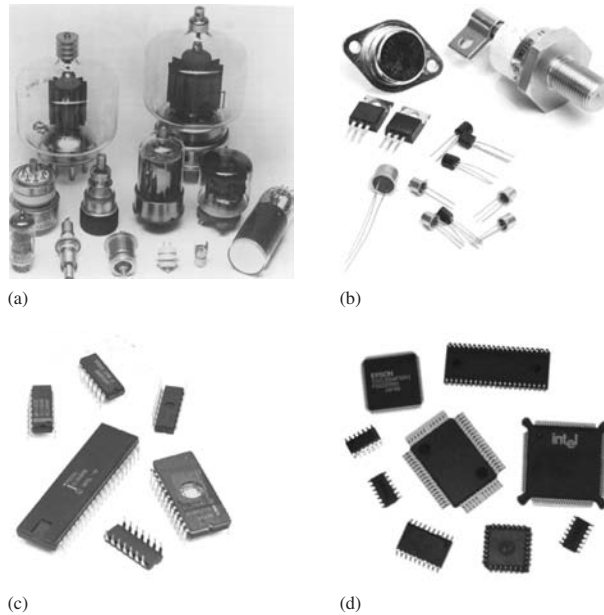


**Figure 1.3** Comparison of (a) vacuum tubes, (b) individual transistors, (c) integrated circuits in dual-in-line packages (DIPs), and (d) ICs in surface mount packages.

Source: (a) Courtesy ARRL Handbook for Radio Amateurs, 1992

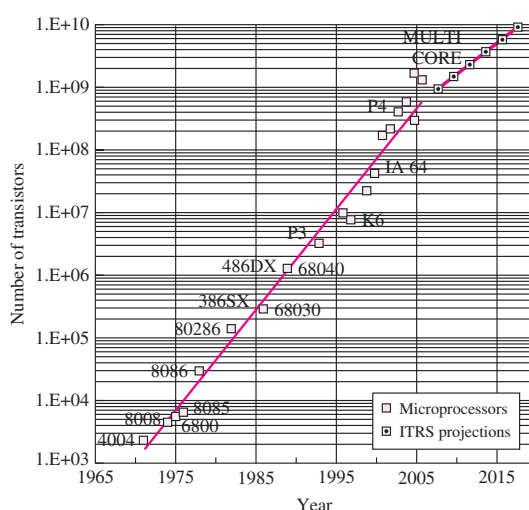


**Figure 1.4** Microprocessor complexity versus time.

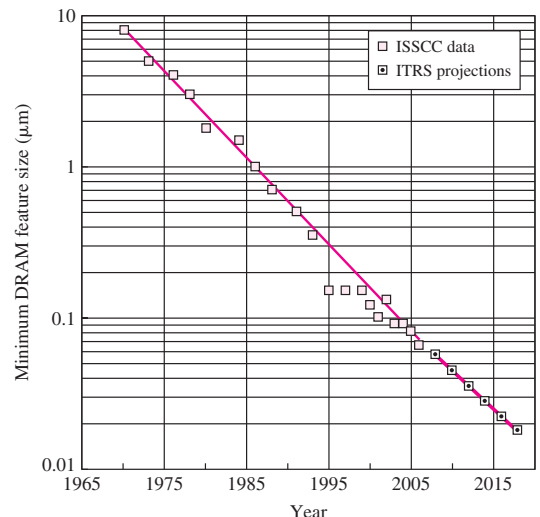


**Figure 1.5** DRAM feature size versus year.

a factor of one million as depicted in Fig. 1.4. Similarly, memory density has grown by a factor of more than 10 million from a 64-bit chip in 1968 to the announcement of 4-Gbit chip production in the late 2009.

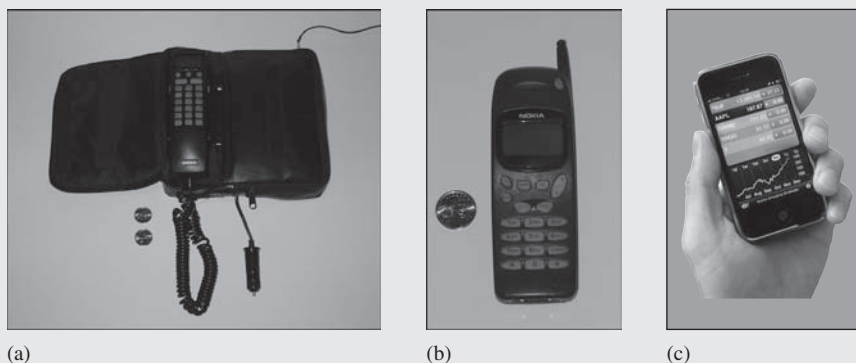
Since the commercial introduction of the integrated circuit, these increases in density have been achieved through a continued reduction in the minimum line width, or **minimum feature size**, that can be defined on the surface of the integrated circuit (see Fig. 1.5). Today most corporate semiconductor laboratories around the world are actively working on deep submicron processes with feature sizes below  $50 \mu\text{m}$ —less than one two-hundredth the diameter of a human hair.

As the miniaturization process has continued, a series of commonly used abbreviations has evolved to characterize the various levels of integration. Prior to the invention of the integrated circuit, electronic systems were implemented in discrete form. Early ICs, with fewer than 100 components, were characterized as **small-scale integration**, or **SSI**. As density increased, circuits became identified as **medium-scale integration (MSI)**, 100–1000 components/chip), **large-scale integration (LSI**,  $10^3 - 10^4$  components/chip), and **very-large-scale integration (VLSI**,  $10^4 - 10^9$  components/chip). Today discussions focus on **ultra-large-scale integration (ULSI)** and **giga-scale integration (GSI**, above  $10^9$  components/chip).

## ELECTRONICS IN ACTION

### *Cellular Phone Evolution*

The impact of technology scaling is ever present in our daily lives. One example appears visually in the pictures of cellular phone evolution below. Early mobile phones were often large and had to be carried in a relatively large pouch (hence the term “bag phone”). The next generation of analog phones could easily fit in your hand, but they had poor battery life caused by their analog communications technology. Implementations of second- and third-generation digital cellular technology are considerably smaller and have much longer battery life. As density continues to increase, additional functions such as personal digital assistants (PDA), cameras and GPS are integrated with the digital phone.



A decade of cellular phone evolution: (a) early Uniden “bag phone,” (b) Nokia analog phone, and (c) Apple iPhone.  
Source: (c) iPhone: © Lourens Smak/Alamy/RF

Cell phones also represent excellent examples of the application of **mixed-signal** integrated circuits that contain both analog and digital circuitry on the same chip. ICs in the cell phone contain analog radio frequency receiver and transmitter circuitry, analog-to-digital and digital-to-analog converters, CMOS logic and memory, and power conversion circuits.

## 1.2 CLASSIFICATION OF ELECTRONIC SIGNALS

The signals that electronic devices are designed to process can be classified into two broad categories: analog and digital. **Analog signals** can take on a continuous range of values, and thus represent continuously varying quantities; purely **digital signals** can appear at only one of several discrete levels. Examples of these types of signals are described in more detail in the next two subsections, along with the concepts of digital-to-analog and analog-to-digital conversion, which make possible the interface between the two systems.

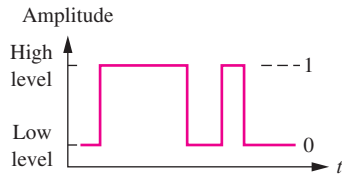


**Figure 1.6** A time-varying binary digital signal.

### 1.2.1 DIGITAL SIGNALS

When we speak of digital electronics, we are most often referring to electronic processing of **binary digital signals**, or signals that can take on only one of two discrete amplitude levels as illustrated in Fig. 1.6. The status of binary systems can be represented by two symbols: a logical 1 is assigned to represent one level, and a logical 0 is assigned to the second level.<sup>2</sup> The two logic states generally correspond to two separate voltages— $V_H$  and  $V_L$ —representing the high and low amplitude levels, and a number of voltage ranges are in common use. Although  $V_H = 5\text{ V}$  and  $V_L = 0\text{ V}$  represented the primary standard for many years, these have given way to lower voltage levels because of power consumption and semiconductor device limitations. Systems employing  $V_H = 3.3, 2.5,$  and  $1.5\text{ V}$ , with  $V_L = 0\text{ V}$ , are now used in many types of electronics.

However, binary voltage levels can also be negative or even bipolar. One high-performance logic family called ECL uses  $V_H = -0.8\text{ V}$  and  $V_L = -2.0\text{ V}$ , and the early standard RS-422 and RS-232 communication links between a small computer and its peripherals used  $V_H = +12\text{ V}$  and  $V_L = -12\text{ V}$ . In addition, the time-varying binary signal in Fig. 1.6 could equally well represent the amplitude of a current or that of an optical signal being transmitted down a fiber in an optical digital communication system. The more recent USB and Firewire standards returned to the use of a single positive supply voltage.

Part II of this text discusses the design of a number of families of digital circuits using various semiconductor technologies. These include CMOS,<sup>3</sup> NMOS, and PMOS logic, which use field-effect transistors, and the TTL and ECL families, which are based on bipolar transistors.

### 1.2.2 ANALOG SIGNALS

Although quantities such as electronic charge and electron spin are truly discrete, much of the physical world is really analog in nature. Our senses of vision, hearing, smell, taste, and touch are all analog processes. Analog signals directly represent variables such as temperature, humidity, pressure, light intensity, or sound—all of which may take on any value, typically within some finite range. In reality, classification of digital and analog signals is largely one of perception. If we look at a digital signal similar to the one in Fig. 1.6 with an oscilloscope, we find that it actually makes a continuous transition between the high and low levels. The signal cannot make truly abrupt transitions between two levels. Designers of high-speed digital systems soon realize that they are really dealing with analog signals. The time-varying voltage or current plotted in Fig. 1.7 could be the electrical representation of temperature, flow rate, or pressure versus time, or the continuous audio output from a microphone. Some analog transducers produce output *voltages* in the range of 0 to 5 or 0 to 10 V, whereas others are designed to produce an output *current* that ranges between 4 and 20 mA. At the other extreme, signals brought in by a radio antenna can be as small as a fraction of a microvolt.

To process the information contained in these analog signals, electronic circuits are used to selectively modify the amplitude, phase, and frequency content of the signals. In addition, significant

<sup>2</sup> This assignment facilitates the use of Boolean algebra, reviewed in Chapter 6.

<sup>3</sup> For now, let us accept these initials as proper names without further definition. The details of each of these circuits are developed in Part II.

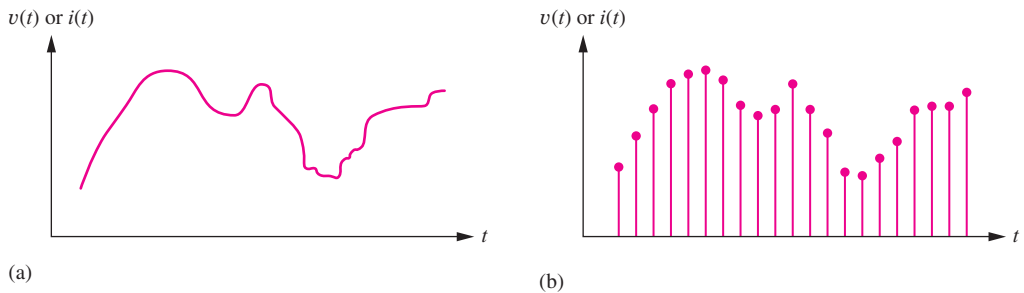


**Figure 1.7** (a) A continuous analog signal; (b) sampled data version of signal in (a).

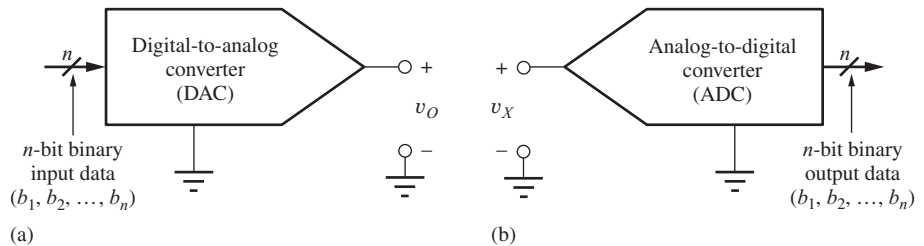


**Figure 1.8** Block diagram representation for a (a) D/A converter and a (b) A/D converter.

increases in the voltage, current, and power level of the signal are usually needed. All these modifications to the signal characteristics are achieved using various forms of amplifiers, and Part III of this text discusses the analysis and design of a wide range of amplifiers using operational amplifiers and bipolar and field-effect transistors.

### 1.2.3 A/D AND D/A CONVERTERS—BRIDGING THE ANALOG AND DIGITAL DOMAINS

For analog and digital systems to be able to operate together, we must be able to convert signals from analog to digital form and vice versa. We sample the input signal at various points in time as in Fig. 1.7(b) and convert or quantize its amplitude into a digital representation. The quantized value can be represented in binary form or can be a decimal representation as given by the display on a digital multimeter. The electronic circuits that perform these translations are called digital-to-analog (D/A) and analog-to-digital (A/D) converters.

#### Digital-to-Analog Conversion

The **digital-to-analog converter**, often referred to as a **D/A converter** or **DAC**, provides an interface between the digital signals of computer systems and the continuous signals of the analog world. The D/A converter takes digital information, most often in binary form, as input and generates an output voltage or current that may be used for electronic control or analog information display. In the DAC in Fig. 1.8(a), an  $n$ -bit binary input word ( $b_1, b_2, \dots, b_n$ ) is treated as a binary fraction and multiplied by a full-scale reference voltage  $V_{FS}$  to set the output of the D/A converter. The behavior of the DAC can be expressed mathematically as

$$v_O = (b_1 2^{-1} + b_2 2^{-2} + \dots + b_n 2^{-n}) V_{FS} \quad \text{for } b_i \in \{1, 0\} \quad (1.1)$$

Examples of typical values of the full-scale voltage  $V_{FS}$  are 1, 2, 5, 5.12, 10, and 10.24 V. The smallest voltage change that can occur at the output takes place when the **least significant bit**  $b_n$ , or **LSB**, in the digital word changes from a 0 to a 1. This minimum voltage change is also referred to as the **resolution of the converter** and is given by

$$V_{LSB} = 2^{-n} V_{FS} \quad (1.2)$$

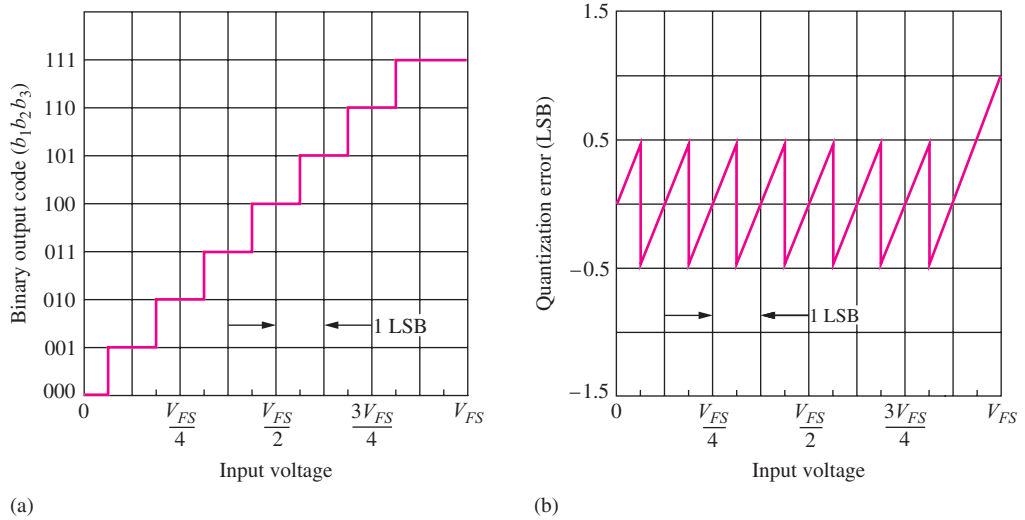


**Figure 1.9** (a) Input–output relationship and (b) quantization error for 3-bit ADC.

At the other extreme,  $b_1$  is referred to as the **most significant bit**, or **MSB**, and has a weight of one-half  $V_{FS}$ .

**EXERCISE:** A 10-bit D/A converter has  $V_{FS} = 5.12 \text{ V}$ . What is the output voltage for a binary input code of (1100010001)? What is  $V_{\text{LSB}}$ ? What is the size of the MSB?

**ANSWERS:** 3.925 V; 5 mV; 2.56 V

### Analog-to-Digital Conversion

The **analog-to-digital converter (A/D converter)** or **ADC** is used to transform analog information in electrical form into digital data. The ADC in Fig. 1.8(b) takes an unknown continuous analog input signal, usually a voltage  $v_X$ , and converts it into an  $n$ -bit binary number that can be easily manipulated by a computer. The  $n$ -bit number is a binary fraction representing the ratio between the unknown input voltage  $v_X$  and the converter's full-scale voltage  $V_{FS}$ .

For example, the input–output relationship for an ideal 3-bit A/D converter is shown in Fig. 1.9(a). As the input increases from zero to full scale, the output digital code word stair-steps from 000 to 111.<sup>4</sup> The output code is constant for an input voltage range equal to 1 LSB of the ADC. Thus, as the input voltage increases, the output code first underestimates and then overestimates the input voltage. This error, called **quantization error**, is plotted against input voltage in Fig. 1.9(b).

For a given output code, we know only that the value of the input voltage lies somewhere within a 1-LSB quantization interval. For example, if the output code of the 3-bit ADC is 100, corresponding to a voltage  $V_{FS}/2$ , then the input voltage can be anywhere between  $\frac{7}{16}V_{FS}$  and  $\frac{9}{16}V_{FS}$ , a range of  $V_{FS}/8 \text{ V}$  or 1 LSB. From a mathematical point of view, the ADC circuitry in Fig. 1.8(b) picks the values of the bits in the binary word to minimize the magnitude of the quantization error  $v_e$  between the unknown input voltage  $v_X$  and the nearest quantized voltage level:

$$v_e = |v_X - (b_1 2^{-1} + b_2 2^{-2} + \dots + b_n 2^{-n}) V_{FS}| \quad (1.3)$$

<sup>4</sup> The binary point is understood to be to the immediate left of the digits of the code word. As the code word stair-steps from 000 to 111, the binary fraction steps from 0.000 to 0.111.

**EXERCISE:** An 8-bit A/D converter has  $V_{FS} = 5$  V. What is the digital output code word for an input of 1.2 V? What is the voltage range corresponding to 1 LSB of the converter?

**ANSWERS:** 00111101; 19.5 mV

### 1.3 NOTATIONAL CONVENTIONS

In many circuits we will be dealing with both dc and time-varying values of voltages and currents. The following standard notation will be used to keep track of the various components of an electrical signal. Total quantities will be represented by lowercase letters with capital subscripts, such as  $v_T$  and  $i_T$  in Eq. (1.4). The dc components are represented by capital letters with capital subscripts as, for example,  $V_{DC}$  and  $I_{DC}$  in Eq. (1.4); changes or variations from the dc value are represented by signal components  $v_{sig}$  and  $i_{sig}$ .

$$v_T = V_{DC} + v_{sig} \quad \text{or} \quad i_T = I_{DC} + i_{sig} \quad (1.4)$$

As examples, the total base-emitter voltage  $v_{BE}$  of a transistor and the total drain current  $i_D$  of a field-effect transistor are written as

$$v_{BE} = V_{BE} + v_{be} \quad \text{and} \quad i_D = I_D + i_d \quad (1.5)$$

Unless otherwise indicated, the equations describing a given network will be written assuming a consistent set of units: volts, amperes, and ohms. For example, the equation  $5 \text{ V} = (10,000 \Omega)I_1 + 0.6 \text{ V}$  will be written as  $5 = 10,000I_1 + 0.6$ .

The fourth upper/lowercase combination, such as  $V_{be}$  or  $I_d$ , is reserved for the amplitude of a sinusoidal signal's phasor representation as defined in Section 1.7.

**EXERCISE:** Suppose the voltage at a circuit node is described by

$$v_A = (5 \sin 2000\pi t + 4 + 3 \cos 1000\pi t) \text{ V}$$

What are the expressions for  $V_A$  and  $v_a$ ?

**ANSWERS:**  $V_A = 4 \text{ V}$ ;  $v_a = (5 \sin 2000\pi t + 3 \cos 1000\pi t) \text{ V}$

### Resistance and Conductance Representations

In the circuits throughout this text, resistors will be indicated symbolically as  $R_x$  or  $r_x$ , and the values will be expressed in  $\Omega$ ,  $\text{k}\Omega$ ,  $\text{M}\Omega$ , and so on. During analysis, however, it may be more convenient to work in terms of conductance with the following convention:

$$G_x = \frac{1}{R_x} \quad \text{and} \quad g_\pi = \frac{1}{r_\pi} \quad (1.6)$$

For example, conductance  $G_x$  always represents the reciprocal of the value of  $R_x$ , and  $g_\pi$  represents the reciprocal of  $r_\pi$ . The values next to a resistor symbol will always be expressed in terms of resistance ( $\Omega$ ,  $\text{k}\Omega$ ,  $\text{M}\Omega$ ).

### Dependent Sources

In electronics, **dependent** (or **controlled**) **sources** are used extensively. Four types of dependent sources are summarized in Fig. 1.10, in which the standard diamond shape is used for controlled sources. The **voltage-controlled current source (VCCS)**, **current-controlled current source (CCCS)**, and **voltage-controlled voltage source (VCVS)** are used routinely in this text to model

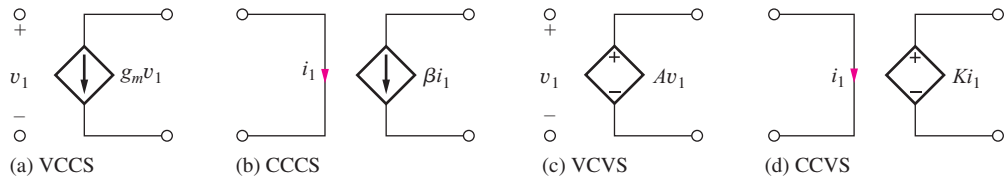


**Figure 1.10** Controlled sources. (a) Voltage-controlled current source (VCCS). (b) Current-controlled current source (CCCS). (c) Voltage-controlled voltage source (VCVS). (d) Current-controlled voltage source (CCVS).

transistors and amplifiers or to simplify more complex circuits. Only the **current-controlled voltage source (CCVS)** sees limited use.

## 1.4 PROBLEM-SOLVING APPROACH

Solving problems is a centerpiece of an engineer's activity. As engineers, we use our creativity to find new solutions to problems that are presented to us. A well-defined approach can aid significantly in solving problems. The examples in this text highlight an approach that can be used in all facets of your career, as a student and as an engineer in industry. The method is outlined in the following nine steps:

1. State the **problem** as clearly as possible.
2. List the **known information and given data**.
3. Define the **unknowns** that must be found to solve the problem.
4. List your **assumptions**. You may discover additional assumptions as the analysis progresses.
5. Develop an **approach** from a group of possible alternatives.
6. Perform an **analysis** to find a solution to the problem. As part of the analysis, be sure to draw the circuit and label the variables.
7. **Check the results.** Has the problem been solved? Is the math correct? Have all the unknowns been found? Have the assumptions been satisfied? Do the results satisfy simple consistency checks?
8. **Evaluate the solution.** Is the solution realistic? Can it be built? If not, repeat steps 4–7 until a satisfactory solution is obtained.
9. **Computer-aided analysis.** SPICE and other computer tools are highly useful to check the results and to see if the solution satisfies the problem requirements. Compare the computer results to your hand results.

To begin solving a problem, we must try to understand its details. The first four steps, which attempt to clearly define the problem, can be the most important part of the solution process. Time spent understanding, clarifying, and defining the problem can save much time and frustration.

The first step is to write down a statement of the problem. The original problem description may be quite vague; we must try to understand the problem as well as, or even better than, the individual who posed the problem. As part of this focus on understanding the problem, we list the information that is known and unknown. Problem-solving errors can often be traced to imprecise definition of the unknown quantities. For example, it is very important for analysis to draw the circuit properly and to clearly label voltages and currents on our circuit diagrams.

Often there are more unknowns than constraints, and we need engineering judgment to reach a solution. Part of our task in studying electronics is to build up the background for selecting between various alternatives. Along the way, we often need to make approximations and assumptions that simplify the problem or form the basis of the chosen approach. It is important to state these assumptions, so that we can be sure to check their validity at the end. Throughout this text you will encounter opportunities to make assumptions. Most often, you should make assumptions that simplify your computational effort yet still achieve useful results.

The exposition of the known information, unknowns, and assumptions helps us not only to better understand the problem but also to think about various alternative solutions. We must choose the approach that appears to have the best chance of solving the problem. There may be more than one satisfactory approach. Each person will view the problem somewhat differently, and the approach that is clearest to one individual may not be the best for another. Pick the one that seems best to you. As part of defining the approach, be sure to think about what computational tools are available to assist in the solution, including MATLAB®, Mathcad®, spreadsheets, SPICE, and your calculator.

Once the problem and approach are defined as clearly as possible, then we can perform any analysis required and solve the problem. After the analysis is completed we need to check the results. A number of questions should be resolved. First, have all the unknowns been found? Do the results make sense? Are they consistent with each other? Are the results consistent with assumptions used in developing the approach to the problem?

Then we need to evaluate the solution. Are the results viable? For example, are the voltage, current, and power levels reasonable? Can the circuit be realized with reasonable yield with real components? Will the circuit continue to function within specifications in the face of significant component variations? Is the cost of the circuit within specifications? If the solution is not satisfactory, we need to modify our approach and assumptions and attempt a new solution. An iterative solution is often required to meet the specifications in realistic design situations. SPICE and other computer tools are highly useful for checking results and ensuring that the solution satisfies the problem requirements.

The solutions to the examples in this text have been structured following the problem-solving approach introduced here. Although some examples may appear trivial, the power of the structured approach increases as the problem becomes more complex.

## WHAT ARE REASONABLE NUMBERS?

Part of our results check should be to decide if the answer is “reasonable” and makes sense. Over time we must build up an understanding of what numbers are reasonable. Most solid-state devices that we will encounter are designed to operate from voltages ranging from a battery voltage of 1 V on the low end to no more than 40–50 V<sup>5</sup> at the high end. Typical power supply voltages will be in the 10- to 20-V range, and typical resistance values encountered will range from tens of  $\Omega$  up to many G $\Omega$ .

Based on our knowledge of dc circuits, we should expect that the voltages in our circuits not exceed the power supply voltages. For example, if a circuit is operating from +8- and -5-V supplies, all of our calculated dc voltages must be between -5 and +8 V. In addition, the peak-to-peak amplitude of an ac signal should not exceed 13 V, the difference of the two supply voltages. With a 10-V supply, the maximum current that can go through a 100- $\Omega$  resistor is 100 mA; the current through a 10-M $\Omega$  resistor can be no more than 1  $\mu$ A. Thus we should remember the following “rules” to check our results:

1. With few exceptions, the dc voltages in our circuits cannot exceed the power supply voltages. The peak-to-peak amplitude of an ac signal should not exceed the difference of the power supply voltages.
2. The currents in our circuits will range from microamperes to no more than a hundred milliamperes or so.

---

<sup>5</sup> The primary exception is in the area of power electronics, where one encounters much larger voltages and currents than the ones discussed here.

## 1.5 IMPORTANT CONCEPTS FROM CIRCUIT THEORY

Analysis and design of electronic circuits make continuous use of a number of important techniques from basic network theory. Circuits are most often analyzed using a combination of **Kirchhoff's voltage law**, abbreviated **KVL**, and **Kirchhoff's current law**, abbreviated **KCL**. Occasionally, the solution relies on systematic application of **nodal** or **mesh analysis**. **Thévenin** and **Norton circuit transformations** are often used to help simplify circuits, and the notions of voltage and current division also represent basic tools of analysis. Models of active devices invariably involve dependent sources, as mentioned in the last section, and we need to be familiar with dependent sources in all forms. Amplifier analysis also uses two-port network theory. A review of two-port networks is deferred until the introductory discussion of amplifiers in Chapter 10. If the reader feels uncomfortable with any of the concepts just mentioned, this is a good time for review. To help, a brief review of these important circuit techniques follows.

### 1.5.1 VOLTAGE AND CURRENT DIVISION

Voltage and current division are highly useful circuit analysis techniques that can be derived directly from basic circuit theory. They are both used routinely throughout this text, and it is very important to be sure to understand the conditions for which each technique is valid! Examples of both methods are provided next.

**Voltage division** is demonstrated by the circuit in Fig. 1.11(a) in which the voltages  $v_1$  and  $v_2$  can be expressed as

$$v_1 = i_i R_1 \quad \text{and} \quad v_2 = i_i R_2 \quad (1.7)$$

Applying KVL to the single loop,

$$v_i = v_1 + v_2 = i_i(R_1 + R_2) \quad \text{and} \quad i_i = \frac{v_i}{R_1 + R_2} \quad (1.8)$$

Combining Eqs. (1.7) and (1.8) yields the basic voltage division formula:

$$v_1 = v_i \frac{R_1}{R_1 + R_2} \quad \text{and} \quad v_2 = v_i \frac{R_2}{R_1 + R_2} \quad (1.9)$$

For the resistor values in Fig. 1.11(a),

$$v_1 = 10 \text{ V} \frac{8 \text{ k}\Omega}{8 \text{ k}\Omega + 2 \text{ k}\Omega} = 8.00 \text{ V} \quad \text{and} \quad v_2 = 10 \text{ V} \frac{2 \text{ k}\Omega}{8 \text{ k}\Omega + 2 \text{ k}\Omega} = 2.00 \text{ V} \quad (1.10)$$

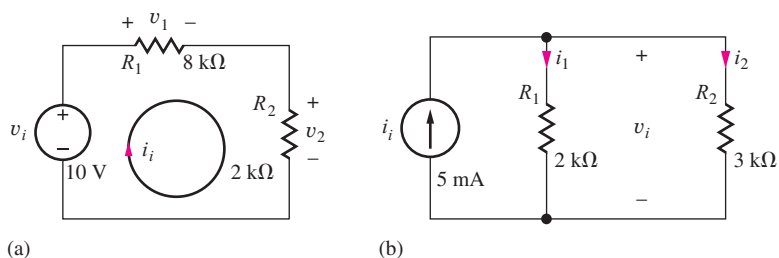
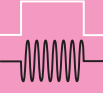


Figure 1.11 (a) A resistive voltage divider, (b) Current division in a simple network.


**DESIGN NOTE**

Note that the voltage divider relationships in Eq. (1.9) can be applied only when the current through the two resistor branches is the same. Also, note that the formulas are correct if the resistances are replaced by complex impedances and the voltages are represented as **phasors**.

$$\mathbf{V}_1 = \mathbf{V}_S \frac{Z_1}{Z_1 + Z_2} \quad \text{and} \quad \mathbf{V}_2 = \mathbf{V}_S \frac{Z_2}{Z_1 + Z_2}$$

**Current division** is also very useful. Let us find the currents  $i_1$  and  $i_2$  in the circuit in Fig. 1.11(b). Using KCL at the single node,

$$i_i = i_1 + i_2 \quad \text{where } i_1 = \frac{v_i}{R_1} \text{ and } i_2 = \frac{v_i}{R_2} \quad (1.11)$$

and solving for  $v_S$  yields

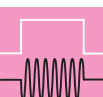
$$v_i = i_i \frac{1}{\frac{1}{R_1} + \frac{1}{R_2}} = i_i \frac{R_1 R_2}{R_1 + R_2} = i_i (R_1 \parallel R_2) \quad (1.12)$$

in which the notation  $R_1 \parallel R_2$  represents the parallel combination of resistors  $R_1$  and  $R_2$ . Combining Eqs. (1.11) and (1.12) yields the current division formulas:

$$i_1 = i_i \frac{R_2}{R_1 + R_2} \quad \text{and} \quad i_2 = i_i \frac{R_1}{R_1 + R_2} \quad (1.13)$$

For the values in Fig. 1.11(b),

$$i_1 = 5 \text{ mA} \frac{3 \text{ k}\Omega}{2 \text{ k}\Omega + 3 \text{ k}\Omega} = 3.00 \text{ mA} \quad i_2 = 5 \text{ mA} \frac{2 \text{ k}\Omega}{2 \text{ k}\Omega + 3 \text{ k}\Omega} = 2.00 \text{ mA}$$


**DESIGN NOTE**

It is important to note that the same voltage must appear across both resistors in order for the current division expressions in Eq. (1.13) to be valid. Here again, the formulas are correct if the resistances are replaced by complex impedances and the currents are represented as **phasors**.

$$\mathbf{I}_1 = \mathbf{I}_S \frac{Z_2}{Z_1 + Z_2} \quad \text{and} \quad \mathbf{I}_2 = \mathbf{I}_S \frac{Z_1}{Z_1 + Z_2}$$

### 1.5.2 THÉVENIN AND NORTON CIRCUIT REPRESENTATIONS

Let us now review the method for finding **Thévenin** and **Norton equivalent circuits**, including a dependent source; the circuit in Fig. 1.12(a) serves as our illustration. Because the linear network in the dashed box has only two terminals, it can be represented by either the Thévenin or Norton equivalent circuits in Figs. 1.12(b) and 1.12(c). The work of Thévenin and Norton permits us to reduce complex circuits to a single source and equivalent resistance. We illustrate these two important techniques with the next four examples.

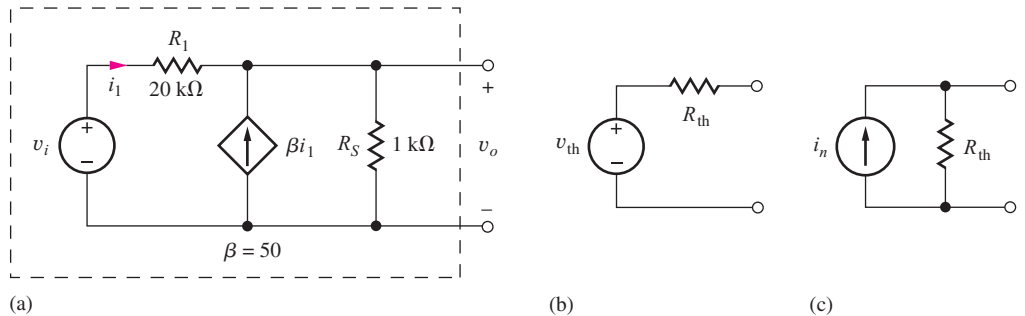


**Figure 1.12** (a) Two-terminal circuit and its (b) Thévenin and (c) Norton equivalents.

**EXAMPLE 1.1** THÉVENIN AND NORTON EQUIVALENT CIRCUITS

Let's practice finding the Thévenin and Norton equivalent circuits for the network in Fig. 1.12(a).

**PROBLEM** Find the Thévenin and Norton equivalent representations for the circuit in Fig. 1.12(a).

**SOLUTION** Known Information and Given Data: Circuit topology and values appear in Fig. 1.12(a).

**Unknowns:** Thévenin equivalent voltage  $v_{th}$ , Thévenin equivalent resistance  $R_{th}$ , and Norton equivalent current  $i_n$ .

**Approach:** Voltage source  $v_{\text{th}}$  is defined as the open-circuit voltage at the terminals of the circuit.  $R_{\text{th}}$  is the equivalent at the terminals of the circuit terminals with all independent sources set to zero. Source  $i_n$  represents the short-circuit current available at the output terminals and is equal to  $v_{\text{th}}/R_{\text{th}}$ .

**Assumptions:** None

**Analysis:** We will first find the value of  $v_{th}$ , then  $R_{th}$  and finally  $i_n$ . Open-circuit voltage  $v_{th}$  can be found by applying KCL at the output terminals.

$$\beta i_1 = \frac{v_o - v_i}{R_1} + \frac{v_o}{R_S} = G_1(v_o - v_i) + G_S v_o \quad (1.14)$$

by applying the notational convention for conductance from Sec. 1.3 ( $G_S = 1/R_S$ ).

Current  $i_1$  is given by

$$i_1 = G_1(v_i - v_\rho) \quad (1.15)$$

Substituting Eq. (1.15) into Eq. (1.14) and combining terms yields

$$G_1(\beta + 1)v_i = [G_1(\beta + 1) + G_S]v_o \quad (1.16)$$

The Thévenin equivalent output voltage is then found to be

$$v_o = \frac{G_1(\beta + 1)}{[G_1(\beta + 1) + G_s]} v_i = \frac{(\beta + 1)R_S}{[(\beta + 1)R_S + R_1]} v_i \quad (1.17)$$

where the second relationship was found by multiplying numerator and denominator by  $(R_1 R_S)$ . For the values in this problem,

$$v_o = \frac{(50+1)1\text{ k}\Omega}{[(50+1)1\text{ k}\Omega + 20\text{ k}\Omega]} v_i = 0.718 v_i \quad \text{and} \quad v_{\text{th}} = 0.718 v_i \quad (1.18)$$

$R_{\text{th}}$  represents the equivalent resistance present at the output terminals with all independent sources set to zero. To find the **Thévenin equivalent resistance**  $R_{\text{th}}$ , we first set the independent sources in the network to zero. Remember, however, that any dependent sources must remain active. A test voltage or current source is then applied to the network terminals and the corresponding current or voltage calculated. In Fig. 1.13  $v_i$  is set to zero, voltage source  $v_x$  is applied to the network, and the current  $i_x$  must be determined so that

$$R_{\text{th}} = \frac{v_x}{i_x} \quad (1.19)$$

can be calculated.

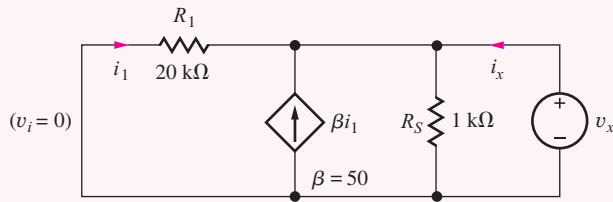


Figure 1.13 A test source  $v_x$  is applied to the network to find  $R_{\text{th}}$ .

$$i_x = -i_1 - \beta i_1 + G_S v_x \quad \text{in which } i_1 = -G_1 v_x \quad (1.20)$$

Combining and simplifying these two expressions yields

$$i_x = [(\beta + 1)G_1 + G_S]v_x \quad \text{and} \quad R_{\text{th}} = \frac{v_x}{i_x} = \frac{1}{(\beta + 1)G_1 + G_S} \quad (1.21)$$

The denominator of Eq. (1.21) represents the sum of two conductances, which corresponds to the parallel combination of two resistances. Therefore, Eq. (1.21) can be rewritten as

$$R_{\text{th}} = \frac{1}{(\beta + 1)G_1 + G_S} = \frac{R_S \frac{R_1}{(\beta + 1)}}{R_S + \frac{R_1}{(\beta + 1)}} = R_S \left| \left( \frac{R_1}{(\beta + 1)} \right) \right| \quad (1.22)$$

For the values in this example,

$$R_{\text{th}} = R_S \left| \left( \frac{R_1}{(\beta + 1)} \right) \right| = 1 \text{ k}\Omega \left| \left( \frac{20 \text{ k}\Omega}{(50 + 1)} \right) \right| = 1 \text{ k}\Omega \parallel 392 \Omega = 282 \Omega \quad (1.23)$$

Norton source in represents the short circuit current available from the original network. Since we already have the Thévenin equivalent circuit, we can use it to fid the value of  $i_n$ .

$$i_n = \frac{v_{\text{th}}}{R_{\text{th}}} = \frac{0.718v_i}{282\Omega} = 2.55 \times 10^{-3}v_i$$

The Thévenin and Norton equivalent circuits for Fig. 1.12 calculated in the previous example appear for comparison in Fig. 1.14.

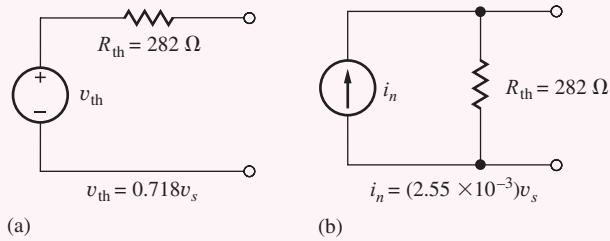


**Figure 1.14** Completed (a) Thévenin and (b) Norton equivalent circuits for the two-terminal network in Fig. 1.12(a).

**Check of Results:** We have found the three unknowns required. A recheck of the calculations indicates they are done correctly. The value of  $v_{th}$  is the same order of magnitude as  $v_i$ , so its value should not be unusually large or small. The value of  $R_{th}$  is less than 1 k $\Omega$ , which seems reasonable, since we should not expect the resistance to exceed the value of  $R_S$  that appears in parallel with the output terminals. We can double-check everything by directly calculating  $i_n$  from the original circuit. If we short the output terminals in Fig. 1.12, we find the short-circuit current (See Ex. 1.2) to be  $i_n = (\beta + 1) v_i / R_1 = 2.55 \times 10^{-3} v_i$  and in agreement with the other method.

**EXAMPLE 1.2** NORTON EQUIVALENT CIRCUIT

Practice finding the Norton equivalent circuit for a network containing a dependent source.

**PROBLEM** Find the Norton equivalent (Fig. 1.12(c)) for the circuit in Fig. 1.12(a).

**SOLUTION** **Known Information and Given Data:** Circuit topology and circuit values appear in Fig. 1.12(a). The value of  $R_{th}$  was calculated in the previous example.

**Unknowns:** Norton equivalent current  $i_n$ .

**Approach:** The Norton equivalent current is found by determining the current coming out of the network when a short circuit is applied to the terminals.

**Assumptions:** None.

**Analysis:** For the circuit in Fig. 1.15, the output current will be

$$j_n \equiv j_1 + \beta i_1 \quad \text{and} \quad j_1 \equiv G_1 v_i \quad (1.24)$$

The short circuit across the output forces the current through  $R_S$  to be 0. Combining the two expressions in Eq. (1.24) yields

$$i_n = (\beta + 1)G_1 v_i = \frac{(\beta + 1)}{R_1} v_i \quad (1.25)$$

or

$$i_n = \frac{(50 + 1)}{29\text{ k}\Omega} v_i = \frac{v_i}{392\text{ }\Omega} = (2.55 \text{ mS}) v_i \quad (1.26)$$

The resistance in the Norton equivalent circuit also equals  $R_{th}$  found in Eq. (1.23).

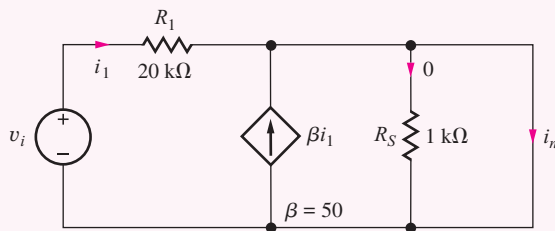
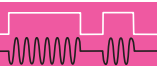
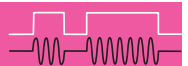


**Figure 1.15** Circuit for determining short-circuit output current.

**Check of Results:** We have found the Norton equivalent current. Note that  $v_{\text{th}} = i_n R_{\text{th}}$  and this result can be used to check the calculations:  $i_n R_{\text{th}} = (2.55 \text{ mS})v_s(282 \Omega) = 0.719 v_s$ , which agrees within round-off error with the previous example.



## ELECTRONICS IN ACTION

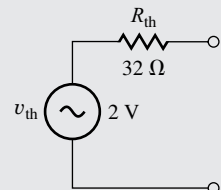


### Player Characteristics

The headphone amplifier in a personal music player represents an everyday example of a basic audio amplifier. The traditional audio band spans the frequencies from 20 Hz to 20 kHz, a range that extends beyond the hearing capability of most individuals at both the upper and lower ends.

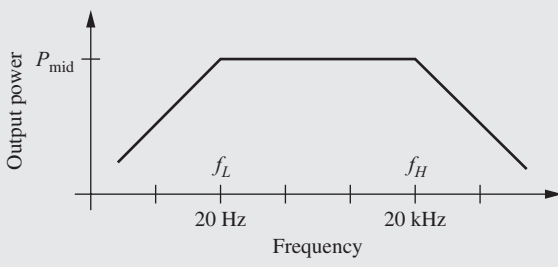


iPod: © The McGraw-Hill Companies, Inc./Jill Braaten, photographer



Thévenin equivalent circuit for output stage

The characteristics of the Apple iPod in the accompanying figure are representative of a high quality audio output stage in an MP3 player or a computer sound card. The output can be represented by a Thévenin equivalent circuit with  $v_{\text{th}} = 2 \text{ V}$  and  $R_{\text{th}} = 32 \text{ ohms}$ , and the output stage is designed to deliver a power of approximately 15 mW into each channel of a headphone with a matched impedance of 32 ohms. The output power is approximately constant over the 20 Hz–20 kHz frequency range. At the lower and upper cutoff frequencies,  $f_L$  and  $f_H$ , the output power will be reduced by 3 dB, a factor of 2.



Power versus frequency for an audio amplifier

The distortion characteristics of the amplifier are also important, and this is an area that often distinguishes one sound card or MP3 player from another. A good audio system will have a total harmonic distortion (THD) specification of less than 0.1 percent at full power.

## 1.6 FREQUENCY SPECTRUM OF ELECTRONIC SIGNALS

**Fourier analysis** and the **Fourier series** represent extremely powerful tools in electrical engineering. Results from Fourier theory show that complicated signals are actually composed of a continuum of sinusoidal components, each having a distinct amplitude, frequency, and phase. The **frequency spectrum** of a signal presents the amplitude and phase of the components of the signal versus frequency.

Nonrepetitive signals have continuous spectra with signals that may occupy a broad range of frequencies. For example, the amplitude spectrum of a television signal measured during a small time interval is depicted in Fig. 1.16. The TV video signal is designed to occupy the frequency range from 0 to 4.5 MHz.<sup>6</sup> Other types of signals occupy different regions of the frequency spectrum. Table 1.3 identifies the frequency ranges associated with various categories of common signals.

In contrast to the continuous spectrum in Fig. 1.16, Fourier series analysis shows that *any periodic signal*, such as the square wave of Fig. 1.17, contains spectral components only at discrete frequencies<sup>7</sup> that are related directly to the period of the signal. For example, the square wave of Fig. 1.17 having an amplitude  $V_O$  and period  $T$  can be represented by the Fourier series

$$v(t) = V_{DC} + \frac{2V_O}{\pi} \left( \sin \omega_o t + \frac{1}{3} \sin 3\omega_o t + \frac{1}{5} \sin 5\omega_o t + \dots \right) \quad (1.27)$$

in which  $\omega_o = 2\pi/T$  (rad/s) is the **fundamental radian frequency** of the square wave. We refer to  $f_o = 1/T$  (Hz) as the **fundamental frequency** of the signal, and the frequency components at  $2f_o$ ,  $3f_o$ ,  $4f_o$ , ... are called the second, third, fourth, and so on **harmonic frequencies**.

<sup>6</sup> This signal is combined with a much higher carrier frequency prior to transmission.

<sup>7</sup> There are an infinite number of components, however.

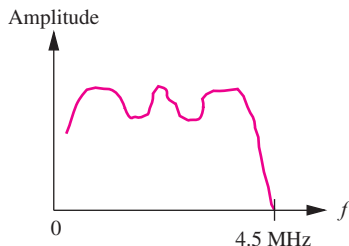


**Figure 1.16** Spectrum of a TV signal.

**TABLE 1.3**  
Frequencies Associated with Common Signals

CATEGORY	FREQUENCY RANGE
Audible sounds	20 Hz – 20 kHz
Baseband video (TV) signal	0 – 4.5 MHz
AM radio broadcasting	540 – 1600 kHz
High-frequency radio communications	1.6 – 54 MHz
VHF television (Channels 2–6)	54 – 88 MHz
FM radio broadcasting	88 – 108 MHz
VHF radio communication	108 – 174 MHz
VHF television (Channels 7–13)	174 – 216 MHz
Maritime and government communications	216 – 450 MHz
Business communications	450 – 470 MHz
UHF television (Channels 14–69)	470 – 806 MHz
Fixed and mobile communications including allocations for analog and digital cellular	806 – 902 MHz
Telephones, personal communications, and other	928 – 960 MHz
Wireless devices	1710 – 1990 MHz
Satellite television	2310 – 2690 MHz
Wireless devices	3.7 – 4.2 GHz
Wireless devices	5.0 – 5.5 GHz

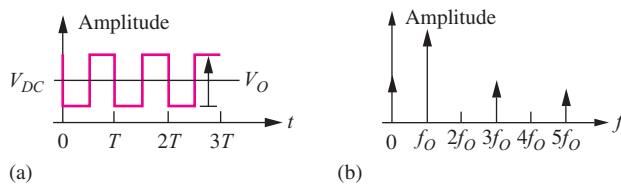


**Figure 1.17** A periodic signal (a) and its amplitude spectrum (b).

## 1.7 AMPLIFIERS

The characteristics of analog signals are most often manipulated using linear amplifiers that affect the amplitude and/or phase of the signal without changing its frequency. Although a complex signal may have many individual components, as just described in Sec. 1.6, linearity permits us to use the **superposition principle** to treat each component individually.

For example, suppose the amplifier with voltage gain  $A$  in Fig. 1.18(a) is fed a sinusoidal input signal component  $v_i$  with amplitude  $V_i$ , frequency  $\omega_i$ , and phase  $\phi$ :

$$v_i = V_i \sin(\omega_i t + \phi) \quad (1.28)$$

Then, if the amplifier is linear, the output corresponding to this signal component will also be a sinusoidal signal at the same frequency but with a different amplitude and phase:

$$v_o = V_o \sin(\omega_i t + \phi + \theta) \quad (1.29)$$

Using phasor notation, the input and output signals would be represented as

$$\mathbf{V}_i = V_i \angle \phi \quad \text{and} \quad \mathbf{V}_o = V_o \angle (\phi + \theta) \quad (1.30)$$

The **voltage gain** of the amplifier is defined in terms of these phasors:

$$A = \frac{\mathbf{V}_o}{\mathbf{V}_i} = \frac{V_o \angle (\phi + \theta)}{V_i \angle \phi} = \frac{V_o}{V_i} \angle \theta \quad (1.31)$$

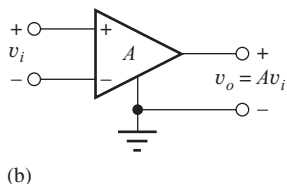
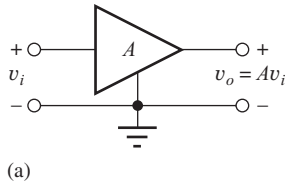


**Figure 1.18** (a) Symbol for amplifier with single input and voltage gain  $A$ ; (b) differential amplifier having two inputs and gain  $A$ .

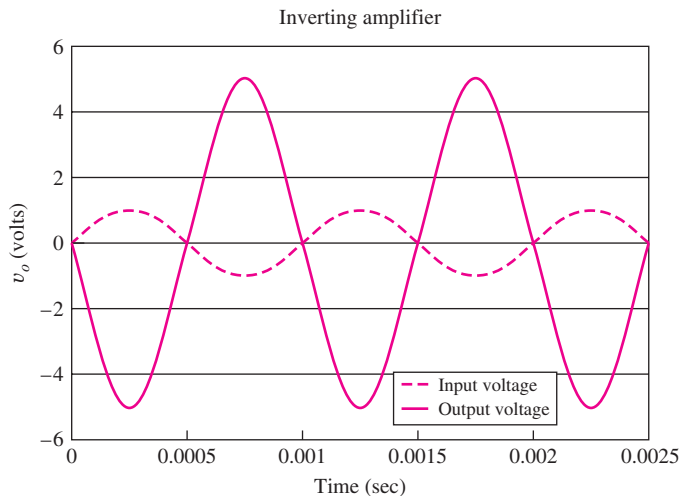


**Figure 1.19** Input and output voltage waveforms for an amplifier with gain  $A_v = -5$  and  $v_i = 1 \sin 2000\pi t$  V.

This amplifier has a voltage gain with magnitude equal to  $V_o/V_i$  and a phase shift of  $\theta$ . In general, both the magnitude and phase of the voltage gain will be a function of frequency. Note that amplifiers also often provide current gain and power gain as well as voltage gain, but these concepts will not be explored further until Chapter 10.

The curves in Fig. 1.19 represent the input and output voltage waveforms for an inverting amplifier with  $A_v = -5$  and  $v_i = 1 \sin 2000\pi t$  V. Both the factor of five increase in signal amplitude and the  $180^\circ$  phase shift (multiplication by  $-1$ ) are apparent in the graph.

At this point, a note regarding the phase angle is needed. In Eqs. (1.28) and (1.29),  $\omega t$ ,  $\phi$ , and  $\theta$  must have the same units. With  $\omega t$  normally expressed in radians,  $\phi$  should also be in radians. However, in electrical engineering texts,  $\phi$  is often expressed in degrees. We must be aware of this mixed system of units and remember to convert degrees to radians before making any numeric calculations.

**EXERCISE:** The input and output voltages of an amplifier are expressed as

$$v_i = 0.001 \sin(2000\pi t) \text{ V} \quad \text{and} \quad v_o = -5 \cos(2000\pi t + 25^\circ) \text{ V}$$

in which  $v_i$  and  $v_o$  are specified in volts when  $t$  is seconds. What are  $V_i$ ,  $V_o$ , and the voltage gain of the amplifier?

**ANSWERS:**  $0.001 \angle 0^\circ$ ;  $5 \angle -65^\circ$ ;  $5000 \angle -65^\circ$

### 1.7.1 IDEAL OPERATIONAL AMPLIFIERS

The **operational amplifier**, “op amp” for short, is a fundamental building block in electronic design and is discussed in most introductory circuit courses. A brief review of the ideal op amp is provided here; an in-depth study of the properties of ideal and nonideal op amps and the circuits used to build the op amp itself are the subjects of Chapters 11, 12, 15, and 16. Although it is impossible to realize the **ideal operational amplifier**, its use allows us to quickly understand the basic behavior to be expected from a given circuit and serves as a model to help in circuit design.

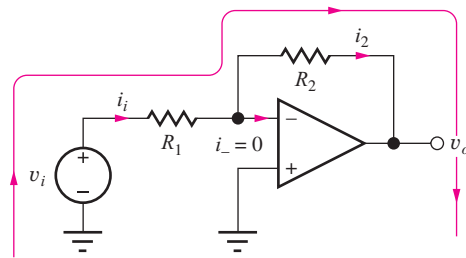


**Figure 1.20** Inverting amplifier using op amp.

From our basic circuit courses, we may recall that op amps are differential (or difference) amplifiers that respond to the signal voltage that appears between the + and – input terminals of the amplifier depicted in Fig. 1.18(b). Ideal op amps are assumed to have infinite **voltage gain** and infinite **input resistance**, and these properties lead to two special assumptions that are used to analyze circuits containing ideal op amps:

1. The voltage difference across the input terminals is zero; that is,  $v_- = v_+$ .
2. Both input currents are zero.

### Applying the Assumptions—The Inverting Amplifier

The classic **inverting amplifier** circuit will be used to refresh our memory of the analysis of circuits employing op amps. The inverting amplifier is built by grounding the positive input of the operational amplifier and connecting resistors  $R_1$  and  $R_2$ , called the **feedback network**, between the inverting input and the signal source and amplifier output node, respectively, as in Fig. 1.20. Note that the ideal op amp is represented by a triangular amplifier symbol without a gain  $A$  indicated.

Our goal is to determine the voltage gain  $A_v$  of the overall amplifier, and to find  $A_v$ , we must find a relationship between  $v_i$  and  $v_o$ . One approach is to write an equation for the single loop shown in Fig. 1.20:

$$v_i - i_1 R_1 - i_2 R_2 - v_o = 0 \quad (1.32)$$

Now we need to express  $i_1$  and  $i_2$  in terms of  $v_i$  and  $v_o$ . By applying KCL at the inverting input to the amplifier, we see that  $i_2$  must equal  $i_1$  because Assumption 2 states that  $i_-$  must be zero:

$$i_1 = i_2 \quad (1.33)$$

Current  $i_1$  can be written in terms of  $v_i$  as

$$i_1 = \frac{v_i - v_-}{R_1} \quad (1.34)$$

where  $v_-$  is the voltage at the inverting input (negative input) of the op amp. But Assumption 1 states that the input voltage between the op amp terminals must be zero, so  $v_-$  must be zero because the positive input is grounded. Therefore

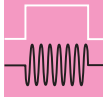
$$i_1 = \frac{v_i}{R_1} \quad (1.35)$$

Combining Eqs. (1.32)–(1.35), the voltage gain is given by

$$A_v = \frac{v_o}{v_i} = -\frac{R_2}{R_1} \quad (1.36)$$

Referring to Eq. (1.36), we should note several things. The voltage gain is negative, indicative of an inverting amplifier with a  $180^\circ$  phase shift between its input and output signals. In addition, the magnitude of the gain can be greater than or equal to 1 if  $R_2 \geq R_1$  (the most common case), but it can also be less than 1 for  $R_2 < R_1$ .

In the amplifier circuit in Fig. 1.20, the inverting-input terminal of the operational amplifier is at ground potential, 0 V, and is referred to as a **virtual ground**. The ideal operational amplifier adjusts its output to whatever voltage is necessary to force  $v_-$  to be zero.


**DESIGN NOTE** VIRTUAL GROUND IN OP AMP CIRCUITS

Although the inverting input represents a virtual ground, it is *not* connected directly to ground (there is no direct dc path for current to reach ground). Shorting this terminal to ground for analysis purposes is a common error that must be avoided.

**EXERCISE:** The amplifier in Fig. 1.20 has a gain of  $-5$  with  $R_1 = 10 \text{ k}\Omega$ . What is the value of  $R_2$ ?

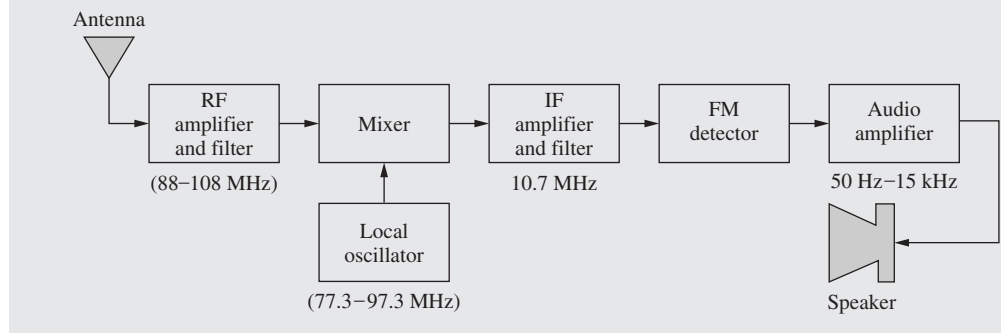
**ANSWER:**  $50 \text{ k}\Omega$


**ELECTRONICS IN ACTION**


### *Amplifiers in a Familiar Electronic System—The FM Stereo Receiver*

The block diagram of an FM radio receiver is an example of an electronic system that uses a number of amplifiers. The signal from the antenna can be very small, often in the microvolt range. The signal's amplitude and power level are increased sequentially by three groups of amplifiers: the radio frequency (RF), intermediate frequency (IF), and audio amplifiers. At the output, the amplifier driving the loudspeaker could be delivering a  $100 \text{ W}$  audio signal to the speaker, whereas the power originally available from the antenna may amount to only picowatts.

The local oscillator, which tunes the radio receiver to select the desired station, represents another special application of amplifiers; these are investigated in Chapters 12 and 15. The mixer circuit actually changes the frequency of the incoming signal and is thus a nonlinear circuit. However, its design draws heavily on linear amplifier circuit concepts. Finally, the FM detector may be formed from either a linear or nonlinear circuit. Chapters 10 to 17 provide in-depth exploration of the design techniques used in linear amplifiers and oscillators and the foundation needed to understand more complex circuits such as mixers, modulators, and detectors.



Block diagram for an FM radio receiver.

### 1.7.2 AMPLIFIER FREQUENCY RESPONSE

In addition to modifying the voltage, current, and/or power level of a given signal, amplifiers are often designed to selectively process signals of different frequency ranges. Amplifiers are classified into a number of categories based on their frequency response; five possible categories are shown in Fig. 1.21. The **low-pass amplifier**, Fig. 1.21(a), passes all signals below some upper cutoff frequency  $f_H$ , whereas the **high-pass amplifier**, Fig. 1.21(b), amplifies all signals above the lower cutoff frequency  $f_L$ . The **band-pass amplifier** passes all signals between the two cutoff frequencies  $f_L$  and  $f_H$ , as in Fig. 1.21(c). The **band-reject amplifier** in Fig. 1.21(d) rejects all signals having

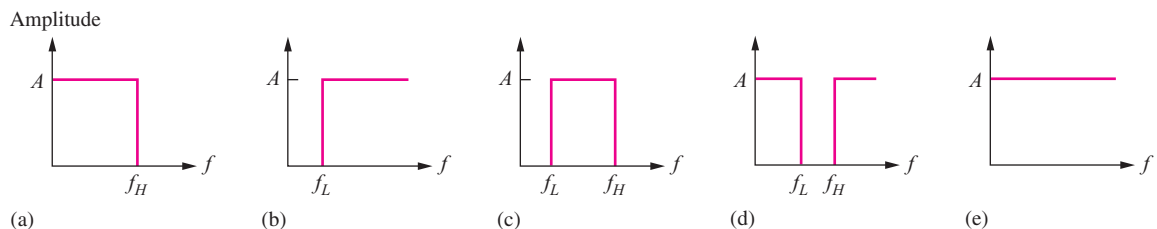


**Figure 1.21** Ideal amplifier frequency responses: (a) low-pass, (b) high-pass, (c) band-pass, (d) band-reject, and (e) all-pass characteristics.

frequencies lying between  $f_L$  and  $f_H$ . Finally, the **all-pass amplifier** in Fig. 1.21(e) amplifies signals at any frequency. The all-pass amplifier is actually used to tailor the phase of the signal rather than its amplitude. Circuits that are designed to amplify specific ranges of signal frequencies are usually referred to as **filters**.

**EXERCISE:** (a) The band-pass amplifier in Fig. 1.21(c) has  $f_L = 1.5$  kHz,  $f_H = 2.5$  kHz, and  $A = 10$ . If the input voltage is given by

$$v_s = [0.5 \sin(2000\pi t) + \sin(4000\pi t) + 1.5 \sin(6000\pi t)] \text{ V}$$

what is the output voltage of the amplifier?

(b) Suppose the same input signal is applied to the low-pass amplifier in Fig. 1.21(a), which has  $A = 6$  and  $f_H = 1.5$  kHz. What is the output voltage?

**ANSWERS:** 10.0  $\sin 4000\pi t$  V; 3.00  $\sin 2000\pi t$  V

## 1.8 ELEMENT VARIATIONS IN CIRCUIT DESIGN

Whether a circuit is built in discrete form or fabricated as an integrated circuit, the passive components and semiconductor device parameters will all have **tolerances** associated with their values. Discrete resistors can be purchased with a number of different tolerances including  $\pm 10$  percent,  $\pm 5$  percent,  $\pm 1$  percent, or better, whereas resistors in ICs can exhibit wide variations ( $\pm 30$  percent). Capacitors often exhibit asymmetrical tolerance specifications such as  $+20$  percent/ $-50$  percent, and power supply voltage tolerances are often specified in the range of 1–10 percent. For the semiconductor devices that we shall study in Chapters 3–5, device parameters may vary by 30 percent or more.

In addition to this initial value uncertainty due to tolerances, the values of the circuit components and parameters will vary with temperature and circuit age. It is important to understand the effect of these element changes on our circuits and to be able to design circuits that will continue to operate correctly in the face of such element variations. We will explore two analysis approaches, worst-case analysis and Monte Carlo analysis, that can help quantify the effects of tolerances on circuit performance.

### 1.8.1 MATHEMATICAL MODELING OF TOLERANCES

A mathematical model for symmetrical parameter variations is

$$P_{\text{nom}}(1 - \varepsilon) \leq P \leq P_{\text{nom}}(1 + \varepsilon) \quad (1.37)$$

in which  $P_{\text{nom}}$  is the nominal specification for the parameter such as the resistor value or independent source value, and  $\varepsilon$  is the fractional tolerance for the component. For example, a resistor  $R$  with

**nominal value** of  $10\text{ k}\Omega$  and a 5 percent tolerance could exhibit a resistance anywhere in the following range:

$$10,000\ \Omega(1 - 0.05) \leq R \leq 10,000\ \Omega(1 + 0.05)$$

or

$$9500\ \Omega \leq R \leq 10,500\ \Omega$$

**EXERCISE:** A  $39\text{-k}\Omega$  resistor has a 10 percent tolerance. What is the range of resistor values corresponding to this resistor? Repeat for a  $3.6\text{-k}\Omega$  resistor with a 1 percent tolerance.

**ANSWERS:**  $35.1 \leq R \leq 42.9\text{ k}\Omega$ ;  $3.56 \leq R \leq 3.64\text{ k}\Omega$ .

## 1.8.2 WORST-CASE ANALYSIS

**Worst-case analysis** is often used to ensure that a design will function under a given set of component variations. Worst-case analysis is performed by choosing values of the various components that make a desired variable (such as voltage, current, power, gain, or bandwidth) as large and as small as possible. These two limits are usually found by analyzing a circuit with the values of the various circuit elements pushed to their extremes. Although a design based on the worst case is often too conservative and represents “overdesign,” it is important to understand the technique and its limitations. An easy way to explore worst-case analysis is with an example.

### EXAMPLE 1.3 WORST-CASE ANALYSIS

Here we apply worst-case analysis to a simple voltage divider circuit.

**PROBLEM** Find the nominal and worst-case values (highest and lowest) of output voltage  $V_O$  and source current  $I_I$  for the voltage divider circuit of Fig. 1.22.

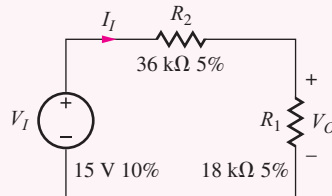


Figure 1.22 Resistor voltage divider circuit with tolerances.

**SOLUTION** **Known Information and Given Data:** We have been given the voltage divider circuit in Fig. 1.22; the 15-V source  $V_I$  has a 10 percent tolerance; resistor  $R_1$  has a nominal value of  $18\text{ k}\Omega$  with a 5 percent tolerance; resistor  $R_2$  has a nominal value of  $36\text{ k}\Omega$  with a 5 percent tolerance. Expressions for  $V_O$  and  $I_I$  are

$$V_O = V_I \frac{R_1}{R_1 + R_2} \quad \text{and} \quad I_I = \frac{V_I}{R_1 + R_2} \quad (1.38)$$

**Unknowns:**  $V_O^{\text{nom}}$ ,  $V_O^{\text{max}}$ ,  $V_O^{\text{min}}$ ,  $I_I^{\text{nom}}$ ,  $I_I^{\text{max}}$ ,  $I_I^{\text{min}}$

**Approach:** Find the nominal values of  $V_O$  and  $I_I$  with all circuit elements set to their nominal (ideal) values. Find the worst-case values by selecting the individual voltage and resistance values that force  $V_O$  and  $I_I$  to their extremes. Note that the values selected for the various circuit elements to produce  $V_O^{\text{max}}$  will most likely differ from those that produce  $I_I^{\text{max}}$ , and so on.

**Assumptions:** None.

**Analysis: (a) Nominal Values**

The nominal value of voltage  $V_O$  is found using the nominal values for all the parameters:

$$V_O^{\text{nom}} = V_I^{\text{nom}} \frac{R_1^{\text{nom}}}{R_1^{\text{nom}} + R_2^{\text{nom}}} = 15 \text{ V} \frac{18 \text{ k}\Omega}{18 \text{ k}\Omega + 36 \text{ k}\Omega} = 5 \text{ V} \quad (1.39)$$

Similarly, the nominal value of source current  $I_I$  is

$$I_I^{\text{nom}} = \frac{V_S^{\text{nom}}}{R_1^{\text{nom}} + R_2^{\text{nom}}} = \frac{15 \text{ V}}{18 \text{ k}\Omega + 36 \text{ k}\Omega} = 278 \mu\text{A} \quad (1.40)$$

**(b) Worst-Case Limits**

Now let us find the **worst-case values (the largest and smallest possible values)** of voltage  $V_O$  and current  $I_I$  that can occur for the given set of element tolerances. First, the values of the components will be selected to make  $V_O$  as large as possible. However, it may not always be obvious at first to which extreme to push the individual component values. Rewriting Eq. (1.38) for voltage  $V_O$  will help:

$$V_O = V_I \frac{R_1}{R_1 + R_2} = \frac{V_I}{1 + R_2/R_1} \quad (1.41)$$

In order to make  $V_O$  as large as possible, the numerator of Eq. (1.41) should be large and the denominator small. Therefore,  $V_I$  and  $R_1$  should be chosen to be as large as possible and  $R_2$  as small as possible. Conversely, in order to make  $V_O$  as small as possible,  $V_I$  and  $R_1$  must be small and  $R_2$  must be large. Using this approach, the maximum and minimum values of  $V_O$  are

$$V_O^{\text{max}} = \frac{15 \text{ V}(1.1)}{1 + \frac{36 \text{ k}\Omega(0.95)}{18 \text{ k}\Omega(1.05)}} = 5.87 \text{ V} \quad \text{and} \quad V_O^{\text{min}} = \frac{15 \text{ V}(0.9)}{1 + \frac{36 \text{ k}\Omega(1.05)}{18 \text{ k}\Omega(0.95)}} = 4.20 \text{ V} \quad (1.42)$$

The maximum value of  $V_O$  is 17 percent greater than the nominal value of 5 V, and the minimum value is 16 percent below the nominal value.

The worst-case values of  $I_I$  are found in a similar manner but require different choices for the values of the resistors:

$$I_I^{\text{max}} = \frac{V_I^{\text{max}}}{R_1^{\text{min}} + R_2^{\text{min}}} = \frac{15 \text{ V}(1.1)}{18 \text{ k}\Omega(0.95) + 36 \text{ k}\Omega(0.95)} = 322 \mu\text{A} \quad (1.43)$$

$$I_I^{\text{min}} = \frac{V_I^{\text{min}}}{R_1^{\text{max}} + R_2^{\text{max}}} = \frac{15 \text{ V}(0.9)}{18 \text{ k}\Omega(1.05) + 36 \text{ k}\Omega(1.05)} = 238 \mu\text{A}$$

The maximum of  $I_I$  is 16 percent greater than the nominal value, and the minimum value is 14 percent less than nominal.

**Check of Results:** The nominal and worst-case values have been determined and range 14–17 percent above and below the nominal values. We have three circuit elements that are varying, and the sum of the three tolerances is 20 percent. Our worst-case values differ from the nominal case by somewhat less than this amount, so the results appear reasonable.

**EXERCISE:** Find the nominal and worst-case values of the power delivered by source  $V_1$  in Fig. 1.22.

**ANSWERS:** 4.17 mW, 3.21 mW, 5.31 mW.



## DESIGN NOTE BE WARY OF WORST-CASE DESIGN

In a real circuit, the parameters will be randomly distributed between the limits, and it is unlikely that the various components will all reach their extremes at the same time. Thus the worst-case analysis technique will overestimate (often badly) the extremes of circuit behavior, and a design based on worst-case analysis usually represents an unnecessary overdesign that is more costly than necessary to achieve the specifications with satisfactory yield. A better, although more complex, approach is to attack the problem statistically using Monte Carlo analysis. However, if every circuit must work no matter what, worst-case analysis may be appropriate.

### 1.8.3 MONTE CARLO ANALYSIS

**Monte Carlo analysis** uses randomly selected versions of a given circuit to predict its behavior from a statistical basis. For Monte Carlo analysis, a value for each of the elements in the circuit is selected at random from the possible distributions of parameters, and the circuit is then analyzed using the randomly selected element values. Many such randomly selected realizations (“cases” or “instances”) of the circuit are generated, and the statistical behavior of the circuit is built up from analysis of the many test cases. Obviously, this is a good use of the computer. Before proceeding, we need to refresh our memory concerning a few results from probability and random variables.

#### Uniformly Distributed Parameters

In this section, the variable parameters will be assumed to be uniformly distributed between the two extremes. In other words, the probability that any given value of the parameter will occur is the same. In fact, when the parameter tolerance expression in Eq. (1.37) was first encountered, most of us probably visualized it in terms of a uniform distribution.

The probability density function  $p(r)$  for a uniformly distributed resistor  $r$  is represented graphically in Fig. 1.23(a). The probability that a resistor value lies between  $r$  and  $(r + dr)$  is equal to  $p(r) dr$ . The total probability  $P$  must equal unity, so

$$P = \int_{-\infty}^{+\infty} p(r) dr = 1 \quad (1.44)$$

Using this equation with the uniform probability density of Fig. 1.23(a) yields  $p(r) = \frac{1}{2\varepsilon R_{\text{nom}}}$  as indicated in the figure.

Monte Carlo analysis can be readily implemented with a spreadsheet, MATLAB®, Mathcad®, or another computer program using the **uniform random number generators** that are built into the software. Successive calls to these random number generators produce a sequence of **pseudo-random numbers** that are uniformly distributed between 0 and 1 with a mean of 0.5 as in Fig. 1.23(b).

For example, the Excel® spreadsheet contains the function called RAND() (used with a null argument), whereas MATLAB uses rand,<sup>8</sup> and Mathcad uses rnd(1). These functions generate random numbers with the distribution in Fig. 1.23(b). Other software products contain random number

<sup>8</sup> In MATLAB, rand generates a single random number, rand( $n$ ) is an  $n \times n$  matrix of random numbers, and rand ( $n, m$ ) is an  $n \times m$  matrix of random numbers. In Mathcad, rnd( $x$ ) returns a number uniformly distributed between 0 and  $x$ .

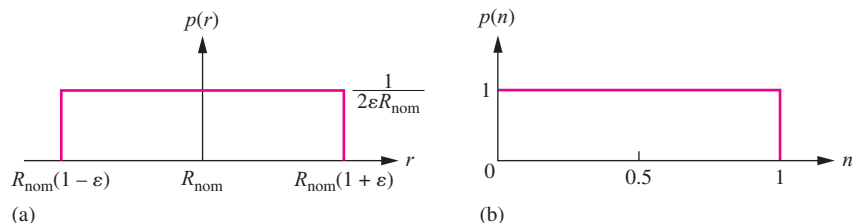


**Figure 1.23** (a) Probability density function for a uniformly distributed resistor; (b) probability density function for a random variable uniformly distributed between 0 and 1.

generators with similar names. In order to use `RAND()` to generate the distribution in Fig. 1.23(a), the mean must be centered at  $R_{\text{nom}}$  and the width of the distribution set to  $(2\varepsilon) \times R_{\text{nom}}$ :

$$R = R_{\text{nom}}(1 + 2\varepsilon(\text{RAND}() - 0.5)) \quad (1.45)$$

Now let us see how we use Eq. (1.45) in implementing a Monte Carlo analysis.

### EXAMPLE 1.4 MONTE CARLO ANALYSIS

Now we will apply Monte Carlo analysis to the voltage divider circuit.

**PROBLEM** Perform a Monte Carlo analysis of the circuit in Fig. 1.22. Find the mean, standard deviation, and largest and smallest values for  $V_O$ ,  $I_S$ , and the power delivered from the source.

**SOLUTION** **Known Information and Given Data:** The voltage divider circuit appears in Fig. 1.22. The 15 V source  $V_I$  has a 10 percent tolerance, resistor  $R_1$  has a nominal value of 18 k $\Omega$  with a 5 percent tolerance, and resistor  $R_2$  has a nominal value of 36 k $\Omega$  with a 5 percent tolerance. Expressions for  $V_O$ ,  $I_I$ , and  $P_I$  are

$$V_O = V_I \frac{R_1}{R_1 + R_2} \quad I_I = \frac{V_I}{R_1 + R_2} \quad P_I = V_I I_I$$

**Unknowns:** The mean, standard deviation, and largest and smallest values for  $V_O$ ,  $I_I$ , and  $P_I$ .

**Approach:** To perform a Monte Carlo analysis of the circuit in Fig. 1.22, we assign randomly selected values to  $V_I$ ,  $R_1$ , and  $R_2$  and then use the values to determine  $V_O$  and  $I_S$ . Using Eq. (1.45) with the tolerances specified in Fig. 1.22, the power supply and resistor values are represented as

1.  $V_I = 15(1 + 0.2(\text{RAND}() - 0.5))$
2.  $R_1 = 18,000(1 + 0.1(\text{RAND}() - 0.5))$
3.  $R_2 = 36,000(1 + 0.1(\text{RAND}() - 0.5))$

Note that each variable must invoke a separate call of the function `RAND()` so that the random values will be independently selected. The random elements in Eqs. (1.46) are then used to evaluate the equations that characterize the circuit, including the power delivered from the source:

4.  $V_O = V_I \frac{R_1}{R_1 + R_2}$
5.  $I_I = \frac{V_s}{R_1 + R_2}$
6.  $P_I = V_I I_I$

This example will utilize a spreadsheet. However, any number of computer tools could be used: MATLAB®, Mathcad®, C++, SPICE, or the like.

**Assumptions:** The parameters are uniformly distributed between their means. A 100-case analysis will be performed.

**Analysis:** The spreadsheet used in this analysis appears in Table 1.4. Equation sets (1.46) and (1.47) are entered into the first row of the spreadsheet, and then that row may be copied into as many additional rows as the number of statistical cases that are desired. The analysis is automatically repeated for the random selections to build up the statistical distributions, with each row representing one analysis of the circuit. At the end of the columns, the mean, standard deviation, and minimum and maximum values can all be calculated using built-in spreadsheet functions, and the overall spreadsheet data can be used to build histograms for the circuit performance. A portion of the spreadsheet output for 100 cases of the circuit of Fig. 1.22 is shown in Table 1.4.

**TABLE 1.4**

TOLERANCE	$V_I$ (V)	$R_1$ ( $\Omega$ )	$R_2$ ( $\Omega$ )	$V_O$ (V)	$I_I$ (A)	$P$ (W)
	10.00%	5.00%	5.00%			
Case 1	15.94	17,248	35,542	5.21	3.02E – 04	4.81E – 03
2	14.90	18,791	35,981	5.11	2.72E – 04	4.05E – 03
3	14.69	18,300	36,725	4.89	2.67E – 04	3.92E – 03
4	16.34	18,149	36,394	5.44	3.00E – 04	4.90E – 03
5	14.31	17,436	37,409	4.55	2.61E – 04	3.74E – 03
...						
95	16.34	17,323	36,722	5.24	3.02E – 04	4.94E – 03
96	16.38	17,800	35,455	5.47	3.08E – 04	5.04E – 03
97	15.99	17,102	35,208	5.23	3.06E – 04	4.89E – 03
98	14.06	18,277	35,655	4.76	2.61E – 04	3.66E – 03
99	13.87	17,392	37,778	4.37	2.51E – 04	3.49E – 03
Case 100	15.52	18,401	34,780	5.37	2.92E – 04	4.53E – 03
Avg	14.88	17,998	36,004	4.96	2.76E – 04	4.12E – 03
Nom.	15.00	18,000	36,000	5.00	2.78E – 04	4.17E – 03
Stdev	0.86	476	976	0.30	1.73E – 05	4.90E – 04
Max	16.46	18,881	37,778	5.70	3.10E – 04	5.04E – 03
WC-Max	16.50	18,900	37,800	5.87	3.22E – 04	—
Min	13.52	17,102	34,201	4.37	2.42E – 04	3.29E – 03
WC-Min	13.50	17,100	34,200	4.20	2.38E – 04	—

**Check of Results:** The average values for  $V_O$  and  $I_I$  are 4.96 V and 276  $\mu$ A, respectively, which are close to the values originally estimated from the nominal circuit elements. The averages will more closely approach the nominal values as the number of cases used in the analysis is increased. The standard deviations are 0.30 V and 17.3  $\mu$ A, respectively.

A histogram (generated with MATLAB® hist( $x$ ,  $n$ )) of the results of a 1000-case simulation of the output voltage in the same problem appears in Fig. 1.24. Note that the overall distribution is becoming Gaussian in shape with the peak in the center near the mean value. The worst-case values calculated earlier are several standard deviations from the mean and lie outside the minimum and maximum values that occurred even in this 1000-case Monte Carlo analysis.

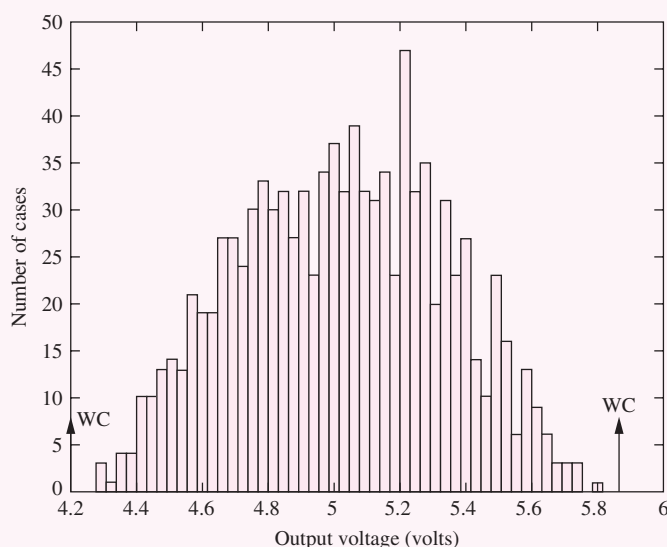


Figure 1.24 Histogram of a 1000-case simulation.

Some implementations of the SPICE circuit analysis program, PSPICE® for example, actually contain a Monte Carlo option in which a full circuit simulation is automatically performed for any number of randomly selected test cases. These programs, which provide a powerful tool for much more complex statistical analysis than is possible by hand, can perform statistical estimates of delay, frequency response, and the like for circuits with many elements.

#### 1.8.4 TEMPERATURE COEFFICIENTS

In the real world, all physical circuit elements change value as the temperature changes. Our circuit designs must continue to operate properly as the temperature changes. For example, the temperature range for commercial products is typically 0 to 70°C, whereas the standard military temperature range is –55 to +85°C. Other environments, such as the engine compartment of an automobile, can be even more extreme.

##### Mathematical Model

The basic mathematical model for incorporating element variation with temperature is

$$P = P_{\text{nom}}(1 + \alpha_1 \Delta T + \alpha_2 \Delta T^2) \quad \text{and} \quad \Delta T = T - T_{\text{nom}} \quad (1.48)$$

Coefficients  $\alpha_1$  and  $\alpha_2$  represent the first- and second-order<sup>9</sup> **temperature coefficients**, and  $\Delta T$  represents the difference between the actual temperature  $T$  and the temperature at which the nominal value is specified:

$$P = P_{\text{nom}} \quad \text{for} \quad T = T_{\text{nom}} \quad (1.49)$$

Common values for the magnitude of  $\alpha_1$  range from 0 to plus or minus several thousand parts per million per degree C ( $1000 \text{ ppm}/^\circ\text{C} = 0.1\%/\text{ }^\circ\text{C}$ ). For example, nichrome resistors are highly stable and can exhibit a **temperature coefficient of resistance (TCR =  $\alpha_1$ )** of only 50 ppm/ $^\circ\text{C}$ . In contrast, diffused resistors in integrated circuits may have  $\alpha_1$  as large as several thousand ppm/ $^\circ\text{C}$ . Most elements will also exhibit some curvature in their characteristics as a function of temperature, and  $\alpha_2$  will be nonzero, although small. We will neglect  $\alpha_2$  unless otherwise stated.

<sup>9</sup> Higher-order temperature dependencies can also be included.

### SPICE Model

Most SPICE programs contain models for the temperature dependencies of many circuit elements. For example, the temperature-dependent SPICE model for the resistor is equivalent to that given in Eq. (1.48):

$$R(T) = R(TNOM) * [1 + TC1 * (T - TNOM) + TC2 * (T - TNOM)^2] \quad (1.50)$$

in which the SPICE parameters are defined as follows:

$TNOM$  = temperature at which the nominal resistor value is measured

$T$  = temperature at which the simulation is performed

$TC1$  = first-order temperature coefficient

$TC2$  = second-order temperature coefficient

## EXAMPLE 1.5 TCR ANALYSIS

Find the value of a resistor at various temperatures.

**PROBLEM** A diffused resistor has a nominal value of  $10\text{ k}\Omega$  at a temperature of  $25^\circ\text{C}$  and has a TCR of  $+1000\text{ ppm}/^\circ\text{C}$ . Find its resistance at  $40$  and  $75^\circ\text{C}$ .

**SOLUTION** **Known Information and Given Data:** The resistor's nominal value is  $10\text{ k}\Omega$  at  $T = 25^\circ\text{C}$ . The TCR is  $1000\text{ ppm}/^\circ\text{C}$ .

**Unknowns:** The resistor values at  $40$  and  $75^\circ\text{C}$ .

**Approach:** Use the known values to evaluate Eq. (1.48).

**Assumptions:** Based on the TCR statement,  $\alpha_1 = 1000\text{ ppm}/^\circ\text{C}$  and  $\alpha_2 = 0$ .

**Analysis:** The TCR of  $+1000\text{ ppm}/^\circ\text{C}$  corresponds to

$$\alpha_1 = \frac{10^3}{10^6} \frac{1}{^\circ\text{C}} = 10^{-3}/^\circ\text{C}$$

The resistor value at  $40^\circ\text{C}$  would be

$$R = 10\text{ k}\Omega \left[ 1 + \frac{10^{-3}}{^\circ\text{C}} (40 - 25)^\circ\text{C} \right] = 10.15\text{ k}\Omega$$

and at  $75^\circ\text{C}$  the value would be

$$R = 10\text{ k}\Omega \left[ 1 + \frac{10^{-3}}{^\circ\text{C}} (75 - 25)^\circ\text{C} \right] = 10.5\text{ k}\Omega$$

**Check of Results:**  $1000\text{ ppm}/^\circ\text{C}$  corresponds to  $0.1\%/\text{ }^\circ\text{C}$  or  $10\text{ }\Omega/\text{ }^\circ\text{C}$  for the  $10\text{-k}\Omega$  resistor. A  $15^\circ\text{C}$  temperature change should shift the resistor value by  $150\text{ }\Omega$ , whereas a  $50^\circ\text{C}$  change should change the value by  $500\text{ }\Omega$ . Thus the answers appear correct.

**EXERCISE:** What will the resistor value in Ex. 1.5 be for  $T = -55^\circ\text{C}$  and  $T = +85^\circ\text{C}$ ?

**ANSWERS:**  $9.20\text{ k}\Omega$ ,  $10.6\text{ k}\Omega$ .

## 1.9 NUMERIC PRECISION

Many numeric calculations will be performed throughout this book. Keep in mind that the circuits being designed can all be built in discrete form in the laboratory or can be implemented in integrated circuit form. In designing circuits, we will be dealing with components that have tolerances ranging from less than  $\pm 1$  percent to greater than  $\pm 50$  percent, and calculating results to a precision of more than three significant digits represents a meaningless exercise except in very limited circumstances. Thus, the results in this text are consistently represented with three significant digits: 2.03 mA, 5.72 V, 0.0436  $\mu$ A, and so on. For example, see the answers in Eqs. (1.18), (1.23), and so on.

## SUMMARY

- The age of electronics began in the early 1900s with Pickard's creation of the crystal diode detector, Fleming's invention of the diode vacuum tube, and then Deforest's development of the triode vacuum tube. Since that time, the electronics industry has grown to account for as much as 10 percent of the world gross domestic product.
- The real catalysts for the explosive growth of electronics occurred following World War II. The first was the invention of the bipolar transistor by Bardeen, Brattain, and Shockley in 1947; the second was the simultaneous invention of the integrated circuit by Kilby and by Noyce and Moore in 1958.
- Integrated circuits quickly became a commercial reality, and the complexity, whether measured in memory density (bits/chip), microprocessor transistor count, or minimum feature size, has changed exponentially since the mid-1960s. We are now in an era of giga-scale integration (GSI), having already put lower levels of integration—SSI, MSI, LSI, VLSI, and ULSI—behind us.
- Electronic circuit design deals with two major categories of signals. Analog electrical signals may take on any value within some finite range of voltage or current. Digital signals, however, can take on only a finite set of discrete levels. The most common digital signals are binary signals, which are represented by two discrete levels.
- Bridging between the analog and digital worlds are the digital-to-analog and analog-to-digital conversion circuits (DAC and ADC, respectively). The DAC converts digital information into an analog voltage or current, whereas the ADC creates a digital number at its output that is proportional to an analog input voltage or current.
- Fourier demonstrated that complex signals can be represented as a linear combination of sinusoidal signals. Analog signal processing is applied to these signals using linear amplifiers; these modify the amplitude and phase of analog signals. Linear amplifiers do not alter the frequency content of the signal, changing only the relative amplitudes and phases of the frequency components.
- Amplifiers are often classified by their frequency response into low-pass, high-pass, band-pass, band-reject, and all-pass categories. Electronic circuits that are designed to amplify specific ranges of signal frequencies are usually referred to as filters.
- Solving problems is one focal point of an engineer's career. A well-defined approach can help significantly in solving problems, and to this end, a structured problem-solving approach has been introduced in this chapter as outlined in these nine steps. Throughout the rest of this text, the examples will follow this problem-solving approach:
  1. State the **problem** as clearly as possible.
  2. List the **known information and given data**.

3. Define the **unknowns** that must be found to solve the problem.
  4. List your **assumptions**. You may discover additional assumptions as the analysis progresses.
  5. Select and develop an **approach** from a list of possible alternatives.
  6. Perform an **analysis** to find a solution to the problem.
  7. **Check the results.** Is the math correct? Have all the unknowns been found? Do the results satisfy simple consistency checks?
  8. **Evaluate the solution.** Is the solution realistic? Can it be built? If not, repeat steps 4–7 until a satisfactory solution is obtained.
  9. Use **computer-aided analysis** to check the results and to see if the solution satisfies the problem requirements.
- Our circuit designs will be implemented using real components whose initial values differ from those of the design and that change with time and temperature. Techniques for analyzing the influence of element tolerances on circuit performance include the worst-case analysis and statistical Monte Carlo analysis methods. Most circuit analysis programs include the ability to specify temperature dependencies for most circuit elements.
  - In worst-case analysis, element values are simultaneously pushed to their extremes, and the resulting predictions of circuit behavior are often overly pessimistic.
  - The Monte Carlo method analyzes a large number of randomly selected versions of a circuit to build up a realistic estimate of the statistical distribution of circuit performance. Random number generators in high-level computer languages, spreadsheets, Mathcad®, or MATLAB® can be used to randomly select element values for use in Monte Carlo analysis. Some circuit analysis packages such as PSPICE® provide a Monte Carlo analysis option as part of the program.

## KEY TERMS

All-pass amplifier	Fundamental frequency
Analog signal	Fundamental radian frequency
Analog-to-digital converter (A/D converter or ADC)	Giga-scale integration (GSI)
Band-pass amplifier	Harmonic frequency
Band-reject amplifier	High-pass amplifier
Binary digital signal	Ideal operational amplifier
Bipolar transistor	Integrated circuit (IC)
Current-controlled current source (CCCS)	Input resistance
Current-controlled voltage source (CCVS)	Inverting amplifier
Current division	Kirchhoff's current law (KCL)
Dependent (or controlled) source	Kirchhoff's voltage law (KVL)
Digital signal	Large-scale integration (LSI)
Digital-to-analog converter (D/A converter or DAC)	Least significant bit (LSB)
Diode	Low-pass amplifier
Feedback network	Medium-scale integration (MSI)
Filters	Mesh analysis
Fourier analysis	Minimum feature size
Fourier series	Monte Carlo analysis
Frequency spectrum	Most significant bit (MSB)
	Nodal analysis
	Nominal value

Norton circuit transformation	Tolerance
Norton equivalent circuit	Transistor
Operational amplifier (op amp)	Triode
Phasor	Ultra-large-scale integration (ULSI)
Problem-solving approach	Uniform random number generator
Quantization error	Vacuum diode
Random numbers	Vacuum tube
Resolution of the converter	Very-large-scale integration (VLSI)
Small-scale integration (SSI)	Virtual ground
Superposition principle	Voltage-controlled current source (VCCS)
Temperature coefficient	Voltage-controlled voltage source (VCVS)
Temperature coefficient of resistance (TCR)	Voltage division
Thévenin circuit transformation	Voltage gain
Thévenin equivalent circuit	Worst-case analysis
Thévenin equivalent resistance	

## REFERENCES

1. W. F. Brinkman, D. E. Haggan, and W. W. Troutman, "A History of the Invention of the Transistor and Where It Will Lead Us," *IEEE Journal of Solid-State Circuits*, vol. 32, no. 12, pp. 1858–65, December 1997.
2. [www.pbs.org/transistor/sitemap.html](http://www.pbs.org/transistor/sitemap.html).
3. *CIA Factbook*, [www.cia.gov](http://www.cia.gov).
4. *Fortune Global 500*, [www.fortune.com](http://www.fortune.com).
5. *Fortune 500*, [www.fortune.com](http://www.fortune.com).
6. J. T. Wallmark, "The Field-Effect Transistor—An Old Device with New Promise," *IEEE Spectrum*, March 1964.
7. IEEE: [www.ieee.org](http://www.ieee.org).
8. ISSCC: [www.sscs.org](http://www.sscs.org).
9. IEDM: [www.ieee.org](http://www.ieee.org).
10. International Technology Roadmap for Semiconductors: [public.itrs.net](http://public.itrs.net).
11. Frequency allocations: [www.fcc.org](http://www.fcc.org).

## ADDITIONAL READING

- Commemorative Supplement to the Digest of Technical Papers, 1993 IEEE International Solid-State Circuits Conference Digest*, vol. 36, February 1993.
- Digest of Technical Papers of the IEEE Custom Integrated International Circuits Conference*, September of each year.
- Digest of Technical Papers of the IEEE International Electronic Devices Meeting*, December of each year.
- Digest of Technical Papers of the IEEE International Solid-State Circuits Conference*, February of each year.
- Digest of Technical Papers of the IEEE International Symposia on VLSI Technology and Circuits*, June of each year.
- Electronics*, Special Commemorative Issue, April 17, 1980.
- Garratt, G. R. M. *The Early History of Radio from Faraday to Marconi*. London: Institution of Electrical Engineers (IEE), 1994.
- "200 Years of Progress." *Electronic Design* 24, no. 4, February 16, 1976.

## PROBLEMS

### 1.1 A Brief History of Electronics: From Vacuum Tubes to Ultra-Large-Scale Integration

- 1.1. Make a list of 20 items in your environment that contain electronics. A PC and its peripherals are considered one item. (Do not confuse electromechanical timers, common in clothes dryers or the switch in a simple thermostat, with electronic circuits.)
- 1.2. The straight line in Fig. 1.4 is described by  $N = 1610 \times 10^{0.1548(\text{Year}-1970)}$ . Based on a straight-line projection of this figure, what will be the number of transistors in a microprocessor in the year 2020?
- 1.3. The change in memory density with time can be described by  $B = 19.97 \times 10^{0.1977(\text{Year}-1960)}$ . If a straight-line projection is made using this equation, what will be the number of memory bits/chip in the year 2020?
- 1.4. (a) How many years does it take for memory chip density to increase by a factor of 2, based on the equation in Prob. 1.3? (b) By a factor of 10?
- 1.5. (a) How many years does it take for microprocessor circuit density to increase by a factor of 2, based on the equation in Prob. 1.2? (b) By a factor of 10?
- 1.6. If you make a straight-line projection from Fig. 1.5, what will be the minimum feature size in integrated circuits in the year 2025? The curve can be described by  $F = 8.00 \times 10^{-0.05806(\text{Year}-1970)} \mu\text{m}$ . Do you think this is possible? Why or why not?
- 1.7. Based on Fig. 1.4, how many processors will we be able to place on one chip in the year 2020?
- 1.8. The filament of a small vacuum tube uses a power of approximately 1.5 W. Suppose that 268 million of these tubes are used to build the equivalent of a 256 Mb memory. How much power is required for this memory? If this power is supplied from a 220 V ac source, what is the current required by this memory?

### 1.2 Classification of Electronic Signals

- 1.9. Classify each of the following as an analog or digital quantity: (a) status of a light switch, (b) status of

a thermostat, (c) water pressure, (d) gas tank level, (e) bank overdraft status, (f) light bulb intensity, (g) stereo volume, (h) full or empty cup, (i) room temperature, (j) TV channel selection, and (k) tire pressure.

- 1.10. A 12-bit D/A converter has a full scale voltage of 10.00 V. What is the voltage corresponding to the LSB? To the MSB? What is the output voltage if the binary input code is equal to (100100100101)?
- 1.11. A 10-bit D/A converter has a full scale voltage of 2.5 V. What is the voltage corresponding to the LSB? What is the output voltage if the binary input code is equal to (0101100100)?
- 1.12. An 8-bit A/D converter has  $V_{FS} = 5$  V. What is the value of the voltage corresponding to the LSB? If the input voltage is 2.97 V, what is the binary output code of the converter?
- 1.13. A 15-bit A/D converter has  $V_{FS} = 10$  V. What is the value of the LSB? If the input voltage is 6.85 V, what is the binary output code of the converter?
- 1.14. (a) A digital multimeter is being designed to have a readout with four decimal digits. How many bits will be required in its A/D converter? (b) Repeat for six decimal digits.
- 1.15. A 12-bit ADC has  $V_{FS} = 5.12$  V and the output code is (101110111010). What is the size of the LSB for the converter? What range of input voltages corresponds to the ADC output code?

### 1.3 Notational Conventions

- 1.16. If  $i_B = 0.003(1 + \cos 1000t)$  A, what are  $I_B$  and  $i_b$ ?
- 1.17. If  $v_{GS} = (2.5 + 0.5u(t - 1) + 0.1 \cos 2000\pi t)$  V, what are  $V_{GS}$  and  $v_{gs}$ ? [ $u(t)$  is the unit step function.]
- 1.18. If  $V_{CE} = 4$  V and  $v_{ce} = (2 \cos 5000t)$  V, write the expression for  $v_{CE}$ .
- 1.19. If  $V_{DS} = 5$  V and  $v_{ds} = (2 \sin 2500t + 4 \sin 1000t)$  V, write the expression for  $v_{DS}$ .

### 1.5 Important Concepts from Circuit Theory

- 1.20. Use voltage and current division to find  $V_1$ ,  $V_2$ ,  $I_2$ , and  $I_3$  in the circuit in Fig. P1.21 if  $V = 1$  V,  $R_1 = 24$  k $\Omega$ ,  $R_2 = 30$  k $\Omega$ , and  $R_3 = 11$  k $\Omega$ .

- 1.21. Use voltage and current division to find  $V_1$ ,  $V_2$ ,  $I_2$ , and  $I_3$  in the circuit in Fig. P1.21 if  $V = 8$  V,  $R_1 = 24 \text{ k}\Omega$ ,  $R_2 = 30 \text{ k}\Omega$ , and  $R_3 = 11 \text{ k}\Omega$ .

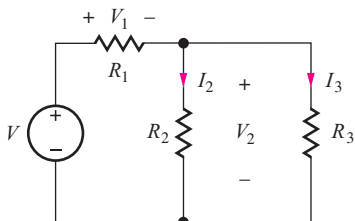


Figure P1.21

- 1.22. Use current and voltage division to find  $I_1$ ,  $I_2$ , and  $V_3$  in the circuit in Fig. P1.23 if  $I = 300 \mu\text{A}$ ,  $R_1 = 150 \text{ k}\Omega$ ,  $R_2 = 68 \text{ k}\Omega$ , and  $R_3 = 82 \text{ k}\Omega$ .

- 1.23. Use current and voltage division to find  $I_1$ ,  $I_2$ , and  $V_3$  in the circuit in Fig. P1.23 if  $I = 5 \text{ mA}$ ,  $R_1 = 2.4 \text{ k}\Omega$ ,  $R_2 = 5.6 \text{ k}\Omega$ , and  $R_3 = 3.9 \text{ k}\Omega$ .

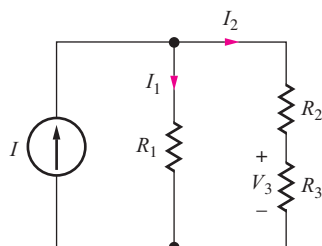


Figure P1.23

- 1.24. Find the Norton equivalent representation of the circuit in Fig. P1.25 if  $g_m = 0.025 \text{ S}$  and  $R_1 = 10 \text{ k}\Omega$ .

- 1.25. Find the Thévenin equivalent representation of the circuit in Fig. P1.25 if  $g_m = 0.002 \text{ S}$  and  $R_1 = 75 \text{ k}\Omega$ .

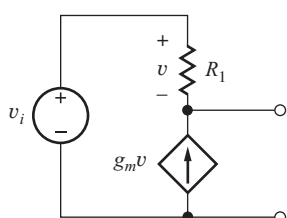
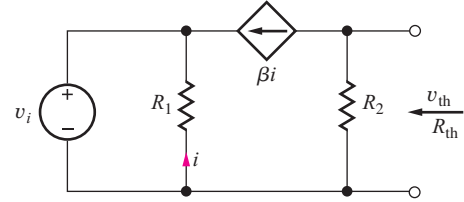
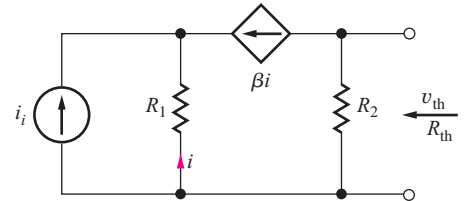


Figure P1.25

- 1.26. Find the Thévenin equivalent representation of the circuit in Fig. P1.26(a) if  $\beta = 150$ ,  $R_1 = 100 \text{ k}\Omega$ , and  $R_2 = 39 \text{ k}\Omega$ . (b) Repeat for the circuit in Fig. P1.26(b).



(a)



(b)

Figure P1.26

- 1.27. Find the Norton equivalent representation of the circuit in Fig. P1.26(a) if  $\beta = 120$ ,  $R_1 = 75 \text{ k}\Omega$ , and  $R_2 = 56 \text{ k}\Omega$ .

- 1.28. What is the resistance presented to source  $v_s$  by the circuit in Fig. P1.26(a) if  $\beta = 75$ ,  $R_1 = 100 \text{ k}\Omega$ , and  $R_2 = 39 \text{ k}\Omega$ ?

- 1.29. Find the Thévenin equivalent representation of the circuit in Fig. P1.29 if  $g_m = .0025 \text{ S}$ ,  $R_1 = 200 \text{ k}\Omega$ , and  $R_2 = 1.5 \text{ M}\Omega$ .

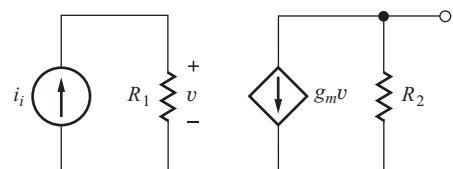


Figure P1.29

- 1.30. (a) What is the equivalent resistance between terminals A and B in Fig. P1.30? (b) What is the equivalent resistance between terminals C and D? (c) What is the equivalent resistance between terminals E and F?

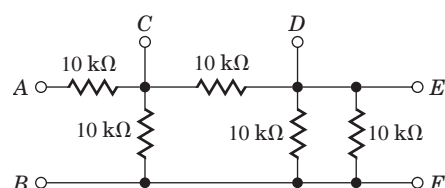


Figure P1.30

- 1.31. (a) Find the Thévenin equivalent circuit for the network in Fig. P1.31. (b) What is the Norten equivalent circuit?

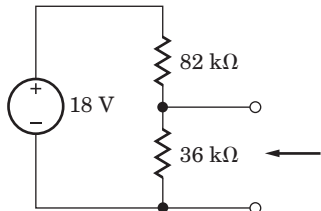


Figure P1.31

- 1.32. (a) Find the Thévenin equivalent circuit for the network in Fig. P1.32. (b) What is the Norten equivalent circuit?

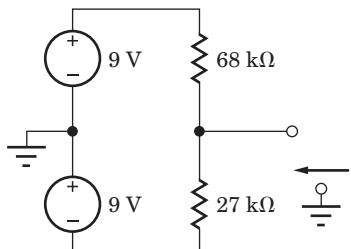


Figure P1.32

## 1.6 Frequency Spectrum of Electronic Signals

- 1.33. A signal voltage is expressed as  $v(t) = (5 \sin 4000\pi t + 3 \cos 2000\pi t)$  V. Draw a graph of the amplitude spectrum for  $v(t)$  similar to the one in Fig. 1.17(b).
- \*1.34. Voltage  $v_1 = 2 \sin 20,000\pi t$  is multiplied by voltage  $v_2 = 2 \sin 2000\pi t$ . Draw a graph of the amplitude spectrum for  $v = v_1 \times v_2$  similar to the one in Fig. 1.17(b). (Note that multiplication is a nonlinear mathematical operation. In electronics it is often called *mixing* because it produces a signal that contains output frequencies that are not in the input signal but depend directly on the input frequencies.)

## 1.7 Amplifiers

- 1.35. The input and output voltages of an amplifier are expressed as  $v_s = 10^{-4} \sin(2 \times 10^7 \pi t)$  V and  $v_o = 4 \sin(2 \times 10^7 \pi t + 56^\circ)$  V. What are the magnitude and phase of the voltage gain of the amplifier?
- \*1.36. The input and output voltages of an amplifier are expressed as

$$v_s = [10^{-3} \sin(3000\pi t) + 2 \times 10^{-3} \sin(5000\pi t)] \text{ V}$$

$$\text{and } v_o = [10^{-2} \sin(3000\pi t - 45^\circ) + 10^{-1} \sin(5000\pi t - 12^\circ)] \text{ V}$$

- (a) What are the magnitude and phase of the voltage gain of the amplifier at a frequency of 2500 Hz? (b) At 1500 Hz?

- 1.37. What is the voltage gain of the amplifier in Fig. 1.20 if (a)  $R_1 = 14 \text{ k}\Omega$  and  $R_2 = 560 \text{ k}\Omega$ ? (b) For  $R_1 = 18 \text{ k}\Omega$  and  $R_2 = 360 \text{ k}\Omega$ ? (c) For  $R_1 = 1.8 \text{ k}\Omega$  and  $R_2 = 62 \text{ k}\Omega$ ?
- 1.38. Write an expression for the output voltage  $v_o(t)$  of the circuit in Fig. 1.20 if  $R_1 = 910 \Omega$ ,  $R_2 = 7.5 \text{ k}\Omega$ , and  $v_s(t) = (0.01 \sin 750\pi t)$  V. Write an expression for the current  $i_s(t)$ .
- 1.39. Find an expression for the voltage gain  $A_v = v_o/v_i$  for the amplifier in Fig. P1.39.

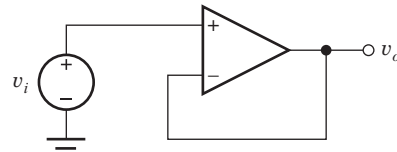


Figure P1.39

- 1.40. Find an expression for the voltage gain  $A_v = v_o/v_i$  for the amplifier in Fig. P1.40.

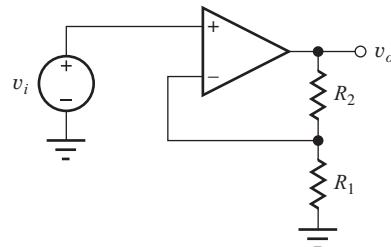


Figure P1.40

- 1.41. Write an expression for the output voltage  $v_o(t)$  of the circuit in Fig. P1.41 if  $R_1 = 2 \text{ k}\Omega$ ,  $R_2 = 10 \text{ k}\Omega$ ,  $R_3 = 51 \text{ k}\Omega$ ,  $v_1(t) = (0.01 \sin 3770t)$  V, and  $v_2(t) = (0.05 \sin 10,000t)$  V. Write an expression for the voltage appearing at the inverting input ( $v_-$ ).

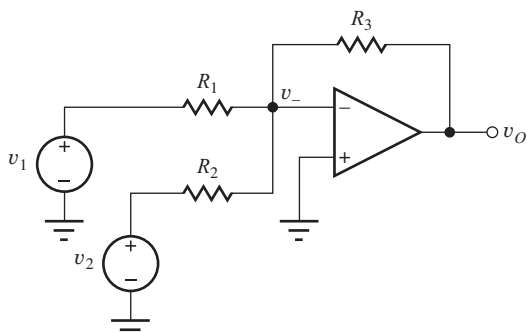


Figure P1.41

- 1.42. The circuit in Fig. P1.42 can be used as a simple 3-bit digital-to-analog converter (DAC). The individual bits of the binary input word ( $b_1 b_2 b_3$ ) are used to control the position of the switches, with the resistor connected to 0 V if  $b_i = 0$  and connected to  $V_{\text{REF}}$  if  $b_i = 1$ . (a) What is the output voltage for the DAC as shown with input data of (011) if  $V_{\text{REF}} = 5.0$  V? (b) Suppose the input data change to (100). What will be the new output voltage? (c) Make a table giving the output voltages for all eight possible input combinations.

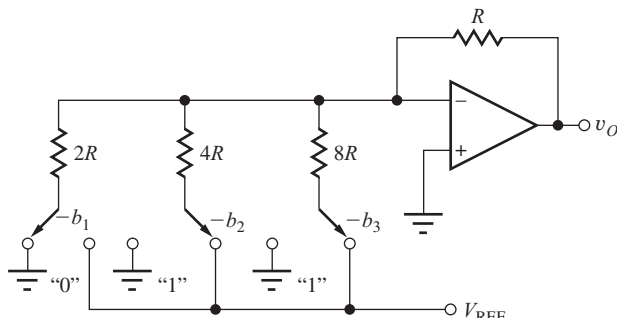


Figure P1.42

### Amplifier Frequency Response

- 1.43. An amplifier has a voltage gain of zero for frequencies below 1000 Hz, and zero gain for frequencies above 5000 Hz. In between these two frequencies the amplifier has a gain of 20. Classify this amplifier.
- 1.44. An amplifier has a voltage gain of 10 for frequencies below 6000 Hz, and zero gain for frequencies above 6000 Hz. Classify this amplifier.
- 1.45. The amplifier in Prob. 1.44 has an input signal given by  $v_s(t) = (5 \sin 2000\pi t + 3 \cos 8000\pi t + 2 \cos 15000\pi t)$  V. Write an expression for the output voltage of the amplifier.

$2 \cos 15000\pi t)$  V. Write an expression for the output voltage of the amplifier.

- 1.46. An amplifier has a voltage gain of 16 for frequencies above 10 kHz, and zero gain for frequencies below 10 kHz. Classify this amplifier.
- 1.47. The amplifier in Prob. 1.43 has an input signal given by  $v_s(t) = (0.5 \sin 2500\pi t + 0.75 \cos 8000\pi t + 0.6 \cos 12,000\pi t)$  V. Write an expression for the output voltage of the amplifier.
- 1.48. The amplifier in Prob. 1.46 has an input signal given by  $v_s(t) = (0.5 \sin 2500\pi t + 0.75 \cos 8000\pi t + 0.8 \cos 12,000\pi t)$  V. Write an expression for the output voltage of the amplifier.
- 1.49. An amplifier has an input signal that can be represented as

$$v(t) = \frac{4}{\pi} \left( \sin \omega_o t + \frac{1}{3} \sin 3\omega_o t + \frac{1}{5} \sin 5\omega_o t \right) \text{V}$$

where  $\omega_o = 1000$  Hz

- (a) Use MATLAB to plot the signal for  $0 \leq t \leq 5$  ms. (b) The signal  $v(t)$  is amplified by an amplifier that provides a voltage gain of 5 at all frequencies. Plot the output voltage for this amplifier for  $0 \leq t \leq 5$  ms. (c) A second amplifier has a voltage gain of 5 for frequencies below 2000 Hz but zero gain for frequencies above 2000 Hz. Plot the output voltage for this amplifier for  $0 \leq t \leq 5$  ms. (d) A third amplifier has a gain of 5 at 1000 Hz, a gain of 3 at 3000 Hz, and a gain of 1 at 5000 Hz. Plot the output voltage for this amplifier for  $0 \leq t \leq 5$  ms.

### 1.8 Element Variations in Circuit Design

- 1.50. (a) A 4.7-kΩ resistor is purchased with a tolerance of 1 percent. What is the possible range of values for this resistor? (b) Repeat for a 5 percent tolerance. (c) Repeat for a 10 percent tolerance.
- 1.51. A 10,000 μF capacitor has an asymmetric tolerance specification of  $+20\%/-50\%$ . What is the possible range of values for this capacitor?
- 1.52. The power supply voltage for a circuit must vary by no more than 50 mV from its nominal value of 1.8 V. What is its tolerance specification?
- 1.53. An 8200-Ω resistor is purchased with a tolerance of 10 percent. It is measured with an ohmmeter and found to have a value of 7905 Ω. Is this resistor within its specification limits? Explain your answer.
- 1.54. (a) The output voltage of a 5-V power supply is measured to be 5.30 V. The power supply has a 5 percent tolerance specification. Is the supply

operating within its specification limits? Explain your answer. (b) The voltmeter that was used to make the measurement has a 1.5 percent tolerance. Does that change your answer? Explain.

- 1.55. A resistor is measured and found to have a value of  $6066 \Omega$  at  $0^\circ\text{C}$  and  $6562 \Omega$  at  $100^\circ\text{C}$ . What are the temperature coefficient and nominal value for the resistor? Assume  $T_{\text{NOM}} = 27^\circ\text{C}$ .
- 1.56. Find the worst-case values of  $I_1$ ,  $I_2$ , and  $V_3$  for the circuit in Prob. 1.22 if the resistor tolerances are 5 percent and the current source tolerance is 2 percent.
- 1.57. Find the worst-case values of  $V_1$ ,  $I_2$ , and  $I_3$  for the circuit in Prob. 1.20 if the resistor tolerances are 10 percent and the voltage source tolerance is 5 percent.
- 1.58. Find the worst-case values for the Thévenin equivalent resistance for the circuit in Prob. 1.25 if the resistor tolerance is 20 percent and the tolerance on  $g_m$  is also 20 percent.

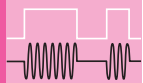
- 1.59. Perform a 200-case Monte Carlo analysis for the circuit in Prob. 1.56 and compare the results to the worst-case calculations.

- 1.60. Perform a 200-case Monte Carlo analysis for the circuit in Prob. 1.57 and compare the results to the worst-case calculations.

## 1.9 Numeric Precision

- 1.61. (a) Express the following numbers to three significant digits of precision: 3.2947, 0.995171,  $-6.1551$ . (b) To four significant digits. (c) Check these answers using your calculator.
- 1.62. (a) What is the voltage developed by a current of  $1.763 \text{ mA}$  in a resistor of  $20.70 \text{ k}\Omega$ ? Express the answer with three significant digits. (b) Express the answer with two significant digits. (c) Repeat for  $I = 102.1 \mu\text{A}$  and  $R = 97.80 \text{ k}\Omega$ .

# CHAPTER 2



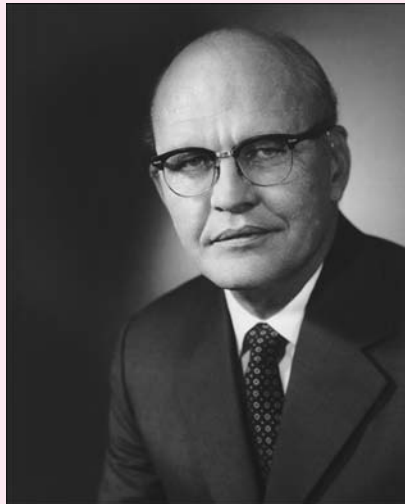
## SOLID-STATE ELECTRONICS

### CHAPTER OUTLINE

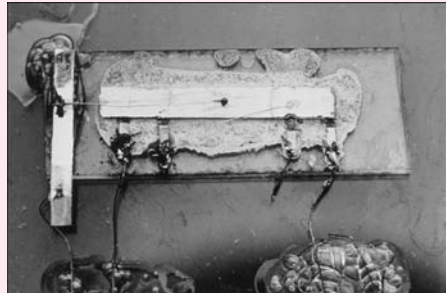
- 2.1 Solid-State Electronic Materials 44
- 2.2 Covalent Bond Model 45
- 2.3 Drift Currents and Mobility in Semiconductors 48
- 2.4 Resistivity of Intrinsic Silicon 50
- 2.5 Impurities in Semiconductors 51
- 2.6 Electron and Hole Concentrations in Doped Semiconductors 52
- 2.7 Mobility and Resistivity in Doped Semiconductors 55
- 2.8 Diffusion Currents 59
- 2.9 Total Current 60
- 2.10 Energy Band Model 61
- 2.11 Overview of Integrated Circuit Fabrication 64
  - Summary 67
  - Key Terms 68
  - Reference 69
  - Additional Reading 69
  - Important Equations 69
  - Problems 70

### CHAPTER GOALS

- Explore the characteristics of semiconductors and discover how engineers control semiconductor properties to fabricate electronic devices
- Characterize resistivity and insulators, semiconductors, and conductors
- Develop the covalent bond and energy band models for semiconductors
- Understand the concepts of bandgap energy and intrinsic carrier concentration
- Explore the behavior of the two charge carriers in semiconductors—electrons and holes
- Discuss acceptor and donor impurities in semiconductors
- Learn to control the electron and hole populations using impurity doping
- Understand drift and diffusion currents in semiconductors
- Explore the concepts of low-field mobility and velocity saturation
- Discuss the dependence of mobility on doping level
- Explore basic IC fabrication processes

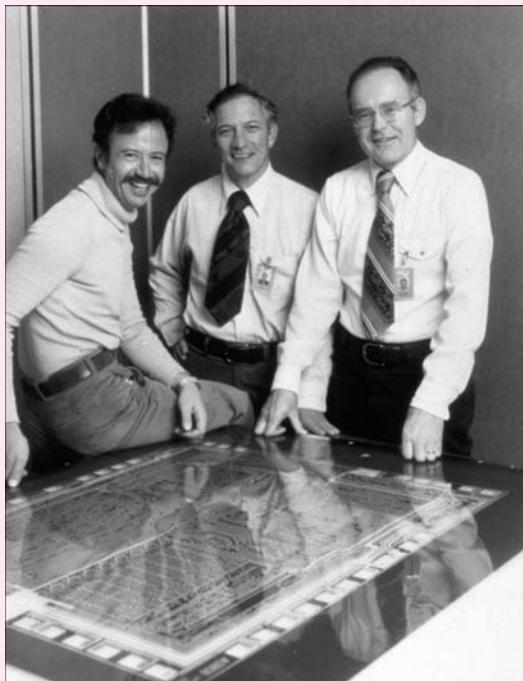


Jack St. Clair Kilby.  
*Courtesy of Texas Instruments*



The Kilby integrated circuit.  
*Courtesy of Texas Instruments*

Jack Kilby from Texas Instruments Inc. and Gordon Moore and Robert Noyce from Fairchild Semiconductor pioneered the nearly simultaneous development of the integrated circuit in the late 1950s. After years of litigation, the basic integrated circuit patents of Jack Kilby and Texas Instruments were upheld, and also finally recognized in Japan in 1994. Gordon E. Moore, Robert Noyce, and Andrew S. Grove founded the Intel Corporation in 1968. Kilby shared the 2000 Nobel prize in physics for invention of the integrated circuit.



Andy Grove, Robert Noyce, and Gordon Moore with Intel 8080 processor rubylith in 1978.  
*Courtesy of Intel Corporation*

**A**s discussed in Chapter 1, the evolution of solid-state materials and the subsequent development of the technology for integrated circuit fabrication have revolutionized electronics and made possible the modern information and technological revolution. Using silicon as well as other crystalline semiconductor materials, we can now fabricate integrated circuits (ICs) that have more than billions of electronic components on a single  $2\text{ cm} \times 2\text{ cm}$  die. Most of us have some familiarity with the very high-speed microprocessor and memory components that form the building blocks for personal computers and workstations. Consider for a moment the content of a 1-gigabit memory chip. The memory array alone on this chip will contain more than  $10^9$  transistors and  $10^9$  capacitors—more than 2 billion electronic components on a single die!

Our ability to build such phenomenal electronic system components is based on a detailed understanding of solid-state physics as well as on development of fabrication processes necessary to turn the theory into a manufacturable reality. Integrated circuit manufacturing is an excellent example of a process requiring a broad understanding of many disciplines. IC fabrication requires knowledge of physics, chemistry, electrical engineering, mechanical engineering, materials engineering, and metallurgy, to mention just a few disciplines. The breadth of understanding required is a challenge, but it makes the field of solid-state electronics an extremely exciting and vibrant area of specialization.

It is possible to explore the behavior of electronic circuits from a “black box” perspective, simply trusting a set of equations that model the terminal voltage and current characteristics of each of the electronic devices. However, understanding the underlying behavior of the devices leads a designer to develop an intuition that extends beyond the simplified models of a black box approach. Building our models from fundamentals enables us to understand the limitations and appropriate

uses of particular models. This is especially true when we experimentally observe deviations from our model predictions. One goal of this chapter is to develop a basic understanding of the underlying operational principles of semiconductor devices that enables us to place our simplified models in the appropriate context.

The material in this chapter provides the background necessary for understanding the behavior of the solid-state devices presented in subsequent chapters. We begin our study of solid-state electronics by exploring the characteristics of crystalline materials, with an emphasis on silicon, the most commercially important semiconductor. We look at electrical conductivity and resistivity and discuss the mechanisms of electronic conduction. The technique of impurity doping is discussed, along with its use in controlling conductivity and resistivity type.

## 2.1 SOLID-STATE ELECTRONIC MATERIALS

Electronic materials generally can be divided into three categories: **insulators**, **conductors**, and **semiconductors**. The primary parameter used to distinguish among these materials is the **resistivity**  $\rho$ , with units of  $\Omega \cdot \text{cm}$ . As indicated in Table 2.1, insulators have resistivities greater than  $10^5 \Omega \cdot \text{cm}$ , whereas conductors have resistivities below  $10^{-3} \Omega \cdot \text{cm}$ . For example, diamond, one of the highest quality insulators, has a very large resistivity,  $10^{16} \Omega \cdot \text{cm}$ . On the other hand, pure copper, a good conductor, has a resistivity of only  $3 \times 10^{-6} \Omega \cdot \text{cm}$ . Semiconductors occupy the full range of resistivities between the insulator and conductor boundaries; moreover, the resistivity can be controlled by adding various impurity atoms to the semiconductor crystal.

**Elemental semiconductors** are formed from a single type of atom (column IV of the periodic table of elements; see Table 2.2), whereas **compound semiconductors** can be formed from combinations of elements from columns III and V or columns II and VI. These later materials are often referred to as III–V (3–5) or II–VI (2–6) compound semiconductors. Table 2.3 presents some of the most useful possibilities. There are also ternary materials such as mercury cadmium telluride, gallium aluminum arsenide, gallium indium arsenide, and gallium indium phosphide.

Historically, germanium was one of the first semiconductors to be used. However, it was rapidly supplanted by silicon, which today is the most important semiconductor material. Silicon has a wider bandgap energy,<sup>1</sup> enabling it to be used in higher-temperature applications than germanium, and oxidation forms a stable insulating oxide on silicon, giving silicon significant processing advantages over germanium during fabrication of ICs. In addition to silicon, gallium arsenide, indium phosphide, silicon carbide, and silicon germanium are commonly encountered today, although germanium is still used in some limited applications. Silicon germanium has emerged as an important material over the last decade or so, and silicon germanium technology has been used to achieve record high frequency performance in silicon-based bipolar transistors.

The compound semiconductor materials gallium arsenide (GaAs) and indium phosphide (InP) are the most important material for optoelectronic applications, including light-emitting diodes (LEDs), lasers, and photodetectors.

**TABLE 2.1**  
Electrical Classification of Solid Materials

MATERIALS	RESISTIVITY ( $\Omega \cdot \text{cm}$ )
Insulators	$10^5 < \rho$
Semiconductors	$10^{-3} < \rho < 10^5$
Conductors	$\rho < 10^{-3}$

<sup>1</sup> The meaning of bandgap energy is discussed in detail in Secs. 2.2 and 2.10.

**TABLE 2.2**  
Portion of the Periodic Table, Including the Most Important Semiconductor Elements (shaded)

	IIIA	IVA	VA	VIA
	5 10.811 <b>B</b> Boron	6 12.01115 <b>C</b> Carbon	7 14.0067 <b>N</b> Nitrogen	8 15.9994 <b>O</b> Oxygen
IIB	13 26.9815 <b>Al</b> Aluminum	14 28.086 <b>Si</b> Silicon	15 30.9738 <b>P</b> Phosphorus	16 32.064 <b>S</b> Sulfur
	30 65.37 <b>Zn</b> Zinc	31 69.72 <b>Ga</b> Gallium	32 72.59 <b>Ge</b> Germanium	33 74.922 <b>As</b> Arsenic
	48 112.40 <b>Cd</b> Cadmium	49 114.82 <b>In</b> Indium	50 118.69 <b>Sn</b> Tin	51 121.75 <b>Sb</b> Antimony
	80 200.59 <b>Hg</b> Mercury	81 204.37 <b>Tl</b> Thallium	82 207.19 <b>Pb</b> Lead	83 208.980 <b>Bi</b> Bismuth
				84 (210) <b>Po</b> Polonium

**TABLE 2.3**  
Semiconductor Materials

SEMICONDUCTOR	BANDGAP ENERGY $E_G$ (eV)
Carbon (diamond)	5.47
Silicon	1.12
Germanium	0.66
Tin	0.082
Gallium arsenide	1.42
Gallium nitride	3.49
Indium phosphide	1.35
Boron nitride	7.50
Silicon carbide	3.26
Silicon germanium	1.10
Cadmium selenide	1.70

Many research laboratories are exploring the formation of diamond, boron nitride, silicon carbide, and silicon germanium materials. Diamond and boron nitride are excellent insulators at room temperature, but they, as well as silicon carbide, can be used as semiconductors at much higher temperatures ( $600^{\circ}\text{C}$ ). Adding a small percentage (<10 percent) of germanium to silicon has been shown recently to offer improved device performance in a process compatible with normal silicon processing. Because of its performance advantages, this SiGe technology [1] has rapidly been introduced into fabrication of devices for RF (radio-frequency) applications, particularly for use in the telecommunications marketplace.

**EXERCISE:** What are the chemical symbols for antimony, arsenic, aluminum, boron, gallium, germanium, indium, phosphorus, and silicon?

**ANSWERS:** Sb, As, Al, B, Ga, Ge, In, P, Si

## 2.2 COVALENT BOND MODEL

Atoms can bond together in **amorphous**, **polycrystalline**, or **single-crystal** forms. Amorphous materials have a disordered structure, whereas polycrystalline material consists of a large number of small crystallites. Most of the useful properties of semiconductors, however, occur in high-purity, single-crystal material. Silicon—column IV in the periodic table—has four **electrons** in the outer shell. Single-crystal material is formed by the covalent bonding of each silicon atom with its four nearest neighbors in a highly regular three-dimensional array of atoms, as shown in Fig. 2.1. Much of the behavior we discuss can be visualized using the simplified two-dimensional **covalent bond model** of Fig. 2.2.

At temperatures approaching absolute zero, all the electrons reside in the covalent bonds shared between the atoms in the array, with no electrons free for conduction. The outer shells of the silicon atoms are full, and the material behaves as an insulator. As the temperature increases, thermal energy is added to the crystal and some bonds break, freeing a small number of electrons for conduction, as

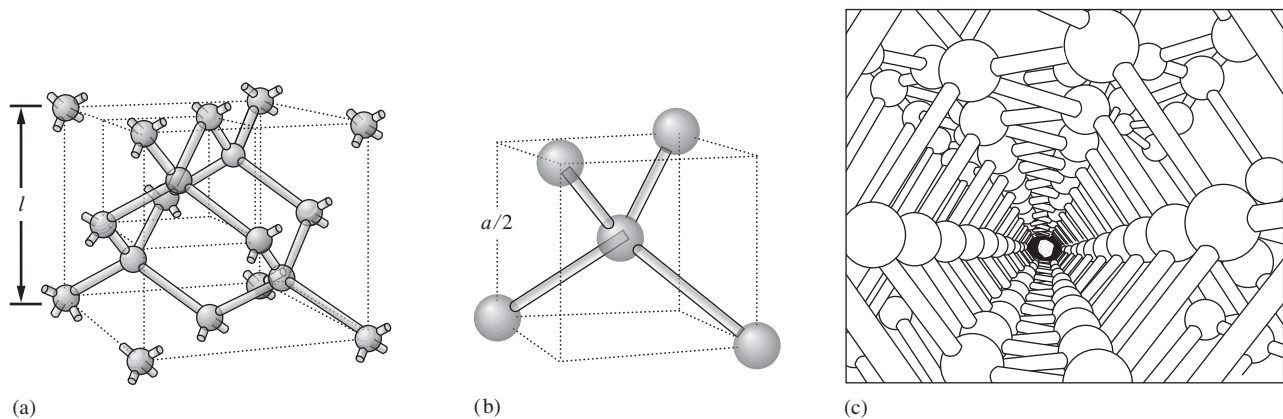


**Figure 2.1** Silicon crystal lattice structure. (a) Diamond lattice unit cell. The cube side length  $l = 0.543$  nm. (b) Enlarged top corner of the diamond lattice, showing the four nearest neighbors bonding within the structure.  
Source: (c) From Sze, Semiconductor Devices: Physics and Technology. Copyright © 1985 John Wiley & Sons. Reprinted by permission.

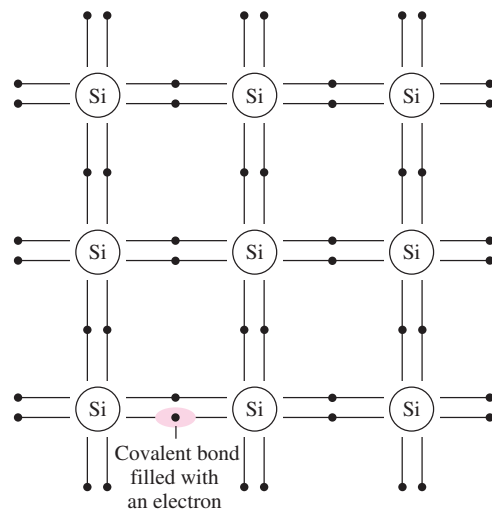


**Figure 2.2** Two-dimensional silicon lattice with shared covalent bonds. At temperatures approaching absolute zero, 0 K, all bonds are filled, and the outer shells of the silicon atoms are completely full.

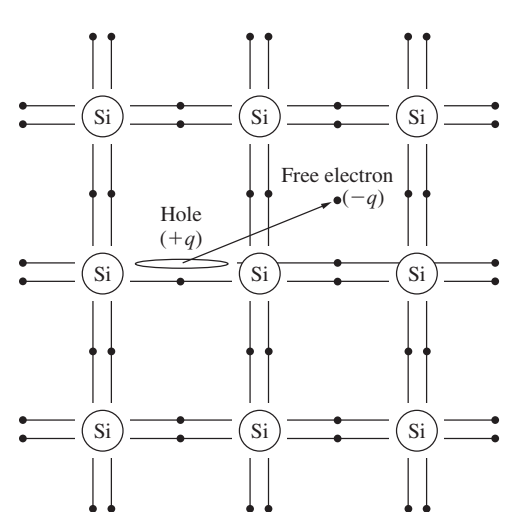


**Figure 2.3** An electron–hole pair is generated whenever a covalent bond is broken.

in Fig. 2.3. The density of these free electrons is equal to the **intrinsic carrier density**  $n_i$  ( $\text{cm}^{-3}$ ), which is determined by material properties and temperature:

$$n_i^2 = B T^3 \exp\left(-\frac{E_G}{kT}\right) \quad \text{cm}^{-6} \quad (2.1)$$

where  $E_G$  = semiconductor bandgap energy in eV (electron volts)

$k$  = Boltzmann's constant,  $8.62 \times 10^{-5}$  eV/K

$T$  = absolute temperature, K

$B$  = material-dependent parameter,  $1.08 \times 10^{31} \text{ K}^{-3} \cdot \text{cm}^{-6}$  for Si

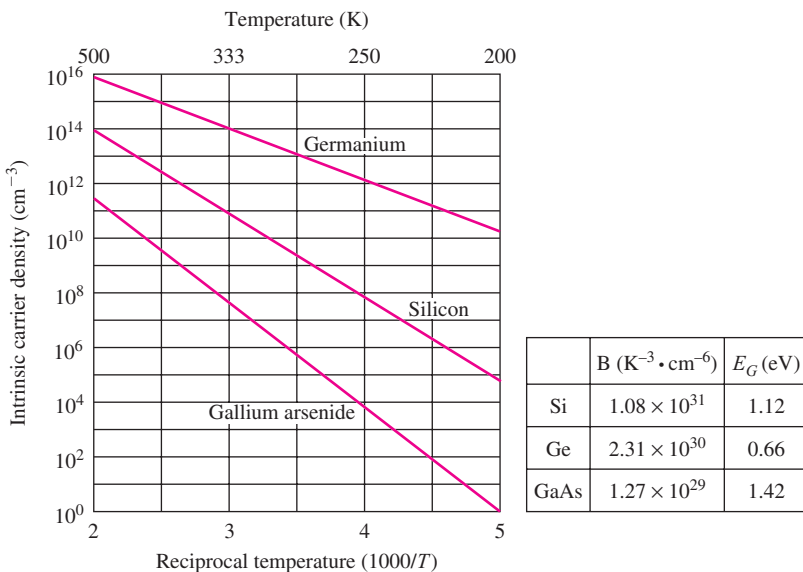


Figure 2.4 Intrinsic carrier density versus temperature from Eq. (2.1).

**Bandgap energy**  $E_G$  is the minimum energy needed to break a covalent bond in the semiconductor crystal, thus freeing electrons for conduction. Table 2.3 lists values of the bandgap energy for various semiconductors.

The *density of conduction (or free) electrons* is represented by the symbol  $n$  (electrons/cm<sup>3</sup>), and for **intrinsic material**  $n = n_i$ . The term *intrinsic* refers to the generic properties of pure material. Although  $n_i$  is an intrinsic property of each semiconductor, it is extremely temperature-dependent for all materials. Figure 2.4 has examples of the strong variation of intrinsic carrier density with temperature for germanium, silicon, and gallium arsenide.

### EXAMPLE 2.1 INTRINSIC CARRIER CONCENTRATION

Calculate the theoretical value of  $n_i$  in silicon at room temperature.

**PROBLEM** Calculate the value of  $n_i$  in silicon at room temperature (300 K).

**SOLUTION** **Known Information and Given Data:** Equation (2.1) defines  $n_i$ ,  $B$ , and  $k$ .  $E_G = 1.12$  eV from Table 2.3.

**Unknowns:** Intrinsic carrier concentration  $n_i$ .

**Approach:** Calculate  $n_i$  by evaluating Eq. (2.1).

**Assumptions:**  $T = 300$  K at room temperature.

**Analysis:**

$$n_i^2 = 1.08 \times 10^{31} (K^{-3} \cdot cm^{-6})(300 K)^3 \exp \left[ \frac{-1.12 \text{ eV}}{(8.62 \times 10^{-5} \text{ eV/K})(300 K)} \right]$$

$$n_i^2 = 4.52 \times 10^{19}/cm^6 \quad \text{or} \quad n_i = 6.73 \times 10^9/cm^3$$

**Check of Results:** The desired unknown has been found, and the value agrees with the results graphed in Fig. 2.4.

**Discussion:** For simplicity, in subsequent calculations we use  $n_i = 10^{10}/\text{cm}^3$  as the room temperature value of  $n_i$  for silicon. The density of silicon atoms in the crystal lattice is approximately  $5 \times 10^{22}/\text{cm}^3$ . We see from this example that only one bond in approximately  $10^{13}$  is broken at room temperature.

**EXERCISE:** Calculate the value of  $n_i$  in germanium at a temperature of 300 K.

**ANSWER:**  $2.27 \times 10^{13}/\text{cm}^3$

A second charge carrier is actually formed when the covalent bond in Fig. 2.3 is broken. As an electron, which has charge  $-q$  equal to  $-1.602 \times 10^{-19} \text{ C}$ , moves away from the covalent bond, it leaves behind a **vacancy** in the bond structure in the vicinity of its parent silicon atom. The vacancy is left with an effective charge of  $+q$ . An electron from an adjacent bond can fill this vacancy, creating a new vacancy in another position. This process allows the vacancy to move through the crystal. The moving vacancy behaves just as a particle with charge  $+q$  and is called a **hole**. **Hole density** is represented by the symbol  $p$  ( $\text{holes}/\text{cm}^3$ ).

As already described, two charged particles are created for each bond that is broken: one electron and one hole. For intrinsic silicon,  $n = n_i = p$ , and the product of the electron and hole concentrations is

$$pn = n_i^2 \quad (2.2)$$

The  **$pn$  product** is given by Eq. (2.2) whenever a semiconductor is in **thermal equilibrium**. (This very important result is used later.) In thermal equilibrium, material properties are dependent only on the temperature  $T$ , with no other form of stimulus applied. Equation (2.2) does not apply to semiconductors operating in the presence of an external stimulus such as an applied voltage or current or an optical excitation.

**EXERCISE:** Calculate the intrinsic carrier density in silicon at 50 K and 325 K. On the average, what is the length of one side of the cube of silicon that is needed to find one electron and one hole at  $T = 50 \text{ K}$ ?

**ANSWERS:**  $4.34 \times 10^{-39}/\text{cm}^3$ ;  $4.01 \times 10^{10}/\text{cm}^3$ ;  $6.13 \times 10^{10} \text{ m}$

## 2.3 DRIFT CURRENTS AND MOBILITY IN SEMICONDUCTORS

### 2.3.1 DRIFT CURRENTS

Electrical resistivity  $\rho$  and its reciprocal, **conductivity**  $\sigma$ , characterize current flow in a material when an electric field is applied. Charged particles move or *drift* in response to the electric field, and the resulting current is called *drift current*. The **drift current density**  $j$  is defined as

$$j = Qv \quad (\text{C}/\text{cm}^3)(\text{cm}/\text{s}) = \text{A}/\text{cm}^2 \quad (2.3)$$

where  $j$  = current density<sup>2</sup>, the charge in coulombs moving through an area of unit cross section

$Q$  = charge density<sup>2</sup>, the charge in a unit volume

$v$  = velocity of charge in an electric field

<sup>2</sup> Note that “density” has different meanings based on the context. Current density involves a cross-sectional area, whereas charge density is a volumetric quantity.

In order to find the charge density, we explore the structure of silicon using both the covalent bond model and (later) the energy band model for semiconductors. Next, we relate the velocity of the charge carriers to the applied electric field.

### 2.3.2 MOBILITY

We know from electromagnetics that charged particles move in response to an applied electric field. This movement is termed **drift**, and the resulting current flow is known as **drift current**. Positive charges drift in the same direction as the electric field, whereas negative charges drift in a direction opposed to the electric field. At low fields carrier drift velocity  $v$  (cm/s) is proportional to the electric field  $E$  (V/cm); the constant of proportionality is called the **mobility  $\mu$** :

$$v_n = -\mu_n E \quad \text{and} \quad v_p = \mu_p E \quad (2.4)$$

where  $v_n$  = velocity of electrons (cm/s)

$v_p$  = velocity of holes (cm/s)

$\mu_n$  = **electron mobility**,  $1350 \text{ cm}^2/\text{V} \cdot \text{s}$  in intrinsic Si

$\mu_p$  = **hole mobility**,  $500 \text{ cm}^2/\text{V} \cdot \text{s}$  in intrinsic Si

Conceptually, holes are localized to move through the covalent bond structure, but electrons are free to move about the crystal. Thus, one might expect hole mobility to be less than electron mobility.

**EXERCISE:** Calculate the velocity of a hole in an electric field of  $10 \text{ V/cm}$ . What is the electron velocity in an electric field of  $1000 \text{ V/cm}$ ? The voltage across a resistor is  $1 \text{ V}$ , and the length of the resistor is  $2 \mu\text{m}$ . What is the electric field in the resistor?

**ANSWERS:**  $5.00 \times 10^3 \text{ cm/s}$ ;  $1.35 \times 10^6 \text{ cm/s}$ ;  $5.00 \times 10^3 \text{ V/cm}$

### 2.3.3 VELOCITY SATURATION

From physics, we know that the velocity of carriers cannot increase indefinitely, certainly not beyond the speed of light. In silicon, for example, the linear velocity-field relationship assumed in Eq. (2.4) is valid only for fields below approximately  $5000 \text{ V/cm}$  or  $0.5 \text{ V}/\mu\text{m}$ . As the electric field increases above this value, the velocity of both holes and electrons begins to saturate, as indicated in Fig. 2.5. At low fields, the slope of the characteristic represents the mobility, as defined by Eq. (2.4). For fields above approximately  $3 \times 10^4 \text{ V/cm}$  in silicon, carrier velocity approaches the **saturated drift velocity  $v_{\text{sat}}$** . For electrons and holes in silicon,  $v_{\text{sat}}$  is approximately  $10^7 \text{ cm/s}$ . The velocity saturation phenomenon ultimately places an upper limit on the frequency response of solid-state devices.

**EXERCISE:** (a) What are the maximum drift velocities for electrons and holes in germanium. What are the low field mobilities? (b) What is the maximum drift velocity for electrons in gallium arsenide? What is the electron mobility in gallium arsenide?

**ANSWERS:**  $6 \times 10^6 \text{ cm/s}$ ,  $4300 \text{ cm}^2/\text{V} \cdot \text{s}$ ,  $2100 \text{ cm}^2/\text{V} \cdot \text{s}$ ;  $2 \times 10^7 \text{ cm/s}$ ,  $8500 \text{ cm}^2/\text{V} \cdot \text{s}$

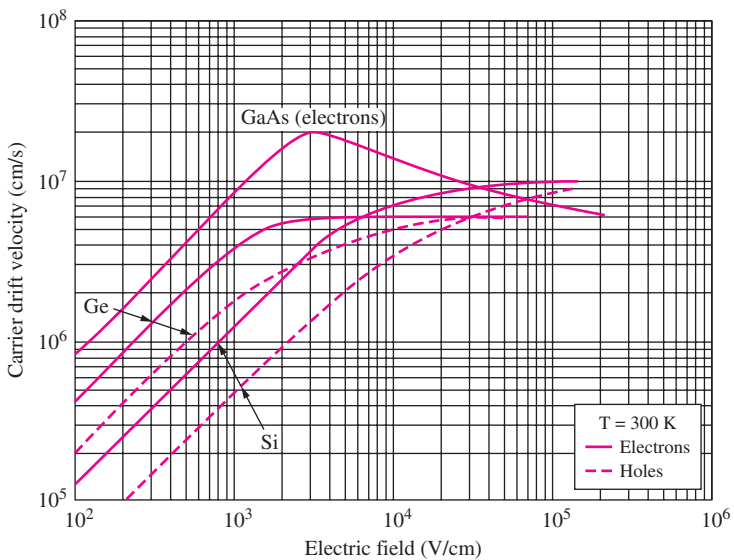


**Figure 2.5** Carrier velocity versus electric field in semiconductors at 300 K.

Source: Semiconductor Devices: Physics and Technology by S. M. Sze © 1985 Reproduced with permission of John Wiley & Sons, Inc.

## 2.4 RESISTIVITY OF INTRINSIC SILICON

We are now in a position to calculate the electron and hole drift current densities  $j_n^{\text{drift}}$  and  $j_p^{\text{drift}}$ . For simplicity, we assume a one-dimensional current and avoid the vector notation of Eqs. (2.3) and (2.4):

$$\begin{aligned} j_n^{\text{drift}} &= Q_n v_n = (-qn)(-\mu_n E) = qn\mu_n E \quad \text{A/cm}^2 \\ j_p^{\text{drift}} &= Q_p v_p = (+qp)(+\mu_p E) = qp\mu_p E \quad \text{A/cm}^2 \end{aligned} \quad (2.5)$$

in which  $Q_n = (-qn)$  and  $Q_p = (+qp)$  represent the charge densities ( $\text{C}/\text{cm}^3$ ) of electrons and holes, respectively. The total drift current density is then given by

$$j_T^{\text{drift}} = j_n + j_p = q(n\mu_n + p\mu_p)E = \sigma E \quad (2.6)$$

This equation defines  $\sigma$ , the **electrical conductivity**:

$$\sigma = q(n\mu_n + p\mu_p) \quad (\Omega \cdot \text{cm})^{-1} \quad (2.7)$$

Resistivity  $\rho$  is the reciprocal of conductivity:

$$\rho = \frac{1}{\sigma} \quad (\Omega \cdot \text{cm}) \quad (2.8)$$

The unit of resistivity, the Ohm-cm, may seem strange to many of us, but from Eq. (2.6),  $\rho$  represents the ratio of electric field to drift current density. The resistivity unit is therefore

$$\rho = \frac{E}{j_T^{\text{drift}}} \quad \text{and} \quad \frac{\text{V}/\text{cm}}{\text{A}/\text{cm}^2} = \Omega \cdot \text{cm} \quad (2.9)$$

**EXAMPLE 2.2****RESISTIVITY OF INTRINSIC SILICON**

Here we determine if intrinsic silicon is an insulator, semiconductor, or conductor at room temperature by calculating its resistivity.

**PROBLEM** Find the resistivity of intrinsic silicon at room temperature and classify it as an insulator, semiconductor or conductor.

**SOLUTION** **Known Information and Given Data:** The room temperature mobilities for intrinsic silicon were given right after Eq. (2.4). For intrinsic silicon, the electron and hole densities are both equal to  $n_i$ .

**Unknowns:** Resistivity  $\rho$  and classification.

**Approach:** The conductivity and resistivity can be found using Eqs. (2.7) and (2.8), respectively. The results are then compared to the definitions in Table 2.1.

**Assumptions:** Temperature is unspecified; assume “room temperature” with  $n_i = 10^{10}/\text{cm}^3$ .

**Analysis:** For intrinsic silicon, the charge density of electrons is given by  $Q_n = -qn_i$ , whereas the charge density for holes is  $Q_p = +qn_i$ . Substituting the given values into Eq. (2.7) yields

$$\begin{aligned}\sigma &= (1.60 \times 10^{-19})[(10^{10})(1350) + (10^{10})(500)] \quad (\text{C})(\text{cm}^{-3})(\text{cm}^2/\text{V} \cdot \text{s}) \\ &= 2.96 \times 10^{-6} \quad (\Omega \cdot \text{cm})^{-1}\end{aligned}$$

The resistivity  $\rho$  is equal to the reciprocal of the conductivity, so for intrinsic silicon

$$\rho = \frac{1}{\sigma} = 3.38 \times 10^5 \quad \Omega \cdot \text{cm}$$

From Table 2.1, we see that intrinsic silicon can be characterized as an insulator, albeit near the low end of the insulator resistivity range.

**Check of Results:** The resistivity has been found, and intrinsic silicon is a poor insulator.

**EXERCISE:** Find the resistivity of intrinsic silicon at 400 K and classify it as an insulator, semiconductor, or conductor. Use the mobility values from Ex. 2.2.

**ANSWERS:**  $1450 \Omega \cdot \text{cm}$ , semiconductor

**EXERCISE:** Calculate the resistivity of intrinsic silicon at 50 K if the electron mobility is  $6500 \text{ cm}^2/\text{V} \cdot \text{s}$  and the hole mobility is  $2000 \text{ cm}^2/\text{V} \cdot \text{s}$ . Classify the material.

**ANSWER:**  $1.69 \times 10^{53} \Omega \cdot \text{cm}$ , insulator

## 2.5 IMPURITIES IN SEMICONDUCTORS

The real advantages of semiconductors emerge when **impurities** are added to the material in minute but well-controlled amounts. This process is called **impurity doping**, or just **doping**, and the material that results is termed a **doped semiconductor**. Impurity doping enables us to change the resistivity

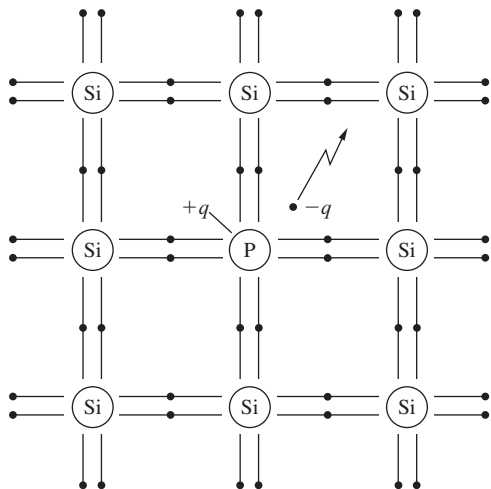


**Figure 2.6** An extra electron is available from a phosphorus donor atom.

over a very wide range and to determine whether the electron or hole population controls the resistivity of the material. The following discussion focuses on silicon, although the concepts of impurity doping apply equally well to other materials. The impurities that we use with silicon are from columns III and V of the periodic table.

### 2.5.1 DONOR IMPURITIES IN SILICON

**Donor impurities** in silicon are from column V, having five valence electrons in the outer shell. The most commonly used elements are phosphorus, arsenic, and antimony. When a donor atom replaces a silicon atom in the crystal lattice, as shown in Fig. 2.6, four of the five outer shell electrons fill the covalent bond structure; it then takes very little thermal energy to free the extra electron for conduction. At room temperature, essentially every donor atom contributes (donates) an electron for conduction. Each donor atom that becomes ionized by giving up an electron will have a net charge of  $+q$  and represents an immobile fixed charge in the crystal lattice.

### 2.5.2 ACCEPTOR IMPURITIES IN SILICON

**Acceptor impurities** in silicon are from column III and have one less electron than silicon in the outer shell. The primary acceptor impurity is boron, which is shown in place of a silicon atom in the lattice in Fig. 2.7. Because boron has only three electrons in its outer shell, a vacancy exists in the bond structure, and it is easy for a nearby electron to move into this vacancy, creating another vacancy in the bond structure. This mobile vacancy represents a hole that can move through the lattice, as illustrated in Fig. 2.7(a) and (b), and the hole may simply be visualized as a particle with a charge of  $+q$ . Each impurity atom that becomes ionized by accepting an electron has a net charge of  $-q$  and is immobile in the lattice, as in Fig. 2.7(a).

## 2.6 ELECTRON AND HOLE CONCENTRATIONS IN DOPED SEMICONDUCTORS

We now discover how to calculate the **electron** and **hole concentrations** in a semiconductor containing donor and acceptor impurities. In doped material, the electron and hole concentrations are no longer equal. If  $n > p$ , the material is called ***n*-type**, and if  $p > n$ , the material is referred to as

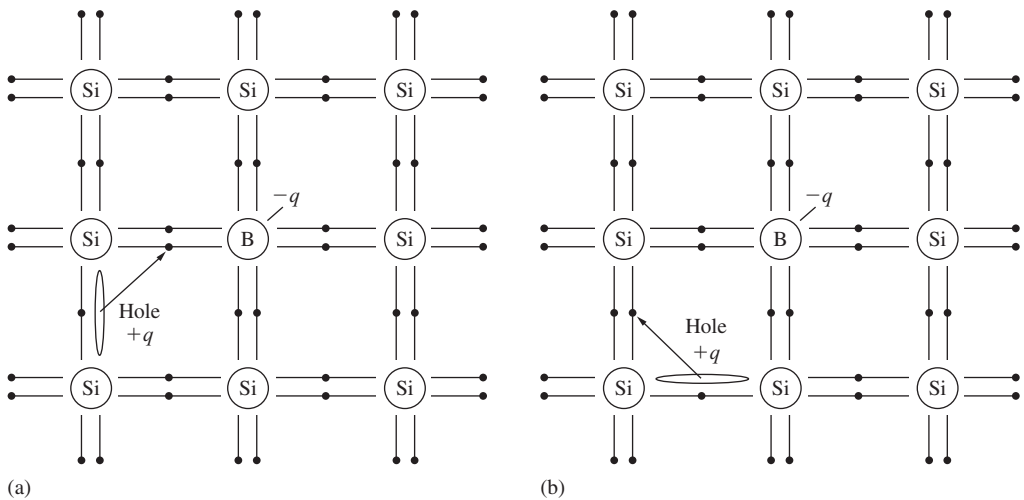


**Figure 2.7** (a) A hole is created after boron atom accepts an electron. The ionized boron atom represents an immobilized charge of  $-q$ . The vacancy in the silicon bond structure represents a mobile hole with charge  $+q$ . (b) Mobile hole moving through the silicon lattice.

**p-type.** The carrier with the larger population is called the **majority carrier**, and the carrier with the smaller population is termed the **minority carrier**.

To make detailed calculations of electron and hole densities, we need to keep track of the donor and acceptor impurity concentrations:

$N_D$  = donor impurity concentration atoms/cm<sup>3</sup>

Two additional pieces of information are needed. First, the semiconductor material must remain charge neutral, which requires that the sum of the total positive charge and negative charge be zero. Ionized donors and holes represent positive charge, whereas ionized acceptors and electrons carry negative charge. Thus **charge neutrality** requires

$$q(N_D + p - N_A - n) = 0 \quad (2.10)$$

Second, the product of the electron and hole concentrations in intrinsic material was given in Eq. (2.2) as  $pn = n_i^2$ . It can be shown theoretically that  $pn = n_i^2$  even for doped semiconductors in thermal equilibrium, and Eq. (2.2) is valid for a very wide range of doping concentrations.

### 2.6.1 *n*-TYPE MATERIAL ( $N_P > N_A$ )

Solving Eq. (2.2) for  $p$  and substituting into Eq. (2.10) yields a quadratic equation for  $n$ :

$$n^2 - (N_D - N_A)n - n_i^2 = 0$$

Now solving for  $n$ ,

$$n = \frac{(N_D - N_A) + \sqrt{(N_D - N_A)^2 + 4n_i^2}}{2} \quad \text{and} \quad p = \frac{n_i^2}{n} \quad (2.11)$$

In practical situations  $(N_D - N_A) \gg 2n_i$ , and  $n$  is given approximately by  $n \cong (N_D - N_A)$ . The formulas in Eq. (2.11) should be used for  $N_D \geq N_A$ .

### 2.6.2 *p*-TYPE MATERIAL ( $N_A > N_D$ )

For the case of  $N_A > N_D$ , we substitute for  $n$  in Eq. (2.10) and use the quadratic formula to solve for  $p$ :

$$p = \frac{(N_A - N_D) + \sqrt{(N_A - N_D)^2 + 4n_i^2}}{2} \quad \text{and} \quad n = \frac{n_i^2}{p} \quad (2.12)$$

Again, the usual case is  $(N_A - N_D) \gg 2n_i$ , and  $p$  is given approximately by  $p \cong (N_A - N_D)$ . Equation (2.12) should be used for  $N_A > N_D$ .

Because of practical process-control limitations, impurity densities that can be introduced into the silicon lattice range from approximately  $10^{14}$  to  $10^{21}$  atoms/cm<sup>3</sup>. Thus,  $N_A$  and  $N_D$  normally will be much greater than the intrinsic carrier concentration in silicon at room temperature. From the preceding approximate expressions, we see that the majority carrier density is set directly by the net impurity concentration:  $p \cong (N_A - N_D)$  for  $N_A > N_D$  or  $n \cong (N_D - N_A)$  for  $N_D > N_A$ .



### DESIGN NOTE PRACTICAL DOPING LEVELS

In both *n*- and *p*-type semiconductors, the majority carrier concentrations are established “at the factory” by the engineer’s choice of  $N_A$  and  $N_D$  and are independent of temperature over a wide range. In contrast, the minority carrier concentrations, although small, are proportional to  $n_i^2$  and highly temperature dependent. For practical doping levels,

$$\text{For } n\text{-type } (N_D > N_A): \quad n \cong N_D - N_A \quad p = \frac{n_i^2}{N_D - N_A}$$

$$\text{For } p\text{-type } (N_A > N_D): \quad p \cong N_A - N_D \quad n = \frac{n_i^2}{N_A - N_D}$$

Typical values of doping fall in this range:

$$10^{14}/\text{cm}^3 \leq |N_A - N_D| \leq 10^{21}/\text{cm}^3$$

### EXAMPLE 2.3

### ELECTRON AND HOLE CONCENTRATIONS

Calculate the electron and hole concentrations in a silicon sample containing both acceptor and donor impurities.

**PROBLEM** Find the type and electron and hole concentrations in a silicon sample at room temperature if it is doped with a boron concentration of  $10^{16}/\text{cm}^3$  and a phosphorus concentration of  $2 \times 10^{15}/\text{cm}^3$ .

**SOLUTION** **Known Information and Given Data:** Boron and phosphorus doping concentrations and room temperature operation are specified.

**Unknowns:** Electron and hole concentrations ( $n$  and  $p$ ).

**Approach:** Identify the donor and acceptor impurity concentrations and use their values to find  $n$  and  $p$  with Eq. (2.11) or Eq. (2.12), as appropriate.

**Assumptions:** At room temperature,  $n_i = 10^{10}/\text{cm}^3$ .

**Analysis:** Using Table 2.2 we find that boron is an acceptor impurity and phosphorus is a donor impurity. Therefore

$$N_A = 10^{16}/\text{cm}^3 \quad \text{and} \quad N_D = 2 \times 10^{15}/\text{cm}^3$$

Since  $N_A > N_D$ , the material is *p*-type, and we have  $(N_A - N_D) = 8 \times 10^{15}/\text{cm}^3$ . For  $n_i = 10^{10}/\text{cm}^3$ ,  $(N_A - N_D) \gg 2n_i$ , and we can use the simplified form of Eq. (2.12):

$$p \cong (N_A - N_D) = 8.00 \times 10^{15} \text{ holes/cm}^3$$

$$n = \frac{n_i^2}{p} = \frac{10^{20}/\text{cm}^6}{8.00 \times 10^{15}/\text{cm}^3} = 1.25 \times 10^4 \text{ electrons/cm}^3$$

**Check of Results:** We have found the electron and hole concentrations. We can double check the  $pn$  product:  $pn = 10^{20}/\text{cm}^6$ , which is correct.

**EXERCISE:** Find the type and electron and hole concentrations in a silicon sample at a temperature of 400 K if it is doped with a boron concentration of  $10^{16}/\text{cm}^3$  and a phosphorus concentration of  $2 \times 10^{15}/\text{cm}^3$ .

**ANSWERS:**  $8.00 \times 10^{15}/\text{cm}^3$ ,  $6.75 \times 10^8/\text{cm}^3$

**EXERCISE:** Silicon is doped with an antimony concentration of  $2 \times 10^{16}/\text{cm}^3$ . Is antimony a donor or acceptor impurity? Find the electron and hole concentrations at 300 K. Is this material *n*- or *p*-type?

**ANSWERS:** Donor;  $2 \times 10^{16}/\text{cm}^3$ ;  $5 \times 10^3/\text{cm}^3$ ; *n*-type

One might ask why we care about the minority carriers if they are so small in number. Indeed, we find shortly that semiconductor resistivity is controlled by the majority carrier concentration, and in Chapter 4 we find that field-effect transistors (FETs) are also majority carrier devices. However, the characteristics of diodes and bipolar junction transistors, discussed in Chapters 3 and 5, respectively, depend strongly on the minority carrier populations. Thus, to be able to design a variety of solid-state devices, we must understand how to manipulate both the majority and minority carrier concentrations.

## 2.7 MOBILITY AND RESISTIVITY IN DOPED SEMICONDUCTORS

The introduction of impurities into a semiconductor such as silicon actually degrades the mobility of the carriers in the material. Impurity atoms have slightly different sizes than the silicon atoms that they replace and hence disrupt the periodicity of the lattice. In addition, the impurity atoms are ionized and represent regions of localized charge that were not present in the original crystal. Both these effects cause the electrons and holes to scatter as they move through the semiconductor and reduce the mobility of the carriers in the crystal.

Figure 2.8 shows the dependence of mobility on the *total* impurity doping density  $N_T = (N_A + N_D)$  in silicon. We see that mobility drops rapidly as the doping level in the crystal increases. Mobility in heavily doped material can be more than an order of magnitude less than that in lightly doped material. On the other hand, doping vastly increases the density of majority carriers in the semiconductor material and thus has a dramatic effect on resistivity that overcomes the influence of decreased mobility.

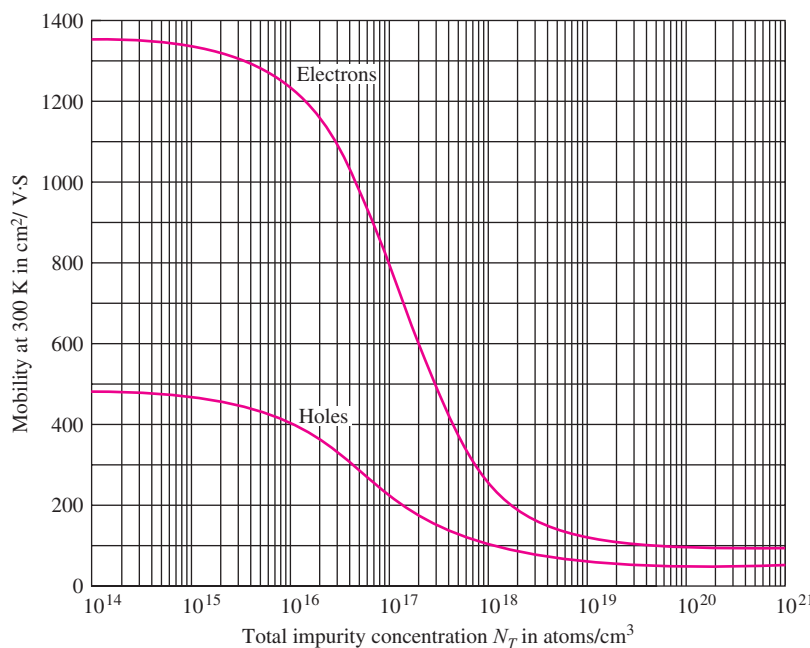


**Figure 2.8** Dependence of electron and hole mobility on total impurity concentration in silicon at 300 K.

Mobility approximations

$$\mu_n = 92 + \frac{1270}{1 + \left( \frac{N_T}{1.3 \times 10^{17}} \right)^{0.91}}$$

$$\mu_p = 48 + \frac{447}{1 + \left( \frac{N_T}{6.3 \times 10^{16}} \right)^{0.76}}$$

**EXERCISE:** What are the electron and hole mobilities in a silicon sample with an acceptor impurity density of  $10^{16}/\text{cm}^3$ ?

**ANSWERS:**  $1250 \text{ cm}^2/\text{V} \cdot \text{s}$ ;  $400 \text{ cm}^2/\text{V} \cdot \text{s}$

**EXERCISE:** What are the electron and hole mobilities in a silicon sample with an acceptor impurity density of  $4 \times 10^{16}/\text{cm}^3$  and a donor impurity density of  $6 \times 10^{16}/\text{cm}^3$ ?

**ANSWERS:**  $800 \text{ cm}^2/\text{V} \cdot \text{s}$ ,  $230 \text{ cm}^2/\text{V} \cdot \text{s}$

Remember that impurity doping also determines whether the material is *n*- or *p*-type, and simplified expressions can be used to calculate the conductivity of most extrinsic material. Note that  $\mu_n n \gg \mu_p p$  in the expression for  $\sigma$  in Ex. 2.4. For doping levels normally encountered, this inequality will be true for *n*-type material, and  $\mu_p p \gg \mu_n n$  will be valid for *p*-type material. The majority carrier concentration controls the conductivity of the material so that

$$\begin{aligned} \sigma &\cong q\mu_n n \cong q\mu_n(N_D - N_A) && \text{for } n\text{-type material} \\ \sigma &\cong q\mu_p p \cong q\mu_p(N_A - N_D) && \text{for } p\text{-type material} \end{aligned} \quad (2.13)$$

We now explore the relationship between doping and resistivity with an example.

## EXAMPLE 2.4

### RESISTIVITY CALCULATION OF DOPED SILICON

This example contrasts the resistivity of doped silicon to that of pure silicon.

**PROBLEM** Calculate the resistivity of silicon doped with a donor density  $N_D = 2 \times 10^{15}/\text{cm}^3$ . What is the material type? Classify the sample as an insulator, semiconductor, or conductor.

**SOLUTION** **Known Information and Given Data:**  $N_D = 2 \times 10^{15}/\text{cm}^3$ .

**Unknowns:** Resistivity  $\rho$ , which also requires us to find the hole and electron concentrations ( $p$  and  $n$ ) and mobilities ( $\mu_p$  and  $\mu_n$ ); material type.

**Approach:** Use the doping concentration to find  $n$  and  $p$  and  $\mu_n$  and  $\mu_p$ ; substitute these values into the expression for  $\sigma$ .

**Assumptions:** Since  $N_A$  is not mentioned, assume  $N_A = 0$ . Assume room temperature with  $n_i = 10^{10}/\text{cm}^3$ .

**Analysis:** In this case,  $N_D > N_A$  and much much greater than  $n_i$ , so

$$n = N_D = 2 \times 10^{15} \text{ electron/cm}^3$$

$$p = \frac{n_i^2}{n} = 10^{20}/2 \times 10^{15} = 5 \times 10^4 \text{ holes/cm}^3$$

Because  $n > p$ , the silicon is  $n$ -type material. From Fig. 2.8, the electron and hole mobilities for an impurity concentration of  $2 \times 10^{15}/\text{cm}^3$  are

$$\mu_n = 1320 \text{ cm}^2/\text{V} \cdot \text{s} \quad \mu_p = 460 \text{ cm}^2/\text{V} \cdot \text{s}$$

The conductivity and resistivity are now found to be

$$\sigma = 1.6 \times 10^{19}[(1320)(2 \times 10^{15}) + (460)(5 \times 10^4)] = 0.422 (\Omega \cdot \text{cm})^{-1}$$

and

$$\rho = 1/\sigma = 2.37 \Omega \cdot \text{cm}$$

This silicon sample is a semiconductor.

**Check of Results:** We have found the required unknowns.

**Discussion:** Comparing these results to those for intrinsic silicon, we note that the introduction of a minute fraction of impurities into the silicon lattice has changed the resistivity by 5 orders of magnitude, changing the material in fact from an insulator to a midrange semiconductor. Based upon this observation, it is not unreasonable to assume that additional doping can change silicon into a conductor (see the exercise following Ex. 2.5). Note that the doping level in this example represents a replacement of less than  $10^{-5}$  percent of the atoms in the silicon crystal.

## EXAMPLE 2.5 WAFER DOPING—AN ITERATIVE CALCULATION

Solutions to many engineering problems require iterative calculations as well as the integration of mathematical and graphical information.

**PROBLEM** An  $n$ -type silicon wafer has a resistivity of  $0.054 \Omega \cdot \text{cm}$ . What is the donor concentration  $N_D$ ?

**SOLUTION** **Known Information and Given Data:** The wafer is  $n$ -type silicon; resistivity is  $0.054 \Omega \cdot \text{cm}$ .

**Unknowns:** Doping concentration  $N_D$  required to achieve the desired resistivity.

**Approach:** For this problem, an iterative trial-and-error solution is necessary. Because the resistivity is low, it should be safe to assume that

$$\sigma = q\mu_n n = q\mu_n N_D \quad \text{and} \quad \mu_n N_D = \frac{\sigma}{q}$$

We know that  $\mu_n$  is a function of the doping concentration  $N_D$ , but the functional dependence may be available only in graphical form. This is an example of a type of problem often encountered in engineering. The solution requires an iterative trial-and-error approach involving both mathematical and graphical evaluations. To solve the problem, we need to establish a logical progression of steps in which the choice of one parameter enables us to evaluate other parameters that lead to the solution. One method for this problem is

1. Choose a value of  $N_D$ .
2. Find  $\mu_n$  from the mobility graph.
3. Calculate  $\mu_n N_D$ .
4. If  $\mu_n N_D$  is not correct, go back to step 1.

Obviously, we hope we can make educated choices that will lead to convergence of the process after a few trials.

**Assumptions:** Assume the wafer contains only donor impurities.

**Analysis:** For this problem,

$$\frac{\sigma}{q} = (0.054 \times 1.6 \times 10^{-19})^{-1} = 1.2 \times 10^{20} (\text{V} \cdot \text{s} \cdot \text{cm})^{-1}$$

Choosing a first guess of  $N_D = 1 \times 10^{16}/\text{cm}^3$ :

TRIAL	$N_D$ ( $\text{cm}^{-3}$ )	$\mu_n$ ( $\text{cm}^2/\text{V} \cdot \text{s}$ )	$\mu_n N_D$ ( $\text{V} \cdot \text{s} \cdot \text{cm}$ ) $^{-1}$
1	$1 \times 10^{16}$	1250	$1.3 \times 10^{19}$
2	$1 \times 10^{18}$	260	$2.5 \times 10^{20}$
3	$1 \times 10^{17}$	80	$8.0 \times 10^{19}$
4	$5 \times 10^{17}$	380	$3.8 \times 10^{20}$
5	$4 \times 10^{17}$	430	$1.7 \times 10^{20}$
6	$2 \times 10^{17}$	600	$1.2 \times 10^{20}$

After six iterations, we find  $N_D = 2 \times 10^{17}$  donor atoms/ $\text{cm}^3$ .

**Check of Results:** We have found the only unknown.  $N_D = 2 \times 10^{17}/\text{cm}^3$  is in the range of practically achievable doping. See the Design Note in Sec. 2.6. Numeric approximations for the mobility dependence upon doping appear in Fig. 2.8. For  $N_D = 2 \times 10^{17}/\text{cm}^3$ , the calculated mobility is  $604 \text{ cm}^2/\text{V}\cdot\text{s}$ , in agreement with our iterative analysis.

**EXERCISE:** What is the minimum value of donor doping required to convert silicon to a conductor at room temperature? What is the resistivity?

**ANSWER:**  $6.25 \times 10^{19}/\text{cm}^3$  with  $\mu_n \approx 100 \text{ cm}^2/\text{V} \cdot \text{s}$ ,  $0.001 \Omega\cdot\text{cm}$

**EXERCISE:** Silicon is doped with a phosphorus concentration of  $2 \times 10^{16}/\text{cm}^3$ . What are  $N_A$  and  $N_D$ ? What are the electron and hole mobilities? What are the mobilities if boron in a concentration of  $3 \times 10^{16}/\text{cm}^3$  is added to the silicon? What are the resistivities?

**ANSWERS:**  $N_A = 0/\text{cm}^3$ ;  $N_D = 2 \times 10^{16}/\text{cm}^3$ ;  $\mu_n = 1160 \text{ cm}^2/\text{V} \cdot \text{s}$ ,  $\mu_p = 370 \text{ cm}^2/\text{V} \cdot \text{s}$ ;  $\mu_n = 980 \text{ cm}^2/\text{V} \cdot \text{s}$ ;  $\mu_p = 290 \text{ cm}^2/\text{V} \cdot \text{s}$ ;  $0.27 \Omega\cdot\text{cm}$ ;  $0.46 \Omega\cdot\text{cm}$

**EXERCISE:** Silicon is doped with a boron concentration of  $4 \times 10^{18}/\text{cm}^3$ . Is boron a donor or acceptor impurity? Find the electron and hole concentrations at 300 K. Is this material *n*-type or *p*-type? Find the electron and hole mobilities. What is the resistivity of the material?

**ANSWERS:** Acceptor;  $n = 25/\text{cm}^3$ ,  $p = 4 \times 10^{18}/\text{cm}^3$ ; *p*-type;  $\mu_n = 150 \text{ cm}^2/\text{V}\cdot\text{s}$  and  $\mu_p = 70 \text{ cm}^2/\text{V}\cdot\text{s}$ ;  $0.022 \Omega\cdot\text{cm}$

**EXERCISE:** Silicon is doped with an indium concentration of  $7 \times 10^{19}/\text{cm}^3$ . Is indium a donor or acceptor impurity? Find the electron and hole concentrations, the electron and hole mobilities, and the resistivity of this silicon material at 300 K. Is this material *n*- or *p*-type?

**ANSWERS:** Acceptor;  $n = 1.4/\text{cm}^3$ ,  $p = 7 \times 10^{19}/\text{cm}^3$ ;  $\mu_n = 100 \text{ cm}^2/\text{V}\cdot\text{s}$  and  $\mu_p = 50 \text{ cm}^2/\text{V}\cdot\text{s}$ ;  $\rho = 0.00179 \Omega\cdot\text{cm}$ ; *p*-type

## 2.8 DIFFUSION CURRENTS

As already described, the electron and hole populations in a semiconductor are controlled by the impurity doping concentrations  $N_A$  and  $N_D$ . Up to this point we have tacitly assumed that the doping is uniform in the semiconductor, but this need not be the case. Changes in doping are encountered often in semiconductors, and there will be gradients in the electron and hole concentrations. Gradients in these free carrier densities give rise to a second current flow mechanism, called **diffusion**. The free carriers tend to move (diffuse) from regions of high concentration to regions of low concentration in much the same way as a puff of smoke in one corner of a room rapidly spreads throughout the entire room.

A simple one-dimensional gradient in the electron or hole density is shown in Fig. 2.9. The gradient in this figure is positive in the  $+x$  direction, but the carriers diffuse in the  $-x$  direction, from high to low concentration. Thus the **diffusion current densities** are proportional to the negative of the carrier gradient:

$$\begin{aligned} j_p^{\text{diff}} &= (+q)D_p \left( -\frac{\partial p}{\partial x} \right) = -q D_p \frac{\partial p}{\partial x} & \text{A/cm}^2 \\ j_n^{\text{diff}} &= (-q)D_n \left( -\frac{\partial n}{\partial x} \right) = +q D_n \frac{\partial n}{\partial x} \end{aligned} \quad (2.14)$$

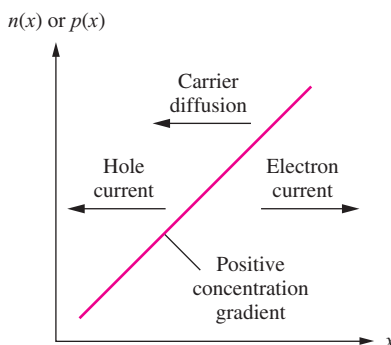


Figure 2.9 Carrier diffusion in the presence of a concentration gradient.

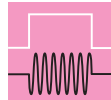
The proportionality constants  $D_p$  and  $D_n$  are the **hole** and **electron diffusivities**, with units ( $\text{cm}^2/\text{s}$ ). Diffusivity and mobility are related by **Einstein's relationship**:

$$\frac{D_n}{\mu_n} = \frac{kT}{q} = \frac{D_p}{\mu_p} \quad (2.15)$$

The quantity ( $kT/q = V_T$ ) is called the **thermal voltage**  $V_T$ , and its value is approximately 0.025 V at room temperature. We encounter the parameter  $V_T$  in several different contexts throughout this book. Typical values of the diffusivities (also referred to as the **diffusion coefficients**) in silicon are in the range 2 to 35  $\text{cm}^2/\text{s}$  for electrons and 1 to 15  $\text{cm}^2/\text{s}$  for holes at room temperature.

**EXERCISE:** Calculate the value of the thermal voltage  $V_T$  for  $T = 50 \text{ K}$ ,  $300 \text{ K}$ , and  $400 \text{ K}$ .

**ANSWERS:** 4.3 mV; 25.8 mV; 34.5 mV



### DESIGN NOTE THERMAL VOLTAGE $V_T$

$$V_T = kT/q = 0.0258 \text{ V at } 300 \text{ K}$$

**EXERCISE:** What are the maximum values of the room temperature values (300 K) of the diffusion coefficients for electrons and holes in silicon based on the mobilities in Fig. 2.8?

**ANSWERS:** Using  $V_T = 25.8 \text{ mV}$ ;  $35.1 \text{ cm}^2/\text{s}$ ,  $12.8 \text{ cm}^2/\text{s}$

**EXERCISE:** An electron gradient of  $+10^{16}/(\text{cm}^3 \cdot \mu\text{m})$  exists in a semiconductor. What is the diffusion current density at room temperature if the electron diffusivity =  $20 \text{ cm}^2/\text{s}$ ? Repeat for a hole gradient of  $+10^{20}/\text{cm}^4$  with  $D_p = 4 \text{ cm}^2/\text{s}$ .

**ANSWER:**  $+320 \text{ A/cm}^2$ ;  $-64 \text{ A/cm}^2$

## 2.9 TOTAL CURRENT

Generally, currents in a semiconductor have both drift and diffusion components. The total electron and hole current densities  $j_n^T$  and  $j_p^T$  can be found by adding the corresponding drift and diffusion components from Eqs. (2.5) and (2.14):

$$j_n^T = q\mu_n nE + qD_n \frac{\partial n}{\partial x} \quad \text{and} \quad j_p^T = q\mu_p pE - qD_p \frac{\partial p}{\partial x} \quad (2.16)$$

Using Einstein's relationship from Eq. (2.15), Eq. (2.16) can be rewritten as

$$j_n^T = q\mu_n n \left( E + V_T \frac{1}{n} \frac{\partial n}{\partial x} \right) \quad \text{and} \quad j_p^T = q\mu_p p \left( E - V_T \frac{1}{p} \frac{\partial p}{\partial x} \right) \quad (2.17)$$

Equation (2.16) or (2.17) combined with Gauss' law

$$\nabla \cdot (\varepsilon E) = Q \quad (2.18)$$

where  $\varepsilon$  = permittivity (F/cm),  $E$  = electric field (V/cm), and  $Q$  = charge density (C/cm<sup>3</sup>)

gives us a powerful mathematics approach for analyzing the behavior of semiconductors and forms the basis for many of the results presented in later chapters.

## 2.10 ENERGY BAND MODEL

This section discusses the **energy band model** for a semiconductor, which provides a useful alternative view of the electron–hole creation process and the control of carrier concentrations by impurities. Quantum mechanics predicts that the highly regular crystalline structure of a semiconductor produces periodic quantized ranges of allowed and disallowed energy states for the electrons surrounding the atoms in the crystal. Figure 2.10 is a conceptual picture of this band structure in the semiconductor, in which the regions labeled **conduction band** and **valence band** represent allowed energy states for electrons. Energy  $E_V$  corresponds to the top edge of the valence band and represents the highest permissible energy for a valence electron. Energy  $E_C$  corresponds to the bottom edge of the conduction band and represents the lowest available energy level in the conduction band. Although these bands are shown as continuums in Fig. 2.10, they actually consist of a very large number of closely spaced, discrete energy levels.

Electrons are not permitted to assume values of energy lying between  $E_C$  and  $E_V$ . The difference between  $E_C$  and  $E_V$  is called the *bandgap energy*  $E_G$ :

$$E_G = E_C - E_V \quad (2.19)$$

Table 2.3 listed examples of the bandgap energy for a number of semiconductors.

### 2.10.1 ELECTRON–HOLE PAIR GENERATION IN AN INTRINSIC SEMICONDUCTOR

In silicon at very low temperatures ( $\approx 0$  K), the valence band states are completely filled with electrons, and the conduction band states are completely empty, as shown in Fig. 2.11. The semiconductor

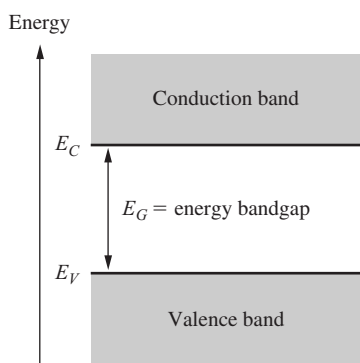


**Figure 2.10** Energy band model for a semiconductor with bandgap  $E_G$ .

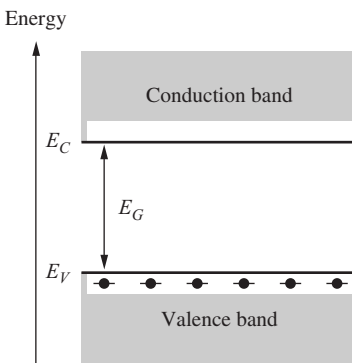


**Figure 2.11** Semiconductor at 0 K with filled valence band and empty conduction band. This figure corresponds to the bond model in Fig. 2.2.

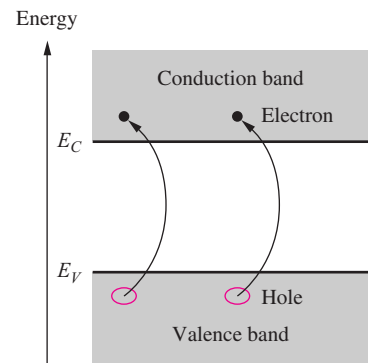


**Figure 2.12** Creation of electron–hole pair by thermal excitation across the energy bandgap. This figure corresponds to the bond model of Fig. 2.3.

in this situation does not conduct current when an electric field is applied. There are no free electrons in the conduction band, and no holes exist in the completely filled valence band to support current flow. The band model of Fig. 2.11 corresponds directly to the completely filled bond model of Fig. 2.2.

As temperature rises above 0 K, thermal energy is added to the crystal. A few electrons gain the energy required to surmount the energy bandgap and jump from the valence band into the conduction band, as shown in Fig. 2.12. Each electron that jumps the bandgap creates an electron–hole pair. This **electron–hole pair generation** situation corresponds directly to that presented in Fig. 2.3.

### 2.10.2 ENERGY BAND MODEL FOR A DOPED SEMICONDUCTOR

Figures 2.13 to 2.15 present the band model for **extrinsic material** containing donor and/or acceptor atoms. In Fig. 2.13, a concentration  $N_D$  of donor atoms has been added to the semiconductor. The donor atoms introduce new localized energy levels within the bandgap at a **donor energy level**  $E_D$  near the conduction band edge. The value of  $(E_C - E_D)$  for phosphorus is approximately 0.045 eV, so it takes very little thermal energy to promote the extra electrons from the donor sites into the conduction band. The density of conduction-band states is so high that the probability of finding an electron in a donor state is practically zero, except for heavily doped material (large  $N_D$ ) or at very low temperature. Thus at room temperature, essentially all the available donor electrons are free for conduction. Figure 2.13 corresponds to the bond model of Fig. 2.6.

In Fig. 2.14, a concentration  $N_A$  of acceptor atoms has been added to the semiconductor. The acceptor atoms introduce energy levels within the bandgap at the **acceptor energy level**  $E_A$  near the valence band edge. The value of  $(E_A - E_V)$  for boron is approximately 0.044 eV, and it takes very little thermal energy to promote electrons from the valence band into the acceptor energy levels. At room temperature, essentially all the available acceptor sites are filled, and each promoted electron creates a hole that is free for conduction. Figure 2.14 corresponds to the bond model of Fig. 2.7.

### 2.10.3 COMPENSATED SEMICONDUCTORS

The situation for a **compensated semiconductor**, one containing both acceptor and donor impurities, is depicted in Fig. 2.15 for the case in which there are more donor atoms than acceptor atoms. Electrons seek the lowest energy states available, and they fall from donor sites, filling all the available acceptor sites. The remaining free electron population is given by  $n = (N_D - N_A)$ .

The energy band model just discussed represents a conceptual model that is complementary to the covalent bond model of Sec. 2.2. Together they help us visualize the processes involved in creating holes and electrons in doped semiconductors.

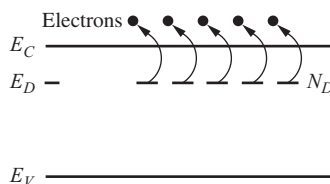


**Figure 2.13** Donor level with activation energy ( $E_C - E_D$ ). This figure corresponds to the bond model of Fig. 2.6.

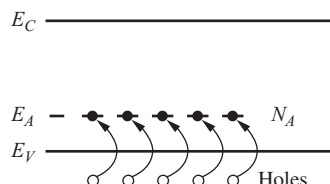


**Figure 2.14** Acceptor level with activation energy ( $E_A - E_V$ ). This figure corresponds to the bond model of Fig. 2.7(b).

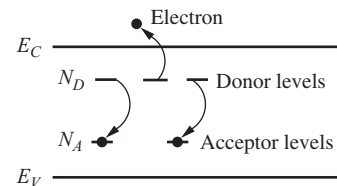


**Figure 2.15** Compensated semiconductor containing both donor and acceptor atoms with  $N_D > N_A$ .

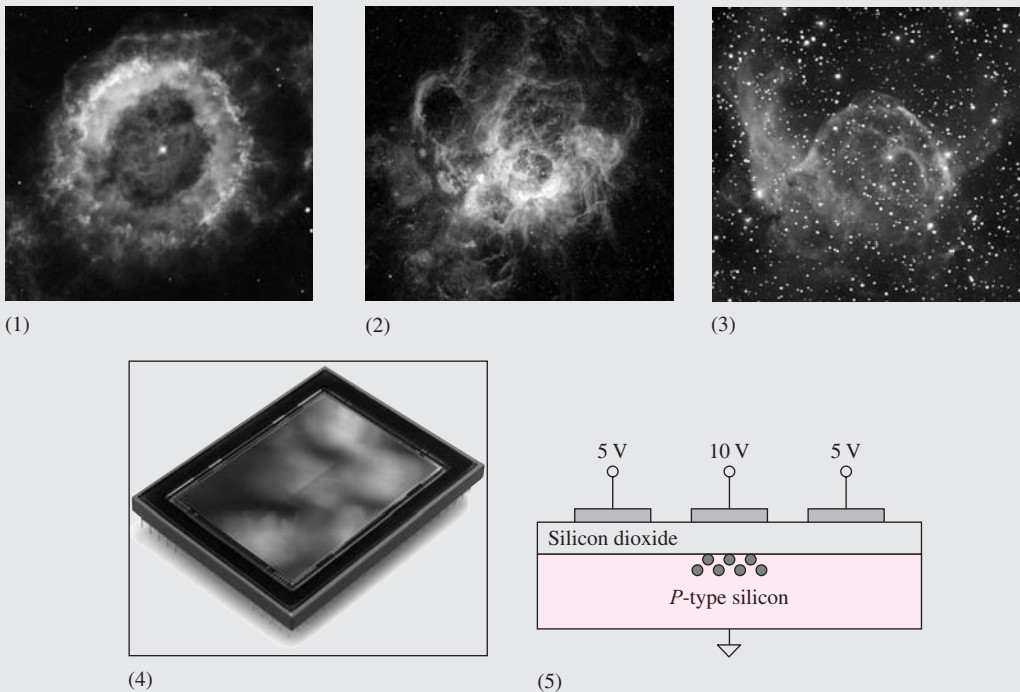


## ELECTRONICS IN ACTION

### *CCD Cameras*

Modern astronomy is highly dependent on microelectronics for both the collection and analysis of astronomical data. Tremendous advancements in astronomy have been made possible by the combination of electronic image capture and computer analysis of the acquired images.

In the case of optical telescopes, the Charge-Coupled Device (CCD) camera converts photons to electrical signals that are then formed into a computer image. Like other photo-detector circuits, the CCD captures electrons that are generated when incident photons interact with the semiconductor material and create hole-electron pairs as in Fig. 2.12. A two-dimensional array of as many as several million CCD cells is formed on a single chip, similar to the one shown below. CCD imagers are especially important to astronomers because of their very high sensitivity and low electronic noise.



A simplified view of a CCD cell is shown here. A group of electrons have accumulated under the middle electrode due to the higher voltage present. The electrons are held within the semiconductor by the combination of the insulating silicon-dioxide layer and the fields created by the electrodes. The more incident light, the more electrons are captured. To read the charge out of the cell, the electrode voltages are manipulated to move the charge from electrode to electrode until it is converted to a voltage at the edge of the imaging array. The astronomical images were acquired with CCD cameras located on the Hubble Space Telescope.

---

Source: (1) NGC6369: The Little Ghost Nebula. Credit: Hubble Heritage Team, NASA; (2) NGC604: Giant Stellar Nursery. Credit: H. Yang (UIUC), HST, NASA; (3) NGC2359: Thors Helmet. Credits: Christine and David Smith, Steve Mandel, Adam Block (KPNO Visitor Program), NOAO, AURA, NSF. (4) The chip pictured above is a 33 MegaPixel Dalsa CCD image sensor and is reprinted here with permission from the Dalsa Corporation.

## 2.11 OVERVIEW OF INTEGRATED CIRCUIT FABRICATION

Before we leave this chapter, we explore how an engineer uses selective control of semiconductor doping to form a simple electronic device. We do this by exploring the basic fabrication steps utilized to fabricate a solid-state diode. These ideas help us understand the characteristics of many electronic devices that depend strongly on the physical structure of the device.

Complex solid-state devices and circuits are fabricated through the repeated application of a number of basic IC processing steps including oxidation, photolithography, etching, ion implantation, diffusion, evaporation, sputtering, chemical vapor deposition, and epitaxial growth. **Silicon dioxide** ( $\text{SiO}_2$ ) layers are formed by heating silicon wafers to a high temperature (1000 to 1200°C) in the presence of pure oxygen or water vapor. This process is called **oxidation**. Thin layers of metal films are deposited through **evaporation** by heating the metal to its melting point in a vacuum. In contrast, both conducting metal films and insulators can be deposited through a process called **sputtering**, which uses physical ion bombardment to effect transfer of atoms from a source target to the wafer surface.

Thin films of polysilicon, silicon dioxide, and **silicon nitride** can all be formed through **chemical vapor deposition** (CVD), in which the material is precipitated from a gaseous mixture directly onto the surface of the silicon wafer. Shallow *n*- and *p*-type layers are formed by **ion implantation**, where the wafer is bombarded by high-energy (50-keV to 1-MeV) acceptor or donor impurity atoms generated by a high-voltage particle accelerator. A greater depth of the impurity layers can be achieved by **diffusion** of the impurities at high temperatures, typically 1000 to 1200°C, in either an inert or oxidizing environment. Bipolar processes, as well as some CMOS processes, employ the **epitaxial growth** technique to form thin high-quality layers of crystalline silicon on top of the wafer. The epitaxial layer replicates the crystal structure of the original silicon substrate.

To build integrated circuits, localized *n*- and *p*-type regions must be formed selectively in the silicon surface. Silicon dioxide, silicon nitride, **polysilicon**, **photoresist**, and other materials can all be used to block out areas of the wafer surface to prevent penetration of impurity atoms during implantation and/or diffusion. **Masks** containing window patterns to be opened in the protective layers are produced using a combination of computer-aided design systems and photographic reduction techniques. The patterns are transferred from the mask to the wafer surface through the use of high-resolution optical photographic techniques, a process called **photolithography**. The windows defined by the masks are cut through the protective layers by wet-chemical **etching** using acids or by dry-plasma etching.

The fabrication steps just outlined can be combined in many different ways to form integrated circuits. A simple example is contained in Figs. 2.16 and 2.17. Here we wish to form, and make contact to a localized *p*-type region in the surface of an *n*-type silicon wafer. In Fig. 2.17(a), a 500  $\mu\text{m}$  thick silicon wafer has been oxidized to form a thin layer of silicon dioxide (1  $\mu\text{m}$ ), and a layer of photoresist has been applied to the top of the  $\text{SiO}_2$ . The photoresist is exposed by shining light through a mask that contains patterns to be transferred to the wafer. After exposure and development, this photoresist (called positive resist) has an opening where it was exposed, as in Fig. 2.17(b). Next, the oxide is etched away using the photoresist as a barrier layer, leaving a window through both the photoresist and oxide layers, as in Fig. 2.17(c). Acceptor impurities are now implanted into the silicon through the window, but are blocked everywhere else by the barrier formed by the photoresist and oxide layers. After photoresist removal, a localized *p*-type region exists in the silicon below the window in the  $\text{SiO}_2$ , as in Fig. 2.17(d). The *p*-type region will extend from a few tenths of a micron to at most a few microns below the silicon surface.

Oxide is regrown on the wafer surface and coated with a new layer of photoresist, as indicated in Fig. 2.17(e). Contact windows are exposed through a second mask. The structure in Fig. 2.17(f) results following completion of the photolithography step and subsequent etching of the contact windows in the oxide. Contacts will be made to both the *n*-type substrate and the *p*-type region through these openings. Next, an aluminum layer is evaporated onto the silicon wafer and once again coated with photoresist as in Fig. 2.17(g). A third mask and photolithography step are used to transfer

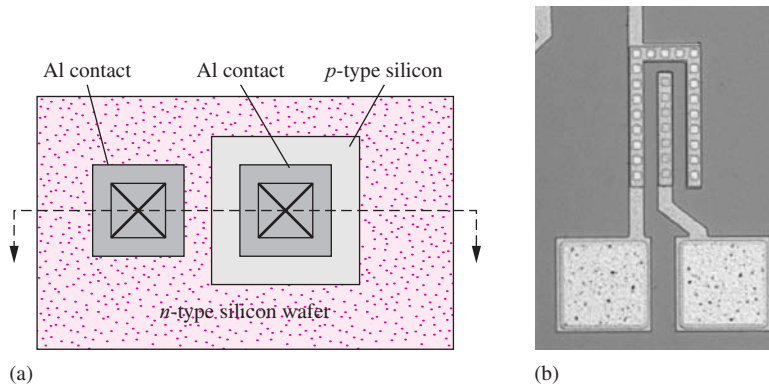


**Figure 2.16** (a) Top view of the *pn* diode structure formed by fabrication steps in Fig. 2.17.  
(b) Photomicrograph of an actual diode.

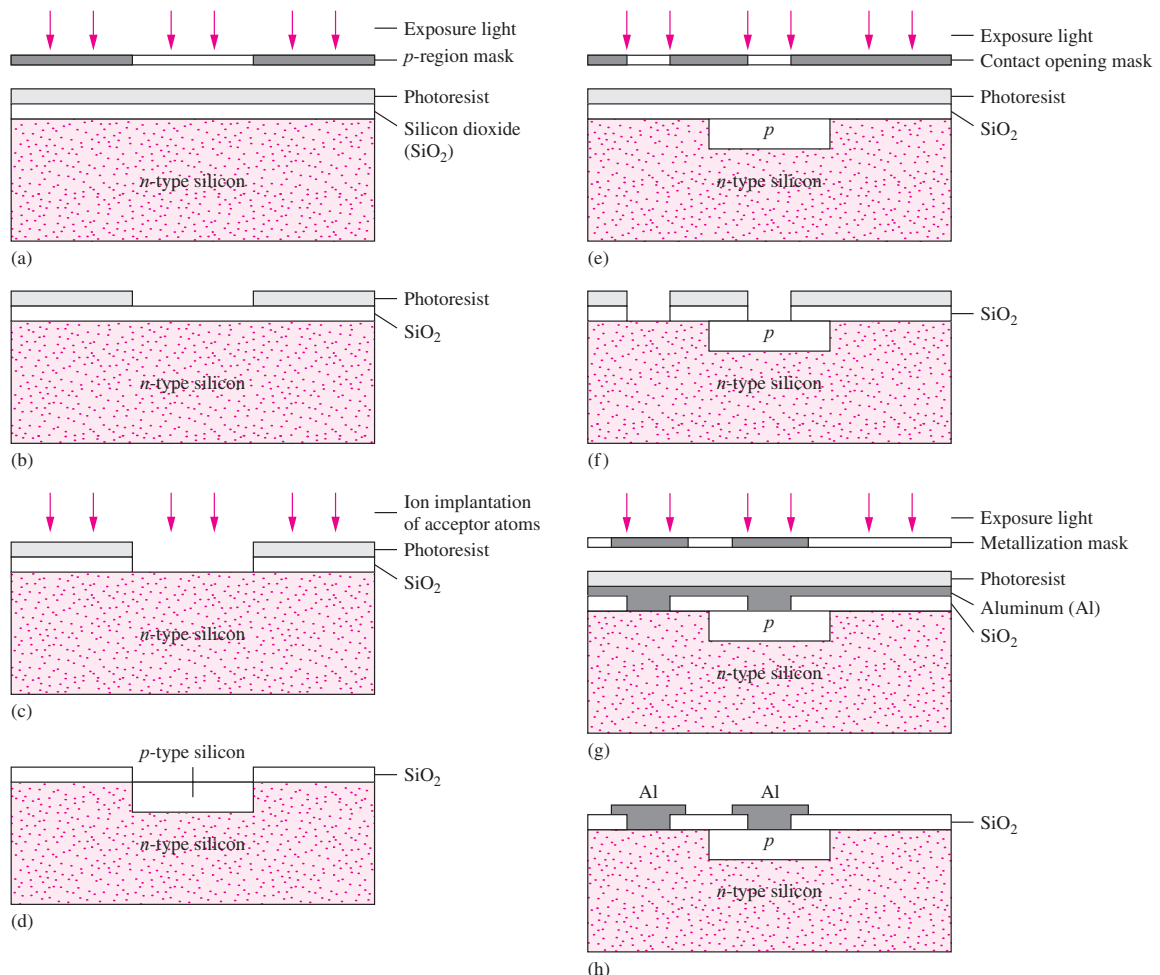


**Figure 2.17** Silicon wafer (a) at first mask exposure step, (b) after exposure and development of photoresist, (c) following etching of silicon dioxide, and (d) after implantation/diffusion of acceptor impurity and resist removal. (e) Exposure of contact opening mask (f) after resist development and etching of contact openings. (g) Exposure of metal mask. (h) Final structure after etching of aluminum and resist removal.

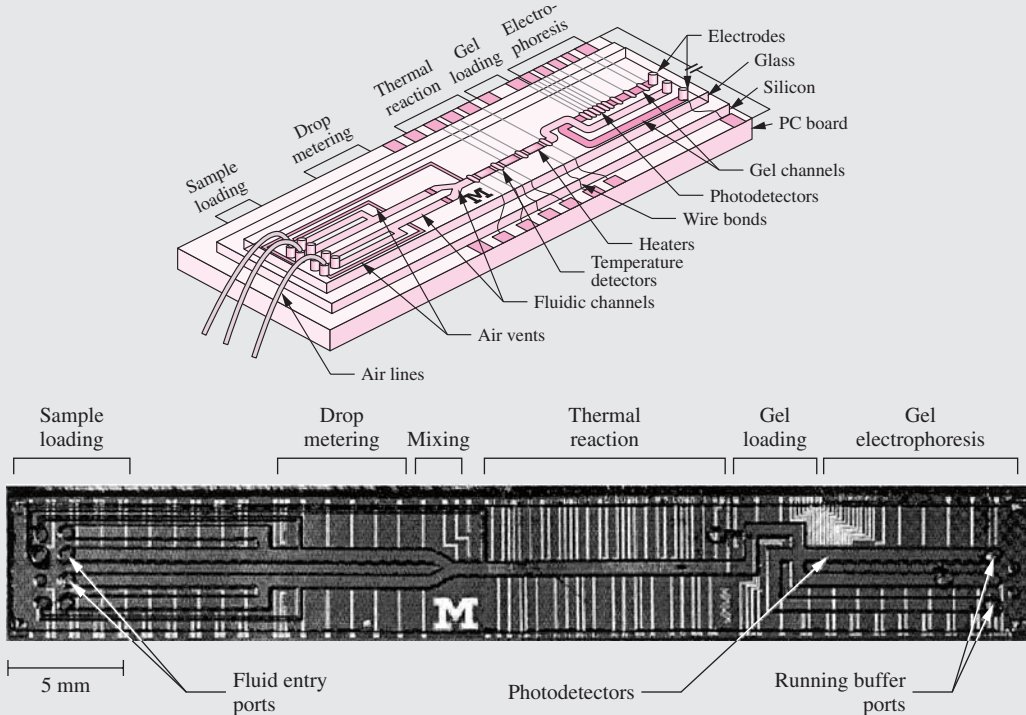
the desired metallization pattern to the wafer surface, and then the aluminum is etched away wherever it is not coated with resist. The completed structure appears in Fig. 2.17(h) and corresponds to the top view in Fig. 2.16. Aluminum contacts have been made to both the *n*-type substrate and the *p*-type region. We have just stepped through the fabrication of our first solid-state device—a *pn* junction diode! Study of the characteristics, operation, and application of diodes is the topic of Chapter 3. Figure 2.16(b) is a photomicrograph of an actual diode.

## ELECTRONICS IN ACTION

### *Lab-on-a-chip*

The photo below<sup>1</sup> illustrates the integration of silicon microelectronic circuits, microfluidics, and a printed circuit board to realize a nanoliter DNA analysis device. DNA fluid samples are introduced at one end of the device, metered into nanoliter sized droplets, and propelled along a fluidic channel where the sample is mixed with other materials, heated, and optically stimulated. Integrated optical detectors are used to measure the resulting fluorescence for detection of target genetic bio-materials.

Devices such as the one below are revolutionizing health-care by improving our understanding of disease and disease mechanisms, enabling rapid diagnostics and providing for the screening of large numbers of potential treatments in a low-cost fashion. Bioengineering and in particular the application of microelectronics to health-care and life sciences is a rapidly growing and exciting field.



<sup>1</sup> Mark A. Burns, Brian N. Johnson, Sundaresh N. Brahmasandra, Kalyan Handique, James R. Webster, Madhavi Krishnan, Timothy S. Sammarco, Piu M. Man, Darren Jones, Dylan Heldsinger, Carlos H. Mastrangelo, David T. Burke, "An Integrated Nanoliter DNA Analysis Device," *Science*, vol. 282, no. 5388, 16 Oct 1998. Reprinted by permission from AAAS.

## SUMMARY

- Materials are found in three primary forms: amorphous, polycrystalline, and crystalline. An amorphous material is a totally disordered or random material that shows no short range order. In polycrystalline material, large numbers of small crystallites can be identified. A crystalline material exhibits a highly regular bonding structure among the atoms over the entire macroscopic crystal.
- Electronic materials can be separated into three classifications based on their electrical resistivity. Insulators have resistivities above  $10^5 \Omega \cdot \text{cm}$ , whereas conductors have resistivities below  $10^{-3} \Omega \cdot \text{cm}$ . Between these two extremes lie semiconductor materials.
- Today's most important semiconductor is silicon (Si), which is used for fabrication of very-large-scale-integrated (VLSI) circuits. Two compound semiconductor materials, gallium arsenide (GaAs) and indium phosphide (InP), are the most important materials for optoelectronic applications including light-emitting diodes (LEDs), lasers, and photodetectors.
- The highly useful properties of semiconductors arise from the periodic nature of crystalline material, and two conceptual models for these semiconductors were introduced: the covalent bond model and the energy band model.
- At very low temperatures approaching 0 K, all the covalent bonds in a semiconductor crystal will be intact and the material will actually be an insulator. As temperature is raised, the added thermal energy causes a small number of covalent bonds to break. The amount of energy required to break a covalent bond is equal to the bandgap energy  $E_G$ .
- When a covalent bond is broken, two charge carriers are produced: an electron, with charge  $-q$ , that is free to move about the conduction band; and a hole, with charge  $+q$ , that is free to move through the valence band.
- Pure material is referred to as intrinsic material, and the electron density  $n$  and hole density  $p$  in an intrinsic material are both equal to the intrinsic carrier density  $n_i$ , which is approximately equal to  $10^{10}$  carriers/cm<sup>3</sup> in silicon at room temperature. In a material in thermal equilibrium, the product of the electron and hole concentrations is a constant:  $pn = n_i^2$ .
- The hole and electron concentrations can be significantly altered by replacing small numbers of atoms in the original crystal with impurity atoms. Silicon, a column IV element, has four electrons in its outer shell and forms covalent bonds with its four nearest neighbors in the crystal. In contrast, the impurity elements (from columns III and V of the periodic table) have either three or five electrons in their outer shells.
- In silicon, column V elements such as phosphorus, arsenic, and antimony, with an extra electron in the outer shell, act as donors and add electrons directly to the conduction band. A column III element such as boron has only three outer shell electrons and creates a free hole in the valence band.
- The donor and acceptor impurity densities are usually represented by  $N_D$  and  $N_A$ , respectively.
- If  $n$  exceeds  $p$ , the semiconductor is referred to as  $n$ -type material, and electrons are the majority carriers and holes are the minority carriers. If  $p$  exceeds  $n$ , the semiconductor is referred to as  $p$ -type material, and holes become the majority carriers and electrons the minority carriers.
- Electron and hole currents each have two components: a drift current and a diffusion current.
- Drift current is the result of carrier motion caused by an applied electric field. Drift currents are proportional to the electron and hole mobilities ( $\mu_n$  and  $\mu_p$ , respectively).
- Diffusion currents arise from gradients in the electron or hole concentrations. The magnitudes of the diffusion currents are proportional to the electron and hole diffusivities ( $D_n$  and  $D_p$ , respectively).
- Diffusivity and mobility are related by the Einstein relationship:  $D/\mu = kT/q$ . The expression  $kT/q$  has units of voltage and is often referred to as the thermal voltage  $V_T$ . Doping the semiconductor disrupts the periodicity of the crystal lattice, and the mobility—and hence diffusivity—both decrease monotonically as the impurity doping concentration is increased.

- The ability to add impurities to change the conductivity type and to control hole and electron concentrations is at the heart of our ability to fabricate high-performance, solid-state devices and high-density integrated circuits. In the next several chapters, we see how this capability is used to form diodes, field-effect transistors (FETs), and bipolar junction transistors (BJTs).
- Complex solid-state devices and circuits are fabricated through the repeated application of a number of basic IC processing steps, including oxidation, photolithography, etching, ion implantation, diffusion, evaporation, sputtering, chemical vapor deposition (CVD), and epitaxial growth.
- To build integrated circuits, localized *n*- and *p*-type regions must be formed selectively in the silicon surface. Silicon dioxide, silicon nitride, polysilicon, photoresist, and other materials can all be used to block out areas of the wafer surface to prevent penetration of impurity atoms during implantation and/or diffusion. Masks containing window patterns to be opened in the protective layers are produced using a combination of computer-aided design systems and photographic reduction techniques. The patterns are transferred from the mask to the wafer surface through the use of high-resolution photolithography.

## KEY TERMS

Acceptor energy level	Hole
Acceptor impurities	Hole concentration
Acceptor impurity concentration	Hole density
Amorphous material	Hole diffusivity
Bandgap energy	Hole mobility
Charge neutrality	Impurities
Chemical vapor deposition	Impurity doping
Compensated semiconductor	Insulator
Compound semiconductor	Intrinsic carrier density
Conduction band	Intrinsic material
Conductivity	Ion implantation
Conductor	Majority carrier
Covalent bond model	Mask
Diffusion	Minority carrier
Diffusion coefficients	Mobility
Diffusion current density	<i>n</i> -type material
Donor energy level	Oxidation
Donor impurities	<i>p</i> -type material
Donor impurity concentration	Photolithography
Doped semiconductor	Photoresist
Doping	<i>pn</i> product
Drift current density	Polycrystalline material
Einstein's relationship	Polysilicon
Electrical conductivity	Resistivity
Electron	Saturated drift velocity
Electron concentration	Semiconductor
Electron diffusivity	Silicon dioxide
Electron–hole pair generation	Silicon nitride
Electron mobility	Single-crystal material
Elemental semiconductor	Sputtering
Energy band model	Thermal equilibrium
Epitaxial growth	Thermal voltage
Etching	Vacancy
Evaporation	Valence band
Extrinsic material	

## REFERENCE

1. J. D. Cressler, "Re-Engineering Silicon: SiGe Heterojunction Bipolar Technology," *IEEE Spectrum*, pp. 49–55, March 1995.

## ADDITIONAL READING

- Jaeger, R. C. *Introduction to Microelectronic Fabrication*, 2d ed. Prentice-Hall, Reading, MA: 2001.  
 Campbell, S. A. *The Science and Engineering of Microelectronic Fabrication*, 2nd ed. Oxford University Press, New York: 2001.  
 Yang, E. S. *Microelectronic Devices*. McGraw-Hill, New York: 1988.  
 Pierret, R. F. *Semiconductor Fundamentals*, 2d ed. Prentice-Hall, Reading, MA: 1988.  
 Sze, S. M. *Physics of Semiconductor Devices*. Wiley, New York: 1982.

## IMPORTANT EQUATIONS

$$n_i^2 = BT^3 \exp\left(-\frac{E_G}{kT}\right) \quad \text{cm}^{-6} \quad (2.1)$$

where  $E_G$  = semiconductor bandgap energy in eV (electron volts)

$k$  = Boltzmann's constant,  $8.62 \times 10^{-5}$  eV/K ( $1.38 \times 10^{-23}$  J/K)

$T$  = absolute temperature, K

$B$  = material-dependent parameter,  $1.08 \times 10^{31}/\text{K}^{-3} \cdot \text{cm}^{-6}$  for Si

$$\sigma = q(n\mu_n + p\mu_p) \quad (\Omega \cdot \text{cm})^{-1} \quad (2.7)$$

### Doped Semiconductors

$$q(N_D + p - N_A - n) = 0 \quad (2.10)$$

### n-Type Material ( $N_D > N_A$ )

$$n = \frac{(N_D - N_A) + \sqrt{(N_D - N_A)^2 + 4n_i^2}}{2} \quad \text{and} \quad p = \frac{n_i^2}{n} \quad (2.11)$$

### p-Type Material ( $N_A > N_D$ )

$$p = \frac{(N_A - N_D) + \sqrt{(N_A - N_D)^2 + 4n_i^2}}{2} \quad \text{and} \quad n = \frac{n_i^2}{p} \quad (2.12)$$

### Currents

$$\begin{aligned} j_n^{\text{drift}} &= Q_n v_n = (-qn)(-\mu_n E) = qn\mu_n E & \text{A/cm}^2 \\ j_p^{\text{drift}} &= Q_p v_p = (+qp)(+\mu_p E) = qp\mu_p E & \text{A/cm}^2 \end{aligned} \quad (2.5)$$

$$\begin{aligned} j_p^{\text{diff}} &= (+q)D_p \left( -\frac{\partial p}{\partial x} \right) = -qD_p \frac{\partial p}{\partial x} & \text{A/cm}^2 \\ j_n^{\text{diff}} &= (-q)D_n \left( -\frac{\partial n}{\partial x} \right) = +qD_n \frac{\partial n}{\partial x} \end{aligned} \quad (2.14)$$

$$j_n^T = q\mu_n n E + qD_n \frac{\partial n}{\partial x} \quad \text{and} \quad j_p^T = q\mu_p p E - qD_p \frac{\partial p}{\partial x} \quad (2.16)$$

## PROBLEMS

### 2.1 Solid-State Electronic Materials

- 2.1. Pure aluminum has a resistivity of  $2.83 \mu\Omega \cdot \text{cm}$ . Based on its resistivity, should aluminum be classified as an insulator, semiconductor, or conductor?
- 2.2. The resistivity of silicon dioxide is  $10^{15} \Omega \cdot \text{cm}$ . Is this material a conductor, semiconductor, or insulator?
- 2.3. An aluminum interconnection line in an integrated circuit can be operated with a current density up to  $10 \text{ MA/cm}^2$ . If the line is  $5 \mu\text{m}$  wide and  $1 \mu\text{m}$  high, what is the maximum current permitted in the line?

### 2.2 Covalent Bond Model

- 2.4. An aluminum interconnection line runs diagonally from one corner of a  $20 \text{ mm} \times 20 \text{ mm}$  silicon integrated circuit die to the other corner. (a) What is the resistance of this line if it is  $1 \mu\text{m}$  thick and  $5 \mu\text{m}$  wide? (b) Repeat for a  $0.5 \mu\text{m}$  thick line. The resistivity of pure aluminum is  $2.82 \mu\Omega\text{-cm}$ .
- 2.5. Copper interconnections have been introduced into state-of-the-art ICs because of its lower resistivity. Repeat Prob. 2.4 for pure copper with a resistivity of  $1.66 \mu\Omega\text{-cm}$ .
- 2.6. Calculate the intrinsic carrier densities in silicon and germanium at (a)  $77 \text{ K}$ , (b)  $300 \text{ K}$ , and (c)  $500 \text{ K}$ . Use the information from the table in Fig. 2.4.
- 2.7. (a) At what temperature will  $n_i = 10^{13}/\text{cm}^3$  in silicon? (b) Repeat the calculation for  $n_i = 10^{15}/\text{cm}^3$ .
- 2.8. Calculate the intrinsic carrier density in gallium arsenide at (a)  $300 \text{ K}$ , (b)  $100 \text{ K}$ , (c)  $450 \text{ K}$ . Use the information from the table in Fig. 2.4.
- 2.9. Use Eq. (2.1) to calculate the actual temperature that corresponds to the value  $n_i = 10^{10}/\text{cm}^3$  in silicon.

### 2.3 Drift Currents and Mobility in Semiconductors

- 2.10. Electrons and holes are moving in a uniform, one-dimensional electric field  $E = +2500 \text{ V/cm}$ . The electrons and holes have mobilities of  $700$  and  $250 \text{ cm}^2/\text{V} \cdot \text{s}$ , respectively. What are the electron and hole velocities? If  $n = 10^{17}/\text{cm}^3$  and  $p = 10^3/\text{cm}^3$ , what are the electron and hole current densities?

- 2.11. The maximum drift velocities of electrons and holes in silicon are approximately  $10^7 \text{ cm/s}$ . What are the electron and hole current densities if  $n = 10^{18}/\text{cm}^3$  and  $p = 10^2/\text{cm}^3$ ? What is the total current density?
- 2.12. A current density of  $-2000 \text{ A/cm}^2$  exists in a semiconductor having a charge density of  $0.01 \text{ C/cm}^3$ . What are the carrier velocities?
- 2.13. The maximum drift velocity of electrons in silicon is  $10^7 \text{ cm/s}$ . If the silicon has a charge density of  $0.4 \text{ C/cm}^3$ , what is the maximum current density in the material?
- 2.14. A silicon sample is supporting an electric field of  $-2000 \text{ V/cm}$ , and the mobilities of electrons and holes are  $1000$  and  $400 \text{ cm}^2/\text{V} \cdot \text{s}$ , respectively. What are the electron and hole velocities? If  $p = 10^{17}/\text{cm}^3$  and  $n = 10^3/\text{cm}^3$ , what are the electron and hole current densities?
- 2.15. (a) A voltage of  $5 \text{ V}$  is applied across a  $10\text{-}\mu\text{m}$ -long region of silicon. What is the electric field? (b) Suppose the maximum field allowed in silicon is  $10^5 \text{ V/cm}$ . How large a voltage can be applied to the  $10\text{-}\mu\text{m}$  region?
- 2.16. The maximum drift velocity for holes in silicon is  $10^7 \text{ cm/s}$ . If the hole density in a sample is  $10^{19}/\text{cm}^3$ , what is the maximum hole current density? If the sample has a cross section of  $1 \mu\text{m} \times 25 \mu\text{m}$ , what is the maximum current?

### 2.4 Resistivity of Intrinsic Silicon

- 2.17. At what temperature will intrinsic silicon become an insulator, based on the definitions in Table 2.1? Assume that  $\mu_n = 2000 \text{ cm}^2/\text{V} \cdot \text{s}$  and  $\mu_p = 750 \text{ cm}^2/\text{V} \cdot \text{s}$ .
- 2.18. At what temperature will intrinsic silicon become a conductor based on the definitions in Table 2.1? Assume that  $\mu_n = 100 \text{ cm}^2/\text{V} \cdot \text{s}$  and  $\mu_p = 50 \text{ cm}^2/\text{V} \cdot \text{s}$ . (Note that silicon melts at  $1430 \text{ K}$ .)

### 2.5 Impurities in Semiconductors

- 2.19. Draw a two-dimensional conceptual picture [similar to Fig. 2.6] of the silicon lattice containing one donor atom and one acceptor atom in adjacent lattice positions. Are there any free electrons or holes?

- 2.20. Crystalline germanium has a lattice similar to that of silicon. (a) What are the possible donor atoms in Ge based on Table 2.2? (b) What are the possible acceptor atoms in Ge based on Table 2.2?
- 2.21. GaAs is composed of equal numbers of atoms of gallium and arsenic in a lattice similar to that of silicon. (a) Suppose a silicon atom replaces a gallium atom in the lattice. Do you expect the silicon atom to behave as a donor or acceptor impurity? Why? (b) Suppose a silicon atom replaces an arsenic atom in the lattice. Do you expect the silicon atom to behave as a donor or acceptor impurity? Why?
- 2.22. InP is composed of equal atoms of indium and phosphorus in a lattice similar to that of silicon. (a) Suppose a germanium atom replaces an indium atom in the lattice. Do you expect the germanium atom to behave as a donor or acceptor impurity? Why? (b) Suppose a germanium atom replaces a phosphorus atom in the lattice. Do you expect the germanium atom to behave as a donor or acceptor impurity? Explain.
- 2.23. A current density of 10,000 A/cm<sup>2</sup> exists in a 0.02- $\Omega \cdot \text{cm}$  *n*-type silicon sample. What is the electric field needed to support this drift current density?
- 2.24. The maximum drift velocity of carriers in silicon is approximately 10<sup>7</sup> cm/s. What is the maximum drift current density that can be supported in *n*-type silicon with a doping of 10<sup>17</sup>/cm<sup>3</sup>?
- 2.25. Silicon is doped with 10<sup>16</sup> boron atoms/cm<sup>3</sup>. How many boron atoms will be in a silicon region that is 0.5  $\mu\text{m}$  long, 5  $\mu\text{m}$  wide, and 0.5  $\mu\text{m}$  deep?
- 2.29. Silicon is doped with  $5 \times 10^{17}$  boron atoms/cm<sup>3</sup> and  $2 \times 10^{17}$  phosphorus atoms/cm<sup>3</sup> (a) Is this *n*- or *p*-type silicon? (b) What are the hole and electron concentrations at room temperature?
- 2.30. Suppose a semiconductor has  $N_D = 10^{16}/\text{cm}^3$ ,  $N_A = 5 \times 10^{16}/\text{cm}^3$ , and  $n_i = 10^{11}/\text{cm}^3$ . What are the electron and hole concentrations?
- 2.31. Suppose a semiconductor has  $N_A = 10^{15}/\text{cm}^3$ ,  $N_D = 10^{14}/\text{cm}^3$ , and  $n_i = 5 \times 10^{13}/\text{cm}^3$ . What are the electron and hole concentrations?
- 2.32. Suppose a semiconductor has  $N_A = 2 \times 10^{17}/\text{cm}^3$ ,  $N_D = 3 \times 10^{17}/\text{cm}^3$ , and  $n_i = 10^{17}/\text{cm}^3$ . What are the electron and hole concentrations?

## 2.7 Mobility and Resistivity in Doped Semiconductors

- 2.33. Silicon is doped with a donor concentration of  $5 \times 10^{16}/\text{cm}^3$ . Find the electron and hole concentrations, the electron and hole mobilities, and the resistivity of this silicon material at 300 K. Is this material *n*- or *p*-type?
- 2.34. Silicon is doped with an acceptor concentration of  $2.5 \times 10^{18}/\text{cm}^3$ . Find the electron and hole concentrations, the electron and hole mobilities, and the resistivity of this silicon material at 300 K. Is this material *n*- or *p*-type?
- 2.35. Silicon is doped with an indium concentration of  $8 \times 10^{19}/\text{cm}^3$ . Is indium a donor or acceptor impurity? Find the electron and hole concentrations, the electron and hole mobilities, and the resistivity of this silicon material at 300 K. Is this material *n*- or *p*-type?
- 2.36. A silicon wafer is uniformly doped with  $4.5 \times 10^{16}$  phosphorus atoms/cm<sup>3</sup> and  $5.5 \times 10^{16}$  boron atoms/cm<sup>3</sup>. Find the electron and hole concentrations, the electron and hole mobilities, and the resistivity of this silicon material at 300 K. Is this material *n*- or *p*-type?
- 2.37. Repeat Example 2.5 for *p*-type silicon. Assume that the silicon contains only acceptor impurities. What is the acceptor concentration  $N_A$ ?
- 2.38. Repeat Ex. 2.5 using the equations presented with the graph in Fig. 2.8.
- 2.39. Repeat Prob. 2.37 using the equations presented with the graph in Fig. 2.8.
- \*2.40. A *p*-type silicon wafer has a resistivity of 0.5  $\Omega \cdot \text{cm}$ . It is known that silicon contains only

## 2.6 Electron and Hole Concentrations in Doped Semiconductors

- 2.26. Silicon is doped with  $3 \times 10^{17}$  arsenic atoms/cm<sup>3</sup>. (a) Is this *n*- or *p*-type silicon? (b) What are the hole and electron concentrations at room temperature? (c) What are the hole and electron concentrations at 250 K?
- 2.27. Silicon is doped with  $6 \times 10^{18}$  boron atoms/cm<sup>3</sup>. (a) Is this *n*- or *p*-type silicon? (b) What are the hole and electron concentrations at room temperature? (c) What are the hole and electron concentrations at 200 K?
- 2.28. Silicon is doped with  $2 \times 10^{18}$  arsenic atoms/cm<sup>3</sup> and  $8 \times 10^{18}$  boron atoms/cm<sup>3</sup>. (a) Is this *n*- or *p*-type silicon? (b) What are the hole and electron concentrations at room temperature?

acceptor impurities. What is the acceptor concentration  $N_A$ ?

- \*2.41. It is conceptually possible to produce extrinsic silicon with a higher resistivity than that of intrinsic silicon. How would this occur?
- \*2.42.  $n$ -type silicon wafers with a resistivity of  $3.0 \Omega \cdot \text{cm}$  are needed for integrated circuit fabrication. What donor concentration  $N_D$  is required in the wafers? Assume  $N_A = 0$ .
- 2.43. (a) What is the minimum donor doping required to convert silicon into a conductor based on the definitions in Table 2.1? (b) What is the minimum acceptor doping required to convert silicon into a conductor?
- 2.44. A silicon sample is doped with  $5.0 \times 10^{19}$  donor atoms/cm<sup>3</sup> and  $5.0 \times 10^{19}$  acceptor atoms/cm<sup>3</sup>. (a) What is its resistivity? (b) Is this an insulator, conductor, or semiconductor? (c) Is this intrinsic material? Explain your answers.
- \*2.45. Measurements of a silicon wafer indicate that it is  $p$ -type with a resistivity of  $1 \Omega \cdot \text{cm}$ . It is also known that it contains only boron impurities. (a) What additional acceptor concentration must be added to the sample to change its resistivity to  $0.25 \Omega \cdot \text{cm}$ ? (b) What concentration of donors would have to be added to the original sample to change the resistivity to  $0.25 \Omega \cdot \text{cm}$ ? Would the resulting material be classified as  $n$ - or  $p$ -type silicon?
- \*2.46. A silicon wafer has a doping concentration of  $1 \times 10^{16}$  phosphorus atoms/cm<sup>3</sup>. (a) Determine the conductivity of the wafer. (b) What concentration of boron atoms must be added to the wafer to make the conductivity equal to  $4.0 (\Omega \cdot \text{cm})^{-1}$ ?
- \*2.47. A silicon wafer has a background concentration of  $1 \times 10^{16}$  boron atoms/cm<sup>3</sup>. (a) Determine the conductivity of the wafer. (b) What concentration of phosphorus atoms must be added to the wafer to make the conductivity equal to  $5.5 (\Omega \cdot \text{cm})^{-1}$ ?

## 2.8 Diffusion Currents

- 2.48. Make a table of the values of thermal voltage  $V_T$  for  $T = 50 \text{ K}, 75 \text{ K}, 100 \text{ K}, 150 \text{ K}, 200 \text{ K}, 250 \text{ K}, 300 \text{ K}, 350 \text{ K}, \text{ and } 400 \text{ K}$ .
- 2.49. The electron concentration in a region of silicon is shown in Fig. P2.49. If the electron mobility is  $350 \text{ cm}^2/\text{V} \cdot \text{s}$  and the width  $W_B = 0.5 \mu\text{m}$ , determine the electron diffusion current density. Assume room temperature.

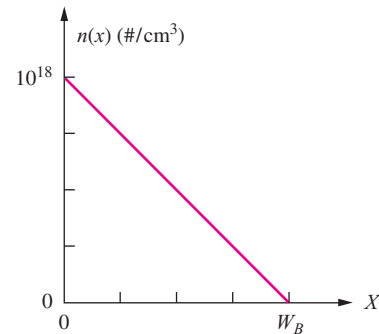


Figure P2.49

- 2.50. Suppose the hole concentration in silicon sample is described mathematically by

$$p(x) = 10^5 + 10^{19} \exp\left(-\frac{x}{L_p}\right) \text{ holes/cm}^3, x \geq 0$$

in which  $L_p$  is known as the diffusion length for holes and is equal to  $2.0 \mu\text{m}$ . Find the diffusion current density for holes as a function of distance for  $x \geq 0$  if  $D_p = 15 \text{ cm}^2/\text{s}$ . What is the diffusion current at  $x = 0$  if the cross-sectional area is  $10 \mu\text{m}^2$ ?

## 2.9 Total Current

- \*2.51. A  $5\text{-}\mu\text{m}$ -long block of  $p$ -type silicon has an acceptor doping profile given by  $N_A(x) = 10^{14} + 10^{18} \exp(-10^4 x)$ , where  $x$  is measured in cm. Use Eq. (2.17) to demonstrate that the material must have a nonzero internal electric field  $E$ . What is the value of  $E$  at  $x = 0$  and  $x = 5 \mu\text{m}$ ? (Hint: In thermal equilibrium, the total electron and total hole currents must each be zero.)
- 2.52. Figure P2.52 gives the electron and hole concentrations in a  $2\text{-}\mu\text{m}$ -wide region of silicon. In addition, there is a constant electric field of  $20 \text{ V/cm}$  present in the sample. What is the total current density at  $x = 0$ ? What are the individual drift and diffusion components of the hole and electron current

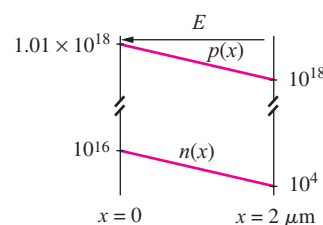


Figure P2.52

densities at  $x = 1.0 \mu\text{m}$ ? Assume that the electron and hole mobilities are 350 and  $150 \text{ cm}^2/\text{V} \cdot \text{s}$ , respectively.

## 2.10 Energy Band Model

- 2.53. Draw a figure similar to Fig. 2.15 for the case  $N_A > N_D$  in which there are two acceptor atoms for each donor atom.
- \*2.54. Electron–hole pairs can be created by means other than the thermal activation process as described in Figs. 2.3 and 2.12. For example, energy may be added to electrons through optical means by shining light on the sample. If enough optical energy is absorbed, electrons can jump the energy bandgap, creating electron–hole pairs. What is the maximum wavelength of light that we should expect silicon to be able to absorb? (*Hint:* Remember from physics that energy  $E$  is related to wavelength  $\lambda$  by  $E = hc/\lambda$  in which Planck's constant  $h = 6.626 \times 10^{-34} \text{ J} \cdot \text{s}$  and the velocity of light  $c = 3 \times 10^{10} \text{ cm/s}$ .)

## 2.11 Overview of Integrated Circuit Fabrication

- 2.55. Draw the cross section for a  $pn$  diode similar to that in Fig. 2.17(h) if the fabrication process utilizes a  $p$ -type substrate in place of the  $n$ -type substrate depicted in Fig. 2.17.

- 2.56. To ensure that a good ohmic contact is formed between aluminum and  $n$ -type silicon, an additional doping step is added to the diode in Fig. 2.17(h) to place an  $n+$  region beneath the left-hand contact as in Fig. P2.56. Where might this step go in the process flow in Fig. 2.17? Draw a top and side view of a mask that could be used in the process.

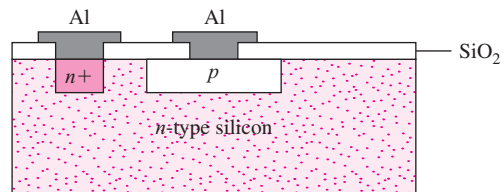
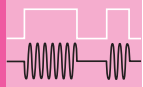


**Figure P2.56**

## Miscellaneous

- 2.57. Single crystal silicon consists of three-dimensional arrays of the basic unit cell in Fig. 2.1(a). (a) How many atoms are in each unit cell? (b) What is volume of the unit cell in cm<sup>3</sup>? (c) Show that the atomic density of silicon is  $5 \times 10^{22} \text{ atoms/cm}^3$ . (d) The density of silicon is  $2.33 \text{ g/cm}^3$ . What is the mass of one unit cell? (e) Based on your calculations here, what is the mass of a proton? Assume that protons and neutrons have the same mass and that electrons are much much lighter. Is your answer reasonable? Explain.

# CHAPTER 3



## SOLID-STATE DIODES AND DIODE CIRCUITS

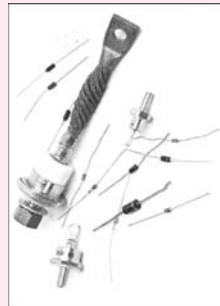
### CHAPTER OUTLINE

- 3.1 The *pn* Junction Diode 75
- 3.2 The *i-v* Characteristics of the Diode 80
- 3.3 The Diode Equation: A Mathematical Model for the Diode 82
- 3.4 Diode Characteristics Under Reverse, Zero, and Forward Bias 85
- 3.5 Diode Temperature Coefficient 88
- 3.6 Diodes Under Reverse Bias 89
- 3.7 *pn* Junction Capacitance 92
- 3.8 Schottky Barrier Diode 93
- 3.9 Diode SPICE Model and Layout 94
- 3.10 Diode Circuit Analysis 96
- 3.11 Multiple-Diode Circuits 106
- 3.12 Analysis of Diodes Operating in the Breakdown Region 109
- 3.13 Half-Wave Rectifier Circuits 113
- 3.14 Full-Wave Rectifier Circuits 123
- 3.15 Full-Wave Bridge Rectification 125
- 3.16 Rectifier Comparison and Design Tradeoffs 125
- 3.17 Dynamic Switching Behavior of the Diode 129
- 3.18 Photo Diodes, Solar Cells, and Light-Emitting Diodes 130
- Summary 133
- Key Terms 134
- Reference 135
- Additional Reading 135
- Problems 135

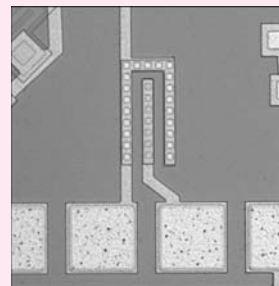
### CHAPTER GOALS

- Understand diode structure and basic layout
- Develop electrostatics of the *pn* junction
- Explore various diode models including the mathematical model, the ideal diode model, and the constant voltage drop model
- Understand the SPICE representation and model parameters for the diode
- Define regions of operation of the diode, including forward and reverse bias and reverse breakdown
- Apply the various types of models in circuit analysis
- Explore different types of diodes including Zener, variable capacitance, and Schottky barrier diodes as well as solar cells and light emitting diodes (LEDs)
- Discuss the dynamic switching behavior of the *pn* junction diode

- Explore diode rectifiers
- Practice simulating diode circuits using SPICE



Photograph of an assortment of diodes



Fabricated Diode

The first electronic circuit element that we explore is the solid-state *pn* junction diode. The diode is an extremely important device in its own right with many important applications including ac-dc power conversion (rectification), solar power generation and high frequency mixers for RF communications. In addition, the *pn* junction diode is a fundamental building block for other solid-state devices. In later chapters, we will find that two closely coupled diodes are used to form the bipolar junction transistor (BJT), and two diodes form an integral part of the metal-oxide-semiconductor field-effect transistor (MOSFET), and the junction field-effect transistor (JFET). Gaining an understanding of diode characteristics is prerequisite to understanding the behavior of the field-effect and bipolar transistors that are used to realize both digital logic circuits and analog amplifiers.

The *pn* junction diode is formed by fabricating adjoining regions of *p*-type and *n*-type semiconductor material. Another type of diode, called the Schottky barrier diode, is formed by a non-ohmic contact between a metal such as aluminum, palladium, or platinum and an *n*-type or *p*-type semiconductor. Both types of solid-state diodes are discussed in this chapter. The vacuum diode, which was used before the advent of semiconductor diodes, still finds application in very high voltage situations.

The *pn* junction diode is a nonlinear element, and for many of us, this will be our first encounter with a nonlinear device. The diode is a two-terminal circuit element similar to a resistor, but its *i-v* characteristic, the relationship between the current through the element and the voltage across the element, is not a straight line. This nonlinear

behavior allows electronic circuits to be designed to provide many useful operations, including rectification, mixing (a form of multiplication), and wave shaping. Diodes can also be used to perform elementary logic operations such as the AND and OR functions.

## T

his chapter begins with a basic discussion of the structure and behavior of the *pn* junction diode and its terminal characteristics. Next is an introduction to the concept of modeling, and several different models for the diode are introduced and used to analyze the behavior of diode circuits. We begin to develop the intuition needed to make choices between models of various complexities in order to simplify electronic circuit analysis and design. Diode circuits are then explored, including the detailed application of the diode in rectifier circuits. The characteristics of Zener diodes, photo diodes, solar cells, and light-emitting diodes are also discussed.

### 3.1 THE *pn* JUNCTION DIODE

The ***pn* junction diode** is formed by fabrication of a *p*-type semiconductor region in intimate contact with an *n*-type semiconductor region, as illustrated in Fig. 3.1. The diode is constructed using the impurity doping process discussed in Chapter 2.

An actual diode can be formed by starting with an *n*-type wafer with doping  $N_D$  and selectively converting a portion of the wafer to *p*-type by adding acceptor impurities with  $N_A > N_D$ . The point at which the material changes from *p*-type to *n*-type is called the metallurgical junction. The *p*-type region is also referred to as the **anode** of the diode, and the *n*-type region is called the **cathode** of the diode.

Figure 3.2 gives the circuit symbol for the diode, with the left-hand end corresponding to the *p*-type region of the diode and the right-hand side corresponding to the *n*-type region. We will see shortly that the “arrow” points in the direction of positive current in the diode.

#### 3.1.1 *pn* JUNCTION ELECTROSTATICS

Consider a *pn* junction diode similar to Fig. 3.1 having  $N_A = 10^{17}/\text{cm}^3$  on the *p*-type side and  $N_D = 10^{16}/\text{cm}^3$  on the *n*-type side. The hole and electron concentrations on the two sides of the junction will be

$$\begin{aligned} \text{p-type side: } p_p &= 10^{17} \text{ holes/cm}^3 & n_p &= 10^3 \text{ electrons/cm}^3 \\ \text{n-type side: } p_n &= 10^4 \text{ holes/cm}^3 & n_n &= 10^{16} \text{ electrons/cm}^3 \end{aligned} \quad (3.1)$$

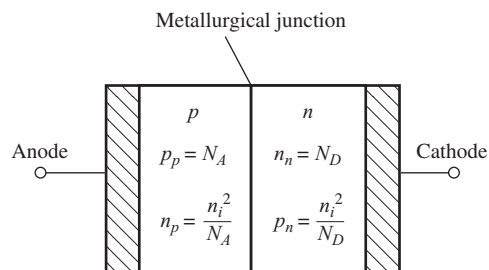


Figure 3.1 Basic *pn* junction diode.

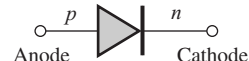
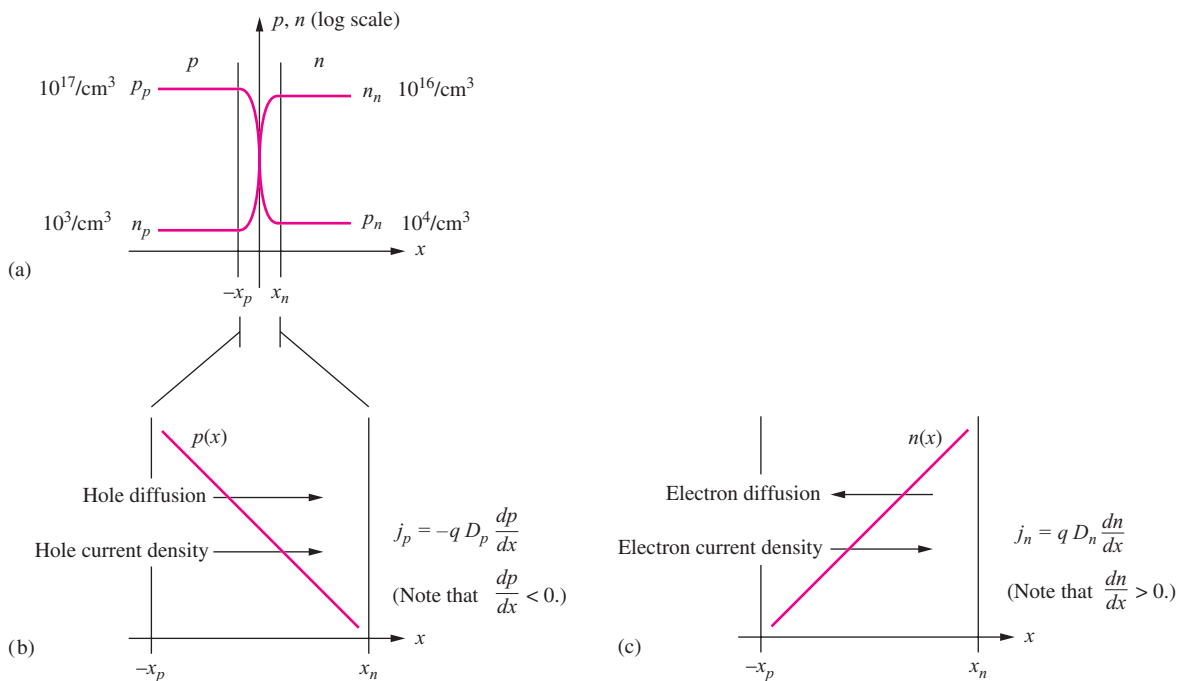


Figure 3.2 Diode circuit symbol.



**Figure 3.3** (a) Carrier concentrations; (b) Hole diffusion current in the space charge region; (c) Electron diffusion current in the space charge region.

As shown in Fig. 3.3(a), a very large concentration of holes exists on the *p*-type side of the metallurgical junction, whereas a much smaller hole concentration exists on the *n*-type side. Likewise, there is a very large concentration of electrons on the *n*-type side of the junction and a very low concentration on the *p*-type side.

From our knowledge of diffusion from Chapter 2, we know that mobile holes will diffuse from the region of high concentration on the *p*-type side toward the region of low concentration on the *n*-type side and that mobile electrons will diffuse from the *n*-type side to the *p*-type side, as in Figs. 3.3(b) and (c). If the diffusion processes were to continue unabated, there would eventually be a uniform concentration of holes and electrons throughout the entire semiconductor region, and the *pn* junction would cease to exist. Note that the two diffusion current densities are both directed in the positive  $x$  direction, but this is inconsistent with zero current in the open-circuited terminals of the diode.

A second, competing process must be established to balance the diffusion current. The competing mechanism is a drift current, as discussed in Chapter 2, and its origin can be understood by focusing on the region in the vicinity of the **metallurgical junction** shown in Fig. 3.4. As mobile holes move out of the *p*-type material, they leave behind immobile negatively charged acceptor atoms. Correspondingly, mobile electrons leave behind immobile ionized donor atoms with a localized positive charge. A **space charge region (SCR)**, depleted of mobile carriers, develops in the region immediately around the metallurgical junction. This region is also often called the **depletion region**, or **depletion layer**.

From electromagnetics, we know that a region of space charge  $\rho_c$  ( $\text{C}/\text{cm}^3$ ) will be accompanied by an electric field  $E$  measured in  $\text{V}/\text{cm}$  through Gauss' law,

$$\nabla \cdot E = \frac{\rho_c}{\varepsilon_s} \quad (3.2)$$

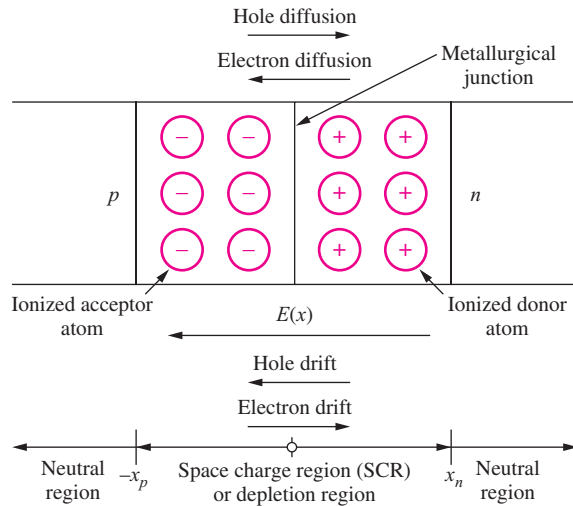


**Figure 3.4** Space charge region formation near the metallurgical junction.

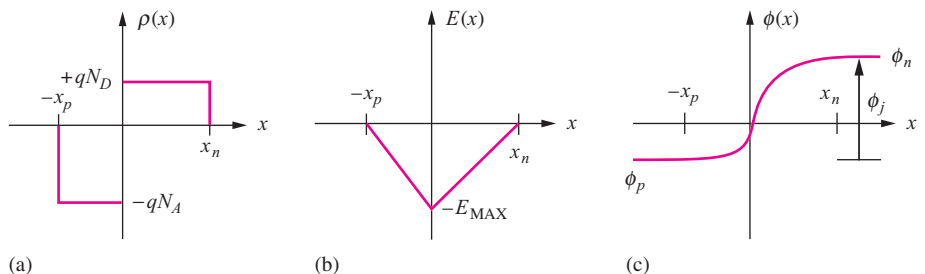


**Figure 3.5** (a) Charge density ( $C/cm^3$ ), (b) electric field ( $V/cm$ ), and (c) electrostatic potential ( $V$ ) in the space charge region of a *pn* junction.

written assuming a constant semiconductor permittivity  $\varepsilon_s$  ( $F/cm$ ). In one dimension, Eq. (3.2) can be rearranged to give

$$E(x) = \frac{1}{\varepsilon_s} \int \rho_c(x) dx \quad (3.3)$$

Figure 3.5 illustrates the space charge and electric field in the diode for the case of uniform (constant) doping on both sides of the junction. As illustrated in Fig. 3.5(a), the value of the space charge density on the *p*-type side will be  $-qN_A$  and will extend from the metallurgical junction at  $x = 0$  to  $-x_p$ , whereas that on the *n*-type side will be  $+qN_D$  and will extend from 0 to  $+x_n$ . The overall diode must be charge neutral, so

$$qN_Ax_p = qN_Dx_n \quad (3.4)$$

The electric field is proportional to the integral of the space charge density and will be zero in the (charge) neutral regions outside of the depletion region. Using this zero-field boundary condition yields the triangular electric field distribution in Fig. 3.5(b).

Figure 3.5(c) represents the integral of the electric field and shows that a **built-in potential** or **junction potential**  $\phi_j$ , exists across the *pn* junction space charge region according to

$$\phi_j = - \int E(x) dx \quad V \quad (3.5)$$

$\phi_j$  represents the difference in the internal chemical potentials between the *n* and *p* sides of the diode, and it can be shown [1] to be given by

$$\phi_j = V_T \ln \left( \frac{N_A N_D}{n_i^2} \right) \quad (3.6)$$

where the **thermal voltage**  $V_T = kT/q$  was originally defined in Chapter 2.

Equations (3.3) to (3.5) can be used to determine the total width of the depletion region  $w_{do}$  in terms of the built-in potential:

$$w_{do} = (x_n + x_p) = \sqrt{\frac{2\epsilon_s}{q} \left( \frac{1}{N_A} + \frac{1}{N_D} \right) \phi_j} \quad \text{m} \quad (3.7)$$

From Eq. (3.7), we see that the doping on the more lightly doped side of the junction will be the most important in determining the **depletion-layer width**.

### EXAMPLE 3.1 DIODE SPACE CHARGE REGION WIDTH

When diodes are actually fabricated, the doping levels on opposite sides of the *pn* junction tend to be quite asymmetric, and the resulting depletion layer tends to extend primarily on one side of the junction and is referred to as a “one-sided” step junction or one-sided abrupt junction. The *pn* junction that we analyze provides an example of the magnitudes of the distances involved in such a *pn* junction.

**PROBLEM** Calculate the built-in potential and depletion-region width for a silicon diode with  $N_A = 10^{17}/\text{cm}^3$  on the *p*-type side and  $N_D = 10^{20}/\text{cm}^3$  on the *n*-type side.

**SOLUTION** **Known Information and Given Data:** On the *p*-type side,  $N_A = 10^{17}/\text{cm}^3$ ; on the *n*-type side,  $N_D = 10^{20}/\text{cm}^3$ . Theory describing the *pn* junction is given by Eqs. (3.4) through (3.7).

**Unknowns:** Built-in potential  $\phi_j$  and depletion-region width  $w_{do}$

**Approach:** Find the built-in potential using Eq. (3.6); use  $\phi_j$  to calculate  $w_{do}$  in Eq. (3.7).

**Assumptions:** The diode operates at room temperature operation with  $V_T = 0.025$  V. There are only donor impurities on the *n*-type side and acceptor impurities on the *p*-type side of the junction. The doping levels are constant on each side of the junction.

**Analysis:** The built-in potential is given by

$$\phi_j = V_T \ln \left( \frac{N_A N_D}{n_i^2} \right) = (0.025 \text{ V}) \ln \left[ \frac{(10^{17}/\text{cm}^3)(10^{20}/\text{cm}^3)}{(10^{20}/\text{cm}^6)} \right] = 0.979 \text{ V}$$

For silicon,  $\epsilon_s = 11.7\epsilon_0$ , where  $\epsilon_0 = 8.85 \times 10^{-14}$  F/cm represents the permittivity of free space.

$$w_{do} = \sqrt{\frac{2\epsilon_s}{q} \left( \frac{1}{N_A} + \frac{1}{N_D} \right) \phi_j}$$

$$w_{do} = \sqrt{\frac{2 \cdot 11.7 \cdot (8.85 \times 10^{-14} \text{ F/cm})}{1.60 \times 10^{-19} \text{ C}} \left( \frac{1}{10^{17}/\text{cm}^3} + \frac{1}{10^{20}/\text{cm}^3} \right) 0.979 \text{ V}} = 0.113 \mu\text{m}$$

**Check of Results:** The built-in potential should be less than the bandgap of the material. For silicon the bandgap is approximately 1.2 V (see Table 2.3), so  $\phi_j$  appears reasonable. The depletion-layer width seems quite small, but a double check of the numbers indicates that the calculation is correct.

**Discussion:** The numbers in this example are fairly typical of a *pn* junction diode. For the normal doping levels encountered in solid-state diodes, the built-in potential ranges between 0.5 V and 1.0 V, and the total depletion-layer width  $w_{do}$  can range from a fraction of 1  $\mu\text{m}$  in heavily doped diodes to tens of microns in lightly doped diodes.

**EXERCISE:** Calculate the built-in potential and depletion-region width for a silicon diode if  $N_A$  is increased to  $2 \times 10^{18}/\text{cm}^3$  on the *p*-type side and  $N_D = 10^{20}/\text{cm}^3$  on the *n*-type side.

**ANSWERS:** 1.05 V; 0.0263  $\mu\text{m}$

### 3.1.2 INTERNAL DIODE CURRENTS

Remember that the electric field  $E$  points in the direction that a positive carrier will move, so electrons drift toward the positive  $x$  direction and holes drift in the negative  $x$  direction in Fig. 3.4. The carriers drift in directions opposite the diffusion of the same carrier species. Because the terminal currents must be zero, a dynamic equilibrium is established in the junction region. Hole diffusion is precisely balanced by hole drift, and electron diffusion is exactly balanced by electron drift. This balance is stated mathematically in Eq. (3.8), in which the total hole and electron current densities must each be identically zero:

$$j_n^T = qn\mu_n E + qD_n \frac{\partial n}{\partial x} = 0 \quad \text{and} \quad j_p^T = qp\mu_p E - qD_p \frac{\partial p}{\partial x} = 0 \quad \text{A/cm}^2 \quad (3.8)$$

The difference in potential in Fig. 3.5(c) represents a barrier to both hole and electron flow across the junction. When a voltage is applied to the diode, the potential barrier is modified, and the delicate balances in Eq. (3.8) are disturbed, resulting in a current in the diode terminals.

#### EXAMPLE 3.2 DIODE ELECTRIC FIELD AND SPACE-CHARGE REGION EXTENTS

Now we find the value of the electric field in the diode and the size of the individual depletion layers on either side of the *pn* junction.

**PROBLEM** Find  $x_n$ ,  $x_p$ , and  $E_{\text{MAX}}$  for the diode in Ex. 3.1.

**SOLUTION** **Known Information and Given Data:** On the *p*-type side,  $N_A = 10^{17}/\text{cm}^3$ ; on the *n*-type side,  $N_D = 10^{20}/\text{cm}^3$ . Theory describing the *pn* junction is given by Eqs. (3.4) through (3.7). From Ex. 3.1,  $\phi_j = 0.979$  V and  $w_{do} = 0.113 \mu\text{m}$ .

**Unknowns:**  $x_n$ ,  $x_p$ , and  $E_{\text{MAX}}$

**Approach:** Use Eqs. (3.4) and (3.7) to find  $x_n$  and  $x_p$ ; use Eq. (3.5) to find  $E_{\text{MAX}}$ .

**Assumptions:** Room temperature operation

**Analysis:** Using Eq. (3.4), we can write

$$w_{do} = x_n + x_p = x_n \left( 1 + \frac{N_D}{N_A} \right) \quad \text{and} \quad w_{do} = x_n + x_p = x_p \left( 1 + \frac{N_A}{N_D} \right)$$

Solving for  $x_n$  and  $x_p$  gives

$$x_n = \frac{w_{do}}{\left(1 + \frac{N_D}{N_A}\right)} = \frac{0.113 \mu\text{m}}{\left(1 + \frac{10^{20}/\text{cm}^3}{10^{17}/\text{cm}^3}\right)} = 1.13 \times 10^{-4} \mu\text{m}$$

and

$$x_p = \frac{w_{do}}{\left(1 + \frac{N_A}{N_D}\right)} = \frac{0.113 \mu\text{m}}{\left(1 + \frac{10^{17}/\text{cm}^3}{10^{20}/\text{cm}^3}\right)} = 0.113 \mu\text{m}$$

Equation (3.5) indicates that the built-in potential is equal to the area under the triangle in Fig. 3.5(b). The height of the triangle is  $(-E_{\text{MAX}})$  and the base of the triangle is  $x_n + x_p = w_{do}$ :

$$\phi_j = \frac{1}{2} E_{\text{MAX}} w_{do} \quad \text{and} \quad E_{\text{MAX}} = \frac{2\phi_j}{w_{do}} = \frac{2(0.979 \text{ V})}{0.113 \mu\text{m}} = 173 \text{ kV/cm}$$

**Check of Results:** From Eqs. (3.3) and (3.4),  $E_{\text{MAX}}$  can also be found from the doping levels and depletion-layer widths on each side of the junction. The equation in the next exercise can be used as a check of the answer.

**EXERCISE:** Using Eq. (3.3) and Fig. 3.5(a) and (b), show that the maximum field is given by

$$E_{\text{MAX}} = \frac{qN_A x_p}{\epsilon_s} = \frac{qN_D x_n}{\epsilon_s}$$

Use this formula to find  $E_{\text{MAX}}$ .

**ANSWER:** 175 kV/cm

**EXERCISE:** Calculate  $E_{\text{MAX}}$ ,  $x_p$ , and  $x_n$  for a silicon diode if  $N_A = 2 \times 10^{18}/\text{cm}^3$  on the *p*-type side and  $N_D = 10^{20}/\text{cm}^3$  on the *n*-type side. Use  $\phi_j = 1.05 \text{ V}$  and  $w_{do} = 0.0263 \mu\text{m}$ .

**ANSWERS:** 799 kV/cm;  $5.06 \times 10^{-4} \mu\text{m}$ ;  $0.0258 \mu\text{m}$

## 3.2 THE *i-v* CHARACTERISTICS OF THE DIODE

The diode is the electronic equivalent of a mechanical check valve—it permits current to flow in one direction in a circuit, but prevents movement of current in the opposite direction. We will find that this nonlinear behavior has many useful applications in electronic circuit design. To understand this phenomenon, we explore the relationship between the current in the diode and the voltage applied to the diode. This information, called the *i-v* characteristic of the diode, is first presented graphically and then mathematically in this section and Sec. 3.3.

The current in the diode is determined by the voltage applied across the diode terminals, and the diode is shown with a voltage applied in Fig. 3.6. Voltage  $v_D$  represents the voltage applied to the diode terminals;  $i_D$  is the current through the diode. The neutral regions of the diode represent a low resistance to current, and essentially all the external applied voltage is dropped across the space charge region.

The applied voltage disturbs the balance between the drift and diffusion currents at the junction specified in the two expressions in Eq. (3.8). A positive applied voltage reduces the potential barrier for electrons and holes, as in Fig. 3.7, and current easily crosses the junction. A negative voltage

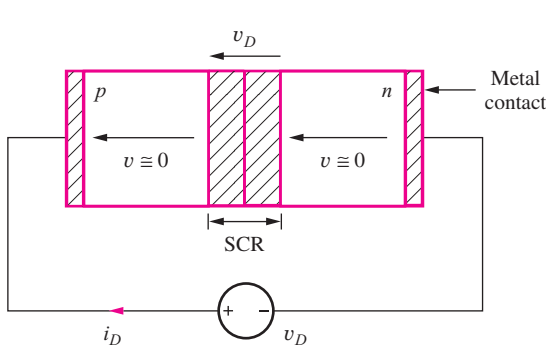


**Figure 3.6** Diode with external applied voltage  $v_D$ .

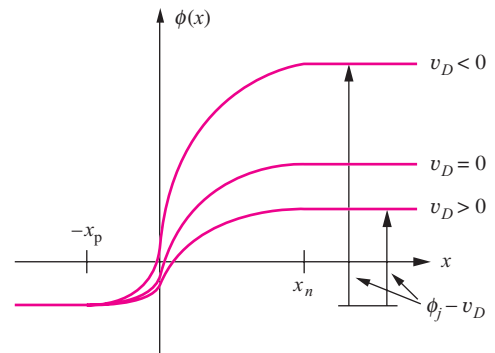


**Figure 3.7** Electrostatic junction potential for different applied voltages.

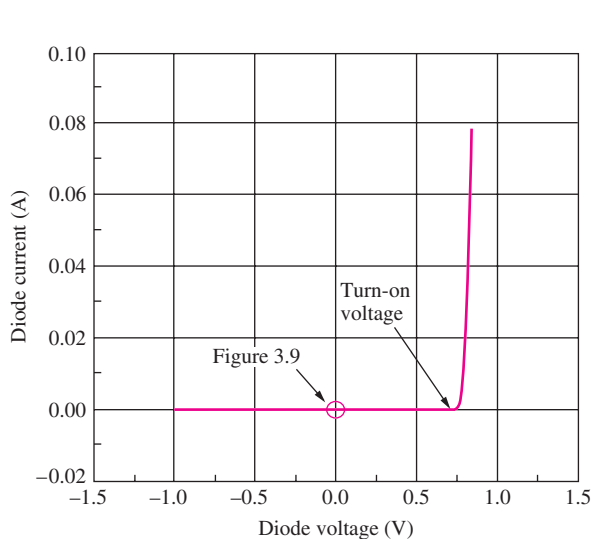


**Figure 3.8** Graph of the  $i$ - $v$  characteristics of a  $pn$  junction diode.

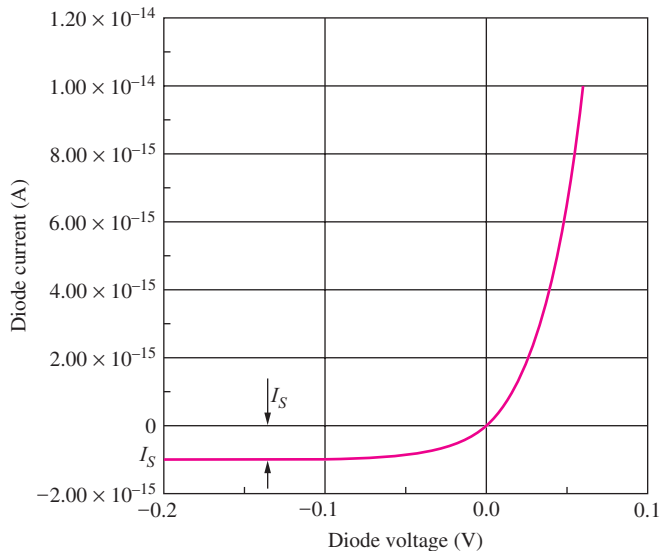


**Figure 3.9** Diode behavior near the origin with  $I_S = 10^{-15}$  A and  $n = 1$ .

increases the potential barrier, and although the balance in Eq. (3.8) is disturbed, the increased barrier results in a very small current.

The most important details of the diode  $i$ - $v$  characteristic appear in Fig. 3.8. The diode characteristic is definitely not linear. For voltages less than zero, the diode is essentially nonconducting, with  $i_D \cong 0$ . As the voltage increases above zero, the current remains nearly zero until the voltage  $v_D$  exceeds approximately 0.5 to 0.7 V. At this point, the diode current increases rapidly, and the voltage across the diode becomes almost independent of current. The voltage required to bring the diode into significant conduction is often called either the **turn-on** or **cut-in voltage** of the diode.

Figure 3.9 is an enlargement of the region around the origin in Fig. 3.8. We see that the  $i$ - $v$  characteristic passes through the origin; the current is zero when the voltage is zero. For negative voltages the current is not actually zero but reaches a limiting value labeled as  $-I_S$  for voltages less than  $-0.1$  V.  $I_S$  is called the **reverse saturation current**, or just **saturation current**, of the diode.

### 3.3 THE DIODE EQUATION: A MATHEMATICAL MODEL FOR THE DIODE

When performing both hand and computer analysis of circuits containing diodes, it is very helpful to have a mathematical representation, or model, for the  $i$ - $v$  characteristics depicted in Fig. 3.8. In fact, solid-state device theory has been used to formulate a mathematical expression that agrees amazingly well with the measured the  $i$ - $v$  characteristics of the  $pn$  junction diode. We study this extremely important formula called the **diode equation** in this section.

A voltage is applied to the diode in Fig. 3.10; in the figure the diode is represented by its circuit symbol from Fig. 3.2. Although we will not attempt to do so here, Eq. (3.8) can be solved for the hole and electron concentrations and the terminal current in the diode as a function of the voltage  $v_D$  across the diode. The resulting diode equation, given in Eq. (3.9), provides a **mathematical model** for the  $i$ - $v$  characteristics of the diode:

$$i_D = I_S \left[ \exp \left( \frac{q v_D}{n k T} \right) - 1 \right] = I_S \left[ \exp \left( \frac{v_D}{n V_T} \right) - 1 \right] \quad (3.9)$$

where  $I_S$  = reverse saturation current of diode (A)

$T$  = absolute temperature (K)

$v_D$  = voltage applied to diode (V)

$n$  = nonideality factor (dimensionless)

$q$  = electronic charge ( $1.60 \times 10^{-19}$  C)

$V_T = kT/q$  = thermal voltage (V)

$k$  = Boltzmann's constant ( $1.38 \times 10^{-23}$  J/K)

The total current through the diode is  $i_D$ , and the voltage drop across the diode terminals is  $v_D$ . Positive directions for the terminal voltage and current are indicated in Fig. 3.10.  $V_T$  is the thermal voltage encountered previously in Chapter 2 and will be assumed equal to 0.025 V at room temperature.  $I_S$  is the (reverse) saturation current of the diode encountered in Fig. 3.9, and  $n$  is a dimensionless parameter discussed in more detail shortly. The saturation current is typically in the range

$$10^{-18} \text{ A} \leq I_S \leq 10^{-9} \text{ A} \quad (3.10)$$

From device physics, it can be shown that the diode saturation current is proportional to  $n_i^2$ , where  $n_i$  is the density of electrons and holes in intrinsic semiconductor material. After reviewing Eq. (2.1) in Chapter 2, we realize that  $I_S$  will be strongly dependent on temperature. Additional discussion of this temperature dependence is in Sec. 3.5.

Parameter  $n$  is termed the **nonideality factor**. For most silicon diodes,  $n$  is in the range 1.0 to 1.1, although it approaches a value of 2 in diodes operating at high current densities. From this point on, we assume that  $n = 1$  unless otherwise indicated, and the diode equation will be written as

$$i_D = I_S \left[ \exp \left( \frac{v_D}{V_T} \right) - 1 \right] \quad (3.11)$$

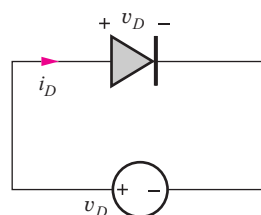


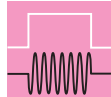
Figure 3.10 Diode with applied voltage  $v_D$ .

It is difficult to distinguish small variations in the value of  $n$  from an uncertainty in our knowledge in the absolute temperature. This is one reason that we will assume that  $n = 1$  in this text. The problem can be investigated further by working the next exercise.

**EXERCISE:** For  $n = 1$  and  $T = 300$  K,  $n(KT/q) = 25.8$  mV. Verify this calculation. Now, suppose  $n = 1.03$ . What temperature gives the same value for  $nV_T$ ?

**ANSWER:** 291 K

The mathematical model in Eq. (3.11) provides a highly accurate prediction of the  $i$ - $v$  characteristics of the  $pn$  junction diode. The model is useful for understanding the detailed behavior of diodes. It also provides a basis for understanding the  $i$ - $v$  characteristics of the bipolar transistor in Chapter 5.



### DESIGN NOTE

The static  $i$ - $v$  characteristics of the diode are well-characterized by three parameters: Saturation current  $I_S$ , temperature via the thermal voltage  $V_T$ , and nonideality factor  $n$ .

$$i_D = I_S \left[ \exp \left( \frac{v_D}{nV_T} \right) - 1 \right]$$

### EXAMPLE 3.3 DIODE VOLTAGE AND CURRENT CALCULATIONS

In this example, we calculate some typical values of diode voltages for several different current levels and types of diodes.

**PROBLEM** (a) Find the diode voltage for a silicon diode with  $I_S = 0.1$  fA operating at room temperature at a current of 300  $\mu$ A. What is the diode voltage if  $I_S = 10$  fA? What is the diode voltage if the current increases to 1 mA?

(b) Find the diode voltage for a silicon power diode with  $I_S = 10$  nA and  $n = 2$  operating at room temperature at a current of 10 A.

(c) A silicon diode is operating with a temperature of 50°C and the diode voltage is measured to be 0.736 V at a current of 2.50 mA. What is the saturation current of the diode?

**SOLUTION (a)** **Known Information and Given Data:** The diode currents are given and the saturation current parameter  $I_S$  is specified.

**Unknowns:** Diode voltage at each of the operating currents

**Approach:** Solve Eq. (3.9) for the diode voltage and evaluate the expression at each operating current.

**Assumptions:** At room temperature, we will use  $V_T = 0.025$  V = 1/40 V; assume  $n = 1$ , since it is not specified otherwise; assume dc operation:  $i_D = I_D$  and  $v_D = V_D$ .

**Analysis:** Solving Eq. (3.9) for  $V_D$  with  $I_D = 0.1 \text{ fA}$  yields

$$V_D = n V_T \ln \left( 1 + \frac{I_D}{I_S} \right) = 1(0.025 \text{ V}) \ln \left( 1 + \frac{3 \times 10^{-4} \text{ A}}{10^{-16} \text{ A}} \right) = 0.718 \text{ V}$$

For  $I_S = 10 \text{ fA}$ :

$$V_D = n V_T \ln \left( 1 + \frac{I_D}{I_S} \right) = 1(0.025 \text{ V}) \ln \left( 1 + \frac{3 \times 10^{-4} \text{ A}}{10^{-14} \text{ A}} \right) = 0.603 \text{ V}$$

For  $I_D = 1 \text{ mA}$  with  $I_S = 0.1 \text{ fA}$ :

$$V_D = n V_T \ln \left( 1 + \frac{I_D}{I_S} \right) = 1(0.025 \text{ V}) \ln \left( 1 + \frac{10^{-3} \text{ A}}{10^{-16} \text{ A}} \right) = 0.748 \text{ V}$$

**Check of Results:** The diode voltages are all between 0.5 V and 1.0 V and are reasonable (the diode voltage should not exceed the bandgap for  $n = 1$ ).

### SOLUTION (b)

**Known Information and Given Data:** The diode current is given and the values of the saturation current parameter  $I_S$  and  $n$  are both specified.

**Unknowns:** Diode voltage at the operating current

**Approach:** Solve Eq. (3.9) for the diode voltage and evaluate the resulting expression.

**Assumptions:** At room temperature, we will use  $V_T = 0.025 \text{ V} = 1/40 \text{ V}$ .

**Analysis:** The diode voltage will be

$$V_D = n V_T \ln \left( 1 + \frac{I_D}{I_S} \right) = 2(0.025 \text{ V}) \ln \left( 1 + \frac{10 \text{ A}}{10^{-8} \text{ A}} \right) = 1.04 \text{ V}$$

**Check of Results:** Based on the comment at the end of part (a) and realizing that  $n = 2$ , voltages between 1 V and 2 V are reasonable for power diodes operating at high currents.

### SOLUTION (c)

**Known Information and Given Data:** The diode current is 2.50 mA and voltage is 0.736 V. The diode is operating at a temperature of 50°C.

**Unknowns:** Diode saturation current  $I_S$

**Approach:** Solve Eq. (3.9) for the saturation current and evaluate the resulting expression. The value of the thermal voltage  $V_T$  will need to be calculated for  $T = 50^\circ\text{C}$ .

**Assumptions:** The value of  $n$  is unspecified, so assume  $n = 1$ .

**Analysis:** Converting  $T = 50^\circ\text{C}$  to Kelvins,  $T = (273 + 50) \text{ K} = 323 \text{ K}$ , and

$$V_T = \frac{kT}{q} = \frac{(1.38 \times 10^{-23} \text{ J/K})(323 \text{ K})}{1.60 \times 10^{-19} \text{ eV}} = 27.9 \text{ mV}$$

Solving Eq. (3.9) for  $I_S$  yields

$$I_S = \frac{I_D}{\exp \left( \frac{V_D}{n V_T} \right) - 1} = \frac{2.5 \text{ mA}}{\exp \left( \frac{0.736 \text{ V}}{0.0279 \text{ V}} \right) - 1} = 8.74 \times 10^{-15} \text{ A} = 8.74 \text{ fA}$$

**Check of Results:** The saturation current is within the range of typical values specified in Eq. (3.10).

**EXERCISE:** A diode has a reverse saturation current of 40 fA. Calculate  $i_D$  for diode voltages of 0.55 and 0.7 V. What is the diode voltage if  $i_D = 6$  mA?

**ANSWERS:** 143  $\mu$ A; 57.9 mA; 0.643 V

### 3.4 DIODE CHARACTERISTICS UNDER REVERSE, ZERO, AND FORWARD BIAS

When a dc voltage or current is applied to an electronic device, we say that we are providing a dc bias or simply a **bias** to the device. As we develop our electronics expertise, choosing the bias will be important to all of the circuits that we analyze and design. We will find that bias determines device characteristics, power dissipation, voltage and current limitations, and other important circuit parameters. For a diode, there are three important bias conditions. **Reverse bias** and **forward bias** correspond to  $v_D < 0$  V and  $v_D > 0$  V, respectively. The **zero bias** condition, with  $v_D = 0$  V, represents the boundary between the forward and reverse bias regions. When the diode is operating with reverse bias, we consider the diode “off” or nonconducting because the current is very small. For forward bias, the diode is usually in a highly conducting state and is considered “on.”

#### 3.4.1 REVERSE BIAS

For  $v_D < 0$ , the diode is said to be operating under reverse bias. Only a very small reverse leakage current, approximately equal to  $I_S$ , flows through the diode. This current is small enough that we usually think of the diode as being in the nonconducting or off state when it is reverse-biased. For example, suppose that a dc voltage  $V = -4V_T = -0.1$  V is applied to the diode terminals so that  $v_D = -0.1$  V. Substituting this value into Eq. (3.11) gives

$$i_D = I_S \left[ \exp\left(\frac{v_D}{V_T}\right) - 1 \right] = I_S [\exp(-4)^{\text{negligible}} - 1] \approx -I_S \quad (3.12)$$

because  $\exp(-4) = 0.018$ . For a reverse bias greater than  $4V_T$ —that is,  $v_D \leq -4V_T = -0.1$  V—the exponential term  $\exp(v_D/V_T)$  is much less than 1, and the diode current will be approximately equal to  $-I_S$ , a very small current. The current  $I_S$  was identified in Fig. 3.9.

**EXERCISE:** A diode has a reverse saturation current of 5 fA. Calculate  $i_D$  for diode voltages of  $-0.04$  V and  $-2$  V (see Sec. 3.6).

**ANSWERS:**  $-3.99$  fA;  $-5$  fA

The situation depicted in Fig. 3.9 and Eq. (3.12) actually represents an idealized picture of the diode. In a real diode, the reverse leakage current is several orders of magnitude larger than  $I_S$  due to the generation of electron–hole pairs within the depletion region. In addition,  $i_D$  does not saturate but increases gradually with reverse bias as the width of the depletion layer increases with reverse bias. (See Sec. 3.6.1).

#### 3.4.2 ZERO BIAS

Although it may seem to be a trivial result, it is important to remember that the  $i$ - $v$  characteristic of the diode passes through the origin. For zero bias with  $v_D = 0$ , we find  $i_D = 0$ . Just as for a resistor, there must be a voltage across the diode terminals in order for a nonzero current to exist.

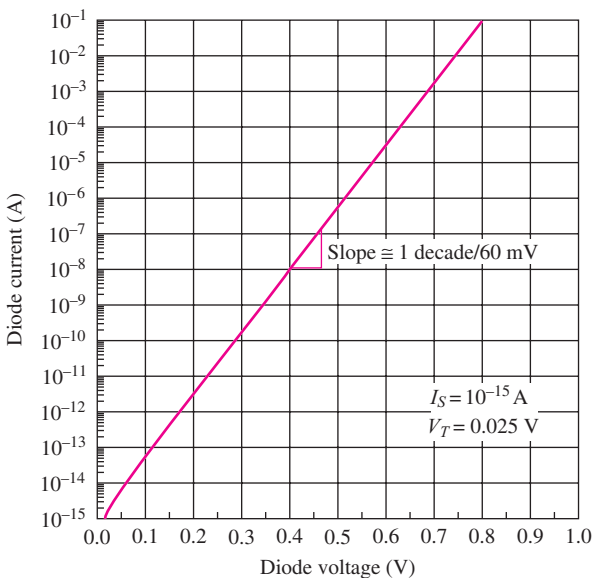


**Figure 3.11** Diode  $i$ - $v$  characteristic on semilog scale.

### 3.4.3 FORWARD BIAS

For the case  $v_D > 0$ , the diode is said to be operating under forward bias, and a large current can be present in the diode. Suppose that a voltage  $v_D \geq +4V_T = +0.1$  V is applied to the diode terminals. The exponential term  $\exp(v_D/V_T)$  is now much greater than 1, and Eq. (3.9) reduces to

$$i_D = I_S \left[ \exp\left(\frac{v_D}{V_T}\right) - 1 \right] \cong I_S \exp\left(\frac{v_D}{V_T}\right) \quad (3.13)$$

The diode current grows exponentially with applied voltage for a forward bias greater than approximately  $4V_T$ .

The diode  $i$ - $v$  characteristic for forward voltages is redrawn in semilogarithmic form in Fig. 3.11. The straight line behavior predicted by Eq. (3.13) for voltages  $v_D \geq 4V_T$  is apparent. A slight curvature can be observed near the origin, where the  $-1$  term in Eq. (3.13) is no longer negligible. The slope of the graph in the exponential region is very important. Only a 60-mV increase in the forward voltage is required to increase the diode current by a factor of 10. This is the reason for the almost vertical increase in current noted in Fig. 3.8 for voltages above the turn-on voltage.

#### EXAMPLE 3.4

#### DIODE VOLTAGE CHANGE VERSUS CURRENT

The slope of the diode  $i$ - $v$  characteristic is an important number for circuit designers to remember.

**PROBLEM** Use Eq. (3.13) to accurately calculate the voltage change required to increase the diode current by a factor of 10.

**SOLUTION** **Known Information and Given Data:** The current changes by a factor of 10.

**Unknowns:** The diode voltage change corresponding to a one decade change in current; the saturation current has not been given.

**Approach:** Form an expression for the ratio of two diode currents using the diode equation. The saturation current will cancel out and is not needed.

**Assumptions:** Room temperature operation with  $V_T = 25.0 \text{ mV}$ ; Assume  $I_D \gg I_S$ .

**Analysis:** Let

$$i_{D1} = I_S \exp\left(\frac{v_{D1}}{V_T}\right) \quad \text{and} \quad i_{D2} = I_S \exp\left(\frac{v_{D2}}{V_T}\right)$$

Taking the ratio of the two currents and setting it equal to 10 yields

$$\frac{i_{D2}}{i_{D1}} = \exp\left(\frac{v_{D2} - v_{D1}}{V_T}\right) = \exp\left(\frac{\Delta v_D}{V_T}\right) = 10 \quad \text{and} \quad \Delta v_D = V_T \ln 10 = 2.3V_T$$

Therefore  $\Delta V_D = 2.3V_T = 57.5 \text{ mV}$  (or approximately 60 mV) at room temperature.

**Check of Results:** The result is consistent with the logarithmic plot in Fig. 3.11. The diode voltage changes approximately 60 mV for each decade change in forward current.

**EXERCISE:** A diode has a saturation current of 2 fA. (a) What is the diode voltage at a diode current of 40  $\mu\text{A}$  (assume  $V_T = 25.0 \text{ mV}$ )? Repeat for a diode current of 400  $\mu\text{A}$ . What is the difference in the two diode voltages? (b) Repeat for  $V_T = 25.8 \text{ mV}$ .

**ANSWER:** 0.593 V, 0.651 V, 57.6 mV; 0.612 V, 0.671 V, 59.4 mV

## DESIGN NOTE

The diode voltage changes by approximately *60 mV per decade* change in diode current. Sixty mV/decade often plays an important role in our thinking about the design of circuits containing both diodes and bipolar transistors and is a good number to remember.

Figure 3.12 compares the characteristics of three diodes with different values of saturation current. The saturation current of diode A is 10 times larger than that of diode B, and the saturation current of diode B is 10 times that of diode C. The spacing between each pair of curves is

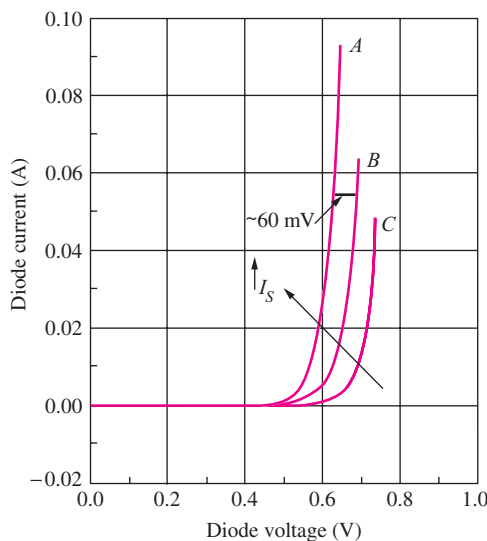
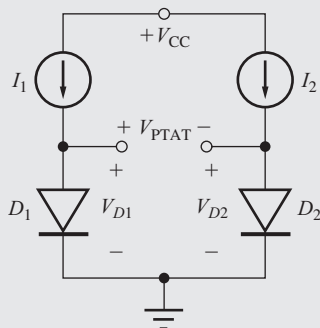


**Figure 3.12** Diode characteristics for three different reverse saturation currents (a)  $10^{-12} \text{ A}$ , (b)  $10^{-13} \text{ A}$ , and (c)  $10^{-14} \text{ A}$ .

### The PTAT Voltage and Electronic Thermometry

The well-defined temperature dependence of the diode voltage discussed in Secs. 3.3–3.5 is actually used as the basis for most digital thermometers. We can build a simple electronic thermometer based on the circuit shown here in which two identical diodes are biased by current sources  $I_1$  and  $I_2$ .



Digital thermometer: © Spike Mafford/Getty Images/RF.

If we calculate the difference between the diode voltages using Eq. (3.14), we discover a voltage that is directly proportional to absolute temperature (PTAT), referred to as the PTAT voltage or  $V_{\text{PTAT}}$ :

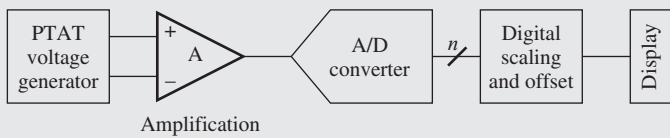
$$V_{\text{PTAT}} = V_{D1} - V_{D2} = V_T \ln \left( \frac{I_{D1}}{I_S} \right) - V_T \ln \left( \frac{I_{D2}}{I_S} \right) = V_T \ln \left( \frac{I_{D1}}{I_{D2}} \right) = \frac{kT}{q} \ln \left( \frac{I_{D1}}{I_{D2}} \right)$$

The PTAT voltage has a temperature coefficient given by

$$\frac{dV_{\text{PTAT}}}{dT} = \frac{k}{q} \ln \left( \frac{I_{D1}}{I_{D2}} \right) = \frac{V_{\text{PTAT}}}{T}$$

By using two diodes, the temperature dependence of  $I_S$  has been eliminated from the equation. For example, suppose  $T = 295$  K,  $I_{D1} = 250$   $\mu\text{A}$ , and  $I_{D2} = 50$   $\mu\text{A}$ . Then  $V_{\text{PTAT}} = 40.9$  mV with a temperature coefficient of  $+0.139$  mV/K.

This simple but elegant PTAT voltage circuit forms the heart of most of today's highly accurate electronic thermometers as depicted in the block diagram here. The analog PTAT voltage is amplified and then converted to a digital representation by an A/D converter. The digital output is scaled and offset to properly represent either the Fahrenheit or Celsius temperature scales and appears on an alphanumeric display. The scaling and offset shift can also be done in analog form prior to the A/D conversion operation.



Block diagram of a digital thermometer.

approximately 60 mV. If the saturation current of the diode is reduced by a factor of 10, then the diode voltage must increase by approximately 60 mV to reach the same operating current level. Figure 3.12 also shows the relatively low sensitivity of the forward diode voltage to changes in the parameter  $I_S$ . For a fixed diode current, a change of two orders of magnitude in  $I_S$  results in a diode voltage change of only 120 mV.

### 3.5 DIODE TEMPERATURE COEFFICIENT

Another important number to keep in mind is the temperature coefficient associated with the diode voltage  $v_D$ . Solving Eq. (3.11) for the diode voltage under forward bias

$$v_D = V_T \ln \left( \frac{i_D}{I_S} + 1 \right) = \frac{kT}{q} \ln \left( \frac{i_D}{I_S} + 1 \right) \cong \frac{kT}{q} \ln \left( \frac{i_D}{I_S} \right) \quad \text{V} \quad (3.14)$$

and taking the derivative with respect to temperature yields

$$\frac{dv_D}{dT} = \frac{k}{q} \ln \left( \frac{i_D}{I_S} \right) - \frac{kT}{q} \frac{1}{I_S} \frac{dI_S}{dT} = \frac{v_D}{T} - V_T \frac{1}{I_S} \frac{dI_S}{dT} = \frac{v_D - V_{GO} - 3V_T}{T} \quad \text{V/K} \quad (3.15)$$

where it is assumed that  $i_D \gg I_S$  and  $I_S \propto n_i^2$ . In the numerator of Eq. (3.15),  $v_D$  represents the diode voltage,  $V_{GO}$  is the voltage corresponding to the silicon bandgap energy at 0 K, ( $V_{GO} = E_G/q$ ), and  $V_T$  is the thermal potential. The last two terms result from the temperature dependence of  $n_i^2$  as defined by Eq. (2.2). Evaluating the terms in Eq. (3.15) for a silicon diode with  $v_D = 0.65$  V,  $E_G = 1.12$  eV, and  $V_T = 0.025$  V yields

$$\frac{dv_D}{dT} = \frac{(0.65 - 1.12 - 0.075) \text{ V}}{300 \text{ K}} = -1.82 \text{ mV/K} \quad (3.16)$$

#### DESIGN NOTE

The forward voltage of the diode decreases as temperature increases, and the diode exhibits a temperature coefficient of approximately  $-1.8 \text{ mV/}^\circ\text{C}$  at room temperature.

**EXERCISE:** (a) Verify Eq. (3.15) using the expression for  $n_i^2$  from Eq. (2.2). (b) A silicon diode is operating at  $T = 300$  K, with  $i_D = 1$  mA, and  $v_D = 0.680$  V. Use the result from Eq. (3.16) to estimate the diode voltage at 275 K and at 350 K.

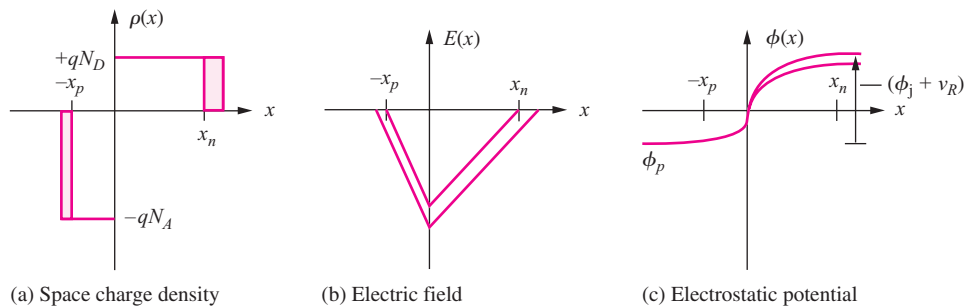
**ANSWERS:** 0.726 V; 0.589 V

### 3.6 DIODES UNDER REVERSE BIAS

We must be aware of several other phenomena that occur in diodes operated under reverse bias. As depicted in Fig. 3.13, the reverse voltage  $v_R$  applied across the diode terminals is dropped across the space charge region and adds directly to the built-in potential of the junction:

$$v_j = \phi_j + v_R \quad \text{for } v_R > 0 \quad (3.17)$$

The increased voltage results in a larger internal electric field that must be supported by additional charge in the depletion layer, as defined by Eqs. (3.2) to (3.5). Using Eq. (3.7) with the voltage

Figure 3.13 The *pn* junction diode under reverse bias.

from Eq. (3.17), the general expression for the depletion-layer width  $w_d$  for an applied reverse-bias voltage  $v_R$  becomes

$$w_d = (x_n + x_p) = \sqrt{\frac{2\epsilon_s}{q} \left( \frac{1}{N_A} + \frac{1}{N_D} \right) (\phi_j + v_R)}$$

or

$$w_d = w_{do} \sqrt{1 + \frac{v_R}{\phi_j}} \quad \text{where } w_{do} = \sqrt{\frac{2\epsilon_s}{q} \left( \frac{1}{N_A} + \frac{1}{N_D} \right) \phi_j} \quad (3.18)$$

The width of the space charge region increases approximately in proportion to the square root of the applied voltage.

**EXERCISE:** The diode in Ex. 3.1 had a zero-bias depletion-layer width of 0.113  $\mu\text{m}$  and a built-in voltage of 0.979 V. What will be the depletion-layer width for a 10-V reverse bias? What is the new value of  $E_{\text{MAX}}$ ?

**ANSWERS:** 0.378  $\mu\text{m}$ ; 581 kV/cm

### 3.6.1 SATURATION CURRENT IN REAL DIODES

The reverse saturation current actually results from the thermal generation of hole-electron pairs in the depletion region that surrounds the *pn* junction and is therefore proportional to the volume of the depletion region. Since the depletion-layer width increases with reverse bias, as described by Eq. (3.18), the reverse current does not truly saturate, as depicted in Fig. 3.9 and Eq. (3.9). Instead, there is gradual increase in reverse current as the magnitude of the reverse bias voltage is increased.

$$I_S = I_{SO} \sqrt{1 + \frac{v_R}{\phi_j}} \quad (3.19)$$

Under forward bias, the depletion-layer width changes very little, and  $I_S = I_{SO}$  for forward bias.

**EXERCISE:** A diode has  $I_{SO} = 10 \text{ fA}$  and a built-in voltage of 0.8 V. What is  $I_S$  for a reverse bias of 10 V?

**ANSWER:** 36.7 fA

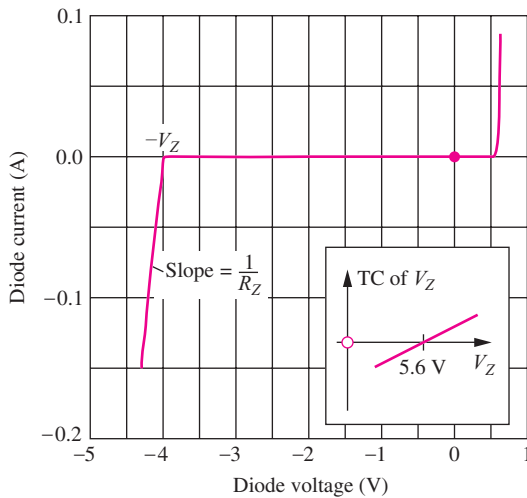


**Figure 3.14**  $i$ - $v$  characteristic of a diode including the reverse-breakdown region. The inset shows the temperature coefficient (TC) of  $V_Z$ .

### 3.6.2 REVERSE BREAKDOWN

As the reverse voltage increases, the electric field within the device grows, and the diode eventually enters the **breakdown region**. The onset of the breakdown process is fairly abrupt, and the current increases rapidly for any further increase in the applied voltage, as shown in the  $i$ - $v$  characteristic of Fig. 3.14.

The magnitude of the voltage at which breakdown occurs is called the **breakdown voltage**  $V_Z$  of the diode and is typically in the range  $2 \text{ V} \leq V_Z \leq 2000 \text{ V}$ . The value of  $V_Z$  is determined primarily by the doping level on the more lightly doped side of the  $pn$  junction, but the heavier the doping, the smaller the breakdown voltage of the diode.

Two separate breakdown mechanisms have been identified: *avalanche breakdown* and *Zener breakdown*. These are discussed in the following two sections.

#### Avalanche Breakdown

Silicon diodes with breakdown voltages greater than approximately 5.6 V enter breakdown through a mechanism called **avalanche breakdown**. As the width of the depletion layer increases under reverse bias, the electric field increases, as indicated in Fig. 3.13. Free carriers in the depletion region are accelerated by this electric field, and as the carriers move through the depletion region, they collide with the fixed atoms. At some point, the electric field and the width of the space charge region become large enough that some carriers gain energy sufficient to break covalent bonds upon impact, thereby creating electron–hole pairs. The new carriers created can also accelerate and create additional electron–hole pairs through this **impact-ionization process**, as illustrated in Fig. 3.15.

#### Zener Breakdown

True **Zener breakdown** occurs only in heavily doped diodes. The high doping results in a very narrow depletion-region width, and application of a reverse bias causes carriers to tunnel directly between the conduction and valence bands, again resulting in a rapidly increasing reverse current in the diode.

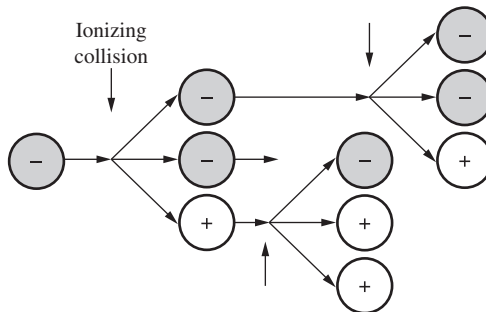


**Figure 3.15** The avalanche breakdown process. (Note that the positive and negative charge carriers will actually be moving in opposite directions in the electric field in the depletion region.)

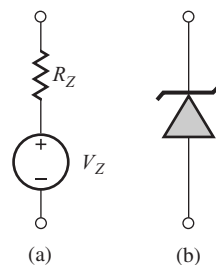


**Figure 3.16** (a) Model for reverse-breakdown region of diode. (b) Zener diode symbol.

### Breakdown Voltage Temperature Coefficient

We can differentiate between the two types of breakdown because the breakdown voltages associated with the two mechanisms exhibit opposite temperature coefficients (TC). In avalanche breakdown,  $V_Z$  increases with temperature; in Zener breakdown,  $V_Z$  decreases with temperature. For silicon diodes, a zero temperature coefficient is achieved at approximately 5.6 V. The avalanche breakdown mechanism dominates in diodes that exhibit breakdown voltages of more than 5.6 V, whereas diodes with breakdown voltages below 5.6 V enter breakdown via the Zener mechanism.

### 3.6.3 DIODE MODEL FOR THE BREAKDOWN REGION

In breakdown, the diode can be modeled by a voltage source of value  $V_Z$  in series with resistor  $R_Z$ , which sets the slope of the  $i$ - $v$  characteristic in the breakdown region, as indicated in Fig. 3.14. The value of  $R_Z$  is normally small ( $R_Z \leq 100 \Omega$ ), and the reverse current flowing in the diode must be limited by the external circuit or the diode will be destroyed.

From the  $i$ - $v$  characteristic in Fig. 3.14 and the model in Fig. 3.16, we see that the voltage across the diode is almost constant, independent of current, in the reverse-breakdown region. Some diodes are actually designed to be operated in **reverse breakdown**. These diodes are called **Zener diodes**<sup>1</sup> and have the special circuit symbol given in Fig. 3.16(b). Links to data sheets for a series of zener diode can be found on the MCD website.



## 3.7 *pn* JUNCTION CAPACITANCE

Forward- and reverse-biased diodes have a capacitance associated with the *pn* junction. This capacitance is important under dynamic signal conditions because it prevents the voltage across the diode from changing instantaneously.

### 3.7.1 REVERSE BIAS

Under reverse bias,  $w_d$  increases beyond its zero-bias value, as expressed by Eq. (3.18), and hence the amount of charge in the depletion region also increases. Since the charge in the diode is changing with voltage, a capacitance results. Using Eqs. (3.4) and (3.7), the total space charge on the *n*-side of the diode is given by

$$Q_n = q N_D x_n A = q \left( \frac{N_A N_D}{N_A + N_D} \right) w_d A \quad C \quad (3.20)$$

<sup>1</sup> The term *Zener diode* is typically used to refer to diodes that breakdown by either the Zener or avalanche mechanism.

where  $A$  is the cross-sectional area of the diode and  $w_d$  is described by Eq. (3.18). The capacitance of the reverse-biased  $pn$  junction is given by

$$C_j = \frac{dQ_n}{dv_R} = \frac{C_{jo}A}{\sqrt{1 + \frac{v_R}{\phi_j}}} \quad \text{where } C_{jo} = \frac{\epsilon_s}{w_{do}} \quad \text{F/cm}^2 \quad (3.21)$$

in which  $C_{jo}$  represents the **zero-bias junction capacitance** per unit area of the diode.

Equation (3.21) shows that the capacitance of the diode changes with applied voltage. The capacitance decreases as the reverse bias increases, exhibiting an inverse square root relationship. This voltage-controlled capacitance can be very useful in certain electronic circuits. Diodes can be designed with impurity profiles (called *hyper-abrupt profiles*) specifically optimized for operation as voltage-controlled capacitors. As for the case of Zener diodes, a special symbol exists for the variable capacitance diode, as shown in Fig. 3.17. Remember that this diode is designed to be operated under reverse bias, but it conducts in the forward direction. Links to data sheets for a series of variable capacitance diodes can be found on the MCD website.



**Figure 3.17** Circuit symbol for the variable capacitance diode (varactor).



**EXERCISE:** What is the value of  $C_{jo}$  for the diode in Ex. 3.1? What is the zero bias value of  $C_j$  if the diode junction area is  $100 \mu\text{m} \times 125 \mu\text{m}$ ? What is the capacitance at a reverse bias of 5 V?

**ANSWERS:**  $91.7 \text{ nf/cm}^2$ ;  $11.5 \text{ pF}$ ;  $4.64 \text{ pF}$

### 3.7.2 FORWARD BIAS

When the diode is operating under forward bias, additional charge is stored in the neutral regions near the edges of the space charge region. The amount of charge  $Q_D$  stored in the diode is proportional to the diode current:

$$Q_D = i_D \tau_T \quad \text{C} \quad (3.22)$$

The proportionality constant  $\tau_T$  is called the diode **transit time** and ranges from  $10^{-15}$  s to more than  $10^{-6}$  s (1 fs to 1  $\mu\text{s}$ ) depending on the size and type of diode. Because we know that  $i_D$  is dependent on the diode voltage through the diode equation, there is an additional capacitance, the **diffusion capacitance**  $C_D$ , associated with the forward region of operation:

$$C_D = \frac{dQ_D}{dv_D} = \frac{(i_D + I_S)\tau_T}{V_T} \cong \frac{i_D \tau_T}{V_T} \quad \text{F} \quad (3.23)$$

in which  $V_T$  is the thermal voltage. The diffusion capacitance is proportional to current and can become quite large at high currents.

**EXERCISE:** A diode has a transit time of 10 ns. What is the diffusion capacitance of the diode for currents of 10  $\mu\text{A}$ , 0.8 mA, and 50 mA at room temperature?

**ANSWERS:** 4 pF; 320 pF; 20 nF

## 3.8 SCHOTTKY BARRIER DIODE

In a  $p^+n$  junction diode, the  $p$ -side is a highly doped region (a conductor), and one might wonder if it could be replaced with a metallic layer. That is in fact the case, and in the **Schottky barrier diode**, one of the semiconductor regions of the  $pn$  junction diode is replaced by a non-ohmic rectifying

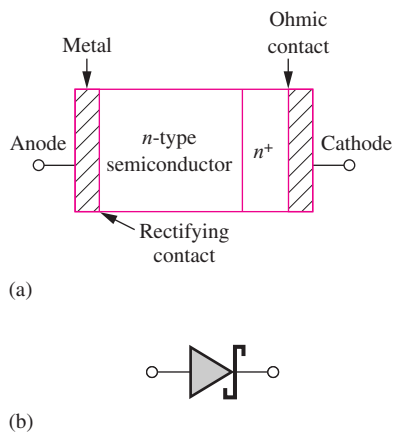


**Figure 3.18** (a) Schottky barrier diode structure. (b) Schottky diode symbol.

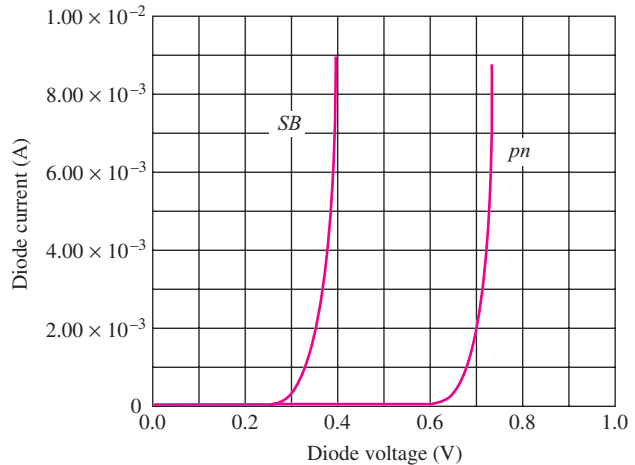


**Figure 3.19** Comparison of *pn* junction (*pn*) and Schottky barrier diode (*SB*) *i*-*v* characteristics.

metal contact, as indicated in Fig. 3.18. It is easiest to form a Schottky contact to *n*-type silicon, and for this case the metal region becomes the diode anode. An  $n^+$  region is added to ensure that the cathode contact is ohmic. The symbol for the Schottky barrier diode appears in Fig. 3.18(b).

The Schottky diode turns on at a much lower voltage than its *pn*-junction counterpart, as indicated in Fig. 3.19. It also has significantly reduced internal charge storage under forward bias. We encounter an important use of the Schottky diode in bipolar logic circuits in Chapter 9. Schottky diodes also find important applications in high-power rectifier circuits and fast switching applications.

### 3.9 DIODE SPICE MODEL AND LAYOUT

The circuit in Fig. 3.20 represents the diode model that is included in SPICE programs. Resistance  $R_S$  represents the inevitable series resistance that always accompanies fabrication of, and making contacts to, a real device structure. The current source represents the ideal exponential behavior of the diode as described by Eq. 3.12 and **SPICE parameters IS, N, and  $V_T$** . The model equation for  $i_D$  also includes a second term, not shown here, that models the effects of carrier generation in the space charge region in a manner similar to Eq. (3.19).

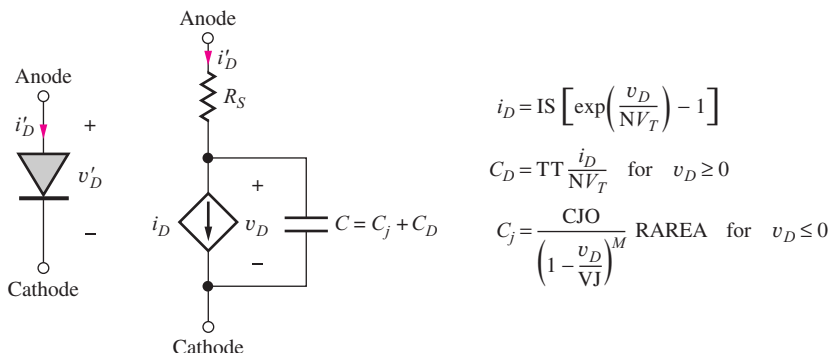


**Figure 3.20** Diode equivalent circuit and simplified versions of the model equations used in SPICE programs.

The capacitor specification includes the depletion-layer capacitance for the reverse-bias region modeled by **SPICE parameters CJO, VJ, and M**, as well as the diffusion capacitance associated with the junction under forward bias and defined by  $N$  and the transit-time parameter TT. In SPICE, the “junction grading coefficient” is an adjustable parameter. Using the typical value of  $M = 0.5$  results in Eq. (3.21).



**EXERCISE:** Find the default values of the seven parameters in Table 3.1 for the SPICE program that you use in class. Compare to the values in Table 3.1.

**TABLE 3.1**  
SPICE Diode Parameter Equivalences

PARAMETER	OUR TEXT	SPICE	TYPICAL DEFAULT VALUES
Saturation current	$I_S$	IS	10 fA
Ohmic series resistance	$R_S$	RS	0 Ω
Ideality factor or emission coefficient	$n$	N	1
Transit time	$\tau_T$	TT	0 sec
Zero-bias junction capacitance for a unit area diode RAREA = 1	$C_{jo} \cdot A$	CJO	0 F
Built-in potential	$\phi_j$	VJ	1 V
Junction grading coefficient	—	M	0.5
Relative junction area	—	RAREA	1

### Diode Layout

Figure 3.21(a) shows the layout of a simple diode fabricated by forming a *p*-type diffusion in an *n*-type silicon wafer, as outlined in Chapter 2. This diode has a long rectangular *p*-type diffusion to increase the value of  $I_S$ , which is proportional to the junction area. Multiple contacts are formed to the *p*-type anode, and the *p*-region is surrounded by a collar of contacts to the *n*-type region.

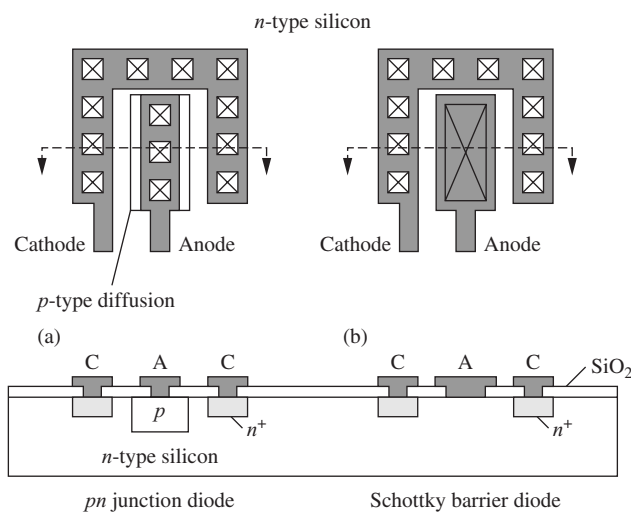


**Figure 3.21** Layout of (a) a *pn* junction diode and (b) a metal-semiconductor Schottky diode. (See top view of diode in Chapter 3 opener.)

Both these sets of contacts are used to minimize the value of the extrinsic series resistance  $R_S$  of the diode, as included in the model in Fig. 3.20. Identical contacts are used so that they all tend to etch open at the same time during the fabrication process. The use of multiple identical contacts also facilitates calculation of the overall contact resistance. Heavily doped  $n$ -type regions are placed under the  $n$ -region contacts to ensure formation of an ohmic contact and prevent formation of a Schottky barrier diode.

A conceptual drawing of a metal-semiconductor or Schottky diode also appears in Fig. 3.21(b) in which the aluminum metallization acts as the anode of the diode and the  $n$ -type semiconductor is the diode cathode. Careful attention to processing details is needed to form a diode rather than just an ohmic contact.

### 3.10 DIODE CIRCUIT ANALYSIS

We now begin our analysis of circuits containing diodes and introduce simplified circuit models for the diode. Figure 3.22 presents a series circuit containing a voltage source, resistor, and diode. Note that  $V$  and  $R$  may represent the Thévenin equivalent of a more complicated two-terminal network. Also note the notational change in Fig. 3.22. In the circuits that we analyze in the next few sections, the applied voltage and resulting diode voltage and current will all be dc quantities. (Recall that the dc components of the total quantities  $i_D$  and  $v_D$  are indicated by  $I_D$  and  $V_D$ , respectively.)

One common objective of diode circuit analysis is to find the **quiescent operating point** (Q-point), or **bias point**, for the diode. The Q-point consists of the dc current and voltage ( $I_D$ ,  $V_D$ ) that define the point of operation on the diode's  $i$ - $v$  characteristic. We start the analysis by writing the loop equation for the circuit of Fig. 3.22:

$$V = I_D R + V_D \quad (3.24)$$

Equation (3.24) represents a constraint placed on the diode operating point by the circuit elements. The diode  $i$ - $v$  characteristic in Fig. 3.8 represents the allowed values of  $I_D$  and  $V_D$  as determined by the solid-state diode itself. Simultaneous solution of these two sets of constraints defines the Q-point.

We explore several methods for determining the solution to Eq. (3.24), including graphical analysis and the use of models of varying complexity for the diode. These techniques will include

- Graphical analysis using the load-line technique.
- Analysis with the mathematical model for the diode.
- Simplified analysis with an ideal diode model.
- Simplified analysis using the constant voltage drop model.

#### 3.10.1 LOAD-LINE ANALYSIS

In some cases, the  $i$ - $v$  characteristic of the solid-state device may be available only in graphical form, as in Fig. 3.23. We can then use a graphical approach (**load-line analysis**) to find the simultaneous solution of Eq. (3.24) with the graphical characteristic. Equation (3.24) defines the **load line** for the

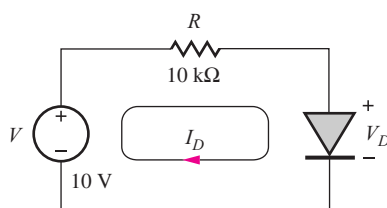


**Figure 3.22** Diode circuit containing a voltage source and resistor.

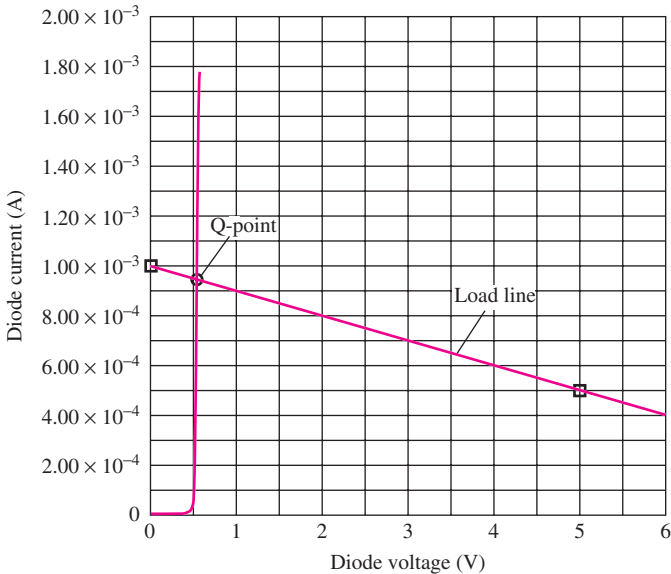


**Figure 3.23** Diode  $i$ - $v$  characteristic and load line.

diode. The Q-point can be found by plotting the graph of the load line on the  $i$ - $v$  characteristic for the diode. The intersection of the two curves represents the quiescent operating point, or Q-point, for the diode.

### EXAMPLE 3.5 LOAD-LINE ANALYSIS

The graphical load-line approach is an important concept for visualizing the behavior of diode circuits as well as for estimating the actual Q-point.

**PROBLEM** Use load-line analysis to find the Q-point for the diode circuit in Fig. 3.22 using the  $i$ - $v$  characteristic in Fig. 3.23.

**SOLUTION** **Known Information and Given Data:** The diode  $i$ - $v$  characteristic is presented graphically in Fig. 3.23. Diode circuit is given in Fig. 3.22 with  $V = 10$  V and  $R = 10$  k $\Omega$ .

**Unknowns:** Diode Q-point ( $I_D$ ,  $V_D$ ).

**Approach:** Write the load-line equation and find two points on the load line that can be plotted on the graph in Fig. 3.23. The Q-point is at the intersection of the load line with the diode  $i$ - $v$  characteristic.

**Assumptions:** Diode temperature corresponds to the temperature at which the graph in Fig. 3.23 was measured.

**Analysis:** Using the values from Fig. 3.22, Eq. (3.24) can be rewritten as

$$10 = 10^4 I_D + V_D \quad (3.25)$$

Two points are needed to define the line. The simplest choices are

$$I_D = (10 \text{ V}/10 \text{ k}\Omega) = 1 \text{ mA} \quad \text{for} \quad V_D = 0 \quad \text{and} \quad V_D = 10 \text{ V} \quad \text{for} \quad I_D = 0$$

Unfortunately, the second point is not in the range of the graph presented in Fig. 3.23, but we are free to choose any point that satisfies Eq. (3.25). Let's pick  $V_D = 5$  V:

$$I_D = (10 - 5)V/10^4 \Omega = 0.5 \text{ mA} \quad \text{for } V_D = 5$$

These points and the resulting load line are plotted in Fig. 3.23. The Q-point is given by the intersection of the load line and the diode characteristic:

$$\text{Q-point} = (0.95 \text{ mA}, 0.6 \text{ V})$$

**Check of Results:** We can double check our result by substituting the diode voltage found from the graph into Eq. (3.25) and calculating  $I_D$ . Using  $V_D = 0.6$  V in Eq. (3.25) yields an improved estimate for the Q-point: (0.94 mA, 0.6 V). [We could also substitute 0.95 mA into Eq. (3.25) and calculate  $V_D$ .]

**Discussion:** Note that the values determined graphically are not quite on the load line since they do not precisely satisfy the load-line equation. This is a result of the limited precision that we can obtain by reading the graph.

**EXERCISE:** Repeat the load-line analysis if  $V = 5$  V and  $R = 5 \text{ k}\Omega$ .

**ANSWERS:** (0.88 mA, 0.6 V)



**EXERCISE:** Use SPICE to find the Q-point for the circuit in Fig. 3.22. Use the default values of parameters in your SPICE program.

**ANSWERS:** (935  $\mu$ A, 0.653 V) for  $I_S = 10 \text{ fA}$  and  $T = 300 \text{ K}$

### 3.10.2 ANALYSIS USING THE MATHEMATICAL MODEL FOR THE DIODE

We can use our mathematical model for the diode to approach the solution of Eq. (3.25) more directly. The particular diode characteristic in Fig. 3.23 is represented quite accurately by diode Eq. (3.11), with  $I_S = 10^{-13}$  A,  $n = 1$ , and  $V_T = 0.025$  V:

$$I_D = I_S \left[ \exp\left(\frac{V_D}{V_T}\right) - 1 \right] = 10^{-13} [\exp(40V_D) - 1] \quad (3.26)$$

Eliminating  $I_D$  by substituting Eq. (3.26) into Eq. (3.25) yields

$$10 = 10^4 \cdot 10^{-13} [\exp(40V_D) - 1] + V_D \quad (3.27)$$

The expression in Eq. (3.27) is called a *transcendental equation* and does not have a closed-form analytical solution, so we settle for a numerical answer to the problem.

One approach to finding a numerical solution to Eq. (3.27) is through simple trial and error. We can guess a value of  $V_D$  and see if it satisfies Eq. (3.27). Based on the result, a new guess can be formulated and Eq. (3.27) evaluated again. The human brain is quite good at finding a sequence of values that will converge to the desired solution.

On the other hand, it is often preferable to use a computer to find the solution to Eq. (3.27), particularly if we need to find the answer to several different problems or parameter sets. The computer, however, requires a much more well-defined iteration strategy than brute force trial and error.

We can develop an iterative solution method for the diode circuit in Fig. 3.22 by creating a linear model for the diode equation in the vicinity of the diode Q-point as depicted in Fig. 3.24(a). First

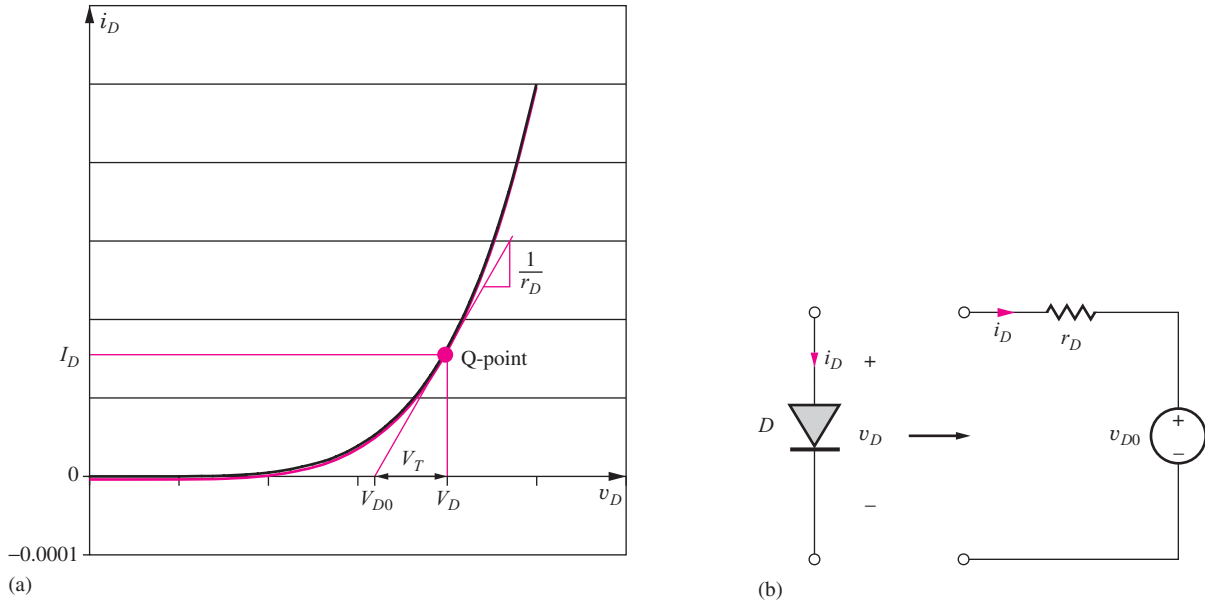


**Figure 3.24** (a) Diode behavior around the Q-Point. (b) Linear model for the diode at the Q-Point.

we find the slope of the diode characteristic at the operating point:

$$g_D = \left. \frac{\partial i_D}{\partial v_D} \right|_{Q-Pr} = \frac{I_S}{V_T} \exp \left( \frac{V_D}{V_T} \right) = \frac{I_D + I_S}{V_T} \cong \frac{I_D}{V_T} \quad \text{and} \quad r_D = \frac{1}{g_D} = \frac{V_T}{I_D} \quad (3.28)$$

Slope  $g_D$  is called the diode conductance, and its reciprocal  $r_D$  is termed the diode resistance. Next we can use the slope to find the  $x$ -axis intercept point  $V_{D0}$ :

$$V_{D0} = V_D - I_D R_D = V_D - V_T \quad (3.29)$$

$V_{D0}$  and  $r_D$  represent a two-element linear circuit model for the diode as in Fig. 3.24(b), and this circuit model replaces the diode in the single loop circuit in Fig. 3.25.

Now we can use an iterative process to find the Q-point of the diode in the circuit.

1. Pick a starting guess for  $I_D$ .
2. Calculate the diode voltage using  $V_D = V_T \ln \left( 1 + \frac{I_D}{I_S} \right)$ .
3. Calculate the values of  $V_{D0}$  and  $r_D$ .
4. Calculate a new estimate for  $I_D$  from the circuit in Fig. 3.25(b):  $I_D = \frac{V - V_{D0}}{R + r_D}$ .
5. Repeat steps 2–4 until convergence is obtained.

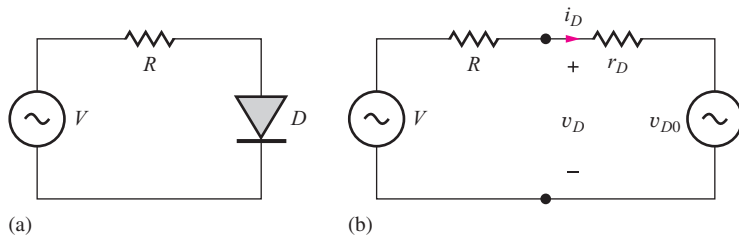


**Figure 3.25** (a) Diode circuit. (b) Circuit with two-element diode model.

**TABLE 3.2**  
Example of Iterative Analysis

$I_D$ (A)	$V_D$ (V)	$R_D$ ( $\Omega$ )	$V_{D0}$ (V)
1.0000E-03	0.5756	25.80	0.5498
9.4258E-04	0.5742	27.37	0.5484
9.4258E-04	0.5742	27.37	0.5484

Table 3.2 presents the results of performing the above iteration process using a spreadsheet. The diode current and voltage converge rapidly in only three iterations.

Note that one can achieve answers to an almost arbitrary precision using the numerical approach. However, in most real circuit situations, we will not have an accurate value for the saturation current of the diode, and there will be significant tolerances associated with the sources and passive components in the circuit. For example, the saturation current specification for a given diode type may vary by factors ranging from 10:1 to as much as 100:1. In addition, resistors commonly have  $\pm 5$  percent or  $\pm 10$  percent tolerances, and we do not know the exact operating temperature of the diode (remember the  $-1.8$  mV/K temperature coefficient) or the precise value of the parameter  $n$ . Hence, it does not make sense to try to obtain answers with a precision of more than a few significant digits.

An alternative to the use of a spreadsheet is to write a simple program using a high-level language. The solution to Eq. (3.28) also can be found using the “solver” routines in many calculators, which use iteration procedures more sophisticated than that just described. MATLAB also provides the function fzero, which will calculate the zeros of a function as outlined in Example 3.6.

**EXERCISE:** An alternative expression (another transcendental equation) for the basic diode circuit can be found by eliminating  $V_D$  in Eq. (3.25) using Eq. (3.14). Show that the result is

$$10 = 10^4 I_D + 0.025 \ln \left( 1 + \frac{I_D}{I_S} \right)$$

### EXAMPLE 3.6 SOLUTION OF THE DIODE EQUATION USING MATLAB

MATLAB is one example of a computer tool that can be used to find the solution to transcendental equations.

**PROBLEM** Use MATLAB to find the solution to Eq. (3.27).

**SOLUTION** **Known Information and Given Data:** Diode circuit in Fig. 3.22 with  $V = 10$  V,  $R = 10$  k $\Omega$ ,  $I_S = 10^{-13}$  A,  $n = 1$ , and  $V_T = 0.025$  V

**Unknowns:** Diode voltage  $V_D$

**Approach:** Create a MATLAB “M-File” describing Eq. (3.27). Execute the program to find the diode voltage.

**Assumptions:** Room temperature operation with  $V_T = 1/40$  V

**Analysis:** First, create an M-file for the function ‘diode’:

```
function xd = diode(vd)
xd = 10 - (10^(-9)) * (exp(40 * vd) - 1) - vd;
```

Then find the solution near 1 V:

`fzero('diode',1)`

*Answer:* 0.5742 V

**Check of Results:** The diode voltage is positive and in the range of 0.5 to 0.8 V, which is expected for a diode. Substituting this value of voltage into the diode equation yields a current of 0.944 mA. This answer appears reasonable since we know that the diode current cannot exceed  $10\text{ V}/10\text{ k}\Omega = 1.0\text{ mA}$ , which is the maximum current available from the circuit.



**EXERCISE:** Use the MATLAB to find the solution to

$$10 = 10^4 I_D + 0.025 \ln\left(1 + \frac{I_D}{I_S}\right) \quad \text{for } I_S = 10^{-13} \text{ A}$$

**ANSWER:** 942.6  $\mu\text{A}$

### EXAMPLE 3.7

#### EFFECT OF DEVICE TOLERANCES ON DIODE Q-POINTS

Let us now see how sensitive our Q-point results are to the exact value of the diode saturation current.

**PROBLEM** Suppose that there is a tolerance on the value of the saturation current such that the value is given by

$$I_S^{\text{nom}} = 10^{-15} \text{ A} \quad \text{and} \quad 2 \times 10^{-16} \text{ A} \leq I_S \leq 5 \times 10^{-15} \text{ A}$$

Find the nominal, smallest, and largest values of the diode voltage and current in the circuit in Fig. 3.22.

**SOLUTION** **Known Information and Given Data:** The nominal and worst-case values of saturation current are given as well as the circuit values in Fig. 3.22.

**Unknowns:** Nominal and worst-case values for the diode Q-point: ( $I_D$ ,  $V_D$ )

**Approach:** Use MATLAB or the solver on our calculator to find the diode voltages and then the currents for the nominal and worst-case values of  $I_S$ . Note from Eq. (3.24) that the maximum value of diode voltage corresponds to minimum current and vice versa.

**Assumptions:** Room temperature operation with  $V_T = 0.025\text{ V}$ ; The voltage and resistance in the circuit do not have tolerances associated with them.

**Analysis:** For the nominal case, Eq. (3.28) becomes

$$f = 10 - 10^4(10^{-15})[\exp(40V_D) - 1] - V_D$$

for which the solver yields

$$V_D^{\text{nom}} = 0.689 \text{ V} \quad \text{and} \quad I_D^{\text{nom}} = \frac{(10 - 0.689) \text{ V}}{10^4 \Omega} = 0.931 \text{ mA}$$

For the minimum  $I_S$  case, Eq. (3.28) is

$$f = 10 - 10^4(2 \times 10^{-16})[\exp(40V_D) - 1] - V_D$$

and the solver yields

$$V_D^{\max} = 0.729 \text{ V} \quad \text{and} \quad I_D^{\min} = \frac{(10 - 0.729) \text{ V}}{10^4 \Omega} = 0.927 \text{ mA}$$

Finally, for the maximum value of  $I_S$ , Eq. (3.28) becomes

$$f = 10 - 10^4(5 \times 10^{-15})[\exp(40V_D) - 1] - V_D$$

and the solver gives

$$V_D^{\min} = 0.649 \text{ V} \quad \text{and} \quad I_D^{\max} = \frac{(10 - 0.649) \text{ V}}{10^4 \Omega} = 0.935 \text{ mA}$$

**Check of Results:** The diode voltages are positive and in the range of 0.5 to 0.8 V which is expected for a diode. The diode currents are all less than the short circuit current available from the voltage source ( $10 \text{ V}/10 \text{ k}\Omega = 1.0 \text{ mA}$ ).

**Discussion:** Note that even though the diode saturation current in this circuit changes by a factor of 5:1 in either direction, the current changes by less than  $\pm 0.5\%$ . As long as the driving voltage in the circuit is much larger than the diode voltage, the current should be relatively insensitive to changes in the diode voltage or the diode saturation current.

**EXERCISE:** Find  $V_D$  and  $I_D$  if the upper limit on  $I_S$  is increased to  $10^{-14} \text{ A}$ .

**ANSWERS:**  $0.6316 \text{ V}; 0.9368 \text{ A}$



**EXERCISE:** Use the Solver function in your calculator to find the solution to

$$10 = 10^4 I_D + 0.025 \ln\left(1 + \frac{I_D}{I_S}\right) \quad \text{for } I_S = 10^{-13} \text{ A} \quad \text{and} \quad I_S = 10^{-15} \text{ A}$$

**ANSWER:**  $0.9426 \text{ mA}; 0.9311 \text{ mA}$

### 3.10.3 THE IDEAL DIODE MODEL

Graphical load-line analysis provides insight into the operation of the diode circuit of Fig. 3.22, and the mathematical model can be used to provide more accurate solutions to the load-line problem. The next method discussed provides simplified solutions to the diode circuit of Fig. 3.22 by introducing simplified diode circuit models of varying complexity.

The diode, as described by its  $i$ - $v$  characteristic in Fig. 3.8 or by Eq. (3.11), is obviously a nonlinear device. However, most, if not all, of the circuit analysis that we have learned in electrical engineering thus far assumed that the circuits were composed of linear elements. To use this wealth of analysis techniques, we will use **piecewise linear** approximations to the diode characteristic.

The **ideal diode model** is the simplest model for the diode. The  $i$ - $v$  characteristic for the **ideal diode** in Fig. 3.26 consists of two straight-line segments. If the diode is conducting a forward or positive current (forward-biased), then the voltage across the diode is zero. If the diode is reverse-biased, with  $v_D < 0$ , then the current through the diode is zero. These conditions can be stated mathematically as

$$v_D = 0 \quad \text{for } i_D > 0 \quad \text{and} \quad i_D = 0 \quad \text{for } v_D \leq 0$$

The special symbol in Fig. 3.26 is used to represent the ideal diode in circuit diagrams.

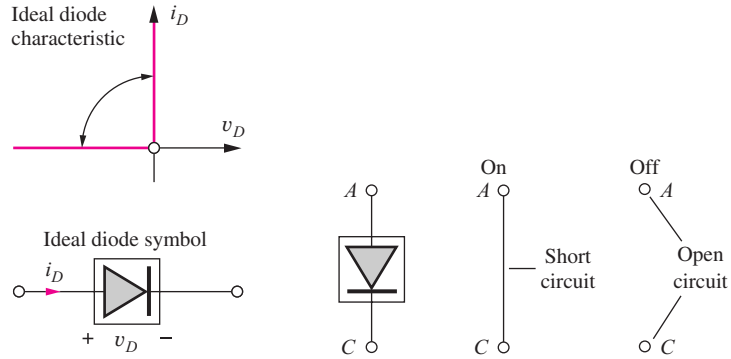


**Figure 3.26** (a) Ideal diode  $i$ - $v$  characteristics and circuit symbol. (b) Circuit models for on and off states of the ideal diode.

We can now think of the diode as having two states. The diode is either conducting in the *on* state, or nonconducting and *off*. For circuit analysis, we use the models in Fig. 3.26(b) for the two states. If the diode is on, then it is modeled by a “short” circuit, a wire. For the off state, the diode is modeled by an “open” circuit, no connection.

### Analysis Using the Ideal Diode Model

Let us now analyze the circuit of Fig. 3.22 assuming that the diode can be modeled by the ideal diode of Fig. 3.26(b). The diode has two possible states, and our analysis of diode circuits proceeds as follows:

1. Select a model for the diode.
2. Identify the anode and cathode of the diode and label the diode voltage  $v_D$  and current  $i_D$ .
3. Make an (educated) guess concerning the region of operation of the diode based on the circuit configuration.
4. Analyze the circuit using the diode model appropriate for the assumption in step 3.
5. Check the results to see if they are consistent with the assumptions.

For this analysis, we select the ideal diode model. The diode in the original circuit is replaced by the ideal diode, as in Fig. 3.27(b). Next we must guess the state of the diode. Because the voltage source appears to be trying to force a positive current through the diode, our first guess will be to assume that the diode is on. The ideal diode of Fig. 3.27(b) is replaced by its piecewise linear model for the on region in Fig. 3.28, and the diode current is given by

$$I_D = \frac{(10 - 0) \text{ V}}{10 \text{ k}\Omega} = 1.00 \text{ mA}$$

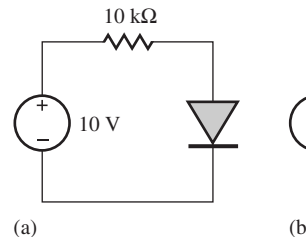


**Figure 3.27** (a) Original diode circuit. (b) Circuit modeled by an ideal diode.

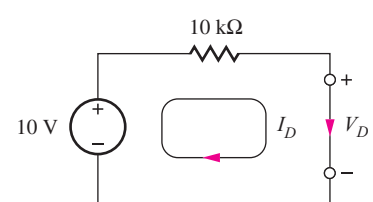


**Figure 3.28** Ideal diode replaced with its model for the on state.

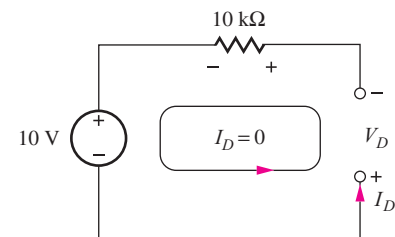
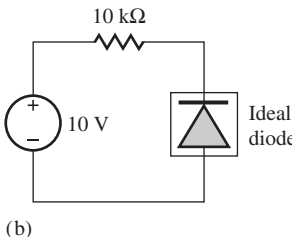
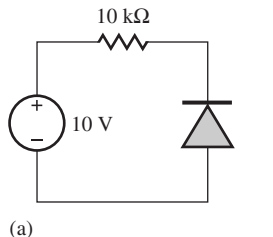


**Figure 3.29** (a) Circuit with reverse-biased diode. (b) Circuit modeled by ideal diode.

**Figure 3.30** Ideal diode replaced with its model for the off region.

The current  $I_D \geq 0$ , which is consistent with the assumption that the diode is on. The Q-point is therefore equal to (1 mA, 0 V). Based on the ideal diode model, we find that the diode is forward-biased and operating with a current of 1 mA.

#### Analysis of a Circuit Containing a Reverse-Biased Diode

A second circuit example in which the diode terminals have been reversed appears in Fig. 3.29; the ideal diode model is again used to model the diode [Fig. 3.29(b)]. The voltage source now appears to be trying to force a current backward through the diode. Because the diode cannot conduct in this direction, we assume the diode is off. The ideal diode of Fig. 3.29(b) is replaced by the open circuit model for the off region, as in Fig. 3.30.

Writing the loop equation for this case,

$$10 + V_D + 10^4 I_D = 0$$

Because  $I_D = 0$ ,  $V_D = -10$  V. The calculated diode voltage is negative, which is consistent with the starting assumption that the diode is off. The Q-point is (0, -10 V). The analysis shows that the diode in the circuit of Fig. 3.29 is indeed reverse-biased.

Although these two problems may seem rather simple, the complexity of diode circuit analysis increases rapidly as the number of diodes increases. If the circuit has  $N$  diodes, then the number of possible states is  $2^N$ . A circuit with 10 diodes has 1024 different possible circuits that could be analyzed! Only through practice can we develop the intuition needed to avoid analysis of many incorrect cases. We analyze more complex circuits shortly, but first let's look at a slightly better piecewise linear model for the diode.

#### 3.10.4 CONSTANT VOLTAGE DROP MODEL

We know from our earlier discussion that there is a small, nearly constant voltage across the forward-biased diode. The ideal diode model ignores the presence of this voltage. However, the piecewise linear model for the diode can be improved by adding a constant voltage  $V_{on}$  in series with the ideal diode, as shown in Fig. 3.31(b). This is the **constant voltage drop (CVD) model**.  $V_{on}$  offsets the

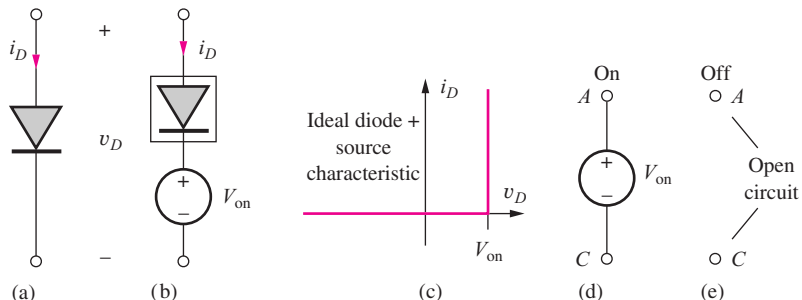


**Figure 3.31** Constant voltage drop model for diode. (a) Actual diode. (b) Ideal diode plus voltage source  $V_{on}$ . (c) Composite  $i$ - $v$  characteristic. (d) CVD model for the on state. (e) Model for the off state.

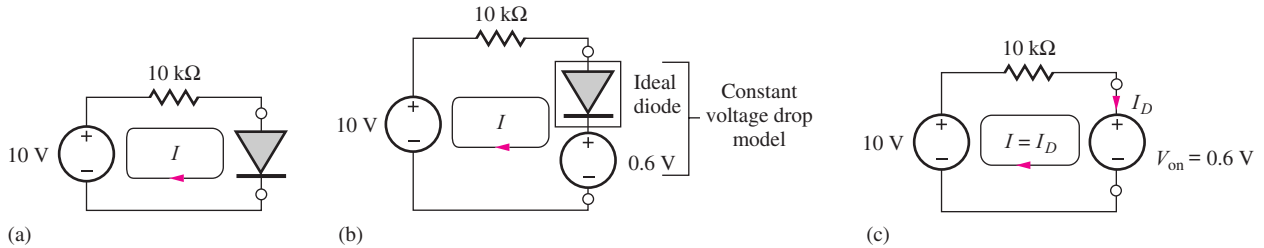


**Figure 3.32** Diode circuit analysis using constant voltage drop model. (a) Original diode circuit. (b) Circuit with diode replaced by the constant voltage drop model. (c) Circuit with ideal diode replaced by the piecewise linear model.

$i$ - $v$  characteristic of the ideal diode, as indicated in Fig. 3.31(c). The piecewise linear models for the two states become a voltage source  $V_{on}$  for the on state and an open circuit for the off state. We now have

$$v_D = V_{on} \quad \text{for } i_D > 0 \quad \text{and} \quad i_D = 0 \quad \text{for } v_D \leq V_{on}$$

We may consider the ideal diode model to be the special case of the constant voltage drop model for which  $V_{on} = 0$ . From the  $i$ - $v$  characteristics presented in Fig. 3.8, we see that a reasonable choice for  $V_{on}$  is 0.6 to 0.7 V. We use a voltage of 0.6 V as the turn-on voltage for our diode circuit analysis.

### Diode Analysis with the Constant Voltage Drop Model

Let us analyze the diode circuit from Fig. 3.22 using the CVD model for the diode. The diode in Fig. 3.32(a) is replaced by its CVD model in Fig. 3.32(b). The 10-V source once again appears to be forward biasing the diode, so assume that the diode is on, resulting in the simplified circuit in Fig. 3.32(c). The diode current is given by

$$I_D = \frac{(10 - V_{on}) \text{ V}}{10 \text{ k}\Omega} = \frac{(10 - 0.6) \text{ V}}{10 \text{ k}\Omega} = 0.940 \text{ mA} \quad (3.30)$$

which is slightly smaller than that predicted by the ideal diode model but quite close to the exact result found earlier.

### 3.10.5 MODEL COMPARISON AND DISCUSSION

We have analyzed the circuit of Fig. 3.22 using four different approaches; the various results appear in Table 3.3. All four sets of predicted voltages and currents are quite similar. Even the simple ideal diode model only overestimates the current by less than 10 percent compared to the mathematical model. We see that the current is quite insensitive to the actual choice of diode voltage. This is a result of the exponential dependence of the diode current on voltage as well as the large source voltage (10 V) in this particular circuit.

Rewriting Eq. (3.31),

$$I_D = \frac{10 - V_{on}}{10 \text{ k}\Omega} = \frac{10 \text{ V}}{10 \text{ k}\Omega} \left(1 - \frac{V_{on}}{10}\right) = (1.00 \text{ mA}) \left(1 - \frac{V_{on}}{10}\right) \quad (3.31)$$

**TABLE 3.3**  
Comparison of Diode Circuit Analysis Results

ANALYSIS TECHNIQUE	DIODE CURRENT	DIODE VOLTAGE
Load-line analysis	0.94 mA	0.6 V
Mathematical model	0.942 mA	0.547 V
Ideal diode model	1.00 mA	0 V
Constant voltage drop model	0.940 mA	0.600 V

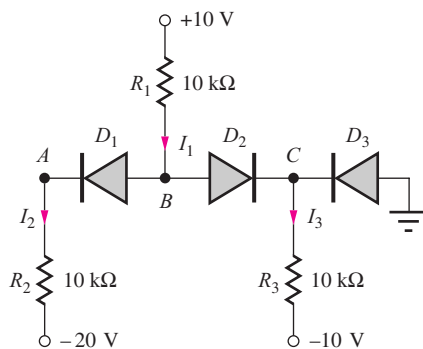


**Figure 3.33** Example of a circuit containing three diodes.

**TABLE 3.4**  
Possible Diode States  
for Circuit in Fig. 3.33

$D_1$	$D_2$	$D_3$
Off	Off	Off
Off	Off	On
Off	On	Off
Off	On	On
On	Off	Off
On	Off	On
On	On	Off
On	On	On

we see that the value of  $I_D$  is approximately 1 mA for  $V_{on} \ll 10$  V. Variations in  $V_{on}$  have only a small effect on the result. However, the situation would be significantly different if the source voltage were only 1 V for example (see Prob. 3.68).

### 3.11 MULTIPLE-DIODE CIRCUITS

The load-line technique is applicable only to single-diode circuits, and the mathematical model, or numerical iteration technique, becomes much more complex for circuits with more than one nonlinear element. In fact, the SPICE electronic circuit simulation program referred to throughout this book is designed to provide numerical solutions to just such complex problems. However, we also need to be able to perform hand analysis to predict the operation of multidiode circuits as well as to build our understanding and intuition for diode circuit operation. In this section we discuss the use of the simplified diode models for hand analysis of more complicated diode circuits.

As the complexity of diode circuits increases, we must rely on our intuition to eliminate unreasonable solution choices. Even so, analysis of diode circuits often requires several iterations. Intuition can only be developed over time by working problems, and here we analyze a circuit containing three diodes.

Figure 3.33 is an example of a circuit with several diodes. In the analysis of this circuit, we will use the CVD model to improve the accuracy of our hand calculations.

#### EXAMPLE 3.8 ANALYSIS OF A CIRCUIT CONTAINING THREE DIODES

Now we will attempt to find the solution for a three-diode circuit. Our analysis will employ the CVD model.

**PROBLEM** Find the Q-points for the three diodes in Fig. 3.33. Use the constant voltage drop model for the diodes.

**SOLUTION Known Information and Given Data:** Circuit topology and element values in Fig. 3.33

**Unknowns:**  $(I_{D1}, V_{D1}), (I_{D2}, V_{D2}), (I_{D3}, V_{D3})$

**Approach:** With three diodes, there are the eight On/Off combinations indicated in Table 3.4. A common method that we often use to find a starting point is to consider the circuit with all the

diodes in the off state as in Fig 3.34(a). Here we see that the circuit produces large forward biases across  $D_1$ ,  $D_2$  and  $D_3$ . So our second step will be to assume that all the diodes are on.

**Assumptions:** Use the constant voltage drop model with  $V_{on} = 0.6$  V.

**Analysis:** The circuit is redrawn using the CVD diode models in Fig. 3.34(b). Here we skipped the step of physically drawing the circuit with the ideal diode symbols but instead incorporated the piecewise linear models directly into the figure. Working from right to left, we see that the voltages at nodes  $C$ ,  $B$ , and  $A$  are given by

$$V_C = -0.6 \text{ V} \quad V_B = -0.6 + 0.6 = 0 \text{ V} \quad V_A = 0 - 0.6 = -0.6 \text{ V}$$

With the node voltages specified, it is easy to find the current through each resistor:

$$\begin{aligned} I_1 &= \frac{10 - 0}{10 \text{ k}\Omega} \text{ V} = 1 \text{ mA} & I_2 &= \frac{-0.6 - (-20)}{10 \text{ k}\Omega} \text{ V} = 1.94 \text{ mA} \\ I_3 &= \frac{-0.6 - (-10)}{10 \text{ k}\Omega} \text{ V} = 0.94 \text{ mA} \end{aligned} \quad (3.32)$$

Using Kirchhoff's current law, we also have

$$I_2 = I_{D1} \quad I_1 = I_{D1} + I_{D2} \quad I_3 = I_{D2} + I_{D3} \quad (3.33)$$

Combining Eqs. (3.32) and (3.33) yields the three diode currents:

$$I_{D1} = 1.94 \text{ mA} > 0 \checkmark \quad I_{D2} = -0.94 \text{ mA} < 0 \times \quad I_{D3} = 1.86 \text{ mA} > 0 \checkmark \quad (3.34)$$

**Check of Results:**  $I_{D1}$  and  $I_{D3}$  are greater than zero and therefore consistent with the original assumptions. However,  $I_{D2}$ , which is less than zero, represents a contradiction.

**SECOND ITERATION** For our second attempt, let us assume  $D_1$  and  $D_3$  are on and  $D_2$  is off, as in Fig. 3.35(a). We now have

$$+10 - 10,000I_1 - 0.6 - 10,000I_2 + 20 = 0 \quad \text{with } I_1 = I_{D1} = I_2 \quad (3.35)$$

which yields

$$I_{D1} = \frac{29.4}{20 \text{ k}\Omega} \text{ V} = 1.47 \text{ mA} > 0 \checkmark$$

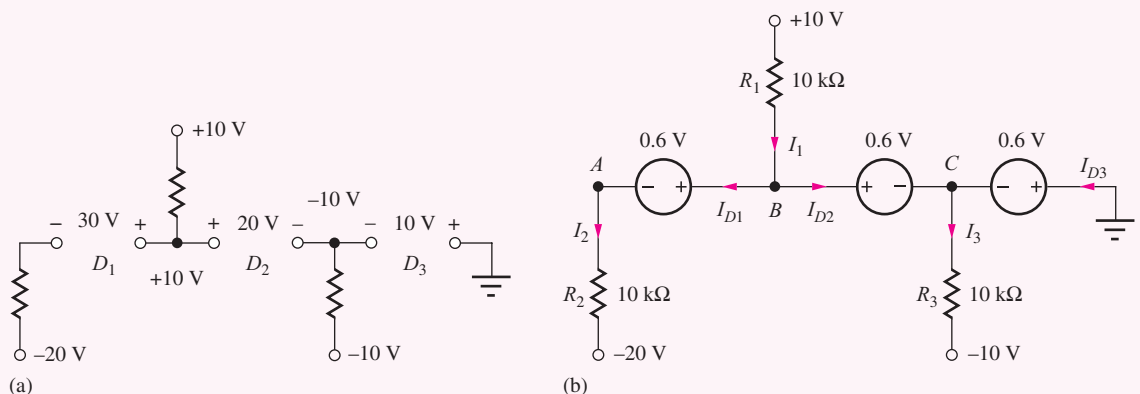


**Figure 3.34** (a) Three diode circuit model with all diodes off. (b) Circuit model for circuit of Fig. 3.33 with all diodes on.

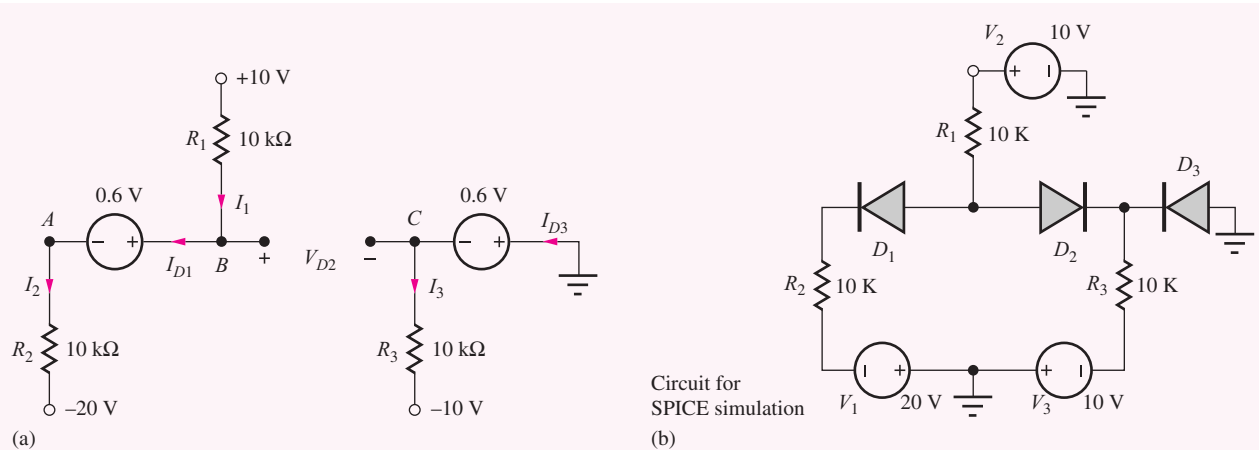


**Figure 3.35** (a) Circuit with diodes  $D_1$  and  $D_3$  on and  $D_2$  off.

Also

$$I_{D3} = I_3 = \frac{-0.6 - (-10)}{10} \frac{\text{V}}{\text{k}\Omega} = 0.940 \text{ mA} > 0 \checkmark$$

The voltage across diode  $D_2$  is given by

$$V_{D2} = 10 - 10,000I_1 - (-0.6) = 10 - 14.7 + 0.6 = -4.10 \text{ V} < 0 \checkmark$$

**Check of Results:**  $I_{D1}$ ,  $I_{D3}$ , and  $V_{D2}$  are now all consistent with the circuit assumptions, so the Q-points for the circuit are

$$D_1: (1.47 \text{ mA}, 0.6 \text{ V}) \quad D_2: (0 \text{ mA}, -4.10 \text{ V}) \quad D_3: (0.940 \text{ mA}, 0.6 \text{ V})$$

**Discussion:** The Q-point values that we would have obtained using the ideal diode model are (see Prob. 3.79):

$$D_1: (1.50 \text{ mA}, 0 \text{ V}) \quad D_2: (0 \text{ mA}, -5.00 \text{ V}) \quad D_3: (1.00 \text{ mA}, 0 \text{ V})$$

The values of  $I_{D1}$  and  $I_{D3}$  differ by less than 6 percent. However, the reverse-bias voltage on  $D_2$  differs by 20 percent. This shows the difference that the choice of models can make. The results from the circuit using the CVD model should be a more accurate estimate of how the circuit will actually perform than would result from the ideal diode case. Remember, however, that these calculations are both just approximations based on our models for the actual behavior of the real diode circuit.

**Computer-Aided Analysis:** SPICE analysis yields the following Q-points for the circuit in Fig. 3.35(b): (1.47 mA, 0.665 V), (-4.02 pA, -4.01 V), (0.935 mA, 0.653 V). Device parameter and Q-point information are found directly using the SHOW and SHOWMOD commands in SPICE. Or, voltmeters and ammeters (zero-valued current and voltage sources) can be inserted in the circuit in some implementations of SPICE. Note that the -4 pA current in  $D_2$  is much larger than the reverse saturation current of the diode (IS defaults to 10 fA), and results from a more complete SPICE model in the author's version of SPICE.

**EXERCISE:** Find the Q-points for the three diodes in Fig. 3.33 if  $R_1$  is changed to  $2.5 \text{ k}\Omega$ .

**ANSWERS:** (2.13 mA, 0.6 V); (1.13 mA, 0.6 V); (0 mA, -1.27 V)



**EXERCISE:** Use SPICE to calculate the Q-points of the diodes in the previous exercise. Use  $I_S = 1 \text{ fA}$ .

**ANSWERS:** (2.12 mA, 0.734 V); (1.12 mA, 0.718 V); (0 mA, -1.19 V)

## 3.12 ANALYSIS OF DIODES OPERATING IN THE BREAKDOWN REGION

Reverse breakdown is actually a highly useful region of operation for the diode. The reverse breakdown voltage is nearly independent of current and can be used as either a voltage regulator or voltage reference. Thus, it is important to understand the analysis of diodes operating in reverse breakdown.

Figure 3.36 is a single-loop circuit containing a 20-V source supplying current to a Zener diode with a reverse breakdown voltage of 5 V. The voltage source has a polarity that will tend to reverse-bias the diode. Because the source voltage exceeds the Zener voltage rating of the diode,  $V_Z = 5 \text{ V}$ , we should expect the diode to be operating in its breakdown region.

### 3.12.1 LOAD-LINE ANALYSIS

The  $i$ - $v$  characteristic for this Zener diode is given in Fig. 3.37, and load-line analysis can be used to find the Q-point for the diode, independent of the region of operation. The normal polarities for  $I_D$  and  $V_D$  are indicated in Fig. 3.36, and the loop equation is

$$-20 = V_D + 5000I_D \quad (3.36)$$

In order to draw the load line, we choose two points on the graph:

$$V_D = 0, I_D = -4 \text{ mA} \quad \text{and} \quad V_D = -5 \text{ V}, I_D = -3 \text{ mA}$$

In this case the load line intersects the diode characteristic at a Q-point in the breakdown region: (-2.9 mA, -5.2 V).

### 3.12.2 ANALYSIS WITH THE PIECEWISE LINEAR MODEL

The assumption of reverse breakdown requires that the diode current  $I_D$  be less than zero or that the Zener current  $I_Z = -I_D > 0$ . We will analyze the circuit with the piecewise linear model and test this condition to see if it is consistent with the reverse-breakdown assumption.

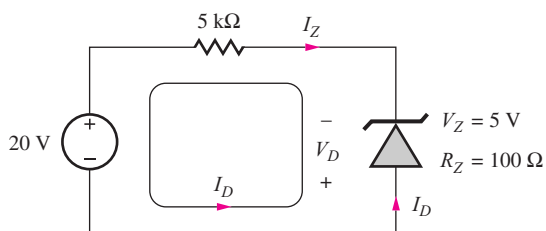


**Figure 3.36** Circuit containing a Zener diode with  $V_Z = 5 \text{ V}$  and  $R_Z = 100 \Omega$ .

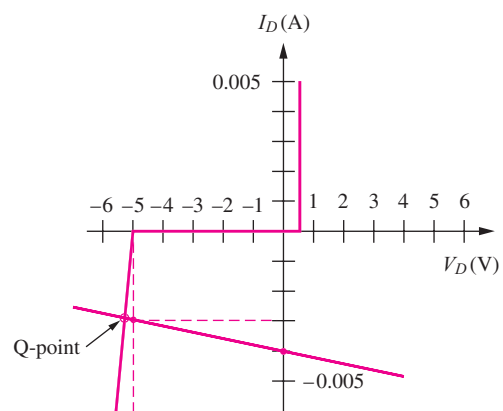


**Figure 3.37** Load line for Zener diode.

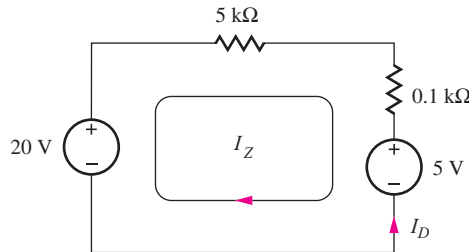


**Figure 3.38** Circuit with piecewise linear model for Zener diode. Note that the diode model is valid only in the breakdown region of the characteristic.

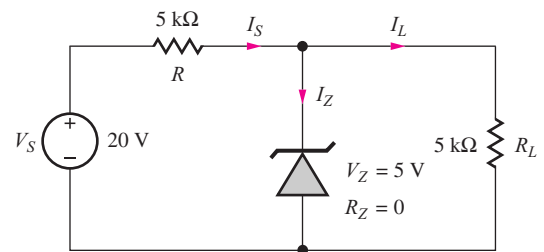


**Figure 3.39** Zener diode voltage regulator circuit.

In Fig. 3.38, the Zener diode has been replaced with its piecewise linear model from Fig. 3.16 in Sec. 3.6, with  $V_Z = 5 \text{ V}$  and  $R_Z = 100 \Omega$ . Writing the loop equation this time in terms of  $I_Z$ :

$$20 - 5100I_Z - 5 = 0 \quad \text{or} \quad I_Z = \frac{(20 - 5) \text{ V}}{5100 \Omega} = 2.94 \text{ mA} \quad (3.37)$$

Because  $I_Z$  is greater than zero ( $I_D < 0$ ), the solution is consistent with our assumption of Zener breakdown operation.

It is worth noting that diodes have three possible states when the breakdown region is included, further increasing analysis complexity.

### 3.12.3 VOLTAGE REGULATION

A useful application of the Zener diode is as a **voltage regulator**, as shown in the circuit of Fig. 3.39. The function of the Zener diode is to maintain a constant voltage across load resistor  $R_L$ . As long as the diode is operating in reverse breakdown, a voltage of approximately  $V_Z$  will appear across  $R_L$ . To ensure that the diode is operating in the Zener breakdown region, we must have  $I_Z > 0$ .

The circuit of Fig. 3.39 has been redrawn in Fig. 3.40 with the model for the Zener diode, with  $R_Z = 0$ . Using nodal analysis, the Zener current is expressed by  $I_Z = I_S - I_L$ . The currents  $I_S$  and  $I_L$  are equal to

$$I_S = \frac{V_S - V_Z}{R} = \frac{(20 - 5) \text{ V}}{5 \text{ k}\Omega} = 3 \text{ mA} \quad \text{and} \quad I_L = \frac{V_Z}{R_L} = \frac{5 \text{ V}}{5 \text{ k}\Omega} = 1 \text{ mA} \quad (3.38)$$

resulting in a Zener current  $I_Z = 2 \text{ mA}$ .  $I_Z > 0$ , which is again consistent with our assumptions. If the calculated value of  $I_Z$  were less than zero, then the Zener diode no longer controls the voltage across  $R_L$ , and the voltage regulator is said to have “dropped out of regulation.”

For proper regulation to take place, the Zener current must be positive,

$$I_Z = I_S - I_L = \frac{V_S}{R} - V_Z \left( \frac{1}{R} + \frac{1}{R_L} \right) > 0 \quad (3.39)$$

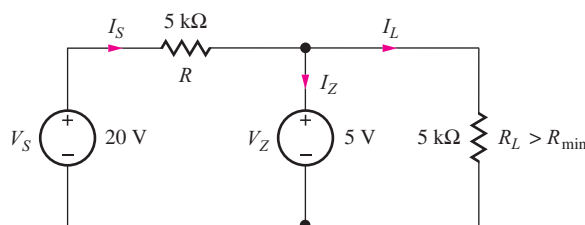


**Figure 3.40** Circuit with a constant voltage model for the Zener diode.

Solving for  $R_L$  yields a lower bound on the value of load resistance for which the Zener diode will continue to act as a voltage regulator.

$$R_L > \frac{R}{\left(\frac{V_S}{V_Z} - 1\right)} = R_{\min} \quad (3.40)$$

**EXERCISE:** What is the value of  $R_{\min}$  for the Zener voltage regulator circuit in Figs. 3.39 and 3.40? What is the output voltage for  $R_L = 1 \text{ k}\Omega$ ? For  $R_L = 2 \text{ k}\Omega$ ?

**ANSWERS:**  $1.67 \text{ k}\Omega$ ;  $3.33 \text{ V}$ ;  $5.00 \text{ V}$

### 3.12.4 ANALYSIS INCLUDING ZENER RESISTANCE

The voltage regulator circuit in Fig. 3.39 has been redrawn in Fig. 3.41 and now includes a nonzero Zener resistance  $R_Z$ . The output voltage is now a function of the current  $I_Z$  through the Zener diode. For small values of  $R_Z$ , however, the change in output voltage will be small.

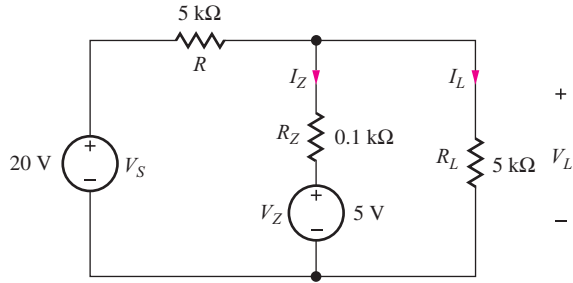


Figure 3.41 Zener diode regulator circuit, including Zener resistance.

### EXAMPLE 3.9 DC ANALYSIS OF A ZENER DIODE REGULATOR CIRCUIT

Find the operating point for a Zener-diode-based voltage regulator circuit.

**PROBLEM** Find the output voltage and Zener diode current for the Zener diode regulator in Figs. 3.39 to 3.41 if  $R_Z = 100 \Omega$  and  $V_Z = 5 \text{ V}$ .

**SOLUTION** **Known Information and Given Data:** Zener diode regulator circuit as modeled in Fig. 3.41 with  $V_S = 20 \text{ V}$ ,  $R = 5 \text{ k}\Omega$ ,  $R_Z = 0.1 \text{ k}\Omega$ , and  $V_Z = 5 \text{ V}$

**Unknowns:**  $V_L$ ,  $I_Z$

**Approach:** The circuit contains a single unknown node voltage  $V_L$ , and a nodal equation can be written to find the voltage. Once  $V_L$  is found,  $I_Z$  can be determined using Ohm's law.

**Assumptions:** Use the piecewise linear model for the diode as drawn in Fig. 3.41.

**Analysis:** Writing the nodal equation for  $V_L$  yields

$$\frac{V_L - 20 \text{ V}}{5000 \Omega} + \frac{V_L - 5 \text{ V}}{100 \Omega} + \frac{V_L}{5000 \Omega} = 0$$

Multiplying the equation by 5000  $\Omega$  and collecting terms gives

$$52V_L = 270 \text{ V} \quad \text{and} \quad V_L = 5.19 \text{ V}$$

The Zener diode current is equal to

$$I_Z = \frac{V_L - 5 \text{ V}}{100 \Omega} = \frac{5.19 \text{ V} - 5 \text{ V}}{100 \Omega} = 1.90 \text{ mA} > 0$$

**Check of Results:**  $I_Z > 0$  confirms operation in reverse breakdown. We see that the output voltage of the regulator is slightly higher than for the case with  $R_Z = 0$ , and the Zener diode current is reduced slightly. Both changes are consistent with the addition of  $R_Z$  to the circuit.

**Computer-Aided Analysis:** We can use SPICE to simulate the Zener circuit if we specify the breakdown voltage using SPICE parameters BV, IBV, and RS. BV sets the breakdown voltage, and IBV represents the current at breakdown. Setting BV = 5 V, and RS = 100  $\Omega$  and letting IBV default to 1 mA yields  $V_L = 5.21 \text{ V}$  and  $I_Z = 1.92 \text{ mA}$ , which agree well with our hand calculations. A transfer function analysis from  $V_S$  to  $V_L$  gives a sensitivity of 21 mV/V and an output resistance of 108  $\Omega$ . The meaning of these numbers is discussed in the next section.

**EXERCISE:** Find  $V_L$ ,  $I_Z$ , and the Zener power dissipation in Fig. 3.41 if  $R = 1 \text{ k}\Omega$ .

**ANSWERS:** 6.25 V; 12.5 mA; 78.1 mW

### 3.12.5 LINE AND LOAD REGULATION

Two important parameters characterizing a voltage regulator circuit are **line regulation** and **load regulation**. Line regulation characterizes how sensitive the output voltage is to input voltage changes and is expressed as mV/V or as a percentage. Load regulation characterizes how sensitive the output voltage is to changes in the load current withdrawn from the regulator and has the units of Ohms.

$$\text{Line regulation} = \frac{dV_L}{dV_S} \quad \text{and} \quad \text{Load regulation} = \frac{dV_L}{dI_L} \quad (3.41)$$

We can find expressions for these quantities from a straight forward analysis of the circuit in Fig. 3.41 similar to that in Ex. 3.9:

$$\frac{V_L - V_S}{R} + \frac{V_L - V_Z}{R_Z} + I_L = 0 \quad (3.42)$$

For a fixed load current, we find the line regulation is

$$\text{Line regulation} = \frac{R_Z}{R + R_Z} \quad (3.43)$$

and for changes in  $I_L$ ,

$$\text{Load regulation} = -(R_Z \parallel R) \quad (3.44)$$

The load regulation should be recognized as the Thévenin equivalent resistance looking back into the regulator from the load terminals.

**EXERCISE:** What are the values of the load and line regulation for the circuit in Fig. 3.41?

**ANSWERS:** 19.6 mV/V; 98.0  $\Omega$ . Note that these agree with the SPICE results in Ex. 3.9.

### 3.13 HALF-WAVE RECTIFIER CIRCUITS

Rectifiers represent an application of diodes that we encounter frequently every day, but they may not be recognized as such. The basic **rectifier circuit** converts an ac voltage to a pulsating dc voltage. A filter is then added to eliminate the ac components of the waveform and produce a nearly constant dc voltage output. Virtually every electronic device that is plugged into the wall utilizes a rectifier circuit to convert the 120-V, 60-Hz ac power line source to the various dc voltages required to operate electronic devices such as personal computers, audio systems, radio receivers, televisions, and the like. All of our battery chargers and “wall-warts” contain rectifiers. As a matter of fact, the vast majority of electronic circuits are powered by a dc source, usually based on some form of rectifier.

This section explores half-wave rectifier circuits with capacitor filters that form the basis for many dc power supplies. Up to this point, we have looked at only steady-state dc circuits in which the diode remained in one of its three possible states (on, off, or reverse breakdown). Now, however, the diode state will be changing with time, and a given piecewise linear model for the circuit will be valid for only a certain time interval.

#### 3.13.1 HALF-WAVE RECTIFIER WITH RESISTOR LOAD

A single diode is used to form the **half-wave rectifier circuit** in Fig. 3.42. A sinusoidal voltage source  $v_I = V_p \sin \omega t$  is connected to the series combination of diode  $D_1$  and load resistor  $R$ . During the first half of the cycle, for which  $v_I > 0$ , the source forces a current through diode  $D_1$  in the forward direction, and  $D_1$  will be on. During the second half of the cycle,  $v_I < 0$ . Because a negative current cannot exist in the diode (unless it is in breakdown), it turns off. These two states are modeled in Fig. 3.43 using the ideal diode model.

When the diode is on, voltage source  $v_S$  is connected directly to the output and  $v_O = v_I$ . When the diode is off, the current in the resistor is zero, and the output voltage is zero. The input and output voltage waveforms are shown in Fig. 3.44(b), and the resulting current is called pulsating

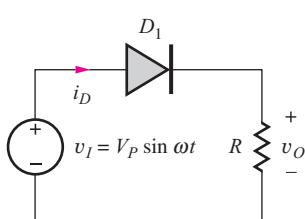


**Figure 3.42** Half-wave rectifier circuit.

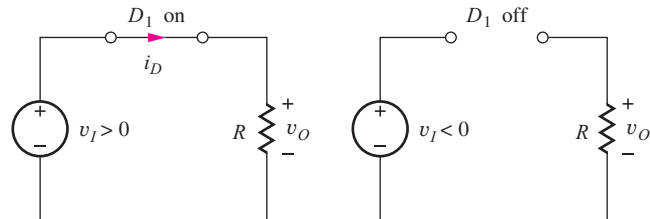


**Figure 3.43** Ideal diode models for the two half-wave rectifier states.

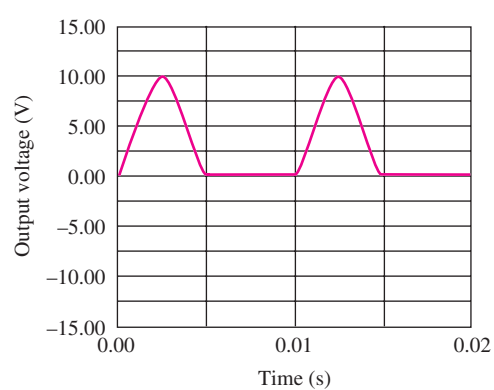
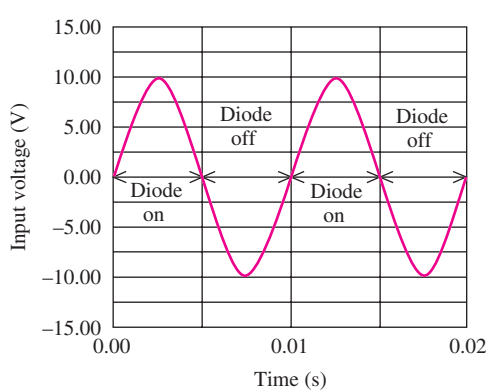


**Figure 3.44** Sinusoidal input voltage  $v_S$  and pulsating dc output voltage  $v_O$  for the half-wave rectifier circuit.

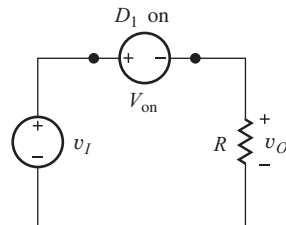


**Figure 3.45** CVD model for the rectifier on state.

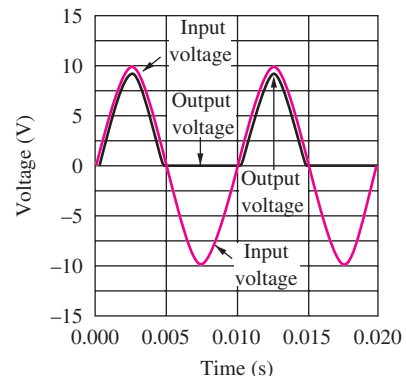


**Figure 3.46** Half-wave rectifier output voltage with  $V_P = 10$  V and  $V_{on} = 0.7$  V.

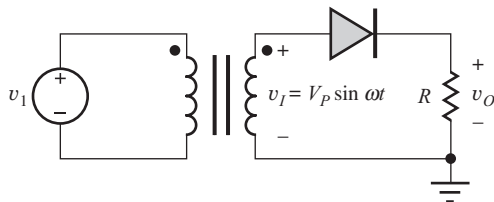


**Figure 3.47** Transformer-driven half-wave rectifier.

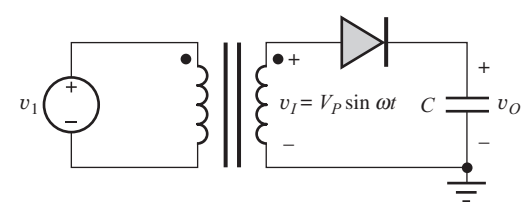


**Figure 3.48** Rectifier with capacitor load (peak detector).

direct current. In this circuit, the diode is conducting 50 percent of the time and is off 50 percent of the time.

In some cases, the forward voltage drop across the diode can be important. Figure 3.45 shows the circuit model for the on-state using the CVD model. For this case, the output voltage is one diode-drop smaller than the input voltage during the conduction interval:

$$v_O = (V_P \sin \omega t) - V_{on} \quad (3.45)$$

The output voltage remains zero during the off-state interval. The input and output waveforms for the half-wave rectifier, including the effect of  $V_{on}$ , are shown in Fig. 3.46 for  $V_P = 10$  V and  $V_{on} = 0.7$  V.

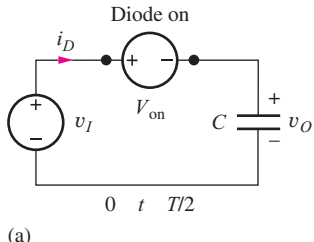
In many applications, a transformer is used to convert from the 120-V ac, 60-Hz voltage available from the power line to the desired ac voltage level, as in Fig. 3.47. The transformer can step the voltage up or down depending on the application; it also enhances safety by providing isolation from the power line. From circuit theory we know that the output of an ideal transformer can be represented by an ideal voltage source, and we use this knowledge to simplify the representation of subsequent rectifier circuit diagrams.

The unfiltered output of the half-wave rectifier in Fig. 3.42 or 3.47 is not suitable for operation of most electronic circuits because constant power supply voltages are required to establish proper bias for the electronic devices. A **filter capacitor** (or more complex circuit) can be added to filter the output of the circuit in Figs. 3.47 to remove the time-varying components from the waveform.

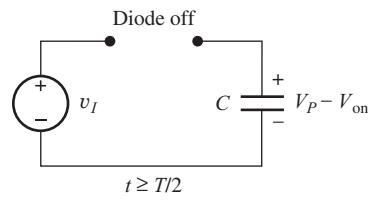
### 3.13.2 RECTIFIER FILTER CAPACITOR

To understand operation of the rectifier filter, we first consider operation of the **peak-detector** circuit in Fig. 3.48. This circuit is similar to that in Fig. 3.47 except that the resistor is replaced with a capacitor  $C$  that is initially discharged [ $v_O(0) = 0$ ].

Models for the circuit with the diode in the on and off states are in Fig. 3.49, and the input and output voltage waveforms associated with this circuit are in Fig. 3.50. As the input voltage starts to



(a)



(b)

**Figure 3.49** Peak-detector circuit models (constant voltage drop model). (a) The diode is on for  $0 \leq t \leq T/2$ . (b) The diode is off for  $t > T/2$ .

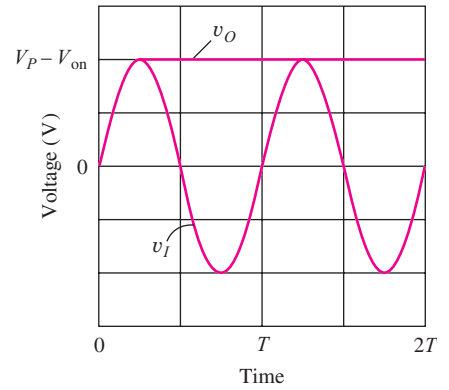


**Figure 3.50** Input and output waveforms for the peak-detector circuit.

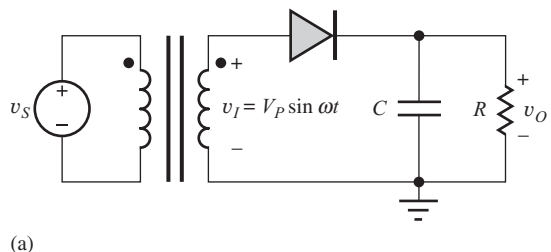
rise, the diode turns on and connects the capacitor to the source. The capacitor voltage equals the input voltage minus the voltage drop across the diode.

At the peak of the input voltage waveform, the current through the diode tries to reverse direction because  $i_D = C[d(v_I - V_{on})/dt] < 0$ , the diode cuts off, and the capacitor is disconnected from the rest of the circuit. There is no circuit path to discharge the capacitor, so the voltage on the capacitor remains constant. Because the amplitude of the input voltage source  $v_S$  can never exceed  $V_P$ , the capacitor remains disconnected from  $v_S$  for  $t > T/2$ . Thus, the capacitor in the circuit in Fig. 3.48 charges up to a voltage one diode-drop below the peak of the input waveform and then remains constant, thereby producing a dc output voltage

$$V_{dc} = V_P - V_{on} \quad (3.46)$$

### 3.13.3 HALF-WAVE RECTIFIER WITH RC LOAD

To make use of this output voltage, a load must be connected to the circuit as represented by the resistor  $R$  in Fig. 3.51. Now there is a path available to discharge the capacitor during the time the diode is not conducting. Models for the conducting and nonconducting time intervals are shown in

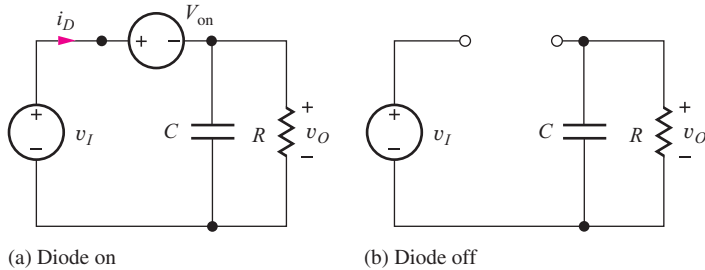


(a)



(b)

**Figure 3.51** (a) Half-wave rectifier circuit with filter capacitor. (b) A-175,000- $\mu$ F, 15-V filter capacitor. Capacitance tolerance is  $-10\%$ ,  $+75\%$ .



(a) Diode on

(b) Diode off

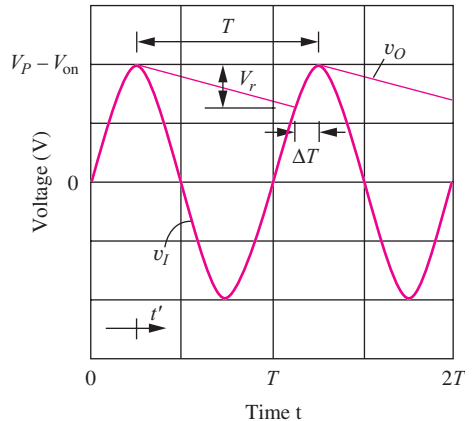
**Figure 3.52** Half-wave rectifier circuit models.**Figure 3.53** Input and output voltage waveforms for the half-wave rectifier circuit.

Fig. 3.52; the waveforms for the circuit are shown in Fig. 3.53. The capacitor is again assumed to be initially discharged. During the first quarter cycle, the diode conducts, and the capacitor is rapidly charged toward the peak value of the input voltage source. The diode cuts off at the peak of  $v_I$ , and the capacitor voltage then discharges exponentially through the resistor  $R$ , as governed by the circuit in Fig. 3.52(b). The discharge continues until the voltage  $v_I - v_{\text{on}}$  exceeds the output voltage  $v_O$ , which occurs near the peak of the next cycle. The process is then repeated once every cycle.

### 3.13.4 RIPPLE VOLTAGE AND CONDUCTION INTERVAL

The output voltage is no longer constant as in the ideal peak-detector circuit but has a **ripple voltage**  $V_r$ . In addition, the diode only conducts for a short time  $\Delta T$  during each cycle. This time  $\Delta T$  is called the **conduction interval**, and its angular equivalent is the **conduction angle**  $\theta_c$  where  $\theta_c = \omega \Delta T$ . The variables  $\Delta T$ ,  $\theta_c$ , and  $V_r$  are important values related to dc power supply design, and we will now develop expressions for these parameters.

During the discharge period, the voltage across the capacitor is described by

$$v_o(t') = (V_p - V_{\text{on}}) \exp\left(-\frac{t'}{RC}\right) \quad \text{for } t' = \left(t - \frac{T}{4}\right) \geq 0 \quad (3.47)$$

We have referenced the  $t'$  time axis to  $t = T/4$  to simplify the equation. The ripple voltage  $V_r$  is given by

$$V_r = (V_p - V_{\text{on}}) - v_o(t') = (V_p - V_{\text{on}}) \left[ 1 - \exp\left(-\frac{T - \Delta T}{RC}\right) \right] \quad (3.48)$$

A small value of  $V_r$  is desired in most power supply designs; a small value requires  $RC$  to be much greater than  $T - \Delta T$ . Using  $\exp(-x) \approx 1 - x$  for small  $x$  results in an approximate expression for the ripple voltage:

$$V_r \approx (V_p - V_{\text{on}}) \frac{T}{RC} \left(1 - \frac{\Delta T}{T}\right) \quad (3.49)$$

A small ripple voltage also means  $\Delta T \ll T$ , and the final simplified expression for the ripple voltage becomes

$$V_r \approx \frac{(V_p - V_{\text{on}})}{R} \frac{T}{C} \quad (3.50)$$

The approximation of the exponential used in Eqs. (3.49) and (3.50) is equivalent to assuming that the capacitor is being discharged by a constant current so that the discharge waveform is a straight line. The ripple voltage  $V_r$  can be considered to be determined by an equivalent dc current equal to

$$I_{dc} = \frac{V_p - V_{on}}{R} \quad (3.51)$$

discharging the capacitor  $C$  for a time period  $T$  (that is,  $\Delta V = (I_{dc}/C) T$ ).

Approximate expressions can also be obtained for conduction angle  $\theta_C$  and conduction interval  $\Delta T$ . At time  $t = \frac{5}{4}T - \Delta T$ , the input voltage just exceeds the output voltage, and the diode has is conducting. Therefore,  $\theta = \omega t = 5\pi/2 - \theta_C$  and

$$V_p \sin\left(\frac{5}{2}\pi - \theta_C\right) - V_{on} = (V_p - V_{on}) - V_r \quad (3.52)$$

Remembering that  $\sin(5\pi/2 - \theta_C) = \cos \theta_C$ , we can simplify the above expression to

$$\cos \theta_C = 1 - \frac{V_r}{V_p} \quad (3.53)$$

For small values of  $\theta_C$ ,  $\cos \theta_C \cong 1 - \theta_C^2/2$ . Solving for the conduction angle and conduction interval gives

$$\theta_C = \sqrt{\frac{2V_r}{V_p}} \quad \text{and} \quad \Delta T = \frac{\theta_C}{\omega} = \frac{1}{\omega} \sqrt{\frac{2V_r}{V_p}} \quad (3.54)$$

### EXAMPLE 3.10 HALF-WAVE RECTIFIER ANALYSIS

Here we see an illustration of numerical results for a half-wave rectifier with a capacitive filter.

**PROBLEM** Find the value of the dc output voltage, dc output current, ripple voltage, conduction interval, and conduction angle for a half-wave rectifier driven from a transformer having a secondary voltage of 12.6 V<sub>rms</sub> (60 Hz) with  $R = 15 \Omega$  and  $C = 25,000 \mu\text{F}$ . Assume the diode on-voltage  $V_{on} = 1 \text{ V}$ .

**SOLUTION** **Known Information and Given Data:** Half-wave rectifier circuit with  $RC$  load as depicted in Fig. 3.51; Transformer secondary voltage is 12.6 V<sub>rms</sub>, operating frequency is 60 Hz,  $R = 15 \Omega$ , and  $C = 25,000 \mu\text{F}$ .

**Unknowns:** dc output voltage  $V_{dc}$ , output current  $I_{dc}$ , ripple voltage  $V_r$ , conduction interval  $\Delta T$ , conduction angle  $\theta_C$

**Approach:** Given data can be used directly to evaluate Eqs. (3.46), (3.50), (3.51), and (3.54).

**Assumptions:** Diode on-voltage is 1 V. Remember that the derived results assume the ripple voltage is much less than the dc output voltage ( $V_r \ll V_{dc}$ ) and the conduction interval is much less than the period of the ac signal ( $\Delta T \ll T$ ).

**Analysis:** The ideal dc output voltage in the absence of ripple is given by Eq. (3.46):

$$V_{dc} = V_p - V_{on} = (12.6\sqrt{2} - 1) \text{ V} = 16.8 \text{ V}$$

The nominal dc current delivered by the supply is

$$I_{dc} = \frac{V_p - V_{on}}{R} = \frac{16.8 \text{ V}}{15 \Omega} = 1.12 \text{ A}$$

The ripple voltage is calculated using Eq. (3.50) with the discharge interval  $T = 1/60 \text{ s}$ :

$$V_r \cong \frac{(V_p - V_{on})}{R} \frac{T}{C} = \frac{16.8 \text{ V}}{15 \Omega} \frac{\frac{1}{60} \text{ s}}{2.5 \times 10^{-2} \text{ F}} = 0.747 \text{ V}$$

The conduction angle is calculated using Eq. (3.54)

$$\theta_c = \omega \Delta T = \sqrt{\frac{2V_r}{V_p}} = \sqrt{\frac{2 \cdot 0.75}{17.8}} = 0.290 \text{ rad or } 16.6^\circ$$

and the conduction interval is

$$\Delta T = \frac{\theta_c}{\omega} = \frac{\theta_c}{2\pi f} = \frac{0.29}{120\pi} = 0.769 \text{ mS}$$

**Check of Results:** The ripple voltage represents 4.4 percent of the dc output voltage. Thus the assumption that the voltage is approximately constant is justified. The conduction time is 0.769 mS out of a total period  $T = 16.7 \text{ ms}$ , and the assumption that  $\Delta T \ll T$  is also satisfied.

**Discussion:** From this example, we see that even a 1-A power supply requires a significant filter capacitance  $C$  to maintain a low ripple percentage. In this case,  $C = 0.025 \text{ F} = 25,000 \mu\text{F}$ .

**EXERCISE:** Find the value of the dc output voltage, dc output current, ripple voltage, conduction interval, and conduction angle for a half-wave rectifier that is being supplied from a transformer having a secondary voltage of  $6.3 \text{ V}_{\text{rms}}$  (60 Hz) with  $R = 0.5 \Omega$  and  $C = 500,000 \mu\text{F}$ . Assume the diode on voltage  $V_{on} = 1 \text{ V}$ .

**ANSWERS:** 7.91 V; 15.8 A; 0.527; 0.912 ms;  $19.7^\circ$

**EXERCISE:** What are the values of the dc output voltage and dc output current for a half-wave rectifier that is being supplied from a transformer having a secondary voltage of  $10 \text{ V}_{\text{rms}}$  (60 Hz) and a  $2-\Omega$  load resistor? Assume the diode on voltage  $V_{on} = 1 \text{ V}$ . What value of filter capacitance is required to have a ripple voltage of no more than  $0.1 \text{ V}$ ? What is the conduction angle?

**ANSWERS:** 13.1 V; 6.57 A; 1.10 F;  $6.82^\circ$

### 3.13.5 DIODE CURRENT

In rectifier circuits, a nonzero current is present in the diode for only a very small fraction of the period  $T$ , yet an almost constant dc current is flowing out of the filter capacitor to the load. The total charge lost from the capacitor during each cycle must be replenished by the current through the diode during the short conduction interval  $\Delta T$ , which leads to high peak diode currents. Figure 3.54 shows

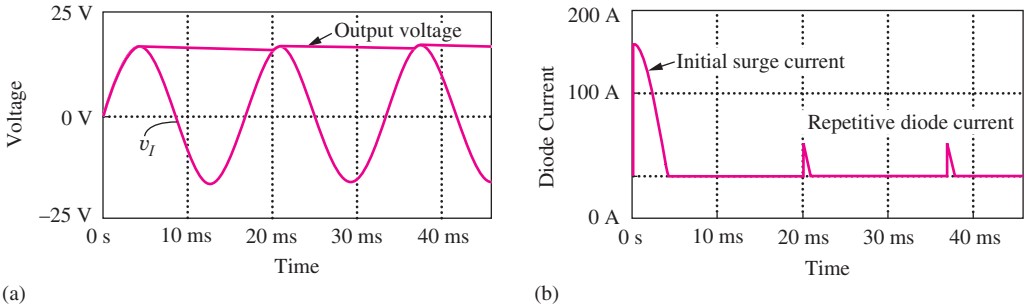


**Figure 3.54** SPICE simulation of the half-wave rectifier circuit. (a) Voltage waveforms (b) Diode current.

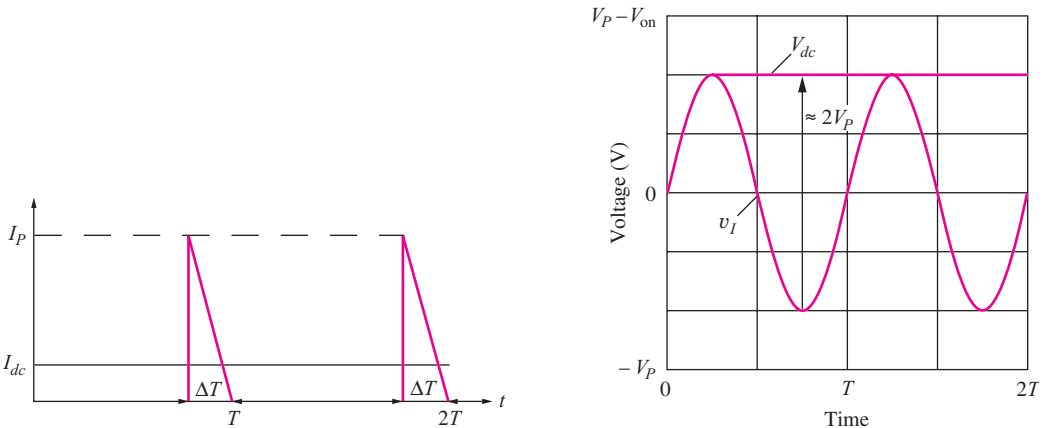


**Figure 3.55** Triangular approximation to diode current pulse.

**Figure 3.56** Peak reverse voltage across the diode in a half-wave rectifier.

the results of SPICE simulation of the diode current. The repetitive current pulse can be modeled approximately by a triangle of height  $I_P$  and width  $\Delta T$ , as in Fig. 3.55.

Equating the charge supplied through the diode during the conduction interval to the charge lost from the filter capacitor during the complete period yields

$$Q = I_P \frac{\Delta T}{2} = I_{dc} T \quad \text{or} \quad I_P = I_{dc} \frac{2T}{\Delta T} \quad (3.55)$$

Here we remember that the integral of current over time represents charge  $Q$ . Therefore the charge supplied by the triangular current pulse in Fig. 3.55 is given by the area of the triangle,  $I_P \Delta T / 2$ .

For Ex. 3.10, the peak diode current would be

$$I_P = 1.12 \frac{2 \cdot 16.7}{0.769} = 48.6 \text{ A} \quad (3.56)$$

which agrees well with the simulation results in Fig. 3.55. The diode must be built to handle these high peak currents, which occur over and over. This high peak current is also the reason for the relatively large choice of  $V_{on}$  used in Ex. 3.10 (See Prob. 3.88).

**EXERCISE:** (a) What is the forward voltage of a diode operating at a current of 48.6 A at 300 K if  $I_S = 10^{-15}$  A? (b) At 50 C?

**ANSWERS:** 0.994 V; 1.07 V

### 3.13.6 SURGE CURRENT

When the power supply is first turned on, the capacitor is completely discharged, and there will be an even larger current through the diode, as is visible in Fig. 3.54. During the first quarter cycle, the current through the diode is given approximately by

$$i_d(t) = i_c(t) \cong C \left[ \frac{d}{dt} V_P \sin \omega t \right] = \omega C V_P \cos \omega t \quad (3.57)$$

The peak value of this initial **surge current** occurs at  $t = 0^+$  and is given by

$$I_{SC} = \omega C V_P = 2\pi(60 \text{ Hz})(0.025 \text{ F})(17.8 \text{ V}) = 168 \text{ A}$$

Using the numbers from Ex. 3.7 yields an initial surge current of almost 170 A! This value, again, agrees well with the simulation results in Fig. 3.54. If the input signal  $v_I$  does not happen to be crossing through zero when the power supply is turned on, the situation can be even worse, and rectifier diodes selected for power supply applications must be capable of withstanding very large surge currents as well as the large repetitive current pulses required each cycle.

In most practical circuits, the surge current will be large but cannot actually reach the values predicted by Eq. (3.57) because of series resistances in the circuit that we have neglected. The rectifier diode itself will have an internal series resistance (review the SPICE model in Sec. 3.9 for example), and the transformer will have resistances associated with both the primary and secondary windings. A total series resistance in the secondary of only a few tenths of an ohm will significantly reduce both the surge current and peak repetitive current in the circuit. In addition, the large time constant associated with the series resistance and filter capacitance causes the rectifier output to take many cycles to reach its steady state voltage. (See SPICE simulation problems at the end of this chapter.)

### 3.13.7 PEAK-INVERSE-VOLTAGE (PIV) RATING

We must also be concerned about the breakdown voltage rating of the diodes used in rectifier circuits. This breakdown voltage is called the **peak-inverse-voltage (PIV)** rating of the rectifier diode. The worst-case situation for the half-wave rectifier is depicted in Fig. 3.56 in which it is assumed that the ripple voltage  $V_r$  is very small. When the diode is off, as in Fig. 3.52(b), the reverse bias across the diode is equal to  $V_{dc} - v_I$ . The worst case occurs when  $v_I$  reaches its negative peak of  $-V_P$ . The diode must therefore be able to withstand a reverse bias of at least

$$\text{PIV} \geq V_{dc} - v_I^{\min} = V_P - V_{on} - (-V_P) = 2V_P - V_{on} \cong 2V_P \quad (3.58)$$

From Eq. (3.58), we see that diodes used in the half-wave rectifier circuit must have a PIV rating equal to twice the peak voltage supplied by the source  $v_I$ . The PIV value corresponds to the minimum value of Zener breakdown voltage for the rectifier diode. A safety margin of at least 25 to 50 percent is usually specified for the diode PIV rating in power supply designs.

### 3.13.8 DIODE POWER DISSIPATION

In high-current power supply applications, the power dissipation in the rectifier diodes can become significant. The average power dissipation in the diode is defined by

$$P_D = \frac{1}{T} \int_0^T v_D(t)i_D(t) dt \quad (3.59)$$

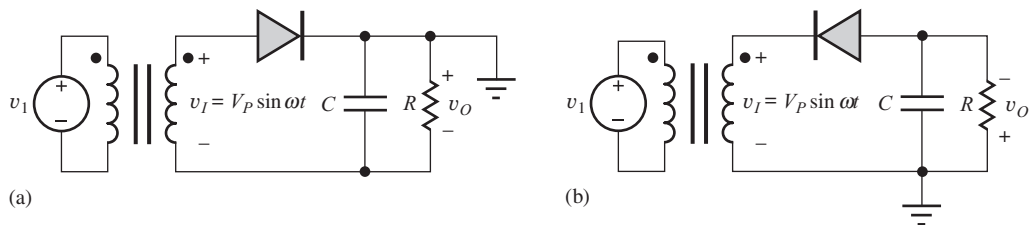


**Figure 3.57** Half-wave rectifier circuits that develop negative output voltages.

This expression can be simplified by assuming that the voltage across the diode is approximately constant at  $v_D(t) = V_{on}$  and by using the triangular approximation to the diode current  $i_D(t)$  shown in Fig. 3.55. Eq. (3.59) becomes

$$P_D = \frac{1}{T} \int_0^T V_{\text{on}} i_D(t) dt = \frac{V_{\text{on}}}{T} \int_{T-\Delta T}^T i_D(t) dt = V_{\text{on}} \frac{I_P}{2} \frac{\Delta T}{T} = V_{\text{on}} I_{\text{dc}} \quad (3.60)$$

Using Eq. (3.55) we see that the power dissipation is equivalent to the constant dc output current multiplied by the on-voltage of the diode. For the half-wave rectifier example,  $P_D = (1 \text{ V})(1.1 \text{ A}) = 1.1 \text{ W}$ . This rectifier diode would probably need a heat sink to maintain its temperature at a reasonable level.

Another source of power dissipation is caused by resistive loss within the diode. Diodes have a small internal series resistance  $R_S$ , and the average power dissipation in this resistance can be calculated using

$$P_D = \frac{1}{T} \int_0^T i_D^2(t) R_S dt \quad (3.61)$$

Evaluation of this integral (left for Prob. 3.93) for the triangular current wave form in Fig. 3.55 yields

$$P_D = \frac{1}{3} I_P^2 R_S \frac{\Delta T}{T} = \frac{4}{3} \frac{T}{\Delta T} I_{dc}^2 R_S \quad (3.62)$$

Using the number from the rectifier example with  $R_S = 0.20 \Omega$  yields  $P_D = 7.3 \text{ W}$ ! This is significantly greater than the component of power dissipation caused by the diode on-voltage calculated using Eq. (3.60). The component of power dissipation described by Eq. (3.62) can be reduced by minimizing the peak current  $I_P$  through the use of the minimum required size of filter capacitor or by using the full-wave rectifier circuits, which are discussed in Sec. 3.14.

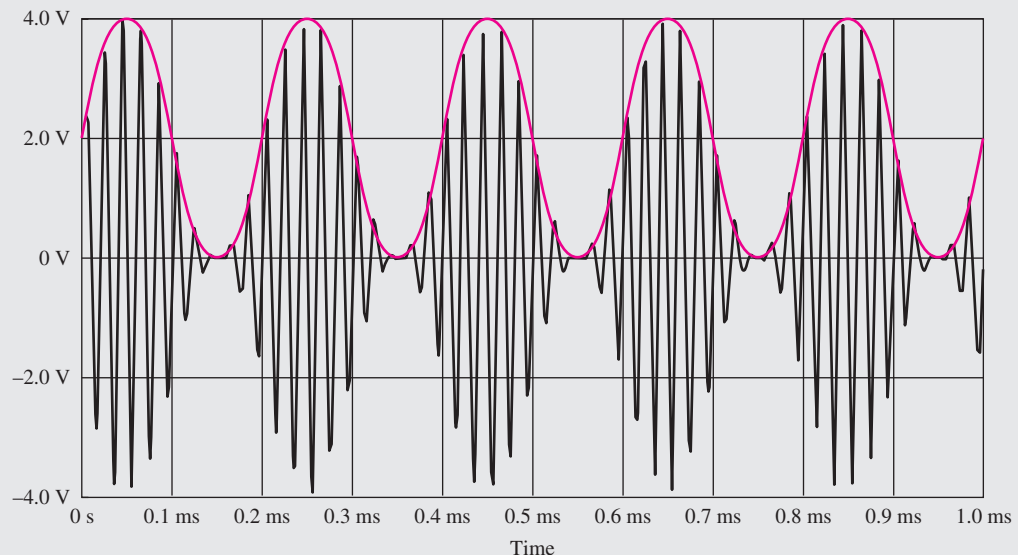
### 3.13.9 HALF-WAVE RECTIFIER WITH NEGATIVE OUTPUT VOLTAGE

The circuit of Fig. 3.51 can also be used to produce a negative output voltage if the top rather than the bottom of the capacitor is grounded, as depicted in Fig. 3.57(a). However, we usually draw the circuit as in Fig. 3.57(b). These two circuits are equivalent. In the circuit in Fig. 3.57(b), the diode conducts on the negative half cycle of the transformer voltage  $v_I$ , and the dc output voltage is  $V_{dc} = -(V_P - V_{on})$ .

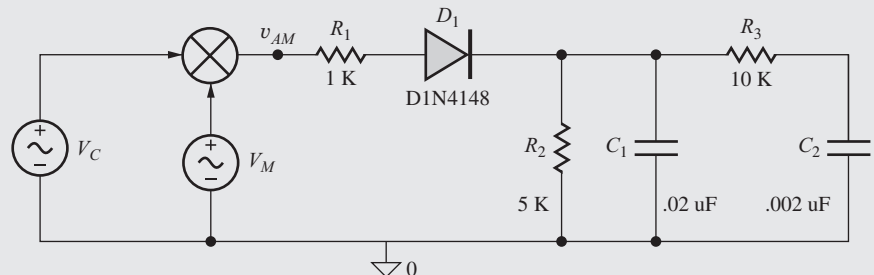


### AM Demodulation

The waveform for a 100% amplitude modulated (AM) signal is shown in the figure below and described mathematically by  $v_{AM} = 2 \sin \omega_C t (1 + \sin \omega_M t)$  V in which  $\omega_C$  is the carrier frequency ( $f_C = 50$  kHz) and  $\omega_M$  is the modulating frequency ( $f_M = 5$  kHz). The envelope of



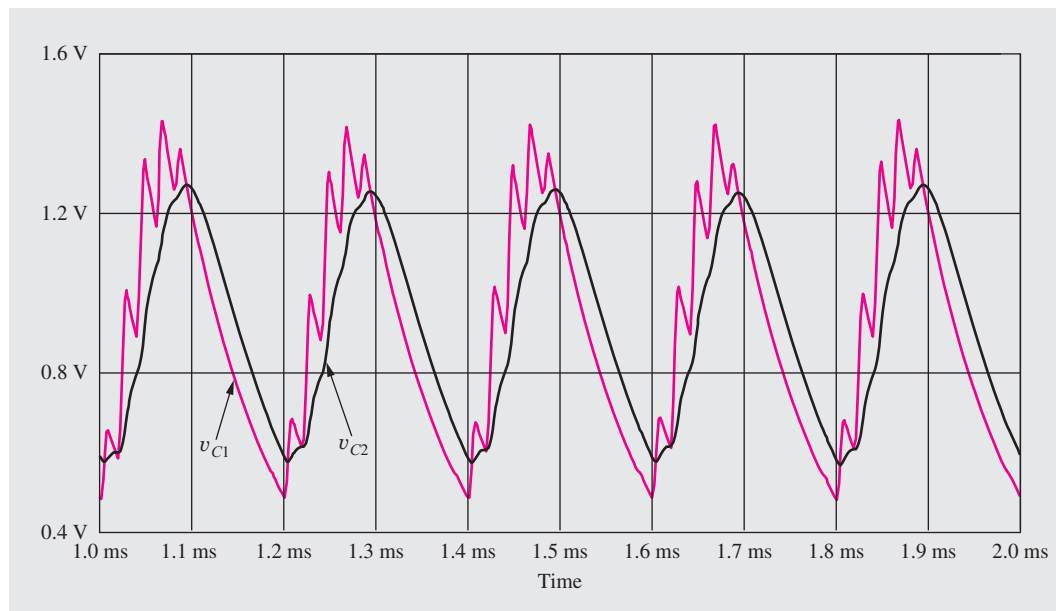
the AM signal contains the information being transmitted, and the envelope can be recovered from the signal using a simple half-wave rectifier. In the SPICE circuit below, the signal to be demodulated is applied as the input signal to the rectifier, and the rectifier, and the  $R_2C_1$  time



constant is set to filter out the carrier frequency but follow the signal's envelope. Additional filtering is provided by the low-pass filter formed by  $R_3$  and  $C_2$ . SPICE simulation results appear below along with the results of a Fourier analysis of the demodulated signal. The plots of  $v_{C1}$  and  $v_{C2}$  represent the voltages across capacitors  $C_1$  and  $C_2$  respectively.

**SPICE Results  
for Spectral  
Content of  
 $v_{C2}$  (V)**

5 kHz	0.330
10 kHz	0.046
15 kHz	0.006
20 kHz	0.001
—	
45 kHz	0.006
50 kHz	0.007
55 kHz	0.004



### 3.14 FULL-WAVE RECTIFIER CIRCUITS

**Full-wave rectifier circuits** cut the capacitor discharge time in half and offer the advantage of requiring only one-half the filter capacitance to achieve a given ripple voltage. The full-wave rectifier circuit in Fig. 3.58 uses a **center-tapped transformer** to generate two voltages that have equal amplitudes but are 180 degrees out of phase. With voltage  $v_I$  applied to the anode of  $D_1$ , and  $-v_I$  applied to the anode of  $D_2$ , the two diodes form a pair of half-wave rectifiers operating on alternate half cycles of the input waveform. Proper phasing is indicated by the dots on the two halves of the transformer.

For  $v_I > 0$ ,  $D_1$  will be functioning as a half-wave rectifier, and  $D_2$  will be off, as indicated in Fig. 3.59. The current exits the upper terminal of the transformer, goes through diode  $D_1$ , through the  $RC$  load, and returns back into the center tap of the transformer.

For  $v_I < 0$ ,  $D_1$  will be off, and  $D_2$  will be functioning as a half-wave rectifier as indicated in Fig. 3.60. During this portion of the cycle, the current path leaves the bottom terminal of the transformer, goes through  $D_2$ , down through the  $RC$  load, and again returns into the transformer center tap. The current direction in the load is the same during both halves of the cycle; one-half of the transformer is utilized during each half cycle.

The load, consisting of the filter capacitor  $C$  and load resistor  $R$ , now receives two current pulses per cycle, and the capacitor discharge time is reduced to less than  $T/2$ , as indicated in the graph.

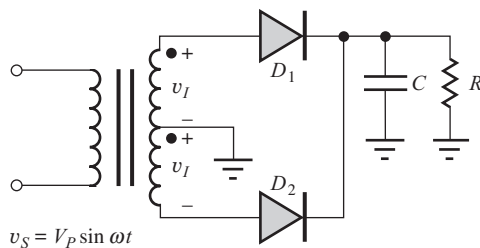


**Figure 3.58** Full-wave rectifier circuit using two diodes and a center-tapped transformer. This circuit produces a positive output voltage.

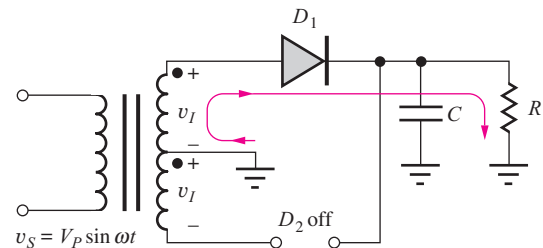


**Figure 3.59** Equivalent circuit for  $v_I > 0$ .

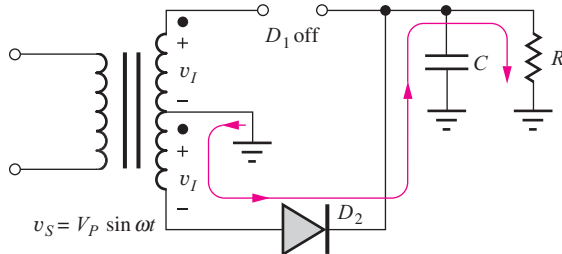


**Figure 3.60** Equivalent circuit for  $v_I < 0$ .

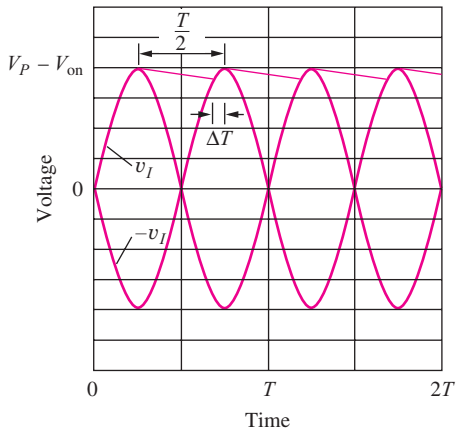


**Figure 3.61** Voltage waveforms for the full-wave rectifier.

in Fig. 3.61. An analysis similar to that for the half-wave rectifier yields the same formulas for dc output voltage, ripple voltage, and  $\Delta T$ , except that the discharge interval is  $T/2$  rather than  $T$ . For a given capacitor value, the ripple voltage is one-half as large, and the conduction interval and peak current are reduced. The peak-inverse-voltage waveform for each diode is similar to the one shown in Fig. 3.56 for the half-wave rectifier, with the result that the PIV rating of each diode is the same as in the half-wave rectifier. These results are summarized in Eqs. (3.63) to (3.67) for  $v_S = V_P \sin \omega t$ :

#### Full-Wave Rectifier Equations:

$$V_{dc} = V_P - V_{on} \quad (3.63)$$

$$V_r = \frac{(V_P - V_{on})}{R} \frac{T}{2C} \quad (3.64)$$

$$\Delta T = \frac{1}{\omega} \sqrt{\frac{T}{RC}} \frac{(V_P - V_{on})}{V_P} = \frac{1}{\omega} \sqrt{\frac{2V_r}{V_P}} \quad (3.65)$$

$$\theta_c = \omega \Delta T = \sqrt{\frac{2V_r}{V_P}} \quad I_P = I_{DC} \frac{T}{\Delta T} \quad (3.66)$$

$$PIV = 2V_P \quad (3.67)$$

### 3.14.1 FULL-WAVE RECTIFIER WITH NEGATIVE OUTPUT VOLTAGE

By reversing the polarity of the diodes, as in Fig. 3.62, a full-wave rectifier circuit with a negative output voltage is realized. Other aspects of the circuit remain the same as the previous full-wave rectifiers with positive output voltages.

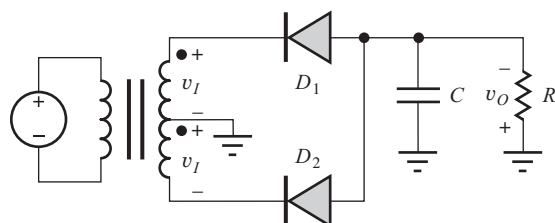


**Figure 3.62** Full-wave rectifier with negative output voltage.

### 3.15 FULL-WAVE BRIDGE RECTIFICATION

The requirement for a center-tapped transformer in the full-wave rectifier can be eliminated through the use of two additional diodes in the **full-wave bridge rectifier circuit** configuration shown in Fig. 3.63. For  $v_I > 0$ ,  $D_2$  and  $D_4$  will be on and  $D_1$  and  $D_3$  will be off, as indicated in Fig. 3.64. Current exits the top of the transformer, goes through  $D_2$  into the  $RC$  load, and returns to the transformer through  $D_4$ . The full transformer voltage, now minus two diode voltage drops, appears across the load capacitor yielding a dc output voltage

$$V_{dc} = V_P - 2V_{on} \quad (3.68)$$

The peak voltage at node 1, which represents the maximum reverse voltage appearing across  $D_1$ , is equal to  $(V_P - V_{on})$ . Similarly, the peak reverse voltage across diode  $D_4$  is  $(V_P - 2V_{on}) - (-V_{on}) = (V_P - V_{on})$ .

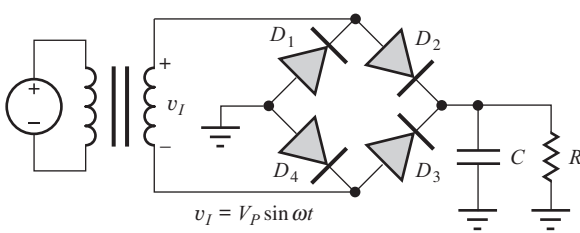


Figure 3.63 Full-wave bridge rectifier circuit with positive output voltage.

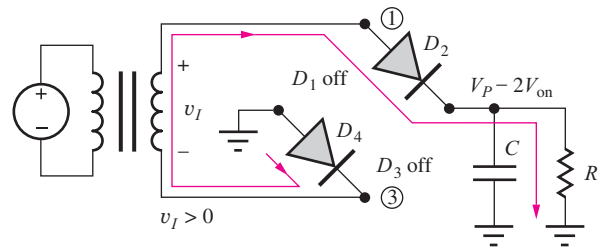


Figure 3.64 Full-wave bridge rectifier circuit for  $v_I > 0$ .

For  $v_I < 0$ ,  $D_1$  and  $D_3$  will be on and  $D_2$  and  $D_4$  will be off, as depicted in Fig. 3.65. Current leaves the bottom of the transformer, goes through  $D_3$  into the  $RC$  load, and back through  $D_1$  to the transformer. The full transformer voltage is again being utilized. The peak voltage at node 3 is now equal to  $(V_P - V_{on})$  and is the maximum reverse voltage appearing across  $D_4$ . Similarly, the peak reverse voltage across diode  $D_2$  is  $(V_P - 2V_{on}) - (-V_{on}) = (V_P - V_{on})$ .

From the analysis of the two half cycles, we see that each diode must have a PIV rating given by

$$\text{PIV} = V_P - V_{on} \cong V_P \quad (3.69)$$

As with the previous rectifier circuits, a negative output voltage can be generated by reversing the direction of the diodes, as in the circuit in Fig. 3.66.

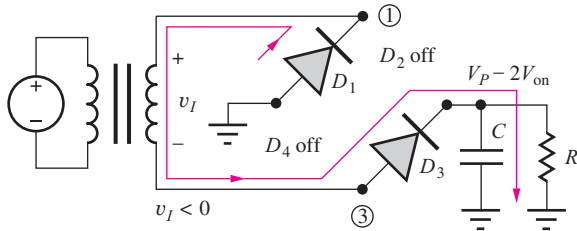


Figure 3.65 Full-wave bridge rectifier circuit for  $v_I < 0$ .

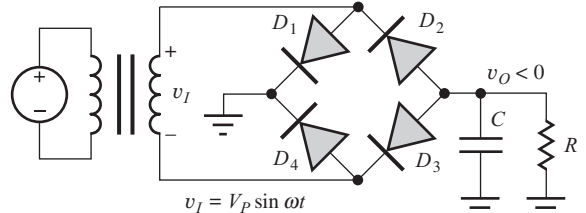


Figure 3.66 Full-wave bridge rectifier circuit with  $v_O < 0$ .

### 3.16 RECTIFIER COMPARISON AND DESIGN TRADEOFFS

Table 3.5 summarizes the characteristics of the half-wave, full-wave, and full-wave bridge rectifiers introduced in Secs. 3.13 to 3.15. The filter capacitor often represents a significant economic factor in terms of cost, size, and weight in the design of **rectifier circuits**. For a given ripple voltage, the value

**TABLE 3.5**  
Comparison of Rectifiers with Capacitive Filters

RECTIFIER PARAMETER	HALF-WAVE RECTIFIER	FULL-WAVE RECTIFIER	FULL-WAVE BRIDGE RECTIFIER
Filter capacitor	$C = \frac{V_p - V_{on}}{V_r} \frac{T}{R}$	$C = \frac{V_p - V_{on}}{V_r} \frac{T}{2R}$	$C = \frac{V_p - 2V_{on}}{V_r} \frac{T}{2R}$
PIV rating	$2V_p$	$2V_p$	$V_p$
Peak diode current (constant $V_r$ )	Highest $I_p$	Reduced $\frac{I_p}{2}$	Reduced $\frac{I_p}{2}$
Surge Current	Highest	Reduced ( $\propto C$ )	Reduced ( $\propto C$ )
Comments	Least complexity	Smaller capacitor Requires center-tapped transformer Two diodes	Smaller capacitor Four diodes No center tap on transformer

of the filter capacitor required in the full-wave rectifier is one-half that for the half-wave rectifier.

The reduction in peak current in the full-wave rectifier can significantly reduce heat dissipation in the diodes. The addition of the second diode and the use of a center-tapped transformer represent additional expenses that offset some of the advantage. However, the benefits of full-wave rectification usually outweigh the minor increase in circuit complexity.

The bridge rectifier eliminates the need for the center-tapped transformer, and the PIV rating of the diodes is reduced, which can be particularly important in high-voltage circuits. The cost of the extra diodes is usually negligible, particularly since four-diode bridge rectifiers can be purchased in single-component form.

## DESIGN EXAMPLE 3.11

### RECTIFIER DESIGN

Now we will use our rectifier theory to design a rectifier circuit that will provide a specified output voltage and ripple voltage.

**PROBLEM** Design a rectifier to provide a dc output voltage of 15 V with no more than 1 percent ripple at a load current of 2 A.

**SOLUTION** **Known Information and Given Data:**  $V_{dc} = 15$  V,  $V_r < 0.15$  V,  $I_{dc} = 2$  A

**Unknowns:** Circuit topology, transformer voltage, filter capacitor, diode PIV rating, diode repetitive current rating, diode surge current rating.

**Approach:** Use given data to evaluate rectifier circuit equations. Let us choose a full-wave bridge topology that requires a smaller value of filter capacitance, a smaller diode PIV voltage, and no center tap in the transformer.

**Assumptions:** Assume diode on-voltage is 1 V. The ripple voltage is much less than the dc output voltage ( $V_r \ll V_{dc}$ ), and the conduction interval should be much less than the period of the ac signal ( $\Delta T \ll T$ ).

**Analysis:** The required transformer voltage is

$$V = \frac{V_P}{\sqrt{2}} = \frac{V_{dc} + 2V_{on}}{\sqrt{2}} = \frac{15 + 2}{\sqrt{2}} \text{ V} = 12.0 \text{ V}_{\text{rms}}$$

The filter capacitor is found using the ripple voltage, output current, and discharge interval:

$$C = I_{dc} \left( \frac{T/2}{V_r} \right) = 2 \text{ A} \left( \frac{1}{120} \text{ s} \right) \left( \frac{1}{0.15 \text{ V}} \right) = 0.111 \text{ F}$$

To find  $I_P$ , the conduction time is calculated using Eq. (3.54)

$$\Delta T = \frac{1}{\omega} \sqrt{\frac{2V_r}{V_P}} = \frac{1}{120\pi} \sqrt{\frac{2(0.15) \text{ V}}{17 \text{ V}}} = 0.352 \text{ ms}$$

and the peak repetitive current is found to be

$$I_P = I_{dc} \left( \frac{2}{\Delta T} \right) \left( \frac{T}{2} \right) = 2 \text{ A} \frac{(1/60) \text{ s}}{0.352 \text{ ms}} = 94.7 \text{ A}$$

The surge current estimate is

$$I_{\text{surge}} = \omega C V_P = 120\pi(0.111)(17) = 711 \text{ A}$$

The minimum diode PIV is  $V_P = 17 \text{ V}$ . A choice with a safety margin would be  $\text{PIV} > 20 \text{ V}$ . The repetitive current rating should be 95 A with a surge current rating of 710 A. Note that both of these calculations overestimate the magnitude of the currents because we have neglected series resistance of the transformer and diode. The minimum filter capacitor needs to be 111,000  $\mu\text{F}$ . Assuming a tolerance of -30 percent, a nominal filter capacitance of 160,000  $\mu\text{F}$  would be required.

**Check of Results:** The ripple voltage is designed to be 1 percent of the dc output voltage. Thus the assumption that the voltage is approximately constant is justified. The conduction time is 0.352 mS out of a total period  $T = 16.7 \text{ mS}$ . Thus the assumption that  $\Delta T \ll T$  is satisfied.

**Computer-Aided Analysis:** This design example represents an excellent place where simulation can be used to explore the magnitude of the diode currents and improve the design so that we don't over specify the rectifier diodes. A SPICE simulation with  $R_S = 0.1 \Omega$ ,  $n = 2$ ,  $I_S = 1 \mu\text{A}$ , and a transformer series resistance of  $0.1 \Omega$  yields a number of unexpected results:  $I_P = 11 \text{ A}$ ,  $I_{\text{surge}} = 70 \text{ A}$ , and  $V_{dc} = 13 \text{ V}$ ! The surge current and peak repetitive current are both reduced by almost an order of magnitude compared to our hand calculations! In addition the output voltage is lower than expected. If we think further, a peak current of 11 A will cause a peak voltage drop of 2.2 V across the total series resistance of  $0.2 \Omega$ , so it should not be surprising that the output voltage is 2 V lower than originally expected. The series resistances actually help to reduce the stress on the diodes. The time constant of the series resistance and the filter capacitor is 0.44 s, so the circuit takes many cycles to reach the steady state output voltage.

**EXERCISE:** Repeat the rectifier design assuming the use of a half-wave rectifier.

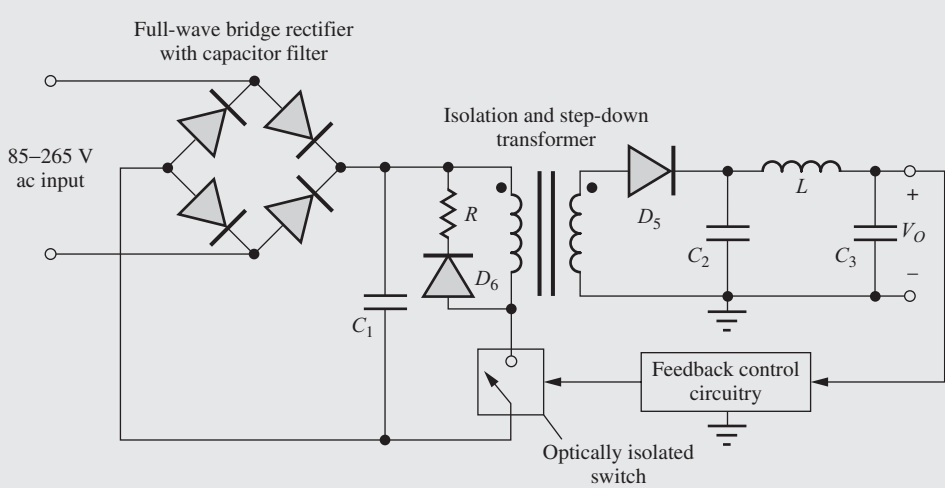
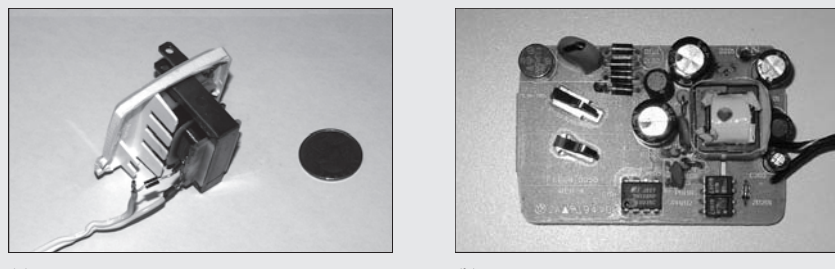
**ANSWERS:**  $V = 11.3 \text{ V}_{\text{rms}}$ ;  $C = 222,000 \mu\text{F}$ ;  $I_P = 184 \text{ A}$ ;  $I_{\text{SC}} = 1340 \text{ A}$



### Power Cubes and Cell Phone Chargers

We actually encounter the unfiltered transformer driven half-wave rectifier circuit depicted in Fig. 3.47 frequently in our everyday lives in the form of “power cubes” and battery chargers for many portable electronic devices. An example is shown in the accompanying figure. The power cube contains only a small transformer and rectifier diode. The transformer is wound with small wire and has a significant resistance in both the primary and secondary windings. In the transformer in the photograph, the primary resistance is  $600\ \Omega$  and the secondary resistance is  $15\ \Omega$ , and these resistances actually help provide protection from failure of the transformer windings. Load resistance  $R$  in Fig. 3.47 represents the actual electronic device that is receiving power from the power cube and may often be a rechargeable battery. In some cases, a filter capacitor may be included as part of the circuit that forms the load for the power cube.

Part (c) of the figure below shows a much more complex device used for recharging the batteries in a cell phone. The simplified schematic in part (c) utilizes a full-wave bridge rectifier with filter capacitor connected directly to the ac line. The rectifier’s high voltage output is filtered by capacitor  $C_1$  and feeds a switching regulator consisting of a switch, the transformer driving a half-wave rectifier with pi-filter ( $D_5$ ,  $C_2$ ,  $L$ , and  $C_3$ ), and a feedback circuit that controls the output voltage by modulating the duty cycle of the switch. The transformer steps down the voltage and provides isolation from the high voltage ac line input. Diode  $D_6$  and  $R$  clamp the inductor voltage when the switch opens. The feedback signal path is isolated from the input using an optical isolator. (See Electronics in Action in Chapter 5 for discussion of an optical isolator.) Note the wide range of input voltages accommodated by the circuit.



(a) Inside a simple power cube. (b) Cell phone charger. (c) Simplified schematic for the cell-phone charger.

### 3.17 DYNAMIC SWITCHING BEHAVIOR OF THE DIODE

Up to this point, we have tacitly assumed that diodes can turn on and off instantaneously. However, an unusual phenomenon characterizes the dynamic switching behavior of the *pn* junction diode. SPICE simulation is used to illustrate the switching of the diode in the circuit in Fig. 3.67, in which diode  $D_1$  is being driven from voltage source  $v_1$  through resistor  $R_1$ .

The source is zero for  $t < 0$ . At  $t = 0$ , the source voltage rapidly switches to +1.5 V, forcing a current into the diode to turn it on. The voltage remains constant until  $t = 7.5$  ns. At this point the source switches to -1.5 V in order to turn the diode back off.

The simulation results are presented in Fig. 3.68. Following the voltage source change at  $t = 0+$ , the current increases rapidly. The internal capacitance of the diode prevents the diode voltage from changing instantaneously. The current actually overshoots its final value and then decreases as the diode turns on and the diode voltage increases to approximately 0.7 V. At any given time, the current flowing into the diode is given by

$$i_D(t) = \frac{v_1(t) - v_D(t)}{0.75 \text{ k}\Omega} \quad (3.70)$$

The initial peak of the current occurs when  $v_1$  reaches 1.5 V and  $v_D$  is still nearly zero:

$$i_{D\max} = \frac{1.5 \text{ V}}{0.75 \text{ k}\Omega} = 2.0 \text{ mA} \quad (3.71)$$

After the diode voltage reaches its final value with  $V_{on} \approx 0.7 \text{ V}$ , the current stabilizes at a forward current  $I_F$  of

$$I_F = \frac{1.5 - 0.7}{0.75 \text{ k}\Omega} = 1.1 \text{ mA} \quad (3.72)$$

At  $t = 7.5$  ns, the input source rapidly changes polarity to -1.5 V, and a surprising thing happens. The diode current also rapidly reverses direction and is much greater than the reverse saturation current of the diode! The diode does not turn off immediately. In fact, the diode actually

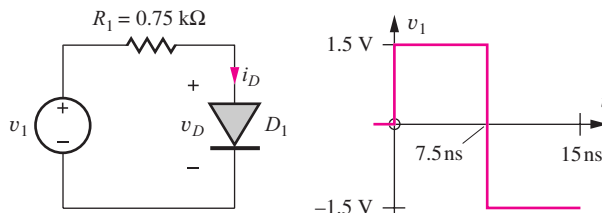


Figure 3.67 Circuit used to explore diode-switching behavior.

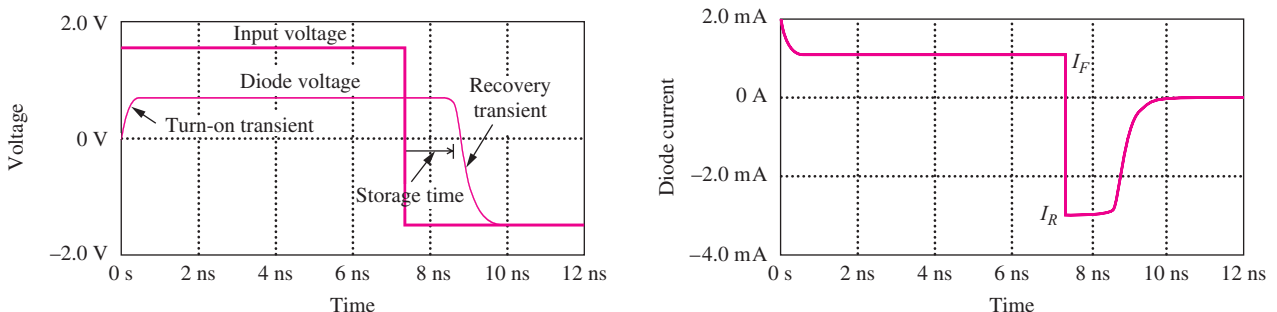


Figure 3.68 SPICE simulation results for the diode circuit in Fig. 3.67. (The diode transit time is equal to 5 ns.)

remains forward-biased by the charge stored in the diode, with  $v_D = V_{on}$ , even though the current has changed direction! The reverse current  $I_R$  is equal to

$$I_R = \frac{-1.5 - 0.7}{0.75 \text{ k}\Omega} = -2.9 \text{ mA} \quad (3.73)$$

The current remains at  $-2.9 \text{ mA}$  for a period of time called the diode **storage time**  $\tau_S$ , during which the internal charge stored in the diode is removed. Once the stored charge has been removed, the voltage across the diode begins to drop and charges toward the final value of  $-1.5 \text{ V}$ . The current in the diode drops rapidly to zero as the diode voltage begins to fall.

The turn-on time and recovery time are determined primarily by the charging and discharging of the nonlinear depletion-layer capacitance  $C_j$  through the resistance  $R_S$ . The storage time is determined by the diode transit time defined in Eq. (3.22) and by the values of the forward and reverse currents  $I_F$  and  $I_R$ :

$$\tau_S = \tau_T \ln \left[ 1 - \frac{I_F}{I_R} \right] = 5 \ln \left[ 1 - \frac{1.1 \text{ mA}}{-2.9 \text{ mA}} \right] \text{ ns} = 1.6 \text{ ns} \quad (3.74)$$

The SPICE simulation in results Fig. 3.68 agree well with this value.

Always remember that solid-state devices do not turn off instantaneously. The unusual storage time behavior of the diode is an excellent example of the switching delays that occur in *pn* junction devices in which carrier flow is dominated by the minority-carrier diffusion process. This behavior is not present in field-effect transistors, in which current flow is dominated by majority-carrier drift.

## 3.18 PHOTO DIODES, SOLAR CELLS, AND LIGHT-EMITTING DIODES

Several other important applications of diodes include photo detectors in communication systems, solar cells for generating electric power, and light-emitting diodes (LEDs). These applications all rely on the solid-state diode's ability to interact with optical photons.

### 3.18.1 PHOTO DIODES AND PHOTODETECTORS

If the depletion region of a *pn* junction diode is illuminated with light of sufficiently high frequency, the photons can provide enough energy to cause electrons to jump the semiconductor bandgap, creating electron–hole pairs. For photon absorption to occur, the incident photons must have an energy  $E_p$  that exceeds the bandgap of the semiconductor:

$$E_p = h\nu = \frac{hc}{\lambda} \geq E_G \quad (3.75)$$

where  $h$  = Planck's constant ( $6.626 \times 10^{-34} \text{ J} \cdot \text{s}$ )  $\lambda$  = wavelength of optical illumination

$\nu$  = frequency of optical illumination  $c$  = velocity of light ( $3 \times 10^8 \text{ m/s}$ )

The  $i$ - $v$  characteristic of a diode with and without illumination is shown in Fig. 3.69. The original diode characteristic is shifted vertically downward by the photon-generated current. Photon absorption creates an additional current crossing the *pn* junction that can be modeled by a current source  $i_{PH}$  in parallel with the *pn* junction diode, as shown in Fig. 3.70.

Based on this model, we see that the incident optical signal can be converted to an electrical signal voltage using the simple **photodetector circuit** in Fig. 3.71. The diode is reverse-biased to enhance the width and electric field in the depletion region. The photon-generated current  $i_{PH}$  will flow through resistor  $R$  and produce an output signal voltage given by

$$v_o = i_{PH}R \quad (3.76)$$

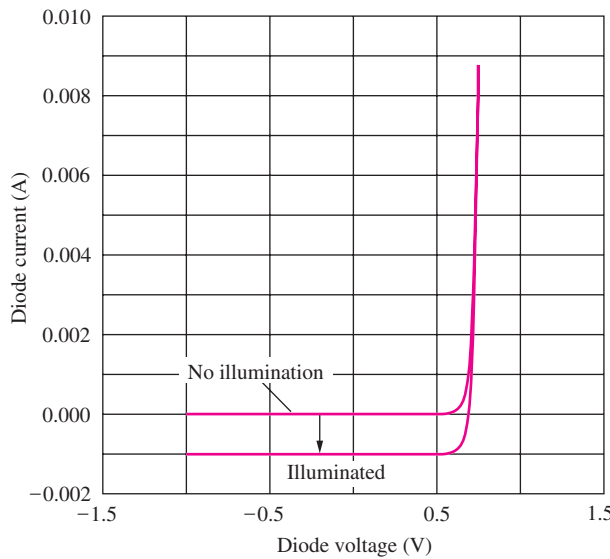


**Figure 3.69** Diode  $i$ - $v$  characteristic with and without optical illumination.

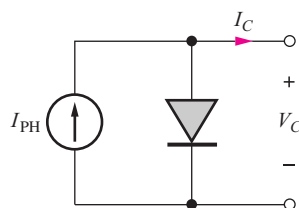


**Figure 3.72**  $pn$  Diode under steady-state illumination as a solar cell.

In optical fiber communication systems, the amplitude of the incident light is modulated by rapidly changing digital data, and  $i_{PH}$  is a time-varying signal. The time-varying signal voltage at  $v_o$  is fed to additional electronic circuits to demodulate the signal and recover the original data that were transmitted down the optical fiber.

### 3.18.2 POWER GENERATION FROM SOLAR CELLS

In **solar cell** applications, the optical illumination is constant, and a dc current  $I_{PH}$  is generated. The goal is to extract power from the cell, and the  $i$ - $v$  characteristics of solar cells are usually plotted in terms of the cell current  $I_C$  and cell voltage  $V_C$ , as defined in Fig. 3.72.

The  $i$ - $v$  characteristic of the  $pn$  junction used for solar cell applications is plotted in terms of these terminal variables in Fig. 3.73. Also indicated on the graph are the short-circuit current  $I_{SC}$ ,

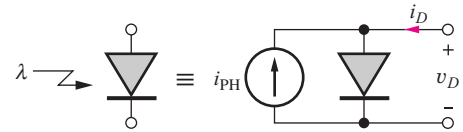


**Figure 3.70** Model for optically illuminated diode.  $i_{PH}$  represents the current generated by absorption of photons in the vicinity of the  $pn$  junction.

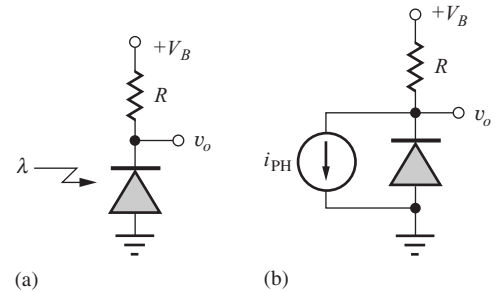


**Figure 3.71** Basic photodetector circuit (a) and model (b).

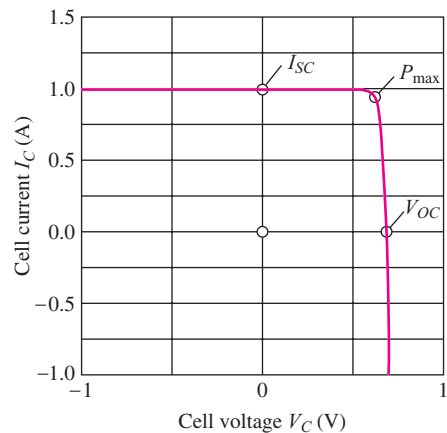


**Figure 3.73** Terminal characteristics for a  $pn$  junction solar cell.



## ELECTRONICS IN ACTION

### Solar Power for the Home

The following photo shows Auburn University's entry in the 2002 Solar Decathlon competition sponsored by the US Dept. of Energy and its private-sector partners BP Solar, The Home Depot, Electronic Data Systems (EDS), and the American Institute of Architects. Solar energy represents a clean and renewable source of power that significantly reduces pollutant emissions. For the competition, the solar energy available within the footprint of the house had to supply the total energy requirements for an entire home. The solar array on top of the house consists of 36 panels, connected as eighteen parallel strings of two panels each. Each solar panel (BP3160) is a series connection of 72 polycrystalline-silicon solar cells that can be represented by the simple model in Figs. 3.72 and 3.73, and each panel is specified to have an open-circuit voltage of 44.2 V and a short-circuit current of 4.8 A. The complete array produces a maximum power of 5.74 kW at an output voltage of 70 V and a current of 82 A. The solar cells charge batteries that drive ac inverters to supply 110/220-V 60-Hz power to the house. Note that two separate solar water heating panels are also visible on the roof of the building in the photograph.



Auburn University's award-winning entry in the 2002 Solar Decathlon.

the open-circuit voltage  $V_{OC}$ , and the maximum power point  $P_{max}$ .  $I_{SC}$  represents the maximum current available from the cell, and  $V_{OC}$  is the voltage across the open-circuited cell when all the photo current is flowing into the internal  $pn$  junction. For the solar cell to supply power to an external circuit, the product  $I_C \times V_C$  must be positive, corresponding to the first quadrant of the characteristic. An attempt is made to operate the cell near the point of maximum output power  $P_{max}$ .

### 3.18.3 LIGHT-EMITTING DIODES (LEDS)

**Light-emitting diodes**, or **LEDs**, rely on the annihilation of electrons and holes through recombination rather than on the generation of carriers, as in the case of the photo diode. When a hole and electron recombine, an energy equal to the bandgap of the semiconductor can be released in the form of a photon. This recombination process is present in the forward-biased  $pn$  junction diode. In silicon, the recombination process actually involves the interaction of photons and lattice vibrations

called phonons. The optical emission process in silicon is not nearly as efficient as that in the III-V compound semiconductor GaAs or the ternary materials such as  $\text{GaIn}_{1-x}\text{As}_x$  and  $\text{GaIn}_{1-x}\text{P}_x$ . LEDs in these compound semiconductor materials provide visible illumination, and the color of the output can be controlled by varying the fraction  $x$  of arsenic or phosphorus in the material.

## SUMMARY

In this chapter we investigated the detailed behavior of the solid-state diode.

- A  $pn$  junction diode is created when  $p$ -type and  $n$ -type semiconductor regions are formed in intimate contact with each other. In the  $pn$  diode, large concentration gradients exist in the vicinity of the metallurgical junction, giving rise to large electron and hole diffusion currents.
- Under zero bias, no current can exist at the diode terminals, and a space charge region forms in the vicinity of the  $pn$  junction. The region of space charge results in both a built-in potential and an internal electric field, and the internal electric field produces electron and hole drift currents that exactly cancel the corresponding components of diffusion current.
- When a voltage is applied to the diode, the balance in the junction region is disturbed, and the diode conducts a current. The resulting  $i$ - $v$  characteristics of the diode are accurately modeled by the diode equation:

$$i_D = I_S \left[ \exp \left( \frac{v_D}{n V_T} \right) - 1 \right]$$

where  $I_S$  = reverse saturation current of the diode

$n$  = nonideality factor (approximately 1)

$V_T = kT/q$  = thermal voltage (0.025 V at room temperature)

- Under reverse bias, the diode current equals  $-I_S$ , a very small current.
- For forward bias, however, large currents are possible, and the diode presents an almost constant voltage drop of 0.6 to 0.7 V.
- At room temperature, an order of magnitude change in diode current requires a change of less than 60 mV in the diode voltage. At room temperature, the silicon diode voltage exhibits a temperature coefficient of approximately  $-1.8 \text{ mV}^{\circ}\text{C}$ .
- One must also be aware of the reverse-breakdown phenomenon that is not included in the diode equation. If too large a reverse voltage is applied to the diode, the internal electric field becomes so large that the diode enters the breakdown region, either through Zener breakdown or avalanche breakdown. In the breakdown region, the diode again represents an almost fixed voltage drop, and the current must be limited by the external circuit or the diode can easily be destroyed.
- Diodes called Zener diodes are designed to operate in breakdown and can be used in simple voltage regulator circuits. Line regulation and load regulation characterize the change in output voltage of a power supply due to changes in input voltage and output current, respectively.
- As the voltage across the diode changes, the charge stored in the vicinity of the space charge region of the diode changes, and a complete diode model must include a capacitance. Under reverse bias, the capacitance varies inversely with the square root of the applied voltage. Under forward bias, the capacitance is proportional to the operating current and the diode transit time. These capacitances prevent the diode from turning on and off instantaneously and cause a storage time delay during turn-off.

- Direct use of the nonlinear diode equation in circuit calculations usually requires iterative numeric techniques. Several methods for simplifying the analysis of diode circuits were discussed, including the graphical load-line method and use of the ideal diode and constant voltage drop models.
- SPICE circuit analysis programs include a comprehensive built-in model for the diode that accurately reproduces both the ideal and nonideal characteristics of the diode and is useful for exploring the detailed behavior of circuits containing diodes.
- Important applications of diodes include half-wave, full-wave, and full-wave bridge rectifier circuits used to convert from ac to dc voltages in power supplies. Simple power supply circuits use capacitive filters, and the design of the filter capacitor determines power supply ripple voltage and diode conduction angle. Diodes used as rectifiers in power supplies must be able to withstand large peak repetitive currents as well as surge currents when the power supplies are first turned on. The reverse-breakdown voltage of rectifier diodes is referred to as the peak-inverse-voltage, or PIV, rating of the diode.
- Real diodes cannot turn on or off instantaneously because the internal capacitances of the diodes must be charged and discharged. The turn-on time is usually quite short, but diodes that have been conducting turn off much less abruptly. It takes time to remove stored charge within the diode, and this time delay is characterized by storage time  $\tau_s$ . During the storage time, it is possible for large reverse currents to occur in the diode.
- Finally, the ability of the *pn* junction device to generate and detect light was discussed, and the basic characteristics of photo diodes, solar cells, and light-emitting diodes were presented.

## KEY TERMS

Anode	Light-emitting diode (LED)
Avalanche breakdown	Line regulation
Bias current and voltage	Load line
Breakdown region	Load-line analysis
Breakdown voltage	Load regulation
Built-in potential (or voltage)	Mathematical model
Cathode	Metallurgical junction
Center-tapped transformer	Nonideality factor ( $n$ )
Conduction angle	Peak detector
Conduction interval	Peak inverse voltage (PIV)
Constant voltage drop (CVD) model	Photodetector circuit
Cut-in voltage	Piecewise linear model
Depletion layer	<i>pn</i> junction diode
Depletion-layer width	Q-point
Depletion region	Quiescent operating point
Diffusion capacitance	Rectifier circuits
Diode equation	Reverse bias
Diode SPICE parameters (IS, RS, N, TT, CJO, VJ, M)	Reverse breakdown
Filter capacitor	Reverse saturation current ( $I_S$ )
Forward bias	Ripple current
Full-wave bridge rectifier circuit	Ripple voltage
Full-wave rectifier circuit	Saturation current
Half-wave rectifier circuit	Schottky barrier diode
Ideal diode	Solar cell
Ideal diode model	Space charge region (SCR)
Impact-ionization process	Storage time
Junction potential	Surge current
	Thermal voltage ( $V_T$ )

Transit time	Zener breakdown
Turn-on voltage	Zener diode
Voltage regulator	Zero bias
Voltage transfer characteristic (VTC)	Zero-bias junction capacitance

## REFERENCE

1. G. W. Neudeck, *The PN Junction Diode*, 2d ed. Pearson Education, Upper Saddle River, NJ: 1989.

## ADDITIONAL READING

- PSPICE, ORCAD, now owned by Cadence Design Systems, San Jose, CA.  
 LTspice available from Linear Technology Corp.  
 Tina-TI SPICE-based analog simulation program available from Texas Instruments.  
 T. Quarles, A. R. Newton, D. O. Pederson, and A. Sangiovanni-Vincentelli, *SPICE3 Version 3f3 User's Manual*. UC Berkeley: May 1993.  
 A. S. Sedra, and K. C. Smith. *Microelectronic Circuits*. 5th ed. Oxford University Press, New York: 2004.

## PROBLEMS

### 3.1 The *pn* Junction Diode

- 3.1. A diode is doped with  $N_A = 10^{19}/\text{cm}^3$  on the *p*-type side and  $N_D = 10^{18}/\text{cm}^3$  on the *n*-type side.  
 (a) What is the depletion-layer width  $w_{do}$ ? (b) What are the values of  $x_p$  and  $x_n$ ? (c) What is the value of the built-in potential of the junction? (d) What is the value of  $E_{MAX}$ ? Use Eq. (3.3) and Fig. 3.5.
- 3.2. A diode is doped with  $N_A = 10^{18}/\text{cm}^3$  on the *p*-type side and  $N_D = 10^{15}/\text{cm}^3$  on the *n*-type side.  
 (a) What are the values of  $p_p$ ,  $p_n$ ,  $n_p$ , and  $n_n$ ? (b) What are the depletion-region width  $w_{do}$  and built-in voltage?
- 3.3. Repeat Prob. 3.2 for a diode with  $N_A = 10^{16}/\text{cm}^3$  on the *p*-type side and  $N_D = 10^{19}/\text{cm}^3$  on the *n*-type side.
- 3.4. Repeat Prob. 3.2 for a diode with  $N_A = 10^{18}/\text{cm}^3$  on the *p*-type side and  $N_D = 10^{18}/\text{cm}^3$  on the *n*-type side.
- 3.5. Repeat Prob. 3.2 for a diode with  $N_D = 10^{20}/\text{cm}^3$  on the *n*-type side and  $N_A = 10^{18}/\text{cm}^3$  on the *p*-type side.
- 3.6. A diode has  $w_{do} = 0.4 \mu\text{m}$  and  $\phi_j = 0.85 \text{ V}$ .  
 (a) What reverse bias is required to triple the depletion-layer width? (b) What is the depletion region width if a reverse bias of 7 V is applied to the diode?
- 3.7. A diode has  $w_{do} = 1 \mu\text{m}$  and  $\phi_j = 0.6 \text{ V}$ .  
 (a) What reverse bias is required to double the

- depletion-layer width? (b) What is the depletion region width if a reverse bias of 12 V is applied to the diode?
- 3.8. Suppose a drift current density of  $2000 \text{ A/cm}^2$  exists in the neutral region on the *n*-type side of a diode that has a resistivity of  $0.5 \Omega \cdot \text{cm}$ . What is the electric field needed to support this drift current density?
  - 3.9. Suppose a drift current density of  $5000 \text{ A/cm}^2$  exists in the neutral region on the *p*-type side of a diode that has a resistivity of  $2.5 \Omega \cdot \text{cm}$ . What is the electric field needed to support this drift current density?
  - 3.10. The maximum velocity of carriers in silicon is approximately  $10^7 \text{ cm/s}$ . What is the maximum drift current density that can be supported in a region of *p*-type silicon with a doping of  $4 \times 10^{17}/\text{cm}^3$ ?
  - 3.11. The maximum velocity of carriers in silicon is approximately  $10^7 \text{ cm/s}$ . What is the maximum drift current density that can be supported in a region of *n*-type silicon with a doping of  $5 \times 10^{15}/\text{cm}^3$ ?
  - \*\*3.12. Suppose that  $N_A(x) = N_o \exp(-x/L)$  in a region of silicon extending from  $x = 0$  to  $x = 12 \mu\text{m}$ , where  $N_o$  is a constant. Assume that  $p(x) = N_A(x)$ . Assuming that  $j_p$  must be zero in thermal equilibrium, show that a built-in electric field must exist and find its value for  $L = 1 \mu\text{m}$  and  $N_o = 10^{18}/\text{cm}^3$ .

- 3.13. What carrier gradient is needed to generate a diffusion current density of  $j_n = 2000 \text{ A/cm}^2$  if  $\mu_n = 500 \text{ cm}^2/\text{V} \cdot \text{s}$ ?
- 3.14. Use the solver routine in your calculator to find the solution to Eq. (3.25) for  $I_S = 10^{-16} \text{ A}$ .
- 3.15. Use a spreadsheet to iteratively find the solution to Eq. 3.25 for  $I_S = 10^{-13} \text{ A}$ .
- 3.16. (a) Use MATLAB or MATHCAD to find the solution to Eq. 3.25 for  $I_S = 10^{-13} \text{ A}$ . (b) Repeat for  $I_S = 10^{-15} \text{ A}$ .

### 3.2 – 3.4 The $i$ - $v$ Characteristics of the Diode; The Diode Equation: A Mathematical Model for the Diode; and Diode Characteristics Under Reverse, Zero, and Forward Bias

- 3.17. To what temperature does  $V_T = 0.025 \text{ V}$  actually correspond? What is the value of  $V_T$  for temperatures of  $-55^\circ\text{C}$ ,  $0^\circ\text{C}$ , and  $+85^\circ\text{C}$ ?
- 3.18. (a) Plot a graph of the diode equation similar to Fig. 3.8 for a diode with  $I_S = 10^{-12} \text{ A}$  and  $n = 1$ . (b) Repeat for  $n = 2$ . (c) Repeat (a) for  $I_S = 10^{-14} \text{ A}$ .
- 3.19. A diode has  $n = 1.05$  at  $T = 320 \text{ K}$ . What is the value of  $n \cdot V_T$ ? What temperature would give the same value of  $n \cdot V_T$  if  $n = 1.00$ ?
- 3.20. Plot the diode current for a diode with  $I_{SO} = 11 \text{ fA}$  and  $\phi_j = 0.8$  for  $-10 \text{ V} \leq v_D \leq 0 \text{ V}$  using Eq. 3.19.
- \*3.21. What are the values of  $I_S$  and  $n$  for the diode in the graph in Fig. P3.21? Assume  $V_T = 0.025 \text{ V}$ .

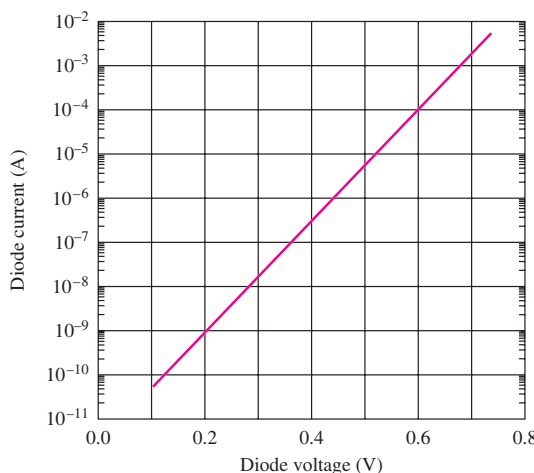


Figure P3.21

- 3.22. A diode has  $I_S = 10^{-17} \text{ A}$  and  $n = 1.07$ . (a) What is the diode voltage if the diode current is  $70 \mu\text{A}$ ? (b) What is the diode voltage if the diode current is

$5 \mu\text{A}$ ? (c) What is the diode current for  $v_D = 0 \text{ V}$ ? (d) What is the diode current for  $v_D = -0.075 \text{ V}$ ? (e) What is the diode current for  $v_D = -5 \text{ V}$ ?

- 3.23. A diode has  $I_S = 10^{-18} \text{ A}$  and  $n = 1$ . (a) What is the diode voltage if the diode current is  $100 \mu\text{A}$ ? (b) What is the diode voltage if the diode current is  $10 \mu\text{A}$ ? (c) What is the diode current for  $v_D = 0 \text{ V}$ ? (d) What is the diode current for  $v_D = -0.06 \text{ V}$ ? (e) What is the diode current for  $v_D = -4 \text{ V}$ ?
- 3.24. A diode has  $I_S = 10^{-16} \text{ A}$  and  $n = 1$ . (a) What is the diode current if the diode voltage is  $0.675 \text{ V}$ ? (b) What will be the diode voltage if the current increases by a factor of 3?
- 3.25. A diode has  $I_S = 10^{-10} \text{ A}$  and  $n = 2$ . (a) What is the diode voltage if the diode current is  $40 \text{ A}$ ? (b) What is the diode voltage if the diode current is  $100 \text{ A}$ ?
- 3.26. A diode is operating with  $i_D = 300 \mu\text{A}$  and  $v_D = 0.75 \text{ V}$ . (a) What is  $I_S$  if  $n = 1$ ? (b) What is the diode current for  $v_D = -3 \text{ V}$ ?
- 3.27. A diode is operating with  $i_D = 2 \text{ mA}$  and  $v_D = 0.82 \text{ V}$ . (a) What is  $I_S$  if  $n = 1$ ? (b) What is the diode current for  $v_D = -5 \text{ V}$ ?
- 3.28. The saturation current for diodes with the same part number may vary widely. Suppose it is known that  $10^{-14} \text{ A} \leq I_S \leq 10^{-12} \text{ A}$ . What is the range of forward voltages that may be exhibited by the diode if it is biased with  $i_D = 1 \text{ mA}$ ?
- 3.29. A diode is biased by a 0.9-V dc source, and its current is found to be  $100 \mu\text{A}$  at  $T = 315 \text{ K}$ . (a) At what temperature will the current double? (b) At what temperature will the current be  $50 \mu\text{A}$ ?
- \*\*3.30. The  $i$ - $v$  characteristic for a diode has been measured under carefully controlled temperature conditions ( $T = 307 \text{ K}$ ), and the data are in Table P3.30.

**TABLE P3.30**  
Diode  $i$ - $v$  Measurements

DIODE VOLTAGE	DIODE CURRENT
0.500	$6.591 \times 10^{-7}$
0.550	$3.647 \times 10^{-6}$
0.600	$2.158 \times 10^{-5}$
0.650	$1.780 \times 10^{-4}$
0.675	$3.601 \times 10^{-4}$
0.700	$8.963 \times 10^{-4}$
0.725	$2.335 \times 10^{-3}$
0.750	$6.035 \times 10^{-3}$
0.775	$1.316 \times 10^{-2}$

Use a spreadsheet or MATLAB to find the values of  $I_S$  and  $n$  that provide the best fit of the diode equation to the measurements in the least-squares sense. [That is, find the values of  $I_S$  and  $n$  that minimize the function  $M = \sum_{m=1}^n (i_D^m - I_{Dm})^2$ , where  $i_D$  is the diode equation from Eq. (3.1) and  $I_{Dm}$  are the measured data.] For your values of  $I_S$  and  $n$ , what is the minimum value of  $M = \sum_{m=1}^n (i_D^m - I_{Dm})^2$ ?

### 3.5 Diode Temperature Coefficient

- 3.31. What is the value of  $V_T$  for temperatures of  $-40^\circ\text{C}$ ,  $0^\circ\text{C}$ , and  $+50^\circ\text{C}$ ?
- 3.32. A diode has  $I_S = 10^{-15} \text{ A}$  and  $n = 1$ . (a) What is the diode voltage if the diode current is  $100 \mu\text{A}$  at  $T = 25^\circ\text{C}$ ? (b) What is the diode voltage at  $T = 50^\circ\text{C}$ ? Assume the diode voltage temperature coefficient is  $-1.8 \text{ mV/K}$  at  $0^\circ\text{C}$ .
- 3.33. A diode with  $I_S = 2.5 \times 10^{-16} \text{ A}$  at  $30^\circ\text{C}$  is biased at a current of  $1 \text{ mA}$ . (a) What is the diode voltage? (b) If the diode voltage temperature coefficient is  $-2 \text{ mV/K}$ , what will be the diode voltage at  $50^\circ\text{C}$ ?
- 3.34. A diode has  $I_S = 10^{-15} \text{ A}$  and  $n = 1$ . (a) What is the diode voltage if the diode current is  $250 \mu\text{A}$  at  $T = 25^\circ\text{C}$ ? (b) What is the diode voltage at  $T = 85^\circ\text{C}$ ? Assume the diode voltage temperature coefficient is  $-2 \text{ mV/K}$  at  $55^\circ\text{C}$ .
- \*3.35. The temperature dependence of  $I_S$  is described approximately by

$$I_S = CT^3 \exp\left(-\frac{E_G}{kT}\right)$$

What is the diode voltage temperature coefficient based on this expression and Eq. (3.15) if  $E_G = 1.21 \text{ eV}$ ,  $V_D = 0.7 \text{ V}$ , and  $T = 300 \text{ K}$ ?

- 3.36. The saturation current of a silicon diode is described by the expression in Prob. 3.35. (a) What temperature change will cause  $I_S$  to double? (b) To increase by 10 times? (c) To decrease by 100 times?

### 3.6 Diodes Under Reverse Bias

- 3.37. A diode has  $w_{do} = 1 \mu\text{m}$  and  $\phi_j = 0.8 \text{ V}$ . (a) What is the depletion layer width for  $V_R = 5 \text{ V}$ ? (b) For  $V_D = -10 \text{ V}$ ?
- 3.38. A diode has a doping of  $N_D = 10^{20}/\text{cm}^3$  on the  $n$ -type side and  $N_A = 10^{18}/\text{cm}^3$  on the  $p$ -type side. What are the values of  $w_{do}$  and  $\phi_j$ ? What is the value of  $w_d$  at a reverse bias of  $5 \text{ V}$ ? At  $25 \text{ V}$ ?
- 3.39. A diode has a doping of  $N_D = 10^{15}/\text{cm}^3$  on the  $n$ -type side and  $N_A = 10^{16}/\text{cm}^3$  on the  $p$ -type

side. What are the values of  $w_{do}$  and  $\phi_j$ ? What is the value of  $w_d$  at a reverse bias of  $10 \text{ V}$ ? At  $100 \text{ V}$ ?

- \*3.40. A diode has  $w_{do} = 1 \mu\text{m}$  and  $\phi_j = 0.6 \text{ V}$ . If the diode breaks down when the internal electric field reaches  $300 \text{ kV/cm}$ , what is the breakdown voltage of the diode?
- \*3.41. Silicon breaks down when the internal electric field exceeds  $300 \text{ kV/cm}$ . At what reverse bias do you expect the diode of Prob. 3.2 to break down?
- 3.42. What are the breakdown voltage  $V_Z$  and Zener resistance  $R_Z$  of the diode depicted in Fig. P3.42?

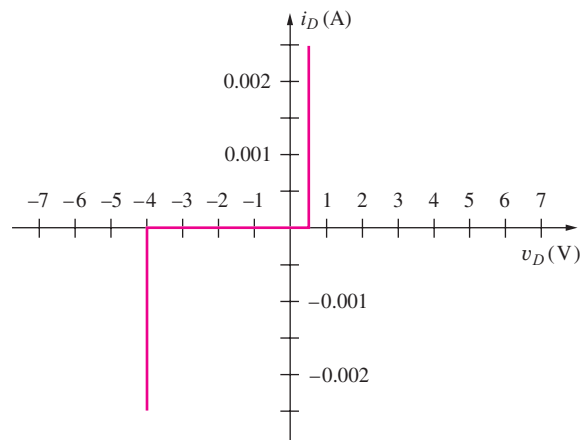


Figure P3.42

- \*\*3.43. A diode is fabricated with  $N_A \gg N_D$ . What value of doping is required on the lightly doped side to achieve a reverse-breakdown voltage of  $1000 \text{ V}$  if the semiconductor material breaks down at a field of  $300 \text{ kV/cm}$ ?

- ### 3.7 $pn$ Junction Capacitance
- 3.44. What is the zero-bias junction capacitance per  $\text{cm}^2$  for a diode with  $N_A = 10^{18}/\text{cm}^3$  on the  $p$ -type side and  $N_D = 10^{15}/\text{cm}^3$  on the  $n$ -type side. What is the diode capacitance with a  $9 \text{ V}$  reverse bias if the diode area is  $0.02 \text{ cm}^2$ ?
  - 3.45. What is the zero-bias junction capacitance/ $\text{cm}^2$  for a diode with  $N_A = 10^{15}/\text{cm}^3$  on the  $p$ -type side and  $N_D = 10^{20}/\text{cm}^3$  on the  $n$ -type side? What is the diode capacitance with a  $3\text{-V}$  reverse bias if the diode area is  $0.05 \text{ cm}^2$ ?
  - 3.46. A diode is operating at a current of  $200 \mu\text{A}$ . (a) What is the diffusion capacitance if the diode transit time is  $100 \text{ ps}$ ? (b) How much charge is stored in the diode? (c) Repeat for  $i_D = 5 \text{ mA}$ .

- 3.47. A diode is operating at a current of 1 A. (a) What is the diffusion capacitance if the diode transit time is 10 ns? (b) How much charge is stored in the diode? (c) Repeat for  $i_D = 100$  mA.
- 3.48. A square *pn* junction diode is 5 mm on a side. The *p*-type side has a doping concentration of  $10^{19}/\text{cm}^3$  and the *n*-type side has a doping concentration of  $10^{16}/\text{cm}^3$ . What is the zero-bias capacitance of the diode? What is the capacitance at a reverse bias of 4 V?
- 3.49. A *pn* junction diode has a cross-sectional area of  $10^4 \mu\text{m}^2$ . The *p*-type side has a doping concentration of  $10^{19}/\text{cm}^3$  and the *n*-type side has a doping concentration of  $10^{17}/\text{cm}^3$ . What is the zero-bias capacitance of the diode? What is the capacitance at a reverse bias of 5 V?
- 3.50. A variable capacitance diode with  $C_{jo} = 39 \text{ pF}$  and  $\phi_j = 0.80 \text{ V}$  is used to tune a resonant LC circuit as shown in Fig. P3.50. The impedance of the RFC (radio frequency choke) can be considered infinite. What are the resonant frequencies ( $f_o = \frac{1}{2\pi\sqrt{LC}}$ ) for  $V_{DC} = 1 \text{ V}$  and  $V_{DC} = 9 \text{ V}$ ?

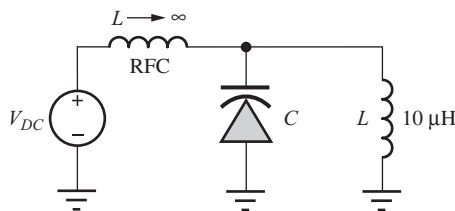


Figure P3.50

### 3.8 Schottky Barrier Diode

- 3.51. A Schottky barrier diode is modeled by the diode equation in Eq. (3.11) with  $I_S = 10^{-11} \text{ A}$ . (a) What is the diode voltage at a current of 4 mA? (b) What would be the voltage of a *pn* junction diode with  $I_S = 10^{-14} \text{ A}$  operating at the same current?
- 3.52. Suppose a Schottky barrier diode can be modeled by the diode equation in Eq. (3.11) with  $I_S = 10^{-7} \text{ A}$ . (a) What is the diode voltage at a current of 50 A? (b) What would be the voltage of a *pn* junction diode with  $I_S = 10^{-15} \text{ A}$  and  $n = 2$ ?

### 3.9 Diode SPICE Model and Layout

- 3.53. (a) A diode has  $I_S = 5 \times 10^{-16} \text{ A}$  and  $R_S = 10 \Omega$  and is operating at a current of 1 mA at room temperature. What are the values of  $V_D$  and  $V'_D$ ? (b) Repeat for  $R_S = 100 \Omega$ .

- 3.54. A *pn* diode has a resistivity of  $2 \Omega \cdot \text{cm}$  on the *p*-type side and  $0.01 \Omega \cdot \text{cm}$  on the *n*-type side. What is the value of  $R_S$  for this diode if the cross-sectional area of the diode is  $0.01 \text{ cm}^2$  and the lengths of the *p*- and *n*-sides of the diode are each  $250 \mu\text{m}$ ?
- \*3.55. A diode fabrication process has a specific contact resistance of  $10 \Omega \cdot \mu\text{m}^2$ . If the contacts are each  $1 \mu\text{m} \times 1 \mu\text{m}$  in size, what are the total contact resistances associated with the anode and cathode contacts to the diode in Fig. 3.21(a).
- 3.56. (a) Estimate the area of the diode in Fig. 3.21(a) if the contact dimensions are  $1 \mu\text{m} \times 1 \mu\text{m}$ . (b) Repeat for  $0.13 \mu\text{m} \times 0.13 \mu\text{m}$  contacts.

### 3.10 Diode Circuit Analysis Load-Line Analysis

- 3.57. (a) Plot the load line and find the Q-point for the diode circuit in Fig. P3.57 if  $V = 10 \text{ V}$  and  $R = 5 \text{ k}\Omega$ . Use the *i-v* characteristic in Fig. P3.42. (b) Repeat for  $V = -10 \text{ V}$  and  $R = 5 \text{ k}\Omega$ . (c) Repeat for  $V = -2 \text{ V}$  and  $R = 2 \text{ k}\Omega$ .

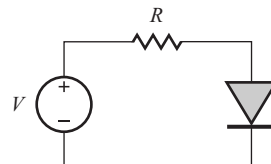


Figure P3.57

- 3.58. (a) Plot the load line and find the Q-point for the diode circuit in Fig. P3.57 if  $V = 5 \text{ V}$  and  $R = 10 \text{ k}\Omega$ . Use the *i-v* characteristic in Fig. P3.42. (b) Repeat for  $V = -6 \text{ V}$  and  $R = 3 \text{ k}\Omega$ . (c) Repeat for  $V = -3 \text{ V}$  and  $R = 3 \text{ k}\Omega$ .
- 3.59. Simulate the circuit in Prob. 3.57 with SPICE and compare the results to those in Prob. 3.57. Use  $I_S = 10^{-15} \text{ A}$ .
- 3.60. Use the *i-v* characteristic in Fig. P3.42. (a) Plot the load line and find the Q-point for the diode circuit in Fig. P3.57 if  $V = 6 \text{ V}$  and  $R = 4 \text{ k}\Omega$ . (b) For  $V = -6 \text{ V}$  and  $R = 3 \text{ k}\Omega$ . (c) For  $V = -3 \text{ V}$  and  $R = 3 \text{ k}\Omega$ . (d) For  $V = 12 \text{ V}$  and  $R = 8 \text{ k}\Omega$ . (e) For  $V = -25 \text{ V}$  and  $R = 10 \text{ k}\Omega$ .
- 3.61. (a) Plot the load line and find the Q-point for the diode circuit in Fig. P3.57 if  $V = -10 \text{ V}$  and  $R = 10 \text{ k}\Omega$ . Use the *i-v* characteristic in Fig. P3.42. (b) Repeat for  $V = 10 \text{ V}$  and  $R = 10 \text{ k}\Omega$ . (c) Repeat for  $V = -4 \text{ V}$  and  $R = 2 \text{ k}\Omega$ .

### Iterative Analysis and the Mathematical Model

- 3.62. (a) Use direct trial and error to find the solution to the diode circuit in Fig. 3.22 using Eq. (3.27).
- 3.63. Repeat the iterative procedure used in the spreadsheet in Table 3.2 for initial guesses of  $1 \mu\text{A}$ ,  $5 \text{ mA}$ , and  $5 \text{ A}$  and  $0 \text{ A}$ . How many iterations are required for each case? Did any problem arise? If so, what is the source of the problem?
- 3.64. A diode has  $I_S = 0.1 \text{ fA}$  and is operating at  $T = 300 \text{ K}$ . (a) What are the values of  $V_{DO}$  and  $r_D$  if  $I_D = 100 \mu\text{A}$ ? (b) If  $I_D = 2.5 \text{ mA}$ ? (c) If  $I_D = 20 \text{ mA}$ ?
- 3.65. (a) Use the iterative procedure in the spreadsheet in Table 3.2 to find the diode current and voltage for the circuit in Fig. 3.22 if  $V = 7.5 \text{ V}$  and  $R = 3 \text{ k}\Omega$ . (b) Repeat for  $V = 2.5 \text{ V}$  and  $R = 15 \text{ k}\Omega$ .
- 3.66. (a) Use the iterative procedure in the spreadsheet in Table 3.2 to find the diode current and voltage for the circuit in Fig. 3.22 if  $V = 3 \text{ V}$  and  $R = 15 \text{ k}\Omega$ . (b) Repeat for  $V = 1 \text{ V}$  and  $R = 6.2 \text{ k}\Omega$ .
- 3.67. Use MATLAB or MATHCAD to numerically find the Q-point for the circuit in Fig. 3.22 using the equation in the exercise on page 100.

### Ideal Diode and Constant Voltage Drop Models

- \*3.68. Find the Q-point for the circuit in Fig. 3.22 using the same four methods as in Sec. 3.10 if the voltage source is  $1 \text{ V}$ . Compare the answers in a manner similar to Table 3.3.
- 3.69. Find the Q-point for the diode in Fig. P3.69 using (a) the ideal diode model and (b) the constant voltage drop model with  $V_{on} = 0.6 \text{ V}$ . (c) Discuss the results. Which answer do you feel is most correct? (d) Use iterative analysis to find the actual Q-point if  $I_S = 1 \text{ fA}$ .

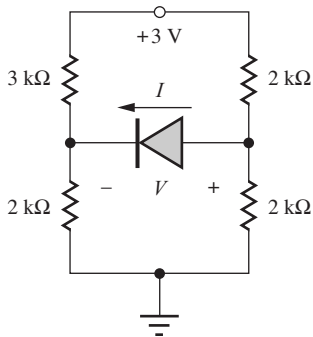


Figure P3.69

- 3.70. (a) Find the worst-case values of the Q-point current for the diode in Fig. P3.69 using the ideal diode model if the resistors all have 10 percent tolerances. (b) Repeat using the CVD model with  $V_{on} = 0.6 \text{ V}$ .
- 3.71. Simulate the circuit of Fig. P3.69 and find the diode Q-point. Compare the results to those in Prob. 3.69.
- 3.72. (a) Find  $I$  and  $V$  in the four circuits in Fig. P3.72 using the ideal diode model. (b) Repeat using the constant voltage drop model with  $V_{on} = 0.7 \text{ V}$ .

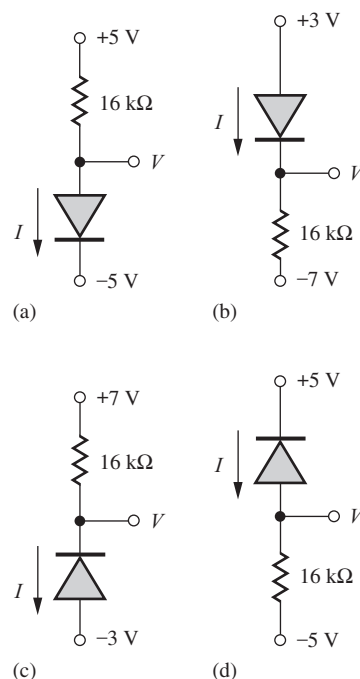
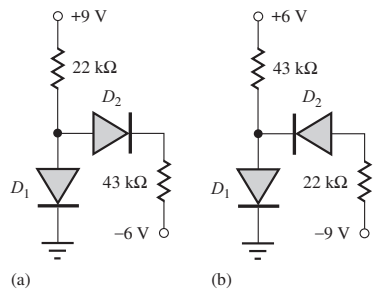


Figure P3.72

- 3.73. (a) Find  $I$  and  $V$  in the four circuits in Fig. P3.72 using the ideal diode model if the resistor values are changed to  $100 \text{ k}\Omega$ . (b) Repeat using the constant voltage drop model with  $V_{on} = 0.6 \text{ V}$ .

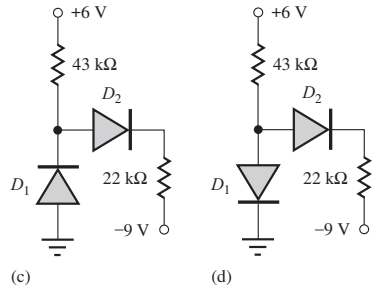
### 3.11 Multiple Diode Circuits

- 3.74. Find the Q-points for the diodes in the four circuits in Fig. P3.74 using (a) the ideal diode model and (b) the constant voltage drop model with  $V_{on} = 0.65 \text{ V}$ .



(a)

(b)

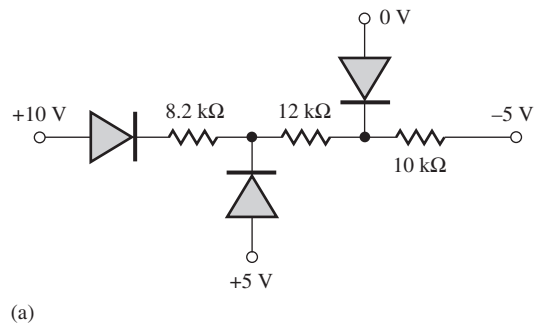


(c)

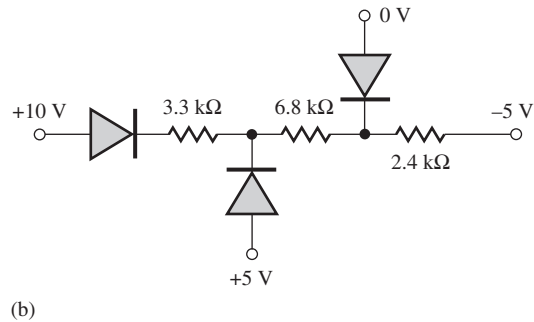
(d)

**Figure P3.74**

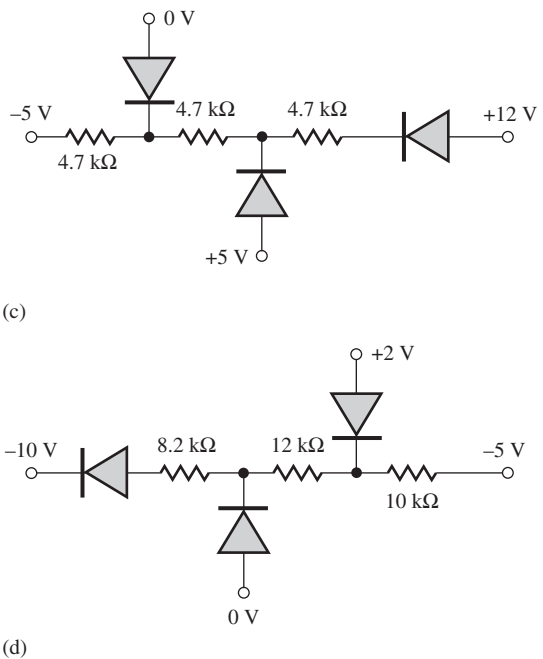
- 3.75. Find the Q-points for the diodes in the four circuits in Fig. P3.74 if the values of all the resistors are changed to  $15\text{ k}\Omega$  using (a) the ideal diode model and (b) the constant voltage drop model with  $V_{\text{on}} = 0.65\text{ V}$ .
- 3.76. Find the Q-point for the diodes in the circuits in Fig. P3.76 using the ideal diode model.



(a)



(b)



(c)

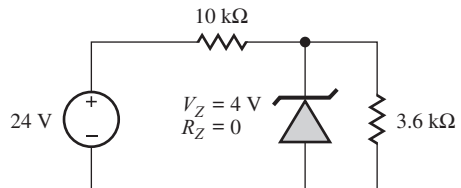
(d)

**Figure P3.76**

- 3.77. Find the Q-point for the diodes in the circuits in Fig. P3.76 using the constant voltage drop model with  $V_{\text{on}} = 0.65\text{ V}$ .
- 3.78. Simulate the diode circuits in Fig. P3.76 and compare your results to those in Prob. 3.76.
- 3.79. Verify that the values presented in Ex. 3.8 using the ideal diode model are correct.
- 3.80. Simulate the circuit in Fig. 3.33 and compare to the results in Ex. 3.8.

### 3.12 Analysis of Diodes Operating in the Breakdown Region

- 3.81. Draw the load line for the circuit in Fig. P3.81 on the characteristics in Fig. P3.42 and find the Q-point.

**Figure P3.81**

- 3.82. Find the Q-point for the Zener diode in Fig. P3.81.
- 3.83. What is maximum load current  $I_L$  that can be drawn from the Zener regulator in Fig. P3.83 if it is to

maintain a regulated output? What is the minimum value of  $R_L$  that can be used and still have a regulated output voltage?

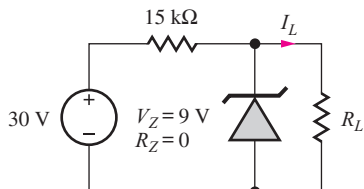


Figure P3.83

- 3.84. What is power dissipation in the Zener diode in Fig. P3.83 for  $R_L = \infty$ ?
- 3.85. Load resistor  $R_L$  in Fig. P3.83 is  $10 \text{ k}\Omega$ . What are the nominal and worst-case values of Zener diode current and power dissipation if the power supply voltage, Zener breakdown voltage and resistors all have 5 percent tolerances?
- 3.86. What is power dissipation in the Zener diode in Fig. P3.86 for (a)  $R_L = 100 \Omega$ ? (b)  $R_L = \infty$ ?

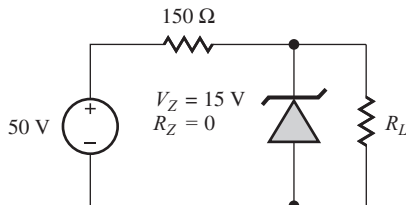


Figure P3.86

- 3.87. Load resistor  $R_L$  in Fig. P3.86 is  $100 \Omega$ . What are the nominal and worst-case values of Zener diode current and power dissipation if the power supply voltage, Zener breakdown voltage, and resistors all have 10 percent tolerances?

### 3.13 Half-Wave Rectifier Circuits

- 3.88. A power diode has a reverse saturation current of  $10^{-9} \text{ A}$  and  $n = 2$ . What is the forward voltage drop at the peak current of  $48.6 \text{ A}$  that was calculated in the example in Sec. 3.13.5?
- 3.89. A power diode has a reverse saturation current of  $10^{-8} \text{ A}$  and  $n = 1.6$ . What is the forward voltage drop at the peak current of  $100 \text{ A}$ ? What is the power dissipation in the diode in a half-wave rectifier application operating at  $60 \text{ Hz}$  if the series resistance is  $0.01 \Omega$  and the conduction time is  $1 \text{ ms}$ ?
- \*3.90. (a) Use a spreadsheet or MATLAB or write a computer program to find the numeric solution to the

conduction angle equation for a  $60 \text{ Hz}$  half-wave rectifier circuit that uses a filter capacitance of  $100,000 \mu\text{F}$ . The circuit is designed to provide  $5 \text{ V}$  at  $5 \text{ A}$ . {That is, solve  $[(V_P - V_{on}) \exp(-t/RC)] = V_P \cos \omega t - V_{on}]$ . Be careful! There are an infinite number of solutions to this equation. Be sure your algorithm finds the desired answer to the problem.} Assume  $V_{on} = 1 \text{ V}$ . (b) Compare to calculations using Eq. (3.57).

- 3.91. What is the actual average value (the dc value) of the rectifier output voltage for the waveform in Fig. P3.91 if  $V_r$  is 5 percent of  $V_P - V_{on} = 18 \text{ V}$ ?

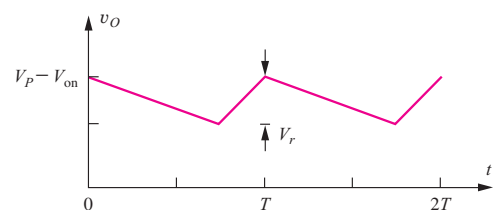


Figure P3.91

- 3.92. Draw the voltage waveforms, similar to those in Fig. 3.53, for the negative output rectifier in Fig. 3.57(b).
- \*3.93. Show that evaluation of Eq. (3.61) will yield the result in Eq. (3.62).
- 3.94. The half-wave rectifier in Fig. P3.94 is operating at a frequency of  $60 \text{ Hz}$ , and the rms value of the transformer output voltage  $v_I$  is  $12.6 \text{ V} \pm 10\%$ . What are the nominal and worst case values of the dc output voltage  $V_O$  if the diode voltage drop is  $1 \text{ V}$ ?

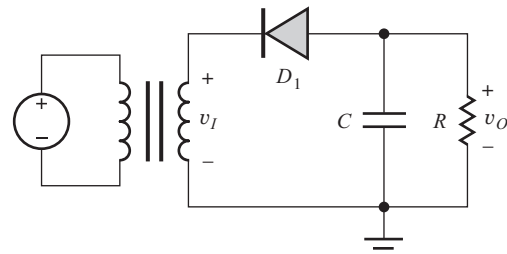


Figure P3.94

- 3.95. The half-wave rectifier in Fig. P3.94 is operating at a frequency of  $60 \text{ Hz}$ , and the rms value of the transformer output voltage is  $6.3 \text{ V}$ . (a) What is the value of the dc output voltage  $V_O$  if the diode voltage drop is  $1 \text{ V}$ ? (b) What is the minimum value of  $C$  required to maintain the ripple voltage to less than  $0.25 \text{ V}$  if  $R = 0.5 \Omega$ ? (c) What is the PIV

rating of the diode in this circuit? (d) What is the surge current when power is first applied? (e) What is the amplitude of the repetitive current in the diode?

- 3.96. Simulate the behavior of the half-wave rectifier in Fig. P3.94 for  $v_I = 10 \sin 120\pi t$ ,  $R = 0.025 \Omega$  and  $C = 0.5 \text{ F}$ . (Use  $IS = 10^{-10} \text{ A}$ ,  $RS = 0$ , and  $\text{RELTOL} = 10^{-6}$ .) Compare the simulated values of dc output voltage, ripple voltage, and peak diode current to hand calculations. Repeat simulation with  $R_S = 0.02 \Omega$ .
- 3.97. (a) Repeat Prob. 3.95 for a frequency of 400 Hz.  
(b) Repeat Prob. 3.95 for a frequency of 70 kHz.
- 3.98. For the Zener regulated power supply in Fig. P3.98, the rms value of  $v_I$  is 15 V, the operating frequency is 60 Hz,  $R = 100 \Omega$ ,  $C = 1000 \mu\text{F}$ , the on-voltage of diodes  $D_1$  and  $D_2$  is 0.75 V, and the Zener voltage of diode  $D_3$  is 15 V. (a) What type of rectifier is used in this power supply circuit? (b) What is the dc voltage at  $V_1$ ? (c) What is the dc output voltage  $V_O$ ? (d) What is the magnitude of the ripple voltage at  $V_1$ ? (e) What is the minimum PIV rating for the rectifier diodes? (f) Draw a new version of the circuit that will produce an output voltage of  $-15 \text{ V}$ .

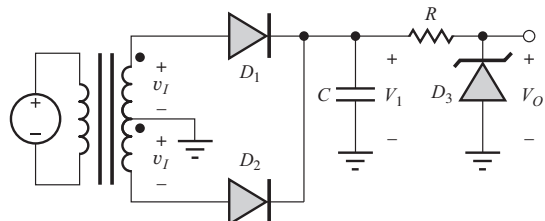


Figure P3.98

- 3.99. A 3.3-V, 30-A dc power supply is to be designed with a ripple of less than 2.5 percent. Assume that a half-wave rectifier circuit (60 Hz) with a capacitor filter is used. (a) What is the size of the filter capacitor  $C$ ? (b) What is the PIV rating for the diode? (c) What is the rms value of the transformer voltage needed for the rectifier? (d) What is the value of the peak repetitive diode current in the diode? (e) What is the surge current at  $t = 0^+$ ?
- 3.100. A 2800-V, 2-A, dc power supply is to be designed with a ripple voltage  $\leq 0.5$  percent. Assume that a half-wave rectifier circuit (60 Hz) with a capacitor filter is used. (a) What is the size of the filter capacitor  $C$ ? (b) What is the minimum PIV rating for the diode? (c) What is the rms value of the trans-

former voltage needed for the rectifier? (d) What is the peak value of the repetitive current in the diode? (e) What is the surge current at  $t = 0^+$ ?

- \*3.101. Draw the voltage waveforms at nodes  $v_O$  and  $v_1$  for the “voltage-doubler” circuit in Fig. P3.101 for the first two cycles of the input sine wave. What is the steady-state output voltage if  $V_P = 17 \text{ V}$ ?

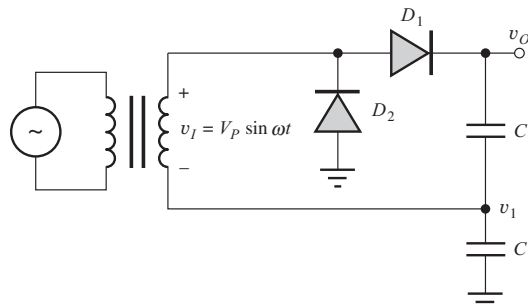


Figure P3.101

- 3.102. Simulate the voltage-doubler rectifier circuit in Fig. P3.101 for  $C = 500 \mu\text{F}$  and  $v_I = 1500 \sin 2\pi(60)t$  with a load resistance of  $R_L = 3000 \Omega$  added between  $v_O$  and ground. Calculate the ripple voltage and compare to the simulation.
- 3.103. Simulate the AM demodulator in the EIA on page 122. Compare the spectra of the voltages across the two capacitors.

### 3.14 Full-Wave Rectifier Circuits

- 3.104. The full-wave rectifier in Fig. P3.104 is operating at a frequency of 60 Hz, and the rms value of the transformer output voltage is 18 V. (a) What is the value of the dc output voltage if the diode voltage drop is 1 V? (b) What is the minimum value of  $C$  required to maintain the ripple voltage to less than 0.25 V if  $R = 0.5 \Omega$ ? (c) What is the PIV rating of the diode in this circuit? (d) What is the surge current when power is first applied? (e) What is the amplitude of the repetitive current in the diode?

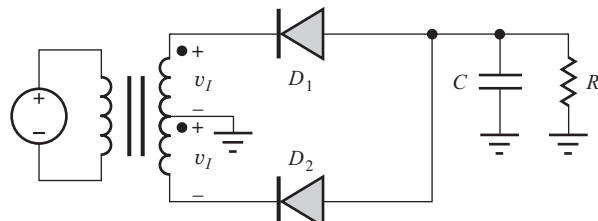


Figure P3.104

- 3.105. Repeat Prob. 3.104 if the rms value of the transformer output voltage  $v_I$  is 10 V.

- 3.106. Simulate the behavior of the full-wave rectifier in Fig. P3.104 for  $R = 3 \Omega$  and  $C = 22,000 \mu\text{F}$ . Assume that the rms value of  $v_I$  is 10.0 V and the frequency is 400 Hz. (Use  $\text{IS} = 10^{-10} \text{ A}$ ,  $\text{RS} = 0$ , and  $\text{RELTOL} = 10^{-6}$ .) Compare the simulated values of dc output voltage, ripple voltage, and peak diode current to hand calculations. Repeat simulation with  $R_S = 0.25$ .
- 3.107. Repeat Prob. 3.99 for a full-wave rectifier circuit.
- 3.108. Repeat Prob. 3.100 for a full-wave rectifier circuit.
- \*3.109. The full-wave rectifier circuit in Fig. P3.109(a) was designed to have a maximum ripple of approximately 1 V, but it is not operating properly. The measured waveforms at the three nodes in the circuit are shown in Fig. P3.109(b). What is wrong with the circuit?

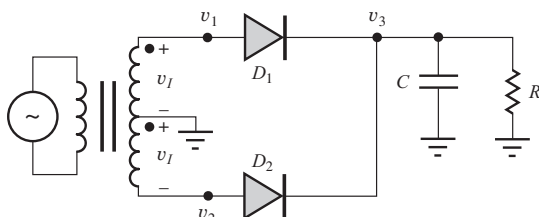


Figure P3.109(a)

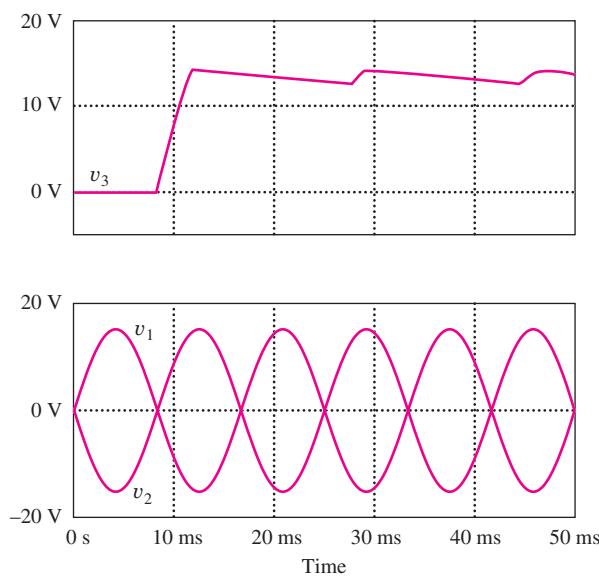


Figure P3.109(b) Waveforms for the circuit in Fig. P3.109(a).

### 3.15 Full-Wave Bridge Rectification

- 3.110. Repeat Prob. 3.104 for a full-wave bridge rectifier circuit. Draw the circuit.

- 3.111. Repeat Prob. 3.99 for a full-wave bridge rectifier circuit. Draw the circuit.
- 3.112. Repeat Prob. 3.100 for a full-wave bridge rectifier circuit. Draw the circuit.
- \*3.113. What are the dc output voltages  $V_1$  and  $V_2$  for the rectifier circuit in Fig. P3.113 if  $v_I = 40 \sin 377t$  and  $C = 20,000 \mu\text{F}$ ?

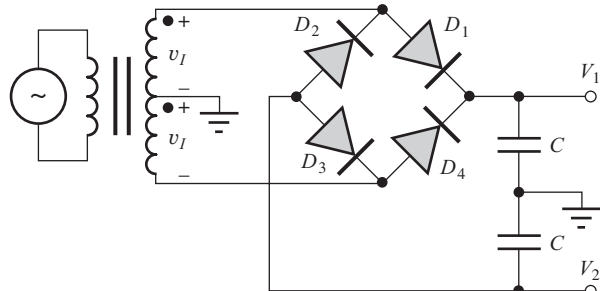


Figure P3.113

- 3.114. Simulate the rectifier circuit in Fig. P3.113 for  $C = 100 \text{ mF}$  and  $v_I = 40 \sin 2\pi(60)t$  with a  $500\text{-}\Omega$  load connected between each output and ground.
- 3.115. Repeat Prob. 3.104 if the full-wave bridge circuit is used instead of the rectifier in Fig. P3.104. Draw the circuit!

### 3.16 Rectifier Comparison and Design Tradeoffs

- 3.116. A 3.3-V, 15-A dc power supply is to be designed to have a ripple voltage of no more than 10 mV. Compare the pros and cons of implementing this power supply with half-wave, full-wave, and full-wave bridge rectifiers.
- 3.117. A 200-V, 3-A dc power supply is to be designed with less than a 2 percent ripple voltage. Compare the pros and cons of implementing this power supply with half-wave, full-wave, and full-wave bridge rectifiers.
- 3.118. A 3000-V, 1-A dc power supply is to be designed with less than a 4 percent ripple voltage. Compare the pros and cons of implementing this power supply with half-wave, full-wave, and full-wave bridge rectifiers.

### 3.17 Dynamic Switching Behavior of the Diode

- \*3.119. (a) Calculate the current at  $t = 0^+$  in the circuit in Fig. P3.119. (b) Calculate  $I_F$ ,  $I_R$ , and the storage time expected when the diode is switched off if  $\tau_T = 7 \text{ ns}$ .

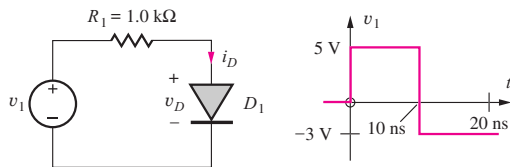
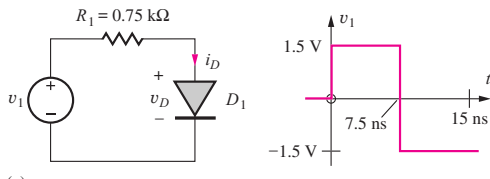


Figure P3.119

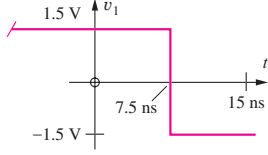
- 3.120. (a) Simulate the switching behavior of the circuit in Fig. P3.119. (b) Compare the simulation results to the hand calculations in Prob. 3.119.

- \*3.121. (a) Calculate the current at \$t = 0^+\$ in the circuit in Fig. P3.119 if \$R\_1\$ is changed to \$5 \Omega\$. (b) Calculate \$I\_F\$, \$I\_R\$, and the storage time expected when the diode is switched off at \$t = 10 \mu\text{s}\$ if \$\tau\_T = 250 \text{ nS}\$.

- \*\*3.122. The simulation results presented in Fig. 3.68 were performed with the diode transit time \$\tau\_T = 5 \text{ ns}\$. (a) Repeat the simulation of the diode circuit in Fig. 3.122(a) with the diode transit time changed to \$\tau\_T = 50 \text{ ns}\$. Does the storage time that you observe change in proportion to the value of \$\tau\_T\$ in your simulation? Discuss. (b) Repeat the simulation with the input voltage changed to the one in Fig. P3.122(b), in which it is assumed that \$v\_1\$ has been at 1.5 V for a long time, and compare the results to those obtained in (a). What is the reason for the difference between the results in (a) and (b)?



(a)



(b)

Figure 3.122

### 3.18 Photo Diodes, Solar Cells, and LEDs

- \*3.123. The output of a diode used as a solar cell is given by

$$I_C = 1 - 10^{-15}[\exp(40V_C) - 1] \text{ amperes}$$

What operating point corresponds to \$P\_{\max}\$? What is \$P\_{\max}\$? What are the values of \$I\_{SC}\$ and \$V\_{OC}\$?

- \*3.124. Three diodes are connected in series to increase the output voltage of a solar cell. The individual outputs of the three diodes are given by

$$I_{C1} = 1.05 - 10^{-15}[\exp(40V_{C1}) - 1] \text{ A}$$

$$I_{C2} = 1.00 - 10^{-15}[\exp(40V_{C2}) - 1] \text{ A}$$

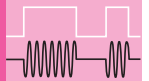
$$I_{C3} = 0.95 - 10^{-15}[\exp(40V_{C3}) - 1] \text{ A}$$

(a) What are the values of \$I\_{SC}\$ and \$V\_{OC}\$ for the series connected cell? (b) What is the value of \$P\_{\max}\$?

- \*\*3.125. The bandgaps of silicon and gallium arsenide are 1.12 eV and 1.42 eV, respectively. What are the wavelengths of light that you would expect to be emitted from these devices based on direct recombination of holes and electrons? To what “colors” of light do these wavelengths correspond?

- \*\*3.126. Repeat Prob. 3.125 for Ge, GaN, InP, InAs, BN, SiC and CdSe.

# CHAPTER 4



## FIELD-EFFECT TRANSISTORS

### CHAPTER OUTLINE

- 4.1 Characteristics of the MOS Capacitor 146
- 4.2 The NMOS Transistor 148
- 4.3 PMOS Transistors 161
- 4.4 MOSFET Circuit Symbols 163
- 4.5 Capacitances in MOS Transistors 165
- 4.6 MOSFET Modeling in SPICE 167
- 4.7 MOS Transistor Scaling 169
- 4.8 MOS Transistor Fabrication and Layout Design Rules 172
- 4.9 Biasing the NMOS Field-Effect Transistor 176
- 4.10 Biasing the PMOS Field-Effect Transistor 188
- 4.11 The Junction Field-Effect Transistor (JFET) 190
- 4.12 JFET Modeling in SPICE 197
- 4.13 Biasing the JFET and Depletion-Mode MOSFET 198  
Summary 200  
Key Terms 202  
References 203  
Problems 204

### CHAPTER GOALS

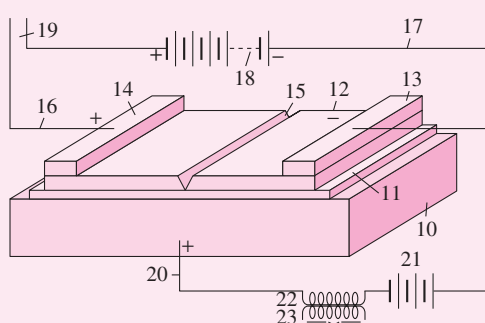
- Develop a qualitative understanding of the operation of the MOS field-effect transistor
- Define and explore FET characteristics in the cutoff, triode, and saturation regions of operation
- Develop mathematical models for the current-voltage ( $i$ - $v$ ) characteristics of MOSFETs and JFETs
- Introduce the graphical representations for the output and transfer characteristic descriptions of electron devices
- Catalog and contrast the characteristics of both NMOS and PMOS enhancement-mode and depletion-mode FETs
- Learn the symbols used to represent FETs in circuit schematics
- Investigate circuits used to bias the transistors into various regions of operation
- Learn the basic structure and mask layout for MOS transistors and circuits
- Explore the concept of MOS device scaling

- Contrast three- and four-terminal device behavior
- Understand sources of capacitance in MOSFETs
- Explore FET Modeling in SPICE

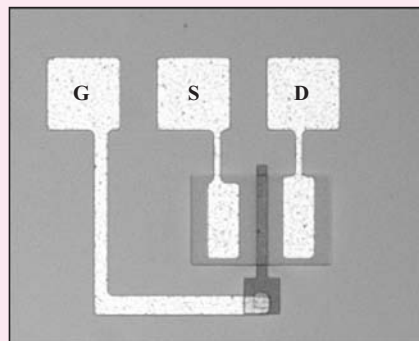
In this chapter we begin to explore the field-effect transistor or FET. The FET has emerged as the dominant device in modern integrated circuits and is present in the vast majority of semiconductor products produced today. The ability to dramatically shrink the size of the FET device has made possible handheld computational power unimagined just 20 years ago.

As noted in Chapter 1, various versions of the field-effect device were conceived by Lilienfeld in 1928, Heil in 1935, and Shockley in 1952, well before the technology to produce such devices existed. The first successful metal-oxide-semiconductor field-effect transistors, or MOSFETs, were fabricated in the late 1950s, but it took nearly a decade to develop reliable commercial fabrication processes for MOS devices. Because of fabrication-related difficulties, MOSFETs with a *p*-type conducting region, PMOS devices, were the first to be commercially available in IC form, and the first microprocessors were built using PMOS processes. By the late 1960s, understanding and control of fabrication processes had improved to the point that devices with an *n*-type conducting region, NMOS transistors, could be reliably fabricated in large numbers, and NMOS rapidly supplanted PMOS technology because the improved mobility of the NMOS device translated directly into higher circuit performance. By the mid 1980s, power had become a severe problem, and the low-power characteristics of complementary MOS or CMOS devices caused a rapid shift to that technology even though it was a more complex and costly process. Today CMOS technology, which utilizes both NMOS and PMOS transistors, is the dominant technology in the electronics industry.

An additional type of FET, the junction field-effect transistor or JFET, is based upon a *pn* junction structure and is typically found in analog applications including the design of op amps and RF circuits.



Drawing from Lillienfeld patent [1]



Top view of a simple MOSFET

**C**hapter 4 explores the characteristics of the **metal-oxide-semiconductor field-effect transistor (MOSFET)** that is without doubt the most commercially successful solid-state device. It is the primary component in high-density VLSI chips, including microprocessors and memories. A second type of FET, the **junction field-effect transistor (JFET)**, is based on a *pn* junction structure and finds application particularly in analog and RF circuit design.

**P-channel MOS (PMOS) transistors** were the first MOS devices to be successfully fabricated in large-scale integrated (LSI) circuits. Early microprocessor chips used PMOS technology. Greater performance was later obtained with the commercial introduction of **n-channel MOS (NMOS)** technology, using both enhancement-mode and ion-implanted depletion-mode devices.

This chapter discusses the qualitative and quantitative *i-v* behavior of FETs and investigates the differences between the various types of transistors. Techniques for biasing the transistors in various regions of operation are also presented.

Early integrated circuit chips contained only a few transistors, whereas today, the National Technology Roadmap for Semiconductors (NTRS [2]) projects the existence of chips with greater than 10 billion transistors by the year 2020! This phenomenal increase in transistor density has been the force behind the explosive growth of the electronics industry outlined in Chapter 1 that has been driven by our ability to reduce (scale) the dimensions of the transistor without compromising its operating characteristics.

Although the bipolar junction transistor or BJT was successfully reduced to practice before the FET, the FET is conceptually easier to understand and is by far the most commercially important device. Thus, we consider it first. The BJT is discussed in detail in Chapter 5.

## 4.1 CHARACTERISTICS OF THE MOS CAPACITOR

At the heart of the MOSFET is the **MOS capacitor** structure depicted in Fig. 4.1. Understanding the qualitative behavior of this capacitor provides a basis for understanding operation of the MOSFET. The MOS capacitor is used to induce charge at the interface between the semiconductor and oxide. The top electrode of the MOS capacitor is formed of a low-resistivity material, typically aluminum or heavily doped polysilicon (polycrystalline silicon). We refer to this electrode as the **gate (G)** for reasons that become apparent shortly. A thin insulating layer, typically silicon dioxide, isolates the gate from the substrate or body—the semiconductor region that acts as the second electrode of the capacitor. Silicon dioxide is a stable, high-quality electrical insulator readily formed by thermal oxidation of the silicon substrate. The ability to form this stable high-quality insulator is one of the basic reasons that silicon is the dominant semiconductor material today. The semiconductor region may be *n*- or *p*-type. A *p*-type substrate is depicted in Fig. 4.1.

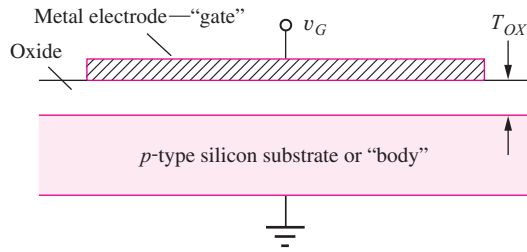


**Figure 4.1** MOS capacitor structure on *p*-type silicon.

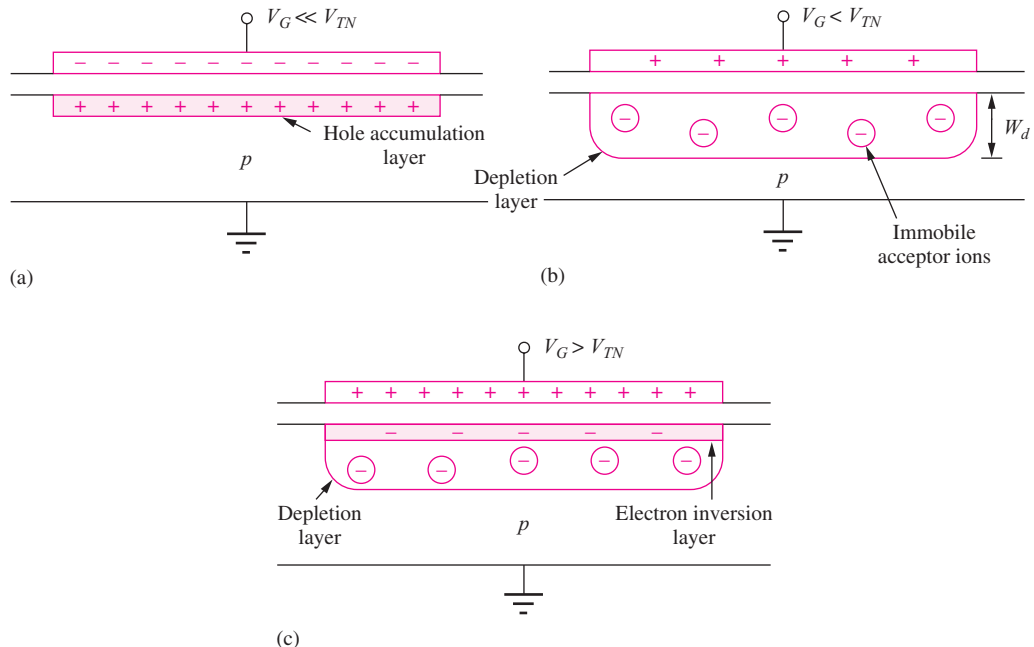


**Figure 4.2** MOS capacitor operating in (a) accumulation, (b) depletion, and (c) inversion. Parameter  $V_{TN}$  in the figure is called the threshold voltage and represents the voltage required to just begin formation of the inversion layer.

The semiconductor forming the bottom electrode of the capacitor typically has a substantial resistivity and a limited supply of holes and electrons. Because the semiconductor can therefore be depleted of carriers, as discussed in Chapter 2, the capacitance of this structure is a nonlinear function of voltage. Figure 4.2 shows the conditions in the region of the substrate immediately below the gate electrode for three different bias conditions: accumulation, depletion, and inversion.

#### 4.1.1 ACCUMULATION REGION

The situation for a large negative bias on the gate with respect to the substrate is indicated in Fig. 4.2(a). The large negative charge on the metallic gate is balanced by positively charged holes attracted to the silicon-silicon dioxide interface directly below the gate. For the bias condition shown, the hole density at the surface exceeds that which is present in the original *p*-type substrate, and the surface is said to be operating in the **accumulation region** or just in **accumulation**. This majority carrier accumulation layer is extremely shallow, effectively existing as a charge sheet directly below the gate.

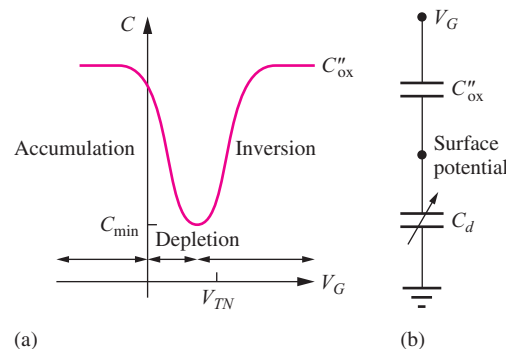


**Figure 4.3** (a) Low frequency capacitance-voltage ( $C$ - $V$ ) characteristics for a MOS capacitor on a  $p$ -type substrate. (b) Series capacitance model for the  $C$ - $V$  characteristic.

### 4.1.2 DEPLETION REGION

Now consider the situation as the gate voltage is slowly increased. First, holes are repelled from the surface. Eventually, the hole density near the surface is reduced below the majority-carrier level set by the substrate doping level, as depicted in Fig. 4.2(b). This condition is called **depletion** and the region, the **depletion region**. The region beneath the metal electrode is depleted of free carriers in much the same way as the depletion region that exists near the metallurgical junction of the  $pn$  junction diode. In Fig. 4.2(b), positive charge on the gate electrode is balanced by the negative charge of the ionized acceptor atoms in the depletion layer. The depletion-region width  $w_d$  can range from a fraction of a micron to tens of microns, depending on the applied voltage and substrate doping levels.

### 4.1.3 INVERSION REGION

As the voltage on the top electrode increases further, electrons are attracted to the surface. At some particular voltage level, the electron density at the surface exceeds the hole density. At this voltage, the surface has inverted from the  $p$ -type polarity of the original substrate to an  $n$ -type **inversion layer**, or **inversion region**, directly underneath the top plate as indicated in Fig. 4.2(c). This inversion region is an extremely shallow layer, existing as a charge sheet directly below the gate. In the MOS capacitor, the high density of electrons in the inversion layer is supplied by the electron–hole generation process within the depletion layer.

The positive charge on the gate is balanced by the combination of negative charge in the inversion layer plus negative ionic acceptor charge in the depletion layer. The voltage at which the surface inversion layer just forms plays an extremely important role in field-effect transistors and is called the **threshold voltage**  $V_{TN}$ .

Figure 4.3 depicts the variation of the capacitance of the NMOS structure with gate voltage. At voltages well below threshold, the surface is in accumulation, corresponding to Fig. 4.2(a), and the capacitance is high and determined by the **oxide thickness**. As the gate voltage increases, the surface depletion layer forms as in Fig. 4.2(b), the effective separation of the capacitor plates increases, and the capacitance decreases. The total capacitance can be modeled as the series combination of the fixed oxide capacitance  $C''_{ox}$  and the voltage dependent depletion-layer capacitance  $C_d$ , as in Fig. 4.3(b). The inversion layer forms at the surface as  $V_G$  exceeds threshold voltage  $V_{TN}$ , as in Fig. 4.2(c), and the capacitance rapidly increases back to the value determined by the oxide layer thickness.

## 4.2 THE NMOS TRANSISTOR

A MOSFET is formed by adding two heavily doped  $n$ -type ( $n^+$ ) diffusions to the cross section of Fig. 4.1, resulting in the structure in Fig. 4.4. The diffusions provide a supply of electrons that can readily move under the gate as well as terminals that can be used to apply a voltage and cause a current in the channel region of the transistor.

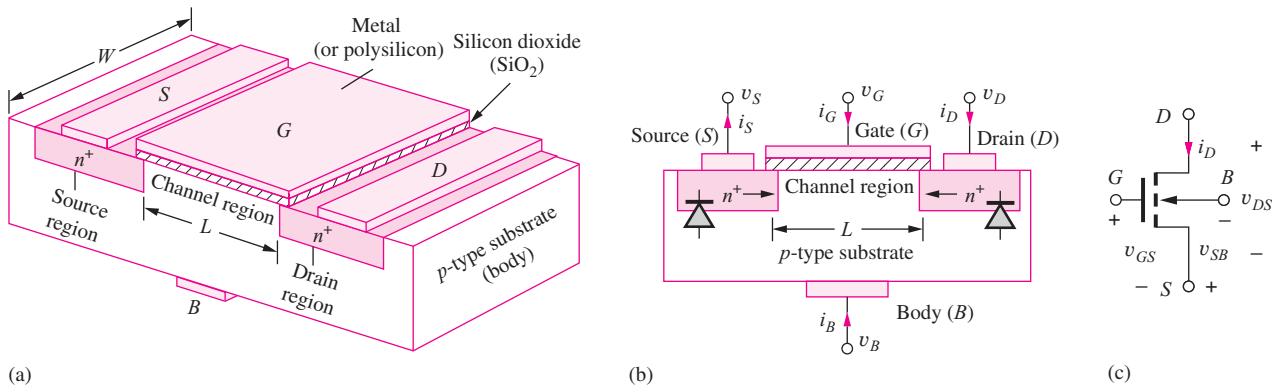


**Figure 4.4** (a) NMOS transistor structure; (b) cross section; and (c) circuit symbol for the four-terminal NMOSFET.

Figure 4.4 shows a planar view, cross section, and circuit symbol of an **n-channel MOSFET**, usually called an **NMOS transistor**, or **NMOSFET**. The central region of the NMOSFET is the MOS capacitor discussed in Sec. 4.1, and the top electrode of the capacitor is called the **gate**. The two heavily doped *n*-type regions (*n*<sup>+</sup> regions), called the **source (S)** and **drain (D)**, are formed in the *p*-type substrate and aligned with the edge of the gate. The source and drain provide a supply of carriers so that the inversion layer can rapidly form in response to the gate voltage. The substrate of the NMOS transistor represents a fourth device terminal and is referred to synonymously as the **substrate terminal**, or the **body terminal (B)**.

The terminal voltages and currents for the NMOS device are defined in Figs. 4.4(b) and (c). Drain current  $i_D$ , source current  $i_S$ , gate current  $i_G$ , and body current  $i_B$  are all defined, with the positive direction of each current indicated for an NMOS transistor. The important terminal voltages are the gate-source voltage  $v_{GS} = v_G - v_S$ , the drain-source voltage  $v_{DS} = v_D - v_S$ , and the source-bulk voltage  $v_{SB} = v_S - v_B$ . These voltages are all positive during normal operation of the NMOSFET.

Note that the source and drain regions form *pn* junctions with the substrate. These two junctions are kept reverse-biased at all times to provide isolation between the junctions and the substrate as well as between adjacent MOS transistors. Thus, the bulk voltage must be less than or equal to the voltages applied to the source and drain terminals to ensure that these *pn* junctions are properly reverse-biased.

The semiconductor region between the source and drain regions directly below the gate is called the **channel region** of the FET, and two dimensions of critical import are defined in Fig. 4.4. **L** represents the **channel length**, which is measured in the direction of current in the channel. **W** is the **channel width**, which is measured perpendicular to the direction of current. In this and later chapters we will find that choosing the values for **W** and **L** is an important aspect of the digital and analog IC designer's task.

#### 4.2.1 QUALITATIVE *i-v* BEHAVIOR OF THE NMOS TRANSISTOR

Before attempting to derive an expression for the current-voltage characteristic of the NMOS transistor, let us try to develop a qualitative understanding of what we might expect by referring to Fig. 4.5. In the figure, the source, drain, and body of the NMOSFET are all grounded.

For a dc gate-source voltage,  $v_{GS} = V_{GS}$ , well below threshold voltage  $V_{TN}$ , as in Fig. 4.5(a), back-to-back *pn* junctions exist between the source and drain, and only a small leakage current can flow between these two terminals. For  $V_{GS}$  near but still below threshold, a depletion region forms beneath the gate and merges with the depletion regions of the source and drain, as indicated in Fig. 4.5(b). The depletion region is devoid of free carriers, so a current still does not appear between the source and drain. Finally, when the gate-channel voltage exceeds the threshold voltage  $V_{TN}$ , as

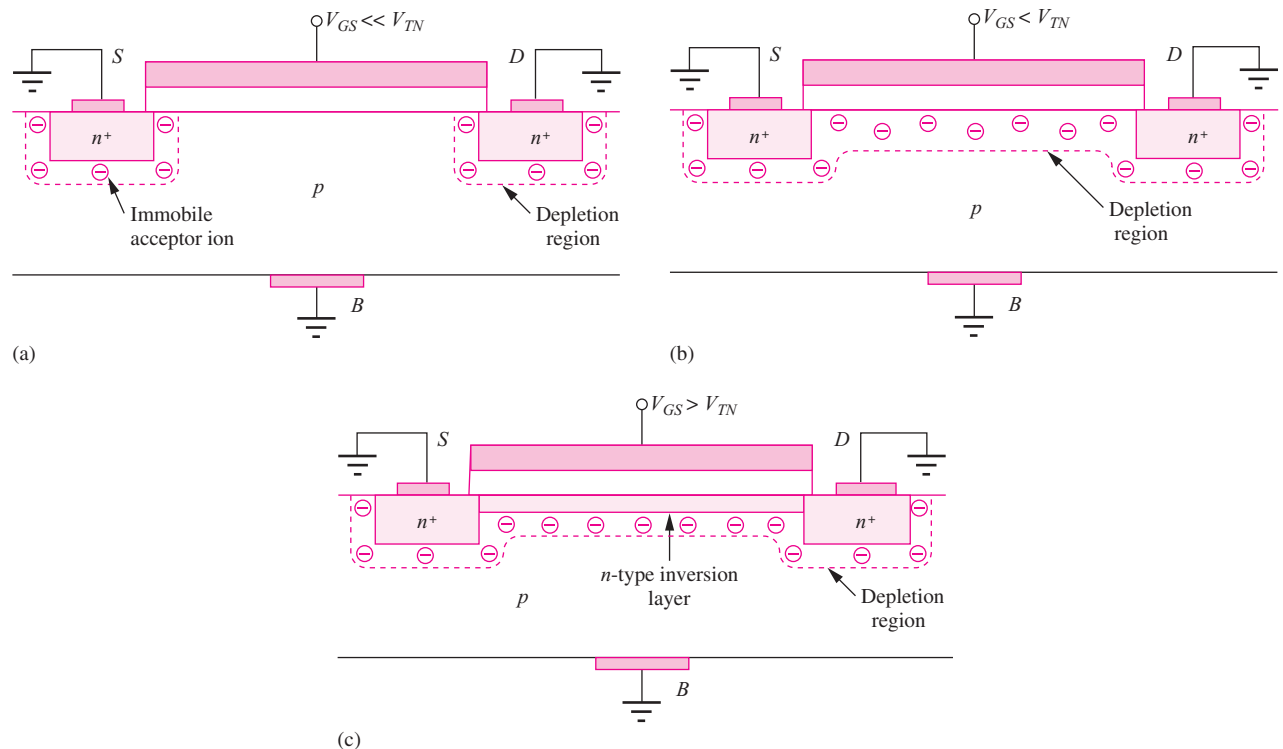


Figure 4.5 (a)  $V_{GS} \ll V_{TN}$ . (b)  $V_{GS} < V_{TN}$ . (c)  $V_{GS} > V_{TN}$ .

in Fig. 4.5(c), electrons flow in from the source and drain to form an inversion layer that connects the  $n^+$  source region to the  $n^+$  drain. A resistive connection, the channel, exists between the source and drain terminals.

If a positive voltage is now applied between the drain and source terminals, electrons in the channel inversion layer will drift in the electric field, creating a current in the terminals. Positive current in the NMOS transistor enters the drain terminal, travels down the channel, and exits the source terminal, as indicated by the polarities in Fig. 4.4(b). The gate terminal is insulated from the channel; thus, there is no dc gate current, and  $i_G = 0$ . The drain-bulk and source-bulk (and induced channel-to-bulk)  $pn$  junctions must be reverse-biased at all times to ensure that only a small reverse-bias leakage current exists in these diodes. This current is usually negligible with respect to the channel current  $i_D$  and is neglected. Thus we assume that  $i_B = 0$ .

In the device in Fig. 4.5, a channel must be induced by the applied gate voltage for conduction to occur. The gate voltage “enhances” the conductivity of the channel; this type of MOSFET is termed an **enhancement-mode device**. Later in this chapter we identify an additional type of MOSFET called a **depletion-mode device**. In Sec. 4.2.2, we develop a mathematical model for the current in the terminals of the NMOS device in terms of the applied voltages.

#### 4.2.2 TRIODE<sup>1</sup> REGION CHARACTERISTICS OF THE NMOS TRANSISTOR

We saw in Sec. 4.2.1 that both  $i_G$  and  $i_B$  are zero. Therefore, the current entering the drain in Fig. 4.4 must be equal to the current leaving the source:

$$i_S = i_D \quad (4.1)$$

<sup>1</sup> This region of operation is also referred to as the “linear region.” We will use triode region to avoid confusion with the concept of linear amplification introduced later in the text.

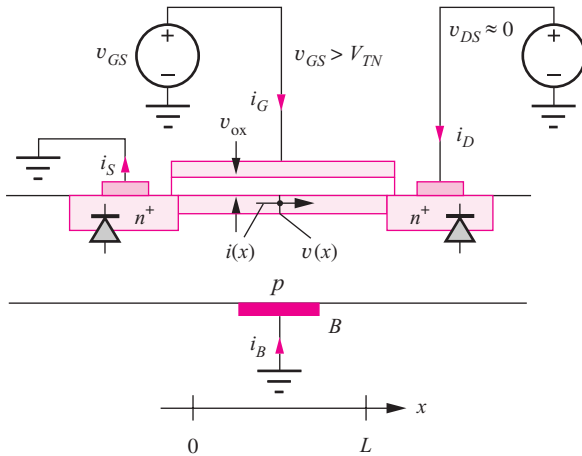


**Figure 4.6** Model for determining  $i$ - $v$  characteristics of the NMOS transistor.

An expression for the drain current  $i_D$  can be developed by considering the transport of charge in the channel in Fig. 4.6, which is depicted for a small value of  $v_{DS}$ . The electron charge per unit length (a line charge — C/cm) at any point in the channel is given by

$$Q' = -WC''_{ox}(v_{ox} - V_{TN}) \quad \text{C/cm for } v_{ox} \geq V_{TN} \quad (4.2)$$

where  $C''_{ox} = \epsilon_{ox}/T_{ox}$ , the oxide capacitance per unit area (F/cm<sup>2</sup>)

$\epsilon_{ox}$  = oxide permittivity (F/cm)       $T_{ox}$  = oxide thickness (cm)

For silicon dioxide,  $\epsilon_{ox} = 3.9\epsilon_0$ , where  $\epsilon_0 = 8.854 \times 10^{-14}$  F/cm.

The voltage  $v_{ox}$  represents the voltage across the oxide and will be a function of position in the channel:

$$v_{ox} = v_{GS} - v(x) \quad (4.3)$$

where  $v(x)$  is the voltage at any point  $x$  in the channel referred to the source. Note that  $v_{ox}$  must exceed  $V_{TN}$  for an inversion layer to exist, so  $Q'$  will be zero until  $v_{ox} > V_{TN}$ . At the source end of the channel,  $v_{ox} = v_{GS}$ , and it decreases to  $v_{ox} = v_{GS} - v_{DS}$  at the drain end of the channel.

The electron drift current at any point in the channel is given by the product of the charge per unit length times the velocity  $v_x$ :

$$i(x) = Q'(x)v_x(x) \quad (4.4)$$

The charge  $Q'$  is represented by Eq. (4.2), and the velocity  $v_x$  of electrons in the channel is determined by the electron mobility and the transverse electric field in the channel:

$$i(x) = Q'v_x = [-WC''_{ox}(v_{ox} - V_{TN})](-\mu_n E_x) \quad (4.5)$$

The transverse field is equal to the negative of the spatial derivative of the voltage in the channel

$$E_x = -\frac{dv(x)}{dx} \quad (4.6)$$

Combining Eqs. (4.3) to (4.6) yields an expression for the current at any point in the channel:

$$i(x) = -\mu_n C''_{ox} W [v_{GS} - v(x) - V_{TN}] \frac{dv(x)}{dx} \quad (4.7)$$

We know the voltages applied to the device terminals are  $v(0) = 0$  and  $v(L) = v_{DS}$ , and we can integrate Eq. (4.7) between 0 and  $L$ :

$$\int_0^L i(x) dx = - \int_0^{v_{DS}} \mu_n C''_{\text{ox}} W [v_{GS} - v(x) - V_{TN}] dv(x) \quad (4.8)$$

Because there is no mechanism to lose current as it goes down the channel, the current must be equal to the same value  $i_D$  at every point  $x$  in the channel,  $i(x) = i_D$ , and Eq. (4.8) finally yields

$$i_D = \mu_n C''_{\text{ox}} \frac{W}{L} \left( v_{GS} - V_{TN} - \frac{v_{DS}}{2} \right) v_{DS} \quad (4.9)$$

The value of  $\mu_n C''_{\text{ox}}$  is fixed for a given technology and cannot be changed by the circuit designer. For circuit analysis and design purposes, Eq. (4.9) is therefore most often written as

$$i_D = K'_n \frac{W}{L} \left( v_{GS} - V_{TN} - \frac{v_{DS}}{2} \right) v_{DS} \quad \text{or just} \quad i_D = K_n \left( v_{GS} - V_{TN} - \frac{v_{DS}}{2} \right) v_{DS} \quad (4.10)$$

where  $K_n = K'_n W/L$  and  $K'_n = \mu_n C''_{\text{ox}}$ . Parameters  $K_n$  and  $K'_n$  are called **transconductance parameters** and both have units of A/V<sup>2</sup>.

Equation (4.10) represents the classic expression for the drain-source current for the NMOS transistor in its **linear region** or **triode region** of operation, in which a resistive channel directly connects the source and drain. This resistive connection will exist as long as the voltage across the oxide exceeds the threshold voltage at every point in the channel:

$$v_{GS} - v(x) \geq V_{TN} \quad \text{for } 0 \leq x \leq L \quad (4.11)$$

The voltage in the channel is maximum at the drain end where  $v(L) = v_{DS}$ . Thus, Eqs. (4.9) and (4.10) are valid as long as

$$v_{GS} - v_{DS} \geq V_{TN} \quad \text{or} \quad v_{GS} - V_{TN} \geq v_{DS} \quad (4.12)$$

Recapitulating for the triode region,

$$i_D = K'_n \frac{W}{L} \left( v_{GS} - V_{TN} - \frac{v_{DS}}{2} \right) v_{DS} \quad \text{for } v_{GS} - V_{TN} \geq v_{DS} \geq 0 \quad \text{and} \quad K'_n = \mu_n C''_{\text{ox}} \quad (4.13)$$

Equation (4.13) is used frequently in the rest of this text. Commit it to memory!

Some additional insight into the mathematical model can be gained by regrouping the terms in Eq. (4.13):

$$i_D = \left[ C''_{\text{ox}} W \left( v_{GS} - V_{TN} - \frac{v_{DS}}{2} \right) \right] \left( \mu_n \frac{v_{DS}}{L} \right) \quad (4.14)$$

For small drain-source voltages, the first term represents the average charge per unit length in the channel because the average channel voltage  $\overline{v(x)} = v_{DS}/2$ . The second term represents the drift velocity in the channel, where the average electric field is equal to the total voltage  $v_{DS}$  across the channel divided by the channel length  $L$ .

We should note that the term *triode region* is used because the drain current of the FET depends on the drain voltage of the transistor, and this behavior is similar to that of the electronic vacuum triode that appeared many decades earlier (see Table 1.2 — Milestones in Electronics).

Note also that the **quiescent operating point** or **Q-point** of the FET is given by  $(I_D, V_{DS})$ .

**EXERCISE:** Calculate  $K'_n$  for a transistor with  $\mu_n = 500 \text{ cm}^2/\text{V} \cdot \text{s}$  and  $T_{ox} = 25 \text{ nm}$ .

**ANSWER:**  $69.1 \mu\text{A/V}^2$

**EXERCISE:** An NMOS transistor has  $K'_n = 50 \mu\text{A/V}^2$ . What is the value of  $K_n$  if  $W = 20 \mu\text{m}$ ,  $L = 1 \mu\text{m}$ ? If  $W = 60 \mu\text{m}$ ,  $L = 3 \mu\text{m}$ ? If  $W = 10 \mu\text{m}$ ,  $L = 0.25 \mu\text{m}$ ?

**ANSWERS:**  $1000 \mu\text{A/V}^2$ ;  $1000 \mu\text{A/V}^2$ ;  $2000 \mu\text{A/V}^2$

**EXERCISE:** Calculate the drain current in an NMOS transistor for  $V_{GS} = 0, 1 \text{ V}, 2 \text{ V}$ , and  $3 \text{ V}$ , with  $V_{DS} = 0.1 \text{ V}$ , if  $W = 10 \mu\text{m}$ ,  $L = 1 \mu\text{m}$ ,  $V_{TN} = 1.5 \text{ V}$ , and  $K'_n = 25 \mu\text{A/V}^2$ . What is the value of  $K_n$ ?

**ANSWERS:**  $0; 0; 11.3 \mu\text{A}; 36.3 \mu\text{A}; 250 \mu\text{A/V}^2$

### 4.2.3 ON RESISTANCE

The  $i$ - $v$  characteristics in the triode region generated from Eq. (4.13) are drawn in Fig. 4.7 for the case of  $V_{TN} = 1 \text{ V}$  and  $K_n = 250 \mu\text{A/V}^2$ . The curves in Fig. 4.7 represent a portion of the common-source **output characteristics** for the NMOS device. The output characteristics for the MOSFET are graphs of drain current  $i_D$  as a function of drain-source voltage  $v_{DS}$ . A family of curves is generated, with each curve corresponding to a different value of gate-source voltage  $v_{GS}$ . The output characteristics in Fig. 4.7 appear to be a family of nearly straight lines, hence the alternate name **linear region** (of operation). However, some curvature can be noted in the characteristics, particularly for  $V_{GS} = 2 \text{ V}$ .

Let us explore the triode region behavior in more detail using Eq. (4.9). For small drain-source voltages such that  $v_{DS}/2 \ll v_{GS} - V_{TN}$ , Eq. (4.9) can be reduced to

$$i_D \cong \mu_n C''_{ox} \frac{W}{L} (v_{GS} - V_{TN}) v_{DS} \quad (4.15)$$

in which the current  $i_D$  through the MOSFET is directly proportional to the voltage  $v_{DS}$  across the MOSFET. The FET behaves much like a resistor connected between the drain and source terminals, but the resistor value can be controlled by the gate-source voltage. It has been said that this voltage-controlled resistance behavior originally gave rise to the name transistor, a contraction of “transfer-resistor.”

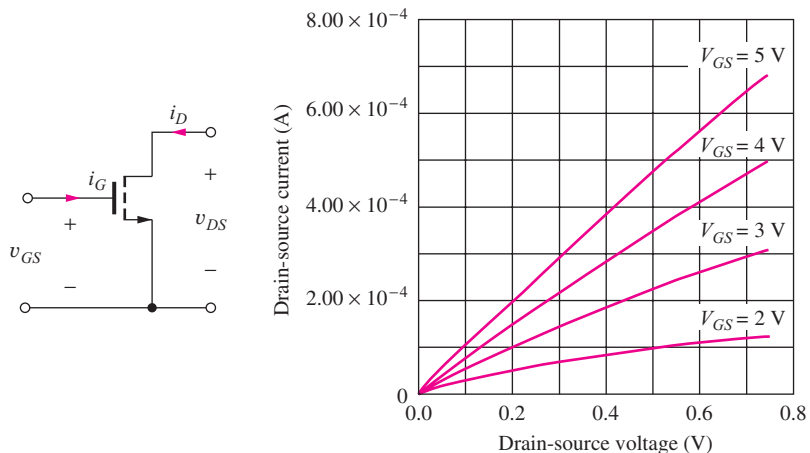


**Figure 4.7** NMOS  $i$ - $v$  characteristics in the triode region ( $V_{SB} = 0$ ). A three-terminal NMOS circuit symbol is often used when  $v_{SB} = 0$ .

The resistance of the FET in the triode region near the origin, called the **on-resistance**  $R_{\text{on}}$ , is defined in Eq. (4.16) and can be found by taking the derivative of Eq. (4.13):

$$R_{\text{on}} = \left[ \frac{\partial i_D}{\partial v_{DS}} \Big|_{v_{DS} \rightarrow 0} \right]_{Q-pt}^{-1} = \frac{1}{K'_n \frac{W}{L} (V_{GS} - V_{TN} - V_{DS})} \Bigg|_{v_{DS} \rightarrow 0} = \frac{1}{K'_n \frac{W}{L} (V_{GS} - V_{TN})} \quad (4.16)$$

We will find that the value of  $R_{\text{on}}$  plays a very important role in the operation of MOS logic circuits in Chapters 6–8. Note that  $R_{\text{on}}$  is also equal to the ratio  $v_{DS}/i_D$  from Eq. (4.15).

Near the origin, the  $i$ - $v$  curves are indeed straight lines. However, curvature develops as the assumption  $v_{DS} \ll v_{GS} - V_{TN}$  starts to be violated. For the lowest curve in Fig. 4.7,  $V_{GS} - V_{TN} = 2 - 1 = 1$  V, and we should expect linear behavior only for values of  $v_{DS}$  below 0.1 to 0.2 V. On the other hand, the curve for  $V_{GS} = 5$  V exhibits quasi-linear behavior throughout most of the range of Fig. 4.7. Note that a three-terminal NMOS circuit symbol is often used (see Figs. 4.7 and 4.8) when the bulk terminal is connected to the source terminal forcing  $v_{SB} = 0$ .

**EXERCISE:** Calculate the on-resistance of an NMOS transistor for  $V_{GS} = 2$  V and  $V_{GS} = 5$  V if  $V_{TN} = 1$  V and  $K_n = 250 \mu\text{A/V}^2$ . What value of  $V_{GS}$  is required for an on-resistance of  $2 \text{ k}\Omega$ ?

**ANSWERS:**  $4 \text{ k}\Omega$ ;  $1 \text{ k}\Omega$ ;  $3\text{V}$

#### 4.2.4 SATURATION OF THE $i$ - $v$ CHARACTERISTICS

As discussed, Eq. (4.13) is valid as long as the resistive channel region directly connects the source to the drain. However, an unexpected phenomenon occurs in the MOSFET as the drain voltage increases above the triode region limit in Eq. (4.13). The current does not continue to increase, but instead saturates at a constant value. This unusual behavior is depicted in the  $i$ - $v$  characteristics in Fig. 4.8 for several fixed gate-source voltages.

We can try to understand the origin of the current saturation by studying the device cross sections in Fig. 4.9. In Fig. 4.9(a), the MOSFET is operating in the triode region with  $v_{DS} < v_{GS} - V_{TN}$ , as discussed previously. In Fig. 4.9(b), the value of  $v_{DS}$  has increased to  $v_{DS} = v_{GS} - V_{TN}$ , for which the channel just disappears at the drain. Figure 4.9(c) shows the channel for an even larger value of

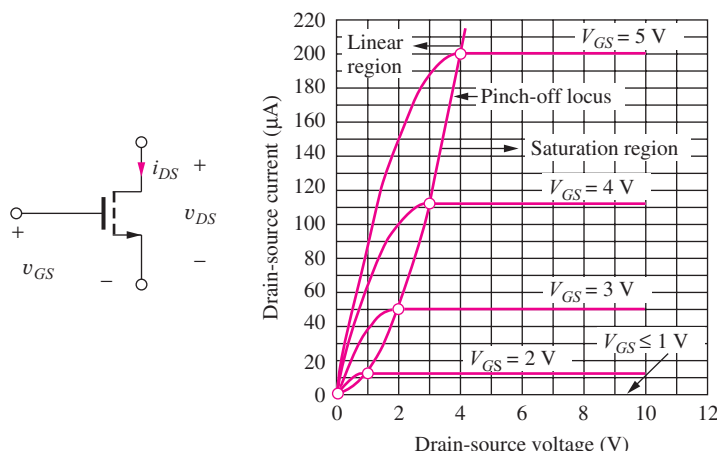


**Figure 4.8** Output characteristics for an NMOS transistor with  $V_{TN} = 1$  V and  $K_n = 25 \times 10^{-6} \text{ A/V}^2 (v_{SB} = 0)$ . A three-terminal NMOS circuit symbol is used when  $v_{SB} = 0$ .

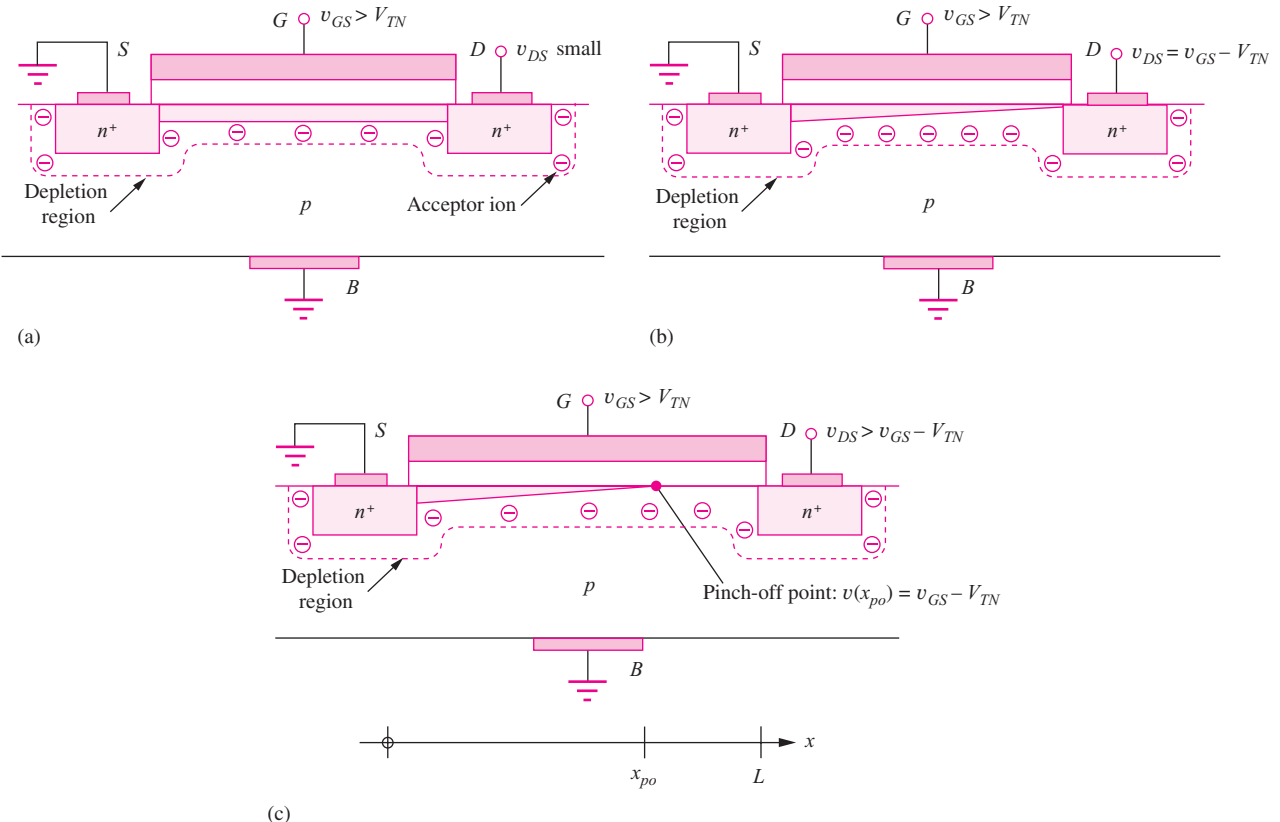


**Figure 4.9** (a) MOSFET in the linear region. (b) MOSFET with channel just pinched off at the drain. (c) Channel pinch-off for  $v_{DS} > v_{GS} - V_{TN}$ .

$v_{DS}$ . The channel region has disappeared, or *pinched off*, before reaching the drain end of the channel, and the resistive channel region is no longer in contact with the drain. At first glance, one may be inclined to expect that the current should become zero in the MOSFET; however, this is not the case. As depicted in Fig. 4.9(c), the voltage at the **pinch-off point** in the channel is always equal to

$$v_{GS} - v(x_{po}) = V_{TN} \quad \text{or} \quad v(x_{po}) = v_{GS} - V_{TN}$$

There is still a voltage equal to  $v_{GS} - V_{TN}$  across the inverted portion of the channel, and electrons will be drifting down the channel from left to right. When the electrons reach the pinch-off point, they are injected into the depleted region between the end of the channel and the drain, and the electric field in the depletion region then sweeps these electrons on to the drain. Once the channel has reached pinch-off, the voltage drop across the inverted channel region is constant; hence, the drain current becomes constant and independent of drain-source voltage.

This region of operation of the MOSFET is often referred to as either the **saturation region** or the **pinch-off region** of operation. However, we will learn a different meaning for saturation when we discuss bipolar transistors in the next chapter. On the other hand, operation beyond pinchoff is the regime that we most often use for analog amplification, and in Part III we will use the term **active region** to refer to this region for both MOS and bipolar devices.

#### 4.2.5 MATHEMATICAL MODEL IN THE SATURATION (PINCH-OFF) REGION

Now let us find an expression for the MOSFET drain current in the pinched-off channel. The drain-source voltage just needed to pinch off the channel at the drain is  $v_{DS} = v_{GS} - V_{TN}$ , and

substituting this value into Eq. (4.13) yields an expression for the NMOS current in the saturation region of operation:

$$i_D = \frac{K'_n}{2} \frac{W}{L} (v_{GS} - V_{TN})^2 \quad \text{for } v_{DS} \geq (v_{GS} - V_{TN}) \geq 0 \quad (4.17)$$

This is the classic square-law expression for the drain-source current for the  $n$ -channel MOSFET operating in pinch-off. The current depends on the square of  $v_{GS} - V_{TN}$  but is now independent of the drain-source voltage  $v_{DS}$ . Equation (4.17) is *also used* frequently in the rest of this text. Be sure to commit it to memory!

The value of  $v_{DS}$  for which the transistor saturates is given the special name  $v_{DSAT}$  defined by

$$v_{DSAT} = v_{GS} - V_{TN} \quad (4.18)$$

and  $v_{DSAT}$  is referred to as the **saturation voltage**, or **pinch-off voltage**, of the MOSFET. Equation (4.17) can be interpreted in a manner similar to that of Eq. (4.14):

$$i_D = \left( C''_o W \frac{v_{GS} - V_{TN}}{2} \right) \left( \mu_n \frac{v_{GS} - V_{TN}}{L} \right) \quad (4.19)$$

The inverted channel region has a voltage of  $v_{GS} - V_{TN}$  across it, as depicted in Fig. 4.9(c). Thus, the first term represents the magnitude of the average electron charge in the inversion layer, and the second term is the magnitude of the velocity of electrons in an electric field equal to  $(v_{GS} - V_{TN})/L$ .

An example of the overall output characteristics for an NMOS transistor with  $V_{TN} = 1$  V and  $K_n = 25 \mu\text{A}/\text{V}^2$  appeared in Fig. 4.8, in which the locus of pinch-off points is determined by  $v_{DS} = v_{DSAT}$ . To the left of the **pinch-off locus**, the transistor is operating in the triode region, and it is operating in the saturation region for operating points to the right of the locus. For  $v_{GS} \leq V_{TN} = 1$  V, the transistor is cut off, and the drain current is zero. As the gate voltage is increased in the saturation region, the curves spread out due to the square-law nature of Eq. (4.17).

Figure 4.10 gives an individual output characteristic for  $V_{GS} = 3$  V, showing the behavior of the individual triode and saturation region equations. The triode region expression given in Eq. (4.13) is represented by the inverted parabola in Fig. 4.10. Note that it does not represent a valid model for the  $i$ - $v$  behavior for  $V_{DS} > V_{GS} - V_{TN} = 2$  V for this particular device. Note also that the maximum drain voltage must never exceed the Zener breakdown voltage of the drain-substrate  $pn$  junction diode.

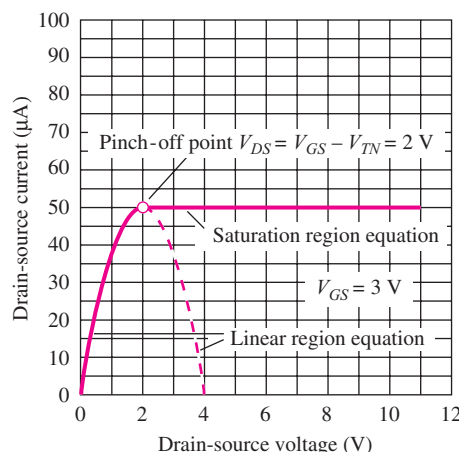


**Figure 4.10** Output characteristic showing intersection of the triode (linear) region and saturation region equations at the pinch-off point.

**EXERCISE:** Calculate the drain current for an NMOS transistor operating with  $V_{GS} = 5 \text{ V}$  and  $V_{DS} = 10 \text{ V}$  if  $V_{TN} = 1 \text{ V}$  and  $K_n = 1 \text{ mA/V}^2$ . What is the  $W/L$  ratio of this device if  $K'_n = 40 \mu\text{A/V}^2$ ? What is  $W$  if  $L = 0.35 \mu\text{m}$ ?

**ANSWERS:** 8.00 mA; 25/1; 8.75  $\mu\text{m}$

#### 4.2.6 TRANSCONDUCTANCE

An important characteristic of transistors is the **transconductance** given the symbol  $g_m$ . The transconductance of the MOS devices relates the change in drain current to a change in gate-source voltage. For the saturation region:

$$g_m = \left. \frac{di_D}{dv_{GS}} \right|_{Q-pt} = K'_n \frac{W}{L} (V_{GS} - V_{TN}) = \frac{2I_D}{V_{GS} - V_{TN}} \quad (4.20)$$

where we have taken the derivative of Eq. (4.17) and evaluated the result at the Q-point. We encounter  $g_m$  frequently in electronics, particularly during our study of analog circuit design. The larger the device transconductance, the more gain we can expect from an amplifier that utilizes the transistor. It is interesting to note that  $g_m$  is the reciprocal of the on-resistance defined in Eq. (4.16).

**EXERCISE:** Find the drain current and transconductance for an NMOS transistor operating with  $V_{GS} = 2.5 \text{ V}$ ,  $V_{TN} = 1 \text{ V}$ , and  $K_n = 1 \text{ mA/V}^2$ .

**ANSWERS:** 1.13 mA; 1.5 mS

#### 4.2.7 CHANNEL-LENGTH MODULATION

The output characteristics of the device in Fig. 4.8 indicate that the drain current is constant once the device enters the saturation region of operation. However, this is not quite true. Rather, the  $i-v$  curves have a small positive slope, as indicated in Fig. 4.11(a). The drain current increases slightly as the drain-source voltage increases. The increase in drain current visible in Fig. 4.11 is the result of a phenomenon called **channel-length modulation**, which can be understood by referring

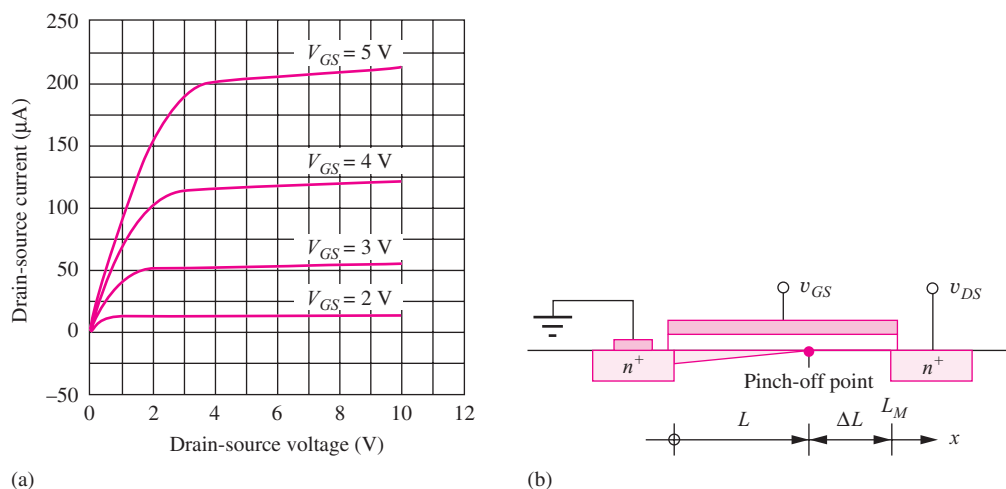


**Figure 4.11** (a) Output characteristics including the effects of channel-length modulation. (b) Channel-length modulation.

to Fig. 4.11(b), in which the channel region of the NMOS transistor is depicted for the case of  $v_{DS} > v_{DSAT}$ . The channel pinches off before it makes contact with the drain. Thus, the actual length of the resistive channel is given by  $L = L_M - \Delta L$ . As  $v_{DS}$  increases above  $v_{DSAT}$ , the length of the depleted channel region  $\Delta L$  also increases, and the effective value of  $L$  decreases. Therefore, the value of  $L$  in the denominator of Eq. (4.17) actually has a slight inverse dependence on  $v_{DS}$ , leading to an increase in drain current increases as  $v_{DS}$  increases. The expression in Eq. (4.17) can be heuristically modified to include this drain-voltage dependence as

$$i_D = \frac{K'_n}{2} \frac{W}{L} (v_{GS} - V_{TN})^2 (1 + \lambda v_{DS}) \quad (4.21)$$

in which  $\lambda$  is called the **channel-length modulation parameter**. The value of  $\lambda$  is dependent on the channel length, and typical values are  $0 \text{ V}^{-1} \leq \lambda \leq 0.2 \text{ V}^{-1}$ . In Fig. 4.11,  $\lambda$  is approximately  $0.01 \text{ V}^{-1}$ , which yields a 10 percent increase in drain current for a drain-source voltage change of 10 V.

**EXERCISE:** Calculate the drain current for an NMOS transistor operating with  $V_{GS} = 5 \text{ V}$  and  $V_{DS} = 10 \text{ V}$  if  $V_{TN} = 1 \text{ V}$ ,  $K_n = 1 \text{ mA/V}^2$ , and  $\lambda = 0.02 \text{ V}^{-1}$ . What is  $I_D$  for  $\lambda = 0$ ?

**ANSWERS:** 9.60 mA; 8.00 mA

**EXERCISE:** Calculate the drain current for the NMOS transistor in Fig. 4.11 operating with  $V_{GS} = 4 \text{ V}$  and  $V_{DS} = 5 \text{ V}$  if  $V_{TN} = 1 \text{ V}$ ,  $K_n = 25 \mu\text{A/V}^2$ , and  $\lambda = 0.01 \text{ V}^{-1}$ . Repeat for  $V_{GS} = 5 \text{ V}$  and  $V_{DS} = 10 \text{ V}$ .

**ANSWERS:** 118  $\mu\text{A}$ ; 220  $\mu\text{A}$

#### 4.2.8 TRANSFER CHARACTERISTICS AND DEPLETION-MODE MOSFETS

The output characteristics in Figs. 4.7 and 4.11 represented our first look at graphical representations of the  $i$ - $v$  characteristics of the transistor. The output characteristics plot drain current versus drain-source voltage for fixed values of the gate-source voltage. The second commonly used graphical format, called the **transfer characteristic**, plots drain current versus gate-source voltage for a fixed drain-source voltage. An example of this form of characteristic is given in Fig. 4.12 for two NMOS transistors in the pinch-off region. Up to now, we have been assuming that the threshold voltage of the NMOS transistor is positive, as in the right-hand curve in Fig. 4.12. This curve corresponds to an enhancement-mode device with  $V_{TN} = +2 \text{ V}$ . Here we can clearly see the turn-on of the transistor as  $v_{GS}$  increases. The device is off (nonconducting) for  $v_{GS} \leq V_{TN}$ , and it starts to conduct as  $v_{GS}$  exceeds  $V_{TN}$ . The curvature reflects the square-law behavior of the transistor in the saturation region as described by Eq. (4.17).

However, it is also possible to fabricate NMOS transistors with values of  $V_{TN} \leq 0$ . These transistors are called **depletion-mode MOSFETs**, and the transfer characteristic for such a device with  $V_{TN} = -2 \text{ V}$  is depicted in the left-hand curve in Fig. 4.12(a). Note that a nonzero drain current exists in the depletion-mode MOSFET for  $v_{GS} = 0$ ; a negative value of  $v_{GS}$  is required to turn the device off.

The cross section of the structure of a depletion-mode NMOSFET is shown in Fig. 4.12(b). A process called *ion implantation* is used to form a built-in *n*-type channel in the device so that the source and drain are connected through the resistive channel region. A negative voltage must be applied to the gate to deplete the *n*-type channel region and eliminate the current path between the source and drain (hence the name depletion-mode device). In Chapter 6 we will see that the ion-implanted depletion-mode device played an important role in the evolution of MOS logic circuits. The addition of the depletion-mode MOSFET to NMOS technology provided substantial performance improvement, and it was a rapidly accepted change in technology in the mid 1970s.

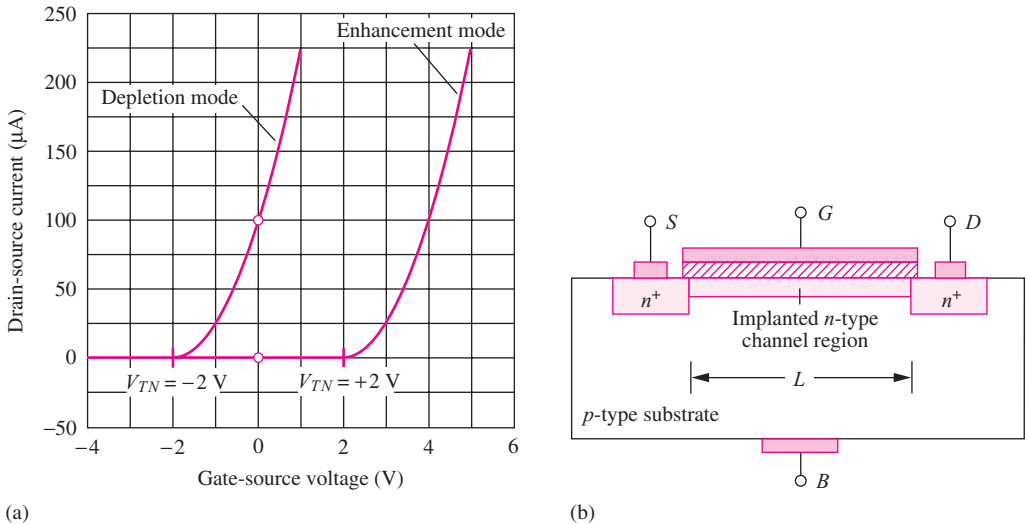


**Figure 4.12** (a) Transfer characteristics for enhancement-mode and depletion-mode NMOS transistors. (b) Cross section of a depletion-mode NMOS transistor.

**EXERCISE:** Calculate the drain current for the NMOS depletion-mode transistor in Fig. 4.12 for  $V_{GS} = 0$  V if  $K_n = 50 \mu\text{A/V}^2$ . Assume the transistor is in the pinch-off region. What value of  $V_{GS}$  is required to achieve the same current in the enhancement-mode transistor in the same figure?

**ANSWERS:** 100  $\mu$ A; 4 V

**EXERCISE:** Calculate the drain current for the NMOS depletion-mode transistor in Fig. 4.12 for  $V_{GS} = +1$  V if  $K_n = 50 \mu\text{A/V}^2$ . Assume the transistor is in the pinch-off region.

**ANSWER:** 225  $\mu$ A

## 4.2.9 BODY EFFECT OR SUBSTRATE SENSITIVITY

Thus far, it has been assumed that the source-bulk voltage  $v_{SB}$  is zero. With  $v_{SB} = 0$ , the MOSFET behaves as if it were a three-terminal device. However, we find many circuits, particularly in ICs, in which the bulk and source of the MOSFET must be connected to different voltages so that  $v_{SB} \neq 0$ . A nonzero value of  $v_{SB}$  affects the  $i$ - $v$  characteristics of the MOSFET by changing the value of the threshold voltage. This effect is called **substrate sensitivity**, or **body effect**, and can be modeled by

$$V_{TN} = V_{TO} + \gamma (\sqrt{v_{SB} + 2\phi_F} - \sqrt{2\phi_F}) \quad (4.22)$$

where  $V_{TO}$  = zero-substrate-bias value for  $V_{TN}$  (V)

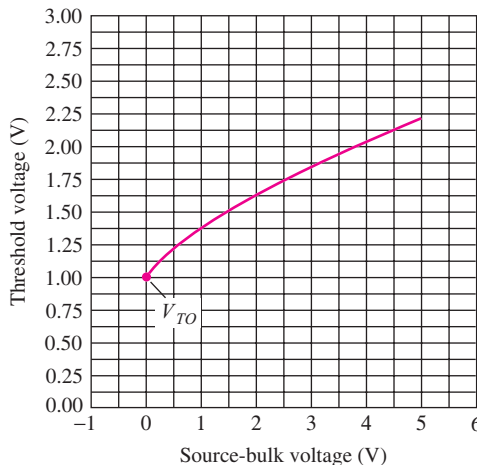
$\gamma$  = body-effect parameter ( $\sqrt{\text{V}}$ )

$2\phi_F$  = surface potential parameter (V)

Parameter  $\gamma$  determines the intensity of the body effect, and its value is set by the relative sizes of the oxide and depletion-layer capacitances  $C''_{ox}$  and  $C_d$  in Fig. 4.3. The surface potential represents the approximate voltage across the depletion layer at the onset of inversion. For typical NMOS transistors,  $-5 \text{ V} \leq V_{TO} \leq +5 \text{ V}$ ,  $0 \leq \gamma \leq 3\sqrt{\text{V}}$ , and  $0.3 \text{ V} \leq 2\phi_F \leq 1 \text{ V}$ .

We use  $2\phi_F = 0.6 \text{ V}$  throughout the rest of this text, and Eq. (4.22) will be represented as

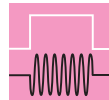
$$V_{TN} = V_{TO} + \gamma (\sqrt{v_{SB} + 0.6} - \sqrt{0.6}) \quad (4.23)$$



$$V_{TN} = V_{TO} + \gamma(\sqrt{v_{SB} + 2\phi_F} - \sqrt{2\phi_F})$$

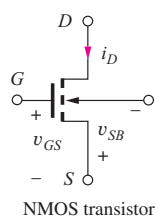
**Figure 4.13** Threshold variation with source-bulk voltage for an NMOS transistor, with  $V_{TO} = 1$  V,  $2\phi_F = 0.6$  V and  $\gamma = 0.75\sqrt{V}$ .

Figure 4.13 plots an example of the threshold-voltage variation with source-bulk voltage for an NMOS transistor, with  $V_{TO} = 1$  V and  $\gamma = 0.75\sqrt{V}$ . We see that  $V_{TN} = V_{TO} = 1$  V for  $v_{SB} = 0$  V, but the value of  $V_{TN}$  more than doubles for  $v_{SB} = 5$  V. In Chapter 6, we will see that this behavior can have a significant impact on the design of MOS logic circuits.



### DESIGN NOTE

The mathematical model for the NMOS transistor in its various regions of operation is summarized in the equation set below and should be committed to memory!



- + For all regions,

$$K_n = K'_n \frac{W}{L} \quad K'_n = \mu_n C''_{ox} \quad i_G = 0 \quad i_B = 0 \quad (4.24)$$

- Cutoff region:

$$i_D = 0 \quad \text{for } v_{GS} \leq V_{TN} \quad (4.25)$$

Triode region:

$$i_D = K_n \left( v_{GS} - V_{TN} - \frac{v_{DS}}{2} \right) v_{DS} \quad \text{for } v_{GS} - V_{TN} \geq v_{DS} \geq 0 \quad (4.26)$$

Saturation region:

$$i_D = \frac{K_n}{2} (v_{GS} - V_{TN})^2 (1 + \lambda v_{DS}) \quad \text{for } v_{DS} \geq (v_{GS} - V_{TN}) \geq 0 \quad (4.27)$$

Threshold voltage:

$$V_{TN} = V_{TO} + \gamma (\sqrt{v_{SB} + 2\phi_F} - \sqrt{2\phi_F}) \quad (4.28)$$

$V_{TN} > 0$  for enhancement-mode NMOS transistors. Depletion-mode NMOS devices can also be fabricated, and  $V_{TN} \leq 0$  for these transistors.

**EXERCISE:** Calculate the threshold voltage for the MOSFET of Fig. 4.13 for source-bulk voltages of 0 V, 1.5 V, and 3 V.

**ANSWERS:** 1.00 V; 1.51 V; 1.84 V

**EXERCISE:** What is the region of operation and drain current of an NMOS transistor having  $V_{TN} = 1$  V,  $K_n = 1$  mA/V<sup>2</sup>, and  $\lambda = 0.02$  V<sup>-1</sup> for (a)  $V_{GS} = 0$  V,  $V_{DS} = 1$  V; (b)  $V_{GS} = 2$  V,  $V_{DS} = 0.5$  V; (c)  $V_{GS} = 2$  V,  $V_{DS} = 2$  V?

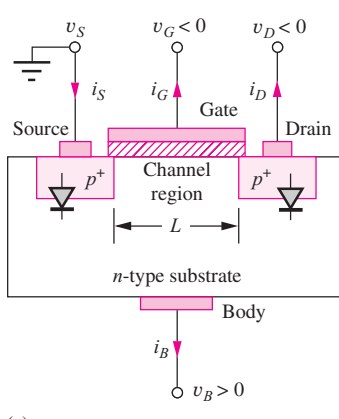
**ANSWERS:** (a) cutoff, 0 A; (b) triode, 375  $\mu$ A; (c) saturation, 520  $\mu$ A

### 4.3 PMOS TRANSISTORS

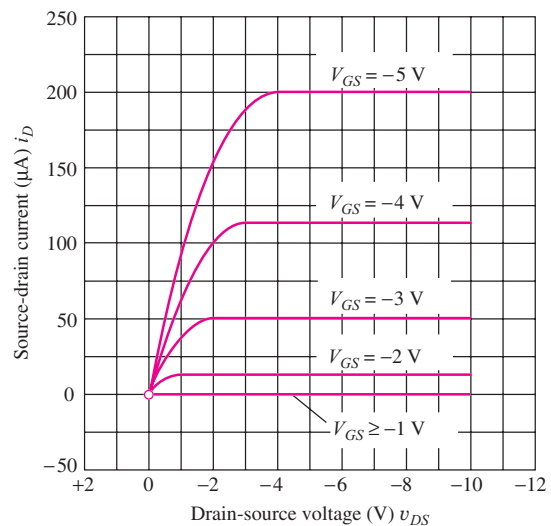
MOS transistors with *p*-type channels (PMOS transistors) can also easily be fabricated. In fact, as mentioned earlier, the first commercial MOS transistors and integrated circuits used PMOS devices because it was easier to control the fabrication process for PMOS technology. The PMOS device is built by forming *p*-type source and drain regions in an *n*-type substrate, as depicted in the device cross section in Fig. 4.14(a).

The qualitative behavior of the transistor is essentially the same as that of an NMOS device except that the normal voltage and current polarities are reversed. The normal directions of current in the **PMOS transistor** are indicated in Fig. 4.14. A negative voltage on the gate relative to the source ( $v_{GS} < 0$ ) is required to attract holes and create a *p*-type inversion layer in the channel region. To initiate conduction in the enhancement-mode PMOS transistor, the gate-source voltage must be more negative than the threshold voltage of the *p*-channel device, denoted by  $V_{TP}$ . To keep the source-substrate and drain-substrate junctions reverse-biased,  $v_{SB}$  and  $v_{DB}$  must also be less than zero. This requirement is satisfied by  $v_{DS} \leq 0$ .

An example of the output characteristics for an enhancement-mode PMOS transistor is given in Fig. 4.14(b). For  $v_{GS} \geq V_{TP} = -1$  V, the transistor is off. For more negative values of  $v_{GS}$ , the drain current increases in magnitude. The PMOS device is in the triode region for small values of  $V_{DS}$ , and the saturation of the characteristics is apparent at larger  $V_{DS}$ . The curves look just like those for



(a)



(b)

**Figure 4.14** (a) Cross section of an enhancement-mode PMOS transistor. (b) Output characteristics for a PMOS transistor with  $V_{TP} = -1$  V.

the NMOS device except for sign changes on the values of  $v_{GS}$  and  $v_{DS}$ . This is a result of assigning the positive current direction to current exiting from the drain terminal of the PMOS transistor.

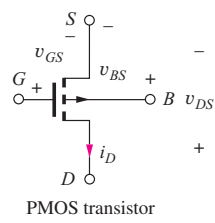
## DESIGN NOTE

The mathematical model for the PMOS transistor in its various regions of operation is summarized in the equation set below and should be committed to memory!

### PMOS TRANSISTOR MATHEMATICAL MODEL SUMMARY

Equations (4.29) through (4.33) represent the complete model for the  $i-v$  behavior of the PMOS transistor.

For all regions,



$$K_p = K'_p \frac{W}{L} \quad K'_p = \mu_p C''_{\text{ox}} \quad i_G = 0 \quad i_B = 0 \quad (4.29)$$

Cutoff region:

$$i_D = 0 \quad \text{for } V_{GS} \geq V_{TP} \quad (4.30)$$

Triode region:

$$i_D = K_p \left( v_{GS} - V_{TP} - \frac{v_{DS}}{2} \right) v_{DS} \quad \text{for } 0 \leq |v_{DS}| \leq |v_{GS} - V_{TP}| \quad (4.31)$$

Saturation region:

$$i_D = \frac{K_p}{2} (v_{GS} - V_{TP})^2 (1 + \lambda |v_{DS}|) \quad \text{for } |v_{DS}| \geq |v_{GS} - V_{TP}| \geq 0 \quad (4.32)$$

Threshold voltage:

$$V_{TP} = V_{TO} - \gamma (\sqrt{v_{BS} + 2\phi_F} - \sqrt{2\phi_F}) \quad (4.33)$$

For the enhancement-mode PMOS transistor,  $V_{TP} < 0$ . Depletion-mode PMOS devices can also be fabricated;  $V_{TP} \geq 0$  for these devices.

Various authors have different ways of writing the equations that describe the PMOS transistor. Our choice attempts to avoid as many confusing minus signs as possible. The drain-current expressions for the PMOS transistor are written in similar form to those for the NMOS transistor except that the drain-current direction is reversed and the values of  $v_{GS}$  and  $v_{DS}$  are now negative quantities. A sign must still be changed in the expressions, however. The parameter  $\gamma$  is normally specified as a positive value for both  $n$ - and  $p$ -channel devices, and a positive bulk-source potential will cause the PMOS threshold voltage to become more negative.

An important parametric difference appears in the expressions for  $K_p$  and  $K_n$ . In the PMOS device, the charge carriers in the channel are holes, so current is proportional to hole mobility  $\mu_p$ . Hole mobility is typically only 40 percent of the electron mobility, so for a given set of voltage bias conditions, the PMOS device will conduct only 40 percent of the current of the NMOS device! Higher current capability leads to higher frequency operation in both digital and analog circuits. Thus, NMOS devices are preferred over PMOS devices in many applications.

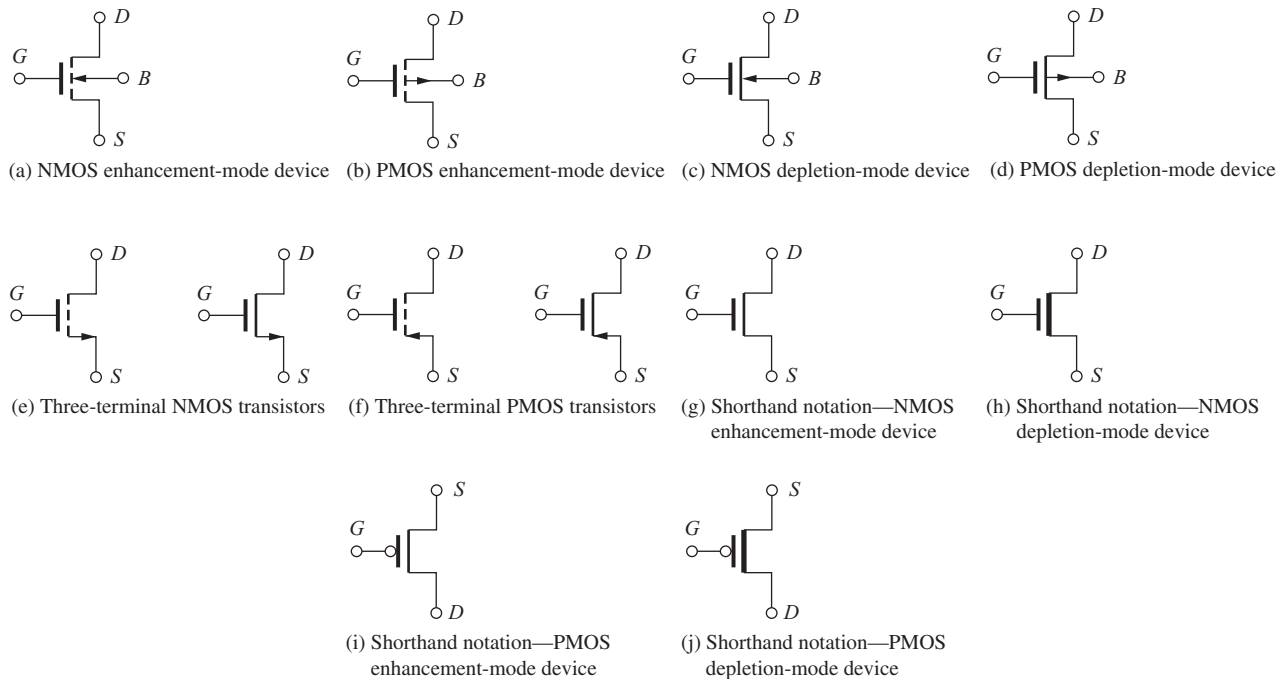


**Figure 4.15** (a)–(f) IEEE Standard MOS transistor circuit symbols. (g)–(j) Other commonly used symbols.

**EXERCISE:** What is the region of operation and drain current of a PMOS transistor having  $V_{TP} = -1$  V,  $K_p = 0.4$  mA/V<sup>2</sup>, and  $\lambda = 0.02$  V<sup>-1</sup> for (a)  $V_{GS} = 0$  V,  $V_{DS} = -1$  V; (b)  $V_{GS} = -2$  V,  $V_{DS} = -0.5$  V; (c)  $V_{GS} = -2$  V,  $V_{DS} = -2$  V?

**ANSWERS:** (a) cutoff, 0 A; (b) triode, 150  $\mu$ A; (c) saturation, 208  $\mu$ A

## 4.4 MOSFET CIRCUIT SYMBOLS

Standard circuit symbols for four different types of MOSFETs are given in Fig. 4.15: (a) NMOS enhancement-mode, (b) PMOS enhancement-mode, (c) NMOS depletion-mode, and (d) PMOS depletion-mode transistors. The four terminals of the MOSFET are identified as source ( $S$ ), drain ( $D$ ), gate ( $G$ ), and bulk ( $B$ ). The arrow on the **bulk terminal** indicates the polarity of the bulk-drain, bulk-source, and bulk-channel  $pn$  junction diodes; the arrow points inward for an NMOS device and outward for the PMOS transistor. Enhancement-mode devices are indicated by the dashed line in the channel region, whereas depletion-mode devices have a solid line, indicating the existence of the built-in channel. The gap between the gate and channel represents the insulating oxide region. Table 4.1 summarizes the threshold-voltage values for the four types of NMOS and PMOS transistors.

In many circuit applications, the MOSFET substrate terminal is connected to its source. The shorthand notation in Fig. 4.15(e) and 4.15(f) is often used to represent these three-terminal MOSFETs. The arrow identifies the source terminal and points in the direction of normal positive current.

**TABLE 4.1**  
Categories of MOS transistors

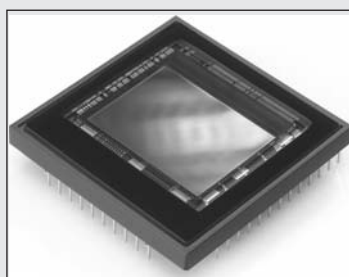
	NMOS DEVICE	PMOS DEVICE
Enhancement-mode	$V_{TN} > 0$	$V_{TP} < 0$
Depletion-mode	$V_{TN} \leq 0$	$V_{TP} \geq 0$



### CMOS Camera on a Chip

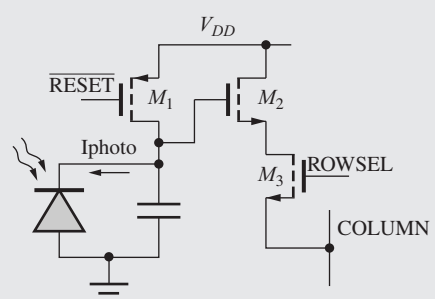
Earlier in this text we examined the CCD image sensor widely used in astronomy. Although the CCD imager produces very high quality images, it requires an expensive specialized manufacturing process, complex control circuitry, and consumes a substantial amount of power. In the early 1990s, designers began developing techniques to integrate photo-detection circuitry onto inexpensive mainstream digital CMOS processes. In 1993, Dr. Eric Fossum's group at the Jet Propulsion Laboratory announced a CMOS digital camera on a chip. Since that time, many companies have designed camera chips that are based on mainstream CMOS processes, allowing the merging of many camera functions onto a single chip.

Pictured here is a photo of such a chip from Dalsa Corporation.<sup>1</sup> The device produces full color images and has 4 million pixels in a  $2352 \times 1728$  imaging array.



Dalsa 4 MegaPixel CMOS color image sensor

*Copyright © DALSA. Reprinted by permission*



Basic photo diode pixel architecture.

A typical photodiode-based imaging pixel is also shown above. After asserting the **RESET** signal, the storage capacitor is fully charged to  $V_{DD}$  through transistor  $M_1$ . The reset signal is then removed, and light incident on the photodiode generates a photo current that discharges the capacitor. Different light intensities produce different voltages on the capacitor at the end of the light integration time. To read the stored value, the row select (ROWSEL) signal is asserted, and the capacitor voltage is driven onto the COLUMN bus via transistors  $M_2$  and  $M_3$ .

In many designs random variations in the device characteristics will cause variations in the signal produced by each pixel for the same intensity of incident light. To correct for many of these variations, a technique known as *correlated double sampling* is used. After the signal level is read from a pixel, the pixel is reset and then read again to acquire a baseline signal. The baseline signal is subtracted from the desired signal, thereby removing the non-uniformities and noise sources which are common to both of the acquired signals.

Chips like this one are now common in digital cameras and digital camcorders. These now-common and inexpensive portable devices are enabled by the integration of analog photo-sensitive pixel structures with mainstream CMOS processes.

<sup>1</sup> The chip pictured above is a Dalsa 4 MegaPixel CMOS color image sensor. The image is courtesy of the Dalsa Corporation.

To further add to the confusing array of symbols that the circuit designer must deal with, a number of additional symbols are used in other texts and reference books and in papers in technical journals. The wide diversity of symbols is unfortunate, but it is a fact of life that circuit designers must accept. For example, if one tires of drawing the dashed line for the enhancement-mode device as well as the substrate arrow, one arrives at the NMOS transistor symbol in Fig. 4.15(g); the channel line is

then thickened to represent the NMOS depletion-mode device, as in Fig. 4.15(h). In a similar vein, the symbol in Fig. 4.15(i) represents the enhancement-mode PMOS transistor, and the corresponding depletion-mode PMOS device appears in Fig. 4.15(j). In the last two symbols, the circles represent a carry-over from logic design and are meant to indicate the logical inversion operation. We explore this more fully in Part II of this book. The symbols in Figs. 4.15(g) and (i) commonly appear in books discussing VLSI logic design.

The symmetry of MOS devices should be noted in the cross sections of Figs. 4.4 and 4.14. The terminal that is acting as the drain is actually determined by the applied potentials. Current can traverse the channel in either direction, depending on the applied voltage. For NMOS transistors, the  $n^+$  region that is at the highest voltage will be the drain, and the one at the lowest voltage will be the source. For the PMOS transistor, the  $p^+$  region at the lowest voltage will be the drain, and the one at the highest voltage will be the source. In later chapters, we shall see that this symmetry is highly useful in certain applications, particularly in MOS logic and dynamic random-access memory (DRAM) circuits.

### DESIGN NOTE MOS DEVICE SYMMETRY

The MOS transistor terminal that is acting as the drain is actually determined by the applied potentials. Current can traverse the channel in either direction, depending on the applied voltage.

## 4.5 CAPACITANCES IN MOS TRANSISTORS

Every electronic device has internal capacitances that limit the high-frequency performance of the particular device. In logic applications, these capacitances limit the switching speed of the circuits, and in amplifiers, the capacitances limit the frequency at which useful amplification can be obtained. Thus knowledge of the origin and modeling of these capacitances is quite important, and an introductory discussion of the capacitances of the MOS transistor appears in this section.

### 4.5.1 NMOS TRANSISTOR CAPACITANCES IN THE TRIODE REGION

Figure 4.16(a) shows the various capacitances associated with the MOS field-effect transistor operating in the triode region, in which the resistive channel region connects the source and drain.

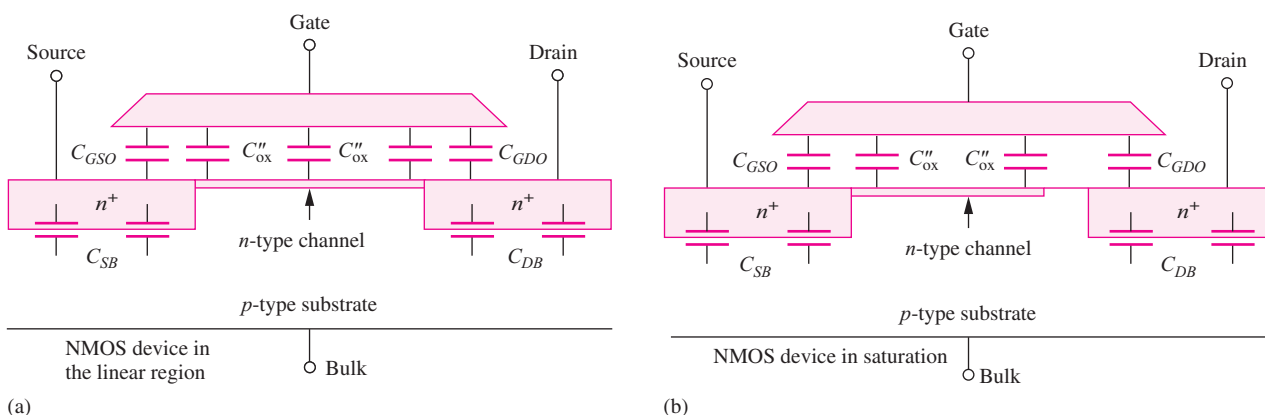


Figure 4.16 (a) NMOS capacitances in the linear region. (b) NMOS capacitances in the active region.

A simple model for these capacitances was presented by Meyer [4]. The total gate-channel capacitance  $C_{GC}$  is equal to the product of the **gate-channel capacitance** per unit area  $C''_{ox}$  ( $\text{F/m}^2$ ) and the area of the gate:

$$C_{GC} = C''_{ox} WL \quad (4.34)$$

In the Meyer model for the triode region,  $C_{GC}$  is partitioned into two equal parts. The **gate-source capacitance**  $C_{GS}$  and the **gate-drain capacitance**  $C_{GD}$  each consist of one-half of the gate-channel capacitance plus the overlap capacitances  $C_{GSO}$  and  $C_{GDO}$  associated with the gate-source or gate-drain regions:

$$\begin{aligned} C_{GS} &= \frac{C_{GC}}{2} + C_{GSO}W = C''_{ox} \frac{WL}{2} + C_{GSO}W \\ C_{GD} &= \frac{C_{GC}}{2} + C_{GDO}W = C''_{ox} \frac{WL}{2} + C_{GDO}W \end{aligned} \quad (4.35)$$

The overlap capacitances arise from two sources. First, the gate is actually not perfectly aligned to the edges of the source and drain diffusion but overlaps the diffusions somewhat. In addition, fringing fields between the gate and the source and drain regions contribute to the values of  $C_{GSO}$  and  $C_{GDO}$ .

The **gate-source** and **gate-drain overlap capacitances**  $C_{GSO}$  and  $C_{GDO}$  are normally specified as oxide capacitances per unit width ( $\text{F/m}$ ). Note that  $C_{GS}$  and  $C_{GD}$  each have a component that is proportional to the area of the gate and one proportional to the width of the gate.

The capacitances of the reverse-biased *pn* junctions, indicated by the **source-bulk** and **drain-bulk capacitances**  $C_{SB}$  and  $C_{DB}$ , respectively, exist between the source and drain diffusions and the substrate of the MOSFET. Each capacitance consists of a component proportional to the junction bottom area of the source ( $A_S$ ) or drain ( $A_D$ ) region and a sidewall component that is proportional to the perimeter of the source ( $P_S$ ) or drain ( $P_D$ ) junction region:

$$C_{SB} = C_J A_S + C_{JSW} P_S \quad C_{DB} = C_J A_D + C_{JSW} P_D \quad (4.36)$$

Here  $C_J$  is called the junction bottom capacitance per unit area ( $\text{F/m}^2$ ), and  $C_{JSW}$  is the junction sidewall capacitance per unit length.  $C_{SB}$  and  $C_{DB}$  will be present regardless of the region of operation. Note that the junction capacitances are voltage dependent [see Eq. (3.21)].

## 4.5.2 CAPACITANCES IN THE SATURATION REGION

In the saturation region of operation, depicted in Fig. 4.16(b), the portion of the channel beyond the pinch-off point disappears. The Meyer models for the values of  $C_{GS}$  and  $C_{GD}$  become

$$C_{GS} = \frac{2}{3} C_{GC} + C_{GSO}W \quad \text{and} \quad C_{GD} = C_{GDO}W \quad (4.37)$$

in which  $C_{GS}$  now contains two-thirds of  $C_{GC}$ , but only the overlap capacitance contributes to  $C_{GD}$ . Now  $C_{GD}$  is directly proportional to  $W$ , whereas  $C_{GS}$  retains a component dependent on  $W \times L$ .

## 4.5.3 CAPACITANCES IN CUTOFF

In the cutoff region of operation, depicted in Fig. 4.17, the conducting channel region is gone. The values of  $C_{GS}$  and  $C_{GD}$  now contain only the overlap capacitances:

$$C_{GS} = C_{GSO}W \quad \text{and} \quad C_{GD} = C_{GDO}W \quad (4.38)$$

In the cutoff region, a small capacitance  $C_{GB}$  appears between the gate and bulk terminal, as indicated in Fig. 4.17.

$$C_{GB} = C_{GBO}L \quad (4.39)$$

in which  $C_{GBO}$  is the **gate-bulk capacitance per unit length**.

It should be clear from Eqs. (4.34) to (4.39) that MOSFET capacitances depend on the region of operation of the transistor and are nonlinear functions of the voltages applied to the terminals of

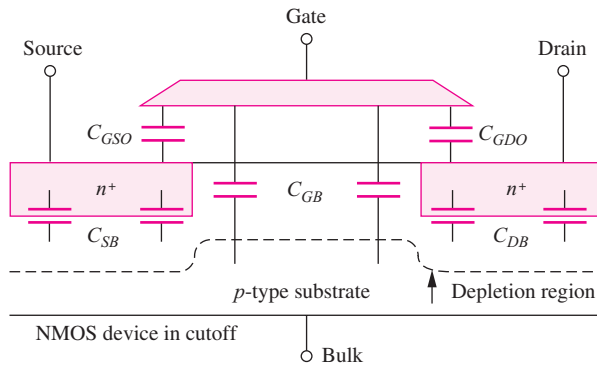


**Figure 4.17** NMOS capacitances in the cutoff region.

the device. In subsequent chapters we analyze the impact of these capacitances on the behavior of digital and analog circuits. Complete models for these nonlinear capacitances are included in circuit simulation programs such as SPICE, and circuit simulation is an excellent tool for exploring the detailed impact of these capacitances on circuit performance.

**EXERCISE:** Calculate  $C_{GS}$  and  $C_{GD}$  for a transistor operating in the triode and saturation regions if  $C_{ox}'' = 200 \mu\text{F/m}^2$ ,  $C_{GSO} = C_{GDO} = 300 \text{ pF/m}$ ,  $L = 0.5 \mu\text{m}$ , and  $W = 5 \mu\text{m}$ .

**ANSWERS:** 1.75 fF, 1.75 fF; 1.83 fF, 1.5 fF

## 4.6 MOSFET MODELING IN SPICE

The SPICE circuit analysis program is used to simulate more complicated circuits and to make much more detailed calculations than we can perform by hand analysis. The circuit representation for the MOSFET model that is implemented in SPICE is given in Fig. 4.18, and as we can observe, the model uses quite a number of circuit elements in an attempt to accurately represent the characteristics of a real MOSFET. For example, small resistances  $R_S$  and  $R_D$  appear in series with the external MOSFET source and drain terminals, and diodes are included between the source and drain regions and the

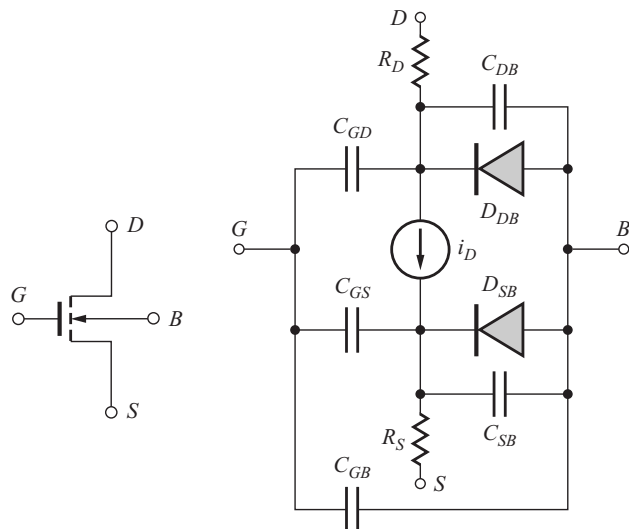


**Figure 4.18** SPICE model for the NMOS transistor.

**TABLE 4.2**  
SPICE Parameter Equivalences

PARAMETER	OUR TEXT	SPICE	DEFAULT
Transconductance	$K'_n$ or $K'_p$	KP	$20 \mu\text{A}/\text{V}^2$
Threshold voltage	$V_{TN}$ or $V_{TP}$	VT	—
Zero-bias threshold voltage	$V_{TO}$	VTO	1V
Surface potential	$2\phi_F$	PHI	0.6 V
Body effect	$\gamma$	GAMMA	0
Channel length modulation	$\lambda$	LAMBDA	0
Mobility	$\mu_n$ or $\mu_p$	UO	$600 \text{ cm}^2/\text{V} \cdot \text{s}$
Gate-drain capacitance per unit width	$C_{GDO}$	CGDO	0
Gate-source capacitance per unit width	$C_{GSO}$	CGSO	0
Gate-bulk capacitance per unit length	$C_{GBO}$	CGBO	0
Junction bottom capacitance per unit area	$C_J$	CJ	0
Grading coefficient	MJ	MJ	$0.5 \text{ V}^{0.5}$
Sidewall capacitance	$C_{JSW}$	CJSW	0
Sidewall grading coefficient	MJSW	MJSW	$0.5 \text{ V}^{0.5}$
Oxide thickness	$T_{ox}$	TOX	100 nm
Junction saturation current	$I_S$	IS	$10 \text{ fA}$
Built-in potential	$\phi_j$	PB	0.8 V
Ohmic drain resistance	—	RD	0
Ohmic source resistance	—	RS	0

substrate. The need for the power of the computer is clear here. It would be virtually impossible for us to use this sophisticated a model in our hand calculations.

As many as 20 different MOSFET models [5] of varying complexity are built into various versions of the SPICE simulation program, and they are denoted by “Level=Model\_Number”. The levels each have a unique mathematical formulation for current source  $i_D$  and for the various device capacitances. The model we have studied in this chapter is the most basic model and is referred to as the Level-1 model (LEVEL=1). Largely because of a lack of standard parameter usage at the time SPICE was first written, as well as the limitations of the programming languages originally used, the parameter names that appear in the models often differ from those used in this text and throughout the literature. The LEVEL=1 model is coded into SPICE using the following formulas, which are the similar to those we have already studied.

Table 4.2 contains the equivalences of the **SPICE model** parameters and our equations summarized in Sec. 4.2. Typical and default values of the SPICE model parameters can be found in Table 4.2. A similar model is used for the PMOS transistor, but the polarities of the voltages and currents, and the directions of the diodes, are reversed.

$$\text{Triode region: } i_D = \text{KP} \frac{W}{L} \left( v_{GS} - \text{VT} - \frac{v_{DS}}{2} \right) v_{DS} (1 + \text{LAMBDA} \cdot v_{DS}) \quad (4.40)$$

$$\text{Saturation region: } i_D = \frac{\text{KP}}{2} \frac{W}{L} (v_{GS} - \text{VT})^2 (1 + \text{LAMBDA} \cdot v_{DS}) \quad (4.40)$$

$$\text{Threshold voltage: } \text{VT} = \text{VTO} + \gamma (\sqrt{v_{SB} + \text{PHI}} - \sqrt{\text{PHI}})$$

Notice that the SPICE level-1 description includes the addition of channel-length modulation to the triode region expression. Also, be sure not to confuse SPICE threshold voltage **VT** with thermal voltage  $V_T$ .

The junction capacitances are modeled in SPICE by a generalized form of the capacitance expression in Eq. (3.21)

$$C_J = \frac{C_{JO}}{\left(1 + \frac{v_R}{PB}\right)^{MJ}} \quad \text{and} \quad C_{JSW} = \frac{C_{JSWO}}{\left(1 + \frac{v_R}{PB}\right)^{MJSW}} \quad (4.41)$$

in which  $v_R$  is the reverse bias across the  $pn$  junction.

**EXERCISE:** What are the values of SPICE model parameters **KP**, **LAMBDA**, **VTO**, **PHI**, **W**, and **L** for a transistor with the following characteristics:  $V_{TN} = 1$  V,  $K_n = 150$   $\mu\text{A}/\text{V}^2$ ,  $W = 1.5$   $\mu\text{m}$ ,  $L = 0.25$   $\mu\text{m}$ ,  $\lambda = 0.0133$   $\text{V}^{-1}$ , and  $2\phi_F = 0.6$  V?

**ANSWERS:** 150  $\mu\text{A}/\text{V}^2$ ; 0.0133  $\text{V}^{-1}$ ; 1 V; 0.6 V; 1.5  $\mu\text{m}$ ; 0.25  $\mu\text{m}$  (specified in SPICE as 150U; 0.0133; 1; 0.6; 1.5U; 0.25U)

## 4.7 MOS TRANSISTOR SCALING

In Chapter 1, we discussed the phenomenal increase in integrated circuit density and complexity. These changes have been driven by our ability to aggressively scale the physical dimensions of the MOS transistor. A theoretical framework for MOSFET miniaturization was first provided by Dennard, Gaensslen, Kuhn, and Yu [6, 7]. The basic tenant of the theory is to require that the electrical fields be maintained constant within the device as the geometry is changed. Thus, if a physical dimension is reduced by a factor of  $\alpha$ , then the voltage applied across that dimension must also be decreased by the same factor.

### 4.7.1 DRAIN CURRENT

These rules are applied to the transconductance parameter and triode region drain current expressions for the MOSFET in Eq. (4.42) in which the three physical dimensions,  $W$ ,  $L$ , and  $T_{ox}$  are all reduced by the factor  $\alpha$ , and each of the voltages including the threshold voltage is reduced by the same factor.

$$\begin{aligned} K_n^* &= \mu_n \frac{\epsilon_{ox}}{T_{ox}/\alpha} \frac{W/\alpha}{L/\alpha} = \alpha \mu_n \frac{\epsilon_{ox}}{T_{ox}} \frac{W}{L} = \alpha K_n \\ i_D^* &= \mu_n \frac{\epsilon_{ox}}{T_{ox}/\alpha} \frac{W/\alpha}{L/\alpha} \left( \frac{v_{GS}}{\alpha} - \frac{V_{TN}}{\alpha} - \frac{v_{DS}}{2\alpha} \right) \frac{v_{DS}}{\alpha} = \frac{i_D}{\alpha} \end{aligned} \quad (4.42)$$

We see that scaled transconductance  $K_n^*$  is increased by the scale factor  $\alpha$ , whereas the scaled drain current is reduced from the original value by the scale factor.

### 4.7.2 GATE CAPACITANCE

In a similar manner, the total gate-channel capacitance of the device is also found to be reduced by  $\alpha$ :

$$C_{GC}^* = (C_{ox}'')^* W^* L^* = \frac{\epsilon_{ox}}{T_{ox}/\alpha} \frac{W/\alpha}{L/\alpha} = \frac{C_{GC}}{\alpha} \quad (4.43)$$

In Chapter 6 we will demonstrate that the delay of logic gates is limited by the transistor's ability to charge and discharge the capacitance associated with the circuit. Based on  $i = C dv/dt$ , an estimate of the delay of a scaled logic circuit is

$$\tau^* = C_{GC}^* \frac{\Delta V^*}{i_D^*} = \frac{C_{GC}}{\alpha} \frac{\Delta V/\alpha}{i_D/\alpha} = \frac{\tau}{\alpha} \quad (4.44)$$

We find that circuit delay is also improved by the scale factor  $\alpha$ .

### 4.7.3 CIRCUIT AND POWER DENSITIES

As we scale down the dimensions by  $\alpha$ , the number of circuits in a given area will increase by a factor of  $\alpha^2$ . An important concern in scaling is therefore what happens to the power per circuit, and hence the power per unit area (power density) as dimensions are reduced. The total power supplied to a transistor circuit will be equal to the product of the supply voltage and the transistor drain current:

$$P^* = V_{DD}^* i_D^* = \left( \frac{V_{DD}}{\alpha} \right) \left( \frac{i_D}{\alpha} \right) = \frac{P}{\alpha^2}$$

and

$$\frac{P^*}{A^*} = \frac{P^*}{W^*L^*} = \frac{P/\alpha^2}{(W/\alpha)(L/\alpha)} = \frac{P}{WL} = \frac{P}{A} \quad (4.45)$$

The result in Eq. (4.45) is extremely important. It indicates that the power per unit area remains constant if a technology is properly scaled. Even though we are increasing the number of circuits by  $\alpha^2$ , the total power for a given size integrated circuit die will remain constant. Violation of the **scaling theory** over many years, by maintaining a constant 5-V power supply as dimensions were reduced, led to unmanageable power levels in integrated circuits. The power problem was finally resolved by changing from NMOS to CMOS technology, and then by reducing the power supply voltages.

### 4.7.4 POWER-DELAY PRODUCT

A useful figure of merit for comparing logic families is the **power-delay product** (PDP), which is discussed in more detail in Chapters 6 to 9. The product of power and delay time represents energy, and the power-delay product represents a measure of the energy required to perform a simple logic operation.

$$PDP^* = P^* \tau^* = \frac{P}{\alpha^2} \frac{\tau}{\alpha} = \frac{PDP}{\alpha^3} \quad (4.46)$$

The PDP figure of merit shows the full power of technology scaling. The power-delay product is reduced by the cube of the scaling factor.

Each new generation of lithography technology corresponds to a scale factor  $\alpha = \sqrt{2}$ . Therefore each new technology generation increases the potential number of circuits per chip by a factor of 2 and improves the PDP by a factor of almost 3. Table 4.3 summarizes the performance changes achieved with **constant electric field scaling**.

**EXERCISE:** A MOS technology is scaled from a 1- $\mu\text{m}$  feature size to 0.25  $\mu\text{m}$ . What is the increase in the number of circuits/cm<sup>2</sup>? What is the improvement in the power-delay product?

**ANSWERS:** 16 times; 64 times

**TABLE 4.3**  
Constant Electric Field Scaling Results

PERFORMANCE MEASURE	SCALE FACTOR	PERFORMANCE MEASURE	SCALE FACTOR
Area/circuit	$1/\alpha^2$	Circuit delay	$1/\alpha$
Transconductance parameter	$\alpha$	Power/circuit	$1/\alpha^2$
Current	$1/\alpha$	Power/unit area (power density)	1
Capacitance	$1/\alpha$	Power-delay product (PDP)	$1/\alpha^3$

**EXERCISE:** Suppose that the voltages are not scaled as the dimensions are reduced by a factor of  $\alpha$ ? How does the drain current of the transistor change? How do the power/circuit and power density scale?

**ANSWERS:**  $I_D^* = \alpha I_D$ ;  $P^* = \alpha P$ ;  $P^*/A^* = \alpha^3 P!!$

### 4.7.5 CUTOFF FREQUENCY

The ratio of transconductance  $g_m$  to gate-channel capacitance  $C_{GC}$  represents the highest useful frequency of operation of the transistor, and this ratio is called the cutoff frequency  $f_T$  of the device. The cutoff frequency represents the highest frequency at which the transistor can provide amplification. We can find  $f_T$  for the MOSFET by combining Eqs. (4.20) and (4.34):

$$f_T = \frac{1}{2\pi} \frac{g_m}{C_{GC}} = \frac{1}{2\pi} \frac{\mu_n}{L^2} (V_{GS} - V_{TN}) \quad (4.47)$$

Here we see clearly the advantage of scaling the channel length of MOSFET. The cutoff frequency improves with the square of the reduction in channel length.

**EXERCISE:** (a) A MOSFET has a mobility of  $500 \text{ cm}^2/\text{V}\cdot\text{s}$  and channel length of  $1 \mu\text{m}$ . What is its cutoff frequency if the gate voltage exceeds the threshold voltage by  $1 \text{ V}$ ? (b) Repeat for a channel length of  $0.25 \mu\text{m}$ .

**ANSWERS:** (a)  $7.96 \text{ GHz}$ ; (b)  $127 \text{ GHz}$

### 4.7.6 HIGH FIELD LIMITATIONS

Unfortunately the assumptions underlying constant-field scaling have often been violated due to a number of factors. For many years, the supply voltage was maintained constant at a standard level of  $5 \text{ V}$ , while the dimensions of the transistor were reduced, thus increasing the electric fields within the MOSFET. Increasing the electric field in the device can reduce long-term reliability and ultimately lead to breakdown of the gate oxide or  $pn$  junction.

High fields directly affect MOS transistor mobility in two ways. The first effect is a reduction in the mobility of the MOS transistor due to increasing carrier scattering at the channel oxide interface. The second effect of high electric fields is to cause a breakdown of the linear mobility-field relationship as discussed in Chapter 2. At low fields, carrier velocity is directly proportional to electric field, as assumed in Eq. (4.5), but for fields exceeding approximately  $10^5 \text{ V/cm}$ , the carriers reach a maximum velocity of approximately  $10^7 \text{ cm/s}$  called the saturation velocity  $v_{SAT}$  (see Fig. 2.5). Both mobility reduction and velocity saturation tend to linearize the drain current expressions for the MOSFET. The results of these effects can be incorporated into the drain current model for the MOSFET as indicated in Eqs. (4.48) and (4.49) in which the expression for carrier velocity is replaced with the maximum velocity limit  $v_{SAT}$ :

$$i_D = Q_n v_n = \frac{C''_{ox} W}{2} (v_{GS} - V_{TN}) v_n \text{ and } v_n = \mu_n \frac{v_{DS}}{L} \rightarrow v_{SAT} \quad (4.48)$$

This modification causes the square-law behavior to disappear from the saturation region equation:

$$\text{Saturation region: } i_D = \frac{C''_{ox} W}{2} (v_{GS} - V_{TN}) v_{SAT} \quad (4.49)$$

**EXERCISE:** A MOSFET has a channel length of  $1 \mu\text{m}$ . What value of  $V_{DS}$  will cause the electrons to reach saturation velocity? Repeat for a channel length of  $0.1 \mu\text{m}$ .

**ANSWERS:**  $10 \text{ V}, 1 \text{ V}$

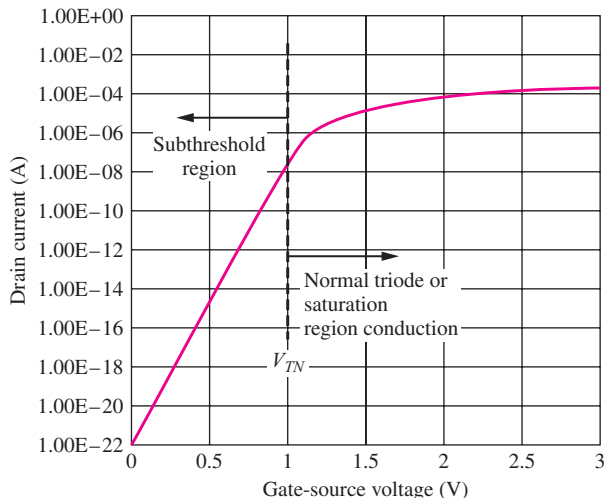


Figure 4.19 Subthreshold conduction in an NMOS transistor with  $V_{TN} = 1$  V.

#### 4.7.7 SUBTHRESHOLD CONDUCTION

In our discussion of the MOSFET thus far, we have assumed that the transistor turns off abruptly as the gate-source voltage drops below the threshold voltage. In reality, this is not the case. As depicted in Fig. 4.19, the drain current decreases exponentially for values of  $v_{GS}$  less than  $V_{TN}$  (referred to as the **subthreshold region**), as indicated by the region of constant slope in the graph. A measure of the rate of turn off of the MOSFET in the subthreshold region is specified as the reciprocal of the slope (1/S) in mV/decade of current change. Typical values range from 60 to 120 mV/decade. The value depends on the relative magnitudes of  $C''_{ox}$  and  $C_d$  in Fig. 4.3(b).

From Eq. (4.42), we see that the threshold voltage of the transistor should be reduced as the dimensions are reduced. However, the subthreshold region does not scale properly, and the curve in Fig. 4.19 tends to shift horizontally as  $V_{TN}$  is decreased. The reduced threshold increases the leakage current in “off” devices, which ultimately limits data storage time in the dynamic memory cells (see Chapter 8) and can play an important role in limiting battery life in low-power portable devices.

**EXERCISE:** (a) What is the leakage current in the device in Fig. 4.19 for  $V_{GS} = 0.25$  V? (b) Suppose the transistor in Fig. 4.19 had  $V_{TN} = 0.5$  V. What will be the leakage current for  $V_{GS} = 0$  V? (c) A memory chip uses  $10^9$  of the transistors in part (b). What is the total leakage current if  $V_{GS} = 0$  V for all the transistors?

**ANSWERS:** (a)  $\cong 10^{-18}$  A; (b)  $\cong 10^{-15}$  A; (c)  $\cong 1$   $\mu$ A

#### 4.8 MOS TRANSISTOR FABRICATION AND LAYOUT DESIGN RULES<sup>2</sup>

In addition to choosing the circuit topology, the MOS integrated circuit designer must pick the values of the  $W/L$  ratios of the transistors and develop a layout for the circuit that ensures that it will achieve the performance specifications. Design of the layout of transistors and circuits in integrated form is constrained by a set of rules termed the **design rules** or **ground rules**. These rules are

<sup>2</sup> Jaeger, Richard C., *Introduction to Microelectronic Fabrication: Volume 5 of Modular Series on Solid State Devices*, 2nd edition, © 2002. Electronically reproduced by permission of Pearson Education, Inc., Upper Saddle River, New Jersey.

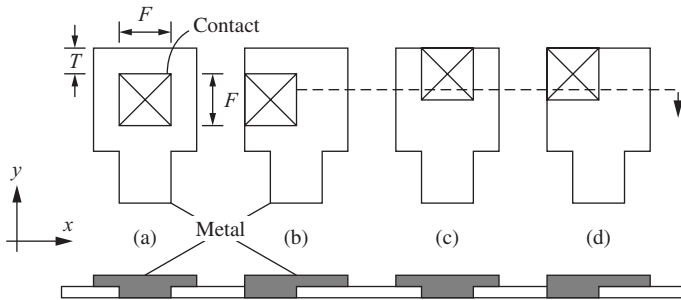


**Figure 4.20** Misalignment of a metal pattern over a contact opening: (a) desired alignment, (b) one possible worst-case misalignment in the  $x$  direction, (c) one possible worst-case misalignment in the  $y$  direction, and (d) misalignment in both directions.

technology specific and specify minimum sizes, spacings and overlaps for the various shapes that define transistors. The sets of rules are different for MOS and bipolar processes, for MOS processes designed specifically for logic and memory, and even for similar processes from different companies.

#### 4.8.1 MINIMUM FEATURE SIZE AND ALIGNMENT TOLERANCE

Processes are defined around a **minimum feature size**  $F$ , which represents the width of the smallest line or space that can be reliably transferred to the surface of a wafer using a given generation of lithographic manufacturing tools. To produce a basic set of ground rules, we must also know the maximum misalignment which can occur between two mask levels during fabrication. For example, Fig. 4.20(a) shows the nominal position of a metal line aligned over a contact window (indicated by the box with an  $\times$  in it). The metal overlaps the contact window by at least one **alignment tolerance**  $T$  in all directions. During the fabrication process, alignment will not be perfect, and the actual structure may exhibit misalignment in the  $x$  or  $y$  directions or both. Figures 4.20(b) through 4.20(d) show the result of one possible set of worst-case alignments of the patterns in the  $x$ ,  $y$ , and both directions simultaneously. Our set of design rules assume that  $T$  is the same in both directions. Transistors designed with our ground rules may fail to operate properly if the misalignment exceeds tolerance  $T$ .

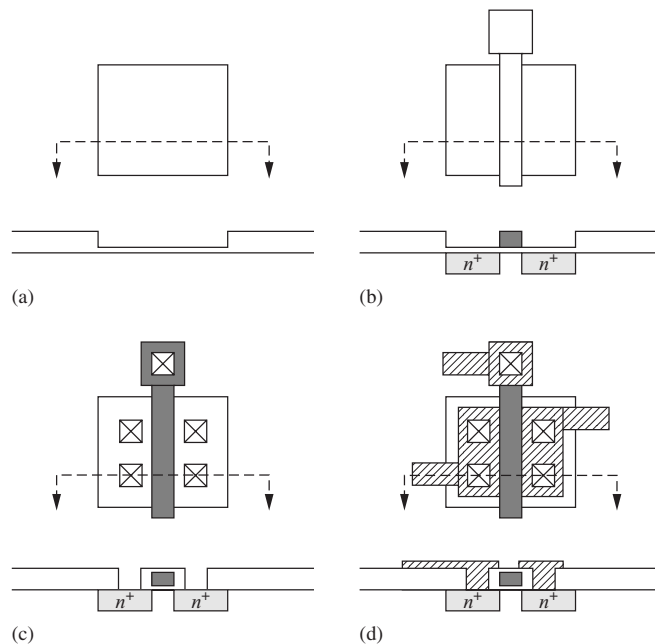
#### 4.8.2 MOS TRANSISTOR LAYOUT

Figure 4.21 outlines the process and mask sequence used to fabricate a basic polysilicon-gate transistor. The first mask defines the active area, or thin oxide region of the transistor, and the second mask defines the polysilicon gate of the transistor. The channel region of the transistor is actually produced by the intersection of these first two mask layers; the source and/or drain regions are formed wherever the active layer (mask 1) is *not* covered by the gate layer (mask 2). The third and fourth masks delineate the contact openings and the metal pattern. The overall mask sequence is

Active area mask	Mask 1
Polysilicon-gate mask	Mask 2—align to mask 1
Contact window mask	Mask 3—align to mask 2
Metal mask	Mask 4—align to mask 3

The alignment sequence must be specified to properly account for alignment tolerances in the ground rules. In this particular example, each mask is aligned to the one used in the preceding step, but this is not always the case.

We will now explore a set of design rules similar in concept to those developed by Mead and Conway [3]. These ground rules were designed to permit easy translation of a design from one generation of technology to another by simply changing the size of one parameter  $\Lambda$ . To achieve this goal, the rules are quite forgiving in terms of the mask-to-mask alignment tolerance.



**Figure 4.21** (a) Active area mask, (b) gate mask, (c) contact opening mask, (d) metal mask.

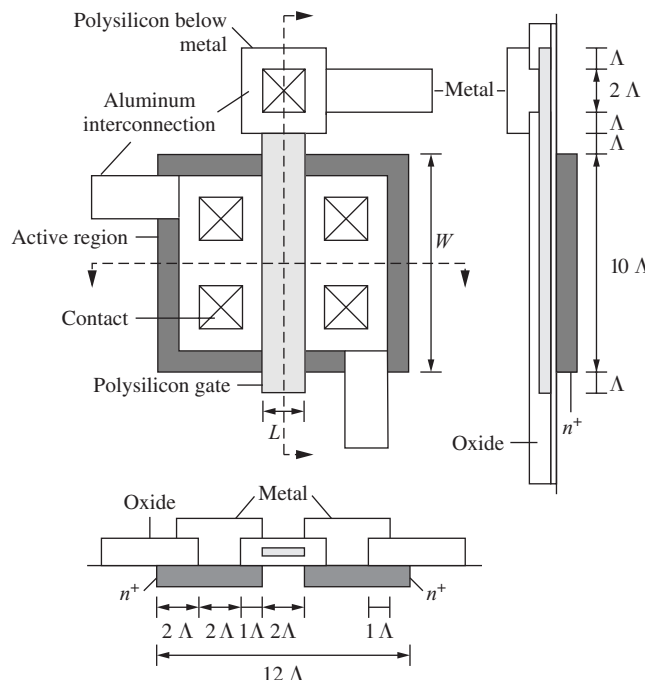


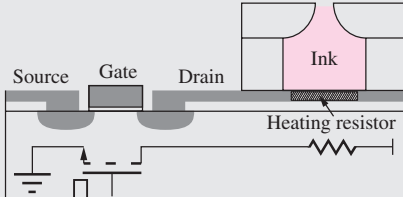
**Figure 4.22** Composite top view and cross sections of a transistor with  $W/L = 5/1$  demonstrating a basic set of ground rules.

A composite set of rules for a transistor is shown graphically in Fig. 4.22 in which the minimum feature size  $F = 2\Lambda$  and the alignment tolerance  $T = F/2 = \Lambda$ . (Parameter  $\Lambda$  could be 0.5, 0.25, or  $0.1\text{ }\mu\text{m}$ , for example.) Note that an alignment tolerance equal to one-half the minimum feature size is a very forgiving alignment tolerance.

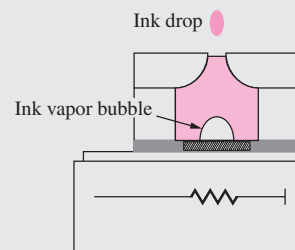
## ELECTRONICS IN ACTION

### *Thermal Inkjet Printers*

Inkjet printers have moved from a few niche applications in the 1960s to a widespread, mainstream consumer presence. Thermal inkjet technology was invented in 1979 at Hewlett-Packard Laboratories. Since that time, inkjet technology has evolved to the point where modern thermal inkjet printers deliver 10–20 picoliter droplets at rates of several kHz. Integration of the ink handling structures with microelectronics has been an important component of this evolution. Early versions of thermal inkjet printers had drive electronics that were separate from the ink delivery devices. Through the use of MEMS (micro-electro-mechanical system) technology, it has been possible to combine MOS transistors onto the same substrate with the ink handling structures.



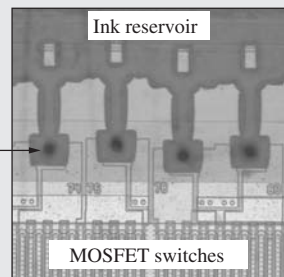
Simplified diagram of thermal inkjet structure integrated with MOS drive transistors. A voltage pulse on the gate causes  $I^2R$  heating in the resistor.



Heat from power dissipated in the resistor vaporizes a small amount of ink causing the ejection of an ink droplet out of the nozzle.



© 1994–2006 Hewlett-Packard Company.  
All Rights Reserved.



Photomicrograph of inkjet print head

This diagram is a simplified illustration of a merged thermal inkjet system. A MOSFET transistor is located in the left segment of the silicon substrate. A metal layer connects the drain of the transistor to the thin-film resistive heating material directly under the ink cavity. When the gate of the transistor is driven with a voltage pulse, current passes through the resistor leading to a rapid heating of the ink in the cavity. The temperature of the ink in contact with the resistor increases until a small portion of the ink vaporizes. The vapor bubble forces an ink drop to be ejected from the nozzle at the top of the ink cavity and onto the paper. (In practice, the drops are directed down onto the paper.) At the end of the gate drive pulse, the resistor cools and the vapor bubble collapses, allowing more ink to be drawn into the cavity from an ink reservoir.

Due to the high densities and resolutions made possible by the merging of control and drive electronics with the printing structures, inkjet printers are now capable of generating photo-quality images at reasonable costs. As we will see throughout this text, making high-technology affordable and widely available is a common trait of microelectronics-based systems.

For the transistor in Fig. 4.22, all linewidths and spaces must be a minimum feature size of  $2 \text{ \AA}$ . Square contacts are a minimum feature size of  $2 \text{ \AA}$  in each dimension. To ensure that the metal completely covers the contact for worst-case misalignment, a  $1 \text{ \AA}$  border of metal is required around the contact region. The polysilicon gate must overlap the edge of the active area and the contact openings by  $1 \text{ \AA}$ . However, because of the potential for tolerance accumulation during successive misalignments of masks 2 and 3, the contacts must be inside the edges of the active area by  $2 \text{ \AA}$ .

The transistor in Fig. 4.22 has a  $W/L$  ratio of  $10 \text{ \AA}/2 \text{ \AA}$  or  $5/1$ , and the total active area is  $120 \text{ \AA}^2$ . Thus the active channel region represents approximately 17 percent of the total area of the transistor. Note that the polysilicon gate defines the edges of the source and/or drain regions and results in “self-alignment” of the edges of the gate to the edges of the channel region. Self-alignment of the gate to the channel reduces the size of the transistor and minimizes the “overlap capacitances” associated with the transistor.

**EXERCISE:** What is the active area of the transistor in Fig. 4.22 if  $\Lambda = 0.125 \mu\text{m}$ ? What are the values of  $W$  and  $L$  for the transistor? What is the area of the transistor gate region? How many of these transistors could be packed together on a  $1 \text{ cm} \times 1 \text{ cm}$  integrated circuit die if the active areas of the individual transistors must be spaced apart by a minimum of  $4 \text{ \AA}$ ?

**ANSWERS:**  $1.88 \mu\text{m}^2$ ;  $1.25 \mu\text{m}$ ;  $0.25 \mu\text{m}$ ;  $0.31 \mu\text{m}^2$ ; 28.6 million

## 4.9 BIASING THE NMOS FIELD-EFFECT TRANSISTOR

As stated before, the MOS circuit designer has the flexibility to choose the circuit topology and  $W/L$  ratios of the devices in the circuit, and to a lesser extent, the voltages applied to the devices. As designers, we need to develop a mental catalog of useful circuit configurations, and we begin by looking at several basic circuits for biasing the MOSFET.

### 4.9.1 WHY DO WE NEED BIAS?

We have found that the MOSFET has three regions of operation: cutoff, triode, and saturation. For circuit applications, we want to establish a well-defined **quiescent operating point**, or **Q-point**, for the MOSFET in a particular region of operation. The Q-point for the MOSFET is represented by the dc values ( $I_D$ ,  $V_{DS}$ ) that locate the operating point on the MOSFET output characteristics. [In reality, we need the three values ( $I_D$ ,  $V_{DS}$ ,  $V_{GS}$ ), but two are enough to calculate the third if we know the region of operation of the device.]

For binary logic circuits investigated in detail in Part II of this text, the transistor acts as an “on-off” switch, and the Q-point is set to be in either the cutoff region (“off”) or the triode region (“on”). For example, let us explore the circuit in Fig. 4.23(a) that can be used as either a logic inverter or a linear amplifier depending upon our choice of operating points. The voltage transfer characteristic (VTC) for the circuit appears in Fig. 4.24(a). For low values of  $v_{GS}$ , the MOSFET is off, and the output voltage is  $5 \text{ V}$ , corresponding to a binary “1” in a logic application. As  $v_{GS}$  increases, the output begins to drop and finally reaches its “on-state” voltage of  $0.65 \text{ V}$  for  $v_{GS} = 5 \text{ V}$ . This voltage would correspond to a “0” in binary logic. These two logic states are also shown on the transistor output characteristics in Fig. 4.24(b). When the transistor is “on,” it conducts a substantial current, and  $v_{DS}$  falls to  $0.65 \text{ V}$ . When the transistor is off,  $v_{DS}$  equals  $5 \text{ V}$ . We study the design of logic gates in detail in Chapters 6–9.

For amplifier applications, the Q-point is located in the region of high slope (high gain) near the center of the voltage transfer characteristic, also indicated in Fig. 4.24(a). At this operating point, the transistor is operating in saturation, the region in which high voltage, current and/or power gain can be achieved. To establish this Q-point, a **dc bias**  $V_{GS}$  is applied to the gate as in Fig. 4.23(b), and

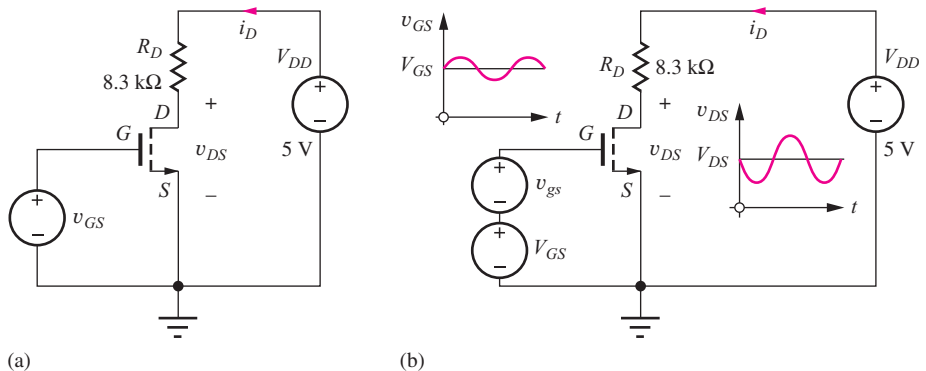


**Figure 4.23** (a) Circuit for a logic inverter. (b) The same transistor used as a linear amplifier.

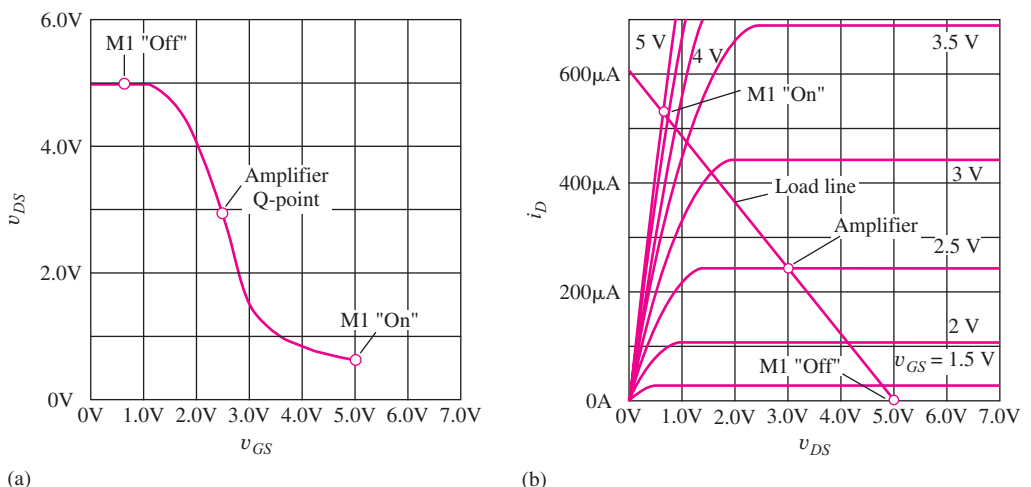


**Figure 4.24** (a) Voltage transfer characteristic (VTC) with quiescent operating points (Q-points) corresponding to an “on-switch,” an amplifier, and an “off-switch.” (b) The same three operating points located on the transistor output characteristics.

a small ac signal  $v_{gs}$  is added to vary the gate voltage around the bias value.<sup>3</sup> The variation in total gate-source voltage  $v_{GS}$  causes the drain current to change, and an amplified replica of the ac input voltage appears at the drain. Our study of the design of transistor amplifiers begins in Chapter 13.

The straight line connecting the Q-points in Figure 4.24(b) is the *load line* that was first encountered in Chapter 3. The dc load line plots the permissible values of  $I_D$  and  $V_{DS}$  as determined by the external circuit. In this case, the load line equation is given by

$$V_{DD} = I_D R_D + V_{DS}$$

For hand analysis and design of Q-points, channel-length modulation is usually ignored by assuming  $\lambda = 0$ . A review of Fig. 4.11 indicates that including  $\lambda$  changes the drain current by less than 10 percent. Generally, we do not know the values of transistor parameters to this accuracy, and the tolerances on both discrete or integrated circuit elements may be as large as 30 to 50 percent. If you explore some transistor specification sheets (see the JaegerBlalock website), you will discover parameters that have a 4 or 5 to 1 spread in values. You will also find parameters with only a minimum

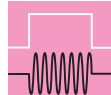
<sup>3</sup> Remember  $v_{GS} = V_{GS} + v_{gs}$ .

or maximum value specified. Thus, neglecting  $\lambda$  will not significantly affect the validity of our analysis. Also, many bias circuits involve feedback which further reduces the influence of  $\lambda$ . On the other hand, in Part III we will see that  $\lambda$  can play an extremely important role in limiting the voltage gain of analog amplifier circuits, and the effect of  $\lambda$  must often be included in the analysis of these circuits.

To analyze circuits containing MOSFETs, we must first assume a region of operation, just as we did to analyze diode circuits in Chapter 3. The bias circuits that follow will most often be used to place the transistor Q-point in the saturation region, and by examining Eq. (4.27) with  $\lambda = 0$ , we see that we must know the gate-source voltage  $V_{GS}$  to calculate the drain current  $I_D$ . Then, once we know  $I_D$ , we can find  $V_{DS}$  from the constraints of Kirchhoff's voltage law. Thus our most frequently used analysis approach will be to first find  $V_{GS}$  and then to use its value to find the value of  $I_D$ .  $I_D$  will then be used to calculate  $V_{DS}$ .

### Menu for Bias Analysis

1. Assume a region of operation (Most often the saturation region).
2. Use circuit analysis to find  $V_{GS}$ .
3. Use  $V_{GS}$  to calculate  $I_D$ , and  $I_D$  to determine  $V_{DS}$ .
4. Check the validity of the operating region assumptions.
5. Change assumptions and analyze again if necessary.



### DESIGN NOTE SATURATION BY CONNECTION!

When making bias calculations for analysis or design, it is useful to remember that an NMOS enhancement-mode device that is operating with  $V_{DS} = V_{GS}$  will always be in the pinch-off region. The same is true for an enhancement-mode PMOS transistor.

To demonstrate this result, it is easiest to keep the signs straight by considering an NMOS device with dc bias. For pinch-off, it is required that

$$V_{DS} \geq V_{GS} - V_{TN}$$

But if  $V_{DS} = V_{GS}$ , this condition becomes

$$V_{DS} \geq V_{DS} - V_{TN} \quad \text{or} \quad V_{TN} \geq 0$$

which is always true if  $V_{TN}$  is a positive number.  $V_{TN} > 0$  corresponds to an NMOS enhancement-mode device. Thus an enhancement-mode device operating with  $V_{DS} = V_{GS}$  is always in the saturation region! Similar arguments hold true for enhancement-mode PMOS devices.

### 4.9.2 CONSTANT GATE-SOURCE VOLTAGE BIAS

A basic bias circuit for the NMOS transistor is shown in Fig. 4.25, in which dc voltage source  $V_{GG}$  is used to establish a fixed gate-source bias for the MOSFET, source  $V_{DD}$  supplies drain current to

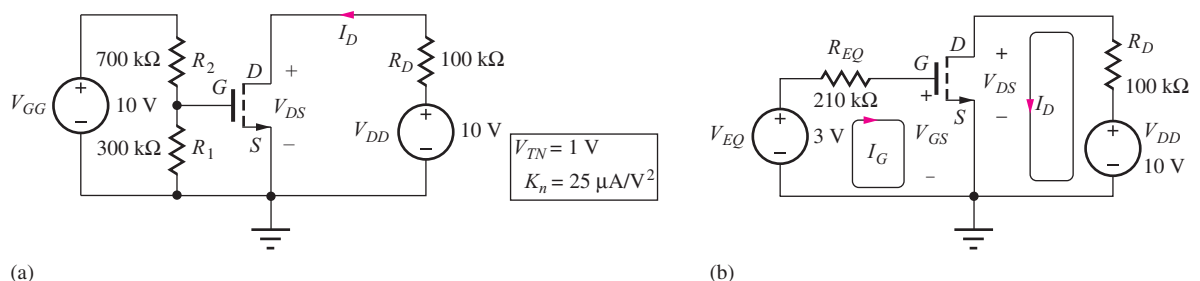


**Figure 4.25** (a) Constant gate-voltage bias using a voltage divider. (b) Simplified MOSFET bias circuit.

the NMOS transistor through resistor  $R_D$ , and the value of  $R_D$  determines  $V_{DS}$ . This circuit is used to introduce a number of concepts related to biasing, but we shall find that it is not a very useful circuit in practical applications.

### EXAMPLE 4.1 CONSTANT GATE-SOURCE VOLTAGE BIAS

**PROBLEM** (a) Find the quiescent operating point Q-point ( $I_D$ ,  $V_{DS}$ ) for the MOSFET in the fixed gate bias circuit in Fig. 4.25. Neglect channel-length modulation. (b) Find the Q-point if  $\lambda = 0.02 \text{ V}^{-1}$ .

**SOLUTION Known Information and Given Data:** Circuit schematic in Fig. 4.25 with  $V_{DD} = 10 \text{ V}$ ,  $V_{GG} = 10 \text{ V}$ ,  $R_1 = 300 \text{ k}\Omega$ ,  $R_2 = 700 \text{ k}\Omega$ ,  $R_D = 100 \text{ k}\Omega$ ,  $V_{TN} = 1 \text{ V}$ ,  $K_n = 25 \mu\text{A/V}^2$ ,  $I_G = 0$ ,  $I_B = 0$ , and  $\lambda = 0.02 \text{ V}^{-1}$ .

**Unknowns:**  $I_D$ ,  $V_{DS}$ , and  $V_{GS}$

**Approach:** We can find the Q-point using the mathematical model for the NMOS transistor. We must assume a region of operation, determine the Q-point, and then see if the resulting Q-point is consistent with the assumed region of operation.

**Assumptions:** (a) We will assume that the MOSFET is pinched-off:  $I_D = (K_n/2)(V_{GS} - V_{TN})^2$ . Remember, we ignore  $\lambda$  in hand bias calculations. This assumption simplifies the mathematics because  $I_D$  is then modeled as being independent of  $V_{DS}$ .

**Analysis:** From the drain current expression and given data, we see that if we first find  $V_{GS}$ , then we can use it to find  $I_D$ . First label the variables in the circuit including  $I_D$ ,  $V_{DS}$ , and  $V_{GS}$ . Then to simplify the analysis, we replace the gate-bias network consisting of  $V_{GG}$ ,  $R_1$ , and  $R_2$  with its Thévenin equivalent circuit as in Fig. 4.25(b) in which

$$V_{EQ} = \frac{R_1}{R_1 + R_2} V_{GG} = 3 \text{ V} \quad \text{and} \quad R_{EQ} = \frac{R_1 R_2}{R_1 + R_2} = 210 \text{ k}\Omega$$

We apply Kirchhoff's voltage law (KVL) to the loop containing the gate-source terminals of the device (referred to here as the input loop):

$$V_{EQ} = I_G R_{EQ} + V_{GS} \quad (4.50)$$

But, we know that  $I_G = 0$  for the MOSFET, so that  $V_{GS} = V_{EQ} = 3 \text{ V}$ . We can now find  $I_D$  using the transistor parameters from Fig. 4.25 will  $\lambda = 0$ :

$$I_D = \frac{K_n}{2} (V_{GS} - V_{TN})^2 = \frac{25 \times 10^{-6}}{2} \frac{\text{A}}{\text{V}^2} (3 - 1)^2 \text{ V}^2 = 50 \mu\text{A}$$

To determine  $V_{DS}$  we write a loop equation including the drain-source terminals of the device (referred to here as the output loop):

$$V_{DD} = I_D R_D + V_{DS} \quad (4.51)$$

Again substituting the values from Fig. 4.25,

$$V_{DS} = 10 \text{ V} - (50 \times 10^{-6} \text{ A})(10^5 \Omega) = 5.00 \text{ V}$$

**Check of Results:** We have  $V_{DS} = 5 \text{ V}$  and  $V_{GS} - V_{TN} = 2 \text{ V}$ . Since  $V_{DS}$  exceeds  $V_{GS} - V_{TN}$ , the transistor is indeed pinched-off and in the saturation region. Thus, the Q-point is (50.0  $\mu\text{A}$ , 5.00 V) with  $V_{GS} = 3 \text{ V}$ .

**Assumptions:** (b) Assume that the MOSFET is in the pinch-off region. But now

$$I_D = \frac{K_n}{2}(V_{GS} - V_{TN})^2(1 + \lambda V_{DS}).$$

**Analysis:** To find  $V_{DS}$ , we still have

$$V_{DS} = V_{DD} - I_D R_D$$

Combining this equation with the expression for the drain current and substituting the values from Fig. 4.25 yields

$$V_{DS} = 10 - \frac{(25 \times 10^{-6})(10^5)}{2}(3 - 1)^2(1 + 0.02 V_{DS})$$

in which the units have been eliminated for simplicity. Solving for  $V_{DS}$  yields  $V_{DS} = 4.55\text{ V}$ . Using this value to calculate the drain current gives

$$I_D = \frac{25 \times 10^{-6}}{2}(3 - 1)^2[1 + 0.02(4.55)] = 54.5\text{ }\mu\text{A}$$

**Check of Results:** We see that  $V_{DS} = 4.55\text{ V}$  exceeds  $V_{GS} - V_{TN} = 2\text{ V}$  so that the transistor is indeed pinched-off. Thus, the saturation region assumption is justified. The final Q-point is ( $54.5\text{ }\mu\text{A}$ ,  $4.55\text{ V}$ ).

**Discussion:** For  $\lambda = 0.02\text{ V}^{-1}$ , we see that the Q-point values have each changed by approximately 10 percent from ( $50\text{ }\mu\text{A}$ ,  $5\text{ V}$ ) to ( $54.5\text{ }\mu\text{A}$ ,  $4.55\text{ V}$ ). From a practical point of view, the tolerances on circuit element and transistor parameter values will completely swamp out these small differences. Therefore we gain little from the additional complexity of including  $\lambda$  in our hand calculations. Note that, although this particular calculation including  $\lambda$  may have seemed relatively painless, the relative ease is an artifact of this particular circuit. Including  $\lambda$  in calculations for other bias circuits is considerably more difficult. On the other hand, if we use a circuit analysis program to perform the calculations, we might as well include  $\lambda$ . Although this circuit introduces a number of concepts related to biasing, it is not a very useful circuit in practical applications because the Q-point is very sensitive to variations in the values of the transistor parameters. If the value of  $V_{GS}$  is fixed in the drain current expression, then  $I_D$  varies in direct proportion to  $K_n$  and depends on the square of changes in  $V_{TN}$ . The bias circuits that we will explore in Exs. 4.3 and 4.7 provide a much reduced sensitivity of the Q-point to changes in device parameters and are preferred methods of biasing the transistor.

**EXERCISE:** Find the Q-point for the circuit in Fig. 4.25 if  $R_D$  is changed to  $50\text{ k}\Omega$ , and  $\lambda = 0$ .

**ANSWER:** ( $50.0\text{ }\mu\text{A}$ ,  $7.50\text{ V}$ )

**EXERCISE:** Find the Q-point for the circuit in Fig. 4.25 if  $R_1 = 270\text{ k}\Omega$ ,  $R_2 = 750\text{ k}\Omega$ ,  $R_D = 100\text{ k}\Omega$ , and  $\lambda = 0$ .

**ANSWER:** ( $33.9\text{ }\mu\text{A}$ ,  $6.61\text{ V}$ )

**EXERCISE:** Suppose that  $K_n = 30\text{ }\mu\text{A/V}^2$  instead of  $25\text{ }\mu\text{A/V}^2$  as in Ex. 4.1(a). What are the new values of  $V_{GS}$ ,  $I_D$ , and  $V_{DS}$ ?

**ANSWER:** ( $3\text{ V}$ ,  $60.0\text{ }\mu\text{A}$ ,  $4\text{ V}$ ) (Note in this circuit that  $I_D$  is directly proportional to  $K_n$ .)

**EXERCISE:** Suppose that  $V_{TN}$  is 1.5 V instead of 1 V in Ex. 4.1(a). What are the new values of  $V_{GS}$ ,  $I_D$ , and  $V_{DS}$ ?

**ANSWER:** (3 V, 28.1  $\mu$ A, 7.19 V) (We see that the current is also quite sensitive to the value of  $V_{TN}$ .)

**EXERCISE:** Repeat the channel length modulation calculation for  $\lambda = 0.01 \text{ V}^{-1}$ . What are the new values of  $I_D$  and  $V_{DS}$ ?

**ANSWER:** (52.4  $\mu$ A, 4.76 V)

### 4.9.3 LOAD LINE ANALYSIS FOR THE Q-POINT

The Q-point for the MOSFET circuit in Fig. 4.25 can also be found graphically with a load-line method very similar to the one used for analysis of diode circuits in Sec. 3.10. The graphical approach helps us visualize the operating point of the device and its location relative to the boundaries between the cutoff, triode and pinch-off regions of operation.

#### EXAMPLE 4.2 LOAD LINE ANALYSIS

**PROBLEM** Use load line analysis to locate the Q-point for the MOSFET in the fixed gate bias circuit in Fig. 4.25.

**SOLUTION Known Information and Given Data:** Circuit schematic in Fig. 4.25 with  $V_{DD} = 10 \text{ V}$ ,  $V_{EQ} = 3 \text{ V}$ ,  $R_{EQ} = 210 \text{ k}\Omega$ ,  $R_D = 100 \text{ k}\Omega$ ,  $V_{TN} = 1 \text{ V}$ ,  $K_n = 25 \mu\text{A/V}^2$ ,  $I_G = 0$ , and  $I_B = 0$

**Unknowns:** Q-point = ( $I_D$ ,  $V_{DS}$ )

**Approach:** We need to find an equation for the load line,  $I_D = f(V_{DS})$ , so that it can be plotted on the output  $i-v$  characteristics. The Q-point can then be located on the output characteristics. Equation (4.51) represents the *load line* for this MOSFET circuit and is repeated here:

$$V_{DD} = I_D R_D + V_{DS}$$

**Assumptions:** We have already found  $V_{GS} = 3 \text{ V}$  using the techniques in Ex. 4.1(a).

**Analysis:** For the values for the circuit in Fig. 4.25, the load line equation becomes

$$10 = 10^5 I_D + V_{DS}$$

Just as for the diode circuits in Sec. 3.10, the load line is constructed by finding two points on the line: for  $V_{DS} = 0$ ,  $I_D = 100 \mu\text{A}$ , and for  $I_D = 0$ ,  $V_{DS} = 10 \text{ V}$ . The resulting line is drawn on the output characteristics of the MOSFET in Fig. 4.26. The family of NMOS curves intersects the load line at many different points (actually infinitely many since each possible gate voltage corresponds to a different curve). The gate-source voltage is the parameter that determines which of the intersection points is the actual Q-point. In this circuit, we already found  $V_{GS} = 3 \text{ V}$ ; the Q-point is indicated by the circle in the Fig. 4.26. Reading the values from the graph yields  $V_{DS} = 5 \text{ V}$  and  $I_D = 50 \mu\text{A}$ .

**Check of Results:** This is the same Q-point that we found using our mathematical model for the MOSFET.

**Discussion:** From the graph, we can immediately see that the Q-point is in the saturation region of the transistor output characteristics. The Q-point is fairly well centered in the saturation region of operation, and the drain-source voltage is 3 V greater than that required to saturate the device.

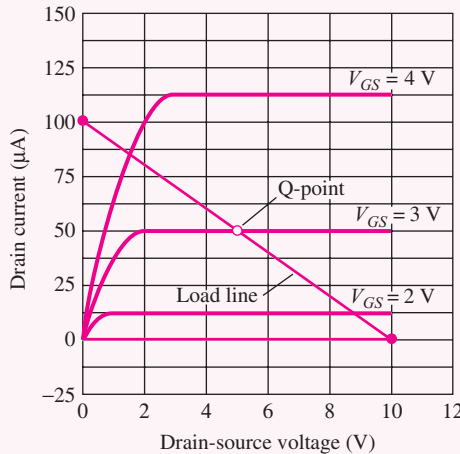


Figure 4.26 Load line for the circuit in Fig. 4.25.

Although we will seldom actually solve bias problems using graphical techniques, it is very useful to visualize the location of the Q-point in terms of the load line on the output characteristics as in Fig. 4.26. We can readily see if the device is operating in the triode or saturation regions as well as how far the operating point is from the boundaries between the various regions of operation.

**EXERCISE:** Draw the new load line and find the Q-point if  $R_D$  is changed to  $66.7\text{ k}\Omega$ .

**ANSWER:** (50  $\mu\text{A}$ , 6.7 V)

#### 4.9.4 FOUR-RESISTOR BIASING

The circuit in Fig. 4.25 provides a fixed gate-source bias voltage to the transistor. Theoretically, this works fine. However, in practice the values of  $K_n$ ,  $V_{TN}$ , and  $\lambda$  for the MOSFET will not be known with high precision and the Q-point is not well-controlled. In addition, we must be concerned about resistor and power supply tolerances (you may wish to review Sec. 1.8) as well as component value drift with both time and temperature in an actual circuit. Four-resistor bias provides a well-stabilized Q-point.

#### EXAMPLE 4.3 FOUR-RESISTOR BIAS CIRCUIT

The most general and important bias method that we will encounter is the **four-resistor bias** circuit in Fig. 4.27(a). The addition of the fourth resistor  $R_S$  helps stabilize the MOSFET Q-point in the face of many types of circuit parameter variations. This bias circuit is actually a form of *feedback circuit*, which will be studied in great detail in Part III of this text. Also observe that a single voltage source  $V_{DD}$  is now used to supply both the gate-bias voltage and the drain current. The four-resistor bias circuit is most often used to place the transistor in the saturation region of operation for use as an amplifier for analog signals.

**PROBLEM** Find the Q-point = ( $I_D$ ,  $V_{DS}$ ) for the MOSFET in the four resistor bias circuit in Fig. 4.27.

**SOLUTION** **Known Information and Given Data:** Circuit schematic in Fig. 4.27 with  $V_{DD} = 10\text{ V}$ ,  $R_1 = 1\text{ M}\Omega$ ,  $R_2 = 1.5\text{ M}\Omega$ ,  $R_D = 75\text{ k}\Omega$ ,  $R_S = 39\text{ k}\Omega$ ,  $K_n = 25\text{ }\mu\text{A/V}^2$ , and  $V_{TN} = 1\text{ V}$

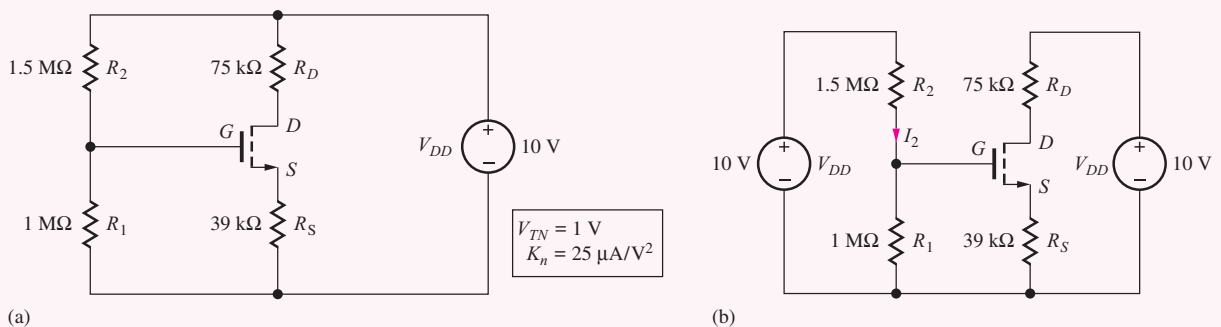


**Figure 4.27** (a) Four-resistor bias network for a MOSFET. (b) Equivalent circuit with replicated sources.

**Unknowns:** Q-point =  $(I_D, V_{DS}, V_{GS})$ , and region of operation

**Approach:** We can find the Q-point using the mathematical model for the NMOS transistor. We assume a region of operation, determine the Q-point, and check to see if the resulting Q-point is consistent with the assumed region of operation.

**Assumptions:** The first step in our Q-point analysis of the equivalent circuit in Fig. 4.27 is to assume that the transistor is saturated (remember to use  $\lambda = 0$ ):

$$I_D = \frac{K_n}{2}(V_{GS} - V_{TN})^2 \quad (4.52)$$

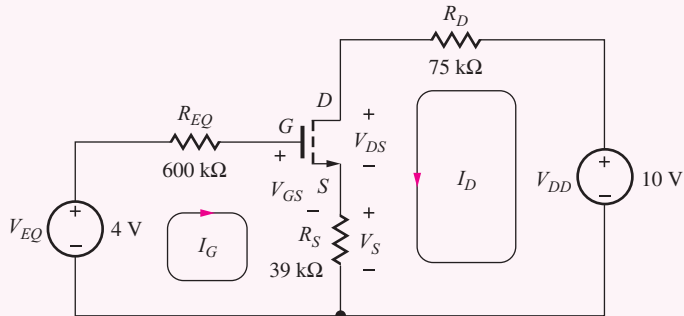


**Figure 4.28** Equivalent circuit for the four-resistor bias network.

Also,  $I_G = 0 = I_B$ . Using the  $\lambda = 0$  assumption simplifies the mathematics because  $I_D$  is then modeled as being independent of  $V_{DS}$ .

**Analysis:** To find  $I_D$ , the gate-source voltage must be determined, and we begin by simplifying the circuit. In the equivalent circuit in Fig. 4.27(b), the voltage source  $V_{DD}$  has been split into two equal-valued sources, and we recognize that the gate-bias voltage is determined by  $V_{EQ}$  and  $R_{EQ}$ , exactly as in Fig. 4.25. After the Thévenin transformation is applied to this circuit, the resulting equivalent circuit is given in Fig. 4.28 in which the variables have been clearly labeled. This is the final circuit to be analyzed.

Detailed analysis begins by writing the input loop equation containing  $V_{GS}$ :

$$V_{EQ} = I_G R_{EQ} + V_{GS} + (I_G + I_D) R_S \quad \text{or} \quad V_{EQ} = V_{GS} + I_D R_S \quad (4.53)$$

because we know that  $I_G = 0$ . Substituting Eq. (4.52) into Eq. (4.53) yields

$$V_{EQ} = V_{GS} + \frac{K_n R_s}{2} (V_{GS} - V_{TN})^2 \quad (4.54)$$

and solving for  $V_{GS}$  using the quadratic equation yields

$$V_{GS} = V_{TN} + \frac{1}{K_n R_S} (\sqrt{1 + 2K_n R_S (V_{EQ} - V_{TN})} - 1) \quad (4.55)$$

Substitution of this result back into Eq. (4.54) gives us  $I_D$ :

$$I_D = \frac{1}{2K_n R_S^2} (\sqrt{1 + 2K_n R_S (V_{EQ} - V_{TN})} - 1)^2 \quad (4.56)$$

The second part of the Q-point,  $V_{DS}$ , can now be determined by writing the “output” loop equation including the drain-source terminals of the device.

$$V_{DD} = I_D R_D + V_{DS} + (I_G + I_D) R_S \quad \text{or} \quad V_{DS} = V_{DD} - I_D (R_D + R_S) \quad (4.57)$$

Equation (4.57) has been simplified since we know  $I_G = 0$ .

For the specific values in Fig. 4.28 with  $V_{TN} = 1$ ,  $K_n = 25 \mu\text{A}/\text{V}^2$ ,  $V_{EQ} = 4 \text{ V}$  and  $V_{DD} = 10 \text{ V}$ , the Q-point values are

$$I_D = \frac{1}{2(25 \times 10^{-6})(39 \times 10^3)^2} (\sqrt{1 + 2(25 \times 10^{-6})(39 \times 10^3)(4 - 1)} - 1)^2 = 34.4 \mu\text{A}$$

$$V_{DS} = 10 - 34.4 \mu\text{A}(75 \text{ k}\Omega + 39 \text{ k}\Omega) = 6.08 \text{ V}$$

**Check of Results:** Checking the saturation region assumption for  $V_{DS} = 6.08 \text{ V}$ , we have

$$V_{GS} - V_{TN} = \frac{1}{K_n R_S} (\sqrt{1 + 2K_n R_S (V_{EQ} - V_{TN})} - 1) = 1.66 \text{ V} \quad \text{so} \quad V_{DS} > (V_{GS} - V_{TN}) \quad \checkmark$$

The saturation region assumption is consistent with the resulting Q-point: (34.4  $\mu\text{A}$ , 6.08 V) with  $V_{GS} = 2.66 \text{ V}$ .

**Discussion:** The four-resistor bias circuit is one of the best for biasing transistors in discrete circuits. The bias point is well stabilized with respect to device parameter variations and temperature changes. The four-resistor bias circuit is most often used to place the transistor in the saturation region of operation for use as an amplifier for analog signals, and as mentioned at the beginning of this example, the bias circuit in Fig. 4.27 represents a type of feedback circuit that uses negative feedback to stabilize the operating point. The operation of this feedback mechanism can be viewed in the following manner. Suppose for some reason that  $I_D$  begins to increase. Equation (4.53) indicates that an increase in  $I_D$  must be accompanied by a decrease in  $V_{GS}$  since  $V_{EQ}$  is fixed. But, this decrease in  $V_{GS}$  will tend to restore  $I_D$  back to its original value [see Eq. (4.52)]. This is negative feedback in action!

Note that this circuit uses the three-terminal representation for the MOSFET, in which it is assumed that the bulk terminal is tied to the source. If the bulk terminal is instead grounded, the analysis becomes more complex because the threshold voltage is then a function of the voltage developed at the source terminal of the device. This case will be investigated in more detail in Ex. 4.4. Let us now use the computer to explore the impact of neglecting  $\lambda$  in our hand analysis.

**Computer-Aided Analysis:** If we use SPICE to simulate the circuit using a LEVEL = 1 model and the parameters from our hand analysis ( $K_P = 25 \mu\text{A}/\text{V}^2$  and  $V_{TO} = 1 \text{ V}$ ), we get exactly the same Q-point (34.4  $\mu\text{A}$ , 6.08 V). If we add  $LAMBDA = 0.02 \text{ V}^{-1}$ , SPICE yields a new Q-point of (35.9  $\mu\text{A}$ , 5.91 V). The Q-point values change by less than 5 percent, a value that is well below our uncertainty in the device parameter and resistor values in a real situation.

**EXERCISE:** Use the quadratic equation to derive Eq. (4.55) and then verify the result given in Eq. (4.55)

**EXERCISE:** Suppose  $K_n$  increases to  $30 \mu\text{A}/\text{V}^2$  for the transistor in Fig. 4.28. What is the new Q-point for the circuit?

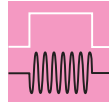
**ANSWER:** ( $36.8 \mu\text{A}$ ,  $5.81 \text{ V}$ )

**EXERCISE:** Suppose  $V_{TN}$  changes from  $1 \text{ V}$  to  $1.5 \text{ V}$  for the MOSFET in Fig. 4.28. What is the new Q-point for the circuit?

**ANSWER:** ( $26.7 \mu\text{A}$ ,  $6.96 \text{ V}$ )

**EXERCISE:** Find the Q-point in the circuit in Fig. 4.28 if  $R_S$  is changed to  $62 \text{ k}\Omega$ .

**ANSWER:** ( $25.4 \mu\text{A}$ ,  $6.52 \text{ V}$ )



## DESIGN NOTE

The Q-point values ( $I_D$ ,  $V_{DS}$ ) for the MOS transistor using the four-resistor bias network are

$$I_D = \frac{1}{2K_n R_S^2} \left( \sqrt{1 + 2K_n R_S (V_{EQ} - V_{TN})} - 1 \right)^2 \quad \text{and} \quad V_{DS} = V_{DD} - I_D (R_D + R_S)$$

where  $V_{EQ}$  is the Thévenin equivalent voltage between the gate terminal and ground.

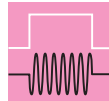
**EXERCISE:** Show that the actual Q-point in the circuit in Fig. 4.27 for  $R_1 = 1 \text{ M}\Omega$ ,  $R_2 = 1.5 \text{ M}\Omega$ ,  $R_S = 1.8 \text{ k}\Omega$ , and  $R_D = 39 \text{ k}\Omega$  is ( $99.5 \mu\text{A}$ ,  $5.95 \text{ V}$ ).

**EXERCISE:** Find the Q-point in the circuit in Fig. 4.26 for  $R_1 = 1.5 \text{ M}\Omega$ ,  $R_2 = 1 \text{ M}\Omega$ ,  $R_S = 22 \text{ k}\Omega$ , and  $R_D = 18 \text{ k}\Omega$ .

**ANSWER:** ( $99.1 \mu\text{A}$ ,  $6.04 \text{ V}$ )

**EXERCISE:** Redesign the values of  $R_1$  and  $R_2$  to set the bias current to  $2 \mu\text{A}$  while maintaining  $V_{EQ} = 6 \text{ V}$ . What is the value of  $R_{EQ}$ ?

**ANSWER:**  $3 \text{ M}\Omega$ ,  $2 \text{ M}\Omega$ ,  $1.2 \text{ M}\Omega$



## DESIGN NOTE

Resistors  $R_1$  and  $R_2$  in Fig. 4.27 are required to set the value of  $V_{EQ}$ , but the current in the resistors does not contribute directly to operation of the transistor. Thus we would like to minimize the current “lost” through  $R_1$  and  $R_2$ . The sum ( $R_1 + R_2$ ) sets the current in the gate bias resistors. As a rule of thumb,  $R_1 + R_2$  is usually chosen to limit the current to no more than a few percent of the value of the drain current. In Fig. 4.26, the value of current  $I_2$  is 4 percent of the drain current  $I_2 = 10 \text{ V}/(1 \text{ M}\Omega + 1.5 \text{ M}\Omega) = 4 \mu\text{A}$ .

**EXAMPLE 4.4 ANALYSIS INCLUDING BODY EFFECT**

The NMOS transistor in Fig. 4.28 was connected as a three-terminal device. This example explores how the Q-point is altered when the substrate is connected as shown in Fig. 4.29.

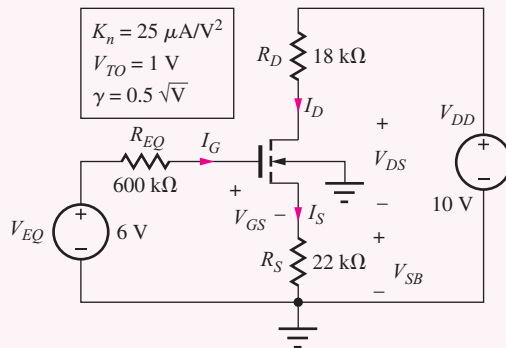


**Figure 4.29** MOSFET with redesigned bias circuit.

**PROBLEM** Find the Q-point =  $(I_D, V_{DS})$  for the MOSFET in the four-resistor bias circuit in Fig. 4.29 including the influence of body effect on the transistor threshold.

**SOLUTION** **Known Information and Given Data:** The circuit schematic in Fig. 4.29 with  $V_{EQ} = 6 \text{ V}$ ,  $R_{EQ} = 600 \text{ k}\Omega$ ,  $R_S = 22 \text{ k}\Omega$ ,  $R_D = 18 \text{ k}\Omega$ ,  $K_n = 25 \mu\text{A}/\text{V}^2$ ,  $V_{TO} = 1 \text{ V}$ , and  $\gamma = 0.5 \text{ V}^{-1}$

**Unknowns:**  $I_D$ ,  $V_{DS}$ ,  $V_{GS}$ ,  $V_{BS}$ ,  $V_{TN}$ , and region of operation

**Approach:** In this case, the source-bulk voltage,  $V_{SB} = I_S R_S = I_D R_S$ , is no longer zero, and we must solve the following set of equations:

$$\begin{aligned} V_{GS} &= V_{EQ} - I_D R_S & V_{SB} &= I_D R_S \\ V_{TN} &= V_{TO} + \gamma (\sqrt{V_{SB} + 2\phi_F} - \sqrt{2\phi_F}) & (4.58) \\ I_D &= \frac{K_n}{2} (V_{GS} - V_{TN})^2 \end{aligned}$$

Although it may be possible to solve these equations analytically, it will be more expedient to find the Q-point by iteration using the computer with a spreadsheet, MATLAB, MATHCAD, or with a calculator.

**Assumptions:** Saturation region operation with  $I_G = 0$ ,  $I_B = 0$ , and  $2\phi_F = 0.6 \text{ V}$

**Analysis:** Using the assumptions and values in Fig. 4.29, Eq. set (4.58) becomes

$$\begin{aligned} V_{GS} &= 6 - 22,000 I_D & V_{SB} &= 22,000 I_D \\ V_{TN} &= 1 + 0.5 (\sqrt{V_{SB} + 0.6} - \sqrt{0.6}) & I'_D &= \frac{25 \times 10^{-6}}{2} (V_{GS} - V_{TN})^2 \quad (4.59) \end{aligned}$$

and the drain-source voltage is found from

$$V_{DS} = V_{DD} - I_D (R_D + R_S) = 10 - 40,000 I_D \quad (4.60)$$

The expressions in Eq. (4.59) have been arranged in a logical order for an iterative solution:

1. Estimate the value of  $I_D$ .
2. Use  $I_D$  to calculate the values of  $V_{GS}$  and  $V_{SB}$ .
3. Calculate the resulting value of  $V_{TN}$  using  $V_{SB}$ .
4. Calculate  $I'_D$  using the results of steps 1 to 3, and compare to the original estimate for  $I_D$ .
5. If the calculated value of  $I'_D$  is not equal to the original estimate for  $I_D$ , then go back to step 1.

In this case, no specific method for choosing the improved estimate for  $I_D$  is provided (although the problem could be structured to use Newton's method), but it is easy to converge to the solution after a few trials, using the power of the computer to do the calculations. (Note that the SPICE circuit analysis program can also do the job for us.)

Table 4.4 shows the results of using a spreadsheet to iteratively find the solution to Eqs. (4.59) and (4.60) by trial and error. The first iteration sequence used by the author is shown; it converges to a drain current of 88.0  $\mu$ A and drain-source voltage of 6.48 V. Care must be exercised to be sure that the spreadsheet equations are properly formulated to account for all regions of operation. In particular,  $I_D = 0$  if  $V_{GS} < V_{TN}$ .

**TABLE 4.4**  
Four-Resistor Bias Iteration

$I_D$	$I_D R_S$	$V_{GS}$	$V_{TN}$	$I'_D$	$V_{DS}$
1.000E-04	2.200	3.800	1.449	6.907E-05	6.000
9.000E-05	1.980	4.020	1.416	8.477E-05	6.400
8.000E-05	1.760	4.240	1.381	1.022E-04	6.800
8.100E-05	1.782	4.218	1.384	1.004E-04	6.760
8.200E-05	1.804	4.196	1.388	9.856E-05	6.720
⋮	⋮	⋮	⋮	⋮	⋮
8.800E-05	1.936	4.064	1.409	8.812E-05	6.480
8.805E-05	1.937	4.063	1.409	8.803E-05	6.478
8.804E-05	1.937	4.063	1.409	8.805E-05	6.478

**Check of Results:** For this design, we now have

$$V_{DS} = 6.48 \text{ V}, V_{GS} - V_{TN} = 2.56 \text{ V} \quad \text{and} \quad V_{DS} > (V_{GS} - V_{TN}) \quad \checkmark$$

The saturation region assumption is consistent with the solution, and the Q-point is (88.0  $\mu$ A, 6.48 V).

**Discussion:** Now that the analysis is complete, we see that the presence of body effect in the circuit has caused the threshold voltage to increase from 1 V to 1.41 V and the drain current to decrease by approximately 12 percent from 100  $\mu$ A to 88  $\mu$ A.



**EXERCISE:** Find the new drain current in the circuit in Fig. 4.29 if  $\gamma = 0.75\sqrt{V}$ .

**ANSWER:** 83.2  $\mu$ A

Examples 4.1 through 4.4 represent but a few of the many possible ways to bias an NMOS transistor. Nevertheless, the examples have demonstrated the techniques that we need to analyze most of the circuits we will encounter. The four-resistor and two-resistor bias circuits are most often encountered in discrete design, whereas current sources and current mirrors, introduced in Chapter 15, find extensive application in integrated circuit design.

## 4.10 BIASING THE PMOS FIELD-EFFECT TRANSISTOR

CMOS technology, which uses a combination of NMOS and PMOS transistors, is the dominant IC technology in use today, and it is thus very important to know how to bias both types of devices. PMOS bias techniques mirror those used in the previous NMOS bias examples. In the circuits that follow, you will observe that the source of the PMOS transistor will be consistently drawn at the top of the device since the source of the PMOS device is normally connected to a potential that is higher than the drain. This is in contrast to the NMOS transistor in which the drain is connected to a more positive voltage than the source. The PMOS model equations were summarized in Sec. 4.3. Remember that the drain current  $I_D$  is positive when coming out of the drain terminal of the PMOS device, and the values of  $V_{GS}$  and  $V_{DS}$  will be negative.

### EXAMPLE 4.5

#### FOUR-RESISTOR BIAS FOR THE PMOS FET

The four-resistor bias circuit in Fig. 4.30 functions in a manner similar to that used for the NMOS device in Ex. 4.3. In the circuit in Fig. 4.30(a), a single voltage source  $V_{DD}$  is used to supply both the gate-bias voltage and the source-drain current.  $R_1$  and  $R_2$  form the gate voltage divider circuit.  $R_S$  sets the source/drain current, and  $R_D$  determines the source-drain voltage.

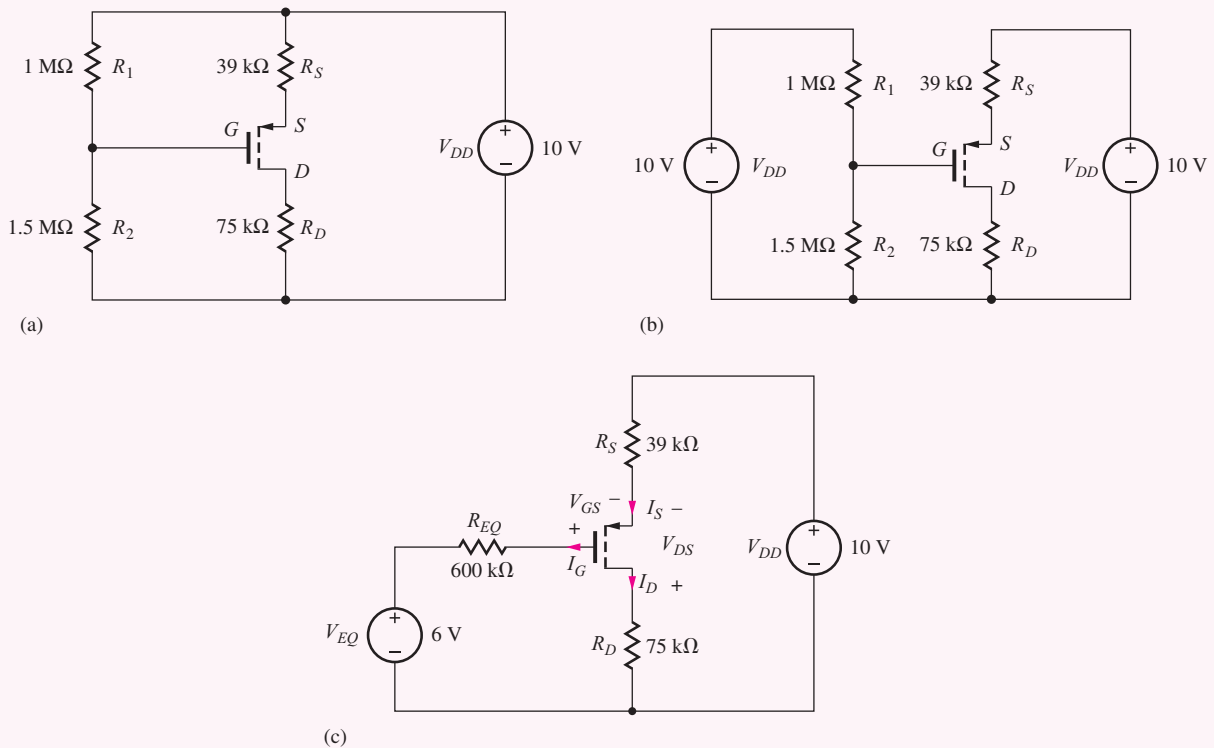


Figure 4.30 Four-resistor bias for a PMOS transistor.

**PROBLEM** Find the quiescent operating point Q-point ( $I_D$ ,  $V_{DS}$ ) for the PMOS transistor in the four resistor bias circuit in Fig. 4.30.

**SOLUTION** **Known Information and Given Data:** Circuit schematic in Fig. 4.30 with  $V_{DD} = 10 \text{ V}$ ,  $R_1 = 1 \text{ M}\Omega$ ,  $R_2 = 1.5 \text{ M}\Omega$ ,  $R_D = 75 \text{ k}\Omega$ ,  $R_S = 39 \text{ k}\Omega$ ,  $K_P = 25 \mu\text{A/V}^2$ ,  $V_{TP} = -1 \text{ V}$ , and  $I_G = 0$

**Unknowns:**  $I_D$ ,  $V_{DS}$ ,  $V_{GS}$ , and the region of operation

**Approach:** We can find the Q-point using the mathematical model for the PMOS transistor. We assume a region of operation, determine the Q-point, and check to see if the Q-point is consistent with the assumed region of operation. First find the value of  $V_{GS}$ ; use  $V_{GS}$  to find  $I_D$ ; use  $I_D$  to find  $V_{DS}$ .

**Assumptions:** Assume that the transistor is operating in the saturation region (Once again, remember to use  $\lambda = 0$ )

$$I_D = \frac{K_p}{2} (V_{GS} - V_{TP})^2 \quad (4.61)$$

**Analysis:** We begin by simplifying the circuit. In the equivalent circuit in Fig. 4.30(b), the voltage source has been split into two equal-valued sources, and in Fig. 4.30(c), the gate-bias circuit is replaced by its Thévenin equivalent

$$V_{EQ} = 10 \text{ V} \frac{1.5 \text{ M}\Omega}{1 \text{ M}\Omega + 1.5 \text{ M}\Omega} = 6 \text{ V} \quad \text{and} \quad R_{EQ} = 1 \text{ M}\Omega \parallel 1.5 \text{ M}\Omega = 600 \text{ k}\Omega$$

Figure 4.30(c) represents the final circuit to be analyzed (be sure to label the variables). Note that this circuit uses the three-terminal representation for the MOSFET, in which it is assumed that the bulk terminal is tied to the source. If the bulk terminal were connected to  $V_{DD}$ , the analysis would be similar to that used in Ex. 4.4 because the threshold voltage would then be a function of the voltage developed at the source terminal of the device.

To find  $I_D$ , the gate-source voltage must be determined, and we write the input loop equation containing  $V_{GS}$ :

$$V_{DD} = I_S R_S - V_{GS} + I_G R_G + V_{EQ} \quad (4.62)$$

Because we know that  $I_G = 0$  and therefore  $I_S = I_D$ , Eq. (4.62) can be reduced to

$$V_{DD} - V_{EQ} = I_D R_S - V_{GS} \quad (4.63)$$

Substituting Eq. (4.61) into Eq. (4.63) yields

$$V_{DD} - V_{EQ} = \frac{K_p R_S}{2} (V_{GS} - V_{TP})^2 - V_{GS} \quad (4.64)$$

and we again have a quadratic equation to solve for  $V_{GS}$ . For the values in Fig. 4.30 with  $V_{TP} = -1 \text{ V}$  and  $K_p = 25 \mu\text{A/V}^2$ ,

$$10 - 6 = \frac{(25 \times 10^{-6})(3.9 \times 10^4)}{2} (V_{GS} + 1)^2 - V_{GS}$$

and

$$V_{GS}^2 - 0.051V_{GS} - 7.21 = 0 \quad \text{for which} \quad V_{GS} = +2.71 \text{ V}, -2.66 \text{ V}$$

For  $V_{GS} = +2.71 \text{ V}$ , the PMOS FET would be cut off because  $V_{GS} > V_{TP} (= -1 \text{ V})$ . Therefore,  $V_{GS} = -2.66 \text{ V}$  must be the answer we seek, and  $I_D$  is found using Eq. (4.61):

$$I_D = \frac{25 \times 10^{-6}}{2} (-2.66 + 1)^2 = 34.4 \mu\text{A}$$

The second part of the Q-point,  $V_{DS}$ , can now be determined by writing a loop equation including the source-drain terminals of the device:

$$V_{DD} = I_S R_S - V_{DS} + I_D R_D \quad \text{or} \quad V_{DD} = I_D (R_S + R_D) - V_{DS} \quad (4.65)$$

Eq. (4.65) has been simplified since we know that  $I_S = I_D$ . Substituting the values from the circuit gives

$$10 \text{ V} = (34.4 \mu\text{A})(39 \text{ k}\Omega + 75 \text{ k}\Omega) - V_{DS} \quad \text{or} \quad V_{DS} = -6.08 \text{ V}$$

**Check of Results:** We have

$$V_{DS} = -6.08 \text{ V} \quad \text{and} \quad V_{GS} - V_{TP} = -2.66 \text{ V} + 1 \text{ V} = -1.66 \text{ V}$$

and  $|V_{DS}| > |V_{GS} - V_{TP}|$ . Therefore the saturation region assumption is consistent with the resulting Q-point ( $34.4 \mu\text{A}$ ,  $-6.08 \text{ V}$ ) with  $V_{GS} = -2.66 \text{ V}$ .

**Evaluation and Discussion:** As mentioned in Ex. 4.3, the bias circuit in Fig. 4.30 uses negative feedback to stabilize the operating point. Suppose  $I_D$  begins to increase. Since  $V_{EQ}$  is fixed, an increase in  $I_D$  will cause a decrease in the magnitude of  $V_{GS}$  [see Eq. (4.63)], and this decrease will tend to restore  $I_D$  back to its original value.

**EXERCISE:** Find the Q-point in the circuit in Fig. 4.30 if  $R_S$  is changed to  $62 \text{ k}\Omega$ .

**ANSWER:** ( $25.4 \mu\text{A}$ ,  $-6.52 \text{ V}$ )



**EXERCISE:** (a) Use SPICE to find the Q-point in the circuit in Fig. 4.30. (b) Repeat if  $R_S$  is changed to  $62 \text{ k}\Omega$ . (c) Repeat parts (a) and (b) with  $\lambda = 0.02$ .

**ANSWERS:** (a) ( $34.4 \mu\text{A}$ ,  $-6.08 \text{ V}$ ); (b) ( $25.4 \mu\text{A}$ ,  $-6.52 \text{ V}$ ); (c) ( $35.9 \mu\text{A}$ ,  $-5.91 \text{ V}$ ), ( $26.3 \mu\text{A}$ ,  $-6.39 \text{ V}$ )

## 4.11 THE JUNCTION FIELD-EFFECT TRANSISTOR (JFET)

Another type of field-effect transistor can be formed without the need for an insulating oxide by using  $pn$  junctions, as illustrated in Fig. 4.31. This device, the **junction field-effect transistor**, or **JFET**, consists of an  $n$ -type block of semiconductor material and two  $pn$  junctions that form the gate. Although less prevalent than MOSFETs, JFETs have many applications in both integrated and discrete circuit design, particularly in analog and RF applications. In integrated circuits, JFETs are most often found in BiFET processes, which combine bipolar transistors with JFETs. The JFET provides a device with much lower input current and much higher input impedance than that typically achieved with the bipolar transistor.

In the  **$n$ -channel JFET**, current again enters the channel region at the drain and exits from the source. The resistance of the channel region is controlled by changing the physical width

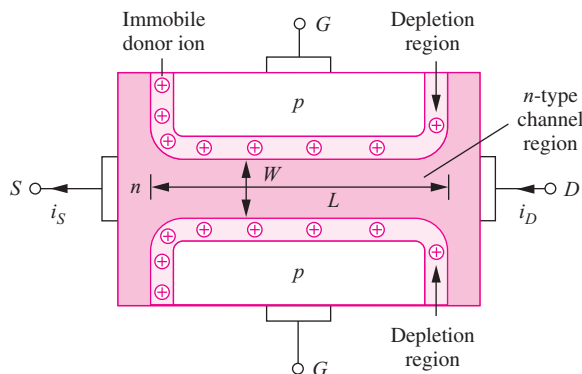


**Figure 4.31** Basic  $n$ -channel JFET structure and important dimensions. (Note that for clarity the depletion layer in the  $p$ -type material is not indicated in the figure.)

of the channel through modulation of the depletion layers that surround the *pn* junctions between the gate and the channel (see Sec. 3.1 and 3.6). In its triode region, the JFET can be thought of as simply a voltage-controlled resistor with its channel resistance determined by

$$R_{CH} = \frac{\rho}{t} \frac{L}{W} \quad (4.66)$$

where  $\rho$  = resistivity of the channel region

$L$  = channel length

$W$  = width of channel between the *pn* junction depletions regions

$t$  = depth of channel into the page

When a voltage is applied between the drain and source, the channel resistance determines the current.

With no bias applied, as in Fig. 4.31, a resistive channel region exists connecting the drain and source. Application of a reverse bias to the gate-channel diodes will cause the depletion layers to widen, reducing the channel width and decreasing the current. Thus, the JFET is inherently a depletion-mode device — a voltage must be applied to the gate to turn the device off.

The JFET in Fig. 4.31 is drawn assuming one-sided step junctions ( $N_A \gg N_D$ ) between the gate and channel in which the depletion layers extend only into the channel region of the device (see Sec. 3.1 and 3.6). Note how an understanding of the physics of the *pn* junction is used to create the JFET.

### 4.11.1 THE JFET WITH BIAS APPLIED

Figure 4.32(a) shows a JFET with 0 V on the drain and source and with the gate voltage  $v_{GS} = 0$ . The channel width is  $W$ . During normal operation, a reverse bias must be maintained across the *pn* junctions to provide isolation between the gate and channel. This reverse bias requires  $v_{GS} \leq 0$  V.

In Fig. 4.32(b),  $v_{GS}$  has decreased to a negative value, and the depletion layers have increased in width. The width of the channel has now decreased, with  $W' < W$ , increasing the resistance of the channel region; see Eq. (4.66). Because the gate-source junction is reverse-biased, the gate current will equal the reverse saturation current of the *pn* junction, normally a very small value, and we will assume that  $i_G \cong 0$ .

For more negative values of  $v_{GS}$ , the channel width continues to decrease, increasing the resistance of the channel region. Finally, the condition in Fig. 4.32(c) is reached for  $v_{GS} = V_P$ , the pinch-off voltage;  $V_P$  is the (negative) value of gate-source voltage for which the conducting channel region completely disappears. The channel becomes pinched-off as the depletion regions from the two *pn* junctions merge at the center of the channel. At this point, the resistance of the channel region has become infinitely large. Further increases in  $v_{GS}$  do not substantially affect the internal appearance of the device in Fig. 4.33(c). However,  $v_{GS}$  must not exceed the reverse breakdown voltage of the gate-channel junction.

### 4.11.2 JFET CHANNEL WITH DRAIN-SOURCE BIAS

Figures 4.33(a) to 4.33(c) show conditions in the JFET for increasing values of drain-source voltage  $v_{DS}$  and a fixed value of  $v_{GS}$ . For a small value of  $v_{DS}$ , as in Fig. 4.33(a), the resistive channel connects the source and drain, the JFET is operating in its triode region, and the drain current will be dependent on the drain-source voltage  $v_{DS}$ . Assuming  $i_G = 0$ , the current entering the drain must exit from the source, as in the MOSFET. Note, however, that the reverse bias across the gate-channel junction is larger at the drain end of the channel than at the source end, and so the depletion layer is wider at the drain end of the device than at the source end. For increasing values of  $v_{DS}$ , the depletion layer at the drain becomes wider and wider until the channel pinches off near the drain, as in Fig. 4.33(b). Pinch-off first occurs for

$$v_{GS} - v_{DSP} = V_P \quad \text{or} \quad v_{DSP} = v_{GS} - V_P \quad (4.67)$$

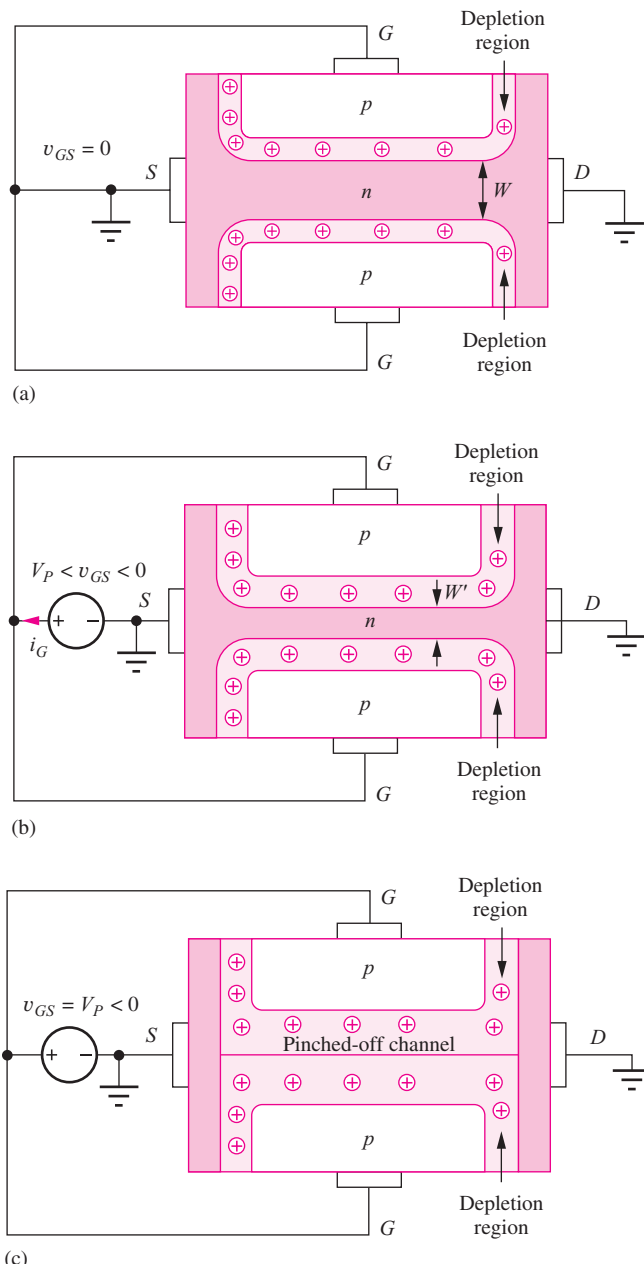


**Figure 4.32** (a) JFET with zero gate-source bias. (b) JFET with negative gate-source voltage that is less negative than the pinch-off voltage  $V_P$ . Note  $W' < W$ . (c) JFET at pinch-off with  $v_{GS} = V_P$ .

in which  $v_{DSP}$  is the value of drain voltage required to just pinch off the channel. Once the JFET channel pinches-off, the drain current saturates, just as for the MOSFET. Electrons are accelerated down the channel, injected into the depletion region, and swept on to the drain by the electric field.

Figure 4.33(c) shows the situation for an even larger value of  $v_{DS}$ . The pinch-off point moves toward the source, shortening the length of the resistive channel region. Thus, the JFET suffers from channel-length modulation in a manner similar to that of the MOSFET.

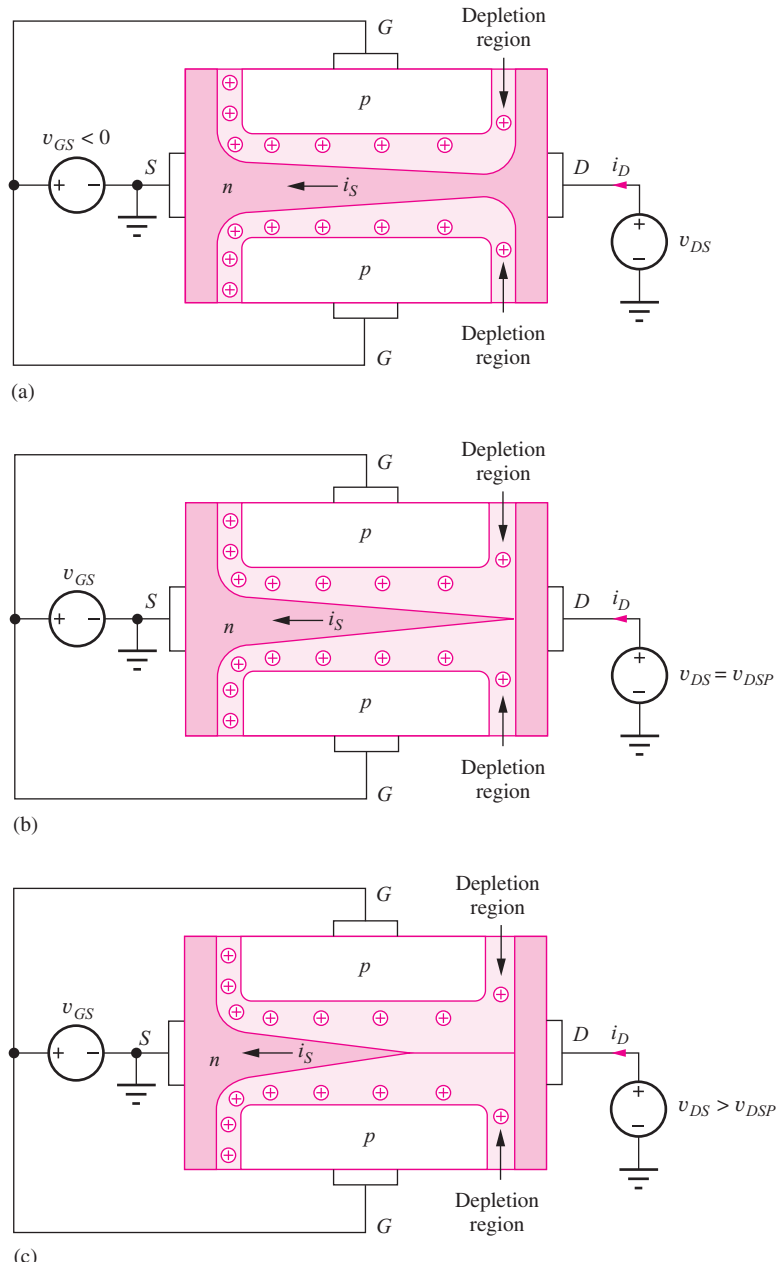


**Figure 4.33** (a) JFET with small drain source. (b) JFET with channel just at pinch-off with  $v_{DS} = v_{DSP}$ . (c) JFET with  $v_{DS}$  greater than  $v_{DSP}$ .

### 4.11.3 n-CHANNEL JFET I-V CHARACTERISTICS

Since the structure of the JFET is considerably different from the MOSFET, it is quite surprising that the  $i$ - $v$  characteristics are virtually identical. We will rely on this similarity and not try to derive the JFET equations here. However, although mathematically equivalent, the equations for the JFET are usually written in a form slightly different from those of the MOSFET. We can develop this form starting with the saturation region expression for a MOSFET, in which the threshold voltage  $V_{TN}$  is

replaced with the pinch-off voltage  $V_P$ :

$$i_D = \frac{K_n}{2}(v_{GS} - V_P)^2 = \frac{K_n}{2}(-V_P)^2 \left(1 - \frac{v_{GS}}{V_P}\right)^2 \quad \text{or} \quad i_D = I_{DSS} \left(1 - \frac{v_{GS}}{V_P}\right)^2 \quad (4.68)$$

in which the parameter  $I_{DSS}$  is defined by

$$I_{DSS} = \frac{K_n}{2} V_P^2 \quad \text{or} \quad K_n = \frac{2I_{DSS}}{V_P^2} \quad (4.69)$$

The pinch-off voltage  $V_P$  typically ranges from 0 to  $-25$  V, and the value of  $I_{DSS}$  can range from  $10\ \mu\text{A}$  to more than  $10$  A.

If we include channel-length modulation, the expression for the drain current in pinch-off (saturation) becomes

$$I_D = I_{DSS} \left(1 - \frac{v_{GS}}{V_P}\right)^2 (1 + \lambda v_{DS}) \quad \text{for} \quad v_{DS} \geq v_{GS} - V_P \geq 0 \quad (4.70)$$

The transfer characteristic for a JFET operating in pinch-off, based on Eq. (4.70), is shown in Fig. 4.34.  $I_{DSS}$  is the current in the JFET for  $v_{GS} = 0$  and represents the maximum current in the device under normal operating conditions because the gate diode should be kept reverse-biased, with  $v_{GS} \leq 0$ .

The overall output characteristics for an  $n$ -channel JFET are reproduced in Fig. 4.35 with  $\lambda = 0$ . We see that the drain current decreases from a maximum of  $I_{DSS}$  toward zero as  $v_{GS}$  ranges from zero to the negative pinch-off voltage  $V_P$ .

The triode region of the device is also apparent in Fig. 4.35 for  $v_{DS} \leq v_{GS} - V_P$ . We can obtain an expression for the triode region of the JFET using the equation for the MOSFET triode region.

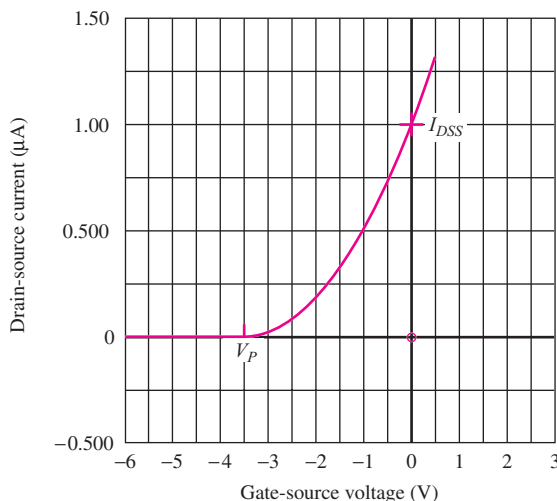


**Figure 4.34** Transfer characteristic for a JFET operating in pinch-off with  $I_{DSS} = 1\ \text{mA}$  and  $V_P = -3.5\ \text{V}$ .

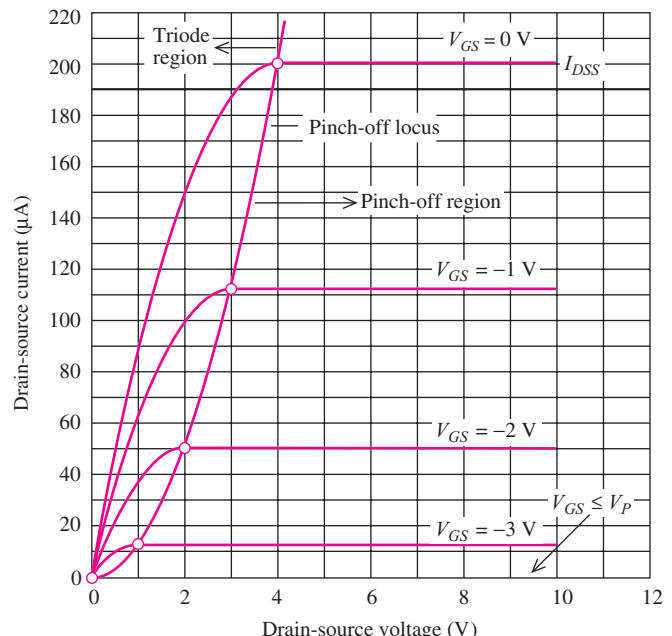


**Figure 4.35** Output characteristics for a JFET with  $I_{DSS} = 200\ \mu\text{A}$  and  $V_P = -4\ \text{V}$ .

Substituting for  $K_n$  and  $V_{TN}$  in Eq. (4.26) yields

$$i_D = \frac{2I_{DSS}}{V_P^2} \left( v_{GS} - V_P - \frac{v_{DS}}{2} \right) v_{DS} \quad \text{for } v_{GS} \geq V_P \quad \text{and} \quad v_{GS} - V_P \geq v_{DS} \geq 0 \quad (4.71)$$

Equations (4.70) and (4.71) represent our mathematical model for the *n*-channel JFET.

**EXERCISE:** (a) Calculate the current for the JFET in Fig. 4.34 for  $V_{GS} = -2$  V and  $V_{DS} = 3$  V. What is the minimum drain voltage required to pinch off the JFET? (b) Repeat for  $V_{GS} = -1$  V and  $V_{DS} = 6$  V. (c) Repeat for  $V_{GS} = -2$  V and  $V_{DS} = 0.5$  V.

**ANSWERS:** (a) 184  $\mu$ A, 1.5 V; (b) 510  $\mu$ A, 2.5 V; (c) 51.0  $\mu$ A, 1.5 V

**EXERCISE:** (a) Calculate the current for the JFET in Fig. 4.35 for  $V_{GS} = -2$  V and  $V_{DS} = 0.5$  V. (b) Repeat for  $V_{GS} = -1$  V and  $V_{DS} = 6$  V.

**ANSWERS:** (a) 21.9  $\mu$ A; (b) 113  $\mu$ A

#### 4.11.4 THE *p*-CHANNEL JFET

A *p*-channel version of the JFET can be fabricated by reversing the polarities of the *n*- and *p*-type regions in Fig. 4.31, as depicted in Fig. 4.36. As for the PMOS FET, the direction of current in the channel is opposite to that of the *n*-channel device, and the signs of the operating bias voltages will be reversed.

#### 4.11.5 CIRCUIT SYMBOLS AND JFET MODEL SUMMARY

The circuit symbols and terminal voltages and currents for *n*-channel and *p*-channel JFETs are presented in Fig. 4.37. The arrow identifies the polarity of the gate-channel diode. The JFET structures in Figs. 4.31 and 4.36 are inherently symmetric, as were those of the MOSFET, and the source and drain are actually determined by the voltages in the circuit in which the JFET is used. However, the arrow that indicates the gate-channel junction is often offset to indicate the preferred source terminal of the device.

A summary of the mathematical models for the *n*-channel and *p*-channel JFETs follows. Because the JFET is a three-terminal device, the pinch-off voltage is independent of the terminal voltages.

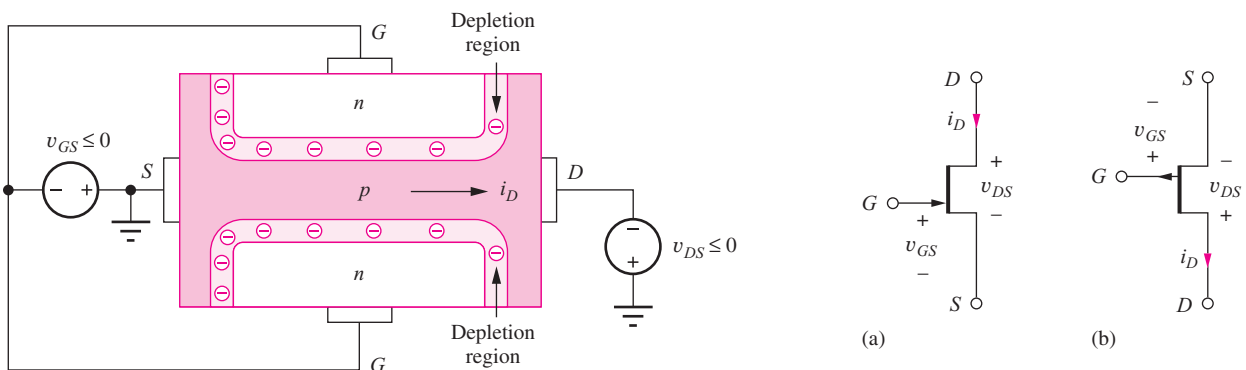


Figure 4.36 *p*-channel JFET with bias voltages.

Figure 4.37 (a) *n*-channel and (b) *p*-channel JFET circuit symbols.

### ***n*-CHANNEL JFET**

For all regions,

$$i_G = 0 \quad \text{for} \quad v_{GS} \leq 0 \quad (4.72)$$

Cutoff region:

$$i_D = 0 \quad \text{for} \quad v_{GS} \leq V_P \quad (V_P < 0) \quad (4.73)$$

Triode region:

$$i_D = \frac{2I_{DSS}}{V_P^2} \left( v_{GS} - V_P - \frac{v_{DS}}{2} \right) v_{DS} \quad \text{for} \quad v_{GS} \geq V_P \quad \text{and} \quad v_{GS} - V_P \geq v_{DS} \geq 0 \quad (4.74)$$

Pinch-off region:

$$i_D = I_{DSS} \left( 1 - \frac{v_{GS}}{V_P} \right)^2 (1 + \lambda v_{DS}) \quad \text{for} \quad v_{DS} \geq v_{GS} - V_P \geq 0 \quad (4.75)$$


---

### ***p*-CHANNEL JFET**

For all regions,

$$i_G = 0 \quad \text{for} \quad v_{GS} \geq 0 \quad (4.76)$$

Cutoff region:

$$i_D = 0 \quad \text{for} \quad v_{GS} \geq V_P \quad (V_P > 0) \quad (4.77)$$

Triode region:

$$i_D = \frac{2I_{DSS}}{V_P^2} \left( v_{GS} - V_P - \frac{v_{DS}}{2} \right) v_{DS} \quad \text{for} \quad v_{GS} \leq V_P \quad \text{and} \quad |v_{GS} - V_P| \geq |v_{DS}| \geq 0 \quad (4.78)$$

Pinch-off region:

$$i_D = I_{DSS} \left( 1 - \frac{v_{GS}}{V_P} \right)^2 (1 + \lambda |v_{DS}|) \quad \text{for} \quad |v_{DS}| \geq |v_{GS} - V_P| \geq 0 \quad (4.79)$$


---

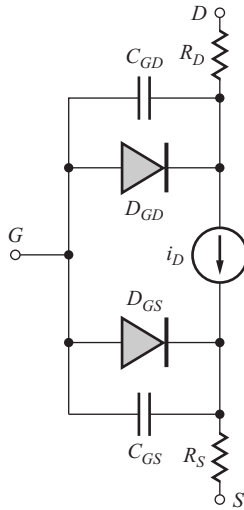
Overall, JFETs behave in a manner very similar to that of depletion-mode MOSFETs, and the JFET is biased in the same way as a depletion-mode MOSFET. In addition, most circuit designs must ensure that the gate-channel diode remains reverse-biased. This is not a concern for the MOSFET. In certain circumstances, however, forward bias of the JFET diode can actually be used to advantage. For instance, we know that a silicon diode can be forward-biased by up to 0.4 to 0.5 V without significant conduction. In other applications, the gate diode can be used as a built-in diode clamp, and in some oscillator circuits, forward conduction of the gate diode is used to help stabilize the amplitude of the oscillation. This effect is explored in more detail during the discussion of oscillator circuits in Chapter 18.

#### **4.11.6 JFET CAPACITANCES**

The gate-source and gate-drain capacitances of the JFET are determined by the depletion-layer capacitances of the reverse-biased *pn* junctions forming the gate of the transistor and will exhibit a bias dependence similar to that described by Eq. (3.21) in Chapter 3.

**EXERCISE:** (a) Calculate the drain current for a *p*-channel JFET described by  $I_{DSS} = 2.5 \text{ mA}$  and  $V_P = 4 \text{ V}$  and operating with  $V_{GS} = 3 \text{ V}$  and  $V_{DS} = -3 \text{ V}$ . What is the minimum drain-source voltage required to pinch off the JFET? (b) Repeat for  $V_{GS} = 1 \text{ V}$  and  $V_{DS} = -6 \text{ V}$ . (c) Repeat for  $V_{GS} = 2 \text{ V}$  and  $V_{DS} = -0.5 \text{ V}$ .

**ANSWERS:** (a)  $156 \mu\text{A}, -1.00 \text{ V}$ ; (b)  $1.41 \text{ mA}, -3.00 \text{ V}$ ; (c)  $273 \mu\text{A}, -2.00 \text{ V}$



## 4.12 JFET MODELING IN SPICE

The circuit representation for the basic JFET model that is implemented in SPICE is given in Fig. 4.38. As for the MOSFET, the JFET model contains a number of additional parameters in an attempt to accurately represent the real device characteristics. Small resistances  $R_S$  and  $R_D$  appear in series with the JFET source and drain terminals, diodes are included between the gate and internal source and drain terminals, and device capacitances are included in the model.

The model for  $i_D$  is an adaptation of the MOSFET model and uses some of the parameter names and formulas from the MOSFET as can be observed in Eq. (4.80).

$$\text{Triode region: } i_D = 2 \cdot \text{BETA} \left( v_{GS} - \text{VTO} - \frac{v_{DS}}{2} \right) v_{DS} (1 + \text{LAMBDA} \cdot v_{DS}) \quad \text{for } v_{GS} - \text{VTO} \geq v_{DS} \geq 0 \quad (4.80)$$

$$\text{Pinch-off region: } i_D = \text{BETA} (v_{GS} - \text{VTO})^2 (1 + \text{LAMBDA} \cdot v_{DS}) \quad \text{for } v_{DS} \geq v_{GS} - \text{VTO} \geq 0$$

The transconductance parameter BETA is related to the JFET parameters by

$$\text{BETA} = \frac{I_{DSS}}{V_P^2} \quad (4.81)$$

The SPICE description adds a channel-length modulation term to the triode region expression. An additional quirk is that the value of VTO is always specified as a positive number for both *n*- and *p*-channel JFETs. Table 4.5 contains the equivalences of the SPICE model parameters and our equations summarized at the end of the previous section. Typical and default values of the SPICE model parameters can also be found in Table 4.5. For more detail see [5].

**TABLE 4.5**  
SPICE JFET Parameter Equivalences

PARAMETER	OUR TEXT	SPICE	DEFAULT
Transconductance	—	BETA	$100 \mu\text{A/V}^2$
Zero-bias drain current	$I_{DSS}$	—	—
Pinch-off voltage	$V_P$	VTO	$-2 \text{ V}$
Channel length modulation	$\lambda$	LAMBDA	0
Zero-bias gate-drain capacitance	$C_{GD}$	CGD	0
Zero-bias gate-source capacitance	$C_{GS}$	CGS	0
Gate-bulk capacitance per unit width	$C_{GBO}$	CGBO	0
Ohmic drain resistance	—	RD	0
Ohmic source resistance	—	RS	0
Gate diode saturation current	$I_S$	IS	$10 \text{ fA}$

**EXERCISE:** An *n*-channel JFET is described by  $I_{DSS} = 2.5 \text{ mA}$ ,  $V_P = -2 \text{ V}$ , and  $\lambda = 0.025 \text{ V}^{-1}$ . What are the values of BETA and VTO for this transistor?

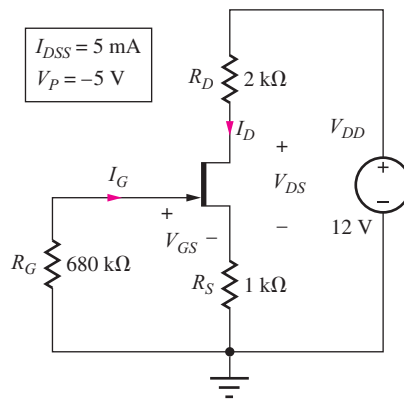
**ANSWERS:**  $625 \mu\text{A}$ ;  $2 \text{ V}$ ;  $0.025 \text{ V}^{-1}$

**EXERCISE:** A *p*-channel JFET is described by  $I_{DSS} = 5 \text{ mA}$ ,  $V_P = 2 \text{ V}$ , and  $\lambda = 0.02 \text{ V}^{-1}$ . What are the values of BETA and VTO for this transistor?

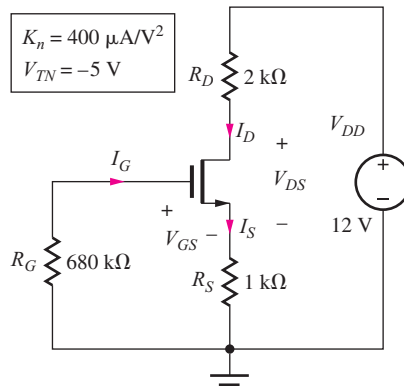
**ANSWERS:**  $1.25 \text{ mA}$ ;  $2 \text{ V}$ ;  $0.02 \text{ V}^{-1}$

## 4.13 BIASING THE JFET AND DEPLETION-MODE MOSFET

The basic bias circuit for an *n*-channel JFET or depletion-mode MOSFET appears in Fig. 4.39. Because depletion-mode transistors conduct for  $v_{GS} = 0$ , a separate gate bias voltage is not required, and the bias circuit requires one less resistor than the four-resistor bias circuit discussed earlier in this chapter. In the circuits in Fig. 4.39, the value of  $R_S$  will set the source and drain currents, and the sum of  $R_S$  and  $R_D$  will determine the drain-source voltage.  $R_G$  is used to provide a dc connection



(a)



(b)

**Figure 4.39** Bias circuits for (a) *n*-channel JFET and (b) depletion-mode MOSFET.

between the gate and ground while maintaining a high resistance path for ac signal voltages that may be applied to the gate (in amplifier applications, for example). In some cases, even  $R_G$  may be omitted.

## EXAMPLE 4.6 BIASING THE JFET AND DEPLETION-MODE MOSFET

Biasing of JFETs and depletion-mode MOSFETs is very similar, and this example presents a set of bias calculations for the two devices.

**PROBLEM** Find the quiescent operating point for the circuit in Fig. 4.39(a).

**SOLUTION Known Information and Given Data:** Circuit topology in Fig. 4.39(a) with  $V_{DD} = 12$  V,  $R_D = 2 \text{ k}\Omega$ ,  $R_G = 680 \text{ k}\Omega$ ,  $I_{DSS} = 5 \text{ mA}$ , and  $V_P = -5 \text{ V}$

**Unknowns:**  $V_{GS}$ ,  $I_D$ ,  $V_{DS}$

**Approach:** Analyze the input loop to find  $V_{GS}$ . Use  $V_{GS}$  to find  $I_D$ , and  $I_D$  to determine  $V_{DS}$ .

**Assumptions:** The JFET is pinched-off, the gate-channel junction is reverse biased, and the reverse leakage current of the gate is negligible.

**Analysis:** Write the input loop equation including  $V_{GS}$ :

$$I_G R_G + V_{GS} + I_S R_S = 0 \quad \text{or} \quad V_{GS} = -I_D R_S \quad (4.82)$$

Equation (4.82) was simplified since  $I_G = 0$  and  $I_S = I_D$ . By assuming the JFET is in the pinch-off region and using Eq. (4.69), Eq. (4.82) becomes

$$V_{GS} = -I_{DSS} R_S \left( 1 - \frac{V_{GS}}{V_P} \right)^2 \quad (4.83)$$

Substituting in the circuit and transistor values into Eq. (4.83) yields

$$V_{GS} = -(5 \times 10^{-3} \text{ A})(1000 \Omega) \left( 1 - \frac{V_{GS}}{-5 \text{ V}} \right)^2 \quad \text{or} \quad V_{GS}^2 + 15V_{GS} + 25 = 0 \quad (4.84)$$

which has the roots  $-1.91$  and  $-13.1$  V. The second value is more negative than the pinch-off voltage of  $-5$  V, so the transistor would be cutoff for this value of  $V_{GS}$ . Therefore  $V_{GS} = -1.91$  V, and the drain and source currents are

$$I_D = I_S = \frac{1.91 \text{ V}}{1 \text{ k}\Omega} = 1.91 \text{ mA}$$

The drain-source voltage is found by writing the output loop equation:

$$V_{DD} = I_D R_D + V_{DS} + I_S R_S \quad (4.85)$$

which can be rearranged to yield

$$V_{DS} = V_{DD} - I_D(R_D + R_S) = 12 - (1.91 \text{ mA})(3 \text{ k}\Omega) = 6.27 \text{ V}$$

**Check of Results:** Our analysis yields

$$V_{GS} - V_P = -1.91 \text{ V} - (-5 \text{ V}) = +3.09 \text{ V} \quad \text{and} \quad V_{DS} = 6.27 \text{ V}$$

Because  $V_{DS}$  exceeds  $(V_{GS} - V_P)$ , the device is pinched off. In addition, the gate-source junction is reverse biased by 1.91 V. So, the JFET Q-point is (1.91 mA, 6.27 V).

**Discussion:** Because depletion-mode transistors conduct for  $v_{GS} = 0$ , a separate gate bias voltage is not required, and the bias circuit requires one less resistor than the four-resistor bias circuit discussed earlier in this chapter. The circuitry for biasing depletion-mode MOSFETs is identical as indicated in Fig. 4.39(b) — see the exercises after this example.

**Computer-Aided Analysis:** SPICE analysis yields the same Q-point as our hand calculations. If we add  $\lambda = 0.02 \text{ V}^{-1}$ , the Q-point shifts to (2.10 mA, 5.98 V). It is helpful to add a voltmeter to the circuit to directly measure  $V_{DS}$ .

**EXERCISE:** What are the values of VTO, BETA, and LAMBDA used in the simulation in the last example?

**ANSWERS:** -5 V; 0.2 mA; 0.02  $\text{V}^{-1}$

**EXERCISE:** Show that the expression for the gate-source voltage of the MOSFET in Fig. 4.39(b) is identical to Eq. (4.83). Find the Q-point for the MOSFET and show that it is the same as that for the JFET.

**EXERCISE:** What is the Q-point for the JFET in Fig. 4.39(a) if  $V_{DD} = 9 \text{ V}$ ?

**ANSWER:** (1.91 mA, 3.27 V)

**EXERCISE:** Find the Q-point in the circuit in Fig. 4.39(a) if  $R_S$  is changed to 2 k $\Omega$ .

**ANSWER:** (1.25 mA, 4.00 V)

**EXERCISE:** (a) Suppose the gate diode of the JFET in Fig. 4.39(a) has a reverse saturation current of 10 nA. Since the diode is reverse biased,  $I_G = -10 \text{ nA}$ . What is the voltage at the gate terminal of the transistor? [See Eq. (4.84)]. What is the new value of  $V_{GS}$ ? What will be the new Q-point of the JFET? (b) Repeat if the saturation current is 1  $\mu\text{A}$ .

**ANSWERS:** (a) +6.80 mV, -1.91 V, (1.91 mA, 6.27 V); (b) 0.680 V, -1.64 V, (2.26 mA, 5.22 V)

## SUMMARY

- This chapter discussed the structures and  $i-v$  characteristics of two types of field-effect transistors (FETs): the metal-oxide-semiconductor FET, or MOSFET, and the junction FET, or JFET.
- At the heart of the MOSFET is the MOS capacitor, formed by a metallic gate electrode insulated from the semiconductor by an insulating oxide layer. The potential on the gate controls the carrier

concentration in the semiconductor region directly beneath the gate; three regions of operation of the MOS capacitor were identified: accumulation, depletion, and inversion.

- A MOSFET is formed when two  $pn$  junctions are added to the semiconductor region of the MOS capacitor. The junctions act as the source and drain terminals of the MOS transistor and provide a ready supply of carriers for the channel region of the MOSFET. The source and drain junctions must be kept reverse-biased at all times in order to isolate the channel from the substrate.
- MOS transistors can be fabricated with either  $n$ - or  $p$ -type channel regions and are referred to as NMOS or PMOS transistors, respectively. In addition, MOSFETs can be fabricated as either enhancement-mode or depletion-mode devices.
- For an enhancement-mode device, a gate-source voltage exceeding the threshold voltage must be applied to the transistor to establish a conducting channel between source and drain.
- In the depletion-mode device, a channel is built into the device during its fabrication, and a voltage must be applied to the transistor's gate to quench conduction.
- The JFET uses  $pn$  junctions to control the resistance of the conducting channel region. The gate-source voltage modulates the width of the depletion layers surrounding the gate-channel junctions and thereby changes the width of the channel region. A JFET can be fabricated with either  $n$ - or  $p$ -type channel regions, but because of its structure, the JFET is inherently a depletion-mode device.
- Both the MOSFET and JFET are symmetrical devices. The source and drain terminals of the device are actually determined by the voltages applied to the terminals. For a given geometry and set of voltages, the  $n$ -channel transistor will conduct two to three times the current of the  $p$ -channel device because of the difference between the electron and hole mobilities in the channel.
- Although structurally different, the  $i-v$  characteristics of MOSFETs and JFETs are very similar, and each type of FET has three regions of operation.
  - In cutoff, a channel does not exist, and the terminal currents are zero.
  - In the triode region of operation, the drain current in the FET depends on both the gate-source and drain-source voltages of the transistor. For small values of drain-source voltage, the transistor exhibits an almost linear relationship between its drain current and drain-source voltage. In the triode region, the FET can be used as a voltage-controlled resistor, in which the on-resistance of the transistor is controlled by the gate-source voltage of the transistor. Because of this behavior, the name *transistor* was developed as a contraction of "transfer resistor."
  - For values of drain-source voltage exceeding the pinch-off voltage, the drain current of the FET becomes almost independent of the drain-source voltage. In this region, referred to variously as the pinch-off region, the saturation region, or the active region, the drain-source current exhibits a square-law dependence on the voltage applied between the gate and source terminals. Variations in drain-source voltage do cause small changes in drain current in saturation due to channel-length modulation.
- Mathematical models for the  $i-v$  characteristics of both MOSFETs and JFETs were presented. The MOSFET is actually a four-terminal device and has a threshold voltage that depends on the source-bulk voltage of the transistor.
  - Key parameters for the MOSFET include the transconductance parameters  $K_n$  or  $K_p$ , the zero-bias threshold voltage  $V_{TO}$ , body effect parameter  $\gamma$ , and channel-length modulation parameter  $\lambda$  as well as the width  $W$  and length  $L$  of the channel.

- The JFET was modeled as a three-terminal device with constant pinch-off voltage. Key parameters for the JFET include saturation current  $I_{DSS}$ , pinch-off voltage  $V_P$ , and channel-length modulation parameter  $\lambda$ .
- A variety of examples of bias circuits were presented, and the mathematical model was used to find the quiescent operating point, or Q-point, for various types of MOSFETs. The Q-point represents the dc values of drain current and drain-source voltage: ( $I_D$ ,  $V_{DS}$ ).
- The  $i$ - $v$  characteristics are often displayed graphically in the form of either the output characteristics, that plot  $i_D$  versus  $v_{DS}$ , or the transfer characteristics, that graph  $i_D$  versus  $v_{GS}$ . Examples of finding the Q-point using graphical load-line and iterative numerical analyses were discussed. The examples included application of the field-effect transistor as both electronic current and voltage sources.
- The most important bias circuit in discrete design is the four-resistor circuit which yields a well-stabilized operating point.
- The gate-source, gate-drain, drain-bulk, source-bulk, and gate-bulk capacitances of MOS transistors were discussed, and the Meyer model for the gate-source and gate-bulk capacitances was introduced. All the capacitances are nonlinear functions of the terminal voltages of the transistor. The capacitances of the JFET are determined by the capacitance of the reverse-biased gate-channel junctions and also exhibit a nonlinear dependence on the terminal voltages of the transistor.
- Complex models for MOSFETs and JFETs are built into SPICE circuit analysis programs. These models contain many circuit elements and parameters to attempt to model the true behavior of the transistor as closely as possible.
- Part of the IC designer's job often includes layout of the transistors based on a set of technology-specific ground rules that define minimum feature dimensions and spaces between features.
- Constant electric field scaling provides a framework for proper miniaturization of MOS devices in which the power density remains constant as the transistor density increases. In this case, circuit delay improves directly with the scale factor  $\alpha$ , whereas the power-delay product improves with the cube of  $\alpha$ .
- The cutoff frequency  $f_T$  of the transistor represents the highest frequency at which the transistor can provide amplification. Cutoff frequency  $f_T$  improves directly with the scale factor.
- The electric fields in small devices can become very high, and the carrier velocity tends to saturate at fields above 10 kV/cm. Subthreshold leakage current becomes increasingly important as devices are scaled to small dimension.

## KEY TERMS

Accumulation	Channel-length modulation
Accumulation region	Channel-length modulation parameter $\lambda$
Active region	Channel region
Alignment tolerance $T$	Channel width $W$
Body effect	Constant electric field scaling
Body-effect parameter $\gamma$	Current sink
Body terminal ( $B$ )	Current source
Bulk terminal ( $B$ )	Cutoff frequency
$C_{GS}$ , $C_{GD}$ , $C_{GB}$ , $C_{DB}$ , $C_{SB}$ , $C''_{ox}$ , $C_{GDO}$ , $C_{GSO}$	Depletion
Capacitance per unit width	Depletion-mode device
Channel length $L$	Depletion-mode MOSFETs

Depletion region	Output characteristics
Design rules	Output resistance
Drain ( $D$ )	Overlap capacitance
Electronic current source	Oxide thickness
Enhancement-mode device	$p$ -channel MOS (PMOS)
Field-effect transistor (FET)	PHI
Four-resistor bias	Pinch-off locus
Gate ( $G$ )	Pinch-off point
Gate-channel capacitance $C_{GC}$	Pinch-off region
Gate-drain capacitance $C_{GD}$	PMOS transistor
Gate-source capacitance $C_{GS}$	Power delay product
Ground rules	Quiescent operating point
High field limitations	Q-point
Inversion layer	Saturation region
Inversion region	Saturation voltage
KP	Scaling theory
$K'_n, K'_p$	Small-signal output resistance
LAMDA, $\lambda$	SPICE MODELS
Triode region	Source ( $S$ )
Metal-oxide-semiconductor field-effect transistor (MOSFET)	Substrate sensitivity
Minimum feature size $F$	Substrate terminal
Mirror ratio	Surface potential parameter $2\phi_F$
MOS capacitor	Subthreshold region
$n$ -channel MOS (NMOS)	Threshold voltage $V_{TN}, V_{TP}$
$n$ -channel MOSFET	Transconductance $g_m$
$n$ -channel transistor	Transconductance parameter — $K'_n, K'_p$ , KP
NMOSFET	Transfer characteristic
NMOS transistor	Triode region
On-resistance ( $R_{on}$ )	$V_{TN}, V_{TP}$ , VT, VTO
	Zero-substrate-bias value for $V_{TN}$

## REFERENCES

1. U. S. Patent 1,900,018. Also see 1,745,175 and 1,877,140.
2. National Technology Road Map for Semiconductors, public.itrs.net
3. Carver Mead and Lynn Conway, *Introduction to VLSI Systems*, Addison Wesley, Reading, Massachusetts: 1980.
4. J. E. Meyer, “MOS models and circuit simulations,” *RCA Review*, vol. 32, pp. 42–63, March 1971.
5. B. M. Wilamowski and R. C. Jaeger, *Computerized Circuit Analysis Using SPICE Programs*, McGraw-Hill, New York: 1997.
6. R. H. Dennard, F. H. Gaensslen, L. Kuhn, and H. N. Yu, “Design of micron MOS switching devices,” *IEEE IEDM Digest*, pp. 168–171, December 1972.
7. R. H. Dennard, F. H. Gaensslen, H-N. Yu, V. L. Rideout, E. Bassous and A. R. LeBlanc, “Design of ion-implanted MOSFET’s with very small physical dimensions,” *IEEE J. Solid-State Circuits*, vol. SC-9, no. 5, pp. 256–268, October 1974.

## PROBLEMS

Use the parameters in Table 4.6 as needed in the problems here.

**TABLE 4.6**  
MOS Transistor Parameters

	NMOS DEVICE	PMOS DEVICE
$V_{TO}$	+0.75 V	-0.75 V
$\gamma$	$0.75\sqrt{V}$	$0.5\sqrt{V}$
$2\phi_F$	0.6 V	0.6 V
$K'$	$100 \mu\text{A/V}^2$	$40 \mu\text{A/V}^2$

$$\varepsilon_{ox} = 3.9 \varepsilon_o \text{ and } \varepsilon_s = 11.7 \varepsilon_o \text{ where } \varepsilon_o = 8.854 \times 10^{-14} \text{ F/cm}$$

### 4.1 Characteristics of the MOS Capacitor

- 4.1. (a) The MOS capacitor in Fig. 4.1 has  $V_{TN} = 1$  V and  $V_G = 2$  V. To what region of operation does this bias condition correspond? (b) Repeat for  $V_G = -2$  V. (c) Repeat for  $V_G = 0.5$  V.
- 4.2. Calculate the capacitance of an MOS capacitor with an oxide thickness  $T_{ox}$  of (a) 50 nm, (b) 25 nm, (c) 10 nm, and (d) 5 nm.
- 4.3. The minimum value of the depletion-layer capacitance can be estimated using an expression similar to Eq. (3.18):  $C_d = \varepsilon_S / x_d$  in which the depletion-layer width is  $x_d \cong \sqrt{\frac{2\varepsilon_S}{qN_B}}(0.75 \text{ V})$  and  $N_B$  is the substrate doping. Estimate  $C_d$  for  $N_B = 10^{15}/\text{cm}^3$ .

### 4.2 The NMOS Transistor

#### Triode (Linear) Region Characteristics

- 4.4. Calculate  $K'_n$  for an NMOS transistor with  $\mu_n = 500 \text{ cm}^2/\text{V} \cdot \text{s}$  for an oxide thickness of (a) 40 nm, (b) 20 nm, (c) 10 nm, and (d) 5 nm.
- 4.5. (a) What is the charge density ( $\text{C}/\text{cm}^2$ ) in the channel if the oxide thickness is 25 nm and the oxide voltage exceeds the threshold voltage by 1 V? (b) Repeat for a 10-nm oxide and a bias 1.5 V above threshold.
- 4.6. (a) What is the electron velocity in the channel if  $\mu_n = 500 \text{ cm}^2/\text{V} \cdot \text{s}$  and the electric field is 5000 V/cm? (b) Repeat for  $\mu_n = 400 \text{ cm}^2/\text{V} \cdot \text{s}$  with a field of 2000 V/cm.
- 4.7. Equation (4.2) indicates that the charge/unit · length in the channel of a pinched-off

transistor decreases as one proceeds from source to drain. However, our text argued that the current entering the drain terminal is equal to the current exiting from the source terminal. How can a constant current exist everywhere in the channel between the drain and source terminals if the first statement is indeed true?

- 4.8. An NMOS transistor has  $K'_n = 200 \mu\text{A/V}^2$ . What is the value of  $K_n$  if  $W = 60 \mu\text{m}$ ,  $L = 3 \mu\text{m}$ ? If  $W = 3 \mu\text{m}$ ,  $L = 0.15 \mu\text{m}$ ? If  $W = 10 \mu\text{m}$ ,  $L = 0.25 \mu\text{m}$ ?
- 4.9. Calculate the drain current in an NMOS transistor for  $V_{GS} = 0, 1 \text{ V}, 2 \text{ V}$ , and  $3 \text{ V}$ , with  $V_{DS} = 0.25 \text{ V}$ , if  $W = 5 \mu\text{m}$ ,  $L = 0.5 \mu\text{m}$ ,  $V_{TN} = 0.80 \text{ V}$ , and  $K'_n = 200 \mu\text{A/V}^2$ . What is the value of  $K_n$ ?
- 4.10. Calculate the drain current in an NMOS transistor for  $V_{GS} = 0, 1 \text{ V}, 2 \text{ V}$ , and  $3 \text{ V}$ , with  $V_{DS} = 0.1 \text{ V}$ , if  $W = 10 \mu\text{m}$ ,  $L = 0.2 \mu\text{m}$ ,  $V_{TN} = 1.0 \text{ V}$ , and  $K'_n = 250 \mu\text{A/V}^2$ . What is the value of  $K_n$ ?
- 4.11. Identify the source, drain, gate, and bulk terminals and find the current  $I$  in the transistors in Fig. P4.11. Assume  $V_{TN} = 0.70 \text{ V}$ .

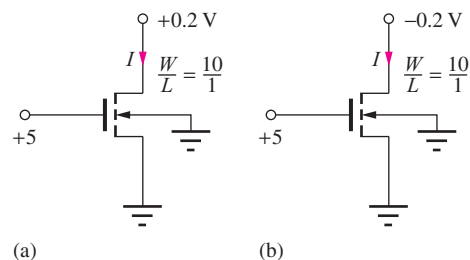


Figure P4.11

- 4.12. (a) What is the current in the transistor in Fig. P4.11(a) if the 0.2 V is changed to 0.5 V? Assume  $V_{TN} = 0.70 \text{ V}$ . (b) Repeat if the gate voltage is changed to 3 V and the other voltage remains at 0.2 V?
- 4.13. (a) What is the current in the transistor in Fig. P4.11(b) if -0.2 V is changed to -0.5 V? Assume  $V_{TN} = 0.75 \text{ V}$ . (b) If the gate voltage is changed to 3 V and the upper terminal voltage is replaced by -1 V?
- 4.14. (a) Design a transistor (choose  $W$ ) to have  $K_n = 4 \text{ mA/V}^2$  if  $L = 0.5 \mu\text{m}$ . (See Table 4.6.) (b) Repeat for  $K_n = 750 \mu\text{A/V}^2$ .

## On Resistance

- 4.15. What is the on-resistance of an NMOS transistor with  $W/L = 100/1$  if  $V_{GS} = 5$  V and  $V_{TN} = 0.65$  V? (b) If  $V_{GS} = 2.5$  V and  $V_{TN} = 0.50$  V? (See Table 4.6.)
- 4.16. (a) What is the  $W/L$  ratio required for an NMOS transistor to have an on-resistance of  $500 \Omega$  when  $V_{GS} = 5$  V and  $V_{SB} = 0$ ? (b) Repeat for  $V_{GS} = 3.3$  V.
- 4.17. Suppose that an NMOS transistor must conduct a current  $I_D = 10$  A with  $V_{DS} \leq 0.1$  V when it is on. What is the maximum on-resistance of the transistor? If  $V_G = 5$  V is used to turn on the transistor and  $V_{TN} = 2$  V, what is the minimum value of  $K_n$  required to achieve the required on-resistance?

## Saturation of the $i$ - $v$ Characteristics

- \*4.18. The output characteristics for an NMOS transistor are given in Fig. P4.18. What are the values of  $K_n$  and  $V_{TN}$  for this transistor? Is this an enhancement-mode or depletion-mode transistor? What is  $W/L$  for this device?

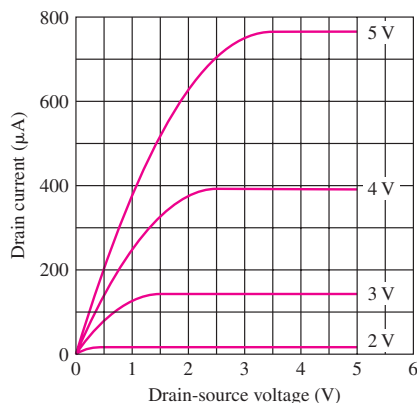


Figure P4.18

- 4.19. Add the  $V_{GS} = 3.5$  V and  $V_{GS} = 4.5$  V curves to the  $i$ - $v$  characteristic of Fig. P4.18. What are the values of  $i_{DSAT}$  and  $v_{DSAT}$  for these new curves?
- 4.20. Calculate the drain current in an NMOS transistor for  $V_{GS} = 0, 1$  V, 2 V, and 3 V, with  $V_{DS} = 3.3$  V, if  $W = 5 \mu\text{m}$ ,  $L = 0.5 \mu\text{m}$ ,  $V_{TN} = 1$  V, and  $K'_n = 375 \mu\text{A/V}^2$ . What is the value of  $K_n$ ? Check the saturation region assumption.
- 4.21. Calculate the drain current in an NMOS transistor for  $V_{GS} = 0, 1$  V, 2 V, and 3 V, with  $V_{DS} = 4$  V, if  $W = 10 \mu\text{m}$ ,  $L = 1 \mu\text{m}$ ,  $V_{TN} = 1.5$  V, and  $K'_n = 200 \mu\text{A/V}^2$ . What is the value of  $K_n$ ? Check the saturation region assumption.

## Regions of Operation

- 4.22. Find the region of operation and drain current in an NMOS transistor with  $K'_n = 200 \mu\text{A/V}^2$ ,  $W/L = 10/1$ ,  $V_{TN} = 0.75$  V and (a)  $V_{GS} = 2$  V and  $V_{DS} = 2.5$  V, (b)  $V_{GS} = 2$  V and  $V_{DS} = 0.2$  V, (c)  $V_{GS} = 0$  V and  $V_{DS} = 4$  V. (d) Repeat for  $K'_n = 300 \mu\text{A/V}^2$ .
- 4.23. Identify the region of operation of an NMOS transistor with  $K_n = 400 \mu\text{A/V}^2$  and  $V_{TN} = 0.7$  V for (a)  $V_{GS} = 3.3$  V and  $V_{DS} = 3.3$  V, (b)  $V_{GS} = 0$  V and  $V_{DS} = 3.3$  V, (c)  $V_{GS} = 2$  V and  $V_{DS} = 2$  V, (d)  $V_{GS} = 1.5$  V and  $V_{DS} = 0.5$ , (e)  $V_{GS} = 2$  V and  $V_{DS} = -0.5$  V, and (f)  $V_{GS} = 3$  V and  $V_{DS} = -3$  V.
- 4.24. Identify the region of operation of an NMOS transistor with  $K_n = 250 \mu\text{A/V}^2$  and  $V_{TN} = 1$  V for (a)  $V_{GS} = 5$  V and  $V_{DS} = 6$  V, (b)  $V_{GS} = 0$  V and  $V_{DS} = 6$  V, (c)  $V_{GS} = 2$  V and  $V_{DS} = 2$  V, (d)  $V_{GS} = 1.5$  V and  $V_{DS} = 0.5$ , (e)  $V_{GS} = 2$  V and  $V_{DS} = -0.5$  V, and (f)  $V_{GS} = 3$  V and  $V_{DS} = -6$  V.
- 4.25. (a) Identify the source, drain, gate, and bulk terminals for the transistor in the circuit in Fig. P4.25. Assume  $V_{DD} > 0$ . (b) Repeat for  $V_{DD} < 0$ . (c) An issue occurs with operation of the circuit in Fig. P4.25 with  $V_{DD} < 0$ . What is the problem?

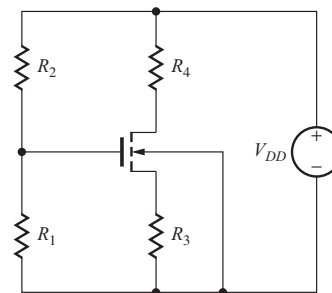


Figure P4.25

- 4.26. (a) Identify the source, drain, gate, and bulk terminals for each of the transistors in the circuit in Fig. P4.26(a). Assume  $V_{DD} > 0$ . (b) Repeat for the circuit in Fig. P4.26(b).

## Transconductance

- 4.27. Calculate the transconductance for an NMOS transistor for  $V_{GS} = 2$  V and 3.3 V, with  $V_{DS} = 3.3$  V, if  $W = 20 \mu\text{m}$ ,  $L = 1 \mu\text{m}$ ,  $V_{TN} = 0.7$  V, and  $K'_n = 250 \mu\text{A/V}^2$ . Check the saturation region assumption.
- 4.28. (a) Estimate the transconductance for the transistor in Fig. P4.18 for  $V_{GS} = 4$  V and  $V_{DS} = 4$  V.

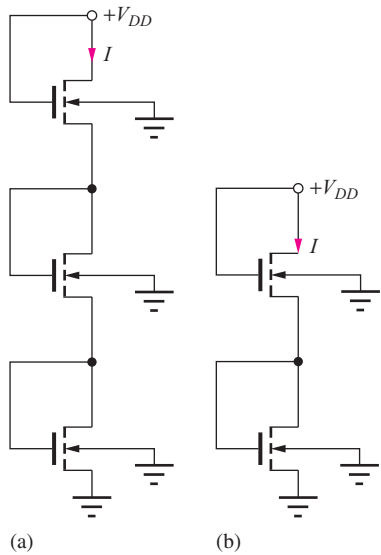


Figure P4.26

(Hint:  $g_m \cong \Delta i_D / \Delta V_{GS}$ .) (b) Repeat for  $V_{GS} = 3$  V and  $V_{DS} = 4.5$  V.

- 4.29. Find an expression for the transconductance of the MOSFET in the linear region. What is the transconductance of the MOSFET in Prob. 4.27 with  $V_{GS} = 2$  V and 3.3 V with  $V_{DS} = 1$  V?

### Channel-Length Modulation

- 4.30. (a) Calculate the drain current in an NMOS transistor if  $K_n = 500 \mu\text{A}/\text{V}^2$ ,  $V_{TN} = 1$  V,  $\lambda = 0.02 \text{ V}^{-1}$ ,  $V_{GS} = 4$  V, and  $V_{DS} = 5$  V. (b) Repeat assuming  $\lambda = 0$ .
- 4.31. (a) Calculate the drain current in an NMOS transistor if  $K_n = 250 \mu\text{A}/\text{V}^2$ ,  $V_{TN} = 0.75$  V,  $\lambda = 0.025 \text{ V}^{-1}$ ,  $V_{GS} = 5$  V, and  $V_{DS} = 6$  V. (b) Repeat assuming  $\lambda = 0$ .
- 4.32. (a) Find the drain current for the transistor in Fig. P4.32 if  $\lambda = 0$ . (b) Repeat if  $\lambda = 0.025 \text{ V}^{-1}$ . (c) Repeat part (a) if the  $W/L$  ratio is changed to 25/1.

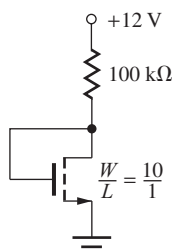


Figure P4.32

- 4.33. (a) Find the drain current for the transistor in Fig. P4.32 if  $\lambda = 0$  and the  $W/L$  ratio is changed to 20/1. (b) Repeat if  $\lambda = 0.020 \text{ V}^{-1}$ .
- 4.34. (a) Find the current  $I$  in Fig. P4.34 if  $V_{DD} = 10$  V and  $\lambda = 0$ . Both transistors have  $W/L = 10/1$ . (b) What is the current if both transistors have  $W/L = 20/1$ . (c) Repeat part (a) for  $\lambda = 0.04 \text{ V}^{-1}$ .

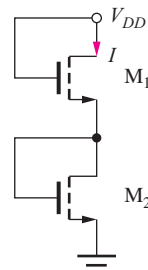


Figure P4.34

- 4.35. (a) Find the currents in the two transistors in Fig. P4.34 if  $(W/L)_1 = 10/1$ ,  $(W/L)_2 = 40/1$ , and  $\lambda = 0$  for both transistors. (b) Repeat for  $(W/L)_2 = 40/1$  and  $(W/L)_1 = 10/1$ . (c) Repeat part (a) if  $\lambda = 0.05/\text{V}$  for both transistors.
- 4.36. (a) Find the currents in the two transistors in Fig. P4.34 if  $(W/L)_1 = 25/1$ ,  $(W/L)_2 = 12.5/1$  and  $\lambda = 0$  for both transistors. (b) Repeat part (a) if  $\lambda = 0.05/\text{V}$  for both transistors.

### Transfer Characteristics and the Depletion-Mode MOSFET

- 4.37. (a) Calculate the drain current in an NMOS transistor if  $K_n = 250 \mu\text{A}/\text{V}^2$ ,  $V_{TN} = -3$  V,  $\lambda = 0$ ,  $V_{GS} = 0$  V, and  $V_{DS} = 6$  V. (b) Repeat assuming  $\lambda = 0.025 \text{ V}^{-1}$ .
- 4.38. (a) Calculate the drain current in an NMOS transistor if  $K_n = 250 \mu\text{A}/\text{V}^2$ ,  $V_{TN} = -2$  V,  $\lambda = 0$ ,  $V_{GS} = 5$  V, and  $V_{DS} = 6$  V. (b) Repeat assuming  $\lambda = 0.03 \text{ V}^{-1}$ .
- 4.39. An NMOS depletion-mode transistor is operating with  $V_{DS} = V_{GS} > 0$ . What is the region of operation for this device?
- 4.40. (a) Find the Q-point for the transistor in Fig. P4.40(a) if  $V_{TN} = -2$  V. (b) Repeat for  $R = 50 \text{ k}\Omega$  and  $W/L = 20/1$ . (c) Repeat parts (a) & (b) for Fig. 4.40(b).
- 4.41. (a) Find the Q-point for the transistor in Fig. P4.40(a) if  $V_{TN} = -1$  V and  $W/L$  is changed to 20/1. (b) Repeat for Fig. P4.40(b).

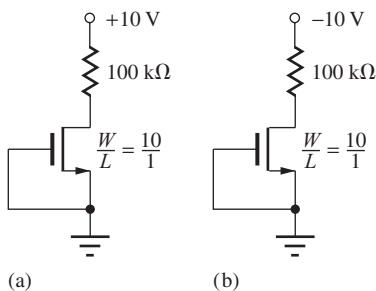


Figure P4.40

**Body Effect or Substrate Sensitivity**

- 4.42. Repeat Problem 4.20 with for  $V_{SB} = 1.25$  V with the values from Table 4.6.
- 4.43. Repeat Prob. 4.21 for  $V_{SB} = 1.5$  V with the values from Table 4.6.
- 4.44. (a) An NMOS transistor with  $W/L = 8/1$  has  $V_{TO} = 1$  V,  $2\phi_F = 0.6$  V, and  $\gamma = 0.7 \sqrt{V}$ . The transistor is operating with  $V_{SB} = 3$  V,  $V_{GS} = 2.5$  V, and  $V_{DS} = 5$  V. What is the drain current in the transistor? (b) Repeat for  $V_{DS} = 0.5$  V.
- 4.45. An NMOS transistor with  $W/L = 16.8/1$  has  $V_{TO} = 1.5$  V,  $2\phi_F = 0.75$  V, and  $\gamma = 0.5 \sqrt{V}$ . The transistor is operating with  $V_{SB} = 4$  V,  $V_{GS} = 2$  V, and  $V_{DS} = 5$  V. What is the drain current in the transistor? (b) Repeat for  $V_{DS} = 0.5$  V.
- 4.46. A depletion-mode NMOS transistor has  $V_{TO} = -1.5$  V,  $2\phi_F = 0.75$  V, and  $\gamma = 1.5 \sqrt{V}$ . What source-bulk voltage is required to change this transistor into an enhancement-mode device with a threshold voltage of +0.85 V?
- \*4.47. The measured body-effect characteristic for an NMOS transistor is given in Table 4.7. What are

**TABLE 4.7**

$V_{SB}$ (V)	$V_{TN}$ (V)
0	0.710
0.5	0.912
1.0	1.092
1.5	1.232
2.0	1.377
2.5	1.506
3.0	1.604
3.5	1.724
4.0	1.822
4.5	1.904
5.0	2.005

the best values of  $V_{TO}$ ,  $\gamma$ , and  $2\phi_F$  (in the least-squares sense—see Prob. 3.30) for this transistor?

**4.3 PMOS Transistors**

- 4.48. Calculate  $K'_p$  for a PMOS transistor with  $\mu_p = 200 \text{ cm}^2/\text{V} \cdot \text{s}$  for an oxide thickness of (a) 50 nm, (b) 20 nm, (c) 10 nm, and (d) 5 nm.
- \*4.49. The output characteristics for a PMOS transistor are given in Fig. P4.49. What are the values of  $K_p$  and  $V_{TP}$  for this transistor? Is this an enhancement-mode or depletion-mode transistor? What is the value of  $W/L$  for this device?

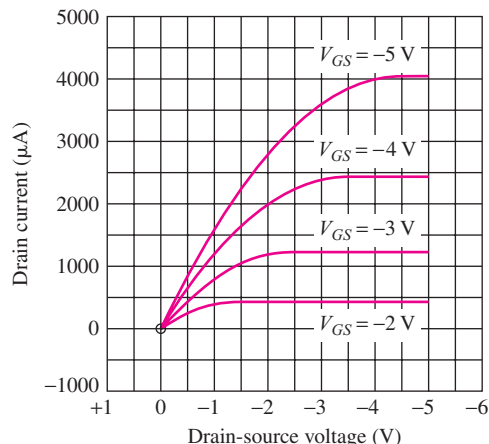


Figure P4.49

- 4.50. Add the  $V_{GS} = -3.5$  V and  $V_{GS} = -4.5$  V curves to the  $i-v$  characteristic of Fig. P4.49. What are the values of  $i_{DSAT}$  and  $v_{DSAT}$  for these new curves?
- 4.51. Find the region of operation and drain current in a PMOS transistor with  $W/L = 20/1$  for  $V_{BS} = 0$  V and (a)  $V_{GS} = -1.1$  V and  $V_{DS} = -0.2$  V and (b)  $V_{GS} = -1.3$  V and  $V_{DS} = -0.2$  V. (c) Repeat parts (a) and (b) for  $V_{BS} = 1$  V.
- 4.52. (a) What is the  $W/L$  ratio required for an PMOS transistor to have an on-resistance of  $2 \text{ k}\Omega$  when  $V_{GS} = -5$  V and  $V_{BS} = 0$ ? Assume  $V_{TP} = -0.70$  V. (b) Repeat for an NMOS transistor with  $V_{GS} = +5$  V and  $V_{BS} = 0$ . Assume  $V_{TN} = 0.70$  V.
- 4.53. (a) What is the  $W/L$  ratio required for a PMOS transistor to have an on-resistance of  $1 \Omega$  when  $V_{GS} = -5$  V and  $V_{SB} = 0$ ? Assume  $V_{TP} = -0.70$  V. (b) Repeat for an NMOS transistor with  $V_{GS} = +5$  V and  $V_{BS} = 0$ . Assume  $V_{TN} = 0.70$  V.
- 4.54. (a) Calculate the on-resistance for a PMOS transistor having  $W/L = 200/1$  and operating with  $V_{GS} = -5$  V and  $V_{TP} = -0.75$  V. (b) Repeat for

a similar NMOS transistor with  $V_{GS} = 5$  V and  $V_{TN} = 0.75$  V. (c) What  $W/L$  ratio is required for the PMOS transistor to have the same  $R_{on}$  as the NMOS transistor in (b)?

- 4.55. (a) Identify the source, drain, gate, and bulk terminals for the transistors in the two circuits in Fig. P4.55(a). Assume  $V_{DD} = 10$  V. (b) Repeat for Fig. P4.55(b).

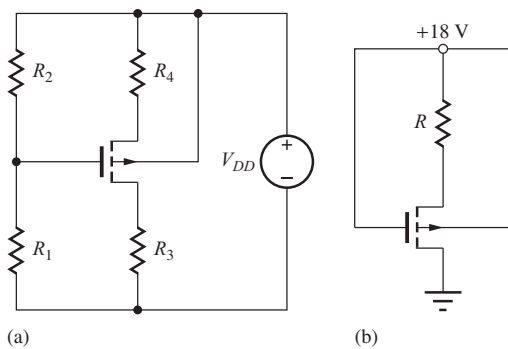


Figure P4.55

- 4.56. What is the on-resistance and voltage  $V_O$  for the parallel combination of the NMOS ( $W/L = 10/1$ ) and PMOS ( $W/L = 25/1$ ) transistors in Fig. P4.56 for  $V_{IN} = 0$  V? (b) For  $V_{IN} = 5$  V? This circuit is called a transmission-gate.

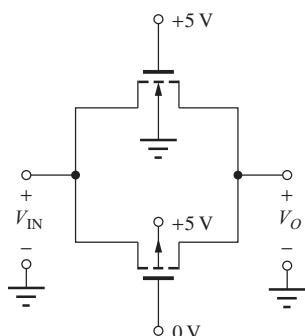


Figure P4.56

- 4.57. Suppose a PMOS transistor must conduct a current  $I_D = 0.5$  A with  $V_{SD} \leq 0.1$  V when it is on. What is the maximum on-resistance? If  $V_G = 0$  V is used to turn on the transistor with  $V_S = 10$  V and  $V_{TP} = -2$  V, what is the minimum value of  $K_p$  required to achieve the required on-resistance?
- 4.58. A PMOS transistor is operating with  $V_{BS} = 0$  V,  $V_{GS} = -1.5$  V, and  $V_{DS} = -0.5$  V. What are the region of operation and drain current in this device if  $W/L = 40/1$ ?

- 4.59. A PMOS transistor is operating with  $V_{BS} = 4$  V,  $V_{GS} = -1.5$  V, and  $V_{DS} = -4$  V. What are the region of operation and drain current in this device if  $W/L = 25/1$ ?

#### 4.4 MOSFET Circuit Symbols

- 4.60. The PMOS transistor in Fig. P4.55(a) is conducting current. Is  $V_{TP} > 0$  or  $V_{TP} < 0$  for this transistor? Based on this value of  $V_{TP}$ , what type transistor is in the circuit? Is the proper symbol used in this circuit for this transistor? If not, what symbol should be used?
- 4.61. The PMOS transistor in Fig. P4.55(b) is conducting current. Is  $V_{TP} > 0$  or  $V_{TP} < 0$  for this transistor? Based on this value of  $V_{TP}$ , what type transistor is in the circuit? Is the proper symbol used in this circuit for this transistor? If not, what symbol should be used?
- 4.62. (a) Redraw the circuits in Fig. P4.55(a) with a three-terminal PMOS transistor with its body connected to its source. (b) Repeat for Fig. P4.55(b).
- 4.63. Redraw the circuit in Fig. 4.27 with a four-terminal NMOS transistor with its body connected to  $-3$  V.
- 4.64. Redraw the circuit in Fig. 4.28 with a four-terminal NMOS transistor with its body connected to  $-5$  V.

#### 4.5 Capacitances in MOS Transistors

- 4.65. Calculate  $C''_{ox}$  and  $C_{GC}$  for an MOS transistor with  $W = 10$   $\mu\text{m}$  and  $L = 0.25$   $\mu\text{m}$  with an oxide thickness of (a) 50 nm, (b) 20 nm, (c) 10 nm, and (d) 5 nm.
- 4.66. Calculate  $C''_{ox}$  and  $C_{GC}$  for an MOS transistor with  $W = 5$   $\mu\text{m}$  and  $L = 0.5$   $\mu\text{m}$  with an oxide thickness of (a) 25 nm and (b) 10 nm.
- 4.67. In a certain MOSFET, the value of  $C'_{OL}$  can be calculated using an effective overlap distance of 0.5  $\mu\text{m}$ . What is the value of  $C'_{OL}$  for an oxide thickness of 10 nm.
- 4.68. What are the values of  $C_{GS}$  and  $C_{GD}$  for a transistor with  $C''_{ox} = 1.4 \times 10^{-3}$   $\text{F/m}^2$  and  $C'_{OL} = 5 \times 10^{-9}$   $\text{F/m}$  if  $W = 10$   $\mu\text{m}$  and  $L = 1$   $\mu\text{m}$  operating in (a) the triode region, (b) the saturation region, and (c) cutoff?
- 4.69. A large-power MOSFET has an effective gate area of  $60 \times 10^6$   $\mu\text{m}^2$ . What is the value of  $C_{GC}$  if  $T_{ox}$  is 100 nm?
- 4.70. (a) Find  $C_{GS}$  and  $C_{GD}$  for the transistor in Fig. 4.22 for the triode region if  $\Lambda = 0.5$   $\mu\text{m}$ ,  $T_{ox} = 150$  nm,

and  $C_{GSO} = C_{GDO} = 20 \text{ pF/m}$ . (b) Repeat for the saturation region. (c) Repeat for the cutoff region.

- 4.71. (a) Repeat Prob. 4.70 for a transistor similar to Fig. 4.22 but with  $W/L = 10/1$ . (b) With  $W/L = 100/1$ . Assume  $L = 1 \mu\text{m}$ .
- 4.72. Find  $C_{SB}$  and  $C_{DB}$  for the transistor in Fig. 4.22 if  $\Lambda = 0.5 \mu\text{m}$ , the substrate doping is  $10^{16}/\text{cm}^3$ , the source and drain doping is  $10^{20}/\text{cm}^3$ , and  $C_{JSW} = C_J \times (5 \times 10^{-4} / \text{cm})$ .

## 4.6 MOSFET Modeling in SPICE

- 4.73. What are the values of SPICE model parameters KP, LAMBDA, VTO, PHI, W, and L for a transistor with the following characteristics:  $V_{TN} = 0.7 \text{ V}$ ,  $K_n = 175 \mu\text{A/V}^2$ ,  $W = 5 \mu\text{m}$ ,  $L = 0.25 \mu\text{m}$ ,  $\lambda = 0.02 \text{ V}^{-1}$ , and  $2\phi_F = 0.8 \text{ V}$ ?
- 4.74. What are the values of SPICE model parameters KP, LAMBDA, VTO, W and L for the transistor in Fig. 4.7 if  $K'_n = 50 \mu\text{A/V}^2$  and  $L = 0.5 \mu\text{m}$ ?
- 4.75. What are the values of SPICE model parameters KP, LAMBDA, VTO, W and L for the transistor in Fig. 4.8 if  $K'_n = 10 \mu\text{A/V}^2$  and  $L = 0.6 \mu\text{m}$ ?
- 4.76. (a) What are the values of SPICE model parameters VTO, PHI, and GAMMA for the transistor in Fig. 4.13? (b) Repeat for the transistor in Prob. 4.45.
- 4.77. What are the values of SPICE model parameters KP, LAMBDA, VTO, W and L, for the transistor in Fig. 4.14 if  $K'_p = 10 \mu\text{A/V}^2$  and  $L = 0.5 \mu\text{m}$ ?
- 4.78. What are the values of SPICE model parameters KP, LAMBDA, VTO, W and L, for the transistor in Fig. 4.24(b) if  $K'_n = 25 \mu\text{A/V}^2$  and  $L = 0.6 \mu\text{m}$ ?

## 4.7 MOS Transistor Scaling

- 4.79. (a) A transistor has  $T_{ox} = 40 \text{ nm}$ ,  $V_{TN} = 1 \text{ V}$ ,  $\mu_n = 500 \text{ cm}^2/\text{V} \cdot \text{s}$ ,  $L = 2 \mu\text{m}$ , and  $W = 20 \mu\text{m}$ . What are  $K_n$  and the saturated value of  $i_D$  for this transistor if  $V_{GS} = 4 \text{ V}$ ? (b) The technology is scaled by a factor of 2. What are the new values of  $T_{ox}$ ,  $W$ ,  $L$ ,  $V_{TN}$ ,  $V_{GS}$ ,  $K_n$ , and  $i_D$ ?
- 4.80. (a) A transistor has an oxide thickness of 20 nm with  $L = 1 \mu\text{m}$  and  $W = 20 \mu\text{m}$ . What is  $C_{GC}$  for this transistor? (b) The technology is scaled by a factor of 2. What are the new values of  $T_{ox}$ ,  $W$ ,  $L$ , and  $C_{GC}$ ?
- 4.81. Show that the cutoff frequency of a PMOS device is given by  $f_T = \frac{1}{2\pi} \frac{\mu_p}{L^2} |V_{GS} - V_{TP}|$ .

- 4.82. (a) An NMOS device has  $\mu_n = 400 \text{ cm}^2/\text{V} \cdot \text{s}$ . What is the cutoff frequency for  $L = 1 \mu\text{m}$  if the transistor is biased at 1 V above threshold? What would be the cutoff frequency of a similar PMOS device if  $\mu_p = 0.4 \mu_n$ ? (b) Repeat for  $L = 0.1 \mu\text{m}$ .

- 4.83. An NMOS transistor has  $T_{ox} = 80 \text{ nm}$ ,  $\mu_n = 400 \text{ cm}^2/\text{V} \cdot \text{s}$ ,  $L = 0.1 \mu\text{m}$ ,  $W = 2 \mu\text{m}$ , and  $V_{GS} - V_{TN} = 2 \text{ V}$ . (a) What is the saturation region current predicted by Eq. (4.17)? (b) What is the saturation current predicted by Eq. (4.49) if we assume  $v_{SAT} = 10^7 \text{ cm/s}$ ?
- 4.84. The NMOS transistor in Fig. 4.19 is biased with  $V_{GS} = 0 \text{ V}$ . What is the drain current? (b) What is the drain current if the threshold voltage is reduced to 0.5 V?

## 4.8 MOS Transistor Fabrication and Layout Design Rules

- 4.85. Layout a transistor with  $W/L = 10/1$  similar to Fig. 4.22. What fraction of the total area does the channel represent?
- 4.86. Layout a transistor with  $W/L = 5/1$  similar to Fig. 4.22 using  $T = F = 2 \Lambda$ . What fraction of the total area does the channel represent?
- 4.87. Layout a transistor with  $W/L = 5/1$  similar to Fig. 4.22 but change the alignment so that masks 2, 3, and 4 are all aligned to mask 1. What fraction of the total area does the channel represent?
- 4.88. Layout a transistor with  $W/L = 5/1$  similar to Fig. 4.22 but change the alignment so that mask 3 is aligned to mask 1. What fraction of the total area does the channel represent?

## 4.9 Biasing the NMOS Field-Effect Transistor Load Line Analysis

- 4.89. Draw the load line for the circuit in Fig. P4.89 on the output characteristics in Fig. P4.18 and locate the Q-point. Assume  $V_{DD} = +4 \text{ V}$ . What is the operating region of the transistor?
- 4.90. Draw the load line for the circuit in Fig. P4.89 on the output characteristics in Fig. P4.18 and locate the Q-point. Assume  $V_{DD} = +5 \text{ V}$  and the resistor is changed to  $8.3 \text{ k}\Omega$ . What is the operating region of the transistor?
- 4.91. Draw the load line for the circuit in Fig. P4.91 on the output characteristics in Fig. P4.18 and locate the Q-point. Assume  $V_{DD} = +6 \text{ V}$ . What is the operating region of the transistor?

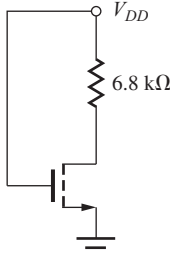


Figure P4.89

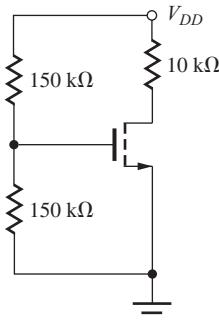


Figure P4.91

- 4.92. Draw the load line for the circuit in Fig. P4.91 on the output characteristics in Fig. P4.18 and locate the Q-point. Assume  $V_{DD} = +8$  V. What is the operating region of the transistor?

### Four-Resistor Biasing

- 4.93. (a) Find the Q-point for the transistor in Fig. P4.93 for  $R_1 = 100$  kΩ,  $R_2 = 220$  kΩ,  $R_3 = 24$  kΩ,  $R_4 = 12$  kΩ, and  $V_{DD} = 10$  V. Assume that  $V_{TO} = 1$  V,  $\gamma = 0$ , and  $W/L = 6/1$ . (b) Repeat for  $W/L = 12/1$ .

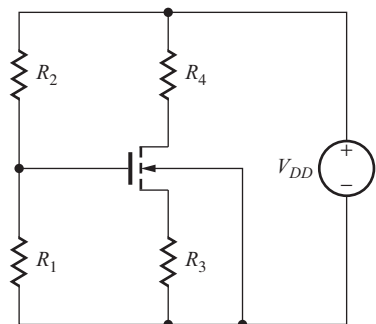


Figure P4.93

- 4.94. Repeat Prob. 4.93(a) if all resistor values are increased by a factor of 10.
- 4.95. Repeat Prob. 4.93(a) if all resistor values are reduced by a factor of 10 and  $W/L = 20/1$ . (b) Repeat for  $W/L = 60/1$ .
- 4.96. Repeat Prob. 4.93 with  $V_{DD} = 12$  V.
- 4.97. Find the Q-point for the transistor in Fig. P4.93 for  $R_1 = 200$  kΩ,  $R_2 = 430$  kΩ,  $R_3 = 47$  kΩ,  $R_4 = 24$  kΩ, and  $V_{DD} = 12$  V. Assume that  $V_{TO} = 1$  V,  $\gamma = 0$ , and  $W/L = 5/1$ . (b) Repeat for  $W/L = 15/1$ .
- 4.98. Use SPICE to simulate the circuit in Prob. 4.93 and compare the results to hand calculations.

4.99. Use SPICE to simulate the circuit in Prob. 4.96 and compare the results to hand calculations.

4.100. Use SPICE to simulate the circuit in Prob. 4.97 and compare the results to hand calculations.

4.101. The drain current in the circuit in Fig. 4.25 was found to be 50 μA. The gate bias circuit in the example could have been designed with many different choices for resistors  $R_1$  and  $R_2$ . Some possibilities for  $(R_1, R_2)$  are (3 kΩ, 7 kΩ), (12 kΩ, 28 kΩ), (300 kΩ, 700 kΩ), and (1.2 MΩ, 2.8 MΩ). Which of these choices would be the best and why?

\*4.102. Suppose the design of Ex. 4.4 is implemented with  $V_{EQ} = 4$  V,  $R_S = 1.7$  kΩ, and  $R_D = 38.3$  kΩ. (a) What would be the Q-point if  $K_n = 35$  μA/V<sup>2</sup>? (b) If  $K_n = 25$  μA/V<sup>2</sup> but  $V_{TN} = 0.75$  V?

4.103. (a) Simulate the circuit in Ex. 4.3 and compare the results to the calculations. (b) Repeat for the circuit design in Ex. 4.4.

4.104. Design a four-resistor bias network for an NMOS transistor to give a Q-point of (500 μA, 5 V) with  $V_{DD} = 15$  V and  $R_{EQ} \cong 600$  kΩ. Use the parameters from Table 4.6.

4.105. Design a four-resistor bias network for an NMOS transistor to give a Q-point of (250 μA, 3 V) with  $V_{DD} = 9$  V and  $R_{EQ} \cong 250$  kΩ. Use the parameters from Table 4.6.

4.106. Design a four-resistor bias network for an NMOS transistor to give a Q-point of (100 μA, 4 V) with  $V_{DD} = 12$  V and  $R_{EQ} \cong 250$  kΩ. Use the parameters from Table 4.6.

### Depletion-Mode Devices

4.107. What is the Q-point of the transistor in Fig. P4.93 if  $R_1 = 470$  kΩ,  $R_2 = \infty$ ,  $R_3 = 27$  kΩ,  $R_4 = 51$  kΩ, and  $V_{DD} = 12$  V for  $V_{TN} = -4$  V and  $K_n = 600$  μA/V<sup>2</sup>.

4.108. What is the Q-point of the transistor in Fig. P4.93 if  $R_1 = 1$  MΩ,  $R_2 = \infty$ ,  $R_3 = 10$  kΩ,  $R_4 = 5$  kΩ, and  $V_{DD} = 15$  V for  $V_{TN} = -5$  V and  $K_n = 1$  mA/V<sup>2</sup>.

\*4.109. Design a bias network for a depletion-mode NMOS transistor to give a Q-point of (2 mA, 5 V) with  $V_{DD} = 15$  V if  $V_{TN} = -2.5$  V and  $K_n = 250$  μA/V<sup>2</sup>. (Hint: You may wish to consider the four-resistor bias network.)

4.110. Design a bias network for a depletion-mode NMOS transistor to give a Q-point of (250 μA, 5 V) with  $V_{DD} = 15$  V if  $V_{TN} = -4$  V and  $K_n = 1$  mA/V<sup>2</sup>.

## Two-Resistor Biasing

The two-resistor bias circuit represents a simple alternative strategy for biasing the MOS transistor.

- 4.111. (a) Find the Q-point for the transistor in the circuit in Fig. P4.111(a) if  $V_{DD} = +12$  V. (b) Repeat for the circuit in Fig. P4.111(b).

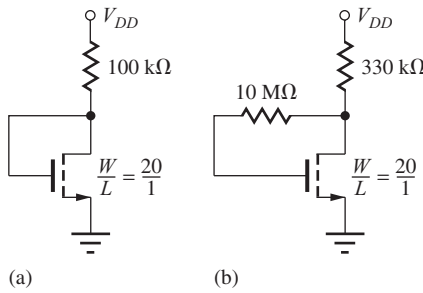


Figure P4.111

- 4.112. (a) Find the Q-point for the transistor in the circuit in Fig. P4.111(a) if  $V_{DD} = +12$  V and  $W/L$  is changed to 101? (b) Repeat for the circuit in Fig. P4.111(b).
- 4.113. (a) Find the Q-point for the transistor in the circuit in Fig. P4.111(b) if  $V_{DD} = +15$  V. (b) Repeat for  $V_{DD} = +15$  V with  $W/L$  is changed to 25/1?
- 4.114. (a) Find the Q-point for the transistor in the circuit in Fig. P4.111(b) if  $V_{DD} = +12$  V and the 330 kΩ resistor is increased to 470 kΩ. (b) Repeat if the 10 MΩ resistor is reduced to 2 MΩ.

## Body Effect

- 4.115. Find the solution to Eq. set (4.58) using MATLAB.  
■ (b) Repeat for  $\gamma = 0.75 \sqrt{V}$ .
- 4.116. Find the solution to Eq. set (4.58) using a spreadsheet if  $\gamma = 0.75 \sqrt{V}$ . (b) Repeat for  $\gamma = 1.25 \sqrt{V}$ .
- 4.117. Redesign the values of  $R_S$  and  $R_D$  in the circuit in Ex. 4.4 to compensate for the body effect and restore the Q-point to its original value (100 μA, 6 V).
- 4.118. Find the Q-point for the transistor in Fig. P4.93 for  $R_1 = 100$  kΩ,  $R_2 = 220$  kΩ,  $R_3 = 24$  kΩ,  $R_4 = 12$  kΩ, and  $V_{DD} = 12$  V. Assume that  $V_{TO} = 1$  V,  $\gamma = 0.6 \sqrt{V}$ , and  $W/L = 5/1$ .  
\*\*4.119. (a) Repeat Prob. 4.118 with  $\gamma = 0.75 \sqrt{V}$ . (b) Repeat Prob. 4.118 with  $R_4 = 24$  kΩ.
- 4.120. (a) Use SPICE to simulate the circuit in Prob. 4.118 and compare the results to hand calculations.

- (b) Repeat for Prob. 4.119(a). (c) Repeat for Prob. 4.119(b).

- 4.121. Simulate the circuit in Prob. 4.93 using (a)  $\gamma = 0$  and (b)  $\gamma = 0.5 \text{ V}^{-0.5}$  and  $2\phi_F = 0.6$  V and compare the results. Does our neglect of body effect in hand calculations appear to be justified?
- 4.122. Simulate the circuit in Prob. 4.94 using (a)  $\gamma = 0$  and (b)  $\gamma = 0.5 \text{ V}^{-0.5}$  and  $2\phi_F = 0.6$  V and compare the results. Does our neglect of body effect in hand calculations appear to be justified?
- 4.123. Simulate the circuit in Prob. 4.95 using (a)  $\gamma = 0$  and (b)  $\gamma = 0.5 \text{ V}^{-0.5}$  and  $2\phi_F = 0.6$  V and compare the results. Does our neglect of body effect in hand calculations appear to be justified?
- 4.124. Simulate the circuit in Prob. 4.96 using (a)  $\gamma = 0$  and (b)  $\gamma = 0.5 \text{ V}^{-0.5}$  and  $2\phi_F = 0.6$  V and compare the results. Does our neglect of body effect in hand calculations appear to be justified?

## General Bias Problems

- 4.125. (a) Find the current  $I$  in Fig. P4.125 if  $V_{DD} = 5$  V assuming that  $\gamma = 0$ ,  $V_{TO} = 1$  V, and the transistors both have  $W/L = 20/1$ . (b) Repeat for  $V_{DD} = 10$  V.  
\*(c) Repeat part (a) with  $\gamma = 0.5 \sqrt{V}$ .

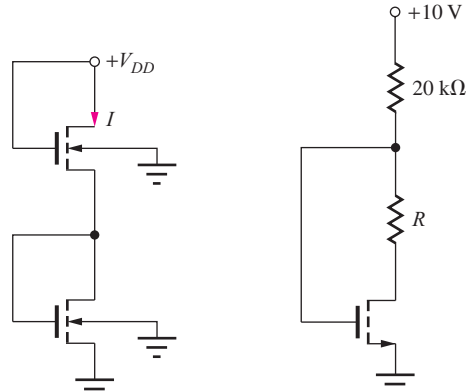


Figure P4.125

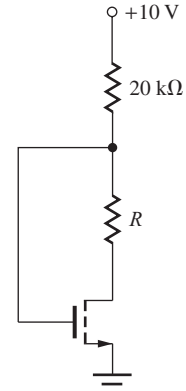


Figure P4.127

- 4.126. Find the Q-point for the transistor in Fig. P4.127 if  $R = 10$  kΩ,  $V_{TO} = 1$  V, and  $W/L = 4/1$ .
- 4.127. Find the Q-point for the transistor in Fig. P4.127 if  $R = 20$  kΩ,  $V_{TO} = 1$  V, and  $W/L = 2/1$ .
- 4.128. (a) Find the current  $I$  in Fig. P4.128 assuming that  $\gamma = 0$  and  $W/L = 20/1$  for each transistor. (b) Repeat part (a) for  $W/L = 50/1$ . \*(c) Repeat part (a) with  $\gamma = 0.5 \sqrt{V}$ .
- 4.129. (a) Simulate the circuit in Fig. P4.128 using SPICE and compare the results to those of Prob. 4.128(a).

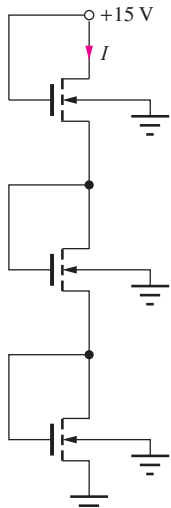


Figure P4.128

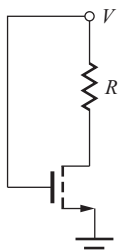


Figure P4.130

(b) Repeat for Prob. 4.128(b). \*\*(c) Repeat for Prob. 4.128(c).

- 4.130. What value of  $W/L$  is required to set  $V_{DS} = 0.50$  V in the circuit in Fig. P4.130 if  $V = 5$  V and  $R = 68$  k $\Omega$ ?  
 4.131. What value of  $W/L$  is required to set  $V_{DS} = 0.25$  V in the circuit in Fig. P4.130 if  $V = 3.3$  V and  $R = 160$  k $\Omega$ ?

#### 4.10 Biasing the PMOS Field-Effect Transistor

- 4.132. (a) Find the Q-point for the transistor in Fig. P4.132(a) if  $V_{DD} = -15$  V,  $R = 75$  k $\Omega$ , and  $W/L = 1/1$ . (b) Find the Q-point for the transistor in Fig. P4.132(b) if  $V_{DD} = -15$  V,  $R = 75$  k $\Omega$ , and  $W/L = 1/1$ .

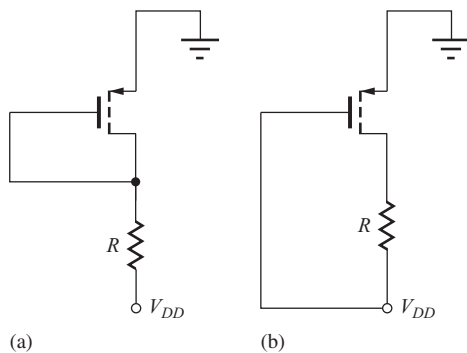


Figure P4.132

- 4.133. Simulate the circuits in Prob. 4.132 with  $V_{DD} = -15$  V and compare the Q-point results to hand calculations.

- \*4.134. (a) Find current  $I$  and voltage  $V_o$  in Fig. P4.134(a) if  $W/L = 20/1$  for both transistors and  $V_{DD} = 10$  V. (b) What is the current if  $W/L = 80/1$ ? (c) Repeat for the circuit in Fig. P4.134(b).

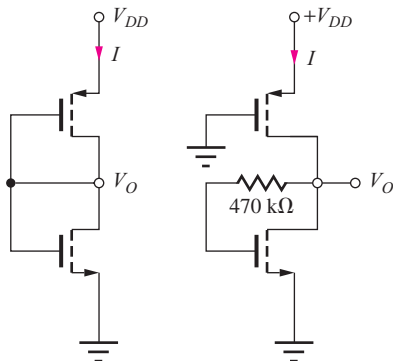


Figure P4.134

- 4.135. (a) Find the current  $I$  in Fig. P4.135 assuming that  $\gamma = 0$  and  $W/L = 40/1$  for each transistor. (b) Repeat part (a) for  $W/L = 75/1$ . \*\*(c) Repeat part (a) with  $\gamma = 0.5\sqrt{V}$ .

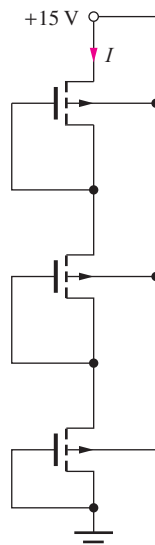


Figure P4.135

- \*4.136. (a) Simulate the circuit in Prob. 4.135(a) and compare the results to those of Prob. 4.135(a). (b) Repeat for Prob. 4.135(b). (c) Repeat for Prob. 4.135(c).

- 4.137. Draw the load line for the circuit in Fig. P4.137 on the output characteristics in Fig. P4.49 and locate the Q-point. What is the operating region of the transistor?

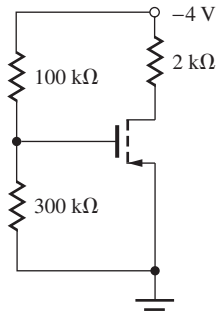


Figure P4.137

- 4.138. (a) Find the Q-point for the transistor in Fig. P4.138 if  $R = 50 \text{ k}\Omega$ . Assume that  $\gamma = 0$  and  $W/L = 20/1$ . (b) What is the permissible range of values for  $R$  if the transistor is to remain in the saturation region?

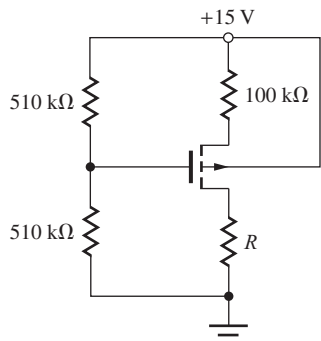


Figure P4.138

- 4.139. Simulate the circuit of Prob. 4.138(a) and find the Q-point. Compare the results to hand calculations.

- \*4.140. (a) Find the Q-point for the transistor in Fig. P4.138 if  $R = 43 \text{ k}\Omega$ . Assume that  $\gamma = 0.5 \sqrt{V}$  and  $W/L = 20/1$ . (b) What is the permissible range of values for  $R$  if the transistor is to remain in the saturation region?

- 4.141. Simulate the circuit of Prob. 4.140(a) and find the Q-point. Compare the results to hand calculations.

- 4.142. (a) Find the Q-point for the transistor in Fig. P4.142 if  $V_{DD} = 14 \text{ V}$ ,  $R = 100 \text{ k}\Omega$ ,  $W/L = 10/1$ , and  $\gamma = 0$ . (b) Repeat for  $\gamma = 1 \sqrt{V}$ .

- 4.143. Find the Q-point current for the transistor in Fig. P4.138 if all resistors are reduced by a factor of 2. Assume saturation region operation. What value of  $R$  is needed to set  $V_{DS} = -5 \text{ V}$ . Assume that  $\gamma = 0$  and  $W/L = 40/1$ .

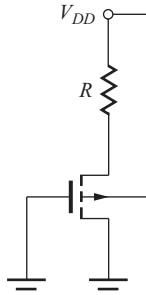


Figure P4.142

- 4.144. Repeat Prob. 4.143 if  $\gamma = 0.5 \sqrt{V}$  and  $W/L = 40/1$ .
- 4.145. (a) Find the Q-point current for the transistor in Fig. P4.138 if the upper 510-kΩ resistor is changed to 270 kΩ. Assume that the transistor is saturated,  $\gamma = 0$ , and  $W/L = 20/1$ . (b) What is the permissible range of values for  $R$  if the transistor is to remain in the saturation region?
- 4.146. Repeat Prob. 4.145 if  $\gamma = 0.5 \sqrt{V}$ .
- 4.147. (a) Design a four-resistor bias network for a PMOS transistor to give a Q-point of  $(500 \mu\text{A}, -3 \text{ V})$  with  $V_{DD} = -9 \text{ V}$  and  $R_{EQ} \geq 1 \text{ M}\Omega$ . Use the parameters from Table 4.6. (b) Repeat for an NMOS transistor with  $V_{DS} = +3 \text{ V}$  and  $V_{DD} = +9 \text{ V}$ .
- 4.148. (a) Design a four-resistor bias network for a PMOS transistor to give a Q-point of  $(1 \text{ mA}, -5 \text{ V})$  with  $V_{DD} = -15 \text{ V}$  and  $R_{EQ} \geq 100 \text{ k}\Omega$ . Use the parameters from Table 4.6. (b) Repeat for an NMOS transistor with  $V_{DS} = +6 \text{ V}$  and  $V_{DD} = +15 \text{ V}$ .
- 4.149. Find the Q-point for the transistor in Fig. P4.149 if  $V_{TO} = +4 \text{ V}$ ,  $\gamma = 0$ , and  $W/L = 10/1$ .

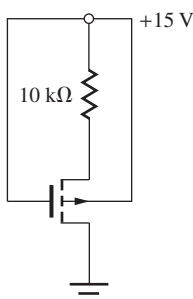


Figure P4.149

- 4.150. Find the Q-point for the transistor in Fig. P4.149 if  $V_{TO} = +4 \text{ V}$ ,  $\gamma = 0.25 \sqrt{V}$ , and  $W/L = 10/1$ .

- 4.151. Find the Q-point for the transistor in Fig. P4.151 if  $V_{TO} = -1$  V and  $W/L = 10/1$ .

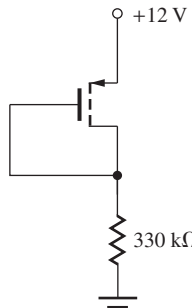


Figure P4.151

- 4.152. Find the Q-point for the transistor in Fig. P4.151 if  $V_{TO} = -3$  V and  $W/L = 30/1$ .  
 4.153. What is the Q-point for each transistor in Fig. P4.153?

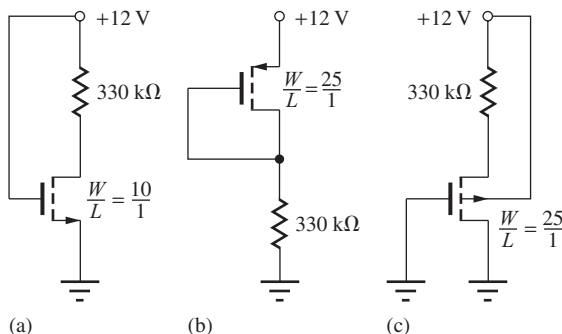


Figure P4.153

#### 4.11 The Junction Field-Effect Transistor (JFET)

- 4.154. The JFET in Fig. P4.154 has  $I_{DSS} = 500 \mu\text{A}$  and  $V_P = -3$  V. Find the Q-point for the JFET for (a)  $R = 0$  and  $V = 5$  V (b)  $R = 0$  and  $V = 0.25$  V, and (c)  $R = 8.2 \text{ k}\Omega$  and  $V = 5$  V.  
 4.155. Find the Q-point for the JFET in Fig. P4.155 if  $I_{DSS} = 5 \text{ mA}$  and  $V_P = -5$  V.  
 4.156. Find the on-resistance of the JFET in Fig. P4.156 if  $I_{DSS} = 1 \text{ mA}$  and  $V_P = -5$  V. Repeat for  $I_{DSS} = 100 \mu\text{A}$  and  $V_P = -2$  V.

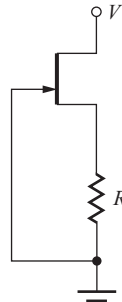


Figure 4.154

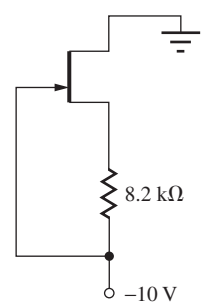


Figure 4.155

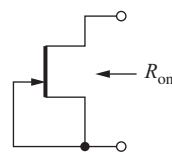


Figure 4.156

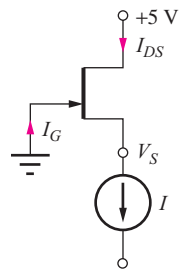


Figure 4.157

- 4.157. The JFET in Fig. P4.157 has  $I_{DSS} = 1 \text{ mA}$  and  $V_P = -4$  V. Find  $I_D$ ,  $I_G$ , and  $V_S$  for the JFET if (a)  $I = 0.5 \text{ mA}$  and (b)  $I = 2 \text{ mA}$ .  
 \*4.158. The JFETs in Fig. P4.158 have  $I_{DSS1} = 200 \mu\text{A}$ ,  $V_{P1} = -2$  V,  $I_{DSS2} = 500 \mu\text{A}$ , and  $V_{P2} = -4$  V. (a) Find the Q-point for the two JFETs if  $V = 9$  V. (b) What is the minimum value of  $V$  that will ensure that both  $J_1$  and  $J_2$  are in pinch-off?  
 \*4.159. The JFETs in Fig. P4.159 have  $I_{DSS} = 200 \mu\text{A}$  and  $V_P = +2$  V. (a) Find the Q-point for the two JFETs if  $R = 10 \text{ k}\Omega$  and  $V = 15$  V. (b) What is the minimum value of  $V$  that will ensure that both  $J_1$  and  $J_2$  are in pinch-off if  $R = 10 \text{ k}\Omega$ ?

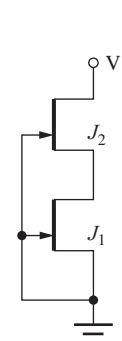


Figure 4.158

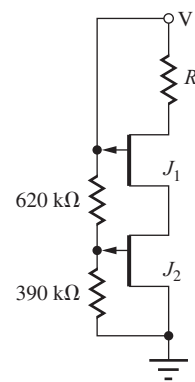
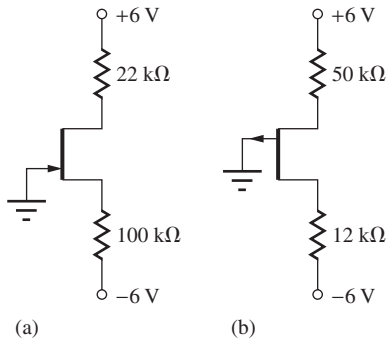


Figure 4.159

- 4.160. (a) The JFET in Fig. P4.160(a) has  $I_{DSS} = 250 \mu\text{A}$  and  $V_P = -2 \text{ V}$ . Find the Q-point for the JFET.  
 (b) The JFET in Fig. P4.160(b) has  $I_{DSS} = 250 \mu\text{A}$  and  $V_P = +2 \text{ V}$ . Find the Q-point for the JFET.

4.161. Simulate the circuit in Prob. 4.160(a) and compare the results to hand calculations. (b) Repeat for Prob. 4.160(b).



**Figure 4.160**

- 4.162. The JFET in Fig. P4.161 has  $I_{DSS} = 250 \mu\text{A}$  and  $V_P = -2 \text{ V}$ . Find the Q-point for JFET for (a)  $R = 100 \text{ k}\Omega$  and (b)  $R = 10 \text{ k}\Omega$ .

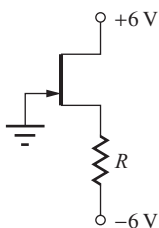


Figure 4.161

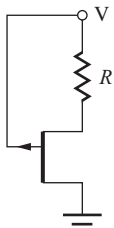


Figure 4.162

- 4.163. The JFET in Fig. P4.162 has  $I_{DSS} = 500 \mu\text{A}$  and  $V_P = +3 \text{ V}$ . Find the Q-point for JFET for (a)  $R = 0$  (b)  $R = 10 \text{ k}\Omega$ , and (c)  $R = 100 \text{ k}\Omega$ .

4.164. Simulate the circuit in Prob. 4.158(a) and compare the results to hand calculations.

4.165. Simulate the circuit in Prob. 4.159(a) and compare the results to hand calculations.

4.166. Use SPICE to plot the  $i-v$  characteristic for the circuit in Fig. P4.158 for  $0 \leq V \leq 15 \text{ V}$  if the JFETs have  $I_{DSS1} = 200 \mu\text{A}$ ,  $V_{P1} = -2 \text{ V}$ ,  $I_{DSS2} = 500 \mu\text{A}$ , and  $V_{P2} = -4 \text{ V}$ .

- 4.167 The circuit in Fig. P4.167 is a voltage regulator utilizing an ideal op amp. (a) Find the output voltage of the circuit if the Zener diode voltage is 5 V. (b) What are the current in the Zener diode and the drain current in the NMOS transistor? (c) What is the op amp output voltage if the MOSFET has  $V_{TN} = 1.25$  V and  $K_n = 150 \text{ mA/V}^2$ ?

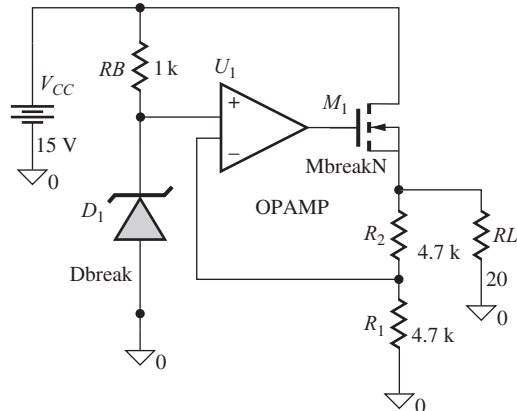


**Figure 4.167**

- 4.168 The circuit in Fig. P4.168 is a current regulator utilizing an ideal op amp. (a) Find the current in the Zener diode and the drain current in the NMOS transistor if the Zener voltage is 6.8 V. (b) What is the op amp output voltage if the MOSFET has  $V_{TN} = 1.25$  V and  $K_n = 75$  mA/V<sup>2</sup>?

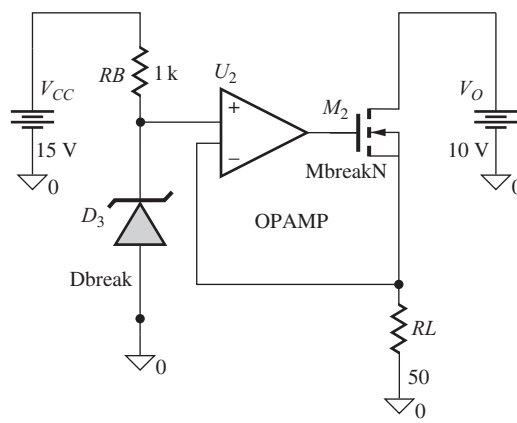


**Figure 4.168**

- 4.169 The circuit in Fig. P4.169 is a voltage regulator utilizing an ideal op amp. (a) Find the output voltage of the circuit if the Zener diode voltage is 5 V. (b) What are the current in the Zener diode and the drain current in the PMOS transistor? (c) What is the op amp output voltage if the MOSFET has  $V_{TP} = -1.5$  V and  $K_n = 50 \text{ mA/V}^2$ ?

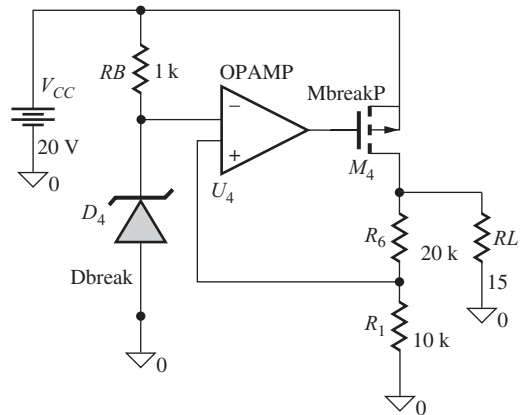
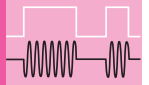


Figure 4.169

# CHAPTER 5



## BIPOLAR JUNCTION TRANSISTORS

### CHAPTER OUTLINE

- 5.1 Physical Structure of the Bipolar Transistor 218
- 5.2 The Transport Model for the *npn* Transistor 219
- 5.3 The *pnp* Transistor 225
- 5.4 Equivalent Circuit Representations for the Transport Models 227
- 5.5 The *i-v* Characteristics of the Bipolar Transistor 228
- 5.6 The Operating Regions of the Bipolar Transistor 230
- 5.7 Transport Model Simplifications 231
- 5.8 Nonideal Behavior of the Bipolar Transistor 245
- 5.9 Transconductance 252
- 5.10 Bipolar Technology and SPICE Model 253
- 5.11 Practical Bias Circuits for the BJT 256
- 5.12 Tolerances in Bias Circuits 266
  - Summary 272
  - Key Terms 274
  - References 274
  - Problems 275

### CHAPTER GOALS

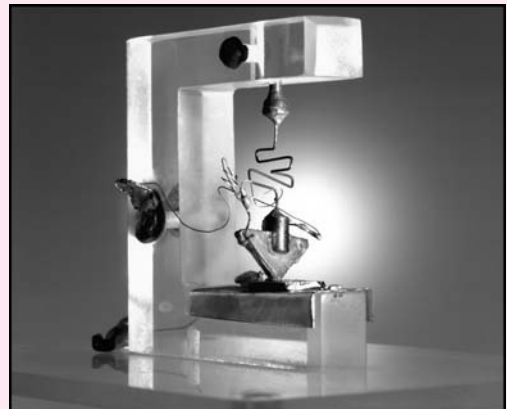
- Explore the physical structure of the bipolar transistor
- Understand bipolar transistor action and the importance of carrier transport across the base region
- Study the terminal characteristics of the BJT
- Explore the differences between *npn* and *pnp* transistors
- Develop the Transport model for the bipolar device
- Define the four regions of operation of the BJT
- Explore model simplifications for each region of operation
- Understand the origin and modeling of the Early effect
- Present the SPICE model for the bipolar transistor
- Provide examples of worst-case and Monte Carlo analysis of bias circuits

November 2007 was the 60th anniversary of the discovery of the bipolar transistor by John Bardeen and Walter Brattain at Bell Laboratories. In a matter of a few months, William Shockley managed to develop a theory describing the operation of the bipolar junction transistor. Only a few years later in 1956, Bardeen, Brattain, and Shockley received the Nobel Prize in Physics for the discovery of the transistor.



John Bardeen, William Shockley, and Walter Brattain in Brattain's Laboratory in 1948.

*Reprinted with permission of Alacatel-Lucent USA Inc.*



The first germanium bipolar transistor

*Reprinted with permission of Alacatel-Lucent USA Inc.*

In June 1948, Bell Laboratories held a major press conference to announce the discovery (which of course went essentially unnoticed by the public). Later in 1952, Bell Laboratories, operating under legal consent decrees, made licenses for the transistor available for the modest fee of \$25,000 plus future royalty payments. About this time, Gordon Teal, another member of the solid-state group, left Bell Laboratories to work on the transistor at Geophysical Services Inc., which subsequently became Texas Instruments (TI). There he made the first silicon transistors, and

TI marketed the first all transistor radio. Another of the early licensees of the transistor was Tokyo Tsushin Kogyo which became the Sony Company in 1955. Sony subsequently sold a transistor radio with a marketing strategy based upon the

idea that everyone could now have their own personal radio; thus was launched the consumer market for transistors. A very interesting account of these and other developments can be found in [1, 2] and their references.

**F**ollowing its invention and demonstration in the late 1940s by Bardeen, Brattain, and Shockley at Bell Laboratories, the **bipolar junction transistor**, or **BJT**, became the first commercially successful three-terminal solid-state device. Its commercial success was based on its structure. In the structure of the BJT, the active base region of the transistor is below the surface of the semiconductor material, making it much less dependent on surface properties and cleanliness. Thus, it was initially easier to manufacture BJTs than MOS transistors, and commercial bipolar transistors were available in the late 1950s. The first integrated circuits, resistor-transistor logic gates, and operational amplifiers consisting of a few transistors and resistors appeared in the early 1960s.

While the FET has become the dominant device technology in modern integrated circuits, bipolar transistors are still widely used in both discrete and integrated circuit design. In particular, the BJT is still the preferred device in many applications that require high speed and/or high precision. Typical of these application areas are circuits for the growing families of wireless computing and communication products, and silicon-germanium (SiGe) BJTs offer the highest operating frequencies of any silicon transistor.

The bipolar transistor is composed of a sandwich of three doped semiconductor regions and comes in two forms: the *npn* transistor and the *pnp* transistor. Performance of the bipolar transistor is dominated by *minority-carrier* transport via diffusion and drift in the central region of the transistor. Because carrier mobility and diffusivity are higher for electrons than holes, the *npn* transistor is an inherently higher-performance device than the *pnp* transistor. In Part III of this book, we will learn that the bipolar transistor typically offers a much higher voltage gain capability than the FET. On the other hand, the BJT input resistance is much lower, because a current must be supplied to the control electrode.

Our study of the BJT begins with a discussion of the *npn* transistor, followed by a discussion of the *pnp* device. The **transport model**, a simplified version of the Gummel-Poon model, is developed and used as our mathematical model for the behavior of the BJT. Four regions of operation of the BJT are defined and simplified models developed for each region. Examples of circuits that can be used to bias the bipolar transistor are presented. The chapter closes with a discussion of the worst-case and Monte Carlo analyses of the effects of tolerances on bias circuits.

## 5.1 PHYSICAL STRUCTURE OF THE BIPOLAR TRANSISTOR

The bipolar transistor structure consists of three alternating layers of *n*- and *p*-type semiconductor material. These layers are referred to as the **emitter (E)**, **base (B)**, and **collector (C)** of the transistor. Either an *npn* or a *pnp* transistor can be fabricated. The behavior of the device can be seen from the simplified cross section of the *npn* transistor in Fig. 5.1(a). During normal operation, a majority of the current enters the collector terminal, crosses the base region, and exits from the emitter terminal. A small current also enters the base terminal, crosses the base-emitter junction of the transistor, and exits the emitter.

The most important part of the bipolar transistor is the active base region between the dashed lines directly beneath the heavily doped (*n*+) emitter. Carrier transport in this region dominates the *i-v* characteristics of the BJT. Figure 5.1(b) illustrates the rather complex physical structure actually used to realize an *npn* transistor in integrated circuit form. Most of the structure in Fig. 5.1(b) is required to fabricate the external contacts to the collector, base, and emitter regions and to isolate one bipolar transistor from another. In the *npn* structure shown, collector current  $i_C$  and base current  $i_B$  enter the

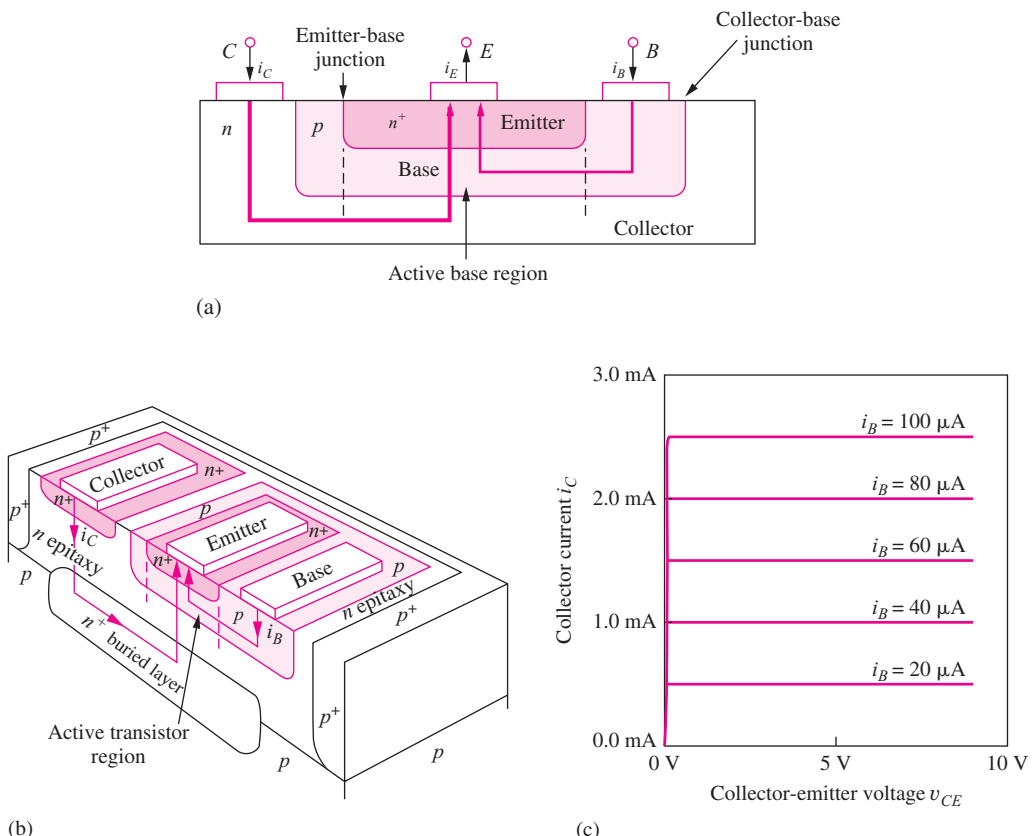


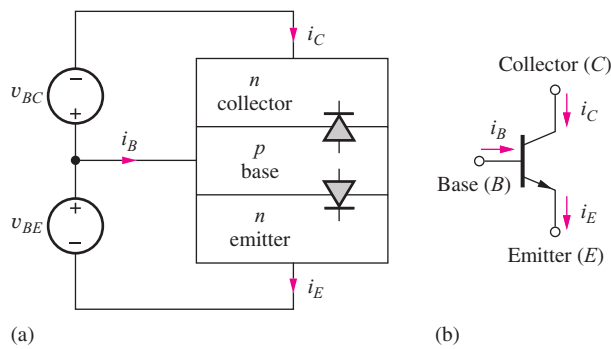
**Figure 5.1** (a) Simplified cross section of an *n**p**n* transistor with currents that occur during “normal” operation. (b) Three-dimensional view of an integrated *n**p**n* bipolar junction transistor. (c) Output characteristics of an *n**p**n* transistor.

collector (*C*) and base (*B*) terminals of the transistor, and emitter current  $i_E$  exits from the emitter (*E*) terminal. An example of the **output characteristics** of the bipolar transistor appears in Fig. 5.1(c), which plots collector current  $i_C$  versus collector-emitter voltage  $v_{CE}$  with base current as a parameter. The characteristics exhibit an appearance very similar to the output characteristics of the field-effect transistor. We find that a primary difference, however, is that a significant current must be supplied to the base of the device, whereas the dc gate current of the FET is zero. In the sections that follow, a mathematical model is developed for these *i-v* characteristics for both *n**p**n* and *p**n**p* transistors.

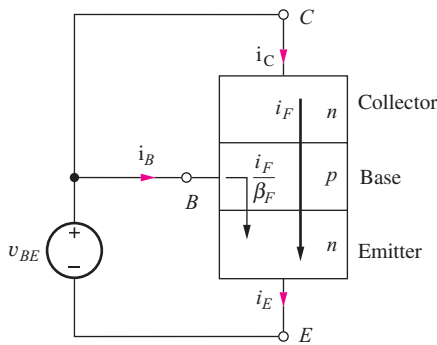
## 5.2 THE TRANSPORT MODEL FOR THE *n**p**n* TRANSISTOR

Figure 5.2 is a conceptual model for the active region of the *n**p**n* bipolar junction transistor structure. At first glance, the BJT appears to simply be two *pn* junctions connected back to back. However, the central region (the base) is very thin (0.1 to 100  $\mu$ m), and the close proximity of the two junctions leads to coupling between the two diodes. This coupling is the essence of the bipolar device. The lower *n*-type region (the emitter) injects electrons into the *p*-type base region of the device. Almost all these injected electrons travel across the narrow base region and are removed (or collected) by the upper *n*-type region (the collector).

The three terminal currents are the **collector current**  $i_C$ , the **emitter current**  $i_E$ , and the **base current**  $i_B$ . The base-emitter voltage  $v_{BE}$  and the base-collector voltage  $v_{BC}$  applied to the two *pn* junctions in Fig. 5.2 determine the magnitude of these three currents in the bipolar transistor and



**Figure 5.2** (a) Idealized npn transistor structure for a general-bias condition. (b) Circuit symbol for the npn transistor.



**Figure 5.3** npn transistor with \$v\_{BE}\$ applied and \$v\_{BC} = 0\$.

**TABLE 5.1**  
Common-Emitter and Common-Base  
Current Gain Comparison

\$\alpha_F\$ or \$\alpha_R\$	\$\beta_F = \frac{\alpha_F}{1 - \alpha_F}\$ or \$\beta_R = \frac{\alpha_R}{1 - \alpha_R}\$
0.1	0.11
0.5	1
0.9	9
0.95	19
0.99	99
0.998	499

are defined as positive when they forward-bias their respective *pn* junctions. The arrows indicate the directions of positive current in most *npn* circuit applications. The circuit symbol for the *npn* transistor appears in Fig. 5.2(b). The arrow part of the symbol identifies the emitter terminal and indicates that dc current normally exits the emitter of the *npn* transistor.

### 5.2.1 FORWARD CHARACTERISTICS

To facilitate both hand and computer analysis, we need to construct a mathematical model that closely matches the behavior of the transistor, and equations that describe the static *i-v* characteristics of the device can be constructed by summing currents within the transistor structure.<sup>1</sup> In Fig. 5.3, an arbitrary voltage \$v\_{BE}\$ is applied to the base-emitter junction, and the voltage applied to the base-collector junction is set to zero. The base-emitter voltage establishes emitter current \$i\_E\$, which equals the total current crossing the base-emitter junction. This current is composed of two components. The largest portion, the **forward-transport current** \$i\_F\$, enters the collector, travels completely across the very narrow base region, and exits the emitter terminal. The collector current \$i\_C\$ is equal to \$i\_F\$, which has the form of an ideal diode current

$$i_C = i_F = I_S \left[ \exp \left( \frac{v_{BE}}{V_T} \right) - 1 \right] \quad (5.1)$$

<sup>1</sup> The differential equations that describe the internal physics of the BJT are linear second-order differential equations. These equations are linear in terms of the hole and electron concentrations; the currents are directly related to these carrier concentrations. Thus, superposition can be used with respect to the currents flowing in the device.

The parameter  $I_S$  is the **transistor saturation current**—that is, the saturation current of the bipolar transistor.  $I_S$  is proportional to the cross-sectional area of the active base region of the transistor, and can have a wide range of values:

$$10^{-18} \text{ A} \leq I_S \leq 10^{-9} \text{ A}$$

In Eq. (5.1),  $V_T$  should be recognized as the thermal voltage introduced in Chapter 2 and given by  $V_T = kT/q = 0.025 \text{ V}$  at room temperature.

In addition to  $i_F$ , a second, much smaller component of current crosses the base-emitter junction. This current forms the base current  $i_B$  of the transistor, and it is directly proportional to  $i_F$ :

$$i_B = \frac{i_F}{\beta_F} = \frac{I_S}{\beta_F} \left[ \exp \left( \frac{v_{BE}}{V_T} \right) - 1 \right] \quad (5.2)$$

Parameter  $\beta_F$  is called the **forward (or normal)<sup>2</sup> common-emitter current gain**. Its value typically falls in the range

$$10 \leq \beta_F \leq 500$$

Emitter current  $i_E$  can be calculated by treating the transistor as a super node for which

$$i_C + i_B = i_E \quad (5.3)$$

Adding Eqs. (5.1) and (5.2) together yields

$$i_E = \left( I_S + \frac{I_S}{\beta_F} \right) \left[ \exp \left( \frac{v_{BE}}{V_T} \right) - 1 \right] \quad (5.4)$$

which can be rewritten as

$$i_E = I_S \left( \frac{\beta_F + 1}{\beta_F} \right) \left[ \exp \left( \frac{v_{BE}}{V_T} \right) - 1 \right] = \frac{I_S}{\alpha_F} \left[ \exp \left( \frac{v_{BE}}{V_T} \right) - 1 \right] \quad (5.5)$$

The parameter  $\alpha_F$  is called the **forward (or normal)<sup>3</sup> common-base current gain**, and its value typically falls in the range

$$0.95 \leq \alpha_F < 1.0$$

The parameters  $\alpha_F$  and  $\beta_F$  are related by

$$\alpha_F = \frac{\beta_F}{\beta_F + 1} \quad \text{or} \quad \beta_F = \frac{\alpha_F}{1 - \alpha_F} \quad (5.6)$$

Equations (5.1), (5.2), and (5.5) express the fundamental physics-based characteristics of the bipolar transistor. The three terminal currents are all exponentially dependent on the base-emitter voltage of the transistor. This is a much stronger nonlinear dependence than the square-law behavior of the FET.

For the bias conditions in Fig. 5.3, the transistor is actually operating in a region of high current gain, called the **forward-active region<sup>4</sup>** of operation, which is discussed more fully in Sec. 5.9. Three extremely useful auxiliary relationships are valid in the forward-active region. The first two

<sup>2</sup>  $\beta_N$  is sometimes used to represent the normal common-emitter current gain.

<sup>3</sup>  $\alpha_N$  is sometimes used to represent the normal common-base current gain.

<sup>4</sup> Four regions of operation are fully defined in Sec. 5.6.

can be found from the ratio of the collector and base current in Eqs. (5.1) and (5.2):

$$\frac{i_C}{i_B} = \beta_F \quad \text{or} \quad i_C = \beta_F i_B \quad \text{and} \quad i_E = (\beta_F + 1)i_B \quad (5.7)$$

using Eq. (5.3). The third relationship is found from the ratio of the collector and emitter currents in Eqs. (5.1) and (5.5):

$$\frac{i_C}{i_E} = \alpha_F \quad \text{or} \quad i_C = \alpha_F i_E \quad (5.8)$$

Equation (5.7) expresses important and useful properties of the bipolar transistor: The transistor “amplifies” (magnifies) its base current by the factor  $\beta_F$ . Because the current gain  $\beta_F \gg 1$ , injection of a small current into the base of the transistor produces a much larger current in both the collector and the emitter terminals. Equation (5.8) indicates that the collector and emitter currents are almost identical, because  $\alpha_F \cong 1$ .

### 5.2.2 REVERSE CHARACTERISTICS

Now consider the transistor in Fig. 5.4, in which voltage  $v_{BC}$  is applied to the base-collector junction, and the base-emitter junction is zero-biased. The base-collector voltage establishes the collector current  $i_C$ , now crossing the base-collector junction. The largest portion of the collector current, the reverse-transport current  $i_R$ , enters the emitter, travels completely across the narrow base region, and exits the collector terminal. Current  $i_R$  has a form identical to  $i_F$ :

$$i_R = I_S \left[ \exp \left( \frac{v_{BC}}{V_T} \right) - 1 \right] \quad \text{and} \quad i_E = -i_R \quad (5.9)$$

except the controlling voltage is now  $v_{BC}$ .

In this case, a fraction of the current  $i_R$  must also be supplied as base current through the base terminal:

$$i_B = \frac{i_R}{\beta_R} = \frac{I_S}{\beta_R} \left[ \exp \left( \frac{v_{BC}}{V_T} \right) - 1 \right] \quad (5.10)$$

Parameter  $\beta_R$  is called the **reverse (or inverse)<sup>5</sup> common-emitter current gain**.

In Chapter 4, we discovered that the FET was an inherently symmetric device. For the bipolar transistor, Eqs. (5.1) and (5.9) show the symmetry that is inherent in the current that traverses the base region of the bipolar transistor. However, the impurity doping levels of the emitter and collector regions of the BJT structure are quite asymmetric, and this fact causes the base currents in the

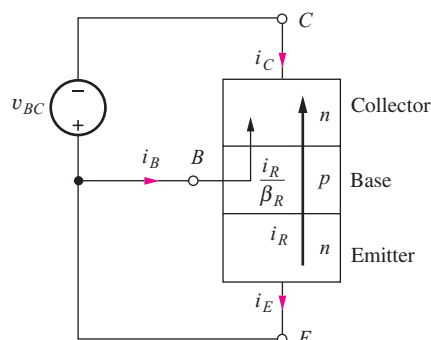


**Figure 5.4** Transistor with  $v_{BC}$  applied and  $v_{BE} = 0$ .

<sup>5</sup>  $\beta_I$  is sometimes used to represent the inverse common-emitter current gain.

forward and reverse modes to be significantly different. For typical BJTs,  $0 < \beta_R \leq 10$  whereas  $10 \leq \beta_F \leq 500$ .

The collector current in Fig. 5.4 can be found by combining the base and emitter currents, as was done to obtain Eq. (5.5):

$$i_C = -\frac{I_S}{\alpha_R} \left[ \exp \left( \frac{v_{BC}}{V_T} \right) - 1 \right] \quad (5.11)$$

in which the parameter  $\alpha_R$  is called the **reverse (or inverse)<sup>6</sup> common-base current gain**:

$$\alpha_R = \frac{\beta_R}{\beta_R + 1} \quad \text{or} \quad \beta_R = \frac{\alpha_R}{1 - \alpha_R} \quad (5.12)$$

Typical values of  $\alpha_R$  fall in the range

$$0 < \alpha_R \leq 0.95$$

Values of the common-base current gain  $\alpha$  and the common-emitter current gain  $\beta$  are compared in Table 5.1 on page 220. Because  $\alpha_F$  is typically greater than 0.95,  $\beta_F$  can be quite large. Values ranging from 10 to 500 are quite common for  $\beta_F$ , although it is possible to fabricate special-purpose transistors<sup>7</sup> with  $\beta_F$  as high as 5000. In contrast,  $\alpha_R$  is typically less than 0.5, which results in values of  $\beta_R$  of less than 1.

**EXERCISE:** (a) What values of  $\beta$  correspond to  $\alpha = 0.970, 0.993, 0.250$ ? (b) What values of  $\alpha$  correspond to  $\beta = 40, 200, 3$ ?

**ANSWERS:** (a) 32.3; 142; 0.333 (b) 0.976; 0.995; 0.750

### 5.2.3 THE COMPLETE TRANSPORT MODEL EQUATIONS FOR ARBITRARY BIAS CONDITIONS

Combining the expressions for the two collector, emitter, and base currents from Eqs. (5.1) and (5.11), (5.4) and (5.9), and (5.2) and (5.10) yields expressions for the total collector, emitter, and base currents for the *npn* transistor that are valid for the completely general-bias voltage situation in Fig. 5.2:

$$\begin{aligned} i_C &= I_S \left[ \exp \left( \frac{v_{BE}}{V_T} \right) - \exp \left( \frac{v_{BC}}{V_T} \right) \right] - \frac{I_S}{\beta_R} \left[ \exp \left( \frac{v_{BC}}{V_T} \right) - 1 \right] \\ i_E &= I_S \left[ \exp \left( \frac{v_{BE}}{V_T} \right) - \exp \left( \frac{v_{BC}}{V_T} \right) \right] + \frac{I_S}{\beta_F} \left[ \exp \left( \frac{v_{BE}}{V_T} \right) - 1 \right] \\ i_B &= \frac{I_S}{\beta_F} \left[ \exp \left( \frac{v_{BE}}{V_T} \right) - 1 \right] + \frac{I_S}{\beta_R} \left[ \exp \left( \frac{v_{BC}}{V_T} \right) - 1 \right] \end{aligned} \quad (5.13)$$

From this equation set, we see that three parameters are required to characterize an individual BJT:  $I_S$ ,  $\beta_F$ , and  $\beta_R$ . (Remember that temperature is also an important parameter because  $V_T = kT/q$ .)

The first term in both the emitter and collector current expressions in Eqs. (5.13) is

$$i_T = I_S \left[ \exp \left( \frac{v_{BE}}{V_T} \right) - \exp \left( \frac{v_{BC}}{V_T} \right) \right] \quad (5.14)$$

which represents the current being transported completely across the base region of the transistor. Equation (5.14) demonstrates the symmetry that exists between the base-emitter and base-collector voltages in establishing the dominant current in the bipolar transistor.

<sup>6</sup>  $\alpha_I$  is sometimes used to represent the inverse common-base current gain.

<sup>7</sup> These devices are often called “super-beta” transistors.

Equations (5.13) actually represent a simplified version of the more complex **Gummel-Poon model** [3, 4] and form the heart of the BJT model used in the SPICE simulation program. The full Gummel-Poon model accurately describes the characteristics of BJTs over a wide range of operating conditions, and it has largely supplanted its predecessor, the **Ebers-Moll model** [5] (see Prob. 5.23).

### EXAMPLE 5.1 TRANSPORT MODEL CALCULATIONS

The advantage of the full transport model is that it can be used to estimate the currents in the bipolar transistor for any given set of bias voltages.

**PROBLEM** Use the transport model equations to find the terminal voltages and currents in the circuit in Fig. 5.5 in which an *npn* transistor is biased by two dc voltage sources.

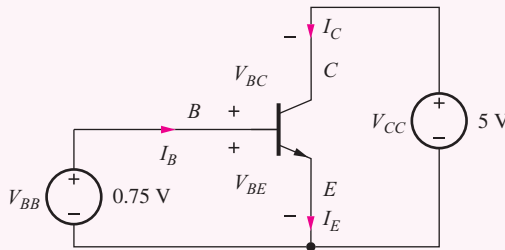


Figure 5.5 *npn* transistor circuit example:  $I_S = 10^{-16}$  A,  $\beta_F = 50$ ,  $\beta_R = 1$ .

**SOLUTION** **Known Information and Given Data:** The *npn* transistor in Fig. 5.5 is biased by two dc sources  $V_{BB} = 0.75$  V and  $V_{CC} = 5.0$  V. The transistor parameters are  $I_S = 10^{-16}$  A,  $\beta_F = 50$ , and  $\beta_R = 1$ .

**Unknowns:** Junction bias voltages  $V_{BE}$  and  $V_{BC}$ ; emitter current  $I_E$ , collector current  $I_C$ , base current  $I_B$

**Approach:** Determine  $V_{BE}$  and  $V_{BC}$  from the circuit. Use these voltages and the transistor parameters to calculate the currents using Eq. (5.13).

**Assumptions:** The transistor is modeled by the transport equations and is operating at room temperature with  $V_T = 25.0$  mV.

**Analysis:** In this circuit, the base emitter voltage  $V_{BE}$  is set directly by source  $V_{BB}$ , and the base collector voltage is the difference between  $V_{BB}$  and  $V_{CC}$ :

$$V_{BE} = V_{BB} = 0.75 \text{ V}$$

$$V_{BC} = V_{BB} - V_{CC} = 0.75 \text{ V} - 5.00 \text{ V} = -4.25 \text{ V}$$

Substituting these voltages into Eqs. (5.13) along with the transistor parameters yields

$$i_C = 10^{-16} \text{ A} \left[ \exp\left(\frac{0.75 \text{ V}}{0.025 \text{ V}}\right) - \exp\left(\frac{-4.75 \text{ V}}{0.025 \text{ V}}\right)^0 \right] - \frac{10^{-16}}{1} \text{ A} \left[ \exp\left(\frac{-4.75 \text{ V}}{0.025 \text{ V}}\right)^0 - 1 \right]$$

$$i_E = 10^{-16} \text{ A} \left[ \exp\left(\frac{0.75 \text{ V}}{0.025 \text{ V}}\right) - \exp\left(\frac{-4.75 \text{ V}}{0.025 \text{ V}}\right)^0 \right] + \frac{10^{-16}}{50} \text{ A} \left[ \exp\left(\frac{0.75 \text{ V}}{0.025 \text{ V}}\right) - 1 \right]$$

$$i_B = \frac{10^{-16}}{50} \text{ A} \left[ \exp\left(\frac{0.75 \text{ V}}{0.025 \text{ V}}\right) - 1 \right] + \frac{10^{-16}}{1} \text{ A} \left[ \exp\left(\frac{-4.75 \text{ V}}{0.025 \text{ V}}\right)^0 - 1 \right]$$

and evaluating these expressions gives

$$I_C = 1.07 \text{ mA} \quad I_E = 1.09 \text{ mA} \quad I_B = 21.4 \mu\text{A}$$

**Check of Results:** The sum of the collector and base currents equals the emitter current as required by KCL for the transistor treated as a super node. Also, the terminal currents range from microamperes to milliamperes, which are reasonable for most transistors.

**Discussion:** Note that the collector-base junction in Fig. 5.5 is reverse-biased, so the terms containing  $V_{BC}$  become negligibly small. In this example, the transistor is biased in the forward-active region of operation for which

$$\beta_F = \frac{I_C}{I_B} = \frac{1.07 \text{ mA}}{0.0214 \text{ mA}} = 50 \quad \text{and} \quad \alpha_F = \frac{I_C}{I_E} = \frac{1.07 \text{ mA}}{1.09 \text{ mA}} = 0.982$$

**EXERCISE:** Repeat the example problem for  $I_S = 10^{-15} \text{ A}$ ,  $\beta_F = 100$ ,  $\beta_R = 0.50$ ,  $V_{BE} = 0.70 \text{ V}$ , and  $V_{CC} = 10 \text{ V}$ .

**ANSWERS:**  $I_C = 1.45 \text{ mA}$ ,  $I_E = 1.46 \text{ mA}$ , and  $I_B = 14.5 \mu\text{A}$

In Secs. 5.5 to 5.11 we completely define four different regions of operation of the transistor and find simplified models for each region. First, however, let us develop the transport model for the *pnp* transistor in a manner similar to that for the *npn* transistor.

### 5.3 THE *pnp* TRANSISTOR

In Chapter 4, we found we could make either NMOS or PMOS transistors by simply interchanging the *n*- and *p*-type regions in the device structure. One might expect the same to be true of bipolar transistors, and we can indeed fabricate *pnp* transistors as well as *npn* transistors.

The *pnp* transistor is fabricated by reversing the layers of the transistor, as diagrammed in Fig. 5.6. The transistor has been drawn with the emitter at the top of the diagram, as it appears in most circuit diagrams throughout this book. The arrows again indicate the normal directions of positive current in the *pnp* transistor in most circuit applications. The voltages applied to the two *pn* junctions are the emitter-base voltage  $v_{EB}$  and the collector-base voltage  $v_{CB}$ . These voltages are again positive when they forward-bias their respective *pn* junctions. Collector current  $i_C$  and base current  $i_B$  exit the transistor terminals, and the emitter current  $i_E$  enters the device. The circuit symbol for the *pnp*

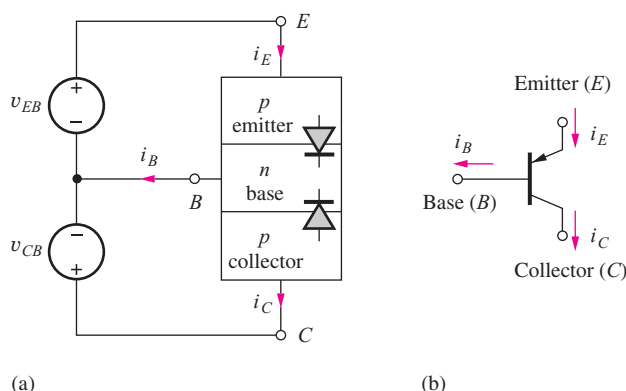


**Figure 5.6** (a) Idealized *pnp* transistor structure for a general-bias condition. (b) Circuit symbol for the *pnp* transistor.

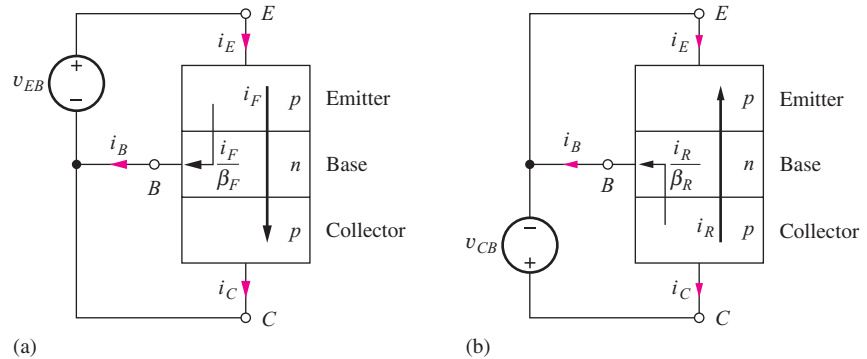


**Figure 5.7** (a) *pnp* transistor with  $v_{EB}$  applied and  $v_{CB} = 0$ . (b) *pnp* transistor with  $v_{CB}$  applied and  $v_{EB} = 0$ .

transistor appears in Fig. 5.6(b). The arrow identifies the emitter of the *pnp* transistor and points in the direction of normal positive-emitter current.

Equations that describe the static  $i$ - $v$  characteristics of the *pnp* transistor can be constructed by summing currents within the structure just as for the *npn* transistor. In Fig. 5.7(a), voltage  $v_{EB}$  is applied to the emitter-base junction, and the collector-base voltage is set to zero. The emitter-base voltage establishes forward-transport current  $i_F$  that traverses the narrow base region and base current  $i_B$  that crosses the emitter-base junction of the transistor:

$$i_C = i_F = I_S \left[ \exp \left( \frac{v_{EB}}{V_T} \right) - 1 \right] \quad i_B = \frac{i_F}{\beta_F} = \frac{I_S}{\beta_F} \left[ \exp \left( \frac{v_{EB}}{V_T} \right) - 1 \right] \quad (5.15)$$

and

$$i_E = i_C + i_B = I_S \left( 1 + \frac{1}{\beta_F} \right) \left[ \exp \left( \frac{v_{EB}}{V_T} \right) - 1 \right]$$

In Fig. 5.7(b), a voltage  $v_{CB}$  is applied to the collector-base junction, and the emitter-base junction is zero-biased. The collector-base voltage establishes the reverse-transport current  $i_R$  and base current  $i_B$ :

$$\begin{aligned} -i_E &= i_R = I_S \left[ \exp \left( \frac{v_{CB}}{V_T} \right) - 1 \right] \\ i_B &= \frac{i_R}{\beta_R} = \frac{I_S}{\beta_R} \left[ \exp \left( \frac{v_{CB}}{V_T} \right) - 1 \right] \\ i_C &= -I_S \left( 1 + \frac{1}{\beta_R} \right) \left[ \exp \left( \frac{v_{CB}}{V_T} \right) - 1 \right] \end{aligned} \quad (5.16)$$

where the collector current is given by  $i_C = i_E - i_B$ .

For the general-bias voltage situation in Fig. 5.6, Eqs. (5.15) and (5.16) are combined to give the total collector, emitter, and base currents of the *pnp* transistor:

$$\begin{aligned} i_C &= I_S \left[ \exp \left( \frac{v_{EB}}{V_T} \right) - \exp \left( \frac{v_{CB}}{V_T} \right) \right] - \frac{I_S}{\beta_R} \left[ \exp \left( \frac{v_{CB}}{V_T} \right) - 1 \right] \\ i_E &= I_S \left[ \exp \left( \frac{v_{EB}}{V_T} \right) - \exp \left( \frac{v_{CB}}{V_T} \right) \right] + \frac{I_S}{\beta_F} \left[ \exp \left( \frac{v_{EB}}{V_T} \right) - 1 \right] \\ i_B &= \frac{I_S}{\beta_F} \left[ \exp \left( \frac{v_{EB}}{V_T} \right) - 1 \right] + \frac{I_S}{\beta_R} \left[ \exp \left( \frac{v_{CB}}{V_T} \right) - 1 \right] \end{aligned} \quad (5.17)$$

These equations represent the simplified Gummel-Poon or transport model equations for the *pnp* transistor and can be used to relate the terminal voltages and currents of the *pnp* transistor for any general-bias condition. Note that these equations are identical to those for the *npn* transistor except that  $v_{EB}$  and  $v_{CB}$  replace  $v_{BE}$  and  $v_{BC}$ , respectively, and are a result of our careful choice for the direction of positive currents in Figs. 5.2 and 5.6.

**EXERCISE:** Find  $I_C$ ,  $I_E$ , and  $I_B$  for a *pnp* transistor if  $I_S = 10^{-16} \text{ A}$ ,  $\beta_F = 75$ ,  $\beta_R = 0.40$ ,  $V_{EB} = 0.75 \text{ V}$ , and  $V_{CB} = +0.70 \text{ V}$ .

**ANSWERS:**  $I_C = 0.563 \text{ mA}$ ,  $I_E = 0.938 \text{ mA}$ ,  $I_B = 0.376 \text{ mA}$

## 5.4 EQUIVALENT CIRCUIT REPRESENTATIONS FOR THE TRANSPORT MODELS

For circuit simulation, as well as hand analysis purposes, the transport model equations for the *npn* and *pnp* transistors can be represented by the equivalent circuits shown in Fig. 5.8(a) and (b), respectively. In the *npn* model in Fig. 5.8(a), the total transport current  $i_T$  traversing the base is determined by  $I_S$ ,  $v_{BE}$ , and  $v_{BC}$ , and is modeled by the current source  $i_T$ :

$$i_T = i_F - i_R = I_S \left[ \exp\left(\frac{v_{BE}}{V_T}\right) - \exp\left(\frac{v_{BC}}{V_T}\right) \right] \quad (5.18)$$

The diode currents correspond directly to the two components of the base current:

$$i_B = \frac{I_S}{\beta_F} \left[ \exp\left(\frac{v_{BE}}{V_T}\right) - 1 \right] + \frac{I_S}{\beta_R} \left[ \exp\left(\frac{v_{BC}}{V_T}\right) - 1 \right] \quad (5.19)$$

Directly analogous arguments hold for the circuit elements in the *pnp* circuit model of Fig. 5.8(b).

**EXERCISE:** Find  $i_T$  if  $I_S = 10^{-15} \text{ A}$ ,  $V_{BE} = 0.75 \text{ V}$ , and  $V_{BC} = -2.0 \text{ V}$ .

**ANSWER:** 10.7 mA

**EXERCISE:** Find the dc transport current  $i_T$  for the transistor in Example 5.1 on page 224.

**ANSWER:**  $i_T = 1.07 \text{ mA}$

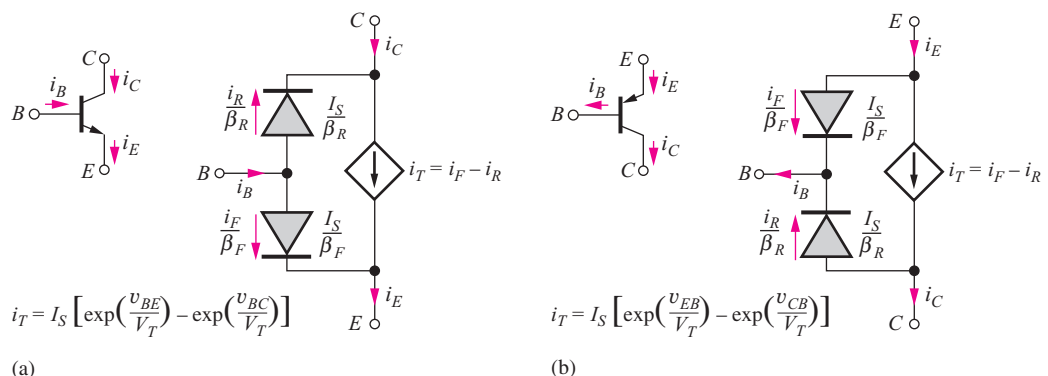


**Figure 5.8** (a) Transport model equivalent circuit for the *npn* transistor. (b) Transport model equivalent circuit for the *pnp* transistor.

## 5.5 THE $i$ - $v$ CHARACTERISTICS OF THE BIPOLAR TRANSISTOR

Two complementary views of the  $i$ - $v$  behavior of the BJT are represented by the device's **output characteristic** and **transfer characteristic**. (Remember that similar characteristics were presented for the FETs in Chapter 4.) The output characteristics represent the relationship between the collector current and collector-emitter or collector-base voltage of the transistor, whereas the transfer characteristic relates the collector current to the base-emitter voltage. A knowledge of both  $i$ - $v$  characteristics is basic to understanding the overall behavior of the bipolar transistor.

### 5.5.1 OUTPUT CHARACTERISTICS

Circuits for measuring or simulating the **common-emitter output characteristics** are shown in Fig. 5.9. In these circuits, the base of the transistor is driven by a constant current source, and the output characteristics represent a graph of  $i_C$  vs.  $v_{CE}$  for the *npn* transistor (or  $i_C$  vs.  $v_{EC}$  for the *pnp*) with base current  $i_B$  as a parameter. Note that the Q-point ( $I_C$ ,  $V_{CE}$ ) or ( $I_C$ ,  $V_{EC}$ ) locates the BJT operating point on the output characteristics.

First, consider the *npn* transistor operating with  $v_{CE} \geq 0$ , represented by the first quadrant of the graph in Fig. 5.10. For  $i_B = 0$ , the transistor is nonconducting or cut off. As  $i_B$  increases above 0,  $i_C$  also increases. For  $v_{CE} \geq v_{BE}$ , the *npn* transistor is in the forward-active region, and collector current is independent of  $v_{CE}$  and equal to  $\beta_F i_B$ . Remember, it was demonstrated earlier that  $i_C \cong \beta_F i_B$  in the forward-active region. For  $v_{CE} \leq v_{BE}$ , the transistor enters the **saturation region** of operation in which the total voltage between the collector and emitter terminals of the transistor is small.

It is important to note that the saturation region of the BJT does not correspond to the saturation region of the FET. The forward-active region (or just **active region**) of the BJT corresponds to the saturation region of the FET. When we begin our discussion of amplifiers in Part III, we will simply apply the term active region to both devices. The active region is the region most often used in transistor implementations of amplifiers.

In the third quadrant for  $v_{CE} \leq 0$ , the roles of the collector and emitter reverse. For  $v_{BE} \leq v_{CE} \leq 0$ , the transistor remains in saturation. For  $v_{CE} \leq v_{BE}$ , the transistor enters the **reverse-active region**, in which the  $i$ - $v$  characteristics again become independent of  $v_{CE}$ , and now  $i_C \cong -(\beta_R + 1)i_B$ . The reverse-active region curves have been plotted for a relatively large value of reverse

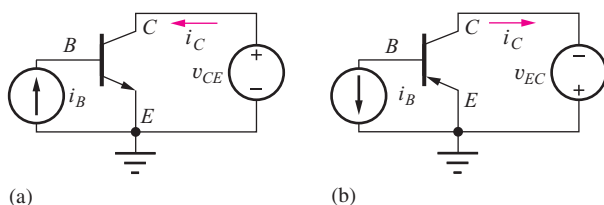


**Figure 5.9** Circuits for determining common-emitter output characteristics: (a) *npn* transistor, (b) *pnp* transistor.

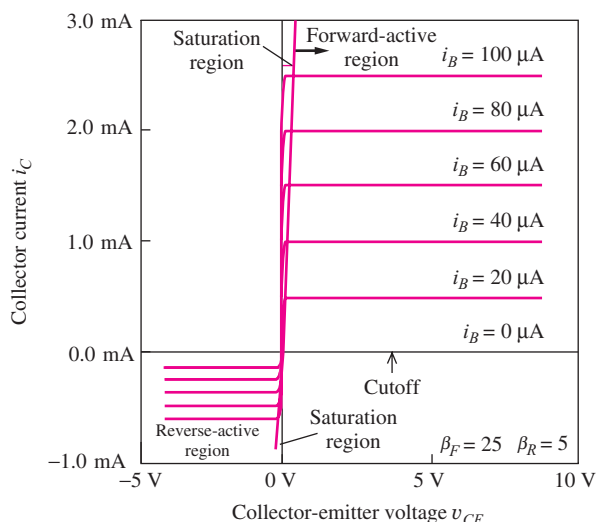


**Figure 5.10** Common-emitter output characteristics for the bipolar transistor ( $i_C$  vs.  $v_{CE}$  for the *npn* transistor or  $i_C$  vs.  $v_{EC}$  for the *pnp* transistor).

common-emitter current gain,  $\beta_R = 5$ , to enhance their visibility. As noted earlier, the reverse-current gain  $\beta_R$  is often less than 1.

Using the polarities defined in Fig. 5.9(b) for the *pnp* transistor, the output characteristics will appear exactly the same as in Fig. 5.10, except that the horizontal axis will be the voltage  $v_{EC}$  rather than  $v_{CE}$ . Remember that  $i_B > 0$  and  $i_C > 0$  correspond to currents exiting the base and collector terminals of the *pnp* transistor.

Circuits for measuring or simulating the **common-base output characteristics** of the *npn* and *pnp* transistors are shown in Fig. 5.11. In these circuits, the emitter of the transistor is driven by a constant current source, and the output characteristics plot  $i_C$  vs.  $v_{CB}$  for the *npn* (or  $i_C$  vs.  $v_{BC}$  for the *pnp*), with the emitter-current  $i_E$  as a parameter. For  $v_{CB} \geq 0$  V in Fig. 5.12, the transistor operates in the forward-active region with  $i_C$  independent of  $v_{CB}$ , and we saw earlier that  $i_C \cong i_E$ . For  $v_{CB}$  less than zero, the base-collector diode of the transistor becomes forward-biased, and the collector current grows exponentially (in the negative direction) as the base-collector diode begins to conduct.

Using the polarities defined in Fig. 5.11(b) for the *pnp* transistor, the output characteristics appear exactly the same as in Fig. 5.12, except that the horizontal axis is the voltage  $v_{BC}$  rather than  $v_{CB}$ . Again, remember that  $i_B > 0$  and  $i_C > 0$  correspond to currents exiting the emitter and collector terminals of the *pnp* transistor.

### 5.5.2 TRANSFER CHARACTERISTICS

The **common-emitter transfer characteristic** of the BJT defines the relationship between the collector current and the base-emitter voltage of the transistor. An example of the transfer characteristic for an *npn* transistor is shown in graphical form in Fig. 5.13, with both linear and semilog scales for

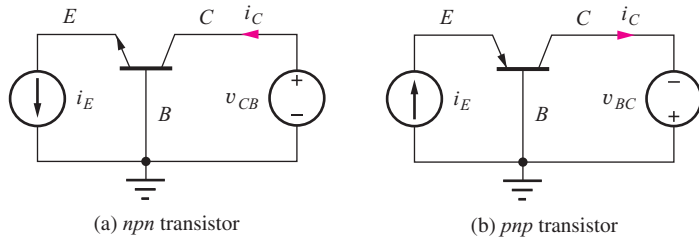


**Figure 5.11** Circuits to determine common-base output characteristics.

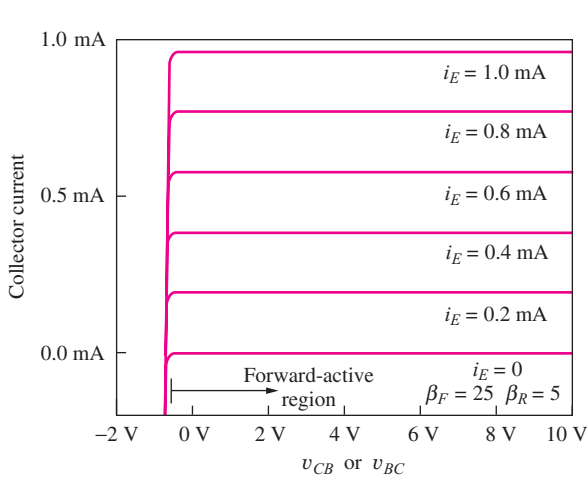


**Figure 5.12** Common-base output characteristics for the bipolar transistor ( $i_C$  vs.  $v_{CB}$  for the *npn* transistor or  $i_C$  vs.  $v_{BC}$  for the *pnp* transistor).

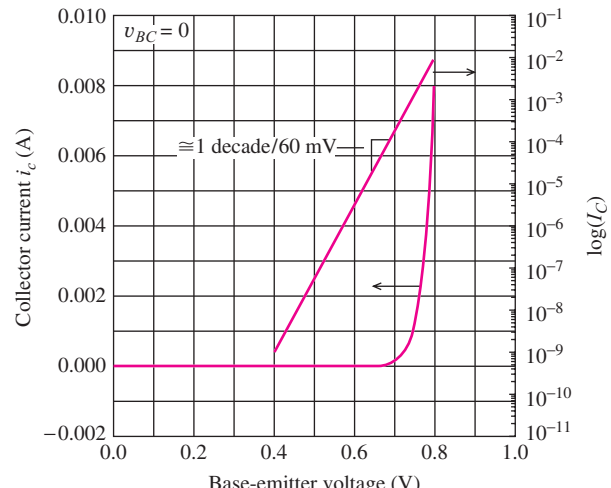


**Figure 5.13** BJT transfer characteristic in the forward-active region.

the particular case of  $v_{BC} = 0$ . The transfer characteristic is virtually identical to that of a  $pn$  junction diode. This behavior can also be expressed mathematically by setting  $v_{BC} = 0$  in the collector-current expression in Eq. (5.13):

$$i_C = I_S \left[ \exp \left( \frac{v_{BE}}{V_T} \right) - 1 \right] \quad (5.20)$$

Because of the exponential relationship in Eq. (5.20), the semilog plot exhibits the same slope as that for a  $pn$  junction diode. Only a 60-mV change in  $v_{BE}$  is required to change the collector current by a factor of 10, and for a fixed collector current, the base-emitter voltage of the silicon BJT will exhibit a  $-1.8\text{-mV}/^\circ\text{C}$  temperature coefficient, just as for the silicon diode (see Sec. 3.5).

**EXERCISE:** What base-emitter voltage  $V_{BE}$  corresponds to  $I_C = 100 \mu\text{A}$  in an  $npn$  transistor at room temperature if  $I_S = 10^{-16} \text{ A}$ ? For  $I_C = 1 \text{ mA}$ ?

**ANSWERS:** 0.691 V; 0.748 V

## 5.6 THE OPERATING REGIONS OF THE BIPOLAR TRANSISTOR

In the bipolar transistor, each  $pn$  junction may be independently forward-biased or reverse-biased, so there are four possible regions of operation, as defined in Table 5.2. The operating point establishes the region of operation of the transistor and can be defined by any two of the four terminal voltages or currents. The characteristics of the transistor are quite different for each of the four regions of operation, and in order to simplify our circuit analysis task, we need to be able to make an educated guess as to the region of operation of the BJT.

When both junctions are reverse-biased, the transistor is essentially nonconducting or *cut off* (**cutoff region**) and can be considered an open switch. If both junctions are forward-biased, the transistor is operating in the **saturation region**<sup>8</sup> and appears as a closed switch. Cutoff and saturation (colored in Table 5.2) are most often used to represent the two states in binary logic circuits implemented with BJTs. For example, switching between these two operating regions occurs in the transistor-transistor logic circuits that we shall study in Chapter 9 on bipolar logic circuits.

**TABLE 5.2**  
Regions of Operation of the Bipolar Transistor

BASE-EMITTER JUNCTION	BASE-COLLECTOR JUNCTION	
	Reverse Bias	Forward Bias
Forward Bias	Forward-active region (Normal-active region) (Good amplifier)	Saturation region* (Closed switch)
Reverse Bias	Cutoff region (Open switch)	Reverse-active region (Inverse-active region) (Poor amplifier)

\* It is important to note that the saturation region of the bipolar transistor does *not* correspond to the saturation region of the FET. This unfortunate use of terms is historical in nature and something we just have to accept.

<sup>8</sup> It is important to again note that the saturation region of the bipolar transistor does *not* correspond to the saturation region of the FET. This unfortunate use of terms is historical in nature and something we just have to accept.

In the **forward-active region** (also called the **normal-active region** or **just active region**), in which the base-emitter junction is forward-biased and the base-collector junction is reverse-biased, the BJT can provide high current, voltage, and power gains. The forward-active region is most often used to achieve high-quality amplification. In addition, in the fastest form of bipolar logic, called emitter-coupled logic, the transistors switch between the cutoff and the forward-active regions.

In the **reverse-active region** (or **inverse-active region**), the base-emitter junction is reverse-biased and the base-collector junction is forward-biased. In this region, the transistor exhibits low current gain, and the reverse-active region is not often used. However, we will see an important application of the reverse-active region in transistor-transistor logic circuits in Chapter 9. Reverse operation of the bipolar transistor has also found use in analog-switching applications.

The transport model equations describe the behavior of the bipolar transistor for any combination of terminal voltages and currents. However, the complete sets of equations in (5.13) and (5.17) are quite imposing. In subsequent sections, bias conditions specific to each of the four regions of operation will be used to obtain simplified sets of relationships that are valid for the individual regions. The Q-point for the BJT is  $(I_C, V_{CE})$  for the *npn* transistor and  $(I_C, V_{EC})$  for the *pnp*.

**EXERCISE:** What is the region of operation of (a) an *npn* transistor with  $V_{BE} = 0.75$  V and  $V_{BC} = -0.70$  V? (b) A *pnp* transistor with  $V_{CB} = 0.70$  V and  $V_{EB} = 0.75$  V?

**ANSWERS:** Forward-active region; saturation region

## 5.7 TRANSPORT MODEL SIMPLIFICATIONS

The complete sets of Transport Model Equations developed in Sections 5.2 and 5.3 describe the behavior of the *npn* and *pnp* transistors for any combination of terminal voltages and currents, and these equations are indeed the basis for the models used in SPICE circuit simulation. However, the full sets of equations are quite imposing. Now we will explore simplifications that can be used to reduce the complexity of the model descriptions for each of the four different regions of operation identified in Table 5.2.

### 5.7.1 SIMPLIFIED MODEL FOR THE CUTOFF REGION

The easiest region to understand is the cutoff region, in which both junctions are reverse-biased. For an *npn* transistor, the cutoff region requires  $v_{BE} \leq 0$  and  $v_{BC} \leq 0$ . Let us further assume that

$$v_{BE} < -\frac{4kT}{q} \quad \text{and} \quad v_{BC} < -4\frac{kT}{q} \quad \text{where } -4\frac{kT}{q} = -0.1V$$

These two conditions allow us to neglect the exponential terms in Eqs. (5.13), yielding the following simplified equations for the *npn* terminal currents in cutoff:

$$\begin{aligned} i_C &= I_S \left[ \exp\left(\frac{v_{BE}}{V_T}\right)^0 - \exp\left(\frac{v_{BC}}{V_T}\right)^0 \right] - \frac{I_S}{\beta_R} \left[ \exp\left(\frac{v_{BC}}{V_T}\right)^0 - 1 \right] \\ i_E &= I_S \left[ \exp\left(\frac{v_{BE}}{V_T}\right)^0 - \exp\left(\frac{v_{BC}}{V_T}\right)^0 \right] + \frac{I_S}{\beta_F} \left[ \exp\left(\frac{v_{BE}}{V_T}\right)^0 - 1 \right] \\ i_B &= \frac{I_S}{\beta_F} \left[ \exp\left(\frac{v_{BE}}{V_T}\right)^0 - 1 \right] + \frac{I_S}{\beta_R} \left[ \exp\left(\frac{v_{BC}}{V_T}\right)^0 - 1 \right] \end{aligned} \quad (5.21)$$

or

$$i_C = +\frac{I_S}{\beta_R} \quad i_E = -\frac{I_S}{\beta_F} \quad i_B = -\frac{I_S}{\beta_F} - \frac{I_S}{\beta_R}$$

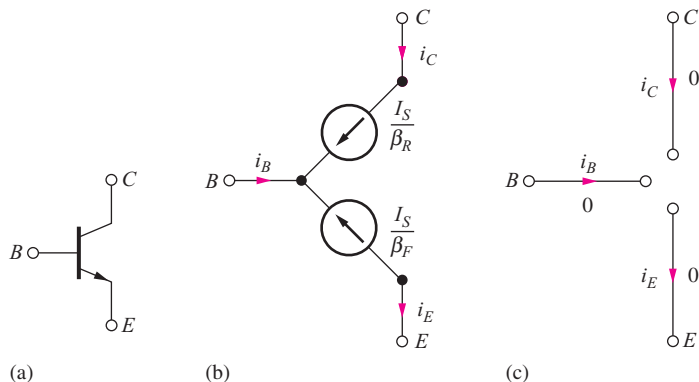


**Figure 5.14** Modeling the *npn* transistor in cutoff: (a) *npn* transistor, (b) constant leakage current model, (c) open-circuit model.

In cutoff, the three terminal currents— $i_C$ ,  $i_E$ , and  $i_B$ —are all constant and smaller than the saturation current  $I_S$  of the transistor. The simplified model for this situation is shown in Fig. 5.14(b). In cutoff, only very small leakage currents appear in the three transistor terminals. In most cases, these currents are negligibly small and can be assumed to be zero.

We usually think of the transistor operating in the cutoff region as being “off” with essentially zero terminal currents, as indicated by the three-terminal open-circuit model in Fig. 5.14(c). The cutoff region represents an open switch and is used as one of the two states required for binary logic circuits.

## EXAMPLE 5.2 A BJT BIASED IN CUTOFF

Cutoff represents the “off state” in switching applications, so an understanding of the magnitudes of the currents involved is important. In this example, we explore how closely the “off state” approaches zero.

**PROBLEM** Figure 5.15 is an example of a circuit in which the transistor is biased in the cutoff region. Estimate the currents using the simplified model in Fig. 5.14, and compare to calculations using the full transport model.

**SOLUTION** **Known Information and Given Data:** From the figure,  $I_S = 10^{-16} \text{ A}$ ,  $\alpha_F = 0.95$ ,  $\alpha_R = 0.25$ ,  $V_{BE} = 0 \text{ V}$ ,  $V_{BC} = -5 \text{ V}$

**Unknowns:**  $I_C$ ,  $I_B$ ,  $I_E$

**Approach:** First analyze the circuit using the simplified model of Fig. 5.14. Then, compare the results to calculations using the voltages to simplify the transport equations.

**Assumptions:**  $V_{BE} = 0 \text{ V}$ , so the “diode” terms containing  $V_{BE}$  are equal to 0.  $V_{BC} = -5 \text{ V}$ , which is much less than  $-4kT/q = -100 \text{ mV}$ , so the transport model equations can be simplified.

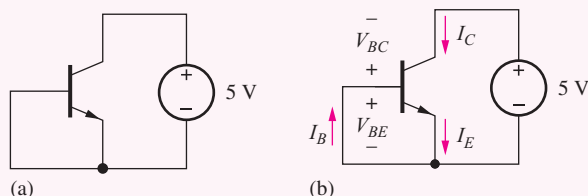


**Figure 5.15** (a) *npn* transistor bias in the cutoff region. (For calculations, use  $I_S = 10^{-16} \text{ A}$ ,  $\alpha_F = 0.95$ ,  $\alpha_R = 0.25$ .) (b) Normal current directions.

**Analysis:** The voltages  $V_{BE} = 0$  and  $V_{BC} = -5$  V are consistent with the definition of the cutoff region. If we use the open-circuit model in Fig. 5.14(c), the currents  $I_C$ ,  $I_E$ , and  $I_B$  are all predicted to be zero.

To obtain a more exact estimate of the currents, we use the transport model equations. For the circuit in Fig. 5.15, the base-emitter voltage is exactly zero, and  $V_{BC} \ll 0$ . Therefore, Eqs. (5.13) reduce to

$$I_C = I_S \left( 1 + \frac{1}{\beta_R} \right) = \frac{I_S}{\alpha_R} = \frac{10^{-16} \text{ A}}{0.25} = 4 \times 10^{-16} \text{ A}$$

$$I_E = I_S = 10^{-16} \text{ A} \quad \text{and} \quad I_B = -\frac{I_S}{\beta_R} = -\frac{10^{-16} \text{ A}}{\frac{1}{3}} = -3 \times 10^{-16} \text{ A}$$

The calculated currents in the terminals are very small but nonzero. Note, in particular, that the base current is not zero and that small currents exit both the emitter and base terminals of the transistor.

**Check of Results:** As a check on our results, we see that Kirchhoff's current law is satisfied for the transistor treated as a super node:  $i_C + i_B = i_E$ .

**Discussion:** The voltages  $V_{BE} = 0$  and  $V_{BC} = -5$  V are consistent with the definition of the cutoff region. Thus, we expect the currents to be negligibly small. Here again we see an example of the use of different levels of modeling to achieve different degrees of precision in the answer  $[(I_C, I_E, I_B) = (0, 0, 0)$  or  $(4 \times 10^{-16} \text{ A}, 10^{-16} \text{ A}, -3 \times 10^{-16} \text{ A})]$ .

**EXERCISE:** Calculate the values of the currents in the circuit in Fig. 5.15(a) if the value of the voltage source is changed to 10 V and (b) if the base-emitter voltage is set to -3 V using a second voltage source.

**ANSWERS:** (a) No change; (b) 0.300 fA, 5.26 aA, -0.305 fA

## 5.7.2 MODEL SIMPLIFICATIONS FOR THE FORWARD-ACTIVE REGION

Arguably the most important region of operation of the BJT is the forward-active region, in which the emitter-base junction is forward-biased and the collector-base junction is reverse-biased. In this region, the transistor can exhibit high voltage and current gains and is useful for analog amplification. From Table 5.2, we see that the forward-active region of an *n*p*n* transistor corresponds to  $v_{BE} \geq 0$  and  $v_{BC} \leq 0$ . In most cases, the forward-active region will have

$$v_{BE} > 4 \frac{kT}{q} = 0.1 \text{ V} \quad \text{and} \quad v_{BC} < -4 \frac{kT}{q} = -0.1 \text{ V}$$

and we can assume that  $\exp(-v_{BC}/V_T) \ll 1$  just as we did in simplifying Eq. Set (5.21). This simplification yields:

$$\begin{aligned} i_C &= I_S \exp \left( \frac{v_{BE}}{V_T} \right) + \frac{I_S}{\beta_R} \\ i_E &= \frac{I_S}{\alpha_F} \exp \left( \frac{v_{BE}}{V_T} \right) + \frac{I_S}{\beta_F} \\ i_B &= \frac{I_S}{\beta_F} \exp \left( \frac{v_{BE}}{V_T} \right) - \frac{I_S}{\beta_F} - \frac{I_S}{\beta_R} \end{aligned} \tag{5.22}$$

The exponential term in each of these expressions is usually huge compared to the other terms. By neglecting the small terms, we find the most useful simplifications of the BJT model for the forward-active region:

$$i_C = I_S \exp\left(\frac{v_{BE}}{V_T}\right) \quad i_E = \frac{I_S}{\alpha_F} \exp\left(\frac{v_{BE}}{V_T}\right) \quad i_B = \frac{I_S}{\beta_F} \exp\left(\frac{v_{BE}}{V_T}\right) \quad (5.23)$$

In these equations, the fundamental, exponential relationship between all the terminal currents and the base-emitter voltage  $v_{BE}$  is once again clear. In the forward-active region, the terminal currents all have the form of diode currents in which the controlling voltage is the base-emitter junction potential. It is also important to note that the currents are all independent of the base-collector voltage  $v_{BC}$ . The collector current  $i_C$  can be modeled as a voltage-controlled current source that is controlled by the base-emitter voltage and independent of the collector voltage.

By taking ratios of the terminal currents in Eq. (5.23), two important auxiliary relationships for the forward-active region are found:

$$i_C = \alpha_F i_E \quad \text{and} \quad i_C = \beta_F i_B \quad (5.24)$$

Observing that  $i_E = i_C + i_B$  and using Eq. (5.24) yields a third important result:

$$i_E = (\beta_F + 1)i_B \quad (5.25)$$

The results from Eqs. (5.24) and (5.25) are placed in a circuit context in the next two examples from Fig. 5.16.



### DESIGN FORWARD-ACTIVE REGION NOTE

Operating points in the forward-active region are normally used for linear amplifiers. Our dc model for the forward-active region is quite simple:

$$I_C = \beta_F I_B \quad \text{and} \quad I_E = (\beta_F + 1)I_B \quad \text{with} \quad V_{BE} \cong 0.7 \text{ V.}$$

Forward-active operation requires  $V_{BE} > 0$  and  $V_{CE} \geq V_{BE}$ .

### EXAMPLE 5.3

### FORWARD-ACTIVE REGION OPERATION WITH Emitter CURRENT BIAS

Current sources are widely utilized for biasing in circuit design, and such a source is used to set the Q-point current in the transistor in Fig. 5.16(a).

**PROBLEM** Find the emitter, base and collector currents, and base-emitter voltage for the transistor biased by a current source in Fig. 5.16(a).

**SOLUTION** **Known Information and Given Data:** An *n*p*n* transistor biased by the circuit in Fig. 5.16(a) with  $I_S = 10^{-16}$  A and  $\alpha_F = 0.95$ . From the circuit,  $V_{BC} = V_B - V_C = -5$  V and  $I_E = +100$   $\mu$ A.

**Unknowns:**  $I_C$ ,  $I_B$ ,  $V_{BE}$

**Approach:** Show that the transistor is in the forward-active region of operation and use Eqs. (5.23) to (5.25) to find the unknown currents and voltage.

**Assumptions:** Room temperature operation with  $V_T = 25.0$  mV

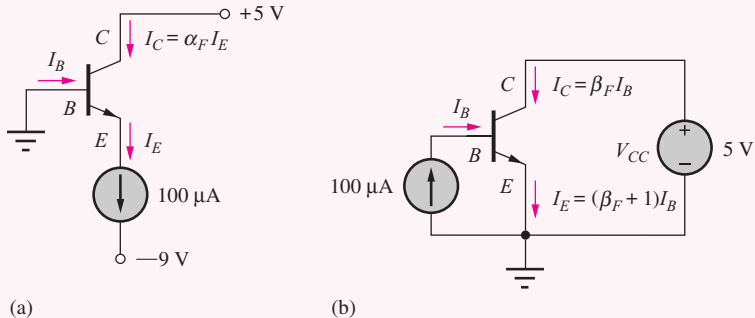


**Figure 5.16** Two *npn* transistors operating in the forward-active region ( $I_S = 10^{-16}$  A and  $\alpha_F = 0.95$  are assumed for the example calculations).

**Analysis:** From the circuit, we observe that the emitter current is forced by the current source to be  $I_E = +100 \mu\text{A}$ , and the current source will forward-bias the base-emitter diode. Study of the mathematical model in Eq. (5.13) also confirms that the base-emitter voltage must be positive (forward bias) in order for the emitter current to be positive. Thus, we have  $V_{BE} > 0$  and  $V_{BC} < 0$ , which correspond to the forward-active region of operation for the *npn* transistor.

The base and collector currents can be found using Eqs. (5.24) and (5.25) with  $I_E = 100 \mu\text{A}$ :

$$I_C = \alpha_F I_E = 0.95 \cdot 100 \mu\text{A} = 95 \mu\text{A}$$

$$\text{Solving for } \beta_F \text{ gives} \quad \beta_F = \frac{\alpha_F}{1 - \alpha_F} = \frac{0.95}{1 - .95} = 19 \quad \beta_F + 1 = 20$$

$$I_B = \frac{I_E}{\beta_E + 1} = \frac{100 \mu A}{20} = 5 \mu A$$

The base-emitter voltage is found from the emitter current expression in Eq. (5.23):

$$V_{BE} = V_T \ln \frac{\alpha_F I_E}{I_S} = (0.025 \text{ V}) \ln \frac{0.95(10^{-4} \text{ A})}{10^{-16} \text{ A}} = 0.690 \text{ V}$$

**Check of Results:** As a check on our results, we see that Kirchhoff's current law is satisfied for the transistor treated as a super node:  $i_C + i_B = i_E$ . Also we can check  $V_{BE}$  using both the collector and base current expressions in Eq. (5.23).

**Discussion:** We see that most of the current being forced or “pulled” out of the emitter by the current source comes directly through the transistor from the collector. This is the common-base mode in which  $i_C = \alpha_E i_E$  with  $\alpha_E \approx 1$ .

**EXERCISE:** Calculate the values of the currents and base-emitter voltage in the circuit in Fig. 5.16(a) if (a) the value of the voltage source is changed to 10 V. (b) The transistor's common-emitter current gain is increased to 50.

**ANSWERS:** (a) No change; (b) 100  $\mu$ A, 1.96  $\mu$ A, 98.0  $\mu$ A, 0.690 V

**EXAMPLE 5.4 FORWARD-ACTIVE REGION OPERATION WITH BASE CURRENT BIAS**

A current source is used to bias the transistor into the forward-active region in Fig. 5.16(b).

**PROBLEM** Find the emitter, base and collector currents, and base-emitter and base-collector voltages for the transistor biased by the base current source in Fig. 5.16(b).

**SOLUTION** **Known Information and Given Data:** An *npn* transistor biased by the circuit in Fig. 5.16(b) with  $I_S = 10^{-16}$  A and  $\alpha_F = 0.95$ . From the circuit,  $V_C = +5$  V and  $I_B = +100$   $\mu$ A.

**Unknowns:**  $I_C$ ,  $I_B$ ,  $V_{BE}$ ,  $V_{BC}$

**Approach:** Show that the transistor is in the forward-active region of operation and use Eqs. (5.23) to (5.25) to find the unknown currents and voltage.

**Assumptions:** Room temperature operation with  $V_T = 25.0$  mV

**Analysis:** In the circuit in Fig. 5.16(b), base current  $I_B$  is now forced to equal 100  $\mu$ A by the ideal current source. This current enters the base and will exit the emitter, forward-biasing the base-emitter junction. From the mathematical model in Eq. (5.13), we see that positive base current can occur for positive  $V_{BE}$  and positive  $V_{BC}$ . However, we have  $V_{BC} = V_B - V_C = V_{BE} - V_C$ . Since the base-emitter diode voltage will be approximately 0.7 V, and  $V_C = 5$  V,  $V_{BC}$  will be negative (e.g.,  $V_{BC} \cong 0.7 - 5.0 = -4.3$  V). Thus we have  $V_{BE} > 0$  and  $V_{BC} < 0$ , which corresponds to the forward-active region of operation for the *npn* transistor, and the collector and emitter currents can be found using Eqs. (5.24) and (5.25) with  $I_B = 100$   $\mu$ A:

$$I_C = \beta_F I_B = 19 \cdot 100 \mu\text{A} = 1.90 \text{ mA}$$

$$I_E = (\beta_F + 1)I_B = 20 \cdot 100 \mu\text{A} = 2.00 \text{ mA}$$

The base-emitter voltage can be found from the collector current expression in Eq. (5.23):

$$V_{BE} = V_T \ln \frac{I_C}{I_S} = (0.025 \text{ V}) \ln \frac{1.9 \times 10^{-3} \text{ A}}{10^{-16} \text{ A}} = 0.764 \text{ V}$$

$$V_{BC} = V_B - V_C = V_{BE} - V_C = 0.764 - 5 = -4.24 \text{ V}$$

**Check of Results:** As a check on our results, we see that Kirchhoff's current law is satisfied for the transistor treated as a super node:  $i_C + i_B = i_E$ . Also we can check the value of  $V_{BE}$  using either the emitter or base current expressions in Eq. (5.23). The calculated values of  $V_{BE}$  and  $V_{BC}$  correspond to forward-active region operation.

**Discussion:** A large amplification of the current takes place when the current source is injected into the base terminal in Fig. 5.16(b) in contrast to the situation when the source is connected to the emitter terminal in Fig. 5.16(a).

**EXERCISE:** Calculate the values of the currents and base-emitter voltage in the circuit in Fig. 5.16(b) if (a) the value of the voltage source is changed to 10 V. (b) The transistor's common-emitter current gain is increased to 50.

**ANSWERS:** (a) No change; (b) 5.00 mA, 100  $\mu$ A, 5.10 mA, 0.789 V, -4.21 V

**EXERCISE:** What is the minimum value of  $V_{CC}$  that corresponds to forward-active region bias in Fig. 5.16(b)?

**ANSWERS:**  $V_{BE} = 0.764$  V

As illustrated in Examples 5.3 and 5.4, Eqs. (5.24) and (5.25) can often be used to greatly simplify the analysis of circuits operating in the forward-active region. However, remember this caveat well: **The results in Eqs. (5.24) and (5.25) are valid only for the forward-active region of operation!**

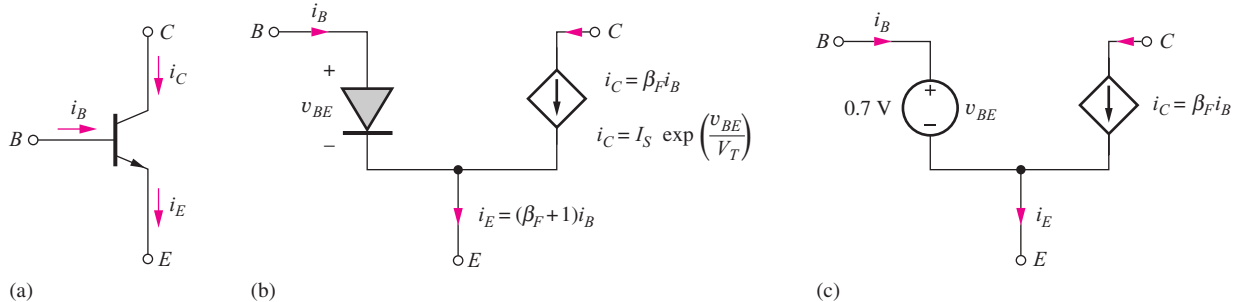


**Figure 5.17** (a) *npn* transistor. (b) Simplified model for the forward-active region. (c) Further simplification for the forward-active region using the CVD model for the diode.

Based on Eq. (5.24), the BJT is often considered a current-controlled device. However, from Eqs. (5.23), we see that the fundamental physics-based behavior of the BJT in the forward-active region is that of a (nonlinear) voltage-controlled current source. The base current should be considered as an unwanted defect current that must be supplied to the base in order for the transistor to operate. In an ideal BJT,  $\beta_F$  would be infinite, the base current would be zero, and the collector and emitter currents would be identical, just as for the FET. (Unfortunately, it is impossible to fabricate such a BJT.)

Equations (5.23) lead to the simplified circuit model for the forward-active region shown in Fig. 5.17. The current in the base-emitter diode is amplified by the common-emitter current gain  $\beta_F$  and appears in the collector terminal. However, remember that the base and collector currents are exponentially related to the base-emitter voltage. Because the base-emitter diode is forward-biased in the forward-active region, the transistor model of Fig. 5.17(b) can be further simplified to that of Fig. 5.17(c), in which the diode is replaced by its constant voltage drop (CVD) model, in this case  $V_{BE} = 0.7$  V. The dc base and emitter voltages differ by the 0.7-V diode voltage drop in the forward-active region.

### EXAMPLE 5.5 FORWARD-ACTIVE REGION BIAS USING TWO POWER SUPPLIES

Analog circuits frequently operate from a pair of positive and negative power supplies so that bipolar input and output signals can easily be accommodated. The circuit in Fig. 5.18 provides one possible circuit configuration in which the resistor and -9-V source replace the current source utilized in Fig. 5.16(a). Collector resistor  $R_C$  has been added to reduce the collector-emitter voltage.

**PROBLEM** Find the Q-point for the transistor in the circuit in Fig. 5.18.

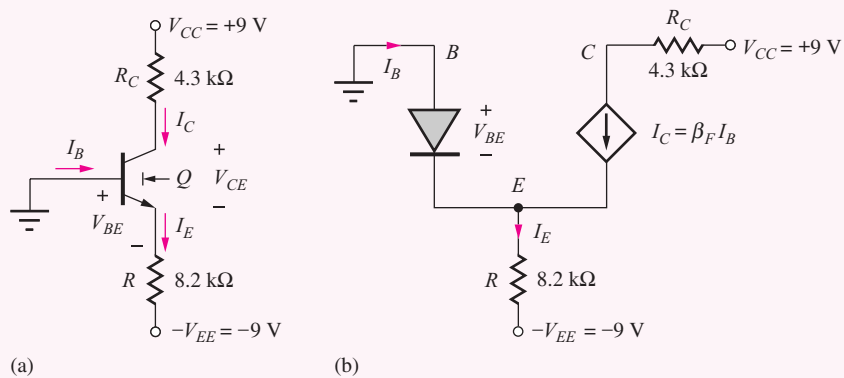


**Figure 5.18** (a) *npn* Transistor circuit (assume  $\beta_F = 50$  and  $\beta_R = 1$ ). (b) Simplified model for the forward-active region.

**SOLUTION** **Known Information and Given Data:** *npn* transistor in the circuit in Fig. 5.18(a) with  $\beta_F = 50$  and  $\beta_R = 1$

**Unknowns:** Q-point ( $I_C$ ,  $V_{CE}$ )

**Approach:** In this circuit, the base-collector junction will tend to be reverse-biased by the 9-V source. The combination of the resistor and the -9-V source will force a current out of the emitter and forward-bias the base-emitter junction. Thus, the transistor appears to be biased in the forward-active region of operation.

**Assumptions:** Assume forward-active region operation; since we do not know the saturation current, assume  $V_{BE} = 0.7$  V; use the simplified model for the forward-active region to analyze the circuit as in Fig. 5.18(b).

**Analysis:** The currents can now be found by using KVL around the base-emitter loop:

$$V_{BE} + 8200I_E - V_{EE} = 0$$

$$\text{For } V_{BE} = 0.7 \text{ V}, 0.7 + 8200I_E - 9 = 0 \quad \text{or} \quad I_E = \frac{8.3 \text{ V}}{8200 \Omega} = 1.01 \text{ mA}$$

At the emitter node,  $I_E = (\beta_F + 1)I_B$ , so

$$I_B = \frac{1.02 \text{ mA}}{50 + 1} = 19.8 \mu\text{A} \quad \text{and} \quad I_C = \beta_F I_B = 0.990 \text{ mA}$$

Because all the currents are positive, the assumption of forward-active region operation was correct. The collector-emitter voltage is equal to

$$V_{CE} = V_{CC} - I_C R_C - (-V_{BE}) = 9 - .990 \text{ mA}(4.3 \text{ k}\Omega) + 0.7 = 5.44 \text{ V}$$

The Q-point is (0.990 mA, 5.44 V).

**Check of Results:** We see that KVL is satisfied around the output loop containing the collector-emitter voltage:  $+9 - V_{RC} - V_{CE} - V_R - (-9) = 9 - 4.3 - 5.4 - 8.3 + 9 = 0$ . We must check the forward-active region assumption:  $V_{CE} = 5.4$  V which is greater than  $V_{BE} = 0.7$  V. Also,  $I_C + I_B = I_E$ .

**Discussion:** In this circuit, the combination of the resistor and the -9-V source replace the current source that was used to bias the transistor in Fig. 5.16(a).

**Computer-Aided Analysis:** SPICE contains a built-in model for the bipolar transistor that will be discussed in detail in Sec. 5.10. SPICE simulation with the default *npn* transistor model yields a Q-point that agrees well with our hand analysis: (0.993 mA, 5.50 V).

**EXERCISE:** (a) Find the Q-point in Ex. 5.5 if the resistor is changed to 5.6 kΩ. (b) What value of  $R$  is required to set the current to approximately 100 μA in the original circuit?

**ANSWERS:** (a) (1.45 mA, 3.5 V); (b) 82 kΩ.

Figure 5.19 displays the results of simulation of the collector current of the transistor in Fig. 5.18 versus the supply voltage  $V_{CC}$ . For  $V_{CC} > 0$ , the collector-base junction will be reverse-biased, and the transistor will be in the forward-active region. In this region, the circuit behaves essentially as a 1-mA ideal current source in which the output current is independent of  $V_{CC}$ . Note that the circuit

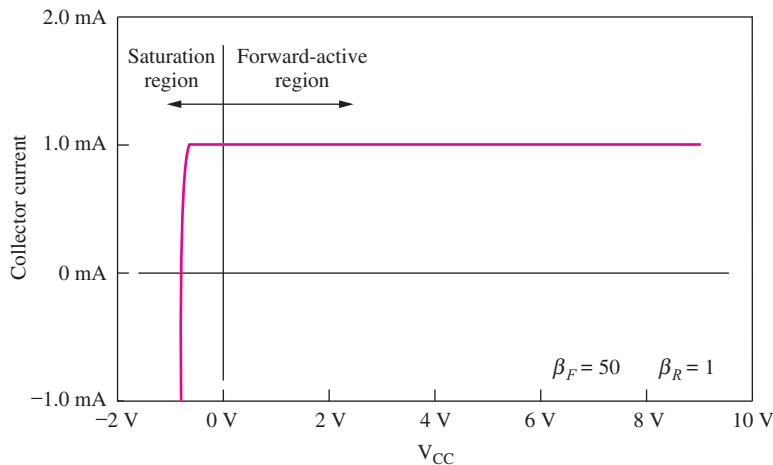


**Figure 5.19** Simulation of output characteristics of circuit of Fig. 5.18(a).

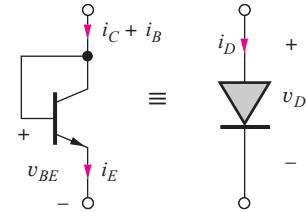


**Figure 5.20** Diode-connected transistor.

actually behaves as a current source for  $V_{CC}$  down to approximately  $-0.5$  V. By the definitions in Table 5.2, the transistor enters saturation for  $V_{CC} < 0$ , but the transistor does not actually enter heavy saturation until the base-collector junction begins to conduct for  $V_{BC} \geq +0.5$  V.

**EXERCISE:** Find the three terminal currents in the transistor in Fig. 5.18 if the  $8.2\text{ k}\Omega$  resistor value is changed to  $5.6\text{ k}\Omega$ .

**ANSWER:**  $1.48\text{ mA}$ ,  $29.1\text{ }\mu\text{A}$ ,  $1.45\text{ mA}$ .

**EXERCISE:** What are the actual values of  $V_{BE}$  and  $V_{CE}$  for the transistor in Fig. 5.18(a) if  $I_S = 5 \times 10^{-16}$  A? (Note that an iterative solution is necessary.)

**ANSWERS:**  $0.708\text{ V}$ ,  $5.44\text{ V}$

### 5.7.3 DIODES IN BIPOLAR INTEGRATED CIRCUITS

In integrated circuits, we often want the characteristics of a diode to match those of the BJT as closely as possible. In addition, it takes about the same amount of area to fabricate a diode as a full bipolar transistor. For these reasons, a diode is usually formed by connecting the base and collector terminals of a bipolar transistor, as shown in Fig. 5.20. This connection forces  $v_{BC} = 0$ .

Using the transport model equations for BJT with this boundary condition yields an expression for the terminal current of the “diode”:

$$i_D = (i_C + i_B) = \left( I_S + \frac{I_S}{\beta_F} \right) \left[ \exp \left( \frac{v_{BE}}{V_T} \right) - 1 \right] = \frac{I_S}{\alpha_F} \left[ \exp \left( \frac{v_D}{V_T} \right) - 1 \right] \quad (5.26)$$

The terminal current has an  $i-v$  characteristic corresponding to that of a diode with a reverse saturation current that is determined by the BJT parameters. This technique is often used in both analog and digital circuit design; we will see many examples of its use in the analog designs in Part III.

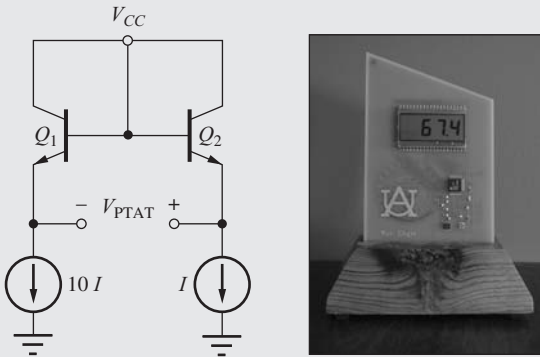
**EXERCISE:** What is the equivalent saturation current of the diode in Fig. 5.20 if the transistor is described by  $I_S = 2 \times 10^{-14}$  A and  $\alpha_F = 0.95$ ?

**ANSWER:**  $21\text{ fA}$



### The Bipolar Transistor PTAT Cell

The diode version of the PTAT cell that generates an output voltage proportional to absolute temperature was introduced back in Chapter 3. We can also easily implement the PTAT cell using two bipolar transistors as shown in the figure here in which two identical bipolar transistors are biased in the forward-active region by current sources with a 10:1 current ratio.



The PTAT voltage is given by

$$V_{\text{PTAT}} = V_{E2} - V_{E1} = (V_{CC} - V_{BE2}) - (V_{CC} - V_{BE1}) = V_{BE1} - V_{BE2}$$

$$V_{\text{PTAT}} = V_T \ln \left( \frac{10I}{I_S} \right) - V_T \ln \left( \frac{I}{I_S} \right) = \frac{kT}{q} \ln(10)$$

The bipolar PTAT cell is the circuit most commonly used in electronic thermometry.

#### 5.7.4 SIMPLIFIED MODEL FOR THE REVERSE-ACTIVE REGION

In the reverse-active region, also called the inverse-active region, the roles of the emitter and collector terminals are reversed. The base-collector diode is forward-biased and the base-emitter junction is reverse-biased, and we can assume that  $\exp(v_{BE}/V_T) \ll 1$  for  $v_{BE} < -0.1$  V just as we did in simplifying Eq. Set (5.21). Applying this approximation to Eq. (5.13) and neglecting the  $-1$  terms relative to the exponential terms yields the simplified equations for the reverse-active region:

$$i_C = -\frac{I_S}{\alpha_R} \exp \left( \frac{v_{BC}}{V_T} \right) \quad i_E = -I_S \exp \left( \frac{v_{BC}}{V_T} \right) \quad i_B = \frac{I_S}{\beta_R} \exp \left( \frac{v_{BC}}{V_T} \right) \quad (5.27)$$

Ratios of these equations yield  $i_E = -\beta_R i_B$  and  $i_E = \alpha_R i_C$ .

Equations (5.27) lead to the simplified circuit model for the reverse-active region shown in Fig. 5.21. The base current in the base-collector diode is amplified by the reverse common-emitter current gain  $\beta_R$  and enters the emitter terminal.

In the reverse-active region, the base-collector diode is now forward-biased, and the transistor model of Fig. 5.21(b) can be further simplified to that of Fig. 5.21(c), in which the diode is replaced by its CVD model with a voltage of 0.7 V. The base and collector voltages differ only by one 0.7-V diode drop in the reverse-active region.

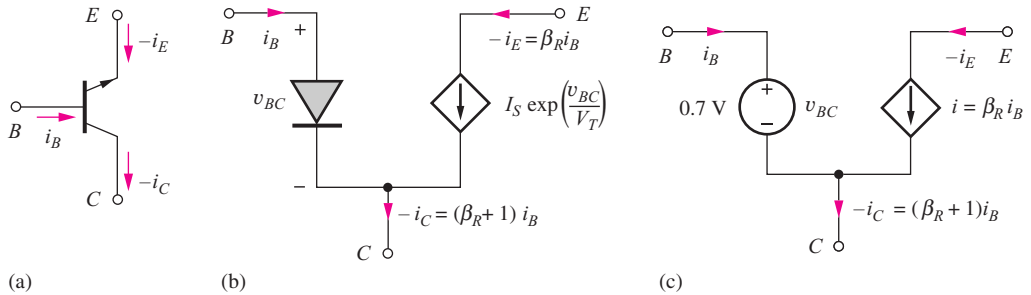


**Figure 5.21** (a) *npn* transistor in the reverse active region. (b) Simplified circuit model for the reverse-active region. (c) Further simplification in the reverse-active region using the CVD model for the diode.

### EXAMPLE 5.6 REVERSE-ACTIVE REGION ANALYSIS

Although the reverse active region is not often used, one does encounter it fairly frequently in the laboratory. If the transistor is inadvertently plugged in upside down, for example, the transistor will be operating in the reverse-active region. On the surface, the circuit will seem to be working but not very well. It is useful to be able to recognize when this error has occurred.

**PROBLEM** The collector and emitter terminals of the *npn* transistor in Fig. 5.18 have been interchanged in the circuit in Fig. 5.22 (perhaps the transistor was plugged into the circuit backwards by accident). Find the new Q-point for the transistor in the circuit in Fig. 5.22.

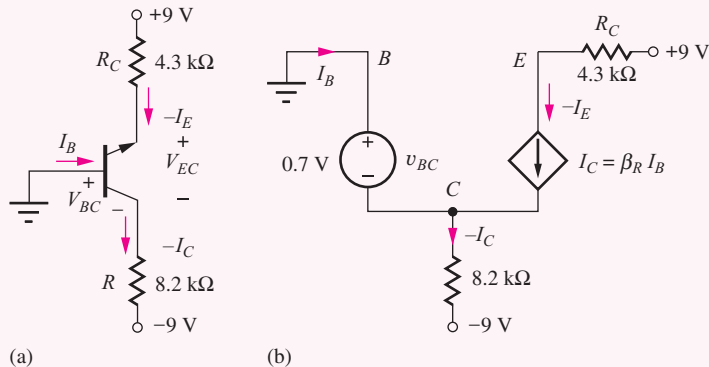


**Figure 5.22** (a) Circuit of Fig. 5.18 with *npn* transistor orientation reversed. (b) Circuit simplification using the model for the reverse-active region. (Analysis of the circuit uses  $\beta_F = 50$  and  $\beta_R = 1$ .)

**SOLUTION** **Known Information and Given Data:** *npn* transistor in the circuit in Fig. 5.22 with  $\beta_F = 50$  and  $\beta_R = 1$

**Unknowns:** Q-point ( $I_C$ ,  $V_{CE}$ )

**Approach:** In this circuit, the base-emitter junction is reverse-biased by the 9-V source ( $V_{BE} = V_B - V_E = -9$  V). The combination of the 8.2-kΩ resistor and the -9-V source will pull a current *out* of the collector and forward-bias the base-collector junction. Thus, the transistor appears to be biased in the reverse-active region of operation.

**Assumptions:** Assume reverse-active region operation; since we do not know the saturation current, assume  $V_{BC} = 0.7$  V; use the simplified model for the reverse-active region to analyze the circuit as in Fig. 5.22(b).

**Analysis:** The current exiting from the collector ( $-I_C$ ) is now equal to

$$(-I_C) = \frac{-0.7 \text{ V} - (-9 \text{ V})}{8200 \Omega} = 1.01 \text{ mA}$$

The current through the 8.2-k $\Omega$  resistor is unchanged compared to that in Fig. 5.18. However, significant differences exist in the currents in the base terminal and the +9-V source. At the collector node,  $(-I_C) = (\beta_R + 1)I_B$ , and at the emitter,  $(-I_E) = \beta_R I_B$ :

$$I_B = \frac{1.01 \text{ mA}}{2} = 0.505 \text{ mA} \quad \text{and} \quad -I_E = (1)I_B = 0.505 \text{ mA}$$

$$V_{EC} = 9 - 4300(0.505 \text{ mA}) - (-0.7 \text{ V}) = 7.5 \text{ V}$$

**Check of Results:** We see that KVL is satisfied around the output loop containing the collector-emitter voltage:  $+9 - V_{CE} - V_R - (-9) = 9 - 9.7 - 8.3 + 9 = 0$ . Also,  $I_C + I_B = I_E$ , and the calculated current directions are all consistent with the assumption of reverse-active region operation. Finally  $V_{EB} = 9 - 43 \text{ k}\Omega (0.505 \text{ mA}) = 6.8 \text{ V}$ .  $V_{EB} > 0 \text{ V}$ , and the reverse active assumption is correct.

**Discussion:** Note that the base current is much larger than expected, whereas the current entering the upper terminal of the device is much smaller than would be expected if the transistor were in the circuit as originally drawn in Fig. 5.18. These significant differences in current often lead to unexpected shifts in voltage levels at the base and collector terminals of the transistor in more complicated circuits.

**Computer-Aided Design:** The built-in SPICE model is valid for any operating region, and simulation with the default model gives results very similar to hand calculations.

## DESIGN NOTE

Note that the currents for reverse-active region operation are usually very different from those found for forward-active region operation in Fig. 5.18. These drastic differences are often useful in debugging circuits that we have built in the lab and can be used to discover transistors that have been improperly inserted into a circuit breadboard.

**EXERCISE:** Find the three terminal currents in the transistor in Fig. 5.22 if the resistor value is changed to 5.6 k $\Omega$ .

**ANSWER:** 1.48 mA, 0.741 mA, 0.741 mA

### 5.7.5 MODELING OPERATION IN THE SATURATION REGION

The fourth and final region of operation is called the saturation region. In this region, both junctions are forward-biased, and the transistor typically operates with a small voltage between collector and emitter terminals. In the saturation region, the dc value of  $v_{CE}$  is called the **saturation voltage** of the transistor:  $v_{CESAT}$  for the *npn* transistor or  $v_{ECSAT}$  for the *pnp* transistor.

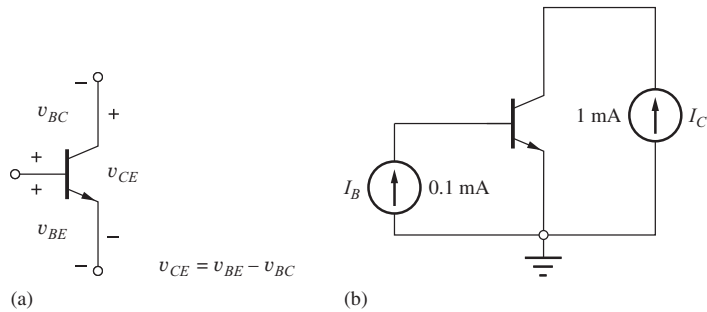


**Figure 5.23** (a) Relationship between the terminal voltages of the transistor. (b) Circuit for Example 5.8.

In order to determine  $v_{CESAT}$ , we assume that both junctions are forward-biased so that  $i_C$  and  $i_B$  from Eqs. (5.13) can be approximated as

$$\begin{aligned} i_C &= I_S \exp\left(\frac{v_{BE}}{V_T}\right) - \frac{I_S}{\alpha_R} \exp\left(\frac{v_{BC}}{V_T}\right) \\ i_B &= \frac{I_S}{\beta_F} \exp\left(\frac{v_{BE}}{V_T}\right) + \frac{I_S}{\beta_R} \exp\left(\frac{v_{BC}}{V_T}\right) \end{aligned} \quad (5.28)$$

Simultaneous solution of these equations using  $\beta_R = \alpha_R/(1 - \alpha_R)$  yields expressions for the base-emitter and base-collector voltages:

$$v_{BE} = V_T \ln \frac{i_B + (1 - \alpha_R)i_C}{I_S \left[ \frac{1}{\beta_F} + (1 - \alpha_R) \right]} \quad \text{and} \quad v_{BC} = V_T \ln \frac{i_B - \frac{i_C}{\beta_F}}{I_S \left[ \frac{1}{\alpha_R} \right] \left[ \frac{1}{\beta_F} + (1 - \alpha_R) \right]} \quad (5.29)$$

By applying KVL to the transistor in Fig. 5.23, we find that the collector-emitter voltage of the transistor is  $v_{CE} = v_{BE} - v_{BC}$ , and substituting the results from Eqs. (5.29) into this equation yields an expression for the saturation voltage of the *npn* transistor:

$$v_{CESAT} = V_T \ln \left[ \left( \frac{1}{\alpha_R} \right) \frac{1 + \frac{i_C}{(\beta_R + 1)i_B}}{1 - \frac{i_C}{\beta_F i_B}} \right] \quad \text{for } i_B > \frac{i_C}{\beta_F} \quad (5.30)$$

This equation is important and highly useful in the design of saturated digital switching circuits. For a given value of collector current, Eq. (5.30) can be used to determine the base current required to achieve a desired value of  $v_{CESAT}$ .

Note that Eq. (5.30) is valid only for  $i_B > i_C/\beta_F$ . This is an auxiliary condition that can be used to define saturation region operation. The ratio  $i_C/\beta_F$  represents the base current needed to maintain transistor operation in the forward-active region. If the base current exceeds the value needed for forward-active region operation, the transistor will enter saturation. The actual value of  $i_C/i_B$  is often called the **forced beta**  $\beta_{FOR}$  of the transistor, where  $\beta_{FOR} \leq \beta_F$ .

### EXAMPLE 5.7 SATURATION VOLTAGE CALCULATION

The BJT saturation voltage is important in many switching applications. Here we find an example of the value of the saturation voltage for a forced beta of 10.

**PROBLEM** Calculate the saturation voltage for an *npn* transistor with  $I_C = 1 \text{ mA}$ ,  $I_B = 0.1 \text{ mA}$ ,  $\beta_F = 50$ , and  $\beta_R = 1$ .

**SOLUTION** **Known Information and Given Data:** An *npn* transistor is operating with  $I_C = 1 \text{ mA}$ ,  $I_B = 0.1 \text{ mA}$ ,  $\beta_F = 50$ , and  $\beta_R = 1$

**Unknowns:** Collector-emitter voltage of the transistor

**Approach:** Because  $I_C/I_B = 10 < \beta_F$ , the transistor will indeed be saturated. Therefore we can use Eq. (5.30) to find the saturation voltage.

**Assumptions:** Room temperature operation with  $V_T = 0.025 \text{ V}$

**Analysis:** Using  $\alpha_R = \beta_R/(\beta_R + 1) = 0.5$  and  $I_C/I_B = 10$  yields

$$v_{CESAT} = (0.025 \text{ V}) \ln \left[ \left( \frac{1}{0.5} \right) \frac{1 + \frac{1 \text{ mA}}{2(0.1 \text{ mA})}}{1 - \frac{1 \text{ mA}}{50(0.1 \text{ mA})}} \right] = 0.068 \text{ V}$$

**Check of Results:** A small, nearly zero, value of saturation voltage is expected; thus the calculated value appears reasonable.

**Discussion:** We see that the value of  $V_{CE}$  in this example is indeed quite small. However, it is nonzero even for  $i_C = 0$  [see Prob. 5.58]! It is impossible to force the forward voltages across both *pn* junctions to be exactly equal, which is a consequence of the asymmetric values of the forward and reverse current gains. The existence of this small voltage “offset” is an important difference between the BJT and the MOSFET. In the case of the MOSFET, the voltage between drain and source becomes zero when the drain current is zero.

**Computer-Aided Analysis:** We can simulate the situation in this example by driving the base of the BJT with one current source and the collector with a second. (This is one of the few circuit situations in which we can force a current into the collector using a current source.) SPICE yields  $V_{CESAT} = 0.070 \text{ V}$ . The default temperature in SPICE is  $27^\circ\text{C}$ , and the slight difference in  $V_T$  accounts for the difference between SPICE result and our hand calculations.

**EXERCISE:** What is the saturation voltage in Ex. 5.7 if the base current is reduced to  $40 \mu\text{A}$ ?

**ANSWER:**  $99.7 \text{ mV}$

**EXERCISE:** Use Eqs. (5.29) to find  $V_{BESAT}$  and  $V_{BCSAT}$  for the transistor in Ex. 5.7 if  $I_S = 10^{-15} \text{ A}$ .

**ANSWERS:**  $0.694 \text{ V}$ ,  $0.627 \text{ V}$

Figure 5.24 shows the simplified model for the transistor in saturation in which the two diodes are assumed to be forward-biased and replaced by their respective on-voltages. The forward voltages

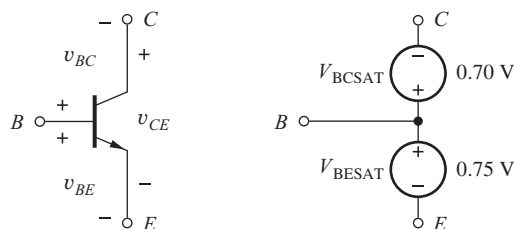
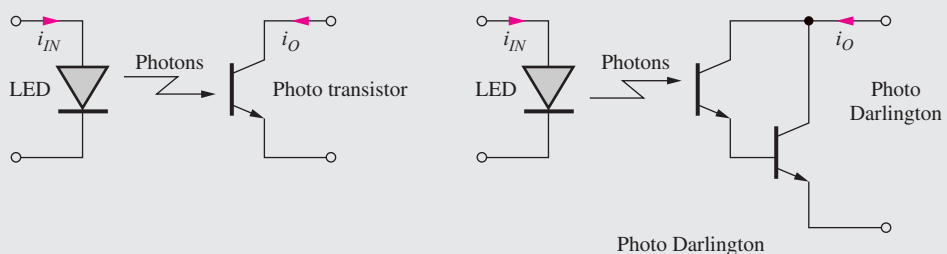


**Figure 5.24** Simplified model for the *npn* transistor in saturation.


**ELECTRONICS IN ACTION**
***Optical Isolators***

The optical isolator drawn schematically here represents a highly useful circuit that behaves much like a single transistor, but provides a very high breakdown voltage and low capacitance between its input and output terminals. Input current  $i_{IN}$  drives a light emitting diode (LED) whose output illuminates the base region of an *npn* transistor. Energy lost by the photons creates hole-electron pairs in the base of the *npn*. The holes represent base current that is then amplified by the current gain  $\beta_F$  of the transistor, whereas the electrons simply become part of the collector current.



The output characteristics of the optical isolator are very similar to those of a BJT operating in the active region in Fig. 5.10. However, the conversion of photons to hole-electron pairs is not very efficient in silicon, and the current transfer ratio,  $\beta_F = i_O/i_{IN}$ , of the optical isolator is often only around unity. The “Darlington connection” of two transistors (see Prob. 15.56), is often used to improve the overall current gain of the isolator. In this case, the output current is increased by the current gain of the second transistor.

The dc isolation provided by such devices can exceed a thousand volts and is limited primarily by the spacing of the pins and the characteristics of the circuit board that the isolator is mounted upon. ac isolation is limited to the low picofarad range by stray capacitance between the input and outputs pins.

of both diodes are normally higher in saturation than in the forward-active region, as indicated in the figure by  $V_{BESAT} = 0.75$  V and  $V_{BCSAT} = 0.7$  V. In this case,  $V_{CESAT}$  is 50 mV. In saturation, the terminal currents are determined by the external circuit elements; no simplifying relationships exist between  $i_C$ ,  $i_B$ , and  $i_E$  other than  $i_C + i_B = i_E$ .

## 5.8 NONIDEAL BEHAVIOR OF THE BIPOLAR TRANSISTOR

As with all devices, the BJT characteristics deviate from our ideal mathematical models in a number of ways. The emitter-base and collector-base diodes that form the bipolar transistor have finite reverse breakdown voltages (See Section 3.6.2) that we must carefully consider when choosing a transistor or the power supplies for our circuits. There are also capacitances associated with each of the diodes, and these capacitances place limitations on the high frequency response of the transistor. In addition, we know that holes and electrons in semiconductor materials have finite velocities. Thus, it takes time for the carriers to move from the emitter to the collector, and this time delay places an additional limit on the upper frequency of operation of the bipolar transistor. Finally, the output characteristics of the BJT exhibit a dependence on collector-emitter voltage similar to the channel-length modulation effect that occurs in the MOS transistor (Section 4.2.7). This section considers each of these limitations in more detail.

### 5.8.1 JUNCTION BREAKDOWN VOLTAGES

The bipolar transistor is formed from two back-to-back diodes, each of which has a Zener breakdown voltage associated with it. If the reverse voltage across either *pn* junction is too large, the corresponding diode will break down. In the transistor structure in Fig. 5.1, the emitter region is the most heavily doped region and the collector is the most lightly doped region. These doping differences lead to a relatively low breakdown voltage for the base-emitter diode, typically in the range of 3 to 10 V. On the other hand, the collector-base diode can be designed to break down at much larger voltages.<sup>9</sup> Transistors can be fabricated with collector-base breakdown voltages as high as several hundred volts.

Transistors must be selected with breakdown voltages commensurate with the reverse voltages that will be encountered in the circuit. In the forward-active region, for example, the collector-base junction is operated under reverse bias and must not break down. In the cutoff region, both junctions are reverse-biased, and the relatively low breakdown voltage of the emitter-base junction must not be exceeded.

### 5.8.2 MINORITY-CARRIER TRANSPORT IN THE BASE REGION

Current in the BJT is predominantly determined by the transport of *minority carriers* across the base region. In the *npn* transistor in Fig. 5.25, transport current  $i_T$  results from the diffusion of minority carriers—electrons in the *npn* transistor or holes in the *pnp*—across the base. Base current  $i_B$  is composed of hole injection back into the emitter and collector, as well as a small additional current  $I_{REC}$  needed to replenish holes lost to recombination with electrons in the base. These three components of base current are shown in Fig. 5.25(a).

An expression for the transport current  $i_T$  can be developed using our knowledge of carrier diffusion and the values of base-emitter and base-collector voltages. It can be shown from device physics (beyond the scope of this text) that the voltages applied to the base-emitter and base-collector junctions define the minority-carrier concentrations at the two ends of the base region through these relationships:

$$n(0) = n_{bo} \exp\left(\frac{v_{BE}}{V_T}\right) \quad \text{and} \quad n(W_B) = n_{bo} \exp\left(\frac{v_{BC}}{V_T}\right) \quad (5.31)$$

in which  $n_{bo}$  is the **equilibrium electron density** in the *p*-type base region.

The two junction voltages establish a minority-carrier concentration gradient across the base region, as illustrated in Fig. 5.25(b). For a narrow base, the minority-carrier density decreases linearly

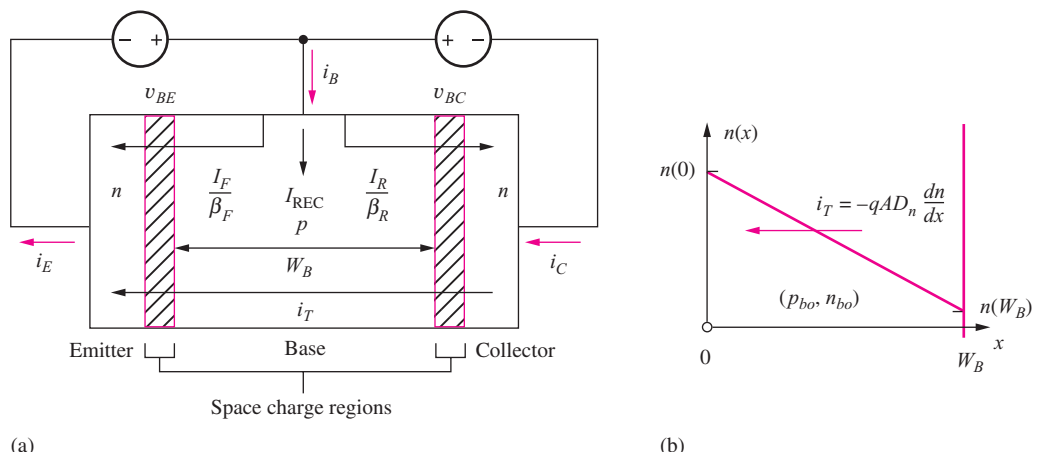


**Figure 5.25** (a) Currents in the base region of an *npn* transistor. (b) Minority-carrier concentration in the base of the *npn* transistor.

<sup>9</sup> Specially designed power transistors may have breakdown voltages in the 1000-V range.

across the base, and the diffusion current in the base can be calculated using the diffusion current expression in Eq. (2.14):

$$i_T = -qAD_n \frac{dn}{dx} = +qAD_n \frac{n_{bo}}{W_B} \left[ \exp\left(\frac{v_{BE}}{V_T}\right) - \exp\left(\frac{v_{BC}}{V_T}\right) \right] \quad (5.32)$$

where  $A$  = cross-sectional area of base region and  $W_B$  = **base width**. Because the carrier gradient is negative, electron current  $i_T$  is directed in the negative  $x$  direction, exiting the emitter terminal (positive  $i_T$ ).

Comparing Eqs. (5.32) and (5.19) yields a value for the bipolar transistor saturation current  $I_S$ :

$$I_S = qAD_n \frac{n_{bo}}{W_B} = \frac{qAD_n n_i^2}{N_{AB} W_B} \quad (5.33a)$$

where  $N_{AB}$  = doping concentration in base of transistor,  $n_i$  = intrinsic-carrier concentration ( $10^{10}/\text{cm}^3$ ), and  $n_{bo} = n_i^2/N_{AB}$  using Eq. (2.12).

The corresponding expression for the saturation current of the *pnp* transistor is

$$I_S = qAD_p \frac{p_{bo}}{W_B} = \frac{qAD_p n_i^2}{N_{DB} W_B} \quad (5.33b)$$

Remembering from Chapter 2 that mobility  $\mu$ , and hence diffusivity  $D = (kT/q)\mu$  ( $\text{cm}^2/\text{s}$ ), is larger for electrons than holes ( $\mu_n > \mu_p$ ), we see from Eqs. (5.33) that the *npn* transistor will conduct a higher current than the *pnp* transistor for a given set of applied voltages.

**EXERCISE:** (a) What is the value of  $D_n$  at room temperature if  $\mu_n = 500 \text{ cm}^2/\text{V} \cdot \text{s}$ ? (b) What is  $I_S$  for a transistor with  $A = 50 \mu\text{m}^2$ ,  $W = 1 \mu\text{m}$ ,  $D_n = 12.5 \text{ cm}^2/\text{s}$  and  $N_{AB} = 10^{18}/\text{cm}^3$ ?

**ANSWERS:** 12.5  $\text{cm}^2/\text{s}$ ;  $10^{-18} \text{ A}$

### 5.8.3 BASE TRANSIT TIME

To turn on the bipolar transistor, minority-carrier charge must be introduced into the base to establish the carrier gradient in Fig. 5.25(b). The **forward transit time**  $\tau_F$  represents the time constant associated with storing the required charge  $Q$  in the base region and is defined by

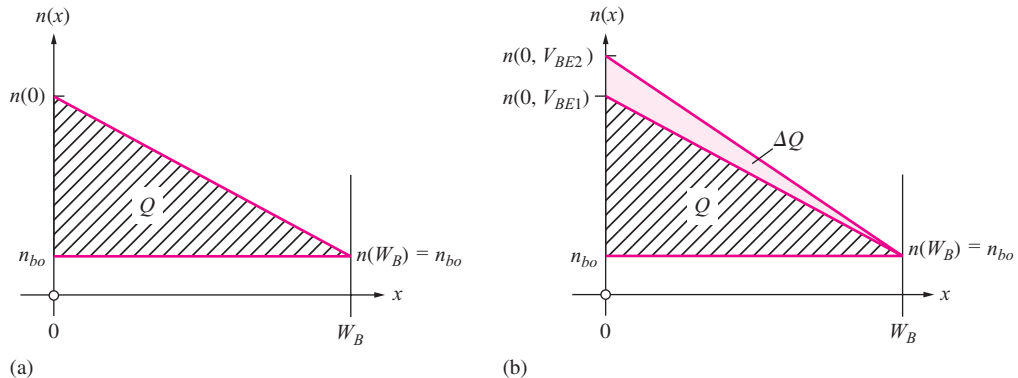
$$\tau_F = \frac{Q}{I_T} \quad (5.34)$$

Figure 5.26 depicts the situation in the neutral base region of an *npn* transistor operating in the forward-active region with  $v_{BE} > 0$  and  $v_{BC} = 0$ . The area under the triangle represents the excess minority charge  $Q$  that must be stored in the base to support the diffusion current. For the dimensions in Fig. 5.26 and using Eq. (5.31),

$$Q = qA[n(0) - n_{bo}] \frac{W_B}{2} = qAn_{bo} \left[ \exp\left(\frac{v_{BE}}{V_T}\right) - 1 \right] \frac{W_B}{2} \quad (5.35)$$

For the conditions in Fig. 5.26(a),

$$i_T = \frac{qAD_n}{W_B} n_{bo} \left[ \exp\left(\frac{v_{BE}}{V_T}\right) - 1 \right] \quad (5.36)$$



**Figure 5.26** (a) Excess minority charge  $Q$  stored in the bipolar base region. (b) Stored charge  $Q$  changes as  $v_{BE}$  changes.

Substituting Eqs. (5.35) and (5.36) into Eq. (5.34), the forward transit time for the *npn* transistor is found to be

$$\tau_F = \frac{W_B^2}{2D_n} = \frac{W_B^2}{2V_T\mu_n} \quad (5.37a)$$

The corresponding expression for the transit time of the *pnp* transistor is

$$\tau_F = \frac{W_B^2}{2D_p} = \frac{W_B^2}{2V_T\mu_p} \quad (5.37b)$$

The base transit time can be viewed as the average time required for a carrier emitted by the emitter to arrive at the collector. Hence, one would not expect the transistor to be able to reproduce frequencies with periods that are less than the transit time, and the base transit time in Eq. (5.37) places an upper limit on the useful operating frequency  $f$  of the transistor,

$$f \leq \frac{1}{2\pi\tau_F} \quad (5.38)$$

From Eq. (5.37), we see that the transit time is inversely proportional to the minority-carrier mobility in the base, and the difference between electron and hole mobility leads to an inherent frequency and speed advantage for the *npn* transistor. Thus, an *npn* transistor may be expected to be 2 to 2.5 times as fast as a *pnp* transistor for a given geometry and doping. Equation (5.37) also indicates the importance of shrinking the base width  $W_B$  of the transistor as much as possible. Early transistors had base widths of 10  $\mu\text{m}$  or more, whereas the base width of transistors in research laboratories today is 0.1  $\mu\text{m}$  (100 nm) or less.

### EXAMPLE 5.8 SATURATION CURRENT AND TRANSIT TIME

Device physics has provided us with expressions that can be used to estimate transistor saturation current and transit time based on a knowledge of physical constants and structural device information. Here we find representative values of  $I_S$  and  $\tau_F$  for a bipolar transistor.

**PROBLEM** Find the saturation current and base transit time for an *npn* transistor with a 100  $\mu\text{m} \times 100 \mu\text{m}$  emitter region, a base doping of  $10^{17}/\text{cm}^3$ , and a base width of 1  $\mu\text{m}$ . Assume  $\mu_n = 500 \text{ cm}^2/\text{V} \cdot \text{s}$ .

**SOLUTION** **Known Information and Given Data:** Emitter area = 100  $\mu\text{m} \times 100 \mu\text{m}$ ,  $N_{AB} = 10^{17}/\text{cm}^3$ ,  $W_B = 1 \mu\text{m}$ ,  $\mu_n = 500 \text{ cm}^2/\text{V} \cdot \text{s}$

**Unknowns:** Saturation current  $I_S$ ; transit time  $\tau_F$

**Approach:** Evaluate Eqs. (5.33) and (5.37) using the given data.

**Assumptions:** Room temperature operation with  $V_T = 0.025$  V and  $n_i = 10^{10}/\text{cm}^3$

**Analysis:** Using Eq. (5.33) for  $I_S$ ,

$$I_S = \frac{qAD_n n_i^2}{N_{AB} W_B} = \frac{(1.6 \times 10^{-19} \text{ C})(10^{-2} \text{ cm})^2 \left(0.025 \text{ V} \times 500 \frac{\text{cm}^2}{\text{V} \cdot \text{s}}\right) \left(\frac{10^{20}}{\text{cm}^6}\right)}{\left(\frac{10^{17}}{\text{cm}^3}\right)(10^{-4} \text{ cm})} = 2 \times 10^{-15} \text{ A}$$

in which  $D_n = (kT/q)\mu_n$  has been used [remember Eq. (2.15)].

Using Eq. (5.37),

$$\tau_F = \frac{W_B^2}{2V_T \mu_n} = \frac{(10^{-4} \text{ cm})^2}{2(0.025 \text{ V}) \left(500 \frac{\text{cm}^2}{\text{V} \cdot \text{s}}\right)} = 4 \times 10^{-10} \text{ s}$$

**Check of Results:** The calculations appear correct, and the value of  $I_S$  is within the range given in Sec. 5.2.

**Discussion:** Operation of this particular transistor is limited to frequencies below  $f = 1/(2\pi\tau_F) = 400$  MHz.

#### 5.8.4 DIFFUSION CAPACITANCE

Capacitances are circuit elements that limit the high-frequency performance of MOS and bipolar devices. For the base-emitter voltage and hence the collector current in the BJT to change, the charge stored in the base region also must change, as illustrated in Fig. 5.26(b). This change in charge with  $v_{BE}$  can be modeled by a capacitance  $C_D$ , called the **diffusion capacitance**, placed in parallel with the forward-biased base-emitter diode as defined by

$$C_D = \frac{dQ}{dv_{BE}} \Big|_{\text{Q-point}} = \frac{1}{V_T} \frac{qAn_{bo}W_B}{2} \exp\left(\frac{V_{BE}}{V_T}\right) \quad (5.39)$$

This equation can be rewritten as

$$C_D = \frac{1}{V_T} \left[ \frac{qAD_n n_{bo}}{W_B} \exp\left(\frac{V_{BE}}{V_T}\right) \right] \left( \frac{W_B^2}{2D_n} \right) \cong \frac{I_T}{V_T} \tau_F \quad (5.40)$$

Because the transport current actually represents the collector current in the forward-active region, the expression for the diffusion capacitance is normally written as

$$C_D = \frac{I_C}{V_T} \tau_F \quad (5.41)$$

From Eq. (5.41), we see that the diffusion capacitance  $C_D$  is directly proportional to current and inversely proportional to temperature  $T$ . For example, a BJT operating at a current of 1 mA with  $\tau_F = 4 \times 10^{-10}$  s has a diffusion capacitance of

$$C_D = \frac{I_C}{V_T} \tau_F = \frac{10^{-3} \text{ A}}{0.025 \text{ V}} (4 \times 10^{-10} \text{ s}) = 16 \times 10^{-12} \text{ F} = 16 \text{ pF}$$

This is a substantial capacitance, but it can be even larger if the transistor is operating at significantly higher currents.

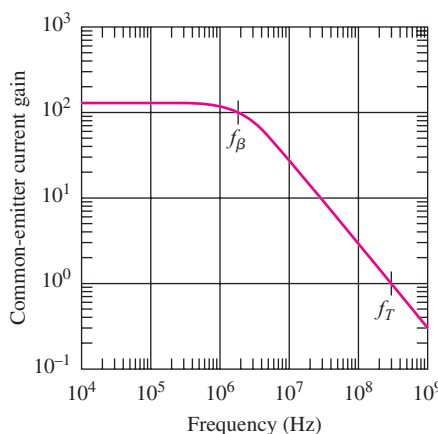


**Figure 5.27** Magnitude of the common-emitter current gain  $\beta$  vs. frequency.

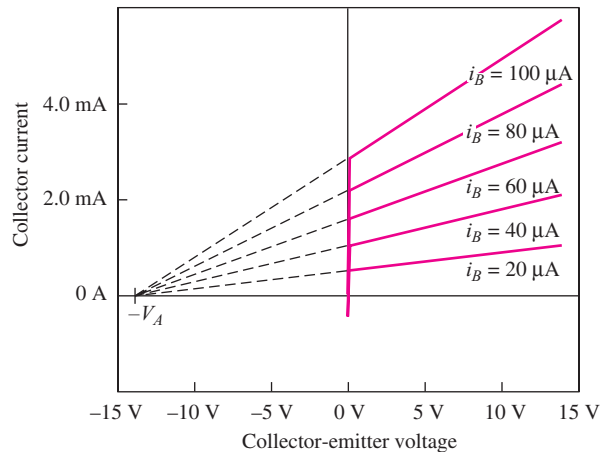


**Figure 5.28** Transistor output characteristics identifying the Early voltage  $V_A$ .

**EXERCISE:** Calculate the value of the diffusion capacitance for a power transistor operating at a current of 10 A and a temperature of 100°C if  $\tau_F = 4 \text{ nS}$ .

**ANSWERS:** 1.24  $\mu\text{F}$  — a significant capacitance!

### 5.8.5 FREQUENCY DEPENDENCE OF THE COMMON-EMITTER CURRENT GAIN

The forward-biased diffusion and reverse-biased  $pn$  junction capacitances of the bipolar transistor cause the current gain of the transistor to be frequency-dependent. An example of this dependence is given in Fig. 5.27. At low frequencies, the current gain has a constant value  $\beta_F$ , but as frequency increases, the current gain begins to decrease. The **unity-gain frequency**  $f_T$  is defined to be the frequency at which the magnitude of the current gain is equal to 1. The behavior in the graph is described mathematically by

$$\beta(f) = \frac{\beta_F}{\sqrt{1 + \left(\frac{f}{f_\beta}\right)^2}} \quad (5.42)$$

where  $f_\beta = f_T/\beta_F$  is the  **$\beta$ -cutoff frequency**. For the transistor in Fig. 5.27,  $\beta_F = 125$  and  $f_T = 300 \text{ MHz}$ .

**EXERCISE:** What is the  $\beta$ -cutoff frequency for the transistor in Fig. 5.27?

**ANSWER:** 2.4 MHz

### 5.8.6 THE EARLY EFFECT AND EARLY VOLTAGE

In the transistor output characteristics in Figs. 5.11 and 5.12, the current saturated at a constant value in the forward-active region. However, in a real transistor, there is actually a positive slope to the characteristics, as shown in Fig. 5.28. The collector current is not truly independent of  $v_{CE}$ . Note that this situation is the same as that found for the MOSFET in saturation.

It has been observed experimentally that when the output characteristic curves are extrapolated back to the point of zero collector current, the curves all intersect at a common point,  $v_{CE} = -V_A$ .

This phenomenon is called the **Early effect** [4], and the voltage  $V_A$  is called the **Early voltage** after James Early from Bell Laboratories, who first identified the source of the behavior. A relatively small value of Early voltage (14 V) has been used in Fig. 5.28 to exaggerate the characteristics. Values for the Early voltage more typically fall in the range

$$10 \text{ V} \leq V_A \leq 200 \text{ V}$$

### 5.8.7 MODELING THE EARLY EFFECT

The dependence of the collector current on collector-emitter voltage is easily included in the simplified mathematical model for the forward-active region of the BJT by modifying Eqs. (5.23) as follows:

$$\begin{aligned} i_C &= I_S \left[ \exp \left( \frac{v_{BE}}{V_T} \right) \right] \left[ 1 + \frac{v_{CE}}{V_A} \right] \\ \beta_F &= \beta_{FO} \left[ 1 + \frac{v_{CE}}{V_A} \right] \\ i_B &= \frac{I_S}{\beta_{FO}} \left[ \exp \left( \frac{v_{BE}}{V_T} \right) \right] \end{aligned} \quad (5.43)$$

$\beta_{FO}$  represents the value of  $\beta_F$  extrapolated to  $v_{CE} = 0$ . In these expressions, the collector current and current gain now have the same dependence on  $v_{CE}$ , but the base current remains independent of  $v_{CE}$ . This is consistent with Fig. 5.28, in which the separation of the constant-base-current curves in the forward-active region increases as  $v_{CE}$  increases, indicating that the current gain  $\beta_F$  is increasing with  $v_{CE}$ .

**EXERCISE:** A transistor has  $I_S = 10^{-15} \text{ A}$ ,  $\beta_{FO} = 75$ , and  $V_A = 50 \text{ V}$  and is operating with  $v_{BE} = 0.7 \text{ V}$  and  $v_{CE} = 10 \text{ V}$ . What are  $i_B$ ,  $\beta_F$ , and  $i_C$ ? What would be  $\beta_F$  and  $i_C$  if  $V_A = \infty$ ?

**ANSWERS:** 19.3  $\mu\text{A}$ , 90, 1.74 mA; 75, 1.45 mA

### 5.8.8 ORIGIN OF THE EARLY EFFECT

Modulation of the base width  $W_B$  of the transistor by the collector-base voltage is the cause of the Early effect. As the reverse bias across the collector-base junction increases, the width of the collector-base depletion layer increases, and the width  $W_B$  of the base decreases. This mechanism, termed **base-width modulation**, is depicted in Fig. 5.29, in which the collector-base space charge

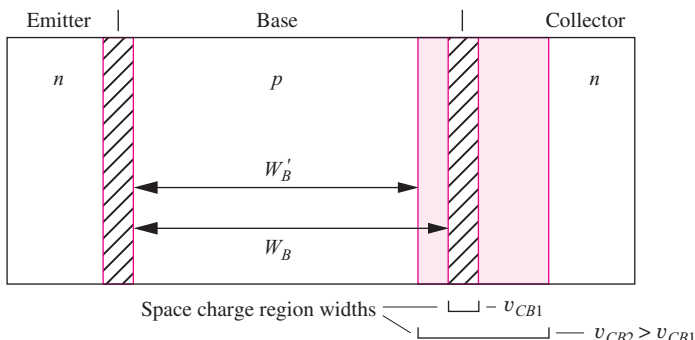


Figure 5.29 Base-width modulation, or Early effect.

region width is shown for two different values of collector-base voltage corresponding to effective base widths of  $W_B$  and  $W'_B$ . Equation (5.32) demonstrated that collector current is inversely proportional to the base width  $W_B$ , so a decrease in  $W_B$  results in an increase in transport current  $i_T$ . This decrease in  $W_B$  as  $V_{CB}$  increases is the cause of the Early effect.

The Early effect reduces the output resistance of the bipolar transistor and places an important limit on the amplification factor of the BJT. These limitations are discussed in detail in Part III, Chapter 13. Note that both the Early effect in the BJT and channel-length modulation in the MOSFET are similar in the sense that the nonzero slope of the output characteristics is related to changes in a characteristic length within the device as the voltage across the output terminals of the transistor changes.

## 5.9 TRANSCONDUCTANCE

The important transistor parameter, **transconductance**  $g_m$ , was introduced during our study of the MOSFET in Chapter 4. For the bipolar transistor,  $g_m$  relates changes in  $i_C$  to changes in  $v_{BE}$  and is defined by

$$g_m = \left. \frac{di_C}{dv_{BE}} \right|_{Q\text{-point}} \quad (5.44)$$

For Q-points in the forward-active region, Eq. (5.44) can be evaluated using the collector-current expression from Eq. (5.23):

$$g_m = \left. \frac{d}{dv_{BE}} \left\{ I_S \exp \left( \frac{v_{BE}}{V_T} \right) \right\} \right|_{Q\text{-point}} = \frac{1}{V_T} I_S \exp \left( \frac{V_{BE}}{V_T} \right) = \frac{I_C}{V_T} \quad (5.45)$$

Equation (5.45) represents the fundamental relationship for the transconductance of the bipolar transistor, in which we find  $g_m$  is directly proportional to collector current. This is an important result that is used many times in bipolar circuit design. It is worth noting that the expression for the transit time defined in Eq. (5.41) can be rewritten as

$$\tau_F = \frac{C_D}{g_m} \quad \text{or} \quad C_D = g_m \tau_F \quad (5.46)$$

### DESIGN NOTE

#### BIPOLAR TRANSCONDUCTANCE

$$g_m = \frac{I_C}{V_T}$$

The BJT transconductance is substantially higher than that of the FET for a given operating current. This difference will be discussed in more detail in Chapters 13 and 14.

### DESIGN NOTE

#### TRANSIT TIME

$$\tau_F = \frac{C_D}{g_m}$$

Transit time  $\tau_F$  places an upper limit on the frequency response of the bipolar device.

**EXERCISE:** What is the value of the BJT transconductance  $g_m$  at  $I_C = 100 \mu\text{A}$  and  $I_C = 1 \text{ mA}$ ? What is the value of the diffusion capacitance for each of these currents if the base transit time is 25 psec?

**ANSWERS:** 4 mS; 40 mS; 0.1 pF; 1.0 pF

## 5.10 BIPOLAR TECHNOLOGY AND SPICE MODEL

In order to create a comprehensive simulation model of the bipolar transistor, our knowledge of the physical structure of the transistor is coupled with the transport model expressions and experimental observations. We typically start with a circuit representation of our mathematical model that describes the intrinsic behavior of the transistor, and then add additional elements to model parasitic effects introduced by the actual physical structure. Remember, in any case, that our SPICE models represent only lumped element equivalent circuits for the distributed structure that we actually fabricate.

Although we will seldom use the equations that make up the simulation model in hand calculations, awareness and understanding of the equations can help when SPICE generates unexpected results. This can happen when we attempt to use a device in an unusual way, or the simulator may produce a circuit result that does not fit within our understanding of the device behavior. Understanding the internal model in SPICE will help us interpret whether our knowledge of the device is wrong or if the simulation has some built-in assumptions that may not be consistent with a particular application of the device.

### 5.10.1 QUALITATIVE DESCRIPTION

A detailed cross section of the classic *npn* structure from Fig. 5.1 is given in Fig. 5.30(a), and the corresponding SPICE circuit model appears in Fig. 5.30(b). Circuit elements  $i_C$ ,  $i_B$ ,  $C_{BE}$ , and  $C_{BC}$  describe the intrinsic transistor behavior that we have discussed thus far. Current source  $i_C$  represents the current transported across the base from collector to emitter, and current source  $i_B$  models the total base current of the transistor. **Base-emitter** and **base-collector** capacitances  $C_{BE}$  and  $C_{BC}$  include

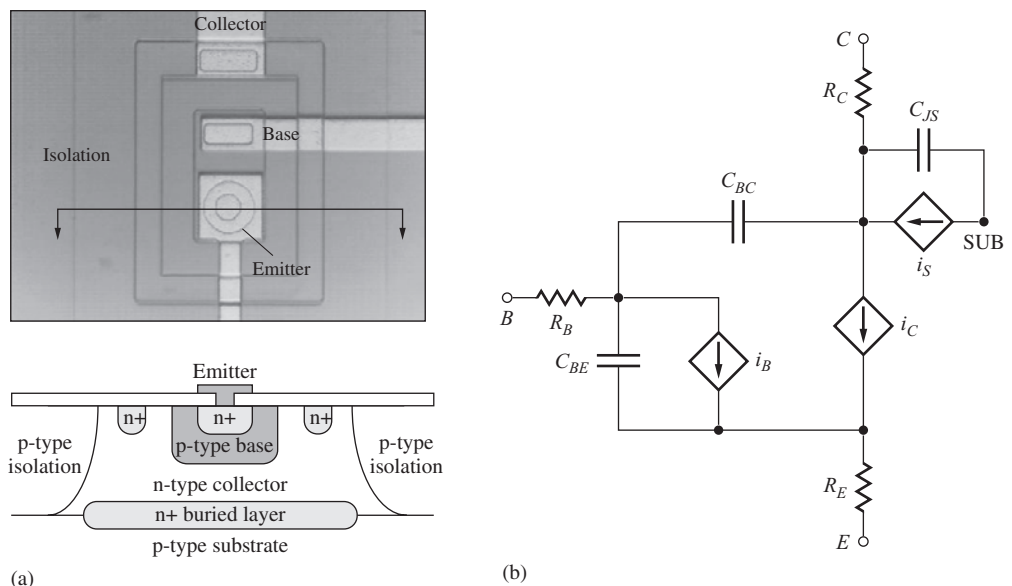


**Figure 5.30** (a) Top view and cross section of a junction-isolated transistor. (b) SPICE model for the *npn* transistor.

models for the diffusion capacitances and the junction capacitances associated with the base-emitter and base-collector diodes.

Additional circuit elements are added to account for nonideal characteristics of the real transistor. The physical structure has a large-area *pn* junction that isolates the collector from the substrate of the transistor and separates one transistor from the next. The primary components related to this junction are diode current  $i_S$  and capacitance  $C_{JS}$ . Base resistance  $R_B$  accounts for the resistance between the external base contact and the intrinsic base region of the transistor. Similarly, collector current must pass through  $R_C$  on its way to the active region of the collector-base junction, and  $R_E$  models any extrinsic emitter resistance present in the device.

### 5.10.2 SPICE MODEL EQUATIONS

The SPICE models are comprehensive but quite complex. Even the model equations presented below represent simplified versions of the actual models. Table 5.3 defines the SPICE parameters that are used in these expressions. More complete descriptions can be found in [7].

The collector and base currents are given by

$$i_C = \frac{(i_F - i_R)}{KBQ} - \frac{i_R}{BR} - i_{RG} \quad \text{and} \quad i_B = \frac{i_F}{BF} + \frac{i_R}{BR} + i_{FG} + i_{RG}$$

**TABLE 5.3**

Bipolar Device Parameters for Circuit Simulation (*npn/pnp*)

PARAMETER	NAME	DEFAULT	TYPICAL VALUES
Saturation current	IS	$10^{-16}$ A	$3 \times 10^{-17}$ A
Forward current gain	BF	100	100
Forward emission coefficient	NF	1	1.03
Forward Early voltage	VAF	$\infty$	75 V
Forward knee current	IKF	$\infty$	0.05 A
Reverse knee current	IKR	$\infty$	0.01 A
Reverse current gain	BR	1	0.5
Reverse emission coefficient	NR	1	1.05
Base resistance	RB	0	$250 \Omega$
Collector resistance	RC	0	$50 \Omega$
Emitter resistance	RE	0	$1 \Omega$
Forward transit time	TF	0	0.15 nS
Reverse transit time	TR	0	15 nS
Base-emitter leakage saturation current	ISE	0	1 pA
Base-emitter leakage emission coefficient	NE	1.5	1.4
Base-emitter junction capacitance	CJE	0	0.5 pF
Base-emitter junction potential	PHIE	0.8 V	0.8 V
Base-emitter grading coefficient	ME	0.5	0.5
Base-collector leakage saturation current	ISC	0	1 pA
Base-collector leakage emission coefficient	NC	1.5	1.4
Base-collector junction capacitance	CJC	0	1 pF
Base-collector junction potential	PHIC	0.75 V	0.7 V
Base-collector grading coefficient	MC	0.33	0.33
Substrate saturation current	ISS	0	1 fA
Substrate emission coefficient	NS	1	1
Collector-substrate junction capacitance	CJS	0	3 pF
Collector-substrate junction potential	VJS	0.75 V	0.75 V
Collector-substrate grading coefficient	MJS	0	0.5

in which the forward and reverse components of the transport current are

$$i_F = IS \cdot \left[ \exp \left( \frac{v_{BE}}{NF \cdot V_T} \right) - 1 \right] \quad \text{and} \quad i_R = IS \cdot \left[ \exp \left( \frac{v_{BC}}{NR \cdot V_T} \right) - 1 \right] \quad (5.47)$$

Base current  $i_B$  includes two added terms to model additional space-charge region currents associated with the base-emitter and base-collector junctions:

$$i_{FG} = ISE \cdot \left[ \exp \left( \frac{v_{BE}}{NE \cdot V_T} \right) - 1 \right] \quad \text{and} \quad i_{RG} = ISC \cdot \left[ \exp \left( \frac{v_{BC}}{NC \cdot V_T} \right) - 1 \right]$$

Another new addition is the KBQ term that includes voltages VAF and VAR to model the Early effect in both the forward and reverse modes, as well as “knee current” parameters IKF and IKR that model current gain fall-off at high operating currents. This phenomenon is discussed in more detail in Chapter 13.

$$\text{KBQ} = \left( \frac{1}{2} \right) \frac{1 + \left[ 1 + 4 \left( \frac{i_F}{IKF} + \frac{i_R}{IKR} \right) \right]^{NK}}{1 + \frac{v_{CB}}{\text{VAF}} + \frac{v_{EB}}{\text{VAR}}}$$

Note as well that the Early effect is cast in terms of  $v_{BC}$  rather than  $v_{CE}$  as we have used in Eq. (5.43).

The substrate junction current is expressed as

$$i_S = ISS \cdot \left[ \exp \left( \frac{v_{\text{SUB-C}}}{NS \cdot V_T} \right) - 1 \right]$$

The three device capacitances in Fig. 5.30(b) are represented by

$$C_{BE} = \frac{i_F}{NE \cdot V_T} \text{TF} + \frac{\text{CJE}}{\left( 1 - \frac{v_{BE}}{\text{PHIE}} \right)^{\text{MJE}}} \quad \text{and} \quad C_{BC} = \frac{i_R}{NC \cdot V_T} \text{TR} + \frac{\text{CJC}}{\left( 1 - \frac{v_{BC}}{\text{PHIC}} \right)^{\text{MJC}}}$$

$$C_{JS} = \frac{\text{CJS}}{\left( 1 + \frac{v_{\text{SUB-C}}}{\text{VJS}} \right)^{\text{MJS}}} \quad (5.48)$$

$C_{BE}$  and  $C_{BC}$  consist of two terms representing the diffusion capacitance (modeled by TF and NE or TR and NC) and depletion-region capacitance (modeled by CJE, PHIE, and MJE or CJC, PHIC, and MJC). The substrate diode is normally reverse biased, so it is modeled by just the depletion-layer capacitance (CJS, VJS, and MJS). The base, collector, and emitter series resistances are RB, RC, and RE, respectively.

The SPICE model for the *pnp* transistor is similar to that presented in Fig. 5.30(b) except for reversal of the current sources and of the positive polarity for the transistor currents and voltages.

### 5.10.3 HIGH-PERFORMANCE BIPOLAR TRANSISTORS

Modern transistors designed for high-speed switching and analog RF applications use combinations of sophisticated shallow and deep trench isolation processes to reduce the device capacitances and minimize the transit times. These devices typically utilize polysilicon emitters, have extremely narrow bases, and may incorporate SiGe base regions. A layout and cross section of a very high frequency, trench-isolated SiGe bipolar transistors appears in Fig. 5.31. In the research laboratory, SiGe transistors have already exhibited cutoff frequencies in excess of 300 GHz.

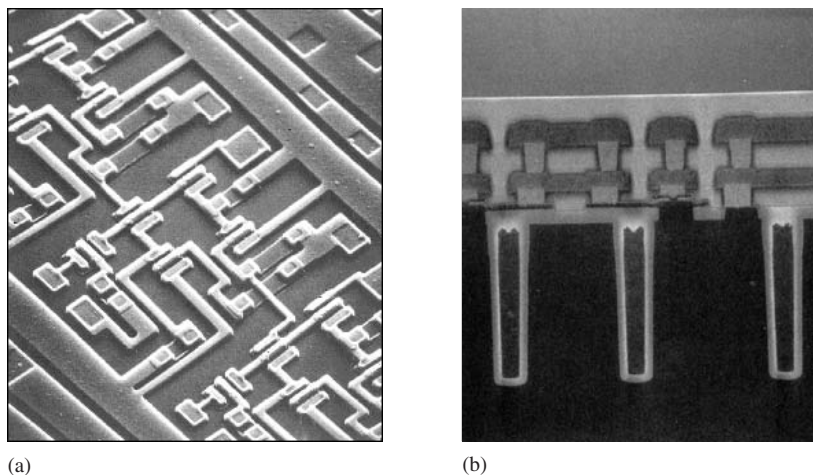


**Figure 5.31** (a) Top view of a high-performance trench-isolated integrated circuit. (b) Cross section of a high-performance trench-isolated bipolar transistor. Copyright ©1995, IEEE. Reprinted with permission from [8].

**EXERCISE:** A bipolar transistor has a current gain of 80, a collector current of  $350 \mu\text{A}$  for  $V_{BE} = 0.68 \text{ V}$ , and an Early voltage of  $70 \text{ V}$ . What are the values of SPICE parameters BF, IS, and VAF? Assume  $T = 27^\circ\text{C}$ .

**ANSWERS:** 80,  $1.35 \text{ fA}$ ,  $70 \text{ V}$

## 5.11 PRACTICAL BIAS CIRCUITS FOR THE BJT

The goal of biasing is to establish a known **quiescent operating point**, or **Q-point** that represents the initial operating region of the transistor. In the bipolar transistor, the Q-point is represented by the dc values of the collector-current and collector-emitter voltage ( $I_C, V_{CE}$ ) for the *npn* transistor, or emitter-collector voltage ( $I_C, V_{EC}$ ) for the *pnp*.

Logic gates and linear amplifiers use very different operating points. For example, the circuit in Fig. 5.32(a) can be used as either a logic inverter or a linear amplifier depending upon our choice of operating points. The voltage transfer characteristic (VTC) for the circuit appears in Fig. 5.33(a), and the corresponding output characteristics and load line appear in Fig. 5.33(b). For low values of  $v_{BE}$ , the transistor is nearly cut off, and the output voltage is  $5 \text{ V}$ , corresponding to a binary “1” in a logic applications. As  $v_{BE}$  increases above  $0.6 \text{ V}$ , the output drops quickly and reaches its “on-state” voltage of  $0.18 \text{ V}$  for  $v_{BE}$  greater than  $0.8 \text{ V}$ . The BJT is now operating in its saturation region, and the small “on-voltage” would correspond to a “0” in binary logic. These two logic states are also shown on the transistor output characteristics in Fig. 5.33(b). When the transistor is “on,” it conducts a substantial current, and  $v_{CE}$  falls to  $0.18 \text{ V}$ . When the transistor is off,  $v_{CE}$  equals  $5 \text{ V}$ . We study the design of logic gates in detail in Chapters 6–9.

For amplifier applications, the Q-point is located in the region of high slope (high gain) of the voltage transfer characteristic, also indicated in Fig. 5.33(a). At this operating point, the transistor is operating in the forward-active region, the region in which high voltage, current and/or power gain can be achieved. To establish this Q-point, a **dc bias**  $V_{BE}$  is applied to the base as in Fig. 5.32(b), and a small ac signal  $v_{be}$  is added to vary the base voltage around the bias value.<sup>10</sup> The variation in total base-emitter voltage  $v_{BE}$  causes the collector current to change, and an amplified replica of the

<sup>10</sup> Remember  $v_{BE} = V_{BE} + v_{be}$ .

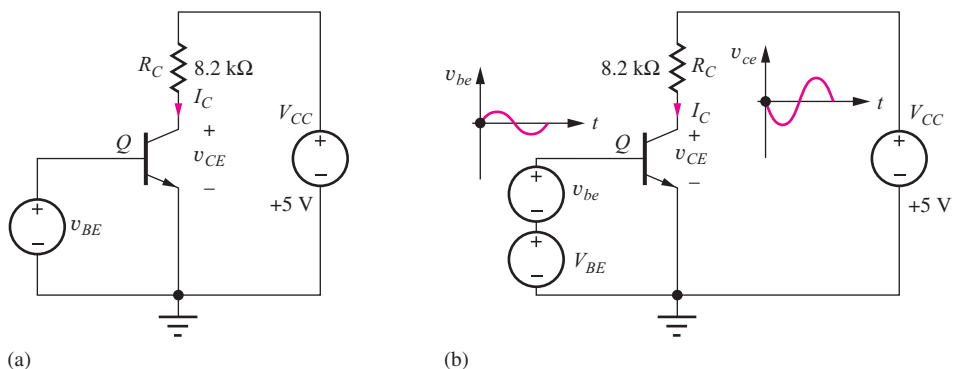


**Figure 5.32** (a) Circuit for a logic inverter. (b) The same transistor used as a linear amplifier.

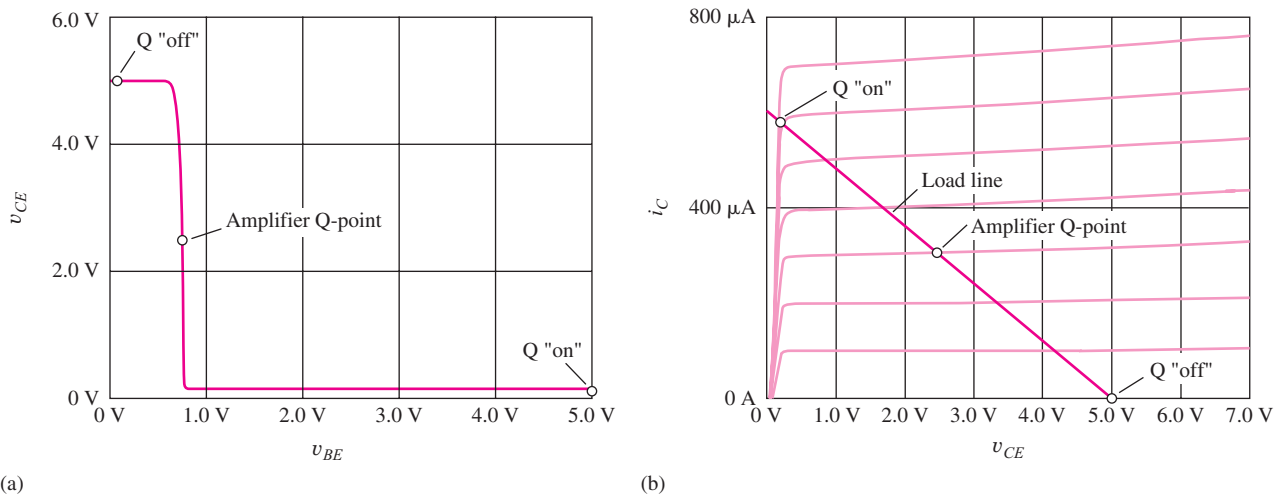


**Figure 5.33** (a) Voltage transfer characteristic (VTC) with quiescent operating points (Q-points) corresponding to an “on-switch,” an amplifier, and an “off switch.” (b) The same three operating points located on the transistor output characteristics.

ac input voltage appears at the collector. Our study of the design of transistor amplifiers begins in Chapter 13 of this text.

In Secs. 5.6 to 5.10, we presented simplified models for the four operating regions of the BJT. In general, we will not explicitly insert the simplified circuit models for the transistor into the circuit but instead will use the mathematical relationships that were derived for the specific operating region of interest. For example, in the forward-active region, the results  $V_{BE} = 0.7 \text{ V}$  and  $I_C = \beta_F I_B$  will be utilized to directly simplify the circuit analysis.

In the dc biasing examples that follow, the Early voltage is assumed to be infinite. In general, including the Early voltage in bias circuit calculations substantially increases the complexity of the analysis but typically changes the results by less than 10 percent. In most cases, the tolerances on the values of resistors and independent sources will be 5 to 10 percent, and the transistor current-gain  $\beta_F$  may vary by a factor of 4:1 to 10:1. For example, the current gain of a transistor may be specified to be a minimum of 50 with a typical value of 100 but no upper bound specified. These tolerances will swamp out any error due to neglect of the Early voltage. Thus, basic hand design will be done ignoring the Early effect, and if more precision is needed, the calculations can be refined through SPICE analysis.

### 5.11.1 FOUR-RESISTOR BIAS NETWORK

Because of the BJT's exponential relationship between current and voltage and its strong dependence on temperature  $T$ , the constant  $V_{BE}$  form of biasing utilized in Fig. 5.32 does not represent a practical technique. One of the best circuits for stabilizing the Q-point of a transistor is the four-resistor bias network in Fig. 5.34.  $R_1$  and  $R_2$  form a resistive voltage divider across the power supplies (12 V and 0 V) and attempt to establish a fixed voltage at the base of transistor  $Q_1$ .  $R_E$  and  $R_C$  are used to define the emitter current and collector-emitter voltage of the transistor.

Our goal is to find the Q-point of the transistor: ( $I_C$ ,  $V_{CE}$ ). The first steps in analysis of the circuit in Fig. 5.34(a) are to split the power supply into two equal voltages, as in Fig. 5.34(b), and then to simplify the circuit by replacing the base-bias network by its Thévenin equivalent circuit, as shown in Fig. 5.34(c).  $V_{EQ}$  and  $R_{EQ}$  are given by

$$V_{EQ} = V_{CC} \frac{R_1}{R_1 + R_2} \quad R_{EQ} = \frac{R_1 R_2}{R_1 + R_2} \quad (5.49)$$

For the values in Fig. 5.34(c),  $V_{EQ} = 4$  V and  $R_{EQ} = 12 \text{ k}\Omega$ .

Detailed analysis begins by assuming a region of operation in order to simplify the BJT model equations. Because the most common region of operation for this bias circuit is the forward-active

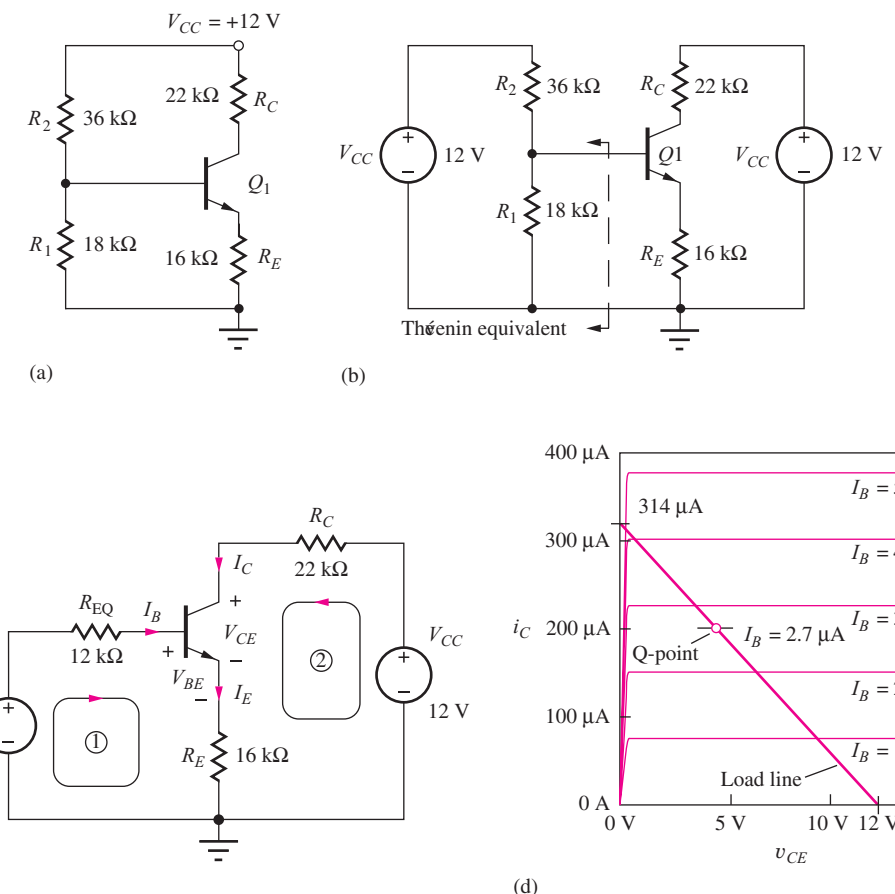


**Figure 5.34** (a) The four-resistor bias network. (Assume  $\beta_F = 75$  for analysis.) (b) Four-resistor bias circuit with replicated sources. (c) Thévenin simplification of the four-resistor bias network. (Assume  $\beta_F = 75$ .) (d) Load line for the four-resistor bias circuit.

region, we will assume it to be the region of operation. Using Kirchhoff's voltage law around loop 1:

$$V_{EQ} = I_B R_{EQ} + V_{BE} + I_E R_E = I_B R_{EQ} + V_{BE} + (\beta_F + 1) I_B R_E \quad (5.50)$$

Solving for  $I_B$  yields

$$I_B = \frac{V_{EQ} - V_{BE}}{R_{EQ} + (\beta_F + 1) R_E} \quad \text{where} \quad V_{BE} = V_T \ln \left( \frac{I_B}{I_S/\beta_F} + 1 \right) \quad (5.51)$$

Unfortunately, combining these expressions yields a transcendental equation. However, if we assume an approximate value of  $V_{BE}$ , then we can find the collector and emitter currents using our auxillary relationships  $I_C = \beta_F I_B$  and  $I_E = (\beta_F + 1) I_B$ :

$$I_C = \frac{V_{EQ} - V_{BE}}{\frac{R_{EQ}}{\beta_F} + \frac{(\beta_F + 1)}{\beta_F} R_E} \quad \text{and} \quad I_E = \frac{V_{EQ} - V_{BE}}{\frac{R_{EQ}}{(\beta_F + 1)} + R_E} \quad (5.52)$$

For large current gain ( $\beta_F \gg 1$ ), Eqs. (5.51) and (5.52) simplify to

$$I_E \cong I_C \cong \frac{V_{EQ} - V_{BE}}{\frac{R_{EQ}}{\beta_F} + R_E} \quad \text{with} \quad I_B \cong \frac{V_{EQ} - V_{BE}}{R_{EQ} + \beta_F R_E} \quad (5.53)$$

Now that  $I_C$  is known, we can use loop 2 to find collector-emitter voltage  $V_{CE}$ :

$$V_{CE} = V_{CC} - I_C R_C - I_E R_E = V_{CC} - I_C \left( R_C + \frac{R_E}{\alpha_F} \right) \quad (5.54)$$

since  $I_E = I_C / \alpha_F$ . Normally  $\alpha_F \cong 1$ , and Eq. (5.54) can be simplified to

$$V_{CE} \cong V_{CC} - I_C (R_C + R_E) \quad (5.55)$$

For the circuit in Fig. 5.34, we are assuming forward-active region operation with  $V_{BE} = 0.7$  V, and the Q-point values ( $I_C$ ,  $V_{CE}$ ) are

$$I_C \cong \frac{V_{EQ} - V_{BE}}{\frac{R_{EQ}}{\beta_F} + R_E} = \frac{(4 - 0.7)\text{V}}{\frac{12\text{k}\Omega}{75} + 16\text{k}\Omega} = 204 \mu\text{A} \quad \text{with} \quad I_B = \frac{204 \mu\text{A}}{75} = 2.72 \mu\text{A}$$

$$V_{CE} \cong V_{CC} - I_C (R_C + R_E) = 12 - 2.04 \mu\text{A} (22\text{k}\Omega + 16\text{k}\Omega) = 4.25 \text{V}$$

A more precise estimate using Eqs. (5.52) and (5.54) gives a Q-point of (202  $\mu\text{A}$ , 4.30 V). Since we don't know the actual value of  $V_{BE}$ , and haven't considered any tolerances, the approximate expressions give excellent engineering results.

All the calculated currents are greater than zero, and using the result in Eq. (5.54),  $V_{BC} = V_{BE} - V_{CE} = 0.7 - 4.32 = -3.62$  V. Thus, the base-collector junction is reverse-biased, and the assumption of forward-active region operation was correct. The Q-point resulting from our analysis is (204  $\mu\text{A}$ , 4.25 V).

Before leaving this bias example, let us draw the load line for the circuit and locate the Q-point on the output characteristics. The load-line equation for this circuit already appeared as Eq. (5.52):

$$V_{CE} = V_{CC} - \left( R_C + \frac{R_E}{\alpha_F} \right) I_C = 12 - 38,200 I_C \quad (5.56)$$

Two points are needed to plot the load line. Choosing  $I_C = 0$  yields  $V_{CE} = 12$  V, and picking  $V_{CE} = 0$  yields  $I_C = 314 \mu\text{A}$ . The resulting load line is plotted on the transistor common-emitter output characteristics in Fig. 5.34(d). The base current was already found to be 2.7  $\mu\text{A}$ , and the intersection of the  $I_B = 2.7\text{-}\mu\text{A}$  characteristic with the load line defines the Q-point. In this case we must estimate the location of the  $I_B = 2.7\text{-}\mu\text{A}$  curve.

**EXERCISE:** Find the values of  $I_B$ ,  $I_C$ ,  $I_E$  and  $V_{CE}$  using the exact expressions in Eqs. (5.51), (5.52) and (5.54).

**ANSWERS:** 2.69  $\mu\text{A}$ , 202  $\mu\text{A}$ , 204  $\mu\text{A}$ , 4.28 V

**EXERCISE:** Find the Q-point for the circuit in Fig. 5.34(d) if  $R_1 = 180 \text{ k}\Omega$  and  $R_2 = 360 \text{ k}\Omega$ .

**ANSWERS:** (185  $\mu\text{A}$ , 4.93 V)

## DESIGN NOTE

Good engineering approximations for the Q-point in the four-resistor bias circuit for the bipolar transistor are:

$$I_C \cong \frac{\frac{V_{EQ} - V_{BE}}{R_{EQ}}}{\frac{V_{EQ} - V_{BE}}{R_E} + R_E} \cong \frac{V_{EQ} - V_{BE}}{R_E} \quad \text{and} \quad V_{CE} \cong V_{CC} - I_C(R_C + R_E)$$

### 5.11.2 DESIGN OBJECTIVES FOR THE FOUR-RESISTOR BIAS NETWORK

Now that we have analyzed a circuit involving the four-resistor bias network, let us explore the design objectives of this bias technique through further simplification of the expression for the collector and emitter currents in Eq. (5.53) by assuming that  $R_{EQ}/\beta_F \ll R_E$ . Then,

$$I_E \cong I_C \cong \frac{V_{EQ} - V_{BE}}{R_E} \quad (5.57)$$

The value of the Thévenin equivalent resistance  $R_{EQ}$  is normally designed to be small enough to neglect the voltage drop caused by the base current flowing through  $R_{EQ}$ . Under these conditions,  $I_C$  and  $I_E$  are set by the combination of  $V_{EQ}$ ,  $V_{BE}$ , and  $R_E$ . In addition,  $V_{EQ}$  is normally designed to be large enough that small variations in the assumed value of  $V_{BE}$  will not materially affect the value of  $I_E$ .

In the original bias circuit reproduced in Fig. 5.35, the assumption that the voltage drop  $I_B R_{EQ} \ll (V_{EQ} - V_{BE})$  is equivalent to assuming  $I_B \ll I_2$  so that  $I_1 \cong I_2$ . For this case, the base current of  $Q_1$  does not disturb the voltage divider action of  $R_1$  and  $R_2$ . Using the approximate expression in Eq. (5.55) estimates the emitter current in the circuit in Fig. 5.34 to be

$$I_C \cong I_E \cong \frac{4 \text{ V} - 0.7 \text{ V}}{16,000 \Omega} = 206 \mu\text{A}$$

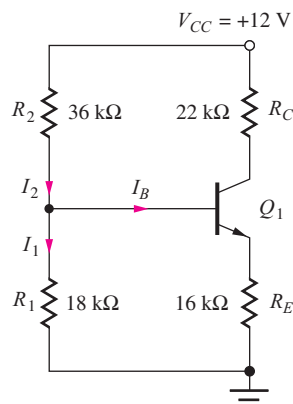


Figure 5.35 Currents in the base-bias network.

which is essentially the same as the result that was calculated using the more exact expression. This is the result that should be achieved with a proper bias network design. If the Q-point is independent of  $I_B$ , it will also be independent of current gain  $\beta$  (a poorly controlled transistor parameter). The emitter current will then be approximately the same for a transistor with a current gain of 50 or 500.

Generally, a very large number of possible combinations of  $R_1$  and  $R_2$  will yield the desired value of  $V_{EQ}$ . An additional constraint is needed to finalize the design choice. A useful choice is to limit the current used in the base-voltage-divider network by choosing  $I_2 \leq I_C/5$ . This choice ensures that the power dissipated in bias resistors  $R_1$  and  $R_2$  is less than 20 percent of the total quiescent power consumed by the circuit and at the same time ensures that  $I_2 \gg I_B$  for  $\beta \geq 50$ .

**EXERCISE:** Show that choosing  $I_2 = I_C/5$  is equivalent to setting  $I_2 = 10I_B$  when  $\beta_F = 50$ .

**EXERCISE:** Find the Q-point for the circuit in Fig. 5.34(a) if  $\beta_F$  is 500.

**ANSWERS:** (206  $\mu\text{A}$ , 4.18 V)

## DESIGN EXAMPLE 5.9 FOUR-RESISTOR BIAS DESIGN

Here we explore the design of the network most commonly utilized to bias the BJT — the four-resistor bias circuit.

**PROBLEM** Design a four resistor bias circuit to give a Q-point of (750  $\mu\text{A}$ , 5 V) using a 15-V supply with an *npn* transistor having a minimum current gain of 100.

**SOLUTION** **Known Information and Given Data:** The bias circuit in Fig. 5.35 with  $V_{CC} = 15$  V; the *npn* transistor has  $\beta_F = 100$ ,  $I_C = 750 \mu\text{A}$ , and  $V_{CE} = 5$  V.

**Unknowns:** Base voltage  $V_B$ , voltages across resistors  $R_E$  and  $R_C$ ; values for  $R_1$ ,  $R_2$ ,  $R_C$ , and  $R_E$

**Approach:** First, partition  $V_{CC}$  between the collector-emitter voltage of the transistor and the voltage drops across  $R_C$  and  $R_E$ . Next, choose currents  $I_1$  and  $I_2$  for the base bias network. Finally, use the assigned voltages and currents to calculate the unknown resistor values.

**Assumptions:** The transistor is to operate in the forward-active region. The base-emitter voltage of the transistor is 0.7 V. The Early voltage is infinite.

**Analysis:** To calculate values for the resistors, we must know the voltage across the emitter and collector resistors and the voltage  $V_B$ .  $V_{CE}$  is designed to be 5 V. One common choice is to divide the remaining power supply voltage ( $V_{CC} - V_{CE}$ ) = 10 V equally between  $R_E$  and  $R_C$ . Thus,  $V_E = 5$  V and  $V_C = 5 + V_{CE} = 10$  V. The values of  $R_C$  and  $R_E$  are then given by

$$R_C = \frac{V_{CC} - V_C}{I_C} = \frac{5 \text{ V}}{750 \mu\text{A}} = 6.67 \text{ k}\Omega \quad \text{and} \quad R_E = \frac{V_E}{I_E} = \frac{5 \text{ V}}{758 \mu\text{A}} = 6.60 \text{ k}\Omega$$

The base voltage is given by  $V_B = V_E + V_{BE} = 5.7$  V. For forward-active region operation, we know that  $I_B = I_C/\beta_F = 750 \mu\text{A}/100 = 7.5 \mu\text{A}$ . Now choosing  $I_2 = 10I_B$ , we have  $I_2 = 75 \mu\text{A}$ ,  $I_1 = 9I_B = 67.5 \mu\text{A}$ , and  $R_1$  and  $R_2$  can be determined:

$$R_1 = \frac{V_B}{9I_B} = \frac{5.7 \text{ V}}{67.5 \mu\text{A}} = 84.4 \text{ k}\Omega \quad R_2 = \frac{V_{CC} - V_B}{10I_B} = \frac{15 - 5.7 \text{ V}}{75 \mu\text{A}} = 124 \text{ k}\Omega \quad (5.58)$$

**Check of Results:** We have  $V_{BE} = 0.7$  V and  $V_{BC} = 5.7 - 10 = -4.3$  V, which are consistent with the forward-active region assumption.

**Discussion:** The values calculated above should yield a Q-point very close to the design goals. However, if we were going to build this circuit in the laboratory, we must use standard values for the resistors. In order to complete the design, we refer to the table of resistor values in Appendix A. There we find that the closest available values are  $R_1 = 82 \text{ k}\Omega$ ,  $R_2 = 120 \text{ k}\Omega$ ,  $R_E = 6.8 \text{ k}\Omega$ , and  $R_C = 6.8 \text{ k}\Omega$ .

**Computer-Aided Analysis:** SPICE can now be used as a tool to check our design. The final design using these values appears in Fig. 5.36 for which SPICE (with  $I_S = 2 \times 10^{-15} \text{ A}$ ) predicts the Q-point to be  $(734 \mu\text{A}, 4.97 \text{ V})$ , with  $V_{BE} = 0.65 \text{ V}$ . We neglected the Early effect in our hand calculations, but SPICE represents an easy way to check this assumption. If we set  $V_A = 75 \text{ V}$  in SPICE, keeping the other parameters the same, the new Q-point is  $(737 \mu\text{A}, 4.93 \text{ V})$ . Clearly, the changes caused by the Early effect are negligible.

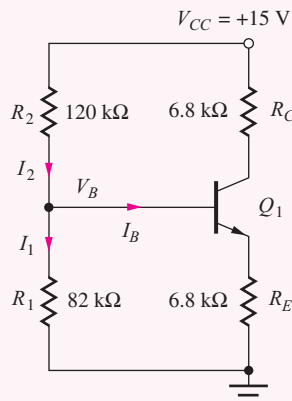
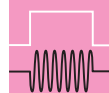


Figure 5.36 Final bias circuit design for a Q-point of  $(750 \mu\text{A}, 5 \text{ V})$ .

**EXERCISE:** Redesign the four resistor bias circuit to yield  $I_C = 75 \mu\text{A}$  and  $V_{CE} = 5 \text{ V}$ .

**ANSWERS:**  $(66.7 \text{ k}\Omega, 66.0 \text{ k}\Omega, 844 \text{ k}\Omega, 1.24 \text{ M}\Omega) \rightarrow (68 \text{ k}\Omega, 68 \text{ k}\Omega, 820 \text{ k}\Omega, 1.20 \text{ M}\Omega)$



## DESIGN NOTE FOUR-RESISTOR BIAS DESIGN

- Choose the Thévenin equivalent base voltage  $V_{EQ}$ : 
$$\frac{V_{CC}}{4} \leq V_{EQ} \leq \frac{V_{CC}}{2}$$
- Select  $R_1$  to set  $I_1 = 9I_B$ : 
$$R_1 = \frac{V_{EQ}}{9I_B}$$
- Select  $R_2$  to set  $I_2 = 10I_B$ : 
$$R_2 = \frac{V_{CC} - V_{EQ}}{10I_B}$$
- $R_E$  is determined by  $V_{EQ}$  and the desired collector current: 
$$R_E \cong \frac{V_{EQ} - V_{BE}}{I_C}$$
- $R_C$  is determined by the desired collector-emitter voltage: 
$$R_C \cong \frac{V_{CC} - V_{CE}}{I_C} - R_E$$

### EXAMPLE 5.10 ANALYSIS OF A TRANSISTOR OPERATING IN SATURATION

This example demonstrates an analysis in which the assumption of forward-active region operation is discovered to be incorrect, and a second analysis iteration is required. We explore the impact of changing the collector resistor in the circuit of Fig. 5.34(a) from  $22\text{ k}\Omega$  to  $56\text{ k}\Omega$ , as shown in Fig. 5.37. (Perhaps the resistor color code was misread by the builder of the circuit.)

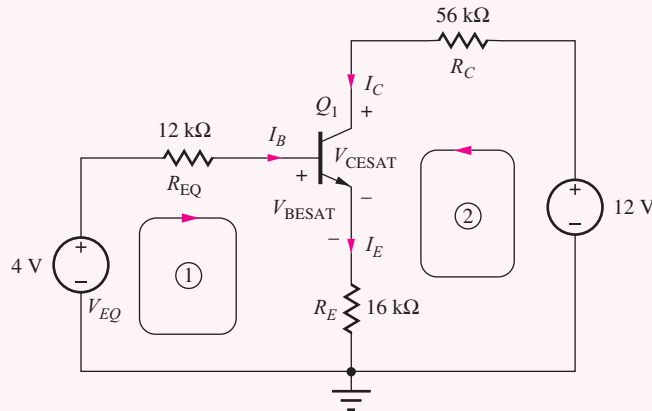


Figure 5.37 Bias circuit with collector resistor  $R_C$  increased to  $56\text{ k}\Omega$  ( $\beta_F = 75$ ).

**PROBLEM** Find the Q-point for the transistor in Fig. 5.37.

**SOLUTION Known Information and Given Data:** Simplified equivalent circuit in Fig. 5.37 with  $V_{EQ} = 4\text{ V}$ ,  $R_{EQ} = 12\text{ k}\Omega$ ,  $V_{CC} = 12\text{ V}$ ,  $R_E = 16\text{ k}\Omega$ , and  $R_C = 56\text{ k}\Omega$

**Unknowns:**  $I_C$ ,  $V_{CE}$

**Approach:** Assume a region of operation and calculate the Q-point; check answer to see if it is consistent with the assumptions. Analyze the input loop to find  $I_B$ ,  $I_C$ , and  $I_E$ . Use currents in the output loop to find  $V_{CE}$ .

**Assumptions:** Forward-active region of operation with  $V_{BE} = 0.7\text{ V}$ ;  $V_A = \infty$

**Analysis:** The analysis starts by analyzing input loop 1 in Fig. 5.37, which is identical to that in Fig. 5.34(c). Therefore  $I_B$  is determined by Eq. (5.51) with  $\beta_F = 75$ :

$$I_B = \frac{4\text{ V} - 0.7\text{ V}}{1.21 \times 10^6 \Omega} = 2.73 \mu\text{A} \quad I_C = \beta_F I_B = 205 \mu\text{A}$$

$$I_E = (\beta_F + 1)I_B = 208 \mu\text{A}$$

Using loop 2 to determine an expression for  $V_{CE}$  as in Eq. (5.52) yields:

$$V_{CE} = V_{CC} - \left( R_C + \frac{R_E}{\alpha_F} \right) I_C = 12 - 72,200 I_C = -2.80 \text{ V} \text{—Oops!}$$

The calculated Q-point is  $(-2.80\text{ V}, 205 \mu\text{A})$ .

**Check of Results:** The calculated value of  $V_{CE}$  is negative, which violates the assumption of forward-active region operation that requires  $V_{CE} \geq V_{BE}$ . (In addition, it is physically impossible for  $V_{CE}$  to become negative in this circuit.) Therefore, we must choose a new region of operation and reanalyze the circuit.

**Analysis—Second Iteration:** Because  $V_{CE}$  was found to be negative, our second analysis attempt will assume that  $Q_1$  is saturated ( $V_{CE}$  as small as possible). We will need to assume a value for  $V_{CESAT}$ .) Writing a new set of equations for loops 1 and 2:

$$\begin{aligned} 4 &= 12,000I_B + V_{BESAT} + 16,000I_E \\ 12 &= 56,000I_C + V_{CESAT} + 16,000I_E \end{aligned} \quad (5.59)$$

If we substitute assumed values of  $V_{BESAT} = 0.75$  V and  $V_{CESAT} = 0.05$  V, and use  $I_E = I_B + I_C$ , then simultaneous solution of Eqs. (5.57) gives

$$I_C = 160 \mu\text{A} \quad I_B = 24 \mu\text{A} \quad \text{and} \quad I_E = I_C + I_B = 184 \mu\text{A}$$

The Q-point is (0.05 V, 160  $\mu\text{A}$ ).

**Check of Results:** The three terminal currents are all positive, and  $I_C/I_B < \beta_F$  (that is,  $\beta_{FOR} < \beta_F$ ). Therefore, the assumption of saturation region operation is correct. The values of  $V_{BESAT}$  and  $V_{CESAT}$  can be calculated using Eqs. (5.57) as a check on the hand analysis and are found to be close to the assumed values:  $V_{BESAT} = 0.77$  V and  $V_{CESAT} = 0.096$  V.

**Discussion:** This problem provides an example in which the initial assumed region of operation was incorrect, and a second analysis iteration was required to find the correct Q-point.

**Computer-Aided Analysis:** This problem is another good place to use SPICE analysis to check our hand calculations. SPICE simulation yields

$$I_C = 160 \mu\text{A} \quad I_B = 28 \mu\text{A} \quad I_E = 188 \mu\text{A}$$

The slight discrepancies are caused by the differences in  $V_{BESAT}$  and  $V_{CESAT}$  between our hand analysis and SPICE.

**EXERCISE:** What is the largest value for resistor  $R_C$  that can be used in the circuit in Fig. 5.37 if the transistor is to remain biased in the forward-active region ( $V_{CE} = 0.7$  V)?

**ANSWER:** 38.9 k $\Omega$

**EXERCISE:** Substitute  $I_C$ ,  $I_B$ , and  $I_E$  into Eqs. (5.57) and verify the values of  $V_{BESAT}$  and  $V_{CESAT}$ .

### EXAMPLE 5.11 TWO-RESISTOR BIASING

In this example, we analyze a two-resistor circuit used to bias a pnp transistor. (A similar circuit can also be used for npn biasing.)

**PROBLEM** Find the Q-point for the *pnp* transistor in the two-resistor bias circuit in Fig. 5.38. Assume  $\beta_F = 50$ .

**SOLUTION** **Known Information and Given Data:** Two-resistor bias circuit in Fig. 5.38 with a *pnp* transistor with  $\beta_F = 50$

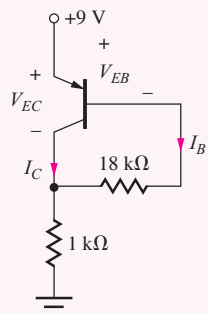
**Unknowns:**  $I_C$ ,  $V_{CE}$

**Approach:** Assume a region of operation and analyze the circuit to determine the Q-point; check answer to see if it is consistent with the assumptions.

**Assumptions:** Forward-active region operation with  $V_{EB} = 0.7$  V and  $V_A = \infty$

**Analysis:** The voltages and currents are first carefully labeled as in Fig. 5.38. To find the Q-point, an equation is written involving  $V_{EB}$ ,  $I_B$ , and  $I_C$ :

$$9 = V_{EB} + 18,000I_B + 1000(I_C + I_B) \quad (5.60)$$



Applying the assumption of forward-active region operation with  $\beta_F = 50$  and  $V_{EB} = 0.7$  V,

$$9 = 0.7 + 18,000I_B + 1000(51)I_B \quad (5.61)$$

and

$$I_B = \frac{9 \text{ V} - 0.7 \text{ V}}{69,000 \Omega} = 120 \mu\text{A} \quad I_C = 50I_B = 6.01 \text{ mA} \quad (5.62)$$

**Figure 5.38** Two-resistor bias circuit with a *pnp* transistor.

The emitter-collector voltage is given by

$$V_{EC} = 9 - 1000(I_C + I_B) = 2.88 \text{ V} \quad \text{and} \quad V_{BC} = 2.18 \text{ V} \quad (5.63)$$

The Q-point is  $(I_C, V_{EC}) = (6.01 \text{ mA}, 2.88 \text{ V})$ .

**Check of Results:** Because  $I_B$ ,  $I_C$ , and  $V_{BC}$  are all greater than zero, the assumption of forward-active region operation is valid, and the Q-point is correct.

**Computer-Aided Analysis:** For this circuit, SPICE simulation yields (6.04 mA, 2.95 V), which agrees with the Q-point found from our hand calculations.

**EXERCISE:** What is the Q-point if the 18 kΩ resistor is increased to 36 kΩ?

**ANSWER:** (4.77 mA, 4.13 V)

**EXERCISE:** Draw the two-resistor bias circuit (a “mirror image” of Fig. 5.38) that would be used to bias an *npn* transistor from a single +9-V supply using the same two resistor values as in Fig. 5.38.

**ANSWER:** See circuit topology in Fig. P5.96.

The bias circuit examples that have been presented in this section have only scratched the surface of the possible techniques that can be used to bias *npn* and *pnp* transistors. However, the analysis techniques have illustrated the basic approaches that need to be followed in order to determine the Q-point of any bias circuit.

**TABLE 5.4**

BJT Iterative Bias Solution  $I_S = 10^{-15} A$ ,  
 $V_T = 25 \text{ mV}$

$V_{BE}$ (V)	$I_C$ (A)	$V'_{BE}$ (V)
0.7000	2.015E-04	0.6507
0.6507	2.046E-04	0.6511
0.6511	2.045E-04	0.6511

### 5.11.3 ITERATIVE ANALYSIS OF THE FOUR-RESISTOR BIAS CIRCUIT

To find  $I_C$  in the circuit in Fig. 5.34, we need to find a solution to the following pair of equations:

$$I_C = \frac{V_{EQ} - V_{BE}}{\frac{R_{EQ}}{\beta_F} + \frac{(\beta_F + 1)}{\beta_F} R_E} \quad \text{where} \quad V_{BE} = V_T \ln \left( \frac{I_C}{I_S} + 1 \right) \quad (5.64)$$

In the analysis presented in Section 5.11, we avoided the problems associated with solving the resulting transcendental equation by assuming that we knew an approximate value for  $V_{BE}$ . However, we can find a numerical solution to these two equations with a simple iterative process.

1. Guess a value for  $V_{BE}$ .
2. Calculate the corresponding value of  $I_C$  using  $I_C = \frac{V_{EQ} - V_{BE}}{\frac{R_{EQ}}{\beta_F} + \frac{(\beta_F + 1)}{\beta_F} R_E}$ .
3. Update the estimate for  $V_{BE}$  as  $V'_{BE} = V_T \ln \left( \frac{I_C}{I_S} + 1 \right)$ .
4. Repeat steps 2 and 3 until convergence is obtained.

Table 5.4 presents the results of this iterative method showing convergence in only three iterations. This rapid convergence occurs because of the very steep nature of the  $I_C - V_{BE}$  characteristic.

One might ask if this result is better than the one obtained earlier in Section 5.11.1. As in most cases, the results are only as good as the input data. Here we need to accurately know the values of saturation current  $I_S$  and temperature  $T$  in order to calculate  $V_{BE}$ . In the earlier solution we simply estimated  $V_{BE}$ . In reality, we seldom will know exact values of either  $I_S$  or  $T$ , so we most often are just satisfied with a direct estimate for  $V_{BE}$ .

**EXERCISE:** Repeat the iterative analysis above to find the values of  $I_C$  and  $V_{BE}$  if  $V_T = 25.8 \text{ mV}$ .

**ANSWERS:**  $203.3 \mu\text{A}$ ,  $0.6718 \text{ V}$

### 5.12 TOLERANCES IN BIAS CIRCUITS

When a circuit is actually built in discrete form in the laboratory or fabricated as an integrated circuit, the components and device parameters all have tolerances associated with their values. Discrete resistors can easily be purchased with 10 percent, 5 percent, or 1 percent tolerances, whereas typical resistors in ICs can exhibit even wider variations ( $\pm 30$  percent). Power supply voltage tolerances are often 5 to 10 percent.

For a given bipolar transistor type, parameters such as current gain may cover a range of 5:1 to 10:1, or may be specified with only a nominal value and lower bound. The BJT (or diode) saturation current may vary by a factor varying from 10:1 to 100:1, and the Early voltage may vary by  $\pm 20$  percent. In FET circuits, the values of threshold voltage and the transconductance parameter can vary widely, and in op-amp circuits all the op-amp parameters (for example, open-loop gain, input resistance, output resistance, input bias current, unity gain frequency, and the like) typically exhibit wide specification ranges.

In addition to these initial value uncertainties, the values of the circuit components and parameters change as temperature changes and the circuit ages. It is important to understand the effect of these variations on our circuits and be able to design circuits that will continue to operate correctly in the face of these element variations. Worst-case analysis and Monte Carlo analysis, introduced in Chapter 1, are two approaches that can be used to quantify the effects of tolerances on circuit performance.

### 5.12.1 WORST-CASE ANALYSIS

**Worst-case analysis** is often used to ensure that a design will function under an expected set of component variations. In Q-point analysis, for example, the values of components are simultaneously pushed to their various extremes in order to determine the worst possible range of Q-point values. Unfortunately, a design based on worst-case analysis is usually an unnecessary overdesign and economically undesirable, but it is important to understand the technique and its limitations.

#### EXAMPLE 5.12 WORST-CASE ANALYSIS OF THE FOUR-RESISTOR BIAS NETWORK

Now we explore the application of worst-case analysis to the four-resistor bias network with a given set of tolerances assigned to the elements. In Ex. 5.13, the bounds generated by the worst-case analysis will be compared to a statistical sample of the possible network realizations using Monte Carlo analysis.

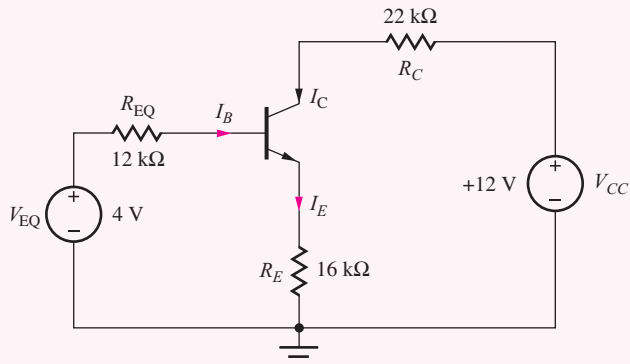


Figure 5.39 Simplified four-resistor bias circuit of Fig. 5.34(c) assuming nominal element values.

**PROBLEM** Find the worst-case values of  $I_C$  and  $V_{CE}$  for the transistor in Fig. 5.39. The circuit in Fig. 5.39 is the simplified version of the four-resistor bias circuit in Figs. 5.33. Assume that the 12-V power supply has a 5 percent tolerance and the resistors have 10 percent tolerances. Also, assume that the transistor current gain has a nominal value of 75 with a 50 percent tolerance.

**SOLUTION** **Known Information and Given Data:** Simplified version of the four-resistor bias circuit in Fig. 5.39; 5 percent tolerance on  $V_{CC}$ ; 10 percent tolerance for each resistor; current  $\beta_{FO} = 75$  with a 50 percent tolerance

**Unknowns:** Minimum and maximum values of  $I_C$  and  $V_{CE}$

**Approach:** Find the worst-case values of  $V_{EQ}$  and  $R_{EQ}$ ; use the results to find the extreme values of the base and collector current; use the collector current values to find the worst-case values of collector-emitter voltage

**Assumptions:** To simplify the analysis, assume that the voltage drop in  $R_{EQ}$  can be neglected and  $\beta_F$  is large so that  $I_C$  is given by

$$I_C \cong I_E = \frac{V_{EQ} - V_{BE}}{R_E} \quad (5.65)$$

Assume  $V_{BE}$  is fixed at 0.7 V.

**Analysis:** To make  $I_C$  as large as possible,  $V_{EQ}$  should be at its maximum extreme and  $R_E$  should be a minimum value. To make  $I_C$  as small as possible,  $V_{EQ}$  should be minimum and  $R_E$  should be a maximum value. Variations in  $V_{BE}$  are assumed to be negligible but could also be included if desired.

The extremes of  $R_E$  are  $0.9 \times 16 \text{ k}\Omega = 14.4 \text{ k}\Omega$ , and  $1.1 \times 16 \text{ k}\Omega = 17.6 \text{ k}\Omega$ . The extreme values of  $V_{EQ}$  are somewhat more complicated:

$$V_{EQ} = V_{CC} \frac{R_1}{R_1 + R_2} = \frac{V_{CC}}{1 + \frac{R_2}{R_1}} \quad (5.66)$$

To make  $V_{EQ}$  as large as possible, the numerator of Eq. (5.66) should be large and the denominator small. Therefore,  $V_{CC}$  and  $R_1$  must be as large as possible and  $R_2$  as small as possible. Conversely, to make  $V_{EQ}$  as small as possible,  $V_{CC}$  and  $R_1$  must be small and  $R_2$  must be large. Using this approach, the maximum and minimum values of  $V_{EQ}$  are

$$V_{EQ}^{\max} = \frac{12 \text{ V}(1.05)}{1 + \frac{36 \text{ k}\Omega(0.9)}{18 \text{ k}\Omega(1.1)}} = 4.78 \text{ V} \quad \text{and} \quad V_{EQ}^{\min} = \frac{12 \text{ V}(0.95)}{1 + \frac{36 \text{ k}\Omega(1.1)}{18 \text{ k}\Omega(0.9)}} = 3.31 \text{ V}$$

Substituting these values in Eq. (5.62) gives the following extremes for  $I_C$ :

$$I_C^{\max} = \frac{4.78 \text{ V} - 0.7 \text{ V}}{14,400 \text{ }\Omega} = 283 \text{ }\mu\text{A} \quad \text{and} \quad I_C^{\min} = \frac{3.31 \text{ V} - 0.7 \text{ V}}{17,600 \text{ }\Omega} = 148 \text{ }\mu\text{A}$$

The worst-case range of  $V_{CE}$  will be calculated in a similar manner, but we must be careful to watch for possible cancellation of variables:

$$V_{CE} = V_{CC} - I_C R_C - I_E R_E \cong V_{CC} - I_C R_C - \frac{V_{EQ} - V_{BE}}{R_E} R_E \quad (5.67)$$

$$V_{CE} \cong V_{CC} - I_C R_C - V_{EQ} + V_{BE}$$

The maximum value of  $V_{CE}$  in Eq. (5.67) occurs for minimum  $I_C$  and minimum  $R_C$  and vice versa. Using (5.67), the extremes of  $V_{CE}$  are

$$V_{CE}^{\max} \cong 12 \text{ V}(1.05) - (148 \text{ }\mu\text{A})(22 \text{ k}\Omega \times 0.9) - 3.31 \text{ V} + 0.7 \text{ V} = 7.06 \text{ V} \quad \checkmark$$

$$V_{CE}^{\min} \cong 12 \text{ V}(0.95) - (283 \text{ }\mu\text{A})(22 \text{ k}\Omega \times 1.1) - 4.78 \text{ V} + 0.7 \text{ V} = 0.471 \text{ Saturated!}$$

**Check of Results:** The transistor remains in the forward-active region for the upper extreme, but the transistor saturates (weakly) at the lower extreme. Because the forward-active region

assumption is violated in the latter case, the calculated values of  $V_{CE}$  and  $I_C$  would not actually be correct for this case.

**Discussion:** Note that the worst-case values of  $I_C$  differ by a factor of almost 2:1! The maximum  $I_C$  is 38 percent greater than the nominal value of 210  $\mu\text{A}$ , and the minimum value is 37 percent below the nominal value. The failure of the bias circuit to maintain the transistor in the desired region of operation for the worst-case values is evident.

### 5.12.2 MONTE CARLO ANALYSIS

In a real circuit, the parameters will have some statistical distribution, and it is unlikely that the various components will all reach their extremes at the same time. Thus, the worst-case analysis technique will overestimate (often badly) the extremes of circuit behavior. A better approach is to attack the problem statistically using the method of Monte Carlo analysis.

As discussed in Chapter 1, **Monte Carlo analysis** uses randomly selected versions of a given circuit to predict its behavior from a statistical basis. For Monte Carlo analysis, values for each parameter in the circuit are selected at random from the possible distributions of parameters, and the circuit is then analyzed using the randomly selected element values. Many random parameter sets are generated, and the statistical behavior of the circuit is built up from analysis of the many test cases.

In Ex. 5.13, an Excel spreadsheet will be used to perform a Monte Carlo analysis of the four-resistor bias circuit. As discussed in Chapter 1, Excel contains the function RAND(), which generates random numbers uniformly distributed between 0 and 1, but for Monte Carlo analysis, the mean must be centered on  $R_{\text{nom}}$  and the width of the distribution set to  $(2\varepsilon) \times R_{\text{nom}}$ :

$$R = R_{\text{nom}}[1 + 2\varepsilon(\text{RAND}() - 0.5)] \quad (5.68)$$

### EXAMPLE 5.13 MONTE CARLO ANALYSIS OF THE FOUR-RESISTOR BIAS NETWORK

Now, let us compare the worst-case results from Ex. 5.12 to a statistical sample of 500 randomly generated realizations of the transistor embedded in the four-resistor bias network.

**PROBLEM** Perform a Monte Carlo analysis to determine statistical distributions for the collector current and collector-emitter voltage for the four-resistor circuit in Figs. 5.34 and 5.39 with a 5 percent tolerance on  $V_{CC}$ , 10 percent tolerances for each resistor and a 50 percent tolerance on the current gain  $\beta_{FO} = 75$ .

**SOLUTION** **Known Information and Given Data:** Circuit in Fig. 5.34(a) as simplified in Fig. 5.39; 5 percent tolerance on the 12-V power supply  $V_{CC}$ ; 10 percent tolerance on each resistor; current  $\beta_{FO} = 75$  with a 50 percent tolerance

**Unknowns:** Statistical distributions of  $I_C$  and  $V_{CE}$

**Approach:** To perform a Monte Carlo analysis of the circuit in Fig. 5.34, random values are assigned to  $V_{CC}$ ,  $R_1$ ,  $R_2$ ,  $R_C$ ,  $R_E$ , and  $\beta_F$  and then used to determine  $I_C$  and  $V_{CE}$ . A spreadsheet is used to make the repetitive calculations. Since the computer is performing the calculations, the most exact formulas will be used in the analyses.

**Assumptions:**  $V_{BE}$  is fixed at 0.7 V. Random values are statistically independent of each other.

**Computer-Aided Analysis:** Using the tolerances from the worst-case analysis, the power supply, resistors, and current gain are represented as

1.  $V_{CC} = 12(1 + 0.1(\text{RAND}() - 0.5))$
  2.  $R_1 = 18,000(1 + 0.2(\text{RAND}() - 0.5))$
  3.  $R_2 = 36,000(1 + 0.2(\text{RAND}() - 0.5))$
  4.  $R_E = 16,000(1 + 0.2(\text{RAND}() - 0.5))$
  5.  $R_C = 22,000(1 + 0.2(\text{RAND}() - 0.5))$
  6.  $\beta_F = 75(1 + (\text{RAND}() - 0.5))$
- (5.69)

Remember, each variable evaluation must invoke a separate call of the function RAND() so that the random values will be independent of each other.

In the spreadsheet results presented in Fig. 5.40, the random elements in Eqs. (5.69) are used to evaluate the equations that characterize the bias circuit:

$$\begin{aligned}
 7. \quad V_{EQ} &= V_{CC} \frac{R_1}{R_1 + R_2} & 10. \quad I_C &= \beta_F I_B \\
 8. \quad R_{EQ} &= \frac{R_1 R_2}{R_1 + R_2} & 11. \quad I_E &= \frac{I_C}{\alpha_F} \\
 9. \quad I_B &= \frac{V_{EQ} - V_{BE}}{R_{EQ} + (\beta_F + 1)R_E} & 12. \quad V_{CE} &= V_{CC} - I_C R_C - I_E R_E
 \end{aligned}
 \quad (5.70)$$

Because the computer is doing the work, the complete expressions rather than the approximate relations for the various calculations are used in Eqs. (5.70).<sup>11</sup> Once Eqs. (5.69) and (5.70) have been entered into one row of the spreadsheet, that row can be copied into as many additional rows as the number of statistical cases that are desired. The analysis is automatically repeated for the random selections to build up the statistical distributions, with each row representing one analysis of the circuit. At the end of the columns, the mean and standard deviation can be calculated using built-in spreadsheet functions, and the overall spreadsheet data can be used to build histograms for the circuit performance.

An example of a portion of the spreadsheet output for 25 cases of the circuit in Fig. 5.39 is shown in Fig. 5.40, whereas the full results of the analysis of 500 cases of the four-resistor bias circuit are given in the histograms for  $I_C$  and  $V_{CE}$  in Fig. 5.41. The mean values for  $I_C$  and  $V_{CE}$  are 207  $\mu\text{A}$  and 4.06 V, respectively, which are close to the values originally estimated from the nominal circuit elements. The standard deviations are 19.6  $\mu\text{A}$  and 0.64 V, respectively.

**Check of Results and Discussion:** The worst-case calculations from Sec. 5.12.1 are indicated by the arrows in the figures. It can be seen that the worst-case values of  $V_{CE}$  lie well beyond the edges of the statistical distribution, and that saturation does not actually occur for the worst statistical case evaluated. If the Q-point distribution results in the histograms in Fig. 5.41 were not sufficient to meet the design criteria, the parameter tolerances could be changed and the Monte Carlo simulation redone. For example, if too large a fraction of the circuits failed to be within some specified limits, the tolerances could be tightened by specifying more expensive, higher accuracy resistors.

<sup>11</sup> Note that  $V_{BE}$  could also be treated as a random variable.

Monte Carlo Spreadsheet											
Case #	$V_{CC}$ (1)	$R_1$ (2)	$R_2$ (3)	$R_E$ (4)	$R_C$ (5)	$\beta_F$ (6)	$V_{EQ}$ (7)	$R_{EQ}$ (8)	$I_B$ (9)	$I_C$ (10)	$V_{CE}$ (12)
1	12.277	16827	38577	15780	23257	67.46	3.729	11716	2.87E-06	1.93E-04	4.687
2	12.202	18188	32588	15304	23586	46.60	4.371	11673	5.09E-06	2.37E-04	2.891
3	11.526	16648	35643	14627	20682	110.73	3.669	11348	1.87E-06	2.07E-04	4.206
4	11.658	17354	33589	14639	22243	44.24	3.971	11442	5.00E-06	2.21E-04	3.420
5	11.932	19035	32886	16295	20863	62.34	4.374	12056	3.61E-06	2.25E-04	3.500
6	11.857	18706	32615	15563	21064	60.63	4.322	11888	3.83E-06	2.32E-04	3.286
7	11.669	18984	39463	17566	21034	42.86	3.790	12818	4.07E-06	1.75E-04	4.859
8	12.222	19291	37736	15285	22938	63.76	4.135	12765	3.53E-06	2.25E-04	3.577
9	11.601	17589	34032	17334	23098	103.07	3.953	11596	1.85E-06	1.90E-04	3.873
10	11.533	17514	33895	17333	19869	71.28	3.929	11547	2.63E-06	1.88E-04	4.505
11	11.436	19333	34160	15107	22593	68.20	4.133	12346	3.34E-06	2.28E-04	2.797
12	11.962	18810	33999	15545	22035	53.69	4.261	12110	4.25E-06	2.28E-04	3.330
13	11.801	19610	37917	14559	21544	109.65	4.023	12925	2.11E-06	2.31E-04	3.426
14	12.401	17947	34286	15952	21086	107.84	4.261	11780	2.09E-06	2.26E-04	4.002
15	11.894	16209	35321	17321	23940	45.00	3.741	11111	3.89E-06	1.75E-04	4.607
16	12.329	16209	37873	16662	23658	112.01	3.695	11351	1.63E-06	1.83E-04	4.923
17	11.685	19070	35267	15966	21864	64.85	4.101	12377	3.29E-06	2.13E-04	3.559
18	11.456	18096	37476	15529	20141	91.14	3.730	12203	2.17E-06	1.98E-04	4.370
19	12.527	18752	38261	15186	21556	69.26	4.120	12584	3.26E-06	2.26E-04	4.180
20	12.489	17705	36467	17325	20587	83.95	4.082	11919	2.35E-06	1.97E-04	4.979
21	11.436	18773	34697	16949	21848	65.26	4.015	12182	3.01E-06	1.96E-04	3.768
22	11.549	16830	38578	16736	19942	109.22	3.508	11718	1.57E-06	1.71E-04	5.247
23	11.733	16959	39116	15944	21413	62.82	3.548	11830	2.86E-06	1.80E-04	4.965
24	11.738	18486	35520	17526	20455	70.65	4.018	12158	2.70E-06	1.90E-04	4.457
25	11.679	18908	38236	15160	21191	103.12	3.864	12652	2.05E-06	2.12E-04	3.958
Mean	11.848	18014	35102	15973	21863	67.30	4.024	11885	3.44E-06	2.09E-04	3.880
Std. Dev.	0.296	958	2596	1108	1309	23.14	0.264	520	1.14E-06	2.18E-05	0.657

(X) = Equation number in text

**Figure 5.40** Example of a Monte Carlo analysis using a spreadsheet.

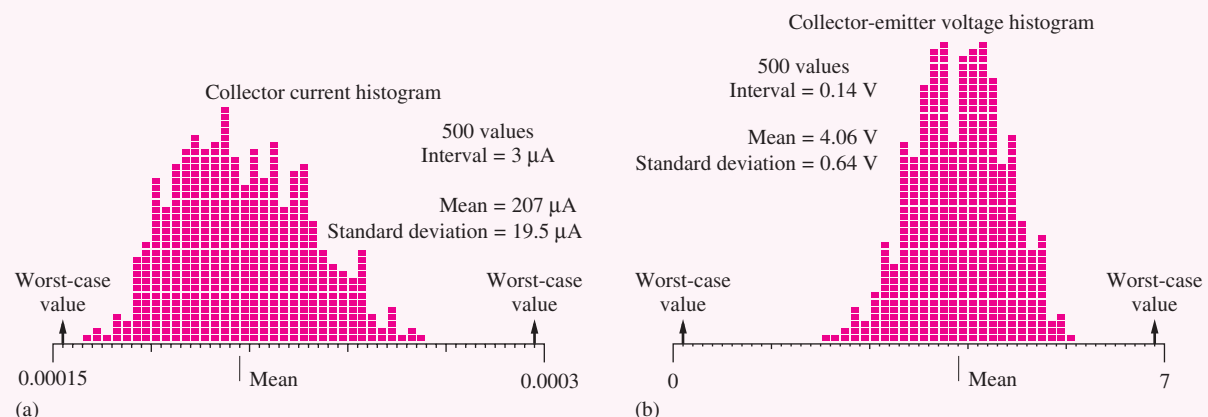


**Figure 5.41** (a) Collector-current histogram. (b) Collector-emitter voltage histogram.

Some implementations of the SPICE circuit analysis program actually contain a Monte Carlo option in which a full circuit simulation is automatically performed for any number of randomly selected test cases. These programs are a powerful tool for performing much more complex statistical analysis than is possible by hand. Using these programs, statistical estimates of delay, frequency response, and so on of circuits with large numbers of transistors can be performed.

## SUMMARY

- The bipolar junction transistor (BJT) was invented in the late 1940s at the Bell Telephone Laboratories by Bardeen, Brattain, and Shockley and became the first commercially successful three-terminal solid-state device.
- Although the FET has become the dominant device technology in modern integrated circuits, bipolar transistors are still widely used in both discrete and integrated circuit design. In particular, the BJT is still the preferred device in many applications that require high speed and/or high precision such as op-amps, A/D and D/A converters, and wireless communication products.
- The basic physical structure of the BJT consists of a three-layer sandwich of alternating  $p$ - and  $n$ -type semiconductor materials and can be fabricated in either  $npn$  or  $pnp$  form.
- The emitter of the transistor injects carriers into the base. Most of these carriers traverse the base region and are collected by the collector. The carriers that do not completely traverse the base region give rise to a small current in the base terminal.
- A mathematical model called the transport model (a simplified Gummel-Poon model) characterizes the  $i$ - $v$  characteristics of the bipolar transistor for general terminal voltage and current conditions. The transport model requires three unique parameters to characterize a particular BJT: the saturation current  $I_S$  and the forward and reverse common-emitter current gains  $\beta_F$  and  $\beta_R$ .
- $\beta_F$  is a relatively large number, ranging from 20 to 500, and characterizes the significant current amplification capability of the BJT. Practical fabrication limitations cause the bipolar transistor structure to be inherently asymmetric, and the value of  $\beta_R$  is much smaller than  $\beta_F$ , typically between 0 and 10.

- SPICE circuit analysis programs contain a comprehensive built-in model for the transistor that is an extension of the transport model.
- Four regions of operation — cutoff, forward-active, reverse-active, and saturation — were identified for the BJT based on the bias voltages applied to the base-emitter and base-collector junctions. The transport model can be simplified for each individual region of operation.
- The cutoff and saturation regions are most often used in switching applications and logic circuits. In cutoff, the transistor approximates an open switch, whereas in saturation, the transistor represents a closed switch. However, in contrast to the “on” MOSFET, the saturated bipolar transistor has a small voltage, the collector-emitter saturation voltage  $V_{CESAT}$ , between its collector and emitter terminals, even when operating with zero collector current.
- In the forward-active region, the bipolar transistor can provide high voltage and current gain for amplification of analog signals. The reverse-active region finds limited use in some analog- and digital-switching applications.
- The  $i$ - $v$  characteristics of the bipolar transistor are often presented graphically in the form of the output characteristics,  $i_C$  versus  $v_{CE}$  or  $v_{CB}$ , and the transfer characteristics,  $i_C$  versus  $v_{BE}$  or  $v_{EB}$ .
- In the forward-active region, the collector current increases slightly as the collector-emitter voltage increases. The origin of this effect is base-width modulation, known as the Early effect, and it can be included in the model for the forward-active region through addition of the parameter called the Early voltage  $V_A$ .
- The collector current of the bipolar transistor is determined by minority-carrier diffusion across the base of the transistor, and expressions were developed that relate the saturation current and base transit time of the transistor to physical device parameters. The base width plays a crucial role in determining the base transit time and the high-frequency operating limits of the transistor.
- Minority-carrier charge is stored in the base of the transistor during its operation, and changes in this stored charge with applied voltage result in diffusion capacitances being associated with forward-biased junctions. The value of the diffusion capacitance is proportional to the collector current  $I_C$ .
- Capacitances of the bipolar transistor cause the current gain to be frequency-dependent. At the beta cutoff frequency  $f_\beta$ , the current gain has fallen to 71 percent of its low frequency value, whereas the value of the current gain is only 1 at the unity-gain frequency  $f_T$ .
- The transconductance  $g_m$  of the bipolar transistor in the forward-active region relates differential changes in collector current and base-emitter voltage and was shown to be directly proportional to the dc collector current  $I_C$ .
- Design of the four-resistor network was investigated in detail. The four-resistor bias circuit provides highly stable control of the Q-point and is the most important bias circuit for discrete design.
- Techniques for analyzing the influence of element tolerances on circuit performance include the worst-case analysis and statistical Monte Carlo analysis methods. In worst-case analysis, element values are simultaneously pushed to their extremes, and the resulting predictions of circuit behavior are often overly pessimistic. The Monte Carlo method analyzes a large number of randomly selected versions of a circuit to build up a realistic estimate of the statistical distribution of circuit performance. Random number generators in high-level computer languages, spreadsheets, or MATLAB can be used to randomly select element values for use in the Monte Carlo analysis. Some circuit analysis packages such as PSPICE provide a Monte Carlo analysis option as part of the program.

## KEY TERMS

Base	Forward transport current
Base current	Gummel-Poon model
Base width	Inverse-active region
Base-collector capacitance	Inverse common-emitter current gain
Base-emitter capacitance	Inverse common-base current gain
Base-width modulation	Monte Carlo analysis
$\beta$ -cutoff frequency $f_\beta$	Normal-active region
Bipolar junction transistor (BJT)	Normal common-emitter current gain
Collector	Normal common-base current gain
Collector current	<i>n-p-n</i> transistor
Common-base output characteristic	Output characteristic
Common-emitter output characteristic	<i>p-n-p</i> transistor
Common-emitter transfer characteristic	Quiescent operating point
Cutoff region	Q-point
Diffusion capacitance	Reverse-active region
Early effect	Reverse common-base current gain $\alpha_R$
Early voltage $V_A$	Reverse common-emitter current gain $\beta_R$
Ebers-Moll model	Saturation region
Emitter	Saturation voltage
Emitter current	SPICE model parameters BF, IS, VAF
Equilibrium electron density	Transconductance
Forced beta	Transfer characteristic
Forward-active region	Transistor saturation current
Forward common-emitter current gain $\beta_F$	Transport model
Forward common-base current gain $\alpha_F$	Unity-gain frequency $f_T$
Forward transit time $\tau_F$	Worst-case analysis

## REFERENCES

1. William F. Brinkman, “The transistor: 50 glorious years and where we are going,” *IEEE International Solid-State Circuits Conference Digest*, vol. 40, pp. 22–26, February 1997.
2. William F. Brinkman, Douglas E. Haggan, William W. Troutman, “A history of the invention of the transistor and where it will lead us,” *IEEE Journal of Solid-State Circuits*, vol. 32, pp. 1858–1865, December 1997.
3. H. K. Gummel and H. C. Poon, “A compact bipolar transistor model,” *ISSCC Digest of Technical Papers*, pp. 78, 79, 146, February 1970.
4. H. K. Gummel, “A charge control relation for bipolar transistors,” *Bell System Technical Journal*, January 1970.
5. J. J. Ebers and J. L. Moll, “Large signal behavior of junction transistors,” *Proc. IRE.*, pp. 1761–1772, December 1954.
6. J. M. Early, “Effects of space-charge layer widening in junction transistors,” *Proc. IRE.*, pp. 1401–1406, November 1952.
7. B. M. Wilamowski and R. C. Jaeger, *Computerized Circuit Analysis Using SPICE Programs*, McGraw-Hill, New York: 1997.
8. J. D. Cressler, “Reengineering silicon: SiGe heterojunction bipolar technology,” *IEEE Spectrum*, pp. 49–55, March 1995.

## PROBLEMS

If not otherwise specified, use  $I_S = 10^{-16} \text{ A}$ ,  $V_A = 50 \text{ V}$ ,  $\beta_F = 100$ ,  $\beta_R = 1$ , and  $V_{BE} = 0.70 \text{ V}$ .

### 5.1 Physical Structure of the Bipolar Transistor

- 5.1. Figure P5.1 is a cross section of an *npn* bipolar transistor similar to that in Fig. 5.1. Indicate the letter (*A* to *G*) that identifies the base contact, collector contact, emitter contact, *n*-type emitter region, *n*-type collector region, and the active or intrinsic transistor region.

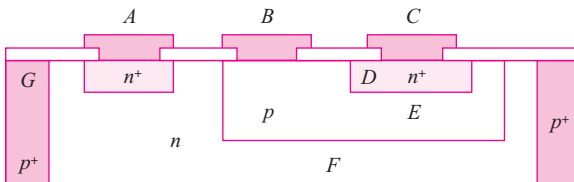


Figure P5.1

### 5.2 The Transport Model for the *npn* Transistor

- 5.2. (a) Label the collector, base, and emitter terminals of the transistor in the circuit in Fig. P5.2. (b) Label the base-emitter and base-collector voltages,  $V_{BE}$  and  $V_{BC}$ , respectively. (c) If  $V = 0.650 \text{ V}$ ,  $I_C = 275 \mu\text{A}$ , and  $I_B = 3 \mu\text{A}$ , find the values of  $I_S$ ,  $\beta_F$ , and  $\beta_R$  for the transistor if  $\alpha_R = 0.55$ .

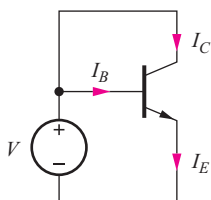


Figure P5.2

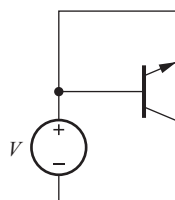


Figure P5.3

- 5.3. (a) Label the collector, base, and emitter terminals of the transistor in the circuit in Fig. P5.3. (b) Label the base-emitter and base-collector voltages,  $V_{BE}$  and  $V_{BC}$ , and the positive directions of the collector, base, and emitter currents. (c) If  $V = 0.615 \text{ V}$ ,  $I_E = -275 \mu\text{A}$ , and  $I_B = 125 \mu\text{A}$ , find the values of  $I_S$ ,  $\beta_F$ , and  $\beta_R$  for the transistor if  $\alpha_F = 0.975$ .

- 5.4. Fill in the missing entries in Table 5.P1.

TABLE 5.P1

$\alpha$	$\beta$
	0.200
0.400	
0.750	10.0
0.980	
	200
	1000
0.9998	

- 5.5. (a) Find the current  $I_{CBS}$  in Fig. P5.5(a). (Use the parameters specified at the beginning of the problem set.) (b) Find the current  $I_{CBO}$  and the voltage  $V_{BE}$  in Fig. P5.5(b).

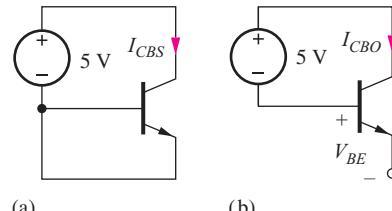


Figure P5.5

- 5.6. For the transistor in Fig. P5.6,  $I_S = 5 \times 10^{-16} \text{ A}$ ,  $\beta_F = 100$ , and  $\beta_R = 0.25$ . (a) Label the collector, base, and emitter terminals of the transistor. (b) What is the transistor type? (c) Label the base-emitter and base-collector voltages,  $V_{BE}$  and  $V_{BC}$ , respectively, and label the normal directions for  $I_E$ ,  $I_C$ , and  $I_B$ . (d) What is the relationship between  $V_{BE}$  and  $V_{BC}$ ? (e) Write the simplified form of the transport model equations that apply to this particular circuit configuration. Write an expression for  $I_E/I_B$ . Write an expression for  $I_E/I_C$ . (f) Find the values of  $I_E$ ,  $I_C$ ,  $I_B$ ,  $V_{BC}$ , and  $V_{BE}$ .

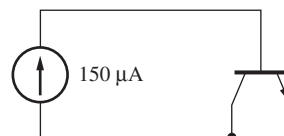


Figure P5.6

- 5.7. For the transistor in Fig. P5.7,  $I_S = 4 \times 10^{-16}$  A,  $\beta_F = 100$ , and  $\beta_R = 0.25$ . (a) Label the collector, base, and emitter terminals of the transistor. (b) What is the transistor type? (c) Label the base-emitter and base-collector voltages,  $V_{BE}$  and  $V_{BC}$ , and the normal directions for  $I_E$ ,  $I_C$ , and  $I_B$ . (d) Find the values of  $I_E$ ,  $I_C$ ,  $I_B$ ,  $V_{BC}$ , and  $V_{BE}$  if  $I = 175$   $\mu$ A.

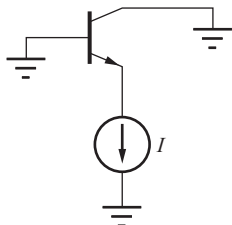


Figure P5.7

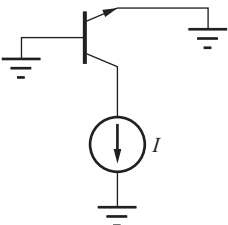


Figure P5.8

- 5.8. For the transistor in Fig. P5.8,  $I_S = 4 \times 10^{-16}$  A,  $\beta_F = 100$ , and  $\beta_R = 0.25$ . (a) Label the collector, base, and emitter terminals of the transistor. (b) What is the transistor type? (c) Label the base-emitter and base-collector voltages,  $V_{BE}$  and  $V_{BC}$ , and label the normal directions for  $I_E$ ,  $I_C$ , and  $I_B$ . (d) Find the values of  $I_E$ ,  $I_C$ ,  $I_B$ ,  $V_{BC}$ , and  $V_{BE}$  if  $I = 175$   $\mu$ A.
- 5.9. The *npn* transistor is connected in a “diode” configuration in Fig. P5.9(a). Use the transport model equations to show that the  $i$ - $v$  characteristics of this connection are similar to those of a diode as defined by Eq. (3.11). What is the reverse saturation current of this “diode” if  $I_S = 4 \times 10^{-15}$  A,  $\beta_F = 100$ , and  $\beta_R = 0.25$ ?

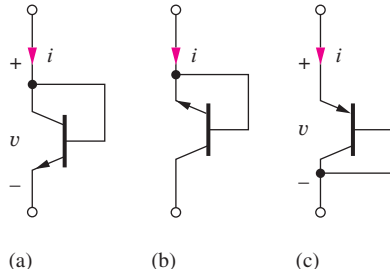


Figure P5.9

- 5.10. The *npn* transistor is connected in an alternate “diode” configuration in Fig. P5.9(b). Use the transport model equations to show that the  $i$ - $v$  characteristics of this connection are similar to those of a diode as defined by Eq. (3.11). What is the reverse saturation current of this “diode” if  $I_S = 5 \times 10^{-16}$  A,  $\beta_F = 60$ , and  $\beta_R = 3$ ?

- 5.11. Calculate  $i_T$  for an *npn* transistor with  $I_S = 10^{-15}$  A for (a)  $V_{BE} = 0.70$  V and  $V_{BC} = -3$  V and (b)  $V_{BC} = 0.70$  V and  $V_{BE} = -3$  V.

- 5.12. Calculate  $i_T$  for an *npn* transistor with  $I_S = 10^{-16}$  A for (a)  $V_{BE} = 0.75$  V and  $V_{BC} = -3$  V and (b)  $V_{BC} = 0.75$  V and  $V_{BE} = -3$  V.

### 5.3 The *pnp* Transistor

- 5.13. Figure P5.13 is a cross section of a *pnp* bipolar transistor similar to the *npn* transistor in Fig. 5.1. Indicate the letter (*A* to *G*) that represents the base contact, collector contact, emitter contact, *p*-type emitter region, *p*-type collector region, and the active or intrinsic transistor region.

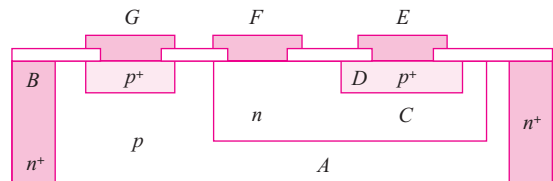


Figure P5.13

- 5.14. For the transistor in Fig. P5.14(a),  $I_S = 4 \times 10^{-16}$  A,  $\alpha_F = 0.985$ , and  $\alpha_R = 0.25$ . (a) What type of transistor is in this circuit? (b) Label the collector, base, and emitter terminals of the transistor. (c) Label the emitter-base and collector-base voltages, and label the normal direction for  $I_E$ ,  $I_C$ , and  $I_B$ . (d) Write the simplified form of the transport model equations that apply to this particular circuit configuration. Write an expression for  $I_E/I_C$ . Write an expression for  $I_E/I_B$ . (e) Find the values of  $I_E$ ,  $I_C$ ,  $I_B$ ,  $\beta_F$ ,  $\beta_R$ ,  $V_{EB}$ , and  $V_{CB}$ .

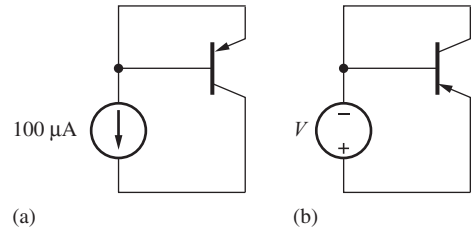


Figure P5.14

- 5.15. (a) Label the collector, base and, emitter terminals of the transistor in the circuit in Fig. P5.14(b). (b) Label the emitter-base and collector-base voltages,  $V_{EB}$  and  $V_{CB}$ , and the normal directions for  $I_E$ ,  $I_C$ , and  $I_B$ . (c) If  $V = 0.640$  V,  $I_C = 300$   $\mu$ A,

and  $I_B = 4 \mu\text{A}$ , find the values of  $I_S$ ,  $\beta_F$ , and  $\beta_R$  for the transistor if  $\alpha_R = 0.2$ .

- 5.16. Repeat Prob. 5.9 for the “diode-connected” *pnp* transistor in Fig. P5.9(c).
- 5.17. For the transistor in Fig. P5.17,  $I_S = 5 \times 10^{-16} \text{ A}$ ,  $\beta_F = 75$ , and  $\beta_R = 4$ . (a) Label the collector, base, and emitter terminals of the transistor. (b) What is the transistor type? (c) Label the emitter-base and collector-base voltages, and label the normal direction for  $I_E$ ,  $I_C$ , and  $I_B$ . (d) Write the simplified form of the transport model equations that apply to this particular circuit configuration. Write an expression for  $I_E/I_B$ . Write an expression for  $I_E/I_C$ . (e) Find the values of  $I_E$ ,  $I_C$ ,  $I_B$ ,  $V_{CB}$ , and  $V_{EB}$ .

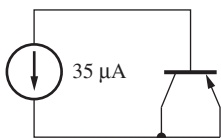


Figure P5.17

- 5.18. For the transistor in Fig. P5.18(a),  $I_S = 5 \times 10^{-16} \text{ A}$ ,  $\beta_F = 100$ , and  $\beta_R = 5$ . (a) Label the collector, base, and emitter terminals of the transistor. (b) What is the transistor type? (c) Label the emitter-base and collector-base voltages,  $V_{EB}$  and  $V_{CB}$ , and the normal directions for  $I_E$ ,  $I_C$ , and  $I_B$ . (d) Find the values of  $I_E$ ,  $I_C$ ,  $I_B$ ,  $V_{CB}$ , and  $V_{EB}$  if  $I = 300 \mu\text{A}$ .

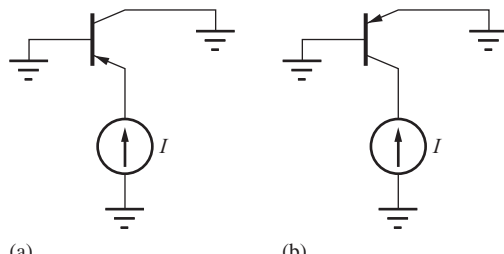


Figure P5.18

- 5.19. For the transistor in Fig. P5.18(b),  $I_S = 5 \times 10^{-16} \text{ A}$ ,  $\beta_F = 75$ , and  $\beta_R = 1$ . (a) Label the collector, base,

and emitter terminals of the transistor. (b) What is the transistor type? (c) Label the emitter-base and collector-base voltages,  $V_{EB}$  and  $V_{CB}$ , and label the normal directions for  $I_E$ ,  $I_C$ , and  $I_B$ . (d) Find the values of  $I_E$ ,  $I_C$ ,  $I_B$ ,  $V_{CB}$ , and  $V_{EB}$  if  $I = 300 \mu\text{A}$ .

- 5.20. Calculate  $i_T$  for a *pnp* transistor with  $I_S = 5 \times 10^{-16} \text{ A}$  for (a)  $V_{EB} = 0.70 \text{ V}$  and  $V_{CB} = -3 \text{ V}$  and (b)  $V_{CB} = 0.70 \text{ V}$  and  $V_{EB} = -3 \text{ V}$ .

## 5.4 Equivalent Circuit Representations for the Transport Models

- 5.21. Calculate the values of  $i_T$  and the two diode currents for the equivalent circuit in Fig. 5.8(a) for an *npn* transistor with  $I_S = 4 \times 10^{-16} \text{ A}$ ,  $\beta_F = 80$ , and  $\beta_R = 2$  for (a)  $V_{BE} = 0.73 \text{ V}$  and  $V_{BC} = -3 \text{ V}$  and (b)  $V_{BC} = 0.73 \text{ V}$  and  $V_{BE} = -3 \text{ V}$ .
- 5.22. Calculate the values of  $i_T$  and the two diode currents for the equivalent circuit in Fig. 5.8(b) for a *pnp* transistor with  $I_S = 3 \times 10^{-15} \text{ A}$ ,  $\beta_F = 60$ , and  $\beta_R = 3$  for (a)  $V_{EB} = 0.68 \text{ V}$  and  $V_{CB} = -3 \text{ V}$  and (b)  $V_{CB} = 0.68 \text{ V}$  and  $V_{EB} = -3 \text{ V}$ .
- 5.23. The Ebers-Moll model was one of the first mathematical models used to describe the characteristics of the bipolar transistor. Show that the *npn* Transport Model equations can be transformed into the Ebers-Moll equations below. (*Hint:* Add and subtract 1 from the collector and emitter current expressions in Eqs. (5.13).)

$$\begin{aligned} i_E &= I_{ES} \left[ \exp \left( \frac{v_{BE}}{V_T} \right) - 1 \right] - \alpha_R I_{CS} \left[ \exp \left( \frac{v_{BC}}{V_T} \right) - 1 \right] \\ i_C &= \alpha_F I_{ES} \left[ \exp \left( \frac{v_{BE}}{V_T} \right) - 1 \right] - I_{CS} \left[ \exp \left( \frac{v_{BC}}{V_T} \right) - 1 \right] \\ i_B &= (1 - \alpha_F) I_{ES} \left[ \exp \left( \frac{v_{BE}}{V_T} \right) - 1 \right] + (1 - \alpha_R) I_{CS} \left[ \exp \left( \frac{v_{BC}}{V_T} \right) - 1 \right] \\ \alpha_F I_{ES} &= \alpha_R I_{CS} \end{aligned}$$

- 5.24. What are the values of  $\alpha_F$ ,  $\alpha_R$ ,  $I_{ES}$  and  $I_{CS}$  for an *npn* transistor with  $I_S = 2 \times 10^{-15} \text{ A}$ ,  $\beta_F = 100$  and  $\beta_R = 0.5$ ? Show that  $\alpha_F I_{ES} = \alpha_R I_{CS}$ .
- 5.25. The Ebers-Moll model was one of the first mathematical models used to describe the characteristics of the bipolar transistor. Show that the *pnp* Transport Model equations can be transformed into the Ebers-Moll equations that follow. (*Hint:* Add and subtract 1 from the collector and emitter current expressions in Eqs. (5.17).)

$$\begin{aligned} i_E &= I_{ES} \left[ \exp \left( \frac{v_{EB}}{V_T} \right) - 1 \right] - \alpha_R I_{CS} \left[ \exp \left( \frac{v_{CB}}{V_T} \right) - 1 \right] \\ i_C &= \alpha_F I_{ES} \left[ \exp \left( \frac{v_{EB}}{V_T} \right) - 1 \right] - I_{CS} \left[ \exp \left( \frac{v_{CB}}{V_T} \right) - 1 \right] \quad \alpha_F I_{ES} = \alpha_R I_{CS} \\ i_B &= (1 - \alpha_F) I_{ES} \left[ \exp \left( \frac{v_{EB}}{V_T} \right) - 1 \right] + (1 - \alpha_R) I_{CS} \left[ \exp \left( \frac{v_{CB}}{V_T} \right) - 1 \right] \end{aligned}$$

## 5.5 The $i$ - $v$ Characteristics of the Bipolar Transistor

- \*5.26. The common-emitter output characteristics for an *npn* transistor are given in Fig. P5.26. What are the values of  $\beta_F$  at (a)  $I_C = 5$  mA and  $V_{CE} = 5$  V? (b)  $I_C = 7$  mA and  $V_{CE} = 7.5$  V? (c)  $I_C = 10$  mA and  $V_{CE} = 14$  V?

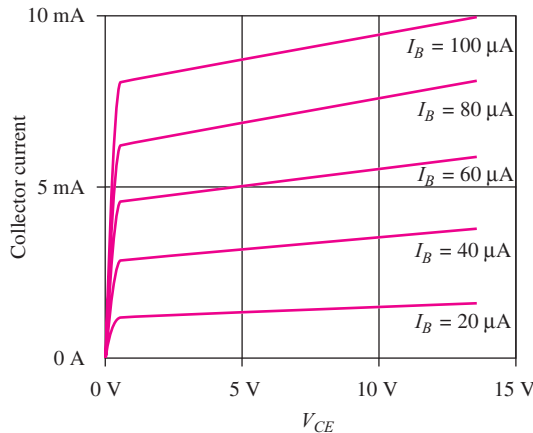


Figure P5.26

- 5.27. Plot the common-emitter output characteristics for an *npn* transistor having  $I_S = 1$  fA,  $\beta_{FO} = 75$ , and  $V_A = 50$  V for six equally spaced base current steps ranging from 0 to 200  $\mu$ A and  $V_{CE}$  ranging from 0 to 10 V.
- 5.28. Use SPICE to plot the common-emitter output characteristics for the *npn* transistor in Prob. 5.27.
- 5.29. Use SPICE to plot the common-base output characteristics for an *npn* transistor having  $I_S = 1$  fA,  $\beta_{FO} = 75$ , and  $V_A = 50$  V for six equally spaced emitter current steps ranging from 0 to 2 mA and  $V_{CB}$  ranging from 0 to 10 V.
- 5.30. Plot the common-emitter output characteristics for a *pnp* transistor having  $I_S = 1$  fA,  $\beta_{FO} = 75$ , and  $V_A = 50$  V for six equally spaced base current steps ranging from 0 to 250  $\mu$ A and  $V_{EC}$  ranging from 0 to 10 V.

- 5.31. Use SPICE to plot the common-emitter output characteristics for the *pnp* transistor in Prob. 5.30.

- 5.32. Use SPICE to plot the common-base output characteristics for an *pnp* transistor having  $I_S = 1$  fA,  $\beta_{FO} = 75$ , and  $V_A = 50$  V for six equally spaced emitter current steps ranging from 0 to 2 mA and  $V_{BC}$  ranging from 0 to 10 V.

- 5.33. What is the reciprocal of the slope (in mV/decade) of the logarithmic transfer characteristic for an *npn* transistor in the common-emitter configuration at a temperature of (a) 200 K, (b) 250 K, (c) 300 K and (d) 350 K?

## Junction Breakdown Voltages

- \*5.34. In the circuits in Fig. P5.9, the Zener breakdown voltages of the collector-base and emitter-base junctions of the transistors are 60 V and 5 V, respectively. What is the Zener breakdown voltage for each “diode” connected transistor configuration?

- 5.35. In the circuits in Fig. P5.35, the Zener breakdown voltages of the collector-base and emitter-base junctions of the *npn* transistors are 50 V and 6.3 V, respectively. What is the current in the resistor in each circuit? (*Hint:* The equivalent circuits for the transport model equations may help in visualizing the circuit.)

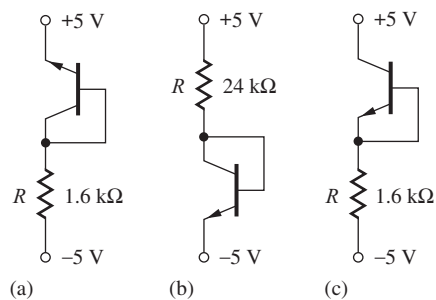


Figure P5.35

- 5.36. An *npn* transistor is biased as indicated in Fig. 5.9(a). What is the largest value of  $V_{CE}$  that can

be applied without junction breakdown if the breakdown voltages of the collector-base and emitter-base junctions of the *npn* transistors are 60 V and 5 V, respectively?

- \*5.37. (a) For the circuit in Fig. P5.37, what is the maximum value of  $I$  according to the transport model equations if  $I_S = 1 \times 10^{-16}$  A,  $\beta_F = 50$ , and  $\beta_R = 0.5$ ? (b) Suppose that  $I = 1$  mA. What happens to the transistor? (*Hint:* The equivalent circuits for the transport model equations may help in visualizing the circuit.)

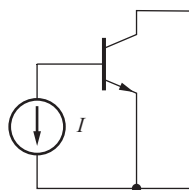


Figure P5.37

## 5.6 The Operating Regions of the Bipolar Transistor

- 5.38. Indicate the region of operation in the following table for an *npn* transistor biased with the indicated voltages.

BASE-EMITTER VOLTAGE	BASE-COLLECTOR VOLTAGE	
	0.7 V	-5.0 V
-5.0 V		
0.7 V		

- 5.39. (a) What are the regions of operation for the transistors in Fig. P5.9? (b) In Fig. P5.46(a)? (c) In Fig. P5.49? (d) In Fig. P5.62?
- 5.40. (a) What is the region of operation for the transistor in Fig. P5.5(a)? (b) In Fig. P5.5(b)?
- 5.41. (a) What is the region of operation for the transistor in Fig. P5.6? (b) In Fig. P5.7? (c) In Fig. P5.8?
- 5.42. Indicate the region of operation in the following table for a *pnp* transistor biased with the indicated voltages.

EMITTER-BASE VOLTAGE	COLLECTOR-BASE VOLTAGE	
	0.7 V	-0.65 V
0.7 V		
-0.65 V		

- 5.43. (a) What is the region of operation for the transistor in Fig. P5.2? (b) In Fig. P5.3?
- 5.44. (a) What is the region of operation for the transistor in Fig. P5.14(a)? (b) In Fig. P5.14(b)?
- 5.45. (a) What is the region of operation for the transistor in Fig. P5.17? (b) In Fig. P5.18(a)? (c) In Fig. P5.18(b).

## 5.7 Transport Model Simplifications Cutoff Region

- 5.46. (a) What are the three terminal currents  $I_E$ ,  $I_B$ , and  $I_C$  in the transistor in Fig. P5.46(a) if  $I_S = 1 \times 10^{-16}$  A,  $\beta_F = 75$ , and  $\beta_R = 4$ ? (b) Repeat for Fig. P5.46(b).
- \*\*5.47. An *npn* transistor with  $I_S = 5 \times 10^{-16}$  A,  $\alpha_F = 0.95$  and  $\alpha_R = 0.5$  is operating with  $V_{BE} = 0.3$  V and  $V_{BC} = -5$  V. This transistor is not truly operating in the region defined to be cutoff, but we still say the transistor is off. Why? Use the transport model equations to justify your answer. In what region is the transistor actually operating according to our definitions?

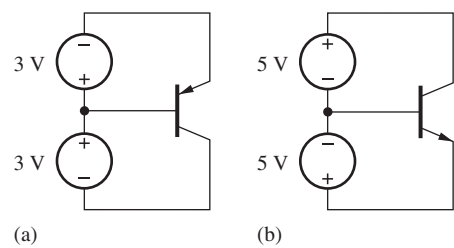


Figure P5.46

## Forward-Active Region

- 5.48. What are the values of  $\beta_F$  and  $I_S$  for the transistor in Fig. P5.48?
- 5.49. What are the values of  $\beta_F$  and  $I_S$  for the transistor in Fig. P5.49?

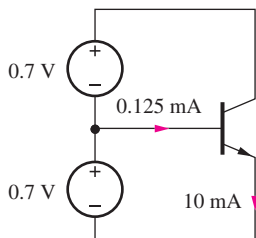


Figure P5.48

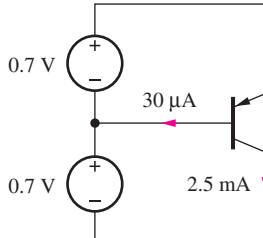


Figure P5.49

- 5.50. What are the emitter, base, and collector currents in the circuit in Fig. 5.18 if  $V_{EE} = 3.3$  V,  $R = 47$  k $\Omega$ , and  $\beta_F = 80$ ?
- \*\*5.51. A transistor has  $f_T = 500$  MHz and  $\beta_F = 75$ . (a) What is the  $\beta$ -cutoff frequency  $f_\beta$  of this transistor? (b) Use Eq. (5.42) to find an expression for the frequency dependence of  $\alpha_F$ —that is,  $\alpha_F(f)$ . [Hint: Write an expression for  $\beta(s)$ .] What is the  $\alpha$ -cutoff frequency for this transistor?
- \*5.52. (a) Start with the transport model equations for the *pnp* transistor, Eqs. (5.17), and construct the simplified version of the *pnp* equations that apply to the forward-active region [similar to Eqs. (5.23)]. (b) Draw the simplified model for the *pnp* transistor similar to the *npn* version in Fig. 5.21(c).

### Reverse-Active Region

- 5.53. What are the values of  $\beta_R$  and  $I_S$  for the transistor in Fig. P5.53?
- 5.54. What are the values of  $\beta_R$  and  $I_S$  for the transistor in Fig. P5.54?

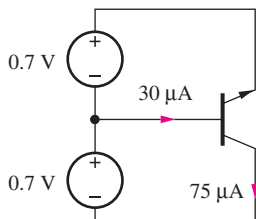


Figure P5.53

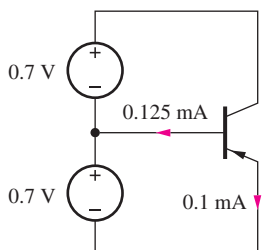


Figure P5.54

- 5.55. Find the emitter, base, and collector currents in the circuit in Fig. 5.22 if the negative power supply is  $-3.3$  V,  $R = 56$  k $\Omega$ , and  $\beta_R = 0.75$ .

### Saturation Region

- 5.56. What is the saturation voltage of an *npn* transistor operating with  $I_C = 1$  mA and  $I_B = 1$  mA if  $\beta_F = 50$  and  $\beta_R = 2$ ? What is the forced  $\beta$  of this transistor? What is the value of  $V_{BE}$  if  $I_S = 10^{-15}$  A?

5.57. Derive an expression for the saturation voltage  $V_{ECSAT}$  of the *pnp* transistor in a manner similar to that used to derive Eq. (5.30).

- 5.58. (a) What is the collector-emitter voltage for the transistor in Fig. P5.58(a) if  $I_S = 5 \times 10^{-16}$  A,  $\alpha_F = 0.99$ , and  $\alpha_R = 0.5$ ? (b) What is the emitter-collector voltage for the transistor in Fig. P5.59(b) for the same transistor parameters?

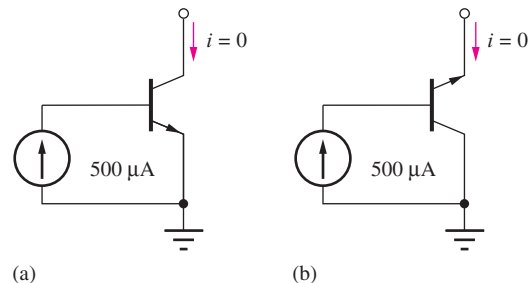


Figure P5.58

- 5.59. Repeat Prob. 5.58 for  $\alpha_F = 0.95$  and  $\alpha_R = 0.33$ .
- 5.60. (a) What base current is required to achieve a saturation voltage of  $V_{CESAT} = 0.1$  V in an *npn* power transistor that is operating with a collector current of 20 A if  $\beta_F = 15$  and  $\beta_R = 0.9$ ? What is the forced  $\beta$  of this transistor? (b) Repeat for  $V_{CESAT} = 0.04$  V.
- \*\*5.61. An *npn* transistor with  $I_S = 1 \times 10^{-16}$  A,  $\alpha_F = 0.975$ , and  $\alpha_R = 0.5$  is operating with  $V_{BE} = 0.70$  V and  $V_{BC} = 0.50$  V. By definition, this transistor is operating in the saturation region. However, in the discussion of Fig. 5.19 it was noted that this transistor actually behaves as if it is still in the forward-active region even though  $V_{BC} > 0$ . Why? Use the transport model equations to justify your answer.
- 5.62. The current  $I$  in both circuits in Fig. P5.62 is 175  $\mu$ A. Find the value of  $V_{BE}$  for both circuits if  $I_S = 4 \times 10^{-16}$  A,  $\beta_F = 50$ , and  $\beta_R = 0.5$ . What is  $V_{CESAT}$  in Fig. P5.62(b)?

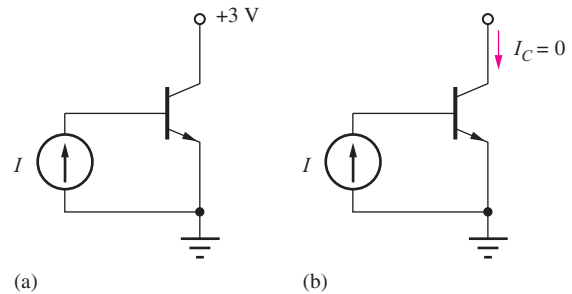


Figure P5.62

## Diodes in Bipolar Integrated Circuits

- 5.63. Derive the result in Eq (5.26) by applying the circuit constraints to the transport equations.
- 5.64. What is the reverse saturation current of the diode in Fig. 5.20 if the transistor is described by  $I_S = 10^{-15}$  A,  $\alpha_R = 0.20$ , and  $\alpha_F = 0.98$ ?
- 5.65. The two transistors in Fig. P5.65 are identical. What is the collector current of  $Q_2$  if  $I = 25 \mu\text{A}$  and  $\beta_F = 60$ ?

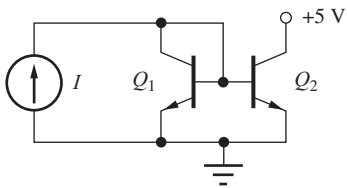


Figure P5.65

## 5.8 Nonideal Behavior of the Bipolar Transistor

- 5.66. Calculate the diffusion capacitance of a bipolar transistor with a forward transit time  $\tau_F = 50 \text{ ps}$  for collector currents of (a)  $2 \mu\text{A}$ , (b)  $200 \mu\text{A}$ , (c)  $20 \text{ mA}$ .
- 5.67. (a) What is the forward transit time  $\tau_F$  for an *npn* transistor with a base width  $W_B = 0.5 \mu\text{m}$  and a base doping of  $10^{18}/\text{cm}^3$ ? (b) Repeat the calculation for a *pnp* transistor.
- 5.68. A transistor has a dc current gain of 200 and a current gain of 10 at 75 MHz. What are the unity-gain and beta-cutoff frequencies of the transistor?
- 5.69. A transistor has  $f_T = 900 \text{ MHz}$  and  $f_\beta = 5 \text{ MHz}$ . What is the dc current gain of the transistor? What is the current gain of the transistor at 50 MHz? At 250 MHz?
- 5.70. What is the saturation current for a transistor with a base doping of  $6 \times 10^{18}/\text{cm}^3$ , a base width of  $0.4 \mu\text{m}$ , and a cross-sectional area of  $25 \mu\text{m}^2$ ?
- 5.71. An *npn* transistor is needed that will operate at a frequency of at least 5 GHz. What base width is required for the transistor if the base doping is  $5 \times 10^{18}/\text{cm}^3$ ?

## The Early Effect and Early Voltage

- 5.72. An *npn* transistor is operating in the forward-active region with a base current of  $3 \mu\text{A}$ . It is found that  $I_C = 240 \mu\text{A}$  for  $V_{CE} = 5 \text{ V}$  and  $I_C = 265 \mu\text{A}$  for  $V_{CE} = 10 \text{ V}$ . What are the values of  $\beta_{FO}$  and  $V_A$  for this transistor?

- 5.73. An *npn* transistor with  $I_S = 4 \times 10^{-16} \text{ A}$ ,  $\beta_F = 100$ , and  $V_A = 65 \text{ V}$  is biased in the forward-active region with  $V_{BE} = 0.72 \text{ V}$  and  $V_{CE} = 10 \text{ V}$ . (a) What is the collector current  $I_C$ ? (b) What would be the collector current  $I_C$  if  $V_A = \infty$ ? (c) What is the ratio of the two answers in parts (a) and (b)?
- 5.74. The common-emitter output characteristics for an *npn* transistor are given in Fig. P5.26. What are the values of  $\beta_{FO}$  and  $V_A$  for this transistor?
- 5.75. (a) Recalculate the currents in the transistor in Fig. 5.16 if  $I_S = 5 \times 10^{-16} \text{ A}$ ,  $\beta_{FO} = 19$ , and  $V_A = 50 \text{ V}$ . What is  $V_{BE}$ ? (b) What was  $V_{BE}$  for  $V_A = \infty$ ?
- 5.76. Recalculate the currents in the transistor in Fig. 5.18 if  $\beta_{FO} = 50$  and  $V_A = 50 \text{ V}$ .
- 5.77. Repeat Prob. 5.65 if  $V_A = 50 \text{ V}$  and  $V_{BE} = 0.7 \text{ V}$ .

## 5.9 Transconductance

- 5.78. What is the transconductance of an *npn* transistor operating at 350 K and a collector current of (a)  $10 \mu\text{A}$ , (b)  $100 \mu\text{A}$ , (c)  $1 \text{ mA}$ , and (d)  $10 \text{ mA}$ ? (e) Repeat for a *pnp* transistor.
- 5.79. What is the diffusion capacitance for an *npn* transistor with  $\tau_F = 10 \text{ psec}$  if it is operating at 300 K with a collector currents of  $1 \mu\text{A}$ ,  $1 \text{ mA}$ , and  $10 \text{ mA}$ ?

## 5.10 Bipolar Technology and SPICE Model

- 5.80. (a) Find the default values of the following parameters for the generic *npn* transistor in the version of SPICE that you use in class: IS, BF, BR, VAF, VAR, TF, TR, NF, NE, RB, RC, RE, ISE, ISC, ISS, IKF, IKR, CJE, CJC. (Note: The values in Table 5.P1 may not agree exactly with your version of SPICE.) (b) Repeat for the generic *pnp* transistor.
- 5.81. A SPICE model for a bipolar transistor has a forward knee current  $IKF = 10 \text{ mA}$  and  $NK = 0.5$ . How much does the KBQ factor reduce the collector current of the transistor in the forward-active region if  $i_F$  is (a)  $1 \text{ mA}$ ? (b)  $10 \text{ mA}$ ? (c)  $50 \text{ mA}$ ?
- 5.82. Plot a graph of KBQ versus  $i_F$  for an *npn* transistor with  $IKF = 40 \text{ mA}$  and  $NK = 0.5$ . Assume forward-active region operation with  $VAF = \infty$ .

## 5.11 Practical Bias Circuits for the BJT

### Four-Resistor Biasing

- 5.83. (a) Find the Q-point for the circuit in Fig. P5.83(a). Assume that  $\beta_F = 50$  and  $V_{BE} = 0.7 \text{ V}$ . (b) Repeat the calculation if all the resistor values are decreased

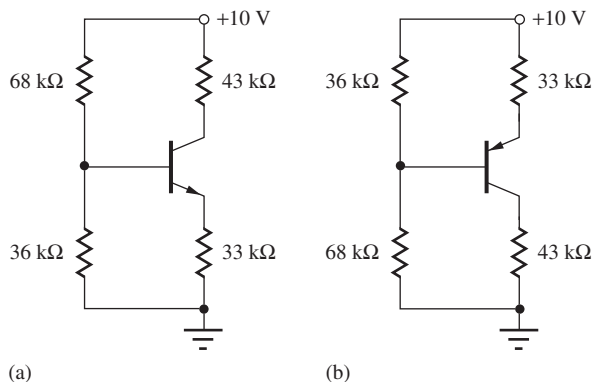


Figure P5.83

by a factor of 5. (c) Repeat if all the resistor values are increased by a factor of 5. (d) Find the Q-point in part (a) using the numerical iteration method if  $I_S = 0.5 \text{ fA}$  and  $V_T = 25.8 \text{ mV}$ .

- 5.84. (a) Find the Q-point for the circuit in Fig. 5.83(a) if the 33-kΩ resistor is replaced with a 22-kΩ resistor. Assume that  $\beta_F = 75$ .
- 5.85. (a) Find the Q-point for the circuit in Fig. P5.83(b). Assume  $\beta_F = 50$  and  $V_{BE} = 0.7 \text{ V}$ . (b) Repeat if all the resistor values are decreased by a factor of 5. (c) Repeat if all the resistor values are increased by a factor of 5. (d) Find the Q-point in part (a) using the numerical iteration method if  $I_S = 0.4 \text{ fA}$  and  $V_T = 25.8 \text{ mV}$ .
- 5.86. (a) Find the Q-point for the circuit in Fig. P5.83(b) if the 33-kΩ resistor is replaced with a 22-kΩ resistor. Assume  $\beta_F = 75$  and  $V_{BE} = 0.7 \text{ V}$ . (b) Repeat if all the resistor values are decreased by a factor of 5. (c) Repeat if all the resistor values are increased by a factor of 5. (d) Find the Q-point in part (a) using the numerical iteration method if  $I_S = 1 \text{ fA}$  and  $V_T = 25.8 \text{ mV}$ .
- 5.87. (a) Simulate the circuits in Fig. P5.83 and compare the SPICE results to your hand calculations of the Q-point. Use  $I_S = 1 \times 10^{-16} \text{ A}$ ,  $\beta_F = 50$ ,  $\beta_R = 0.25$ , and  $V_A = \infty$ . (b) Repeat for  $V_A = 60 \text{ V}$ . (c) Repeat (a) for the circuit in Fig. 5.34(c). (d) Repeat (b) for the circuit in Fig. 5.34(c).
- 5.88. Find the Q-point in the circuit in Fig. 5.34 if  $R_1 = 120 \text{ k}\Omega$ ,  $R_2 = 270 \text{ k}\Omega$ ,  $R_E = 100 \text{ k}\Omega$ ,  $R_C = 150 \text{ k}\Omega$ ,  $\beta_F = 100$ , and the positive power supply voltage is 15 V.
- 5.89. Find the Q-point in the circuit in Fig. 5.34 if  $R_1 = 6.2 \text{ k}\Omega$ ,  $R_2 = 13 \text{ k}\Omega$ ,  $R_C = 5.1 \text{ k}\Omega$ ,  $R_E =$

$7.5 \text{ k}\Omega$ ,  $\beta_F = 100$ , and the positive power supply voltage is 10 V.

- 5.90. (a) Design a four-resistor bias network for an *npn* transistor to give  $I_C = 1 \text{ mA}$ ,  $V_{CE} = 5 \text{ V}$ , and  $V_E = 3 \text{ V}$  if  $V_{CC} = 12 \text{ V}$  and  $\beta_F = 100$ . (b) Replace your exact values with the nearest values from the resistor table in Appendix C and find the resulting Q-point.
- 5.91. (a) Design a four-resistor bias network for an *npn* transistor to give  $I_C = 10 \mu\text{A}$  and  $V_{CE} = 6 \text{ V}$  if  $V_{CC} = 18 \text{ V}$  and  $\beta_F = 75$ . (b) Replace your exact values with the nearest values from the resistor table in Appendix C and find the resulting Q-point.
- 5.92. (a) Design a four-resistor bias network for a *pnp* transistor to give  $I_C = 11 \text{ mA}$  and  $V_{EC} = 5 \text{ V}$  if  $V_{RE} = 1 \text{ V}$ ,  $V_{CC} = -15 \text{ V}$  and  $\beta_F = 50$ . (b) Replace your exact values with the nearest values from the resistor table in Appendix C and find the resulting Q-point.
- 5.93. (a) Design a four-resistor bias network for a *pnp* transistor to give  $I_C = 850 \mu\text{A}$ ,  $V_{EC} = 2 \text{ V}$ , and  $V_E = 1 \text{ V}$  if  $V_{CC} = 5 \text{ V}$  and  $\beta_F = 60$ . (b) Replace your exact values with the nearest values from the resistor table in Appendix C and find the resulting Q-point.
- ### Load Line Analysis
- \*5.94. Find the Q-point for the circuit in Fig. P5.94 using the graphical load-line approach. Use the characteristics in Fig. P5.26.
- \*5.95. Find the Q-point for the circuit in Fig. P5.95 using the graphical load-line approach. Use the characteristics in Fig. P5.26, assuming that the graph is a plot of  $i_C$  vs.  $v_{EC}$  rather than  $i_C$  vs.  $v_{CE}$ .

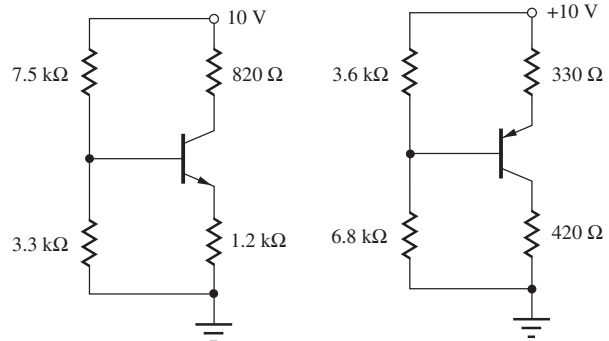


Figure P5.94

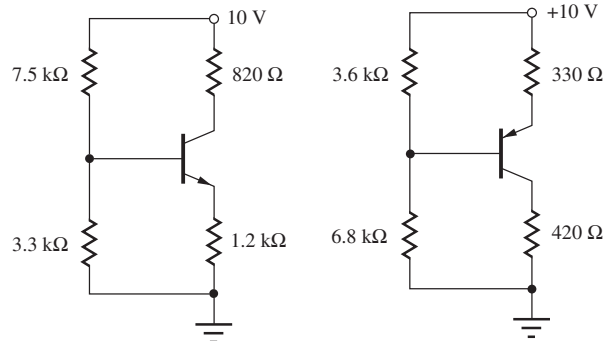


Figure P5.95

## Bias Circuits and Applications

- 5.96. Find the Q-point for the circuit in Fig. P5.96 for  
 (a)  $\beta_F = 40$ , (b)  $\beta_F = 120$ , (c)  $\beta_F = 250$ ,  
 (d)  $\beta_F = \infty$ . (e) Find the Q-point in part (a) using  
 the numerical iteration method if  $I_S = 0.5 \text{ fA}$   
 and  $V_T = 25.8 \text{ mV}$ . (f) Find the Q-point in part (c)  
 using the numerical iteration method if  $I_S = 0.5 \text{ fA}$   
 and  $V_T = 25.8 \text{ mV}$ .
- \*5.97. Write the load-line expression for the circuit in Fig. P5.96. Draw the load line on the characteristics in Fig. P5.26. Find the Q-point by drawing a curve that plots  $I_B$  vs.  $V_{CE}$ .

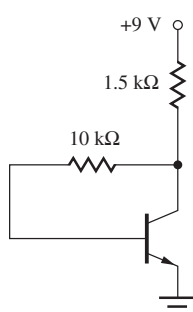


Figure P5.96

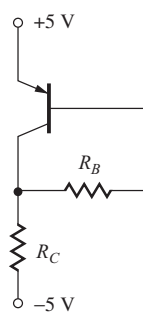


Figure P5.98

- 5.98. Design the bias circuit in Fig. P5.98 to give a Q-point of  $I_C = 10 \text{ mA}$  and  $V_{CE} = 3 \text{ V}$  if the transistor current gain  $\beta_F = 60$ . What is the Q-point if the current gain of the transistor is actually 40?
- 5.99. Design the bias circuit in Fig. P5.99 to give a Q-point of  $I_C = 20 \mu\text{A}$  and  $V_{CE} = 0.90 \text{ V}$  if the transistor current gain is  $\beta_F = 50$  and  $V_{BE} = 0.65 \text{ V}$ . What is the Q-point if the current gain of the transistor is actually 125?
- \*5.100. (a) Find the Q-point for the circuit in Fig. P5.100 if the Zener diode has  $V_Z = 5 \text{ V}$  and  $R_C = 500 \Omega$ . Use  $\beta_F = 100$ . (b) Find the Q-point in part (a) using the numerical iteration method if  $I_S = 0.5 \text{ fA}$  and  $V_T = 25.8 \text{ mV}$ .

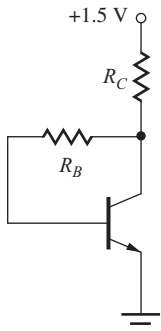


Figure P5.99

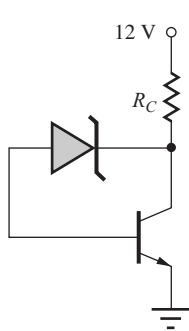


Figure P5.100

## Bias Circuit Applications

- 5.101. The Zener diode in Fig. P5.101 has  $V_Z = 6 \text{ V}$  and  $R_Z = 100 \Omega$ . What is the output voltage if  $I_L = 20 \text{ mA}$ ? Use  $I_S = 1 \times 10^{-16} \text{ A}$ ,  $\beta_F = 50$ , and  $\beta_R = 0.5$  to find a precise answer.

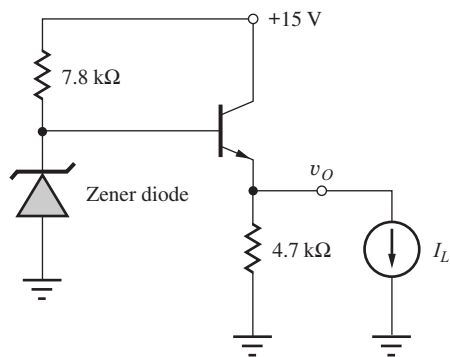


Figure P5.101

- \*5.102. Create a model for the Zener diode and simulate the circuit in Prob. P5.101. Compare the SPICE results to your hand calculations. Use  $I_S = 1 \times 10^{-16} \text{ A}$ ,  $\beta_F = 50$ , and  $\beta_R = 0.5$ .
- \*\*5.103. The circuit in Fig. P5.103 has  $V_{EQ} = 7 \text{ V}$  and  $R_{EQ} = 100 \Omega$ . What is the output resistance  $R_o$  of this circuit for  $i_L = 20 \text{ mA}$  if  $R_o$  is defined as  $R_o = -dv_O/di_L$ ? Assume  $\beta_F = 50$ .

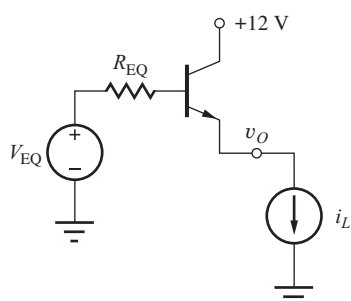


Figure P5.103

- 5.104. What is the output voltage  $v_O$  in Fig. P5.104 if the op-amp is ideal? What are the values of the emitter current and the total current supplied by the 15-V source? Assume  $\beta_F = 60$ . What is the op-amp output voltage?

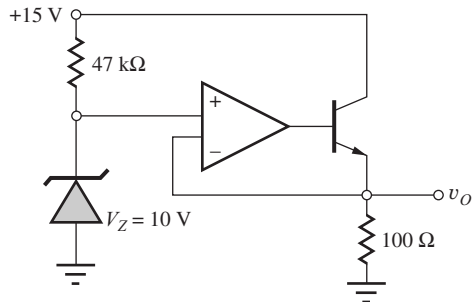


Figure P5.104

- 5.105. What is the output voltage  $v_O$  in Fig. P5.105 if the op-amp is ideal? What are the values of the emitter current and the total current supplied by the 15-V source? Assume  $\beta_F = 40$ . What is the op-amp output voltage?

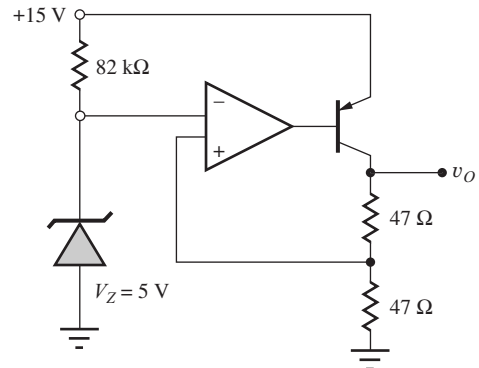
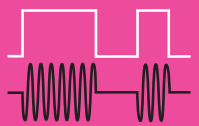


Figure P5.105

## PART TWO **DIGITAL ELECTRONICS**



CHAPTER 6  
**INTRODUCTION TO DIGITAL ELECTRONICS 287**

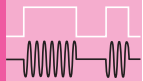
CHAPTER 7  
**COMPLEMENTARY MOS (CMOS) LOGIC DESIGN 367**

CHAPTER 8  
**MOS MEMORY AND STORAGE CIRCUITS 416**

CHAPTER 9  
**BIPOLAR LOGIC CIRCUITS 460**

*This page intentionally left blank*

# CHAPTER 6



## INTRODUCTION TO DIGITAL ELECTRONICS

### CHAPTER OUTLINE

- 6.1 Ideal Logic Gates 289
- 6.2 Logic Level Definitions and Noise Margins 289
- 6.3 Dynamic Response of Logic Gates 293
- 6.4 Review of Boolean Algebra 295
- 6.5 NMOS Logic Design 297
- 6.6 Transistor Alternatives to the Load Resistor 306
- 6.7 NMOS Inverter Summary and Comparison 323
- 6.8 NMOS NAND and NOR Gates 324
- 6.9 Complex NMOS Logic Design 328
- 6.10 Power Dissipation 333
- 6.11 Dynamic Behavior of MOS Logic Gates 337
- 6.12 PMOS Logic 349
  - Summary 352
  - Key Terms 354
  - References 355
  - Additional Reading 355
  - Problems 355

### CHAPTER GOALS

- Introduce binary digital logic concepts
- Explore the voltage transfer characteristics of ideal and nonideal inverters
- Define logic levels and logic states at the input and output of logic gates
- Present goals for logic gate design
- Understand the need for noise rejection and the concept of noise margin; present examples of noise margin calculations
- Introduce measures of dynamic performance of logic gates including rise time, fall time, propagation delay, and power-delay product
- Review Boolean algebra and the NOT, OR, AND, NOR, and NAND functions
- Learn basic inverter design; discover why transistors are used in place of resistors
- Explore simple transistor implementations of the inverter
- Explore the design of MOS logic gates employing single transistor types—either NMOS or PMOS transistors (known as single-channel technology)
- Understand design and performance differences between saturated load, linear load, depletion-mode, and pseudo NMOS load circuits

- Learn to design multiinput NAND and NOR gates
- Learn to design complex logic gates including sum-of-products representations
- Develop expressions and approximation techniques for calculating rise time, fall time, and propagation delay of the various single-channel logic families

Digital electronics has had a profound effect on our lives through the pervasive application of microprocessors and microcontrollers in consumer and industrial products. The microprocessor chip forms the heart of personal computers and workstations, and digital signal processing is the basis of modern telecommunications. Microcontrollers are found in everything from CD/MP3 players to refrigerators to washing machines to vacuum cleaners, and in today's luxury automobiles often more than 50 microprocessors work together to control the vehicle. In fact, as much as 40 to 50 percent of the total cost of luxury cars is projected to come from electronics in the near future.

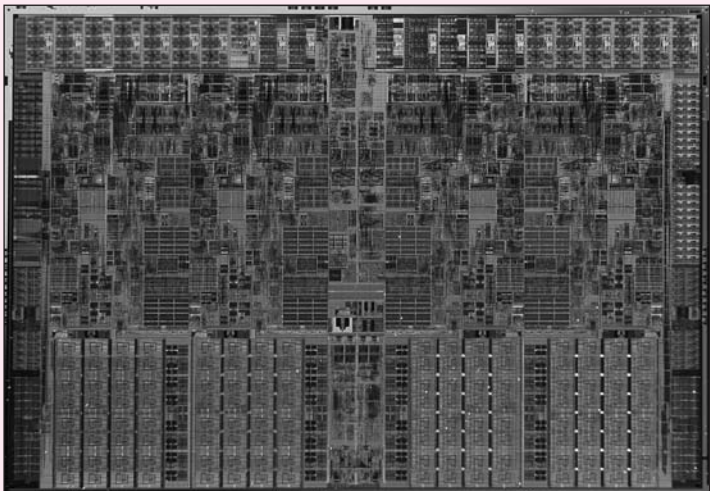
The digital electronics market is dominated by far by **complementary MOS, or CMOS, technology**. However, as pointed out in previous chapters, the first successful manufacturing processes were developed for bipolar devices, and the first integrated circuits utilized bipolar transistors. The rapid advance in the application of digital electronics was facilitated by circuit designers who developed early bipolar logic families called resistor-transistor logic (RTL) and diode-transistor logic (DTL). These families were subsequently replaced with highly robust bipolar logic families including **transistor-transistor logic (TTL)** and **emitter-coupled logic (ECL)** that could be easily interconnected to form highly reliable digital systems. High-performance forms of TTL and ECL remain in use today.

It took almost a decade to develop viable MOS manufacturing processes. The first high-density MOS integrated circuits utilizing PMOS technology appeared around 1970. The landmark development of the microprocessor is attributed to Ted Hoff who convinced Intel to develop the 4-bit 4004 microprocessor chip containing approximately of 2300 transistors that was introduced in 1971 [1]. As with many advances, work on single-chip processors advanced



Intel Founders Andy Grove, Robert Noyce, and Gordon Moore with rubylith layout of 8080 microprocessor.

*Photo Courtesy of Intel Corporation*



Intel® Core™ i7 Processor Nehalem Die.

*Copyright © Intel Corporation.*

rapidly in research and development laboratories around the world. In the following 30 years, the industry went on to develop microprocessor chips of incredible complexity. As this edition is written, chips employing more than one billion transistors have been introduced, and the ITRS projections in Chapter 1 predict microprocessors with more than 10 billion transistors will appear by the year 2018.

By the mid 1970s, PMOS was being rapidly replaced by the higher-performance NMOS technology. The Intel 8080, 8085, and 8086 were all implemented in NMOS logic. A significant advance in NMOS circuit performance was achieved with the introduction of the depletion-mode load device, and this work was formally recognized when Dr. Toshiaki Masuhara of Hitachi received the 1990 IEEE Solid-State Circuits Award for this work.

But by the mid 1980s, power dissipation levels associated with NMOS microprocessors had reached unmanageable levels, and the industry made a transition to CMOS technology almost overnight. CMOS has remained the dominant technology since that time. Chapter 7 is dedicated to CMOS logic design.

In this chapter, we begin our study of digital logic circuits with the introduction of a number of important concepts and definitions related to logic circuits. Then the chapter looks in detail at the design of MOS logic circuits built using only a single transistor type—either NMOS or PMOS—referred to as “single channel technology.” Pseudo NMOS utilizes a PMOS load transistor and provides a bridge to modern Complementary MOS (CMOS) logic that uses both NMOS and PMOS transistors, as discussed in Chapter 7. MOS memory and storage circuits are introduced in Chapter 8, and bipolar logic circuits are discussed in Chapter 9.

**T**his chapter explores the requirements and general characteristics of digital logic gates and then investigates the detailed implementation of logic gates in MOS technologies. The initial discussion in this chapter focuses on the characteristics of the inverter. Important logic levels associated with binary logic are defined, and the concepts of the voltage transfer characteristic and noise margin are introduced. Later, the temporal behavior and time delays of the gates are addressed. A short review of Boolean algebra, used for representation and analysis of logic functions, is included. NMOS inverters

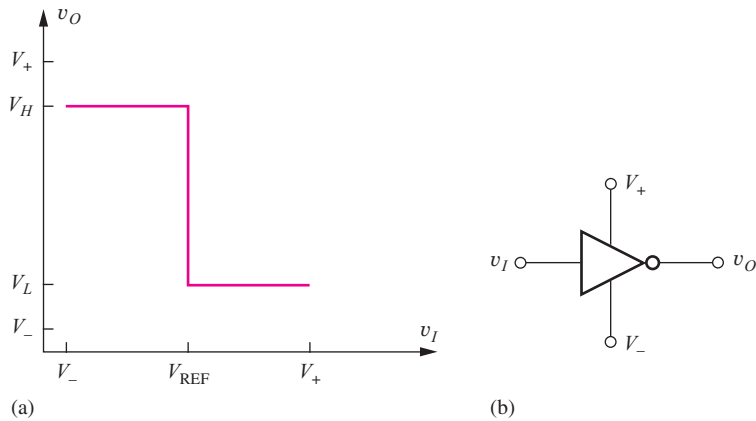


**Figure 6.1** (a) Voltage transfer characteristic for an ideal inverter. (b) Inverter logic symbol.

with various types of load elements are studied in detail, including static design and behavior in the time domain. In integrated circuits, transistors replace resistors as load devices in order to minimize circuit area. NAND, NOR, and complex gate implementations are based upon the basic inverter designs.

## 6.1 IDEAL LOGIC GATES

We begin our discussion of logic gates by considering the characteristics of the ideal logical inverter. Although we cannot achieve the ideal behavior, the concepts and definitions form the basis for our study of actual circuit implementations of MOS and bipolar logic families in Chapters 6–9.

In the discussions in this book, we limit consideration to binary logic, which requires only two discrete states for operation. In addition, the positive logic convention will be used throughout: The higher voltage level will correspond to a logic 1, and the lower voltage level will correspond to a logic 0.

The logic symbol and **voltage transfer characteristic (VTC)** for an ideal inverter are given in Fig. 6.1. The positive and negative power supplies, shown explicitly as  $V_+$  and  $V_-$ , respectively, are not included in most logic diagrams. For input voltages  $v_I$  below the **reference voltage**  $V_{REF}$ , the output  $v_O$  will be in the **high logic level at the gate output**  $V_H$ . As the input voltage increases and exceeds  $V_{REF}$ , the output voltage changes abruptly to the **low logic level at the gate output**  $V_L$ . The output voltages corresponding to  $V_H$  and  $V_L$  generally fall between the supply voltages  $V_+$  and  $V_-$  but may not be equal to either voltage. For an input equal to  $V_+$  or  $V_-$ , the output does not necessarily reach either  $V_-$  or  $V_+$ . The actual levels depend on the individual logic family, and the reference voltage  $V_{REF}$  is determined by the internal circuitry of the gate.

In most digital designs, the power supply voltage is predetermined either by technology constraints or system-level power supply criteria. For example,  $V_+ = 5.0$  V (with  $V_- = 0$ ) represented the standard power supply for logic for many years. However, because of the power-dissipation, heat-removal, and breakdown-voltage limitations of advanced technology, many ICs now operate from supply voltages of 1.8 to 3.3 V, and many low-power systems must be designed to operate from voltages as low as 1.0 to 1.5 V.

## 6.2 LOGIC LEVEL DEFINITIONS AND NOISE MARGINS

Now, let us look at electronic implementations of the inverter in Fig. 6.2. Conceptually, the basic inverter circuit consists of a load resistor and a switch controlled by the input voltage  $v_I$ , as indicated in Fig. 6.2(b). When closed, the switch forces  $v_O$  to  $V_L$ , and when open, the resistor sets the output to  $V_H$ . In Fig. 6.2(b), for example,  $V_L = 0$  V and  $V_H = V_+$ .

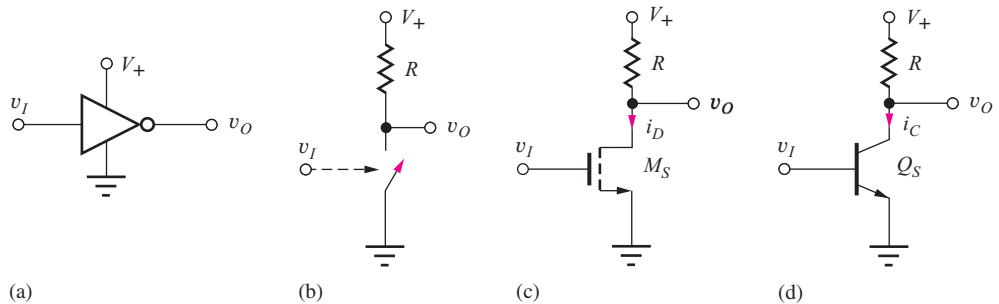


**Figure 6.2** (a) Inverter operating with power supplies of 0 V and  $V_+$ . (b) Simple inverter circuit comprising a load resistor and switch. (c) Inverter with NMOS transistor switch. (d) Inverter with BJT switch.

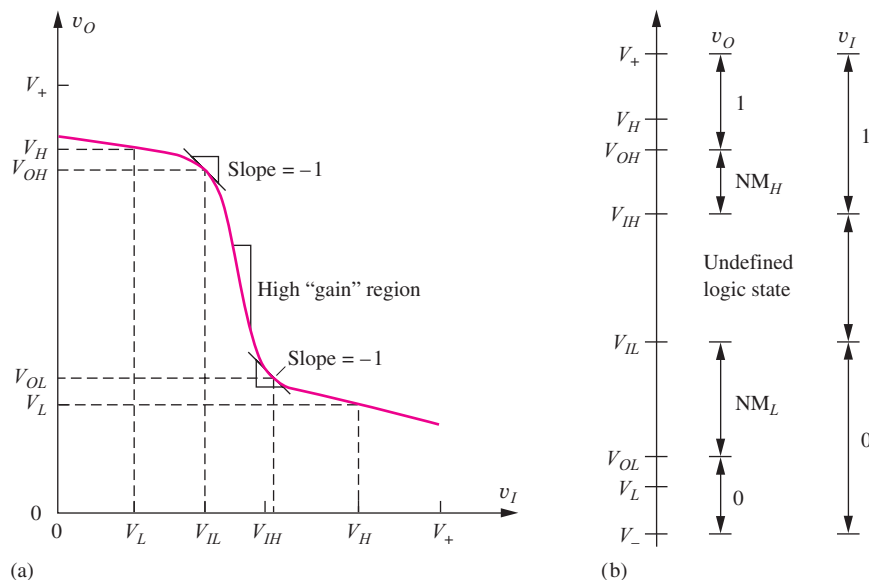


**Figure 6.3** (a) Voltage transfer characteristic for the inverters in Fig. 6.2 with  $V_- = 0$ . (b) Voltage levels and logic state relationships for positive logic.

The voltage-controlled switch can be realized by either the MOS transistor in Fig. 6.2(c) or the bipolar transistor in Fig. 6.2(d). Transistors  $M_S$  and  $Q_S$  switch between two states: nonconducting or “off,” and conducting or “on”. Load resistor  $R$  sets the output voltage to  $V_H = V_+$  when switching transistor  $M_S$  or  $Q_S$  is off. If the input voltage exceeds the threshold voltage of  $M_S$  or the turn-on voltage of the base-emitter junction of  $Q_S$ , the transistors conduct a current that causes the output voltage to drop to  $V_L$ . When transistors are used as switches, as in Figs. 6.2(c) and (d),  $V_L \neq 0$  V. Detailed discussion of the design of these circuits appears later in this chapter and in Chapter 9.

In an actual inverter circuit, the transition between  $V_H$  and  $V_L$  does not occur in the abrupt manner indicated in Fig. 6.1 but is more gradual, as indicated by the more realistic transfer characteristic shown in Fig. 6.3(a). A single, well-defined value of  $V_{REF}$  does not exist. Instead, several additional input voltage levels are important.

When the input  $v_I$  is below the **input low-logic-level**  $V_{IL}$ , the output is defined to be in the high-output or 1 state. As the input voltage increases, the output voltage  $v_O$  falls until it reaches the low output or 0 state as  $v_I$  exceeds the voltage of the **input high-logic-level**  $V_{IH}$ . The input voltages  $V_{IL}$  and  $V_{IH}$  are defined by the points at which the slope of the voltage transfer characteristic equals  $-1$ .

Voltages below  $V_{IL}$  are reliably recognized as logic 0s at the input of a logic gate, and voltages above  $V_{IH}$  are recognized reliably as logic 1s at the input. Voltages corresponding to the region between  $V_{IL}$  and  $V_{IH}$  do not represent valid logic input levels and generate logically indeterminate output voltages. The transition region of high negative slope between these two points<sup>1</sup> represents an undefined logic state. The voltages labeled as  $V_{OL}$  and  $V_{OH}$  represent the gate output voltages at the  $-1$  slope points and correspond to input levels of  $V_{IH}$  and  $V_{IL}$ , respectively.

In Part III of this book, we will find that the region of the VTC with a high negative slope between  $V_{IL}$  and  $V_{IH}$  corresponds to a large “voltage gain,” and we actually use this region for amplification of analog signals. The gain is the slope of the voltage transfer characteristic. The higher the gain, the narrower will be the voltage range corresponding to the undefined logic state in Fig. 6.3.

An alternate representation of the voltages and voltage ranges appears in Fig. 6.3(b), along with quantities that represent the voltage noise margins. The various terms are defined more fully next.

### 6.2.1 LOGIC VOLTAGE LEVELS

- $V_L$  The nominal voltage corresponding to a low-logic state at the output of a logic gate for  $v_I = V_H$ . Generally,  $V_- \leq V_L$ .
- $V_H$  The nominal voltage corresponding to a high-logic state at the output of a logic gate for  $v_I = V_L$ . Generally,  $V_H \leq V_+$ .
- $V_{IL}$  The maximum input voltage that will be recognized as a low input logic level.
- $V_{IH}$  The minimum input voltage that will be recognized as a high input logic level.
- $V_{OH}$  The output voltage corresponding to an input voltage of  $V_{IL}$ .
- $V_{OL}$  The output voltage corresponding to an input voltage of  $V_{IH}$ .

For subsequent discussions of MOS logic,  $V_-$  will usually be taken to be 0 V, and  $V_+$  will be either 2.5 V or 3.3 V. Five volts was commonly used in bipolar logic. However, other values are possible. For example, emitter-coupled logic, discussed in Chapter 9 has historically used  $V_+ = 0$  V and  $V_- = -5.2$  V or  $-4.5$  V, and low-power ECL gates have been developed to operate with a total supply voltage span of only 2 V.

### 6.2.2 NOISE MARGINS

The **noise margin in the high state**  $\text{NM}_H$  and the **noise margin in the low state**  $\text{NM}_L$  represent “safety margins” that prevent the gate from producing erroneous logic decisions in the presence of noise sources. The noise margins are needed to absorb voltage differences that may arise between the outputs and inputs of various logic gates due to a variety of sources. These may be extraneous signals coupled into the gates or simply parameter variations between gates in a logic family.

Figure 6.4 shows several interconnected inverters and illustrates why noise margin is important. The signal and power interconnections on a printed circuit board or integrated circuit, which we most often draw as zero resistance wires (or short circuits), really consist of distributed *RLC* networks. In Fig. 6.4 the output of the first inverter,  $v_{O1}$ , and the input of the second inverter,  $v_{I2}$ , are not necessarily equal. As logic signals propagate from one logic gate to the next, their characteristics become degraded by the resistance, inductance, and capacitance of the interconnections ( $R$ ,  $L$ ,  $C$ ). Rapidly switching signals may induce transient voltages and currents directly onto nearby signal lines through capacitive and inductive coupling indicated by  $C_c$  and  $M$ . In an RF environment, the interconnections may even act as small antennae that can couple additional extraneous signals into the logic circuitry. Similar problems occur in the power distribution network. Both direct current and transient currents during gate switching generate voltage drops across the various components ( $R_p$ ,  $L_p$ ,  $C_p$ ) of the power distribution network.

---

<sup>1</sup> This region corresponds to a region of relatively high voltage gain. See Probs. 6.6 and 6.7.

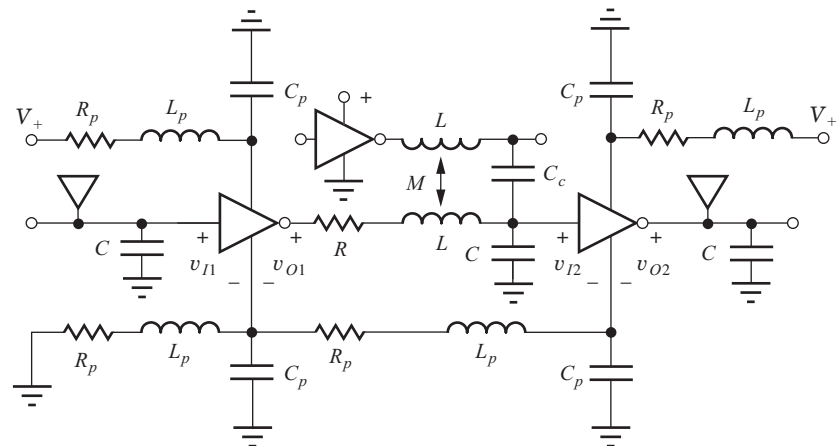


**Figure 6.4** Inverters embedded in a signal and power and distribution network.

Noise margins also absorb parameter variations that occur between individual logic gates. During manufacture, there will be unavoidable variations in device and circuit parameters, and variations will occur in the power supply voltages and operating temperature during application of the logic circuits. Normally, the logic manufacturer specifies worst-case values for  $V_H$ ,  $V_L$ ,  $V_{IL}$ ,  $V_{OL}$ ,  $V_{IH}$ , and  $V_{OH}$ . In our analysis, however, we will generally restrict ourselves to finding nominal values of these voltages.

There are a number of different ways to define the noise margin [2–4] of a logic gate. In this text, we will use a definition based on the input and output voltages at the  $-1$  slope points on the inverter voltage transfer characteristic, as identified in Fig. 6.3:

$NM_L$  The noise margin associated with a low input level is defined by

$$NM_L = V_{IL} - V_{OL} \quad (6.1)$$

$NM_H$  The noise margin associated with a high input level is defined by

$$NM_H = V_{OH} - V_{IH} \quad (6.2)$$

The noise margins represent the voltages necessary to upset the logic levels in a long chain (actually an infinite chain) of inverters, or in the cross-coupled flip-flop storage elements that we explore in Chapter 8. The definitions in Eqs. (6.1) and (6.2) can be shown [2–4] to maximize the sum of the two noise margins. These definitions provide a reasonable metric for comparing the noise margins of different logic families and are relatively easy to understand and calculate.

**EXERCISE:** A certain TTL gate has the following values for its logic levels:  $V_{OH} = 3.6$  V,  $V_{OL} = 0.4$  V,  $V_{IH} = 2.0$  V,  $V_{IL} = 0.8$  V. What are the noise margins for this TTL gate?

**ANSWERS:**  $NM_H = 1.6$  V;  $NM_L = 0.4$  V

### 6.2.3 LOGIC GATE DESIGN GOALS

As we explore the design of logic gates, we should keep in mind a number of goals.

- From Fig. 6.1, we see that the ideal logic gate is a highly nonlinear device that attempts to quantize the input signal into two discrete output levels. In the actual gate in Figs. 6.2 and 6.3, we should strive to minimize the width of the undefined input voltage range, and the noise margins should generally be as large as possible.

2. Logic gates should be unidirectional in nature. The input should control the output to produce a well-defined logic function. Voltage changes at the output of a gate should not affect the input side of the circuit.
3. The logic levels must be regenerated as the signal passes through the gate. In other words, the voltage levels at the output of one gate must be compatible with the input voltage levels of the same or similar logic gates.
4. The output of one gate should also be capable of driving the inputs of more than one gate. The number of inputs that can be driven by the output of a logic gate is called the **fan-out** capability of that gate. The term **fan in** refers to the number of input signals that may be applied to the input of a gate.
5. In most design situations, the logic gate should consume as little power (and area in an IC design) as needed to meet the speed requirements of the design.

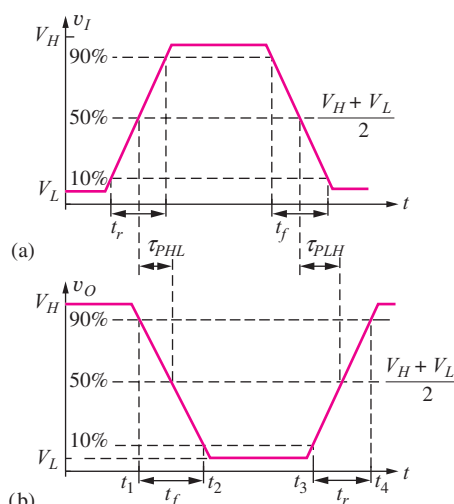
## 6.3 DYNAMIC RESPONSE OF LOGIC GATES

In today's environment, even the general public is familiar with the significant increase in logic performance as we are bombarded with marketing of the latest microprocessors in terms of their clock frequencies, 1 GHz, 2 GHz, 3 GHz, and so on. The clock rate of a processor is ultimately set by the dynamic performance of the individual logic circuits. In engineering terms, the time domain performance of a logic family is cast in terms of its average propagation delay, rise time, and fall time as defined in this section.

Figure 6.5 shows idealized time domain waveforms for an inverter. The input and output signals are switching between the two static logic levels  $V_L$  and  $V_H$ . Because of capacitances in the circuits, the waveforms exhibit nonzero rise and fall times, and propagation delays occur between the switching times of the input and output waveforms.

### 6.3.1 RISE TIME AND FALL TIME

The **rise time**  $t_r$  for a given signal is defined as the time required for the signal to make the transition from the “10 percent point” to the “90 percent point” on the waveform, as indicated in Fig. 6.5, whereas the **fall time**  $t_f$  is defined as the time required for the signal to make the transition between the 90 percent point and the 10 percent point on the waveform. The voltages corresponding to the 10 percent and 90 percent points are defined in terms of  $V_L$  and  $V_H$  and the logic swing  $\Delta V$ :



$$\begin{aligned} V_{10\%} &= V_L + 0.1 \Delta V \\ V_{90\%} &= V_L + 0.9 \Delta V = V_H - 0.1 \Delta V \\ \Delta V &= V_H - V_L \end{aligned} \quad (6.3)$$

**Figure 6.5** Switching waveforms for an *idealized* inverter: (a) input voltage signal, (b) output voltage waveform.

where  $\Delta V = V_H - V_L$ . Rise and fall times usually have unequal values; the characteristic shapes of the input and output waveforms also differ.

### 6.3.2 PROPAGATION DELAY

Propagation delay is measured as the difference in time between the input and output signals reaching the “**50 percent points**” in their respective transitions. The 50 percent point is the voltage level corresponding to one-half the total transition between  $V_H$  and  $V_L$ :

$$V_{50\%} = \frac{V_H + V_L}{2} \quad (6.4)$$

The **propagation delay** on the **high-to-low output transition** is  $\tau_{PHL}$  and that of the **low-to-high transition** is  $\tau_{PLH}$ . In the general case, these two delays will not be equal, and the **average propagation delay**  $\tau_P$  is defined by

$$\tau_P = \frac{\tau_{PLH} + \tau_{PHL}}{2} \quad (6.5)$$

Average propagation delay is another figure of merit that is commonly used to compare the performance of different logic families. In Chapters 6, 7, and 9, we explore the propagation delays for various MOS and bipolar logic circuits.

**EXERCISE:** Suppose the waveforms in Fig. 6.5 are those of an ECL gate with  $V_L = -2.6$  V and  $V_H = -0.6$  V, and  $t_1 = 100$  ns,  $t_2 = 105$  ns,  $t_3 = 150$  ns, and  $t_4 = 153$  ns. What are the values of  $V_{10\%}$ ,  $V_{90\%}$ ,  $V_{50\%}$ ,  $t_r$ , and  $t_f$ ?

**ANSWERS:**  $-2.4$  V;  $-0.8$  V;  $-1.6$  V; 3 ns; 5 ns

### 6.3.3 POWER-DELAY PRODUCT

The overall performance of a logic family is ultimately determined by how much energy is required to change the state of the logic circuit. The traditional metric for comparing various logic families is the power-delay product, which tells us the amount of energy that is required to perform a basic logic operation.

Figure 6.6 shows the behavior of the average propagation delay of a general logic gate versus the average power supplied to the gate. The power consumed by a gate can be changed by increasing or decreasing the sizes of the transistors and resistors in the gate or by changing the power supply voltage. At low power levels, gate delay is dominated by inter gate wiring capacitance, and the delay decreases as power increases. As device size and power are increased further, circuit delay becomes limited by the inherent speed of the electronic switching devices, and the delay becomes independent of power. In bipolar logic technology, the properties of the transistors begin to degrade at even higher power levels, and the delay can actually become worse as power increases further, as indicated in Fig. 6.6.

In the low power region, the propagation delay decreases in direct proportion to the increase in power. This behavior corresponds to a region of constant **power-delay product (PDP)**,

$$PDP = P\tau_P \quad (6.6)$$

in which  $P$  is the average power dissipated by the logic gate. The PDP represents the energy (Joules) required to perform a basic logic operation.

Early logic families had power-delay products of 10 to 100 pJ ( $1\text{ pJ} = 10^{-12}\text{ J}$ ), whereas many of today’s IC logic families now have PDPs in the 10 to 100 fJ range ( $1\text{ fJ} = 10^{-15}\text{ J}$ ). It has been estimated that the minimum energy required to reliably differentiate two logic states is on the order of  $(\ln 2)kT$ , which is approximately  $4 \times 10^{-20}\text{ J}$  at room temperature [5]. Thus even today’s best logic families have power-delay products that are many orders of magnitude from the ultimate limit [6].

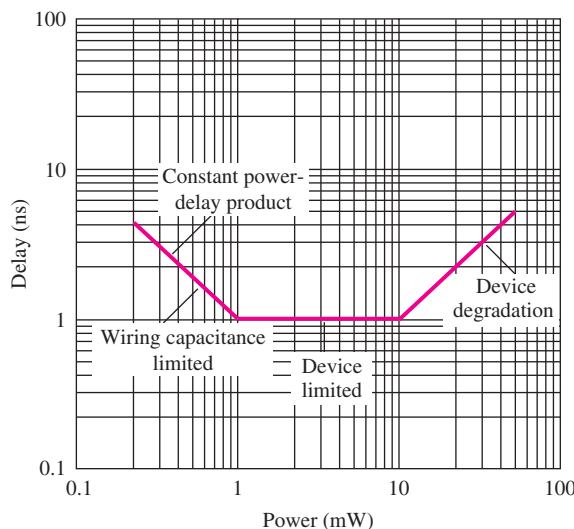


Figure 6.6 Logic gate delay versus power dissipation.

**TABLE 6.2**  
NOT, OR, AND Gate Truth Tables

		NOT (INVERTER)	OR GATE	AND GATE
B	A	$Z = \bar{A}$	$Z = A + B$	$Z = AB$
0	0	0	0	0
0	1	1	1	0
1	0	0	1	0
1	1	1	1	1

**TABLE 6.1**  
Basic Boolean Operations

OPERATION	BOOLEAN REPRESENTATION
NOT	$Z = \bar{A}$
OR	$Z = A + B$
AND	$Z = A \cdot B = AB$
NOR	$Z = \overline{A + B}$
NAND	$Z = \overline{A \cdot B} = \overline{AB}$

**TABLE 6.3**  
NOR and NAND Gate Truth Table

		NOR	NAND
A	B	$Z = \overline{A + B}$	$Z = \overline{AB}$
0	0	1	1
0	1	0	1
1	0	0	1
1	1	0	0

**EXERCISE:** (a) What is the power-delay product at low power for the logic gate characterized by Fig. 6.6? (b) What is the PDP at  $P = 3$  mW? (c) At 20 mW?

**ANSWERS:** 1 pJ; 3 pJ; 40 pJ

## 6.4 REVIEW OF BOOLEAN ALGEBRA

In order to be able to effectively deal with logic system analysis and design, we need a mathematical representation for networks of logic gates. Fortunately, way back in 1849, G. Boole [7] presented a powerful mathematical formulation for dealing with logical thought and reasoning, and the formal algebra we use today to manipulate binary logic expressions is known as **Boolean algebra**. Tables 6.1 to 6.3 and the following discussion summarize Boolean algebra.

Table 6.1 lists the basic logic operations that we need. The logic function at the gate output is represented by variable  $Z$  and is a function of logical input variables  $A$  and  $B$ :  $Z = f(A, B)$ . To perform general logic operations, a logic family must provide logical inversion (NOT) plus at least one other function of two input variables, such as the OR or AND functions. We will find in Chapter 7 that NMOS logic can easily be used to implement NOR gates as well as NAND gates, and in Chapter 9 we will see that the basic TTL gate provides a NAND function whereas OR/NOR logic is provided by the basic ECL gate. Note in Table 6.1 that the NOT function is equivalent to the output of either a single input NOR gate or NAND gate.

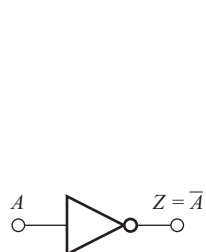
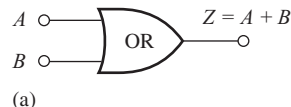
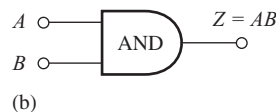


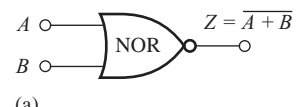
Figure 6.7 Inverter symbol.



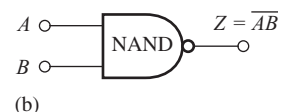
(a)



(b)

Figure 6.8 (a) OR gate symbol.  
(b) AND gate symbol.

(a)



(b)

Figure 6.9 (a) NOR gate symbol.  
(b) NAND gate symbol.

**TABLE 6.4**  
Useful Boolean Identities

$A + 0 = A$	$A \cdot 1 = A$	Identity operation
$A + B = B + A$	$AB = BA$	Commutative law
$A + (B + C) = (A + B) + C$	$A(BC) = (AB)C$	Associative law
$A + BC = (A + B)(A + C)$	$A(B + C) = AB + AC$	Distributive law
$A + \overline{A} = 1$	$A \cdot \overline{A} = 0$	Complements
$A + A = A$	$A \cdot A = A$	Idempotency
$A + 1 = 1$	$A \cdot 0 = 0$	Null elements
$\overline{A + B} = \overline{AB}$	$\overline{AB} = \overline{A} + \overline{B}$	DeMorgan's theorem

**Truth tables** and logic symbols for the five functions in Table 6.1 appear in Tables 6.2 and 6.3 and Figs. 6.7 to 6.9. The truth table presents the output  $Z$  for all possible combinations of the input variables  $A$  and  $B$ . The inverter,  $Z = \overline{A}$ , has a single input, and the output represents the logical inversion or complement of the input variable, as indicated by the overbar (Table 6.2; Fig. 6.7).

Table 6.2 presents the truth tables for a two-input **OR gate** and a two-input **AND gate**, respectively, and the corresponding logic symbols appear in Fig. 6.8. The OR operation is indicated by the  $+$  symbol; its output  $Z$  is a 1 when either one or both of the input variables  $A$  or  $B$  is a 1. The output is a 0 only if both inputs are 0. The AND operation is indicated by the  $\cdot$  symbol, as in  $A \cdot B$ , or in a more compact form as simply  $AB$ , and the output  $Z$  is a 1 only if both the input variables  $A$  and  $B$  are in the 1 state. If either input is 0, then the output is 0. We shall use  $AB$  to represent  $A$  AND  $B$  throughout the rest of this text.

Table 6.3 gives the truth tables for the two-input NOR gate and the two-input NAND gate, respectively, and the logic symbols appear in Fig. 6.9. These functions represent the complements of the OR and AND operations—that is, the OR or AND operations followed by logical inversion. The NOR operation is represented as  $Z = \overline{A + B}$ , and its output  $Z$  is a 1 only if both inputs are 0. For the NAND operation,  $Z = \overline{AB}$ , output  $Z$  is a 1 except when both the input variables  $A$  or  $B$  are in the 1 state.

In this chapter and Chapter 8, we will find that a major advantage of MOS logic is its capability to readily form more complex logic functions, particularly logic expressions represented in a complemented **sum-of-products** or **AND-OR-INVERT** (AOI) form:

$$Z = \overline{AB + CD + E} \quad \text{or} \quad Z = \overline{ABC + DE} \quad (6.7)$$

The Boolean identities that are shown in Table 6.4 can be very useful in finding simplified logic expressions, such as those expressions in Eq. (6.7). This table includes the identity operations as well as the basic commutative, associative, and distributive laws of Boolean algebra.

### EXAMPLE 6.1 LOGIC EXPRESSION SIMPLIFICATION

Here is an example of the use of Boolean identities to simplify a logic expression.

**PROBLEM** Use the Boolean relationships in Table 6.4 to show that the expression

$$Z = A\bar{B}C + ABC + \bar{A}BC \quad \text{can be reduced to} \quad Z = (A + B)C.$$

**SOLUTION** **Known Information and Given Data:** Two expressions for  $Z$  just given; Boolean identities in Table 6.4.

**Unknowns:** Proof that  $Z$  is equivalent to  $(A + B)C$

**Approach:** Apply various identities from Table 6.4 to simplify the formula for  $Z$

**Assumptions:** None

**Analysis:**

$$\begin{aligned} Z &= A\bar{B}C + ABC + \bar{A}BC \\ Z &= A\bar{B}C + ABC + ABC + \bar{A}BC && \text{using } ABC = ABC + ABC \\ Z &= A(\bar{B} + B)C + (\bar{A} + A)BC && \text{using distributive law} \\ Z &= A(1)C + (1)BC && \text{using } (\bar{B} + B) = (B + \bar{B}) = 1 \\ Z &= AC + BC && \text{since } A(1)C = AC(1) = AC \\ Z &= (A + B)C && \text{using distributive law} \end{aligned}$$

**Check of Results:** We have reached the desired answer. A double check indicates the sequence of steps appears valid.

**EXERCISE:** Simplify the logic expression  $Z = (A + B)(B + C)$

**ANSWER:**  $Z = B + AC$

## 6.5 NMOS LOGIC DESIGN

The rest of Chapter 6 focuses on understanding the design of MOS logic gates that use  $n$ -channel MOS transistors (NMOS logic) and  $p$ -channel MOS transistors (PMOS logic). Study of these circuits provides a background for understanding many important logic circuit concepts as well as the improvements gained by going to CMOS circuitry, which is the topic for Chapter 7. The discussion begins by investigating the design of the MOS inverter in order to gain an understanding of its voltage transfer characteristic and noise margins. Inverters with four different NMOS load configurations are considered: the resistor load, saturated load, linear load, and depletion-mode load circuits. In addition, pseudo NMOS is a modern extension of classic NMOS logic that uses a PMOS transistor as a load device. NOR, NAND, and more complex logic gates can be easily designed as simple extensions of the reference inverter designs. Later, the rise time, fall time, and propagation delays of the gates are analyzed.

The drain current of the MOS device depends on its gate-source voltage  $v_{GS}$ , drain-source voltage  $v_{DS}$ , and source-bulk voltage  $v_{SB}$ , and on the device parameters, which include the transconductance parameter  $K'_n$ , threshold voltage  $V_{TN}$ , and width-to-length or **W/L ratio**. The power supply voltage constrains the range of  $v_{GS}$  and  $v_{DS}$ , and the technology sets the values of  $K'_n$  and  $V_{TN}$ . Thus, the

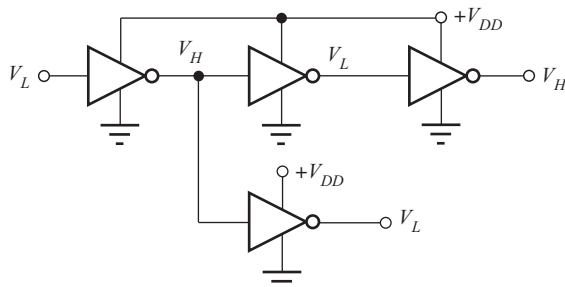


**Figure 6.10** A network of inverters.

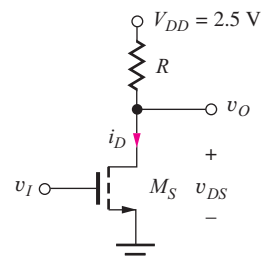


**Figure 6.11** NMOS inverter with resistor load.

circuit designer's job is to choose the circuit topology and the  $W/L$  ratios of the MOS transistors to achieve the desired logic function.

In most logic design situations, the power supply voltage is predetermined by either technology reliability constraints or system-level criteria. For example, as mentioned in Sec. 6.1,  $V_{DD}^2 = 5.0$  V was the standard power supply for logic for many years. However, 1.8–3.3 V power supply levels are gaining widespread use. In addition, many portable low-power systems, such as cell phones and PDAs, must operate from battery voltages as low as 1.0 to 1.5 V.

We begin our study of MOS logic circuit design by considering the detailed design of the NMOS inverter with the resistor load that was introduced in Chapter 5. Although we will seldom use this exact circuit, it provides a good basis for understanding operation of the basic logic gate. In integrated logic circuits, the load resistor occupies too much silicon area, and is replaced by a second MOS transistor. NMOS "load devices" can be connected in three different configurations called the saturated load, linear load, and depletion-mode load circuits, whereas pseudo NMOS uses a PMOS load device. We will explore the design of the NMOS load configurations in detail in this and Secs. 6.6 through 6.7.

### 6.5.1 NMOS INVERTER WITH RESISTIVE LOAD

Complex digital systems can consist of millions of logic gates, and it is helpful to remember that each individual logic gate is generally interconnected in a larger network. The output of one logic gate drives the input of another logic gate, as shown schematically by the four inverters in Fig. 6.10. Thus, a gate has  $v_O = V_H$  when an input voltage  $v_I = V_L$  is applied to its input, and vice versa.

The basic inverter circuit shown in Fig. 6.11 consists of an NMOS switching device  $M_S$  designed to force  $v_O$  to  $V_L$  and a **resistor load** element to "pull" the output up toward the power supply  $V_{DD}$ . The NMOS transistor is designed to switch between the triode region for  $v_I = V_H$  and the cutoff (nonconducting) state for  $v_I = V_L$ . The circuit designer must choose the values of the load resistor  $R$  and the  $W/L$  ratio of **switching transistor**  $M_S$  so the inverter meets a set of design specifications. In this case, these two design variables permit us to choose the  $V_L$  level and set the total power dissipation of the logic gate.

Let us explore the inverter operation by considering the requirements for the design of such a logic gate. Writing an equation for the output voltage for the circuit in Fig. 6.11, we find

$$v_O = v_{DS} = V_{DD} - i_D R \quad (6.8)$$

When the input voltage is at a low state,  $v_I = V_L$ ,  $M_S$  should be cut off with  $i_D = 0$ , so that

$$v_O = V_{DD} = V_H \quad (6.9)$$

Thus, in this particular logic circuit, the value of  $V_H$  is set by the power supply voltage  $V_{DD} = 2.5$  V.

<sup>2</sup>  $V_{DD}$  and  $V_{SS}$  have traditionally been used to denote the positive and negative power supply voltages in MOS circuits.

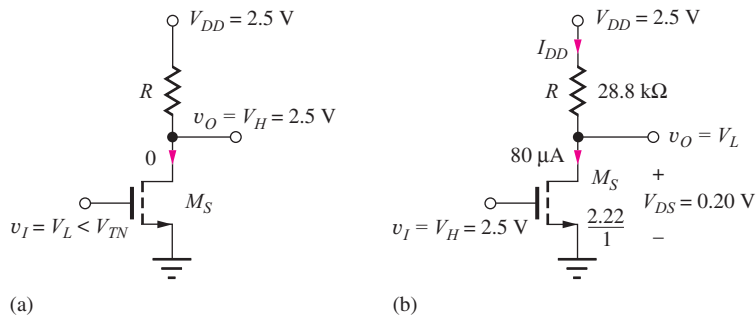


**Figure 6.12** Inverters in the (a)  $v_I = V_L(0)$  and (b)  $v_I = V_H(1)$  logic states.

To ensure that transistor  $M_S$  is cut off when the input is equal to  $V_L$ , as in Fig. 6.12(a), the gate-source voltage of  $M_S$  ( $v_{GS} = V_L$ ) must be less than its threshold voltage  $V_{TN}$ . For  $V_{TN} = 0.6$  V, a normal design point would be for  $V_L$  to be in the range of 25 to 50 percent of  $V_{TN}$  or 0.15 to 0.30 V to ensure adequate noise margins. Let us assume a design value of  $V_L = 0.20$  V.

### DESIGN NOTE DESIGN OF $V_L$

To ensure that switching transistor  $M_S$  is cut off when the input is in the low logic state,  $V_L$  is designed to be 25 to 50 percent of the threshold voltage of switch  $M_S$ . This choice also provides a reasonable value for noise margin  $\text{NM}_L$ .

### 6.5.2 DESIGN OF THE $W/L$ RATIO OF $M_S$

The value of  $W/L$  required to set  $V_L = 0.20$  V can be calculated if we know the parameters of the MOS device. For now, the values  $V_{TN} = 0.6$  V and  $K'_n = 100 \times 10^{-6}$  A/V<sup>2</sup> will be used. In addition, we need to know a value for the desired operating current of the inverter. The current is determined by the permissible power dissipation of the NMOS gate when  $v_O = V_L$ . Using  $P = 0.20$  mW (see Probs. 6.1 and 6.2),<sup>3</sup> the current in the gate can be found from  $P = V_{DD} \times I_{DD}$ . For our circuit,

$$0.20 \times 10^{-3} = 2.5 \times I_{DD} \quad \text{or} \quad I_{DD} = 80 \mu\text{A}$$

Now we can determine the value for the  $W/L$  ratio of the NMOS switching device from the MOS drain current expression using the circuit conditions in Fig. 6.12(b). In this case, the input is set equal to  $V_H = 2.5$  V, and the output of the inverter should then be at  $V_L$ . The expression for the drain current in the triode region of the device is used because  $v_{GS} - V_{TN} = 2.5$  V - 0.6 V = 1.9 V, and  $v_{DS} = V_L = 0.20$  V, yielding  $v_{DS} < v_{GS} - V_{TN}$ .

$$i_D = K'_n \left( \frac{W}{L} \right)_S (v_{GS} - V_{TN} - 0.5v_{DS}) v_{DS} \quad (6.10)$$

or

$$8 \times 10^{-5} \text{ A} = \left( 100 \times 10^{-6} \frac{\text{A}}{\text{V}^2} \right) \left( \frac{W}{L} \right)_S (2.5 \text{ V} - 0.6 \text{ V} - 0.10 \text{ V})(0.20 \text{ V})$$

Solving Eq. (6.10) for  $(W/L)_S$  gives  $(W/L)_S = 2.22/1$ .

<sup>3</sup> It would be worth exploring these problems before continuing.

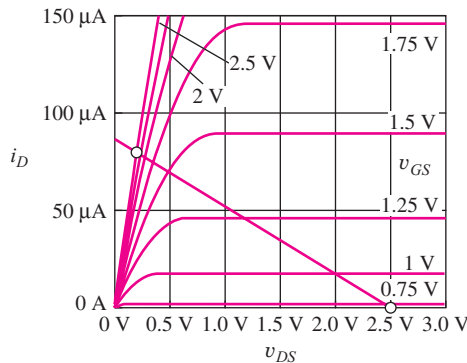


Figure 6.13 MOSFET output characteristics and load line.

### 6.5.3 LOAD RESISTOR DESIGN

The value of the load resistor  $R$  is chosen to limit the current when  $v_O = V_L$  and is found from

$$R = \frac{V_{DD} - V_L}{I_{DD}} = \frac{(2.5 - 0.20) \text{ V}}{8 \times 10^{-5} \text{ A}} = 28.8 \text{ k}\Omega \quad (6.11)$$

These design values are shown in the circuit in Fig. 6.12(b).

**EXERCISE:** Redesign the logic gate in Fig. 6.12 to operate at a power of 0.4 mW while maintaining  $V_L = 0.20$  V.

**ANSWER:**  $(W/L)_S = 4.44/1$ ;  $R = 14.4 \text{ k}\Omega$

### 6.5.4 LOAD-LINE VISUALIZATION

An important way to visualize the operation of the inverter is to draw the load line on the MOS transistor output characteristics as in Fig. 6.13. Equation (6.8), repeated here, represents the equation for the load line:

$$v_{DS} = V_{DD} - i_D R$$

When the transistor is cut off,  $i_D = 0$  and  $v_{DS} = V_{DD} = 2.5$  V, and when the transistor is on, the MOSFET is operating in the triode region, with  $v_{GS} = V_H = 2.5$  V and  $v_{DS} = v_O = V_L = 0.20$  V. The MOSFET switches between the two operating points on the load line, as indicated by the circles in Fig. 6.13. At the right-hand end of the load line, the MOSFET is cut off. At the Q-point near the left end of the load line, the MOSFET represents a relatively low resistance, and the current is determined primarily by the load resistance. (Note how the Q-point is nearly independent of  $v_{GS}$ .)

## DESIGN EXAMPLE 6.2

### DESIGN OF AN INVERTER WITH RESISTIVE LOAD

Design a resistively loaded NMOS inverter to operate from a 3.3-V power supply.

**PROBLEM** Design an inverter with a resistive load for  $V_{DD} = 3.3$  V and  $P = 0.1$  mW with  $V_L = 0.2$  V. Assume  $K'_n = 60 \mu\text{A}/\text{V}^2$  and  $V_{TN} = 0.75$  V.

**SOLUTION** **Known Information and Given Data:** Circuit topology in Fig. 6.11;  $V_{DD} = 3.3$  V,  $P = 0.1$  mW,  $V_L = 0.2$  V,  $K'_n = 60 \mu\text{A}/\text{V}^2$ , and  $V_{TN} = 0.75$  V

**Unknowns:** Value of load resistor  $R$ ;  $W/L$  ratio of switching transistor  $M_S$

**Approach:** Use the power dissipation specification to find the current  $I_{DD}$  for  $v_O = V_L$ . Use  $V_{DD}$ ,  $V_L$ , and  $I_{DD}$  to calculate  $R$ . Determine  $V_H$ . Use  $V_H$ ,  $V_L$ , and  $I_{DD}$  to find  $(W/L)_S$ .

**Assumptions:**  $M_S$  is off for  $v_I = V_L$ ;  $M_S$  is in the triode region for  $v_O = V_L$ .

**Analysis:** Using the power specification with the inverter circuit in Fig. 6.11, we have

$$I_{DD} = \frac{P}{V_{DD}} = \frac{10^{-4} \text{ W}}{3.3 \text{ V}} = 30.3 \mu\text{A} \quad R = \frac{V_{DD} - V_L}{I_{DD}} = \frac{3.3 - 0.2}{30.3} \frac{\text{V}}{\mu\text{A}} = 102 \text{ k}\Omega$$

For  $v_I = V_L = 0.2 \text{ V}$ , the MOSFET will be off since  $0.2 \text{ V}$  is less than the threshold voltage, and the output high level will be  $V_H = V_{DD} = 3.3 \text{ V}$ . The triode region expression for the MOSFET drain current with  $v_{GS} = v_I = V_H$  and  $v_{DS} = v_O = V_L$  is

$$I_D = K'_n \left( \frac{W}{L} \right)_S \left( V_H - V_{TN} - \frac{V_L}{2} \right) V_L$$

Equating this expression to the drain current yields

$$30.3 \mu\text{A} = (60 \times 10^{-6}) \left( \frac{W}{L} \right)_S \left( 3.3 - 0.75 - \frac{0.2}{2} \right) 0.2 \rightarrow \left( \frac{W}{L} \right)_S = \frac{1.03}{1}$$

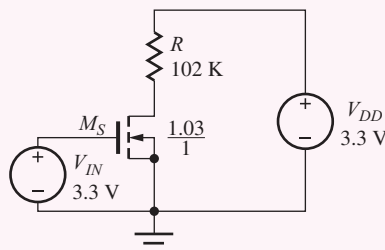
Thus our completed design values are  $R = 102 \text{ k}\Omega$  and  $(W/L)_S = 1.03/1$ .

**Check of Results:** We should check the triode region assumption for the MOSFET for  $v_O = V_L$ :  $V_{GS} - V_{TN} = 3.3 - 0.75 = 2.55 \text{ V}$ , which is indeed greater than  $V_{DS} = 0.2 \text{ V}$ . Let us also double check the value of  $W/L$  by using it to calculate the drain current:

$$I_D = (60 \times 10^{-6}) \left( \frac{1.03}{1} \right) \left( 3.3 - 0.75 - \frac{0.2}{2} \right) 0.2 = 30.3 \mu\text{A} \quad \checkmark$$

**Discussion:** This new design for reduced power from a higher supply voltage requires a larger value of load resistor to limit the current, but a smaller device to conduct the reduced level of current.

**Computer-Aided Analysis:** Let us verify our design values with SPICE. The circuit drawn with a schematic capture tool is given below. The NMOS transistor uses the LEVEL = 1 model with  $K_P = 6.0E-5$ ,  $VTO = 1$ ,  $W = 1.03\text{U}$ , and  $L = 1\text{U}$ . The Q-point of the transistor is  $(30.4 \mu\text{A}, 0.201 \text{ V})$ , which agrees with the design specifications.



**EXERCISE:** (a) Redesign the inverter in Ex. 6.2 to have  $V_L = 0.1 \text{ V}$  with  $R = 102 \text{ k}\Omega$ . (b) Verify your design with SPICE.

**ANSWER:**  $(W/L)_S = 2.09/1$

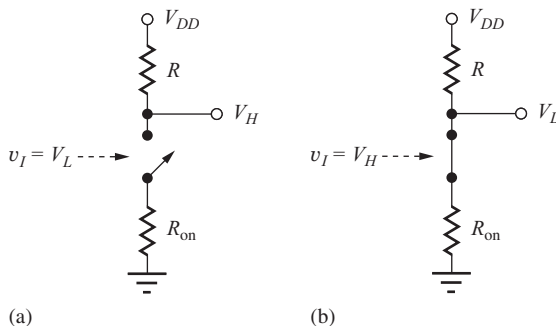


**Figure 6.14** Simplified representation of an inverter: (a) the off or nonconducting state, (b) the on or conducting state.

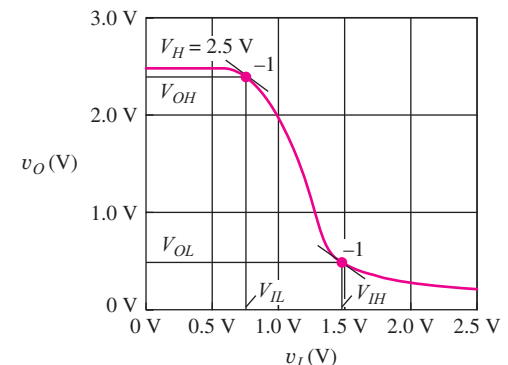


**Figure 6.15** Simulated voltage transfer characteristic of an NMOS inverter with resistive load.

### 6.5.5 ON-RESISTANCE OF THE SWITCHING DEVICE

When the logic gate output is in the low state, the output voltage can also be calculated from a resistive voltage divider formed by the load resistor  $R$  and the **on-resistance**  $R_{\text{on}}$  of the MOSFET, as in Fig. 6.14.

$$V_L = V_{DD} \frac{R_{on}}{R_{on} + R} = V_{DD} \frac{1}{1 + \frac{R}{R_{on}}} \quad (6.12)$$

where

$$R_{\text{on}} = \frac{v_{DS}}{i_D} = \frac{1}{K'_n \frac{W}{L} \left( v_{GS} - V_{TN} - \frac{v_{DS}}{2} \right)} \quad (6.13)$$

$R_{on}$  must be much smaller than  $R$  in order for  $V_L$  to be small. It is important to recognize that  $R_{on}$  represents a nonlinear resistor because the value of  $R_{on}$  is dependent on  $v_{DS}$ , the voltage across the resistor terminals. All the NMOS gates that we study in this chapter demonstrate “**ratioed logic**”—that is, designs in which the on-resistance of the switching transistor must be much smaller than that of the load resistor in order to achieve a small value of  $V_L$  ( $R_{on} \ll R$ ).

**EXAMPLE 6.3** ON-RESISTANCE CALCULATION

Find the on-resistance for the MOSFET in the completed inverter design in Fig. 6.12(b).

**PROBLEM** What is the value of the on-resistance for the NMOS FET in Fig. 6.12 when the output voltage is at  $V_L$ ?

**SOLUTION** Known Information and Given Data:  $K'_n = 100 \mu\text{A}/\text{V}^2$ ,  $V_{TN} = 0.60 \text{ V}$ ,  $W/L = 2.22/1$ ,  $V_{DS} = V_L = 0.20 \text{ V}$

**Unknowns:** On-resistance of the switching transistor.

**Approach:** Use the known values to evaluate Eq. (6.13).

**Assumptions:** The transistor is in the triode region of operation.

**Analysis:**  $R_{\text{on}}$  can be found using Eq. (6.13).

$$R_{on} = \frac{1}{\left(100 \times 10^{-6} \frac{\text{A}}{\text{V}^2}\right) \left(\frac{2.22}{1}\right) \left(2.5 - 0.60 - \frac{0.20}{2}\right) \text{V}} = 2.50 \text{ k}\Omega$$

**Check of Results:** We can check this value by using it to calculate  $V_L$ :

$$V_L = V_{DD} \frac{R_{on}}{R_{on} + R} = 2.5 \text{ V} \frac{2.5 \text{ k}\Omega}{2.5 \text{ k}\Omega + 28.8 \text{ k}\Omega} = 0.20 \text{ V}$$

$R_{on} = 2.5 \text{ k}\Omega$  does indeed give the correct value of  $V_L$ . Note that  $R_{on} \ll R$ . Checking the triode region assumption:  $V_{GS} - V_{TN} = 2.5 - 0.6 = 1.9 \text{ V}$  and  $V_{DS} = V_L = 0.20 \text{ V}$ . ✓

**EXERCISE:** What value of  $R_{on}$  is needed to set  $V_L = 0.15 \text{ V}$  in Ex. 6.3? What is the new value of  $W/L$  needed for the MOSFET to achieve this value of  $R_{on}$ ?

**ANSWERS:** 1.84 kΩ; 2.98/1

**EXERCISE:** What is the value of  $R_{on}$  for the MOSFET in Ex. 6.2? Use  $R_{on}$  to find  $V_L$ .

**ANSWERS:** 6.61 kΩ; 0.201 V

## 6.5.6 NOISE MARGIN ANALYSIS

Figure 6.15 is a SPICE simulation of the voltage transfer function for the completed inverter design from Fig. 6.12. Now we are in a position to find the values of  $V_{IL}$ ,  $V_{OL}$ ,  $V_{IH}$ , and  $V_{OH}$  that correspond to the points at which the slope of the voltage transfer characteristic for the inverter is equal to  $-1$ , as defined in Sec. 6.2.

## 6.5.7 CALCULATION OF $V_{IL}$ AND $V_{OH}$

Our analysis begins with the expression for the load line, repeated here from Eq. (6.8):

$$v_O = V_{DD} - i_D R \quad (6.14)$$

Referring to Fig. 6.15 with  $v_I = V_{IL}$ ,  $v_{GS}$  is small and  $v_{DS}$  is large, so we expect the MOSFET to be operating in saturation, with drain current given by

$$i_D = (K_n/2)(v_{GS} - V_{TN})^2 \quad \text{where } K_n = K'_n(W/L) \text{ and } v_{GS} = v_I$$

Substituting this expression for  $i_D$  in load-line Eq. (6.14),

$$v_O = V_{DD} - \frac{K_n}{2}(v_I - V_{TN})^2 R \quad (6.15)$$

and taking the derivative of  $v_O$  with respect to  $v_I$  results in

$$\frac{dv_O}{dv_I} = -K_n(v_I - V_{TN})R \quad (6.16)$$

Setting this derivative equal to  $-1$  for  $v_I = V_{IL}$  yields

$$V_{IL} = V_{TN} + \frac{1}{K_n R} \quad \text{with} \quad V_{OH} = V_{DD} - \frac{1}{2K_n R} \quad (6.17)$$

We see that the value of  $V_{IL}$  is slightly greater than  $V_{TN}$ , since the input must exceed  $V_{TN}$  for  $M_S$  to begin conduction, and  $V_{OH}$  is slightly less than  $V_{DD}$ . The  $1/K_n R$  terms represent the ratio of the transistor's transconductance parameter to the value of the load resistor. As  $K_n$  increases for a given value of  $R$ ,  $V_{IL}$  decreases and  $V_{OH}$  increases.

**EXERCISE:** Show that  $(1/K_n R)$  has the units of voltage.

### 6.5.8 CALCULATION OF $V_{IH}$ AND $V_{OL}$

For  $v_I = V_{IH}$ ,  $v_{GS}$  is large and  $v_{DS}$  is small, so we now expect the MOSFET to be operating in the triode region with drain current given by  $i_D = K_n[v_{GS} - V_{TN} - (v_{DS}/2)]v_{DS}$ . Substituting this expression for  $i_D$  into Eq. (6.14) and realizing that  $v_O = v_{DS}$  yields

$$v_O = V_{DD} - K_n R \left( v_I - V_{TN} - \frac{v_O}{2} \right) v_O \quad \text{or} \quad \frac{v_O^2}{2} - v_O \left[ v_I - V_{TN} + \frac{1}{K_n R} \right] + \frac{V_{DD}}{K_n R} = 0 \quad (6.18)$$

Solving for  $v_O$  and then setting  $dv_O/dv_I = -1$  for  $v_I = V_{IH}$  yields

$$V_{IH} = V_{TN} - \frac{1}{K_n R} + 1.63 \sqrt{\frac{V_{DD}}{K_n R}} \quad \text{with} \quad V_{OL} = \sqrt{\frac{2V_{DD}}{3K_n R}} \quad (6.19)$$

Combining the results from Eqs. (6.17) and (6.19) yields expressions for the noise margins:

$$\text{NM}_H = V_{DD} - V_{TN} + \frac{1}{2K_n R} - 1.63 \sqrt{\frac{V_{DD}}{K_n R}} \quad \text{and} \quad \text{NM}_L = V_{TN} + \frac{1}{K_n R} - \sqrt{\frac{2V_{DD}}{3K_n R}} \quad (6.20)$$

The product  $K_n R$  compares the drive capability of the MOSFET to the resistance of the load resistor, and the noise margins increase as  $K_n R$  increases for typical values of  $K_n R$  greater than two.

#### EXAMPLE 6.4 NOISE MARGIN CALCULATION FOR THE RESISTIVE LOAD INVERTER

Find the noise margins associated with the inverter design in Fig. 6.12(b).

**PROBLEM** Calculate  $K_n R$  and the noise margins for the inverter in Fig. 6.12(b).

**SOLUTION** **Known Information and Given Data:** The NMOS inverter circuit with resistor load in Fig. 6.11 with  $R = 28.8 \text{ k}\Omega$ ,  $(W/L)_S = 2.22/1$ ,  $K'_n = 100 \mu\text{A/V}^2$ , and  $V_{TN} = 0.60 \text{ V}$

**Unknowns:** The values of  $K_n R$ ,  $V_{IL}$ ,  $V_{OH}$ ,  $V_{IH}$ ,  $V_{OL}$ ,  $\text{NM}_L$ , and  $\text{NM}_H$

**Approach:** Use the given data to evaluate Eqs. (6.17) and (6.18). Use the results to find the noise margins:  $\text{NM}_H = V_{OH} - V_{IH}$  and  $\text{NM}_L = V_{IL} - V_{OL}$ .

**Assumptions:** Equation (6.17) assumes saturation region operation; Eq. (6.18) assumes triode region operation.

**Analysis:** For the inverter design in Fig. 6.12(b),

$$V_{TN} = 0.6 \text{ V} \quad K'_n \frac{W}{L} = 100 \left( \frac{2.22}{1} \right) \frac{\mu\text{A}}{\text{V}^2} = 222 \frac{\mu\text{A}}{\text{V}^2} \quad R = 28.8 \text{ k}\Omega \quad K_n R = 6.39$$

Evaluating Eq. (6.17),

$$V_{IL} = 0.6 + \frac{1}{(222 \mu\text{A})(28.8 \text{ k}\Omega)} = 0.756 \text{ V} \quad \text{and} \quad V_{OH} = 2.5 - \frac{1}{2(222 \mu\text{A})(28.8 \text{ k}\Omega)} = 2.42 \text{ V}$$

and Eq. (6.18),

$$V_{IH} = 0.6 - \frac{1}{(222 \mu\text{A})(28.8 \text{ k}\Omega)} + 1.63 \sqrt{\frac{2.5}{(222 \mu\text{A})(28.8 \text{ k}\Omega)}} = 1.46 \text{ V}$$

$$V_{OL} = \sqrt{\frac{2(2.5)}{3(222 \mu\text{A})(28.8 \text{ k}\Omega)}} = 0.51 \text{ V}$$

The noise margins are found to be

$$NM_H = 2.42 - 1.46 = 0.96 \text{ V} \quad \text{and} \quad NM_L = 0.76 - 0.51 = 0.25 \text{ V}$$

**Check of Results:** The values of  $V_{IL}$ ,  $V_{OH}$ ,  $V_{IH}$ , and  $V_{OL}$  all agree well with the simulation results in Fig. 6.15. Equation (6.17) is based on the assumption of saturation region operation. We should check to see if this assumption is consistent with the results in Eq. (6.17):  $v_{DS} = 2.42$  and  $v_{GS} - V_{TN} = 0.76 - 0.6 = 0.16$ . Because  $v_{DS} > (v_{GS} - V_{TN})$ , our assumption was correct. Similarly, Eq. (6.18) is based on the assumption of triode region operation. Checking this assumption, we have  $v_{DS} = 0.51$  and  $v_{GS} - V_{TN} = 1.46 - 0.6 = 0.86$ . Since  $v_{DS} < (v_{GS} - V_{TN})$ , our assumption was correct.

**Discussion:** Our analysis indicates that a long chain of inverters can tolerate electrical noise and process variations equivalent to 0.25 V in the low-input state and 0.96 V in the high state. Note that it is common for the values of the two noise margins to be unequal, as illustrated here.

**EXERCISE:** (a) Find the noise margins for the inverter in Ex. 6.2. (b) Verify your results with SPICE.

**ANSWERS:**  $NM_L = 0.32 \text{ V}$ ;  $NM_H = 1.45 \text{ V}$  ( $V_{IL} = 0.090 \text{ V}$ ,  $V_{OH} = 3.22 \text{ V}$ ,  $V_{IH} = 1.77 \text{ V}$ ,  $V_{OL} = 0.591 \text{ V}$ )

As mentioned earlier,  $V_{IL}$ ,  $V_{OL}$ ,  $V_{IH}$ , and  $V_{OH}$ , as specified by a manufacturer, actually represent guaranteed specifications for a given logic family and take into account the full range of variations in technology parameters, temperature, power supply, loading conditions, and so on. In Ex. 6.4, we have computed only  $V_{IL}$ ,  $V_{OL}$ ,  $V_{IH}$ , and  $V_{OH}$  and the noise margins under nominal conditions at room temperature.

### 6.5.9 LOAD RESISTOR PROBLEMS

The NMOS inverter with resistive load has been used to introduce the concepts associated with static logic gate design. Although a simple discrete component logic gate could be built using this circuit, IC realizations do not use resistive loads because the resistor would take up far too much area.

To explore the load resistor problem further, consider the rectangular block of semiconductor material in Fig. 6.16 with a resistance given by

$$R = \frac{\rho L}{t W} \quad (6.21)$$

where  $\rho$  = resistivity, and  $L$ ,  $W$ ,  $t$  are the length, width, and thickness of the resistor, respectively. In an integrated circuit, a resistor might typically be fabricated with a thickness of  $1 \mu\text{m}$  in a silicon region with a resistivity of  $0.001 \Omega \cdot \text{cm}$ . For these parameters, the  $28.8\text{-k}\Omega$  load resistor in the

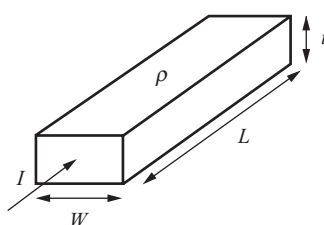


Figure 6.16 Geometry for a simple rectangular resistor.

previous section would require the ratio of  $L / W$  to be

$$\frac{L}{W} = \frac{Rt}{\rho} = \frac{(2.88 \times 10^4 \Omega)(1 \times 10^{-4} \text{ cm})}{0.001 \Omega \cdot \text{cm}} = \frac{2880}{1}$$

If the resistor width  $W$  were made a minimum line width of  $1 \mu\text{m}$ , which we will call the **minimum feature size  $F$** , then the length  $L$  would be  $2880 \mu\text{m}$ , and the area would be  $2880 \mu\text{m}^2$ .

For the switching device  $M_S$ ,  $W/L$  was found to be  $2.22/1$ . If the device channel length is made equal to the minimum feature size of  $1 \mu\text{m}$ , then the gate area of the NMOS device is only  $2.22 \mu\text{m}^2$ . Thus, the load resistor would consume more than 1000 times the area of the switching transistor  $M_S$ . This is simply not an acceptable utilization of area in IC design. The solution to this problem is to replace the load resistor with a transistor.

## 6.6 TRANSISTOR ALTERNATIVES TO THE LOAD RESISTOR

Six different alternatives for replacing the load resistor with a three-terminal MOSFET are shown in Fig. 6.17. When we replace the load resistor with a transistor, we are replacing the two terminal resistor with a three-terminal (or actually four-terminal) MOSFET, and we must decide where to connect the extra terminals. Current in the NMOS transistor goes from drain to source, so these terminals attach to the terminals where the resistor was removed. However, there are a number of possibilities for the gate terminal as indicated in the figure.

One possibility is to connect the gate to the source as in Fig. 6.17(a). However, for this case  $v_{GS} = 0$ , and MOSFET  $M_L$  will be nonconducting, assuming it is an enhancement-mode device with  $V_{TN} > 0$ . A similar problem exists if the gate is grounded as in Fig. 6.17(b). Here again, the connection forces  $v_{GS} \leq 0$ , and the load device is always turned off. Neither of these two

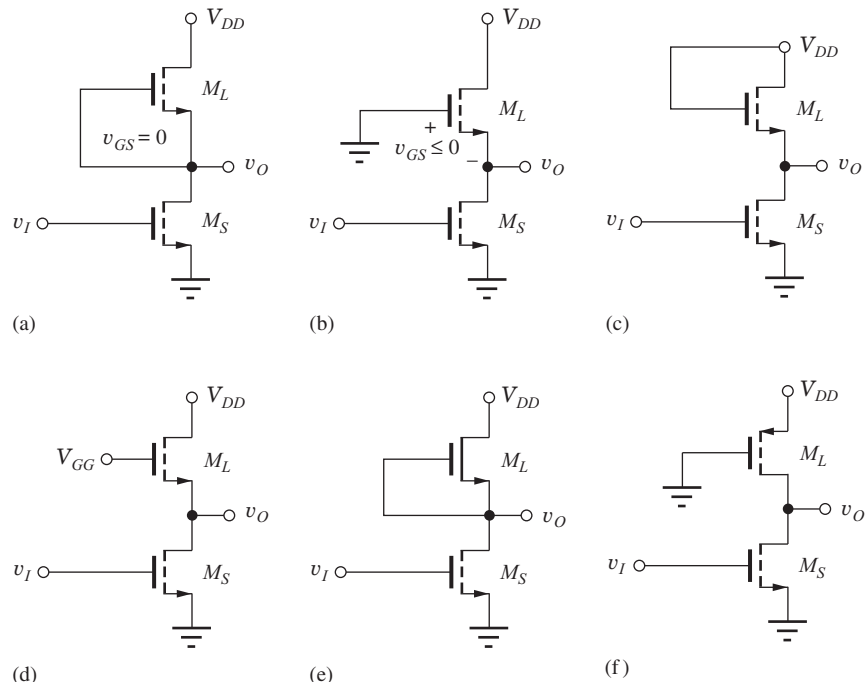


**Figure 6.17** NMOS inverter load device options: (a) NMOS inverter with gate of the load device connected to its source, (b) NMOS inverter with gate of the load device grounded, (c) saturated load inverter, (d) linear load inverter, (e) depletion load inverter, and (f) pseudo NMOS inverter. Note that (a) and (b) are not useful with enhancement-mode transistors.

alternatives work because an enhancement-mode NMOS device can never conduct current under these conditions.

The next three sections present an overview of the behavior of the circuits in Figs. 6.17(c–e). Saturated load logic, Fig. 6.17(c), played an important role in the history of electronic circuits. This form of logic was used in the design of early microprocessors, first in PMOS and then in NMOS technology. We briefly explore its static design in the next section. The characteristics of the linear load, Fig. 6.17(d), and depletion load, Fig. 6.17(e), technologies are outlined in Sections 6.6.2 and 6.6.3. The pseudo NMOS circuit in Fig. 6.17(f) is often encountered today in CMOS design, and a detailed discussion of its design appears in Section 6.6.4.

### 6.6.1 THE NMOS SATURATED LOAD INVERTER

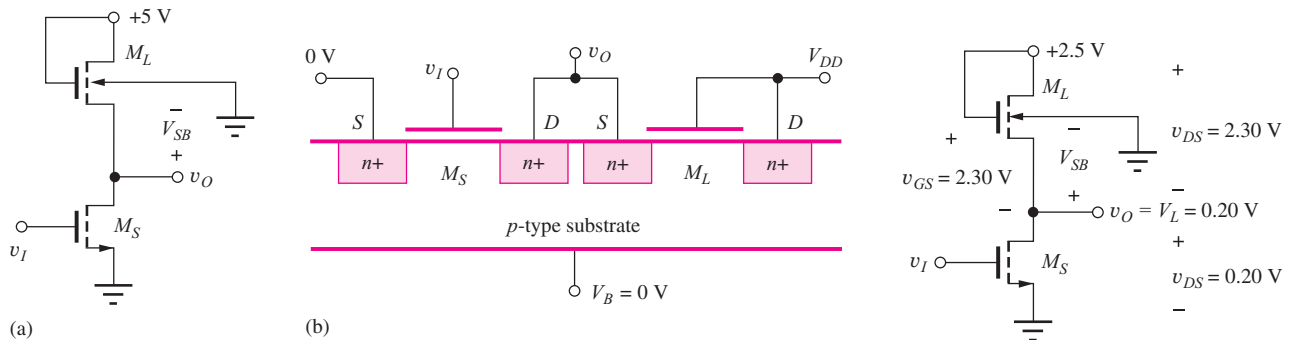
The first workable circuit alternative, used in NMOS (and earlier in PMOS) logic design, appears in Fig. 6.17(c). Here  $v_{DS} = v_{GS}$ , and since the connection forces the enhancement-mode load transistor to always operate in the saturation region,<sup>4</sup> we refer to this circuit as the **saturated load inverter**.

Figure 6.18(a) shows the actual circuit diagram for the saturated load inverter, and Fig. 6.18(b) gives the cross section of the inverter implementation in integrated circuit form. Here we see a very important aspect of the structure. The substrate is common to both transistors; thus, the substrate voltage must be the same for both  $M_S$  and  $M_L$  in the inverter, and the substrate terminal of  $M_L$  cannot be connected to its source as originally indicated in Fig. 6.17(c). This extra substrate terminal is most commonly connected to ground (0 V) (although voltages of  $-5$  V and  $-8$  V have been used in the past). For a substrate voltage of 0 V,  $v_{SB}$  for the switching device is always zero, but  $v_{SB}$  for the load device  $M_L$  changes as  $v_O$  changes. In fact,  $v_{SB} = v_O$ , as indicated in Fig. 6.18(a). The threshold voltages of transistors  $M_S$  and  $M_L$  will no longer be the same, and we will indicate the different values by  $V_{TNS}$  and  $V_{TNL}$ , respectively.

For the design of the saturated load inverter, we use the same circuit conditions that were used for the case of the resistive load ( $I_{DD} = 80 \mu\text{A}$  with  $V_{DD} = 2.5$  V and  $V_L = 0.20$  V). We first choose the  $W/L$  ratio of  $M_L$  to limit the operating current and power in the inverter. Because  $M_L$  is forced to operate in saturation by the circuit connection, its drain current is given by

$$i_D = \frac{K'_n}{2} \left( \frac{W}{L} \right)_L (v_{GS} - V_{TNL})^2 \quad (6.22)$$

For the circuit conditions in Fig. 6.19, load device  $M_L$  has  $v_{GS} = 2.30$  V when  $v_O = 0.20$  V.



**Figure 6.18** (a) Saturated load inverter. (b) Cross section of two integrated MOSFETs forming an inverter.

**Figure 6.19** Saturated load inverter with  $v_O = V_L$ .

<sup>4</sup> Since  $v_{GS} = V_{DS}$ , we have  $v_{GS} - V_{TN} = v_{DS} - V_{TN} < v_{DS}$  for  $V_{TN} > 0$ .

**TABLE 6.5**

NMOS ENHANCEMENT-MODE DEVICE PARAMETERS	NMOS DEPLETION-MODE DEVICE PARAMETERS	PMOS ENHANCEMENT-MODE DEVICE PARAMETERS
$V_{TO}$	0.6 V	-0.6 V
$\gamma$	$0.5\sqrt{V}$	$0.75\sqrt{V}$
$2\phi_F$	0.6 V	0.70 V
$K'_n$	$100 \mu A/V^2$	$40 \mu A/V^2$

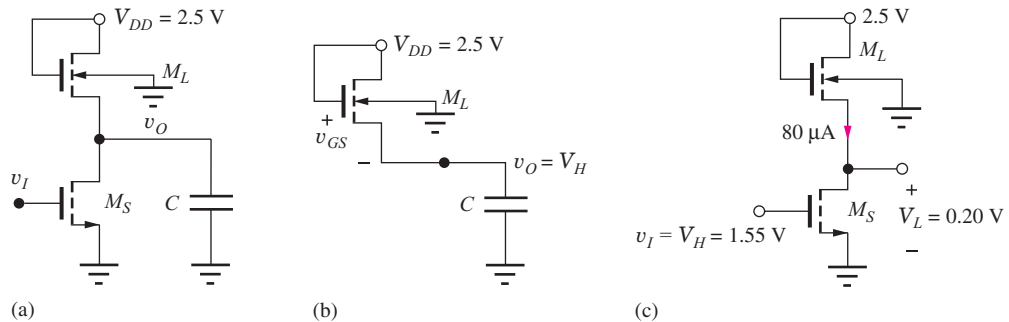


**Figure 6.20** (a) Inverter with load capacitance. (b) High output level is reached when  $v_I = V_L$  and  $M_S$  is off. (c) Bias conditions used to determine  $(W/L)_S$ .

Before we can calculate  $W/L$ , we must find the value of threshold voltage  $V_{T_{NL}}$ , which is determined by the body effect relation represented by Eq. (4.23) in Chapter 4:

$$V_{TN} = V_{TO} + \gamma (\sqrt{v_{SB} + 2\phi_F} - \sqrt{2\phi_F}) \quad (6.23)$$

where  $V_{TO}$  = zero bias value of  $V_{TN}$  (V)

$\gamma$  = body effect parameter ( $\sqrt{V}$ )

$2\phi_F$  = surface potential parameter (V)

For the rest of the discussion in this chapter, we use the set of device parameters given in Table 6.5.

For the load transistor, we have  $v_{SB} = v_S - v_B = 0.20 \text{ V} - 0 \text{ V} = 0.20 \text{ V}$ , and

$$V_{T_{NL}} = 0.6 + 0.5(\sqrt{0.20 + 0.6} - \sqrt{0.6}) = 0.660 \text{ V}$$

Now, we can find the  $W/L$  ratio for the load transistor:

$$\left(\frac{W}{L}\right)_L = \frac{2i_D}{K'_n(v_{GS} - V_{TN})^2} = \frac{2 \cdot 80 \mu A}{100 \frac{\mu A}{V^2} (2.30 - 0.66)^2} = \frac{1}{1.68} \quad (6.24)$$

Note that the length of this load device is larger than its width. In most digital IC designs, one of the two dimensions will be made as small as possible corresponding to the minimum feature size in one direction. The  $W/L$  ratio is usually written with the smallest number normalized to unity. For  $L = 1 \mu\text{m}$ , the gate area of  $M_L$  is now only  $1.68 \mu\text{m}^2$ , which is comparable to the area of  $M_S$ .

### Calculation of $V_H$

Unfortunately, the use of the saturated load device has a detrimental effect on other characteristics of the logic gate. The value of  $V_H$  will no longer be equal to  $V_{DD}$ . In order to understand this effect, it is helpful to imagine a capacitive load attached to the logic gate, as in Fig. 6.20. Consider the logic gate with  $v_I = V_L$  so that  $M_S$  is turned off. When  $M_S$  turns off, load device  $M_L$  charges capacitor  $C$  until the current through  $M_L$  becomes zero, which occurs when  $v_{GS} = V_{TN}$ :

$$v_{GS} = V_{DD} - V_H = V_{TN} \quad \text{or} \quad V_H = V_{DD} - V_{TN} \quad (6.25)$$

Thus, for the NMOS saturated load inverter, the output voltage reaches a maximum value equal to one threshold voltage drop below the power supply voltage  $V_{DD}$ . Without body effect, the output voltage in Fig. 6.20 would reach  $V_H = 2.5 - 0.6 = 1.9$  V, which represents a substantial degradation in  $V_H$  compared to the resistive load inverter with  $V_H = 2.5$  V.

However, body effect makes the situation even worse. As the output voltage increases toward  $V_H$ ,  $v_{SB}$  increases, the threshold voltage increases above  $V_{TO}$  (see Eq. 6.23), and the steady-state value of  $V_H$  is degraded further. When  $v_O$  reaches  $V_H$ , Eq. (6.26) must be true because  $v_{SB} = V_H$ :

$$V_H = V_{DD} - V_{TNL} = V_{DD} - [V_{TO} + \gamma(\sqrt{V_H + 2\phi_F} - \sqrt{2\phi_F})] \quad (6.26)$$

Using Eq. (6.26) with the parameters from Table 6.5 and  $V_{DD} = 2.5$  V, we can solve for  $V_H$ , which yields the following equation:

$$(V_H - 1.9 - 0.5\sqrt{0.6})^2 = 0.25(V_H + 0.6)$$

We can find the value of  $V_H$  using the solver in our calculator or by rearranging this equation into a quadratic equation. Either method yields  $V_H = 1.55$  V or  $V_H = 3.27$  V. In this circuit, the steady-state value of  $V_H$  cannot exceed power supply voltage  $V_{DD}$  (actually it cannot exceed  $V_{DD} - V_{TNL}$ ), so the answer must be  $V_H = 1.55$  V. We can check our result for  $V_H$  by computing the threshold voltage of the load device using Eq. (6.23):

$$V_{TNL} = 0.6 \text{ V} + 0.5\sqrt{V}(\sqrt{(1.55 + 0.6) \text{ V}} - \sqrt{0.6 \text{ V}}) = 0.95 \text{ V}$$

and

$$V_H = V_{DD} - V_{TNL} = 2.5 - 0.95 = 1.55 \text{ V} \quad \checkmark$$

which checks with the previous calculation of  $V_H$ .

**EXERCISE:** Use your solver to find the two roots of Eq. (6.26) for the values used above.

### Calculation of $(W/L)_S$

Now we are in a position to complete the inverter design by calculating  $W/L$  for the switching transistor. The bias conditions for  $v_O = V_L$  appear in Fig. 6.20(c) in which the drain current of  $M_S$  must equal the design value of 80  $\mu\text{A}$ . For  $V_{GS} = 1.55$  V,  $V_{DS} = 0.20$  V, and  $V_{TNS} = 0.6$  V, the switching transistor is operating in the triode region. Therefore,

$$i_D = K'_n \left( \frac{W}{L} \right)_S \left( v_{GS} - V_{TNS} - \frac{v_{DS}}{2} \right) v_{DS}$$

$$80 \mu\text{A} = 100 \frac{\mu\text{A}}{\text{V}^2} \left( \frac{W}{L} \right)_S \left( 1.55 - 0.6 - \frac{0.20}{2} \right) 0.20 \text{ V}^2 \quad \text{and} \quad \left( \frac{W}{L} \right)_S = \frac{4.71}{1}$$

The final inverter design appears in Fig. 6.21 in which  $(W/L)_S = 4.71/1$  and  $(W/L)_L = 1/1.68$ . Note that the size of  $M_S$  has increased because of the reduction in the value of  $V_H$ .

**EXERCISE:** Find  $V_H$  for the inverter in Fig. 6.18(a) if  $V_{TO} = 0.75$  V. Assume the other parameters remain constant.

**ANSWER:** 1.43 V

**EXERCISE:** (a) What value of  $(W/L)_S$  is required to achieve  $V_L = 0.15$  V in Fig. 6.20? Assume that  $i_D = 80 \mu\text{A}$ . What is the new value of  $V_{TNL}$  for  $v_O = V_L$ ? What value of  $(W/L)_L$  is required to set  $i_D = 80 \mu\text{A}$  for  $V_L = 0.15$  V? (b) Repeat for  $V_L = 0.10$  V.

**ANSWER:** (a) 6.10/1, 0.646 V, 1/1.82; (b) 8.89/1, 0.631 V, 1/1.96

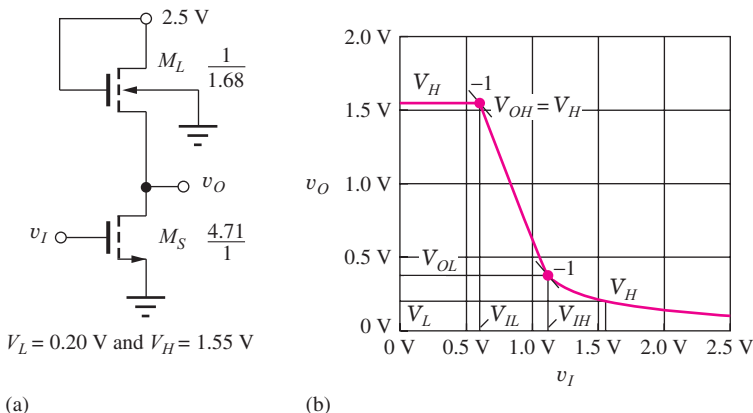


**Figure 6.21** (a) Completed inverter design with saturated load devices. (b) SPICE simulation of the voltage transfer function for the NMOS inverter with saturated load.

Figure 6.21 shows the results of SPICE simulation of the voltage transfer function for the final design. For low values of input voltage, the output is constant at 1.55 V. As the input voltage increases, the slope of the transfer function abruptly changes at the point at which the switching transistor begins to conduct as the input voltage exceeds the threshold voltage of \$M\_S\$. As the input voltage continues to increase, the output voltage decreases rapidly and ultimately reaches the design value of 0.20 V for an input of 1.55 V.



### DESIGN NOTE STATIC LOGIC INVERTER DESIGN STRATEGY

- Given design values of \$V\_{DD}\$, \$V\_L\$, and power level, find \$I\_{DD}\$ from \$V\_{DD}\$ and the power.
- Calculate load resistor value or \$(W/L)\_L\$ for the load transistor based on design values of \$V\_L\$ and \$I\_{DD}\$.
- Assume switching transistor \$M\_S\$ is off, and find the high output voltage level \$V\_H\$.
- Apply \$V\_H\$ to the inverter input and calculate \$(W/L)\_S\$ of the switching transistor based upon design values of \$V\_L\$ and \$I\_{DD}\$.
- Check operating region assumptions for \$M\_S\$ and \$M\_L\$ for \$v\_O = V\_L\$.
- Check overall design with SPICE simulation.

### DESIGN EXAMPLE 6.5

Now let's design a saturated load inverter to operate from a 3.3-V supply including the influence of body effect on the transistor design.

**PROBLEM** Design a saturated load inverter similar to that of Fig. 6.21 with \$V\_{DD} = 3.3\$ V and \$V\_L = 0.2\$ V. Assume \$I\_{DD} = 60 \mu\text{A}\$, \$K'\_n = 50 \mu\text{A}/\text{V}^2\$, \$V\_{TN} = 0.75\$ V, \$\gamma = 0.5 \sqrt{\text{V}}\$, and \$2\phi\_F = 0.6\$ V.

**SOLUTION** **Known Information and Given Data:** Circuit topology in Fig. 6.21; \$V\_{DD} = 3.3\$ V, \$I\_{DD} = 60 \mu\text{A}\$, \$V\_L = 0.2\$ V, \$K'\_n = 50 \mu\text{A}/\text{V}^2\$, \$V\_{TO} = 0.75\$ V, \$\gamma = 0.5 \sqrt{\text{V}}\$, and \$2\phi\_F = 0.6\$ V

**Unknowns:** \$W/L\$ ratios of the load and switching transistors \$M\_S\$ and \$M\_L\$

**Approach:** First determine \$V\_H\$ including the influence of body effect on the load transistor threshold voltage by evaluating Eq. (6.26). Use \$I\_D\$ and the voltages in the circuit to find \$(W/L)\_L\$. Use \$V\_H\$ and the specified values of \$V\_L\$ and \$I\_D\$ to find \$(W/L)\_S\$.

**Assumptions:**  $M_S$  is off for  $v_I = V_L$ . For  $v_O = V_L$ ,  $M_S$  is in the triode region, and  $M_L$  is in the saturation region.

**Analysis:** The transistor operating conditions for the load and switching transistors appear in the (a) part of the circuit below for  $v_O = V_L$ . To find the  $W/L$  ratio for the load device, the saturation region expression is evaluated at a drain current of 60  $\mu\text{A}$ . We must recalculate the threshold voltage since the body voltage of the load is 0.2 V when  $v_O = V_L = 0.2 \text{ V}$ .

$$I_{DL} = \frac{K'_n}{2} \left( \frac{W}{L} \right)_L (V_{GSL} - V_{TNL})^2$$

$$V_{TNL} = 0.75 + 0.5(\sqrt{0.2+0.6} - \sqrt{0.6}) = 0.81 \text{ V}$$

$$60 \mu\text{A} = \frac{50 \frac{\mu\text{A}}{\text{V}^2}}{2} \left( \frac{W}{L} \right)_L (3.3 - 0.2 - 0.81)^2 \rightarrow \left( \frac{W}{L} \right)_L = \frac{1}{2.19}$$

In order to find  $W/L$  for the switching transistor, we first need to find the value of  $V_H$ . For the values associated with this technology, Eq. (6.26) becomes

$$V_H = 3.3 - [0.75 + 0.5(\sqrt{V_H+0.6} - \sqrt{0.6})]$$

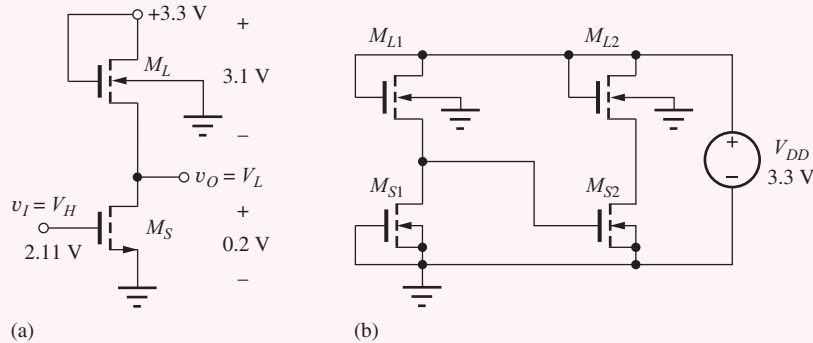
and rearranging this equation gives

$$V_H^2 - 6.125V_H + 8.476 = 0 \quad \text{for which} \quad V_H = 2.11 \text{ V, } 4.01 \text{ V}$$

Since  $V_H$  cannot exceed  $V_{DD}$ , the correct choice must be  $V_H = 2.11 \text{ V}$ . Note that an extra digit was included in the calculation to increase the precision of the result.

The triode region expression for the switching transistor drain current with  $v_I = V_H$  and  $v_O = V_L$  is

$$I_{DS} = K'_n \left( \frac{W}{L} \right)_S \left( V_H - V_{TN} - \frac{V_L}{2} \right) V_L$$



Equating this expression to the drain current yields

$$60 \mu\text{A} = (50 \times 10^{-6}) \left( \frac{W}{L} \right)_S \left( 2.11 - 0.75 - \frac{0.2}{2} \right) 0.2 \rightarrow \left( \frac{W}{L} \right)_S = \frac{4.76}{1}$$

Our completed design values are  $(W/L)_S = 4.76/1$  and  $(W/L)_L = 1/2.19$ .

**Check of Results:** We must check the triode and saturation region assumptions for the two MOSFETs: For the switch,  $V_{GS} - V_{TN} = 2.11 - 0.75 = 1.36 \text{ V}$ , which is greater than  $V_{DS} = 0.2 \text{ V}$ , and the triode region assumption is correct. For the load device,  $V_{GS} - V_{TN} = 3.1 - 0.81 = 2.29 \text{ V}$

and  $V_{DS} = 3.1$  V, which is consistent with the saturation region of operation. We can double check our  $V_H$  calculation by using it to find the threshold of  $M_L$ :

$$V_{T_{NL}} = 0.75 + 0.5(\sqrt{2.11 + 0.6} - \sqrt{0.6}) = 1.19 \text{ V}$$

This is correct since  $V_H + V_{T_{NL}} = 2.11 + 1.19 = 3.3$  V, which must equal the value of  $V_{DD}$ .

Let us also double check the values of  $W/L$  by using them to recalculate the drain currents:

$$I_{DS} = (50 \times 10^{-6}) \left( \frac{4.76}{1} \right) \left( 2.11 - 0.75 - \frac{0.2}{2} \right) 0.2 = 60.0 \mu\text{A} \quad \checkmark$$

$$I_{DL} = \frac{50 \frac{\mu\text{A}}{\text{V}^2}}{2} \left( \frac{1}{2.19} \right) (3.3 - 0.2 - 0.81)^2 = 59.9 \mu\text{A} \quad \checkmark$$

Both results agree within round off error.

**Computer-Aided Analysis:** To verify our design with SPICE, we draw the circuit with a schematic capture tool, as in part (b) of the figure on the previous page. Two inverters are cascaded in order to get both  $V_H$  and  $V_L$  with one simulation. The NMOS transistors use the LEVEL = 1 model with  $K_P = 5.0E-5$ ,  $VTO = 0.75$  V,  $GAMMA = 0.5$ , and  $\Phi_I = 0.6$  V. The transistor sizes are specified as  $W = 4.76$  U and  $L = 1$  U for  $M_S$ , and  $W = 1$  U and  $L = 2.19$  U for  $M_L$ . SPICE dc analysis gives  $V_H = 2.11$  V and  $V_L = 0.196$  V. The drain current of transistor  $M_{S2}$  is  $60.1 \mu\text{A}$ . All the values agree with the design specifications.

**EXERCISE:** Redesign the inverter in Ex. 6.5 to have  $V_L = 0.1$  V.

**ANSWER:**  $(W/L)_S = 9.16/1$ ;  $(W/L)_L = 1/2.44$  (Note  $V_{T_{NL}} = 0.781$  V)

## EXAMPLE 6.6

### LOGIC LEVEL ANALYSIS FOR THE SATURATED LOAD INVERTER

Finding the logic levels associated with someone else's design involves a somewhat different thought process than that used in designing our own inverter. Here we find  $V_H$  and  $V_L$  for a specified inverter design.

**PROBLEM** Find the high and low logic levels and the power supply current for a saturated load inverter with  $(W/L)_S = 10/1$  and  $(W/L)_L = 2/1$ . The inverter operates with  $V_{DD} = 2.5$  V. Assume  $K'_n = 100 \mu\text{A}/\text{V}^2$ ,  $V_{TO} = 0.60$  V,  $\gamma = 0.5\sqrt{V}$ , and  $2\phi_F = 0.6$  V.

**SOLUTION** **Known Information and Given Data:** Circuit topology in Fig. 6.18(a);  $V_{DD} = 2.5$  V,  $(W/L)_S = 10/1$ ,  $(W/L)_L = 2/1$ ,  $K'_n = 100 \mu\text{A}/\text{V}^2$ ,  $V_{TO} = 0.60$  V,  $\gamma = 0.5\sqrt{V}$ , and  $2\phi_F = 0.6$  V

**Unknowns:**  $V_H$ ,  $V_L$ , and  $I_{DD}$  for both logic states

**Approach:** First, determine  $V_H$ . Include the influence of body effect on the load transistor threshold voltage by solving Eq. (6.26). Use  $V_H$  and the specified transistor parameters to find  $V_L$  by equating the drain currents in the switching and load transistors. Use  $V_L$  to find the  $I_{DS}$ .

**Assumptions:**  $M_S$  is off for  $v_I = V_L$ . For  $v_O = V_L$ ,  $M_S$  operates in the triode region, and  $M_L$  is in the saturation region.

**Analysis:** First we find  $V_H$ , and then we use it to find  $V_L$ . For the values associated with this technology, Eq. (6.26) becomes

$$V_H = 2.5 - [0.60 + 0.5(\sqrt{V_H + 0.6} - \sqrt{0.6})]$$

Rearranging this equation gives

$$V_H^2 - 4.824V_H + 5.082 = 0 \quad \text{for which} \quad V_H = 3.27 \text{ V or } 1.55 \text{ V}$$

Since,  $V_H$  cannot exceed  $V_{DD}$ , the correct choice must be  $V_H = 1.55 \text{ V}$ . Note that an extra digit was included in the calculation to increase the precision of the result. Since  $M_S$  is off, there is no path for current from  $V_{DD}$  and  $I_{DD} = 0$  for  $v_O = V_H$ .

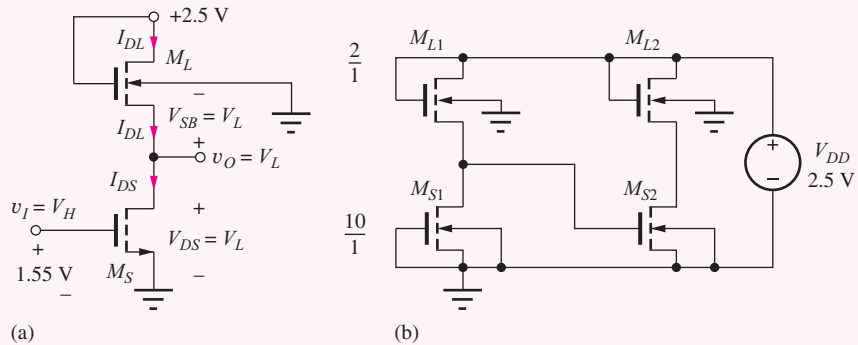
At this point we should check our result to avoid propagation of errors in our calculations. We can use  $V_H$  to find  $V_{T_{NL}}$  and see if it is consistent with the value of  $V_H$ :

$$V_{T_{NL}} = 0.60 + 0.5(\sqrt{1.55 + 0.6} - \sqrt{0.6}) = 0.946 \text{ V}$$

$$V_H = 2.5 - 0.946 = 1.55 \text{ V}$$

We see that the value of  $V_H$  is correct.

To find  $V_L$ , we use the condition that  $I_{DS}$  must equal  $I_{DL}$  in the steady state. The load transistor is saturated by connection, and we expect the switching transistor to be in the triode region since its drain-source voltage should be small. ( $V_{DS} = V_L$ .)



For  $I_{DS} = I_{DL}$ , we have  $K'_n \left( \frac{10}{1} \right) \left( V_{GSS} - V_{TNS} - \frac{V_L}{2} \right) V_L = \frac{K'_n}{2} \left( \frac{2}{1} \right) (2.5 - V_L - V_{T_{NL}})^2$  where

$$V_{T_{NL}} = 0.60 + 0.5(\sqrt{V_L + 0.6} - \sqrt{0.6})$$

From the circuit shown,  $V_{GSS} = 1.55 \text{ V}$  and  $V_{TNS} = 0.60 \text{ V}$ , since there will be no body effect in  $M_S$ . Unfortunately,  $V_{T_{NL}}$  is a function of the unknown voltage  $V_L$ , since the source-bulk voltage of  $M_L$  is equal to  $V_L$ .

**Approach 1:** Since we expect  $V_L$  to be small, its effect on  $V_{T_{NL}}$  will also be small, and one approach to finding  $V_L$  is to simply ignore body effect in the load transistor. For this case, equating  $I_{DS}$  and  $I_{DL}$  gives

$$K'_n \left( \frac{10}{1} \right) \left( 1.55 - 0.6 - \frac{V_L}{2} \right) V_L = \frac{K'_n}{2} \left( \frac{2}{1} \right) (2.5 - V_L - 0.6)^2$$

which can be rearranged to yield a quadratic equation for which  $V_L = 1.80 \text{ V}$  or  $0.33 \text{ V}$ . We must choose  $V_L = 0.33 \text{ V}$  since the other root is not consistent with the assumed regions of operation of the transistors. For this value of  $V_L$ , the current in  $M_S$  is

$$I_{DS} = \left( 100 \frac{\mu\text{A}}{\text{V}^2} \right) \left( \frac{10}{1} \right) \left( 1.55 - 0.6 - \frac{0.33}{2} \right) (0.33) \text{ V}^2 = 259 \mu\text{A}$$

**Approach 2:** For a more exact result, we can find the simultaneous solution to the drain current and threshold voltage equations with the solver in a calculator, with a spreadsheet, or by direct iteration. The result is  $V_L = 0.290$  V with  $V_{TNL} = 0.68$  V. Using the value of  $V_L$ , we can find the current in  $M_S$ :

$$I_{DS} = \left(100 \frac{\mu\text{A}}{\text{V}^2}\right) \left(\frac{10}{1}\right) \left(1.55 - 0.6 - \frac{0.29}{2}\right) (0.29) \text{ V}^2 = 234 \mu\text{A}$$

The approximate values in Approach 1 overestimate the more exact values in Approach 2 by approximately 10 percent. In most cases, this would be a negligible error.

**Check of Results:** Note that we double checked the value of  $V_H$  earlier. For  $V_L$ , we should check our triode and saturation region assumptions for the two MOSFETs: For the switching transistor,  $V_{GS} - V_{TN} = 1.55 - 0.6 = 0.96$  V, which is greater than  $V_{DS} = 0.29$  V, and the triode region assumption is correct. For the load device,  $V_{GS} - V_{TN} = 2.5 - 0.29 - 0.68 = 1.53$  V and  $V_{DS} = 2.5 - 0.29 = 2.21$ , which are consistent with the saturation region of operation. We can further check our results by finding the drain current in  $M_L$ :

$$I_{DL} = \left(\frac{100}{2} \frac{\mu\text{A}}{\text{V}^2}\right) \left(\frac{2}{1}\right) (2.5 - 0.29 - 0.68)^2 = 234 \mu\text{A}$$

This value agrees with  $I_{DS}$  within round-off error.

**Computer-Aided Analysis:** To verify our design with SPICE, we draw the circuit with a schematic capture tool, as in part (b) of the figure on the previous page. Two inverters are cascaded in order to get both  $V_H$  and  $V_L$  with one simulation. The gate of MS1 is grounded to force MS1 to be off. The NMOS transistors use the LEVEL = 1 model with KP = 10E-5, VTO = 0.60 V, GAMMA = 0.5, and PHI = 0.6 V. The transistor sizes are specified as W = 10 U and L = 1 U for  $M_S$ , and W = 2 U and L = 1 U for  $M_L$ . SPICE dc analysis gives  $V_H = 1.55$  V and  $V_L = 0.289$  V. The current in  $V_{DD}$  is 234  $\mu\text{A}$ . All the values agree with the hand calculations.

**EXERCISE:** Use the “Solver” on your calculator to find  $V_H$  in Ex. 6.6.

**EXERCISE:** Repeat the calculations with  $\gamma = 0$ . Check your results with SPICE.

**ANSWERS:** 1.90 V; 0 A; 0.235 V; 278  $\mu\text{A}$

### Noise Margin Analysis

Detailed analysis of the noise margins for saturated load inverters operating from low power supply voltages is very tedious and results in expressions that yield little additional insight into the behavior of the inverter. So here we explore the values of  $V_{IL}$ ,  $V_{OH}$ ,  $V_{IH}$ , and  $V_{OL}$  based upon the SPICE simulation results presented in Fig. 6.21. Remember that these voltages are defined by the points in the voltage transfer characteristic at which the slope is  $-1$ . Looking at Fig. 6.21, we see that the slope of the VTC abruptly changes at the point where  $M_S$  just begins to conduct. This occurs for  $v_I = V_{TN}$  and defines  $V_{IL}$  and  $V_{OH}$ . Therefore,  $V_{IL} = V_{TNS} = 0.6$  V, and  $V_{OH} = V_H = 1.55$  V. The values of  $V_{IH}$  and  $V_{OL}$  are found from the graph at the second point where the slope is  $-1$ . Reading the values from the graph yields  $V_{IH} \cong 1.12$  V and  $V_{OL} \cong 0.38$  V.<sup>5</sup>

The noise margins for this saturated load inverter are

$$\text{NM}_H = V_{OH} - V_{IH} = 1.55 - 1.12 = 0.33 \text{ V}$$

$$\text{NM}_L = V_{IL} - V_{OL} = 0.60 - 0.38 = 0.22 \text{ V}$$

<sup>5</sup> Note that we can have SPICE estimate the derivative of the VTC numerically by plotting the output  $D(V_O)/D(V_I)$  for example, and we can quite accurately locate the points for which the slope is  $-1$ .

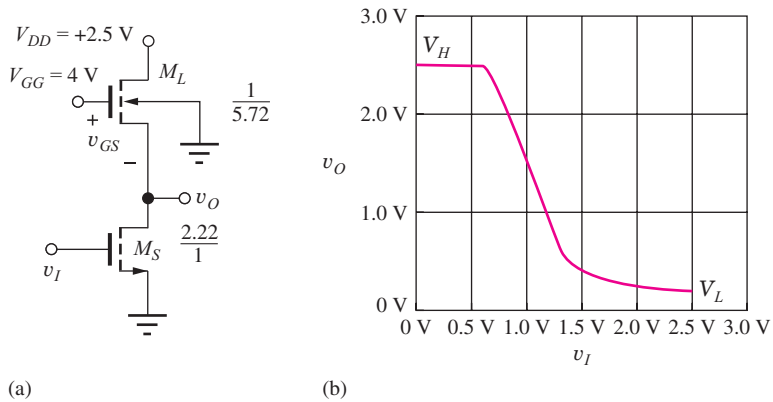


**Figure 6.22** (a) Linear load inverter design. (b) Linear load inverter VTC.

Let's compare these values to those of the resistive load inverter ( $\text{NM}_H = 0.96\text{ V}$ ,  $\text{NM}_L = 0.25\text{ V}$ ). The reduction in  $V_H$  caused by the saturated load device has significantly reduced the value of  $\text{NM}_H$ , whereas the value of  $\text{NM}_L$  is very similar since  $M_S$  has been designed to maintain the same value of  $V_L$ .

### 6.6.2 NMOS INVERTER WITH A LINEAR LOAD DEVICE

Figure 6.17(d) provides a second workable choice for the load transistor  $M_L$ . In this case, the gate of the load transistor is connected to a separate voltage  $V_{GG}$  as in Fig. 6.22(a).  $V_{GG}$  is normally chosen to be at least one threshold voltage greater than the supply voltage  $V_{DD}$ :

$$V_{GG} \geq V_{DD} + V_{T_{NL}}$$

For this value of  $V_{GG}$ , the output voltage in the high output state  $V_H$  is equal to  $V_{DD}$  since  $i_D = 0$  for  $v_{DS} = 0$  and  $v_{DS} = V_{DD} - V_H$ .

The region of operation of  $M_L$  in Fig. 6.22 can be found by comparing  $V_{GS} - V_{T_{NL}}$  to  $V_{DS}$ . For the load device with its output at  $v_O$  and  $V_{GG} \geq V_{DD} + V_{T_{NL}}$ :

$$\begin{aligned} v_{GS} - V_{T_{NL}} &= V_{GG} - v_O - V_{T_{NL}} \\ &\geq V_{DD} + V_{T_{NL}} - v_O - V_{T_{NL}} \\ &\geq V_{DD} - v_O \end{aligned} \quad (6.27)$$

So  $v_{GS} - V_{T_{NL}} \geq V_{DD} - v_O$ , but  $v_{DS} = V_{DD} - v_O$ , which demonstrates that the load device always operates in the triode (linear) region.

The  $W/L$  ratios for  $M_S$  and  $M_L$  can be calculated using methods similar to those in the previous sections; the results are shown in Fig. 6.22. Because  $V_H$  is now equal to  $V_{DD} = 2.5\text{ V}$ ,  $M_S$  is again 2.22/1. However, for  $v_O = V_L$ ,  $v_{GS}$  of  $M_L$  is large, and  $(W/L)_L$  must be set to (1/5.72) in order to limit the current to the desired level. (Verification of these values is left for Prob. 6.76.)

Introduction of the additional power supply voltage  $V_{GG}$  overcomes the reduced output voltage problem associated with the saturated load device. However, the cost of the additional power supply level, as well as the increased wiring congestion introduced by distribution of the extra supply voltage to every logic gate, cause this form of load topology to rarely be used.

**EXERCISE:** Estimate the values of  $V_{IL}$ ,  $V_{OH}$ ,  $V_{IH}$ ,  $V_{OL}$ ,  $\text{NM}_H$  and  $\text{NM}_L$  for the linear load inverter using the graph in Fig. 6.22(b).

**ANSWERS:** 0.64 V, 2.42 V, 1.46 V, 0.52 V, 0.12 V, 0.96 V.

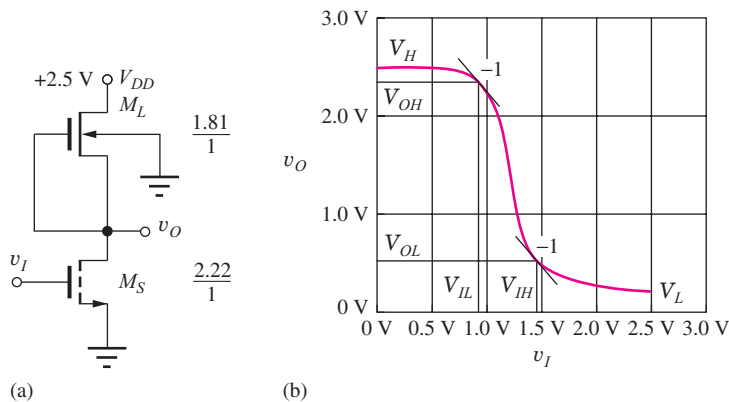


**Figure 6.23** (a) NMOS inverter with depletion-mode load. (b) SPICE simulation results for the voltage transfer function of the NMOS depletion-load inverter of part (a).

### 6.6.3 NMOS INVERTER WITH A DEPLETION-MODE LOAD

The saturated load and linear load circuits were developed for use in early integrated circuits because all the devices had the same threshold voltages in the first PMOS and NMOS technologies. However, once ion-implantation technology was perfected, it became possible to selectively adjust the threshold of the load transistors to alter their characteristics to become those of NMOS depletion-mode devices with \$V\_{TN} < 0\$, and the use of the circuit in Fig. 6.23(a) became feasible.

The circuit topology for the NMOS inverter with a depletion-mode load device is shown in Fig. 6.23(a). Because the threshold voltage of the NMOS depletion-mode device is negative, a channel exists even for \$v\_{GS} = 0\$, and the load device conducts current until its drain-source voltage becomes zero. When the switching device \$M\_S\$ is off (\$v\_I = V\_L\$), the output voltage rises to its final value of \$V\_H = V\_{DD}\$.

For \$v\_I = V\_H\$, the output is low at \$v\_O = V\_L\$. In this state, current is limited by the depletion-mode load device, and it is normally designed to operate in the saturation region, requiring:

$$v_{DS} \geq v_{GS} - V_{TDL} = 0 - V_{TDL} \quad \text{or} \quad v_{DS} \geq -V_{TDL}$$

#### Design of the \$W/L\$ Ratios of \$M\_L\$

As an example of inverter design, if we assume \$V\_{DD} = 2.5\text{ V}\$, \$V\_L = 0.20\text{ V}\$, and \$V\_{TDL} = -1\text{ V}\$, then the drain-source voltage for the load device with \$v\_O = V\_L\$ is \$V\_{DS} = 2.30\text{ V}\$, which is greater than \$-V\_{TDL} = 1\text{ V}\$, and the MOSFET operates in the saturation region. The drain current of the depletion-mode load device operating in the saturation region with \$V\_{GS} = 0\$ is given by

$$i_{DL} = \frac{K'_n}{2} \left( \frac{W}{L} \right)_L (v_{GSL} - V_{TDL})^2 = \frac{K'_n}{2} \left( \frac{W}{L} \right)_L (V_{TDL})^2 \quad (6.28)$$

Just as for the case of the saturated load inverter, body effect must be taken into account in the depletion-mode MOSFET, and we must calculate \$V\_{TDL}\$ before \$(W/L)\_L\$ can be properly determined. For depletion-mode devices, we use the parameters in Table 6.5, and

$$V_{TDL} = -1\text{ V} + 0.5 \sqrt{V} (\sqrt{(0.20 + 0.6)\text{ V}} - \sqrt{0.6\text{ V}}) = -0.94\text{ V}$$

Using our previous design current of \$80\text{ }\mu\text{A}\$ with \$K'\_n = 100\text{ }\mu\text{A/V}^2\$ and the depletion-mode threshold voltage of \$-0.94\text{ V}\$, we find \$(W/L)\_L = 1.81/1\$.

#### Design of the \$W/L\$ Ratio of \$M\_S\$

When \$v\_I = V\_H = V\_{DD}\$, the switching device once again has the full supply voltage applied to its gate, and its \$W/L\$ ratio will be identical to the design of the NMOS logic gate with resistor

load:  $(W/L)_S = 2.22/1$ . The completed depletion-mode load inverter design appears in Fig. 6.23, and the logic levels of the final design are  $V_L = 0.20$  V and  $V_H = 2.5$  V.

Figure 6.23 shows the results of SPICE simulation of the voltage transfer function for the final inverter design with the depletion-mode load. For low values of input voltage, the output is 2.5 V. As the input voltage increases, the slope of the transfer function gradually changes as the switching transistor begins to conduct for an input voltage exceeding the threshold voltage. As the input voltage continues to increase, the output voltage decreases rapidly and ultimately reaches the design value of 0.20 V for an input of 2.5 V.

### Noise Margin Analysis

As for the saturated load inverter, detailed analysis of the noise margins for depletion load inverters operating from low power supply voltages is very tedious. So here we explore the values of  $V_{IL}$ ,  $V_{OH}$ ,  $V_{IH}$ , and  $V_{OL}$  based upon the SPICE simulation results presented in Fig. 6.23. Remember that these voltages are defined by the points in the voltage transfer characteristic at which the slope is  $-1$ . Reading values from Fig. 6.23, we estimate  $V_{IL} = 0.93$  V and  $V_{OH} = 2.35$  V, and  $V_{IH} \cong 1.45$  V and  $V_{OL} \cong 0.50$  V.

The noise margins for this saturated load inverter are

$$NM_H = V_{OH} - V_{IH} = 2.35 - 1.45 = 0.90 \text{ V}$$

$$NM_L = V_{IL} - V_{OL} = 0.93 - 0.50 = 0.43 \text{ V}$$

Compared to the noise margins of the resistive load inverter ( $NM_H = 0.96$  V,  $NM_L = 0.25$  V), we see that  $NM_H$  is similar and  $NM_L$  has actually improved.

## DESIGN EXAMPLE 6.7

### NMOS INVERTER WITH DEPLETION-MODE LOAD

Now we will redesign the depletion-load inverter for operation with 3.3-V power supply voltage.

**PROBLEM** Design the inverter with depletion-mode load of Fig. 6.23 for operation with  $V_{DD} = 3.3$  V. Assume  $V_{TO} = 0.6$  V for the switching transistor and  $V_{TO} = -1$  V for the depletion-mode load. Keep the other design parameters the same (i.e.,  $V_L = 0.20$  V and  $P = 0.20$  mW).

**SOLUTION** **Known Information and Given Data:** Circuit topology in Fig. 6.23;  $V_{DD} = 3.3$  V,  $P = 0.20$  mW,  $V_L = 0.20$  V,  $K'_n = 100 \mu\text{A}/\text{V}^2$ ,  $V_{TOS} = 0.60$  V,  $V_{TOL} = -1$  V,  $\gamma = 0.5 \sqrt{\text{V}}$ , and  $2\phi_F = 0.6$  V for both transistor types

**Unknowns:** Power supply current  $I_{DD}$ ,  $W/L$  ratios of the load and switching transistors  $M_S$  and  $M_L$

**Approach:** Find  $V_H$ . Use  $V_H$ ,  $I_{DD}$ , and the specified value of  $V_L$  to find  $(W/L)_S$ . Calculate  $V_{TNL}$ . Use  $I_{DD}$ ,  $V_{TNL}$ , and the voltages in the circuit to find  $(W/L)_L$ .

**Assumptions:**  $M_S$  is off for  $v_I = V_L$ . For  $v_O = V_L$ ,  $M_S$  is in the triode region, and  $M_L$  is in the saturation region.

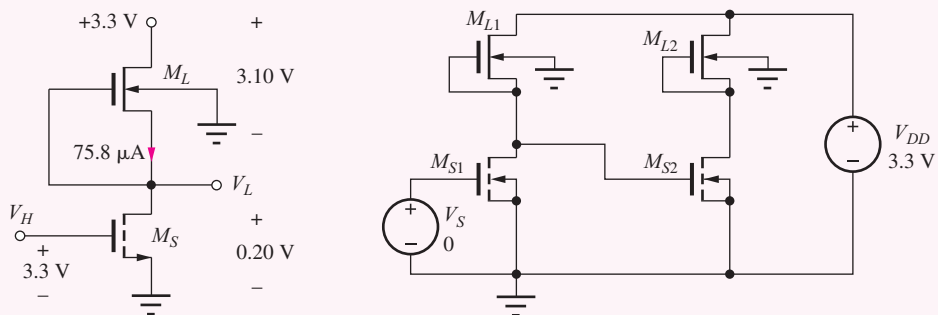
**Analysis:** First, we need to know the power supply current for  $v_O = V_L$  in order to calculate the  $W/L$  ratios of both transistors.

$$I_{DD} = \frac{P}{V_{DD}} = \frac{0.20 \text{ mW}}{3.3 \text{ V}} = 60.6 \mu\text{A}$$

The value of  $V_H$  will be equal to  $V_{DD}$  as long as the threshold of the depletion-mode device remains negative for  $v_O = V_{DD}$ . Checking the value of  $V_{TNL}$ :

$$V_{TNL} = -1 + 0.5(\sqrt{3.3 + 0.6} - \sqrt{0.6}) = -0.40 \text{ V} \quad \checkmark$$

Therefore,  $V_H = V_{DD} = 3.3$  V. Now the size of the switching transistor can be determined. The transistor has  $V_{GS} = V_H = 3.3$  V and  $V_{DS} = V_L = 0.20$  V, as shown in the figure.



$$60.6 \mu\text{A} = 100 \mu\text{A} \left( \frac{W}{L} \right)_S \left( 3.3 - 0.6 - \frac{0.20}{2} \right) 0.20 \rightarrow \left( \frac{W}{L} \right)_S = \frac{1.17}{1}$$

In order to design the load transistor, we calculate its threshold voltage with  $v_O = V_L = 0.20$  V, and then use  $V_{TNL}$  to find  $W/L$  (note that  $V_{SB} = V_L = 0.20$  V):

$$V_{TNL} = -1 + 0.5(\sqrt{0.20 + 0.6} - \sqrt{0.6}) = -0.940 \text{ V}$$

$$60.6 \mu\text{A} = \frac{100 \mu\text{A}}{2} \left( \frac{W}{L} \right)_L (-0.94)^2 \rightarrow \left( \frac{W}{L} \right)_L = \frac{1.37}{1}$$

**Check of Results:** We must check the triode and saturation region assumptions for the two MOSFETs. For the switch,  $V_{GS} - V_{TN} = 3.3 - 0.60 = 2.7$  V, which is greater than  $V_{DS} = 0.20$  V, and the triode region assumption is correct. For the load device,  $V_{GS} - V_{TN} = 0 - (-0.93) = 0.93$  V, and  $V_{DS} = 3.3 - 0.20 = 3.10$  V, which are consistent with the saturation region of operation. Let us also double check the values of  $W/L$  by directly calculating the drain currents:

$$I_{DS} = (100 \times 10^{-6}) \left( \frac{1.17}{1} \right) \left( 3.3 - 0.60 - \frac{0.20}{2} \right) 0.20 = 60.8 \mu\text{A} \quad \checkmark$$

$$I_{DL} = \frac{100 \frac{\mu\text{A}}{\text{V}^2}}{2} \left( \frac{1.37}{1} \right) [0 - (-0.94)]^2 = 60.5 \mu\text{A} \quad \checkmark$$

Both results agree within round-off error.

**Computer-Aided Analysis:** Let us verify our design with SPICE. Here again, two inverters are cascaded in order to get both  $V_H$  and  $V_L$  with one simulation. The enhancement-mode transistors use the LEVEL = 1 model with KP = 1E-4, VTO = 0.60 V, GAMMA = 0.5, and PHI = 0.6 V. For the depletion mode devices, VTO is changed to VTO = -1.0 V. The transistor sizes are specified as W = 1.17 U and L = 1 U for  $M_S$ , and W = 1.37 U and L = 1 U for  $M_L$ . SPICE gives  $V_H = 3.30$  V and  $V_L = 0.20$  V with  $I_D = 60.6 \mu\text{A}$  for transistor  $M_{S2}$ . All the values confirm our design calculations.

**EXERCISE:** What are the new  $W/L$  ratios for the transistors in Ex. 6.7 if  $V_{TOL} = -1.5$  V?

**ANSWERS:**  $(W/L)_S = 1.17/1$ ;  $(W/L)_L = 1/1.72$

### 6.6.4 STATIC DESIGN OF THE PSEUDO NMOS INVERTER

It is also possible to replace the load resistor with a PMOS transistor with its source connected to  $V_{DD}$ , its drain is connected to the output node, and its gate connected to ground, as in Fig. 6.24. This circuit has become known as **pseudo NMOS** since circuit operation is very similar to that of NMOS logic even though it is usually found embedded in CMOS designs that we will study in detail in Chapter 7.

In order to design the circuit, we use the same circuit conditions that were used for the case of the resistive load. ( $I_{DD} = 80 \mu\text{A}$ ,  $V_{DD} = 2.5$  V and  $V_L = 0.20$  V). First we choose the  $W/L$  ratio of the PMOS load device to limit the operating current in the inverter. Then we calculate the size of  $M_S$  required to achieve the specified value of  $V_L$ . (Note that neither transistor suffers from any body effect since the bulk terminals of both transistors are connected to their respective sources. This is an important advantage of the PMOS load transistor in comparison to NMOS load devices.)

#### Calculation of $(W/L)_P$ and $(W/L)_S$

For the PMOS device in Fig. 6.24, we see that  $V_{GS} = -V_{DD}$ , and the transistor will be in the conducting state. Since  $V_{DS} = 0.2 - 2.5 = -2.3$  V and  $V_{GS} - V_{TP} = -2.5 - (-0.6) = -1.9$  V, the transistor will be saturated ( $|V_{DS}| > |V_{GS} - V_{TP}|$ —see Section 4.2). We need to find the value of  $W/L$  that sets the PMOS drain current to  $80 \mu\text{A}$ :

$$i_D = \frac{K'_p}{2} \left( \frac{W}{L} \right)_P (V_{GS} - V_{TP})^2 \quad \text{or} \quad 80 \mu\text{A} = \frac{1}{2} \left( 40 \frac{\mu\text{A}}{V^2} \right) \left( \frac{W}{L} \right)_P [-2.5 - (-0.6)]^2 V^2$$

which gives  $\left( \frac{W}{L} \right)_P = \frac{1.11}{1}$ .

#### Calculation of $V_H$ and $(W/L)_S$

In order to calculate  $(W/L)_S$ , we need to determine the high output level  $V_H$ , since this is the voltage that is used to drive switching transistor  $M_S$  to achieve  $v_O = V_L$ . As shown in Fig. 6.24(b), the PMOS load transistor has a fixed value of  $V_{GS} = -2.5$  V. Thus it will always be in the conducting state. With  $M_S$  off, current will flow through the PMOS device to charge the output node until the drain-source voltage  $V_{DS}$  of the transistor collapses to zero. Thus,  $V_H = V_{DD}$ , just as for the inverter with the resistor load.

Now, the conditions for switching transistor  $M_S$  with  $v_O = V_L$  in Fig. 6.24(a) are  $V_{GS} = V_H = 2.5$  V and  $V_{DS} = V_L = 0.20$  V with  $i_D = 80 \mu\text{A}$ . These are identical to those of the switching

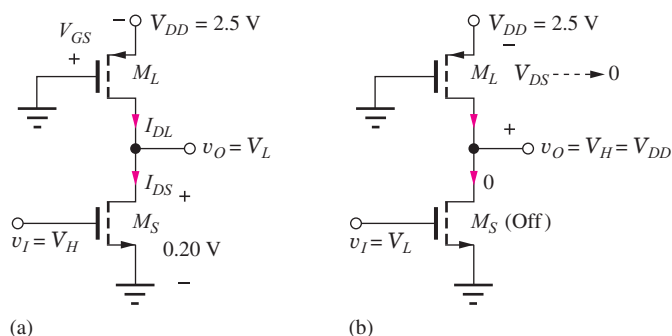
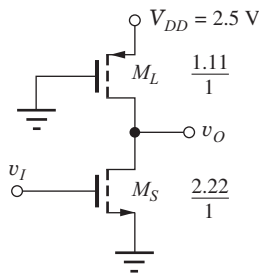
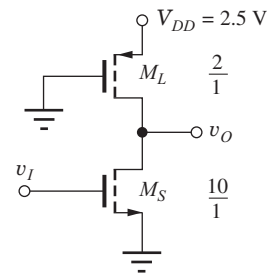


Figure 6.24 Pseudo NMOS Inverter with (a)  $v_I = V_H$  and (b)  $v_I = V_L$ .



**Figure 6.25** Completed pseudo NMOS inverter design.



**Figure 6.26** Pseudo NMOS inverter used in Ex. 6.8.

transistor in the resistor load inverter in Section 6.5.2. Thus,  $(W/L)_S = 2.22/1$ . The completed pseudo NMOS inverter design appears in Fig. 6.25.

**EXERCISE:** Verify the value of  $(W/L)_S$  by calculating the drain current of  $M_S$ .

### EXAMPLE 6.8

#### LOGIC LEVEL ANALYSIS FOR THE PSEUDO NMOS INVERTER

Finding the logic levels associated with someone else's inverter design involves a different thought process than that required to design the inverter. Here we find  $V_H$  and  $V_L$  for a specified inverter design.

**PROBLEM** Find the high and low logic levels and the power supply current for the pseudo NMOS inverter in Fig. 6.26 with  $(W/L)_S = 10/1$  and  $(W/L)_L = 2/1$ . The inverter operates with  $V_{DD} = 2.5$  V. Assume  $K'_n = 100 \mu\text{A}/\text{V}^2$ ,  $V_{TN} = 0.60$  V,  $K'_p = 40 \mu\text{A}/\text{V}^2$ ,  $V_{TP} = -0.60$  V.

**SOLUTION** **Known Information and Given Data:** Circuit topology in Fig. 6.26;  $V_{DD} = 2.5$  V,  $(W/L)_N = 10/1$ ,  $(W/L)_P = 2/1$ ,  $K'_n = 100 \mu\text{A}/\text{V}^2$ ,  $V_{TN} = 0.60$  V,  $K'_p = 40 \mu\text{A}/\text{V}^2$ , and  $V_{TP} = -0.60$  V.

**Unknowns:**  $V_H$ ,  $V_L$ ,  $I_{DD}$  for both logic states

**Approach:** First determine  $V_H$ . Use  $V_H$  and the specified transistor parameters to find  $V_L$  by equating the drain currents in the switching and load transistors. Use  $V_L$  to find power supply current  $I_{DD}$  which is equal to switching transistor drain current  $I_{DS}$ .

**Assumptions:**  $M_S$  is off for  $v_I = V_L$ . For  $v_O = V_L$ ,  $M_S$  operates in the triode region, and  $M_L$  is in the saturation region.

**Analysis:** First we find  $V_H$ , and then we use it to find  $V_L$ . For the pseudo NMOS logic gate,  $V_H = V_{DD}$ . Thus, for our circuit,  $V_H = 2.5$  V. To find  $V_L$ , we use the condition that the two transistor drain currents must be equal in the steady state:  $I_{DS} = I_{DL}$ . For  $v_O = V_L$ , we expect that the load transistor will be saturated since the magnitude of its drain-source voltage is large ( $V_{DS} = V_L - V_{DD}$ ), and we expect the switching transistor to be in the triode region since its drain-source voltage will be small ( $V_{DS} = V_L$ ). For  $I_{DS} = I_{DL}$ , we have

$$K'_n \left( \frac{10}{1} \right) \left( V_{GSN} - V_{TN} - \frac{V_L}{2} \right) V_L = \frac{K'_p}{2} \left( \frac{2}{1} \right) (V_{GSP} - V_{TP})^2$$

For the circuit in Fig. 6.24,  $V_{GSN} = 2.5$  V and  $V_{GSP} = -2.5$  V, and

$$100 \frac{\mu\text{A}}{\text{V}^2} \left( \frac{10}{1} \right) \left( 2.5 - 0.6 - \frac{V_L}{2} \right) V_L = \frac{40 \mu\text{A}}{2 \text{ V}^2} \left( \frac{2}{1} \right) (-2.5 - (-0.6))^2$$

which can be rearranged to yield a quadratic equation:

$$12.5V_L^2 - 47.5V_L + 3.61 = 0 \quad \text{for which} \quad V_L = 0.0776 \text{ V, } 3.72 \text{ V.}$$

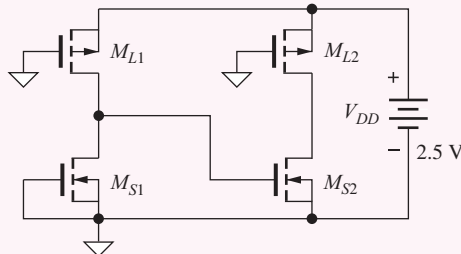
$V_L = 3.72 \text{ V}$  exceeds the 2.5-V power supply, so that answer must be discarded. Hence the answer must be  $V_L = 0.0776 \text{ V}$ . For this value of  $V_L$ , the current in  $M_S$  is

$$I_{DS} = \left( 100 \frac{\mu\text{A}}{V^2} \right) \left( \frac{10}{1} \right) \left( 2.5 - 0.6 - \frac{0.0776}{2} \right) (0.0776)V^2 = 144 \mu\text{A}$$

**Check of Results:** For  $V_L$ , we should check our triode and saturation region assumptions for the two MOSFETs: For the switching transistor,  $V_{GS} - V_{TN} = 2.5 - 0.6 = 1.90 \text{ V}$  which is greater than  $V_{DS} = 0.078 \text{ V}$ , and the triode region assumption is correct. For the load device,  $V_{GS} - V_{TN} = -2.5 - (-0.6) = -1.9 \text{ V}$ , and  $V_{DS} = 0.078 - 2.5 = -2.42$ , which are consistent with the saturation region of operation. We can further check our results by finding the drain current in  $M_L$ :

$$I_{DL} = \left( \frac{40 \mu\text{A}}{2 V^2} \right) \left( \frac{2}{1} \right) (-2.5 + 0.6)^2 = 144 \mu\text{A} \quad \text{which agrees with } I_{DS}.$$

**Computer-Aided Analysis:** To verify our design with SPICE, we draw the circuit with a schematic capture tool. Two inverters are cascaded in order to get both  $V_H$  and  $V_L$  with one simulation. The gate of  $MS_1$  is grounded to force  $MS_1$  to be off. The NMOS transistor uses the LEVEL = 1 model with  $KP = 10E-5$ ,  $VTO = 0.60 \text{ V}$ ,  $GAMMA = 0.5$  and  $PHI = 0.6 \text{ V}$ , and the PMOS parameters are  $KP = 4E-5$ ,  $VTO = -0.60 \text{ V}$ ,  $GAMMA = 0.5$  and  $PHI = 0.6 \text{ V}$ . The transistor sizes are specified as  $W = 10 \text{ U}$  and  $L = 1 \text{ U}$  for  $M_S$ , and  $W = 2 \text{ U}$  and  $L = 1 \text{ U}$  for  $M_L$ . SPICE gives  $V_H = 2.50 \text{ V}$  and  $V_L = 0.0776 \text{ V}$ . The current in  $V_{DD}$  is  $144 \mu\text{A}$ . All the values agree with the hand calculations.



**EXERCISE:** Use the “Solver” in your calculator to check the value of  $V_L$  found in Section 6.7.2.

**EXERCISE:** Repeat the calculations with  $(W/L)_S = 5/1$ . Check your results with SPICE.

**ANSWERS:** 2.50 V, 0.159 V, 144  $\mu\text{A}$ .

### Noise Margin Analysis for the Pseudo NMOS Inverter

Let us now find the noise margins for the pseudo NMOS inverter. We need to calculate the values of  $V_{IL}$ ,  $V_{OL}$ ,  $V_{IH}$ , and  $V_{OH}$  and remember these voltages are defined by the points on the voltage transfer characteristic at which the slope  $dv_O/dv_I = -1$ , as indicated on the graph in Fig. 6.27.

First let us find  $V_{IL}$  and  $V_{OH}$ . We need to find a relationship between  $v_I$  and  $v_O$  that we can differentiate. Remember that the drain currents in the switching and load devices must be equal at all points on the static VTC. Also, at  $v_I = V_{IL}$  the input will be at a relatively low voltage, and the

output will be a relatively high voltage. Thus, we guess that  $M_S$  will be operating in the saturation region and that  $M_L$  will operate in the triode region. Setting  $i_{DS} = i_{DL}$  yields

$$\frac{K_S}{2}(v_I - V_{TN})^2 = K_L \left( -V_{DD} - V_{TP} - \frac{v_O - V_{DD}}{2} \right) (v_O - V_{DD})$$

with

$$K_S = K'_n \left( \frac{W}{L} \right)_S \quad \text{and} \quad K_L = K'_p \left( \frac{W}{L} \right)_L \quad (6.29)$$

The point of interest is  $\frac{\partial v_O}{\partial v_I} = -1$ , but solving for the value of  $v_O$  would be quite tedious. Since we expect the derivatives to be smooth, continuous, and nonzero, we will assume that  $\frac{\partial v_O}{\partial v_I} = \left( \frac{\partial v_I}{\partial v_O} \right)^{-1}$  and solve for  $v_I$  in terms of  $v_O$ :

$$v_I = V_{TN} + \frac{1}{\sqrt{K_R}} \sqrt{[2(V_{DD} + V_{TP}) - (V_{DD} - v_O)](V_{DD} - v_O)} \quad \text{where} \quad K_R = \frac{K_S}{K_L}$$

Evaluating the derivative is still quite tedious, so only the results are given here:<sup>6</sup>

$$V_{IL} = V_{TN} + \frac{(V_{DD} + V_{TP})}{\sqrt{K_R^2 + K_R}} \quad \text{and} \quad V_{OH} = V_{DD} - (V_{DD} + V_{TP}) \left( 1 - \sqrt{\frac{K_R}{K_R + 1}} \right) \quad (6.30)$$

For the inverter design of Fig. 6.26 with  $V_{DD} = 2.5$  V,  $V_{TP} = -0.6$  V and  $K_R = (2.22)(100)/(1.11)(40) = 5$ , we find

$$V_{IL} = 0.6 + \frac{(2.5 - 0.6)}{\sqrt{(5)^2 + 5}} = 0.95 \text{ V} \quad \text{and} \quad V_{OH} = 2.5 - (2.5 - 0.6) \left( 1 - \sqrt{\frac{5}{5+1}} \right) = 2.33 \text{ V}$$

These values appear reasonable. The input must exceed the threshold voltage of the NMOS transistor before it begins to conduct, so  $V_{IL}$  should be somewhat larger than  $V_{TN}$ , and the value of  $V_{OH}$  should be somewhat below  $V_{DD}$  as in Fig. 6.27.

With these values we can check our assumptions of the operating regions of  $M_S$  and  $M_L$ . For the NMOS switching transistor,  $V_{GS} - V_{TN} = 0.95 - 0.6 = 0.35$  V and  $V_{DS} = 2.33$  V. Since  $V_{DS} > V_{GS} - V_{TN}$ , the saturation region assumption was correct. For the PMOS load device,  $V_{GS} - V_{TP} = -2.5 - (-0.6) = -1.9$  V and  $V_{DS} = 2.33 - 2.5 = -0.17$  V. Since the magnitude of  $V_{DS}$  is less than that of  $V_{GS} - V_{TP}$ , the triode region assumption was correct.

A similar process is used to find  $V_{IH}$  and  $V_{OL}$ . We again observe that the drain currents in the switching and load devices must be equal. At  $v_I = V_{IH}$ , the input will be at a relatively high voltage, and the output will be at a relatively low voltage. Thus, we guess that  $M_S$  will operate in the triode region and  $M_L$  will be in the saturation region. Equating drain currents in the switching and load transistors yields

$$K_S \left( v_I - V_{TN} - \frac{v_O}{2} \right) v_O = \frac{K_L}{2} (-V_{DD} - V_{TP})^2 \quad (6.31)$$

We again assume that  $\frac{\partial v_O}{\partial v_I} = \left( \frac{\partial v_I}{\partial v_O} \right)^{-1}$  and solve for  $v_I$  in terms of  $v_O$ :

$$v_I = V_{TN} + \frac{v_O}{2} + \frac{(V_{DD} + V_{TP})^2}{2K_R} \left( \frac{1}{v_O} \right) \quad \text{where} \quad K_R = \frac{K_S}{K_L} \quad (6.32)$$

---

<sup>6</sup> The details of the derivation can be found on the MCD website.

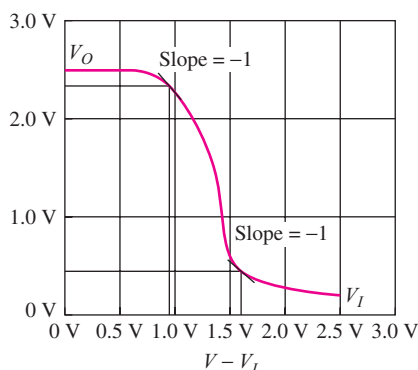


**Figure 6.27** PSPICE simulation of the voltage transfer function for the pseudo NMOS inverter.

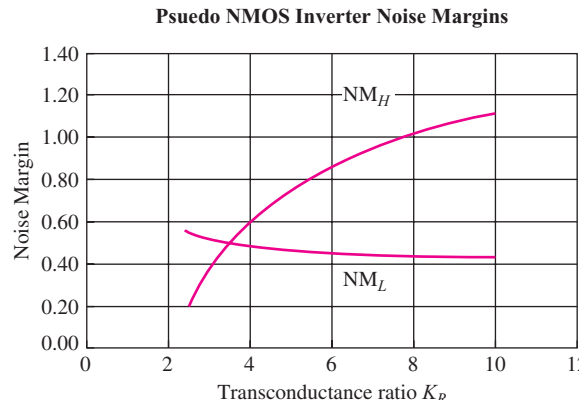


**Figure 6.28** Noise margins versus transconductance ratio  $K_R$  for the pseudo NMOS inverter with  $V_{DD} = 2.5$  V,  $V_{TN} = 0.6$  V and  $V_{TP} = -0.6$  V.

Taking the derivative

$$\frac{\partial v_1}{\partial v_O} = \frac{1}{2} - \frac{1}{2K_R} \frac{(V_{DD} + V_{TP})^2}{v_O^2} \quad (6.33)$$

and setting it equal to  $-1$  at  $v_O = V_{OL}$  yields

$$-1 = \frac{1}{2} - \frac{1}{2K_R} \frac{(V_{DD} + V_{TP})^2}{V_{OL}^2} \quad \text{or} \quad V_{OL} = \frac{V_{DD} + V_{TP}}{\sqrt{3K_R}}$$

Substituting this result in Eq. (6.32) with  $v_I = V_{IH}$  gives

$$V_{IH} = V_{TN} + \frac{2(V_{DD} + V_{TP})}{\sqrt{3K_R}} = V_{TN} + 2V_{OL} \quad (6.34)$$

For the inverter design of Fig. 6.26,

$$V_{OL} = \frac{V_{DD} + V_{TP}}{\sqrt{3K_R}} = \frac{(2.5 - 0.6)}{\sqrt{3(5)}} = 0.491 \text{ V} \quad \text{and} \quad V_{IH} = 0.6 + 2(0.49) = 1.58 \text{ V} \quad (6.35)$$

With these values we should again check our assumptions of the operating regions of  $M_S$  and  $M_L$ . For the NMOS switching transistor,  $V_{GS} - V_{TN} = 1.58 - 0.6 = 0.98$  V and  $V_{DS} = 0.491$  V. Since  $V_{DS} < V_{GS} - V_{TN}$ , the triode region assumption was correct. For the PMOS load device,  $V_{GS} - V_{TP} = -2.5 - (-0.6) = -1.9$  V and  $V_{DS} = 0.491 - 2.5 = -2.01$  V. Since the magnitude of  $V_{DS}$  exceeds that of  $V_{GS} - V_{TP}$ , the saturation region assumption was correct. In Fig. 6.27, it can be seen that these calculated values of  $V_{IL}$ ,  $V_{OL}$ ,  $V_{IH}$  and  $V_{OH}$  all agree well with SPICE simulation results.

The noise margins for this pseudo NMOS inverter are

$$NM_H = V_{OH} - V_{IH} = 2.33 - 1.58 = 0.75 \text{ V}$$

$$NM_L = V_{IL} - V_{OL} = 0.95 - 0.49 = 0.46 \text{ V}$$

With Eqs. (6.30)–(6.35), we can easily explore the dependence of the noise margins on transconductance ratio  $K_R$ , and the results are plotted in Fig. 6.28. High-state noise margin  $NM_H$  increases monotonically as the drive capacity of switching transistor  $M_S$ , and hence  $K_R$ , increases, whereas  $NM_L$  gradually decreases.

## 6.7 NMOS INVERTER SUMMARY AND COMPARISON

Figure 6.29 and Table 6.6 summarize the NMOS inverter designs discussed in Secs. 6.5 and 6.6. The gate with the resistive load takes up too much area to be implemented in IC form. The saturated load configuration is the simplest circuit, using only NMOS transistors. However, it has a disadvantage

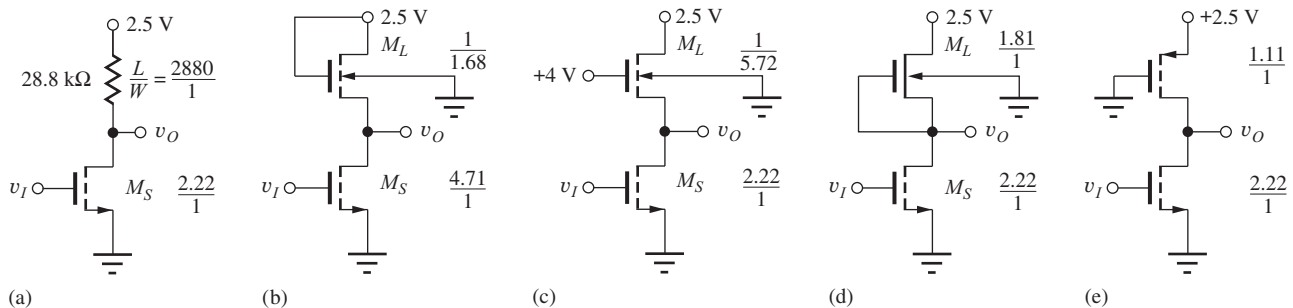


**Figure 6.29** Comparison of various NMOS inverter designs: (a) Inverter with resistor load, (b) saturated load inverter, (c) linear load inverter, (d) inverter with depletion-mode load, (e) pseudo NMOS inverter.

**TABLE 6.6**  
Inverter Characteristics

	INVERTER WITH RESISTOR LOAD	SATURATED LOAD INVERTER	LINEAR LOAD INVERTER	INVERTER WITH DEPLETION-MODE LOAD	PSEUDO NMOS INVERTER
$V_H$	2.50 V	1.55 V	2.50 V	2.50 V	2.50 V
$V_L$	0.20 V	0.20 V	0.20 V	0.20 V	0.20 V
$N_{ML}$	0.25 V	0.22 V	0.12 V	0.43 V	0.46 V
$N_{MH}$	0.96 V	0.33 V	0.96 V	0.90 V	0.75 V
Relative Area ( $\mu\text{m}^2$ )	2880	6.39	7.94	4.03	3.33

that the high logic state no longer reaches the power supply. Also, in Sec. 6.11, the speed of the saturated load gate will be demonstrated to be poorer than that of other circuit implementations. The linear load circuit solves the logic level and speed problems but requires an additional costly power supply voltage that causes wiring congestion problems in IC designs.

Following successful development of the ion-implantation process and invention of depletion-mode load technology, NMOS circuits with depletion-mode load devices quickly became the circuit of choice. From Fig. 6.29 and Table 6.6, we see that the additional process complexity is traded for a simple inverter topology that gives  $V_H = V_{DD}$  with small overall transistor sizes. At the same time, the depletion-load gate yields the best combination of noise margins. At the end of the chapter, we will find that the depletion load gate also yields the highest speed of the four circuit configurations. The depletion-mode load in Sec. 6.11 tends to act as a current source during most of the output transition, and it offers high speed with significantly reduced area compared to the other purely NMOS inverter circuits. In pseudo NMOS, the PMOS load transistor acts as a current source during much of the output transition, and it offers the best speed with smallest area. We will refer to the gate designs of Fig. 6.29 as our **reference inverter designs** and use these circuits as the basis for more complex designs in subsequent sections.

Because of its many advantages, depletion-mode NMOS logic was the dominant technology for many years in the design of microprocessors. However, the large static power dissipation inherent in NMOS logic eventually limited further increases in IC chip density, and a rapid shift took place to the more complex CMOS technology, which is discussed in detail in the next chapter.

## 6.8 NMOS NAND AND NOR GATES

A complete logic family must provide not only the logical inversion function but also the ability to form some combination of at least two input variables such as the AND or OR function. In NMOS logic, an additional transistor can be added to the simple inverter to form either a NOR or

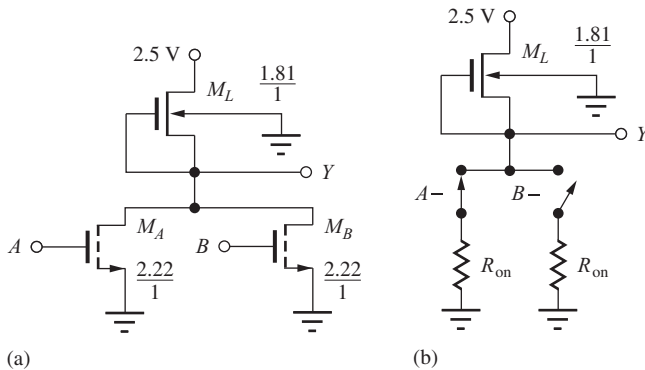


**Figure 6.30** (a) Two-input NMOS NOR gate:  $Y = \overline{A + B}$ . (b) Simplified model with switching transistor A on.

**TABLE 6.7**  
NOR Gate Truth Table

A	B	$Y = \overline{A + B}$
0	0	1
0	1	0
1	0	0
1	1	0

a NAND logic gate. The NOR gate represents the combination of an OR operation followed by inversion, and the NAND function represents the AND operation followed by inversion. One of the advantages of MOS logic is the ease with which both the NOR and NAND functions can be implemented. The switching devices inherently provide the inversion operation, whereas series and parallel combinations of transistors produce the AND and OR operations, respectively.

In the following discussion, remember that we use the positive logic convention to relate voltage levels to logic variables: a high logic level corresponds to a logical 1 and a low logic level corresponds to a logical 0:

$$V_H \equiv 1 \quad \text{and} \quad V_L \equiv 0$$

### 6.8.1 NOR GATES

In Fig. 6.30, switching transistor  $M_S$  of the inverter has been replaced with two devices,  $M_A$  and  $M_B$ , to form a two-input NOR gate. If either one, or both, of the inputs  $A$  and  $B$  is in the high logic state, a current path will exist through at least one of the two switching devices, and the output will be in the low logic state. Only if inputs  $A$  and  $B$  are both in the low state will the output of the gate be in the high logic state. The truth table for this gate, Table 6.7, corresponds to that of the NOR function  $Y = \overline{A + B}$ .

We will pick the size of the devices in our logic gates based on the reference inverter design defined at the end of Sec. 6.7 [Fig. 6.29(d)]. The size of the various transistors must be chosen to ensure that the gate meets the desired logic level and power specifications under the worst-case set of logic inputs.

Consider the simplified schematic for the two-input NOR gate in Fig. 6.30(b). The worst-case condition for the output low state occurs when either  $M_A$  or  $M_B$  is conducting alone, so the on-resistance  $R_{on}$  of each individual transistor must be chosen to give the desired low output level. Thus,  $(W/L)_A$  and  $(W/L)_B$  should each be equal to the size of  $M_S$  in the reference inverter (2.22/1). If  $M_A$  and  $M_B$  both happen to be conducting ( $A = 1$  and  $B = 1$ ), then the combined on-resistance will be equivalent to  $R_{on}/2$ , and the actual output voltage will be lower than the original design value of  $V_L = 0.20$  V.

When either  $M_A$  or  $M_B$  is conducting alone, the current is limited by the load device, and the voltages are exactly the same as in the reference inverter.<sup>7</sup> Thus, the  $W/L$  ratio of the load device is the same as in the reference inverter (1.81/1). The completed NOR gate design is given in Fig. 6.30(a).

<sup>7</sup> Actually, the worst-case situation for current in the load device occurs when  $M_A$  and  $M_B$  are both on because the voltage is slightly higher across the load device, and its value of  $V_{SB}$  is smaller. However, this effect is small enough to be neglected. See Prob. 6.97.

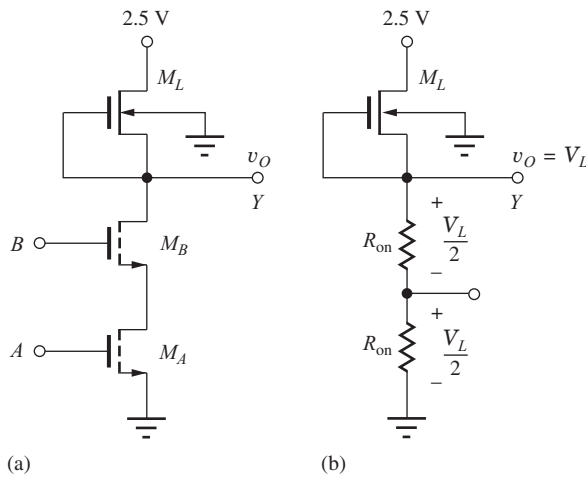


Figure 6.31 Two-input NMOS NAND gate:  $Y = \overline{AB}$ .

**TABLE 6.8**  
NAND Gate Truth Table

A	B	$Y = \overline{AB}$
0	0	1
0	1	1
1	0	1
1	1	0

**EXERCISE:** Draw the schematic of a three-input NOR gate. What are the  $W/L$  ratios for the transistors based on Fig. 6.30?

**ANSWERS:** Add a third transistor  $M_C$  between the output mode and ground.  $1.81/1; 2.22/1; 2.22/1; 2.22/1$ .

## 6.8.2 NAND GATES

In Fig. 6.31(a), a second NMOS transistor has been added in series with the original switching device of the basic inverter to form a two-input NAND gate. Now, if inputs  $A$  and  $B$  are *both* in a high logic state, a current path exists through the series combination of the two switching devices, and the output is in a low logic state. If either input  $A$  or input  $B$  is in the low state, then the conducting path is broken and the output of the gate is in the high state. The truth table for this gate, Table 6.8, corresponds to that of the NAND function  $Y = \overline{AB}$ .

### Selecting the Sizes of the Switching Transistors

The sizes of the devices in the NAND logic gate are again chosen based on the reference inverter design from Fig. 6.29(d). The  $W/L$  ratios of the various transistors must be selected to ensure that the gate still meets the desired logic level and power specifications under the worst-case set of logic inputs. Consider the simplified schematic for the two-input NAND gate in Fig. 6.31(b). The output low state occurs when both  $M_A$  and  $M_B$  are conducting. The combined on-resistance will now be equivalent to  $2R_{on}$ , where  $R_{on}$  is the on-resistance of each individual transistor conducting alone. In order to achieve the desired low level,  $(W/L)_A$  and  $(W/L)_B$  must both be approximately twice as large as the  $W/L$  ratio of  $M_S$  in the reference inverter because the on-resistance of each device in the triode region is inversely proportional to the  $W/L$  ratio of the transistor:

$$R_{on} = \frac{v_{DS}}{i_D} = \frac{1}{K'_n \frac{W}{L} \left( v_{GS} - V_{TN} - \frac{v_{DS}}{2} \right)} \quad (6.36)$$

A second way to approach the choice of device sizes is to look at the voltage across the two switching devices when  $v_O$  is in the low state. For our design,  $V_L = 0.20\text{ V}$ . If we assume that one-half of this voltage is dropped across each of the switching transistors and that  $(v_{GS} - V_{TN}) \gg v_{DS}/2$ ,

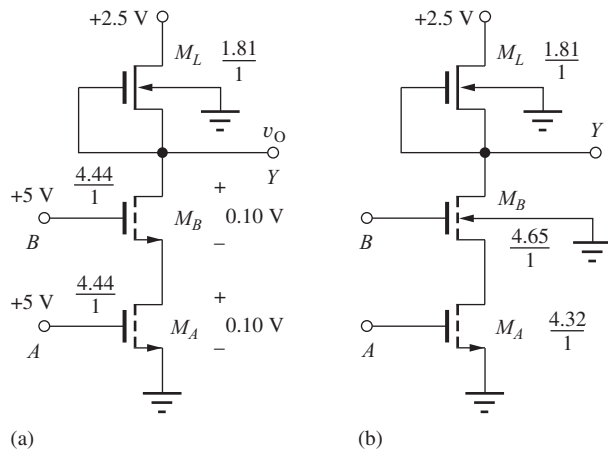


**Figure 6.32** NMOS NAND gate:  $Y = \overline{AB}$ : (a) approximate design, (b) corrected design.

then it can be seen from

$$i_D = K'_n \left( \frac{W}{L} \right)_S (v_{GS} - V_{TN} - 0.5v_{DS})v_{DS} \cong K'_n \left( \frac{W}{L} \right)_S (v_{GS} - V_{TN})v_{DS} \quad (6.37)$$

that the  $W/L$  of the transistors must be approximately doubled in order to keep the current at the same value. Figure 6.32(a) shows the NAND gate design based on these arguments.

Two approximations have crept into this analysis. First, the source-bulk voltages of the two transistors are not equal, and therefore the values of the threshold voltages are slightly different for  $M_A$  and  $M_B$ . Second,  $V_{GSA} \neq V_{GSB}$ . From Fig. 6.32(a),  $V_{GSA} = 2.5$  V, but  $V_{GSB} = 2.4$  V. The results of taking these two effects into account are shown in Fig. 6.32(b). (Verification of these  $W/L$  values is left for Prob. (6.82). The corrected device sizes have changed by only a small amount. The approximate results in Fig. 6.32(a) represent an adequate level of design for most purposes.

### Choosing the Size of the Load Device

When both  $M_A$  and  $M_B$  are conducting, the current is limited by the load device, but the voltages applied to the load device are exactly the same as those in the reference inverter design. Thus, the  $W/L$  ratio of the load device is the same as in the reference inverter. The completed NAND gate design, based on the simplified device sizing, is given in Fig. 6.32(a).

**EXERCISE:** Draw the schematic of a three-input NAND gate. What are the  $W/L$  ratios for the transistors based on Fig. 6.32(a)?

**ANSWERS:** 1.81/1; 6.66/1; 6.66/1; 6.66/1

### 6.8.3 NOR AND NAND GATE LAYOUTS IN NMOS DEPLETION-MODE TECHNOLOGY

Sample layouts for two-input NOR and two-input NAND gates appear in Fig. 6.33 based on ground rules similar to those discussed in Chapter 4. The metal overlap has been reduced in the layout to make the figure clearer.

The NOR gate has the sources and drains of switching transistors  $A$  and  $B$  connected in parallel using the  $n^+$  layer. The source of the load device is also connected to the common drain region of the switching transistors using the  $n^+$  layer. The gate of the load device is connected to the switching transistors using the metal layer, which also is the output terminal.

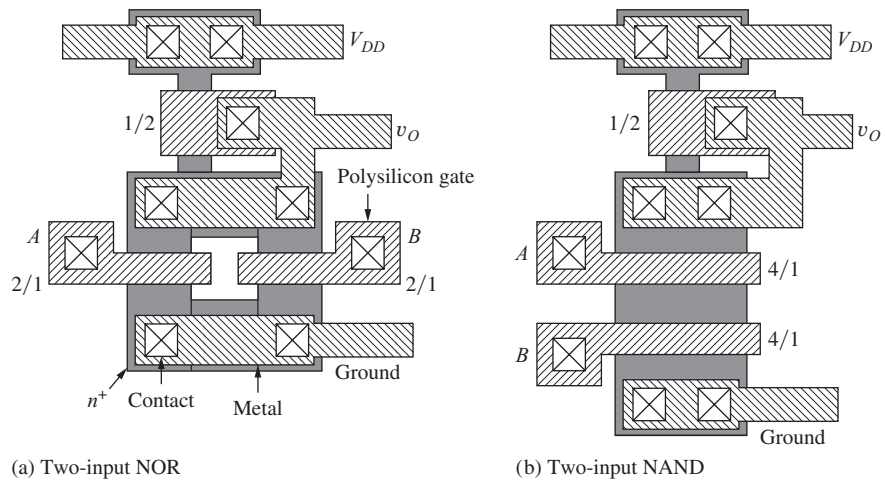


**Figure 6.33** Possible layouts for (a) two-input NOR gate and (b) two-input NAND gate.

Input transistors  $A$  and  $B$  are stacked above each other in the NAND gate layout. Note that the source of transistor  $A$  and the drain of transistor  $B$  are the same  $n^+$  region; no contacts are required between the transistors. The widths of transistors  $A$  and  $B$  have been made twice as wide to maintain the desired low output level, whereas the size of the load transistor remains unchanged.

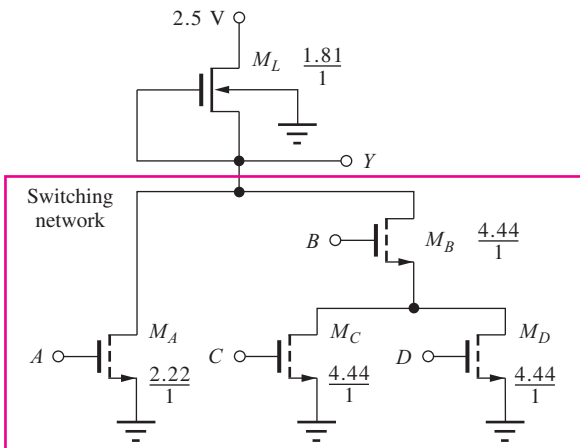


**Figure 6.34** Complex NMOS logic gate:  $Y = \overline{A + BC + BD}$ .

## 6.9 COMPLEX NMOS LOGIC DESIGN

A major advantage of MOS logic over most forms of bipolar logic comes through the ability to directly combine NAND and NOR gates into more complex configurations. Three examples of **complex logic gate** design are discussed in this section.

Consider the circuit in Fig. 6.34. The output  $Y$  will be in a low state whenever a conducting path is developed through the switching transistor network. For this circuit, the output voltage will be low if any one of the following paths is conducting:  $A$  or  $BC$  ( $B$  and  $C$ ) or  $BD$  ( $B$  and  $D$ ). The output  $Y$  is represented logically as

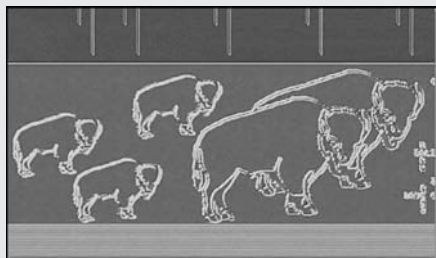
$$Y = \overline{A + BC + BD} \quad \text{or} \quad Y = \overline{A + B(C + D)}$$



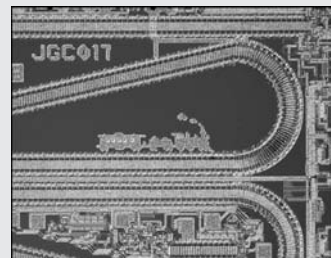
## ELECTRONICS IN ACTION

### Silicon Art

Successful integrated circuit designers are typically a very creative group of people. In the course of a large chip design project, engineers generate numerous innovations. The process involves many long hours leading up to the release of the chip layout data to manufacturing.



A small herd of buffalo added to a Hewlett-Packard 64-bit combinatorial divider created by HP engineer Dick Vlach.



A train found on an analog shift register from a LeCroy MVV200 integrated circuit.



A roadrunner drawn in aluminum on silicon by Dan Zuras of Hewlett-Packard.



A compass placed on a prototype optical navigation chip by Hewlett-Packard Labs designer Travis Blalock.

As the end of the design process nears, exhausted designers often want to add a more personal imprint on their work. Traditionally this has taken the form of using patterns in the metal layers of the chip layout to create graphical images relating to the chip's internal code name.

Sadly, most modern IC foundries are now forbidding designers to express themselves in this way over concerns about design rule violations and potential processing problems. Designers tell us that this has forced them to become covert with their doodles and they are sometimes embedding the graphics directly into functional design structures.



which directly implements a complemented **sum-of-products logic function**. This logic gate is most commonly referred to as the **AND-OR-INVERT** or **AOI** gate, and it is widely used as one of the basic building blocks in chips such as field programmable logic arrays (FPGAs). The AND terms ( $A^8, BC, BD$ ) are formed by vertical stacking of two transistors. These paths are then placed in parallel to form the OR function, and the logic gate inherently provides the logical inversion.

<sup>8</sup>  $A = A \cdot 1$

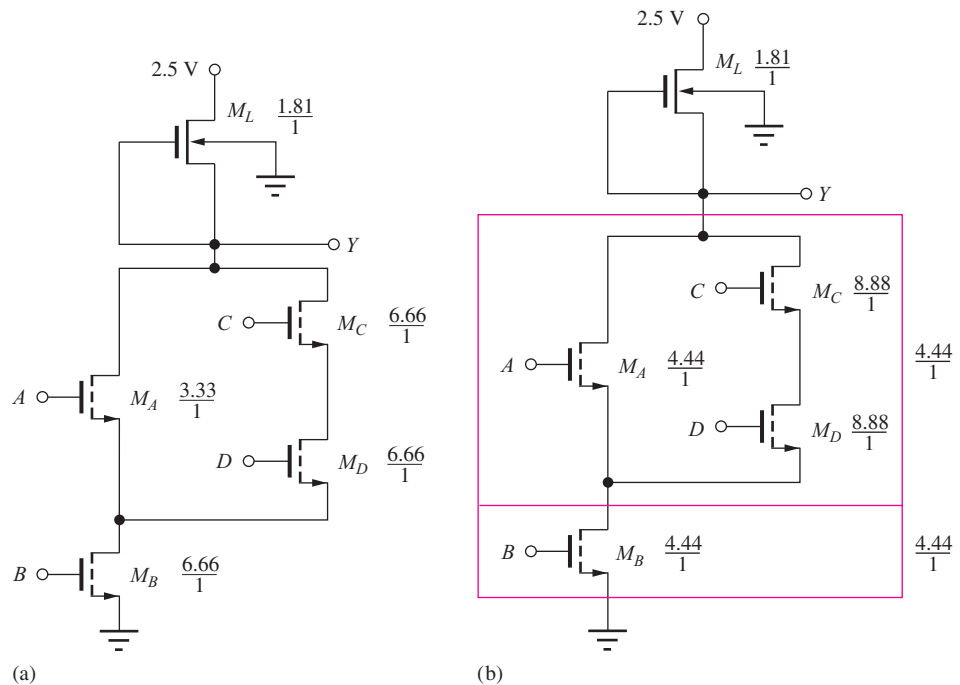


**Figure 6.35** (a) NMOS implementation of  $Y = \overline{AB + CDB}$  or  $Y = \overline{(A + CD)B}$ . (b) An alternate transistor sizing for the logic gate in (a).

In the final minimum size version in Fig. 6.34, it is recognized that transistor  $B$  need not be replicated. Device sizing is again based on the worst-case logic state situations. Referring to the reference inverter design, device  $M_A$  must have  $W/L = 2.22/1$  because it must be able to maintain the output at 0.20 V when it is the only device that is conducting. In the other two paths,  $M_B$  will appear in series with either  $M_C$  or  $M_D$ . Thus, in the worst case, there will be two devices in series in this path, and the simplest choice will be  $M_B = M_C = M_D = 4.44/1$ . The load device size remains unchanged.

The circuit in Fig. 6.35 provides a second example of transistor sizing in complex logic gates. There are two possible conducting paths through the switching transistor network:  $AB$  ( $A$  and  $B$ ) or  $CDB$  ( $C$  and  $D$  and  $B$ ). The output will be low if either path is conducting, resulting in

$$Y = \overline{AB + CDB} \quad \text{or} \quad Y = \overline{(A + CD)B}$$

Transistor sizing can be done in two ways. In the first method, we find the worst-case path in terms of transistor count. For this example, path  $CDB$  has three transistors. By making each transistor three times the size of the reference switching transistor, the  $CDB$  path will have an on-resistance equivalent to that of  $M_S$  in the reference inverter. Thus, each of the three transistors should have  $W/L = 6.66/1$ .

The second path contains transistors  $M_A$  and  $M_B$ . In this path, we want the sum of the on-resistances of the devices to be equal to the on-resistance of  $M_S$  in the reference inverter:

$$\frac{R_{\text{on}}}{\left(\frac{W}{L}\right)_A} + \frac{R_{\text{on}}}{\left(\frac{W}{L}\right)_B} = \frac{R_{\text{on}}}{\left(\frac{W}{L}\right)_S} \quad (6.38)$$

In Eq. (6.38),  $R_{on}$  represents the on-resistance of a transistor with  $W/L = 1/1$ . Because  $(W/L)_B$  has already been chosen,

$$\frac{R_{on}}{\left(\frac{W}{L}\right)_A} + \frac{R_{on}}{6.66} = \frac{R_{on}}{2.22} \quad (6.39)$$

Solving for  $(W/L)_A$  yields a value of  $3.33/1$ . Because the operating current of the gate is to be the same as the reference inverter, the geometry of the load device remains unchanged. The completed design values appear in Fig. 6.35(a).

A slightly different approach is used to determine the transistor sizes for the same logic gate in Fig. 6.35(b). The switching circuit can be partitioned into two sub-networks connected in series: transistor  $B$  in series with the parallel combination of  $A$  and  $CD$ . We make the equivalent on-resistance of these two subnetworks equal. Because the two subnetworks are in series,  $(W/L)_B = 2(2.22/1) = 4.44/1$ . Next, the on-resistance of each path through the  $(A + CD)$  network should also be equivalent to that of a  $4.44/1$  device. Thus  $(W/L)_A = 4.44/1$  and  $(W/L)_C = (W/L)_D = 8.88/1$ . These results appear in Fig. 6.35(b).

### Selecting Between the Two Designs

If the unity dimension corresponds to the minimum feature size  $F$ , then the total gate area of the switching transistors for the design in Fig. 6.35(b) is  $28.5F^2$ . The previous implementation of Fig. 6.35(a) had a total gate area of  $25.1F^2$ . With this yardstick, the second design requires 13 percent more area than the first. Minimum area utilization is often a key consideration in IC design, and the device sizes in Fig. 6.35(a) would be preferred over those in Fig. 6.35(b).

## DESIGN EXAMPLE 6.9

### TRANSISTOR SIZING IN COMPLEX LOGIC GATES

**PROBLEM** Choose the transistor sizes for a complex logic gate based on a given reference inverter design.

**SOLUTION** Find the logic expression for the gate in Fig. 6.36. Design the  $W/L$  ratios of the transistors based on the pseudo NMOS reference inverter in Fig. 6.29(e).

**Known Information and Given Data:** Logic circuit diagram in Fig. 6.36; reference inverter design in Fig. 6.29(e) with  $(W/L)_S = 2.22/1$  and  $(W/L)_L = 1.11/1$ .

**Unknowns:** Logic expression for output  $Y$ ;  $W/L$  ratios for all the transistors

**Approach:** Identify the conducting paths that force the output low; output  $Y$  can be represented as a complemented sum-of-products function of the conducting path descriptions. Size the transistors in each path to yield the same on-resistance as the reference inverter.

**Assumptions:** Neglect the effects of the non-zero source-bulk voltages on the switching transistors. Neglect  $V_{GS}$  differences among the switching transistors.

**Analysis:** Comparing the circuit in Fig. 6.36 to that in 6.35, we see that a fifth transistor has been added to the switching network. Now there are *four* possible conducting paths through the switching transistor network:  $AB$  or  $CDB$  or  $CE$  or  $ADE$ . The output will be low when any one of these paths is conducting, resulting in

$$Y = \overline{AB + CDB + CE + ADE}$$

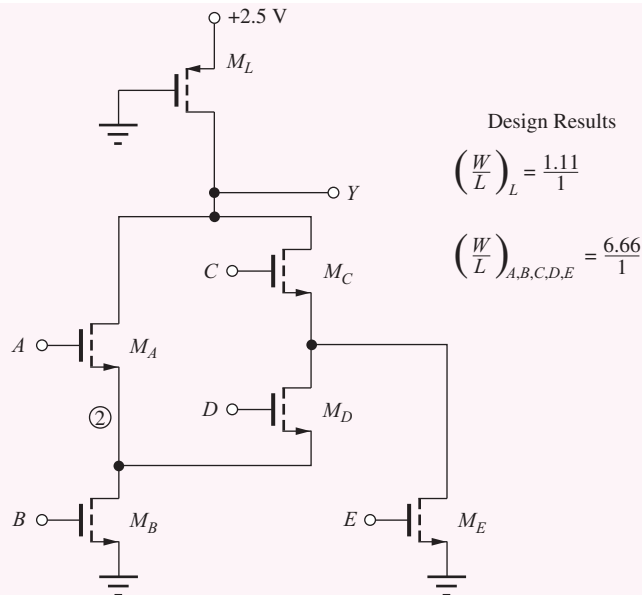


**Figure 6.36** NMOS implementation of  $Y = \overline{AB} + C\overline{D}\overline{B} + C\overline{E} + \overline{A}\overline{D}\overline{E}$ .

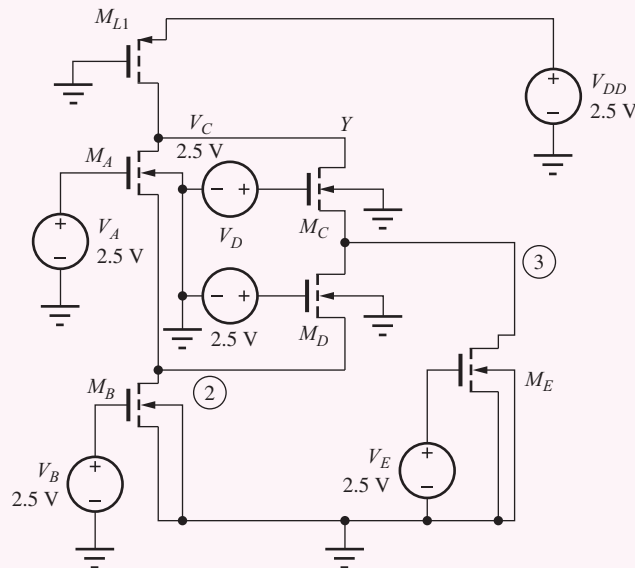
We desire the current and power to be the same in the circuit when the output is in the low state. Thus the load device will be identical to that of the inverter. The switching transistor network cannot be broken into series and parallel branches, and transistor sizing will follow the worst-case path approach. Path  $CDB$  has three transistors in series, so each  $W/L$  will be set to three times that of the switching transistor in the reference inverter, or  $6.66/1$ . Path  $ADE$  also has three transistors in series, and, because  $D$  has  $(W/L) = 6.66/1$ , the  $W/L$  ratios of  $A$  and  $E$  can also be  $6.66/1$ . All transistors are now  $6.66/1$  devices.

**Check of Results:** The remaining paths,  $AB$  and  $CE$ , must be checked to ensure that the low output level will be properly maintained. Each has two transistors with  $W/L = 6.66/1$  in series for an equivalent  $W/L = 3.33/1$ . Because the  $W/L$  of  $3.33/1$  is greater than  $2.22/1$ , the low output state will be maintained at  $V_L < 0.20$  V when paths  $AB$  or  $CE$  are conducting alone.

**Discussion:** Note that the current traverses transistor  $D$  in one direction when path  $CDB$  is conducting, but in the opposite direction when path  $ADE$  is active! Remember from the device cross section in Fig. 6.18(b) that the MOS transistor is a symmetrical device. The only way to actually tell the drain terminal from the source terminal is from the values of the applied potentials. For the NMOS transistor, the drain terminal will be the terminal at the higher voltage, and the source terminal will be the terminal at the lower potential. This bidirectional nature of the MOS transistor is also a key to the design of high-density dynamic random access memories (DRAMs), which are discussed in Chapter 8.

**Computer-Aided Design:** Now we can use SPICE to find the actual values of  $V_L$  for different input combinations, including the influence of body effect and nonzero source voltages on the operation of the gate. For the circuit below with  $VTO = 0.60$ ,  $KP = 100E-6$ ,  $GAMMA = 0.5$ ,  $PHI = 0.6$ ,  $W = 6.66$  U, and  $L = 1$  U for the switching devices and  $VTO = -0.6$ ,  $KP = 40E-6$ ,  $GAMMA = 0.5$ ,  $PHI = 0.6$ ,  $W = 1.11$  U, and  $L = 1$  U for the load device, SPICE gives these results:

ABCDE	Y (mV)	NODE 2 (mV)	NODE 3 (mV)	$I_{DD}$ ( $\mu$ A)
11000	132	64.4	0	80.1
01110	203	64.4	132	80.1
00101	132	0	64.4	80.1
11111	64.6	31.9	31.9	80.1



**EXERCISE:** (a) Calculate the power supply current  $I_{DD}$  if the voltage at node Y is 203 mV. (b) Repeat for 132 mV. (c) Repeat for 64.4 mV.

**ANSWERS:** (a) 80.1  $\mu$ A; (b) 80.1  $\mu$ A; (c) 80.1  $\mu$ A

**EXERCISE:** Make a complete table for node voltages Y, 2, and 3 and  $I_{DD}$  for all 32 possible combinations of inputs for the circuit in Ex. 6.9. Fill in the table entries based on the SPICE simulation results presented in the example.

## 6.10 POWER DISSIPATION

In this section we consider the two primary contributions to power dissipation in NMOS inverters. The first is the steady-state power dissipation that occurs when the logic gate output is stable in either the high or low states. The second is power that is dissipated in order to charge and discharge the total equivalent load capacitance during dynamic switching of the logic gate.

### 6.10.1 STATIC POWER DISSIPATION

The overall **static power dissipation** of a logic gate is the average of the power dissipations of the gate when its output is in the low state and the high state. The power supplied to the logic gate is expressed as  $P = V_{DD}i_{DD}$ , where  $i_{DD}$  is the current provided by the source  $V_{DD}$ . In the circuits considered so far,  $i_{DD}$  is equal to the current through the load device, and the total power supplied by source  $V_{DD}$  is dissipated in the load and switching transistors. The average power dissipation

depends on the fraction of time that the output spends in the two logic states. If we assume that the average logic gate spends one-half of the time in each of the two output states (a 50 percent duty cycle), then the average power dissipation is given by

$$P_{av} = \frac{V_{DD}I_{DDH} + V_{DD}I_{DDL}}{2} \quad (6.40)$$

where  $I_{DDH}$  = current in gate for  $v_O = V_H$

$I_{DDL}$  = current for  $v_O = V_L$

For the NMOS logic gates considered in this chapter, the current in the gate becomes zero when the  $v_O$  reaches  $V_H$ . Thus,  $I_{DDH} = 0$ , and the average power dissipation becomes equal to one-half the power dissipation when the output is low, given by

$$P_{av} = \frac{V_{DD}I_{DDL}}{2} \quad (6.41)$$

If some other duty factor is deemed more appropriate (for example, 33 percent), it simply changes the factor of 2 in the denominator of Eq. (6.41).

**EXERCISE:** What is the average power dissipation of the gates in Fig. 6.29?

**ANSWER:** 0.10 mW

## 6.10.2 DYNAMIC POWER DISSIPATION

A second, very important source of power dissipation is **dynamic power dissipation**, which occurs during the process of charging and discharging the load capacitance of a logic gate. Consider the simple circuit in Fig. 6.37(a), in which a capacitor is being charged toward positive voltage  $V_{DD}$  through a nonlinear resistor (such as an MOS load device).

Let us assume the capacitor is initially discharged; at  $t = 0$  the switch closes, and the capacitor then charges toward its final value. We also assume that the nonlinear element continues to deliver current until the voltage across it reaches zero (for example, a depletion-mode NMOS or PMOS load). The total energy  $E_D$  delivered by the source is given by

$$E_D = \int_0^\infty P(t) dt \quad (6.42)$$

The power  $P(t) = V_{DD}i(t)$ , and because  $V_{DD}$  is a constant,

$$E_D = V_{DD} \int_0^\infty i(t) dt \quad (6.43)$$

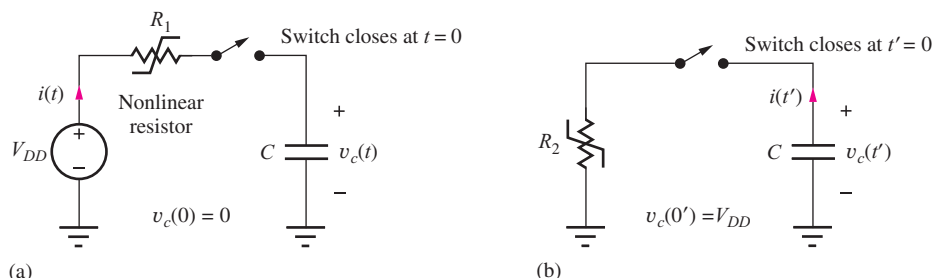


**Figure 6.37** Simple circuit model for dynamic power calculation: (a) charging  $C$ , (b) discharging  $C$ .

The current supplied by source  $V_{DD}$  is also equal to the current in capacitor  $C$ , and so

$$E_D = V_{DD} \int_0^\infty C \frac{dv_C}{dt} dt = CV_{DD} \int_{V_C(0)}^{V_C(\infty)} dv_C \quad (6.44)$$

Integrating from  $t = 0$  to  $t = \infty$ , with  $V_C(0) = 0$  and  $V_C(\infty) = V_{DD}$  results in

$$E_D = CV_{DD}^2 \quad (6.45)$$

We also know that the energy  $E_S$  stored in capacitor  $C$  is given by

$$E_S = \frac{CV_{DD}^2}{2} \quad (6.46)$$

and thus the energy  $E_L$  lost in the resistive element must be

$$E_L = E_D - E_S = \frac{CV_{DD}^2}{2} \quad (6.47)$$

Now consider the circuit in Fig. 6.37(b), in which the capacitor is initially charged to  $V_{DD}$ . At  $t' = 0$ , the switch closes and the capacitor discharges toward zero through another nonlinear resistor (such as an enhancement-mode MOS transistor). Again, we wait until the capacitor reaches its final value,  $V_C = 0$ . The energy  $E_S$  that was stored on the capacitor has now been completely dissipated in the resistor. The total energy  $E_{TD}$  dissipated in the process of first charging and then discharging the capacitor is equal to

$$E_{TD} = \frac{CV_{DD}^2}{2} + \frac{CV_{DD}^2}{2} = CV_{DD}^2 \quad (6.48)$$

Thus, every time a logic gate goes through a complete switching cycle, the transistors within the gate dissipate an energy equal to  $E_{TD}$ . Logic gates normally switch states at some relatively high frequency  $f$  (switching events/second), and the dynamic power  $P_D$  dissipated by the logic gate is then

$$P_D = CV_{DD}^2 f \quad (6.49)$$

In effect, an average current equal to  $(CV_{DD}f)$  is supplied from source  $V_{DD}$ .

**EXERCISE:** What is the dynamic power dissipated by alternately charging and discharging a 1-pF capacitor between 2.5 V and 0 V at a frequency of 32 MHz? At 3.2 GHz?

**ANSWER:** 200  $\mu$ W, 20 mW

Note that the power dissipation in the first part of previous exercise is the same as the static power dissipation that we allocated to the  $v_O = V_L$  state in our original NMOS logic gate design. In high-speed logic systems, the dynamic component of power can become dominant—we see in Chapter 7 that this is in fact the primary source of power dissipation in CMOS logic gates!

### 6.10.3 POWER SCALING IN MOS LOGIC GATES

During logic design in complex systems, gates with various power dissipations are often needed to provide different levels of drive capability and to drive different values of load capacitance at different speeds. For example, consider the saturated load inverter in Fig. 6.38(a). The static power dissipation is determined when  $v_O = V_L$ .  $M_S$  is operating in the linear region,  $M_L$  is saturated, and

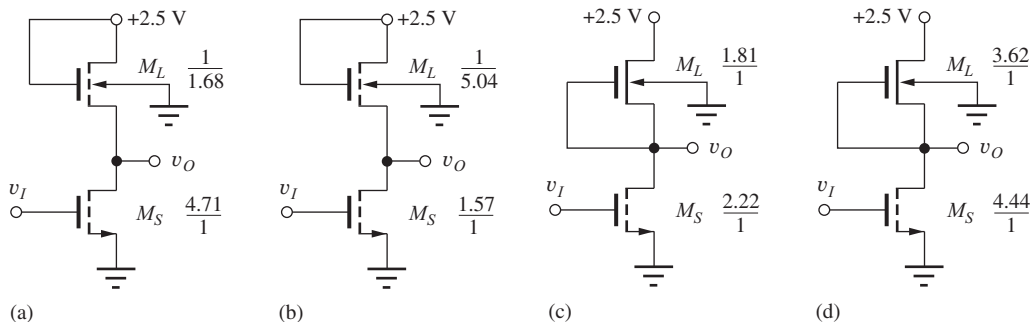


**Figure 6.38** Inverter power scaling. The NMOS inverter of (b) operates at one-third the power of circuit (a), and the NMOS inverter of (d) operates at twice the power of circuit (c).

the drain currents of the two transistors are given by

$$i_{DL} = \frac{K'_n}{2} \left( \frac{W}{L} \right)_L (v_{GSL} - V_{TNL})^2$$

$$i_{DS} = K'_n \left( \frac{W}{L} \right)_S \left( v_{GSS} - V_{TNS} - \frac{v_{DSS}}{2} \right) v_{DSS} \quad (6.50)$$

in which the  $W/L$  ratios have been chosen so that  $i_{DS} = i_{DL}$  for  $v_O = V_L$ . For fixed voltages, both drain currents are directly proportional to their respective  $W/L$  ratios. If we double the  $W/L$  ratio of the load device *and* the switching device, then the drain currents both double, with no change in operating voltage levels.

Or, if we reduce the  $W/L$  ratios of both the load device and the switching device by a factor of 3, then the drain currents are both reduced by a factor of 3, with no change in operating voltage levels. Thus, if the  $W/L$  ratios of  $M_L$  and  $M_S$  are changed by the same factor, the power level of the gate can easily be scaled up and down without affecting the values of  $V_H$  and  $V_L$ . With this technique, the inverter in Fig. 6.38(b) has been designed to operate at one-third the power of the inverter of Fig. 6.38(a) by reducing the value of  $W/L$  of each device by a factor of 3. This **power scaling** is a property of ratioed logic circuits. The power level can be scaled up or down without disturbing the voltage levels of the design.

Similar arguments can be used to scale the power levels of any of the NMOS gate configurations that we have studied, and the depletion-mode load inverter in Fig. 6.38(d) has been designed to operate at twice the power of the inverter of that of Fig. 6.38(c) by increasing the value of  $W/L$  of each device by a factor of 2. As we will see shortly, this same technique can also be used to scale the dynamic response time of the inverter to compensate for various capacitive load conditions.

**EXERCISE:** What are the new  $W/L$  ratios for the transistors in the gate in Fig. 6.38(a) for a power of 0.1 mW?

**ANSWERS:** 1/3.36 and 2.36/1

**EXERCISE:** What are the new  $W/L$  ratios for the transistors in the gate in Fig. 6.38(c) for a power of 4 mW?

**ANSWERS:** 36.2/1 and 44.4/1

**EXERCISE:** What are the  $W/L$  ratios of the transistors in the gate in Fig. 6.35(a) required to reduce the power by a factor of three while maintaining the same value of  $V_t$ ?

**ANSWERS:** 1/1.66; 1.11/1; 2.22/1; 2.22/1; 2.22/1

## 6.11 DYNAMIC BEHAVIOR OF MOS LOGIC GATES

Thus far in this chapter the discussion has been concerned with only the static design of NMOS logic gates. The time domain response, however, plays an extremely important role in the application of logic circuits. There are delays between input changes and output transitions in logic circuits because every node is shunted by capacitance to ground and is not able to change voltage instantaneously. This section reviews the sources of capacitance in the MOS circuit and then explores the dynamic or time-varying behavior of logic gates. Calculations of rise time  $t_r$ , fall time  $t_f$ , and the average propagation delay  $\tau_p$  (all defined in Sec. 6.3) are presented, and expressions are then developed for estimating the response time of various inverter configurations.

### 6.11.1 CAPACITANCES IN LOGIC CIRCUITS

Figure 6.39(a) shows two NMOS inverters including the various capacitances associated with each transistor. These capacitances were introduced in Sec. 4.5. Each device has capacitances between its gate-source, gate-drain, source-bulk, and drain-bulk terminals. Some of the capacitances do not appear in the schematic because they are shorted out by the various circuit connections (for example,  $C_{SB1}, C_{GS2}, C_{SB3}, C_{GS4}$ ). In addition to the **MOS device capacitances**, the figure includes a wiring capacitance  $C_W$ , representing the capacitance of the electrical interconnection between the two logic gates. For simplicity in analyzing the delay times in logic circuits, the capacitances on a given node will be lumped together into a fixed effective nodal capacitance  $C$ , as indicated in Fig. 6.39(b), and our hand analysis will cast the behavior of circuits in terms of this effective capacitance  $C$ . The MOS

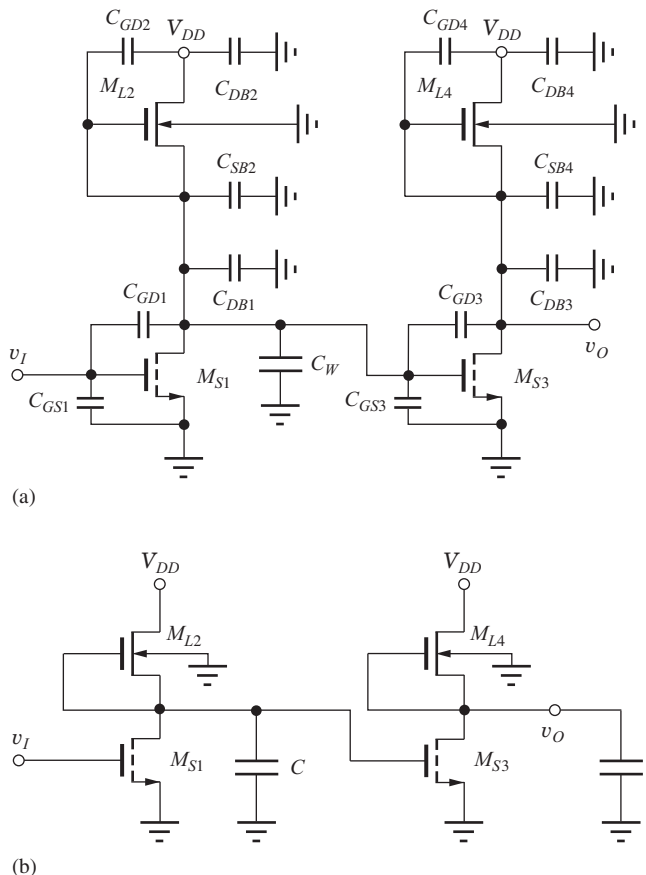


**Figure 6.39** (a) Capacitances associated with an inverter pair. (b) Lumped-load capacitance model for inverters.

device capacitances are nonlinear functions of the various node voltages; they are highly dependent on circuit layout in an integrated circuit. We will not attempt to find a precise expression for  $C$  in terms of all the capacitances in Fig. 6.39(a), but we assume that we have an estimate for the value of  $C$ . Simulation tools exist that will extract values of  $C$  from a given IC layout, and more accurate predictions of time-domain behavior can be obtained using SPICE circuit simulations.

### Fan-Out Limitations in NMOS Logic

Since no dc current needs to be supplied to the input of an NMOS logic gate, the fan-out of an MOS logic gate is not limited by static design constraints. (But this is not the case for bipolar design discussed later in Chapter 9.) However, as more and more gates are attached to a given output as in Figs. 6.39 or 6.10, the value of capacitor  $C$  increases, and the temporal responses of the circuit will decrease accordingly. Thus the fan-out will be limited by how much degradation can be tolerated in the time delays of the circuit.

### Capacitance Estimates

We can make a basic estimate for the load capacitance  $C_L$  in terms of the fanout of the gates:

$$C_L = C_{\text{out}} + FO \times C_{\text{in}} + C_W \quad (6.51)$$

where  $C_{\text{out}}$  is the capacitance looking into the output of the gate,  $C_{\text{in}}$  is the capacitance looking into the input of the gate,  $C_W$  is the capacitance of the wiring that connects one gate to the next, and  $FO$  is the fanout. The “unloaded delay” of an inverter is found for a fanout of one with zero wiring capacitance.

For the circuit in Fig. 6.39, we get the following estimates for the output and input capacitances of the logic gate:

$$C_{\text{out}} \cong C_{GD1} + C_{DB1} + C_{SB2} + C_{GD2} \quad \text{and} \quad C_{\text{in}} \cong C_{GS3} + 2C_{GD3} \quad (6.52)$$

For  $C_{\text{in}}$ , the factor of two is an approximate number that is included because the voltage change across  $C_{GD3}$  is twice the input logic swing.

### 6.11.2 DYNAMIC RESPONSE OF THE NMOS INVERTER WITH A RESISTIVE LOAD

Figure 6.40 shows the circuit from our earlier discussion of the inverter with a resistive load. For hand analysis, the logic input signal is represented by an ideal step function, and we now calculate the rise time, fall time, and delay times for this inverter.

#### Calculation of $t_r$ and $\tau_{PLH}$

For analysis of the rise time, assume that the input and output voltages have reached their steady-state levels for  $t < 0$ :  $v_I = V_H = 2.5$  V and  $v_O = V_L = 0.20$  V. At  $t = 0$ , the input drops from  $v_I = 2.5$  V to  $v_I = 0.20$  V. Because the gate-source voltage of the switching transistor drops below  $V_{TNS}$ , the MOS transistor abruptly stops conducting. The output then charges from  $v_O = V_L = 0.20$  V to

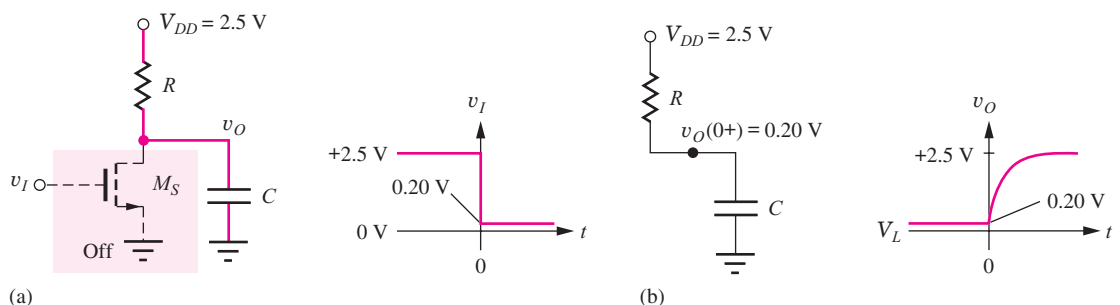


Figure 6.40 Model for rise time in resistively loaded inverter.

$v_O = V_H = V_{DD} = 2.5$  V. In this case, the waveform is that of the simple  $RC$  network formed by the load resistor  $R$  and the load capacitor  $C$ . Using our knowledge of single-time constant circuits:

$$v_O(t) = V_F - (V_F - V_I) \exp\left(-\frac{t}{RC}\right) = V_F - \Delta V \exp\left(-\frac{t}{RC}\right) \quad (6.53)$$

where  $V_F$  is the final value of the capacitor voltage,  $V_I$  is the initial capacitor voltage, and  $\Delta V = (V_F - V_I)$  is the change in the capacitor voltage. For the inverter in Fig. 6.40,  $V_F = 2.5$  V,  $V_I = 0.20$  V, and  $\Delta V = 2.30$  V.

The rise time is determined by the difference between the time  $t_1$  when  $v_O(t_1) = V_I + 0.1 \Delta V$  and the time  $t_2$  when  $v_O(t_2) = V_I + 0.9 \Delta V$ . Using Eq. (6.53),

$$\begin{aligned} V_I + 0.1 \Delta V &= V_F - \Delta V \exp\left(\frac{-t_1}{RC}\right) \quad \text{yields} \quad t_1 = -RC \ln 0.9 \\ V_I + 0.9 \Delta V &= V_F - \Delta V \exp\left(\frac{-t_2}{RC}\right) \quad \text{yields} \quad t_2 = -RC \ln 0.1 \end{aligned}$$

and

$$t_r = t_2 - t_1 = RC \ln 9 = 2.2RC \quad (6.54)$$

The delay time  $\tau_{PLH}$  is determined by  $v_O(\tau_{PLH}) = V_I + 0.5 \Delta V$ , which yields

$$\tau_{PLH} = -RC \ln 0.5 = 0.69RC \quad (6.55)$$

Equations (6.54) and (6.55) represent the classical expressions for the rise time and propagation delay for an  $RC$  network. Similar analyses show that  $t_f = 2.2RC$  and  $\tau_{PHL} = 0.69RC$ . Remember that these expressions apply only to the simple  $RC$  network.

## DESIGN NOTE

The rise and fall times and propagation delays for an  $RC$  network are given by

$$t_r = t_f = 2.2RC \quad \tau_{PLH} = \tau_{PHL} = 0.69RC$$

**EXERCISE:** Find  $t_r$  and  $\tau_{PLH}$  for the resistively loaded inverter with  $C = 0.2$  pF and  $R = 28.8$  k $\Omega$ .

**ANSWERS:** 12.7 ns; 3.97 ns

**EXERCISE:** Derive expressions for the fall time and high-to-low propagation delay for an  $RC$  network.

**ANSWERS:**  $t_f = 2.2RC$ ;  $\tau_{PHL} = 0.69RC$

### Calculation of $\tau_{PHL}$ and $t_f$

Now consider the other switching situation, with  $v_I = V_L = 0.20$  V and  $v_O = V_H = 2.5$  V, as displayed in Fig. 6.41. At  $t = 0$ , the input abruptly changes from  $v_I = 0.20$  V to  $v_I = 2.5$  V. At  $t = 0^+$ ,  $M_S$  has  $v_{GS} = 2.5$  V and  $v_{DS} = 2.5$  V, so it conducts heavily and discharges the capacitance until the value of  $v_O$  reaches  $V_L$ .

Figure 6.42 shows the currents  $i_R$  and  $i_D$  in the load resistor and switching transistor as a function of  $v_O$  during the transition between  $V_H$  and  $V_L$ . The current available to discharge the capacitor  $C$  is the difference in these two currents:

$$i_C = i_D - i_R$$

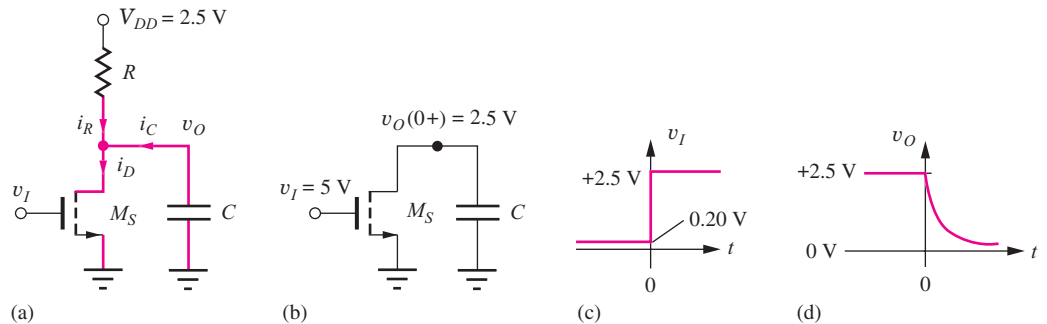


Figure 6.41 Simplified circuit for determining  $t_f$  and  $\tau_{PHL}$ .  $v_I(0^+) = V_H = V_{DD}$ .

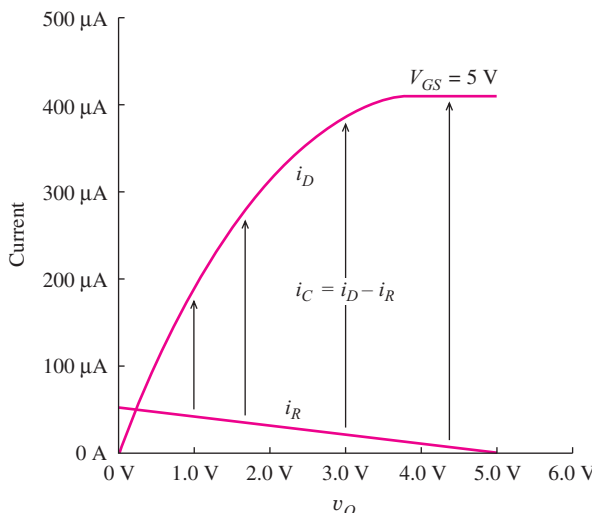


Figure 6.42 Drain current and resistor current versus  $v_O$ .

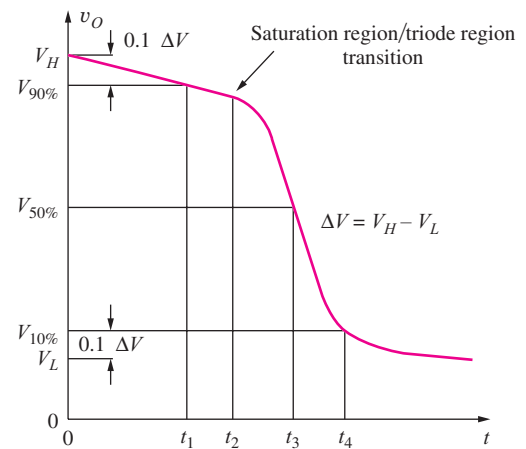
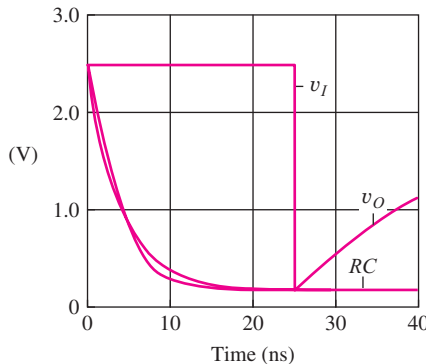


Figure 6.43 Times needed for calculation of  $\tau_{PHL}$  and  $t_f$  for the inverter. Fall time  $t_f = t_4 - t_1$ ; propagation delay  $\tau_{PHL} = t_3$ .

Because the load element is a resistor, the current in the resistor increases linearly as  $v_O$  goes from  $V_H$  to  $V_L$ . However, when  $M_S$  first turns on, a large drain current occurs, rapidly discharging the load capacitance  $C$ .  $V_L$  is reached when the current through the capacitor becomes zero and  $i_R = i_D$ . Note that the drain current is much greater than the current in the resistor for most of the period of time corresponding to  $\tau_{PHL}$ . This leads to values of  $\tau_{PHL}$  and  $t_f$  that are much shorter than  $\tau_{PLH}$  and  $t_r$  associated with the rising output waveform. This behavior is characteristic of NMOS (or PMOS) logic circuits. Another way to visualize this difference is to remember that the on-resistance of the MOS transistor must be much smaller than  $R$  in order to force  $V_L$  to be a low value. Thus, the apparent “time constant” for the falling waveform will be much smaller than that of the rising waveform.

An exact calculation of  $t_f$  and  $\tau_{PHL}$  is much more complicated than that for a fixed resistor charging the load capacitance because the NMOS transistor changes regions of operation during the voltage transition as shown in Fig. 6.43. At time  $t_2$ , the transistor moves from the saturation region of operation to the triode region, and the differential equation that models the  $V_H$  to  $V_L$  transition changes at that point. An example of these direct calculations can be found in the previous editions of this text or on the website. However, even those “exact” calculations only represent approximations because of the assumptions involved.

Rather than following this more involved approach, we can get very usable estimates for  $t_f$  and  $\tau_{PHL}$  by defining an effective value for the on-resistance of the MOS transistor. Throughout the transient, the on-resistance of the transistor is continually changing as the drain-source voltage of the



**Figure 6.44** SPICE simulation of high-to-low output transient for the resistor load inverter with  $C = 1 \text{ pF}$  and its effective constant on-resistance approximation.

transistor changes. The effective on-resistance will be chosen to minimize the difference between the MOS and exponential transient curves, and it will then be used with Eqs. (6.54) and (6.55) to find  $t_f$  and  $\tau_{PHL}$ .

First, let us simplify our model for the circuit. From Fig. 6.42, we can see that  $i_D \gg i_R$  except for  $v_O$  very near  $V_L$ . Therefore, the current through the resistor will be neglected so that we can assume that all the drain current of the NMOS transistor is available to discharge the load capacitance, as in Fig. 6.41(b). The input signal  $v_I$  is assumed to be a step function changing to  $v_I = 2.5 \text{ V}$  at  $t = 0$ . At  $t = 0$ , the output voltage  $V_C$  on the capacitor is  $V_H = V_{DD} = 2.5 \text{ V}$ , and the gate voltage is forced to  $V_G = 2.5 \text{ V}$ .

Figure 6.44 displays a SPICE simulation of the high-to-low transition for the resistor load inverter with  $R = 28.8 \text{ k}\Omega$  and  $(W/L)_S = 2.22/1$ . Superimposed on this plot is the transient for the exponential discharge of an  $RC$  network with a constant value of  $R$ . We see that the actual discharge curve is very similar to a purely exponential decay. The effective value of on-resistance used in this simulation is

$$R = R_{\text{eff}} = 1.7R_{\text{onS}} \quad \text{where} \quad R_{\text{onS}} = \frac{1}{K_n(V_H - V_{TNS})} \quad (6.56)$$

where the factor of 1.7 minimizes the integral of the magnitude of the errors between the MOS and exponential transient curves.  $R_{\text{onS}}$  represents the on-resistance of the switching transistor as originally defined in Eq. (4.16) with  $v_{GS} = V_H$ . Substituting  $R = R_{\text{eff}}$  into the equations for  $t_f$  and  $\tau_{PHL}$  (see the design note below Eq. (6.55)) yields

$$\tau_{PHL} = 0.69(1.7R_{\text{onS}})C \cong 1.2R_{\text{onS}}C \quad \text{and} \quad t_f = 2.2(1.7R_{\text{onS}})C \cong 3.7R_{\text{onS}}C \quad (6.57)$$

## EXAMPLE 6.10 DYNAMIC PERFORMANCE OF THE INVERTER WITH RESISTOR LOAD

Find numerical values for the dynamic performance measures of the reference inverter in Fig. 6.29(a).

**PROBLEM** Find  $t_f$ ,  $t_r$ ,  $\tau_{PLH}$ ,  $\tau_{PHL}$ , and  $\tau_p$  for the resistively loaded inverter in Fig. 6.29 with  $C = 0.5 \text{ pF}$  and  $R = 28.8 \text{ k}\Omega$ .

**SOLUTION** **Known Information and Given Data:** Basic resistively loaded inverter circuit in Fig. 6.29;  $R = 28.8 \text{ k}\Omega$ ,  $C = 0.5 \text{ pF}$ ,  $V_{DD} = 2.5 \text{ V}$ ,  $W/L = 2.22/1$ ,  $V_H = 2.5 \text{ V}$ ,  $V_L = 0.20 \text{ V}$ , and  $K_S = (2.22)(100 \times 10^{-6} \text{ A/V}^2)$

**Unknowns:**  $t_f$ ,  $t_r$ ,  $\tau_{PLH}$ ,  $\tau_{PHL}$ , and  $\tau_p$

**Approach:** Find  $t_r$  and  $\tau_{PLH}$  using Eqs. (6.54) and (6.55); calculate  $R_{\text{onS}}$  and use it to evaluate Eq. (6.57);  $\tau_p = (\tau_{PLH} + \tau_{PHL})/2$

**Assumptions:** None

**Analysis:** For the resistive load inverter, the rise time and low-to-high propagation delay are

$$t_r = 2.2RC = 2.2(28.8 \text{ k}\Omega)(0.5 \text{ pF}) = 31.7 \text{ ns}$$

$$\tau_{PLH} = 0.69RC = 0.69(28.8 \text{ k}\Omega)(0.5 \text{ pF}) = 9.94 \text{ ns}$$

To find  $t_f$  and  $\tau_{PHL}$ , we first calculate the value of  $R_{onS}$ :

$$R_{onS} = \frac{1}{K_S(V_H - V_{TNS})} = \frac{1}{(2.22) \left( 100 \frac{\mu\text{A}}{\text{V}^2} \right) (2.5 - 0.6) \text{ V}} = 2.37 \text{ k}\Omega$$

Substituting the data values into Eq. (6.57):

$$\tau_{PHL} = 1.2R_{onS}C = 1.2(2.37 \text{ k}\Omega)(0.5 \text{ pF}) = 1.42 \text{ ns}$$

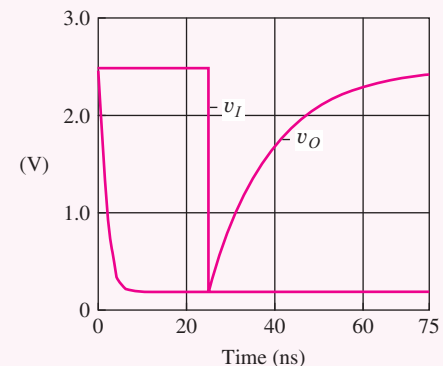
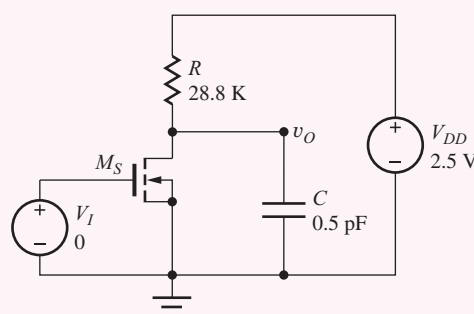
$$t_f = 3.7R_{onS}C = 3.7(2.37 \text{ k}\Omega)(0.5 \text{ pF}) = 4.39 \text{ ns}$$

$$\tau_P = \frac{\tau_{PHL} + \tau_{PLH}}{2} = \frac{9.94 + 1.42}{2} \text{ ns} = 5.68 \text{ ns}$$

**Check of Results:** A double check of the arithmetic indicates our calculations are correct. We see the expected asymmetry in the rise and fall times as well as in the two propagation delay values.

**Discussion:** Remember that the asymmetry in the rise and fall times and in  $\tau_{PLH}$  and  $\tau_{PHL}$  will occur in all NMOS (or PMOS) logic gates because the switching device must have a much smaller on-resistance than that of the load in order to produce the desired value of  $V_L$ . We see that  $\tau_{PLH}$  is approximately 7 times  $\tau_{PHL}$  and that  $t_r$  is more than 7 times  $t_f$ !

**Computer-Aided Analysis:** Let us check our hand calculations using the SPICE transient simulation capability. In the circuit schematic,  $V_I$  is a pulse source with an initial value of 0, peak value of 2.5 V, zero delay time, 0.1-ns rise time, 0.1-ns fall time, 24.9-ns pulse width, and a 100-ns period. Note the pulse width is chosen so that the rise time plus the pulse width add up to a convenient value of 25 ns. The rise and fall times for  $V_I$  are chosen to be much smaller than those expected for the inverter. The transient simulation parameters are a start time of zero, stop time of 100 ns and a time step of 0.025 ns.



The SPICE results yield values that are very similar to our hand calculations:  $t_f = 3.9 \text{ ns}$ ,  $\tau_{PHL} = 1.6 \text{ ns}$ ,  $t_r = 31 \text{ ns}$ , and  $\tau_{PLH} = 10 \text{ ns}$ . (Note: In order to extract these values from the simulation one must expand the scale for the falling portion of the waveform.)

**EXERCISE:** Recalculate the values of  $t_f$ ,  $t_r$ ,  $\tau_{PHL}$ ,  $\tau_{PLH}$ , and  $\tau_P$  if C is decreased to 0.25 pF.

**ANSWERS:** 2.20 ns; 15.8 ns; 0.71 ns; 4.97 ns; 2.84 ns

### 6.11.3 PSEUDO NMOS INVERTER

Because of its important relationship to CMOS design, we will develop estimates for the delays of the pseudo NMOS inverter. The conditions for the two switching transients appear in Fig. 6.45, and the time response for this inverter can quite easily be found based upon the results from the previous section. In Fig. 6.45(b), we assume that  $i_{DL} \ll i_{DS}$ , so that the full drain current of switching transistor  $M_S$  is available to discharge the capacitor from  $V_H$  to  $V_L$ , and the gate-source voltage of  $M_S$  is  $v_{GS} = V_H = V_{DD}$ . These conditions are exactly the same as those for the resistor load inverter depicted in Fig. 6.41. Thus the expressions for  $\tau_{PHL}$  and  $t_f$  are the same as in Eq. (6.57):

$$\tau_{PHL} = 0.69(1.7R_{onS})C \cong 1.2R_{onS}C \quad \text{and} \quad t_f = 2.2(1.7R_{onS})C \cong 3.7R_{onS}C$$

with

$$R_{onS} = \frac{1}{K_n(V_H - V_{TNS})} = \frac{1}{K_n(V_{DD} - V_{TNS})} \quad (6.58)$$

The situation for the low-to-high transient is the same as given in Fig. 6.40(a–b) in which we assume a step change in the input from  $V_H$  to  $V_L$  at  $t = 0$ . The switching transistor turns off abruptly, and the load device charges the capacitor from  $V_L$  to  $V_H$ . We see that the operating conditions for the PMOS transistor are similar to those in Fig. 6.45(b): the source-gate voltage is equal to  $V_{DD}$ , and the source-drain voltage changes from a large voltage toward zero. Thus the expressions in Eq. (6.58) can be used to obtain  $\tau_{PLH}$  and  $t_r$  with suitable changes in subscripts:

$$\tau_{PLH} = 0.69(1.7R_{onL})C \cong 1.2R_{onL}C \quad \text{and} \quad t_r = 2.2(1.7R_{onL})C \cong 3.7R_{onL}C$$

with

$$R_{onL} = \frac{1}{K_p|V_{DD} - V_{TNL}|} \quad (6.59)$$

Figure 6.46 presents SPICE simulation results for the pseudo NMOS Inverter from Fig. 6.29(e) with  $(W/L)_S = 2.22/1$ ,  $(W/L)_L = 1.11/1$  and  $C = 1$  pF. Based upon the data from the SPICE output file,  $\tau_{PHL} = 3.25$  ns,  $t_f = 7.8$  ns,  $\tau_{PLH} = 15.0$  ns, and  $t_r = 35.0$  ns, whereas Eqs. 6.58 and 6.59 predict

$$R_{onS} = \frac{1}{K_n(V_{DD} - V_{TNS})} = \frac{1}{(100 \mu\text{A}/\text{V}^2)(2.22/1)(2.5 - 0.6)\text{V}} = 2.37 \text{ k}\Omega$$

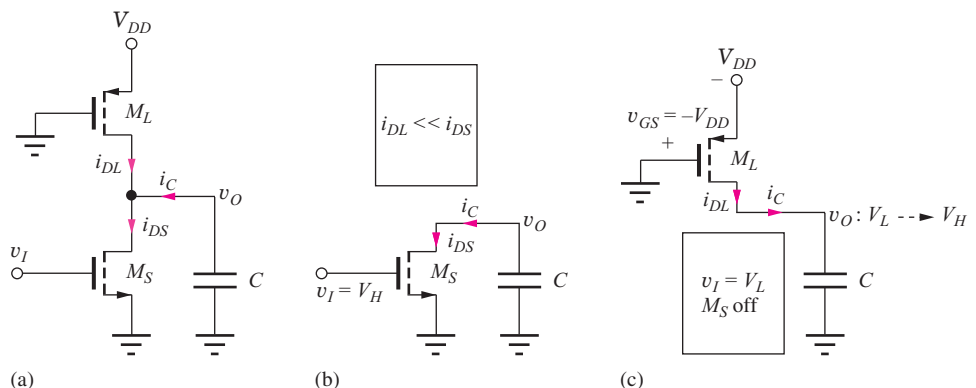
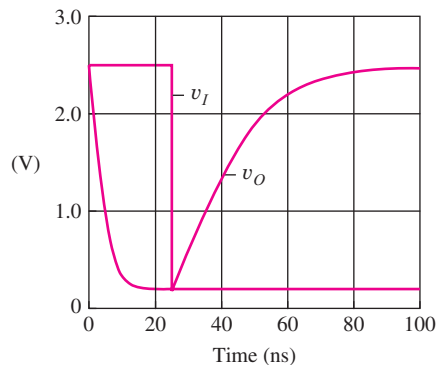


Figure 6.45 (a) Pseudo NMOS logic gate. (b)  $V_H$  to  $V_L$  transient. (c)  $V_L$  to  $V_H$  transient.



**Figure 6.46** SPICE simulation of the pseudo NMOS Inverter with a 1 pF load.

**TABLE 6.9**  
NMOS Inverter Time Delays\*

	$\tau_{PHL}$	$\tau_{PLH}$	$t_f$	$t_r$
Resistor load	0.31 ns	2.3 ns	0.71 ns	9.9 ns
Pseudo NMOS	0.33 ns	1.5 ns	0.77 ns	3.7 ns
Depletion load	0.31 ns	2.5 ns	0.74 ns	4.6 ns
Saturated load	0.33 ns	1.7 ns	0.71 ns	13.7 ns
Linear load	0.31 ns	2.3 ns	0.72 ns	9.8 ns

\*Circuits from Fig. 6.29 with  $C = 0.1 \text{ pF}$

$$R_{onL} = \frac{1}{K_n |V_{DD} - V_{TNL}|} = \frac{1}{(40 \mu\text{A}/\text{V}^2)(1.11/1)(2.5 - 0.6)\text{V}} = 11.9 \text{ k}\Omega$$

$$\tau_{PHL} = 1.2R_{onS}C = 1.2(2.37 \text{ k}\Omega)(1 \text{ pF}) = 2.84 \text{ ns} \quad t_f = 3.7R_{onS}C = 8.77 \text{ ns}$$

$$\tau_{PLH} = 1.2R_{onL}C = 1.2(11.9 \text{ k}\Omega)(1 \text{ pF}) = 14.3 \text{ ns} \quad t_f = 3.7R_{onL}C = 44.0 \text{ ns}$$

We see that the analytic expressions provide reasonable estimates for time response of the inverter. The largest error occurs from overestimating the long tail on the rise time.

**EXERCISE:** Estimate  $\tau_{PHL}$ ,  $t_f$ ,  $\tau_{PLH}$  and  $t_r$  from Fig. 6.46.

**ANSWERS:** 3 ns; 7 ns; 15 ns; 35 ns

#### 6.11.4 A FINAL COMPARISON OF NMOS INVERTER DELAYS

Rather than spend additional time developing closed-form expressions for the other less important NMOS logic gates, we will instead compare the delays of all five NMOS inverter configurations using the results of SPICE simulations that appear in Table 6.9. In this table we observe that the gates all have nearly the same values for both  $\tau_{PHL}$  and  $t_f$ . This occurs since the switching transistors have each been designed with equal on-resistances in order to achieve the same value of  $V_L$ . Note that if we crudely assume that the charging current from the switching transistor<sup>9</sup> is constant, we find

$$I_D = \left( \frac{100 \mu\text{A}}{2 \text{ V}^2} \right) \left( \frac{2.22}{1} \right) (2.5 - 0.6)^2 \text{ V}^2 = 401 \mu\text{A} \quad (6.60)$$

$$\tau_{PHL} \cong \frac{C}{I_D} \left( \frac{\Delta V}{2} \right) = \left( \frac{0.1 \text{ pF}}{40 \mu\text{A}} \right) \left( \frac{2.5 - 0.2}{2} \right) = 0.29 \text{ ns}$$

which represents only a slightly optimistic estimate for the propagation delays.

We also see that the values of  $\tau_{PLH}$  are similar with the exception of the saturated load and pseudo NMOS inverters. As we shall see, the pseudo NMOS inverter has the best drive current by far, whereas the reduced logic swing ( $\Delta V = 1.35 \text{ V}$  versus  $2.3 \text{ V}$  for the other inverters) is responsible for the faster response of the saturated load inverter. All the loads deliver the same charging current at the start of the low-high transient (i.e.,  $80 \mu\text{A}$ ), and if we assume that the charging current from

<sup>9</sup> The switching transistors are all saturated at the start of the transition.

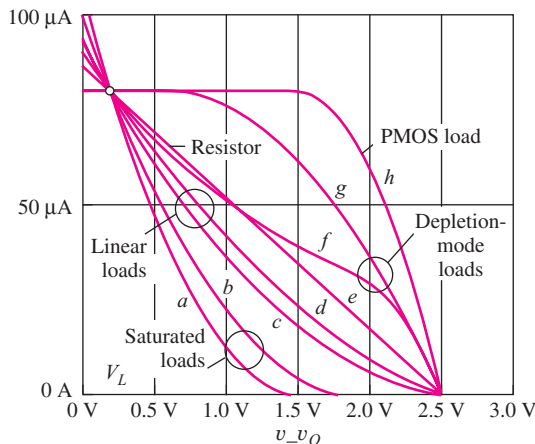


**Figure 6.47** A comparison of NMOS inverter load device characteristics with current normalized to  $80 \mu\text{A}$  for  $v_o = V_L = 0.20 \text{ V}$ . (a) Saturated load including body effect, (b) saturated load without body effect, (c) linear load with body effect, (d) linear load without body effect, (e)  $28.8\text{-k}\Omega$  load resistor, (f) depletion-mode load with body effect, (g) depletion-mode load with no body effect, (h) PMOS load transistor for the pseudo NMOS inverter.

**TABLE 6.10**  
NMOS Inverter Time Delays

	$\tau_{PHL}$	$\tau_{PLH}$	$t_f$	$t_r$
Resistor load	$1.2R_{onS}C$	$0.69RC$	$3.7R_{onS}C$	$2.2RC$
Pseudo NMOS	$1.2R_{onS}C$	$1.2R_{onL}C$	$3.7R_{onS}C$	$3.7R_{onL}C$
Depletion load	$1.2R_{onS}C$	$3.6R_{onL}C$	$3.7R_{onS}C$	$8.1R_{onL}C$
Saturated load	$1.2R_{onS}C$	$3.0R_{onL}C$	$3.7R_{onS}C$	$11.9R_{onL}C$
Linear load	$1.2R_{onS}C$	$0.69R_{onL}C$	$3.7R_{onS}C$	$3.7R_{onL}C$

$$R_{onS} = \frac{1}{K_S(V_H - V_{TNS})}$$

$$R_{onL} = \frac{1}{K_L|V_{GS} - V_{TNL}|}$$

the load is constant during the  $\tau_{PLH}$  time, we get

$$\begin{aligned} \tau_{PLH} &\cong \frac{C}{I} \left( \frac{\Delta V}{2} \right) = \left( \frac{0.1 \text{ pF}}{80 \mu\text{A}} \right) \left( \frac{2.5 - 0.2}{2} \right) = 1.44 \text{ ns (pseudo NMOS)} \\ \tau_{PLH} &\cong \frac{C}{I} \left( \frac{\Delta V}{2} \right) = \left( \frac{0.1 \text{ pF}}{80 \mu\text{A}} \right) \left( \frac{1.55 - 0.2}{2} \right) = 0.84 \text{ ns (saturated load inverter)} \end{aligned} \quad (6.61)$$

These simple calculations again represent an optimistic approximation that underestimates the simulated values of the propagation delays.

The largest differences in the delay times appear in the rise time results and are due to the widely differing current carrying capability of the various load transistors as the output rises from  $V_L$  to  $V_H$  as depicted in Fig. 6.47. The transistor sizes have been chosen so that the current in each device is  $80 \mu\text{A}$  when  $v_o$  is at the output low level of  $0.20 \text{ V}$ , and the drive current of each device decreases as the output voltage rises. The PMOS load provides the largest current whereas the saturated load is the weakest. As a reference for comparison, curve (e) is the straight line corresponding to the constant  $28.8\text{-k}\Omega$  load resistor. Note that body effect significantly degrades the characteristics of the saturated, linear, and depletion-mode load devices.

Both saturated load characteristics (a and b in Fig. 6.47) deliver substantially less current than the resistor throughout the full output voltage transition. Thus, we expect gates with saturated loads to have the poorest values of  $t_r$ . We also can observe that the load current of the saturated load devices goes to zero before the output reaches  $2.5 \text{ V}$ . The linear loads c and d are an improvement over the saturated load devices but still provide less current than the resistor load. The depletion-mode load devices f and g provide the largest current throughout the transition, and thus they should exhibit the smallest value of  $t_r$ . The ideal depletion-mode load g would deliver substantially more current than the resistor load. However, body effect significantly degrades the current source characteristics of the depletion-mode device. We can clearly see the substantial current advantage offered by the PMOS load device that leads to the improvements in  $t_r$  and  $\tau_{PLH}$  in Table 6.9.

Table 6.10 presents the inverter delay equations presented earlier in the chapter as well as similar approximations for the temporal responses of the other inverters. Each of the time responses

is determined by an  $RC$  product consisting of the load capacitance and the effective on-resistance of either the switching transistor or the load device. The constants multiplying the  $RC$  product are determined by the nonlinear behavior of the transistors.

As we should expect from our knowledge of RC networks, all the delays are directly proportional to the load capacitance  $C$  and to the effective resistance of the switching and load transistors. Note that the time responses are inversely proportional to carrier mobility since the on-resistances contain mobility in  $K_S$  and  $K_L$ . Thus, we expect NMOS logic to be approximately 2.5 times faster than PMOS circuits operating at equivalent voltages. This fact was the main reason for the rapid switch to NMOS technology from PMOS as soon as the manufacturing problems were overcome.

### 6.11.5 SCALING BASED UPON REFERENCE CIRCUIT SIMULATION

In many practical cases, particularly for advanced processes, we will not have closed-form expressions for the delay of a reference inverter. The models for the  $i-v$  characteristics may be too cumbersome for use in hand calculations, or the models may only exist in tabular form. In this case, we base our designs on scaling the results of circuit simulation of a reference inverter with a known load capacitance. Obviously we need values of the actual capacitive load that may be initially estimated from expected device sizes, and then later improved with CAD tools that extract the capacitance from the integrated circuit layout. We can then scale the inverter to achieve the desired delay with the new level of capacitive load.

Even though the delay expressions that have been developed using our first order  $i-v$  models are no longer quantitatively accurate for state-of-the-art technologies, for example, 65 nm CMOS, two important relationships continue to be true: delay remains proportional to the total load capacitance  $C_L$  and inversely proportional to the  $(W/L)$ . So for proper scaling, the size of the devices must be increased (i.e., increase the power of the gate) to decrease the propagation delay, and must also be increased to drive a larger capacitance. Thus the new values  $(W/L)'$  are related to the reference values  $(W/L, C_{L\text{ref}}, \tau_{P\text{ref}})$  by

$$\tau'_P = \frac{\left(\frac{W}{L}\right)}{\left(\frac{W}{L}\right)'} \times \left(\frac{C'_L}{C_{L\text{ref}}}\right) \times \tau_{P\text{ref}} \quad \text{or} \quad \left(\frac{W}{L}\right)' = \left(\frac{W}{L}\right) \times \left(\frac{\tau_{P\text{ref}}}{\tau'_P}\right) \times \left(\frac{C'_L}{C_{L\text{ref}}}\right) \quad (6.62)$$

The scaling results are often improved by building up a library of reference gates including not only the inverter but also a range of multi-input (2, 3, 4, etc.) NAND, NOR, and AOI gates for example. This latter technique helps account for the many components that contribute to the effective load capacitances.

### 6.11.6 RING OSCILLATOR MEASUREMENT OF INTRINSIC GATE DELAY

A common method of measuring the average propagation delay  $\tau_{P0}$  of a reference inverter is to construct a long ring of inverters as shown in Fig. 6.48. This can be done in hardware on an IC or as a simulation exercise. The circuit is called a **ring oscillator**, and the number of inverters must be an odd in order to ensure oscillation. The waveform at the output of any inverter will be similar to a square wave with a period  $T$  equal to two trips around the ring,

$$T = N (\tau_{PLH} + \tau_{PHL}) = 2N \times \tau_{P0} \quad (6.63)$$

where  $\tau_{P0}$  is the average propagation delay of the unloaded inverter ( $FO = 1, C_W = 0$ ).

**EXERCISE:** What is the frequency of oscillation of a 401-stage ring oscillator with an inverter propagation delay of 1 ns?

**ANSWER:** 1.25 MHz

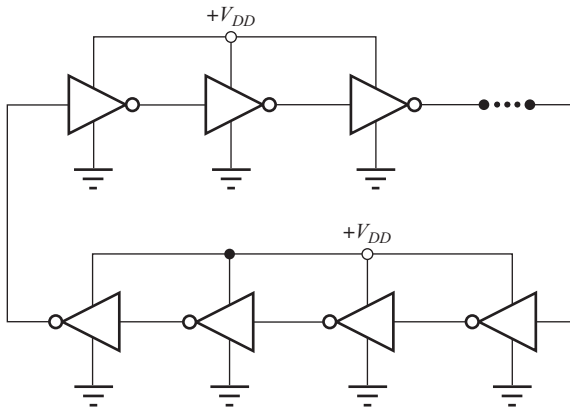


**Figure 6.48** Ring oscillator formed from a long chain of an *odd* number of inverters.

### 6.11.7 UNLOADED INVERTER DELAY

The reference inverter delay is ultimately limited by the characteristics of the transistors and the available power supply voltage. For example, consider a chain of NMOS inverters whose propagation delay is given by  $\tau_P = kR_{on}C$  where  $k$  depends upon the inverter technology as in Table 6.10. If we assume that the total load capacitance is dominated by the input capacitance  $C_{in}$  of the inverter, then we can find a limiting expression for the intrinsic propagation delay  $\tau_{P0}$  of the inverter:

$$\tau_{P0} = kR_{on}C \cong kR_{on}C_{in} \propto \frac{C''_{ox} \cdot W \cdot L}{\mu_n C''_{ox} \frac{W}{L} (V_{DD} - V_{TN})}$$

or

$$\tau_{P0} \propto \frac{L^2}{\mu_n (V_{DD} - V_{TN})} \quad (6.64)$$

In Eq. (6.64), we have used our standard expression for  $R_{on}$  and assumed that the input capacitance of the inverter is proportional to the gate area of the inverter. From Eq. (6.64), we see that the fundamental inverter delay is proportional to the square of the channel length, inversely proportional to mobility and power supply voltage, but independent of inverter width. It is clear why logic designers try to use the shortest available channel length whenever possible! In reality, the intrinsic inverter delay will be larger than that predicted by Eq. (6.64) since we have neglected the output capacitance in our derivation.

**EXERCISE:** What is the value of  $t_{P0}$  for a technology with  $L = 250$  nm,  $\mu_n = 500$  cm<sup>2</sup>/V-s,  $V_{DD} = 3.3$  V and  $V_{TN} = V_{DD}/4$ .

**ANSWER:** 50.5 ps

## DESIGN EXAMPLE 6.11

### PROPAGATION DELAY DESIGN FOR AN INVERTER

The logic gates that drive signals off an integrated-circuit chip are typically loaded by relatively large capacitances. This example determines the size of an inverter that is required to drive a large load capacitor with a small value of propagation delay.

**PROBLEM** Design a pseudo NMOS inverter to provide an average propagation delay of 2 ns when driving a 5-pF capacitor. Use the reference inverter design in Fig. 6.29 as described by the equations in Table 6.10. Find the rise and fall times for the logic gate.

**Known Information and Given Data:** Pseudo NMOS reference inverter design in Fig. 6.29(e) with  $C = 5 \text{ pF}$ ,  $V_{DD} = 2.5 \text{ V}$ ,  $K'_n = 100 \mu\text{A/V}^2$ ,  $V_{TNS} = 0.6 \text{ V}$ ,  $V_{TNL} = -0.6 \text{ V}$ ,  $V_H = 2.5 \text{ V}$ ,  $V_L = 0.20 \text{ V}$ ,  $(W/L)_S = 2.22/1$ , and  $(W/L)_L = 1.11/1$

**Unknowns:**  $(W/L)_S$ ,  $(W/L)_L$ ,  $t_f$ , and  $t_r$

**Approach:** (a) Use the results in Table 6.10 to find the required values of  $R_{onL}$  and  $R_{onS}$ . Determine the  $W/L$  ratios from the on-resistance values and the reference inverter design. (b) A second method is to scale the inverter based upon the results in Table 6.9.

**Assumptions:** Remember, there are many assumptions built into the various equations.

**SOLUTION** (a) **Direct Approach:** Using the equations in Table 6.10 for the pseudo NMOS inverter, we can write an expression for the average propagation delay.

$$\tau_P = \frac{1.2R_{onS}C + 1.2R_{onL}C}{2} = \frac{0.6C}{K_n} \left[ \frac{1}{(V_{DD} - V_{TN})} + \frac{1}{\frac{K_p}{K_n}| - V_{DD} - V_{TP}|} \right]$$

Using the parameters from the reference inverter design, we can solve for the  $W/L$  ratios of the two transistors:

$$\left( \frac{W}{L} \right)_S = \frac{0.6(5 \text{ pF})}{2 \text{ ns} (10^{-4} \text{ A/V}^2)} \left[ \frac{1}{(2.5 - 0.6)} + \frac{1}{\frac{1.11(40)}{2.22(100)} | - 2.5 - (-0.6)|} \right] = \frac{47.4}{1}$$

$$\left( \frac{W}{L} \right)_L = \frac{1}{2} \left( \frac{W}{L} \right)_S = \frac{23.7}{1}$$

The rise and fall times can be estimated using the equations in Table 6.10.

$$t_f = 3.7R_{onL}C = 3.7 \frac{5 \text{ pF}}{47.4(100 \mu\text{A/V}^2)(2.5 - 0.6) \text{ V}} = 2.05 \text{ ns}$$

$$t_r = 3.7R_{onL}C = 3.7 \frac{5 \text{ pF}}{23.7(40 \mu\text{A/V}^2)(2.5 - 0.6) \text{ V}} = 10.3 \text{ ns}$$

(b) **Scaling Approach:** SPICE results for the propagation delays of the inverters appear in Table 6.9. For the Psuedo NMOS gate we have

$$\tau_{PHL} = 0.33 \text{ ns} \quad \tau_{PLH} = 1.5 \text{ ns} \quad \tau_P = \frac{0.33 + 1.5}{2} \text{ ns} = 0.915 \text{ ns}$$

We need to reduce the size of the devices (i.e., reduce the power of the gate) to increase the propagation delay, and we need to increase the size of the devices to drive the larger capacitance. Thus the new  $W/L$  values are related to the reference values by

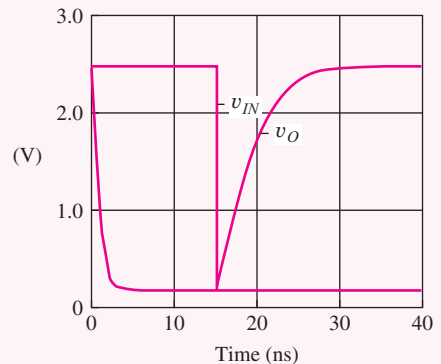
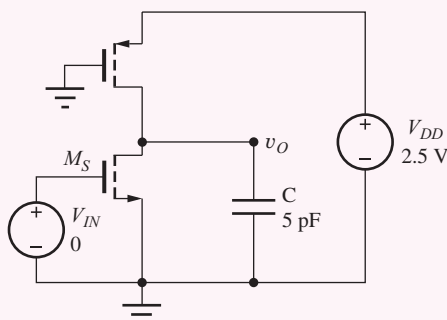
$$\left( \frac{W}{L} \right)' = \left( \frac{W}{L} \right) \times \left( \frac{0.915 \text{ ns}}{2 \text{ ns}} \right) \times \left( \frac{5 \text{ pF}}{0.1 \text{ pF}} \right) = 22.9 \left( \frac{W}{L} \right)$$

$$\left( \frac{W}{L} \right)_N = 22.9 \times \frac{2.22}{1} = \frac{50.8}{1} \quad \text{and} \quad \left( \frac{W}{L} \right)_P = 22.9 \times \frac{1.11}{1} = \frac{25.4}{1}$$

**Check of Results:** We have found the unknowns, and the values appear reasonable. The best check will be to simulate the transient response of the new inverter design using SPICE. The values in solution (b) differ slightly from those in (a). The (b) results are based upon SPICE simulation, whereas the ones in (a) use approximate formulas.

**Discussion:** Large transistor sizes are required to achieve the low propagation delay with a large capacitive load. The input capacitance to this inverter will also be large and require another large driver stage. The optimum form of these “cascade” buffers will be described in Chapter 7.

**Computer-Aided Analysis:** Now we confirm the behavior of our design using SPICE transient simulation. In the circuit schematic,  $V_{IN}$  is a pulse source with initial value of 0.2 V, peak value of 2.5 V, zero delay time, 0.10-ns rise time, 0.10-ns fall time, 14.9-ns pulse width, and a 40-ns period. The pulse width is chosen so that the rise time plus the pulse width add up to a convenient value of 15 ns. The rise and fall times for  $V_{IN}$  are chosen to be much smaller than the expected values of the inverter rise and fall times. The transient simulation parameters are a start time of zero, a stop time of 40 ns, and a time step of 0.025 ns.



From the graph of the transient response, we find  $\tau_{PHL} = 0.75$  ns and  $\tau_{PLH} = 3.5$  ns, yielding  $\tau_p = 2.1$  ns. The rise and fall times are 8.0 ns and 1.8 ns, respectively. The values all agree well with the design goals and estimates.

**EXERCISE:** What is the static power dissipation in the inverter in Ex. 6.11? What is the dynamic power dissipation if the inverter is switching on and off every 2 ns?

**ANSWERS:** 2.14 mW; 13.2 mW

**EXERCISE:** What would be the transistor sizes in Ex. 6.11 if the inverter was required to drive 20 pF with an average propagation delay of 1 ns (a 1-GHz rate)? What is the dynamic power consumption of this inverter?

**ANSWERS:** 379/1; 189/1; 0.11 W

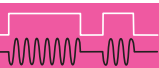
## 6.12 PMOS LOGIC

In the previous sections of this chapter, we have concentrated on understanding NMOS logic circuits. However, as already mentioned several times, PMOS logic historically preceded NMOS logic, but was quickly replaced by the higher-performance NMOS logic as soon as NMOS technology could be reliably manufactured. This section presents a brief discussion of PMOS logic circuits.

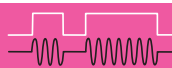
### 6.12.1 PMOS INVERTERS

PMOS logic circuits mirror those presented for NMOS logic as exhibited in Fig. 6.49 which presents the PMOS equivalents of the inverter designs in Fig. 6.29. In these circuits, the power supply has been changed to  $-2.5$  V and each NMOS transistor has been replaced with a PMOS device.

Each circuit has been designed to have the same power level as the equivalent NMOS circuit:  $P = 0.20$  mW. Note that for the circuit in Fig. 6.49(a),  $V_L = -2.5$  V and  $V_H = -0.20$  V. In the saturated load circuit in Fig. 6.49(b),  $V_L = -1.55$  V and  $V_H = -0.20$  V, assuming the value of  $V_{TP} = -0.6$  V. The  $W/L$  ratios have been found by simply scaling the  $W/L$  ratios of the NMOS inverters by the mobility ratio  $\mu_n/\mu_p = 2.5$ , not by going through detailed calculations.



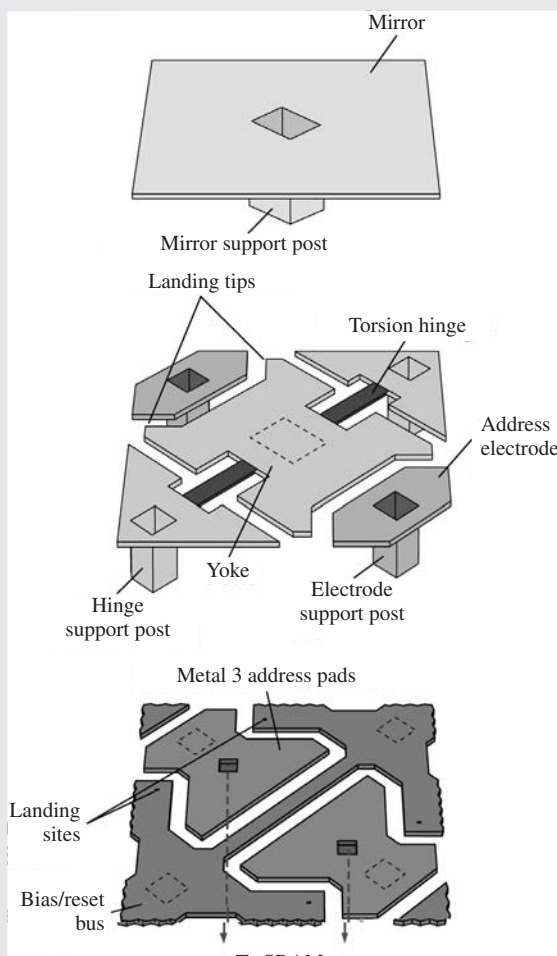
## ELECTRONICS IN ACTION



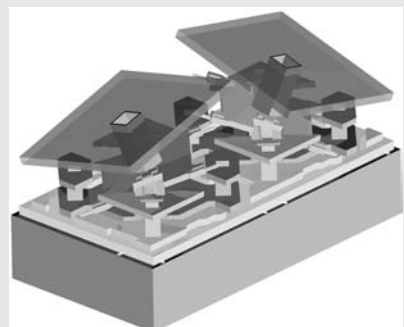
### **MEMS-Based Computer Projector**

Microelectromechanical systems (MEMS) devices are becoming increasingly important in a variety of applications. MEMS allow one to design mechanical devices controllable by electrical signals and micromachined using tools and techniques similar to those used in the microelectronics industry. MEMS devices are used in applications such as air-bag accelerometers, radio frequency filters, and electrically addressable light modulators.

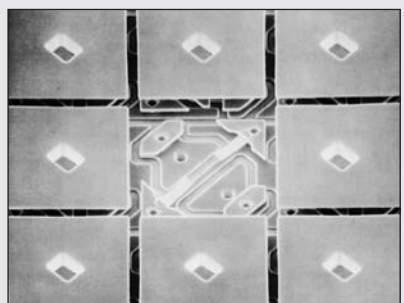
These figures show a MEMS-based technology developed at Texas Instruments and used at the core of many computer-driven projectors. The device has a large array of 12 to 16  $\mu\text{m}$  mirrors, each of which is controlled by a CMOS SRAM memory cell located underneath each mirror. The mirror rotates about the torsion hinge shown. Depending on the digital value stored



(a)



(b)



(c)

(a) Details of the micro-mirror pixel structure. (b) Three-dimensional view of two adjacent pixels. (c) Magnified view of 9 micro-mirror pixels. The middle mirror and yoke have been removed.

in each cell, voltages are driven onto the address electrodes creating electrostatic forces that rotate the mirror into one of two positions. Combined with the appropriate optics, light is directed onto the device and reflected onto a projection screen. Writing appropriate data values in each pixel allows any arbitrary pattern to be created on the screen.

This scheme allows one to turn on or off each pixel. To also include grayscale, the ON time of each pixel is varied by writing different data into the cells during a single display interval. If a mirror is held in the ON position for 20 percent of a display interval, the human eye will perceive a pixel with an intensity of 20 percent. Color is created by a sequence of red, green, and blue illumination sources used in rapid sequence to create three sequential color frames. Again, the eye integrates the three color signals and creates the perception of a vast palette of colors. A few projection systems use three separate display chips to create the three-color image frames simultaneously, allowing for greater total optical power to be projected onto very large screens.

The combination of microscale movable mirrors with microelectronics has made possible a new technique for the projection of high resolution and high quality digital images and video. The integration of MEMS and microelectronics is enabling new applications in fields as diverse as medicine, science, transportation, and consumer electronics.

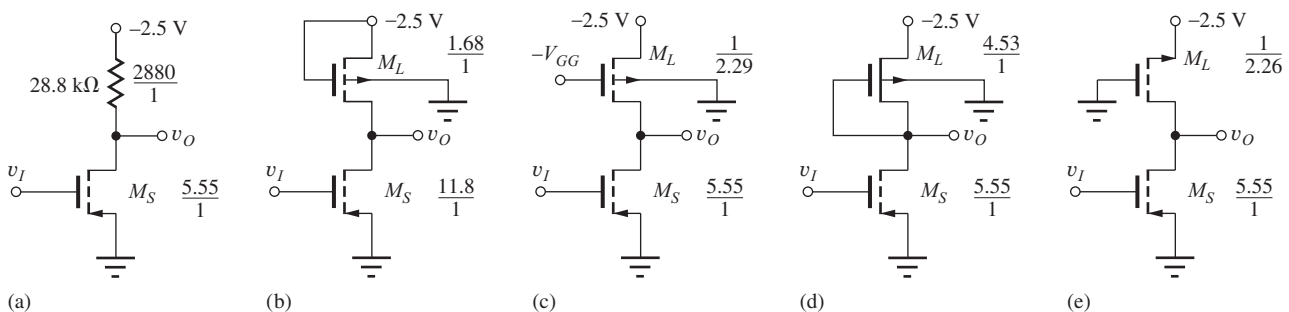


**Figure 6.49** PMOS inverters: (a) resistive load, (b) saturated load, (c) linear load, (d) depletion-mode load, and (e) pseudo PMOS.

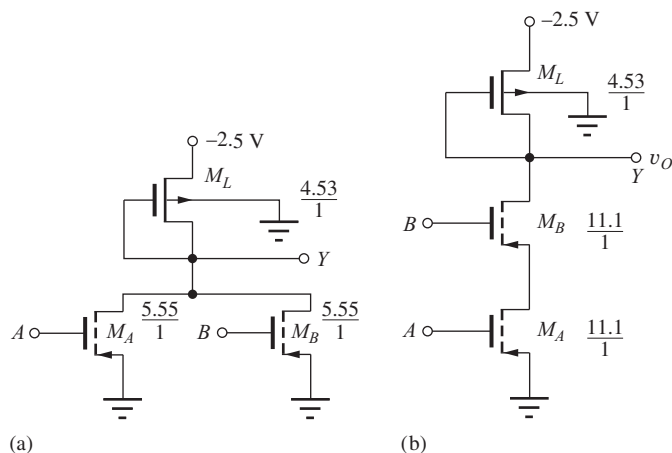


**Figure 6.50** Two-input PMOS gates: (a) NOR gate and (b) NAND gate.

### 6.12.2 NOR AND NAND GATES

The PMOS NOR and NAND gates in Fig. 6.50 mirror the NMOS circuits in Figs. 6.30 and 6.31. The power supply has been changed to  $-2.5$  V, and each NMOS transistor has been replaced with a PMOS device. The  $W/L$  ratios are scaled by the mobility ratio of 2.5. Complex logic gates are built up in a manner analogous to the NMOS case. As noted previously, NMOS logic will have a  $2.5 \times$  speed advantage over PMOS logic for a given capacitance and gate size. The various delay times can be calculated using the formulas presented in Table 6.10.

## SUMMARY

Chapter 6 introduced a number of concepts and definitions that form a basis for logic gate design. NMOS technology was then used as a vehicle to explore detailed logic circuit design. The geometry of the load device,  $(W/L)_L$ , is designed to limit the current and power dissipation of the logic gate to the desired level, whereas the geometry of the switching device,  $(W/L)_S$ , is chosen to provide the desired value of  $V_L$ . Transistors are usually designed with either  $W$  or  $L$  set equal to the minimum feature size achievable in a given technology.

- *Boolean algebra:* Boolean algebra, developed by G. Boole in the mid-1800s, is a powerful mathematical tool for manipulating binary logic expressions. Basic logic gates provide some combination of the NOT, AND, OR, NAND, or NOR logic functions. A complete logic family must provide at least the NOT function and either the AND or OR functions.
- *Binary logic states:* Binary logic circuits use two voltage levels to represent the Boolean logic variables 1 and 0. In the positive logic convention used throughout this book, the more positive voltage represents a 1, and the more negative level represents a 0. The output of an ideal logic gate would take on only two possible voltage levels:  $V_H$  corresponding to the 1 state, and  $V_L$  corresponding to the 0 state.
- *Logic state transitions:* The output of the ideal gate would abruptly change state as the input crossed through a fixed reference voltage  $V_{REF}$ . However, such an abrupt transition cannot be achieved (it requires infinite gain devices). Logic gates implemented with electronic circuits can only approximate this ideal behavior. The transition between states as the input voltage changes is much more gradual, and a precise reference voltage is not defined.  $V_{IL}$  and  $V_{IH}$  are defined by the input voltages at which the slope of the voltage transfer characteristic is equal to  $-1$ , and these voltages define the boundaries of the transition region between the logical 1 and 0 levels.
- *Noise margins:* Noise margins are very important in logic gates and represent a measure of the gate's ability to reject extraneous signals. The high-state and low-state noise margins are defined by  $NM_H = V_{OH} - V_{IH}$  and  $NM_L = V_{IL} - V_{OL}$ , respectively. Voltages  $V_{OL}$  and  $V_{OH}$  represent the gate output voltages at the  $-1$  slope points and correspond to input levels  $V_{IH}$  and  $V_{IL}$ , respectively. The unwanted signals can be voltages or currents coupled into the circuit from adjacent logic gates, from the power distribution network, or by electromagnetic radiation. The noise margins must also absorb manufacturing process tolerance variations and power supply voltage variations.
- *Logic design goals:* Keep in mind a number of logic gate design goals.
  1. The logic gate should quantize the input signal into two discrete output levels and minimize the width of the undefined input voltage range.
  2. The gate should be unidirectional in nature.
  3. Logic levels must be regenerated as the signal passes through the gate.
  4. Logic gates should have significant fan-in and fan-out capability.
  5. Minimum power and area should be used to meet the speed requirements of the design. Noise margins generally should be as large as possible.

- *Logic delays:* In the time domain, the transition between logic states cannot occur instantaneously. Capacitances exist in any real circuit and slow down the state transitions, thereby degrading the logic signals. Rise time  $t_r$  and fall time  $t_f$  characterize the time required for a given signal to change between the 0 and 1 or 1 and 0 states, respectively, and the average propagation delay  $\tau_P$  characterizes the time required for the output of a given gate to respond to changes in its input signals. The propagation delays on the high-to-low ( $\tau_{PHL}$ ) and low-to-high ( $\tau_{PLH}$ ) transitions are typically not equal, and  $\tau_P$  is equal to the average of these two values.
- *Power-delay product:* The power-delay product PDP, expressed in picojoules (pJ) or femtojoules (fJ), is an important figure of merit for comparing logic families. At low power levels, the power-delay product is a constant, and the propagation delay of a given logic family decreases as power is increased. At intermediate power levels, the propagation delay becomes independent of power level, and at high power levels, the propagation delay may degrade as power is increased.
- *NMOS inverter with resistor load:* Basic inverter design was introduced by considering the static behavior of an inverter using an NMOS switching transistor and a resistor load. Although simple in concept, the resistor is not feasible for use as a load element in ICs because it consumes too much area.
- *IC inverters:* In integrated circuits, the resistor load in the logic gate is replaced with a second MOS transistor, and four possibilities were investigated in detail: the saturated load device, the linear load device, the depletion-mode load device, and the pseudo NMOS inverter.
  - *Saturated load:* The saturated load device is the most economical configuration because it does not require any modification to the basic MOS fabrication process.
  - *Linear load:* The linear load configuration offers improved performance but requires an additional power supply voltage, which is both expensive and causes substantial wiring congestion in ICs.
  - *Depletion-mode load:* Depletion-mode load circuits require additional processing in order to create MOSFETs with a second value of threshold voltage. However, substantial performance improvement can be obtained, and NMOS depletion-mode load technology was the workhorse of the microprocessor industry for many years.
  - *Pseudo NMOS Inverter:* A PMOS transistor is used as the load device in this logic family. Pseudo NMOS is a high-performance form of NMOS logic that is most commonly found embedded in today's CMOS IC chip designs.
- *NOR and NAND gates:* Multi-input NOR and NAND gates can both easily be implemented in MOS logic. The NOR gate is formed by placing additional transistors in parallel with the switching transistor of the basic inverter, whereas the NAND gate is formed by several switching devices connected in series.
- *Complex logic gates:* An advantage of MOS logic is its ability to implement complex sum-of-products and product-of-sums logic equations in a single logic gate, by utilizing both parallel and series connections of the switching transistors. A single load device is required for each logic gate, and one switching transistor is required for each logic input variable.
- *Reference inverter based design:* Once the reference inverter for a logic family is designed, NAND, NOR, and complex gates can all be designed by applying simple scaling rules to the geometry of the reference inverter.
- *MOS body effect:* The influence of the MOSFET body effect cannot be avoided in integrated circuits, and it plays an important role in the design of NMOS (or PMOS) logic gates. Body effect reduces the value of  $V_H$  in saturated load logic and generally degrades the current delivery capability of all the load device configurations, thereby increasing the delay of all the logic gates. The MOS body effect has a minor influence on the design of the  $W/L$  ratios of the switching transistors in complex logic gates.

- *Rise time, fall time, and propagation delay:* Equations were developed for the rise time, fall time, and propagation delays of the various types of NMOS logic gates, and it was shown that all the time delays of MOS logic circuits are directly proportional to the total equivalent capacitance connected to the output node of the gate. The total effective capacitance is a complicated function of operating point and is due to the capacitance of the interconnections between gates as well as the capacitances of the MOS devices, which include the gate-source ( $C_{GS}$ ), gate-drain ( $C_{GD}$ ), drain-bulk ( $C_{DB}$ ), and source-bulk ( $C_{SB}$ ) capacitances.
- *Static and dynamic power dissipation:* Power dissipation of a logic gate has a static component and a dynamic component. Dynamic power dissipation is proportional to the switching frequency of the logic gate, the total capacitance, and the square of the logic voltage swing. At low switching frequencies, static power dissipation is most important, but at high switching rates the dynamic component becomes dominant. For a given load capacitance, the power and speed of a logic gate can be changed by proportionately scaling the geometry of the load and switching transistors. For example, doubling the  $W/L$  ratios of all devices doubles the power of the gate without changing the static voltage levels of the design. This behavior is characteristic of “ratioed” MOS logic.
- *PMOS logic:* PMOS logic gates are mirror images of the NMOS gates. In order to equal the performance of NMOS, the size of the transistors must be increased in order to compensate for the lower mobility of holes compared to electrons.

## KEY TERMS

AND gate	Power scaling
Average propagation delay ( $\tau_p$ )	Propagation delay—high-to-low transition ( $\tau_{PHL}$ )
Boolean algebra	Propagation delay—low-to-high transition ( $\tau_{PLH}$ )
Complementary MOS (CMOS) technology	Pseudo NMOS inverter
Complex logic gates	Ratioed logic
Depletion load inverter	Reference inverter design
Dynamic power dissipation	Reference voltage ( $V_{REF}$ )
Emitter-coupled logic (ECL)	Resistor load inverter
Fall time $t_f$	Rise time $t_r$
Fan in	Saturated load inverter
Fan out	Single-channel technology
High logic level at the gate input ( $V_{IH}$ )	Static power dissipation
High logic level at the gate output ( $V_H$ )	Sum-of-products logic function
Linear load inverter	Switching transistor
Load transistor	Transistor-transistor logic (TTL)
Low logic level at the gate input ( $V_{IL}$ )	Truth table
Low logic level at the gate output ( $V_L$ )	$V_{OH}$ —The output voltage corresponding to an input voltage of $V_{IL}$
Minimum feature size ( $F$ )	$V_{OL}$ —The output voltage corresponding to an input voltage of $V_{IH}$
MOS device capacitances	Voltage transfer characteristic (VTC)
NAND gate	10 percent point
Noise margin in the high state ( $NM_H$ )	50 percent point
Noise margin in the low state ( $NM_L$ )	90 percent point
NOR gate	$W/L$ ratio
On-resistance	
OR gate	
Output high logic level ( $V_H$ )	
Output low logic level ( $V_L$ )	
Power-delay product (PDP)	

## REFERENCES

1. "The 4004 Microprocessor of FAggin, Hoff, Mazor and Shima," *IEEE Solid-State Circuits Magazine*, vol. 1, no. 1, Winter 2009.
2. J. R. Houser, "Noise margin criteria for digital logic circuits," *IEEE Trans. on Education*, vol. 36, no. 4, pp. 363–368, November 1993.
3. C. F. Hill, "Noise margin and noise immunity in logic circuits," *Microelectronics*, vol. 1, pp. 16–21, April 1968.
4. J. Lohstroh, E. Seevinck, and J. Degroot, "Worst-case static noise margin criteria for logic circuits and their mathematical equivalence," *IEEE J. of Solid-State Circuits*, vol. SC-18, no. 6, pp. 803–806, December 1983.
5. J. D. Meindl and J. A. Davis, "The fundamental limit on binary switching energy for terascale integration (TSI)," *IEEE J. of Solid-State Circuits*, vol. 35, no. 10, pp. 1515–1516, October 2000.
6. R. M. Swanson and J. D. Meindl, "Ion-implanted complementary MOS transistors in low-voltage circuits," *IEEE J. of Solid-State Circuits*, vol. SC-7, no. 2, pp. 146–153, April 1972.
7. G. Boole, *An Investigation of the Laws of Thought, on Which Are Founded the Mathematical Theories of Logic and Probability*, 1849. Reprinted by Dover Publications, Inc., New York: 1954.

## ADDITIONAL READING

Nelson, V. P., et al. *Analysis and Design of Logic Circuits*. Prentice-Hall, Englewood Cliffs, N.J.: 1995.

## PROBLEMS

Use  $K'_n = 100 \mu\text{A/V}^2$ ,  $K'_p = 40 \mu\text{A/V}^2$ ,  $V_{TN} = 0.6 \text{ V}$ , and  $V_{TP} = -0.6 \text{ V}$  unless otherwise indicated.

### General Introduction

- 6.1. Integrated circuit chips packaged in plastic can typically dissipate only 1 W per chip. Suppose we have an IC design that must fit on one chip and requires 100,000 logic gates. (a) What is the average power that can be dissipated by each logic gate on the chip? (b) If a supply voltage of 2.5 V is used, how much current can be used by each gate? Assume a 50 percent duty cycle.
- 6.2. A high-performance microprocessor design requires 100 million logic gates and is placed in a package that can dissipate 100 W. (a) What is the average power that can be dissipated by each logic gate on the chip? (b) If a supply voltage of 2.5 V is used, how much current can be used by each gate? Assume a 25 percent duty cycle. (c) What is the total current required by the IC chip?

### Ideal Gates, Logic Level Definitions, and Noise Margins

- 6.3. (a) The ideal inverter in Fig. 6.2(b) has  $R = 100 \text{ k}\Omega$  and  $V_+ = 2.5 \text{ V}$ . What are  $V_H$  and  $V_L$ ? What is the power dissipation of the gate for  $v_O = V_H$  and  $v_O = V_L$ ? (b) Repeat for  $V_+ = 3.3 \text{ V}$ .

- 6.4. Plot a graph of the voltage transfer characteristic for an ideal inverter with  $V_+ = 2.5 \text{ V}$ ,  $V_- = 0 \text{ V}$ , and  $V_{\text{REF}} = 0.8 \text{ V}$ . Assume  $V_H = V_+$  and  $V_L = V_-$ .
- 6.5. (a) Plot a graph of the overall voltage transfer function for two cascaded ideal inverters if each individual inverter has a voltage transfer characteristic as defined in Prob. 6.4. (b) What is the overall logic expression  $Z = f(A)$  for the two cascaded inverters?
- 6.6. Plot a graph of the voltage gain  $A_v$  of the ideal inverter in Fig. 6.1 as a function of input voltage  $v_I$ . ( $A_v = dv_O/dv_I$ )
- 6.7. The voltage transfer characteristic for an inverter is given in Fig. P6.7. What are  $V_H$ ,  $V_L$ ,  $V_{IH}$ ,  $V_{IL}$ ? Plot the voltage gain  $A_v$  of the inverter ( $A_v = dv_O/dv_I$ ) as a function of  $v_I$ .

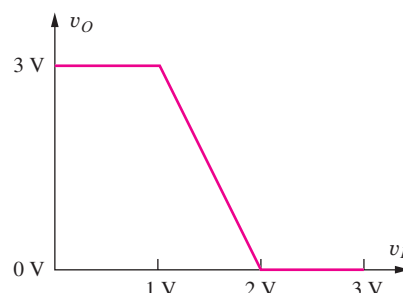


Figure P6.7

- 6.8. Plot a graph of the overall voltage transfer characteristic for two cascaded inverters if each individual inverter has the voltage transfer function defined in Fig. P6.7.
- 6.9. Suppose  $V_H = 5 \text{ V}$ ,  $V_L = 0 \text{ V}$ , and  $V_{\text{REF}} = 2.0 \text{ V}$  for the ideal logic gate in Fig. 6.1. What are the values of  $V_{IH}$ ,  $V_{OL}$ ,  $V_{IL}$ ,  $V_{OH}$ ,  $\text{NM}_H$ , and  $\text{NM}_L$ ?
- 6.10. Suppose  $V_H = 3.3 \text{ V}$  and  $V_L = 0 \text{ V}$  for the ideal logic gate in Fig. 6.1. Considering noise margins, what would be the best choice of  $V_{\text{REF}}$ , and why did you make this choice?
- 6.11. The static voltage transfer characteristic for a practical CMOS inverter is given in Fig. P6.11. Estimate the values of  $V_H$ ,  $V_L$ ,  $V_{OH}$ ,  $V_{OL}$ ,  $V_{IH}$ ,  $V_{IL}$ ,  $\text{NM}_H$ , and  $\text{NM}_L$ .

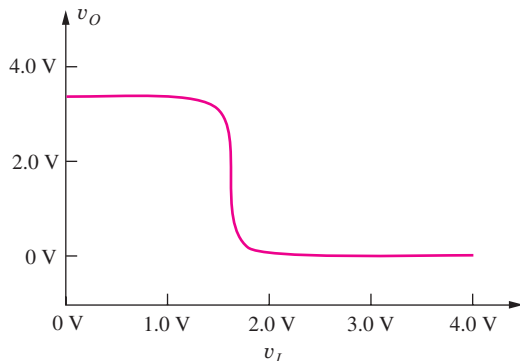


Figure P6.11

- 6.12. The graph in Fig. P6.12 gives the results of a SPICE simulation of an inverter. What are  $V_H$  and  $V_L$  for this gate?

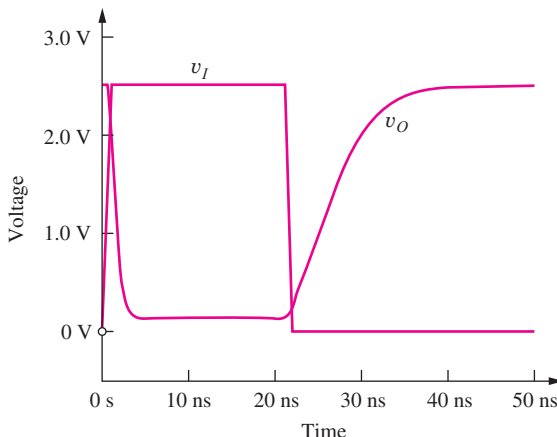


Figure P6.12

- 6.13. The graph in Fig. P6.13 gives the results of a SPICE simulation of an inverter. What are  $V_H$  and  $V_L$  for this gate?

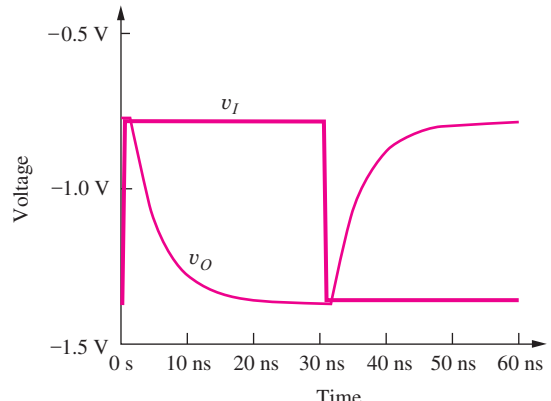


Figure P6.13

- 6.14. An ECL gate exhibits the following characteristics:  $V_{OH} = -0.8 \text{ V}$ ,  $V_{OL} = -2.0 \text{ V}$ , and  $\text{NM}_H = \text{NM}_L = 0.5 \text{ V}$ . What are the values of  $V_{IH}$  and  $V_{IL}$ ?

### Dynamic Response of Logic Gates

- 6.15. A logic family has a power-delay product of 100 fJ. If a logic gate consumes a power of 100  $\mu\text{W}$ , estimate the propagation delay of the logic gate.
- 6.16. Plot the power-delay product versus power for the logic gate with the power-delay characteristic depicted in Fig. 6.6.
- 6.17. A 1-GHz processor has  $10^9$  logic gates with an average propagation delay of 150 ps. If the package can dissipate 50 W, what is the average power per gate assuming a 33 percent duty cycle? What is the power-delay product?
- 6.18. Integrated circuit chips packaged in plastic can typically dissipate only 1 W per chip. Suppose we have an IC design that must fit on one chip and requires 500,000 logic gates. (a) What is the average power that can be dissipated by each logic gate on the chip? (b) If a supply voltage of 2.5 V is used, how much current can be used by each gate? Assume a 50 percent duty cycle. (c) If the average gate delay for these circuits must be 2 ns, what is the power-delay product required for the circuits in this design?
- 6.19. A high-performance microprocessor design requires 200 million logic gates and is placed in a package that can dissipate 100 W. (a) What is the average power that can be dissipated by each logic gate on the chip? (b) If a supply voltage of 1.8 V is used, how much current can be used by each gate? Assume a 20 percent duty cycle. (c) If the average gate delay for these circuits must be 1 ns, what is

the power-delay product required for the circuits in this design?

- \*6.20. (a) Derive an expression for the rise time of the circuit in Fig. P6.20(a) in terms of the circuit time constant. Assume that  $v(t)$  is a 1-V step function, changing state at  $t = 0$ . (b) Derive a similar expression for the fall time of the capacitor voltage in Fig. P6.20(b) if the capacitor has an initial voltage of 1 V at  $t = 0$ .

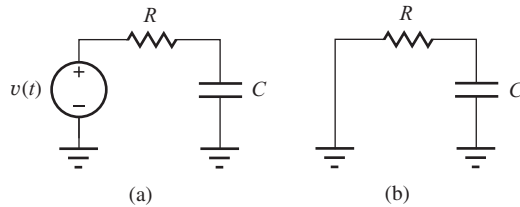


Figure P6.20

- 6.21. The graph in Fig. P6.12 gives the results of a SPICE simulation of an inverter. (a) What are  $V_H$  and  $V_L$  for this gate? (b) What are the rise and fall times for  $v_I$  and  $v_O$ ? (c) What are the values of  $\tau_{PHL}$  and  $\tau_{PLH}$ ? (d) What is the average propagation delay for this gate?
- 6.22. The graph in Fig. P6.13 gives the results of a SPICE simulation of an inverter. (a) What are  $V_H$  and  $V_L$  for this gate? (b) What are the rise and fall times for  $v_I$  and  $v_O$ ? (c) What are the values of  $\tau_{PHL}$  and  $\tau_{PLH}$ ? (d) What is the average propagation delay for this gate?

#### 6.4 Review of Boolean Algebra

- 6.23. Use the results in Table 6.2 to prove that  $(A + B) \cdot (A + C) = A + BC$ .
- 6.24. Use the results in Table 6.2 to simplify the logic expression  $Z = \bar{A}\bar{B}C + ABC + \bar{A}BC + A\bar{B}C$ .
- 6.25. Make a truth table for the expression in Prob. 6.24.
- 6.26. Use the results in Table 6.2 to simplify the logic expression  $Z = AB\bar{C} + ABC + \bar{A}BC$ .
- 6.27. Make a truth table for the expression in Prob. 6.26.
- 6.28. Make a truth table and write an expression for the two logic functions in Fig. P6.28.

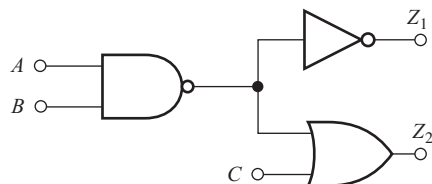


Figure P6.28

- 6.29. Make a truth table and write an expression for the logic function in Fig. P6.29.

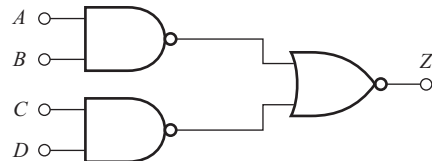


Figure P6.29

- 6.30. (a) What is the fan out of the NAND gate in Fig. P6.28? (b) Of each NAND gate in Fig. P6.29?

#### General Problems

- 6.31. A high-speed microprocessor must drive a 64-bit data bus in which each line has a capacitive load  $C$  of 40 pF, and the logic swing is 3.3 V. The bus drivers must discharge the load capacitance from 3.3 V to 0 V in 0.8 ns, as depicted in Fig. P6.31. Draw the waveform for the current in the output of the bus driver as a function of time for the indicated waveform. What is the peak current in the microprocessor chip if all 64 drivers are switching simultaneously?

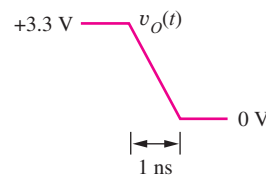
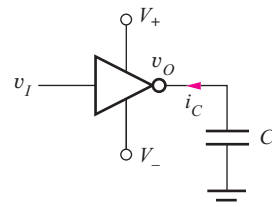


Figure P6.31 Bus driver and switching waveform.

- 6.32. Repeat Prob. 6.31 for a processor with a 1-GHz clock. Assume that the fall time must be 0.1 ns instead of 1 ns, as depicted in Fig. P6.31.
- \*6.33. A particular interconnection between two logic gates in an IC chip runs one-half the distance across a 7.5-mm-wide die. The interconnection line is insulated from the substrate by silicon dioxide. If the line is 1.5  $\mu\text{m}$  wide and the oxide ( $\epsilon_{\text{ox}} = 3.9\epsilon_0$  and  $\epsilon_0 = 8.85 \times 10^{-14} \text{ F/cm}$ ) beneath the line is

1  $\mu\text{m}$  thick, what is the total capacitance of this line assuming that the capacitance is three times that predicted by the parallel plate capacitance formula? Assume that the silicon beneath the oxide represents a conducting ground plane.

- \*\*6.34. Ideal constant-electric-field scaling of a MOS technology reduces all the dimensions and voltages by the same factor  $\alpha$ . Assume that the circuit delay  $\Delta T$  can be estimated from

$$\Delta T = C \frac{\Delta V}{I}$$

in which the capacitance  $C$  is proportional to the total gate capacitance of the MOS transistor,  $C = C_{\text{ox}}'' WL$ ,  $\Delta V$  is the logic swing, and  $I$  is the MOS-FET drain current in saturation. Show that constant-field scaling results in a reduction in delay by a factor of  $\alpha$  and a reduction in power by a factor of  $\alpha^2$  so that the PDP is reduced by a factor of  $\alpha^3$ . Show that the power density actually remains constant under constant-field scaling.

- \*\*6.35 For many years, MOS devices were scaled to smaller and smaller dimensions without changing the power supply voltage. Suppose that the width  $W$ , length  $L$ , and oxide thickness  $T_{\text{ox}}$  of a MOS transistor are all reduced by a factor of 2. Assume that  $V_{TN}$ ,  $v_{GS}$ , and  $v_{DS}$  remain the same. (a) Calculate the ratio of the drain current of the scaled device to that of the original device. (b) By what factor has the power dissipation changed? (c) By what factor has the value of the total gate capacitance changed? (d) By what factor has the circuit delay  $\Delta T$  changed? (Use the delay formula in Prob. 6.34)

## 6.5 NMOS Logic Design

- 6.36. Integrated circuit chips packaged in plastic DIPs (dual-in-line packages) can typically dissipate 1 W per chip. Suppose that we have an IC design that must fit on one chip and requires two million logic gates. Assume that one-third the logic gates on the chip are conducting current at any given time. (a) What is the average power that can be dissipated by each logic gate on the chip? (b) If a supply voltage of 1.8 V is used, how much current can be used by each gate?
- 6.37. A high-performance microprocessor design requires 20 million logic gates and will be placed in a package that can dissipate 20 W. (a) What is the average power that can be dissipated by each logic gate on the chip? (b) If a supply voltage of 1.8 V is used, how much current can be used by each gate?

Assume that one-third of the logic gates on the chip are in the conducting state at any given time.

### Resistor Load Inverter

- 6.38. Design a resistive load inverter to operate from a 2.0-V power supply with a power dissipation of 50  $\mu\text{W}$ .
- 6.39. (a) Find  $V_H$ ,  $V_L$ , and the power dissipation (for  $v_O = V_L$ ) for the logic inverter with resistor load in Fig. P6.39(a). (b) Repeat for Fig. P6.39(b).

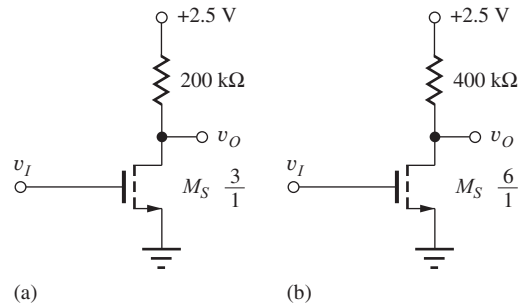


Figure P6.39

- 6.40. (a) What should be the value of  $W/L$  for the transistor in Fig. 6.39(b) if it is to have the same value of  $V_L$  as the inverter in Fig. 6.39(a)? (a) What should be the value of  $W/L$  for the transistor in Fig. 6.39(a) if it is to have the same value of  $V_L$  as the inverter in Fig. 6.39(b)?
- 6.41. (a) The load resistor in Fig. 6.39(a) is changed to 100 k $\Omega$ . What should be the new value of  $W/L$  if  $V_L$  is to remain unchanged? (b) What is the new value of  $V_H$ ? (c) The load resistor in Fig. 6.39(b) is changed to 200 k $\Omega$ . What should be the new value of  $W/L$  if  $V_L$  is to remain unchanged?
- 6.42. A manufacturing problem caused  $V_{TN} = 0.8$  V instead of 0.6 V for the inverter in Fig. P6.39(a). (a) What are the values of  $V_H$ ,  $V_L$ , and power dissipation? (b) Repeat for  $V_{TN} = 0.4$  V.
- 6.43. (a) What are the noise margins for the circuit in Fig. P6.39(a)? (b) Fig. P6.39(b)?
- 6.44. (a) Find  $V_H$ ,  $V_L$ , and the power dissipation (for  $v_O = V_L$ ) for the logic inverter with resistor load in Fig. P6.39(b). (b) A manufacturing problem caused  $V_{TN} = 0.5$  V instead of 0.6 V. What are the new values of  $V_H$ ,  $V_L$ , and power dissipation? (c) Repeat for  $V_{TN} = 0.7$  V.
- 6.45. (a) What is the minimum value of  $K_n R$  required for both noise margins to be positive in the inverter in Ex. 6.4? (b) What is  $V_L$  for this value of  $K_n R$ ? (c) What value of  $W/L$  corresponds to the value of

$K_n R$  in part (a)? (d) What is the value of  $R_{on}$  for the transistor?

- 6.46. (a) What are the noise margins for the circuit in Fig. P6.39(b)? (b) What value of  $W/L$  will result in  $N_{ML} = 0$  for the resistive load inverter in Fig. P6.39(b)?
- 6.47. Plot the noise margins of the inverter in Ex. 6.4 as a function of  $W/L$  of the switching transistor.
- 6.48. Find the nominal and worst-case values for the noise margins of the inverter in Ex. 6.4 if the threshold voltage has a tolerance of 10 percent, the power supply has a 5 percent tolerance, and  $K_n$  and  $R$  both have 30 percent tolerances.
- 6.49. (a) Perform a 1000 case Monte Carlo analysis for the noise margins of the inverter in Ex. 6.4 if the threshold voltage has a tolerance of 10 percent, the power supply has a 5 percent tolerance and  $K_n$  and  $R$  both have 30 percent tolerances. What are the nominal, minimum and maximum values of  $N_{ML}$  and  $N_{MH}$ ? (b) Compare the results to those of Prob. 6.48.
- 6.50. The resistive load inverter in Fig. 6.12 is to be redesigned for  $V_L = 0.5$  V. (a) What are the new values of  $R$  and  $(W/L)_S$  assuming that the power dissipation remains the same? (b) What are the values of  $N_{ML}$  and  $N_{MH}$ ?
- 6.51. (a) Redesign the resistive load inverter of Fig. 6.12 for operation at a power level of 0.30 mW with  $V_{DD} = 3.3$  V. Assume  $V_{TO} = 0.7$  V. Keep the other design parameters the same. What is the new size of  $M_S$  and the value of  $R$ ? (b) What are the values for  $N_{MH}$  and  $N_{ML}$ ?
- 6.52. (a) Design an inverter with a resistive load for  $V_{DD} = 2.0$  V and  $V_L = 0.15$  V. Assume  $I_{DD} = 10 \mu\text{A}$ ,  $K'_n = 75 \mu\text{A/V}^2$ , and  $V_{TN} = 0.6$  V. (b) Confirm the validity of your design with SPICE.
- 6.53. Design an inverter with a resistive load for  $V_{DD} = 3$  V and  $V_L = 0.30$  V. Assume  $I_{DD} = 33 \mu\text{A}$ ,  $K'_n = 60 \mu\text{A/V}^2$ , and  $V_{TN} = 0.75$  V. (b) Confirm the validity of your design with SPICE.

## 6.6 Transistor Alternatives to Resistor Load

- 6.54. (a) Calculate the on-resistance of an NMOS transistor with  $W/L = 10/1$  for  $V_{GS} = 5$  V,  $V_{SB} = 0$ ,  $V_{TO} = 1$  V, and  $V_{DS} = 0$  V. (b) Calculate the on-resistance of a PMOS transistor with  $W/L = 10/1$  for  $V_{SG} = 5$  V,  $V_{SB} = 0$ ,  $V_{TO} = -1$  V, and  $V_{SD} = 0$  V. (c) What do we mean when we say that a transistor is “on” even though  $I_D$  and  $V_{DS} = 0$ ?

(d) What must be the  $W/L$  ratios of the NMOS and PMOS transistors if they are to have the same on-resistance as parts (a) and (b) with  $|V_{GS}| = 3.0$  V?

## Saturated Load Inverter

- 6.55. Find  $V_H$  for an NMOS logic gate with a saturated load if  $V_{TO} = 0.5$  V,  $\gamma = 0.85 \sqrt{V}$ ,  $2\phi_F = 0.6$  V, and  $V_{DD} = 2.5$  V.
- 6.56. Find  $V_H$  for an NMOS logic gate with a saturated load if  $V_{TO} = 0.75$  V,  $\gamma = 0.75 \sqrt{V}$ ,  $2\phi_F = 0.7$  V, and  $V_{DD} = 3.0$  V.
- 6.57. Find  $V_H$  for an NMOS logic gate with a saturated load if  $V_{TO} = 0.6$  V,  $\gamma = 0.6 \sqrt{V}$ ,  $2\phi_F = 0.6$  V, and  $V_{DD} = 3.3$  V.
- 6.58. Suppose there is a 30 percent tolerance on the value of  $K'_n$  in the inverter in Fig. 6.21. What are the worst-case values of  $V_H$ ,  $V_L$ , and the power in the circuit? Assume the two transistors in the circuit are matched (i.e., they have the same value of  $K'_n$ ).
- 6.59. Find  $V_H$ ,  $V_L$ , and the power dissipation (for  $v_O = V_L$ ) for the logic inverter with the saturated load in Fig. P6.59. Assume  $\gamma = 0$ .

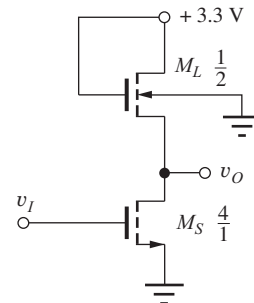


Figure P6.59

- 6.60. Repeat Prob. 6.59 if  $\gamma = 0.6$ .
- 6.61. Suppose there is a 30 percent tolerance on the value of  $K'_n$  in the inverter in Fig. P6.59. What are the worst-case values of  $V_H$ ,  $V_L$  and the power in the circuit? Assume the two transistors in the circuit are matched (i.e., they have the same value of  $K'_n$ ).
- 6.62. A manufacturing problem caused  $V_{TN} = 0.8$  V instead of 0.6 V in the inverter in Fig. P6.59. What are the new values of  $V_H$ ,  $V_L$ , and power dissipation? (c) Repeat for  $V_{TN} = 0.4$  V.
- \*6.63. What are the noise margins for the circuit in Fig. P6.59?
- 6.64. (a) Find  $V_H$ ,  $V_L$ , and the power dissipation (for  $v_O = V_L$ ) for the logic inverter with the saturated load in Fig. P6.59 if the transistor sizes are changed

to  $(W/L)_S = 8/1$  and  $(W/L)_L = 1/1$ . (b) What are the noise margins for the circuit? (c) A manufacturing problem caused  $V_{TN} = 0.7$  V instead of 0.6 V. What are the new values of  $V_H$ ,  $V_L$ , and power dissipation?

- 6.65. Redesign the NMOS logic gate with saturated load of Fig. 6.21 to give  $V_L = 0.3$  V and  $P = 0.4$  mW for  $v_O = V_L$ .
- 6.66. (a) Redesign the saturated load inverter of Fig. 6.21 for operation at a power level of 0.25 mW with  $V_{DD} = 3.3$  V. Assume  $V_{TO} = 0.7$  V. Keep the other design parameters the same. What are the new sizes of  $M_L$  and  $M_S$ ? (b) What are the new values for  $NM_H$  and  $NM_L$ ?
- 6.67. (a) Design a saturated load inverter similar to that of Fig. 6.17(c) with  $V_{DD} = 3.3$  V and  $V_L = 0.2$  V. Assume  $I_{DD} = 75 \mu\text{A}$ . (b) Recalculate the values of  $W/L$  including body effect, as in Fig. 6.21.
- 6.68. (a) Design a saturated load inverter similar to that of Fig. 6.17(c) with  $V_{DD} = 2.0$  V and  $V_L = 0.15$  V. Assume  $I_{DD} = 25 \mu\text{A}$  and  $V_{TN} = 0.6$  V. (b) Recalculate the values of  $W/L$  including body effect, as in Fig. 6.21 if  $V_{TO} = 0.6$  V,  $\gamma = 0.6 \sqrt{V}$ , and  $2\phi_F = 0.6$  V. (c) Confirm the validity of your designs with SPICE.
- 6.69. The logic input of the saturated load inverter of Fig. 6.21 is connected to 2.5 V. What is  $v_O$  for this input voltage? (This problem will probably require an iterative solution.)
- 6.70. The saturated load inverter of Fig. 6.29(b) was designed using  $K'_n = 100 \mu\text{A/V}^2$ , but due to process variations during fabrication, the value actually turned out to be  $K'_n = 125 \mu\text{A/V}^2$ . What will be the new values of  $V_H$ ,  $V_L$ , and the power dissipation in the gate for this new value of  $K'_n$ ?
- 6.71. The saturated load inverter of Fig. 6.29(b) was designed using  $K'_n = 100 \mu\text{A/V}^2$ , but due to process variations during fabrication, the value actually turned out to be  $K'_n = 75 \mu\text{A/V}^2$ . What will be the new values of  $V_H$ ,  $V_L$ , and the power dissipation in the gate for this new value of  $K'_n$ ?
- 6.72. The inverter designs in Fig. 6.29 assume  $\lambda = 0$ . (a) Does  $V_H$  depend upon the value of  $\lambda$ ? (b) Use SPICE to find  $I_{DD}$  and  $V_L$  for the saturated load inverter in Fig. 6.29(b) if  $\lambda = 0.02$ ,  $0.05$ , and  $0.1 \text{ V}^{-1}$ .
- \*\*6.73. Plot the noise margins for the saturated load inverter similar to the design of Fig. 6.29(b) versus

$K_R = K_S/K_L$  (see the graph in Fig. 6.28). Note that  $V_L$  will be changing.

- 6.74. Find the slope of the voltage transfer characteristic (i.e., the voltage gain) at the input voltage for which  $v_O = v_I$  in the inverter in Fig. 6.21.
- 6.75. Find the slope of the voltage transfer characteristic (i.e., the voltage gain) at the input voltage for which  $v_O = v_I$  in the inverter in Fig. P6.59.

### NMOS Inverter with a Linear Load Device

- 6.76. Calculate the  $W/L$  ratio for the linear load device using the circuit and device parameters that apply to Sec. 6.8, and show that the values presented in Fig. 6.22 are correct.
- 6.77. What is the minimum value of  $V_{GG}$  required for linear region operation of  $M_L$  in Fig. 6.29(c) if  $V_{TO} = 0.8$  V,  $\gamma = 0.5 \sqrt{V}$ , and  $2\phi_F = 0.6$  V.
- 6.78. The linear load inverter in Fig. 6.29(c) was designed using  $K'_n = 100 \mu\text{A/V}^2$ . (a) What will be the new values of  $V_H$ ,  $V_L$ , and the power dissipation in this gate if  $K'_n = 70 \mu\text{A/V}^2$ ? (b) Repeat for  $K'_n = 130 \mu\text{A/V}^2$ .
- 6.79. Find  $V_H$ ,  $V_L$ , and the power dissipation (for  $v_O = V_{OL}$ ) for the linear load inverter in Fig. P6.79.

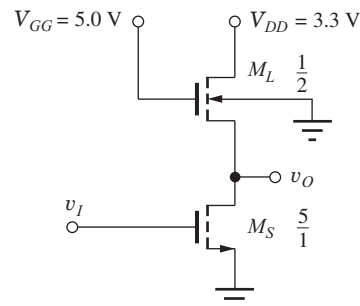


Figure P6.79

- 6.80. What is the minimum value of  $V_{GG}$  in the circuit in Fig. P6.79 if  $V_{TO} = 0.6$  V,  $\gamma = 0.6 \sqrt{V}$ , and  $2\phi_F = 0.6$  V.
- 6.81. The linear load inverter in Fig. P6.79 was designed using  $K'_n = 100 \mu\text{A/V}^2$ . (a) What will be the new values of  $V_H$ ,  $V_L$  and the power dissipation in this gate if  $K'_n = 130 \mu\text{A/V}^2$ ? (b) Repeat for  $K'_n = 70 \mu\text{A/V}^2$ .
- 6.82. (a) Design a linear load inverter similar to that of Fig. P6.79 with  $V_{DD} = 3.3$  V,  $V_L = 0.20$  V, and  $P = 300 \mu\text{W}$ . Assume  $V_{TO} = 0.6$  V,  $\gamma = 0.6 \sqrt{V}$ ,  $2\phi_F = 0.6$  V. (b) Confirm the validity of your design using SPICE.

- 6.83. Repeat Probs. 6.79 and 6.80 if  $V_{DD}$  and  $V_{GG}$  are changed to 2.5 V and 3.5 V respectively.

### NMOS Inverter with a Depletion-Mode Load

- 6.84. We know that body effect deteriorates the behavior of NMOS logic gates with depletion-mode loads. Assume that the depletion-mode load device has  $V_{TO} = -1$  V and is operating in an inverter circuit with  $V_{DD} = 2.5$  V. What is the largest value of the body-effect parameter  $\gamma$  that still will allow  $V_{OH} = V_{DD}$ ? Assume  $2\phi_F = 0.6$  V.
- 6.85. (a) Redesign the inverter with depletion-mode load of Fig. 6.29(d) for operation with  $V_{DD} = 3.3$  V. Assume  $V_{TO} = 0.6$  V for the switching transistor and  $V_{TO} = -1$  V,  $\gamma = 0.5 \sqrt{V}$ , and  $2\phi_F = 0.6$  V for the depletion-mode load. Design for  $V_L = 0.20$  V and  $P = 0.25$  mW.
- 6.86. (a) The depletion load inverter of Fig. 6.29(d) was designed using  $K'_n = 100 \mu\text{A}/\text{V}^2$ , but due to process variations during fabrication, the value actually turned out to be  $K'_n = 80 \mu\text{A}/\text{V}^2$ . What will be the new values of  $V_H$ ,  $V_L$ , and the power dissipation in the gate for this new value of  $K'_n$ ? (b) Repeat for  $K'_n = 120 \mu\text{A}/\text{V}^2$ .
- 6.87. (a) Design a depletion-load inverter to operate with  $V_{DD} = 3.3$  V,  $V_L = 0.20$  V, and  $P = 250 \mu\text{W}$ . Assume  $V_{TO} = -2$  V,  $\gamma = 0.5 \sqrt{V}$ , and  $2\phi_F = 0.6$  V for the load transistor and  $V_{TO} = 0.6$  V for  $M_S$ . (b) Confirm the validity of your design using SPICE.
- 6.88. The inverter designs in Fig. 6.29 assume  $\lambda = 0$ . (a) Does  $V_H$  depend upon the value of  $\lambda$ ? (b) Use SPICE to find  $I_{DD}$  and  $V_L$  for the depletion-load inverter in Fig. 6.29(d) if  $\lambda = 0.02$ ,  $0.05$ , and  $0.1 \text{ V}^{-1}$ .
- 6.89. Find the slope of the voltage transfer characteristic (i.e., the voltage gain) at the input voltage for which  $v_O = v_I$  in the inverter in Fig. 6.29(d).

### Pseudo NMOS Inverter

- 6.90. (a) The inverter in Fig. 6.29(e) is to be redesigned to have  $V_L = 0.25$  V. What is the new value of  $(W/L)_S$ ? (b) What are the noise margins for the new design?
- 6.91. (a) Due to process variations, the value of  $K'_n$  for the NMOS transistor in Fig. 6.29(e) was found to be  $K'_n = 120 \mu\text{A}/\text{V}^2$  instead of  $100 \mu\text{A}/\text{V}^2$ . What are the new values of  $V_L$  and  $I_{DD}$ ? (b) What are the new values of the noise margins? (c) Repeat parts (a) and (b) for  $K'_n = 80 \mu\text{A}/\text{V}^2$ .

- 6.92. (a) Due to process variations, the NMOS threshold voltage for the inverter in Fig. 6.29(e) was found to be  $V_{TN} = 0.5$  V instead of 0.6 V. What are the new values of  $V_L$  and  $I_{DD}$ ? (b) What are the new values of the noise margins? (c) Repeat parts (a) and (b) for  $V_{TN} = 0.7$  V.
- 6.93. (a) Due to process variations, the value of  $K'_p$  for the PMOS transistor in Fig. 6.29(e) was found to be  $K'_p = 50 \mu\text{A}/\text{V}^2$  instead of  $40 \mu\text{A}/\text{V}^2$ . What are the new values of  $V_L$  and  $I_{DD}$ ? (b) What are the new values of the noise margins? (c) Repeat parts (a) and (b) for  $K'_p = 30 \mu\text{A}/\text{V}^2$ .
- 6.94. (a) Due to process variations, the PMOS threshold voltage for the inverter in Fig. 6.29(e) was found to be  $V_{TP} = -0.5$  V instead of  $-0.6$  V. What are the new values of  $V_L$  and  $I_{DD}$ ? (b) What are the new values of the noise margins? (c) Repeat parts (a) and (b) for  $V_{TP} = -0.7$  V.
- 6.95. (a) Design a pseudo NMOS inverter to operate from  $V_{DD} = 1.8$  V with  $V_L = 0.2$  V and a power of  $100 \mu\text{W}$ . Assume  $V_{TN} = 0.5$  V and  $V_{TP} = -0.5$  V. (b) Find the noise margins for your design.
- 6.96. (a) Design a pseudo NMOS inverter to operate from  $V_{DD} = 3.0$  V with  $V_L = 0.3$  V and a power of  $200 \mu\text{W}$ . (b) Find the noise margins for your design.

### 6.8 NMOS NAND and NOR Gates

- 6.97. (a) What is the value of  $V_L$  in the two-input NOR gate in Fig. 6.30(a) when both  $A = 1$  and  $B = 1$ ? (b) What is the current in  $V_{DD}$  for this input condition?
- 6.98. The design value for  $V_L$  was 0.2 V in the NAND gate in Fig. 6.32(a). What is the actual value of  $V_L$ ?
- 6.99. Calculate the  $W/L$  ratios of the switching devices in the NAND gate in Fig. 6.32(b) and verify that they are correct.
- \*\*6.100. The two-input NAND gate in Fig. 6.32 was designed with equal values of  $R_{on}$  (approximately equal voltage drops) in the two series-connected switching transistors, but an infinite number of other choices are possible. Show that the equal  $R_{on}$  design requires the minimum total gate area for the switching transistors.
- 6.101. Draw the schematic for a four-input NAND gate with a depletion-mode load device. What are the  $W/L$  ratios of all the transistors, based on the reference inverter in Fig. 6.32?

- 6.102. Draw the schematic for a four-input NOR gate with a saturated load device. What are the  $W/L$  ratios of all the transistors, based on the reference inverter in Fig. 6.29?
- 6.103. (a) Draw the schematic for a three-input pseudo NMOS NOR gate. Choose the device sizes based upon the reference inverter in Fig. 6.29. (b) What is  $V_L$  if all the logic inputs are equal to 1?
- 6.104. (a) Draw the schematic for a three-input pseudo NMOS NAND gate. Choose the device sizes based upon the reference inverter in Fig. 6.29. Ignore body effect in your design. (b) What is  $V_L$  if all the logic inputs are equal to 1? Do not ignore body effect. (c) Redesign the sizes of the three switching transistors to account for body effect.
- 6.105. Draw the layout of a two-input NOR gate similar to that in Fig. 6.33(a) but use a saturated load device. Be sure to scale the transistor sizes properly based on Fig. 6.29(b).
- 6.106. (a) Draw the layout of a three-input NOR gate similar to that in Fig. 6.33(a). Be sure to scale the transistor sizes properly. (b) Draw the layout of a three-input NAND gate similar to that in Fig. 6.33(b). Be sure to scale the transistor sizes properly.

## 6.9 Complex NMOS Logic

- 6.107. (a) What is the logic function that is implemented by the gate in Fig. P6.107? (b) What are the  $W/L$

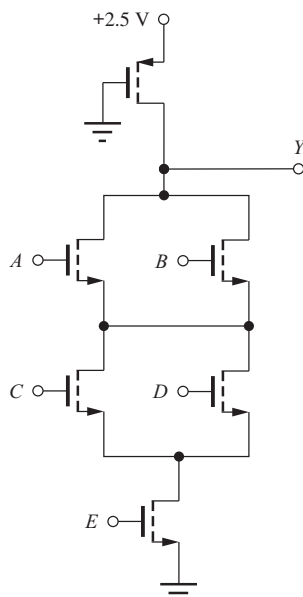


Figure P6.107

ratios for the transistors, based on the reference inverter design of Fig. 6.29(d)?

- 6.108. (a) Redraw the circuit in Fig. P6.107 using a saturated load transistor. (b) What is the logic function of the new circuit? (c) What are the  $W/L$  ratios of the transistors based upon the reference inverter design in Fig. 6.29(b)?
- 6.109. (a) What is the logic function that is implemented by the gate in Fig. P6.109? (b) What are the  $W/L$  ratios for the transistors, based on the reference inverter design of Fig. 6.29(d)?

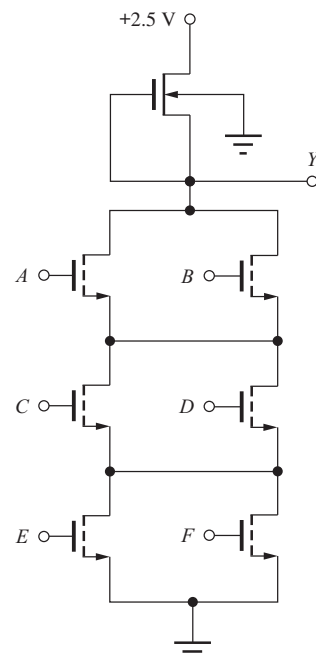


Figure P6.109

- 6.110. (a) Redraw the circuit in Fig. P6.109 using a saturated load transistor. (b) What is the logic function of the new circuit? (c) What are the  $W/L$  ratios of the transistors based upon the reference inverter design in Fig. 6.29(b)?
- 6.111. (a) What is the logic function that is implemented by the gate in Fig. P6.111? (b) What are the  $W/L$  ratios for the transistors if the gate is to dissipate three times as much power as the reference inverter design of Fig. 6.29(d)?
- 6.112. (a) Redraw the circuit in Fig. P6.111 using a saturated load transistor. (b) What is the logic function of the new circuit? (c) What are the  $W/L$  ratios of the transistors based on the reference inverter design in Fig. 6.29(b)?

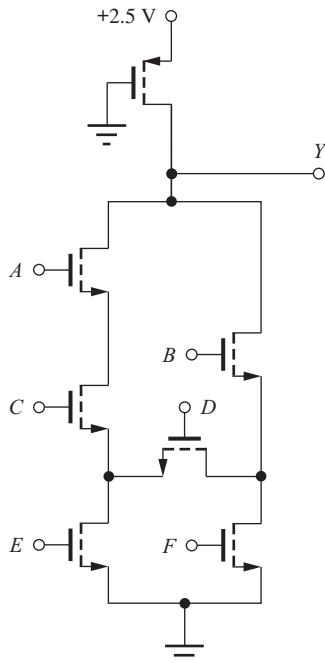


Figure P6.111

- 6.113. Design a depletion-load gate that implements the logic function  $Y = \overline{A[B + C(D + E)]}$ , based on the reference inverter design of Fig. 6.29(d).
- 6.114. Design a saturated-load gate that implements the logic function  $Y = \overline{A(BC + DE)}$ , based on the reference inverter design of Fig. 6.29(b).
- 6.115. Design a pseudo NMOS gate that implements the logic function  $Y = \overline{A(BC + DE)}$  and consumes one-half the power of the reference inverter design of Fig. 6.29(e).
- 6.116. Design a pseudo NMOS gate that implements the logic function  $Y = \overline{A(B + CD) + E}$ , based on the reference inverter design of Fig. 6.29(e).
- 6.117. What is the logic function for the gate in Fig. P6.117? What are the  $W/L$  ratios of the transistors that form the gate if the gate is to consume twice as much power as the reference inverter in Fig. 6.29(d)?
- 6.118. (a) Design a depletion-load gate that implements the logic function  $Y = \overline{A(B + CD) + E}$ , based on the reference inverter design of Fig. 6.29(d). (b) Re-design the  $W/L$  ratios of this gate to account for body effect and differences in values of  $V_{DS}$  for the various transistors.
- 6.119. Recalculate the  $W/L$  ratios of the transistors in the gate in Fig. 6.34 to account for the body effect and differences in the  $V_{DS}$  of the various transistors.

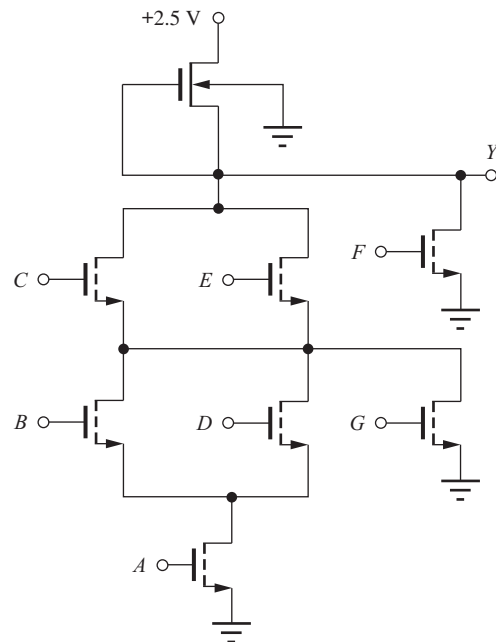


Figure P6.117

- \*6.120. Recalculate the  $W/L$  ratios of the transistors in the gate in Fig. 6.35(a) to account for the body effect and differences in the  $V_{DS}$  of the various transistors.
  - \*6.121. Recalculate the  $W/L$  ratios of the transistors in the gate in Fig. 6.35(b) to account for the body effect and differences in the  $V_{DS}$  of the various transistors.
  - \*6.122. Recalculate the  $W/L$  ratios of the transistors in the gate in Fig. 6.36 to account for the body effect and differences in the  $V_{DS}$  of the various transistors.
  - \*\*6.123. (a) What is the truth table for the logic function  $Y$  for the gate in Fig. P6.123? (b) Write an expression for the logical output of this gate. (c) What are the sizes of the transistors  $M_S$  and  $M_P$  in order for  $V_L \leq 0.20$  V? (d) Qualitatively describe how the sizes of  $M_S$  and  $M_P$  will change if body effect is included in the models for the transistors. (e) What is the name for this logic function?
  - 6.124. (a) Estimate the value of  $V_L$  in Fig. 6.36 if all five switching transistors are “on” by finding the equivalent value of  $R_{on}$  for the switching tree. (b) Compare your calculation to SPICE results.
- ### 6.10 Power Dissipation
- 6.125. Scale the sizes of the resistors and transistors in the five inverters in Fig. 6.29 to change the power dissipation level to 2 mW.

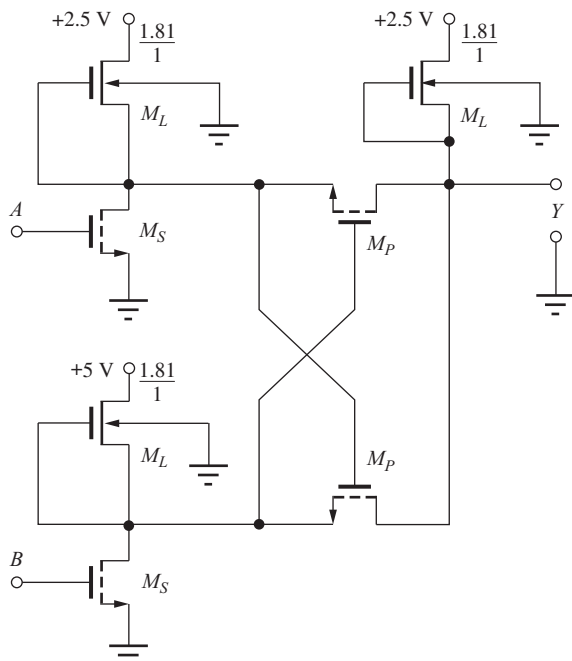


Figure P6.123

- 6.126. What are the  $W/L$  ratios of the transistors in the gate in Fig. P6.117 if the gate is to consume three times as much power as the reference inverter in Fig. 6.29(d)?
- 6.127. What are the  $W/L$  ratios for the transistors in Fig. P6.109 if the gate is to dissipate one-fifth as much power as the reference inverter design of Fig. 6.29(d)?
- 6.128. (a) Scale the transistor sizes in Fig. 6.35(a) to increase the gate power by a factor of four. (b) Scale the transistor sizes in Fig. 6.35(a) to decrease the gate power by a factor of four.
- 6.129. (a) Scale the transistor sizes in Fig. 6.35(b) to decrease the gate power by a factor of 8. (b) Scale the transistor sizes in Fig. 6.35(b) to increase the gate power by a factor of 3.5.
- 6.130. (a) Scale the transistor sizes in Fig. 6.36 to triple the gate power. (b) Scale the transistor sizes in Fig. 6.36 to decrease the gate power by a factor of four.
- 6.131. For the saturated load inverter, we found  $V_H \neq V_{DD}$  and  $V_L \neq 0$ . Find a new general expression (similar to Eq. 6.49) for the dynamic power dissipation of a logic gate in terms of  $V_H$ ,  $V_L$  and/or  $\Delta V$ .
- \*6.132. For many years, MOS devices were scaled to smaller and smaller dimensions without changing the power supply voltage. Suppose that the width  $W$ ,

length  $L$ , and oxide thickness  $t_{ox}$  are all reduced by a factor of 2. Assume that  $V_{TN}$ ,  $v_{GS}$ , and  $v_{DS}$  remain the same. Calculate the ratio of the drain current of the scaled device to that of the original device. How has the power dissipation changed?

- 6.133. A high-speed NMOS microprocessor has a 64-bit address bus and performs a memory access every 50 ns. Assume that all address bits change during every memory access, and that each bus line represents a load of 10 pF. (a) How much power is being dissipated by the circuits that are driving these signals if the power supply is 2.5 V? (b) 3.3 V?

### 6.11 Dynamic Behavior of MOS Logic Gates

- 6.134. A logic family has a power-delay product of 100 fJ. If a logic gate consumes a power of 100  $\mu$ W, what is the expected propagation delay of the logic gate?
- 6.135. The graph in Fig. P6.135 gives the results of a SPICE simulation of an inverter. (a) What are the rise and fall times for  $v_I$  and  $v_O$ ? (b) What are the values of  $\tau_{PHL}$  and  $\tau_{PLH}$ ? (c) What is the average propagation delay for this gate?

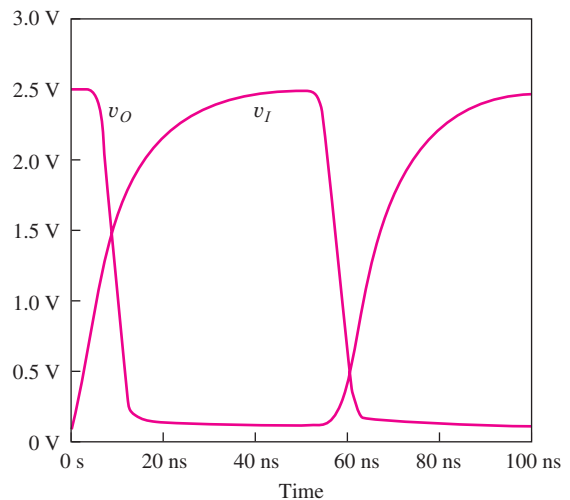


Figure P6.135

- \*\*6.136. Derive Eq. 6.63 for an  $N$ -stage ring oscillator by adding together the total number of  $\tau_{PHL}$  and  $\tau_{PLH}$  delays that occur in two round trips through the oscillator.
- 6.137. (a) Suppose that a ring oscillator contains 301 inverters and the average propagation delay of an inverter is 100 ps. What will be the period of the square wave generated by the oscillator? (b) What

is the frequency of oscillator? (c) Why should the number of inverters be odd? What could happen if an even number of inverters were used in the ring oscillator?

- 6.138. (a) The input capacitance for a gate can be written as  $C_{in} = k_1 C_{GS} + k_2 C_{GD}$ . Use SPICE to determine  $k_1$  and  $k_2$  for a resistively loaded NMOS logic gate. (b) Repeat for a psuedo NMOS circuit.

### Resistor Load

- 6.139. What are the rise time, fall time, and average propagation delay of the NMOS gate in Fig. 6.12(b) if a load capacitance  $C = 0.5 \text{ pF}$  is attached to the output of the gate?
- 6.140. What are the rise time, fall time, and average propagation delay of the NMOS gate in Fig. 6.12(b) if a load capacitance  $C = 0.5 \text{ pF}$  is attached to the output of the gate and  $V_{DD}$  is increased to 3.3 V?
- 6.141. Design an NMOS inverter with resistor load to have an average propagation delay of 2.5 ns with a capacitive load of 1 pF by scaling the reference inverter based upon the results in Table 6.9. What is the average power dissipation of this gate with a 33 percent duty cycle?
- 6.142. Repeat Prob. 6.141 to achieve an average propagation delay of 2 ns with a 0.4 pF load. What is the average power dissipation of this gate with a 20 percent duty cycle?
- 6.143. Repeat the simulation of Ex. 6.10 with  $\lambda = 0.04 \text{ V}$ . Compare the new values rise time, fall time, and propagation delays with those of the example.

### Saturated Load

- 6.144. (a) What are the rise and fall times and average propagation delay of the NMOS gate in Fig. P6.144 if  $C = 0.5 \text{ pF}$  and  $V_{DD} = 2.5 \text{ V}$ ? Use the estimates in Table 6.10. (b) What are the rise and fall times

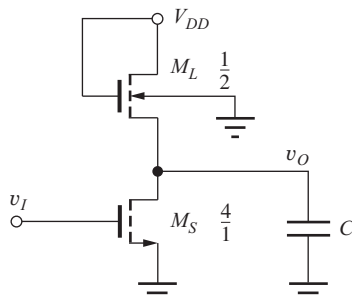


Figure P6.144

and average propagation delays of the NMOS gate in Fig. P6.144 if  $C = 0.3 \text{ pF}$  and  $V_{DD} = 3.3 \text{ V}$ ? Use Table 6.10.

- 6.145. Design an NMOS saturated load inverter ( $V_{DD} = 2.5 \text{ V}$ ,  $V_L = 0.25 \text{ V}$ ) to have an average propagation delay of 2 ns with a capacitive load of 1 pF. What is the average static power dissipation of this gate? Make use of Table 6.9.

### Linear Load

- 6.146. What are the rise and fall times and average propagation delay for the linear load inverter in Fig. 6.29(c) with a load capacitance of 0.7 pF? Use Table 6.10.
- 6.147. Use SPICE to determine the characteristics of the NMOS inverter with a linear load device for the design given in Fig. 6.29. (a) Simulate the voltage transfer function. (b) Determine  $t_r$ ,  $t_f$ ,  $\tau_{PHL}$ , and  $\tau_{PLH}$  for this inverter with a square wave input and  $C = 0.15 \text{ pF}$ .

### Depletion-Mode Load

- 6.148. What are the sizes of the transistors in the NMOS depletion-mode load inverter if it must drive a 1-pF capacitance with an average propagation delay of 3 ns? Assume  $V_{DD} = 3.0 \text{ V}$  and  $V_L = 0.25 \text{ V}$ . What are the rise and fall times for the inverter? Use  $V_{TNL} = -3 \text{ V}$  ( $\gamma = 0$ ). Make use of Table 6.10.
- 6.149. Design an NMOS depletion load inverter ( $V_{DD} = 3.3 \text{ V}$ ,  $V_L = 0.20 \text{ V}$ ,  $V_{TNS} = 0.75 \text{ V}$ ,  $V_{TNL} = -2 \text{ V}$ ,  $\gamma = 0$ ) to have an average propagation delay of 1 ns with a capacitive load of 0.2 pF. What is the average static power dissipation of this gate? Use the results in Table 6.9.

### A Final Comparison of Load Devices

- 6.150. Currents in the various load devices are shown in Fig. 6.47. The resistor load has a value of  $28.8 \text{ k}\Omega$ . The  $W/L$  ratios of the devices were chosen to set the current in each load device to  $80 \mu\text{A}$  when  $v_O = V_L = 0.20 \text{ V}$ . Calculate the values of the  $W/L$  ratios of the load devices that were used in the figure for the: (a) saturated load device including body effect, (b) saturated load device with no body effect, (c) linear load device including body effect, (d) linear load device with no body effect, (e) depletion-mode load device including body effect, (f) depletion-mode load with no body effect (g) pseudo NMOS load.

### 6.12 PMOS Problems

- 6.151. Design five PMOS logic gates similar to the ones in Fig. 6.29. Do not do a complete mathematical redesign, but design the PMOS circuits by scaling the  $W/L$  ratios in Fig. 6.29, assuming that  $K'_p = 40 \mu\text{A}/\text{V}^2$ .
- \*6.152. What are the values of  $V_L$  and  $V_H$  for the inverter in Fig. P6.152?

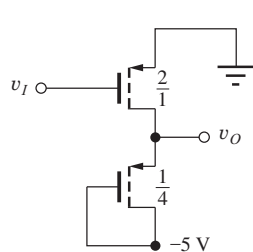


Figure P6.152

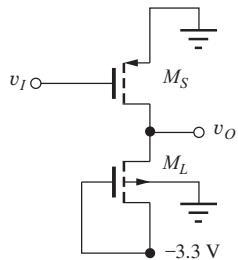


Figure P6.153

- 6.153. Design the transistors in the inverter of Fig. P6.153 so that  $V_H = -0.33 \text{ V}$  and the power dissipation = 0.1 mW. Use the values in Table 6.5 on page 308.
- 6.154. What are the values of  $V_H$  and  $V_L$  for the inverter of Fig. P6.154? Use the values in Table 6.5 on page 308.

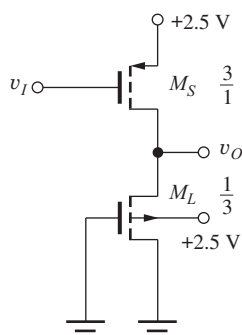


Figure P6.154

- 6.155. What is the logic function  $Y$  for the gate in Fig. P6.155?

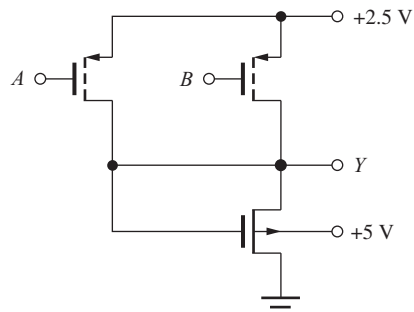


Figure P6.155

- 6.156. What is the logic function  $Y$  for the gate in Fig. P6.156?

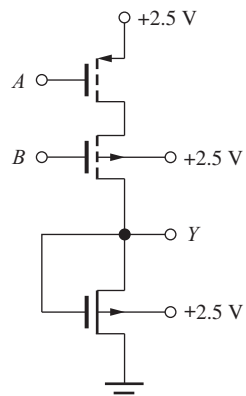
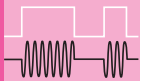


Figure P6.156

- 6.157. Simulate the voltage transfer characteristic for the PMOS gate in Fig. P6.152, and compare the results to those of Prob. 6.152.
- 6.158. Simulate the voltage transfer characteristic for the PMOS gate in Fig. P6.153, and compare the results to those of Prob. 6.153.
- 6.159. Simulate the delay of the PMOS gate in Fig. P6.152 with a load capacitance of 1 pF, and determine the rise time, fall time, and average propagation delay.
- 6.160. Simulate the delay of the PMOS gate in Fig. P6.153 with a load capacitance of 1 pF, and determine the rise time, fall time, and average propagation delay.

# CHAPTER 7



## COMPLEMENTARY MOS (CMOS) LOGIC DESIGN

### CHAPTER OUTLINE

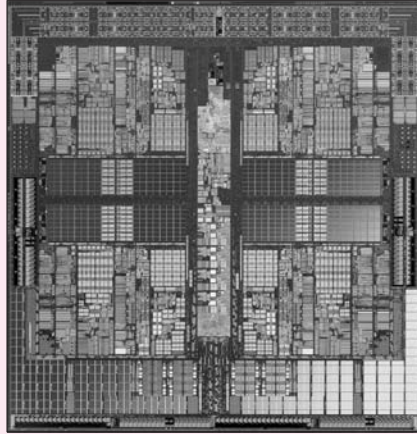
- 7.1 CMOS Inverter Technology 368
- 7.2 Static Characteristics of the CMOS Inverter 370
- 7.3 Dynamic Behavior of the CMOS Inverter 375
- 7.4 Power Dissipation and Power Delay Product in CMOS 380
- 7.5 CMOS NOR and NAND Gates 384
- 7.6 Design of Complex Gates in CMOS 388
- 7.7 Minimum Size Gate Design and Performance 393
- 7.8 Dynamic Domino CMOS Logic 395
- 7.9 Cascade Buffers 397
- 7.10 The CMOS Transmission Gate 400
- 7.11 CMOS Latchup 401
- Summary 404
- Key Terms 405
- References 406
- Problems 406

### CHAPTER GOALS

From Chapter 7, we shall gain a basic understanding of the design of CMOS logic and memory circuits.

- Introduce CMOS Logic Gates
- Explore the voltage transfer characteristics of CMOS inverters
- Learn to design CMOS inverter, NOR, and NAND gates
- Learn to design complex CMOS logic gates
- Explore sources of static and dynamic power dissipation in CMOS logic
- Develop expressions for the rise time, fall time, propagation delay, and power-delay product of CMOS logic
- Develop expressions for CMOS noise margins
- Introduce the concept of dynamic logic and domino CMOS logic techniques
- Learn to design “cascade buffers” for driving high load capacitances
- Explore layout of CMOS inverters and logic gates
- Understand the problem of “latchup” in CMOS technology

Today, **Complementary MOS**, or CMOS, is by far the dominant integrated circuit technology. CMOS logic was first described by Wanlass and Sah in 1963 [1], but for many



Quad-Core AMD Operton™ Processor die plot.  
Copyright © 2009 Advanced Micro Devices, Inc.

years, CMOS technology was only available in unit-logic form, with several gates packaged together in a single dual in-line package (DIP). CMOS circuitry requires both NMOS and PMOS transistors to be built into the same substrate, and this increase in process complexity leads to higher-cost circuits. In addition, standard CMOS gates require more transistors than the corresponding NMOS or PMOS logic gates, and thereby require more silicon area to implement. Larger silicon area contributes further to increased cost.

The increased cost that results from CMOS fabrication and circuit complexities represented the primary reason why CMOS technology was not widely used in integrated circuits. CMOS was utilized in applications that required extremely low power and where the increased cost could be justified.

However, as mentioned in Chapter 6, power levels associated with NMOS microprocessors reached crisis levels by the mid 1980s, with power dissipations as high as 50 W per chip or more. To solve the static power dissipation problem, the microprocessor industry rapidly moved to CMOS technology. Today, CMOS is the industrywide standard technology, and this important circuit innovation was recognized by the presentation of the 1991 IEEE Solid-State Circuits Society Field Award to Frank Wanlass for his invention of CMOS logic.

In Chapter 7, we investigate the design of CMOS logic circuits, starting with characterization of the CMOS inverter, and followed by a discussion of the design of NOR, NAND, and complex gates based on a CMOS reference inverter. CMOS gate design is shown to be determined primarily by logic delay considerations. CMOS noise margins and power-delay products are discussed, and the transmission gate is also introduced.

The physical structure of CMOS technology is presented, and parasitic bipolar transistors are shown to exist within the integrated CMOS structure. If these bipolar devices become active, a potentially destructive phenomenon called latchup can occur.

## 7.1 CMOS INVERTER TECHNOLOGY

As noted, CMOS requires a fabrication technology that can produce both NMOS and PMOS transistors together on one IC substrate, and the basic IC structure used to accomplish this task is shown in Fig. 7.1. In this cross section, NMOS transistors are shown fabricated in a normal manner in a *p*-type silicon substrate. A lightly doped *n*-type region, called the *n*-well, is formed in the *p*-type substrate, and PMOS transistors are then fabricated in the *n*-well region, which becomes the body of the PMOS device. Note that a large-area diode exists between the *n*-well and *p*-type substrate. This *pn* diode must always be kept reverse-biased by the proper connection of  $V_{DD}$  and  $V_{SS}$  (for example, 2.5 V and 0 V).

The connections between the transistors needed to form a CMOS inverter are shown in Fig. 7.1 and correspond to the circuit schematic for the CMOS inverter in Fig. 7.2(a). The inverter circuit consists of one NMOS and one PMOS transistor similar to pseudo NMOS introduced in Chapter 6. The NMOS transistor functions in a manner identical to that of the switching device in NMOS gates. However, in CMOS, the PMOS load device is also switched on and off under control of the logic input signal  $v_I$ .

The CMOS logic gate can be conceptually modeled by the circuit in Fig. 7.2(b), in which the position of the two switches is controlled by the input voltage  $v_I$ . In an ideal inverter, there would never be a conducting path between the positive and negative power supplies under steady-state conditions. When the NMOS transistor is on, the PMOS transistor is off; if the PMOS transistor is on, the NMOS device is off. In an actual inverter, input  $v_I$  cannot abruptly jump from  $V_L$  to  $V_H$  or  $V_H$  to  $V_L$ , and there will be a period of time during the input voltage transition when both transistors are on and a conducting path exists between  $V_{DD}$  and ground (This is discussed further in Section 7.4).

In the CMOS inverter of Fig. 7.2, the source of the PMOS transistor is connected to  $V_{DD}$ , the source of the NMOS transistor is connected to  $V_{SS}$  (0 V in this case), and the drain terminals of the two MOSFETs are connected together to form the output node. Also, the substrates of both the NMOS and PMOS transistors are connected to their respective sources, so body effect is eliminated in both devices.

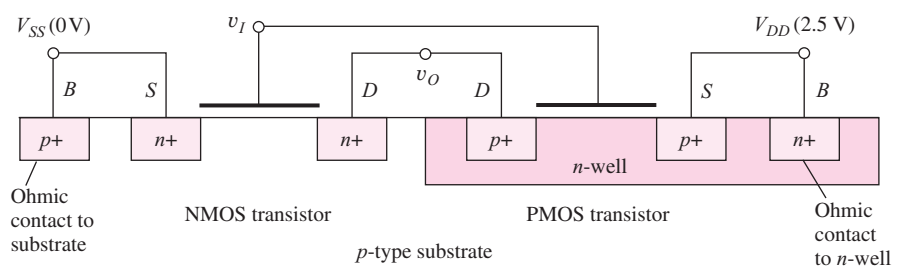


**Figure 7.1** *n*-well CMOS structure for forming both NMOS and PMOS transistors in a single silicon substrate.

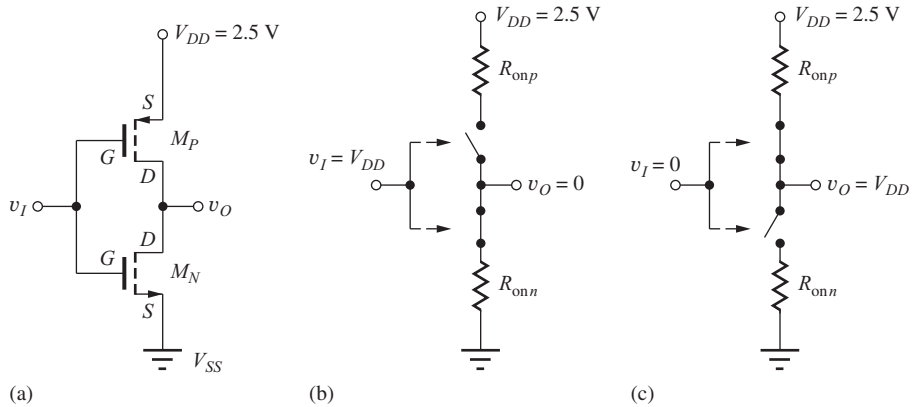


**Figure 7.2** (a) A CMOS inverter uses one NMOS and one PMOS transistor. (b) A simplified model of the inverter for a high input level. The output is forced to zero through the on-resistance of the NMOS transistor. (c) Simplified model of the inverter for a low input level. The output is pulled to  $V_{DD}$  through the on-resistance of the PMOS transistor.

**TABLE 7.1**  
CMOS Transistor Parameters

	NMOS DEVICE	PMOS DEVICE
$V_{TO}$	0.6 V	-0.6 V
$\gamma$	$0.50 \sqrt{V}$	$0.75 \sqrt{V}$
$2\phi_F$	0.60 V	0.70 V
$K'$	$100 \mu\text{A}/\text{V}^2$	$40 \mu\text{A}/\text{V}^2$

Simplified models for the CMOS inverter operation appear in Fig. 7.2(b) and 7.2(c). The input signal controls the state of the two switches that effectively work as a single-pole double-throw switch. In Fig. 7.2(b), the input is at a high input level ( $v_I = V_{DD}$ ), and the output is connected to ground through the on-resistance of the NMOS transistor. In Fig. 7.2(c), the input is at a low input level ( $v_I = 0$ ), and the output is connected to  $V_{DD}$  through the on-resistance of the PMOS transistor.

Before we explore the design of the CMOS inverter, we need parameters for the CMOS devices, as given in Table 7.1. The NMOS parameters are the same as those given in Chapter 6. In CMOS technology, the transistors are normally designed to have equal and opposite threshold voltages: for example,  $V_{TON} = +0.6$  V and  $V_{TOP} = -0.6$  V. Remember that  $K'_n = \mu_n C_{ox}''$  and  $K'_p = \mu_p C_{ox}$  and that hole mobility in the channel of the PMOSFET is approximately 40 percent of the electron mobility in the NMOSFET channel. The values in Table 7.1 reflect this difference because the value of  $K'$  for the NMOS device is shown as 2.5 times that for the PMOS transistor. Processing differences are also reflected in the different values for  $\gamma$  and  $2\phi_F$  in the two types of transistors.

Remember that the threshold voltage of the NMOS transistor is denoted by  $V_{TN}$  and that of the PMOS transistor by  $V_{TP}$ :

$$V_{TN} = V_{TON} + \gamma_n (\sqrt{V_{SBN} + 2\phi_{FN}} - \sqrt{2\phi_{FN}}) \quad (7.1)$$

and

$$V_{TP} = V_{TOP} - \gamma_p (\sqrt{V_{BSP} + 2\phi_{FP}} - \sqrt{2\phi_{FP}})$$

For  $v_{SBN} = 0$ ,  $V_{TN} = V_{TON}$ , and for  $v_{BSP} = 0$ ,  $V_{TP} = V_{TOP}$ .

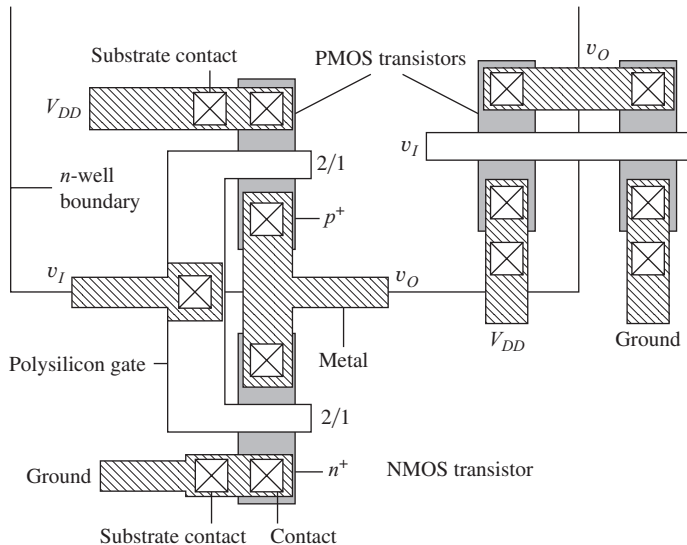


**Figure 7.3** Layout of two CMOS inverters.

**EXERCISES:** (a) What are the values of  $K_p$  and  $K_n$  for transistors with  $W/L = 20/1$ ? (b) An NMOS transistor has  $V_{SB} = 2.5$  V. What is the value of  $V_{TN}$ ? (c) A PMOS transistor has  $V_{BS} = 2.5$  V. What is the value of  $V_{TP}$ ?

**ANSWERS:** (a)  $800 \mu\text{A/V}^2$ ,  $2 \text{ mA/V}^2$ ; (b)  $1.09$  V; (c)  $-1.31$  V

### 7.1.1 CMOS INVERTER LAYOUT

Two possible layouts for CMOS inverters appear in Fig. 7.3. In the left-hand layout, the lower transistor is the NMOS device in the  $p$ -type substrate, whereas the upper transistor is the PMOS device, which is within the boundary of the  $n$ -well. The polysilicon gates of the two transistors are connected together to form the input  $v_I$ , and the drain diffusions of the two transistors are connected together by the metallization to form output  $v_O$ . The sources of the NMOS and PMOS devices are at the bottom and top of the drawing, respectively, and are connected to the ground and power supply buss metallization. Each device has a local substrate contact connected to the source of the transistor. In this particular layout, each transistor has a  $W/L$  of  $2/1$ . In the right-hand layout, the two transistors appear side by side with a common polysilicon gate running through both. Various options for the design of the  $W/L$  ratios of the transistors are a major focus of the rest of this chapter.

## 7.2 STATIC CHARACTERISTICS OF THE CMOS INVERTER

We now explore the static behavior of CMOS logic gates by looking at the CMOS inverter in Fig. 7.4 where  $C$  represents the equivalent capacitance connected to the output of the inverter (See Section 6.11.1). First, consider the inverter with an input  $v_I = +2.5$  V (1 state), as shown in Fig. 7.4(a). For this input condition,  $v_{GS} = +2.5$  V for the NMOS transistor, and  $v_{GS} = 0$  V for the PMOS transistor. For the NMOS device,  $v_{GS} > V_{TN}$  (0.6 V), so a channel exists in the NMOS transistor, but the PMOS transistor is off because  $v_{GS} = 0$  V for the PMOS device. Thus, load capacitor  $C$  discharges through the NMOS transistor, and  $v_O$  reaches 0 V. Because the PMOS transistor is off, a dc current path does not exist through  $M_N$  and  $M_P$ ! A simplified equivalent circuit for the inverter for a high input level appears in Fig. 7.4(b). The output capacitance  $C$  is discharged to zero through the on-resistance of the NMOS transistor. Current continues in the NMOS device until  $v_{DS} = 0$ .

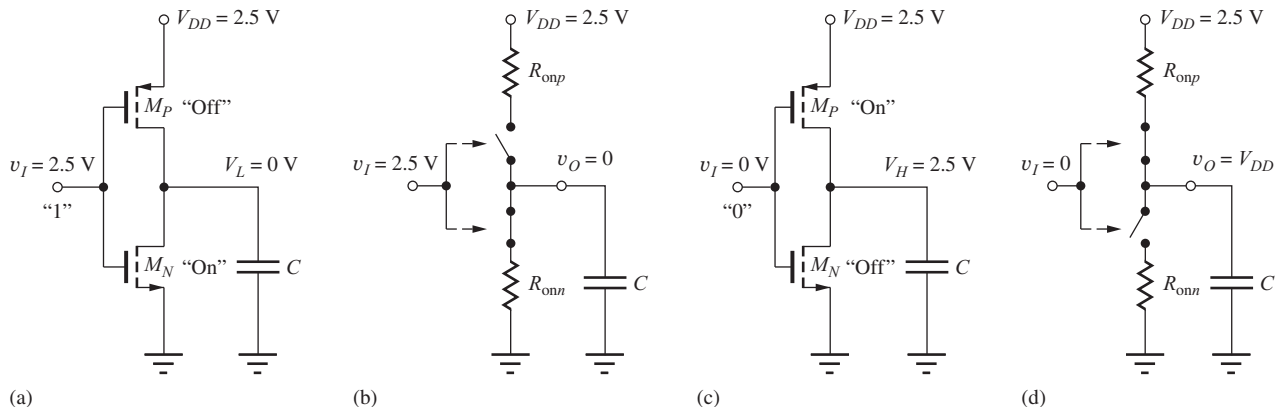


**Figure 7.4** (a) CMOS inverter with the input high.  $M_N$  is on and  $M_P$  is off. (b) Simplified model of the inverter for a high input level. Output capacitance  $C$  is discharged to zero through the on-resistance of the NMOS transistor. (c) CMOS inverter with the input low.  $M_N$  is off and  $M_P$  is on. (d) Simplified model of the inverter for a low input level. Output capacitance  $C$  is charged to  $V_{DD}$  through the on-resistance of the PMOS transistor.

If  $v_I$  is now set to 0 V (0 state), as in Fig. 7.4(c),  $v_{GS}$  becomes 0 V for the NMOS transistor, and it is cut off. For the PMOS transistor,  $v_{GS} = -2.5 \text{ V}$ , a channel exists in the PMOS transistor, and load capacitor  $C$  charges to the positive power supply voltage  $V_{DD}$  (2.5 V). Once a steady-state condition is reached, the currents in  $M_N$  and  $M_P$  must both be zero because the NMOS transistor is off. The corresponding simplified equivalent circuit for the inverter with a low input level appears in Fig. 7.4(d). In this case, we see that the capacitance  $C$  is charged to  $V_{DD}$  through the on-resistance of the PMOS transistor.

Several important characteristics of the CMOS inverter are evident. The values of  $V_H$  and  $V_L$  are equal to the positive and negative power supply voltages, and the logic swing  $\Delta V$  is equal to the full power supply span. For the circuit in Fig. 7.4,  $V_H = 2.5 \text{ V}$ ,  $V_L = 0 \text{ V}$ , and the logic swing  $\Delta V = 2.5 \text{ V}$ . Of even greater importance is the observation that the static power dissipation is zero because the dc current is zero in both logic states!

### 7.2.1 CMOS VOLTAGE TRANSFER CHARACTERISTICS

Figure 7.5 shows the result of simulation of the voltage transfer characteristic (VTC) of a **symmetrical CMOS inverter**, designed with  $K_P = K_N$ . The VTC can be divided into five different regions, as shown in the figure and summarized in Table 7.2. For an input voltage less than  $V_{TN} = 0.6 \text{ V}$  in region 1, the NMOS transistor is off, and the output is maintained at  $V_H = 2.5 \text{ V}$  by the PMOS device.

Similarly, for an input voltage greater than  $(V_{DD} - |V_{TP}|)$  (1.9 V) in region 5, the PMOS device is off, and the output is maintained at  $V_L = 0 \text{ V}$  by the NMOS transistor. In region 2, the NMOS transistor is saturated, and the PMOS transistor is in the triode region. For the input voltage near  $V_{DD}/2$  (region 3), both transistors are operating in the saturation region. The boundary between regions 2 and 3 is defined by the boundary between the saturation and triode regions of operation for the PMOS transistor. Saturation of the PMOS device requires  $|v_{DS}| \geq |v_{GS} - V_{TP}|$ :

$$(2.5 - v_O) \geq (2.5 - v_I) - 0.6 \quad \text{or} \quad v_O \leq v_I + 0.6 \quad (7.2)$$

In a similar manner, the boundary between regions 3 and 4 is defined by saturation of the NMOS device:

$$v_{DS} \geq v_{GS} - V_{TN} \quad \text{or} \quad v_O \geq v_I - 0.6 \quad (7.3)$$

In region 4, the voltages place the NMOS transistor in the triode region, and the PMOS transistor remains saturated.

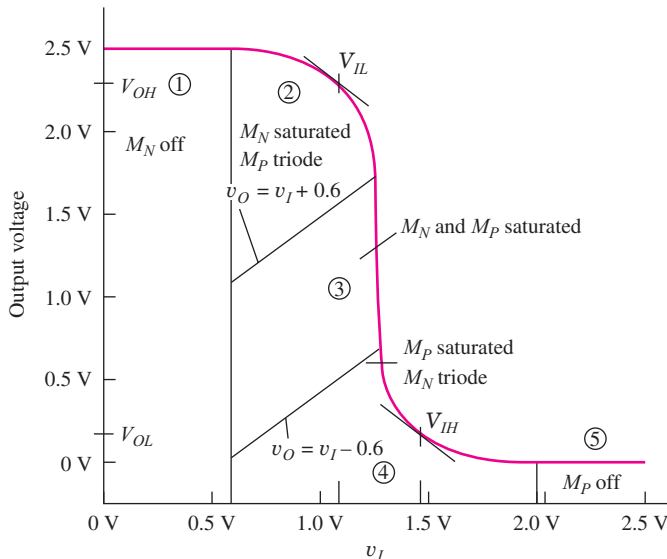


**Figure 7.5** CMOS voltage transfer characteristic may be broken down into the five regions outlined in Table 7.2.

**TABLE 7.2**

Regions of Operation of Transistors in a Symmetrical CMOS Inverter

REGION	INPUT VOLTAGE $v_I$	OUTPUT VOLTAGE $v_O$	NMOS TRANSISTOR	PMOS TRANSISTOR
1	$v_I \leq V_{TN}$	$V_H = V_{DD}$	Cutoff	Triode
2	$V_{TN} < v_I \leq v_O + V_{TP}$	High	Saturation	Triode
3	$v_I \cong V_{DD}/2$	$V_{DD}/2$	Saturation	Saturation
4	$v_O + V_{TN} < v_I \leq (V_{DD} -  V_{TP} )$	Low	Triode	Saturation
5	$v_I \geq (V_{DD} -  V_{TP} )$	$V_L = 0$	Triode	Cutoff

**EXERCISE:** Suppose  $v_I = 1$  V for the CMOS inverter in Fig. 7.4. (a) What is the range of values of  $v_O$  for which  $M_N$  is saturated and  $M_P$  is in the triode region? (b) For which values are both transistors saturated? (c) For which values is  $M_P$  saturated and  $M_N$  in the triode region?

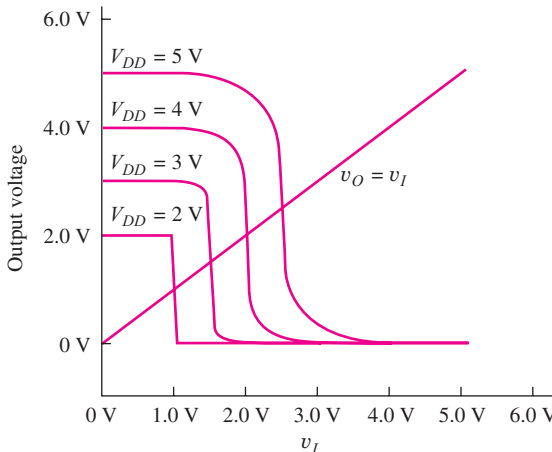
**ANSWERS:** (1.6 V  $\leq v_O \leq 2.5$  V); (0.4 V  $\leq v_O \leq 1.6$  V); (0 V  $\leq v_O \leq 0.4$  V)

**EXERCISE:** The  $(W/L)_N$  of  $M_N$  in Fig. 7.4 is 10/1. What is the value of  $(W/L)_P$  required to form a symmetrical inverter?

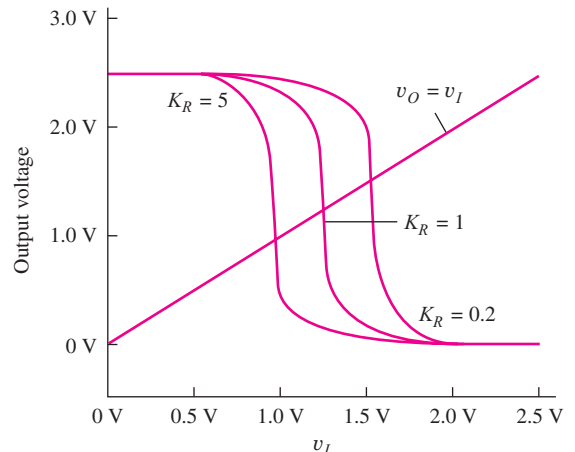
**ANSWER:** 25/1

Figure 7.6 shows the results of simulation of the voltage transfer characteristics for a CMOS inverter with a symmetrical design ( $K_p = K_n$ ) for several values of  $V_{DD}$ . Note that the output voltage levels  $V_H$  and  $V_L$  are always determined by the two power supplies. As the input voltage rises from 0 to  $V_{DD}$ , the output remains constant for  $v_I < V_{TN}$  and  $v_I > (V_{DD} - |V_{TP}|)$ . For this symmetrical design case, the transition between  $V_H$  and  $V_L$  is centered at  $v_I = V_{DD}/2$ . The straight line on the graph represents  $v_O = v_I$ , which occurs for  $v_I = V_{DD}/2$  for the symmetrical inverter.

If  $K_p \neq K_n$ , then the transition shifts away from  $V_{DD}/2$ . To simplify notation, a parameter  $K_R$  is defined:  $K_R = K_n/K_p$ .  $K_R$  represents the relative current drive capability of the NMOS



**Figure 7.6** Voltage transfer characteristics for a symmetrical CMOS inverter ( $K_R = 1$ ) with  $V_{DD} = 5$  V, 4 V, 3 V, and 2 V.



**Figure 7.7** CMOS voltage transfer characteristics for  $K_R = 5$ , 1, and 0.2 for  $V_{DD} = 2.5$  V.  $K_R = K_n/K_p$ .

and PMOS devices in the inverter. Voltage transfer characteristics for inverters with  $K_R = 5$ , 1, and 0.2 are shown in Fig. 7.7. For  $K_R > 1$ , the NMOS current drive capability exceeds that of the PMOS transistor, so the transition region shifts to  $v_I < V_{DD}/2$ . Conversely, for  $K_R < 1$ , PMOS current drive capability is greater than that of the NMOS device, and the transition region occurs for  $v_I > V_{DD}/2$ .

As discussed briefly in Chapter 4, FETs do not actually turn off abruptly as indicated in Eq. (4.9), but conduct small currents for gate-source voltages below threshold. This characteristic enables a CMOS inverter to function at very low supply voltages. In fact, it has been shown that the minimum supply voltage for operation of CMOS is only  $[2V_T \ln(2)]$  V [2, 3]. At room temperature, this voltage is less than 40 mV!

**EXERCISES:** Equate the expressions for the drain currents of  $M_N$  and  $M_P$  to show that  $v_O = v_I$  occurs for a voltage equal to  $V_{DD}/2$  in a symmetrical inverter. What voltage corresponds to  $v_O = v_I$  in an inverter with  $K_R = 10$  and  $V_{DD} = 4$  V? For  $K_R = 0.1$  and  $V_{DD} = 4$  V?

**ANSWER:** 1.27 V, 2.73 V

## 7.2.2 NOISE MARGINS FOR THE CMOS INVERTER

Because of the importance of the CMOS logic family, we explore the noise margins of the inverter in some detail.  $V_{IL}$  and  $V_{IH}$  are identified graphically in Figs. 7.5 and 7.8 as the points at which the voltage transfer characteristic has a slope of  $-1$ . First, we will find  $V_{IH}$ .

For  $v_I$  near  $V_{IH}$ ,  $v_{DS}$  of  $M_P$  will be large and that of  $M_N$  will be small. Therefore, we assume that the PMOS device is saturated, and the NMOS device is in its triode region. The two drain currents must be equal, so  $i_{DN} = i_{DP}$ , and

$$K_n \left( v_I - V_{TN} - \frac{v_O}{2} \right) (v_O) = \frac{K_p}{2} (v_I - V_{DD} - V_{TP})^2 \quad (7.4)$$

For  $M_N$ ,  $v_{GS} = v_I$  and  $v_{DS} = v_O$ . For  $M_P$ ,  $v_{GS} = v_I - V_{DD}$  and  $v_{DS} = v_O - V_{DD}$ . Now

$$K_R (2v_I - 2V_{TN} - v_O) (v_O) = (v_I - V_{DD} - V_{TP})^2 \quad (7.5)$$

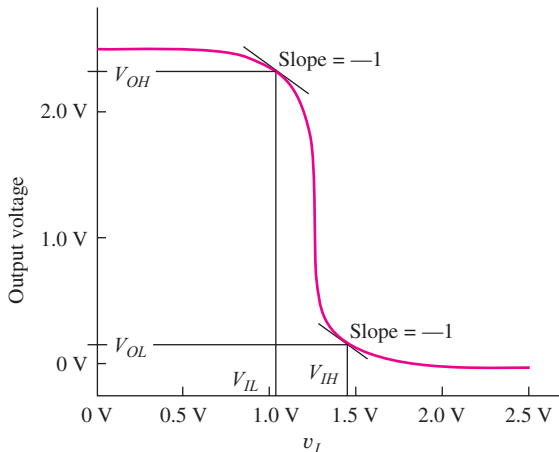


**Figure 7.8** CMOS voltage transfer characteristic, with  $V_{IL}$  and  $V_{IH}$  indicated.

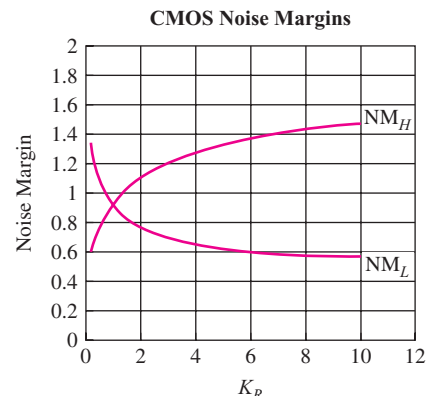


**Figure 7.9** Noise margins versus  $K_R$  for the CMOS inverter with  $V_{DD} = 2.5\text{ V}$  and  $V_{TN} = -V_{TP} = 0.6\text{ V}$ .  $K_R = K_n/K_p$ .

in which  $K_R = K_n/K_p$ . Solving for  $v_O$  yields

$$v_O = (v_I - V_{TN}) \pm \sqrt{(v_I - V_{TN})^2 - \frac{(v_I - V_{DD} - V_{TP})^2}{K_R}} \quad (7.6)$$

Taking the derivative with respect to  $v_I$  and setting it equal to  $-1$  at  $v_I = V_{IH}$  is quite involved (and is most easily done with a symbolic algebra package<sup>1</sup> on the computer), but eventually yields this result:

$$V_{IH} = \frac{2K_R(V_{DD} - V_{TN} + V_{TP})}{(K_R - 1)\sqrt{1 + 3K_R}} - \frac{(V_{DD} - K_R V_{TN} + V_{TP})}{K_R - 1} \quad (7.7)$$

The value of  $V_{OL}$  corresponding to  $V_{IH}$  is

$$V_{OL} = \frac{(K_R + 1)V_{IH} - V_{DD} - K_R V_{TN} - V_{TP}}{2K_R} \quad (7.8)$$

For the special case of  $K_R = 1$ ,

$$V_{IH} = \frac{5V_{DD} + 3V_{TN} + 5V_{TP}}{8} \quad \text{and} \quad V_{OL} = \frac{V_{DD} - V_{TN} + V_{TP}}{8} \quad (7.9)$$

$V_{IL}$  can be found in a similar manner using  $i_{DN} = i_{DP}$ . For  $v_I$  near  $V_{IL}$ , the  $v_{DS}$  of  $M_P$  will be small and that of  $M_N$  will be large, so we assume that the NMOS device is saturated and the PMOS device is in its linear region. Equating drain currents:

$$\begin{aligned} K_p \left( v_I - V_{DD} - V_{TP} - \frac{v_O - V_{DD}}{2} \right) (v_O - V_{DD}) &= \frac{K_n}{2} (v_I - V_{TN})^2 \\ \text{or} \quad (2v_I - V_{DD} - 2V_{TP} - v_O)(v_O - V_{DD}) &= K_R(v_I - V_{TN})^2 \end{aligned} \quad (7.10)$$

Again, we solve for  $v_O$ , take the derivative with respect to  $v_I$ , and set the result equal to  $-1$  at  $v_I = V_{IL}$ . This process yields

$$V_{IL} = \frac{2\sqrt{K_R}(V_{DD} - V_{TN} + V_{TP})}{(K_R - 1)\sqrt{K_R + 3}} - \frac{(V_{DD} - K_R V_{TN} + V_{TP})}{K_R - 1} \quad (7.11)$$

<sup>1</sup> For example, Mathematica, MAPLE, Macsyma, and so on.

The value of  $V_{OH}$  corresponding to  $V_{IL}$  is given by

$$V_{OH} = \frac{(K_R + 1)V_{IL} + V_{DD} - K_R V_{TN} - V_{TP}}{2} \quad (7.12)$$

For the special case of  $K_R = 1$ ,

$$V_{IL} = \frac{3V_{DD} + 5V_{TN} + 3V_{TP}}{8} \quad \text{and} \quad V_{OH} = \frac{7V_{DD} + V_{TN} - V_{TP}}{8} \quad (7.13)$$

The noise margins for  $K_R = 1$  are found using the results in Eqs. (7.9) and (7.13):

$$NM_H = \frac{V_{DD} - V_{TN} - 3V_{TP}}{4} \quad \text{and} \quad NM_L = \frac{V_{DD} + 3V_{TN} + V_{TP}}{4} \quad (7.14)$$

For  $V_{DD} = 2.5$  V,  $V_{TN} = 0.6$  V, and  $V_{TP} = -0.6$  V, the noise margins are both equal to 0.93 V.

Figure 7.9 is a graph of the CMOS noise margins versus  $K_R$  from Eqs. (7.7–7.12) for the particular case  $V_{DD} = 2.5$  V,  $V_{TN} = 0.6$  V, and  $V_{TP} = -0.6$  V. For a symmetrical inverter design ( $K_R = 1$ ), the noise margins are both equal to 0.93 V, in agreement with the results already presented.

**EXERCISE:** What is the value of  $K_R$  for a CMOS inverter in which  $(W/L)_P = (W/L)_N$ ? Calculate the noise margins for this value of  $K_R$  with  $V_{DD} = 2.5$  V,  $V_{TN} = 0.6$  V, and  $V_{TP} = -0.6$  V.

**ANSWERS:** 2.5;  $NM_L = 0.728$  V,  $NM_H = 1.15$  V

## 7.3 DYNAMIC BEHAVIOR OF THE CMOS INVERTER

Static power dissipation and the values of  $V_H$  and  $V_L$  do not really represent design parameters in CMOS circuits as they did for NMOS and PMOS logic. Instead, the choice of sizes of the NMOS and PMOS transistors is dictated by the dynamic behavior of the logic gate—namely, by the desired average propagation delay  $\tau_p$ .

### 7.3.1 PROPAGATION DELAY ESTIMATE

We can get an estimate of the propagation delay in the CMOS inverter by studying the circuit in Fig. 7.10, in which the inverter is driven by an ideal step function. For  $t < 0$ , the NMOS transistor is off and the PMOS transistor is on, forcing the output into the high state with  $v_O = V_H = V_{DD}$ . At  $t = 0$ , the input abruptly changes from 0 V to 2.5 V, and for  $t = 0^+$ , the NMOS transistor is on ( $v_{GS} = +2.5$  V) and the PMOS transistor is off ( $v_{SG} = 0$  V). Thus, the circuit simplifies to that in Fig. 7.10(b). The capacitor voltage is equal to  $V_{DD}$  at  $t = 0^+$  and begins to fall as  $C$  is discharged through the NMOS transistor. The NMOS device starts conduction in the saturation region with  $v_{DS} = v_{GS} = V_{DD}$  and enters the triode region of operation when  $v_{DS} = (v_{GS} - V_{TN}) = (V_{DD} - V_{TN})$ . The NMOS device continues to discharge  $C$  until its  $v_{DS}$  becomes zero. Therefore,  $V_L = 0$  V.

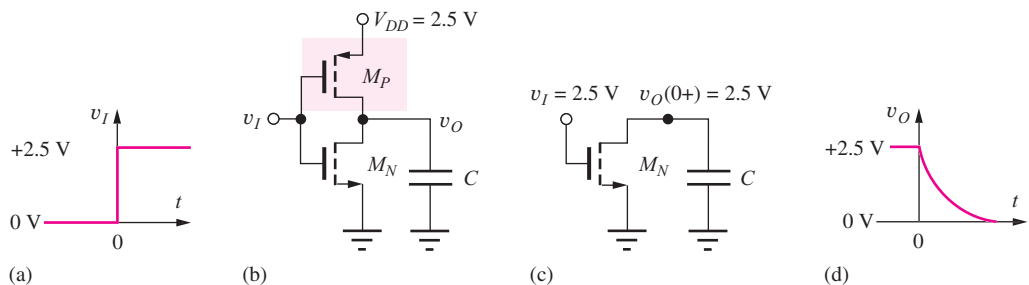
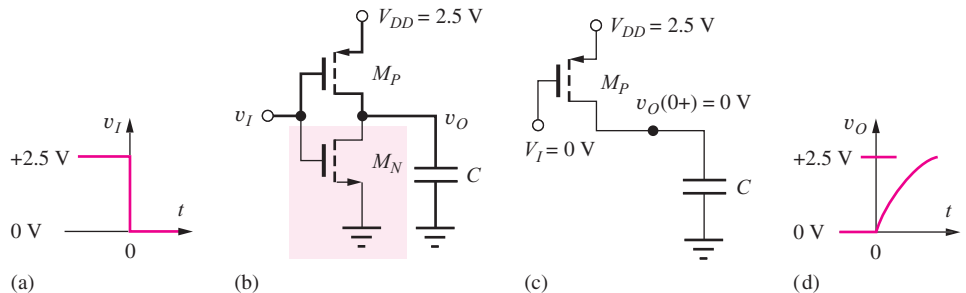


Figure 7.10 High-to-low output transition in a CMOS inverter.



**Figure 7.11** Low-to-high output transition in a CMOS inverter.

A significant amount of effort can be saved by realizing that the set of operating conditions in Fig. 7.10 is exactly the same as was used to determine  $\tau_{PHL}$  for the NMOS inverter with a resistive load. Using Eq. (6.57),

$$\tau_{PHL} = 1.2R_{on}C \quad \text{where} \quad R_{on} = \frac{1}{K_n(V_H - V_{TN})} \quad (7.15)$$

For the CMOS inverter with  $V_H = 2.5$  V and  $V_{TN} = 0.6$  V,  $\tau_{PHL}$  becomes

$$\tau_{PHL} = 1.2R_{on}C = \frac{0.63C}{K_n} \quad (7.16)$$

Now consider the inverter driven by a step function that switches from +2.5 V to 0 V at  $t = 0$ , as in Fig. 7.11. For  $t < 0$ , the PMOS transistor is off and the NMOS transistor is on, forcing the output into the low state with  $v_O = V_L = 0$ . At  $t = 0$ , the input abruptly changes from 2.5 V to 0 V. For  $t = 0^+$ , the PMOS transistor will be on ( $v_{GS} = -2.5$  V) and the NMOS transistor will be off ( $v_{GS} = 0$  V). Thus, the circuit simplifies to that in Fig. 7.11(b). The voltage on the capacitor at  $t = 0^+$  is equal to zero, and it begins to rise toward  $V_{DD}$  as charge is supplied through the PMOS transistor. The PMOS device begins conduction in the saturation region and subsequently enters the triode region of operation. This device continues to conduct until  $v_{DS}$  becomes zero, when  $v_O = V_H = V_{DD}$ . The same set of equations that was used to arrive at Eqs. (7.15) and (7.16) applies to this circuit, and for the CMOS inverter with  $V_{DD} = 2.5$  V and  $V_{TP} = -0.6$  V,  $\tau_{PLH}$  becomes

$$\tau_{PLH} = 1.2R_{onp}C \quad \text{for} \quad R_{onp} = \frac{1}{K_p(V_H + V_{TP})} \quad \text{and} \quad \tau_{PLH} = \frac{0.63C}{K_p} \quad (7.17)$$

The only difference between Eqs. (7.16) and (7.18) is the value of  $R_{on}$  and  $R_{onp}$ . From Table 7.1, we expect  $K'_n$  to be approximately 2.5 times the value of  $K'_p$ . In CMOS, a “symmetrical” inverter with  $\tau_{PLH} = \tau_{PHL}$  can be designed if we set  $(W/L)_P = (K'_n/K'_p)(W/L)_N = 2.5(W/L)_N$  in order to compensate for the difference in mobilities. Because of the layout design rules in many MOS technologies, it is often convenient to design the smallest transistor with  $(W/L) = (2/1)$ . We use the symmetrical inverter design in Fig. 7.12, which has  $(W/L)_N = (2/1)$  and  $(W/L)_P = (5/1)$  as our **CMOS reference inverter** in the subsequent design of more complex CMOS logic gates.

Because we have designed this gate to have  $\tau_{PLH} = \tau_{PHL}$ , the average propagation delay is given by

$$\tau_P = \frac{\tau_{PHL} + \tau_{PLH}}{2} = \tau_{PHL} = 1.2R_{on}C \quad (7.18)$$

**EXERCISE:** Calculate the average propagation delay of the reference inverter in Fig. 7.12 for  $C = 1$  pF.

**ANSWER:** 3.16 ns

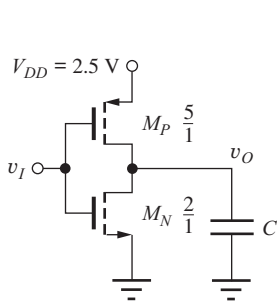


**Figure 7.12** Symmetrical reference inverter design.

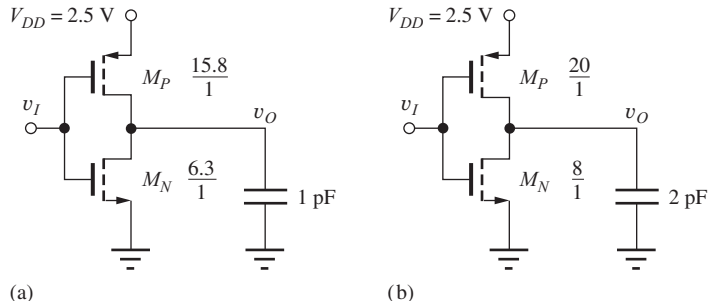


**Figure 7.13** Scaled inverters: (a)  $\tau_p = 1$  ns, (b)  $\tau_p = 1.6$  ns.

### 7.3.2 RISE AND FALL TIMES

The rise and fall times for the CMOS gate can also be found using our results for the NMOS inverter. Based upon Eq. (6.57), we see that the fall time is approximately three times  $\tau_{PHL}$ , and because of the symmetry of the CMOS gate, the rise time is three times  $\tau_{PLH}$ :

$$t_f = 3\tau_{PHL} \quad \text{and} \quad t_r = 3\tau_{PLH} \quad (7.19)$$

Based on the results of the preceding exercise for the 1-pF load capacitance, the expected rise and fall times are 9.5 ns.

### 7.3.3 PERFORMANCE SCALING

Once we have characterized the delay of a single inverter design by analysis or simulation, we can easily scale the size (i.e.,  $W/L$ ) of the inverter to achieve different levels of performance and account for changes in the load capacitance. Even though the delay expressions that have been developed using our first order i-v models may no longer be quantitatively accurate for state-of-the-art technologies, for example, 65 nm CMOS, two important relationships continue to be true: delay remains proportional to the total load capacitance  $C_L$  and inversely proportional to the  $(W/L)$ . So for proper scaling, the size of the devices must be increased (i.e., increase the power of the gate) to decrease the propagation delay, and must also be increased to drive a larger capacitance. Thus the new values  $(W/L)'$  are related to the reference values  $(W/L, C_{L\text{ref}}, \tau_{P\text{ref}})$  by

$$\tau'_p = \left(\frac{W}{L}\right)' \times \left(\frac{C'_L}{C_{L\text{ref}}}\right) \times \tau_{P\text{ref}} \quad \text{or} \quad \left(\frac{W}{L}\right)' = \left(\frac{W}{L}\right) \times \left(\frac{\tau_{P\text{ref}}}{\tau'_p}\right) \times \left(\frac{C'_L}{C_{L\text{ref}}}\right) \quad (7.20)$$

For example, the inverter in Fig. 7.13(a) has a delay of 1 ns because the  $W/L$  ratios of both transistors are 3.16 times larger than those in the reference inverter design in Fig. 7.12. The inverter in Fig. 7.13(b) has a delay of 1.6 ns because its transistors are four times larger than those in the reference inverter, but it is driving twice as much capacitance:

$$\tau'_p = \frac{\left(\frac{2}{1}\right)}{\left(\frac{8}{1}\right)} \times \left(\frac{2 \text{ pF}}{1 \text{ pF}}\right) \times 3.16 \text{ ns} = 1.58 \text{ ns}$$

**EXERCISE:** An inverter must drive a 5-pF load capacitance with  $\tau_p = 1$  ns. Scale the reference inverter to achieve this delay.

**ANSWER:**  $(W/L)_P = 78.8/1$  and  $(W/L)_N = 31.5/1$

## DESIGN REFERENCE INVERTER DESIGN

### EXAMPLE 7.1

In this example, we design a reference inverter to achieve a desired value of delay.

**DESIGN SPECIFICATIONS** Design a reference inverter to achieve a delay of 250 ps when driving a 0.2-pF load using a 3.3-V power supply. Assume that the threshold voltages of the CMOS technology are  $V_{TN} = -V_{TP} = 0.75$  V.

**SOLUTION** **Specifications and Known Information:**  $V_{DD} = 3.3$  V,  $C = 0.2$  pF,  $\tau_p = 250$  ps,  $V_{TN} = -V_{TP} = 0.75$  V

**Unknowns:**  $(W/L)_n, (W/L)_p$

**Approach:** Use Eq. (7.15) to find the value of  $R_{on}$  and  $(W/L)_n; (W/L)_p = 2.5(W/L)_n$ .

**Assumptions:** A symmetrical inverter design is desired; the  $K'$  values are the same as Table 7.1:  $K'_n = 100 \mu\text{A}/\text{V}^2$ ,  $K'_p = 40 \mu\text{A}/\text{V}^2$

**Analysis:** Using Eq. (7.15),

$$R_{on} = \frac{\tau_{PHL}}{1.2C} = \frac{250 \times 10^{-12}\text{sec}}{1.2(0.2 \times 10^{-12} \text{ F})} = 1040 \Omega$$

$$\left(\frac{W}{L}\right)_n = \frac{1}{R_{on} K'_n (V_{DD} - V_{TN})} = \frac{1}{(1040 \Omega) \left(100 \frac{\mu\text{A}}{\text{V}^2}\right) (3.3 - 0.75) \text{ V}} = \frac{3.77}{1}$$

$$\left(\frac{W}{L}\right)_p = \frac{K'_n}{K'_p} \left(\frac{W}{L}\right)_n = 2.5 \left(\frac{W}{L}\right)_n = \frac{9.43}{1}$$

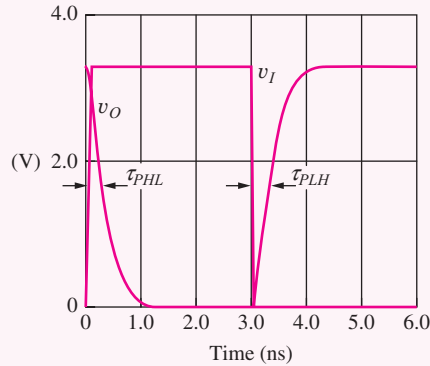
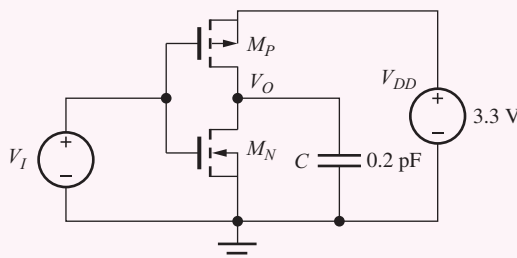
**Check of Results:** Let us double check the value of on-resistance for the PMOS device:

$$R_{onp} = \frac{1}{K_p(V_{DD} + V_{TP})} = \frac{1}{(9.43) \left(40 \frac{\mu\text{A}}{\text{V}^2}\right) (3.3 - 0.75) \text{ V}} = 1040 \Omega \quad \checkmark$$

**Discussion:** The on-resistances are equal, so the rise and fall times should be the same. The  $R_{on}C$  time constant is 208 ps, which appears consistent with our design goal.

**Computer-Aided Analysis:** Our design is checked in the SPICE circuit below. Source  $V_I$  is a pulse source, and the output waveform is the voltage across the capacitor. From the output waveforms, we find symmetrical propagation delays of approximately 280 ps. Our approximation in Eq. (7.15) is slightly optimistic in its estimate of  $\tau_p$ , because it assumes an ideal step function as an input.

PULSE SOURCE DESCRIPTION (VS)		SIMULATION PARAMETERS	
Initial voltage	0	Start time	0
Peak voltage	3.3 V	Stop time	6 ns
Delay time	0		
Rise time	50 ps		
Fall time	50 ps		
Pulse width	2.95 ns		
Pulse period	6 ns		



**EXERCISE:** Based upon the simulation results in Ex. 7.1, what  $W/L$  ratios are required to actually achieve an average propagation delay of 250 psec?

**ANSWERS:** 4.22/1, 10.6/1

**EXERCISE:** What would be the  $W/L$  ratios in Ex. 7.1 if the threshold voltages of the transistors were +0.5 V and -0.5 V?

**ANSWERS:** 3.43/1, 8.59/1

### 7.3.4 DELAY OF CASCDED INVERTERS

Obviously, the ideal step-function input waveform used in the analysis leading to Eq. (7.15) cannot be achieved in real circuits. The waveforms will have nonzero rise and fall times, and the propagation delay estimate given by Eq. (7.15) will be more optimistic than the delay encountered in actual circuits. Let us use SPICE to help improve the propagation delay design equation through simulation of the cascade of five identical inverters shown in Fig. 7.14(a). The first inverter is driven by a pulse with a 5-ns width, a 10-ns period, and rise and fall times of 2 ps.

The outputs of the five inverters are shown in the waveforms in Fig. 7.14(b). The propagation time between the step input and the output of the first inverter is approximately 0.28 ns, in agreement with the design of Ex. 7.1. However, the delay times of the other four inverters are significantly slower because of the rise and fall times of the waveforms driving each successive inverter. Looking

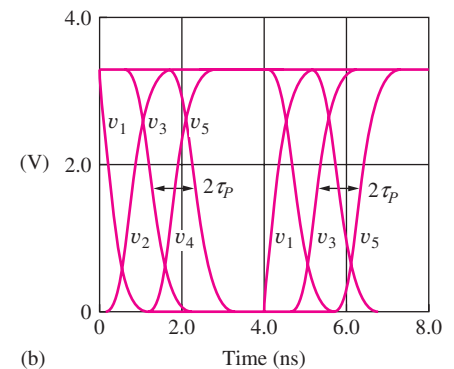
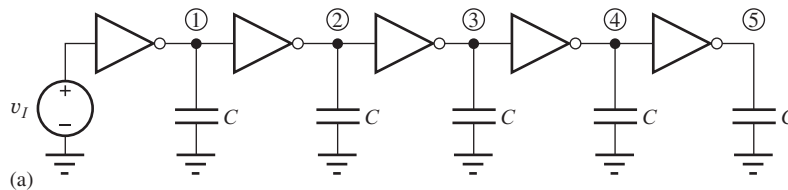


**Figure 7.14** (a) Cascade of five identical inverters. (b) Output waveforms for five inverters using design from Ex. 7.1.  $V_I$  is a step function,  $V_{DD} = 3.3$  V and  $C = 0.2$  pF.

at every other inverter, we see that the waveforms are very similar and quickly reach a periodic state. The average delay time through each inverter pair is 1 ns, corresponding to  $\tau_{PHL} = \tau_{PLH} = 0.5$  ns. This value is approximately two times that predicted by Eq. (7.15). We also find that the rise and fall times are approximately two times the propagation delays. Based on these results, we modify our design estimate for the propagation delays and rise and fall times to be

$$\begin{aligned}\tau_{PHL} &\cong 2.4R_{on}C & R_{on} &= \frac{1}{K_n(V_{DD} - V_{TN})} & \tau_{PLH} &\cong 2.4R_{op}C & R_{op} &= \frac{1}{K_p(V_{DD} + V_{TP})} \\ t_r &= 2\tau_{PLH} & t_f &= 2\tau_{PHL} \end{aligned}\quad (7.21)$$

**EXERCISE:** What are the new equations [similar to Eqs. (7.16) and (7.17)] for  $\tau_{PHL}$  and  $\tau_{PLH}$  for  $V_{DD} = 2.5$  V,  $V_{TN} = 0.6$  V, and  $V_{TP} = -0.6$  V?

**ANSWERS:**  $\tau_{PHL} = 2.4R_{on}C = 1.26C/K_n$ ,  $\tau_{PLH} = 2.4R_{op}C = 1.26C/K_p$

**EXERCISE:** What are the new equations [similar to Eqs. (7.16) and (7.17)] for  $\tau_{PHL}$  and  $\tau_{PLH}$  for  $V_{DD} = 3.3$  V,  $V_{TN} = 0.75$  V, and  $V_{TP} = -0.75$  V?

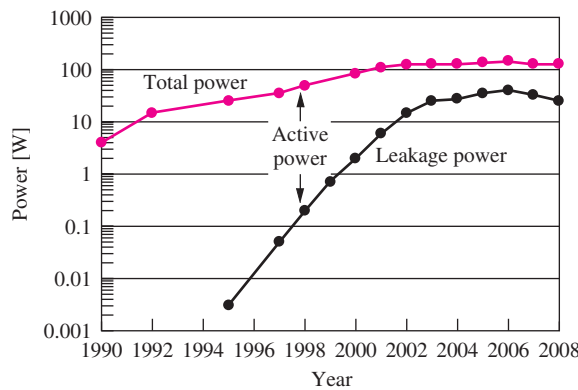
**ANSWERS:**  $\tau_{PHL} = 2.4R_{on}C = 0.94C/K_n$ ,  $\tau_{PLH} = 2.4R_{op}C = 0.94C/K_p$

## 7.4 POWER DISSIPATION AND POWER DELAY PRODUCT IN CMOS

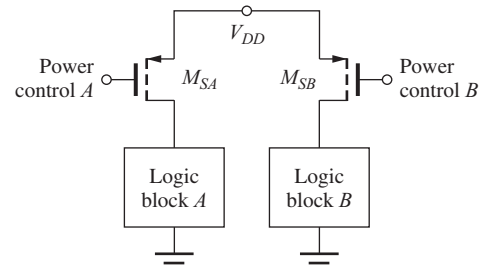
### 7.4.1 STATIC POWER DISSIPATION

CMOS logic is often considered to have zero static power dissipation. When the CMOS inverter is resting in either logic state, no direct current path exists between the two power supplies ( $V_{DD}$  and ground). However in both very low power applications as well as state-of-the-art multicore microprocessor designs, static power dissipation can be extremely important. The actual static power dissipation is nonzero due to subthreshold conduction (see Sec. 4.10.7) as well as the leakage currents associated with the reverse-biased drain-to-substrate junctions of the NMOS and PMOS transistors and the large area of reverse-biased  $n$ -well (or  $p$ -well) regions. The leakage current of these  $pn$  junctions flows between the supplies and contributes directly to static power dissipation. Power lost due to leakage is approaching 30 percent of total chip power dissipation in microprocessors implemented in sub 0.1- $\mu$ m logic technologies as in Fig. 7.15(a)!

New circuit techniques are continually being invented to minimize static power dissipation. One straight-forward example appears in Fig. 7.15(b) in which large PMOS transistors are added to



(a)



(b)

**Figure 7.15** (a) Power trends in microprocessors, IntelCorporation. Courtesy of Stefan Rusu. (b) Static power reduction can be achieved by selectively turning power off to inactive logic blocks.

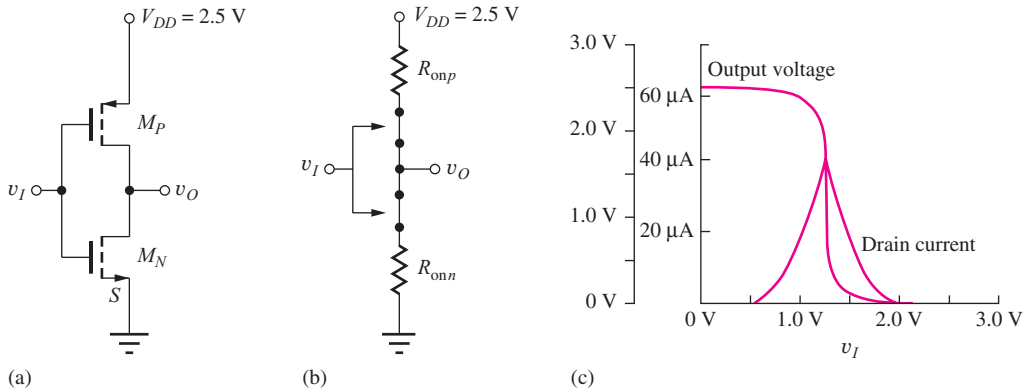


**Figure 7.16** (a) CMOS inverter. (b) Switch and on-resistance model for the inverter with  $V_{TN} \leq v_I \leq V_{DD} - |V_{TP}|$ . (c) Supply current versus input voltage for a symmetrical CMOS inverter.

control the power to logic blocks. Power to inactive blocks can be turned off under either hardware or software control. The logic block can be a small number of gates or a much larger function, such as a multiplier or arithmetic logic unit (ALU) or even a CPU in chips containing multiple processor cores. When the PMOS switch is off, it is the only device that contributes to leakage and static power dissipation. Software techniques are also being employed to dynamically power down unneeded hardware during program execution.

#### 7.4.2 DYNAMIC POWER DISSIPATION

Dynamic power dissipation represents the power associated with switching a logic gate between states. There are two components of dynamic power dissipation in CMOS logic gates. As the gate charges and discharges load capacitance  $C$  at frequency  $f$ , the power dissipation is equal to that given by Eq. (6.49) in Chapter 6:

$$P_D = CV_{DD}^2 f \quad (7.22)$$

Power  $P_D$  is usually the largest component of power dissipation in CMOS gates operating at high frequency.

A second mechanism for power dissipation also occurs during switching of the CMOS logic gate and can be explored by referring to Fig. 7.16, which shows the current through a symmetrical CMOS inverter (with  $C = 0$ ) as a function of the input voltage  $v_I$ . The current is zero for  $v_I < V_{TN}$  and  $v_I > (V_{DD} - |V_{TP}|)$  because either the NMOS or PMOS transistor is off for these conditions. However, in a logic gate we realize that input  $v_I$  does not make an abrupt jump between  $V_H$  and  $V_L$ , but instead makes a smooth transition between the two input states. During the input transition when  $V_{TN} \leq v_I \leq V_{DD} - |V_{TP}|$ , both transistor switches are on as in Fig. 7.16(b), and a current path exists through both the NMOS and PMOS devices. The current reaches a peak for  $v_I = v_O = V_{DD}/2$ . As  $v_I$  increases further, the current decreases back to zero. In the time domain, a pulse of current occurs between the power supplies as the output switches state, as shown in Fig. 7.17. In very high-speed CMOS circuits, this second component of dynamic power dissipation can approach 20 to 30 percent of that given by Eq. (7.22).

In the technical literature, this current pulse between supplies is often referred to as a “short circuit current.” This reference is a misnomer, however, because the current is limited by the device characteristics and a true short circuit does not actually exist between the power supplies.

**EXERCISE:** Calculate the value of the maximum current similar to that in Fig. 7.16 for the inverter design in Fig. 7.12.

**ANSWER:** 42.3 \$\mu\$A

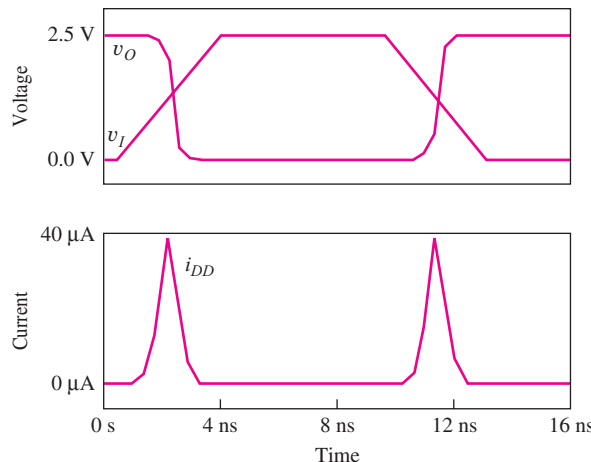


**Figure 7.17** SPICE simulation of the transient current pulses between the power supplies during switching of a CMOS inverter.

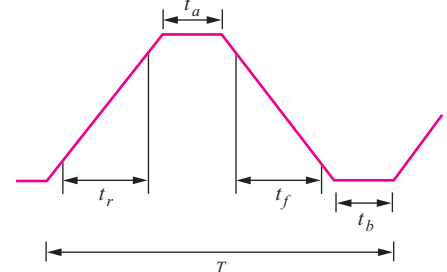


**Figure 7.18** CMOS switching waveform at high frequency.

#### 7.4.3 POWER-DELAY PRODUCT

The **power-delay product (PDP)**, defined in Sec. 6.3, is an important figure of merit for comparing various logic technologies:

$$\text{PDP} = P_{\text{av}} \tau_P \quad (7.23)$$

For CMOS operating at high frequency, the power consumed when charging and discharging the load capacitance \$C\$ is usually the dominant source of power dissipation. For this case, \$P\_{\text{av}} = CV\_{DD}^2 f\$. The switching frequency \$f = (1/T)\$ can be related to the rise time \$t\_r\$, fall time \$t\_f\$, and the propagation delay \$\tau\_P\$ of the CMOS waveform by referring to Fig. 7.18, in which we see that the period \$T\$ must satisfy

$$T \geq t_r + t_a + t_f + t_b \quad (7.24)$$

For the highest possible switching frequency, times \$t\_a\$ and \$t\_b\$ approach 0, and the rise and fall times account for approximately 80 percent of the total transition time. Assuming a symmetrical inverter design with equal rise and fall times and using Eqs. (7.21) permits Eq. (7.24) to be approximated by

$$T \geq \frac{2t_r}{0.8} = \frac{2(2\tau_P)}{0.8} = 5\tau_P \quad (7.25)$$

A lower bound on the power-delay product for CMOS is then given by

$$\text{PDP} \geq \frac{CV_{DD}^2}{5\tau_P} \tau_P = \frac{CV_{DD}^2}{5} \quad (7.26)$$

The importance of using lower power supply voltages is obvious in Eq. (7.26), from which we see that the PDP is reduced in proportion to the square of any reduction in power supply. Moving from a power supply voltage of 5 V to one of 3.3 V reduces the power-delay product by a factor of 2.5. The importance of reducing the capacitance is also clear in Eq. (7.26). The lower the effective load capacitance, the smaller the power-delay product.

**EXERCISE:** (a) What is the power-delay product for the symmetrical reference inverter in Fig. 7.12 operating from \$V\_{DD} = 2.5\$ V and driving an average load capacitance of 100 fF? (b) Repeat for a 3.3-V supply. (c) Repeat for a 1.8 V supply.

**ANSWERS:** 130 fJ; 220 fJ; 65 fJ

## ELECTRONICS IN ACTION

### **CMOS-The Enabler for Handheld Technologies**

Starting with science fiction stories of the 1940s, moving on to space-going movies of the 50s and 60s, and eventually finding its way into the Star Trek voyages, powerful handheld sensing, computing, and communication technologies have been a dream of many an author. Enabling those dreams has also been the goal of many microelectronic circuit designers in the last 30 years. The beginnings of the integrated circuit era in the 1960s gave us a peek at the possibilities, but the realization was still elusive due to a lack of functional density and power consumption too high to enable battery powered operation.

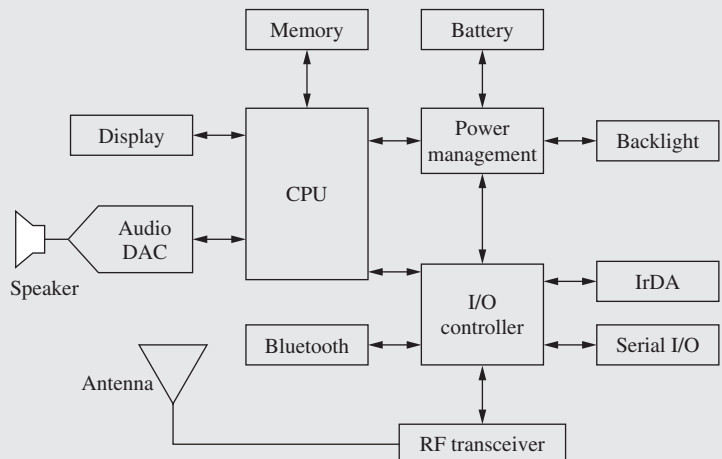
In the 1980s, CMOS technologies became widely available. Finally, we had a technology that promised to combine high computational power and low power consumption in a way that would lead to the handheld devices envisioned by authors years ago. As CMOS transistors continued to be scaled to smaller and smaller sizes during the 1990s, handheld devices such as cell phones, GPS receivers, and PDAs were introduced and rapidly improved from year to year.

Cell phones are highly complex devices and typically include a central processing unit (CPU), memory, input/output circuits, RF transceiver, power management, touchscreen, liquid-crystal display, and various optional modules such as Bluetooth radio, infrared, and other interfaces. In total, a cell phone will typically contain millions of transistors. The extremely low standby current of CMOS logic enables the designer to build complex capabilities that only dissipate significant power when activated.

Throughout this chapter, we have assumed that a CMOS transistor has zero current when the gate-source voltage is less than the threshold voltage. This property is responsible for the extremely low standby-power dissipation of CMOS logic. However, in practice, the current is not exactly zero; a small sub-threshold current (approximately  $10^{-11}$  –  $10^{-9}$  amps) flows when the device is OFF (See Fig. 4.19). This would seem to be an insignificant current, but when multiplied by gate counts in the millions, it can add up to a sizable limitation on battery lifetime. Modern sub 100 nm gate-length processes have such a large sub-threshold leakage current that designers are being forced to invent new logic forms to reduce the leakage currents, and processes are being modified to incorporate multiple thresholds to better control the leakage current power dissipation. These new CMOS logic forms build on the logic topologies developed in this chapter and are a topic of advanced VLSI design courses.



(a) BlackBerry: © The McGraw-Hill Companies, Inc./L. Niki, photographer



(b) PDA Block Diagram

## 7.5 CMOS NOR AND NAND GATES

The next several sections explore the design of CMOS gates, including the NOR gate, the NAND gate, and complex CMOS gates. The structure of a general static CMOS logic gate is given in Fig. 7.19 and consists of an NMOS transistor-switching network and a PMOS transistor-switching network. For each logic input variable in a CMOS gate, there is one transistor in the NMOS network and one transistor in the PMOS network. Thus, a CMOS logic gate has two transistors for every input variable. When a static conducting path exists through the NMOS network, a path must not exist through the PMOS network and vice versa. In other words, the conducting paths must represent logical complements of each other. CMOS forms an unusually powerful logic family because it is easy to realize both NOR and NAND gates as well as much more complex logic functions in a single gate. In Secs. 7.5.1 and 7.5.2, we will look at the NOR and NAND gate design. Then more complex gate design will be discussed.

### 7.5.1 CMOS NOR GATE

The realization of a two-input CMOS **NOR gate** is shown in Fig. 7.19 (b) in which the output should be low when either input  $A$  or input  $B$  is high. Thus the NMOS portion of the gate is identical to that of the NMOS NOR gate. However, in the CMOS gate, we must ensure that a static current path does not exist through the logic gate, and this requires the use of two PMOS transistors in series in the PMOS transistor network.

The complementary nature of the conducting paths can be seen in Table 7.3. A conducting path exists through the NMOS network for  $A = 1$  or  $B = 1$ , as indicated by the highlighted entries in the table. However, a path exists through the PMOS network only when both  $A = 0$  and  $B = 0$  (no conducting path through the NMOS network).

In general, a parallel path in the NMOS network corresponds to a series path in the PMOS network, and a series path in the NMOS network corresponds to a parallel path in the PMOS

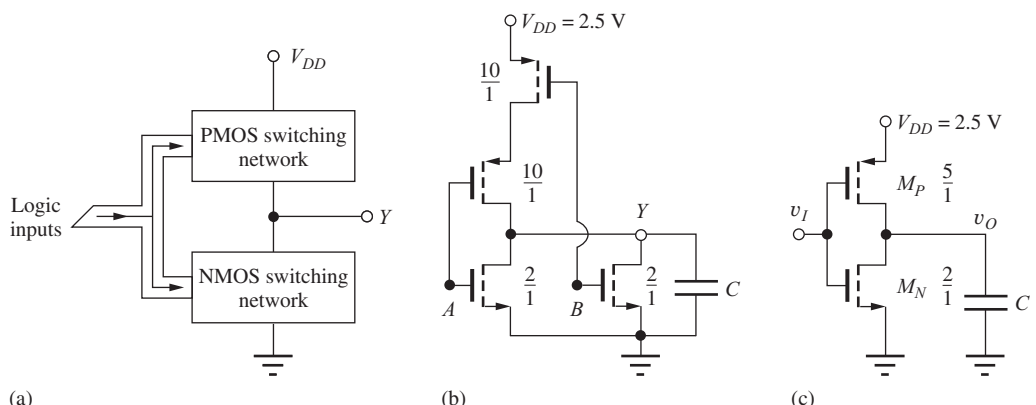


**Figure 7.19** (a) Basic CMOS logic gate structure. (b) Two-input CMOS NOR gate and reference inverter.

**TABLE 7.3**  
CMOS NOR Gate Truth Table and Transistor States

$A$	$B$	$Y = \overline{A + B}$	NMOS-A	NMOS-B	PMOS-A	PMOS-B
0	0	1	Off	Off	On	On
0	1	0	Off	On	On	Off
1	0	0	On	Off	Off	On
1	1	0	On	On	Off	Off

network. (Bridging paths correspond to bridging paths in both networks.) We will study a rigorous method for implementing these two switching networks in Sec. 7.6.

### Transistor Sizing

We can determine the sizes of the transistors in the two-input NOR gate by using our knowledge of NMOS gate design. In the CMOS case, one approach is to maintain the delay times equal to the reference inverter design under the worst-case input conditions. For the NMOS network with  $AB = 10$  or  $01$ , transistor  $A$  or transistor  $B$  must individually be capable of discharging load capacitance  $C$ , so each must be the same size as the NMOS device of the reference inverter. The PMOS network conducts only when  $AB = 00$  and there are two PMOS transistors in series. To maintain the same **on-resistance** as the reference inverter, each PMOS device must be twice as large:  $(W/L)_P = 2(5/1) = 10/1$ . The resulting  $W/L$  ratios are indicated in Fig. 7.19(b).

### Body Effect

In the preceding design, we ignored the influence of body effect. In the series-connected PMOS network, the source of the PMOS transistor connected to input  $A$  cannot actually be connected to its substrate. During switching, its threshold voltage changes as its source-to-bulk voltage changes. However, once the steady-state condition is reached, with  $v_O = V_H$ , for example, all the PMOS source and drain nodes will be at a voltage equal to  $V_{DD}$ . Thus, the total on-resistance of the PMOS transistors is not affected by the body effect once the final logic level is reached. During the transient response, however, the threshold voltage changes as a function of time, and  $|V_{TP}| > |V_{TOP}|$ , which slows down the rise time of the gate slightly. An investigation of this effect is left for Probs. 7.66 to 7.69.

### Two-Input NOR Gate Layout

A possible layout for the two-input NOR gate is shown in Fig. 7.20. The two NMOS transistors are formed in the substrate, and each has a  $2/1$   $W/L$  ratio. The PMOS transistors, each with  $W/L = 10/1$ , are located in a common  $n$ -well. Note that the drain of the upper PMOS device is merged with the source of the lower PMOS device to form the connection between these two transistors. No contacts or metal are required to make this connection.

The gates of the NMOS and PMOS transistors are connected together with the metal level at inputs  $A$  and  $B$ , and the drains of three transistors are connected together by the metal layer to form output  $Y$ . Local substrate contacts are provided next to the sources of the NMOS transistors and the upper PMOS device. Note the much larger area taken up by the PMOS devices caused by the symmetrical gate design specification.

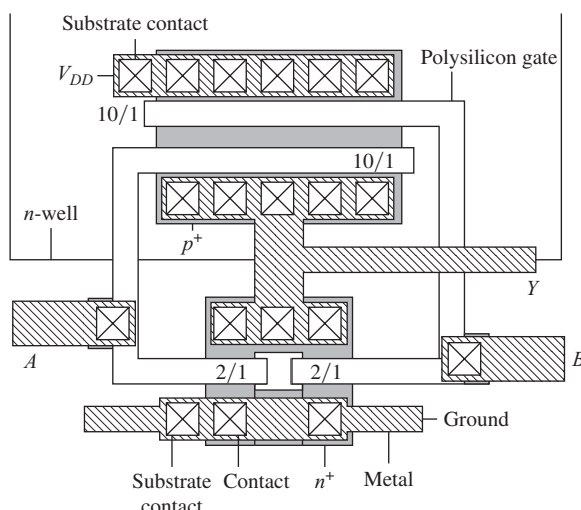


**Figure 7.20** Layout of symmetrical two-input CMOS NOR gate. Note the large area of the PMOS transistors relative to the NMOS devices.

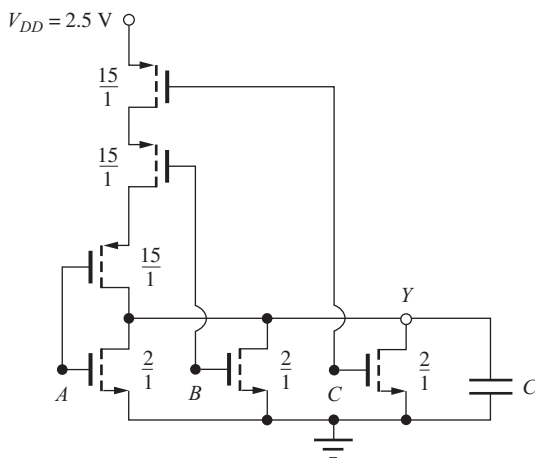


**Figure 7.21** Three-input CMOS NOR gate.

**TABLE 7.4**  
Three-Input NOR Gate Truth Table

$A$	$B$	$C$	$Y = \overline{A + B + C}$
0	0	0	1
0	0	1	0
0	1	0	0
0	1	1	0
1	0	0	0
1	0	1	0
1	1	0	0
1	1	1	0

### Three-Input NOR Gate

Figure 7.21(a) is the schematic for a three-input version of the NOR gate, and Table 7.4 is the truth table. As in the case of the NMOS gate, the output is low when NMOS transistor  $A$  or transistor  $B$  or transistor  $C$  is conducting. The only time that a conducting path exists through the PMOS network is for  $A = B = C = 0$ . The NMOS transistors must each individually be able to discharge the load capacitance in the desired time, so the  $W/L$  ratios are each 2/1 based on our reference inverter design in Fig. 7.19. The PMOS network now has three devices in series, so each must be three times as large as the reference inverter device ( $W/L = 15/1$ ).

It is possible to find the PMOS network directly from the truth table. From Table 7.3 for the two-input NOR gate, we see that  $Y = \overline{A \cdot B}$  and, using the identities in Table 6.4, the expression for  $\overline{Y} = A + B$ . For the three-input NOR gate described by Table 7.4,  $Y = \overline{A \cdot B \cdot C}$  and  $\overline{Y} = A + B + C$ . The PMOS network directly implements the logic function  $Y = \overline{A \cdot B \cdot C}$ , written in terms of the complements of the input variables, and the NMOS network implements the logic function  $\overline{Y} = A + B + C$ , written in terms of the uncomplemented input variables. In effect, the PMOS transistors directly complement the input variables for us! The two functions  $\overline{Y}$  and  $Y$  for the NMOS and PMOS networks need to be written in minimum form in order to have the minimum number of transistors in the two networks.

The complementing effect of the PMOS devices has led to a shorthand representation for CMOS logic gates that is used in many VLSI design texts. This notation is shown by the right-hand symbol in the transistor pairs in Fig. 7.22(a) and 7.22(b). The NMOS and PMOS transistor symbols differ only by the circle at the input of the PMOS gate. This circle identifies the PMOS transistor and

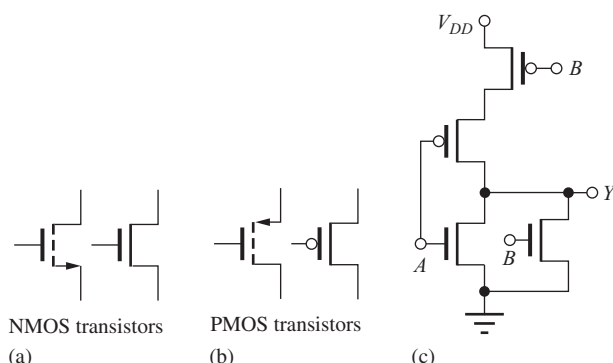


**Figure 7.22** Shorthand notation for (a) NMOS and (b) PMOS transistors. (c) Two-input CMOS NOR gate using shorthand transistor symbols.

indicates the logical inversion operation that is occurring to the input variable. In this book, however, we will continue to use the standard symbols.

### 7.5.2 CMOS NAND GATES

The NAND gate is also easy to realize in CMOS, and the structure and truth table for a two-input static CMOS NAND gate are given in Fig. 7.23 and Table 7.5, respectively. From the truth table for the NAND gate, we see that  $Y = \overline{AB}$ , and the output should be low only when both input  $A$  and input  $B$  are high. Thus, the NMOS switching network is identical to that of the NMOS NAND gate with transistors  $A$  and  $B$  in series.

Expanding the equation for  $Y$  in terms of complemented variables, we have  $Y = \overline{A} + \overline{B}$ . If either input  $A$  or input  $B$  is low, the output must be pulled high through a PMOS transistor, resulting in two transistors in parallel in the PMOS switching network. Once again, there is one transistor in the NMOS network and one transistor in the PMOS network for each logic input variable.

#### Transistor Sizing

We determine the sizes of the transistors in the two-input NAND gate by again using our knowledge of NMOS design. There are two transistors in series in the NMOS network, so each should be twice as large as in the reference inverter or 4/1. In the PMOS network, each transistor must individually be capable of discharging load capacitance  $C$ , so each must be the same size as the PMOS device in the reference inverter. These  $W/L$  ratios are indicated in Fig. 7.23.

#### The Multi-Input NAND Gate

As another example, the circuit for a five-input NAND gate is given in Fig. 7.24. The NMOS network consists of a series stack of five transistors with one MOS device for each input variable. The PMOS

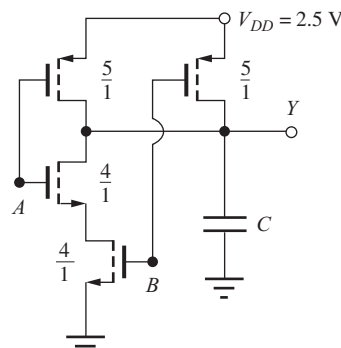


**Figure 7.23** Two-input CMOS NAND gate and reference inverter.

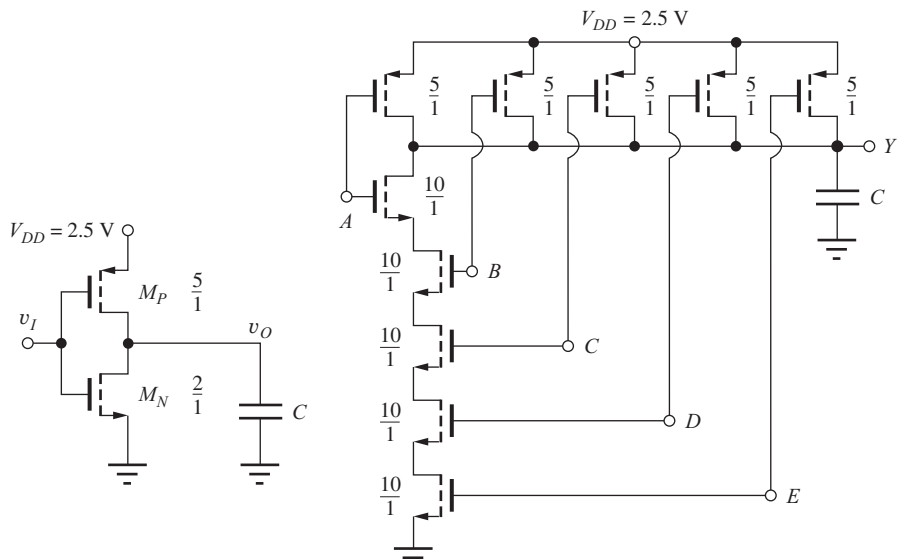


**Figure 7.24** Five-input CMOS NAND gate:  $Y = \overline{ABCDE}$ .

**TABLE 7.5**  
CMOS NAND Gate Truth Table and Transistor States

$A$	$B$	$Y = \overline{AB}$	NMOS-A	NMOS-B	PMOS-A	PMOS-B
0	0	1	Off	Off	On	On
0	1	1	Off	On	On	Off
1	0	1	On	Off	Off	On
1	1	0	On	On	Off	Off

network consists of a group of PMOS devices in parallel, also with one transistor for each input. To maintain the speed on the high-to-low transition in the five-input gate, the NMOS transistors must each be five times larger than that of the reference inverter, whereas the PMOS transistors are each identical to that of the reference inverter.

**EXERCISE:** Draw a four-input NAND gate similar to the five-input gate in Fig. 7.24. What are the *W/L* ratios of the transistors?

**ANSWERS:** 8/1; 5/1

## 7.6 DESIGN OF COMPLEX GATES IN CMOS

Just as with NMOS design, the real power of CMOS is not realized if the designer uses only NANDs, NORs, and inverters. The ability to implement **complex logic gates** directly in CMOS is an advantage for CMOS design, just as it is in NMOS. This section investigates complex gate design through Design Examples 7.2 and 7.3.

### DESIGN EXAMPLE 7.2 COMPLEX CMOS LOGIC GATE DESIGN

This example presents the design of a CMOS logic gate with the same logic function as the NMOS design from Fig. 6.34 in Chapter 6. A graphical approach for relating NMOS and PMOS transistor networks is introduced as part of the example.

#### DESIGN SPECIFICATIONS

Design a CMOS logic gate logic that implements the function  $Y = \overline{A + BC + BD}$ .

#### SOLUTION

**Specifications and Known Information:** Logic function  $Y = \overline{A + B(C + D)}$  and  $\overline{Y} = A + B(C + D)$ . The NMOS network in Fig. 7.25(a) for  $\overline{Y}$  is exactly the same as that of the corresponding NMOS gate in Fig. 6.34.

**Unknowns:** Topology of the PMOS network; *W/L* ratios of all the transistors

**Approach:** In this case, we already have the NMOS network (Fig. 6.34) but need to construct the corresponding PMOS network. A new graphical method for finding the PMOS network will be introduced for this design. Once the PMOS circuit topology is found, then the transistor *W/L* values can be determined.

**Assumptions:** Use a symmetrical design based on the reference inverter in Fig. 7.12.

**Analysis:** In this case, we have been given the NMOS network. First we construct a graph of the NMOS network, which is shown in Fig. 7.25(b). Each node in the NMOS network corresponds to a node in the graph, including node 0 for ground and node 2 for the output. Each NMOS transistor is represented by an arc connecting the source and drain nodes of the transistors and is labeled with the logical input variable.

Next, we construct the PMOS network directly from the graph of the NMOS network. First, place a new node inside of every enclosed path [nodes 4 and 5 in Fig. 7.25(c)] in the NMOS graph. In addition, two exterior nodes are needed: one representing the output and one representing  $V_{DD}$  [nodes 2' and 3 in Fig. 7.25(c)]. An arc, ultimately corresponding to a PMOS transistor, is then added to the graph for each arc in the NMOS graph. The new arcs cut through the NMOS arcs and connect the pairs of nodes that are separated by the NMOS arcs. A given PMOS arc has the same logic label as the NMOS arc that is intersected. This construction results in a minimum PMOS

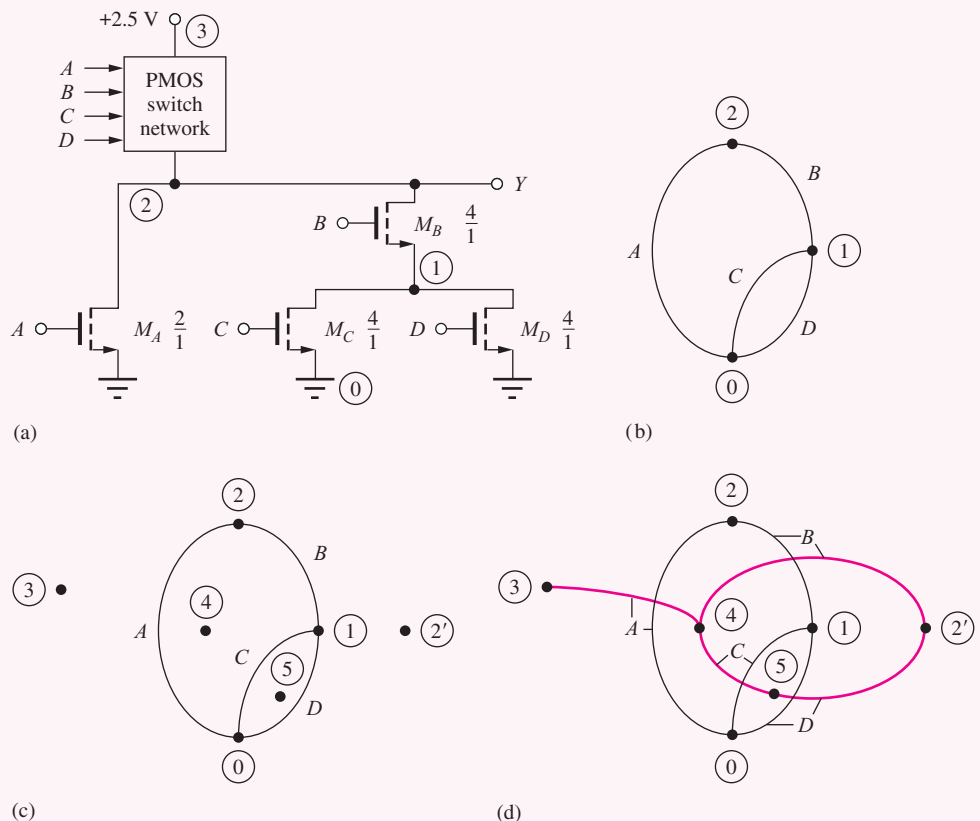


**Figure 7.25** Steps in constructing graphs for NMOS and PMOS networks. (a) NMOS network. (b) NMOS graph. (c) NMOS graph with new nodes added. (d) Graph with PMOS arcs added.

logic network, which has only one PMOS transistor per logic input. The completed graph is given in Fig. 7.25(d), and the corresponding PMOS network is shown in Fig. 7.26. A transistor is added to the PMOS switching network corresponding to each arc in the PMOS graph. Note that nodes 2 and 2' represent the same output node.

To complete the design of this CMOS gate, we must choose the  $W/L$  ratios of the transistors. In the NMOS switching network, the worst-case path contains two transistors in series, and transistors  $B$ ,  $C$ , and  $D$  should each be twice as large as those of the reference inverter. Transistor  $A$  should be the same size as the NMOS transistor in the reference inverter because it must be able to discharge the load capacitance by itself. In the PMOS switching network, the worst-case path has three transistors in series, and PMOS transistors  $A$ ,  $C$ , and  $D$  should be three times as large as the PMOS device in the reference inverter. The size of transistor  $B$  is determined using the on-resistance method from Eq. (6.38), in which  $R_{\text{on}}$  represents the on-resistance of a reference transistor with  $W/L = 1/1$ :

$$\frac{R_{\text{on}}}{\left(\frac{15}{1}\right)} + \frac{R_{\text{on}}}{\left(\frac{W}{L}\right)_B} = \frac{R_{\text{on}}}{\left(\frac{5}{1}\right)} \quad \text{or} \quad \left(\frac{W}{L}\right)_B = \frac{7.5}{1}$$

The completed design appears in Fig. 7.26.

Figure 7.26(b) gives a second implementation of the same logic network; here nodes 2 and 3 in the PMOS graph have been interchanged. The conducting paths through the PMOS network are identical, and hence the logic function is also the same.

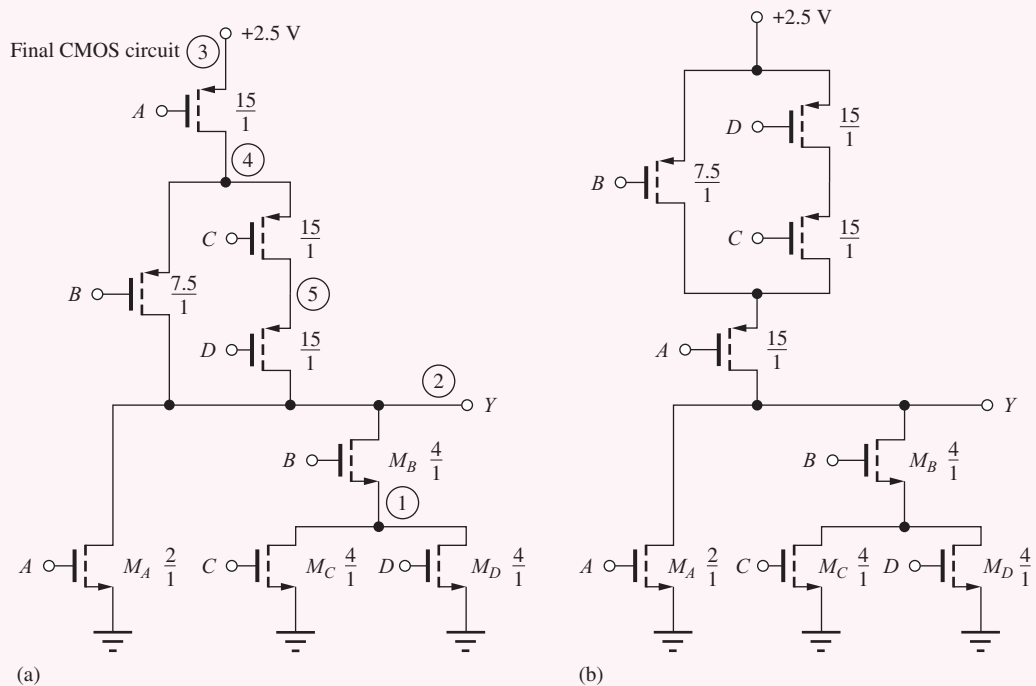


Figure 7.26 (a) CMOS implementation of  $Y = \overline{A} + BC + \overline{BD}$ . (b) Circuit equivalent to gate in Fig. 7.26(a).

**Check of Results:** Another approach can be used to check the PMOS network topology. Note that the PMOS network implements the function obtained by expanding  $Y$  as a product of sums:

$$Y = \overline{A} + B(C + D) = \overline{A} \cdot (\overline{B} + \overline{C} \overline{D})$$

The inversion of each variable is provided directly by the PMOS transistor (remember the transistor symbol introduced in Fig. 7.22). A conducting path is formed through the PMOS network when  $A$  is conducting, and either  $B$  is conducting, or  $C$  and  $D$  are both conducting. The network structure appears to be correct. Thus, in summary, the NMOS network implements  $Y$  as a sum-of-products, whereas the PMOS network implements the function  $Y$  as a product-of-sums in the complemented variables.

**Discussion:** Note that the PMOS network in Fig. 7.26 could also be obtained from the NMOS network by successive application of the series/parallel transformation rule. The NMOS network consists of two parallel branches: transistors  $A$  and transistors  $B, C$ , and  $D$ . The PMOS network, therefore, has two branches in series, one with transistor  $A$  and a second representing the branch with  $B, C$ , and  $D$ . The second branch in the NMOS network is the series combination of transistor  $B$  and a third branch consisting of the parallel combination of  $C$  and  $D$ . In the PMOS network, this corresponds to transistor  $B$  in parallel with the series combination of transistors  $C$  and  $D$ . This process can be used to create the PMOS network from the NMOS network, or vice versa. However, it can run into trouble when bridging branches are present, as in Ex. 7.3.

**EXERCISE:** Draw another version of the circuit in Fig. 7.26(b).

**ANSWER:** The position of PMOS transistors  $C$  and  $D$  may be interchanged in Fig. 7.26(a) or (b). Another possibility is to interchange the position of the NMOS transistors forming the  $B(C + D)$  subnetwork.

## DESIGN EXAMPLE 7.3 COMPLEX CMOS GATE WITH A BRIDGING TRANSISTOR

### DESIGN SPECIFICATIONS

In this example, we design a CMOS logic gate with the same logic function as the NMOS design from Fig. 6.36 in Chapter 6. In this example, the logic gate contains a bridging transistor.

### SOLUTION

**Specifications and Known Information:**  $Y = \overline{AB + CE + ADE + CDB}$  or  $\overline{Y} = AB + CE + ADE + CDB$ . The NMOS network implementation of  $\overline{Y}$  is exactly the same as that of the NMOS gate in Fig. 6.36.

**Unknowns:** Topology of the PMOS network;  $W/L$  ratios of all the transistors

**Approach:** We have the NMOS network and need to construct the corresponding PMOS network. Use the graphical method introduced in Ex. 7.2 to find the PMOS network. Once the PMOS circuit topology is found, the transistor  $W/L$  values can be determined.

**Assumptions:** Use a symmetrical design based upon the reference inverter in Fig. 7.12.

**Analysis:** Figure 7.27(b) is the graph of the NMOS network. The corresponding graph for the PMOS network is constructed in Fig. 7.27(c): new nodes 5 and 6 are added inside the enclosed

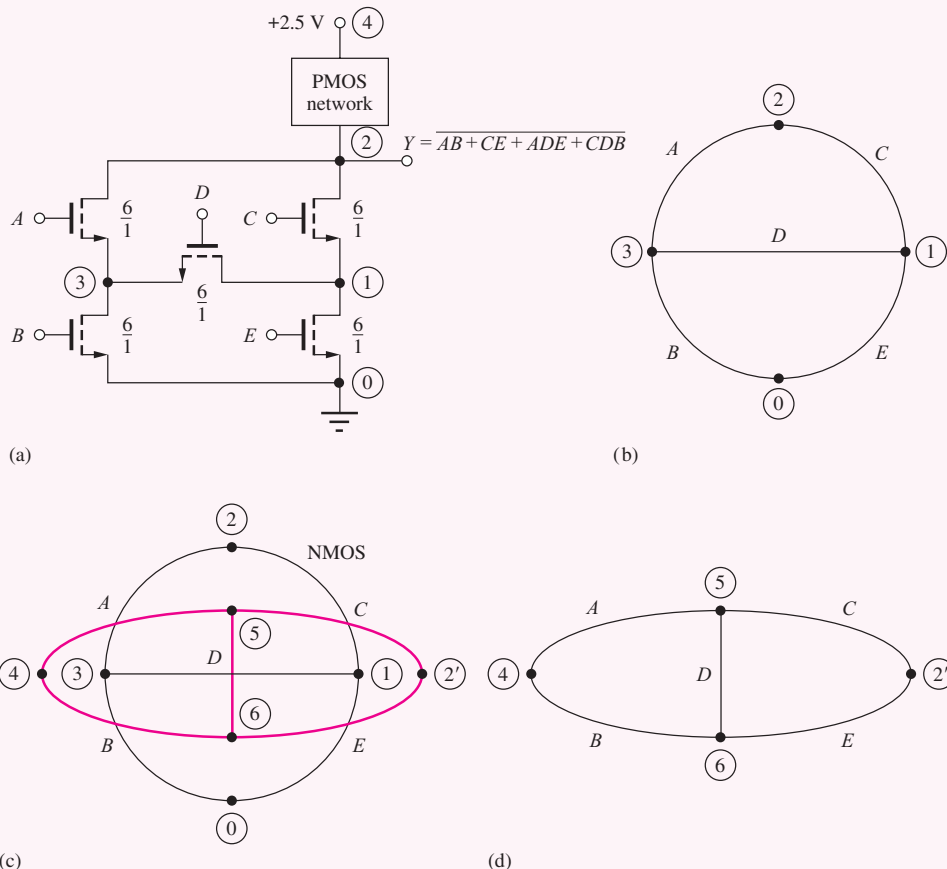


**Figure 7.27** (a) NMOS portion of CMOS gate. (b) Graph for NMOS network. (c) Construction of the PMOS graph. (d) Resulting graph for the PMOS network.

paths formed by arcs *ACD* and *BED* in Fig. 7.27(b), and nodes 2' and 4 are added to represent the output and power supply. New arcs are added for each transistor. The resulting CMOS gate design is given in Fig. 7.28. In this unusual case, the NMOS and PMOS network topologies are identical. Transistor *D* is a bridging transistor in both networks. The worst-case path in each network contains three devices in series, and all the transistors in the CMOS gate are three times the size of the corresponding transistors in the reference inverter.

**Check of Results:** A recheck of our work finds no errors.

**Discussion:** For this case, it is not easy to check our work using the series/parallel transformations because of the bridging transistor in the network.

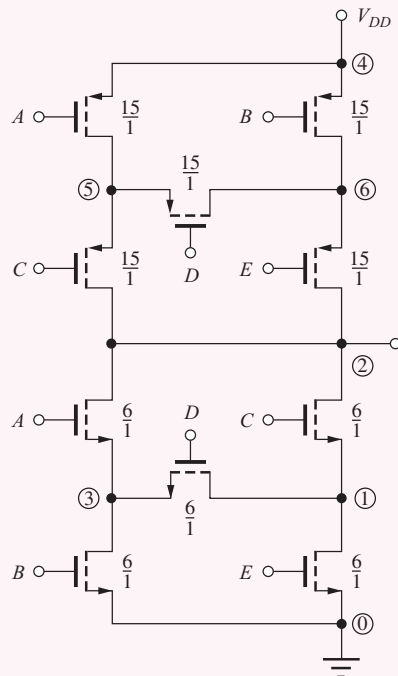


Figure 7.28 CMOS implementation of  
 $Y = \overline{AB} + CE + ADE + \overline{CDB}$ .

**EXERCISE:** Draw another version of the circuit in Fig. 7.28.

**ANSWER:** Either one or both of the NMOS and PMOS switching networks can be rearranged. In the NMOS network, the positions of transistors *A* and *B* and transistors *C* and *E* can be interchanged. Note that both of these changes must be done to retain the correct logic function. In the PMOS network, the positions of transistors *A* and *C* and transistors *B* and *E* can be interchanged. Again, both sets of changes must occur together.

**EXERCISE:** What are the sizes of transistors in part (b) of the figure on the next page based upon the symmetrical reference inverter in Fig. 7.12?

**ANSWER:** 4/1, 2/1, 15/1

**EXERCISE:** Draw the logic diagram and transistor implementation for a (2-2-2) AOI (see page 394).

**ANSWER:** Add a second input labeled  $F$  to the lower AND gate in the logic diagram. Add NMOS transistor  $F$  in series with transistor  $E$  in the NMOS tree and PMOS transistor  $F$  in parallel with transistor  $E$  in the PMOS network.

## 7.7 MINIMUM SIZE GATE DESIGN AND PERFORMANCE

Because there is one NMOS and one PMOS transistor for each logic input variable in static CMOS, there is an area penalty in CMOS logic with respect to NMOS logic that requires only a single-load device regardless of the number of input variables. In addition, series paths in the PMOS or NMOS switching networks require large devices in order to maintain logic delay. (See Fig. 7.20.) However, in most logic designs, only the critical logic delay paths need to be scaled to maintain maximum performance. If gate delay is not the primary concern, then considerable area savings can be achieved if all transistors are made of minimum geometry. For example, the gate from Fig. 7.26 is shown implemented with minimum size transistors in Fig. 7.29. Here, area is being traded directly for increased logic delay. The total gate area for Fig. 7.29 is  $16F^2$ , where  $F$  is the minimum feature size, whereas that of Fig. 7.26 is  $66.5F^2$ , an area four times larger.

Let us estimate the worst-case propagation delay of this minimum size logic gate relative to our reference inverter design. In the NMOS switching network, the worst-case path contains two transistors in series, with  $W/L = 2/1$ , which is equivalent to the  $R_{on}$  of a 1/1 device, as compared to the reference inverter in which  $W/L = 2/1$ . Thus, the high-to-low propagation delay for this gate is twice that of the symmetrical reference inverter  $\tau_{PHLI} : \tau_{PHL} = 2\tau_{PHLI}$ . The worst-case path in the PMOS switching network contains three minimum geometry transistors in series, yielding an

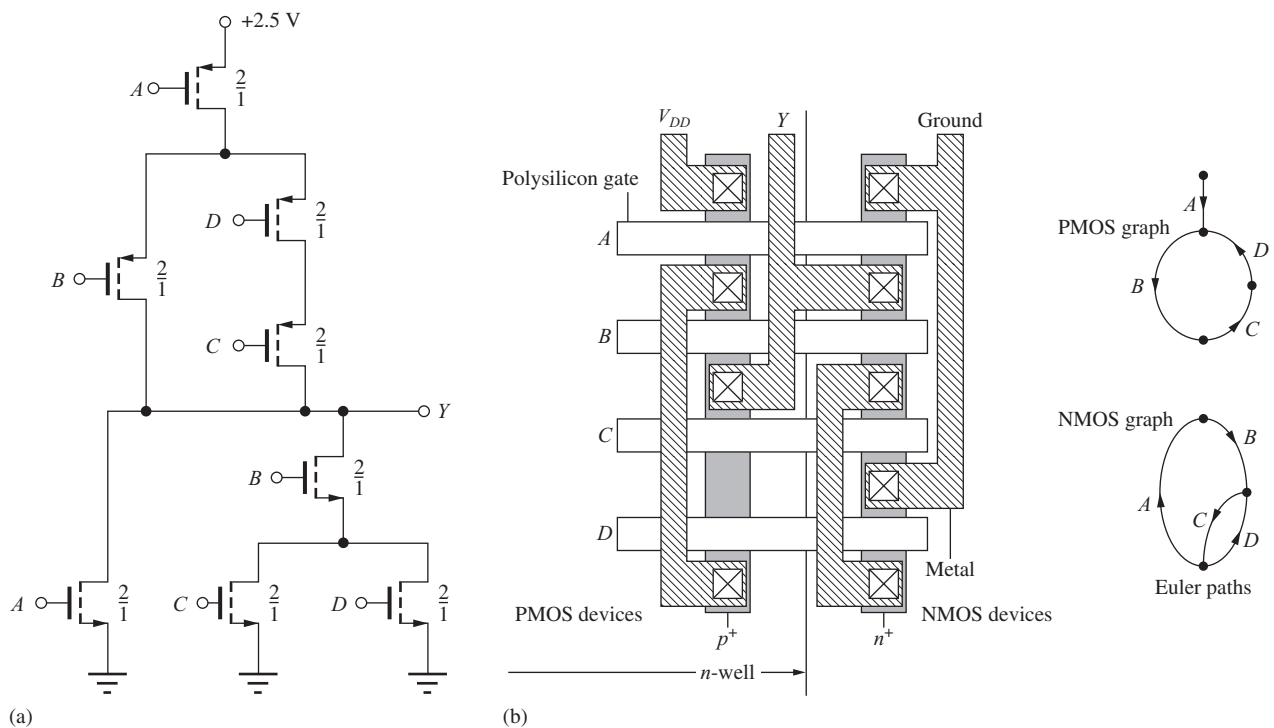
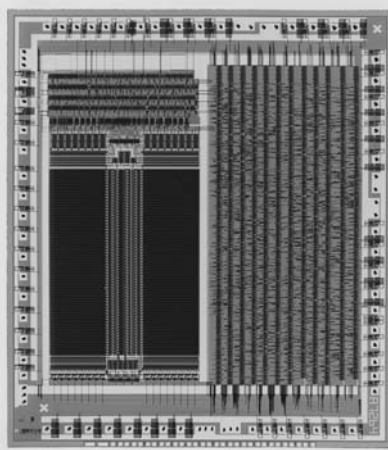


**Figure 7.29** (a) Minimum size implementation of a complex CMOS gate. (b) Layout of complex CMOS gate in (a).



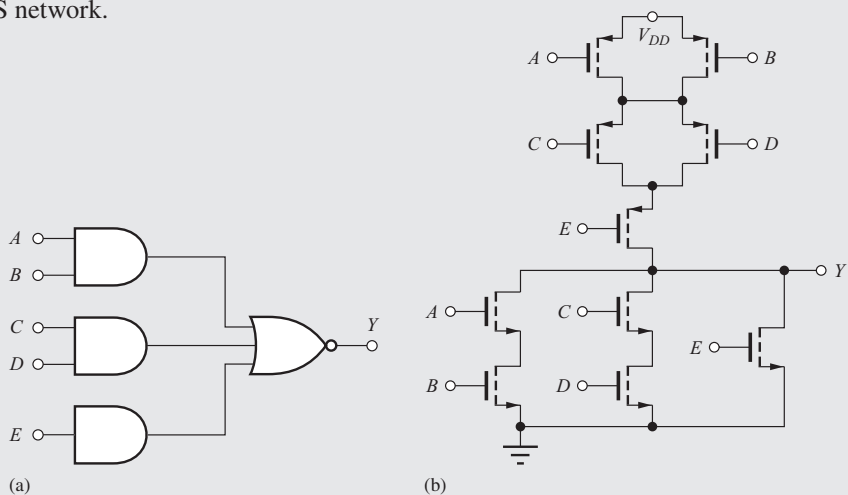
### And-Or-Invert Gates in a Standard Cell Library

The Standard Cell design approach utilizes a library of predesigned logic blocks that are placed and interconnected on a chip by the circuit designer or more often by automated design tools. The library contains a large number of cells ranging from basic logic gates to multipliers, ALU's, shifters, CPU cores, and memories, for example. The resulting integrated circuit chips have a highly regular appearance, as can be observed in the photograph below.



Die photograph courtesy of Professor Charles E. Stroud, ECE Department, Auburn University.

The And-Or-Invert or AOI gate introduced in Chapter 6 (page 296) represents a basic logic block that is widely used in Standard Cell designs. The logic diagram and its transistor implementation for a (2-2-1) AOI gate that implements  $\overline{Y} = AB + CD + \overline{E}$  appear below. The 2-2-1 notation represents the input configuration for the gate: two 2-input ANDs and one 1-input AND. In the transistor realization, the NMOS switching tree is the same as would be used in the corresponding NMOS gate. The PMOS tree implements  $Y = (\overline{A} + \overline{B})(\overline{C} + \overline{D})(\overline{E})$ . The three parallel branches in the NMOS network are replaced by three series branches in the PMOS network, and the AND branches in the NMOS network become OR branches in the PMOS network.



(a) Logic diagram for a (2-2-1) AOI gate. (b) Transistor implementation of  $Y = \overline{AB} + \overline{CD} + \overline{E}$ .

effective  $W/L$  ratio of  $2/3$ , versus  $5/1$  for the reference inverter. The low-to-high propagation delay is related to that of the reference inverter  $\tau_{PLHI}$  by

$$\tau_{PLH} = \frac{\left(\frac{5}{1}\right)}{\left(\frac{2}{3}\right)} \tau_{PLHI} = 7.5 \tau_{PLHI}$$

The average propagation delay of the minimum size logic gate is

$$\tau_p = \frac{(\tau_{PLH} + \tau_{PHL})}{2} = \frac{(2\tau_{PLHI} + 7.5\tau_{PLHI})}{2} = \frac{9.5\tau_{PLHI}}{2} = 4.75\tau_{PLHI}$$

We find that the propagation delay of the minimum size gate will be 4.75 times slower than the reference inverter design when driving the same load capacitance and will be highly assymetrical.

Layout of the gate in Fig. 7.29 is implemented by two vertical linear arrays of transistors with common horizontal polysilicon gate stripes. The diffusions between various transistors are interconnected on the metal level to create the desired circuit. This layout strategy requires identification of an “Euler path” in the graphs of the PMOS and NMOS switching trees. The **Euler path** connects all the transistors in the graph of the NMOS or PMOS network, but must pass through each transistor once and only once. The path may go through a given node more than once. To create the layout in Fig. 7.29, the Euler paths in both the NMOS and PMOS networks must have the same transistor order—in this case the paths have the common order  $ABCD$ .

## 7.8 DYNAMIC DOMINO CMOS LOGIC

Dynamic logic circuits were first developed as a means of reducing power in PMOS and NMOS logic, but they are also highly useful in CMOS design. **Dynamic logic** uses separate **precharge** and **evaluation phases** governed by a system clock signal to eliminate the dc current path that exists in single-channel static logic gates. However, the logical outputs are now valid only during a portion of the evaluation phase of the clock. In addition, static power represents only one component of power dissipation in high-speed systems, and the power required to drive the clock signals that must connect to every dynamic logic gate can be significant. Early PMOS and NMOS dynamic circuits used complicated two-phase and four-phase clocking techniques. However, a more recently developed form of dynamic CMOS logic called **Domino CMOS** is based on a single clock signal.

The circuit in Fig. 7.30 represents a general gate in domino CMOS. Operation of the domino CMOS circuit begins with the clock signal in the low state.  $M_{NC}$  is off, which disables the current path to ground through the logic function block  $F$ . The same clock signal turns on  $M_{PC}$ , pulling node 4 high to  $V_{DD}$  and forcing the inverter output low.

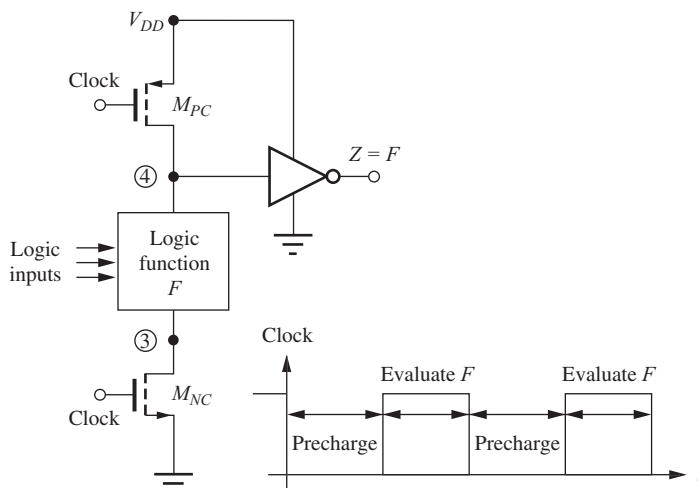
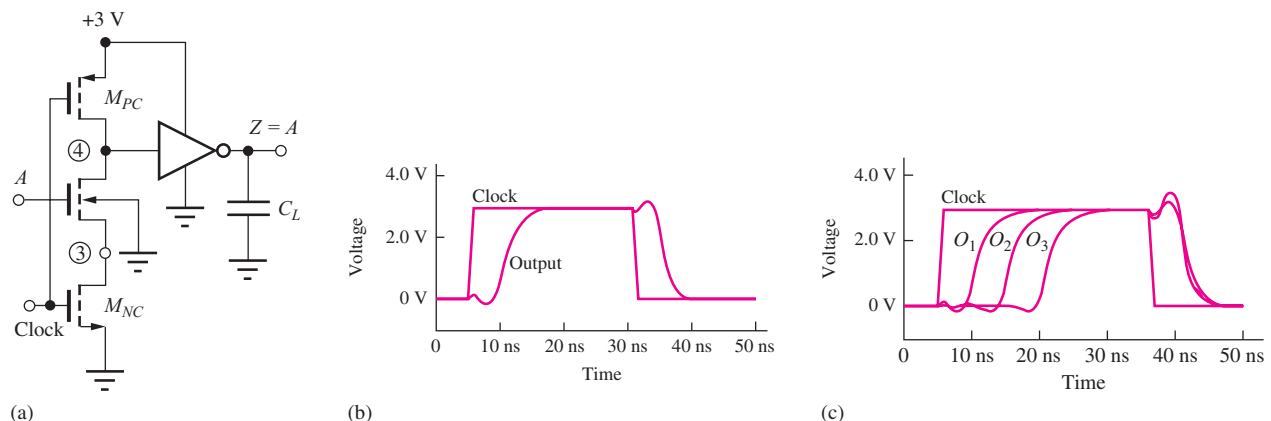


Figure 7.30 Dynamic domino CMOS logic.



**Figure 7.31** (a) Domino CMOS gate with a single input. (b) Waveforms for the clocked domino circuit. (c) Outputs of three cascaded domino CMOS gates.

When the clock signal goes high, the capacitance at node 4 is selectively discharged. If a conducting path exists through the logic network  $F$  (that is, if  $F = 1$ ), then node 4 is discharged to zero, and the output of the inverter rises to a 1 level. If  $F = 0$ , no discharge path exists, the voltage at node 4 remains high, and the output of the inverter remains at 0.

Simulated waveforms for the single-input domino CMOS gate in Fig. 7.31(a) are shown in Fig. 7.31(b) for the case of  $A = 1$ . After the clock goes high, the output rises following the delay to discharge the capacitances at nodes 3 and 4 plus the delay through the inverter. The output drops back to zero following the clock signal's return to zero.

The inputs to a given domino CMOS gate, generated by other domino gates, make only low-to-high transitions following the clock transition, and the functional evaluation during the positive clock phase ripples through the gates like a series of dominos falling over—hence the name domino logic. Figure 7.31(c) shows the ripple-through effect for the case of three domino gates in series. Output  $O_1$  follows the rising edge of the clock and drives the input of  $O_2$ , and output  $O_2$  responds to the change in  $O_1$ . Note that the outputs are all reset to zero at the same time, following the falling edge of the clock.

External inputs that are not from other domino gates must remain stable during the evaluation phase of the clock. As with most CMOS circuits, power dissipation is set by the dynamic power consumed in charging and discharging the capacitances at the various nodes. A major advantage of the domino CMOS circuit is the requirement for only two PMOS transistors per logic stage, no matter how complex the function  $F$ .

The observant reader has probably noticed that domino CMOS gates do not form a complete logic family because only true output functions are available. However, this does not represent a problem in system designs in which a register transfer structure exists, as in Fig. 7.32. In this logic structure, data are stored in a static register (1), which can be designed to produce both true and complemented data values at its outputs. Domino CMOS performs the combinational logic functions on the positive

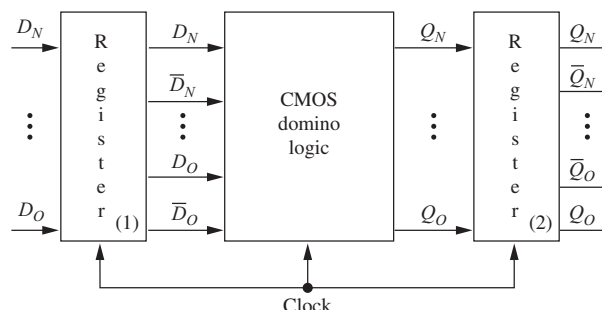


**Figure 7.32** Section of logic in a complex digital system.

phase of the clock signal, and the results of the logic operations are clocked into register (2) on the falling edge of the clock signal.

**EXERCISE:** (a) Draw the circuit schematic for a domino CMOS gate for  $Z = AB + C$ . (b) What power is required in a domino CMOS clock driver circuit that drives a 50-pF load at 10 MHz if  $V_{DD} = 5$  V?

**ANSWER:** Transistor A in Fig. 7.31 is replaced with a three-transistor NMOS structure for  $AB + C$ . 12.5 mW

## 7.9 CASCADE BUFFERS

In today's high-density ICs, the input capacitance of a logic gate may be in the range of only 10 to 100 fF, and the propagation delay of a CMOS gate driving such a small load capacitance can be well below 1 ns. However, there are many cases in which a much higher load capacitance is encountered. For example, the wordlines in RAMs and ROMs represent relatively large capacitances; long interconnection lines and internal data buses in microprocessors also represent significant load capacitances. In addition, the circuits that drive off-chip data buses may encounter capacitances as large as 10 to 50 pF, a capacitance 1000 times larger than the internal load capacitance. We know that the propagation delay of a CMOS gate is proportional to its load capacitance, so if a minimum size inverter is used to drive such a large capacitance, then the delay will be extremely long. If the inverter is scaled up in size to reduce its own delay, then its input capacitance increases, slowing down the propagation delay of the previous stage.

### 7.9.1 CASCADE BUFFER DELAY MODEL

It has been shown [4, 5] that a minimum overall delay can be achieved by using an optimized cascade of several inverter stages, as depicted in Fig. 7.33. The  $W/L$  ratios of the transistors are increased by **taper factor**  $\beta$  in each successive inverter stage in order to drive the large load capacitance. In this analysis, the load capacitance is  $C_L = \beta^N C_o$ , in which  $C_o$  is the input capacitance of the normal reference inverter stage and  $N$  is the number of stages in the **cascade buffer**. The analysis is simplified by assuming that the total capacitance at a given node is dominated by the input capacitance of the next inverter. Thus, the capacitive load on the first inverter is  $\beta C_o$ , the load on the second inverter is  $\beta^2 C_o$ , and so on. If the propagation delay of the unit size inverter driving a load capacitance of  $C_o$  is  $\tau_o$ , then the delay of each inverter stage will be  $\beta \tau_o$ , and the total propagation delay of the  $N$ -stage buffer will be

$$\tau_B = N\beta\tau_o \quad (7.27)$$

in which

$$\beta^N = \frac{C_L}{C_o} \quad \text{or} \quad \beta = \left( \frac{C_L}{C_o} \right)^{1/N} \quad (7.28)$$

Substituting this result into Eq. (7.27) yields an expression for the total propagation delay of the buffer:

$$\tau_B = N \left( \frac{C_L}{C_o} \right)^{1/N} \tau_o \quad (7.29)$$

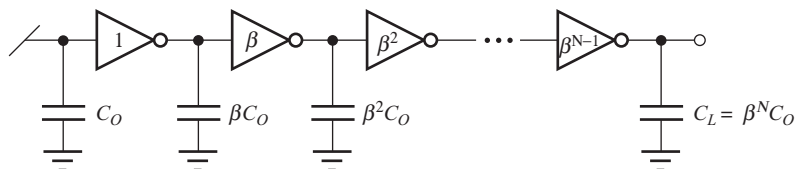


Figure 7.33 Cascade buffer for driving large capacitive loads.

In Eq. (7.29),  $N$  increases as additional stages are added to the buffer, but the value of the capacitance ratio term decreases with increasing  $N$ . The opposite behavior of these two factors leads to the existence of an optimum value of  $N$  for a given capacitance ratio.

### 7.9.2 OPTIMUM NUMBER OF STAGES

The number of stages that minimizes the overall buffer delay can be found by differentiating Eq. (7.29) with respect to  $N$  and setting the derivative equal to zero. The optimization can be simplified by taking logarithms of both sides of Eq. (7.29) before taking the derivative:

$$\ln \tau_B = \ln N + \frac{1}{N} \ln \left( \frac{C_L}{C_o} \right) + \ln \tau_o \quad (7.30)$$

Taking the derivative with respect to  $N$  and setting it equal to zero gives the optimum value of  $N$ :

$$\frac{d \ln \tau_B}{dN} = \frac{1}{N} - \frac{1}{N^2} \ln \left( \frac{C_L}{C_o} \right) \quad \text{and} \quad N_{\text{opt}} = \ln \left( \frac{C_L}{C_o} \right) \quad (7.31)$$

Substituting  $N_{\text{opt}}$  into Eqs. (7.28) into (7.29) yields the optimum value of the taper factor  $\beta_{\text{opt}}$  and the optimum buffer delay  $\tau_{B_{\text{opt}}}$ :

$$\beta_{\text{opt}} = \left( \frac{C_L}{C_o} \right)^{[1/\ln(C_L/C_o)]} = \varepsilon \quad \text{and} \quad \tau_{B_{\text{opt}}} = \varepsilon \tau_o \ln \left( \frac{C_L}{C_o} \right) \quad (7.32)$$

The optimum value of the taper factor is equal to the natural base  $\varepsilon \cong 2.72$ .

## DESIGN EXAMPLE 7.4 CASCADE BUFFER DESIGN

In digital chip designs, such as microprocessors and memory chips, we often design circuits that must drive high-capacitance loads. This example designs a buffer to drive a 50-pF load.

**DESIGN SPECIFICATIONS** Design a cascade buffer to drive a load capacitance of 50 pF if  $C_o = 50$  fF. Find the overall delay for the buffer design for a 3.3-V supply with  $V_{TN} = 0.75$  V and  $V_{TP} = -0.75$  V.

**SOLUTION** **Specifications and Known Information:**  $C_L = 50$  pF; technology has  $C_o = 50$  fF.

**Unknowns:** The number of stages  $N$ , taper factor  $\beta$ , and relative size of each inverter in the cascade buffer; overall buffer delay

**Approach:** Select the number of stages  $N$  needed using the result in Eq. (7.31). Calculate the taper factor using the selected value of  $N$ . Scale the reference inverter using  $N$ .

**Assumptions:** The value of  $C_o$  (50 fF) is known for the symmetrical reference inverter in Fig. 7.12.

**Analysis:** The optimum value of  $N$  is  $N_{\text{opt}} = \ln C_L/C_o = \ln(1000) = 6.91$ , and the optimum delay is  $\tau_{B_{\text{opt}}} = 6.91 \times (2.72) \times t_o = 18.8t_o$ .  $N$  must be an integer, but either  $N = 6$  or  $N = 7$  can be used because the delay minimum is quite broad, as illustrated by the following numeric results. Using these two values of  $N$  yields

$$N = 6: \quad \tau_B = 6(1000^{1/6})\tau_o = 19.0\tau_o$$

$$N = 7: \quad \tau_B = 7(1000^{1/7})\tau_o = 18.8\tau_o$$

Little speed is lost by using the smaller value of  $N$ . The choice between  $N = 6$  and  $N = 7$  will usually be made based on buffer area. For  $N = 6$ , the taper factor  $\beta$  is found using Eq. (7.28):

$$\beta = \left( \frac{C_L}{C_o} \right)^{1/N} = \left( \frac{50 \text{ pF}}{50 \text{ fF}} \right)^{1/6} = (1000)^{1/6} = \sqrt{10} = 3.16$$

Each successive stage of the cascade buffer is 3.16 times larger than the preceding stage, and the result appears in Fig. 7.34. The transistor sizes (NMOS, PMOS) for the six inverters are (2/1, 5/1), (6.33/1, 15.8/1), (20/1, 50/1), (63.3/1, 158/1), (200/1, 500/1), and (633/1, 1580/1).

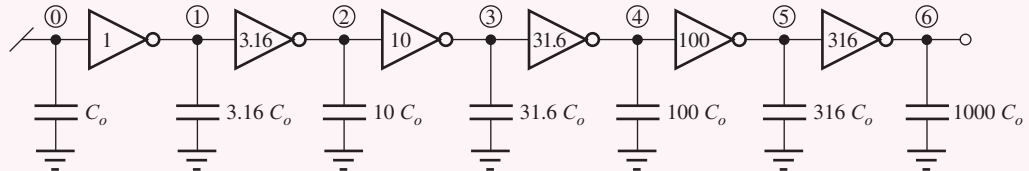


**Figure 7.34** Optimum buffer design.

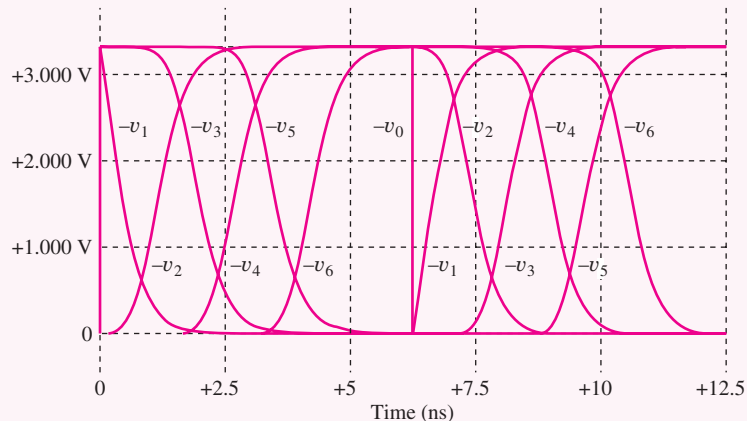
For  $N = 6$ , we already found  $\tau_B = 19.0\tau_o$ , and we need the value of  $\tau_o$ . For the symmetrical inverter designs,

$$\tau_o \approx \frac{2.4C}{K_n(V_{DD} - V_{TN})} = \frac{2.4(50 \text{ fF})}{2(100 \mu\text{A/V}^2)(3.3 - 0.75)} = 0.24 \text{ ns}$$

and the estimated buffer delay is  $\tau_B = 4.5 \text{ ns}$ .

**Check of Results:** A recheck of calculations indicates the work is correct. We now check the overall buffer delay using SPICE.

**Computer-Aided Analysis:** The output waveforms for the cascade buffer in Fig. 7.34 appear below. The first inverter is driven by a pulse having a 6.25-ns width, a 12.5-ns period, and rise and fall times of 2 ps. The propagation delay of the full buffer is 4 ns. This is slightly shorter than our estimate because the delay of the first inverter is shortened by the fast rise and fall times of the input signal. The delay between the output of inverters 1 and 6 should be  $15.8\tau_o = 3.8 \text{ ns}$ , and SPICE also yields an identical result.



**Discussion:** The buffer optimization just discussed is based on a set of very simple assumptions for the change in nodal capacitance with buffer size. Many refinements to this analysis have been published in the literature, and those more complex analyses indicate that the optimum tapering factor lies between 3 and 4. The results in Eqs. (7.28), (7.29), and (7.31) should be used as an initial guide, with the final design determined using circuit simulation based on a given set of device and technology parameters.

**EXERCISE:** Suppose we try to drive the 50-pF capacitance in Ex. 7.4 by adding only one additional buffer stage, i.e.,  $N = 2$ . What is the relative size of the buffer stage? What is the overall delay?

**ANSWERS:** 31.6,  $63.2\tau_o$

**EXERCISE:** Prove that  $z^{1/\ln z} = e$ .

**EXERCISE:** What would be the relative inverter sizes for the cascade buffer example if  $N$  were chosen to be 7? Compare the total buffer area for  $N = 6$  and  $N = 7$ .

**ANSWERS:** 1, 2.68, 7.20, 19.3, 51.8, 139, 372; 462 times the unit inverter area versus 593 times

## 7.10 THE CMOS TRANSMISSION GATE

The CMOS transmission gate in Fig. 7.35 is a circuit useful in both analog and digital design. The circuit consists of NMOS and PMOS transistors, with source and drain terminals connected in parallel and gate terminals driven by opposite phase logic signals indicated by  $A$  and  $\bar{A}$ . The transmission gate is used so often that it is given the special circuit symbol shown in Fig. 7.35(c). For  $A = 0$ , both transistors are off, and the transmission gate represents an open circuit.

When the transmission gate is in the conducting state ( $A = 1$ ), the input and output terminals are connected together through the parallel combination of the on-resistances of the two transistors, and the transmission gate represents a *bidirectional* resistive connection between the input and output terminals. The individual on-resistances  $R_{onp}$  and  $R_{onn}$ , as well as the equivalent on-resistance  $R_{EQ}$ , all vary as a function of the input voltage  $v_I$ , as shown in Fig. 7.36. The value of  $R_{EQ}$  is equal to the parallel combination of  $R_{onp}$  and  $R_{onn}$ :

$$R_{EQ} = \frac{R_{onp} R_{onn}}{R_{onp} + R_{onn}} \quad (7.33)$$

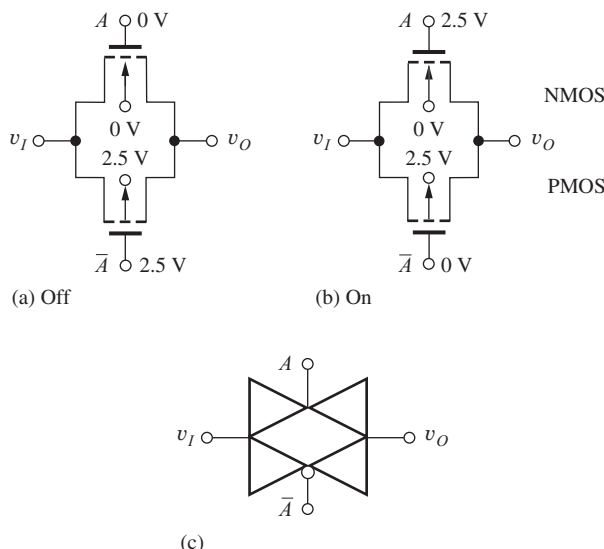


**Figure 7.35** CMOS transmission gate in (b) on state and (a) off state. (c) Special circuit symbol for the transmission gate.

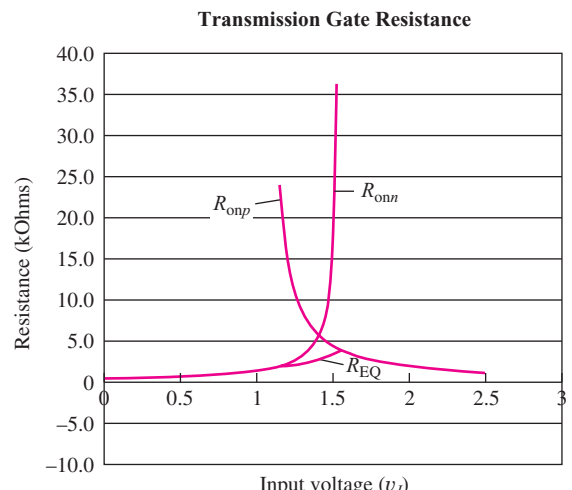


**Figure 7.36** On-resistance of a transmission gate versus input voltage  $v_I$  including body effect using the values from Table 7.1 and  $(W/L)_N = (W/L)_P = 10/1$ . The maximum value of  $R_{EQ}$  is approximately 4 kΩ.

In Fig. 7.36, the PMOS transistor is cut off ( $R_{onp} = \infty$ ) for  $v_I \leq 1.05$  V, and the NMOS transistor is cut off for  $v_I \geq 1.56$  V. For the parameters used in Fig. 7.36, the equivalent on-resistance is always less than 4 k $\Omega$ , but it can be made smaller by increasing the  $W/L$  ratios of the  $n$ - and  $p$ -channel transistors.

**EXERCISE:** What  $W/L$  ratios are required in the transmission gate in Fig. 7.36 to ensure that  $R_{EQ} \leq 1$  k $\Omega$  if the  $W/L$  ratios of both transistors are the same?

**ANSWER:**  $W/L = 40/1$

## 7.11 CMOS LATCHUP

The basic CMOS structure has a potentially destructive failure mechanism called **latchup** that was a major concern in early implementations and helped delay adoption of the technology. By the mid-1980s, technological solutions were developed that effectively suppress the latchup phenomenon. However, it is important to understand the source of the problem that arises from the complex nature of the CMOS integrated structure that produces **parasitic bipolar transistors**. These bipolar transistors are normally off but can conduct under some transient fault conditions.

In the cross section of the CMOS structure in Fig. 7.37(a), a *pnp* transistor is formed by the source region of the PMOS transistor, the *n*-well, and the *p*-type substrate, and an *npn* transistor is formed by the source region of the NMOS transistor, the *p*-type substrate, and the *n*-well. The physical structure connects the *npn* and *pnp* transistors together in the equivalent circuit shown in Fig. 7.38(b).  $R_n$  and  $R_p$  model the series resistances existing between the external power supply connections and the internal base terminals of the bipolar transistors.

If the currents in  $R_n$  and  $R_p$  in the circuit model in Fig. 7.37(b) are zero, then the base-emitter voltages of both bipolar transistors are zero, and both devices are off. The total supply voltage ( $V_{DD} - V_{SS}$ ) appears across the reverse-biased well-to-substrate junction that forms the collector-base junction of the two parasitic bipolar transistors. However, if a current should develop in the base of either the *npn* or the *pnp* transistor, latchup can be triggered, and high currents can destroy the structure. One source of current is the leakage across the large area *pn*-junction formed between the *n*-well and substrate. Another source is a transient that momentarily forward biases the drain

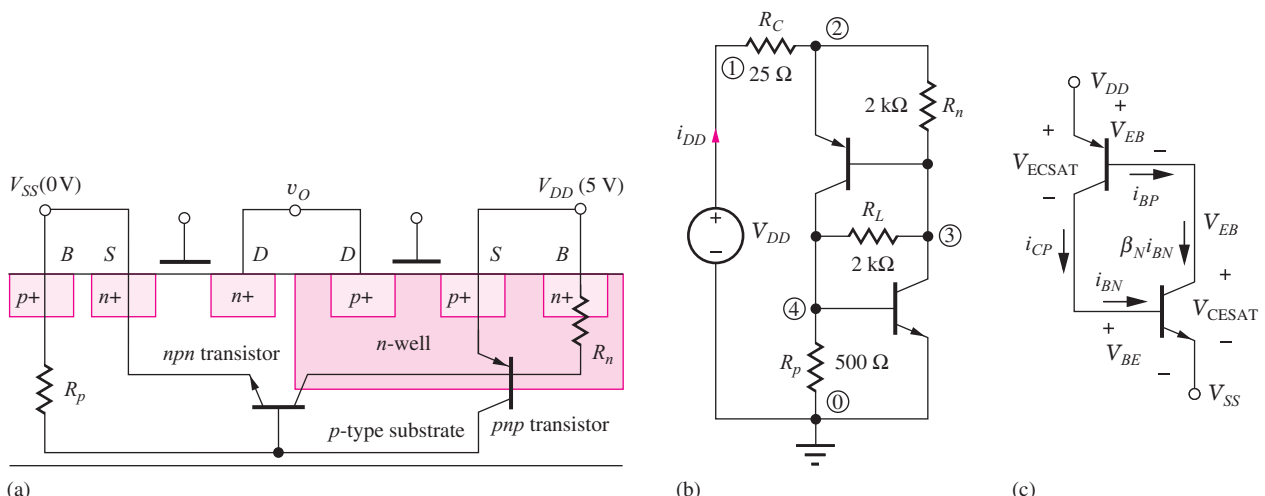


**Figure 7.37** (a) CMOS structure with parasitic *npn* and *pnp* transistors identified. (b) Circuit including shunting resistors  $R_n$  and  $R_p$  for SPICE simulation. See text for description of  $R_L$ . (c) Regenerative structure formed by parasitic *npn* and *pnp* transistors.

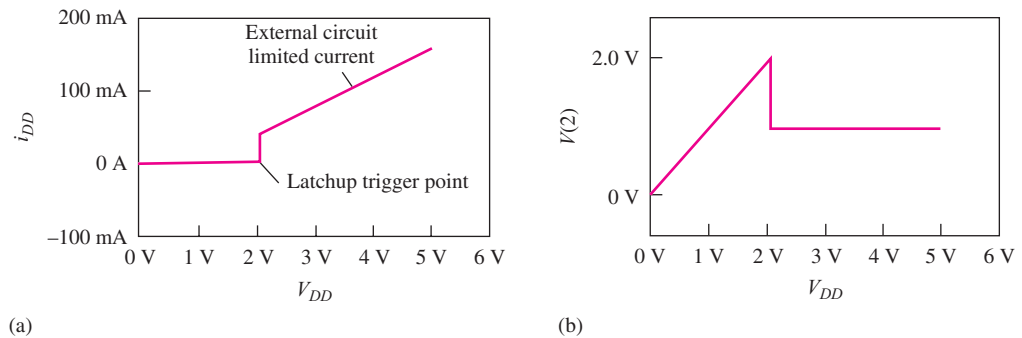


**Figure 7.38** SPICE simulation of latchup in the circuit of Fig. 7.37(a): (a) current from  $V_{DD}$ , (b) voltage at node 2.

substrate diode of the one of the MOS transistors. Once latchup is triggered, the current is limited only by the external circuit components.

The problem can be more fully understood by referring to Fig. 7.37(c), in which  $R_n$  and  $R_p$  have been neglected for the moment. Suppose a base current  $i_{BN}$  begins to flow in the base of the *npn* transistor. This base current is amplified by the *npn* current gain  $\beta_N$  and must be supplied from the base of the *pnp* transistor. The *pnp* base current is then amplified further by the current gain  $\beta_P$  of the *pnp* transistor, yielding a collector current equal to

$$i_{CP} = \beta_P i_{BP} = \beta_P (\beta_N i_{BN}) \quad (7.34)$$

However, the *pnp* collector current  $i_{CP}$  is also equal to the *npn* base current  $i_{BN}$ . If the product of the two current gains  $\beta_P \beta_N$  exceeds unity, then all the currents will grow without bound. This situation is called *latchup*. Once the circuit has entered the latchup state, both transistors enter their low impedance state, and the voltage across the structure collapses to one diode drop plus one emitter collector voltage:

$$V = V_{EB} + V_{CESAT} = V_{BE} + V_{ECSAT} \quad (7.35)$$

Shunting resistors  $R_n$  and  $R_p$  shown in Fig. 7.37 actually play an important role in determining the latchup conditions in a real CMOS structure. As mentioned before, latchup would not occur in an ideal structure for which  $R_n = 0 = R_p$ , and modern CMOS technology uses special substrates and processing to minimize the values of these two resistors.

The results of SPICE simulation of the behavior of the circuit in Fig. 7.37(b) for representative circuit elements are presented in Fig. 7.38. Resistor  $R_L$  is added to the circuit to provide a leakage path across the collector-base junctions to initiate the latchup phenomenon in the simulation. Prior to latchup in Fig. 7.38, all currents are very small, and the voltage at node 2 is directly proportional to the input voltage  $V_{DD}$ . At the point that latchup is triggered, the voltage across the CMOS structure collapses to approximately 0.8 V, and the current increases abruptly to  $(V_{DD} - 0.8)/R_C$ . The current level is limited only by the external circuit component values. Large currents cause high power dissipation that can rapidly destroy most CMOS structures.

Under normal operating conditions, latchup does not occur. However, if a fault or transient occurs that causes one of the source or drain diffusions to momentarily exceed the power supply voltage levels, then latchup can be triggered. Ionizing radiation or intense optical illumination are two other possible sources of latchup initiation.

Note that this section actually introduced another form of modeling. Figure 7.37(a) is a cross section of a complex three-dimensional distributed structure, whereas Figs. 7.37(b) and 7.37(c) are attempts to represent or model this complex structure using a simplified network of discrete transistors and resistors. Note, too, that Fig. 7.37(b) is only a crude model of the real situation, so significant deviations between model predictions and actual measurements should not be surprising. It is easy to forget that circuit schematics generally represent only idealized models for the behavior of highly complex circuits.

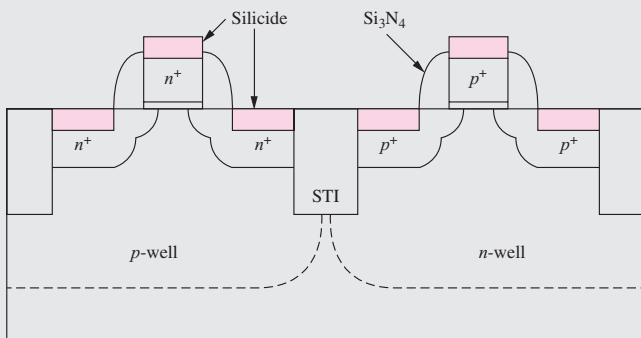


## ELECTRONICS IN ACTION

### High Performance CMOS Technologies<sup>1</sup>

#### Shallow Trench Isolation

Advanced processes with deep submicron feature sizes make use of shallow trench isolation (STI) as depicted in the twin-well process shown in the first figure below. Both the NMOS and PMOS devices are bounded by the STI oxide region. The STI in combination with a heavily doped substrate mitigates problems with latchup by substantially reducing the current gain of the bipolar devices and decreasing the value of the shunt resistances. Lightly-doped-drain (LDD) extensions can be noted on both devices as well as the silicon nitride spacers around the perimeter of the gate. Self-aligned metallic silicide layers are used to reduce the effective sheet resistance of the polysilicon gate as well as the source and drain regions. This type of CMOS process is being used to fabricate deep submicron CMOS devices.



CMOS technology employing shallow trench isolation.<sup>2</sup>

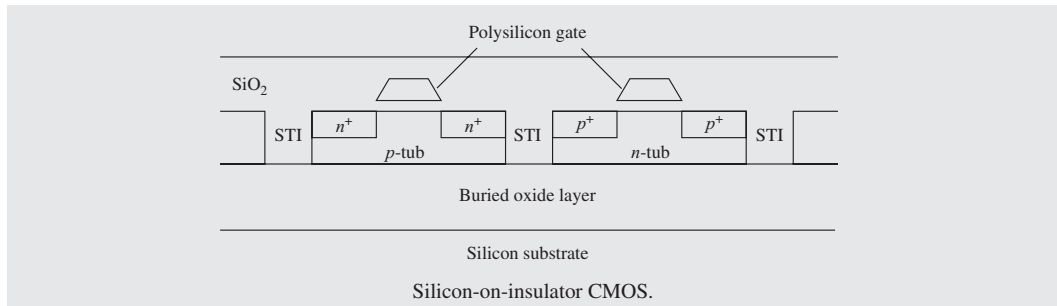
#### Silicon-on-Insulator

Insulating substrates provide the ultimate in device isolation and freedom from latchup problems by completely separating the NMOS and PMOS devices. The earliest efforts to achieve an insulating substrate grew thin layers ( $< 10 \mu\text{m}$ ) of single crystal silicon on a sapphire substrate that provides a reasonable match to the silicon crystal lattice. NMOS and PMOS devices were fabricated in the silicon film to produce a CMOS technology. This technology was termed silicon-on-sapphire, or simply SOS, technology. These early attempts were plagued by problems at the silicon-sapphire interface, but the problems were eventually controlled well enough to produce a manufacturable, although high-cost, technology.

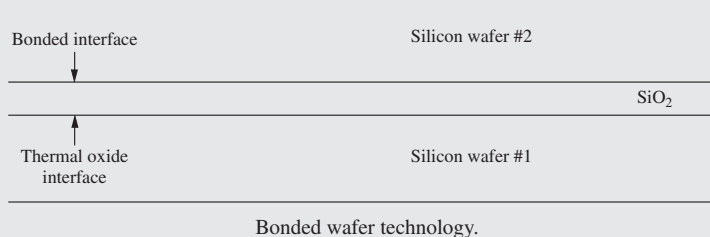
The ability to produce a highly controlled silicon-silicon dioxide interface has led to newer forms of silicon-on-insulator, or SOI, processes. High-energy ion-implantation can be used to place oxygen atoms in a layer well below the surface of a lightly doped silicon wafer. Following implantation, the wafers are annealed at elevated temperature to produce a buried oxide layer as depicted in the next figure. This technology is often referred to as SIMOX, separation by implanted oxygen. Twin tubs are then formed in the lightly doped substrate and separated by trench isolation. NMOS and PMOS devices are fabricated in the tubs to complete the SOI CMOS process.

<sup>1</sup> Jaeger, Richard C., *Introduction to Microelectronic Fabrication: Volume 5 of Modular Series on Solid State Devices*, 2nd edition, © 2002. Electronically reproduced by permission of Pearson Education, Inc., Upper Saddle River, New Jersey.

<sup>2</sup> Adapted from S. Yang et al., "A High Performance 180 nm Generation Logic Technology," IEEE IEDM Digest, Figure 1, pp. 197-200, December 1998. Copyright © 1998 IEEE. Reprinted with Permission.



Silicon wafer-to-wafer bonding, originally developed for use with micro-electro-mechanical systems (MEMS) has also been used to fabricate SOI substrates. To begin, a silicon wafer is oxidized to form an insulating  $\text{SiO}_2$  layer as depicted in the final figure. A second silicon wafer is brought in contact with the oxidized surface, and annealed at elevated temperature to form a bond between the two wafers. Surface cleanliness is of extreme importance to the success of this process. After the bonding is completed, the upper silicon layer is thinned by chemical etching and/or mechanical polishing until a few-micron-thick desired silicon layer remains.



These CMOS technologies provide a number of performance enhancements. The leakage of the large area  $pn$  junction associated with the traditional CMOS “well” is eliminated, thereby reducing power. Latchup is effectively eliminated, and junction capacitances are minimized resulting in high-speed circuits.

## SUMMARY

- **CMOS inverters:** In this chapter, we discussed the design of CMOS logic circuits beginning with the design of a reference inverter. The shape of the voltage transfer characteristic (VTC) of the CMOS inverter is almost independent of power supply voltage, and the noise margins of a symmetrical inverter can approach one-half the power supply voltage. The design of the  $W/L$  ratios of the transistors in a CMOS gate is determined primarily by the desired propagation delay  $\tau_p$ , which is related directly to the device parameters  $K'_n$ ,  $V_{TN}$ ,  $K'_p$ , and  $V_{TP}$ , and the total load capacitance  $C$ .
- **CMOS logic gates:** In CMOS logic, each gate contains both an NMOS and a PMOS switching network, and every logical input is connected to at least one NMOS and one PMOS transistor. NAND gates, NOR gates, and complex CMOS logic gates can all be designed using the reference inverter concept, similar to that introduced in Chapter 6. As for NMOS circuitry, complex CMOS gates can directly implement Boolean logic equations expressed in a sum-of-products form. In contrast to NMOS logic, which has highly asymmetric rise and fall times, symmetrical inverters in which  $t_f$  and  $t_r$  are equal can easily be designed in CMOS, although there can be a significant area penalty. A number of examples of styles for the layout of CMOS inverters and more complex logic gates were presented.

- *Body effect:* Body effect has a smaller influence on CMOS design than on NMOS design because the source-bulk voltages of all the transistors in a CMOS gate become zero in the steady state. However, the source-bulk voltages are nonzero during switching transients, and the body effect degrades the rise and fall times and propagation delays of CMOS logic.
- *Dynamic power dissipation and power delay product:* Except for very low power applications, CMOS power dissipation is determined by the energy required to charge and discharge the effective load capacitance at the desired switching frequency. A simple expression for the power-delay product of CMOS was developed. For a given capacitive load, the power and delay of the CMOS gate may be scaled up or down by simply modifying the  $W/L$  ratios of the NMOS and PMOS transistors.
- *Static power dissipation:* For low-power applications, particularly where battery life is important, leakage current from subthreshold conduction and the reverse-biased wells and drain-substrate junctions can become an important source of power dissipation. This leakage current places a lower bound on the power required to operate a CMOS circuit.
- *“Short circuit” current:* During switching of the CMOS logic gate, a pulse of current occurs between the positive and negative power supplies. This current causes an additional component of power dissipation in the CMOS gate that can be as much as 20 to 30 percent of the dissipation resulting from charging and discharging the load capacitance.
- *Cascade buffers:* High capacitance loads are often encountered in logic design, and cascade buffers are used to minimize the propagation delay associated with driving these large capacitance values. Cascade buffers are widely used in wordline drivers and for on-chip and off-chip bus driver applications.
- *Dynamic logic:* Dynamic logic circuits, such as domino CMOS, operate on two phases—a precharge phase and a logic evaluation phase. This circuit family requires only two PMOS transistors in each gate (including the output inverter), thus reducing the silicon area overhead traditionally associated with static CMOS logic circuits. Dynamic circuits are also used to reduce power consumption in many applications.
- *The CMOS transmission gate:* A bidirectional circuit element, the CMOS transmission gate that utilizes the parallel connection of an NMOS and a PMOS, transistor, was introduced. When the transmission gate is on, it provides a low-resistance connection between its input and output terminals over the entire input voltage range. We will find the transmission gate used in circuit implementations of both the D latch and the master-slave D flip-flop in Chapter 8. It has also been widely used in analog multiplexers.
- *Latchup:* An important potential failure mechanism in CMOS is the phenomenon called latchup, which is caused by the existence of parasitic *n-p-n* and *p-n-p* bipolar transistors in the CMOS structure. A lumped circuit model for latchup was developed and used to simulate the latchup behavior of a CMOS inverter. Special substrates and IC processing are used to minimize the possibility of latchup in modern CMOS technologies.

## KEY TERMS

Cascade buffer	Evaluation phase
CMOS transmission gate	Fall time
CMOS reference inverter	Latchup
Complementary MOS (CMOS)	NAND gate
Complex logic gate	NOR gate
Domino CMOS	On-resistance
Dynamic logic	Parasitic bipolar transistors
Euler path	Power-delay product

Precharge phase  
Propagation delay  
Rise time

Symmetrical CMOS inverter  
Taper factor  
Transmission gate

## REFERENCES

1. F. M. Wanlass and C. T. Sah, "Nanowatt logic using field-effect metal-oxide-semiconductor triodes," *IEEE International Solid-State Circuits Conference Digest*, vol. VI, pp. 32–33, February 1963.
2. J. D. Meindl and J. A. Davis, "The fundamental limit on binary switching energy for terascale integration (TSI)," *IEEE Journal of Solid-State Circuits*, vol. 35, no. 10, pp. 1515–1516, October 2000.
3. R. M. Swanson and J. D. Meindl, "Ion-implanted complementary MOS transistors in low-voltage circuits," *IEEE Journal of Solid-State Circuits*, vol. SC-7, no. 2, pp. 146–153, April 1972.
4. H. C. Lin and L. W. Linholm, "An optimized output stage for MOS integrated circuits," *IEEE Journal of Solid-State Circuits*, vol. 10, pp. 106–109, April 1975.
5. R. C. Jaeger, "Comments on An optimized output stage for MOS integrated circuits," *IEEE Journal of Solid-State Circuits*, vol. 10, pp. 185–186, June 1975.

## PROBLEMS

Use  $K'_n = 100 \mu\text{A/V}^2$ ,  $K'_p = 40 \mu\text{A/V}^2$ ,  $V_{TN} = 0.6 \text{ V}$ , and  $V_{TP} = -0.6 \text{ V}$  unless otherwise indicated. For simulation purposes, use the values in Appendix B.

### 7.1 CMOS Inverter Technology

- 7.1. Calculate the values of  $K'_n$  and  $K'_p$  for NMOS and PMOS transistors with a gate oxide thickness of 100 Å. Assume that  $\mu_n = 500 \text{ cm}^2/\text{V} \cdot \text{s}$ ,  $\mu_p = 200 \text{ cm}^2/\text{V} \cdot \text{s}$ , and the relative permittivity of the gate oxide is 3.9. ( $\epsilon_0 = 8.854 \times 10^{-14} \text{ F/cm}$ ).
- 7.2. Draw a cross section similar to that in Fig. 7.1 for a CMOS process that uses a *p*-well instead of an *n*-well. Show the connections for a CMOS inverter, and draw an annotated version of the corresponding circuit schematic. (*Hint:* Start with an *n*-type substrate and interchange all the *n*- and *p*-type regions.)
- \*7.3. (a) The *n*-well in a CMOS process covers an area of  $1 \text{ cm} \times 0.5 \text{ cm}$ , and the junction saturation current density is  $500 \text{ pA/cm}^2$ . What is the total leakage current of the reverse-biased well? (b) Suppose the drain and source regions of the NMOS and PMOS transistors are  $2 \mu\text{m} \times 5 \mu\text{m}$ , and the saturation current density of the junctions is  $100 \text{ pA/cm}^2$ . If the chip has 20 million inverters, what is the total leakage current due to the reverse-biased

junctions when  $v_O = 2.5 \text{ V}$ ? Assume  $V_{DD} = 2.5 \text{ V}$  and  $V_{SS} = 0 \text{ V}$ . (c) When  $v_O = 0 \text{ V}$ ?

- \*7.4. A particular interconnection between two logic gates in an IC chip runs one-half the distance across a 10-mm-wide die. If the line is  $1 \mu\text{m}$  wide and the oxide ( $\epsilon_r = 3.9$ ,  $\epsilon_0 = 8.854 \times 10^{-14} \text{ F/cm}$ ) beneath the line is  $1 \mu\text{m}$  thick, what is the total capacitance of this line, assuming that the capacitance is three times that predicted by the parallel plate capacitance formula? Assume that the silicon beneath the oxide represents a conducting ground plane.
- 7.5. The CMOS inverter in Fig. P7.5 has  $V_{DD} = 2.5 \text{ V}$  and  $V_{SS} = 0 \text{ V}$ . What are the values of  $V_H$  and  $V_L$  for this inverter? (b) Repeat for  $V_{DD} = 1.8 \text{ V}$ .

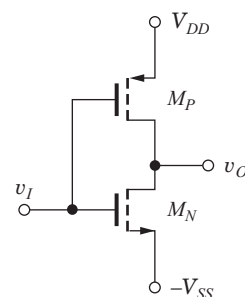


Figure P7.5

- 7.6. The CMOS inverter in Fig. P7.5 has  $V_{DD} = 3.3 \text{ V}$ ,  $V_{SS} = 0 \text{ V}$ ,  $(W/L)_N = 4/1$ , and  $(W/L)_P = 10/1$ .

What are the values of  $V_H$  and  $V_L$  for this inverter?  
 (b) Repeat for  $(W/L)_N = 6/1$  and  $(W/L)_P = 15/1$ .

- 7.7. The CMOS inverter in Fig. P7.5 has  $V_{DD} = 2.5$  V,  $V_{SS} = 0$  V,  $(W/L)_N = 4/1$ , and  $(W/L)_P = 10/1$ . What are the values of  $V_H$  and  $V_L$  for this inverter?  
 (b) Repeat for  $(W/L)_N = 4/1$  and  $(W/L)_P = 4/1$ .
- 7.8. The CMOS inverter in Fig. P7.5 has  $V_{DD} = 3.3$  V and  $V_{SS} = 0$  V. If  $V_{TN} = 0.75$  V and  $V_{TP} = -0.75$  V, what are the regions of operation of the transistors for (a)  $V_I = V_L$ ? (b)  $V_I = V_H$ ?  
 (c)  $V_I = V_O = 1.65$  V?
- 7.9. The CMOS inverter in Fig. P7.5 has  $V_{DD} = 2.5$  V and  $V_{SS} = 0$  V. If  $V_{TN} = 0.60$  V and  $V_{TP} = -0.60$  V, what are the regions of operation of the transistors for (a)  $V_I = V_L$ ? (b)  $V_I = V_H$ ?  
 (c)  $V_I = V_O = 1.25$  V?
- 7.10. (a) The CMOS inverter in Fig. P7.5 with  $(W/L)_N = 20/1$  and  $(W/L)_P = 50/1$  is operating with  $V_{DD} = 0$  V and  $-V_{SS} = -5.2$  V. What are  $V_L$  and  $V_H$ ? (b) If  $(W/L)_N = 10/1$  and  $(W/L)_P = 10/1$ ?
- 7.11. (a) Calculate the voltage at which  $v_O = v_I$  for a CMOS inverter with  $K_n = K_p$ . (*Hint:* Always remember that  $i_{DN} = i_{DP}$ .) Use  $V_{DD} = 2.5$  V,  $V_{TN} = 0.6$  V,  $V_{TP} = -0.6$  V. (b) What is the current  $I_{DD}$  from the power supply for  $v_O = v_I$  if  $(W/L)_N = 2/1$ ? (c) Repeat the calculation in (a) for a CMOS inverter with  $K_n = 2.5K_p$ . (d) What is the current  $I_{DD}$  from the power supply for  $v_O = v_I$  if  $(W/L)_N = 2/1$ ?
- 7.12. (a) Repeat Prob. 7.11 for  $V_{DD} = 1.8$  V,  $V_{TN} = 0.5$  V and  $V_{TP} = -0.5$  V. (b) Repeat Prob. 7.11 for  $V_{DD} = 2.5$  V,  $V_{TN} = 0.75$  V and  $V_{TP} = -0.65$  V.  
 (c) Repeat Prob. 7.11 for  $V_{DD} = 2.5$  V,  $V_{TN} = 0.65$  V and  $V_{TP} = -0.75$  V.
- 7.13. (a) Repeat Prob. 7.11 for  $V_{DD} = 3.3$  V,  $V_{TN} = 0.75$  V, and  $V_{TP} = -0.75$  V. (b) Repeat Prob. 7.11 for  $V_{DD} = 2.5$  V,  $V_{TN} = 0.60$  V, and  $V_{TP} = -0.50$  V.

## 7.2 Static Characteristics of the CMOS Inverter

- 7.14. Simulate the VTC for a CMOS inverter with  $K_n = 2.5K_p$ . Find the input voltage for which  $v_O = v_I$  and compare to the value calculated by hand. Use  $V_{DD} = 2.5$  V.
- 7.15. (a) The CMOS gate in Fig. P7.15 is called pseudo-NMOS. Find  $V_H$  and  $V_L$  for this gate. (b) Repeat for  $V_{DD} = 2.5$  V. (c) Repeat for  $V_{DD} = 1.8$  V.

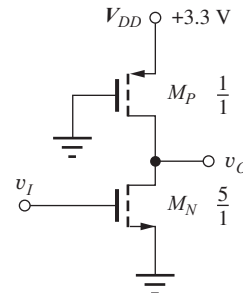


Figure P7.15

- 7.16. What is the switching threshold (where does  $v_I = v_O$ ) for a minimum size inverter in which both  $W/L$  ratios are  $2/1$  if  $V_{DD} = 2.5$  V and  $V_{TN} = -V_{TP} = 0.6$  V?
- 7.17. What are the noise margins of a minimum size CMOS inverter in which both  $W/L$  ratios are  $2/1$  and  $V_{DD} = 2.5$  V and  $V_{TN} = -V_{TP} = 0.6$  V?
- 7.18. What is the switching threshold (where does  $v_I = v_O$ ) for a minimum size inverter in which both  $W/L$  ratios are  $2/1$  if  $V_{DD} = 1.8$  V and  $V_{TN} = -V_{TP} = 0.5$  V?
- 7.19. What are the noise margins for a symmetrical CMOS inverter operating with  $V_{DD} = 3.3$  V and  $V_{TN} = -V_{TP} = 0.75$  V? (b) Repeat for a CMOS inverter having  $(W/L)_N = (W/L)_P$  operating with  $V_{DD} = 3.3$  V and  $V_{TN} = -V_{TP} = 0.75$  V.
- 7.20. Use SPICE to plot the VTC for a CMOS inverter with  $(W/L)_N = 2/1$ ,  $(W/L)_P = 5/1$ ,  $V_{DD} = 3.3$  V,  $V_{SS} = 0$  V,  $V_{TN} = 0.75$  V, and  $V_{TP} = -0.75$  V. Repeat if the threshold voltages are mismatched with values  $V_{TN} = 0.85$  V and  $V_{TP} = 0.65$  V. Repeat for  $(W/L)_N = 2/1$  and  $(W/L)_P = 4/1$  with the original threshold voltages. Plot the three curves on one graph.
- 7.21. (a) Plot a graph of the noise margins of the CMOS inverter (similar to Fig. 7.9) for  $V_{DD} = 3.3$  V,  $V_{TN} = 0.75$  V, and  $V_{TP} = -0.75$  V. (b) Repeat for  $V_{DD} = 2.0$  V,  $V_{TN} = 0.50$  V, and  $V_{TP} = -0.50$  V.
- 7.22. The outputs of two CMOS inverters are accidentally tied together, as shown in Fig. P7.22. What is the voltage at the common output node if the NMOS and PMOS transistors have  $W/L$  ratios of  $20/1$  and  $40/1$ , respectively? What is the current in the circuit?
- \*\*7.23. A CMOS inverter is to be designed to drive a single TTL inverter (which will be studied in Chapter 9). When  $v_O = V_L$ , the CMOS inverter must

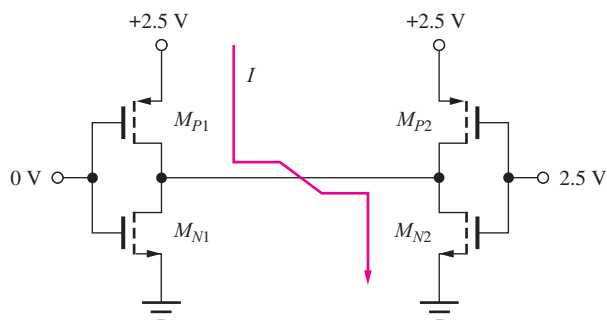


Figure P7.22

sink a current of 1.5 mA and maintain  $V_L \leq 0.6$  V. When  $v_O \geq V_H$ , the CMOS inverter must source a current of 60  $\mu$ A and maintain  $V_H \geq 2.4$  V. What are the minimum  $W/L$  ratios of the NMOS and PMOS transistors required to meet these specifications? Assume  $V_{DD} = 5$  V.

### 7.3 Dynamic Behavior of the CMOS Inverter

- 7.24. (a) What are the rise time, fall time, and average propagation delay for a symmetrical CMOS inverter with  $(W/L)_N = 2/1$ ,  $(W/L)_P = 5/1$ ,  $V_{DD} = 2.5$  V, and  $C = 0.20$  pF? (b) Repeat for  $V_{DD} = 2.0$  V. (c) Repeat for  $V_{DD} = 1.8$  V.
- 7.25. (a) Repeat problem 7.24(a) if the inverter is asymmetrical with  $V_{TN} = 0.65$  V and  $V_{TP} = -0.55$  V. What is the switching threshold  $v_I$  (where does  $v_O = v_I$ )? (b) Repeat for  $V_{DD} = 1.8$  V. (c) Repeat for  $V_{DD} = 3.3$  V.
- 7.26. (a) Repeat problem 7.24(a) if the inverter is asymmetrical with  $V_{TN} = 0.55$  V and  $V_{TP} = -0.65$  V. What is the switching threshold  $v_I$  (where does  $v_O = v_I$ )? (b) Repeat for  $V_{DD} = 1.8$  V. (c) Repeat for  $V_{DD} = 3.3$  V.
- 7.27. What are the rise time, fall time, and average propagation delay for a minimum size CMOS inverter in which both  $W/L$  ratios are 2/1? Assume a load capacitance of 0.4 pF and  $V_{DD} = 2.5$  V.
- 7.28. Repeat problem 7.27 if  $V_{TN} = 0.65$  V and  $V_{TP} = -0.55$  V. What is the switching threshold  $v_I$  ( $v_O = v_I$ ) of the inverter?
- 7.29. What are the rise time, fall time, and average propagation delay for a symmetrical CMOS inverter with  $(W/L)_N = 2/1$ ,  $(W/L)_P = 5/1$ ,  $C = 0.20$  pF,  $V_{DD} = 3.3$  V,  $V_{TN} = 0.75$  V, and  $V_{TP} = -0.75$  V?
- 7.30. What are the rise time, fall time, and average propagation delay for a symmetrical CMOS inverter with  $(W/L)_N = 2/1$ ,  $(W/L)_P = 5/1$ ,  $C = 0.15$  pF,  $V_{DD} = 2.5$  V,  $V_{TN} = 0.60$  V, and  $V_{TP} = -0.60$  V?
- 7.31. What are the sizes of the transistors in the CMOS inverter if it must drive a 1-pF capacitance with an average propagation delay of 3 ns? Design the inverter for equal rise and fall times. Use  $V_{DD} = 2.5$  V,  $V_{TN} = 0.6$  V,  $V_{TP} = -0.6$  V.
- 7.32. Design an asymmetrical inverter to meet the delay specification in Prob. 7.31 with  $(W/L)_P = (W/L)_N$ .
- 7.33. Design a symmetrical CMOS reference inverter to provide a delay of 1 ns when driving a 10-pF load. (a) Assume  $V_{DD} = 2.5$  V. (b) Assume  $V_{DD} = 3.3$  V and  $V_{TN} = -V_{TP} = 0.75$  V.
- 7.34. Design an asymmetrical inverter to meet the delay specification in Prob. 7.33 with  $(W/L)_P = 2(W/L)_N$ .
- 7.35. Design a symmetrical CMOS reference inverter to provide a propagation delay of 200 ps for a load capacitance of 100 fF. Use  $V_{DD} = 1.5$  V,  $V_{TN} = 0.50$  V, and  $V_{TP} = -0.50$  V.
- 7.36. Design an asymmetrical inverter to meet the delay specification in Prob. 7.35 with  $(W/L)_P = (W/L)_N$ .
- 7.37. Design a symmetrical CMOS reference inverter to provide a propagation delay of 400 ps for a load capacitance of 100 fF. Use  $V_{DD} = 2.5$  V,  $V_{TN} = 0.60$  V, and  $V_{TP} = -0.60$  V.
- 7.38. Design an asymmetrical inverter to meet the delay specification in Prob. 7.37 with  $(W/L)_P = (W/L)_N$ .
- 7.39. (a) Scale the reference inverter in Fig. 7.12 to achieve a 0.4 ns delay with  $C = 2$  pF. (b) What is the delay of the new inverter if  $C = 3$  pF?
- 7.40. (a) Scale the reference inverter in Fig. 7.12 to achieve a 0.3 ns delay with  $C = 0.5$  pF. (b) What is the delay of the new inverter if  $C = 1.5$  pF?
- \*7.41. Use SPICE to determine the characteristics of the CMOS inverter for the design given in Fig. 7.12 if  $C = 100$  fF. (a) Simulate the voltage transfer function. (b) Determine  $t_r$ ,  $t_f$ ,  $\tau_{PHL}$ , and  $\tau_{PLH}$  for this inverter with a square wave input. What must be the total effective load capacitance  $C$  based on the propagation delay formula developed in the text?
- \*\*7.42. Use SPICE to simulate the behavior of a chain of five CMOS inverters similar to those in Fig. 7.13(b). The input to the first inverter should be a square wave with 0.1-ns rise and fall times and a period

of 100 ns. (a) Calculate  $t_r$ ,  $t_f$ ,  $\tau_{PHL}$ , and  $\tau_{PLH}$  using the input and output waveforms from the first inverter in the chain and compare your results to the formulas developed in the text. (b) Determine  $t_r$ ,  $t_f$ ,  $\tau_{PHL}$ , and  $\tau_{PLH}$  from the waveforms at the input and output of the fourth inverter in the chain, and compare your results to the formulas developed in the text. (c) Discuss the differences between the results in (a) and (b).

## 7.4 Power Dissipation and Power Delay Product in CMOS

- 7.43. A high-performance CMOS microprocessor design requires 500 million logic gates and will be placed in a package that can dissipate 100 W. (a) What is the average power that can be dissipated by each logic gate on the chip? (b) If a supply voltage of 1.8 V is used, what is the average current that must be supplied to the chip?
- 7.44. A certain packaged IC chip can dissipate 5 W. Suppose we have a CMOS IC design that must fit on one chip and requires 5 million logic gates. What is the average power that can be dissipated by each logic gate on the chip? If the average gate must switch at 5 MHz, what is the maximum capacitive load on a gate for  $V_{DD} = 3.3$  V, 2.5 V and 1.8 V.
- 7.45. (a) The *n*-well in a CMOS process covers an area of  $5 \text{ mm} \times 10 \text{ mm}$ , and the saturation current density of the junction is  $400 \text{ pA/cm}^2$ . What is the total leakage current of the reverse-biased well? (b) Suppose the drain and source regions of the NMOS and PMOS transistors are each  $0.5 \mu\text{m} \times 1.25 \mu\text{m}$  in size, and the saturation current density of the junction is  $150 \text{ pA/cm}^2$ . If the chip has 200 million inverters, what is the total leakage current when  $v_O = 2.5 \text{ V}$ ? Assume  $V_{DD} = 2.5 \text{ V}$ . (b) Repeat for  $v_O = 0 \text{ V}$ .
- 7.46. A high-speed CMOS microprocessor has a 64-bit address bus and performs a memory access every 2 ns. Assume that all address bits change during every memory access and that each bus line represents a load of  $25 \text{ pF}$ . (a) How much power is being dissipated by the circuits that are driving these signals if the power supply is 2.5 V? (b) Repeat for 3.3 V.
- \*7.47. (a) A CMOS inverter has  $(W/L)_N = 15/1$ ,  $(W/L)_P = 15/1$ , and  $V_{DD} = 3.3 \text{ V}$ . What is the peak current in the logic gate and at what input voltage does it occur? (b) Repeat for  $V_{DD} = 2.5 \text{ V}$ .
- 7.48. (a) Repeat Prob. 7.47(a) for  $V_{DD} = 1.8 \text{ V}$ . (b) Repeat for  $V_{DD} = 2.5 \text{ V}$ ,  $V_{TN} = 0.55 \text{ V}$ , and  $V_{TP} = -0.65 \text{ V}$ .
- \*7.49. (a) A CMOS inverter has  $(W/L)_N = 2/1$ ,  $(W/L)_P = 5/1$ , and  $V_{DD} = 3.3 \text{ V}$ . Assume  $V_{TN} = -V_{TP} = 0.7 \text{ V}$ . What is the peak current in the logic gate and at what input voltage does it occur? (b) Repeat for  $V_{DD} = 2.0 \text{ V}$  with  $V_{TN} = -V_{TP} = 0.5 \text{ V}$ .
- 7.50. (a) Repeat Prob. 7.49(a) for  $V_{DD} = 2.0 \text{ V}$ ,  $V_{TN} = 0.45 \text{ V}$ , and  $V_{TP} = -0.55 \text{ V}$ . (b) Repeat Prob. 7.49(a) for  $V_{DD} = 2.0 \text{ V}$ ,  $V_{TN} = 0.55 \text{ V}$ , and  $V_{TP} = -0.45 \text{ V}$ .
- 7.51. What is the power-delay product for the inverter in Prob. 7.24? How much power does the inverter dissipate if it is switching at a frequency of 100 MHz?
- 7.52. (a) What is the power-delay product for the inverter in Prob. 7.29? (b) Estimate the maximum switching frequency for this inverter. (c) How much power does the inverter dissipate if it is switching at the frequency found in (b)?
- 7.53. (a) What is the power-delay product for the inverter in Prob. 7.30? (b) Estimate the maximum switching frequency for this inverter. (c) How much power does the inverter dissipate if it is switching at the frequency found in (b)?
- 7.54. Plot the power-delay characteristic for the CMOS inverter family based on an inverter design in which  $(W/L)_N = (W/L)_P$ . Assume the load capacitance  $C = 0.2 \text{ pF}$ . Use  $V_{DD} = 2.5 \text{ V}$  and vary the power by changing the  $W/L$  ratios.
- \*\*7.55. Ideal constant-electric-field scaling of a MOS technology reduces all the dimensions and voltages by the same factor  $\alpha$ . Assume that the capacitor  $C$  in Eq. (7.31) is proportional to the total gate capacitance of the MOS transistor:  $C = C''_{ox} W/L$ , and show that constant-field scaling results in a reduction of the PDP by a factor of  $\alpha^3$ .
- \*\*7.56. For many years, MOS technology was scaled by reducing all the dimensions by the same factor  $\alpha$ , but keeping the voltages constant. Assume that the capacitor  $C$  in Eq. (7.31) is proportional to the total gate capacitance of the MOS transistor:  $C = C''_{ox} WL$ , and show that this geometry scaling results in a reduction of the PDP by a factor of  $\alpha$ .
- \*\*7.57. Use SPICE to simulate the behavior of a chain of five CMOS inverters with the same design as in Fig. 7.12 with  $C = 0.25 \text{ pF}$ . The input to the first inverter should be a square wave with 0.1-ns rise

and fall times and a period of 30 ns. (a) Calculate  $t_r$ ,  $t_f$ ,  $\tau_{PHL}$ , and  $\tau_{PLH}$  using the input and output waveforms from the first inverter in the chain, and compare your results to the formulas developed in the text. (b) Determine  $t_r$ ,  $t_f$ ,  $\tau_{PHL}$ , and  $\tau_{PLH}$  from the waveforms at the input and output of the fourth inverter in the chain, and compare your results to the formulas developed in the text. (c) Discuss the differences between the results in (a) and (b).

- \*\*7.58. Use SPICE to simulate the behavior of a chain of five CMOS inverters with the same design as in Fig. 7.12 with  $C = 1 \text{ pF}$ . The input to the first inverter should be a square wave with 0.1-ns rise and fall times and a period of 40 ns. (a) Determine  $t_r$ ,  $t_f$ ,  $\tau_{PHL}$ , and  $\tau_{PLH}$  from the waveforms at the input and output of the fourth inverter in the chain, and compare your results to the formulas developed in the text. (b) Repeat the simulation for  $(W/L)_P = (W/L)_N = 2/1$ , and compare the results to those obtained in (a).

## 7.5 CMOS NOR and NAND Gates

- 7.59. (a) Draw the circuit schematic for a four-input NOR gate. What are the  $W/L$  ratios of the transistors based on the reference inverter design in Fig. 7.12? (b) What should be the  $W/L$  ratios if the NOR gate must drive twice the load capacitance with the same delay as the reference inverter?
- 7.60. Draw the circuit schematic of a four-input NOR gate. Suppose the PMOS transistors are chosen to have  $(W/L)_P = 2/1$ . What are the corresponding  $W/L$  ratios of the NMOS devices, if the gate is to have symmetrical delay characteristics?
- 7.61. Draw the circuit schematic of a three-input NOR gate. Suppose the PMOS transistors are chosen to have  $(W/L)_P = 2/1$ . What are the corresponding  $W/L$  ratios of the NMOS devices, if the gate is to have symmetrical delay characteristics?
- 7.62. (a) Draw the circuit schematic for a four-input NAND gate. What are the  $W/L$  ratios of the transistors based on the reference inverter design in Fig. 7.12? (b) What should be the  $W/L$  ratios if the NOR gate must drive three times the load capacitance with the same delay as the reference inverter?
- 7.63. Draw the circuit schematic of a four-input NAND gate. Suppose the NMOS transistors are chosen to have  $(W/L)_N = 2/1$ . What are the corresponding  $W/L$  ratios of the PMOS devices, if the gate is to have symmetrical delay characteristics?

7.64. Draw the circuit schematic of a three-input NAND gate. Suppose the NMOS transistors are chosen to have  $(W/L)_N = 2/1$ . What are the corresponding  $W/L$  ratios of the PMOS devices, if the gate is to have symmetrical delay characteristics?

7.65. Design a circuit to multiply two one-bit numbers. (*Hint:* Construct a truth table for output bit  $M$  based on two inputs  $A$  and  $B$ .) Choose the  $W/L$  ratios based on the inverter in Fig. 7.12.

- \*\*7.66. Use SPICE to determine the characteristics of the two-input CMOS NOR gate given in Fig. 7.19 with a load capacitance of 1 pF. Assume that  $\gamma = 0$  for all transistors. (a) Simulate the voltage transfer function by varying the voltage at input  $A$  with the voltage at input  $B$  fixed at 2.5 V. (b) Repeat the simulation in (a) but now vary the voltage at input  $B$  with the voltage at input  $A$  fixed at 2.5 V. Plot the results from (a) and (b) and note any differences. (c) Determine  $t_r$ ,  $t_f$ ,  $\tau_{PHL}$ , and  $\tau_{PLH}$  for this inverter with a square wave input at input  $A$  with the voltage at input  $B$  fixed at 2.5 V. (d) Determine  $t_r$ ,  $t_f$ ,  $\tau_{PHL}$ , and  $\tau_{PLH}$  for this inverter with a square wave input at input  $B$  with the voltage at input  $A$  fixed at 2.5 V. (e) Compare the results from (c) and (d). (f) Determine  $t_r$ ,  $t_f$ ,  $\tau_{PHL}$ , and  $\tau_{PLH}$  for this inverter with a single square wave input applied to both inputs  $A$  and  $B$ . Compare the results to those in (c) and (d).

\*\*7.67. Repeat (a) and (b), Prob. 7.66, using the nonzero values for the parameter  $\gamma$  from the device parameter tables.

- \*\*7.68. Use SPICE to determine the characteristics of the two-input CMOS NAND gate given in Fig. 7.23 with a load capacitance of 1 pF. Assume that  $\gamma = 0$  for all transistors. (a) Simulate the voltage transfer function by varying the voltage at input  $A$  with the voltage at input  $B$  fixed at 2.5 V. (b) Repeat the simulation in (a) but now vary the voltage at input  $B$  with the voltage at input  $A$  fixed at 2.5 V. Plot the results from (a) and (b) and note any differences. (c) Determine  $t_r$ ,  $t_f$ ,  $\tau_{PHL}$ , and  $\tau_{PLH}$  for this inverter with a square wave input at input  $A$  with the voltage at input  $B$  fixed at 2.5 V. (d) Determine  $t_r$ ,  $t_f$ ,  $\tau_{PHL}$ , and  $\tau_{PLH}$  for this inverter with a square wave input at input  $B$  with the voltage at input  $A$  fixed at 2.5 V. (e) Compare the results from (c) and (d). (f) Determine  $t_r$ ,  $t_f$ ,  $\tau_{PHL}$ , and  $\tau_{PLH}$  for this inverter with a single square wave input applied to both inputs  $A$  and  $B$ . Compare the results to those in (c) and (d).

- \*\*7.69. Repeat (a) and (b), Prob. 7.68, using the nonzero values for the parameter  $\gamma$  from the device parameter tables.

## 7.6 Design of Complex Gates in CMOS

- 7.70. What are the worst case rise and fall times and average propagation delays of the CMOS gate in Fig. 7.26(b) for a load capacitance of 1.25 pF?
- 7.71 (a) What is the equivalent  $W/L$  ratio of the NMOS switching network in Fig. 7.26(b) when all of the NMOS transistors are on? (b) Repeat for the PMOS network.
- \*\*7.72. (a) How many transistors are needed to implement the CMOS gate in Fig. 7.29 using depletion-mode NMOS? (b) Compare the total gate area of the CMOS and NMOS designs if they are both designed for a 10-ns average propagation delay for a load capacitance of 1 pF.
- 7.73. (a) What is the logic function implemented by the gate in Fig. P7.73? (b) Design the PMOS transistor network. Select the device sizes for both the NMOS and PMOS transistors to give a delay similar to that of the CMOS reference inverter.  $C$  is the same. (c) What is the equivalent  $W/L$  ratio of the NMOS switching network when all of the NMOS transistors are on? (d) Repeat for the PMOS network.

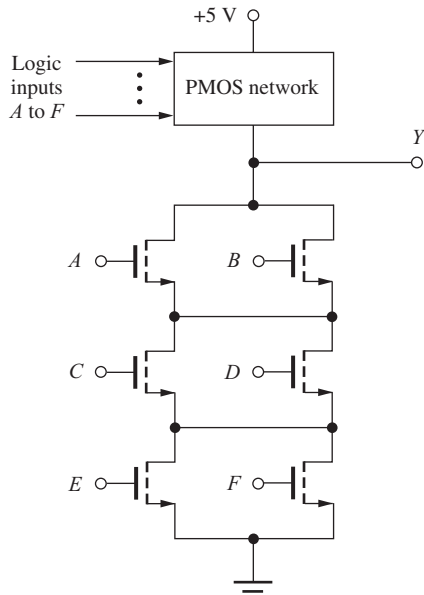


Figure P7.73

- 7.74. (a) What is the logic function implemented by the gate in Fig. P7.74? (b) Design the PMOS transistor

network. Select the device sizes for both the NMOS and PMOS transistors to give a delay of approximately one-half the delay of the CMOS reference inverter.  $C$  is the same. (c) What is the equivalent  $W/L$  ratio of the NMOS switching network when all of the NMOS transistors are on? (d) Repeat for the PMOS network.

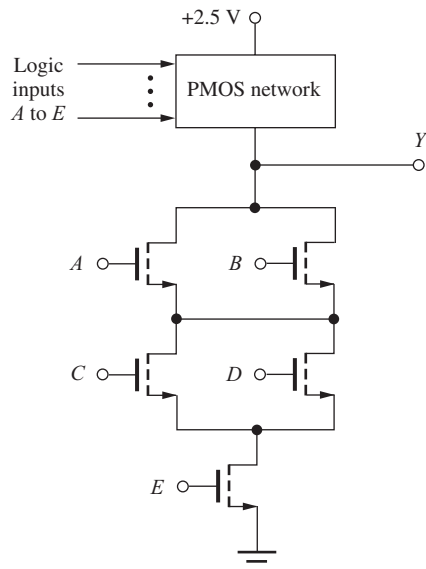


Figure P7.74

- 7.75. (a) What is the logic function implemented by the gate in Fig. P7.75? (b) Design the PMOS transistor network. Select the device sizes for both the NMOS

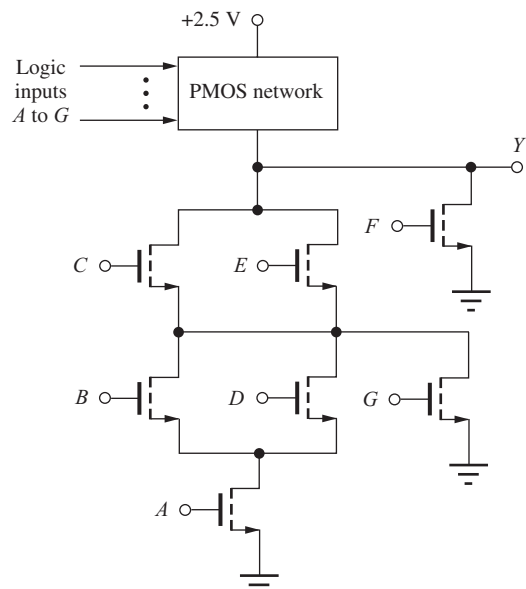


Figure P7.75

and PMOS transistors to give a delay of approximately one-half the delay of the CMOS reference inverter.  $C$  is the same. (c) What is the equivalent  $W/L$  ratio of the NMOS switching network when all of the NMOS transistors are on? (d) Repeat for the PMOS network.

- 7.76. (a) What is the logic function implemented by the gate in Fig. P7.76? (b) Design the NMOS transistor network. Select the device sizes for both the NMOS and PMOS transistors to give a delay similar to that of the CMOS reference inverter.  $C$  is the same. (c) What is the equivalent  $W/L$  ratio of the PMOS switching network when all of the PMOS transistors are on? (d) Repeat for the NMOS network.

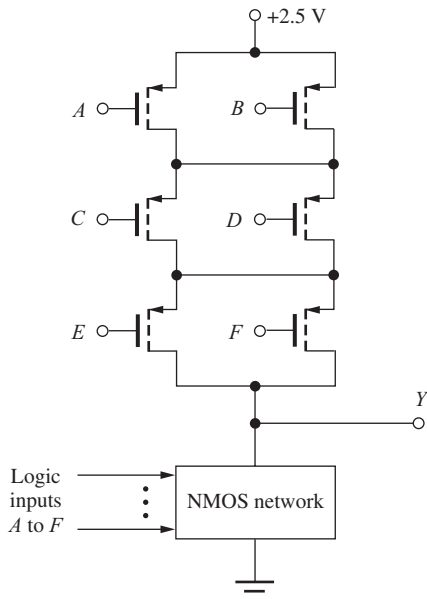


Figure P7.76

- 7.77. (a) What is the logic function implemented by the gate in Fig. P7.77? (b) Design the NMOS transistor network. Select the device sizes for both the NMOS and PMOS transistors to give a delay of approximately one-fourth the delay of the CMOS reference inverter.  $C$  is the same. (c) What is the equivalent  $W/L$  ratio of the PMOS switching network when all of the PMOS transistors are on? (d) Repeat for the NMOS network.
- 7.78. Draw the logic diagram and transistor implementation for a (2-3-1) AOI gate. Use the graphical approach to design the PMOS network. Choose the size of the transistors based upon the reference inverter in Fig. 7.12.

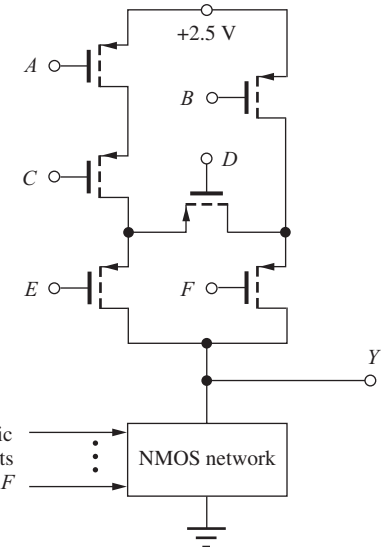


Figure P7.77

- 7.79. Draw the logic diagram and transistor implementation for a (3-2-3-1) AOI gate. Use the graphical approach to design the PMOS network. Choose the size of the transistors based upon the reference inverter in Fig. 7.12.
- 7.80. (a) Draw the NMOS and PMOS graphs for the (2-2-1) AOI in the Electronics in Action figure on page 394. (b) Find an Euler path for this circuit if it exists. (c) Draw the NMOS and PMOS graphs for a (2-2-2) AOI. (d) Find an Euler path for part (d) if it exists.
- 7.81. Redraw Fig. 7.28 and highlight the conducting path(s) for the following sets of inputs for ABCDE: (a) 10011, (b) 10001, (c) 11101, (d) 00010.
- 7.82. Draw the circuit for Prob. 7.73 and highlight the conducting path(s) for the following sets of inputs for ABCDEF: (a) 100110, (b) 011001, (c) 010101, (d) 110011.
- 7.83. Design a CMOS logic gate that implements the logic function  $Y = \overline{A(BC + DE)}$  and is twice as fast as the CMOS reference inverter when loaded by a capacitance of  $2C$ .
- 7.84. Design a CMOS logic gate that implements the logic function  $Y = \overline{ABC + DE}$ , based on the CMOS reference inverter. Select the transistor sizes to give the same delay as that of the reference inverter if the load capacitance is the same as that of the reference inverter.

- 7.85. Design a CMOS logic gate that implements the logic function  $Y = \overline{A(B + CD)} + \overline{E}$  and has the same logic delay as the CMOS reference inverter when driving a capacitance of  $4C$ .
- 7.86. Design a CMOS logic gate that implements the logic function  $Y = A(\overline{B} + C(D + E))$ , based on the CMOS reference inverter. Select the transistor sizes to give the same delay as that of the reference inverter if the load capacitance is the same as that of the reference inverter.
- 7.87. Design a complex gate implementation of a one-bit half adder for which the sum bit is described by  $S = X \oplus Y$ , and the carry bit is given by  $C = A \cdot B$ . Choose the  $W/L$  ratios based on the reference inverter design in Fig. 7.12. Assume that true and complement values of each variable are available as inputs. (Note: Two gate designs are needed, one for  $S$  and one for  $C$ .)
- 7.88. Design a complex gate implementation of a 1-bit full adder for which the  $i$ th sum bit is described by  $S_i = X_i \oplus Y_i \oplus C_{i-1}$ , and the  $i$ th carry bit is given by  $C_i = X_i \cdot Y_i + X_i \cdot C_{i-1} + Y_i \cdot C_{i-1}$ . Choose the  $W/L$  ratios based upon the reference inverter design in Fig. 7.12. Assume that true and complement values of each variable are available as inputs. (Note: Two gate designs are needed, one for  $S_i$  and one for  $C_i$ .)
- 7.89. Design a complex gate implementation of a 2-bit parallel multiplier. [Note: The circuit should produce a 4-bit output (e.g.,  $11_2 \times 11_2 = 1001_2$ ), and a separate circuit should be designed for each output bit.] Choose the  $W/L$  ratios based on the inverter in Fig. 7.12.

## 7.7 Minimum Size Gate Design and Performance

- 7.90. The five-input NAND gate in Fig. 7.24 is implemented with transistors all having  $W/L = 2/1$ . What is the propagation delay for this gate for a load capacitance  $C = 180 \text{ fF}$ ? Assume  $V_{DD} = 2.5 \text{ V}$ . What would be the delay of the reference inverter for  $C = 180 \text{ fF}$ ?
- 7.91. The three-input NOR gate in Fig. 7.21 is implemented with transistors all having  $W/L = 2/1$ . What is the propagation delay for this gate for a load capacitance  $C = 400 \text{ fF}$ ? Assume  $V_{DD} = 2.5 \text{ V}$ . What would be the delay of the reference inverter for  $C = 400 \text{ fF}$ ?
- 7.92. A (2-3-1) AOI is implemented with transistors all having  $W/L = 2/1$ . What are the worst-case val-

ues of  $\tau_{PLH}$  and  $\tau_{PHL}$  if  $V_{DD} = 2.5 \text{ V}$  and  $C = 350 \text{ fF}$ ?

- 7.93. A (2-2-2) AOI is implemented with transistors all having  $W/L = 2/1$ . What are the worst-case values of  $\tau_{PLH}$  and  $\tau_{PHL}$  if  $V_{DD} = 2.5 \text{ V}$  and  $C = 200 \text{ fF}$ ?
- 7.94. What are the worst-case values of  $\tau_{PHL}$  and  $\tau_{PLH}$  for the gate in Fig. 7.28 when it is implemented using only 2/1 transistors and drives a load capacitance of  $0.5 \text{ pF}$ ? Assume  $V_{DD} = 2.5 \text{ V}$ .
- 7.95. What is the worst-case value of  $\tau_{PHL}$  for the gate in Fig. P7.73 when it is implemented using only 2/1 transistors and drives a load capacitance of  $0.5 \text{ pF}$ ? Assume  $V_{DD} = 2.5 \text{ V}$ .
- 7.96. (a) Use a transient simulation in SPICE to find the average propagation delay of a cascade connection of 10 minimum size inverters ( $W/L = 2/1$ ) in series. Assume each has a capacitive load  $C$  of  $200 \text{ fF}$  and  $V_{DD} = 2.5 \text{ V}$ . (b) Repeat for a cascade of 10 symmetrical reference inverters with the same design as in Fig. 7.12, and compare the average propagation delays.

## 7.8 Dynamic Domino CMOS Logic

- 7.97. (a) Draw the circuit schematic for a two-input domino CMOS NOR gate. Assume that true and complement values of each variable are available as inputs. (b) Repeat for a two-input domino CMOS NAND gate.
- 7.98. (a) Draw the circuit schematic for a two-input domino CMOS OR gate. Assume that true and complement values of each variable are available as inputs. (b) Repeat for a two-input domino CMOS AND gate.
- 7.99. (a) Draw the circuit schematic for a three-input domino CMOS NOR gate. Assume that true and complement values of each variable are available as inputs. (b) Repeat for a three-input domino CMOS NAND gate.
- 7.100. (a) Draw the circuit schematic for a three-input domino CMOS OR gate. Assume that true and complement values of each variable are available as inputs. (b) Repeat for a three-input domino CMOS AND gate.
- 7.101. Draw the circuit schematic for a (2-2-2) AOI in domino CMOS.
- 7.102. Draw the circuit schematic for a (3-2-1) AOI in domino CMOS.

- \*7.103. (a) Suppose that inputs  $A_0$ ,  $A_1$ , and  $A_2$  are all 0 in the domino CMOS gate in Fig. P7.103, and the clock has just changed to the evaluate phase. If  $A_0$  now changes to a 1, what happens to the voltage at node  $B$  if  $C_1 = 2C_2$ ? (*Hint:* Charge sharing occurs between  $C_1$  &  $C_2$ .) (b) Now  $A_1$  changes to a 1. What happens to the voltage at node  $B$  if  $C_3 = C_2$ ? (c) If the output inverter is a symmetrical design, what is the minimum ratio of  $C_1/C_2$  (assume  $C_3 = C_2$ ) for which the gate maintains a valid output?  $V_{DD} = 2.5$  V

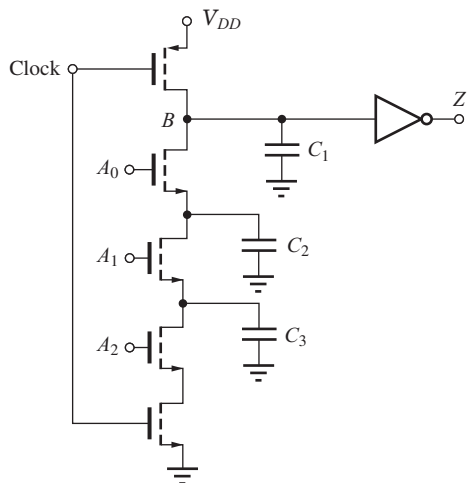


Figure P7.103

- 7.104. Draw the mirror image of the gate in Fig. P7.102 by replacing NMOS transistors with PMOS transistors and vice versa. Assume the logic inputs remain the same and write an expression for the logic function  $Z$ .
- 7.105. Draw the circuit schematic for a domino CMOS gate that implements the sum of products (SOP) logic function  $Z = AB + CD$ . Assume that true and complement values of each variable are available as inputs.
- 7.106. Draw the circuit schematic for a domino CMOS gate that implements the product of sums (POS) logic function  $Z = (A + B)(C + D)$ . Assume that true and complement values of each variable are available as inputs.
- 7.107. Draw the circuit schematic for a domino CMOS gate that implements the sum-of-products (SOP) logic function  $Z = AB + CD + EF$ . Assume that true and complement values of each variable are available as inputs. (Remember DeMorgan's theorem.)

- 7.108. Draw the circuit schematic for a domino CMOS gate that implements the product-of-sums (POS) logic function  $Z = (A + B)(C + D)(E + F)$ . Assume that true and complement values of each variable are available as inputs. (Remember DeMorgan's theorem.)

## 7.9 Cascade Buffers

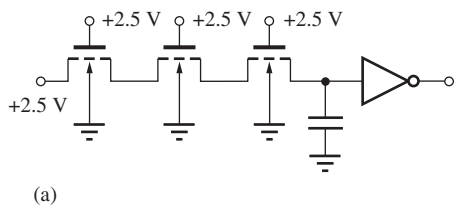
- 7.109. Design an optimized cascade buffer to drive a load capacitance of  $5000C_o$ . (a) What is the optimum number of stages? (b) What are the relative sizes of each inverter in the chain (see Fig. 7.33)? (c) What is the delay of the buffer in terms of  $\tau_o$ ?
- 7.110. Design an optimized cascade buffer to drive a load capacitance of  $10 \text{ pF}$  if the capacitance of the symmetrical reference inverter is  $80 \text{ fF}$ . What is the optimum number of stages? What are the relative sizes of each inverter in the chain? What is the total delay of the buffer for  $V_{DD} = 2.5$  V?
- 7.111. Design an optimized cascade buffer to drive a load capacitance of  $40 \text{ pF}$  if the capacitance of a symmetrical reference inverter is  $50 \text{ fF}$ . What is the optimum number of stages? What are the relative sizes of each inverter in the chain? What is the total delay of the buffer for  $V_{DD} = 2.5$  V?
- \*\*7.112. Assume that the area of each inverter in a cascade buffer is proportional to the taper factor  $\beta$  and that the unit size inverter has an area  $A_o$ . Write an expression for the total area of an  $N$ -stage cascade buffer. In the example in Fig. 7.34, buffers with  $N = 6$  and  $N = 7$  have approximately the same delay. Compare the area of these two buffer designs using your formula.

## 7.10 The CMOS Transmission Gate

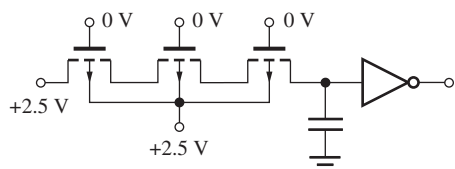
- 7.113. (a) Calculate the on-resistance of an NMOS transistor with  $W/L = 20/1$  for  $V_{GS} = 2.5$  V,  $V_{SB} = 0$  V, and  $V_{DS} = 0$  V. (b) Calculate the on-resistance of a PMOS transistor with  $W/L = 20/1$  for  $V_{SG} = 2.5$  V,  $V_{SB} = 0$  V, and  $V_{SD} = 0$  V. (c) What do we mean when we say that a transistor is “on” even though  $I_D$  and  $V_{DS} = 0$ ?
- 7.114. Calculate the maximum and minimum values of the equivalent on-resistance for the transmission gate in Fig. 7.36.
- 7.115. (a) What is the largest value of the on-resistance of a transmission gate with  $W/L = 10/1$  for both transistors if the input voltage range is  $0 \leq v_I \leq 1$  V and the power supply is 2.5 V? At what input

voltage does it occur? (b) Repeat for  $0 \leq v_I \leq 2.5$  V.

- 7.116. A certain analog multiplexer application requires the equivalent on-resistance  $R_{EQ}$  of a transmission gate to always be less than  $250 \Omega$  for  $0 \leq v_I \leq 2.5$  V. What are the minimum values of  $W/L$  for the NMOS and PMOS transistors if  $V_{TON} = 0.75$  V,  $V_{TOP} = -0.75$  V,  $\gamma = 0.5\sqrt{V}$ ,  $2\phi_F = 0.6$  V,  $K'_p = 40 \mu\text{A}/\text{V}^2$ , and  $K'_n = 100 \mu\text{A}/\text{V}^2$ ?
- 7.117. (a) What are the voltages at the nodes in the pass-transistor networks in Fig. P7.117. For NMOS transistors, use  $V_{TO} = 0.70$  V,  $\gamma = 0.6\sqrt{V}$ , and  $2\phi_F = 0.6$  V. For PMOS transistors,  $V_{TO} = -0.70$  V and  $\gamma = 0.5\sqrt{V}$ . (b) What would be the voltages if transmission gates were used in place of each transistor?



(a)



(b)

**Figure P7.117**

### 7.11 CMOS Latchup

- 7.118. Simulate CMOS latchup using the circuit in Fig. 7.37(b) and plot graphs of the voltages at nodes 2, 3, and 4 as well as the current supplied by  $V_{DD}$ . Discuss the behavior of the voltages and identify important voltage levels, current levels, and slopes on the graphs.

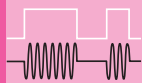
- 7.119. Repeat Prob. 7.118 if the values of  $R_n$  and  $R_p$  are reduced by a factor of 10.

- 7.120. Draw the cross section and equivalent circuit, similar to Fig. 7.37, for a *p*-well CMOS technology.

### Additional Problems

- 7.121. (a) Verify Eq. (7.9). (b) Verify Eq. (7.13).
- \*\*7.122. (a) Calculate the sensitivity  $S_{K_n}^{\tau_p} = (K_n/\tau_p)(d\tau_p/dK_n)$  of the propagation delay  $\tau_p$  in Eq. (7.18) to changes in  $K_n$ . If the IC processing causes  $K_n$  to be 25 percent below its nominal value, what will be the percentage change in  $\tau_p$ ? (b) Calculate the sensitivity  $S_{V_{TN}}^{\tau_p} = (V_{TN}/\tau_p)(d\tau_p/dV_{TN})$  of the propagation delay  $\tau_p$  in Eq. (7.18) to changes in  $V_{TN}$ . If the IC processing causes  $V_{TN}$  to change from a nominal value of 0.75 V to 0.85 V, what will be the percentage change in  $\tau_p$ ?
- 7.123. Calculate logic delay versus input signal rise time for a minimum size inverter with a load capacitance of 1 pF for  $0.1 \text{ ns} \leq t_r \leq 5 \text{ ns}$ .
- 7.124. An NMOS transistor is to be used as a power switch to disable one core of a multicore processor chip that operates from a 2.5 V power supply. When the core is enabled, its current is 4 A. What is the  $W/L$  ratio of the NMOS transistor if the voltage drop across the transistor must be less than 100 mV? If  $L = 1 \mu\text{m}$ , estimate the area of the transistor.
- 7.125. CMOS with a PDP of 50 fJ is to be used in a chip design that requires 100 million gates. The chip will be placed in a package that can safely dissipate 40 W. What is the minimum logic gate delay that can be used in the design if all the gates operate at the same speed and 20 percent of the gates are switching at any given time?

# CHAPTER 8



## MOS MEMORY AND STORAGE CIRCUITS

### CHAPTER OUTLINE

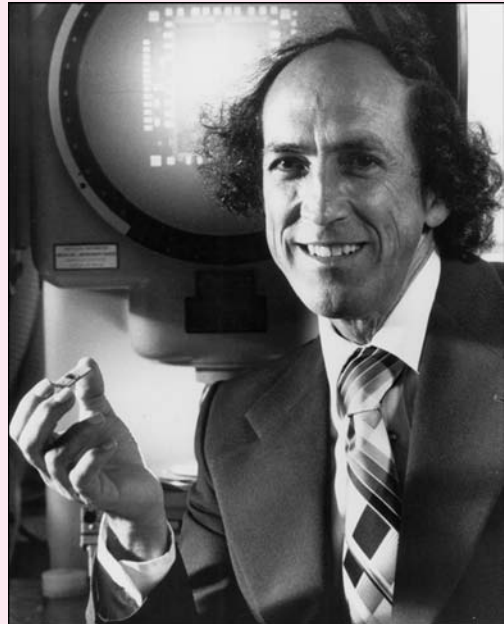
- 8.1 Random-Access Memory (RAM) 417
- 8.2 Static Memory Cells 419
- 8.3 Dynamic Memory Cells 428
- 8.4 Sense Amplifiers 434
- 8.5 Address Decoders 440
- 8.6 Read-Only Memory (ROM) 444
- 8.7 Flip-Flops 447
- Summary 451
- Key Terms 452
- References 452
- Problems 453

### CHAPTER GOALS

From Chapter 8, we shall gain a basic understanding of the design of computer memory and storage circuits including

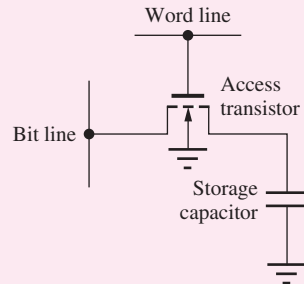
- Overall memory chip organization
- Static memory circuits using the six-transistor cell
- Dynamic memory circuits including the one-transistor and four-transistor cells
- Sense amplifier circuits required to detect the information stored in the memory cells
- Row and address decoders used to select cells from large memory arrays
- The implementation of various types of flip-flops used in CPU registers
- Pass transistor logic
- Read only memory

For many years, high-density memory has served as the IC industry's vehicle for driving technology to ever smaller dimensions. In the mid-1960s, the first random-access memory (RAM) chip using MOS technology [1] was discussed at the IEEE International Solid-State Circuits Conference (ISSCC) [2], and in 1974 the first commercial 1024-bit (1-Kb) memory was introduced [3]. By 2000, experimental 1-gigabit (Gb) chips had been described at the ISSCC, and the technology for future 1-Gb memories had been discussed at the IEEE International Electron Devices Meeting (IEDM)[4]. Thus, just 30 years after the introduction of the first commercial MOS RAM chips, chips have been



Robert H. Dennard, inventor of the 1-transistor DRAM cell

*Courtesy of IBM Archives*



1-T DRAM cell.

demonstrated with more than 1 million times the storage capacity of the original RAMs.

The circuit that made these incredible memory chips possible is called the **one-transistor dynamic RAM cell** or 1-T DRAM. This elegant circuit, which requires only one transistor and one capacitor to store a single bit of information [1], was invented in 1966 by Robert H. Dennard of the IBM Thomas J. Watson Research Center. In this circuit,

patented in 1968, the binary information is temporarily stored as a charge on the capacitor, and the data must be periodically refreshed in order to prevent information loss. In addition, the process of reading the data out of most DRAM circuits destroys the information, and the data must be put back into memory as part of the read operation. At

the time of the invention, Dennard and a few of his colleagues were probably the only ones that believed the circuit could be made to actually work. Today, there are arguably more 1-T DRAM bits in the world than any other electronic circuit.

## 8.1 RANDOM ACCESS MEMORY

Thus far, our study of logic circuits concentrated on understanding the design of basic inverters and combinational logic circuits. In addition to logic, however, digital systems generally require data storage capability in the form of high-speed registers, high-density **random-access memory (RAM)**, and **read-only memory (ROM)**.

In digital systems, the term RAM is used to refer to memory with both read and write capability. This is the type of memory used when information needs to be changed with great frequency. The data in any given storage location in RAM can be directly read or altered just as quickly as the information at any other location.

Early memory designs were **static RAM** or **SRAM** circuits in which the information remains stored in memory as long as the power supply voltage is maintained. The SRAM cell requires the equivalent of six transistors per memory bit and features nondestructive readout of its stored information.

In the **dynamic RAM** or **DRAM** circuit, information is temporarily stored as a charge on a capacitor, and the data must be periodically refreshed in order to prevent information loss. The process of reading the data out of most DRAMs destroys the information, and the data must be put back into memory as part of the read operation.

Because the SRAM cell takes up considerably more area than the DRAM cell, an SRAM memory chip typically has only one-fourth the number of bits as a DRAM memory of the same technology generation. For example, using the same IC technology, it would be possible to fabricate a 256-Mb DRAM and a 64-Mb SRAM. The majority of RAM chips with densities below 4 Mb have provided a single output bit, but because the capacity of recent memory chips has become so large, the external interface to many memory chips is now designed to be four, eight, or more bits wide.

Read-only memories or ROMs, also sometimes called **read-only storage**, or **ROS**, represent another important class of memory. In these memories, data is permanently stored within the physical structure of the array. However, ROM technology can also be used to perform logic using the programmable logic array, or PLA, structure. Digital systems also require high-speed storage in the form of individual flip-flops and registers, and this chapter concludes with a discussion of the basic circuits used to realize RS and D flip-flops.

### 8.1.1 RANDOM ACCESS MEMORY (RAM) ARCHITECTURE

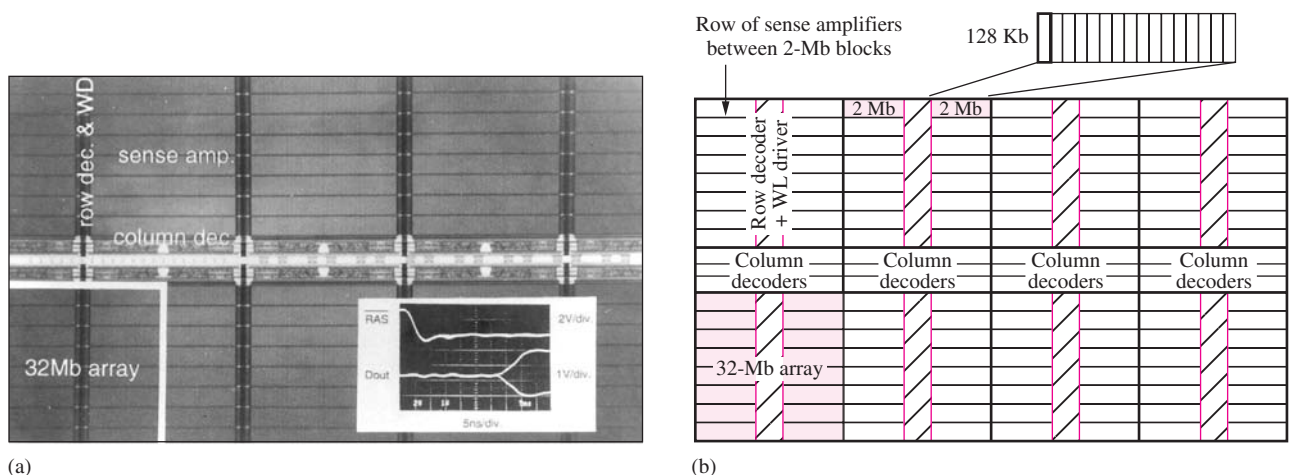
Random-access memory (RAM) provides the high-speed temporary storage used in digital computers, and digital systems have an almost insatiable demand for RAM. Today's high-function image processing and publishing software often require many tens of megabytes of RAM for operation, and the operating systems may require gigabytes. Thus, it is common even for a personal computer to have a gigabyte (GB) (1 byte = 8 bits) or more of RAM. In contrast, high-end computer mainframes contain multigigabytes of RAM.

It is mind-boggling to realize that a single 1-Gb memory chip contains 128 MB of storage and that the chips contain more than 2 billion electronic components that must all be working! Only the very regular repetitive structure of the memory array permits the design and realization of such complex IC chips. This section explores the basic structure of an IC memory; subsequent sections look at individual memory cells and subcircuits in more detail.

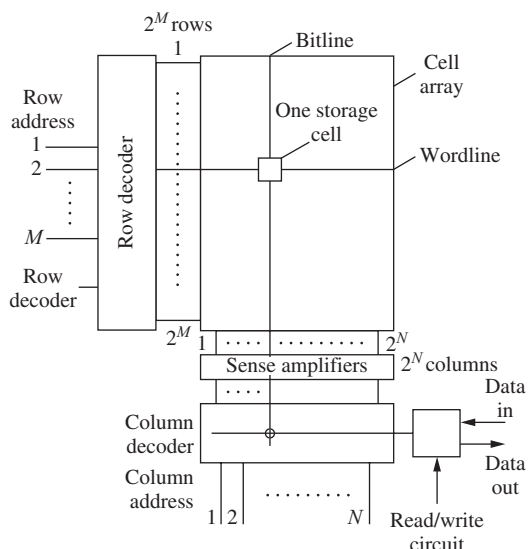
### 8.1.2 A 256-Mb MEMORY CHIP

Figure 8.1(a) is a microphotograph of a 256-Mb memory chip [8] and its block structure. Internally, the 256-Mb array is divided into eight 32-Mb subarrays. To select a group of bits within the large array, the memory address is selected by **column** and **row address decoders**. In Fig. 8.1, the column decoders occupy the center of the die and separate it into upper and lower halves. Row decoders and **wordline drivers** bisect each 32-Mb subarray. Each 32-Mb subarray is further subdivided into 16 2-Mb sections, each of which contains 16 blocks of 128 kilobits (Kb). The 128-Kb array represents the basic building block of this 256-Mb memory.

Figure 8.2 is a block diagram of a basic memory array that could correspond to one of the 128-Kb ( $2^{17}$ -bit) subarrays in Fig. 8.1. The array contains  $2^{M+N}$  storage locations, and the address is split into  $M$  bits of row address plus  $N$  bits of column address. Each  $(M + N)$ -bit address corresponds to a single storage location or memory cell within the array. For the 128-Kb memory segment in Fig. 8.1,



**Figure 8.1** 256-Mb RAM chip: (a) RAM micrograph and measured output waveforms, (b) functional identification of areas of the chip. Micrograph from Mikio Asakura et al., 1994 ISSCC Digest of Technical Papers, February 1994, Vol. 37. Copyright © 1994 IEEE. Reprinted with permission.



**Figure 8.2** Block diagram of a basic memory array.

$M = 10$  and  $N = 7$ . When a given bit is addressed, information can be written into the storage cell or the contents of the cell may be read out. Each 128-Kb array has a set of **sense amplifiers** to read and write the information of the selected memory cells.

When a row is selected, the contents of a 128-bit-wide word ( $2^7$ ) are actually accessed in parallel. These horizontal rows are normally referred to as **wordlines (WL)**. The lines running in the vertical direction contain the cell data and are called **bitlines (BL)**. One or two bitlines may run through each cell, and bitlines can be shared between adjacent cells. The 7-bit column address is used to select the individual bit or group of bits that is actually transferred to the output during a **read operation**, or modified during a **write operation**.

In addition to the storage array, memory chips require several other types of peripheral circuits. Address decoder circuits are required to select the desired row and column. In addition, the wordlines present heavy capacitive loads to the address decoders, and special wordline driver circuits are needed to drive these lines. Also, during a read operation the signal coming from the cell can be quite small, and sense amplifiers are required to detect the state of the memory cell and restore the signal to a full logic level for use in the external interface. The next several sections explore the individual circuits used to implement static and dynamic memory cells as well as sense amplifier and address decoder circuits. Both static and dynamic decoder circuits are discussed.

**EXERCISE:** (a) How many 128-Kb segments form the 256-Mb memory? (b) A 1-Gb memory made by doubling the dimensions of the main arrays in Fig. 8.1 (32 Mb  $\rightarrow$  128 Mb, 2 Mb  $\rightarrow$  8 Mb, 128 Kb  $\rightarrow$  512 Kb). How many 512 Kb segments are required in the 1-Gb memory?

**ANSWERS:** 2048; 2048

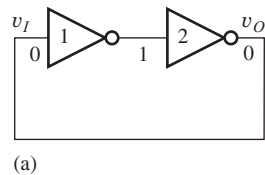
## 8.2 STATIC MEMORY CELLS

The basic electronic storage element consists of two inverters in series, with the output of the second inverter connected back to the input of the first, as shown in Fig. 8.3. If the input of the first inverter is a 0, as in Fig. 8.3(a), then its output will be a 1 and the output of the second inverter will be a 0. In Fig. 8.3(b), an alternate representation of the circuit in Fig. 8.3(a), the input of the first inverter is a 1, its output is a 0, and the output of the second inverter is a 1. For both cases, the output of the second inverter is connected back to the input of the first inverter to form a logically stable configuration. These circuits have two stable states and are termed **bistable circuits**. The pair of **cross-coupled inverters** is also often called a **latch**. The latch is a circuit that we also often use to study the noise margin of logic gates [16, 17].

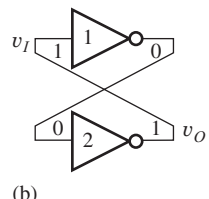
The behavior of the circuit can be understood more completely by looking at the voltage transfer characteristic (VTC) in Fig. 8.4 for two cascaded inverters. A line with unity slope has been drawn on the figure, indicating three possible operating points with  $v_O = v_I$ . The points with  $v_O = V_L$  and  $v_O = V_H$  are the two stable Q-points already noted and represent the two data states of the binary latch.

However, the third point, corresponding to the midpoint of the VTC ( $v_O \cong 1.5$  V), represents an **unstable equilibrium point**. It is unstable in the sense that any disturbance to the voltages in the circuit will cause the latch to quickly make a transition to one of its two stable operating points. For example, suppose the inverter is operating with  $v_I = v_O = 1.5$  V, and then the input increases slightly. The output will immediately move toward  $V_H$  due to the large positive gain of the circuit. A small negative change from the 1.5-V equilibrium point would drive the output immediately to  $V_L$ . Using nonlinear analysis techniques beyond the scope of this text, it can actually be shown that any imbalance in the voltages between the two output nodes of the latch will be reinforced; the node at the higher potential will become a logic 1, and the node at the lower potential will become a logic 0.

The two stable points in the VTC are obviously useful for storing binary data. However, in Sec. 8.4 we will see that the latch can be forced to operate at the unstable equilibrium point and find that this third point is highly useful in designing sense amplifiers.



(a)



(b)

**Figure 8.3** Two inverters forming a static storage element or latch.

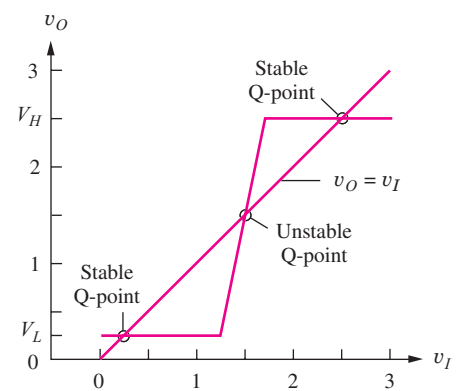


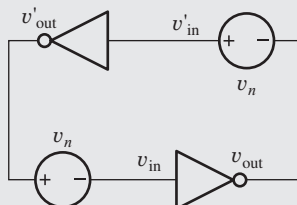
**Figure 8.4** VTC for two inverters in series, indicating the three possible operating points for a latch with  $v_O = v_I$ .



### A Second Look at Noise Margins

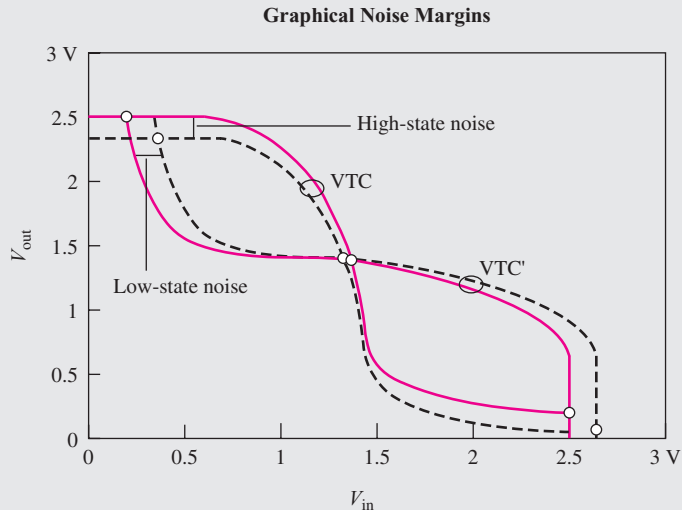
In Chapters 6 and 7, a noise margin analysis based upon finding the points at which the slope of the inverter VTC is equal to  $-1$  was utilized because it is relatively straight forward to apply and understand. The method also gives reasonable values for the noise margins of the gates that were being considered. However, it does not produce reasonable results in certain circumstances.<sup>1</sup> A generally applicable method based upon graphical analysis is outlined below.

Noise margin can be interpreted as the amount of noise ( $v_n$ ) needed to upset the state of a latch formed by a cross-coupled inverter pair as in the accompanying schematic. First, we plot the VTC of the inverter in the normal manner as  $v_{out}$  vs.  $v_{in}$ . In the latch schematic we see that  $v_{out}$  becomes  $v'_{in}$  and  $v_{in}$  comes from  $v'_{out}$ , so the VTC is plotted a second time with the  $v_{out}$  and  $v_{in}$  axes interchanged. The accompanying graphs were plotted with a spreadsheet using data from a SPICE simulation of the VTC for a psuedo NMOS inverter. The points on the graphs where the curves cross correspond to the Q-points in Fig. 8.4. The stable Q-points correspond to  $V_H$  and  $V_L$ . The effect of noise is to collapse the separation between the two curves. (Note that the two noise voltage polarities in the schematic are chosen to degrade the input voltages of both inverters.) It can be seen from the figure that if the two shifts due to high-state and low-state noise are sufficiently large, the two curves will no longer intersect in two stable points, resulting in a logic state upset for the latch. This upset can occur for various combinations of high-state and low-state noise.

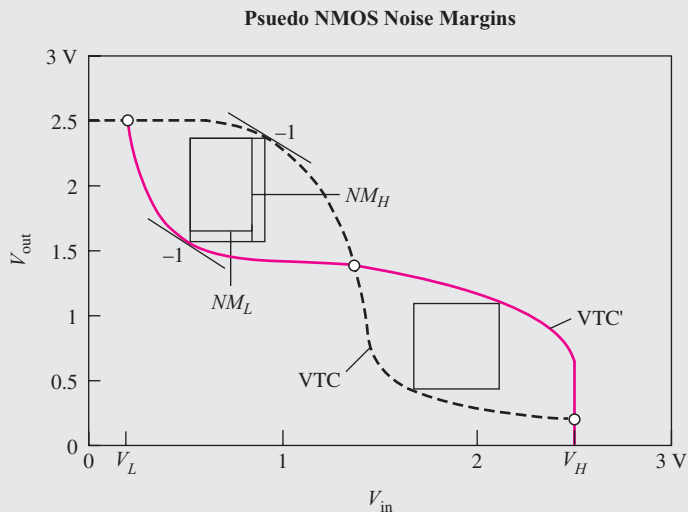


Cross-coupled inverter pair forming a latch including noise sources.

<sup>1</sup>J. R. Hauser, "Noise margin criteria for digital logic circuits," *IEEE Trans. on Education*, vol. 36, no. 4, pp. 363–368, November 1993.



To find the noise margins, we construct a rectangle that is bounded by the two VTC curves as depicted in the second graph. For example, if we want to find the noise margins that are equivalent to those presented earlier in Chapters 6 and 7, then the opposite corners of the rectangle must touch the two VTCs at the points where the slope is  $-1$ . The width of the rectangle represents  $NM_L$  ( $0.42$  V), and the height of the rectangle represents  $NM_H$  ( $0.75$  V); both values are close to the results in Table 6.6. It has been shown<sup>2</sup> that the definition employing the  $-1$  slope condition is equivalent to maximizing the sum of  $NM_H$  and  $NM_L$ .



Graphical plot of the standard VTC and VTC' with interchanged axes.

However, many other definitions of noise margin can be used. If we construct the largest square that is bounded by the two VTC curves, as in right-hand square in the graph, then we have found the largest value of noise margins for which  $NM_L = NM_H$  ( $0.58$  V). Note that values of  $V_{IH}$ ,  $V_{IL}$ ,  $V_{OH}$ , and  $V_{OL}$  are a function of the noise margin definition. Another possible definition of noise margin is obtained by finding the values of  $NM_L$  and  $NM_H$  that maximize the area of the rectangle embedded within the two VTC curves.

<sup>2</sup>J. Lohstroh, "Static and dynamic noise margins of logic circuits," *IEEE Journal of Solid-State Circuits*, vol. SC-14, pp. 591–598, June 1979.

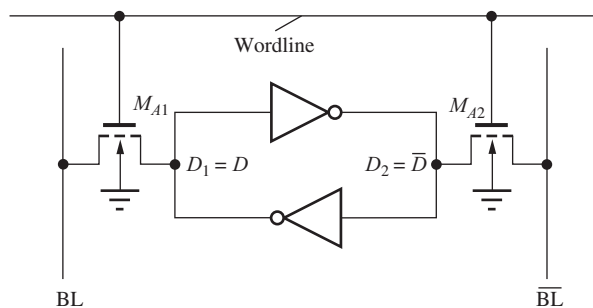


**Figure 8.5** Basic memory cell formed from the two-inverter latch and two access transistors  $M_{A1}$  and  $M_{A2}$ .

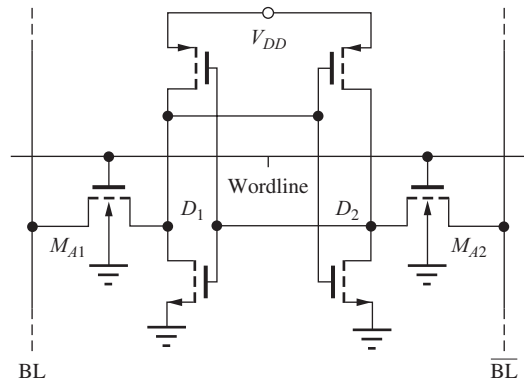


**Figure 8.6** Six-transistor CMOS memory cell.

### 8.2.1 MEMORY CELL ISOLATION AND ACCESS — THE 6-T CELL

The cross-coupled inverter pair is the basic storage element needed in Fig. 8.2 to build a static memory. In Fig. 8.5, two additional transistors are added to the latch to isolate it from other memory cells and to provide a path for information to be written to and read from the memory cell. In NMOS or CMOS technology, each inverter requires two transistors, so the memory circuit in Fig. 8.5 is usually referred to as the **six-transistor (6-T) SRAM cell**. Note that the 6-T cell provides both true and complemented data outputs,  $D$  and  $\bar{D}$ .

Figure 8.6 is a 6-T CMOS cell implementation. The advantage of CMOS inverters is that only very small leakage currents exist in the cell since a static current path does not exist through either inverter. Because of higher mobility and lower on-resistance for a given  $W/L$  ratio, the access devices  $M_{A1}$  and  $M_{A2}$  are shown as NMOS transistors in all the circuits in this chapter. However, PMOS transistors can successfully be used in some designs.

The 6-T cell presents an interesting set of conflicting design requirements. During the read operation, the state of the memory cell must be determined through the access transistors without upsetting the data in the cell. However, during a write operation, the data in the cell must be forced to the desired state using the same access devices. The design of these cells is explored in more detail in the next two subsections. In the following discussion, a 0 in the memory cell will correspond to a low level (0 V) on the left-hand data storage node ( $D_1$ ) and a high level ( $V_{DD}$ ) on the right-hand data node ( $D_2$ ); a 1 in the memory cell will correspond to a high level ( $V_{DD}$ ) at  $D_1$  and a low level (0 V) at  $D_2$ .

**EXERCISES:** (a) How many storage cells are actually in a 256-Mb memory? (b) Suppose a 256-Mb memory is to use the cells in Fig. 8.6, and the total static power consumption of the memory must be  $\leq 50$  mW with a 3.3-V power supply. What is the permissible leakage current in each cell?

**ANSWERS:** 268,435,456; 56.4 pA

**EXERCISE:** Draw a version of the storage cell in Fig. 8.6 with PMOS access transistors.

**ANSWER:** Simply reverse the direction of the substrate arrows in the access devices ( $M_{A1}$  and  $M_{A2}$ ), and connect the substrates to  $V_{DD}$ .

### 8.2.2 THE READ OPERATION

Figure 8.7 is a 6-T CMOS memory cell in the 0 state, in which  $V_{DD}$  has been chosen to be 3 V. Although a number of different strategies can be used to read the state of the cell, we will assume that

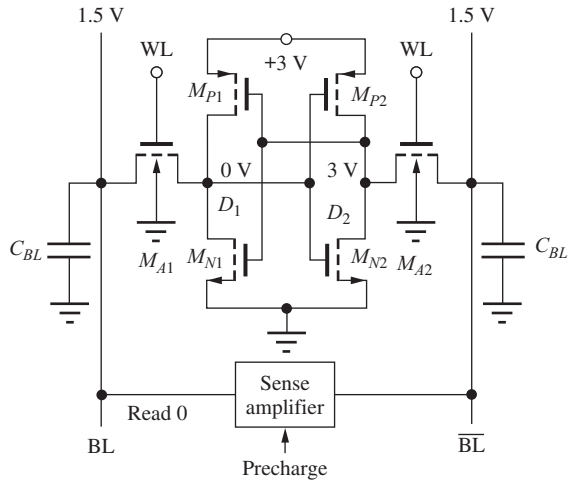


**Figure 8.7** Reading data from a 6-T cell with a 0 stored in the cell.

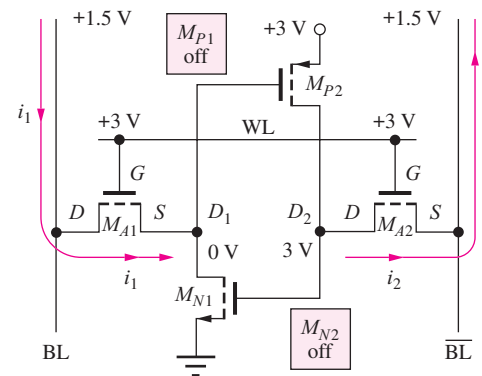


**Figure 8.8** Conditions immediately following activation of the wordline.

both bitlines are initially precharged to approximately one-half  $V_{DD}$  by the sense amplifier circuitry, while  $M_{A1}$  and  $M_{A2}$  are turned off by holding the wordline WL at 0 V. The exact precharge level is determined by the sense amplifiers and is discussed in the next section. Precharge levels equal to  $V_{DD}$ ,  $\frac{1}{2}V_{DD}$ , and  $\frac{2}{3}V_{DD}$  have all been proposed for memory design.

Once the bitline voltages have been precharged to the desired level, cell data can be accessed through transistors  $M_{A1}$  and  $M_{A2}$  by raising the wordline voltage to a high logic level (3 V). The conditions immediately following initiation of such a read operation are shown in Fig. 8.8, in which the substrate terminals of the access transistors have been omitted for clarity.<sup>3</sup>  $M_{P1}$  and  $M_{N2}$  are off.  $M_{A1}$  will be operating in the triode region (for typical values of  $V_{TN}$ ) because  $V_{GS} = 3$  V and  $V_{DS} = 1.5$  V, and current  $i_1$  enters the cell from the bitline into the cell.  $M_{A2}$  is saturated because both  $V_{GS}$  and  $V_{DS}$  are equal to 1.5 V, and the current  $i_2$  exits cell into  $\overline{BL}$ .

As current increases through  $M_{A1}$  and  $M_{A2}$ , the voltage on data node  $D_1$  tends to rise, and the voltage at  $D_2$  tends to fall. For the data stored in the cell not to be disturbed, a conservative design ensures that the voltage at  $D_1$  remains below the threshold voltage of  $M_{N2}$ , and that the voltage at  $D_2$  remains high enough ( $> 3 - |V_{TP}|$ ) to maintain  $M_{P1}$  off. Currents  $i_1$  and  $i_2$  in the two bitlines cause the sense amplifier to rapidly assume the same state as the data stored in the cell, and the BL and  $\overline{BL}$  voltages become 0 V and 3 V, respectively.

The voltages in the circuit after the sense amplifier reaches steady-state are shown in Fig. 8.9. The bitline voltages match the original cell voltages, and the bistable latch in the storage cell has restored the cell voltages to the original full logic levels. In the final steady-state condition, both  $M_{A1}$  and  $M_{A2}$  will be on in the triode region but not conducting current because  $V_{DS} = 0$ .

It is important to note in Fig. 8.8 that the source terminal of  $M_{A1}$  is connected to the cell, whereas the source of  $M_{A2}$  is connected to the bitline. This is an example of the bidirectional nature of the FET. Remember that the source and drain of the FET are always determined by the relative polarities of the voltages in the circuit.

Rather than try to analyze the details of this complex circuit by hand, the waveforms resulting from a SPICE simulation of the 6-T circuit are presented in Fig. 8.10. The simulation assumes a total capacitance on each bitline of 500 fF, and the  $W/L$  ratios of all transistors in the memory cell are 1/1. In Fig. 8.10, the bitlines can be observed to be precharged to slightly less than one-half  $V_{DD}$ ,

<sup>3</sup> Note that the capacitances at nodes  $D_1$  and  $D_2$  prevent the voltages at these nodes from changing at  $t = 0^+$ .

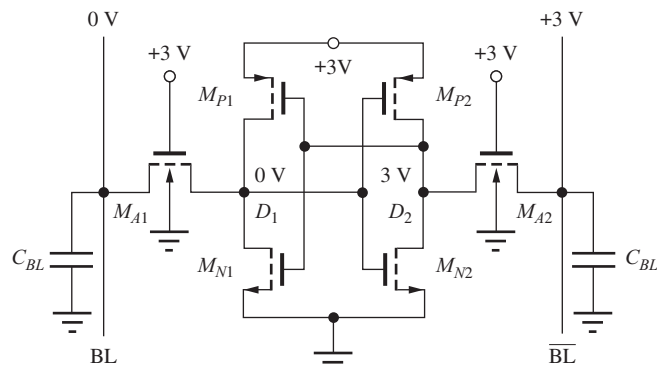


**Figure 8.9** Final state after the sense amplifier has reached steady-state.

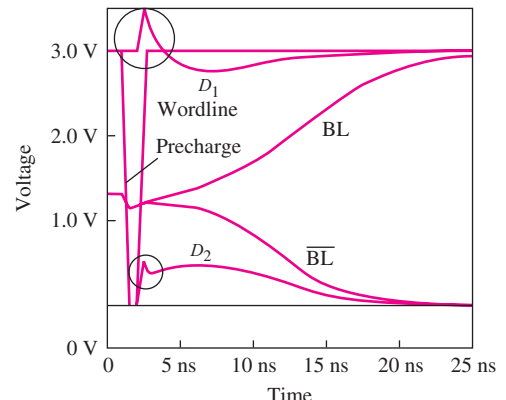


**Figure 8.10** SPICE memory cell waveforms during a read operation.

approximately 1.3 V. At  $t = 1$  ns, the precharge signal is turned off, and at  $t = 2$  ns the wordline begins its transition from 0 V to 3 V. As the two access transistors turn on, BL and  $\overline{BL}$  begin to diverge as the sense amplifier responds and reinforces the data stored in the cell. As the bitlines increase further, the cell voltages at  $D_1$  and  $D_2$  return to the full 3 V and 0 V levels. The state of the memory cell is disturbed, but not destroyed, during the read operation. Thus the 6-T cell provides data storage with nondestructive readout.

Note that the time delay from the midpoint of the wordline transition to the point when the bitlines reach full logic levels is approximately 20 ns. Also, the two rapid positive transients at  $D_1$  and  $D_2$  (in the circles) result from direct coupling of the rapid transition of the wordline signal through the MOSFET gate capacitances to the internal nodes of the latch. This capacitive coupling of the wordline signal causes the initial transients both to be in the same direction.  $D_1$  actually goes above the 3-V supply, and the designer must ensure that the breakdown voltages of the transistors are not exceeded. (A large transient could potentially initiate latchup as discussed in the previous Chapter.)

Reading a 1 stored in the memory cell in Fig. 8.11 simply reverses the conditions in Figs. 8.7 to 8.10. The two cell currents  $i_1$  and  $i_2$  reverse directions, and the sense amplifier flips to the opposite state. Note that the source and drain terminals and direction of current in the two access transistors have all reversed.

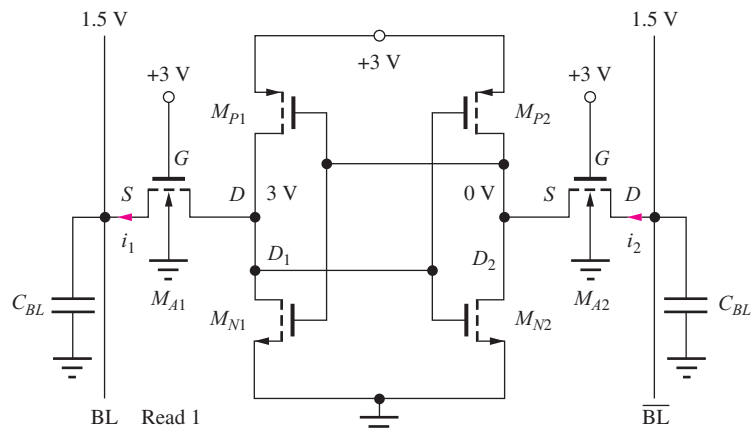


**Figure 8.11** Reading data from 6-T cell with a 1 stored in the cell.

**EXAMPLE 8.1****CURRENTS IN THE 6-T STATIC MEMORY CELL**

This example demonstrates calculation of the currents in the access transistors in the six-transistor memory cell during a read operation.

**PROBLEM** Calculate bitline currents  $i_1$  and  $i_2$  in Fig. 8.8 immediately following activation of the wordline. Assume  $W/L = 1/1$  for all devices and use  $K'_n = 60 \mu\text{A}/\text{V}^2$ ,  $V_{TO} = 0.7 \text{ V}$ ,  $\gamma = 0.5 \text{ V}^{1/2}$ , and  $2\phi_F = 0.6 \text{ V}$ .

**SOLUTION** **Known Information and Given Data:** The circuit is the six-transistor memory cell in Figs. 8.7 and 8.8 with 0 V initially stored at  $D_1$  and 3 V at  $D_2$ . All  $W/L$  values are 1/1;  $K'_n = 60 \mu\text{A}/\text{V}^2$ ,  $V_{TO} = 0.7 \text{ V}$ ,  $\gamma = 0.5 \text{ V}^{1/2}$ , and  $2\phi_F = 0.6 \text{ V}$ .

**Unknowns:** Find currents  $i_1$  and  $i_2$  just after the wordline is activated.

**Approach:** “Activation” of the wordline means the wordline has just stepped from 0 V to 3 V. Current is supplied to the drain of  $M_{A1}$  from the left-hand bitline BL, and, at the right-hand side, current exits the source of  $M_{A2}$  onto  $\overline{\text{BL}}$ . The currents are set by these two transistors. Note that the drain-source voltages of  $M_{N1}$  and  $M_{P2}$  are both zero, so that the drain currents in these two devices must be zero. First we find the terminal voltages for  $M_{A1}$  and  $M_{A2}$  from Fig. 8.8. Then we use the terminal voltages to find the region of operation of each device. Once the region of operation has been identified, the drain currents are found using the equation appropriate for the region of operation.

**Assumptions:** The wordline voltage change is a step function that occurs at  $t = 0$ .

**Analysis:** At  $t = 0^+$ , the wordline has just stepped from 0 V to 3 V, and current goes from left-hand bitline BL into the drain of  $M_{A1}$ . Referring to the conditions in Fig. 8.8, we see that the source of  $M_{A1}$  is at 0 V, the drain is at 1.5 V, and the gate is at 3 V. Since the source is at 0 V,  $V_{TN} = V_{TO}$ ,  $V_{GS} - V_{TN} = (3 - 0) - 0.7 = 2.3 \text{ V}$ , and  $V_{DS} = 1.5 - 0 = 1.5 \text{ V}$ . Thus, the device is in the triode region of operation, and the drain current is given by

$$i_1(0^+) = K'_n \left( \frac{W}{L} \right) \left( V_{GS} - V_{TN} - \frac{V_{DS}}{2} \right) V_{DS} = \left( \frac{60 \mu\text{A}}{\text{V}^2} \right) \left( \frac{1}{1} \right) \left( 3 - 0.7 - \frac{1.5}{2} \right) 1.5 \text{ V}^2 = 140 \mu\text{A}$$

At the right-hand bitline, current exits the source of  $M_{A2}$  onto  $\overline{\text{BL}}$ . Referring again to the conditions in Fig. 8.8, the drain of  $M_{A2}$  is at 3 V, the source is at 1.5 V, and the gate is at 3 V. Since the source of  $M_{A2}$  is not at 0 V, we must find its threshold voltage using Eq. (4.20).

$$V_{TN} = V_{TO} + \gamma (\sqrt{v_{SB} + 2\phi_F} - \sqrt{2\phi_F}) = 0.7 + 0.5(\sqrt{1.5 + 0.6} - \sqrt{0.6}) = 1.04 \text{ V}$$

To find the region of operation, we have  $V_{GS} - V_{TN} = (3 - 1.5) - 1.04 = 0.46 \text{ V}$ , and  $V_{DS} = 3 - 1.5 = 1.5 \text{ V}$ . Thus,  $M_{A2}$  is in the saturation region of operation for which the drain current is given by

$$i_2(0^+) = \frac{K'_n}{2} \left( \frac{W}{L} \right) (V_{GS} - V_{TN})^2 = \left( \frac{60 \mu\text{A}}{2 \text{ V}^2} \right) \left( \frac{1}{1} \right) (1.5 - 1.04)^2 = 6.35 \mu\text{A}$$

We have found the two required currents  $i_1(0^+) = 140 \mu\text{A}$  and  $i_2(0^+) = 6.35 \mu\text{A}$ . Note that the current on the left-hand side is more than 20 times that on the right. Thus, the sense amplifier will have a significant current difference on which to make a decision.

**Check of Results:** We have found the two required currents, and the values appear reasonable (they are both in the  $\mu\text{A}$  to  $\text{mA}$  range).

**Discussion:** Note that the terminals identified as the drain and source of  $M_{A1}$  and  $M_{A2}$  are different in the two devices and are determined by the potentials at the various nodes. If the opposite state were stored in the memory cell, then the source and drain terminal identifications would be reversed. At this point, we should be puzzled about where the currents that we have calculated are actually going. Since the voltage across  $M_{N1}$  and  $M_{P2}$  are zero at  $t = 0^+$ , the drain-source currents are zero in these devices. The initial currents in  $M_{A1}$  and  $M_{A2}$  begin to charge and discharge the capacitances at nodes  $D_1$  and  $D_2$ , respectively. As the voltages change at nodes  $D_1$  and  $D_2$ , transistors  $M_{N1}$  and  $M_{P2}$  begin to conduct current.

**EXERCISE:** Find bitline currents  $i_1$  and  $i_2$  in Fig. 8.8 immediately following activation of the wordline. Assume  $W/L = 1/1$  for all devices, and use  $V_{DD} = 5$  V,  $W/L = 5$  V, the bitline voltages are 2.5 V,  $K'_n = 60 \mu\text{A/V}^2$ ,  $V_{TO} = 1$  V,  $\gamma = 0.6 \text{ V}^{1/2}$ , and  $2\phi_F = 0.6$  V.

**ANSWERS:** 413  $\mu\text{A}$ ; 24.7  $\mu\text{A}$  ( $V_{TN} = 1.592$  V)

### 8.2.3 WRITING DATA INTO THE 6-T CELL

For a write operation, the bitlines are initialized with the data that is to be written into the cell. In Fig. 8.12, a zero is being written into a cell that already contains a zero. It can be seen that the access transistors both have  $V_{DS} = 0$ . The currents  $i_1$  and  $i_2$  are zero, and virtually nothing happens, except for the transients that occur due to internode coupling of the wordline signal through the MOS transistor capacitances (see Prob. 8.8).

The more interesting case is shown in Fig. 8.13, in which the state of the cell must be changed. When the wordline is raised to 3 V, access transistor  $M_{A1}$  conducts current in the saturation region, with  $V_{GS} = 3$  V and  $V_{DS} = 3$  V, and the voltage at  $D_1$  tends to discharge toward 0 through  $M_{A1}$ . Access transistor  $M_{A2}$  is also in saturation, with  $V_{GS} = 3$  V and  $V_{DS} = 3$  V, and the voltage at  $D_2$  initially tends to charge toward a voltage of  $(3 - V_{TN})$  V. As soon as the voltage at  $D_2$  exceeds that at  $D_1$ , positive feedback takes over, and the cell rapidly completes the transition to the new desired state, with  $D_1 = 0$  V and  $D_2 = 3$  V.

Figure 8.14 shows waveforms from a SPICE simulation of this write operation. As the wordline transition begins at  $t = 0.5$  ns, the fixed levels on the bitlines are transferred to nodes  $D_1$  and  $D_2$  through the two access transistors. Minimum area transistors are normally used throughout the

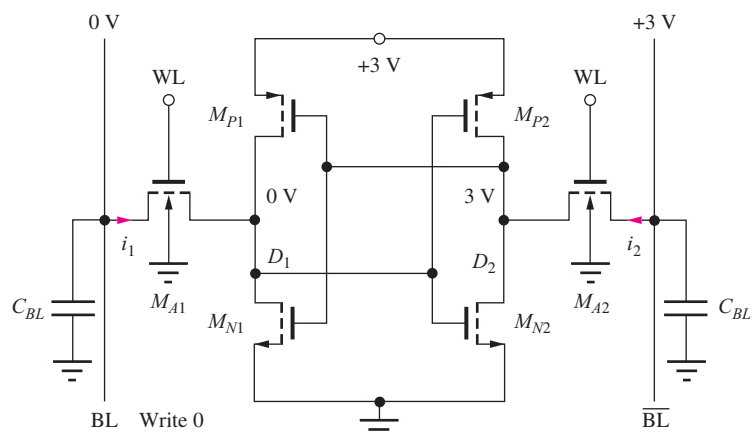
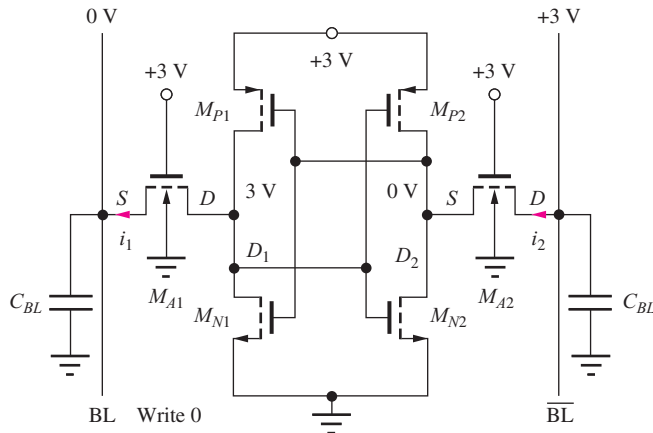
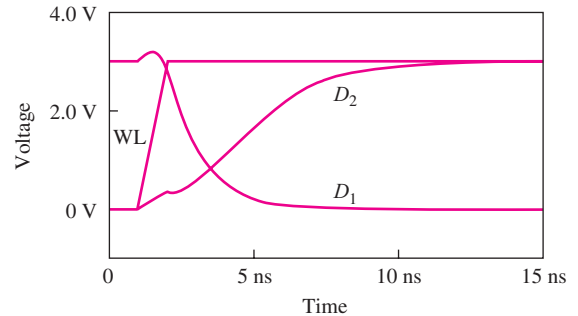


Figure 8.12 A memory cell set up for a write 0 operation with a 0 already stored in the cell.



**Figure 8.13** A memory cell set up for a write 0 operation with a 1 previously stored in the cell.



**Figure 8.14** SPICE bitline and data node waveforms as a 0 is written into the 6-T cell in Fig. 8.13.

memory cell array, and the capacitances on the memory cell nodes are quite small. This small nodal capacitance is the reason why the voltages at  $D_1$  and  $D_2$  reach the desired state in approximately 10 ns in this simulation.

In the simulation results in Fig. 8.14, the bitlines were connected to ideal voltage sources. However, in a real memory implementation, the two bitlines will be driven by logic buffers, and the current driving capability of the buffer must exceed that of the inverters in the RAM cell in order for data to be written into the cell. The buffer must “overpower” the state of the memory cell.

## EXAMPLE 8.2 INITIAL MEMORY CELL CURRENTS DURING A WRITE OPERATION

This example calculates of the currents in a 6-T memory cell when the state of the cell is being changed.

**PROBLEM** Find bitline currents  $i_1$  and  $i_2$  in Fig. 8.13 immediately following activation of the wordline. Assume  $W/L = 1/1$  for all devices and use  $K'_n = 60 \mu\text{A}/\text{V}^2$ ,  $V_{TO} = 0.7 \text{ V}$ ,  $\gamma = 0.5 \text{ V}^{1/2}$ , and  $2\phi_F = 0.6 \text{ V}$ .

**SOLUTION** **Known Information and Given Data:** The circuit is the six-transistor memory cell in Fig. 8.13 with 3 V stored at  $D_1$  and 0 V at  $D_2$ . The state of the cell is to be changed, so the left-hand bitline is set to 0 V and the right-hand bitline is set to 3 V prior to activation of the wordline. All  $W/L$  values are 1/1;  $K'_n = 60 \mu\text{A}/\text{V}^2$ ,  $V_{TO} = 0.7 \text{ V}$ ,  $\gamma = 0.5 \text{ V}^{1/2}$ , and  $2\phi_F = 0.6 \text{ V}$ . “Activation” of the wordline means that it changes from 0 V to +3 V.

**Unknowns:** Find currents  $i_1$  and  $i_2$  just after the wordline is activated.

**Approach:** At  $t = 0^+$ , the wordline has just completed a step from 0 V to 3 V, and current will exit the cell through  $M_{A1}$  and enter the cell through  $M_{A2}$ . At  $t = 0^+$ , the drain currents in  $M_{N1}$ ,  $M_{N2}$ ,  $M_{P1}$ , and  $M_{P2}$  are all zero since either the gate-source voltage is zero or the drain-source voltage is zero for all four of these devices. The initial cell currents are set by transistors  $M_{A1}$  and  $M_{A2}$ . First we find the terminal voltages for  $M_{A1}$  and  $M_{A2}$  from Fig. 8.13, and then we use the terminal voltages to find the region of operation of each device. Once the region of operation has been identified, we calculate the drain currents using the equation appropriate for the region of operation.

**Assumptions:** The wordline voltage change is a step function that occurs at  $t = 0$ .

**Analysis:** At  $t = 0^+$ , the wordline has just stepped from 0 V to 3 V. In Fig. 8.13, we see that the drain terminals of  $M_{A1}$  and  $M_{A2}$  are both at 3 V, the source terminals are both at 0 V and the gate terminals are both at 3 V. The bias conditions for both transistors are identical. Since the source terminal of each transistor is at 0 V,  $V_{TN} = V_{TO}$ , and we have  $V_{GS} - V_{TN} = (3 - 0) - 0.7 = 2.3$  V and  $V_{DS} = 3 - 0 = 3$  V. Thus, the devices are in saturation, and the drain currents are given by

$$i_1(0^+) = i_2(0^+) = \frac{K'_n}{2} \left( \frac{W}{L} \right) (V_{GS} - V_{TN})^2 = \left( \frac{60 \mu\text{A}}{2 \text{V}^2} \right) \left( \frac{1}{1} \right) (3 - 0.7)^2 = 158 \mu\text{A}$$

**Check of Results:** We have found the two unknown currents, and the values appear reasonable (they are both in the  $\mu\text{A}$  to mA range).

**Discussion:** Note once again that the terminals identified as the drain and source of  $M_{A1}$  and  $M_{A2}$  are different in the two devices and are determined solely by the potentials at the various nodes. Again, we may be puzzled about where the currents that we have calculated are actually going. The initial currents in  $M_{A1}$  and  $M_{A2}$  begin to discharge and charge the capacitances at nodes  $D_1$  and  $D_2$ , respectively, to begin the process of changing the information stored in the cell.

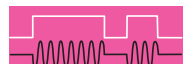
**EXERCISE:** Find bitline currents  $i_1$  and  $i_2$  in Fig. 8.13 immediately following activation of the wordline. Assume  $W/L = 1/1$  for all devices, and use  $V_{DD} = 5$  V,  $W/L = 5$  V, bitline voltages = 2.5 V,  $K'_n = 60 \mu\text{A/V}^2$ ,  $V_{TO} = 1$  V,  $\gamma = 0.6 \text{ V}^{1/2}$ , and  $2\phi_F = 0.6$  V.

**ANSWERS:** 480  $\mu\text{A}$ ; 480  $\mu\text{A}$

### 8.3 DYNAMIC MEMORY CELLS

As long as power is applied to static memory cells, the information stored in the cells should be retained. In addition, static cells feature nondestructive readout of data from the cell. Although voltage levels in the cell are disturbed during the read operation, the cross-coupled latch automatically restores the levels once the access transistors are turned off.

However, much smaller memory cells can be built if the requirement for static data storage is relaxed. These memory cells are referred to as dynamic memory, and the most important dynamic random-access memory cell is the one-transistor cell. The operation of the 1-T cell is explored in the next several subsections.

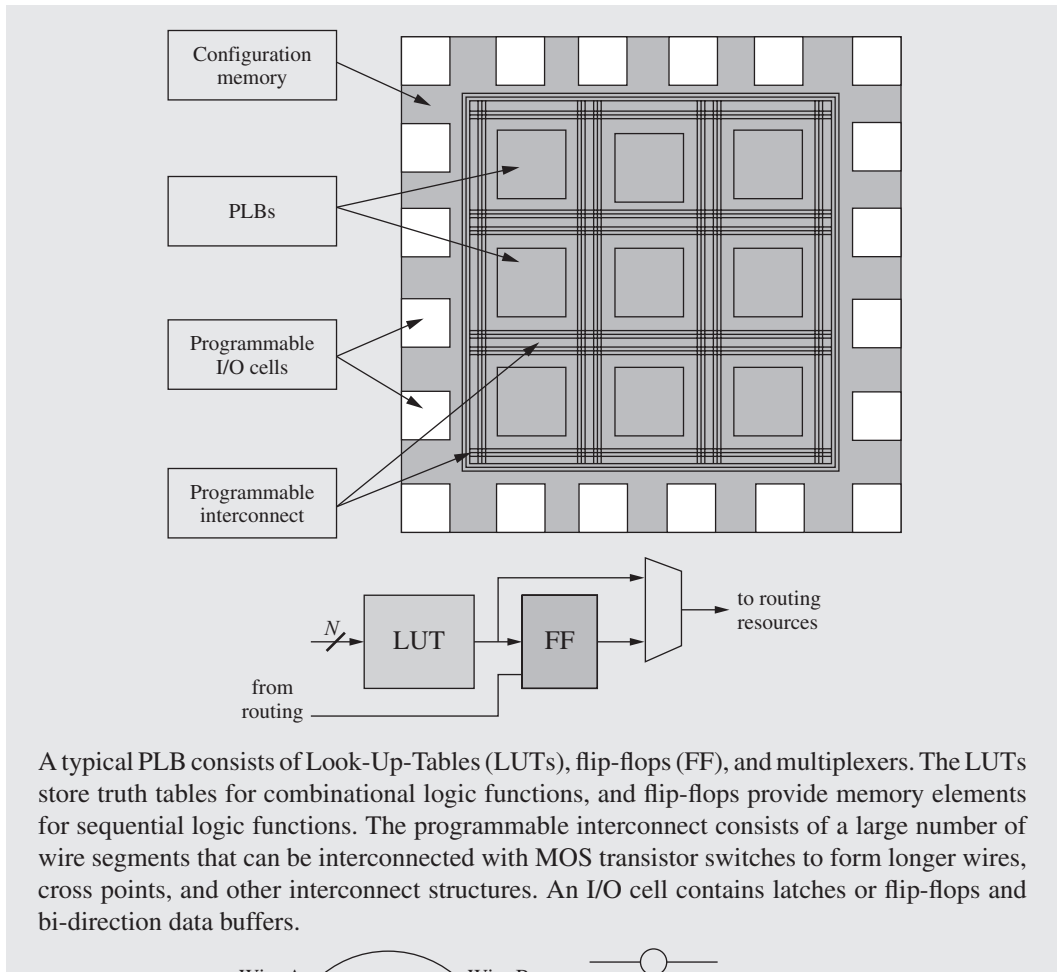


#### ELECTRONICS IN ACTION

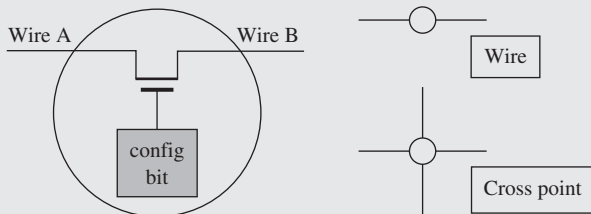


##### Field Programmable Gate Arrays (FPGAs)

Field programmable gate arrays (FPGAs) are widely used in electronic prototype development as well as in many completed products in which the volume and/or time schedule cannot justify the cost of custom integrated circuit development. FPGAs consist of a two-dimensional array of programmable logic blocks (PLBs), programmable input/output cells, and programmable interconnects that are controlled by the contents of a configuration memory that defines the logic functions of the PLBs, the I/O cells, and the interconnections between the PLBs and I/O cells. The configuration memory is loaded with the bit patterns required to define and connect the desired functions. Changing the configuration memory data changes the system function and, in some FPGAs, can even be done while the FPGA is operating without destroying the contents of RAMs and other memory elements on the chip.



A typical PLB consists of Look-Up-Tables (LUTs), flip-flops (FF), and multiplexers. The LUTs store truth tables for combinational logic functions, and flip-flops provide memory elements for sequential logic functions. The programmable interconnect consists of a large number of wire segments that can be interconnected with MOS transistor switches to form longer wires, cross points, and other interconnect structures. An I/O cell contains latches or flip-flops and bi-direction data buffers.



FPGAs have grown from relatively simple devices to extremely complex system chips as the density of integrated circuit technology has increased. Some chips contain general purpose microprocessor and DSP cores.

### Current FPGA Characteristics

- 10 M—1 B transistors
- 32 Kb to 82 Mb of configuration memory
- 100—26,000 PLBs per FPGA
- 50—400 wire segments/PLB
- 80—3300 switches/PLB
- 50—1200 I/O cells per FPGA

Drawings and data courtesy of Professor Charles E. Stroud, ECE Department, Auburn University.

### 8.3.1 THE ONE-TRANSISTOR CELL

In the 1-T cell in Fig. 8.15, data is stored as the presence or absence of charge on **cell capacitor**  $C_C$ . Because leakage currents exist in the drain-bulk and source-bulk junctions of the transistor and in the transistor channel, the information stored on  $C_C$  is eventually corrupted. To prevent this loss of information, the state of the cell is periodically read and then written back into the cell to reestablish the desired cell voltages. This operation is referred to as the **refresh operation**. Each storage cell in a DRAM typically must be refreshed every 2 to 10 ms.

### 8.3.2 DATA STORAGE IN THE 1-T CELL

In the analysis that follows, a 0 will be represented by 0 V on capacitor  $C_C$ , and a 1 will be represented by a high level on  $C_C$ . These data are written into the 1-T cell by placing the desired voltage level on the single bitline and turning on access transistor  $M_A$ .

#### Storing a 0

Consider first the situation for storing a 0 in the cell, as in Fig. 8.16. In this case, the bitline is held at 0 V, and the bitline terminal of the MOSFET acts as the source of the FET. The gate is raised to  $V_{DD} = 3$  V. If the cell voltage is already zero, then the drain-source voltage of the MOSFET is zero, and the current is zero. If the cell contains a 1 with  $v_C > 0$ , then the MOSFET completely discharges  $C_C$ , also yielding  $v_C = 0$ .

The cell voltage waveform resulting from writing a zero into a cell containing a one is given in Fig. 8.17(b). The initial capacitor voltage, calculated in the next section, is rapidly discharged by the access transistor.

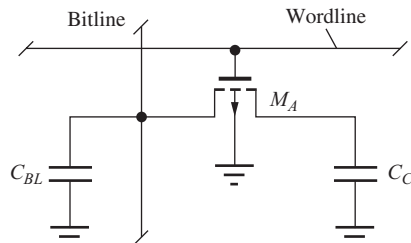


**Figure 8.15** One-transistor (1-T) storage cell in which binary data is represented by the presence or absence of charge on  $C_C$ .

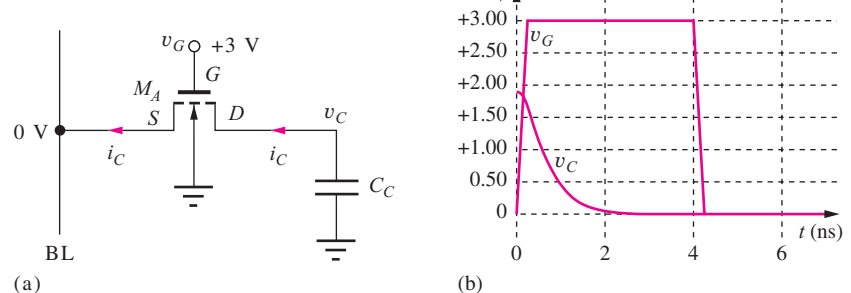


**Figure 8.16** (a) Writing a 0 into the 1-T cell. (b) Waveform during WRITE operation.

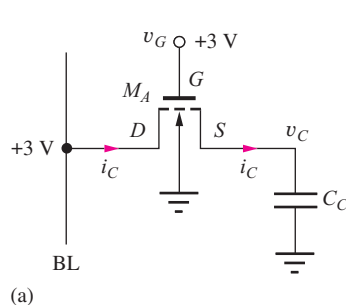


**Figure 8.17** (a) Conditions for writing a 1 into the 1-T cell. (b) Waveform during WRITE operation.

**EXERCISE:** (a) What is the cell current  $i_C$  in Fig. 8.16 just after access transistor  $M_A$  is turned on if  $V_C = 1.9$  V,  $K_n = 60 \mu\text{A/V}^2$ , and  $V_{TO} = 0.7$  V? (b) Estimate the fall time of the voltage on the capacitor using Eqs. (7.15) and (7.20), with  $C_C = 50$  fF.

**ANSWERS:** 154  $\mu\text{A}$ ; 1.30 ns

### Storing a 1

Now consider the case of writing a 1 into the 1-T cell in Fig. 8.17. The bitline is first set to  $V_{DD}$  (3 V), and the wordline is then raised to  $V_{DD}$ . The bitline terminal of  $M_A$  acts as its drain, and the cell capacitance terminal acts as the FET source. Because  $V_{DS} = V_{GS}$ , and  $M_A$  is an enhancement mode device,  $M_A$  will operate in the saturation region. If a full 1 level already exists in the cell, then the current is zero in  $M_A$ . However, if  $V_C$  is less than a full 1 level, current through  $M_A$  will charge up the capacitor to a potential one threshold voltage below the gate voltage.

We see from this analysis that the voltage levels corresponding to 0 and 1 in the 1-T cell are 0 V and  $V_G - V_{TN}$ . The threshold voltage must be evaluated for a source-bulk voltage equal to  $V_C$ :

$$V_C = V_G - V_{TN} = V_G - [V_{TO} + \gamma(\sqrt{V_C + 2\phi_F} - \sqrt{2\phi_F})] \quad (8.1)$$

Note that Eq. (8.1) is identical to Eq. (6.26) used to determine  $V_H$  for the saturated load NMOS logic circuit.

Once again we see the important use of the bidirectional characteristics of the MOSFET. Charge must be able to flow in both directions through the transistor in order to write the desired data into the cell. To read the data, current must also be able to change directions.

The waveform for writing a one into the 1-T cell appears in Fig. 8.17(b). Note the relatively long time required to reach final value. This is exactly the same situation as the long transient tail observed on the low-to-high transition in NMOS saturated load logic. However, access transistor  $M_A$  can be turned off at the 10-ns point without significant loss in cell voltage.

**EXERCISE:** Find the cell voltage  $V_C$  if  $V_{DD} = 3$  V,  $V_{TO} = 0.7$  V,  $\gamma = 0.5 \sqrt{\text{V}}$ , and  $2\phi_F = 0.6$  V. What is  $V_C$  if  $\gamma = 0$ ?

**ANSWERS:** 1.89 V; 2.3 V

**EXERCISE:** If a cell is in a 1 state, how many electrons are stored on the cell capacitor if  $C_C = 25$  fF?

**ANSWER:**  $2.95 \times 10^5$  electrons

The results in the preceding exercises are typical of the situation for the 1 level in the cell. A significant part of the power supply voltage is lost because of the threshold voltage of the MOSFET, and the body effect has an important role in further reducing the cell voltage for the 1 state. If there were no body effect in the first exercise, then  $V_C$  would increase to 2.3 V.

### 8.3.3 READING DATA FROM THE 1-T CELL

To read the information from the 1-T cell, the bitline is first precharged (**bitline precharge**) to a known voltage, typically  $V_{DD}$  or one-half  $V_{DD}$ . The access transistor is then turned on, and the cell capacitance is connected to the bitline through  $M_A$ . A phenomenon called **charge sharing** occurs. The total charge, originally stored separately on the **bitline capacitance**  $C_{BL}$  and cell capacitance  $C_C$ , is shared between the two capacitors following the switch closure, and the voltage on the bitline changes slightly. The magnitude and sign of the change are related to the stored information.

Detailed behavior of data readout can be understood using the circuit model in Fig. 8.18. Before access transistor  $M_A$  is turned on, the switch is open, and the total initial charge  $Q_I$  on the two

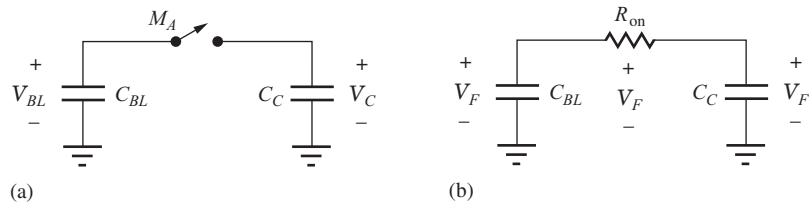


**Figure 8.18** Model for charge sharing between the 1-T storage cell capacitance and the bitline capacitance: (a) circuit model before activation of access transistor, (b) circuit following closure of access switch.

capacitors is

$$Q_I = C_{BL}V_{BL} + C_CV_C \quad (8.2)$$

After access transistor  $M_A$  is activated, corresponding to closing the switch, current through the on-resistance of  $M_A$  equalizes the voltage on the two capacitors. The final value of the stored charge  $Q_F$  is given by

$$Q_F = (C_{BL} + C_C)V_F \quad (8.3)$$

Because no mechanism for charge loss exists,  $Q_F$  must equal  $Q_I$ . Equating Eqs. (8.2) and (8.3) and solving for  $V_F$  yields

$$V_F = \frac{C_{BL}V_{BL} + C_CV_C}{C_{BL} + C_C} \quad (8.4)$$

The signal to be detected is the change in the voltage on the bitline from its initial precharged value:

$$\Delta V = V_F - V_{BL} = \frac{C_C}{C_{BL} + C_C}(V_C - V_{BL}) = \frac{(V_C - V_{BL})}{\frac{C_{BL}}{C_C} + 1} \quad (8.5)$$

Equation (8.5) can be used to guide our selection of the precharge voltage. If  $V_{BL}$  is set midway between the 1 and 0 levels, then  $\Delta V$  will be positive if a 1 is stored in the cell and negative if a 0 is stored. Study of Eq. (8.5) also shows that the signal voltage  $\Delta V$  can be quite small. Equal and opposite voltages are exactly what we desire for driving sense amplifiers with differential inputs. If there are 128 rows in our memory array, then there will be 128 access transistors connected to the bitline, and the ratio of bitline capacitance to cell capacitance can be quite large. If we assume that  $C_{BL} \gg C_C$ , Eq. (8.4) shows that the final voltage on the bitline and cell is

$$V_F = \frac{C_{BL}V_{BL} + C_CV_C}{C_{BL} + C_C} \cong V_{BL} \quad (8.6)$$

Thus, the content of the cell is destroyed during the process of reading the data from the cell—the 1-T cell is a cell with destructive readout. To restore the original contents following a read operation, the data must be written back into the cell.

Except for the case of an ideal switch, charge transfer cannot occur instantaneously. If the on-resistance were constant, the voltages and currents in the circuit in Fig. 8.18 would change exponentially with a time constant  $\tau$  determined by  $R_{on}$  and the series combination of  $C_{BL}$  and  $C_C$ :

$$\tau = R_{on} \frac{C_C C_{BL}}{C_C + C_{BL}} \cong R_{on} C_C \quad \text{for } C_{BL} \gg C_C \quad (8.7)$$

**EXERCISE:** (a) Find the change in bitline voltage for a memory array in which  $C_{BL} = 49 C_C$  if the bitline is precharged midway between the voltages corresponding to a 1 and a 0. Assume that 0 V corresponds to a 0 and 1.9 V corresponds to a 1. (b) What is  $\tau$  if  $R_{on} = 5 \text{ k}\Omega$  and  $C_C = 25 \text{ fF}$

**ANSWERS:** +19.0 mV, -19.0 mV; 0.125 ns

The preceding exercise reinforces the fact that the voltage change that must be detected by the sense amplifier for a 1-T cell is quite small. Designing a sense amplifier to rapidly detect this small change is one of the major challenges of DRAM design. Also, note that the **charge transfer** occurs rapidly.

### 8.3.4 THE FOUR-TRANSISTOR CELL

We saw earlier that the 6-T static cell provides a large signal current to drive the sense amplifiers. This is one reason why static memory designs generally provide shorter access times than dynamic memories. The **four-transistor (4-T) cell** in Fig. 8.19 is a compromise between the 6-T and 1-T cells. The load devices of the 6-T cell are eliminated, and the information is stored on the capacitances at the interior nodes. The cross-coupled transistors provide high current for sensing, as well as both true and complemented outputs. If BL,  $\overline{BL}$ , and the wordline are all forced high, the two access transistors temporarily act as load devices for the 4-T cell, and the cell levels are automatically refreshed.

The conditions for writing information into the 4-T cell using a 3-V power supply are shown in Fig. 8.20. Following wordline activation, node  $D$  charges up to  $3 - V_{TN} = 1.9$  V through access transistor  $M_{A1}$ , and node  $\overline{D}$  discharges to 0 V through  $M_{A2}$  and  $M_{N2}$ . The regenerative nature of the two cross-coupled transistors enhances the speed of the write operation.

Figure 8.21 shows conditions during a read operation, in which the bitline capacitances have been precharged to 1.5 V. The voltages stored in the cell initially force  $M_{N1}$  to be off and  $M_{N2}$  on. When the wordline is raised to 3 V, charge sharing occurs on BL, and the  $D$  node drops to approximately 1.5 V. However, the voltage on BL rapidly divides between  $M_{A2}$  and  $M_{N2}$ . In a conservative design, the  $W/L$  ratios of  $M_{N2}$  and  $M_{A2}$  keep the voltage at  $\overline{D}$  from exceeding the threshold voltage of  $M_{N1}$ .

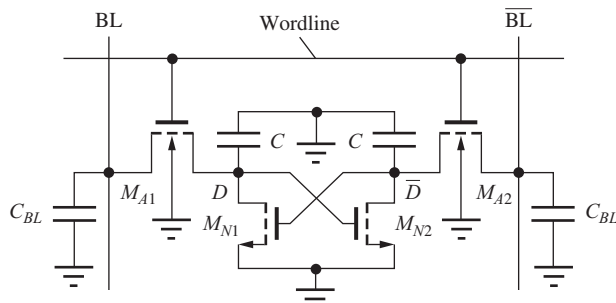


**Figure 8.19** Four-transistor (4-T) dynamic memory cell.

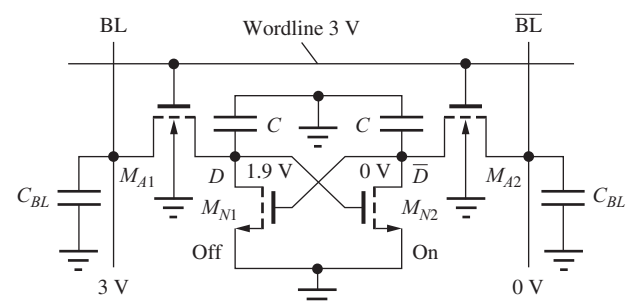


**Figure 8.20** Writing data into the 4-T memory cell.

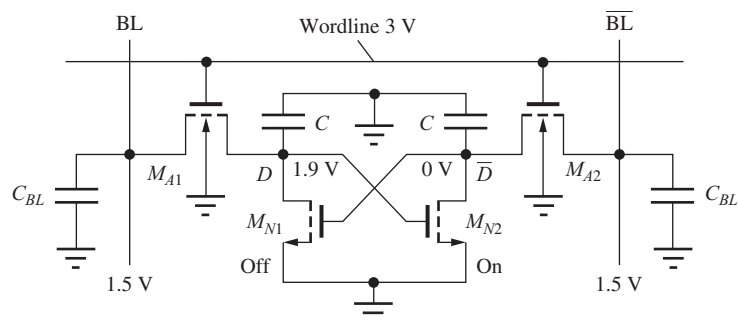


**Figure 8.21** Reading data from the 4-T cell.

to ensure that  $M_{N1}$  remains off. As the sense amplifier responds and drives the bitlines to 0 and 3 V, the 1 level within the cell is also restored to its original value through the access transistors. When the wordline drops, the cross-coupled transistors fully discharge the 0 node to 0 V.

**EXERCISE:** What is the drain current of  $M_{A2}$  in Fig. 8.21 just after the wordline is raised to 3 V if all the devices have  $W/L = 2/1$ ? Use  $K'_n = 60 \mu\text{A}/\text{V}^2$ ,  $V_{TO} = 0.7 \text{ V}$ ,  $\gamma = 0.5 \sqrt{\text{V}}$ , and  $2\phi_F = 0.6 \text{ V}$ .

**ANSWER:** 280  $\mu\text{A}$

## 8.4 SENSE AMPLIFIERS

The sense amplifiers for the cells discussed in the previous sections must detect the small currents that run through the access transistors of the cell, or the small voltage difference that arises from charge sharing, and then must rapidly amplify the signal up to full on-chip logic levels. One sense amplifier is associated with each bitline or bitline pair. The regenerative properties of the latch circuit are used to achieve high-speed sensing.

### 8.4.1 A SENSE AMPLIFIER FOR THE 6-T CELL

A basic sense amplifier that can be used with the 6-T cell consists of a two-inverter latch plus an additional **precharge transistor**, as shown in Fig. 8.22. Transistor  $M_{PC}$  is used to force the latch to operate at the unstable equilibrium point, originally noted in Fig. 8.4 with equal voltages at BL and  $\overline{\text{BL}}$ . When the precharge device is on, it operates in the triode region and represents a low-resistance connection between the two bitlines. As long as transistor  $M_{PC}$  is on, the two nodes of the sense amplifier are forced to remain at equal voltages.

Figure 8.23 shows waveforms from a SPICE simulation of the precharge operation. The voltages on BL and  $\overline{\text{BL}}$  begin at 0 V and 3 V. These levels are arbitrary, but they result from a preceding

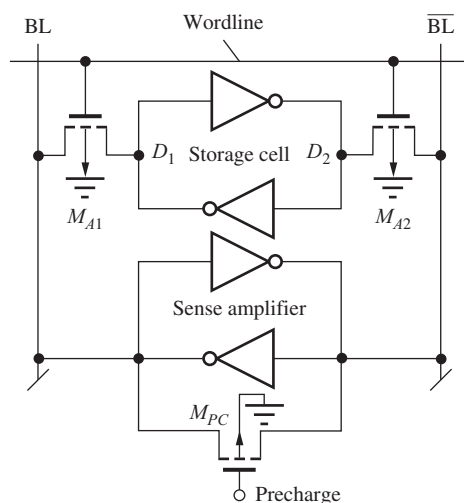


**Figure 8.22** Memory array that includes a sense amplifier.

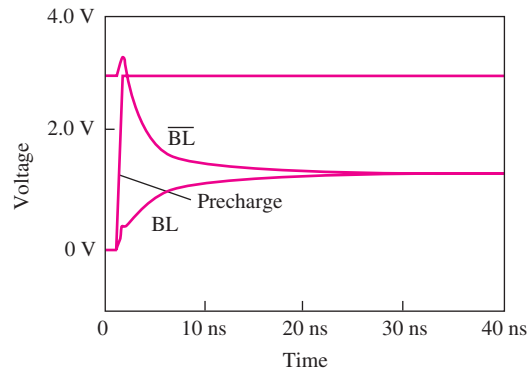


**Figure 8.23** Results of SPICE simulation of the bitline voltage waveforms during the precharge operation.

read or write operation. At  $t = 1$  ns, the precharge signal turns on, forcing the two bitlines toward the same potential. The time required for the latch to reach the  $v_O = v_I$  state in the simulation, approximately 30 ns, is limited by the  $W/L$  ratio of the precharge device, the capacitance of the bitlines, and the current drive capability of the inverters in the latch. In the simulation in Fig. 8.23, the precharge transistor is a 50/1 device,  $C_{BL} = 500$  fF, and all devices in the sense amplifier have  $W/L = 50/1$ . One problem with this simple sense amplifier is its relatively slow precharge of the bitlines. Precharge must remain active until the bitline voltages are equal, or sensing errors may occur.

Once equilibrium is reached, the precharge transistor can be turned off, and the precharge level will be maintained temporarily on the bitline capacitances. The wordline can then be activated to read the cell, as demonstrated previously in Fig. 8.10.

### EXAMPLE 8.3 CURRENT AND POWER IN THE PRECHARGED SENSE AMPLIFIER

This example evaluates the currents in a sense amplifier during the precharge phase, when significant power can be consumed.

**PROBLEM** Find the currents in the transistors in the latch in Fig. 8.22 when the precharge transistor is turned on and the circuit has reached a steady-state condition. Use  $V_{DD} = 3$  V and assume  $W/L = 2/1$  for all devices; for the NMOS transistors,  $K'_n = 60 \mu\text{A}/\text{V}^2$ ,  $V_{TO} = 0.7$  V,  $\gamma = 0.5 \text{ V}^{1/2}$ , and  $2\phi_F = 0.6$  V; for the PMOS devices,  $K'_p = 25 \mu\text{A}/\text{V}^2$ ,  $V_{TO} = -0.7$  V,  $\gamma = 0.75 \text{ V}^{1/2}$ , and  $2\phi_F = 0.6$  V.

**SOLUTION** **Known Information and Given Data:** The sense amplifier utilizes a two-inverter latch with a precharge transistor, as in Fig. 8.22, with  $V_{DD} = 3$  V. All  $W/L$  values are 2/1; for the NMOS transistors,  $K'_n = 60 \mu\text{A}/\text{V}^2$ ,  $V_{TO} = 0.7$  V,  $\gamma = 0.5 \text{ V}^{1/2}$ , and  $2\phi_F = 0.6$  V; for the PMOS devices,  $K'_p = 25 \mu\text{A}/\text{V}^2$ ,  $V_{TO} = -0.7$  V,  $\gamma = 0.75 \text{ V}^{1/2}$ , and  $2\phi_F = 0.6$  V.

**Unknowns:** Find the drain currents in the transistors and the power dissipated by the sense amplifier.

**Approach:** The four-transistor latch is forced to the unstable equilibrium point by the precharge transistor  $M_{PC}$ . Because of the circuit symmetry, the two output voltages will be the same and the current through  $M_{PC}$  will be zero when the steady-state condition is reached. The output voltages are found by equating the drain currents of the two transistors. We must identify the region of operation of the devices and can then calculate the drain currents using the equation appropriate for the region of operation. Once the output voltages are determined, they will be used to find the drain currents.

**Assumptions:** Each inverter forming the latch is composed of the two-transistor CMOS inverter in Fig. 7.2(a).

**Analysis:** Since the output voltages will be the same on both sides of the latch,  $V_{GS} = V_{DS}$  for the NMOS devices, and  $V_{SG} = V_{SD}$  for the PMOS devices. Hence, we immediately know that all the transistors are saturated! We also note that all the source-body voltages are zero, allowing us to disregard the body effect in the calculation. Since the drain current of  $M_{PC}$  is zero due to its zero drain-source voltage, the drain currents of the PMOS and NMOS transistors must be identical on both sides of the latch. The source gate voltage of the NMOS device is  $V_O$  and that of the PMOS device is  $3 \text{ V} - V_O$ . Equating the two drain currents yields a single quadratic equation

that can be solved for  $V_O$ :

$$\frac{K'_p}{2} \left( \frac{W}{L} \right) (V_{SG} + V_{TP})^2 = \frac{K'_n}{2} \left( \frac{W}{L} \right) (V_{GS} - V_{TN})^2$$

$$\frac{1}{2} \left( \frac{25 \mu\text{A}}{\text{V}^2} \right) \left( \frac{2}{1} \right) (3 - V_O - 0.7)^2 = \frac{1}{2} \left( \frac{60 \mu\text{A}}{\text{V}^2} \right) \left( \frac{2}{1} \right) (V_O - 0.7)^2$$

$$35V_O^2 + 31V_O - 102.9 = 0 \rightarrow V_O = 1.33 \text{ V}$$

The NMOS drain current is then

$$i_D = \frac{1}{2} \left( \frac{60 \mu\text{A}}{\text{V}^2} \right) \left( \frac{2}{1} \right) (1.33 - 0.7)^2 = 23.6 \mu\text{A}$$

The currents on both sides of the cell are equal, so the power dissipation is

$$P = 2i_D V_{DD} = 2(23.5 \mu\text{A})(3 \text{ V}) = 0.140 \text{ mW}$$

**Check of Results:** We have found the two required currents and the power dissipation. As a check, we can independently calculate the PMOS drain current

$$i_D = \frac{1}{2} \left( \frac{25 \mu\text{A}}{\text{V}^2} \right) \left( \frac{2}{1} \right) (3 - 1.33 - 0.7)^2 = 23.5 \mu\text{A}$$

which agrees with the NMOS calculation for the NMOS device.

**Discussion:** Although the power in this simple sense amplifier appears to be small, we must realize that thousands of these sense amplifiers can be simultaneously active in a large memory chip, so that the power dissipation is extremely important. For example, if  $2^{10} = 1024$  of these sense amplifiers are on at once, then the power would be 144 mW. To minimize this power, the amount of time that these latches remain in the precharge state must be minimized. More complex clocked sense amplifiers have been developed to minimize this component of power dissipation.

**EXERCISE:** Repeat Ex. 8.3 if the transistors all have  $W/L = 5/1$ .

**ANSWERS:** 59.0  $\mu\text{A}$ ; 0.350 mW

**EXERCISE:** Repeat Ex. 8.3 if  $V_{DD}$  is changed to 2.5 V with  $V_{TON} = 0.6 \text{ V}$  and  $V_{TOP} = -0.6 \text{ V}$ .

**ANSWERS:** 15.6  $\mu\text{A}$ ; 78.0  $\mu\text{W}$  ( $V_O = 1.11 \text{ V}$ )

#### 8.4.2 A SENSE AMPLIFIER FOR THE 1-T CELL

The two-inverter latch that was used with the 6-T static memory cell in Fig. 8.22 can also be used as the sense amplifier for the 1-T cell. The 1-T cell and a latch with precharge transistor  $M_{PC}$  are shown attached to the bitline in Fig. 8.24, and the waveforms associated with the sensing operation are shown in Fig. 8.25. Because the cross-coupled latch is highly sensitive, it remains connected across two bitlines in order to balance the capacitive load on the two nodes of the latch and to share the sense amplifier between two columns of cells.

In the circuit in Fig. 8.24, the 1-T cell is shown connected to BL. In most designs, a dummy cell with its own access transistor and storage capacitor would be connected to  $\overline{\text{BL}}$  to try to balance the

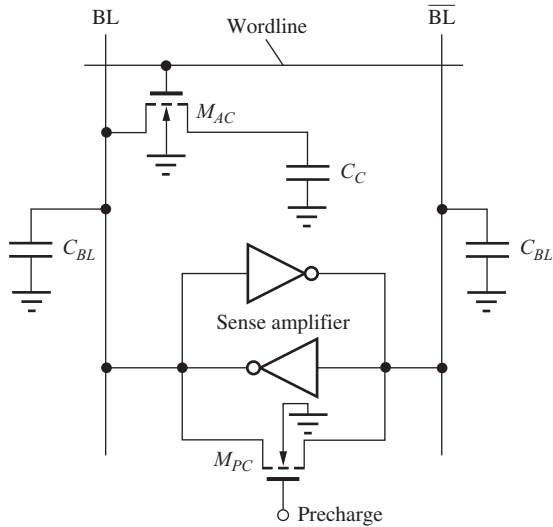


**Figure 8.24** Simple sense amplifier for the 1-T cell.

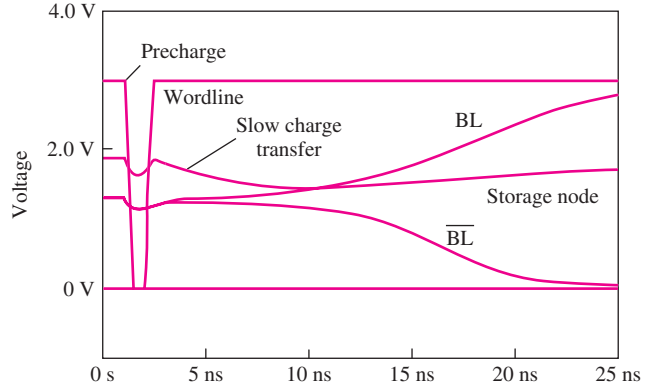


**Figure 8.25** Single-ended sensing of the 1-T cell.

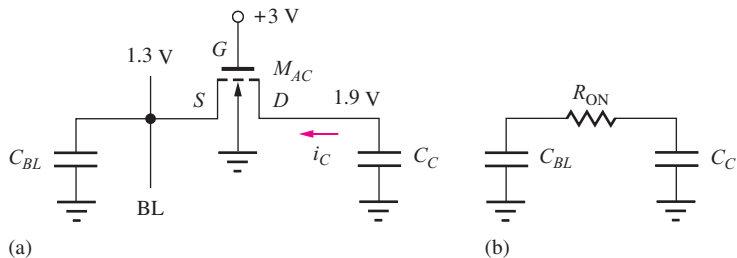


**Figure 8.26** Voltages on the access transistor immediately following activation of the wordline.

switching transients on the two sides of the latch, as well as to improve the response time of the sense amplifier. Use of the dummy cell is discussed in more detail in the section on clocked sense amplifiers.

During the **precharge phase** of the circuit, as shown by the waveforms in Fig. 8.25, the bitlines are forced to a level determined by the relative  $W/L$  ratios of the NMOS and PMOS transistors in the sense amplifier. Following turnoff of the precharge transistor, the data in the storage cells is accessed by raising the wordline, enabling charge sharing between cell capacitance  $C_C$  and bitline capacitance  $C_{BL}$ . In the simulation, the sense amplifier amplifies the small difference and generates almost the full 3-V logic levels on the two bitlines in approximately 25 ns.

A closer inspection of the bitline waveform indicates that the desired charge sharing is actually not occurring in this circuit. The voltage on the storage node does not drop instantaneously because of the large on-resistance of the access transistor. Let us explore this problem further by looking at the voltages applied to the access transistor immediately following activation of the wordline, as in Fig. 8.26.

$$\text{For } M_{AC}: \quad V_{TN} = 0.70 + 0.5(\sqrt{1.3 + 0.6} - \sqrt{0.6}) = 1.0 \text{ V}$$

$$V_{GS} = 3 - 1.3 = 1.7 \text{ V} \quad \text{and} \quad V_{DS} = 1.9 - 1.3 = 0.6 \text{ V}$$

Because  $V_{GS} > V_{DS}$ , the transistor is operating in the triode region as desired, but for these voltages, the initial current through the MOSFET is quite small. Assuming  $W/L = 1/1$ ,

$$i_D = K'_n \frac{W}{L} \left( v_{GS} - V_{TN} - \frac{v_{DS}}{2} \right) v_{DS} = (60 \times 10^{-6}) \left( \frac{1}{1} \right) \left( 1.7 - 1.0 - \frac{0.6}{2} \right) 0.6 = 14.4 \mu\text{A}$$

A measure of the charge-sharing response time is the initial discharge rate of the cell capacitance, given by  $\Delta v/\Delta t = i_D/C_C$ . In the simulation,  $C_C = 25 \text{ fF}$  and the initial discharge rate is  $0.24 \text{ V/ns}$ . This relatively low discharge rate is responsible for the incomplete charge transfer and shallow slope on the storage node waveform. Even though charge sharing is not complete in this circuit, the small initial current drawn from the storage cell is still enough to unbalance the sense amplifier and cause it to reach the proper final state.

**EXERCISE:** What are the initial values of  $R_{on}$  and  $\tau = R_{on}C_C$  in the circuit in Fig. 8.26?

**ANSWERS:**  $23.8 \text{ k}\Omega$ ,  $0.59 \text{ ns}$

### 8.4.3 THE BOOSTED WORDLINE CIRCUIT

In high-speed memory circuits, every fraction of a nanosecond is precious, and some DRAM designs use a separate voltage level for the wordline. The additional level raises the voltage corresponding to a 1 level in the 1-T cell and substantially increases  $i_D$  during cell access. The waveforms for the circuit of Fig. 8.24 are repeated in Fig. 8.27 for the case in which the wordline is driven to  $+5 \text{ V}$  instead of  $+3 \text{ V}$  (referred to as a **boosted wordline**). In this case the cell voltage becomes  $3.7 \text{ V}$  and the initial current from the cell is increased to  $216 \mu\text{A}$ , 15 times larger (see Prob. 8.17)! A much more rapid charge transfer is evident in the storage node waveform in Fig. 8.27, where the sense amplifier has developed a  $1.5\text{-V}$  difference between the two bitlines approximately  $10 \text{ ns}$  after the wordline is raised. In the original case in Fig. 8.25, approximately  $15 \text{ ns}$  were required to reach the same bitline differential.

### 8.4.4 CLOCKED CMOS SENSE AMPLIFIERS

In the sense amplifiers in Figs. 8.22 and 8.24, there is considerable current between the two power supplies during the precharge phase. In addition, a relatively long time is required for precharge. Because a large number of sense amplifiers will be active simultaneously — 128 in the 256-Mb memory chip example — minimizing power dissipation in the individual sense amplifier is an important design consideration. By introducing a more sophisticated clocking scheme, sense amplifier power dissipation can be reduced.

**Clocked sense amplifiers** were originally introduced in NMOS technology to reduce power dissipation in saturated load and depletion-mode load sense circuits. The same techniques are also routinely used in CMOS sense amplifiers; an example of such a circuit is shown in Fig. 8.28. For sensing 1-T cells, a dummy cell is used that has one-half the capacitance of the 1-T cell. In Fig. 8.28, the bottom plate of all the capacitors has been connected to  $V_{DD}$  instead of to  $0 \text{ V}$ . This change represents another design alternative but does not alter the basic theory of operation.

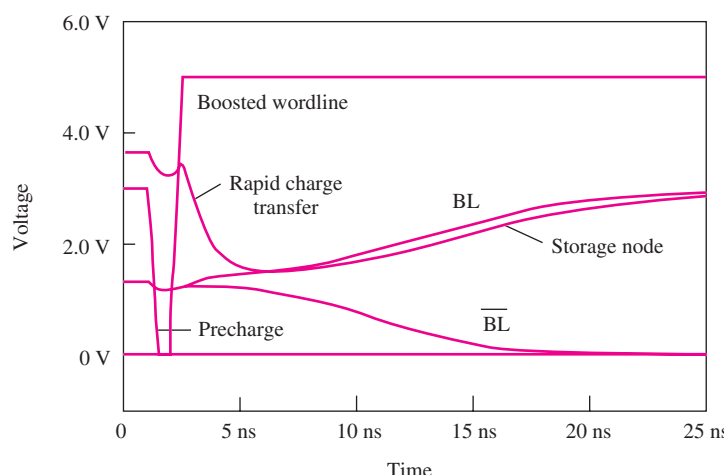


**Figure 8.27** 1-T sensing with wordline voltage boosted to  $5 \text{ V}$ .

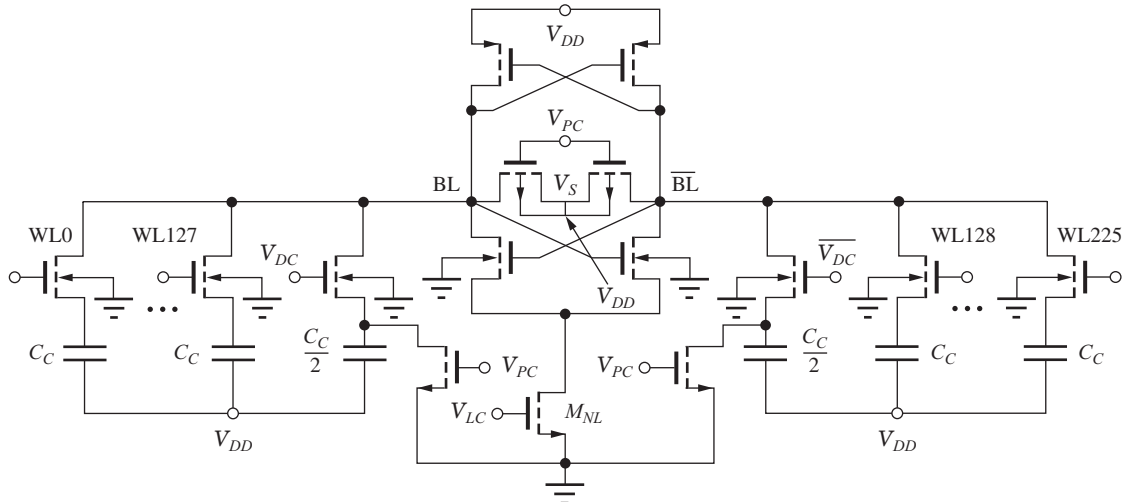


**Figure 8.28** Clocked CMOS sense amplifier showing an array of 1-T memory cells and a dummy cell on each side of the sense amplifier. The right-hand dummy cell ( $C_C/2$ ) is used with cells 0 to 127 and the left-hand dummy cell is used with cells 128 to 255.

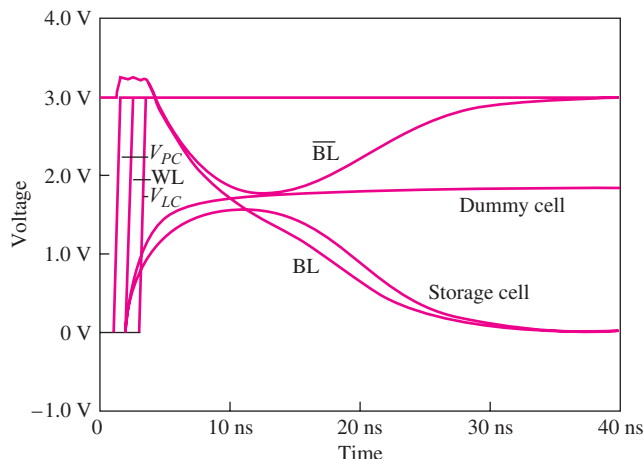


**Figure 8.29** Simulated behavior of the clocked CMOS sense amplifier.

During precharge,  $V_{PC}$  is held at 0 V, and the bitlines are precharged to  $V_{DD}$  through the two PMOS transistors. After the precharge signal is removed, the access transistor of the addressed cell is activated, and the corresponding bitline drops slightly. The magnitude of the change depends on the data stored in the cell. A relatively large change occurs if cell voltage is 0, and a small change occurs if the cell voltage is  $V_{DD} - V_{TN}$ .

A dummy cell is required in this circuit to ensure that a voltage difference of the proper polarity will always develop between the two bitlines following cell access. Dummy cell capacitance is designed to be one-half the capacitance of the data storage cell, and cell voltage is always preset to 0 V by  $V_{PC}$ . During charge sharing, the selected dummy cell causes the corresponding bitline to drop by an amount equal to one-half the voltage drop that occurs when a 0 is stored in the 1-T cell. Thus, a positive voltage difference exists between BL and  $\overline{BL}$  if a 1 is stored in the 1-T cell, and a negative difference exists if a 0 is stored in the cell.

Following charge sharing, the lower part of the CMOS latch is activated by turning on  $M_{NL}$ , and the small difference between the two bitline voltages is amplified by the full cross-coupled CMOS latch. Simulated waveforms for the clocked CMOS sense amplifier are shown in Fig. 8.29. For clarity, the three clock signals, precharge  $V_{PC}$ , wordline WL, and latch clock  $V_{LC}$  have each been staggered

by 1 ns in the simulation. Note that both BL and  $\overline{BL}$  are driven above 3 V by the coupling of the clock signal to the bitlines, but the voltage difference is maintained, and the latch responds properly.

No static current paths exist through the latch during the precharge period, and hence only transient switching currents exist in the sense amplifier. Although there are many variants and refinements to the circuit in Fig. 8.28, the basic circuit ideas presented here form the heart of the sense amplifiers in most dynamic RAMs.

To achieve high-speed precharge and sensing with minimum size transistors, the bitline capacitance  $C_{BL}$  in either static or dynamic RAMs must be kept as small as possible. This requirement restricts the number of cells that can be connected to each bitline. Many clever techniques have been developed to segment the bitlines in order to reduce the size of  $C_{BL}$ , and the interested reader is referred to the references. In particular, information can be found in the annual digests of the IEEE International Solid-State Circuits Conference [2], the Custom Integrated Circuits Conference (CICC) [9], and the Symposium on VLSI Circuits [10], as well as in the yearly Special Issues of the *IEEE Journal of Solid State Circuits* [11]. New information on memory-cell technology is discussed yearly at the IEEE International Electron Devices Meeting [4], the Symposium on VLSI Technology [10], and in the *IEEE Transactions on Electron Devices* [12].

## 8.5 ADDRESS DECODERS

Two additional major blocks in design of a memory are the *row address* and *column address decoders* shown in the block diagram in Fig. 8.2. The row address circuits decode the row address information to determine the single wordline that is to be activated. The decoded column address information is then used to select a bit or group of bits from the selected word. This section first explores NOR and NAND row address decoders and then discusses the use of an NMOS pass-transistor tree decoder for selecting the desired data from the wide internal memory word. Dynamic logic techniques for implementing these decoders are also introduced.

### 8.5.1 NOR DECODER

Figure 8.30 is the schematic for a 2-bit **NOR decoder**. The circuit must fully decode all possible combinations of the input variables and is equivalent to at least four 2-input NOR gates ( $2^N$  N-input gates in the general case). In the circuit, true and complemented address information is fed through an array of NMOS transistors. Each row of the decoder contains two FETs, with each gate connected to one of the desired address bits or its complement and the two drains connected in parallel to the output line being enabled. At the end of each row is a depletion-mode load device to pull the row output high, which occurs only if all the inputs to that row are low. Only one output line will be high for any given combination of input variables; the rest will be low. Each row corresponds to one possible address combination.

**EXERCISE:** What are the sizes of the transistors for the NOR decoder in Fig. 8.30 based on the reference inverter in Fig. 6.29(d)? What is the static power dissipation of this decoder?

**ANSWERS:** Depletion-mode load devices: 1.81/1; NMOS switching devices: 2.22/1; 1.00 mW

### 8.5.2 NAND DECODER

Figure 8.31 is a NAND version of the same decoder. Again, true and complemented address information is fed through the array. For the **NAND decoder**, all outputs are high except for the single row in which the transistor gates are all at a 1 level. Because additional driver circuits are normally required between the decoder and the highly capacitive wordline, the logical inversion that is needed to actually drive wordlines in a memory array is easily accommodated. As for standard NOR and

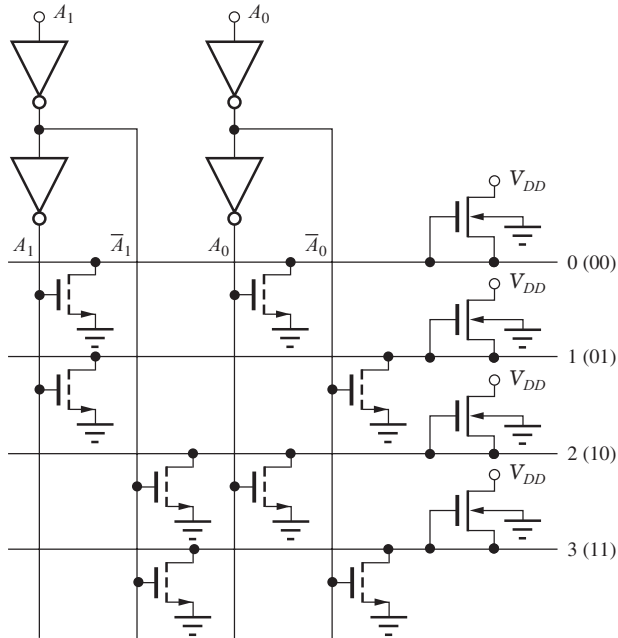


Figure 8.30 NMOS static NOR address decoder.

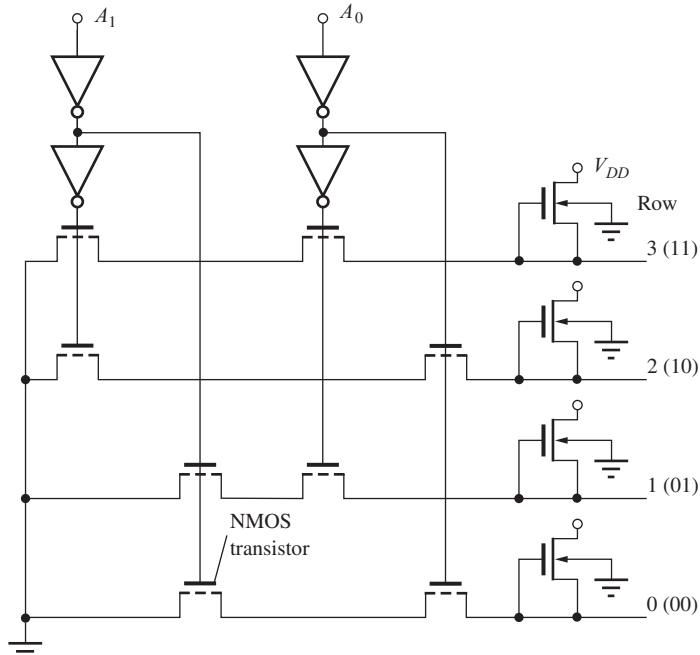


Figure 8.31 NMOS NAND decoder circuit.

NAND gates, the stacked series structure of the NAND gate tends to be slower than the corresponding parallel NOR structure, particularly if minimum-size devices are used throughout the decoder.

The NMOS static decoder circuits in Figs. 8.30 and 8.31 cause power consumption problems in high-density memories. In the memory array, 1 wordline will be high for a given address, and \$2^N - 1\$ will be low. For static NMOS circuits, \$2^N - 1\$ of the individual NOR gates in the NOR decoder

$$\text{Row } 0 = \overline{\bar{A}_1 + A_0}$$

$$\text{Row } 1 = \overline{\bar{A}_1 + \bar{A}_0}$$

$$\text{Row } 2 = \overline{\bar{A}_1 + A_0}$$

$$\text{Row } 3 = \overline{\bar{A}_1 + \bar{A}_0}$$

dissipate power simultaneously. A similar problem occurs if NMOS inverters are used at the output of the NAND decoder.

Standard CMOS circuits offer low power dissipation but cause layout and area problems when there are a large number of inputs, because each input must be connected to both an NMOS and a PMOS transistor, which doubles the number of devices in the array. A full CMOS decoder can be more efficiently implemented as a combination of an NMOS NOR array and a PMOS NAND array. However, because memories are generally used in clocked systems, they can use dynamic decoders, which consume low power and require only a few PMOS transistors. We introduce these next.

**EXERCISE:** What are the sizes of the load devices in the NAND decoder in Fig. 8.31 if the  $W/L$  ratios of the switching devices are all 2/1? Base your design on the reference inverter in Fig. 6.29(d).

**ANSWER:** 1.63/1

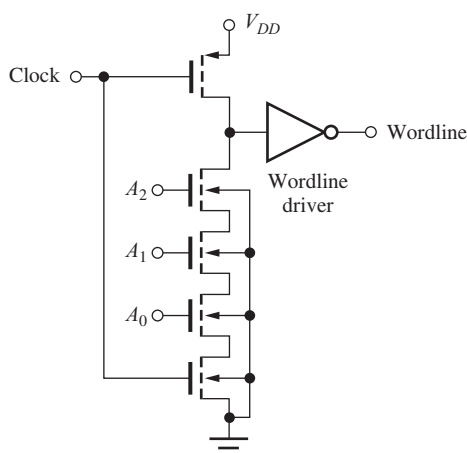


Figure 8.32 One row of a 3-bit NAND decoder in domino CMOS logic.

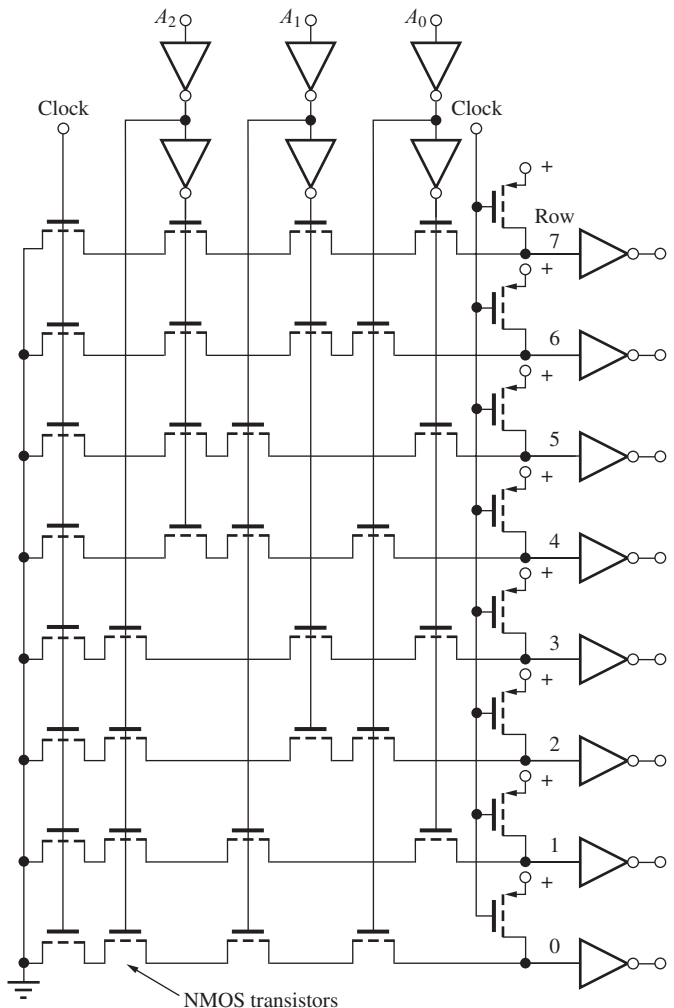


Figure 8.33 Complete 3-bit domino CMOS NAND address decoder.

### 8.5.3 DECODERS IN DOMINO CMOS LOGIC

**Domino CMOS**, introduced in the last chapter in Sec. 7.8, is highly useful in the design of compact decoder circuits for memory circuits. As an example, Fig. 8.32 is the schematic for one row of a domino CMOS NAND decoder for a 3-bit address. In this circuit, a discharge path exists through the function block only for address  $A_0A_1A_2 = 111$ , and only the single-addressed wordline makes a low-to-high transition at the output of the inverter. This structure ensures that the voltage changes on only one of the high-capacitance wordlines during a given row access. The output inverter can be designed to drive the high-capacitance load by utilizing the cascade buffer techniques that we studied in Sec. 7.9 of the last chapter.

Figure 8.33 is the circuit schematic for a full 3-bit address decoder using the NAND decoder array of Fig. 8.31; here the load devices in Fig. 8.32 have been replaced with clocked PMOS transistors, and an NMOS clock transistor has been added to the beginning of each row. A CMOS inverter is connected to each output line to complete the domino CMOS implementation.

### 8.5.4 PASS-TRANSISTOR COLUMN DECODER

The column address decoder of the memory in Fig. 8.2 must choose a group of data bits—usually 1, 4, or 8 bits—from the much wider word that has been selected by the row address decoder. Another form of data selection circuit using NMOS **pass-transistor logic** is shown in Fig. 8.34. For a large number of data bits, the pass-transistor circuit technique requires far fewer transistors than would the more direct approach using standard NOR and NAND gates.

The pass-transistor decoder structure is quite similar to an analog multiplexer in which the transistors behave as switches. “On” switches pass the data from one node to the next, whereas “off” switches prevent the data transfer. In the pass-transistor implementation, true and complement address information is fed through a transistor array, with one level of the array corresponding to each address bit. Although all transistors with a logic 1 on their respective gates will be on, the tree structure ensures that only a single path is completed through the array for each combination of inputs. In Fig. 8.34, an address of 101 is provided to the array, and the transistors indicated in blue all have a logic 1 on their respective gates, creating a conducting channel region in each. In this case, a completed conducting path connects input column 5 to the data output.

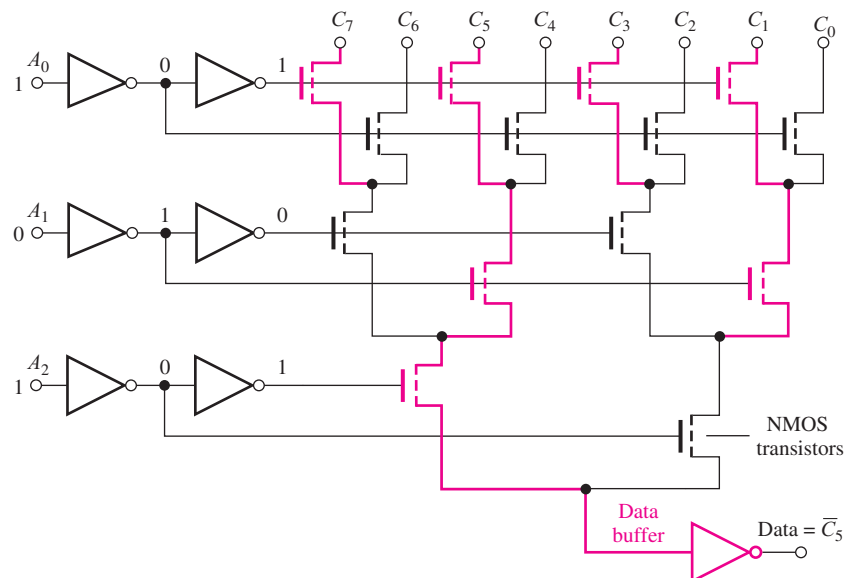
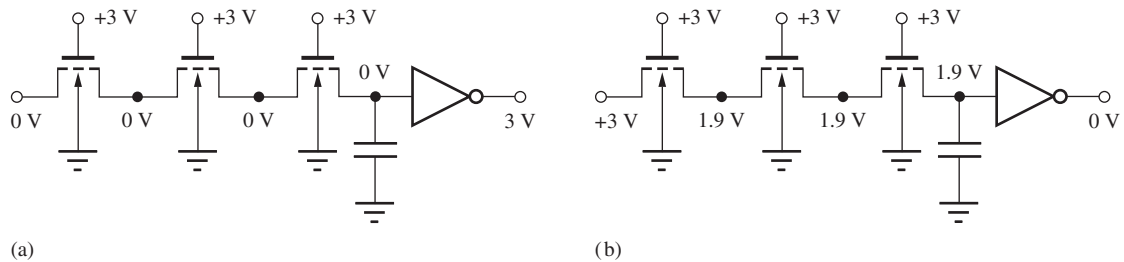


Figure 8.34 3-bit column data selector using pass-transistor logic.



**Figure 8.35** Data transmission through the pass-transistor decoder: (a) 0 input data, (b) 1 input data.

Examples of the conducting paths through a three-level pass-transistor array for input data of 0 and 1 are shown in Fig. 8.35 for the case of  $V_{DD} = 3$  V. For a 0 input equal to 0 V, the output node capacitor  $C$  is discharged to zero through the series combination of the three pass transistors. However, for a 1 input voltage of 3 V, the output of the first pass transistor is one threshold voltage below the gate voltage of 3 V. Using the NMOS parameters from earlier in the chapter, we find that the output voltage is

$$V_O = V_G - V_{TN} = 3 - 1.1 = 1.9 \text{ V}$$

The other node voltages can reach this same potential, so the output capacitance will charge to  $V_G - V_{TN} = 1.9$  V, regardless of the number of levels in the array. The data buffer at the output must be designed to have a switching threshold below 1.9 V in order to properly restore the logic level at the output.

Full logic levels can also be achieved in pass-transistor logic for both 1 and 0 inputs by replacing each NMOS transistor with a CMOS transmission gate. However, this significantly increases the area and complexity of the design with little actual benefit because the data buffer can easily be designed to compensate for the loss in signal level through the NMOS (or PMOS) pass-transistor array. In addition to doubling the number of transistors in the array, the full CMOS version requires distribution of both true and complement address information to each transmission gate. However, design techniques to simplify the layout of CMOS transmission gate arrays do exist [13].

**EXERCISE:** What are the voltage levels at the nodes in Fig. 8.35(a) and 8.35(b) if the gate voltages are 5 V instead of 3 V? Assume  $V_{TO} = 0.70$  V,  $\gamma = 0.5 \sqrt{V}$ , and  $2\phi_F = 0.6$  V. What is the largest  $\gamma$  for which the output of the pass-transistor is at least 3 V?

**ANSWERS:** 0 V, 3.00 V;  $1.16 \sqrt{V}$

**EXERCISE:** What would be the actual voltage at the output of the CMOS inverter in Fig. 8.35(b) if the inverter utilized a symmetrical design operating from a 3-V supply and  $V_{TN} = -V_{TP} = 0.7$  V?

**ANSWER:** 68.6 mV

## 8.6 READ-ONLY MEMORY (ROM)

Read-only memory (ROM) is another form of memory often required in digital systems, and many common applications exist. Many microprocessors use microcoded instruction sets that reside in ROM, and a portion of the operating system for personal computers usually resides in ROM. The fixed programs for microcontrollers, often called *firmware*, are also typically stored in ROM, and

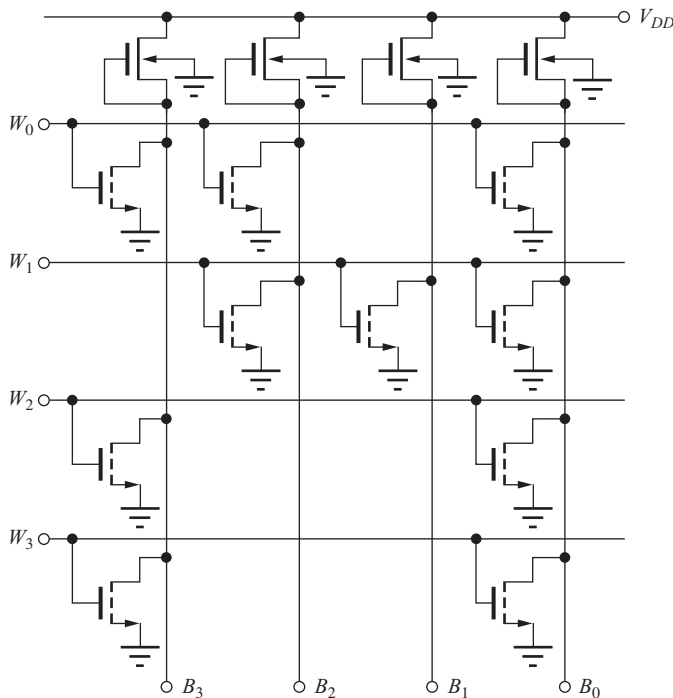


**Figure 8.36** Basic structure of an NMOS static ROM with four 4-bit words:  
 $W_0 = 0010$ ;  $W_1 = 1000$ ;  $W_2 = 0110$ ;  $W_3 = 0110$ .

**TABLE 8.1**  
 Contents of ROM in Fig. 8.36

WORD	DATA
0	0010
1	1000
2	0110
3	0110

cartridges for home video games are simply ROMs that contain the firmware programs that define the characteristics of the particular game. Plug-in modules for hand-held scientific calculators are another application of read-only memory.

Most ROMs are organized as an array of  $2^N$  words, where each word contains the number of bits required by the intended application. Common values are 4, 8, 12, 16, 18, 24, 32, 48, 64, and so on. Figure 8.36 shows the structure of a static NMOS ROM using depletion-mode load devices. This particular ROM contains four 4-bit words. Each column corresponds to 1 bit of the stored word, and an individual word  $W_i$  is selected when the corresponding wordline is raised to a 1 state by an address decoder similar to that in RAM. For example, this ROM could be driven by a NOR decoder circuit similar to Fig. 8.30.

An NMOS transistor can be placed at the intersection of each row and column within the array. In this ROM, the gate of the transistor is tied to the wordline and the drain is connected to the output data line. If connections to an NMOS transistor exist at a given array site, then the corresponding output data line is pulled low when the word is selected. If no FET exists, then the data line is maintained at a high level by the load device. Thus, the presence of an FET corresponds to a 0 stored in the array and the absence of an FET corresponds to a 1 stored in ROM. The particular data pattern stored in the array is often referred to as the **array personalization**. Table 8.1 contains the contents of the ROM array in Fig. 8.36.

Information can be personalized in the ROM array in many ways; we mention three possibilities here. Suppose an FET is fabricated at every possible site within the array. One method of storing the desired data is to eliminate the contact between the drain and data line wherever a 1 bit is to be stored. This design yields a high capacitance on the wordline because a gate is connected to the wordline at every possible site, but a low capacitance exists on the output line because only selected drain diffusions are connected to the output lines. A second technique is to use ion implantation to alter the MOSFET threshold voltage of the FETs wherever a 1 is to be stored. If the threshold is raised

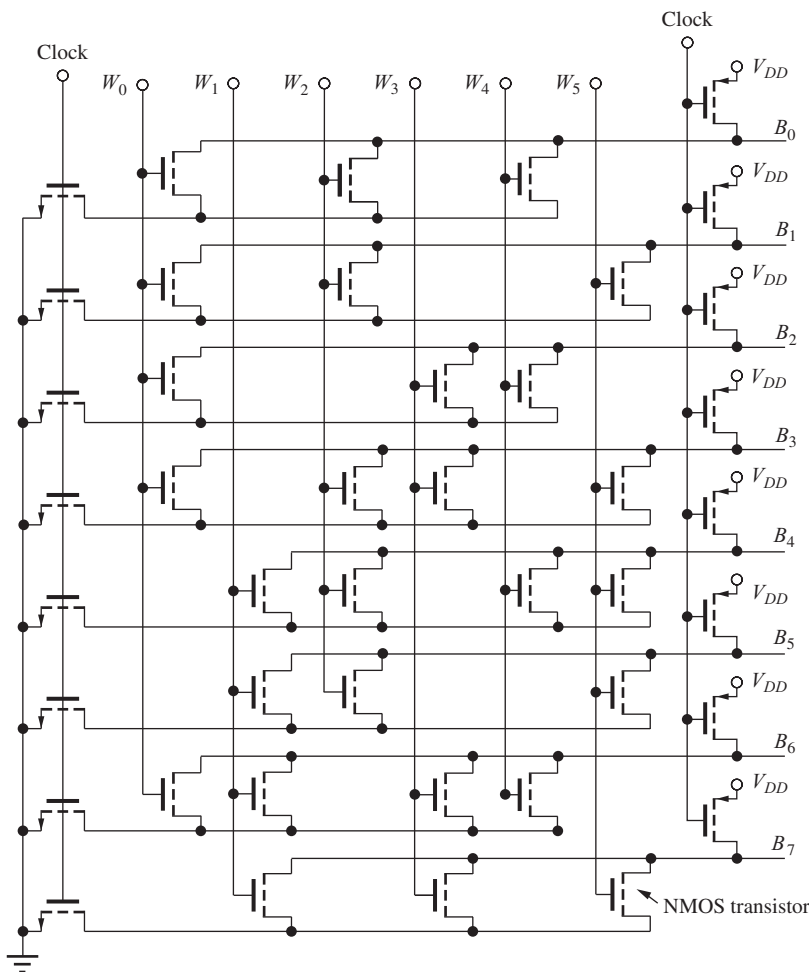


**Figure 8.37** Domino CMOS ROM containing six 8-bit words. The array contains NMOS transistors in which substrate connections have been eliminated for clarity.

high enough, then the MOSFET cannot be turned on, and therefore cannot pull the corresponding data line low. A third method is to personalize the array by eliminating gate contacts instead of drain contacts.

Standard NMOS ROM circuits exhibit substantial static power dissipation. To eliminate this power dissipation, ROMs can be designed using dynamic circuitry such as domino CMOS, as demonstrated by the ROM in Fig. 8.37, which contains six 8-bit words. When the clock signal is low, the capacitance on the output data lines is precharged high. As the clock is raised to a high level, the PMOS transistors turn off, and the data bits of the addressed word are selectively discharged to zero if a transistor connection exists at a given intersection point in the array. A full domino implementation will add an inverter to each output bitline. Table 8.2 lists the contents of the ROM personalization in Fig. 8.37.

The ROMs in Figs. 8.36 and 8.37 use the NOR gate structure and are often called NOR arrays. It is also possible to use a NAND array structure, as shown in Fig. 8.38. In the NAND array, all the wordlines except the desired word are raised high. Thus, all the MOSFETs in the array are turned on except for the unselected row. If a MOSFET exists at a given cross-point in the unselected row, then the conducting path is broken, and the data for that column will be a 1. If the MOSFET has been

**TABLE 8.2**  
Contents of ROM in Fig. 8.37

WORD	DATA
0	10110000
1	00001111
2	11000100
3	00110011
4	10101010
5	01000101

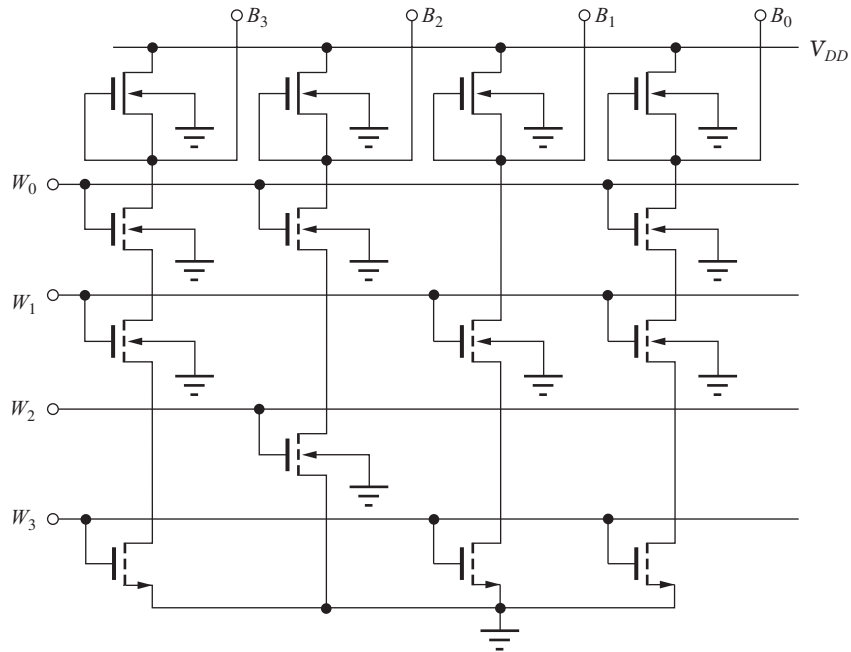


**Figure 8.38** ROM based on a NAND array.

replaced by a connection (possibly resistive)—by making the MOSFET a depletion-mode device for example—then the corresponding data bit will be pulled low. Note that the NAND ROM array could be driven directly by the NAND decoder in Fig. 8.31.

**EXERCISE:** Draw the schematic of an additional row in the ROM in Fig. 8.37 with contents of 11001101. What are the contents of the ROM in Fig. 8.38?

**ANSWERS:** NMOS transistors connected to  $B_5$ ,  $B_4$ , and  $B_1$ ; (0010, 0100, 1011, 0100)

The ROMs already mentioned are all personalized at the mask level, which must be done during IC design and subsequent fabrication. If a design error occurs, the IC must be redesigned and the complete fabrication process repeated. To solve this problem, **programmable read-only memories (PROMs)**, which can be programmed once from the external terminals, have been developed. **Erasable programmable read-only memories (EPROMs)** are another type of ROM. These can be erased using intense ultraviolet light and reprogrammed many times. **Electrically erasable read-only memories (EEPROMs)** can be both erased and reprogrammed from the external terminals. High-density **flash memories** allow selective electrical erasure and reprogramming of large blocks of cells.

## 8.7 FLIP-FLOPS

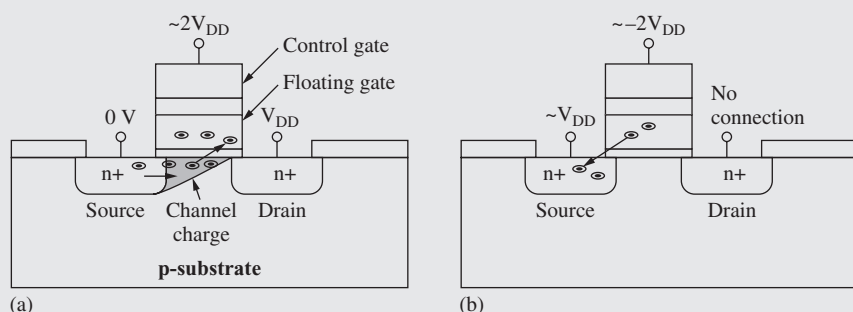
Temporary storage in the form of high-speed registers is another requirement in most digital systems. The external data interface to these registers may be in either parallel or serial form and includes various **flip-flops (FFs)** and shift registers. There are many different types of flip-flops and shift registers, and this section presents several examples of circuits that can be used in static parallel registers. However, an exhaustive discussion of the various possibilities is not attempted.


**ELECTRONICS IN ACTION**
**Flash Memory**

The ever increasing number of handheld, low-power devices has given rise to a new class of memory devices known as flash memory. Cell phones maintain phone number lists as well as configuration information, digital cameras store pictures on flash memory cards, digital audio players use flash memory for storage, and most computer users carry flash memory drives in their pockets. All of these devices need to maintain stored information with no applied power but can be both read and written when powered.



Flash memory is a type of electrically erasable, programmable ROM (EEPROM). As seen below, the basic storage cell is similar to a MOSFET with two gates, but one gate is electrically floating. The *write* process involves placing negative charge on the floating gate by driving a large positive voltage on the control gate and a positive drain-source voltage across the device. The positive control gate voltage inverts the MOSFET channel, and the large drain-source voltage accelerates electrons through the channel to the drain. The electrons gain so much kinetic energy that they are known as ‘hot’ electrons; they have the same energy as they would have if the device temperature were much higher. The vertical field created by the large control voltage captures some of the ‘hot’ electrons, and they tunnel through the thin oxide to the floating gate.



Flash memory cell structure and control voltages during write operation (left) and read operation.

Erasure occurs by removing the negative charge with a process known as Fowler-Nordheim tunneling.<sup>4</sup> The source is driven positive, and the control gate is set to a large negative voltage. This creates an electric field that causes electrons to slowly tunnel from the floating gate to the source. Unlike the *write* operation, the *erase* operation for flash memory is performed on a large number of cells simultaneously. This is done to amortize the rather slow erasure time over many cells, reducing the effective per cell erasure time.

The presence or absence of charge on the floating gate changes the effective threshold voltage of the control gate. Reading the state of the memory cell is done by driving the control gate with an appropriate voltage and measuring the resulting drain-source current.

Due to the proliferation of handheld digital devices, the market for flash memory products is expected to be more than \$50 billion dollars by 2012. This is another example of the microelectronics industry inventing a solution to a market need and rapidly creating an entirely new market segment.

<sup>4</sup> Lenzlinger, M. and Snow, E. H., "Fowler-Nordheim Tunneling into Thermally Grown  $\text{SiO}_2$ ," *Journal of Applied Physics*, vol. 40, No. 1, January 1967, pp. 278–283.

### 8.7.1 RS FLIP-FLOP

The **RS (reset-set) flip-flop (RS-FF)** can be formed in a straightforward manner by using either two NOR gates or two NAND gates to replace the inverters in the simple latch. The desired state is stored by setting ( $Q = 1$ ) or resetting ( $Q = 0$ ) the flip-flop with the RS control inputs.

Figure 8.39 is the circuit for an RS-FF constructed using two-input CMOS NOR gates and corresponding to the truth table in Table 8.3. If the R and S inputs are low, they are both inactive, and the previously stored state of the flip-flop is maintained. However, if S is high and R is low, output  $\bar{Q}$  is forced low, and  $Q$  then becomes high, setting the latch. If R is high and S is low, node  $Q$  is low, and  $\bar{Q}$  is then forced high, resetting the latch. Finally, if both R and S are high, both output nodes are forced low, and the final state is determined by the input that is maintained high for the longest period of time. The RS = 11 state is usually avoided in logic design.

The RS-FF can also be implemented using two-input NAND gates, as shown in Fig. 8.40 and Table 8.4. In this case, the latch maintains its state as long as both the  $\bar{R}$  and  $\bar{S}$  inputs are high, thus maintaining a conducting channel in both NMOS transistors. If the  $\bar{R}$  input is set to 0 and  $\bar{S}$  is a 1, then the  $\bar{Q}$  output becomes a 1, causing the  $Q$  output to be reset to 0. If  $\bar{R}$  returns to a 1, the reset condition is maintained within the latch. If the  $\bar{S}$  input becomes a 0, and  $\bar{R}$  remains a 1, the  $Q$  output is set to a 1 and the  $\bar{Q}$  output becomes 0. If  $\bar{S}$  returns to a 1, the latch remains "set." In the NAND implementation, both outputs are forced to 1 when  $\bar{R}$  and  $\bar{S}$  are both 0.

The flip-flops in Figs. 8.39 and 8.40 utilize full CMOS implementations of the NOR and NAND gates. If static power dissipation can be tolerated when the R and S inputs are both active, then the simplified implementation of Fig. 8.41 can be used. This is essentially the two-inverter latch used in the static memory circuits, with R and S transistors added to force either the  $Q$  or  $\bar{Q}$  output low. If both R and S are 1, both outputs will be 0, and both load devices and the R and S transistors will conduct current. PMOS transistors can also be used to replace the NMOS RS transistors to pull  $Q$  or  $\bar{Q}$  toward  $V_{DD}$ .

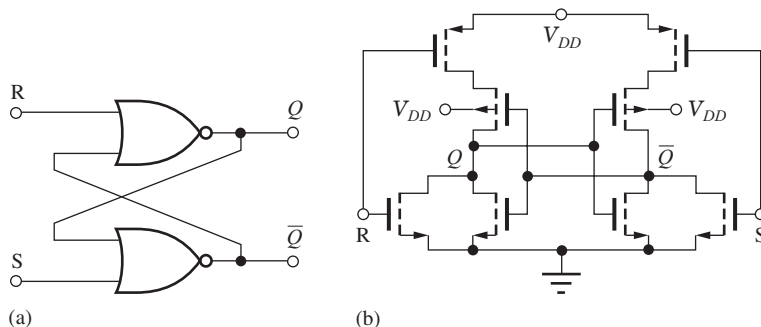
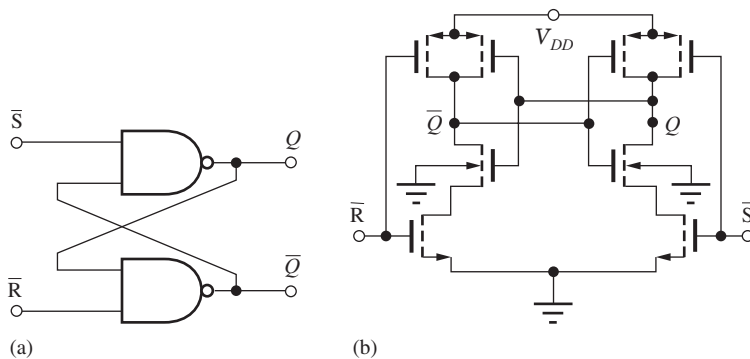


Figure 8.39 (a) RS flip-flop using NOR gates. (b) RS flip-flop using two CMOS NOR gates.

**TABLE 8.3**  
**NOR RS Flip-Flop**

R	S	Q	$\bar{Q}$
0	0	$Q$	$\bar{Q}$
0	1	1	0
1	0	0	1
1	1	0	0



**Figure 8.40** (a) A NAND  $\bar{RS}$  flip-flop. (b)  $\bar{RS}$  flip-flop implemented with two CMOS NAND gates.

**TABLE 8.4**  
NAND RS Flip-Flop

$\bar{R}$	$\bar{S}$	$Q$	$\bar{Q}$
1	1	$Q$	$\bar{Q}$
0	1	0	1
1	0	1	0
0	0	1	1

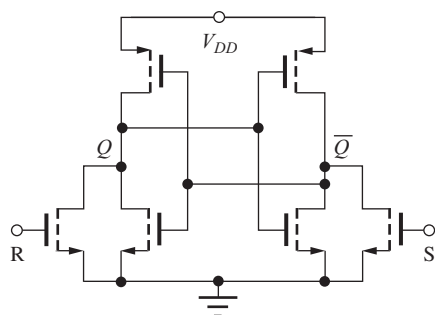


**Figure 8.41** Simplified RS flip-flop using two NOR gates.

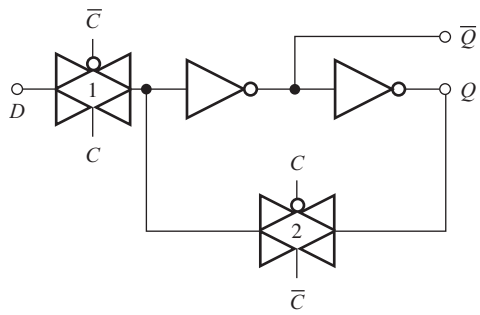


**Figure 8.42** D latch.

### 8.7.2 THE D-LATCH USING TRANSMISSION GATES

The CMOS transmission gate introduced in Sec. 7.10 is used to implement another basic form of storage element called the **D latch**, as shown in Fig. 8.42. When the clock input  $C = 1$ , transmission gate 1 is on and transmission gate 2 is off. The state of the  $D$  input is stored on the capacitance at the input of the first inverter and transferred through the inverter pair to the  $\bar{Q}$  and  $Q$  outputs. The  $Q$  output equals the  $D$  input as long as  $C = 1$ . When the clock changes state to  $C = 0$ , the  $D$  input is disabled, and the state of the inverter pair is latched through transmission gate 2. The state at  $Q$  and  $\bar{Q}$  remains constant as long as  $C = 0$ .

### 8.7.3 A MASTER-SLAVE D FLIP-FLOP

The **master-slave D flip-flop (D-FF)** in Fig. 8.43 is a storage element in which the data is stable during both **phases of the clock**. Master-slave D-FFs can be directly cascaded to form a shift register. This D-FF is formed by a cascade connection of two D-type latches operating on opposite phases of the clock.

When the clock  $C = 1$ , transmission gates 1 and 4 are closed and 2 and 3 are open, resulting in the simplified circuit in Fig. 8.43(b). The  $D$  input is connected to the input of the first inverter pair, and the  $D$  input data appears at the output of the second inverter. The second pair of inverters is connected as a latch, holding the information previously placed on the input to the second inverter pair.

When the clock changes states and  $C = 0$ , as depicted in Fig. 8.43(c), transmission gate 1 disables the  $D$  input, and transmission gate 2 latches the information that was on the  $D$  input just before the clock state change. During the clock transition, data from the  $D$  input is maintained temporarily on the nodal capacitances associated with the first two inverters. Transmission gate 3

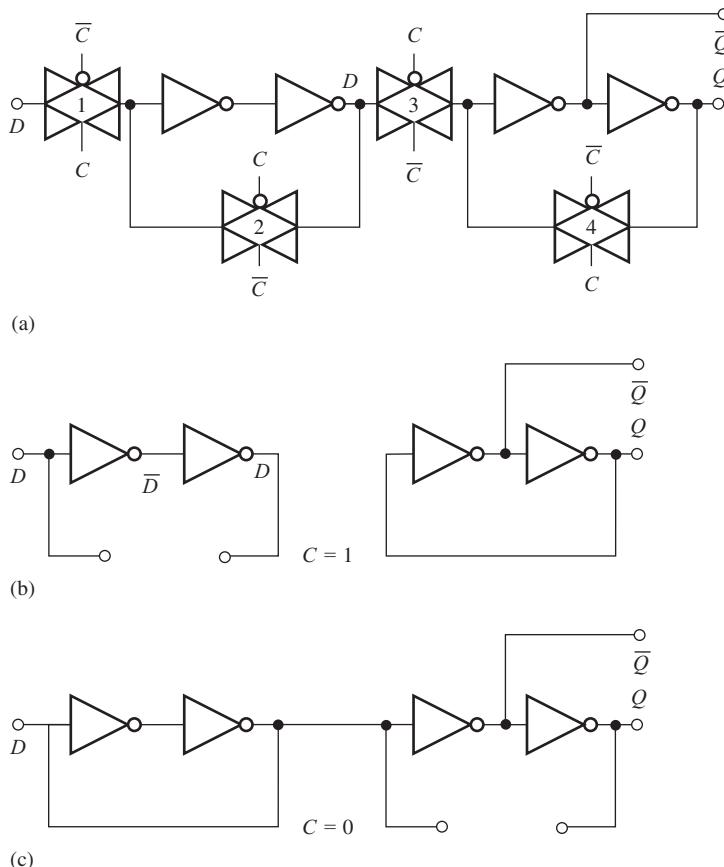


**Figure 8.43** Master-slave D flip-flop. (a) Complete master-slave D flip-flop. (b) D flip-flop with  $C = 1$ . (c) D flip-flop with  $C = 0$ .

propagates the stored data onto the  $\bar{Q}$  and  $Q$  outputs.  $Q$  is now equal to the data originally on the  $D$  input when  $C$  was equal to 1.

Note that the data at the output of the master-slave flip-flop is constant during both phases of the clock, except for the time required for the latches to change state. A path should never exist completely from the  $D$  input to the  $Q$  or  $\bar{Q}$  outputs.

## SUMMARY

- *Memory organization:* In Chapter 8, we have explored basic MOS memory circuits, including both random-access memory (RAM) and read-only memory (ROM), sometimes called read-only storage (ROS). The internal organization of IC memories was presented, and examples of the major building blocks of a memory chip, including row and column address decoders, sense amplifiers, wordline drivers, and output buffers were investigated.
- *Static RAM cells:* A six-transistor cell is normally used as the storage element in the SRAM, and the integrity of the stored data is maintained as long as power is applied to the circuit.
- *Dynamic RAM cells:* The one-transistor cell is utilized in most high-density dynamic RAM (DRAM) designs. Dynamic memory circuits store the information temporarily as the charge on

a capacitor, and the data must be periodically refreshed to prevent loss of the information. Read operations also destroy the data in the cell, and it must be written back into the cell as part of the read cycle. Dynamic memories can also be based on four-transistor dynamic memory cells.

- *Decoder design:* Static NAND and NOR array structures are often utilized in address decoder circuits. Dynamic domino CMOS, introduced in Chapter 7 can also be used effectively to reduce power consumption in many applications; a domino CMOS decoder was presented.
- *Pass transistors:* Pass-transistor logic was introduced as one method for simplifying the design of the column decoding circuitry in a RAM.
- *ROMs:* The structure of read only memory or ROM is very similar to that of RAM, but the data is embedded in the physical design of the circuitry.
- *Register elements:* Bistable storage elements based on the cross-coupled inverter pair were introduced, including the RS flip-flop, the dynamic D flip-flop or D latch, and the master-slave flip-flop. Flip-flops use the two stable equilibrium points of a cross-coupled pair of inverters to represent the binary data.
- *Sense amplifiers:* The bistable latch also forms the heart of many sense amplifier circuits, and the unstable equilibrium point of the latch plays a key role in the design of high-speed sensing circuits. Both static and clocked dynamic sense amplifiers can be used in memory designs.

## KEY TERMS

Array personalization	Latch
Bistable circuit	Master-slave D flip-flop (D-FF)
Bitline	NAND decoder
Bitline precharge	NOR decoder
Bitline capacitance	One-transistor (1-T) cell
Boosted wordline	Pass-transistor logic
Cell capacitor	Precharge phase
Charge sharing	Precharge transistor
Charge transfer	Programmable read-only memory (PROM)
Clocked sense amplifier	Random-access memory (RAM)
Clock phases	Read-only memory (ROM)
Column address decoder	Read-only storage (ROS)
Cross-coupled inverter	Read operation
Domino CMOS	Refresh operation
Dynamic random-access memory (DRAM)	Row address decoder
D latch	RS flip-flop (RS-FF)
Electrically erasable read-only memory (EEROM)	Sense amplifier
Erasable programmable read-only memory (EPROM)	Six-transistor (6-T) SRAM cell
Flash memory	Static random-access memory (SRAM)
Flip-flop (FF)	Unstable equilibrium point
Four-transistor (4-T) cell	Wordline
	Wordline driver
	Write operation

## REFERENCES

1. J. Wood and R. G. Wood, “The use of insulated-gate field-effect transistors in digital storage systems,” *ISSCC Digest of Technical Papers*, pp. 82–83, February 1965.
2. *Digest of Technical Papers of the IEEE International Solid-State Circuits Conference (ISSCC)*, February of each year.

3. W. M. Regitz and J. A. Karp, "A three-transistor cell, 1024-bit, 500 ns MOS RAM," *ISSCC Digest of Technical Papers*, pp. 36–39, February 1970.
4. *Digest of the IEEE International Electron Devices Meeting (IEDM)*, December of each year.
5. Robert H. Dennard; patent 3,387,286 assigned to the IBM Corporation.
6. H. C. Lin and L. W. Linholm, "An optimized output stage for MOS integrated circuits," *IEEE JSSC*, vol. SC-10, pp. 106–109, April 1975.
7. R. C. Jaeger, "Comments on 'An optimized output stage for MOS integrated circuits,'" *IEEE JSSC*, vol. SC-10, pp. 185–186, June 1975.
8. Mikio Asakura et al., "A 34 ns 256 Mb DRAM with boosted sense-ground scheme," *ISSCC Digest of Technical Papers*, pp. 140–141, 324, February 1994.
9. *Digest of the IEEE Custom Integrated Circuits Conference*, April of each year.
10. *Digests of the Symposium on VLSI Circuits and the Symposium on VLSI Technology*, June of each year.
11. *IEEE Journal of Solid-State Circuits*, monthly.
12. *IEEE Transactions on Electron Devices*, monthly.
13. Carver Mead and Lynn Conway, *Introduction to VLSI Systems*, Addison-Wesley, Reading, MA: 1980.
14. R. M. Swanson and J. D. Meindl, "Ion-implanted complementary MOS transistors in low-voltage circuits," *IEEE Journal of Solid-State Circuits*, vol. SC-7, no. 2, pp. 146–152, April 1972.
15. J. D. Meindl and J. A. Davis, "The fundamental limit on binary switching energy for terascale integration," *IEEE Journal of Solid-State Circuits*, vol. SC-35, no. 10, pp. 1515–1516, October 2000.
16. J. R. Houser, "Noise margin criteria for digital logic circuits," *IEEE Trans. on Education*, vol. 36, no. 4, pp. 363–368, November 1993.
17. J. Lohstroh, E. Seevinck, and J. Degroot, "Worst-case static noise margin criteria for logic circuits and their mathematical equivalence," *IEEE Journal of Solid-State Circuits*, vol. SC-18, no. 6, pp. 803–806, December 1983.

## PROBLEMS

Unless otherwise specified, use  $K'_n = 100 \mu\text{A/V}^2$ ,  $K'_p = 40 \mu\text{A/V}^2$ ,  $V_{TON} = 0.7 \text{ V}$ ,  $V_{TOP} = -0.7 \text{ V}$ ,  $\gamma = 0.5 \sqrt{\text{V}}$ ,  $2\phi_F = 0.6 \text{ V}$ . For simulation, use the models in Appendix B.

### 8.1 Random-Access Memory (RAM)

- 8.1. (a) How many bits are actually in a 256-Mb memory chip? In a 1-Gb chip? (b) How many 128-Kb blocks must be replicated to form the 256-Mb memory in Fig. 8.1?
- 8.2. How much leakage is permitted per memory cell in a 256-Mb static CMOS memory chip if the total standby current of the memory is to be less than 1 mA? (b) Repeat for a 4-Gb memory.
- 8.3. Suppose a memory chip has a 128-bit-wide external memory bus. What is the power dissipated driving the memory bus at a 1-GHz data rate if each bus line

has 10 pF of capacitance, and the voltage is 1.8 V?  
 (b) Repeat for 3 GHz and 1.8 V.

- 8.4. Suppose that each cell in a 1-Gbit memory chip must be refreshed every 10 ms. What is the power dissipated in refreshing the chip if the cell capacitance is 100 fF and the cell voltage is 2.5 V? Assume that 50 percent of the cells have 1 bits stored and that the cell voltage is completely discharged and restored during the refresh operation.

### 8.2 Static Memory Cells

- 8.5. Find the voltages corresponding to  $D$  and  $\bar{D}$  in an NMOS memory cell with resistor loads in place of the PMOS transistors in Fig. 8.6 if  $R = 10^{10} \Omega$ ,  $V_{DD} = 3 \text{ V}$ , and  $W/L = 2/1$ . Use  $V_{TO} = 0.75 \text{ V}$ ,  $\gamma = 0.5 \sqrt{\text{V}}$ , and  $2\phi_F = 0.6 \text{ V}$ .
- \*8.6. Assume that the two bitlines are fixed at 1.5 V in the circuit in Figs. 8.7 and 8.8 and that a steady-state

condition has been reached, with the wordline voltage equal to 3 V. Assume that the inverter transistors all have  $W/L = 1/1$ ,  $V_{TN} = 0.7$  V,  $V_{TP} = -0.7$  V, and  $\gamma = 0$ . What is the largest value of  $W/L$  for  $M_{A1}$  and  $M_{A2}$  (use the same value) that will ensure that the voltage at  $D_1 \leq 0.7$  V and the voltage at  $D_2 \geq 2.3$  V?

- \*8.7. Simulate the response time of the 6-T cell in Fig. 8.6 from an initial condition of  $D_1 = 1.55$  V and  $D_2 = 1.45$  V with the access transistors off. How long does it take for the cell voltages to reach 90 percent of their final values? Use  $V_{DD} = 3$  V and a symmetrical cell design, with  $W/L$  of the NMOS transistors = 2/1. Use the SPICE models from Appendix B.
- 8.8. Simulate and plot a graph of the transients that occur when writing a 0 into a cell containing a 0, as in Fig. 8.12. Discuss the results.

### 8.3 Dynamic Memory Cells

- 8.9. The 1-T cell in Fig. P8.9 uses a bitline voltage of 2.5 V and a wordline voltage of 2.5 V. (a) What are the cell voltages stored on  $C_C$  for a 1 and 0 if  $V_{TO} = 0.6$  V,  $\gamma = 0.5\sqrt{V}$ , and  $2\phi_F = 0.6$  V? (b) What would be the minimum wordline voltage needed in order for the cell voltage to reach 2.5 V for a 1?

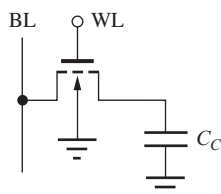


Figure P8.9

- 8.10. Repeat Prob. 8.9 if the bitline and wordline voltages are 1.8 V.
- 8.11. Substrate leakage currents usually tend to destroy only one of the two possible states in the 1-T cell. For the circuit in Fig. P8.9, which level is the most sensitive to leakage currents and why?
- 8.12. Find an expression for the energy that is lost during the charge redistribution for reading out the data in the 1-T? (a) How much energy is lost if  $V_C = 1.9$  V,  $V_{BL} = 1$  V, and  $C_C = 25$  fF. State your assumptions. (b) Suppose a 128 Mb memory using these cells is refreshed every 5 ms. What is the average power consumed by the charge redistribution operation?

- \*8.13. The gate-source and drain-source capacitances of the MOSFET in Fig. P8.9 are each 100 fF, and  $C_C = 75$  fF. The bitline and wordline have been stable at 2.5 V for a long time. The wordline signal is shown in Fig. P8.13. What is the voltage stored on  $C_C$  before the wordline drops? Estimate the drop in voltage on the  $C_C$  due to coupling of the wordline signal through the gate-source capacitance. Use  $V_{TO} = 0.70$  V,  $\gamma = 0.5\sqrt{V}$ , and  $2\phi_F = 0.6$  V.

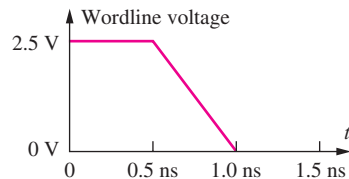


Figure P8.13

- 8.14. A 1-T cell has  $C_C = 60$  fF and  $C_{BL} = 7.5$  pF. (a) If the bitlines are precharged to 2.5 V, and the cell voltage is 0 V, what is the change in bitline voltage  $\Delta V$  following cell access? (b) What is the final voltage in the cell?
- 8.15. A 1-T cell memory can be fabricated using PMOS transistors in the array shown in Fig. P8.15. (a) What are the voltages stored on the capacitor corresponding to logic 0 and 1 levels for a technology using  $V_{DD} = 3.3$  V? (b) Repeat for  $V_{DD} = 2.5$  V.

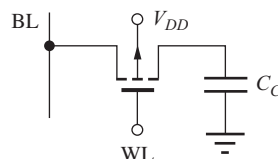


Figure P8.15

- 8.16. The bottom electrode of the storage capacitor in the 1-T cell is often connected to a voltage  $V_{PP}$  rather than ground, as shown in Fig. P8.16. Suppose that  $V_{PP} = 5$  V. (a) What are the voltages stored in the cell at node  $V_C$  for 0 = 0 V on the bitline and 1 = 3 V on the bitline? Assume the wordline can be driven to 3 V. (b) Which level will deteriorate due to leakage in this cell?

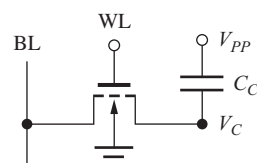


Figure P8.16

- 8.17. (a) Calculate the cell voltage for the boosted wordline version of the 1-T cell in Fig. 8.24 and show that the value in the text is correct. (b) Verify that the value of the current entering the sense amplifier node from the 1-T cell immediately following activation of the wordline is 216  $\mu\text{A}$ .
- \*8.18. The 1-T cell in Fig. P8.18 uses bitline and wordline voltages of 0 V and 5 V. (a) What are the cell voltages stored on  $C_C$  for a 1 and 0 if  $V_{TO} = -0.80 \text{ V}$ ,  $\gamma = 0.65 \text{ V}^{0.5}$ , and  $2\phi_F = 0.6 \text{ V}$ ? (b) What would be the minimum wordline voltage needed for the stored cell voltage to reach 0 V for a 0 state?

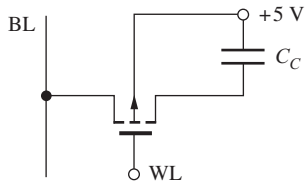


Figure P8.18

- \*8.19. In the discussion of the 1-T cell in the text, an improvement factor of 15 was stated for current drive from the boosted wordline cell compared to the normal cell. How much of this factor of 15 is attributable to the increased  $V_{DS}$  across the access transistor, and what portion is attributable to the increased gate voltage?
- 8.20. Simulate the refresh operation of the 4-T dynamic cell in Fig. P8.20. For initial conditions, assume that node  $D$  has decreased to 1 V, and node  $\bar{D}$  is at 0 V. Use  $BL = 3 \text{ V}$ ,  $\bar{BL} = 3 \text{ V}$ ,  $W/L = 2/1$  for all transistors, and the bitline capacitance is 500 fF.

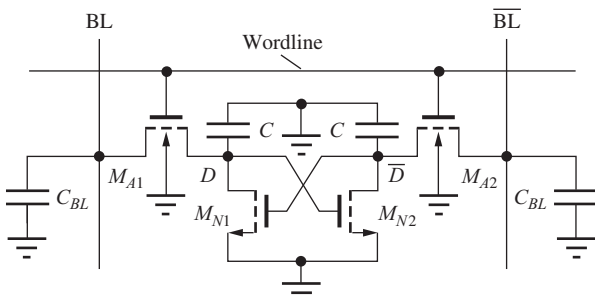


Figure P8.20

- \*\*8.21. Simulate the read access operation of the 4-T cell in Fig. P8.21 and discuss the waveforms that you obtain. What is the access time of the cell from the

time the wordline is activated until the data is valid at the output of the sense amplifier? Use  $W/L = 2/1$  for all devices, and assume  $C_{BL} = 1 \text{ pF}$ , with  $V_{DD} = 3 \text{ V}$ .

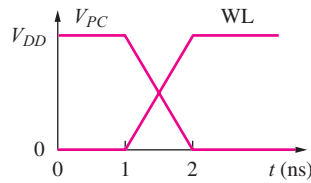
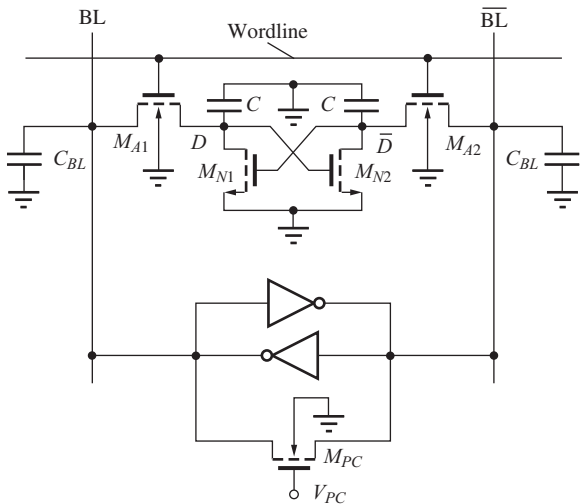


Figure P8.21

#### 8.4 Sense Amplifiers

- 8.22. A simple CMOS sense amplifier is shown in Fig. P8.22. Suppose  $V_{DD} = 2.5 \text{ V}$  and the  $W/L$  ratios of all the NMOS and PMOS transistors are 5/1 and 10/1, respectively. What is the total current through the sense amplifier when the precharge transistor is on? How much power will be consumed by 1024 of these sense amplifiers operating simultaneously?

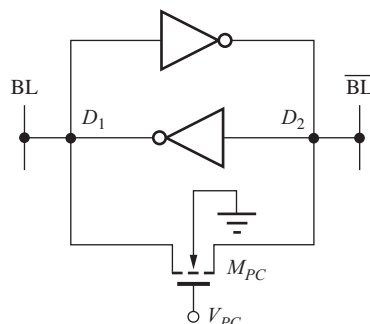


Figure P8.22

- \*\*8.23. The two bitlines in Fig. 8.29 are driven above  $V_{DD}$  by capacitive coupling of the precharge signal through the gate capacitance of the precharge device. (a) Calculate the expected voltage change  $\Delta V$  on the bitlines due to this coupling and compare to the simulation results in the figure. (b) What is the largest possible value of  $\Delta V$ ? See Appendix B for transistor models. Use  $C_{BL} = 500 \text{ fF}$ .

- \*\*8.24. A transient drop can be observed in the waveforms for the two bitlines in Fig. 8.25 due to capacitive coupling of the precharge signal through the gate capacitance of the precharge device. Calculate the expected voltage change  $\Delta V$  on the bitlines due to this coupling and compare to the simulation results in the figure. The BL capacitances are each 500 fF. See Appendix B for transistor models.

- \*\*8.25. Figure P8.25 shows the basic form of a charge-transfer sense amplifier that can be used for amplifying the output of a 1-T cell. Assume that the switch closes at  $t = 0$ , that capacitor  $C_C$  is initially discharged, and that  $C_L$  is initially charged to +3 V. Also assume that charge sharing between  $C_C$  and  $C_{BL}$  occurs instantaneously. Find the total change in the output voltage  $\Delta v_O$  that occurs once the circuit returns to steady-state conditions following the switch closure. Assume  $C_C = 50 \text{ fF}$ ,  $C_{BL} = 1 \text{ pF}$ ,  $C_L = 100 \text{ fF}$ , and  $W/L = 50/1$ . (Hint: The MOSFET will restore the BL potential to the original value, and the total charge that flows out of the source of the FET must be supplied from the drain.)

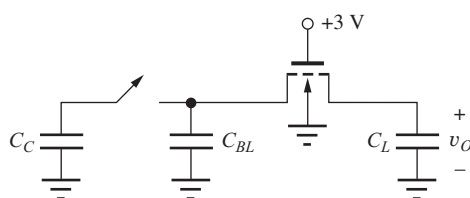


Figure P8.25 Charge transfer sense amplifier.

- 8.26. Simulate the circuit in Fig. P8.25 using a MOSFET ( $W/L = 4/1$ ) for the switch and compare the results to your hand calculations.

- \*\*8.27. Convince yourself of the statement that any voltage imbalance in the cross-coupled latch will be reinforced by simulating the CMOS latch of Fig. P8.27 using the following initial conditions: (a)  $D_1 = 1.45 \text{ V}$  and  $D_2 = 1.55 \text{ V}$ , (b)  $D_1 = 1 \text{ V}$  and  $D_2 = 1.25 \text{ V}$ , (c)  $D_1 = 2.75 \text{ V}$  and  $D_2 = 2.70 \text{ V}$ .

Assume all  $W/L$  ratios are 2/1 and  $V_{DD} = 3.3 \text{ V}$ , and use bitline capacitances of 1 pF.

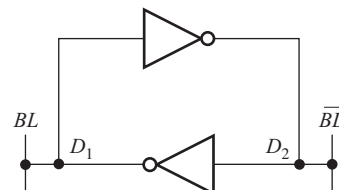


Figure P8.27

- \*8.28. The  $W/L$  ratios of the NMOS and PMOS transistors are 2/1 and 4/1, respectively, in the CMOS inverters in Fig. P8.28. The bitline capacitances are 400 fF,  $W/L$  of  $M_{PC}$  is 10/1, and  $V_{DD} = 3 \text{ V}$ . (a) Simulate the switching behavior of the symmetrical latch and explain the behavior of the voltages at nodes  $D_1$  and  $D_2$ . (b) Now suppose that a design error occurred and the  $W/L$  ratio of  $M_{N2}$  is 2.2/1 instead of 2/1. Simulate the latch again and explain any changes in the behavior of the voltages at nodes  $D_1$  and  $D_2$ .

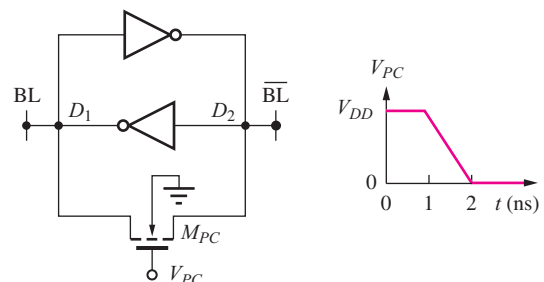


Figure P8.28

- \*8.29. Simulate the response of the NMOS clocked sense amplifier in Fig. P8.29 if  $V_{DD} = 3 \text{ V}$ . What are the final voltage values on the two bitlines? How long does it take for the sense amplifier to develop a

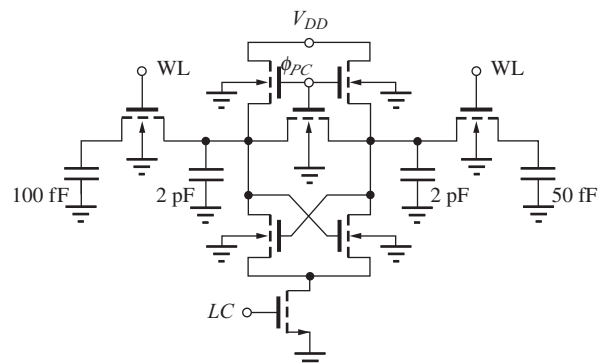


Figure P8.29

difference of 1.5 V between the two bitlines? Assume that all clock signals have amplitudes equal to  $V_{DD}$  and rise or fall times of 1 ns. Assume that the three signals are delayed successively by 0.5 ns in a manner similar to Fig. 8.29.

- \*8.30. Repeat Prob. 8.29 for  $V_{DD} = 5$  V.



- 8.31. Simulate the transfer function of two cascaded CMOS inverters with all 2/1 devices and find the three equilibrium points. Use  $V_{DD} = 3$  V.

- 8.32. (a) Find the noise margins for a memory cell formed from two cross-coupled inverters as defined in Prob. 8.31. Use the method described in the EIA on page 420. (b) Repeat for a symmetrical inverter using a 2/1 NMOS device and a 5/1 PMOS device.

## 8.5 Address Decoders

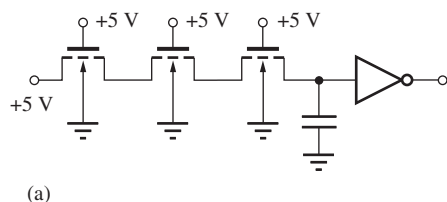
- 8.33. Calculate the number of transistors required to implement a 7-bit column decoder using (a) NMOS pass-transistor logic and (b) standard NOR logic.

- 8.34. (a) How many transistors are required to implement a full 12-bit NOR address decoder similar to that of Fig. 8.30? (b) How many transistors are required to implement a full 12-bit NAND address decoder similar to that of Fig. 8.31?

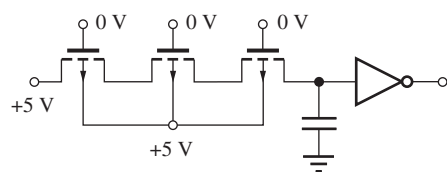
- 8.35. Draw the schematic of a 3-bit OR address decoder using domino CMOS.



- 8.36. What are the voltages at the nodes in the pass-transistor networks in Fig. P8.36? For NMOS transistors, use  $V_{TO} = 0.8$  V,  $\gamma = 0.6\sqrt{V}$ , and  $2\phi_F = 0.6$  V. For PMOS transistors,  $V_{TO} = -0.8$  V and  $\gamma = 0.6\sqrt{V}$ .



(a)



(b)

Figure P8.36

- \*8.37. (a) Suppose that inputs  $A_0$ ,  $A_1$ , and  $A_2$  are all 0 in the domino CMOS gate in Fig. P8.37, and the clock has just changed to the evaluate phase. If  $A_0$  now changes to a 1, what happens to the voltage at node  $B$  if  $C_1 = 2C_2$ ? (Hint: Remember the charge-sharing phenomena.) (b) Now  $A_1$  changes to a 1—what happens to the voltage at node  $B$  if  $C_3 = C_2$ ? (c) If the output inverter is a symmetrical design, what is the minimum ratio of  $C_1/C_2$  (assume  $C_3 = C_2$ ) for which the gate maintains a valid output? Assume  $V_{DD} = 5$  V.

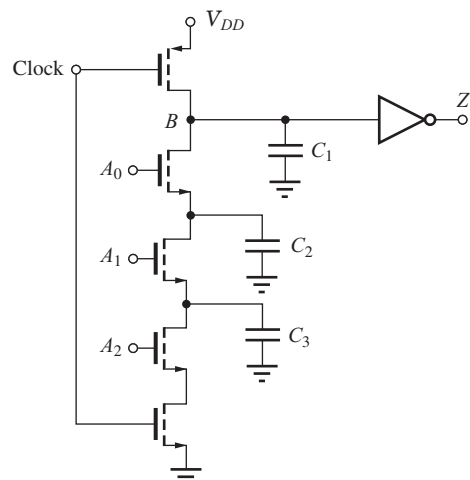


Figure P8.37

- 8.38. Draw the mirror image of the gate in Fig. P8.37 by replacing NMOS transistors with PMOS transistors and vice versa. Assume the logic inputs remain the same and write an expression for the logic function  $Z$ .

## 8.6 Read-Only Memory (ROM)

- 8.39. What are the contents of the ROM in Fig. P8.39? (All FETs are NMOS.)
- 8.40. What are the contents of the ROM in Fig. P8.40? (All FETs are NMOS.)
- 8.41. What are the six output data words for the ROM in Fig. P8.41?
- 8.42. Identify and simulate the worst-case delay path in the ROM in Fig. P8.41.
- 8.43. Redraw the ROM circuit in Fig. 8.36 using pseudo-NMOS circuitry.

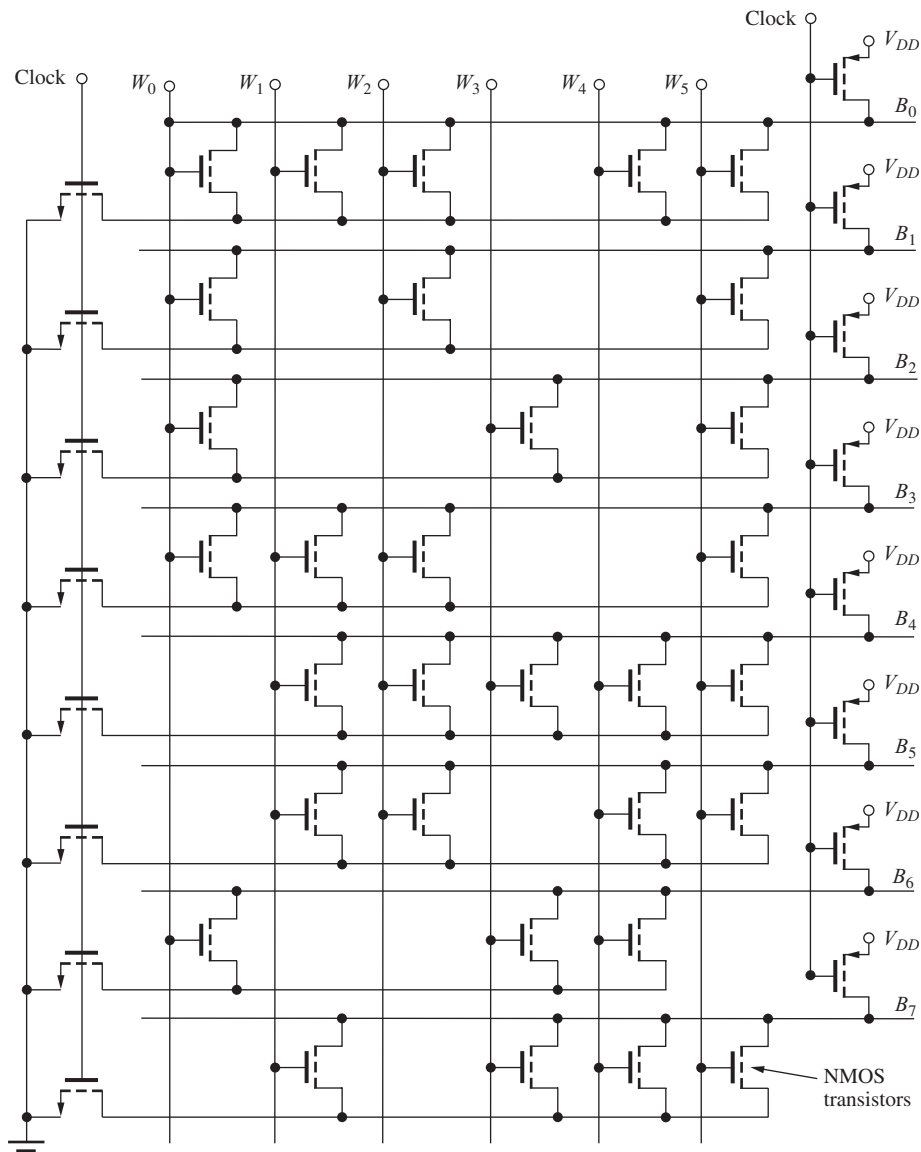


Figure P8.41

## 8.7 Flip-Flops

- 8.44. What are the logic functions of inputs 1 and 2 in the flip-flop in Fig. P8.44?
- 8.45. What is the minimum size of the transistors connected to the R and S inputs in Fig. P8.45 that will ensure that the latch can be forced to the desired state? Do not be concerned with speed of the latch.

8.46. Simulate the propagation delay through the D latch to  $Q$  and  $\bar{Q}$  in Fig. 8.44. Assume that D is stable and the clock signal is a square wave. Assume the transistors all have  $W/L = 2/1$  and use  $V_{DD} = 2.5$  V. Use the transistor models on Appendix B.

8.47. Simulate the master-slave D-flip-flop with the slowly rising clock ( $T = 20 \mu\text{s}$ ) in Fig. P8.47(a). Assume all  $W/L = 2/1$ . What happens to data on the D input? Use the transistor models in Appendix B.

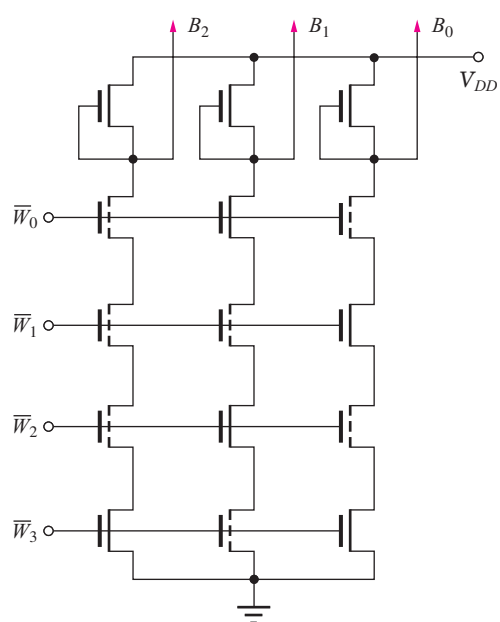


Figure P8.39

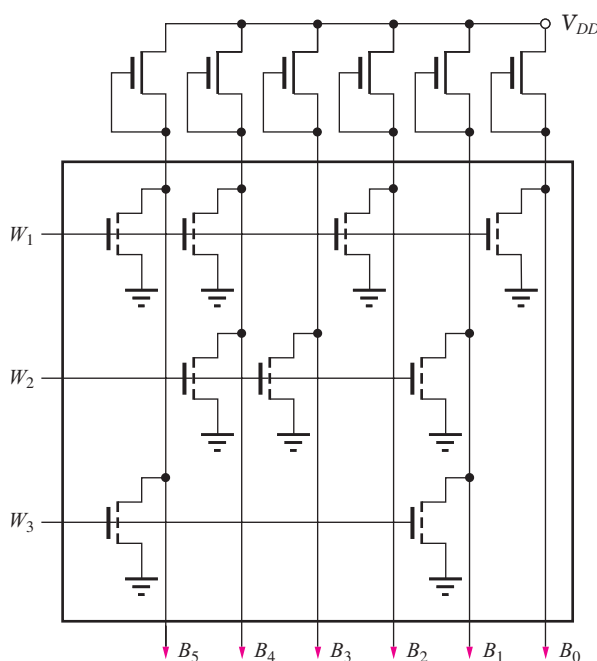


Figure P8.40

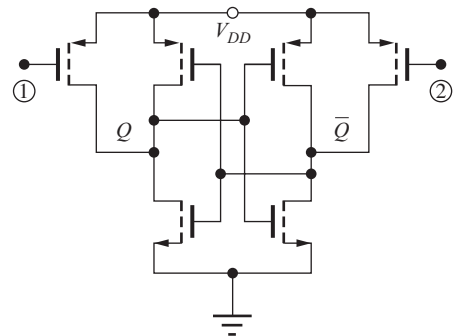


Figure P8.44

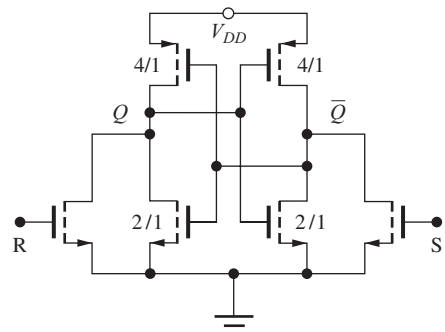


Figure P8.45

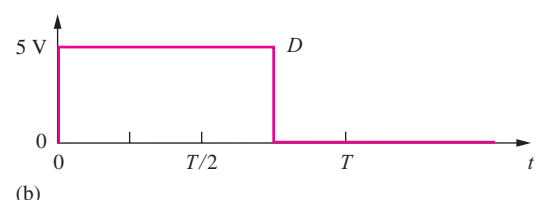
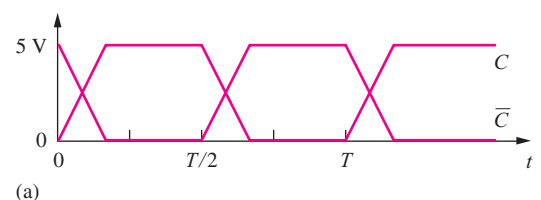
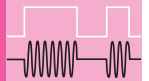


Figure P8.47

# CHAPTER 9



## BIPOLAR LOGIC CIRCUITS

### CHAPTER OUTLINE

- 9.1 The Current Switch (Emitter-Coupled Pair) 461
- 9.2 The Emitter-Coupled Logic (ECL) Gate 464
- 9.3 Noise Margin Analysis for the ECL Gate 467
- 9.4 Current Source Implementation 469
- 9.5 The ECL OR-NOR Gate 471
- 9.6 The Emitter Follower 473
- 9.7 “Emitter Dotting” or “Wired-OR” Logic 476
- 9.8 ECL Power-Delay Characteristics 477
- 9.9 Current-Mode Logic 481
- 9.10 The Saturating Bipolar Inverter 487
- 9.11 A Transistor-Transistor Logic (TTL) Prototype 494
- 9.12 The Standard 7400 Series TTL Inverter 500
- 9.13 Logic Functions in TTL 504
- 9.14 Schottky-Clamped TTL 506
- 9.15 Comparison of the Power-Delay Products of ECL and TTL 508
- 9.16 BiCMOS Logic 509
- Summary 513
- Key Terms 515
- Reference 515
- Additional Reading 515
- Problems 516

### CHAPTER GOALS

From Chapter 9, we shall gain a basic appreciation of the switching characteristics of the bipolar transistor and for the design of the most important bipolar logic circuit families. The material in this chapter includes

- Bipolar current switch circuits
- Emitter-coupled logic (ECL)
- Behavior of the bipolar transistor as a saturated switch
- Transistor-transistor logic (TTL)
- Schottky clamping techniques for preventing saturation
- Operation of the transistor in the inverse-active region
- Current-mode logic
- BiCMOS logic circuits

As mentioned in Chapters 1 and 2, bipolar transistors were the first three-terminal solid-state devices to reach high-volume manufacturing, and in fact the first integrated circuits were bipolar logic circuits. The earliest logic family, built with just resistors and transistors, was called



Photo of a group of TTL unit logic.

resistor-transistor logic or RTL. Later it was discovered that improved logic characteristics could be obtained by adding input diodes to the logic gate, creating a family called diode-transistor logic or DTL. Shortly thereafter, it was realized that the diodes in DTL could be merged and replaced by a multi-input transistor, and this circuit became the basis of transistor-transistor logic — TTL or  $T^2L$ .

TTL evolved into an extremely robust logic family that was very easy to use, and TTL was the dominant logic technology from the mid-1960s through the mid-1980s. A tremendous number of different types of logic gates and system components were made available by the manufacturers. TTL is still widely used today in prototype systems and as “glue” logic in most digital systems.

The second form of bipolar logic that found wide use is emitter-coupled logic or ECL. ECL has traditionally represented the highest-speed form of logic that is available, and it was the technology of choice for large mainframe computers and supercomputers for many years. ECL unit logic families also offer an extremely wide range of logic gates and system building blocks.

Low-voltage and low-power versions of both TTL and ECL were eventually developed for VLSI applications, but still suffered from relatively high levels of power consumption compared to CMOS technology. Today, sub-micron CMOS now offers logic delay performance approaching that of emitter-coupled logic but with much higher circuit density and lower power consumption. Yet,

the high transconductance of the bipolar transistor is still a significant advantage, and a number of semiconductor companies have developed complex BiCMOS processes that add bipolar transistors (often both *npn* and *pnp* devices)

to a full CMOS technology. Silicon-germanium (SiGe) bipolar transistors have been used to achieve record performance in frequency synthesizers and other RF circuits using current-mode logic, an extension of emitter-coupled logic.

## C

Chapter 9 explores details of the two bipolar circuit families that have been used extensively in logic circuit design since the mid-1960s. **Emitter-coupled logic (ECL)** historically has been the fastest form of logic available. The ECL circuit uses bipolar transistors operating in a differential circuit that is often called a current switch. For binary logic operation, two states are needed, and in ECL, the transistors operate in the forward-active region with either a relatively large collector current or a very small collector current, actually near cutoff. The transistors avoid saturation and an attendant delay time that substantially slows down BJT switching speed. **Current-mode logic (CML)** maintains the high speed of ECL but reduces power by stacking several current switch cells on top of each other, effectively reusing the bias current.

**Transistor-transistor logic (TTL or T<sup>2</sup>L)** was the dominant logic family for systems designed through the mid-1980s, when CMOS began to replace it. TTL was the family that established 5 V as the standard power supply level. The main transistors in a TTL switch between the **forward-active**—but essentially nonconducting—and **saturation regions** of operation. In the TTL circuit, we find one of the few actual applications for the **reverse-active region** of operation of the BJT. Because various transistors in the TTL circuit enter saturation, TTL delays tend to be poorer than those that can be achieved with ECL. However, an improved circuit, Schottky-clamped TTL, is substantially faster than standard TTL or can achieve delays similar to standard TTL at much less power dissipation.

## 9.1 THE CURRENT SWITCH (EMITTER-COUPLED PAIR)

We begin our study of bipolar logic circuits with emitter-coupled logic, or ECL. At the heart of an ECL gate is the **current switch circuit** in Fig. 9.1, consisting of two identical transistors,  $Q_1$  and  $Q_2$ , two matched-load resistors,  $R_C$ , and current source  $I_{EE}$ . This circuit is also known as an **emitter-coupled pair**. The input logic signal  $v_I$  is applied to the base of  $Q_1$  and is compared to the **reference voltage**  $V_{REF}$ , that is connected to the base of transistor  $Q_2$ . If  $v_I$  is greater than  $V_{REF}$  by a few hundred millivolts, then the current from source  $I_{EE}$  is supplied through the emitter of  $Q_1$ . If  $v_I$  is less than  $V_{REF}$  by a few hundred millivolts, then the current from source  $I_{EE}$  is supplied by the emitter of  $Q_2$ . Thus input voltage  $v_I$  “switches” the current from source  $I_{EE}$  back and forth between  $Q_1$  and  $Q_2$ . This behavior is conceptually illustrated in Fig. 9.2, in which transistors  $Q_1$  and  $Q_2$  have been replaced by a single-pole, double-throw switch whose position is controlled by the input  $v_I$ .

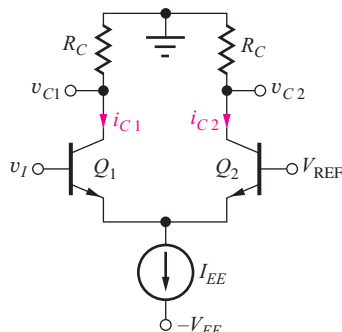


Figure 9.1 Current switch circuit used in an ECL gate.

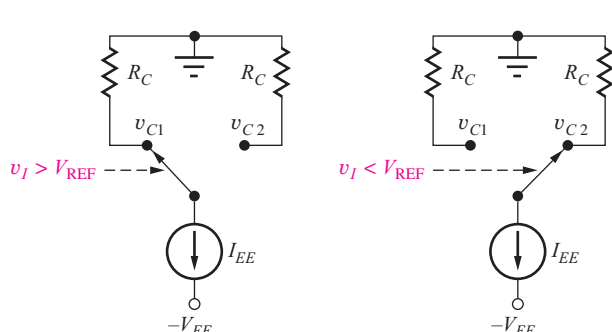


Figure 9.2 Conceptual representation of the current switch.

### 9.1.1 MATHEMATICAL MODEL FOR STATIC BEHAVIOR OF THE CURRENT SWITCH

The behavior of the current switch can be understood in more detail using the transport model for the forward-active region from Chapter 5, in which the collector currents in the two transistors are represented by

$$i_{C1} = I_S \exp\left(\frac{v_{BE1}}{V_T}\right) \quad \text{and} \quad i_{C2} = I_S \exp\left(\frac{v_{BE2}}{V_T}\right) \quad (9.1)$$

It is assumed in Eq. (9.1) that  $v_{BE} > 4V_T$ . If the transistors are identical, so that the saturation currents are the same, then the ratio of these two collector currents can be written as

$$\frac{i_{C2}}{i_{C1}} = \frac{I_S \exp\left(\frac{v_{BE2}}{V_T}\right)}{I_S \exp\left(\frac{v_{BE1}}{V_T}\right)} = \exp\left(\frac{v_{BE2} - v_{BE1}}{V_T}\right) = \exp\left(-\frac{\Delta v_{BE}}{V_T}\right) \quad (9.2)$$

Now, suppose that  $v_{BE2}$  exceeds  $v_{BE1}$  by 300 mV:  $\Delta v_{BE} = (v_{BE1} - v_{BE2}) = -0.3$  V. For  $V_T = 0.025$  V, we find that  $i_{C2}$  is approximately  $1.6 \times 10^5$  times bigger than  $i_{C1}$ .<sup>1</sup> However, if  $v_{BE1}$  exceeds  $v_{BE2}$  by 300 mV, then  $i_{C1}$  will be  $1.6 \times 10^5$  times larger than  $i_{C2}$ . Thus, the assumption that all the current from the source  $I_{EE}$  is switched from one side to the other appears justified for a few-hundred-millivolt difference in  $v_{BE}$ .

A useful expression for the normalized difference in collector currents can be derived from Eq. (9.1):

$$\frac{i_{C1} - i_{C2}}{i_{C1} + i_{C2}} = \frac{\exp\left(\frac{v_{BE1}}{V_T}\right) - \exp\left(\frac{v_{BE2}}{V_T}\right)}{\exp\left(\frac{v_{BE1}}{V_T}\right) + \exp\left(\frac{v_{BE2}}{V_T}\right)} = \tanh\left(\frac{v_{BE1} - v_{BE2}}{2V_T}\right) \quad (9.3)$$

Using Kirchhoff's current law at the emitter node yields

$$i_{E1} + i_{E2} = I_{EE} \quad \text{so that} \quad i_{C1} + i_{C2} = \alpha_F I_{EE} \quad (9.4)$$

since  $i_C = \alpha_F i_E$  in the forward-active region, and assuming matched devices with identical current gains. Combining Eqs. (9.3) and (9.4) gives the desired result for the collector current difference in terms of the difference in base-emitter voltages:

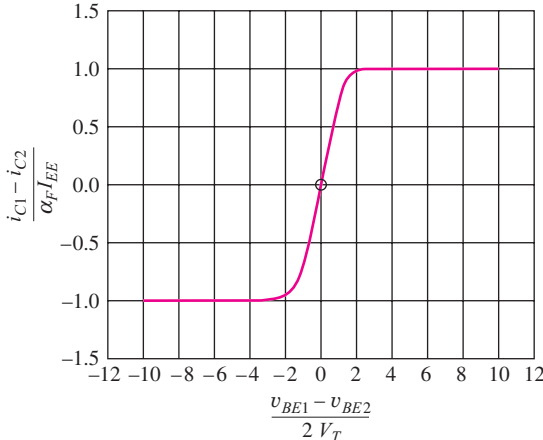
$$i_{C1} - i_{C2} = \alpha_F I_{EE} \tanh\left(\frac{v_{BE1} - v_{BE2}}{2V_T}\right) \quad (9.5)$$

Figure 9.3 plots a graph of Eq. (9.5) in normalized form, showing that only a small voltage change is required to switch the current from one collector to the other. Ninety-nine percent of the current switches for  $|\Delta v_{BE}| > 4.6V_T$  (130 mV)! We see that a relatively small voltage change is required to completely switch the current from one side to the other in the current switch. This small voltage change directly contributes to the high speed of ECL logic gates.

**EXERCISE:** Calculate the ratio  $i_{C2}/i_{C1}$  for  $(v_{BE2} - v_{BE1}) = 0.2$  V, 0.3 V and 0.4 V.

**ANSWERS:**  $2.98 \times 10^3$ ;  $1.63 \times 10^5$ ;  $8.89 \times 10^6$

<sup>1</sup> Remember that one decade of current change in a BJT corresponds to approximately a 60-mV change in  $v_{BE}$ , so a factor of  $10^5$  is precisely the change we expect for a  $\Delta V_{BE}$  of 300 mV.



**Figure 9.3** Normalized collector current difference versus  $\Delta v_{BE}/2V_T$  for the bipolar current switch.

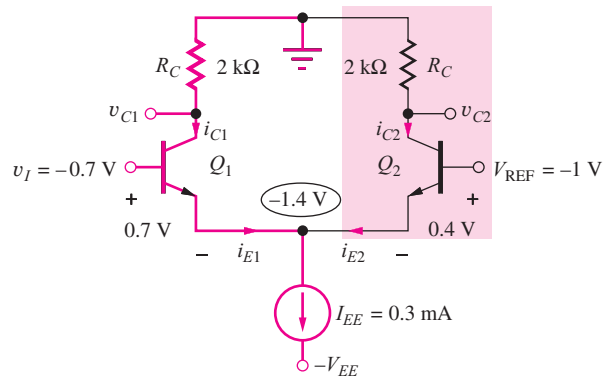


**Figure 9.4** Current switch circuit with  $v_I > V_{\text{REF}}$ .  $Q_1$  is conducting;  $Q_2$  is “off.”

### 9.1.2 CURRENT SWITCH ANALYSIS FOR $v_I > V_{\text{REF}}$

Now let us explore the actual current switch circuit for the case of  $v_I = V_{\text{REF}} + 0.3 \text{ V} = -0.7 \text{ V}$ , as in Fig. 9.4. From Fig. 9.3 we expect 0.3 V to be more than enough to fully switch the current. In this design,  $V_{\text{REF}}$  has been selected to be  $-1.0 \text{ V}$  (the reasons for this choice will become clear shortly). Because  $v_I > V_{\text{REF}}$ , we assume that  $Q_2$  is off ( $i_{C2} = 0$ ) and  $Q_1$  is conducting in the forward-active region with  $V_{BE1} = 0.7 \text{ V}$ . Applying Kirchhoff’s voltage law to the circuit in Fig. 9.4:

$$\begin{aligned} v_I - v_{BE1} + v_{BE2} - V_{\text{REF}} &= 0 \\ (V_{\text{REF}} + 0.3 \text{ V}) - (0.7) + v_{BE2} - V_{\text{REF}} &= 0 \quad \text{and} \quad v_{BE2} = 0.4 \text{ V} \end{aligned} \quad (9.6)$$

The base-emitter voltage difference is given by  $v_{BE1} - v_{BE2} = 300 \text{ mV}$ , so essentially all the current  $I_{EE}$  switches to the emitter of  $Q_1$ , and  $Q_2$  is nearly cut off. [However,  $Q_2$  is actually still in the forward-active region by our strict definition of the regions of operation for the bipolar transistor ( $v_{BE} \geq 0, v_{BC} \leq 0$ ].

At the emitter node, we have  $i_{E1} \cong I_{EE}$  because  $i_{E2} \cong 0$  and the output voltages  $v_{C1}$  and  $v_{C2}$  at the two collectors are given by

$$v_{C1} = -i_{C1}R_C = -\alpha_F i_{E1}R_C \cong -\alpha_F I_{EE}R_C \quad (9.7)$$

$$v_{C2} = -i_{C2}R_C = -\alpha_F i_{E2}R_C \cong 0 \quad (9.8)$$

in which  $i_C = \alpha_F i_E$  in the forward-active region. For  $\alpha_F \cong 1$ , the two output voltages become

$$v_{C1} = -i_{C1}R_C \cong -I_{EE}R_C \quad \text{and} \quad v_{C2} = -i_{C2}R_C = 0 \quad (9.9)$$

For the circuit in Fig. 9.4,  $I_{EE} = 0.3 \text{ mA}$  and  $R_C = 2 \text{ k}\Omega$ , and

$$v_{C1} = -0.6 \text{ V} \quad \text{and} \quad v_{C2} = 0 \text{ V} \quad (9.10)$$

#### Check of Forward-Active Region Assumptions

Now we can check our assumptions concerning the forward-active region of operation. For  $Q_1$ ,  $v_{BC1} = v_{B1} - v_{C1} = -0.7 \text{ V} - (-0.6 \text{ V}) = -0.1 \text{ V}$ , and the collector-base junction is indeed reverse-biased. We assumed that the emitter-base junction was forward-biased, so the assumption of forward-active region is consistent with our circuit analysis. For  $Q_2$ ,  $v_{BC2} = -1.0 \text{ V} - (0 \text{ V}) = -1.0 \text{ V}$  and  $v_{BE2} = 0.4 \text{ V}$ , so  $Q_2$  is also in the forward-active region, although, it is conducting a negligibly small current.

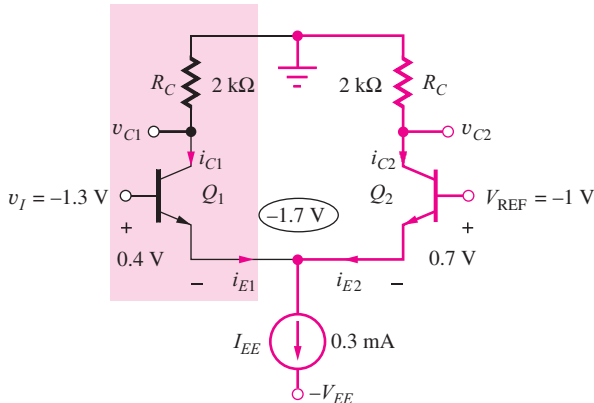


**Figure 9.5** Current switch circuit with  $v_I < V_{\text{REF}}$ .  $Q_2$  is conducting;  $Q_1$  is “off.”

**TABLE 9.1**  
Current Switch Voltage Levels

$v_I$ ( $V_{\text{REF}} = -1.0 \text{ V}$ )	$v_{C1}$	$v_{C2}$
$V_{\text{REF}} + 0.3 \text{ V} = -0.7 \text{ V}$	$-0.6 \text{ V}$	$0 \text{ V}$
$V_{\text{REF}} - 0.3 \text{ V} = -1.3 \text{ V}$	$0 \text{ V}$	$-0.6 \text{ V}$

### 9.1.3 CURRENT SWITCH ANALYSIS FOR $v_I < V_{\text{REF}}$

The second logic state occurs for  $v_I = V_{\text{REF}} - 0.3 \text{ V} = -1.3 \text{ V}$ , as in Fig. 9.5. Because  $v_I < V_{\text{REF}}$ , we assume that  $Q_2$  is conducting in the forward-active region, with  $v_{BE2} = 0.7 \text{ V}$ . Kirchhoff's voltage law again requires

$$v_I - v_{BE1} + v_{BE2} - V_{\text{REF}} = 0$$

which yields

$$(V_{\text{REF}} - 0.3 \text{ V}) - v_{BE1} + (0.7) - V_{\text{REF}} = 0 \quad \text{and} \quad v_{BE1} = 0.4 \text{ V}$$

$v_{BE1}$  is much less than  $v_{BE2}$ , so now  $i_{E1} \cong 0$ , and  $i_{E2} \cong I_{EE}$ . The output voltages at  $v_{C1}$  and  $v_{C2}$  are given by

$$\begin{aligned} v_{C1} &= -i_{C1}R_C = -\alpha_F i_{E1}R_C \cong 0 \\ v_{C2} &= -i_{C2}R_C = -\alpha_F i_{E2}R_C \cong -\alpha_F I_{EE}R_C = -0.6 \text{ V} \end{aligned} \tag{9.11}$$

for  $\alpha_F \cong 1$ .

The results from Eqs. (9.10) and (9.11) are combined in Table 9.1. We see there are two discrete voltage levels at the two outputs,  $0 \text{ V}$  and  $-0.6 \text{ V}$ , that can correspond to a logic 1 and a logic 0, respectively. Note, however, that the voltages at the outputs of the current switch do not match the input voltages used at  $v_I$ . Thus, this current switch circuit fails to meet one of the important criteria for logic gates set forth in Sec. 6.2.3: The logic levels must be restored as the signal goes through the gate. That is, the voltage levels at the output of a logic gate must be compatible with the levels used at the input of the gate.

**EXERCISE:** Redesign the circuit in Fig. 9.4 to reduce the power by a factor of five while maintaining the same voltage levels.

**ANSWER:**  $R_C = 10 \text{ k}\Omega$ ,  $I_{EE} = 60 \mu\text{A}$

## 9.2 THE Emitter-Coupled Logic (ECL) GATE

We observe in Table 9.1 that the high and low logic levels at the input and output of the current switch differ by exactly one base-emitter voltage drop ( $0.7 \text{ V}$ ), which leads to the circuit of the complete ECL inverter in Fig. 9.6. Two transistors,  $Q_3$  and  $Q_4$ , have been added, and their base-emitter junctions

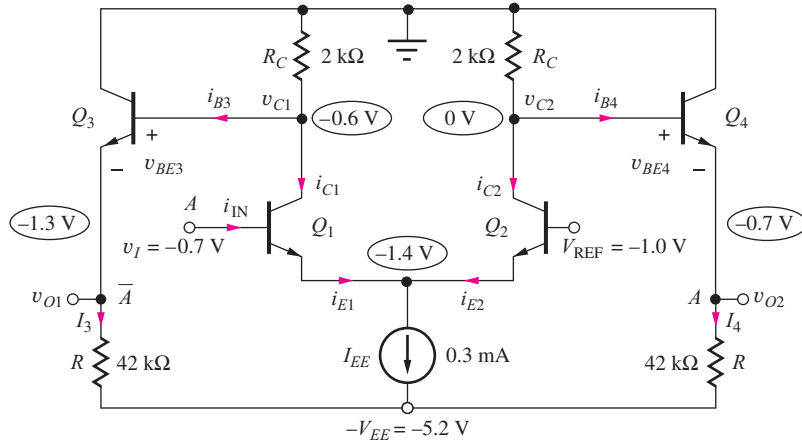


Figure 9.6 Emitter-coupled logic circuit with  $v_I = V_H$ .

are used to shift the output voltages down by one base-emitter drop. These transistors act as **level shifters** in the circuit and are usually called emitter followers. The emitter-followers also give the circuit a high fanout capability.

### 9.2.1 ECL GATE WITH $v_I = V_H$

To understand how the level-shifting operation takes place in the ECL circuit, consider the case for  $v_I = V_H = -0.7$  V indicated in Fig. 9.6. Equations for the output voltages  $v_{O1}$  and  $v_{O2}$  can be written as

$$v_{O1} = v_{C1} - v_{BE3} \quad \text{and} \quad v_{O2} = v_{C2} - v_{BE4} \quad (9.12)$$

in which each output is now one base-emitter voltage drop below the corresponding collector level. Expanding the expressions for the collector voltages in terms of the transistor currents yields

$$v_{O1} = -(i_{C1} + i_{B3})R_C - v_{BE3} \quad \text{and} \quad v_{O2} = -(i_{C2} + i_{B4})R_C - v_{BE4}$$

where the base currents are given by

$$i_{B3} = \frac{I_3}{\beta_F + 1} \quad \text{and} \quad i_{B4} = \frac{I_4}{\beta_F + 1}$$

In a typical digital IC technology,  $\beta_F \geq 20$  and  $i_B R_C$  is designed to be much less than  $v_{BE}$ . Then

$$v_{O1} \cong -i_{C1}R_C - v_{BE3} = -0.6 - 0.7 = -1.3 \text{ V}$$

and

$$v_{O2} \cong -i_{C2}R_C - v_{BE4} = 0 - 0.7 = -0.7 \text{ V} \quad (9.13)$$

For sufficiently large  $\beta_F$ , the addition of  $Q_3$  and  $Q_4$  does not change the voltage at  $v_{C1}$  or  $v_{C2}$ .

The base-collector voltages of  $Q_3$  and  $Q_4$  will be  $-0.6$  V and  $0$  V, respectively, and the two emitter resistors  $R$  set up an average current of  $0.1$  mA in the emitters of  $Q_3$  and  $Q_4$ :

$$I_{E3} = \frac{-1.3 - (-5.2)}{42} \frac{\text{V}}{\text{k}\Omega} = 92.9 \mu\text{A} \quad \text{and} \quad I_{E4} = \frac{-0.7 - (-5.2)}{42} \frac{\text{V}}{\text{k}\Omega} = 107 \mu\text{A} \quad (9.14)$$

Thus, both  $Q_3$  and  $Q_4$  are in the forward-active region, so  $v_{BE3} = v_{BE4} = 0.7$  V has been used.

**EXERCISE:** What are the base currents  $i_{B3}$  and  $i_{B4}$  in Fig. 9.6 if  $\beta_F = 20$ ? Compare  $i_B R_C$  to  $V_{BE}$ .

**ANSWERS:**  $4.42 \mu\text{A}, 5.10 \mu\text{A}, 8.84 \text{ mV} \ll 0.7 \text{ V}, 10.2 \text{ mV} \ll 0.7 \text{ V}$

### 9.2.2 ECL GATE WITH $v_I = V_L$

For  $v_I = V_L = -1.3$  V, the outputs change state, and:

$$\begin{aligned} v_{O1} &\cong -i_{C1}R_C - v_{BE3} = 0 - 0.7 = -0.7 \text{ V} \\ v_{O2} &\cong -i_{C2}R_C - v_{BE4} = -0.6 - 0.7 = -1.3 \text{ V} \end{aligned} \quad (9.15)$$

### 9.2.3 INPUT CURRENT OF THE ECL GATE

In NMOS and CMOS logic circuits, the inputs are normally connected to FET gates, and the static input current to the logic gate is zero. In bipolar logic circuits, however, there is a nonzero current in the input. For the ECL gate in Fig. 9.6, the input current  $i_{IN}$  is equal to the base current of  $Q_1$ . When  $Q_1$  is conducting ( $v_I = -0.7$  V), the input current is given by

$$i_{IN} = i_{B1} = \frac{i_{E1}}{\beta_F + 1} = \frac{0.3 \text{ mA}}{21} = 14.3 \mu\text{A} \quad (9.16)$$

whereas  $i_{IN} \cong 0$  when  $Q_1$  is off ( $v_I = -1.3$  V). Thus, a circuit that is providing an input to an ECL gate must be capable of supplying 14.3  $\mu\text{A}$  to each input that it drives.

### 9.2.4 ECL SUMMARY

Table 9.2 summarizes the behavior of the basic ECL inverter in Fig. 9.6. The requirement for level compatibility between the input and output voltages is now met. For this ECL gate design,

$$V_H = -0.7 \text{ V}, V_L = -1.3 \text{ V}, \text{ and } \Delta V = V_H - V_L = 0.6 \text{ V} \quad (9.17)$$

To provide symmetrical noise margins, the reference voltage  $V_{REF}$  is normally centered midway between the two logic levels:

$$V_{REF} = \frac{V_H + V_L}{2} = -1.0 \text{ V} \quad (9.18a)$$

In the design in Fig. 9.6, the logic signal swings symmetrically above and below  $V_{REF}$  by one-half the logic swing, or 0.3 V. Note that the logic swing  $\Delta V$  is just equal to the voltage drop developed across the load resistor  $R_C$ :

$$\Delta V = I_{EE}R_C \quad (9.18b)$$

Several important observations can be made at this point. If the input at  $v_I$  is now defined as the logic variable  $A$ , then the output at  $v_{O1}$  corresponds to  $\bar{A}$ , but the output at  $v_{O2}$  corresponds to  $A!$  A complete ECL gate generates both true and complement outputs for a given logic function. Having both true and complement outputs available can often reduce the total number of logic gates required to implement a given logic function.

A second observation relates to the speed of emitter-coupled logic. The transistors remain in the forward-active region at all times. The “off” transistor is actually conducting current but at a very low level, and it is ready to switch rapidly into high conduction for a base-emitter voltage change of only a few tenths of a volt. The transistors avoid the saturation region, which substantially slows down the switching speed of the bipolar transistor. (A detailed discussion of this problem is in Sec. 9.9.) The reduced logic swing of ECL also contributes to its high speed, and the small  $\Delta V$  reduces the dynamic power required to charge and discharge the load capacitances.

**TABLE 9.2**  
ECL Voltage Levels and Input Current

$v_I$	$v_{O1}$	$v_{O2}$	$i_{IN}$
$V_{REF} + 0.3 \text{ V} = -0.7 \text{ V}$	-1.3 V	-0.7 V	+14.3 $\mu\text{A}$
$V_{REF} - 0.3 \text{ V} = -1.3 \text{ V}$	-0.7 V	-1.3 V	0

Another benefit of ECL is the nearly constant power supply current maintained by the current sources in Fig. 9.6, regardless of the gate's logic state. This constant supply current reduces noise in the power distribution network.

**EXERCISE:** Find  $V_H$ ,  $V_L$ ,  $V_{\text{REF}}$ , and  $\Delta V$  for the ECL gate in Fig. 9.6 if  $I_{EE}$  is changed to 0.2 mA.

**ANSWERS:**  $-0.7 \text{ V}$ ,  $-1.1 \text{ V}$ ,  $-0.9 \text{ V}$ ,  $0.4 \text{ V}$

## 9.3 NOISE MARGIN ANALYSIS FOR THE ECL GATE

The simulated VTC for the ECL gate is given in Fig. 9.7, in which both outputs switch between the two logic levels specified in Table 9.2. The two outputs remain constant until the input comes within approximately 100 mV of the reference voltage, and then they rapidly change states as the input voltage changes by an additional 200 mV. The approach to finding the values of  $V_{IH}$  and  $V_{IL}$  and the noise margins is similar to that used for NMOS and CMOS circuits, but the algebra is simpler.

### 9.3.1 $V_{IL}$ , $V_{OH}$ , $V_{IH}$ , AND $V_{OL}$

$V_{IH}$  and  $V_{IL}$  are defined by the points at which  $\partial v_{O1}/\partial v_I = -1$  for the inverting output or  $\partial v_{O2}/\partial v_I = +1$  for the noninverting output. Writing the expression for  $v_{O1}$  in Fig. 9.6 yields

$$v_{O1} = v_{C1} - v_{BE3} = -(i_{C1} + i_{B3})R_C - v_{BE3} \quad (9.19)$$

and taking the derivative with respect to  $v_I$  gives

$$\frac{\partial v_{O1}}{\partial v_I} = -R_C \frac{\partial i_{C1}}{\partial v_I} \quad (9.20)$$

The base current and base-emitter voltage of  $Q_3$  are constant because  $i_{E3} = I_3$ , a constant current. An expression for  $i_{C1}$  in terms of  $v_I$  can be obtained using the same procedure as that used to derive Eqs. (9.2) and (9.3):

$$\frac{i_{C1}}{i_{C1} + i_{C2}} = \frac{1}{1 + \exp\left(\frac{v_{BE2} - v_{BE1}}{V_T}\right)} \quad \text{and} \quad i_{C1} = \frac{\alpha_F I_{EE}}{1 + \exp\left(\frac{v_{BE2} - v_{BE1}}{V_T}\right)} \quad (9.21)$$

because  $i_{C1} + i_{C2} = \alpha_F I_{EE}$ . Equation (9.6) can be rearranged to yield a relationship between the input voltage and the base-emitter voltages:

$$v_{BE2} - v_{BE1} = V_{\text{REF}} - v_I \quad (9.22)$$

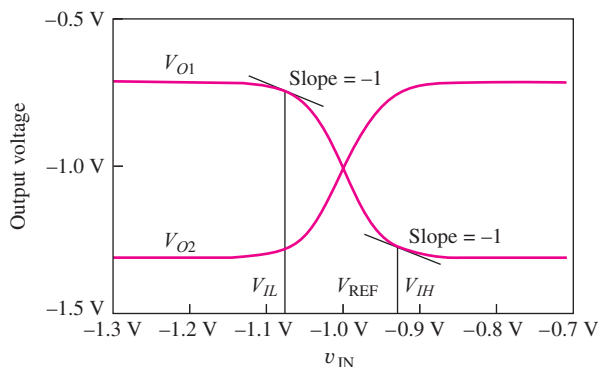


Figure 9.7 SPICE simulation results for ECL voltage transfer function.

Rewriting  $i_{C1}$  from Eq. (9.21):

$$i_{C1} = \frac{\alpha_F I_{EE}}{1 + \exp\left(\frac{V_{REF} - v_I}{V_T}\right)} \quad (9.23)$$

Taking the derivative and substituting the result in Eq. (9.20) yields

$$\frac{\partial v_{O1}}{\partial v_I} = \frac{-\left(\frac{1}{V_T}\right)i_{C1}R_C}{\left[1 + \exp\left(\frac{v_I - V_{REF}}{V_T}\right)\right]} \quad (9.24)$$

At  $v_I = V_{IL}$ ,  $v_I < V_{REF}$ ,  $\exp[(v_I - V_{REF})/V_T] \ll 1$ , and Eq. (9.24) simplifies to

$$\frac{\partial v_{O1}}{\partial v_I} \cong -\left(\frac{1}{V_T}\right)i_{C1}R_C = -1 \quad \text{or} \quad i_{C1} = \frac{V_T}{R_C} \quad (9.25)$$

Using Eq. (9.2),

$$V_{REF} - V_{IL} = V_T \ln\left(\frac{I_{EE} - i_{C1}}{i_{C1}}\right) = V_T \ln\left(\frac{\frac{I_{EE}}{R_C} - \frac{V_T}{R_C}}{\frac{V_T}{R_C}}\right) \quad (9.26)$$

Solving for  $V_{IL}$  yields

$$V_{IL} = V_{REF} - V_T \ln\left(\frac{I_{EE}R_C}{V_T} - 1\right) = V_{REF} - V_T \ln\left(\frac{\Delta V}{V_T} - 1\right) \quad (9.27)$$

and

$$V_{OH} = V_H - i_{C1}R_C = V_H - V_T$$

Using symmetry, or a similar analysis, the value of  $V_{IH}$  is

$$V_{IH} = V_{REF} + V_T \ln\left(\frac{I_{EE}R_C}{V_T} - 1\right) = V_{REF} + V_T \ln\left(\frac{\Delta V}{V_T} - 1\right) \quad (9.28)$$

and

$$V_{OL} = V_L + i_{C1}R_C = V_L + V_T$$

### 9.3.2 NOISE MARGINS

The noise margins are found using Eqs. (9.27) and (9.28):

$$NM_L = V_{IL} - V_{OL} = V_{REF} - V_T \ln\left(\frac{\Delta V}{V_T} - 1\right) - \left(V_{REF} - \frac{\Delta V}{2} + V_T\right)$$

and

$$NM_L = \frac{\Delta V}{2} - V_T \left[1 + \ln\left(\frac{\Delta V}{V_T} - 1\right)\right] \quad (9.29)$$

By symmetry,

$$NM_H = \frac{\Delta V}{2} - V_T \left[1 + \ln\left(\frac{\Delta V}{V_T} - 1\right)\right] \quad (9.30)$$

Using the values from Fig. 9.6, we find

$$NM_H = NM_L = \frac{0.6 \text{ V}}{2} - 0.025 \text{ V} \left[1 + \ln\left(\frac{0.6}{0.025} - 1\right)\right] = 0.197 \text{ V}$$

$V_{IL}$  occurs at an input voltage approximately 78 mV below  $V_{REF}$ , and  $V_{IH}$  occurs at an input voltage approximately 78 mV above  $V_{REF}$ . These numbers are in excellent agreement with the circuit simulation results in Fig. 9.7, and the high and low state noise margins are both equal to approximately 0.20 V.

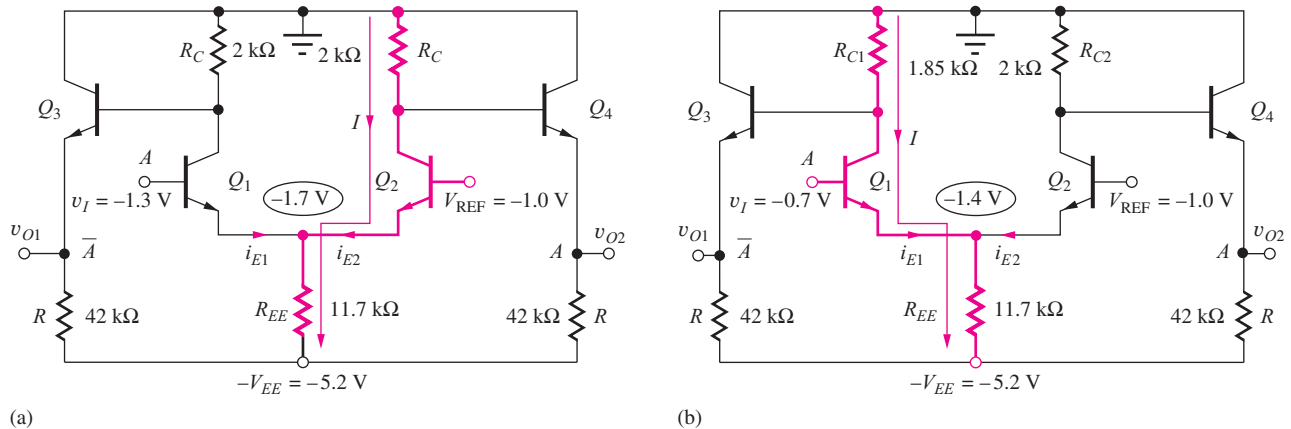


**Figure 9.8** (a) ECL gate with current source  $I_{EE}$  replaced by a resistor. (b) Modification of one of the collector-load resistors.

**EXERCISE:** What are the noise margins for the circuit in Fig. 9.6 if  $I_{EE}$  is changed to 0.2 mA?

**ANSWER:** 0.107 V

**EXERCISE:** Evaluate the required derivative and demonstrate that Eq. 9.24 is correct.

## 9.4 CURRENT SOURCE IMPLEMENTATION

Source  $I_{EE}$  in Fig. 9.6 is often replaced by a resistor, as in Fig. 9.8(a). For  $v_I = -1.3\text{ V}$ , the voltage at the emitters of  $Q_1$  and  $Q_2$  is the same as that in Fig. 9.5,  $-1.7\text{ V}$ , and the value of  $R_{EE}$  required to set the emitter current  $i_{E2}$  to 0.3 mA is

$$R_{EE} = \frac{[-1.7 - (-5.2)]\text{ V}}{0.3 \text{ mA}} = 11.7 \text{ k}\Omega$$

The use of resistor  $R_{EE}$  is normally accompanied by a slight modification in the value of the resistor connected to the collector of  $Q_1$ . Referring to Fig. 9.8(b) for the case of  $v_I = -0.7\text{ V}$ , we find that the voltage at the emitters of  $Q_1$  and  $Q_2$  is  $-1.4\text{ V}$ , and hence the emitter current has changed slightly due to the voltage change across resistor  $R_{EE}$ :

$$i_E = \frac{[-1.4 - (-5.2)]\text{ V}}{11.7 \text{ k}\Omega} = 0.325 \text{ mA}$$

Because the emitter current increases, the value of  $R_{C1}$  must be decreased to maintain a constant logic swing  $\Delta V$ . The new value of the resistor  $R_{C1}$  in the collector of  $Q_1$  is

$$R_{C1} = \frac{0.6 \text{ V}}{0.325 \text{ mA}} = 1.85 \text{ k}\Omega$$

The corrected design values appear in the circuit in Fig. 9.8(b).

### DESIGN ECL GATE DESIGN EXAMPLE 9.1

In this example, we design the resistors in the ECL gate so that the gate can operate from a reduced supply voltage of  $-3.3\text{ V}$ .

**PROBLEM** Redesign the ECL gate in Fig. 9.8(b) to work from a  $-3.3\text{-V}$  supply.

**SOLUTION** **Known Information and Given Data:** Circuit topology in Fig. 9.8(b).

**Unknowns:** Values of resistors  $R_{EE}$ ,  $R_{C1}$ ,  $R_{C2}$ , and  $R$

**Approach:** Determine the new voltage and current in each resistor, and then calculate the required value of resistance.

**Assumptions:** Maintain the same currents and values of  $V_H$  and  $V_L$  as in the design in Fig. 9.8(b):  $V_H = -0.7$  V,  $V_L = -1.3$  V,  $\Delta V = 0.6$  V,  $V_{REF} = -1.0$  V,  $I_{E2} = 0.3$  mA, and the average emitter follower current is 0.1 mA.

**Analysis:** For  $v_I = -1.3$  V as in Fig. 9.8(a),  $Q_1$  is off and  $Q_2$  is conducting. The voltage at the emitter of  $Q_2$  is  $V_{E2} = -1 - 0.7 = -1.7$  V, and the value of  $R_{EE}$  is given by

$$R_{EE} = \frac{-1.7 - (-3.3)}{0.3} \frac{\text{V}}{\text{mA}} = 5.33 \text{ k}\Omega$$

The value of  $R_{C2}$  is given by

$$R_{C2} = \frac{\Delta V}{I_{C2} + I_{B4}} = \frac{\Delta V}{I_{C2} + I_{B2} + (I_{B4} - I_{B2})} \cong \frac{\Delta V}{I_{E2}} = \frac{0.6 \text{ V}}{0.3 \text{ mA}} = 2.00 \text{ k}\Omega$$

in which the difference in the base currents between  $Q_4$  and  $Q_2$  is neglected.

For  $v_I = -0.7$  V, as in Fig 9.8(b),  $Q_2$  is off and  $Q_1$  is conducting. The voltage at the emitter of  $Q_2$  is  $V_{E2} = -0.7 - 0.7 = -1.4$  V, and the value of  $I_{E1}$  is

$$I_{E1} = \frac{-1.4 - (-3.3)}{2.00} \frac{\text{V}}{\text{k}\Omega} = 357 \mu\text{A}$$

The value of  $R_{C1}$  is given by

$$R_{C1} = \frac{\Delta V}{I_{C1} + I_{B3}} \cong \frac{\Delta V}{I_{E1}} = \frac{0.6 \text{ V}}{0.357 \text{ mA}} = 1.68 \text{ k}\Omega$$

The value of  $R$  is determined by the mean output voltage and current:

$$R = \frac{\frac{V_H + V_L}{2} - (-V_{EE})}{I_{E3}} \cong \frac{-1 + 3.3}{0.1} \frac{\text{V}}{\text{mA}} = 23 \text{ k}\Omega$$

**Check of Results:** We have found the four resistor values required to complete the design. Let us check the results using alternate methods of calculation. Since the voltage and current in  $R_{C2}$  have not changed, the value should be unchanged, as we calculated. For  $v_I = V_H$ ,  $R_{C1}$  and  $R_{EE}$  are conducting approximately the same current. So, the voltage across  $R_{C1}$  should be equal to

$$\Delta V = R_{C1} \frac{V_{R_{EE}}}{R_{EE}} = 1.68 \text{ k}\Omega \frac{1.9 \text{ V}}{5.33 \text{ k}\Omega} = 0.599 \text{ V}$$

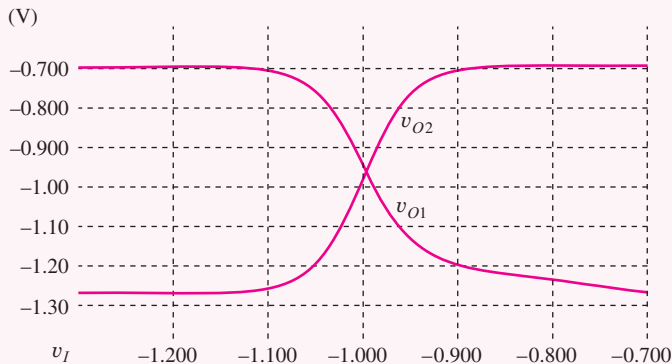
which is correct (0.6 V) within round-off error. The resistors  $R$  should be proportional to the voltage across them

$$R = \frac{-1 - (3.3)}{-1 - (5.2)} (42 \text{ k}\Omega) = 23 \text{ k}\Omega$$

which again agrees with the earlier calculation.

**Discussion and Computer-Aided Analysis:** The simulated outputs for our new design are given below using  $IS = 0.3$  fA,  $BF = 40$ , and  $BR = 0.25$ . By design, we expect the VTC results to be essentially the same as those in Fig. 9.7, and the two graphs appear very similar. However, we

should immediately note that asymmetries exist. The transfer function in Fig. 9.7 was generated with an ideal current source bias, whereas in this circuit the current in  $R_{EE}$  is different for the two logic states. In this circuit, the values of  $R_{C1}$  and  $R_{C2}$  are different, which causes the two transition slopes to be different. The circuit asymmetry causes the intersection of the two curves to shift slightly away from the  $v_I = -1\text{-V}$  point. The values of  $V_H$  and  $V_L$  are  $-0.694$  and  $-1.27$  V, respectively.



**EXERCISE:** Calculate the power dissipation and noise margins for the new ECL design.

**ANSWERS:** 1.65 mW, 1.84 mW; 0.20 V, 0.20 V

**EXERCISE:** What are the values of  $V_{IL}$  and  $V_{IH}$  from the VTC simulation in Design Ex. 9.1? What are the noise margins based on these values?

**ANSWERS:**  $-1.08$  V,  $-0.91$  V;  $0.19$  V,  $0.21$  V

**EXERCISE:** Redesign the ECL gate in Design Ex. 9.1 to reduce the power by a factor of 3.

**ANSWERS:**  $6.00$  k $\Omega$ ,  $5.04$  k $\Omega$ ,  $16.0$  k $\Omega$ ,  $69$  k $\Omega$



**EXERCISE:** Simulate the circuit in Design Ex. 9.1 with  $R_{EE}$  replaced by a 0.3-mA current source. Then change  $R_{C1}$  to  $2$  k $\Omega$  and simulate the circuit again. Note the differences in the various VTCs.

**EXERCISE:** What are the new values of  $R_{EE}$  and  $R_{C1}$  for the circuit in Fig. 9.8(b) if  $I_{EE}$  is changed to  $0.2$  mA and  $R_{C2} = 2$  k $\Omega$ ?

**ANSWERS:**  $18.0$  k $\Omega$ ,  $1.89$  k $\Omega$

## 9.5 THE ECL OR-NOR GATE

In order to have a complete logic family, ECL must provide either the OR or AND function in addition to logical inversion, and the ECL inverter becomes an OR-NOR gate through the addition of transistors in parallel with the original input transistor of the inverter, as in Fig. 9.9(a). If any one of the inputs ( $A$  or  $B$  or  $C$ ) is at a high input level ( $v_I > V_{REF}$ ), then the current from source  $I_{EE}$  will be switched into collector node  $v_{C1}$ , output  $Y_1$  will drop to a low level, and output  $Y_2$  will rise to a high level.  $Y_1$  therefore represents a NOR output, and  $Y_2$  is an OR output:

$$Y_1 = \overline{A + B + C} \quad \text{and} \quad Y_2 = A + B + C$$

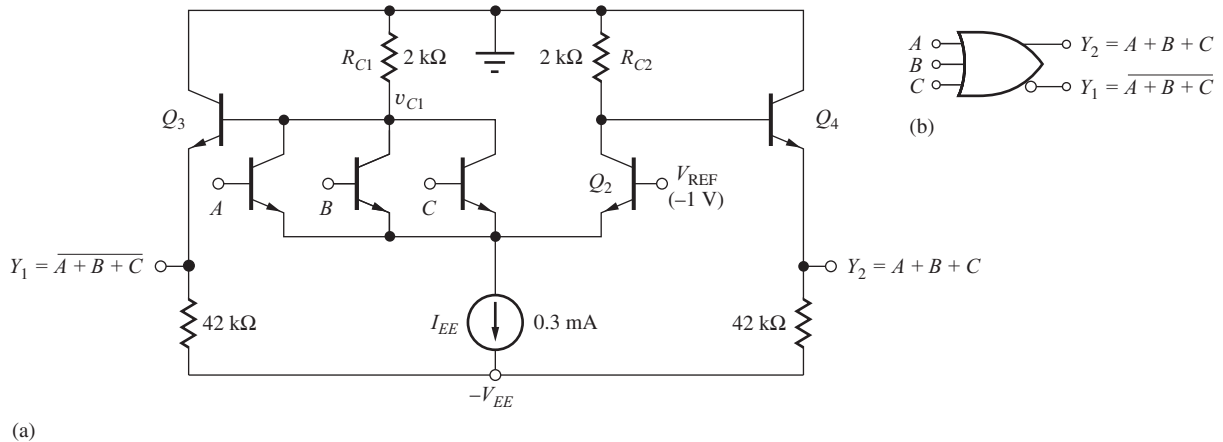


Figure 9.9 (a) Three-input ECL OR-NOR gate and (b) logic symbol.

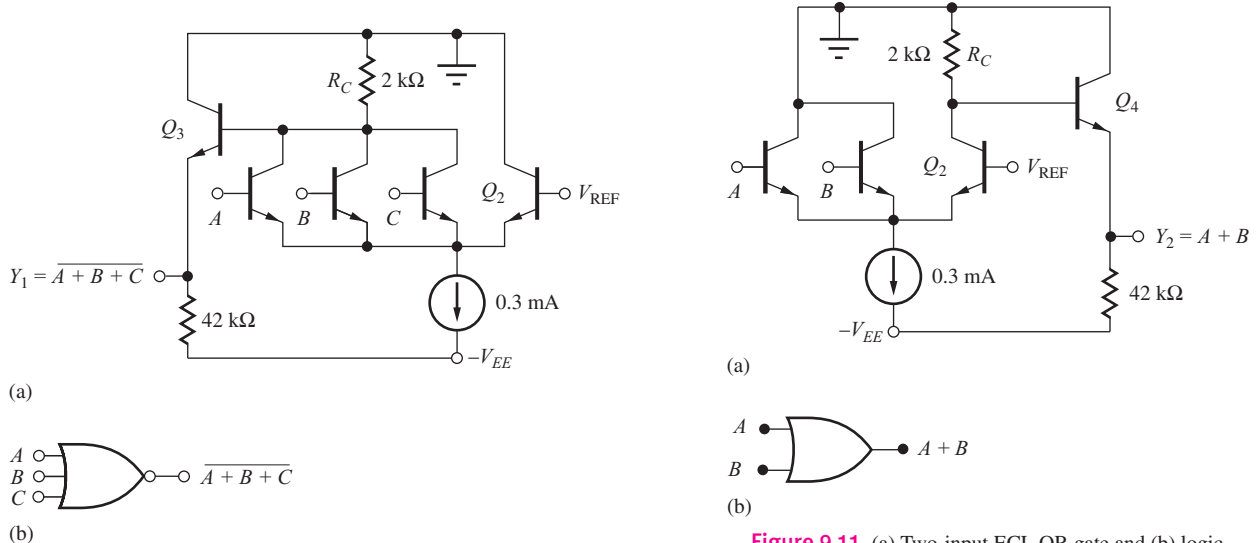


Figure 9.10 (a) Three-input ECL NOR gate and (b) logic symbol.

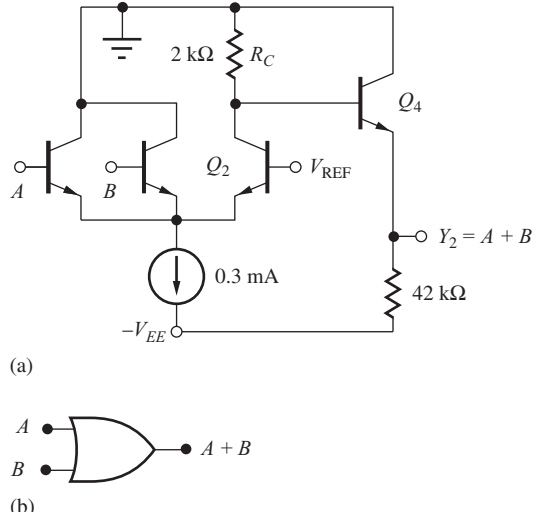
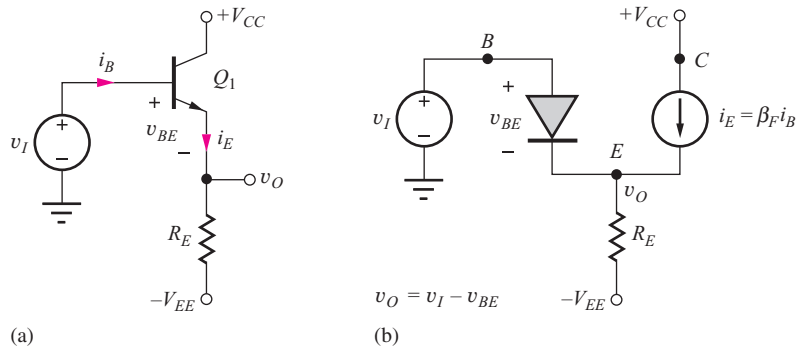


Figure 9.11 (a) Two-input ECL OR gate and (b) logic symbol.

The logic symbol in Fig. 9.9(b) is used for the dual output OR-NOR gate. The NOR output is marked by the small circle, which indicates the complemented or inverted output. The full ECL gate produces both true and complemented outputs. However, not every gate need be implemented this way. For example, the three-input logic gate in Fig. 9.10 has been designed with only the NOR output available; the two-input gate in Fig. 9.11 provides only the OR function. Note that the resistor in the collector of \$Q\_2\$ is not needed in Fig. 9.10 and has been eliminated. Similarly, the left-hand collector resistor is eliminated from the circuit in Fig. 9.11.

**EXERCISES:** What are the new values of \$R\_{C1}\$ and \$R\_{C2}\$ for the circuit in Fig. 9.9 if \$I\_{EE}\$ is replaced by a \$11.7\text{-k}\Omega\$ resistor? Assume \$V\_{REF} = -1\text{ V}\$ and \$V\_{EE} = -5.2\text{ V}\$. What is the new value of \$R\_C\$ for the circuit in Fig. 9.10 if \$I\_{EE}\$ is replaced by a \$11.7\text{-k}\Omega\$ resistor? Assume \$V\_{REF} = -1\text{ V}\$ and \$V\_{EE} = -5.2\text{ V}\$.

**ANSWERS:** 1.85 k\$\Omega\$, 2.00 k\$\Omega\$; 1.85 k\$\Omega\$



**Figure 9.12** (a) Emitter follower and (b) transport model for the forward-active region.

**EXERCISE:** What is the new value of \$R\_C\$ for the circuit in Fig. 9.11 if \$I\_{EE}\$ is replaced by a 11.7-k\$\Omega\$ resistor? Assume \$V\_{REF} = -1\$ V and \$V\_{EE} = -5.2\$ V.

**ANSWER:** 2.00 k\$\Omega\$

## 9.6 THE Emitter FOLLOWER

Let us now look in more detail at the operation of the emitter followers that provide the level-shifting function in the ECL gate. An emitter follower is shown biased by emitter resistor \$R\_E\$ in Fig. 9.12(a). For \$v\_I \leq V\_{CC}\$, \$Q\_1\$ operates in the forward-active region because its base-collector voltage is negative, and current comes out of the emitter through resistor \$R\_E\$. The behavior of the emitter follower can be better understood by replacing \$Q\_1\$ with its model for the forward-active region, as in Fig. 9.12(b).

Using Kirchhoff's voltage law:

$$v_O = v_I - v_{BE} \quad (9.31)$$

Although the emitter current of the transistor changes as the output voltage changes,

$$i_E = \frac{v_O - (-V_{EE})}{R_E} = \frac{v_O + V_{EE}}{R_E} \quad (9.32)$$

\$v\_{BE}\$ does not change significantly<sup>2</sup> because of the logarithmic dependence of \$v\_{BE}\$ on \$i\_E\$, as obtained from Eq. (9.1):

$$v_{BE} = V_T \ln \left( \frac{\alpha_F i_E}{I_S} \right) \quad (9.33)$$

So the difference between the input and output voltages is approximately constant,

$$v_O = v_I - v_{BE} \cong v_I - 0.7 \text{ V}$$

Thus, the voltage at the emitter “follows” the voltage at the input, but with a fixed offset equal to one base-emitter diode voltage. This is also clearly evident in Fig. 9.12(b), in which the base and emitter terminals are connected together through the base-emitter diode.

The voltage transfer characteristic for the emitter follower appears in Fig. 9.13. The output voltage \$v\_O\$ at the emitter follows the input voltage with a slope of +1 and a fixed offset voltage equal to \$V\_{BE} \cong 0.7\$ V. For positive inputs, the output follows the input voltage until the BJT begins to enter saturation at the point when \$v\_I\$ exceeds \$V\_{CC}\$. The maximum output voltage occurs when the transistor saturates with \$v\_O = V\_{CC} - V\_{CESAT}\$ and \$v\_I = V\_{CC} - v\_{CESAT} + v\_{BE}\$. At this point, the

<sup>2</sup> Remember that a factor of 10 change in \$i\_E\$ requires only a 60-mV change in \$v\_{BE}\$ at room temperature.

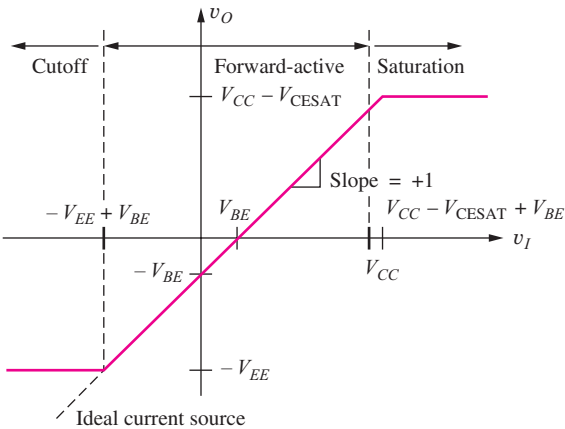
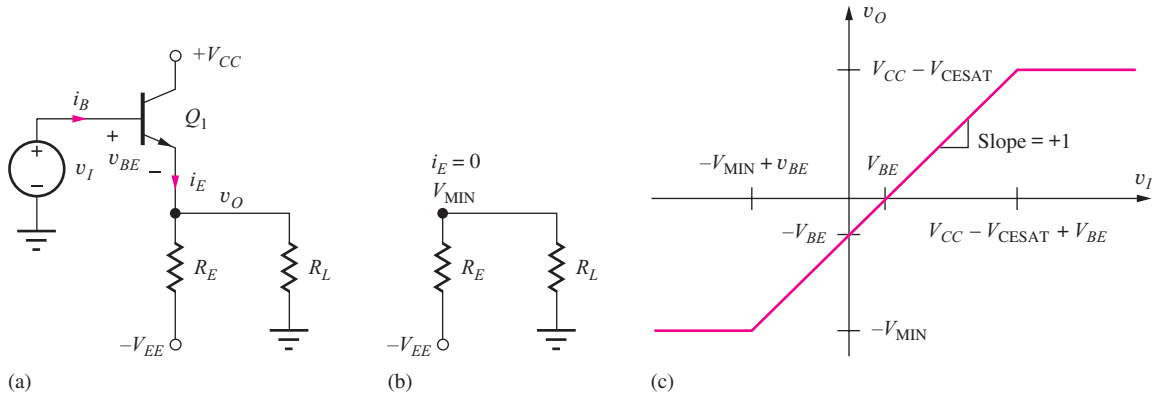


Figure 9.13 Voltage transfer characteristic for the emitter follower.

Figure 9.14 (a) Emitter follower with load resistor  $R_L$  added; (b) circuit with  $Q_1$  cut off; (c) voltage transfer function for emitter follower with load resistor.

input voltage is approximately one diode-drop above  $V_{CC}$ ! Any further increase in  $v_I$  will destroy the bipolar transistor.

The minimum output voltage is set by the negative power supply. The total emitter current  $i_E$  cannot become negative, so  $Q_1$  turns off as input  $v_I$  falls below  $(-V_{EE} + 0.7 \text{ V})$ , and the output becomes  $-V_{EE}$ .

**EXERCISE:** What value of  $R_E$  is required to set  $i_E = 0.3 \text{ mA}$  for  $v_I = 0$  in the emitter follower if  $-V_{EE} = -5.2 \text{ V}$ ?

**ANSWER:**  $15.0 \text{ k}\Omega$

### 9.6.1 Emitter Follower with a Load Resistor

An external load resistor is often connected to an emitter follower, as shown by  $R_L$  in Fig. 9.14(a). The addition of  $R_L$  sets a new limit  $V_{\text{MIN}}$  on the negative output swing of the emitter follower.  $V_{\text{MIN}}$  represents the Thévenin equivalent voltage at  $v_O$  for  $i_E = 0$ , as in Fig. 9.14(b):

$$V_{\text{MIN}} = \frac{R_L}{R_L + R_E}(-V_{EE}) \quad (9.34)$$

For  $V_I > V_{MIN} + v_{BE}$ , the behavior of the emitter follower is the same as discussed previously. However, for  $v_O$  to drop below  $V_{MIN}$ , emitter current  $i_E$  has to be negative, which is impossible in this circuit. The modified VTC for the emitter follower is shown in Fig. 9.14(c), in which the minimum output voltage is now  $V_{MIN}$ .

**EXERCISE:** If  $R_E = 15 \text{ k}\Omega$ ,  $V_{CC} = 0 \text{ V}$ , and  $-V_{EE} = -5.2 \text{ V}$ , what is the minimum output voltage of the emitter follower in Fig. 9.14(a) if  $R_L = \infty$ ? If  $R_L = 10 \text{ k}\Omega$ ?

**ANSWERS:**  $-5.20 \text{ V}; -2.08 \text{ V}$

## DESIGN EXAMPLE 9.2

### EMITTER FOLLOWER DESIGN

Emitter followers are widely used to buffer analog signals such as sine waves, and this example investigates the design of a circuit in such an application.

**PROBLEM** An emitter follower has an input voltage  $v_I = 3 \sin 2000\pi t \text{ V}$ . Design an emitter follower to deliver this signal to a  $5\text{-k}\Omega$  load resistor. The available power supplies are  $\pm 5 \text{ V}$ .

**SOLUTION** **Known Information and Given Data:** An emitter follower circuit is specified;  $v_I = 3 \sin 2000\pi t \text{ V}$ ; power supply voltages are  $+5 \text{ V}$  and  $-5 \text{ V}$ ; the load resistor is  $5 \text{ k}\Omega$ .

**Unknowns:** Bias circuit and operating current for the transistor

**Approach:** The simplest circuit implementation is that of Fig. 9.14(a) in which we need to choose only the value of  $R_E$ . First determine the required output voltage range; then calculate the required value of emitter resistance.

**Assumptions:** Use the emitter follower circuit biased with resistor  $R_E$  as in Fig. 9.14.

**Analysis:** The minimum value of  $v_I$  is  $-3 \text{ V}$ , and the minimum value of  $v_O$  will be one base-emitter diode drop ( $0.7 \text{ V}$ ) below this voltage or  $-3.7 \text{ V}$ . Using Eq. (9.34):

$$-3.7 \text{ V} = \frac{5 \text{ k}\Omega}{5 \text{ k}\Omega + R_E} (-5 \text{ V}) \rightarrow R_E = 1.76 \text{ k}\Omega$$

The nearest 5 percent resistor value is  $1.8 \text{ k}\Omega$ , but this value is too large since  $1.76 \text{ k}\Omega$  represents the maximum allowable value for  $R_E$ . So we choose  $R_E = 1.6 \text{ k}\Omega$ , the nearest smaller value.

**Check of Results:** We have found the resistor required for the design. Let us use the value to check the minimum output voltage.

$$V_{MIN} = \frac{5 \text{ k}\Omega}{5 \text{ k}\Omega + 1.6 \text{ k}\Omega} (-5 \text{ V}) = -3.79 \text{ V} \quad \checkmark$$

We have not checked the maximum input condition and really need to be sure that the transistor is in the forward-active region. The maximum input voltage is  $+3 \text{ V}$ , and the collector voltage is fixed at  $+5 \text{ V}$ . Therefore the base-collector junction remains reverse-biased throughout the full input signal range.

**Discussion:** Let us explore the currents in the transistor at the Q-point and the extremes of the input voltage. The current in the emitter follower is given by

$$i_E = \frac{v_O - (-V_{EE})}{R_E} - \frac{v_O}{R_L} = \frac{v_O + V_{EE}}{R_E} - \frac{v_O}{R_L}$$

The Q-point current is defined as the current for  $v_I = 0$  for which  $v_O = -0.7$  V:

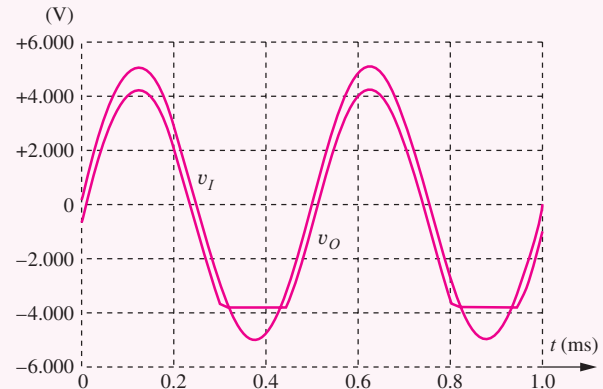
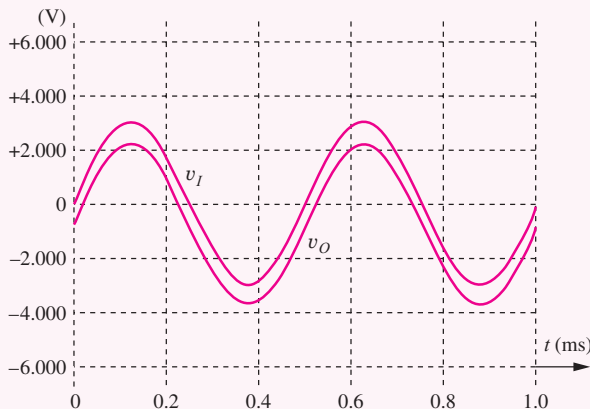
$$i_E = \frac{-0.7 + 5 \text{ V}}{1.6 \text{ k}\Omega} - \frac{0.7 \text{ V}}{5 \text{ k}\Omega} = 2.55 \text{ mA}$$

The minimum and maximum emitter follower currents are

$$i_E^{\min} = \frac{-3.7 \text{ V} - (-5 \text{ V})}{1.6 \text{ k}\Omega} - \frac{3.7 \text{ V}}{5 \text{ k}\Omega} = 72.5 \mu\text{A} \quad \text{and} \quad i_E^{\max} = \frac{+2.3 \text{ V} + 5 \text{ V}}{1.6 \text{ k}\Omega} - \frac{2.3 \text{ V}}{5 \text{ k}\Omega} = 4.10 \text{ mA}$$

Use of the 1.6-k $\Omega$  emitter resistor causes a nonzero emitter current to flow in the transistor for  $v_I = -3$  V so that the transistor remains in the forward-active region rather than entering cutoff at the minimum value of output voltage. This is the preferred situation in the design of the emitter follower. However, the minimum current is a relatively small fraction of the Q-point current. We might consider decreasing the value of  $R_E$  somewhat further to increase this current (e.g., 1.5 k $\Omega$  or 1.3 k $\Omega$ ) to provide a design safety margin.

**Computer-Aided Analysis:** The results of two simulations are given here. For the design input,  $v_I = 3 \sin 4000\pi t$  V, the output follows the input as desired. Note that the input and output are simply shifted by the base-emitter voltage drop (approximately 0.7 V). However, if the input is increased above the 3 V design limit, the waveform becomes distorted. The second graph presents the results for  $v_I = 5 \sin 4000\pi t$  V. The follower circuit is unable to replicate the input as it becomes more negative than -3 V.



**EXERCISE:** What is the power dissipation at the Q-point of the emitter follower in Design Ex. 9.2? Assume  $\beta_F = 50$ . What is the minimum emitter follower current if  $R_E$  is changed to 1.3 k $\Omega$ ? What is the power dissipation at the Q-point for  $R_E = 1.3$  k $\Omega$ ?

**ANSWERS:** 14.4 mW; 260  $\mu$ A; 17.7 mW

**EXERCISE:** (a) If  $R_L = 10$  k $\Omega$ ,  $V_{CC} = 5$  V, and  $-V_{EE} = -5.2$  V, what value of  $R_E$  is required to achieve  $V_{MIN} = -4$  V? (b) What is the value of  $i_E$  for  $v_O = 0$  V, -4 V, and +4 V?

**ANSWERS:** 3.00 k $\Omega$ ; 1.73 mA, 0 A, 3.47 mA

## 9.7 “EMITTER DOTTING” OR “WIRED-OR” LOGIC

In most logic circuits including NMOS, CMOS, and TTL, the outputs of two logic gates cannot be directly connected together. (See Prob. 7.22.) However, it is possible to tie the outputs of emitter followers together, and this capability provides a powerful enhancement to the logic function of ECL.

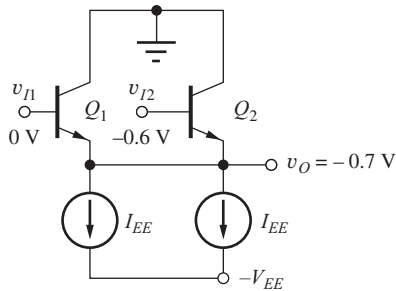


**Figure 9.15** Parallel connection of two emitter followers.

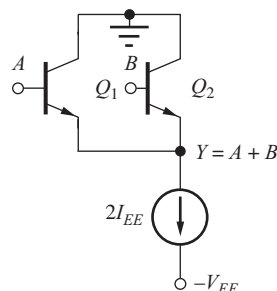


**Figure 9.16** ‘Wired-OR’ connection of emitter followers.

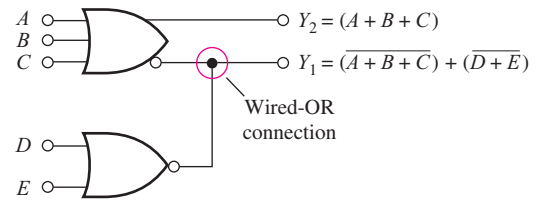


**Figure 9.17** ‘Wired-OR’ connection of two ECL logic gates.

### 9.7.1 PARALLEL CONNECTION OF Emitter-FOLLOWER OUTPUTS

Consider the circuit of Fig. 9.15, with the input voltages as shown. The output follows the most positive input voltage (minus the 0.7-V base-emitter offset), whereas the transistor with the lower input voltage operates near cutoff. For the specific example in Fig. 9.15, the input voltage to  $Q_2$  is at  $-0.6\text{ V}$ . If  $Q_2$  were conducting, then its emitter would be one diode drop below its base at  $-1.3\text{ V}$ . However, the input to  $Q_1$  is  $0\text{ V}$ , and its emitter can only drop down to  $-0.7\text{ V}$ . Thus, the output is at  $-0.7\text{ V}$ . The base-emitter voltage of transistor  $Q_2$  is forced to become  $-0.1\text{ V}$ , and  $Q_2$  is cut off. Note that because  $Q_2$  is cut off, the emitter of  $Q_1$  must now supply the current of both current sources,  $i_{E1} = 2I_{EE}$ .

### 9.7.2 THE WIRED-OR LOGIC FUNCTION

Now, suppose that one emitter-follower input corresponds to the logic variable  $A$ , and the second input corresponds to logic variable  $B$ , as in Fig. 9.16. The output will be high if either  $A$  or  $B$  is high, whereas the output will be low only if both  $A$  and  $B$  are low. This corresponds to the OR function:  $Y = A + B$ . The logical OR function can be obtained by simply connecting the outputs of two ECL gates. This is a powerful additional feature provided by the ECL logic family.

A simple example is provided in the logic circuit in Fig. 9.17, in which the outputs of two ECL gates are connected to provide the logic function  $Y_1 = \overline{(A + B + C)} + \overline{(D + E)}$ . The upper gate also provides a second output,  $Y_2 = A + B + C$ .

The **wired-OR logic** function in ECL represents an example of the reason we need to understand the internal circuitry associated with various logic families. We cannot arbitrarily connect the outputs of all types of logic gates together. In many other logic families, the wired-OR function is not permitted. If we connect the outputs, the logic levels will not be valid, and the logic gate may even be destroyed in some cases.

## 9.8 ECL POWER-DELAY CHARACTERISTICS

As pointed out in the chapters on MOS logic design, the power-delay product (PDP) is an important figure of merit for comparing logic families. In this section, we first explore the power dissipation of the ECL gate and then characterize its delay at low power. The results are then combined to form the power-delay product.

### 9.8.1 POWER DISSIPATION

The static power dissipation of the ECL gate is easily calculated based on our original inverter circuit, shown in Fig. 9.18. The total current  $I$  in the inverter is independent of the logic state within the gate:  $I = I_{EE} + I_3 + I_4$ . Thus, the average ECL power dissipation  $\langle P \rangle$  is independent of logic state and is equal to

$$\langle P \rangle = V_{EE}(I_{EE} + I_3 + I_4) \quad (9.35)$$

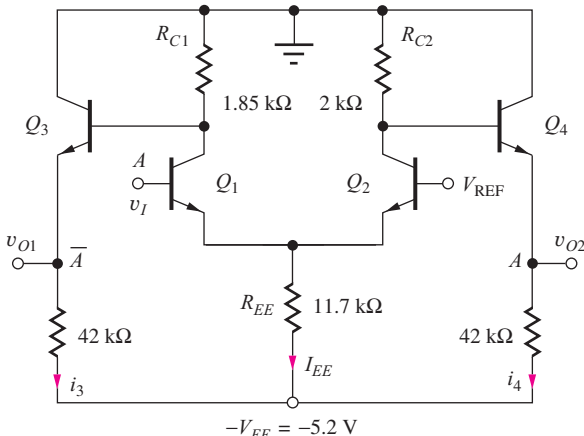


**Figure 9.18** ECL gate with resistor biasing.

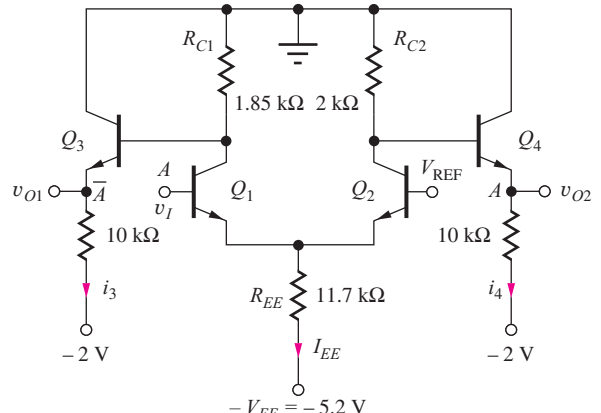


**Figure 9.19** ECL circuit with reduced power in the emitter followers

For the circuit in Fig. 9.18, we remember that the sum  $i_3 + i_4 = 0.2$  mA is a constant regardless of input state, and the average value of the current  $I_{FE}$  is

$$\langle I_{EE} \rangle = \frac{0.300 + 0.325}{2} \text{ mA} = 0.313 \text{ mA} \quad (9.36)$$

based on a 50 percent logic state duty cycle. Thus, the average power dissipation is  $\langle P \rangle = (5.2 \text{ V})(0.200 + 0.313 \text{ mA}) = 2.7 \text{ mW}$ .

**EXERCISE:** Scale the resistors in the ECL gate in Fig. 9.18 to reduce the power by a factor of 10.

**ANSWERS:** 20 k $\Omega$ , 18.5 k $\Omega$ , 117 k $\Omega$ , 420 k $\Omega$

### Power Reduction

Note that 40 percent of the power in the circuits in Fig. 9.18 is dissipated in the emitter-follower stages. Two techniques have been used to reduce the power consumption in more advanced ECL gates. The first is to simply return the emitter-follower resistors to a second, less negative power supply, such as the  $-2\text{-V}$  supply in Fig. 9.19. The resistors in the emitters of  $Q_3$  and  $Q_4$  have been changed to  $10\text{ k}\Omega$  to keep the currents in  $Q_3$  and  $Q_4$  equal to  $0.1\text{ mA}$ . The power dissipation in this circuit is reduced by 33 percent to

$$P = 5.2(0.313) + 2(0.1) = 1.8 \text{ mW} \quad (9.37)$$

This method, however, requires the cost of another power supply and its associated wiring for power distribution.

Another power-reduction technique is illustrated in Fig. 9.20, in which the resistors that supply current to the emitter followers are now connected between each input and the  $-5.2\text{-V}$  supply. In Fig. 9.15, we saw that one emitter follower would have to supply the current of multiple current sources when the wired-OR function was used. Using the repartitioned circuit in Fig. 9.20, the emitter follower current is always equal to the current of only one of the original emitter followers. This redesign significantly reduces the overall power consumption in large logic networks. However, any output that does not drive the input of another logic gate needs to have an external termination resistor connected from its output to the negative power supply.

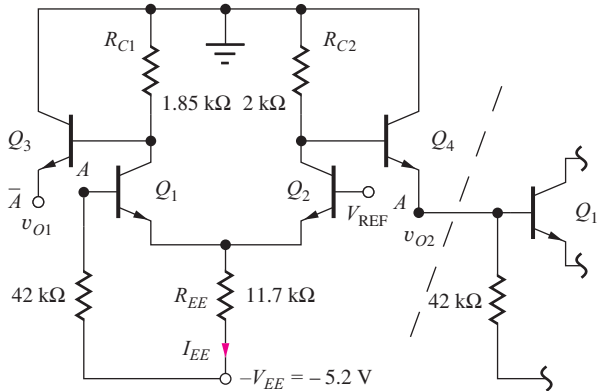


**Figure 9.20** Repartitioned ECL gate.

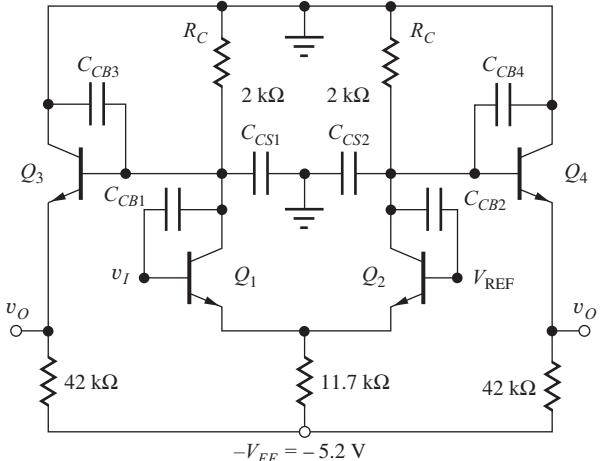


**Figure 9.21** ECL inverter with capacitances at the collector nodes of the current switch.

### 9.8.2 GATE DELAY

The capacitances that dominate the delay of the ECL inverter at low power levels have been added to the circuit in Fig. 9.21. The symbol  $C_{CB}$  represents the capacitance of the reverse-biased collector-base junction, and  $C_{CS}$  represents the capacitance between the collector and the substrate of the transistor. Transistors  $Q_1$  and  $Q_2$  switch the current  $I_{EE}$  back and forth very rapidly in response to the input  $v_I$ . The emitter followers can supply large amounts of current to quickly charge any load capacitances connected to the two outputs.

At low power, the speed of the ECL gate is dominated by the  $R_C - C_L$  time constant at the collectors of  $Q_1$  and  $Q_2$ , and the response of the inverter can be modeled by the simple  $RC$  circuit in Fig. 9.22, in which  $R_C$  is the collector-load resistance and  $C_L$  is the effective load capacitance at the collector node of  $Q_2$ , given by

$$C_L = C_{CS2} + C_{CB2} + C_{CB4} \quad (9.38)$$

The load capacitance consists of the base-collector capacitances of  $Q_2$  and  $Q_4$  plus the collector-substrate capacitance of  $Q_2$ .

For the negative-going transient, the capacitor is initially discharged, and current  $-I_{EE}$  is switched into the node at  $t = 0$ . The voltage at node  $v_{C2}$  is described by

$$v_{C2}(t) = -I_{EE} R_C \left[ 1 - \exp \left( -\frac{t}{R_C C_L} \right) \right] \quad (9.39)$$

The collector-node voltage exponentially approaches the final value of  $-I_{EE} R_C$ . The actual output voltage at  $v_O$  is level-shifted down by one 0.7-V drop by the emitter follower.

The propagation-delay time is the time required for the output to make 50 percent of its transition<sup>3</sup>:

$$v_{C2}(\tau_{PHL}) = -\frac{I_{EE} R_C}{2} \quad \text{and} \quad \tau_{PHL} = 0.69 R_C C_L \quad (9.40)$$

For the positive-going transition, the capacitor is initially charged to the negative voltage  $-I_{EE} R_C$ . At  $t = 0$ , the current source is switched off, and the capacitor simply discharges through  $R_C$ :

$$v_{C2}(t) = -I_{EE} R_C \exp \left( -\frac{t}{R_C C_L} \right) \quad (9.41)$$

<sup>3</sup> See Section 6.11.2.

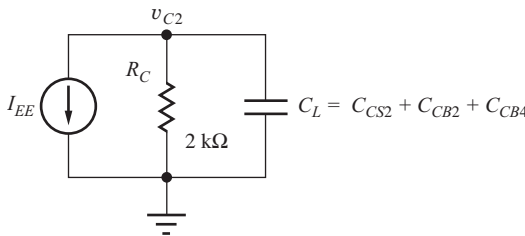


**Figure 9.22** Simplified model for the dynamic response of an ECL gate.

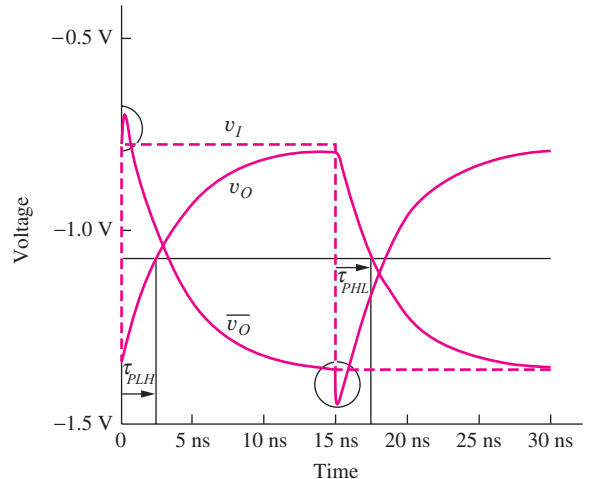


**Figure 9.23** Simulated switching waveforms for the ECL inverter of Fig. 9.21.

For this case, the propagation delay is

$$v_{C2}(\tau_{PLH}) = -\frac{I_{EE} R_C}{2} \quad \text{and} \quad \tau_{PLH} = 0.69 R_C C_L \quad (9.42)$$

Using Eqs. (9.40) and (9.42), the average propagation delay of the ECL gate is

$$\tau_p = \frac{\tau_{PHL} + \tau_{PLH}}{2} = 0.69 R_C C_L \quad (9.43)$$

Figure 9.23 shows the results of simulation of the switching behavior of the ECL gate in Fig. 9.21. In this case, the transistor capacitances are  $C_{CB} = 0.5 \text{ pF}$  and  $C_{CS} = 1.0 \text{ pF}$ . For  $R_C = 2 \text{ k}\Omega$ , the two propagation-delay times from Eqs. (9.40) and (9.42) are estimated to be 2.8 ns. This prediction agrees very well with the waveforms in Fig. 9.23.

Note the two transient “spikes” (circled in Fig. 9.23) that show up on the  $\bar{v}_O$  output coinciding with the switching points on the input waveform. These spikes do not show up on the  $v_O$  output. The transients are in the same direction as the input signal change and result from the coupling of the input waveform directly through capacitance  $C_{BC1}$  to the inverting output. A similar path to the noninverting output does not exist. This is another good illustration of detailed simulation results that one should always try to understand. Such unusual observations should be studied to determine if they are real effects or some artifact of the simulation tool, as well as to understand how they might affect the performance of the circuit.

### 9.8.3 POWER-DELAY PRODUCT

Using the values calculated from Eqs. (9.35) and (9.43) for the gate in Fig. 9.21, the power-delay product is  $2.6 \text{ mW} \times 2.8 \text{ ns}$ , or 7.3 pJ. From Eq. (9.43), we see that the propagation delay of the inverter for a given capacitance is directly proportional to the choice of  $R_C$ , and we know  $R_C$  is related to the logic swing and current  $I_{EE}$  by  $R_C = \Delta V / I_{EE}$ . Assuming that we want to keep the logic swing and the noise margins constant, then we can reduce  $R_C$  only if we increase the current  $I_{EE}$  and hence the power of the gate. This illustrates the direct power-delay trade-off involved in gate design because  $I_{EE}$  accounts for most of the power in the ECL logic gate.

The analysis presented in the previous section was valid for operation in the region of constant power-delay product. However, as power is increased, the effect of charge storage in the BJT (discussed in detail in Sec. 9.9) becomes more and more important, and the delay of the ECL gate enters

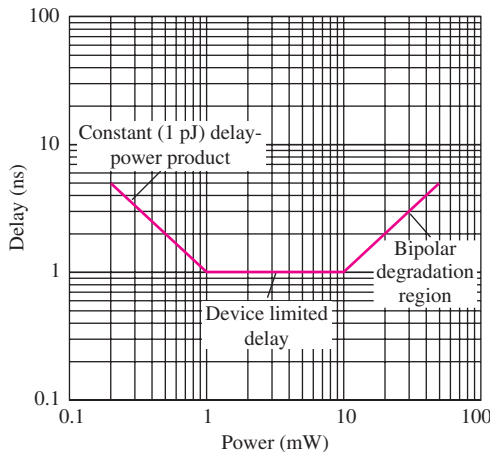


**Figure 9.24** Delay versus power behavior for bipolar logic.

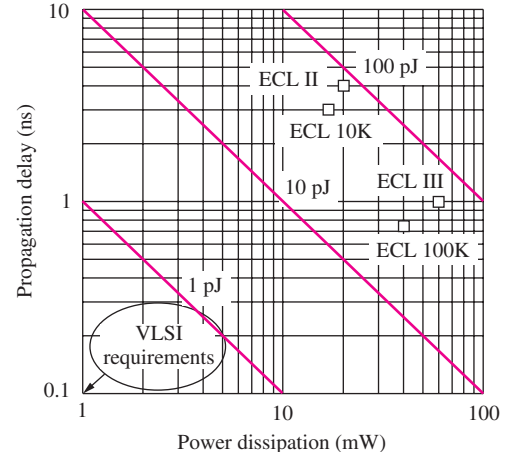


**Figure 9.25** Power-delay characteristics for various ECL gates. VLSI requirements are less than 100 fJ.

a region in which it becomes independent of power. Finally, at even higher power levels, the delay starts to degrade as the  $f_T$  of the BJT falls. These three regions are shown in Fig. 9.24.

Figure 9.25 summarizes the power-delay characteristics of a number of commercial ECL unit logic gates as well as the requirements for high-performance circuits for use in high-density IC chips. The more recent ECL unit logic families offer subnanosecond performance but consume relatively large amounts of power in order to reliably drive the large off-chip capacitances associated with printed circuit board mounting and interconnect. The large power-delay products are not usable for VLSI circuit densities. Much lower power-delay products are associated with state-of-the-art on-chip logic circuits that benefit from smaller capacitive loads as well as significantly improved bipolar device technology.

**EXERCISE:** What are the delay and power-delay product for the ECL gate in Fig. 9.21 if  $I_{EE}$  is changed to 0.5 mA, but the logic swing is maintained the same?

**ANSWERS:** 1.66 ns, 6.0 pJ

## 9.9 CURRENT MODE LOGIC

The power-delay product of standard ECL is too high to permit the use of ECL in high density integrated circuits. However a second generation of current switch circuits called *current mode logic* (CML) was developed with significantly improved PDP characteristics. In this circuit, the bias current is effectively reused by stacking current switch pairs on top of each other as shown in the two-input gates of Fig. 9.26. Let us first explore the logic behavior of these circuits, and then we will look at the various voltage levels associated with the logic inputs and outputs.

### 9.9.1 CML LOGIC GATES

The circuits in Fig. 9.26 each employ two levels of current switching in which each switch pair is driven differentially by true and complement values of the logic variables. First consider the circuit in Fig. 9.26(a). If  $A$  and  $B$  are both logic ones (high level), bias current  $I_{EE}$  will be diverted through  $Q_1$  and then  $Q_3$  to collector resistor  $R_{C1}$ , output  $\bar{Y}$  will be low, and  $Y$  will be high. Therefore  $Y = AB$  and  $\bar{Y} = \bar{A}\bar{B}$ , and the gate in Fig. 9.26(a) implements the AND-NAND functions at its two outputs. The OR-NOR functions are achieved with the same circuit topology but with the inputs and outputs

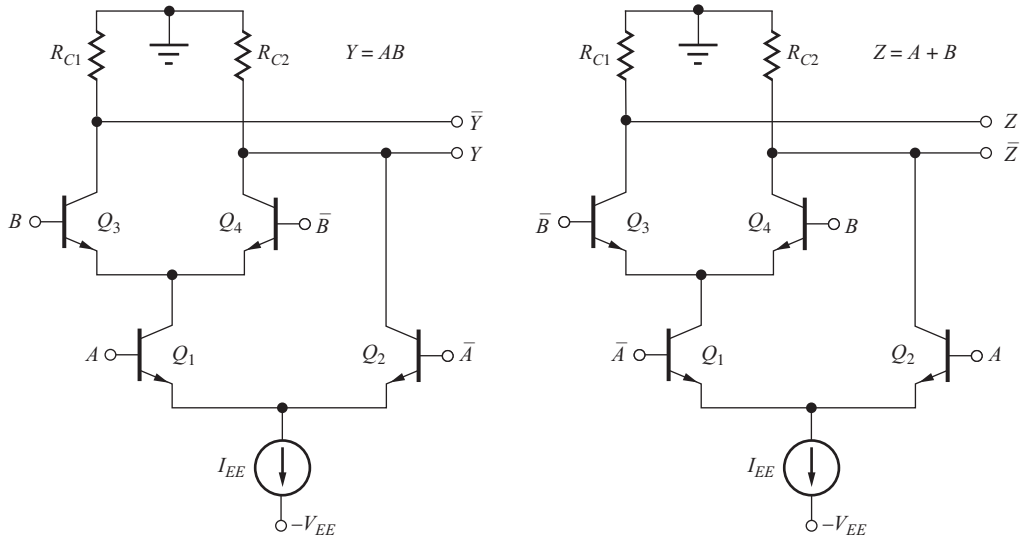


**Figure 9.26** Basic current mode logic (CML) gate. (a) AND-NAND gate. (b) OR-NOR gate.

interchanged as in Fig. 9.26(b). Output  $Z$  will be low, and  $\bar{Z}$  will be high, when both  $\bar{A}$  and  $\bar{B}$  are high. Thus  $\bar{Z} = \bar{A}\bar{B} = \bar{A} + \bar{B}$  and  $Z = A + B$ .

### 9.9.2 CML LOGIC LEVELS

Now let us find the voltage levels in this circuit. At the output,  $I_{EE}$  appears in one collector resistor, and zero current is in the other collector resistor. Thus the two logic levels are the same as those in the current switch in Fig. 9.1:  $V_H = 0$  V and  $V_L = -I_{EE}R_C$ . In CML circuits,  $V_L$  is often chosen to be  $-400$  mV, which is more than enough to completely switch the currents with good noise margin. The logic levels are centered about an equivalent bias level (common-mode level) of  $(V_H + V_L)/2 = -200$  mV.

To prevent saturation of the transistors, we level-shift the output to the proper voltage to drive the two different input levels with the emitter-follower circuit in Fig. 9.27. At the level-B node,  $V_{BH} = -0.7$  V and  $V_{BL} = -1.1$  V for  $v_{in}$  at  $V_H$  and  $V_L$  respectively. At the level-A node,  $V_{AH} = -1.4$  V and  $V_{AL} = -1.8$  V. The corresponding bias levels are  $-0.20$  V,  $-0.90$  V, and  $-1.60$  V. If all the bipolar transistors in the circuit have the same emitter areas, then we choose  $I_{EF} = I_{EE}/2$  to match the base-emitter voltage drops.

Now we can check saturation of  $Q_3$ . If the  $\bar{Y}$  output is at  $-0.4$  V and the  $B$  input is at  $-0.7$  V, then the collector-base diode is reverse-biased by  $0.3$  V and the transistor is not saturated. Next suppose the  $A$  input of  $Q_1$  is at  $-1.4$  V. Either the  $B$  or the  $\bar{B}$  input will be at  $-0.7$  V, so that the collector of transistor  $Q_1$  will be at  $-0.7 - 0.7 = -1.4$  V, and the collector-base diode is operating at zero bias. Thus the transistor is not saturated. Note that in the steady state, one side of each transistor pair is always at a high level. Thus the emitter node of each transistor pair does not change level except during the switching transients, and little power is lost charging and discharging the capacitances at the emitter nodes.

### 9.9.3 $V_{EE}$ SUPPLY VOLTAGE

With the  $A$  input at  $-1.4$  V, the emitter of transistor  $Q_1$  will be at  $-2.1$  V. An additional diode drop will be required to operate a bipolar transistor current source, so the minimum value of  $V_{EE}$  will be  $2.8$  V.

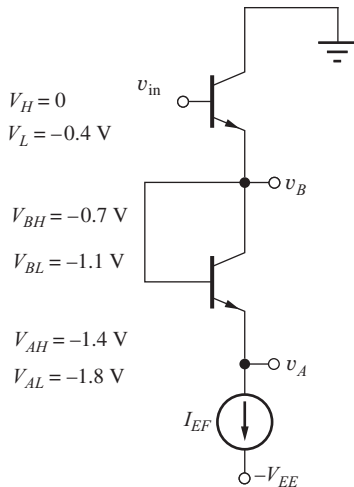


**Figure 9.27** CML level shifting with  $v_{BE} = 0.7 \text{ V}$ .

**EXERCISE:** What are the values of the collector resistors in Fig. 9.26 if  $V_{EE} = 2.8 \text{ V}$ ,  $I_{EE} = 500 \mu\text{A}$  and  $V_L = -0.4 \text{ V}$ ? What is the power in the circuits in Fig. 9.26 not including the level shifter? What is the power-delay product if  $\tau_P = 50 \text{ psec}$ ?

**ANSWER:**  $800\Omega$ ;  $1.4 \text{ mW}$ ;  $70 \text{ fJ}$

**EXERCISE:** What is the value of  $I_{EF}$ ? What is the power in the level shifter in Fig. 9.27?

**ANSWER:**  $250 \mu\text{A}$ ;  $0.7 \text{ mW}$

**EXERCISE:** What are the three bias levels and  $V_{EE}$  in the circuit in Fig. 9.26 if the design is changed to have  $V_L = -0.2 \text{ V}$ ?

**ANSWER:**  $-0.1 \text{ V}$ ,  $-0.8 \text{ V}$ ,  $-1.4 \text{ V}$ ,  $-2.1 \text{ V}$

#### 9.9.4 HIGHER-LEVEL CML

The circuits in Fig. 9.26 can easily be extended to more inputs and can implement more complex logic functions. Figure 9.28 is the schematic of a three-input AND-NAND gate ( $Y = ABC$ ). Each additional input level comes at a cost of one more diode drop of power supply voltage. Even so, CML gates with four inputs are used in some circuits.

Examples of complex CML logic gate implementations are the two-input XOR circuit depicted in Fig. 9.29, and the CML D-latch in Fig. 9.30. Note that the storage element of the latch is formed by the cross-coupled inverter pair formed by  $Q_5$ ,  $Q_6$  and the two collector resistors. When the CLK input is high, the output tracks the  $D$  input; the outputs are latched when CLK goes low. Transistors  $Q_5$  and  $Q_6$  are actually permitted to enter the saturation region, but are not heavily saturated (see Section 9.9.4).

**EXERCISE:** What are the three bias levels and  $V_{EE}$  in the circuit in Fig. 9.28 if  $V_L = -0.4 \text{ V}$ ?

**ANSWER:**  $-0.2 \text{ V}$ ,  $-0.9 \text{ V}$ ,  $-1.6 \text{ V}$ ,  $-2.3 \text{ V}$ ,  $-3.0 \text{ V}$

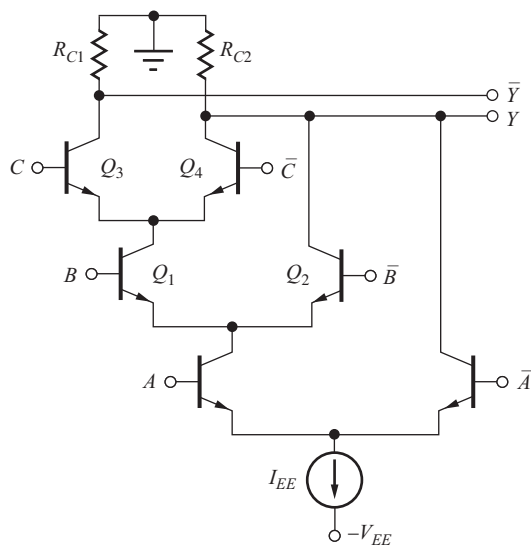


Figure 9.28 Three-input CML OR gate.

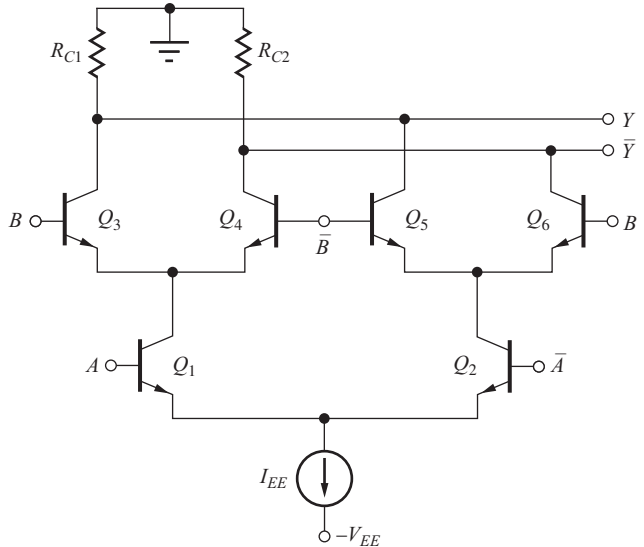


Figure 9.29 Two-input Exclusive-OR gate.

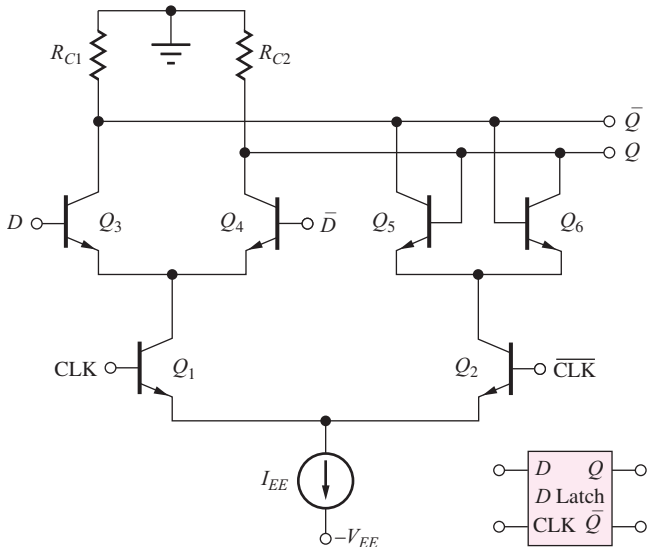


Figure 9.30 CML D-latch.

### 9.9.5 CML POWER REDUCTION

Power is a critical issue in high-density integrated circuits and using our knowledge of bipolar transistor behavior, we can change the CML design to significantly reduce  $V_{EE}$  and the power consumption. A one-diode level shift can be eliminated by driving the  $B$ -level inputs directly from the gate outputs, forcing the current-switch transistors to enter “weak” saturation. This technique is used in the  $D$ -latch in Fig. 9.30. For this case, the minimum operating voltage is  $V_{EE}^{\min} = NV_{BE} + \Delta V + V_{IEE}$

where  $N$  is the number of logic input levels,  $DV$  is the logic swing, and  $V_{I_{EE}}$  is the minimum operating voltage required across current source  $I_{EE}$ .

We also know that the dynamic power depends upon the square of the logic swing. Therefore the value of  $V_L$  is often reduced to save additional power. For example, the value of  $V_L$  can be reduced to  $-0.2$  V in the  $D$ -latch in the Fig. 9.30. When the collector of  $Q_3$  is at  $-0.2$  V and the  $D$  input is at  $0$  V, then the collector-base diode of  $Q_3$  is forward-biased by  $0.2$  V. Although technically saturated, we realize that the diode does not conduct any substantial current at this small value of forward bias. Thus, the transistor is not heavily saturated, and any added storage delay is minimal. So now  $V_{DH} = V_H = 0$  V, and  $V_{DL} = V_L = -0.2$  V. The CLK-level voltages are shifted down by one diode drop to  $V_{CLKH} = -0.7$  V, and  $V_{CLKL} = -0.9$  V. The emitter voltage of  $Q_1$  will be  $-1.4$  V, and  $V_{EE}$  can be reduced to  $2.1$  V or less.

Here we see the strong interaction between device knowledge and circuit design! Understanding the saturation behavior of the BJT has permitted a clever circuit design in which the power supply is reduced from  $2.8$  V to  $2.1$  V yielding a 25 percent power savings for a given operating current!

In a BiCMOS technology that includes MOSFETs, we can save another several tenths of a volt by using an NMOS transistor as a current source with  $V_{DS} = 0.4$  V. Then  $V_{EE}$  can be reduced by an additional  $0.3$  V. Using these techniques, state-of-the-art CML circuits implemented in SiGe technology can yield 10 psec delays at a power of  $2$  mW.

### 9.9.6 NMOS CML

Current mode logic can also be implemented in MOS technology as depicted in Fig. 9.31. Operation is very similar to the bipolar versions. NMOS current switch pairs are driven differentially by the true and complement logic inputs and switch the bias current to one output or the other yielding  $V_H = 0$  and  $V_L = -I_{EE} R_D$ . The power supply is limited by the required gate-source and drain-source voltages, but with proper design, the drain-source voltage required for active region operation of each MOSFET can be reduced to a few tenths of a volt.

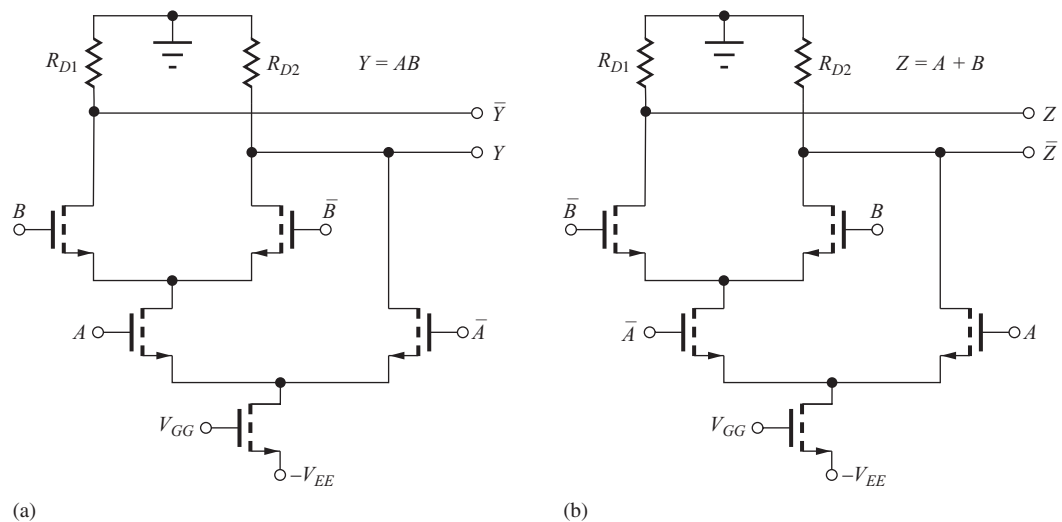
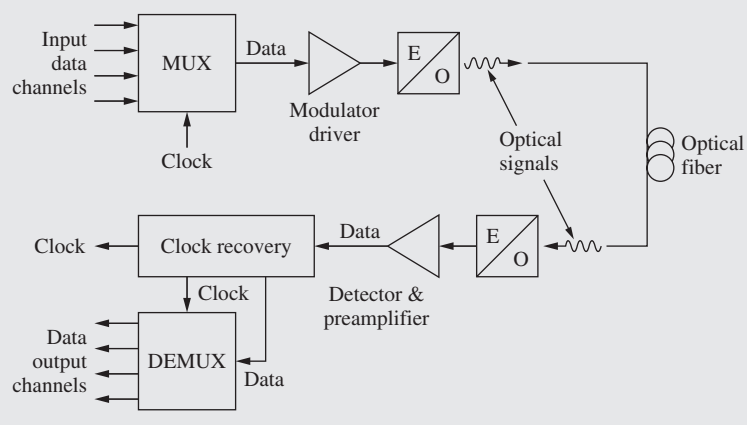


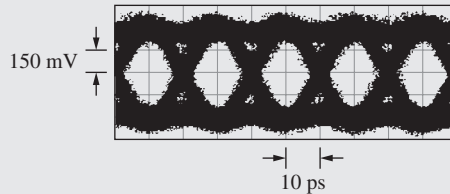
Figure 9.31 NMOS CML gates. (a) AND-NAND. (b) OR-NOR.


**ELECTRONICS IN ACTION**
***Electronics for Optical Communications***

Optical fiber communication systems provide the backbone of today's high bandwidth Internet and cellular communication systems. For example, in the OC-192 and OC-768 links, digital information is modulated onto optical carriers generated by solid-state lasers operating at data rates of 10 Gb/s and 40 Gb/s, respectively. Extremely high speed electronic circuits are required at both ends of the optical fiber link to convert from electrical to optical (E/O) and optical to electrical (O/E) form. These interface circuits include the data multiplexers and de-multiplexers, modulators, detectors, preamplifiers and clock recovery circuits shown in the accompanying figure. Because of the very high speed requirements, the circuit implementations are typically based on current-mode logic (CML) circuits using bipolar transistors with  $f_T$ 's in the 50-200 GHz range. Versions of the circuits have been implemented using silicon BJTs,<sup>1</sup> Indium Phosphide (InP) heterojunction bipolar transistors (HBTs),<sup>2</sup> and HBTs in Silicon Germanium (SiGe—"Siggy").<sup>3</sup>



(a)



(b)

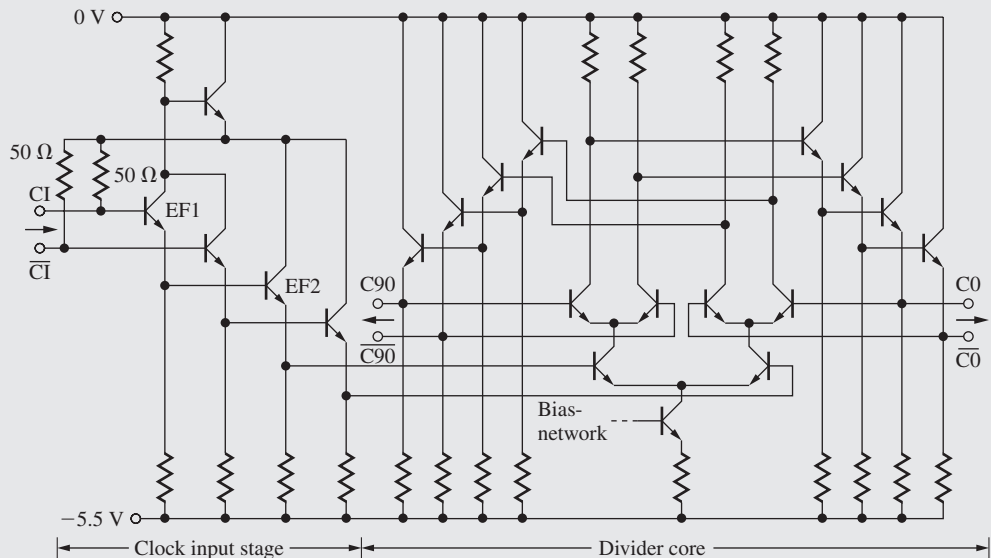
(a) Block diagram of a 40 Gb/s optical fiber communication system. (b) Eye diagram at data output of 2/1 MUX running at 50 Gb/s. (a) and (b): Copyright ©1996 IEEE. Reprinted with permission from [1].

<sup>1</sup> Alfred Felder, Michael Möller, Josef Popp, Josef Böck, and Hans-Martin Rein, "46 Gb/s DEMUX, 50 Gb/s MUX, and 30 GHz Static Frequency Divider in Silicon Bipolar Technology, *IEEE Journal Of Solid-State Circuits*, vol. 31, no. 4, pp. 481–486, April 1996.

<sup>2</sup> Mario Reinhold, Claus Dorschky, Eduard Rose, Rajasekhar Pullela, Peter Mayer, Frank Kunz, Yves Baeyens, Thomas Link, and John-Paul Mattia, "A Fully Integrated 40-Gb/s Clock and Data Recovery IC With 1:4 DEMUX in SiGe Technology, *IEEE Journal Of Solid-State Circuits*, vol. 36, no. 12, pp. 1937–1945, December, 2001.

<sup>3</sup> Y. Baeyens, G. Georgiou, J. S. Weiner, A. Leven, V. Houtsma, P. Paschke, Q. Lee, R. F. Kopf, Y. Yang, L. Chua, C. Chen, C. T. Liu, and Y. Chen, "InP D-HBT ICs for 40-Gb/s and higher bitrate lightwave transceivers," *IEEE Journal of Solid-State Circuits*, vol. 37, no. 9, pp. 1152–1159, September 2002.

On the receiver side of the optical fiber system, the digital signal appearing at the output of the detector and preamplifier contains a combination of both data and clock information. The clock is first separated from the data and then used to synchronize the data recovery process. The clock recovery circuit shown represents one example of the use of CML circuitry. The differential input signal is buffered by two-stages of emitter-followers. The output of the second pair of emitter followers drives the input of an CML flip-flop divider formed from three current switch circuits. The output of the current switches is buffered and level-shifted by additional pairs of emitter followers and fed back to the upper pair of current switches to form the flip-flop. The clock recovery circuit produces two differential clock signals with a  $90^\circ$  phase separation (quadrature) at the  $C0/\bar{C}0$  and  $C90/\bar{C}90$  outputs. See the Electronics in Action topics in Chapters 12 and 16 for a further discussion of detector and amplifier interface circuitry for optical communications.



ECL clock-recovery circuit using SiGe HBT's Copyright © 2001 IEEE. Reprinted with permission from (2).

## 9.10 THE SATURATING BIPOLAR INVERTER

At the heart of many bipolar logic gates is the simple saturating bipolar inverter circuit in Fig. 9.32, which uses a single BJT switching device  $Q_2$  to pull  $v_O$  down to  $V_L$  and a resistor load element to pull the output up to the power supply  $V_{CC}$ . The input voltage  $v_I$  and the base current  $i_B$  supplied to the base of the bipolar transistor will be designed to switch  $Q_2$  between the saturation and nonconducting states.

For analysis and design of saturating BJT circuits, we use the transistor parameters in Table 9.3. The base-emitter or base-collector voltages in the forward- or reverse-active regions are assumed to be 0.7 V. However, when a transistor saturates, its base-emitter voltage increases slightly, and  $V_{BESAT} = 0.8$  V will be used for the base-emitter voltage of a saturated transistor. Our BJT circuits will be designed to have a worst-case  $V_{CESAT} = 0.15$  V. Transistors in most logic technologies are optimized for speed, and current gain is often compromised, as indicated by the relatively low value of  $\beta_F$  in Table 9.3.  $\beta_R$  typically ranges between 0.1 and 2. Up to now, we have not found a use for the reverse-active region of operation, but as we shall see in Sec. 9.11, it plays a very important role in TTL circuits.

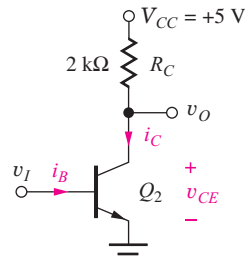


**Figure 9.32** Single transistor bipolar inverter and device parameters.

**TABLE 9.3**  
BJT Parameters

$I_S$	$10^{-15}$ A
$\beta_F$	40
$\beta_R$	0.25
$V_{BE}$	0.70 V
$V_{BESAT}$	0.80 V
$V_{CESAT}$	0.15 V

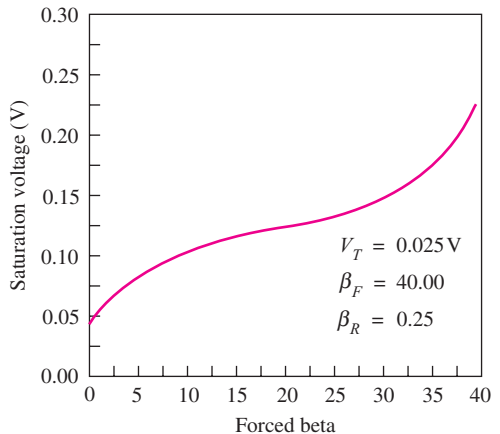


**Figure 9.33** Saturation voltage  $V_{CESAT}$  versus forced beta  $i_C/i_B$ .

### 9.10.1 STATIC INVERTER CHARACTERISTICS

Writing the equation for the output voltage of the inverter in Fig. 9.32, we find

$$v_O = V_{CC} - i_C R_C \quad (9.44)$$

If the base-emitter voltage ( $v_{BE} = v_I$ ) is several hundred millivolts less than the normal turn-on voltage of the base-emitter junction (0.6 to 0.7 V), then  $Q_2$  will be nearly cut off, with  $i_C \cong 0$ . Equivalently, if the input base current  $i_B$  is zero, then  $Q_2$  will be near cutoff. For either case,

$$v_O = V_H \cong V_{CC} \quad (9.45)$$

In this particular logic circuit, the value of  $V_H$  is set by the power supply voltage:  $V_H = 5$  V.

The low-state output level is set by the saturation voltage of the bipolar transistor,  $V_L = V_{CESAT}$ . To ensure saturation, as discussed in Sec. 5.7.5, we require that

$$i_B > \frac{i_{CMAX}}{\beta_F} \quad \text{where} \quad i_{CMAX} = \frac{V_{CC} - V_{CESAT}}{R_C} \cong \frac{V_{CC}}{R_C} \quad (9.46)$$

For the circuit in Fig. 9.32,  $i_{CMAX} = 2.43$  mA, assuming  $V_{CESAT} = 0.15$  V. Using  $\beta_F = 40$ , the transistor will be saturated for

$$i_B > \frac{2.43 \text{ mA}}{40} = 60.8 \mu\text{A}$$

**EXERCISE:** Estimate the static power dissipation of the inverter in Fig. 9.32 for  $v_O = V_H$  and  $v_O = V_L$ . What value of  $R_C$  is required to reduce the power dissipation by a factor of 10?

**ANSWERS:** 0, 12.1 mW; 20 kΩ

### 9.10.2 SATURATION VOLTAGE OF THE BIPOLAR TRANSISTOR

An expression for the **saturation voltage** of the BJT in terms of its base and collector currents was derived in Eq. (5.30) and is repeated here:

$$V_{CESAT} = V_T \ln \left[ \left( \frac{1}{\alpha_R} \right) \frac{1 + \frac{i_C}{(\beta_R + 1)i_B}}{1 - \frac{i_C}{\beta_F i_B}} \right] = V_T \ln \left[ \left( \frac{1}{\alpha_R} \right) \frac{1 + \frac{\beta_{FOR}}{(\beta_R + 1)}}{1 - \frac{\beta_{FOR}}{\beta_F}} \right] \quad \text{for } i_B > \frac{i_C}{\beta_F} \quad (9.47)$$

Recall that the ratio  $i_C/i_B$  is the forced beta  $\beta_{FOR}$  and that  $i_C/i_B = \beta_F$  is true only for the forward-active region. Note that Eq. (9.47) is no longer valid for  $i_C/i_B = \beta_F$ .

Equation (9.47) is plotted as a function of  $\beta_{FOR} = i_C/i_B$  in Fig. 9.33. As  $i_B$  becomes very large or  $i_C$  becomes very small,  $\beta_{FOR}$  approaches zero, and  $V_{CESAT}$  reaches its minimum value:

$$V_{CESAT}^{\text{MIN}} = V_T \ln \left( \frac{1}{\alpha_R} \right) \quad (9.48)$$

The minimum value of  $V_{CESAT}$  is approximately 40 mV for the transistor depicted in Fig. 9.33.

For the more general case,  $i_{C\text{MAX}}$  is known from Eq. (9.46), and Eq. (9.47) can be used to ensure that our circuit design supplies enough base current to saturate the transistor to the desired level. As assumed earlier,  $V_{CESAT} \leq 0.15$  V. Solving Eq. (9.47) for  $i_C/i_B$ ,

$$\frac{i_C}{i_B} \leq \beta_F \left[ \frac{1 - \frac{1}{\alpha_R \Gamma}}{1 + \frac{\beta_F}{\beta_R \Gamma}} \right] \quad \text{where } \Gamma = \exp(V_{CESAT}/V_T) \quad (9.49)$$

Using Eq. (9.49) with  $i_C = 2.43$  mA and the values from Table 9.3, reaching  $V_{CESAT} = 0.15$  V requires  $i_C/i_B \leq 28.3$  or  $i_B \geq 86$   $\mu$ A.

## DESIGN EXAMPLE 9.3

### BIPOLAR TRANSISTOR SATURATION VOLTAGE

In this example, we will choose the base current required to achieve a desired saturation voltage in a power transistor used in a switching application.

**PROBLEM** A bipolar power transistor has a forward current gain of 20 and an inverse current gain of 0.1. How much base current is required to achieve a saturation voltage of 0.1 V at a collector current of 10 A?

**SOLUTION** **Known Information and Given Data:** Bipolar transistor with  $\beta_F = 20$ ,  $\beta_R = 0.1$ , and  $I_C = 10$  A

**Unknowns:** Base current  $I_B$  required to achieve the desired “on-voltage”

**Approach:** Find  $\Gamma$  and calculate  $I_B$  based on Eq. (9.49).

**Assumptions:** Current gain values are independent of current; room temperature operation with  $V_T = 25$  mV

**Analysis:** Let us first check to be sure that  $V_{CESAT} = 0.1$  V is possible:

$$V_{CEMIN} = V_T \ln \frac{1}{\alpha_R} = V_T \ln \left( \frac{\beta_R + 1}{\beta_R} \right) = 0.025 \text{ V} \ln \left( \frac{0.1 + 1}{0.1} \right) = 0.025 \text{ V} \ln(11) = 0.06 \text{ V}$$

Since 60 mV is less than the required saturation voltage of 0.1 V, we can proceed. Using Eq. (9.49) to find  $\Gamma$  yields

$$\Gamma = \exp \left( \frac{V_{CESAT}}{V_T} \right) = \exp \left( \frac{0.1 \text{ V}}{0.025 \text{ V}} \right) = 54.6$$

and solving the same equation set for  $I_B$  yields

$$I_B \geq \frac{I_C}{\beta_F} \left[ \frac{1 + \frac{\beta_F}{\beta_R \Gamma}}{1 - \frac{1}{\alpha_R \Gamma}} \right] = \frac{10 \text{ A}}{20} \left[ \frac{1 + \frac{20}{0.1(54.6)}}{1 - \frac{11}{54.6}} \right] = 2.92 \text{ A}$$

A minimum base current of 2.92 A is required to achieve the saturation voltage of 100 mV. Note that an additional safety margin should be used in the design of the base current drive circuit.

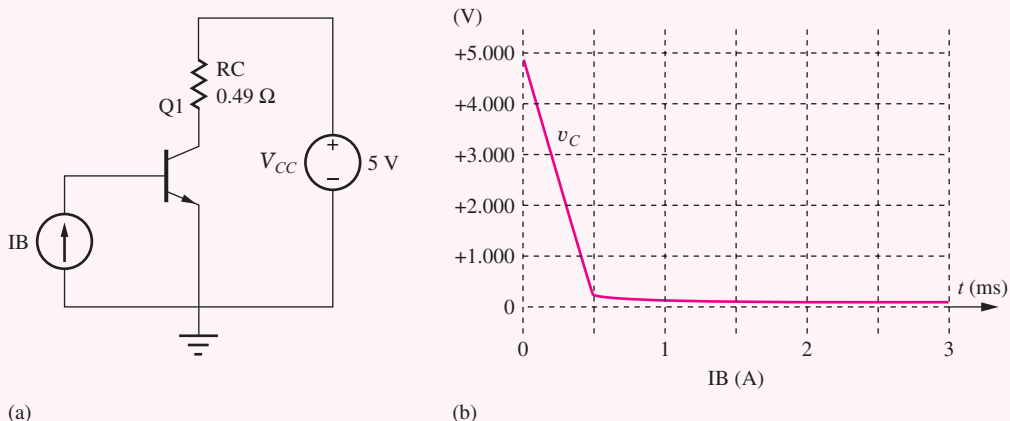
**Check of Results:** The forced beta is

$$\beta_{\text{FOR}} = \frac{I_C}{I_B} = \frac{10}{2.92} = 3.43$$

and the collector-emitter voltage of the saturated transistor will be

$$V_{\text{CESAT}} = V_T \ln \left[ \left( \frac{1}{\alpha_R} \right) \frac{1 + \frac{\beta_{\text{FOR}}}{\beta_R + 1}}{1 - \frac{\beta_{\text{FOR}}}{\beta_F}} \right] = 0.025 \text{ V} \ln \left[ (11) \frac{1 + \frac{3.43}{0.1 + 1}}{1 - \frac{3.43}{20}} \right] = 0.100 \text{ V} \quad \checkmark$$

**Computer-Aided Analysis and Discussion:** SPICE simulation uses the circuit shown here in which current source  $I_B$  is swept from 0 to 4 A.  $V_{CC}$  is chosen arbitrarily to be 5 V, and  $RC$  is selected so that the collector current will be 10 A when  $v_C = 0.1$  V. The default *npm* model is used with the parameters set as  $\text{BF} = 20$ ,  $\text{BR} = 0.1$ , and  $\text{IS} = 10 \text{ fA}$ . The output voltage doesn't reach 0.1 V until  $I_B = 3.37$  A. We should ask ourselves why there is such a discrepancy. The answer lies in our choice of the value of the thermal voltage. Remember that the temperature in SPICE defaults to  $T = 27^\circ\text{C}$ . If we recalculate the required base current using  $V_T = 25.8 \text{ mV}$ , we find the base current should be at least 3.33 A.



Note that the transistor enters saturation as the base current exceeds approximately 0.5 A, but the base current must increase to 3.4 A to force  $V_{\text{CESAT}}$  to reach 0.1 V. At a forced beta of 15 ( $I_B = 0.667$  A),  $V_{\text{CESAT}}$  is 0.16 V.

**EXERCISE:** Recalculate the minimum value of  $I_B$  and  $\beta_{\text{FOR}}$  assuming  $V_T = 25.8 \text{ mV}$ .

**ANSWER:** 3.33 A; 3.00

**EXERCISE:** What is the minimum base current required in Design Ex. 9.3 if  $\beta_R$  of the transistor changes to 0.2?

**ANSWER:** 1.59 A

**EXERCISE:** What minimum base current is required to achieve a saturation voltage of 0.15 in Design Ex. 9.3?

**ANSWER:** 0.769 A

**EXERCISE:** What is the minimum saturation voltage of a power transistor having  $\beta_R = 0.05$  and operating at a junction temperature of 150°C?

**ANSWER:** 111 mV

### 9.10.3 LOAD-LINE VISUALIZATION

As presented in Chapter 6, an important way of visualizing inverter operation is to look at the load line, Eq. (9.44), drawn on the BJT transistor output characteristics, as in Fig. 9.34. The BJT switches between the two operating points on the load line indicated by the circles in Fig. 9.34. At the right-hand end of the load line, the BJT is cut off, with  $i_C = 0$  and  $v_{CE} = 5$  V. At the Q-point near the left end of the load line, the BJT represents a low resistance in the saturation region, with  $v_O = V_{CESAT}$ . Note that the current in saturation is limited primarily by the load resistance and is nearly independent of the base current.

**EXERCISE:** A transistor must reach a saturation voltage  $\leq 0.1$  V with  $I_C = 10$  mA. What are the maximum value of  $\beta_{FOR}$  and the minimum value of the base current? Use the transistor parameters from Table 9.3.

**ANSWERS:** 9.24, 1.08 mA

### 9.10.4 SWITCHING CHARACTERISTICS OF THE SATURATED BJT

A very important change occurs in the switching characteristics of bipolar transistors when they saturate. The excess base current that drives the transistor into saturation causes additional charge storage in the base region of the transistor. This charge must be removed before the transistor can

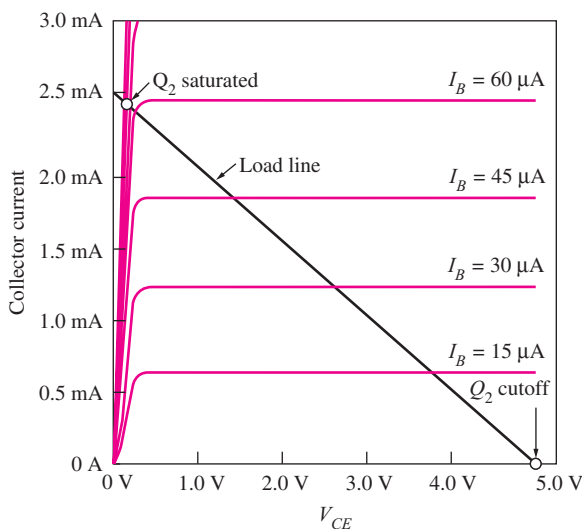
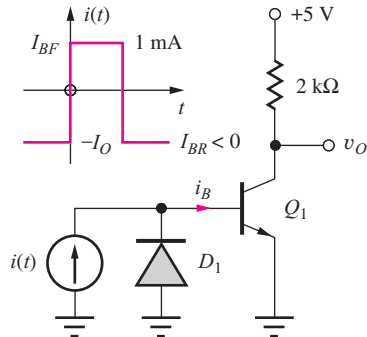
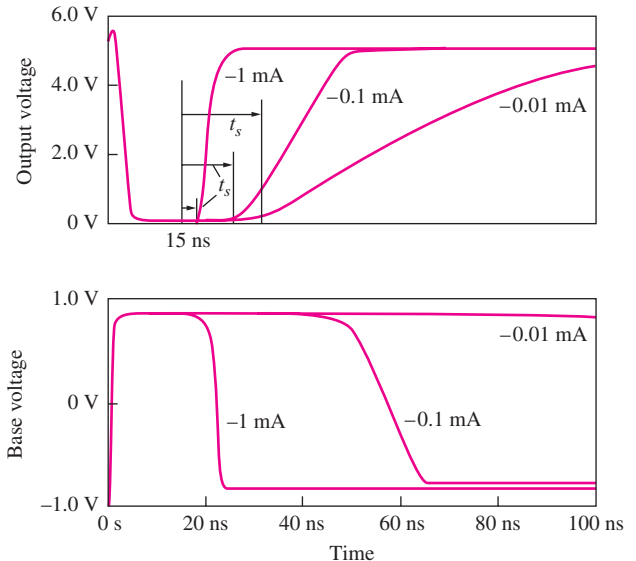


Figure 9.34 BJT output characteristics and load line.



**Figure 9.35** Bipolar inverter with current source drive.



**Figure 9.36** Switching behavior for the BJT inverter for three values of reverse base current:  $I_{BR} = -1 \text{ mA}$ ,  $-0.1 \text{ mA}$ , and  $-0.01 \text{ mA}$ .

turn off, and an extra delay time, termed the **storage time  $t_s$** , appears in the switching characteristic of the saturated BJT.

We illustrate the problem through the circuit simulation results presented in Fig. 9.36 for the inverter circuit in Fig. 9.35, in which the BJT is driven by a current source that forces current  $I_{BF}$  into the base to turn the transistor on and pulls current  $I_{BR}$  out of the base to turn the transistor back off. Negative base current can only occur in the *n-p-n* transistor during the transient that removes charge from the base. Diode  $D_1$  is added to the circuit to provide a steady-state path for the negative source current because we know that the *n-p-n* transistor cannot support a large negative steady-state base current without junction breakdown.

Referring to Figs. 9.35 and 9.36 at  $t = 0$ , we see that the current source forces a base current  $I_{BF} = 1 \text{ mA}$  into the transistor, rapidly charging the base-emitter capacitance and supplying charge to the base. The BJT turns on and saturates within approximately 5 ns. At  $t = 15 \text{ ns}$ , the direction of the current source reverses, and simulation results are shown for three different values of reverse current. For a small reverse current ( $0.01 \text{ mA}$ ), electron-hole recombination in the base is the only mechanism available to remove the excess base charge. The transistor turns off very slowly because of the slow decay of the charge stored on the base-emitter junction capacitance. As the reverse base current is increased, both storage time and rise time are substantially reduced.

Observe the behavior of the voltage at the base of the transistor. The base voltage remains constant at  $+0.85 \text{ V}$  until the excess **stored base charge** has been removed from the base. Then the base voltage can drop, and the transistor turns off. Note that the base voltage is still above  $0.8 \text{ V}$  at  $t = 100 \text{ ns}$  for the smallest reverse base current!

The storage time  $t_s$  can be calculated from this formula [1]:

$$t_s = \tau_s \ln \left( \frac{I_{BF} - I_{BR}}{\frac{i_{CMAX}}{\beta_F} - I_{BR}} \right) \quad \text{with} \quad \tau_s = \frac{\alpha_F(\tau_F + \alpha_R \tau_R)}{1 - \alpha_F \alpha_R} \quad (9.50)$$

in which  $\tau_s$  is called the **storage time constant**.  $I_{BF}$  and  $I_{BR}$  are the forward and reverse base currents defined in Fig. 9.35, and  $\alpha_F$  and  $\alpha_R$  are the forward and reverse common-base current gains. Note that the value of  $I_{BR}$  is negative.

The constants  $\tau_F$  and  $\tau_R$  are called the **forward** and **reverse transit times** for the transistor and determine the amount of charge stored in the base in the forward- and reverse-active modes of operation— $Q_F$  and  $Q_R$ , respectively:

$$Q_F = i_F \tau_F \quad \text{and} \quad Q_R = i_R \tau_R \quad (9.51)$$

In Eq. (9.51),  $i_F$  and  $i_R$  are the forward and reverse current components from the transport model.

The storage time constant quantifies the amount of excess charge, over and above that needed to support the actual collector current, stored in the base when the bipolar transistor enters saturation:

$$Q_{XS} = \tau_S \left( i_B - \frac{i_{CMAX}}{\beta_F} \right) \quad (9.52)$$

The storage time  $t_S$  represents a significant degradation in the speed of the BJT when it tries to come out of saturation, as can be seen in Fig. 9.36 and Ex. 9.4.

## EXAMPLE 9.4 STORAGE TIME CALCULATIONS

In this example, we calculate the impact of the reverse turnoff current on the transistor storage time.

**PROBLEM** Calculate the storage time constant and storage times for the three currents used in Figs. 9.35 and 9.36 if  $\alpha_F = 0.976$ ,  $\alpha_R = 0.20$ ,  $\tau_F = 0.25$  ns, and  $\tau_R = 25$  ns.

**SOLUTION** **Known Information and Given Data:** Circuit in Fig. 9.35; transistor parameters  $\alpha_F = 0.976$ ,  $\alpha_R = 0.20$ ,  $\tau_F = 0.25$  ns, and  $\tau_R = 25$  ns; a forward current ( $I_{BF}$ ) of 1 mA and reverse turnoff currents ( $I_{BR}$ ) of  $-1$  mA,  $-0.1$  mA, and  $-0.01$  mA

**Unknowns:** Storage time constant  $\tau_S$  and storage times for the three turnoff conditions

**Approach:** Use Eq. (9.50) to find the storage time constant and then to calculate the storage time for the three different turnoff currents.

**Assumptions:** None

**Analysis:** Equation (9.50) gives  $\tau_S = \frac{0.976(0.25 \text{ ns} + 0.20(25 \text{ ns}))}{1 - 0.976(0.20)} = 6.4 \text{ ns}$

In order to evaluate Eq. (9.50) we need values for  $i_{CMAX}$  and  $\beta_F$ . Equation (9.46) defines the value of  $i_{CMAX}$ ,

$$i_{CMAX} \approx \frac{V_{CC}}{R_C} = \frac{5 \text{ V}}{2 \text{ k}\Omega} = 2.5 \text{ mA} \quad \text{and} \quad \beta_F = \frac{\alpha_F}{1 - \alpha_F} = \frac{0.976}{1 - 0.976} = 40.7$$

Using Eq. (9.50) with  $\tau_S = 6.4$  ns,  $I_{BR} = 1$  mA, and  $I_{BR} = -0.01$  mA,  $-0.1$  mA, and  $-1.0$  mA yields

$$t_S = (6.4 \text{ ns}) \ln \left[ \frac{\frac{1 - (-0.01)}{2.5} \text{ mA}}{\frac{40.7}{2.5} - (-0.01) \text{ mA}} \right] = 17.0 \text{ ns} \quad t_S = (6.4 \text{ ns}) \ln \left[ \frac{\frac{1 - (-0.1)}{2.5} \text{ mA}}{\frac{40.7}{2.5} - (-0.1) \text{ mA}} \right] = 12.3 \text{ ns}$$

$$t_S = (6.4 \text{ ns}) \ln \left[ \frac{\frac{1 - (-1)}{2.5} \text{ mA}}{\frac{40.7}{2.5} - (-1) \text{ mA}} \right] = 4.06 \text{ ns}$$

**Check of Results:** A double check of the calculations indicates they are correct, and the values agree well with the storage times that can be observed in Fig. 9.36.

**EXERCISE:** What value of  $i_{BR}$  is required to achieve a storage time of 1 ns in the circuit in Fig. 9.35? Use the transistor parameters from Ex. 9.4.

**ANSWER:**  $-5.49 \text{ mA}$

**EXERCISE:** For Ex. 9.4, calculate the excess charge stored in the base and compare to  $Q_F$ .

**ANSWERS:**  $6.01 \text{ pC}$ ,  $0.625 \text{ pC}$ ,  $Q_{XS} \gg Q_F$

## 9.11 A TRANSISTOR-TRANSISTOR LOGIC (TTL) PROTOTYPE

Now that we have studied the characteristics of the saturating transistor inverter, we have the knowledge in place to understand the behavior of transistor-transistor logic or TTL. For years, TTL has been a workhorse technology for implementing digital functions and for providing “glue logic” necessary in microprocessor system design. TTL is interesting from another point of view since it is the only circuit that we shall encounter that makes use of transistors operating in all four regions of operation—forward-active, reverse-active, saturation, and cutoff. In this section and Secs. 9.11 to 9.14, we will first explore a simplified TTL prototype, and then move to analysis of the full standard TTL logic gate, as well as other members of the TTL logic family.

Figure 9.37 is the prototype for a low power TTL inverter. Transistor  $Q_1$  has been added to the inverter of Fig. 9.32 to control the supply of base current to  $Q_2$ . Input voltage  $v_I$  causes the current  $i_{B1}$  to switch between either the base-emitter diode or the base-collector diode of  $Q_1$ . We first explore circuit behavior for  $v_I = V_L$ , find  $V_H$ , and then use it to study the circuit for  $v_I = V_H$ .

### 9.11.1 TTL INVERTER FOR $v_I = V_L$

The input to the TTL gate in Fig. 9.38 is set to  $V_L = V_{CESAT1} = 0.15$ . The +5-V supply tends to force current  $i_{B1}$  down through the  $4\text{-k}\Omega$  resistor and into the base of  $Q_1$ , turning on the base-emitter diode of  $Q_1$ . Transistor  $Q_1$  attempts to pull a collector current  $i_{C1} = \beta_F i_{B1}$  out of the base of  $Q_2$ , but only leakage currents can flow in the reverse direction from the base. Therefore,  $i_{C1} \cong 0$ . Because  $Q_1$  is operating with  $\beta_F i_B > i_C$ , it saturates, with both junctions being forward-biased. Thus the voltage at the base of  $Q_2$  is given by

$$v_{BE2} = v_I + V_{CESAT1} = 0.15 + 0.04 = 0.19 \text{ V} \quad (9.53)$$

where  $V_{CESAT1} = 0.04 \text{ V}$  has been used because  $i_{C1} \cong 0$  (see Fig. 9.33). Since  $v_{BE2}$  is only 0.19 V,  $Q_2$  does not conduct any substantial collector current (although it technically remains in the forward-active region—see Prob. 9.69), and the output voltage will be  $v_O \cong V_{CC} = 5 \text{ V}$ .

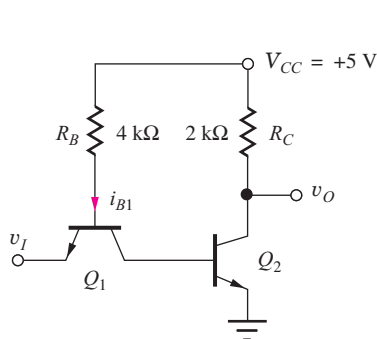


Figure 9.37 TTL inverter prototype.

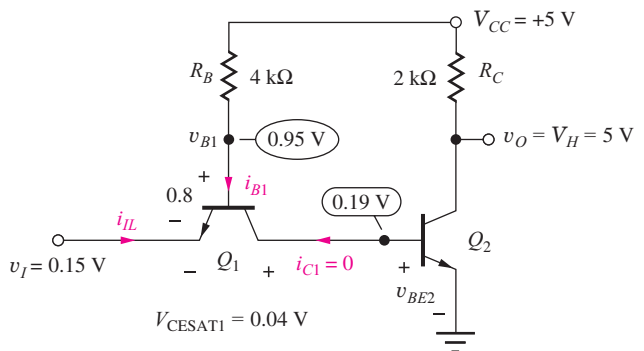


Figure 9.38 TTL gate with input  $v_I = V_L$ .

Base current  $i_{B1}$  is given by

$$i_{B1} = \frac{5 - v_{B1}}{4 \text{ k}\Omega} \quad \text{where } v_{B1} = v_1 + V_{\text{BESAT}} = 0.95 \text{ V for } V_{\text{BESAT}} = 0.8 \text{ V} \quad (9.54)$$

For the gate in Fig. 9.38, we find that  $i_{B1} = 1.01 \text{ mA}$ . This current enters the base and exits the emitter of  $Q_1$ . For this TTL gate, the input current for the low input state is  $i_{IL} = -i_{E1}$ , or

$$-i_{IL} = i_{E1} = (i_{B1} + i_{C1}) \cong i_{B1} = \frac{5 - v_{B1}}{4 \text{ k}\Omega} = \frac{5 - 0.95}{4 \text{ k}\Omega} = 1.01 \text{ mA} \quad (9.55)$$

This is a logic gate characteristic that we have not seen before. In TTL, there is a relatively large current that the input signal source  $v_I$  must absorb. We shall see shortly how this current limits the fanout of the TTL gate.

**EXERCISE:** What are the values of  $V_{BE2}$  and  $i_{IL}$  in Fig. 9.38 if  $\beta_R = 2$ ?

**ANSWERS:** 0.19 V, -1.01 mA

### 9.11.2 TTL INVERTER FOR $v_I = V_H$

$V_H = 5 \text{ V}$  is applied as the input to the inverter in Fig. 9.39. Because the emitter of  $Q_1$  is at 5 V, base current  $i_{B1}$  cannot enter the base-emitter diode; it instead forward-biases the base-collector diode. Transistor  $Q_1$  enters the reverse-active region with the base-collector junction forward-biased and the base-emitter junction reverse-biased. Base current  $i_{B1}$  causes a current  $(\beta_R + 1)i_{B1}$  to exit the collector terminal, and this current becomes the base current of  $Q_2$ . In addition, a current  $\beta_R i_{B1}$  enters the emitter terminal, and this current represents the input current  $i_{IH}$  for the input high state. A small value of  $\beta_R$  is desired to keep  $i_{IH}$  low.

$$i_{B2} = (\beta_R + 1)i_{B1} \quad \text{and} \quad i_{IH} = +\beta_R i_{B1} \quad (9.56)$$

For proper circuit operation,  $i_{B2} = (\beta_R + 1)i_{B1}$  is designed to be much greater than  $i_{C2}/\beta_F$ ,  $Q_2$  saturates, and its base-emitter voltage becomes 0.8 V. The voltage  $v_{B1} = v_{BC1} + V_{\text{BESAT2}} = 0.7 + 0.8 = 1.5 \text{ V}$ . The base current of  $Q_1$  is now

$$i_{B1} = \frac{(5 - 1.5) \text{ V}}{4 \text{ k}\Omega} = 0.875 \text{ mA} \quad \text{and} \quad i_{IH} = \beta_R i_{B1} = 0.25(0.875 \text{ mA}) = 0.219 \text{ mA} \quad (9.57)$$

Evaluating Eq. (9.56), we find that the base current of  $Q_2$  is

$$i_{B2} = (\beta_R + 1)i_{B1} = (1.25)0.875 \text{ mA} = 1.09 \text{ mA} \quad (9.58)$$

Current  $i_{B2}$  is much greater than the 86  $\mu\text{A}$  required to saturate  $Q_2$ , as we calculated immediately following Eq. (9.49). The forced beta in this circuit is  $\beta_{\text{FOR}} = 2.43 \text{ mA}/1.09 \text{ mA} = 2.22$ , and

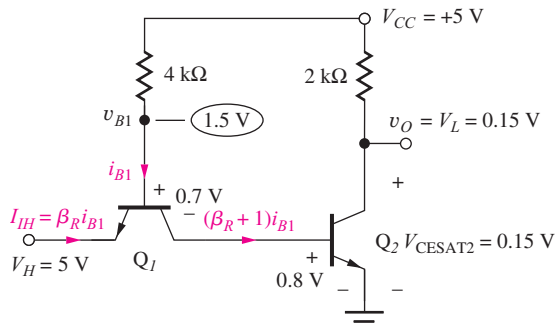


Figure 9.39 TTL gate with input  $v_I = V_H$ .

Eq. (9.47) indicates that  $Q_2$  actually has  $V_{CESAT2} = 67 \text{ mV}$ . The additional base current just calculated is needed to ensure that the  $V_{CESAT}$  specification is met when the inverter must drive a large fanout.

**EXERCISE:** What would be the values of  $v_{BE2}$  and  $i_{IH}$  in Fig. 9.39 if  $\beta_{R1} = 2$ ?

**ANSWERS:** 0.80 V, 1.75 mA

### 9.11.3 POWER IN THE PROTOTYPE TTL GATE

Now we explore the power dissipation in the TTL gate for the two logic states. For  $v_I = 5 \text{ V}$  and  $v_O = V_L$ , as in Fig. 9.40(a), the total power being consumed by the gate is

$$P_L = V_{CC}i_{CC} + v_I i_{IH} = V_{CC}(i_{C2} + i_{B1}) + v_I i_{IH} \quad (9.59)$$

For the circuit in Fig. 9.40(a),  $P_L = 5 \text{ V}(2.4 \text{ mA} + 0.88 \text{ mA} + 0.22 \text{ mA}) = 17.6 \text{ mW}$ .

For  $v_I = V_L$  and  $v_O = V_H$ , as in Fig. 9.34(b), the power being consumed by the gate is

$$P_H = V_{CC}i_{CC} + v_I i_{IL} = V_{CC}i_{B1} + v_I i_{IL} \quad (9.60)$$

For the values in Fig. 9.40(b),  $P_H = 5 \text{ V}(1.0 \text{ mA}) + 0.15 \text{ V}(-1.0 \text{ mA}) = 4.85 \text{ mW}$ . Assuming that the gate spends 50 percent of the time in each state (a 50 percent duty cycle), the average power dissipation  $\langle P \rangle$  is

$$\langle P \rangle = \frac{17.6 + 4.85}{2} \text{ mW} = 11.2 \text{ mW}$$

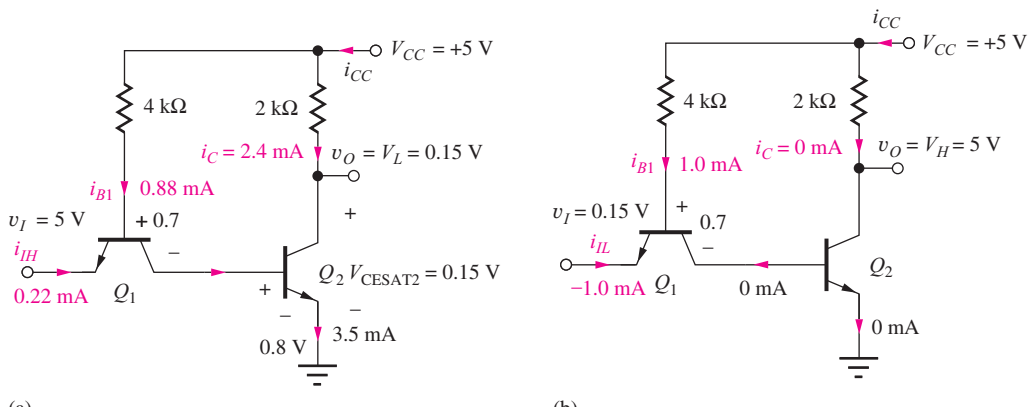
### 9.11.4 $V_{IH}$ , $V_{IL}$ , AND NOISE MARGINS FOR THE TTL PROTOTYPE

Figure 9.41 shows the results of circuit simulation of the VTC for the TTL inverter of Figs. 9.37 to 9.39. As expected,  $V_H$  is equal to  $V_{CC}$ . For  $v_O = V_L$ , the output transistor is heavily saturated, with  $V_L < 0.1 \text{ V}$ . The transition region between  $V_H$  and  $V_L$  is quite narrow, which is a result of the exponential characteristics of the BJT.

As can be observed in the VTC, the difference between  $V_{IH}$  and  $V_{IL}$  is only slightly larger than 0.1 V (although large enough to change  $i_C$  by a factor of more than 50!). Calculating the exact input voltages for which the slope of the VTC equals  $-1$  is complex, but a simplified analysis of the circuit in Fig. 9.42 yields the approximate location of the  $V_{IH}$  and  $V_{IL}$  transition points.

For an input voltage near  $V_L$ ,  $Q_1$  is saturated and the voltage at the base of  $Q_2$  is given by

$$v_{BE2} = v_I + V_{CESAT1} = v_I + 0.04 \text{ V} \quad (9.61)$$



**Figure 9.40** (a) Currents in the prototype inverter for  $v_O = V_L$ . (b) Currents in the TTL gate for  $v_I = V_L$ .

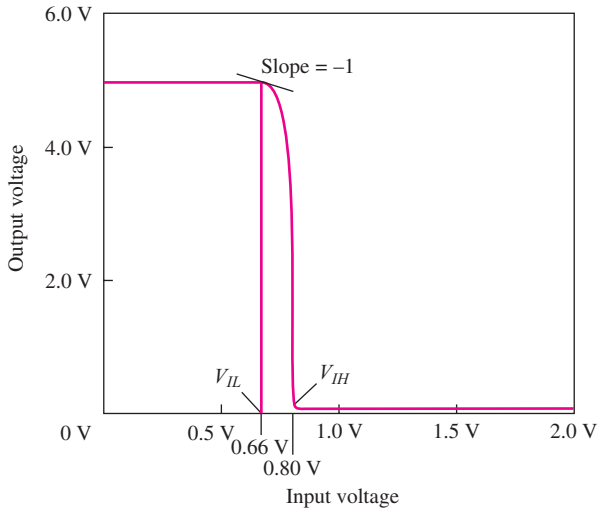


Figure 9.41 SPICE simulation of the VTC of the prototype TTL gate.

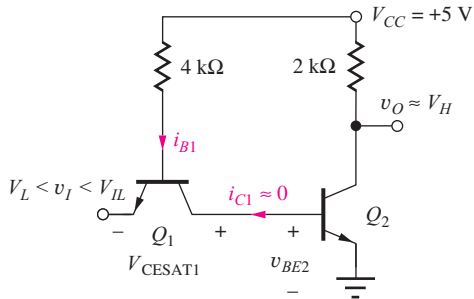


Figure 9.42 TTL gate with input  $v_I$  below  $V_{IL}$ .

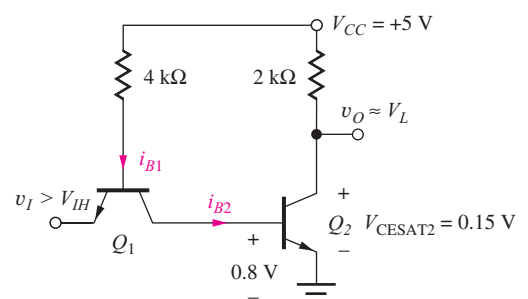


Figure 9.43 TTL gate with input  $v_I$  above  $V_{IH}$ .

using the actual value of saturation voltage from Fig. 9.33 for  $i_{C1} = 0$ . Because of the exponential turn-on of the transistor, the slope of the VTC changes rapidly at the point at which  $Q_2$  just begins to conduct as  $v_{BE2}$  reaches 0.7 V, and this point marks  $V_{IL}$ :

$$V_{IL} \cong 0.7 - V_{CESAT1} = 0.66 \text{ V} \quad (9.62)$$

Near  $V_{IL}$ ,  $Q_1$  is saturated, and the collector voltage of  $Q_1$  follows the voltage applied to the emitter.

Calculation of the value of  $V_{OH}$  corresponding to  $V_{IL}$  is very similar to the method used to obtain Eq. (9.27), and  $V_{OH}$  is very close to  $V_H$ :

$$V_{OH} \cong V_H - V_T \cong V_H = 5 \text{ V} \quad (9.63)$$

We see that this value agrees well with the simulation results in Fig. 9.41.

Similar arguments yield an approximate value of  $V_{IH}$ . In Fig. 9.43, the input voltage is above  $V_{IH}$ , and the base-emitter voltage of  $Q_2$  is given by  $V_{BESAT2} = 0.8 \text{ V}$ . As the input decreases, the output remains at  $V_{CESAT}$  until current begins to be diverted away from the base of  $Q_2$ . This occurs approximately as the base-emitter and base-collector voltages of  $Q_1$  become equal, or  $v_I = 0.8 \text{ V}$  (see Prob. 9.71). Thus, we expect  $V_{IH}$  to be given approximately by

$$V_{IH} \cong V_{BESAT2} = 0.8 \text{ V} \quad (9.64)$$

Calculation of the value of  $V_{OL}$  is more complex and will not be attempted here. However, we see from the results in Fig. 9.41 that  $V_{OL}$  is very close to  $V_L$ , and we will incur little error if we use

$V_L$  for our estimate of  $V_{OL}$ :

$$V_{OL} \cong V_L = V_{CESAT2} = 0.15 \text{ V} \quad (9.65)$$

These approximate values for  $V_{IH}$  and  $V_{IL}$ , based on Eqs. (9.62) and (9.64), agree well with the simulation results in Fig. 9.41. These estimates are accurate because of the exponential behavior of the BJT. Less than a 60-mV change in  $v_{BE}$  changes  $i_C$  by a factor of 10, so the estimates of  $V_{IH}$  and  $V_{IL}$  should not be in error by more than  $\pm 60 \text{ mV}$ .

Using Eqs. (9.62) and (9.64) with the values of  $V_{OH}$  and  $V_{OL}$  yields

$$NM_L \cong 0.66 - 0.15 = 0.51 \text{ V} \quad \text{and} \quad NM_H \cong 5.0 - 0.8 = 4.2 \text{ V} \quad (9.66)$$

### 9.11.5 PROTOTYPE INVERTER SUMMARY

Figure 9.44 is a summary of the static characteristics of the prototype TTL inverter.  $V_H$  is equal to the power supply voltage of 5 V, and an input of this value produces an output low state of  $V_L \leq 0.15 \text{ V}$ . The highly asymmetrical noise margins are  $NM_L = 0.51 \text{ V}$  and  $NM_H = 4.2 \text{ V}$ . When the input is high, a current of 0.22 mA enters the TTL input, and when the input is low, a current of 1.0 mA exits from the input.

### 9.11.6 FANOUT LIMITATIONS OF THE TTL PROTOTYPE

For NMOS, CMOS, and ECL logic, fanout restrictions were not investigated in detail because the input current to the various logic gates was zero, as for the case of NMOS and CMOS, or it was a very small base current, as for the case of ECL. However, a substantial current exists in the input terminal of the TTL inverter for both input states, as summarized in Fig. 9.44. This input current limits the number of gates that can be connected to the output of an individual TTL logic gate. Both logic states must be checked to see which set of conditions actually limits the fanout of the gate.

#### Fanout Limit for $v_o = V_L$

$N$  inverters are shown connected to the output of one TTL inverter in Fig. 9.45. The maximum value of  $N$  is termed the **fanout** capability of the TTL gate.  $N$  can be determined from the conditions required to maintain  $Q_2$  in saturation with  $V_{CESAT2} \leq 0.15 \text{ V}$ .

Referring to Fig. 9.45, the collector current of  $Q_2$  is given by

$$i_C = i_R + N(1.01 \text{ mA}) = 2.43 \text{ mA} + N(1.01 \text{ mA}) \quad (9.67)$$

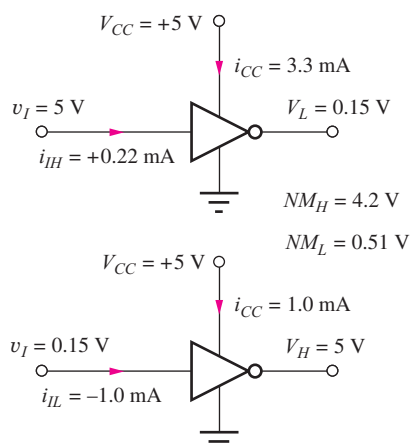


Figure 9.44 Summary of TTL prototype inverter characteristics.

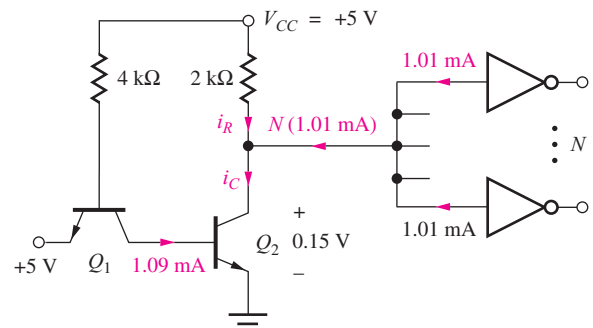


Figure 9.45 Fanout conditions for  $v_o = V_L$ .

In Sec. 9.10 we found that a forced beta  $\beta_{FOR} \leq 28.3$  was required to maintain  $V_{CESAT} \leq 0.15$  V. Also, the base current of  $Q_2$  was previously found to be 1.09 mA for  $v_I = 5$  V, so the collector current must satisfy

$$i_C \leq 28.3i_B = 28.3 \times 1.09 \text{ mA} = 30.8 \text{ mA}$$

or

$$2.43 \text{ mA} + N(1.01 \text{ mA}) \leq 30.8 \text{ mA} \quad \text{and} \quad N \leq 28.1 \quad (9.68)$$

Because the number of gates must be an integer, the fanout capability of this gate is  $N = 28$  for the output in the low state. This result indicates that the prototype TTL gate can drive a valid low output into 28 gates, a relatively large fanout capability.

### Fanout Limit for $v_O = V_H$

The circuit conditions for  $v_I = 0.15$  V and  $v_O = V_H$  are given in Fig. 9.46. At the output node, the collector current of  $Q_2$  is zero, but the input currents of the  $N$  inverters must be supplied through the  $2\text{-k}\Omega$  load resistor. The resulting expression for  $v_O$  becomes:

$$v_O = 5 - 2000i_R = 5 - N(2000 \Omega)(0.22 \text{ mA}) = 5 - N(0.44) \text{ V} \quad (9.69)$$

Each added fanout connection causes the output voltage to drop an additional 0.44 V below 5 V.

To determine  $N$ , we must understand how far  $v_O$  can drop without having a detrimental effect on the inverters connected to the output. The inverter circuit with  $v_I \cong V_{IH}$  is redrawn in Fig. 9.47.  $Q_1$  is operating in the reverse-active region, and its collector current,  $i_C = -(\beta_R + 1)i_{B1}$ , is independent of the base-emitter voltage as long as the base-emitter junction is reverse-biased. Therefore, the base current of  $Q_2$  will be constant as long as  $v_{BE1} = (v_{B1} - v_I) \leq 0$ , which requires  $v_I \geq 1.5$  V. Combining this limit with Eq. (9.69) enables us to determine the fanout  $N$ :

$$5 - N(2000 \Omega)(0.22 \text{ mA}) \geq 1.5 \quad \text{or} \quad N \leq 7.95 \quad (9.70)$$

For the output voltage in the high state, the fanout  $N$  must not exceed 7.95. Because  $N$  must once again be an integer, the maximum fanout is limited to 7. Further, because the overall fanout specification for the TTL gate must be the smallest  $N$  that works properly regardless of logic state, the fanout for the prototype TTL inverter must be specified as  $N = 7$ .

**EXERCISE:** What value is the maximum value of  $\beta_R$  in the TTL prototype gate if we desire  $N = 5$ ?  $N = 10$ ?

**ANSWERS:** 0.4; 0.2

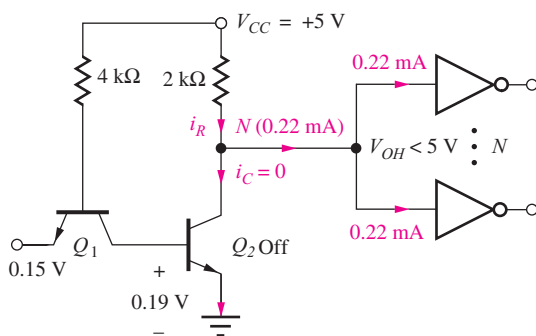


Figure 9.46 Fanout conditions for  $v_O = V_H$ .

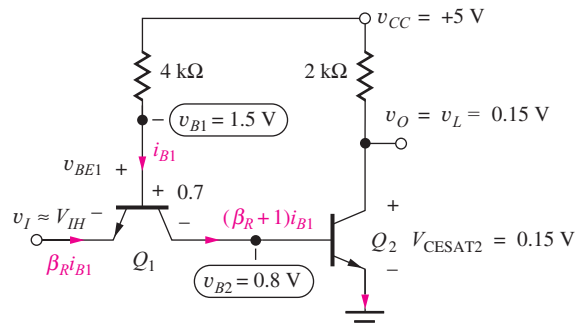


Figure 9.47 Circuit for determining  $V_H$  limitations.

**EXERCISE:** How much base current is available to saturate  $Q_2$  if  $\beta_R = 2$  in Fig. 9.47? What is the fanout capability of the TTL prototype for the  $v_O = V_L$  state for  $V_{CESAT} = 0.15$  V as in Fig. 9.41 if  $\beta_R = 2$ ?

**ANSWERS:** 2.63 mA; 71

## 9.12 THE STANDARD 7400 SERIES TTL INVERTER

The TTL gate described thus far has been a prototype for understanding the more complex gate that forms standard TTL logic. This basic circuit is also useful for low-level on-chip applications. However, with an overdriven transistor  $Q_2$  to pull the output down, but only the 2-k $\Omega$  load resistor to pull the output up, the dynamic response of this gate will be highly asymmetric, as was the case for NMOS logic. In addition, the prototype circuit has a limited fanout capability and is quite sensitive to the value of  $\beta_R$ .

The circuit for the classical TTL inverter shown in Fig. 9.48 solves these problems. This circuit is typically found in TTL unit logic in which several identical gates are packaged together in a single **dual-in-line package**, or **DIP**. Input transistor  $Q_1$  operates in exactly the same manner as  $Q_1$  in the prototype gate, and  $Q_2$  forces the output low to  $V_{CESAT2}$ . The load resistor is replaced with an **active pull-up circuit** formed by transistor  $Q_4$  and diode  $D_1$ . Inverter  $Q_3$  and  $D_1$  are required to ensure that  $Q_4$  is turned off when  $Q_2$  is turned on and vice versa.

### 9.12.1 ANALYSIS FOR $v_I = V_L$

Figure 9.49 is the full TTL circuit with an input voltage of 0.15 V. Base current  $i_{B1}$  causes  $Q_1$  to saturate, with  $i_{C1} \cong 0$  and  $V_{CESAT1} = 0.04$  V. The emitter current is equal to the base current given by

$$i_{E1} \cong i_{B1} = \frac{(5 - 0.8 - 0.15) \text{ V}}{4 \text{ k}\Omega} = 1.0 \text{ mA} \quad (9.71)$$

The voltage  $v_{B3}$  at the base of  $Q_3$  is approximately  $0.15 \text{ V} + 0.04 \text{ V} = 0.19 \text{ V}$ , which keeps both  $Q_2$  and  $Q_3$  off because 0.19 V is less than one base-emitter voltage drop, and two are required to turn on both  $Q_2$  and  $Q_3$  ( $v_{BE2} + v_{BE3} = 1.4 \text{ V}$ ).

Because  $Q_2$  and  $Q_3$  are off with  $i_{C2}$  and  $i_{C3}$  approximately zero, the output portion of the gate may be simplified to the circuit of Fig. 9.50. In this circuit, base current is supplied to  $Q_4$  through

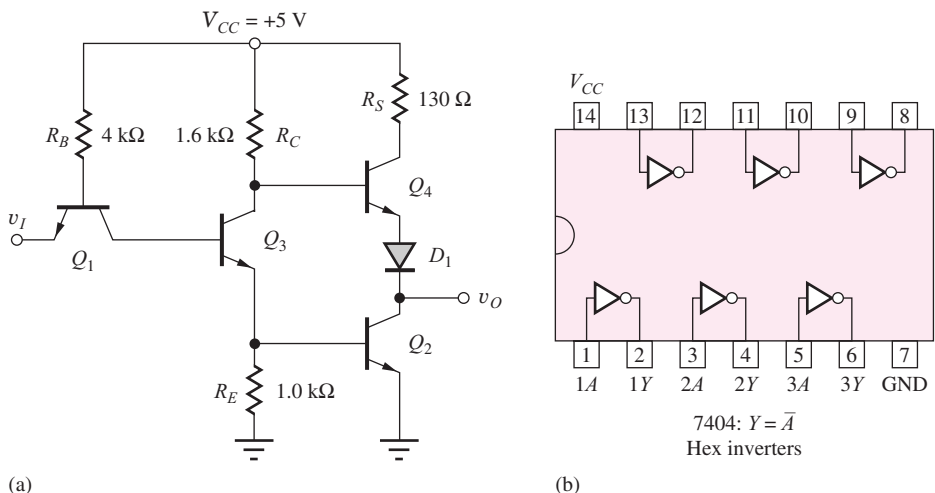
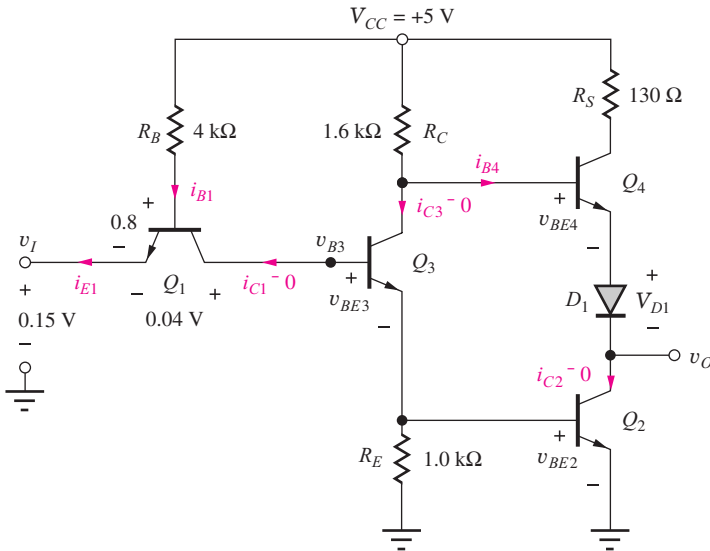
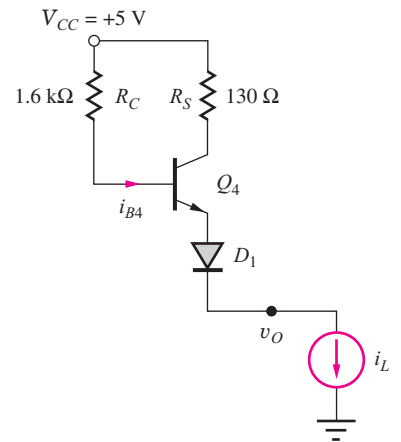


Figure 9.48 (a) Standard TTL inverter. (b) 7404 hex inverter.

Figure 9.49 Standard TTL inverter with  $v_I = 0.15$  V.Figure 9.50 Simplified TTL output stage for  $v_O = V_H$ .

resistor  $R_C$ , and the output reaches

$$v_O = 5 - i_{B4} R_C - v_{BE4} - v_{D1} \quad (9.72)$$

For normal values of load current  $i_L$ , modeled by the current source in Fig. 9.50, the voltage drop in  $R_C$  is usually negligible, and the nominal value of  $V_{OH}$  is

$$V_H \cong 5 - v_{BE4} - v_{D1} = 5 - 0.7 - 0.7 = 3.6 \text{ V} \quad (9.73)$$

The 130- $\Omega$  resistor  $R_S$  is added to the circuit to protect transistor  $Q_4$  from accidental short circuits to ground. Resistor  $R_S$  allows  $Q_4$  to saturate and limits the power dissipation in the transistor. For example, if  $v_O$  is connected directly to ground, then the current through  $Q_4$  and  $D_1$  will be limited to approximately

$$i_{C4} = \frac{V_{CC} - V_{CESAT4} - V_{D1}}{R_S} \quad \text{and} \quad i_{C4} \leq \frac{(5 - 0 - 0.7) \text{ V}}{130 \Omega} = 33.1 \text{ mA} \quad (9.74)$$

**EXERCISES:** What is  $i_L$  if  $Q_4$  remains in the forward-active region when  $v_O$  is shorted to ground? Use  $\beta_F = 40$ . What is the maximum value of  $i_L$  for which  $v_O \geq 3$  V if  $\beta_{F4} = 40$ ? Is  $Q_4$  in the forward-active region at this value of  $i_C$ ?

**ANSWERS:** 92.3 mA; 9.22 mA; no

### 9.12.2 ANALYSIS FOR $v_I = V_H$

$V_H$  is now applied as the input to the TTL circuit in Fig. 9.51. This input level exceeds the voltage required at the base of  $Q_3$  to turn on both  $Q_2$  and  $Q_3$ , ( $v_{B3} \geq v_{BE3} + v_{BE2}$ ), and the base current to  $Q_3$  becomes

$$i_{B3} = (\beta_R + 1)i_{B1} = (\beta_R + 1) \frac{V_{CC} - v_{BC1} - v_{BESAT3} - v_{BESAT2}}{R_B} \quad (9.75)$$

or

$$i_{B3} = (0.25 + 1) \frac{(5 - 0.7 - 0.8 - 0.8) \text{ V}}{4 \text{ k}\Omega} = 0.84 \text{ mA}$$

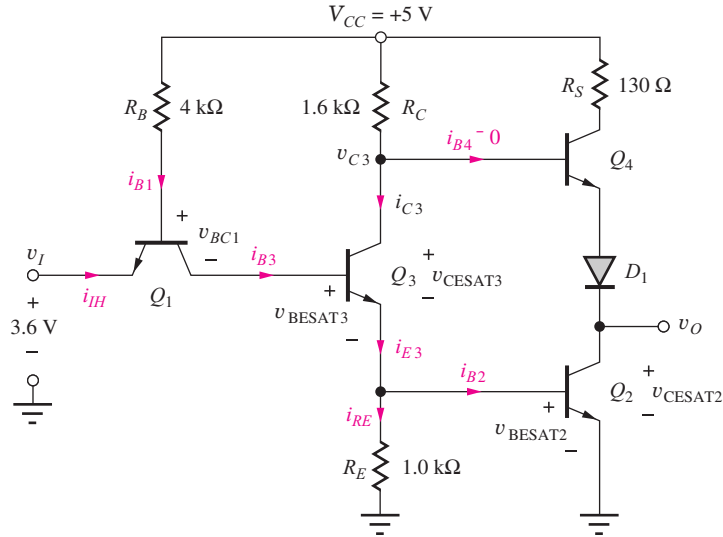


Figure 9.51 Standard TTL inverter with  $v_I = V_H$ .

Both  $Q_2$  and  $Q_3$  are designed to saturate, so both base-emitter voltages are assumed to be 0.8 V in Eq. (9.75). For this case, the input current entering the emitter is

$$i_{IH} = -i_{E1} = \beta_R i_{B1} = 0.25(0.68 \text{ mA}) = 0.17 \text{ mA} \quad (9.76)$$

The base current of  $Q_2$  ultimately determines the fanout limit of this TTL gate; it is given by

$$i_{B2} = i_{E3} - i_{RE} = i_{C3} + i_{B3} - i_{RE} \quad (9.77)$$

Currents  $i_{RE}$  and  $i_{C3}$  are given by

$$\begin{aligned} i_{RE} &= \frac{V_{\text{BESAT}_2}}{R_E} = \frac{0.8 \text{ V}}{1.0 \text{ K}} = 0.80 \text{ mA} \\ i_{C3} &= \frac{5 - V_{\text{CESAT}_3} - V_{\text{BESAT}_2}}{1.6 \text{ K}} = \frac{5 - 0.15 - 0.8}{1.6 \text{ K}} = 2.53 \text{ mA} \end{aligned} \quad (9.78)$$

and

$$i_{B2} = (2.53 + 0.84 - 0.80) \text{ mA} = 2.57 \text{ mA} \quad (9.79)$$

in which it has been assumed that  $Q_4$  is off with  $i_{B4} = 0$ .

The assumption that  $Q_4$  is off can be checked by calculating the voltage  $v_{C3} - v_O$ :

$$\begin{aligned} v_{C3} - v_O &= (V_{\text{CESAT}_3} + V_{\text{BESAT}_2}) - (V_{\text{CESAT}_2}) \\ &= 0.80 + 0.15 - 0.15 = 0.80 \text{ V} \end{aligned} \quad (9.80)$$

This voltage, 0.8 V, must be shared by the base-emitter junction of  $Q_4$  and diode  $D_1$ , but it is not sufficient to turn on the series combination of the two. However, if  $D_1$  were not present, the full 0.8 V would appear across the base-emitter junction of  $Q_4$ , and it would saturate. Thus,  $D_1$  must be added to the circuit to ensure that  $Q_4$  is off when  $Q_2$  and  $Q_3$  are saturated.

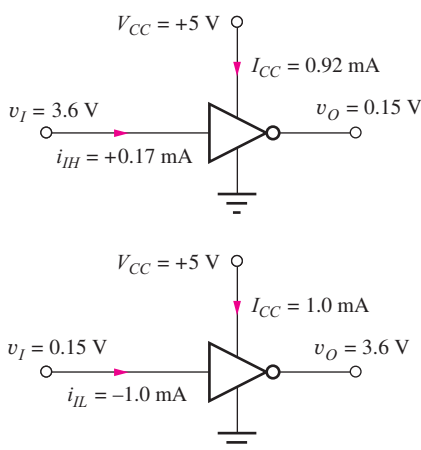


**Figure 9.52** Voltage and current summary for standard TTL.

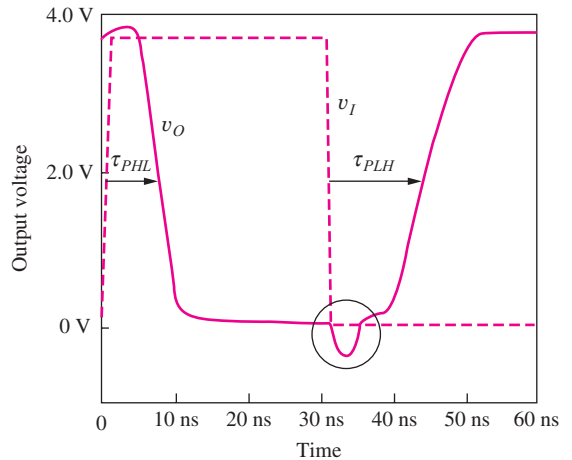


**Figure 9.53** SPICE simulation of the full TTL inverter propagation delay.  $\tau_{PHL} = 6 \text{ ns}$ ;  $\tau_{PLH} = 10 \text{ ns}$ .

### 9.12.3 POWER CONSUMPTION

Figure 9.52 summarizes the voltages and currents in the TTL gate. Assuming a 50 percent duty cycle, the average power consumed by the TTL gate is

$$\langle P \rangle = \frac{P_{OL} + P_{OH}}{2} \quad (9.81)$$

$$\langle P \rangle = \frac{[5 \text{ V}(0.92 \text{ mA}) + 3.6 \text{ V}(0.17 \text{ mA})] + [5 \text{ V}(1.0 \text{ mA}) + 0.15 \text{ V}(-1.0 \text{ mA})]}{2}$$

$$\langle P \rangle = 5.03 \text{ mW}$$

### 9.12.4 TTL PROPAGATION DELAY AND POWER-DELAY PRODUCT

Analysis of the propagation delay of the TTL inverter is fairly complex because several saturating transistors are involved. Therefore, we investigate the behavior by looking at the results of simulation. From Fig. 9.53, the average propagation delay is approximately

$$\tau_P = \frac{\tau_{PHL} + \tau_{PLH}}{2} = \frac{6 + 14}{2} \text{ ns} = 10 \text{ ns} \quad (9.82)$$

This value represents the nominal delay of standard TTL.

On the high-to-low transition, transistor  $Q_1$  must come out of saturation and enter the reverse-active mode, while  $Q_2$  and  $Q_3$  must go from near cutoff to saturation. For the low-to-high transition,  $Q_2$  and  $Q_3$  must both come out of saturation. Thus, we may expect one storage time delay for the first case and two storage time delays for the second. Thus,  $\tau_{PLH}$  should be greater than  $\tau_{PHL}$ , as in the simulation results.

Using these simulation results and the power calculated from Eq. (9.81), we estimate the rather large power-delay product for the standard TTL gate to be

$$PDP = (5.0 \text{ mW})(10 \text{ ns}) = 50 \text{ pJ} \quad (9.83)$$

### 9.12.5 TTL VOLTAGE TRANSFER CHARACTERISTIC AND NOISE MARGINS

Figure 9.54 gives the results of simulation of the VTC for the TTL inverter. The various break points in the characteristic can be easily identified in a manner similar to that used for the TTL prototype gate. As the input voltage increases to become equal to 0.7 V, base current begins to enter  $Q_3$ . The emitter voltage of  $Q_3$  starts to rise, and its collector voltage begins to fall.  $Q_4$  functions as an emitter

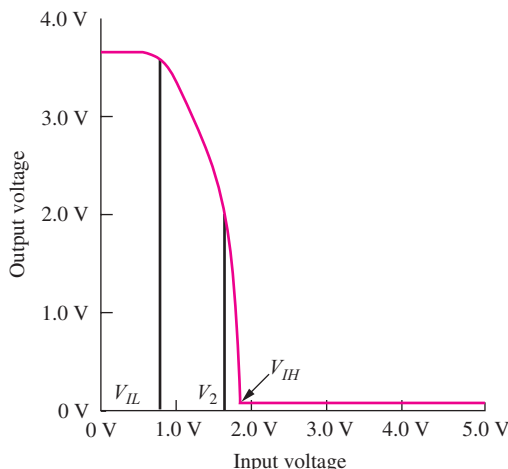


Figure 9.54 SPICE simulation of the VTC for the TTL gate in Fig. 9.48.

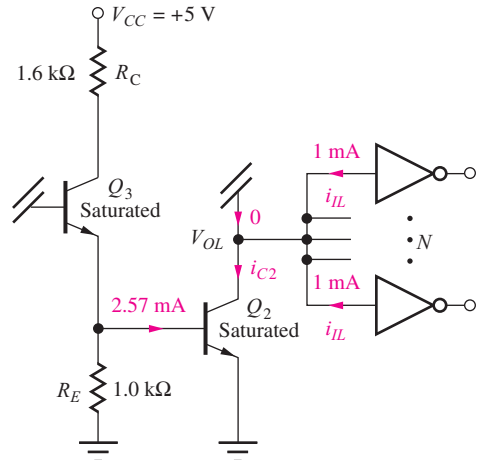


Figure 9.55 Fanout conditions for  $v_o = V_{OL}$ .

follower, and the output drops as the collector voltage of  $Q_3$  falls. As  $Q_3$  turns on, the slope changes abruptly, giving  $V_{IL} \cong 0.7$  V.

As the input voltage (and the voltage at  $v_{B3}$ ) approaches 1.5 V, there is enough voltage to both saturate  $Q_3$  and turn on  $Q_2$ . As  $Q_2$  turns on and  $Q_3$  saturates, turning off  $Q_4$ , the output voltage drops more abruptly, causing break point  $V_2$  in the curve. In Fig. 9.54 it can be seen that  $V_{IH} \cong 1.8$  V, which is slightly larger than  $V_{BESAT3} + V_{BESAT2}$ , the voltage at  $v_{B3}$  for which both  $Q_2$  and  $Q_3$  are heavily saturated. For this voltage,  $Q_1$  is coming out of heavy saturation and starting to operate in the reverse-active mode.

Using  $V_{IL} = 0.7$  V,  $V_{OL} = 0.15$  V,  $V_{IH} = 1.8$  V, and  $V_{OH} = 3.5$  V yields

$$NM_L = 0.7\text{ V} - 0.15\text{ V} = 0.55\text{ V} \quad \text{and} \quad NM_H = 3.5\text{ V} - 1.8\text{ V} = 1.7\text{ V} \quad (9.84)$$

### 9.12.6 FANOUT LIMITATIONS OF STANDARD TTL

The active pull-up circuit can supply relatively large amounts of current with the output changing very little (see Probs. 9.95 to 9.99), so the fanout becomes limited by the current sinking capability of  $Q_2$ . For  $v_o = V_L$ ,  $Q_4$  and  $D_1$  are off, and the collector current of  $Q_2$  is equal to the input currents of the  $N$  gates connected to the output, as shown in Fig. 9.55:

$$Ni_{IL} \leq \beta_{FOR}i_{B2} \quad \text{or} \quad N(1\text{ mA}) \leq 28.3(2.57\text{ mA}) \quad \text{and} \quad N \leq 72.7 \quad (9.85)$$

Using the transistor parameters in Table 9.3 with this circuit yields a fanout limit of 72. However, from Eq. (9.77), we see that the fanout is sensitive to the actual values of  $\beta_R$ ,  $R_B$ , and  $R_E$ . The parameters of the transistors in the standard TTL IC process are somewhat different from those in Table 9.3, and the specifications must be guaranteed over a wide range of temperature, supply voltages, and IC process variations. Thus, the fanout of standard TTL is actually specified to be  $N \leq 10$ .

## 9.13 LOGIC FUNCTIONS IN TTL

Now, we will explore multi-input gates but will begin our discussion with the prototype TTL gate in order to simplify the discussion. The TTL inverter becomes a two-input gate with the addition of a second transistor in parallel with transistor  $Q_1$ , as drawn in the schematic in Fig. 9.56. If either the emitter of  $Q_{1A}$  or the emitter of  $Q_{1B}$  is in a low state, then base current  $i_B$  will be diverted out of the corresponding emitter terminal, the base current of  $Q_2$  will be negligibly small, and the output will be high. Base current will be supplied to  $Q_2$ , and the output will be low, only if both inputs  $A$  and  $B$  are high. Table 9.4 is the truth table for this gate and corresponds to a two-input NAND gate.

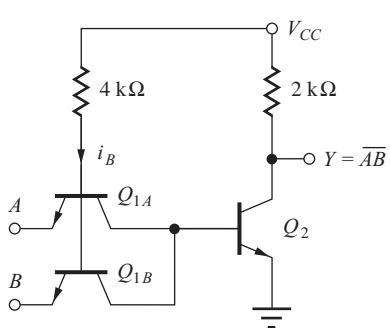
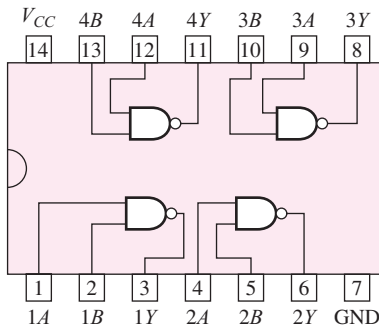


**Figure 9.56** Two-input prototype TTL NAND gate:  $Y = \overline{AB}$ .



7400:  $Y = \overline{AB}$   
Quadruple two-input NAND gates

**TABLE 9.4**  
Two-Input NAND Gate Truth Table

A	B	$Y = \overline{AB}$
0	0	1
0	1	1
1	0	1
1	1	0

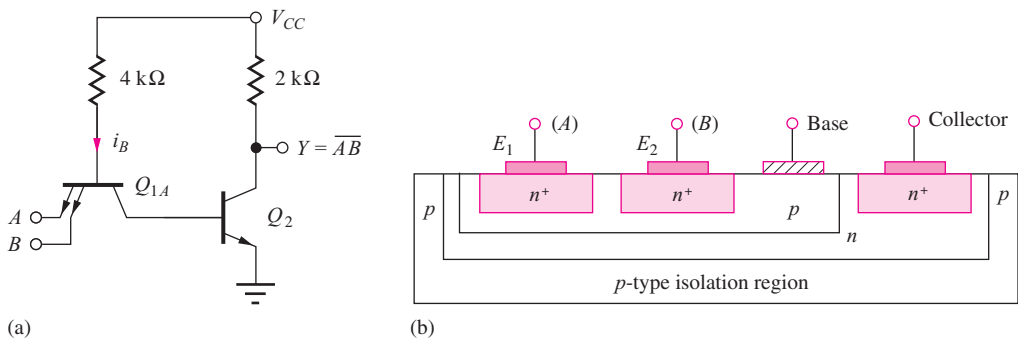


**Figure 9.57** (a) Multi-emitter realization of the two-input NAND gate. (b) Merged structure for two-emitter bipolar transistor.

### 9.13.1 MULTI-EMITTER INPUT TRANSISTORS

Standard TTL logic families provide gates with eight or more inputs. An eight-input gate conceptually has eight transistors in parallel. However, because the input transistors all have common base and collector connections, these devices are actually implemented as a single multi-emitter transistor, which is usually drawn as shown in the two-input NAND gate diagram in Fig. 9.57(a).

The concept of the **merged transistor structure** for a multi-emitter transistor appears in Fig. 9.57(b), in which the two-emitter transistor with merged base and collector regions takes up far less area than two individual transistors would require.

### 9.13.2 TTL NAND GATES

A complete standard three-input TTL NAND gate is shown in the schematic in Fig. 9.58. If any one of the three input emitters is low, then the base current to transistor  $Q_3$  will be zero, and the output will be high, yielding  $Y = \overline{ABC}$ . The behavior of the rest of the gate is identical to that described in the discussion of Figs. 9.48 to 9.55.

Although the basic TTL gate provides the NAND function, other logic operations can be implemented with the addition of more transistors. One example is shown in Fig. 9.59, in which the input circuitry of  $Q_1$  and  $Q_3$  is replicated to provide the **AND-OR-Invert**, or **AOI**, logic function (a complemented **sum-of-products** function). This five-input gate provides the logic function  $Y = \overline{ABC} + \overline{DE}$ .

TTL also has several power options, including standard, high-power, and low-power versions, in which the resistor values are modified to change the power level and hence the gate delay. **Low-power TTL** has a delay of approximately 30 ns, and the **high-power TTL** series (54H/74H) has a delay of approximately 7 ns.

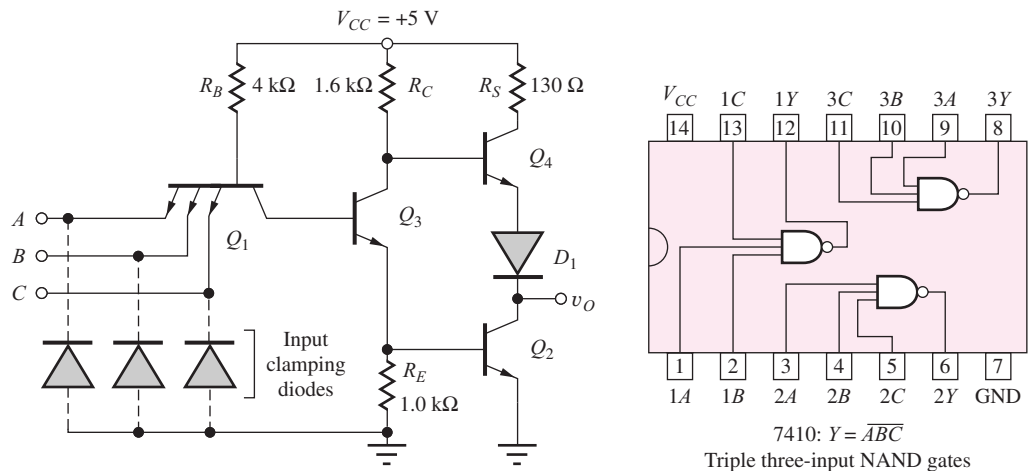


**Figure 9.58** Standard TTL three-input NAND gate.

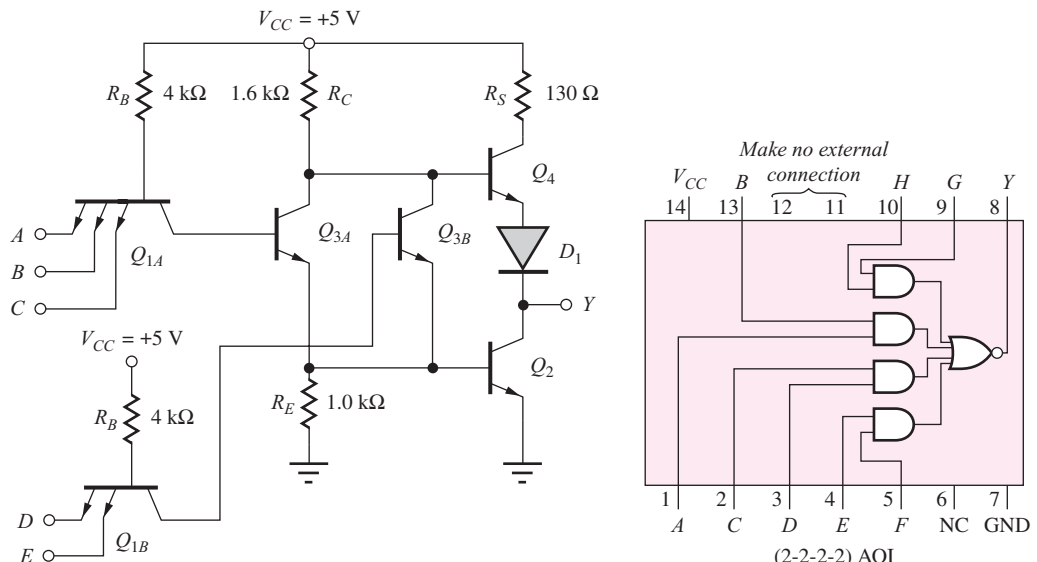


**Figure 9.59** TTL AND-OR-Invert (AOI) gate:  $Y \equiv \overline{ABC + DE}$ .

### 9.13.3 INPUT CLAMPING DIODES

In Fig. 9.53, we observe a negative-going transient on the output signal near  $t = 15$  ns, which resulted from the rapid input signal transition. Another source of such transients is “ringing,” which results from high-speed signals exciting the distributed  $L-C$  interconnection network between logic gates, as diagrammed in Fig. 6.4. To prevent large excursions of the inputs below ground level, which can damage the TTL input transistors, a diode is usually added to each input to clamp the input signal to no more than one diode-drop below ground potential. These input **clamping diodes** are added to the TTL NAND gate schematic in Fig. 9.58.

## 9.14 SCHOTTKY-CLAMPED TTL

As discussed in Sec. 9.11, saturation of the transistors in TTL logic substantially slows down the dynamic response of the logic gates. The **Schottky-clamped transistor** drawn in Fig. 9.60(a) was

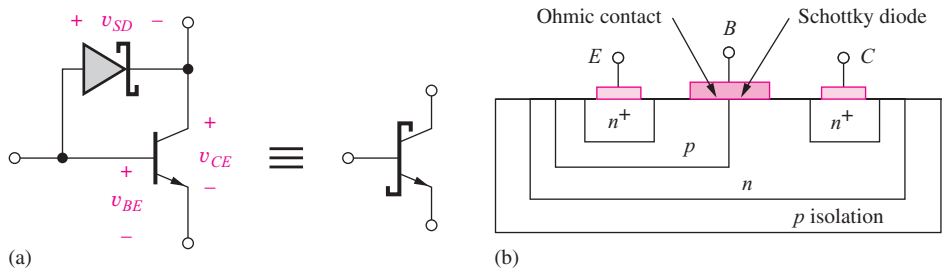


**Figure 9.60** (a) Schottky-clamped transistor. (b) Cross section of the merged Schottky diode and bipolar transistor structure.

developed to solve this problem. The Schottky-clamped transistor consists of a metal semiconductor **Schottky barrier diode** in parallel with the collector-base junction of the bipolar transistor.

When conducting, the forward voltage drop of the Schottky diode is designed to be approximately 0.45 V, so it will turn on before the collector-base diode of the bipolar transistor becomes strongly forward-biased. Referring to Fig. 9.60(a), we see that

$$v_{CE} = v_{BE} - v_{SD} = 0.70 - 0.45 = 0.25 \text{ V} \quad (9.86)$$

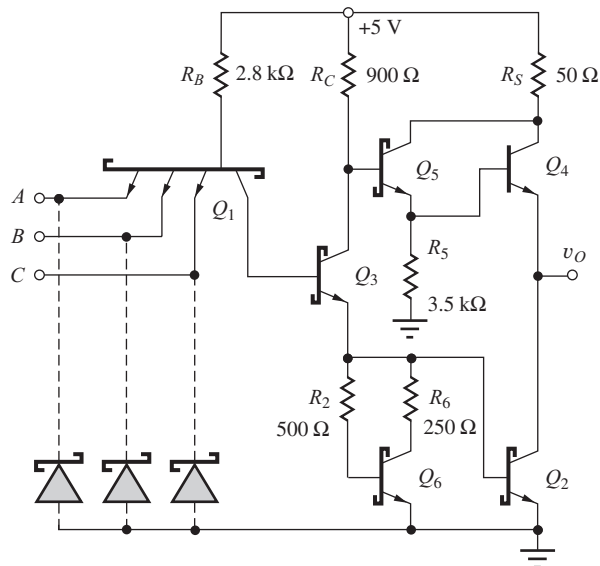
The Schottky diode prevents the BJT from going into deep saturation by diverting excess base current through the Schottky diode and around the BJT. Because the BJT is prevented from entering heavy saturation, 0.7 V has been used for the value of  $v_{BE}$  in Eq. (9.86).

A cross section of the structure used to fabricate the Schottky transistor is given in Fig. 9.60(b). Conceptually, an aluminum base contact overlaps the collector-base junction, forming an ohmic contact to the *p*-type base region and a Schottky diode to the more lightly doped *n*-type collector region. (Remember that aluminum is a *p*-type dopant in silicon.) This is another example of the novel merged structures that can be fabricated using IC technology.

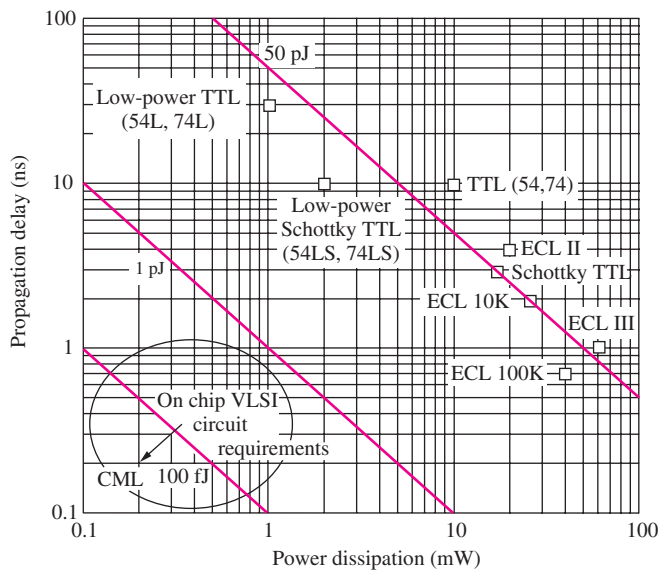
Invention of this circuit required a good understanding of the exponential dependence of the BJT collector current on base-emitter voltage as well as knowledge of the differences between Schottky and *pn* junction diodes. Successful manufacture of the circuit relies on tight process control to maintain the desired difference between the forward drops of the base-collector and Schottky diodes.

Figure 9.61 is the schematic for a full three-input Schottky TTL NAND gate. Each saturating transistor in the original gate— $Q_1$ ,  $Q_2$ , and  $Q_3$ —is replaced with a Schottky transistor.  $Q_6$ ,  $R_2$ , and  $R_6$  replace the resistor  $R_E$  in the original TTL gate and eliminate the first “knee” voltage corresponding to  $V_{IL}$  in the VTC in Fig. 9.54. Thus, the transition region for the Schottky TTL is considerably narrower than for the original TTL circuit (see Prob. 9.118).  $Q_5$  provides added drive to emitter follower  $Q_4$  and eliminates the need for the series output diode  $D_1$  in the original TTL gate.  $Q_4$  cannot saturate in this circuit because the smallest value for  $v_{CB4}$  is the positive voltage  $V_{CESAT5}$ , so it is not a Schottky transistor. The input clamp diodes are replaced with Schottky diodes to eliminate charge storage delays in these diodes.

The use of Schottky transistors substantially improves the speed of the gate, reducing the nominal delay for the standard Schottky TTL series gate (54S/74S) to 3 ns at a power dissipation of approximately 15 mW. An extremely popular TTL family is **low-power Schottky TTL** (54LS/74LS), which provides the delay of standard TTL (10 ns) but at only one-fifth the power. The resistor values are increased to decrease the power, but speed is maintained at lower power by eliminating the storage times associated with saturating transistors. This family is widely used to replace standard TTL because it offers the same delay at substantially less power. As IC technology has continued to improve, the complexity and performance of TTL has also continued to increase. Advanced Schottky logic (ALS) and advanced low-power Schottky logic families were introduced with improved power-delay characteristics.



**Figure 9.61** Schottky TTL NAND gate.



**Figure 9.62** Power-delay products for various commercial unit-logic families.

## 9.15 COMPARISON OF THE POWER-DELAY PRODUCTS OF ECL AND TTL

Figure 9.62 is a comparison of the power versus delay characteristics of a number of the ECL and TTL unit-logic families that have been produced. ECL, with its nonsaturating transistors and low logic swing, is generally faster than TTL, although one can see the performance overlap between generations that occurred for ECL II versus Schottky TTL, for example. A new generation of IC technology and better circuit techniques achieve higher speed circuits for a given power level. However, for high-density integrated circuits, significant improvements in power and power-delay products are required, as indicated by the circle in the lower left-hand corner of Fig. 9.62. For example, CML based upon SiGe HBT technology with 200 GHz  $f_T$  transistors can achieve a PDP of 100 fJ or less.

## 9.16 BiCMOS LOGIC

There have been numerous attempts to combine various bipolar and FET technologies in order to realize the advantages of both types of transistors in a single process. For example, the BiFET process combines BJTs and JFETs and has often been used in analog circuits. BiCMOS processes combine the *n*- and *p*-channel transistors from CMOS with bipolar transistors, and the most sophisticated forms of BiCMOS include both *npn* and *pnp* transistors. BiCMOS is a complex technology, but it permits one to use the bipolar and MOS transistors wherever they provide the most advantage. In BiCMOS logic gates, MOS transistors are typically used to provide high-impedance inputs with the power of MOS NAND, NOR, and complex gate implementations. Bipolar transistors are then used to provide high-output-current capacity for driving high-capacitance loads. BiCMOS is also highly useful in “mixed signal” designs that combine both analog and digital signal processing.

For many years, BiCMOS was considered a niche technology. There was strong debate whether the performance advantages were real and worth the additional process complexity and cost. However, the demand for ever higher microprocessor performance as well as the requirements for mixed-signal system-on-a-chip components has led to the development of BiCMOS processes by many companies, including IBM, Intel, and Texas Instruments, to name a few. Today, BiCMOS is used

in high-performance processors, in mixed-signal ICs, and in advanced silicon-germanium (SiGe) processes. Silicon-germanium BiCMOS is the highest performance silicon-based technology available today. CML is often implemented in SiGe BiCMOS in which NMOS transistors are used to implement low voltage current sources, and the BJT are used for the current switches. Delays of 5–10 ps per logic level can be achieved.

With fully complementary MOS and bipolar devices available, the circuit design possibilities become almost endless. One need only search through the topic of BiCMOS in the *IEEE Journal of Solid-State Circuits*, for example, to discover the wide variety of novel circuits proposed for use with BiCMOS technology. Here we will attempt to get a flavor for how BJT and MOS devices can be combined to achieve improved logic performance. In Part III of this book we explore some of the possibilities that BiCMOS offers the analog circuit designer.

### 9.16.1 BiCMOS BUFFERS

Let us start by seeing how we can add bipolar transistors to improve performance of the CMOS inverter. The bipolar transistor offers high current gain and higher transconductance than the FET for a given operating current and can therefore rapidly charge and discharge large capacitances. On the other hand, the very high input impedance of the MOS device requires very little driving power, and CMOS gates provide ease of implementation of complex logic functions. Thus BJTs are used in the output stage of the on- and off-chip buffers used to drive high-capacitance busses. These buffers replace the large-area cascade buffer designs that are required to drive large capacitances in standard CMOS technology.

A basic BiCMOS buffer is shown in Fig. 9.63 in which a complementary *npn/pnp* pair of emitter followers,  $Q_4$  and  $Q_3$ , is driven by a standard CMOS inverter. Operation of the circuit for the two logic states is outlined in Fig. 9.64. Figure 9.64(a) shows the circuit following a low-to-high transition of input  $v_I$ . PMOS transistor  $M_2$  is off, and NMOS transistor  $M_1$  turns on, providing a path for the base current  $i_{BP}$  of *pnp*  $Q_3$ . The base current is amplified by the *pnp* current gain ( $\beta_F + 1$ ), and the resulting emitter current rapidly discharges the load capacitance to a voltage approximately equal to  $V_{EB3}$ . At the beginning of the transition, the NMOS transistor also provides a reverse base current path to quickly turn off *npn* transistor  $Q_4$  and discharge the equivalent capacitance at the bases of the BJTs.

Circuit operation for the opposite input transition is shown in Fig. 9.64(b). When  $v_I$  returns to zero, NMOS transistor  $M_1$  is cut off. PMOS transistor  $M_2$  turns on and supplies forward base current to *npn* transistor  $Q_4$  as well as reverse base current to the *pnp* transistor.  $Q_3$  turns off, and the *npn* device rapidly charges load capacitor  $C$  to a high logic level approximately equal to  $V_{DD} - V_{BE4}$ .

In order to charge or discharge the load capacitance, the CMOS inverter must supply only base current to the bipolar transistors and current to the equivalent capacitance of the bases of  $Q_3$  and

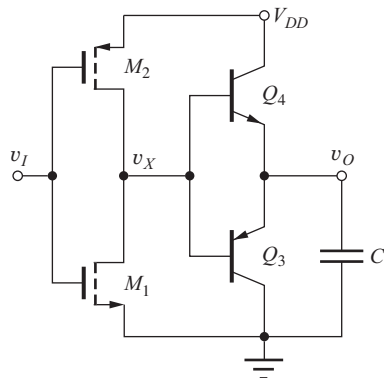


**Figure 9.63** BiCMOS buffer employing complementary emitter followers.

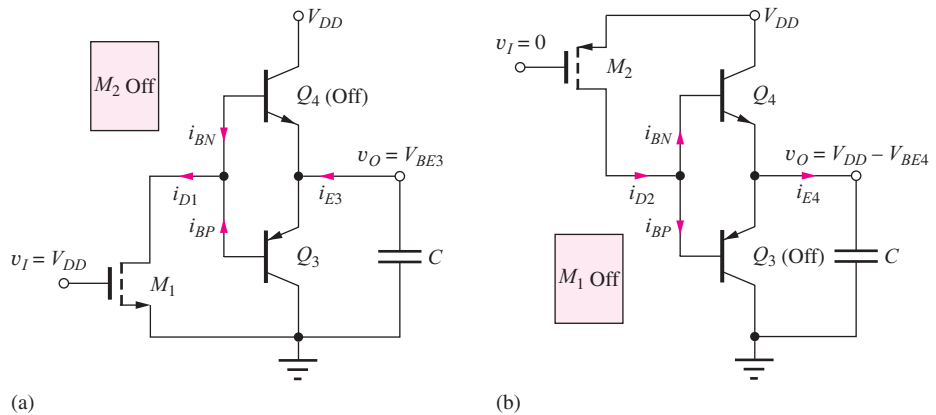


**Figure 9.64** BiCMOS buffer (a) following low-to-high input transition and (b) after high-to-low input transition.

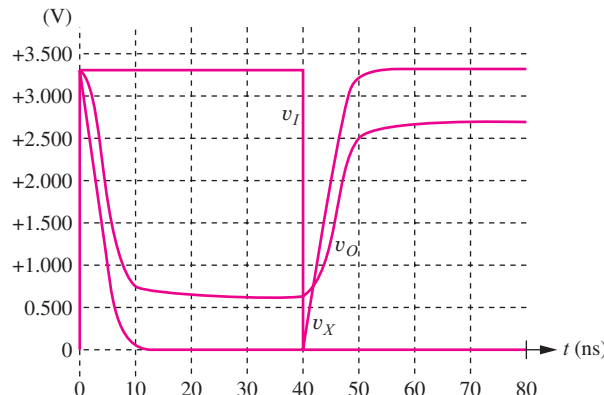


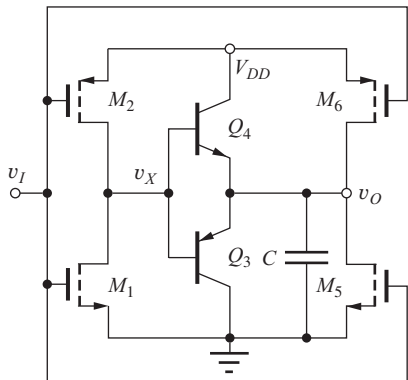
**Figure 9.65** Simulation results for the BiCMOS gate in Fig. 9.63 with  $C = 2 \text{ pF}$  and  $W/L = 6/1$  and  $15/1$  for the NMOS and PMOS transistors, respectively.  $V_{DD} = 3.3 \text{ V}$ .

$Q_4$ . Note in this circuit that the base-emitter junctions of  $Q_3$  and  $Q_4$  are connected in parallel. When the  $npn$  base-emitter junction is forward biased, the  $pnp$  base-emitter junction is reverse-biased and vice versa. So, the  $pnp$  must be off when the  $npn$  is on, and the  $npn$  must be off when the  $pnp$  is on. Furthermore, neither collector-base junction can become forward biased, so the bipolar transistors can never saturate, and storage time delays are eliminated, enabling high-speed operation.

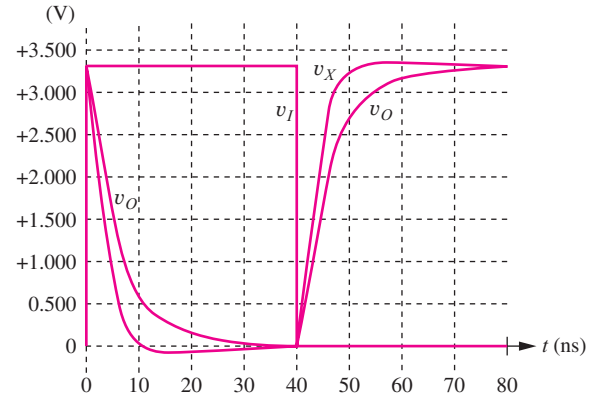
We see that the overall circuit behaves as an inverter. The input is a standard CMOS inverter, and the bipolar output configuration is a noninverting follower. Thus the two-stage combination forms an inverter. Note, however, that the logic levels have deteriorated. The high logic level is now one base emitter voltage drop below the power supply,  $V_H \cong V_{DD} - V_{BE4}$ , and the low logic level is  $V_L \cong V_{EB3}$ . This loss of logic swing ( $\Delta V \cong V_{DD} - 1.4 \text{ V}$ ) is undesirable, particularly as power-supply voltages are reduced.

Figure 9.65 presents the results of SPICE simulations for the BiCMOS circuit in Fig. 9.63 with  $V_{DD} = 3.3 \text{ V}$  and  $C = 2 \text{ pF}$ . After the initial transient,  $V_L$  and  $V_H$  are  $0.62 \text{ V}$  and  $2.68 \text{ V}$ , respectively. The propagation delay is approximately  $6 \text{ ns}$ .

The full logic swing can be restored using various techniques. One approach is shown in Fig. 9.66 in which the output of an auxiliary inverter, composed of transistors  $M_5$  and  $M_6$ , is connected in parallel with the output of the emitter followers. The bipolar transistors charge and discharge the load capacitance rapidly through most of the transition, and then the CMOS devices take over near



**Figure 9.66** BiCMOS buffer with an auxiliary inverter to restore full logic swing.



**Figure 9.67** Simulation results for buffer in Fig. 9.66 with  $W/L = 12/1$  and  $30/1$  for  $M_5$  and  $M_6$ , respectively.  $V_{DD} = 3.3$  V.

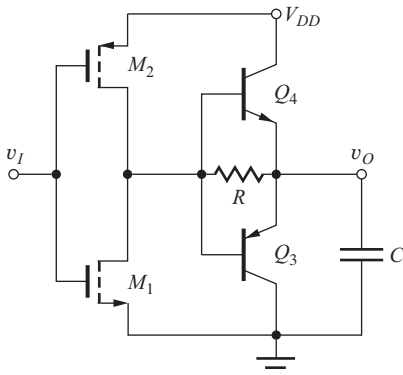


**Figure 9.68** BiCMOS buffer using a resistor to increase logic swing.

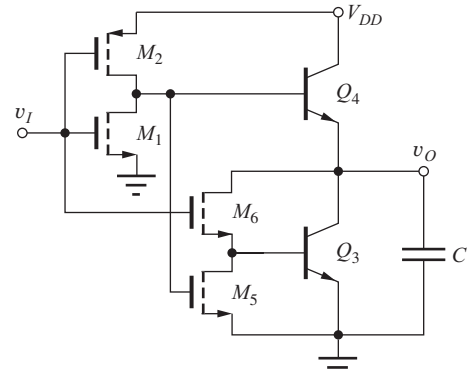


**Figure 9.69** BiNMOS buffer.

the end of the transition and force the capacitor to charge fully to  $V_{DD}$  or discharge completely to ground potential. The results of simulation of the circuit in Fig. 9.66 appear in Fig. 9.67. The auxiliary CMOS inverter restores the full logic swing.

A second method is to simply place a resistor in parallel with the base-emitter junctions of the emitter followers as shown in Fig. 9.68. The resistor path permits the final voltage on the capacitor to reach 0 or  $V_{DD}$ .

### 9.16.2 BiNMOS INVERTERS

Simplified BiCMOS process implementations include high-performance *n*p*n* devices but not *p*n*p* transistors. This places restrictions on the circuitry that can be designed, and the resulting BiCMOS circuits are sometimes referred to as BiNMOS rather than BiCMOS. BiNMOS gates use *n*p*n* transistors to drive the load capacitance in a manner that is similar to the “totem-pole” output stage of the TTL gate, as shown in the schematic in Fig. 9.69. Here *n*p*n* transistor  $Q_4$  functions as an emitter follower to assist in charging load capacitor  $C$  toward  $V_{DD}$ , and transistor  $Q_3$  is used to discharge  $C$ .

The CMOS drive circuits must provide forward base-current drive to only one of the *n*p*n* transistors at a time. With the input high as in Fig. 9.70(a), the CMOS inverter output will be low, and transistors  $M_2$  and  $M_5$  will both be off. NMOS transistor  $M_6$  provides a base-current path

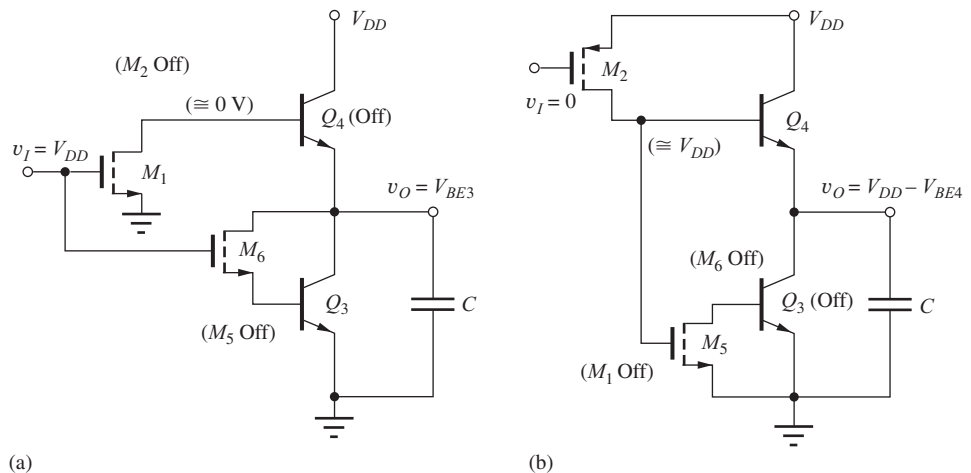


**Figure 9.70** BiNMOS buffer (a) following low-to-high input transition ( $M_2$  and  $M_5$  are cut off) and (b) after high-to-low input transition ( $M_1$  and  $M_6$  are cut off).

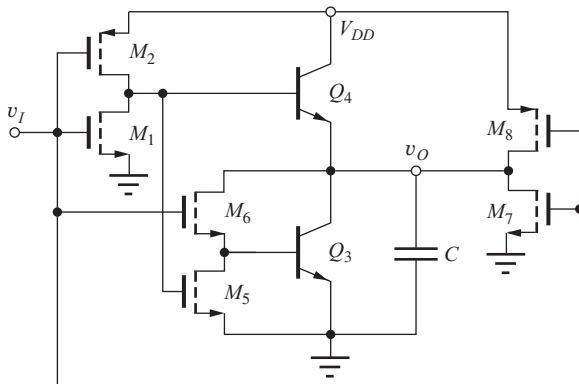


**Figure 9.71** Full swing BiNMOS inverting buffer.

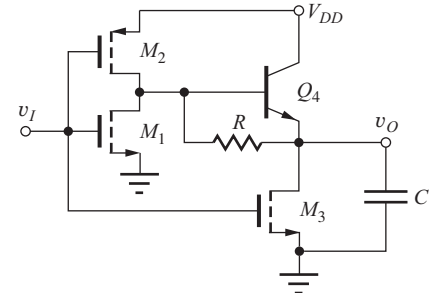


**Figure 9.72** BiNMOS buffer employing a single *npn* transistor.

from the output node to the base of  $Q_3$ , and  $Q_3$  discharges the load capacitance. At the same time,  $M_1$  provides a path for reverse base current to speed up the turn off of transistor  $Q_4$ . With  $M_6$  connected between the collector and base of  $Q_3$ , the BJT cannot saturate, and the output low level is approximately  $V_{BE3}$ .

For the low-input state in Fig. 9.70(b), the CMOS inverter output will be high, and transistors  $M_1$  and  $M_6$  will be cut off. PMOS transistor  $M_2$  provides base current to  $Q_4$ . This current is amplified, and the emitter follower action of  $Q_4$  charges up capacitor  $C$  to the high logic level:  $V_H \cong V_{DD} - V_{BE4}$ . Transistor  $M_6$  turns off, removing the path for forward base current to  $Q_3$ . Although the circuit would function logically without transistor  $M_5$ , it is added to provide a reverse base-current path to ensure rapid turn off of  $Q_3$ .

This BiNMOS gate suffers from the reduced logic swing problems just as the circuit in Fig. 9.63. However, the solution to this problem is similar. Figure 9.71 shows the addition of an auxiliary inverter ( $M_6$  and  $M_7$ ) that forces  $V_H$  and  $V_L$  to equal the full power supply levels.

A simplified BiNMOS gate appears in Fig. 9.72. Here NMOS device  $M_3$  is used to discharge the load capacitance, and the *npn* transistor is only used to assist in the low-to-high transition. Resistor

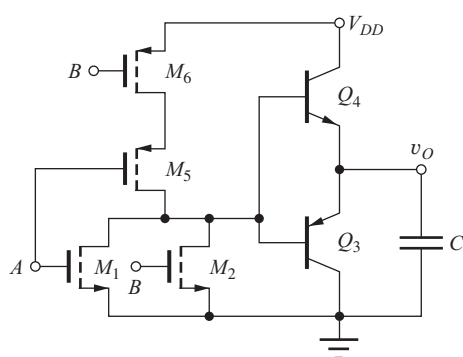


**Figure 9.73** Two-input BiCMOS NOR gate.

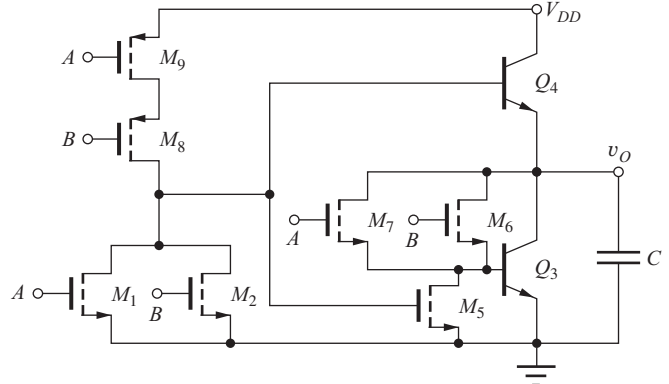


**Figure 9.74** Two-Input BiNMOS NOR gate.

$R$  is added to increase the value of  $V_H$ . The resistor can be implemented by a MOS transistor biased in the linear region.

### 9.16.3 BiCMOS LOGIC GATES

Although this section has focused on BiCMOS inverter circuitry, additional logic function may easily be added by converting the CMOS inverters to more complex gates. Examples of two-input NOR gates appear in Figs. 9.73 and 9.74. The BiCMOS NOR gate simply adds the complementary bipolar follower stage to the standard CMOS NOR gate as in Fig. 9.73. A NAND gate is constructed in a similar manner.

The BiNMOS NOR gate in Fig. 9.74 requires a little more effort since base current must be provided to  $Q_3$  when either input  $A$  or input  $B$  is high. Thus the two transistors designated as  $M_6$  and  $M_7$  are required.

**EXERCISE:** (a) Draw the circuit for a two-input BiCMOS NAND gate. (b) Draw the schematic for a two-input BiNMOS NAND gate.

## SUMMARY

The two commercially most important forms of bipolar logic are emitter-coupled logic (ECL) and transistor-transistor logic (TTL or T<sup>2</sup>L). In this chapter, we examined simple prototype circuits for the ECL and TTL gates, and then we explored the full gate structures.

- **ECL:** ECL logic has traditionally operated from a negative supply voltage, typically  $-5.2$  V, and  $V_H$  and  $V_L$  are therefore negative. The voltage transfer characteristic for the ECL gate was investigated, and the ECL logic swing  $\Delta V$  is relatively small, ranging between  $0.2$  V and  $0.8$  V with noise margins approaching  $\Delta V/2$ . The ECL gate introduced two new circuit techniques, the current switch and the emitter-follower circuit, and also requires a reference voltage circuit. ECL logic gates generate both true and complement outputs, and the basic ECL gate provides the OR-NOR logic functions. Standard ECL unit-logic families provide delays in the  $0.25$ - to  $5$ -ns range with a power-delay product of approximately  $50$  pJ.
- **Current switches:** The current switch consists of two matched BJTs and a current source. This circuit rapidly switches the bias current back and forth between the two transistors, based on a comparison of the logic input signal with a reference voltage. In the ECL gate, the transistors actually switch between two points in the forward-active region, which is one reason why ECL

is the highest speed form of bipolar logic. A second factor is the relatively small logic swing, typically in the 0.4- to 0.8-V range. The low ECL logic swing results in noise margins of a few tenths of a volt. ECL is somewhat unusual compared to the other logic families that have been studied in that it is typically designed to operate from a single negative power supply, historically  $-5.2$  V, and  $V_H$  and  $V_L$  are both negative voltages.

- *Emitter followers:* In the emitter-follower circuit, the output signal replicates the input signal except for a fixed offset equal to one base-emitter diode voltage, approximately 0.7 V. In ECL, this fixed-voltage offset is used to provide the level-shifting function needed to ensure that the logic levels at the input and output of the gates are the same. The emitter followers permit additional logic power through the use of the “wired-OR” circuit technique.
- *Current Mode Logic:* CML utilizes two or more levels of stacked BJT current switches to produce extremely high-speed logic circuits with power-delay products suitable for integration in high density ICs. The gates produce true and complement outputs and can directly implement NOR/OR and AND/NAND gates as well as complex logic functions. Stacking effectively reuses the current and reduces power. The power supply voltage depends upon the number of logic levels used in the design and ranges from 2.0–3.3 V. CML can also be implemented with MOS transistors.
- *TTL circuits:* Classical TTL circuits operate from a single 5-V supply and provide a logic swing of approximately 3.5 V, with noise margins exceeding 1 V. During operation, the transistors in standard TTL circuits switch between the cutoff and saturation regions of operation. Basic TTL gates realize multi-input NAND functions; however, more complex gates can be used to realize almost any desired logic function. Standard TTL unit-logic families provide delays in the 3- to 30-ns range, with a power-delay product of approximately 50 pJ. Schottky diodes are used to prevent BJT saturation and speed up the TTL logic circuits.
- *BJT saturation region:* The collector-emitter saturation voltage of the BJT is controlled by the value of the forced beta, defined as  $\beta_{FOR} = i_C / i_B$ . The transistor enters saturation if the base current exceeds the value needed to support the collector current (that is,  $i_B > i_C / \beta_F$  so that  $\beta_{FOR} < \beta_F$ ). An undesirable result of saturation is storage of excess charge in the base region of the transistor. The time needed to remove the excess charge can cause the BJT to turn off slowly. This delayed turnoff response is characterized by the storage time  $t_S$  and is proportional to the value of the storage time constant  $\tau_S$ , which determines the magnitude of the excess charge stored in the base during saturation.
- *Schottky-clamped transistors:* The Schottky-clamped transistor merges a standard bipolar transistor with a Schottky diode and was developed as a way to prevent saturation in bipolar transistors. The Schottky diode diverts excess base current around the base-collector diode of the BJT and prevents heavy saturation of the device. Schottky TTL circuits offer considerable improvement in speed compared to standard TTL for a given power dissipation because storage time delays are eliminated.
- *Inverse operation:* The input transistors in a TTL gate operate in the reverse-active mode when the input is in the high state. This is the only use of this mode of operation that we encounter in this text.
- *Fanout:* The TTL gate has relatively large input currents for both high- and low-input voltages. The input current is positive for high-input levels and negative for low-input levels. This input current limits the fanout capability of the gate, and the fanout capability of TTL was analyzed in detail. At the output of the TTL gate, another emitter follower can be found. The emitter follower provides the high-current drive needed to support large fanouts as well as to rapidly pull up the output.
- *TTL family members:* TTL gates are available in many forms, including standard, low-power, high-power, Schottky, low-power Schottky, advanced Schottky, and advanced low-power Schottky

versions. Standard TTL has essentially been replaced by low-power Schottky (54LS/74LS) TTL, which provides similar delay but at reduced power. Schottky TTL (54S/74S) provides a high-speed alternative for circuits with critical speed requirements.

- *Power delay products:* The standard ECL and TTL unit-logic families have relatively large power-delay products (20 to 100 pJ), which are not suitable for high-density VLSI chip designs. VLSI circuit densities require subpicojoule power-delay products; simplified circuit designs with much lower values of power-delay product are required for VLSI applications. Low-voltage forms of TTL and ECL have been designed for VLSI applications, but for the most part they have been replaced by CMOS circuitry.
- *BiCMOS:* BiCMOS is a highly complex integrated circuit technology, but it provides the advantages of both bipolar and MOS transistors. Full BiCMOS technologies provide NMOS, PMOS, *npn*, and *pnp* transistors. Thus the circuit designer has maximum flexibility to choose the best device for each place in a circuit. In BiCMOS logic gates, MOS transistors are typically used to provide high-impedance inputs with the simplicity of MOS NAND, NOR, and complex gate implementations. Bipolar transistors are used to provide high-output-current capacity for driving large load capacitances. BiCMOS is also highly useful for “mixed-signal” designs that combine both analog and digital signal processing. Simplified BiCMOS technologies add *npn* transistors to the CMOS process, and the resulting circuits are often referred to as BiNMOS instead of BiCMOS.

## KEY TERMS

Active pull-up circuit	Merged transistor structure
AND-OR-Invert (AOI) logic	Reference voltage
Base-emitter saturation voltage ( $V_{BESAT}$ )	Reverse-active region
Collector-emitter saturation voltage ( $V_{CESAT}$ )	Reverse transit time
Clamping diodes	Saturation region
Current switch circuit	Saturation voltage
Dual-in-line package (DIP)	Schottky barrier diode
Emitter-coupled logic (ECL)	Schottky-clamped transistor
Emitter-coupled pair	Schottky TTL inverter
Emitter dotting	Stored base charge
Emitter follower	Storage time $t_s$
Fanout	Storage time constant $\tau_s$
Forward-active region	Sum-of-products logic function
Forward transit time	Temperature compensation
High-power TTL	Transistor-transistor logic (TTL, T <sup>2</sup> L)
Level shifter	$V_{BESAT}$
Low-power TTL	Wired-OR logic
Low-power Schottky TTL	

## REFERENCES

1. Hodges, D. A. and H. G. Jackson, *Analysis and Design of Digital Integrated Circuits*, Second Edition, McGraw-Hill, New York: 1988.
2. Martin, K., *Digital Integrated Circuit Design*, Oxford University Press, New York, NY: 2000.

## ADDITIONAL READING

- Haznedar, H. *Digital Microelectronics*, Benjamin/Cummings, Redwood City, CA: 1991.  
 Glasford, G. M. *Digital Electronic Circuits*, Prentice-Hall, Englewood Cliffs, NJ: 1988.  
 J. N. Rabaey, A. Chandrakasan and B. Nikolic', *Digital Integrated Circuits — A Design Perspective*, Second Edition, Prentice Hall, Upper Saddle River, NJ: 2003.

## PROBLEMS

For SPICE simulations, use the device parameters in Appendix B. For hand calculations, use the values in Table 9.3 on page 488.

### 9.1 The Current Switch (Emitter-Coupled Pair)

- 9.1. What are the voltages at  $v_{C1}$  and  $v_{C2}$  in the circuit in Fig. P9.1 for  $v_I = -1.6$  V if  $I_{EE} = 2.0$  mA,  $R_C = 350 \Omega$ , and  $V_{REF} = -1.25$  V?

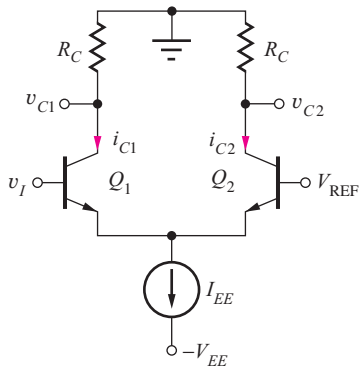


Figure P9.1

- 9.2. (a) What value of  $v_I$  is required in Fig. P9.1 to switch 99.5 percent of the current  $I_{EE}$  into transistor  $Q_1$  if  $V_{REF} = -1.25$  V? What value of  $v_I$  will switch 99.5 percent of  $I_{EE}$  into transistor  $Q_2$ ? (b) Repeat part (a) if  $V_{REF} = -2$  V.
- 9.3. What are the voltages at  $v_{C1}$  and  $v_{C2}$  in the circuit in Fig. P9.1 for  $v_I = -1.6$  V,  $I_{EE} = 2.5$  mA,  $R_C = 600 \Omega$ , and  $V_{REF} = -2$  V?
- 9.4. What are the voltages at  $v_{C1}$  and  $v_{C2}$  in the circuit in Fig. P9.4 for  $v_I = -1.7$  V,  $I_{EE} = 0.3$  mA,  $R_1 = 3.33 \text{ k}\Omega$ ,  $R_C = 2 \text{ k}\Omega$ , and  $V_{REF} = -2$  V?
- \*9.5. A bipolar transistor is operating with  $v_{BE} = +0.7$  V and  $v_{BC} = +0.3$  V. By the strict definitions given in the chapter on bipolar transistors, this transistor is operating in the saturation region. Use the transport equations to demonstrate that it actually behaves as if it is still in the forward-active region. Discuss this result. (You may use  $I_S = 10^{-15}$  A,  $\alpha_F = 0.98$ , and  $\alpha_R = 0.2$ .)
- \*\*9.6. A low-voltage current switch is shown in Fig. P9.6. (a) What are the voltage levels corresponding to  $V_H$  and  $V_L$  at  $v_{O2}$ ? (b) Do these voltage levels appear to be compatible with the levels needed at the

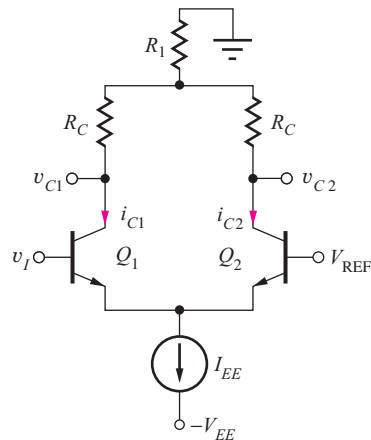


Figure P9.4

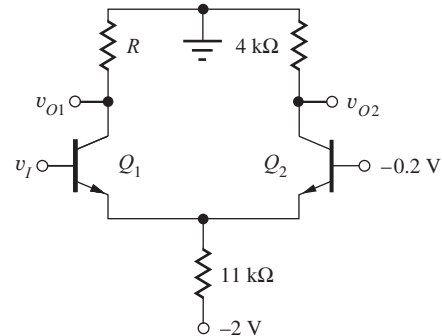


Figure P9.6

- input  $v_I$ ? Why? (c) What is the value of  $R$ ? (d) For  $v_I = V_H$  from part (a), what are the regions of operation of transistors  $Q_1$  and  $Q_2$ ? (e) For  $v_I = V_L$  from part (a), what are the regions of operation of transistors  $Q_1$  and  $Q_2$ ? (f) Your answers in parts (c) and (d) should have involved regions other than the forward-active region. Discuss whether this appears to represent a problem in this circuit.

- 9.7. (a) What is the average power in the current switch in Fig. P9.6? Assume  $v_I$  spends 50 percent of the time in each logic state. (b) Redesign the resistor values to reduce the power by a factor of five.

### 9.2 The Emitter-Coupled Logic (ECL) Gate

- 9.8. The values of  $I_{EE}$ ,  $R_C$ , and  $I_3$  and  $I_4$  in Fig. 9.6 are changed to 1 mA, 600  $\Omega$ , and 0.3 mA, respectively. What are the new values of  $V_H$ ,  $V_L$ ,  $V_{REF}$ , and  $\Delta V$ ?
- 9.9. The values of  $I_{EE}$  and  $R_C$  in Fig. 9.6 are changed to 5 mA and 200  $\Omega$ , respectively. What are the new values of  $V_H$ ,  $V_L$ ,  $V_{REF}$ , and  $\Delta V$ ?

- 9.10. Redesign the values of resistors and current sources in Fig. 9.6 to increase the power consumption by a factor of 3. The values of  $V_H$  and  $V_L$  should remain constant.
- 9.11. Redesign the circuit of Fig. 9.6 to have a logic swing of 0.8 V. Maintain the same power. (a) What are the new values of  $V_H$ ,  $V_L$ ,  $V_{\text{REF}}$ , and the resistors? (b) What are the values of the noise margins? (c) What is the minimum value of  $V_{CB}$  for  $Q_1$  and  $Q_2$ ? Do the values of  $V_{CB}$  represent a problem?
- \*9.12. Redesign the circuit of Fig. 9.6 to have a logic swing of 0.8 V. Use the same currents. (a) What are the new values of  $V_H$ ,  $V_L$ ,  $V_{\text{REF}}$ , and the resistors? (b) What are the values of the noise margins? (c) What is the minimum value of  $V_{CB}$  for  $Q_1$  and  $Q_2$ ? Do the values of  $V_{CB}$  represent a problem?
- 9.13. Emitter followers are added to the outputs of the circuit in Fig. P9.4 in the same manner as in Fig. 9.6. (a) Draw the new circuit. (b) If  $I_{EE} = 0.3 \text{ mA}$ ,  $R_1 = 3.33 \text{ k}\Omega$ ,  $R_C = 2 \text{ k}\Omega$ , and  $V_{\text{REF}} = -2 \text{ V}$ , what are the values of  $V_H$ ,  $V_L$ , and the logic swing  $\Delta V$ ? (c) Are the input and output levels of this gate compatible with each other?
- 9.14. Emitter followers are added to the outputs of the circuit in Fig. P9.4 in the same manner as in Fig. 9.6. (a) Draw the new circuit. (b) What are the values of  $R_C$ ,  $V_H$ ,  $V_L$ , and  $V_{\text{REF}}$  if  $I_{EE} = 1.5 \text{ mA}$ ,  $R_1 = 800 \Omega$ , and  $\Delta V = 0.4 \text{ V}$ ?
- \*\*9.15. Calculate the fanout for the ECL inverter in Fig. P9.6 at room temperature for  $\beta_F = 30$ . Define the fanout  $N$  to be equal to the number of inverters for which the  $V_H$  level deteriorates by no more than one  $V_T$ . (*Hint:* At  $v_O2$ ,  $\Delta V_H = \Delta V_{BE4} + \Delta i_{B4} R_C$ ) Do we need to consider the case for  $v_O = V_L$ ? Why?

### 9.3–9.4 $V_{IH}$ , $V_{IL}$ , and Noise Margin Analysis for the ECL Gate and Current Source Implementation

- 9.16. Change the values of resistors and current sources in Fig. 9.8(b) to reduce the power consumption by a factor of 6. The values of  $V_H$  and  $V_L$  should remain constant.
- 9.17. (a) Redesign the values of resistors and current sources in Fig. 9.8(b) to increase the power consumption by a factor of 6. The values of  $V_H$  and  $V_L$  should remain constant. (b) Change the values of resistors and current sources in Fig. 9.8(b) to reduce the power consumption by a factor of 4. The values of  $V_H$  and  $V_L$  should remain constant.
- 9.18. What are the values of  $V_H$ ,  $V_L$ ,  $V_{\text{REF}}$ ,  $\Delta V$ , the noise margins, and the average power dissipation for the circuit in Fig. P9.18?

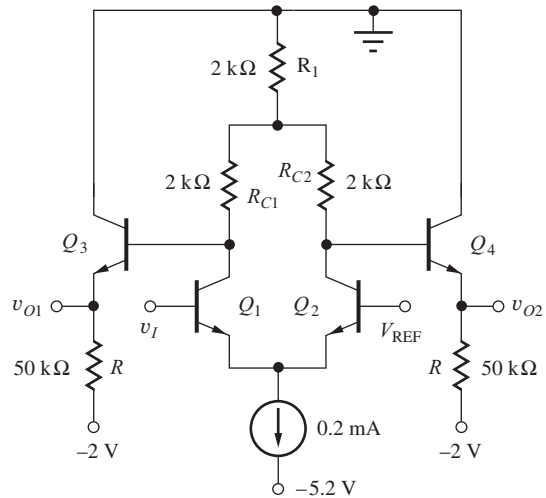


Figure P9.18

- 9.19. What is the minimum logic swing  $\Delta V$  required for an ECL gate to have a noise margin of 0.1 V at room temperature?
- \*9.20. Suppose the values of resistors in Fig. 9.8(a) all increase in value by 20 percent. (a) How do the values of  $V_H$ ,  $V_L$ , and the noise margins change? (b) Repeat part (a) for the circuit of Fig. 9.8(b).
- 9.21. Redesign the circuit of Fig. 9.8(b) to have a logic swing of 0.8 V. Use the same power. (a) What are the new values of  $V_H$ ,  $V_L$ ,  $V_{\text{REF}}$ , and the resistors? (b) What are the values of the noise margins? (c) What is the minimum value of  $V_{CB}$  for  $Q_1$  and  $Q_2$ ? Do the values of  $V_{CB}$  represent a problem?
- 9.22. Redesign the circuit of Fig. 9.8(b) to have a logic swing of 0.8 V. Use the same currents. (a) What are the new values of  $V_H$ ,  $V_L$ ,  $V_{\text{REF}}$ , and the resistors? (b) What are the values of the noise margins? (c) What is the minimum value of  $V_{CB}$  for  $Q_1$  and  $Q_2$ ? Do the values of  $V_{CB}$  represent a problem?
- \*\*9.23. Suppose that an ECL gate is to be designed to operate over the  $-55^\circ\text{C}$  to  $+75^\circ\text{C}$  temperature range and must maintain a minimum noise margin of 0.1 V over that full range. What is the value of the logic swing of this ECL gate at room temperature?
- 9.24. Replace the current source in Fig. P9.18 with a resistor. Assume  $V_{\text{REF}} = -1.3 \text{ V}$ . Do any of the three collector resistors need to be changed? If so, what are the new values?

- \*9.25. The current source for a current switch is implemented with a transistor and three resistors, as in Fig. P9.25. What is the current  $I_{EE}$ ? What is the minimum permissible value of  $V_{REF}$  if transistor  $Q_S$  is to remain in the forward-active region? Assume that  $\beta_F$  is large. (See Section 5.11.)

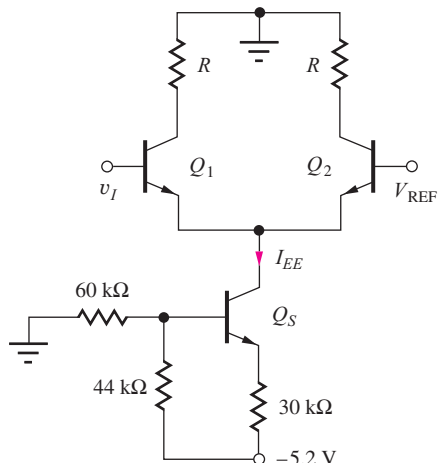


Figure P9.25

- 9.26. Design a 0.2-mA electronic current source to replace the ideal source in Fig. P9.18. Use the circuit topology from Fig. P9.25 (e.g.,  $Q_S$  and its three bias resistors). The base bias network should not use more than 20  $\mu$ A of current.
- 9.27. Simulate the voltage transfer characteristic of the ECL inverter in Fig. 9.8(b) at  $T = -55^\circ\text{C}$ ,  $25^\circ\text{C}$ , and  $85^\circ\text{C}$ . Use a constant voltage source for  $V_{REF}$ . What are  $V_H$ ,  $V_L$ , and the noise margins at the three temperatures?

## 9.5 The ECL OR-NOR Gate

- 9.28. Draw the schematic of a four-input ECL NOR gate.
- 9.29. Draw the schematic of a five-input ECL OR gate.
- 9.30.  $V_{CC} = +1 \text{ V}$  and  $V_{EE} = -2.5 \text{ V}$  in the ECL gate in Fig. P9.30. (a) Find  $V_H$  and  $V_L$  at the emitter of  $Q_5$ . (b) What is the value of  $R$  required to give the same voltage levels at the emitter of  $Q_1$ ?
- 9.31.  $V_{CC} = +1.3 \text{ V}$  and  $V_{EE} = -3.2 \text{ V}$  in the ECL gate in Fig. P9.30 (a) Find  $V_H$  and  $V_L$  at the emitter of  $Q_5$ . (b) What value of  $R$  is required to give the same voltage levels at the emitter of  $Q_1$ ?

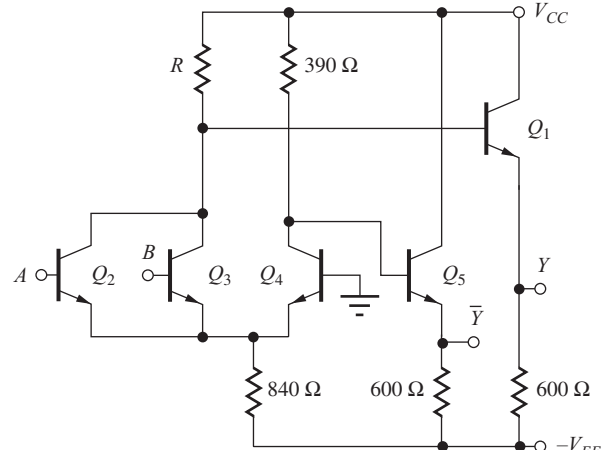


Figure P9.30

- 9.32. (a) Only the OR output is needed in the circuit of Fig. P9.30. Redraw the circuit, eliminating the unneeded components. Use  $V_{CC} = +1.3 \text{ V}$  and  $V_{EE} = -3.2 \text{ V}$ . (b) Repeat part (a) if only the NOR output is needed.

## 9.6 The Emitter Follower

- 9.33. In the circuit in Fig. P9.33,  $\beta_F = 50$ ,  $V_{CC} = +5 \text{ V}$ ,  $-V_{EE} = -5 \text{ V}$ ,  $I_{EE} = 2.5 \text{ mA}$ , and  $R_L = 1.2 \text{ k}\Omega$ . What is the minimum voltage at  $v_O$ ? What are the emitter, base, and collector currents if  $v_I = +4 \text{ V}$ ?

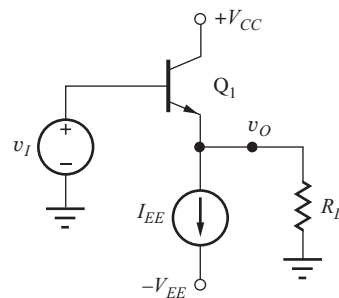


Figure P9.33

- 9.34. The input voltage  $v_I$  for the circuit in Fig. P9.33 is a symmetrical 1-kHz triangular signal ranging between  $+3 \text{ V}$  and  $-3 \text{ V}$ . (a) Sketch the output voltage  $v_O$  if  $\beta_F = 40$ ,  $V_{CC} = +4 \text{ V}$ ,  $-V_{EE} = -4 \text{ V}$ ,  $I_{EE} = 4 \text{ mA}$ , and  $R_L = 1 \text{ k}\Omega$ . (b) Repeat for  $I_{EE} = 2 \text{ mA}$ . (c) What is the minimum value of  $I_{EE}$  needed to insure that the output voltage is an undistorted replica of the input voltage?

- 9.35. Simulate the circuit in Prob. 9.34 using SPICE.

- 9.36. The input voltage for the circuit in Fig. P9.33 is  $v_I = -1 + \sin 2000\pi t$  V. (a) Write an expression for the output voltage  $v_O$  if  $\beta_F = 40$ ,  $V_{CC} = 0$  V,  $-V_{EE} = -3$  V,  $I_{EE} = 0.2$  mA, and  $R_L = 20$  k $\Omega$ . (b) What is the minimum value of  $I_{EE}$  needed to insure that the output voltage is an undistorted replica of the input voltage?
- 9.37. Simulate the circuit in Prob. 9.36 using SPICE.
- 9.38. In the circuit in Fig. P9.33,  $\beta_F = 40$ ,  $V_{CC} = 0$  V,  $-V_{EE} = -15$  V, and  $R_L = 1$  k $\Omega$ . What is the minimum value of  $I_{EE}$  required for the circuit to work properly for  $-10$  V  $\leq v_I \leq 0$  V?
- 9.39. In the circuit in Fig. P9.33,  $\beta_F = 40$ ,  $V_{CC} = +1.5$  V,  $-V_{EE} = -1.5$  V,  $I_{EE} = 0.5$  mA, and  $R_L = 1$  k $\Omega$ . (a) What range of values is permitted for  $v_I$  if  $Q_1$  is to stay within the forward-active region of operation? (b) What is the minimum value of  $I_{EE}$  required for the circuit to work properly for  $-1.5$  V  $\leq v_I \leq +1.5$  V.
- 9.40. In the circuit in Fig. P9.40,  $R_L = 2$  k $\Omega$ ,  $V_{CC} = 15$  V, and  $-V_{EE} = -15$  V. (a) What is the maximum value of  $R_E$  that can be used if  $v_O$  is to reach  $-12.5$  V? (b) What is the emitter current of  $Q_1$  when  $v_O = +12.5$  V?

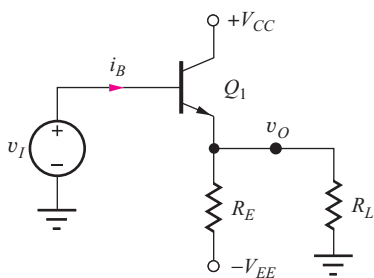


Figure P9.40

- 9.41. In the circuit in Fig. P9.40,  $\beta_F = 100$ ,  $V_{CC} = 0$  V,  $-V_{EE} = -15$  V, and  $R_L = 4.7$  k $\Omega$ . (a) What is the maximum value of  $R_E$  that can be used for the circuit to work properly for  $-10$  V  $\leq v_I \leq 0$  V? (b) What is the emitter current of  $Q_1$  when  $v_I = 0$  V? (c) For  $v_I = -10$  V?
- 9.42. In the circuit in Fig. P9.40,  $\beta_F = 100$ ,  $V_{CC} = 0$  V,  $-V_{EE} = -6$  V,  $R_E = 1.3$  k $\Omega$ ,  $R_L = 4.7$  k $\Omega$ , and  $v_I = -1.5 + 1.5 \sin 2000\pi t$  V. (a) Plot the output voltage versus time. (b) Write an expression for the output voltage. (c) What is the maximum value of emitter current and for what value of  $v_I$  does it occur? (d) What is the minimum value of

emitter current, and for what value of  $v_I$  does it occur? (e) What is the maximum value of  $R_E$  that can be used for the output voltage to be an undistorted replica of the input voltage?

- 9.43. (a) Simulate the circuit in Prob. 9.42 for  $0 \leq t \leq 3$  ms. (b) Repeat the simulation if  $R_E$  is changed to 4.7 k $\Omega$ .

### 9.7 "Emitter Dotting" or "Wired-OR" Logic

- 9.44. The two outputs of the inverter in Fig. 9.6 are accidentally connected together. What will be the output voltage for  $v_I = -0.7$  V? For  $v_I = -1.3$  V? What will be the currents in transistors  $Q_3$  and  $Q_4$  for each case?
- 9.45. What are the logic functions for  $Y$  and  $Z$  in Fig. P9.45?

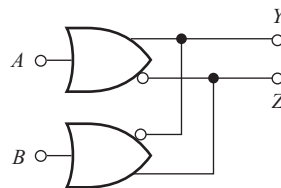


Figure P9.45

- \*9.46. Draw the full circuit schematic for an ECL implementation of the logic function  $Y = A + B + (C + D)$  using a wired-OR connection of two ECL gates.

### 9.8 ECL Power-Delay Characteristics

- 9.47. The logic swing in the inverter in Fig. P9.21 is reduced by a factor of 2 by reducing the value of all the current sources by a factor of 2 and changing  $V_{REF}$ . What is the new value of  $V_{REF}$ ? What is the new value of the power-delay product?
- 9.48. The logic swing in the inverter in Fig. 9.21 is reduced by a factor of 2 by reducing the value of  $R_C$  and changing  $V_{REF}$ . What is the new value of  $V_{REF}$ ? What is the new value of the power-delay product?
- 9.49. Suppose the ECL inverter in Figs. 9.21 and 9.23 must operate at a power of 20  $\mu$ W. If the current sources are scaled by the same factor, and the capacitances and voltage levels remain the same, what is the new propagation delay of the inverter?
- \*9.50. (a) The logic circuit in Fig. P9.50 represents an alternate form of an ECL gate. If  $V_{EE} = -3.3$  V,  $V_{REF} = -1.0$  V,  $R_B = 3.2$  k $\Omega$ , and  $R_E = 1.6$  k $\Omega$ , find the values of  $V_L$ ,  $V_H$ , and the power consumption in the gate. What are the values of  $R_{C1}$  and  $R_{C2}$ ?

- (b) What are the logic function descriptions for the two outputs? (c) Compare the number of transistors in this gate with a standard ECL gate providing the same logic function.

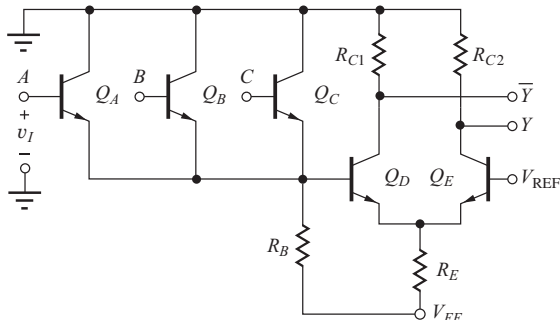


Figure P9.50

- \*9.51. Assume that you need 0.6 V across  $R_E$  to properly stabilize the current in the modified ECL gate in Fig. P9.50. Design the resistors in the gate for a logic swing of 0.4 V and an average current of 1 mA through  $R_B$  and  $R_E$ . What are the minimum values of  $V_{EE}$  and the value of  $V_{REF}$ ?
- 9.52. Use SPICE and the values in Prob. P9.50 to find the propagation delay of the gate in Fig. P9.50.
- 9.53. Redesign the ECL inverter in Fig. 9.18 to change the average power dissipation to 1 mW. Scale the power in the current switch and the emitter followers by the same factor.
- 9.54. The power supply  $-V_{EE}$  in Fig. 9.19 is changed to  $-2$  V. What are the new values of  $R_{EE}$  and  $R_{C1}$  required to keep the logic levels and logic swing unchanged? What is the new power dissipation?
- \*9.55. What type of logic gate is the circuit in Fig. P9.55? What logic function is provided at the output  $Y$ ?

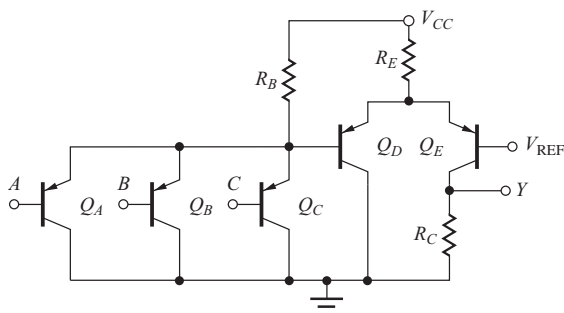


Figure P9.55

- \*9.56. Design the circuit in Fig. P9.55 to provide a logic swing of 0.6 V from a power supply of  $+3$  V. The

power consumption should average 1 mW, with 90 percent of the power consumed by  $Q_D$  and  $Q_E$ .

- 9.57. (a) Use SPICE to find the propagation delay of the gate in Prob. 9.56. (b) In Prob. 9.4. (c) In Fig. P9.18.

## 9.9 Current Mode Logic (CML)

- 9.58 Find the truth table and logic expression for  $Y$  in the gate in Fig. 9.29 and show that it is an XOR gate. What is the function at  $\bar{Y}$ ?
- 9.59 The BJT in a CML gate has a saturation current of 0.1 fA. (a) Find the emitter, collector, and base currents of the transistor if  $V_{BE} = 0.7$  V and  $V_{BC} = 0.4$  V. (b) What are the currents if  $V_{BC} = 0$  V?
- 9.60 The SiGe HBT in a CML gate has a saturation current of 1 aA. (a) Find the emitter, collector and base currents of the transistor if  $V_{BE} = 0.85$  V and  $V_{BC} = 0.2$  V. (b) What are the currents if  $V_{BC} = 0$  V?
- 9.61 High-density SiGe ICs employ transistors with very small emitter areas and achieve cutoff frequencies exceeding 150 GHz. At a bias current of 400  $\mu$ A, the base emitter voltages are approximately 0.9 V. What are the logic levels associated with the output and inputs of the gate in Fig. 9.28 if  $V_L = -0.2$  V? What is the minimum value of  $V_{EE}$  if the voltage across the current source is 0.4 V?
- 9.62 Draw the circuit schematic for a three-input CML XOR gate.
- 9.63 What is the logic function for the circuit in Fig. P9.63.

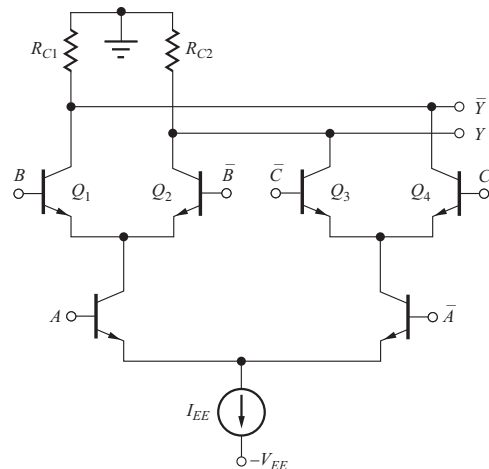


Figure P9.63

- 9.64 What is the logic function for the circuit in Fig. P9.63 if the inputs to  $Q_3$  and  $Q_4$  are interchanged?
- 9.65 Design a CML gate that implements  $Y = \bar{A}\bar{C} + B$ .
- 9.66 Design a CML gate that implements  $Y = B(\bar{A} + C)$ .
- 9.67 Draw the circuit schematic for a two-input NMOS CML XOR gate.
- 9.68 Suppose  $V_{GG}$  is chosen so that the current in  $M_5$  in Fig. 9.31 is 100  $\mu\text{A}$  and the drain resistors are 8  $\text{k}\Omega$ . What are the voltage levels at the outputs and the  $A$  and  $B$  inputs if each transistor is to remain in the saturation region? What is the minimum value of  $V_{EE}$ ? Assume  $K'_n = 100 \mu\text{A}/\text{V}^2$  and  $W/L = 2/1$  for each transistor.

## 9.10 The Saturating Bipolar Inverter

- 9.69. Calculate the collector and base currents in a bipolar transistor operation with  $v_{BE} = 0.20 \text{ V}$  and  $v_{BC} = -4.8 \text{ V}$ . Use the BJT parameters from Table 9.3.
- 9.70. What is the value of  $V_{CESAT}$  of transistor  $Q_1$  in Fig. 9.39 based on Eq. (9.47) and the BJT parameters from Table 9.3.
- 9.71. (a) What is the ratio  $i_C/i_E$  in Fig. P9.71 for  $v_I = 0.8 \text{ V}$ ? If needed, you may use the parameters in Table 9.3. (b) For  $v_I = 0.6 \text{ V}$ ? (c) For  $v_I = 1.0 \text{ V}$ ? (d) What is the dc input voltage  $v_I$  required for  $i_C/i_E = -1$ ?

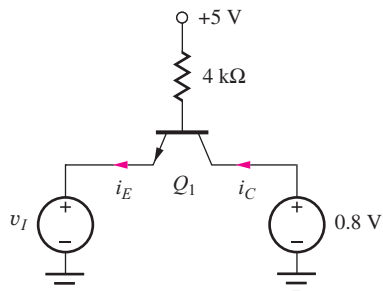


Figure P9.71

- 9.72. (a) What is the base-emitter voltage in the circuit in Fig. P9.72? Use the transport equations and the

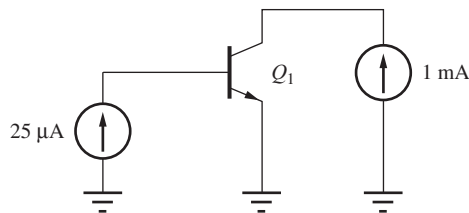


Figure P9.72

transistor parameters from Table 9.3. (b) What is the base-emitter voltage if  $\beta_F = 80$ ? (c) What is  $V_{BE}$  if  $I_B$  is increased to 1 mA and  $\beta_F = 40$ ?

- 9.73. What is  $V_{CESAT}$  for the transistor in Fig. P9.72 if  $\beta_F = 60$  and  $\beta_R = 1$ ? (b) If  $\beta_F = 60$ ,  $\beta_R = 1$ , and the 25- $\mu\text{A}$  current source is increased to 40  $\mu\text{A}$ ?
- 9.74. (a) What is the minimum value of  $V_{CESAT}$  at room temperature in a BJT if  $\beta_F = 20$  and  $\beta_R = 1$ ? (b) At 180 °C?
- 9.75. What is  $V_{CESAT}$  for the transistor in Fig. P9.72 if  $\beta_F = 50$  and  $\beta_R = 2$ ? (b) If  $\beta_F = 100$  and  $\beta_R = 2$ ?
- 9.76. (a) What base current is required to reach  $V_{CESAT} = 0.2 \text{ V}$  in the circuit in Fig. 9.32? (b) To reach  $V_{CESAT} = 0.1 \text{ V}$ ?
- 9.77. What base current is required to reach  $V_{CESAT} = 0.1 \text{ V}$  in the circuit in Fig. 9.32 if  $R_C$  is changed to 3.9  $\text{k}\Omega$ ?
- 9.78. Calculate the value of  $v_{CE}$  for the two circuits in Fig. P9.78.

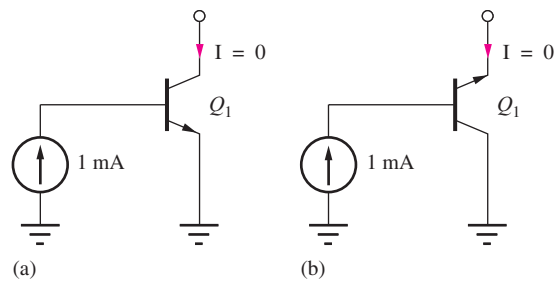


Figure P9.78

- 9.79. Calculate the storage time for the inverter in Fig. 9.35 if  $I_{BF} = 2.5 \text{ mA}$ ,  $I_{BR} = -0.5 \text{ mA}$ ,  $\tau_F = 0.4 \text{ ns}$ , and  $\tau_R = 12 \text{ ns}$ . Use Table 9.3.

## 9.11 A Transistor-Transistor Logic (TTL) Prototype

- 9.80. What are the worst-case minimum and maximum values of the power consumed by the gate in Fig. 9.37 if the 2- $\text{k}\Omega$  and 4- $\text{k}\Omega$  resistors have a tolerance of  $\pm 20$  percent?
- \*9.81. Suppose the TTL circuit in Fig. 9.37 is operated with  $V_{CC} = +3.3 \text{ V}$ . What are the new values of  $V_H$ ,  $V_L$ ,  $V_{IH}$ ,  $V_{IL}$ , and fanout for this gate?
- \*\*9.82. A fixed value for  $V_L$  was assumed in the analysis of the prototype TTL gate in Fig. 9.39. However, an exact value can be found by the simultaneous solution of Eqs. (9.44) and (9.47) if we assume that  $i_{B2} = 1.09 \text{ mA}$  is constant. Find the actual  $V_L$  level

for the circuit in Fig. 9.39 using an iterative numerical solution of these two equations.

- 9.83. A low-power TTL gate is shown in Fig. P9.83. Find  $V_H$ ,  $V_L$ ,  $V_{IL}$ ,  $V_{IH}$ , and the noise margins for this circuit.

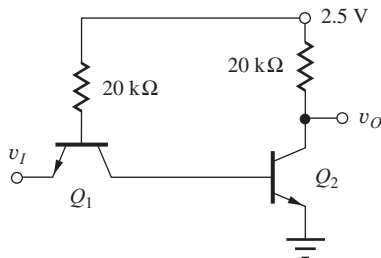


Figure P9.83

- \*9.84. A low-power TTL gate similar to the gate in Fig. P9.83 is needed for a VLSI design. These supply voltages are being considered: 0.5, 1.0, 1.5, 2.0, and 2.5 V. Which of these voltages represents the minimum supply needed for the circuit to operate properly? Why?

- 9.85. Scale the resistors in the TTL prototype in Fig. 9.37 to change the power of the gate to 1.0 mW.

- 9.86. (a) Use SPICE to determine the average propagation delay for the TTL prototype of Fig. 9.37. (b) Repeat for the scaled gate design from Prob. 9.85.

- \*9.87. The TTL prototype in Fig. 9.37 is operated from  $V_{DD} = 3.0$  V. (a) Based on the results in Fig. 9.41, draw the new VTC. (b) What are approximate values of the new  $V_{IL}$  and  $V_{IH}$ ? (c) What are the new values of the noise margins?

- \*9.88. The inverter in Fig. P9.88(a) is a member of the diode-transistor logic (DTL) family that was used prior to the invention of TTL. (a) Find  $V_H$  and  $V_L$  for the circuit in Fig. P9.88(a). What are the input currents in the two logic states? (b) What is the fanout limit for the DTL inverter? (c) Compare the

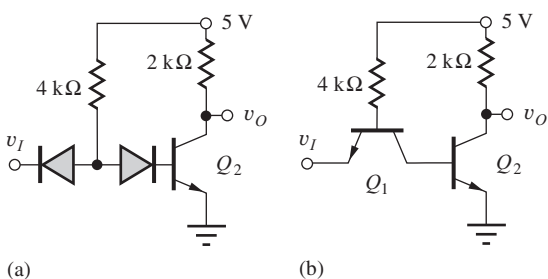


Figure P9.88

values from parts (a) and (b) to those for the circuit in Fig. P9.88(b).

- \*9.89. The inverter in Fig. P9.88(a) is a member of the diode-transistor logic (DTL) family that was used prior to the invention of TTL. Sketch the VTC and compare to the VTC for the circuit in Fig. P9.90(b).

- \*9.90. The inverter in Fig. P9.88(a) is a member of the diode-transistor logic (DTL) family that was used before the introduction of TTL. Simulate the VTC of the DTL inverter and compare to that of the circuit in Fig. P9.88(b). Discuss the location of the break points in the characteristic.

- \*9.91. Simulate the propagation delay of the two inverters in Fig. P9.88. Discuss the reasons for any differences that are observed. (Hint: Calculate the values of  $I_{BR}$  available to bring  $Q_2$  out of saturation and calculate the storage times in the two inverters.)

- \*\*9.92. The circuits in Fig. P9.92 are members of the diode-transistor logic (DTL) family that was used before the invention of TTL. (a) Simulate the propagation delay of the two DTL inverters in Fig. P9.92. Discuss the reasons for any differences that are observed. What is the function of the 1-kΩ resistor in Fig. P9.92(b), and why is it important? (Hint: Calculate the values of  $I_{BR}$  available to bring  $Q_2$  out of saturation and calculate the storage times in the two inverters.)

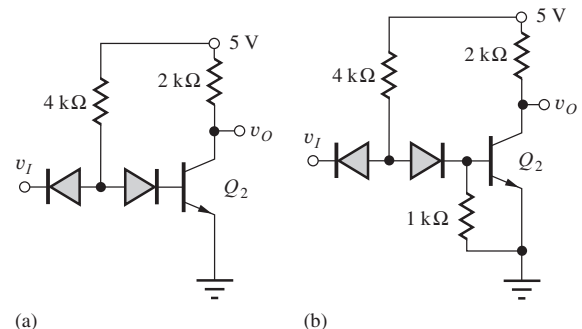


Figure P9.92

- \*9.93. Sketch the VTC for the simplified TTL gate in Fig. P9.93. Discuss the relationship between the observed break points in the VTC to the switching points of the various transistors. Estimate the noise margins.

- 9.94. Simulate the VTC for the simplified TTL gate in Fig. P9.93. Discuss the relationship between the observed break points in the VTC to the switching points of the various transistors. What are the noise margins?

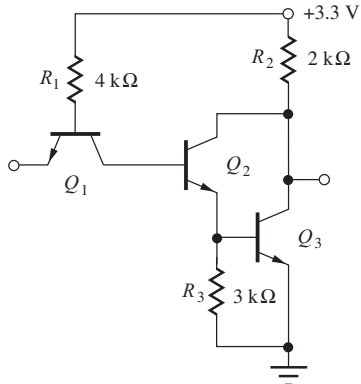


Figure P9.93

### Fanout Limitations of the TTL Prototype

- \*9.95. What is the minimum value of the fanout specification for the gate in Fig. 9.37 if the 2-k $\Omega$  and 4-k $\Omega$  resistors have a tolerance of  $\pm 20$  percent? Assume the resistors in each gate track each other.
- 9.96. A fabrication process control problem causes  $\beta_F = 25$  and  $\beta_R = 1$  in the transistors used in the TTL circuit in Fig. 9.37. What is the new value of the fanout?
- 9.97. The fanout for the circuit in Fig. 9.37 was calculated to be 7. Redesign the value of  $R_B$  to increase the fanout to 10.
- 9.98. (a) What is the fanout limit in the prototype TTL gate in Fig. 9.37 if  $V_{CESAT2}$  is required to be less than 0.1 V? (b) What are the input current  $i_{IH}$  and fanout limit for  $v_I = V_{OH}$  if  $\beta_{R1} = 2$ ?
- 9.99. What is the fanout limit in the prototype TTL gate in Fig. 9.37 if  $V_{CC}$  is changed to 3.3 V?

### 9.12 The Standard 7400 Series TTL Inverter

- 9.100. Suppose the output in Fig. P9.100 is accidentally shorted to ground. (a) Calculate the emitter current in the circuit if  $R_S = 0$  and  $\beta_F = 100$ . (b) Repeat for  $R_S = 130\ \Omega$ .
- 9.101. Calculate the power dissipation in the circuit in both parts of Prob. 9.100.
- 9.102. Use SPICE to plot  $v_O$  versus  $I_L$  for the circuit in Fig. P9.100.
- \*9.103. Simulate the voltage transfer characteristic for the modified TTL gate in Fig. P9.103. Discuss why the first “knee” voltage at  $V_2$  in Fig. 9.54 has been eliminated.
- 9.104. Calculate the currents in transistors  $Q_1$  to  $Q_4$  in a low-power version of the TTL gate in Fig. 9.48 in

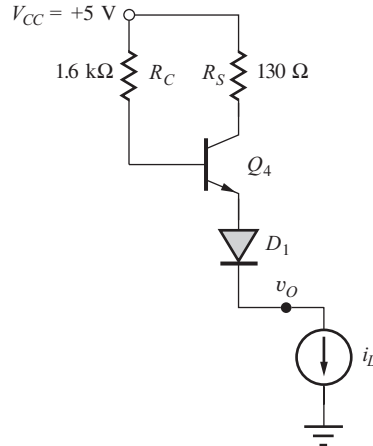


Figure P9.100

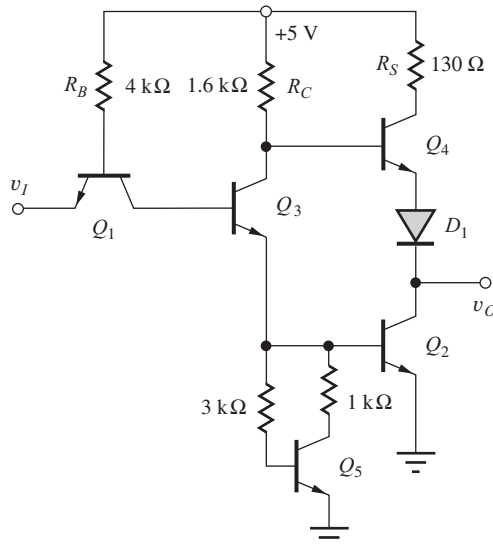


Figure P9.103

which  $R_B = 20\text{ k}\Omega$ ,  $R_C = 8\text{ k}\Omega$ ,  $R_E = 5\text{ k}\Omega$ , and  $R_S = 650\ \Omega$  for (a)  $v_I = V_H$  and (b)  $v_I = V_L$ .

- 9.105. Simulate the voltage transfer characteristic for the low-power TTL gate in Prob. 9.104 for  $T = 25^\circ\text{C}$ .
- 9.106. Simulate the voltage transfer characteristic for the low-power TTL gate in Prob. 9.104 for  $T = -55^\circ\text{C}$ ,  $+25^\circ\text{C}$ , and  $+85^\circ\text{C}$ .

### Fanout Limitations of Standard TTL

- \*9.107. Calculate the fanout limit for  $v_O = V_H$  for the standard TTL gate in Fig. 9.58. Assume that  $V_H$  must not drop below 2.4 V.
- \*9.108. Calculate the fanout limit for the standard TTL gate in Fig. 9.58 if  $R_B = 5\text{ k}\Omega$ ,  $R_C = 2\text{ k}\Omega$ ,

$R_E = 1.25 \text{ k}\Omega$ ,  $\beta_R = 0.05$ , and  $\beta_F = 20$ . Assume that  $V_H$  must not drop below 2.4 V.

- \*9.109. Plot the fanout of the standard TTL gate of Fig. 9.58 versus  $\beta_R$  for  $\beta_R$  ranging between 0 and 5.
- \*9.110. (a) Calculate  $V_H$  and  $V_L$  for the inverter in Fig. P9.110. (b) What are the input currents in the two logic states? (c) What is the fanout capability of the gate?

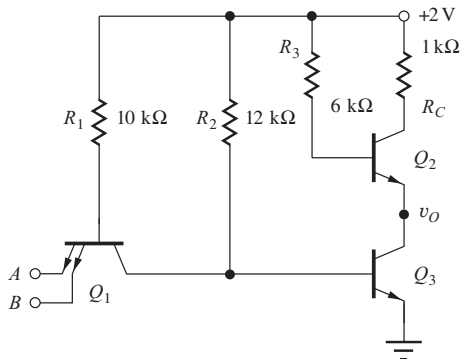


Figure P9.110

- \*9.111. (a) Calculate  $V_H$  and  $V_L$  for the inverter in Fig. P9.111. (b) What are the input currents in the two logic states? (c) What is the fanout capability of the gate?

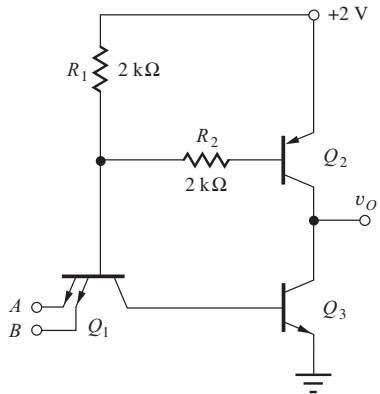


Figure P9.111

### 9.13 Logic Functions in TTL

- 9.112. Use the graphical technique described in the EIA in Chapter 8 to find the noise margins for the standard TTL gate.
- \*9.113. The circuit in Fig. P9.113 can be considered a member of the diode-transistor logic (DTL) family. (a) What is the logic function of this gate? (b) Calculate  $V_H$  and  $V_L$  for this DTL inverter. (c) What are the input currents in the two logic states? (d) Sketch

the VTC and compare to the VTC for the standard TTL circuit.

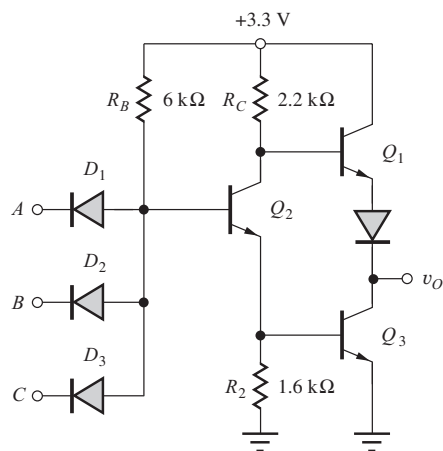


Figure P9.113

- \*9.114. For the circuit in Fig. P9.114,  $R_1 = 4 \text{ k}\Omega$ ,  $R_2 = 4 \text{ k}\Omega$ ,  $R_3 = 4.3 \text{ k}\Omega$ ,  $R_4 = 10 \text{ k}\Omega$ ,  $R_5 = 5 \text{ k}\Omega$ , and  $R_6 = 5 \text{ K}$ . (a) What is the logic function  $Y$ ? (b) What are the values of  $V_L$  and  $V_H$ ? (c) What are the input currents in the high- and low-input states?

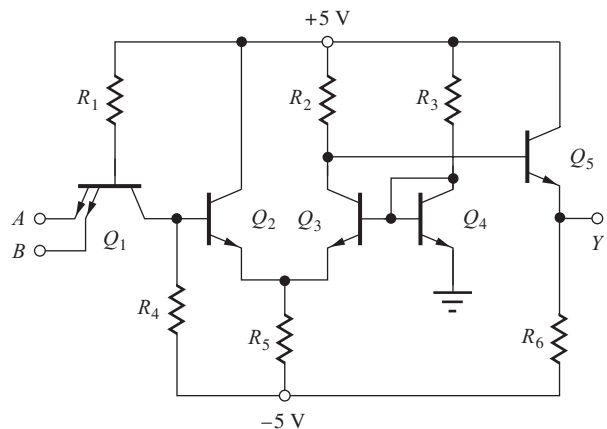


Figure P9.114

### 9.14 Schottky-Clamped TTL

- 9.115. (a) Find  $V_H$  and  $V_L$  for the Schottky DTL gate in Fig. P9.115. (b) What are the input currents in the two logic states? (c) What is the fanout of the gate?
- 9.116. Prior to the availability of Schottky diodes, the *Baker clamp* circuit in Fig. P9.116 was used to prevent saturation. What is the collector-emitter voltage of the transistor in this circuit assuming that  $i_B > i_C/\beta_F$ ? What are  $i_{D1}$ ,  $i_{D2}$ , and  $i_C$  if  $i_{BB} = 250 \mu\text{A}$ ,  $i_{CC} = 1 \text{ mA}$ ,  $\beta_F = 20$ , and  $\beta_R = 2$ ?

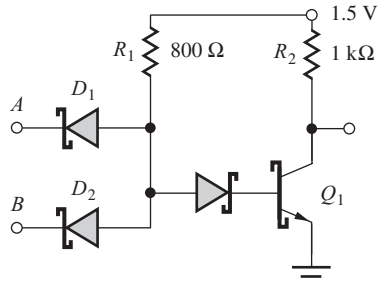


Figure P9.115

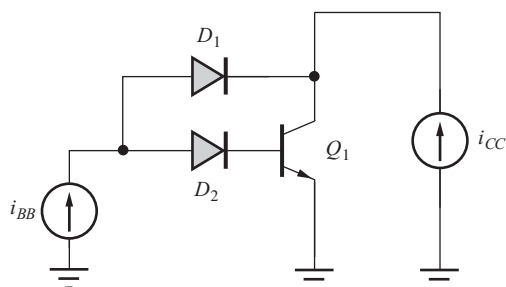


Figure P9.116

- \*9.117. Calculate the currents in  $Q_1$  to  $Q_6$  in the Schottky TTL gate in Fig. 9.61 for (a) all inputs at  $V_H$  and (b) all inputs at  $V_L$ .
- 9.118. Simulate the voltage transfer characteristic and propagation delay for the Schottky TTL gate in Fig. 9.61.
- 9.119. What is the logic function of the gate in Fig. P9.119. Find  $V_H$ ,  $V_L$ , and  $V_{REF}$  for the circuit, assuming  $V_{EE} = -3 \text{ V}$ ,  $R_C = 3.3 \text{ k}\Omega$ , and  $R_E = 2.4 \text{ k}\Omega$ . Assume  $V_{BE} = 0.7$  and  $V_D = 0.4 \text{ V}$  for the Schottky diode.

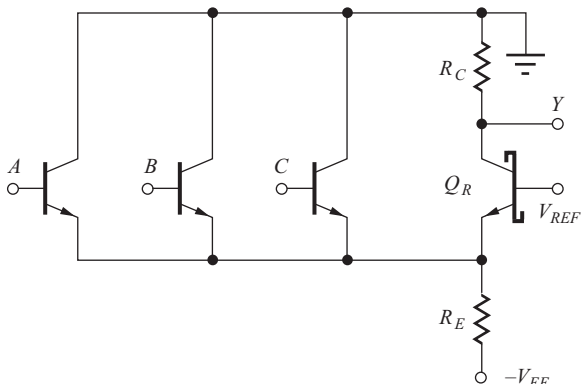


Figure P9.119

- \*9.120. What is the logic function of the gate in Fig. P9.120. Find  $V_H$ ,  $V_L$ , and  $V_{REF}$  for the circuit, assuming

$V_{EE} = -3 \text{ V}$ ,  $R_C = 0.54 \text{ k}\Omega$ , and  $R_E = 0.75 \text{ k}\Omega$ . Assume  $V_{BE} = 0.7$  and  $V_D = 0.4 \text{ V}$  for the Schottky diode.

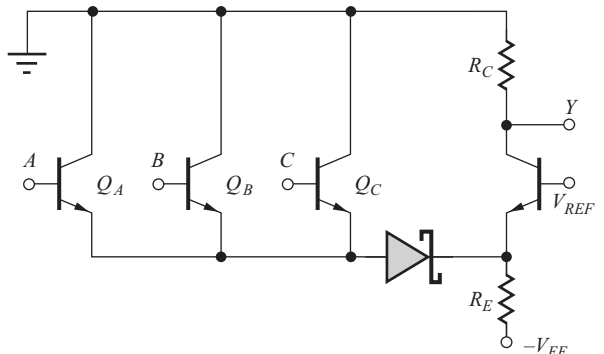


Figure P9.120

- 9.121. Estimate  $i_B$  and  $i_C$  of the Schottky transistor in Fig. P9.121 if the external collector terminal is open. Assume the forward voltage of the Schottky diode is 0.45 V.

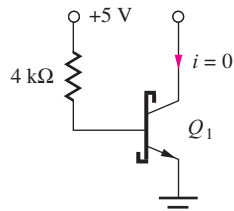


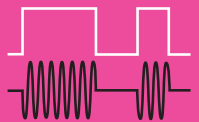
Figure P9.121

### 9.15 Comparison of Power-Delay Products of ECL and TTL

- 9.122. The power dissipation of a particular IC chip is 50 W, and the chip will contain 50 million logic gates. The gates must have an average propagation delay of 1 ns. (a) What is the power-delay product of the logic family? (b) What is the lowest PDP that can be plotted on the graph in Fig. 9.62?
- 9.123. The power dissipation of a particular IC chip is limited to 100 W, and the chip will contain 250 million logic gates. The gates must have an average propagation delay of 0.25 ns. (a) What is the power-delay product of the logic family? (b) What is the lowest PDP that can be plotted on the graph in Fig. 9.62?
- 9.124. A low-power ECL gate has a 0.5-pJ PDP. (a) What will be the gate delay for a gate operating at a power level of 0.3 mW? (b) What power is required for the gate to achieve a delay of 1 ns?

- 9.125. The 74LS gate in Fig. 9.62 is redesigned to operate at a power of 5 mW. (a) What is the gate delay of the new design? Assume a constant power-delay product. (b) What power is required to achieve a delay of 0.3 ns?
- 9.126. The ECL-100K gate in Fig. 9.62 is redesigned to operate at a power of 10 mW. (a) What is the gate delay of the new design? Assume a constant power-delay product. (b) What power is required to achieve a delay of 0.2 ns?
- 9.127. CML with a PDP of 25 fJ is to be used in a chip design that requires 50,000 gates. The chip will be placed in a package that can safely dissipate 20 W. What is the minimum logic gate delay that can be used in the design if all the gates operate at the same speed?
- 9.16 BiCMOS Logic**
- 9.128. (a) Simulate the VTC for the BiNMOS buffer in Fig. 9.69 if the  $W/L$  ratios of all the transistors are 10/1. (b) Use SPICE to find the propagation delays for  $C = 2 \text{ pF}$ . Use the BJT parameters from the simulation for Fig. 9.23.
- 9.129. (a) Simulate the VTC for the BiNMOS buffer in Fig. 9.72 if the  $W/L$  ratios of all the transistors are 10/1. (b) Use SPICE to find the propagation delays for  $C = 2 \text{ pF}$ . Use the BJT parameters from the simulation for Fig. 9.23.
- 9.130. Add MOS transistors to the circuit in Fig. 9.68 to create a two-input BiCMOS NAND gate.
- 9.131. Add MOS transistors to the circuit in Fig. 9.69 to create a two-input BiCMOS NAND gate.
- 9.132. (a) Add MOS transistors to the circuit in Fig. 9.72 to create a two-input BiNMOS NOR gate. (b) Add MOS transistors to the circuit in Fig. 9.72 to create a two-input BiCMOS NAND gate.
- 9.133. Simulate the VTC for the BiCMOS NOR gate in Fig. 9.73 if the  $W/L$  ratios of the NMOS transistors are 4/1 and those of the PMOS transistors are 10/1. (b) Use SPICE to find the propagation delays for  $C = 2 \text{ pF}$ . Use the BJT parameters from the simulation for Fig. 9.23.

## PART THREE **ANALOG ELECTRONICS**



CHAPTER 10  
**ANALOG SYSTEMS AND IDEAL OPERATIONAL AMPLIFIERS 529**

CHAPTER 11  
**NONIDEAL OPERATIONAL AMPLIFIERS AND FEEDBACK AMPLIFIER STABILITY 600**

CHAPTER 12  
**OPERATIONAL AMPLIFIER APPLICATIONS 697**

CHAPTER 13  
**SMALL-SIGNAL MODELING AND LINEAR AMPLIFICATION 786**

CHAPTER 14  
**SINGLE-TRANSISTOR AMPLIFIERS 857**

CHAPTER 15  
**DIFFERENTIAL AMPLIFIERS AND OPERATIONAL AMPLIFIER DESIGN 968**

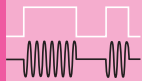
CHAPTER 16  
**ANALOG INTEGRATED CIRCUIT DESIGN TECHNIQUES 1046**

CHAPTER 17  
**AMPLIFIER FREQUENCY RESPONSE 1128**

CHAPTER 18  
**TRANSISTOR FEEDBACK AMPLIFIERS AND OSCILLATORS 1228**

*This page intentionally left blank*

# CHAPTER 10



## ANALOG SYSTEMS AND IDEAL OPERATIONAL AMPLIFIERS

### CHAPTER OUTLINE

10.1	An Example of an Analog Electronic System	530
10.2	Amplification	531
10.3	Two-Port Models for Amplifiers	537
10.4	Mismatched Source and Load Resistances	541
10.5	Introduction to Operational Amplifiers	544
10.6	Distortion in Amplifiers	548
10.7	Differential Amplifier Model	549
10.8	Ideal Differential and Operational Amplifiers	551
10.9	Analysis of Circuits Containing Ideal Operational Amplifiers	552
10.10	Frequency Dependent Feedback	568
	Summary	586
	Key Terms	588
	References	588
	Problems	589

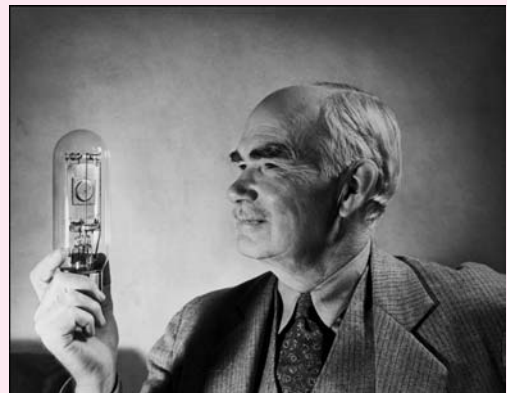
- Factors that must be considered in the design of circuits using operational amplifiers

Invention of the Audion tube by Lee DeForest in 1906 was a milestone event in electronics as it represented the first device that provided amplification with reasonable isolation between the input and output [1–4]. Amplifiers today, most often in solid-state form, play a key role in the multitude of electronic devices that we encounter in our daily activities, even in devices that we often think are digital in nature. Examples include cell phones, disk drives, digital audio and DVD players, and global positioning systems. All these devices utilize amplifiers to transform very small analog signals to levels where they can be reliably

### CHAPTER GOALS

Chapter 10 begins our study of the circuits used for analog electronic signal processing. We will develop an understanding of concepts related to linear amplification and circuits containing ideal operational amplifiers.

- Voltage gain, current gain, and power gain
- Gain conversion to decibel representation
- Input resistance and output resistance
- Transfer functions and Bode plots
- Low-pass and high-pass amplifiers
- Cutoff frequencies and bandwidth
- Biasing for linear amplification
- Distortion in amplifiers
- Use of ac and transfer function (TF) analyses in SPICE
- Behavior and characteristics of ideal differential and operational amplifiers (op amps)
- Techniques used to analyze circuits containing ideal op amps
- Techniques used to determine voltage gain, input resistance, and output resistance of general amplifier circuits
- Classic op amp circuits, including the inverting, noninverting, and summing amplifiers, the voltage follower, and the integrator



Lee deForest and the Audion.  
Courtesy of © Bettmann/Corbis.

converted into digital form. Analog circuit technology also lies at the heart of the interface between the analog and digital portions of these devices in the form of analog-to-digital (A/D) and digital-to-analog (D/A) converters. Every day the world is becoming connected through an increasing variety of communications links. Optical fiber systems, cable modems, digital subscriber lines, and wireless communications technologies rely on amplifiers to both generate and then detect extremely small signals containing the transmitted information.

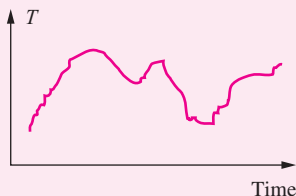


**Figure 10.1** Temperature vs. time — a continuous analog signal.

In Part II, we explored the analysis and design of circuits used to manipulate information in discrete form—that is, binary data. However, much information about the world around us, such as temperature, humidity, pressure, velocity, light intensity, sound, and so on, is “analog” in nature, may take on any value within some continuous range, and can be represented by the analog signal in Fig. 10.1. In electrical form, these signals may be the output of transducers that measure pressure, temperature, or flow rate, or the audio signal from a microphone or stereo amplifier. The characteristics of these signals are most often manipulated using linear amplifiers, which change the amplitude and/or phase of a signal.

Today we recognize it is frequently advantageous to do as much signal processing as possible in the digital domain.

Because of noise and dynamic range considerations, most A/D and D/A converters have full-scale ranges of 1–5 volts, whereas signals in sensor, transducer, communications, and many other applications are typically at much lower levels. For example, temperature sensor outputs may be less than 1 mV/ $^{\circ}$ C, and cell phones and satellite radios require sensitivities in the microvolt range. Thus, we require the use of amplifiers to increase the voltage, current, and/or power levels of these signals. At the same time, amplifiers are used to limit (filter) the frequency content of the signals.

Part III of this text explores the design of amplifiers that are required in all these applications. Most of these devices mentioned in the previous paragraphs employ “mixed signal” designs that require a knowledge of both analog and digital circuitry as well as the A/D and D/A conversion interfaces between the two.

This chapter begins our detailed study of the behavior of ideal operational amplifiers, or op amps, that today represent fundamental building blocks of analog circuit design. The name *operational amplifier* originates from its historic use to perform specific electronic functions in analog computers, and this chapter introduces the classic op amp circuits that realize the scaling, inverting, summation, integration, differentiation and filtering functions.

## 10.1 AN EXAMPLE OF AN ANALOG ELECTRONIC SYSTEM

We begin exploring some of the uses for analog amplifiers by examining a familiar electronic system, the FM stereo receiver, shown schematically in Fig. 10.2. This figure is representative of the FM receiver in our automobiles, as well as that in our home audio systems. At the receiving antenna are **very high frequency**, or **VHF**,<sup>1</sup> radio signals in the 88- to 108-MHz range that contain the information for at least two channels of stereo music.<sup>2</sup> In our FM receiver, these signals may have amplitudes as small as 1  $\mu$ V and often reach the receiver input through a 50- or 75- $\Omega$  coaxial cable. At the output of the receiver are audio amplifiers that develop the voltage and current necessary to deliver 100 W of power to the 8- $\Omega$  speakers in the 50- to 15,000-Hz audio frequency range.

This receiver is a complex analog system that provides many forms of analog signal processing, some linear and some nonlinear (see Table 10.1). For example, the amplitude of the signal must be increased at **radio** and **audio frequencies** (**RF** and **AF**, respectively). Large overall voltage, current, and power gains are required to go from the very small signal received from the antenna to the 100-W audio signal delivered to the speaker. The input of the receiver is often designed to match the 75- $\Omega$  impedance of the coaxial transmission line coming from the antenna.

In addition, we usually want only one station to be heard at a time. The desired signal must be selected from the multitude of signals appearing at the antenna, and the receiver requires circuits with high frequency selectivity at its input. An adjustable frequency signal source, called the *local*

<sup>1</sup> The radio spectrum is traditionally divided into different frequency bands: RF, or radio frequency (0.5–50 MHz); VHF, or very high frequency (50–150 MHz); UHF, or ultra high frequencies (150–1000 MHz); and so on. Today, however, RF is commonly used to refer to the whole radio spectrum from 0.5 MHz to 10 GHz and higher. (See Sec. 1.6.)

<sup>2</sup> A satellite radio receiver is very similar except the input frequencies range from 1–5 GHz.

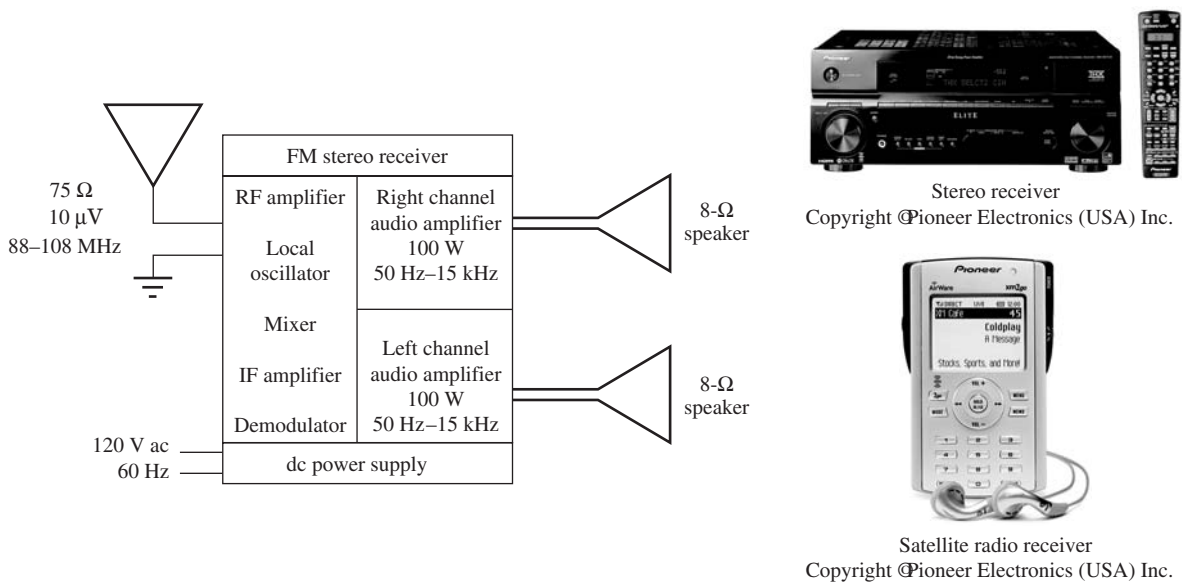


Figure 10.2 FM stereo receiver.

**TABLE 10.1**  
**FM Stereo Receiver**

LINEAR CIRCUIT FUNCTIONS	NONLINEAR CIRCUIT FUNCTIONS
Radio frequency amplification	dc power supply (rectification)
Audio frequency amplification	Frequency conversion (mixing)
Frequency selection (tuning)	Detection/demodulation
Impedance matching ( $75\text{-}\Omega$ input)	
Tailoring audio frequency response	
Local oscillator	

*oscillator*, is also needed to tune the receiver. The electronic implementations of all these functions are based on **linear amplifiers**.

In most receivers, the incoming signal frequency is changed, through a process called *mixing*, to a lower **intermediate frequency (IF)**,<sup>3</sup> where the audio information can be readily separated from the RF carrier through a process called *demodulation*. Mixing and demodulation are two basic examples of nonlinear analog signal processing. But even these nonlinear circuits are based on linear amplifier designs. Finally, the dc voltages needed to power the system are obtained using the nonlinear rectifier circuits described in Chapter 3.

## 10.2 AMPLIFICATION

Linear amplifiers are an extremely important class of circuits, and most of Part III discusses various aspects of their analysis and design. As an introduction to amplification, let us concentrate on one of the channels of the audio portion of the FM receiver in Fig. 10.3. In this figure, the input to the stereo amplifier channel is represented by the Thévenin equivalent source  $v_i$  and source resistor  $R_I$ . The speaker at the output is modeled by an  $8\text{-}\Omega$  resistor.

<sup>3</sup> Common IF frequencies are 11.7 MHz, 455 kHz, and 262 kHz.

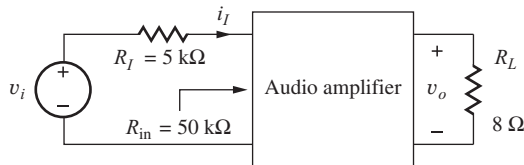


**Figure 10.3** Audio amplifier channel from FM receiver.

Based on Fourier analysis, we know that a complex periodic signal  $v_i$  can be represented as the sum of many individual sine waves:

$$v_i = \sum_{j=1}^{\infty} V_j \sin(\omega_j t + \phi_j) \quad (10.1)$$

where  $V_j$  = amplitude of  $j$ th component of signal,  $\omega_j$  is the radian frequency, and  $\phi_j$  is the phase.

If the amplifier is linear, the principle of superposition applies, so that each signal component can be treated individually and the results summed to find the complete signal. For simplicity in our analysis, we will consider only the  $i$ th component of the signal, with frequency  $\omega_i$  and amplitude  $V_i$ :

$$v_i = V_i \sin \omega_i t \quad (10.2)$$

For this example, we assume  $V_i = 0.001$  V, 1 mV; because this signal serves as our reference input, we can assume  $\phi_i = 0$  without loss of generality.

The output of the linear amplifier is a sinusoidal signal at the same frequency but with a different amplitude  $V_o$  and phase  $\theta$ :

$$v_o = V_o \sin(\omega_i t + \theta) \quad (10.3)$$

The amplifier output power is

$$P_o = \left( \frac{V_o}{\sqrt{2}} \right)^2 \frac{1}{R_L} \quad (10.4)$$

(Remember from circuit theory that the quantity  $V_o/\sqrt{2}$  in this equation represents the rms value of the sinusoidal voltage signal.) For an amplifier delivering 100 W to the 8-Ω load, the amplitude of the output voltage is

$$V_o = \sqrt{2 P_o R_L} = \sqrt{2 \times 100 \times 8} = 40 \text{ V}$$

This output power level also requires an output current

$$i_o = I_o \sin(\omega_i t + \theta) \quad (10.5)$$

with an amplitude

$$I_o = \frac{V_o}{R_L} = \frac{40 \text{ V}}{8 \Omega} = 5 \text{ A}$$

Note that because the load element is a resistor,  $i_o$  and  $v_o$  have the same phase.

### 10.2.1 VOLTAGE GAIN

For sinusoidal signals, the **voltage gain**  $A_v$  of an amplifier is defined in terms of the **phasor representations** of the input and output voltages. Using  $\sin \omega t = \text{Im}[e^{j\omega t}]$  as our reference, the phasor representation of  $v_i$  is  $\mathbf{v}_i = V_i \angle 0^\circ$  and that for  $v_o$  is  $\mathbf{v}_o = V_o \angle \theta$ . Similarly,  $\mathbf{i}_i = I_i \angle 0^\circ$  and

$i_o = I_o \angle \theta$ . The voltage gain is then expressed by the phasor ratio:

$$A_v = \frac{v_o}{v_i} = \frac{V_o \angle \theta}{V_i \angle 0} = \frac{V_o}{V_i} \angle \theta \quad \text{or} \quad |A_v| = \frac{V_o}{V_i} \quad \text{and} \quad \angle A_v = \theta \quad (10.6)$$

For the audio amplifier in Fig. 10.3, the magnitude of the required voltage gain is

$$|A_v| = \frac{V_o}{V_i} = \frac{40 \text{ V}}{10^{-3} \text{ V}} = 4 \times 10^4$$

We will find that the amplifier building blocks studied in the next several chapters have either  $\theta = 0^\circ$  or  $\theta = 180^\circ$  for frequencies in the “midband” range of the amplifier. (Midband will be defined later in Sec. 10.10.4.)

We will find in subsequent chapters that achieving this level of voltage gain usually requires several stages of amplification. Be sure to note that the magnitude of the gain is defined by the amplitudes of the signals and is a constant; it is *not* a function of time! For the rest of this section, we concentrate on the magnitudes of the gains, saving a more detailed consideration of amplifier phase for Sec. 10.10.

### 10.2.2 CURRENT GAIN

The audio amplifier in our example requires a substantial increase in current level as well. The input current is determined by the **source resistance**  $R_I$  and the **input resistance**  $R_{in}$  of the amplifier. When we write the input current as  $i_i = I_i \sin \omega_i t$ , the amplitude of the current is

$$I_i = \frac{V_i}{R_I + R_{in}} = \frac{10^{-3} \text{ V}}{5 \text{ k}\Omega + 50 \text{ k}\Omega} = 1.82 \times 10^{-8} \text{ A} \quad (10.7)$$

The phase  $\phi = 0$  because the circuit is purely resistive.

The **current gain** is defined as the ratio of the phasor representations of  $i_o$  and  $i_i$ :

$$A_i = \frac{i_o}{i_i} = \frac{I_o \angle \theta}{I_i \angle 0} = \frac{I_o}{I_i} \angle \theta \quad (10.8)$$

The magnitude of the overall current gain is equal to the ratio of the amplitudes of the output and input currents:

$$|A_i| = \frac{I_o}{I_i} = \frac{5 \text{ A}}{1.82 \times 10^{-8} \text{ A}} = 2.75 \times 10^8$$

This level of current gain also requires several stages of amplification.

### 10.2.3 POWER GAIN

The power delivered to the amplifier input is quite small, whereas the power delivered to the speaker is substantial. Thus, the amplifier also exhibits a very large power gain. **Power gain**  $A_P$  is defined as the ratio of the output power  $P_o$  delivered to the load, to the power  $P_i$  delivered from the source:

$$A_P = \frac{P_o}{P_i} = \frac{\frac{V_o}{\sqrt{2}} \frac{I_o}{\sqrt{2}}}{\frac{V_i}{\sqrt{2}} \frac{I_i}{\sqrt{2}}} = \frac{V_o}{V_i} \frac{I_o}{I_i} = |A_v| |A_i| \quad (10.9)$$

Note from Eq. (10.9) that either rms or peak values of voltage and current may be used to define power gain as long as the choice is applied consistently at the input and output of the amplifier. (This is also true for  $A_v$  and  $A_i$ .) For our ongoing example, we find the power gain to be a very large number:

$$A_P = \frac{40 \times 5}{10^{-3} \times 1.82 \times 10^{-8}} = 1.10 \times 10^{13}$$

**EXERCISE:** (a) Verify that  $|A_P| = |A_v| |A_i|$ . (b) An amplifier must deliver 20 W to a  $16\text{-}\Omega$  speaker. The sinusoidal input signal source can be represented as a 5-mV source in series with a  $10\text{-k}\Omega$  resistor. If the input resistance of the amplifier is  $20\text{ k}\Omega$ , what are the voltage, current, and power gains required of the overall amplifier?

**ANSWERS:** 5060,  $9.49 \times 10^6$ ,  $4.80 \times 10^{10}$

### 10.2.4 THE DECIBEL SCALE

The various gain expressions often involve some rather large numbers, and it is customary to express the values of voltage, current, and power gain in terms of the **decibel**, or **dB** (one-tenth of a Bel):

$$A_{P\text{dB}} = 10 \log A_P \quad A_{v\text{dB}} = 20 \log |A_v| \quad A_{i\text{dB}} = 20 \log |A_i| \quad (10.10)$$

The number of decibels is 10 times the base 10 logarithm of the arithmetic power ratio, and decibels are added and subtracted just like logarithms to represent multiplication and division. Because power is proportional to the square of both voltage and current, a factor of 20 appears in the expressions for  $A_{v\text{dB}}$  and  $A_{i\text{dB}}$ .

Table 10.2 has a number of useful examples. From this table, we can see that an increase in voltage or current gain by a factor of 10 corresponds to a change of 20 dB, whereas a factor of 10 increase in power gain corresponds to a change of 10 dB. A factor of 2 corresponds to a 6-dB change in voltage or current gain or a 3-dB change in power gain. In the chapters that follow, the various gains routinely are expressed interchangeably in terms of arithmetic values or dB, so it is important to become comfortable with the conversions in Eqs. (10.10) and Table 10.2.

**EXERCISE:** Express the voltage gain, current gain, and power gain in the exercise at the end of Sec. 10.2.3 in dB.

**ANSWERS:** 74.1 dB, 140 dB, 107 dB

**EXERCISE:** Express the voltage gain, current gain, and power gain of the amplifier in Fig. 10.3 in dB.

**ANSWERS:** 92.0 dB, 169 dB, 130 dB

**TABLE 10.2**  
Expressing Gain in Decibels

	$ GAIN $	$A_{v\text{dB}}$ or $A_{i\text{dB}}$	$A_{P\text{dB}}$
	1000	60 dB	30 dB
	500	54 dB	27 dB
	300	50 dB	25 dB
$A_{v\text{dB}} = 20 \log  A_v $	100	40 dB	20 dB
$A_{i\text{dB}} = 20 \log  A_i $	20	26 dB	13 dB
$A_{P\text{dB}} = 10 \log A_P$	10	20 dB	10 dB
	$\sqrt{10} = 3.16$	10 dB	5 dB
	2	6 dB	3 dB
	1	0 dB	0 dB
	0.5	-6 dB	-3 dB
	0.1	-20 dB	-10 dB

### EXAMPLE 10.1 IMPEDANCE LEVEL TRANSFORMATION

Let's explore another example of what an amplifier might do for us. Suppose we have a signal  $v_i = 0.1 \sin 2000\pi t$  volts from some transducer (e.g., a microphone in a computer or the output of a digital-to-analog converter) with a Thévenin equivalent source resistance  $R_I$  of  $2\text{ k}\Omega$ , and we'd like to listen to that signal with a  $32\text{-}\Omega$  ear bud, represented by the load  $R_L$ , as depicted by the circuit model in Fig. 10.4. Unfortunately, only a very small fraction of the transducer voltage will get to the load because of the large impedance mismatch between the  $2\text{-k}\Omega$  source resistance and the  $32\text{-}\Omega$  load resistance.

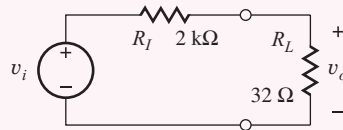


**Figure 10.4** Circuit model for transducer connected directly to a load.

Since we are dealing with a resistive network, the output voltage will also be a sine wave with the same phase as the input,  $v_o = V_o \sin 2000\pi t$  volts, and the amplitude of the output voltage is found using voltage division:

$$V_o = V_i \frac{R_L}{R_I + R_L} = 0.1V \left( \frac{32\Omega}{2032\Omega} \right) = 1.58 \text{ mV} \quad (10.11)$$

The signal is reduced by a factor of almost 100 and will probably be inaudible. We can use an amplifier to solve this problem as depicted in Fig. 10.5. Here we are using a *two-port model* for the amplifier consisting of an *input resistance*  $R_{\text{in}}$ , a *voltage gain*  $A$ , and an *output resistance*  $R_{\text{out}}$ .

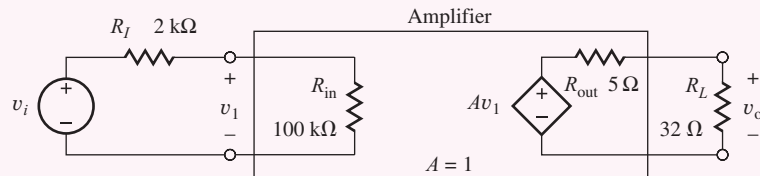


**Figure 10.5** Circuit model with amplifier inserted in the network.

Let us assume (arbitrarily for the moment) that  $R_{\text{in}} = 100\text{ k}\Omega$ ,  $A = 1$  (0 dB) and  $R_{\text{out}} = 5\Omega$ , and recalculate the output voltage using voltage division:

$$V_o = AV_1 \frac{R_L}{R_{\text{out}} + R_L} \quad \text{and} \quad V_1 = V_i \frac{R_{\text{in}}}{R_I + R_{\text{in}}} \quad (10.12)$$

Combining and evaluating these expressions yields

$$V_o = A_v \left( V_i \frac{R_{\text{in}}}{R_I + R_{\text{in}}} \right) \left( \frac{R_L}{R_{\text{out}} + R_L} \right) = 1(0.1V) \left( \frac{100\text{k}\Omega}{102\text{k}\Omega} \right) \left( \frac{32\Omega}{37\Omega} \right) = 84.8 \text{ mV} \quad (10.13)$$

and the actual output signal is  $v_o = 84.8 \sin 2000\pi t$  mV. Now we have succeeded in applying about 85 percent of the signal to the desired load, the earphone. The power delivered to the earphone is still fairly small:

$$P_o = \frac{V_o^2}{2R_L} = \frac{(84.8 \text{ mV})^2}{2(32\Omega)} = 0.112 \text{ mW} \quad (10.14)$$

If we would like to increase the power in the earphone, we can increase the voltage gain of the amplifier. Suppose we increase the internal gain of the amplifier by 26 dB and see what happens.

We must convert  $A$  from dB and then repeat the calculations:

$$\begin{aligned} A &= 10^{\frac{26}{20}} = 20.0 \\ V_o &= 20(0.1 \text{ V}) \left( \frac{100 \text{ k}\Omega}{102 \text{ k}\Omega} \right) \left( \frac{32 \Omega}{37 \Omega} \right) = 1.709 \text{ V} \\ P_o &= \frac{(1.709 \text{ V})^2}{2(32 \Omega)} = 45.2 \text{ mW} \end{aligned} \quad (10.15)$$

Now we have a substantial audio signal in our earphone (possibly near the specification limit of the earphone).

In Ex. 10.1, we have used an amplifier to provide an impedance level transformation as well as increasing the signal power applied to the ear bud. The amplifier “buffers” the signal source from the low impedance ( $32\text{-}\Omega$ ) load. These are only two of the many uses of amplifiers. One of the most common additional applications is to taylor the frequency response of the signal. In this case the amplifier circuitry becomes a *filter*.

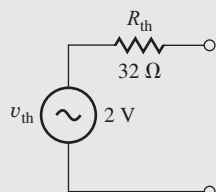
## ELECTRONICS IN ACTION

### *Player Characteristics*

The headphone amplifier in a personal music player represents an everyday example of a basic audio amplifier. The traditional audio band spans the frequencies from 20 Hz to 20 kHz, a range that extends beyond the hearing capability of most individuals at both the upper and lower ends.



Black Apple iPod  
on display  
©The McGraw-Hill  
Companies, Inc./Jill  
Braaten, photographer



Thévenin equivalent  
circuit for output stage

The characteristics of the Apple iPod in the accompanying figure are representative of a high quality audio output stage in an MP3 player or a computer sound card. The output can be represented by a Thévenin equivalent circuit with  $v_{th} = 2 \text{ V}$  and  $R_{th} = 32 \text{ ohms}$ , and the output stage is designed to deliver a power of approximately 15 mW into each channel of a headphone with a matched impedance of 32 ohms. The output power is approximately constant over the 20 Hz–20 kHz frequency range.

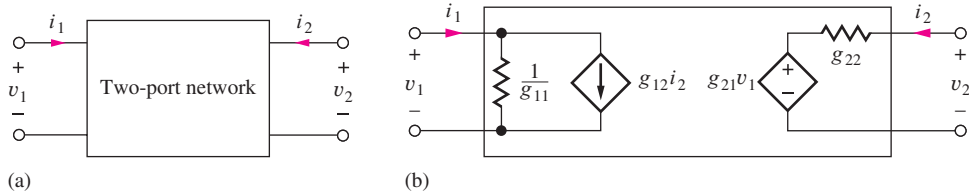


**Figure 10.6** (a) Two-port network representation. (b) Two port *g*-parameter representation.

## 10.3 TWO-PORT MODELS FOR AMPLIFIERS

The simple three-element model for the amplifier in Fig. 10.5, which we introduced in Ex. 10.1, is referred to as a *two-port network* or just a *two-port* in electrical circuits texts and is very useful for modeling the behavior of amplifiers in complex systems. We can use the two-port to provide a relatively simple representation of a much more complicated circuit. Thus, the two-port helps us hide or encapsulate the complexity of the circuit so we can more easily manage the overall analysis and design. One important limitation must be remembered, however. The two-ports we use are linear network models, and are valid under small-signal conditions that will be fully discussed in Chapter 13.

From network theory, we know that two-port networks can be represented in terms of **two-port parameters**: the *g*-, *h*-, *y*-, *z*-, *s*- and *abcd*-parameters. Note in these two-port representations that \$(v\_1, i\_1)\$ and \$(v\_2, i\_2)\$ represent the signal components of the voltages and currents at the two ports of the network. We will focus on the *g*-parameter description. The other parameter sets are discussed on the website for this text.



### 10.3.1 THE *g*-PARAMETERS

The ***g*-parameter** description is one of the most commonly used two-port representations for a voltage amplifier:

$$\begin{aligned} \mathbf{i}_1 &= g_{11}\mathbf{v}_1 + g_{12}\mathbf{i}_2 \\ \mathbf{v}_2 &= g_{21}\mathbf{v}_1 + g_{22}\mathbf{i}_2 \end{aligned} \quad (10.16)$$

Figure 10.6(b) is a network representation of these equations.

The *g*-parameters are determined from a given network using a combination of **open-circuit** (\$i = 0\$) and **short-circuit** (\$v = 0\$) **termination** conditions by applying these parameter definitions:

$$\begin{aligned} g_{11} &= \left. \frac{\mathbf{i}_1}{\mathbf{v}_1} \right|_{\mathbf{i}_2=0} = \text{open-circuit input conductance} \\ g_{12} &= \left. \frac{\mathbf{i}_1}{\mathbf{i}_2} \right|_{\mathbf{v}_1=0} = \text{reverse short-circuit current gain} \\ g_{21} &= \left. \frac{\mathbf{v}_2}{\mathbf{v}_1} \right|_{\mathbf{i}_2=0} = \text{forward open-circuit voltage gain} \\ g_{22} &= \left. \frac{\mathbf{v}_2}{\mathbf{i}_2} \right|_{\mathbf{v}_1=0} = \text{short-circuit output resistance} \end{aligned} \quad (10.17)$$

Unfortunately, the classic *g*-parameter notation doesn't provide much support for our intuition, so the more descriptive representation that was used in Ex. 10.1 is described by Eq. (10.18) and Fig. 10.7.

$$\begin{aligned} v_1 &= i_1 R_{in} \\ v_2 &= A v_1 + i_2 R_{out} \end{aligned} \quad (10.18)$$

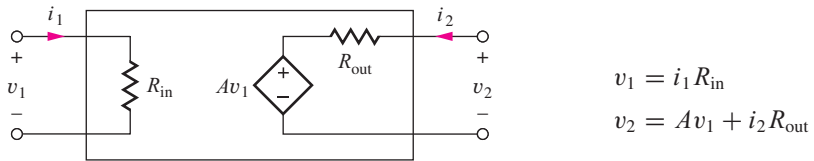


Figure 10.7 Simplified two-port with more intuitive notation, and “ $g_{12}$ ” = 0.

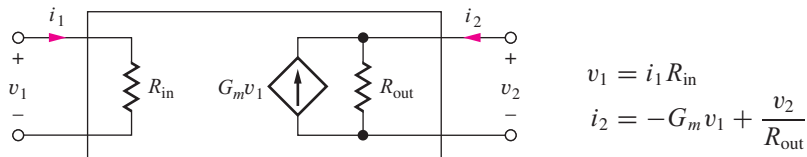


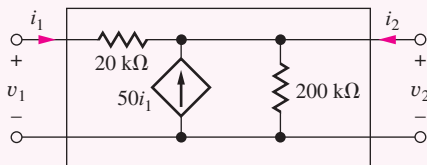
Figure 10.8 Norton transformation of the circuit in Fig. 10.7 in which  $G_m = \frac{A}{R_{\text{out}}}$ .

$R_{\text{in}}$  represents the input resistance to the amplifier,  $A$  is the voltage gain when there is no external load on the amplifier, and  $R_{\text{out}}$  is the output resistance of the amplifier. In a normal amplifier design, we desire the forward gain ( $g_{21}$ ) to be much larger than the reverse gain ( $g_{12}$ ), that is,  $g_{21} \gg g_{12}$ , and Eq. (10.18) and Fig. 10.7 show the simplified two-port representation in which the reverse gain  $g_{12}$  is assumed to be zero. Figure 10.8 presents an alternate two-port representation that we shall encounter frequently in our transistor circuits. In this equivalent circuit, the output port components have been found using Norton's theorem that yields  $G_m = A v_1 / R_{\text{out}}$ .

### EXAMPLE 10.2 FINDING A SET OF $g$ -PARAMETERS

This example calculates a set of  $g$ -parameters for a network containing a dependent current source. We encounter this type of circuit often in analog circuit analysis and design because our models for both bipolar and field-effect transistors contain dependent current sources.

**PROBLEM** Find the  $g$ -parameters for the circuit shown here. Include  $g_{12}$  for completeness, and compare it to  $g_{21}$ .



**SOLUTION** **Known Information and Given Data:** Circuit as given in the problem statement including element values;  $g$ -parameter definitions in Eq. (10.17)

**Unknowns:** Values of the four  $g$ -parameters

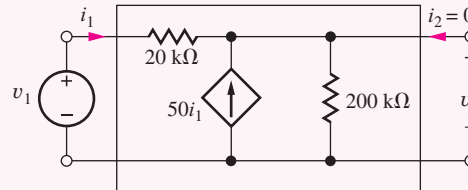
**Approach:** Apply the boundary conditions specified for each  $g$ -parameter and use circuit analysis to find the values of the four parameters. Note that each set of boundary conditions applies to two parameters.

**Assumptions:** None

**Analysis —  $g_{11}$  and  $g_{21}$ :** Looking at the definitions of the  $g$ -parameters,

$$G_{\text{in}} = g_{11} = \left. \frac{\mathbf{i}_1}{\mathbf{v}_1} \right|_{\mathbf{i}_2=0} \quad \text{and} \quad A = g_{21} = \left. \frac{\mathbf{v}_2}{\mathbf{v}_1} \right|_{\mathbf{i}_2=0}$$

we see that  $g_{11}$  and  $g_{21}$  use the same boundary conditions. We apply voltage  $\mathbf{v}_1$  to the input port, and the output port is open circuited (i.e.,  $\mathbf{i}_2$  is set to zero), as in the figure here.



**$g_{11}$ :** Writing an equation around the input loop and applying KCL at the output node yields

$$\mathbf{v}_1 = (2 \times 10^4) \mathbf{i}_1 + (\mathbf{i}_1 + 50\mathbf{i}_1)(200 \text{ k}\Omega)$$

$$G_{\text{in}} = \frac{\mathbf{i}_1}{\mathbf{v}_1} = \frac{1}{2 \times 10^4 \Omega + 51(200 \text{ k}\Omega)} = \frac{1}{10.2 \text{ M}\Omega} = 9.79 \times 10^{-8} \text{ S}$$

**$g_{21}$ :** Since the external port current  $\mathbf{i}_2$  is zero, the voltage  $\mathbf{v}_2$  is given by

$$\mathbf{v}_2 = (\mathbf{i}_1 + 50\mathbf{i}_1)(200 \text{ k}\Omega) = \mathbf{i}_1(51)(200 \text{ k}\Omega)$$

and  $\mathbf{i}_1$  can be related to  $\mathbf{v}_1$  using  $g_{11}$ :

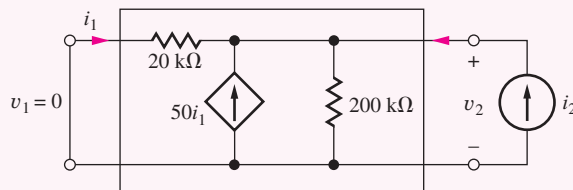
$$\mathbf{v}_2 = (g_{11}\mathbf{v}_1)(51)(200 \text{ k}\Omega)$$

$$A = \frac{\mathbf{v}_2}{\mathbf{v}_1} = g_{11}(51)(200 \text{ k}\Omega) = (9.79 \times 10^{-8} \text{ S})(51)(200 \text{ k}\Omega) = +0.998$$

**Analysis —  $g_{12}$  and  $g_{22}$ :** Looking again at the definitions of the  $g$ -parameters, we see that  $g_{12}$  and  $g_{22}$  use the same boundary condition.

$$g_{12} = \left. \frac{\mathbf{i}_1}{\mathbf{i}_2} \right|_{\mathbf{v}_1=0} \quad \text{and} \quad R_{\text{out}} = g_{22} = \left. \frac{\mathbf{v}_2}{\mathbf{i}_2} \right|_{\mathbf{v}_1=0}$$

A current source  $\mathbf{i}_2$  is applied to the output port, and the input port is short-circuited (i.e.,  $\mathbf{v}_1$  is set to zero) as shown in this figure:



**$g_{22}$ :** With  $\mathbf{v}_1 = 0$ , we see that the network is just a single-node circuit. Writing a nodal equation for  $\mathbf{v}_2$  yields

$$(\mathbf{i}_2 + 50\mathbf{i}_1) = \frac{\mathbf{v}_2}{200 \text{ k}\Omega} + \frac{\mathbf{v}_2}{20 \text{ k}\Omega}$$

But,  $\mathbf{i}_1$  can be written directly in terms of  $\mathbf{v}_2$  as  $i_1 = -v_2/20 \text{ k}\Omega$ . Combining these two equations yields the short-circuit output resistance  $g_{22}$ :

$$\mathbf{i}_2 = \frac{\mathbf{v}_2}{200 \text{ k}\Omega} + \frac{\mathbf{v}_2}{20 \text{ k}\Omega} + 50 \frac{\mathbf{v}_2}{20 \text{ k}\Omega} \quad \text{and} \quad R_{\text{out}} = \frac{\mathbf{v}_2}{\mathbf{i}_2} = \frac{1}{\frac{1}{200 \text{ k}\Omega} + \frac{51}{20 \text{ k}\Omega}} = 391 \Omega$$

$g_{12}$ : The reverse short-circuit current gain  $g_{12}$  can be found using the preceding results:

$$\mathbf{i}_1 = -\frac{\mathbf{v}_2}{20 \text{ k}\Omega} = -\frac{R_{\text{out}} \mathbf{i}_2}{20 \text{ k}\Omega} \quad \text{and} \quad g_{12} = \frac{\mathbf{i}_1}{\mathbf{i}_2} = -\frac{391 \Omega}{20 \text{ k}\Omega} = -0.0196$$

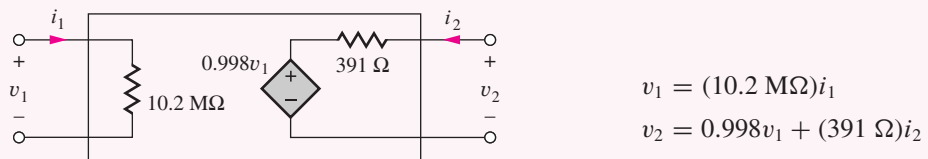
The final  $g$ -parameter equations for the network are

$$\mathbf{i}_1 = 9.79 \times 10^{-8} \mathbf{v}_1 - 1.96 \times 10^{-2} \mathbf{i}_2$$

$$\mathbf{v}_2 = 0.998 \mathbf{v}_1 + 3.91 \times 10^2 \mathbf{i}_2$$

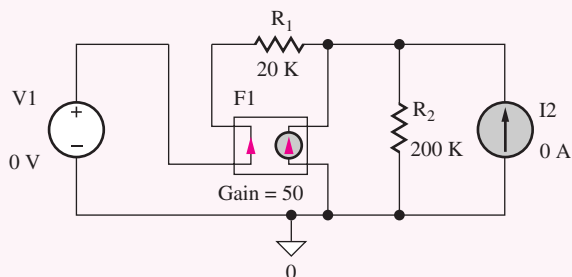
**Check of Results:** The results are confirmed below using SPICE.

**Discussion:** Note that the values of  $R_{\text{in}} = 10.2 \text{ M}\Omega$  and  $R_{\text{out}} = 391 \Omega$  differ greatly from any of the resistor values in the network. This is a result of the action of the dependent current source and is an important effect that we will see throughout the analysis of analog transistor circuits. Here we see that  $g_{12}$  is indeed small and that  $g_{12} \ll g_{21}$ . The simplified mathematical and two-port models for the circuit become



We will make use of this observation when we study feedback.

**Computer-Aided Analysis:** Numerical values for two-port parameters can easily be found using the transfer function (TF) analysis capability of SPICE. In order to find the  $g$ -parameters for the circuit in this example, we drive the network with voltage source  $V1$  at the input and current source  $I2$  at the output, as in the figure here. These choices correspond to the boundary conditions in the definitions of the  $g$ -parameters.



Both independent sources are assigned zero values. The TF analysis calculates how variables change in response to changes in an independent source. Therefore, a starting point of zero is fine. The zero value sources directly satisfy the boundary conditions required to calculate the  $g$ -parameters.

Two TF analyses are used—one to find  $g_{11}$  and  $g_{21}$  and a second to find  $g_{12}$  and  $g_{22}$ . The first analysis requests calculation of the transfer function from source V1 to the voltage at the output node, and SPICE will calculate three quantities: the value of the transfer function, resistance at the input source node, and resistance at the output node. The SPICE results are transfer function = 0.998, input resistance =  $10.2\text{ M}\Omega$ , and output resistance =  $391\text{ }\Omega$ . Parameter  $g_{21}$  is the open-circuit voltage gain, which agrees with the hand calculations, and  $g_{11}$  is the input conductance equal to the reciprocal of  $10.2\text{ M}\Omega$ , again in agreement with our hand calculations.

The second analysis requests the transfer function from source I2 to (the current in) source V1. The results from SPICE are transfer function = 0.0196 and input resistance =  $391\text{ }\Omega$ . In this case, the output resistance (at V1) cannot be calculated because V1 represents a short at the input. Note that parameter  $g_{12}$  is the negative of the TF value. The sign difference arises from the passive sign convention assumed by SPICE in which positive current is directed downward through source V1. Parameter  $g_{22}$  is the  $391\text{-}\Omega$  resistance presented to source I2, which is the “input resistance” in this calculation. We find precise agreement with our hand calculations. It is important to remember that the SPICE TF analysis is a form of dc analysis and should not be used in networks containing capacitors and inductors.

**EXERCISE:** Find the  $g$ -parameters for the circuit in Ex. 10.2 if the  $200\text{-k}\Omega$  resistor is replaced with a  $50\text{-k}\Omega$  resistor, and the dependent source is changed to  $75i_1$ .

**ANSWERS:**  $2.62 \times 10^{-7}\text{ S}$ ; 0.995,  $-0.0131$ ;  $3.82\text{ mS}(1/262\Omega)$

**EXERCISE:** Confirm your calculations in the previous exercise using SPICE.

## DESIGN NOTE

Remember, the transfer function analysis in SPICE is a dc analysis and should not be used in circuits containing capacitors and inductors!

## 10.4 MISMATCHED SOURCE AND LOAD RESISTANCES

In introductory circuit theory, the maximum power transfer theorem is usually discussed. Maximum power transfer occurs when the source and load resistances are matched (equal in value). In most amplifier applications, however, the opposite situation is desired. A completely mismatched condition is used at both the input and output ports of the amplifier.

To understand the statement above, let's further consider the voltage amplifier in Fig. 10.9, which has the same structure as the one in Ex. 10.1. The input to the two-port is a Thévenin equivalent representation of the input source, and the output is connected to a load represented by resistor  $R_L$ .

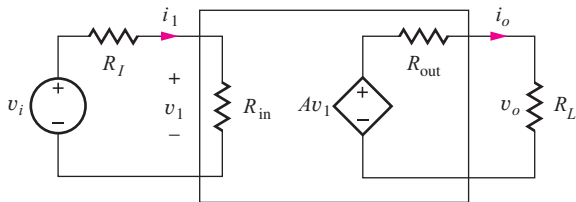


**Figure 10.9** Two-port representation of an amplifier with source and load connected.

To find the voltage gain, voltage division is applied to each loop:

$$\mathbf{v}_o = A\mathbf{v}_1 \frac{R_L}{R_{out} + R_L} \quad \text{and} \quad \mathbf{v}_1 = \mathbf{v}_i \frac{R_{in}}{R_I + R_{in}} \quad (10.19)$$

Combining these two equations yields an expression for the magnitude of the voltage gain  $A_v$ :

$$|A_v| = \frac{V_o}{V_i} = A \frac{R_{in}}{R_I + R_{in}} \frac{R_L}{R_{out} + R_L} \quad (10.20)$$

To achieve maximum voltage gain, the resistors should satisfy  $R_{in} \gg R_I$  and  $R_{out} \ll R_L$ . For this case,

$$|A_v| \cong A \quad (10.21)$$

The situation described by these two equations is a totally mismatched condition at both the input and the output ports. An **ideal voltage amplifier** satisfies the conditions in Eq. (10.20) with  $R_{in} = \infty$  and  $R_{out} = 0$ .

The magnitude of the current gain of the amplifier in Fig. 10.9 can be expressed as

$$|A_i| = \frac{I_o}{I_1} = \frac{\frac{V_o}{R_L}}{\frac{V_i}{R_I + R_{in}}} = \frac{V_o}{V_i} \frac{R_I + R_{in}}{R_L} \quad \text{or} \quad |A_i| = |A_v| \frac{R_I + R_{in}}{R_L} \quad (10.22)$$

**EXERCISE:** Write an expression for the power gain of the amplifier in Fig. 10.9 in terms of the voltage gain.

**ANSWER:**  $A_P = A_v^2 \frac{R_I + R_{in}}{R_L}$

**EXERCISE:** Suppose the audio amplifier in Fig. 10.3 can be modeled by  $R_{in} = 50 \text{ k}\Omega$  and  $R_{out} = 0.5 \Omega$ . What value of open-circuit gain  $A$  is required to achieve an output power of 100 W if  $v_i = 0.001 \sin 2000\pi t$ ? How much power is being dissipated in  $R_{out}$ ? What is the current gain?

**ANSWERS:** 46,800 (93.4 dB); 6.25 W;  $2.75 \times 10^8$  (169 dB)

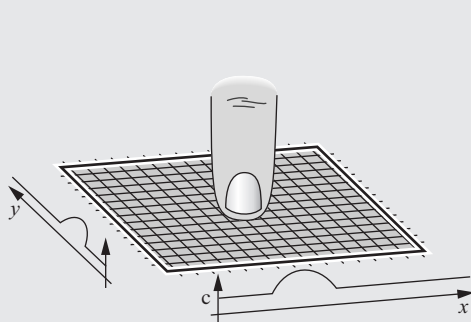
**EXERCISE:** Repeat the preceding exercise if the input and output ports are matched to the source and load respectively (that is,  $R_{in} = 5 \text{ k}\Omega$  and  $R_{out} = 8 \Omega$ ). (It should become clear why we don't design  $R_{out}$  to match the load resistance.)

**ANSWERS:** 160,000 (104 dB); 100 W;  $5 \times 10^7$  (153 dB)



## Laptop Computer Touchpad

An essential element of a graphical user interface is a pointing device. This was clear to Douglas Engelbart in the late 1960s during his experimentation with graphical computer interfaces. In order to provide the feeling that a user was directly manipulating objects on the screen, Engelbart invented the computer mouse in 1968. It did not move into the computing mainstream until the introduction of the Apple Macintosh in 1984. As integrated circuit technology advanced and made possible the creation of laptop computers, it became necessary to develop a pointing device that was contained within the form factor of the laptop computer but maintained the ‘connective’ feel between the user and the computer interface. Trackballs were used in early machines, but they didn’t allow the intuitive  $x$ - $y$  hand displacement feedback of the mouse. Trackballs were also prone to accumulation of dirt and other debris which reduced their robustness.



Touch screens were available in the early 1980s, but they required non-robust resistive membranes and/or expensive fabrication techniques. In the early 1990s, Synaptics Corporation developed the capacitive sensing touchpad. A simplified drawing of a capacitive touchpad is shown above. A thin insulating surface covers an  $x$ - $y$  grid of wires. When a finger is placed on or near the surface, the capacitance of the wires directly underneath is changed. By measuring the capacitance between the wires and ground, it is possible to detect the presence of an object. If the capacitance measurement is performed with each of the wires in sequence, a capacitance versus position profile is developed. Calculating the centroid of the broad profile allows the system to form a precise indication of finger position over the touchpad.

The measurement itself can be done in a number of ways. The capacitance could be part of a tuned circuit to control the frequency of an oscillator. One could drive the capacitance with a sinusoid current and measure the peak-to-peak value of the resulting voltage. Or, as is the case with most touchpads, a step voltage is driven onto the wire and the resulting charging current is integrated. The magnitude of the integral is proportional to capacitance. Once again, integrated circuit technology made the device practical and inexpensive. A significant number of wires is required to achieve adequate resolution. If implemented with discrete components, the switches, signal routing, and signal processing would be large and expensive. A single mixed-signal CMOS integrated circuit, integrating precision analog circuits and digital processing, was designed to provide all of the necessary functionality, as well as to provide a digital interface that is easily incorporated into a computer. Bridging the gap between real world analog information and digital computers is an important and recurring theme in analog microelectronics.

## 10.5 INTRODUCTION TO OPERATIONAL AMPLIFIERS

Now that we've explored some of the utility of amplifiers, we will study the characteristics and applications of an extremely important building block called the operational amplifier. In later chapters, we will investigate transistor circuits that are utilized to implement more complex circuits such as the operational amplifier.

The **operational amplifier**, or **op amp**, is a fundamental building block of analog circuit design. The name "operational amplifier" originates from the use of this type of amplifier to perform specific electronic circuit functions or operations, such as scaling, summation, and integration, in analog computers.

Integrated circuit operational amplifiers evolved rapidly following development of the first bipolar integrated circuit processes in the 1960s. Although early IC amplifier designs offered little if any performance improvements over tube-type designs and discrete semiconductor realizations and were somewhat "delicate," they offered significant advantages in physical size, cost, and power consumption. The  $\mu$ A709, introduced by Fairchild Semiconductor in 1965, was one of the first widely used general-purpose IC operational amplifiers. IC op amp circuits improved quickly, and the now-classic Fairchild  $\mu$ A741 amplifier design, which appeared in the late 1960s, is a robust amplifier with excellent characteristics for general-purpose applications. The internal circuit design of these op amps used 20 to 50 bipolar transistors. Later designs improved performance in most specification areas. Today there is an almost overwhelming array of operational amplifiers from which to choose (see Figure 10.10).

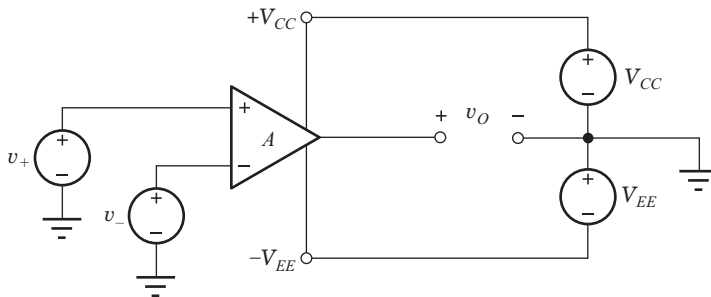
The rest of this chapter explores the characteristics of operational amplifiers and op amp circuits. A number of basic circuit applications are discussed, including inverting and noninverting amplifiers, the summing amplifier, the integrator, and basic filters. Limitations caused by the nonideal behavior of the operational amplifier are discussed in Chapter 11, including finite gain, bandwidth, input and output resistances, common-mode rejection, offset voltage, bias current, and stability. Chapter 12 presents a variety of op amp applications.

### 10.5.1 THE DIFFERENTIAL AMPLIFIER

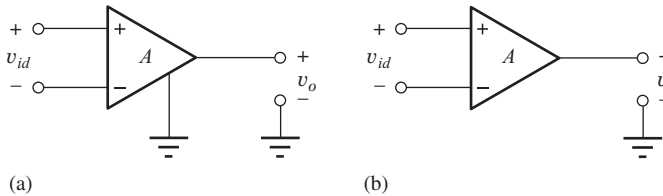
The operational amplifier is a form of **differential amplifier** that responds to the difference of two input signals (and hence is sometimes referred to as a difference amplifier) and represents an extremely useful class of circuits. For example, they are used as error amplifiers in almost all



Figure 10.10 Discrete operational amplifiers.



**Figure 10.11** The differential amplifier, including power supplies.



**Figure 10.12** (a) Amplifier without power supplies explicitly included.  
(b) Differential amplifier with implied ground connection.

electronic feedback and control systems, and operational amplifiers themselves are in fact very high performance versions of the differential amplifier. Thus, we begin our study of op amps by exploring the characteristics of the basic differential amplifier shown in schematic form in Fig. 10.11.

The amplifier has two inputs, to which the input signals  $v_+$  and  $v_-$  are connected, and a single output  $v_O$ , all referenced to the common (ground) terminal between the two power supplies  $V_{CC}$  and  $V_{EE}$ . In most applications,  $V_{CC} \geq 0$  and  $-V_{EE} \leq 0$ , and the voltages are often symmetric—that is,  $\pm 5\text{ V}, \pm 12\text{ V}, \pm 15\text{ V}, \pm 18\text{ V}, \pm 22\text{ V}$ , and so on. These power supply voltages limit the output voltage range:  $-V_{EE} \leq v_O \leq V_{CC}$ . For simplicity, the amplifier is most often drawn without explicitly showing the power supplies, as in Fig. 10.12(a), or the ground connection, as in Fig. 10.12(b)—but we must remember that the power and ground terminals are always present in the implementation of a real circuit.

### 10.5.2 DIFFERENTIAL AMPLIFIER VOLTAGE TRANSFER CHARACTERISTIC

The **voltage transfer characteristic** or **VTC** for a differential amplifier biased by power supplies  $V_{CC}$  and  $-V_{EE}$  is shown in Fig. 10.13. The VTC graphs the total output voltage  $v_O$  versus the total differential input voltage  $v_{ID}$ . In this particular case,  $V_{CC}$  and  $-V_{EE}$  are symmetrical 10-V supplies, and thus the output voltage is restricted to  $-10\text{ V} \leq v_O \leq +10\text{ V}$ .

Because of the power supply limits, we see that the input–output relationship is linear over only a limited region of the characteristic. Using our standard notation introduced in Chapter 1, the total input voltage  $v_{ID}$  is represented as the sum of two components:

$$v_{ID} = V_{ID} + v_{id} \quad (10.23)$$

in which  $V_{ID}$  represents the dc value of  $v_{ID}$ , and  $v_{id}$  is the signal component of the input voltage. Similarly, the total output voltage is represented by

$$v_O = V_O + v_o \quad (10.24)$$

in which  $V_O$  represents the dc value of the output voltage, and  $v_o$  is the signal component of the output voltage. For the amplifier to provide linear amplification of the signal  $v_{id}$ , the total input signal must be biased by the dc voltage  $V_{ID}$  into the central high-slope region of the characteristic.

### 10.5.3 VOLTAGE GAIN

The voltage gain  $A$  of an amplifier describes the relation between changes in the input signal and changes in the output signal and is defined by the *slope* of the amplifier's VTC, evaluated for an

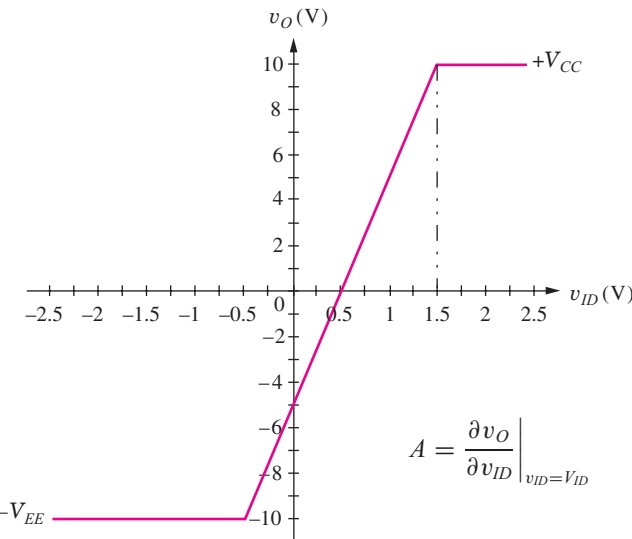


**Figure 10.13** Voltage transfer characteristic (VTC) for a differential amplifier with  $V_{CC} = 10$  V,  $-V_{EE} = -10$  V and gain  $A = +10$  (20 dB).

input voltage equal to the dc bias voltage  $V_{ID}$ :

$$A = \left. \frac{\partial v_O}{\partial v_{ID}} \right|_{v_{ID}=V_{ID}} \quad (10.25)$$

For the VTC in Fig. 10.13,

$$A = \frac{10 - 0}{1.5 - 1} \left( \frac{V}{V} \right) = +10 \quad \text{or} \quad A_{dB} = 20 \log(10) = 20 \text{ dB} \quad (10.26)$$

Note that the gain is **not** equal to the ratio of the total output voltage to the total input voltage! For example, for  $v_{ID} = +1$  V,

$$\frac{v_O}{v_{ID}} = \frac{5}{1} = +5 \neq A \quad (10.27)$$

The slope of the VTC in Fig. 10.13 is everywhere  $\geq 0$ , so the amplifier input and output are in phase; this amplifier is a **noninverting amplifier**. If the slope had been negative, then the input and output signals would be  $180^\circ$  out of phase, and the amplifier would be characterized as an **inverting amplifier**.

### Signal Amplification

A graphical representation of the VTC with a sinusoidal input signal and sinusoidal output signal appears in Fig. 10.14 in which  $v_{ID1}$  and  $v_{O1}$  are given by

$$v_{ID1} = 1 + 0.25 \sin 2000\pi t \text{ volts} \quad \text{and} \quad v_{O1} = 5 + 2.5 \sin 2000\pi t \text{ volts} \quad (10.28)$$

Notice also that there is a limited range of input voltage for which the amplifier will behave in a linear manner. For an input bias of 1 V as in Eq. (10.28) and Fig. 10.14, the maximum input voltage signal amplitude must be less than 0.5 V, which corresponds to a maximum output signal amplitude of 5 V.

If the ac input signal exceeds 0.5 V, then the top part of the output signal will be clipped off. Figure 10.15 presents the results of SPICE simulation of the amplifier VTC in Fig. 10.14 with the input signal in Eq. (10.28) and  $v_{ID2} = 1 + 1.5 \sin 2000\pi t$  volts. As  $v_{ID2}$  exceeds 1.5 V, the output

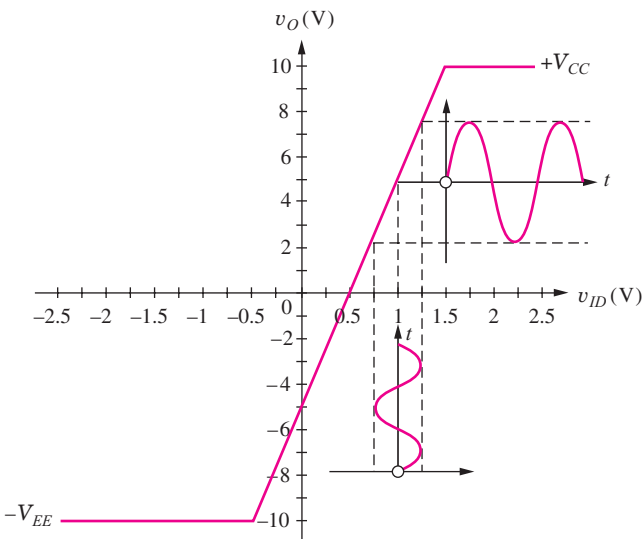


**Figure 10.14** Graphical interpretation voltage transfer characteristic (VTC) with a sinusoidal input signal applied.

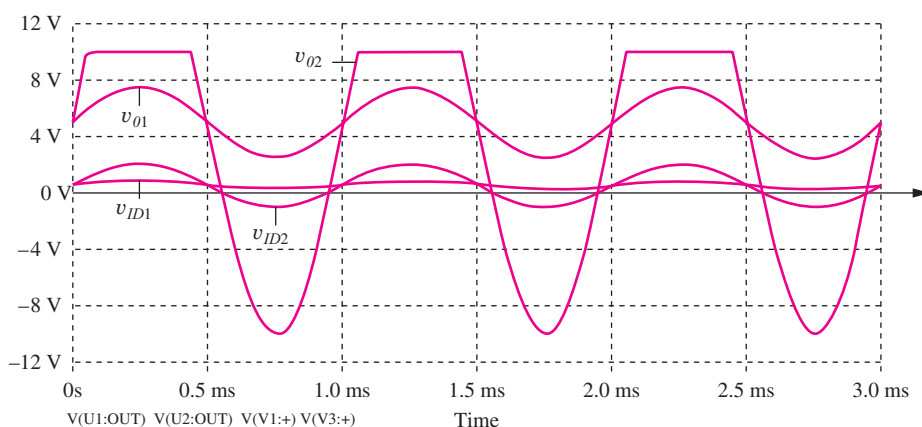


**Figure 10.15** SPICE simulation results for the amplifier VTC in Fig. 10.14 for two input signals:  $v_{ID1} = 1 + 0.25 \sin 2000\pi t$  volts and  $v_{ID2} = 1 + 1.5 \sin 2000\pi t$  volts. The amplifier is operating in a linear manner for input one, but is driven into nonlinear operation by input signal two.

stays constant at +10 V. Any further increase in input voltage results in no change in the output voltage! The voltage gain in this region is zero because the slope of the VTC is 0.

**EXERCISE:** (a) What input bias point should be chosen for the amplifier in Fig. 10.13 to provide the maximum possible linear input signal magnitude? What are the maximum input and output signal amplitudes? (b) What is the voltage gain if the amplifier input is biased at  $V_D = -1.0$  V?

**ANSWERS:** 0.5 V,  $|v_i| \leq 1.0$  V; 10 V; 0

**EXERCISE:** Write an expression for  $v_O(t)$  for the amplifier in Fig. 10.13 if  $v_{ID}(t) = (0.25 + 0.75 \sin 1000\pi t)$  V. What dc bias appears as part of the output voltage?

**ANSWER:**  $(-2.5 + \sin 1000\pi t)$  V; -2.5 V

## 10.6 DISTORTION IN AMPLIFIERS

As mentioned in Sec. 10.5, if the input signal is too large, then the output waveform will be significantly distorted since the gain for positive values of the input signal will be different from the gain for negative values. In Fig. 10.15, the top of the largest waveform appears “flattened,” and there is a slope discontinuity in the waveform.

A measure of the distortion in such a signal is given by its **total harmonic distortion** (THD), which compares the undesired harmonic content of a signal to the desired component. If we expand the Fourier series representation for a signal  $v(t)$ , we have

$$v(t) = V_0 + V_1 \sin(\omega_o t + \phi_1) + V_2 \sin(2\omega_o t + \phi_2) + V_3 \sin(3\omega_o t + \phi_3) + \dots$$

dc	desired	2nd harmonic	3rd harmonic	
	output	distortion	distortion	(10.29)

The signal at frequency  $\omega_o$  is the desired output that has the same frequency as the input signal. The terms at  $2\omega_o$ ,  $3\omega_o$ , etc. represent second-, third-, and higher-order harmonic distortion. The percent THD is defined by

$$\text{THD\%} = 100\% \times \frac{\sqrt{\sum_{n=2}^{\infty} V_n^2}}{V_1} \quad (10.30)$$

The numerator of this expression combines the amplitudes of the individual distortion terms in rms form, whereas the denominator contains only the desired component. Normally, only the first few terms are important in the numerator. For example, SPICE Fourier analysis yields this representation for the distorted signal in Fig. 10.15,

$$v(t) = 2.46 + 10.6 \sin(2000\pi t) + 2.67 \sin(4000\pi t + 90^\circ) \\ + 0.886 \sin(6000\pi t) + 0.177 \sin(8000\pi t + 90^\circ) + 0.372 \sin(10000\pi t)$$

for which the total distortion is approximately

$$\text{THD} \cong 100\% \times \frac{\sqrt{2.67^2 + 0.886^2 + 0.177^2 + 0.372^2}}{3} = 26.8\%$$

This value of THD represents a large amount of distortion, which is clearly visible in Fig. 10.15. Good distortion levels are well below 1 percent and are not readily apparent to the eye.

**EXERCISE:** Use MATLAB or Mathcad to plot both the distorted output signal in Fig. 10.15 and its reconstruction described by  $v(t)$ .

```
ANSWER: wt = 2000*pi*linspace(0,.002,1024);
v = min(10,(5+15*sin(wt));
f = 2.46+10.6*sin(wt)+2.67*cos(2*wt)+0.866*sin(3*wt)+0.177*cos(4*wt)
+0.372*sin(5*wt);
plot(wt,v,wt,f)
```

(Note the close match between the two curves with only a few components of the series.)

**EXERCISE:** Use MATLAB to find the Fourier representation for  $v(t)$ .

**ANSWER:**

```
wt = 2000*pi*linspace(0,.001,512);
v = min(10,(5+15*sin(wt));
s = fft(v)/512;
mag=sqrt(s.*conj(s))
mag(1:10)
```

(Note that the `fft` function in MATLAB generates the coefficients for the complex Fourier series.)

## 10.7 DIFFERENTIAL AMPLIFIER MODEL

For purposes of signal analysis, the differential amplifier can be represented by its input resistance  $R_{id}$ , output resistance  $R_o$ , and controlled voltage source  $A v_{id}$ , as in Fig. 10.16. This is the two-port representation introduced to Sec. 10.3.

$A$  = voltage gain (open-circuit voltage gain)

$v_{id} = (v_+ - v_-)$  = differential input signal voltage

$R_{id}$  = amplifier input resistance

$R_o$  = amplifier output resistance

(10.31)

The signal voltage developed at the output of the amplifier is in phase with the voltage applied to the + input terminal and  $180^\circ$  out of phase with the signal applied to the – input terminal. The  $v_+$  and  $v_-$  terminals are therefore referred to as the **noninverting input** and **inverting input**, respectively.

In a typical application, the amplifier is driven by a signal source having a Thévenin equivalent voltage  $v_i$  and resistance  $R_I$  and is connected to a load represented by the resistor  $R_L$ , as in Fig. 10.17. For this simple circuit, the input voltage  $v_{id}$  and the output voltage can be written in terms of the circuit elements as

$$v_{id} = v_i \frac{R_{id}}{R_{id} + R_I} \quad \text{and} \quad v_o = A v_{id} \frac{R_L}{R_o + R_L} \quad (10.32)$$

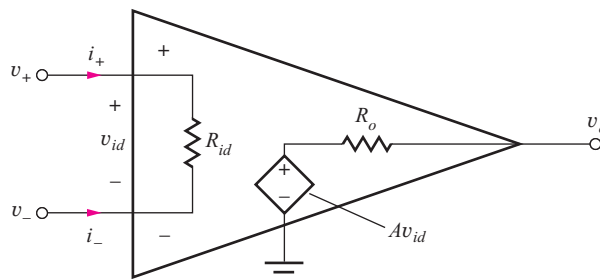


Figure 10.16 Differential amplifier.

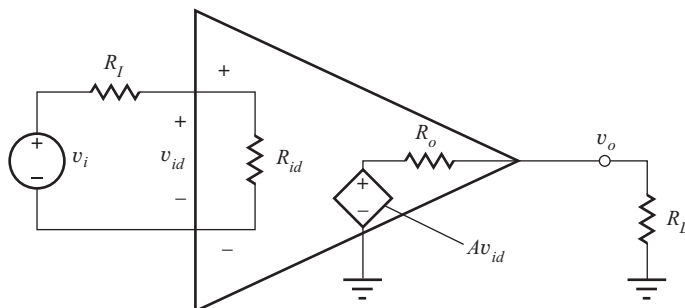


Figure 10.17 Amplifier with source and load attached.

Combining Eqs. (10.32) yields an expression for the overall voltage gain of the amplifier circuit in Fig. 10.17 for arbitrary values of  $R_I$  and  $R_L$ :

$$A_v = \frac{\mathbf{v}_o}{\mathbf{v}_i} = A \frac{R_{id}}{R_I + R_{id}} \frac{R_L}{R_o + R_L} \quad (10.33)$$

Operational amplifier circuits are most often **dc-coupled amplifiers**, and the signals  $v_o$  and  $v_i$  may in fact have a dc component that represents a dc shift of the input away from the Q-point. The op amp amplifies not only the ac components of the signal but also this dc component. We must remember that the ratio needed to find  $A_v$ , as indicated in Eq. (10.33), is determined by the amplitude and phase of the individual signal components and is not a time-varying quantity, but  $\omega = 0$  is a valid signal frequency! Recall from Chapter 1 that  $v_i$ ,  $v_o$ ,  $i_2$  and so on represent our signal voltages and currents and are generally functions of time:  $v_i(t)$ ,  $v_o(t)$ ,  $i_2(t)$ . But whenever we do algebraic calculations of voltage gain, current gain, input resistance, output resistance, and so on, we must use **phasor** representations of the individual signal components in our calculations:  $\mathbf{v}_i$ ,  $\mathbf{v}_o$ ,  $\mathbf{i}_2$ . Signals  $v_i(t)$ ,  $v_o(t)$ ,  $i_2(t)$  and so on may be composed of many individual signal components, one of which may be a dc shift away from the Q-point value.

### EXAMPLE 10.3 VOLTAGE GAIN ANALYSIS

Find the gain of a differential amplifier including the effects of load and source resistance.

**PROBLEM** Calculate the voltage gain for an amplifier with the following parameters:  $A = 100$ ,  $R_{id} = 100 \text{ k}\Omega$ , and  $R_o = 100 \Omega$ , with  $R_I = 10 \text{ k}\Omega$  and  $R_L = 1000 \Omega$ . Express the result in dB.

**SOLUTION** **Known Information and Given Data:**  $A = 100$ ,  $R_{id} = 100 \text{ k}\Omega$ ,  $R_o = 100 \Omega$ ,  $R_I = 10 \text{ k}\Omega$ , and  $R_L = 1000 \Omega$

**Unknown:** Voltage gain  $A_v$

**Approach:** Evaluate the expression in Eq. (10.33). Convert answer to dB.

**Assumptions:** None

**Analysis:** Using Eq. (10.33),

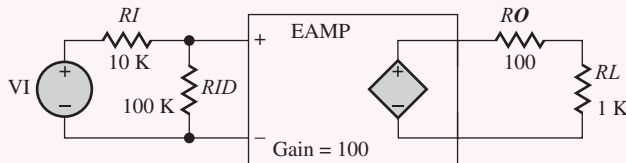
$$A_v = 100 \left( \frac{100 \text{ k}\Omega}{10 \text{ k}\Omega + 100 \text{ k}\Omega} \right) \left( \frac{1000 \Omega}{100 \Omega + 1000 \Omega} \right) = 82.6$$

$$A_{v\text{dB}} = 20 \log |A_v| = 20 \log |82.6| = 38.3 \text{ dB}$$

**Check of Results:** We have found the only unknown requested.

**Discussion:** The amplifier's internal voltage gain capability is  $A = 100$ , but an overall gain of only 82.6 is being realized because a portion of the signal source voltage ( $\approx 9$  percent) is being dropped across  $R_I$ , and part of the internal amplifier voltage ( $A v_{id}$ ) (also  $\approx 9$  percent) is being lost across  $R_o$ .

**Computer-Aided Analysis:** The SPICE circuit is shown here, and a transfer function analysis from source VI to the output node is used to characterize the amplifier in this example.



The SPICE results are transfer function = 82.6, input resistance = 110 k $\Omega$ , and output resistance = 90.9  $\Omega$ .  $A_v$  equals the value of the transfer function, the resistance at the terminals of VI is the input resistance, and the output resistance represents the total resistance at the output node. The voltage gain agrees with our hand analysis.

## 10.8 IDEAL DIFFERENTIAL AND OPERATIONAL AMPLIFIERS

An ideal differential amplifier would produce an output that depends only on the voltage difference  $v_{id}$  between its two input terminals, and this voltage would be independent of source and load resistances. Referring to Eq. (10.33), we see that this behavior can be achieved if the input resistance of the amplifier is infinite and the output resistance is zero (as pointed out previously in Sec. 10.4). For this case, Eq. (10.33) reduces to

$$v_o = A v_{id} \quad \text{or} \quad A_v = \frac{v_o}{v_{id}} = A \quad (10.34)$$

and the full differential amplifier gain is realized.  $A$  is referred to as either the **open-circuit voltage gain** or **open-loop gain** of the amplifier and represents the maximum voltage gain available from the device.

As introduced earlier in this chapter, we often want to achieve a completely mismatched resistance condition in voltage amplifier applications ( $R_{id} \gg R_s$  and  $R_o \ll R_L$ ), so that maximum voltage gain in Eq. (10.34) can be achieved. For the mismatched case, the overall amplifier gain is independent of the source and load resistances, and multiple amplifier stages can be cascaded without concern for interaction between stages.

As noted earlier, the term “operational amplifier” grew from use of these high-performance amplifiers to perform specific electronic circuit functions or operations, such as scaling, summation, and integration, in analog computers. The operational amplifier used in these applications is an ideal differential amplifier with an additional property: infinite voltage gain. Although it is impossible to realize the **ideal operational amplifier**, its conceptual use allows us to understand the basic performance to be expected from a given analog circuit and serves as a model to help in circuit design. Once the properties of the ideal amplifier and its use in basic circuits are understood, then various ideal assumptions can be removed in order to understand their effect on circuit performance.

### 10.8.1 ASSUMPTIONS FOR IDEAL OPERATIONAL AMPLIFIER ANALYSIS

The ideal operational amplifier is a special case of the ideal difference amplifier in Fig. 10.16, in which  $R_{id} = \infty$ ,  $R_o = 0$ , and, most importantly, voltage gain  $A = \infty$ . Infinite gain leads to the first of two assumptions used to analyze circuits containing ideal op amps. Solving for  $v_{id}$  in Eq. (10.34),

$$v_{id} = \frac{v_o}{A} \quad \text{and} \quad \lim_{A \rightarrow \infty} v_{id} = 0 \quad (10.35)$$

If  $A$  is infinite, then the input voltage  $v_{id}$  will be zero for any finite output voltage. We will refer to this condition as **Assumption 1** for ideal op-amp circuit analysis.

An infinite value for the input resistance  $R_{id}$  forces the two input currents  $i_+$  and  $i_-$  to be zero, which will be **Assumption 2** for analysis of ideal op amp circuits. These two results, combined with Kirchhoff's voltage and current laws, form the basis for analysis of all ideal op amp circuits.

As just described, the two primary assumptions used for analysis of circuits containing ideal op amps are:

1. Input voltage difference is zero:  $v_{id} = 0$
  2. Input currents are zero:  $i_+ = 0$  and  $i_- = 0$
- (10.36)

Infinite gain and infinite input resistance are the explicit characteristics that lead to Assumptions 1 and 2. However, the ideal operational amplifier actually has quite a number of additional implicit properties, but these assumptions are seldom clearly stated. They are

- Infinite common-mode rejection
- Infinite power supply rejection
- Infinite output voltage range (not limited by  $-V_{EE} \leq v_O \leq V_{CC}$ )
- Infinite output current capability
- Infinite open-loop bandwidth
- Infinite slew rate
- Zero output resistance
- Zero input-bias currents and offset current
- Zero input-offset voltage

These terms may be unfamiliar at this point, but they will all be defined and discussed in detail in Chapter 11.

**EXERCISE:** Suppose an amplifier is operating with  $v_o = +10$  V. What is the input voltage  $v_{id}$  if  
 (a)  $A = 100$ ? (b)  $A = 10,000$ ? (c)  $A = 120$  dB?

**ANSWERS:** (a) 100 mV; (b) 1.00 mV; (c) 10.0  $\mu$ V



## DESIGN NOTE

Two assumptions are used for analysis of ideal operational amplifier circuits:

1. The differential input voltage of the op amp will be zero:  $v_{id} = 0$ .
2. The currents in both amplifier input terminals are zero:  $i_+ = 0$  and  $i_- = 0$ .

## 10.9 ANALYSIS OF CIRCUITS CONTAINING IDEAL OPERATIONAL AMPLIFIERS

This section introduces a number of classic operational amplifier circuits, including the basic inverting and noninverting amplifiers; the unity-gain buffer, or voltage follower; the summing and difference amplifiers; the low-pass filter; the integrator; and the differentiator. Analysis of these various circuits demonstrates use of the two ideal op amp assumptions in combination with Kirchhoff's voltage and current laws (KVL and KCL, respectively). These classic op amp circuits are a fundamental part of our circuit design toolbox that we need to build more complex analog systems.

### 10.9.1 THE INVERTING AMPLIFIER

An **inverting-amplifier** circuit is built by grounding the positive input of the operational amplifier and connecting resistors  $R_1$  and  $R_2$ , called the **feedback network**, between the inverting input and the signal source and amplifier output node, respectively, as in Fig. 10.18. We wish to find a set of two-port parameters that characterize the overall circuit, including the open-circuit voltage gain  $A_v$ , input resistance  $R_{\text{in}}$ , and output resistance  $R_{\text{out}}$ .

#### Inverting Amplifier Voltage Gain

We begin by determining the voltage gain. To find  $A_v$ , we need a relationship between  $v_i$  and  $v_o$ , which we can find by writing an equation for the single loop shown in Fig. 10.19.

$$v_i - i_1 R_1 - i_2 R_2 - v_o = 0 \quad (10.37)$$

Applying KCL at the inverting input to the amplifier yields a relationship between  $i_1$  and  $i_2$

$$i_1 = i_- + i_2 \quad \text{or} \quad i_1 = i_2 \quad (10.38)$$

since Assumption 2 states that  $i_-$  must be zero. Equation (10.37) then becomes

$$v_i - i_1 R_1 - i_1 R_2 - v_o = 0 \quad (10.39)$$

Now, current  $i_1$  can be written in terms of  $v_i$  as

$$i_1 = \frac{v_i - v_-}{R_1} \quad (10.40)$$

where  $v_-$  is the voltage at the inverting input (negative input) of the op amp. But, Assumption 1 states that the input voltage  $v_{id}$  must be zero, so  $v_-$  must also be zero because the positive input is grounded:

$$v_{id} = v_+ - v_- = 0 \quad \text{but} \quad v_+ = 0 \quad \text{so} \quad v_- = 0$$

Because  $v_- = 0$ ,  $i_1 = v_i/R_1$ , and Eq. (10.39) reduces to

$$-v_i \frac{R_2}{R_1} - v_o = 0 \quad \text{or} \quad v_o = -v_i \frac{R_2}{R_1} \quad (10.41)$$

The voltage gain is given by

$$A_v = \frac{v_o}{v_i} = -\frac{R_2}{R_1} \quad (10.42)$$

Referring to Eq. (10.42), we should note several things. The voltage gain is negative, indicative of an inverting amplifier with a  $180^\circ$  phase shift between dc or sinusoidal input and output signals. In addition, the magnitude of the gain can be greater than or equal to 1 if  $R_2 \geq R_1$  (the most common case), but it can also be less than 1 for  $R_1 > R_2$ . The inverting amplifier in Fig. 10.18 employs *negative feedback* in which a portion of the output signal is “fed back” to the op amp’s negative input terminal through resistor  $R_2$ . Negative feedback is a requirement for stability of the feedback amplifier and will be discussed in more detail in Chapter 11.

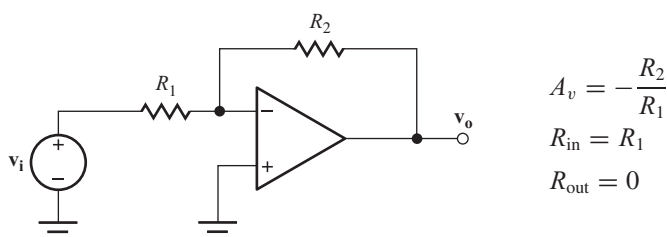


Figure 10.18 Inverting-amplifier circuit.

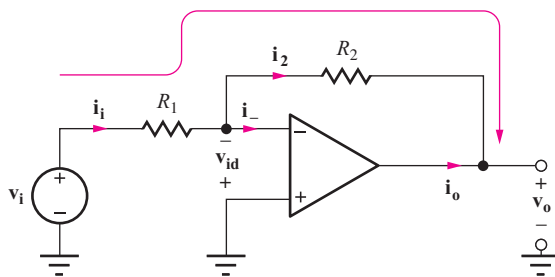
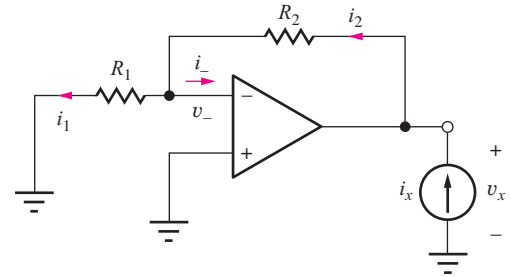


Figure 10.19 Inverting-amplifier circuit.

Figure 10.20 Test current applied to the amplifier to determine the output resistance:  $R_{\text{out}} = v_x/i_x$ .

### Understanding Inverting Amplifier Operation

In the amplifier circuit in Figs. 10.18 and 10.19, the inverting-input terminal of the operational amplifier is at ground potential, 0 V, and is referred to as a **virtual ground**. The ideal operational amplifier adjusts its output to whatever voltage is necessary to force the differential input voltage to zero. Because of the virtual ground at the inverting input, input voltage  $v_i$  appears directly across resistor  $R_1$  and establishes an input current  $v_i/R_1$ . The op amp forces this input current to flow through  $R_2$  developing a voltage drop of  $v_i \cdot (R_2/R_1)$ . Thus  $v_o = -v_i(R_2/R_1)$  and  $A_v = -(R_2/R_1)$ .

Note however, that although the inverting input represents a virtual ground, it is *not* connected directly to ground (there is no direct dc path for current to reach ground). Shorting this terminal to ground for analysis purposes is a common error that must be avoided.

**EXERCISE:** Find  $A_v$ ,  $v_o$ ,  $i_i$ , and  $i_o$  for the amplifier in Fig. 10.19 if  $R_1 = 68 \text{ k}\Omega$ ,  $R_2 = 360 \text{ k}\Omega$ , and  $v_i = 0.5 \text{ V}$ .

**ANSWERS:**  $-5.29$ ,  $-2.65 \text{ V}$ ,  $7.35 \mu\text{A}$ ,  $-7.35 \mu\text{A}$

### Input and Output Resistances of the Ideal Inverting Amplifier

The input resistance  $R_{\text{in}}$  of the overall amplifier is found directly from Eq. (10.40). Since  $v_- = 0$  (virtual ground),

$$R_{\text{in}} = \frac{v_i}{i_i} = R_1 \quad (10.43)$$

The output resistance  $R_{\text{out}}$  is the Thévenin equivalent resistance at the output terminal; it is found by applying a test signal current source to the output of the amplifier circuit and determining the voltage, as in Fig. 10.20. All other *independent* voltage and current sources in the circuit must be turned off, and so  $v_i$  is set to zero in Fig. 10.20.

The output resistance of the overall amplifier is defined by

$$R_{\text{out}} = \frac{v_x}{i_x} \quad (10.44)$$

Writing a single-loop equation for Fig. 10.20 gives

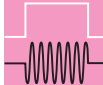
$$v_x = i_2 R_2 + i_1 R_1 \quad (10.45)$$

but  $i_1 = i_2$  because  $i_- = 0$  based on op-amp Assumption 2. Therefore,

$$v_x = i_1 (R_2 + R_1) \quad (10.46)$$

However,  $i_1$  must be zero because Assumption 1 tells us that  $v_- = 0$ . Thus,  $v_x = 0$  independent of the value of  $i_x$ , and

$$R_{\text{out}} = 0 \quad (10.47)$$


**DESIGN  
NOTE**

For the **ideal inverting amplifier**, the closed-loop voltage gain  $A_v$ , input resistance  $R_{\text{in}}$ , and output resistance  $R_{\text{out}}$  are:

$$A_v = -\frac{R_2}{R_1} \quad R_{\text{in}} = R_1 \quad R_{\text{out}} = 0$$

## DESIGN INVERTING AMPLIFIER DESIGN

### EXAMPLE 10.4

Design an op amp inverting amplifier to meet a pair of specifications.

**PROBLEM** Design an inverting amplifier (i.e., choose the values of  $R_1$  and  $R_2$ ) to have an input resistance of 20 kΩ and a gain of 40 dB.

**SOLUTION** **Known Information and Given Data:** In this case, we are given the values for the gain and input resistance, and the amplifier circuit configuration has also been specified: op amp inverting amplifier topology; voltage gain = 20 dB;  $R_{\text{in}} = 20 \text{ k}\Omega$ .

**Unknowns:** Values of  $R_1$  and  $R_2$  required to achieve the specifications

**Approach:** Based on Eqs. (10.42) and (10.43), we see that the input resistance is controlled by  $R_1$ , and the voltage gain is set by  $R_2/R_1$ . First find the value of  $R_1$ ; then use it to find the value of  $R_2$ .

**Assumptions:** The op amp is ideal so that Eqs. (10.42) and (10.43) apply.

**Analysis:** We must convert the gain from dB before we use it in the calculations:

$$|A_v| = 10^{40 \text{ dB}/20 \text{ dB}} = 100 \quad \text{so} \quad A_v = -100$$

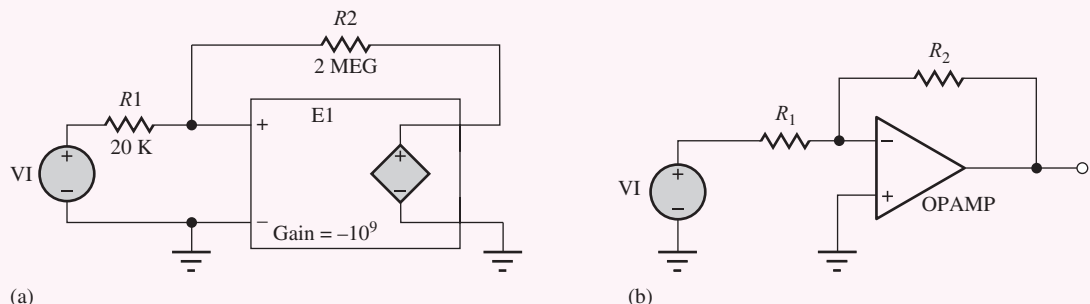
The minus sign is added since an inverting amplifier is specified. Using Eqs. (10.43) and Eq. (10.42):

$$R_1 = R_{\text{in}} = 20 \text{ k}\Omega \quad \text{and} \quad A_v = -\frac{R_2}{R_1} \rightarrow R_2 = 100R_1 = 2 \text{ M}\Omega$$

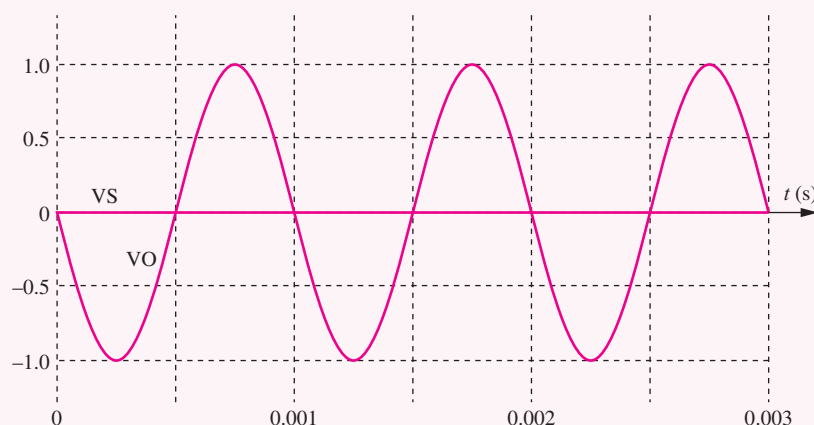
**Check of Results:** We have found all the answers requested.

**Evaluation and Discussion:** Looking at Appendix A, we find that 20 kΩ and 2 MΩ represent standard 5 percent resistor values, and our design is complete. (Murphy has been on our side for a change.) Note in this example, that we have two design constraints and two resistors to choose.

**Computer-Aided Analysis:** In the SPICE circuit shown here in (a), the op amp is modeled by VCVC E1. In SPICE, we cannot set the gain of E1 to infinity. To approximate the ideal op amp, a value of  $-10^9$  is assigned to E1. Remember that  $R_2 = 2 \text{ MEG}$ , not  $2\text{M} = 0.002 \Omega$ ! A transfer function analysis from source VS to the output node is used to characterize the gain of the amplifier. A transient analysis gives the output voltage. VS is defined to have zero voltage offset, a 10 mV amplitude and a frequency of 1000 Hz ( $V = 0.01 \sin 2000\pi t$ ). The transient solution starts at  $T = 0$ , stops at  $T = 0.003$  s and uses a time step of 1 μs.



The SPICE results are: transfer function =  $-100$ , input resistance =  $20\text{ k}\Omega$ , and output resistance =  $0$ . These values confirm our design, and the output signal is an inverted 1-V, 1000-Hz sine wave, as expected. Note that the small input signal is actually present but hard to see on the graph because of the scale.



An alternate SPICE circuit appears in (b) in which a built-in OPAMP model is used. The adjustable parameters for this model are the voltage gain and two power supply voltages that need not be the same. Thus OPAMP models the voltage transfer characteristic presented in Fig. 10.13.

**EXERCISE:** If  $V_I = 2\text{ V}$ ,  $R_1 = 4.7\text{ k}\Omega$ , and  $R_2 = 24\text{ k}\Omega$ , find  $I_I$ ,  $I_2$ ,  $I_O$ , and  $V_O$  in Fig. 10.19. Why is the symbol  $V_I$  being used instead of  $v_i$ , and so on?

**ANSWERS:**  $0.426\text{ mA}$ ,  $0.426\text{ mA}$ ,  $-0.426\text{ mA}$ ,  $-10.2\text{ V}$ ; the problem is stated specifically in terms of dc values.

## 10.9.2 THE TRANSRESISTANCE AMPLIFIER — A CURRENT-TO-VOLTAGE CONVERTER

In the inverting amplifier, the input voltage source injects a current into the summing junction through resistor  $R_1$ . If we instead inject the current directly from a current source as in Fig. 10.21, we form a **transresistance amplifier**, also called a **current-to-voltage (I-V) converter**. This circuit is widely used in receivers in fiber-optic communication systems.

Following the inverting amplifier analysis, we have

$$i_2 = i_1 \quad i_2 = -\frac{v_o}{R_2} \quad \text{and} \quad A_{tr} = \frac{v_o}{i_i} = -R_2 \quad (10.48)$$

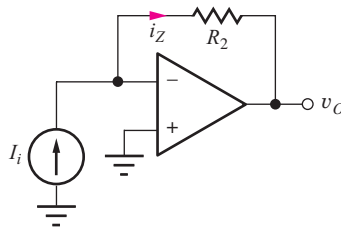


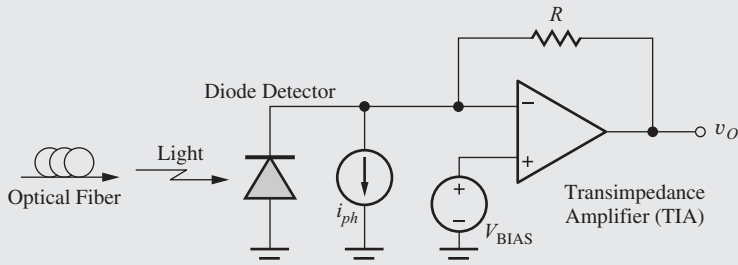
**Figure 10.21** Transresistance amplifier.

The gain  $A_{tr}$  is the ratio of  $v_o$  to  $i_i$  and has units of resistance. Since the inverting input terminal is a virtual ground, the input resistance is zero, and zero output resistance appears at the output terminal of the ideal op amp.

### ELECTRONICS IN ACTION

#### Fiber Optic Receiver

Interface circuits for optical communications were introduced in the Electronics in Action feature in Chapter 9. One of the important electronic blocks on the receiver side of such a fiber optic communication link is the circuit that performs the optical-to-electrical (O/E) signal conversion, and a common approach is shown in the accompanying figure. Light exiting the optical fiber is incident upon a photodiode (see Sec. 3.18) that generates photocurrent  $i_{ph}$  as modeled by the current source in the figure. This photocurrent flows through feedback resistor  $R$  and generates a signal voltage at the output given by  $v_o = i_{ph}R$ . The voltage  $V_{BIAS}$  can be used to provide reverse bias to the photodiode. In this case, the total output voltage is  $v_o = V_{BIAS} + i_{ph}R$ .



Optical-to-electrical interface for fiber optic data transmission.

Since the input to the amplifier is a current and the output is a voltage, the gain  $A_{tr} = v_o / i_{ph}$  has the units of resistance, and the amplifier is referred to as a transresistance or (more generally) a transimpedance amplifier (TIA). The operational amplifier shown in the circuit must have an extremely wideband and linear design. The requirements are particularly stringent in OC-768 systems in which 40-GHz signals coming from the optical fiber must be amplified without the addition of any significant phase distortion.

#### DESIGN NOTE

The gain of the *ideal transresistance amplifier* is set by feedback resistor  $R_2$ , and the input and output resistances are both zero:

$$A_{tr} = -R_2 \quad R_{in} = 0 \quad R_{out} = 0$$

**EXERCISE:** We wish to convert a  $25 \mu\text{A}$  sinusoidal current to a voltage with an amplitude of  $5 \text{ V}$  using a transresistance amplifier. What value of  $R_2$  is required? If  $i_i = 50 \sin 2000\pi t \mu\text{A}$ , what is the amplifier output voltage?

**ANSWERS:**  $200 \text{ k}\Omega$ ;  $v_o = -10 \sin 2000\pi t \text{ V}$

### 10.9.3 THE NONINVERTING AMPLIFIER

The operational amplifier can also be used to construct a **noninverting amplifier** utilizing the circuit schematic in Fig. 10.22. The input signal is applied to the positive or (noninverting) input terminal of the operational amplifier, and a portion of the output signal is fed back to the negative input terminal (negative feedback).

Analysis of the circuit is performed by relating the voltage at  $v_1$  to both input voltage  $v_i$  and output voltage  $v_o$ . Because Assumption 2 states that input current  $i_-$  is zero,  $v_1$  can be related to the output voltage through the voltage divider formed by  $R_1$  and  $R_2$ :

$$v_1 = v_o \frac{R_1}{R_1 + R_2} \quad (10.49)$$

Writing an equation around the loop including  $v_i$ ,  $v_{id}$ , and  $v_1$  yields a relation between  $v_1$  and  $v_i$ :

$$v_i - v_{id} = v_1 \quad (10.50)$$

However, Assumption 1 requires  $v_{id} = 0$ , so

$$v_i = v_1 \quad (10.51)$$

Combining Eqs. (10.49) and (10.51) and solving for  $v_o$  in terms of  $v_i$  gives

$$v_o = v_i \frac{R_1 + R_2}{R_1} \quad (10.52)$$

which yields an expression for the voltage gain of the noninverting amplifier:

$$A_v = \frac{v_o}{v_i} = \frac{R_1 + R_2}{R_1} = 1 + \frac{R_2}{R_1} \quad (10.53)$$

Note that the gain is positive and must be greater than or equal to 1 because  $R_1$  and  $R_2$  are positive numbers for real resistors.

#### Understanding Noninverting Amplifier Operation

Since the voltage across the inputs of the op amp must be zero (Assumption 1), input voltage  $v_i$  appears directly across resistor  $R_1$  and establishes a current  $v_i/R_1$ . This current flows down through  $R_2$  developing a scaled replica of  $v_i$  {i.e.,  $v_i \cdot (R_2/R_1)$ } across  $R_2$ . The output is the sum of the voltages across  $R_1$  and  $R_2$  yielding  $v_o = v_i + v_i(R_2/R_1)$  and  $A_v = 1 + R_2/R_1$ .

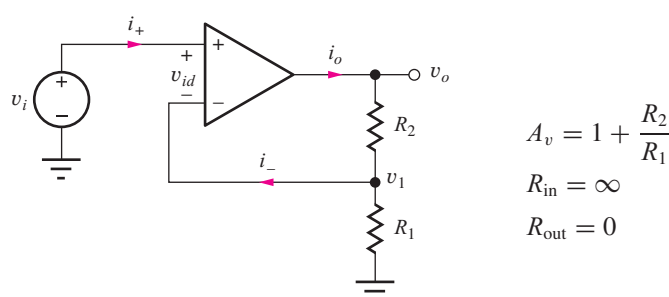


Figure 10.22 Noninverting amplifier configuration.

### EXAMPLE 10.5 NONINVERTING AMPLIFIER ANALYSIS

Determine the characteristics of a noninverting amplifier with feedback resistors specified.

**PROBLEM** Find the voltage gain  $A_v$ , output voltage  $v_o$ , and output current  $i_o$  for the amplifier in Fig. 10.22 if  $R_1 = 3 \text{ k}\Omega$ ,  $R_2 = 43 \text{ k}\Omega$ , and  $v_i = +0.1 \text{ V}$ .

**SOLUTION** **Known Information and Given Data:** Noninverting amplifier circuit with  $R_1 = 3 \text{ k}\Omega$ ,  $R_2 = 43 \text{ k}\Omega$ , and  $v_i = +0.1 \text{ V}$

**Unknowns:** Voltage gain  $A_v$ , output voltage  $v_o$ , and output current  $i_o$

**Approach:** Use Eq. (10.53) to find the voltage gain. Use the gain to calculate the output voltage. Use the output voltage and KCL to find  $i_o$ .

**Assumptions:** The op amp is ideal.

**Analysis:** Using Eq. (10.53),

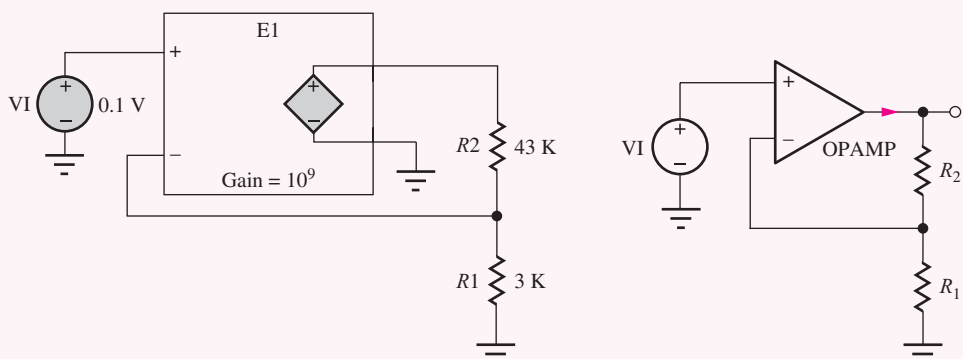
$$A_v = 1 + \frac{R_2}{R_1} = 1 + \frac{43 \text{ k}\Omega}{3 \text{ k}\Omega} = +15.3 \quad \text{and} \quad v_o = A_v v_i = (15.3)(0.1 \text{ V}) = 1.53 \text{ V}$$

Since the current  $i_- = 0$ ,

$$i_o = \frac{v_o}{R_2 + R_1} = \frac{1.53 \text{ V}}{43 \text{ k}\Omega + 3 \text{ k}\Omega} = 33.3 \mu\text{A}$$

**Check of Results:** We have found all the answers requested. SPICE is used to check the results.

**Computer-Aided Analysis:** The noninverting amplifier is characterized using a combination of an operating point analysis and a transfer function analysis. The gain of E1 of the op amp is set to  $10^9$  to model the ideal op amp. The transfer function analysis results are: transfer function = +15.3, input resistance =  $10^{20} \Omega$ , and output resistance = 0. The dc output voltage is 1.53 V, and the current in source E1 is  $-33.3 \mu\text{A}$ . These values agree with our hand analysis. Note that  $10^{20}$  is the representation of infinity in this particular version of SPICE, and the current in E1 is negative because SPICE uses the passive sign convention which assumes that positive current enters the positive terminal of E1.



**EXERCISE:** What are the voltage gain  $A_v$ , output voltage  $v_o$ , and output current  $i_o$  for the amplifier in Fig. 10.22 if  $R_1 = 2 \text{ k}\Omega$ ,  $R_2 = 36 \text{ k}\Omega$ , and  $v_i = -0.2 \text{ V}$ ?

**ANSWERS:** +19.0; -3.80 V; -100  $\mu\text{V}$

### Input and Output Resistances of the Noninverting Amplifier

Using Assumption 2,  $i_+ = 0$ , we find that the input resistance of the noninverting amplifier is given by

$$R_{\text{in}} = \frac{v_i}{i_+} = \infty \quad (10.54)$$

To find the output resistance, a test current is applied to the output terminal, and the source  $v_i$  is set to 0 V. The resulting circuit is identical to that in Fig. 10.20, so the output resistance of the noninverting amplifier is also zero.

$$R_{\text{out}} = 0 \quad (10.55)$$

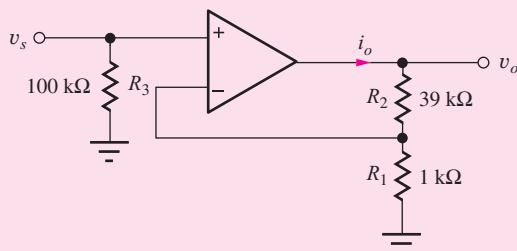
### DESIGN NOTE

For the **ideal noninverting amplifier**, the closed-loop voltage gain  $A_v$ , input resistance  $R_{\text{in}}$ , and output resistance  $R_{\text{out}}$  are:

$$A_v = 1 + \frac{R_2}{R_1} \quad R_{\text{in}} = \infty \quad R_{\text{out}} = 0$$

**EXERCISE:** Draw the circuit used to determine the output resistance of the noninverting amplifier and convince yourself that it is indeed the same as Fig. 10.20.

**EXERCISE:** What are the voltage gain in dB and the input resistance of the amplifier shown here? If  $v_i = 0.25 \text{ V}$ , what are the values of  $v_o$  and  $i_o$ ?



**ANSWERS:** 32.0 dB, 100  $\text{k}\Omega$ ; +10.0 V, 0.250 mA

**EXERCISE:** Design a noninverting amplifier (choose  $R_1$  and  $R_2$  from Appendix A) to have a gain of 54 dB, and the current  $i_o \leq 0.1 \text{ mA}$  when  $v_o = 10 \text{ V}$ .

**ANSWERS:** Two possibilities of many: (220  $\Omega$  and 110  $\text{k}\Omega$ ) or (200  $\Omega$  and 100  $\text{k}\Omega$ )

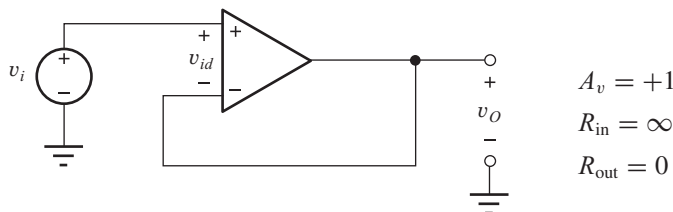


Figure 10.23 Unity-gain buffer (voltage follower).

#### 10.9.4 THE UNITY-GAIN BUFFER, OR VOLTAGE FOLLOWER

A special case of the noninverting amplifier, known as the **unity-gain buffer**, or **voltage follower**, is shown in Fig. 10.23, in which the value of  $R_1$  is infinite and that of  $R_2$  is zero. Substituting these values in Eq. (10.53) yields  $A_v = 1$ . An alternative derivation can be obtained by writing a single-loop equation for Fig. 10.23:

$$v_i - v_{id} = v_o \quad \text{or} \quad v_o = v_i \quad \text{and} \quad A_v = 1 \quad (10.56)$$

because the ideal operational amplifier forces  $v_{id}$  to be zero.

Why is such an amplifier useful? The ideal unity-gain buffer provides a gain of 1 with infinite input resistance and zero output resistance and therefore provides a tremendous impedance-level transformation while maintaining the level of the signal voltage. Many transducers represent high-source impedances and cannot supply any significant current to drive a load. The ideal unity-gain buffer does not require any input current, yet can drive any desired load resistance without loss of signal voltage. Thus, the unity-gain buffer is found in many sensor and data acquisition applications.

This circuit is also often used as a building block within more complex circuits. It is used to transfer a voltage from one point in the circuit to another point without directly connecting the points together, thus buffering the first point from the loading of the second.

#### Understanding Voltage Follower Operation

The operation of this circuit is quite simple. The voltage across the inputs of the op amp must be zero (Assumption 1). Therefore the output voltage must equal (follow) the input voltage.

#### Summary of Ideal Inverting and Noninverting Amplifier Characteristics

Table 10.3 summarizes the properties of the ideal inverting and noninverting amplifiers; the properties are recapitulated here. The gain of the noninverting amplifier must be greater than or equal to 1, whereas the inverting amplifier can be designed with a gain magnitude greater than or less than unity (as well as exactly 1). The gain of the inverting amplifier is negative, indicating a  $180^\circ$  phase inversion between input and output voltages.

The input resistance represents an additional major difference between the two amplifiers.  $R_{in}$  is extremely large for the noninverting amplifier but is relatively low for the inverting amplifier, limited by the value of  $R_1$ . The output resistance of both ideal amplifiers is zero.

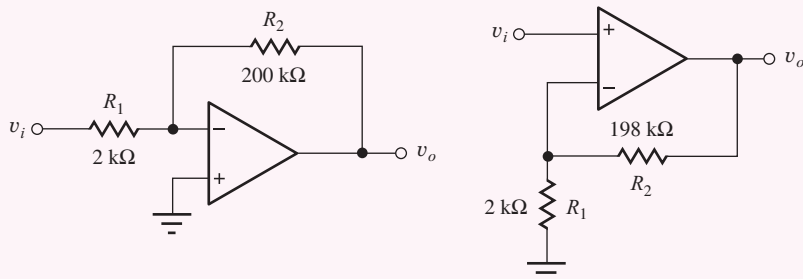
**TABLE 10.3**  
Summary of the Ideal Inverting and Noninverting Amplifiers

	INVERTING AMPLIFIER	NONINVERTING AMPLIFIER
Voltage gain $A_v$	$-\frac{R_2}{R_1}$	$1 + \frac{R_2}{R_1}$
Input resistance $R_{in}$	$R_1$	$\infty$
Output resistance $R_{out}$	0	0

### EXAMPLE 10.6 INVERTING AND NONINVERTING AMPLIFIER COMPARISON

This example compares the characteristics of the inverting and noninverting amplifier configurations.

**PROBLEM** Explore the differences between the inverting and noninverting amplifiers in the figure here. Each amplifier is designed to have a gain of 40 dB.



**SOLUTION** **Known Information and Given Data:** Inverting amplifier topology with  $R_1 = 2 \text{ k}\Omega$  and  $R_2 = 200 \text{ k}\Omega$ ; noninverting amplifier topology with  $R_1 = 2 \text{ k}\Omega$  and  $R_2 = 198 \text{ k}\Omega$ .

**Unknowns:** Voltage gains, input resistances and output resistances for the two amplifier circuits

**Approach:** Use the given data to evaluate the amplifier formulas that have already been derived for the two topologies.

**Assumptions:** The operational amplifiers are ideal.

**Analysis:**

$$\text{Inverting amplifier: } A_v = -\frac{200 \text{ k}\Omega}{2 \text{ k}\Omega} = -100 \text{ or } 40 \text{ dB}$$

$$R_{\text{in}} = 2 \text{ k}\Omega \quad \text{and} \quad R_{\text{out}} = 0 \Omega$$

$$\text{Noninverting amplifier: } A_v = 1 + \frac{198 \text{ k}\Omega}{2 \text{ k}\Omega} = +100 \text{ or } 40 \text{ dB}$$

$$R_{\text{in}} = \infty \quad \text{and} \quad R_{\text{out}} = 0 \Omega$$

**Check of Results:** We have indeed found all the answers requested. A second check indicates the calculations are correct.

**TABLE 10.4**  
Numeric Comparison of the Ideal Inverting and Noninverting Amplifiers

	INVERTING AMPLIFIER	NONINVERTING AMPLIFIER
Voltage gain $A_v$	-100 (40 dB)	+100 (40 dB)
Input resistance $R_{\text{in}}$	2 kΩ	$\infty$
Output resistance $R_{\text{out}}$	0	0

**Evaluation and Discussion:** Table 10.4 lists the characteristics of the two amplifier designs. In addition to the sign difference in the gain of the two amplifiers, we see that the input resistance of the inverting amplifier is only 2 kΩ, whereas that of the noninverting amplifier is infinite. Note that the noninverting amplifier achieves our ideal voltage amplifier goals with  $R_{\text{in}} = \infty$  and  $R_{\text{out}} = 0 \Omega$ .

**EXERCISE:** What are the voltage gain  $A_v$ , input resistance  $R_{in}$ , output voltage  $v_o$ , and output current  $i_o$  for the amplifiers in Ex. 10.6 if  $R_1 = 1.5 \text{ k}\Omega$ ,  $R_2 = 30 \text{ k}\Omega$ , and  $v_i = 0.15 \text{ V}$ ?

**ANSWERS:**  $-20.0$ ,  $1.5 \text{ k}\Omega$ ,  $-3.00 \text{ V}$ ,  $-100 \mu\text{A}$ ;  $+21$ ,  $\infty$ ,  $+3.15 \text{ V}$ ,  $+100 \mu\text{A}$

**EXERCISE:** Use SPICE transfer function analysis to confirm the analysis in Ex. 10.6.

**EXERCISE:** Add a resistor to the noninverting amplifier circuit to change its input resistance to  $2 \text{ k}\Omega$ .

**ANSWER:** Set resistor  $R_3 = 2 \text{ k}\Omega$  in the schematic on page 560.

### 10.9.5 THE SUMMING AMPLIFIER

Operational amplifiers can also be used to combine signals using the **summing-amplifier** circuit depicted in Fig. 10.24. Here, two input sources  $v_1$  and  $v_2$  are connected to the inverting input of the amplifier through resistors  $R_1$  and  $R_2$ . Because the negative amplifier input represents a virtual ground, the currents  $i_1$  and  $i_2$  are forced to flow through resistors  $R_1$  and  $R_2$ , respectively. These currents sum at the inverting input node to form the total inverting current  $i_- = i_1 + i_2$ .

$$i_1 = \frac{v_1}{R_1} \quad i_2 = \frac{v_2}{R_2} \quad i_- = i_1 + i_2 = \frac{v_1}{R_1} + \frac{v_2}{R_2} \quad (10.57)$$

Because  $i_- = 0$ ,  $i_3 = i_1 + i_2$ , and substituting Eq. (10.57) into this expression yields

$$v_o = -\left(\frac{R_3}{R_1}v_1 + \frac{R_3}{R_2}v_2\right) \quad (10.58)$$

The output voltage sums the scaled replicas of the two input voltages, and the scale factors for the two inputs may be independently adjusted through the choice of resistors  $R_1$  and  $R_2$ . These two inputs can be scaled independently because of the virtual ground maintained at the inverting-input terminal of the op amp.

The inverting-amplifier input node is also commonly called the **summing junction** because currents  $i_1$  and  $i_2$  are “summed” at this node and forced through the feedback resistor  $R_3$ . Although the amplifier in Fig. 10.24 has only two inputs, any number of inputs can be connected to the summing junction through additional resistors. A simple digital-to-analog converter can be formed in this way (see the EIA below and Prob. 10.70).

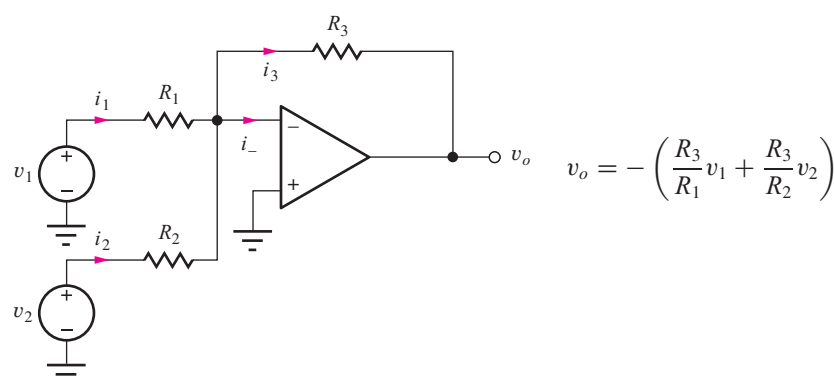


Figure 10.24 The summing amplifier.

**EXERCISE:** What is the summing amplifier output voltage  $v_o$  in Fig. 10.24 if  $v_1 = 2 \sin 1000\pi t$  V,  $v_2 = 4 \sin 2000\pi t$  V,  $R_1 = 1 \text{ k}\Omega$ ,  $R_2 = 2 \text{ k}\Omega$ , and  $R_3 = 3 \text{ k}\Omega$ ? What are the input resistances presented to sources  $v_1$  and  $v_2$ ? What is the current supplied by the op amp output terminal?

**ANSWERS:**  $(-6 \sin 1000\pi t - 6 \sin 2000\pi t)$  V;  $1 \text{ k}\Omega$ ,  $2 \text{ k}\Omega$ ;  $(-2 \sin 1000\pi t - 2 \sin 2000\pi t)$  mA



## ELECTRONICS IN ACTION

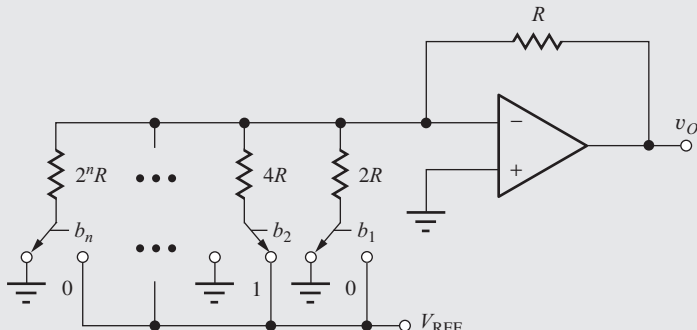


### Digital-to-Analog Converter (DAC) Circuits

One of the simplest digital-to-analog converter (DAC) circuits, known as the **weighted resistor DAC**, is based upon the summing amplifier concept that we just encountered in Section 10.9.5. The DAC utilizes a binary-weighted resistor network, a reference voltage  $V_{\text{REF}}$ , and a group of single-pole, double-throw switches that are usually implemented using MOS transistors. Binary input data controls the switches, with a logical 1 indicating that the switch is connected to  $V_{\text{REF}}$  and a logical 0 corresponding to a switch connected to ground. Successive resistors are weighted progressively by a factor of 2, thereby producing the desired binary weighted contributions to the output:

$$v_O = (b_1 2^{-1} + b_2 2^{-2} + \cdots + b_n 2^{-n}) V_{\text{REF}} \quad \text{for } b_i \in \{1, 0\}$$

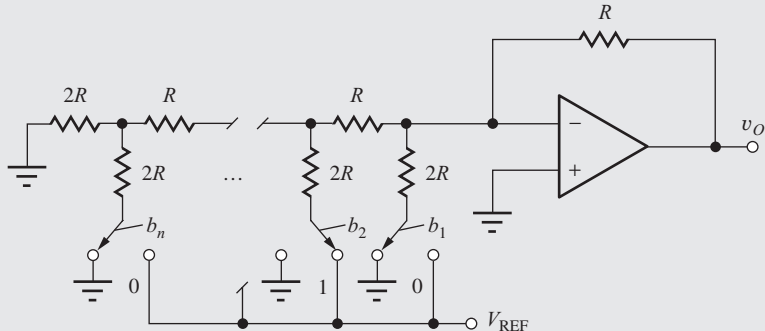
Bit  $b_1$  has the highest weight and is referred to as the **most significant bit (MSB)**, whereas bit  $b_n$  has the smallest weight and is referred to as the **least significant bit (LSB)**.



An  $n$ -bit weighted-resistor DAC.

Several problems arise in building a DAC using the weighted-resistor approach. The primary difficulty is the need to maintain accurate resistor ratios over a very wide range of resistor values (e.g., 4096 to 1 for a 12-bit DAC). Linearity and gain errors occur when the resistor ratios are not perfectly maintained. In addition, because the switches are in series with the resistors, their on-resistance must be very low, and they should have zero offset voltage. The designer can meet these last two requirements by using good MOSFETs (or JFETs) as switches, and the  $(W/L)$  ratios of the FETs can be scaled with bit position to equalize the resistance contributions of the switches. However, the wide range of resistor values is not suitable for monolithic converters of moderate to high resolution. We should also note that the current drawn from the voltage reference varies with the binary input pattern. This varying current causes a change in voltage drop in the Thévenin equivalent source resistance of the voltage reference and can lead to data-dependent errors sometimes called **superposition errors**.

The **R-2R ladder** avoids the problem of a wide range of resistor values. It is well-suited to integrated circuit realization because it requires matching of only two resistor values,  $R$  and  $2R$ . The value of  $R$  typically ranges from  $2\text{k}\Omega$  to  $10\text{k}\Omega$ . By forming successive Thévenin equivalents proceeding from left to right at each node in the ladder, we can show that the contribution of each bit is reduced by a factor of 2 going from the MSB to LSB. Like the weighted-resistor DAC, this network requires switches with low on-resistance and zero offset voltage, and the current drawn from the reference still varies with the input data pattern.



*n*-bit DAC using an R-2R ladder.

### 10.9.6 THE DIFFERENCE AMPLIFIER

Except for the summing amplifier, all the circuits thus far have had a single input. However, the operational amplifier may itself be used in a **difference amplifier** configuration, which amplifies the difference between two input signals as shown schematically in Fig. 10.25. Our analysis begins by relating the output voltage to the voltage at  $v_-$  as

$$v_o = v_- - i_2 R_2 = v_- - i_1 R_2 \quad (10.59)$$

because  $i_2 = i_1$  since  $i_-$  must be zero. The current  $i_1$  can be written as

$$i_1 = \frac{v_1 - v_-}{R_1} \quad (10.60)$$

Combining Eqs. (10.59) and (10.60) yields

$$v_o = v_- - \frac{R_2}{R_1}(v_1 - v_-) = \left( \frac{R_1 + R_2}{R_1} \right) v_- - \frac{R_2}{R_1} v_1 \quad (10.61)$$

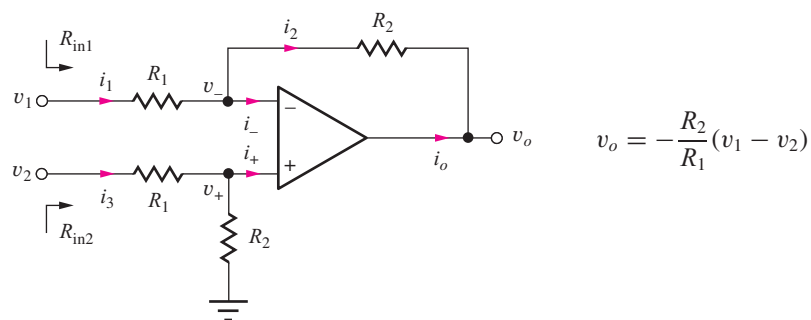


**Figure 10.25** Circuit for the difference amplifier.

Because the voltage between the op amp input terminals must be zero,  $v_- = v_+$ , and the current  $i_+$  is also zero,  $v_+$  can be written using the voltage division formula as

$$v_+ = \frac{R_2}{R_1 + R_2} v_2 \quad (10.62)$$

Substituting Eq. (10.62) into Eq. (10.61) yields the final result

$$v_o = \left( -\frac{R_2}{R_1} \right) (v_1 - v_2) \quad (10.63)$$

Thus, the circuit in Fig. 10.25 amplifies the difference between  $v_1$  and  $v_2$  by a factor that is determined by the ratio of resistors  $R_2$  and  $R_1$ . For  $R_2 = R_1$ ,

$$v_o = -(v_1 - v_2) \quad (10.64)$$

This particular circuit is sometimes called a **differential subtractor**.

The input resistance of this circuit is limited by resistors  $R_2$  and  $R_1$ . Input resistance  $R_{in2}$ , presented to source  $v_2$ , is simply the series combination of  $R_2$  and  $R_1$  because  $i_+$  is zero. For  $v_2 = 0$ , input resistance  $R_{in1}$  equals  $R_1$  because the circuit reduces to the inverting amplifier under this condition. However, for the general case, the input current  $i_1$  is a function of both  $v_1$  and  $v_2$ .

### Understanding Differential Amplifier Circuit Operation

Probably the easiest way to understand how the differential amplifier operates is to employ superposition. If input  $v_2$  is set to zero, then the circuit behaves as an inverting amplifier with gain  $-R_2/R_1$ . If  $v_1$  is set to zero, then  $v_2$  is attenuated by the voltage divider at the amplifier input formed by  $R_1$  and  $R_2$ , and then amplified by a noninverting amplifier gain of  $1 + R_2/R_1$ . The total output is the sum of the outputs from the two individual inputs acting alone.

$$\text{For } v_2 = 0, v_{o1} = -\frac{R_2}{R_1} v_1 \quad \text{For } v_1 = 0, v_{o2} = +\left(\frac{R_2}{R_1 + R_2}\right) \left(1 + \frac{R_2}{R_1}\right) v_2 = +\frac{R_2}{R_1} v_2$$

Combining these results yields

$$v_o = v_{o1} + v_{o2} = -\frac{R_2}{R_1} (v_1 - v_2)$$

### EXAMPLE 10.7 DIFFERENCE AMPLIFIER ANALYSIS

Here we find the various voltages and currents within the single op amp difference amplifier circuit with a specific set of input voltages.

**PROBLEM** Find the values of  $V_o$ ,  $V_+$ ,  $V_-$ ,  $I_1$ ,  $I_2$ ,  $I_3$ , and  $I_o$  for the difference amplifier in Figure 10.25 with  $V_1 = 5$  V,  $V_2 = 3$  V,  $R_1 = 10$  k $\Omega$ , and  $R_2 = 100$  k $\Omega$ .

**SOLUTION** **Known Information and Given Data:** The input voltages, resistor values, and circuit topology are specified.

**Unknowns:**  $V_o$ ,  $V_+$ ,  $V_-$ ,  $I_1$ ,  $I_2$ ,  $I_3$ , and  $I_o$

**Approach:** We must use circuit analysis (KCL and KVL) coupled with the ideal op amp assumptions to determine the various voltages and currents, but we must find the node voltages in order to find the currents.

**Assumptions:** Since the op amp is ideal, we know  $I_+ = 0 = I_-$ , and  $V_+ = V_-$ .

**Analysis:** Since  $I_+ = 0$ ,  $V_+$  can be found directly by voltage division,

$$V_+ = V_2 \frac{R_2}{R_1 + R_2} = 3 \text{ V} \frac{100 \text{ k}\Omega}{10 \text{ k}\Omega + 100 \text{ k}\Omega} = 2.73 \text{ V} \quad \text{and} \quad V_- = 2.73 \text{ V}$$

$V_O$  can be related to  $V_1$  using Kirchhoff's voltage law:

$$V_1 - I_1 R_1 - I_2 R_2 - V_O = 0$$

We know that  $I_- = 0$ , and  $I_2 = I_1$ . We can find  $I_1$  since we know the values of  $V_1$ ,  $V_-$ , and  $R_1$ :

$$I_1 = \frac{V_1 - V_-}{R_1} = \frac{5 \text{ V} - 2.73 \text{ V}}{10 \text{ k}\Omega} = 227 \mu\text{A} \quad \text{and} \quad I_2 = 227 \mu\text{A}$$

Then the output voltage can be found

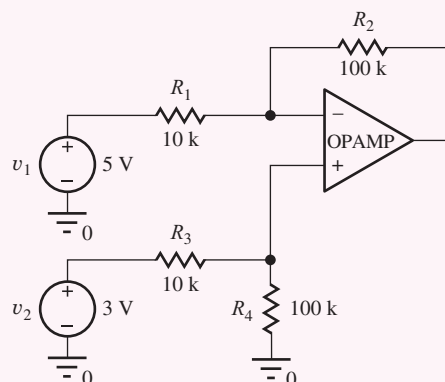
$$V_O = V_1 - I_1 R_1 - I_2 R_2 = V_1 - I_1(R_1 + R_2)$$

$$V_O = 5 \text{ V} - (227 \mu\text{A})(110 \text{ k}\Omega) = -20.0 \text{ V}$$

The op amp output current is  $I_O = -I_2 = -227 \mu\text{A}$ .

**Check of Results:** We have indeed found all the answers requested. The values of the voltages and currents all appear reasonable. This circuit is a difference amplifier that should amplify the difference in its inputs by the gain of  $-R_2/R_1 = -10$ . The output should be  $-10(5 - 3) = -20 \text{ V}$ . ✓

**Computer-Aided Analysis:** SPICE can be used to check our calculations using the circuit below. The ideal op amp is modeled by OPAMP with a gain of 120 dB. An operating point analysis produces voltages that agree with our hand analysis:  $V_+ = V_- = 2.73 \text{ V}$ ,  $V_O = -20 \text{ V}$ ,  $I_1 = 227 \mu\text{A}$ , and  $I_O = -227 \mu\text{A}$ , ( $I(E1) = 227 \mu\text{A}$ ).



**EXERCISE:** What is the current exiting the positive terminal of source  $V_2$  in Ex. 10.7?

**ANSWER:**  $27.3 \mu\text{A}$

**EXERCISE:** What are the voltage gain  $A_v$ , output voltage  $V_O$ , output current  $I_O$ , and the current in source  $V_2$  for the amplifier in Ex. 10.7 if  $V_1 = 3 \text{ V}$  and  $V_2 = 5 \text{ V}$ ?

**ANSWERS:**  $-10$ ;  $20.0 \text{ V}$ ;  $+154 \mu\text{A}$ ,  $45.5 \mu\text{A}$

**EXERCISE:** What are the voltage gain  $A_v$ , output voltage  $V_o$  and output current  $I_o$  for the amplifier in Fig. 10.25 if  $R_1 = 2 \text{ k}\Omega$ ,  $R_2 = 36 \text{ k}\Omega$ ,  $V_1 = 8 \text{ V}$ , and  $V_2 = 8.25 \text{ V}$ ?

**ANSWERS:**  $-18.0$ ;  $4.50 \text{ V}$ ;  $-92.0 \mu\text{A}$

## 10.10 FREQUENCY DEPENDENT FEEDBACK

Although the operational-amplifier circuit examples thus far have used only resistors in the feedback network, other passive elements or even solid-state devices can be part of the feedback path. The general case of the inverting configuration with passive feedback is shown in Fig. 10.26, in which resistors  $R_1$  and  $R_2$  have been replaced by general impedances  $Z_1(s)$  and  $Z_2(s)$ , which may now be a function of frequency. (Note that resistive feedback is just a special case of the amplifier in Fig. 10.26.)

The gain of this amplifier can be described by its **transfer function** in the frequency domain in which  $s = \sigma + j\omega$  represents the complex frequency variable:

$$A_v(s) = \frac{V_o(s)}{V_i(s)} \quad (10.65)$$

General amplifier transfer functions can be quite complicated, having many poles and zeros, but their overall behavior can be broken down into a number of categories including low-pass, high-pass, and band-pass amplifiers to name a few. In the next several sections we will review Bode plots for low-pass and high-pass amplifiers. Other types of transfer functions will be discussed in later chapters.

### 10.10.1 BODE PLOTS

When we explore the characteristics of amplifiers, we are usually interested in the behavior of the transfer function for physical frequencies  $\omega$ —that is, for  $s = j\omega$ , and the transfer function can then be represented in polar form by its **magnitude**  $|A_v(j\omega)|$  and **phase angle**  $\angle A_v(j\omega)$ , which are both functions of frequency:

$$A_v(j\omega) = |A_v(j\omega)| \angle A_v(j\omega) \quad (10.66)$$

It is often convenient to display this information separately in a graphical form called a **Bode plot**. The Bode plot displays the magnitude of the transfer function in dB and the phase in degrees (or radians) versus a logarithmic frequency scale. Bode plots for low-pass and high-pass amplifiers are discussed in the next section.

### 10.10.2 THE LOW-PASS AMPLIFIER

Circuits that amplify signals over a range of frequencies including dc are an extremely important class of circuits and are referred to as low-pass amplifiers. For instance, most operational amplifiers are designed as low-pass amplifiers. The simplest low-pass amplifier circuit is described by the

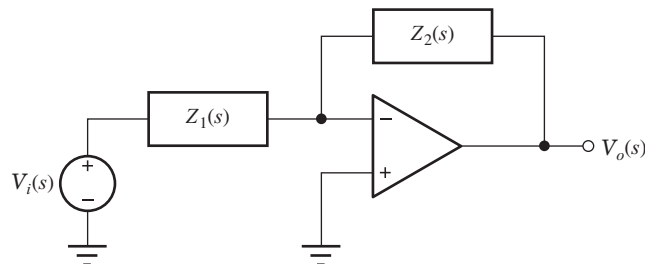
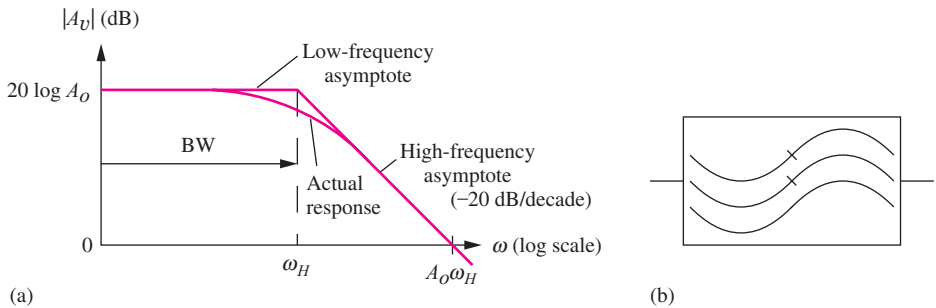


Figure 10.26 Generalized inverting-amplifier configuration.



**Figure 10.27** (a) Low-pass amplifier:  $BW = \omega_H$  and  $GBW = A_o\omega_H$ . (b) Low-pass filter symbol.

single-pole<sup>4</sup> transfer function

$$A_v(s) = \frac{A_o\omega_H}{s + \omega_H} = \frac{A_o}{1 + \frac{s}{\omega_H}} \quad (10.67)$$

in which  $A_o$  is the low-frequency gain and  $\omega_H$  represents the cutoff frequency of this low-pass amplifier. Let us first explore the behavior of the magnitude of  $A_v(s)$  and then look at the phase response.

### Magnitude Response

Substituting  $s = j\omega$  into Eq. (10.67) and finding the magnitude of the function  $A_v(j\omega)$  yields

$$|A_v(j\omega)| = \left| \frac{A_o\omega_H}{j\omega + \omega_H} \right| = \frac{|A_o\omega_H|}{\sqrt{\omega^2 + \omega_H^2}} \quad (10.68)$$

The Bode magnitude plot is given in terms of dB:

$$|A_v(j\omega)|_{dB} = 20 \log |A_o\omega_H| - 20 \log \sqrt{\omega^2 + \omega_H^2} \quad (10.69)$$

For a given set of numeric values, Eq. (10.69) can be easily evaluated and plotted using a package such as MATLAB or a spreadsheet, and results in the graph in Fig. 10.27.

For the general case, the graph is conveniently plotted in terms of its asymptotic behavior at low and high frequencies. For low frequencies,  $\omega \ll \omega_H$ , the magnitude is approximately constant:

$$\left. \frac{A_o\omega_H}{\sqrt{\omega^2 + \omega_H^2}} \right|_{\omega \ll \omega_H} \approx \frac{A_o\omega_H}{\sqrt{\omega_H^2}} = A_o \quad \text{or} \quad (20 \log A_o) \text{ dB} \quad (10.70)$$

At frequencies well below  $\omega_H$ , the gain of the amplifier is constant and equal to  $A_o$ , which corresponds to the horizontal asymptote in Fig. 10.27. Signals at frequencies below  $\omega_H$  are amplified by the gain  $A_o$ . In fact, the gain of this amplifier is constant down to dc ( $\omega = 0$ )!

However, as  $\omega$  exceeds  $\omega_H$ , the gain of the amplifier begins to decrease (high-frequency roll-off). For sufficiently high frequencies,  $\omega \gg \omega_H$ , the magnitude can be approximated by

$$\left. \frac{A_o\omega_H}{\sqrt{\omega^2 + \omega_H^2}} \right|_{\omega \gg \omega_H} \approx \frac{A_o\omega_H}{\sqrt{\omega^2}} = \frac{A_o\omega_H}{\omega} \quad (10.71)$$

and converting Eq. (10.70) to dB yields

$$|A_v(j\omega)|_{dB} \cong \left( 20 \log A_o - 20 \log \frac{\omega}{\omega_H} \right) \text{ dB} \quad (10.72)$$

<sup>4</sup> A general low-pass amplifier may have many poles. The single-pole version is the simplest approximation to the ideal low-pass characteristic described in Chapter 1.

For frequencies much greater than  $\omega_H$ , the transfer function decreases at a rate of 20 dB per decade increase in frequency, as indicated by the high-frequency asymptote in Fig. 10.27. Obviously,  $\omega_H$  plays an important role in characterizing the amplifier; this critical frequency is called the **upper-cutoff frequency** of the amplifier. At  $\omega = \omega_H$ , the gain of the amplifier is

$$|A_v(j\omega_H)| = \frac{A_o\omega_H}{\sqrt{\omega_H^2 + \omega_H^2}} = \frac{A_o}{\sqrt{2}} \quad \text{or} \quad [(20 \log A_o) - 3] \text{ dB} \quad (10.73)$$

and  $\omega_H$  is sometimes referred to as the **upper -3-dB frequency** of the amplifier.  $\omega_H$  is also often termed the **upper half-power point** of the amplifier because the output power of the amplifier, which is proportional to the square of the voltage, is reduced by a factor of 2 at  $\omega = \omega_H$ . Note that when the expressions for the two asymptotes given in Eqs. (10.70) and (10.71) are equated, they intersect precisely at  $\omega = \omega_H$ .

### Bandwidth

The gain of the amplifier in Fig. 10.27 is approximately uniform (it varies by less than 3 dB) for all frequencies below  $\omega_H$ . This is called a **low-pass amplifier**. The **bandwidth (BW)** of an amplifier is defined by the range of frequencies in which the amplification is approximately constant; it is expressed in either radians/second or Hz. For the low-pass amplifier,

$$\text{BW} = \omega_H \text{ (rad/s)} \quad \text{or} \quad \text{BW} = f_H = \frac{\omega_H}{2\pi} \text{ Hz} \quad (10.74)$$

### Gain-Bandwidth Product

The **gain-bandwidth product** is often used as a figure-of-merit for comparing amplifiers, and for a low-pass amplifier it is simply the product of the low-frequency gain and the bandwidth of the amplifier:

$$\text{GBW} = A_o\omega_H \quad (10.75)$$

For a single-pole, low-pass characteristic, the GBW also represents the **unity-gain** frequency  $\omega_T$  of the amplifier, the frequency at which the magnitude of the gain becomes 1 or 0 dB. We can find  $\omega_T$  using Eq. (10.71) for  $\omega \gg \omega_H$ :

$$|A_v(j\omega_T)| = 1 \quad \text{or} \quad \frac{A_o\omega_H}{\omega_T} = 1 \quad \text{and} \quad \omega_T = A_o\omega_H \quad (10.76)$$

**EXERCISE:** Find the low-frequency gain, cutoff frequency, bandwidth, and gain-bandwidth product of the low-pass amplifier with the following transfer function:

$$A_v(s) = -\frac{2\pi \times 10^6}{(s + 5000\pi)}$$

**ANSWERS:** -400, 2.5 kHz, 2.5 kHz, 1 MHz

### Phase Response

The phase behavior versus frequency is also of interest in many applications and later will be found to be of great importance to the stability of feedback amplifiers. Again substituting  $s = j\omega$  in Eq. (10.66), the phase response of the low-pass amplifier is found to be

$$\angle A_v(j\omega) = \angle \frac{A_o}{1 + j \frac{\omega}{\omega_H}} = \angle A_o - \tan^{-1} \left( \frac{\omega}{\omega_H} \right) \quad (10.77)$$

The phase angle of  $A_o$  is  $0^\circ$  if  $A_o$  is positive and  $180^\circ$  if  $A_o$  is negative.

**TABLE 10.5**  
Inverse Tangent

$\omega$	$\tan^{-1} \frac{\omega}{\omega_C}$
$0.01 \omega_C$	$0.057^\circ$
$0.1 \omega_C$	$5.7^\circ$
$\omega_C$	$45^\circ$
$10 \omega_C$	$84.3^\circ$
$100 \omega_C$	$89.4^\circ$

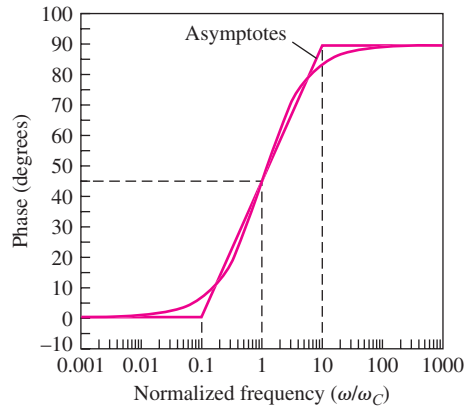


**Figure 10.28** Phase versus normalized frequency ( $\omega/\omega_C$ ) resulting from a single inverse tangent term  $+\tan^{-1}(\omega/\omega_C)$ . The straight-line approximation is also given.

The frequency-dependent phase term associated with each pole or zero in a transfer function involves the evaluation of the inverse tangent function, as in Eq. (10.77). Important values appear in Table 10.5, and a graph of the complete inverse tangent function is given in Fig. 10.28. At the pole or zero frequency indicated by critical frequency  $\omega_C$ , the magnitude of the phase shift is  $45^\circ$ . One decade below  $\omega_C$ , the phase is  $5.7^\circ$ , and one decade above  $\omega_C$ , the phase is  $84.3^\circ$ . Two decades away from  $\omega_C$ , the phase approaches its asymptotic limits of  $0^\circ$  and  $90^\circ$ . Note that the phase response can also be approximated by the three straight-line segments in Fig. 10.28, in a manner similar to the asymptotes of the magnitude response.

The phase of more complex transfer functions with multiple poles and zeros is simply given by the appropriate sum and differences of inverse tangent functions. However, they are most easily evaluated with a computer or calculator.

### EXAMPLE 10.8 THE RC LOW-PASS FILTER

An *RC* low-pass network is a simple but important passive circuit that we will encounter in the upcoming chapters.

**PROBLEM** Find the voltage transfer function  $V_o/V_i$  for the low-pass network in the figure below.

$$V_o = V_i \frac{\frac{R_2/sC}{R_2 + 1/sC}}{R_1 + \frac{R_2/sC}{R_2 + 1/sC}}$$

$$\frac{V_o}{V_i} = \left( \frac{R_2}{R_1 + R_2} \right) \left( \frac{1}{1 + \frac{s}{\omega_H}} \right)$$

**SOLUTION Known Information and Given Data:** Circuit as given above in the problem statement.

**Unknowns:** Voltage transfer function  $V_o/V_i$

**Approach:** Find the transfer function by applying voltage division in the frequency domain ( $s$  domain). Remember that the impedance of the capacitor is  $1/sC$ .

**Assumptions:** None

**Analysis:** Direct application of voltage division yields the equations next to the schematic, where the upper cutoff frequency is

$$\omega_H = \frac{1}{(R_1 \parallel R_2)C}$$

**Check of Results:** For  $s \ll \omega_H$ , the gain through the network is  $R_2/(R_1 + R_2)$ , which is correct.

**Discussion:** The cutoff frequency  $\omega_H$  occurs at the frequency for which the reactance of the capacitor equals the parallel combination of resistors  $R_1$  and  $R_2$ :  $1/\omega_H C = R_1 \parallel R_2$ .  $R_1 \parallel R_2$  represents the Thévenin equivalent resistance present at the capacitor terminals. For  $\omega \ll \omega_H$ , the impedance of the capacitor is negligible with respect to the resistance in the circuit.

**EXERCISE:** What is the cutoff frequency for the low-pass circuit in Ex. 10.8 if  $R_1 = 1 \text{ k}\Omega$ ,  $R_2 = 100 \text{ k}\Omega$ , and  $C = 200 \text{ pF}$ ?

**ANSWER:** 804 kHz

### 10.10.3 THE HIGH-PASS AMPLIFIER

A second basic single-pole transfer function is the high-pass characteristic, which includes a single pole plus a zero at the origin. We most often find this function combined with the low-pass function to form **band-pass amplifiers**. In fact a true high-pass characteristic is impossible to obtain since we will see that it requires infinite bandwidth. The best we can hope to do is approximate the high-pass characteristic over some finite range of frequencies.

The transfer function for a single-pole **high-pass amplifier** can be written as

$$A_v(s) = \frac{A_o s}{s + \omega_L} = \frac{A_o}{1 + \frac{\omega_L}{s}} \quad (10.78)$$

and for  $s = j\omega$  the magnitude of Eq. (10.78) is

$$|A_v(j\omega)| = \left| \frac{A_o j\omega}{j\omega + \omega_L} \right| = \frac{A_o \omega}{\sqrt{\omega^2 + \omega_L^2}} = \frac{A_o}{\sqrt{1 + \left(\frac{\omega_L}{\omega}\right)^2}} \quad (10.79)$$

The Bode magnitude plot for this function is depicted in Fig. 10.29. In this case, the gain of the amplifier is constant for all frequencies above the **lower-cutoff frequency  $\omega_L$** . At frequencies high enough to satisfy  $\omega \gg \omega_L$ , the magnitude can be approximated by

$$\left. \frac{A_o \omega}{\sqrt{\omega^2 + \omega_L^2}} \right|_{\omega \gg \omega_L} \cong \frac{A_o \omega}{\sqrt{\omega^2}} = A_o \quad \text{or} \quad (20 \log A_o) \text{ dB} \quad (10.80)$$

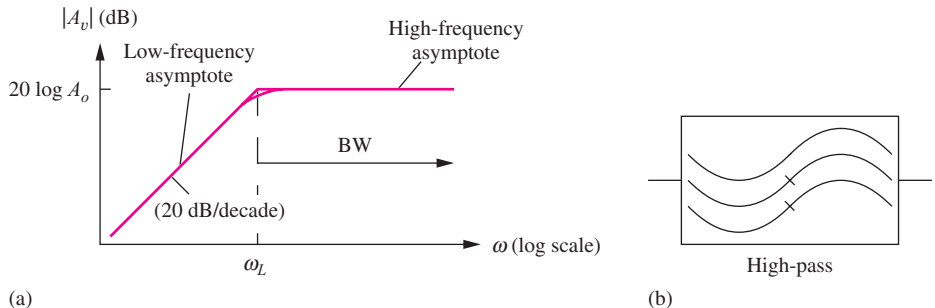


**Figure 10.29** (a) High-pass amplifier. (b) High-pass filter symbol.

For  $\omega$  exceeding  $\omega_L$ , the gain is constant at gain  $A_0$ . At frequencies well below  $\omega_L$ ,

$$\left. \frac{A_o\omega}{\sqrt{\omega^2 + \omega_L^2}} \right|_{\omega \ll \omega_L} \cong \frac{A_o\omega}{\sqrt{\omega_L^2}} = \frac{A_o\omega}{\omega_L} \quad (10.81)$$

Converting Eq. (10.81) to dB yields

$$|A_v(j\omega)| \cong (20 \log A_o) + 20 \log \frac{\omega}{\omega_1} \quad (10.82)$$

At frequencies below  $\omega_L$ , the gain increases at a rate of 20 dB per decade increase in frequency.  
**At critical frequency**  $\omega = \omega_L$ ,

$$|A_v(j\omega_L)| = \frac{A_o \omega_L}{\sqrt{\omega_L^2 + \omega_o^2}} = \frac{A_o}{\sqrt{2}} \quad \text{or} \quad [(20 \log A_o) - 3] \text{ dB} \quad (10.83)$$

The gain is again 3 dB below its midband value. Besides being called the lower-cutoff frequency,  $\omega_L$  is referred to as the **lower -3-dB frequency** or the **lower half-power point**.

The high-pass amplifier provides approximately uniform gain at all frequencies above  $\omega_L$ , and its bandwidth is therefore infinite:

$$\text{BW} \equiv \infty = \rho_L \equiv \infty \quad (10.84)$$

The phase dependence of the high-pass amplifier is found by evaluating the phase of  $A_v(j\omega)$  from Eq. (10.78):

$$\text{and } \angle A_v(j\omega) = \angle \frac{A_o j\omega}{j\omega + \omega_l} = \angle A_o + 90^\circ - \tan^{-1} \left( \frac{\omega}{\omega_l} \right) \quad (10.85)$$

This phase expression is similar to that of the low-pass amplifier, except for a  $+90^\circ$  shift due to the  $s$  term in the numerator.

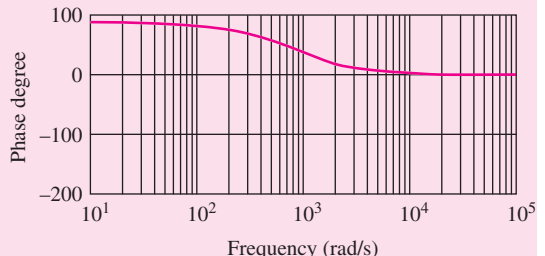
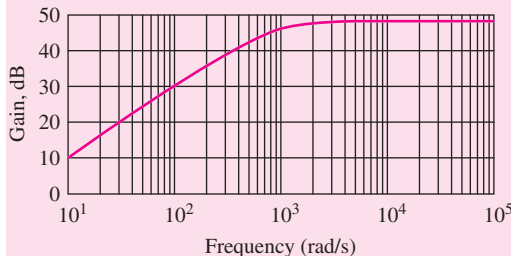
**EXERCISE:** Find the midband gain, cutoff frequency, and bandwidth of the amplifier with this transfer function:

$$A_v(s) = \frac{250s}{(s + 250\pi)}$$

**ANSWERS:** 250; 125 Hz;  $\infty$

**EXERCISE:** Use MATLAB to produce a Bode plot of this transfer function.

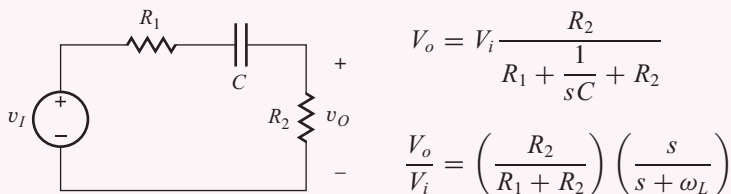
**ANSWER:**  $w = \text{logspace}(1,5,100)$   
 $\text{bode}([250\ 0],[1\ 250*\pi],w)$



### EXAMPLE 10.9 THE RC HIGH-PASS FILTER

The *RC* high-pass network is another important passive circuit that we will encounter in the upcoming chapters.

**PROBLEM** Find the voltage transfer function  $V_o/V_i$  for the high-pass network in the figure below.



**SOLUTION** **Known Information and Given Data:** Circuit as given in the problem statement.

**Unknowns:** Voltage transfer function  $V_o/V_i$

**Approach:** Find the transfer function by applying voltage division in the frequency domain ( $s$  domain). Remember that the impedance of the capacitor is  $1/sC$ .

**Assumptions:** None

**Analysis:** Direct application of voltage division yields the equation next to the circuit schematic, where the lower cutoff frequency is

$$\omega_L = \frac{1}{(R_1 + R_2)C}$$

**Check of Results:** For  $\omega \gg \omega_L$ , the gain through the network is  $R_2/(R_1 + R_2)$ , which is correct.

**Discussion:** Cutoff frequency  $\omega_L$  occurs at the frequency for which the reactance of the capacitor equals the sum of resistors  $R_1$  and  $R_2$ , which represents the Thévenin equivalent resistance at the capacitor terminals:  $1/\omega_L C = R_1 + R_2$ . For  $\omega \gg \omega_L$ , the impedance of the capacitor is negligible with respect to the resistance in the circuit.

**EXERCISE:** What is the cutoff frequency for the high-pass circuit in Ex. 10.9 if  $R_1 = 1 \text{ k}\Omega$ ,  $R_2 = 100 \text{ k}\Omega$ , and  $C = 0.1 \mu\text{F}$ ?

**ANSWER:** 15.8 Hz

#### 10.10.4 BAND-PASS AMPLIFIERS

Many amplifiers combine low-pass and high-pass characteristics to form a bandpass amplifier as shown in the graph in Fig. 10.30. For example, audio amplifiers are often designed to only pass frequencies in the 20 Hz–20 kHz range. In this case, the lower and upper cutoff frequencies  $f_L$  and  $f_H$  would be set to 20 Hz and 20 kHz respectively. The region of constant gain between  $\omega_L$  and  $\omega_H$  is referred to as midband.

The transfer function for a basic **band-pass amplifier** can be constructed from the product of the low-pass and high-pass transfer functions from Eqs. (10.67) and (10.78):

$$A_v(s) = \frac{A_o s \omega_H}{(s + \omega_L)(s + \omega_H)} = A_o \frac{s}{(s + \omega_L)} \frac{1}{\left(\frac{s}{\omega_H} + 1\right)} \quad (10.86)$$

The **midband** range of frequencies is defined by  $\omega_L \leq \omega \leq \omega_H$ , for which

$$|A_v(j\omega)| \cong A_o \quad (10.87)$$

$A_o$  represents the gain in this midband region and is called the **midband gain**:  $A_{\text{mid}} = A_o$ .

The mathematical expression for the magnitude of  $A_v(j\omega)$  is

$$|A_v(j\omega)| = \left| \frac{A_o j\omega \omega_H}{(j\omega + \omega_L)(j\omega + \omega_H)} \right| = \frac{A_o \omega \omega_H}{\sqrt{(\omega^2 + \omega_L^2)(\omega^2 + \omega_H^2)}} \quad (10.88)$$

or

$$|A_v(j\omega)| = \frac{A_{\text{mid}}}{\sqrt{\left(1 + \frac{\omega_L^2}{\omega^2}\right)\left(1 + \frac{\omega^2}{\omega_H^2}\right)}} \quad (10.89)$$

The expression in Eq. (10.89) has been written in a form that exposes the gain in the midband region.

At both  $\omega_L$  and  $\omega_H$ , it is easy to show, assuming  $\omega_L \ll \omega_H$ , that

$$|A_v(j\omega_L)| = \frac{A_o}{\sqrt{2}} = |A(j\omega_H)| \quad \text{or} \quad [(20 \log A_o) - 3] \text{ dB} \quad (10.90)$$

The gain is 3 dB below the midband gain at both critical frequencies. The region of approximately uniform gain (that is, the region of less than 3 dB variation) extends from  $\omega_L$  to  $\omega_H$  ( $f_L$  to  $f_H$ ), and hence the bandwidth of the band-pass amplifier is

$$\text{BW} = f_H - f_L = \frac{\omega_H - \omega_L}{2\pi} \quad (10.91)$$

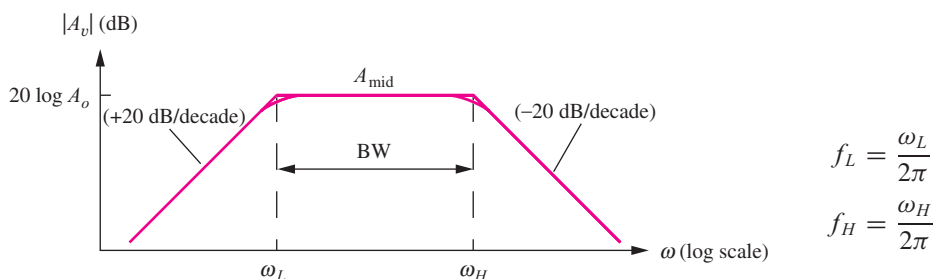


Figure 10.30 Band-pass amplifier.

Evaluating the phase of  $A_v(j\omega)$  from Eq. (10.86),

$$\angle A_v(j\omega) = \angle A_o + 90^\circ - \tan^{-1} \left( \frac{\omega}{\omega_L} \right) - \tan^{-1} \left( \frac{\omega}{\omega_H} \right) \quad (10.92)$$

An example of this phase response is in the next exercise.

### EXAMPLE 10.10 TRANSFER FUNCTION EVALUATION

This example is included to help refresh our memory on calculations involving complex numbers.

**PROBLEM** Find the magnitude and phase of this voltage transfer function for  $\omega = 0$  and  $\omega = 3$  rad/s.

$$A_v(s) = 50 \frac{s^2 + 4}{s^2 + 2s + 2}$$

**SOLUTION** **Known Information and Given Data:** Transfer function describing the voltage gain

**Unknowns:** Magnitude and phase of  $A_v(j0)$  and  $A_v(j3)$

**Approach:** Substitute  $s = j\omega$  into the expression for  $A_v(s)$  and simplify. Substitute  $\omega = 0$  and  $\omega = 3$  into the resulting expressions. Then find magnitude and phase of the resulting complex numbers.

**Assumptions:** We remember how to do arithmetic with complex numbers.

**Analysis:** Inserting  $s = j\omega$  into  $A_v(s)$  and rearranging yields

$$A_v(j\omega) = 50 \frac{\omega^2 - 4}{(\omega^2 - 2) - j(2\omega)}$$

The magnitude and phase of this expression are

$$|A_v(j\omega)| = 50 \frac{|\omega^2 - 4|}{\sqrt{(\omega^2 - 2)^2 + 4\omega^2}} \quad \text{and} \quad \angle A_v(j\omega) = \angle(\omega^2 - 4) - \tan^{-1} \left( \frac{-2\omega}{\omega^2 - 2} \right)$$

Substituting  $\omega = 0$  gives

$$|A_v(j\omega)| = \frac{200}{\sqrt{4}} = 100 \quad \text{or} \quad 40.0 \text{ dB}$$

$$\angle A_v(j\omega) = \angle(200) - \tan^{-1}(-0) = 0^\circ$$

Substituting  $\omega = 3$  gives

$$|A_v(j3)| = \frac{250}{\sqrt{49 + 36}} = 27.1 \quad \text{or} \quad 28.7 \text{ dB}$$

$$\angle A_v(j\omega) = \angle(250) - \tan^{-1} \left( \frac{-6}{7} \right) = 0^\circ - (-40.6) = 40.6^\circ$$

**Check of Results:** We can easily check the results using MATLAB or a calculator. With MATLAB,

```

h = freqs([50 0 200], [1 2 2], [0 3]);
abs(h)
angle (h) * 180/pi

```

The results confirm the preceding analysis.

**EXERCISE:** Find the magnitude and phase of the voltage gain in Ex. 10.10 for  $\omega = 1 \text{ rad/s}$  and  $\omega = 5 \text{ rad/s}$ .

**ANSWERS:** 36.5 dB,  $-63.4^\circ$ ; 32.4 dB,  $23.5^\circ$

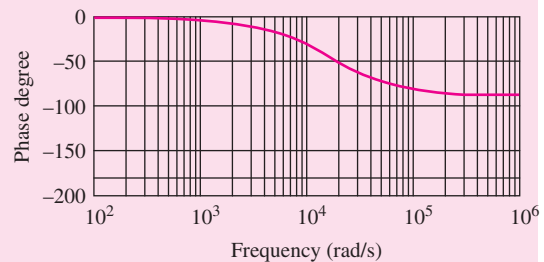
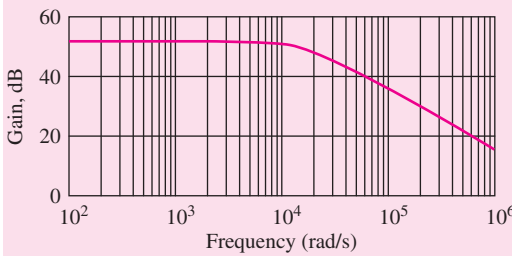
**EXERCISE:** Find the magnitude and phase of the following transfer function for  $\omega = 0.95, 1.0$ , and  $1.10$ .

$$A_v(s) = 20 \frac{s^2 + 1}{s^2 + 0.1s + 1}$$

**ANSWERS:** 14.3,  $-44.3^\circ$ ; 0,  $-90^\circ$ ; 17.7,  $+27.6^\circ$

**EXERCISE:** Make a Bode plot of the following  $A_v(s)$  using MATLAB:  $A_v(s) = -\frac{2\pi \times 10^6}{(s + 5000\pi)}$

**ANSWER:** `w = logspace(2, 6, 100)`  
`bode(2*pi*1e6,[1 5000*pi],w)`



**EXERCISE:** Find the midband gain, lower- and upper-cutoff frequencies, and bandwidth of the amplifier with the following transfer function:

$$A_v(s) = -\frac{2 \times 10^7 s}{(s + 100)(s + 50000)}$$

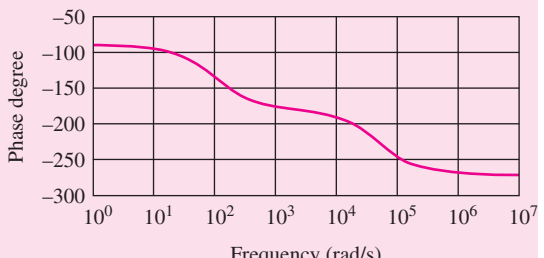
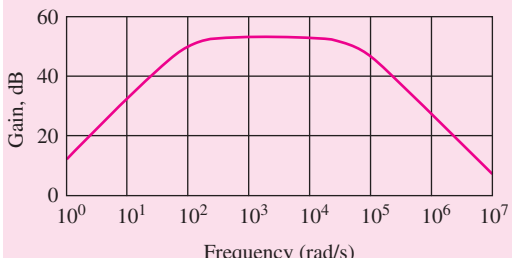
**ANSWERS:** 52 dB; 15.9 Hz; 7.96 kHz; 7.94 kHz

**EXERCISE:** Write an expression for the phase of the transfer function above. What is the phase shift for  $w = 0, 100, 50,000$ , and  $\infty$ ?

**ANSWERS:**  $\angle A_v(j\omega) = -90^\circ - \tan^{-1} \left( \frac{\omega}{100} \right) - \tan^{-1} \left( \frac{\omega}{50000} \right); -90^\circ, -135^\circ, -225^\circ, -270^\circ$

**EXERCISE:** Use MATLAB or another computer program to produce a Bode plot of the previous transfer function.

**ANSWER:** `w = logspace(0, 7, 150)`  
`bode([-2e7 0],[1 50,100 5e6],w)`



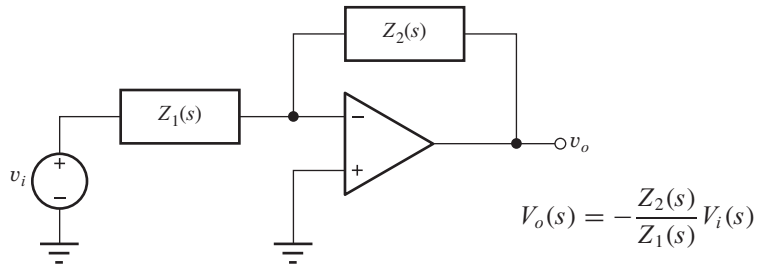


**Figure 10.31** Generalized inverting-amplifier configuration.

### 10.10.5 AN ACTIVE LOW-PASS FILTER

Now let us return to considering the generalized inverting-amplifier circuit in Fig. 10.31. The gain of the amplifier in this figure is obtained in a manner identical to that in the resistive-feedback case. Replacing  $R_1$  by  $Z_1$  and  $R_2$  by  $Z_2$  in Eq. (10.41) yields the transfer function  $A_v(s)$ :

$$A_v(s) = \frac{\mathbf{V}_o(s)}{\mathbf{V}_i(s)} = -\frac{Z_2(s)}{Z_1(s)} \quad (10.93)$$

One useful circuit involving frequency-dependent feedback is the single-pole, **low-pass filter** in Fig. 10.32, for which

$$Z_1(s) = R_1 \quad \text{and} \quad Z_2(s) = \frac{\frac{1}{R_2 s C}}{\frac{1}{R_2} + \frac{1}{sC}} = \frac{R_2}{sCR_2 + 1} \quad (10.94)$$

Substituting the results from Eq. (10.94) into Eq. (10.93) yields an expression for the voltage transfer function for the low-pass filter.

$$A_v(s) = -\frac{R_2}{R_1} \frac{1}{(1 + sR_2C)} = -\frac{R_2}{R_1} \frac{1}{\left(1 + \frac{s}{\omega_H}\right)} \quad \text{where} \quad \omega_H = 2\pi f_H = \frac{1}{R_2 C} \quad (10.95)$$

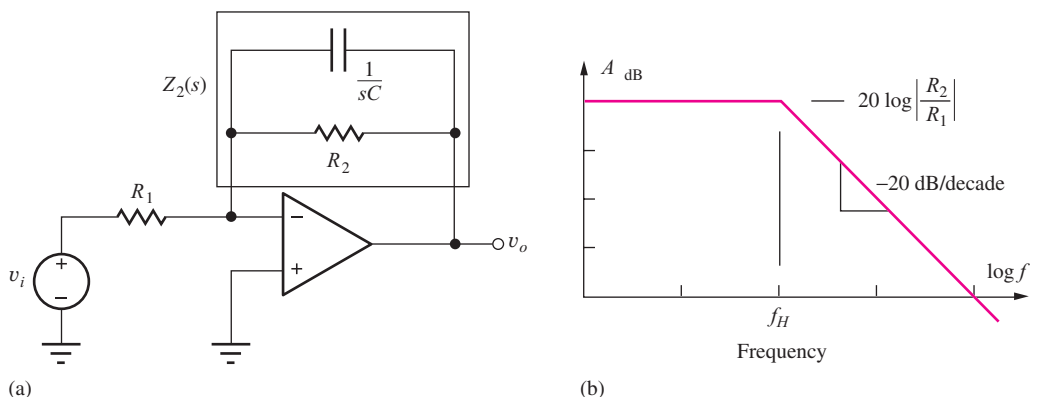


**Figure 10.32** (a) Inverting amplifier with frequency-dependent feedback. (b) Bode plot of the voltage gain of the low-pass filter.

Figure 10.32(b) is the asymptotic Bode plot of the magnitude of the gain in Eq. (10.95). The transfer function exhibits a low-pass characteristic with a single pole at frequency  $\omega_H$ , the upper-cutoff frequency ( $-3$  dB point) of the low-pass filter. At frequencies below  $\omega_H$ , the amplifier behaves as an inverting amplifier with gain set by the ratio of resistors  $R_2$  and  $R_1$ ; at frequencies above  $\omega_H$ , the amplifier response rolls off at a rate of  $-20$  dB/decade.

Note from Eq. (10.95) that the low-frequency gain and the cutoff frequency can be set independently in this **low-pass filter**. Indeed, because there are three elements —  $R_1$ ,  $R_2$ , and  $C$  — the input resistance ( $R_{in} = R_1$ ) can be a third design parameter. Since the inverting input terminal is at  $0$  V (remember it is a virtual ground),  $R_{in} = R_1$ . Filters that employ gain elements such as op amps or transistors are often referred to as **active filters**.

### Understanding Low-Pass Filter Operation

The low-pass filter circuit functions in manner similar to the inverting amplifier. The virtual ground at the inverting input causes input voltage  $V_i$  to appear directly across resistor  $R_1$  establishing an input current  $V_i/R_1$  (using frequency domain notation). The op amp forces this input current to flow out through  $Z_2$  developing a voltage drop of  $(V_i/R_1) \cdot Z_2$  across  $Z_2$ . Because of the virtual ground,  $v_o = -(V_i/R_1) \cdot Z_2$ , and the gain is  $-Z_2/R_1$  as expressed in Eq. (10.94).

At low frequencies (below  $\omega_H$ ), the amplifier operates as an inverting amplifier with gain of  $-R_2/R_1$ , since the capacitive reactance ( $1/\omega C$ ) is much larger than that of  $R_2$  and can be neglected. As frequencies increase, the magnitude of the impedance of the parallel combination of  $R_2$  and  $C$  falls, reducing the gain. At high frequencies, the impedance of  $C$  becomes small,  $R_2$  can be neglected, and the gain falls at a rate of  $20$  dB per decade as  $(1/\omega C)$  decreases.

## DESIGN ACTIVE LOW-PASS FILTER DESIGN

### EXAMPLE 10.11

Design a single-pole low-pass filter using the single op-amp circuit in Fig. 10.32(a) to meet a given cutoff frequency specification.

**PROBLEM** Design an active low-pass filter (choose the values of  $R_1$ ,  $R_2$ , and  $C$ ) with  $f_H = 2$  kHz,  $R_{in} = 5\text{ k}\Omega$ , and  $A_v = 40$  dB.

**SOLUTION** **Known Information and Given Data:** In this case, we are given the values for the bandwidth, gain and input resistance ( $f_H = 2$  kHz,  $R_{in} = 5\text{ k}\Omega$ , and  $A_v = 40$  dB), and the amplifier circuit configuration has also been specified. However, we must convert the gain from dB to purely numeric form before we use it in the calculations:

$$|A_v| = 10^{40\text{ dB}/20\text{ dB}} = 100$$

**Unknowns:** Find the values of  $R_1$ ,  $R_2$ , and  $C$ .

**Approach:** Use the single-pole low-pass filter circuit in Fig. 10.32(a). The three specifications should uniquely determine the three unknowns. We will use  $R_{in}$  to determine  $R_1$ ,  $R_1$  to find  $R_2$ , and  $R_2$  to find  $C$ .

**Assumptions:** The op amp is ideal. Note that the specified gain actually represents the low-frequency gain of the amplifier and that a gain of either  $+100$  or  $-100$  will satisfy the gain specification.

**Analysis:** Since the inverting input represents a virtual ground, the input resistance is set directly by  $R_1$  so that

$$R_1 = R_{\text{in}} = 5 \text{ k}\Omega$$

and

$$|A_v| = \frac{R_2}{R_1} \rightarrow R_2 = 100R_1 = 500 \text{ k}\Omega$$

The value of  $C$  can now be determined from the  $f_H$  specification:

$$C = \frac{1}{2\pi f_H R_2} = \frac{1}{2\pi(2 \text{ kHz})(500 \text{ k}\Omega)} = 1.59 \times 10^{-10} \text{ F} = 159 \text{ pF}$$

Looking at Appendix A, we find the nearest values for  $R_1$  and  $R_2$  are 5.1 k $\Omega$  and 510 k $\Omega$ . In most applications, an input resistance of 5.1 k $\Omega$  (set by  $R_1$ ) would be acceptable since it is only 2 percent higher than the design specification of 5 k $\Omega$ . Recalculating the value of  $C$  using the new value of  $R_2$  yields

$$C = \frac{1}{2\pi f_H R_2} = \frac{1}{2\pi(2 \text{ kHz})(510 \text{ k}\Omega)} = 156 \text{ pF}$$

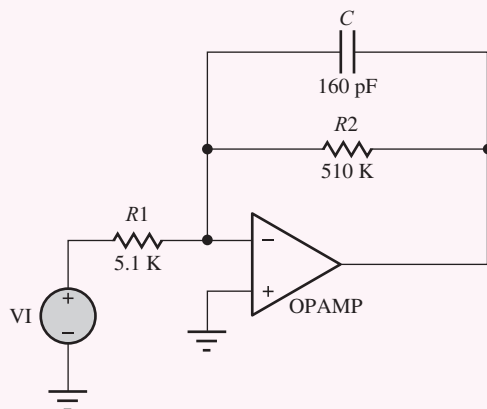
The closest capacitor value is 160 pF, which will lower  $f_H$  to 1.95 kHz. A second choice would be 150 pF for which  $f_H = 2.08$  kHz.

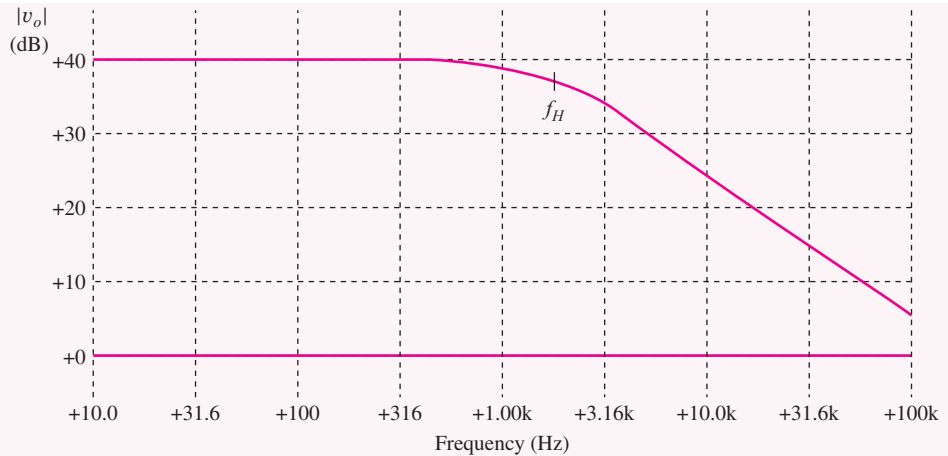
**Final Design:**  $R_1 = 5.1 \text{ k}\Omega$ ,  $R_2 = 510 \text{ k}\Omega$ , and  $C = 160 \text{ pF}$ , yielding a slightly smaller bandwidth than the design specification.

**Check of Results:** We have found the three required values. The SPICE analysis here confirms the design.

**Discussion:** A third but more costly option would be to use a parallel combination of two capacitors, 100 pF and 56 pF. In a similar vein,  $R_1$  and  $R_2$  could be synthesized from the series combination of two resistors (e.g.,  $R_1 = 4.7 \text{ k}\Omega + 300 \Omega$ ). It might be preferable to just use more expensive 1 percent resistors with  $R_1 = 4.99 \text{ k}\Omega$  and  $R_2 = 499 \text{ k}\Omega$ . In order to select between these options, one would need to know more details about the application. Note that trying to use an exact values of  $R$  and  $C$  doesn't provide much benefit if the resistor and capacitor tolerances are 5, 10, or 20 percent.

**Computer-Aided Analysis:** An ac analysis of the low-pass filter circuit is performed using the equivalent circuit below. The op amp gain is set to  $10^6$  (120 dB). The frequency response parameters are Start Frequency = 10 Hz, Stop Frequency = 100 KHz with 10 frequency points per decade. From the graph,  $A_v = 40 \text{ dB}$  and  $f_H = 1.95 \text{ kHz}$  as designed.





**EXERCISE:** Design an active low-pass filter (choose the values of  $R_1$ ,  $R_2$ , and  $C$ ) with  $f_H = 3 \text{ kHz}$ ,  $R_{in} = 10 \text{ k}\Omega$ , and  $A_v = 26 \text{ dB}$ .

**ANSWERS:** Calculated values:  $10 \text{ k}\Omega$ ,  $200 \text{ k}\Omega$ ,  $265 \text{ pF}$ ; Appendix A values:  $10 \text{ k}\Omega$ ,  $200 \text{ k}\Omega$ ,  $270 \text{ pF}$

### 10.10.6 AN ACTIVE HIGH-PASS FILTER

We can also create an active high-pass filter by changing the form of impedances in the generalized inverting amplifier as in Fig. 10.33(a). Here  $Z_1$  is replaced by the series combination of capacitor  $C$  and resistor  $R_1$ , and  $Z_2$  is resistor  $R_2$ :

$$Z_1 = R_1 + \frac{1}{sC} = \frac{sCR_1 + 1}{sC} \quad \text{and} \quad Z_2 = R_2 \quad (10.96)$$

Substituting the results from Eq. (10.96) into Eq. (10.93) produces the voltage transfer function for the high-pass filter.

$$A_v(s) = -\frac{Z_2}{Z_1} = -\frac{R_2}{R_1} \frac{sCR_1}{sCR_1 + 1} = -\frac{R_2}{R_1} \frac{1}{1 + \frac{s}{\omega_L}} = \frac{A_o}{1 + \frac{s}{\omega_L}} \quad (10.97)$$

where  $A_o = -\frac{R_2}{R_1}$  and  $\omega_L = 2\pi f_L = \frac{1}{R_1 C}$

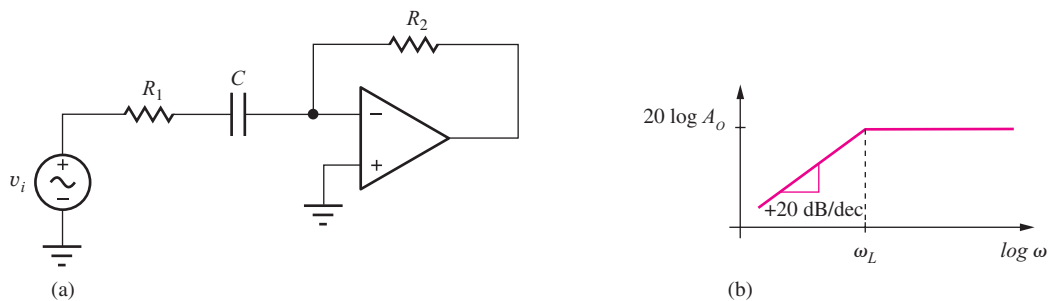


Figure 10.33 (a) Active high-pass filter circuit. (b) Bode plot for high-pass filter.

Figure 10.33(b) is the asymptotic Bode plot of the magnitude of the gain in Eq. (10.97). The transfer function exhibits a high-pass characteristic with a single pole at frequency  $\omega_L$ , the lower cutoff frequency of the high-pass filter. At frequencies above  $\omega_L$ , the amplifier behaves as an inverting amplifier with gain set by the ratio of resistors  $R_2$  and  $R_1$ ; at frequencies below  $\omega_L$ , the amplifier rolls off at a rate of 20 dB/dec.

Realization of the transfer function in Eq. (10.99) and Fig. 10.33(b) is based upon use of an ideal operational amplifier with infinite bandwidth. In reality, we can only approximate the characteristic over a limited frequency range with a real op amp that has finite bandwidth. We will reexamine the behavior of a number of our basic building block circuits including low-pass and high-pass filters in Chapter 11 when we consider the frequency response limitations of op amps.

### Understanding High-Pass Filter Operation

Once again, this filter circuit functions in manner similar to the inverting amplifier. The virtual ground at the inverting input causes input voltage  $V_i$  to appear directly across the series combination of resistor  $R_1$  and  $C$  establishing an input current  $V_i/Z_1$ . The op amp forces this input current to flow out through  $R_2$  developing a voltage drop of  $(V_i/Z_1) \cdot R_2$  across  $R_2$ . Because of the virtual ground,  $v_o = -(V_i/Z_1) \cdot R_2$ , and the gain is  $-R_2/Z_1$  as expressed in Eq. (10.97).

At high frequencies (above  $\omega_L$ ), the amplifier operates as an inverting amplifier with gain of  $-R_2/R_1$ , because the capacitive reactance  $(1/\omega C)$  is much smaller than that of  $R_1$  and can be neglected. At low frequencies, the impedance of  $C$  becomes large,  $R_1$  can be neglected, and the gain falls at a rate of 20 dB/decade as the value of  $(1/\omega C)$  increases.

**EXERCISE:** Design an active high-pass filter (choose the values of  $R_1$ ,  $R_2$  and  $C$ ) with  $f_L = 5$  kHz, a high frequency gain of 20 dB, and an input resistance of 18 k $\Omega$  at high frequencies.

**ANSWERS:** Calculated values: 18 k $\Omega$ , 180 k $\Omega$ , 1770 pF; Appendix A values: 18 k $\Omega$ , 180 k $\Omega$ , 1800 pF.

### 10.10.7 THE INTEGRATOR

The **integrator** is another highly useful building block formed from an operational amplifier with frequency-dependent feedback. In the integrator circuit, feedback-resistor  $R_2$  is replaced by capacitor  $C$ , as in Fig. 10.34. This circuit provides an opportunity to explore op amp circuit analysis in the time domain (for frequency-domain analysis, see Prob. 10.112(a)).

Because the inverting-input terminal represents a virtual ground,

$$i_i = \frac{v_i}{R} \quad \text{and} \quad i_c = -C \frac{dv_o}{dt} \quad (10.98)$$

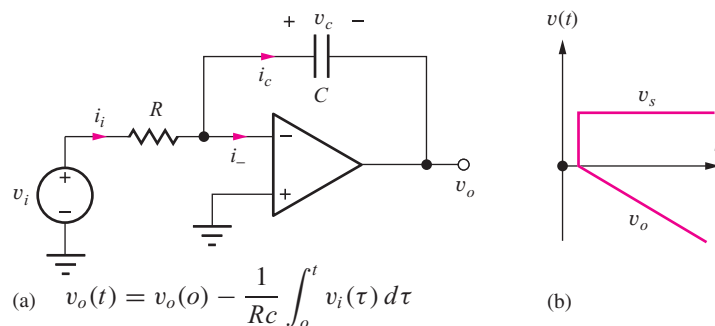


Figure 10.34 (a) The integrator circuit. (b) Output voltage for a step-function input with  $v_C(0) = 0$ .

For an ideal op amp,  $i_- = 0$ , so  $i_c$  must equal  $i_i$ . Equating the two expressions in Eq. (10.98) and integrating both sides yields

$$\int dv_o = \int -\frac{1}{RC} v_i d\tau \quad \text{or} \quad v_o(t) = v_o(0) - \frac{1}{RC} \int_0^t v_i(\tau) d\tau \quad (10.99)$$

in which the initial value of the output voltage is determined by the voltage on the capacitor at  $t = 0$ :  $v_o(0) = -V_c(0)$ . Thus the voltage at the output of this circuit at any time  $t$  represents the initial capacitor voltage minus the integral of the input signal from the start of the integration interval, chosen in this case to be  $t = 0$ .

### Understanding Integrator Circuit Operation

The virtual ground at the inverting input of the op amp causes input voltage  $V_i$  to appear directly across resistor  $R$  establishing an input current  $V_i/R$ . As the input current flows out through  $C$ , the capacitor accumulates a charge equal to the integral of the current,  $Q_C = \frac{1}{C} \int i \cdot dt$ , and the overall scale factor becomes  $-1/RC$ .

**EXERCISE:** Suppose the input voltage  $v_i(t)$  to an integrator is a 500-Hz square wave with a peak-to-peak amplitude of 10 V and 0 dc value. Choose the values of  $R$  and  $C$  in the integrator so that the peak output voltage will be 10 V and  $R_{in} = 10 \text{ k}\Omega$ .

**ANSWERS:**  $10 \text{ k}\Omega, 0.05 \mu\text{F}$



### ELECTRONICS IN ACTION

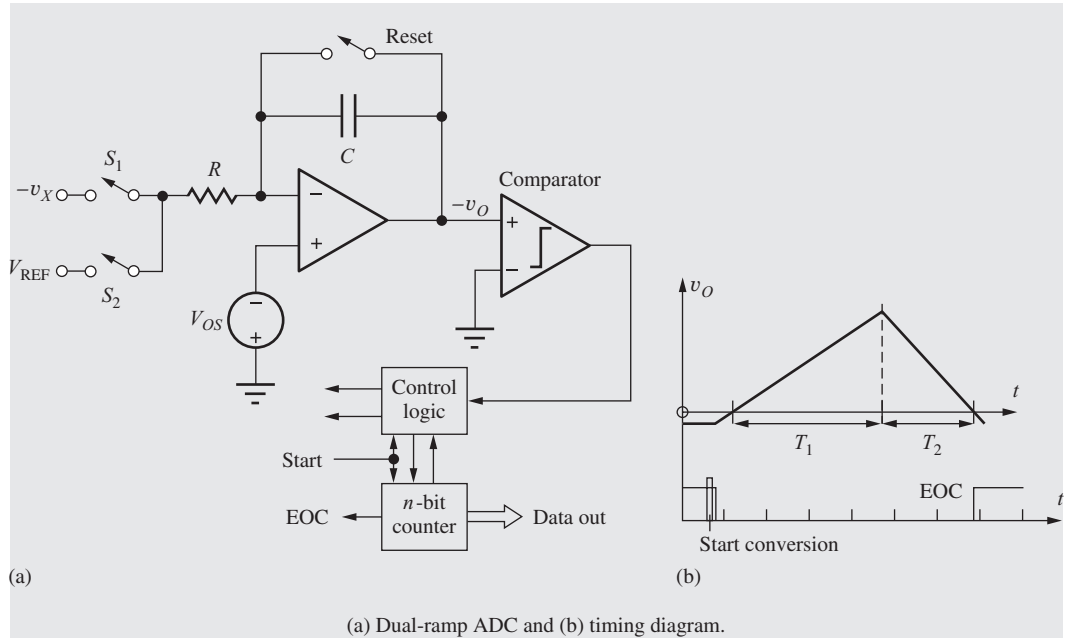


#### Dual-Ramp or Dual-Slope Analog-to-Digital Converters (ADCs)

The dual-ramp or dual-slope analog-to-digital converter is widely used as the ADC in data acquisition systems, digital multimeters, and other precision instruments. The heart of the dual-ramp converter is the integrator circuit discussed in Section 10.10.7. As illustrated in the circuit schematic on the next page, the conversion cycle consists of two separate integration intervals.



Agilent Digital Multimeter  
©Agilent Technologies 2006. All Rights Reserved.



(a) Dual-ramp ADC and (b) timing diagram.

First, unknown voltage  $v_X$  is integrated for a known period of time  $T_1$ . The value of this integral is then compared to that of a known reference voltage  $V_{REF}$ , which is integrated for a variable length of time  $T_2$ .

At the start of conversion the counter is reset, and the integrator is reset to a slightly negative voltage. The unknown input  $v_X$  is connected to the integrator input through switch  $S_1$ . Unknown voltage  $v_X$  is integrated for a fixed period of time  $T_1 = 2^n T_C$ , which begins when the integrator output crosses through zero where  $T_C$  is the period of the clock. At the end of time  $T_1$ , the counter overflows, causing  $S_1$  to be opened and the reference input  $V_{REF}$  to be connected to the integrator input through  $S_2$ . The integrator output then decreases until it crosses back through zero, and the comparator changes state, indicating the end of the conversion. The counter continues to accumulate pulses during the down ramp, and the final number in the counter represents the quantized value of the unknown voltage  $v_X$ .

Circuit operation forces the integrals over the two time periods to be equal:

$$\frac{1}{RC} \int_0^{T_1} v_X(t) dt = \frac{1}{RC} \int_{T_1}^{T_1+T_2} V_{REF} dt$$

$T_1$  is set equal to  $2^n T_C$  because the unknown voltage  $v_X$  was integrated over the amount of time needed for the  $n$ -bit counter to overflow. Time period  $T_2$  is equal to  $N T_C$ , where  $N$  is the number accumulated in the counter during the second phase of operation.

Recalling the mean-value theorem from calculus, we have

$$\frac{1}{RC} \int_0^{T_1} v_X(t) dt = \frac{\langle v_X \rangle}{RC} T_1 \quad \text{and} \quad \frac{1}{RC} \int_{T_1}^{T_1+T_2} V_{REF}(t) dt = \frac{V_{REF}}{RC} T_2$$

because  $V_{REF}$  is a constant. Equating these last two results, we find the average value of the input  $\langle v_X \rangle$  to be

$$\frac{\langle v_X \rangle}{V_{REF}} = \frac{T_2}{T_1} = \frac{N}{2^n}$$

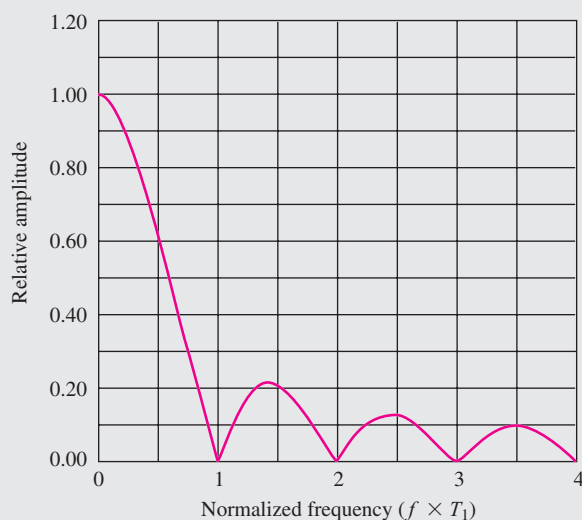
assuming that the  $RC$  product remains constant throughout the complete conversion cycle. The absolute values of  $R$  and  $C$  do not enter directly into the relation between  $v_X$  and  $V_{FS}$ . The digital output word represents the average value of  $v_X$  during the first integration phase. Thus,  $v_X$  can change during the conversion cycle of this converter without destroying the validity of the quantized output value.

The conversion time  $T_T$  requires  $2^n$  clock periods for the first integration period, and  $N$  clock periods for the second integration period. Thus the conversion time is variable and given by  $T_T = (2^n + N)T_C \leq 2^{n+1}T_C$  because the maximum value of  $N$  is  $2^n$ .

The dual ramp is a widely used converter. Although much slower than other forms of converters, the dual-ramp converter offers excellent linearity. By combining its integrating properties with careful design, one can obtain accurate conversion at resolutions exceeding 20 bits, but at relatively low conversion rates. In a number of recent converters and instruments, the basic dual-ramp converter has been modified to include extra integration phases for automatic offset voltage elimination. These devices are often called *quad-slope* or *quad-phase converters*. Another converter, the *triple ramp*, uses coarse and fine down ramps to greatly improve the speed of the integrating converter (by a factor of  $2^{n/2}$  for an  $n$ -bit converter).

### Normal-Mode Rejection

As mentioned before, the quantized output of the dual-ramp converter represents the average of the input during the first integration phase. The integrator operates as a low-pass filter with the normalized transfer function shown in the accompanying figure. Sinusoidal input signals, whose frequencies are exact multiples of the reciprocal of the integration time  $T_1$ , have integrals of zero value and do not appear at the integrator output. This property is used in many digital multimeters, which are equipped with dual-ramp converters having an integration time that is some multiple of the period of the 50- or 60-Hz power-line frequency. Noise sources with frequencies at multiples of the power-line frequency are therefore rejected by these integrating ADCs. This property is usually termed **normal-mode rejection**.



Normal-mode rejection for an integrating ADC.

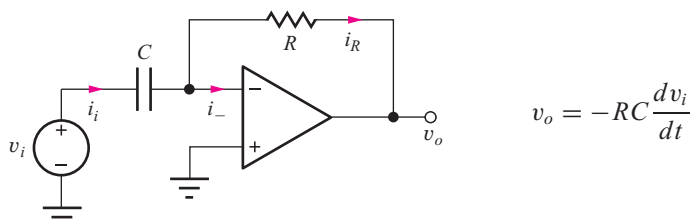


Figure 10.35 Differentiator circuit.

### 10.10.8 THE DIFFERENTIATOR

The derivative operation can also be provided by an op amp circuit. The **differentiator** is obtained by interchanging the resistor and capacitor of the integrator as drawn in Fig. 10.35. The circuit is less often used than the integrator because the derivative operation is an inherently “noisy” operation; that is, the high-frequency components of the input signal are emphasized. Analysis of the circuit is similar to that of the integrator. Since the inverting-input terminal represents a virtual ground,

$$i_i = C \frac{dv_i}{dt} \quad \text{and} \quad i_R = -\frac{v_o}{R} \quad (10.100)$$

Since  $i_- = 0$ , the currents  $i_i$  and  $i_R$  must be equal, and

$$v_o = -RC \frac{dv_i}{dt} \quad (10.101)$$

The output voltage is a scaled version of the derivative of the input voltage.

#### Understanding Differentiator Circuit Operation

The virtual ground at the inverting input of the op amp causes input voltage  $v_i$  to appear directly across capacitor  $C$ , establishing an input current that is proportional to the derivative of  $v_i$ . This current flows out through  $R$  yielding an output voltage that is a scaled version of the derivative of the input voltage.

Thinking in the frequency domain, the reactance of the capacitor ( $1/\omega C$ ) decreases as frequency increases. Therefore the input current, and the scaled output voltage, both increase directly with frequency, yielding a frequency dependence that corresponds to a differentiator.

**EXERCISE:** What is the output voltage of the circuit in Fig. 10.35 if  $R = 20 \text{ k}\Omega$ ,  $C = 0.02 \mu\text{F}$ , and  $v_i = 2.5 \sin 2000\pi t \text{ V}$ ?

**ANSWER:**  $-6.28 \cos 2000\pi t \text{ V}$

## SUMMARY

- This chapter introduced important characteristics of linear amplifiers and explored simplified models for the amplifiers. The operational amplifier, or op amp, was then introduced, and our circuit toolkit was expanded to include a number of classic op-amp-based building blocks. The op amp represents an extremely important tool for implementing basic amplifiers and more complex electronic circuits. Voltage gain  $A_v$ , current gain  $A_i$ , power gain  $A_P$ , input resistance, and output

resistance were all defined. Gains are expressed in terms of the phasor representations of sinusoidal signals or as transfer functions using Laplace transforms. The magnitudes of the gains are often expressed in terms of the logarithmic decibel or dB scale.

- Linear amplifiers can be conveniently modeled using two-port representations. The  $g$ -parameters are of particular interest for describing amplifiers in this text. In most of the amplifiers we consider, the 1–2 parameter (i.e.,  $g_{12}$ ) will be neglected. These networks were recast in terms of input resistance  $R_{\text{in}}$ , output resistance  $R_{\text{out}}$ , and open-circuit voltage gain  $A$ . Ideal voltage amplifiers have  $R_{\text{in}} = \infty$  and  $R_{\text{out}} = 0$ .
- Linear amplifiers can be used to tailor the magnitude and/or phase of sinusoidal signals and are often characterized by their frequency response. Low-pass and high-pass characteristics were discussed. The characteristics of these amplifiers are conveniently displayed in graphical form as a Bode plot, which presents the magnitude (in dB) and phase (in degrees) of a transfer function versus a logarithmic frequency scale. Bode plots can be created easily using MATLAB.

In an amplifier, the midband gain  $A_{\text{mid}}$  represents the maximum gain of the amplifier. At the upper- and lower-cutoff frequencies —  $f_H$  and  $f_L$ , respectively — the voltage gain is equal to  $A_{\text{mid}}/\sqrt{2}$  and is 3 dB below its midband value ( $20 \log |A_{\text{mid}}|$ ). The bandwidth of the amplifier extends from  $f_L$  to  $f_H$  and is defined as  $\text{BW} = f_H - f_L$ .

- An amplifier must be properly biased to ensure that it operates in its linear region. The choice of bias point of the amplifier, its Q-point, can affect both the gain of the amplifier and the size of the input signal range for which linear amplification will occur. Improper choice of bias point can lead to nonlinear operation of an amplifier and distortion of the signal. One measure of linearity of a signal is its percent total harmonic distortion (THD).
- Ideal operational amplifiers are assumed to have infinite gain and zero input current, and circuits containing these amplifiers were analyzed using two primary assumptions:
  1. The differential input voltage is zero:  $v_{id} = 0$ .
  2. The input currents are zero:  $i_+ = 0$  and  $i_- = 0$ .
- Assumptions 1 and 2, combined with Kirchhoff's voltage and current laws, are used to analyze the ideal behavior of circuit building blocks based on operational amplifiers. Constant feedback with resistive voltage dividers is used in the inverting and noninverting amplifier configurations, the voltage follower, the difference amplifier, and the summing amplifier, whereas frequency-dependent feedback is used in the integrator, low-pass filter, high-pass filter, and differentiator circuits.
- Infinite gain and input resistance are the explicit characteristics that lead to Assumptions 1 and 2. However, many additional properties are implicit characteristics of ideal operational amplifiers; these assumptions are seldom clearly stated, though. They are
  - Infinite common-mode rejection
  - Infinite power supply rejection
  - Infinite output voltage range
  - Infinite output current capability
  - Infinite open-loop bandwidth
  - Infinite slew rate
  - Zero output resistance
  - Zero input-bias currents
  - Zero input-offset voltage

These limitations will be explained in detail in the next two chapters.

## KEY TERMS

Active filters	Low-pass amplifier
Audio frequency (AF)	Low-pass filter
Band-pass amplifier	Magnitude
Bandwidth	Midband gain
Bias	Most significant bit (MSB)
Bode plot	Noninverting amplifier
Closed-loop amplifier	Noninverting input
Closed-loop gain	Normal mode rejection
Comparator	Open-circuit input conductance
Critical frequency	Open-circuit input resistance
Current amplifier	Open-circuit termination
Current gain ( $A_i$ )	Open-circuit voltage gain
Decibel (dB)	Open-loop gain
dc-coupled amplifier	Operational amplifier (op amp)
Difference amplifier	Output resistance
Differential amplifier	Phase angle
Differential-mode gain	Phasor representation
Differential-mode input resistance	Power gain ( $A_P$ )
Differential-mode input voltage	R-2R ladder
Differentiator	Radio frequency (RF)
Digital-to-analog converter (DAC or D/A converter)	Short-circuit output conductance
Dual-ramp (dual slope) ADC	Short-circuit output resistance
Feedback amplifier	Short-circuit termination
Gain-bandwidth product	Single-pole frequency response
<i>g</i> -parameters	Source resistance ( $R_S$ )
High-pass amplifier	Summing amplifier
High-pass filter	Summing junction
Ideal operational amplifier	Total harmonic distortion
Input resistance ( $R_{in}$ )	Transfer function
Integrator	Two-port model
Intermediate frequency (IF)	Two-port network
Inverted R-2R ladder	Unity-gain buffer
Inverting amplifier	Upper-cutoff frequency
Inverting input	Upper half-power point
Least significant bit (LSB)	Upper $-3$ -dB frequency
Inverting amplifier	Very high frequency
Linear amplifier	Virtual ground
Lower-cutoff frequency	Voltage amplifier
Lower half-power point	Voltage follower
Lower $-3$ -dB frequency	Voltage gain

## REFERENCES

1. Tom Lewis, *Empire on the Air: The Men Who Made Radio*, Harper Collins: 1991.
2. James A. Hijiya, *Lee de Forest and the Fatherhood of Radio*, Lehigh University Press: 1992.
3. Thomas H. Lee, "A Non Linear History of Radio," Chapter 1 in *The Design of CMOS Radio-Frequency Integrated Circuits*, Cambridge University Press: 1998.
4. National Geographic Society, *Those Inventive Americans*, (Editor and Publisher, 1971). pp. 182–187 (Lee de Forest by Howard J. Lewis).

## ADDITIONAL READING

- Franco, Sergio, *Design with Operational Amplifiers and Analog Integrated Circuits*, Third Edition, McGraw-Hill, New York: 2001.
- Gray, P. R., P. J. Hurst, S. H. Lewis, and R. G. Meyer, *Analysis and Design of Analog Integrated Circuits*, Fourth Edition, John Wiley and Sons, New York: 2001.
- Kennedy, E. J. *Operational Amplifier Circuits—Theory and Applications*. Holt, Rinehart, and Winston, New York: 1988.

## PROBLEMS

### 10.1 An Example of an Analog Electronic System

- 10.1. In addition to those given in the introduction, list 15 physical variables in your everyday life that can be represented as continuous analog signals.

### 10.2 Amplification

- 10.2. Convert the following to decibels: (a) voltage gains of 120, -60, 50,000, -100,000, 0.90; (b) current gains of 600, 3000, -10<sup>6</sup>, 200,000, 0.95; (c) power gains of 2 × 10<sup>9</sup>, 4 × 10<sup>5</sup>, 6 × 10<sup>8</sup>, 10<sup>10</sup>.
- 10.3. Express the voltage, current, and power gains in Ex. 10.1 in dB.
- 10.4. For what value of voltage gain  $A_v$  does  $A_v = 20 \log(A_v)$ ?
- 10.5. Suppose the input and output voltages of an amplifier are given by

$$v_I = 1 \sin(1000\pi t) + 0.333 \sin(3000\pi t) + 0.200 \sin(5000\pi t) \text{ V}$$

and

$$\begin{aligned} v_O &= 2 \sin\left(1000\pi t + \frac{\pi}{6}\right) \\ &\quad + \sin\left(3000\pi t + \frac{\pi}{6}\right) \\ &\quad + \sin\left(5000\pi t + \frac{\pi}{6}\right) \text{ V} \end{aligned}$$

(a) Plot the input and output voltage waveforms of  $v_I$  and  $v_O$  for  $0 \leq t \leq 4$  ms. (b) What are the amplitudes, frequencies, and phases of the individual signal components in  $v_I$ ? (c) What are the amplitudes, frequencies, and phases of the individual signal components in  $v_O$ ? (d) What are the voltage gains at the three frequencies? (e) Is this a linear amplifier?

- 10.6. What are the voltage gain, current gain, and power gain required of the amplifier in Fig. 10.3 if  $V_i = 2.5$  mV and the desired output power is 30 W?

- 10.7. What are the voltage gain, current gain, and power gain required of the amplifier in Fig. 10.3 if  $V_i = 20$  mV,  $R_L = 2$  kΩ, and the output power is 20 mW?
- 10.8. The output of a PC sound card was set to be a 1-kHz sine wave with an amplitude of 1 V using MATLAB. The outputs were monitored with an oscilloscope and ac voltmeter. (a) For the left channel, the rms value of the open-circuit output voltage at 1 kHz was measured to be 0.760 V, and it dropped to 0.740 V with a 1040-Ω load resistor attached. Draw the Thévenin equivalent circuit representation for the left output of the sound card (i.e., What are  $v_{th}$  and  $R_{th}$ ?). (b) For the right channel, the rms value of the open-circuit output voltage at 1 kHz was measured to be 0.768 V, and it dropped to 0.721 V with a 430-Ω load resistor attached. Draw the Thévenin equivalent circuit representation for the output of the right channel. (c) What were the values of the measured amplitudes of the two open-circuit output voltages? What percent error was observed between the actual voltage and the desired voltage as defined by MATLAB? (c) Go to the lab and determine the Thévenin equivalent output voltage and resistance for the sound card in your laptop PC.
- 10.9. Suppose that each output channel of a computer's sound card can be represented by a 1-V ac source in series with a 32-Ω resistor. Each channel of the amplifier in the external speakers has an input resistance of 20 kΩ, and must deliver 5 W into an 8-Ω speaker. (a) What are the voltage gain, current gain, and power gain required of the amplifier? (b) What would be a reasonable dc power supply voltage for this amplifier?
- 10.10. The amplifier in a battery-powered device is being designed to deliver 0.1 W to a set of headphones. The impedance of the headphones can be chosen to be 8 Ω, 32 Ω, or 1000 Ω. Calculate the voltage and current required to deliver 0.1 W to each of these

resistances. Which resistance seems the best choice for a battery powered application?

### 10.3 Two-Port Models for Amplifiers

- 10.11. Calculate the  $g$ -parameters for the circuit in Fig. P10.11.

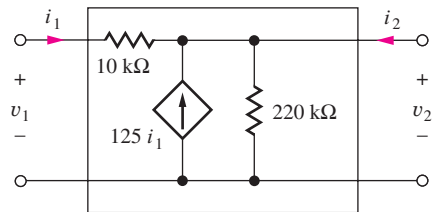


Figure P10.11

- 10.12. (a) Use SPICE transfer function analysis to find the  $g$ -parameters for the circuit in Fig. P10.11.

- 10.13. Calculate the  $g$ -parameters for the circuit in Fig. P10.13.

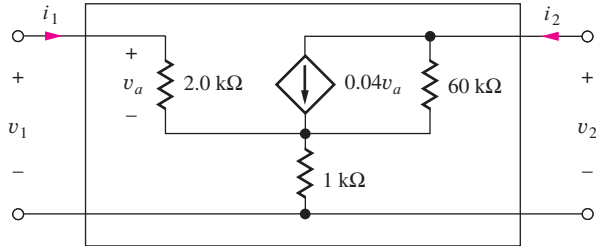


Figure P10.13

- 10.14. Calculate the  $g$ -parameters for the circuit in Fig. P10.14.

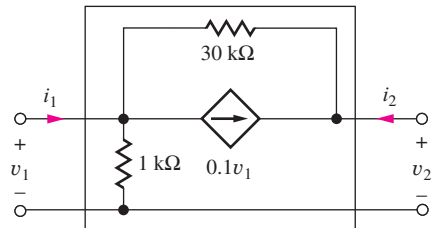


Figure P10.14

- 10.15. Use SPICE transfer function analysis to find the  $g$ -parameters for the circuit in Fig. P10.14.

### 10.4 Mismatched Source and Load Resistances

- 10.16. An amplifier connected in the circuit in Fig. P10.16 has the two-port parameters listed below, with  $R_I = 1 \text{ k}\Omega$  and  $R_L = 16 \text{ }\Omega$ . (a) Find the overall voltage gain  $A_v$ , current gain  $A_i$ , and power gain  $A_P$  for the amplifier and express the results in dB. (b) What is

the amplitude  $V_i$  of the sinusoidal input signal  $v_i$  needed to deliver 1 W to the  $16\text{-}\Omega$  load resistor? (c) How much power is dissipated in the amplifier when 1 W is delivered to the load resistor?

$$\text{Input resistance } R_{in} = 1 \text{ M}\Omega$$

$$\text{Output resistance } R_{out} = 0.5 \text{ }\Omega$$

$$A = 50 \text{ dB}$$

$$v_i = V_i \sin \omega t$$

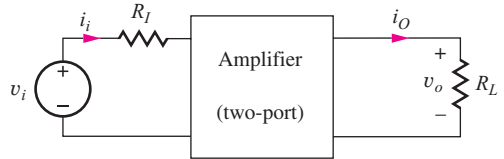


Figure P10.16

- 10.17. Suppose that the amplifier of Fig. P10.16 has been designed to match the source and load resistances with the parameters below. (a) What is the amplitude of the input signal  $v_i$  needed to deliver 1 W to the  $16\text{-}\Omega$  load resistor? (b) How much power is dissipated in the amplifier when 1 W is delivered to the load resistor?

$$\text{Input resistance } R_{in} = 1 \text{ k}\Omega$$

$$\text{Output resistance } R_{out} = 16 \text{ }\Omega$$

$$A = 50 \text{ dB}$$

- 10.18. The headphone amplifier in a battery-powered device has an output resistance of  $28 \text{ }\Omega$  and is designed to deliver 0.1 W to the headphones. If the resistance of the headphones is  $24 \text{ }\Omega$ , calculate the voltage and current required from the dependent voltage source ( $A_v$  in our model) to deliver 0.1 W to the headphones. How much power is delivered from dependent source? How much power is lost in the output resistance?

- 10.19. Repeat Prob. 10.18 if the headphones have a resistance of  $1000 \text{ }\Omega$ .

- 10.20. For the circuit in Fig. 10.9,  $R_I = 1 \text{ k}\Omega$ ,  $R_L = 16 \text{ }\Omega$ , and  $A = -2000$ . What values of  $R_{in}$  and  $R_{out}$  will produce maximum power in the load resistor  $R_L$ ? What is the maximum power that can be delivered to  $R_L$  if  $v_i$  is a sine wave with an amplitude of  $10 \text{ mV}$ ? What is the power gain of this amplifier?

- 10.21. For the circuit in Fig. 10.9,  $R_I = 1 \text{ k}\Omega$ ,  $R_{in} = 30 \text{ k}\Omega$ ,  $R_{out} = 100 \text{ }\Omega$ , and  $R_L = 2 \text{ k}\Omega$ . What value of  $A$  is required to produce a voltage gain of  $74 \text{ dB}$  if the amplifier is to be an inverting amplifier ( $\theta = 180^\circ$ )?

- 10.22. The circuit in Fig. P10.22 represents a two-port model for a current amplifier. Write expressions for input current  $i_1$ , output current  $i_o$  and the current gain  $A_i = I_o/I_s$ . What values of  $R_{in}$  and  $R_{out}$  provide maximum magnitude for the current gain?

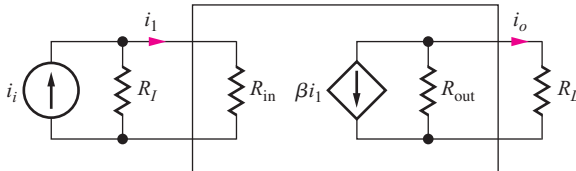


Figure P10.22

- 10.23. For the circuit in Fig. P10.22,  $R_I = 100 \text{ k}\Omega$ ,  $R_L = 10 \text{ k}\Omega$ , and  $\beta = 4000$ . What values of  $R_{in}$  and  $R_{out}$  will produce maximum power in the load resistor  $R_L$ ? What is the maximum power that can be delivered to  $R_L$  if  $i_i$  is a sine wave with an amplitude of  $1 \mu\text{A}$ ? What is the power gain of this amplifier?
- 10.24. For the circuit in Fig. P10.22,  $R_I = 200 \text{ k}\Omega$ ,  $R_{in} = 10 \text{ k}\Omega$ ,  $R_{out} = 300 \text{ k}\Omega$ , and  $R_L = 47 \text{ k}\Omega$ . What value of  $\beta$  is required to produce a current gain of 150?

- \*10.25. For the circuit in Fig. 10.9, show that

$$A_{PdB} = A_{vdB} - 10 \log \left( \frac{R_L}{R_S + R_{in}} \right)$$

and

$$A_{PdB} = A_{idB} + 10 \log \left( \frac{R_L}{R_S + R_{in}} \right)$$

- 10.26. Two amplifiers are connected in series, or cascaded, in the circuit in Fig. P10.26. If  $R_I = 1 \text{ k}\Omega$ ,  $R_{in} = 5 \text{ k}\Omega$ ,  $R_{out} = 500 \Omega$ ,  $R_L = 500 \Omega$ , and  $A = -1200$ , what are the voltage gain, current gain, and power gain of the overall amplifier?

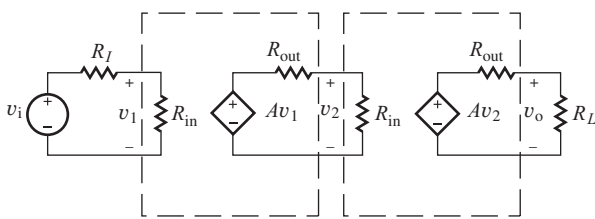


Figure P10.26

## 10.5 Introduction to Operational Amplifiers

- 10.27. The circuit inside the box in Fig. P10.27 contains only resistors and diodes. The terminal  $V_O$  is connected to some point in the circuit inside the box.
- (a) Is the largest possible value of  $V_O$  most nearly  $0 \text{ V}$ ,  $-9 \text{ V}$ ,  $+6 \text{ V}$ , or  $+15 \text{ V}$ ? Why? (b) Is the

smallest possible value of  $V_O$  most nearly  $0 \text{ V}$ ,  $-9 \text{ V}$ ,  $+6 \text{ V}$ , or  $+15 \text{ V}$ ? Why?

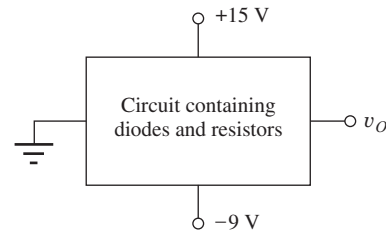


Figure P10.27

- 10.28. (a) The input voltage applied to the amplifier in Fig. P10.28 is  $v_I = V_B + V_M \sin 1000t$ . What is the voltage gain of the amplifier for small values of  $V_M$  if  $V_B = 0.6 \text{ V}$ ? What is the maximum value of  $V_M$  that can be used and still have an undistorted sinusoidal signal at  $v_O$ ? (b) Write expressions for  $v_I(t)$  and  $v_O(t)$ .

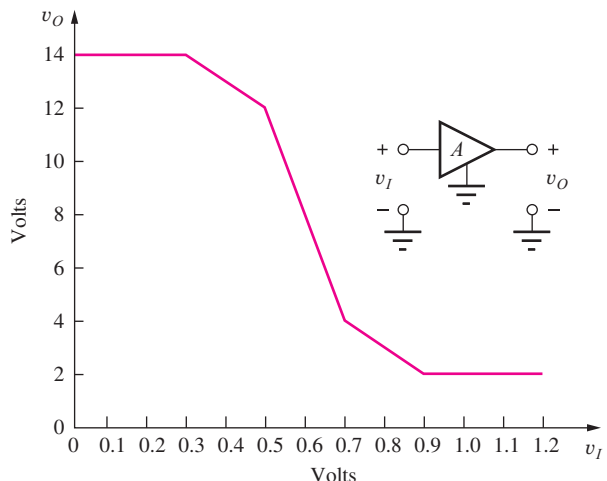


Figure P10.28

- 10.29. (a) Repeat Prob. 10.28 for  $V_B = 0.8 \text{ V}$ . (b) For  $V_B = 0.2 \text{ V}$ .
- 10.30. (a) Repeat Prob. 10.28 for  $V_B = 0.5 \text{ V}$ . (b) For  $V_B = 1.1 \text{ V}$ .
- 10.31. The input voltage applied to the amplifier in Fig. P10.28 is  $v_I = (0.6 + 0.1 \sin 1000t) \text{ V}$ .
- (a) Write expressions for the output voltage.
- (b) Draw a graph of two cycles of the output voltage.
- (c) Calculate the first five spectral components of this signal. You may use MATLAB or other computer analysis tools.

- \*10.32. The input voltage applied to the amplifier in Fig. P10.28 is  $v_I = (0.5 + 0.1 \sin 1000t) \text{ V}$ .

- (a) Write expressions for the output voltage.  
 (b) Draw a graph of two cycles of the output voltage.  
 (c) Calculate the first five spectral components of this signal. You may use MATLAB or other computer analysis tools.

## 10.6 Distortion in Amplifiers

- 10.33. The input signal to an audio amplifier is described by  $v_I = (0.5 + 0.25 \sin 1200\pi t)$  V, and the output is described by  $v_O = (2 + 4 \sin 1200\pi t + 0.8 \sin 2400\pi t + 0.4 \sin 3600\pi t)$  V. What is the voltage gain of the amplifier? What order harmonics are present in the signal? What is the total harmonic distortion in the output signal?
- 10.34. The input signal to an audio amplifier is a 1-kHz sine wave with an amplitude of 4 mV, and the output is described by  $v_O = (5 \sin 2000\pi t + 0.5 \sin 6000\pi t + 0.20 \sin 10,000\pi t)$  V. What is the voltage gain of the amplifier? What order harmonics are present in the signal? What is the total harmonic distortion in the output signal?
- 10.35. (a) Use the FFT capability of MATLAB to find the Fourier series representation of  $v(t)$  in Fig. 10.5(b).  
 (b) Use MATLAB to find the coefficients of the first three terms of the Fourier series for  $v(t)$  by evaluating the integral expression for the coefficients.
- 10.36. MATLAB limits the output of a sound signal to unity (1 V). Any signal value above this limit will be clipped (set to 1). (a) Use MATLAB to plot the following waveform:  $y = \max(-1, \min(1, 1.5 \sin(1400\pi t)))$ . (b) Use MATLAB to find the total harmonic distortion in waveform  $y$ . (c) Use the sound output on your computer to listen to and compare the following signals:  $y = 1 \sin 1400\pi t$ ,  $y = 1.5 \sin 1400\pi t$ , and  $y = \max(-1, \min(1, 1.5 \sin(1400\pi t)))$ . Describe what you hear.
- 10.37. Suppose the VTC for an amplifier is described by  $v_O = 10 \tanh(2v_I)$  volts. (a) Plot the VTC.  
 (b) Calculate the distortion based upon the first three frequency components in the output if  $v_I = 0.75 \sin 2000\pi t$  volts.

## 10.7 The Differential Amplifier Model

- 10.38. A differential amplifier connected in the circuit in Fig. P10.38 has the parameters listed below with  $R_I = 5 \text{ k}\Omega$  and  $R_L = 1 \text{ k}\Omega$ . (a) Find the overall voltage gain  $A_v$ , current gain  $A_i$ , and power gain  $A_P$  for the amplifier, and express the results in dB.

- (b) What is the amplitude  $V_I$  of the sinusoidal input signal needed to develop a 10-V peak-to-peak signal at  $v_o$ ?

$$\text{Input resistance } R_{id} = 1 \text{ M}\Omega$$

$$\text{Output resistance } R_o = 25 \text{ }\Omega$$

$$A = 60 \text{ dB}$$

$$v_i = V_I \sin \omega t$$

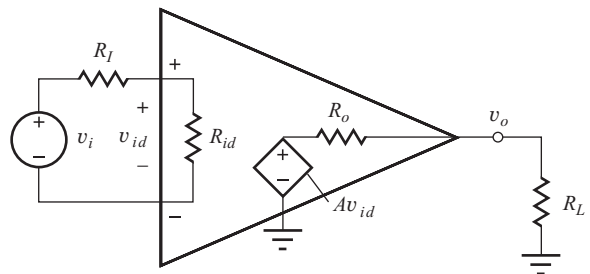


Figure P10.38

- 10.39. Suppose that the amplifier in Fig. P10.38 has been designed to match the source and load resistances in Prob. 10.38 with the parameters below. (a) What is the amplitude of the input signal  $v_i$  needed to develop a 15-V peak-to-peak signal at  $v_o$ ? (b) How much power is dissipated in the amplifier when 0.5 W is delivered to the load resistor?

$$\text{Input resistance } R_{id} = 5 \text{ k}\Omega$$

$$\text{Output resistance } R_o = 1 \text{ k}\Omega$$

$$A = 30 \text{ dB}$$

- 10.40. An amplifier has a sinusoidal output signal and is delivering 100 W to a  $50\text{-}\Omega$  load resistor. What output resistance is required if the amplifier is to dissipate no more than 2 W in its own output resistance?
- 10.41. The input to an amplifier comes from a transducer that can be represented by a 1-mV voltage source in series with a  $50\text{-k}\Omega$  resistor. What input resistance is required of the amplifier for  $v_{id} \geq 0.99 \text{ mV}$ ?

## 10.8 Ideal Differential and Operational Amplifiers

- 10.42. Suppose a differential amplifier has  $A = 120 \text{ dB}$ , and it is operating in a circuit with an open-circuit output voltage  $v_o = 15 \text{ V}$ . What is the input voltage  $v_{id}$ ? How large must the voltage gain be to make  $v_{id} \leq 1 \mu\text{V}$ ? What is the input current  $i_+$  if  $R_{id} = 1 \text{ M}\Omega$ ?

- 10.43. An almost ideal op amp has an open-circuit output voltage  $v_o = 10$  V and a gain  $A = 106$  dB. What is the input voltage  $v_{id}$ ? How large must the voltage gain be to make  $v_{id} \leq 1 \mu\text{V}$ ?

## 10.9 Analysis of Circuits Containing Ideal Operational Amplifiers

### Inverting Amplifiers

- 10.44. (a) What are the voltage gain, input resistance, and output resistance of the amplifier in Fig. P10.44 if  $R_1 = 4.7 \text{ k}\Omega$  and  $R_2 = 220 \text{ k}\Omega$ ? Express the voltage gain in dB. (b) Repeat for  $R_1 = 47 \text{ k}\Omega$  and  $R_2 = 2.2 \text{ M}\Omega$ .

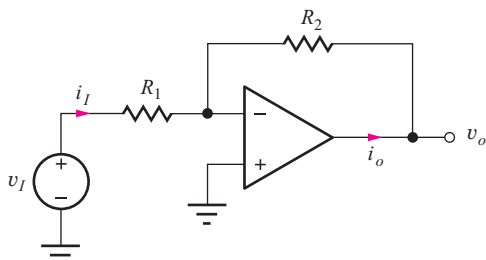


Figure P10.44

- 10.45. What are the voltage gain, input resistance, and output resistance of the amplifier in Fig. P10.44 if  $R_1 = 12 \text{ k}\Omega$  and  $R_2 = 120 \text{ k}\Omega$ ? (b) Repeat for  $R_1 = 140 \text{ k}\Omega$  and  $R_2 = 330 \text{ k}\Omega$ ? (c) Repeat for  $R_1 = 4.3 \text{ k}\Omega$  and  $R_2 = 240 \text{ k}\Omega$ ?
- 10.46. Write an expression for the output voltage  $v_o(t)$  of the circuit in Fig. P10.44 if  $R_1 = 750 \Omega$ ,  $R_2 = 8.2 \text{ k}\Omega$ , and  $v_i(t) = (0.05 \sin 4638t) \text{ V}$ . Write an expression for the current  $i_I(t)$ .
- 10.47.  $R_1 = 22 \text{ k}\Omega$  and  $R_2 = 110 \text{ k}\Omega$  in the amplifier circuit in Fig. P10.44. (a) What is the output voltage if  $v_i = 0$ ? (b) What is the output voltage if a dc signal  $V_I = 0.22 \text{ V}$  is applied to the circuit? (c) What is the output voltage if an ac signal  $v_I = 0.15 \sin 2500 \pi t \text{ V}$  is applied to the circuit? (d) What is the output voltage if the input signal is  $v_I = 0.22 - 0.15 \sin 2500 \pi t \text{ V}$ ? (e) What is the input current  $i_I$  for parts (b), (c), and (d). (f) What is the op amp output current  $i_O$  for the input signals in parts (b), (c), and (d)? (g) What is the voltage at the inverting input of the op amp for the input signal in part (d)?
- 10.48. The amplifier in Fig. P10.44 has  $R_1 = 10 \text{ k}\Omega$ ,  $R_2 = 100 \text{ k}\Omega$  and operates from  $\pm 12\text{-V}$  power supplies. (a) If  $v_I = 0.5 + V_I \sin 5000 \pi t$  volts, write an

expression for the output voltage. (b) What is the maximum value of  $V_I$  for an undistorted output? (c) Repeat if  $v_I = -0.25 + V_I \sin 2000 \pi t$  volts.

- 10.49. The amplifier in Fig. P10.44 has  $R_1 = 7.5 \text{ k}\Omega$ ,  $R_2 = 150 \text{ k}\Omega$  and operates from  $\pm 10\text{-V}$  power supplies. (a) If  $v_I = -0.2 + V_I \sin 2000 \pi t$  volts, write an expression for the output voltage. (b) What is the maximum value of  $V_I$  for an undistorted output? (c) Repeat if  $v_I = 0.6 + V_I \sin 2000 \pi t$  volts.
- 10.50. The amplifier in Fig. P10.44 has  $R_1 = 8.2 \text{ k}\Omega$ ,  $R_2 = 160 \text{ k}\Omega$  and operates from  $\pm 12\text{-V}$  power supplies. (a) What is the voltage gain  $A_v = v_o/v_i$  of the circuit? (b) Suppose input source  $v_i$  is not ideal but actually has a  $1.5 \text{ k}\Omega$  source resistance. What is the voltage gain  $A_v = v_o/v_i$ ?
- 10.51. The amplifier in Prob. 10.44(a) utilizes resistors with 10 percent tolerances. What are the nominal and worst-case values of the voltage gain and input resistance?
- 10.52. (a) The amplifier in Prob. 10.45(a) utilizes resistors with 5 percent tolerances. What are the nominal and worst-case values of the voltage gain and input resistance? (b) Repeat for Prob. 10.45(b). (c) Repeat for Prob. 10.45(c).
- 10.53. Design an inverting amplifier with an input resistance of  $30 \text{ k}\Omega$  and a gain of 26 dB. Choose values from the 1-percent resistor table in Appendix A.
- 10.54. Design an inverting amplifier with an input resistance of  $1.5 \text{ k}\Omega$  and a gain of 40 dB. Choose values from the 1-percent resistor table in Appendix A.
- 10.55. Design an inverting amplifier with an input resistance of  $100 \text{ k}\Omega$  and a gain of 12 dB. Choose values from the 1-percent resistor table in Appendix A.
- 10.56. Find the voltage gain, input resistance, and output resistance for the circuits in Fig. P10.56.

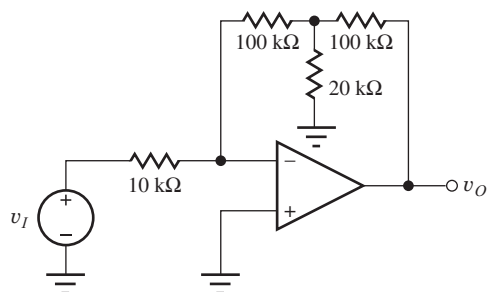


Figure P10.56

### Transresistance Amplifiers

- 10.57. Find an expression for the output voltage  $v_o$  in Fig. P10.57.

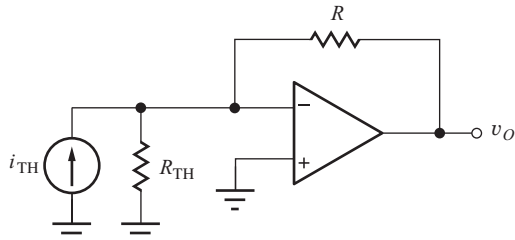


Figure P10.57

- 10.58. Convert the inverting amplifier in Fig. 10.18 to the transresistance amplifier in Fig. P10.56 using a Norton transformation of  $v_i$  and  $R_1$ . What are the expressions for  $i_{TH}$  and  $R_{TH}$ ? Write an expression for the gain  $v_o/v_i$ .
- 10.59. The current generated by some transducer falls in the range of  $\pm 2.5 \mu\text{A}$ , and its source resistance is  $200 \text{ k}\Omega$ . A transresistance amplifier is needed to convert the current to a voltage between  $\pm 5 \text{ V}$ . What value of  $R$  is required?

### Noninverting Amplifiers

- 10.60. What are the voltage gain, input resistance, and output resistance of the amplifier in Fig. P10.60 if  $R_1 = 8.2 \text{ k}\Omega$  and  $R_2 = 680 \text{ k}\Omega$ ? Express the voltage gain in dB.

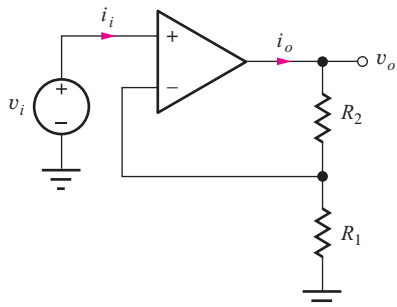


Figure P10.60

- 10.61. Write an expression for the output voltage  $v_o(t)$  of the circuit in Fig. P10.60 if  $R_1 = 910 \Omega$ ,  $R_2 = 8.2 \text{ k}\Omega$ , and  $v_i(t) = (0.04 \sin 9125t) \text{ V}$ .
- 10.62. What are the voltage gain, input resistance, and output resistance of the amplifier in Fig. P10.60 if  $R_1 = 24 \text{ k}\Omega$  and  $R_2 = 120 \text{ k}\Omega$ ? (b) Repeat for  $R_1 = 15 \text{ k}\Omega$  and  $R_2 = 300 \text{ k}\Omega$ . (c) Repeat for  $R_1 = 3.3 \text{ k}\Omega$  and  $R_2 = 360 \text{ k}\Omega$ .

- 10.63.  $R_1 = 22 \text{ k}\Omega$  and  $R_2 = 330 \text{ k}\Omega$  in the amplifier circuit in Fig. P10.60. (a) What is the output voltage if  $v_i = 0$ ? (b) What is the output voltage if a dc signal  $V_i = 0.33 \text{ V}$  is applied to the circuit? (c) What is the output voltage if an ac signal  $v_i = 0.18 \sin 3250 \pi t \text{ V}$  is applied to the circuit? (d) What is the output voltage if the input signal is  $v_i = 0.33 - 0.18 \sin 3250\pi t \text{ V}$ ? (e) Write an expression for the input current  $i_I$  for parts (b), (c), and (d). (f) Write an expression for the op amp output current  $i_O$  for the input signals in parts (b), (c) and (d). (g) What is the voltage at the inverting input of the op amp for the input signal in part (d)?

- \*10.64. (a) What are the gain, input resistance, and output resistance of the amplifier in Fig. P10.64 if  $R_1 = 180 \Omega$  and  $R_2 = 47 \text{ k}\Omega$ ? Express the gain in dB. (b) If the resistors have 10 percent tolerances, what are the worst-case values (highest and lowest) of gain that could occur? (c) What are the resulting positive and negative tolerances on the voltage gain with respect to the ideal value? (d) What is the ratio of the largest to the smallest voltage gain? (e) Perform a 500-case Monte Carlo analysis of this circuit. What percentage of the circuits has a gain within  $\pm 5$  percent of the nominal design value?

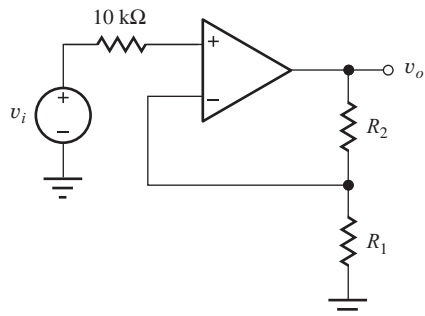
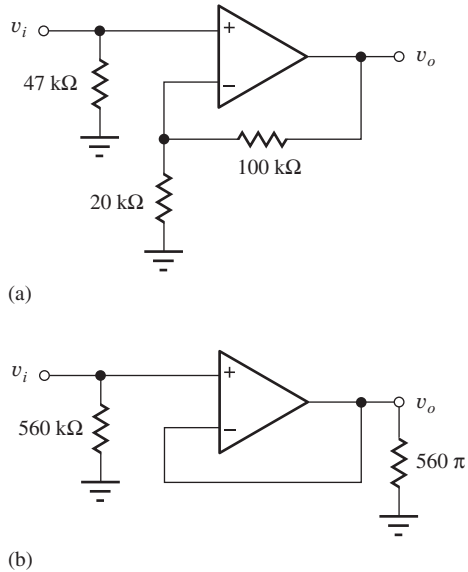


Figure P10.64

- 10.65. Design a noninverting amplifier with a gain of 32 dB. Choose values from the 1-percent resistor table in Appendix A, and use values that are no smaller than  $2 \text{ k}\Omega$ .
- 10.66. Design a noninverting amplifier with an input resistance of  $100 \text{ k}\Omega$  and a gain of 6 dB. Choose values from the 1-percent resistor table in Appendix A, and use values that are no smaller than  $2 \text{ k}\Omega$ .
- 10.67. Design a noninverting amplifier with a gain of 33 dB. Choose values from the 1-percent resistor table in Appendix A, and use values that are no smaller than  $1 \text{ k}\Omega$ .

- 10.68. What are the gain, input resistance, and output resistance for the circuits in Fig. P10.68.



**Figure P10.68**

### Summing Amplifiers

- 10.69. Write an expression for the output voltage  $v_o(t)$  of the circuit in Fig. P10.69 if  $R_1 = 1\text{ k}\Omega$ ,  $R_2 = 2\text{ k}\Omega$ ,  $R_3 = 47\text{ k}\Omega$ ,  $v_1(t) = (0.01 \sin 3770t)$  V, and  $v_2(t) = (0.04 \sin 10000t)$  V. Write an expression for the voltage appearing at the summing junction ( $v_-$ ).

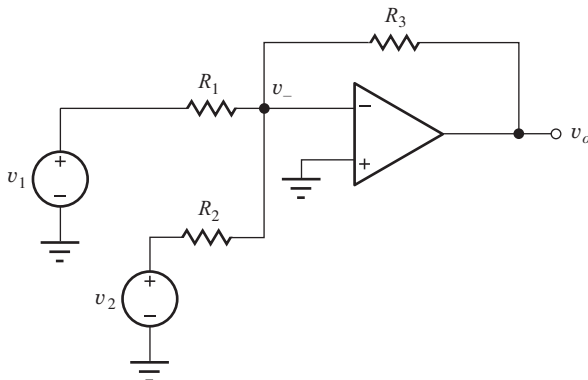


**Figure P10.69**

- 10.70. The summing amplifier can be used as a digitally controlled volume control using the circuit in Fig. P10.70. The individual bits of the 4-bit binary input word ( $b_1 b_2 b_3 b_4$ ) are used to control the position of the switches with the resistor connected to 0 V if  $b_i = 0$  and connected to the input signal  $v_I$  if

$b_i = 1$ . (a) What is the output voltage  $v_O$  with the data input 0110 if  $v_I = 1 \sin 4000\pi t$  V? (b) Suppose the input changes to 1011. What will be the new output voltage? (c) Make a table giving the output voltages for all 16 possible input combinations.

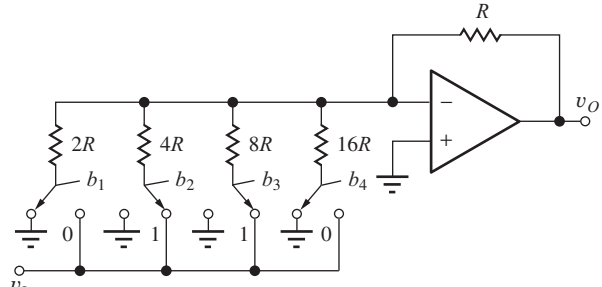


**Figure P10.70**

- 10.71. The switches in Fig. P10.70 can be implemented using MOSFETs, as shown in Fig. P10.71. What are the  $W/L$  ratios of the transistors if the on-resistance of the transistor is to be less than 1 percent of the resistor  $2R = 10\text{ k}\Omega$ ? Use  $V_{REF} = 3.0$  V. Assume that the voltage applied to the gate of the MOSFET is 5 V when  $b_1 = 1$  and 0 V when  $b_1 = 0$ . For the MOSFET,  $V_{TN} = 1$  V,  $K'_n = 50 \mu\text{A/V}^2$ ,  $2\phi_F = 0.6$  V, and  $\gamma = 0.5 \sqrt{V}$ .

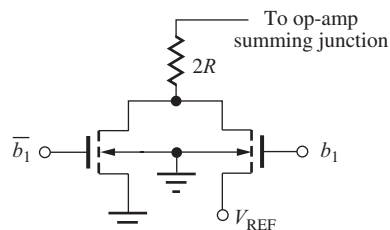


**Figure P10.71**

### Difference Amplifier

- 10.72. (a) What is the gain of the circuit in Fig. P10.72 if  $A_v = v_o / (v_1 - v_2)$  and  $R = 10\text{ k}\Omega$ ? (b) What is the input resistance presented to  $v_2$ ? (c) What is the input resistance at terminal  $v_1$ ? (d) What is the output voltage if  $v_1 = 3$  V and  $v_2 = 1.5 \cos 8300\pi t$  V? (e) What is the output voltage if  $v_1 = [3 - 1.5 \cos 8300\pi t]$  V and  $v_2 = 1.5 \sin 8300\pi t$  V?

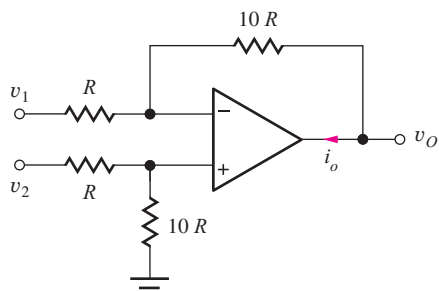


Figure P10.72

- 10.73. (a) What are the voltages at all the nodes in the difference amplifier in Fig. P10.72 if  $V_1 = 3.2$  V,  $V_2 = 3.1$  V, and  $R = 100$  k $\Omega$ ? (b) What is amplifier output current  $I_O$ ? (c) What are the currents entering the circuit from  $v_1$  and  $v_2$ ?
- 10.74. Find  $v_O$ ,  $i_1$  and  $i_2$  for the difference amplifier in Fig. P10.72 if  $v_1 = 2 \sin 1000\pi t$  V,  $v_2 = (2 \sin 1000\pi t + 2 \sin 2000\pi t)$  V, and  $R = 15$  k $\Omega$ .

### 10.10 Frequency-Dependent Feedback Amplifier Transfer Functions and Frequency Response

- \*10.75. Find the poles and zeros of the following transfer functions:

(a)  $A_i(s)$ 

$$= -\frac{3 \times 10^9 s^2}{(s^2 + 51s + 50)(s^2 + 13,000s + 3 \times 10^7)}$$

\*(b)  $A_v(s)$ 

$$= -\frac{10^5(s^2 + 51s + 50)}{s^5 + 1000s^4 + 50,000s^3 + 20,000s^2 + 13,000s + 3 \times 10^7}$$

- 10.76. What are  $A_{\text{mid}}$  in dB,  $f_H$ ,  $f_L$ , and the BW in Hz for the amplifier described by

$$A_v(s) = \frac{2\pi \times 10^7 s}{(s + 20\pi)(s + 2\pi \times 10^4)}$$

What type of amplifier is this?

- 10.77. What are  $A_{\text{mid}}$  in dB,  $f_H$ ,  $f_L$ , and the BW in Hz for the amplifier described by

$$A_v(s) = \frac{10^4 s}{s + 200\pi}$$

What type of amplifier is this?

- 10.78. What are  $A_{\text{mid}}$  in dB,  $f_H$ ,  $f_L$ , and the BW in Hz for the amplifier described by

$$A_v(s) = \frac{2\pi \times 10^6}{s + 200\pi}$$

What type of amplifier is this?

- 10.79. What are  $A_{\text{mid}}$  in dB,  $f_H$ ,  $f_L$ , the BW in Hz, and the  $Q$  for the amplifier described by

$$A_v(s) = -\frac{10^7 s}{s^2 + 10^5 s + 10^{14}}$$

What type of amplifier is this?

- 10.80. What are  $A_{\text{mid}}$  in dB,  $f_H$ ,  $f_L$ , and the BW in Hz for the amplifier described by

$$A_v(s) = -20 \frac{s^2 + 10^{12}}{s^2 + 10^4 s + 10^{12}}$$

What type of amplifier is this?

- \*10.81. What are  $A_{\text{mid}}$  in dB,  $f_H$ ,  $f_L$ , and the BW in Hz for the amplifier described by

$$A_v(s) = \frac{4\pi^2 \times 10^{14} s^2}{(s + 20\pi)(s + 50\pi)(s + 2\pi \times 10^5)(s + 2\pi \times 10^6)}$$

What type of amplifier is this?

- 10.82. Use MATLAB, a spreadsheet, or other computer program to generate a Bode plot of the magnitude and phase of the transfer function in Prob. 10.76.

- 10.83. Use MATLAB, a spreadsheet, or other computer program to generate a Bode plot of the magnitude and phase of the transfer function in Prob. 10.77.

- 10.84. Use MATLAB, a spreadsheet, or other computer program to generate a Bode plot of the magnitude and phase of the transfer function in Prob. 10.78.

- 10.85. Use MATLAB, a spreadsheet, or other computer program to generate a Bode plot of the magnitude and phase of the transfer function in Prob. 10.79.

- 10.86. Use MATLAB, a spreadsheet, or other computer program to generate a Bode plot of the magnitude and phase of the transfer function in Prob. 10.80.

- 10.87. Use MATLAB, a spreadsheet, or other computer program to generate a Bode plot of the magnitude and phase of the transfer function in Prob. 10.81.

- 10.88. The voltage gain of an amplifier is described by the transfer function in Prob. 10.76 and has an input  $v_i = 0.002 \sin \omega t$  V. Write an expression for the amplifier's output voltage at a frequency of (a) 5 Hz, (b) 500 Hz, (c) 50 kHz.

- 10.89. The voltage gain of an amplifier is described by the transfer function in Prob. 10.77 and has an input  $v_i = 0.3 \sin \omega t$  mV. Write an expression for the amplifier's output voltage at a frequency of (a) 1 Hz, (b) 50 Hz, (c) 5 kHz.

- 10.90. The voltage gain of an amplifier is described by the transfer function in Prob. 10.78 and has an input  $v_i = 10 \sin \omega t \mu\text{V}$ . Write an expression for the amplifier's output voltage at a frequency of (a) 2 Hz, (b) 2 kHz, (c) 200 kHz.
- 10.91. The voltage gain of an amplifier is described by the transfer function in Prob. 10.79 and has an input  $v_i = 0.004 \sin \omega t \text{ V}$ . Write an expression for the amplifier's output voltage at a frequency of (a) 1.59 MHz, (b) 1 MHz, (c) 5 MHz.
- 10.92. The voltage gain of an amplifier is described by the transfer function in Prob. 10.80 and has an input  $v_i = 0.25 \sin \omega t \text{ V}$ . Write an expression for the amplifier's output voltage at a frequency of (a) 159 kHz, (b) 50 kHz, (c) 200 kHz.
- 10.93. The voltage gain of an amplifier is described by the transfer function in Prob. 10.81 and has an input  $v_i = 0.002 \sin \omega t \text{ V}$ . Write an expression for the amplifier's output voltage at a frequency of (a) 5 Hz, (b) 500 Hz, (c) 50 kHz.
- 10.94. (a) Write an expression for the transfer function of a low-pass voltage amplifier with a gain of 26 dB and  $f_H = 5 \text{ MHz}$ . (b) Repeat if the amplifier exhibits a phase shift of  $180^\circ$  at  $f = 0$ .
- 10.95. (a) Write an expression for the transfer function of a voltage amplifier with a gain of 40 dB,  $f_L = 200 \text{ Hz}$ , and  $f_H = 100 \text{ kHz}$ . (b) Repeat if the amplifier exhibits a phase shift of  $180^\circ$  at  $f = 0$ .
- 10.96. (a) What is the bandwidth of the low-pass amplifier described by

$$A_v(s) = A_o \left( \frac{\omega_1}{s + \omega_1} \right)^3$$

if  $A_o = -2000$  and  $\omega_1 = 50,000\pi$ . (b) Make a Bode plot of this transfer function. What is the slope of the magnitude plot for  $\omega \gg \omega_H$  in dB/dec?

- \*10.97. The input to a low-pass amplifier with a gain of 10 dB is

$$v_S = 1 \sin(1000\pi t) + 0.333 \sin(3000\pi t) + 0.200 \sin(5000\pi t) \text{ V}$$

(a) If the phase shift of the amplifier at 500 Hz is  $10^\circ$ , what must be the phase shift at the other two frequencies if the shape of the output waveform is to be the same as that of the input waveform? Write an expression for the output signal. (b) Use the computer to check your answer by plotting the input and output waveforms.

## Low-Pass Filters

- 10.98. Find the midband gain in dB and the upper cut-off frequency for the low-pass filter in Ex. 10.8 if  $R_1 = 1 \text{ k}\Omega$ ,  $R_2 = 1.5 \text{ k}\Omega$ , and  $C = 0.01 \mu\text{F}$ .
- 10.99. Find the midband gain in dB and the upper cut-off frequency for the low-pass filter in Ex. 10.8 if  $R_1 = 10 \text{ k}\Omega$ ,  $R_2 = 100 \text{ k}\Omega$ , and  $C = 0.01 \mu\text{F}$ .
- 10.100. (a) Design a low-pass filter using the circuit in Ex. 10.8 to provide a loss of no more than 0.5 dB at low frequencies and a cutoff frequency of 20 kHz if  $R_1 = 560 \Omega$ . (b) Pick standard values from the tables in Appendix A.
- 10.101. (a) What are the low-frequency voltage gain (in dB) and cutoff frequency  $f_H$  for the amplifier in Fig. 10.32 if  $R_1 = 2 \text{ k}\Omega$ ,  $R_2 = 10 \text{ k}\Omega$ , and  $C = 0.001 \mu\text{F}$ ? (b) Repeat for  $R_1 = 2.7 \text{ k}\Omega$ ,  $R_2 = 56 \text{ k}\Omega$ , and  $C = 100 \text{ pF}$ .
- 10.102. (a) Design a low-pass amplifier (i.e., choose  $R_1$ ,  $R_2$ , and  $C$ ) to have a low-frequency input resistance of  $10 \text{ k}\Omega$ , a midband gain of 20 dB, and a bandwidth of 20 kHz. (b) Choose element values from the tables in Appendix A.
- 10.103. What are  $A_{\text{mid}}$  in dB,  $f_H$ ,  $f_L$ , and the BW in Hz for the amplifier described by

$$A_v(s) = \frac{2\pi \times 10^6}{s + 200\pi}$$

What type of amplifier is this?

## High-Pass Filters

- 10.104. Find the midband gain in dB and the upper cut-off frequency for the high-pass filter in Ex. 10.9 if  $R_1 = 8.2 \text{ k}\Omega$ ,  $R_2 = 20 \text{ k}\Omega$ , and  $C = 0.01 \mu\text{F}$ .
- 10.105. Find the midband gain in dB and the upper cutoff frequency for the high-pass filter in Ex. 10.9 if  $R_1 = 10 \text{ k}\Omega$ ,  $R_2 = 78 \text{ k}\Omega$ , and  $C = 0.01 \mu\text{F}$ .
- 10.106. (a) Design a high-pass filter using the circuit in Ex. 10.9 to provide a loss of no more than 0.5 dB at high frequencies and a cutoff frequency of 20 kHz if  $R_1 = 330 \Omega$ . (b) Pick standard values from the tables in Appendix A.
- 10.107. What are the high-frequency voltage gain (in dB) and cutoff frequency  $f_L$  for the amplifier in Fig. 10.33 if  $R_1 = 4.2 \text{ k}\Omega$ ,  $R_2 = 20 \text{ k}\Omega$ , and  $C = 0.002 \mu\text{F}$ ? (b) Repeat for  $R_1 = 2.7 \text{ k}\Omega$ ,  $R_2 = 56 \text{ k}\Omega$ , and  $C = 560 \text{ pF}$ .
- 10.108. (a) Design a high-pass filter (choose  $R_1$ ,  $R_2$ , and  $C$ ) to have a high frequency input resistance of  $10 \text{ k}\Omega$ , a gain of 20 dB, and a lower cutoff

frequency of 1 kHz. (b) Choose element values from the tables in Appendix A.

- 10.109. What are  $A_{mid}$  in dB,  $f_H$ ,  $f_L$ , and the BW in Hz for the amplifier described by

$$A_v(s) = \frac{10^4 s}{s + 200\pi}$$

What type of amplifier is this?

### Integrator

- 10.110. The input voltage to the integrator circuit in Fig. 10.34 is given by  $v_i = 0.1 \sin 2000\pi t$  V. What is the output voltage if  $R = 10$  k $\Omega$ ,  $C = 0.005$   $\mu$ F, and  $v_o(0) = 0$ ?
- 10.111. The input voltage to the integrator circuit in Fig. 10.34 is a rectangular pulse with an amplitude of 5 V and a width 1 ms. Draw the waveform at the output of the integrator if the pulse starts at  $t = 0$ ,  $R = 10$  k $\Omega$ , and  $C = 0.1$   $\mu$ F. Assume  $v_o = 0$  for  $t \leq 0$ .
- \*10.112. (a) What is the voltage transfer  $V_o(s)/V_i(s)$  function for the integrator in Fig. 10.34. (b) What is the voltage transfer function for the circuit in Fig. P10.112?

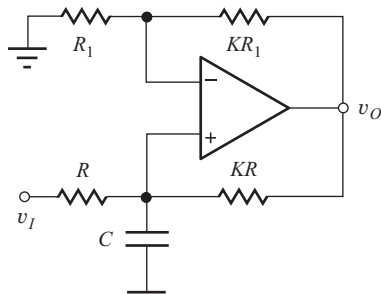


Figure P10.112

### Differentiator

- 10.113. What is the transfer function  $T(s) = V_O(s)/V_S(s)$  for the differentiator circuit in Fig. 10.33?
- 10.114. What is the output voltage of the differentiator circuit in Fig. 10.33 if  $v_S(t) = 2 \cos 3000\pi t$  V with  $C = 0.02$   $\mu$ F and  $R = 100$  k $\Omega$ ?
- 10.115. What is the transfer function  $A_v(s) = V_o(s)/V_i(s)$  for the circuit in Fig. P10.115? Draw a Bode Plot for the transfer function.

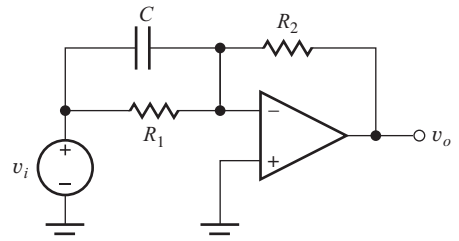
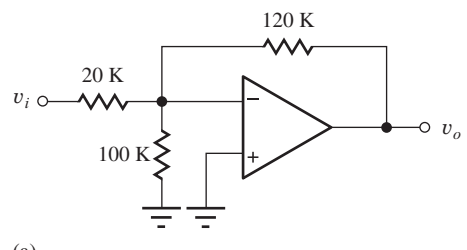


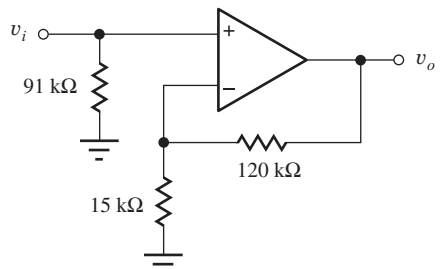
Figure P10.115

### General OP AMP Problems

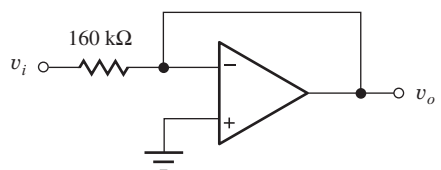
- 10.116. Find the voltage gain, input resistance, and output resistance for the circuits in Fig. P10.116.



(a)



(b)



(c)

Figure P10.116

- \*10.117. (a) What is the output current  $I_O$  in the circuit of Fig. P10.117 if  $-V_{EE} = -10$  V and  $R = 10$   $\Omega$ ? Assume that the MOSFET is saturated. (b) What is the minimum voltage  $V_{DD}$  needed to saturate the MOSFET if  $V_{TN} = 2.5$  V and  $K_n = 0.25$  A/V<sup>2</sup>. (c) What must be the power dissipation rating of resistor  $R$ ?

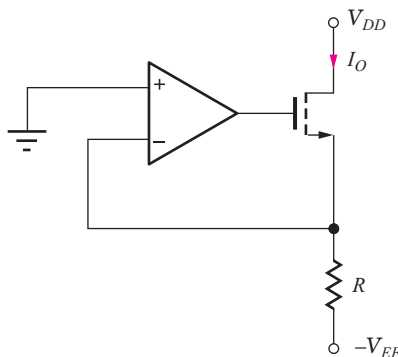


Figure P10.117

- \*10.118. (a) What is the output current  $I_O$  in the circuit in Fig. P10.118 if  $-V_{EE} = -15$  V and  $R = 30 \Omega$ ? Assume that the BJT is in the forward-active region and  $\beta_F = 30$ . (b) What is the voltage at the output of the operational amplifier if the saturation current  $I_S$  of the BJT is  $10^{-13}$  A? (c) What is the minimum voltage  $V_{CC}$  needed for forward-active region operation of the bipolar transistor? (d) Find the power dissipation rating of the resistor  $R$ . How much power is dissipated in the transistor if  $V_{CC} = 15$  V?

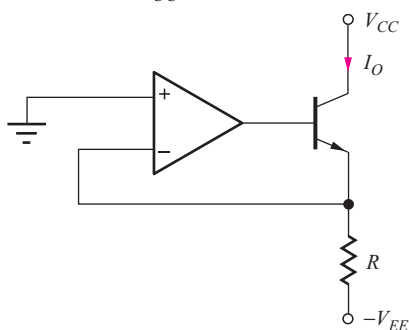


Figure P10.118

- 10.119. What is the transfer function for the voltage gain of the amplifier in Fig. P10.119?

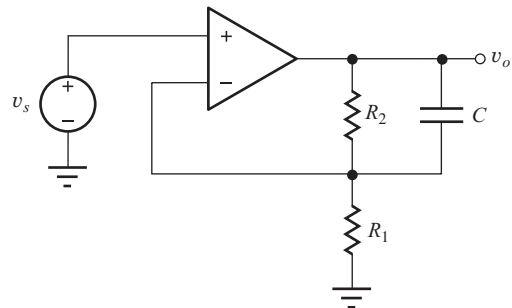


Figure P10.119

- \*10.120. The low-pass filter in Fig. P10.120 has  $R_1 = 10 \text{ k}\Omega$ ,  $R_2 = 330 \text{ k}\Omega$ , and  $C = 100 \text{ pF}$ . If the tolerances of the resistors are  $\pm 10$  percent and that of the capacitor is  $+20$  percent/ $-50$  percent, what are the nominal and worst-case values of the low-frequency gain and cutoff frequency?

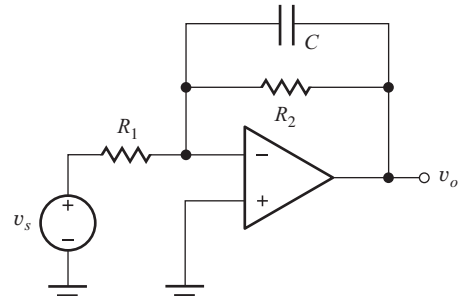
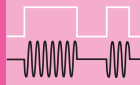


Figure P10.120 Low-pass filter

# CHAPTER 11



## NONIDEAL OPERATIONAL AMPLIFIERS and FEEDBACK AMPLIFIER STABILITY

### CHAPTER OUTLINE

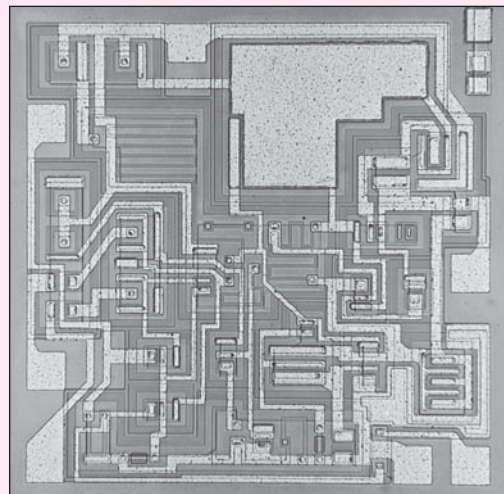
- 11.1 Classic Feedback Systems 601
- 11.2 Analysis of Circuits Containing Nonideal Operational Amplifiers 603
- 11.3 Series and Shunt Feedback Circuits 615
- 11.4 A Unified Approach to Feedback Amplifier Calculations 616
- 11.5 Series-Shunt Feedback—Voltage Amplifiers 617
- 11.6 Shunt-Shunt Feedback—Transresistance Amplifiers 624
- 11.7 Series-Series Feedback—Transconductance Amplifiers 629
- 11.8 Shunt-Series Feedback—Current Amplifiers 633
- 11.9 Finding the Loop Gain Using Successive Voltage and Current Injection 638
- 11.10 Distortion Reduction Through the Use of Feedback 641
- 11.11 DC Error Sources and Output Range Limitations 642
- 11.12 Common-Mode Rejection and Input Resistance 650
- 11.13 Frequency Response and Bandwidth of Operational Amplifiers 659
- 11.14 Stability of Feedback Amplifiers 671
  - Summary 682
  - Key Terms 684
  - References 684
  - Problems 685

### CHAPTER GOALS

- Study nonideal operational amplifier behavior
- Demonstrate techniques used to analyze circuits containing nonideal op amps
- Determine the voltage gain, input resistance, and output resistance of general amplifier circuits
- Explore common-mode rejection limitations and the effect of common-mode input resistance
- Learn how to model dc errors including offset voltage, input bias current, and input offset current
- Explore limits imposed by power supply voltages and finite output current capability
- Model amplifier limitations due to limited bandwidth and slew rate of the op amp

- Perform SPICE simulation of nonideal op amp circuits
- Understand the topologies and characteristics of the series-shunt, shunt-shunt, series-series, and shunt-series feedback configurations
- Develop techniques for analysis of feedback amplifiers including the effects of circuit loading
- Understand the effects of feedback on frequency response and feedback amplifier stability
- Define phase and gain margins
- Learn to interpret feedback amplifier stability in terms of Nyquist and Bode plots
- Use SPICE ac and transfer function analyses to characterize feedback amplifiers
- Develop techniques to determine the loop-gain of closed-loop amplifiers using SPICE simulation or measurement

Chapter 10 explored the characteristics of circuits employing ideal operational amplifiers having infinite gain, zero input current, and zero output resistance. Real operational amplifiers, on the other hand, do not exhibit any of these



uA741 Die Photograph (Courtesy of Fairchild Semiconductor)

ideal characteristics. In fact, they have a significant number of additional limitations as tabulated in the next column.

- Finite open loop gain
- Finite input resistance
- Nonzero output resistance
- Offset voltage
- Input bias and offset currents
- Limited output voltage range
- Limited output current capability
- Finite common-mode rejection
- Finite power supply rejection
- Limited bandwidth
- Limited slew rate

There are literally hundreds of commercial hybrid and integrated circuit operational amplifiers available to the engineer for use in circuit design. The only way to choose among this large set of options is to fully understand the characteristics and limitations of real operational amplifiers. Thus, this chapter explores the impact of these limitations in detail and demonstrates the approaches used to analyze circuits employing nonideal op amps. Generally, we look at the effect of each of the nonideal characteristics independently, while assuming the others are still ideal. Then we can combine the results to understand how the circuits behave in general.

To better understand the impact of nonideal op amp characteristics on circuit performance, we will start by reviewing the classic theory of negative feedback in electronic systems that was first developed by Harold Black of the Bell

Telephone System [1-3]. In 1928, he invented the feedback amplifier to stabilize the gain of early telephone repeaters. Today, some form of feedback is used in virtually every electronic system. This chapter formally develops the concept of feedback, which is an invaluable tool in the design of electronic systems. Valuable insight into the operation of many common electronic circuits can be gained by recasting the circuits as feedback amplifiers.

Several of the advantages of negative feedback were actually uncovered during the discussion of ideal operational amplifier circuit design in Chapter 10. Generally, feedback can be used to achieve a trade-off between gain and many of the other properties of amplifiers:

- *Gain stability:* Feedback reduces the sensitivity of gain to variations in the values of transistor parameters and circuit elements.
- *Input and output impedances:* Feedback can increase or decrease the input and output resistances of an amplifier.
- *Bandwidth:* The bandwidth of an amplifier can be extended using feedback.
- *Nonlinear distortion:* Feedback reduces the effects of nonlinear distortion.

Feedback may also be **positive** (or **regenerative**), and we explore the use of positive feedback in sinusoidal **oscillator circuits** in Chapter 12. Positive feedback in amplifiers is usually undesirable. Excess phase shift in a feedback amplifier may cause the feedback to become regenerative and cause the feedback amplifier to break into oscillation, a situation that we must know how to avoid!

## 11.1 CLASSIC FEEDBACK SYSTEMS

Classic feedback systems are described by the block diagram in Fig. 11.1. This diagram may represent a simple feedback amplifier or a complex feedback control system. It consists of an amplifier with transfer function  $A(s)$ , referred to as the **open-loop amplifier**, a **feedback network** with transfer function  $\beta(s)$ , and a summing block indicated by  $\Sigma$ . The variables in this diagram are represented as voltages but could equally well be currents or even other physical quantities such as temperature, velocity, distance, and so on.

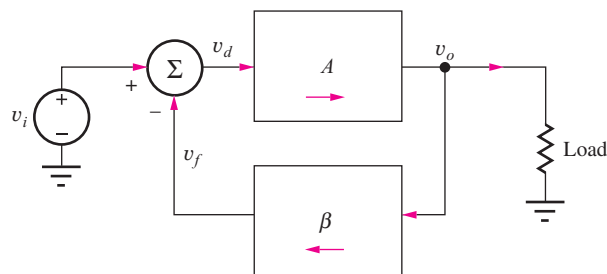


**Figure 11.1** Classic block diagram for a feedback system.

### 11.1.1 CLOSED-LOOP GAIN ANALYSIS

In Fig. 11.1, the input to the open-loop amplifier  $A$  is provided by the summing block, that develops the difference between the input signal  $v_i$  and the feedback signal  $v_f$ :

$$v_d = v_i - v_f \quad (11.1)$$

The output signal is equal to the product of the open-loop amplifier gain and the input signal  $v_d$ :

$$v_o = A v_d \quad (11.2)$$

The signal fed back to the input is given by

$$v_f = \beta v_o \quad (11.3)$$

Combining Eqs. (11.1) to (11.3) and solving for the overall voltage gain of the system yields the classic expression for the **closed-loop gain** of a feedback amplifier:

$$A_v = \frac{v_o}{v_i} = \frac{A}{1 + A\beta} = \frac{1}{\beta} \left( \frac{A\beta}{1 + A\beta} \right) = A_v^{\text{ideal}} \left( \frac{T}{1 + T} \right) \quad (11.4)$$

where  $A_v$  is the **closed-loop gain**,  $A$  is usually called the **open-loop gain**, and the product  $T = A\beta$  is defined as the **loop gain** or **loop transmission**.  $A_v^{\text{ideal}}$  is the **ideal gain** that would be achieved if the op amp were ideal.

Remember in Chapter 10 that the linear amplifier circuits all assumed that the circuit was connected correctly with negative feedback. For the block diagram in Fig. 11.1, negative feedback requires  $T > 0$ , whereas  $T < 0$  corresponds to a positive feedback condition. We will investigate some circuits called multivibrators that employ positive feedback in Chapter 12. We will explore the concepts of positive and negative feedback in more depth in this chapter and in Chapter 12.

A number of assumptions are implicit in this derivation. It is assumed that the blocks can be interconnected, as shown in Fig. 11.1, without affecting each other. That is, connecting the feedback network and the load to the output of the amplifier does not change the characteristics of the amplifier, nor does the interconnection of the summer, feedback network, and input of the open-loop amplifier modify the characteristics of either the amplifier or feedback network. In addition, it is tacitly assumed that signals flow only in the forward direction through the amplifier, and only in the reverse direction through the feedback network, as indicated by the arrows in Fig. 11.1.

Implementation of the block diagram in Fig. 11.1 with operational amplifiers having large input resistances, low output resistances, and essentially zero reverse-voltage gain is one method of satisfying these unstated assumptions. However, most general amplifiers and feedback networks do not necessarily satisfy these assumptions. In the next several sections we explore analysis and design of more general feedback systems that do not satisfy the implicit restrictions just outlined.

### 11.1.2 GAIN ERROR

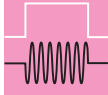
In high precision applications it is important to know, or to control by design, just how far the actual gain in Eq. (11.4) deviates from the ideal value of the gain. The **gain error (GE)** is defined as the difference between the ideal gain and the actual gain:

$$\text{GE} = (\text{ideal gain}) - (\text{actual gain}) = A_v^{\text{ideal}} - A_v = \frac{A_v^{\text{ideal}}}{1 + T} \quad (11.5)$$

This error is more often expressed as a fractional error or percentage, and the **fractional gain error (FGE)** is defined as

$$\text{FGE} = \frac{(\text{ideal gain}) - (\text{actual gain})}{(\text{ideal gain})} = \frac{A_v^{\text{ideal}} - A_v}{A_v^{\text{ideal}}} = \frac{1}{1 + T} \approx \frac{1}{T} \text{ for } T \gg 1 \quad (11.6)$$

For  $T \gg 1$ , we see that the value of FGE is determined by the reciprocal of the loop gain.


**DESIGN  
NOTE**

If the maximum fractional gain error is given as a design specification, then the value of the FGE places a lower bound on the value of the loop gain.

## 11.2 ANALYSIS OF CIRCUITS CONTAINING NONIDEAL OPERATIONAL AMPLIFIERS

In Chapter 10 we always assumed that the open-loop gain  $A$  of the op amp was infinite, which simplified the circuit analysis. If we take the limit of the expression in Eq. (11.4) as  $A$ , and therefore  $T$ , approach infinity

$$\lim_{A \rightarrow \infty} A_v = \lim_{T \rightarrow \infty} A_v^{\text{Ideal}} \left( \frac{T}{1+T} \right) = A_v^{\text{Ideal}} \quad (11.7)$$

we see that the closed-loop voltage gain equals the ideal gain (in this case the reciprocal of the feedback factor  $\beta$ ) and is independent of the characteristics of the op amp! This independence is one goal of feedback amplifier design. From our work in Chapter 10, we recognize that  $A_v^{\text{Ideal}} = 1/\beta$  represents the gain of the noninverting amplifier circuit employing an ideal amplifier.

In the next several sections, we remove various ideal assumptions as we explore the effects of finite open-loop gain, finite input resistance, and nonzero output resistance on the overall characteristics of the inverting and noninverting amplifiers that were introduced in Chapter 10, and see how close we can come to achieving our ideal goals.

### 11.2.1 FINITE OPEN-LOOP GAIN

A real operational amplifier provides a large but noninfinite gain. Op amps are commercially available with minimum open-loop gains of 80 dB (10,000) to over 120 dB (1,000,000). The finite open-loop gain contributes to deviations of the closed-loop gain, input resistance, and output resistance from those presented for the ideal amplifiers in Chapter 10.

#### Noninverting Amplifier

Evaluation of the closed-loop gain for the noninverting amplifier of Fig. 11.2 provides our first example of amplifier calculations involving nonideal amplifiers. In Fig. 11.2, the output voltage of

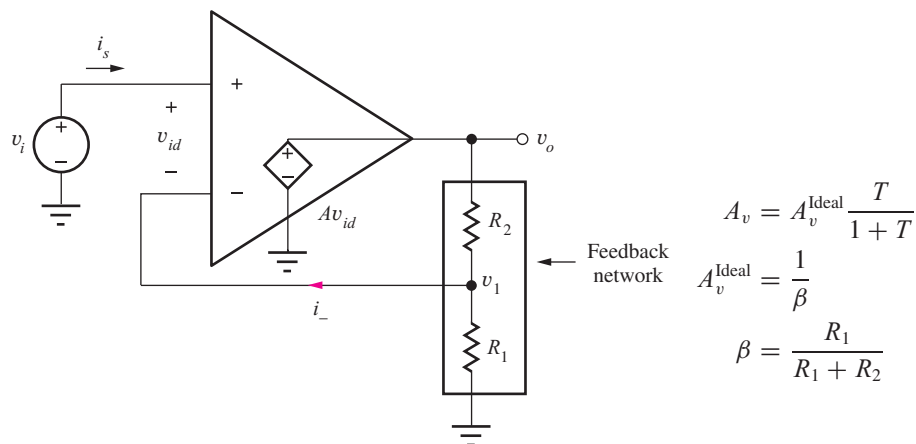


Figure 11.2 Operational amplifier with finite open-loop gain  $A$ .

the amplifier is given by

$$\mathbf{v}_o = A\mathbf{v}_{id} \quad \text{where} \quad \mathbf{v}_{id} = \mathbf{v}_i - \mathbf{v}_1 \quad (11.8)$$

Because  $i_- = 0$  by ideal op-amp Assumption 2 (see Eq. (10.36)),  $v_1$  is set by the voltage divider formed by resistors  $R_1$  and  $R_2$ :

$$\mathbf{v}_1 = \frac{R_1}{R_1 + R_2} \mathbf{v}_o = \beta \mathbf{v}_o \quad \text{where} \quad \beta = \frac{R_1}{R_1 + R_2} \quad (11.9)$$

The parameter  $\beta$  is called the **feedback factor** and represents the fraction of the output voltage that is fed back to the input from the output. Combining the last two equations gives

$$\mathbf{v}_o = A(\mathbf{v}_i - \beta \mathbf{v}_o) \quad (11.10)$$

and solving for  $\mathbf{v}_o$  yields the classic **feedback amplifier** voltage-gain formula in Eq. (11.11).

$$A_v = \frac{\mathbf{v}_o}{\mathbf{v}_i} = \frac{A}{1 + A\beta} = \frac{1}{\beta} \left( \frac{A\beta}{1 + A\beta} \right) = A_v^{\text{Ideal}} \left( \frac{T}{1 + T} \right) \quad (11.11)$$

The product  $A\beta$  is called the **loop gain** (or **loop transmission  $T$** ) and plays an important role in feedback amplifiers. For  $T \gg 1$ ,  $A_v$  approaches the ideal gain expression found previously:

$$A_v^{\text{Ideal}} = \frac{1}{\beta} = 1 + \frac{R_2}{R_1} \quad (11.12)$$

The voltage  $\mathbf{v}_{id}$  across the op amp input is given by

$$\mathbf{v}_{id} = \frac{\mathbf{v}_o}{A} = \frac{1}{A} \left( \frac{A}{1 + A\beta} \mathbf{v}_i \right) = \frac{\mathbf{v}_i}{1 + T} \quad (11.13)$$

Although  $\mathbf{v}_{id}$  is no longer zero, it is small for large values of the loop gain  $T$ . Thus, when we apply an input voltage  $\mathbf{v}_i$ , only a small portion of it appears across the input terminals.

### Inverting Amplifier

Evaluation of the closed-loop gain of the inverting amplifier in Fig. 11.3 is similar to that of the noninverting amplifier but yields a slightly different form of answer. In this case, the output voltage is

$$\mathbf{v}_o = A\mathbf{v}_{id} = -A\mathbf{v}_- \quad (11.14)$$

and the voltage at the inverting input terminal can be found using superposition:

$$\text{For } \mathbf{v}_o = 0, \text{ then } \mathbf{v}_- = \mathbf{v}_i \frac{R_2}{R_1 + R_2} \quad \text{and for } \mathbf{v}_i = 0, \text{ then } \mathbf{v}_- = \mathbf{v}_o \frac{R_1}{R_1 + R_2} \quad (11.15)$$

Combining these results yields

$$\mathbf{v}_- = \mathbf{v}_i \frac{R_2}{R_1 + R_2} + \mathbf{v}_o \frac{R_1}{R_1 + R_2} \quad (11.16)$$

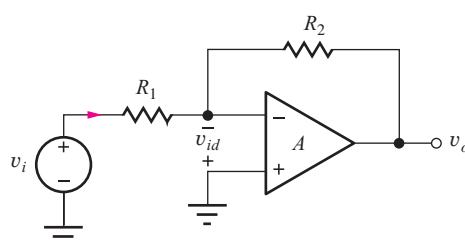


**Figure 11.3** Inverting amplifier circuit.

After some additional algebra, the closed-loop gain can be written as

$$A_v = \frac{v_o}{v_i} = -\frac{R_2}{R_1} \left( \frac{A\beta}{1 + A\beta} \right) = A_v^{\text{ideal}} \left( \frac{T}{1 + T} \right) \quad (11.17)$$

where  $A_v^{\text{ideal}} = R_2/R_1$ ,  $T = A\beta$  and  $\beta = R_1/(R_1 + R_2)$ . First note that the expression for the feedback factor  $\beta$ , which represents the portion of the output voltage that is fed back to the input, is the same as we found for the noninverting amplifier, i.e.  $\beta$  is independent of the configuration! In addition, as the loop-gain approaches infinity, we find that the ideal gain is again the same as we calculated in Chapter 10:

$$A_v^{\text{ideal}} = \lim_{A \rightarrow \infty} A_v = \lim_{T \rightarrow \infty} \left( -\frac{R_2}{R_1} \right) \left( \frac{T}{1 + T} \right) = -\frac{R_2}{R_1} \quad (11.18)$$

The residual voltage across the op amp input terminals is

$$v_{id} = \frac{v_o}{A} = \frac{1}{A} \left( -\frac{R_2}{R_1} \frac{A\beta}{1 + A\beta} v_i \right) = -\frac{R_2}{R_1} \frac{\beta}{1 + A\beta} v_i \cong -\frac{R_2}{R_1} \frac{v_i}{A} \quad (11.19)$$

in which the approximation holds for large loop-gain  $T$ . Once again, only a very small portion of input signal  $v_i$  appears across the op amp input terminals.

**EXERCISE:** Suppose  $A = 10^5$ ,  $\beta = 1/100$ , and  $v_s = 100 \text{ mV}$ . What are  $A_v^{\text{ideal}}$ ,  $T$ ,  $A_v$ ,  $v_o$ , and  $v_{id}$  for the noninverting amplifier.

**ANSWERS:** 100, 99.9, 10.0 V, 100  $\mu\text{V}$  ( $v_{id}$  is small but nonzero)

**EXERCISE:** Repeat the previous exercise for the inverting amplifier.

**ANSWERS:** -99, 1000, -98.9, -9.90 V, -99.0  $\mu\text{V}$



**EXERCISE:** What are the nominal, minimum, and maximum values of the open-loop gain at 25°C for an OP-27 operational amplifier?

**ANSWERS:** With 15-V supplies: 1,000,000; 1,800,000; no maximum value specified

**EXERCISE:** What value of open-loop gain is guaranteed for the OP-27 op amp over the full temperature range with a load resistance of at least 2 k $\Omega$ ?

**ANSWER:** 600,000 with 15-V power supplies

## EXAMPLE 11.1 GAIN ERROR ANALYSIS

Characterize the gain and gain error of a noninverting amplifier implemented with a finite gain operation amplifier.

**PROBLEM** A noninverting amplifier is designed to have a gain of 200 (46 dB) and is built using an operational amplifier with an open-loop gain of 80 dB. Find the values of the ideal gain, the actual gain, and the gain error. Express the gain error in percent.

**SOLUTION** **Known Information and Given Data:** Design a noninverting amplifier circuit with closed-loop gain of 46 dB. The open-loop gain of the op amp is 10,000 (80 dB).

**Unknowns:** Values of the ideal gain, the actual gain, and the gain error in percent

**Approach:** First, we need to clarify the meaning of some terminology. We normally design an amplifier to produce a given value of ideal gain, and then determine the deviations to be expected from the ideal case. So, when it is said that this amplifier is designed to have a gain of 200, we set  $\beta = \frac{1}{200}$ . We do not normally try to adjust the design values of  $R_1$  and  $R_2$  to try to compensate for the finite open-loop gain of the amplifier. One reason is that we do not know the exact value of the gain  $A$  but generally only know its lower bound. Also, the resistors we use have tolerances, and their exact values are also unknown.

**Assumptions:** The op amp is ideal except for its finite open-loop gain.

**Analysis:** The ideal gain of the circuit is 200, so  $\beta = 1/200$  and  $T = 10^4/200 = 50$ . The actual gain and FGE are given by

$$A_v = A_v^{\text{Ideal}} \frac{T}{1+T} = 200 \left( \frac{50}{51} \right) = 196 \quad \text{and} \quad \text{FGE} = \frac{200 - 196}{200} = 0.02 \text{ or } 2\%$$

**Check of Results:** The three unknown values have been found. The value of  $A_v^{\text{Ideal}}$  is slightly less than  $A_v$  and therefore appears to be a reasonable result.

**Discussion:** The actual gain is 196, representing a 2 percent error from the ideal design gain of 200. Note that this gain error expression does not include the effects of resistor tolerances, which are an additional source of gain error in an actual circuit. If the gain must be more precise, a higher-gain op amp must be used, or the resistors can be replaced by a potentiometer so the gain can be adjusted manually. But note that the gain will still change with temperature.

**Computer Aided Analysis:** The circuit in Ex. 10.5 can be used to check the results of this example by setting  $R_1 = 1 \text{ k}\Omega$ ,  $R_2 = 199 \text{ k}\Omega$ , and the gain of  $E_1$  to 10,000. A transfer function analysis gives  $A_v = 196$ , in agreement with our hand calculations.

**EXERCISE:** A noninverting amplifier is designed with  $R_1 = 1 \text{ k}\Omega$ ,  $R_2 = 39 \text{ k}\Omega$ , and an op amp with an open-loop gain of 80 dB. What are the loop gain, closed-loop gain, ideal gain and fractional gain error of the amplifier?

**ANSWER:** 250, +39.8, +40.0, 0.4 percent

**EXERCISE:** Repeat the previous exercise for the inverting amplifier.

**ANSWERS:** -38.8, -39.0, 0.398 percent

### 11.2.2 NONZERO OUTPUT RESISTANCE

The next effect we explore is the influence of a nonzero output resistance on the characteristics of the inverting and noninverting closed-loop amplifiers. In this case, we assume that the op amp has a nonzero output resistance  $R_o$  as well as a finite open-loop gain  $A$ . (As we shall see, finite gain must also be assumed; otherwise, we would get the same output resistance as for the ideal case.)

To determine the (Thévenin equivalent) output resistances of the two amplifiers in Fig. 11.4, each output terminal is driven with a test signal source  $v_x$  (a current source could also be used), and the current  $i_x$  is calculated; all other independent sources in the network must be turned off. The

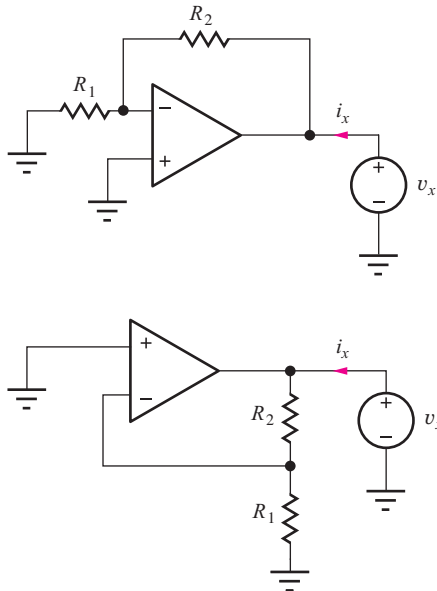
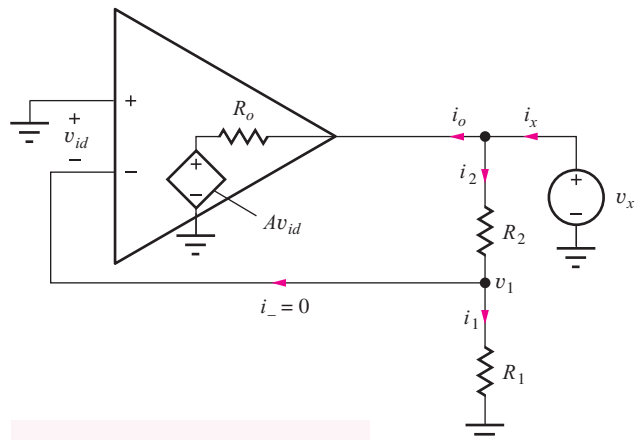


**Figure 11.4** Circuits for determining output resistances of the inverting and noninverting amplifiers.



$$R_{\text{out}} = \frac{R_o}{1 + A\beta} \parallel (R_1 + R_2)$$

**Figure 11.5** Circuit explicitly showing amplifier with  $A$  and  $R_o$ .

output resistance is then given by

$$R_{\text{out}} = \frac{V_x}{I_x} \quad (11.20)$$

By studying Fig. 11.4 we observe that the two amplifier circuits are identical for the output resistance calculation. Thus, analysis of the circuit in Fig. 11.5 gives the expression for  $R_{\text{out}}$  for both the inverting and noninverting amplifiers.

Analysis begins by expressing currents  $I_x$  and  $I_o$  as

$$I_x = I_o + I_2 \quad \text{and} \quad I_o = \frac{V_x - A V_{id}}{R_o} \quad (11.21)$$

Current  $I_2$  can be found from

$$V_x = I_2 R_2 + I_1 R_1 \quad \text{or} \quad I_2 = \frac{V_x}{R_1 + R_2} \quad (11.22)$$

because  $I_1 = I_2$  due to op amp Assumption 2:  $i_- = 0$ . The input voltage  $V_{id}$  is equal to  $-V_1$ , and because  $i_- = 0$ ,

$$V_1 = \frac{R_1}{R_1 + R_2} V_x = \beta V_x \quad (11.23)$$

Combining Eqs. (11.21) through (11.23) yields

$$\frac{1}{R_{\text{out}}} = \frac{I_x}{V_x} = \frac{1 + A\beta}{R_o} + \frac{1}{R_1 + R_2} \quad (11.24)$$

Equation (11.24) represents the output conductance of the amplifier and corresponds to the sum of the conductances of two parallel resistors. Thus, the output resistance can be expressed as

$$R_{\text{out}} = \frac{R_o}{1 + A\beta} \parallel (R_1 + R_2) \quad (11.25)$$

The output resistance in Eq. (11.25) represents the series combination of  $R_1$  and  $R_2$  in parallel with a resistance  $R_o/(1 + A\beta)$  that represents the output resistance of the operational amplifier including the effects of feedback. In almost every practical situation, the value of  $R_o/(1 + A\beta)$  is much less than that of  $(R_1 + R_2)$ , and the output resistance expression in Eq. (11.25) simplifies to

$$R_{\text{out}} \cong \frac{R_o}{1 + A\beta} = \frac{R_o}{1 + T} \quad (11.26)$$

An example of the degree of dominance of the resistance term in Eq. (11.26) is given in Example 11.2.

Note that the output resistance would be zero if  $A$  were assumed to be infinite in Eqs. (11.25) or (11.26). This is the reason why the analysis must simultaneously account for both finite  $A$  and nonzero  $R_o$ .



**EXERCISE:** What are the nominal, minimum, and maximum values of the open-loop gain and output resistance for an OP-77E operational amplifier (see MCD website)?

**ANSWERS:** 12,000,000 (142 dB); 5,000,000 (134 dB); no maximum value specified; 60  $\Omega$ ; no minimum or maximum value specified.

## EXAMPLE 11.2 OP AMP OUTPUT RESISTANCE

Perform a numeric calculation of the output resistance of a noninverting amplifier implemented using an op amp with a finite open-loop gain and nonzero output resistance.

**PROBLEM** A noninverting amplifier is constructed with  $R_1 = 1 \text{ k}\Omega$  and  $R_2 = 39 \text{ k}\Omega$  using an operational amplifier with an open-loop gain of 80 dB and an output resistance of 50  $\Omega$ . Find the output resistance of the noninverting amplifier.

**SOLUTION** **Known Information and Given Data:** Noninverting op amp amplifier circuit with  $R_1 = 1 \text{ k}\Omega$ ,  $R_2 = 39 \text{ k}\Omega$ ,  $A = 10,000$ , and  $R_o = 50 \Omega$ .

**Unknowns:** Output resistance of the overall amplifier

**Approach:** Use known values to evaluate Eq. (11.25)

**Assumptions:** The op amp is ideal except for finite gain and nonzero output resistance.

**Analysis:** Evaluating Eq. (11.25):

$$1 + A\beta = 1 + A \frac{R_1}{R_1 + R_2} = 1 + 10^4 \frac{1 \text{ k}\Omega}{1 \text{ k}\Omega + 39 \text{ k}\Omega} = 251$$

and

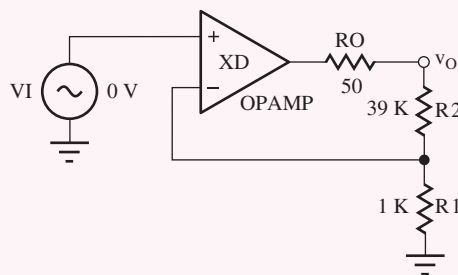
$$R_{\text{out}} = \frac{50 \Omega}{251} \parallel (40 \text{ k}\Omega) = 0.199 \Omega \parallel 40 \text{ k}\Omega = 0.198 \Omega$$

**Check of Results:** The unknown value of output resistance has been calculated. The value is much smaller than the value of  $R_o$ , which is expected.

**Evaluation and Discussion:** We see that the effect of the feedback in the circuits in Fig. 11.4 is to reduce the output resistance of the closed-loop amplifier far below that of the individual op amp

itself. In fact, the output resistance is quite small and represents a good practical approximation to that of an ideal amplifier ( $R_{out} = 0$ ). This is a characteristic of shunt feedback at the output port, in which the feedback network is in parallel with the port. **Shunt feedback** tends to lower the resistance at a port, whereas feedback in series with a port, termed **series feedback**, tends to raise the resistance at that port. The properties of series and shunt feedback are explored in greater detail later in this chapter.

**Computer-Aided Design:** The output resistance of the noninverting amplifier can be simulated by adding the output resistance  $R_O$  to the circuit of Ex. 10.5 as indicated in the figure. The gain of the OP AMP is set to 10,000. A transfer function analysis from  $V_I$  to output node  $v_o$  gives a gain of +39.8 and an output resistance of  $0.199 \Omega$ .



**EXERCISE:** What value of open-loop gain is required to achieve an output resistance of  $0.1 \Omega$  in the amplifier in Ex. 11.2.

**ANSWER:** 20,000

**EXERCISE:** Calculate the value of closed-loop gain in Ex. 11.2 and verify that the simulation result is correct.

**EXERCISE:** Suppose the resistors in Ex. 11.2 both have 5 percent tolerances. What are the worst-case (highest and lowest) values of gain that can be expected if the open-loop gain were infinite? What is the gain error for each of these two cases?

**ANSWERS:** 44.1, 36.2, 4.20(10.5 percent), -3.60(-9.5 percent)

## DESIGN OPEN-LOOP GAIN DESIGN

### EXAMPLE 11.3

In this example, we find the value of open-loop gain required to meet an amplifier output resistance specification.

**PROBLEM** Design a noninverting amplifier to have a gain of 35 dB and an output resistance of no more than  $0.2 \Omega$ . The only op amp available has an output resistance of  $250 \Omega$ . What is the minimum open-loop gain of the op amp that will meet the design requirements?

**SOLUTION** **Known Information and Given Data:** For the noninverting amplifier: ideal gain = 35 dB, closed-loop output resistance =  $0.2 \Omega$ . For the operational amplifier used to realize the noninverting amplifier: open-loop output resistance =  $250 \Omega$ .

**Unknowns:** Open-loop gain  $A$  of the op amp

**Approach:** The required value of operational amplifier gain can be found using Eq. (11.26), in which all the variables are known except  $A$ .

**Assumptions:** The operational amplifier is ideal except for finite open-loop gain and nonzero output resistance.

**Analysis:** The closed-loop output resistance is given by

$$R_{\text{out}} = \frac{R_o}{1 + A\beta} \leq 0.2 \Omega$$

$R_o$  and  $R_{\text{out}}$  are given, and  $\beta$  is determined by the desired gain:

$$R_o = 250 \Omega \quad R_{\text{out}} = 0.2 \Omega \quad \beta = \frac{1}{|A_v|}$$

We must convert the gain from dB before we use it in the calculations:

$$|A_v| = 10^{35 \text{ dB}/20 \text{ dB}} = 56.2 \quad \text{and} \quad \beta = \frac{1}{|A_v|} = \frac{1}{56.2}$$

The minimum value of the open-loop gain  $A$  can now be determined from the  $R_{\text{out}}$  specification:

$$A \geq \frac{1}{\beta} \left( \frac{R_o}{R_{\text{out}}} - 1 \right) = 56.2 \left( \frac{250}{0.2} - 1 \right) = 7.03 \times 10^4$$

$$A_{\text{dB}} = 20 \log(7.03 \times 10^4) = 96.9 \text{ dB}$$

**Check of Results:** We have found the required unknown value.

**Discussion:** By exploring the world wide web, we see that op amps are available with 100 dB gain. So the value required by our design is achievable.

**Computer-Aided Analysis:** If we change the parameter values in the circuit in Ex. 11.2 and rerun the simulation, we will see if we meet the output resistance specification. Using  $R_1 = 10 \text{ k}\Omega$ ,  $R_2 = 552 \text{ k}\Omega$ , and  $R_O = 250 \Omega$  with the OP AMP gain set to  $7.03E4$ , the SPICE transfer function analysis yields  $A_v = 56.2$  and  $R_{\text{out}} = 0.200 \Omega$ . The values of  $R_1$  and  $R_2$  were deliberately chosen to be large so that they would not materially affect the output resistance. We see from the voltage gain result that we have chosen the correct value for the ratio  $R_2/R_1$ .

**EXERCISE:** A noninverting amplifier must have a closed-loop gain of 40 dB and an output resistance of less than  $0.1 \Omega$ . The only op amp available has an output resistance of  $200 \Omega$ . What is the minimum open-loop gain of the op amp that will meet the requirements?

**ANSWER:** 106 dB

### 11.2.3 FINITE INPUT RESISTANCE

Next we explore the effect of the finite input resistance of the operational amplifier on the open-loop input resistances of the noninverting and inverting amplifier configurations. In this case, we shall find that the results are greatly different for the two amplifiers.

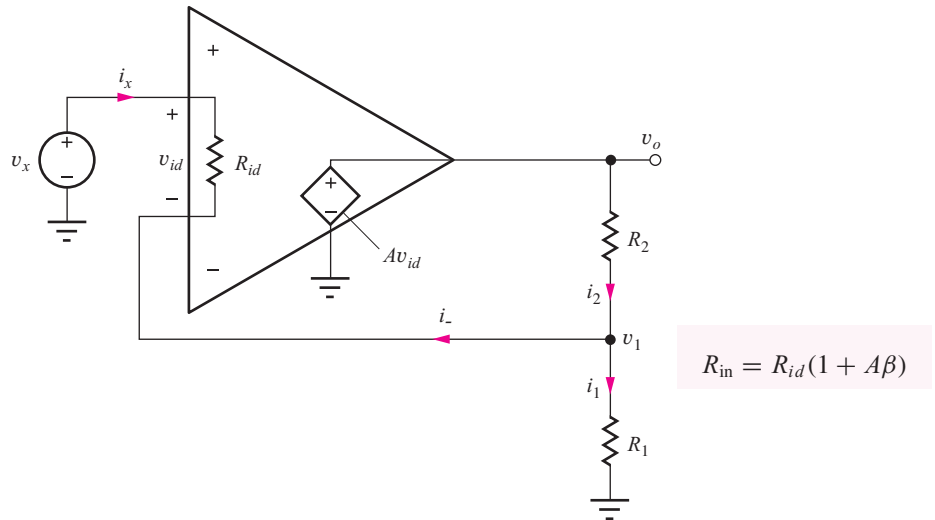


**Figure 11.6** Input resistance of the noninverting amplifier.

### Input Resistance for the Noninverting Amplifier

Let us first consider the noninverting amplifier circuit in Fig. 11.6, in which test source  $v_x$  is applied to the input. To find  $R_{in}$ , we must calculate the current  $\mathbf{i}_x$  given by

$$\mathbf{i}_x = \frac{\mathbf{v}_x - \mathbf{v}_1}{R_{id}} \quad (11.27)$$

Voltage  $\mathbf{v}_1$  is equal to

$$\mathbf{v}_1 = \mathbf{i}_1 R_1 = (\mathbf{i}_2 - \mathbf{i}_-) R_1 \cong \mathbf{i}_2 R_1 \quad (11.28)$$

which has been simplified by assuming that the input current  $\mathbf{i}_-$  to the op amp can still be neglected with respect to  $\mathbf{i}_2$ . We will check this assumption shortly. The assumption is equivalent to saying that  $\mathbf{i}_1 \cong \mathbf{i}_2$  and permits the voltage  $\mathbf{v}_1$  to again be written in terms of the resistive voltage divider as

$$\mathbf{v}_1 \cong \frac{R_1}{R_1 + R_2} \mathbf{v}_o = \beta \mathbf{v}_o = \beta (A \mathbf{v}_{id}) = A\beta (\mathbf{v}_x - \mathbf{v}_1) \quad (11.29)$$

Solving for  $\mathbf{v}_1$  in terms of  $\mathbf{v}_x$  yields

$$\mathbf{v}_1 = \frac{A\beta}{1 + A\beta} \mathbf{v}_x \quad (11.30)$$

and substituting this result into Eq. (12.17) yields an expression for  $R_{in}$

$$\mathbf{i}_x = \frac{\mathbf{v}_x - \frac{A\beta}{1 + A\beta} \mathbf{v}_x}{R_{id}} = \frac{\mathbf{v}_x}{(1 + A\beta) R_{id}} \quad \text{and} \quad R_{in} = R_{id}(1 + A\beta) = R_{id}(1 + T) \quad (11.31)$$

Note from Eq. (11.31) that the input resistance can be very large—much larger than that of the op amp itself.  $R_{id}$  is often large ( $1 \text{ M}\Omega$  to  $1 \text{ T}\Omega$ ) to start with, and it is multiplied by the loop gain  $T$ , which is typically designed to be much greater than 1. If the loop-gain approaches infinity in Eq. (11.31) the input resistance also approaches its ideal value of infinity. Although the actual value of  $R_{in}$  cannot reach infinity in real circuits, it can be extremely large in value. This large input resistance occurs since only a small portion of the applied voltage  $v_x$  actually appears across  $R_{id}$ . Thus the input current is very small, and the overall input resistance becomes very high.



**EXERCISE:** What are the nominal, minimum, and maximum values of the open-loop gain and input resistance for an AD745 operational amplifier (see MCD website)? Repeat for the input resistance of the OP-27.

**ANSWERS:** 132 dB; 120 dB; no maximum value specified;  $10^{10} \Omega$ ; minimum and maximum values not specified;  $6 \text{ M}\Omega$ ;  $1.3 \text{ M}\Omega$ ; no maximum specified.

## EXAMPLE 11.4 NONINVERTING AMPLIFIER INPUT RESISTANCE

Find a numeric value for the input resistance of a noninverting feedback amplifier circuit.

**PROBLEM** The noninverting amplifier in Fig. 11.6 is built with an op amp having an input resistance of  $2 \text{ M}\Omega$  and an open-loop gain of 90 dB. What is the amplifier input resistance if  $R_1 = 20 \text{ k}\Omega$  and  $R_2 = 510 \text{ k}\Omega$ ?

**SOLUTION** **Known Information and Given Data:** A noninverting feedback amplifier circuit is built with feedback resistors  $R_1 = 20 \text{ k}\Omega$  and  $R_2 = 510 \text{ k}\Omega$ . For the op amp:  $A = 90 \text{ dB}$ ,  $R_{id} = 2 \text{ M}\Omega$

**Unknown:** Closed-loop amplifier input resistance  $R_{in}$

**Approach:** In this case, we are given the values necessary to directly evaluate Eq. (11.31) including  $A$ ,  $R_{id}$ , and the two feedback resistors.

**Assumptions:** The operational amplifier is ideal except for finite open-loop gain and finite input resistance.

**Analysis:** In order to evaluate Eq. (11.31) we must find  $\beta$ , which is determined by the feedback resistors

$$\beta = \frac{R_1}{R_1 + R_2} = \frac{20 \text{ k}\Omega}{20 \text{ k}\Omega + 510 \text{ k}\Omega} = \frac{1}{26.5}$$

We must also convert the gain from dB before we use it in the calculations:

$$R_{id} = 2 \text{ M}\Omega \quad \text{and} \quad A = 10^{90 \text{ dB}/20 \text{ dB}} = 31,600$$

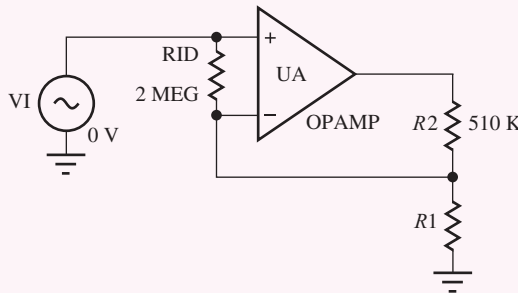
The closed-loop input resistance is given by

$$R_{in} = R_{id}(1 + A\beta) = 2 \text{ M}\Omega \left[ 1 + \frac{31,600}{26.5} \right] = 2.39 \times 10^9 \Omega = 2.39 \text{ G}\Omega$$

**Check of Results:** We have found the only unknown value. The value is large as expected from our analysis of the noninverting amplifier.

**Discussion:** The calculated input resistance of the noninverting amplifier is very large (although not infinite as for case of an ideal op amp). In fact, the calculated value of  $R_{in}$  is so large that we must consider other factors that may limit the actual input resistance. These include surface leakage of the printed circuit board in which the op amp is mounted as well as common-mode input resistance of the op amp itself, which we discuss in Sec. 11.12.4.

**Computer-Aided Analysis:** To check our result with SPICE, we add RID = 2 MEG to the noninverting amplifier circuit model as shown below (with the OP AMP gain set to 31,600) and perform a transfer function analysis. The results are  $A_v = 26.5$  and  $R_{in} = 2.39 \text{ G}\Omega$  confirming our hand calculations.



**EXERCISE:** Suppose a noninverting amplifier has  $R_{id} = 1 \text{ M}\Omega$ , with  $R_1 = 10 \text{ k}\Omega$ ,  $R_2 = 390 \text{ k}\Omega$ , and the open-loop gain is 80 dB. What is the input resistance of the overall amplifier? What are the currents  $I_-$  and  $I_1$  for a dc input voltage  $V_s = 1 \text{ V}$ ? Is  $I_- \ll I_1$ ?

**ANSWERS:**  $251 \text{ M}\Omega$ ;  $-3.98 \text{ nA}$ ,  $100 \mu\text{A}$ ; yes

For the numbers in the preceding exercise, it is easy to see that the current  $\mathbf{i}_-$ , which equals  $-\mathbf{i}_x$ , is small compared to the current through  $R_2$  and  $R_1$  (see Prob. 11.16). Thus, our simplifying assumption that led to Eqs. (11.28) and (11.29) is well justified.

### Input Resistance for the Inverting-Amplifier Configuration

The input resistance of the inverting amplifier can be determined using the circuit in Fig. 11.7(a) and is defined by

$$R_{in} = \frac{\mathbf{v}_x}{\mathbf{i}_x} \quad (11.32)$$

Test signal  $\mathbf{v}_x$  can be expressed as

$$\mathbf{v}_x = \mathbf{i}_x R_1 + \mathbf{v}_- \quad \text{and} \quad R_{in} = R_1 + \frac{\mathbf{v}_-}{\mathbf{i}_x} \quad (11.33)$$

The total input resistance  $R_{in}$  is equal to  $R_1$  plus the resistance looking into the inverting terminal of the operational amplifier, which can be found using the circuit in Fig. 11.7(b). The input current in Fig. 11.7(b) is

$$\mathbf{i}_1 = \mathbf{i}_- + \mathbf{i}_2 = \frac{\mathbf{v}_1}{R_{id}} + \frac{\mathbf{v}_1 - \mathbf{v}_o}{R_2} = \frac{\mathbf{v}_1}{R_{id}} + \frac{\mathbf{v}_1 + A\mathbf{v}_1}{R_2} \quad (11.34)$$

Using this result, the input conductance can be written as

$$G_1 = \frac{\mathbf{i}_1}{\mathbf{v}_1} = \frac{1}{R_{id}} + \frac{1+A}{R_2} \quad (11.35)$$

which represents the sum of two conductances. Thus, the equivalent resistance looking into the inverting-input terminal is the parallel combination of two resistors,

$$R_{id} \parallel \left( \frac{R_2}{1+A} \right) \quad (11.36)$$

and the overall input resistance of the inverting amplifier becomes

$$R_{in} = R_1 + R_{id} \parallel \left( \frac{R_2}{1+A} \right) \quad (11.37)$$

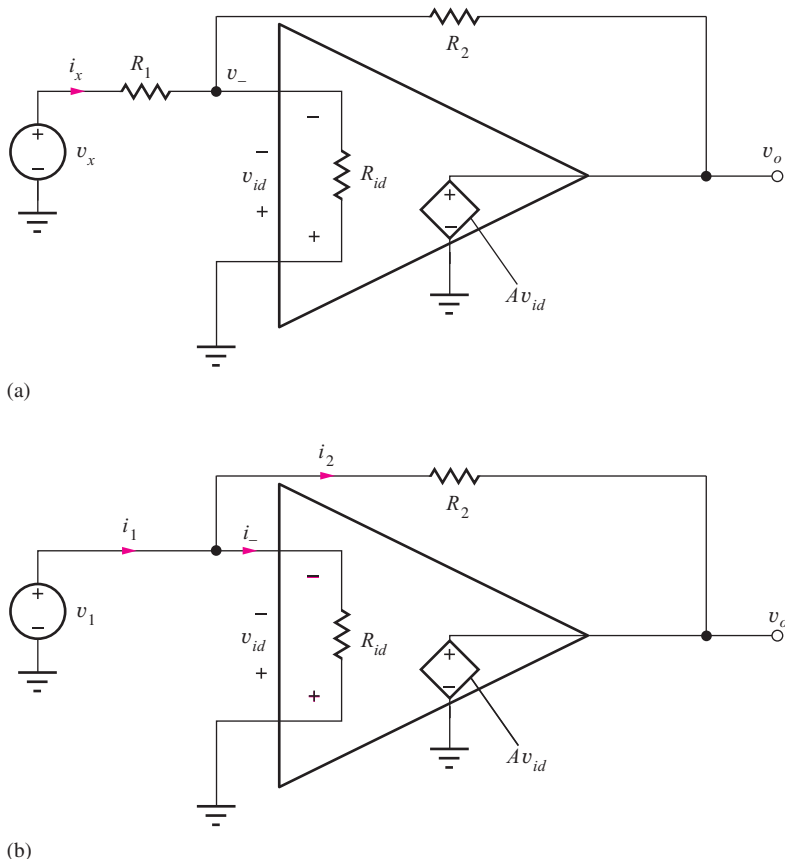


**Figure 11.7** Inverting amplifier input-resistance calculation: (a) complete amplifier, (b) amplifier with  $R_1$  removed.

Normally,  $R_{id}$  will be large and Eq. (11.37) can be approximated by

$$R_{in} \cong R_1 + \left( \frac{R_2}{1 + A} \right) \quad (11.38)$$

For large  $A$  and common values of  $R_2$ , the input resistance approaches the ideal result  $R_{in} \cong R_1$ . In other words, we see that the input resistance is usually dominated by  $R_1$  connected to the quasi virtual ground at the op amp input. (Remember,  $v_{id}$  is no longer exactly zero for a finite-gain amplifier.)

**EXERCISE:** Find the input resistance  $R_{in}$  of an inverting amplifier that has  $R_1 = 1 \text{ k}\Omega$ ,  $R_2 = 100 \text{ k}\Omega$ ,  $R_{id} = 1 \text{ M}\Omega$ , and  $A = 100 \text{ dB}$ . What is the deviation of  $R_{in}$  from its ideal value?

**ANSWERS:**  $1001 \Omega$ ;  $1 \Omega$  out of  $1000 \Omega$  or 0.1 percent

#### 11.2.4 SUMMARY OF NONIDEAL INVERTING AND NONINVERTING AMPLIFIERS

Table 11.1 is a summary of the simplified expressions for the closed-loop voltage gain, input resistance, and output resistance of the inverting and noninverting amplifiers. These equations are most often used in the design of these basic amplifier circuits.

Op amp circuits are usually designed with large loop-gain  $T = A\beta$ ; thus the simplified expressions in Table 11.1 normally apply. Except for very high precision circuits, the gain error caused by finite gain will be negligible, and resistor tolerances are much more likely to be the dominant source of gain error. Large values of  $T$  ensure low values of output resistance, although the output resistances do depend upon the value of  $T$ . The input resistance of the inverting amplifier is approximately equal to  $R_1$ , whereas that of the noninverting amplifier is large, but a direct function of  $T$ .

**TABLE 11.1**  
Inverting and Noninverting Amplifier Summary

$\beta = \frac{R_1}{R_1 + R_2} T = A\beta$	<b>INVERTING AMPLIFIER</b>	<b>NONINVERTING AMPLIFIER</b>
Voltage gain $A_v$	$-\frac{R_2}{R_1} \left( \frac{T}{1+T} \right) \cong -\frac{R_2}{R_1}$	$\left( 1 + \frac{R_2}{R_1} \right) \left( \frac{T}{1+T} \right) \cong 1 + \frac{R_2}{R_1}$
Input resistance $R_{in}$	$R_1 + \left( R_{id} \parallel \frac{R_2}{1+A} \right) \cong R_1$	$R_{id}(1+T)$
Output resistance $R_{out}$	$\frac{R_O}{1+T}$	$\frac{R_O}{1+T}$
Fractional gain error (FGE)	$\frac{1}{1+T}$	$\frac{1}{1+T}$

## 11.3 SERIES AND SHUNT FEEDBACK CIRCUITS

The properties of the feedback amplifier properties summarized earlier in Table 11.1 are characteristics of so-called **series feedback** and **shunt feedback**. When applied to an amplifier port, series feedback generally increases the impedance level. In contrast, shunt feedback decreases the impedance level at the amplifier port.

### 11.3.1 FEEDBACK AMPLIFIER CATEGORIES

The two types of feedback yield  $(2 \times 2)$  or four possible circuit combinations of series and shunt feedback. These circuits are depicted in Fig. 11.8 and characterized in Table 11.2. Each type of feedback will be discussed in detail in the next several sections.

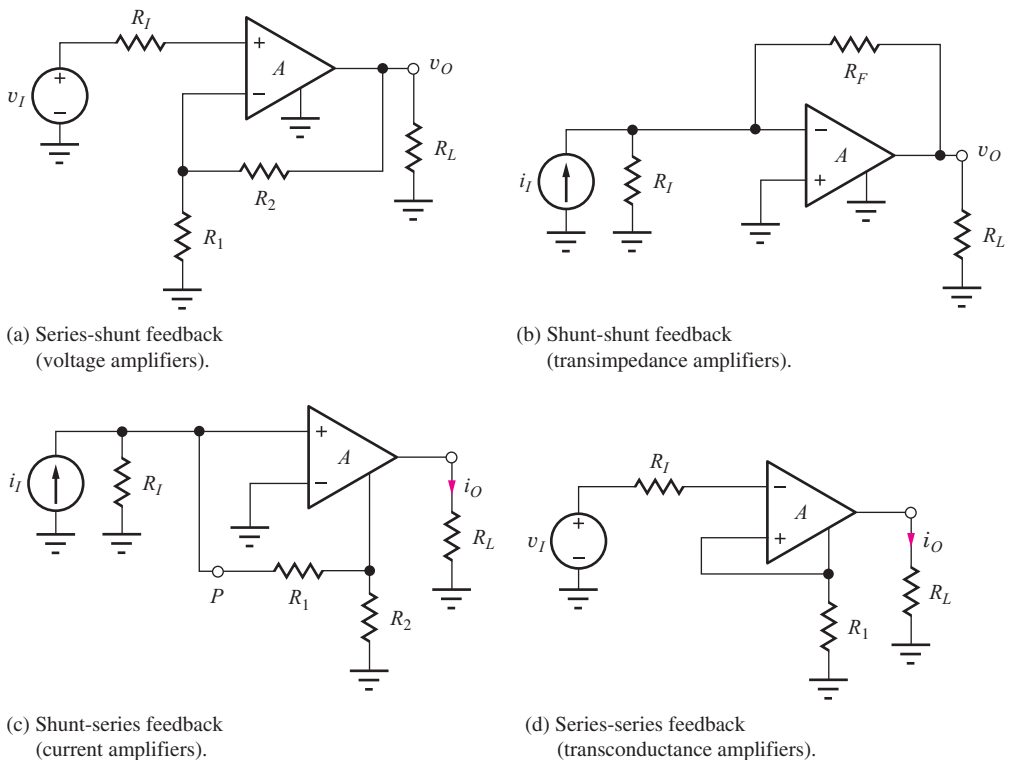


Figure 11.8 Four types of feedback amplifiers.

**TABLE 11.2**  
Feedback Amplifier Categories

FEEDBACK TYPE INPUT-OUTPUT	AMPLIFIER TYPE AND GAIN DEFINITION
Series-shunt	Voltage amplifier: $A_v = \frac{v_o}{v_i}$
Shunt-shunt	Transresistance amplifier: $A_{tr} = \frac{v_o}{i_i}$
Shunt-series	Current amplifier: $A_i = \frac{i_o}{i_i}$
Series-series	Transconductance amplifier: $A_{tc} = \frac{i_o}{v_i}$

### 11.3.2 VOLTAGE AMPLIFIERS—SERIES-SHUNT FEEDBACK

A voltage amplifier should have a high input resistance to measure the desired voltage and a low output resistance to drive the external load. These requirements correspond to the series-shunt feedback circuit shown in Fig. 11.8(a). To achieve the desired behavior, the input ports of the amplifier and feedback network are connected in series, and the output ports are connected in parallel (shunt).

### 11.3.3 TRANSIMPEDANCE AMPLIFIERS—SHUNT-SHUNT FEEDBACK

A transimpedance amplifier converts an input current to an output voltage. Thus it should have a low input resistance to sink the desired current and a low output resistance to drive the external load. These requirements correspond to the shunt-shunt feedback circuit shown in Fig. 11.8(b). To achieve the desired behavior, the input ports of the amplifier and feedback network are connected in parallel, and the output ports are connected in parallel.

### 11.3.4 CURRENT AMPLIFIERS—SHUNT-SERIES FEEDBACK

A current amplifier should provide a low resistance current sink at the input and a high resistance current source at its output. These attributes correspond to the shunt-series feedback as depicted in Fig. 11.8(c). The input ports of the amplifier and feedback network are connected in parallel, and the output ports are connected in series.

### 11.3.5 TRANSCONDUCTANCE AMPLIFIERS—SERIES-SERIES FEEDBACK

The last feedback configuration is the transconductance amplifier that converts an input voltage to an output current. This amplifier should have a high input resistance and a high output resistance and thus corresponds to the series-series feedback circuit in Fig. 11.8(d) in which both the input ports and the output ports of the amplifier and feedback networks are connected in series.

## 11.4 UNIFIED APPROACH TO FEEDBACK AMPLIFIER GAIN CALCULATION

We have already found that loop-gain  $T$  plays a very important role in determining the overall gain, input resistance, and output resistance of feedback amplifiers. We shall see shortly that  $T$  also determines feedback amplifier stability. Because of its importance, we need to understand how to model general feedback amplifiers and to calculate the loop gain directly from the circuit, not only theoretically, but also computationally using SPICE and experimentally based upon actual measurements. For the rest of this chapter, we will adopt a unified method for calculating the gain and terminal resistances associated with feedback amplifiers.

### 11.4.1 CLOSED-LOOP GAIN ANALYSIS

The closed-loop gain of all four feedback configurations in Fig. 11.8 can be written in the single form that we developed earlier in Section 11.2:

$$A_x = A_x^{\text{ideal}} \left( \frac{T}{1+T} \right) \quad (11.39)$$

The ideal gain  $A_x^{\text{ideal}}$  of each amplifier is set by its individual feedback network, and  $T$  is the amplifier's loop gain. In the next several sections, we will calculate  $T$  including the loading effects of  $R_{id}$ ,  $R_o$ ,  $R_I$ ,  $R_L$ , and the feedback network. These loading effects were neglected in our earlier analysis, but they can be important in many real circuit cases.

### 11.4.2 RESISTANCE CALCULATIONS USING BLACKMAN'S THEOREM

R. B. Blackman was one of a group of individuals who first investigated the properties of feedback amplifiers at Bell Laboratories in the 1930s and 1940s [4], and Blackman's Theorem provides a unified way to calculate impedances in feedback circuits. His highly useful result is stated in Eq. (11.40) and provides us with an alternate approach for calculating the input and output resistance [4] of a feedback amplifier.

$$R_X = R_X^D \frac{1 + |T_{SC}|}{1 + |T_{OC}|} \quad (11.40)$$

In this equation,  $R_X$  is the resistance of the closed-loop feedback amplifier looking into one of its ports (any terminal pair),  $R_X^D$  is the resistance looking into the same pair of terminals with the feedback loop disabled,  $T_{SC}$  is the loop-gain with a short-circuit applied to the selected port, and  $T_{OC}$  is the loop gain with the same port open-circuited.

In order to apply Blackman's theorem, first we select the terminals where we desire to find the resistance. For example, we often wish to find the input resistance or the output resistance of a closed-loop feedback amplifier, and the resistance appears between one of the amplifier terminals and ground. Next, we select one of the controlled sources in the equivalent circuit of the amplifier. We use this source to disable the feedback loop, and the source is also used as the reference source for finding the two loop gains  $T_{SC}$  and  $T_{OC}$ . Resistance  $R_X^D$  represents the driving-point resistance at the port of interest calculated with the gain of the controlled source set to zero, whereas  $T_{SC}$  and  $T_{OC}$  are calculated with the port short-circuited and open-circuited, respectively. This procedure is best understood with the aid of several examples in the following section.

## 11.5 SERIES-SHUNT FEEDBACK—VOLTAGE AMPLIFIERS

The noninverting amplifier has been redrawn in Fig. 11.9 to more clearly delineate the series and shunt connections between the amplifier and the feedback network  $F$ . The op amp has been drawn to explicitly include its own input resistance  $R_{id}$  and output resistance  $R_o$ . The feedback network consists of resistors  $R_1$  and  $R_2$ , and its input and output port voltages,  $v_{if}$  and  $v_{of}$ , are defined in the figure. On the left side, applied input voltage  $v_i$  equals the sum of the op amp input voltage and the feedback network voltage:  $v_i = v_{id} + v_{if}$ . Thus there is **series feedback** at the input because the amplifier input and feedback network voltages are in series.

At the output, we see that the feedback network voltage equals the op amp output voltage:  $v_{of} = v_o$ . Thus the amplifier and feedback network are connected in parallel, or shunt, at the output, so we have **shunt feedback** at the output. We refer to this overall configuration as a **series-shunt feedback amplifier**. As summarized previously in Table 11.1, the gain is set by the feedback network, and we expect the input resistance to be increased over that of the op amp itself ( $R_{id}$ ) by the series feedback at the input, and the output resistance is decreased below that of the op amp ( $R_o$ ) by the shunt feedback at the output.

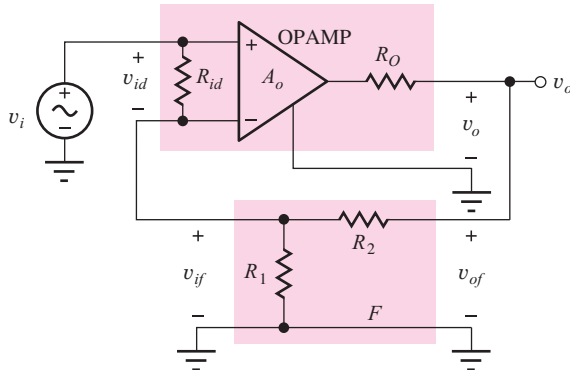


**Figure 11.9** The noninverting amplifier as a series-shunt feedback amplifier.

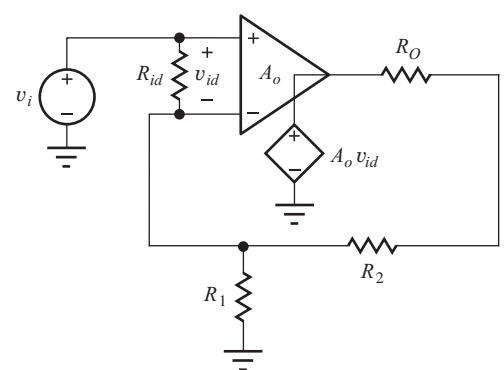


**Figure 11.10** Series-shunt feedback amplifier.

### 11.5.1 CLOSED-LOOP GAIN CALCULATION

In order to find the closed-loop gain for the series-shunt feedback amplifier, we need to evaluate the gain expression from Eq. (11.39) by finding the ideal gain and the loop gain:

$$A_v = A_v^{\text{Ideal}} \left( \frac{T}{1+T} \right) \quad \text{where} \quad A_v^{\text{Ideal}} = 1 + \frac{R_2}{R_1} \quad (11.41)$$

We already know from Chapter 10 that the ideal gain for the noninverting amplifier is given by  $A_v^{\text{Ideal}} = 1 + (R_2/R_1)$ .

Loop gain  $T$  represents the total gain through the amplifier and back around the feedback loop to the input, and we will use Fig. 11.10 to directly calculate the loop gain. To find  $T$ , we disable the feedback loop at some arbitrary point in the circuit, insert a test source into the loop, and calculate the gain around the loop. In the op amp circuit, it is convenient to use the source that already exists within the op amp model. We disable the feedback loop by assuming we know the value of  $v_{id}$  in source  $A_o v_{id}$ , (e.g.,  $v_{id} = 1 \text{ V}$  and  $A_o v_{id} = A_o(1)$ ), and then calculate the value of  $v_{id}$  developed back at the op amp input. The loop gain is then equal to the negative of the ratio of the voltage returned through the loop to the op amp input. The negative sign accounts for the use of negative feedback.

Loop gain  $T$  can now be found by applying voltage division to the circuit in Fig. 11.10 (note that we must also turn off the independent input source  $v_i$  by setting its value to zero):

$$v_{id} = -A_o(1) \frac{(R_1 || R_{id})}{(R_1 || R_{id}) + R_2 + R_o} \quad (11.42)$$

and

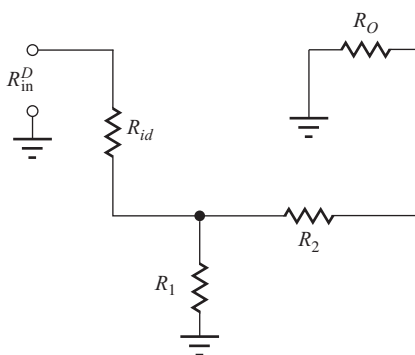
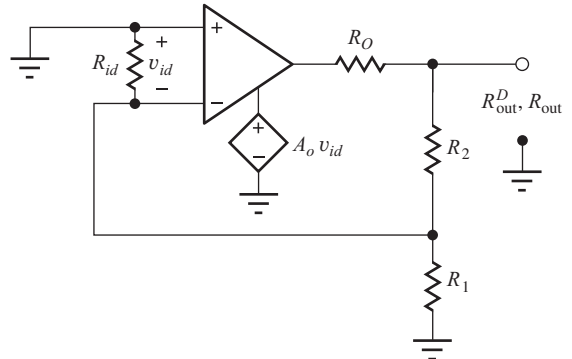
$$T = -\frac{v_{id}}{1} = A_o \frac{R_1 || R_{id}}{(R_1 || R_{id}) + R_2 + R_o} \quad (11.43)$$

Note that the loop gain now incorporates all the nonideal resistance effects.  $R_{id}$  appears in parallel with  $R_1$  of the feedback network, and  $R_o$  appears in series with  $R_2$ . If  $R_{id} || R_1 \gg (R_2 + R_o)$ , then  $T$  approaches  $A_o$ . Otherwise,  $T < A_o$ .

### 11.5.2 INPUT RESISTANCE CALCULATIONS

Next let us find the input resistance of the series-shunt feedback amplifier by applying Blackman's theorem from Eq. (11.40):

$$R_{\text{in}} = R_{\text{in}}^D \frac{1 + |T_{SC}|}{1 + |T_{OC}|} \quad (11.44)$$

Figure 11.11 Circuit for finding  $R_{in}^D$ .Figure 11.12 Circuit for finding  $R_{out}^D$ .

$R_{in}$  is the resistance of the closed-loop feedback amplifier looking into any pair of terminals (a port),  $R_{in}^D$  is the resistance looking into the same terminals with the feedback loop disabled,  $T_{SC}$  is the loop gain with a short circuit applied to the port, and  $T_{OC}$  is the loop gain with the same port open.

In the series-shunt circuit, the input resistance is the resistance appearing between the non-inverting input terminal and ground.  $R_{in}^D$  is found using the circuit in Fig. 11.11 in which the feedback loop has been disabled by setting  $A_o = 0$ , and the input resistance can then be written directly as

$$R_{in}^D = R_{id} + [R_1||(R_2 + R_o)] \quad (11.45)$$

To find  $T_{SC}$ , the input terminals in the original circuit are shorted, and we recognize that the circuit is identical to the one used to find the loop gain  $T$  in Eq. (11.43). Therefore  $|T_{SC}| = T$ . To find  $T_{OC}$ , the input terminals are open-circuited. Then no current can flow through  $R_{id}$ , voltage  $v_{id}$  must be zero, and  $T_{OC} = 0$  in Fig. 11.10. The final expression for the input resistance becomes

$$R_{in} = R_{in}^D \frac{1 + |T_{SC}|}{1 + |T_{OC}|} = R_{in}^D \frac{1 + T}{1 + 0} = [R_{id} + R_1||(R_2 + R_o)](1 + T) \quad (11.46)$$

Compared to the results in Table 11.1, the input resistance now includes the additional influence of  $R_1$ ,  $R_2$ , and  $R_o$  and the modified value of  $T$ .

### 11.5.3 OUTPUT RESISTANCE CALCULATIONS

Again, applying Blackman's theorem gives

$$R_{out} = R_{out}^D \frac{1 + |T_{SC}|}{1 + |T_{OC}|} \quad (11.47)$$

Be sure to note that the values of  $T_{SC}$  and  $T_{OC}$  depend upon the selected terminal pair, and the values in Eq. (11.47) will most likely differ from those just found in the previous section!

The output resistance is the resistance appearing between the amplifier output terminal and ground. We find  $R_{out}^D$  using the circuit in Fig. 11.12 in which we can disable the feedback by setting  $A_o = 0$ . The resistance can then be written directly as

$$R_{out}^D = R_o||(R_2 + R_1||R_{id}) \quad (11.48)$$

For  $T_{SC}$ , output terminal  $v_o$  is connected directly to ground, shorting out the feedback loop. Thus  $T_{SC} = 0$ . To find  $T_{OC}$ , the output terminals are open-circuited. Now we recognize that the circuit is identical to the one used to find the loop gain  $T$  in Eq. (11.43), and  $|T_{OC}| = T$ . The final expression

for the output resistance becomes

$$R_{\text{out}} = R_{\text{out}}^D \frac{1 + |T_{SC}|}{1 + |T_{OC}|} = R_{\text{out}}^D \frac{1 + 0}{1 + T} = \frac{R_o || (R_2 + R_1 || R_{id})}{1 + T} \quad (11.49)$$

Compared to the results in Table 11.1, the input resistance now includes the additional influence of  $R_1$ ,  $R_2$ , and  $R_{id}$  as well as the modified value of  $T$ . Note that the values of  $T_{SC}$  and  $T_{OC}$  are opposite from those found for the input resistance calculation.

During analysis of the impact of finite gain, finite input resistance, and nonzero output resistance on the characteristics of the closed-loop amplifiers at the beginning of this chapter, we assumed in several cases that the input current to the op amp was negligible with respect to the current in the feedback network, which is equivalent to assuming that  $R_{id}$  is much greater than  $R_1$ . However, our loop-gain analysis allows us to directly account for the impact of both  $R_{id}$  and  $R_o$  on the feedback amplifier's gain with no approximations, and it is directly extendable to include any number of additional resistances (See Ex. 11.5). Note that if  $R_{id} \gg R_1$  and  $R_1 + R_2 \gg R_o$ , then  $T = A_o \beta$ .

#### 11.5.4 SERIES-SHUNT FEEDBACK AMPLIFIER SUMMARY

The direct loop-gain analysis of the characteristics of the series-shunt feedback amplifier yielded the following results:

$$A_v = \left(1 + \frac{R_2}{R_1}\right) \frac{T}{1 + T} \quad R_{\text{in}} = R_{\text{in}}^D (1 + T) \quad R_{\text{out}} = \frac{R_{\text{out}}^D}{1 + T} \quad (11.50)$$

The expressions in Eq. (11.50) are identical in form to those developed at the beginning of this chapter and summarized in Table 11.2. The overall input resistance is increased by the series feedback at the input, and the output resistance is decreased by the shunt feedback at the output. However, the equations now use the input resistance, output resistance, and loop gain of the amplifier including the effects of all the resistances in the circuit. Application of this theory appears in the next example.

### EXAMPLE 11.5 SERIES-SHUNT FEEDBACK AMPLIFIER ANALYSIS

This example evaluates the closed-loop characteristics of an op-amp-based series-shunt feedback amplifier using the loop-gain approach. The analysis is extended to include a source resistance.

**PROBLEM** Find the closed-loop voltage gain, input resistance, and output resistance for the series-shunt feedback amplifier in Fig. 11.9, if the op amp has an open-loop gain of 80 dB, an input resistance of 25 kΩ, and an output resistance of 1 kΩ. Assume the amplifier is driven by a signal voltage with a 2-kΩ source resistance, and the feedback network is implemented with  $R_2 = 91$  kΩ and  $R_1 = 10$  kΩ.

**SOLUTION** **Known Information and Given Data:** The series-shunt feedback amplifier is drawn in the figure below with the source resistance added. For the op amp:  $A_o = 80$  dB,  $R_{id} = 25$  kΩ, and  $R_o = 1$  kΩ.

**Unknowns:** Closed-loop gain  $A_v$ , closed-loop input resistance  $R_{\text{in}}$ , closed-loop output resistance  $R_{\text{out}}$

**Approach:** Find  $A_v^{\text{ideal}}$ ,  $T$ ,  $R_{\text{in}}^D$ , and  $R_{\text{out}}^D$ . Then calculate the values of the unknowns using the closed-loop feedback amplifier formulae derived in this section.

**Assumptions:** The op amp is ideal except for  $A_o$ ,  $R_{id}$ , and  $R_o$ .

**Analysis:** The amplifier circuit with the addition of  $R_I$  appears in Fig. 11.13 below.

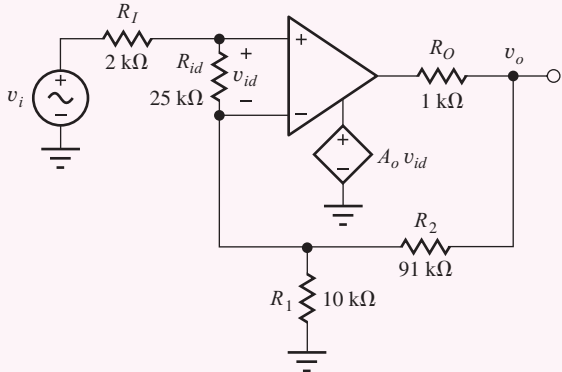


**Figure 11.13** Series-shunt feedback amplifier with source resistance added.

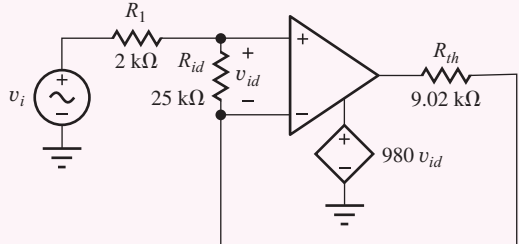


**Figure 11.14** Series-shunt feedback amplifier with Thévenin transformation.

**Amplifier Analysis:** Using Fig. 11.13,

$$A_v^{\text{Ideal}} = 1 + \frac{R_2}{R_1} = 1 + \frac{91 \text{ k}\Omega}{10 \text{ k}\Omega} = 10.1$$

$$R_{\text{in}}^D = R_I + R_{id} + R_1 \parallel (R_2 + R_O)$$

$$R_{\text{in}}^D = 2 \text{ k}\Omega + 25 \text{ k}\Omega + 10 \text{ k}\Omega \parallel (91 \text{ k}\Omega + 1 \text{ k}\Omega) = 36.0 \text{ k}\Omega$$

$$R_{\text{out}}^D = R_O \parallel [R_2 + R_1 \parallel (R_{id} + R_I)]$$

$$R_{\text{out}}^D = 1 \text{ k}\Omega \parallel [91 \text{ k}\Omega + 10 \text{ k}\Omega \parallel (25 \text{ k}\Omega + 2 \text{ k}\Omega)] = 990 \text{ }\Omega$$

The loop gain is most easily found by first taking a Thévenin equivalent of  $R_o$ ,  $R_1$ , and the op amp output source yielding the circuit in Fig. 11.14:

$$v_{th} = A_o v_{id} \frac{R_1}{R_o + R_2 + R_1} = 10^4 v_{id} \frac{10 \text{ k}\Omega}{1 \text{ k}\Omega + 91 \text{ k}\Omega + 10 \text{ k}\Omega} = 980 v_{id}$$

$$R_{th} = R_1 \parallel (R_2 + R_O) = 10 \text{ k}\Omega \parallel (91 \text{ k}\Omega + 1 \text{ k}\Omega) = 9.02 \text{ k}\Omega$$

Now we can assume  $v_{id} = 1$  in  $v_{th}$  and solve for the op amp input voltage  $v_{id}$ :

$$v_{id} = -v_{th} \frac{R_{id}}{R_{th} + R_{id} + R_I} = -980(1) \frac{25 \text{ k}\Omega}{9.02 \text{ k}\Omega + 25 \text{ k}\Omega + 2 \text{ k}\Omega} = -680$$

$$T = -\frac{v_{id}}{1} = 680$$

#### Closed-Loop Amplifier Results:

$$A_v = \left(1 + \frac{R_2}{R_1}\right) \frac{T}{1+T} = \left(1 + \frac{91 \text{ k}\Omega}{10 \text{ k}\Omega}\right) \frac{680}{1+680} = 10.1$$

$$R_{\text{in}} = R_{\text{in}}^D(1+T) = 36.0 \text{ k}\Omega(1+680) = 24.5 \text{ M}\Omega$$

$$R_{\text{out}} = \frac{R_{\text{out}}^D}{1+T} = \frac{990 \text{ }\Omega}{1+680} = 1.45 \text{ }\Omega$$

**Check of Results:** We have found the three unknowns. The loop gain is high, so we expect the closed-loop gain to be approximately 10.1. The calculated input resistance is much larger than that of the op amp itself, and the output resistance is much smaller than that of the op amp. These all agree with our expectations for the series-shunt feedback configuration.

**Discussion:** This analysis demonstrates a direct method for including the effects of nonideal op amp characteristics as well as loading effects of the feedback network and source (and/or load resistors) on the noninverting amplifier configuration. One of the following exercises looks at the impact of adding a load resistor to this amplifier. Note that the low value of  $R_{id}$  relative to  $R_1$ , and  $R_L$  in this problem reduces the loop gain substantially.

**Computer-Aided Analysis:** Our SPICE circuit mirrors the circuit in Fig. 11.13 and augments the built-in OPAMP model with the addition of  $R_{id}$  in parallel with its input and  $R_o$  in series with its output, and the gain is set to 10,000. A transfer function analysis from  $v_i$  to the output voltage yields:  $A_v = 10.09$ ,  $R_{in} = 24.54 \text{ M}\Omega$ , and  $R_{out} = 1.453 \Omega$ . These results agree closely with our hand calculations.

**EXERCISE:** Find the loop gain, closed-loop voltage gain, input resistance, and output resistance for the series-shunt feedback amplifier in Ex. 11.5 if the 2-k $\Omega$  source resistor is eliminated from the amplifier circuit.

**ANSWERS:** 720, 10.1, 24.5 M $\Omega$ , 1.37  $\Omega$

**EXERCISE:** Find the loop gain, closed-loop voltage gain, input resistance, and output resistance for the series-shunt feedback amplifier in Ex. 11.5 if a 5-k $\Omega$  load resistor is connected to the output of the amplifier.

**ANSWERS:** 568, 10.1, 20.5 M $\Omega$ , 1.45  $\Omega$ ; Note that the input resistance is a function of the load resistance  $R_L$ .

**EXERCISE:** What would the closed-loop gain, input resistance, and output resistance of the series-shunt feedback amplifier in the previous exercise have been if the loading effects of the feedback network and  $R_i$  and  $R_L$  had all been ignored?

**ANSWERS:** 10.1, 24.8 M $\Omega$ , 1.01  $\Omega$

**DISCUSSION:** Note that the closed-loop gain is essentially unchanged because of the high value of loop gain, but the values of  $R_{in}$  and  $R_{out}$  differ by substantial percentages. Feedback stabilizes the value of the voltage gain but not those of the input and output resistances.

**EXERCISE:** What are the values of  $A_v$ ,  $R_{in}$ , and  $R_{out}$  if the 2-k $\Omega$  source resistor is changed to 5k $\Omega$  in Fig. 11.14?

**ANSWERS:** 10.1; 15.7 M $\Omega$ ; 1.59  $\Omega$

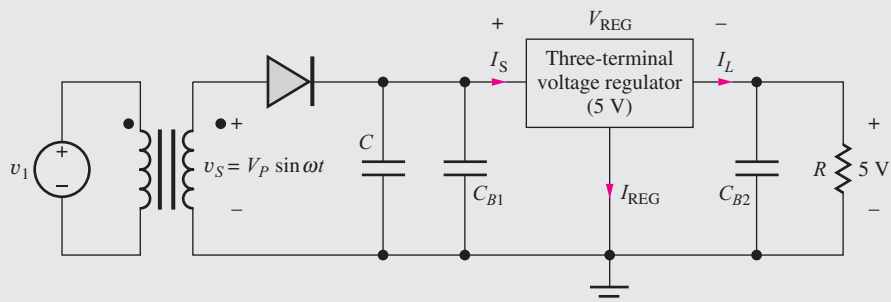
# ELECTRONICS IN ACTION

## *Three-Terminal IC Voltage Regulators*

It is not easy to produce precise output voltages with rectifier circuits, particularly with changing load currents. Specially wound transformers may be required to produce the desired output voltages, and extremely large filter capacitances are required to reduce the output ripple voltage to very small values. A much better approach is to use integrated circuit voltage regulators to set the output voltage and remove the ripple. IC regulators are available with a wide range of fixed output voltages as well as adjustable output versions.

An example of a rectifier circuit with a three-terminal 5-V regulator is shown in the accompanying figure. The regulator uses feedback with high-gain amplifier circuitry to greatly reduce the ripple voltage at the output. **IC voltage regulators** also provide outstanding line and load regulation, maintaining a constant output voltage even though the output current may change by many orders of magnitude. Capacitor  $C$  is the normal rectifier filter capacitor, and  $C_{B1}$  and  $C_{B2}$  (typically 0.001–0.01  $\mu\text{F}$ ) are bypass capacitors that provide a low-impedance path for high-frequency signals and are needed to ensure proper operation of the voltage regulator.

The regulator can reduce the ripple voltage by a factor of 100 to 1000 or more. To minimize power dissipation in the regulator, the rectifier can be designed with a relatively large ripple voltage at the input to the regulator, thus reducing the average input voltage to the regulator. The main design constraint is set by the input-output voltage differential  $V_{\text{REG}}$  across the regulator, which must not fall below a minimum “dropout voltage” value specified for the regulator, typically a few volts. The current  $I_{\text{REG}}$  needed to operate the IC regulator is only a few mA and typically represents a small percentage of the total current supplied by the rectifier:  $I_S = I_L + I_{\text{REG}}$ . An example of a voltage regulator family can be found on the MCD website.

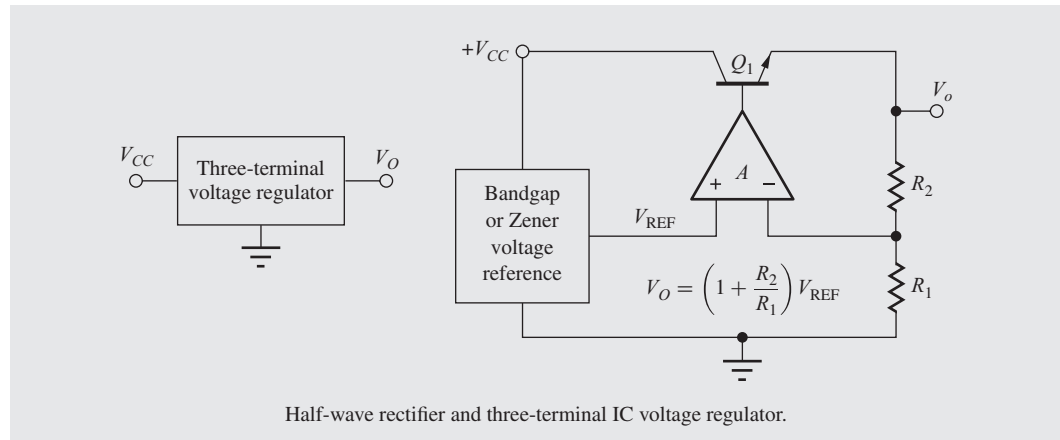


## Half-wave rectifier and three-terminal IC voltage regulator.

A series-shunt feedback amplifier is one common implementation of the three-terminal voltage regulator as in the following figure. The op amp forces the attenuated output voltage to be equal to reference voltage:

$$V_O \left( \frac{R_1}{R_1 + R_2} \right) = V_{\text{REF}} \quad \text{or} \quad V_O = V_{\text{REF}} \left( 1 + \frac{R_2}{R_1} \right)$$

Transistor  $Q_1$ , called a “pass transistor,” is used to increase the regulator’s output current capability far above that of the op amp alone.



## 11.6 SHUNT-SHUNT FEEDBACK—TRANSRESISTANCE AMPLIFIERS

The transresistance amplifier from Chapter 10 is redrawn as a shunt-shunt feedback amplifier in Fig. 11.15a. In this circuit, the input source is represented by its Norton equivalent current  $i_i$  and resistance  $R_I$ , and  $R_{id}$  and  $R_o$  have again been included in the circuit so we can assess their impact on overall feedback amplifier performance. On the input side, the feedback network voltage equals the op amp input voltage:  $v_{if} = -v_{id}$ . Thus the amplifier and feedback network are connected in parallel, so we have **shunt feedback** at the input. At the output,  $v_{of} = v_o$ , so we also have **shunt feedback** at the output. We refer to this overall configuration as a **shunt-shunt feedback amplifier**. In this case, application of feedback results in both a low input resistance and a low output resistance, which is exactly what is required of a transimpedance amplifier (i.e., current in, voltage out).

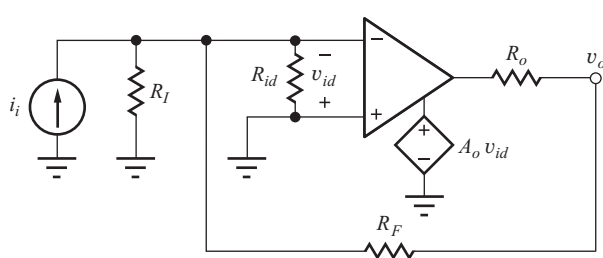
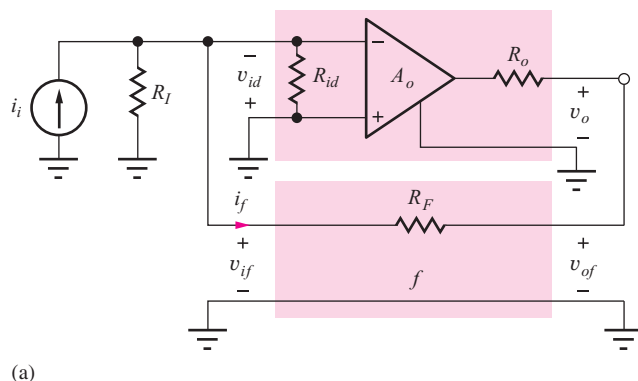


**Figure 11.15** (a) Transresistance amplifier as a shunt-shunt feedback amplifier. (b) Circuit for loop gain calculation.

### 11.6.1 CLOSED-LOOP GAIN CALCULATION

In order to find the closed-loop gain for the shunt-shunt feedback amplifier, we need to evaluate the gain expression from Eq. (11.51) by finding the ideal gain and the loop gain:

$$A_{tr} = A_{tr}^{\text{Ideal}} \left( \frac{T}{1+T} \right) \quad \text{where} \quad A_{tr}^{\text{Ideal}} = -R_F \quad (11.51)$$

We already know from Chapter 10 (Sec. 10.9.2) that the ideal gain for the transresistance amplifier is given by  $A_{tr}^{\text{Ideal}} = -R_F$ .

To find loop-gain  $T$ , the feedback loop is again disabled in Fig. 11.15(b) by arbitrarily setting  $v_{id} = 1$  V in the controlled source, and the value of  $v_{id}$  that actually appears back at the op amp input is calculated. Note that independent input source  $i_i$  is set to zero (an open circuit) in this calculation.  $T$  is then given by  $T = -v_{id}/1$  V, where the value of  $v_{id}$  at the input of the op amp is easily found using voltage division:

$$\begin{aligned} v_{id} &= -A_o(1 \text{ V}) \frac{R_{id} \parallel R_I}{R_o + R_F + (R_{id} \parallel R_I)} \\ T &= -\frac{v_{id}}{(1 \text{ V})} = A_o \frac{R_{id} \parallel R_I}{R_o + R_F + (R_{id} \parallel R_I)} \end{aligned} \quad (11.52)$$

With the aid of Eq. (11.52) we can assess the impact of  $R_I$ ,  $R_F$ ,  $R_{id}$  and  $R_o$  on the loop gain. If the equivalent input resistance ( $R_I \parallel R_{id}$ ) is very large compared to  $R_F + R_o$ , then the loop gain approaches  $A_o$ . If ( $R_I \parallel R_{id}$ ) is not large, then  $T$  can be much smaller than the open-loop gain of the op amp.

### 11.6.2 INPUT RESISTANCE CALCULATIONS

The input resistance of the series-shunt feedback amplifier is found by applying Blackman's theorem from Eq. (11.40):

$$R_{in} = R_{in}^D \frac{1 + |T_{SC}|}{1 + |T_{OC}|} \quad (11.53)$$

in which the input resistance is the resistance appearing between the inverting input terminal and ground.  $R_{in}^D$  is found from the circuit in Fig. 11.15(b) in which the feedback can be disabled by setting  $A_o = 0$ . The expression for  $R_{in}^D$  can then be written directly by inspection as

$$R_{in}^D = R_I \parallel R_{id} \parallel (R_F + R_o) \quad (11.54)$$

To find  $T_{SC}$ , the input terminals are shorted, thereby grounding the inverting input and forcing  $v_{id}$  and  $T_{SC}$  to be 0. To find  $T_{OC}$ , the input terminals are open-circuited, and we see that this is the same circuit used to find loop gain  $T$ . Therefore  $|T_{OC}| = T$ . The final expression for the input resistance becomes

$$R_{in} = R_{in}^D \frac{1 + 0}{1 + T} = \frac{R_I \parallel R_{id} \parallel (R_F + R_o)}{1 + T} \quad (11.55)$$

Compared to the results in Table 11.1, the input resistance now includes the additional influence of  $R_I$ ,  $R_F$ , and  $R_o$  as well as the modified value of  $T$ . In the ideal case,  $T$  approaches infinity, and  $R_{in}$  approaches zero.

### 11.6.3 OUTPUT RESISTANCE CALCULATIONS

For the output resistance case, Blackman's theorem gives

$$R_{out} = R_{out}^D \frac{1 + |T_{SC}|}{1 + |T_{OC}|} \quad (11.56)$$

The output resistance is the resistance appearing between the amplifier output terminal and ground.  $R_{out}^D$  is found using the circuit in Fig. 11.15(b) in which the feedback loop is disabled by setting

$A_o = 0$ . The expression for  $R_{\text{out}}^D$  can then be written directly as

$$R_{\text{out}}^D = R_o \parallel (R_F + R_I \parallel R_{id}) \quad (11.57)$$

For  $T_{SC}$ , output terminal  $v_o$  is connected directly to ground, thereby shorting out the feedback loop. Thus  $T_{SC} = 0$ . To find  $T_{OC}$ , the output terminals are open-circuited. We again recognize that the circuit is identical to the one used to find the loop gain  $T$  in Eq. (11.52), and  $|T_{OC}| = T$ . The final expression for the output resistance becomes

$$R_{\text{out}} = R_{\text{out}}^D \frac{1+0}{1+T} = \frac{R_o \parallel (R_F + R_I \parallel R_{id})}{1+T} \quad (11.58)$$

Compared to the results in Table 11.1, the input resistance now includes the additional influence of  $R_I$ ,  $R_F$  and  $R_{id}$  as well as the modified value of  $T$ . If  $(R_F + R_I \parallel R_{id}) \gg R_o$ , then  $R_{\text{out}}$  approaches  $R_o/(1+T)$ . For infinite  $T$ ,  $R_{\text{out}}$  becomes zero.

#### 11.6.4 SHUNT-SHUNT FEEDBACK AMPLIFIER SUMMARY

The direct loop-gain analysis of the characteristics of the series-shunt feedback amplifier yielded the following results:

$$A_{tr} = (-R_F) \frac{T}{1+T} \quad R_{\text{in}} = \frac{R_{\text{in}}^D}{1+T} \quad R_{\text{out}} = \frac{R_{\text{out}}^D}{1+T} \quad (11.59)$$

The expressions in Eq. (11.59) are identical in form to those developed at the beginning of this chapter and summarized in Table 11.2. The ideal gain is determined by feedback resistor  $R_F$ . The overall input resistance is decreased by the shunt feedback at the input, and the output resistance is decreased by the shunt feedback at the output. However, the equations now use the input resistance, output resistance, and loop gain of the amplifier including the effects of all the resistances in the circuit (see the following example).

**EXERCISE:** Draw the simplified circuits used to find  $R_{\text{in}}^D$  and  $R_{\text{out}}^D$  that result from setting  $A_o$  to zero, and verify the expressions in Eqs. (11.54) and (11.57).

#### EXAMPLE 11.6 SHUNT-SHUNT FEEDBACK AMPLIFIER ANALYSIS

This example evaluates the closed-loop characteristics of an op-amp-based shunt-shunt feedback amplifier by finding the loop gain and applying Blackman's theorem.

**PROBLEM** Find  $I$  and the closed-loop transresistance, input resistance, and output resistance for the shunt-shunt feedback amplifier in Fig. 11.15 if the op amp has an open-loop gain of 80 dB, an input resistance of  $25 \text{ k}\Omega$ , and an output resistance of  $1 \text{ k}\Omega$ . Analyze the circuit with  $R_I = 10 \text{ k}\Omega$ ,  $R_F = 91 \text{ k}\Omega$ , and a  $5\text{-k}\Omega$  load resistance connected to the output.

**SOLUTION** **Known Information and Given Data:** The shunt-shunt feedback amplifier is drawn in Fig. 11.16 with source and load resistances added. For the op amp:  $A_o = 80 \text{ dB}$ ,  $R_{id} = 25 \text{ k}\Omega$  and  $R_o = 1 \text{ k}\Omega$ , and  $R_F = 91 \text{ k}\Omega$ ,  $R_I = 10 \text{ k}\Omega$  and  $R_L = 5 \text{ k}\Omega$ .

**Unknowns:** Closed-loop gain  $A_{tr}$ , closed-loop input resistance  $R_{\text{in}}$ , closed-loop output resistance  $R_{\text{out}}$

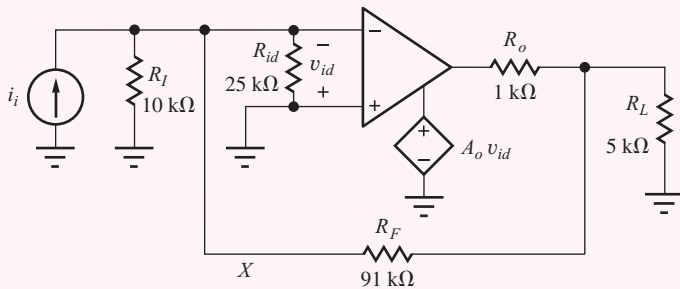


**Figure 11.16** Shunt-shunt feedback amplifier with load resistor added.

**Approach:** Find  $A_{tr}^{\text{ideal}}$ ,  $T$ ,  $R_{\text{in}}^D$ , and  $R_{\text{out}}^D$ . Then calculate the values of the unknowns using the closed-loop feedback amplifier formulae derived in this section.

**Assumptions:** The op amp is ideal except for  $A_o$ ,  $R_{id}$  and  $R_o$ .

**Analysis:** The ideal gain of the amplifier is  $-R_F$ , so

$$A_{tr}^{\text{ideal}} = -R_F = -91 \text{ k}\Omega$$

We must modify the equations derived in the previous section to include the effect of the addition of  $R_L$  to the amplifier:

$$R_{\text{in}}^D = R_I \| R_{id} \| (R_F + R_L \| R_o) = 10 \text{ k}\Omega \| 25 \text{ k}\Omega \| (91 \text{ k}\Omega + 5 \text{k}\Omega \| 1 \text{ k}\Omega) = 6.63 \text{ k}\Omega$$

$$R_{\text{out}}^D = R_L \| R_o \| (R_F + R_I \| R_{id}) = 5 \text{ k}\Omega \| 1 \text{ k}\Omega \| (91 \text{ k}\Omega + 10 \text{ k}\Omega \| 25 \text{ k}\Omega) = 826 \text{ }\Omega$$

The loop gain is most easily found by first taking a Thevenin equivalent (at point  $X$ ) of  $R_F$ ,  $R_o$ ,  $R_L$ , and the op amp output source yielding the result shown in Fig. 11.17.

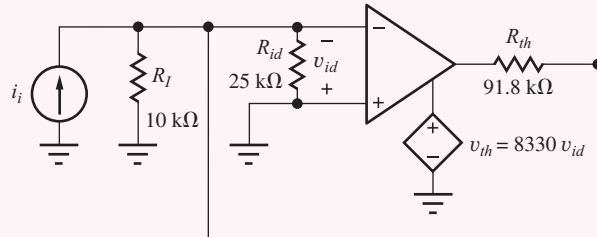


**Figure 11.17** Amplifier following Thevenin transformation.

The Thevenin equivalent voltage and resistance looking back into  $R_F$  are

$$\mathbf{v}_{th} = A_o \mathbf{v}_{id} \frac{R_L}{R_o + R_L} = 10^4 \mathbf{v}_{id} \frac{5 \text{ k}\Omega}{1 \text{ k}\Omega + 5 \text{ k}\Omega} = 8330 \mathbf{v}_{id}$$

$$R_{th} = R_F + R_o \| R_L = 91 \text{ k}\Omega + 1 \text{ k}\Omega \| 5 \text{ k}\Omega = 91.8 \text{ k}\Omega$$

The loop gain is found by setting  $A_o \mathbf{v}_{id} = A_o(1)$  and calculating  $\mathbf{v}_{id}$ :

$$\mathbf{v}_{id} = -\mathbf{v}_{th} \frac{R_I \| R_{id}}{R_{th} + R_I \| R_{id}} = -A_o(1) \frac{R_L}{R_o + R_L} \frac{R_I \| R_{id}}{R_{th} + R_I \| R_{id}}$$

$$T = -\frac{\mathbf{v}_{id}}{\mathbf{v}_{th}} = 10^4 \left( \frac{5 \text{ k}\Omega}{5 \text{ k}\Omega + 1 \text{ k}\Omega} \right) \left( \frac{10 \text{ k}\Omega \| 25 \text{ k}\Omega}{91.8 \text{ k}\Omega + 10 \text{ k}\Omega \| 25 \text{ k}\Omega} \right) = 602$$

**Closed-Loop Amplifier Results:**

$$A_{tr} = A_{tr}^{\text{Ideal}} \frac{T}{1+T} = -91 \text{ k}\Omega \frac{602}{1+602} = -90.9 \text{ k}\Omega$$

$$R_{\text{in}} = \frac{R_{\text{in}}^D}{1+T} = \frac{6.63 \text{ k}\Omega}{603} = 11.0 \text{ }\Omega \quad R_{\text{out}} = \frac{R_{\text{out}}^D}{1+T} = \frac{826 \text{ }\Omega}{603} = 1.37 \text{ }\Omega$$

**Check of Results:** We have found the unknowns. The loop gain is high, so we expect  $A_{tr}$  to be close to the ideal value of  $-91 \text{ k}\Omega$ . The calculated input and output resistances are both much smaller than those of the op amp itself. These all agree with our expectations for the shunt-shunt feedback configuration.

**Discussion:** This analysis illustrates the direct method for including the effects of nonideal op amp characteristics on the shunt-shunt feedback amplifier configuration, as well as the accounting for loading effects of the feedback network and source and load resistors. The first exercise below looks at the errors that occur if these effects are neglected.

Note that the classic inverting amplifier can be transformed into a shunt-shunt feedback amplifier for analysis. The voltage gain, input resistance, and output resistance of the original inverting amplifier can then easily be found directly from the results above. The voltage gain equals the transresistance divided by  $R_I$ :

$$A_v = \frac{v_o}{v_i} = \frac{v_o}{i_i} \cdot \frac{i_i}{v_i} = A_{tr} \cdot \frac{1}{R_I} = -\frac{90.9 \text{ k}\Omega}{10 \text{ k}\Omega} = -9.09$$

$$R_{\text{in}}^{\text{inv}} = R_I + \left( \frac{1}{R_{\text{in}}} - \frac{1}{R_I} \right)^{-1} = 10.0 \text{ k}\Omega \quad \text{and} \quad R'_{\text{out}} = \left( \frac{1}{R_{\text{out}}} - \frac{1}{R_L} \right)^{-1} = 1.37 \text{ }\Omega$$

In the shunt-shunt analysis,  $R_I$  appears in parallel with the amplifier input, whereas it is in series with the input in the inverting amplifier. Thus  $R_{\text{in}}^{\text{inv}}$  is found by first removing  $R_I$  from the parallel combination and then adding it back as a series element. Similarly, the parallel effect of  $R_L$  can be removed directly from the output resistance.

**Computer-Aided Analysis:** Our SPICE circuit mirrors the circuit in Fig. 11.16 and augments the built-in OPAMP model with the addition of  $R_{id}$  in parallel with its input and  $R_o$  in series with its output, and the gain is set to 10,000. A transfer function analysis from  $i_i$  to the voltage across  $R_L$  yields:  $A_{tr} = -90.85 \text{ k}\Omega$ ,  $R_{\text{in}} = 11.00 \text{ }\Omega$  and  $R_{\text{out}} = 1.372 \text{ }\Omega$ . These results agree closely with our hand calculations.

**EXERCISE:** Calculate the loop gain, overall transresistance, input resistance, and output resistance of the transresistance amplifier if the loading effects of  $R_{id}$  and  $R_L$  are neglected.

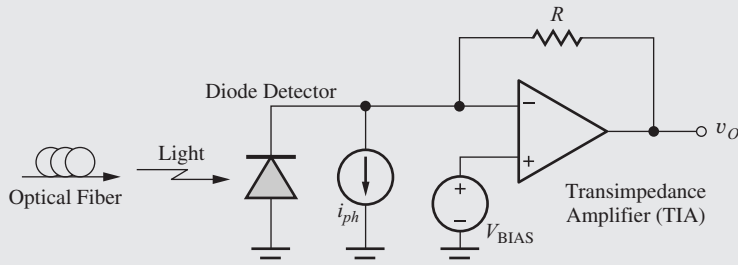
**ANSWERS:**  $T = 980$ ,  $A_{tr} = -90.9 \text{ k}\Omega$ ,  $R_{\text{in}} = 9.20 \text{ }\Omega$ ,  $R_{\text{out}} = 1.01 \text{ }\Omega$

**EXERCISE:** Find the loop gain, closed-loop voltage gain, input resistance and output resistance for the series-shunt feedback amplifier in Ex. 11.5 if the 10-k $\Omega$  source resistor is eliminated from the amplifier circuit.

**ANSWERS:** 720, 10.1, 24.5 M $\Omega$ , 1.37  $\Omega$


**ELECTRONICS IN ACTION**
**Fiber Optic Receiver**

Interface circuits for optical communications were introduced in the Electronics in Action feature in Chapter 9. One of the important electronic blocks on the receiver side of such a fiber optic communication link is the circuit that performs the optical-to-electrical (O/E) signal conversion, and a common approach is shown in the accompanying figure. Light exiting the optical fiber is incident upon a photodiode (see Sec. 3.18) that generates photocurrent  $i_{ph}$  as modeled by the current source in the figure. This photocurrent flows through feedback resistor  $R$  and generates a signal voltage at the output given by  $v_o = i_{ph}R$ . The voltage  $V_{BIAS}$  can be used to provide reverse bias to the photodiode. In this case, the total output voltage is  $v_O = V_{BIAS} + i_{ph}R$ .



Optical-to-electrical interface for fiber optic data transmission.

Since the input to the amplifier is a current and the output is a voltage, the gain  $A_{tr} = v_o / i_{ph}$  has the units of resistance, and the amplifier is referred to as a transresistance or (more generally) a transimpedance amplifier (TIA). The operational amplifier shown in the circuit must have an extremely wideband and linear design. The requirements are particularly stringent in OC-768 systems in which 40-GHz signals coming from the optical fiber must be amplified without the addition of any significant phase distortion.

## 11.7 SERIES-SERIES FEEDBACK—TRANSCONDUCTANCE AMPLIFIERS

In many circuits, we often require a high performance transconductance amplifier that generates an output current that is proportional to the input voltage:  $i_o = A_{tc}v_i$ . In order to accurately measure the input voltage, series feedback is utilized to achieve a high input resistance, and to approximate a current source at the output, series feedback is again utilized to yield a high output resistance. Thus the transconductance amplifier is a **series-series feedback amplifier**. An op amp implementation is depicted in Fig. 11.18 in which the op amp has been drawn to explicitly include its own input resistance  $R_{id}$  and output resistance  $R_o$  and to show its four terminals.

The feedback network consists of only a single resistor  $R_f$ , and its input and output port voltages,  $v_{if}$  and  $v_{of}$ , are defined in the figure. On the left side, the applied input voltage  $v_i$  equals the sum of the op amp input voltage and the feedback network voltage:  $v_i = v_{id} + v_{if}$ . Thus we have **series feedback** at the input because the amplifier input and feedback network voltages are in series. At the output, we see that the output voltage  $v_o$  equals the sum of the op amp output voltage  $v_{op}$  and the feedback network voltage  $v_{of}$ . The amplifier and feedback network are connected in series at both the input and output ports, and this overall configuration represents a **series-series feedback amplifier**.

In order to achieve negative feedback, the negative output terminal must be connected to the noninverting input terminal of the op amp as indicated in the figure.

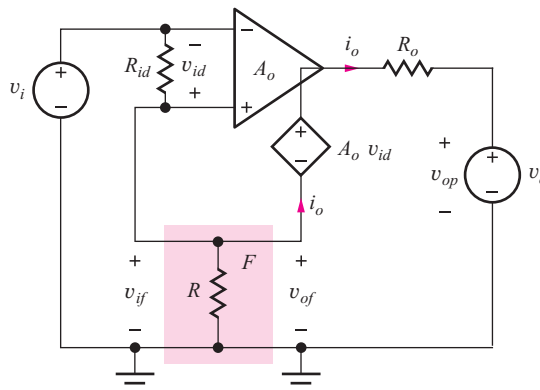


**Figure 11.18** The four-terminal op amp as a series-series feedback amplifier.

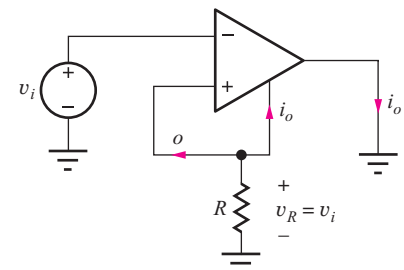


**Figure 11.19** Ideal series-series feedback amplifier.

### 11.7.1 CLOSED-LOOP GAIN CALCULATION

In order to find the closed-loop gain for the series-shunt feedback amplifier, we need to evaluate the gain expression from Eq. (11.39) by finding the ideal gain  $A_{tc}^{\text{Ideal}}$  and the loop gain  $T$ :

$$A_{tc} = A_{tc}^{\text{Ideal}} \left( \frac{T}{1+T} \right) \quad (11.60)$$

The ideal case is depicted in Fig. 11.19. For infinite gain, the op amp input voltage is zero so that  $v_i$  appears directly across resistor  $R$ . Output current  $i_o$  must flow up through  $R$  since the input current to the ideal op amp is zero. Thus  $\mathbf{i}_o = -\mathbf{v}_i/R$  and  $A_{tc}^{\text{Ideal}} = \mathbf{i}_o/\mathbf{v}_i = -1/R$ .

As a reminder, loop gain  $T$  represents the total gain through the amplifier and back around the feedback loop to the input. In the op amp circuit in Fig. 11.18, we can find  $T$  by assuming we know the value of  $\mathbf{v}_{id}$  in source  $A_o \mathbf{v}_{id}$ , (e.g.,  $\mathbf{v}_{id} = 1 \text{ V}$  and  $A_o \mathbf{v}_{id} = A_o(1)$ ), and then calculate the value of  $\mathbf{v}_{id}$  developed at the op amp input. The loop gain is then equal to the negative of the ratio of the voltage returned through the loop to the op amp input.

Loop gain  $T$  can be found by applying voltage division to the circuit (remember the independent input source  $\mathbf{v}_i$  must be turned off by setting its value to zero):

$$\mathbf{v}_{id} = -A_o(1) \frac{(R_{id} \| R)}{(R_{id} \| R) + R_o} \quad \text{and} \quad T = A_o \frac{(R_{id} \| R)}{(R_{id} \| R) + R_o} \quad (11.61)$$

The loop gain expression now incorporates all the nonideal op amp parameters.  $R_{id}$  appears in parallel with  $R$  of the feedback network, and  $R_o$  also affects the loop gain.

### 11.7.2 INPUT RESISTANCE CALCULATION

Next let us find the input resistance of the series-shunt feedback amplifier by applying Blackman's theorem from Eq. (11.40):

$$R_{in} = R_{in}^D \frac{1 + |T_{SC}|}{1 + |T_{OC}|} \quad (11.62)$$

$R_{in}$  represents the resistance appearing between the noninverting input terminal and ground of the closed-loop feedback amplifier,  $R_{in}^D$  is the resistance looking into the same terminals with the feedback loop disabled,  $T_{SC}$  is the loop gain with a short circuit applied to the input port, and  $T_{OC}$  is the loop gain with the input port open.

We find  $R_{in}^D$  using the circuit in Fig. 11.18 in which the feedback is disabled by setting  $A_o = 0$ . The input resistance can then be written directly as

$$R_{in}^D = R_{id} + R \| R_o \quad (11.63)$$

To find  $T_{SC}$ , the input terminals are shorted, and we recognize that the circuit is identical to the one used to find the loop gain  $T$  in Eq. (11.61). Therefore  $|T_{SC}| = T$ . To find  $T_{OC}$ , the input terminals are open-circuited. Then no current can flow through  $R_{id}$ , so the voltage  $v_{id}$  must be zero, and  $T_{OC} = 0$ . The final expression for the input resistance becomes

$$R_{in} = R_{in}^D \frac{1+T}{1+0} = (R_{id} + R \parallel R_o)(1+T) \quad (11.64)$$

We see that the input resistance is increased by  $T$  and can be very high.

### 11.7.3 OUTPUT RESISTANCE CALCULATION

Blackman's theorem gives

$$R_{out} = R_{out}^D \frac{1+|T_{SC}|}{1+|T_{OC}|} \quad (11.65)$$

The output resistance represents the resistance appearing between the amplifier output terminal and ground.  $R_{out}^D$  is found using the circuit in Fig. 11.18 in which we set  $v_i = 0$  and again disable the feedback by setting  $A_o = 0$ . The output resistance can then be written as

$$R_{out}^D = R_o + R \parallel R_{id} \quad (11.66)$$

For  $T_{SC}$ , output terminal  $v_o$  is connected directly to ground, we recognize that the circuit is identical to the one used to find the loop gain  $T$  in Eq. (11.61), and  $|T_{SC}| = T$ . To find  $T_{OC}$ , the output terminals are open-circuited, and no current flows in the circuit. Thus  $T_{OC} = 0$ . The final expression for the output resistance becomes

$$R_{out} = R_{out}^D \frac{1+T}{1+0} = (R_o + R \parallel R_{id})(1+T) \quad (11.67)$$

The output resistance of the op amp is multiplied by  $T$ , and the result can be very high.

### 11.7.4 SERIES-SERIES FEEDBACK AMPLIFIER SUMMARY

The analysis of the characteristics of the series-series feedback amplifier yielded the following results:

$$A_{tc} = \left( -\frac{1}{R} \right) \frac{T}{1+T} \quad R_{in} = R_{in}^D(1+T) \quad R_{out} = R_{out}^D(1+T) \quad (11.68)$$

The transconductance amplifier has a high input resistance, a high output resistance, and the ideal transconductance equals the reciprocal of feedback resistance  $R$ .

## EXAMPLE 11.7 SERIES-SERIES FEEDBACK AMPLIFIER ANALYSIS

This example evaluates the closed-loop characteristics of a op-amp-based series-series feedback amplifier utilizing the loop-gain approach and Blackman's theorem. The analysis is extended to include a source resistance.

**PROBLEM** Find the closed-loop transconductance, input resistance, and output resistance for the series-series feedback amplifier in Fig. 11.18 if the op amp has an open-loop gain of 80 dB, an input resistance of 25 kΩ, and an output resistance of 1 kΩ. Assume the amplifier is driven by a signal voltage with a 10-kΩ source resistance, and the feedback network is implemented with  $R_2 = 91$  kΩ and  $R_1 = 10$  kΩ.

**SOLUTION Known Information and Given Data:** The series-series feedback amplifier is drawn in the figure below with the  $10\text{ k}\Omega$  source resistance added. For the op amp:  $A_o = 80\text{ dB}$ ,  $R_{id} = 25\text{ k}\Omega$  and  $R_o = 1\text{ k}\Omega$ .

**Unknowns:** Closed-loop transconductance  $A_{tc}$ , input resistance  $R_{in}$ , output resistance  $R_{out}$

**Approach:** Find new expressions for  $A_{tc}^{\text{ideal}}$ ,  $T$ ,  $R_{in}^D$ , and  $R_{out}^D$ . Then calculate the values of the unknowns using the closed-loop feedback amplifier formulae derived in this section.

**Assumptions:** The op amp is ideal except for  $A_o$ ,  $R_{id}$  and  $R_o$ .

**Analysis:** The amplifier circuit with the addition of  $R_I$  appears in Fig. 11.20.

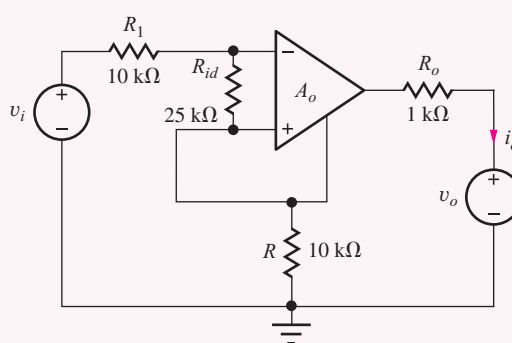


**Figure 11.20** Series-series feedback amplifier with source resistance added.

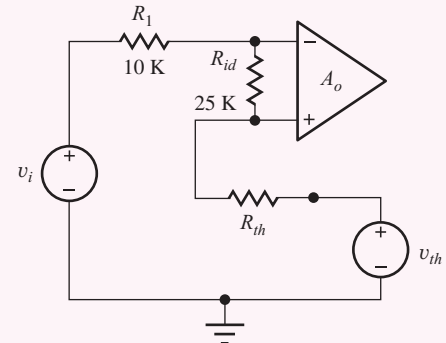


**Figure 11.21** Series-shunt feedback amplifier with Thévenin transformation.

#### Amplifier Analysis:

$$A_{tc}^{\text{ideal}} = -\frac{1}{R} = -\frac{1}{10\text{ k}\Omega} = -10^{-4}\text{ S}$$

$$R_{in}^D = R_I + R_{id} + R \parallel R_o = 10\text{ k}\Omega + 25\text{ k}\Omega + 10\text{ k}\Omega \parallel 1\text{ k}\Omega = 35.9\text{ k}\Omega$$

$$R_{out}^D = R_o + R \parallel (R_{id} + R_I) = 1\text{ k}\Omega + 10\text{ k}\Omega \parallel (25\text{ k}\Omega + 10\text{ k}\Omega) = 8.79\text{ k}\Omega$$

The loop gain is most easily found by first taking a Thévenin equivalent of  $R_o$ ,  $R$ , and the op amp output source with  $v_o = 0$  as depicted in Fig. 11.21.

$$v_{th} = -A_o v_{id} \frac{R}{R + R_o} = -10^4 v_{id} \frac{10\text{ k}\Omega}{10\text{ k}\Omega + 1\text{ k}\Omega} = 9090 v_{id}$$

$$R_{th} = R \parallel R_o = 10\text{ k}\Omega \parallel 1\text{ k}\Omega = 909\text{ }\Omega$$

Now we can assume  $v_{id} = 1$  in  $v_{th}$  and solve for the op amp input voltage  $v_{id}$ :

$$v_{id} = -v_{th} \frac{R_{id}}{R_{th} + R_{id} + R_I} = -9090(1) \frac{25\text{ k}\Omega}{0.909\text{ k}\Omega + 25\text{ k}\Omega + 10\text{ k}\Omega} = -6330$$

$$T = 6330$$

#### Closed-Loop Amplifier Results:

$$A_{tc} = -\frac{1}{R} \left( \frac{T}{1+T} \right) = -\frac{1}{10\text{ k}\Omega} \left( \frac{6330}{1+6330} \right) = -0.100\text{ mS}$$

$$R_{in} = R_{in}^D(1+T) = 35.9\text{ k}\Omega(1+6330) = 227\text{ M}\Omega$$

$$R_{out} = R_{out}^D(1+T) = 8.79\text{ k}\Omega(1+6330) = 55.7\text{ M}\Omega$$

**Check of Results:** The three unknowns have been found. The loop gain is high, so we expect  $A_{tc}$  should be approximately  $-0.1 \text{ mS}$ . The calculated input resistance is much larger than that of the op amp itself, and the output resistance is also much larger than that of the op amp. These all agree with our expectations for the series-series feedback configuration.

**Computer-Aided Analysis:** Our SPICE circuit mirrors the circuit in Fig. 11.20 and augments the built-in OPAMP model with the addition of  $R_{id}$  in parallel with its input and  $R_o$  in series with its output, and the gain is set to 10,000. Zero value voltage source  $v_o$  is added to the circuit in order to use the SPICE transfer function analysis. We must be careful in the description of the circuit for simulation. The op amp model that is being used assumes that its internal controlled source is connected to the reference node (ground). Fortunately, we are free to choose the reference node in a circuit, and the ground connection has been moved from the bottom to the top of resistor  $R$  in Fig. 11.22. A transfer function analysis from  $VI$  to the current in  $VO$  yields the overall transconductance, the input resistance as seen by  $VI$  and the output resistance seen by  $VO$ . The SPICE results are  $A_{tc} = -9.998 \times 10^{-5} \text{ S}$ ,  $R_{in} = 227.3 \text{ M}\Omega$  and  $R_{out} = 55.56 \text{ M}\Omega$ . These results agree closely with our hand calculations.

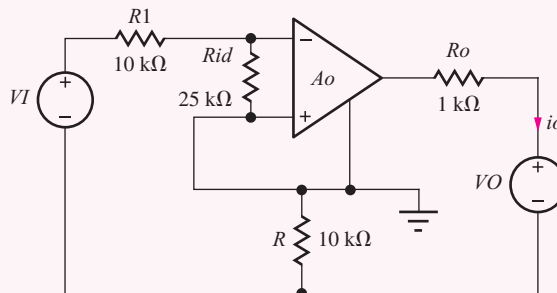


Figure 11.22 Circuit for simulation with new ground reference.

**EXERCISE:** Find the loop gain, closed-loop transconductance, input resistance and output resistance for the series-series feedback amplifier in Ex. 11.7 if the 10-kΩ source resistor is eliminated from the amplifier circuit.

**ANSWERS:** 8770,  $-1.00 \times 10^{-4} \text{ S}$ ,  $227 \text{ M}\Omega$ ,  $71.4 \text{ M}\Omega$ .

## 11.8 SHUNT-SERIES FEEDBACK—CURRENT AMPLIFIERS

The last of the four feedback topologies is the current amplifier that is implemented using the shunt-series feedback configuration. For this case, we need to generate an output current that is proportional to the input current,  $i_o = A_i i_i$ . At the input we want to sense a current, so shunt feedback is utilized to achieve a low input resistance, and the output should approximate a current source, so series feedback is also used at the output to yield high output resistance. The op-amp-based shunt-series feedback amplifier is depicted in Fig. 11.23 in which the op amp input resistance  $R_{id}$  and output resistance  $R_o$  are explicitly shown. Voltage source  $v_o$  is included to identify the output terminals that would normally be connected to an external load.

The feedback network consists of resistors  $R_2$  and  $R_1$ , and its input and output port voltages,  $v_{if}$  and  $v_{of}$ , are defined in the figure. On the left side, the  $v_{id} = v_{if}$ , so we have shunt feedback at the input. The output voltage equals the sum of the op amp output voltage and that of the feedback

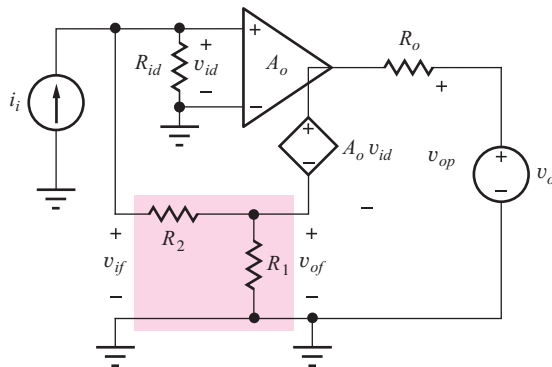


**Figure 11.23** The four-terminal op amp as a shunt-series feedback amplifier.

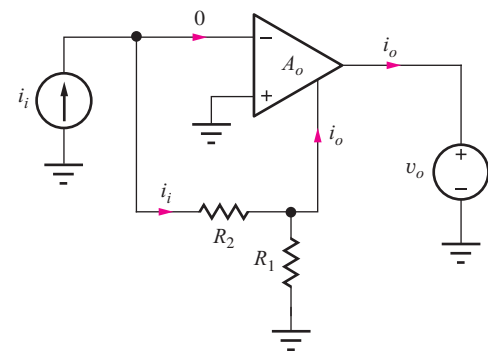


**Figure 11.24** Ideal shunt-series feedback amplifier.

network,  $v_o = v_{op} + v_{of}$ , so there is a series connection at the output. Thus we refer to this overall configuration as a **shunt-series feedback amplifier**.

In order to achieve negative feedback, the negative output terminal must be connected back to the noninverting input terminal of the op amp through the feedback network as indicated in the figure.

### 11.8.1 CLOSED-LOOP GAIN CALCULATION

In order to find the closed-loop current gain  $A_i$  for the series-shunt feedback amplifier, we need to evaluate the gain expression from Eq. (11.39) by finding the ideal current gain  $A_i^{\text{ideal}}$  and the loop gain  $T$ :

$$A_i = A_i^{\text{ideal}} \left( \frac{T}{1+T} \right) \quad (11.69)$$

The ideal case is depicted in Fig. 11.24. The op amp input current is zero, and input current  $i_i$  must go through resistor  $R_2$ . For infinite gain, the op amp input voltage must be zero.

Using these two ideal op amp assumptions, we can find the ideal current gain by writing a loop equation including  $R_2$  and  $R_1$ :

$$\mathbf{i}_i R_2 + (\mathbf{i}_i - \mathbf{i}_o) R_1 = 0 \quad \text{and} \quad A_i^{\text{ideal}} = \frac{\mathbf{i}_o}{\mathbf{i}_i} = 1 + \frac{R_2}{R_1} \quad (11.70)$$

To find  $T$ , we set the value of  $\mathbf{v}_{id}$  in source  $A_o \mathbf{v}_{id}$  to 1 V ( $A_o \mathbf{v}_{id} = A_o(1)$ ), and then calculate the value of  $\mathbf{v}_{id}$  developed at the op amp input. The loop gain is then equal to the negative of the ratio of the voltage returned through the loop to the op amp input. In this case,  $T$  can be found by applying voltage division to the circuit in Fig. 11.23. (Remember independent input source  $\mathbf{v}_i$  must be turned off by setting its value to zero.) First we find the voltage  $\mathbf{v}_1$  across  $R_1$ , and then  $\mathbf{v}_{id}$ :

$$\begin{aligned} \mathbf{v}_1 &= -A_o(1) \frac{[R_1 \parallel (R_2 + R_{id})]}{R_1 \parallel (R_2 + R_{id}) + R_o} \quad \text{and} \quad \mathbf{v}_{id} = \mathbf{v}_1 \left( \frac{R_{id}}{R_2 + R_{id}} \right) \\ T &= A_o \frac{[R_1 \parallel (R_2 + R_{id})]}{R_1 \parallel (R_2 + R_{id}) + R_o} \left( \frac{R_{id}}{R_2 + R_{id}} \right) \end{aligned} \quad (11.71)$$

The loop gain expression now incorporates the nonideal op amp parameters  $A_o$ ,  $R_{id}$ , and  $R_o$ .

### 11.8.2 INPUT RESISTANCE CALCULATION

Next let us find the input resistance of the shunt-series feedback amplifier by applying Blackman's theorem from Eq. (11.40):

$$R_{\text{in}} = R_{\text{in}}^D \frac{1 + |T_{SC}|}{1 + |T_{OC}|} \quad (11.72)$$

$R_{\text{in}}$  represents the resistance appearing between the noninverting input terminal and ground of the closed-loop feedback amplifier,  $R_{\text{in}}^D$  is the resistance looking into the same terminals with the feedback loop disabled,  $T_{SC}$  is the loop gain with a short circuit applied to the input port, and  $T_{OC}$  is the loop gain with the input port open.

We find  $R_{\text{in}}^D$  using the circuit in Fig. 11.23 in which we disable the feedback by setting  $A_o = 0$ . The input resistance can then be written directly as

$$R_{\text{in}}^D = R_{id} \parallel (R_2 + R_1 \parallel R_o) \quad (11.73)$$

To find  $T_{SC}$ , the noninverting input terminal is connected to ground, and  $v_{id}$  is forced to be zero. Thus  $T_{SC} = 0$ . To find  $T_{OC}$ , the input terminals are open-circuited, and we recognize that the circuit is identical to the one used to find the loop gain  $T$  in Eq. (11.71). Therefore  $|T_{OC}| = T$ . The final expression for the input resistance becomes

$$R_{\text{in}} = R_{\text{in}}^D \frac{1 + 0}{1 + T} = \frac{R_{id} \parallel (R_2 + R_1 \parallel R_o)}{1 + T} \quad (11.74)$$

We see that the input resistance is decreased by  $T$  and can be small.

### 11.8.3 OUTPUT RESISTANCE CALCULATION

Blackman's theorem states

$$R_{\text{out}} = R_{\text{out}}^D \frac{1 + |T_{SC}|}{1 + |T_{OC}|} \quad (11.75)$$

The output resistance is the resistance appearing between the amplifier output terminal and ground, the resistance that is presented to source  $v_o$ . We find  $R_{\text{out}}^D$  using the circuit in Fig. 11.23 in which we set  $i_i = 0$  and again disable the feedback by setting  $A_o = 0$ . The output resistance can then be written directly as

$$R_{\text{out}}^D = R_o + R_1 \parallel (R_2 + R_{id}) \quad (11.76)$$

For  $T_{SC}$ , output terminal  $v_o$  is connected directly to ground, and the circuit is identical to the one used to find the loop gain  $T$  in Eq. (11.71). Therefore  $|T_{SC}| = T$ . To find  $T_{OC}$ , the output terminals are open-circuited, and no current flows in the circuit. Thus  $T_{OC} = 0$ . The final expression for the output resistance becomes

$$R_{\text{out}} = R_{\text{out}}^D \frac{1 + T}{1 + 0} = [R_o + R_1 \parallel (R_2 + R_{id})] (1 + T) \quad (11.77)$$

The output resistance is increased by  $T$  and can be very large.

### 11.8.4 SERIES-SERIES FEEDBACK AMPLIFIER SUMMARY

The analysis of the characteristics of the series-series feedback amplifier are summarized in Eq. (11.78):

$$A_i = \left(1 + \frac{R_2}{R_1}\right) \frac{T}{1 + T} \quad R_{\text{in}} = \frac{R_{\text{in}}^D}{(1 + T)} \quad R_{\text{out}} = R_{\text{out}}^D (1 + T) \quad (11.78)$$

The current amplifier has a small input resistance and a large output resistance, and its ideal current gain is  $1 + R_2/R_1$ .

### EXAMPLE 11.8 SHUNT-SERIES FEEDBACK AMPLIFIER ANALYSIS

This example evaluates the closed-loop characteristics of a op-amp-based shunt-series feedback amplifier by applying the loop-gain approach and Blackman's theorem. The analysis is extended to include a source resistance.

**PROBLEM** Find the closed-loop current gain, input resistance, and output resistance for the shunt-series feedback amplifier in Fig. 11.23 if the op amp has an open-loop gain of 80 dB, an input resistance of 25 k $\Omega$ , and an output resistance of 1 k $\Omega$ . Assume the amplifier is driven by a signal current with a 10-k $\Omega$  source resistance, and the feedback network is implemented with  $R_2 = 27$  k $\Omega$  and  $R_1 = 3$  k $\Omega$ .

**SOLUTION Known Information and Given Data:** The shunt-series feedback amplifier is drawn in Fig. 11.25 with the 10 k $\Omega$  source resistance added. For the op amp:  $A_o = 80$  dB,  $R_{id} = 25$  k $\Omega$  and  $R_o = 1$  k $\Omega$ .

**Unknowns:** Closed-loop gain  $A_i$ , closed-loop input resistance  $R_{in}$ , closed-loop output resistance  $R_{out}$

**Approach:** Find new expressions for  $A_i^{\text{ideal}}$ ,  $T$ ,  $R_{in}^D$ , and  $R_{out}^D$  incorporating the influence of  $R_I$ . Then calculate the values of the unknowns using the closed-loop feedback amplifier formulae derived in this section.

**Assumptions:** The op amp is ideal except for  $A_o$ ,  $R_{id}$  and  $R_o$ .

**Analysis:** The amplifier circuit with the addition of  $R_I$  appears in Fig. 11.25.

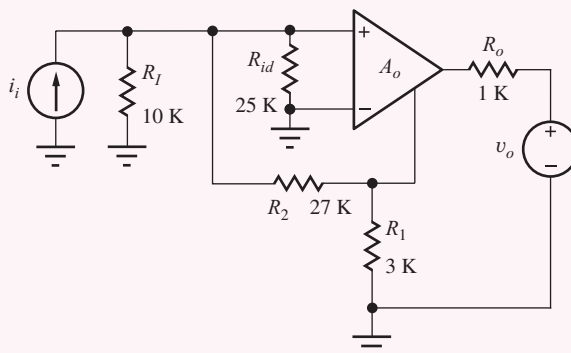


Figure 11.25 Shunt-series feedback amplifier with source resistance added.

**Amplifier Analysis:** In this circuit, we see that  $R_I$  is directly in parallel with  $R_{id}$ . Thus we can use the results from the previous section just by replacing  $R_{id}$  with

$$R'_{id} = R_I \parallel R_{id} = 10 \text{ k}\Omega \parallel 25 \text{ k}\Omega = 7.14 \text{ k}\Omega$$

$$A_i^{\text{ideal}} = 1 + \frac{R_2}{R_1} = 1 + \frac{27 \text{ k}\Omega}{3 \text{ k}\Omega} = +10$$

$$R_{in}^D = R'_{id} \parallel (R_2 + R_1 \parallel R_o) = 7.14 \text{ k}\Omega \parallel (27 \text{ k}\Omega + 3 \text{ k}\Omega \parallel 1 \text{ k}\Omega) = 5.68 \text{ k}\Omega$$

$$R_{out}^D = R_o + R_1 \parallel (R_2 + R'_{id}) = 1 \text{ k}\Omega + 3 \text{ k}\Omega \parallel (27 \text{ k}\Omega + 7.14 \text{ k}\Omega) = 3.76 \text{ k}\Omega$$

The loop gain is found by modifying Eq. (11.71):

$$T = A_o \frac{[R_1|(R_2 + R'_{id})]}{R_1\|(R_2 + R'_{id}) + R_o} \left( \frac{R'_{id}}{R_2 + R'_{id}} \right)$$

$$T = 10^4 \frac{3 \text{k}\Omega \|(27 \text{k}\Omega + 7.14 \text{k}\Omega)}{1 \text{k}\Omega + 3 \text{k}\Omega \|(27 \text{k}\Omega + 7.14 \text{k}\Omega)} \left( \frac{7.14 \text{k}\Omega}{27 \text{k}\Omega + 7.14 \text{k}\Omega} \right) = 1535$$

### Closed-Loop Amplifier Results

$$A_i = +10 \left( \frac{T}{1+T} \right) = +10 \left( \frac{1535}{1+1535} \right) = +9.99$$

$$R_{in} = \frac{R_{in}^D}{(1+T)} = \frac{5.68 \text{k}\Omega}{1536} = 3.70 \text{\Omega}$$

$$R_{out} = R_{out}^D(1+T) = 3.76 \text{k}\Omega(1536) = 5.78 \text{M}\Omega$$

**Check of Results:** We have found the three unknowns. The loop gain is high, so we expect the current gain to be approximately +10. The calculated input resistance is much smaller than that of the op amp itself, and the output resistance is also much larger than that of the op amp. These all agree with our expectations for the series-series feedback configuration.

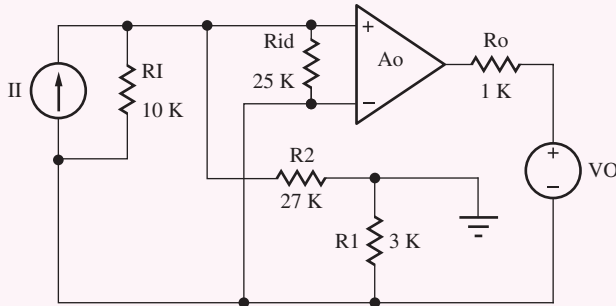


Figure 11.26 Circuit for shunt-series circuit simulation.

**Computer-Aided Analysis:** Our SPICE circuit in Fig. 11.26 augments the built-in OPAMP model with the addition of  $R_{id}$  in parallel with its input and  $R_o$  in series with its output, and the gain is set to 10,000. Zero value voltage source  $VO$  is added to the circuit in order to use the transfer function analysis. We must again be careful in the simulation. The three-terminal op amp model assumes that its internal controlled source is connected to the reference node (ground). Fortunately, we are free to choose the reference node in a circuit, and the ground connection has been moved to the top of resistor  $R_1$  in Fig. 11.26. A transfer function analysis from  $II$  to the current in  $VO$  yields the overall current gain, the input resistance at the terminals of  $II$  and the output resistance at the terminals of  $VO$ . The SPICE results are  $A_i = 9.994 \times 10^{-5} \text{ S}$ ,  $R_{in} = 3.698 \Omega$  and  $R_{out} = 5.773 \text{ M}\Omega$ . These results agree well with our hand calculations.

**EXERCISE:** Find the loop gain, current gain, input resistance, and output resistance for the series-series feedback amplifier in Ex. 11.8 if the 10-kΩ source resistor is eliminated from the amplifier circuit.

**ANSWERS:** 3555, +10.0, 3.71 Ω, 13.7 MΩ.

**EXERCISE:** Find the loop gain, closed-loop current gain, input resistance, and output resistance for the series-series feedback amplifier in Ex. 11.8, if  $R_1$  and  $R_2$  are increased in value by a factor of 10.

**ANSWERS:** 248.5, +9.96, 27.9  $\Omega$ , 7.01 M $\Omega$ .

## 11.9 FINDING THE LOOP GAIN USING SUCCESSIVE VOLTAGE AND CURRENT INJECTION

In many practical cases, particularly when the loop gain is large, the feedback loop cannot be opened to measure the loop gain because a closed loop is required to maintain a correct dc operating point. Another problem is electrical noise, which may cause an open-loop amplifier to saturate. A similar problem occurs in SPICE simulation of high-gain circuits, such as operational amplifiers, in which the circuit amplifies the numerical noise present in the calculations, and the open-loop analysis is unable to converge to a stable operating point. Fortunately, the method of **successive voltage and current injection** [5] can be used to measure the loop gain without opening the feedback loop.

Again consider the basic feedback amplifier in Fig. 11.27. To use the voltage and current injection method, an arbitrary point  $P$  within the feedback loop is selected, and a voltage source  $v_x$  is inserted into the loop, as in Fig. 11.27(a). The two voltages  $v_2$  and  $v_1$  on either side of the inserted source are measured, and  $T_v$  is calculated:

$$T_v = -\frac{v_2}{v_1} \quad (11.79)$$

Next, the voltage source is removed, a current  $i_x$  is injected into the same point  $P$ , and the ratio  $T_i$  of currents  $i_2$  and  $i_1$  is determined.

$$T_i = \frac{i_2}{i_1} \quad (11.80)$$

These two sets of measurements yield two equations in two unknowns: the loop gain  $T$  and the resistance ratio  $R_B/R_A$ .  $R_A$  represents the resistance seen looking to the left from test source  $v_x$ , and  $R_B$  represents the resistance seen looking to the right from the test source.

For the voltage injection case in Fig. 11.27(a),

$$v_1 = iR_A = \frac{-Av_1 + v_x}{R_A + R_B}R_A \quad (11.81)$$

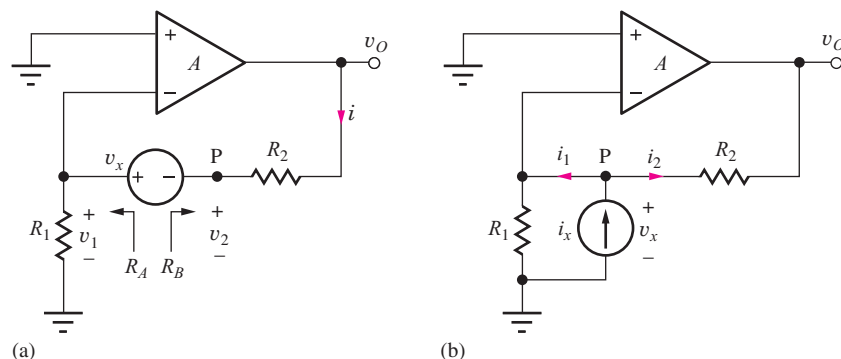


**Figure 11.27** (a) Voltage injection at point  $P$  and (b) current injection at point  $P$ .  $R_{id} = \infty$ .

Solving for  $v_1$  yields

$$v_1 = \frac{\beta}{1 + A\beta} v_x \quad \text{where} \quad \beta = \frac{R_A}{R_A + R_B} \quad (11.82)$$

After some algebra, voltage  $v_2$  is found to be

$$v_2 = v_1 - v_x = \frac{\beta - (1 + A\beta)}{1 + A\beta} v_x \quad (11.83)$$

and  $T_v$  is equal to

$$T_v = \frac{1 + A\beta - \beta}{\beta} \quad (11.84)$$

We recognize the  $A\beta$  product as the loop gain  $T$ , and using  $1/\beta = 1 + R_B/R_A$ ,  $T_v$  can be rewritten as

$$T_v = T \left( 1 + \frac{R_B}{R_A} \right) + \frac{R_B}{R_A} \quad (11.85)$$

The current injection circuit in Fig. 11.27(b) provides the second equation in two unknowns. Injection of current  $i_x$  causes a voltage  $v_x$  to develop across the current generator; currents  $i_1$  and  $i_2$  can each be expressed in terms of this voltage:

$$i_1 = \frac{v_x}{R_A} \quad \text{and} \quad i_2 = \frac{v_x - A v_x}{R_B} = v_x \frac{1 + A}{R_B} \quad (11.86)$$

Taking the ratio of these two expressions yields  $T_i$

$$T_i = \frac{i_2}{i_1} = \frac{\frac{1 + A}{R_B}}{\frac{1}{R_A}} = (1 + A) \frac{R_A}{R_B} = \frac{R_A}{R_B} + A \frac{R_A}{R_B} \quad (11.87)$$

Multiplying the last term by  $\beta$  and again using  $1/\beta = 1 + R_B/R_A$  yields

$$T_i = \frac{R_A}{R_B} + A\beta \frac{R_A}{R_B} \frac{1}{\beta} = \frac{R_A}{R_B} + T \left( 1 + \frac{R_A}{R_B} \right) \quad (11.88)$$

Simultaneous solution of Eqs. (11.85) and (11.88) gives the desired result:

$$T = \frac{T_v T_i - 1}{2 + T_v + T_i} \quad \text{and} \quad \frac{R_B}{R_A} = \frac{1 + T_v}{1 + T_i} \quad (11.89)$$

Using this technique, we can find both the loop gain  $T$  and the resistance (or impedance) ratio at point  $P$ .

Although the resistance ratio would be dominated by  $R_2$  and  $R_1$  in the circuit in Fig. 11.27,  $R_B$  and  $R_A$  in the general case actually represent the two equivalent resistances that would be calculated looking to the right and left of the point  $P$ , where the loop is broken. This fact is illustrated more clearly by the SPICE analysis in Ex. 11.9.

### EXAMPLE 11.9 LOOP GAIN AND RESISTANCE RATIO CALCULATION USING SPICE

We will use SPICE to find the loop gain for an amplifier using the successive voltage and current injection technique.

**PROBLEM** Find the loop gain  $T$  and the resistance ratio for the series-shunt feedback amplifier of Ex. 11.5 using the method of successive voltage and current injection at point  $P$ .

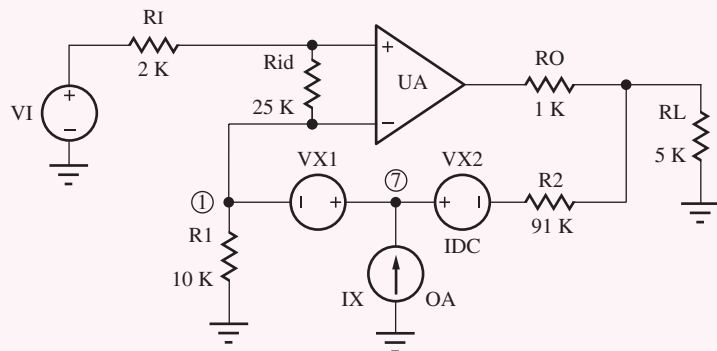
**SOLUTION** **Known Information and Given Data:** Series-shunt feedback amplifier with element values given in Ex. 11.5. Apply the voltage and current injection at point  $P$  between feedback resistors  $R_2$  and  $R_1$ .

**Unknowns:** Loop gain  $T$ ; resistance ratio  $R_B/R_A$

**Approach:** In the dc-coupled case, we can insert zero valued sources into the circuit and use the transfer function capability of SPICE to find the sensitivity of voltages  $v_1$  and  $v_2$  to changes in  $v_x$  and the sensitivity of  $i_1$  and  $i_2$  to changes in  $i_x$ .

**Assumptions:** From Ex. 11.5,  $A_o = 80$  dB,  $R_{id} = 25 \text{ k}\Omega$ ,  $R_o = 1 \text{ k}\Omega$ .

**Analysis:** The amplifier circuit is redrawn below with sources  $VX1$ ,  $VX2$ , and  $IX$  added to the circuit. All three are zero-value sources, which do not affect the Q-point calculations. Source  $VX2$  is added so that current  $I_2$  can be determined by SPICE.



The results of the four SPICE transfer function analyses are

$$\frac{v_7}{v_{x1}} = 0.9999 \quad \frac{v_1}{v_{x1}} = -1.294 \times 10^{-4}$$

$$\frac{i_2}{i_x} = 0.9984 \quad \frac{i_1}{i_x} = 1.628 \times 10^{-3}$$

and the loop gain and resistance ratio calculated using these four values are

$$T_v = -\frac{-0.9999}{1.294 \times 10^{-4}} = 7730 \quad T_i = \frac{0.9984}{1.628 \times 10^{-3}} = 613$$

$$T = \frac{T_v T_i - 1}{2 + T_v + T_i} = \frac{7730(613) - 1}{2 + 7730 + 613} = 568$$

$$\frac{R_B}{R_A} = \frac{1 + T_v}{1 + T_i} = \frac{1 + 7730}{1 + 613} = 12.6$$

**Check of Results:** The value of  $T$  computed by hand in the exercises following Ex. 11.5 was 568 which agrees with the result based on SPICE. Resistances  $R_A$  and  $R_B$  associated with the open feedback loop are identified in Fig. 11.27. Calculating these resistances and their ratio by hand gives

$$R_A = 10 \text{ k}\Omega \| r_\pi = 10 \text{ k}\Omega \| 27 \text{ k}\Omega = 7.30 \text{ k}\Omega$$

$$R_B = R_2 + (R_o \| R_L) = 91 \text{ k}\Omega + (1 \text{ k}\Omega + 5 \text{ k}\Omega) = 91.8 \text{ k}\Omega$$

$$\frac{R_B}{R_A} = 12.6$$

Again, we find good agreement with SPICE.

**Discussion:** The SPICE values and our hand calculations agree closely. As an alternative to using transfer function analyses,  $v_x$  and  $i_x$  can be made 1-V and 1-A ac sources, and two ac analyses can be performed. The ac source method has the advantage that it can find the loop gain and impedance ratio as a function of frequency. We must know the loop gain as a function of frequency in order to determine the stability of a feedback amplifier. This topic is discussed in detail in later in this chapter.

### 11.9.1 SIMPLIFICATIONS

Although analysis of the successive voltage and current injection method was performed using ideal sources, Middlebrook's analysis [5] shows that the technique is valid even if source resistances are included with both  $v_x$  and  $i_x$ . In addition, if point  $P$  is chosen at a position in the circuit where  $R_B$  is zero or  $R_A$  is infinite, then the equations can be simplified and  $T$  can be found from only one measurement. For example, if a point is found where  $R_A$  is infinite, then Eq. (11.85) reduces to  $T = T_v$ . In an ideal op amp circuit, such a point exists at the input of the op amp, as in Fig. 11.28(a).

Alternatively, if a point can be found where  $R_B = 0$ , then Eq. (11.85) also reduces to  $T = T_v$ . In an ideal op amp circuit, such a point exists at the output of the op amp, as in Fig. 11.28(b). A similar set of simplifications can be used for the current injection case. If  $R_A = 0$  or  $R_B$  is infinite, then  $T = T_I$ .

In practice, the conditions  $R_B \gg R_A$  or  $R_A \gg R_B$  are sufficient to permit the use of the simplified expressions [6–8]. In the general case, where these conditions are not met, or we are not sure of the exact impedance levels, then the general method can always be applied.

## 11.10 DISTORTION REDUCTION THROUGH THE USE OF FEEDBACK

Real amplifiers do not have the piece-wise linear voltage transfer functions depicted in Fig. 10.13. Actual VTCs have more of an "S" shape as in Fig. 11.29, and the nonlinearities introduce distortion into the output of the amplifier as discussed in Sec. 10.5. Fortunately, feedback can be used to significantly reduce distortion in amplifiers.

Consider the noninverting amplifier in Fig. 11.30 with an input of  $v_i = V_i \sin \omega_o t$ . Due to distortion, the op amp output will have both the desired output at frequency  $\omega_o$  plus additional unwanted signal components at frequencies other than the input frequency (see Eq. 10.29):

$$v_o(t) = V_1 \sin(\omega_o t + \phi_1) + v_e(t)$$

where

$$v_e(t) = V_2 \sin(2\omega_o t + \phi_2) + V_3 \sin(3\omega_o t + \phi_3) + \dots \quad (11.90)$$

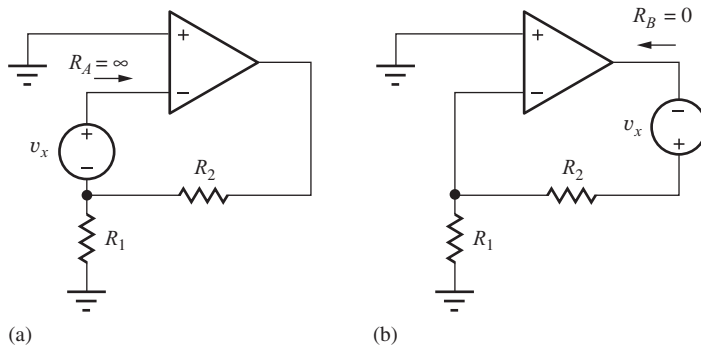


**Figure 11.28** (a) Voltage injection at a point where  $R_A = \infty$  and (b) voltage injection at a point where  $R_B = 0$ . (An ideal op amp is assumed.)

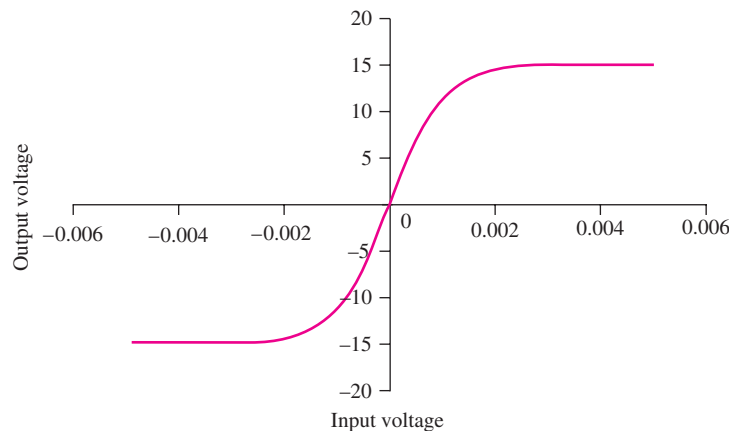


**Figure 11.29** Realistic voltage transfer characteristic.

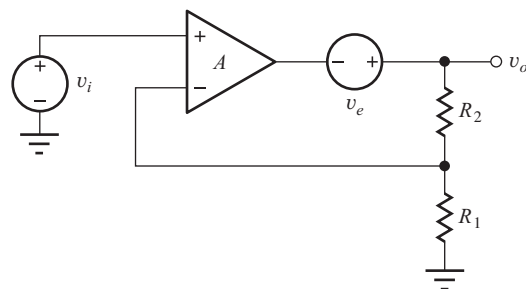


**Figure 11.30** Noninverting amplifier with distortion source added.

We can model this behavior by inserting error source  $v_e$  in series with the output of the op amp as in Fig. 11.30.

Now let us calculate the voltage at the output of the noninverting amplifier. We have

$$v_o = A v_{id} + v_e \quad \text{and} \quad v_{id} = v_i - \beta v_o \quad \text{where} \quad \beta = \frac{R_1}{R_1 + R_2} \quad (11.91)$$

and

$$v_o = \frac{A}{1 + A\beta} v_i + \frac{v_e}{1 + A\beta} \quad (11.92)$$

In the first term, we see that the gain of the amplifier is unchanged, a result we should expect from our knowledge of superposition. In the second term, however, we find that the distortion terms are reduced by the feedback term  $1 + A\beta$ . In fact, in the ideal case distortion would be completely eliminated, since for  $A = \infty$ , the voltage across the op amp input must be zero. Since  $v_i$  contains no distortion terms, output voltage  $v_o$  cannot contain any distortion terms either, because  $\beta v_o$  must equal  $v_i$ . In the real case with finite gain, the distortion is still reduced by the factor  $1 + A\beta$ , which can be very large.

## 11.11 DC ERROR SOURCES AND OUTPUT RANGE LIMITATIONS

An important class of error sources results from the need to bias the internal circuits that form the operational amplifier and from mismatches between pairs of solid-state devices in these circuits. These dc error sources include the input-offset voltage  $V_{OS}$ , the input-bias currents  $I_{B1}$  and  $I_{B2}$ , and the input-offset current  $I_{OS}$ .

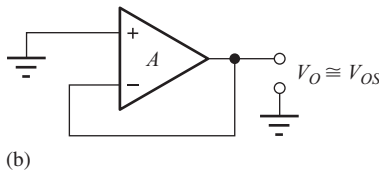
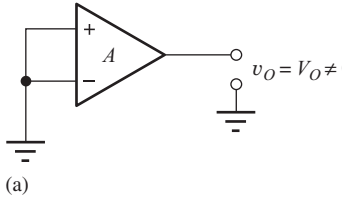


**Figure 11.31** (a) Amplifier with zero input voltage but nonzero output voltage. (Note: The offset voltage cannot be measured in this manner.) (b) Circuit for measuring offset voltage.

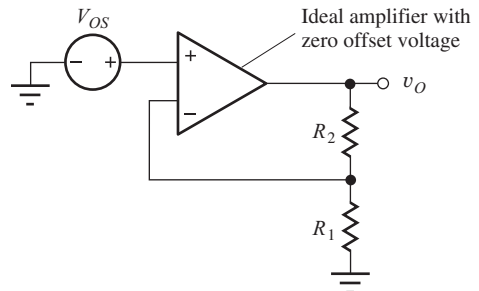


**Figure 11.32** Offset voltage can be modeled by a voltage source  $V_{OS}$  in series with the amplifier input.

### 11.11.1 INPUT-OFFSET VOLTAGE

When the inputs of the amplifier in Fig. 11.31 are both zero, the output of the amplifier is not truly zero but is resting at some nonzero dc voltage level. A small dc voltage seems to have been applied to the input of the amplifier, which is being amplified by the gain.<sup>1</sup> The equivalent dc **input-offset voltage**  $V_{OS}$  is defined as

$$V_{OS} = \left. \frac{V_O}{A} \right|_{v_1=o=v_2} \quad (11.93)$$

The op amp output voltage expression can be modified to include the effects of this offset voltage by adding the  $V_{OS}$  term:

$$v_O = A[v_{ID} + V_{OS}] \quad (11.94)$$

The first term in brackets represents the desired differential input signal to the amplifier, whereas the second term represents the offset-voltage error that corrupts the desired signal.

The offset voltage varies randomly from amplifier to amplifier so the actual sign of  $V_{OS}$  is not known, and only the magnitude of the worst-case offset voltage is specified. Most commercial operational amplifiers have offset-voltage specifications of less than 10 mV, and op amps can easily be purchased with  $V_{OS}$  specified to be less than a few mV. For additional cost, internally trimmed op amps are available with  $V_{OS} < 0.25$  mV.

The offset voltage usually cannot be measured with the operational amplifier connected as depicted in Fig. 11.31(a) because of the high gain of the amplifier. However, the circuit in Fig. 11.31(b) can be used. Here the amplifier is connected as a voltage follower, and the output voltage is equal to the offset voltage of the amplifier (except for the small gain error of the amplifier since  $A \neq \infty$ .)

In Ex. 11.10, the effect of offset voltage is modeled as in Fig. 11.32, in which the offset voltage is represented by a source in series with the input to an otherwise ideal amplifier.  $V_{OS}$  is amplified just as any input signal source, and the dc output voltage of the amplifier in Fig. 11.32 is

$$v_O = \left( 1 + \frac{R_2}{R_1} \right) V_{OS} \quad (11.95)$$

<sup>1</sup> The voltage arises mainly from mismatches in the transistors in the input stage of the operational amplifier. We will explore this problem in Chapter 16.



**EXERCISE:** What are the nominal, minimum, and maximum values of offset voltage for the AD745 operational amplifier at 25°C? (See MCD website for specification sheets.) Repeat for the OP77E.

**ANSWERS:** 0.25 mV, no minimum value specified, 1.0 mV; 10  $\mu$ V, no minimum value specified, 25  $\mu$ V

### EXAMPLE 11.10 OFFSET VOLTAGE ANALYSIS

This example calculates the output voltage of an op amp circuit caused by its offset voltage.

**PROBLEM** Suppose the amplifier in Fig. 11.32 has  $|V_{OS}| \leq 3$  mV and  $R_2$  and  $R_1$  are 99 k $\Omega$  and 1.2 k $\Omega$ , respectively. What is the quiescent dc voltage at the amplifier output?

**SOLUTION** **Known Information and Given Data:** Noninverting amplifier configuration with  $R_1 = 1.2$  k $\Omega$  and  $R_2 = 99$  k $\Omega$ . The amplifier has an equivalent input voltage of  $|V_{OS}| \leq 3$  mV.

**Unknowns:** Amplifier dc output voltage  $V_O$

**Approach:** Use the known values to evaluate Eq. (11.95).

**Assumptions:** The op amp is ideal except for the specified value of nonzero offset voltage.

**Analysis:** Using Eq. (11.95), we find that the output voltage is

$$|V_O| \leq \left(1 + \frac{99 \text{ k}\Omega}{1.2 \text{ k}\Omega}\right) (0.003) = 0.25 \text{ V}$$

**Check of Results:** We have found the value of the only unknown, and the value appears reasonable for standard IC power supplies.

**Discussion:** We do not actually know the sign of  $V_{OS}$  since the  $V_{OS}$  specification represents an upper bound. Therefore we actually know only that

$$-0.25 \text{ V} \leq V_O \leq 0.25 \text{ V}$$

**EXERCISE:** Repeat the calculation in Ex. 11.10 if the noninverting amplifier gain is set to 50 and the offset voltage is 2 mV?

**ANSWER:** 100 mV

### 11.11.2 OFFSET-VOLTAGE ADJUSTMENT

Addition of a potentiometer allows the **offset voltage** of most IC op amps to be manually adjusted to zero. Commercial amplifiers typically provide two terminals to which the potentiometer can be connected, as in Fig. 11.33. The third terminal of the potentiometer is connected to the positive or negative power supply voltage. The potentiometer value depends on the internal design of the amplifier.

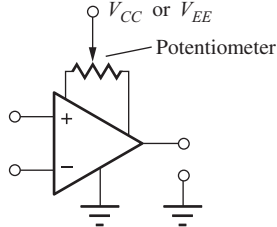


**Figure 11.33** Offset-voltage adjustment of an operational amplifier.

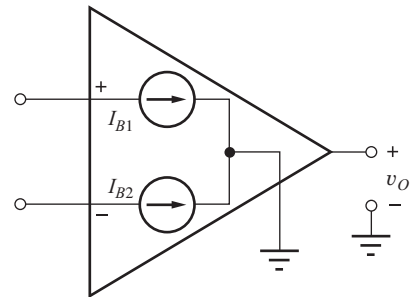
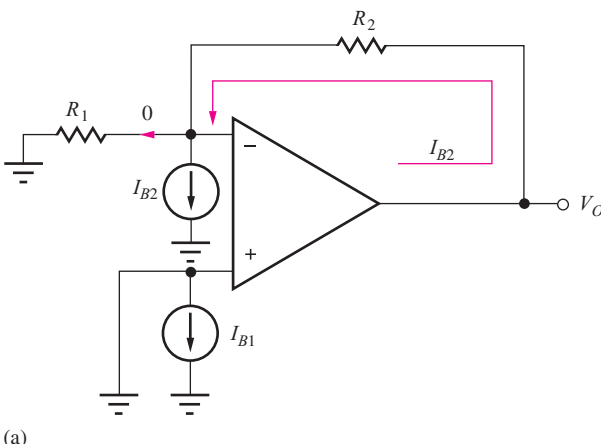
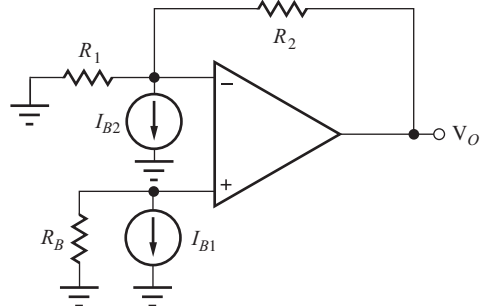


**Figure 11.34** Operational amplifier with input-bias currents modeled by current sources  $I_{B1}$  and  $I_{B2}$ .



(a)



(b)

**Figure 11.35** (a) Inverting amplifier with input-bias currents modeled by current sources  $I_{B1}$  and  $I_{B2}$ . (b) Inverting amplifier with bias current compensation resistor  $R_B$ .

### 11.11.3 INPUT-BIAS AND OFFSET CURRENTS

For the transistors that form the operational amplifier to operate, a small but nonzero dc bias current must be supplied to each input terminal of the amplifier. These currents represent base currents in an amplifier built with bipolar transistors or gate currents in one designed with MOSFETs or JFETs. Although small, the bias and offset currents represent additional sources of error.

The bias currents can be modeled by two current sources  $I_{B1}$  and  $I_{B2}$  connected to the noninverting and inverting inputs of the amplifier, as in Fig. 11.34. The values of  $I_{B1}$  and  $I_{B2}$  are similar but not identical, and the actual direction of the currents depends on the details of the internal amplifier circuit (*npn*, *pnp*, NMOS, PMOS, and so on). The difference between the two bias currents is called the **offset current  $I_{OS}$** .

$$I_{OS} = I_{B1} - I_{B2} \quad (11.96)$$

The offset-current specification for an op amp is normally expressed as an upper bound on the magnitude of  $I_{OS}$ , and the actual sign of  $I_{OS}$  for a given op amp is not known.

In an operational amplifier circuit, the **input-bias currents** produce an undesired voltage at the amplifier output. Consider the inverting amplifier in Fig. 11.35(a) as an example. In this circuit,  $I_{B1}$  is shorted out by the direct connection of the noninverting input to ground and does not affect the circuit. However, because the inverting input represents a virtual ground, the current in  $R_1$  must be

zero, forcing  $I_{B2}$  to be supplied by the amplifier output through  $R_2$ . Thus, the dc output voltage is equal to

$$V_O = I_{B2}R_2 \quad (11.97)$$

The output-voltage error in Eq. (11.97) can be reduced by placing a **bias current compensation resistor**  $R_B$  in series with the noninverting input of the amplifier, as in Fig. 11.35(b). Using analysis by superposition, the output due to  $I_{B1}$  acting alone is

$$V_O = -I_{B1}R_B \left( 1 + \frac{R_2}{R_1} \right) \quad (11.98)$$

The total output voltage is the sum of Eqs. (11.97) and (11.98):

$$V_O^T = I_{B2}R_2 - I_{B1}R_B \left( 1 + \frac{R_2}{R_1} \right) \quad (11.99)$$

If  $R_B$  is set equal to the parallel combination of  $R_1$  and  $R_2$ , then the expression for the output-voltage error reduces to

$$V_O^T = (I_{B2} - I_{B1})R_2 = -I_{OS}R_2 \quad \text{for} \quad R_B = \frac{R_1R_2}{R_1 + R_2} \quad (11.100)$$

The value of the offset current is typically a factor of 5–10 smaller than either of the individual bias currents, so the dc output-voltage error can be substantially reduced by using bias current compensation techniques.

Another example of the problems associated with offset-voltage and bias currents occurs in the integrator circuit in Fig. 11.36. A reset switch has been added to the integrator and is kept closed for  $t < 0$ . With the switch closed, the circuit is equivalent to a voltage follower, and the output voltage  $v_O$  is equal to the offset voltage  $V_{OS}$ . However, when the switch opens at  $t = 0$ , the circuit begins to integrate its own offset-voltage and bias current. Again using superposition analysis, it is easy to show (see Prob. 11.67) that the output voltage becomes

$$v_O(t) = V_{OS} + \frac{V_{OS}}{RC}t + \frac{I_{B2}}{C}t \quad \text{for} \quad t \geq 0 \quad (11.101)$$

The output voltage becomes a ramp with a constant slope determined by the values of  $V_{OS}$  and  $I_{B2}$ . Eventually, the integrator output saturates at a limit set by one of the two power supplies, as discussed in Chapter 10. If an integrator is built in the laboratory without a reset switch, the output is normally found to be resting near one of the power supply voltages.

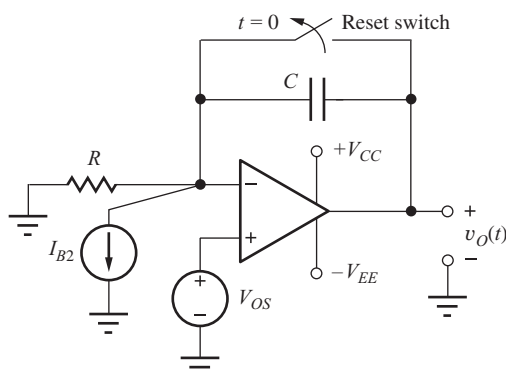


**Figure 11.36** Example of dc offset-voltage and bias current errors in an integrator.



**EXERCISE:** What are the nominal, minimum, and maximum values of the input bias and offset currents for the μA741C operational amplifier (see MCD website for specification sheets)? Repeat for the AD745J.

**ANSWERS:** 80 nA, no minimum value, 500 nA; 20 nA, no minimum value, 200 nA; 150 pA, no minimum value, 400 pA; 40 pA, no minimum value, 150 pA

**EXERCISE:** An inverting amplifier is designed with  $R_1 = 1 \text{ k}\Omega$  and  $R_2 = 39 \text{ k}\Omega$ . What value of resistance should be placed in series with the noninverting input terminal for bias current compensation?

**ANSWERS:** 975 Ω; Note that 1 kΩ is the closest 5 percent resistor value.

**EXERCISE:** An integrator has  $R = 10 \text{ k}\Omega$ ,  $C = 100 \text{ pF}$ ,  $V_{OS} = 1.5 \text{ mV}$ , and  $I_{B2} = 100 \text{ nA}$ . How long will it take  $v_O$  to saturate (reach  $V_{CC}$  or  $V_{EE}$ ) after the power supplies are turned on if  $V_{CC} = V_{EE} = 15 \text{ V}$ ?

**ANSWER:**  $t = 6.0 \text{ ms}$

#### 11.11.4 OUTPUT VOLTAGE AND CURRENT LIMITS

As discussed in Chapter 10, an actual operational amplifier has a limited range of voltage and current capability at its output. For example, the voltage at the output of the amplifier in Fig. 11.37 cannot exceed  $V_{CC}$  or be more negative than  $-V_{EE}$ . In fact, for many real op amps, the output-voltage range is limited to several volts less than the power supply span. For example, the output-voltage limits for a particular op amp might be specified as

$$(-V_{EE} + 1 \text{ V}) \leq v_O \leq (V_{CC} - 2 \text{ V}) \quad (11.102)$$

Commercial operational amplifiers also contain circuits that restrict the magnitude of the current in the output terminal in order to limit power dissipation in the amplifier to protect the amplifier from accidental short circuits. The current-limit specification is often given in terms of the minimum load resistance that an amplifier can drive with a given voltage swing. For example, an amplifier may be guaranteed to deliver an output of  $\pm 10 \text{ V}$  only for a total load resistance  $\geq 5 \text{ k}\Omega$ . This is equivalent to saying that the total output current  $i_O$  is limited to

$$|i_O| \leq \frac{10 \text{ V}}{5 \text{ k}\Omega} = 2 \text{ mA} \quad (11.103)$$

The output-current specification not only affects the size of load resistor that can be connected to the amplifier, it also places lower limits on the value of the feedback resistors  $R_1$  and  $R_2$ . The total

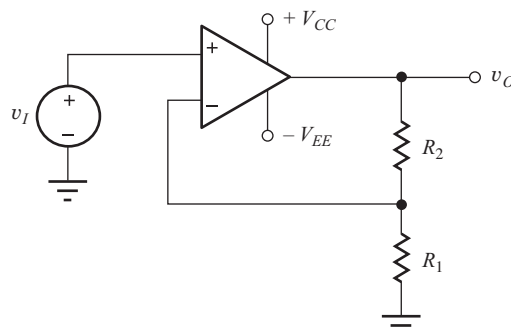
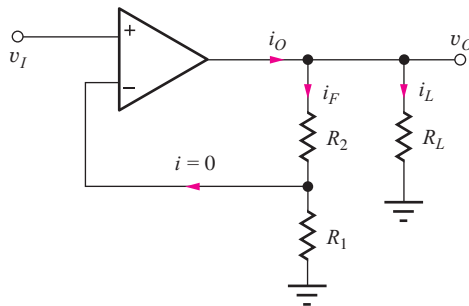
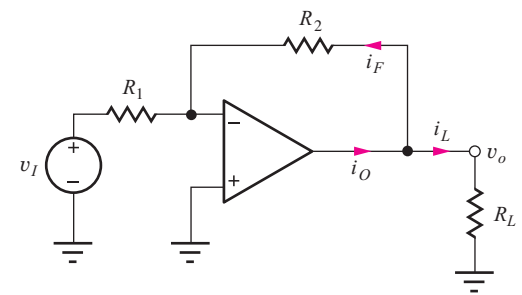


Figure 11.37 Amplifier with power supply voltages indicated.



**Figure 11.38** Output-current limit in the noninverting amplifier.



**Figure 11.39** Output-current limit in the inverting-amplifier circuit.

output current  $i_O$  in Fig. 11.38 is given by  $i_O = i_L + i_F$ , and since the current into the ideal inverting input is zero,

$$i_O = \frac{v_O}{R_L} + \frac{v_O}{R_2 + R_1} = \frac{v_O}{R_{EQ}} \quad (11.104)$$

The amplifier output must supply current not only to the load but also to its own feedback network! From Eq. (11.104), we see that the resistance that the noninverting amplifier must drive is equivalent to the parallel combination of the load resistance and the series combination of  $R_1$  and  $R_2$ :

$$R_{EQ} = R_L \parallel (R_1 + R_2) \quad (11.105)$$

For the case of the inverting amplifier in Fig. 11.39,  $R_{EQ}$  is given by

$$R_{EQ} = R_L \parallel R_1 \quad (11.106)$$

since the inverting-input terminal of the amplifier represents a virtual ground.

The output-current constraint represented by Eqs. (11.105) and (11.106) often helps us choose the size of the feedback resistors during the design process.



**EXERCISE:** What is the maximum guaranteed value for the output current of the OP-27A operational amplifier (see MCD website for specification sheets)?

**ANSWER:** 12 V/2 kΩ = 6 mA

## DESIGN

### EXAMPLE 11.11

Here we explore op amp circuit design including constraints on the output current capability of the op amp.

**PROBLEM** The amplifier in Fig. 11.39 is to be designed to have a gain of 20 dB and must develop a peak output voltage of at least 10 V when connected to a minimum load resistance of 5 kΩ. The op amp output current specification states that the output current must be less than 2.5 mA. Choose acceptable values of  $R_1$  and  $R_2$  from the table of 5 percent resistor values in Appendix A.

**SOLUTION** **Known Information and Given Data:** Inverting amplifier configuration;  $A_v = 20 \text{ dB}$ ,  $|v_o| \leq 10 \text{ V}$  with  $R_L \geq 5 \text{ k}\Omega$ . The magnitude of the op amp output current must not exceed  $2.5 \text{ mA}$ .

**Unknowns:** Feedback resistors  $R_1$  and  $R_2$ . Choose real values from the tables in Appendix A.

**Approach:** The op amp must supply current to both the load resistor and the feedback networks. We must account for both.

**Assumptions:** The op amp is ideal except for its limited output current capability.

**Analysis:** The equivalent load resistance on the amplifier must be greater than  $4 \text{ k}\Omega$ :

$$R_{EQ} \geq \frac{10 \text{ V}}{2.5 \text{ mA}} = 4 \text{ k}\Omega \quad \text{or} \quad R_L \parallel R_2 \geq 4 \text{ k}\Omega$$

Because the minimum value of  $R_L$  is  $5 \text{ k}\Omega$ , the feedback resistor  $R_2$  must satisfy  $R_2 \geq 20 \text{ k}\Omega$ , and we also have  $R_2/R_1 = 10$  because the gain was specified as  $20 \text{ dB}$ . We should allow some safety margin in the value of  $R_2$ . For example, a  $27\text{-k}\Omega$  resistor with a 5 percent tolerance will have a minimum value of  $25.6 \text{ k}\Omega$  and would be satisfactory. A  $22\text{-k}\Omega$  resistor would have a minimum value of  $20.9 \text{ k}\Omega$  and would also meet the specification. A wide range of choices still exists for  $R_1$  and  $R_2$ . Several acceptable choices would be

$$\begin{aligned} R_2 &= 22 \text{ k}\Omega & \text{and} & \quad R_1 = 2.2 \text{ k}\Omega \\ R_2 &= 27 \text{ k}\Omega & \text{and} & \quad R_1 = 2.7 \text{ k}\Omega \\ R_2 &= 47 \text{ k}\Omega & \text{and} & \quad R_1 = 4.7 \text{ k}\Omega \\ R_2 &= 100 \text{ k}\Omega & \text{and} & \quad R_1 = 10 \text{ k}\Omega \end{aligned}$$

Let us select the last choice:  $R_1 = 10 \text{ k}\Omega$  and  $R_2 = 100 \text{ k}\Omega$  to provide an input resistance of  $10 \text{ k}\Omega$ .

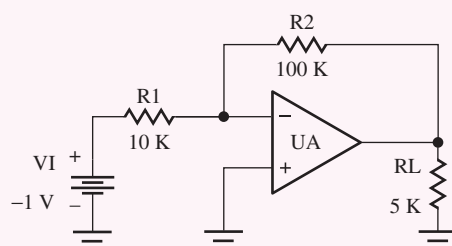
**Check of Results:** The gain is  $-R_2/R_1 = -10$ , which is correct. The maximum output current will be

$$i_o \leq \frac{10 \text{ V}}{100 \text{ k}\Omega} + \frac{10 \text{ V}}{5 \text{ k}\Omega} = 2.1 \text{ mA}$$

which is less than  $2.5 \text{ mA}$  ( $2.2 \text{ mA}$  if we include 5 percent tolerances).

**Discussion:** Note that an input resistance specification would help us decide on a value for  $R_1$ .

**Computer-Aided Design:** SPICE can be used to check our design using the circuit below. The gain of UA is set to  $1E6$  to approximate an ideal op amp. VI is set to  $-1 \text{ V}$  to produce an output of  $+10 \text{ V}$ . Operating point and transfer function analyses yield  $V_o = 10 \text{ V}$ ,  $I_o = 2.1 \text{ mA}$ ,  $A_v = -10$ , and  $R_{in} = 10 \text{ k}\Omega$ , all in agreement with our theory.





**EXERCISE:** What is the maximum guaranteed value for the output current of the AD745J operational amplifier (see MCD website for specification sheets)?

**ANSWER:**  $12 \text{ V}/2 \text{ k}\Omega = 6 \text{ mA}$

**EXERCISE:** Design a noninverting amplifier to have a gain of 20 dB and to develop a peak output voltage of at least 20 V when connected to a load resistance of at least 5 k $\Omega$ . The op amp output current specification states that the output current must be less than 5 mA. Choose acceptable values of  $R_1$  and  $R_2$  from the table of 5 percent resistor values in Appendix A.

**ANSWER:** Some possibilities: 27 k $\Omega$  and 3 k $\Omega$ ; 270 k $\Omega$  and 30 k $\Omega$ ; 180 k $\Omega$  and 20 k $\Omega$ ; *but not* 18 k $\Omega$  and 2 k $\Omega$  because of tolerances.

## 11.12 COMMON-MODE REJECTION AND INPUT RESISTANCE

### 11.12.1 FINITE COMMON-MODE REJECTION RATIO

Unfortunately, the output voltage of the real amplifier in Fig. 11.40 contains components in addition to the scaled replica of the input voltage ( $A v_{id}$ ). In particular, a real amplifier also responds to the signal that is in common to both inputs, called the **common-mode input voltage**  $v_{ic}$  defined as

$$v_{ic} = \left( \frac{v_1 + v_2}{2} \right) \quad (11.107)$$

The common-mode input signal is amplified by the **common-mode gain**  $A_{cm}$  to give an overall output voltage expressed by

$$v_o = A(v_1 - v_2) + A_{cm} \left( \frac{v_1 + v_2}{2} \right) \quad \text{or} \quad v_o = A v_{id} + A_{cm} v_{ic} \quad (11.108)$$

where  $A$  (or  $A_{dm}$ ) = **differential-mode gain**

$A_{cm}$  = common-mode gain

$v_{id} = (v_1 - v_2)$  = differential-mode input voltage

$v_{ic} = \left( \frac{v_1 + v_2}{2} \right)$  = common-mode input voltage

Simultaneous solution of these last two equations allows voltages  $v_1$  and  $v_2$  to be expressed in terms of  $v_{ic}$  and  $v_{id}$  as

$$v_1 = v_{ic} + \frac{v_{id}}{2} \quad \text{and} \quad v_2 = v_{ic} - \frac{v_{id}}{2} \quad (11.109)$$

and the amplifier in Fig. 11.40 can be redrawn in terms of  $v_{ic}$  and  $v_{id}$ , as in Fig. 11.41.

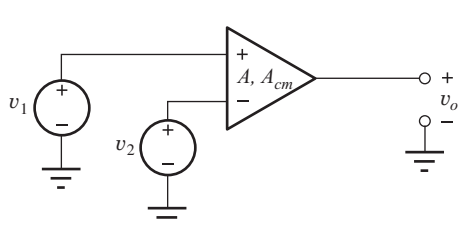


Figure 11.40 Operational amplifier with inputs  $v_1$  and  $v_2$ .

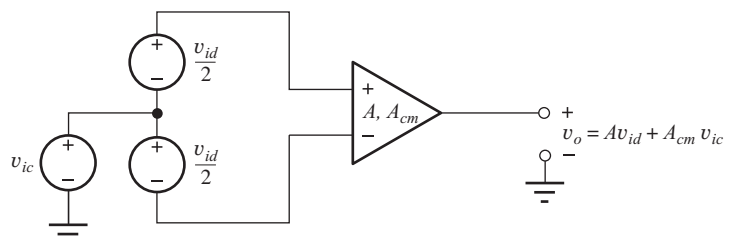


Figure 11.41 Operational amplifier with common-mode and differential-mode inputs shown explicitly.

An ideal amplifier would amplify the **differential-mode input voltage**  $v_{id}$  and totally reject the common-mode input signal ( $A_{cm} = 0$ ), as has been tacitly assumed thus far. However, an actual amplifier has a nonzero value of  $A_{cm}$ , and Eq. (11.108) is often rewritten in a slightly different form by factoring out  $A$ :

$$v_o = A \left[ v_{id} + \frac{A_{cm} v_{ic}}{A} \right] = A \left[ v_{id} + \frac{v_{ic}}{\text{CMRR}} \right] \quad (11.110)$$

In this equation, **CMRR** is the **common-mode rejection ratio**, defined by the ratio of  $A$  and  $A_{cm}$

$$\text{CMRR} = \left| \frac{A}{A_{cm}} \right| \quad (11.111)$$

CMRR is often expressed in dB as

$$\text{CMRR}_{\text{dB}} = 20 \log \left| \frac{A}{A_{cm}} \right| \text{ dB} \quad (11.112)$$

An ideal amplifier has  $A_{cm} = 0$  and therefore infinite CMRR. Actual amplifiers usually have  $A \gg A_{cm}$ , and the CMRR typically falls in the range

$$60 \text{ dB} \leq \text{CMRR}_{\text{dB}} \leq 120 \text{ dB}$$

A value of 60 dB is a relatively poor level of common-mode rejection, whereas achieving 120 dB (or even higher) is possible but difficult. Generally, the sign of  $A_{cm}$  is unknown ahead of time. In addition, CMRR specifications represent a lower bound. An illustration of the problems that can be caused by finite common-mode rejection is given in Ex. 11.12.



**EXERCISE:** What are the nominal, minimum, and maximum values of CMRR for the OP27 operational amplifier. (See MCD website for specification sheets.) Repeat for the AD745.

**ANSWERS:** 126 dB, 114 dB, no maximum value specified; 95 dB, 80 dB, no maximum value specified

### 11.12.2 WHY IS CMRR IMPORTANT?

The common-mode signal concept may initially seem obscure, but we actually encounter common-mode signals quite often. In digital systems, capacitive coupling of high frequency signals between signal lines on a bus or backplane can induce the same signal on more than one line. This induced signal often appears as a common-mode signal. Many high-speed computer buses utilize differential signaling so that the undesired common-mode signals can be eliminated by amplifiers with good CMRR.

Probably the most frequent time that we encounter common-mode signals is when we use instruments to make measurements. Consider the circuit in Fig. 11.42 in which we are trying to measure the

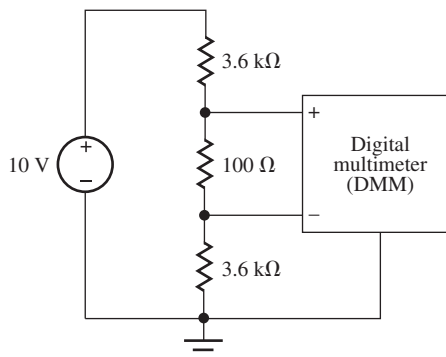


Figure 11.42 Common-mode input in a digital multimeter application.

voltage across the  $100\text{-}\Omega$  resistor with a digital multimeter (DMM). The dc voltage difference across the DMM input terminals (its differential-mode input  $V_{DM}$ ) is easily found by voltage division:

$$V_{DM} = V_+ - V_- = 10 \text{ V} \left( \frac{100 \text{ }\Omega}{7300 \text{ }\Omega} \right) = 0.137 \text{ V}$$

However, there is also a dc common-mode input to the DMM:

$$V_{CM} = \frac{V_+ + V_-}{2} = \frac{1}{2} \left[ 10 \text{ V} \left( \frac{3700 \text{ }\Omega}{7300 \text{ }\Omega} \right) + 10 \text{ V} \left( \frac{3600 \text{ }\Omega}{7300 \text{ }\Omega} \right) \right] = 4.5 \text{ V}$$

Thus our DMM must accurately measure the 0.137 V differential input in the presence of a 4.5 V common-mode input, and this requires the digital multimeter to have good common-mode rejection capability. If we want the common-mode input to produce an error of less than 0.1% in the measurement of the 0.137-V input, we need

$$\frac{4.5}{\text{CMRR}} \leq 10^{-3} \times (0.137 \text{ V}) \quad \text{or} \quad \text{CMRR} \geq 3.28 \times 10^4$$

which represents a CMRR of more than 90 dB.

A similar measurement problem occurs when an oscilloscope is used in its differential mode. In this case, the differential- and common-mode inputs may have high frequency signal components in addition to dc. Unfortunately, good common-mode rejection at high frequencies is difficult to obtain.

### EXAMPLE 11.12 COMMON-MODE ERROR CALCULATION

Calculate the error in a differential amplifier with nonideal values of gain and common-mode rejection.

**PROBLEM** Suppose the amplifier in Fig. 11.40 has a differential-mode gain of 2500 and a CMRR of 80 dB. What is the output voltage if  $v_1 = 5.001 \text{ V}$  and  $v_2 = 4.999 \text{ V}$ ? What is the error introduced by the finite CMRR?

**SOLUTION** **Known Information and Given Data:** For the amplifier in Fig. 11.40:  $A = 2500$ ,  $\text{CMRR} = 80 \text{ dB}$ ,  $v_1 = 5.001 \text{ V}$ , and  $v_2 = 4.999 \text{ V}$ .

**Unknowns:** Output voltage  $v_o$ ; common-mode contribution to the error

**Approach:** Use the known values to evaluate Eq. (11.110)

**Assumptions:** The op amp is ideal except for finite gain and CMRR. The CMRR specification of 80 dB corresponds to  $\text{CMRR} = \pm 10^4$ . Let us assume  $\text{CMRR} = +10^4$  for this example.

**Analysis:** The differential- and common-mode input voltages are

$$v_{id} = 5.001 \text{ V} - 4.999 \text{ V} = 0.002 \text{ V} \quad \text{and} \quad v_{ic} = \frac{5.001 + 4.999}{2} \text{ V} = 5.000 \text{ V}$$

$$\begin{aligned} v_o &= A \left[ v_{id} + \frac{v_{ic}}{\text{CMRR}} \right] = 2500 \left[ 0.002 + \frac{5.000}{10^4} \right] \text{ V} \\ &= 2500[0.002 + 0.0005] \text{ V} = 6.25 \text{ V} \end{aligned}$$

The error introduced by the common-mode input is 25 percent of the differential input voltage.

**Check for Results:** We have found the required unknowns. The output voltage is a reasonable value for power supplies normally used with integrated circuit op amps.

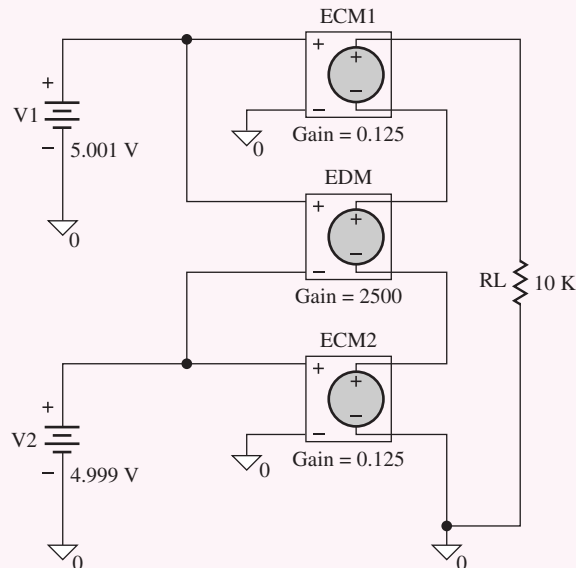
**Evaluation and Discussion:** An ideal amplifier would amplify only  $v_{id}$  and produce an output voltage of 5.00 V. For this particular situation, the output voltage is in error by 25 percent due to the finite common-mode rejection of the amplifier. Common-mode rejection is important in measurements of small voltage differences in the presence of large common-mode voltages, as in the example shown here. Note in this case that

$$A_{cm} = \frac{A}{CMRR} = \frac{2500}{10,000} = 0.25 \text{ or } -12 \text{ dB}$$

**Computer-Aided Analysis:** Let's build a model to simulate this example. The output of the amplifier can be rewritten as

$$v_o = A_{dm}v_{id} + \frac{A_{cm}}{2}v_1 + \frac{A_{cm}}{2}v_2 = 2500v_{id} + 0.125v_1 + 0.125v_2$$

which is implemented below using three voltage-controlled voltage sources. EDM depends on the voltage difference  $V1-V2$ , ECM1 depends on the voltage  $V1$ , and ECM2 depends on the voltage  $V2$ . An operating point analysis confirms our hand analysis with  $v_o = 6.25$  V.  $RL$  is added to have two connections at the output node and does not affect the calculation.



**EXERCISE:** The CMRR specification of 80 dB in Example 11.12 actually corresponds to  $-10^4 \leq CMRR \leq +10^4$ . What range of output voltages may occur?

**ANSWER:**  $3.750 \text{ V} \leq v_o \leq 6.250 \text{ V}$

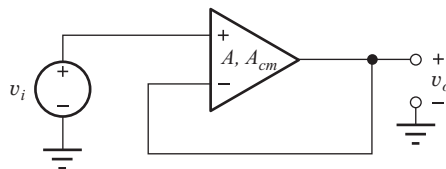


**Figure 11.43** CMRR error in the voltage follower.

### 11.12.3 VOLTAGE-FOLLOWER GAIN ERROR DUE TO CMRR

Finite CMRR can also play an important role in determining the gain error in the voltage-follower circuit in Fig. 11.43, for which

$$v_{id} = v_i - v_o \quad \text{and} \quad v_{ic} = \frac{v_i + v_o}{2}$$

Using Eq. (11.108)

$$v_o = A \left[ (v_i - v_o) + \frac{v_i + v_o}{2 \text{ CMRR}} \right] \quad (11.113)$$

Solving this equation for  $v_o$  yields

$$A_v = \frac{v_o}{v_i} = \frac{A \left[ 1 + \frac{1}{2 \text{ CMRR}} \right]}{1 + A \left[ 1 - \frac{1}{2 \text{ CMRR}} \right]} \quad (11.114)$$

The ideal gain for the voltage follower is unity, so the gain error is equal to

$$GE = 1 - A_v = \frac{1 - \frac{A}{\text{CMRR}}}{1 + A \left[ 1 - \frac{1}{2 \text{ CMRR}} \right]} \cong \frac{1}{A} - \frac{1}{\text{CMRR}} \quad (11.115)$$

Normally, both  $A$  and CMRR will be  $\gg 1$ , so the approximation in Eq. (11.115) is usually valid. The first term in Eq. (11.115) is the error due to the finite gain of the amplifier, as discussed earlier in this chapter, but the second term shows that CMRR may introduce an error of even greater import in the voltage follower.

#### EXAMPLE 11.13 VOLTAGE FOLLOWER GAIN ERROR

Perform a gain error analysis for the unity gain op amp circuit.

**PROBLEM** Calculate the gain error for a voltage follower that is built using an op amp with an open-loop gain of 80 dB and a CMRR of 60 dB.

**SOLUTION** **Known Information and Given Data:** Operational amplifier configured as a voltage follower;  $A = 80 \text{ dB}$ ;  $\text{CMRR} = 60 \text{ dB}$

**Unknowns:** Gain error

**Approach:** Use the known values to evaluate Eq. (11.114).

**Assumptions:** The op amp is ideal except for finite open-loop gain and CMRR. The CMRR specification of 60 dB corresponds to  $\text{CMRR} = \pm 1000$ . Let us assume  $\text{CMRR} = +1000$  for this example. Since both  $A$  and CMRR are much greater than one, we will use the approximate form of Eq. (11.115).

**Analysis:** Equation (12.38) gives a gain error of

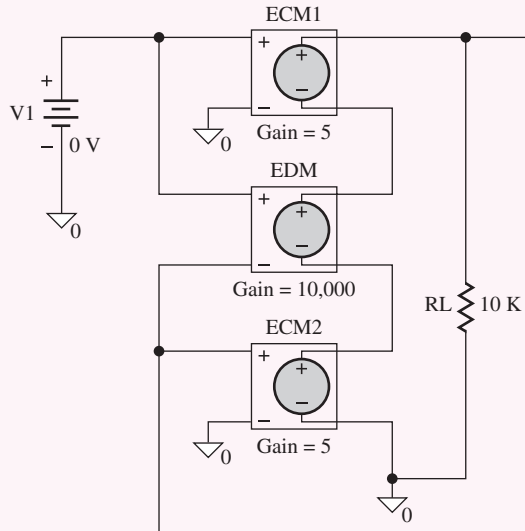
$$GE \cong \frac{1}{10^4} - \frac{1}{10^3} = -9.00 \times 10^{-4} \quad \text{or} \quad -0.090 \text{ percent}$$

**Check of Results:** We have found the desired gain error. However, the sign is negative, which may seem a bit unusual. We better explore this result further.

**Discussion:** In this calculation, the error due to finite CMRR is ten times larger than that due to finite gain. As pointed out above, the gain error is negative, which corresponds to a gain that is greater than 1! Finite open-loop gain alone always causes  $A_v$  to be slightly less than 1. However, for this case,

$$A_v = \frac{A \left[ 1 + \frac{1}{2 \text{ CMRR}} \right]}{1 + A \left[ 1 - \frac{1}{2 \text{ CMRR}} \right]} = \frac{10^4 \left[ 1 + \frac{1}{2(1000)} \right]}{1 + 10^4 \left[ 1 - \frac{1}{2(1000)} \right]} = 1.001$$

**Computer-Aided Analysis:** The amplifier model from the previous example is reconnected in the circuit below as a voltage follower with  $V_1 = 0$ . The gains of EDM, ECM1, and ECM2 are set to 10,000, 5, and 5, respectively. A SPICE transfer function analysis gives a voltage gain of +1.001.



**EXERCISE:** What is the voltage gain in Ex. 11.13 if the CMRR is improved to 80 dB? If the differential-mode gain were only 60 dB?

**ANSWERS:** 1.000; 1.000

We must be aware of errors related to CMRR whenever we are trying to perform precision amplification and measurement. Discussion of CMRR often focuses on amplifier behavior at dc. However, CMRR can be an even greater problem at higher frequencies. **Common-mode rejection** decreases rapidly as frequency increases, typically with a slope of at least  $-20 \text{ dB/decade}$  increase in

frequency. This roll-off of the CMRR can begin at frequencies below 100 Hz. Thus, common-mode rejection at 60 or 120 Hz can be much worse than that specified for dc.

**EXERCISE:** A voltage follower is to be designed to provide a gain error of less than 0.005 percent. Develop a set of minimum required specifications on open-loop gain and CMRR.

**ANSWER:** Several possibilities:  $A = 92 \text{ dB}$ ,  $\text{CMRR} = 92 \text{ dB}$ ;  $A = 100 \text{ dB}$ ,  $\text{CMRR} = 88 \text{ dB}$ ;  $\text{CMRR} = 100 \text{ dB}$ ,  $A = 88 \text{ dB}$ .

#### 11.12.4 COMMON-MODE INPUT RESISTANCE

Up to now, the discussion of the input resistance of an op amp has been limited to the resistance  $R_{id}$ , which is actually the approximate resistance presented to a purely differential-mode input voltage  $v_{id}$ . In Fig. 11.44, two new resistors with value  $2R_{ic}$  have been added to the circuit to model the finite common-mode input resistance of the amplifier.

When a purely common-mode signal  $v_{ic}$  is applied to the input of this amplifier, as depicted in Fig. 11.45, with  $v_{id} = 0$ , the input current is nonzero even though  $R_{id}$  is shorted out. In this situation, the total resistance presented to source  $v_{ic}$  is the parallel combination of the two resistors with value  $2R_{ic}$ , which thus equals  $R_{ic}$ . Therefore,  $R_{ic}$  is the equivalent resistance presented to the common-mode source; it is called the **common-mode input resistance** of the op amp. The value of  $R_{ic}$  is often much greater than that of the **differential-mode input resistance**  $R_{id}$ , typically in excess of  $10^9 \Omega$  ( $1 \text{ G}\Omega$ ).

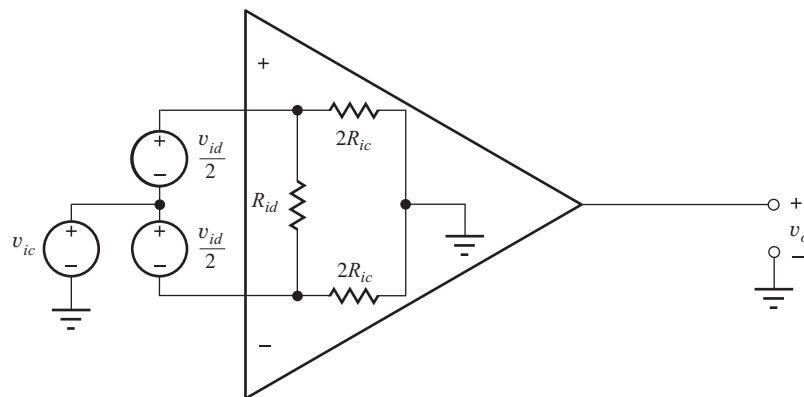


Figure 11.44 Op amp with common-mode input resistances added.

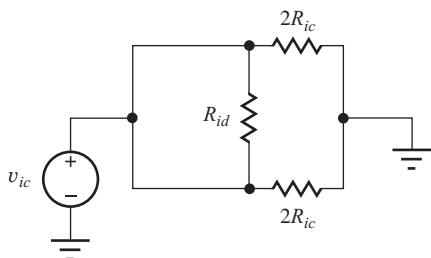


Figure 11.45 Amplifier with only a common-mode input signal present.

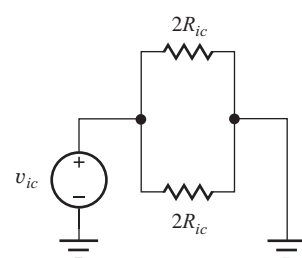


Figure 11.46 Amplifier input for a purely differential-mode input.

From Fig. 11.46, we see that a purely differential-mode input signal actually sees an input resistance equivalent to

$$R_{\text{in}} = R_{id} \parallel 4R_{ic} \quad (11.116)$$

As mentioned, however,  $R_{ic}$  is typically much greater than  $R_{id}$ , and the differential-mode input resistance is approximately equal to  $R_{id}$ .

### 11.12.5 AN ALTERNATE INTERPRETATION OF CMRR

If the differential input voltage  $v_{id}$  is set to zero in Eq. (11.111), then any residual output voltage is due to two equivalent input error voltage contributions:

$$v_O = A \left( V_{OS} + \frac{v_{ic}}{\text{CMRR}} \right) = A(v_{OS}) \quad (11.117)$$

We can view the CMRR as being a measure of how the total offset voltage  $v_{OS}$  changes from its dc value  $V_{OS}$  when a common-mode voltage is applied. We may find CMRR as

$$\text{CMRR} = \frac{v_{OS}}{v_{ic}} \quad \text{or} \quad \text{CMRR}_{\text{dB}} = 20 \log \left| \frac{v_{os}}{v_{ic}} \right|^{-1} \quad (11.118)$$

where the first form has units of  $\mu\text{V/V}$ .

### 11.12.6 POWER SUPPLY REJECTION RATIO

A parameter closely related to CMRR is the **power supply rejection ratio**, or **PSRR**. When power supply voltages change due to long-term drift or the existence of noise on the supplies, the equivalent input-offset voltage changes slightly. PSRR is a measure of the ability of the amplifier to reject these power supply variations.

In a manner similar to the CMRR, the power supply rejection ratio indicates how the offset voltage changes in response to a change in the power supply voltages.

$$\text{PSRR}_+ = \frac{\Delta V_{OS}}{\Delta V_{CC}} \quad \text{and} \quad \text{PSRR}_- = \frac{\Delta V_{OS}}{\Delta V_{EE}} \quad \text{usually expressed in } \frac{\mu\text{V}}{\text{V}} \quad (11.119)$$

PSRR is also often expressed in dB as  $\text{PSRR}_{\text{dB}} = 20 \log |\text{PSRR}|$ .

Generally the PSRR is different for changes in  $V_{CC}$  and  $V_{EE}$ , and the op amp PSRR specification usually represents the poorer of these two values. PSRR values are similar to those of CMRR with typical values ranging from 60 to 120 dB at dc. It is important to note that both CMRR and PSRR fall rapidly as frequency increases.



**EXERCISE:** What are the nominal, minimum, and maximum values of PSRR and CMRR for the OP77E operational amplifier (see MCD website for specification sheets)? Repeat for the AD741C.

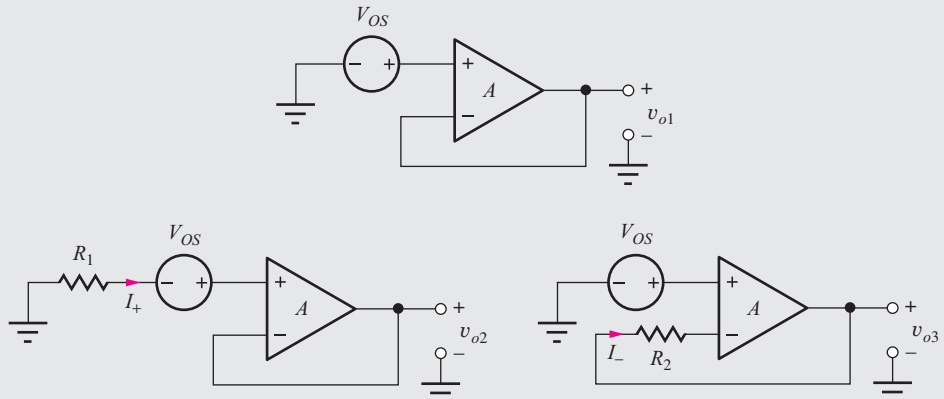
**ANSWERS:** 123 dB, 120 dB, no maximum value specified; 140 dB, 120 dB, no maximum value specified; 90 dB, 76 dB, no maximum value specified; 90 dB, 70 dB, no maximum value specified



### Offset Voltage, Bias Current, and CMRR Measurement

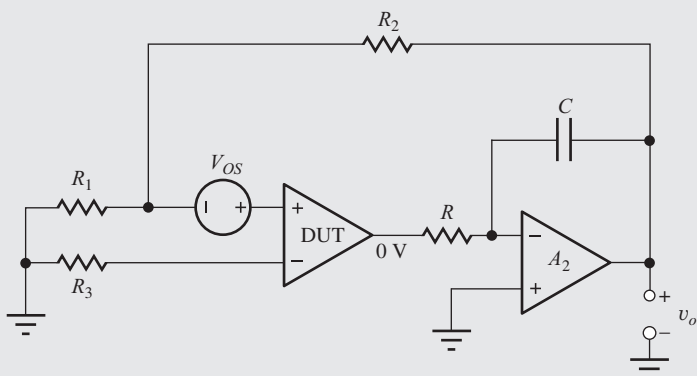
Conceptually, the three circuits in the figure below can be utilized to measure the offset voltage and bias currents of an operational amplifier. The output voltages of the three circuits are

$$V_o = V_{OS} \left( \frac{A}{1+A} \right) \quad V_o = (V_{OS} - I_+ R_1) \left( \frac{A}{1+A} \right) \quad V_o = (V_{OS} - I_- R_2) \left( \frac{A}{1+A} \right)$$



The first circuit produces a dc output voltage that is approximately equal to the offset voltage. Adding  $R_1$  to the circuit allows us to calculate bias current  $I_+$ , since the output voltage changes by approximately  $\Delta V_O = -I_+ R_1$ , whereas adding  $R_2$  to the original circuit permits calculation of bias current  $I_-$ , since the output voltage changes by approximately  $\Delta V_o = +I_- R_2$ . However, all of these measurements suffer from a low value of output voltage and a small gain error.

The next circuit addresses these issues by adding a second amplifier  $A_2$ . At dc, the overall open-loop gain is increased by the open-loop gain of  $A_2$ . The feedback amplifier can then be operated at a large closed-loop gain set by  $R_2$  and  $R_1$  and still have a large loop gain. The second amplifier is operated as an integrator to help stabilize the feedback loop. At dc, the integrator forces the output voltage of the device under test (DUT) to be zero, and the dc output voltage for the improved circuit is  $V_o = V_{OS}(1 + \frac{R_2}{R_1})$  (assuming  $I_+ = 0 = I_-$ ). Resistor ratio  $R_2/R_1$  can be set to increase the output voltage to 10–1000 times  $V_{os}$  and still have a significantly reduced gain error. In this circuit,  $R_3$  is chosen to provide bias current compensation. The bias currents can also be calculated by changing the value of  $R_1$  and  $R_3$ .

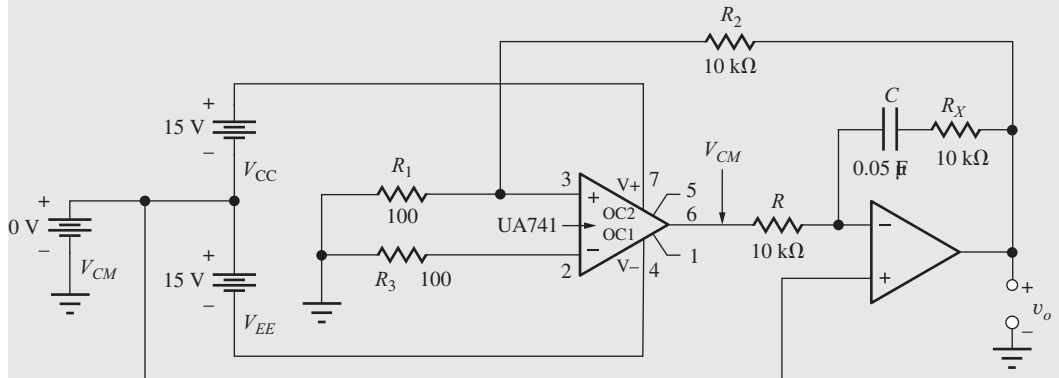


The final circuit extends the technique to include the calculation/measurement of CMRR. A common-mode input voltage is introduced by shifting the voltage at the connection between

the two power supplies  $V_{CC}$  and  $V_{EE}$ . At dc, the integrator forces the output of the first op amp to equal the common-mode voltage  $V_{CM}$ , thereby shifting the operating points of the internal circuits of the op amp in the same manner that occurs for the application of a common-mode input voltage. The output voltage of the circuit including the effect of CMRR and assuming  $T \gg 1$  is

$$V_O \cong \left( V_{OS} + \frac{V_{CM}}{CMRR} \right) \left( 1 + \frac{R_2}{R_1} \right) \quad \text{and} \quad \frac{dV_O}{dV_{CM}} \cong \left( 1 + \frac{R_2}{R_1} \right) \frac{1}{CMRR}$$

Resistor  $R_X$  has been added to the integrator to provide a zero as an additional variable that can be used to stabilize the feedback loop.



In SPICE, we can find the CMRR by using a transfer function analysis between  $V_{CM}$  and output voltage  $V_o$ . As a bonus, the power supply rejection ratios can be found in a similar manner:

$$\frac{dV_O}{dV_{CC}} \cong \left( 1 + \frac{R_2}{R_1} \right) \frac{1}{PSRR_+} \quad \text{and} \quad \frac{dV_O}{dV_{EE}} \cong \left( 1 + \frac{R_2}{R_1} \right) \frac{1}{PSRR_-}$$

Using the circuit above with the  $\mu$ A741 macro model built into SPICE yields the following values:  $V_{OS} = 19.8 \mu\text{V}$ ,  $CMRR = 90.0 \text{ dB}$ ,  $PSRR_+ = 96 \text{ dB}$ ,  $PSRR_- = 96 \text{ dB}$ .

The circuit above is convenient for use in SPICE and can be used in the laboratory. An easier way to implement the common-mode input is by shifting the two power supply voltages by an equal amount, for example from  $\pm 15 \text{ V}$  to  $+20 \text{ V}$  and  $-10 \text{ V}$ . An example of this technique can be found in an Analog Devices application note.<sup>2</sup>

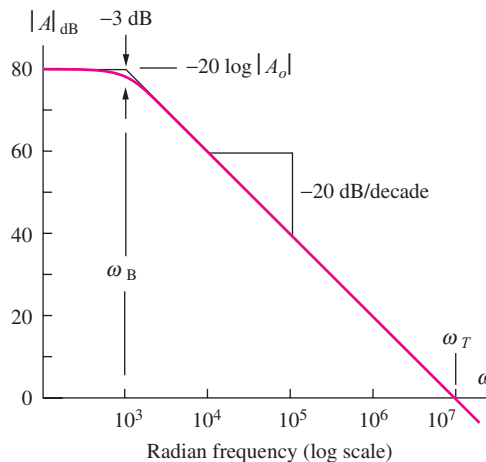
## 11.13 FREQUENCY RESPONSE AND BANDWIDTH OF OPERATIONAL AMPLIFIERS

Up to now we have assumed the op amp to have an ideal frequency response, i.e., infinite bandwidth. However, op amps are made with real electron devices that have internal capacitances, and every node in a real circuit has stray capacitance to ground. These capacitances all act to limit the bandwidth of the op amp. Most general-purpose operational amplifiers are low-pass amplifiers designed to have high gain at dc and a **single-pole frequency response** described by

$$A(s) = \frac{A_o \omega_B}{s + \omega_B} = \frac{\omega_T}{s + \omega_B} \quad (11.120)$$

in which  $A_o$  is the open-loop gain at dc,  $\omega_B$  is the open-loop bandwidth of the op amp, and  $\omega_T$  is called the **unity-gain frequency**, the frequency at which  $|A(j\omega)| = 1$  (0 dB). The magnitude of

<sup>2</sup> "Op Amp common-Mode Rejection Ratio (CMRR)," Analog Devices Tutorial MT-042, see <http://www.analog.com>.



$$A(s) = \frac{A_o \omega_B}{s + 1\omega_B} = \frac{A_o}{1 + \frac{s}{\omega_B}}$$

**Figure 11.47** Voltage gain vs. frequency for an operational amplifier.

Eq. (11.120) versus frequency can be expressed as

$$|A(j\omega)| = \frac{A_o \omega_B}{\sqrt{\omega^2 + \omega_B^2}} = \frac{A_o}{\sqrt{1 + \frac{\omega^2}{\omega_B^2}}} \quad (11.121)$$

An example is depicted graphically in the Bode plot in Fig. 11.47. For  $\omega \ll \omega_B$ , the gain is constant at the dc value  $A_o$ . The bandwidth of the open-loop amplifier, the frequency at which the gain is 3 dB below  $A_o$ , is  $\omega_B$  (or  $f_B = \omega_B/2\pi$ ). In Fig. 11.47,  $A_o = 10,000$  (80 dB) and  $\omega_B = 1000 \text{ rad/s}$  (159 Hz).

At high frequencies,  $\omega \gg \omega_B$ , the transfer function can be approximated by

$$|A(j\omega)| \cong \frac{A_o \omega_B}{\omega} = \frac{\omega_T}{\omega} \quad (11.122)$$

Using Eq. (11.122), we see that the magnitude of the gain is indeed unity at  $\omega = \omega_T$ :

$$|A(j\omega)| = \frac{\omega_T}{\omega} = 1 \quad \text{for } \omega = \omega_T \quad (11.123)$$

Rewriting the result in Eq. (11.123),

$$|A(j\omega)| \omega \cong \omega_T \quad \text{and dividing by } 2\pi \quad |A(j\omega)| f \cong f_T \quad (11.124)$$

The amplifier in Fig. 11.47 has  $\omega_T = 10^7 \text{ rad/s}$ .

The **gain-bandwidth product (GBW)** of the op amp is another figure of merit used to compare amplifiers (high values of GBW are usually preferred), and Eq. (11.125) defines GBW:

$$GBW = |A(j\omega)| \omega \cong \omega_T \quad (11.125)$$

Equation (11.124) states that, for any frequency  $\omega \gg \omega_B$ , the product of the magnitude of amplifier gain and frequency has a constant value equal to the unity-gain frequency  $\omega_T$ . For this reason, the parameter  $\omega_T$  (or  $f_T$ ) is often referred to as the gain-bandwidth product of the amplifier. The important result in Eq. (11.124) is a property of *single-pole* amplifiers that can be represented by transfer functions of the form of Eq. (11.120).

### EXAMPLE 11.14 OP AMP TRANSFER FUNCTION

Determine an op amp transfer function from a given Bode plot.

**PROBLEM** Write the transfer function that describes the frequency-dependent voltage gain of the amplifier in Fig. 11.47.

**SOLUTION** **Known Information and Given Data:** From the figure we see that the amplifier has a single-pole response as modeled by Eq. (11.120).

**Unknowns:** To evaluate the transfer function, we need to find  $A_o$  and  $\omega_B$ .

**Approach:** The values must be found from the graph and converted into proper form before insertion into Eq. (11.120)

**Assumptions:** The amplifier can be modeled by the single-pole formula.

**Analysis:** At low frequencies, the gain asymptotically approaches 80 dB, which must be converted back from dB:

$$A_o = 10^{80 \text{ dB}/20 \text{ dB}} = 10^4$$

The cutoff frequency  $\omega_B$  can also be read directly from the graph and is already in radian form:  $\omega_B = 10^3$  rad/s. Substituting the values of  $A_o$  and  $\omega_B$  into Eq. (11.120) yields the desired transfer function.

$$A_v(s) = \frac{A_o \omega_B}{s + \omega_B} = \frac{10^4(10^3)}{s + 10^3} = \frac{10^7}{s + 10^3}$$

**Check of Results:** We have found the unknown transfer function. We can check the answer for consistency by observing that the numerator value represents the unity-gain frequency  $\omega_T$ . From the graph we see that  $\omega_T$  is indeed  $10^7$  rad/s.

**Discussion:** Note that we often express the frequency values in Hz and that  $A_o f_B = f_T$ .

$$f_B = \frac{\omega_B}{2\pi} = 159 \text{ Hz} \quad \text{and} \quad f_T = \frac{\omega_T}{2\pi} = 1.59 \text{ MHz}$$

**EXERCISE:** An op amp has a gain of 100 dB at dc and a unity-gain frequency of 5 MHz. What is  $f_B$ ? Write the transfer function for the gain of the op amp.

**ANSWER:** 50 Hz;  $A(s) = \frac{10^7 \pi}{s + 100\pi}$



**EXERCISE:** What are the nominal values of open-loop gain and unity-gain frequency for the AD745 operational amplifier (see MCD website for specification sheets)? Write a transfer function for the op amp.

**ANSWERS:** 200,000; 1 MHz;  $A_v(s) = \frac{A_o \omega_B}{s + \omega_B} = \frac{\omega_T}{s + \omega_B} = \frac{2\pi \times 10^6}{s + 10\pi}$

### 11.13.1 FREQUENCY RESPONSE OF THE NONINVERTING AMPLIFIER

We now use the frequency-dependent op-amp gain expression to study the closed-loop frequency response of the noninverting and inverting amplifiers. The closed-loop gain for the noninverting amplifier was found previously to be

$$A_v = \frac{A}{1 + A\beta} \quad \text{where} \quad \beta = \frac{R_1}{R_1 + R_2} \quad (11.126)$$

The algebraic derivation of this gain expression actually placed no restrictions on the functional form of  $A$ . Up to now, we have assumed  $A$  to be a constant, but we can explore the frequency response of the closed-loop feedback amplifier by replacing  $A$  in Eq. (11.126) by the frequency-dependent voltage-gain expression for the op amp, Eq. (11.120):

$$A_v(s) = \frac{A(s)}{1 + A(s)\beta} = \frac{\frac{A_o \omega_B}{s + \omega_B}}{1 + \frac{A_o \omega_B}{s + \omega_B}\beta} = \frac{A_o \omega_B}{s + \omega_B(1 + A_o\beta)} \quad (11.127)$$

Dividing by the factor  $(1 + A_o\beta)\omega_B$ , Eq. (11.127) can be written as

$$A_v(s) = \frac{\frac{A_o}{s}}{\frac{1 + A_o\beta}{s} + 1} = \frac{A_v(0)}{\frac{s}{\omega_H} + 1} \quad (11.128)$$

where the upper-cutoff frequency is

$$\omega_H = \omega_B(1 + A_o\beta) = \omega_T \frac{(1 + A_o\beta)}{A_o} = \frac{\omega_T}{A_v(0)} \quad (11.129)$$

The closed-loop amplifier also has a single-pole response of the same form as Eq. (11.120), but its dc gain and bandwidth are given by

$$A_v(0) = \frac{A_o}{1 + A_o\beta} \quad \text{and} \quad \omega_H = \frac{\omega_T}{A_v(0)} \quad (11.130)$$

For  $A_o\beta \gg 1$ , Eq. (11.129) reduces to

$$A_v(0) \cong \frac{1}{\beta} \quad \text{and} \quad \omega_H \cong \beta\omega_T \quad (11.131)$$

Note that the gain-bandwidth product of the closed-loop amplifier is constant:

$$A_v(0) \omega_H = \omega_T$$

From Eq. (11.130), we see that the gain must be reduced in order to increase  $\omega_H$ , or vice versa. We will explore this in more detail shortly.

The loop gain  $A(s)\beta$  is now also a function of frequency depicted as in Fig. 11.48. At frequencies for which  $|A(j\omega)\beta| \gg 1$ , Eq. (11.126) reduces to  $1/\beta$ , the constant value derived previously for low frequencies. However, at frequencies for which  $|A(j\omega)\beta| \ll 1$ , Eq. (11.126) becomes  $A_v \cong A(j\omega)$ . At low frequencies, the gain is set by the feedback, but at high frequencies, we find that the gain must follow the gain of the amplifier. We should not expect a (negative) feedback amplifier to produce more gain than is available from the open-loop operational amplifier by itself.

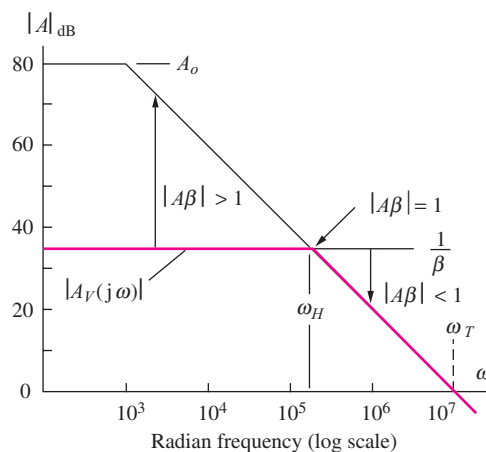


**Figure 11.48** Graphical interpretation of operational amplifier with feedback.

These results are indicated graphically by the bold lines in Fig. 11.48 for an amplifier with  $1/\beta = 35$  dB. Loop gain  $T$  can be expressed as

$$T = A\beta = \frac{A}{\left(\frac{1}{\beta}\right)} \quad \text{and (in dB)} \quad |A\beta|_{\text{dB}} = |A|_{\text{dB}} - \left| \frac{1}{\beta} \right|_{\text{dB}} \quad (11.132)$$

At any given frequency, the magnitude of the loop gain is equal to the difference between  $A_{\text{dB}}$  and  $(1/\beta)_{\text{dB}}$  on the graph. The upper half-power frequency  $\omega_H = \beta\omega_t$  corresponds to the frequency at which  $(1/\beta)$  intersects  $|A(j\omega)|$  corresponding to  $|A\beta| = 1$  (actually  $A\beta \cong -j1 = 1\angle-90^\circ$ ). For the case in Fig. 11.48,  $\beta = 0.0178$  ( $-35$  dB) and  $\omega_H = 0.0178 \times 10^7 = 178 \times 10^3$  rad/s.

### EXAMPLE 11.15 NONINVERTING AMPLIFIER FREQUENCY RESPONSE

Characterize the frequency response of a noninverting amplifier built with a nonideal op amp having limited gain and bandwidth.

**PROBLEM** An op amp has a dc gain of 100 dB and a unity-gain frequency of 10 MHz. (a) What is the bandwidth of the op amp? (b) If the op amp is used to build a noninverting amplifier with a closed-loop gain of 60 dB, what is the bandwidth of the feedback amplifier? (c) Write an expression for the transfer function of the op amp. (d) Write an expression for the transfer function of the noninverting amplifier.

**SOLUTION** **Known Information and Given Data:** We are given  $A_o = 10^5$  (100 dB) and  $f_T = 10^7$  Hz. The desired closed-loop gain is  $A_v = 1000$  (60 dB).

**Unknowns:** (a) Bandwidth  $f_B$  of the operational amplifier, (b) Bandwidth  $f_H$  of the closed-loop amplifier, (c) op amp transfer function, (d) noninverting amplifier transfer function

**Approach:** Evaluate Eqs. (11.126)–(11.131), which model the behavior of the noninverting amplifier.

**Assumptions:** Since we have been given values for  $A_o$  and  $f_T$ , we will assume that the amplifier is described by a single-pole transfer function. The op amp is ideal except for its single pole frequency response.

#### Analysis:

(a) The cutoff frequency of the op amp is  $f_B$ , and its  $-3$ -dB frequency is

$$f_B = \frac{f_T}{A_o} = \frac{10^7 \text{ Hz}}{10^5} = 100 \text{ Hz}$$

(b) Using Eq. (11.129), the bandwidth of the noninverting amplifier is

$$f_H = f_B(1 + A_o\beta) = 100(1 + 10^5 \cdot 10^{-3}) = 10.1 \text{ kHz}$$

in which the feedback factor  $\beta$  is determined by the desired closed-loop gain.

$$\beta = \frac{1}{A_v(0)} = \frac{1}{1000} = 10^{-3}$$

(c) Substituting the values of  $A_o$  and  $\omega_B$  into Eq. (11.120) yields the op amp transfer function.

$$A_v(s) = \frac{A_o\omega_B}{s + \omega_B} = \frac{10^5(2\pi)(10^2)}{s + (2\pi)(10^2)} = \frac{2\pi \times 10^7}{s + 200\pi}$$

(d) Evaluating Eq. (11.127) yields the noninverting amplifier transfer function.

$$A_v(s) = \frac{A_o \omega_B}{s + \omega_B(1 + A_o \beta)} = \frac{10^5 (2\pi)(10^2)}{s + (2\pi)(10^2)[1 + 10^5(10^{-3})]} = \frac{2\pi \times 10^7}{s + 2.02\pi \times 10^4}$$

**Check of Results:** We have found each of the requested answers. The numerators of the transfer functions should be equal to  $\omega_T = 2\pi f_T$  and are correct.  $A_v(0) = 99.0$  is also correct.

**EXERCISE:** An op amp has a dc gain of 90 dB and a unity-gain frequency of 5 MHz. What is the cutoff frequency of the op amp? If the op amp is used to build a noninverting amplifier with a closed-loop gain of 40 dB, what is the bandwidth of the feedback amplifier? Write an expression for the transfer function of the op amp. Write an expression for the transfer function of the noninverting amplifier.

**ANSWERS:** 158 Hz; 50 kHz;  $A(s) = \frac{10^7 \pi}{s + 316\pi}$ ;  $A_v(s) = \frac{10^7 \pi}{s + 10^5 \pi}$

**EXERCISE:** Show that  $A\beta \cong -j1$  at the frequency at which  $(1/\beta)$  intersects  $|A(j\omega)|$ .

### 11.13.2 INVERTING AMPLIFIER FREQUENCY RESPONSE

The frequency response for the inverting-amplifier configuration can be found in a manner similar to that for the noninverting case by substituting the frequency-dependent op amp gain expression, Eq. (11.120), into the equation for the closed-loop gain of the inverting amplifier.

$$\begin{aligned} A_v &= \left(-\frac{R_2}{R_1}\right) \frac{A(s)\beta}{1 + A(s)\beta} \quad \text{where} \quad \beta = \frac{R_1}{R_1 + R_2} \\ \text{or} \quad A_v(s) &= \left(-\frac{R_2}{R_1}\right) \frac{\frac{A_o \omega_B}{s + \omega_B} \beta}{1 + \frac{A_o \omega_B}{s + \omega_B} \beta} = \frac{\left(-\frac{R_2}{R_1}\right) \frac{A_o \beta}{s}}{\frac{\omega_B(1 + A_o \beta)}{s + \omega_B(1 + A_o \beta)} + 1} = -\frac{R_2}{R_1} \frac{A_o \beta \omega_B}{s + \omega_B(1 + A_o \beta)} \end{aligned} \quad (11.133)$$

For  $A_o \beta \gg 1$ , these equations reduce to

$$A_v = \frac{\left(-\frac{R_2}{R_1}\right) \frac{A_o \beta}{\frac{s}{\omega_H} + 1}}{\frac{\omega_H}{\omega_H} + 1} \cong \frac{\left(-\frac{R_2}{R_1}\right)}{\frac{\omega_H}{\omega_H} + 1} \quad \text{and} \quad \omega_H = \frac{\omega_T}{\frac{A_o}{(1 + A_o \beta)}} \cong \beta \omega_T \quad (11.134)$$

where the approximate values hold for  $A_o \beta \gg 1$ . This expression again represents a single-pole transfer function. The gain at low frequencies,  $A_v(0)$ , is set by the resistor ratio  $(-R_2/R_1)$ , and the bandwidth expression is identical to that of the noninverting amplifier,  $\omega_H = \beta \omega_T$ .

The frequency response characteristics of the inverting and noninverting amplifiers are summarized in Table 11.3, in which the expressions have been recast in terms of the ideal value of the gain at low frequencies. The expressions are quite similar. However, for a given value of dc gain, the noninverting amplifier will have slightly greater bandwidth than the inverting amplifier because of the difference in the relation between  $\beta$  and  $A_v(0)$ . The difference is significant only for amplifier stages designed with low values of closed-loop gain.

**TABLE 11.3****Inverting and Noninverting Amplifier Frequency Response Comparison**

$\beta = \frac{R_1}{R_1 + R_2}$	NONINVERTING AMPLIFIER	INVERTING AMPLIFIER
dc gain	$A_v(0) = 1 + \frac{R_2}{R_1}$	$A_v(0) = -\frac{R_2}{R_1}$
Feedback factor	$\beta = \frac{1}{A_v(0)}$	$\beta = \frac{1}{1 +  A_v(0) }$
Bandwidth	$f_B = \beta f_T$	$f_B = \beta f_T$
Input resistance	$R_{ic} \parallel R_{id}(1 + A\beta)$	$R_1 + \left( R_{ID} \parallel \frac{R_2}{1 + A} \right)$
Output resistance	$\frac{R_o}{1 + A\beta}$	$\frac{R_o}{1 + A\beta}$

**EXAMPLE 11.16 INVERTING AMPLIFIER FREQUENCY RESPONSE**

Characterize the frequency response of an inverting amplifier built using a nonideal op amp having limited gain and bandwidth.

**PROBLEM** An op amp has a dc gain of 200,000 and a unity-gain frequency of 500 kHz. (a) What is the cutoff frequency of the op amp? (b) If the op amp is used to build an inverting amplifier with a closed-loop gain of 40 dB, what is the bandwidth of the feedback amplifier? (c) Write an expression for the transfer function of the op amp. (d) Write an expression for the transfer function of the inverting amplifier.

**SOLUTION** **Known Information and Given Data:** For the op amp;  $A_o = 2 \times 10^5$ ,  $f_T = 5 \times 10^5$  Hz; for the inverting amplifier,  $A_v = -100$  (40 dB)

**Unknowns:** (a) Op amp cutoff frequency, (b) inverting amplifier bandwidth, (c) op amp transfer function, (d) inverting amplifier transfer function

**Approach:** Evaluate Eq. (11.120) for the op amp. Evaluate Eqs. (11.133) and (11.134), which model the behavior of the inverting amplifier.

**Assumptions:** The op amp has a single-pole frequency response. Otherwise it is ideal.

**Analysis:**

(a) The cutoff frequency of the op amp is  $f_B$ , its  $-3\text{-dB}$  frequency:

$$f_B = \frac{f_T}{A_o} = \frac{5 \times 10^5 \text{ Hz}}{2 \times 10^5} = 2.5 \text{ Hz}$$

(b) Using Eq. (11.134), the bandwidth of the inverting amplifier is

$$f_H = f_B(1 + A_o\beta) = 2.5 \text{ Hz} \left( 1 + \frac{2 \times 10^5}{101} \right) = 4.95 \text{ kHz}$$

in which the feedback factor  $\beta$  is determined by the desired closed-loop gain (see Table 11.3).

$$\beta = \frac{1}{1 + |A_v(0)|} = \frac{1}{101}$$

(c) Substituting the values of  $A_o$  and  $\omega_B$  into Eq. (12.57) yields the op amp transfer function.

$$A_v(s) = \frac{A_o\omega_B}{s + \omega_B} = \frac{\omega_T}{s + \omega_B} = \frac{(2\pi)(5 \times 10^5)}{s + (2\pi)(2.5)} = \frac{10^6\pi}{s + 5\pi}$$

(d) Evaluating Eq. (11.127) yields the inverting amplifier transfer function:

$$\begin{aligned} A_v(s) &= \left(-\frac{R_2}{R_1}\right) \frac{A_o\beta\omega_B}{s + \omega_B(1 + A_o\beta)} = (-100) \frac{(2 \times 10^5) \left(\frac{1}{101}\right) (2\pi)(2.5)}{s + (2\pi)(2.5) \left(1 + \frac{2 \times 10^5}{101}\right)} \\ &= -\frac{9.90 \times 10^5\pi}{s + 9.91 \times 10^3\pi} \end{aligned}$$

**Check of Results:** We have found the answers to all the unknowns. We can also double check the last transfer function by evaluating its dc gain and bandwidth.

$$A_v(0) = -\frac{9.90 \times 10^5\pi}{9.91 \times 10^3\pi} = -99.9 \quad \text{and} \quad f_H = \frac{9.91 \times 10^3\pi}{2\pi} = 4.96 \text{ kHz}$$

The values agree within round-off error.

**EXERCISE:** An op amp has a dc gain of 90 dB and a unity-gain frequency of 5 MHz. What is the cutoff frequency of the op amp? If the op amp is used to build an inverting amplifier with a closed-loop gain of 50 dB, what is the bandwidth of the feedback amplifier? Write an expression for the transfer function of the op amp. Write an expression for the transfer function of the inverting amplifier.

**ANSWERS:** 158 Hz; 15.8 kHz;  $A(s) = \frac{10^7\pi}{s + 316\pi}$ ;  $A(s) = \frac{10^7\pi}{s + 3.16\pi \times 10^5}$

**EXERCISE:** If the amplifier in Ex. 11.15 is used in a voltage follower, what is its bandwidth? If the amplifier is used in an inverting amplifier with  $A_v = -1$ , what is its bandwidth?

**ANSWERS:** 10 MHz; 5 MHz

### 11.13.3 USING FEEDBACK TO CONTROL FREQUENCY RESPONSE

In the preceding sections, we found that feedback can be used to stabilize the gain and improve the input and output resistances of an amplifier, and that feedback can also be used to trade reduced gain for increased bandwidth in low-pass amplifiers. In this section, we extend the analysis to more general feedback amplifiers.

The closed-loop gain for all the feedback amplifiers in this chapter can be written as

$$A_v = \frac{A}{1 + A\beta} \quad \text{or} \quad A_v(s) = \frac{A(s)}{1 + A(s)\beta(s)} \quad (11.135)$$

Up to now, we have worked with the midband value of  $A$  and assumed it to be a constant. However, we can explore the frequency response of the general closed-loop feedback amplifier by substituting a frequency-dependent voltage gain expression for  $A$  into Eq. (11.135).

Suppose that amplifier  $A$  is an amplifier with cutoff frequencies of  $\omega_H$  and  $\omega_L$  and midband gain  $A_o$  as described by

$$A(s) = \frac{A_o \omega_H s}{(s + \omega_L)(s + \omega_H)} \quad (11.136)$$

Substituting Eq. (11.136) into Eq. (11.135) and simplifying the expression yields

$$A_v(s) = \frac{\frac{A_o \omega_H s}{(s + \omega_L)(s + \omega_H)}}{1 + \frac{A_o \omega_H s}{(s + \omega_L)(s + \omega_H)} \beta} = \frac{A_o \omega_H s}{s^2 + [\omega_L + \omega_H(1 + A_o \beta)]s + \omega_L \omega_H} \quad (11.137)$$

Assuming that  $\omega_H(1 + A_o \beta) \gg \omega_L$ , then dominant-root factorization (see Sec. 17.6.3) yields these estimates of the upper- and lower-cutoff frequencies and bandwidth of the closed-loop feedback amplifier:

$$\begin{aligned} \omega_L^F &\cong \frac{\omega_L \omega_H}{\omega_L + \omega_H(1 + A_o \beta)} \cong \frac{\omega_L}{1 + A_o \beta} \\ \omega_H^F &\cong \omega_L + \omega_H(1 + A_o \beta) \cong \omega_H(1 + A_o \beta) \\ \text{BW}_F &= \omega_H^F - \omega_L^F \cong \omega_H(1 + A_o \beta) \end{aligned} \quad (11.138)$$

The upper- and lower-cutoff frequencies and bandwidth of the feedback amplifier are all improved by the factor  $(1 + A_o \beta)$ . Using the approximations in Eq. (11.138), we find that the transfer function in Eq. (11.137) can be rewritten approximately as

$$A_v(s) \cong \frac{\frac{A_o}{(1 + A_o \beta)} s}{\left(s + \frac{\omega_L}{(1 + A_o \beta)}\right) \left[1 + \frac{s}{\omega_H(1 + A_o \beta)}\right]} \quad (11.139)$$

As expected, the midband gain is stabilized at

$$A_{\text{mid}} = \frac{A_o}{1 + A_o \beta} \cong \frac{1}{\beta} \quad (11.140)$$

It should once again be recognized that the gain-bandwidth product of the closed-loop amplifier remains constant:

$$\text{GBW} = A_{\text{mid}} \times \text{BW}_F \cong \frac{A_o}{1 + A_o \beta} \omega_H(1 + A_o \beta) = A_o \omega_H \quad (11.141)$$

These results are displayed graphically in Fig. 11.49 for an amplifier with  $1/\beta = 20$  dB. The open-loop amplifier has  $A_o = 40$  dB,  $\omega_L = 100$  rad/s, and  $\omega_H = 10,000$  rad/s, whereas the closed-loop amplifier has  $A_v = 19.2$  dB,  $\omega_L = 9.1$  rad/s, and  $\omega_H = 110,000$  rad/s.

**EXERCISE:** An op amp has a dc gain of 100 dB and a unity-gain frequency of 10 MHz. What is the upper-cutoff frequency of the op amp itself? If the op amp is used to build a noninverting amplifier with a closed-loop gain of 60 dB, what is the bandwidth of the feedback amplifier? Write an expression for the transfer function of the op amp. Write an expression for the transfer function of the noninverting amplifier.

**ANSWERS:** 100 Hz; 10 kHz;  $A(s) = 2\pi \times 10^7 / (s + 200\pi)$ ;  $A(s) = 2\pi \times 10^7 / (s + 2\pi \times 10^4)$

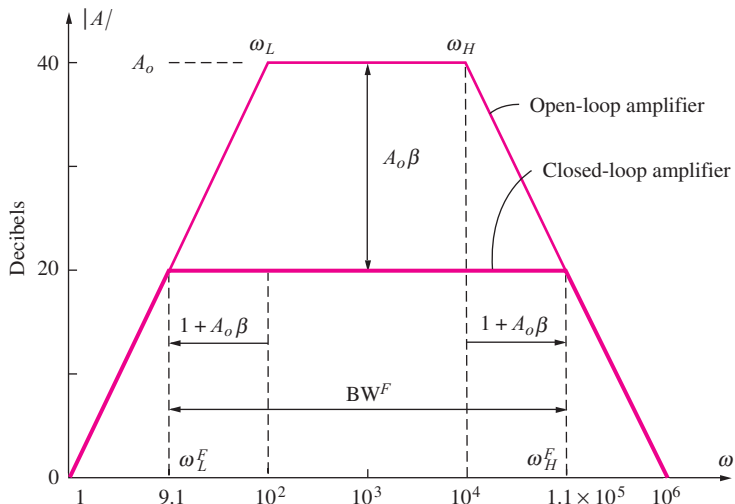


**Figure 11.49** Graphical interpretation of feedback amplifier frequency response.

#### 11.13.4 LARGE-SIGNAL LIMITATIONS—SLEW RATE AND FULL-POWER BANDWIDTH

Up to this point, we have tacitly assumed that the internal circuits that form the operational amplifier can respond instantaneously to changes in the input signal. However, the internal amplifier nodes all have an equivalent capacitance to ground, and only a finite amount of current is available to charge these capacitances. Thus, there will be some limit to the rate of change of voltage on the various nodes. This limit is described by the **slew-rate (SR)** specification of the operational amplifier. The slew rate defines the maximum rate of change of voltage at the output of the operational amplifier. Typical values of slew rate for general-purpose op amps fall into the range

$$0.1 \text{ V}/\mu\text{s} \leq \text{SR} \leq 10 \text{ V}/\mu\text{s}$$

although much higher values are possible in special designs. An example of a slew-rate limited signal at an amplifier output is shown schematically in Fig. 11.50.

For a given frequency, slew rate limits the maximum amplitude of a signal that can be amplified without distortion. Consider a sinusoidal output signal  $v_o = V_M \sin \omega t$ , for example. The maximum

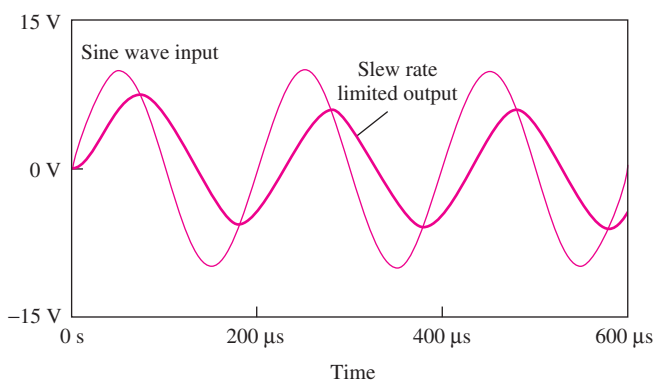


**Figure 11.50** An example of a slew-rate limited output signal.

rate of change of this signal occurs at the zero crossings and is given by

$$\left. \frac{dv_O}{dt} \right|_{\max} = V_M \omega \cos \omega t |_{\max} = V_M \omega \quad (11.142)$$

For no signal distortion, this maximum rate of change must be less than the slew rate:

$$V_M \omega \leq \text{SR} \quad \text{or} \quad V_M \leq \frac{\text{SR}}{\omega} \quad (11.143)$$

The **full-power bandwidth**  $f_M$  is the highest frequency at which a full-scale signal can be developed. Denoting the amplitude of the full-scale output signal by  $V_{FS}$ , the full-power bandwidth can be written as

$$f_M \leq \frac{\text{SR}}{2\pi V_{FS}} \quad (11.144)$$

**EXERCISE:** Suppose that an op amp has a slew rate of 0.5 V/ $\mu$ s. What is the largest sinusoidal signal amplitude that can be reproduced without distortion at a frequency of 20 kHz? If the amplifier must deliver a signal with a 10-V maximum amplitude, what is the full-power bandwidth corresponding to this signal?

**ANSWERS:** 3.98 V; 7.96 kHz

### 11.13.5 MACRO MODEL FOR OPERATIONAL AMPLIFIER FREQUENCY RESPONSE

The actual internal circuit of an operational amplifier may contain from 20 to 100 bipolar and/or field-effect transistors. If the actual circuits were used for each op amp, simulations of complex circuits containing many op amps would be very slow. Simplified circuit representations, called **macro models**, have been developed to model the terminal behavior of the op amp. The two-port model that we used in this chapter is one simple form of macro model. This section introduces a model that can be used for SPICE simulation of the frequency response of circuits utilizing operational amplifiers.

To model the single-pole roll-off, an auxiliary loop consisting of the voltage-controlled voltage source with value  $v_1$  in series with  $R$  and  $C$  is added to the interior of the original two-port, as depicted in Fig. 11.51. The product of  $R$  and  $C$  is chosen to give the desired  $-3$  dB point for the open-loop amplifier. If a voltage source is applied to the input, then the open-circuit voltage gain ( $R_L = \infty$ ) is

$$A_v(s) = \frac{V_o(s)}{V_1(s)} = \frac{A_o \omega_B}{s + \omega_B} \quad \text{where} \quad \omega_B = \frac{1}{RC} \quad (11.145)$$

This interior loop represents a “dummy” circuit added just to model the frequency response; the individual values of  $R$  and  $C$  are arbitrary. For example,  $R = 1 \Omega$  and  $C = 0.0159 \text{ F}$ ,  $R = 1000 \Omega$  and  $C = 15.9 \mu\text{F}$ , or  $R = 1 \text{ M}\Omega$  and  $C = 0.0159 \mu\text{F}$  may all be used to model a cutoff frequency of 10 Hz.

This simple single-pole macro model is utilized in a SPICE simulation in Ex. 11.17 in Sec. 11.14.

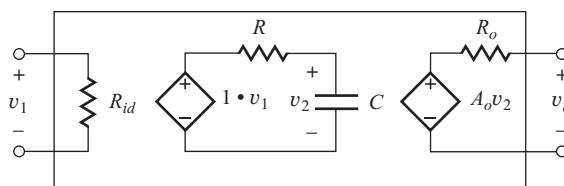


Figure 11.51 Simple macro model for an operational amplifier.



**EXERCISE:** Create a macro model for the OP27 based on Fig. 11.51 (see MCD website for specification sheets). Use the nominal specification values.

**ANSWERS:**  $R_{id} = 6 \text{ M}\Omega$ ,  $R = 2000 \Omega$ ,  $C = 17.9 \mu\text{F}$ ,  $A_o = 1.8 \times 10^6$ ,  $R_o = 70 \Omega$ . The individual values of  $R$  and  $C$  are arbitrary as long as  $RC = (1/8.89 \pi) \text{s}$ .

### 11.13.6 COMPLETE OP AMP MACRO MODELS IN SPICE

Most versions of SPICE contain sophisticated macro models for op amps including descriptions for many commercial op amps. These macro models include all of the nonideal limitations we have discussed in this chapter and contain a large number of parameters that can be adjusted to model op amp behavior. Both three- and five-terminal op amps may be included as shown in Fig. 11.52. An example parameter set is given in Table 11.4. In addition to those discussed previously in this chapter, we see parameters to model multiple poles and a zero in the op amp frequency response, to describe the input capacitance, and to set the input transistors to *n*p*n* or *p*n*p* devices. This choice determines the direction of the input bias current; the bias current goes into the op amp terminals for an *n*-type input and comes out of the terminals for a *p*-type input.

An example of the use of a complete SPICE macro model can also be found in Ex. 11.17 in Sec. 11.14.

### 11.13.7 EXAMPLES OF COMMERCIAL GENERAL-PURPOSE OPERATIONAL AMPLIFIERS

Now that we have explored the theory of circuits using ideal and nonideal operational amplifiers, let us look in more detail at the characteristics of a general-purpose operational amplifier. A portion of the specification sheets for one such commercial op amp, the AD745 series from Analog Devices Corporation, can be found on the MCD website. These amplifiers are fabricated with an IC technology that has both bipolar transistors and JFETs.

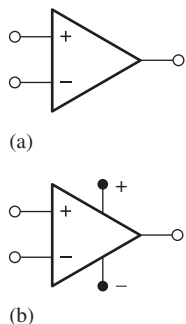


**Figure 11.52** (a) Three-terminal op amp. (b) Five-terminal op amp.

**TABLE 11.4**

Typical Op Amp Macro Model Parameter Set

PARAMETER	TYPICAL VALUE
Differential-mode gain (dc)	106 dB
Differential-mode input resistance	2 MΩ
Input capacitance	1.5 pF
Common-mode rejection ratio	90 dB
Common-mode input resistance	2 GΩ
Output resistance	50 Ω
Input offset voltage	1 mV
Input bias current	80 nA
Input offset current	20 nA
Positive slew rate	0.5 V/μs
Negative slew rate	0.5 V/μs
Maximum output source current	25 mA
Maximum output sink current	25 mA
Input type ( <i>n</i> - or <i>p</i> -type)	<i>n</i> -type
Frequency of first pole	5 Hz
Frequency of zero	5 MHz
Frequency of second pole	2 MHz
Frequency of third pole	20 MHz
Frequency of fourth pole	100 MHz
Power supply voltage (3-pin model)	15 V

Note that many of the specifications are stated in terms of typical values plus either upper or lower bounds. For example, the voltage gain for the AD745J at  $T = 25^\circ\text{C}$  with  $\pm 15\text{-V}$  power supplies is typically 132 dB but has a minimum value of 120 dB and no upper bound. The offset voltage is typically 0.25 mV with an upper bound of 1 mV, but the AD745K version is also available with a typical offset voltage of 0.1 mV and an upper bound of 0.5 mV. The input stage of this amplifier contains JFETs, so the input-bias current is very small at room temperature, and the nominal input resistance is very large.

The minimum common-mode rejection ratio (at dc) is 80 dB, and PSRR and CMRR specifications are the same. With  $\pm 15\text{-V}$  power supplies, the amplifier can handle input signals with a common-mode range of +13.3 and -10.7 V, and the amplifier is guaranteed to develop an output-voltage swing of +12 V with a  $2\text{-k}\Omega$  load resistance.

The AD745J has a minimum gain-bandwidth product (unity-gain frequency  $f_T$ ) of 20 MHz, and a slew rate of  $12.5\text{ V}/\mu\text{s}$ . Considerable additional information is included concerning the performance of the amplifier family over a large range of power supply voltages and temperatures.

## 11.14 STABILITY OF FEEDBACK AMPLIFIERS

Whenever an amplifier is embedded within a feedback network, a question of **stability** arises. Up to this point, it has tacitly been assumed that the feedback is negative. However, as frequency increases, the phase of the loop gain changes, and it is possible for the feedback to become positive at some frequency. If the gain is also greater than or equal to 1 at this frequency, then instability occurs, typically in the form of oscillation.

The locations of the poles of a feedback amplifier can be found by analysis of the closed-loop transfer function described by

$$A_v(s) = \frac{A(s)}{1 + A(s)\beta(s)} = \frac{A(s)}{1 + T(s)} \quad (11.146)$$

The poles occur at the complex frequencies  $s$  for which the denominator becomes zero:

$$1 + T(s) = 0 \quad \text{or} \quad T(s) = -1 \quad (11.147)$$

The particular values of  $s$  that satisfy Eq. (11.147) represent the poles of  $A_v(s)$ . For amplifier stability, the poles must lie in the left half of the  $s$ -plane. Now we discuss two graphical approaches for studying stability using Nyquist and Bode plots.

### 11.14.1 THE NYQUIST PLOT

The **Nyquist plot** is a useful graphical method for qualitatively studying the locations of the poles of a feedback amplifier. The graph represents a mapping of the right half of the  $s$ -plane (RHP) onto the  $T(s)$ -plane, as in Fig. 11.53. Every value of  $s$  in the  $s$ -plane has a corresponding value of  $T(s)$ . The critical issue is whether any value of  $s$  in the RHP corresponds to  $T(s) = -1$ . However, checking every possible value of  $s$  would take a rather long time. Nyquist realized that to simplify the process, we need only plot  $T(s)$  for values of  $s$  on the  $j\omega$  axis

$$T(j\omega) = A(j\omega)\beta(j\omega) = |T(j\omega)| \angle T(j\omega) \quad (11.148)$$

which represents the boundary between the RHP and LHP.  $T(j\omega)$  is normally graphed using the polar coordinate form of Eq. (11.148). If the **-1 point** is enclosed by this boundary, then there must be some value of  $s$  for which  $T(s) = -1$ , a pole exists in the RHP, and the amplifier is not stable.<sup>3</sup> However, if -1 lies outside the interior of the Nyquist plot, then the poles of the closed-loop amplifier are all in the left half-plane, and the amplifier is stable.

---

<sup>3</sup> If we mentally “walk” around the  $s$ -plane, keeping the shaded region on our right, then the corresponding region in the  $T(s)$ -plane will also be on our right as we “walk” in the  $T(s)$ -plane.

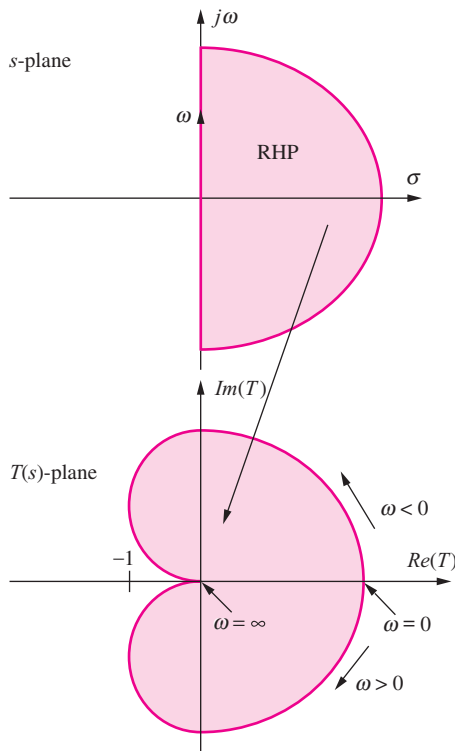


**Figure 11.53** Nyquist plot as a mapping between the  $s$ -plane and the  $T(s)$ -plane.

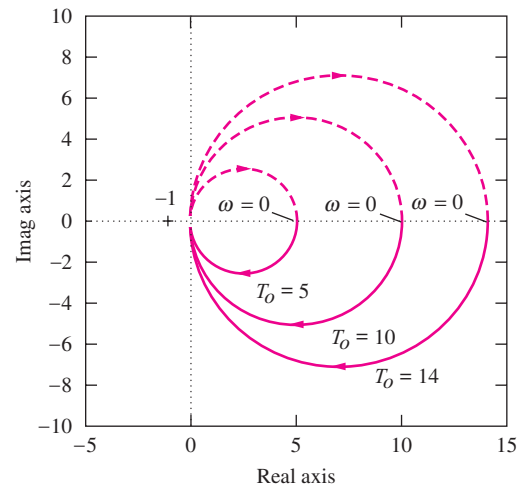


**Figure 11.54** Nyquist plot for first-order  $T(s)$  for  $T_o = 5, 10$ , and  $14$ . (Nyquist plots are easily made using MATLAB. This figure is generated by three simple MATLAB statements: nyquist(14,[1 1]), nyquist(10,[1 1]), and nyquist(5,[1 1]).)

Today, we are fortunate to have computer tools such as MATLAB, which can quickly construct the Nyquist plot for us. These tools eliminate the tedious work involved in creating the graphs so that we can concentrate on interpretation of the information. Let us consider examples of basic first-, second-, and third-order systems.

### 11.14.2 FIRST-ORDER SYSTEMS

In most of the feedback amplifiers we have considered thus far,  $\beta$  was a constant and  $A(s)$  was the frequency-dependent part of the loop gain  $T(s)$ . However, the important thing is the overall behavior of  $T(s)$ . The simplest case of  $T(s)$  is that of a basic low-pass amplifier with a loop-gain described by

$$T(s) = \frac{A_o \omega_o}{s + \omega_o} \beta = \frac{T_o}{s + \omega_o} \quad (11.149)$$

For example, Eq. (11.149) might correspond to a single-pole operational amplifier with resistive feedback. The Nyquist plot for

$$T(j\omega) = \frac{T_o}{j\omega + 1} \quad (11.150)$$

is given in Fig. 11.54. At dc,  $T(0) = T_o$ , whereas for  $\omega \gg 1$ ,

$$T(j\omega) \cong -j \frac{T_o}{\omega} \quad (11.151)$$

As frequency increases, the magnitude monotonically approaches zero, and the phase asymptotically approaches  $-90^\circ$ .

From Eq. (11.149), we see that changing the feedback factor  $\beta$  scales the value of  $T_o = T(0)$ ,

$$T(0) = A_o \omega_o \beta \quad (11.152)$$

but changing  $T(0)$  simply scales the radius of the circle in Fig. 11.54, as indicated by the curves for  $T_o = 5, 10$ , and  $14$ . It is impossible for the graph in Fig. 11.54 to ever enclose the  $T = -1$  point (indicated by the “+” symbol in Fig. 11.54), and the amplifier is stable regardless of the value of  $T_o$ . This is one reason why general-purpose op amps are often internally compensated to have a single-pole low-pass response. Single-pole op amps are stable for any fixed value of  $\beta$ .

### 11.14.3 SECOND-ORDER SYSTEMS AND PHASE MARGIN

A second-order loop-gain function can be described by

$$T(s) = \frac{A_o}{\left(1 + \frac{s}{\omega_1}\right)\left(1 + \frac{s}{\omega_2}\right)} \beta = \frac{T_o}{\left(1 + \frac{s}{\omega_1}\right)\left(1 + \frac{s}{\omega_2}\right)} \quad (11.153)$$

An example appears in Fig. 11.55 for

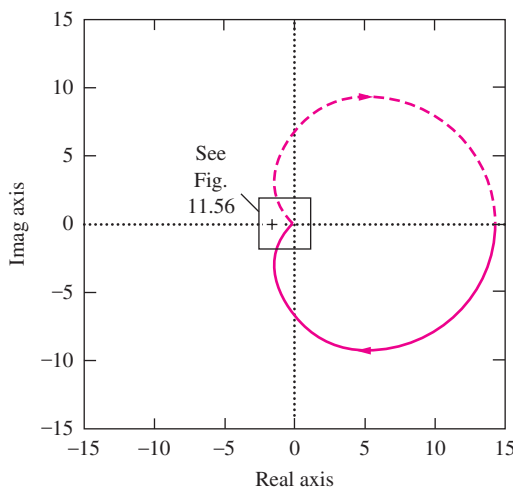
$$T(s) = \frac{14}{(s+1)^2} \quad \text{and} \quad T(j\omega) = \frac{14}{(j\omega+1)^2} \quad (11.154)$$

In this case,  $T_o$  is 14, but at high frequencies

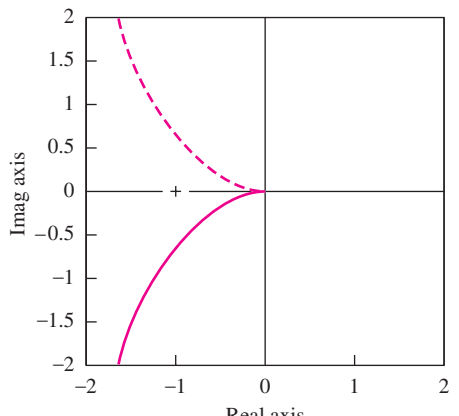
$$T(j\omega) \cong (-j)^2 \frac{14}{\omega^2} = -\frac{14}{\omega^2} \quad (11.155)$$

As frequency increases, the magnitude decreases monotonically from 14 toward 0, and the phase asymptotically approaches  $-180^\circ$ . Again, it is theoretically impossible for this transfer function to encircle the  $-1$  point. However, the second-order system can come arbitrarily close to this point, as indicated in Fig. 11.56, which is a blowup of the Nyquist plot in the region near the  $-1$  point. The larger the value of  $T_o$ , the closer the curve will come to the  $-1$  point. The curve in Fig. 11.56 is plotted for a  $T_o$  value of only 14, whereas an actual op amp circuit could easily have a  $T_o$  value of 1000 or more.

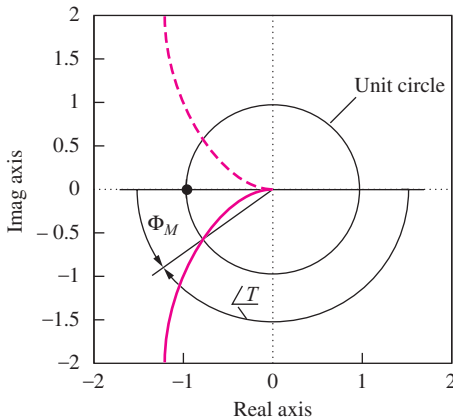
Although technically stable, the second-order system can have essentially zero **phase margin**, as defined in Fig. 11.57. Phase margin  $\Phi_M$  represents the maximum increase in phase shift (phase lag)



**Figure 11.55** Nyquist plot for second-order  $T(s)$ . (Generated using MATLAB command: `nyquist(14,[1 2 1])`.)



**Figure 11.56** Blowup of Fig. 11.55 near the  $-1$  point. The second-order system does not enclose the  $-1$  point but may come arbitrarily close to doing so.

Figure 11.57 Definition of phase margin  $\Phi_M$ .

that can be tolerated before the system becomes unstable.  $\Phi_M$  is defined as

$$\Phi_M = \angle T(j\omega_1) - (-180^\circ) = 180^\circ + \angle T(j\omega_1) \quad \text{where} \quad |T(j\omega_1)| = 1 \quad (11.156)$$

To find  $\Phi_M$ , we first must determine the frequency  $\omega_1$  for which the magnitude of the loop gain is unity, corresponding to the intersection of the Nyquist plot with the unit circle in Fig. 11.57, and then determine the phase shift of  $T$  at this frequency. The difference between this angle and  $-180^\circ$  is  $\Phi_M$ .

Small phase margin leads to excessive peaking in the closed-loop frequency response and undesirable ringing in the step response. In addition, any rotation of the Nyquist plot due to additional phase shift (from poles that may have been neglected in the model, for example) can lead to instability.

#### 11.14.4 STEP RESPONSE AND PHASE MARGIN

We are interested in phase margin not only because of stability concerns but also because phase margin is directly related to the time domain response of the feedback system and its overshoot and settling time. Consider an op amp with a transfer function containing the original low frequency pole  $\omega_B$  plus a second high frequency pole at  $\omega_2$ :

$$A(s) = \frac{A_o \omega_B}{(s + \omega_B)} \frac{\omega_2}{(s + \omega_2)} \quad (11.157)$$

If we assume  $\omega_2 \gg \omega_B$ , then the open-loop bandwidth of the op amp is approximately  $\omega_B$ . For frequency independent feedback  $\beta$ , the closed-loop response is

$$A_{CL} = \frac{A(s)}{1 + A(s)\beta} = \frac{A_o \omega_B \omega_2}{s^2 + s(\omega_B + \omega_2) + \omega_B \omega_2 (1 + A_o \beta)} = \frac{A_o}{1 + A_o \beta} \left( \frac{\omega_n^2}{s^2 + 2\zeta \omega_n s + \omega_n^2} \right)$$

$$\omega_n = \sqrt{\omega_B \omega_2 (1 + A_o \beta)} \quad \text{and} \quad \zeta = \frac{1}{2} \frac{(\omega_B + \omega_2)}{\omega_B \omega_2 (1 + A_o \beta)} = \frac{(\omega_B + \omega_2)}{2\omega_n^2} \quad (11.158)$$

in which two new parameters have been introduced:  $\zeta$  is called the damping coefficient and  $\omega_n$  is the pole frequency of the system. The natural frequencies of the system are given by

$$p_{1,2} = -\zeta \omega_n \pm j \omega_n \sqrt{1 - \zeta^2} \quad (11.159)$$

There are three cases to consider [9] based upon the value of  $\zeta$ :

- (i) Over damped  $\zeta > 1$  (two real poles):  $p_{1,2} = -\omega_n (\zeta \pm \sqrt{\zeta^2 - 1})$

$$v_{od}(t) = V_F \left\{ 1 - \frac{1}{2\sqrt{\zeta^2 - 1}} \left[ \frac{e^{-\omega_n(\zeta - \sqrt{\zeta^2 - 1})t}}{\zeta - \sqrt{\zeta^2 - 1}} - \frac{e^{-\omega_n(\zeta + \sqrt{\zeta^2 - 1})t}}{\zeta + \sqrt{\zeta^2 - 1}} \right] \right\} \quad \text{and} \quad V_F = \frac{A_o}{1 + A_o \beta} V_i \quad (11.160)$$

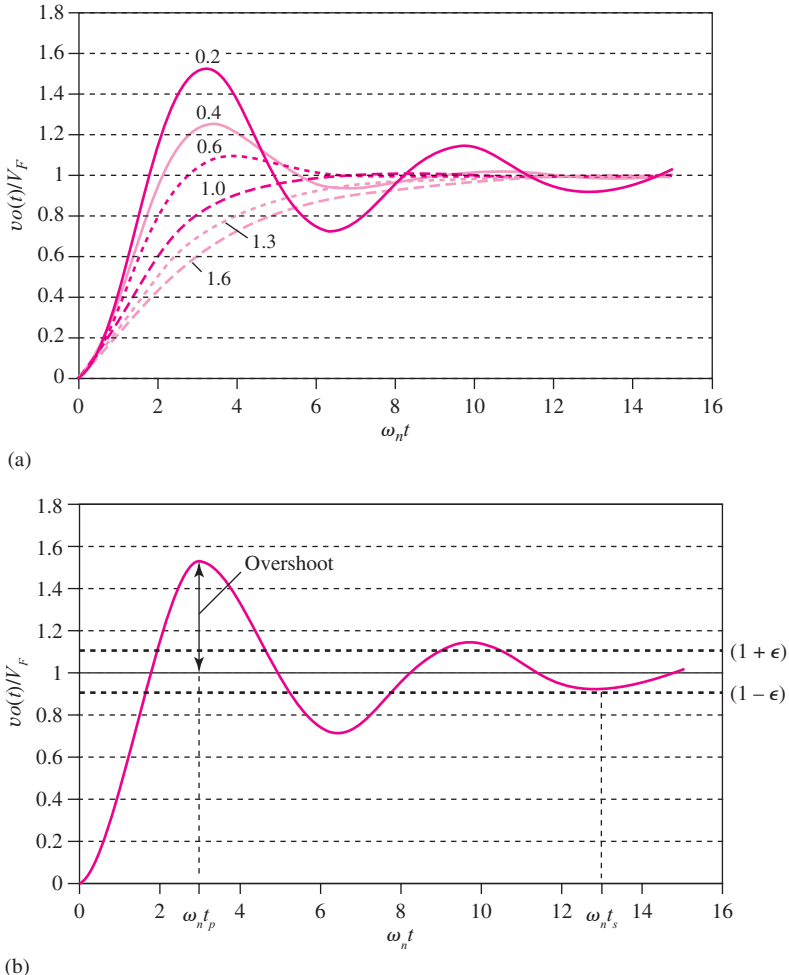


**Figure 11.58** (a) Normalized step response of a second-order system as a function of damping factor  $\zeta$ . (b) Overshoot and settling time for  $\zeta = 0.2$  and  $\epsilon = 0.1$ .

(ii) Critically damped  $\zeta = 1$  (two identical poles):  $p_{1,2} = -\zeta\omega_n$

$$v_{cd}(t) = V_F [1 - (1 + t)\epsilon^{-\zeta\omega_n t}] \quad (11.161)$$

(iii) Under damped  $\zeta > 1$  (complex poles):  $p_{1,2} = -\omega_n\zeta \pm j\omega_n\sqrt{1 - \zeta^2}$

$$v_{ud}(t) = V_F \left[ 1 - \frac{1}{\sqrt{1 - \zeta^2}} \epsilon^{-\zeta\omega_n t} \sin(\sqrt{1 - \zeta^2}\omega_n t + \phi) \right] \quad \phi = \tan^{-1} \left( \frac{\sqrt{1 - \zeta^2}}{\zeta} \right) \quad (11.162)$$

Graphs of the step response of the second-order system<sup>4</sup> as a function of damping factor  $\zeta$  appear in Fig. 11.58(a) with definitions of overshoot and settling time in Fig. 11.58(b). *Overshoot* is a measure of how far the waveform initially exceeds its final value and can be specified as either a fraction or a percentage of final value. The overshoot peaks at time  $t_p$ . In Fig. 11.58(b) for which

<sup>4</sup> Note that for simulations, one must ensure that signals are small enough that the system is behaving linearly and nonlinear slew rate limiting is not occurring in the response.

$\zeta = 0.2$ , the overshoot is 52.7 percent at  $t_p = (3.21/\omega_n)$  seconds.

$$\text{Fractional overshoot} = \frac{\text{Peak value} - \text{Final value}}{\text{Final value}} = \exp\left(-\frac{\pi\zeta}{\sqrt{1-\zeta^2}}\right)$$

$$t_p = \frac{\pi}{\omega_n \sqrt{1-\zeta^2}} \quad (11.163)$$

The time required for the waveform to fall within a given fractional error  $\varepsilon$  of final value is called the *settling time*  $t_s$ . In Fig. 11.58(b), the dashed lines represent 10 percent error bars ( $\varepsilon = 0.1$ ), and the settling time  $t_s$  is slightly less than  $13/\omega_n$  seconds.

An overdamped response ( $\zeta > 1$ ) has no overshoot, but the settling time required to reach within a given error band of final value is the longest. The critically damped response ( $\zeta = 1$ ) has the shortest settling time without overshoot and corresponds to the maximally flat frequency Butterworth response (see Sec. 12.3.1). However, shorter settling time can actually be obtained with an underdamped response ( $\zeta < 1$ ), but the waveform exhibits overshoot and ringing that depend upon damping coefficient  $\zeta$ .

### Unity Gain Frequency and Phase Margin

The phase margin for the system can be found by calculating the unity-gain frequency for the loop gain based upon the transfer function in Eq. (11.157):

$$T(s) = A(s)\beta = \frac{A_o\beta\omega_B\omega_2}{s^2 + s(\omega_B + \omega_2) + \omega_B\omega_2} = \left(\frac{A_o\beta}{1 + A_o\beta}\right) \frac{\omega_n^2}{s^2 + 2\xi\omega_n s + \frac{\omega_n^2}{1+A_o\beta}} \quad (11.164)$$

In order to find the unity-gain frequency for the loop gain, we first must first construct the expression for the magnitude of  $T(j\omega)$  and set it equal to one which yields

$$|T(j\omega_T)| = 1 \Rightarrow \left(\frac{A_o\beta}{1 + A_o\beta}\right)^2 \omega_n^4 = \left(\frac{\omega_n^2}{1 + A_o\beta} - \omega_T^2\right)^2 + 4\xi\omega_n^2\omega_T^2 \quad (11.165)$$

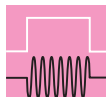
After a considerable amount of algebra [9] and assuming  $A_o\beta \gg 1$ , it can be found that

$$\omega_T = \omega_n \left( \sqrt{4\xi^4 + 1} - 2\xi^2 \right)^{\frac{1}{2}}$$

and

$$\phi_M = \tan^{-1} \frac{2\xi}{\left( \sqrt{4\xi^4 + 1} - 2\xi^2 \right)^{\frac{1}{2}}} = \cos^{-1} \left( \sqrt{4\xi^4 + 1} - 2\xi^2 \right) \quad (11.166)$$

The results in Eqs. (11.163) and (11.166) can be used to relate overshoot, phase margin, and damping coefficient. Sample results appear in Table 11.5. A common design specification is to achieve a minimum phase margin of  $60^\circ$  corresponding to an overshoot of less than 10 percent.



### DESIGN NOTE

A common goal in feedback system design is to achieve a minimum phase margin of  $60^\circ$  that corresponds to an overshoot of less than 10 percent.

**TABLE 11.5**  
Overshoot vs. Phase Margin and Damping Coefficient

OVERSHOOT (%)	PHASE MARGIN ( $^{\circ}$ )	DAMPING COEFFICIENT
1	71	0.83
2	69	0.78
3	67	0.75
5	65	0.69
7	62	0.65
10	59	0.59
20	48	0.46
30	39	0.36
50	24	0.22
70	13	0.11

**EXERCISE:** What damping factor and phase margin is required to achieve an overshoot of no more than 1 percent? How much overshoot will occur with a phase margin of  $45^{\circ}$ ?

**ANSWERS:** 0.826,  $70.9^{\circ}$ ; 23.4 percent

**EXERCISE:** Suppose we desire the amplifier in Fig. 11.58(b) to settle within 10 percent in  $10 \mu\text{sec}$ . What value of  $\omega_n$  is required? If the op amp has  $f_T = 1 \text{ MHz}$  and  $1/\beta = 10$ , what is the value of  $f_2 = \omega_2/2\pi$ ?

**ANSWERS:**  $\geq 1.30 \text{ Mrad/s}$ ;  $\geq 2.69 \text{ MHz}$

### 11.14.5 THIRD-ORDER SYSTEMS AND GAIN MARGIN

Third-order systems described by

$$T(s) = \frac{A_o}{\left(1 + \frac{s}{\omega_1}\right)\left(1 + \frac{s}{\omega_2}\right)\left(1 + \frac{s}{\omega_3}\right)} \beta = \frac{T_o}{\left(1 + \frac{s}{\omega_1}\right)\left(1 + \frac{s}{\omega_2}\right)\left(1 + \frac{s}{\omega_3}\right)} \quad (11.167)$$

can easily have stability problems. Consider the example in Fig. 11.59, for

$$T(s) = \frac{14}{s^3 + s^2 + 3s + 2} \quad (11.168)$$

For this case,  $T(0) = 7$ , and at high frequencies

$$T(j\omega) \cong (-j)^3 \frac{14}{\omega^3} = +j \frac{14}{\omega^3} \quad (11.169)$$

At high frequencies, the polar plot asymptotically approaches zero along the positive imaginary axis, and the plot can enclose the critical  $-1$  point under many circumstances. The particular case in Fig. 11.59 represents an unstable closed-loop system.

**Gain margin** is another important concept and is defined as the reciprocal of the magnitude of  $T(j\omega)$  evaluated at the frequency for which the phase shift is  $180^{\circ}$ :

$$\text{GM} = \frac{1}{|T(j\omega_{180})|} \quad \text{where} \quad \angle T(j\omega_{180}) = -180^{\circ} \quad (11.170)$$

Gain margin is often expressed in dB as  $\text{GM}_{\text{dB}} = 20 \log(\text{GM})$ .

Equation (11.170) is interpreted graphically in Fig. 11.60. If the magnitude of  $T(s)$  is increased by a factor equal to or exceeding the gain margin, then the closed-loop system becomes unstable, because the Nyquist plot then encloses the  $-1$  point.

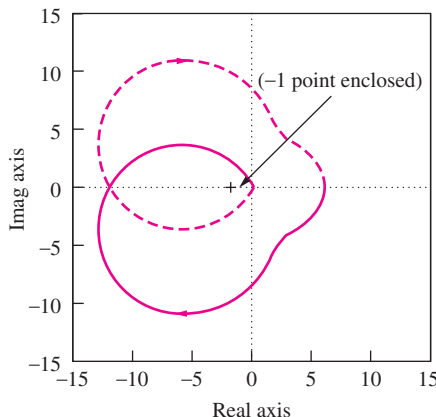


**Figure 11.59** Nyquist plot for third-order  $T(s)$ . (Using MATLAB: `nyquist(14,[1 1 3 2])`.)

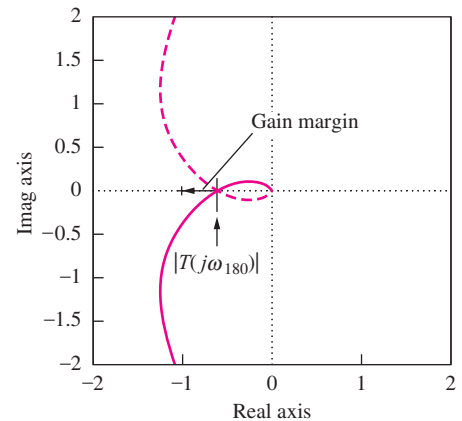


**Figure 11.60** Nyquist plot showing gain margin of a third-order system. (Using MATLAB: `nyquist(5,[1 3 3 1])`.)

**EXERCISE:** Find the gain margin for the system in Fig. 11.60 described by

$$T(s) = \frac{5}{s^3 + 3s^2 + 3s + 1} = \frac{5}{(s+1)^3}$$

**ANSWER:** 4.08 dB

### 11.14.6 DETERMINING STABILITY FROM THE BODE PLOT

Phase and gain margin can also be determined directly from a **Bode plot** of the loop gain, as indicated in Fig. 11.61. This figure represents  $A\beta$  for a third-order transfer function:

$$A\beta = \frac{2 \times 10^{19}}{(s + 10^5)(s + 10^6)(s + 10^7)} = \frac{2 \times 10^{19}}{s^3 + 11.1 \times 10^6 s^2 + 11.1 \times 10^{12} s + 10^{18}}$$

Phase margin is found by first identifying the frequency at which  $|A\beta| = 1$  or 0 dB. For the case in Fig. 11.61, this frequency is approximately  $1.2 \times 10^6$  rad/s. At this frequency, the phase shift is  $-145^\circ$ , and the phase margin is  $\Phi_M = 180^\circ - 145^\circ = 35^\circ$ . The amplifier can tolerate an additional phase shift of approximately  $35^\circ$  before it becomes unstable.

Gain margin is found by identifying the frequency at which the phase shift of the amplifier is exactly  $180^\circ$ . In Fig. 11.61, this frequency is approximately  $3.2 \times 10^6$  rad/s. The loop gain at this frequency is  $-17$  dB, and the gain margin is therefore  $+17$  dB. The gain must increase by 17 dB before the amplifier becomes unstable.

Using a tool like MATLAB, we can easily construct the Bode plot for the gain of the amplifier and use it to determine the range of closed-loop gains for which the amplifier will be stable. Stability can be determined by properly interpreting the Bode magnitude plot. We use this mathematical approach:

$$20 \log |A\beta| = 20 \log |A| - 20 \log \left| \frac{1}{\beta} \right| \quad (11.171)$$

Rather than plotting the loop gain  $A\beta$  itself, the magnitude of the open-loop gain  $A$  and the reciprocal of the feedback factor  $\beta$  are plotted separately. (Remember,  $A_v \cong 1/\beta$ .) The frequency at which these two curves intersect is the point at which  $|A\beta| = 1$ , and the phase margin of the closed-loop amplifier can easily be determined from the phase plot.

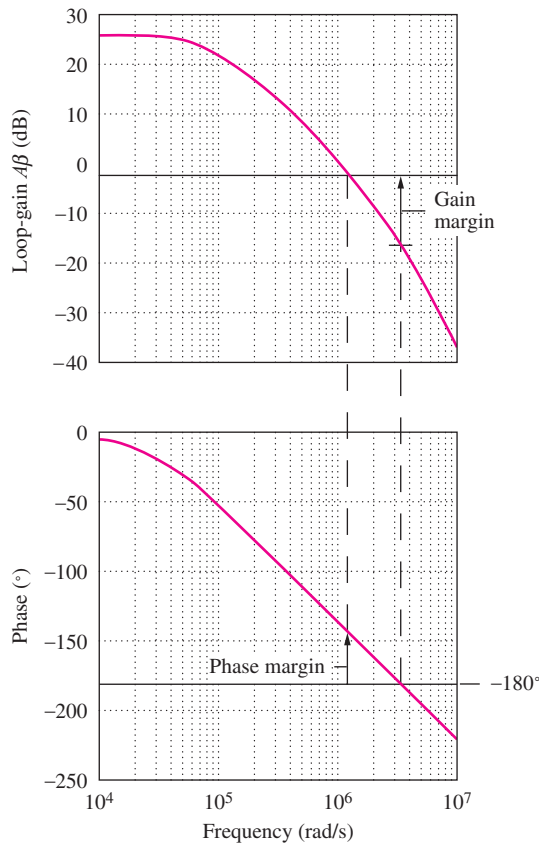


**Figure 11.61** Phase and gain margin on the Bode plot. (Graph plotted using MATLAB: bode(2E19, [1 11.1E6 11.1 E12 1E18]).)

Let us use the Bode plot in Fig. 11.62 as an example. In this case,

$$A(s) = \frac{2 \times 10^{24}}{(s + 10^5)(s + 3 \times 10^6)(s + 10^8)} \quad (11.172)$$

The asymptotes from Eq. (11.172) have also been included on the graph. For simplicity in this example, we assume that the feedback is independent of frequency (for example, a resistive voltage divider) so that  $1/\beta$  is a straight line.

Three closed-loop gains are indicated. For the largest closed-loop gain,  $(1/\beta) = 80$  dB, the phase margin is approximately  $85^\circ$ , and stability is not a problem. The second case corresponds to a closed-loop gain of 50 dB and has a phase margin of only  $15^\circ$ . Although stable, the amplifier operating at a closed-loop gain of 50 dB exhibits significant overshoot and “ringing” in its step response. Finally, if an attempt is made to use the amplifier as a unity gain voltage follower, the amplifier will be unstable (negative phase margin). We see that the phase margin is zero for a closed-loop gain of approximately 35 dB.

Relative stability can be inferred directly from the magnitude plot. If the graphs of  $A$  and  $1/\beta$  intersect at a “rate of closure” of 20 dB/decade, then the amplifier will be stable. However, if the two curves intersect in a region of 40 dB/decade, then the closed-loop amplifier will have poor phase margin (in the best case) or be unstable (in the worst case). Finally, if the rate of closure is 60 dB or greater, the closed-loop system will be unstable. The closure rate criterion is equally applicable to frequency-dependent feedback as well.

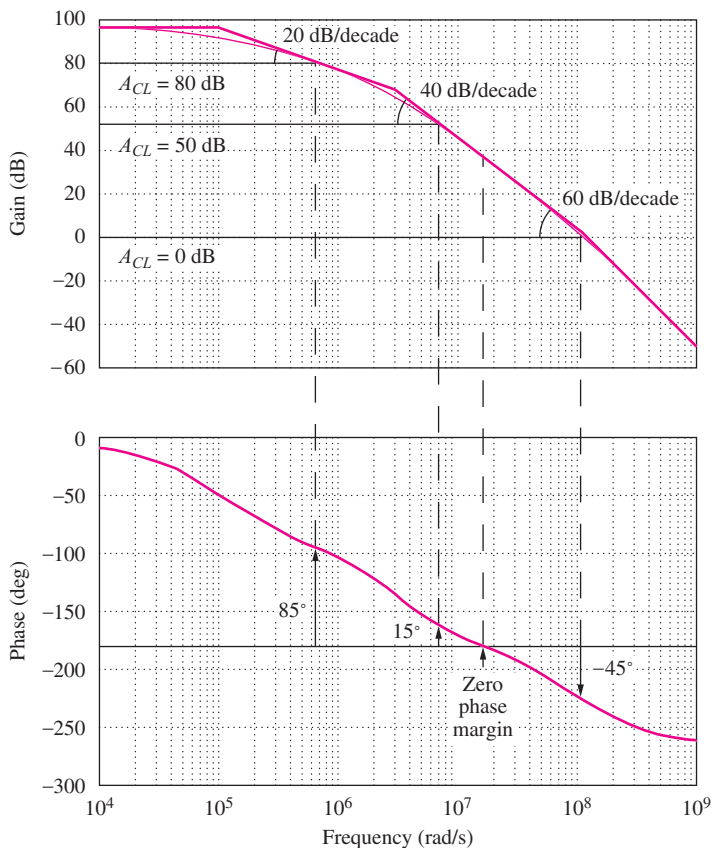


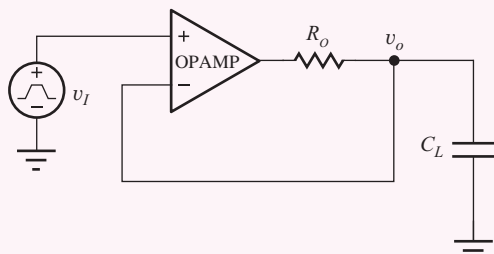
**Figure 11.62** Determining stability from the Bode magnitude plot. Three values of closed-loop gain are indicated: 80 dB, 50 dB, and 0 dB. The corresponding phase margins are 85°, 15° (ringing and overshoot), and -45° (unstable). (Graph plotted using MATLAB: bode(2E24,[1 103.1E6 310.3E12 30E18]).)

### EXAMPLE 11.17 PHASE MARGIN ANALYSIS

Even single-pole op amps can exhibit phase margin problems when driving heavy capacitive loads. This example evaluates the phase margin of the voltage follower with a large load capacitance connected to the output.

**PROBLEM** Find the phase margin for a voltage follower that is driving a  $0.01 \mu\text{F}$  capacitive load. Assume the op amp has an open-loop gain of 100 dB, an  $f_T$  of 1 MHz, and an output resistance of  $250 \Omega$ .

**SOLUTION** **Known Information and Given Data:** The voltage follower with load capacitor  $C_L$  and output resistance  $R_O$  added is drawn in the figure. For the op amp:  $A_o = 100 \text{ dB}$ ,  $f_T = 1 \text{ MHz}$ ,  $C_L = 0.01 \mu\text{F}$  and  $R_o = 250 \Omega$ .



Voltage follower with output resistance and capacitive load.

**Unknowns:** Phase margin for the closed-loop amplifier

**Approach:** Find an expression for the loop gain  $T$ , find the frequency for which  $|T| = 1$ , evaluate the phase at this frequency, and compare it to  $180^\circ$ .

**Assumptions:** The op amp is ideal except for  $A_o$ ,  $f_T$ , and  $R_o$ .

**Analysis:** For the op amp,  $f_B = f_T/A_o = 10^6/10^5 = 10$  Hz.

$$T(s) = A(s)\beta(s) = \frac{A_o}{1 + \frac{s}{\omega_B}} \cdot \frac{1}{1 + sR_oC_L} = \frac{10^5}{1 + \frac{s}{20\pi}} \cdot \frac{1}{1 + \frac{s}{4 \times 10^5}}$$

$$|T(j\omega)| = \frac{10^5}{\sqrt{1 + \left(\frac{\omega}{20\pi}\right)^2} \sqrt{1 + \left(\frac{\omega}{4 \times 10^5}\right)^2}} \quad \angle T(j\omega) = -\tan^{-1}\left(\frac{\omega}{20\pi}\right) - \tan^{-1}\left(\frac{\omega}{4 \times 10^5}\right)$$

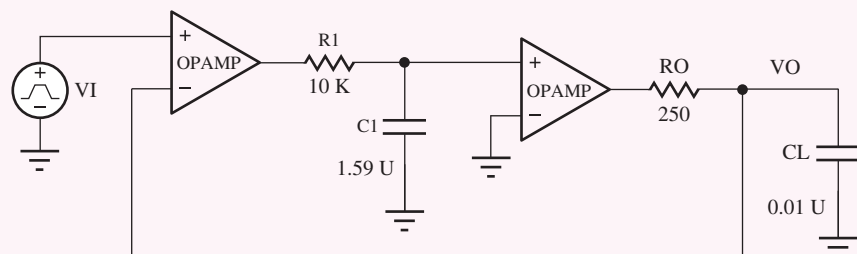
Solving for  $|T(j\omega)| = 1$  using a calculator or spreadsheet yields  $f = 248$  kHz ( $\omega = 1.57$  Mrad/s) and  $\angle T = -166^\circ$ . Thus the phase margin is only  $180^\circ - 166^\circ = 34^\circ$ .

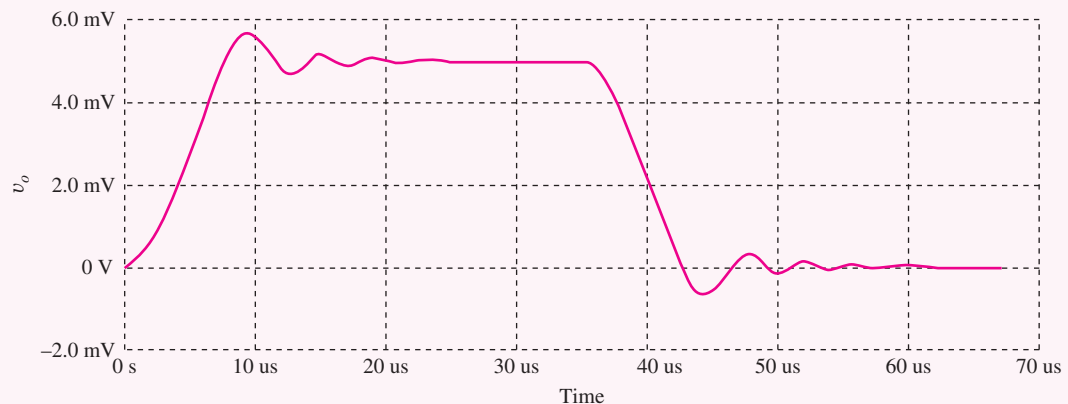
**Check of Results:** We have found the phase margin to be only  $34^\circ$ .

**Discussion:** A second pole is added to the system by the break between the load capacitance and op amp output resistance. Thus the overall feedback amplifier becomes a second-order system, and although it will not oscillate, the phase margin can be poor, and the step response may exhibit overshoot and ringing. Unfortunately, a real op amp has additional poles that can further degrade the phase margin and increase the possibility of oscillation. We can explore this issue further with SPICE simulation.

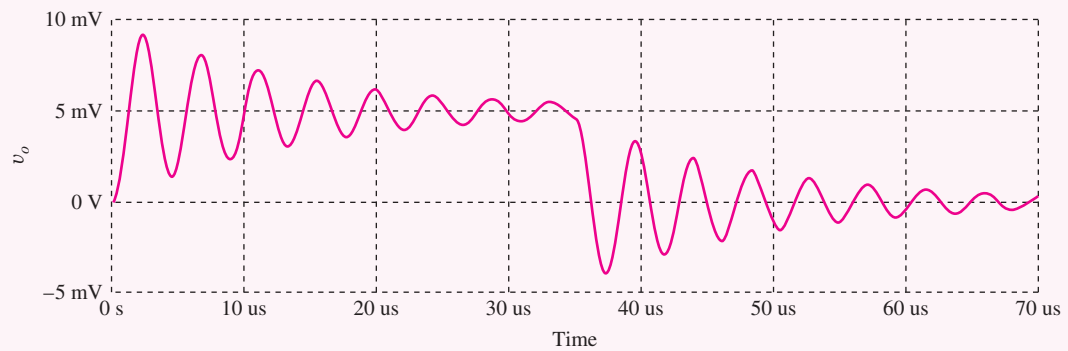
**Computer-Aided Analysis:** First we need to create a simulation model that reflects our analysis. One possibility that employs two op amps is given below. The first op amp is an ideal amplifier with 100 dB gain.  $R_1$  and  $C_1$  are added to model the single op amp pole at 10 Hz, and this “dummy network” is buffered from the output by a second amplifier with its gain set to 1.  $R_o$  and  $C_L$  complete the circuit. A small-signal pulse input with an amplitude of 5mV, a pulse width of 35  $\mu$ s, a period of 70  $\mu$ s, and rise and fall times of 10 ns is used so only a relatively short simulation time is needed.

In the simulated waveform, we observe more than 10 percent overshoot and ringing, and the output takes approximately 30  $\mu$ s to settle to its final value. If we repeat the simulation with the original circuit utilizing a single  $\mu$ A741 op amp, we find the real situation is much worse than our simple model predicts because the  $\mu$ A741 actually contains additional poles at high frequency.





Step response of the circuit model that corresponds to our mathematical analysis.



Simulation results of the original circuit using the  $\mu$ A741 op amp macro model in SPICE.

**EXERCISE:** Estimate the overshoot and calculate the phase margin for simulations in the two figures above.

**ANSWERS:** 14 percent,  $54^\circ$ ; 85 percent,  $6^\circ$

**EXERCISE:** Repeat the simulation to see what happens if the pulse amplitude is changed to 1 V. Explain what you see.

## SUMMARY

The ideal operational amplifier was introduced previously in Chapter 10. Chapter 11 discussed removal of the ideal op amp assumptions, and quantified the effects and limitations caused by the nonideal op amp behavior. The nonideal behavior considered included:

- Finite open-loop gain
- Finite differential-mode input resistance
- Nonzero output resistance

- Offset voltage
  - Input bias and offset currents
  - Limited output voltage range
  - Limited output current capability
  - Finite common-mode rejection
  - Finite common-mode input resistance
  - Finite power supply rejection
  - Limited bandwidth
  - Limited slew rate
- The effect of removing the various ideal operational amplifier assumptions was explored in detail. Expressions were developed for the gain, gain error, input resistance, and output resistance of the closed-loop inverting and noninverting amplifiers, and it was found that the loop gain  $T = A\beta$  plays an important role in determining the value of these closed-loop amplifier parameters.
  - Series and shunt feedback are used to tailor and stabilize the characteristics of feedback amplifiers. Series feedback places the amplifier and feedback network in series and increases the overall impedance level at the series-connected port by  $1 + T$ . Shunt feedback is achieved by placing the amplifier and feedback network in parallel and decreases the impedance level at the shunt-connected port by  $1 + T$ .
  - Feedback amplifiers are placed in four categories based upon the type of feedback utilized at the input and output of the amplifier:
    - Voltage amplifiers utilize series-shunt feedback to achieve high input impedance and low output impedance.
    - Current amplifiers utilize shunt-series feedback to achieve low input impedance and high output impedance.
    - Transresistance amplifiers utilize shunt-shunt feedback to achieve low input impedance and low output impedance.
    - Transconductance amplifiers utilize series-series feedback to achieve high input impedance and high output impedance.
  - The loop gain  $T(s)$  plays an important role in determining the characteristics of feedback amplifiers. For theoretical calculations, the loop gain can be found by breaking the feedback loop at some arbitrary point and directly calculating the voltage returned around the loop. However, both sides of the loop must be properly terminated before the loop-gain calculation is attempted.
  - To find  $T$  in circuits employing op amps, it is convenient to disable the feedback loop by setting  $v_{id} = 1$  V in the controlled source in the model for the op amp (i.e.,  $A_o v_{id} = A_o(1)$ ) and then calculate the value of the  $v_{id}$  that appears at the op amp input.
  - When using SPICE or making experimental measurements, it is often impossible to break the feedback loop. The method of successive voltage and current injection is a powerful technique for determining the loop gain without the need for opening the feedback loop.
  - Whenever feedback is applied to an amplifier, stability becomes a concern. In most cases, a negative or degenerative feedback condition is desired. Stability can be determined by studying the characteristics of the loop gain  $T(s) = A(s)\beta(s)$  of the feedback amplifier as a function of frequency, and stability criteria can be evaluated from either Nyquist diagrams or Bode plots.
  - In the Nyquist case, stability requires that the plot of  $T(j\omega)$  not enclose the  $T = -1$  point.

- On the Bode plot, the asymptotes of the magnitudes of  $A(j\omega)$  and  $1/\beta(j\omega)$  must not intersect with a rate of closure exceeding 20 dB/decade.
- Phase margin and gain margin, which can be found from either the Nyquist or Bode plot, are important measures of stability.
- Phase margin determines the percentage overshoot in the step response of a second-order feedback system. Systems are typically designed to have at least a 60° phase margin.
- The dc error sources, including offset voltage, bias current, and offset current, all limit the dc accuracy of op amp circuits. Real op amps also have limited output voltage and current ranges as well as a finite rate of change of the output voltage called the slew rate. Circuit design options are constrained by these factors.
- The frequency response of basic single-pole operational amplifiers is characterized by two parameters: the open-loop gain  $A_o$  and the gain-bandwidth product  $\omega_T$ . Analysis of the gain and bandwidth of the inverting and noninverting amplifier configurations demonstrated the direct tradeoff between the closed-loop gain and the closed-loop bandwidth of these amplifiers. The gain-bandwidth product is constant, and the closed-loop gain must be reduced in order to increase the bandwidth, or vice versa.
- Simplified macro models are often used for simulation of circuits containing op amps. Simple macro models can be constructed in SPICE using controlled sources, and most SPICE libraries contain comprehensive macro models for a wide range of commercial operational amplifiers.

## KEY TERMS

Bandwidth (BW)	Noninverting amplifier
Bias	Nyquist plot
Bode plot	Open-loop amplifier
Closed-loop gain	Open-loop gain
Closed-loop input resistance	Phase margin
Closed-loop output resistance	Series-series feedback
Decibel (dB)	Series-shunt feedback
Feedback amplifier stability	Short-circuit termination
Feedback network	Shunt-series feedback
Gain-bandwidth product	Shunt connection
Gain margin (GM)	Shunt-shunt feedback
Ideal voltage amplifier	Stability
Input resistance ( $R_{in}$ )	Successive voltage and current injection
Inverting amplifier	Total harmonic distortion
Linear amplifier	Transfer function
Loop gain	Transconductance amplifier
Low-pass amplifier	Transresistance amplifier
Midband gain	Two-port network
–1 Point	Upper-cutoff frequency
Negative feedback	Voltage amplifier

## REFERENCES

1. H. S. Black, “Stabilized feed-back amplifiers,” *Electrical Engineering*, vol. 53, pp. 114–120, Jan. 1934.
2. Harold S. Black, “Inventing the negative feedback amplifier,” *IEEE Spectrum*, vol. 14, pp. 54–60, Dec. 1977. (50th anniversary of Black’s invention of negative feedback amplifier).
3. J. E. Brittain, “Scanning the past: Harold S. Black and the negative feedback amplifier,” *Proc. IEEE*, vol. 85, no. 8, pp. 1335–1336, Aug. 1997.

4. R. B. Blackman, "Effect of feedback on impedance," *Bell System Technical Journal*, vol. 22, no. 3, 1943.
5. R. D. Middlebrook, "Measurement of loop gain in feedback systems," *International Journal of Electronics*, vol. 38, no. 4, pp. 485–512, April 1975. Middlebrook credits a 1965 Hewlett-Packard Application Note as the original source of this technique.
6. R. C. Jaeger, S. W. Director, and A. J. Brodersen, "Computer-aided characterization of differential amplifiers," *IEEE JSSC*, vol. SC-12, pp. 83–86, February 1977.
7. P. J. Hurst, "A comparison of two approaches to feedback circuit analysis," *IEEE Trans. on Education*, vol. 35, pp. 253–261, August 1992.
8. F. Corsi, C. Marzocca, and G. Matarrese, "On impedance evaluation in feedback circuits," *IEEE Trans. on Education*, vol. 45, no. 4, pp. 371–379, November 2002.
9. P. E. Allen and D. R. Holberg, *CMOS Analog Circuit Design*, 2nd ed., Oxford University Press, New York:2002.

## PROBLEMS

### 11.1 Classic Feedback Systems

- 11.1. The classic feedback amplifier in Fig. 11.1 has  $\beta = 0.2$ . What are the loop gain  $T$ , ideal closed-loop gain  $A_v^{\text{ideal}}$ , actual closed-loop gain  $A_v$ , and the fractional gain error FGE if (a)  $A = \infty$ ? (b)  $A = 84 \text{ dB}$ ? (c)  $A = 20$ ?
- 11.2. A voltage follower's closed-loop voltage gain  $A_v$  is described by Eq. (11.4). (a) What is the minimum value of loop gain  $T$  required if the gain error is to be less than 0.01 percent for a voltage follower? (b) What value of open-loop gain  $A$  is required in the amplifier?
- 11.3. A amplifier's closed-loop voltage gain  $A_v$  is described by Eq. (11.4). What is the minimum value of loop gain  $T$  required if the gain error is to be less than 0.2 percent for an ideal gain of 46 dB?
- 11.4. (a) Calculate the sensitivity of the closed-loop gain  $A_v$  with respect to changes in open-loop gain  $A$ ,  $S_A^{A_v}$ , using Eq. (11.4) and the definition of sensitivity given below:

$$S_A^{A_v} = \frac{A}{A_v} \frac{\partial A_v}{\partial A}$$

(b) Use this formula to estimate the percentage change in closed-loop gain if the open-loop gain  $A$  changes by 10 percent for an amplifier with  $A = 100 \text{ dB}$  and  $\beta = 0.01$ .

### 11.2 Nonideal Op-Amp Circuits

- 11.5. A noninverting amplifier is built with  $R_1 = 12 \text{ k}\Omega$  and  $R_2 = 150 \text{ k}\Omega$  using an op amp with an open-

loop gain of 86 dB. What are the closed-loop gain, the gain error, and the fractional gain error for this amplifier? (b) Repeat if  $R_1$  is changed to  $1.2 \text{ k}\Omega$ .

- 11.6. A noninverting amplifier is built with  $R_2 = 47 \text{ k}\Omega$  and  $R_1 = 5.6 \text{ k}\Omega$  using an op amp with an open-loop gain of 100 dB. What are the closed-loop gain, the gain error, and the fractional gain error for this amplifier? (b) Repeat if the open-loop gain is changed to 94 dB.
- 11.7. (a) What value of open-loop gain  $A$  is required of the amplifier in Prob. 11.3 if the amplifier is a noninverting amplifier? (b) If the amplifier is an inverting amplifier?
- 11.8. The feedback amplifier in Fig. P11.8(a) has  $R_1 = 1 \text{ k}\Omega$ ,  $R_2 = 100 \text{ k}\Omega$ ,  $R_f = 0$ , and  $R_L = 10 \text{ k}\Omega$ . (a) What is  $\beta$ ? (b) If  $A = 86 \text{ dB}$ , what are the loop gain  $T$  and the closed loop gain  $A_v$ ? (c) What are the values of GE and FGE?
- 11.9. An inverting amplifier is built with  $R_1 = 22 \text{ k}\Omega$  and  $R_2 = 220 \text{ k}\Omega$  using an op amp with an open-loop gain of 92 dB. What are the closed-loop gain, the gain error, and fractional gain error for this amplifier? (b) Repeat if  $R_1$  is changed to  $1.1 \text{ k}\Omega$ .
- 11.10. The inverting amplifier in Fig. 11.3 is implemented with an op amp with finite gain  $A = 80 \text{ dB}$ . If  $R_1 = 1 \text{ k}\Omega$  and  $R_2 = 100 \text{ k}\Omega$ , what are  $\beta(s)$ ,  $T(s)$ , and  $A_v(s)$ ?
- 11.11. An inverting amplifier is built with  $R_2 = 47 \text{ k}\Omega$  and  $R_1 = 4.7 \text{ k}\Omega$  using an op amp with an open-loop gain of 94 dB. What are the closed-loop gain, the gain error, and fractional gain error for this

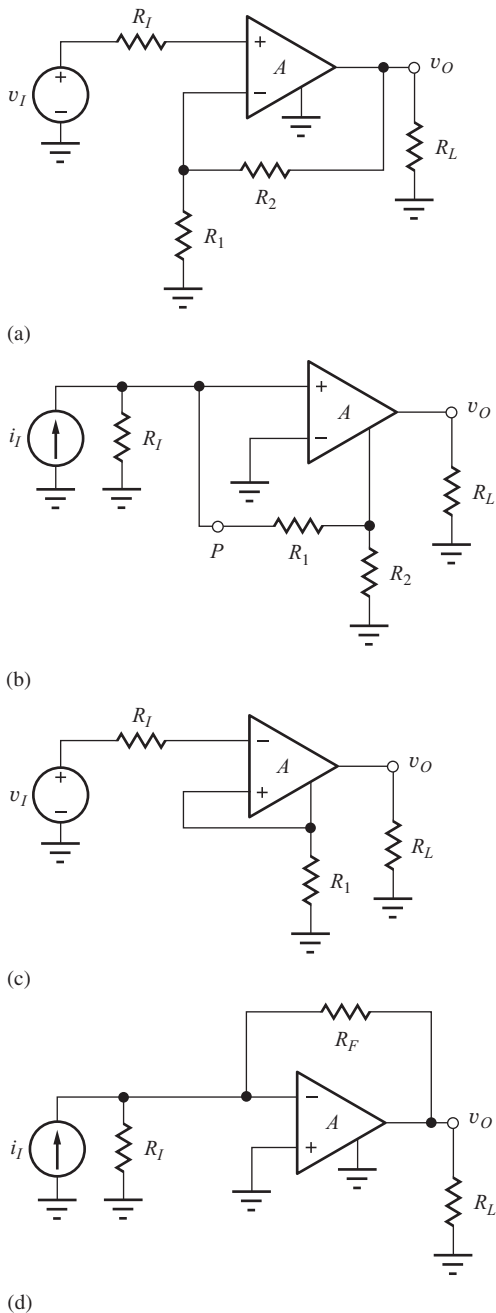


**Figure P11.8** For each amplifier  $A$ :  $A_o = 4000$ ,  $R_{id} = 20 \text{ k}\Omega$ ,  $R_o = 1 \text{ k}\Omega$ .

amplifier? (b) Repeat if the open-loop gain is changed to 100 dB.

- 11.12. A noninverting amplifier is being designed to have a closed-loop gain of 36 dB. What op-amp gain is required to have the gain error less than 0.2 percent?

- 11.13. An inverting amplifier is being built with a closed-loop gain of 43 dB. What op amp gain is required to have the gain error below 0.1 percent?
- 11.14. A noninverting amplifier is built with 0.01 percent precision resistors and designed with  $R_2 = 99R_1$ . What are the nominal and worst-case values of voltage gain if the op amp is ideal? What open-loop gain is required for the op amp if the gain-error due to finite op amp gain is to be less than 0.01 percent?
- 11.15. Repeat the derivation of the output resistance in Fig. 11.5 using a test current source rather than a test voltage source.
- 11.16. Calculate the currents  $i_1$ ,  $i_2$ , and  $i_-$  for the amplifier in Fig. 11.6 if  $v_x = 0.1 \text{ V}$ ,  $R_1 = 1 \text{ k}\Omega$ ,  $R_2 = 47 \text{ k}\Omega$ ,  $R_{id} = 1 \text{ M}\Omega$ , and  $A = 10^5$ . What is  $i_+$ ?
- 11.17. A noninverting amplifier is built with  $R_1 = 12 \text{ k}\Omega$  and  $R_2 = 150 \text{ k}\Omega$  using an op amp with an open-loop gain of 86 dB, an input resistance of 200 k $\Omega$ , and an output resistance of 200  $\Omega$ . What are the closed-loop gain, input resistance, and output resistance for this amplifier? (b) Repeat if  $R_1$  is changed to 1.2 k $\Omega$ .
- 11.18. A noninverting amplifier is built with  $R_2 = 47 \text{ k}\Omega$  and  $R_1 = 5.6 \text{ k}\Omega$  using an op amp with an open-loop gain of 100 dB, an input resistance of 500 k $\Omega$ , and an output resistance of 300  $\Omega$ . What are the closed-loop gain, input resistance, and output resistance for this amplifier? (b) Repeat if the open-loop gain is changed to 94 dB.
- 11.19. An inverting amplifier is built with  $R_2 = 47 \text{ k}\Omega$  and  $R_1 = 2.7 \text{ k}\Omega$  using an op amp with an open-loop gain of 100 dB, an input resistance of 300 k $\Omega$ , and an output resistance of 200  $\Omega$ . What are the closed-loop gain, input resistance, and output resistance for this amplifier? (b) Repeat if the open-loop gain is changed to 94 dB.
- 11.20. An inverting amplifier is built with  $R_2 = 47 \text{ k}\Omega$  and  $R_1 = 4.7 \text{ k}\Omega$  using an op amp with an open-loop gain of 94 dB, an input resistance of 500 k $\Omega$ , and an output resistance of 200  $\Omega$ . What are the closed-loop gain, input resistance, and output resistance for this amplifier? (b) Repeat if the open-loop gain is changed to 100 dB.
- 11.21. An op amp has  $R_{id} = 500 \text{ k}\Omega$ ,  $R_o = 35 \Omega$ , and  $A = 5 \times 10^4$ . You must decide if a single-stage amplifier can be built that meets all of the specifications below. (a) Which configuration (inverting or non-inverting) must be used and why? (b) Assume that the gain specification must be met and show which

of the other specifications can or cannot be met.

$$|A_v| = 200 \quad R_{in} \geq 2 \times 10^8 \Omega \quad R_{out} \leq 0.2 \Omega$$

- 11.22. An op amp has  $R_{id} = 1 \text{ M}\Omega$ ,  $R_o = 100 \Omega$ , and  $A = 1 \times 10^4$ . Can a single-stage amplifier be built with this op amp that meets all of the following specifications? Show which specifications can be met and which cannot.

$$|A_v| = 200 \quad R_{in} \geq 10^8 \Omega \quad R_{out} \leq 0.2 \Omega$$

- 11.23. The overall amplifier circuit in Fig. P11.23 is a two-terminal network.  $R_1 = 6.8 \text{ k}\Omega$  and  $R_2 = 110 \text{ k}\Omega$ . What is its Thévenin equivalent circuit if the operational amplifier has  $A = 5 \times 10^4$ ,  $R_{id} = 1 \text{ M}\Omega$ , and  $R_o = 250 \Omega$ ? What is its Norton equivalent?

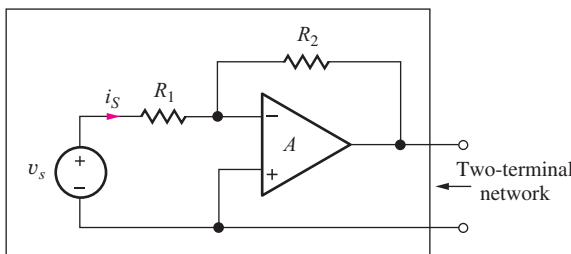


Figure P11.23

- 11.24. The circuit in Fig. P11.24 is a two-terminal network.  $R_1 = 390 \Omega$  and  $R_2 = 56 \text{ k}\Omega$ . What is its Thévenin equivalent circuit if the operational amplifier has  $A = 1 \times 10^4$ ,  $R_{id} = 250 \text{ k}\Omega$ , and  $R_o = 250 \Omega$ ?

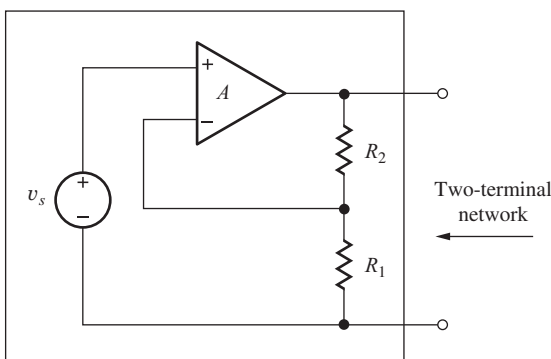


Figure P11.24

- 11.25. A noninverting amplifier is to be designed to have a closed-loop gain of 54 dB. The only op amp that is available has an open-loop gain of 40,000. What must be the tolerance of the feedback resistors if the total gain error must be  $\leq 2$  percent? Assume that the resistors all have the same tolerances.
- 11.26. An inverting amplifier is to be designed to have a closed-loop gain of 60 dB. The only op amp that is available has an open-loop gain of 106 dB.

What is the tolerance of the feedback resistors if the total gain error must be  $\leq 1$  percent? Assume that the resistors all have the same tolerances.

### 11.3–11.4 Feedback Amplifier Characterization

- 11.27. Identify the type of negative feedback that should be used to achieve these design goals: (a) high input resistance and high output resistance, (b) low input resistance and high output resistance, (c) low input resistance and low output resistance, (d) high input resistance and low output resistance.
- 11.28. Identify the type of feedback being used in the four circuits in Fig. P11.8.
- 11.29. Of the four circuits in Fig. P11.8, which tend to provide a high input resistance? (b) Which provide a relatively low input resistance?
- 11.30. Of the four circuits in Fig. P11.8, which tend to provide a high output resistance? (b) Which provide a relatively low output resistance?
- 11.31. An amplifier has an open-loop voltage gain of 90 dB,  $R_{id} = 40 \text{ k}\Omega$ , and  $R_o = 1000 \Omega$ . The amplifier is used in a feedback configuration with a resistive feedback network. (a) What is the largest value of input resistance that can be achieved in the feedback amplifier? (b) What is the smallest value of input resistance that can be achieved? (c) What is the largest value of output resistance that can be achieved? (d) What is the smallest value of output resistance that can be achieved?
- 11.32. An amplifier has an open-loop voltage gain of 90 dB,  $R_{id} = 40 \text{ k}\Omega$ , and  $R_o = 1000 \Omega$ . The amplifier is used in a feedback configuration with a resistive feedback network. (a) What is the largest current gain that can be achieved with this feedback amplifier? (b) What is the largest transconductance that can be achieved with this feedback amplifier?

### 11.5 Voltage Amplifiers—Series-Shunt Feedback

- 11.33. For the circuit in Fig. P11.8(a) find the voltage gain, input resistance, and output resistance of the feedback amplifier. Assume  $R_I = 1 \text{ k}\Omega$ ,  $R_L = 5 \text{ k}\Omega$ ,  $R_1 = 5 \text{ k}\Omega$ , and  $R_2 = 45 \text{ k}\Omega$ .
- 11.34. (a) Find the closed-loop gain for the circuit in Fig. P11.8(a) if  $R_L = 5.6 \text{ k}\Omega$ ,  $R_1 = 4.3 \text{ k}\Omega$ ,  $R_2 = 39 \text{ k}\Omega$ , and  $R_I = 1 \text{ k}\Omega$ .
- 11.35. An op-amp-based noninverting amplifier has  $R_1 = 15 \text{ k}\Omega$ ,  $R_2 = 30 \text{ k}\Omega$ , and  $R_L = 20 \text{ k}\Omega$ . The op

amp has an open-loop gain of 94 dB, an input resistance of 30 k $\Omega$ , and an output resistance of 5 k $\Omega$ . Find the loop gain, ideal voltage gain, actual voltage gain, input resistance, and output resistance for the feedback amplifier.

- 11.36. Find the loop gain, ideal voltage gain, actual voltage gain, input resistance, and output resistance for the feedback amplifier in Ex. 11.5 if a 2-k $\Omega$  load resistor is connected to the output of the amplifier.
- 11.37. (a) Calculate the sensitivity of the closed-loop input resistance of the series-shunt feedback amplifier with respect to changes in open-loop gain  $A$ :

$$S_A^{R_{\text{in}}} = \frac{A}{R_{\text{in}}} \frac{\partial R_{\text{in}}}{\partial A}$$

(b) Use this formula to estimate the percentage change in closed-loop input resistance if the open-loop gain  $A$  changes by 10 percent for an amplifier with  $A = 94$  dB and  $\beta = 0.01$ . (c) Calculate the sensitivity of the closed-loop output resistance of the series-shunt feedback amplifier with respect to changes in open-loop gain  $A$ :

$$S_A^{R_{\text{out}}} = \frac{A}{R_{\text{out}}} \frac{\partial R_{\text{out}}}{\partial A}$$

(d) Use this formula to estimate the percentage change in closed-loop output resistance if the open-loop gain  $A$  changes by 10 percent for an amplifier with  $A = 100$  dB and  $\beta = 0.01$ .

## 11.6 Transresistance Amplifiers—Shunt-Shunt Feedback

- 11.38. Find the loop gain, ideal transresistance, actual transresistance, input resistance, and output resistance for the feedback amplifier in Fig. P11.8(d) with  $R_I = 100$  k $\Omega$ ,  $R_L = 10$  k $\Omega$ , and  $R_F = 10$  k $\Omega$ .
- 11.39. Simulate the amplifier in Prob. 11.38 using SPICE and compare the results to hand calculations.
- 11.40. Find the loop gain, ideal transresistance, actual transresistance, input resistance, and output resistance for the feedback amplifier in Fig. P11.8(d) with  $R_I = 100$  k $\Omega$ ,  $R_L = 5$  k $\Omega$ , and  $R_F = 36$  k $\Omega$ .
- 11.41. Simulate the amplifier in Prob. 11.40 using SPICE and compare the results to hand calculations.
- 11.42. An op-amp-based inverting amplifier has  $R_1 = 15$  k $\Omega$ ,  $R_2 = 30$  k $\Omega$ , and  $R_L = 20$  k $\Omega$ . The op amp has an open-loop gain of 94 dB, an input resistance of 30 k $\Omega$ , and an output resistance of 5 k $\Omega$ . Find the loop gain, ideal voltage gain, actual voltage gain,

input resistance, and output resistance for the feedback amplifier.

## 11.7 Transconductance Amplifiers—Series-Series Feedback

- 11.43. Find the loop gain, ideal transconductance, actual transconductance, input resistance, and output resistance for the feedback amplifier in Fig. P11.8(c) with  $R_I = 15$  k $\Omega$ ,  $R_L = 5$  k $\Omega$ , and  $R_1 = 10$  k $\Omega$ .
- 11.44. Simulate the amplifier in Prob. 11.43 using SPICE and compare the results to hand calculations.
- 11.45. Find the loop gain, ideal transconductance, actual transconductance, input resistance, and output resistance for the feedback amplifier in Fig. P11.8(c) with  $R_I = 15$  k $\Omega$ ,  $R_L = 10$  k $\Omega$ , and  $R_1 = 3$  k $\Omega$ .
- 11.46. Simulate the amplifier in Prob. 11.45 using SPICE and compare the results to hand calculations.
- 11.47. Find the loop gain, ideal transconductance, actual transconductance, input resistance, and output resistance for the feedback amplifier in Ex. 11.7 if a load resistance  $R_L = 5$  k $\Omega$  is connected to the amplifier in place of  $v_o$  in Fig. 11.18.
- 11.48. Find an expression for the loop gain of the low-pass filter in Fig. 10.32 assuming the amplifier has a finite gain  $A_o$ . Show that the gain expression in Eq. (10.95) can be written in the form

$$A_v = A_v^{\text{ideal}} \frac{T}{1 + T}.$$

- 11.49. The integrator in Fig. 10.34 is implemented with an op amp with finite gain  $A = 80$  dB. If  $R = 20$  k $\Omega$  and  $C = 0.01$   $\mu\text{F}$ , what are  $T(s)$  and  $A_v(s)$ ?
- 11.50. The differentiator in Fig. 10.35 is implemented with an op amp with finite gain  $A = 80$  dB. If  $R = 20$  k $\Omega$  and  $C = 0.01$   $\mu\text{F}$ , what are  $T(s)$  and  $A_v(s)$ ?
- 11.51. Find an expression for the loop gain of the integrator in Fig. 10.34 assuming the amplifier has a finite gain  $A_o$ . Show that the integrator voltage gain expression can be written in the form

$$A_v = A_v^{\text{ideal}} \frac{T}{1 + T}.$$

- 11.52. Find an expression for the loop gain of the high-pass filter in Fig. 10.33 assuming the amplifier has a finite gain  $A_o$ . Show that the high-pass filter voltage gain expression can be written in the form

$$A_v = A_v^{\text{ideal}} \frac{T}{1 + T}.$$

## 11.8 Current Amplifiers—Shunt-Series Feedback

- 11.53. Find the loop gain, ideal current gain, actual current gain, input resistance, and output resistance for the feedback amplifier in Fig. P11.8(b) with  $R_I = 150 \text{ k}\Omega$ ,  $R_L = 5 \text{ k}\Omega$ ,  $R_1 = 10 \text{ k}\Omega$  and  $R_2 = 1 \text{ k}\Omega$ .
- 11.54. Simulate the amplifier in Prob. 11.43 using SPICE and compare the results to hand calculations.
- 11.55. Find the loop gain, ideal current gain, actual current gain, input resistance, and output resistance for the feedback amplifier in Fig. P11.8(b) with  $R_I = 100 \text{ k}\Omega$ ,  $R_L = 10 \text{ k}\Omega$ ,  $R_1 = 20 \text{ k}\Omega$  and  $R_2 = 2 \text{ k}\Omega$ .
- 11.56. Simulate the amplifier in Prob. 11.55 using SPICE and compare the results to hand calculations.

## 11.9 Loop Gain Calculations Using SPICE

- 11.57. Verify the value of the loop gain in Ex. 11.5 using successive voltage and current injection at the node connected to the inverting input of the op amp. What is the resistance ratio?
- 11.58. Verify the value of the loop gain in Ex. 11.6 using successive voltage and current injection at the right end of feedback resistor  $R_F$ . What is the resistance ratio?
- 11.59. Verify the value of the loop gain in Ex. 11.7 using successive voltage and current injection at the node connected to the noninverting input of the op amp. What is the resistance ratio?
- 11.60. Verify the value of the loop gain in Ex. 11.8 using successive voltage and current injection between the junction of  $R_2$  and  $R_1$ . What is the resistance ratio?

## 11.10 Distortion Reduction Through the Use of Feedback

- 11.61. The VTC for an amplifier can be expressed as  $v_o = 15 \tanh(1000 v_i) \text{ V}$ . (a) Use MATLAB to find the total harmonic distortion for (a)  $v_i = 0.001 \sin 2000\pi t \text{ V}$ . (b) Repeat for  $v_i = 0.002 \sin 2000\pi t \text{ V}$ .
- 11.62. The VTC for the op amp in the circuit in Fig. 11.30 can be expressed as  $v_o = 15 \tanh(1000 v_i) \text{ V}$  and the closed-loop gain is set to 10. (a) Use MATLAB to find the total harmonic distortion for

$v_i = 1 \sin 2000\pi t \text{ V}$ . (b) Repeat for a closed-loop gain of 50 and  $v_i = 0.2 \sin 2000\pi t \text{ V}$ .

## 11.11 DC Error Sources and Output Range Limitations

- 11.63. Calculate the worst-case output voltage for the circuit in Fig. P11.63 if  $V_{OS} = 1 \text{ mV}$ ,  $I_{B1} = 100 \text{ nA}$ , and  $I_{B2} = 95 \text{ nA}$ . What is the ideal output voltage? What is the total error in this circuit? Is there a better choice for the value of  $R_1$ ? If so, what is the value?

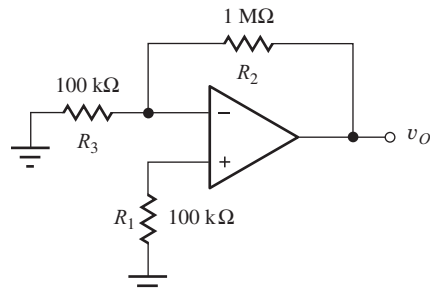


Figure P11.63

- 11.64. Repeat Prob. P11.63 if  $V_{OS} = 10 \text{ mV}$ ,  $I_{B1} = 200 \text{ nA}$ ,  $I_{B2} = 250 \text{ nA}$ , and  $R_2 = 510 \text{ k}\Omega$ ?
- 11.65. The voltage transfer characteristic for an operational amplifier is given in Fig. P11.65. What are the values of gain and offset voltage for this op amp?

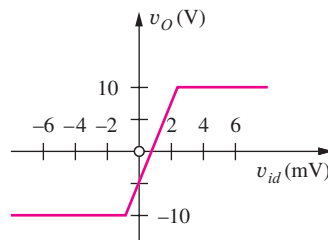


Figure P11.65

- 11.66. Plot voltage gain  $A$  versus  $v_{id}$  for the amplifier voltage transfer characteristic given in Fig. P11.65.
- 11.67. Use superposition to derive the result in Eq. (11.101).
- 11.68. The amplifier in Fig. P11.68 is to be designed to have a gain of 40 dB. What values of  $R_1$  and  $R_2$  should be used in order to meet the gain specification and minimize the effects of bias current errors?
- 11.69. The op amp in the circuit of Fig. P11.69 has an open-loop gain of 10,000, an offset voltage of 1 mV, and an input-bias current of 100 nA. (a) What is

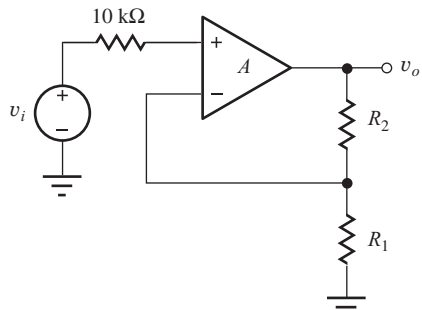


Figure P11.68

the output voltage for an ideal op amp? (b) What is the actual output voltage for the worst-case polarity of offset voltage? (c) What is the percentage error in the output voltage compared to the ideal output voltage?

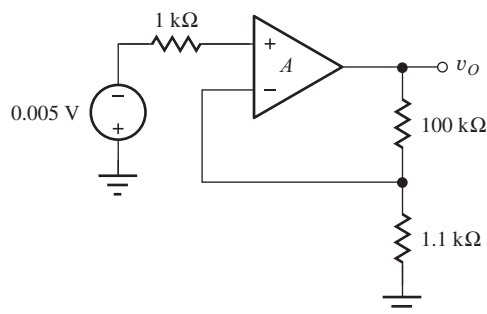


Figure P11.69

### Voltage and Current Limits

- 11.70. The output-voltage range of the op amp in Fig. P11.70 is equal to the power supply voltages. What are the values of  $V_O$  and  $V_-$  for the amplifier if the dc input  $V_S$  is (a)  $-1$  V and (b)  $+2$  V?

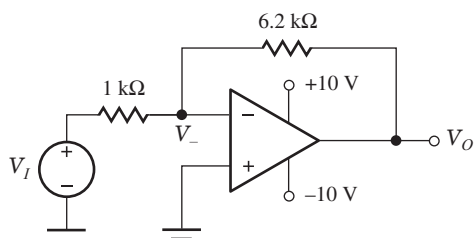


Figure P11.70

- 11.71. Plot a graph of the voltage transfer characteristic for the amplifier in Fig. P11.70.
- 11.72. The 6.2-kΩ resistor in Fig. P11.70 is replaced by a 10-kΩ resistor. What are the values of  $V_o$  and  $V_-$  if the dc input  $V_S$  is (a) 0.5 V and (b) 1.2 V?

- 11.73. Plot a graph of the voltage transfer characteristic for the amplifier in Prob. 11.72.
- 11.74. What are the voltages  $V_O$  and  $V_{ID}$  in the op amp circuit in Fig. P11.74 for dc input voltages of (a)  $V_I = 250$  mV and (b)  $V_I = 500$  mV if the output-voltage range of the op amp is limited to the power supply voltages.
- 11.75. Plot a graph of the voltage transfer characteristic for the amplifier in Fig. P11.74.

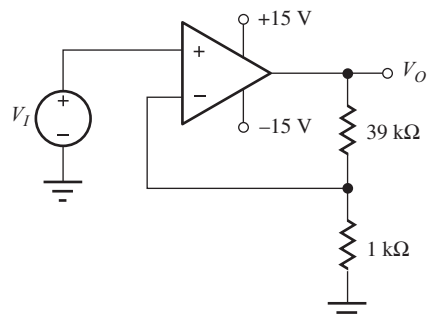


Figure P11.74

- 11.76. Repeat Prob. 11.74 if the 1-kΩ resistor in Fig. P11.74 is replaced by a 910-Ω resistor.
- 11.77. Design a noninverting amplifier with  $A_v = 46$  dB that can deliver a  $\pm 10$ -V signal to a 10-kΩ load resistor. Your op amp can supply only 1.5 mA of output current. Use standard resistor 5 percent values in your design. What is the gain of your design?
- 11.78. Design an inverting amplifier with  $A_v = 40$  dB that can deliver  $\pm 15$  V to a 5-kΩ load resistor. Your op amp can supply only 4 mA of output current. Use standard resistor 5 percent values in your design. What is the gain of your design?
- 11.79. What is the minimum value of  $R$  in the circuit in Fig. P11.79 if the maximum op amp output current is 5 mA and the current gain of the transistor is  $\beta_F \geq 60$ ?

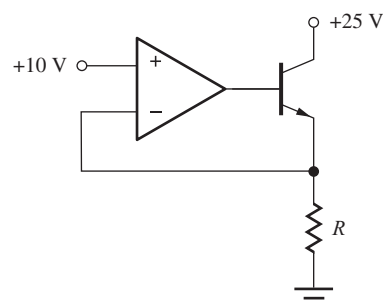


Figure P11.79

- \*11.80. (a) Design a single-stage inverting amplifier with a gain of 46 dB using an operational amplifier. The input resistance should be as low as possible while achieving the op amp output drive capability mentioned here. The amplifier must be able to produce the signal  $v_o = (10 \sin 1000t)$  V at its output when an external load resistance  $R_L \geq 5 \text{ k}\Omega$  is connected to the output of the amplifier. You have an operational amplifier available whose output is guaranteed to deliver  $\pm 10$  V into a  $4\text{-k}\Omega$  load resistance. Otherwise, the amplifier is ideal. (b) If the amplifier input signal is  $v_i = V \sin 1000t$ , what is the largest acceptable value for the input signal amplitude  $V$ ? (c) What is the input resistance of your amplifier?

## 11.12 Common-Mode Rejection and Input Resistance

- 11.81 The resistors in the difference amplifier in Fig. P11.81 are slightly mismatched due to their tolerances. (a) What are the differential-mode and common-mode input voltages if  $v_1 = 3$  V and  $v_2 = 3$  V? (b) What is the output voltage? (c) What would be the output voltage if the resistor pairs were matched? (d) What is the CMRR?

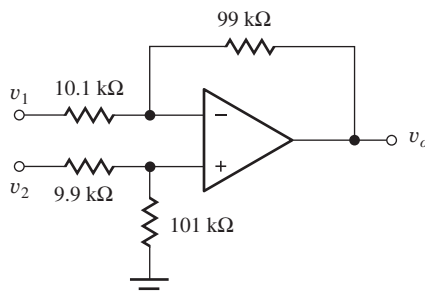


Figure 11.81

- 11.82 The resistors in the difference amplifier in Fig. P11.81 are slightly mismatched due to their tolerances. (a) What is the amplifier output voltage if  $v_1 = 4.05$  V and  $v_2 = 3.95$  V? (b) What would be the output voltage if the resistor pairs were matched? (c) What is the error in amplifying  $(v_1 - v_2)$ ?

- \*11.83. The op amp in the amplifier circuit in Fig. P11.81 is ideal and

$$v_1 = (10 \sin 120\pi t + 0.25 \sin 5000\pi t) \text{ V}$$

$$v_2 = (10 \sin 120\pi t - 0.25 \sin 5000\pi t) \text{ V}$$

- (a) What are the differential-mode and common-mode input voltages to this amplifier? (b) What are

the differential-mode and common-mode gains of this amplifier? (c) What is the common-mode rejection ratio of this amplifier? (d) Find  $v_o$ .

- 11.84. The multimeter in Fig. P11.84 has a common-mode rejection specification of 80 dB. What possible range of voltages can be indicated by the meter?

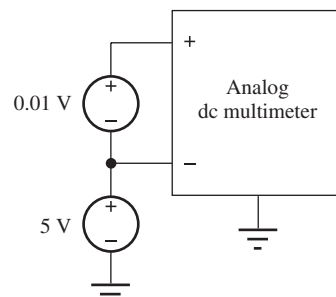


Figure 11.84

- 11.85. (a) We would like to measure the voltage ( $V = V_1 - V_2$ ) appearing across the  $20\text{-k}\Omega$  resistor in Fig. P11.85 with a voltmeter. What is the value of  $V$ ? What is the common-mode voltage associated with  $V(V_{CM} = (V_1 + V_2)/2)$ ? What CMRR is required of the voltmeter if we are to measure  $V$  with an error of less than 0.01 percent? (b) Repeat if the  $10\text{-k}\Omega$  resistor is changed to  $100 \Omega$ .

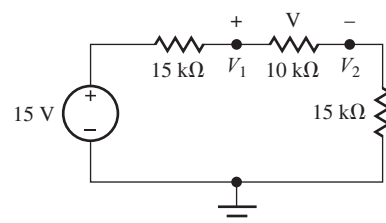


Figure 11.85

- 11.86. The common-mode rejection ratio of the difference amplifier in Fig. P11.86 is most often limited by the mismatch in the resistor pairs and not by the CMRR of the amplifier itself. Suppose that the nominal value of  $R$  is  $10 \text{ k}\Omega$  and its tolerance is 0.05 percent. What is the worst-case value of the CMRR in dB?

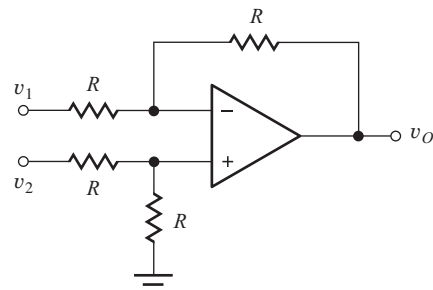


Figure 11.86

- 11.87 What are the values of the common-mode and differential mode input resistances for the amplifier in Fig. P11.81?

### 11.13 Frequency Response and Bandwidth of Operational Amplifier Circuits

- 11.88 (a) A single-pole op amp has an open-loop gain of 100 dB and a unity-gain frequency of 2 MHz. What is the open-loop bandwidth of the op amp? (b) A single-pole op amp has an open-loop gain of 100 dB and a bandwidth of 20 Hz. What is the unity-gain frequency of the op amp? (c) A single-pole op amp has unity-gain-bandwidth product of 30 MHz and a bandwidth of 200 Hz. What is the open-loop gain of the op amp?
- 11.89 A single-pole op amp has an open-loop gain of 100 dB and a unity-gain frequency of 2 MHz. What is the open-loop bandwidth of the op amp?
- 11.90 A single-pole op amp has an open-loop gain of 86 dB and a unity-gain frequency of 1 MHz. What is the open-loop bandwidth of the op amp? (a) The op amp is used in a noninverting amplifier designed to have an ideal gain of 32 dB. What is the bandwidth of the noninverting amplifier? (b) Repeat for an inverting amplifier with an ideal gain of 32 dB.
- 11.91 A single-pole op amp has an open-loop gain of 100 dB and a unity-gain frequency of 5 MHz. What is the open-loop bandwidth of the op amp? (a) The op amp is used in a voltage follower. What is the amplifier's bandwidth? (b) Repeat for a unity-gain inverting amplifier.
- 11.92 A single-pole op amp has an open-loop gain of 100 dB and a unity-gain frequency of 2 MHz. What is the open-loop bandwidth of the op amp? (a) The op amp is used in a voltage follower. What is the amplifier's bandwidth? (b) Repeat for a unity-gain inverting amplifier.
- D11.93 A single-pole op amp has an open-loop gain of 94 dB and a unity-gain frequency of 4 MHz. A noninverting amplifier is needed with bandwidth of at least 20 kHz. (a) What is the maximum closed loop-gain that a noninverting amplifier can have and still meet the frequency response specification? (b) What is the maximum closed loop-gain that an inverting amplifier can have and still meet the frequency response specification?
- 11.94 A single-pole op amp has an open-loop gain of 100 dB and a unity-gain frequency of 5 MHz. What is the open-loop bandwidth of the op amp? (a) The

op amp is used in a noninverting amplifier with a gain of 3. What is the amplifier's bandwidth? (b) Repeat for an inverting amplifier with a gain of 3.

### Using Feedback to Control Frequency Response

- 11.95 The voltage gain of an amplifier is described by

$$A(s) = \frac{2\pi \times 10^{10}s}{(s + 2000\pi)(s + 2\pi \times 10^6)}$$

(a) What are the mid-band gain and upper- and lower-cutoff frequencies of this amplifier? (b) If this amplifier is used in a feedback amplifier with a closed-loop gain of 100, what are the upper- and lower-cutoff frequencies of the closed-loop amplifier? (c) Repeat for a closed-loop gain of 40.

- 11.96 Repeat Prob. 11.95 if the voltage gain of the amplifier is given by

$$A(s) = \frac{2 \times 10^{14}\pi^2}{(s + 2\pi \times 10^3)(s + 2\pi \times 10^5)}$$

- 11.97 Repeat Prob. 11.95 if the voltage gain of the amplifier is given by

$$A(s) = \frac{4\pi^2 \times 10^{18}s^2}{(s + 200\pi)(s + 2000\pi)(s + 2\pi \times 10^6)(s + 2\pi \times 10^7)}$$

- 11.98 Derive an expression for the output impedance  $Z_{out}(s)$  of the inverting and noninverting amplifiers assuming that the op amp has a transfer function given by Eq. (11.120) and an output resistance  $R_o$ .

- 11.99 A single-pole op amp has an open-loop gain of 86 dB, a unity-gain frequency of 5 MHz, and an output resistance of 250 Ω. The op amp is used in an inverting amplifier with an ideal gain of 20. (a) Find an expression for the output impedance of the amplifier. (b) Sketch a Bode plot for the output impedance as a function of frequency.

- S11.100 Use SPICE to make a Bode plot for the amplifier output resistance in Prob. 11.98.

- 11.101 Derive an expression for the input impedance  $Z_{in}(s)$  of the noninverting amplifier assuming that the op amp has a transfer function given by Eq. (11.120) and an input resistance  $R_{id}$ .

- 11.102 A single-pole op amp has an open-loop gain of 86 dB, a unity-gain frequency of 1 MHz, and an input resistance of 100 kΩ. The op amp is used in a noninverting amplifier with an ideal gain of 20. (a) Find an expression for the input impedance of the amplifier. (b) Sketch a Bode plot for the input impedance as a function of frequency.

- S11.103 Use SPICE to make a Bode plot for the amplifier input resistance in Prob. S11.100.
- 11.104 A single-pole op amp has an open-loop gain of 100 dB and a unity-gain frequency of 2 MHz. Find an expression for the transfer function of the low-pass filter in Fig. 10.32 if  $R_1 = 5.1 \text{ k}\Omega$ ,  $R_2 = 51 \text{ k}\Omega$ , and  $C = 1600 \text{ pF}$ . Make a Bode plot comparing the ideal and the actual transfer functions.
- 11.105 A single-pole op amp has an open-loop gain of 86 dB and a unity-gain frequency of 2 MHz. Find an expression for the transfer function of the low-pass filter in Fig. 10.32 if  $R_1 = 5.1 \text{ k}\Omega$ ,  $R_2 = 100 \text{ k}\Omega$  and  $C = 750 \text{ pF}$ . Make a Bode plot comparing the ideal and the actual transfer functions.
- 11.106 A single-pole op amp has an open-loop gain of 86 dB and a unity-gain frequency of 1 MHz. Find an expression for the transfer function of the low-pass filter in Fig. 10.32 if  $R_1 = 1.4 \text{ k}\Omega$ ,  $R_2 = 27 \text{ k}\Omega$ , and  $C = 150 \text{ pF}$ . Make a Bode plot comparing the ideal and the actual transfer functions.
- 11.107 A single-pole op amp has an open-loop gain of 100 dB and a unity-gain frequency of 5 MHz. Find an expression for the transfer function of the integrator in Fig. 10.34 if  $R = 10 \text{ k}\Omega$  and  $C = 0.05 \mu\text{F}$ . Make a Bode plot comparing the ideal and the actual transfer functions.
- 11.108 A single-pole op amp has an open-loop gain of 100 dB and a unity-gain frequency of 1 MHz. Find an expression for the transfer function of the high-pass filter in Fig. 10.33 if  $R_1 = 18 \text{ k}\Omega$ ,  $R_2 = 180 \text{ k}\Omega$ , and  $C = 1800 \text{ pF}$ . Make a Bode plot comparing the ideal and the actual transfer functions.
- 11.109 What are the gain and bandwidth of the amplifier in Fig. P11.109 for the nominal and worst-case values of the feedback resistors if  $A = 50,000$  and  $f_T = 1 \text{ MHz}$ ?

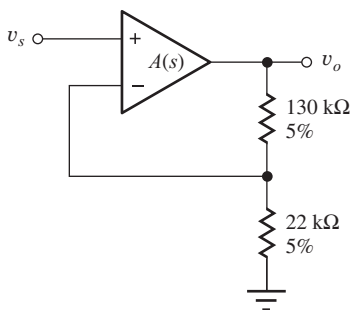


Figure 11.109

- \*\*11.110 Perform a Monte Carlo analysis of the circuit in Fig. P11.109. (a) What are the three sigma limits on the gain and bandwidth of the amplifier if  $A_o = 50,000$  and  $f_T = 1 \text{ MHz}$ ? (b) Repeat if  $A_o$  is uniformly distributed in the interval  $[5 \times 10^4, 1.5 \times 10^5]$  and  $f_T$  is uniformly distributed in the interval  $[10^6, 3 \times 10^6]$ .

### Large Signal Limitations—Slew Rate and Full-Power Bandwidth

- 11.111 (a) An audio amplifier is to be designed to develop a 40-V peak-to-peak sinusoidal signal at a frequency of 20 kHz. What is the slew-rate specification of the amplifier? (b) Repeat for a frequency of 20 Hz.
- 11.112 An amplifier has a slew rate of  $10 \text{ V}/\mu\text{s}$ . What is the full-power bandwidth for signals having an amplitude of 15 V?
- 11.113 An amplifier must reproduce the output waveform in Fig. P11.113. What is its slew rate?

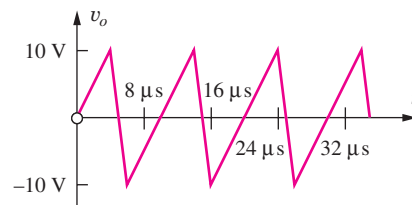


Figure 11.113

### Macro Model for the Operational Amplifier Frequency Response

- 11.114 A single-pole op amp has these specifications:
- $$A_o = 80,000 \quad f_T = 5 \text{ MHz}$$
- $$R_{id} = 250 \text{ k}\Omega \quad R_o = 50 \Omega$$
- (a) Draw the circuit of a macro model for this operational amplifier. (b) Draw the circuit of a macro model for this operational amplifier if the op amp also has  $R_{ic} = 500 \text{ M}\Omega$ .
- 11.115 Draw a macro model for the amplifier in Prob. 11.114, including the additional elements necessary to model  $R_{ic} = 100 \text{ M}\Omega$ ,  $I_{B1} = 105 \text{ nA}$ ,  $I_{B2} = 95 \text{ nA}$ , and  $V_{OS} = 1 \text{ mV}$ .
- \*11.116 A two-pole operational amplifier can be represented by the transfer function

$$A(s) = \frac{A_o \omega_1 \omega_2}{(s + \omega_1)(s + \omega_2)}$$

where

$$A_o = 80,000$$

$$f_1 = 1 \text{ kHz}$$

$$f_2 = 100 \text{ kHz}$$

$$R_{id} = 400 \text{ k}\Omega$$

$$R_o = 75 \Omega$$

Create a macro model for this amplifier. (*Hint:* Consider using two “dummy” loops.)

### Commercial General-Purpose Operational Amplifiers

- 11.117. (a) What are the element values for the macro model in Fig. 11.51 for the AD745J op amp? Use  $R = 1 \text{ k}\Omega$  and the nominal specifications.
- 11.118. (a) What are the worst-case values (minimum or maximum, as appropriate) of the following parameters of the AD745 op amp: open-loop gain, CMRR, PSRR,  $V_{OS}$ ,  $I_{B1}$ ,  $I_{B2}$ ,  $I_{OS}$ ,  $R_{ID}$ , slew rate, gain-bandwidth product, and power supply voltages? (b) Repeat for an LT1028 op amp.

### 11.14 Stability of Feedback Amplifiers

- 11.119. What are the phase and gain margins for the amplifier in Prob. 11.95?
- 11.120. What are the phase and gain margins for the amplifier in Prob. 11.96?
- 11.121. What are the phase and gain margins for the amplifier in Prob. 11.97?
- 11.122. The open-loop gain of an amplifier is described by

$$A(s) = \frac{4 \times 10^{19} \pi^3}{(s + 2\pi \times 10^4)(s + 2\pi \times 10^5)^2}$$

(a) If resistive feedback is used, find the frequency at which the loop gain will have a phase shift of  $180^\circ$ . (b) At what value of closed-loop gain will the amplifier break into oscillation? (c) Is the amplifier stable for larger or smaller values of closed-loop gain?

- 11.123. The open-loop gain of an amplifier is described by

$$A(s) = \frac{4 \times 10^{13} \pi^2}{(s + 2\pi \times 10^3)(s + 2\pi \times 10^4)}$$

(a) Will this amplifier be stable for a closed-loop gain of 4? (b) What is the phase margin?

- 11.124. A single-pole op amp has an open-loop gain of 100 dB and a unity-gain frequency of 1 MHz. (a) The op amp is used to build a noninverting amplifier with an ideal gain of 20 dB. What is the amplifier’s phase margin? (b) Repeat for an ideal gain of 46 dB.

- S11.125 (a) Simulate the amplifier in Prob. 11.124(a) using the SPICE model for the 741 op amp and find the phase margin. Compare with hand calculations in Prob. 11.124. Discuss reasons for differences observed. (b) Repeat for the amplifier in Prob. 11.124(b).

- 11.126. A single-pole op amp has an open-loop gain of 100 dB and a unity-gain frequency of 1 MHz. (a) The op amp is used to build an inverting amplifier with an ideal gain of 20 dB. What is the amplifier’s phase margin? (b) Repeat for an ideal gain of 46 dB.

- S11.127 (a) Simulate the amplifier in Prob. 11.126(a) using the SPICE model for the 741 op amp and find the phase margin. Compare with hand calculations in Prob. 11.126. Discuss reasons for differences observed. (b) Repeat for the amplifier in Prob. 11.126(b).

- 11.128. A single-pole op amp has an open-loop gain of 100 dB and a unity-gain frequency of 5 MHz. (a) If the op amp is used to build a voltage follower, what are its bandwidth and phase margin? (b) Repeat for an inverting amplifier with a gain of 0 dB.

- 11.129. A single-pole op amp has an open-loop gain of 86 dB and a unity-gain frequency of 4 MHz. Find an expression for the transfer function of the low-pass filter in Fig. 10.32 if  $R_1 = 1.4 \text{ k}\Omega$ ,  $R_2 = 27 \text{ k}\Omega$ , and  $C = 150 \text{ pF}$ . What is the filter’s phase margin?

- 11.130. A single-pole op amp has an open-loop gain of 100 dB and a unity-gain frequency of 2 MHz. Find an expression for the transfer function of the integrator in Fig. 10.34 if  $R = 10 \text{ k}\Omega$  and  $C = 0.05 \mu\text{F}$ . What is the integrator’s phase margin?

- 11.131. A single-pole op amp has an open-loop gain of 94 dB and a unity-gain frequency of 3 MHz. Find an expression for the transfer function of the high-pass filter in Fig. 10.33 if  $R_1 = 18 \text{ k}\Omega$ ,  $R_2 = 180 \text{ k}\Omega$ , and  $C = 1800 \text{ pF}$ . What is the filter’s phase margin?

- 11.132. The voltage gain of an amplifier is described by

$$A(s) = \frac{2 \times 10^{14}\pi^2}{(s + 2\pi \times 10^3)(s + 2\pi \times 10^5)}$$

(a) Will this amplifier be stable for a closed-loop gain of 5? (b) What is the phase margin?

- 11.133. (a) Use MATLAB to make a Bode plot for the amplifier in Prob. 11.132 for a closed-loop gain of 5. Is the amplifier stable? What is the phase margin? (b) Repeat for the unity-gain case.
- 11.134. Find the loop gain for an integrator that uses a single-pole op amp with  $A_o = 100$  dB and  $f_T = 1$  MHz. Assume the integrator feedback elements are  $R = 100$  k $\Omega$  and  $C = 0.01$   $\mu$ F. What is the phase margin of the integrator?

- \*11.135. Find the closed-loop transfer function of an integrator that uses a two-pole op amp with  $A_o = 100$  dB,  $f_{p1} = 1$  kHz, and  $f_{p2} = 100$  kHz. Assume the integrator feedback elements are  $R = 100$  k $\Omega$  and  $C = 0.01$   $\mu$ F. What is the phase margin of the integrator?

- \*11.136. (a) Write an expression for the loop gain  $T(s)$  of the amplifier in Fig. P11.136 if  $R_1 = 1$  k $\Omega$ ,  $R_2 = 20$  k $\Omega$ ,  $C_C = 0$ , and the op amp transfer function is

$$A(s) = \frac{2 \times 10^{11}\pi^2}{(s + 2\pi \times 10^2)(s + 2\pi \times 10^4)}$$

(b) Use MATLAB to make a Bode plot of  $T(s)$ . What is the phase margin of this circuit? (c) Can compensation capacitor  $C_C$  be added to achieve a phase margin of  $45^\circ$ ? If so, what is the value of  $C_C$ ?

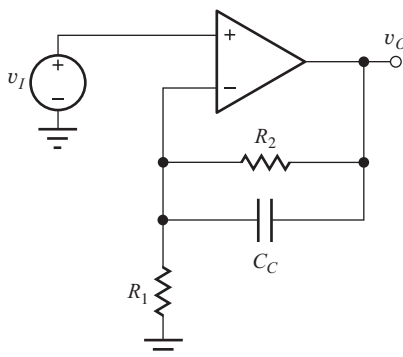


Figure 11.136

- 11.137. (a) Use MATLAB to make a Bode plot for the amplifier in Prob. 11.122. Find the frequency for which the phase shift is  $180^\circ$ . (b) At what value

of closed-loop gain will the amplifier break into oscillation?

- 11.138. Repeat Prob. 11.137 for the amplifier in Prob. 11.95.
- 11.139. Repeat Prob. 11.137 for the amplifier in Prob. 11.96.
- 11.140. Repeat Prob. 11.137 for the amplifier in Prob. 11.97.
- 11.141. Use MATLAB to make a Bode plot for the op amp in Prob. 11.136 for a closed-loop gain of 100. Is the amplifier stable? What is the phase margin? What is the overshoot?
- 11.142. Use MATLAB to make a Bode plot for the integrator in Prob. 11.134. What is the phase margin of the integrator?
- \*11.143. Use MATLAB to make a Bode plot for the integrator in Prob. 11.135. What is the phase margin of the integrator?
- 11.144. The noninverting amplifier in Fig. P11.144 has  $R_1 = 47$  k $\Omega$ ,  $R_2 = 390$  k $\Omega$ , and  $C_S = 45$  pF. Find the phase margin and overshoot of the amplifier if amplifier voltage gain is described by the following transfer function:

$$A(s) = \frac{10^7}{(s + 50)}$$

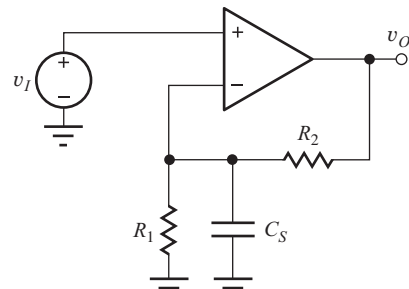


Figure 11.144

- 11.145. Use MATLAB, a spreadsheet, or other computer tool to draw a Bode plot for the low-pass filter circuit in Fig. 10.32 with  $R_1 = 4.3$  k $\Omega$ ,  $R_2 = 82$  k $\Omega$ , and  $C = 200$  pF if the op amp is not ideal but has an open-loop gain  $A_o = 100$  dB and  $f_T = 5$  MHz.
- 11.146. Use MATLAB, a spreadsheet, or other computer tool to draw a Bode plot for the integrator circuit in Fig. 10.34 with  $R_1 = 10$  k $\Omega$ , and  $C = 470$  pF if the op amp is not ideal but has an open-loop gain  $A_o = 100$  dB and  $f_T = 5$  MHz.

- \*11.147. What is the maximum load capacitance  $C_L$  that can be connected to the output of the voltage follower in Fig. P11.147 if the phase margin of the amplifier is to be  $60^\circ$ ? Assume that the amplifier voltage gain is described by this transfer function, and that it has an output resistance of  $R_o = 500 \Omega$ :

$$A(s) = \frac{10^7}{(s + 50)}$$

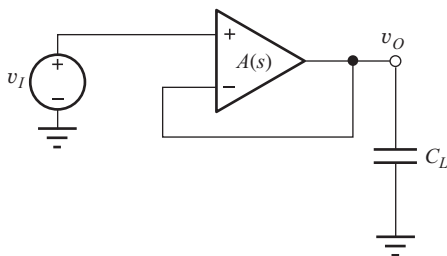


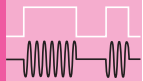
Figure 11.147

- 11.148 Suppose the op amp in Ex. 11.5 has an  $f_T$  of 0.5 MHz. What is the phase margin of the amplifier?
- 11.149 Suppose the op amp in Ex. 11.6 has an  $f_T$  of 2 MHz. What is the phase margin of the amplifier?
- 11.150 Suppose the op amp in Ex. 11.7 has an  $f_T$  of 1 MHz. What is the phase margin of the amplifier?
- 11.151 Suppose the op amp in Ex. 11.8 has an  $f_T$  of 1 MHz. What is the phase margin of the amplifier?
- 11.152 Calculate the phase margin and damping factor that correspond to an overshoot of (a) 0.5 percent, (b) 5 percent, (c) 25 percent.
- 11.153 A two-pole op amp has an open-loop gain of 100 dB and poles at 1000 Hz and 1 MHz. Make a

Bode plot for the gain of the op amp. What is its unity-gain frequency? (a) If the op amp is used to build a voltage follower, what are its bandwidth, phase margin, and overshoot? (b) Repeat for an inverting amplifier with a gain of 0 dB.

- 11.154 The op amp in Prob. 11.153 is used in a noninverting amplifier with a gain of 26 dB. What are the phase margin and overshoot for the amplifier?
- 11.155 An inverting amplifier utilizes the op amp in Prob. 11.153. (a) What closed-loop gain achieves a phase margin of  $45^\circ$ ? What is the overshoot? (b) What closed-loop gain achieves a phase margin of  $60^\circ$ ? What is the overshoot?
- 11.156 A two-pole op amp has an open-loop gain of 120 dB and its unity-gain frequency is 20 MHz. One of the op amp poles is at 2 MHz. What is the frequency of the second pole? (a) What are the bandwidth and phase margin if the op amp is used in an inverting amplifier with a gain 10? (b) What will be the overshoot if the op amp is used in a voltage follower?
- 11.157 A two-pole op amp has an open-loop gain of 94 dB and its first pole occurs at 500 Hz. If the op amp is to be used in a noninverting amplifier with a gain of 2, what is the minimum frequency for the second pole if the phase margin is to be  $60^\circ$ ? (b) Repeat for an inverting amplifier with a gain of 2.
- 11.158 A two-pole op amp has an open-loop gain of 100 dB and its first pole occurs at 100 Hz. The op amp is to be used in a noninverting amplifier with a gain of 5. What is the minimum frequency for the second pole, if the step response is to have an overshoot of less than 5 percent?

# CHAPTER 12



## OPERATIONAL AMPLIFIER APPLICATIONS

### CHAPTER OUTLINE

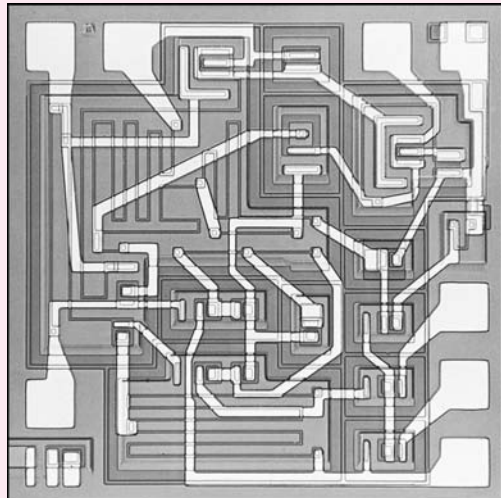
- 12.1 Cascaded Amplifiers 698
- 12.2 The Instrumentation Amplifier 711
- 12.3 Active Filters 714
- 12.4 Switched Capacitor Circuits 728
- 12.5 Digital-to-Analog Conversion 733
- 12.6 Analog-to-Digital Conversion 740
- 12.7 Oscillators 754
- 12.8 Nonlinear Circuit Applications 760
- 12.9 Circuits Using Positive Feedback 763
  - Summary 770
  - Key Terms 772
  - Additional Reading 773
  - Problems 773

### CHAPTER GOALS

In Chapter 12, we hope to achieve an understanding of the following topics:

- Characteristics and design of multistage amplifiers including gain, input resistance, and output resistance
- Frequency response of amplifier cascades
- The instrumentation amplifier
- Op amp based active filters including low-pass, high-pass, band-pass, and band-reject circuits
- Magnitude and frequency scaling of filters
- Switched capacitor circuit techniques
- Analog-to-digital (A/D) and digital-to-analog (D/A) converter specifications
- Basic forms of D/A and A/D converters
- The Barkhausen criteria for oscillation
- Op-amp-based oscillators including the Wein-bridge and phase-shift circuits
- Amplitude stabilization in oscillators
- Precision half-wave and full-wave rectifier circuits
- Circuits employing positive feedback including the Schmitt trigger and the astable and monostable multivibrators
- Voltage comparators

Chapter 12 continues our study of operational amplifier circuits by exploring a number of op amp applications. We frequently encounter a set of specifications that cannot



$\mu$ A709 operational amplifier die photograph.  
(Photo courtesy of Fairchild Semiconductor International.)

be met with a single amplifier stage, and this chapter begins with discussion and an example of multistage amplifier design. This is followed with presentation of a precision instrumentation amplifier circuit that employs three op amps in its realization.

Filters represent an extremely important op amp application, and this chapter discusses op-amp-based active filters including low-pass, high-pass, and band-pass circuits. This is followed with a short introduction to switched capacitor techniques that are widely used to implement modern filters in CMOS technology.

Every day, more and more digital signal processing is utilized to enhance or replace traditional analog functions, and the interface between the analog and digital worlds requires an understanding of analog-to-digital (A/D) and digital-to-analog (D/A) converters. D/A and A/D converter characteristics are delineated, and a number of basic circuit implementations are presented.

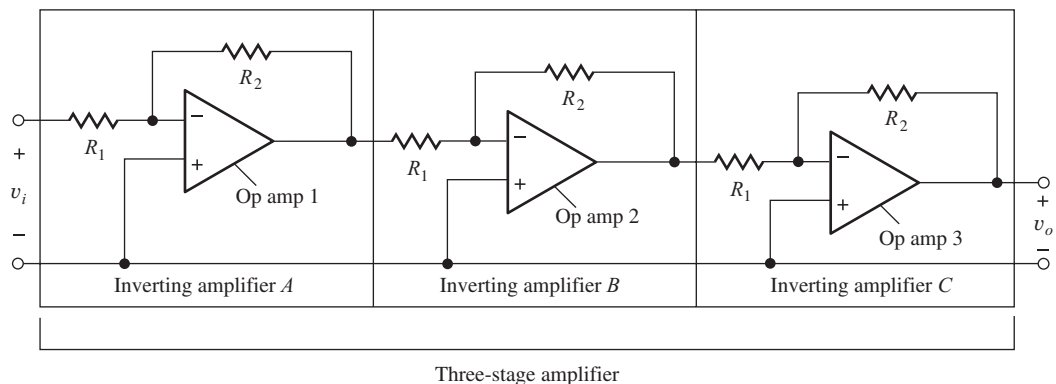
In prior chapters, we generally assumed that the circuits utilized linear negative feedback. In this chapter, we introduce circuits that involve positive feedback including oscillators and multivibrators that are required for signal generation, as well as precision rectifier circuits that employ nonlinear feedback.

## 12.1 CASCADED AMPLIFIERS

Often, a set of design specifications cannot be met using a single amplifier. For example, we cannot simultaneously achieve the desired gain, input resistance, and output resistance, or the required gain and bandwidth at the same time with a just one amplifier.<sup>1</sup> However, the desired specifications can often be met by connecting several amplifiers in cascade as indicated by the three-stage cascade in Fig. 12.1. In this situation, the output of one amplifier stage is connected to the input of the next. If the output resistance of one amplifier is much less than the input resistance of the next,  $R_{\text{out},A} \ll R_{\text{in},B}$  and  $R_{\text{out},B} \ll R_{\text{in},C}$ , then the loading of one amplifier on another can be neglected, and the overall voltage gain is simply the product of the open-circuit voltage gains of the individual stages. In order to understand this behavior more fully, we will represent the amplifiers using their simplified two-port models discussed next.

### 12.1.1 TWO-PORT REPRESENTATIONS

At each level in Fig. 12.1, we represent the “amplifier” as a **two-port model** with a value of voltage gain, input resistance, and output resistance, defined as in Fig. 12.1(b) and (c). Each amplifier



(a)

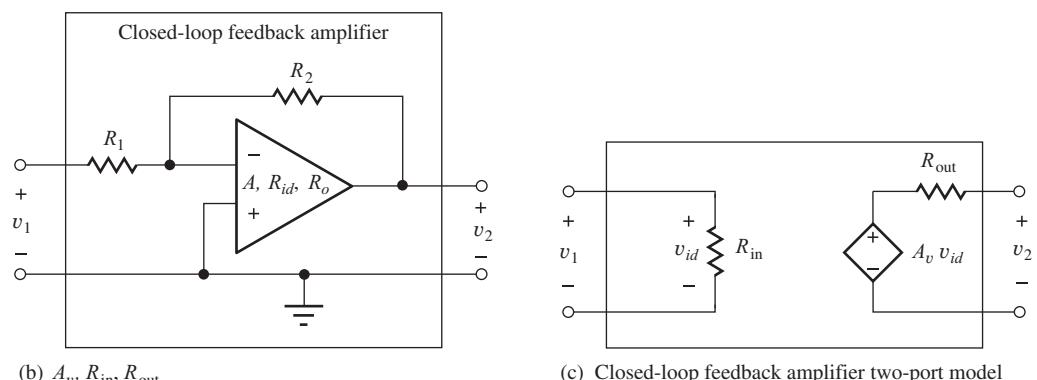


**Figure 12.1** (a) Three-stage amplifier cascade. (b) Inverting amplifier using an operational amplifier. (c) Two-port representation of the overall amplifier.

<sup>1</sup> See Problems 11.21–11.22, for example.

**TABLE 12.1**  
Feedback-Amplifier Terminology Comparison

	VOLTAGE GAIN	INPUT RESISTANCE	OUTPUT RESISTANCE
Open-Loop Amplifier	$A$	$R_{id}$	$R_o$
Closed-Loop Amplifier	$A_v$	$R_{in}$	$R_{out}$

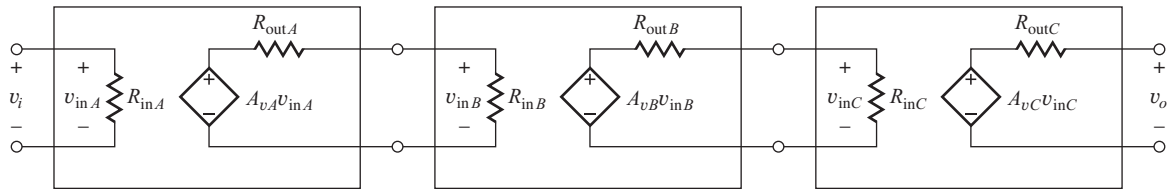


Figure 12.2 Two-port representation for three-stage cascaded amplifier.

stage— $A$ ,  $B$ , and  $C$ —is built using an operational amplifier that has a gain  $A$ , input resistance  $R_{id}$ , and output resistance  $R_o$ . These quantities are usually called the open-loop parameters of the operational amplifier: *open-loop gain*, *open-loop input resistance*, and *open-loop output resistance*. They describe the op amp as a two-port by itself with no external elements connected.

Each single-stage amplifier built from an operational amplifier and the feedback network consisting of  $R_1$  and  $R_2$  is termed a **closed-loop amplifier**. We use  $A_v$ ,  $R_{in}$ , and  $R_{out}$  for each closed-loop amplifier, as well as for the overall composite amplifier. Table 12.1 summarizes this terminology.

### Two-Port Model for the Three-Stage Cascade Amplifier

In Fig. 12.2 each individual amplifier has been replaced by its two-port model. By proceeding through the amplifier from left to right, the overall gain expression can be written as

$$\mathbf{v}_o = A_{vA} \mathbf{v}_i \left( \frac{R_{inB}}{R_{outA} + R_{inB}} \right) A_{vB} \left( \frac{R_{inC}}{R_{outB} + R_{inC}} \right) A_{vC} \quad (12.1)$$

For the voltage amplifiers considered so far, the output resistances are small (zero in the ideal case), so the impedance mismatch requirement is normally met (see Sec. 10.4), and the overall gain of the amplifier cascade is equal to the product of the open-loop gain of the three individual stages:

$$A_v = \frac{\mathbf{v}_o}{\mathbf{v}_i} = A_{vA} \cdot A_{vB} \cdot A_{vC} \quad (12.2)$$

If a test source  $\mathbf{v}_x$  is applied to the input and the input current  $\mathbf{i}_x$  is calculated, we find that  $R_{in}$  of the overall amplifier is determined solely by the input resistance of the first amplifier. In this case,  $R_{in} = \mathbf{v}_x / \mathbf{i}_x = R_{inA}$ . Similarly, if we apply a test source  $\mathbf{v}_x$  at the output and find the current  $\mathbf{i}_x$ , we find that  $R_{out}$  of the overall amplifier is determined only by the output resistance of the last amplifier. In this case,  $R_{out} = R_{outC}$ .



## DESIGN NOTE

The input impedance of an amplifier cascade is set by the input impedance of the first amplifier, and the output impedance of an amplifier cascade is set by the output impedance of the final amplifier in the cascade. A very common mistake is to expect that the input resistance of a cascade of amplifiers results from some combination of the input resistances of all the individual amplifiers, or that the output resistance is a function of the output resistances of all the individual amplifiers.

**EXERCISE:** The amplifier in Fig. 12.1 has  $R_2 = 68 \text{ k}\Omega$  and  $R_1 = 2.7 \text{ k}\Omega$ . What are the values of  $A_{vA}$ ,  $A_{vB}$ ,  $A_{vC}$ ,  $R_{inA}$ ,  $R_{inB}$ ,  $R_{inC}$ , and  $R_{outA}$ ,  $R_{outB}$ ,  $R_{outC}$ , for the amplifier equivalent circuit in Fig. 12.2?

**ANSWERS:**  $-25.2$ ;  $-25.2$ ;  $-25.2$ ;  $2.7 \text{ k}\Omega$ ;  $2.7 \text{ k}\Omega$ ;  $2.7 \text{ k}\Omega$ ;  $0$ ;  $0$ ;  $0$

**EXERCISE:** What are the gain  $A_v$ , input resistance, and output resistance of the three stage amplifier in Fig. 12.1(a) if  $R_2 = 68 \text{ k}\Omega$  and  $R_1 = 2.7 \text{ k}\Omega$ ?

**ANSWERS:**  $(-25.2)^3 = -1.60 \times 10^4$ ;  $2.7 \text{ k}\Omega$ ;  $0$

**EXERCISE:** Suppose the three output resistances in the amplifier in the previous exercise are not zero. What is the largest value of  $R_{out}$  that can be permitted if the gain is not to be reduced by more than 1 percent? Assume that the three output resistance values are the same.

**ANSWER:**  $13.5 \Omega$

### 12.1.2 AMPLIFIER TERMINOLOGY REVIEW

Now that we have analyzed a number of amplifier configurations, let us step back and review the terminology being used. Amplifier terminology is often a source of confusion because the portion of the circuit that is being called an *amplifier* must often be determined from the context of the discussion.

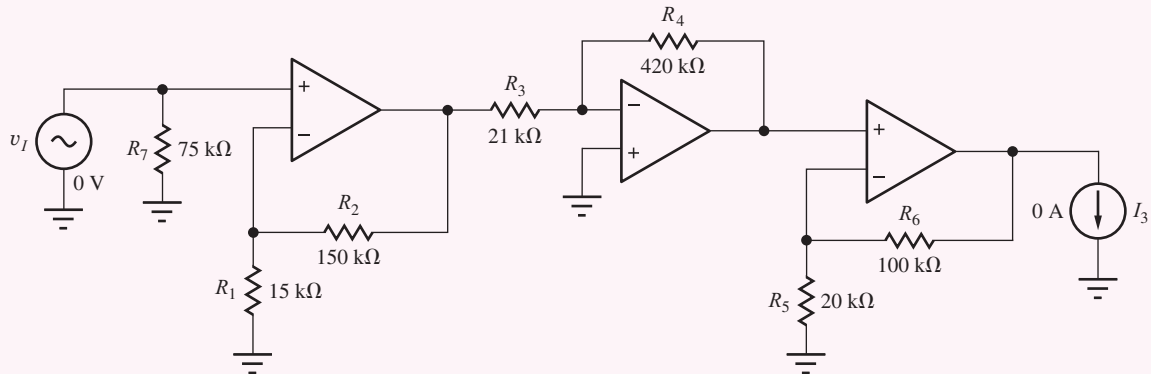
In Fig. 12.1, for example, an overall amplifier (the three-stage amplifier) is formed from the cascade connection of three inverting amplifiers ( $A$ ,  $B$ ,  $C$ ), and each inverting amplifier has been implemented using an operational amplifier (op amp 1, 2, 3). Thus, we can identify at least seven different “amplifiers” in Fig. 12.1: operational amplifiers 1, 2, 3; inverting amplifiers  $A$ ,  $B$ ,  $C$ ; and the composite three-stage amplifier  $ABC$ . Unfortunately, at any given time the “amplifier” that is being referenced must often be inferred from the context of the discussion.

### EXAMPLE 12.1 CASCADED AMPLIFIER CALCULATIONS

This example characterizes a three-stage amplifier cascade and explores effects of power supply limits.

**PROBLEM** The op amps in the circuit on the next page operate from  $\pm 12\text{-V}$  power supplies, but are ideal otherwise. (a) What are the voltage gain, input resistance, and output resistance of the overall amplifier? (b) If input voltage  $v_I = 5 \text{ mV}$ , what are the voltages at each of the 10 nodes in the circuit? (c) Now suppose that  $v_I = 10 \text{ mV}$ . What are the voltages at the outputs of the three op amps? (d) Suppose  $v_I = V_i \sin 2000\pi t$ . What is the largest value of input voltage  $V_i$  that corresponds to linear operation of the amplifier?

**SOLUTION** **Known Information and Given Data:** The three-stage amplifier circuit with resistor values appears below. The op amps are ideal except for power supplies of  $\pm 12$  V.



**Unknowns:** (a) Voltage gain, input resistance, and output resistance of the overall amplifier.  
(b) Voltages at each of the 10 nodes in the circuit with  $v_I = 5$  mV. (c) Voltages at each of the 10 nodes in the circuit with  $v_I = 10$  mV. (d) What is the largest amplitude of a sine wave input voltage that corresponds to linear operation of the amplifier?

**Approach:** Apply the inverting and noninverting amplifier formulas to the individual stages. The gain will be the product of the gains. The input resistance will be the input resistance of the first stage. The output resistance will equal that of the last amplifier.

**Assumptions:** The op amps are ideal except the power supplies are  $\pm 12$  V. The interactions between  $R_{in}$  and  $R_{out}$  for the op amp circuits are negligible. Each op amp is using negative feedback and operating in its linear range.

**Analysis:** The three individual amplifier stages are recognized as noninverting, inverting, and noninverting amplifiers.

(a) Use the expressions in Table 10.3:  $A_v = A_{v1}A_{v2}A_{v3}$

$$A_{v1} = 1 + \frac{R_2}{R_1} \quad A_{v2} = -\frac{R_4}{R_3} \quad A_{v3} = 1 + \frac{R_6}{R_5}$$

$$A_v = \left(1 + \frac{150 \text{ k}\Omega}{15 \text{ k}\Omega}\right) \left(-\frac{420 \text{ k}\Omega}{21 \text{ k}\Omega}\right) \left(1 + \frac{100 \text{ k}\Omega}{20 \text{ k}\Omega}\right) = -1320$$

The input resistance looking into the noninverting input of the first op amp is infinite, but the noninverting input is shunted by the  $75 \text{ k}\Omega$  resistor. Thus,  $R_{in} = 75 \text{ k}\Omega \parallel \infty = 75 \text{ k}\Omega$ . The output resistance is equal to the the output resistance of the third amplifier.  $R_{out} = R_{out3} = 0$

(b)  $v_I = 5.00 \text{ mV}$ ,  $v_{OA} = +11v_I = 55.0 \text{ mV}$ ,  $v_{OB} = -20v_{OA} = -1.10 \text{ V}$ ,  $v_O = +6v_{OB} = -6.60 \text{ V}$

Since the op amps are ideal, there must be zero volts across the input of each op amp:

$$v_{-A} = v_{+A} = +5.00 \text{ mV}, v_{-B} = v_{+B} = 0 \text{ V}, v_{-C} = v_{+C} = -6.60 \text{ V}$$

$$V_+ = +12 \text{ V}, V_- = -12 \text{ V}, V_{gnd} = 0 \text{ V}$$

(c)  $v_I = 10.0 \text{ mV}$ ,  $v_{OA} = +11v_I = 110 \text{ mV}$ ,  $v_{OB} = -20v_{OA} = -2.2 \text{ V}$ ,  $v_O = +6v_{OB} = -13.2 \text{ V} < -12 \text{ V} \rightarrow v_O = -12 \text{ V}$  The output cannot exceed the power supply limits! The first two op amps are operating in their linear regions, so there will be zero volts across the input of the these two op amps:  $v_{-A} = v_{+A} = +10.0 \text{ mV} | v_{-B} = v_{+B} = 0 \text{ V} |$  However, the output of the third amplifier is saturated at  $-12 \text{ V}$ , the gain of the third op amp is 0, and its feedback loop

is “broken.” The inverting and noninverting inputs need no longer be equal.

$$v_{-C} = -12 \text{ V} \frac{20 \text{ k}\Omega}{20 \text{ k}\Omega + 100 \text{ k}\Omega} = -2 \text{ V} \quad V_+ = +12 \text{ V} \quad V_- = -12 \text{ V} \quad V_{gnd} = 0 \text{ V}$$

(d)  $V_i$  must not exceed the voltage that causes the output to just reach the power supply voltages:

$$V_i \leq \left| \frac{12\text{V}}{A_v} \right| = \frac{12}{1320} = 9.09 \text{ mV}$$

**Check of Results:** All the unknowns have been found.  $R_{in}$  should equal the  $75 \text{ k}\Omega$  resistor, and  $R_{out}$  should be very small. For a 5-mV input, the expected output voltage  $v_O = -1320(0.005) = -6.60 \text{ V}$  which checks. For a 10-mV input, the expected output voltage  $v_O = -1320(0.005) = -13.2 \text{ V}$  which is less than the negative the power supply, so  $v_O = -12 \text{ V}$ . The linear range assumption is violated.

**Computer-Aided Analysis and Discussion:** SPICE simulation utilizes a dc analysis with a dc input to find the node voltages and a transfer function analysis from input VI to the voltage across I3, V(I3) to find the gain, input resistance, and output resistance. The OPAMP power supplies are set to  $\pm 12 \text{ V}$ , and the gains default to 120 dB.

SPICE transfer function results are  $A_v = -1320$ ,  $R_{in} = 75 \text{ k}\Omega$ , and  $R_{out} = 0$ , all in agreement with our hand calculations. The computed dc node voltages proceeding from left to right through the circuit are:

dc Node Voltages from SPICE

INPUT CASE	5 mV	10 mV
$v_I$	5.000 mV	10.00 mV
$v_{-A}$	5.000 mV	10.00 mV
$v_{OA}$	55.00 mV	110.0 mV
$v_{-B}$	1.100 $\mu$ V	-2.200 $\mu$ V
$v_{OB}$	-1.100 V	-2.200 V
$v_{-C}$	-1.100 V	-2.000 V
$v_{OC}$	-6.600 V	-12.00 V
$V_+$	+12.00 V	+12.00 V
$V_-$	-12.00 V	-12.00 V
$V_{gnd}$	0.000 V	0.000 V

The computed node voltages agree with our hand calculations to four decimal places except for the voltage at the inverting input of the second amplifier where SPICE yields  $v_{-B} = 1.100 \mu\text{V}$ . Let us try to understand the source of this discrepancy. The amplifiers in SPICE have finite gain of 120 dB. Thus the differential input voltage of the OPAMPS will not be zero. There must be a voltage across the input to generate the nonzero output voltage. The values of  $v_{ID}$  for each op amp will therefore be:

$$v_{IDA} = \frac{55.0 \text{ mV}}{10^6} = 55.0 \text{ nV} \quad v_{IDB} = \frac{-1.1 \text{ V}}{10^6} = -1.10 \mu\text{V} \quad v_{IDC} = \frac{-6.6 \text{ V}}{10^6} = -6.60 \mu\text{V}$$

The voltage at the inverting input of op amp B is the negative of  $v_{IDB}$  which agrees with SPICE. If we calculate  $v_{-A}$  and  $v_{-B}$ , the contributions of  $v_{ID}$  disappear in the round off:

$$v_{-A} = v_I - v_{IDA} = 5.000 \text{ mV} - 55.0 \text{ nV} = 55.00 \text{ mV}$$

$$v_{-C} = v_{OB} - v_{IDC} = -1.100 \text{ V} - (-6.60 \mu\text{V}) = -1.100 \text{ V}$$

For the case with  $v_I = 10 \text{ mV}$ , the node voltages are in agreement with our calculations except for  $v_{-B}$ . Note that the differential input voltage of the third op amp is not zero but equals  $-2.200 \text{ V} - (-2.000) = -0.200 \text{ V}$ ! The output of the op amp cannot reach the value necessary to force  $v_{ID} = 0$ .

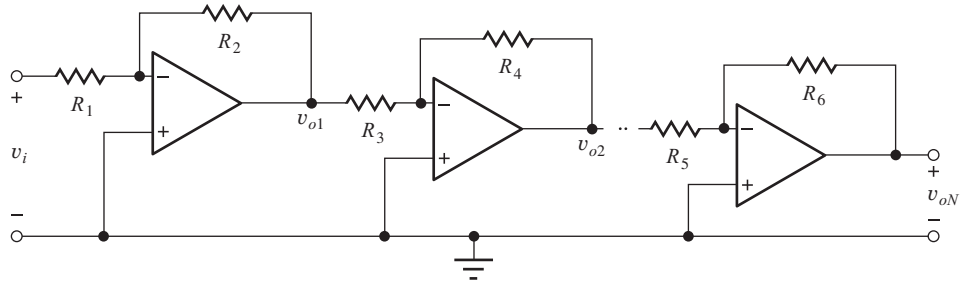


**Figure 12.3** Multistage amplifier cascade.

### 12.1.3 FREQUENCY RESPONSE OF CASCADED AMPLIFIERS

When several amplifiers are connected in cascade, as in Fig. 12.3 for example, the overall transfer function can be written as the product of the transfer functions of the individual stages:

$$A_v(s) = \frac{\mathbf{V}_{oN}(s)}{\mathbf{V}_I(s)} = \frac{\mathbf{V}_{o1}}{\mathbf{V}_I} \frac{\mathbf{V}_{o2}}{\mathbf{V}_{o1}} \cdots \frac{\mathbf{V}_{oN}}{\mathbf{V}_{o(N-1)}} = A_{v1}(s) A_{v2}(s) \cdots A_{vN}(s) \quad (12.3)$$

It is extremely important to remember that this product representation implicitly assumes that the stages do not interact with each other, which can be achieved with  $R_{out} = 0$  or  $R_{in} = \infty$  (that is, the interconnection of the various amplifiers must not alter the transfer function of any of the amplifiers).

In the general case, each amplifier has a different value of dc gain and bandwidth, and the overall transfer function becomes

$$A_v(s) = \frac{A_{v1}(0)}{\left(1 + \frac{s}{\omega_{H1}}\right)} \frac{A_{v2}(0)}{\left(1 + \frac{s}{\omega_{H2}}\right)} \cdots \frac{A_{vN}(0)}{\left(1 + \frac{s}{\omega_{HN}}\right)} \quad (12.4)$$

assuming single-pole amplifiers. The gain at low frequencies ( $s = 0$ ) is

$$A_v(0) = A_{v1}(0) A_{v2}(0) \cdots A_{vN}(0) \quad (12.5)$$

The overall bandwidth of the cascade amplifier is defined to be the frequency at which the voltage gain is reduced by a factor of  $1/\sqrt{2}$  or  $-3$  dB from its low-frequency value. Stated mathematically,

$$|A_v(j\omega_H)| = \frac{|A_{v1}(0) A_{v2}(0) \cdots A_{vN}(0)|}{\sqrt{2}} \quad (12.6)$$

In the general case, hand calculation of  $\omega_H$  based on Eq. (12.6) can be quite tedious, and approximate techniques for estimating  $\omega_H$  will be developed in Chapter 17. With the aid of a computer or calculator, solver routines or iterative trial-and-error can be used directly to find  $\omega_H$ . Example 12.2 uses direct algebraic evaluation of Eq. (12.6) for the case of two amplifiers.

#### EXAMPLE 12.2 TWO-AMPLIFIER CASCADE

Calculate the gain and bandwidth of a two-stage amplifier.

**PROBLEM** Two amplifiers with transfer functions  $A_{v1}(s)$  and  $A_{v2}(s)$  are connected in cascade. What are the dc gain and bandwidth of the overall two-stage amplifier?

$$A_{v1} = \frac{500}{1 + \frac{s}{2000}} \quad \text{and} \quad A_{v2} = \frac{250}{1 + \frac{s}{4000}}$$

**SOLUTION** **Known Information and Given Data:** A cascade connection of two amplifiers; the individual transfer functions are specified for the two amplifiers.

**Unknowns:**  $A_v(0)$  and  $f_H$  for the overall two-stage amplifier

**Approach:** The transfer function for the cascade is given by  $A_v = A_{v1} \times A_{v2}$ . Find  $A_v(0)$ . Apply the definition of bandwidth to find  $f_H$ .

**Assumptions:** The amplifiers are ideal except for their frequency dependencies and can be cascaded without interaction—i.e., the overall gain is equal to the product of the individual transfer functions.

**Analysis:** The overall transfer function is

$$A_v(s) = \left( \frac{500}{1 + \frac{s}{2000}} \right) \left( \frac{250}{1 + \frac{s}{4000}} \right) = \frac{125,000}{\left( 1 + \frac{s}{2000} \right) \left( 1 + \frac{s}{4000} \right)}$$

Calculating the dc gain  $A_v(0)$ :

$$A_v(0) = (500)(250) = 125,000 \text{ or } 102 \text{ dB}$$

Note that  $A_v(0)$  is equal to the product of the dc gains of the two individual amplifiers.

The magnitude of the frequency response for  $s = j\omega$  is

$$|A_v(j\omega)| = \frac{1.25 \times 10^5}{\sqrt{1 + \frac{\omega^2}{2000^2}} \sqrt{1 + \frac{\omega^2}{4000^2}}}$$

and we remember that  $\omega_H$  is defined by

$$|A(j\omega_H)| = \frac{A_{\text{mid}}}{\sqrt{2}} = \frac{A_v(0)}{\sqrt{2}} = \frac{1.25 \times 10^5}{\sqrt{2}}$$

Equating the denominators of these two equations and squaring both sides yields

$$\left( 1 + \frac{\omega_H^2}{2000^2} \right) \left( 1 + \frac{\omega_H^2}{4000^2} \right) = 2$$

which can be rearranged into the following quadratic equation in terms of  $\omega_H^2$ :

$$(\omega_H^2)^2 + 2.00 \times 10^7 (\omega_H^2) - 6.40 \times 10^{13} = 0$$

Using the quadratic formula or our calculator's root-finding routine gives these values for  $\omega_H^2$

$$\omega_H^2 = 2.81 \times 10^6 \quad \text{or} \quad -4.56 \times 10^7$$

The value of  $\omega_H$  must be real, so the only acceptable answer is

$$\omega_H = 1.68 \times 10^3 \quad \text{or} \quad f_H = 267 \text{ Hz}$$

**Check of Results:** The bandwidth of the composite amplifier should be less than that of either individual amplifier:

$$f_{H1} = \frac{2000}{2\pi} = 318 \text{ Hz} \quad \text{and} \quad f_{H2} = \frac{4000}{2\pi} = 637 \text{ Hz}$$

The bandwidth we have calculated is indeed less than for either individual amplifier.

**EXERCISE:** An amplifier is formed by cascading two amplifiers with these transfer functions. What is the gain at low frequencies? What is the gain at  $f_H$ ? What is  $f_H$ ?

$$A_{v1}(s) = \frac{50}{1 + \frac{s}{10,000\pi}} \quad \text{and} \quad A_{v2}(s) = \frac{25}{1 + \frac{s}{20,000\pi}}$$

**ANSWERS:** 1250; 884; 4190 Hz

**EXERCISE:** An amplifier is formed by cascading three amplifiers with the following transfer functions. What is the gain at low frequencies? What is the gain at  $f_H$ ? What is  $f_H$ ?

$$A_{v1}(s) = \frac{-100}{1 + \frac{s}{10,000\pi}}, \quad A_{v2}(s) = \frac{66.7}{1 + \frac{s}{15,000\pi}}, \quad A_{v3}(s) = \frac{50}{1 + \frac{s}{20,000\pi}}$$

**ANSWERS:**  $-3.33 \times 10^5$ ;  $-2.36 \times 10^5$ ; 6900 Hz

### Cascade of Identical Amplifier Stages

For the special case in which a cascade-amplifier configuration is composed of identical amplifiers, then a simple result can be obtained for the bandwidth of the overall amplifier. For  $N$  identical stages,

$$A_v(s) = \left[ \frac{A_{v1}(0)}{1 + \frac{s}{\omega_{H1}}} \right]^N = \frac{[A_{v1}(0)]^N}{\left( 1 + \frac{s}{\omega_{H1}} \right)^N} \quad \text{and} \quad A_v(0) = [A_{v1}(0)]^N \quad (12.7)$$

in which  $A_{v1}(0)$  and  $\omega_{H1}$  are the closed-loop gain and bandwidth of each individual amplifier stage.

The bandwidth  $\omega_H$  of the overall cascade amplifier is determined from

$$|A_v(j\omega_H)| = \frac{[A_{v1}(0)]^N}{\left( \sqrt{1 + \frac{\omega_H^2}{\omega_{H1}^2}} \right)^N} = \frac{[A_{v1}(0)]^N}{\sqrt{2}} \quad (12.8)$$

Solving for  $\omega_H$  in terms of  $\omega_{H1}$  for the cascaded-amplifier bandwidth yields

$$\omega_H = \omega_{H1} \sqrt{2^{1/N} - 1} \quad \text{or} \quad f_H = f_{H1} \sqrt{2^{1/N} - 1} \quad (12.9)$$

The bandwidth of the cascade is less than that of the individual amplifiers. Sample values of the **bandwidth shrinkage factor**  $\sqrt{2^{1/N} - 1}$  are given in Table 12.2.

Although most amplifier designs do not actually cascade identical amplifiers, Eq. (12.9) can be used to help guide the design of a multistage amplifier or, in some cases, to estimate the bandwidth of a portion of a more complex amplifier. (Additional useful results appear in Probs. 12.33 and 12.34.)

**EXERCISE:** Three identical amplifiers are connected in cascade as in Fig. 12.3. Each amplifier has  $A_v = -30$  and  $f_H = 33.3$  kHz. What are the gain and bandwidth of the composite three-stage amplifier?

**ANSWERS:**  $-27,000$ ; 17.0 kHz

**TABLE 12.2**

Bandwidth Shrinkage Factor

$N$	$\sqrt{2^{1/N} - 1}$
1	1
2	0.644
3	0.510
4	0.435
5	0.386
6	0.350
7	0.323

## DESIGN A CASCADE AMPLIFIER DESIGN

### EXAMPLE 12.3

In this example, a spreadsheet is used to assist in the design of a fairly complex multistage amplifier.

**PROBLEM** Design an amplifier to meet these specifications:  $A_v \geq 100$  dB, bandwidth  $\geq 50$  kHz,  $R_{out} \leq 0.1 \Omega$ , and  $R_{in} \geq 20$  k $\Omega$ . Use an operational amplifier with these specifications:  $A_o = 100$  dB,  $f_T = 1$  MHz,  $R_{id} = 1$  G $\Omega$ , and  $R_o = 50 \Omega$ .

**SOLUTION** **Known Information and Given Data:** Op amp and overall amplifier specifications as already tabulated.

**Unknowns:** Choice between inverting and noninverting configurations; gain and bandwidth of each amplifier; feedback resistor values

**Approach:** Because the required value of  $R_{in}$  is relatively low and can be met by a resistor, both the inverting and noninverting amplifier stages should be considered. More than one stage will be required because a single op amp by itself cannot simultaneously meet the specifications for  $A_v$ ,  $f_H$ , and  $R_{out}$ . For example, if we were to use the open-loop op amp by itself, it would provide a gain of 100 dB ( $10^5$ ) but have a bandwidth of only  $f_T/10^5 = 10$  Hz. Thus, we must reduce the gain of each stage in order to increase the bandwidth (i.e., we must trade gain for bandwidth).

For simplicity in the design, we assume that the amplifier will be built from a cascade of  $N$  identical amplifier stages. The design formulas will be set up in a logical order so that we can choose one design variable, and the rest of the equations can then be evaluated based on that single design choice. For this particular design, the gain and bandwidth are the most difficult specifications to achieve, whereas the required input and output resistance specifications are easily met. We can initially force our design to meet either the gain or the bandwidth specification and then find the number of stages that will be required to achieve the other specifications.

**Assumptions:** The design must have the minimum number of stages required to meet the specifications in order to achieve minimum cost.

**Analysis:** In this example, we force the cascade amplifier to meet the gain specification, and then find the number of stages needed to meet the bandwidth by repeated trial and error.

To meet the gain specification, we set the gain of each stage to

$$A_v(0) = \sqrt[N]{10^5}$$

Based on this choice, we can then calculate the other characteristics of the amplifier using this process:

1. Choose  $N$ .
2. Calculate the gain required of each stage  $A_v(0) = \sqrt[N]{10^5}$ .
3. Find  $\beta$  using the numerical result from step 2.
4. Calculate the bandwidth  $f_{H1}$  of each stage.
5. Calculate the bandwidth of  $N$  stages using Eq. (12.9).
6. Using  $A\beta$ , calculate  $R_{out}$  and  $R_{in}$ .
7. See if specifications are met. If not, go back to step 1 and try a new value of  $N$ .

The formulas for the noninverting and inverting amplifiers are slightly different, as summarized in Table 12.3. These formulas have been used for the results tabulated in the spreadsheet in Table 12.4.

From Table 12.4, we see that a cascade of six noninverting amplifiers meets all the specifications, whereas seven inverting amplifier stages are required. This occurs because the inverting

**TABLE 12.3***N*-Stage Cascades of Noninverting and Inverting Amplifiers

$\beta = \frac{R_1}{R_1 + R_2}$	NONINVERTING AMPLIFIER	INVERTING AMPLIFIER
2. Single-stage gain $A_v(0) = \sqrt[N]{10^5}$	$A_v(0) = 1 + \frac{R_2}{R_1}$	$A_v(0) = -\frac{R_2}{R_1}$
3. Feedback factor	$\beta = \frac{1}{A_v(0)}$	$\beta = \frac{1}{1 +  A_v(0) }$
4. Bandwidth of each stage	$f_{H1} = \frac{f_T}{A_o}$	$f_{H1} = \frac{f_T}{A_o}$
	$\frac{1}{1 + A_o\beta}$	$\frac{1}{1 + A_o\beta}$
5. <i>N</i> -stage bandwidth	$f_H = f_{H1}\sqrt{2^{1/N} - 1}$	$f_B = f_{H1}\sqrt{2^{1/N} - 1}$
6. Input resistance	$R_{id}(1 + A_o\beta)$	$R_1$
Output resistance	$\frac{R_o}{1 + A_o\beta}$	$\frac{R_o}{1 + A_o\beta}$

**TABLE 12.4**Design of Cascade of *N* Identical Operational Amplifier Stages**CASCADE OF IDENTICAL NONINVERTING AMPLIFIERS**

NUMBER OF STAGES	$A_V(0)$ GAIN PER STAGE	$f_{H1}$ SINGLE STAGE	$f_H$ <i>N</i> STAGES	$R_{in}$	$R_{out}$
	$1/\beta$	$\beta \times f_T$			
1	1.00E + 05	1.00E + 01	1.000E + 01	2.00E + 09	2.50E + 01
2	3.16E + 02	3.16E + 03	2.035E + 03	3.17E + 11	1.58E - 01
3	4.64E + 01	2.15E + 04	1.098E + 04	2.16E + 12	2.32E - 02
4	1.78E + 01	5.62E + 04	2.446E + 04	5.62E + 12	8.89E - 03
5	1.00E + 01	1.00E + 05	3.856E + 04	1.00E + 13	5.00E - 03
<b>6</b>	<b>6.81E + 00</b>	<b>1.47E + 05</b>	<b>5.137E + 04</b>	<b>1.47E + 13</b>	<b>3.41E - 03</b>
7	5.18E + 00	1.93E + 05	6.229E + 04	1.93E + 13	2.59E - 03
8	4.22E + 00	2.37E + 05	7.134E + 04	2.37E + 13	2.11E - 03

**CASCADE OF IDENTICAL INVERTING AMPLIFIERS**

NUMBER OF STAGES	$A_V(0)$ (1/ $\beta$ ) - 1	$f_{H1}$ SINGLE STAGE	$f_H$ <i>N</i> STAGES	$R_{in}$	$R_{out}$
1	1.00E + 05	1.00E + 01	1.00E + 01	$R_1$	2.50E + 01
2	3.16E + 02	3.15E + 03	2.03E + 03	$R_1$	1.58E - 01
3	4.64E + 01	2.11E + 04	1.08E + 04	$R_1$	2.32E - 02
4	1.78E + 01	5.32E + 04	2.32E + 04	$R_1$	8.89E - 03
5	1.00E + 01	9.09E + 04	3.51E + 04	$R_1$	5.00E - 03
6	6.81E + 00	1.28E + 05	4.48E + 04	$R_1$	3.41E - 03
<b>7</b>	<b>5.18E + 00</b>	<b>1.62E + 05</b>	<b>5.22E + 04</b>	$R_1$	<b>2.59E - 03</b>
8	4.22E + 00	1.92E + 05	5.77E + 04	$R_1$	2.11E - 03

amplifier has a slightly smaller bandwidth than the noninverting amplifier for a given value of closed-loop gain. We are usually interested in the most economical design, so the six-stage amplifier will be chosen. Note that the  $R_{out}$  requirement is met with  $N > 2$  for both amplifiers.

To complete the design, we must choose values for  $R_1$  and  $R_2$ . From Table 12.4, the gain of each stage must be at least 6.81, requiring the resistor ratio  $R_2/R_1$  to be 5.81. Because we will

**TABLE 12.5**  
Cascade of Six Identical Noninverting Amplifiers

NUMBER OF STAGES	$A_v(0)$ GAIN PER STAGE $\beta/\beta$	$N$ STAGE GAIN	$f_{H_1}$		$f_H$ $N$ STAGES	$R_{in}$	$R_{out}$
			SINGLE STAGE $\beta \times f_T$	$f_H$			
6	6.81E + 00	1.00E + 05	1.47E + 05	5.137E + 04	1.47E + 13	3.41E - 03	
6	6.83E + 00	1.02E + 05	1.46E + 05	5.121E + 04	1.46E + 13	3.42E - 03	
6	6.85E + 00	1.04E + 05	1.46E + 05	5.107E + 04	1.46E + 13	3.43E - 03	
6	6.87E + 00	1.05E + 05	1.45E + 05	5.092E + 04	1.46E + 13	3.44E - 03	
6	6.89E + 00	1.07E + 05	1.45E + 05	5.077E + 04	1.45E + 13	3.45E - 03	
6	6.91E + 00	1.09E + 05	1.45E + 05	5.062E + 04	1.45E + 13	3.46E - 03	
6	6.93E + 00	1.11E + 05	1.44E + 05	5.048E + 04	1.44E + 13	3.47E - 03	
6	6.95E + 00	1.13E + 05	1.44E + 05	5.033E + 04	1.44E + 13	3.48E - 03	
6	6.97E + 00	1.15E + 05	1.43E + 05	5.019E + 04	1.43E + 13	3.49E - 03	
6	6.99E + 00	1.17E + 05	1.43E + 05	5.004E + 04	1.43E + 13	3.50E - 03	
6	7.01E + 00	1.19E + 05	1.43E + 05	4.990E + 04	1.43E + 13	3.51E - 03	

probably not be able to find two 5 percent resistors that give a ratio of exactly 5.81, we need to explore the acceptable range for the ratio now that we know we need six stages. In Table 12.5, a spreadsheet is again used to study six-stage amplifier designs having gains ranging from 6.81 to 7.01. As the single-stage gain is increased, the overall bandwidth decreases. From Table 12.5, we see that the specifications will be met for resistor ratios falling between 5.81 and 5.99.

Many acceptable resistor ratios can be found in the table of 5 percent resistors in Appendix C. Picking  $A_v(0) = 6.91$ , a value near the center of the range of acceptable gain and bandwidth, two possible resistor sets are

$$(i) \quad R_1 = 22 \text{ k}\Omega, R_2 = 130 \text{ k}\Omega$$

which gives

$$1 + \frac{R_2}{R_1} = 6.91, A(0) = 101 \text{ dB}, f_H = 50.6 \text{ kHz}, R_{out} = 3.46 \text{ m}\Omega$$

and

$$(ii) \quad R_1 = 5.6 \text{ k}\Omega, R_2 = 33 \text{ k}\Omega$$

which yields

$$1 + \frac{R_2}{R_1} = 6.89, A(0) = 101 \text{ dB}, f_H = 50.8 \text{ kHz}, R_{out} = 3.45 \text{ m}\Omega$$

The overall size of these resistors has been chosen so that the feedback resistors do not heavily load the output of the op amp. For example, the resistor pairs  $R_1 = 220 \Omega$  and  $R_2 = 1.3 \text{ k}\Omega$  or  $R_1 = 56 \Omega$  and  $R_2 = 330 \Omega$ , although providing acceptable resistor ratios, would not be desirable choices for a final design.

**Check of Results:** Based on the spreadsheet results, a design has been found that meets the specifications.

**Discussion:** This example has explored the design of a fairly complex multistage amplifier. Economical design requires the use of the minimum number of amplifier stages. In this case, spreadsheets were used to explore the design space, and the calculations indicated that the specifications could be met with a cascade of six identical noninverting amplifiers. The design was completed through the choice of feedback resistors from the set of available discrete resistor values.

**Computer-Aided Analysis:** With the level of complexity in this example, it would obviously be quite useful to use SPICE to check our final design, and this is done in Ex. 12.4.

**TABLE 12.6**

Cascade of Six Identical Noninverting Amplifiers — Worse-Case Analysis

R VALUES	ONE-STAGE	SIX-STAGE	$f_{H_1}$	$f_H$	$R_{in}$	$R_{out}$
	GAIN	GAIN				
Nominal	6.91E + 00	1.09E + 05	1.45E + 05	5.065E + 04	1.45E + 13	3.45E - 03
Max	7.53E + 00	1.82E + 05	1.33E + 05	4.647E + 04	1.33E + 13	3.77E - 03
Min	6.35E + 00	6.53E + 04	1.58E + 05	5.514E + 04	1.58E + 13	3.17E - 03

### The Influence of Tolerances on Design

Now that we have completed Example 12.3, let us explore the effects of the resistor tolerances on our design. We have chosen resistors that have 5 percent tolerances; Table 12.6 presents the results of calculating the worst-case specifications, in which

$$A_v^{\text{nom}} = 1 + \frac{130 \text{ k}\Omega}{22 \text{ k}\Omega} = 6.91$$

$$A_v^{\text{max}} = 1 + \frac{130 \text{ k}\Omega(1.05)}{22 \text{ k}\Omega(0.95)} = 7.53$$

$$A_v^{\text{min}} = 1 + \frac{130 \text{ k}\Omega(0.95)}{22 \text{ k}\Omega(1.05)} = 6.35$$

The nominal design values easily meet both specifications, with a margin of 9 percent for the gain but only 1.3 percent for the bandwidth. When the resistor tolerances are set to give the largest gain per stage, the gain specification is easily met, but the bandwidth shrinks below the specification limit. At the opposite extreme, the gain of the six stages fails to meet the required specification. This analysis gives us an indication that there may be a problem with the design. Of course, assuming that all the amplifiers reach the worst-case gain and bandwidth limits at the same time is an extreme conclusion. Nevertheless, the nominal bandwidth does not exceed the specification limit by very much.

A Monte Carlo analysis would be much more representative of the actual design results. Such an analysis for 10,000 cases of our six-stage amplifier indicates that if this circuit is built with 5 percent resistors, more than 30 percent of the amplifiers will fail to meet either the gain or bandwidth specification. (The details of this calculation and exact results are left for Prob. 12.33.)

## DESIGN MACRO MODEL APPLICATION

### EXAMPLE 12.4

Use a SPICE op amp macro model to simulate the frequency response of a multistage amplifier.

**PROBLEM:** Use simulation to verify the frequency response of the six-stage amplifier designed in Ex. 12.3.

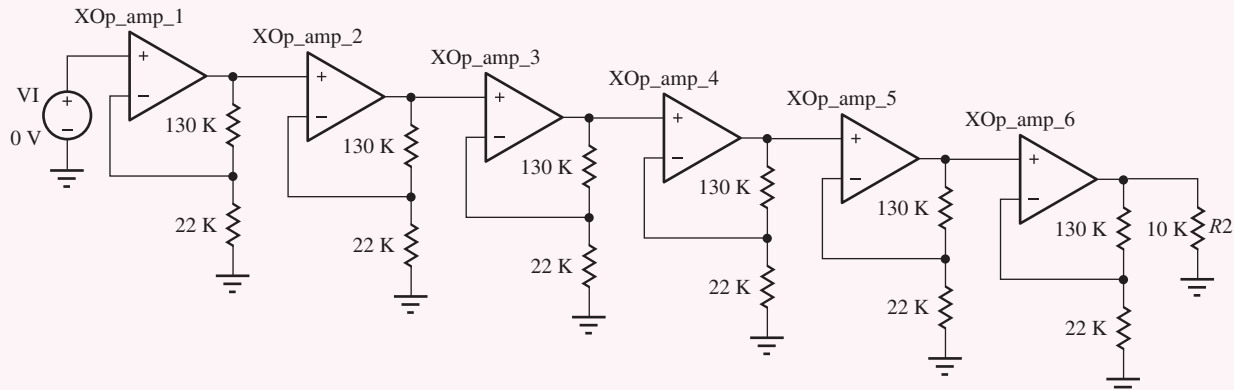
**SOLUTION:** **Known Information and Given Data:** The six-stage noninverting amplifier cascade design from Ex. 12.3 with  $R_1 = 22 \text{ k}\Omega$  and  $R_2 = 130 \text{ k}\Omega$ . The op amp specifications are  $A_o = 100 \text{ dB}$ ,  $f_T = 1 \text{ MHz}$ ,  $R_{id} = 1 \text{ G}\Omega$ , and  $R_o = 50 \Omega$ .

**Unknowns:** A Bode plot of the amplifier frequency response; the values of  $A_v(0)$  and  $f_H$

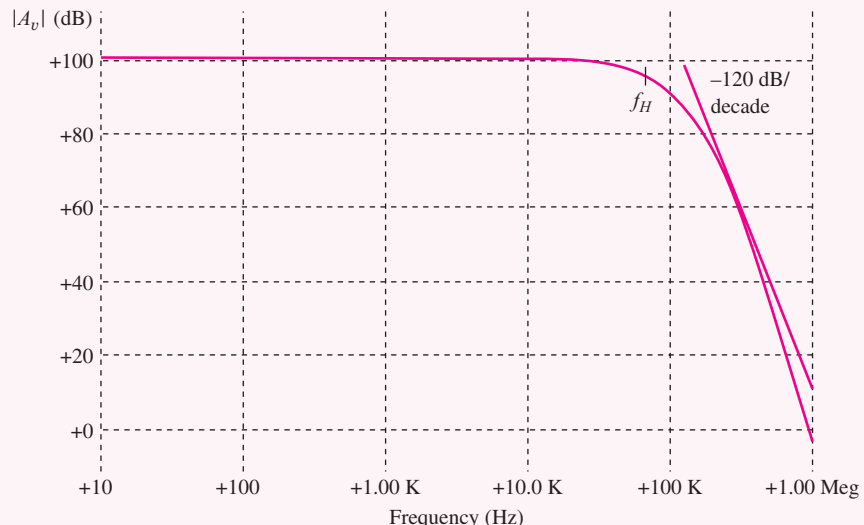
**Approach:** Use a SPICE macro model for the op amp and use it to simulate the frequency response of the six-stage amplifier. Use SPICE subcircuits to simplify the analysis.

**Assumptions:** The amplifier is a single-pole amplifier. Symmetrical 15-V power supplies are available.

**Analysis:** After drawing the circuit with the schematic editor, we need to set the parameters of the SPICE op amp model to agree with our specifications. The differential-mode gain and input resistance and the output resistance are given. We need to calculate the frequency of the first pole:  $f_B = f_T/A_o = 10 \text{ Hz}$ .



VI is an 1-V ac source with a dc value of 0 V. Since the amplifier is dc-coupled, a transfer function analysis from source VI to the output node will give the low-frequency gain, input resistance, and output resistance. An ac analysis using FSTART = 100 Hz, FSTOP = 1 MHz, and 10 frequency points per decade will produce the Bode plot needed to find the bandwidth. The simulation results yield a gain of 100.7 dB,  $R_{in} = 28.9 \text{ T}\Omega$ ,  $R_{out} = 3.52 \text{ m}\Omega$ , and the bandwidth is 54.8 kHz.



**Check of Results:** We see some discrepancies. The gain and output resistance agree with our calculations, but the bandwidth is larger than expected, and the input resistance is far too small. We should immediately be concerned about our simulation results. Indeed, a closer examination of the Bode plot also shows that the high-frequency roll-off is exceeding the  $6(20 \text{ dB/decade}) = 120 \text{ dB/decade}$  slope that we should expect.

**Discussion:** The problems are buried in the macro model in which all of the unspecified parameters have default values. If we look at the op amp model in the version of SPICE used here, we find the default values are the same as given in Table 11.4: common-mode input resistance =  $2 \text{ G}\Omega$ , second pole frequency = 2 MHz, offset voltage = 1 mV, input bias current = 80 nA, input offset current = 20 nA, etc. The input resistance cannot exceed the value set by  $R_{ic}$ , and the bandwidth

and roll-off enhancements are actually caused by the second op amp pole at 2 MHz. If we change  $R_{ic}$  to  $10^{15} \Omega$  and set the higher-order pole frequencies all to 200 MHz, SPICE yields an input resistance of  $28.9 \text{ T}\Omega$  and a bandwidth of 50.4 kHz, close to the expected values. In addition, the high-frequency roll-off rate is 120 dB/decade.

An additional problem was encountered in this simulation. In the initial simulation attempts, very small values of voltage gain were generated. An operating point analysis indicated that several of the op amp output voltages were at large values. Here again, the default parameter settings were causing the problem. This amplifier has very high overall gain, and a 1-mV offset voltage at the input of the first amplifier multiplied by the gain of 100,000 should produce 100 V at the output of the sixth amplifier! In order for the simulation to work, the offset voltage, input bias current, and input offset currents must all be set to zero in our op amp model!

The results discussed in the previous paragraph are also of significant practical interest! If we attempt to build this amplifier, we will encounter exactly the same problem. The offset voltages and input bias currents of the amplifier will cause the individual op amp outputs to saturate against the power supply levels.

**EXERCISE:** Simulate the amplifier with the dc value of  $V_I$  set to 1 mV. What are the op amp output voltages?

**ANSWERS:** 6.91 mV, 47.7 mV, 330 mV, 2.28 V, 15 V, 15 V; the last two are saturated.

## 12.2 THE INSTRUMENTATION AMPLIFIER

We often need to amplify the difference in two signals but cannot use the difference amplifier in Fig. 12.3 because its input resistance is too low. In such a case, we can combine two noninverting amplifiers with a difference amplifier to form the high-performance composite **instrumentation amplifier** depicted in Fig. 12.4.

In this circuit, op amp 3, with resistors  $R_3$  and  $R_4$ , forms a difference amplifier. Using Eq. (10.63), the output voltage  $v_o$  is

$$v_o = \left( -\frac{R_4}{R_3} \right) (v_a - v_b) \quad (12.10)$$

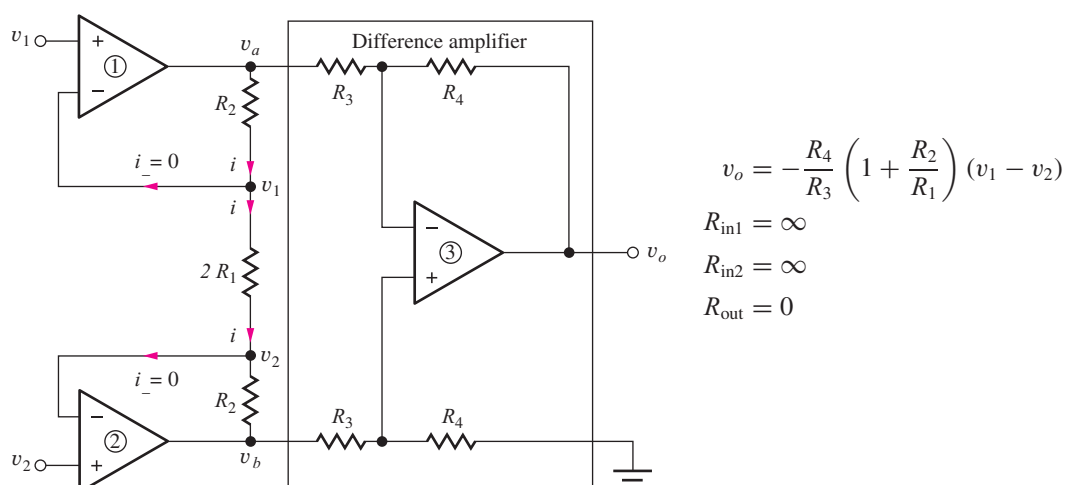


Figure 12.4 Circuit for the instrumentation amplifier.

in which voltages  $\mathbf{v}_a$  and  $\mathbf{v}_b$  are the outputs of the first two amplifiers. Because the  $i_-$  input currents to amplifiers 1 and 2 must be zero, voltages  $\mathbf{v}_a$  and  $\mathbf{v}_b$  are related to each other by

$$\mathbf{v}_a - iR_2 - i(2R_1) - iR_2 = \mathbf{v}_b \quad \text{or} \quad \mathbf{v}_a - \mathbf{v}_b = 2i(R_1 + R_2) \quad (12.11)$$

Since the voltage across the inputs of op amps 1 and 2 must both be zero, the voltage difference ( $\mathbf{v}_1 - \mathbf{v}_2$ ) appears directly across the resistor  $2R_1$ , and

$$i = \frac{\mathbf{v}_1 - \mathbf{v}_2}{2R_1} \quad (12.12)$$

Combining Eqs. (12.10), (12.11), and (12.12) yields a final expression for the output voltage of the instrumentation amplifier:

$$\mathbf{v}_o = -\frac{R_4}{R_3} \left( 1 + \frac{R_2}{R_1} \right) (\mathbf{v}_1 - \mathbf{v}_2) \quad (12.13)$$

The ideal instrumentation amplifier amplifies the difference in the two input signals and provides a gain that is equivalent to the product of the gains of the noninverting and difference amplifiers. The input resistance presented to both input sources is infinite because the input current to both op amps is zero, and the output resistance is forced to zero by the difference amplifier.

### EXAMPLE 12.5 INSTRUMENTATION AMPLIFIER ANALYSIS

The three op amp output voltages are calculated for a specific set of dc input voltages in this example.

**PROBLEM** Find the values of  $V_O$ ,  $V_A$ , and  $V_B$  for the instrumentation amplifier in Fig. 12.4 if  $V_1 = 2.5$  V,  $V_2 = 2.25$  V,  $R_1 = 15$  k $\Omega$ ,  $R_2 = 150$  k $\Omega$ ,  $R_3 = 15$  k $\Omega$ , and  $R_4 = 30$  k $\Omega$ .

**SOLUTION** **Known Information and Given Data:**  $V_1 = 2.5$  V,  $V_2 = 2.25$  V,  $R_1 = 15$  k $\Omega$ ,  $R_2 = 150$  k $\Omega$ ,  $R_3 = 15$  k $\Omega$ , and  $R_4 = 30$  k $\Omega$  for the circuit configuration in Fig. 12.4.

**Unknowns:** The values of  $V_O$ ,  $V_A$ , and  $V_B$

**Approach:** All the values are specified to permit direct use of Eq. (12.13)

**Assumptions:** The op amps are ideal. Therefore  $I_+ = 0 = I_-$  and  $V_+ = V_-$  for each op amp.

**Analysis:** Using Eq. (12.13) with dc values, we find the output voltage is

$$V_O = -\frac{R_4}{R_3} \left( 1 + \frac{R_2}{R_1} \right) (V_1 - V_2) = -\frac{30 \text{ k}\Omega}{15 \text{ k}\Omega} \left( 1 + \frac{150 \text{ k}\Omega}{15 \text{ k}\Omega} \right) (2.5 - 2.25) = -5.50 \text{ V}$$

Since the op amp input currents are zero,  $V_A$  and  $V_B$  can be related directly to the two input voltages and current  $i$

$$V_A = V_1 + IR_2 \quad \text{and} \quad V_B = V_2 - IR_2$$

$$I = \frac{V_1 - V_2}{2R_1} = \frac{2.5 \text{ V} - 2.25 \text{ V}}{2(15 \text{ k}\Omega)} = 8.33 \mu\text{A}$$

$$V_A = 2.5 + (8.33 \mu\text{A})(150 \text{ k}\Omega) = +3.75 \text{ V} \quad V_B = 2.25 - (8.33 \mu\text{A})(150 \text{ k}\Omega) = 1.00 \text{ V}$$

**Check of Results:** The unknowns have all been determined. Let us check to see if these voltages are consistent with the difference amplifier that should amplify its input by a factor of  $-2$ :

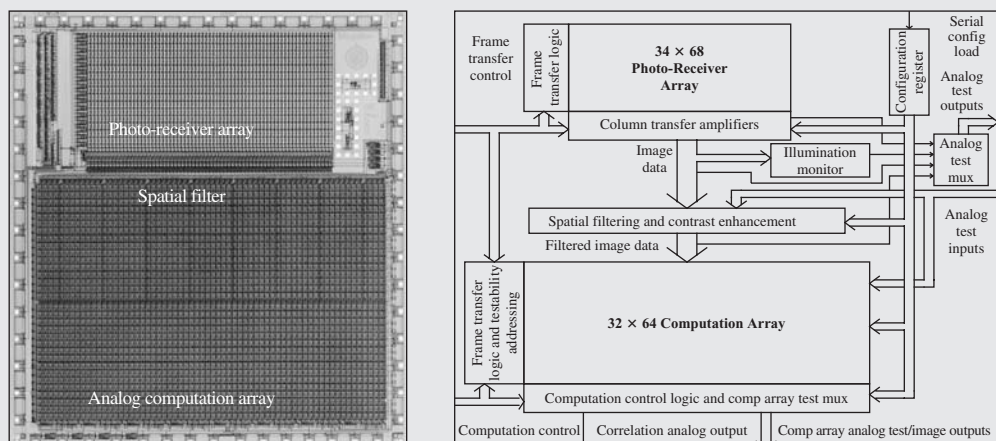
$$V_O = -\frac{R_4}{R_3}(V_A - V_B) = -\frac{30 \text{ k}\Omega}{15 \text{ k}\Omega}(3.75 - 1.00) \text{ V} = -5.50 \text{ V} \quad \checkmark$$

## ELECTRONICS IN ACTION

### **CMOS Navigation Chip Prototype for Optical Mice**

Agilent Technologies has sold over 100 million optical navigation mouse sensors, the devices at the core of most optical mice sold today. However, as is often the case in the engineering world, the navigation technology was originally developed for a different application. In 1993, a group of engineers at Hewlett-Packard Laboratories led by Ross Allen envisioned a handheld, battery powered document scanner that could be moved across a page in a freehand motion and still accurately recover the text. To help make this vision a reality, Travis Blalock and Dick Baumgartner at HP Labs designed a CMOS integrated circuit to optically measure movement of the scanner across the paper. The chip, known as “Magellan” within HP, is shown below.

Similar to digital cameras, the prototype contains a photo-receiver array to acquire images of the scanned surface, which is illuminated and positioned under the chip. The images are then transferred from the photo-receiver array to a computation array. The computation array always contains a reference image and a current image. Two-dimensional cross-correlations are then computed between the two images. The cross-correlation results can then be used to calculate the physical movement between the reference image and current image.



Optical navigation chip photo and block diagram. (Courtesy of Travis N. Blalock)

The Magellan optical navigation chip contains over 6000 operational amplifiers and sample-and-hold circuits, over 2000 photo-transistor amplifiers, and acquires 25,000 images per second. The chip calculates the cross-correlations at a rate of over 1.5 billion computations per second.

After a successful technology demonstration, the prototype was transferred to a product division and modified to create a commercial product. At some point in this process, it was recognized that the optical navigation architecture could be used as the basis for an optical mouse. The navigation chip design was again modified and became the basis of an optical navigation module sold by Agilent Technologies (a spinoff of the Hewlett-Packard company) and is used as the basis of most of the available optical mice on the market today.

**EXERCISE:** Suppose  $v_1$  and  $v_2$  are dc voltages with  $V_1 = 5.001$  V,  $V_2 = 4.999$  V,  $R_1 = 1$  k $\Omega$ ,  $R_2 = 49$  k $\Omega$ ,  $R_3 = 10$  k $\Omega$ , and  $R_4 = 10$  k $\Omega$  in Fig. 12.4. Write expressions for  $V_A$  and  $V_B$ . What are the values of  $V_O$ ,  $V_A$ ,  $V_B$ , and  $I$ ?

**ANSWERS:**  $V_A = V_1 + I R_2$ ,  $V_B = V_2 - I R_2$ ;  $-0.100$  V,  $5.05$  V,  $4.95$  V,  $1.00$   $\mu$ A

## 12.3 ACTIVE FILTERS

Filters come in many forms. We have looked at the characteristics of low-pass, high-pass, band-pass, and band-reject filters in Chapters 1 and 10. The simplest filter implementation uses passive components, resistors, capacitors, and inductors. In integrated circuits, however, inductors are difficult to fabricate, take up significant area, and can only be made with very small values of inductance. With the advent of low-cost high-performance op amps, new circuits were invented that could realize the desired filter characteristics without the use of inductors. These filters utilizing op amps are referred to as **active filters**, and this section discusses examples of active low-pass, high-pass, and band-pass filters. A simple active low-pass filter was discussed in Sec. 10.10.5, but this circuit produced only a single pole. Many of the filters described in this section are more efficient in the sense that the circuits achieve two poles of filtering per op amp. The interested reader can explore the material further in many texts that deal exclusively with active-filter design.

### 12.3.1 LOW-PASS FILTER

A basic two-pole low-pass filter configuration is shown in Fig. 12.5 and is formed from an op amp with two resistors and two capacitors. In this particular circuit, the op amp operates as a voltage follower, which provides unity gain over a wide range of frequencies. The filter uses positive feedback through  $C_1$  at frequencies above dc to realize complex poles without the need for inductors.

Let us now find the transfer function describing the voltage gain of this filter. The ideal op amp forces  $\mathbf{V}_o(s) = \mathbf{V}_2(s)$ , so there are only two independent nodes in the circuit. Writing nodal equations for  $\mathbf{V}_1(s)$  and  $\mathbf{V}_2(s)$  yields

$$\begin{bmatrix} G_1 \mathbf{V}_1(s) \\ 0 \end{bmatrix} = \begin{bmatrix} sC_1 + G_1 + G_2 & -(sC_1 + G_2) \\ -G_2 & sC_2 + G_2 \end{bmatrix} \begin{bmatrix} \mathbf{V}_1(s) \\ \mathbf{V}_2(s) \end{bmatrix} \quad (12.14)$$

and the determinant of this system of equations is

$$\Delta = s^2 C_1 C_2 + s C_2 (G_1 + G_2) + G_1 G_2 \quad (12.15)$$

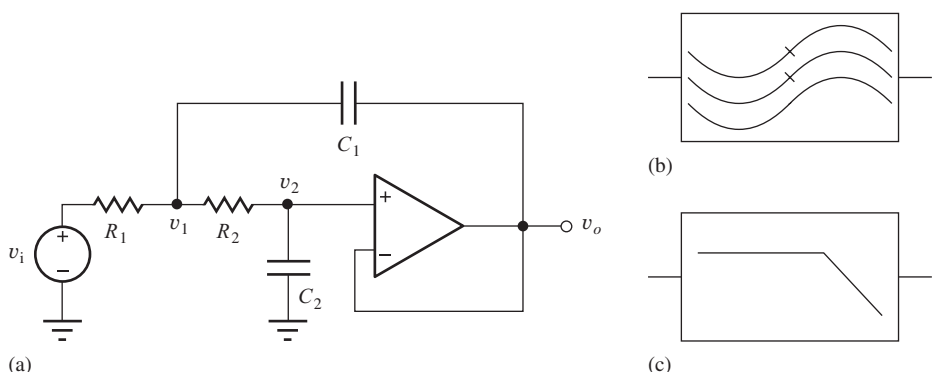


**Figure 12.5** (a) A two-pole low-pass filter. (b) Low-pass filter symbol. (c) Alternate low-pass filter symbol.

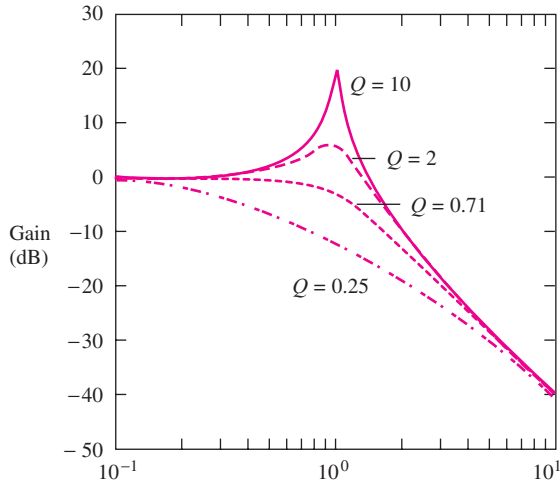


**Figure 12.6** Low-pass filter response<sup>2</sup> for  $\omega_o = 1$  and four values of  $Q$ .

Solving for  $\mathbf{V}_2(s)$  and remembering that  $\mathbf{V}_o(s) = \mathbf{V}_2(s)$  yields

$$\mathbf{V}_o(s) = \mathbf{V}_2(s) = \frac{G_1 G_2}{\Delta} \mathbf{V}_I(s) \quad (12.16)$$

which can be rearranged as

$$A_{LP}(s) = \frac{\mathbf{V}_o(s)}{\mathbf{V}_I(s)} = \frac{1}{s^2 + s \frac{1}{C_1} \left( \frac{1}{R_1} + \frac{1}{R_2} \right) + \frac{1}{R_1 R_2 C_1 C_2}} \quad (12.17)$$

Equation (12.17) is most often written in standard form as

$$A_{LP}(s) = \frac{\omega_o^2}{s^2 + s \frac{\omega_o}{Q} + \omega_o^2} \quad (12.18)$$

in which

$$\omega_o = \frac{1}{\sqrt{R_1 R_2 C_1 C_2}} \quad \text{and} \quad Q = \sqrt{\frac{C_1}{C_2} \frac{\sqrt{R_1 R_2}}{R_1 + R_2}} \quad (12.19)$$

The frequency  $\omega_o$  is referred to as the cutoff frequency of the filter, although the exact value of the cutoff frequency, based on the strict definition of  $\omega_H$ , is equal to  $\omega_o$  only for  $Q = 1/\sqrt{2}$ . At low frequencies—that is,  $\omega \ll \omega_o$ —the filter has unity gain, but for frequencies well above  $\omega_o$ , the filter response exhibits a two-pole roll-off, falling at a rate of 40 dB/decade. At  $\omega = \omega_o$ , the gain of the filter is equal to  $Q$ .

Figure 12.6 shows the response of the filter for  $\omega_o = 1$  and four values of  $Q$ : 0.25,  $1/\sqrt{2}$ , 2, and 10.  $Q = 1/\sqrt{2}$  corresponds to the **maximally flat magnitude** response of a **Butterworth filter**, which gives the maximum bandwidth without a peaked response. For a  $Q$  larger than  $1/\sqrt{2}$ , the filter response exhibits a peaked response that is usually undesirable, whereas a  $Q$  below  $1/\sqrt{2}$  does not take maximum advantage of the filter's bandwidth capability. Because the voltage follower must accurately provide a gain of 1,  $\omega_o$  should be designed to be one to two decades below the unity-gain frequency of the op amp.

From a practical point of view, a much wider selection of resistor values than capacitor values exists, and the filters are often designed with  $C_1 = C_2 = C$ . Then  $\omega_o$  and  $Q$  are adjusted by choosing

<sup>2</sup> Using MATLAB: `Bode(1,[1 0.1 1])`, for example.

different values of  $R_1$  and  $R_2$ . For the equal capacitor design,

$$\omega_o = \frac{1}{C\sqrt{R_1 R_2}} \quad \text{and} \quad Q = \frac{\sqrt{R_1 R_2}}{R_1 + R_2} \quad (12.20)$$

Another practical consideration concerns op amp bias currents. In order to operate properly, the active filter circuits must provide dc paths for the op amp bias currents. In the circuit in Fig. 12.5, the dc current for the noninverting input is supplied from the dc-referenced signal source through  $R_1$  and  $R_2$ . The dc current in the inverting input is supplied from the op amp output.

### DESIGN NOTE

In order for an op amp circuit to operate properly, the feedback network must provide a dc path for the amplifier's input bias currents.

## DESIGN EXAMPLE 12.6 LOW-PASS FILTER DESIGN

**PROBLEM** Determine the capacitor and resistor values required to meet a cutoff frequency specification in a two-pole active low-pass filter.

**SOLUTION** Design a low-pass filter using the circuit in Fig. 12.5 with an upper cutoff frequency of 5 kHz and a maximally flat response.

**Known Information and Given Data:** Second-order active low-pass filter circuit in Fig. 12.6; maximally flat design with  $f_H = 5$  kHz

**Unknowns:**  $R_1$ ,  $R_2$ ,  $C_1$ , and  $C_2$

**Approach:** As mentioned in Sec. 12.3, the maximally flat response for the transfer function in Eq. (12.18) is achieved for  $Q = 1/\sqrt{2}$ . For this case, we also find that  $f_H = f_o$ . Unfortunately, based on Eq. (12.19), the simple equal capacitor design cannot achieve this  $Q$ . We will need to explore another design option.

**Assumptions:** The operational amplifier is ideal.

**Analysis:** From Eq. (12.19), we see that one workable choice for the element values is  $C_1 = 2C_2 = 2C$  and  $R_1 = R_2 = R$ . For these values,

$$R = \frac{1}{\sqrt{2}\omega_o C} \quad \text{and} \quad Q = \frac{1}{\sqrt{2}}$$

but we still have two values to select and only one design constraint. We must call on our engineering judgment to make the design choice. Note that  $1/\omega_o C$  represents the reactance of  $C$  at the frequency  $\omega_o$ , and  $R$  is 30 percent smaller than this value. Thus, the impedance level of the filter is set by the choice of  $C$  (or  $R$ ). If the impedance level is too low, the op amp will not be able to supply the current needed to drive the feedback network.

At 5 kHz, a 0.01- $\mu$ F capacitor has a reactance of 3.18 k $\Omega$ :

$$\frac{1}{\omega_o C} = \frac{1}{10^4 \pi (10^{-8})} = 3180 \Omega$$

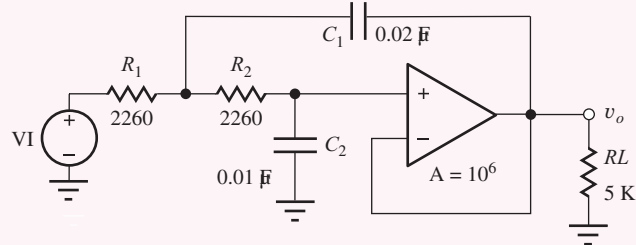
This is a readily available value of capacitance, and so

$$R = \frac{3180 \Omega}{\sqrt{2}} = 2250 \Omega$$

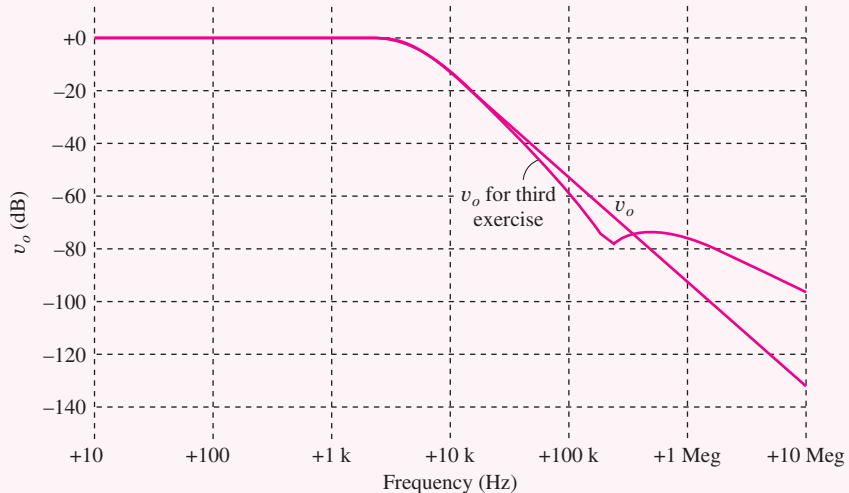
Referring to the precision resistor table in Appendix A, we find that the nearest 1 percent resistor value is  $2260 \Omega$ . The completed design values are

$$R_1 = R_2 = 2.26 \text{ k}\Omega, C_1 = 0.02 \mu\text{F}, C_2 = 0.01 \mu\text{F}$$

**Check of Results:** Using the design values yields  $f_o = 4980 \text{ Hz}$  and  $Q = 0.707$ .



**Discussion and Computer-Aided Analysis:** The frequency response of the filter is simulated using the circuit below. The op amp gain is set to  $10^6$ . An ac analysis is performed with VI as the source with FSTART = 10 Hz, FSTOP = 10 MHz, and 10 simulation points per frequency decade. The gain to the output node is 0 dB and  $f_H = 5 \text{ kHz}$ , in agreement with the design specification. A second simulation result appears in the graph below giving the frequency response for a μA741 op amp.



**EXERCISE:** What is  $A_v(0)$  for the filter design in the above example? Show that  $f_H = f_o$  for the maximally flat design with  $Q = 1/\sqrt{2}$ .

**ANSWER:** +1.00

**EXERCISE:** Redesign the filter in Ex. 12.6 to have an upper cutoff frequency of 10 kHz with a maximally flat response. Keep the impedance level of the filter the same.

**ANSWERS:**  $0.01 \mu\text{F}, 0.005 \mu\text{F}, 2260 \Omega, 2260 \Omega$ .

**EXERCISE:** Starting with Eq. (12.18), show that  $|A_{LP}(j\omega_o)| = Q$ .

**EXERCISE:** Change the cutoff frequency of this filter to 2 kHz by changing the values of  $R_1$  and  $R_2$ . Do not change the  $Q$ .

**ANSWERS:**  $R_1 = R_2 = 5.62 \text{ k}\Omega$

**EXERCISE:** Use the  $Q$  expression in Eq. (12.20) to show that  $Q = 1/\sqrt{2}$  cannot be realized using the equal capacitance design. What is the maximum  $Q$  for  $C_1 = C_2$ ?

**ANSWER:** 0.5

### 12.3.2 A HIGH-PASS FILTER WITH GAIN

A **high-pass filter** can be achieved with the same topology as Fig. 12.5 by interchanging the position of the resistors and capacitors, as shown in Fig. 12.7. In many applications, filters with gain in the midband region are preferred, and the voltage follower in the low-pass filter has been replaced with a noninverting amplifier with a gain of  $K$  in the filter of Fig. 12.7. Gain  $K$  provides an additional degree of freedom in the design of the filter elements. Note that dc paths exist for both op amp input bias currents through resistor  $R_2$  and the two feedback resistors.

The analysis is virtually identical to that of the low-pass filter. Nodes  $v_1$  and  $v_2$  are the only independent nodes because  $v_o = +Kv_2$ , and writing the two nodal equations yields this system of equations:

$$\begin{bmatrix} sC_1\mathbf{V}_1(s) \\ 0 \end{bmatrix} = \begin{bmatrix} s(C_1 + C_2) + G_1 & -(sC_2 + KG_1) \\ -sC_2 & sC_2 + G_2 \end{bmatrix} \begin{bmatrix} \mathbf{V}_1(s) \\ \mathbf{V}_2(s) \end{bmatrix} \quad (12.21)$$

The system determinant is

$$\Delta = s^2C_1C_2 + s(C_1 + C_2)G_2 + sC_2G_1(1 - K) + G_1G_2 \quad (12.22)$$

and the output voltage is

$$\mathbf{V}_o(s) = K\mathbf{V}_2(s) = K \frac{s^2C_1C_2\mathbf{V}_1(s)}{\Delta} \quad (12.23)$$

Combining Eqs. (12.22) and (12.23) yields the filter transfer function that can be written in standard form as

$$A_{HP}(s) = \frac{\mathbf{V}_o(s)}{\mathbf{V}_1(s)} = K \frac{s^2}{s^2 + s\frac{\omega_o}{Q} + \omega_o^2} \quad (12.24)$$

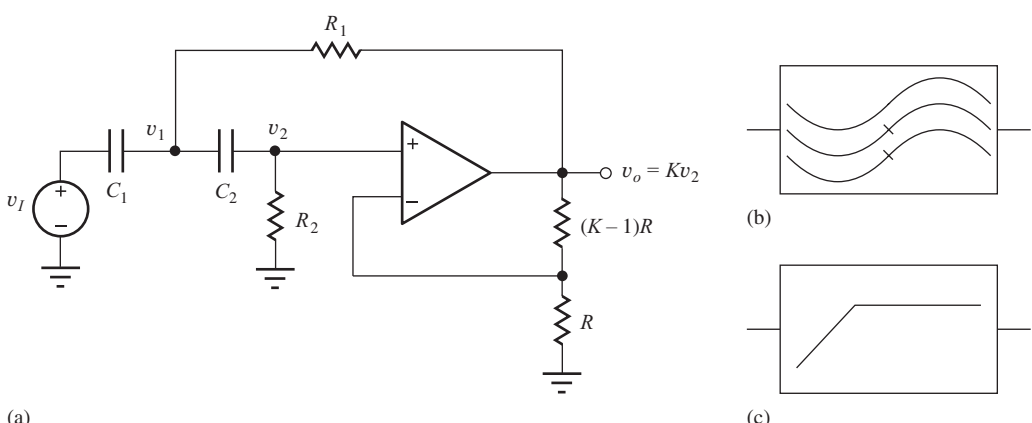


**Figure 12.7** (a) A high-pass filter with gain. (b) High-pass filter symbol. (c) Alternate high-pass filter symbol.

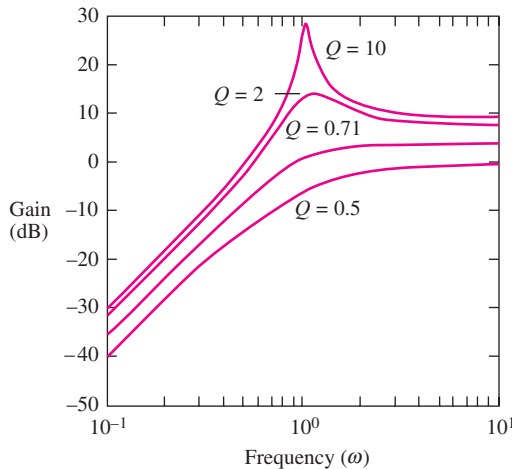


**Figure 12.8** High-pass filter response<sup>3</sup> for  $\omega_o = 1$  and four values of  $Q$ .

in which

$$\omega_o = \frac{1}{\sqrt{R_1 R_2 C_1 C_2}} \quad \text{and} \quad Q = \left[ \sqrt{\frac{R_1}{R_2}} \frac{C_1 + C_2}{\sqrt{C_1 C_2}} + (1 - K) \sqrt{\frac{R_2 C_2}{R_1 C_1}} \right]^{-1} \quad (12.25)$$

For the case  $R_1 = R_2 = R$  and  $C_1 = C_2 = C$ , Eqs. (12.24) and (12.25) can be simplified to

$$A_{HP}(s) = K \frac{s^2}{s^2 + s \frac{3-K}{RC} + \frac{1}{R^2 C^2}} \quad \omega_o = \frac{1}{RC} \quad \text{and} \quad Q = \frac{1}{3-K} \quad (12.26)$$

For this design choice,  $\omega_o$  and  $Q$  can be adjusted independently.

Figure 12.8 shows the high-pass filter responses for a filter with  $\omega_o = 1$  and four values of  $Q$ . The parameter  $\omega_o$  corresponds approximately to the lower-cutoff frequency of the filter, and  $Q = 1/\sqrt{2}$  again represents the maximally flat, or Butterworth, filter response.

The noninverting amplifier circuit in Fig. 12.7 must have  $K \geq 1$ . Note in Eq. (12.26) that  $K = 3$  corresponds to infinite  $Q$ . This situation corresponds to the poles of the filter being exactly on the imaginary axis at  $s = j\omega_o$  and results in sinusoidal oscillation. (Oscillators are discussed later in this chapter.) For  $K > 3$ , the filter poles will be in the right-half plane, and values of  $K \geq 3$  correspond to unstable filters. Therefore,  $1 \leq K < 3$ .

**EXERCISE:** What is the gain at  $\omega = \omega_o$  for the filter described by Eq. (12.26)?

**ANSWER:**  $\frac{K}{3-K}$

**EXERCISE:** The high-pass filter in Fig. 12.7 has been designed with  $C_1 = 0.0047 \mu\text{F}$ ,  $C_2 = 0.001 \mu\text{F}$ ,  $R_1 = 10 \text{ k}\Omega$ , and  $R_2 = 20 \text{ k}\Omega$ , and the amplifier gain is 2. What are  $f_o$  and  $Q$  for this filter?

**ANSWERS:** 5.19 kHz, 0.828

<sup>3</sup> Using MATLAB: `Bode([(3-sqrt(2)) 0 0],[1 sqrt(2) 1])`, for example.

**EXERCISE:** Derive an expression for the sensitivity of  $Q$  with respect to the closed-loop gain  $K$  for the high-pass filter in Fig. 12.7 (See Eq. 12.39). What is the value of sensitivity if  $Q = 1/\sqrt{2}$ ?

**ANSWERS:**  $S_K^Q = (3 - Q); 1.12$

### 12.3.3 BAND-PASS FILTER

A **band-pass filter** can be realized by combining the low-pass and high-pass characteristics of the previous two filters. Figure 12.9 is one possible circuit for such a band-pass filter. In this case, the op amp is used in its inverting configuration; this circuit is sometimes called an “infinite-gain” filter because the full open-loop gain of the op amp, ideally infinity, is utilized. Resistor  $R_3$  is added to provide an extra degree of design freedom so that gain, center frequency, and  $Q$  can be set with a minimum of interaction. Note again that dc paths exist for both op amp input bias currents.

Analysis of the circuit in Fig. 12.9(b) can be reduced to a one-node problem by using op amp theory to relate  $\mathbf{V}_o(s)$  directly to  $\mathbf{V}_1(s)$ :

$$sC_2\mathbf{V}_1(s) = -\frac{\mathbf{V}_o(s)}{R_2} \quad \text{or} \quad \mathbf{V}_1(s) = -\frac{\mathbf{V}_o(s)}{sC_2R_2} \quad (12.27)$$

Using KCL at node  $v_1$ ,

$$G_{\text{th}}\mathbf{V}_{\text{th}} = [s(C_1 + C_2) + G_{\text{th}}]\mathbf{V}_1(s) - sC_1\mathbf{V}_o(s) \quad (12.28)$$

Combining Eqs. (12.27) and (12.28) yields

$$\frac{\mathbf{V}_o(s)}{\mathbf{V}_{\text{th}}(s)} = \frac{-\frac{s}{R_{\text{th}}C_1}}{s^2 + s\frac{1}{R_2}\left(\frac{1}{C_1} + \frac{1}{C_2}\right) + \frac{1}{R_{\text{th}}R_2C_1C_2}} \quad (12.29)$$

The band-pass output can now be expressed as

$$A_{BP}(s) = -\frac{V_o(s)}{V_I(s)} = -\sqrt{\frac{R_3}{R_1 + R_3}\frac{R_2C_2}{R_1C_1}} \frac{s\omega_o}{s^2 + s\frac{\omega_o}{Q} + \omega_o^2} \quad (12.30)$$

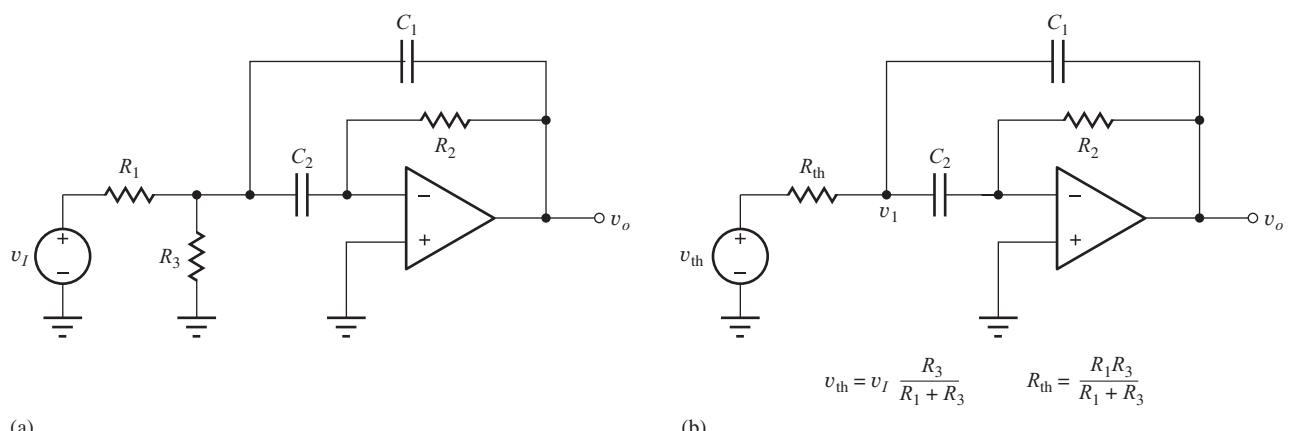


**Figure 12.9** (a) Band-pass filter using inverting op amp configuration. (b) Simplified band-pass filter circuit.

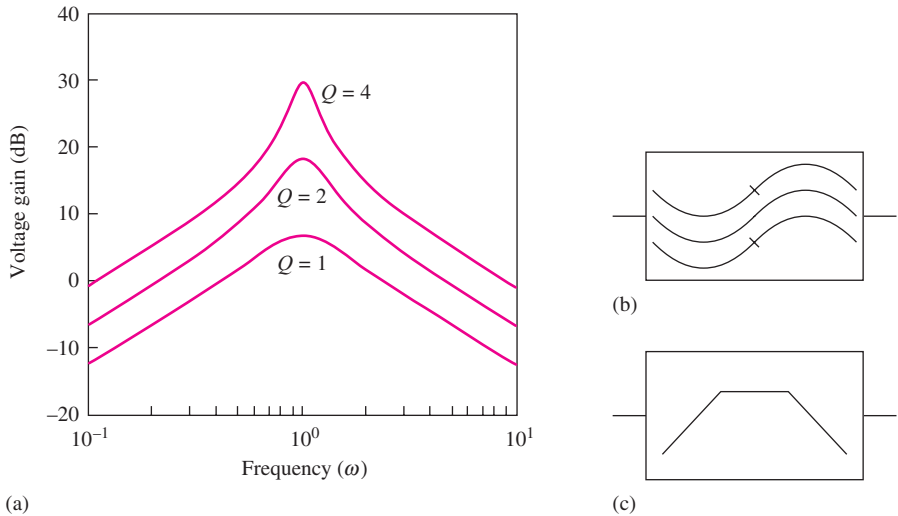


**Figure 12.10** (a) Band-pass filter response<sup>4</sup> for  $\omega_o = 1$  and three values of  $Q$  assuming  $C_1 = C_2$  with  $R_3 = \infty$ . (b) Band-pass filter symbol. (c) Alternate band-pass filter symbol.

with

$$\omega_o = \frac{1}{\sqrt{R_{th} R_2 C_1 C_2}} \quad \text{and} \quad Q = \sqrt{\frac{R_2}{R_{th}} \frac{\sqrt{C_1 C_2}}{C_1 + C_2}} \quad (12.31)$$

If  $C_1$  is set equal to  $C_2 = C$ , then

$$\begin{aligned} \omega_o &= \frac{1}{C \sqrt{R_{th} R_2}} \quad Q = \frac{1}{2} \sqrt{\frac{R_2}{R_{th}}} \quad \text{BW} = \frac{2}{R_2 C} \\ A_{BP}(s) &= - \left( \frac{2Q}{1 + \frac{R_1}{R_3}} \right) \left( \frac{s \omega_o}{s^2 + s \frac{\omega_o}{Q} + \omega_o^2} \right) \quad A_{BP}(\omega_o) = -\frac{1}{2} \left( \frac{R_2}{R_1} \right) \end{aligned} \quad (12.32)$$

The response of the band-pass filter is shown in Fig. 12.10 for  $\omega_o = 1$ ,  $C_1 = C_2$ ,  $R_3 = \infty$ , and three values of  $Q$ . Parameter  $\omega_o$  now represents the center frequency of the band-pass filter. The response peaks at  $\omega_o$ , and the gain at the center frequency is equal to  $2Q^2$ . At frequencies much less than or much greater than  $\omega_o$ , the filter response corresponds to a single-pole high- or low-pass filter, changing at a rate of 20 dB/decade.

**EXERCISE:** The filter in Fig. 12.9 is designed with  $C_1 = C_2 = 0.02 \mu\text{F}$ ,  $R_1 = 2 \text{k}\Omega$ ,  $R_3 = 2 \text{k}\Omega$ , and  $R_2 = 82 \text{k}\Omega$ . What are the values of  $f_o$  and  $Q$ ?

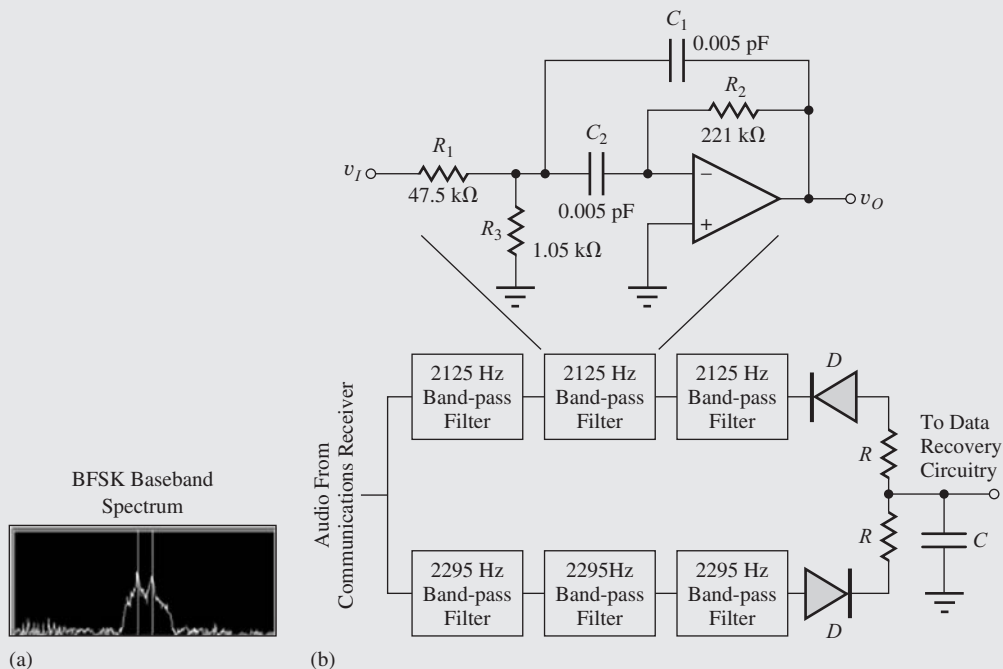
**ANSWERS:** 879 Hz, 4.5

<sup>4</sup> Using MATLAB: `Bode([4 0],[1.5 1])`, for example.



### Band-Pass Filters in BFSK Reception

Binary frequency shift keying (BFSK) is a basic form of modulation that is studied in communications classes and represents a type of communications that is commonly used for radio teletype transmissions in the high-frequency or “short wave” radio bands (3–30 MHz). The signal transmitting the data shifts back and forth between two closely spaced radio frequencies (for example, 18,080,000 Hz and 18,080,170 Hz). In the block diagram in the accompanying figure, a communications receiver that is receiving this transmission produces an audio signal at its output that shifts between 2125 Hz and 2295 Hz (or some other convenient frequency pair separated by a frequency shift of 170 Hz). In the analog signal processing circuit here, six-pole filters are used to separate these two audio tones. Each filter bank consists of a cascade of three, two-pole active band-pass filters as described in Sec. 12.3.3. The outputs of the two filter banks are rectified and filtered by an RC network to form a simple frequency discriminator. The output of the discriminator then drives circuitry that recovers the original data transmission.



These same functions can be performed in the digital domain using digital signal processing (DSP) if the audio signal from the communications receiver is first digitized by an analog-to-digital (A/D) converter.

#### 12.3.4 THE TOW-THOMAS BIQUAD

Many single-amplifier filters do not permit independent design of  $\omega_o$ ,  $Q$ , and midband gain. Multi-amplifier filters trade increased component cost for ease of design and low sensitivity to component variations and can be used to realize the general biquadratic transfer function defined by

$$T(s) = \frac{a_2 s^2 + a_1 s + a_0}{s^2 + \frac{\omega_o}{Q} s + \omega_o^2} \quad (12.33)$$

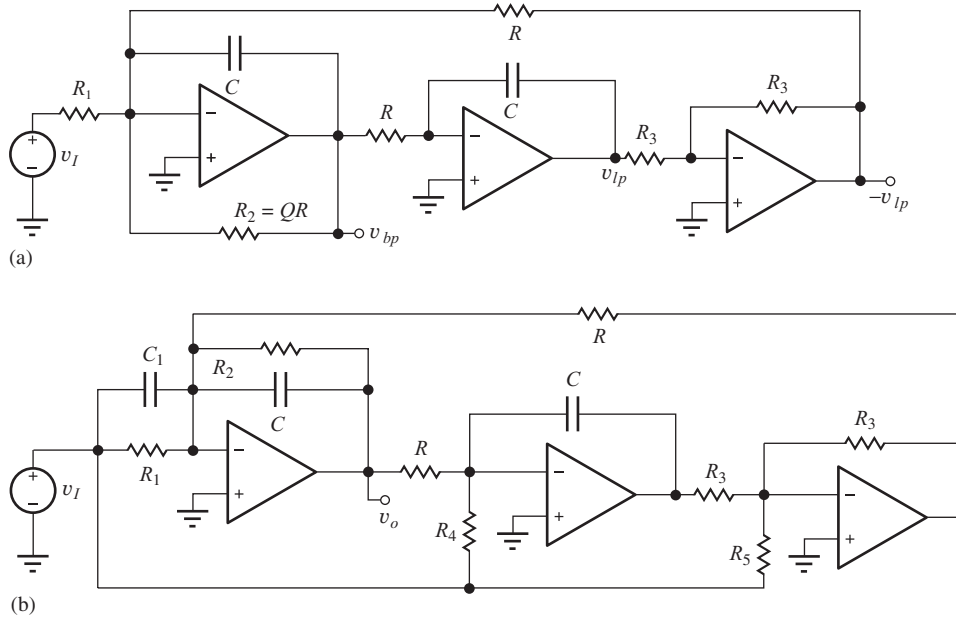


**Figure 12.11** (a) Tow-Thomas filter with band-pass and low-pass outputs. (b) Full Tow-Thomas biquad.

Low-pass, high-pass, band-pass, **all-pass**, and **notch filters** can all be represented by this transfer function with appropriate choices of the numerator coefficients. Compare Eq. (12.33) with Eqs. (12.32), (12.24), and (12.18). Multi-op-amp filters are also used to achieve higher  $Q$ s than are practical with single op amp designs. One example of a two-pole filter using several op amps is the **Tow-Thomas biquad** in Fig. 12.11(a). The Tow-Thomas biquad inherently produces band-pass and low-pass outputs at  $v_{bp}$  and  $v_{lp}$ , respectively, but the other filter functions can easily be obtained with the addition of a few passive components, as in Fig. 12.11(b).

The filter response in Fig. 12.11(a) can be found by treating the first op amp as a multi-input integrator and noting that the third op amp simply forms an inverter with  $V_o(s) = -V_{lp}(s)$ . Using superposition, the output of the first integrator can be written as

$$V_{bp}(s) = -\frac{1}{sR_1C}V_I(s) - \frac{1}{sRC}[-V_{lp}(s)] - \frac{1}{sR_2C}V_{bp}(s) \quad (12.34)$$

$V_{lp}(s)$  and  $V_{bp}(s)$  are related to each other by the second integrator:

$$V_{lp}(s) = -\frac{1}{sRC}V_{bp}(s) \quad (12.35)$$

Combining Eqs. (12.34) and (12.35) and solving for  $V_{bp}(s)$  gives

$$A_{BP}(s) = \frac{V_{bp}(s)}{V_I(s)} = -\frac{\left(\frac{R}{R_1}\right)\frac{s}{RC}}{s^2 + s\left(\frac{R}{R_2}\right)\frac{1}{RC} + \frac{1}{R^2C^2}} = -K \frac{s\omega_o}{s^2 + s\frac{\omega_o}{Q} + \omega_o^2} \quad (12.36)$$

in which

$$K = \left(\frac{R}{R_1}\right) \quad \omega_o = \frac{1}{RC} \quad Q = \frac{R_2}{R} \quad BW = \frac{1}{R_2C}$$

The low-pass output is obtained using Eqs. (12.35) and (12.36):

$$A_{LP}(s) = K \frac{\frac{1}{R^2 C^2}}{s^2 + s \frac{1}{R_2 C} + \frac{1}{R^2 C^2}} = K \frac{\omega_o^2}{s^2 + s \frac{\omega_o}{Q} + \omega_o^2} \quad (12.37)$$

It can be observed that the center frequency  $\omega_o$ ,  $Q$ , and gain  $K$  of the filter are each controlled by separate element values and can all be adjusted independently.

Figure 12.11(b) shows the addition of the components needed to achieve other forms of the biquadratic transfer function. If  $v_O$  is defined as the output of the first amplifier, then

$$A_v(s) = \frac{V_o(s)}{V_I(s)} = -\frac{s^2 \left( \frac{C_1}{C} \right) + \frac{s}{C} \left( \frac{1}{R_1} - \frac{R_3}{RR_5} \right) + \frac{1}{RR_4 C^2}}{s^2 + s \left( \frac{R}{R_2} \right) \frac{1}{RC} + \frac{1}{R^2 C^2}} \quad (12.38)$$

## DESIGN TOW-THOMAS FILTER DESIGN

### EXAMPLE 12.7

In this example, we will design a band-pass filter using the Tow-Thomas circuit.

**PROBLEM** Design a band-pass filter using the Tow-Thomas circuit to meet the following specifications: center frequency = 2000 Hz, bandwidth = 200 Hz, and midband gain = 20.

**SOLUTION** **Known Information and Given Data:** Tow-Thomas filter circuit with a center frequency  $f_o = 2000$  Hz, bandwidth  $BW = 200$  Hz, and midband gain  $|A_v(j\omega_o)| = 20$

**Unknowns:**  $R$ ,  $R_1$ ,  $R_2$ ,  $R_3$ , and  $C$

**Approach:** We are given the circuit topology and the values of center frequency, bandwidth, and midband gain. Also, the  $Q$  of this filter is  $Q = f_o/BW = 10$ . In equation set (12.36), we see we have four circuit values to choose ( $R$ ,  $R_1$ ,  $R_2$ ,  $C$ ), but only three constraints have been specified. This is a situation often encountered in design. In addition, we must pick a value for  $R_3$  that does not directly appear in the band-pass filter equations.

**Assumptions:** The op amps are ideal.

**Analysis:** Let us set up the equations in a logical flow so that one value may be chosen, and it will then determine the others. Based on the values listed in Appendix A, we see that the choices for  $C$  are much more limited than those for the resistors, so we will choose  $C$  first. Then,

$$R = \frac{1}{\omega_o C} \quad R_2 = QR \quad R_1 = -\frac{R_2}{A_v(0)}$$

For the values in this design,

$$R = \frac{1}{4000\pi C} \quad R_2 = 10R \quad R_1 = \frac{R_2}{20} = \frac{R}{2}$$

An additional consideration is the “impedance level” of the filter. Looking at Fig. 12.11(a), we note that the input resistance to the filter is set by  $R_1$ . Also note that the magnitude of the reactance of the capacitor at the center frequency is given by

$$X_C = \frac{1}{\omega_o C} = R = 2R_1$$

As was discussed in Chapter 11, op amps have limited output current drive capability (e.g.,  $R_L > 2 \text{ k}\Omega$  for the LF155 and AD741 amplifiers—see website). The first op amp in the filter must supply ac signal current to the parallel combination of  $R$ ,  $R_2$ , and  $C$ , the second op amp must drive the parallel combination of  $R_3$  and  $C$ , and the third must drive  $R_3$  in parallel with  $R$ . A spreadsheet will help us visualize the design choices.

$C$	$R$	$R_2$	$R_1$	$R \parallel R_2 \parallel X_C$
1.00E - 09	7.96E + 04	7.96E + 05	3.98E + 04	19894
2.00E - 09	3.98E + 04	3.98E + 05	1.99E + 04	9947
2.20E - 09	3.62E + 04	3.62E + 05	1.81E + 04	9043
<b>2.70E - 09</b>	<b>2.95E + 04</b>	<b>2.95E + 05</b>	<b>1.47E + 04</b>	<b>7368</b>
3.30E - 09	2.41E + 04	2.41E + 05	1.21E + 04	6029

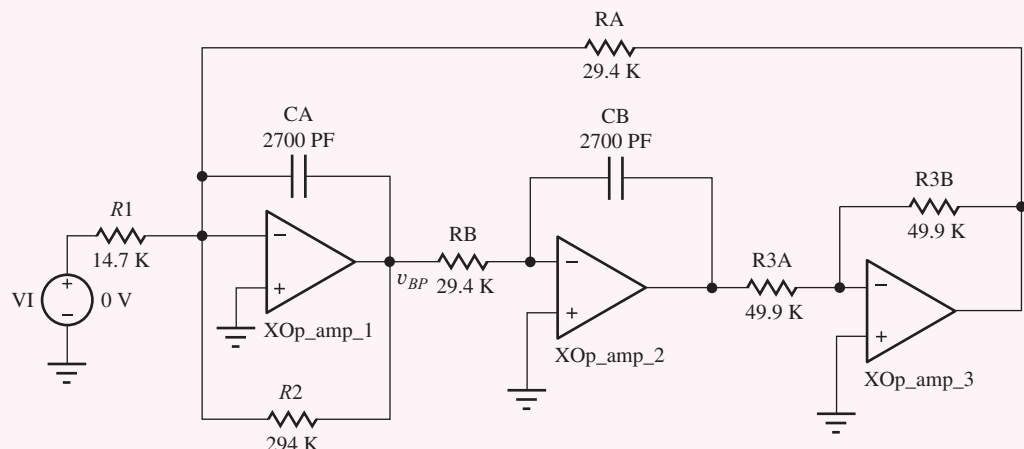
The bold row appears to be one reasonable choice. Based on Appendix A, our design can use  $C = 2700 \text{ pF}$ ,  $R = 29.4 \text{ k}\Omega$ ,  $R_2 = 294 \text{ k}\Omega$ , and  $R_1 = 14.7 \text{ k}\Omega$ . The input resistance of the filter will be  $14.7 \text{ k}\Omega$ , and the load impedance on the first op amp is on the order of  $7.37 \text{ k}\Omega$ . Finally, the choice of  $R_3$  is arbitrary as long as it is large enough not to load down the second and third op amps.  $R_3 = 49.9 \text{ k}\Omega$  is a reasonable choice.

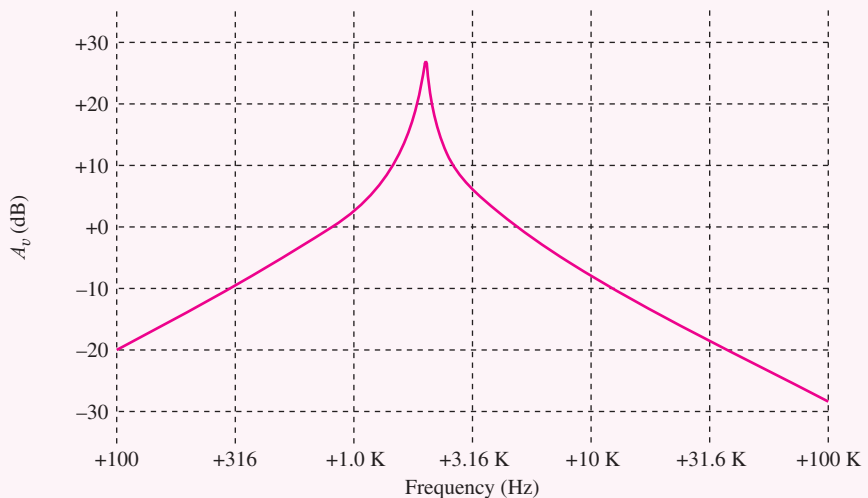
**Check of Results:** Using the standard values selected:

$$A_v(0) = -20.0 \quad f_o = \frac{1}{2\pi(29.4 \text{ k}\Omega)(2700 \text{ pF})} = 2005 \text{ Hz}$$

$$BW = \frac{1}{2\pi(294 \text{ k}\Omega)(2700 \text{ pF})} = 200.5 \text{ Hz}$$

**Computer Aided Design:** The filter response is simulated using the circuit below with these parameters for the op amps: input resistance =  $2 \text{ M}\Omega$ , gain = 106 dB, and output resistance =  $50 \Omega$ . An ac analysis is performed with VI as the input source with FSTART = 100 Hz, FSTOP = 100 kHz, and 10 simulation points per frequency decade. The SPICE results are  $f_o = 1.99 \text{ kHz}$ ,  $BW = 200 \text{ Hz}$ , and gain = 26.7 dB. Note that there is a slight gain enhancement and center frequency shift resulting from the nonideal op amp parameters.





**EXERCISE:** Simulate the filter in Ex. 12.7 with op amps having an open loop gain of 80 dB. What is the filter gain at the center frequency?

**ANSWER:** 31.5 dB.

**EXERCISE:** Redesign the filter in Ex. 12.7 to have a gain of 20 dB at the center frequency.

**ANSWER:** Change  $R_1$  to 29.4 k $\Omega$ .

**EXERCISE:** What standard resistor values would be used if the  $C = 2000$  pF design were utilized in Design Ex. 12.7? What are the center frequency, bandwidth, and voltage gain for that filter design?

**ANSWERS:**  $R = 40.2$  k $\Omega$ ,  $R_2 = 402$  k $\Omega$ ,  $R_1 = 20.0$  k $\Omega$ ,  $R_3 = 49.9$  k $\Omega$  can be used; 1980 Hz, 198 Hz, -20.1

**EXERCISE:** What are the worst-case values of the center frequency, bandwidth, and voltage gain for the filter design in Ex. 12.7 if the capacitor has a tolerance of 2 percent and the resistor tolerances are all 1 percent?

**ANSWERS:** 1946 Hz; 2067 Hz; 195 Hz; 207 Hz; -19.6; -20.4

### 12.3.5 SENSITIVITY

An important concern in the design of active filters is the **sensitivity** of  $\omega_o$  and  $Q$  to changes in passive element values and op amp parameters. The sensitivity of design parameter  $P$  to changes in circuit parameter  $Z$  is defined mathematically as

$$S_Z^P = \frac{\frac{\partial P}{\partial Z}}{\frac{P}{Z}} = \frac{Z}{P} \frac{\partial P}{\partial Z} \quad (12.39)$$

Sensitivity  $S$  represents the fractional change in parameter  $P$  due to a given fractional change in the value of  $Z$ . For example, evaluating the sensitivity of  $\omega_o$  with respect to the values of  $R$  and  $C$  using Eq. (12.19) yields

$$S_R^{\omega_o} = S_C^{\omega_o} = -\frac{1}{2} \quad (12.40)$$

A 2 percent increase in the value of  $R$  or  $C$  will cause a 1 percent decrease in the frequency  $\omega_o$ .

**EXERCISE:** Calculate  $S_{C_1}^Q$  and  $S_{R_2}^Q$  for the low-pass filter using Eq. (12.19) and the values in the example.

**ANSWERS:** +0.5; 0

**EXERCISE:** Calculate  $S_R^{\omega_o}$ ,  $S_C^{\omega_o}$ , and  $S_K^Q$  for the high-pass filter described by Eq. (12.26).

**ANSWERS:** 1; 1;  $K/(3 - K)$

**EXERCISE:** Calculate  $S_{R_1}^{\omega_o}$ ,  $S_{R_2}^{\omega_o}$ ,  $S_{R_3}^{\omega_o}$ ,  $S_C^{\omega_o}$ ,  $S_{R_1}^Q$ ,  $S_{R_2}^Q$ ,  $S_{R_3}^Q$ ,  $S_C^{\omega_o}$  and  $S_C^{BW}$  for the band-pass filter described by Eqs. (12.32).

**ANSWERS:**  $-\frac{1}{2} \frac{R_3}{R_1 + R_3}; -\frac{1}{2}; -\frac{1}{2} \frac{R_1}{R_1 + R_3}; -1; -\frac{1}{2} \frac{R_3}{R_1 + R_3}; +\frac{1}{2}; -\frac{1}{2} \frac{R_1}{R_1 + R_3}; 0; -1$

### 12.3.6 MAGNITUDE AND FREQUENCY SCALING

The values of resistance and capacitance calculated for a given filter design may not always be convenient, or the values may not correspond closely to the standard values that are available. Magnitude scaling can be used to transform the values of the impedances of a filter without changing its frequency response. Frequency scaling, however, allows us to transform a filter design from one value of  $\omega_o$  to another without changing the  $Q$  of the filter.

#### Magnitude Scaling

The magnitude of impedances of a filter may all be increased or decreased by a **magnitude scaling** factor  $K_M$  without changing  $\omega_o$  or  $Q$  of the filter. To scale the magnitude of the impedance of the filter elements, the value of each resistor<sup>5</sup> is multiplied by  $K_M$  and the value of the capacitor is divided by  $K_M$ :

$$R' = K_M R \quad \text{and} \quad C' = \frac{C}{K_M} \quad \text{so that} \quad |Z'_C| = \frac{1}{\omega C'} = \frac{K_M}{\omega C} = K_M |Z_C| \quad (12.41)$$

In all the filters discussed in Sec. 12.3,  $Q$  is determined by ratios of capacitor values and/or resistor values whereas  $\omega_o$  always has the form  $\omega_o = 1/\sqrt{R_1 R_2 C_1 C_2}$ . Applying magnitude scaling to the low-pass filter described by Eq. (12.19) yields

$$\omega'_o = \frac{1}{\sqrt{K_M R_1 (K_M R_2) \frac{C_1}{K_M} \frac{C_2}{K_M}}} = \frac{1}{\sqrt{R_1 R_2 C_1 C_2}} = \omega_o$$

and

$$Q' = \sqrt{\frac{\frac{C_1}{K_M}}{\frac{C_2}{K_M}} \frac{\sqrt{K_M R_1 (K_M R_2)}}{K_M R_1 + K_M R_2}} = \sqrt{\frac{C_1}{C_2} \frac{\sqrt{R_1 R_2}}{R_1 + R_2}} = Q \quad (12.42)$$

Thus, both  $Q$  and  $\omega_o$  are independent of the magnitude scaling factor  $K_M$ .

<sup>5</sup> In  $RLC$  filters, each inductor value is also increased by  $K_M$ :  $L' = K_M L$  so  $|Z'_L| = K_M |Z_L|$ .

**EXERCISE:** The filter in Fig. 12.9 is designed with  $R_1 = R_2 = 2.26 \text{ k}\Omega$ ,  $R_3 = \infty$ ,  $C_1 = 0.02 \mu\text{F}$ , and  $C_2 = 0.01 \mu\text{F}$ . What are the new values of  $C_1$ ,  $C_2$ ,  $R_1$ ,  $R_2$ ,  $f_o$ , and  $Q$  if the impedance magnitude is scaled by a factor of (a) 5 and (b) 0.885?

**ANSWERS:** (a)  $0.004 \mu\text{F}$ ,  $0.002 \mu\text{F}$ ,  $11.3 \text{ k}\Omega$ ,  $11.3 \text{ k}\Omega$ ,  $4980 \text{ Hz}$ ,  $0.707$ ; (b)  $0.0226 \mu\text{F}$ ,  $0.0113 \mu\text{F}$ ,  $2.00 \text{ k}\Omega$ ,  $2.00 \text{ k}\Omega$ ,  $4980 \text{ Hz}$ ,  $0.707$

### Frequency Scaling

The cutoff or center frequencies of a filter may be scaled by a **frequency scaling** factor  $K_F$  without changing the  $Q$  of the filter if each capacitor value is divided by  $K_F$ , and the resistor values are left unchanged.

$$R' = R \quad \text{and} \quad C' = \frac{C}{K_F}$$

Once again, using the low-pass filter as an example yields:

$$\omega'_o = \frac{1}{\sqrt{R_1 R_2 \frac{C_1}{K_F} \frac{C_2}{K_F}}} = \frac{K_F}{\sqrt{R_1 R_2 C_1 C_2}} = K_F \omega_o$$

and

$$Q' = \sqrt{\frac{\frac{C_1}{K_F}}{\frac{C_2}{K_F} \frac{\sqrt{R_1 R_2}}{R_1 + R_2}}} = \sqrt{\frac{C_1}{C_2} \frac{\sqrt{R_1 R_2}}{R_1 + R_2}} = Q \quad (12.43)$$

In this case, we see that the value of  $\omega_o$  is increased by the factor  $K_F$ , but  $Q$  remains unaffected.

**EXERCISE:** The filter in Fig. 12.9 is designed with  $C_1 = C_2 = 0.02 \mu\text{F}$ ,  $R_1 = 2 \text{ k}\Omega$ ,  $R_3 = 2 \text{ k}\Omega$ , and  $R_2 = 82 \text{ k}\Omega$ . (a) What are the values of  $f_o$  and  $Q$ ? (b) What are the new values of  $C_1$ ,  $C_2$ ,  $R_1$ ,  $R_2$ ,  $f_o$ , and  $Q$  if the frequency is scaled by a factor of 4?

**ANSWERS:** 880 Hz, 4.5;  $0.005 \mu\text{F}$ ,  $0.005 \mu\text{F}$ ,  $1 \text{ k}\Omega$ ,  $82 \text{ k}\Omega$ ,  $3.5 \text{ kHz}$ , 4.5.

## 12.4 SWITCHED-CAPACITOR CIRCUITS

As discussed in some detail in Chapter 6, resistors occupy inordinately large amounts of area in integrated circuits, particularly compared to MOS transistors. **Switched-capacitor (SC) circuits** are an elegant way to eliminate the resistors required in filters by replacing those elements with capacitors and switches. The filters become the discrete-time or sampled-data equivalents of the continuous-time filters discussed in Sec. 12.3, and the circuits then become compatible with high-density MOS IC processes. Switched capacitor circuits have become an extremely important and widely used approach to IC filter design. SC circuits provide low-power filters, and CMOS integrated circuits designed for signal processing and communications applications routinely include SC filters as well as SC analog-to-digital and digital-to-analog converters. These circuits will be discussed in Secs. 12.4 and 12.5.

### 12.4.1 A SWITCHED-CAPACITOR INTEGRATOR

A basic building block of SC circuits is the **switched-capacitor integrator** in Fig. 12.12. Resistor  $R$  of the continuous-time integrator is replaced by capacitor  $C_1$  and MOSFET switches  $S_1$  and  $S_2$  in Fig. 12.12(b). The switches are driven by the **two-phase nonoverlapping clock** depicted in Fig. 12.12(c). When phase  $\Phi_1$  is high, switch  $S_1$  is on and  $S_2$  is off, and when phase  $\Phi_2$  is high, switch  $S_2$  is on and  $S_1$  is off, assuming the switches are implemented using NMOS transistors.

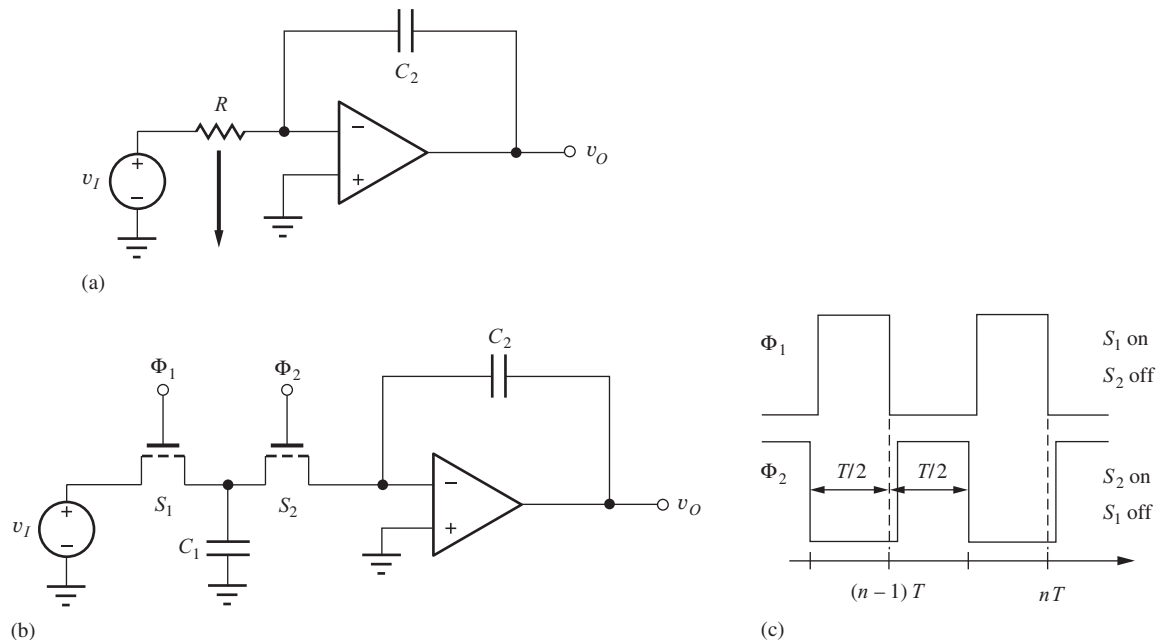


**Figure 12.12** (a) Continuous-time integrator. (b) Switched-capacitor integrator. (c) Two-phase nonoverlapping clock controls the switches of the SC circuit.

Figure 12.13 gives the (piecewise linear) equivalent circuits that can be used to analyze the circuit during the two individual phases of the clock. During phase 1, capacitor  $C_1$  charges up to the value of source voltage  $v_I$  through switch  $S_1$ . At the same time, switch  $S_2$  is open and the output voltage  $v_O$  stored on  $C_2$  remains constant. During phase 2, capacitor  $C_1$  becomes completely discharged because the op amp maintains a virtual ground at its input, and the charge stored on  $C_1$  during the first phase is transferred directly to capacitor  $C_2$  by the current that discharges  $C_1$ .

The charge stored on  $C_1$  while phase 1 is positive ( $S_1$  on) is

$$Q_1 = C_1 V_I \quad (12.44)$$

where  $V_I = v_I[(n-1)T]$  is the voltage stored on  $C_1$  when the switch opens at the end of the sampling interval. The change in charge stored on  $C_2$  during phase 2 is

$$\Delta Q_2 = -C_2 \Delta v_O \quad (12.45)$$

Equating these two equations yields

$$\Delta v_O = -\frac{C_1}{C_2} V_I \quad (12.46)$$

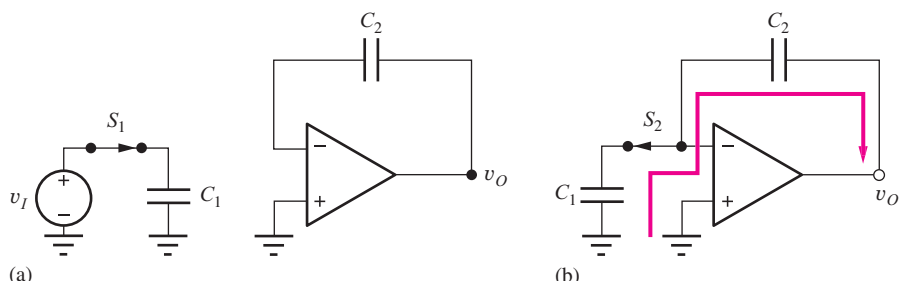


**Figure 12.13** Equivalent circuits during (a) phase 1 and (b) phase 2.

The output voltage at the end of the  $n$ th clock cycle can be written as<sup>6</sup>

$$v_O[nT] = v_O[(n-1)T] - \frac{C_1}{C_2} v_I[(n-1)T] \quad (12.47)$$

During each clock period  $T$ , a packet of charge equal to  $Q_1$  is transferred to storage capacitor  $C_2$ , and the output changes in discrete steps that are proportional to the input voltage with a gain determined by the ratio of capacitors  $C_1$  and  $C_2$ . During phase 1, the input voltage is sampled and the output remains constant. During phase 2, the output changes to reflect the information sampled during phase 1.

An equivalence between the SC integrator and the continuous time integrator can be found by considering the total charge  $Q_I$  that flows from source  $v_I$  through resistor  $R$  during a time interval equal to the clock period  $T$ . Assuming a dc value of  $v_I$  for simplicity,

$$Q_I = IT = \frac{V_I}{R} T \quad (12.48)$$

Equating this charge to the charge stored on  $C_1$  yields

$$\frac{V_I}{R} T = C_1 V_I \quad \text{and} \quad R = \frac{T}{C_1} = \frac{1}{f_C C_1} \quad (12.49)$$

in which  $f_C$  is the clock frequency. For a capacitance  $C_1 = 1 \text{ pF}$  and a switching frequency of 100 kHz, the equivalent resistance  $R = 10 \text{ M}\Omega$ . This large value of  $R$  could not realistically be achieved in an integrated circuit realization of the continuous-time integrator.

**EXERCISE:** The switched capacitor integrator in Fig. 12.12(b) has  $V_I = 0.1 \text{ V}$ ,  $C_1 = 2 \text{ pF}$ , and  $C_2 = 0.5 \text{ pF}$ . What are the output voltages at  $t = T$ ,  $t = 5T$ , and  $t = 9T$  if  $V_O(0) = 0$ ?

**ANSWERS:**  $-0.4 \text{ V}$ ;  $-2.0 \text{ V}$ ;  $-3.6 \text{ V}$

### 12.4.2 NONINVERTING SC INTEGRATOR

Switched-capacitor circuits also provide additional flexibility that is not readily available in continuous-time form. For example, the polarity of a signal can be inverted without the use of an amplifier. In Fig. 12.14, four switches and a floating capacitor are used to realize a **noninverting integrator**.

The circuits valid during the two individual phases appear in Fig. 12.15. During phase 1, switches  $S_1$  are closed, a charge proportional to  $V_I$  is stored on  $C_1$ , and  $v_O$  remains constant. During phase 2, switches  $S_2$  are closed, and a charge packet equal to  $C_1 V_I$  is removed from  $C_2$  instead of being added to  $C_2$  as in the circuit in Fig. 12.12. For the circuit in Fig. 12.14, the output-voltage change at the end of one switch cycle is

$$\Delta v_O = +\frac{C_1}{C_2} V_I \quad (12.50)$$

The capacitances on the source-drain nodes of the MOSFET switches in Fig. 12.12 can cause undesirable errors in the inverting SC integrator circuit. By changing the phasing of the switches, as indicated in Fig. 12.16, the noninverting integrator of Fig. 12.14 can be changed to an inverting integrator. During phase 1 in Fig. 12.17(a), the source is connected through  $C_1$  to the summing junction of the op amp, a charge equivalent to  $C_1 V_I$  is delivered to  $C_2$ , and the output-voltage change

<sup>6</sup> Using z-transform notation, Eq. (12.47) can be written as

$$V_O(z) = z^{-1} V_O(z) - \frac{C_1}{C_2} z^{-1} V_S(z)$$

and the transfer function for the integrator is

$$T(z) = \frac{V_O(z)}{V_S(z)} = \frac{C_1}{C_2} \frac{z^{-1}}{1 - z^{-1}}$$

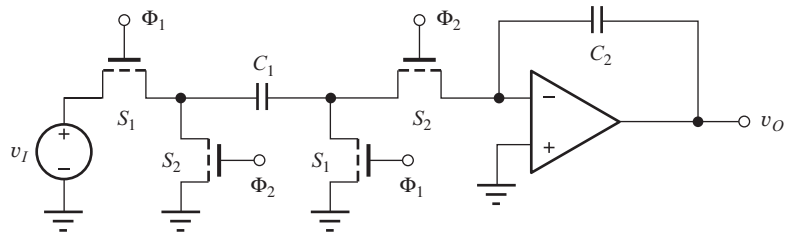


Figure 12.14 Noninverting SC integrator. (All transistors are NMOS devices.)

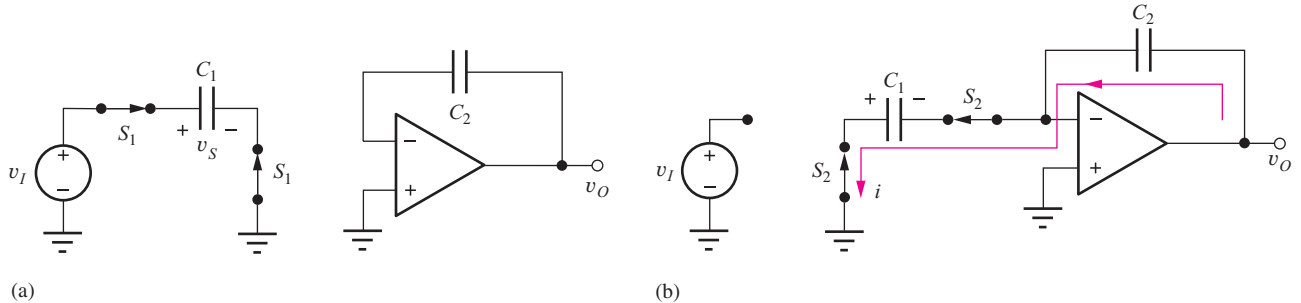


Figure 12.15 Equivalent circuits for the noninverting integrator during (a) phase 1 and (b) phase 2.

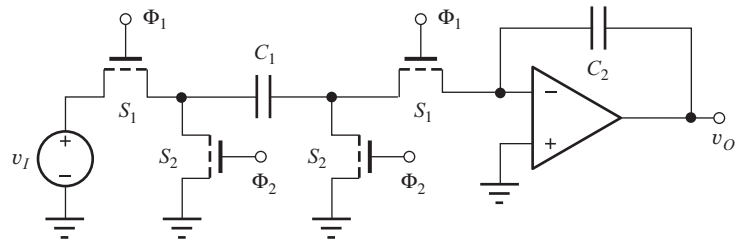


Figure 12.16 Inverting integrator achieved by changing clock phases of the switches.

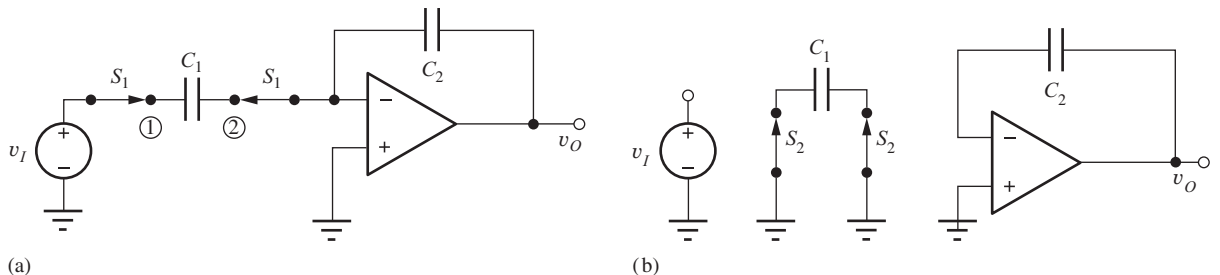
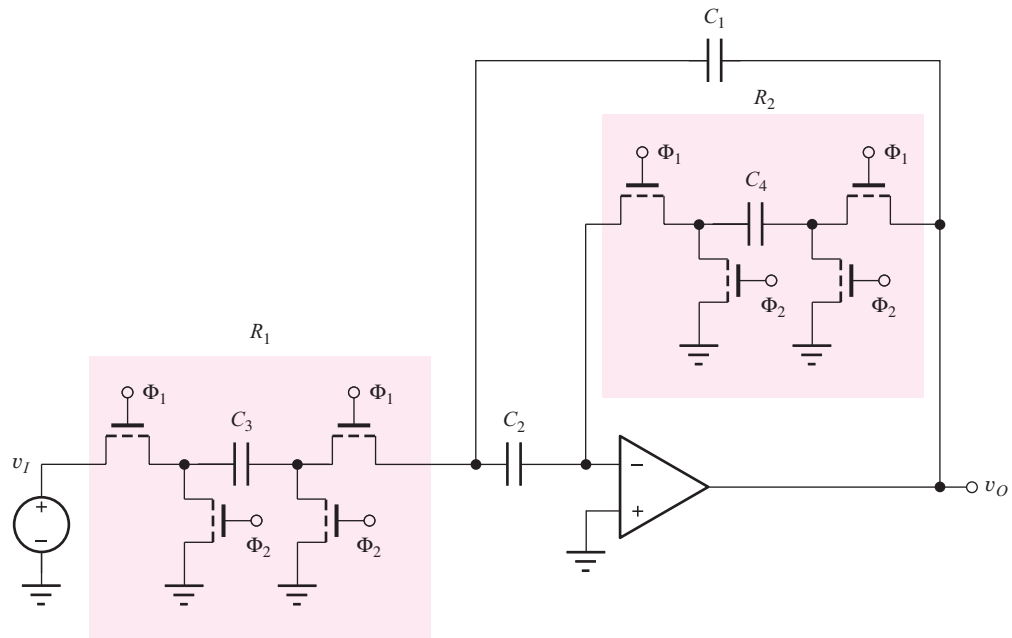


Figure 12.17 (a) Phase 1 of the stray-insensitive inverting integrator. (b) Phase 2 of the stray-insensitive inverting integrator.

is given by Eq. (12.46). During phase 2, Fig. 12.17(b), the source is disconnected,  $v_O$  remains constant, and capacitor  $C_1$  is completely discharged in preparation for the next cycle.

During phase 1, node 1 is driven by voltage source  $v_S$  and node 2 is maintained at zero by the virtual ground at the op amp input. During phase 2, both terminals of capacitor  $C_1$  are forced to zero. Thus, any stray capacitances present at nodes 1 or 2 do not introduce errors into the charge transfer process. A similar set of conditions is true for the noninverting integrator. These two circuits are referred to as **stray-insensitive circuits** and are preferred for use in actual SC circuit implementations.



**Figure 12.18** Switched-capacitor implementation of the second-order band-pass filter in Fig. 12.9.

### 12.4.3 SWITCHED-CAPACITOR FILTERS

Switched-capacitor circuit techniques have been developed to a high level of sophistication and are widely used as filters in audio applications as well as in digital-to-analog and analog-to-digital converter designs. As an example, the SC implementation of the band-pass filter in Fig. 12.9 is shown in Fig. 12.18. For the continuous-time circuit, the center frequency and  $Q$  were described by

$$\omega_o = \frac{1}{\sqrt{R_{th}R_2C_1C_2}} \quad \text{and} \quad Q = \sqrt{\frac{R_2}{R_{th}} \frac{\sqrt{C_1C_2}}{(C_1 + C_2)}} \quad (12.51)$$

In the SC version,

$$R_{th} = \frac{T}{C_3} \quad \text{and} \quad R_2 = \frac{T}{C_4} \quad (12.52)$$

in which  $T$  is the clock period. Substituting these values in Eq. (12.51) gives the equivalent values for the **switched-capacitor filter**:

$$\omega_o = \frac{1}{T} \sqrt{\frac{C_3C_4}{C_1C_2}} = f_c \sqrt{\frac{C_3C_4}{C_1C_2}} \quad \text{and} \quad Q = \sqrt{\frac{C_3}{C_4} \frac{\sqrt{C_1C_2}}{(C_1 + C_2)}} \quad (12.53)$$

Note that the center frequency of this filter is tunable just by changing the clock frequency  $f_c$ , whereas the  $Q$  is independent of frequency. This property can be extremely useful in applications requiring tunable filters. However, since switched-capacitor filters are sampled-data systems, we must remember that the filter's input signal spectrum is limited to  $f \leq f_c/2$  by the sampling theorem.

A more complex example appears in the SC implementation of the Tow-Thomas biquad in Fig. 12.11 given in Fig. 12.19. In this case, the ability to change polarities allows the elimination of one complete operational amplifier in the SC implementation.

**EXERCISE:** What are the values of the center frequency, bandwidth, and voltage gain for the filter design in Fig. 12.18 for  $C_1 = 3 \text{ pF}$ ,  $C_2 = 3 \text{ pF}$ ,  $C_3 = 4 \text{ pF}$ ,  $C_4 = 0.25 \text{ pF}$ , and a clock frequency of 200 kHz?

**ANSWERS:** 10.6 kHz; 5.31 kHz; 16.0

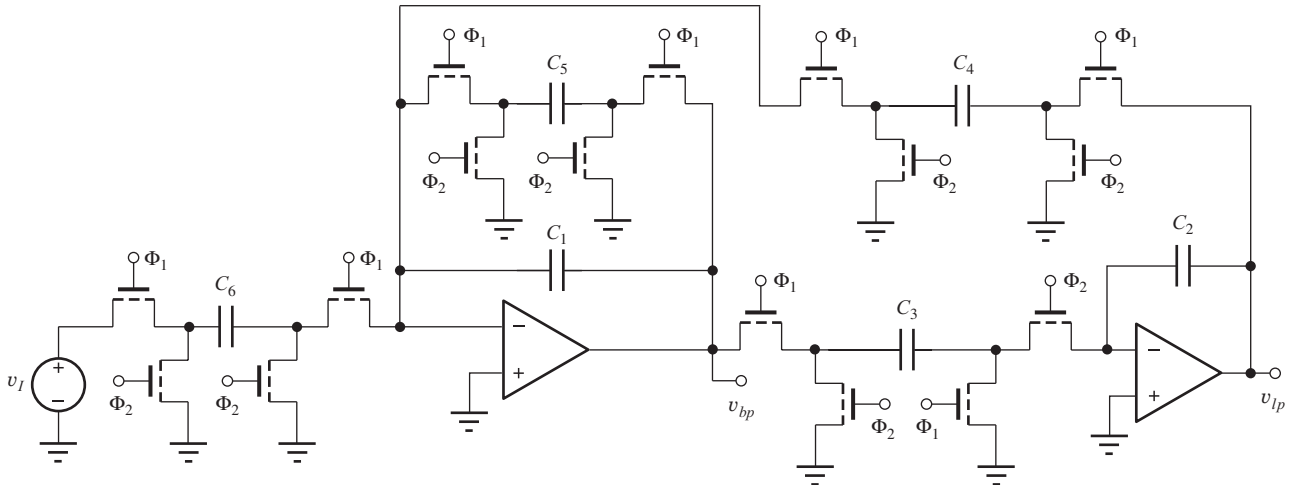


Figure 12.19 Switched-capacitor implementation of the Tow-Thomas biquad.

## 12.5 DIGITAL-TO-ANALOG CONVERSION

As described briefly in Chapter 1, the **digital-to-analog converter**, often referred to as a **D/A converter** or **DAC**, provides an interface between the discrete signals of the digital domain and the continuous signals of the analog world. The D/A converter takes digital information, most often in binary form, as an input and generates an output voltage or current that may then be used for electronic control or information display.

### 12.5.1 D/A CONVERTER FUNDAMENTALS

In the DAC in Fig. 12.20, an  $n$ -bit binary input word  $(b_1, b_2, \dots, b_n)$  is combined with the **dc reference voltage**  $V_{\text{REF}}$  to set the output of the D/A converter. The digital input is treated as a binary fraction with the binary point located to the left of the word. Assuming a voltage output, the behavior of the DAC can be expressed mathematically as

$$v_O = V_{FS}(b_1 2^{-1} + b_2 2^{-2} + \dots + b_n 2^{-n}) + V_{OS} \quad \text{for } b_i \in \{1, 0\} \quad (12.54)$$

The DAC output may also be a current that can be represented as

$$i_O = I_{FS}(b_1 2^{-1} + b_2 2^{-2} + \dots + b_n 2^{-n}) + I_{OS} \quad \text{for } b_i \in \{1, 0\} \quad (12.55)$$

The **full-scale voltage**  $V_{FS}$  or **full-scale current**  $I_{FS}$  is related to the internal reference voltage  $V_{\text{REF}}$  of the converter by

$$V_{FS} = K V_{\text{REF}} \quad \text{or} \quad I_{FS} = G V_{\text{REF}} \quad (12.56)$$

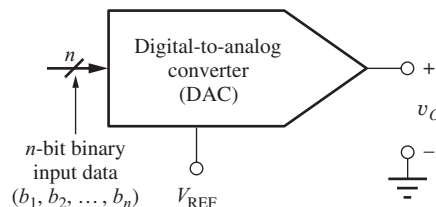


Figure 12.20 D/A converter with voltage output.

in which  $K$  and  $G$  determine the gain of the converter and are often set to a value of 1. Typical values of  $V_{FS}$  are 2.5, 5, 5.12, 10, and 10.24 V, whereas common values of  $I_{FS}$  are 2, 10, and 50 mA.

$V_{OS}$  and  $I_{OS}$  represent the **offset voltage** or **offset current** of the converters, respectively, and characterize the converter output when the digital input code is equal to zero. The offset voltage is normally adjusted to zero, but the offset current of a current output DAC may be deliberately set to a nonzero value. For example, 2 to 10 mA and 10 to 50 mA ranges are used in some process control applications. For now, let us assume that the DAC output is a voltage.

**EXERCISE:** What are the decimal values of the following 8-bit binary fractions? (a) 0.01100001  
(b) 0.10001000.

**ANSWERS:** (a) 0.37890625; (b) 0.5312500

The smallest voltage change that can occur at the DAC output takes place when the **least significant bit (LSB)**  $b_n$  in the digital word changes from a 0 to a 1. This minimum voltage change is also referred to as the **resolution of the converter** and is given by

$$V_{LSB} = 2^{-n} V_{FS} \quad (12.57)$$

At the other extreme,  $b_1$  is referred to as the **most significant bit (MSB)** and has a weight of one-half  $V_{FS}$ .

For example, a 12-bit converter with a full-scale voltage of 10.24 V has an LSB or resolution of 2.500 mV. However, resolution can be stated in different ways. A 12-bit DAC may be said to have 12-bit resolution, a resolution of 0.025 percent of full scale, or a resolution of 1 part in 4096. DACs are available with resolutions ranging from as few as 6 bits to 24 bits. Resolutions of 8 to 12 bits are quite common and economical. Above 12 bits, DACs become more and more expensive, and great care must be taken to truly realize their full precision.

**EXERCISE:** A 12-bit D/A converter has  $V_{REF} = 5.12$  V. What is the output voltage for a binary input code of (101010101010)? What is  $V_{LSB}$ ? What is the size of the MSB?

**ANSWERS:** 3.41250 V, 1.25 mV, 2.56 V

### 12.5.2 D/A CONVERTER ERRORS

Figure 12.21 and columns 1 and 2 in Table 12.7 present the relationship between the digital input code and the analog output voltage for an ideal three-bit DAC. The data points in the figure represent

**TABLE 12.7**  
D/A Converter Transfer Characteristics

BINARY INPUT	IDEAL DAC OUTPUT ( $\times V_{FS}$ )	DAC OF FIG. 12.21 ( $\times V_{FS}$ )	STEP SIZE (LSB)	DIFFERENTIAL LINEARITY ERROR (LSB)	INTEGRAL LINEARITY ERROR (LSB)
000	0.0000	0.0000			0.00
001	0.1250	0.1000	0.80	-0.20	-0.20
010	0.2500	0.2500	1.20	+0.20	0.00
011	0.3750	0.3125	0.50	-0.50	-0.50
100	0.5000	0.5625	2.00	+1.00	+0.50
101	0.6250	0.6250	0.50	-0.50	0.00
110	0.7500	0.8000	1.40	+0.40	+0.40
111	0.8750	0.8750	0.60	-0.40	0.00

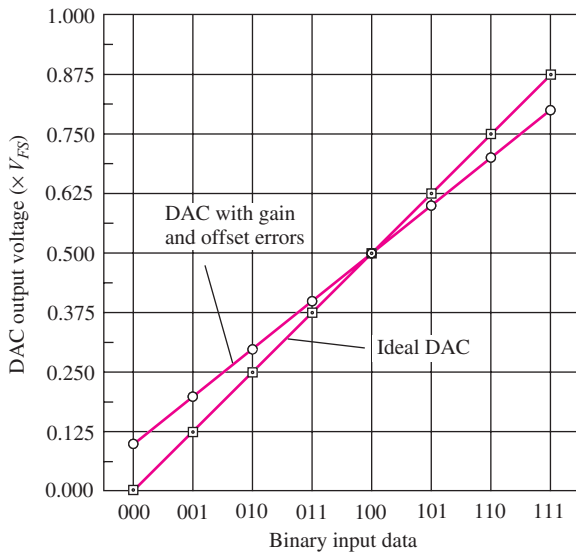


**Figure 12.21** Transfer characteristic for an ideal DAC and a converter with both gain and offset errors.

the eight possible output voltages, which range from 0 to  $0.875 \times V_{FS}$ . Note that the output voltage of the ideal DAC never reaches a value equal to  $V_{FS}$ . The maximum output is always 1 LSB smaller than  $V_{FS}$ . In this case, the maximum output code of 111 corresponds to 7/8 of full scale or  $0.875 V_{FS}$ .

The ideal converter in Fig. 12.21 has been calibrated so that  $V_{OS} = 0$  and 1 LSB is exactly  $V_{FS}/8$ . Figure 12.21 also shows the output of a converter with both gain and offset errors. The **gain error** of the D/A converter represents the deviation of the slope of the converter transfer function from that of the corresponding ideal DAC in Fig. 12.21, whereas the offset voltage is simply the output of the converter for a zero binary input code.

Although the outputs of both converters in Fig. 12.21 lie on a straight line, the output voltages of an actual DAC do not necessarily fall on a straight line. For example, the converter in Fig. 12.22 contains circuit mismatches that cause the output to no longer be perfectly linear. **Integral linearity error**, usually referred to as just **linearity error**, measures the deviation of the actual converter output from a straight line fitted to the converter output voltages. The error is usually specified as a fraction of an LSB or as a percentage of the full-scale voltage.

Table 12.7 lists the linearity errors for the nonlinear DAC in Fig. 12.22. This converter has linearity errors for input codes of 001, 011, 100, and 110. The overall linearity error for the DAC is specified as the magnitude of the largest error that occurs. Hence this converter will be specified as having a linearity error of either 0.5 LSB or 6.25 percent of full-scale voltage. A good converter exhibits a linearity error of less than 0.5 LSB.

A closely related measure of converter performance is the **differential linearity error**. When the binary input changes by 1 bit, the output voltage should change by 1 LSB. A converter's differential linearity error is the magnitude of the maximum difference between each output step of the converter and the ideal step size of 1 LSB. The size of each step and the differential linearity errors of the converter in Fig. 12.22 are also listed in Table 12.7. For instance, the DAC output changes by 0.8 LSB when the input code changes from 000 to 001. The differential linearity error represents the difference between this actual step size and 1 LSB. The integral linearity error for a given binary input represents the sum (integral) of the differential linearity errors for inputs up through the given input.

Another specification that can be important in many applications is **monotonicity**. As the input code to a DAC is increased, the output should increase in a monotonic manner. If this does not

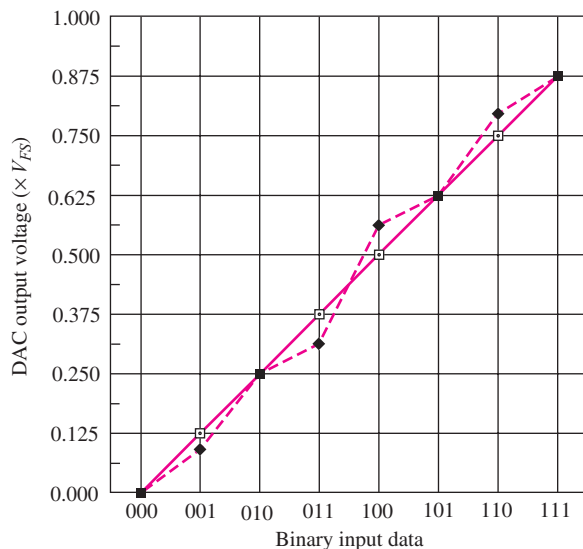


Figure 12.22 D/A converter with linearity errors.

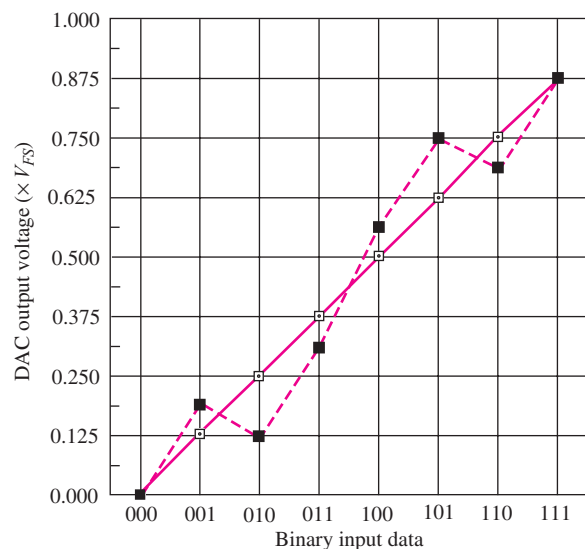


Figure 12.23 DAC with nonmonotonic output.

happen, then the DAC is said to be nonmonotonic. In the nonmonotonic DAC in Fig. 12.23, the output decreases from  $\frac{3}{16}V_{FS}$  to  $\frac{1}{8}V_{FS}$  when the input code changes from 001 to 010. A similar problem occurs for the 101 to 110 transition: In feedback systems, this behavior represents an unwanted  $180^\circ$  phase shift that effectively changes negative feedback to positive feedback and can lead to system instability.

In the upcoming exercise, we will find that this converter has a differential linearity error of 1.5 LSB, whereas the integral linearity error is 1 LSB. A tight linearity error specification does not necessarily guarantee good differential linearity. Although it is possible for a converter to have a differential linearity error of greater than 1 LSB and still be monotonic, a nonmonotonic converter always has a differential linearity error exceeding 1 LSB.

**EXERCISE:** Fill in the missing entries for step size, differential linearity error, and integral linearity error for the converter in Fig. 12.23.

BINARY INPUT	IDEAL DAC OUTPUT ( $\times V_{FS}$ )	ACTUAL DAC EXAMPLE	STEP SIZE (LSB)	DIFFERENTIAL LINEARITY ERROR (LSB)	INTEGRAL LINEARITY ERROR
000	0.0000	0.0000			0.00
001	0.1250	0.2000			
010	0.2500	0.1375			
011	0.3750	0.3125			
100	0.5000	0.5625			
101	0.6250	0.7500			
110	0.7500	0.6875			
111	0.8750	0.8750			0.00

**ANSWERS:** 1.5, -0.5, 1.5; 2.0, 1.5, -0.5, 1.5; 0.5, -1.5, 0.5, 1.0, 0.5, -1.5, 0.5; 0.5, -1.0, -0.5, 0.5, 1.0, -0.5, 0.0

**EXERCISE:** What are the offset voltage and step size for the nonideal converter in Fig. 12.21 if the endpoints are at 0.100 and 0.800  $V_{FS}$ ?

**ANSWERS:** 0.100  $V_{FS}$ , 0.100  $V_{FS}$

### 12.5.3 DIGITAL-TO-ANALOG CONVERTER CIRCUITS

One of the simplest DAC circuits, the **weighted-resistor DAC**, shown in Fig. 12.24, uses the summing amplifier that we encountered earlier in Chapter 10, the reference voltage  $V_{REF}$ , and a weighted-resistor network. The binary input data controls the switches, with a logical 1 indicating that the switch is connected to  $V_{REF}$  and a logical 0 corresponding to a switch connected to ground. Successive resistors are weighted progressively by a factor of 2, thereby producing the desired binary weighted contributions to the output:

$$v_O = (b_1 2^{-1} + b_2 2^{-2} + \cdots + b_n 2^{-n}) V_{REF} \quad \text{for } b_i \in \{1, 0\} \quad (12.58)$$

Differential and integral linearity errors and gain error occur when the resistor ratios are not perfectly maintained. Any op amp offset voltage contributes directly to  $V_{OS}$  of the converter.

Several problems arise in building a DAC using the weighted-resistor approach. The primary difficulty is the need to maintain accurate resistor ratios over a very wide range of resistor values (for example, 4096 to 1 for a 12-bit DAC). In addition, because the switches are in series with the resistors, their on-resistance must be very low and they should have zero offset voltage. The designer can meet these last two requirements by using good MOSFETs or JFETs as switches, and the ( $W/L$ ) ratios of the FETs can be scaled with bit position to equalize the resistance contributions of the switches. However, the wide range of resistor values is not suitable for monolithic converters of moderate to high resolution. We should also note that the current drawn from the voltage reference varies with the binary input pattern. This varying current causes a change in voltage drop in the Thévenin equivalent source resistance of the voltage reference and can lead to data-dependent errors sometimes called **superposition errors**.

**EXERCISE:** Suppose a 1-k $\Omega$  resistor is used for the MSB in an 8-bit converter similar to that in Fig. 12.24. What are the other resistor values?

**ANSWERS:** 2 k $\Omega$ ; 4 k $\Omega$ ; 8 k $\Omega$ ; 16 k $\Omega$ ; 32 k $\Omega$ ; 64 k $\Omega$ ; 128 k $\Omega$ ; 500  $\Omega$

#### The R-2R Ladder

The **R-2R ladder** in Fig. 12.25 avoids the problem of a wide range of resistor values. It is well-suited to integrated circuit realization because it requires matching of only two resistor values,  $R$  and  $2R$ .

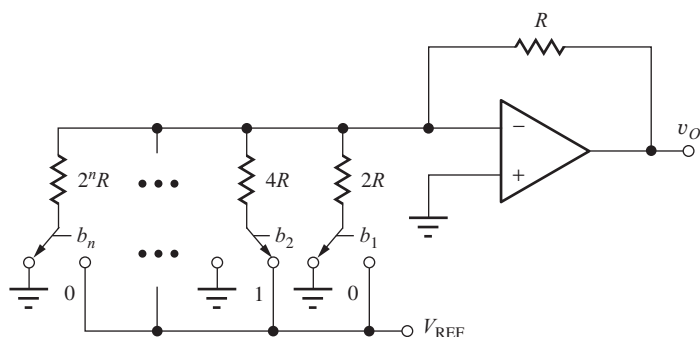
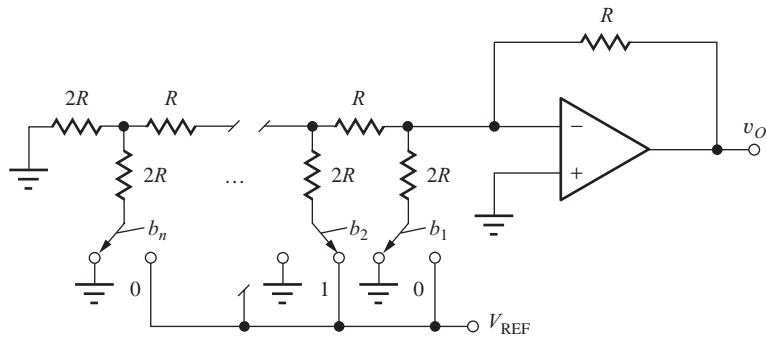


Figure 12.24 An  $n$ -bit weighted-resistor DAC.

Figure 12.25  $n$ -bit DAC using R-2R ladder.

The value of  $R$  typically ranges from  $2\text{ k}\Omega$  to  $10\text{ k}\Omega$ . By forming successive Thévenin equivalents proceeding from left to right at each node in the ladder, we can show that the contribution of each bit is reduced by a factor of 2 going from the MSB to LSB. Like the weighted-resistor DAC, this network requires switches with low on-resistance and zero offset voltage, and the current drawn from the reference still varies with the input data pattern.

**EXERCISE:** What is the total resistance required to build an 8-bit R-2R ladder DAC if  $R = 1\text{ k}\Omega$ ? What is the total resistance required to build an 8-bit weighted resistor D/A converter if  $R = 1\text{ k}\Omega$ ?

**ANSWERS:**  $25\text{ k}\Omega$ ;  $511\text{ k}\Omega$

### Inverted R-2R Ladder

Because the currents in the resistor networks of the DACs in Figs. 12.24 and 12.25 change as the input data changes, power dissipation in the elements of the network changes, which can cause linearity errors in addition to superposition errors. Therefore some monolithic DACs use the configuration in Fig. 12.26, known as the **inverted R-2R ladder**. In this circuit, the currents in the ladder and reference are independent of the digital input because the input data cause the ladder currents to be switched either directly to ground or to the virtual ground input at the input of a current-to-voltage converter. Because both op amp inputs are at ground potential, the ladder currents are independent of switch position. Note that complementary currents,  $I$  and  $\bar{I}$ , are available at the output of the inverted ladder.

The inverted R-2R ladder is a popular DAC configuration, often implemented in CMOS technology. The switches still need to have low on-resistance to minimize errors within the converter.

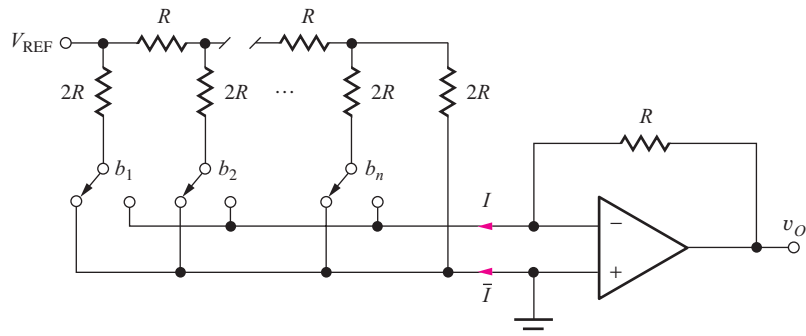
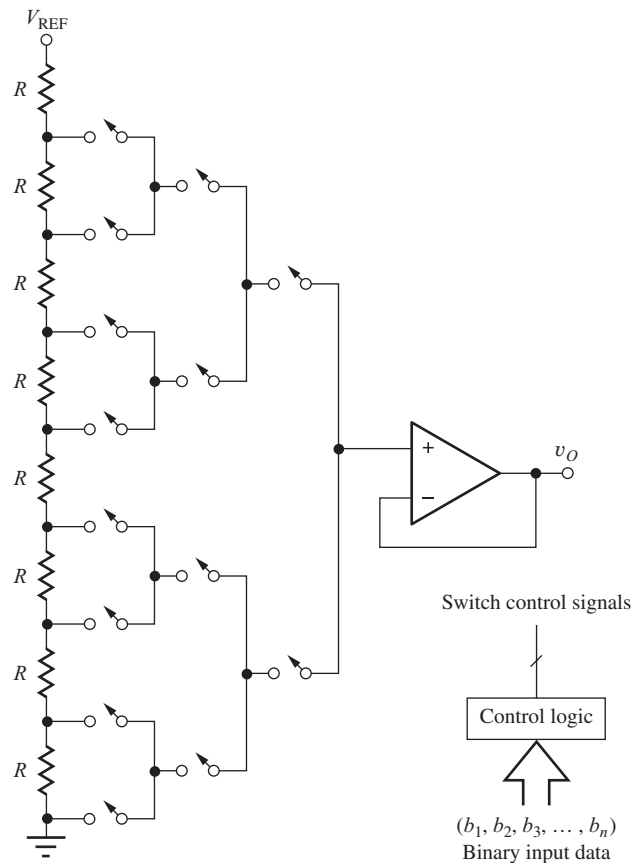


Figure 12.26 D/A converter using the inverted R-2R ladder.



**Figure 12.27** Inherently monotonic 3-bit D/A converter.

The R-2R ladder can be formed of diffused, implanted, or thin-film resistors; the choice depends on both the manufacturer's process technology and the required resolution of the D/A converter.

### An Inherently Monotonic DAC

MOS IC technology has facilitated some unusual approaches to D/A converter design. Figure 12.27 shows a DAC whose output is inherently monotonic. A long resistor string forms a multi-output voltage divider connected between the voltage reference and ground. An analog switch tree connects the desired tap to the input of an operational amplifier operating as a voltage follower. The appropriate switches are closed by a logic network that decodes the binary input data.

Each tap on the resistor network is forced to produce a voltage greater than or equal to that of the taps below it, and the output must therefore increase monotonically as the digital input code increases. An 8-bit version of this converter requires 256 equal-valued resistors and 510 switches, plus the additional decoding logic. This DAC can be fabricated in NMOS or CMOS technology, in which the large number of MOSFET switches and the complex decoding logic are easily realized.

**EXERCISE:** How many resistors and switches are required to implement a 10-bit DAC using the technique in Fig. 12.27?

**ANSWERS:** 1024, 2046

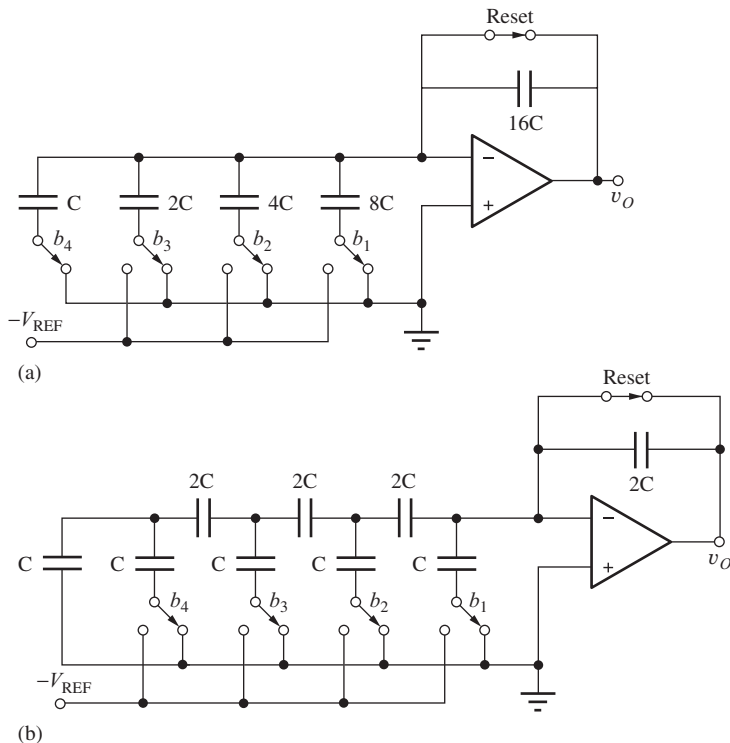


**Figure 12.28** Switched-capacitor D/A converters. (a) Weighted-capacitor DAC; (b) C-2C DAC.

### Switched-Capacitor D/A Converters

D/A converters can be fabricated using only switches, capacitors, and operational amplifiers. Figure 12.28(a) is a **weighted-capacitor DAC**; Fig. 12.28(b) is a **C-2C ladder DAC**. Because these circuits are composed only of switches and capacitors, the only static power dissipation in these circuits occurs in the op amps. However, dynamic switching losses occur just as in CMOS logic (see Sec. 7.4). These circuits represent the direct switched-capacitor (SC) analogs of the weighted-resistor and R-2R ladder techniques presented earlier.

When a switch changes state, current impulses charge or discharge the capacitors in the network. The current impulse is supplied by the output of the operational amplifier and changes the voltage on the feedback capacitor by an amount corresponding to the bit weight of the switch that changed state. These converters consume very little power, even when CMOS operational amplifiers are included on the same chip, and are widely used in VLSI systems.

**EXERCISE:** (a) Suppose that an 8-bit weighted capacitor DAC is fabricated with the smallest unit of capacitance  $C = 1.0 \text{ pF}$ . What is the total capacitance the DAC requires? (b) Repeat for a C-2C ladder DAC. (c) An IC process provides a thin oxide capacitor structure with a capacitance of  $5 \text{ fF}/\mu\text{m}^2$ . How much chip area is required for the C-2C ladder DAC?

**ANSWERS:** 511 pF; 33 pF;  $6600 \mu\text{m}^2$

## 12.6 ANALOG-TO-DIGITAL CONVERSION

As described briefly in Chapter 1, the **analog-to-digital converter**, also known as an **A/D converter** or **ADC**, is used to transform analog information in electrical form into digital data. The ADC in Fig. 12.29 takes an unknown continuous analog input signal, most often a voltage  $v_X$ , and converts it

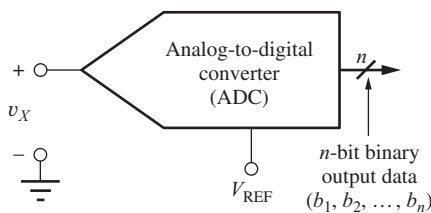


**Figure 12.29** Block diagram representation for an A/D converter.

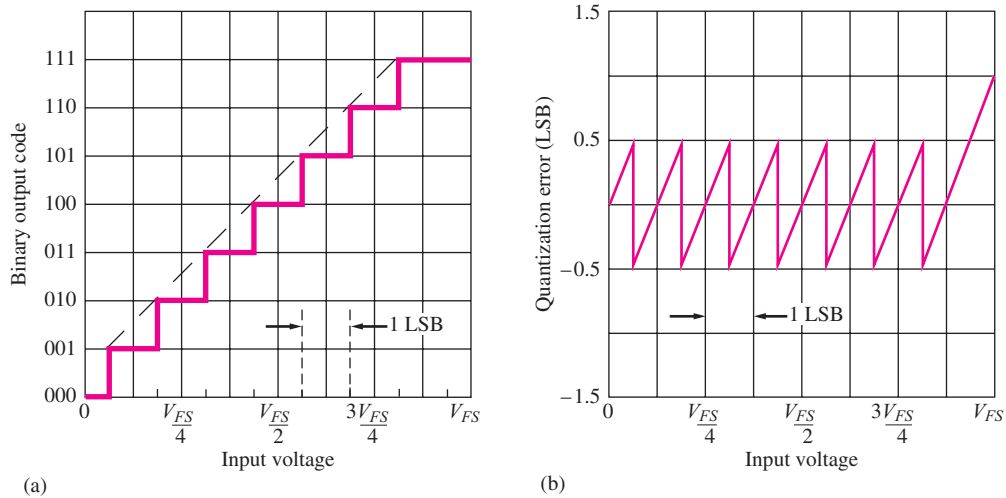


**Figure 12.30** Ideal 3-bit ADC: (a) input-output relationship and (b) quantization error.

into an  $n$ -bit binary number that can be readily manipulated by a digital computer. The  $n$ -bit number is a binary fraction representing the ratio between the unknown input voltage  $v_x$  and the converter's full-scale voltage  $V_{FS} = KV_{REF}$ .

### 12.6.1 A/D CONVERTER FUNDAMENTALS

Figure 12.30(a) is an example of the input-output relationship for an ideal 3-bit A/D converter. As the input increases from zero to full scale, the digital output code word stairsteps from 000 to 111. As the input voltage increases, the output code first underestimates the input voltage and then overestimates the input voltage. This error, called **quantization error**, is plotted against input voltage in Fig. 12.30(b).

For a given output code, we know only that the value of the input voltage  $v_x$  lies somewhere within a 1-LSB quantization interval. For example, if the output code of the 3-bit ADC is (101), then the input voltage can be anywhere between  $\frac{9}{16}V_{FS}$  and  $\frac{11}{16}V_{FS}$ , a range of  $V_{FS}/8$  V equivalent to 1 LSB of the 3-bit converter. From a mathematical point of view, the circuitry of an ideal ADC should be designed to pick the values of the bits in the binary word to minimize the magnitude of the quantization error  $v_e$  between the unknown input voltage  $v_x$  and the nearest quantized voltage level:

$$v_e = |v_x - (b_1 2^{-1} + b_2 2^{-2} + \dots + b_n 2^{-n}) V_{FS}| \quad (12.59)$$

**EXERCISE:** An 8-bit A/D converter has  $V_{REF} = 5$  V. What is the binary output code word for an input of 1.2 V? What is the voltage range corresponding to 1 LSB of the converter?

**ANSWERS:** (00111101); 19.5 mV

**TABLE 12.8**  
A/D Converter Transfer Characteristics

BINARY OUTPUT CODE	IDEAL ADC TRANSITION POINT ( $\times V_{FS}$ )	ADC OF FIG. 12.31 ( $\times V_{FS}$ )	STEP SIZE (LSB)	DIFFERENTIAL LINEARITY ERROR (LSB)	INTEGRAL LINEARITY ERROR (LSB)
000	0.0000	0.0000	0.5	0	0
001	0.0625	0.0625	1.5	0.50	0.5
010	0.1875	0.2500	0.5	-0.50	0
011	0.3125	0.3125	1.0	0	0
100	0.4375	0.4375	1.0	0	0
101	0.5625	0.5625	1.50	0.50	0.5
110	0.6875	0.7500	0.5	-0.50	0
111	0.8125	0.8125	1.5	0	0

### 12.6.2 ANALOG-TO-DIGITAL CONVERTER ERRORS

As shown by the dashed line in Fig. 12.30(a), the code transition points of an ideal converter all fall on a straight line. However, an actual converter has integral and differential linearity errors similar to those of a digital-to-analog converter. Figure 12.31 is an example of the code transitions for a hypothetical nonideal converter. The converter is assumed to be calibrated so that the first and last code transitions occur at their ideal points.

In the ideal case, each code step, other than 000 and 111, would be the same width and should be equal to 1 LSB of the converter. Differential linearity error represents the difference between the actual code step width and 1 LSB, and integral linearity error is a measure of the deviation of the code transition points from their ideal positions. Table 12.8 lists the step size, differential linearity error, and integral linearity error for the converter in Fig. 12.31. Note that the ideal step sizes corresponding to codes 000 and 111 are 0.5 LSB and 1.5 LSB, respectively, because of the desired code transition points. As in D/A converters, the integral linearity error should equal the sum of the differential linearity errors for the individual steps.

Figure 12.32 is an uncalibrated converter with both offset and gain errors. The first code transition occurs at a voltage that is 0.5 LSB too high, representing a converter **offset error** of 0.5 LSB.

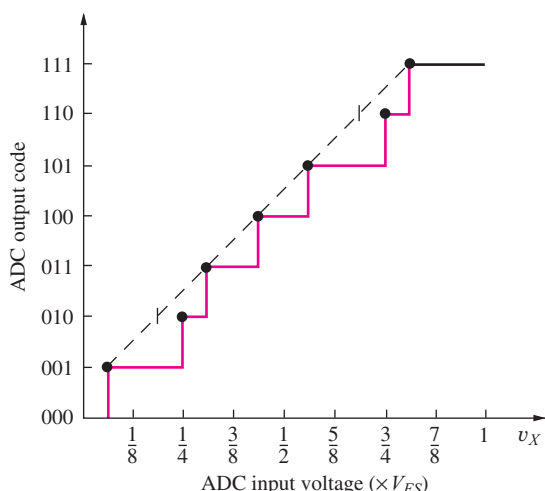


**Figure 12.31** Example of code transitions in a nonideal 3-bit ADC.

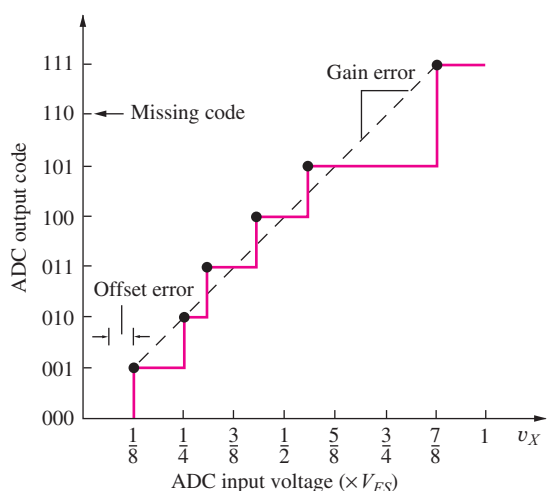


**Figure 12.32** ADC with a missing code.

The slope of the fitted line does not give  $1 \text{ LSB} = V_{FS}/8$ , so the converter also exhibits a gain error.

A new type of error, which is specific to ADCs, can be observed in Fig. 12.32. The output code jumps directly from 101 to 111 as the input passes through  $0.875V_{FS}$ . The output code 110 never occurs, so this converter is said to have a **missing code**. A converter with a differential linearity error of less than 1 LSB does not exhibit missing codes in its input-output function. An ADC can also be **nonmonotonic**. If the output code decreases as the input voltage increases, the converter has a nonmonotonic input–output relationship.

All these deviations from ideal A/D (or D/A) converter behavior are temperature-dependent; hence, converter specifications include temperature coefficients for gain, offset, and linearity. A good converter will be monotonic with less than 0.5 LSB linearity error and no missing codes over its full temperature range.

**EXERCISE:** An A/D converter is used in a digital multimeter (DVM) that displays 6 decimal digits. How many bits are required in the ADC?

**ANSWER:** 20 bits

**EXERCISE:** What are the minimum and maximum code step widths in Fig. 12.32? What are the differential and integral linearity errors for this ADC based on the dashed line in the figure?

**ANSWERS:** 0, 2.5 LSB; 1.5 LSB, 1 LSB

### 12.6.3 BASIC A/D CONVERSION TECHNIQUES

Figure 12.33 shows the basic conversion scheme for a number of analog-to-digital converters. The unknown input voltage  $v_X$  is connected to one input of an analog **comparator**, and a time-dependent reference voltage  $v_{REF}$  is connected to the other input of the comparator. If input voltage  $v_X$  exceeds input  $v_{REF}$ , then the output voltage will be high, corresponding to a logic 1. If input  $v_X$  is less than  $v_{REF}$ , then the output voltage will be low, corresponding to a logic 0.

In performing a conversion, the reference voltage is varied until the unknown input is determined within the quantization error of the converter. Ideally, the logic of the A/D converter will choose a set of binary coefficients  $b_i$  so that the difference between the unknown input voltage  $v_X$  and the final quantized value is less than or equal to 0.5 LSB. In other words, the  $b_i$  will be selected so that

$$\left| v_X - V_{FS} \sum_{i=1}^n b_i 2^{-i} \right| < \frac{V_{FS}}{2^{n+1}} \quad (12.60)$$

The basic difference among the operations of various converters is the strategy that is used to vary the reference signal  $V_{REF}$  to determine the set of binary coefficients  $\{b_i, i = 1 \dots n\}$ .

#### Counting Converter

One of the simplest ways of generating the comparison voltage is to use a digital-to-analog converter. An  $n$ -bit DAC can be used to generate any one of  $2^n$  discrete outputs simply by applying the appropriate digital input word. A direct way to determine the unknown input voltage  $v_X$  is to sequentially compare it to each possible DAC output. Connecting the digital input of the DAC to an  $n$ -bit binary counter enables a step-by-step comparison to the unknown input to be made, as shown in Fig. 12.34.

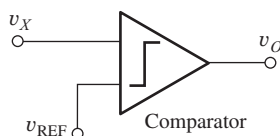


Figure 12.33 Block diagram representation for an A/D converter.

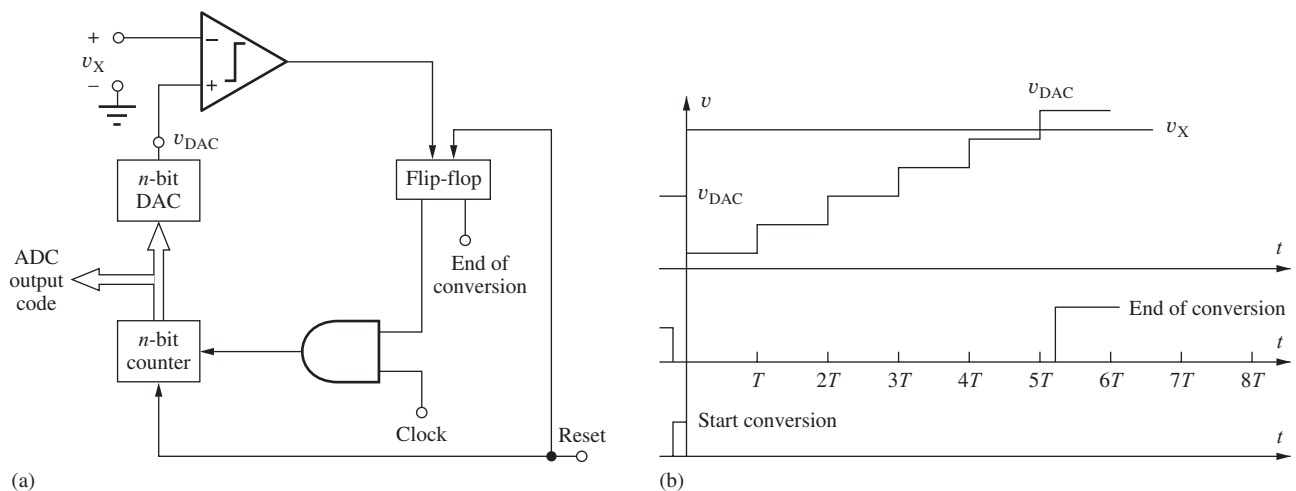


Figure 12.34 (a) Block diagram of the counting ADC. (b) Timing diagram.

A/D conversion begins when a pulse resets the flip-flop and the counter output to zero. Each successive clock pulse increments the counter; the DAC output looks like a staircase during the conversion. When the output of the DAC exceeds the unknown input, the comparator output changes state, sets the flip-flop, and prevents any further clock pulses from reaching the counter. The change of state of the comparator output indicates that the conversion is complete. At this time, the contents of the binary counter represent the converted value of the input signal.

Several features of this converter should be noted. First, the length of the conversion cycle is variable and proportional to the unknown input voltage  $v_X$ . The maximum **conversion time**  $T_T$  occurs for a full-scale input signal and corresponds to  $2^n$  clock periods or

$$T_T \leq \frac{2^n}{f_C} = 2^n T_C \quad (12.61)$$

where  $f_C = 1/T_C$  is the clock frequency. Second, the binary value in the counter represents the smallest DAC voltage that is larger than the unknown input; this value is not necessarily the DAC output which is closest to the unknown input, as was originally desired. Also, the example in Fig. 12.34(b) shows the case for an input that is constant during the conversion period. If the input varies, the binary output will be an accurate representation of the value of the input signal at the instant the comparator changes state.

The advantage of the counting A/D converter is that it requires a minimum amount of hardware and is inexpensive to implement. Some of the least expensive A/D converters have used this technique. The main disadvantage is the relatively low conversion rate for a given D/A converter speed. An  $n$ -bit converter requires  $2^n$  clock periods for its longest conversion.

**EXERCISE:** What is the maximum conversion time for a counting ADC using a 12-bit DAC and a 2-MHz clock frequency? What is the maximum possible number of conversions per second?

**ANSWERS:** 2.05 ms; 488 conversions/second

### Successive Approximation Converter

The **successive approximation converter** uses a much more efficient strategy for varying the reference input to the comparator, one that results in a converter requiring only  $n$  clock periods to complete an  $n$ -bit conversion. Figure 12.35 is a schematic of the operation of a three-bit successive

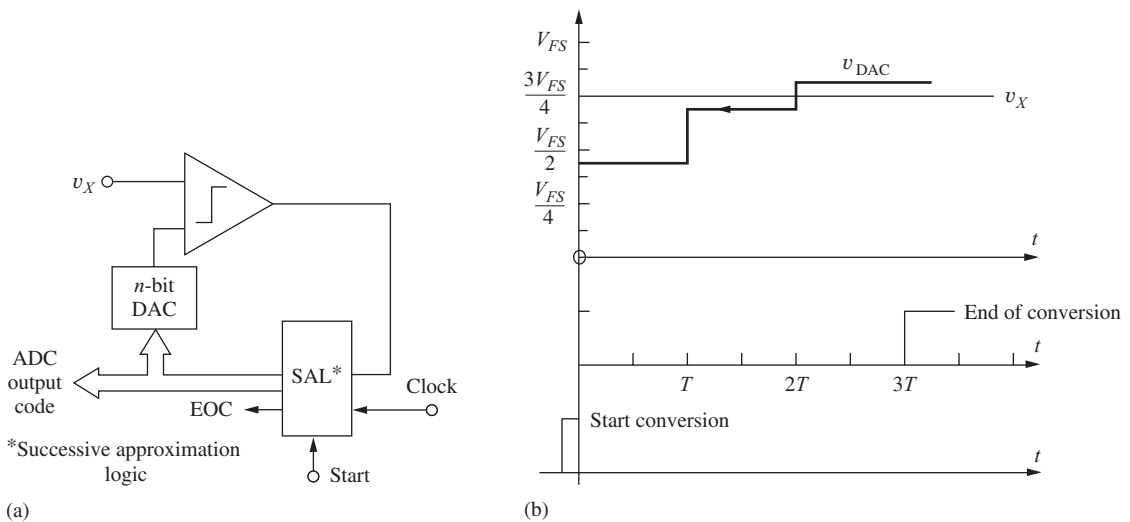


Figure 12.35 (a) Successive approximation ADC. (b) Timing diagram.

approximation converter. A “binary search” is used to determine the best approximation to  $v_X$ . After receiving a start signal, the successive approximation logic sets the DAC output to  $(V_{\text{FS}}/2) - (V_{\text{FS}}/16)$  and, after waiting for the circuit to settle out, checks the comparator output. [The DAC output is offset by  $(-\frac{1}{2}\text{LSB} = -V_{\text{FS}}/16)$  to yield the transfer function of Fig. 12.30.] At the next clock pulse, the DAC output is incremented by  $V_{\text{FS}}/4$  if the comparator output was 1, and decremented by  $V_{\text{FS}}/4$  if the comparator output was 0. The comparator output is again checked, and the next clock pulse causes the DAC output to be incremented or decremented by  $V_{\text{FS}}/8$ . A third comparison is made. The final binary output code remains unchanged if  $v_X$  is larger than the final DAC output or is decremented by 1 LSB if  $v_X$  is less than the DAC output. The conversion is completed following the logic decision at the end of the third clock period for the 3-bit converter, or at the end of  $n$  clock periods for an  $n$ -bit converter.

Figure 12.36 shows the possible code sequences for a 3-bit DAC and the sequence followed for the successive approximation conversion in Fig. 12.35. At the start of conversion, the DAC input is set to 100. At the end of the first clock period, the DAC voltage is found to be less than  $v_X$ , so the DAC code is increased to 110. At the end of the second clock period, the DAC voltage is still found to be too small, and the DAC code is increased to 111. After the third clock period, the DAC voltage is found to be too large, so the DAC code is decremented to yield a final converted value of 110.

Fast conversion rates are possible with a successive approximation ADC. This conversion technique is very popular and used in many 8 to 16-bit converters. The primary factors limiting the speed of this ADC are the time required for the D/A converter output to settle within a fraction of an LSB of  $V_{\text{FS}}$  and the time required for the comparator to respond to input signals that may differ by very small amounts.

**EXERCISE:** What is the conversion time for a successive approximation ADC using a 12-bit DAC and a 2-MHz clock frequency? What is the maximum possible number of conversions per second?

**ANSWERS:** 6.00  $\mu\text{s}$ ; 167,000 conversions/second

In the discussion thus far, it has been tacitly assumed that the input remains constant during the full conversion period. A slowly varying input signal is acceptable as long as it does not change by more than 0.5 LSB ( $V_{\text{FS}}/2^{n+1}$ ) during the conversion time ( $T_T = n/f_C = nT_C$ ). The frequency of a

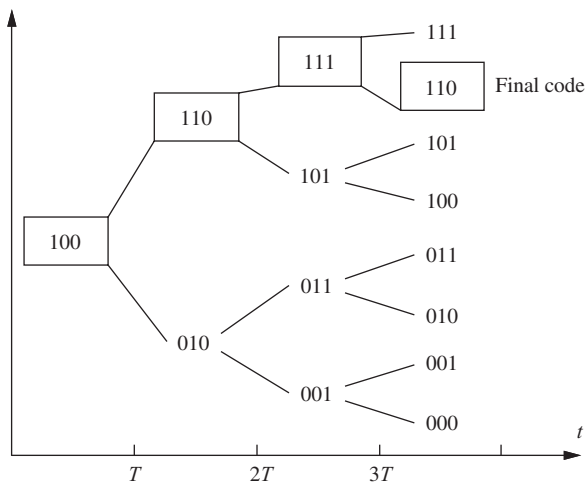


**Figure 12.36** Code sequences for a 3-bit successive approximation ADC.

sinusoidal input signal with a peak-to-peak amplitude equal to the full-scale voltage of the converter must satisfy the following inequality:

$$T_T \left\{ \max \left[ \frac{d}{dt} (V_{FS} \sin \omega_o t) \right] \right\} \leq \frac{V_{FS}}{2^{n+1}} \quad \text{or} \quad \frac{n}{f_C} (V_{FS} \omega_o) \leq \frac{V_{FS}}{2^{n+1}} \quad (12.62)$$

and

$$f_O \leq \frac{f_C}{2^{n+2} n \pi}$$

For a 12-bit converter using a 1-MHz clock frequency,  $f_O$  must be less than 1.62 Hz. If the input changes by more than 0.5 LSB during the conversion process, the digital output of the converter does not bear a precise relation to the value of the unknown input voltage  $v_X$ . To avoid this frequency limitation, a high-speed **sample-and-hold circuit**<sup>7</sup> that samples the signal amplitude and then holds its value constant is usually used ahead of successive approximation ADCs.

### Single-Ramp (Single-Slope) ADC

The discrete output of the D/A converter in the counting ADC can be replaced by a continuously changing analog reference signal, as shown in Fig. 12.37. The reference voltage varies linearly with a well-defined slope from slightly below zero to above  $V_{FS}$ , and the converter is called a **single-ramp**, or **single-slope**, ADC. The length of time required for the reference signal to become equal to the unknown voltage is proportional to the unknown input.

Converter operation begins with a start conversion signal, which resets the binary counter and starts the ramp generator at a slightly negative voltage [see Fig. 12.37(b)]. As the ramp crosses through zero, the output of comparator 2 goes high and allows clock pulses to accumulate in the counter. The number in the counter increases until the ramp output voltage exceeds the unknown  $v_X$ . At this time, the output of comparator 1 goes high and prevents further clock pulses from reaching the counter. The number  $N$  in the counter at the end of the conversion is directly proportional to the input voltage because

$$v_X = KNT_C \quad (12.63)$$

<sup>7</sup> See Additional Reading or the Electronics in Action at the end of this section for examples.

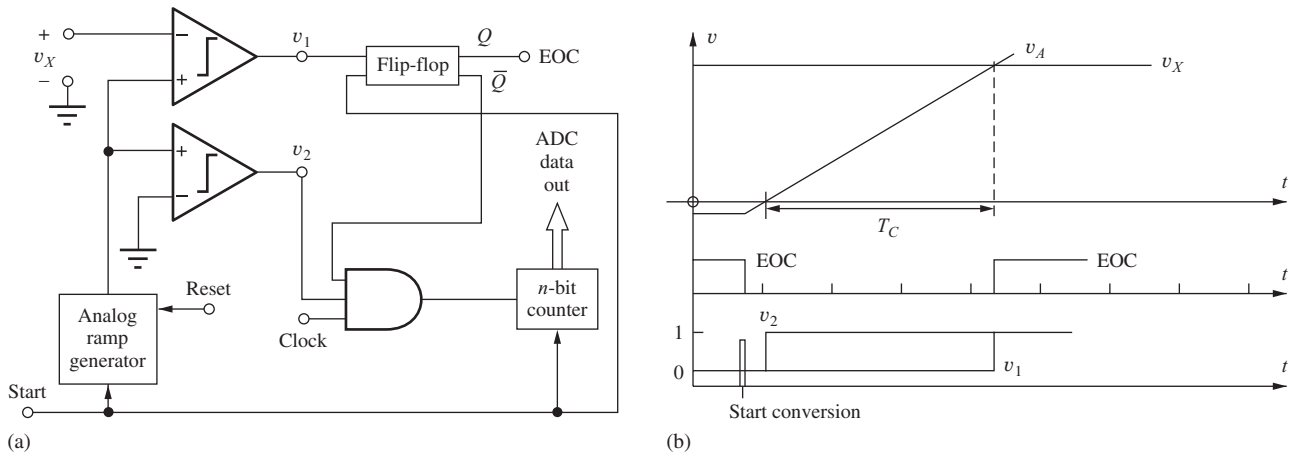


Figure 12.37 (a) Block diagram and (b) timing for a single-ramp ADC.

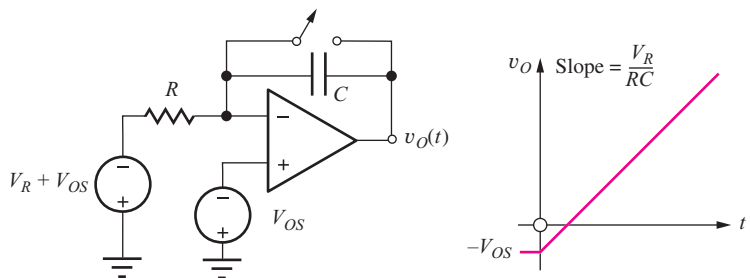


Figure 12.38 Ramp voltage generation using an integrator with constant input.

where  $K$  is the slope of the ramp in volts/second. If the slope of the ramp is chosen to be  $K = V_{FS}/2^n T_C$ , then the number in the counter directly represents the binary fraction equal to  $v_X/V_{FS}$ :

$$\frac{v_X}{V_{FS}} = \frac{N}{2^n} \quad (12.64)$$

The conversion time  $T_T$  of the single-ramp converter is clearly variable and proportional to the unknown voltage  $v_X$ . Maximum conversion time occurs for  $v_X = V_{FS}$ , with

$$T_T \leq 2^n T_C \quad (12.65)$$

As is the case for the **counter-ramp converter**, the counter output represents the value of  $v_X$  at the time that the end-of-conversion signal occurs.

The ramp voltage is usually generated by an integrator connected to a constant reference voltage, as shown in Fig. 12.38. When the reset switch is opened, the output increases with a constant slope given by  $V_R/RC$ :

$$v_O(t) = -V_{OS} + \frac{1}{RC} \int_0^t V_R dt \quad (12.66)$$

The dependence of the ramp's slope on the  $RC$  product is one of the major limitations of the single-ramp A/D converter. The slope depends on the absolute values of  $R$  and  $C$ , which are difficult to maintain constant in the presence of temperature variations and over long periods of time. Because of this problem, the dual-ramp converter in the next section is preferred.

**EXERCISE:** What is the value of  $RC$  for an 8-bit single-ramp ADC with  $V_{FS} = 5.12$  V,  $V_R = 2.000$  V, and  $f_C = 1$  MHz?

**ANSWER:** 0.1 ms

### Dual-Ramp (Dual-Slope) ADC

The **dual-ramp**, or **dual-slope**, **ADC** solves the problems associated with the single-ramp converter and is commonly found in high-precision data acquisition and instrumentation systems. Figure 12.39 illustrates converter operation. The conversion cycle consists of two separate integration intervals. First, unknown voltage  $v_X$  is integrated for a known period of time  $T_1$ . The value of this integral is then compared to that of a known reference voltage  $V_{REF}$ , which is integrated for a variable length of time  $T_2$ .

At the start of conversion the counter is reset, and the integrator is reset to a slightly negative voltage. The unknown input  $v_X$  is connected to the integrator input through switch  $S_1$ . Unknown voltage  $v_X$  is integrated for a fixed period of time  $T_1 = 2^n T_C$ , which begins when the integrator output crosses through zero. At the end of time  $T_1$ , the counter overflows, causing  $S_1$  to be opened and the reference input  $V_{REF}$  to be connected to the integrator input through  $S_2$ . The integrator output then decreases until it crosses back through zero, and the comparator changes state, indicating the end of the conversion. The counter continues to accumulate pulses during the down ramp, and the final number in the counter represents the quantized value of the unknown voltage  $v_X$ .

Circuit operation forces the integrals over the two time periods to be equal:

$$\frac{1}{RC} \int_0^{T_1} v_X(t) dt = \frac{1}{RC} \int_{T_1}^{T_1+T_2} V_{REF} dt \quad (12.67)$$

$T_1$  is set equal to  $2^n T_C$  because the unknown voltage  $v_X$  was integrated over the amount of time needed for the  $n$ -bit counter to overflow. Time period  $T_2$  is equal to  $N T_C$ , where  $N$  is the number accumulated in the counter during the second phase of operation.

Recalling the mean-value theorem from calculus,

$$\frac{1}{RC} \int_0^{T_1} v_X(t) dt = \frac{\langle v_X \rangle}{RC} T_1 \quad (12.68)$$

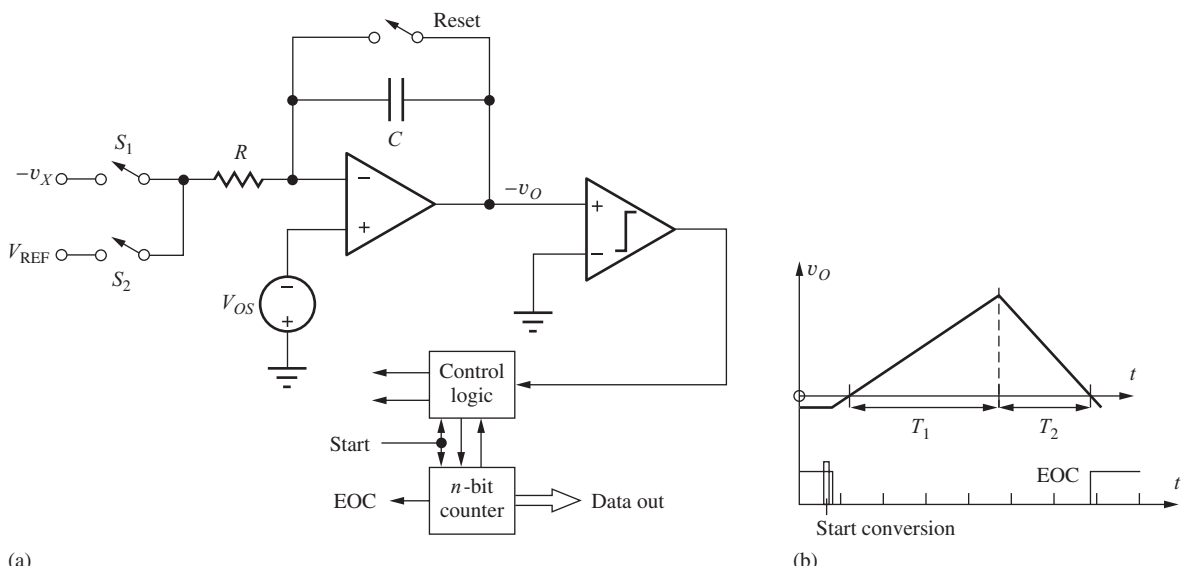


Figure 12.39 (a) Dual-ramp ADC and (b) timing diagram.

and

$$\frac{1}{RC} \int_{T_1}^{T_1+T_2} V_{\text{REF}}(t) dt = \frac{V_{\text{REF}}}{RC} T_2 \quad (12.69)$$

because  $V_{\text{REF}}$  is a constant. Substituting these two results into Eq. (12.67), we find the average value of the input  $\langle v_x \rangle$  to be

$$\frac{\langle v_x \rangle}{V_{\text{REF}}} = \frac{T_2}{T_1} = \frac{N}{2^n} \quad (12.70)$$

assuming that the  $RC$  product remains constant throughout the complete conversion cycle. The absolute values of  $R$  and  $C$  no longer enter directly into the relation between  $v_x$  and  $V_{FS}$ , and the long-term stability problem associated with the single-ramp converter is overcome. Furthermore, the digital output word represents the average value of  $v_x$  during the first integration phase. Thus,  $v_x$  can change during the conversion cycle of this converter without destroying the validity of the quantized output value.

The conversion time  $T_T$  requires  $2^n$  clock periods for the first integration period, and  $N$  clock periods for the second integration period. Thus the conversion time is variable and

$$T_T = (2^n + N)T_C \leq 2^{n+1}T_C \quad (12.71)$$

because the maximum value of  $N$  is  $2^n$ .

**EXERCISE:** What is the maximum conversion time for a 16-bit dual-ramp converter using a 1-MHz clock frequency? What is the maximum conversion rate?

**ANSWERS:** 0.131 s; 7.63 conversions/second

The dual ramp is a widely used converter. Although much slower than the successive approximation converter, the dual-ramp converter offers excellent differential and integral linearity. By combining its integrating properties with careful design, one can obtain accurate conversion at resolutions exceeding 20 bits, but at relatively low conversion rates. In a number of recent converters and instruments, the basic dual-ramp converter has been modified to include extra integration phases for automatic offset voltage elimination. These devices are often called *quad-slope* or *quad-phase converters*. Another converter, the *triple ramp*, uses coarse and fine down ramps to greatly improve the speed of the integrating converter (by a factor of  $2^{n/2}$  for an  $n$ -bit converter).

### Normal-Mode Rejection

As mentioned before, the quantized output of the dual-ramp converter represents the average of the input during the first integration phase. The integrator operates as a low-pass filter with the normalized transfer function shown in Fig. 12.40. Sinusoidal input signals, whose frequencies are exact multiples of the reciprocal of the integration time  $T_1$ , have integrals of zero value and do not appear at the integrator output. This property is used in many digital multimeters, which are equipped with dual-ramp converters having an integration time that is some multiple of the period of the 50- or 60-Hz power-line frequency. Noise sources with frequencies at multiples of the power-line frequency are therefore rejected by these integrating ADCs. This property is usually termed **normal-mode rejection**.

### The Parallel (Flash) Converter

The fastest converters employ substantially increased hardware complexity to perform a parallel rather than serial conversion. The term **flash converter** is sometimes used as the name of the parallel converter because of the device's inherent speed. Figure 12.41 shows a three-bit parallel converter in which the unknown input  $v_x$  is simultaneously compared to seven different reference voltages. The logic network encodes the comparator outputs directly into three binary bits representing the quantized value of the input voltage. The speed of this converter is very fast, limited only by the time

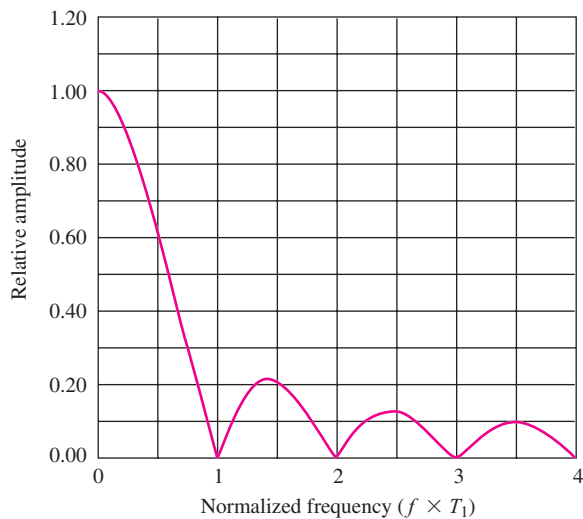


Figure 12.40 Normal-mode rejection for an integrating ADC.

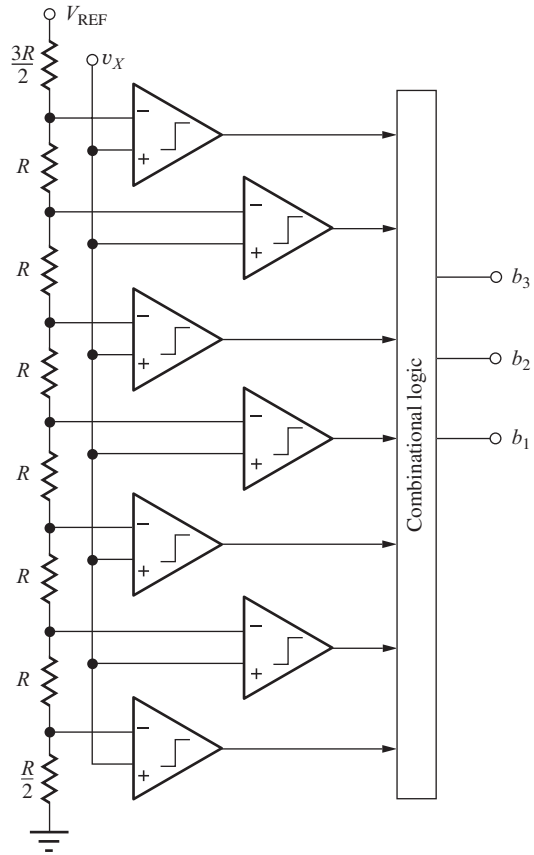


Figure 12.41 3-bit flash ADC.

delays of the comparators and logic network. Also, the output continuously reflects the input signal delayed by the comparator and logic network.

The parallel A/D converter is used when maximum speed is needed and is usually found in converters with resolutions of 10 bits or less because  $2^n - 1$  comparators and reference voltages are needed for an  $n$ -bit converter. Thus the cost of implementing such a converter grows rapidly with resolution. However, converters with 6-, 8-, and 10-bit resolutions have been realized in monolithic IC technology. These converters achieve effective conversion rates as high as  $10^8$ – $10^9$  conversions/second.

**EXERCISE:** How many resistors and comparators are required to implement a 10-bit flash ADC?

**ANSWERS:** 1024 resistors; 1023 comparators

### Delta-Sigma A/D Converters

**Delta-Sigma ( $\Delta-\Sigma$ ) converters** are widely used in today's integrated circuits because they require a minimum of precision components and are easily implemented in switched capacitor form, making them ideal for use in digital signal processing applications. These converters are used in audio as well as high-frequency signal processing applications and mixed-signal integrated circuits.

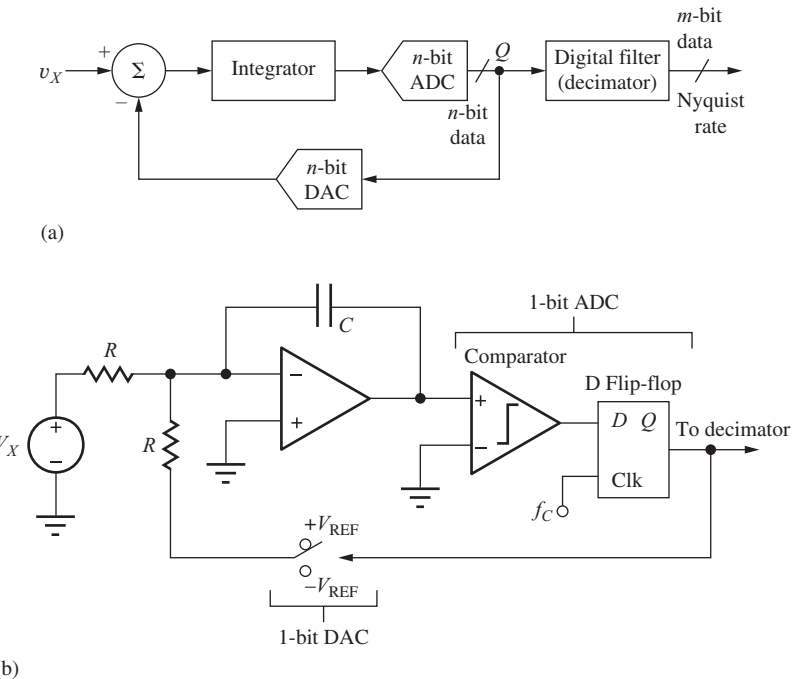


**Figure 12.42** (a) Block diagram of a Delta-Sigma ( $\Delta$ - $\Sigma$ ) ADC. (b) One-bit ( $n = 1$ )  $\Delta$ - $\Sigma$  ADC with utilizing a continuous time integrator.

The basic block diagram for the  $\Delta$ - $\Sigma$  ADC is shown in Fig. 12.42(a). The integrator accumulates the difference between unknown voltage  $v_X$  and the output of an  $n$ -bit D/A converter. The feedback loop forces the average value of the DAC output voltage to be equal to the unknown. In contrast to other types of converters, the internal ADC samples the integrator output at a rate that is much higher than the minimum required by the Nyquist theorem (remember that the sample rate must be at least twice the highest frequency present in the spectrum of the sampled signal). Typical sample rates for  $\Delta$ - $\Sigma$  ADCs range from 16 to 512 times the Nyquist rate, and the  $\Delta$ - $\Sigma$  converter is referred to as an “oversampled” A/D converter. Thus, the converter produces a high-rate stream of  $n$ -bit data words at output  $Q$ . This data stream is then processed by the digital filter to produce a higher resolution ( $m > n$ ) representation of  $v_X$  at the Nyquist rate.

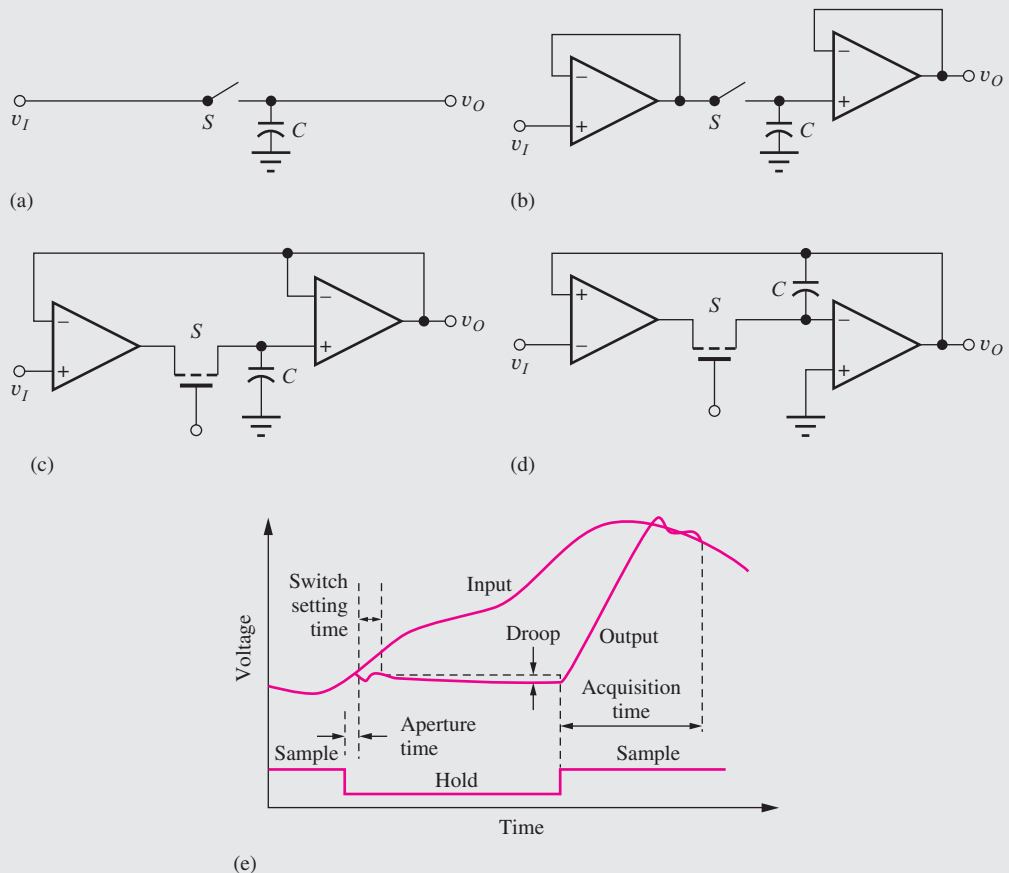
We can explore converter operation in more detail by referring to the implementation in Fig. 12.42(b). This most basic form of the  $\Delta$ - $\Sigma$  converter utilizes a continuous time integrator and 1-bit A/D and D/A converters. The integral of unknown dc voltage  $V_X$  is compared to the average of the D/A output that switches between  $+V_{REF}$  and  $-V_{REF}$ . At the beginning of each clock interval, the 1-bit decides if the output of the integrator is greater than zero ( $Q = 1$ ) or less than zero ( $Q = 0$ ), and the DAC output is set to force the integrator output back toward zero. If  $V_X$  is zero, for example, then the digital output alternates between 0 and 1, spending 50 percent of the time in each state. For other values of  $V_X$ , the switch will spend  $N$  clock periods connected to  $-V_{REF}$  and  $M - N$  clock periods connected to  $+V_{REF}$ , where the choice of the observation interval  $M$  depends on the desired resolution.

We can get a quantitative representation of the output by using the fact that feedback loop attempts to force the integrator output to zero:

$$-V_X \left( \frac{MT_C}{RC} \right) - V_{REF} \left( \frac{NT_C}{RC} \right) + V_{REF} \left[ \frac{(M-N)T_C}{RC} \right] = 0 \quad (12.72)$$


**ELECTRONICS IN ACTION**
**Sample-and-Hold Circuits**

Sample-and-hold (S/H) circuits are used throughout sampled data systems and are needed ahead of many types of analog-to-digital converters in order to prevent the ADC input signal from changing during the conversion time. A switched capacitor S/H circuit was discussed briefly in this chapter following the description of the successive approximation ADC. Several other op amp based S/H circuits are described here.<sup>1</sup>



Sample-and-hold circuits: (a) basic (b) buffered (c) closed-loop (d) integrator (e) waveforms. Copyright IEEE 1974. Reprinted with permission from [1].

The basic sample-and-hold in (a) of the figure includes a sampling switch  $S$  and a capacitor  $C$  that stores the sampled voltage. However, this simple circuit can incur errors due to loading of the signal being sampled. Circuit (b) utilizes voltage followers to solve the problem by buffering both the input to, and the output from, sampling capacitor  $C$ . The closed-loop sample-and-hold circuits in (c) and (d) place  $C$  within a global feedback loop to improve circuit performance. The integrator circuit in (d) greatly increases the effective value of the sampling capacitor. If

<sup>1</sup> K. R. Stafford, P. R. Gray, and R. A. Blanchard, "A complete monolithic sample-and-hold," *IEEE Journal of Solid-State Circuits*, vol. SC-9, no. 6, pp. 381–387, December 1974.

we apply our ideal op amp assumptions to each of the three S/H circuits, we find that both the capacitor and output voltages are always forced to be equal to the input voltage  $v_I$ . It is worth noting that the switched-capacitor circuitry discussed in Section 11.2 utilize the basic sampling circuit in part (a) of the figure.

The graph in part (e) illustrates some of design issues associated with sample-and-hold operation. The aperture time represents the time required for the switching devices to change state between the sample and hold modes. A settling time is then required for the feedback circuits to recover from the switching transients. During the hold mode, the voltage stored on the capacitor can change slightly due to switch leakage and op amp bias currents. This change is referred to as “droop.” Finally, an acquisition time is required for the circuit to catch back up to the input voltage after the circuit switches from hold mode back to sample mode.

or

$$V_X = V_{\text{REF}} \left( \frac{M - 2N}{M} \right) = V_{\text{REF}} \left( 1 - 2 \frac{N}{M} \right) \quad (12.73)$$

where the ratio  $N/M$  represents the average value of the binary bit stream at the output. If we select  $M = 2^m$ , then

$$V_X = \left( \frac{V_{\text{REF}}}{2^m} \right) (2^m - 2N) \quad (12.74)$$

and we see that the LSB is  $V_{\text{REF}}/2^m$ . The effective resolution is determined by how long we are willing to average the output. The simplest (although not necessarily the best) digital filter computes the average described here and converts the 1-bit data stream to  $m$ -bit parallel data words at the Nyquist sample rate. Converter operation is considerably more complex for a time-varying input signal, but the basic ideas are similar.

The circuit can be converted directly to switched capacitor form by replacing the continuous time integrator by the SC integrator in Fig. 12.43. Charge proportional to the input signal is added to the integrator output at each sample time, and a charge given by  $CV_{\text{REF}}$  is added or subtracted at each sample depending on the control sequence applied to the switches.

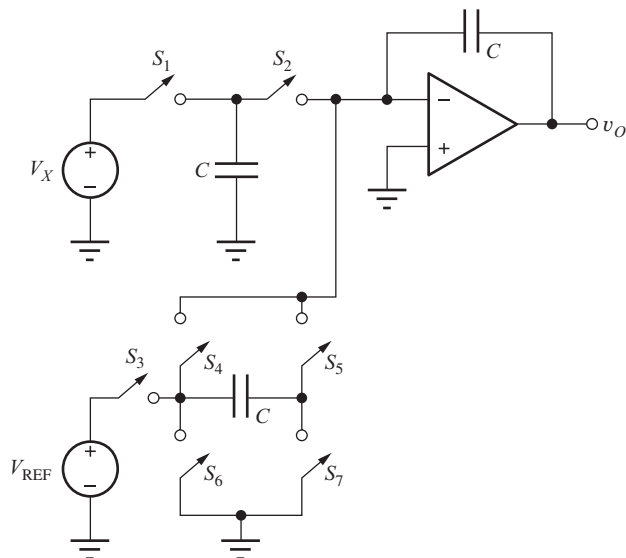


**Figure 12.43** Switched capacitor integrator and reference switch.

One of the advantages of the  $\Delta$ - $\Sigma$  converter is the inherent linearity of using a 1-bit DAC. Since there are only two levels, they must fall on a straight line, although an offset may be involved. For the case of the continuous time integrator, clock jitter still leads to errors. The SC integrator suffers less of a jitter problem as long as the clock interval is long enough for complete charge transfer to occur. The SC converter also offers the advantage of low-power operation.

## 12.7 OSCILLATORS

Oscillators are an important class of feedback circuits that are used for signal generation. In this section, we consider sinusoidal oscillators that are based upon operational amplifiers and represent our first application of positive feedback. Op-amp-based oscillators can be used to generate signals with frequencies of up to approximately one-half of the  $f_T$  of the op amp. Later, in Chapter 18, we will discuss transistor LC oscillators that utilize inductors and capacitors to generate signals with frequencies limited only by the unity-gain frequency of the individual devices. Oscillators using FETs and silicon-germanium BJTs have been shown to operate above 100 GHz!

### 12.7.1 THE BARKHAUSEN CRITERIA FOR OSCILLATION

The oscillator can be described by a positive (or regenerative) feedback system using the block diagram in Fig. 12.44. A frequency-selective feedback network is used, and the oscillator is designed to produce an output even though the input is zero.

For a sinusoidal oscillator, we want the poles of the closed-loop amplifier to be located at a frequency  $\omega_o$ , precisely on the  $j\omega$  axis. These circuits use positive feedback through the frequency-selective feedback network to ensure sustained oscillation at the frequency  $\omega_o$ . Consider the feedback system in Fig. 12.44, which is described by

$$A_v(s) = \frac{A(s)}{1 - A(s)\beta(s)} = \frac{A(s)}{1 - T(s)} \quad (12.75)$$

The use of positive feedback results in the minus sign in the denominator. For sinusoidal oscillations, the denominator of Eq. (12.75) must be zero for a particular frequency  $\omega_o$  on the  $j\omega$  axis:

$$1 - T(j\omega_o) = 0 \quad \text{or} \quad T(j\omega_o) = +1 \quad (12.76)$$

The **Barkhausen criteria for oscillation** are a statement of the two conditions necessary to satisfy Eq. (12.76):

1.  $\angle T(j\omega_o) = 0^\circ$       or even multiples of  $360^\circ - 2n\pi$  rad
2.  $|T(j\omega_o)| = 1$

These two criteria state that the phase shift around the feedback loop must be zero degrees, and the magnitude of the loop gain must be unity. Unity loop gain corresponds to a truly sinusoidal oscillator. A loop gain greater than 1 causes a distorted oscillation to occur.

In Sec. 12.7.2 we look at several  $RC$  oscillators that are useful at frequencies below a few megahertz. In Chapter 18,  $LC$  and crystal oscillators, both suitable for use at much higher frequencies, are presented.

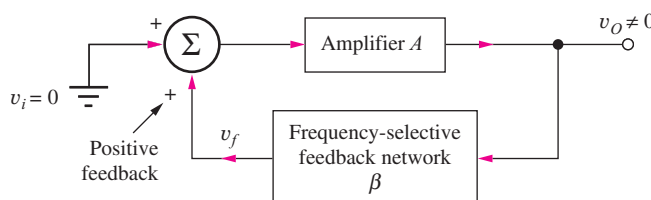
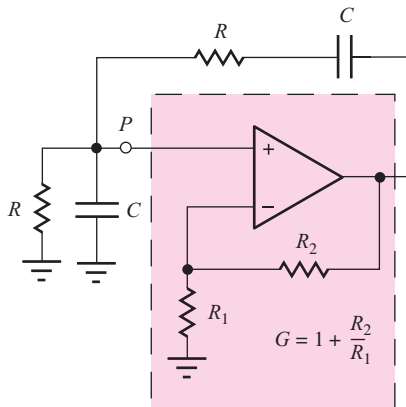
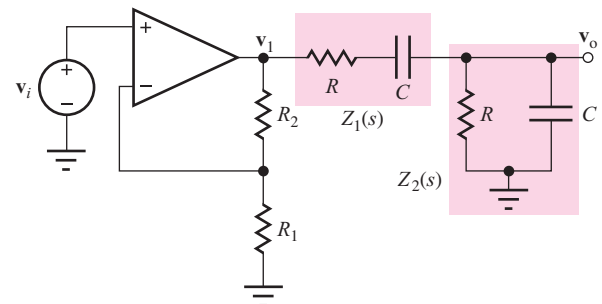


Figure 12.44 Block diagram for a positive feedback system.



**Figure 12.45** Wien-bridge oscillator circuit.



**Figure 12.46** Circuit for finding the loop gain of the Wien-bridge oscillator.

## 12.7.2 OSCILLATORS EMPLOYING FREQUENCY-SELECTIVE RC NETWORKS

RC networks can be used to provide the required frequency-selective feedback at frequencies below a few megahertz. This section introduces two **RC oscillator** circuits: the Wien-bridge oscillator and the phase-shift oscillator. Another example, the quadrature oscillator, is in Prob. 12.97.

### The Wien-Bridge Oscillator

The **Wien-bridge oscillator**<sup>8</sup> in Fig. 12.45 uses two *RC* networks to form the frequency-selective feedback network. The loop gain  $T(s)$  for the Wien-bridge circuit can be found by breaking the loop at point P which represents a convenient point since the op amp represents an open circuit at its noninverting input and does not load the feedback network. The operational amplifier is operating as a noninverting amplifier with a gain  $G = \mathbf{V}_1(s)/\mathbf{V}_I(s) = 1 + R_2/R_1$ . The loop gain can be found from Fig. 12.46 using voltage division between  $Z_1(s)$  and  $Z_2(s)$ :

$$\begin{aligned} V_o(s) &= V_I(s) \frac{Z_2(s)}{Z_1(s) + Z_2(s)} \\ Z_1(s) &= R + \frac{1}{sC} = \frac{sCR + 1}{sC} \quad \text{and} \quad Z_2(s) = R \parallel \frac{1}{sC} = \frac{R}{sCR + 1} \end{aligned} \quad (12.78)$$

Simplifying Eq. (12.78) yields the transfer function for the loop gain:

$$\begin{aligned} \mathbf{V}_o(s) &= G\mathbf{V}_I(s) \frac{sRC}{s^2R^2C^2 + 3sRC + 1} \\ T(s) &= \frac{\mathbf{V}_o(s)}{\mathbf{V}_I(s)} = \frac{sRCG}{s^2R^2C^2 + 3sRC + 1} \end{aligned} \quad (12.79)$$

For  $s = j\omega$ ,

$$T(j\omega) = \frac{j\omega RCG}{(1 - \omega^2 R^2 C^2) + 3j\omega RC} \quad (12.80)$$

<sup>8</sup> A version of this oscillator was the product that launched the Hewlett-Packard Company.

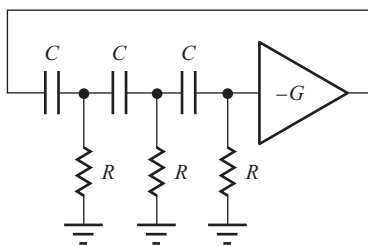


**Figure 12.47** Basic concept for the phase-shift oscillator.

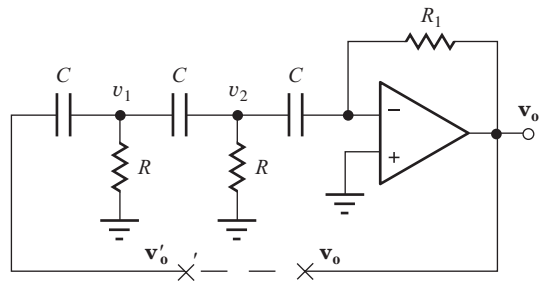


**Figure 12.48** One possible realization of the phase-shift oscillator.

Applying the first Barkhausen criterion, we see that the phase shift will be zero if  $(1 - \omega_o^2 R^2 C^2) = 0$ . At the frequency  $\omega_o = 1/RC$ ,

$$\angle T(j\omega_o) = 0^\circ \quad \text{and} \quad |T(j\omega_o)| = \frac{G}{3} \quad (12.81)$$

At  $\omega = \omega_o$ , the phase shift is zero degrees. If the gain of the amplifier is set to  $G = 3$ , then  $|T(j\omega_o)| = 1$ , and sinusoidal oscillations will be achieved.

The Wien-bridge oscillator is useful up to frequencies of a few megahertz, limited primarily by the characteristics of the amplifier. In signal generator applications, capacitor values are often switched by decade values to achieve a wide range of oscillation frequencies. The resistors can be replaced with potentiometers to provide continuous frequency adjustment within a given range.

### The Phase-Shift Oscillator

A second type of  $RC$  oscillator is the **phase-shift oscillator** depicted in Fig. 12.47. A three-section  $RC$  network is used to achieve a phase shift of  $180^\circ$ , which, added to the  $180^\circ$  phase shift of the inverting amplifier, results in a total phase shift of  $360^\circ$ .

The phase-shift oscillator has many practical implementations. One possible implementation combines a portion of the phase-shift function with an op amp gain block, as in Fig. 12.48. The loop gain can be found by breaking the feedback loop at  $x-x'$  and calculating  $\mathbf{V}_o(s)$  in terms of  $\mathbf{V}'_o(s)$ .

Writing the nodal equations for voltages  $\mathbf{V}_1$  and  $\mathbf{V}_2$ ,

$$\begin{bmatrix} sC\mathbf{V}'_o(s) \\ 0 \end{bmatrix} = \begin{bmatrix} (2sC + G) & -sC \\ -sC & (2sC + G) \end{bmatrix} \begin{bmatrix} \mathbf{V}_1(s) \\ \mathbf{V}_2(s) \end{bmatrix} \quad (12.82)$$

and using standard op amp theory:

$$\frac{\mathbf{V}_o(s)}{\mathbf{V}'_o(s)} = -sCR_1 \quad (12.83)$$

Combining Eqs. (12.82) and (12.83) and solving for  $\mathbf{V}_o(s)$  in terms of  $\mathbf{V}'_o(s)$  yields

$$T(s) = \frac{\mathbf{V}_o(s)}{\mathbf{V}'_o(s)} = -\frac{s^3 C^3 R^2 R_1}{3s^2 R^2 C^2 + 4sRC + 1} \quad (12.84)$$

and

$$T(j\omega) = -\frac{(j\omega)^3 C^3 R^2 R_1}{(1 - 3\omega^2 R^2 C^2) + j4\omega RC} = \frac{j\omega^3 C^3 R^2 R_1}{(1 - 3\omega^2 R^2 C^2) + j4\omega RC} \quad (12.85)$$

We can see from Eq. (12.85) that the phase shift of  $T(j\omega)$  will be zero if the real term in the denominator is zero:

$$1 - 3\omega_o^2 R^2 C^2 = 0 \quad \text{or} \quad \omega_o = \frac{1}{\sqrt{3}RC} \quad (12.86)$$

and

$$T(j\omega_o) = +\frac{\omega_o^2 C^2 R R_1}{4} = +\frac{1}{12} \frac{R_1}{R} \quad (12.87)$$

For  $R_1 = 12R$ , the second Barkhausen criterion is met ( $|T(j\omega_o)| = 1$ ).

### Amplitude Stabilization in RC Oscillators

As power supply voltages, component values, and/or temperature change with time, the loop gain of an oscillator also changes. If the loop gain becomes too small, then the desired oscillation decays; if the loop gain is too large, waveform distortion occurs. Therefore, some form of **amplitude stabilization**, or gain control, is often used in oscillators to automatically control the loop gain and place the poles exactly on the  $j\omega$  axis. Circuits will be designed so when power is first applied, the loop gain will be larger than the minimum needed for oscillation. As the amplitude of the oscillation grows, the gain control circuit reduces the gain to the minimum needed to sustain oscillation.

Two possible forms of amplitude stabilization are shown in Figs. 12.49 to 12.52. In the original Hewlett-Packard Wien-bridge oscillator, resistor  $R_1$  was replaced by a nonlinear element, the light-bulb in Fig. 12.49. The small-signal resistance of the lamp is strongly dependent on the temperature of the filament of the bulb. If the amplitude is too high, the current is too large and the resistance of the lamp increases, thereby reducing the gain. If the amplitude is low, the lamp cools, the resistance decreases, and the loop gain increases. The thermal time constant of the bulb effectively averages the signal current, and the amplitude is stabilized using this clever technique.

In the Wien-bridge circuit in Fig. 12.50, diodes  $D_1$  and  $D_2$  and resistors  $R_1$  to  $R_4$  form an amplitude control network. For a positive output signal at node  $v_O$ , diode  $D_1$  turns on as the voltage across  $R_3$  exceeds the diode turn-on voltage. When the diode is on, resistor  $R_4$  is switched in parallel with  $R_3$ , reducing the effective value of the loop gain. Diode  $D_2$  functions in a similar manner on the negative peak of the signal. The values of the resistors should be chosen so that

$$\frac{R_2 + R_3}{R_1} > 2 \quad \text{and} \quad \frac{R_2 + R_3 \| R_4}{R_1} < 2 \quad (12.88)$$

The first ratio should be set to be slightly greater than 2, and the second to slightly less than 2. Thus, when the diodes are off, the op amp gain is slightly greater than 3, ensuring oscillation, but when one of the diodes is on, the gain is reduced to slightly less than 3.

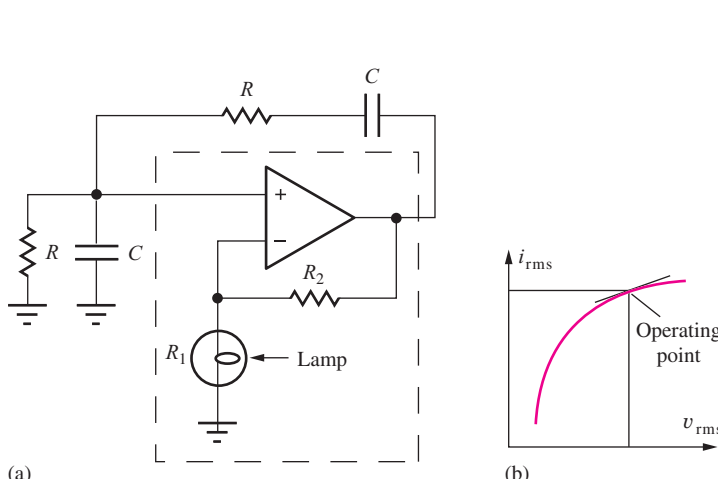


**Figure 12.49** (a) Wien-bridge with amplitude stabilization. (b) Bulb  $i$ - $v$  characteristic.

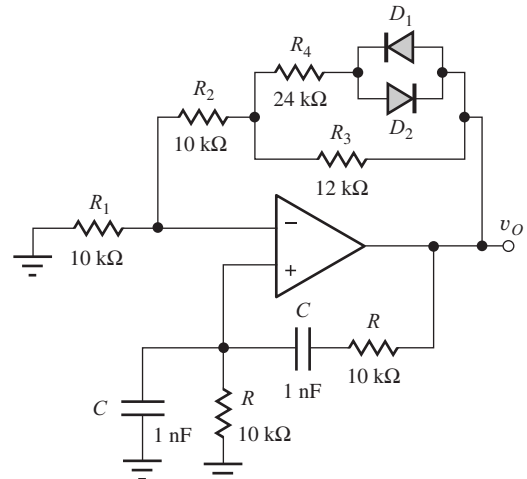


**Figure 12.50** Diode amplitude stabilization of a Wien-bridge oscillator.

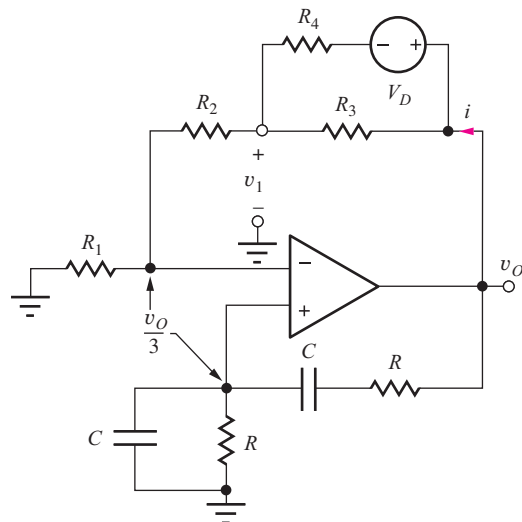


**Figure 12.51** Equivalent circuit with diode  $D_1$  on.

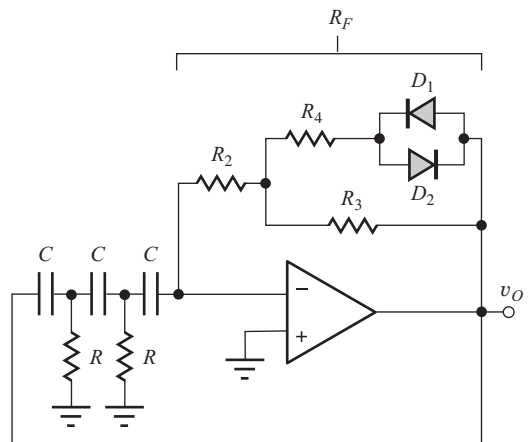


**Figure 12.52** Diode amplitude stabilization of a phase-shift oscillator.

An estimate for the amplitude of oscillation can be determined from the circuit in Fig. 12.51, in which diode  $D_1$  is assumed to be conducting with an on-voltage equal to  $V_D$ . The current  $i$  can be expressed as

$$i = \frac{v_o - v_1}{R_3} + \frac{v_o - v_1 - V_D}{R_4} \quad (12.89)$$

From Eq. (12.81) and ideal op amp behavior, we know that the voltages at both the inverting and noninverting input terminals are equal to one-third of the output voltage. Therefore,

$$v_1 = \frac{v_o}{3} \left( 1 + \frac{R_2}{R_1} \right) \quad (12.90)$$

Combining Eqs. (12.89) and (12.90) and solving for  $v_o$  yields

$$v_o = \frac{3V_D}{\left( 2 - \frac{R_2}{R_1} \right) \left( 1 + \frac{R_4}{R_3} \right) - \frac{R_4}{R_1}} \quad \text{where} \quad \frac{R_2}{R_1} < 2 \quad (12.91)$$

Because the gain control circuit is actually a nonlinear circuit, Eq. (12.91) is only an estimate of the actual output amplitude; nevertheless, it does provide a good basis for circuit design.

A similar amplitude stabilization network is applied to the phase-shift oscillator in Fig. 12.52. In this case, conduction through the diodes adjusts the effective value of the total feedback resistance  $R_F$ , which determines the gain.

**EXERCISE:** What are the amplitude and frequency of oscillation for the Wien-bridge oscillator in Fig. 12.51? Assume  $V_D = 0.6$  V.

**ANSWERS:** 9.95 kHz; 3.0 V

**EXERCISE:** Simulate the Wien-bridge oscillator using SPICE and find the frequency and amplitude of oscillation. Model the op amp using a macromodel with a gain of 100,000.

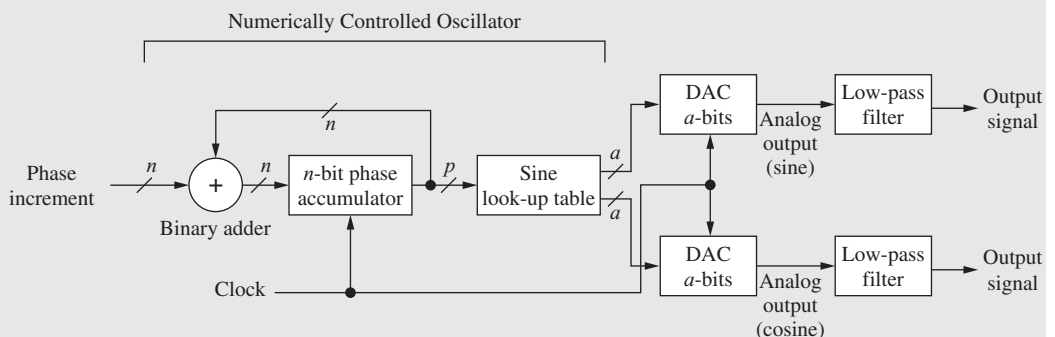
**ANSWERS:** 9.5 kHz; 3 V



## ELECTRONICS IN ACTION

### Numerically Controlled Oscillators and Direct Digital Synthesis

Modern D/A converter technology has advanced to the point that traditional analog feedback oscillators are being replaced with a direct digital synthesizer (DDS) that utilizes numerically controlled oscillators (NCOs) to synthesize the sinusoidal waveforms. The NCO can provide very small frequency step size and high-speed tuning. In the DDS, the signal waveform is constructed in the digital domain, and the analog output signal is produced using a digital-to-analog (DAC) converter followed by a low-pass filter.



The digital NCO consists of an  $n$ -bit phase accumulator and a  $p$ -bit sine look-up table where  $p \leq n$ . To generate a sine wave, an  $n$ -bit phase increment is added to the accumulator during each clock cycle. A full counter ( $2^n$  counts) corresponds to  $2\pi$  radians or 1 cycle of the output sine wave. If the counter is incremented by one at each clock interval, the maximum period  $T_{\max}$  of the output waveform, corresponding to minimum output frequency  $f_{\min}$ , will be

$$T_{\max} = 2^n T_{\text{clk}} \quad \text{or} \quad f_{\min} = \frac{f_{\text{clk}}}{2^n}$$

where  $T_{\text{clk}}$  is the period of the clock, and  $f_{\text{clk}}$  is the clock frequency. This minimum output frequency also represents the frequency resolution of the DDS. To generate higher frequency signals, a larger phase increment  $N$  is added to the phase accumulator at each clock cycle, and  $f_O = Nf_{\min}$ . For example, for  $f_{\text{clk}} = 20$  MHz and  $n = 24$ ,  $f_{\min} \approx 1.192$  Hz. In order to generate a 10-kHz sine wave, a phase increment of 8389 (10,000/1.192) would be added to the counter at each clock cycle. Based upon the Nyquist sampling theorem, the highest frequency that can be generated is one-half of the clock frequency (using  $N = 2^{n/2}$ ), since  $f_{\text{clk}}$  is the update rate of the D/A converter.

In order to reduce the size of the look-up table, only the upper  $p$  bits of the phase accumulator are used to address the sine table. A number of ROM compression techniques are utilized to further reduce the size of the ROM. The output of the sine table is an  $a$ -bit representation of the amplitude of the sine wave where “ $a$ ” corresponds to the number of bits of resolution of the D/A converter. Finite resolution in the representation of both the signal phase and amplitude lead to distortion in the output waveform. The low-pass filter helps to remove distortion and the high-frequency content related to the update rate of the DAC ( $f_{\text{clk}}$ ). Some DDS chips provide two D/A outputs, producing sine and cosine waves with very precise 90-degree phase relationships for the in-phase (I) and quadrature (Q) channels in RF transceivers.

## 12.8 NONLINEAR CIRCUIT APPLICATIONS

Up to this point, we have primarily considered operational amplifier circuits that use passive linear-circuit elements in the feedback network. But many interesting and useful circuits can be constructed using nonlinear elements, such as diodes and transistors in the feedback network. This section explores several examples of such circuits.

Except for oscillators, our op amp circuits thus far have involved only negative feedback configurations, but a number of other important nonlinear circuits employ positive feedback. Section 12.8 looks at this important class of circuits, including op amp implementations of rectifiers, astable and monostable multivibrators, and the Schmitt trigger circuit.

### 12.8.1 A PRECISION HALF-WAVE RECTIFIER

An op amp and diode are combined in Fig. 12.53 to form a **precision half-wave rectifier** circuit. Output  $v_O$  represents a rectified replica of the input signal  $v_I$  without loss of the voltage drop encountered with a normal diode rectifier circuit. The op amp tries to force the voltage across its input terminals to be zero. For  $v_I > 0$ ,  $v_O$  equals  $v_I$ , and  $i > 0$ . Because current  $i_-$  must be zero, diode current  $i_D$  is equal to  $i$ , diode  $D_1$  is forward-biased, and the feedback loop is closed through the diode. However, for negative output voltages, currents  $i$  and  $i_D$  would be less than zero, but negative current cannot go through  $D_1$ . Thus, the diode cuts off ( $i_D = 0$ ), the feedback loop is broken (inactive), and  $v_O = 0$  because  $i = 0$ .

The resulting voltage transfer function for the precision rectifier is shown in Fig. 12.54. For  $v_I \geq 0$ ,  $v_O = v_I$ , and for  $v_I \leq 0$ ,  $v_O = 0$ . The rectification is precise; for  $v_I \geq 0$ , the operational amplifier adjusts its output  $v_1$  to exactly absorb the forward voltage drop of the diode:

$$v_1 = v_O + v_D = v_I + v_D \quad (12.92)$$

This circuit provides accurate rectification even for very small input voltages and is sometimes called a **superdiode**. The primary sources of error are gain error due to the finite gain of the op amp, as well as an offset error due to the offset voltage of the amplifier. These errors were discussed in Chapter 11.

A practical problem occurs in this circuit for negative input voltages. Although the output voltage is zero, as desired for the rectifier, the voltage across the op amp input terminals is now negative, and the output voltage  $v_1$  is saturated at the negative supply limit. Most modern op amps provide input voltage protection and will not be damaged by a large voltage across the input. However, unprotected op amps can be destroyed if the magnitude of the input voltage is larger than a few volts. The saturated output of the op amp is not usually harmful to protected amplifiers, but it does take time for the internal circuits to recover from the saturated condition, thus slowing down the response time of the circuit. It is preferable to prevent the op amp from saturating, if possible.

**EXERCISE:** Suppose diode  $D_1$  in Fig. 12.53 has an “on-voltage” of 0.6 V, and the op amp is operating with  $\pm 10$ -V power supplies. What are the voltages  $v_O$  and  $v_1$  for the circuit if  $v_S = +1$  V? For  $v_S = -1$  V? What is the minimum Zener breakdown voltage for the diode?

**ANSWERS:** +1 V, +1.6 V; 0 V, -10 V; 10 V

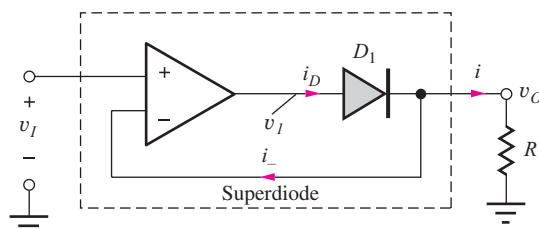


Figure 12.53 Precision half-wave rectifier circuit (or “superdiode”).

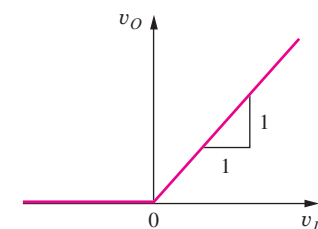


Figure 12.54 Voltage transfer characteristic for the precision rectifier.

### 12.8.2 NONSATURATING PRECISION-RECTIFIER CIRCUIT

The saturation problem can be solved using the circuit given in Fig. 12.55. An inverting-amplifier configuration is used instead of the noninverting configuration, and diode  $D_2$  is added to keep the feedback loop closed when the output of the rectifier is zero.

For positive input voltages depicted in Fig. 12.55(b), the op amp output voltage  $v_1$  becomes negative, forward-biasing diode  $D_2$  so that current  $i_I$  passes through diode  $D_2$  and into the output of the op amp. The inverting input is at virtual ground, the current in  $R_2$  is zero, and the output remains at zero. Diode  $D_1$  is reverse-biased.

For  $v_I < 0$  in Fig. 12.55(c), diode  $D_1$  turns on and supplies current  $i_I$  and load current  $i$ , and  $D_2$  is off. The circuit behaves as an inverting amplifier with gain equal to  $-R_2/R_1$ . Thus, the overall voltage transfer characteristic can be described by

$$v_O = 0 \text{ for } v_I \geq 0 \quad \text{and} \quad v_O = -\frac{R_2}{R_1}v_I \text{ for } v_I \leq 0 \quad (12.93)$$

as shown in Fig. 12.55(d). The output voltage of the op amp itself,  $v_1$ , is one diode-drop below zero for positive input voltages and one diode above the output voltage for negative input voltages. The inverting input is a virtual ground in both cases, and the negative feedback loop is always active: through  $D_1$  and  $R_2$  for  $v_I < 0$  and through  $D_2$  for  $v_I > 0$ .

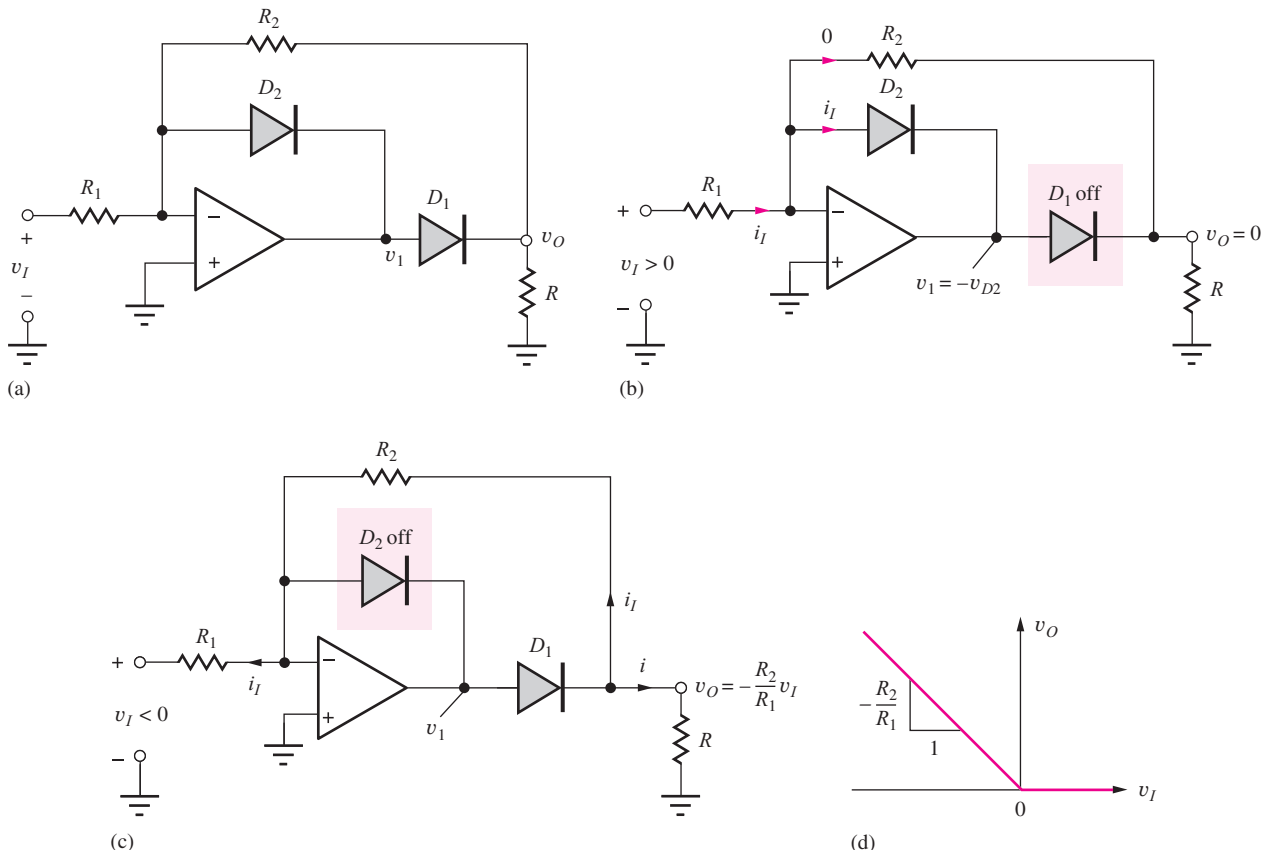


**Figure 12.55** (a) Nonsaturating precision-rectifier circuit. (b) Active feedback elements for  $v_I \geq 0$ . (c) Active feedback elements for  $v_I < 0$ . (d) Improved rectifier voltage transfer characteristic.

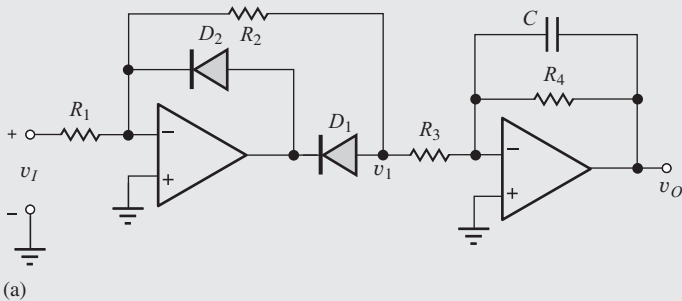


## ELECTRONICS IN ACTION

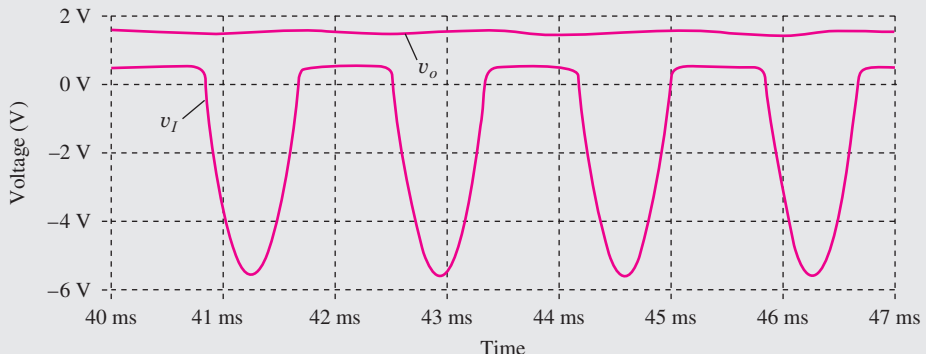
### An AC Voltmeter

The half-wave rectifier circuit can be combined with a low-pass filter to form a basic ac voltmeter circuit, as in Fig. (a). For a sinusoidal input signal with an amplitude  $V_M$  at a frequency  $\omega_o$ , the output voltage  $v_1$  is a rectified sine wave that can be described by its Fourier series as:

$$v_1(t) = - \left( \frac{R_2}{R_1} \right) \left( \frac{V_I}{\pi} \right) \left[ 1 + \frac{\pi}{2} \sin \omega_o t - \sum_{n=2}^{\infty} \frac{1 + \cos n\pi}{(n^2 - 1)} \cos n\omega_o t \right]$$



(a)



(a) AC voltmeter circuit consisting of a half-wave rectifier and low-pass filter. (b) Voltage waveform at rectifier output  $v_1$  for  $v_I = (-5 \sin 120\pi t)$  V with  $R_2 = R_1$ ,  $R_4 = R_3$  and  $f_C = 1.59$  Hz.

If the cutoff frequency of the low-pass filter is chosen such that  $\omega_C \ll \omega_o$ , then the output voltage  $v_O$  will consist primarily of the dc voltage component (see Prob. 12.107) given by

$$v_O = \frac{R_4}{R_3} \left[ \frac{R_2}{R_1} \frac{V_I}{\pi} \right]$$

The voltmeter range (scale factor) can be adjusted through the choice of the four resistors.

**EXERCISE:** Suppose the diodes in Fig. 12.55 have “on-voltages” of 0.6 V, and the op amp is operating with  $\pm 15$ -V power supplies. What are the voltages  $v_O$  and  $v_1$  for the circuit if  $R_1 = 22$  k $\Omega$ ,  $R_2 = 68$  k $\Omega$ , and  $v_S = +2$  V? For  $v_S = -2$  V? Estimate the most negative input voltage for which the circuit will operate properly. What is the minimum Zener breakdown voltage specification for the diodes assuming they are both the same?

**ANSWERS:** 0 V, -0.6 V; +6.18 V, +6.78 V; -4.66 V; 15 V

**EXERCISE:** What is the dc output voltage of the ac voltmeter circuit if  $R_1 = 3.24 \text{ k}\Omega$ ,  $R_2 = 10.2 \text{ k}\Omega$ ,  $R_3 = 20 \text{ k}\Omega$ ,  $R_4 = 20 \text{ k}\Omega$ , and  $V_I = 2 \text{ V}$ ?

**ANSWER:** 2.00 V

## 12.9 CIRCUITS USING POSITIVE FEEDBACK

Up to now, most of our circuits have used negative feedback: A voltage or current proportional to the output signal was returned to the inverting-input terminal of the operational amplifier. However, positive feedback can also be used to perform a number of useful nonlinear functions, and we investigate several possibilities in this final section, including the comparator, Schmitt trigger, and multivibrator circuits.

### 12.9.1 THE COMPARATOR AND SCHMITT TRIGGER

It is often useful to compare a voltage to a known reference level. This can be done electronically using the **comparator** circuit in Fig. 12.56. We want the output of the comparator to be a logic 1 when the input signal exceeds the reference level and a logic 0 when the input is less than the reference level. The basic comparator is simply a very high gain amplifier without feedback, as indicated in Fig. 12.56. For input signals exceeding the reference voltage  $V_{\text{REF}}$ , the output saturates at  $V_{CC}$ ; for input signals less than  $V_{\text{REF}}$ , the output saturates at  $-V_{EE}$ , as indicated in the voltage transfer characteristic in Fig. 12.56.<sup>9</sup> Amplifiers built for use as comparators are specifically designed to be able to saturate at the two voltage extremes without incurring excessive internal time delays.

However, a problem occurs when high-speed comparators are used with noisy signals, as indicated in Fig. 12.57. As the input signal crosses through the reference level, multiple transitions may occur due to noise present on the input. In digital systems, we often want to detect this threshold crossing cleanly by generating only a single transition, and the **Schmitt-trigger** circuit in Fig. 12.58 helps solve this problem.

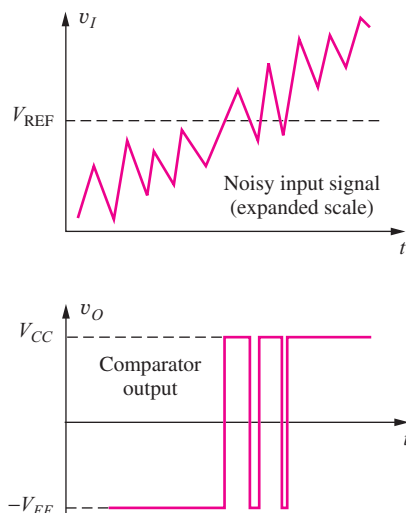
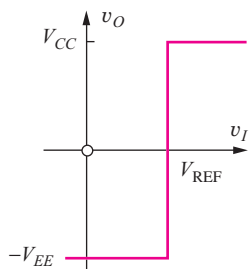
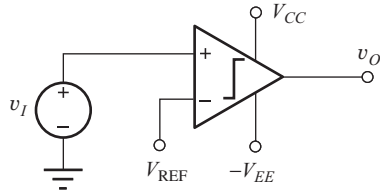


Figure 12.56 Comparator circuit using an infinite-gain amplifier.

Figure 12.57 Comparator response to noisy input signal.

<sup>9</sup> In this section, we assume that the output can reach the supply voltages.

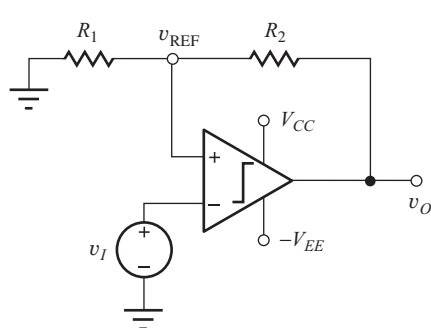


Figure 12.58 Schmitt-trigger circuit.

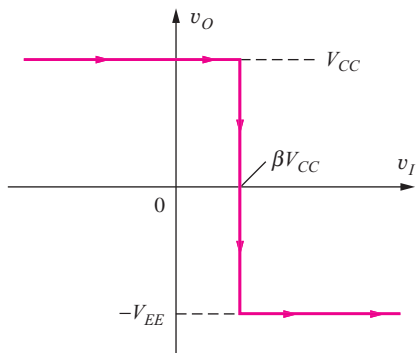
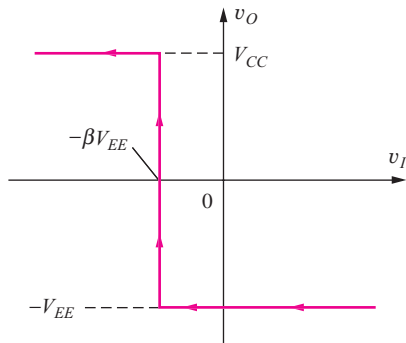
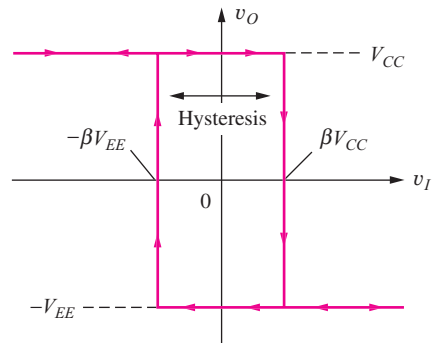
Figure 12.59 Voltage transfer characteristic for the Schmitt trigger as  $v_S$  increases from below  $V_{\text{REF}} = +\beta V_{CC}$ .Figure 12.60 Voltage transfer characteristic for the Schmitt trigger as  $v_S$  decreases from above  $V_{\text{REF}} = -\beta V_{EE}$ .

Figure 12.61 Complete voltage transfer characteristic for the Schmitt trigger.

The Schmitt trigger uses a comparator whose reference voltage is derived from a voltage divider across the output. The input signal is applied to the inverting-input terminal, and the reference voltage is applied to the noninverting input (positive feedback). For positive output voltages,  $V_{\text{REF}} = \beta V_{CC}$ , but for negative output voltages,  $V_{\text{REF}} = -\beta V_{EE}$ , where  $\beta = R_1/(R_1 + R_2)$ . Thus, the reference voltage changes when the output switches state.

Consider the case for an input voltage increasing from below  $V_{\text{REF}}$ , as in Fig. 12.59. The output is at  $V_{CC}$  and  $V_{\text{REF}} = \beta V_{CC}$ . As the input voltage crosses through  $V_{\text{REF}}$ , the output switches state to  $-V_{EE}$ , and the reference voltage simultaneously drops, reinforcing the voltage across the comparator input. In order to cause the comparator to switch states a second time, the input must now drop below  $V_{\text{REF}} = -\beta V_{EE}$ , as depicted in Fig. 12.60.

Now consider the situation as  $v_S$  decreases from a high level, as in the voltage transfer characteristic in Fig. 12.60. The output is at  $-V_{EE}$  and  $V_{\text{REF}} = -\beta V_{EE}$ . As the input voltage crosses through  $V_{\text{REF}}$ , the output switches state to  $V_{CC}$ , and the reference voltage simultaneously increases, again reinforcing the voltage across the comparator input.

The voltage transfer characteristics from Figs. 12.59 and 12.60 are combined to yield the overall voltage transfer characteristic for the Schmitt trigger given in Fig. 12.61. The arrows indicate the portion of the characteristic that is traversed for increasing and decreasing values of the input signal. The Schmitt trigger is said to exhibit **hysteresis** in its VTC, and will not respond to input noise that

has a magnitude  $V_n$  smaller than the difference between the two threshold voltages:

$$V_n < \beta[V_{CC} - (-V_{EE})] = \beta(V_{CC} + V_{EE}) \quad (12.94)$$

The Schmitt trigger with positive feedback is an example of a circuit with two stable states: a **bistable circuit**, or **bistable multivibrator**. Another example of a bistable circuit is the digital storage element usually called the flip-flop (see Chapter 8).

**EXERCISE:** If  $V_{CC} = +10\text{ V} = -V_{EE}$ ,  $R_1 = 1\text{ k}\Omega$ , and  $R_2 = 9.1\text{ k}\Omega$ , what are the values of the switching thresholds for the Schmitt-trigger circuit in Figs. 12.58 through 12.61 and the magnitude of the hysteresis?

**ANSWERS:**  $+0.99\text{ V}$ ;  $-0.99\text{ V}$ ;  $1.98\text{ V}$

## 12.9.2 THE ASTABLE MULTIVIBRATOR

Another type of multivibrator circuit employs a combination of positive and negative feedback and is designed to oscillate and generate a rectangular output waveform. The output of the circuit in Fig. 12.62 has no stable state and is referred to as an **astable multivibrator**.

Operation of the astable multivibrator circuit can best be understood by referring to the waveforms in Fig. 12.63. The output voltage switches periodically (oscillates) between the two output voltages  $V_{CC}$  and  $-V_{EE}$ . Let us assume that the output has just switched to  $v_O = V_{CC}$  at  $t = 0$ . The voltage at the inverting-input terminal of the op amp charges exponentially toward a final value of  $V_{CC}$  with a time constant  $\tau = RC$ . However, when the voltage on the comparator's inverting input exceeds that on the noninverting input, the output switches state. The voltage on the capacitor at the time of the output transition is  $v_C = -\beta V_{EE}$ . Thus, the expression for the voltage on the capacitor can be written as

$$v_C(t) = V_{CC} - (V_{CC} + \beta V_{EE}) \exp\left(-\frac{t}{RC}\right) \quad (12.95)$$

The comparator changes state again at time  $T_1$  when  $v_C(t)$  just reaches  $\beta V_{CC}$ :

$$\beta V_{CC} = V_{CC} - (V_{CC} + \beta V_{EE}) \exp\left(-\frac{T_1}{RC}\right) \quad (12.96)$$

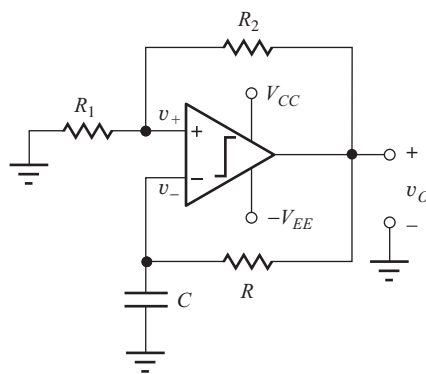


**Figure 12.62** Operational amplifier in an astable multivibrator circuit.

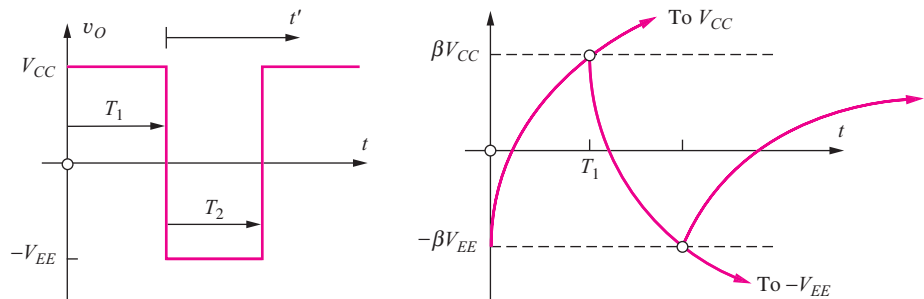


Figure 12.63 Waveforms for the astable multivibrator.

Solving for time  $T_1$  yields

$$T_1 = RC \ln \frac{1 + \beta \left( \frac{V_{EE}}{V_{CC}} \right)}{1 - \beta} \quad (12.97)$$

During time interval  $T_2$ , the output is low and the capacitor discharges from an initial voltage of  $\beta V_{CC}$  toward a final voltage of  $-V_{EE}$ . For this case, the capacitor voltage can be expressed as

$$v_C(t') = -V_{EE} + (V_{EE} + \beta V_{CC}) \exp \left( -\frac{t'}{RC} \right) \quad (12.98)$$

in which  $t' = 0$  at the beginning of the  $T_2$  interval. At  $t' = T_2$ ,  $v_C = -\beta V_{EE}$ ,

$$-\beta V_{EE} = -V_{EE} + (V_{EE} + \beta V_{CC}) \exp \left( -\frac{T_2}{RC} \right) \quad (12.99)$$

and  $T_2$  is equal to

$$T_2 = RC \ln \frac{1 + \beta \left( \frac{V_{CC}}{V_{EE}} \right)}{1 - \beta} \quad (12.100)$$

For the common case of symmetrical power supply voltages,  $V_{CC} = V_{EE}$ , and the output of the astable multivibrator represents a square wave with a period  $T$  given by

$$T = T_1 + T_2 = 2RC \ln \frac{1 + \beta}{1 - \beta} \quad (12.101)$$

**EXERCISE:** What is the frequency of oscillation of the circuit in Fig. 12.62 if  $V_{CC} = +5$  V,  $-V_{EE} = -5$  V,  $R_1 = 6.8$  k $\Omega$ ,  $R_2 = 6.8$  k $\Omega$ ,  $R = 10$  k $\Omega$ , and  $C = 0.001$   $\mu$ F?

**ANSWER:** 45.5 kHz

### 12.9.3 THE MONOSTABLE MULTIVIBRATOR OR ONE SHOT

A third type of multivibrator operates with one stable state and is used to generate a single pulse of known duration following application of a trigger signal. The circuit rests quiescently in its stable state, but can be “triggered” to generate a single transient pulse of fixed duration  $T$ . Once the time  $T$  is past, the circuit returns to the stable state to await another triggering pulse. This **monostable circuit** is variously called a **monostable multivibrator**, a **single shot**, or a **one shot**.

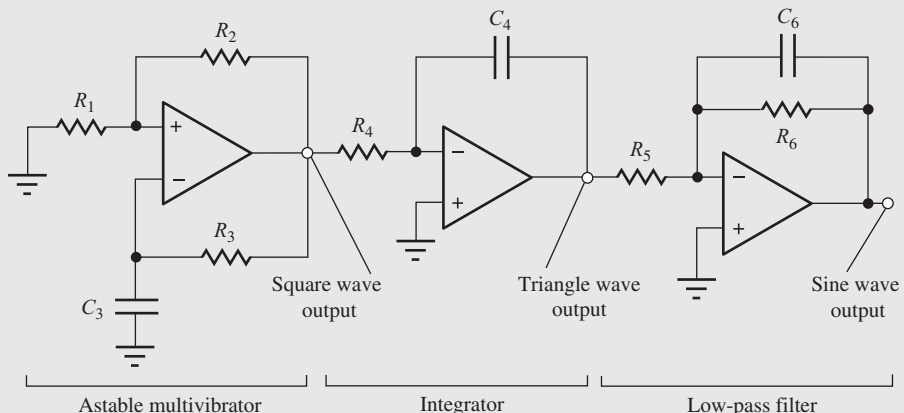
An example of a comparator-based monostable multivibrator circuit is given in Fig. 12.64. Diode  $D_1$  has been added to the astable multivibrator in Fig. 12.62 to couple the triggering signal  $v_T$  into the circuit, and clamping diode  $D_2$  has been added to limit the negative voltage excursion on capacitor  $C$ .



### Function Generators

#### Analog Function Generators

The instrumentation in most introductory electronics laboratories includes some type of low frequency function generator that produces elementary waveforms including square, triangle, and sine wave outputs at frequencies up to a few MHz. For many years, inexpensive versions of these function generators utilized the astable multivibrator to generate the square wave signal as shown in the accompanying figure. The frequency of the multivibrator is varied by changing either  $R_3$  or  $C_3$ .  $C_3$  is often changed in decade steps;  $R_3$  may be varied continuously using a potentiometer. The square wave output of the astable multivibrator drives an op amp integrator circuit to produce a triangular waveform. The output of the integrator can then be passed through a low-pass filter or piecewise linear shaping circuit to produce a low-distortion sine wave.



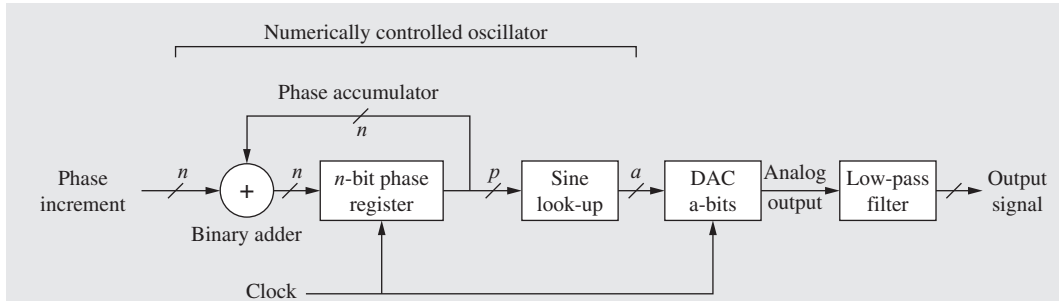
Simple function generator using an astable multivibrator, integrator, and low-pass filter.



Function generator.  
©Agilent Technologies 2006. All Rights Reserved.

#### Direct Digital Synthesis

Today, traditional analog function generators have been largely replaced with instruments based upon direct digital synthesis (DDS) as depicted in the block diagram below. In a DDS, the signal waveform is constructed in the digital domain, and the analog output signal is produced using a digital-to-analog converter followed by a low-pass filter.



The digital portion of the DDS consists of an  $n$ -bit phase accumulator and a sine look-up table. To generate a sine wave, an  $n$ -bit phase increment is added to the accumulator at each clock cycle. A full phase register ( $2^n$ ) corresponds to  $2\pi$  radians or 1 cycle of the output sine wave. If the phase is incremented by one at each clock interval, the maximum period  $T_{\max}$  of the output waveform, corresponding to minimum output frequency  $f_{\min}$ , will be

$$T_{\max} = 2^n T_{\text{clk}} \quad \text{or} \quad f_{\min} = \frac{f_{\text{clk}}}{2^n}$$

where  $T_{\text{clk}}$  is the period of the clock, and  $f_{\text{clk}}$  is the clock frequency. This minimum output frequency also represents the frequency resolution of the DDS. To generate higher frequency signals, a larger phase increment  $N$  is added to the phase at each clock cycle, and  $f_o = Nf_{\min}$ . For example, for  $f_{\text{clk}} = 20$  MHz and  $n = 24$ ,  $f_{\min} \approx 1.192$  Hz. In order to generate a 10 kHz sine wave, a phase increment of 8389(10,000/1.192) would be added to the phase at each clock cycle. Based upon the Nyquist sampling theorem, the highest frequency that can be generated is one-half of the clock frequency (using  $N = 2^{n/2}$ ), since  $f_{\text{clk}}$  is the update rate of the D/A converter.

In order to reduce the size of the look-up table, only the upper  $p$  bits of the phase accumulator are used to address the sine table, and a number of ROM compression techniques are also utilized. The output of the sine table is an  $a$ -bit representation of the amplitude of the sine wave where “ $a$ ” corresponds to the number of bits of resolution of the D/A converter. Finite resolution in the representation of both the signal phase and amplitude lead-to distortion in the output waveform. The low-pass filter helps to remove distortion and the high frequency content related to the update rate of the DAC ( $f_{\text{clk}}$ ).

Direct digital synthesis provides a great deal of flexibility since the digital hardware can create highly complex waveforms in the digital domain. For example, sine and cosine waves can be generated with very precise 90-degree phase relationships, and square and triangular waveforms can be generated by changing the phase update information as a function of time. AM or FM modulated waveforms can also readily be generated with only minor additional complexity.

The circuit rests in its quiescent state with  $v_O = -V_{EE}$ . If the trigger signal voltage  $v_T$  is less than the voltage at node 2,

$$v_T < -\frac{R_1}{R_1 + R_2} V_{EE} = -\beta V_{EE} \quad (12.102)$$

diode  $D_1$  is cut off. Capacitor  $C$  discharges through  $R$  until diode  $D_2$  turns on, clamping the capacitor voltage at one diode-drop  $V_D$  below ground potential. In this condition, the differential-input voltage  $v_{ID}$  to the comparator is given by

$$v_{ID} = -\beta V_{EE} - (-V_D) = -\beta V_{EE} + V_D \quad (12.103)$$

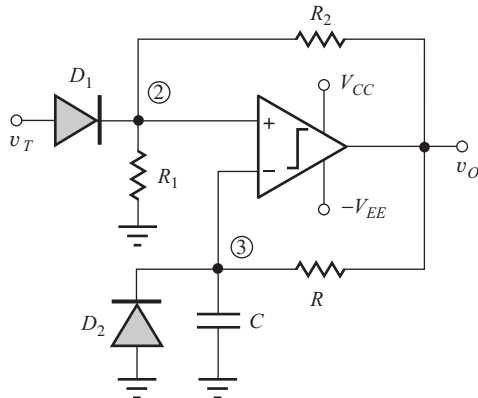


**Figure 12.64** Example of an operational-amplifier monostable-multivibrator circuit.

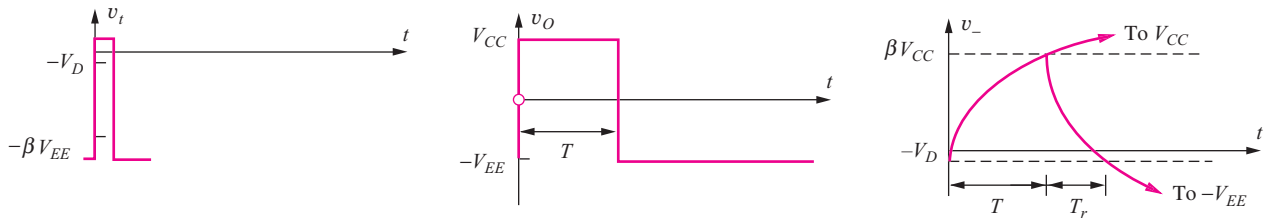


**Figure 12.65** Monostable multivibrator waveforms.

As long as the value of the voltage divider is chosen so that

$$v_{ID} < 0 \quad \text{or} \quad \beta V_{EE} > V_D \quad \text{where } \beta = \frac{R_1}{R_1 + R_2} \quad (12.104)$$

then the output of the circuit will have one stable state.

### Triggering the Monostable Multivibrator

The monostable multivibrator can be triggered by applying a positive pulse to the trigger input  $v_t$ , as shown in the waveforms in Fig. 12.65. As the trigger pulse level exceeds a voltage of  $-\beta V_{EE}$ , diode  $D_1$  turns on and subsequently pulls the voltage at node 2 above that at node 3. At this point, the comparator output changes state, and the voltage at the noninverting-input terminal rises abruptly to a voltage equal to  $+\beta V_{CC}$ . Diode  $D_1$  cuts off, isolating the comparator from any further changes on the trigger input.

The voltage on the capacitor now begins to charge from its initial voltage  $-V_D$  toward a final voltage of  $V_{CC}$  and can be expressed mathematically as

$$v_C(t) = V_{CC} - (V_{CC} + V_D) \exp\left(-\frac{t}{RC}\right) \quad (12.105)$$

where the time origin ( $t = 0$ ) coincides with the start of the trigger pulse. However, the comparator changes state again when the capacitor voltage reaches  $+\beta V_{CC}$ . Thus, the pulse width  $T$  is given by

$$\beta V_{CC} = V_{CC} - (V_{CC} + V_D) \exp\left(-\frac{T}{RC}\right) \quad \text{or} \quad T = RC \ln \frac{1 + \left(\frac{V_D}{V_{CC}}\right)}{1 - \beta} \quad (12.106)$$

The output of the circuit consists of a positive pulse with a fixed duration  $T$  set by the values of  $R_1$ ,  $R_2$ ,  $R$ , and  $C$ .

For a well-defined pulse width to be generated, this circuit should not be retriggered until the voltages on the various nodes have all returned to their quiescent steady-state values. Following the return of the output to  $-V_{EE}$ , the capacitor voltage charges from a value of  $\beta V_{CC}$  toward  $-V_{EE}$ , but reaches steady state when diode  $D_2$  begins to conduct. Thus, the recovery time can be calculated from

$$-V_D = -V_{EE} + (V_{EE} + \beta V_{CC}) \exp\left(-\frac{T_r}{RC}\right) \quad \text{and} \quad T_r = RC \ln \frac{1 + \beta \left(\frac{V_{CC}}{V_{EE}}\right)}{1 - \left(\frac{V_D}{V_{EE}}\right)} \quad (12.107)$$

**EXERCISE:** For the monostable multivibrator circuit in Fig. 12.64,  $V_{CC} = +5\text{ V} = V_{EE}$ ,  $R_1 = 22\text{ k}\Omega$ ,  $R_2 = 18\text{ k}\Omega$ ,  $R = 11\text{ k}\Omega$ , and  $C = 0.002\text{ }\mu\text{F}$ . What is the pulse width of the one shot? What is the minimum time between trigger pulses for this circuit?

**ANSWERS:** 20.4  $\mu\text{s}$ ; 33.4  $\mu\text{s}$

## SUMMARY

Chapter 12 introduced a variety of linear and nonlinear applications of operational amplifiers. Key topics are outlined here.

- It is often impossible to realize a set of amplifier specifications utilizing a single amplifier stage, and we must cascade several stages in order to achieve the desired results.
- Two-port models for cascaded amplifiers can be used to simplify the representation of the overall amplifier.
- A comprehensive example of the design of a multistage amplifier was presented in which a computer spreadsheet was used to explore the design space. The influence of resistor tolerances on this design was also explored.
- The bandwidth of a multistage amplifier is less than the bandwidth of any of the single amplifiers operating alone. An expression was developed for the bandwidth of a cascade of  $N$  identical amplifiers and was cast in terms of the bandwidth shrinkage factor.
- The instrumentation amplifier is a high performance circuit often used in data acquisition systems.
- Active  $RC$  filters including low-pass, high-pass, and band-pass circuits were introduced. These designs use  $RC$  feedback networks and operational amplifiers to replace bulky inductors that would normally be required in  $RLC$  filters designed for the audio range. Single-amplifier active filters employ a combination of negative and positive feedback to realize second-order low-pass, high-pass, and band-pass transfer functions.
- Sensitivity of filter characteristics to passive component and op amp parameter tolerances is an important design consideration. Multiple op amp filters offer low sensitivity and ease of design, compared to their single op amp counterparts.
- Magnitude and frequency scaling can be used to change the impedance level and  $\omega_o$  of a filter without affecting its  $Q$ .
- Switched-capacitor (SC) circuits use a combination of capacitors and switches to replace resistors in integrated circuit filter designs. These filters represent the sampled-data or discrete-time equivalents of the continuous-time  $RC$  filters and are fully compatible with MOS IC technology. Both inverting and noninverting integrators can be implemented using SC techniques.

- Digital-to-analog (D/A) and analog-to-digital (A/D) converters, also known as DACs and ADCs, provide the interface between the digital computer and the world of analog signals. Gain, offset, linearity, and differential linearity errors are important in both types of converters.
- The resolution of A/D and D/A converters is measured in terms of the least significant bit or LSB. The LSB of an  $n$ -bit converter is equal to  $V_{FS}/2^n$ , where  $V_{FS}$  is the full scale voltage range of the converter. The most significant bit or MSB of the converter is equal to  $V_{FS}/2$ .
- Simple MOS DACs can be formed using weighted-resistor, R-2R ladder and inverted R-2R ladder circuits, and MOS transistor switches. The inverted R-2R ladder configuration maintains a constant current within the ladder elements. Switched-capacitor techniques based on weighted-capacitor and C-2C ladder configurations are also widely used in VLSI ICs.
- Good-quality DACs have monotonic input-output characteristics.
- Basic ADC circuits compare an unknown input voltage to a known time-varying reference signal. The reference signal is provided by a D/A converter in the counting and successive approximation converters. The counting converter sequentially compares the unknown to all possible outputs of the D/A converter; a conversion may take as many as  $2^n$  clock periods to complete. The counting converter is simple but relatively slow. The successive approximation converter uses an efficient binary search algorithm to achieve a conversion in only  $n$  clock periods and is a very popular conversion technique.
- In the single- and dual-ramp ADCs, the reference voltage is an analog signal with a well-defined slope, usually generated by an integrator with a constant input voltage. The digital output of the single-ramp converter suffers from its dependence on the absolute values of the integrator time constant. The dual ramp greatly reduces this problem, and can achieve high differential and integral linearity, but with conversion rates of only a few conversions per second. The dual-ramp converter is widely used in high-precision instrumentation systems. Rejection of sinusoidal signals with periods that are integer multiples of the integration time, called normal-mode rejection, is an important feature of integrating converters.
- The fastest A/D conversion technique is the parallel or “flash” converter, which simultaneously compares the unknown voltage to all possible quantized values. Conversion speed is limited only by the speed of the comparators and logic network that form the converter. This high-speed is achieved at a cost of high hardware complexity.
- Good-quality ADCs exhibit linearity and differential linearity errors of less than 1/2 LSB and have no missing codes.
- A/D converters employ circuits called comparators to compare an unknown input voltage with a precision reference voltage. The comparator can be considered to be a high-gain, high-speed op amp designed to operate without feedback.
- In circuits called oscillators, feedback is actually designed to be positive or regenerative so that an output signal can be produced by the circuit without an input being present. The Barkhausen criteria for oscillation state that the phase shift around the feedback loop must be an even multiple of  $360^\circ$  at some frequency, and the loop gain at that frequency must be equal to 1.
- Oscillators use some form of frequency-selective feedback to determine the frequency of oscillation;  $RC$  and  $LC$  networks and quartz crystals can all be used to set the frequency.
- Wien-bridge and phase-shift oscillators are examples of oscillators employing  $RC$  networks to set the frequency of oscillation.
- For true sinusoidal oscillation, the poles of the oscillator must be located precisely on the  $j\omega$  axis in the  $s$ -plane. Otherwise, distortion occurs. To achieve sinusoidal oscillation, some form of amplitude stabilization is normally required. Such stabilization may result simply from the inherent nonlinear characteristics of the transistors used in the circuit, or from explicitly added gain control circuitry.

- Nonlinear circuit applications of operational amplifiers were also introduced including several precision-rectifier circuits.
- Multivibrator circuits are used to develop various forms of electronic pulses. The bistable Schmitt-trigger circuit has two stable states and is often used in place of the comparator in noisy environments. The monostable multivibrator, or one shot, is used to generate a single pulse of known duration, whereas the astable multivibrator has no stable state and oscillates continuously, producing a square wave output.

## KEY TERMS

Active filters	Maximally flat magnitude
Amplitude stabilization	-1 Point
Analog-to-digital converter (ADC or A/D converter)	Missing code
Astable circuit	Monostable circuit
Astable multivibrator	Monostable multivibrator
Band-pass filter	Monotonic converter
Barkhausen criteria for oscillation	Most significant bit (MSB)
Bistable circuit	Negative feedback
Bistable multivibrator	Noninverting integrator
Butterworth filter	Nonmonotonic converter
C-2C ladder DAC	Normal-mode rejection
Comparator	Notch filter
Conversion time	One shot
Counter-ramp converter	Open-circuit voltage gain
Delta-Sigma ADC	Open-loop amplifier
Differential linearity error	Open-loop gain
Differential subtractor	Operational amplifier (op amp)
Digital-to-analog converter (DAC or D/A converter)	Oscillator circuits
Dual-ramp (dual-slope) ADC	Oscillators
Flash converter	Phase-shift oscillator
Frequency scaling	Positive feedback
Full-scale current	Precision half-wave rectifier
Full-scale voltage	Quantization error
Gain error	R-2R ladder
High-pass filter	RC oscillators
Hysteresis	Reference current
Instrumentation amplifier	Reference transistor
Integral linearity error	Reference voltage
Integrator	Regenerative feedback
Inverted R-2R ladder	Resolution of the converter
Inverting amplifier	Sample-and-hold circuit
Inverting input	Schmitt trigger
Least significant bit (LSB)	Sensitivity
Linearity error	Single shot
Loop gain ( $A\beta$ )	Single-ramp (single-slope) ADC
Loop transmission ( $T$ )	Single shot
Low-pass filter	Sinusoidal oscillator
Magnitude scaling	Stray-insensitive circuits
	Successive approximation converter
	Superdiode

Superposition errors  
 Switched-capacitor filters  
 Switched-capacitor integrator  
 Switched-capacitor (SC) circuits  
 Tow-Thomas biquad  
 Triggering

Two-phase nonoverlapping clock  
 Two-port model  
 Weighted-capacitor DAC  
 Weighted-resistor DAC  
 Wien-bridge oscillator

## ADDITIONAL READING

- Franco, Sergio, *Design with Operational Amplifiers and Analog Integrated Circuits*, Third Edition, McGraw-Hill, New York: 2001.
- Ghausi, M. S. and K. R. Laker. *Modern Filter Design—Active RC and Switched Capacitor*. Prentice-Hall, Englewood Cliffs, NJ: 1981.
- Gray, P. R., P. J. Hurst, S. H. Lewis, and R. G. Meyer, *Analysis and Design of Analog Integrated Circuits*, Fourth Edition, John Wiley and Sons, New York: 2001.
- Huelsman, L. P. and P. E. Allen. *Introduction to Theory and Design of Active Filters*. McGraw-Hill, New York: 1980.
- Kennedy, E. J. *Operational Amplifier Circuits—Theory and Applications*. Holt, Rinehart and Winston, New York: 1988.

## PROBLEMS

### 12.1 Cascaded Amplifier

- 12.1. Seven amplifiers were identified in Fig. 12.1. Find two more possibilities.
- 12.2. An amplifier is formed by cascading two operational-amplifier stages, as shown in Fig. P12.2(a). (a) Replace each amplifier stage with its two-port representation. (b) Use the circuit model from part (a) to find the overall two-port representation ( $A_v$ ,  $R_{in}$ ,  $R_{out}$ ) for the complete two-stage amplifier. (c) Draw the circuit of the two-port corresponding to the complete two-stage amplifier.

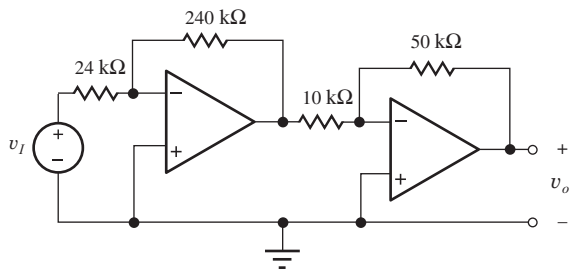


Figure P12.2

- 12.3. An amplifier is formed by cascading three identical operational-amplifier stages, as shown in Fig. P12.3. (a) Replace each op amp circuit with its

two-port representation. (b) Use the circuit model from part (a) to find the overall two-port representation ( $A_v$ ,  $R_{in}$ ,  $R_{out}$ ) for the complete three-stage amplifier. (c) Draw the two-port circuit corresponding to the complete three-stage amplifier.

- 12.4. An amplifier is formed by cascading the two operational amplifier stages shown in Fig. P12.2. What are the voltage gain, input resistance, and output resistance for this amplifier (a) if the op amps are ideal? (b) If the op amps have an open-loop gain of  $10^5$ , an input resistance of  $500 \text{ k}\Omega$ , and an output resistance of  $200 \Omega$ ? (c) Draw the new circuit and repeat (a) and (b) if the two amplifier stages are interchanged.
- 12.5. An amplifier is formed by cascading the two operational amplifier stages shown in Fig. P12.5. What are the voltage gain, input resistance, and output resistance for this amplifier (a) if the op amps are ideal? (b) If the op amps have an open-loop gain of 86 dB, an input resistance of  $250 \text{ k}\Omega$ , and an output resistance of  $100 \Omega$ ? (c) Draw the new circuit and repeat (a) and (b) if the two amplifier stages are interchanged.
- 12.6. An amplifier is formed by cascading the two operational amplifier stages shown in Fig. P12.6. What are the voltage gain, input resistance, and output

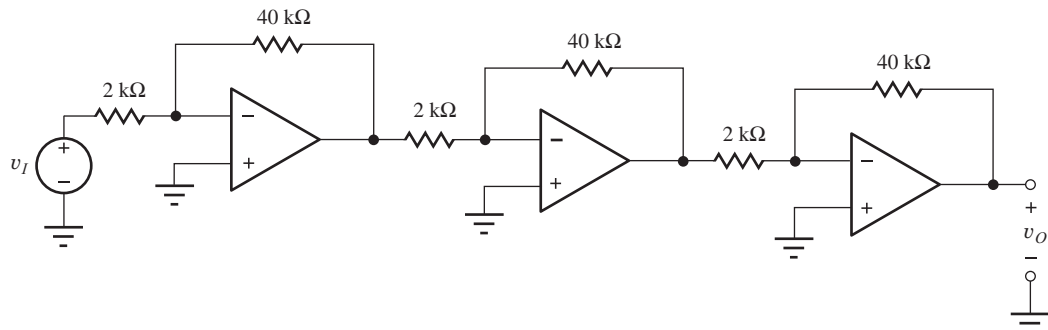


Figure P12.3

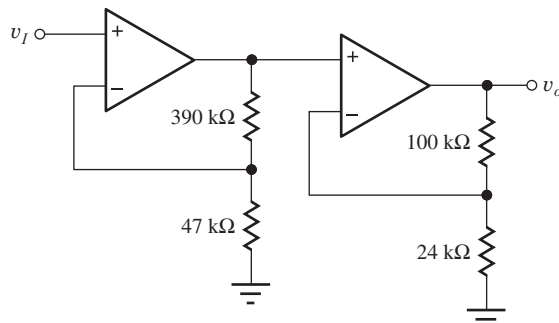
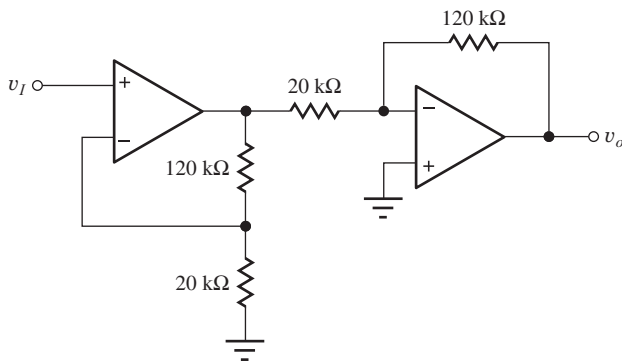


Figure P12.5

resistance for this amplifier (a) if the op amps are ideal? (b) If the op amps have an open-loop gain of 106 dB, an input resistance of  $300 \text{ k}\Omega$ , and an output resistance of  $200 \Omega$ ? (c) Draw the new circuit and repeat (a) and (b) if the two amplifier stages are interchanged.



(c)

Figure P12.6

- 12.7. An amplifier is formed by cascading the three operational amplifier stages shown in Fig. P12.3. What are the voltage gain, input resistance, and output resistance for this amplifier (a) if the op amps are ideal? (b) If the op amps have an open-loop gain of

94 dB, an input resistance of  $400 \text{ k}\Omega$ , and an output resistance of  $250 \Omega$ ?

- 12.8. Assume the op amps in Fig. P12.3 are ideal except for power supply voltages of  $\pm 12 \text{ V}$ . (a) If the input voltage is 1 mV, what are the voltages at the 8 nodes in the circuit? (b) Repeat for an input voltage of 3 mV. (c) Repeat for an input voltage of 2 mV with an open-loop gain of 80 dB.
- 12.9. An amplifier is formed by cascading the three operational amplifier stages shown in Fig. P12.9. What are the voltage gain, input resistance, and output resistance for this amplifier (a) if the op amps are ideal? (b) If the op amps have an open-loop gain of 94 dB, an input resistance of  $400 \text{ k}\Omega$ , and an output resistance of  $250 \Omega$ ?
- 12.10. Assume the op amps in Fig. P12.9 are ideal except for power supply voltages of  $\pm 12 \text{ V}$ . (a) If the input voltage is 5 mV, what are the voltages at the 8 nodes in the circuit? (b) Repeat for an input voltage of 10 mV. (c) Repeat for an input voltage of 10 mV with an open-loop gain of 80 dB.
- 12.11. What are the values of  $A_v$ ,  $R_{in}$ , and  $R_{out}$  for the overall three-stage amplifier in Fig. P12.3 if the 2-kΩ resistors are replaced with 3.9-kΩ resistors?
- 12.12. The 2-kΩ resistors in Fig. P12.3 are to be replaced with a value that gives an overall gain of 40 dB. What is the new resistor value? What is the new value of  $R_{in}$ ?
- 12.13. The op amps in Fig. P12.9 are ideal. What are the nominal, minimum, and maximum values of the voltage gain, input resistance, and output resistance of the overall amplifier if all the resistors have 5 percent tolerances?
- 12.14. The op amps in Fig. P12.14 are ideal (a) What are the voltage gain, input resistance, and output resistance of the overall amplifier? (b) If the input voltage  $v_I = 0.002 \text{ V}$ , what are the voltages at each of the eight nodes in the amplifier circuit?

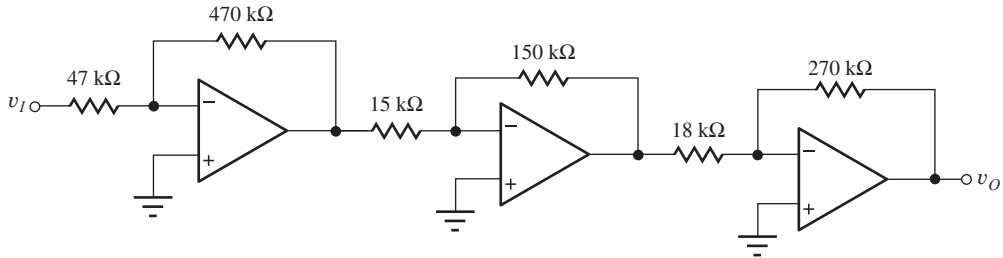


Figure P12.9

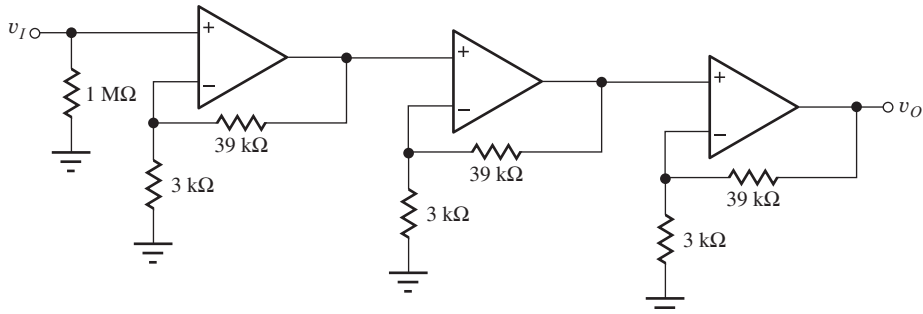


Figure P12.14

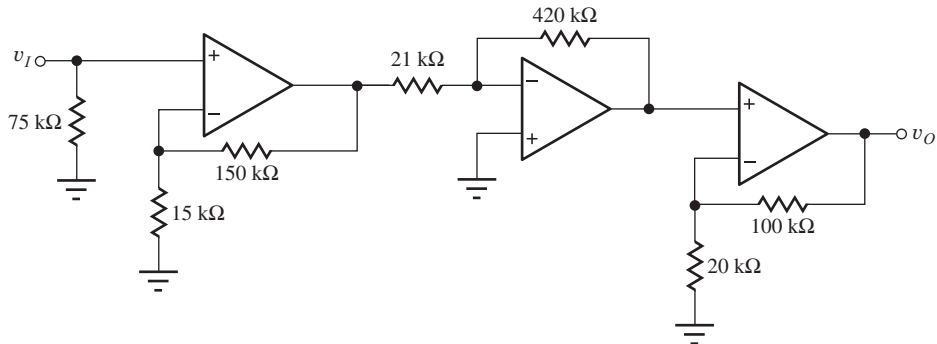


Figure P12.17

- 12.15. Repeat Prob. 12.14 if the 3-k $\Omega$  resistors are all replaced with 1-k $\Omega$  resistors, and the 1-M $\Omega$  resistor is replaced with a 2-M $\Omega$  resistor.
- 12.16. The op amps in Fig. P12.14 are ideal. What are the nominal, minimum, and maximum values of the voltage gain, input resistance, and output resistance of the overall amplifier if all the resistors have 2 percent tolerances?
- 12.17. The op amps in Fig. P12.17 are ideal. (a) What are the voltage gain, input resistance, and output resistance of the overall amplifier? (b) If the input voltage  $v_I = 0.005$  V, what are the voltages at each of the eight nodes in the amplifier circuit?
- 12.18. The op amps in Fig. P12.17 are ideal. What are the nominal, minimum, and maximum values of the voltage gain, input resistance, and output resistance of the overall amplifier if all the resistors have 1 percent tolerances?
- 12.19. What are the gain and bandwidth of the individual stages in the amplifier in Fig. P12.2 if the op amps have an  $A_o = 86$  dB and  $f_T = 4$  MHz? (a) What are the overall gain and bandwidth of the two-stage amplifier? (b) Repeat for the amplifier in Fig. P12.5. (c) Repeat for the amplifier in Fig. P12.6.
- 12.20. (a) What are the gain and bandwidth of the individual amplifier stages in Fig. P12.3 if the op amps have  $A_o = 10^5$  and  $f_T = 3$  MHz? (b) What are the overall gain and bandwidth of the three-stage amplifier?
- 12.21. What are the gain and bandwidth of the individual stages in the amplifier in Fig. P12.14 if the op amps have an  $A_o = 86$  dB and  $f_T = 4$  MHz? What are

the overall gain and bandwidth of the three-stage amplifier?

- 12.22. What are the gain and bandwidth of the individual stages in the amplifier in Fig. P12.17 if the op amps have an  $A_o = 86$  dB and  $f_T = 4$  MHz? What are the overall gain and bandwidth of the three-stage amplifier?
- 12.23. The op-amps in Fig. P12.23 are described by  $A_o = 80$  dB,  $R_{id} = 300$  k $\Omega$ ,  $R_o = 200$   $\Omega$ , and  $f_T = 3$  MHz, and the power supplies are  $\pm 15$  V. (a) What are the voltage gain, input resistance, output resistance, and bandwidth of the overall amplifier? (b) Assume the offset voltage of each op-amp is equivalent to +10 mV at the positive input of the op amp. If the input voltage  $v_I = 0$  V, what are the voltages (three significant digits) at each of the 10 nodes in the amplifier circuit?
- 12.24. What are the nominal, minimum, and maximum values of the voltage gain, input resistance, output resistance, and bandwidth of the overall amplifier in Prob. 12.23 if the resistors all have 10 percent tolerances?

- \*\*12.25. A cascade amplifier is to be designed to meet these specifications:

$$A_v = 5000 \quad R_{in} \geq 10 \text{ M}\Omega \quad R_{out} \leq 0.1 \text{ }\Omega$$

How many amplifier stages will be required if the stages must use an op amp below? Because of bandwidth requirements, assume that no individual stage can have a gain greater than 50.

Op amp specifications:  $A = 85$  dB

$$R_{id} = 1 \text{ M}\Omega$$

$$R_o = 100 \text{ }\Omega$$

$$R_{ic} \geq 1 \text{ G}\Omega$$

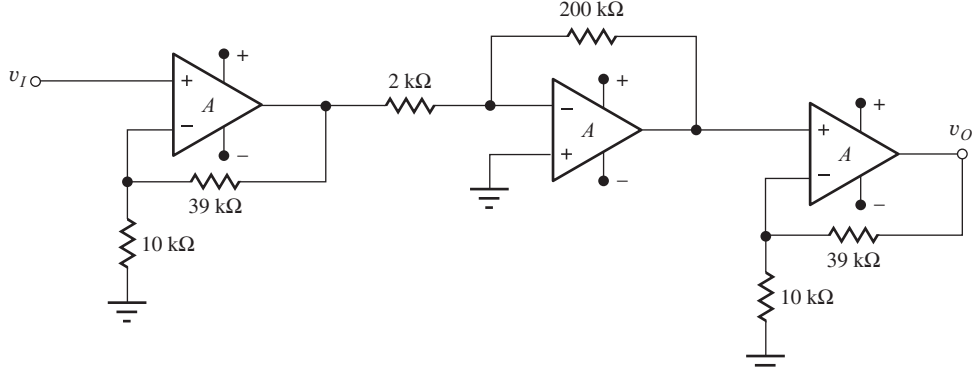


Figure P12.23

\*\*12.26. Use these op amp parameters to design a multistage amplifier that meets the specifications below.

$$A_v = 86 \text{ dB} \pm 1 \text{ dB} \quad R_{in} \geq 10 \text{ k}\Omega$$

$$R_{out} \leq 0.01 \text{ }\Omega \quad f_H \geq 75 \text{ kHz}$$

The amplifier should use the minimum number of op amp stages that will meet the requirements. (A spreadsheet or simple computer program will be helpful in finding the solution.)

$$\text{Op amp specifications: } A_o = 10^5$$

$$R_{id} = 10^9 \text{ }\Omega$$

$$R_o = 50 \text{ }\Omega$$

$$\text{GBW} = 1 \text{ MHz}$$

- \*\*12.27. (a) Design the amplifier in Prob. 12.26, including values for the feedback resistors in each stage.  
 (b) What is the bandwidth of your amplifier if the op amps have  $f_T = 5$  MHz?

- 12.28. Simulate the frequency response of the nominal design of the six-stage cascade amplifier from Table 12.6. Use the macro model in Fig. 11.51 to represent the op amp.

- 12.29. Simulate the frequency response of the six-stage cascade amplifier from Table 12.6 using the μA741 op amp macro model in SPICE.

- 12.30. Use the Monte Carlo analysis capability in PSPICE to simulate 1000 cases of the behavior of the six-stage amplifier in Table 12.6. Assume that all resistors and capacitors have 5 percent tolerances and the open-loop gain and bandwidth of the op amps each has a 50 percent tolerance. Use uniform statistical distributions. What are the lowest and highest observed values of gain and bandwidth for the amplifier?

- 12.31. A cascade amplifier is to be designed to meet these specifications:

$$\begin{aligned}A_v &= 60 \text{ dB} \pm 1 \text{ dB} & R_{in} &= 27 \text{ k}\Omega \\R_{out} &\leq 0.1 \text{ }\Omega & \text{Bandwidth} &= 20 \text{ kHz}\end{aligned}$$

How many amplifier stages will be required if the stages must use these op amp specifications?

Op amp specifications:  $A_o = 85 \text{ dB}$   
 $f_T = 5 \text{ MHz}$   
 $R_o = 100 \Omega$   
 $R_{id} = 1 \text{ M}\Omega$   
 $R_{ic} \geq 1 \text{ G}\Omega$

- 12.32. Design the amplifier in Prob. 12.31, including values for the feedback resistors in each stage.

- \*\*12.33 (a) Perform a Monte Carlo analysis of the six-stage cascade amplifier design resulting from the example in Tables 12.4 and 12.5, and determine the fraction of the amplifiers that will not meet either the gain or bandwidth specifications. Assume the resistors are uniformly distributed between their limits.

$$A_v \geq 100 \text{ dB} \quad \text{and} \quad f_H \geq 50 \text{ kHz}$$

- (b) What tolerance must be used to ensure that less than 0.1 percent of the amplifiers fail to meet both specifications?

The equation here can be used to estimate the location of the half-power frequency for  $N$  closely spaced poles, where  $\overline{f_{H1}}$  is the average of the individual cutoff frequencies of the  $N$  stages and  $f_{H1}^i$  is the cutoff frequency of the  $i$ th individual stage.

$$f_H = \overline{f_{H1}} \sqrt{2^{1/N} - 1}$$

$$\text{where } \overline{f_{H1}} = \frac{1}{N} \sum_{i=1}^N f_{H1}^i$$

- \*\*12.34. (a) Show that the number of stages that optimizes the bandwidth of a cascade of identical noninverting amplifier stages having a total gain  $G$  is given by

$$N = \frac{\ln 2}{\ln \left[ \frac{\ln G}{\ln G - \ln \sqrt{2}} \right]}$$

- (b) Calculate  $N$  for the amplifier in Example 12.3.

## 12.2 Instrumentation Amplifier

- 12.35. What is the voltage gain of the instrumentation amplifier in Fig. 12.4 if  $R_1 = 2 \text{ k}\Omega$ ,  $R_2 = 100 \text{ k}\Omega$ ,  $R_3 = 10 \text{ k}\Omega$ , and  $R_4 = 10 \text{ k}\Omega$ . What is the output

voltage if  $v_1 = (2 + 0.1 \sin 2000\pi t) \text{ V}$  and  $v_2 = 2.1 \text{ V}$ ?

- 12.36. What is the voltage gain of the instrumentation amplifier in Fig. 12.4 if  $R_1 = 20 \text{ k}\Omega$ ,  $R_2 = 100 \text{ k}\Omega$ ,  $R_3 = 10 \text{ k}\Omega$ , and  $R_4 = 20 \text{ k}\Omega$ . What is the output voltage if  $v_1 = (4 - 0.1 \sin 4000\pi t) \text{ V}$  and  $v_2 = 3.5 \text{ V}$ ?

- 12.37. What are the actual values of the two input resistances  $R_{in1}$  and  $R_{in2}$  and the output resistance  $R_{out}$  of the instrumentation amplifier in Fig. 12.4 if it is constructed using operational amplifiers with  $A = 7.5 \times 10^4$ ,  $R_{id} = 1 \text{ M}\Omega$ ,  $R_{ic} = 500 \text{ M}\Omega$ , and  $R_o = 100 \Omega$ ? Assume  $R_1 = 1 \text{ k}\Omega$ ,  $R_2 = 24 \text{ k}\Omega$ , and  $R_3 = R_4 = 10 \text{ k}\Omega$ .

- 12.38. In the instrumentation amplifier in Fig. P12.38,  $v_a = 4.99 \text{ V}$  and  $v_b = 5.01 \text{ V}$ . Find the values of node voltages  $v_1, v_2, v_3, v_4, v_5, v_6, v_o$ , and currents  $i_1, i_2$ , and  $i_3$ . What are the values of the common-mode gain, differential-mode gain, and CMRR of the amplifier? The op amps are ideal.

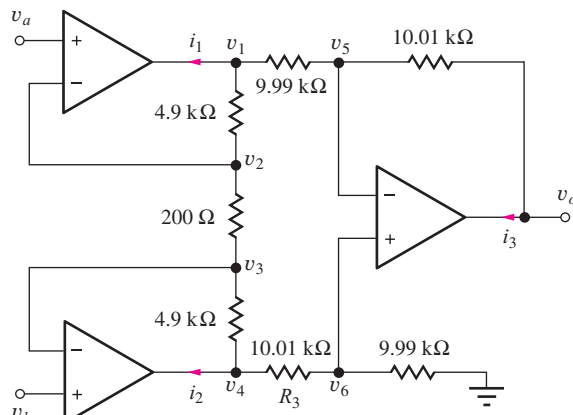


Figure P12.38

- 12.39. Find the values of  $v_1, v_2, v_3, v_4, v_5, v_6, v_o, i_1, i_2$ , and  $i_3$  in the instrumentation amplifier in Fig. P12.38 if  $v_a = 3 \text{ V}$  and  $v_b = 3 \text{ V}$ .

## 12.3 Active Filters

- 12.40. (a) Repeat Design Example 12.6 for a maximally flat second-order low-pass filter with  $f_o = 20 \text{ kHz}$ , using the circuit in Fig. 12.5. Assume  $C = 0.005 \mu\text{F}$ . What is the filter bandwidth? (b) Use frequency scaling to change  $f_o$  to 40 kHz.

- \*12.41. (a) Use MATLAB or other computer tool to make a Bode plot for the response of the filter in Prob. 12.40, assuming the op amp is ideal. (b) Use

SPICE to simulate the characteristics of the filter in Prob. 12.40 using a 741 op amp. (c) Discuss any disagreement between the SPICE results and the ideal response.

- 12.42. Derive an expression for the input impedance of the filter in Fig. 12.5.
- 12.43. Use MATLAB or another computer tool to plot the input impedance of the low-pass filter in Fig. 12.5 versus frequency for  $R_1 = R_2 = 2.26 \text{ k}\Omega$ ,  $C_1 = 0.02 \mu\text{F}$ , and  $C_2 = 0.01 \mu\text{F}$ .
- \*12.44. (a) What is the transfer function for the low-pass filter in Fig. P12.44? (b) What is  $S_C^Q$  for this filter if  $R_1 = R_2$  and  $C_1 = C_2$ ?
- 12.45. What are the expressions for  $S_{R_1}^{\omega_o}$  and  $S_{C_1}^{\omega_o}$  for the high-pass filter of Fig. 12.7?
- 12.46. What is  $S_Q^{\omega_o}$  for the band-pass filter of Fig. 12.9 for  $C_1 = C_2$ ? What is the value for  $f_o = 10 \text{ kHz}$  and  $Q = 10$ ?

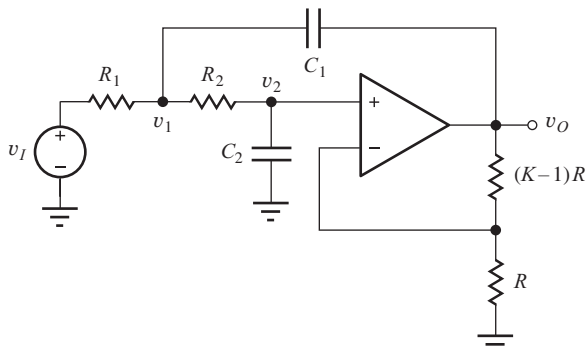


Figure P12.44

- 12.47. Design a maximally flat second-order low-pass filter with a bandwidth of 1 kHz using the circuit in Fig. 12.5.
- 12.48. Design a high-pass filter with a lower-half power frequency of 20 kHz and  $Q = 1$  using the circuit in Fig. 12.7.
- 12.49. (a) Calculate  $f_o$ ,  $Q$ , and the bandwidth for the band-pass filter in Fig. 12.9 if  $R_{th} = 1 \text{ k}\Omega$ ,  $R_2 = 200 \text{ k}\Omega$ , and  $C_1 = C_2 = 220 \text{ pF}$ . (b) Use magnitude scaling to change the element values so that  $R_{th} = 3.3 \text{ k}\Omega$ . (c) Use frequency scaling to double  $f_o$  for the filter in part (a).
- 12.50. (a) Design a band-pass filter with a center frequency of 1 kHz and  $Q = 5$  using the circuit in Fig. 12.9 with  $R_3 = \infty$ . What is the filter bandwidth? (b) Use frequency scaling to change  $f_o$  to 2.25 kHz.

\*12.51. (a) Use MATLAB or another computer tool to make a Bode plot for the response of the filter in Prob. 12.49(a), assuming the op amp is ideal. (b) Use SPICE to simulate the characteristics of the filter in Prob. 12.49(a) using a 741 op amp. (c) Discuss any disagreement between the SPICE results and the ideal response.

- 12.52. (a) Two identical band-pass filters having  $\omega_o = 1$  and  $Q = 3$  are designed using the circuit in Fig. 12.9 with  $C_1 = C_2$  and  $R_3 = \infty$ . If the filters are cascaded, what are the center frequency,  $Q$ , and bandwidth of the overall filter? (b) Write the transfer function for the composite filter.
- 12.53. Use MATLAB or other computer tool to produce a Bode plot for the two-stage filter in Prob. 12.52.
- \*12.54. The first stage of a two-stage filter consists of a band-pass filter with  $f_o = 5 \text{ kHz}$  and  $Q = 5$ . The second stage is also a band-pass filter, but it has  $f_o = 6 \text{ kHz}$  and  $Q = 5$ . If the filters use Fig. 12.9 with  $C_1 = C_2$  and  $R_3 = \infty$ , what are the center frequency,  $Q$ , and bandwidth of the overall filter?
- 12.55. Use MATLAB or another computer tool to produce a Bode plot for the two-stage filter in Prob. 12.54.
- 12.56. Design a band-pass filter with 20-dB gain at  $f_o = 600 \text{ Hz}$ ,  $Q = 5$ , and  $R_{in} = 10 \text{ k}\Omega$  using the Tow-Thomas biquad in Fig. 12.11.
- 12.57. Calculate  $S_C^Q$  for the Tow-Thomas biquad in Fig. 12.11.
- 12.58. Calculate the loop gain of the filter in Fig. P12.44.
- \*12.59. Write an expression for the loop gain of the active low-pass filter in Fig. P12.59.

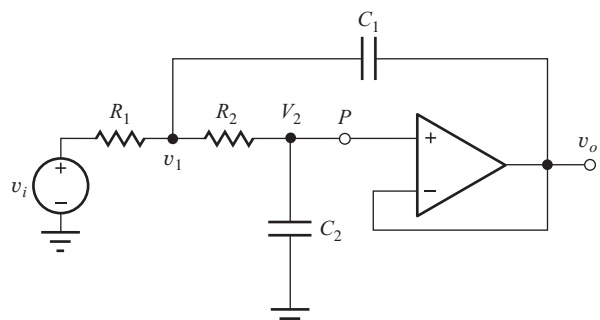


Figure P12.59

- 12.60. Write an expression for the loop gain of the active high-pass filter in Fig. P12.60.

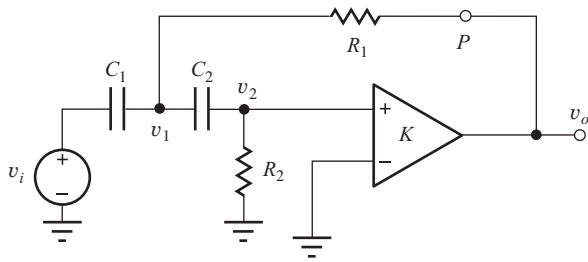


Figure P12.60

## 12.4 Switched-Capacitor Circuits

- 12.61. Draw a graph of the output voltage for the SC integrator in Fig. 12.14 for five clock periods if  $C_1 = 4C_2$ ,  $v_I = 1$  V, and  $v_O(0) = 0$ .
- 12.62. Draw a graph of the output voltage for the SC integrator in Fig. 12.16 for five clock periods if  $C_1 = 4C_2$ ,  $v_I = 1$  V, and  $v_O(0) = 0$ .
- 12.63. (a) Draw a graph of the output voltage for the SC integrator in Fig. 12.14 for five clock periods if  $C_1 = 4C_2$  and  $v_I$  is the signal in Fig. P12.63.  
\*\*(b) Repeat for the integrator in Fig. 12.16.

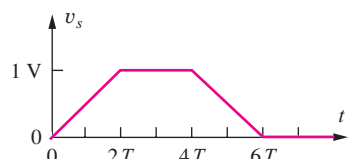


Figure P12.63

- 12.64. (a) What is the output voltage at the end of one clock cycle of the SC integrator in Fig. 12.12 if  $C_1 = 1$  pF,  $C_2 = 0.2$  pF,  $v_I = 1$  V, and there is a stray capacitance  $C_s = 0.1$  pF between each end of capacitor  $C_1$  and ground? What are the gain and gain error of this circuit? (b) Repeat for the integrator in Fig. 12.16.

- \*12.65. (a) Simulate two clock cycles of the integrator of Prob. 12.64(a) using NMOS transistors with  $W/L = 2/1$  and 100-kHz clock signals with rise and fall times of 0.5  $\mu$ s. (b) Repeat for Prob. 12.61(b).

- 12.66. What are the center frequency,  $Q$ , and bandwidth of the switched capacitor band-pass filter in Fig. 12.18 if  $C_1 = 0.4$  pF,  $C_2 = 0.4$  pF,  $C_3 = 1$  pF,  $C_4 = 0.1$  pF, and  $f_c = 100$  kHz?
- 12.67. Draw the circuit for a switched-capacitor implementation of the low-pass filter in Fig. 12.5.

## 12.5 Digital-to-Analog Conversion

- 12.68. Draw the transfer function, similar to Fig. 12.21, for a DAC with  $V_{OS} = 0.5$  LSB and no gain error.
- 12.69. (a) What is the output voltage for the 4-bit DAC in Fig. P12.69, as shown with input data of 0110 if  $V_{REF} = 3.0$  V? (b) Suppose the input data changes to 1001. What will be the new output voltage? (c) Make a table giving the output voltages for all 16 possible input data combinations.

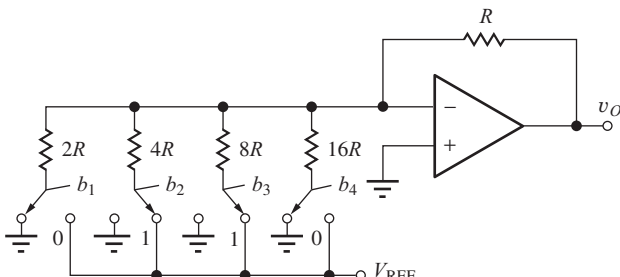


Figure P12.69

- 12.70. The op amp in Fig. P12.69 has an offset voltage of +5 mV and the feedback resistor has a value of  $1.05R$  instead of  $R$ . What are the offset and gain errors of this DAC?
- 12.71. Fill in the missing entries for step size, differential linearity error, and integral linearity error for the DAC in the accompanying table.

BINARY INPUT	DAC OUTPUT VOLTAGES	DIFFERENTIAL LINEARITY ERROR (LSB)			INTEGRAL LINEARITY ERROR
		STEP SIZE (LSB)	(LSB)	(LSB)	
000	0.0000				0.00
001	0.1000				
010	0.3000				
011	0.3500				
100	0.4750				
101	0.6300				
110	0.7250				
111	0.8750				0.00

- 12.72. Use Thévenin equivalent circuits for the R-2R ladder network in Fig. P12.72 to find the output voltage for the four input combinations 0001, 0010, 0100, and 1000 if  $V_{REF} = 5.0$  V.

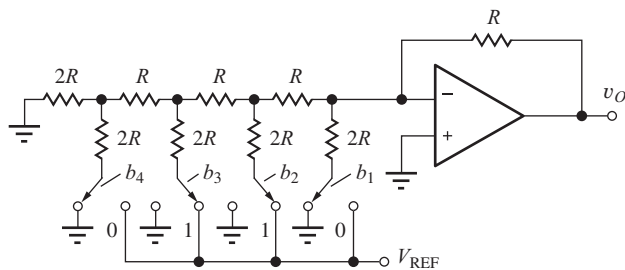


Figure P12.72

- \*12.73. The switches in Fig. P12.67 can be implemented using MOSFETs, as shown in Fig. P12.73. What must be the  $W/L$  ratios of the transistors if the on-resistance of the transistor is to be less than 1 percent of the resistor  $2R = 10\text{ k}\Omega$ ? Use  $V_{\text{REF}} = 3.0\text{ V}$ . Assume that the voltage applied to the gate of the MOSFET is  $5\text{ V}$  when  $b_1 = 1$  and  $0\text{ V}$  when  $b_1 = 0$ . For the MOSFET,  $V_{\text{TN}} = 1\text{ V}$ ,  $K'_n = 50\text{ }\mu\text{A/V}^2$ ,  $2\phi_F = 0.6\text{ V}$ , and  $\gamma = 0.5\sqrt{\text{V}}$ .

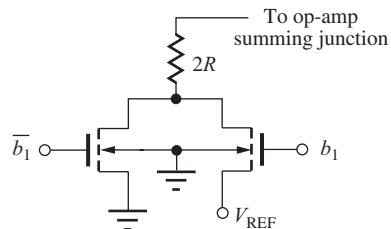


Figure P12.73

- \*12.74. A 3-bit weighted-resistor DAC similar to Fig. 12.24 is made using standard 5 percent resistors with  $R = 1\text{ k}\Omega$ ,  $2R = 2\text{ k}\Omega$ ,  $4R = 3.9\text{ k}\Omega$ , and  $8R = 8.2\text{ k}\Omega$ . (a) Tabulate the nominal output values of this converter in a manner similar to Table 12.8. What are the values of differential linearity and integral linearity errors for the nominal resistor values? (b) What are the worst-case values of linearity error that can occur with the 5 percent resistors? (Note: this converter has a gain error. You must recalculate the “ideal” step size. It is not  $0.1250\text{ V}$ .)

- \*\*12.75. Perform a 200-case Monte Carlo analysis of the DAC in Prob. 12.69 and find the worst-case differential and integral linearity errors for the DAC. Use 5 percent resistor tolerances.

- \*\*12.76. The output voltage of a 3-bit weighted resistor DAC must have an error of no more than 5 percent of  $V_{\text{REF}}$  for any input combination. What can be the tolerances on the resistors  $R$ ,  $2R$ ,  $4R$ , and  $8R$  if each resistor is allowed to contribute approximately the same error to the output voltage?

- 12.77. How many resistors are needed to realize a 10-bit weighted-resistor DAC? What is the ratio of the largest resistor to the smallest resistor?

- \*12.78. Tabulate the output voltages for the eight binary input words for the 3-bit DAC in Fig. P12.78, and find the differential and integral linearity errors if  $V_{\text{REF}} = 5.00\text{ V}$ ,  $R_{\text{REF}} = 250\text{ }\Omega$ , and  $R = 1.2188\text{ k}\Omega$ .

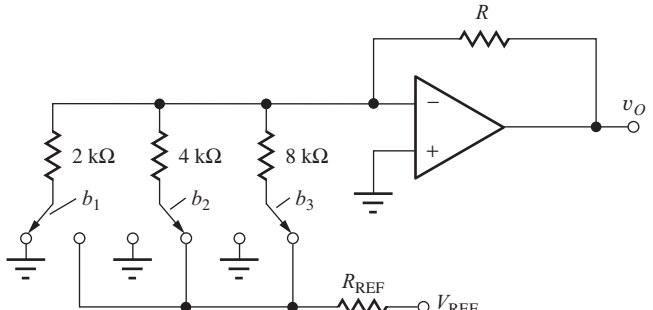


Figure P12.78

- 12.79. Suppose each switch in the DAC in Fig. P12.78 has an on-resistance of  $200\text{ }\Omega$ . (a) What value of  $R$  is required for zero gain error? (b) Find the differential and integral linearity errors if  $V_{\text{REF}} = 5.00\text{ V}$ ,  $R_{\text{REF}} = 0\text{ }\Omega$ . (c) Repeat for  $R_{\text{REF}} = 250\text{ }\Omega$ .

- \*\*12.80. Perform a 200-case Monte Carlo analysis of the DAC in Prob. 12.78 and find the worst-case differential and integral linearity errors for the DAC. Use 10 percent resistor tolerances.

- 12.81. (a) Derive a formula for the total capacitance in an  $n$ -bit weighted-capacitor DAC. (b) In an  $n$ -bit C-2C DAC.

- 12.82. Perform a transient simulation of the C-2C DAC in Fig. 12.28(b) when  $b_3$  switches from a 0 to a 1 and then back to a 0. Use  $C = 0.5\text{ pF}$  with  $V_{\text{REF}} = 5\text{ V}$ , and model the switches with NMOS transistors with  $W/L = 10/1$ , as in Fig. 12.73.

- \*12.83. A 3-bit inverted R-2R ladder with  $R = 2.5\text{ k}\Omega$  and  $V_{BB} = -2.5\text{ V}$  is connected to the input of the op amp in Fig. P12.83. Draw the schematic of the

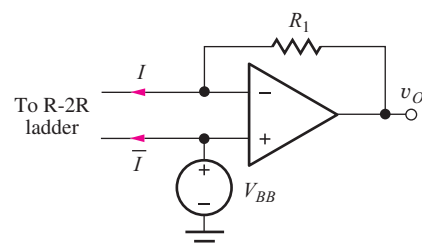


Figure P12.83

complete D/A converter. Make a table of the output voltages versus input code if  $R_1 = 5 \text{ k}\Omega$ .

- \*12.84. Suppose a 10-bit DAC is built using the inherently monotonic circuit technique in Fig. 12.27. (a) If the resistor material has a sheet resistance of  $50 \Omega/\text{square}$ , and  $R = 500 \Omega$ , estimate the number of squares that will be required for the resistor string. (b) If the minimum width of a resistor is  $5 \mu\text{m}$ , what is the required length of the resistor string? Convert this length to inches.

## 12.6 Analog-to-Digital Conversion

- 12.85. A 14-bit ADC with  $V_{FS} = 5.12 \text{ V}$  has an output code of 10101010110010. What is the possible range of input voltages?

- 12.86. A 20-bit ADC has  $V_{FS} = 2 \text{ V}$ . (a) What is the value of the LSB? (b) What is the ADC output code for an input voltage of  $1.630000 \text{ V}$ ? (c) What is the ADC output code for an input voltage of  $0.997003 \text{ V}$ ?

- 12.87. Plot the transfer function and quantization error for an ideal 3-bit ADC that does not have the 0.5 LSB offset shown in Fig. 12.30. (That is, the first code transition occurs for  $v_X = V_{FS}/8$ .) Why is the design in Fig. 12.30 preferred?

- 12.88. A 12-bit counting converter with  $V_{FS} = 10 \text{ V}$  and  $f_c = 1 \text{ MHz}$  has an input voltage  $v_X = 3.760 \text{ V}$ . (a) What is the output code? What is the conversion time  $T_T$  for this value of  $v_X$  if  $f_c = 1 \text{ MHz}$ ? (b) Repeat for  $v_X = 7.333 \text{ V}$ .

- 12.89. A 10-bit counting converter with  $V_{FS} = 5.12 \text{ V}$  uses a clock frequency of  $1 \text{ MHz}$  and has an input voltage  $v_X(t) = 5 \cos 5000\pi t \text{ V}$ . What is the output code? What is the conversion time  $T_T$  for this input voltage?

- 12.90. (a) A 12-bit successive approximation ADC with  $V_{FS} = 2 \text{ V}$  is designed using the circuit in Fig. 12.35. What is the maximum permissible offset voltage of the comparator if this offset error is to be less than 0.1 LSB? (b) Repeat for a 20-bit ADC.

- 12.91. A 16-bit successive approximation ADC is to be designed to operate at 50,000 conversions/second. What is the clock frequency? How rapidly must the unknown and reference voltage switches change state if the switch timing delay is to be equivalent to less than 0.1 LSB time?

- \*12.92. Figure P12.92 is the ramp generator for an integrating converter. (a) If the offset voltage of the op amp

is  $10 \text{ mV}$  and  $V = 3 \text{ V}$ , what is the effective reference voltage of this converter? (b) The integrator is used in a single-slope converter with an integration time of  $1/30 \text{ s}$  and a full-scale voltage of  $5.12 \text{ V}$ . What is the  $RC$  time constant? If  $R = 50 \text{ k}\Omega$ , what is the value of  $C$ ?

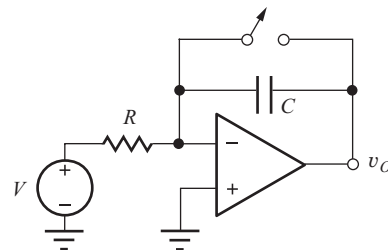


Figure P12.92

- \*\*12.93. A ramp generator using the op amp integrator circuit in Fig. P12.92 is built using an operational amplifier with an open-loop gain  $A_o = 5 \times 10^4$ . A 5-V step function is applied to the input of the integrator at  $t = 0$ . Write an expression for the output of the integrator in the time domain. What is the minimum  $RC$  product if the output ramp is to have an error of less than 1 mV at the end of a 200-ms integration interval?

- 12.94. A 20-bit dual-ramp converter is to have an integration time  $T_1 = 0.2 \text{ s}$ . How rapidly must the unknown and reference voltage switches change state if this timing uncertainty is to be equivalent to less than 0.1 LSB?

- 12.95. Derive the transfer function for the integrator in the dual-ramp converter, and show that it has the functional form of  $|\sin x/x|$ .

- 12.96. Write formulas for the number of resistors and number of comparators that are required to implement an  $n$ -bit flash converter.

## 12.7 Oscillators

### Frequency-Selective RC Networks

- 12.97. The circuit in Fig. P12.97 is called a quadrature oscillator. Derive an expression for its frequency of oscillation. What value of  $R_F$  is required for sinusoidal oscillation?

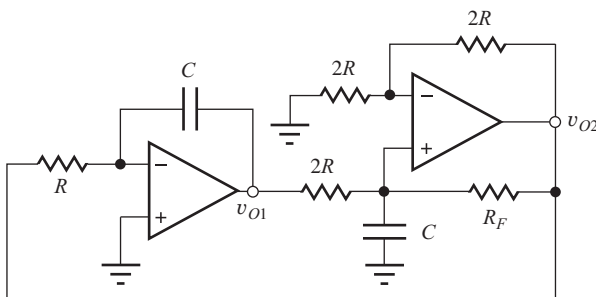


Figure P12.97

- 12.98. Derive an expression for the frequency of oscillation of the three-stage phase-shift oscillator in Fig. P12.98. What is the ratio  $R_2/R_1$  required for oscillation?

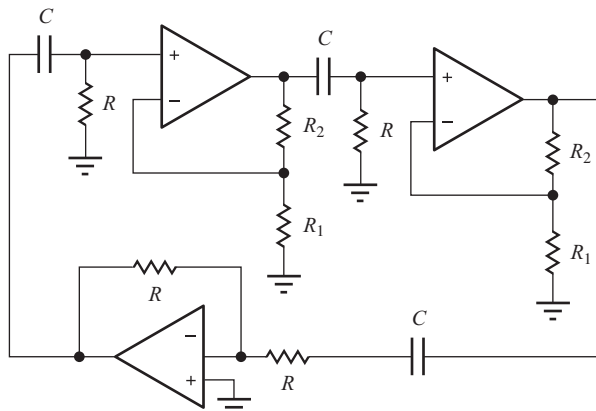


Figure P12.98

- 12.99. Calculate the frequency and amplitude of oscillation of the Wien-bridge oscillator in Fig. 12.50 if  $R = 5 \text{ k}\Omega$ ,  $C = 500 \text{ pF}$ ,  $R_1 = 10 \text{ k}\Omega$ ,  $R_2 = 15 \text{ k}\Omega$ ,  $R_3 = 6.2 \text{ k}\Omega$ , and  $R_4 = 10 \text{ k}\Omega$ .
- 12.100. Use SPICE transient simulation to find the frequency and amplitude of the oscillator in Prob. 12.99. Start the simulation with a 1-V initial condition on the grounded capacitor  $C$ .

- 12.101. Calculate the frequency and amplitude of oscillation of the phase-shift oscillator in Fig. 12.52 if  $R = 5 \text{ k}\Omega$ ,  $C = 1000 \text{ pF}$ ,  $R_2 = 47 \text{ k}\Omega$ ,  $R_3 = 15 \text{ k}\Omega$ , and  $R_4 = 68 \text{ k}\Omega$ .

- 12.102. Use SPICE transient simulation to find the frequency and amplitude of the oscillator in Prob. 12.101. Start the simulation with a 1-V initial condition on the capacitor connected to the inverting input of the amplifier.

- 12.103. Four identical integrators from Fig. 10.34 are cascaded to form an oscillator. (a) Draw the circuit. (b) What is the frequency of oscillation if  $R = 10 \text{ k}\Omega$ ,  $C = 100 \text{ pF}$ , and the op amps are ideal? (c) If the output of the first integrator is  $V_{o1} = 1 \angle 0^\circ$ , what are the phasor representations of the other three output voltages? (d) Add an amplitude stabilization network to one of the amplifiers and design it to set the output voltage to approximately 2 V.
- 12.104. (a) Repeat Prob. 12.103 if the op amps have an open-loop gain of 100 dB and a unity-gain frequency of 750 kHz.

## 12.8 Nonlinear Circuit Applications

### Nonlinear Feedback

- 12.105. Draw the output voltage waveform for the circuit in Fig. P12.105 for the triangular input waveform shown.  $T = 1 \text{ ms}$ .
- \*12.106. The signal  $v_I$  in Fig. P12.105 is used as the input voltage to the circuit in the figure in the EIA box on page 762. What will be the dc component of the voltage waveform at  $v_O$  if  $R_1 = 2.7 \text{ k}\Omega$ ,  $R_2 = 8.2 \text{ k}\Omega$ ,  $R_3 = 10 \text{ k}\Omega$ ,  $R_4 = 10 \text{ k}\Omega$ ,  $C = 0.22 \mu\text{F}$ , and  $T = 1 \text{ ms}$ ?

- \*\*12.107. What must be the cutoff frequency of the low-pass filter in the figure in the EIA box on page 762 if the rms value of the total ac component

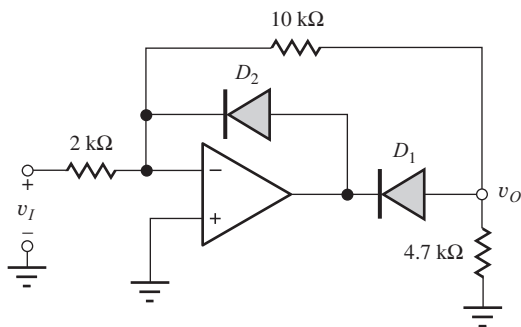
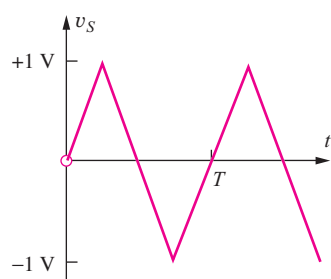


Figure P12.105



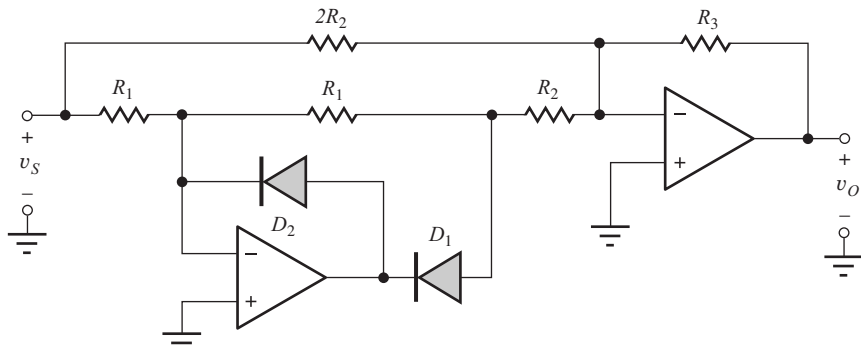


Figure P12.108

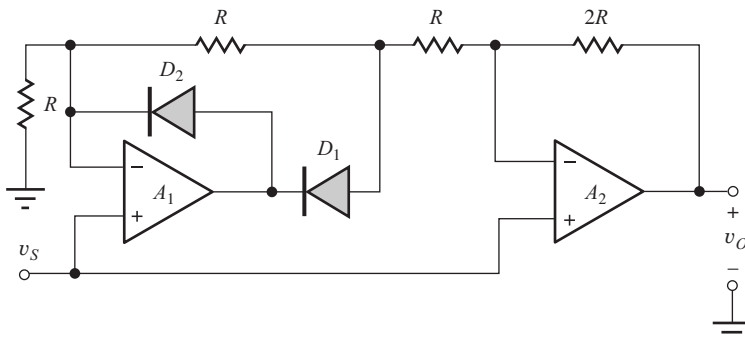


Figure P12.109

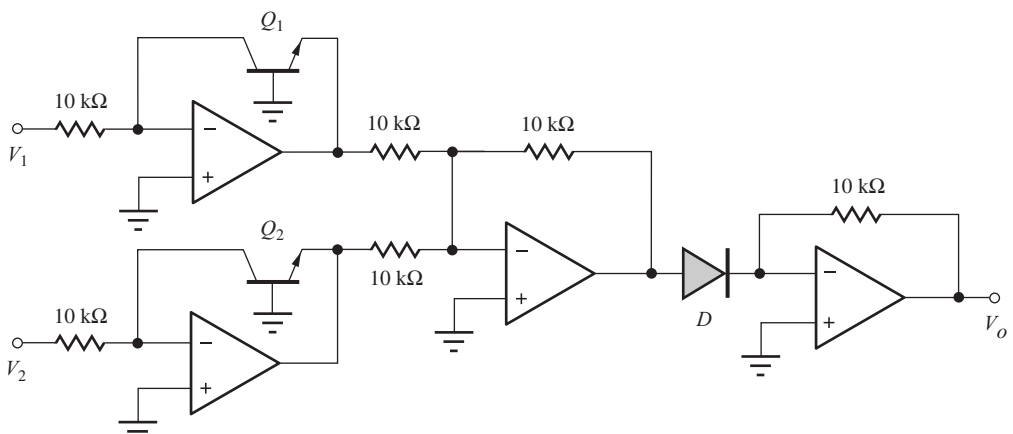


Figure P12.112

in the output voltage must be less than 1 percent of the dc voltage? Assume  $R_1 = R_2$  and  $v_I = -5 \sin 120\pi t$  V.

- 12.108. The triangular waveform in Fig. P12.105 is applied to the circuit in Fig. P12.108. Draw the corresponding output waveform for  $R_3 = R_2$ .
- 12.109. The triangular waveform in Fig. P12.105 is applied to the circuit in Fig. P12.109. Draw the corresponding output waveform.

12.110. Simulate the circuit in Prob. 12.108 using  $R_1 = 10 \text{ k}\Omega$ ,  $R_2 = 10 \text{ k}\Omega$ ,  $R_3 = 10 \text{ k}\Omega$ , and  $R_4 = 10 \text{ k}\Omega$ . Use op amps with  $A_o = 100 \text{ dB}$ .

12.111. Simulate the circuit in Prob. 12.109 for  $R = 10 \text{ k}\Omega$ . Use op amps with  $A_o = 100 \text{ dB}$ .

\*12.112. Write an expression for the output voltage in terms of the input voltage for the circuit in Fig. P12.112. Diode  $D$  is formed from a

diode-connected transistor, and all three transistors are identical.

## 12.9 Circuits Using Positive Feedback

- 12.113. What are the values of the two switching thresholds and hysteresis in the Schmitt-trigger circuit in Fig. P12.113?

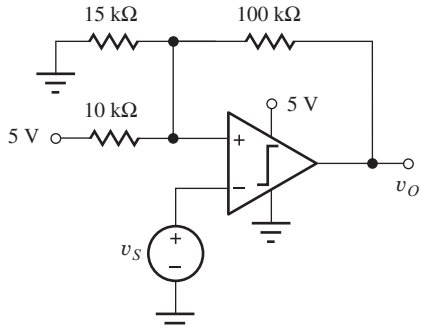


Figure P12.113

- 12.114. What are the switching thresholds and hysteresis for the Schmitt-trigger circuit in Fig. P12.114?

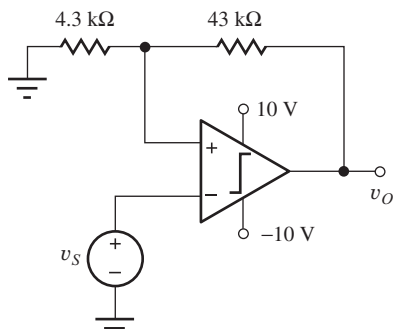


Figure P12.114

- 12.115. What are the switching thresholds and hysteresis for the Schmitt-trigger circuit in Fig. P12.115?

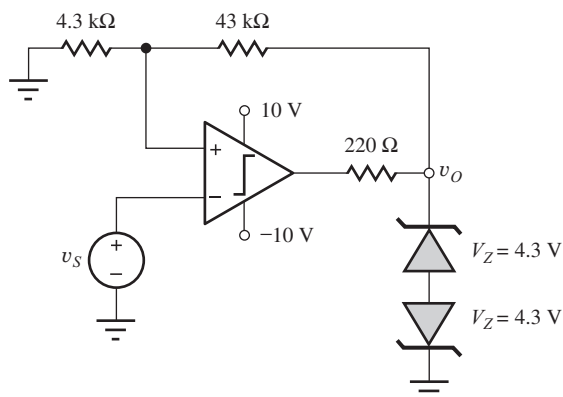


Figure P12.115

- 12.116. Design a Schmitt trigger to have its switching thresholds centered at 1 V with a hysteresis of  $\pm 0.05$  V, using the circuit topology in Fig. P12.113.

- 12.117. What is the frequency of oscillation of the astable multivibrator in Fig. P12.117?

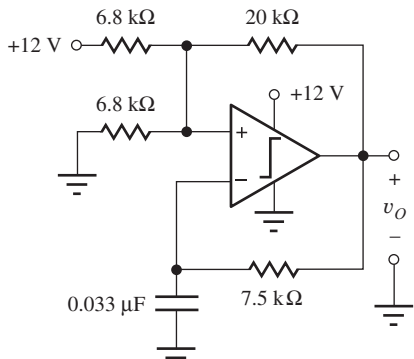


Figure P12.117

- \*\*12.118. Draw the waveforms for the astable multivibrator in Fig. P12.118. What is its frequency of oscillation? (Be careful — think before you calculate!)

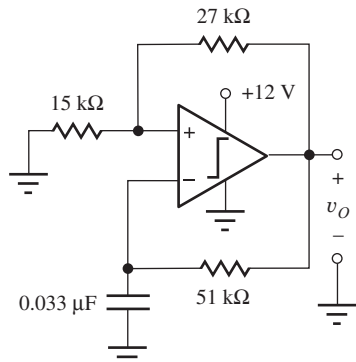
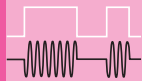


Figure P12.118

- 12.119. (a) Design an astable multivibrator to oscillate at a frequency of 1 kHz. Use the circuit in Fig. 12.62 with symmetric supplies of  $\pm 5$  V. Assume that the total current from the op amp output must never exceed 1 mA. (b) If the resistors have  $\pm 5$  percent tolerances and the capacitors have  $\pm 10$  percent tolerances, what are the worst-case values of oscillation frequency? (c) If the power supplies are actually  $+4.75$  and  $-5.25$  V, what is the oscillation frequency for the nominal resistor and capacitor design values?

- \*\*12.120. The function generator circuit in the EIA on page 767 has been designed to generate a sine wave output voltage with an amplitude of 5 V at a frequency of 1 kHz. The low-pass filter has been designed to have a low-frequency gain of  $-1$  and a cutoff frequency of 1.5 kHz. What are the magnitudes of the undesired frequency components in the output waveform at frequencies of 2 kHz, 3 kHz, and 5 kHz?
- 12.121. Two diodes are added to the circuit in Fig. P12.118 to convert it to a monostable multivibrator similar to the circuit in Fig. 12.64, and the power supplies are changed to  $\pm 10$  V. What are the pulse width and recovery time of the monostable circuit?
- 12.122. Design a monostable multivibrator to have a pulse width of 10  $\mu$ s and a recovery time of 5  $\mu$ s. Use the circuit in Fig. 12.64 with  $\pm 5$  V supplies.

# CHAPTER 13



## SMALL-SIGNAL MODELING AND LINEAR AMPLIFICATION

### CHAPTER OUTLINE

- 13.1 The Transistor as an Amplifier 787
- 13.2 Coupling and Bypass Capacitors 790
- 13.3 Circuit Analysis Using dc and ac Equivalent Circuits 792
- 13.4 Introduction to Small-Signal Modeling 796
- 13.5 Small-Signal Models for Bipolar Junction Transistors 799
- 13.6 The Common-Emitter (C-E) Amplifier 808
- 13.7 Important Limits and Model Simplifications 810
- 13.8 Small-Signal Models for Field-Effect Transistors 815
- 13.9 Summary and Comparison of the Small-Signal Models of the BJT and FET 821
- 13.10 The Common-Source Amplifier 824
- 13.11 Common-Emitter and Common-Source Amplifier Summary 838
- 13.12 Amplifier Power and Signal Range 839  
Summary 843  
Key Terms 844  
Problems 845

### CHAPTER GOALS

In Chapter 13, we develop a basic understanding of the following concepts related to linear amplification:

- Transistors as linear amplifiers
- dc and ac equivalent circuits
- Use of coupling and bypass capacitors and inductors to modify the dc and ac equivalent circuits
- The concept of small-signal voltages and currents
- Small-signal models for diodes and transistors
- Identification of common-emitter and common-source amplifiers
- Amplifier characteristics including voltage gain, input resistance, output resistance, and linear signal range
- Rule-of-thumb estimates for voltage gain of common-emitter and common-source amplifiers
- Improvement of our understanding of the use and differences between the ac small-signal transfer function, and transient analysis capabilities of SPICE

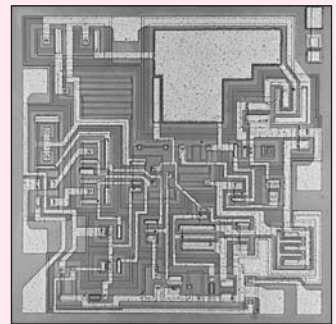
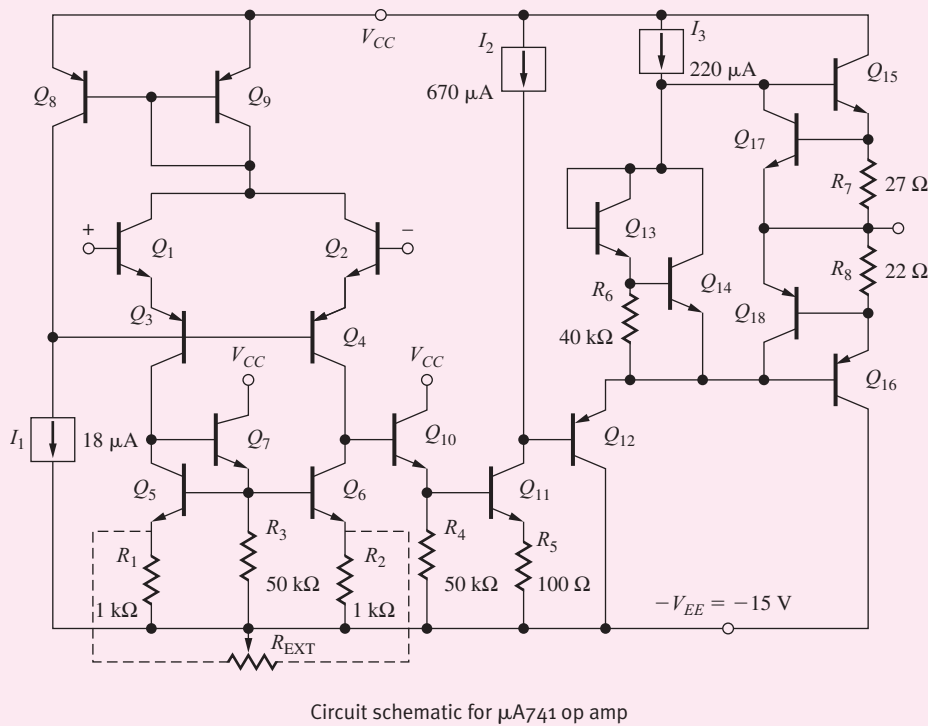
Chapter 13 begins our study of basic amplifier circuits that are used in the design of complex analog components and systems such as high-performance operational amplifiers, analog-to-digital and digital-to-analog converters, audio equipment, compact disk players, wireless devices, cellular telephones, and so on. At first glance, the operational amplifier schematic in the figure here represents an overwhelming interconnection of transistors and passive components. With this chapter, we begin our quest to understand and design a wide variety of such circuits. We will learn to simplify our job by separating the dc and ac circuit analyses.

In order to predict the detailed behavior of the circuit, we must also be able to build mathematical models that describe the circuit. This chapter develops these models. Then over the next several chapters, we become familiar with the basic subcircuits that serve as our electronic tool kit for building more complicated electronic systems. With practice over time, we will be able to spot these basic building blocks in more complex electronic circuits and use our knowledge of the subcircuits to understand the full system.

This chapter introduces the general techniques for employing individual transistors as amplifiers and then studies in detail the operation of the common-emitter bipolar transistor circuit. This is followed by analysis of common-source amplifiers employing MOSFETs. Circuits containing these devices are compared, and expressions are developed for the voltage gain and input and output resistances of the various amplifiers. The advantages and disadvantages of each are discussed in detail.

To simplify the analysis and design processes, the circuits are split into two parts: a dc equivalent circuit used to find the Q-point of the transistor, and an ac equivalent circuit used for analysis of the circuit's response to signal sources. As a by-product of this approach, we discover how capacitors and inductors are used to change the ac and dc circuit topologies.

The ac analysis is based on linearity and requires the use of “small-signal” models that exhibit a linear relation between their terminal voltages and currents. The concept of a small signal is developed, and small-signal models for



$\mu\text{A}741$  Die Photograph (Photo courtesy of Fairchild Semiconductor International)

the diode, bipolar transistor, and MOSFET are all discussed in detail.

Examples of the complete analysis of common-emitter and common-source amplifiers are included in this

chapter. The relationships between the choice of operating point and the small-signal characteristics of the amplifier are developed, as is the relationship between Q-point design and output signal voltage swing.

## 13.1 THE TRANSISTOR AS AN AMPLIFIER

As mentioned in Part I, the bipolar junction transistor is an excellent amplifier when it is biased in the forward-active region of operation; field-effect transistors should be operated in the saturation or pinch-off region in order to be used as amplifiers. For simplicity, we will now refer to bipolar transistors operating in the forward-active region and FETs in the saturation region as simply being in the “**active region**” where they can be used as linear amplifiers. In these regions of operation, the transistors have the capacity to provide high voltage, current, and power gains. This chapter focuses on determining voltage gain, input resistance, and output resistance. We will find that we need the input and output resistance information in order to calculate the lower and upper cutoff frequencies of the amplifiers. Evaluation of current gain and power gain are addressed in later chapters.

We must provide bias to the transistor in order to stabilize the operating point in the active region of operation. Once the dc operating point has been established, we can then use the transistor as an amplifier. The Q-point controls many other amplifier characteristics, including

- Small-signal parameters of the transistor
- Voltage gain, input resistance, and output resistance
- Maximum input and output signal amplitudes
- Power consumption

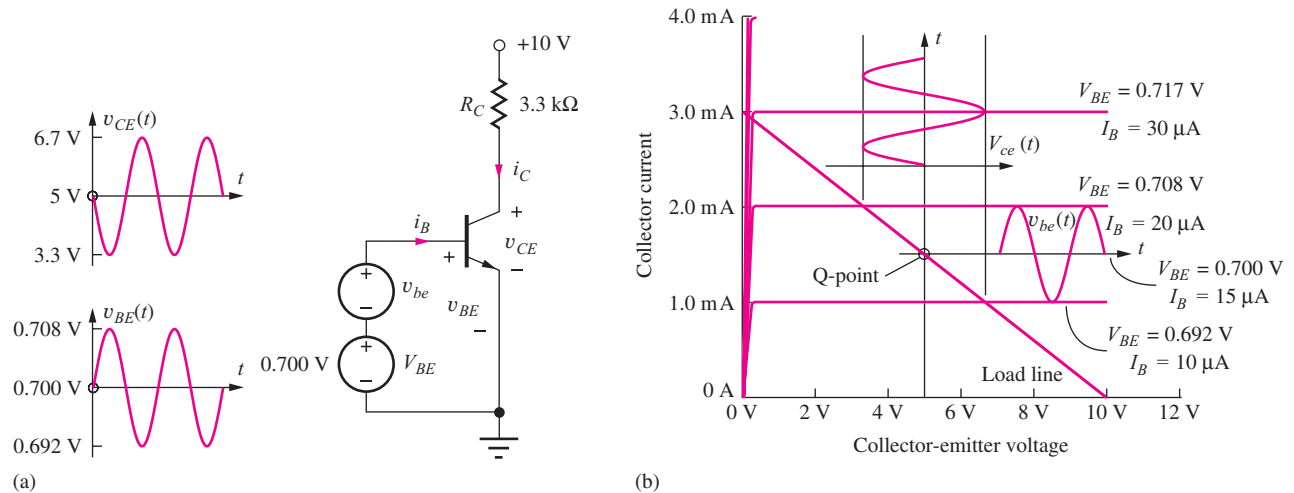


**Figure 13.1** (a) BJT biased in the active region by the voltage source  $V_{BE}$ . A small sinusoidal signal voltage  $v_{be}$  is applied in series with  $V_{BE}$  and generates a similar but larger amplitude waveform at the collector. (b) Load-line, Q-point, and signals for circuit of Fig. 13.1(a).

### 13.1.1 THE BJT AMPLIFIER

To get a clearer understanding of how a transistor can provide linear amplification, let us assume that a bipolar transistor is biased in the active region by the dc voltage source  $V_{BE}$  shown in Fig. 13.1. For this particular transistor, the fixed base-emitter voltage of  $0.700\text{ V}$  sets the Q-point to be  $(I_C, V_{CE}) = (1.5\text{ mA}, 5\text{ V})$  with  $I_B = 15\text{ }\mu\text{A}$ , as indicated in Fig. 13.1(b). Both  $I_B$  and  $V_{BE}$  have been shown as parameters on the output characteristics in Fig. 13.1(b) (usually only  $I_B$  is given).

To provide amplification, a signal must be injected into the circuit in a manner that causes the transistor voltages and currents to vary with the applied signal. For the circuit in Fig. 13.1, the base-emitter voltage is forced to vary about its Q-point value by signal source  $v_{be}$  placed in series with dc bias source  $V_{BE}$ , so the total base-emitter voltage becomes

$$v_{BE} = V_{BE} + v_{be} \quad (13.1)$$

In Fig. 13.1(b), we see that the  $8\text{-mV}$  peak change in base-emitter voltage produces a  $5\text{-}\mu\text{A}$  change in base current and hence a  $500\text{-}\mu\text{A}$  change in collector current ( $i_c = \beta_F i_b$ ).

The collector-emitter voltage of the BJT in Fig. 13.1 can be expressed as

$$v_{CE} = 10 - i_C R_C = 10 - 3300i_C \quad (13.2)$$

The change in collector current develops a time-varying voltage across load resistor  $R_C$  and at the collector terminal of the transistor. The  $500\text{-}\mu\text{A}$  change in collector current develops a  $1.65\text{-V}$  change in collector-emitter voltage.

If these changes in operating currents and voltages are all small enough (“small signals”), then the collector current and collector-emitter voltage waveforms will be undistorted replicas of the input signal. Small-signal operation is device-dependent; it will be precisely defined for the BJT when the small-signal model for the bipolar transistor is introduced.

In Fig. 13.1 we see that a small input voltage change at the base is causing a large voltage change at the collector. The voltage gain for this circuit is defined in terms of the frequency domain (phasor) representation of the signals:

$$A_v = \frac{v_{ce}}{v_{be}} = \frac{1.65 \angle 180^\circ}{0.008 \angle 0^\circ} = 206 \angle 180^\circ = -206 \quad (13.3)$$

The magnitude of the collector-emitter voltage is 206 times larger than the base-emitter signal amplitude; this represents a voltage gain of 206. It is also important to note in Fig. 13.1 that the

output signal voltage decreases as the input signal increases, indicating a  $180^\circ$  phase shift between the input and the output signals. Thus, this transistor circuit is an inverting amplifier. This  $180^\circ$  phase shift is often represented by the minus sign in Eq. (13.3). The transistor in Fig. 13.1 has its emitter connected to ground, and this circuit is known as a **common-emitter amplifier**. Note that Eq. (13.2) represents the load line for this transistor.

**EXERCISE:** The common-emitter current gain  $\beta_F$  of the bipolar transistor is defined by  $\beta_F = I_C/I_B$ . (a) What is the value of  $\beta_F$  for the transistor in Fig. 13.1? (b) The dc collector current of the BJT in the (forward) active region is given by  $I_C = I_S \exp V_{BE}/V_T$ . Use the Q-point data to find the saturation current  $I_S$  of the transistor in Fig. 13.1. (Remember  $V_T = 0.025$  V.) (c) The ratio of  $v_{be}/i_b$  represents the small-signal input resistance  $R_{in}$  of the BJT. What is its value for the transistor in Fig. 13.1? (d) Does the BJT remain in the active region during the full range of signal voltages at the collector? Why? (e) Express the voltage gain in dB.

**ANSWERS:**  $\beta_F = 100$ ;  $I_S = 1.04 \times 10^{-15}$  A;  $R_{in} = 1.6$  k $\Omega$ ; yes,  $v_{CE}^{MIN} > v_{BE} : 3.4$  V > 0.708 V; 46.3 dB.

### 13.1.2 THE MOSFET AMPLIFIER

The amplifier circuit using a MOSFET in Fig. 13.2 is directly analogous to the BJT amplifier circuit in Fig. 13.1. Here the gate-to-source voltage is forced to vary about its Q-point value ( $V_{GS} = 3.5$  V) by signal source  $v_{gs}$  placed in series with dc bias source  $V_{GS}$ . In this case, the total gate-source voltage is

$$v_{GS} = V_{GS} + v_{gs}$$

The resulting signal voltages are superimposed on the MOSFET output characteristics in Fig. 13.2(b).  $V_{GS} = 3.5$  V sets the Q-point ( $I_D$ ,  $V_{DS}$ ) at (1.56 mA, 4.8 V), and the 1-V p-p change in  $v_{GS}$  causes a 1.25-mA p-p change in  $i_D$ .

In this circuit, the drain-source voltage of the MOSFET can be expressed as

$$v_{DS} = 10 - 3300i_D \quad (13.4)$$

The 1.25 mA p-p change in drain current develops a 4.13-V change in the drain-source voltage of the MOSFET. If these changes in operating currents and voltages are again small enough to be considered “small signals,” then the drain-source signal voltage waveform will be an undistorted replica of the

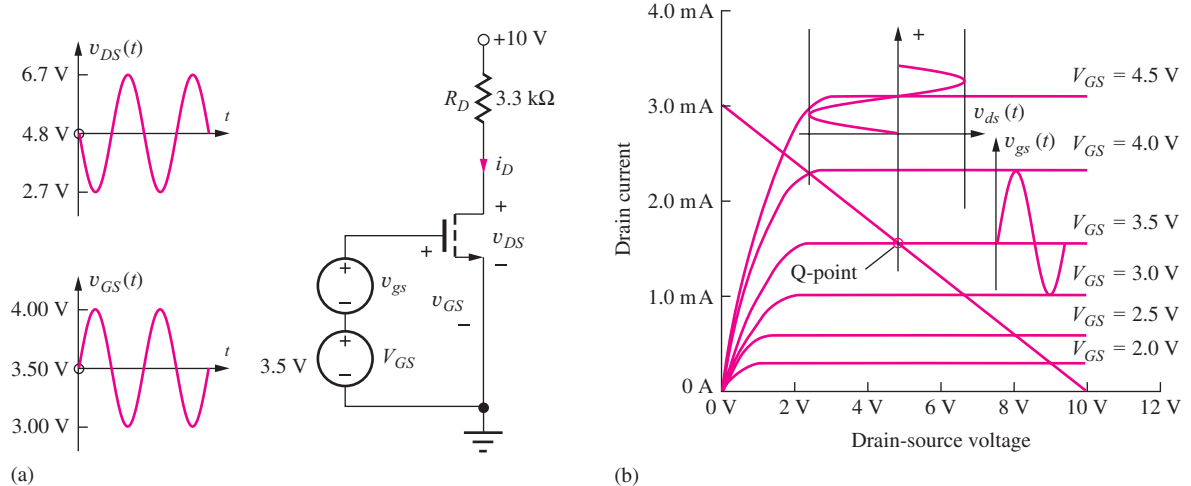


**Figure 13.2** (a) A MOSFET common-source amplifier. (b) Q-point, load line, and signals for the circuit of Fig. 13.2(a).

input signal applied to the gate. The definition of a small-signal is different for the MOSFET than for the BJT, and it will be defined when the MOSFET small-signal model is introduced.

In Fig. 13.2, the input voltage signal applied to the gate is causing a larger voltage change at the drain, and the voltage gain for this circuit is given by

$$A_v = \frac{v_{ds}}{v_{gs}} = \frac{4.13\angle 180^\circ}{1\angle 0^\circ} = 4.13\angle 180^\circ = -4.13 \quad (13.5)$$

In this case, the source of the transistor is grounded, and this circuit is known as a **common-source amplifier**. We see that the common-source configuration also forms an inverting amplifier.

**EXERCISE:** (a) Does the MOSFET in Fig. 13.2 remain in the active region of operation during the full-output signal swing? (b) If the dc drain current of the MOSFET in the active region is given by  $I_D = (K_n/2)(V_{GS} - V_{TN})^2$ , what are the values of the parameter  $K_n$  and threshold voltage  $V_{TN}$  for the transistor in Fig. 13.2? (c) Express the amplifier voltage given in dB.

**ANSWERS:** No, not near the positive peak of  $v_{GS}$ , corresponding to the peak negative excursion of  $v_{DS}$ ;  $K_n = 5 \times 10^4 \text{ A/V}^2$ ,  $V_{TN} = 1 \text{ V}$ ; 12.3 dB

## 13.2 COUPLING AND BYPASS CAPACITORS

The constant base-emitter or gate-source voltage biasing techniques used in Figs. 13.1 and 13.2 are not very desirable methods of establishing the Q-point for a bipolar transistor or FET because the operating point is highly dependent on the transistor parameters. As discussed in detail in Chapters 4 and 5, the four-resistor bias network in Fig. 13.3, is much preferred for establishing a stable Q-point for the transistor.

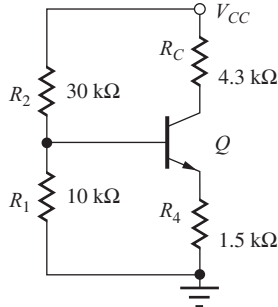
However, to use the transistor as an amplifier, ac signals must be introduced into the circuit, but application of these ac signals must not disturb the dc Q-point that has been established by the bias network. One method of injecting an input signal and extracting an output signal without disturbing the Q-point is to use **ac coupling** through capacitors. The values of these capacitors are chosen to have negligible impedances in the frequency range of interest, but at the same time, the capacitors provide open circuits at dc so the Q-point is not disturbed. When power is first applied to the amplifier circuit, transient currents charge the capacitors, but the final steady-state operating point is not affected.

Figure 13.4 is an example of the use of capacitors; the transistor is biased by the same four-resistor network shown in Fig. 13.3. Input signal  $v_i$  is *coupled* onto the base node of the transistor through capacitor  $C_1$ , and the signal developed at the collector is coupled to load resistor  $R_3$  through capacitor  $C_2$ .  $C_1$  and  $C_2$  are referred to as **coupling capacitors**, or **dc blocking capacitors**.

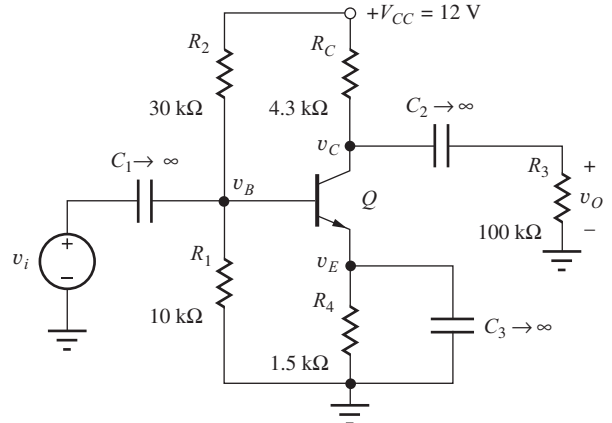
For now, the values of  $C_1$  and  $C_2$  are assumed to be very large, so their reactance ( $1/\omega C$ ) at the signal frequency  $\omega$  will be negligible. This assumption is indicated in the figure by  $C \rightarrow \infty$ . Calculation of more exact values of the capacitors is left until the discussion of amplifier frequency response in Chapters 14 and 17.

Figure 13.4 also shows the use of a third capacitor  $C_3$ , called a **bypass capacitor**. In many circuits, we want to force signal currents to go around elements of the bias network. Capacitor  $C_3$  provides a low impedance path for ac current to “bypass” emitter resistor  $R_4$ . Thus  $R_4$ , which is required for good Q-point stability, can be effectively removed from the circuit when ac signals are considered.

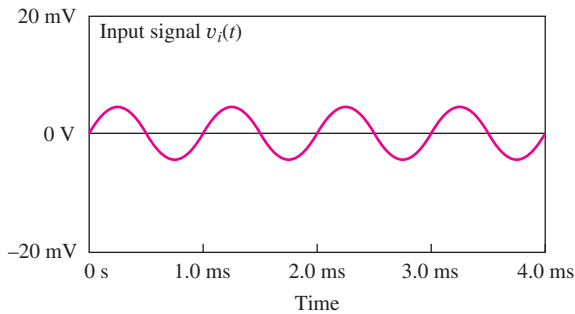
Simulation results of the behavior of this circuit are shown in Fig. 13.5. A 5-mV sine wave signal at a frequency of 1 kHz is applied to the base terminal of transistor  $Q$  through coupling capacitor  $C_1$ ; this signal produces a sinusoidal signal at the collector node with an amplitude of approximately 1.1 V, centered on the Q-point value of  $V_C \cong 5.8$  V. Note once again that there is a  $180^\circ$  phase shift



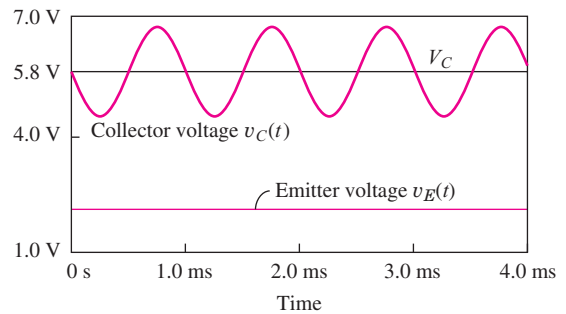
**Figure 13.3** Transistor biased in the active region using the four-resistor bias network (see Sec. 5.11 for an example).



**Figure 13.4** Common-emitter amplifier stage built around the four-resistor bias network.  $C_1$  and  $C_2$  function as coupling capacitors, and  $C_3$  is a bypass capacitor.



(a)



(b)

**Figure 13.5** SPICE simulation results for  $v_S$ ,  $v_C$ , and  $v_E$  for the amplifier in Fig. 13.4 with  $v_I = 0.005 \sin 2000\pi t$  V.

between the input and output voltage signals. These values indicate that the amplifier is providing a voltage gain of

$$A_v = \frac{v_c}{v_i} = \frac{1.1 \angle 180^\circ}{.005 \angle 0^\circ} = 220 \angle 180^\circ = -220. \quad (13.6)$$

In Fig. 13.5, we should also observe that the voltage at the emitter node remains constant at its Q-point value of slightly more than 2 V. The very low impedance of the bypass capacitor prevents any signal voltage from being developed at the emitter. We say that the bypass capacitor maintains an “ac ground” at the emitter terminal. In other words, zero signal voltage appears at the emitter, and the emitter voltage remains constant at its dc Q-point value.

**EXERCISE:** Calculate the Q-point for the bipolar transistor in Fig. 13.3. Use  $\beta_F = 100$ ,  $V_{BE} = 0.7$  V, and  $V_A = \infty$ . What is the value of  $V_B$ ? (See Sec. 5.11.1.)

**ANSWER:** (1.45 mA, 3.41 V); 2.90 V

**EXERCISE:** Write expressions for  $v_C(t)$ ,  $v_E(t)$ ,  $i_c(t)$  and  $v_B(t)$  based on the waveforms shown in Fig. 13.5.

**ANSWERS:**  $v_C(t) = (5.8 - 1.1 \sin 2000\pi t)$  V,  $v_E(t) = 2.20$  V,  $i_c(t) = -0.25 \sin 2000\pi t$  mA;  $v_B(t) = (2.90 + 0.005 \sin 2000\pi t)$  V

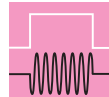
**EXERCISE:** Suppose capacitor  $C_3$  is  $500 \mu\text{F}$ . What is its reactance at a frequency of  $1000$  Hz?

**ANSWER:**  $0.318 \Omega$

### 13.3 CIRCUIT ANALYSIS USING dc AND ac EQUIVALENT CIRCUITS

To simplify the circuit analysis and design tasks, we break the amplifier into two parts, performing separate dc and ac circuit analyses. We find the Q-point of the circuit using the **dc equivalent circuit**—the circuit that is appropriate for steady-state dc analysis. To construct the dc equivalent circuit, we assume that capacitors are open circuits and inductors are short circuits.

Once we have found the Q-point, we determine the response of the circuit to the ac signals using an **ac equivalent circuit**. In constructing the ac equivalent circuit, we assume that the reactance of the coupling and bypass capacitors is negligible at the operating frequency ( $|Z_C| = 1/\omega C = 0$ ), and we replace the capacitors by short circuits. Similarly, we assume the impedance of any inductors in the circuit is extremely large ( $|Z_L| = \omega L \rightarrow \infty$ ), so we replace inductors by open circuits. Because the voltage at a node connected to a dc voltage source cannot change, these points represent grounds in the ac equivalent circuit (i.e., no ac voltage can appear at such a node:  $v_{ac} = 0$ ). Furthermore, the current through a dc current source does not change even if the voltage across the source changes ( $i_{ac} = 0$ ), so we replace dc current sources with open circuits in the ac equivalent circuit.



#### DESIGN NOTE

dc power supply nodes represent grounds and dc current sources represent open circuits in the ac equivalent circuit!

##### 13.3.1 MENU FOR dc AND ac ANALYSIS

First we do a dc analysis to find the Q-point, and then we perform an ac analysis to determine the behavior of the circuit as an amplifier. The Q-point values must be found first because they ultimately determine the ac characteristics of the amplifier. To summarize, our analysis of amplifier circuits is performed using the two-part process listed here.

###### dc Analysis

- Find the dc equivalent circuit by replacing all capacitors with open circuits and inductors by short circuits.
- Find the Q-point from the dc equivalent circuit using the appropriate large-signal model for the transistor.

###### ac Analysis

- Find the ac equivalent circuit by replacing all capacitors by short circuits and all inductors by open circuits. dc voltage sources are replaced by short circuits, and dc current sources are replaced by open circuits in the ac equivalent circuit.
- Replace the transistor by its small-signal model. (The small-signal model is Q-point dependent.)

5. Analyze the ac characteristics of the amplifier using the small-signal ac equivalent circuit from Step 4.
6. If desired, combine the results from Steps 2 and 5 to yield the total voltages and currents in the network.

Since we are most often interested in determining the ac behavior of the circuit, we seldom actually perform this final step of combining the dc and ac results.

### EXAMPLE 13.1 CONSTRUCTING ac AND dc EQUIVALENT CIRCUITS FOR A BJT AMPLIFIER

As has been stated several times, we usually split a circuit into its dc and ac equivalents in order to simplify the analysis or design problem. This is a critical step, since we cannot get the correct answer if the equivalent circuits are improperly constructed.

**PROBLEM** Draw the dc and ac equivalent circuits (menu steps 1 and 3) for the common-emitter amplifier in Fig. 13.6(a). The circuit topology is similar to that in Fig. 13.4 except resistor  $R_I$ , representing the Thévenin equivalent resistance of the signal source, has been added to the circuit. The resistor values have been changed to establish a new operating point.

**SOLUTION** **Known Information and Given Data:** The circuit with element values appears in Fig. 13.6(a).

**Unknowns:** dc equivalent circuit; ac equivalent circuit

**Approach:** Replace capacitors by open circuits to obtain the dc equivalent circuit. Replace capacitors and dc voltage sources by short circuits to obtain the ac equivalent circuit. Combine and simplify resistor combinations wherever possible.

**Assumptions:** Capacitor values are large enough that they can be treated as short circuits in the ac equivalent circuit.

**ANALYSIS** **dc Equivalent Circuit:** The dc equivalent circuit is found by open circuiting all the capacitors in the circuit. We find that the resulting dc equivalent circuit in Fig. 13.6(b) is identical to the four-resistor bias circuit of Fig. 13.3 (also see Sec. 5.11). Opening capacitors  $C_1$  and  $C_2$  disconnects  $v_I$ ,  $R_I$ , and  $R_3$  from the circuit.

**ac Equivalent Circuit:** To construct the ac equivalent circuit, we replace the capacitors by short circuits. Also, the dc voltage source becomes an ac ground in Fig. 13.6(c). In the ac equivalent circuit, source resistance  $R_I$  is now connected directly to the base node, and the external load resistor  $R_3$  is connected directly to the collector node. Figure 13.6(d) is a redrawn version of Fig. 13.6(c). Although these two figures may look different, they are the same circuit! Note that resistor  $R_E$  is shorted out by the presence of bypass capacitor  $C_3$  and has therefore been removed from Fig. 13.6(d). Because the power supply represents an “ac ground,” bias resistors  $R_1$  and  $R_2$  appear in parallel between the base node and ground, and  $R_C$  and  $R_3$  are in parallel at the collector. Do not overlook the fact that only the signal  $v_i$  is included in the ac equivalent circuit!

In Fig. 13.6(e),  $R_1$  and  $R_2$  have been combined into the resistor  $R_B$ , and  $R_C$  and  $R_3$  have been combined into the resistor  $R_L$ :

$$R_B = R_1 \parallel R_2 = 160 \text{ k}\Omega \parallel 300 \text{ k}\Omega = 104 \text{ k}\Omega \quad \text{and} \quad R_L = R_C \parallel R_3 = 22 \text{ k}\Omega \parallel 100 \text{ k}\Omega = 18.0 \text{ k}\Omega$$

**Check of Results:** In this case, the best way to verify our results is to double check our work — everything seems correct.

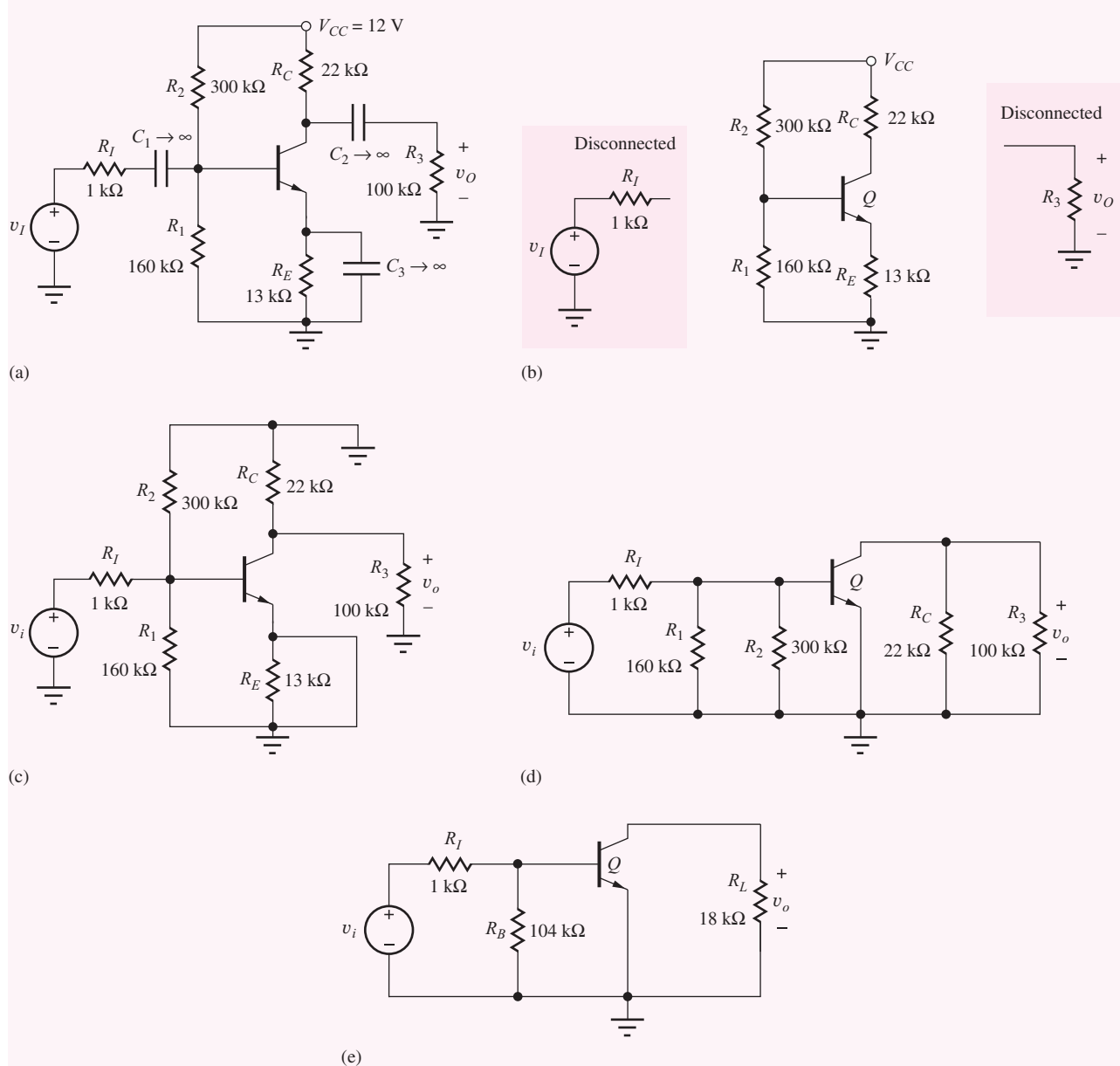


**Figure 13.6** (a) Complete ac-coupled amplifier circuit. (b) Simplified equivalent circuit for dc analysis. (c) Circuit after step 3. Note that the input and output are now  $v_i$  and  $v_o$ . (d) Redrawn version of Fig. 13.6(c). (e) Continued simplification of the ac circuit.

**Discussion:** Notice again how the capacitors have been used to modify the circuit topologies for dc and ac signals.  $C_1$  and  $C_2$  isolate the source and load from the bias circuit at dc. Capacitor  $C_3$  causes the emitter node to be connected directly to ground in the ac circuit, effectively removing  $R_E$  from the circuit.

**EXERCISE:** What are the values of  $R_B$  and  $R_L$  in Fig. 13.6(e) if  $R_1 = 20 \text{ k}\Omega$ ,  $R_2 = 62 \text{ k}\Omega$ ,  $R_C = 8.2 \text{ k}\Omega$ , and  $R_E = 2.7 \text{ k}\Omega$ ?

**ANSWERS:** 15.1 k $\Omega$ ; 7.58 k $\Omega$

### EXAMPLE 13.2 CONSTRUCTING ac AND dc EQUIVALENTS FOR A MOSFET AMPLIFIER

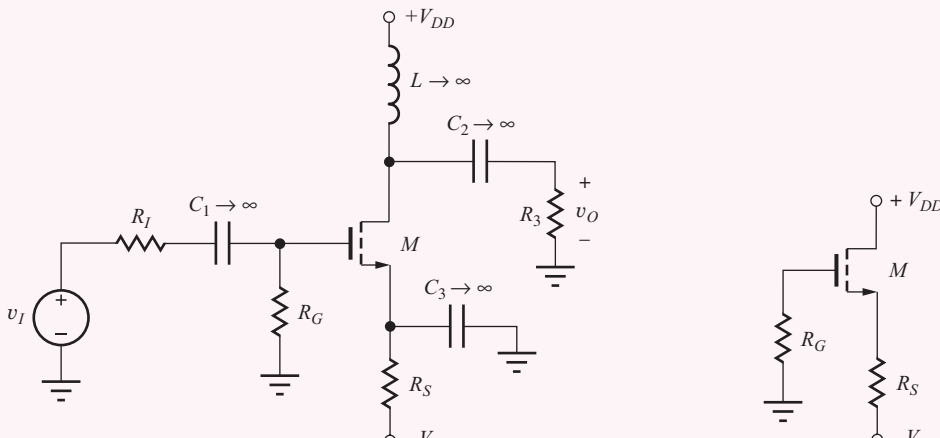
This second example showing how to construct the dc and ac equivalent circuits of an overall amplifier circuit includes the use of a split-supply biasing technique, and an inductor has also been included in the circuit.

**PROBLEM** Draw the dc and ac equivalent circuits (menu steps 1 and 3) for the common-source amplifier in Fig. 13.7(a).

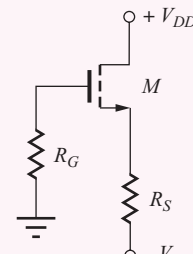
**SOLUTION Known Information and Given Data:** The circuit with labeled elements appears in Fig. 13.7(a).

**Unknowns:** dc equivalent circuit; ac equivalent circuit

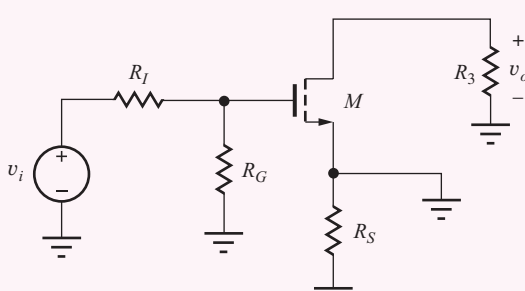
**Approach:** Replace capacitors by open circuits and inductors by short circuits to obtain the dc equivalent circuit. To obtain the ac equivalent circuit, replace capacitors and dc voltage sources by



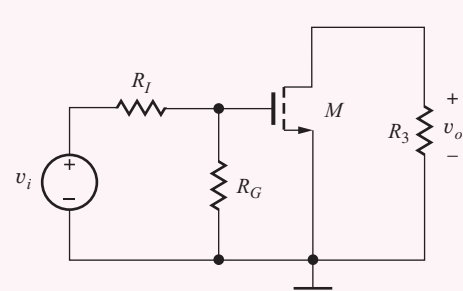
(a)



(b)



(c)



(d)

**Figure 13.7** (a) An amplifier biased by two power supplies. (b) dc Equivalent circuit for Q-point analysis. (c) First step in generating the ac equivalent circuit. (d) Simplified ac equivalent circuit.

short circuits, and current sources and inductors by open circuits. Combine and simplify resistor combinations wherever possible.

**Assumptions:** Capacitor values are large enough that they can be treated as short circuits in the ac equivalent circuit. The inductor value is large enough that it can be treated as an open circuit in the ac equivalent circuit.

**ANALYSIS dc Equivalent Circuit:** The dc equivalent circuit is found by replacing the capacitors by open circuits and the inductor by a short circuit, resulting in the circuit in Fig. 13.7(b). Capacitors  $C_1$  and  $C_2$  again disconnect  $v_I$ ,  $R_I$ , and  $R_3$  from the circuit, and the shorted inductor connects the drain of the transistor directly to  $V_{DD}$ .

**ac Equivalent Circuit:** The ac equivalent circuit in Fig. 13.7(c) is obtained by replacing the capacitors by short circuits and the inductor by an open circuit. Figure 13.7(c) has been redrawn in final simplified form in Fig. 13.7(d). Only signal component  $v_i$  appears in the ac equivalent circuit.

**Check of Results:** For this case, the best way to verify our results is to double check our work—all seems correct.

**Discussion:** Here again, the designer has used the capacitors and inductor to achieve very different circuit topologies for the dc and ac equivalent circuits. Compare Figs. 13.7(b) and 13.7(d).

**EXERCISE:** Redraw the dc and ac equivalent circuits in Fig. 13.7(b) and (d) if  $C_3$  were eliminated from the circuit.

**ANSWERS:** (b) No change, (d) resistor  $R_S$  appears between the MOSFET source and ground (See  $R_E$  in Fig 13.6(e).)

## 13.4 INTRODUCTION TO SMALL-SIGNAL MODELING

For ac analysis, we would like to be able to use our wealth of linear circuit analysis techniques. For this approach to be valid, the signal currents and voltages must be small enough to ensure that the ac circuit behaves in a linear manner. Thus, we must assume that the time-varying signal components are **small signals**. The amplitudes that are considered to be small signals are device-dependent; we will define these as we develop the small-signal models for each device. Our study of **small-signal models** begins with the diode and then proceeds to the bipolar junction transistor and the field-effect transistor.

### 13.4.1 GRAPHICAL INTERPRETATION OF THE SMALL-SIGNAL BEHAVIOR OF THE DIODE

The small-signal model for the diode represents the relationship between small variations in the diode voltage and current around the Q-point values. The total terminal voltage and current for the diode in Fig. 13.8 can be written as  $v_D = V_D + v_d$  and  $i_D = I_D + i_d$  where  $I_D$  and  $V_D$  represent the dc bias point (the Q-point) values, and  $v_d$  and  $i_d$  are small changes away from the Q-point. The changes in voltage and current are depicted graphically in Fig. 13.9. As the diode voltage increases slightly, the current also increases slightly. For small changes,  $i_d$  will be linearly related (i.e., directly proportional) to  $v_d$ , and the proportionality constant is called the diode conductance  $g_d$ :

$$i_d = g_d v_d \quad (13.7)$$

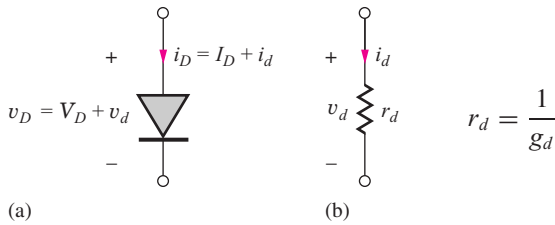


**Figure 13.8** (a) Total diode terminal voltage and current. (b) Small signal model for the diode.

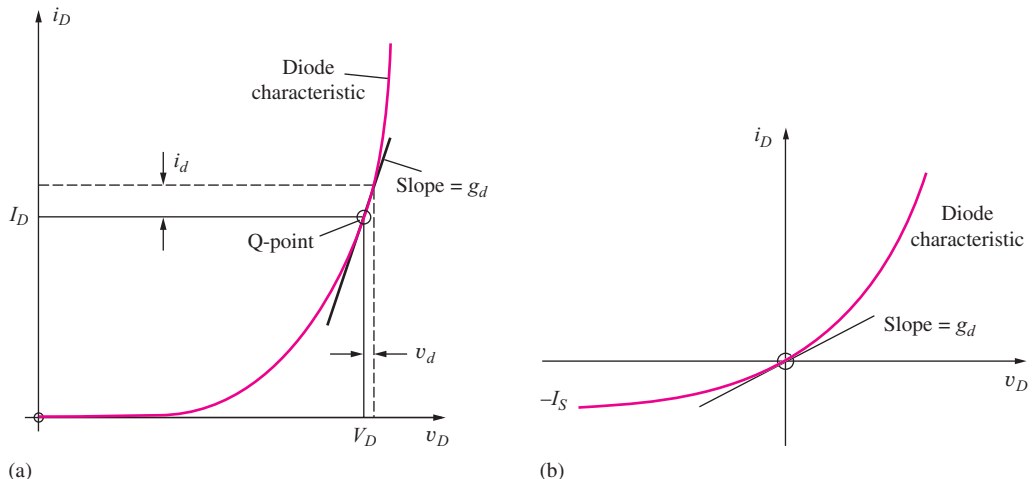


**Figure 13.9** (a) The relationship between small increases in voltage and current above the diode operating point ( $I_D$ ,  $V_D$ ). For small changes  $i_d = g_d v_d$ . (b) The diode conductance is not zero for  $I_D = 0$ .

As depicted graphically in Fig. 13.9(a), diode conductance  $g_d$  actually represents the slope of the diode characteristic evaluated at the Q-point. Stated mathematically,  $g_d$  can be written as

$$g_d = \left. \frac{\partial i_D}{\partial v_D} \right|_{\text{Q-point}} = \left. \frac{\partial}{\partial v_D} \left\{ I_S \left[ \exp \left( \frac{v_D}{V_T} \right) - 1 \right] \right\} \right|_{\text{Q-point}} = \frac{I_S}{V_T} \exp \left( \frac{V_D}{V_T} \right) = \frac{I_D + I_S}{V_T} \quad (13.8)$$

where we have used our mathematical model for  $i_D$ . For forward bias with  $I_D \gg I_S$ , the diode conductance becomes

$$g_d \cong \frac{I_D}{V_T} \quad \text{or} \quad g_d \cong \frac{I_D}{0.025 \text{ V}} = 40I_D \quad (13.9)$$

at room temperature. Note that  $g_d$  is small but not zero for  $I_D = 0$  because the slope of the diode equation is nonzero at the origin, as depicted in Fig. 13.9(b).

### 13.4.2 SMALL-SIGNAL MODELING OF THE DIODE

Now we will use the diode equation to more fully explore the small-signal behavior of the diode and to actually define how large  $v_d$  and  $i_d$  can become before Eq. (13.7) breaks down. A relationship between the ac and dc quantities can be developed directly from the diode equation introduced in Chapter 3:

$$i_D = I_S \left[ \exp \left( \frac{v_D}{V_T} \right) - 1 \right] \quad (13.10)$$

Substituting  $v_D = V_D + v_d$  and  $i_D = I_D + i_d$  into Eq. (13.10) yields

$$I_D + i_d = I_S \left[ \exp \left( \frac{V_D + v_d}{V_T} \right) - 1 \right] = I_S \left[ \exp \left( \frac{V_D}{V_T} \right) \exp \left( \frac{v_d}{V_T} \right) - 1 \right] \quad (13.11)$$

Expanding the second exponential using Maclaurin's series and collecting the dc and signal terms together,

$$I_D + i_d = I_S \left[ \exp \left( \frac{V_D}{V_T} \right) - 1 \right] + I_S \exp \left( \frac{V_D}{V_T} \right) \left[ \frac{v_d}{V_T} + \frac{1}{2} \left( \frac{v_d}{V_T} \right)^2 + \frac{1}{6} \left( \frac{v_d}{V_T} \right)^3 + \dots \right] \quad (13.12)$$

We recognize the first term on the right-hand side of Eq. (13.12) as the dc diode current  $I_D$ :

$$I_D = I_S \left[ \exp \left( \frac{V_D}{V_T} \right) - 1 \right] \quad \text{and} \quad I_S \exp \left( \frac{V_D}{V_T} \right) = I_D + I_S \quad (13.13)$$

Subtracting  $I_D$  from both sides of the equation yields an expression for  $i_d$  in terms of  $v_d$ :

$$i_d = (I_D + I_S) \left[ \frac{v_d}{V_T} + \frac{1}{2} \left( \frac{v_d}{V_T} \right)^2 + \frac{1}{6} \left( \frac{v_d}{V_T} \right)^3 + \dots \right] \quad (13.14)$$

We want the signal current  $i_d$  to be a linear function of the signal voltage  $v_d$ . Using only the first two terms of Eq. (13.14), we find that linearity requires

$$\frac{v_d}{V_T} \gg \frac{1}{2} \left( \frac{v_d}{V_T} \right)^2 \quad \text{or} \quad v_d \ll 2V_T = 0.05 \text{ V} \quad (13.15)$$

If the relationship in Eq. (13.15) is met, then Eq. (13.14) can be written as

$$i_d = (I_D + I_S) \left( \frac{v_d}{V_T} \right) \quad \text{or} \quad i_d = g_d v_d \quad \text{and} \quad i_d = I_D + g_d v_d \quad (13.16)$$

in which  $g_d$  is the **small-signal conductance** of the diode originally given in Eq. (13.8). Equation (13.16) states that the total diode current is the dc current  $I_D$  (at the Q-point) plus a small change in current ( $i_d = g_d v_d$ ) that is linearly related to the small voltage change  $v_d$  across the diode.

The values of the **diode conductance**  $g_d$ , or the equivalent **diode resistance**  $r_d$ , are determined by the operating point of the diode as defined in Eq. (13.9):

$$g_d = \frac{I_D + I_S}{V_T} \cong \frac{I_D}{V_T} = 40I_D \quad \text{and} \quad r_d = \frac{1}{g_d} \quad (13.17)$$

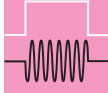
The diode and its corresponding small-signal model, represented by resistor  $r_d$ , are given in Fig. 13.8.

Equation (13.15) defines the requirement for small-signal operation of the diode. The shift in diode voltage away from the Q-point value must be much less than 50 mV. Choosing a factor of 10 as adequate to satisfy the inequality yields  $v_d \leq 0.005$  V for small-signal operation. This is indeed a small voltage change.

Note, however, that the maximum small-signal change in diode voltage represents a significant change in diode current:

$$i_d = g_d v_d = 0.005 \text{ V} \frac{I_D}{0.0025 \text{ V}} = 0.2I_D \quad (13.18)$$

The 5-mV change in diode voltage corresponds to a 20 percent change in the diode current! This large change results from the exponential relationship between voltage and current in the diode.


**DESIGN  
NOTE**

Small changes in diode current and voltage are related by the small-signal conductance of the diode

$$i_d = g_d v_d \quad \text{where} \quad g_d \cong \frac{I_D}{V_T} \cong 40 I_D$$

at room temperature. For small-signal operation,

$$|v_d| \leq 0.005 \text{ V} \quad \text{and} \quad |i_d| \leq 0.20 I_D$$

**EXERCISE:** Calculate the values of the diode resistance  $r_d$  for a diode with  $I_S = 1 \text{ fA}$  operating at  $I_D = 0, 50 \mu\text{A}, 2 \text{ mA}$ , and  $3 \text{ A}$ .

**ANSWERS:**  $25.0 \text{ T}\Omega, 500 \Omega, 12.5 \Omega, 8.33 \text{ m}\Omega$

**EXERCISE:** What is the small-signal diode resistance  $r_d$  at room temperature for  $I_D = 1.5 \text{ mA}$ ? What is the small-signal resistance of this diode at  $T = 100^\circ\text{C}$ ?

**ANSWERS:**  $16.7 \Omega, 21.4 \Omega$

## 13.5 SMALL-SIGNAL MODELS FOR BIPOLAR JUNCTION TRANSISTORS

Now that the concept of small-signal modeling has been introduced, we shall develop the small-signal model for the more complicated bipolar transistor. The BJT is a three-terminal device, and its small-signal model is based on the two-port network representation<sup>1</sup> shown in Fig. 13.10 for which the input port variables are  $v_{be}$  and  $i_b$ , and the output port variables are  $v_{ce}$  and  $i_c$ . A set of two-port equations in terms of these variables can be written as

$$\begin{aligned} i_b &= g_\pi v_{be} + g_r v_{ce} \\ i_c &= g_m v_{be} + g_o v_{ce} \end{aligned} \tag{13.19}$$

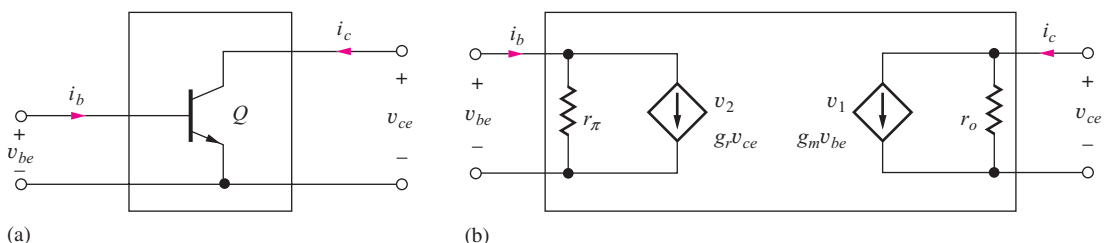


**Figure 13.10** (a) Two-port representation of the  $npn$  transistor. (b) Two-port representation for the transistor in Fig. 13.10(a).

<sup>1</sup> These equations actually represent a  $y$ -parameter two-port network.

The port variables in Fig. 13.10 can be considered to represent either the time-varying portion of the total voltages and currents or small changes in the total quantities away from the Q-point values.

$$\begin{aligned} v_{BE} &= V_{BE} + v_{be} & v_{CE} &= V_{CE} + v_{ce} \\ i_B &= I_B + i_b & i_C &= I_C + i_c \\ \text{or} & & & \\ v_{be} &= \Delta v_{BE} = v_{BE} - V_{BE} & v_{ce} &= \Delta v_{CE} = v_{CE} - V_{CE} \\ i_b &= \Delta i_B = i_B - I_B & i_c &= \Delta i_C = i_C - I_C \end{aligned} \quad (13.20)$$

We can write the  $y$ -parameters in terms of small-signal voltages and currents or in terms of derivatives of the complete port variables, as in Eq. (13.21):

$$\begin{aligned} g_\pi &= \frac{\mathbf{i}_b}{\mathbf{v}_{be}} \Big|_{v_{ce}=0} = \frac{\partial i_B}{\partial v_{BE}} \Big|_{\text{Q-point}} & g_r &= \frac{\mathbf{i}_b}{\mathbf{v}_{ce}} \Big|_{v_{be}=0} = \frac{\partial i_B}{\partial v_{CE}} \Big|_{\text{Q-point}} \\ g_m &= \frac{\mathbf{i}_c}{\mathbf{v}_{be}} \Big|_{v_{ce}=0} = \frac{\partial i_C}{\partial v_{BE}} \Big|_{\text{Q-point}} & g_o &= \frac{\mathbf{i}_c}{\mathbf{v}_{ce}} \Big|_{v_{be}=0} = \frac{\partial i_C}{\partial v_{CE}} \Big|_{\text{Q-point}} \end{aligned} \quad (13.21)$$

Because we have the transport model, Eq. (5.43), which expresses the BJT terminal currents in terms of the terminal voltages, as repeated in Eq. (13.22) for the active region, we use the derivative formulation to determine the  $y$ -parameters for the transistor:

$$\begin{aligned} i_C &= I_S \left[ \exp \left( \frac{v_{BE}}{V_T} \right) \right] \left[ 1 + \frac{v_{CE}}{V_A} \right] & i_B &= \frac{i_C}{\beta_F} = \frac{I_S}{\beta_{FO}} \left[ \exp \left( \frac{v_{BE}}{V_T} \right) \right] \\ \beta_F &= \beta_{FO} \left[ 1 + \frac{v_{CE}}{V_A} \right] \end{aligned} \quad (13.22)$$

Evaluating the various derivatives<sup>2</sup> of Eq. (13.22) yields the parameters for the BJT:

$$\begin{aligned} g_r &= \frac{\partial i_B}{\partial v_{CE}} \Big|_{\text{Q-point}} = 0 \\ g_m &= \frac{\partial i_C}{\partial v_{BE}} \Big|_{\text{Q-point}} = \frac{I_S}{V_T} \left[ \exp \left( \frac{v_{BE}}{V_T} \right) \right] \left[ 1 + \frac{v_{CE}}{V_A} \right]_{\text{Q-point}} = \frac{I_C}{V_T} \\ g_o &= \frac{\partial i_C}{\partial v_{CE}} \Big|_{\text{Q-point}} = \frac{I_S}{V_A} \left[ \exp \left( \frac{V_{BE}}{V_T} \right) \right] = \frac{I_C}{V_A + V_{CE}} \end{aligned} \quad (13.23)$$

Calculation of  $g_\pi$  has been saved until last because it requires a bit more effort and the use of some new information. The current gain of a BJT is actually operating point-dependent, and this dependence should be included when evaluating the derivative needed for  $g_\pi$ :

$$g_\pi = \frac{\partial i_B}{\partial v_{BE}} \Big|_{\text{Q-point}} = \left[ \frac{1}{\beta_F} \frac{\partial i_C}{\partial v_{BE}} - \frac{i_C}{\beta_F^2} \frac{\partial \beta_F}{\partial v_{BE}} \right]_{\text{Q-point}} = \left[ \frac{1}{\beta_F} \frac{\partial i_C}{\partial v_{BE}} - \frac{i_C}{\beta_F^2} \frac{\partial \beta_F}{\partial i_C} \frac{\partial i_C}{\partial v_{BE}} \right]_{\text{Q-point}} \quad (13.24)$$

Factoring out the first term:

$$g_\pi = \frac{1}{\beta_F} \frac{\partial i_C}{\partial v_{BE}} \left[ 1 - \frac{i_C}{\beta_F} \frac{\partial \beta_F}{\partial i_C} \right]_{\text{Q-point}} = \frac{I_C}{\beta_F V_T} \left[ 1 - \left( \frac{i_C}{\beta_F} \frac{\partial \beta_F}{\partial i_C} \right)_{\text{Q-point}} \right] \quad (13.25)$$

<sup>2</sup> We could equally well have taken the direct approach used in analysis of the diode.

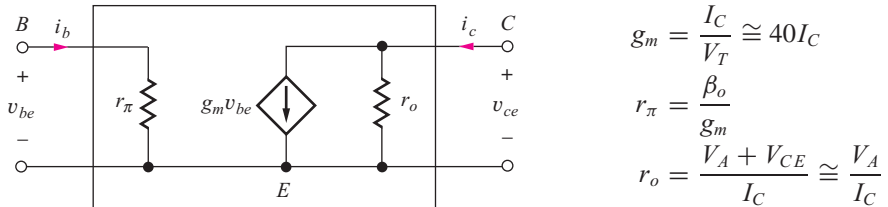


**Figure 13.11** Hybrid-pi small-signal model for the intrinsic bipolar transistor.

Finally, Eq. (13.25) can be simplified by defining a new parameter  $\beta_o$ :

$$g_\pi = \frac{I_C}{\beta_o V_T} \quad \text{where} \quad \beta_o = \frac{\beta_F}{\left[ 1 - I_C \left( \frac{1}{\beta_F} \frac{\partial \beta_F}{\partial i_C} \right)_{\text{Q-point}} \right]} \quad (13.26)$$

$\beta_o$  represents the **small-signal common-emitter current gain** of the bipolar transistor. Equation (13.26) will be discussed in more detail in Sec. 13.5.3.

### 13.5.1 THE HYBRID-PI MODEL

The **hybrid-pi model** is the most widely accepted small-signal model for the bipolar transistor. If one looks at the latest results in analog circuits as published in the *IEEE Journal of Solid-State Circuits*, for example, the analysis will most likely be cast in terms of the hybrid-pi model.<sup>3</sup>

The standard representation of the basic hybrid-pi small-signal model appears in Fig. 13.11, and the expressions for the model elements are given in Eq. (13.27). These results will be used throughout the rest of the text and should be committed to memory.

<b>Transconductance:</b> $g_m = \frac{I_C}{V_T} \cong 40I_C$	<b>Input resistance:</b> $r_\pi = \frac{\beta_o V_T}{I_C} = \frac{\beta_o}{g_m}$	<b>Output resistance:</b> $r_o = \frac{1}{g_o} = \frac{V_A + V_{CE}}{I_C} \cong \frac{V_A}{I_C}$
--	--	--

Arguably the most important small-signal parameter is transconductance  $g_m$ . The transconductance characterizes how the collector current changes in response to a change in the base-emitter voltage, thereby modeling the forward gain of the device. Here again we see the fundamental voltage-controlled current behavior of the bipolar transistor,  $i_c = g_m v_{be}$ . At room temperature,  $V_T \cong 0.025$  mV, and transconductance  $g_m \cong 40I_C$ . Also, collector-emitter voltage  $V_{CE}$  is typically much less than Early voltage  $V_A$ , so we can simplify the expression for the output resistance:  $r_o \cong V_A/I_C$ .

When we change the base-emitter voltage and hence the collector current, we must also supply a change in base current, and resistor  $r_\pi$  characterizes the relationship between changes in  $i_B$  and  $v_{BE}$ . Similarly, when the collector-emitter voltage changes slightly, the collector current changes, and resistor  $r_o$  characterizes the relationship between changes in  $i_c$  and  $v_{ce}$ .

The two-port representation in Fig. 13.11 using these symbols shows the intrinsic low-frequency **hybrid-pi small-signal model** for the bipolar transistor. Additional elements will be added to model frequency dependencies in Chapter 17.

From Eq. (13.27) and Fig. 13.11, we see that the values of the small-signal parameters are controlled explicitly by our choice of Q-point. Transconductance  $g_m$  is directly proportional to the

<sup>3</sup> An alternative model, called the T-model, appears in Prob. 13.64.

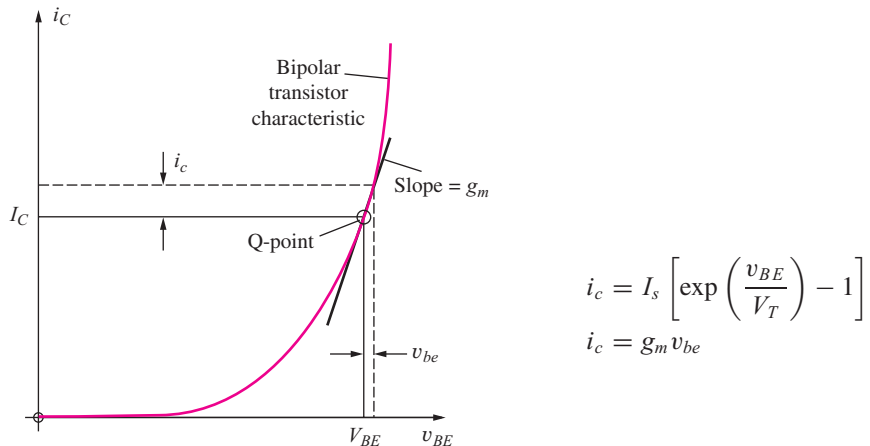


**Figure 13.12** The relationship between small increases in base-emitter voltage and collector current above the BJT operating point ( $I_C$ ,  $V_{CE}$ ). For small changes  $i_c = g_m v_{be}$ .

collector current of the bipolar transistor, whereas input resistance  $r_\pi$  and output resistance  $r_o$  are both inversely proportional to the collector current. The output resistance exhibits a weak dependence on collector-emitter voltage (but generally  $V_{CE} \ll V_A$ ). Note that these parameters are independent of the geometry of the BJT. For example, small high-frequency transistors or large-geometry power devices all have the same value of  $g_m$  for a given collector current.

### 13.5.2 GRAPHICAL INTERPRETATION OF THE TRANSCONDUCTANCE

Figure 13.12 depicts the diode-like exponential relation between total collector current  $i_C$  and total base-emitter voltage  $v_{BE}$  in the bipolar transistor. Transconductance  $g_m$  represents the slope of the  $i_C - v_{BE}$  characteristic at the given operating point (Q-point). For a small increase  $v_{be}$  above the Q-point voltage  $V_{BE}$ , a small corresponding increase  $i_c$  occurs above the Q-point current  $I_C$ . When the small-signal condition  $v_{be} \leq 5$  mV is met, these two changes are linearly related by the transconductance:  $i_c = g_m v_{be}$ .

### 13.5.3 SMALL-SIGNAL CURRENT GAIN

Two important auxiliary relationships also exist between the small-signal parameters. It can be seen in Eq. (13.27) that the parameters  $g_m$  and  $r_\pi$  are related by the small-signal current gain  $\beta_o$ :

$$\beta_o = g_m r_\pi \quad (13.28)$$

As mentioned before, the dc current gain in a real transistor is not constant but is a function of operating current, as indicated in Fig. 13.13. From this figure, we see that

$$\frac{\partial \beta_F}{\partial i_C} > 0 \text{ for } i_C < I_M \quad \text{and} \quad \frac{\partial \beta_F}{\partial i_C} < 0 \text{ for } i_C > I_M$$

where  $I_M$  is the collector current at which  $\beta_F$  is maximum. Thus, for the **small-signal current gain** defined by

$$\beta_o = \frac{\beta_F}{\left[ 1 - I_C \left( \frac{1}{\beta_F} \frac{\partial \beta_F}{\partial i_C} \right)_{\text{Q-point}} \right]} \quad (13.29)$$

$\beta_o > \beta_F$  for  $i_C < I_M$ , and  $\beta_o < \beta_F$  for  $i_C > I_M$ . That is, the ac current gain  $\beta_o$  exceeds the dc current gain  $\beta_F$  when the collector current is below  $I_M$  and is smaller than  $\beta_F$  when  $I_C$  exceeds  $I_M$ . In

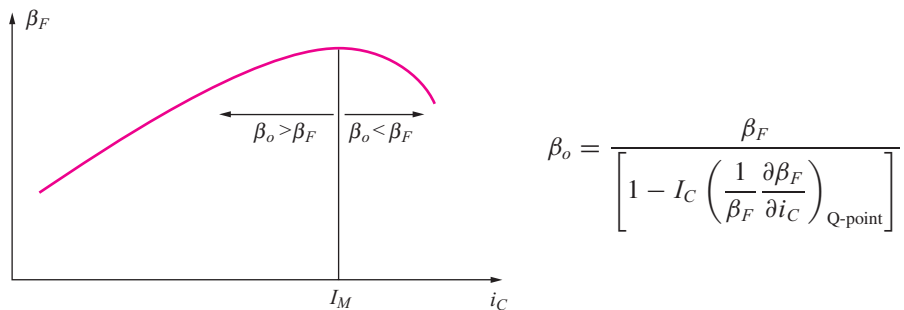


**Figure 13.13** dc current gain versus current for the BJT.

practice, the difference between  $\beta_F$  and  $\beta_o$  is usually ignored, and  $\beta_F$  and  $\beta_o$  are commonly assumed to be the same.

#### 13.5.4 THE INTRINSIC VOLTAGE GAIN OF THE BJT

The second important auxiliary relationship is given by the **intrinsic voltage gain**  $\mu_f$ , which is equal to the product of  $g_m$  and  $r_o$ :

$$\mu_f = g_m r_o = \frac{V_A + V_{CE}}{V_T} \approx \frac{V_A}{V_T} \quad \text{for } V_{CS} \ll V_A \quad (13.30)$$

From Eq. (13.30), the BJT amplification factor can be seen to be almost independent of operating point for  $V_{CE} \ll V_A$ . At room temperature  $\mu_f \approx 40 V_A$ .

We shall find that the amplification factor  $\mu_f$  plays an important role in circuit design, and it appears often in the analysis of amplifier circuits. Parameter  $\mu_f$  represents the maximum voltage gain that the individual transistor can provide and is also referred to as the **amplification factor** of the device. For  $V_A$  ranging from 25 V to 100 V,  $\mu_f$  ranges from 1000 to 4000. Thus, if we are clever enough, we should be able to build a single transistor amplifier with a voltage gain of several thousand. In later chapters, we will explore how this can be achieved.

#### DESIGN NOTE

Remember, the voltage gain of a single transistor amplifier cannot exceed the transistor's intrinsic voltage gain  $\mu_f$ , which ranges from 1000 to 4000 for the bipolar transistor.

$$\mu_f = \frac{V_A + V_{CE}}{V_T} \approx \frac{V_A}{V_T}$$

Table 13.1 displays examples of the variation of the small-signal parameters with operating point. The values of  $g_m$ ,  $r_\pi$ , and  $r_o$  can each be varied over many orders of magnitude by changing the value of the dc collector current corresponding to the Q-point. Note that  $\mu_f$  does not change with the choice of operating point. As we see later in this chapter, this is a very significant difference between the BJT and FET.

It is important to realize that although we developed the small-signal model of the BJT based on analysis of the transistor oriented in the common-emitter configuration in Fig. 13.10, the resulting hybrid-pi model can actually be used in the analysis of any circuit topology. This point will become clearer in Chapter 14.

**TABLE 13.1**BJT Small-Signal Parameters versus Current:  $\beta_o = 100$ ,  $V_A = 75$  V,  $V_{CE} = 10$  V

$I_C$	$g_M$	$r_\pi$	$r_o$	$\mu_f$
1 $\mu$ A	$4 \times 10^{-5}$ S	2.5 M $\Omega$	85 M $\Omega$	3400
10 $\mu$ A	$4 \times 10^{-4}$ S	250 k $\Omega$	8.5 M $\Omega$	3400
100 $\mu$ A	0.004 S	25.0 k $\Omega$	850 k $\Omega$	3400
1 mA	0.04 S	2.5 k $\Omega$	85 k $\Omega$	3400
10 mA	0.40 S	250 $\Omega$	8.5 k $\Omega$	3400

**EXERCISE:** Calculate the values of  $g_m$ ,  $r_\pi$ ,  $r_o$ , and  $\mu_f$  for a bipolar transistor with  $\beta_o = 75$  and  $V_A = 60$  V operating at a Q-point of (50  $\mu$ A, 5 V).

**ANSWERS:** 2.00 mS, 37.5 k $\Omega$ , 1.30 M $\Omega$ , 2600

**EXERCISE:** Calculate the values of  $g_m$ ,  $r_\pi$ ,  $r_o$ , and  $\mu_f$  for a bipolar transistor with  $\beta_o = 50$  and  $V_A = 75$  V operating at a Q-point of (250  $\mu$ A, 15 V).

**ANSWERS:** 10.0 mS, 5.00 k $\Omega$ , 360 k $\Omega$ , 3600

**EXERCISE:** Use graphical analysis to find values of  $\beta_{FO}$ ,  $g_m$ ,  $\beta_o$ , and  $r_o$  at the Q-point for the transistor in Fig. 13.1(b). Calculate the value of  $r_\pi$ .

**ANSWERS:** 100, 62.5 mS, 100,  $\infty$ ; 1.60 k $\Omega$

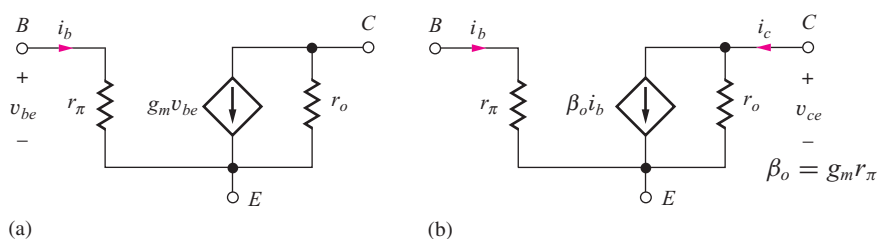
### 13.5.5 EQUIVALENT FORMS OF THE SMALL-SIGNAL MODEL

The small-signal model in Fig. 13.14 includes the voltage-controlled current source  $g_m v_{be}$ . It is often useful in circuit analysis to transform this model into a current-controlled source. Recognizing that the voltage  $v_{be}$  in Fig. 13.13 can be written in terms of the current  $i_b$  as  $v_{be} = i_b r_\pi$ , the voltage-controlled source can be rewritten as

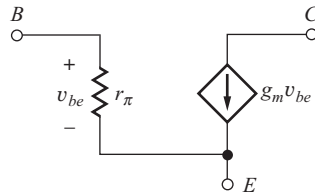
$$g_m v_{be} = g_m r_\pi i_b = \beta_o i_b \quad \text{where} \quad \beta_o = g_m r_\pi \quad (13.31)$$

Figure 13.14(a) and (b) shows the two equivalent forms of the small-signal BJT model. The model in Fig. 13.14(a) recognizes the fundamental voltage-controlled current source nature of the transistor that is explicit in the transport model. From the second model, Fig. 13.14(b), we see that

$$i_c = \beta_o i_b + \frac{v_{ce}}{r_o} \cong \beta_o i_b \quad (13.32)$$



**Figure 13.14** Two equivalent forms of the BJT small-signal model: (a) voltage-controlled current source model, and (b) current-controlled current source model.



**Figure 13.15** Simplified hybrid pi model in which  $r_o$  is neglected.

which demonstrates the auxiliary relationship that  $\mathbf{i}_c \cong \beta_o \mathbf{i}_b$  in the active region of operation. For the most typical case,  $v_{ce}/r_o \ll \beta_o$ . Thus, the basic relationship  $i_C = \beta i_B$  is useful for both ac and dc analysis when the BJT is operating in the active region. We will find that sometimes circuit analysis is more easily performed using the model in Fig. 13.14(a), and at other times more easily performed using the model in Fig. 13.14(b).

### 13.5.6 SIMPLIFIED HYBRID PI MODEL

As we investigate circuit behavior in more detail, we will find that output resistance  $r_o$  often has a relatively minor effect on circuit performance, especially on voltage gain, and we can often greatly simplify our circuit analysis if we neglect the output resistance in our model as shown in Fig. 13.15. Generally, we can make this simplification if the voltage gain of the circuit is much less than the intrinsic voltage gain  $\mu_f$ . So our approach will be to neglect  $r_o$ , then calculate the voltage gain, and see if the result is consistent with the assumption that the voltage gain is much less than  $\mu_f$ . However,  $r_o$  can have a much greater impact on amplifier output resistance calculations, and we must often add it back into the model in order to get nontrivial results. We will see examples of this as we proceed through Chapters 13 and 14.

#### DESIGN NOTE

Output resistance  $r_o$  can be neglected in calculations of voltage gain  $A_v$  as long as  $A_v \ll \mu_f$ .

### 13.5.7 DEFINITION OF A SMALL SIGNAL FOR THE BIPOLAR TRANSISTOR

For small-signal operation, we want the relationship between changes in voltages and currents to be linear. We can find the constraints on the BJT corresponding to small-signal operation using the simplified transport model for the total collector current of the transistor in the active region:

$$i_C = I_S \left[ \exp \left( \frac{v_{BE}}{V_T} \right) \right] = I_S \left[ \exp \left( \frac{V_{BE} + v_{be}}{V_T} \right) \right] \quad (13.33)$$

Rewriting the exponential as a product,

$$i_C = I_C + i_c = \left[ I_S \exp \left( \frac{V_{BE}}{V_T} \right) \right] \left[ \exp \left( \frac{v_{be}}{V_T} \right) \right] = I_C \left[ \exp \left( \frac{v_{be}}{V_T} \right) \right] \quad (13.34)$$

in which it has been recognized that the collector current  $I_C$  is given by

$$I_C = I_S \exp \left( \frac{V_{BE}}{V_T} \right) \quad (13.35)$$

Now, expanding the remaining exponential in Eq. (13.34), its Maclaurin's series yields

$$i_C = I_C \left[ 1 + \frac{v_{be}}{V_T} + \frac{1}{2} \left( \frac{v_{be}}{V_T} \right)^2 + \frac{1}{6} \left( \frac{v_{be}}{V_T} \right)^3 + \dots \right] \quad (13.36)$$

Recognizing  $i_c = I_C - I_C$  yields

$$i_c = I_C \left[ \frac{v_{be}}{V_T} + \frac{1}{2} \left( \frac{v_{be}}{V_T} \right)^2 + \frac{1}{6} \left( \frac{v_{be}}{V_T} \right)^3 + \dots \right] \quad (13.37)$$

Linearity requires that  $i_c$  be proportional to  $v_{be}$ , so we must have

$$\frac{1}{2} \left( \frac{v_{be}}{V_T} \right)^2 \ll \frac{v_{be}}{V_T} \quad \text{or} \quad v_{be} \ll 2V_T \quad (13.38)$$

where higher order terms have been neglected.

From Eq. (13.38), we see that small-signal operation requires the signal applied to the base-emitter junction to be much less than twice the thermal voltage, 50 mV at room temperature. In this book, we assume that a factor of 10 satisfies the condition in Eq. (13.38), and

$$|v_{be}| \leq 0.005 \text{ V} \quad (13.39)$$

is our definition of a **small signal for the BJT**. If the condition in Eq. (13.39) is met, then Eq. (13.36) can be approximated as

$$i_c \cong I_C \left[ 1 + \frac{v_{be}}{V_T} \right] = I_C + \frac{I_C}{V_T} v_{be} = I_C + g_m v_{be} \quad (13.40)$$

and the change in  $i_C$  is directly proportional to the change in  $v_{BE}$  (i.e.,  $i_c = g_m v_{be}$ ). The constant of proportionality is the transconductance  $g_m$ . Note that the quadratic, cubic, and higher-order powers of  $v_{be}$  in Eq. (13.37) are sources of the harmonic distortion that was discussed in Sec. 10.6.

From Eq. (13.39), the signal developed across the base-emitter junction must be no larger than 5 mV to qualify as a small signal! This is indeed small. But note well: We must not infer that signals at other points in the circuit need be small. Referring back to Fig. 13.1, we can see that a 16-mV *p-p* signal  $v_{be}$  generates a 3.3-V *p-p* signal at the collector. This is fortunate because we often want linear amplifiers to develop signals that are many volts in amplitude.

Let us now explore the change in collector current  $i_c$  that corresponds to small-signal operation. Using Eq. (13.40),

$$\frac{i_c}{I_C} = \frac{g_m v_{be}}{I_C} = \frac{v_{be}}{V_T} \leq \frac{0.005}{0.025} = 0.2 \quad (13.41)$$

A 5-mV change in  $v_{BE}$  corresponds to a 20 percent deviation in  $i_C$  from its Q-point value as well as a 20 percent change in  $i_E$  since  $\alpha_F \cong 1$ . Some authors prefer to permit  $|v_{be}| \leq 10$  mV, which corresponds to a 40 percent change in  $i_C$  from the Q-point value. In either case, relatively large changes in voltage can occur at the collector and/or emitter terminals of the transistor when the signal currents  $i_c$  and  $i_e$  flow through resistors external to the transistor.

The strict small-signal guidelines introduced above are frequently violated in practice. The designer must accept the trade-off between a larger signal amplitude and a higher level of distortion. As we move beyond the small-signal limit, our small-signal analysis becomes more approximate. However, our hand analysis still represents a useful estimate of circuit performance that we often refine with detailed transient simulation.

## DESIGN NOTE

The small-signal limit for the bipolar transistor is set by

$$|v_{be}| \leq 0.005 \text{ V} \quad \text{and} \quad |i_c| \leq 0.2I_C$$

**EXERCISE:** Does the amplitude of the signal in Figs. 13.1(a) and 13.1(b) satisfy the requirements for small-signal operation?

**ANSWER:** No,  $v_{be} = 8 \text{ mV}$  exceeds our definition of a small signal.

### 13.5.8 SMALL-SIGNAL MODEL FOR THE *pnp* TRANSISTOR

The small-signal model for the *pnp* transistor is identical to that of the *npn* transistor. At first glance, this fact is surprising to most people because the dc currents flow in opposite directions. The circuits in Fig. 13.16 will be used to help explain this situation.

In Fig. 13.16, the *npn* and *pnp* transistors are each biased by dc current source  $I_B$ , establishing the Q-point current  $I_C = \beta_F I_B$ . In each case a signal current  $i_b$  is also injected *into* the base. For the *npn* transistor, the total base and collector currents are (for  $\beta_o = \beta_F$ ):

$$i_B = I_B + i_b \quad \text{and} \quad i_C = I_C + i_c = \beta_F I_B + \beta_F i_b \quad (13.42)$$

An increase in base current of the *npn* transistor causes an increase in current entering the collector terminal.

For the *pnp* transistor,

$$i_B = I_B - i_b \quad \text{and} \quad i_C = I_C - i_c = \beta_F I_B - \beta_F i_b \quad (13.43)$$

The signal current injected into the base of the *pnp* transistor causes a decrease in the total collector current, which is again equivalent to an increase in the signal current entering the collector. Thus, for both the *npn* and *pnp* transistors, a signal current injected into the base causes a signal current to enter the collector, and the polarities of the current-controlled source in the small-signal model are identical, as in Fig. 13.17.

### 13.5.9 AC ANALYSIS VERSUS TRANSIENT ANALYSIS IN SPICE

Differences between the ac and transient analysis modes in SPICE are a constant source of confusion to new users of electronic simulation tools. ac analysis mirrors our hand calculations with small-signal models. In SPICE ac analysis, the transistors are automatically replaced with their small-signal models, and a linear circuit analysis is then performed. On the other hand, SPICE transient analysis

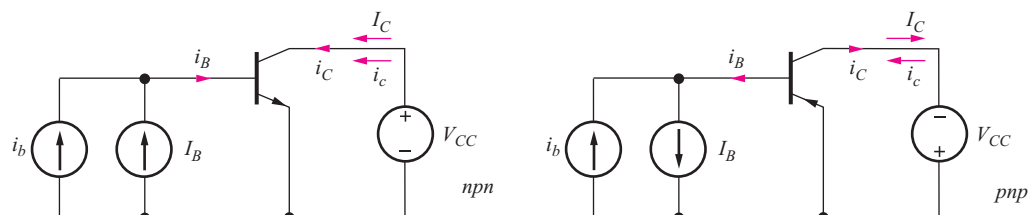


Figure 13.16 dc bias and signal currents for *npn* and *pnp* transistors.

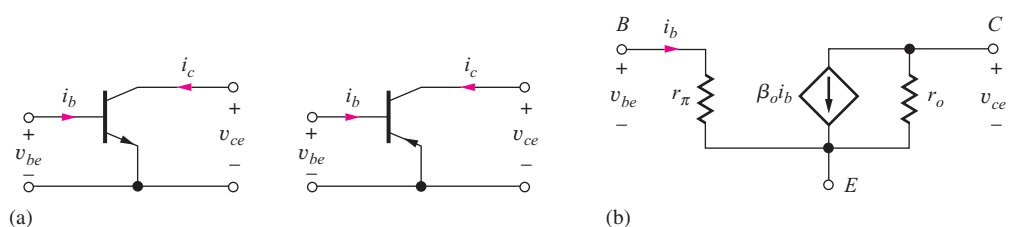


Figure 13.17 (a) Two-port notations for *npn* and *pnp* transistors. (b) The small-signal models are identical.

provides a time-domain representation similar to what we will see when we build the circuit and look at waveforms with an oscilloscope. The built-in models in SPICE attempt to fully account for the nonlinear behavior of the devices. If the small-signal limits are violated, distorted waveforms will result.

Once the circuit is converted to a linearized version, the magnitudes of the sources applied have no small-signal constraints. We typically use a value of 1 V or 1 A for convenience in ac analysis. On the other hand, this large a signal would cause significant distortion in many transient simulations.

## 13.6 THE COMMON-EMITTER (C-E) AMPLIFIER

Now we are in a position to analyze the small-signal characteristics of the complete **common-emitter (C-E) amplifier** shown in Fig. 13.18(a). The ac equivalent circuit of Fig. 13.18(b) was constructed earlier (Ex. 13.1) by assuming that the capacitors all have zero impedance at the signal frequency and the dc voltage source represents an ac ground. For simplicity, we assume that we have found the Q-point and know the values of  $I_C$  and  $V_{CE}$ . In Fig. 13.18(b), resistor  $R_B$  represents the parallel combination of the two base bias resistors  $R_1$  and  $R_2$ ,

$$R_B = R_1 \parallel R_2 \quad (13.44)$$

and  $R_E$  is eliminated by bypass capacitor  $C_3$ .

Before we can develop an expression for the voltage gain of the amplifier, the transistor must be replaced by its small-signal model as in Fig. 13.18(c). A final simplification appears in Fig. 13.18(d), in which the resistor  $R_L$  represents the total equivalent load resistance on the transistor, the parallel

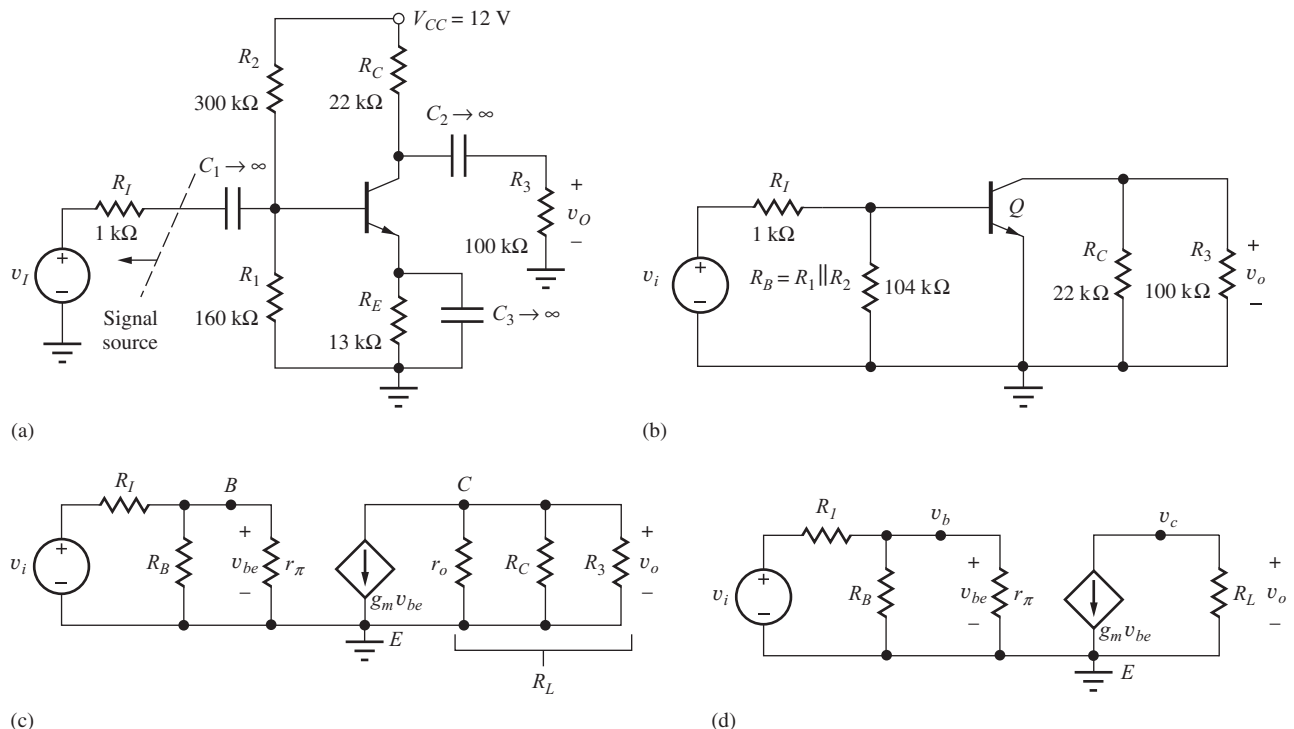


**Figure 13.18** (a) Common-emitter amplifier circuit employing a bipolar transistor. (b) ac Equivalent circuit for the common-emitter amplifier in part (a). The common-emitter connection should now be evident. (c) ac Equivalent circuit with the bipolar transistor replaced by its small-signal model. (d) Final equivalent circuit for ac analysis of the common-emitter amplifier.

combination of  $r_o$ ,  $R_C$  and  $R_3$ :

$$R_L = r_o \parallel R_C \parallel R_3 \quad (13.45)$$

In Fig. 13.18(b) through (d), the reason why this amplifier configuration is called a common-emitter amplifier is apparent. The emitter terminal represents the common connection between the amplifier input and output ports. The input signal is applied to the transistor's base, the output signal appears at the collector, and both the input and output signals are referenced to the (common) emitter terminal.

### 13.6.1 TERMINAL VOLTAGE GAIN

Now we are ready to develop an expression for the overall gain of the amplifier in Fig. 13.18 from signal source  $v_i$  to the output voltage across resistor  $R_3$ . The voltage gain can be written as

$$A_v^{CE} = \frac{v_o}{v_i} = \left( \frac{v_o}{v_b} \right) \left( \frac{v_b}{v_i} \right) = A_{vt}^{CE} \left( \frac{v_b}{v_i} \right) \quad \text{where} \quad A_{vt}^{CE} = \left( \frac{v_o}{v_b} \right) \quad (13.46)$$

$A_{vt}^{CE}$  represents the voltage gain between the base and collector terminals of the transistor, the “**terminal gain**.” We will first find expressions for terminal gain  $A_{vt}^{CE}$  as well as the input resistance at the base of the transistor. Then we can relate  $v_b$  to  $v_i$  to find the overall voltage gain.

In Fig. 13.19, the BJT is replaced with its small-signal model, and the base terminal of the transistor is driven by test source  $v_b$ . Output voltage  $v_o$  is given by

$$v_o = -g_m R_L v_b \quad (13.47)$$

or

$$A_{vt}^{CE} = \frac{v_o}{v_b} = -g_m R_L \quad (13.48)$$

The minus sign indicates that the common-emitter stage is an inverting amplifier in which the input and output are  $180^\circ$  out of phase. The gain is proportional to the product of the transistor transconductance  $g_m$  and load resistor  $R_L$ . This product places an upper bound on the gain of the amplifier, and we will encounter the  $g_m R_L$  product over and over again as we study transistor amplifiers. We will explore gain expression (Eq. 13.48) in more detail shortly.

### 13.6.2 INPUT RESISTANCE

The resistance looking into the base terminal of the transistor  $R_{iB}$  in Fig. 13.19 is simply the ratio of  $v_b$  and  $i_b$ ,

$$R_{iB} = \frac{v_b}{i_b} = r_\pi \quad (13.49)$$

The input resistance looking into the base of the transistor is equal to  $r_\pi$ .

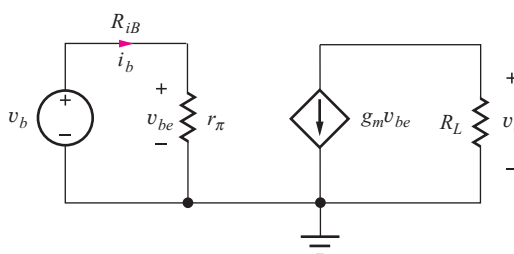


**Figure 13.19** Simplified circuit model for finding the common-emitter terminal voltage gain  $A_{vt}^{CE}$  and input resistance  $R_{iB}$ .

### 13.6.3 SIGNAL SOURCE VOLTAGE GAIN

The overall voltage gain  $A_v^{CE}$  of the amplifier, including the effect of source resistance  $R_I$ , can now be found using the input resistance and terminal gain expressions. Voltage  $v_b$  at the base of the bipolar transistor in Fig. 13.18(d) is related to  $v_i$  by

$$v_b = v_i \frac{R_B \| R_{iB}}{R_I + (R_B \| R_{iB})} \quad (13.50)$$

Combining Eqs. (13.46), (13.48), and (13.50), yields a general expression for the overall voltage gain of the common-emitter amplifier:

$$A_v^{CE} = A_{vt}^{CE} \left( \frac{v_b}{v_i} \right) = -g_m R_L \left[ \frac{R_B \| r_\pi}{R_I + (R_B \| r_\pi)} \right] \quad (13.51)$$

In this expression, we see that the overall voltage gain is equal to the terminal gain  $A_{vt}^{CE}$  reduced by the voltage division between  $R_I$  and the equivalent resistance at the base of the transistor. Terminal gain  $A_{vt}^{CE}$  places an upper limit on the voltage gain since the voltage division factor will be less than one.

## 13.7 IMPORTANT LIMITS AND MODEL SIMPLIFICATIONS

We now explore the limits to the voltage gain of common-emitter amplifiers. First, we will assume that the source resistance is small enough that  $R_I \ll R_B \| R_{iB}$  so that

$$A_v^{CE} \cong A_{vt}^{CE} = -g_m R_L = -g_m (r_o \| R_C \| R_3) \quad (13.52)$$

This approximation is equivalent to saying that the total input signal appears at the base of the transistor. Equation (13.52) states that the terminal voltage gain of the common-emitter stage is equal to the product of the transistor's transconductance  $g_m$  and load resistance  $R_L$ , and the minus sign indicates that the output voltage is “inverted” or  $180^\circ$  out of phase with respect to the input.

Equation (13.52) places an upper limit on the gain we can achieve from a common-emitter amplifier with an external load resistor. The approximations that led to Eq. (13.52) are equivalent to saying that the total input signal appears across  $r_\pi$  as shown in Fig. 13.20.

### 13.7.1 A DESIGN GUIDE FOR THE COMMON-EMITTER AMPLIFIER

In most amplifier designs,  $r_o \gg R_C$  and we try to achieve  $R_3 \gg R_C$ . For these conditions, the load resistance on the collector of the transistor is approximately equal to  $R_C$ , and Eq. (13.52) can be reduced to

$$A_v^{CE} \cong A_{vt}^{CE} = -g_m R_C = -\frac{I_C R_C}{V_T} \quad (13.53)$$

The  $I_C R_C$  product represents the dc voltage dropped across the collector resistor  $R_C$ . Assuming  $I_C R_C = \zeta V_{CC}$  with  $0 \leq \zeta \leq 1$ , and remembering that the reciprocal of  $V_T$  is  $40 \text{ V}^{-1}$ , Eq. (13.53)

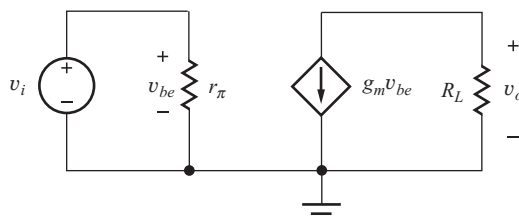


Figure 13.20 Simplified circuit corresponding to Eq. (13.52) with  $R_E = 0$ .

can be rewritten as

$$A_v^{CE} \cong -\frac{I_C R_C}{V_T} \cong -40\zeta V_{CC} \quad \text{with} \quad 0 \leq \zeta \leq 1 \quad (13.54)$$

A common design allocates 1/3 of the power supply voltage across the collector resistor. For this case,  $\zeta = 1/3$ ,  $I_C R_C = V_{CC}/3$ , and Eq. (13.54) becomes  $A_v \cong -13V_{CC}$ . To further account for the approximations that led to this result and produce a number that is easy to remember, we will use this expression for our voltage gain estimate:

$$A_v^{CE} \cong -10V_{CC} \quad \text{for} \quad R_E = 0 \quad (13.55)$$

Equation (13.55) represents our basic rule-of-thumb for the design of resistively loaded common-emitter amplifiers; that is, the magnitude of the voltage gain is approximately equal to 10 times the power supply voltage.<sup>4</sup> We need to know only the supply voltage to make a rough prediction of the gain of the common-emitter amplifier. For a C-E amplifier operating from a 15-V power supply, we estimate the gain to be  $-150$  or  $44$  dB; a C-E amplifier with a 10-V supply would be expected to produce a gain of approximately  $-100$  or  $40$  dB.

### DESIGN NOTE

The magnitude of the voltage gain of a resistively loaded common-emitter amplifier with emitter at ac ground is approximately equal to 10 times the power supply voltage.

$$A_v^{CE} \cong -10V_{CC} \quad \text{for} \quad R_E = 0$$

This result represents an excellent way to quickly check the validity of more detailed calculations. Remember that the rule-of-thumb estimate is not going to be exact, but will predict the order of magnitude of the gain, typically within a factor of two or so.

### A Comparison of $r_o$ and $R_C$

Let us formally compare  $r_o$  to  $R_C$  by multiplying each by the collector current  $I_C$ :

$$I_C r_o = V_A + V_{CE} \cong V_A \quad \text{whereas} \quad I_C R_C \cong V_{CC}/3 \quad (13.56)$$

For typical values, say  $V_A = 75$  V and  $V_{CC} = 15$  V, we see  $I_C R_C \ll I_C r_o$  and  $R_C \ll r_o$ . Therefore we also have

$$g_m R_C \ll g_m r_o \quad \text{or} \quad g_m R_C \ll \mu_f \quad (13.57)$$

From Eq. (13.57), we see we can neglect  $r_o$  any time the voltage gain is much less than  $\mu_f$ .

### DESIGN NOTE

The transistor output resistance  $r_o$  can be neglected in voltage gain calculations whenever the voltage gain is much less than  $\mu_f$ .

<sup>4</sup> For dual power supplies, the corresponding estimate would be  $A_V = -10(V_{CC} + V_{EE})$ .

### 13.7.2 UPPER BOUND ON THE COMMON-EMITTER GAIN

If we can somehow find a circuit in which both  $R_C$  and  $R_3$  are much greater than  $r_o$ <sup>5</sup>, then we achieve the most gain we can possibly get from the transistor:

$$A_v^{CE} \cong -g_m r_o = -\mu_f \quad \text{for} \quad R_C \parallel R_3 \gg r_o \quad (13.58)$$

The gain approaches the intrinsic gain of the transistor ( $\mu_f \approx 40 \text{ V}_A$ ), typically several thousand.

### 13.7.3 SMALL-SIGNAL LIMIT FOR THE COMMON-EMITTER AMPLIFIER

For small-signal operation, the magnitude of the base-emitter voltage  $v_{be}$ , developed across  $r_\pi$  in the small-signal model, must be less than 5 mV (you may wish to review Sec. 13.5.7). This voltage can be found using Eq. (13.50):

$$v_i = v_{be} \left( \frac{R_I + R_B \parallel r_\pi}{R_B \parallel r_\pi} \right) \quad (13.59)$$

Requiring  $|v_{be}|$  in Eq. (13.59) to be less than 5 mV gives

$$\begin{aligned} |v_i| &\leq 0.005 \left( 1 + \frac{R_I}{R_B \parallel r_\pi} \right) \text{ V} \\ v_i &\leq 0.005 \left( 1 + \frac{R_I}{R_B \parallel r_\pi} \right) \text{ V} \cong 0.005 \text{ V} \quad \text{for} \quad R_B \parallel r_\pi \gg R_I \end{aligned} \quad (13.60)$$

### EXAMPLE 13.3 VOLTAGE GAIN OF A COMMON-EMITTER AMPLIFIER

In this example, we find the small-signal parameters of the bipolar transistor and then calculate the voltage gain of a common-emitter amplifier.

**PROBLEM** Calculate the voltage gain of the common-emitter amplifier in Fig. 13.18 if the transistor has  $\beta_F = 100$ ,  $V_A = 75\text{V}$ , and the Q-point is (0.245 mA, 3.39 V). What is the maximum value of  $v_i$  that satisfies the small-signal assumptions? Compare the voltage gain to the common-emitter “rule-of-thumb” gain estimate and the intrinsic gain (amplification factor) of the transistor.

**SOLUTION** **Known Information and Given Data:** Common-emitter amplifier with its ac equivalent circuit given in Fig. 13.18;  $\beta_F = 100$  and  $V_A = 75 \text{ V}$ ; the Q-point is (0.245 mA, 3.39 V);  $R_L = 1 \text{ k}\Omega$ ,  $R_1 = 160 \text{ k}\Omega$ ,  $R_2 = 300 \text{ k}\Omega$ ,  $R_C = 22 \text{ k}\Omega$ ,  $R_E = 13 \text{ k}\Omega$ , and  $R_3 = 100 \text{ k}\Omega$ .

**Unknowns:** Small-signal parameters of the transistor; voltage gain  $A_v^{CE}$ ; small-signal limit for the value of  $v_i$ ; rule-of-thumb estimate; value of  $\mu_f$ .

**Approach:** Use the Q-point information to find  $r_\pi$ . Use the calculated and given values to evaluate the voltage gain expression in Eq. (13.51).

**Assumptions:** The transistor is in the active region, and  $\beta_o = \beta_F$ . The signal amplitudes are low enough to be considered as small signals. Assume  $r_o$  can be neglected.  $T = 300 \text{ K}$ .

**Analysis:** To evaluate Eq. (13.51),

$$A_v^{CE} = -g_m R_L \left[ \frac{R_B \parallel R_{iB}}{R_1 + (R_B \parallel R_{iB})} \right] \quad \text{with} \quad R_B = R_1 \parallel R_2 \quad \text{and} \quad R_{iB} = r_\pi$$

<sup>5</sup> For example, if  $R_3 = \infty$ , and  $R_C$  is replaced with a large value of inductance.

the values of the various resistors and small-signal model parameters are required. We have

$$g_m = 40I_C = 40(0.245 \text{ mA}) = 9.80 \text{ mS} \quad r_\pi = \frac{\beta_o V_T}{I_C} = \frac{100(0.025 \text{ V})}{0.245 \text{ mA}} = 10.2 \text{ k}\Omega$$

$$r_o = \frac{V_A + V_{CE}}{I_C} = \frac{75 \text{ V} + 3.39 \text{ V}}{0.245 \text{ mA}} = 320 \text{ k}\Omega \quad R_{iB} = r_\pi = 10.2 \text{ k}\Omega$$

$$R_B = R_1 \parallel R_2 = 104 \text{ k}\Omega \quad R_L = R_c \parallel R_3 = 18.0 \text{ k}\Omega$$

Using these values,

$$A_v^{CE} = -9.80 \text{ mS} (18 \text{ k}\Omega) \frac{104 \text{ k}\Omega \parallel 10.2 \text{ k}\Omega}{1 \text{ k}\Omega + (104 \text{ k}\Omega \parallel 10.2 \text{ k}\Omega)} = -159 \text{ or } 44.0 \text{ dB}$$

With the emitter bypassed,  $v_{be}$  is given by

$$\mathbf{v}_{be} = \mathbf{v}_i \left[ \frac{R_B \parallel R_{iB}}{R_I + (R_B \parallel R_{iB})} \right] = \mathbf{v}_i \frac{R_B \parallel r_\pi}{R_I + (R_B \parallel r_\pi)} = \mathbf{v}_i \frac{104 \text{ k}\Omega \parallel 10.2 \text{ k}\Omega}{1 \text{ k}\Omega + (104 \text{ k}\Omega \parallel 10.2 \text{ k}\Omega)} = 0.903 \mathbf{v}_i$$

and the small-signal limit for  $v_i$  is

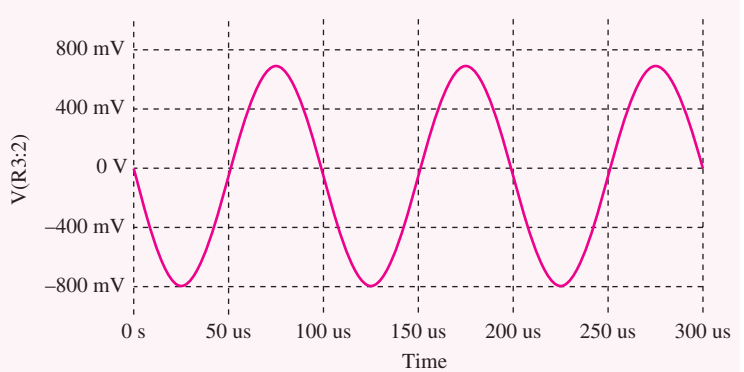
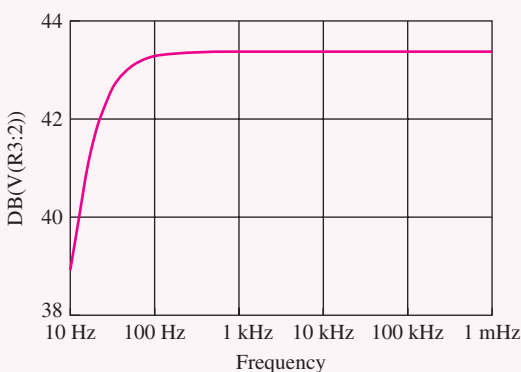
$$|v_i| \leq \frac{0.005 \text{ V}}{0.903} = 5.53 \text{ mV}$$

The rule-of-thumb estimate and intrinsic gain are

$$A_v^{CE} \cong -10(12) = -120 \quad \text{and} \quad \mu_f = 9.80 \text{ mS} (320 \text{ k}\Omega) = 3140$$

**Check of Results:** The calculated voltage gain is similar to the rule-of-thumb estimate so our calculation appears correct. Remember, the rule-of-thumb formula is meant to only be a rough estimate; it will not be exact. The gain is much less than the amplification factor, so the neglect of  $r_o$  is valid.

**Computer-Aided Analysis:** SPICE simulation yields the Q-point (0.248 mA, 3.30 V) that is consistent with the assumed value. The small difference results from  $V_A$  being included in the SPICE simulation and not in our hand calculations. An ac sweep from 10 Hz to 100 kHz with 10 frequency points/decade is used to find the region in which the capacitors are acting as short circuits, and the gain is observed to be constant at 43.4 dB above a frequency of 1 kHz. The voltage gain is slightly less than our calculated value because  $r_o$  was neglected in our calculations. A transient simulation was performed with a 5-mV, 10-kHz sine wave. The output exhibits reasonably good linearity, but the positive and negative amplitudes are slightly different, indicating some waveform distortion. Enabling the Fourier analysis capability of SPICE yields THD = 3.6%.



**Discussion:** Let us complete our discussion of the common-emitter amplifier example by exploring the impact of tolerances on circuit performance. Here we assume that  $V_{CC}$  and all the resistors have 5 percent tolerances, and  $\beta_F$  has a 25 percent tolerance. Tolerances on  $V_{BE}$  and  $V_A$  are not included for simplicity.

The results of a 500-case Monte Carlo analysis appear in the table below. The collector current varies by approximately  $\pm 15$  percent. Fortunately, the transistor's minimum collector-base voltage is  $\pm 1.11$  V, so the transistor remains in the active region. If it were found to be saturated, the circuit would need to be redesigned. The gain varies from  $-125$  to  $-169$ . Most of this variation can be traced to changes in the values of  $R_C$ ,  $R_3$ ,  $I_C$ , and  $\beta_F$ . So if each person in the class were to build this circuit in the lab, we should expect significant variations in Q-point and voltage gain from one individual's circuit to another.

Common-Emitter Amplifier 500-Case Monte Carlo Analysis Results

PARAMETER	NOMINAL VALUE	MAXIMUM VALUE	MINIMUM VALUE
$I_C$ ( $\mu A$ )	245	285	211
$V_{CE}$ (V)	3.40	4.36	2.52
$V_{CB}$ (V)	2.44	3.60	1.11
$A_v^{CE}$	-146	-169	-125
$r_\pi$ ( $k\Omega$ )	10.6	14.2	7.36

**EXERCISE:** What is the terminal voltage gain  $A_{vt}$  ( $-g_m R_L$ ) for the amplifier in Ex. 13.3? The actual gain of the amplifier was only  $-130$ . Where is most of this gain being lost?

**ANSWER:** -222; A significant portion, 42 percent, of the input signal is lost by voltage division between the source resistance  $R_I$  and the amplifier input resistance.

**EXERCISE:** (a) What is the voltage gain in the original circuit if  $\beta_F = 125$ ? (b) Suppose resistors  $R_C$  and  $R_3$  have 10 percent tolerances. What are the worst-case values of voltage gain for this amplifier? (c) Suppose the Q-point current in the original circuit increases to 0.275 mA. What are the new values of  $V_{CE}$  and the voltage gain?

**ANSWERS:** (a) -160; (b) -143, -175; (c) 2.34 V, -179

**EXERCISE:** A common-emitter amplifier similar to Fig. 13.18 is operating from a single +20-V power supply, and the emitter terminal is bypassed by capacitor  $C_3$ . The BJT has  $\beta_F = 100$  and  $V_A = 50$  V and is operating at a Q-point of (100  $\mu A$ , 10 V). The amplifier has  $R_I = 5 k\Omega$ ,  $R_B = 150 k\Omega$ ,  $R_C = 100 k\Omega$ , and  $R_3 = \infty$ . What is the voltage gain predicted using our rule of thumb estimate? What is the actual voltage gain? What is the value of  $\mu_f$  for this transistor?

**ANSWERS:** -200; -278; 2400

## DESIGN NOTE

Remember, the amplification factor  $\mu_f$  places an upper bound on the voltage gain of a single-transistor amplifier. We can't do better than  $\mu_f$ ! For the BJT,

$$\mu_f \cong 40V_A$$

For  $25 V \leq V_A \leq 100 V$ , we have  $1000 \leq \mu_f \leq 4000$ .

**EXERCISE:** Verify the bias point values used in Ex. 13.3 by directly calculating the Q-point.

**EXERCISE:** What value of saturation current  $I_S$  must be used in SPICE to achieve  $V_{BE} = 0.7$  V for  $I_C = 245 \mu\text{A}$ ? Assume a default temperature of 27°C.

**ANSWER:** 0.422 fA

## 13.8 SMALL-SIGNAL MODELS FOR FIELD-EFFECT TRANSISTORS

We now turn our attention to the small-signal model for the field-effect transistor and then use it in Sec. 13.9 to analyze the behavior of the common-source amplifier stage that is the FET version of the common-emitter amplifier. As mentioned earlier for the diode and bipolar transistor, we need to have a linearized model of the field-effect transistor that is valid for small changes in voltages and currents, in order to use our wealth of linear circuit analysis techniques to analyze the ac performance of the circuit. First, we consider the MOSFET as a three-terminal device; we then explore the changes necessary when the MOSFET is operated as a four-terminal device.

### 13.8.1 SMALL-SIGNAL MODEL FOR THE MOSFET

The small-signal model of the MOSFET is based on the two-port network representation in Fig. 13.21 with the input port variables defined as  $v_{gs}$  and  $i_g$  and the output port variables defined as  $v_{ds}$  and  $i_d$ . Rewriting Eq. (13.19) in terms of these variables yields

$$\begin{aligned}\mathbf{i}_g &= g_\pi \mathbf{v}_{gs} + g_r \mathbf{v}_{ds} \\ \mathbf{i}_d &= g_m \mathbf{v}_{gs} + g_o \mathbf{v}_{ds}\end{aligned}\quad (13.61)$$

Remember that the port variables in Fig. 13.21(a) can be considered to represent either the time-varying portion of the total voltages and currents or small changes in the total quantities.

$$\begin{aligned}v_{GS} &= V_{GS} + v_{gs} & v_{DS} &= V_{DS} + v_{ds} \\ i_G &= I_G + i_g & i_{DS} &= I_D + i_d\end{aligned}\quad (13.62)$$

The parameters in Eq. (13.61) can be written in terms of the small-signal variations or in terms of derivatives of the complete port variables, as in Eq. (13.63):

$$\begin{aligned}g_\pi &= \left. \frac{\mathbf{i}_g}{\mathbf{v}_{gs}} \right|_{\mathbf{v}_{ds}=0} = \left. \frac{\partial i_G}{\partial v_{GS}} \right|_{\text{Q-point}} & g_r &= \left. \frac{\mathbf{i}_g}{\mathbf{v}_{ds}} \right|_{\mathbf{v}_{gs}=0} = \left. \frac{\partial i_G}{\partial v_{DS}} \right|_{\text{Q-point}} \\ g_m &= \left. \frac{\mathbf{i}_d}{\mathbf{v}_{gs}} \right|_{\mathbf{v}_{ds}=0} = \left. \frac{\partial i_{DS}}{\partial v_{GS}} \right|_{\text{Q-point}} & g_o &= \left. \frac{\mathbf{i}_d}{\mathbf{v}_{ds}} \right|_{\mathbf{v}_{gs}=0} = \left. \frac{\partial i_{DS}}{\partial v_{DS}} \right|_{\text{Q-point}}\end{aligned}\quad (13.63)$$

We can evaluate these parameters by taking appropriate derivatives of the large-signal model equations for the drain current of the active region MOS transistor, as developed in Chapter 4, and repeated

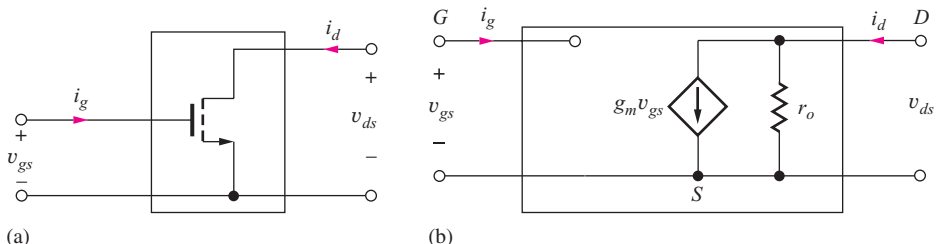


**Figure 13.21** (a) The MOSFET represented as a two-port network. (b) Small-signal model for the three-terminal MOSFET.

here in Eq. (13.64).

$$i_D = \frac{K_n}{2}(v_{GS} - V_{TN})^2(1 + \lambda v_{DS}) \quad (13.64)$$

for  $v_{DS} \geq v_{GS} - V_{TN}$ , and  $i_G = 0$ , where  $K_n = \mu_n C_{ox}(W/L)$ .

$$\begin{aligned} g_\pi &= \left. \frac{\partial i_G}{\partial v_{GS}} \right|_{v_{DS}} = 0 \quad \text{and} \quad g_r = \left. \frac{\partial i_G}{\partial v_{DS}} \right|_{v_{GS}} = 0 \\ g_m &= \left. \frac{\partial i_{DS}}{\partial v_{GS}} \right|_{\text{Q-point}} = K_n(V_{GS} - V_{TN})(1 + \lambda V_{DS}) = \frac{2I_D}{V_{GS} - V_{TN}} \\ g_o &= \left. \frac{\partial i_{DS}}{\partial v_{DS}} \right|_{\text{Q-point}} = \lambda \frac{K_n}{2}(V_{GS} - V_{TN})^2 = \frac{\lambda I_D}{1 + \lambda V_{DS}} = \frac{I_D}{\frac{1}{\lambda} + V_{DS}} \end{aligned} \quad (13.65)$$

Because  $i_G$  is always zero and therefore independent of  $v_{GS}$  and  $v_{DS}$ ,  $g_\pi$  and  $g_r$  are both zero. Remembering that the gate terminal is insulated from the channel by the gate oxide, we can reasonably expect that the input resistance ( $1/g_\pi$ ) of the transistor is infinite.

As for the bipolar transistor,  $g_m$  is called the transconductance, and  $1/g_o$  represents the output resistance of the transistor.

<b>Transconductance:</b>	$g_m = \frac{I_D}{\frac{V_{GS} - V_{TN}}{2}} \quad (13.66)$
<b>Output resistance:</b>	
$r_o = \frac{1}{g_o} = \frac{\frac{1}{\lambda} + V_{DS}}{I_D} \cong \frac{1}{\lambda I_D}$	

The small-signal circuit model for the MOSFET resulting from Eqs. (13.65) and (13.66) appears in Fig. 13.21(b) and contains only the controlled current source and output resistance.

From Eq. (13.66), we see that the values of the small-signal parameters are directly controlled by the design of the Q-point. The form of the equations for  $g_m$  and  $r_o$  of the MOSFET directly mirrors that of the BJT. However, one-half the internal gate drive  $(V_{GS} - V_{TN})/2$  replaces the thermal voltage  $V_T$  in the transconductance expression, and  $1/\lambda$  replaces the Early voltage in the output resistance expression. The value of  $V_{GS} - V_{TN}$  is often a volt or more in MOSFET circuits, whereas  $V_T = 0.025$  V at room temperature. Thus, for a given operating current, the MOSFET can be expected to have a much smaller transconductance than the BJT. However, the value of  $1/\lambda$  is similar to  $V_A$ , so the output resistances are similar for a given operating point  $(I_D, V_{DS}) = (I_C, V_{CE})$ . Here, and similar to the BJT case, drain-source voltage  $V_{DS}$  is typically much less than  $1/\lambda$ , so we can simplify the expression for the output resistance to  $r_o \cong 1/\lambda I_D$ .

The actual dependence of transconductance  $g_m$  on current is not shown explicitly by Eq. (13.66) because  $I_D$  is a function of  $(V_{GS} - V_{TN})$ . Rewriting the expression for  $g_m$  from Eq. (13.65) yields

$$\begin{aligned} g_m &= K_n(V_{GS} - V_{TN})(1 + \lambda V_{DS}) = \sqrt{2K_n I_D (1 + \lambda V_{DS})} \\ g_m &\cong K_n(V_{GS} - V_{TN}) \quad \text{or} \quad g_m \cong \sqrt{2K_n I_D} \end{aligned} \quad (13.67)$$

where the simplifications require  $\lambda V_{DS} \ll 1$ .

Here we see two other important differences between the MOSFET and BJT. The MOSFET transconductance increases only as the square root of drain current, whereas the BJT transconductance is directly proportional to collector current. In addition, the MOSFET transconductance is dependent on the geometry of the transistor because  $K_n \propto W/L$ , whereas the transconductance of the BJT is geometry-independent. It is also worth noting that the current gain of the MOSFET is

infinite. Since the value of  $r_\pi = (1/g_\pi)$  is infinite for the MOSFET, the “current gain”  $\beta_o = g_m r_\pi$  equals infinity as well.

### 13.8.2 INTRINSIC VOLTAGE GAIN OF THE MOSFET

Another important difference between the BJT and MOSFET is the variation of the intrinsic voltage gain  $\mu_f$  with operating point. Using Eq. (13.66) for  $g_m$  and  $r_o$ , we find that the intrinsic voltage gain becomes

$$\mu_f = g_m r_o = \frac{\frac{1}{\lambda} + V_{DS}}{\left(\frac{V_{GS} - V_{TN}}{2}\right)} \quad \text{and} \quad \mu_f \cong \frac{2}{\lambda(V_{GS} - V_{TN})} \cong \frac{1}{\lambda} \sqrt{\frac{2K_n}{I_D}} \quad (13.68)$$

for  $\lambda V_{DS} \ll 1$ .

The value of  $\mu_f$  for the MOSFET decreases as the operating current increases. Thus the larger the operating current of the MOSFET, the smaller its voltage gain capability. In contrast, the intrinsic gain of the BJT is independent of operating point. This is an extremely important difference to keep in mind, particularly during the design process.

Table 13.2 displays examples of the values of the MOSFET small-signal parameters for a variety of operating points. Just as for the bipolar transistor, the values of  $g_m$  and  $r_o$  can each be varied over many orders of magnitude through the choice of Q-point. By comparing the results in Tables 13.1 and 13.2 we see that  $g_m$ ,  $r_o$ , and  $\mu_f$  of the MOSFET are all similar to those of the bipolar transistor at low currents. However, as the drain current increases, the value of  $g_m$  of the MOSFET does not grow as rapidly as for the bipolar transistor, and  $\mu_f$  drops significantly. This particular MOSFET has a significantly lower intrinsic gain than the BJT for currents greater than a few tens of microamperes.

**EXERCISES:** (a) Calculate the values of  $g_m$ ,  $r_o$ , and  $\mu_f$  for a MOSFET transistor with  $K_n = 1 \text{ mA/V}^2$  and  $\lambda = 0.02 \text{ V}^{-1}$  operating at Q-points of  $(250 \mu\text{A}, 5 \text{ V})$  and  $(5 \text{ mA}, 10 \text{ V})$ . (b) Use graphical analysis to find values of  $g_m$  and  $r_o$  at the Q-point for the transistor in Fig. 13.2(b).

**ANSWERS:**  $7.42 \times 10^{-4} \text{ S}$ ,  $220 \text{ k}\Omega$ ,  $163$ ;  $3.46 \times 10^{-3} \text{ S}$ ,  $12.0 \text{ k}\Omega$ ,  $41.5$ ;  $1.3 \times 10^{-3} \text{ S}$ ,  $\infty$

### 13.8.3 DEFINITION OF SMALL-SIGNAL OPERATION FOR THE MOSFET

The limits of linear operation of the MOSFET can be explored using the simplified drain-current expression ( $\lambda = 0$ ) for the MOSFET in the active region:

$$i_D = \frac{K_n}{2}(v_{GS} - V_{TN})^2 \quad \text{for} \quad v_{DS} \geq v_{GS} - V_{TN} \quad (13.69)$$

**TABLE 13.2**

MOSFET Small-Signal Parameters versus Current:  $K_n = 1 \text{ mA/V}^2$ ,  $\lambda = 0.0133 \text{ V}^{-1}$ ,  $V_{DS} = 10 \text{ V}$

$I_D$	$g_m$	$r_\pi$	$r_o$	$\mu_f$
$1 \mu\text{A}$	$4.76 \times 10^{-5} \text{ S}$	$\infty$	$85.2 \text{ M}\Omega$	4060
$10 \mu\text{A}$	$1.51 \times 10^{-4} \text{ S}$	$\infty$	$8.52 \text{ M}\Omega$	1280
$100 \mu\text{A}$	$4.76 \times 10^{-4} \text{ S}$	$\infty$	$852 \text{ k}\Omega$	406
$1 \text{ mA}$	$1.51 \times 10^{-3} \text{ S}$	$\infty$	$85.2 \text{ k}\Omega$	128
$10 \text{ mA}$	$4.76 \times 10^{-3} \text{ S}$	$\infty$	$8.52 \text{ k}\Omega$	40

Expanding this expression using  $v_{GS} = V_{GS} + v_{gs}$  and  $i_D = I_D + i_d$  gives

$$I_D + i_d = \frac{K_n}{2} [(V_{GS} - V_{TN})^2 + 2v_{gs}(V_{GS} - V_{TN}) + v_{gs}^2] \quad (13.70)$$

Recognizing that the dc drain current is equal to  $I_D = (K_n/2)(V_{GS} - V_{TN})^2$  and subtracting this term from both sides of Eq. (13.70) yields an expression for signal current  $i_d$ :

$$i_d = \frac{K_n}{2} [2v_{gs}(V_{GS} - V_{TN}) + v_{gs}^2] \quad (13.71)$$

For linearity,  $i_d$  must be directly proportional to  $v_{gs}$ , which is achieved for

$$v_{gs}^2 \ll 2v_{gs}(V_{GS} - V_{TN}) \quad \text{or} \quad v_{gs} \ll 2(V_{GS} - V_{TN}) \quad (13.72)$$

Using a factor of 10 to satisfy the inequality gives

$$v_{gs} \leq 0.2(V_{GS} - V_{TN}) \quad (13.73)$$

Because the MOSFET can easily be biased with  $(V_{GS} - V_{TN})$  equal to several volts, we see that it can handle much larger values of  $v_{gs}$  than the values of  $v_{be}$  corresponding to the bipolar transistor. This is another fundamental difference between the MOSFET and BJT and can be very important in circuit design, particularly in RF amplifiers, for example.

Now let us explore the change in drain current that corresponds to small-signal operation. Using Eq. (13.73),

$$\frac{i_d}{I_D} = \frac{g_m v_{gs}}{I_D} = \frac{0.2(V_{GS} - V_{TN})}{\frac{V_{GS} - V_{TN}}{2}} \leq 0.4 \quad (13.74)$$

A change of 0.2 ( $V_{GS} - V_{TN}$ ) in  $v_{GS}$  corresponds to a 40 percent deviation in the drain and source currents from the Q-point values.

**EXERCISE:** A MOSFET transistor with  $K_n = 2.0 \text{ mA/V}^2$  and  $\lambda = 0$  is operating at a Q-point of (25 mA, 10 V). What is the largest value of  $v_{gs}$  that corresponds to a small signal? If a BJT is biased at the same Q-point, what is the largest value of  $v_{be}$  that corresponds to a small signal?

**ANSWERS:** 1 V; 0.005 V

### 13.8.4 BODY EFFECT IN THE FOUR-TERMINAL MOSFET

When the body terminal of the MOSFET is not connected to the source terminal, as in Fig. 13.22(a), an additional controlled source must be introduced into the small-signal model. Referring to the simplified drain-current expression for the MOSFET from Sec. 4.2.9:

$$i_D = \frac{K_n}{2}(v_{GS} - V_{TN})^2 \quad \text{and} \quad V_{TN} = V_{TO} + \gamma(\sqrt{v_{SB} + 2\phi_F} - \sqrt{2\phi_F}) \quad (13.75)$$

We recognize that the drain current is dependent on the threshold voltage, and the threshold voltage changes as  $v_{SB}$  changes. Thus, a **back-gate transconductance** can be defined:

$$g_{mb} = \left. \frac{\partial i_D}{\partial v_{BS}} \right|_{\text{Q-point}} = - \left. \frac{\partial i_D}{\partial v_{SB}} \right|_{\text{Q-point}} = - \left( \frac{\partial i_D}{\partial V_{TN}} \right) \left( \frac{\partial V_{TN}}{\partial v_{SB}} \right) \Big|_{\text{Q-point}} \quad (13.76)$$

Evaluating the derivative terms in brackets,

$$\left. \frac{\partial i_D}{\partial V_{TN}} \right|_{\text{Q-point}} = -K_n(V_{GS} - V_{TN}) = -g_m \quad \text{and} \quad \left. \frac{\partial V_{TN}}{\partial v_{SB}} \right|_{\text{Q-point}} = \frac{\gamma}{2\sqrt{V_{SB} + 2\phi_F}} = \eta \quad (13.77)$$

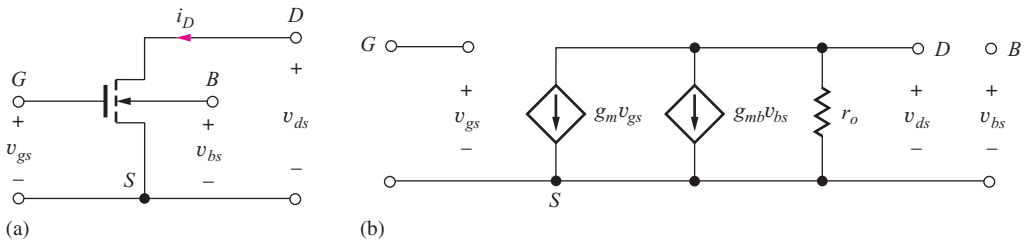


**Figure 13.22** (a) MOSFET as a four-terminal device. (b) Small-signal model for the four-terminal MOSFET.

in which  $\eta$  represents the **back-gate transconductance parameter**. Combining Eqs. (13.77) yields

$$g_{mb} = -(-g_m)\eta \quad \text{or} \quad g_{mb} = +\eta g_m \quad (13.78)$$

for typical values of  $\gamma$  and  $V_{SB}$ ,  $0 \leq \eta \leq 1$ .

We also need to explore the question of whether there is a conductance connected from the bulk terminal to the other terminals. However, the bulk terminal represents a reverse-biased diode between the bulk and channel. Using our small-signal model for the diode, Eq. (13.15), we see that

$$\left. \frac{\partial i_B}{\partial v_{BS}} \right|_{\text{Q-point}} = \frac{I_D + I_S}{V_T} \cong 0 \quad (13.79)$$

because  $I_D \cong -I_S$  for the reverse-biased diode. Thus, there is no conductance indicated between the bulk and source or drain terminals in the small-signal model.

The resulting small-signal model for the four-terminal MOSFET is given in Fig. 13.22(b), in which a second voltage-controlled current source has been added to model the back-gate transconductance  $g_{mb}$ .

**EXERCISE:** Calculate the values of  $\eta$  for a MOSFET transistor with  $\gamma = 0.75 \text{ V}^{0.5}$  and  $2\phi_F = 0.6 \text{ V}$  for  $V_{SB} = 0$  and  $V_{SB} = 3 \text{ V}$ .

**ANSWERS:** 0.48, 0.20

### 13.8.5 SMALL-SIGNAL MODEL FOR THE PMOS TRANSISTOR

Just as was the case for the *pnp* and *npn* transistors, the small-signal model for the PMOS transistor is identical to that of the NMOS device. The circuits in Fig. 13.23 should help reinforce this result.

In Fig. 13.23, the NMOS and PMOS transistors are each biased by the dc voltage source  $V_{GG}$ , establishing Q-point current  $I_D$ . In each case, a signal voltage  $v_{gg}$  is added in series with  $V_{GG}$  so

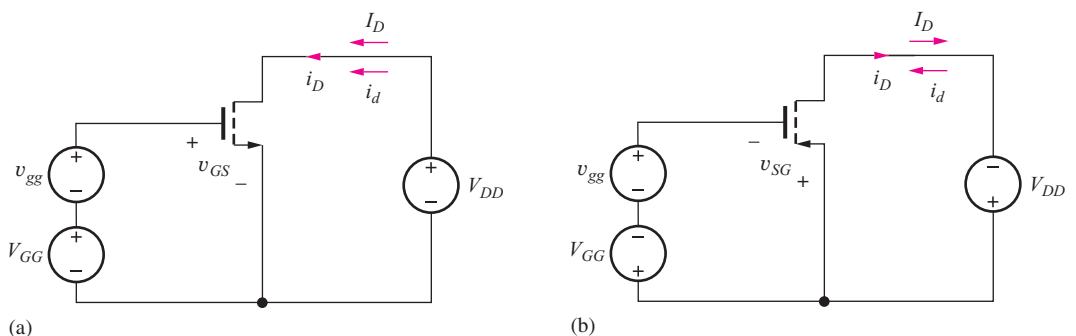


**Figure 13.23** dc Bias and signal currents for (a) NMOS and (b) PMOS transistors.

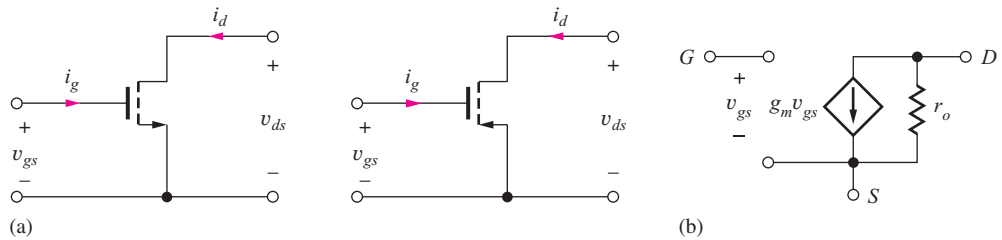


**Figure 13.24** (a) NMOS and PMOS transistors. (b) The small-signal models are identical.

that a positive value of  $v_{gg}$  causes the gate-to-source voltage of each transistor to increase. For the NMOS transistor, the total gate-to-source voltage and drain current are

$$v_{GS} = V_{GG} + v_{gg} \quad \text{and} \quad i_{DS} = I_D + i_d \quad (13.80)$$

and an increase in  $v_{gg}$  causes an increase in current into the drain terminal. For the PMOS transistor,

$$v_{SG} = V_{GG} - v_{gg} \quad \text{and} \quad i_D = I_D - i_d \quad (13.81)$$

A positive signal voltage  $v_{gg}$  reduces the source-to-gate voltage of the PMOS transistor and causes a decrease in the total current exiting the drain terminal. This reduction in total current is equivalent to an increase in the signal current entering the drain.

Thus, for both the NMOS and PMOS transistors, an increase in the value of  $v_{GS}$  causes an increase in current into the drain, and the polarities of the voltage-controlled current source in the small-signal model are identical, as depicted in Fig. 13.24.

### 13.8.6 SMALL-SIGNAL MODEL FOR THE JUNCTION FIELD-EFFECT TRANSISTOR

The drain-current expressions for the JFET and MOSFET can be written in essentially identical form (see Prob. 13.155), so we should not be surprised that the small-signal models also have the same form. For small-signal analysis, we represent the JFET as the two-port network in Fig. 13.25. The small-signal parameters can be determined from the large-signal model given in Chapter 4 for the drain current of the JFET operating in the pinch-off region:

$$i_D = I_{DSS} \left[ 1 - \frac{v_{GS}}{V_P} \right]^2 [1 + \lambda v_{DS}] \quad \text{for } v_{DS} \geq v_{GS} - V_P \quad (13.82)$$

The total gate current  $i_G$  represents the current of the gate-to-channel diode, which we express in terms of the gate-to-source voltage  $v_{GS}$  and saturation current  $I_{SG}$ :

$$i_G = I_{SG} \left[ \exp \left( \frac{v_{GS}}{V_T} \right) - 1 \right] \quad (13.83)$$

Once again using the derivative formulation from Eq. (13.63):

$$g_\pi = \left. \frac{\partial i_G}{\partial v_{GS}} \right|_{Q\text{-point}} = \frac{I_G + I_{SG}}{V_T}$$

$$g_r = \left. \frac{\partial i_G}{\partial v_{DS}} \right|_{Q\text{-point}} = 0$$

$$g_m = y_{21} = \left. \frac{\partial i_D}{\partial v_{GS}} \right|_{Q\text{-point}} = 2 \frac{I_{DSS}}{-V_P} \left[ 1 - \frac{V_{GS}}{V_P} \right] [1 + \lambda V_{DS}] = \frac{I_D}{V_{GS} - V_P} \frac{2}{2}$$

**Figure 13.25** The JFET as a two-port network.

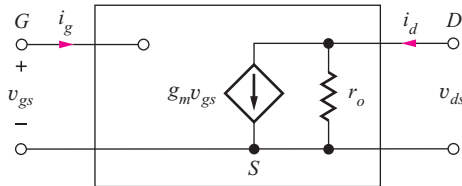


Figure 13.26 Small-signal model for the JFET.

Alternatively,

$$g_m = \frac{2}{|V_P|} \sqrt{I_{DSS} I_D (1 + \lambda V_{DS})} \cong \frac{2}{|V_P|} \sqrt{I_{DSS} I_D} \cong 2 \frac{I_{DSS}}{V_P^2} [V_{GS} - V_P] \quad (13.84)$$

$$g_o = \left. \frac{\partial i_D}{\partial v_{DS}} \right|_{Q\text{-point}} = \lambda I_{DSS} \left[ 1 - \frac{V_{GS}}{V_P} \right]^2 = \frac{\lambda I_D}{1 + \lambda V_{DS}} = \frac{I_D}{\frac{1}{\lambda} + V_{DS}}$$

Because the JFET is normally operated with the gate junction reverse-biased,

$$I_G = -I_{SG} \quad \text{and} \quad r_\pi = \infty \quad (13.85)$$

Thus, the small-signal model for the JFET in Fig. 13.26 is identical to that of the MOSFET, including the formulas used to express  $g_m$  and  $r_o$  when  $V_{TN}$  is replaced by  $V_P$ .

As a result, the definition of a small signal and the expression for the amplification factor  $\mu_f$  are also similar to those of the MOSFET:

$$v_{gs} \leq 0.2(V_{GS} - V_P)$$

and

$$\mu_f = g_m r_o = 2 \frac{\frac{1}{\lambda} + V_{DS}}{V_{GS} - V_P} \cong \frac{2}{\lambda |V_P|} \sqrt{\frac{I_{DSS}}{I_D}} \quad (13.86)$$

**EXERCISES:** Calculate the values of  $g_m$ ,  $r_o$ , and  $\mu_f$  for a JFET with  $I_{DSS} = 5$  mA,  $V_P = -2$  V, and  $\lambda = 0.02$  V $^{-1}$  if it is operating at a Q-point of (2 mA, 5 V). What is the largest value of  $v_{gs}$  that can be considered to be a small signal?

**ANSWERS:**  $3.32 \times 10^{-3}$  S, 27.5 k $\Omega$ , 91; 0.24 V

## 13.9 SUMMARY AND COMPARISON OF THE SMALL-SIGNAL MODELS OF THE BJT AND FET

Table 13.3 is a side-by-side comparison of the small-signal models of the bipolar junction transistor and the field-effect transistor; the table has been constructed to highlight the similarities and differences between the two types of devices.

The transconductance of the BJT is directly proportional to operating current, whereas that of the FET increases only with the square root of current. Both can be represented as the drain current divided by a characteristic voltage:  $V_T$  for the BJT and  $(V_{GS} - V_{TN})/2$  for the MOSFET.

The input resistance of the bipolar transistor is set by the value of  $r_\pi$ , which is inversely proportional to the Q-point current and can be quite small at even moderate currents (1 to 10 mA). On the other hand, the input resistance of the FETs is extremely high, approaching infinity.

**TABLE 13.3**

Small-Signal Parameter Comparison

PARAMETER	BIPOLAR TRANSISTOR	MOSFET	JFET
Transconductance $g_m$	$\frac{I_C}{V_T}$	$\frac{2I_D}{V_{GS} - V_{TN}} \cong \sqrt{2K_n I_D}$	$\frac{2I_D}{V_{GS} - V_P} \cong \frac{2}{ V_P }$
Input resistance	$r_\pi = \frac{\beta_o}{g_m} = \frac{\beta_o V_T}{I_C}$	$\infty$	$\infty$
Output resistance $r_o$	$\frac{V_A + V_{CE}}{I_C} \cong \frac{V_A}{I_C}$	$\frac{\frac{1}{\lambda} + V_{DS}}{I_D} \cong \frac{1}{\lambda I_D}$	$\frac{\frac{1}{\lambda} + V_{DS}}{I_D} \cong \frac{1}{\lambda I_D}$
Intrinsic voltage gain $\mu_f$	$\frac{V_A + V_{CE}}{V_T} \cong \frac{V_A}{V_T}$	$\frac{2 \left( \frac{1}{\lambda} + V_{DS} \right)}{V_{GS} - V_{TN}} \cong \frac{1}{\lambda} \sqrt{\frac{2K_n}{I_D}}$	$\frac{2 \left( \frac{1}{\lambda} + V_{DS} \right)}{V_{GS} - V_P} \cong \frac{2}{\lambda  V_P } \sqrt{\frac{I_{DSS}}{I_D}}$
Small-signal requirement	$v_{be} \leq 0.005 \text{ V}$	$v_{gs} \leq 0.2(V_{GS} - V_{TN})$	$v_{gs} \leq 0.2(V_{GS} - V_P)$
dc i-v active region expressions for use with Table 13.3:			
BJT:	$I_C = I_S \left[ \exp \left( \frac{V_{BE}}{V_T} \right) - 1 \right] \left[ 1 + \frac{V_{CE}}{V_A} \right]$	$V_T = \frac{kT}{q}$	
MOSFET:	$I_D = \frac{K_n}{2} (V_{GS} - V_{TN})^2 (1 + \lambda V_{DS})$	$K_n = \mu_n C_{ox} \frac{W}{L}$	
JFET:	$I_D = I_{DSS} \left( 1 - \frac{V_{GS}}{V_P} \right)^2 (1 + \lambda V_{DS})$		

The expressions for the output resistances of the transistors are almost identical, with the parameter  $1/\lambda$  in the FET taking the place of the Early voltage  $V_A$  of the BJT. The value of  $1/\lambda$  is similar to  $V_A$ , so the output resistances can be expected to be similar in value for comparable operating currents.

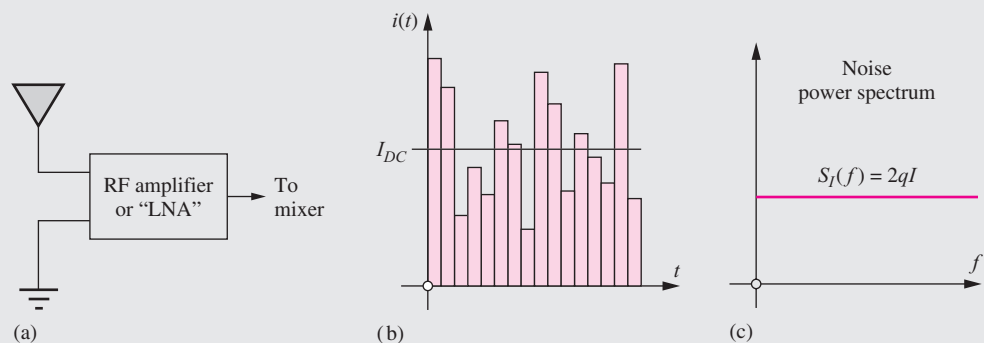
The intrinsic voltage gain of the BJT is nearly independent of operating current and has a typical value of several thousand at room temperature. In contrast,  $\mu_f$  for the FETs is inversely proportional to the square root of operating current and decreases as the Q-point current is raised. At very low currents,  $\mu_f$  of the FETs can be similar to that of the BJT, but in normal operation it is often much smaller and can even fall below 1 for high currents (see Prob. 13.86).

Small-signal operation is dependent on the size of the base-emitter voltage of the BJT or gate-source voltage of the field-effect transistor. The magnitude of voltage that corresponds to small-signal operation can be significantly different for these two devices. For the BJT,  $v_{be}$  must be less than 5 mV. This value is indeed small, and it is independent of Q-point. In contrast, the FET requirement is  $v_{gs} \leq 0.2(V_{GS} - V_{TN})$  or  $0.2(V_{GS} - V_P)$ , which is dependent on bias point and can be designed to be as much as a volt or more.

This discussion highlighted the similarities and differences between the bipolar and field-effect transistors. An understanding of Table 13.3 is extremely important to the design of analog circuits. As we study single and multistage amplifier design in the coming sections and chapters, we will note the effect of these differences and relate them to our circuit designs.

### Noise in Electronic Circuits

The linear signal-level limitations of transistors that we have introduced in this chapter may seem small, but we often deal with signal levels that are far below even the 5-mV  $v_{be}$  limit for the BJT. For example, the radio frequency signals from antennas on our cell phones can be in the microvolt range, and high frequency communications receivers often have minimum detectable signals of less than 0.1  $\mu\text{V}$ ! The minimum detectable signals are set by the noise in the RF amplifiers connected to the antennas. These amplifiers are often referred to as low noise amplifiers, or LNAs, in which the noise actually comes from the transistors and resistors that make up the circuit.



We often think that the dc voltages and currents that we calculate or measure with a dc voltmeter are constants, but they really represent averages of noisy signals. For example, the currents that we encounter in this text are made up of very large numbers of small current pulses due to individual electrons (e.g.,  $1 \mu\text{A} = 6.3 \times 10^{12}$  electrons/sec). The current is constantly fluctuating or varying about the dc value as shown in the graph here, and these fluctuations represent one of the sources of noise in electronic devices. If we somehow listened to this current, it would sound much like rain on a tin roof. The background "din" from the rain is actually made up of the noise from a huge number of individual drops. This form of electronic noise is termed "shot" noise.

We model the noise in electron devices by adding noise voltage and current generators to our circuits. The noise generators represent random signals with zero mean and are therefore characterized by either their rms or mean square values. For example, both the base and collector currents in the bipolar transistor produce shot noise, and the noise is modeled by

$$\overline{i_{cn}^2} = \overline{[i_C(t) - I_C]^2} = 2qI_C B \quad \text{and} \quad \overline{i_{bn}^2} = \overline{[i_B(t) - I_B]^2} = 2qI_B B$$

These sources are referred to as "white noise" sources in which the noise power spectrum is independent of frequency. The mean square value of the noise current is directly proportional to the dc current and depends upon the bandwidth  $B$  (Hz) associated with the measurement. For instance, the rms value of the collector shot noise for  $I_C = 1 \text{ mA}$  and  $B = 1 \text{ kHz}$  would be

$$\sqrt{\overline{i_{cn}^2}} = \sqrt{2(1.6 \times 10^{-19})(10^{-3})(10^3)} = 0.566 \text{ nA}$$

In addition to shot noise, resistors and other resistive elements in electronic circuits exhibit noise due to the thermal agitation of electrons in the resistor. This "thermal" noise or "Johnson" noise is modeled by a noise voltage source in series with the resistor as shown for the base

resistance of the BJT in the figure below (also see Chapter 16). The mean square value of the noise voltage associated with a resistor  $R$  is given by

$$\overline{v_{rn}^2} = 4kT RB$$

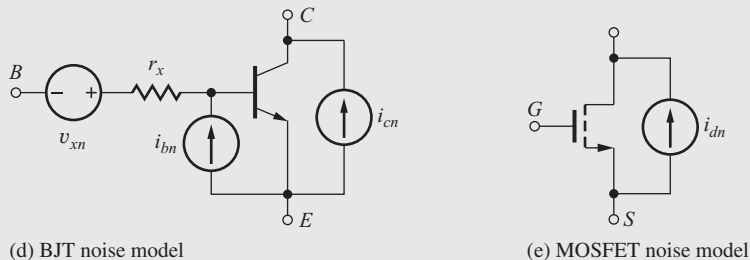
where  $k$  is Boltzmann's constant,  $T$  is absolute temperature, and  $B$  is the bandwidth of interest. For a 1-k $\Omega$  resistor operating at 300 K with  $B = 1$  kHz,

$$\sqrt{\overline{v_{rn}^2}} = \sqrt{4(1.38 \times 10^{-23})(300)(10^3)(10^3)} = 0.129 \mu\text{V}$$

Remembering that the channel region of the MOSFET is really a voltage-controlled resistor, we can model the thermal noise of the channel by a (Norton equivalent) current source whose mean square value is

$$\overline{i_{dn}^2} = \frac{8}{3}kT g_m B$$

The final figure presents our basic transistor noise models. For the BJT, current sources are added to model the shot noise of both the base and collector currents, and the thermal noise



(d) BJT noise model

(e) MOSFET noise model

of the base resistance is also included. For the MOSFET, the thermal noise of the channel is modeled by an equivalent noise current source. These noise models are built into SPICE, and NOISE is one of the analysis options available. For further information on how to make noise calculations and use the noise analysis capability in SPICE, see the MCD website.



## 13.10 THE COMMON-SOURCE AMPLIFIER

Now we are in a position to analyze the small-signal characteristics of the **common-source (C-S) amplifier** shown in Fig. 13.27(a), which uses an enhancement-mode  $n$ -channel MOSFET ( $V_{TN} > 0$ ) in a four-resistor bias network. The ac equivalent circuit of Fig. 13.27(b) is constructed by assuming that the capacitors all have zero impedance at the signal frequency and that the dc voltage sources represent ac grounds. In Fig. 13.27(c), the transistor has been replaced with its small-signal model. Bias resistors  $R_1$  and  $R_2$  appear in parallel and are combined into gate resistor  $R_G$ , and  $R_L$  represents the parallel combination of  $R_D$ ,  $R_3$  and  $r_o$ . In subsequent analysis, we will assume that the voltage gain is much less than the intrinsic voltage gain of the transistor so we can neglect transistor output resistance  $r_o$ . For simplicity at this point, we assume that we have found the Q-point and know the values of  $I_D$  and  $V_{DS}$ .

In Fig. 13.27(b) through (d), the common-source nature of this amplifier should be apparent. The input signal is applied to the transistor's gate terminal, the output signal appears at the drain, and both the input and output signals are referenced to the (common) source terminal. Note that the small-signal models for the MOSFET and BJT are virtually identical at this step, except that  $r_\pi$  is replaced by an open circuit for the MOSFET. Note again that on the signal portion of the input signal appears in the ac circuit model.

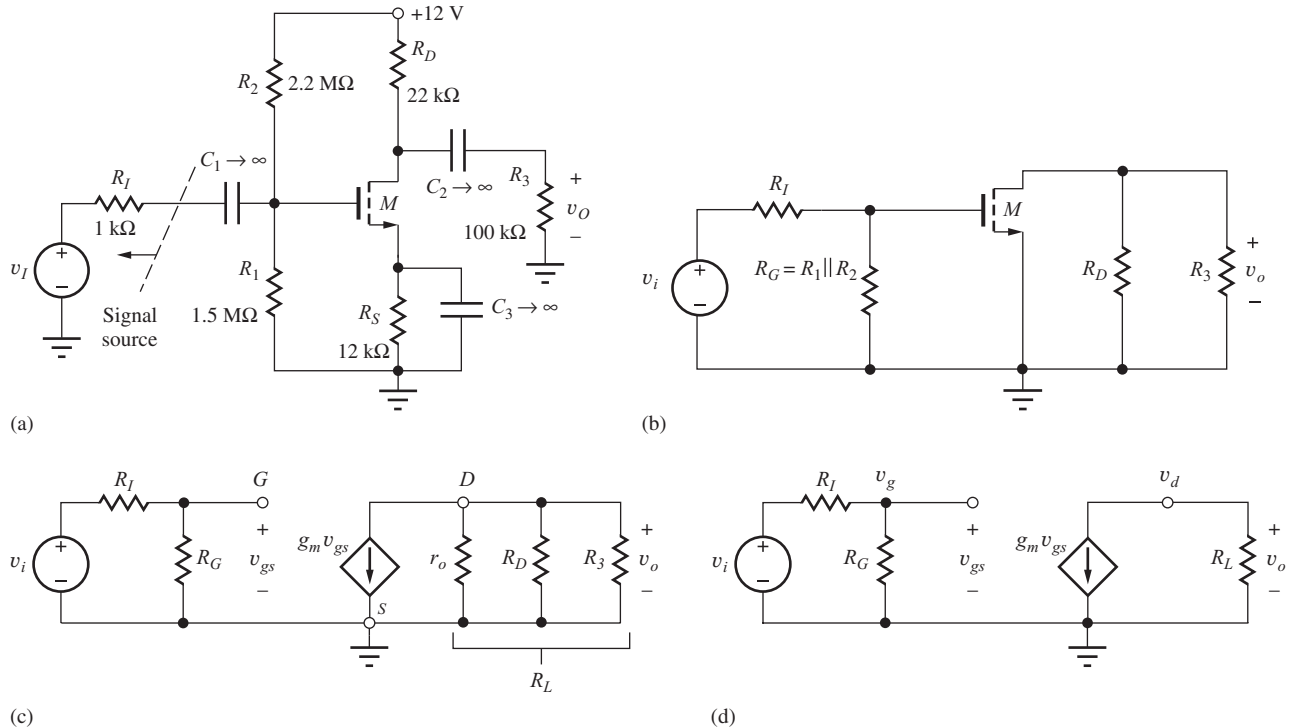


**Figure 13.27** (a) Common-source amplifier circuit employing a MOSFET. (b) ac equivalent circuit for common-source amplifier in part (a). The common-source connection is now apparent. (c) ac Equivalent circuit with the MOSFET replaced by its small-signal model. (d) Final equivalent circuit for ac analysis of the common-source amplifier.

Our first goal is to develop an expression for the voltage gain  $A_v^{CS}$  of the circuit in Fig. 13.27(a) from the source  $v_s$  to the output  $v_o$ . As with the BJT, we will first find the terminal voltage gain  $A_{vt}^{CS}$  between the gate and drain terminals of the transistor. Then, we will use the terminal gain expression to find the gain of the overall amplifier.

### 13.10.1 COMMON-SOURCE TERMINAL VOLTAGE GAIN

Starting with the circuit in Fig. 13.27(d), the terminal voltage gain is defined as

$$A_{vt}^{CS} = \frac{\mathbf{v}_d}{\mathbf{v}_g} = \frac{\mathbf{v}_o}{\mathbf{v}_g} \quad \text{where} \quad \mathbf{v}_o = -g_m \mathbf{v}_{gs} R_L \quad \text{and} \quad A_{vt}^{CS} = -g_m R_L \quad (13.87)$$

### 13.10.2 SIGNAL SOURCE VOLTAGE GAIN FOR THE COMMON-SOURCE AMPLIFIER

Now we can find the overall gain from source  $v_i$  to the voltage across  $R_L$ . The overall gain can be written as

$$A_v^{CS} = \frac{\mathbf{v}_o}{\mathbf{v}_i} = \left( \frac{\mathbf{v}_o}{\mathbf{v}_g} \right) \left( \frac{\mathbf{v}_g}{\mathbf{v}_i} \right) = A_{vt}^{CS} \left( \frac{\mathbf{v}_g}{\mathbf{v}_i} \right) \quad \text{where} \quad \mathbf{v}_g = \mathbf{v}_i \frac{R_G}{R_G + R_I} \quad (13.88)$$

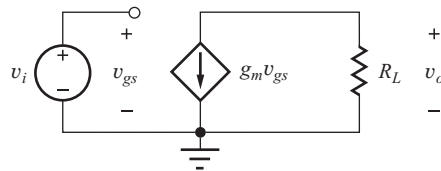


**Figure 13.28** Simplified circuit for  $R_G \gg R_I$  and  $R_s = 0$ .

$v_g$  is related to  $v_i$  by the voltage divider formed by  $R_G$  and  $R_I$ . Combining Eqs. (13.87) and (13.88) yields a general expression for the voltage gain of the common-source amplifier:

$$A_v^{CS} = -g_m R_L \left( \frac{R_G}{R_G + R_I} \right) \quad (13.89)$$

We now explore the limits to the voltage gain of common-source amplifiers using model simplifications for zero and large values of resistance  $R_S$ . First, we will assume that the signal source resistance  $R_I$  is much less than  $R_G$  so that

$$A_v^{CS} \cong A_{vt}^{CS} = -g_m R_L \cong -g_m (R_D \parallel R_3 \parallel r_o) \quad \text{for } R_I \ll R_G \quad (13.90)$$

This approximation is equivalent to saying that the total input signal appears at the gate terminal of the transistor.

Equation (13.87) places an upper limit on the gain we can achieve from a common-source amplifier with an external load resistor. Equation (13.87) states that the terminal voltage gain of the common-source stage is equal to the product of the transistor's transconductance  $g_m$  and load resistance  $R_L$ , and the minus sign indicates that the output voltage is “inverted” or  $180^\circ$  out of phase with respect to the input. The approximations that led to Eq. (13.87) are equivalent to saying that the total input signal appears across  $v_{gs}$  as shown in Fig. 13.28.

### 13.10.3 A DESIGN GUIDE FOR THE COMMON-SOURCE AMPLIFIER

When a resistive load is used with the common-source amplifier, we often try to achieve  $R_3 \gg R_D$ , and normally  $r_o \gg R_D$ . For these conditions, the total load resistance on the collector of the transistor is approximately equal to  $R_D$ , and Eq. (13.90) can be reduced to

$$A_v^{CS} \cong -g_m R_D = -\frac{I_D R_D}{\left( \frac{V_{GS} - V_{TN}}{2} \right)} \quad (13.91)$$

using the expression for  $g_m$  from Eq. (13.65).

The product  $I_D R_D$  represents the dc voltage drop across drain resistor  $R_D$ . This voltage is usually in the range of one-fourth to three-fourths the power supply voltage  $V_{DD}$ . Assuming  $I_D R_D = V_{DD}/2$  and  $V_{GS} - V_{TN} = 1$  V, we can rewrite Eq. (13.91) as

$$A_v^{CS} \cong -\frac{V_{DD}}{V_{GS} - V_{TN}} \cong -V_{DD} \quad (13.92)$$

Equation (13.92) is a basic rule of thumb for the design of the resistively loaded common-source amplifier; its form is very similar to that for the BJT in Eq. (13.52). The magnitude of the gain is approximately the power supply voltage divided by the internal gate drive ( $V_{GS} - V_{TN}$ ) of the MOSFET. For a common-source amplifier operating from a 12-V power supply with a 1-V gate drive, Eq. (13.92) predicts the voltage gain to be  $-12$ .

Note that this estimate is an order of magnitude smaller than the gain for the BJT operating from the same power supply. Equation (13.91) should be carefully compared to the corresponding expression for the BJT, Eq. (13.53). Except in special circumstances, the denominator term  $(V_{GS} - V_{TN})/2$  in Eq. (13.91) for the MOSFET is much greater than the corresponding term  $V_T = 0.025$  V for the BJT, and the MOSFET voltage gain should be expected to be correspondingly lower.



## DESIGN NOTE

The magnitude of the voltage gain of a resistively loaded common-source amplifier with zero source resistance is approximately equal to power supply voltage:

$$A_v^{CS} \cong -V_{DD} \quad \text{for } R_S = 0$$

This result represents an excellent way to quickly check the validity of more detailed calculations.

### 13.10.4 SMALL-SIGNAL LIMIT FOR THE COMMON-SOURCE AMPLIFIER

Using Eq. (13.88) and assuming  $R_G \gg R_I$ ,

$$v_i = v_{gs} \frac{R_I + R_G}{R_G} \cong v_{gs} \quad \text{or} \quad v_i \leq 0.2 (V_{GS} - V_{TN}) \quad (13.93)$$

The permissible input voltage is determined by the design of the bias point.

### EXAMPLE 13.4 VOLTAGE GAIN OF A COMMON-SOURCE AMPLIFIER

In this example, we find the small-signal parameters of the MOSFET and then calculate the voltage gain of a common-source amplifier.

**PROBLEM** (a) Calculate the gain of the common-source amplifier in Fig. 13.27 if the transistor has  $K_n = 0.500 \text{ mA/V}^2$ ,  $V_{TN} = 1 \text{ V}$ , and  $\lambda = 0.0133 \text{ V}^{-1}$ , and the Q-point is  $(0.241 \text{ mA}, 3.81 \text{ V})$ . (b) Compare the result in (a) to the common-source “rule-of-thumb” gain estimate and the amplification factor of the transistor. (c) What is the largest value of  $v_i$  that can be considered to be a small-signal?

**SOLUTION** **Known Information and Given Data:** Common-source amplifier with its ac equivalent circuit given in Fig. 13.27;  $K_n = 0.500 \text{ mA/V}^2$ ,  $V_{TN} = 1 \text{ V}$ , and  $\lambda = 0.0133 \text{ V}^{-1}$ ; the Q-point is  $(0.241 \text{ mA}, 3.64 \text{ V})$ ;  $R_I = 1 \text{ k}\Omega$ ,  $R_1 = 1.5 \text{ M}\Omega$ ,  $R_2 = 2.2 \text{ M}\Omega$ ,  $R_D = 22 \text{ k}\Omega$ ,  $R_3 = 100 \text{ k}\Omega$ ,  $R_S = 12 \text{ k}\Omega$ .

**Unknowns:** Small-signal parameters of the transistor; voltage gain  $A_v$ ; small-signal limit for the value of  $v_i$ ; rule-of-thumb estimate; intrinsic gain

**Approach:** Use the Q-point information to find  $g_m$  and  $r_o$ . Use the calculated and given values to evaluate the voltage gain expression in Eq. (13.89).

**Assumptions:** The transistor is in the active region of operation, and the signal amplitudes are below small-signal limit for the MOSFET. Transistor output resistance  $r_o$  can be neglected.

**Analysis:** (a) Calculating the values of the various resistors and small-signal model parameters yields

$$\begin{aligned} g_m &= \sqrt{2K_n I_{DS}(1 + \lambda V_{DS})} \\ &= \sqrt{2 \left( 5 \times 10^{-4} \frac{\text{A}}{\text{V}^2} \right) (0.241 \times 10^{-3} \text{ A}) \left( 1 + \frac{0.0133}{\text{V}} 3.81 \text{ V} \right)} = 0.503 \text{ mS} \\ r_o &= \frac{\frac{1}{\lambda} + V_{DS}}{I_D} = \frac{\left( \frac{1}{0.0133} + 3.81 \right) \text{ V}}{0.241 \times 10^{-3} \text{ A}} = 328 \text{ k}\Omega \end{aligned}$$

$$R_G = R_1 \| R_2 = 892 \text{ k}\Omega \quad R_L = R_D \| R_3 = 18.0 \text{ k}\Omega$$

$$A_v^{CS} = -g_m R_L \frac{R_G}{R_G + R_I} = -0.503 \text{ mS} (18.0 \text{ k}\Omega) \frac{892 \text{ k}\Omega}{892 \text{ k}\Omega + 1 \text{ k}\Omega} = -9.04 \quad \text{or} \quad 19.1 \text{ dB}$$

(b) Our “rule-of-thumb” estimate for the voltage gain is  $A_v = -V_{DD} = -12$ , which somewhat overestimates the actual gain.

For the given Q-point,

$$V_{GS} - V_{TN} \cong \sqrt{\frac{2I_{DS}}{K_n}} = \sqrt{\frac{2 \times 0.241 \times 10^{-3} \text{ A}}{5 \times 10^{-4} \frac{\text{A}}{\text{V}^2}}} = 0.982 \text{ V}$$

and our simple estimate for the gain is

$$A_v^{CS} \cong -\frac{V_{DD}}{V_{GS} - V_{TN}} = -\frac{12 \text{ V}}{0.982 \text{ V}} = -12.2$$

which is similar to the simple rule-of-thumb estimate.

The amplification factor of the MOSFET is equal to

$$\mu_f = \frac{\frac{1}{\lambda} + V_{DS}}{\frac{V_{GS} - V_{TN}}{2}} = \frac{(75.2 + 3.71) \text{ V}}{0.491} = 161$$

With the source bypassed, essentially all of the input signal appears directly across the gate-source terminals of the transistor. The small-signal limit on the input signal is therefore

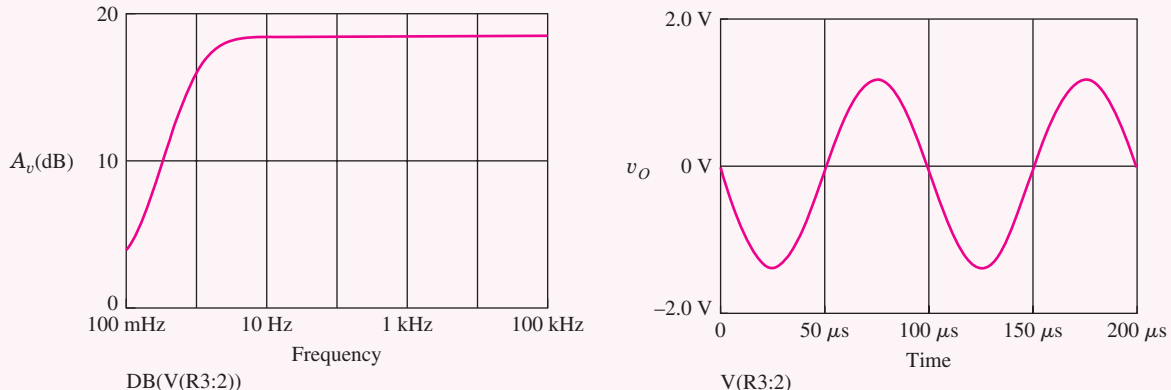
$$|v_{gs}| \leq 0.2(V_{GS} - V_{TN}) = 0.2(0.982 \text{ V}) = 0.196 \text{ V} \quad \text{so} \quad |v_{gs}| \leq 0.196 \text{ V}$$

**Check of Results:** The rule-of-thumb estimates are in reasonable agreement with the actual gains. The voltage gain is much less than the amplification factor, so neglect of  $r_o$  is valid.

**Discussion:** The rule-of-thumb produces a reasonable estimate for the gain of this amplifier. Although the amplification factor for this MOSFET is much smaller than that for the BJT, the gain of this resistively loaded amplifier circuit is still not limited by amplification factor  $\mu_f$ .

**Computer-Aided Analysis:** SPICE simulation yields a Q-point of (0.242 mA, 3.77 V) that is consistent with the assumed value. An ac sweep from 0.1 Hz to 100 kHz with 10 frequency points/decade is used to find the region in which the capacitors are acting as short circuits, and the gain is observed to be constant at 18.7 dB above a frequency of 10 Hz. The voltage gain is slightly

less than our calculated value because  $r_o$  was neglected in our calculations. A transient simulation was performed with a 0.15-V, 10-kHz sine wave. The output exhibits reasonably good linearity, but note that the positive and negative amplitudes are slightly different, indicating some waveform distortion.



**EXERCISE:** Calculate the Q-point for the transistor in Fig. 13.27.

**EXERCISE:** Draw the small-signal ac equivalent circuit for the amplifier in Ex. 13.4 including the transistor output resistance. What is the total load resistance on the transistor? What is the new value of the voltage gain?

**ANSWERS:**  $R_L = r_o \parallel R_D \parallel R_3 = 328 \text{ k}\Omega \parallel 22 \text{ k}\Omega \parallel 100 \text{ k}\Omega = 17.1 \text{ k}\Omega$

$$A_V^{CS} = -0.503 \text{ mS} (17.1 \text{ k}\Omega) \frac{892 \text{ k}\Omega}{892 \text{ k}\Omega + 1 \text{ k}\Omega} = -8.59 \text{ or } 18.7 \text{ dB}$$

**EXERCISE:** Suppose we increase the transconductance parameter of the transistor to  $K_n = 2 \times 10^{-3} \text{ A/V}^2$  by increasing the  $W/L$  ratio of the device. If the drain current is kept the same, find a new estimate for the voltage gain in Ex. 13.4. By what factor was the  $W/L$  ratio increased?

**ANSWERS:** -24.4; 4

### 13.10.5 INPUT RESISTANCES OF THE COMMON-EMITTER AND COMMON-SOURCE AMPLIFIERS

If the voltage gain of the MOSFET amplifier is generally much lower than that of the BJT, there must be other reasons for using the MOSFET. One of the reasons was mentioned earlier: A small signal can be much larger for the MOSFET than for the BJT. Another important difference is in the relative size of the input impedance of the amplifiers. This section explores the input resistances of the common-emitter and common-source amplifiers.

The input resistance  $R_{in}$  to the common-emitter and common-source amplifiers is defined in Figs. 13.29(a) and (b) to be the total resistance looking into the amplifier at coupling capacitor  $C_1$ .  $R_{in}$  represents the total resistance presented to the signal source represented by  $v_I$  and  $R_I$ .

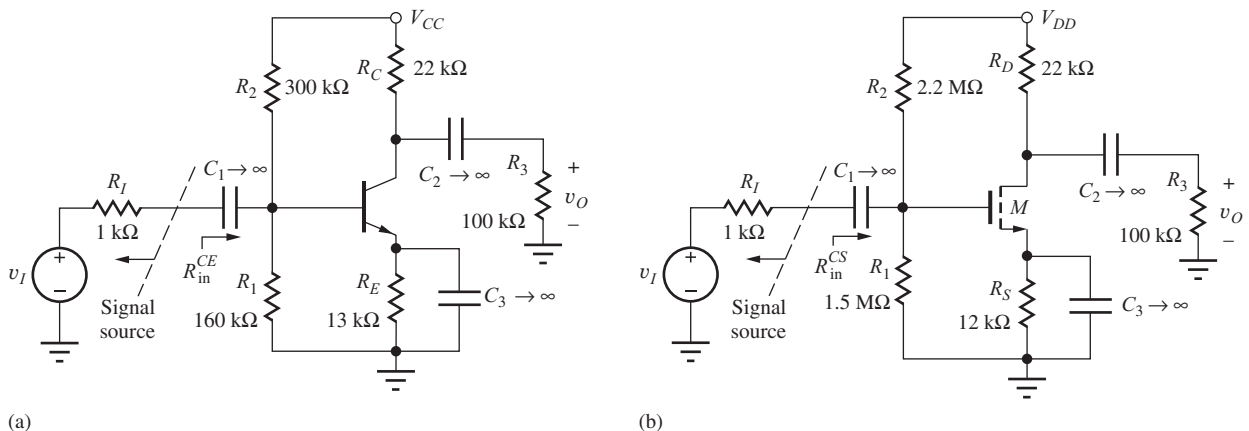


**Figure 13.29** (a) Input resistance definition for the common-emitter amplifier. (b) Input resistance definition for the common-source amplifier.

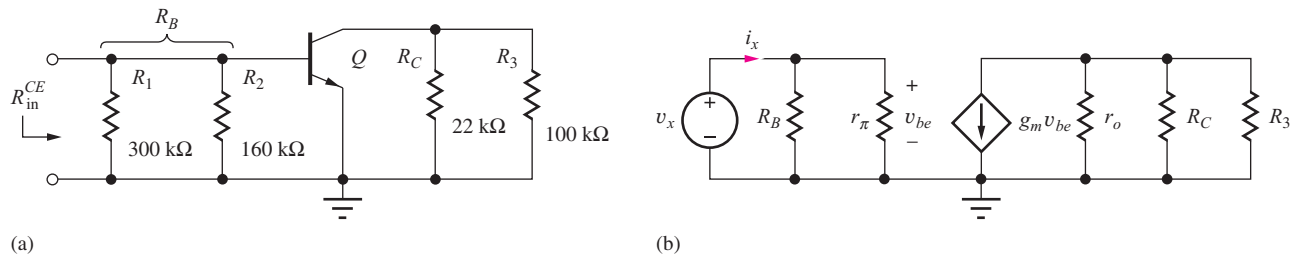


**Figure 13.30** (a) ac Equivalent circuit for the input resistance for the common-emitter amplifier. (b) Small-signal model.

### Common-Emitter Input Resistance

Let us first calculate the input resistance for the common-emitter stage. In Fig. 13.30, the BJT has been replaced by its small-signal model, and the input resistance is found to be

$$v_x = i_x (R_B \parallel r_\pi) \quad \text{and} \quad R_{in}^{CE} = \frac{v_x}{i_x} = R_B \parallel r_\pi = R_1 \parallel R_2 \parallel r_\pi \quad (13.94)$$

$R_{in}$  is equal to the parallel combination of  $r_\pi$  and the two base-bias resistors  $R_1$  and  $R_2$ .

### EXAMPLE 13.5 INPUT RESISTANCE OF THE COMMON-EMITTER AMPLIFIER

Let us calculate  $R_{in}$  for the amplifier in Fig. 13.29 for a given Q-point.

**PROBLEM** (a) Find the input resistance for the common-emitter amplifier in Figs. 13.29 and 13.30. The Q-point is (0.245 mA, 3.39 V). (b) Repeat the calculation if the bypass capacitor is connected between the transistor's emitter and ground.

**SOLUTION** **Known Information and Given Data:** The small-signal circuit topology appears in Fig. 13.31. The Q-point is given as (0.245 mA, 3.39 V). From Fig. 13.30, we have  $R_1 = 160\text{ k}\Omega$ ,  $R_2 = 300\text{ k}\Omega$ , and  $R_3 = 100\text{ k}\Omega$ .

**Unknowns:** Input resistance looking into the common-emitter amplifier.

**Approach:** Find  $r_\pi$  and use Eq. (13.94) to find the input resistance.

**Assumptions:** Small-signal conditions apply,  $\beta_o = 100$ ,  $V_T = 25$  mV

**Analysis:** The values of  $R_B$  and  $r_\pi$  are

$$R_B = R_1 \| R_2 = 160 \text{ k}\Omega \| 300 \text{ k}\Omega = 104 \text{ k}\Omega \quad \text{and} \quad r_\pi = \frac{\beta_o V_T}{I_C} = \frac{100(0.025)}{0.245 \text{ mA}} = 10.2 \text{ k}\Omega$$

$$R_{in}^{CE} = R_B \| R_{iB} = R_B \| r_\pi = 104 \text{ k}\Omega \| 10.2 \text{ k}\Omega = 9.29 \text{ k}\Omega$$

**Check of Results:** The input resistance must be smaller than any one of the resistors  $R_1$ ,  $R_2$ , or  $r_\pi$ , since they all appear in parallel. The calculated value of input resistance is consistent with this observation.

**Discussion:** With the emitter terminal bypassed, the input resistance to the amplifier,  $9.29\text{ k}\Omega$ , is quite low and is dominated by  $r_\pi$ . In the next chapter we will discover how to increase the input resistance of the common-emitter amplifier.

**Computer-Aided Analysis:** (a) We may use an ac analysis of the circuit from Fig.13.30(a) to determine  $R_{in}$  by finding the signal current in source  $v_I$ . (Note that a TF analysis cannot be used because of the presence of capacitors in the network.) The input resistance is equal to the base voltage divided by the current entering the base terminal through  $C_1$ . SPICE yields  $V_B(Q1)I(C1) = 9.80 \text{ k}\Omega$ , which is 5 percent higher than our calculations. This discrepancy results from the values of ac current gain  $\beta_o$  and thermal voltage  $V_T$  used by SPICE, since both differ slightly from our hand calculations.

**EXERCISE:** What is the value of  $R_{in}^{CE}$  if the Q-point is changed to (0.725 mA, 3.86 V)?

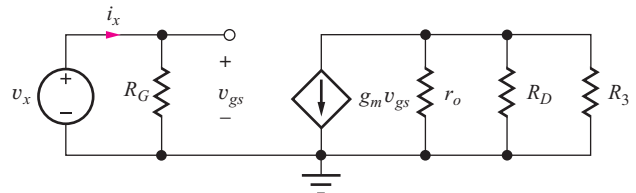
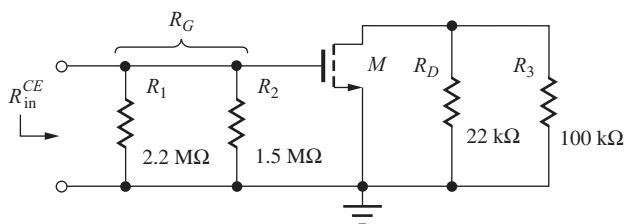
**ANSWER:**  $3.34\text{ k}\Omega$

### Common-Source Input Resistance

Now let us compare the input resistance of the common-source amplifier to that of the common-emitter stage. In Fig. 13.31, the MOSFET in Fig. 13.29 has been replaced by its small-signal model. This circuit is similar to that in Fig. 13.30 except that  $r_\pi \rightarrow \infty$ . Because the gate terminal of the MOSFET itself represents an open circuit, the input resistance of the circuit is simply limited by our value of  $R_G$ :

$$\mathbf{v}_x = \mathbf{i}_x R_G \quad \text{and} \quad R_{in}^{CS} = R_G \quad (13.95)$$

In the C-S amplifier in Figs. 13.29,  $R_G = 2.2\text{ M}\Omega \parallel 1.5\text{ M}\Omega = 892\text{ k}\Omega$ , so  $R_{in}^{CS} = 892\text{ k}\Omega$ . We see that the input resistance of the C-S amplifier can easily be much larger than that of the corresponding C-E stage.



(a)

(b)

**Figure 13.31** (a) ac Equivalent circuits for the input resistance for the common-source amplifiers. (b) Small-signal model.

**EXERCISE:** What is the input resistance of the common-source amplifier in Fig. 13.29(b) if  $R_2 = 1.0 \text{ M}\Omega$  and  $R_1 = 680 \text{ k}\Omega$ ? Is the Q-point of the amplifier changed?

**ANSWERS:** 405  $\text{k}\Omega$ ; no, the Q-point remains the same because  $I_G = 0$  and the dc voltage at the gate is unchanged.

### 13.10.6 COMMON-EMITTER AND COMMON-SOURCE OUTPUT RESISTANCES

The output resistances of the C-E and C-S amplifiers are defined in Figs. 13.32(a) and (b) as the total equivalent resistance looking into the output of the amplifier at coupling capacitor  $C_3$ . The definition of the output resistance is repeated in Fig. 13.33, in which the two amplifiers have been reduced to their ac equivalent circuits. For the output resistance calculation, input source  $v_I$  is set to zero.

#### Output Resistance of the Common-Emitter Amplifier

The transistors are replaced with their small-signal models in Fig 13.34, and test source  $v_x$  is applied to the output in order to calculate the output resistance. For the BJT in Fig. 13.34(a), the current from  $v_x$  is equal to

$$\mathbf{i}_x = \frac{\mathbf{v}_x}{R_C} + \frac{\mathbf{v}_x}{r_o} + g_m \mathbf{v}_{be} \quad (13.96)$$

However, there is no excitation at the base node:

$$\frac{\mathbf{v}_{be}}{R_I} + \frac{\mathbf{v}_{be}}{R_B} + \frac{\mathbf{v}_{be}}{r_\pi} = 0 \quad \text{and} \quad \mathbf{v}_{be} = 0 \quad (13.97)$$

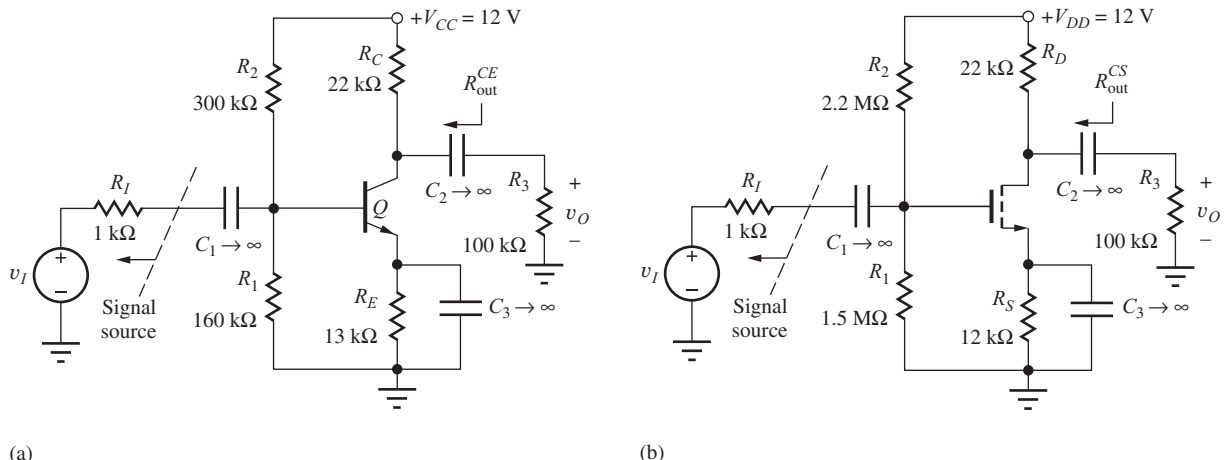


**Figure 13.32** (a) Output resistance definition for the common-emitter amplifier. (b) Output resistance definition for the common-source amplifier.

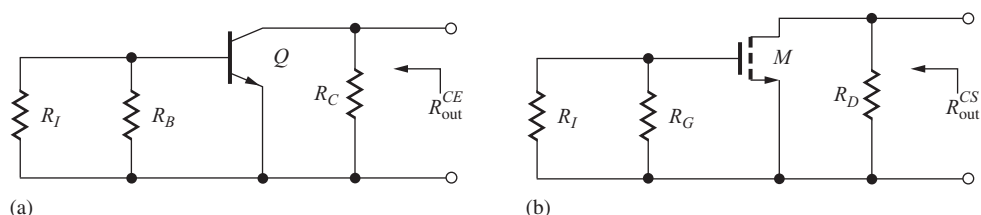


**Figure 13.33** Output resistance definition for (a) common-emitter and (b) common-source amplifiers.

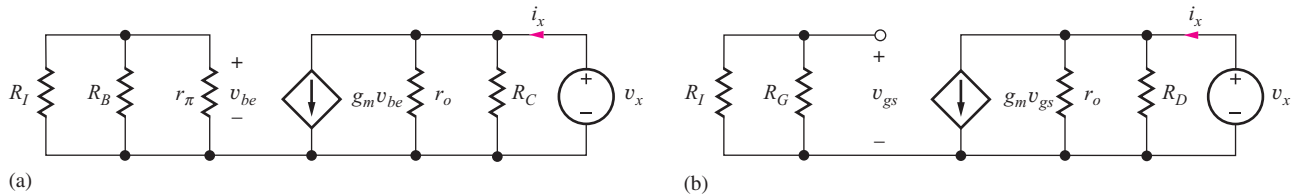


**Figure 13.34** Small signal models for (a) C-E and (b) C-S amplifier output resistance.

Thus,  $g_m v_{be} = 0$ , and the output resistance is equivalent to the parallel combination of  $R_C$  and  $r_o$  given by

$$R_{\text{out}}^{CE} = \frac{v_x}{i_x} = r_o \parallel R_C \quad (13.98)$$

For the common-emitter amplifier in Fig. 13.29(a), we have  $R_{\text{out}}^{CE} = 320 \text{ k}\Omega \parallel 22 \text{ k}\Omega = 20.6 \text{ k}\Omega$  where the value of  $r_o$  was found earlier in Ex. 13.3.

Let us compare the values of  $r_o$  and  $R_C$  by multiplying each by  $I_C$ :

$$I_C r_o = I_C \frac{V_A + V_{CE}}{I_C} \cong V_A \quad \text{and} \quad I_C R_C \cong \frac{V_{CC}}{3} \quad (13.99)$$

As discussed previously, the voltage developed across the collector resistor  $R_C$  is typically 0.25 to 0.75  $V_{CC}$ , but the apparent voltage across  $r_o$  is the Early voltage  $V_A$ . Thus, from the relations in Eq. (13.99), we expect  $r_o \gg R_C$ , and Eq. (13.98) yields  $R_{\text{out}}^{CE} \cong R_C$ .

### Output Resistance of the Common-Source Amplifier

For the MOSFET in Fig. 13.34(b), the analysis is the same. The voltage  $v_{gs}$  will be zero, and  $R_{\text{out}}$  is equal to the parallel combination of  $r_o$  and  $R_D$ :

$$R_{\text{out}}^{CS} = \frac{v_x}{i_x} = r_o \parallel R_D \quad (13.100)$$

For the common-source amplifier in Fig. 13.29(b), we have  $R_{\text{out}}^{CS} = 328 \text{ k}\Omega \parallel 22 \text{ k}\Omega = 20.6 \text{ k}\Omega$  where the value of  $r_o$  was found earlier in Ex. 13.4. Note that the output resistances of the common-emitter and common-source amplifier examples are essentially the same.

Comparing  $r_o$  and  $R_D$  in a manner similar to that for the BJT,

$$I_D r_o = I_D \frac{\frac{1}{\lambda} + V_{DS}}{I_D} \cong \frac{1}{\lambda} \quad \text{and} \quad I_D R_D \cong \frac{V_{DD}}{2} \quad (13.101)$$

where it is assumed that the voltage developed across the drain resistor  $R_D$  is  $V_{DD}/2$ . The effective voltage across  $r_o$  is equivalent to  $1/\lambda$ . Because the value of  $1/\lambda$  is similar to the Early voltage  $V_A$ , we expect  $r_o \gg R_D$ , and Eq. (13.100) can be simplified to  $R_{\text{out}}^{CS} \cong R_D$ . We conclude that, for comparable bias points  $(I_C, V_{CE}) = (I_{DS}, V_{DS})$ , the output resistances of the C-E and C-S stages are similar and limited by the resistors  $R_C$  and  $R_D$ .

### EXAMPLE 13.6 A COMMON-SOURCE AMPLIFIER USING A JFET

Our final example in this chapter is a common-source amplifier using an *n*-channel JFET as depicted in Fig. 13.35. Although not used as often as BJTs and MOSFETs, JFETs do play important roles in analog circuits, both discrete and integrated. Capacitors  $C_1$  and  $C_2$  are used to couple the signal into and out of the amplifier, and bypass capacitor  $C_3$  provides an ac ground at the source of the JFET. The JFET is inherently a depletion-mode device; it requires only three resistors for proper biasing:  $R_G$ ,  $R_4$ , and  $R_D$ .

**PROBLEM** Find the input resistance, output resistance, and voltage gain for the common-source amplifier in Fig. 13.35.

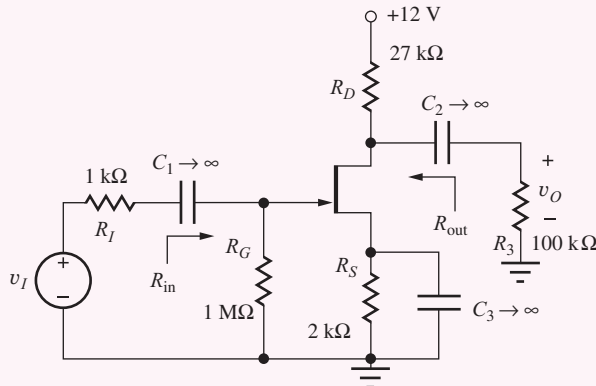


**Figure 13.35** Common-source amplifier using a junction field-effect transistor. For the JFET,  $I_{DSS} = 1 \text{ mA}$ ,  $V_P = -1 \text{ V}$ ,  $\lambda = 0.02 \text{ V}^{-1}$ .

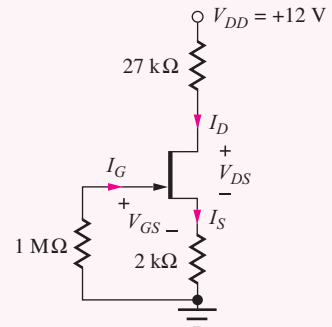


**Figure 13.36** Circuit for determining the Q-point of the JFET.

**SOLUTION** **Known Information and Given Data:** The circuit topology with element values appears in the Fig. 13.35. The transistor parameters are specified in the figure to be  $I_{DSS} = 1 \text{ mA}$ ,  $V_P = -1 \text{ V}$ , and  $\lambda = 0.02 \text{ V}^{-1}$ .

**Unknowns:** Q-point ( $I_D$ ,  $V_{DS}$ ); small-signal parameters,  $R_{in}$ ,  $R_{out}$ , and  $A_v$

**Approach:** To analyze the circuit, we first draw the dc equivalent circuit and find the Q-point. Then we develop the ac equivalent circuit, find the small-signal model parameters, and characterize the small-signal properties of the amplifier.

**Assumptions:** Pinch-off region operation for the JFET;  $\lambda$  can be ignored in dc bias calculations; small-signal operating conditions apply.

**Q-Point Analysis:** The dc equivalent circuit, obtained from Fig. 13.35 by opening the capacitors, appears in Fig. 13.36. Assuming operation in the pinch-off region, the drain current of the JFET is expressed by [see Eq. (4.69)]

$$I_D = I_{DSS} \left( 1 - \frac{V_{GS}}{V_P} \right)^2$$

in which  $\lambda$  is neglected for dc analysis. The gate-source voltage may be related to the drain current by writing a loop equation including  $V_{GS}$ :

$$I_G(10^6) + V_{GS} + I_S(2000) = 0$$

However, the gate current is zero, so  $I_S = I_D$  and  $V_{GS} = -2000I_D$ . Substituting this result and the device parameters into the drain current expression yields a quadratic equation for  $V_{GS}$ :

$$V_{GS} = -(2 \times 10^3)(1 \times 10^{-3}) \left[ 1 - \frac{V_{GS}}{(-1)} \right]^2$$

Rearranging this expression for  $V_{GS}$ , we get

$$2V_{GS}^2 + 5V_{GS} + 2 = 0 \quad \text{and} \quad V_{GS} = -0.50 \text{ V}, -2.0 \text{ V}$$

$V_{GS}$  must be negative but less negative than the pinch-off voltage of the  $n$ -channel JFET, so the  $-0.50\text{-V}$  result must be the correct choice. The corresponding value of  $I_D$  becomes

$$I_D = 10^{-3}\text{A} \left(1 - \frac{-0.50\text{ V}}{-1\text{ V}}\right)^2 = 0.250\text{ mA}$$

$V_{DS}$  can be found by writing the load-line equation for the JFET,

$$12 = 27,000I_D + V_{DS} + 2000I_S$$

Substituting  $I_S = I_D = 250\text{ }\mu\text{A}$  gives the Q-point:

$$(250\text{ }\mu\text{A}, 4.75\text{ V})$$

**Check of Results and Discussion:** As always, we must check the region of operation to be sure our original assumption of pinch-off was correct:

$$V_{DS} \geq V_{GS} - V_P \quad 4.75 > -0.50 - (-1) \quad 4.75 > 0.50 \quad \checkmark$$

In this dc analysis, we neglected the channel-length modulation term since we want to use the lowest complexity model that provides reasonable answers. For this problem, we see that  $\lambda V_{DS}$  is  $(0.02\text{ V}^{-1})(5\text{ V}) = 0.10$ . Including the  $\lambda V_{DS}$  term would change our answers by at most 10 percent but would considerably complicate the dc analysis. In addition, any differences in Q-point values would be less than the total uncertainty in the circuit and device parameter values.

**ac ANALYSIS** As in Ex. 13.3 and Ex. 13.4, we begin the ac analysis by finding the ac equivalent circuit. In Fig. 13.37(a), the capacitors in Fig. 13.35 have been replaced with short circuits, and the dc voltage source has been replaced with a ground connection. The ac equivalent circuit is redrawn in Fig. 13.37(b) by eliminating resistor  $R_4$  and indicating the parallel connection of  $R_D$  and  $R_3$ . We recognize this as a common-source circuit since the source of the JFET is clearly the terminal in common between the input and output ports.

**Small-Signal Parameters and Voltage Gain:** We wish to find the voltage gain from  $v_i$  to  $v_o$  for the amplifier in Fig. 13.37. The output voltage at the drain terminal is related to the voltage at the gate by the terminal gain in Eq. (13.90),  $v_o = -g_m R_L v_{gs}$ , where  $R_L$  is the total load resistance at the drain terminal.  $R_L$  is equal to  $R_{out}$  in parallel with external load resistor  $R_3$ ,  $R_L = R_{out} \parallel R_3$ . Gate-source voltage  $v_{gs}$  is related to  $v_i$  through voltage division between the source resistance  $R_I$  and input

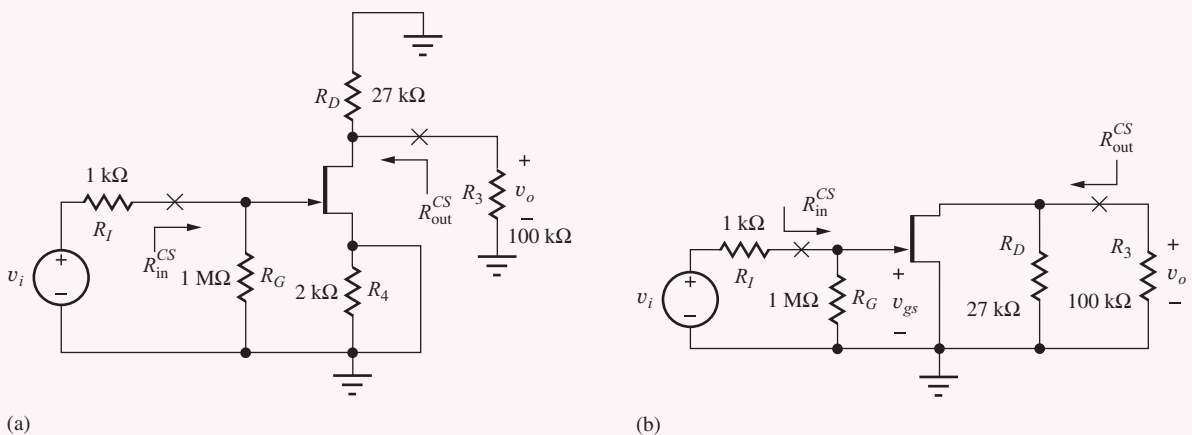


Figure 13.37 (a) Construction of the ac equivalent circuit. (b) Redrawn version of the circuit in (a).

resistance  $R_{in}$ . Combining these results yields an expression for the overall voltage gain:

$$A_v = \frac{v_o}{v_i} = -g_m(R_{out} \parallel R_3) \frac{R_{in}}{R_I + R_{in}} \quad (13.102)$$

The final step prior to mathematical analysis is to find the small-signal model parameters. Using the Q-point values,

$$g_m = \frac{2}{|V_P|} \sqrt{I_{DSS} I_{DS} (1 + \lambda V_{DS})} = \frac{2}{|-1\text{ V}|} \sqrt{(0.001\text{ A})(0.00025\text{ A}) \left(1 + \frac{0.02}{\text{V}} 4.75\text{ V}\right)}$$

$$g_m = 1.05\text{ mS}$$

$$r_o = \frac{\frac{1}{\lambda} + V_{DS}}{I_{DS}} = \frac{(50 + 4.75)\text{ V}}{0.25 \times 10^{-3}\text{ A}} = 219\text{ k}\Omega \quad \mu_f = g_m r_o = 230$$

**Input Resistance:** The amplifier's input resistance is calculated looking into the position of coupling capacitor  $C_1$  in Figs. 13.35 and 13.37, and the equivalent circuit for finding  $R_{in}$  is redrawn in Fig. 13.38. In Fig. 13.38(b), we see that the input resistance is set by gate-bias resistor  $R_G$ , because the input resistance of the JFET itself is infinite:

$$R_{in}^{CS} = R_G = 1\text{ M}\Omega$$

**Output Resistance:** The amplifier's output resistance is calculated looking into the position of coupling capacitor  $C_2$  in Figs. 13.35 and 13.37. The equivalent circuit for calculating  $R_{out}^{CS}$  is presented in the schematic in Fig. 13.39. In Fig. 13.39(b), the voltage  $v_{gs} = 0$ , and the output resistance is equal to the parallel combination of  $R_D$  and  $r_o$ :

$$R_{out}^{CS} = R_D \parallel r_o = 27\text{ k}\Omega \parallel 219\text{ k}\Omega = 24.0\text{ k}\Omega$$

**Voltage gain:** Substituting these values into Eq. (13.102) and solving for the voltage gain gives

$$A_v = \frac{v_o}{v_i} = -(1.05\text{ mS})(24\text{ k}\Omega \parallel 100\text{ k}\Omega) \left(\frac{1\text{ M}\Omega}{1\text{ k}\Omega + 1\text{ M}\Omega}\right) = -20.3$$

Thus, this particular common-source JFET amplifier is an inverting amplifier with a voltage gain of  $-20.3$  or  $26.2\text{ dB}$ .

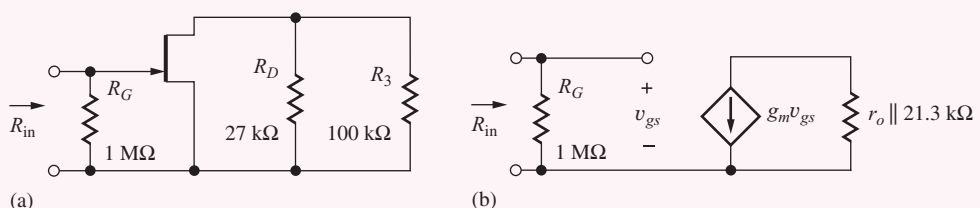


Figure 13.38 (a) ac Equivalent circuit for determining  $R_{in}$ . (b) Small-signal model for the circuit in part (a).

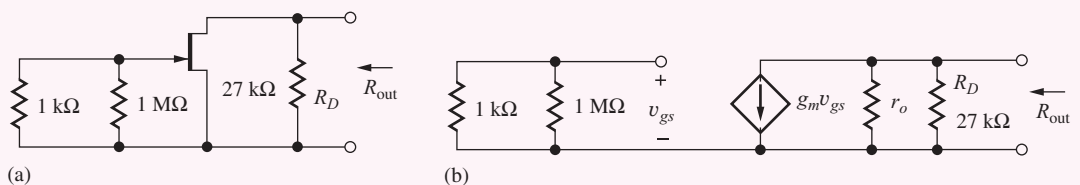
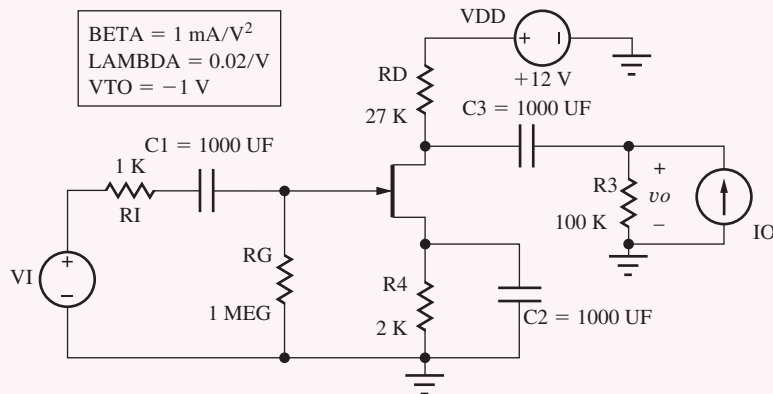


Figure 13.39 (a) ac Equivalent circuit for determining  $R_{out}$ . (b) Small-signal model for circuit in (a).

**Check of Results:** We have found the answers requested in the problem. Our rule-of-thumb estimate for the voltage gain would be  $A_v = -V_{DD} = -12$ , so the calculated gain seems reasonable. Looking at the circuits in Fig. 13.37, we quickly see that the input and output resistances should not exceed  $1 \text{ M}\Omega$  and  $27 \text{ k}\Omega$  respectively, which also agree with our more detailed calculations. In summary, our JFET amplifier provides the following characteristics:

$$A_v = -20.3 \quad R_{\text{in}}^{CS} = 1.00 \text{ M}\Omega \quad R_{\text{out}}^{CS} = 24.0 \text{ k}\Omega$$



**Computer-Aided Analysis:** The JFET parameters must be correctly defined in SPICE. Remember that  $\text{BETA} = I_{DSS}/V_P^2 = 0.001 \text{ A/V}^2$ . SPICE gives the Q-point ( $257 \mu\text{A}$ ,  $5.05 \text{ V}$ ). For ac analysis the capacitors are set to large values so their impedances are small at the frequencies of interest. In this case,  $1000-\mu\text{F}$  capacitors are used. In Chapters 14 and 17, we will find how to choose the values for these capacitors. An ac analysis (DEC, FSTART =  $1 \text{ kHz}$ , FSTOP =  $100 \text{ kHz}$ , and 3 points/decade) with a 1-V value for source  $v_I$  and  $i_o = 0$  yields  $A_v = -20.4$ . The current in source  $v_I$  is  $999 \text{ nA}$  corresponding to a total input resistance of  $1.001 \text{ M}\Omega$ . Subtracting the  $1\text{-k}\Omega$  source resistance yields  $R_{\text{in}} = 1.00 \text{ M}\Omega$ . The output resistance can be found by driving the output with a 1-A ac current source with  $v_I = 0$  yielding a total resistance of  $19.3 \text{ k}\Omega$  at the output node. Removing the influence of the  $100\text{-k}\Omega$  resistance  $R_4$  in parallel with the output node yields  $R_{\text{out}} = 23.9 \text{ k}\Omega$ . Our hand analysis results for the JFET amplifier are confirmed.

**EXERCISE:** What is the amplification factor of the JFET characterized by the parameters in Ex. 13.6? How does  $A_v$  compare to  $\mu_f$ ?

**ANSWERS:** 230;  $|A_v| \ll \mu_f$

**EXERCISE:** What is the largest value of  $v_i$  that corresponds to a small signal for the JFET in this amplifier? What is the largest value of  $v_o$  that corresponds to a small signal in this amplifier?

**ANSWERS:** 100 mV; 2.04 V

**EXERCISE:** Verify the dc and ac analysis using SPICE. Compare the operating points with  $\lambda = 0$  and  $\lambda = 0.02 \text{ V}$ .

**TABLE 13.4**  
Comparison of Three Amplifier Voltage Gains

AMPLIFIER	Q-POINT	$A_v$	$\mu_f$	RULE-OF-THUMB ESTIMATES
BJT	(245 $\mu$ A, 3.39 V)	-159	3140	-120
MOSFET	(241 $\mu$ A, 3.81 V)	-9.04	161	-12
JFET	(250 $\mu$ A, 4.75 V)	-20.4	230	-12

**TABLE 13.5**  
Comparison of Input and Output Resistances

AMPLIFIER	$R_{in}$	$R_B$ or $R_G$	$r_\pi$	$R_{out}$	$R_C$ or $R_D$	$r_o$
BJT	9.29 k $\Omega$	100 k $\Omega$	10.2 k $\Omega$	20.6 k $\Omega$	22 k $\Omega$	320 k $\Omega$
MOSFET	892 k $\Omega$	892 k $\Omega$	$\infty$	20.6 k $\Omega$	22 k $\Omega$	328 k $\Omega$
JFET	1.00 M $\Omega$	1.00 M $\Omega$	$\infty$	24.0 k $\Omega$	27 k $\Omega$	219 k $\Omega$

### 13.10.7 COMPARISON OF THE THREE AMPLIFIER EXAMPLES

Tables 13.4 and 13.5 compare the numerical results for the amplifiers analyzed in Exs. 13.3 through 13.5. The three amplifiers have all been designed to have similar Q-points, as indicated in Table 13.4. In this table, we see that the BJT yields a much higher voltage gain than either of the FET circuits. However, all the voltage gains are well below the value of the amplification factor, which is characteristic of amplifiers with resistive loads in which the gain is limited by the external resistors (that is, in which  $r_o \gg R_C$  or  $R_D$ ).

Table 13.5 compares the input and output resistances. We see that the bipolar input resistance, in this case dominated by the value of  $r_\pi$ , is orders of magnitude smaller than that of the FETs. On the other hand,  $R_{in}$  of the FET stages is limited by the choice of gate-bias resistor  $R_G$ . All the output resistances are limited by the external resistors and are of similar magnitude.

## 13.11 COMMON-EMITTER AND COMMON-SOURCE AMPLIFIER SUMMARY

Table 13.6 presents a comparison of the ac small-signal characteristics of the common-emitter (C-E) and common-source (C-S) amplifiers based on the analyses presented in this chapter. The voltage gain expressions collapse to the same symbolic form, but the values will differ because the value of

**TABLE 13.6**  
Common-Emitter/Common-Source Amplifier Characteristics

	COMMON-EMITTER AMPLIFIER	COMMON-SOURCE AMPLIFIERS
Terminal gain $A_{vt}$	$-g_m R_L$	$-g_m R_L$
Rule-of-thumb estimate for $g_m R_L$	$-10V_{CC}$	$-V_{DD}$
Voltage gain $A_v$	$A_v = \frac{V_o}{V_i} = -g_m (R_{out} \parallel R_3) \left( \frac{R_{in}}{R_I + R_{in}} \right)$	
Input resistance $R_{in}$	$R_B \parallel r_\pi$	$R_G$
Output resistance $R_{out}$	$R_C \parallel r_o \cong R_C$	$R_D \parallel r_o \cong R_D$
Input signal phase	0.005 V	$0.2(V_{GS} - V_{TN})$ or $0.2(V_{GS} - V_P)$

$g_m$  for the BJT is usually much larger than that of the FET for a given operating current. The input resistance of the C-S stages is limited only by the design value of  $R_G$  and can be quite large, whereas the values of  $R_B$  and  $r_\pi$  limit the input resistance of the C-E amplifier to much smaller values. For a given operating point, the output resistances of the C-E and C-S stages are similar because  $R_{out}$  is limited by the collector- or drain-bias resistors  $R_C$  or  $R_D$ .

### 13.11.1 GUIDELINES FOR NEGLECTING THE TRANSISTOR OUTPUT RESISTANCE

In all these amplifier examples, we found that the transistor's own output impedance did not greatly affect the results of the various calculations. The following question naturally arises: Why not just neglect  $r_o$  altogether, which will simplify the analysis? The answer is: The resistance  $r_o$  must be included whenever it makes a difference. We use the following rule: The transistor output resistance  $r_o$  can be neglected in voltage gain calculations as long as the computed value of  $A_v \ll \mu_f$ . However, in Thévenin equivalent resistance calculations  $r_o$  can play a very important role and one must be careful not to overlook limitations due to  $r_o$ . If  $r_o$  is neglected, and an input or output resistance is calculated that is similar to or much larger than  $r_o$ , then the calculation should be rechecked with  $r_o$  included in the circuit. At this point, this procedure may sound mysterious, but in the next several chapters we shall find circuits in which  $r_o$  is very important.



#### DESIGN NOTE

You can neglect the transistor output resistance in voltage gain calculations as long as the computed value is much less than the transistor's amplification factor  $\mu_f$ ! When the output resistance is included in a calculation, we often do not know  $V_{CE}$  or  $V_{DS}$ , and it is perfectly acceptable to use the simplified expression for the output resistances:

$$r_o = \frac{V_A}{I_C} \quad \text{or} \quad r_o = \frac{1}{\lambda I_D}$$

## 13.12 AMPLIFIER POWER AND SIGNAL RANGE

We found in our examples how the selection of Q-point affects the value of the small-signal parameters of the transistors and hence affects the voltage gain, input resistance, and output resistance of common-emitter and common-source amplifiers. For the FET, the choice of Q-point also determines the value of  $v_{gs}$  that corresponds to small-signal operation. Two additional characteristics that are set by Q-point design are discussed in this section. The choice of operating point determines the level of power dissipation in the transistor and overall circuit, and it also determines the maximum linear signal range at the output of the amplifier.

### 13.12.1 POWER DISSIPATION

The static power dissipation of the amplifiers can be determined from the dc equivalent circuits used earlier. The power that is supplied by the dc sources is dissipated in both the resistors and transistors. For the amplifier in Fig. 13.40(a), for example, the power  $P_D$  dissipated in the transistor is the sum of the power dissipation in the collector-base and emitter-base junctions:

$$P_D = V_{CB} I_C + V_{BE} (I_B + I_C) = (V_{CB} + V_{BE}) I_C + V_{BE} I_B$$

or

$$P_D = V_{CE} I_C + V_{BE} I_B \quad \text{where} \quad V_{CE} = V_{CB} + V_{BE}$$

(13.103)

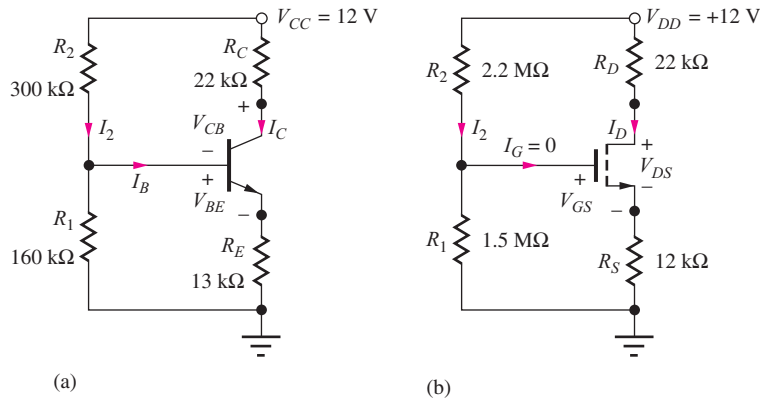


**Figure 13.40** dc Equivalent circuits for the (a) BJT and (b) MOSFET amplifiers from Figs. 13.18(a) and 13.28(a).

The total power  $P_S$  supplied to the amplifier is determined by the currents in the power supply:

$$P_S = V_{CC}(I_C + I_2) \quad (13.104)$$

Similarly for the MOSFET circuit in Fig. 13.40(b), the power dissipated in the transistor is given by

$$P_D = V_{DS}I_D + V_{GS}I_G = V_{DS}I_D \quad (13.105)$$

because the gate current is zero. The total power being supplied to the amplifier is equal to:

$$P_S = V_{DD}(I_D + I_2) \quad (13.106)$$

**EXERCISE:** What power is being dissipated by the bipolar transistor in Fig. 13.40(a)? Assume  $\beta_F = 65$ . What is the total power being supplied to the amplifier? Use the Q-point information given earlier (245  $\mu\text{A}$ , 3.39 V).

**ANSWERS:** 233  $\mu\text{W}$ ; 2.94 mW

**EXERCISE:** What power is being dissipated by the MOSFET in Fig. 13.40(b)? What is the total power being supplied to the amplifier? Use the Q-point information given earlier (241  $\mu\text{A}$ , 3.81 V).

**ANSWERS:** 0.918 mW; 2.93 mW

### 13.12.2 SIGNAL RANGE

We next discuss the relationship between the Q-point and the amplitude of the signals that can be developed at the output of the amplifier. Consider the amplifier in Fig. 13.41 with  $V_{CC} = 12$  V, and the corresponding waveforms, which are given in Fig. 13.42. The collector and emitter voltages at the operating point are 5.9 V and 2.10 V, respectively, and hence the value of  $V_{CE}$  at the Q-point is 3.8 V.

Because the bypass capacitor at the emitter forces the emitter voltage to remain constant, the total collector-emitter voltage can be expressed as

$$v_{CE} = V_{CE} - V_M \sin \omega t \quad (13.107)$$

in which  $V_M \sin \omega t$  is the signal voltage being developed at the collector. The bipolar transistor must remain in the active region at all times, which requires that the collector-emitter voltage remain larger

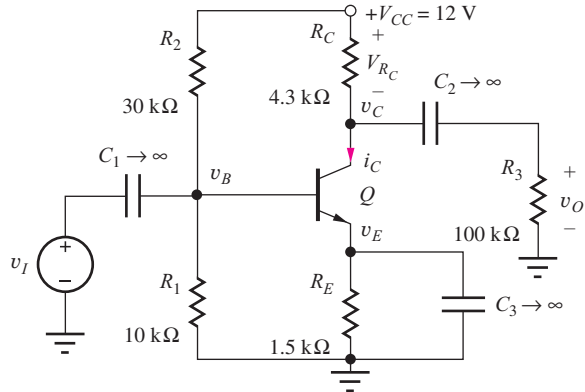


**Figure 13.41** Common-emitter amplifier stage.

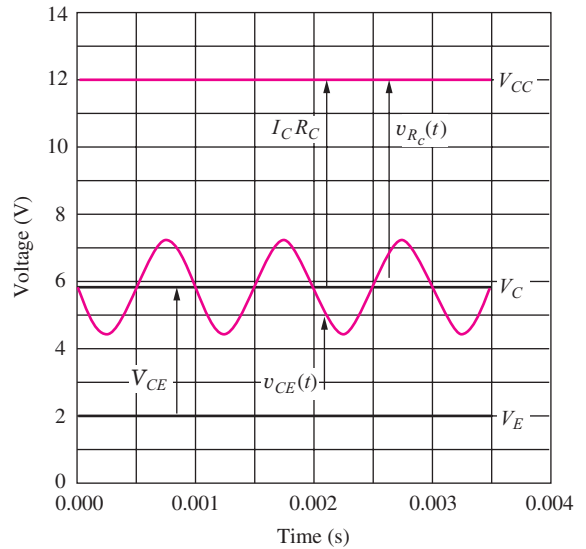


**Figure 13.42** Waveforms for the amplifier in Fig. 13.41.

than base-emitter voltage  $V_{BE}$ :

$$v_{CE} \geq V_{BE} \quad \text{or} \quad v_{CE} \geq 0.7 \text{ V} \quad (13.108)$$

Thus the amplitude of the signal at the collector must satisfy

$$V_M \leq V_{CE} - V_{BE} \quad (13.109)$$

The positive power supply presents an additional limit to the signal swing. Writing an expression for the voltage across resistor  $R_C$ ,

$$v_{R_C}(t) = I_C R_C + V_M \sin \omega t \geq 0 \quad (13.110)$$

In this circuit, the voltage across the resistor cannot become negative; that is, the voltage  $V_C$  at the transistor collector cannot exceed the power supply voltage  $V_{CC}$ . Equation (13.110) indicates that the amplitude  $V_M$  of the ac signal developed at the collector must be smaller than the voltage drop across  $R_C$  at the Q-point:

$$V_M \leq I_C R_C \quad (13.111)$$

Thus, the signal swing at the collector is limited by the smaller of the two limits expressed in Eqs. (13.109) or (13.111):

$$V_M \leq \min[I_C R_C, (V_{CE} - V_{BE})] \quad (13.112)$$

Similar expressions can be developed for field-effect transistor circuits. We must require that the MOSFET remains pinched off, or  $v_{DS}$  must always remain larger than  $v_{GS} - V_{TN}$ .

$$v_{DS} = V_{DS} - V_M \sin \omega t \geq V_{GS} - V_{TN} \quad (13.113)$$

in which it has been assumed that  $v_{gs} \ll V_{GS}$ . In direct analogy to Eq. (13.111) for a BJT circuit, the signal amplitude in the FET case also cannot exceed the dc voltage drop across  $R_D$ :

$$V_M \leq I_D R_D \quad (13.114)$$

So, for the case of the MOSFET,  $V_M$  must satisfy:

$$V_M \leq \min[I_D R_D, (V_{DS} - (V_{GS} - V_{TN}))] \quad (13.115)$$

**EXERCISES:** (a) What is  $V_M$  for the bipolar transistor amplifier in Ex. 13.3? (b) For the MOSFET amplifier in Ex. 13.4?

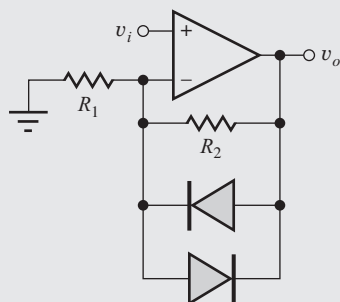
**ANSWERS:** 2.69 V; 2.83 V

## ELECTRONICS IN ACTION

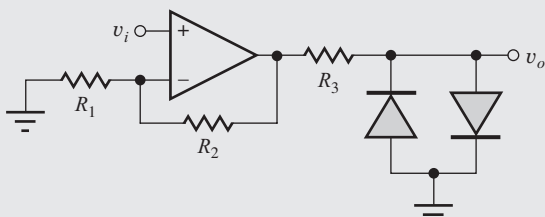
### Electric Guitar Distortion Circuits

For most of this chapter we have focused on small-signal models and gain calculations. However, in some applications, it is desirable to intentionally violate small-signal constraints and generate a distorted waveform. In particular, electric guitars, the mainstay of rock music, intentionally use distortion to enrich the sound. The early Marshall and Fender tube amps, through substantial over-design and the natural characteristics of vacuum tube circuits, generated a rich soft-clipped sound when driven into overload. When excited with the right chords, the tube amplifier distortion can actually generate harmonics that are in-tune and add a great deal to the character of the electric guitar sound.

Modern guitar players use ‘pedal’ boxes to produce distortion and other effects without the excessive power levels required to produce the overdrive sound. Typical forms of these circuits are shown below. The first is an op-amp circuit with a pair of diodes in the feedback network.  $R_2$  is 50 to 200 times larger than  $R_1$ , so the circuit has a large gain. As the voltage across the amplifier exceeds the diode turn-on voltage, the diodes begin to conduct. Since the diode impedance is much less than  $R_2$ , the gain is reduced during diode conduction. The resulting ‘soft’ clipped waveform is shown below.



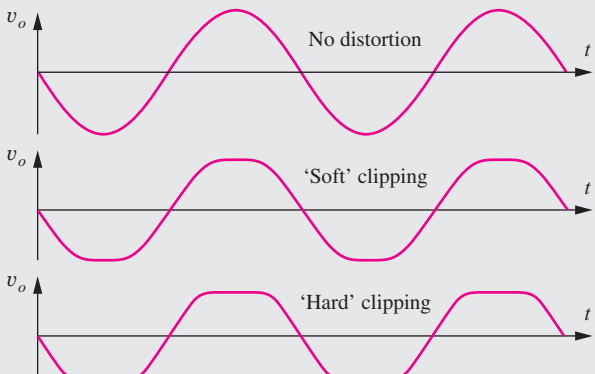
(a) Typical ‘soft’ clipping circuit.



(b) ‘Hard’ clipping circuit.



(c) Royalty-free/Corbis.



(d)

Another form of distortion circuit is the ‘hard’ clipping circuit. The amplifier gain is again set to be quite large, and resistor  $R_3$  is typically a few kilohms. As  $v_o$  exceeds the diode turn-on voltage, the output is clipped to the diode voltage. In this case, the diode current is limited by  $R_3$ , so  $v_o$  changes very little once the diode turns on. This results in a ‘hard’ clipped waveform as seen above. Typically, practical circuits also include some frequency shaping.

From Fourier analysis, we know that any cyclical waveform shape other than an ideal sine wave is composed of a possibly infinite set of harmonics or sine and cosine waves, each at frequencies which are multiples of the fundamental frequency. The sharper the transitions in a waveform, the more harmonic content it contains. The soft clipping circuit creates a waveform with smaller amplitude of harmonics than the hard clipping circuit.

There are also additional tones created by the intermodulation of the incoming frequencies. In these nonlinear clipping circuits, the incoming frequencies mix and give rise to sum and difference frequencies. This is an additional audible effect of the distortion circuits. There are many variations on these simple circuits which produce a wide range of sounds. The guitarist must select between a variety of different distortion and effects devices to create the sound that optimally presents their musical ideas. Additional information can be found through the MCD website.



## SUMMARY

Chapter 13 has initiated our study of the basic amplifier circuits used in the design of more complex analog components and systems such as operational amplifiers, audio amplifiers, and RF communications equipment. The chapter began with an introduction to the use of the transistor as an amplifier, and then explored the operation of the BJT common-emitter (C-E) and FET common-source (C-S) amplifiers. Expressions were developed for the voltage gain and input and output resistances of these amplifiers. Relationships between Q-point design and the small-signal characteristics of the amplifier were discussed.

## POINTS TO REMEMBER

- The BJT common-emitter amplifier can provide good voltage gain but has only a low-to-moderate input resistance.
- In contrast, the FET common-source stage can have very high input resistance but typically provides relatively modest values of voltage gain.
- The output resistances of both C-E and C-S circuits tend to be determined by the resistors in the bias network and are similar for comparable operating points.
- A two-step approach is used to simplify the analysis and design of amplifiers. Circuits are split into two parts: a dc equivalent circuit used to find the Q-point of the transistor, and an ac equivalent circuit used for analysis of the response of the circuit to signal sources. The design engineer often must respond to competing goals in the design of the dc and ac characteristics of the amplifier, and coupling capacitors, bypass capacitors, and inductors are used to change the ac and dc circuit topologies.
- Our ac analyses were all based on linear small-signal models for the transistors. The small-signal models for the diode, bipolar transistor (the hybrid-pi model), MOSFET and JFET were all discussed in detail. The expressions relating the transconductance  $g_m$ , output resistance  $r_o$ , and input resistance  $r_{\pi}$  to the Q-point were all found by evaluating derivatives of the large-signal model equations developed in earlier chapters.
- The small-signal model for the diode is simply a resistor that has a value given by  $r_d = V_T/I_D$ .

- The results in Table 13.3 on page 822 for the three-terminal devices are extremely important. The structure of the models is similar. The transconductance of the BJT is directly proportional to current, whereas that of the FET increases only in proportion to the square root of current. Resistances  $r_\pi$  and  $r_o$  are inversely proportional to Q-point current. Resistor  $r_\pi$  is infinite for the case of the FET, so it does not actually appear in the small-signal model. It was discovered that each device pair, the *npn* and *pnp* BJTs, and the *n*-channel and *p*-channel FETs, has the same small-signal model.
- The small-signal current gain of the BJT was defined as  $\beta_o = g_m r_\pi$ , and its value generally differs from that of the large-signal current gain  $\beta_F$ . The FET exhibits an infinite small-signal current gain at low frequency.
- The intrinsic voltage gain, also known as the amplification factor of the transistor, is defined as  $\mu_f = g_m r_o$  and represents the maximum gain available from the transistor in the C-E and C-S amplifiers. Expressions were evaluated for the intrinsic gain of the BJT and FETs. Parameter  $\mu_f$  was found to be independent of Q-point for the BJT, but for the FET, the amplification factor decreases as operating current increases. For usual operating points,  $\mu_f$  for the BJT will be several thousand, whereas that for the FET ranges between tens and hundreds.
- The definition of a small signal was found to be device-dependent. The signal voltage  $v_d$  developed across the diode must be less than 5 mV in order to satisfy the requirements of a small signal. Similarly, the base-emitter signal voltage  $v_{be}$  of the BJT must be less than 5 mV for small-signal operation. However, FETs can amplify much larger signals without distortion. For the MOSFET,  $v_{gs} \leq 0.2(V_{GS} - V_{TN})$  represent the small-signal limits, respectively, and can be designed to range from 100 mV to more than 1 V. For the JFET,  $v_{gs} \leq 0.2(V_{GS} - V_P)$ .
- Common-emitter and common-source amplifiers were analyzed in detail. Table 13.6 on page 838 is another extremely important table. It summarizes the overall characteristics of these amplifiers. The rule-of-thumb estimates in Table 13.6 were developed to provide quick predictions of the voltage gain of the C-E and C-S stages.
- The chapter closed with a discussion of the relationship between operating point design and the power dissipation and output signal swing of the amplifiers. The amplitude of the signal voltage at the output of the amplifier is limited by the smaller of the Q-point value of the collector-base or drain-gate voltage of the transistor, and by the Q-point value of the voltage across the collector or drain-bias resistors  $R_C$  or  $R_D$ .
- It is extremely important to understand the difference between ac analysis and transient analysis in SPICE. ac analysis assumes that the network is linear and uses small-signal models for the transistors and diodes. Since the circuit is linear, any convenient value can be used for the signal source amplitudes, hence the common choice of 1-V and 1-A sources. In contrast, transient simulations utilize the full large-signal non-linear models of the transistors. If we desire linear behavior in a transient simulation, all signals must satisfy the small-signal constraints.

## KEY TERMS

ac coupling	dc equivalent circuit
ac equivalent circuit	Diode conductance
Amplification factor	Diode resistance
Back-gate transconductance	Hybrid-pi small-signal model
Back-gate transconductance parameter	Input resistance
Bypass capacitor	Intrinsic voltage gain $\mu_f$
Common-emitter (C-E) amplifier	Output resistance $r_o$
Common-source (C-S) amplifier	Signal source voltage gain
Coupling capacitor	Small signal
dc blocking capacitor	Small-signal current gain

Small-signal conductance  
Small-signal models

Terminal voltage gain  
Transconductance  $g_m$

## PROBLEMS

Figures P13.3 through P13.13 are used in a variety of problems in this chapter. Assume all capacitors and inductors have infinite value unless otherwise noted. Assume  $V_{BE} = 0.7$  V and  $\beta_F = \beta_o$  unless otherwise specified.

### 13.1 The Transistor as an Amplifier

- 13.1. (a) Suppose  $v_{be}(t) = 0.005 \sin 2000\pi t$  V in the bipolar amplifier in Fig. 13.1. Write expressions for  $v_{BE}(t)$ ,  $v_{ce}(t)$ , and  $v_{CE}(t)$ . (b) What is the maximum value of  $I_C$  that corresponds to the active region of operation?
- 13.2. (a) Suppose  $v_{gs}(t) = 0.25 \sin 2000\pi t$  V in the MOSFET amplifier in Fig. 13.2. Write expressions for  $v_{GS}(t)$ ,  $v_{ds}(t)$ , and  $v_{DS}(t)$ . (b) What is the maximum value of  $I_D$  that corresponds to the active region of operation?

### 13.2 Coupling and Bypass Capacitors

- 13.3. (a) What are the functions of capacitors  $C_1$ ,  $C_2$ , and  $C_3$  in Fig. P13.3? (b) What is the magnitude of the signal voltage at the top of  $C_3$ ?

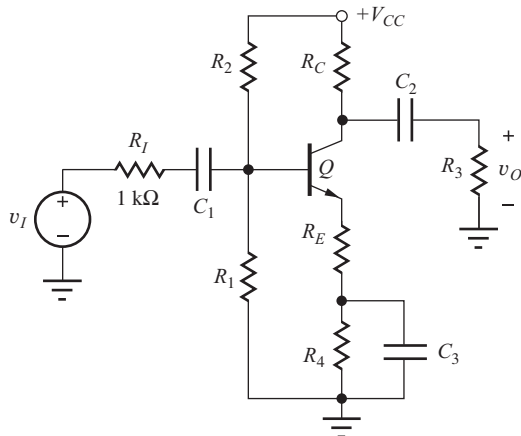


Figure P13.3

- 13.4. Repeat Prob. 13.3 if capacitor  $C_3$  is connected between the transistor's emitter and ground.

- 13.5. (a) What are the functions of capacitors  $C_1$ ,  $C_2$ , and  $C_3$  in Fig. P13.5? (b) What is the magnitude of the signal voltage at the source of  $M_1$ ?

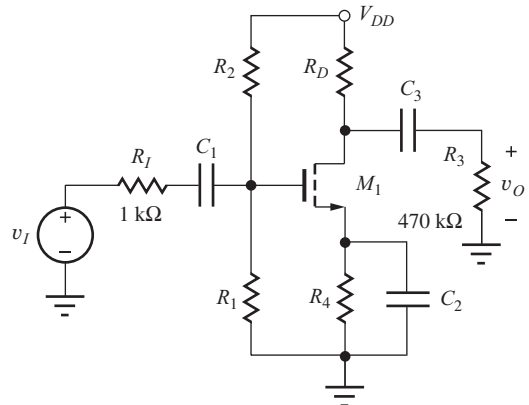


Figure P13.5

- 13.6. (a) What are the functions of capacitors  $C_1$ ,  $C_2$ , and  $C_3$  in Fig. P13.6? (b) What is the magnitude of the signal voltage at the base of  $Q_1$ ?

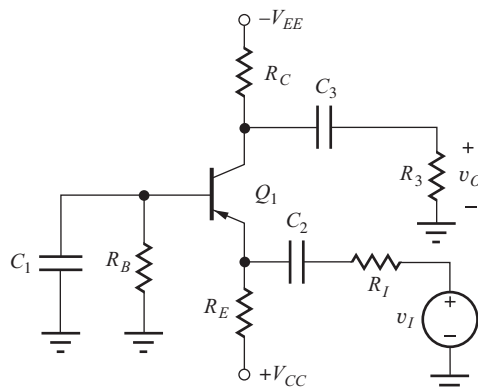


Figure P13.6

- 13.7. (a) What are the functions of capacitors  $C_1$ ,  $C_2$ , and  $C_3$  in Fig. P13.7? (b) What is the magnitude of the signal voltage at the emitter of  $Q_1$ ?

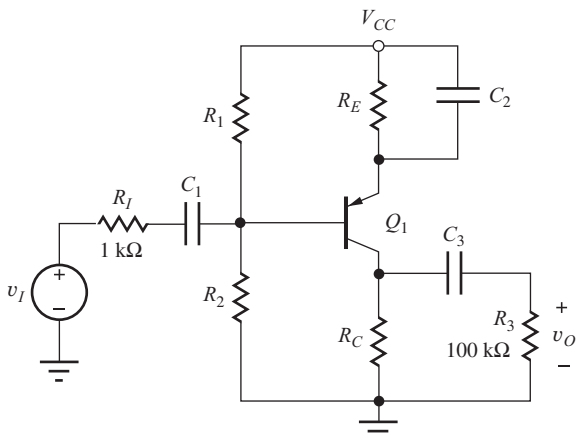


Figure P13.7

- 13.8. (a) What are the functions of capacitors  $C_1$ ,  $C_2$ , and  $C_3$ , in Fig. P13.8? (b) What is the magnitude of the signal voltage at the source of  $M_1$ ?

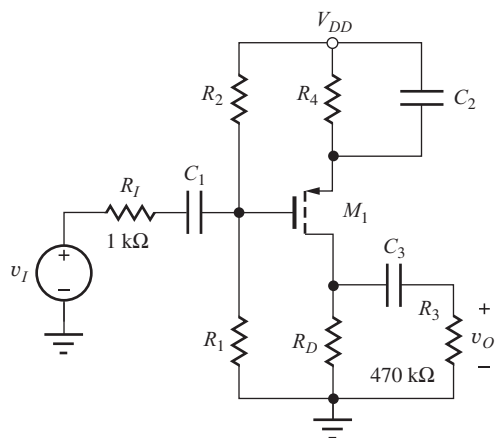


Figure P13.8

- 13.9. What are the functions of capacitors  $C_1$  and  $C_2$  in Fig. P13.9?

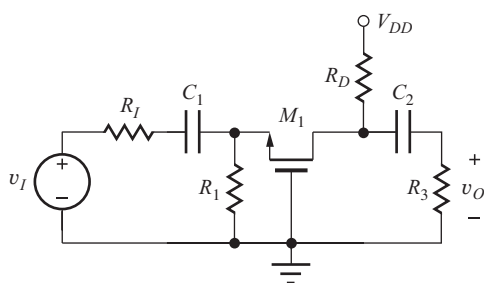


Figure P13.9

- 13.10. What are the functions of capacitors  $C_1$ ,  $C_2$ , and  $C_3$ , in Fig. P13.10? What is the magnitude of the signal voltage at the emitter of  $Q_1$ ?

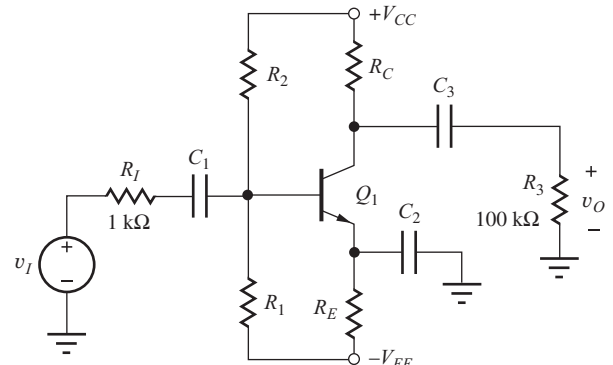


Figure P13.10

- 13.11. What are the functions of capacitors  $C_1$ ,  $C_2$ , and  $C_3$ , in Fig. P13.11? What is the magnitude of the signal voltage at the collector of  $Q_1$ ?

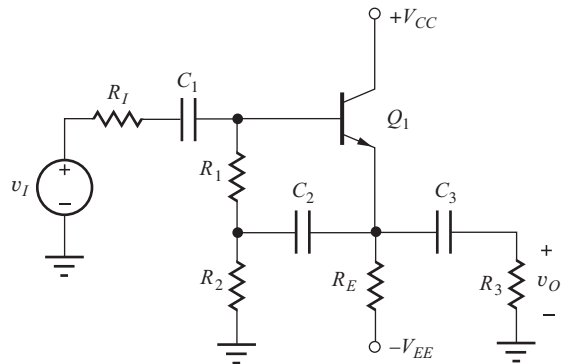


Figure P13.11

- 13.12. What are the functions of capacitors  $C_1$  and  $C_2$  in Fig. P13.12?

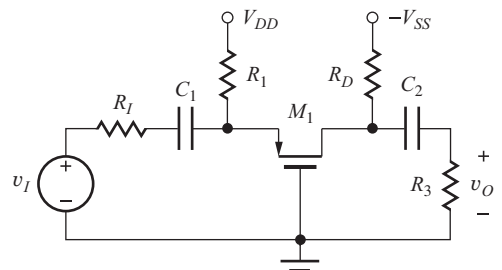


Figure P13.12

- 13.13. Describe the functions of capacitors  $C_1$ ,  $C_2$ , and  $C_3$ , in Fig. P13.13. What is the magnitude of the signal voltage at the upper terminal of  $C_2$ ?

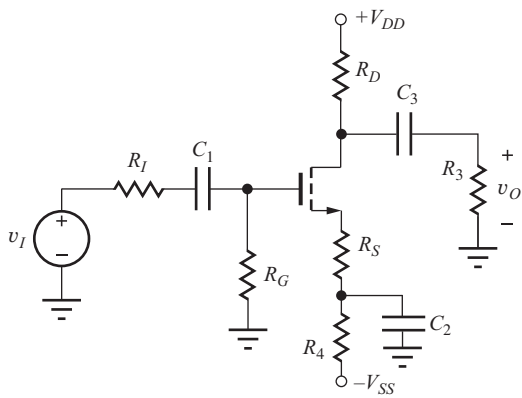


Figure P13.13

- 13.14. What are the functions of capacitors  $C_1$  and  $C_2$  in Fig. P13.14?

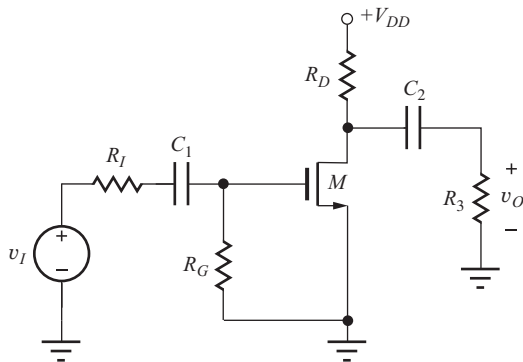


Figure P13.14

- 13.15. The phrase “dc voltage sources represent ac grounds” is used several times in the text. Use your own words to describe the meaning of this statement.

### 13.3 Circuit Analysis Using dc and ac Equivalent Circuits

- 13.16. Draw the dc equivalent circuit and find the Q-point for the amplifier in Fig. P13.10. Assume  $\beta_F = 75$ ,  $V_{CC} = 10$  V,  $-V_{EE} = -10$  V,  $R_I = 1$  k $\Omega$ ,  $R_1 = 5$  k $\Omega$ ,  $R_2 = 10$  k $\Omega$ ,  $R_3 = 24$  k $\Omega$ ,  $R_E = 4$  k $\Omega$ , and  $R_C = 6$  k $\Omega$ .
- 13.17. Use SPICE to find the Q-point for the circuit in Prob. 13.16. Compare the results to the hand calculations in Prob. 13.16.
- 13.18. Draw the dc equivalent circuit and find the Q-point for the amplifier in Fig. P13.14. Assume  $\beta_F = 90$ ,  $V_{CC} = 16$  V,  $R_I = 2$  k $\Omega$ ,  $R_1 = 360$  k $\Omega$ ,

$R_2 = 750$  k $\Omega$ ,  $R_C = 270$  k $\Omega$ ,  $R_E = 8.2$  k $\Omega$ ,  $R_4 = 220$  k $\Omega$ , and  $R_3 = 910$  k $\Omega$ .

- 13.19. (a) Use SPICE to find the Q-point for the circuit in Prob. 13.18. Assume  $V_A = \infty$  and  $I_S = 5$  fA.  
 (b) Repeat with  $V_A = 80$  V and  $I_S = 5$  fA.
- 13.20. Draw the dc equivalent circuit and find the Q-point for the amplifier in Fig. P13.6. Assume  $\beta_F = 65$ ,  $V_{CC} = 5$  V,  $-V_{EE} = -5$  V,  $R_I = 0.47$  k $\Omega$ ,  $R_B = 3$  k $\Omega$ ,  $R_C = 33$  k $\Omega$ ,  $R_E = 68$  k $\Omega$ , and  $R_3 = 120$  k $\Omega$ .
- 13.21. Use SPICE to find the Q-point for the circuit in Prob. 13.20. Compare the results to the hand calculations in Prob. 13.20.
- 13.22. Draw the dc equivalent circuit and find the Q-point for the amplifier in Fig. P13.7. Assume  $\beta_F = 135$  and  $V_{CC} = 10$  V,  $R_I = 20$  k $\Omega$ ,  $R_2 = 62$  k $\Omega$ ,  $R_C = 13$  k $\Omega$ , and  $R_E = 3.9$  k $\Omega$ .
- 13.23. Use SPICE to find the Q-point for the circuit in Prob. 13.22. Compare the results to the hand calculations in Prob. 13.22.
- 13.24. Draw the dc equivalent circuit and find the Q-point for the amplifier in Fig. P13.5. Assume  $K_n = 250$   $\mu\text{A/V}^2$ ,  $V_{TN} = 1$  V,  $V_{DD} = 16$  V,  $R_I = 1$  k $\Omega$ ,  $R_1 = 1$  M $\Omega$ ,  $R_2 = 2.7$  M $\Omega$ ,  $R_D = 82$  k $\Omega$ , and  $R_4 = 27$  k $\Omega$ .
- 13.25. Use SPICE to find the Q-point for the circuit in Prob. 13.24. Compare the results to the hand calculations in Prob. 13.24.
- 13.26. Draw the dc equivalent circuit and find the Q-point for the amplifier in Fig. P13.9. Assume  $K_n = 500$   $\mu\text{A/V}^2$ ,  $V_{TN} = -2$  V,  $V_{DD} = 18$  V,  $R_I = 1$  k $\Omega$ ,  $R_1 = 3.9$  k $\Omega$ ,  $R_D = 4.3$  k $\Omega$ , and  $R_3 = 51$  k $\Omega$ .
- 13.27. Use SPICE to find the Q-point for the circuit in Prob. 13.26. Compare the results to the hand calculations in Prob. 13.26.
- 13.28. Draw the dc equivalent circuit and find the Q-point for the amplifier in Fig. P13.8. Assume  $K_p = 400$   $\mu\text{A/V}^2$ ,  $V_{TP} = -1$  V,  $V_{DD} = 15$  V,  $R_I = 3.3$  M $\Omega$ ,  $R_2 = 3.3$  M $\Omega$ ,  $R_D = 24$  k $\Omega$ , and  $R_4 = 22$  k $\Omega$ .
- 13.29. Use SPICE to find the Q-point for the circuit in Prob. 13.28. Compare the results to the hand calculations in Prob. 13.28.
- 13.30. Draw the dc equivalent circuit and find the Q-point for the amplifier in Fig. P13.11. Assume  $\beta_F = 100$ ,  $V_{CC} = 9$  V,  $-V_{EE} = -9$  V,  $R_I = 1$  k $\Omega$ ,  $R_1 = 43$  k $\Omega$ ,  $R_2 = 43$  k $\Omega$ ,  $R_3 = 24$  k $\Omega$ , and  $R_E = 82$  k $\Omega$ .

- 13.31. Use SPICE to find the Q-point for the circuit in Prob. 13.30. Compare the results to the hand calculations in Prob. 13.30.
- 13.32. Draw the dc equivalent circuit and find the Q-point for the amplifier in Fig. P13.12. Assume  $K_p = 200 \mu\text{A/V}^2$ ,  $V_{TP} = +1 \text{ V}$ ,  $V_{DD} = 15 \text{ V}$ ,  $-V_{SS} = -15 \text{ V}$ ,  $R_1 = 33 \text{ k}\Omega$ ,  $R_D = 22 \text{ k}\Omega$ ,  $R_I = 500 \Omega$ , and  $R_3 = 100 \text{ k}\Omega$ .
- 13.33. Use SPICE to find the Q-point for the circuit in Prob. 13.32. Compare the results to the hand calculations in Prob. 13.32.
- 13.34. Draw the dc equivalent circuit and find the Q-point for the amplifier in Fig. P13.13. Assume  $K_n = 400 \mu\text{A/V}^2$ ,  $V_{TN} = -5 \text{ V}$ ,  $V_{DD} = 16 \text{ V}$ ,  $R_G = 10 \text{ M}\Omega$ ,  $R_D = 3.9 \text{ k}\Omega$ ,  $R_I = 10 \text{ k}\Omega$ ,  $R_1 = 2 \text{ k}\Omega$ ,  $R_S = 1 \text{ k}\Omega$ ,  $R_4 = 1 \text{ k}\Omega$ , and  $R_3 = 36 \text{ k}\Omega$ .
- 13.35. Use SPICE to find the Q-point for the circuit in Prob. 13.34. Compare the results to the hand calculations in Prob. 13.34.
- 13.36. Draw the dc equivalent circuit and find the Q-point for the amplifier in Fig. P13.14. Assume  $V_{DD} = 17.5 \text{ V}$ ,  $K_n = 225 \mu\text{A/V}^2$ ,  $V_{TN} = -3 \text{ V}$ ,  $R_G = 2.2 \text{ M}\Omega$ ,  $R_D = 7.5 \text{ k}\Omega$ ,  $R_I = 10 \text{ k}\Omega$ , and  $R_3 = 220 \text{ k}\Omega$ .
- 13.37. Use SPICE to find the Q-point for the circuit in Prob. 13.36. Compare the results to the hand calculations in Prob. 13.36.
- 13.38. (a) Draw the equivalent circuit used for ac analysis of the circuit in Fig. P13.3. (Use transistor symbols for this part.) Assume all capacitors have infinite value. (b) Redraw the ac equivalent circuit, replacing the transistor with its small-signal model. (c) Identify the function of each capacitor in the circuit (bypass or coupling).
- 13.39. (a) Repeat Prob. 13.38 for the circuit in Fig. P13.6. (b) Repeat Prob. 13.38 for the circuit in Fig. P13.7.
- 13.40. (a) Repeat Prob. 13.38 for the circuit in Fig. P13.10. (b) Repeat Prob. 13.38 for the circuit in Fig. P13.13.
- 13.41. (a) Repeat Prob. 13.38 for the circuit in Fig. P13.5. (b) Repeat Prob. 13.38 for the circuit in Fig. P13.9.
- 13.42. (a) Repeat Prob. 13.38 for the circuit in Fig. P13.8. (b) Repeat Prob. 13.38 for the circuit in Fig. P13.13.
- 13.43. (a) Repeat Prob. 13.38 for the circuit in Fig. P13.13. (b) Repeat Prob. 13.38 for the circuit in Fig. P13.14.
- 13.44. Describe the function of each of the resistors in the circuit in Fig. P13.3.
- 13.45. Describe the function of each of the resistors in the circuit in Fig. P13.6.
- 13.46. Describe the function of each of the resistors in the circuit in Fig. P13.10.
- 13.47. Describe the function of each of the resistors in Fig. P13.10.
- 13.48. Describe the function of each of the resistors in Fig. P13.5.
- 13.49. Describe the function of each of the resistors in Fig. 13.12.
- 13.50. Describe the function of each of the resistors in Fig. 13.14.

### 13.4 Introduction to Small-Signal Modeling

- 13.51. (a) Calculate  $r_d$  for a diode with  $V_D = 0.6 \text{ V}$  if  $I_S = 8 \text{ fA}$ . (b) What is the value of  $r_d$  for  $V_D = 0 \text{ V}$ ? (c) At what voltage does  $r_d$  exceed  $10^{12} \Omega$ ?
- 13.52. What is the value of the small-signal diode resistance  $r_d$  of a diode operating at a dc current of 2 mA at temperatures of (a) 75 K, (b) 100 K, (c) 200 K, (d) 300 K, and (e) 400 K?
- 13.53. (a) Compare  $[\exp(v_d/V_T) - 1]$  to  $v_d/V_T$  for  $v_d = +5 \text{ mV}$  and  $-5 \text{ mV}$ . How much error exists between the linear approximation and the exponential? (b) Repeat for  $v_d = \pm 10 \text{ mV}$ .

### 13.5 Small-Signal Models for Bipolar Junction Transistors

- 13.54. (a) What collector current is required for a bipolar transistor to achieve a transconductance of 40 mS? (b) Repeat for a transconductance of 200  $\mu\text{S}$ . (c) Repeat for a transconductance of 50  $\mu\text{S}$ .
- 13.55. At what Q-point current will  $r_\pi = 10 \text{ k}\Omega$  for a bipolar transistor with  $\beta_o = 85$ ? What are the approximate values of  $g_m$  and  $r_o$  if  $V_A = 100 \text{ V}$ ?
- 13.56. Repeat Prob. 13.55 for  $r_\pi = 1.5 \text{ M}\Omega$  with  $\beta_o = 125$  and  $V_A = 75 \text{ V}$ .
- 13.57. Repeat Prob. 13.56 for  $r_\pi = 220 \text{ k}\Omega$  with  $\beta_o = 100$ .
- 13.58. At what Q-point current will  $r_\pi = 1 \text{ M}\Omega$  for a bipolar transistor with  $\beta_o = 75$ ? What are the values of  $g_m$  and  $r_o$  if  $V_A = 100 \text{ V}$ ?
- 13.59. The following table contains the small-signal parameters for a bipolar transistor. What are the values of  $\beta_F$  and  $V_A$ ? Fill in the values of the missing entries in the table if  $V_{CE} = 10 \text{ V}$ .

**Bipolar Transistor Small-Signal Parameters**

$I_C$ (A)	$g_m$ (S)	$r_\pi$ ( $\Omega$ )	$r_o$ ( $\Omega$ )	$\mu_f$
0.002			50,000	
	0.12	600		
		480,000		

- 13.60. (a) Compare  $[\exp(v_{be}/V_T) - 1]$  to  $v_{be}/V_T$  for  $v_{be} = +5$  mV and  $-5$  mV? How much error exists between the linear approximation and the exponential? (b) Repeat for  $v_{be} = \pm 7.5$  mV. (c) Repeat for  $v_{be} = \pm 2.5$  mV.

- 13.61. The output characteristics of a bipolar transistor appear in Fig. P13.150. (a) What are the values of  $\beta_F$  and  $\beta_o$  at  $I_B = 4$   $\mu$ A and  $V_{CE} = 10$  V? (b) What are the values of  $\beta_F$  and  $\beta_o$  at  $I_B = 8$   $\mu$ A and  $V_{CE} = 10$  V?

- \*\*13.62. (a) Suppose that a BJT is operating with a total collector current given by

$$i_C(t) = 0.001 \exp\left(\frac{v_{be}(t)}{V_T}\right) \text{ Amps}$$

and  $v_{be}(t) = V_M \sin 2000\pi t$  with  $V_M = 5$  mV. What is the value of the dc collector current? Plot the collector current using MATLAB. Use FFT capability of MATLAB to find the amplitude of  $i_c$  at 1000 Hz? At 2000 Hz? At 3000 Hz? (b) Repeat for  $V_M = 50$  mV.

- 13.63. (a) Use SPICE to find the Q-point of the circuit in Fig. P13.10 using the element values in Prob. 13.16. Use the Q-point information from SPICE to calculate the values of the small-signal parameters of transistor  $Q_1$ . Compare the values with those printed out by SPICE and discuss the source of any discrepancies. (b) Repeat part (a) for the circuit in Fig. P13.7 with the element values from Prob. 13.22.

- \*13.64. Another small-signal model, the “T-model” in Fig. P13.64, is of historical interest and quite useful in certain situations. Show that this model is equivalent to the hybrid-pi model if the emitter resistance  $r_e = r_\pi/(\beta_o + 1) = \alpha_o/g_m = V_T/I_E$ . (Hint: Calculate the short-circuit input admittance ( $y_{11}$ ) for both models assuming  $\beta_F = \beta_o$ .)

### 13.6 The BJT Common-Emitter (C-E) Amplifier

- 13.65. The ac equivalent circuit for an amplifier is shown in Fig. P13.65. Assume the capacitors have infinite

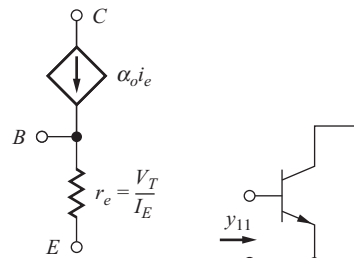


Figure P13.64

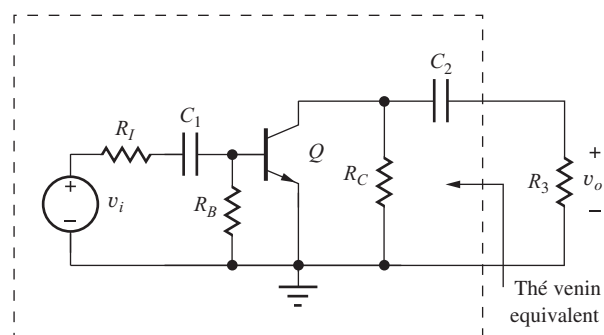


Figure P13.65

value,  $R_S = 750 \Omega$ ,  $R_B = 100 \text{ k}\Omega$ ,  $R_C = 100 \text{ k}\Omega$ , and  $R_3 = 100 \text{ k}\Omega$ . Calculate the voltage gain and input resistance for the amplifier if the BJT Q-point is  $(40 \mu\text{A}, 10 \text{ V})$ . Assume  $\beta_o = 100$  and  $V_A = 75 \text{ V}$ .

- 13.66. What are the worst-case values of voltage gain for the amplifier in Prob. 13.65 if  $\beta_o$  can range from 50 to 100? Assume that the Q-point is fixed.
- 13.67. The ac equivalent circuit for an amplifier is shown in Fig. P13.65. Assume the capacitors have infinite value,  $R_I = 50 \Omega$ ,  $R_B = 4.7 \text{ k}\Omega$ ,  $R_C = 4.3 \text{ k}\Omega$ , and  $R_3 = 10 \text{ k}\Omega$ . Calculate the voltage gain for the amplifier if the BJT Q-point is  $(2.0 \text{ mA}, 7.5 \text{ V})$ . Assume  $\beta_o = 75$  and  $V_A = 50 \text{ V}$ .
- 13.68. The ac equivalent circuit for an amplifier is shown in Fig. P13.68. Assume the capacitors have infinite value,  $R_I = 10 \text{ k}\Omega$ ,  $R_B = 5 \text{ M}\Omega$ ,  $R_C = 1.5 \text{ M}\Omega$  and  $R_3 = 3.3 \text{ M}\Omega$ . Calculate the voltage gain for the amplifier if the BJT Q-point is  $(1 \mu\text{A}, 1.5 \text{ V})$ . Assume  $\beta_o = 40$  and  $V_A = 50 \text{ V}$ .
- 13.69. (a) Rework Prob. 13.68 if  $I_C$  is increased to  $10 \mu\text{A}$ , and the values of  $R_C$ ,  $R_B$  and  $R_3$  are all reduced by a factor of 10. (b) Rework Prob. 13.68 if  $I_C$  is increased to  $100 \mu\text{A}$ , and the values of  $R_C$ ,  $R_B$  and  $R_3$  are all reduced by a factor of 100.

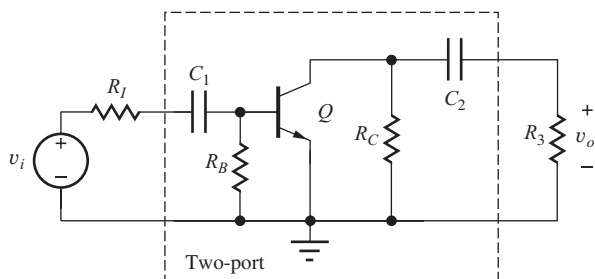


Figure P13.68

- (b) What is the minimum power supply voltage  $V_{CC}$ ?

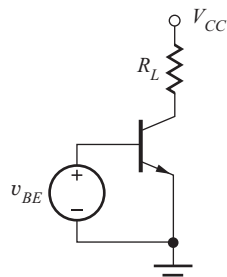


Figure P13.77

- 13.70. Simulate the behavior of the BJT common-emitter amplifier in Fig. 13.18 and compare the results to the calculations in Ex. 13.3. Use  $100 \mu\text{F}$  for all capacitor values and perform the ac analysis at a frequency of 1000 Hz.
- 13.71. (a) Use SPICE to simulate the dc and ac characteristics of the amplifier in Prob. 13.22. What is the Q-point? What is the value of the small-signal voltage gain? Use  $100 \mu\text{F}$  for all capacitor values and perform the ac analysis at a frequency of 1000 Hz.  
(b) Compare the results to hand calculations.
- 13.7 Important Limitations and Model Specifications**
- 13.72. A C-E amplifier is operating from a single 9-V supply. Estimate its voltage gain.
- \*13.73. A C-E amplifier is operating from symmetrical  $\pm 15\text{-V}$  power supplies. Estimate its voltage gain.
- 13.74. A battery-powered amplifier must be designed to provide a gain of 50. Can a single-stage amplifier be designed to meet this goal if it must operate from two  $\pm 1.5\text{-V}$  batteries?
- 13.75. A battery-powered C-E amplifier is operating from a single 1.5-V battery. Estimate its voltage gain. What will the gain be if the battery voltage drops to 1 V?
- \*13.76. An amplifier is required with a voltage gain of 25,000 and will be designed using a cascade of several C-E amplifier stages operating from a single 9-V power supply. Estimate the minimum number of amplifier stages that will be required to achieve this gain.
- \*13.77. The common-emitter amplifier in Fig. P13.77 must develop a 4-V peak-to-peak sinusoidal signal across the  $1\text{-k}\Omega$  load resistor  $R_L$ . (a) What is the minimum collector current  $I_C$  that will satisfy the requirements of small-signal operation of the transistor?
- \*13.78. The common-emitter amplifier in Fig. P13.77 has a voltage gain of 40 dB. What is the amplitude of the largest output signal voltage at the collector that corresponds to small-signal operation?
- \*13.79. A common-emitter amplifier has a gain of 50 dB and is developing a 15-V peak-to-peak ac signal at its output. Is this amplifier operating within its small-signal region? If the input signal to this amplifier is a sine wave, do you expect the output to be distorted? Why or why not?
- 13.80. (a) What is the voltage gain of the common-emitter amplifier in Fig. P13.10? Assume  $\beta_F = 135$ ,  $V_{CC} = V_{EE} = 7.5\text{ V}$ ,  $R_1 = 20\text{ k}\Omega$ ,  $R_2 = 62\text{ k}\Omega$ ,  $R_C = 13\text{ k}\Omega$ , and  $R_E = 3.9\text{ k}\Omega$ .
- 13.81. What is the voltage gain of the amplifier in Fig. P13.7 if  $V_{CC} = 15\text{ V}$ . Use the resistor values from Prob. 13.80.
- 13.82. Resistor  $R_L$  in Fig. P13.77 is replaced with an inductor  $L$ . What is the voltage gain of the circuit at low frequencies for which  $\omega L \gg r_o$ ?
- 13.8 Small-Signal Models for Field-Effect Transistors**
- 13.83. The following table contains the small-signal parameters for a MOS transistor. What are the values of  $K_n$  and  $\lambda$ ? Fill in the values of the missing entries in the table if  $V_{DS} = 6\text{ V}$  and  $V_{TN} = 1\text{ V}$ .

#### MOSFET Small-Signal Parameters

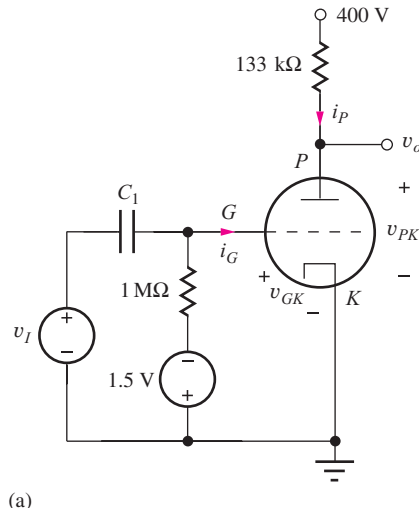
$I_{DS}$	$g_m (\text{s})$	$r_o (\Omega)$	$\mu_f$	SMALL-SIGNAL LIMIT $V_{gs} (\text{V})$
0.8 mA		50,000		
50 $\mu\text{A}$	0.0002			
10 mA				

- 13.84. A MOSFET is needed with  $g_m = 5 \text{ mS}$  at  $V_{GS} - V_{TN} = 0.5 \text{ V}$ . What is  $W/L$  if  $K'_n = 40 \mu\text{A/V}^2$ ?
- 13.85. What value of  $W/L$  is required to achieve  $\mu_f = 200$  in a MOSFET operating at a drain current of  $200 \mu\text{A}$  if  $K'_n = 50 \mu\text{A/V}^2$  and  $\lambda = 0.02/\text{V}$ ? What is the value of  $V_{GS} - V_{TN}$ ?
- 13.86. An  $n$ -channel MOSFET has  $K_n = 250 \mu\text{A/V}^2$ ,  $V_{TN} = 1 \text{ V}$ , and  $\lambda = 0.025 \text{ V}^{-1}$ . At what drain current will the MOSFET no longer be able to provide any voltage gain (that is,  $\mu_F \leq 1$ )?
- 13.87. Compare  $[1 + v_{gs}/(V_{GS} - V_{TN})]^2 - 1$  to  $[2v_{gs}/(V_{GS} - V_{TN})]$  for  $v_{gs} = 0.2 (V_{GS} - V_{TN})$ . How much error exists between the linear approximation and the quadratic expression? Repeat for  $v_{gs} = 0.4 (V_{GS} - V_{TN})$ .
- 13.88. Use SPICE to find the Q-point of the circuit in Prob. 13.24. Use the Q-point information from SPICE to calculate the values of the small-signal parameters of transistor  $M_1$ . Compare the values with those printed out by SPICE and discuss the source of any discrepancies.
- 13.89. Repeat Prob. 13.88 for the circuit in Prob. 13.28.
- 13.90. At approximately what Q-point will  $R_{\text{out}}^{CS} = 100 \text{ k}\Omega$  in a common-source amplifier if the transistor has  $\lambda = 0.02 \text{ V}^{-1}$  and the power supply is 18 V?
- \*13.91. At approximately what Q-point can we achieve an input resistance of  $R_{\text{in}}^{CS} = 2 \text{ M}\Omega$  in a common-source amplifier if the transistor has  $K_n = 500 \mu\text{A/V}^2$ ,  $V_{TN} = 1 \text{ V}$ ,  $\lambda = 0.02 \text{ V}^{-1}$ , and the power supply is 18 V?
- \*\*13.92. Figure P13.92 gives the device characteristics and schematic of an amplifier circuit including a “new”<sup>6</sup> electronic device called a *triode* vacuum tube. (a) Write the equation for the load line for the circuit. (b) What is the Q-point ( $I_P$ ,  $V_{PK}$ )? Assume  $i_G = 0$ . (c) Using the following definitions, find the values of  $g_m$ ,  $r_o$ , and  $\mu_f$ . (d) What is the voltage gain of the circuit?

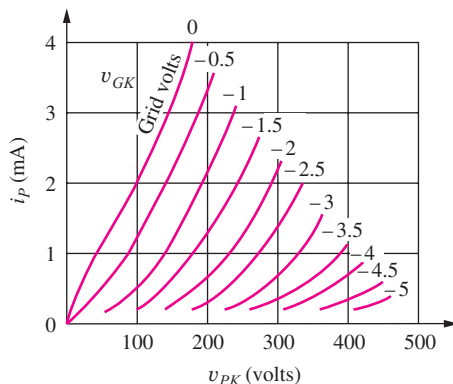
$$g_m = \frac{\Delta i_P}{\Delta v_{GK}} \Big|_{\text{Q-point}}$$

$$r_o = \left( \frac{\Delta i_P}{\Delta v_{PK}} \Big|_{\text{Q-point}} \right)^{-1}$$

$$\mu_f = g_m r_o$$



(a)



(b)

**Figure P13.92** “New” electron device—the triode vacuum tube. (b) Triode output characteristics:  $G$  = grid,  $P$  = plate,  $K$  = cathode.

### 13.9 Summary and Comparison of the Small-Signal Models of the BJT and FET

- 13.93. A circuit is to be biased at a current of  $10 \text{ mA}$  and achieve an input resistance of at least  $1 \text{ M}\Omega$ . Should a BJT or FET be chosen for this circuit and why?
- 13.94. A circuit requires the use of a transistor with a transconductance of  $0.5 \text{ S}$ . A bipolar transistor with  $\beta_F = 60$  and a MOSFET with  $K_n = 25 \text{ mA/V}^2$  are available. Which transistor would be preferred and why?
- 13.95. A BJT has  $V_A = 50 \text{ V}$  and a MOSFET has  $K_n = 25 \text{ mA/V}^2$  and  $\lambda = 0.02 \text{ V}^{-1}$ . At what current level is the intrinsic gain of the MOSFET equal

<sup>6</sup> New to us at least.

to that of the BJT if  $V_{DS} = V_{CE} = 10$  V? What is  $\mu_f$  for the BJT?

- 13.96. A BJT has  $V_A = 50$  V, and a MOSFET has  $\lambda = 0.02/\text{V}$  with  $V_{GS} - V_{TN} = 0.5$  V. What are the intrinsic gains of the two transistors? What are the transconductances if the transistors are both operating at a current of  $200 \mu\text{A}$ ?
- 13.97. An amplifier circuit is needed with an input resistance of  $50 \Omega$ . Should a BJT or MOSFET be chosen for this circuit? Discuss.
- 13.98. (a) We need to amplify a 0.25-V signal by 26 dB. Would a BJT or FET amplifier be preferred? Why? (b) RF amplifiers must often amplify microvolt signals in the presence of many other interfering signals with amplitudes of 100 mV or more. Does an FET or BJT seem most appropriate for this application? Why?

### 13.10 The Common-Source Amplifier

- 13.99. A C-S amplifier is operating from a single 15-V supply with  $V_{GS} - V_{TN} = 1$  V. Estimate its voltage gain.
- 13.100. A common-source amplifier has a gain of 15 dB and is developing a 15-V peak-to-peak ac signal at its output. Is this amplifier operating within its small-signal region? Discuss.
- 13.101. A C-S amplifier is operating from a single 16-V supply. The MOSFET has  $K_n = 1 \text{ mA/V}^2$ . What is the Q-point current required for a voltage gain of 30?
- 13.102. A C-S amplifier is operating from a single 9-V supply. What is the maximum value of  $V_{GS} - V_{TN}$  that can be used if the amplifier must have a gain of at least 30?
- 13.103. A MOSFET common-source amplifier must amplify a sinusoidal ac signal with a peak amplitude of 0.2 V. What is the minimum value of  $V_{GS} - V_{TN}$  for the transistor? If a voltage gain of 35 dB is required, what is the minimum power supply voltage?
- 13.104. A MOSFET common-source amplifier must amplify a sinusoidal ac signal with a peak amplitude of 0.4 V. What is the minimum value of  $V_{GS} - V_{TN}$  for the transistor? If a voltage gain of 20 dB is required, what is the minimum power supply voltage?
- 13.105. An amplifier is required with a voltage gain of 1000 and will be designed using a cascade of sev-

eral C-S amplifier stages operating from a single 10-V power supply. Estimate the minimum number of amplifier stages required to achieve this gain.

- 13.106. What is the voltage gain of the amplifier in Fig. P13.106? Assume  $K_n = 0.500 \text{ mA/V}^2$ ,  $V_{TN} = 1$  V, and  $\lambda = 0.0133 \text{ V}^{-1}$ .

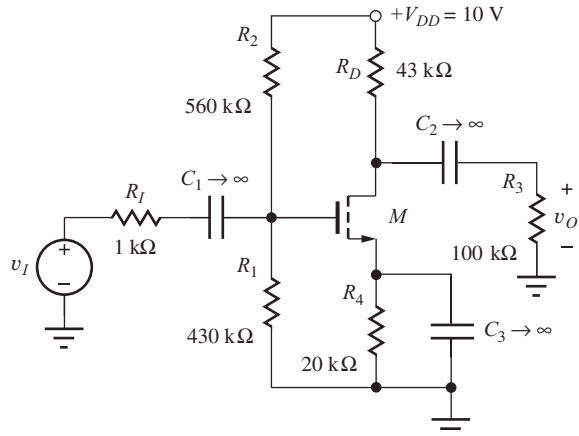


Figure P13.106

- 13.107. The ac equivalent circuit for an amplifier is shown in Fig. P13.107. Assume the capacitors have infinite value,  $R_I = 100 \text{ k}\Omega$ ,  $R_G = 6.8 \text{ M}\Omega$ ,  $R_D = 50 \text{ k}\Omega$ , and  $R_3 = 120 \text{ k}\Omega$ . Calculate the voltage gain for the amplifier if the MOSFET Q-point is  $(100 \mu\text{A}, 5 \text{ V})$ . Assume  $K_n = 500 \mu\text{A/V}^2$  and  $\lambda = 0.02 \text{ V}^{-1}$ .

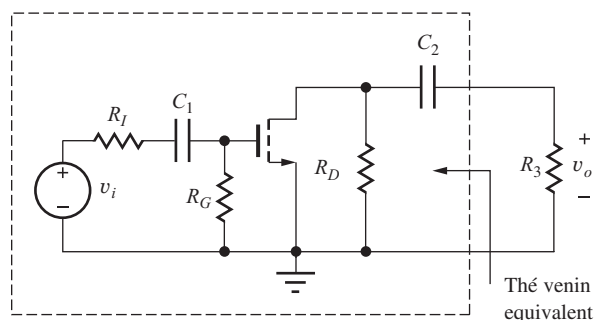


Figure P13.107

- 13.108. What are the worst-case values of voltage gain for the amplifier in Prob. 13.107 if  $K_n$  can range from  $300 \mu\text{A/V}^2$  to  $700 \mu\text{A/V}^2$ ? Assume the Q-point is fixed.
- 13.109. The ac equivalent circuit for an amplifier is shown in Fig. P13.107. Assume the capacitors have infinite value,  $R_I = 100 \text{ k}\Omega$ ,  $R_G = 10 \text{ M}\Omega$ ,

$R_D = 560 \text{ k}\Omega$ , and  $R_3 = 2.2 \text{ M}\Omega$ . Calculate the voltage gain for the amplifier if the MOSFET Q-point is  $(10 \mu\text{A}, 5 \text{ V})$ . Assume  $K_n = 100 \mu\text{A/V}^2$  and  $\lambda = 0.02 \text{ V}^{-1}$ .

- 13.110. The ac equivalent circuit for an amplifier is shown in Fig. P13.110. Assume the capacitors have infinite value,  $R_I = 10 \text{ k}\Omega$ ,  $R_G = 1 \text{ M}\Omega$ ,  $R_D = 3.9 \text{ k}\Omega$ , and  $R_3 = 270 \text{ k}\Omega$ . Calculate the voltage gain for the amplifier if the MOSFET Q-point is  $(2 \text{ mA}, 7.5 \text{ V})$ . Assume  $K_n = 1 \text{ mA/V}^2$  and  $\lambda = 0.015 \text{ V}^{-1}$ .

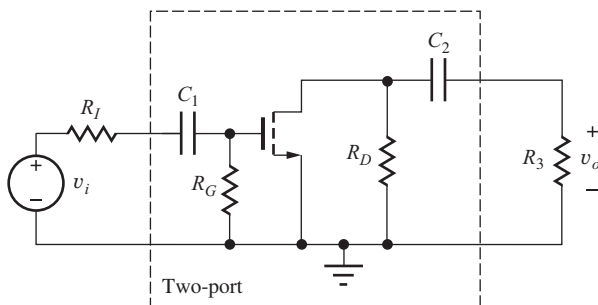


Figure P13.110

- 13.111. Use SPICE to simulate the dc and ac characteristics of the amplifier in Prob. 13.24. What is the Q-point? What are the values of the small-signal voltage gain, input resistance, and output resistance of the amplifier? Use  $100 \mu\text{F}$  for all capacitor values and perform the ac analysis at a frequency of  $1000 \text{ Hz}$ .
- 13.112. Use SPICE to simulate the dc and ac characteristics of the amplifier in Prob. 13.28. What is the Q-point? What are the values of the small-signal voltage gain, input resistance, and output resistance of the amplifier? Use  $100 \mu\text{F}$  for all capacitor values and perform the ac analysis at a frequency of  $1000 \text{ Hz}$ .
- 13.113. Use SPICE to simulate the dc and ac characteristics of the amplifier in Prob. 13.34. What is the Q-point? What are the values of the small-signal voltage gain, input resistance, and output resistance of the amplifier? Use  $100 \mu\text{F}$  for all capacitor values and perform the ac analysis at a frequency of  $1000 \text{ Hz}$ .
- 13.114. Use SPICE to simulate the dc and ac characteristics of the amplifier in Prob. 13.36. What is the Q-point? What are the values of the small-signal voltage gain, input resistance, and output resistance of the amplifier? Use  $100 \mu\text{F}$  for all capacitor values and perform the ac analysis at a frequency of  $1000 \text{ Hz}$ .

values and perform the ac analysis at a frequency of  $1000 \text{ Hz}$ .

### Input and Output Resistances of the Common-Emitter and Common-Source Amplifiers

- 13.115. The ac equivalent circuit for an amplifier is shown in Fig. P13.65. Assume the capacitors have infinite value,  $R_I = 750 \Omega$ ,  $R_B = 100 \text{ k}\Omega$ ,  $R_C = 100 \text{ k}\Omega$ , and  $R_3 = 100 \text{ k}\Omega$ . Calculate the input resistance and output resistance for the amplifier if the BJT Q-point is  $(60 \mu\text{A}, 10 \text{ V})$ . Assume  $\beta_o = 100$  and  $V_A = 75 \text{ V}$ .
- 13.116. The ac equivalent circuit for an amplifier is shown in Fig. P13.65. Assume the capacitors have infinite value,  $R_I = 50 \Omega$ ,  $R_B = 4.7 \text{ k}\Omega$ ,  $R_C = 4.3 \text{ k}\Omega$ , and  $R_3 = 10 \text{ k}\Omega$ . Calculate the input resistance and output resistance for the amplifier if the BJT Q-point is  $(2.5 \text{ mA}, 7.5 \text{ V})$ . Assume  $\beta_o = 75$  and  $V_A = 50 \text{ V}$ .
- 13.117. What are the worst-case values of input resistance and output resistance for the amplifier in Prob. 13.65 if  $\beta_o$  can range from 60 to 100? Assume that the Q-point is fixed.
- 13.118. The ac equivalent circuit for an amplifier is shown in Fig. P13.68. Assume the capacitors have infinite value,  $R_I = 10 \text{ k}\Omega$ ,  $R_B = 5 \text{ M}\Omega$ ,  $R_C = 1.5 \text{ M}\Omega$ , and  $R_3 = 3.3 \text{ M}\Omega$ . Calculate the input resistance and output resistance for the amplifier if the BJT Q-point is  $(1 \mu\text{A}, 1.5 \text{ V})$ . Assume  $\beta_o = 40$  and  $V_A = 50 \text{ V}$ .
- 13.119. (a) Rework Prob. 13.118 if  $I_C$  is increased to  $10 \mu\text{A}$ , and the values of  $R_C$ ,  $R_B$ , and  $R_3$  are all reduced by a factor of 10. (b) Rework Prob. 13.118 if  $I_C$  is increased to  $100 \mu\text{A}$ , and the values of  $R_C$ ,  $R_B$ , and  $R_3$  are all reduced by a factor of 100.
- 13.120. What are the input resistance and output resistance of the amplifier in Prob. 13.106?
- 13.121. Calculate the input and output resistances for the amplifier in Prob. 13.107.
- 13.122. What are the worst-case values of the input and output resistances for the amplifier in Prob. 13.107 if  $K_n$  can range from  $300 \mu\text{A/V}^2$  to  $700 \mu\text{A/V}^2$ ? Assume the Q-point is fixed.
- 13.123. Calculate the input and output resistances for the amplifier in Prob. 13.109.
- 13.124. Calculate the input and output resistances for the amplifier in Prob. 13.110.

- 13.125. Calculate the Thévenin equivalent representation for the amplifier in Prob. 13.67.
- 13.126. Calculate the Thévenin equivalent representation for the amplifier in Prob. 13.65.
- 13.127. Calculate the Thévenin equivalent representation for the amplifier in Prob. 13.109.
- 13.128. Calculate the Thévenin equivalent representation for the amplifier in Prob. 13.107.

### 13.11 Common-Emitter and Common-Source Amplifier Summary

- 13.129. Find the voltage gain, input resistance and output resistance of the C-E stage in Fig. P13.129. Assume  $\beta_F = 65$  and  $V_A = 50$  V.

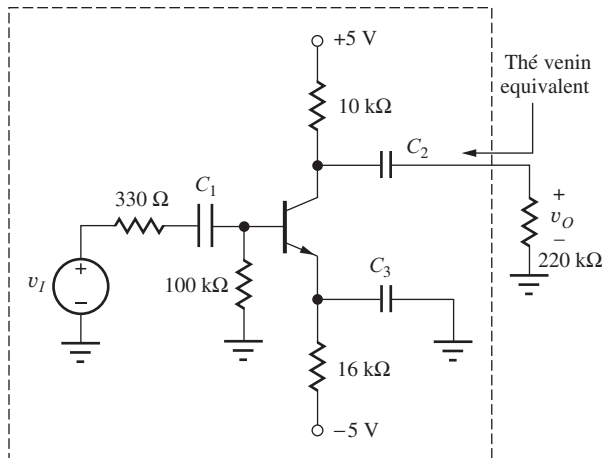


Figure P13.129

- 13.130. Simulate the behavior of the BJT common-emitter amplifier in Fig. P13.129 and compare the results to the calculations in Prob. 13.129. Use  $100 \mu\text{F}$  for all capacitor values and perform the ac analysis at a frequency of 10,000 Hz.
- 13.131. The amplifier in Fig. P13.131 is the bipolar amplifier in Fig. P13.129 with currents reduced by a factor of approximately 10. What are the voltage gain and input resistance and output resistance of this amplifier? Compare to that in Fig. P13.129, and discuss the reasons for any differences in gain.
- 13.132. Simulate the behavior of the BJT common-emitter amplifier in Fig. P13.131 and compare the results to the calculations in Prob. 13.131. Use  $100 \mu\text{F}$  for all capacitor values and perform the ac analysis at a frequency of 1000 Hz.

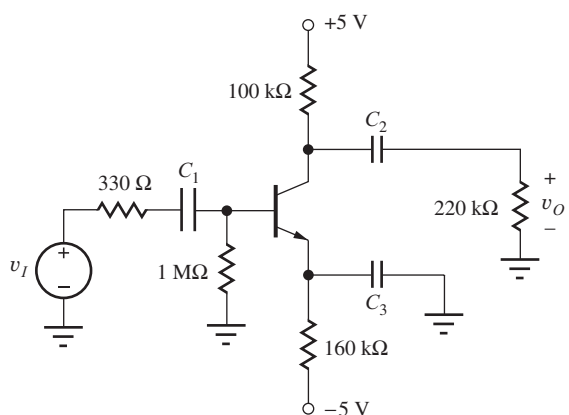


Figure P13.131

- 13.133. Use SPICE to simulate the behavior of the MOSFET common-source amplifier in Fig. 13.32(b) and compare the results to the calculations in the example. Use  $100 \mu\text{F}$  for all capacitor values and perform the ac analysis at a frequency of 1000 Hz.
- 13.134. Use SPICE to simulate the voltage gain and input resistance and output resistance of the amplifier in Prob. 13.106. Use  $100 \mu\text{F}$  for all capacitor values and perform the ac analysis at a frequency of 1000 Hz.

### 13.12 Amplifier Power and Signal Range

- 13.135. Calculate the dc power dissipation in each element in the circuit in Fig. 13.40(a) if  $\beta_F = 65$ . Compare the result to the total power delivered by the sources.
- 13.136. Calculate the dc power dissipation in each element in the circuit in Fig. 13.40(b). Compare the result to the total power delivered by the sources.
- 13.137. Calculate the dc power dissipation in each element in the circuit in Prob. 13.16. Compare the result to the total power delivered by the sources.
- 13.138. Repeat Prob. 13.137 for the circuit in Prob. 13.20.
- 13.139. Repeat Prob. 13.137 for the circuit in Prob. 13.24.
- 13.140. Repeat Prob. 13.137 for the circuit in Prob. 13.28.
- 13.141. Repeat Prob. 13.137 for the circuit in Prob. 13.34.
- \*13.142. A common bias point for a transistor is shown in Fig. P13.142. What is the maximum amplitude signal that can be developed at the collector terminal that will satisfy the small-signal assumptions (in terms of  $V_{CC}$ )?

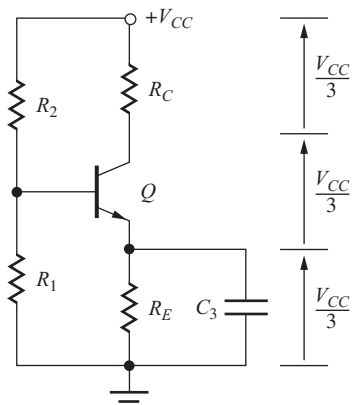


Figure P13.142

- \*13.143. The MOSFET in Fig. P13.143 has \$K\_n = 500 \mu\text{A}/\text{V}^2\$ and \$V\_{TN} = -1.5 \text{ V}\$. What is the largest permissible signal voltage at the drain that will satisfy the requirements for small-signal operation if \$R\_D = 15 \text{ k}\Omega\$? What is the minimum value of \$V\_{DD}\$?

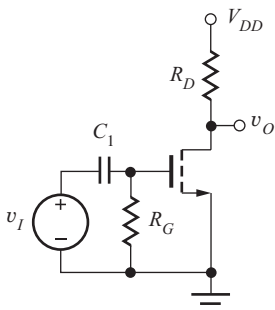


Figure P13.143

- \*13.144. The simple C-E amplifier in Fig. P13.144 is biased with \$V\_{CE} = V\_{CC}/2\$. Assume that the transistor can saturate with \$V\_{CESAT} = 0 \text{ V}\$ and still be

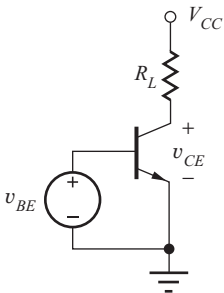


Figure P13.144

operating linearly. What is the amplitude of the largest sine wave that can appear at the output? What is the ac signal power \$P\_{ac}\$ being dissipated in the load resistor \$R\_L\$? What is the total dc power \$P\_S\$ being supplied from the power supply? What is the efficiency \$\varepsilon\$ of this amplifier if \$\varepsilon\$ is defined as \$\varepsilon = 100\% \times P\_{ac}/P\_S\$?

- 13.145. What is the amplitude of the largest ac signal that can appear at the collector of the transistor in Fig. P13.7 that satisfies the small-signal limit? Use the parameter values from Prob. 13.22.
- 13.146. What is the amplitude of the largest ac signal that can appear at the drain of the transistor in Fig. P13.5 that satisfies the small-signal limit? Use the parameter values from Prob. 13.24.
- 13.147. What is the amplitude of the largest ac signal that can appear at the drain of the transistor in Fig. P13.8 that satisfies the small-signal limit? Use the parameter values from Prob. 13.28.
- 13.148. What is the amplitude of the largest ac signal that can appear at the collector of the transistor in Fig. P13.10 that satisfies the small-signal limit? Use the parameter values from Prob. 13.16.
- 13.149. What is the amplitude of the largest ac signal that can appear at the drain of the transistor in Fig. P13.14 that satisfies the small-signal limit? Use the parameter values from Prob. 13.36.
- 13.150. Draw the load line for the circuit in Fig. 13.1 on the output characteristics in Fig. P13.150 for \$V\_{CC} = 20 \text{ V}\$ and \$R\_C = 20 \text{ k}\Omega\$. Locate the Q-point for \$I\_B = 2 \mu\text{A}\$. Estimate the maximum output voltage swing from the characteristics. Repeat for \$I\_B = 5 \mu\text{A}\$.

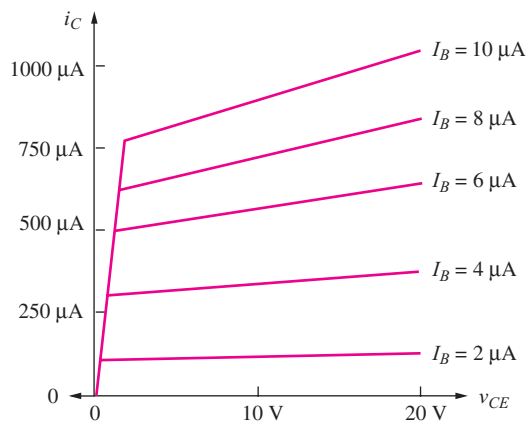


Figure P13.150

### JFET Problems

- 13.151. Describe the functions of capacitors  $C_1$ ,  $C_2$ , and  $C_3$  in Fig. P13.151? What is the magnitude of the signal voltage at the source of  $J_1$ ?

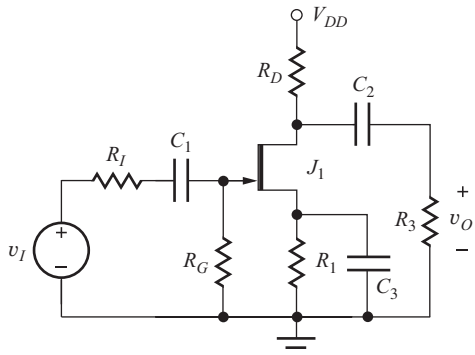


Figure P13.151

- 13.152. What are the functions of capacitors  $C_1$  and  $C_2$  in Fig. P13.152?

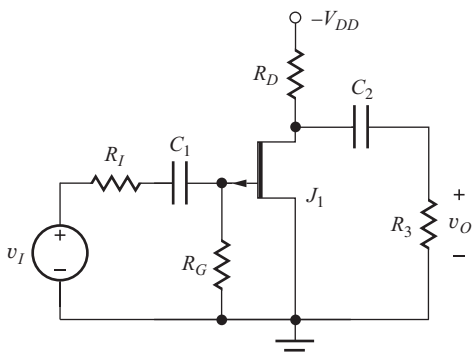


Figure P13.152

- 13.153. The JFET amplifier in Fig. P13.153 must develop a 10-V peak-to-peak sinusoidal signal across the 15-k $\Omega$  load resistor  $R_D$ . What is the minimum drain current  $I_D$  that will satisfy the requirements for small-signal operation of the transistor?

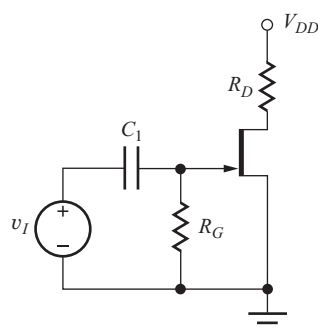


Figure P13.153

- 13.154. The ac equivalent circuit for an amplifier is shown in Fig. P13.154. Assume the capacitors have infinite value,  $R_I = 10\text{ k}\Omega$ ,  $R_G = 1\text{ M}\Omega$ ,  $R_D = 7.5\text{ k}\Omega$ , and  $R_3 = 160\text{ k}\Omega$ . Calculate the voltage gain, input resistance and output resistance for the amplifier if the JFET Q-point is (1 mA, 9 V). Assume  $I_{DSS} = 1\text{ mA}$ ,  $V_P = -3\text{ V}$ , and  $\lambda = 0.015\text{ V}^{-1}$ .

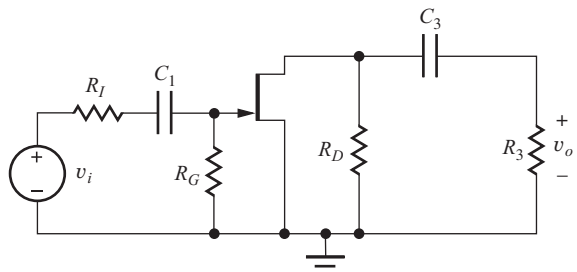
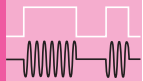


Figure P13.154

- 13.155. Show that the drain-current expression for the JFET can be represented in exactly the same form as that of the MOSFET using the substitutions  $V_P = V_{TN}$  and  $K_n = 2I_{DSS}/V_P^2$ .

# CHAPTER 14



## SINGLE-TRANSISTOR AMPLIFIERS

### CHAPTER OUTLINE

- 14.1 Amplifier Classification 858
- 14.2 Inverting Amplifiers—Common-Emitter and Common-Source Circuits 864
- 14.3 Follower Circuits—Common-Collector and Common-Drain Amplifiers 886
- 14.4 Noninverting Amplifiers—Common-Base and Common-Gate Circuits 894
- 14.5 Amplifier Prototype Review and Comparison 903
- 14.6 Common-Source Amplifiers Using MOS Inverters 907
- 14.7 Coupling and Bypass Capacitor Design 914
- 14.8 Amplifier Design Examples 925
- 14.9 Multistage ac-Coupled Amplifiers 939
- Summary 950
- Key Terms 951
- Additional Reading 952
- Problems 952

### CHAPTER GOALS

In Chapter 14, we fully explore the small-signal characteristics of three families of single-stage amplifiers. We will discover why certain transistor terminals are preferred for signal input whereas others are used for signal outputs. The results define three broad classes of amplifiers.

- Inverting amplifiers—the common-emitter and common-source configurations—that provide high voltage gain with a  $180^\circ$  phase shift
- Followers—the common-collector and common-drain configurations—that provide nearly unity gain similar to the op amp voltage follower
- Noninverting amplifiers—the common-base and common-gate configurations—that provide high voltage gain with no phase shift

For each type of amplifier, we discuss the detailed design of

- Voltage gain and input voltage range
- Current gain
- Input and output resistances
- Coupling and bypass capacitor design and lower cutoff frequency

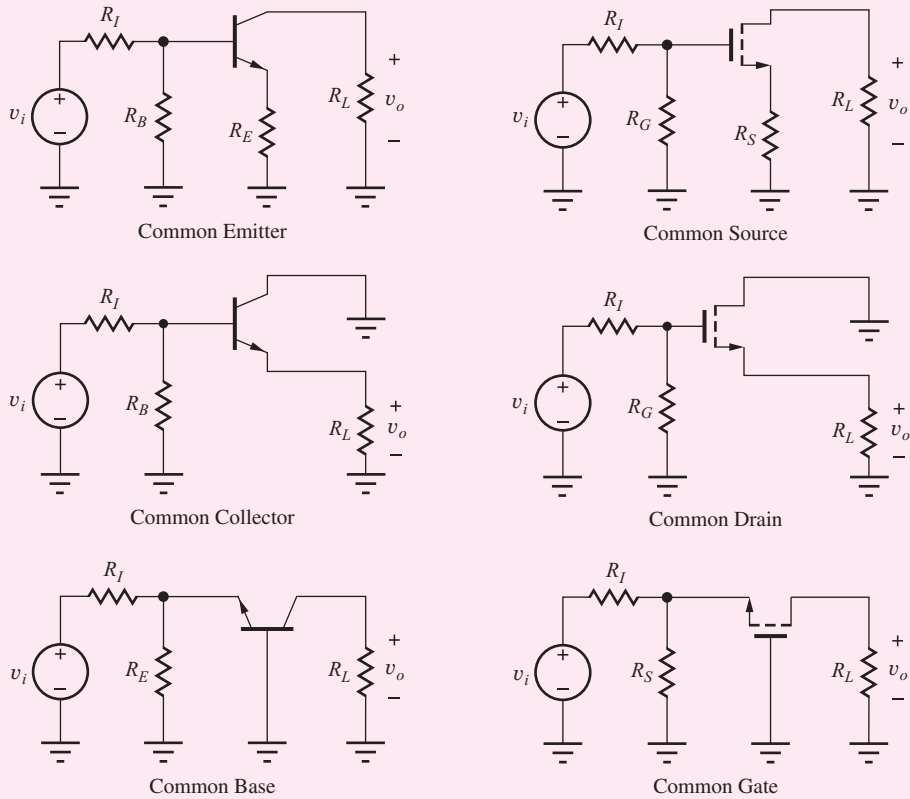
The results become our design toolkit and are used to solve a number of examples of design problems.

As in most chapters, we will continue to increase our understanding of SPICE simulation and interpretation of SPICE results. In particular, we try to understand the differences between

- SPICE ac (small-signal), transient (large signal), and transfer function analysis modes

Chapter 13 introduced the common-emitter and common-source amplifiers, in which the input signal was applied to the base and gate terminals of the BJT and MOSFET, respectively, and the output signal was taken from the collector and drain. However, bipolar and field-effect transistors are three-terminal devices, and this chapter explores the use of other terminals for signal input and output. Three useful amplifier configurations are identified, each using a different terminal as the common or reference terminal. When implemented using bipolar transistors, these are called the common-emitter, common-collector, and common-base amplifiers; the corresponding names for the FET implementations are the common-source, common-drain, and common-gate amplifiers. Each amplifier category provides a unique set of characteristics in terms of voltage gain, input resistance, output resistance, and current gain.

The chapter expands the discussion of the characteristics of the common-emitter and common-source amplifiers, i.e., the inverting amplifiers that were developed in Chapter 13, and then looks in depth at the followers and noninverting amplifiers, focusing on the limits solid-state devices place on individual amplifier performance. Expressions are presented for the properties of each amplifier, and their similarities and differences are discussed in detail in order to build the understanding needed for the circuit design process. The transistor-level results are used throughout this book to analyze and design more complex single-stage and multi-stage amplifiers. We also explore amplifier frequency response at low frequencies and develop design equations useful for choosing coupling and bypass capacitors.



Much discussion is devoted to single-transistor amplifiers because they are the heart of analog design. These single-stage amplifiers are an important part of the basic

“tool set” of analog circuit designers, and a good understanding of their similarities and differences is a prerequisite for more complex amplifier design.

## 14.1 AMPLIFIER CLASSIFICATION

In Chapter 13, the input signal was applied to the base or gate of the transistor, and the output signal was taken from the collector or drain. However, the transistor has three separate terminals that may possibly be used to inject a signal for amplification: the base, emitter, and collector for the BJT; the gate, source, and drain for the FET. We will see shortly that only the base and emitter, or gate and source, are useful as signal insertion points; the collector and emitter, or drain and source, are useful points for signal removal. The examples we use in this chapter of the various amplifier configurations all use the same four-resistor bias circuits shown in Fig. 14.1. Coupling and bypass capacitors are then used to change the signal injection and extraction points and modify the ac characteristics of the amplifiers.

### 14.1.1 SIGNAL INJECTION AND EXTRACTION—THE BJT

For the BJT in Fig. 14.1(a), the large-signal transport model provides guidance for proper location of the input signal. In the forward-active region of the BJT,

$$i_C = I_S \left[ \exp \left( \frac{v_{BE}}{V_T} \right) \right] \quad i_B = \frac{i_C}{\beta_F} = \frac{I_S}{\beta_{FO}} \left[ \exp \left( \frac{v_{BE}}{V_T} \right) \right] \quad i_E = \frac{I_S}{\alpha_F} \left[ \exp \left( \frac{v_{BE}}{V_T} \right) \right] \quad (14.1)$$

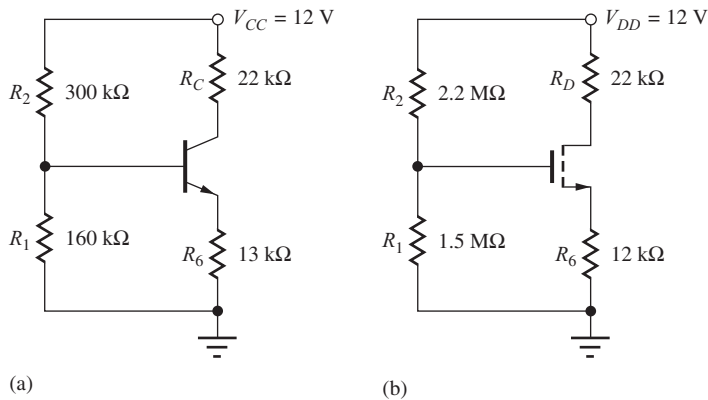


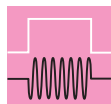
**Figure 14.1** Four-resistor bias circuits for the (a) BJT and (b) MOSFET.

To cause  $i_C$ ,  $i_E$ , and  $i_B$  to vary significantly, we need to change the base-emitter voltage  $v_{BE}$ , which appears in the exponential term. Because  $v_{BE}$  is equivalent to

$$v_{BE} = v_B - v_E \quad (14.2)$$

an input signal voltage can be injected into the circuit to vary the voltage at either the base or the emitter of the transistor. Note that the Early voltage has been omitted from Eq. (14.1), which indicates that varying the collector voltage has no effect on the terminal currents. Thus, the collector terminal is not an appropriate terminal for signal injection. Even for finite values of Early voltage, current variations with collector voltage are small, especially when compared to the exponential dependence of the currents on  $v_{BE}$ —again, the collector is not used as a signal injection point.

Substantial changes in the collector and emitter currents can create large voltage signals across the collector and emitter resistors  $R_C$  and  $R_E$  in Fig. 14.1. Thus, signals can be removed from the amplifier at the collector or emitter terminals. However, because the base current  $i_B$  is a factor of  $\beta_F$  smaller than either  $i_C$  or  $i_E$ , the base terminal is not normally used as an output terminal.



## DESIGN NOTE

The input signal can be applied to the base or emitter terminal of the bipolar transistor, and the output signal can be taken from the collector or emitter. The collector is not used as an input terminal, and the base is not used as an output.

### 14.1.2 SIGNAL INJECTION AND EXTRACTION – THE FET

A similar set of arguments can be used for the FET in Fig. 14.1(b), based on the expression for the  $n$ -channel MOSFET drain current in pinchoff:

$$i_S = i_D = \frac{K_n}{2} (v_{GS} - V_{TN})^2 \quad \text{and} \quad i_G = 0 \quad (14.3)$$

To cause  $i_D$  and  $i_S$  to vary significantly, we need to change the gate-source voltage  $v_{GS}$ . Because  $v_{GS}$  is equivalent to

$$v_{GS} \equiv v_G - v_S \quad (14.4)$$

an input signal voltage can be injected so as to vary either the gate or source voltage of the FET. Varying the drain voltage has only a minor effect (for  $\lambda \neq 0$ ) on the terminal currents, so the drain terminal is not an appropriate terminal for signal injection. As for the BJT, substantial changes in the drain or source currents can develop large voltage signals across resistors  $R_D$  and  $R_6$  in Fig. 14.1(b). However, the gate terminal is not used as an output terminal because the gate current is zero.

In summary, effective amplification requires a signal to be injected into either the base/emitter or gate/source terminals of the transistors in Fig. 14.1; the output signal can be taken from the collector/emitter or drain/source terminals. We do not inject a signal into the collector or drain or extract a signal from the base or gate terminals. These constraints yield three families of amplifiers: the **common-emitter/common-source (C-E/C-S)** circuits that we studied in Chapter 13, the **common-base/common-gate (C-B/C-G)** circuits, and the **common-collector/common-drain (C-C/C-D)** circuits.

These amplifiers are classified in terms of the structure of the ac equivalent circuit; each is discussed in detail in the next several sections. As noted earlier, the circuit examples all use the same four-resistor bias circuits in Fig. 14.1 in order to establish the Q-point of the various amplifiers. Coupling and bypass capacitors are then used to change the ac equivalent circuits. We will find that the ac characteristics of the various amplifiers are significantly different.

**EXERCISE:** Find the Q-points for the transistors in Fig. 14.1 and calculate the small-signal model parameters for the BJT and MOSFET. Use  $\beta_F = 100$ ,  $V_A = 50$  V,  $K_n = 500 \mu\text{A/V}^2$ ,  $V_{TN} = 1$  V, and  $\lambda = 0.02 \text{ V}^{-1}$ . What are the values of  $\mu_f$ ? What is the value of  $V_{GS} - V_{TN}$  for the MOSFET?

**ANSWERS:**

	$I_C / I_D$	$V_{CE} / V_{DS}$	$V_{GS} - V_{TN}$	$g_m$	$r_\pi$	$r_o$	$\mu_f$
BJT	245 $\mu\text{A}$	3.64 V	...	9.80 mS	10.2 k $\Omega$	219 k $\Omega$	2150
FET	241 $\mu\text{A}$	3.81 V	0.982 V	0.491 mS	$\infty$	223 k $\Omega$	110

## DESIGN NOTE

The input signal can be applied to the gate or source terminal of the FET, and the output signal can be taken from the drain or source. The drain is not used as an input terminal, and the gate is not used as an output.

### 14.1.3 COMMON-EMITTER (C-E) AND COMMON-SOURCE (C-S) AMPLIFIERS

The circuits in Fig. 14.2 are generalized versions of the common-emitter and common-source amplifiers discussed in Chapter 13. In these circuits, resistor  $R_6$  in Fig. 14.1 has been split into two parts, with only resistor  $R_4$  bypassed by capacitor  $C_2$ . We gain considerable flexibility in setting the voltage gain, input resistance, and output resistance of the amplifier by not bypassing all of the resistance in the transistor's emitter or source. In the C-E circuit in Fig. 14.2(a), the signal is injected into the base and taken out of the collector of the BJT. The emitter is the common terminal between the input and output ports. In the C-S circuit in Fig. 14.2(b), the signal is injected into the gate and taken out of the drain of the MOSFET; the source is the common terminal between the input and output ports.

The simplified ac equivalent circuits for these amplifiers appear in Figs. 14.2(c) and (d). We see that these network topologies are identical. Resistors  $R_E$  and  $R_S$ , connected between the emitter or source and ground, represent the unbypassed portion of the original bias resistor  $R_6$ . The presence of  $R_E$  and  $R_S$  in the ac equivalent circuits gives an added degree of freedom to the designer, and allows gain to be traded for increased input resistance, output resistance, and input signal range. Our comparative analysis will show that the C-E and C-S circuits can provide moderate-to-high values of voltage, current gain, input resistance, and output resistance.

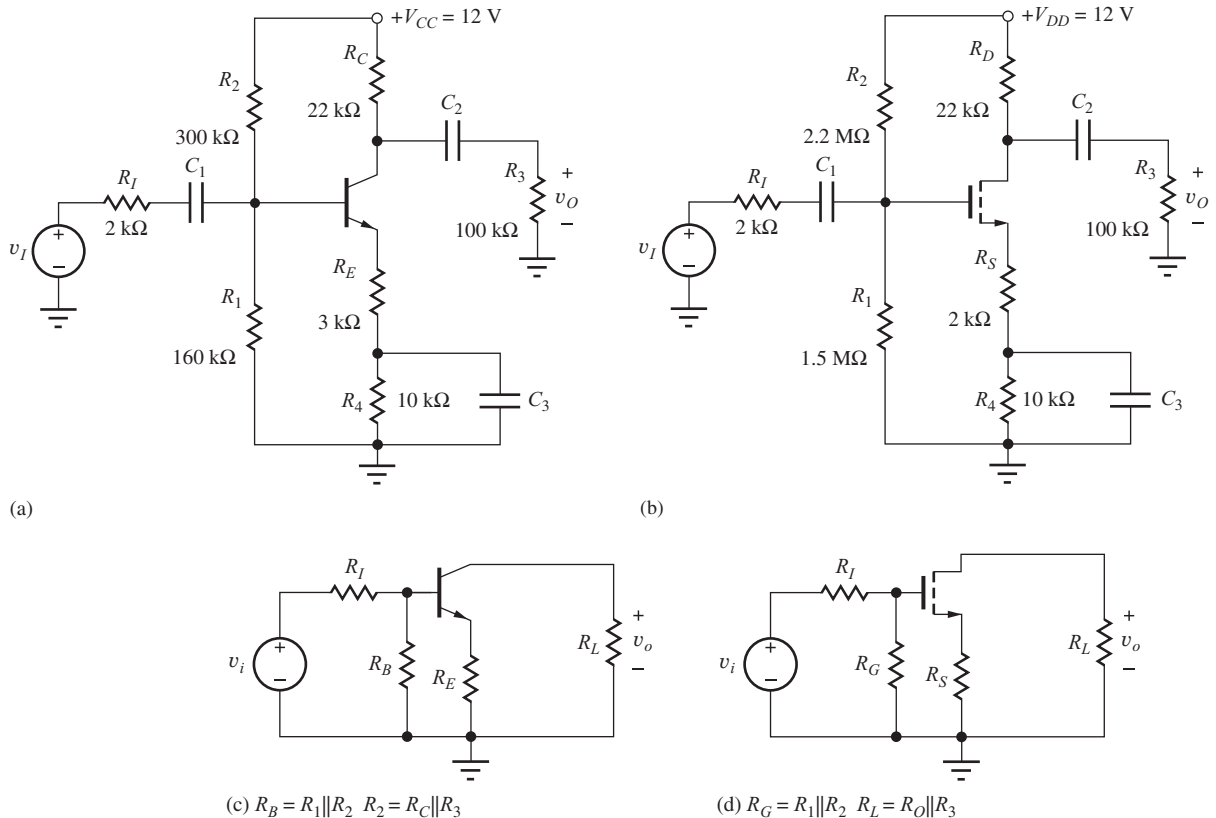


**Figure 14.2** Generalized versions of the (a) common-emitter (C-E) and (b) common-source (C-S) amplifiers. (c) Simplified ac equivalent circuit of the C-E amplifier in (a). (d) Simplified ac equivalent circuit of the C-S amplifier in (b).

**EXERCISE:** Construct the ac equivalent circuit for the C-E and C-S amplifiers in Fig. 14.2, and show that the ac models are correct. What are the values of  $R_B$  or  $R_G$ ,  $R_E$  or  $R_S$ , and  $R_L$ ?

**ANSWERS:** 104 k $\Omega$ , 3.00 k $\Omega$ , 18.0 k $\Omega$ ; 892 k $\Omega$ , 2.00 k $\Omega$ , 18.0 k $\Omega$

**14.1.4 COMMON-COLLECTOR (C-C) AND COMMON-DRAIN (C-D) TOPOLOGIES**  
The C-C and C-D circuits are shown in Fig. 14.3. Here the signal is injected into the base [Fig. 14.3(a)] or gate [Fig. 14.3(b)] and extracted from the emitter or source of the transistors. The collector and drain are bypassed directly to ground by the capacitors  $C_2$  and represent the common terminals between the input and output ports. Once again, the ac equivalent circuits in Figs. 14.3(c) and (d) are identical in structure; the only differences are the resistor and transistor parameter values. Analysis will show that the C-C and C-D amplifiers provide a voltage gain of approximately 1, a high input resistance and a low output resistance. In addition, the input signals to the C-C and C-D amplifiers can be quite large without exceeding the small-signal limits. These amplifiers, often called emitter followers or source followers, are the single-transistor equivalents of the op amp voltage-follower circuit that we studied in Chapter 10.

**EXERCISE:** Construct the ac equivalent circuit for the C-C and C-D amplifiers in Fig. 14.3, and show that the ac models are correct. Verify the values of  $R_B$ ,  $R_G$ , and  $R_L$ .

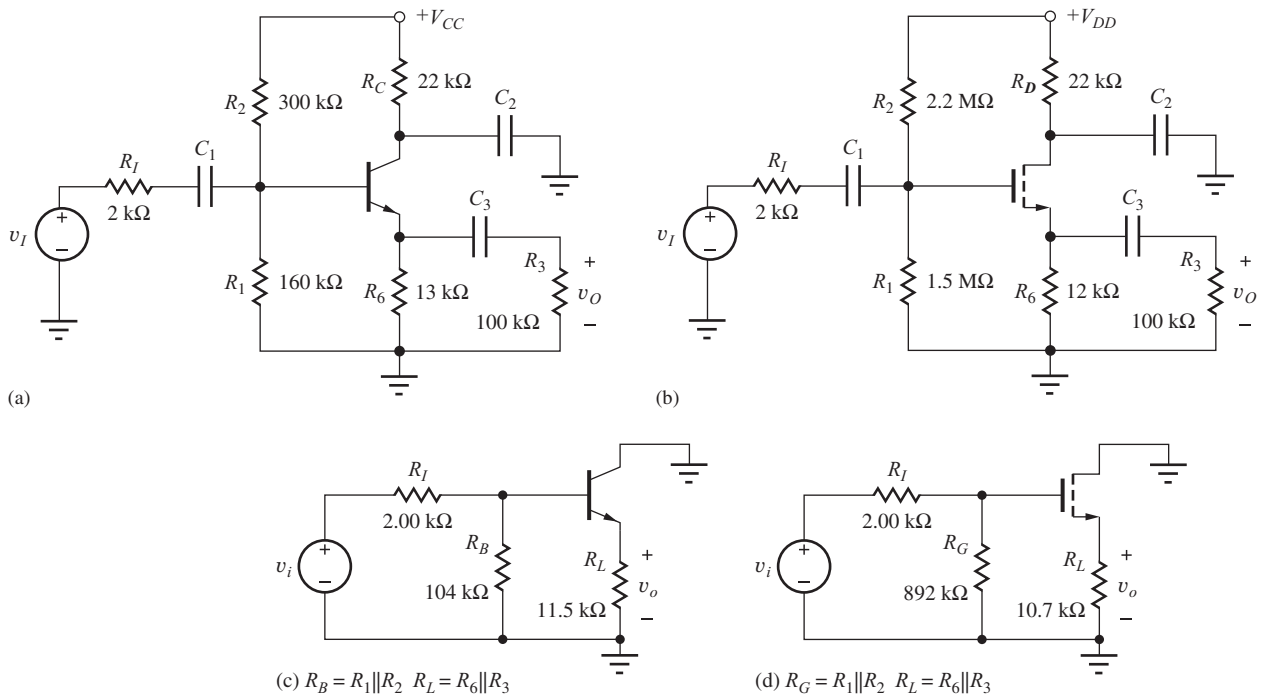


**Figure 14.3** (a) Common-collector (C-C) amplifier. (b) Common-drain (C-D) amplifier. (c) Simplified ac equivalent circuit for the C-C amplifier. (d) Simplified ac equivalent circuit for the C-D amplifier.

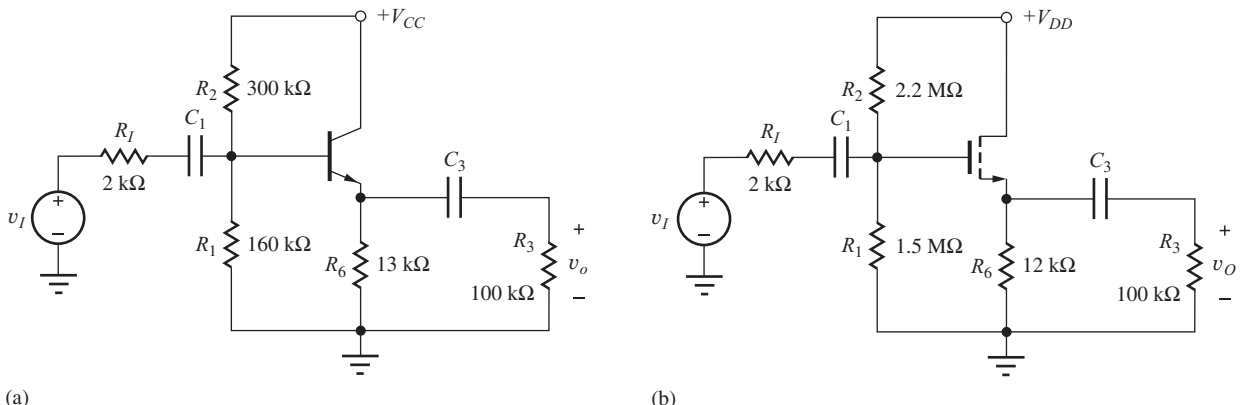


**Figure 14.4** Simplified follower circuits with  $C_2$ ,  $R_C$ , and  $R_D$  eliminated. (a) Common-collector amplifier and (b) common-drain amplifier.

### Circuit Simplification

For economy of design, we certainly do not want to include unneeded components, and the circuits in Fig. 14.3 can actually be simplified. The purpose of capacitor  $C_2$  in the C-C and C-D amplifiers is to provide an ac ground at the collector or drain terminal of the transistor, and since we do not wish to develop a signal voltage at either of these terminals, there is no reason to have resistors  $R_C$  or  $R_D$  in the circuits. We can achieve the desired ac ground by simply connecting the collector and drain terminals directly to  $V_{CC}$  and  $V_{DD}$ , respectively, which eliminates components  $R_C$ ,  $R_D$ , and  $C_2$  from the circuits, as shown in Fig. 14.4.

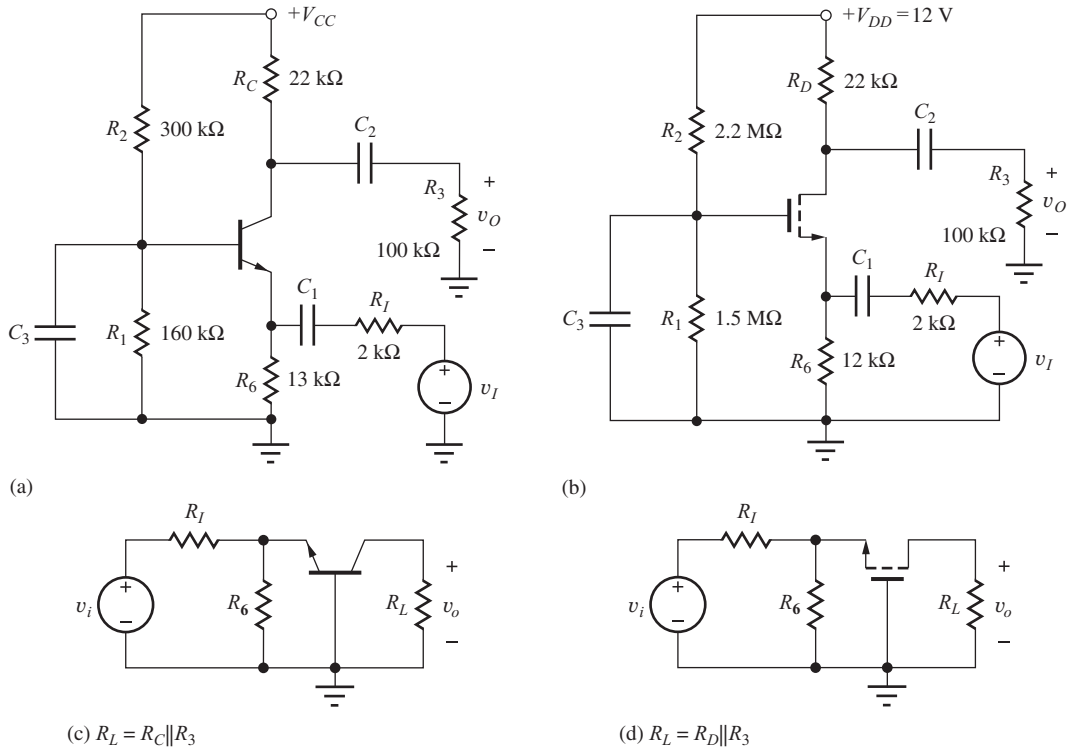


**Figure 14.5** (a) Common-base (C-B) amplifier. (b) Common-gate (C-G) amplifier. (c) Simplified ac equivalent circuit for the C-B amplifier. (d) Simplified ac equivalent circuit for the C-G amplifier.

### 14.1.5 COMMON-BASE (C-B) AND COMMON-GATE (C-G) AMPLIFIERS

The third class of amplifiers contains the C-B and C-G circuits in Fig. 14.5. ac signals are injected into the emitter or source and extracted from the collector or drain of the transistors. The base and gate terminals are connected to signal ground through bypass capacitors  $C_2$ ; these terminals are the common connections between the input and output ports. The resulting ac equivalent circuits in Figs. 14.5(c) and (d) are again identical in structure. Analysis will show that the C-B and C-G amplifiers provide a voltage gain and output resistance very similar to those of the C-E and C-S amplifiers, but they have a much lower input resistance.

Analyses in the next several sections involve the simplified ac equivalent circuits given in Figs. 14.2(c), (d), 14.3(c), (d), and 14.5(c), (d). We assume for purposes of analysis that the circuits have been reduced to these “standard amplifier prototypes.” These circuits are used to delineate the limits that the devices place on performance of the various circuit topologies. The results from these simplified circuits will then be used to analyze and design complete amplifiers.

The circuits in Figs. 14.2 to 14.5 showed only the BJT and MOSFET. The small-signal model of the JFET is identical to that of the three-terminal MOSFET, and the results obtained for the MOSFET amplifiers apply directly to those for the JFETs as well. JFETs can replace the MOSFETs in many circuits.

**EXERCISE:** Construct the ac equivalent circuit for the C-B and C-G amplifiers in Fig. 14.5, and show that the ac models are correct. What are the values of  $R_I$ ,  $R_6$ , and  $R_L$ ?

**ANSWERS:**  $2\text{ k}\Omega$ ,  $13.0\text{ k}\Omega$ ,  $18.0\text{ k}\Omega$ ;  $2\text{ k}\Omega$ ,  $12.0\text{ k}\Omega$ ,  $18.0\text{ k}\Omega$

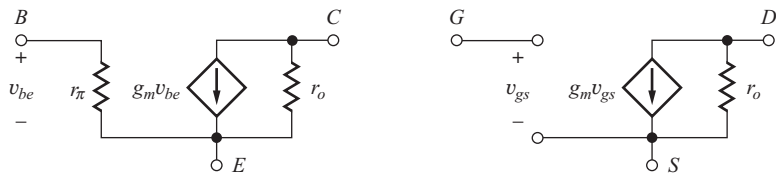


Figure 14.6 Small-signal models for the BJT and MOSFET.

TABLE 14.1

SMALL-SIGNAL PARAMETER	BJT	MOSFET
$g_m$	$\frac{I_C}{V_T} \cong 40I_C$	$\frac{2I_D}{V_{GS} - V_{TN}} \cong \sqrt{2K_n I_D}$
$r_\pi$	$\frac{\beta_o}{g_m}$	$\infty$
$r_o$	$\frac{V_A + V_{CE}}{I_C} \cong \frac{V_A}{I_C}$	$\frac{(1/\lambda) + V_{DS}}{I_D} \cong \frac{1}{\lambda I_D}$
$\beta_o$	$g_m r_\pi$	$\infty$
$\mu_f = g_m r_o$	$\frac{V_A + V_{CE}}{V_T} \cong 40V_A$	$\frac{2}{\lambda(V_{GS} - V_{TN})} \cong \frac{1}{\lambda} \sqrt{\frac{2K_n}{I_D}}$

### 14.1.6 SMALL-SIGNAL MODEL REVIEW

The small-signal models for the BJT and MOSFET appear in Fig. 14.6, and the formulae relating the small-signal model parameters to the Q-point are summarized in Table 14.1.

Again, we recognize that the topologies are very similar, except for the finite value of  $r_\pi$  for the BJT. Due to these similarities, we begin the analyses with that for the bipolar transistor because it has the more general small-signal model; we obtain results for the FET cases from the BJT expressions by taking limits as  $r_\pi$  and  $\beta_o$  approach infinity. In subsequent sections, expressions for the voltage gain, input resistance, output resistance, and current gain are developed for each of the single-transistor amplifiers based upon the small-signal models in Fig. 14.6.

## 14.2 INVERTING AMPLIFIERS—COMMON-EMITTER AND COMMON-SOURCE CIRCUITS

We begin our comparative analysis of the various amplifier families with the common-emitter and common-source amplifiers that we introduced in Chapter 13. The ac equivalent circuits are given in Fig. 14.2 and now include the addition of unbypassed resistors  $R_E$  and  $R_S$ . Here again we note that the topologies are identical. Performance differences arise because of the parametric differences between the transistors used in the circuits. As mentioned above we will analyze the common-emitter amplifier first and then simplify the C-E results for the common-source case.

### 14.2.1 THE COMMON-EMITTER (C-E) AMPLIFIER

Now we are in a position to analyze the small-signal characteristics of the complete **common-emitter (C-E) amplifier** shown in Fig. 14.7(a). The ac equivalent circuit of Fig. 14.7(b) is constructed by assuming that the capacitors all have zero impedance at the signal frequency and the dc voltage

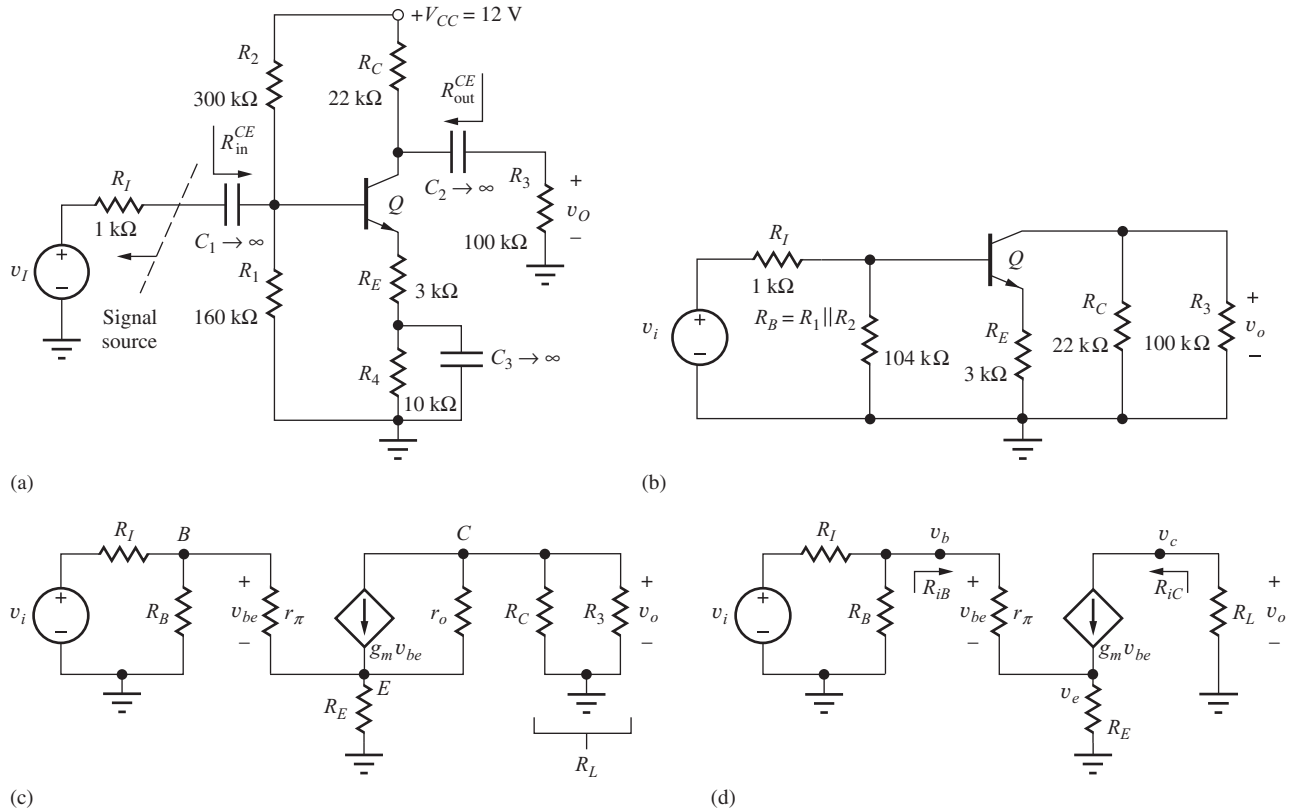


**Figure 14.7** (a) Common-emitter amplifier circuit employing a bipolar transistor. (b) ac Equivalent circuit for the common-emitter amplifier in part (a). The common-emitter connection should now be evident. (c) ac Equivalent circuit with the bipolar transistor replaced by its small-signal model. (d) Final equivalent circuit for ac analysis of the common-emitter amplifier in which  $r_o$  has been neglected.

source represents an ac ground. For simplicity, we assume that we have found the Q-point and know the values of  $I_C$  and  $V_{CE}$ . In Fig. 14.7(b), resistor  $R_B$  represents the parallel combination of the two base bias resistors  $R_1$  and  $R_2$ ,

$$R_B = R_1 \parallel R_2 \quad (14.5)$$

and  $R_4$  is eliminated by bypass capacitor  $C_3$ .

Before we can develop an expression for the voltage gain of the amplifier, the transistor must be replaced by its small-signal model as in Fig. 14.7(c). A final simplification appears in Fig. 14.7(d), in which the resistor  $R_L$  represents the total equivalent load resistance on the transistor, the parallel combination of  $R_C$  and  $R_3$ :

$$R_L = R_C \parallel R_3 \quad (14.6)$$

Note that transistor output resistance  $r_o$  has been neglected in the final circuit in Fig. 14.7(d) as discussed in Sections 13.7 and 13.11.

In Fig. 14.7(b) through (d), the reason why this amplifier configuration is called a common-emitter amplifier is apparent. The emitter portion of the circuit represents the common connection between the amplifier input and output ports. The input signal is applied to the transistor's base, the output signal appears at the collector, and both the input and output signals are referenced to the (common) emitter terminal (through  $R_E$ ).

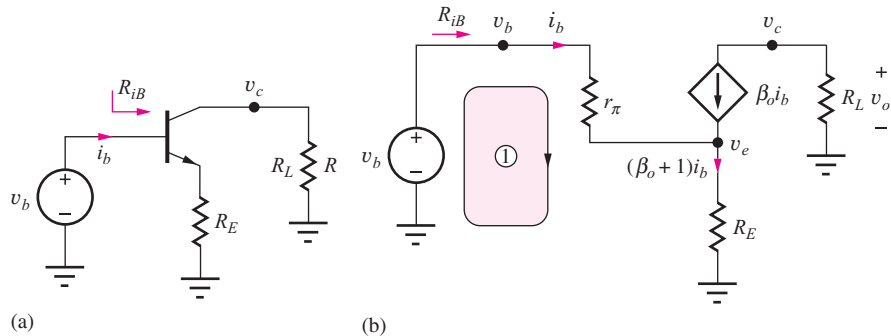


**Figure 14.8** Simplified circuit and small-signal models for finding the common-emitter terminal voltage gain  $A_{vt}^{CE}$  and input resistance  $R_{IB}$ .

## Terminal Voltage Gain

Now we are ready to develop an expression for the overall gain of the amplifier from signal source  $v_i$  to the output voltage across resistor  $R_3$  ( $R_L = R_3 \parallel R_C$ ). The voltage gain can be written as

$$A_v^{CE} = \frac{\mathbf{v}_o}{\mathbf{v}_i} = \begin{pmatrix} \mathbf{v}_c \\ \mathbf{v}_b \end{pmatrix} \begin{pmatrix} \mathbf{v}_b \\ \mathbf{v}_i \end{pmatrix} = A_{vt}^{CE} \begin{pmatrix} \mathbf{v}_b \\ \mathbf{v}_i \end{pmatrix} \quad \text{where} \quad A_{vt}^{CE} = \begin{pmatrix} \mathbf{v}_c \\ \mathbf{v}_b \end{pmatrix} \quad (14.7)$$

$A_{vt}^{CE}$  represents the voltage gain between the base and collector terminals of the transistor, the **“terminal gain.”** We will first find expressions for terminal gain  $A_{vt}^{CE}$  as well as the input resistance at the base of the transistor. Then we can relate  $v_b$  to  $v_i$  to find the overall voltage gain.

In Fig. 14.8, the BJT is replaced with its small-signal model, and the base terminal of the transistor is driven by test source  $v_b$ . Note that the small-signal model has been changed to its current-controlled form, and  $r_o$  is neglected as discussed before. Collector voltage  $v_c$  is given by

$$\mathbf{v}_c = -\beta_\theta \mathbf{i}_b R_L \quad (14.8)$$

We can relate  $i_b$  to base voltage  $v_b$  by writing an equation around loop 1:

$$\mathbf{v}_b = \mathbf{i}_b r_\pi + (\mathbf{i}_b + \beta_o \mathbf{i}_b) R_E = \mathbf{i}_b [r_\pi + (\beta_o + 1) R_E] \quad (14.9)$$

Solving for  $i_b$  and substituting the result in Eq. (14.8) yields

$$A_{vt}^{CE} = \frac{\mathbf{v}_c}{\mathbf{v}_b} = -\frac{\beta_o R_L}{r_\pi + (\beta_o + 1)R_E} \cong -\frac{g_m R_L}{1 + g_m R_E} \quad (14.10)$$

in which the approximation assumes  $\beta_o \gg 1$  and uses  $\beta_o = g_m r_\pi$ .

The minus sign indicates that the common-emitter stage is an inverting amplifier in which the input and output are  $180^\circ$  out of phase. The gain is proportional to the product of the transistor transconductance  $g_m$  and load resistor  $R_L$ . This product places an upper bound on the gain of the amplifier, and we will encounter the  $g_m R_L$  product over and over again as we study transistor amplifiers. We will explore gain expression (Eq. 14.10) in more detail shortly.

## Input Resistance

The resistance looking into the base terminal  $R_{iB}$  in Fig. 14.8 can easily be found by rearranging Eq. (14.9). The input resistance is simply the ratio of  $v_b$  and  $i_b$ ,

$$R_{iB} = \frac{\mathbf{v}_b}{\mathbf{i}_b} = r_\pi + (\beta_o + 1) R_E \cong r_\pi (1 + g_m R_E) \quad (14.11)$$

in which the final approximation again assumes  $\beta_0 \gg 1$  and uses  $\beta_o = g_m r_\pi$ . The input resistance looking into the base of the transistor is equal to  $r_\pi$  plus the resistance reflected into the base by  $R_E$ . The effective value of  $R_E$  is increased by the current gain ( $\beta_0 + 1$ ).

The overall input resistance of the common-emitter amplifier,  $R_{in}^{CE}$ , is defined as the resistance looking into the amplifier at coupling capacitor  $C_1$  and is equal to the parallel combination of  $R_{iB}$  and base bias resistance  $R_B$ :

$$R_{in}^{CE} = R_B \parallel R_{iB} \quad (14.12)$$

### Signal Source Voltage Gain

The overall voltage gain  $A_v^{CE}$  of the amplifier, including the effect of source resistance  $R_I$ , can now be found using the input resistance and terminal gain expressions. Voltage  $v_b$  at the base of the bipolar transistor in Fig. 14.7(d) is related to  $v_i$  by

$$v_b = v_i \frac{R_B \parallel R_{iB}}{R_I + (R_B \parallel R_{iB})} \quad (14.13)$$

Combining Eqs. (14.7), (14.10), and (14.13), yields a general expression for the overall voltage gain of the common-emitter amplifier:

$$A_v^{CE} = A_{vt}^{CE} \left( \frac{v_b}{v_i} \right) = - \left( \frac{g_m R_L}{1 + g_m R_E} \right) \left[ \frac{R_B \parallel R_{iB}}{R_I + (R_B \parallel R_{iB})} \right] \quad (14.14)$$

In this expression, we see that the overall voltage gain is equal to the terminal gain  $A_{vt}^{CE}$  reduced by the voltage division between  $R_I$  and the equivalent resistance at the base of the transistor. Terminal gain  $A_{vt}^{CE}$  places an upper limit on the voltage gain since the voltage division factor will be less than one.

### Important Limits and Model Simplifications

We now explore the limits to the voltage gain of common-emitter amplifiers using model simplifications for large emitter resistance and zero emitter resistance. First, we will assume that the source resistance is small enough that  $R_I \ll R_B \parallel R_{iB}$  so that

$$A_v^{CE} \cong A_{vt}^{CE} = - \frac{g_m R_L}{1 + g_m R_E} \quad \text{for } R_I \ll R_B \parallel R_{iB} \quad (14.15)$$

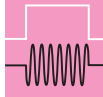
This approximation is equivalent to saying that the total input signal appears at the base of the transistor.

**Zero Resistance in the Emitter** In order to achieve as large a gain as possible, we need to make the denominator in Eq. (14.15) as small as possible, and this is achieved by setting  $R_E = 0$ . The gain is then

$$A_v^{CE} \cong -g_m R_L = -g_m (R_C \parallel R_3) \quad (14.16)$$

which is the expression we found for the basic common-emitter amplifier in Chapter 13. Equation (14.16) states that the terminal voltage gain of the common-emitter stage is equal to the product of the transistor's transconductance  $g_m$  and load resistance  $R_L$ , and the minus sign indicates that the output voltage is “inverted” or  $180^\circ$  out of phase with respect to the input. Equation (14.16) places an upper limit on the gain we can achieve from a common-emitter amplifier with an external load resistor. Remember that we already developed a simple rule-of-thumb estimate for the  $g_m R_L$  product in Chapter 13:

$$g_m R_L \cong 10 V_{CC} \quad (14.17)$$


**DESIGN  
NOTE**

The magnitude of the voltage gain of a resistively loaded common-emitter amplifier with zero emitter resistance is approximately equal to 10 times the power supply voltage.

$$A_v^{CE} \cong -10V_{CC} \quad \text{for } R_E = 0$$

This result represents an excellent way to quickly check the validity of more detailed calculations. Remember that the rule-of-thumb estimate is not going to be exact, but will predict the order of magnitude of the gain, typically within a factor of two or so.

**Large Emitter Resistance** The presence of a nonzero value of emitter resistor  $R_E$  reduces the gain below that given by Eq. (14.16), and another very useful simplification occurs when the  $g_m R_E$  product is much larger than one:

$$A_{vt}^{CE} = -\frac{g_m R_L}{1 + g_m R_E} \cong -\frac{R_L}{R_E} \quad \text{for } g_m R_E \gg 1 \quad (14.18)$$

The gain is now set by the ratio of the load resistor  $R_L$  and emitter resistor  $R_E$ . This is an extremely useful result because the gain is now independent of the transistor characteristics that vary widely from device to device. The result in Eq. (14.18) is very similar to the one obtained for the op-amp inverting amplifier circuit and is a result of feedback introduced by resistor  $R_E$ .

Achieving the simplification in Eq. (14.18) requires  $g_m R_E \gg 1$ . We can relate this product to the dc bias voltage developed across  $R_E$ :

$$g_m R_E = \frac{I_C R_E}{V_T} = \alpha_F \frac{I_E R_E}{V_T} \cong \frac{I_E R_E}{V_T} \quad \text{and we need } I_E R_E \gg V_T \quad (14.19)$$

$I_E R_E$  represents the dc voltage drop across emitter resistor  $R_E$  and must be much greater than 25 mV, for example 0.250 V, a value that is easily achieved.

### Understanding Generalized Common-Emitter Amplifier Operation

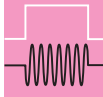
Let us explore common-emitter operation a bit further by looking at the signal voltage developed at the emitter terminal with reference to Fig. 14.8 and Eq. (14.9):

$$\mathbf{v}_e = (\beta_o + 1)\mathbf{i}_b R_E = \frac{(\beta_o + 1)R_E}{r_\pi + (\beta_o + 1)R_E} \mathbf{v}_b \cong \frac{g_m R_E}{1 + g_m R_E} \mathbf{v}_b \cong \mathbf{v}_b \quad \text{for large } g_m R_E \quad (14.20)$$

The voltage  $\mathbf{v}_b$  at the base of the transistor is transferred directly to the emitter, setting up an emitter current of  $\mathbf{v}_b / R_E$ . Essentially all the emitter current must be supplied from the collector yielding a voltage gain equal to the ratio of  $R_L$  to  $R_E$ :

$$\mathbf{i}_e \cong \frac{\mathbf{v}_b}{R_E} \quad \mathbf{v}_o = -\mathbf{i}_c R_L = -\alpha_o \mathbf{i}_e R_L \cong -\mathbf{i}_e R_L \quad \text{and} \quad A_{vt}^{CE} = \frac{\mathbf{v}_o}{\mathbf{v}_b} \cong -\frac{R_L}{R_E} \quad (14.21)$$

This unity signal voltage transfer from base to emitter should not be mysterious. We know that the base and emitter terminals are directly connected by a forward-biased diode whose voltage is virtually constant at 0.7 V. Thus the emitter signal voltage should be approximately the same as the base signal. The voltage transfer between the base and emitter terminals forms the basis of the emitter-follower operation to be discussed in detail in Section 14.3.


**DESIGN  
NOTE**

The gain of the generalized common-emitter amplifier is approximately equal to the ratio of the load and emitter resistors.

$$A_{vt}^{CE} = -\frac{g_m R_L}{1 + g_m R_E} \cong -\frac{R_L}{R_E} \quad \text{for} \quad g_m R_E \gg 1$$

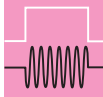
**Small-Signal Limit for the Common-Emitter Amplifier** An important additional benefit of adding resistor  $R_E$  to the circuit is to increase the allowed size of the input signal  $v_b$  at the base. For small-signal operation, the magnitude of the base-emitter voltage  $v_{be}$ , developed across  $r_\pi$  in the small-signal model, must be less than 5 mV (you may wish to review Sec. 13.5.7). This voltage can be found using the input current  $\mathbf{i}_b$  from Eq. (14.9):

$$v_{be} = \mathbf{i}_b r_\pi = v_b \frac{r_\pi}{r_\pi + (\beta_o + 1)R_E} \cong \frac{v_b}{1 + g_m R_E} \quad (14.22)$$

The approximation requires  $\beta_o \gg 1$ . Requiring  $|v_{be}|$  in Eq. (14.22) to be less than 5 mV gives

$$|v_b| \leq 0.005(1 + g_m R_E) \text{ V} \quad (14.23)$$

If  $g_m R_E \gg 1$ , then  $v_b$  can be increased well beyond the 5-mV limit.


**DESIGN  
NOTE**

Use of an emitter resistor in the common-emitter amplifier can significantly increase the input signal range of the amplifier.

$$v_b \leq 0.005 \text{ V}(1 + g_m R_E)$$

### Resistance at the Collector of the Bipolar Transistor

The resistance looking into the collector terminal of the transistor,  $R_{ic}$ , can be found with the aid of the equivalent circuit in Fig. 14.9 in which input source  $v_i$  has been set to zero, and test source  $v_x$  is applied to the collector of the transistor. The Thévenin equivalent resistance on the base is then  $R_{th} = R_B \parallel R_I$ .

$R_{ic}$  equals the ratio of  $v_x$  to  $i_x$ , where  $i_x$  represents the current through independent source  $v_x$ . To find  $i$ , we write an expression for  $v_e$ :

$$v_e = (\beta_o + 1)\mathbf{i}R_E \quad \text{and} \quad \mathbf{i}_x = \beta_o \mathbf{i} \quad (14.24)$$

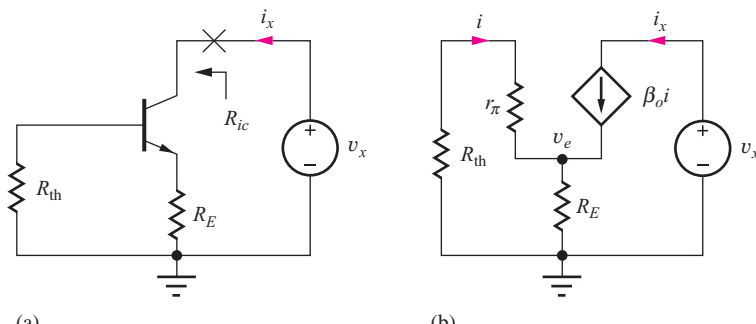


**Figure 14.9** Circuits for calculating the resistance at the collector of the transistor.

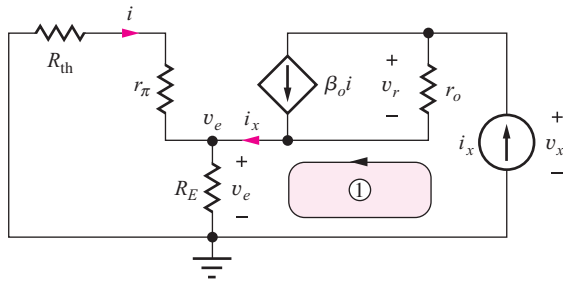


Figure 14.10 Collector resistance with  $r_o$  included.

and realize that the current  $\mathbf{i}$  can also be written directly in terms of  $\mathbf{v}_e$ :

$$\mathbf{i} = -\frac{\mathbf{v}_e}{R_{th} + r_\pi} \quad (14.25)$$

Combining Eqs. (14.24) and (14.25) yields

$$\mathbf{v}_e \left[ 1 + \frac{(\beta_o + 1)R_E}{r_\pi + R_{th}} \right] = 0 \quad \text{and} \quad \mathbf{v}_e = 0 \quad (14.26)$$

Because  $\mathbf{v}_e = 0$ , Eq. (14.25) requires that  $\mathbf{i}$  equal zero as well. Hence,  $\mathbf{i}_x = 0$ , and the output resistance of this circuit is infinite!

On the surface, this result may seem acceptable. However, a red flag should go up. We must be suspicious of the results that indicate resistances are infinite (or zero). Using the simplified circuit model in Fig. 14.9(b), in which  $r_o$  is neglected, has led to an unreasonable result.

We improve our analysis by moving to the next level of model complexity, as shown in Fig. 14.10. For this analysis, the circuit is driven by the test current  $i_x$ , and the voltage  $v_x$  must be determined in order to find  $R_{out}$ .<sup>1</sup>

Summing the voltages around loop 1 and applying KCL at the output node,

$$\mathbf{v}_x = \mathbf{v}_r + \mathbf{v}_e = (\mathbf{i}_x - \beta_o \mathbf{i})r_o + \mathbf{v}_e \quad (14.27)$$

Current  $\mathbf{i}_x$  is forced through the parallel combination of  $(R_{th} + r_\pi)$  and  $R_E$ , so that  $\mathbf{v}_e$  can be expressed as

$$\mathbf{v}_e = \mathbf{i}_x [(R_{th} + r_\pi) \parallel R_E] = \mathbf{i}_x \frac{(R_{th} + r_\pi)R_E}{R_{th} + r_\pi + R_E} \quad (14.28)$$

At the emitter node, current division can be used to find  $\mathbf{i}$  in terms of  $\mathbf{i}_x$ :

$$\mathbf{i} = -\mathbf{i}_x \frac{R_E}{R_{th} + r_\pi + R_E} \quad (14.29)$$

Combining Eqs. (14.27) through (14.29) yields a somewhat messy expression for the output resistance of the C-E amplifier:

$$R_{iC} = r_o \left( 1 + \frac{\beta_o R_E}{R_{th} + r_\pi + R_E} \right) + (R_{th} + r_\pi) \parallel R_E \cong r_o \left( 1 + \frac{\beta_o R_E}{R_{th} + r_\pi + R_E} \right) \quad (14.30)$$

If we now assume that  $(r_\pi + R_E) \gg R_{th}$  and  $r_o \gg R_E$  and remember that  $\beta_o = g_m r_\pi$ , we reach the approximate results that should be remembered:

$$R_{iC} \cong r_o [1 + g_m (R_E \parallel r_\pi)] = r_o + \mu_f (R_E \parallel r_\pi) \quad (14.31)$$

<sup>1</sup> The upcoming sequence of equations has been developed by the author as an “easy” way to derive this result; this approach is not expected to be obvious. Alternatively, the circuit in Fig. 14.10 can be formulated as a two-node problem by combining  $R_{th}$  and  $r_\pi$ .

We should check to see that Eq. (14.31) reduces to the proper result for  $R_E = 0$ ; that is,  $R_{\text{out}} = r_o$ . Since it does, we can feel comfortable that our level of modeling is sufficient to produce a meaningful result.

Equation (14.31) tells us that the output resistance of the common-emitter amplifier is equal to the output resistance  $r_o$  of the transistor itself plus the equivalent resistance  $(R_E \parallel r_\pi)$  multiplied by the amplification factor of the transistor. For  $g_m(R_E \parallel r_\pi) \gg 1$ ,  $R_{\text{out}} \gg r_o$ , we find that the resistance at the collector can be designed to be much greater than the output resistance of the transistor itself!

### Important Limit for the Bipolar Transistor

The finite current gain of the bipolar transistor places an upper bound on the size of  $R_{iC}$  that can be achieved. Referring back to Fig. 14.10, we see that  $r_\pi$  appears in parallel with  $R_E$  when we neglect  $R_{\text{th}}$ . If we let  $R_E \rightarrow \infty$  in Eq. (14.31), we find that the maximum value of output resistance is  $R_{iC} \cong \mu_f r_\pi = \beta_o r_o$ .



## DESIGN NOTE

A quick design estimate for the resistance at the collector of a bipolar transistor with an unbypassed resistor  $R_E$  in the emitter is

$$R_{iC} \cong r_o [1 + g_m(r_\pi \parallel R_E)] \cong \mu_f (r_\pi \parallel R_E) < \beta_o r_o$$

However, remember  $R_{iC}$  can never exceed  $\beta_o r_o$ .

### Output Resistance of the Overall Common-Emitter Amplifier

The output resistance of the overall common-emitter amplifier is defined as the resistance looking into the circuit at input coupling capacitor  $C_2$  in Fig. 14.7(a). Thus  $R_{\text{out}}^{CE}$  equals the parallel combination of collector resistor  $R_C$  and the resistance looking into the collector of the transistor itself,  $R_{iC}$ , as defined in Fig. 14.7(c):

$$R_{\text{out}}^{CE} = R_C \parallel R_{iC} = R_C \parallel r_o \left( 1 + \frac{\beta_o R_E}{R_{\text{th}} + r_\pi + R_E} \right) \quad (14.32)$$

### Terminal Current Gain for the Common-Emitter Amplifier

The **terminal current gain**  $A_{it}$  is defined as the ratio of the current delivered to the load resistor  $R_L$  to the current being supplied to the base terminal. For the C-E amplifier in Fig. 14.11, the current in  $R_L$  is equal to  $i$  amplified by the current gain  $\beta_o$ , yielding a current gain equal to  $-\beta_o$ .

$$A_{it}^{CE} = -\beta_o \quad (14.33)$$

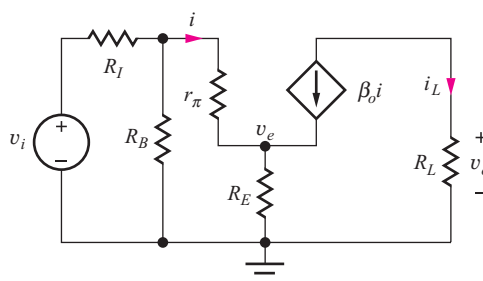


**Figure 14.11** Circuit for calculating C-E current gain.

### EXAMPLE 14.1 VOLTAGE GAIN OF A COMMON-EMITTER AMPLIFIER

In this example, we find the small-signal parameters of the bipolar transistor and then calculate the voltage gain of a common-emitter amplifier.

**PROBLEM** Calculate the voltage gain input resistance, and output resistance of the common-emitter amplifier in Fig. 14.7 if the transistor has  $\beta_F = 100$ ,  $V_A = 75\text{V}$ ,  $\lambda = 0.0133 \text{ V}^{-1}$ , and the Q-point is (0.245 mA, 3.39 V). What is the maximum value of  $v_i$  that satisfies the small-signal assumptions?

**SOLUTION** **Known Information and Given Data:** Common-emitter amplifier with its ac equivalent circuit given in Fig. 13.18;  $\beta_F = 100$  and  $V_A = 75\text{V}$ ; the Q-point is (0.245 mA, 3.39 V);  $R_I = 1\text{k}\Omega$ ,  $R_1 = 160\text{k}\Omega$ ,  $R_2 = 300\text{k}\Omega$ ,  $R_C = 22\text{k}\Omega$ ,  $R_E = 3\text{k}\Omega$ ,  $R_4 = 10\text{k}\Omega$ , and  $R_3 = 100\text{k}\Omega$ .

**Unknowns:** Small-signal parameters of the transistor; voltage gain  $A_v$ ;  $R_{in}^{CE}$ ;  $R_{out}^{CE}$ ; small-signal limit for the value of  $v_i$

**Approach:** Use the Q-point information to find  $g_m$ ,  $r_\pi$  and  $r_o$ . Use the calculated and given values to evaluate the voltage gain expression in Eq. (14.14), and the expressions for  $R_{in}^{CE}$  and  $R_{out}^{CE}$ .

**Assumptions:** The transistor is in the active region, and  $\beta_o = \beta_F$ . The signal amplitudes are low enough to be considered as small signals. Assume  $r_o$  can be neglected.

**Analysis:** (a) To evaluate Eq. (14.14),

$$A_v = - \left( \frac{g_m R_L}{1 + g_m R_E} \right) \left[ \frac{R_B \| R_{iB}}{R_1 + (R_B \| R_{iB})} \right] \quad \text{with} \quad R_B = R_1 \| R_2 \quad \text{and} \quad R_{iB} = r_\pi + (\beta_o + 1) R_E$$

the values of the various resistors and small-signal model parameters are required. We have

$$g_m = 40I_C = 40(0.245\text{mA}) = 9.80\text{mS} \quad r_\pi = \frac{\beta_o V_T}{I_C} = \frac{100(0.025\text{V})}{0.245\text{mA}} = 10.2\text{k}\Omega$$

$$r_o = \frac{V_A + V_{CE}}{I_C} = \frac{75\text{V} + 3.39\text{V}}{0.245\text{mA}} = 320\text{k}\Omega \quad R_{iB} = r_\pi + (\beta_o + 1) R_E = 313\text{k}\Omega$$

$$R_B = R_1 \| R_2 = 104\text{k}\Omega \quad R_L = R_C \| R_3 = 18.0\text{k}\Omega \quad R_{ia} = R_I \| R_B = 0.990\text{k}\Omega$$

Using these values,

$$A_v = - \left( \frac{9.80\text{mS}(18.0\text{k}\Omega)}{1 + 9.80\text{mS}(3.0\text{k}\Omega)} \right) \left[ \frac{104\text{k}\Omega \| 313\text{k}\Omega}{1\text{k}\Omega + (104\text{k}\Omega \| 313\text{k}\Omega)} \right] = -5.80(0.987) = -5.72$$

Thus, the common-emitter amplifier in Fig. 14.7 provides a small-signal voltage gain  $A_v = -5.72$  or 15.1 dB.

The common-emitter amplifier's input and output resistances are found as

$$R_{in}^{CE} = R_B \| R_{iB} = 104\text{k}\Omega \| 313\text{k}\Omega = 78.1\text{k}\Omega \quad \text{and} \quad R_{out}^{CE} = R_C \| R_{iC}$$

$$R_{iC} = R_C \| r_o \left( 1 + \frac{\beta_o R_E}{R_{th} + r_\pi + R_E} \right) = 320\text{k}\Omega \left[ 1 + \frac{100(3\text{k}\Omega)}{0.99\text{k}\Omega + 10.2\text{k}\Omega + 3\text{k}\Omega} \right] = 7.09\text{M}\Omega$$

$$R_{out}^{CE} = 22\text{k}\Omega \| 7.09\text{M}\Omega = 21.9\text{k}\Omega$$

Small-signal operation requires  $|v_{be}| \leq 0.005\text{V}$ . Based on Fig. 14.7, the base-emitter signal voltage can be related to  $v_i$  by

$$v_{be} = v_b \frac{r_\pi}{r_\pi + (\beta_o + 1) R_E} = v_i \left[ \frac{R_B \| R_{iB}}{R_I + R_B \| R_{iB}} \right] \left[ \frac{r_\pi}{r_\pi + (\beta_o + 1) R_E} \right]$$

so that

$$v_i \leq (0.005 \text{ V}) \left[ \frac{R_I + (R_B \parallel R_{iB})}{R_B \parallel R_{iB}} \right] \left[ \frac{r_\pi + (\beta_o + 1)R_E}{r_\pi} \right]$$

$$v_i \leq (0.005 \text{ V}) \left[ \frac{1 \text{ k}\Omega + (104 \text{ k}\Omega \parallel 313 \text{ k}\Omega)}{104 \text{ k}\Omega \parallel 313 \text{ k}\Omega} \right] \left[ \frac{10.2 \text{ k}\Omega + 101(3 \text{ k}\Omega)}{10.2 \text{ k}\Omega} \right] = 0.155 \text{ V}$$

**Check of Results:** We have found the required information. The amplification factor is  $\mu_f = g_m r_o = (9.80 \text{ mS})(320 \text{ k}\Omega) = 3140$ . The magnitude of the voltage gain of a single-transistor amplifier cannot exceed this value. Using the result from Eq. (14.18), we estimate the gain to be  $A_v^{CE} = -R_L/R_E = -18 \text{ k}\Omega/3 \text{ k}\Omega = -6$ . Our answer satisfies both these checks.

We can quickly check our  $R_{iC}$  calculation using the approximation  $R_{iC} \approx \mu_f R_E$ :

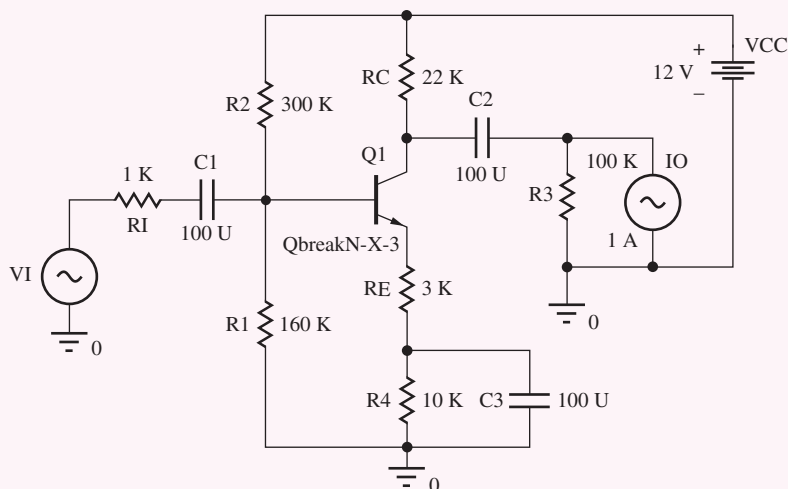
$$R_{iC} \approx \mu_f R_E = (g_m r_o) R_E = (9.80 \text{ mS})(320 \text{ k}\Omega)(3 \text{ k}\Omega) = 9.41 \text{ M}\Omega \quad \text{and} \quad 7.09 \text{ M}\Omega < 9.41 \text{ M}\Omega$$

The estimate of  $R_{iC}$  is somewhat high since  $R_{th}$  and  $r_\pi$  cannot be neglected relative to  $R_E$ .

**Discussion:** Note that the value of the voltage gain ( $A_v = -5.72$ ) is much less than the intrinsic voltage gain ( $\mu_f = 3140$ ), so neglecting  $r_o$  in the calculation should be valid. Note also that the value of  $r_o$  is much greater than the load resistance connected to the collector terminal of the amplifier (18 kΩ). This is also consistent with our being able to neglect  $r_o$  in the voltage gain calculation. The maximum allowed input signal is increased significantly to 0.155 V due to the presence of  $R_E$ .

We also see that we did a lot of work to find out that the output resistance is essentially equal to  $R_C$ . Finally we observe that the value of  $R_{iC}$  is less than 25 percent of the  $\beta_o r_o$  limit of 32 MΩ.

**Computer-Aided Analysis:** Now, let us close up check our hand analysis using the SPICE circuit below in which we must set the transistor parameters to be consistent with our hand analysis in order to achieve a similar Q-point: BF = 100, VAF = 75 V, and IS = 1 fA. We can use an ac analysis to find the voltage gain and will sweep from 1000 Hz to 100 kHz with five frequency points per decade. Several decades are simulated so we can be sure we are in a region where the effects of the capacitors are negligible. The capacitor values must be set to a large number, say 100 μF, so that they will have very small reactance at the simulation frequencies.

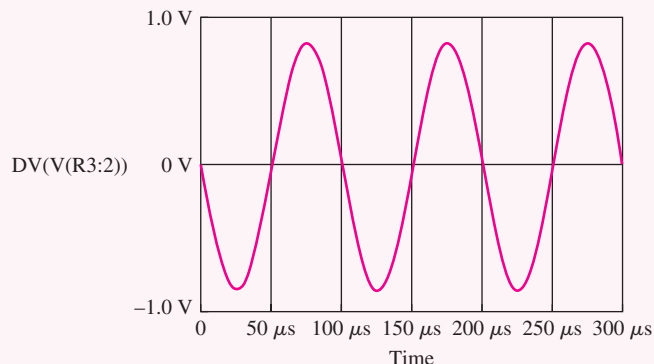


Source VI is the input source and has both an ac value ( $1\angle 0^\circ$ ) for small-signal analysis (ac sweep) and a sine wave component ( $0.15 \sin 20,000 \pi t$ ) for transient simulation. ac current source

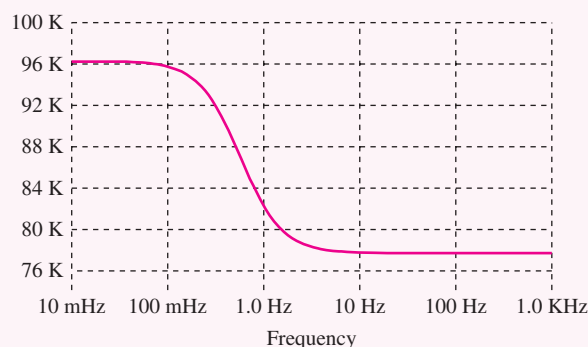
$I_O (1\angle 0^\circ)$  is added to the output in order to find the output resistance. Note that only  $V_I$  or  $I_O$  should have a nonzero value at a given time.

The SPICE results are: Q-point = (0.248 mA, 3.30 V) and  $A_v = -5.67$ . [Note that an alternative method to check our calculations is to use SPICE to perform an ac analysis of the small-signal equivalent circuit in Fig. 14.7(d).]

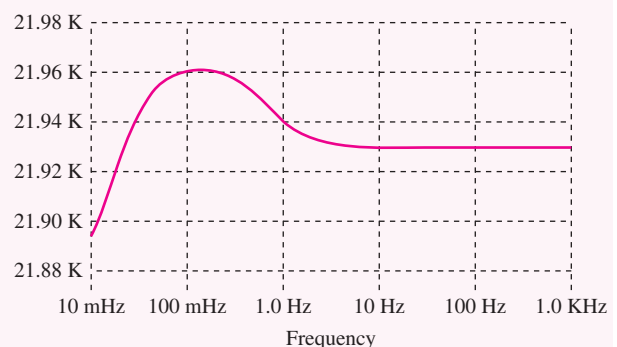
The graph here shows the time-domain response of the amplifier output with an input of 0.15 V obtained with a transient simulation with  $TSTOP = 0.3 \text{ MS}$ . In the graph, we observe good linearity with a gain of  $-5.7$ .



The (frequency dependent) input resistance of the common-emitter amplifier is equal to the voltage at the base node divided by the current entering the node through coupling capacitor  $C_1$ :  $R_{in}^{CE} = V(Q1 : b)/I(C1)$ . As frequency increases, bypass capacitor  $C_3$  becomes effective and the input resistance drops. At frequencies above 10 Hz, the SPICE output becomes constant at  $77.8 \text{ k}\Omega$  in agreement with our hand calculations.



(a) Common-emitter input resistance versus frequency.



(b) Common-emitter output resistance versus frequency.

Similarly, the output resistance of the common-emitter amplifier is equal to the voltage at the collector node divided by the current entering the node through coupling capacitor  $C_2$ :  $R_{out}^{CE} = V(Q1 : c)/I(C2)$ . As bypass capacitor  $C_3$  becomes effective at frequencies above 10 Hz, the SPICE output becomes constant at  $21.9 \text{ k}\Omega$  in agreement with our hand calculations.

The resistance looking into the collector of the transistor itself can be found as  $R_{iC} = VC(Q1)/IC(Q1) = 6.89 \text{ M}\Omega$ . The slight disagreement is due to differences in the calculated Q-point and the small-signal parameters in SPICE.

**EXERCISE:** (a) Suppose resistors  $R_C$ ,  $R_E$ , and  $R_3$  have 10 percent tolerances. What are the worst-case values of voltage gain for this amplifier? (b) What is the voltage gain in the original circuit if  $\beta_o = 125$ ? (c) Suppose the Q-point current in the original circuit increases to 0.275 mA. What are the new values of  $V_{CE}$  and the voltage gain?

**ANSWERS:** (a) -4.75, -6.99; (b) -5.74; (c) 2.34 V, -5.76

**EXERCISE:** What is the value of  $R_{out}$  for the common-emitter amplifier in Ex. 14.1 if  $R_E$  is changed to 2 k $\Omega$ ? Assume the Q-point does not change. Compare the result to the new value of  $\mu_f R_E$ .

**ANSWERS:** 3.31 M $\Omega$ , which is less than 4.30 M $\Omega$

**EXERCISE:** Show that the maximum output resistance for the common-emitter amplifier is  $R_{out} \cong (\beta_o + 1)r_o$  by taking the limit as  $R_E \rightarrow \infty$  in Eq. (14.31).

## EXAMPLE 14.2 COMMON-EMITTER VOLTAGE GAIN WITH BYPASSED Emitter

Now we will find the voltage gain of the amplifier in Ex. 14.1 with bypass capacitor  $C_3$  connected between ground and the emitter terminal of the BJT.

**PROBLEM** (a) Find the voltage gain of the amplifier in Ex. 14.1 with bypass capacitor  $C_3$  connected between ground and the emitter terminal of the BJT. (b) Compare the result in (a) to the common-emitter “rule-of-thumb” gain estimate and the amplification factor of the transistor. (c) Find the new value of the amplifier input and output resistances. (d) Find the value of  $v_i$  that corresponds to the small-signal limit.

**SOLUTION** **Known Information and Given Data:** Common-emitter amplifier in Fig. 14.7 with emitter terminal bypassed to ground. From Ex. 14.1, the Q-point = (0.245 mA, 3.39 V),  $g_m = 9.80$  mS,  $r_\pi = 10.2$  k $\Omega$ , and  $r_o = 320$  k $\Omega$ .

**Unknowns:** Actual voltage gain, rule-of-thumb estimate, amplification factor of the transistor;  $R_{in}^{CE}$ ;  $R_{out}^{CE}$

**Approach:** (a) Evaluate the  $A_v^{CE}$  expression with  $R_E = 0$  (See ac equivalent circuit on next page.). (b) Estimate the voltage gain using  $A_v^{CE} \cong -10V_{CC}$ ; calculate  $\mu_f = g_m r_o$

**Assumptions:** The bipolar transistor is operating in the active region. Signal amplitudes correspond to small-signal conditions. Transistor output resistance  $r_o$  can be neglected.

### Analysis:

(a) With the emitter terminal bypassed to ground,  $R_E = 0$ :

$$R_{iB} = r_\pi + (\beta_o + 1)R_E = r_\pi \quad \text{and} \quad R_B = R_1 \parallel R_2$$

$$A_v^{CE} = -\left(\frac{g_m R_L}{1 + g_m R_E}\right) \left[\frac{R_B \parallel R_{iB}}{R_I + (R_B \parallel R_{iB})}\right] = -g_m R_L \frac{R_B \parallel r_\pi}{R_I + (R_B \parallel r_\pi)}$$

$$A_v^{CE} = -9.80 \text{ mS} (18 \text{ k}\Omega) \frac{104 \text{ k}\Omega \parallel 10.2 \text{ k}\Omega}{1 \text{ k}\Omega + (104 \text{ k}\Omega \parallel 10.2 \text{ k}\Omega)} = -159 \text{ or } 44.0 \text{ dB}$$

(b)  $A_v^{CE} \cong -10(12) = -120$  and  $\mu_f = 9.80 \text{ mS} (320 \text{ k}\Omega) = 3140$

(c) Evaluating the expressions of the C-E amplifier's input and output resistances gives

$$R_{\text{in}}^{CE} = R_B \parallel R_{iB} = 104 \text{ k}\Omega \parallel 10.2 \text{ k}\Omega = 9.29 \text{ k}\Omega$$

$$R_{\text{out}}^{CE} = R_C \parallel R_{iC} = R_C \parallel r_o \cong R_C = 22 \text{ k}\Omega$$

(d) With the emitter bypassed,  $v_{be}$  is given by

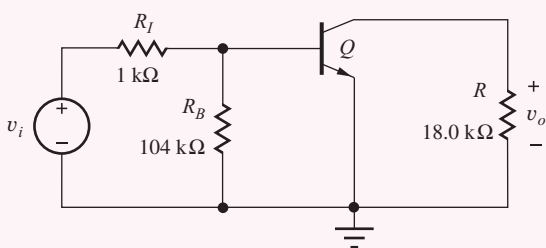
$$v_{be} = v_i \left[ \frac{R_B \parallel R_{iB}}{R_I + (R_B \parallel R_{iB})} \right] = v_i \frac{R_B \parallel r_\pi}{R_I + (R_B \parallel r_\pi)} = v_i \frac{104 \text{ k}\Omega \parallel 10.2 \text{ k}\Omega}{1 \text{ k}\Omega + (104 \text{ k}\Omega \parallel 10.2 \text{ k}\Omega)} = 0.903 v_i$$

and the small-signal limit for  $v_i$  is

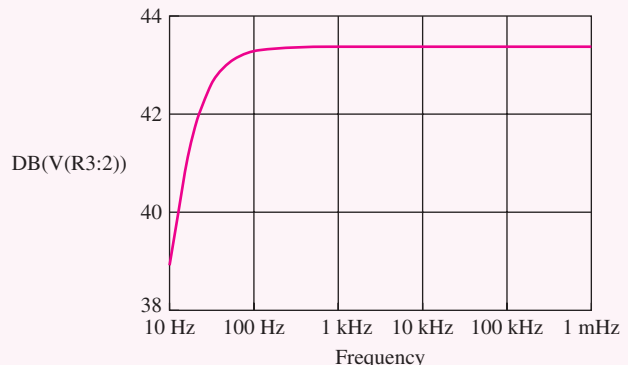
$$|v_i| \leq \frac{0.005 \text{ V}}{0.903} = 5.53 \text{ mV}$$

**Check of Results:** The calculated voltage gain is similar to the rule-of-thumb estimate so our calculation appears correct. Remember, the rule-of-thumb formula is meant to only be a rough estimate; it will not be exact. The gain is much less than the amplification factor, so the neglect of  $r_o$  is valid.

**Computer-Aided Analysis:** SPICE simulation uses the circuit from Example 13.3 with bypass capacitor  $C_3$  connected from the emitter to ground. Simulation yields the Q-point (0.248 mA, 3.30 V) that is consistent with the assumed value. The small difference results from  $V_A$  being included in the SPICE simulation and not in our hand calculations. An ac sweep from 10 Hz to 100 kHz with 10 frequency points/decade is used to find the region in which the capacitors are acting as short circuits, and the gain is observed to be constant at 43.4 dB above a frequency of 1 kHz. The voltage gain is slightly less than our calculated value because  $r_o$  was neglected in our calculations. A transient simulation was performed with a 5-mV, 10-kHz sine wave. The output exhibits reasonably good linearity, but the positive and negative amplitudes are slightly different, indicating some waveform distortion. Enabling the Fourier analysis capability of SPICE yields THD = 3.9%.



ac equivalent circuit with  $R_E = 0$



The (frequency dependent) input resistance of the common-emitter amplifier is equal to the voltage at the base node divided by the current entering the node through coupling capacitor  $C_1$ :  $R_{\text{in}}^{CE} = V(Q1 : b)/I(C1)$ . At frequencies above 10 Hz, the SPICE input becomes constant at 9.80 kΩ in agreement with our hand calculations. Similarly, the output resistance is given by  $R_{\text{out}}^{CE} = V(Q1 : c)/I(C2)$  which becomes constant at 20.6 kΩ for frequencies above 1 kHz. The discrepancies are due to differences in the SPICE values for the Q-point, temperature  $T$ , and the current gain.

**TABLE 14.2**  
Common-Emitter Amplifier Comparison—SPICE Results

	BYPASSED EMITTER ( $R_E = 0$ )	$R_E = 3 \text{ k}\Omega$
$A_v^{CE}$	-159	-5.70
$R_{in}^{CE}$	9.29 k $\Omega$	77.8 k $\Omega$
$R_{out}^{CE}$	20.6 k $\Omega$	21.9 k $\Omega$
$v_i^{\max}, (\text{THD})$	5.53 mV (3.9 %)	155 mV (0.15 %)

### 14.2.2 COMMON-EMITTER EXAMPLE COMPARISON

The results from Examples 14.1 and 14.2 are listed in Table 14.2. Addition of the emitter resistor significantly reduces the voltage gain. This loss in gain is traded for a much higher input resistance and signal handling capability. The output resistances are both set by collector resistor  $R_C$ , so they are approximately the same.

**EXERCISE:** (a) What is the voltage gain  $A_v$  of the amplifier in Ex. 13.3 if  $R_E$  is changed to 1 k $\Omega$ ? Assume the Q-point does not change. (b) What is the new value of  $R_4$  required to maintain the Q-points unchanged in the amplifier?

**ANSWERS:** -15.6, 12 k $\Omega$

**EXERCISE:** What value of saturation current  $I_S$  must be used in SPICE to achieve  $V_{BE} = 0.7 \text{ V}$  for  $I_C = 245 \mu\text{A}$ ? Assume a default temperature of  $27^\circ\text{C}$ .

**ANSWER:** 0.422 fA

**EXERCISE:** A common-emitter amplifier similar to Fig. 14.7 is operating from a single +20-V power supply, and the emitter terminal is bypassed by capacitor  $C_3$ . The BJT has  $\beta_F = 100$  and  $V_A = 50 \text{ V}$  and is operating at a Q-point of (100  $\mu\text{A}$ , 10 V). The amplifier has  $R_I = 5 \text{ k}\Omega$ ,  $R_B = 150 \text{ k}\Omega$ ,  $R_C = 100 \text{ k}\Omega$ , and  $R_3 = \infty$ . What is the voltage gain predicted using our rule of thumb estimate? What is the actual voltage gain? What is the value of  $\mu_f$  for this transistor?

**ANSWERS:** -200; -278; 2400

### DESIGN NOTE

Remember, the amplification factor  $\mu_f$  places an upper bound on the voltage gain of a single-transistor amplifier. We can't do better than  $\mu_f$ ! For the BJT,

$$\mu_f \cong 40V_A$$

For  $25 \text{ V} \leq V_A \leq 100 \text{ V}$ , we have  $1000 \leq \mu_f \leq 4000$ .

### 14.2.3 THE COMMON-SOURCE AMPLIFIER

Now we are in a position to analyze the small-signal characteristics of the **common-source (C-S) amplifier** shown in Fig. 14.12(a), which uses an enhancement-mode *n*-channel MOSFET ( $V_{TN} > 0$ ) in a four-resistor bias network. The ac equivalent circuit of Fig. 14.12(b) is constructed by assuming

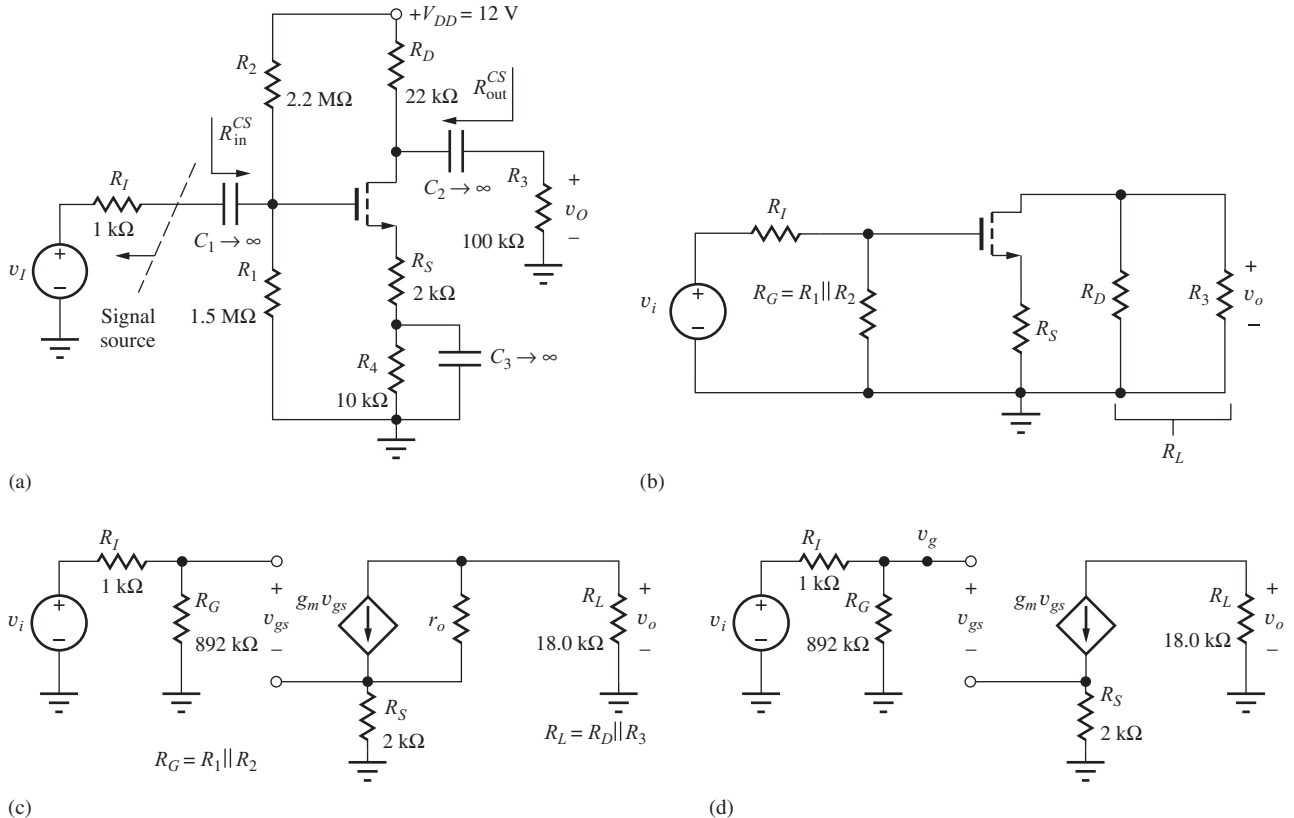


**Figure 14.12** (a) Common-source amplifier circuit employing a MOSFET. (b) ac Equivalent circuit for common-source amplifier in part (a). The common-source connection is now apparent. (c) ac Equivalent circuit with the MOSFET replaced by its small-signal model. (d) Final equivalent circuit for ac analysis of the common-source amplifier in which  $r_o$  is neglected.

that the capacitors all have zero impedance at the signal frequency and that the dc voltage sources represent ac grounds. Bias resistors  $R_1$  and  $R_2$  appear in parallel and are combined into gate resistor  $R_G$ , and  $R_L$  represents the parallel combination of  $R_D$  and  $R_3$ . In Fig. 14.12(c), the transistor has been replaced with its small-signal model. In subsequent analysis, we will assume that the voltage gain is much less than the intrinsic voltage gain of the transistor so we can neglect transistor output resistance  $r_o$ . For simplicity at this point, we assume that we have found the Q-point and know the values of  $I_D$  and  $V_{DS}$ .

In Fig. 14.12(b) through (d), the common-source nature of this amplifier should be apparent. The input signal is applied to the transistor's gate terminal, the output signal appears at the drain, and both the input and output signals are referenced to the (common) source terminal. Note that the small-signal models for the MOSFET and BJT are virtually identical at this step, except that  $r_\pi$  is replaced by an open circuit for the MOSFET.

Our first goal is to develop an expression for the voltage gain  $A_v^{CS}$  of the circuit in Fig. 14.12(a) from the source  $v_s$  to the output  $v_o$ . As with the BJT, we will first find the terminal voltage gain  $A_{vt}^{CS}$  between the gate and drain terminals of the transistor. Then, we will use the terminal gain expression to find the gain of the overall amplifier.

### Common-Source Terminal Voltage Gain

Starting with the circuit in Fig. 14.12(d), the terminal voltage gain is defined as

$$A_{vt}^{CS} = \frac{v_d}{v_g} = \frac{v_o}{v_g} \quad \text{where} \quad v_o = -g_m v_{gs} R_L \quad (14.34)$$

We can relate  $v_{gs}$  to  $v_g$  by applying KVL at the gate of the FET:

$$\mathbf{v}_g = \mathbf{v}_{gs} + g_m \mathbf{v}_{gs} R_S \quad \text{or} \quad \mathbf{v}_{gs} = \frac{\mathbf{v}_g}{1 + g_m R_S} \quad (14.35)$$

Combining Eqs. (14.34) and (14.35) yields an expression for the terminal gain.

$$A_{vt}^{CS} = -\frac{g_m R_L}{1 + g_m R_S} \quad (14.36)$$

### Signal Source Voltage Gain for the Common-Source Amplifier

Now we can find the overall gain from source  $v_i$  to the voltage across  $R_L$ . The overall gain can be written as

$$A_v^{CS} = \frac{v_o}{v_i} = \left( \frac{v_o}{v_g} \right) \left( \frac{v_g}{v_i} \right) = A_{vt}^{CS} = \left( \frac{v_g}{v_i} \right) \quad \text{where} \quad v_g = v_i \frac{R_G}{R_G + R_I} \quad (14.37)$$

in which  $v_g$  is related to  $v_i$  by the voltage divider formed by  $R_G$  and  $R_I$ . Combining Eqs. (14.36) and (14.37) yields a general expression for the voltage gain of the common-source amplifier:

$$A_v^{CS} = -\frac{g_m R_L}{1 + g_m R_S} \left( \frac{R_G}{R_G + R_I} \right) \quad (14.38)$$

We now explore the limits to the voltage gain of common-source amplifiers using model simplifications for zero and large values of resistance  $R_S$ . First, we will assume that the signal source resistance  $R_I$  is much less than  $R_G$  so that

$$A_v^{CS} \cong A_{vt}^{CS} = -\frac{g_m R_L}{1 + g_m R_S} \quad \text{for} \quad R_I \ll R_G \quad (14.39)$$

This approximation is equivalent to saying that the total input signal appears at the gate terminal of the transistor.

### Common-Source Voltage Gain for Large Values of $R_S$

A very useful simplification occurs when  $R_S$  is large enough so that the  $g_m R_S \gg 1$ :

$$A_{vt}^{CS} = -\frac{g_m R_L}{1 + g_m R_S} \cong -\frac{R_L}{R_S} \quad \text{for} \quad g_m R_{EI} \gg 1 \quad \text{and} \quad R_G \gg R_I \quad (14.40)$$

The gain is now set by the ratio of the load resistor  $R_L$  and source resistor  $R_S$ . This is an extremely useful result because the gain is now independent of the transistor characteristics that vary widely from device to device. The result in Eq. (14.40) is very similar to the one that we obtained for the op-amp inverting amplifier circuit and is a result of feedback introduced by resistor  $R_S$ .

Achieving the simplification in Eq. (14.40) requires  $g_m R_S \gg 1$ . We can relate this product to the dc bias voltage developed across  $R_S$ :

$$g_m R_S = \frac{2}{(V_{GS} - V_{TN})} I_D R_S \quad \text{and we need} \quad I_D R_S \gg \frac{V_{GS} - V_{TN}}{2} \quad (14.41)$$

$I_D R_S$  represents the dc voltage drop across source resistor  $R_S$  and must be much greater than half the gate drive of the transistor. This inequality can be achieved, but not as easily as for the case of the BJT.

### Understanding Generalized Common-Source Amplifier Operation

Let us explore common-source operation a bit further by looking at the signal voltage developed at the source terminal of the FET by referencing Fig. 14.12 and Eqs. (14.34) and (14.35):

$$\mathbf{v}_s = g_m \mathbf{v}_{gs} R_S = \frac{g_m R_S}{1 + g_m R_S} \mathbf{v}_g \cong \mathbf{v}_g \quad \text{for large } g_m R_S \quad (14.42)$$

The voltage  $v_g$  at the gate of the transistor is transferred directly to the source, setting up a current of  $v_g/R_S$ . All the source current is supplied from the drain yielding a terminal voltage gain equal to the ratio of  $R_L$  and  $R_S$ :

$$\mathbf{i}_s \cong \frac{\mathbf{v}_g}{R_S} \quad \mathbf{v}_o = -\mathbf{i}_d R_L = -\mathbf{i}_s R_L \quad \text{and} \quad A_{vt}^{CS} = \frac{\mathbf{v}_o}{\mathbf{v}_g} \cong -\frac{R_L}{R_S} \quad (14.43)$$

Unity signal voltage transfer from gate to source should not be mysterious. We know that the gate-source voltage has an approximately constant value of  $V_{GS}$ .<sup>2</sup> Thus the source signal voltage should be approximately the same as the gate signal. This voltage transfer between the gate and source terminals forms the basis of the source-follower operation to be discussed in detail in Section 14.3.



### DESIGN NOTE

The gain of the generalized common-source amplifier is approximately equal to the ratio of the load and emitter resistors.

$$A_{vt}^{CS} = -\frac{g_m R_L}{1 + g_m R_S} \cong -\frac{R_L}{R_S} \quad \text{for } g_m R_S \gg 1$$

#### 14.2.4 SMALL-SIGNAL LIMIT FOR THE COMMON-SOURCE AMPLIFIER

Equation (14.35) presents the general relation for the gate-source signal of the transistor that must be less than  $0.2(V_{GS} - V_{TN})$  for small signal operation:

$$\mathbf{v}_g = \mathbf{v}_{gs} (1 + g_m R_S) < 0.2 (V_{GS} - V_{TN}) (1 + g_m R_S) \quad (14.44)$$

The presence of a resistor in the source can substantially increase the signal handling capability of the common-source amplifier.



### DESIGN NOTE

Use of a source resistor in the common-source amplifier can significantly increase the input signal range of the amplifier.

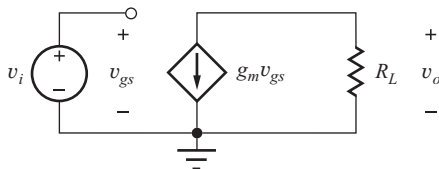
$$v_g \leq 0.2 (V_{GS} - V_{TN}) (1 + g_m R_S)$$

#### Zero Resistance in the Source

In order to achieve as large a gain as possible, we need to make the denominator in Eq. (14.39) as small as possible, and this is achieved by setting  $R_S = 0$ . The gain is then

$$A_v^{CS} \cong -g_m R_L = -g_m (R_D \parallel R_3) \quad \text{for } R_S = 0 \quad (14.45)$$

<sup>2</sup> Remember  $V_{GS} = V_{GS} + v_{gs}$ , and  $v_{gs} \ll V_{GS}$  for small-signal operation.

Figure 14.13 Simplified circuit for  $R_G \gg R_L$  and  $R_s = 0$ .

Equation (14.45) places an upper limit on the gain we can achieve from a common-source amplifier with an external load resistor. Equation (14.45) states that the terminal voltage gain of the common-source stage is equal to the product of the transistor's transconductance  $g_m$  and load resistance  $R_L$ , and the minus sign indicates that the output voltage is “inverted” or  $180^\circ$  out of phase with respect to the input. The approximations that led to Eq. (14.45) are equivalent to saying that the total input signal appears across  $v_{gs}$  as shown in Fig. 14.13.

### Common-Source Input Resistance

If we look in the gate terminal of the circuit in Fig. 14.12(d), we see an open circuit so  $R_{iG} = \infty$ . We can also find  $R_{iG}$  by taking the limit of the common-emitter input resistance as  $r_\pi$  approaches infinity with  $R_E$  replaced by  $R_S$  (and remembering  $\beta_o = g_m r_\pi$ ):

$$R_{iG} = \lim_{r_\pi \rightarrow \infty} R_{iB} = \lim_{r_\pi \rightarrow \infty} [r_\pi + (\beta_o + 1)R_S] = \infty \quad (14.46)$$

The overall input resistance of the common-source amplifier  $R_{\text{in}}^{CS}$  is the resistance looking into the circuit at coupling capacitor  $C_1$ :

$$R_{\text{in}}^{CS} = R_G \parallel R_{iG} = R_G \parallel \infty = R_G \quad (14.47)$$

### Common-Source Output Resistance

The easiest way to find the resistance  $R_{iD}$  looking into the drain terminal of the transistor is to take the limit of the common-emitter output resistance as  $r_\pi$  approaches infinity with  $R_E$  replaced with  $R_S$ :

$$R_{iD} = \lim_{r_\pi \rightarrow \infty} R_{iC} = \lim_{r_\pi \rightarrow \infty} \left[ r_o \left( 1 + \frac{\beta_o R_S}{R_{th} + r_\pi + R_S} \right) \right] = r_o (1 + g_m R_S) = r_o + \mu_f R_S \quad (14.48)$$

The overall output resistance of the common-source amplifier  $R_{\text{out}}^{CS}$  is the resistance looking into the circuit at coupling capacitor  $C_2$ :

$$R_{\text{out}}^{CS} = R_D \parallel R_{iD} = R_D \parallel r_o (1 + g_m R_S) \cong R_D \quad (14.49)$$

The output resistance is approximately equal to the drain resistor  $R_D$ , since  $r_o \gg R_D$ .

### DESIGN NOTE

The equations describing the behavior of the common-source amplifier are the same as those of the common-emitter amplifier in the limit as  $r_\pi$  and  $\beta_o$  approach infinity.

### EXAMPLE 14.3 VOLTAGE GAIN OF A COMMON-SOURCE AMPLIFIER

In this example, we find the small-signal parameters of the MOSFET and then calculate the voltage gain of a common-source amplifier.

**PROBLEM** (a) Calculate the gain, input resistance, and output resistance of the common-source amplifier in Fig. 14.12 if the transistor has  $K_n = 0.500 \text{ mA/V}^2$ ,  $V_{TN} = 1 \text{ V}$ , and  $\lambda = 0.0133 \text{ V}^{-1}$ , and the

Q-point is (0.241 mA, 3.81 V). What is the largest value of  $v_i$  that does not violate the small-signal assumption? (b) Repeat part (a) if bypass capacitor  $C_3$  is connected between the source terminal of the transistor and ground.

**SOLUTION** **Known Information and Given Data:** Common-source amplifier with its ac equivalent circuit given in Fig. 14.12;  $K_n = 0.500 \text{ mA/V}^2$ ,  $V_{TN} = 1 \text{ V}$ , and  $\lambda = 0.0133 \text{ V}^{-1}$ ; the Q-point is (0.241 mA, 3.64 V);  $R_I = 1 \text{ k}\Omega$ ,  $R_1 = 1.5 \text{ M}\Omega$ ,  $R_2 = 2.2 \text{ M}\Omega$ ,  $R_D = 22 \text{ k}\Omega$ ,  $R_3 = 100 \text{ k}\Omega$ ,  $R_S = 2 \text{ k}\Omega$ .

**Unknowns:** Small-signal parameters of the transistor; voltage gain  $A_v$ ; input resistance  $R_{\text{in}}^{CS}$ ; output resistance  $R_{\text{out}}^{CS}$ ; small-signal limit for the value of  $v_i$

**Approach:** Use the Q-point information to find  $g_m$  and  $r_o$ . Use the calculated and given values to evaluate the voltage gain and input and output resistance expression.

**Assumptions:** The transistor is in the active region of operation, and the signal amplitudes are below small-signal limit for the MOSFET.

**Analysis:** We need to evaluate Eq. (14.38):

$$A_v^{CS} = -\frac{g_m R_L}{1 + g_m R_S} \left( \frac{R_G}{R_G + R_I} \right)$$

Calculating the values of the various resistors and small-signal model parameters yields

$$\begin{aligned} g_m &= \sqrt{2K_n I_{DS}(1 + \lambda V_{DS})} \\ &= \sqrt{2 \left( 5 \times 10^{-4} \frac{\text{A}}{\text{V}^2} \right) (0.241 \times 10^{-3} \text{ A}) \left( 1 + \frac{0.0133}{\text{V}} 3.81 \text{ V} \right)} = 0.503 \text{ mS} \end{aligned}$$

$$r_o = \frac{\frac{1}{\lambda} + V_{DS}}{I_D} = \frac{\left( \frac{1}{0.0133} + 3.81 \right) \text{ V}}{0.241 \times 10^{-3} \text{ A}} = 328 \text{ k}\Omega$$

$$R_G = R_1 \| R_2 = 892 \text{ k}\Omega \quad R_L = R_D \| R_3 = 18.0 \text{ k}\Omega$$

$$g_m R_L = 9.05 \quad g_m R_S = 1.01 \quad A_v^{CS} = -\frac{9.05}{1 + 1.01} \left( \frac{892 \text{ k}\Omega}{892 \text{ k}\Omega + 1 \text{ k}\Omega} \right) = -4.50$$

Thus the common-source amplifier in Fig. 14.13 provides a small-signal voltage gain  $A_v = -4.50$  or 13.1 dB.

Based on Eq. (13.82) for small-signal operation, we require

$$v_i \leq 0.2(V_{GS} - V_{TN})(1 + g_m R_S) = 0.2(0.982 \text{ V})(2.01) = 0.395 \text{ V}$$

Thus, the input signal amplitude must not exceed 0.40 V for small-signal operation.

The overall input resistance of the common-source amplifier  $R_{\text{in}}^{CS}$  is set by gate bias resistor  $R_G$ :

$$R_{\text{in}}^{CS} = R_G = 892 \text{ k}\Omega$$

The overall output resistance of the common-source amplifier  $R_{\text{out}}^{CS}$  is approximately equal to the drain bias resistor  $R_D$ :

$$R_{\text{out}}^{CS} = R_D \| r_o(1 + g_m R_S) = 22 \text{ k}\Omega \| 328 \text{ k}\Omega [1 + (0.503 \text{ mS})(2 \text{ k}\Omega)] = 21.3 \text{ k}\Omega$$

(b) When the source is directly bypassed the results become

$$A_v^{CS} = -g_m R_L \left( \frac{R_G}{R_I + R_G} \right) = -9.04 \quad v_i \leq 0.2 (V_{GS} - V_{TN}) = 0.2 (0.982 \text{ V}) = 0.186 \text{ V}$$

$$R_{in}^{CS} = R_G = 892 \text{ k}\Omega \quad R_{out}^{CS} = R_D \| r_o = 22 \text{ k}\Omega \| 328 \text{ k}\Omega = 20.6 \text{ k}\Omega$$

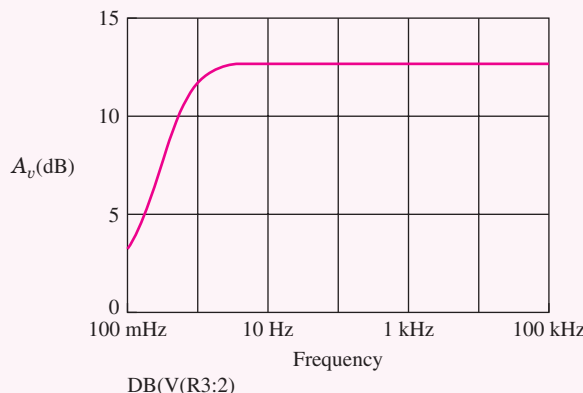
**Check of Results:** We have found all the requested values. The amplification factor for this transistor is  $\mu_f = g_m r_o = 165$ . Our calculated voltage gain is much less than  $\mu_f = 165$ , so neglect of  $r_o$  is justified. With nonzero  $R_S$ , our estimate for the gain is  $-R_L/R_S = -18 \text{ k}\Omega / 2 \text{ k}\Omega = -9.00$ . Our gain is lower than this prediction because the  $g_m R_S$  product is not large compared to one. Checking the active region assumption:  $V_{GS} - V_{TN} = 0.982 \text{ V}$  and  $V_{DS} = 3.81 \text{ V}$ . ✓

**Discussion:** Note that this C-S amplifier has been designed to operate at nearly the same Q-point as the C-E amplifier in Fig. 14.7, and  $R_S$  has been chosen to give about the same gain.

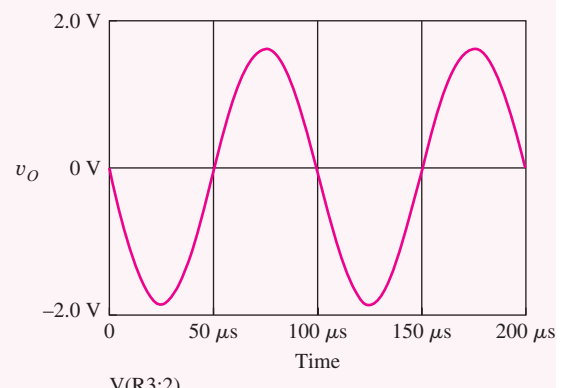
**Computer-Aided Analysis:** (a) A SPICE operating point analysis ( $KP = 0.5 \text{ mA/V}^2$ ,  $VTO = 1 \text{ V}$ ,  $LAMBDA = 0.0133/\text{V}$ ) yields the Q-point of  $(0.242 \text{ mA}, 3.77 \text{ V})$ . The slight variations result from including a nonzero value of  $\lambda$ . ac analysis yields a small-signal gain of  $-4.39$ . SPICE transient simulation results are given in the graphs below at a frequency of  $10 \text{ kHz}$  with  $TSTART = 0$ ,  $TSTOP = 0.2 \text{ MS}$  and  $TSTEP = 0.1 \text{ US}$ . The first graph shows the results of an ac sweep from  $0.1 \text{ Hz}$  to  $100 \text{ kHz}$  with a  $1\text{-V}$  input signal to identify the region (midband) where the capacitors are effectively short circuits. From the graph, we find that the gain is constant at  $-4.39$  frequencies above  $10 \text{ Hz}$ . The second graph shows the result from the transient simulation with a  $0.4\text{-V}$ ,  $10\text{-kHz}$  sine wave as the input. Although this amplitude is at the small signal limit, we do not visually observe any significant distortion in the waveform. SPICE gives the total harmonic distortion as  $2.2$  percent.

The (frequency dependent) input resistance of the common-source amplifier is equal to the voltage at the gate node divided by the current entering the node through coupling capacitor  $C_1 : R_{in}^{CE} = V(M1 : g)/I(C1)$ . At frequencies above  $10 \text{ Hz}$ , the SPICE input becomes constant at  $892 \text{ k}\Omega$  in agreement with our hand calculations. Similarly, the output resistance is given by  $R_{out}^{CS} = V(M1 : d)/I(C2)$  which becomes constant at  $21.3 \text{ k}\Omega$  for frequencies above  $10 \text{ Hz}$ . The discrepancies are due to differences in the SPICE values for the Q-point, temperature  $T$ , and the current gain.

(b) When the source terminal of the transistor is bypassed, SPICE yields the following results:  $A_v^{CS} = -8.61$ ,  $R_{in}^{CS} = 892 \text{ k}\Omega$ ,  $R_{out}^{CS} = 20.6 \text{ k}\Omega$  and the total harmonic distortion is  $3.8$  percent.



Frequency response (as sweep) for a  $1\text{-V}$  ac input signal.



Transient response with  $v_i = 0.4 \sin(20000\pi t) \text{ V}$ .

**EXERCISE:** Calculate the Q-point for the transistor in Fig. 14.12.

**EXERCISE:** Convert the voltage gain in Ex. 14.3 to dB.

**ANSWER:** 13.1 dB

### 14.2.5 COMMON-EMITTER AND COMMON-SOURCE AMPLIFIER CHARACTERISTICS

Table 14.3 summarizes the results for the C-E and C-S amplifiers developed in Chapter 14. In the common-emitter circuit, resistor  $R_E$  adds feedback to the amplifier that reduces the voltage gain by the factor  $(1 + g_m R_E)$ , but increases the transistor's input resistance, output resistance, and input signal range by the same amount. Resistor  $R_S$  has a similar impact on the voltage gain, output resistance, and input signal range of the common-source amplifier. Since the resistance at the gate terminal of the FET is already infinite, the overall input resistance of the C-S amplifier is not affected by  $R_S$ .

**EXERCISE:** (a) What is the voltage gain  $A_v$  of the two amplifiers in Fig. 14.2 if  $R_E$  and  $R_S$  are changed to 1 k $\Omega$ ? Assume the Q-points do not change. (b) What are the new values of  $R_4$  required to maintain the Q-points unchanged in the two amplifiers?

**ANSWERS:** -15.6, -5.9; 12 k $\Omega$ , 11 k $\Omega$

**EXERCISE:** What is the voltage gain  $A_v$  of the two amplifiers in Fig. 14.2 if  $C_3$  is removed from both circuits? What are the estimates for large emitter and large source resistances?

**ANSWERS:** -1.36, -1.28; -1.39, -1.50

**TABLE 14.3**

Common-Emitter/Common-Source Amplifier Design Summary

	COMMON-EMITTER (C-E) AMPLIFIER	COMMON-SOURCE (C-S) AMPLIFIER
Terminal voltage gain	$A_{vt}^{CE} = \frac{V_o}{V_i} = -\frac{g_m R_L}{1 + g_m R_E}$	$A_{vt}^{CS} = \frac{V_o}{V_i} = -\frac{g_m R_L}{1 + g_m R_S}$
Signal source voltage gain	$A_v^{CE} = \frac{V_o}{V_i} = A_{vt}^{CE} \frac{R_B \  R_{iB}}{R_I + R_B \  R_{iB}}$	$A_v^{CS} = \frac{V_o}{V_i} = A_{vt}^{CS} \frac{R_G}{R_I + R_G}$
Rule-of-thumb estimate for $g_m R_L$	$10(V_{CC} + V_{EE})$	$(V_{DD} + V_{SS})$
Input terminal resistance	$R_{iB} = r_\pi(1 + g_m R_E)$	$R_{iG} = \infty$
Output terminal resistance	$R_{iC} = r_o(1 + g_m R_E)$	$R_{iD} = r_o(1 + g_m R_S)$
Amplifier input resistance	$R_{in}^{CE} = R_B \  R_{iB}$	$R_{in}^{CS} = R_G$
Amplifier output resistance	$R_{out}^{CE} = R_C \  R_{iC}$	$R_{out}^{CS} = R_D \  R_{iD}$
Input signal range	$0.005(1 + g_m R_E) \text{ V}$	$0.2(V_{GS} - V_{TN})(1 + g_m R_S)$
Terminal current gain	$\beta_o$	$\infty$

**EXERCISE:** What value of saturation current  $I_S$  must be used in SPICE to achieve  $V_{BE} = 0.7$  V for  $I_C = 245 \mu\text{A}$ ? Assume a default temperature of 27°C.

**ANSWER:** 0.422 fA

**EXERCISE:** Evaluate  $-g_m R_L$  and  $-R_L/R$  for the C-E and C-S amplifiers in Ex. 14.1 and 14.3, and compare the magnitudes to the exact calculations in the examples. ( $R = R_E$  or  $R_S$ )

**ANSWERS:**  $-176, -6.00; -8.84, -9.00; 5.65 < 6.00; 4.46 < 8.84$

### 14.2.6 C-E/C-S AMPLIFIER SUMMARY

The numeric results for the two specific amplifier examples are presented in Table 14.4. The common-emitter and common-source amplifiers have similar voltage gains. The C-E amplifier approaches the  $R_L/R_E$  limit (-6) more closely because  $g_m R_E = 29.4$  for the BJT case, but only 0.982 for the MOSFET. The C-S amplifier provides high input resistance, but that of the BJT amplifier is also substantial due to the  $\mu_f R_E$  term. The output resistance of the C-E and C-S amplifiers use the same. The input signal levels have been increased above the  $R_S$  or  $R_E = 0$  case—again by a substantial amount in the BJT case.

**TABLE 14.4**  
Common-Emitter/Common-Source Amplifier Comparison

	C-E AMPLIFIER	C-S AMPLIFIER
Voltage gain	-5.70	-4.39
Input resistance	77.8 kΩ	892 kΩ
Output resistance	21.9 kΩ	21.3 kΩ
Input signal range	155 mV	395 mV

### 14.2.7 EQUIVALENT TRANSISTOR REPRESENTATION OF THE GENERALIZED C-E/C-S TRANSISTOR

The equations in Table 14.1 can actually provide us with a way to “absorb” resistor  $R$  into the transistor. This action can often simplify our circuit analysis or help provide insight into the operation of a circuit that we haven’t seen before. The process is depicted in Fig. 14.14, in which the original transistor  $Q$  and resistor  $R$  are replaced by a new equivalent transistor  $Q'$ . The small-signal parameters of the new transistor are given by

$$g'_m = \frac{g_m}{1 + g_m R} \quad r'_\pi = r_\pi(1 + g_m R) \quad r'_o = r_o(1 + g_m R) \quad (14.50)$$

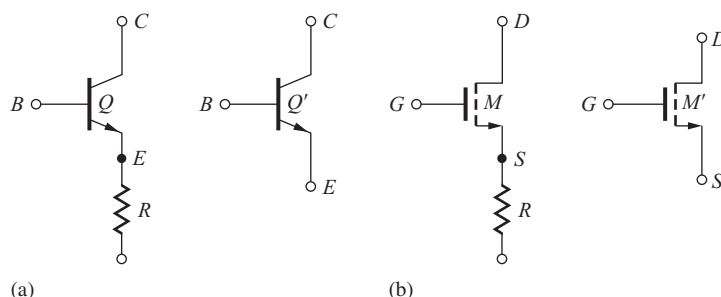


**Figure 14.14** Composite transistor representation of (a) transistor  $Q$  and resistor  $R$ . (b) Transistor  $M$  and resistor  $R$ .

Here we see the direct trade-off between reduced transconductance and increased input and output resistance. It is also important to note, however, that current gain and amplification factor of the transistor are conserved—we cannot exceed the limitations of the transistor itself!

$$\beta'_o = g'_m r'_\pi = \beta_o \quad \text{and} \quad \mu'_f = g'_m r'_o = \mu_f \quad (14.51)$$

Similar results apply to the FET except that the current gain and input resistance are both infinite.

### 14.3 FOLLOWER CIRCUITS—COMMON-COLLECTOR AND COMMON-DRAIN AMPLIFIERS

We now consider a second class of amplifiers, the common-collector (C-C) and common-drain (C-D) amplifiers, as represented by the ac equivalent circuits in Fig. 14.15. We will see that the follower circuits provide high input resistance and low output resistance with a gain of approximately one. The BJT circuit is analyzed first, and then the MOSFET circuit is treated as a special case with  $r_\pi \rightarrow \infty$ .

#### 14.3.1 TERMINAL VOLTAGE GAIN

To find the terminal gain in Fig. 14.15(a), the bipolar transistor is replaced by its small-signal model in Fig. 14.16 ( $r_o$  is again neglected). The output voltage  $v_o$  now appears across load resistor  $R_L$  connected to the emitter of the transistor and is equal to

$$v_o = +(\beta_o + 1)i_b R_L \quad \text{where} \quad R_L = R_3 \parallel R_6 \quad (14.52)$$

The input current is related to applied voltage  $v_b$  by

$$v_b = i_b r_\pi + (\beta_o + 1)i_b R_L = i_b [r_\pi + (\beta_o + 1)R_L] \quad (14.53)$$

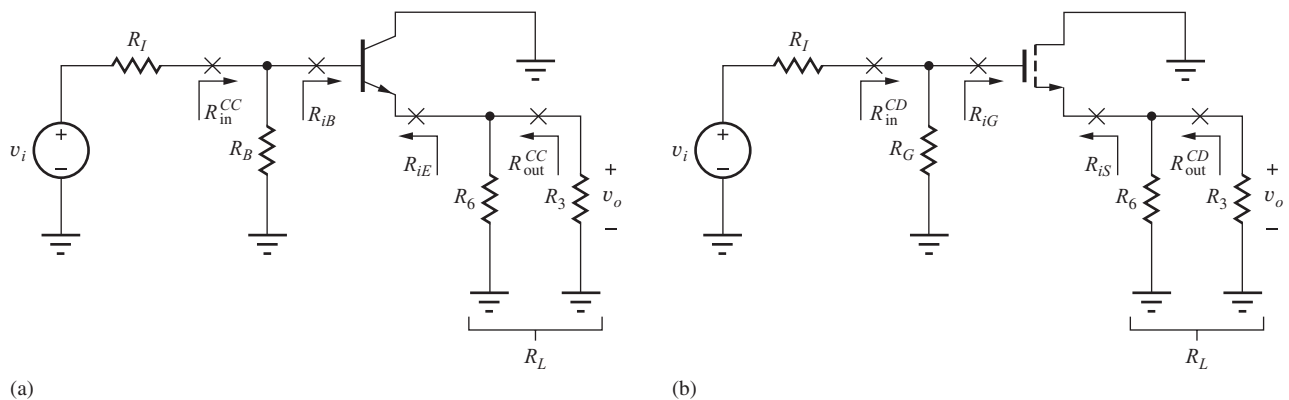


**Figure 14.15** (a) ac equivalent circuit for the C-C amplifier. (b) ac equivalent circuit for the C-D amplifier.

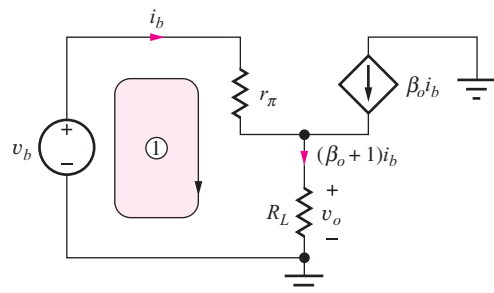


**Figure 14.16** Small-signal model for the C-C amplifier.  $R_L = R_3 \parallel R_6$ .

Combining Eqs. (14.52) and (14.53) yields an expression for the terminal gain of the common-collector amplifier:

$$A_{vt}^{CC} = +\frac{(\beta_o + 1)R_L}{r_\pi + (\beta_o + 1)R_L} \cong +\frac{g_m R_L}{1 + g_m R_L} \quad (14.54)$$

where the approximation holds for large  $\beta_o$ .

Letting  $r_\pi$  (and  $\beta_o$ ) approach infinity in Eq. (14.54) yields the corresponding terminal gain for the FET follower in Fig. 14.15(b):

$$A_{vt}^{CD} = +\frac{g_m R_L}{1 + g_m R_L} \quad (14.55)$$

In most common-collector and common-drain designs,  $g_m R_L \gg 1$ , and Eqs. (14.54) and (14.55) reduce to

$$A_{vt}^{CC} \cong A_{vt}^{CD} \cong 1 \quad (14.56)$$

The C-C and C-D amplifiers both have a gain that approaches 1. That is, the output voltage follows the input voltage, and the C-C and C-D amplifiers are often called **emitter followers** and **source followers**, respectively. In most cases, the BJT does a better job of achieving  $g_m R_L \gg 1$  than does the FET, and the BJT gain is closer to unity than that of the FET. However, in both cases the value of voltage gain typically falls in the range of

$$0.75 \leq A_{vt} \leq 1 \quad (14.57)$$

Obviously,  $A_{vt}$  is much less than the amplification factor  $\mu_f$ , so neglecting  $r_o$  in the model of Fig. 14.16 is valid. Note, however, that  $r_o$  appears in parallel with  $R_L$ , and its effect can be included by replacing  $R_L$  with  $(R_L \parallel r_o)$  in the equations.

### Understanding Follower Operation

Unity signal transfer between the input and output of the follower circuits should not be mysterious. We know that the base and emitter terminals of the BJT are connected by a forward-biased diode whose voltage is virtually constant at 0.7 V. Thus the emitter signal voltage should be approximately the same as the base signal. (Remember that  $v_{BE} = V_{BE} + v_{be}$ , but  $v_{be} \ll V_{BE}$ ). FET followers behave in a similar manner. The gate-source voltage is approximately constant, so the signal voltage at the transistor source should be approximately the same as the applied gate signal. In this case,  $v_{GS} = V_{GS} + v_{gs}$ , but  $v_{gs} \ll V_{GS}$ . Thus the output of either follower should mirror the input with only a dc level shift between the two signals.



## DESIGN NOTE

The terminal gain of single transistor voltage followers is given by

$$A_{vt}^{CC} \cong A_{vt}^{CD} = +\frac{g_m R_L}{1 + g_m R_L} \quad \text{and typically} \quad 0.75 < A_{vt}^{CD} < A_{vt}^{CC} < 1$$

### 14.3.2 INPUT RESISTANCE

The input resistance at the base terminal of the BJT is simply equal to the last term in brackets in Eq. (14.53):

$$R_{iB} = \frac{V_b}{I_b} = r_\pi + (\beta_o + 1)R_L \cong r_\pi(1 + g_m R_L) \quad \text{and} \quad R_{iG} = \infty \quad (14.58)$$

letting  $r_\pi$  approach infinity for the MOSFET. The input resistance of the emitter follower is equal to  $r_\pi$  plus an amplified replica of load resistor  $R_L$ , and can be made quite large. Of course, we see that the input resistance of the source follower is very large.

The overall input resistance  $R_{\text{in}}^{CC}$  to the common-collector amplifier in Fig. 14.15(a) is equal to the parallel combination of bias resistor and the equivalent resistance at the base of the BJT:

$$R_{\text{in}}^{CC} = R_B \parallel R_{iB} = R_B \| r_\pi (1 + g_m R_L) \quad \text{where} \quad R_L = R_6 \parallel R_3 \quad (14.59)$$

The overall input resistance  $R_{\text{in}}^{CD}$  to the common-drain amplifier in Fig. 14.15(b) is equal to the parallel combination of bias resistor and the equivalent resistance at the gate of the FET:

$$R_{\text{in}}^{CD} = R_G \parallel R_{iG} = R_G \parallel \infty = R_G \quad (14.60)$$

### 14.3.3 SIGNAL SOURCE VOLTAGE GAIN

The overall voltage gains from source  $v_i$  in Fig. 14.15 to the output are found using the terminal gain and input resistance expressions

$$A_v^{CC} = \frac{\mathbf{v}_o}{\mathbf{v}_i} = \left( \frac{\mathbf{v}_o}{\mathbf{v}_b} \right) \left( \frac{\mathbf{v}_b}{\mathbf{v}_i} \right) = A_{vt}^{CC} \left( \frac{\mathbf{v}_b}{\mathbf{v}_i} \right)$$

Voltage  $v_b$  at the base of the bipolar transistor in Fig. 14.15 is related to  $v_i$  by

$$\mathbf{v}_b = \mathbf{v}_i \frac{R_B \parallel R_{iB}}{R_I + (R_B \parallel R_{iB})}$$

for  $R_B = R_1 \parallel R_2$ . Combining these expressions,

$$A_v^{CC} = A_{vt}^{CC} \left[ \frac{R_B \parallel R_{iB}}{R_I + (R_B \parallel R_{iB})} \right] \quad (14.61)$$

For the common-source case with infinite input resistance, Eq. (14.61) reduces to

$$A_v^{CD} = A_{vt}^{CD} \left( \frac{R_G}{R_I + R_G} \right) \quad (14.62)$$

### 14.3.4 FOLLOWER SIGNAL RANGE

Because the emitter- and source-follower circuits have a gain approaching unity, only a small portion of the input signal actually appears across the base-emitter or gate-source terminals. Thus, these circuits can be used with relatively large input signals without violating their respective small-signal limits.

The voltage developed across  $r_\pi$  in the small-signal model must be less than 5 mV for small-signal operation of the BJT. An expression for  $v_{be}$  is found in a manner identical to that used to derive Eq. (14.53):

$$\mathbf{v}_{be} = \mathbf{i}_b r_\pi = \mathbf{v}_b \frac{r_\pi}{r_\pi + (\beta_o + 1)R_L} \quad (14.63)$$

Requiring the amplitude of voltage  $\mathbf{v}_{be}$  to be less than 5 mV gives

$$|\mathbf{v}_b| \leq 0.005(1 + g_m R_L) \text{ V} \quad (14.64)$$

for large  $\beta_o$ . Normally,  $g_m R_L \gg 1$ , and the magnitude of  $v_b$  can be increased well beyond the 5-mV limit.

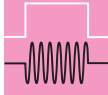
For the case of the FET (letting  $r_\pi \rightarrow \infty$ ), the corresponding expression becomes

$$|\mathbf{v}_{gs}| = \frac{|\mathbf{v}_g|}{1 + g_m R_L} \leq 0.2(V_{GS} - V_{TN}) \quad (14.65)$$

and

$$|\mathbf{v}_g| \leq 0.2(V_{GS} - V_{TN})(1 + g_m R_L) \quad (14.66)$$

which also increases the permissible range for  $v_i$ .


**DESIGN  
NOTE**

An unbypassed resistor  $R$  in series with the emitter or source of a transistor increases the signal handling capability of the amplifier by a factor of approximately  $(1 + g_m R)$ .

**EXERCISE:** What are the largest values of  $v_i$  that correspond to small-signal operation of the amplifiers in Fig. 14.3 if the transistor currents are 0.25 mA and  $V_{GS} - V_{TN} = 1$  V?

**ANSWERS:** 0.580 V; 1.27 V

### 14.3.5 FOLLOWER OUTPUT RESISTANCE

The resistance looking into the emitter terminal can be calculated based on the circuit in Fig. 14.17, in which test source  $v_x$  is applied directly to the emitter terminal. Using KCL at the emitter node yields

$$\mathbf{i}_x = -\mathbf{i} - \beta_o \mathbf{i} = \frac{\mathbf{v}_x}{r_\pi + R_{th}} - \beta_o \left( -\frac{\mathbf{v}_x}{r_\pi + R_{th}} \right) \quad (14.67)$$

Collecting terms and rearranging gives

$$R_{iE} = \frac{r_\pi + R_{th}}{\beta_o + 1} \approx \frac{1}{g_m} + \frac{R_{th}}{\beta_o} \quad (14.68)$$

for  $\beta_o \gg 1$ . Because the current gain is infinite for the FET,

$$R_{iS} = \frac{1}{g_m} \quad (14.69)$$

From Eqs. (14.68) and (14.69), it can be observed that the transistor's output resistance is primarily determined by the reciprocal of the transconductance of the transistor. This is an extremely important result to remember. For the BJT case, an additional term is added, but it is usually small, unless  $R_{th}$  is very large. The value of the output resistance for the C-C and C-D circuits can be quite low. For instance, at a current of 5 mA, the  $g_m$  of the bipolar transistor is  $40 \times 0.005 = 0.2$  S, and  $1/g_m$  is only 5  $\Omega$ .

Using the results above, the overall output resistance of the follower circuits in Fig. 14.9 are also determined primarily by the transistor transconductances,

$$R_{out}^{CC} = R_6 \parallel R_{iE} \approx \frac{1}{g_m} \quad \text{and} \quad R_{out}^{CD} = R_6 \parallel R_{iS} \approx \frac{1}{g_m} \quad (14.70)$$

and can be quite small in value.

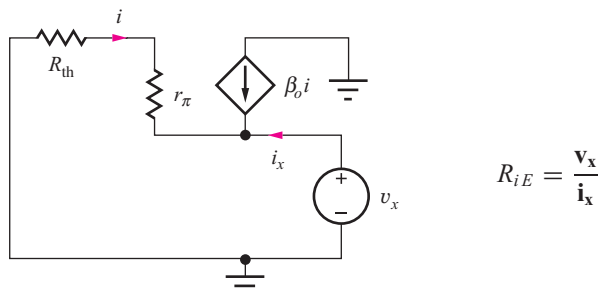


Figure 14.17 C-C/C-D output resistance calculation.

**EXERCISE:** Redraw the small-signal equivalent circuit and derive a new expression for  $R_{iE}$  of the common-collector amplifier including  $r_o$ . Simplify the result.

**ANSWER:**  $R_{iE} = r_o \parallel \left( \frac{1}{g_m} + \frac{R_{th}}{\beta_o} \right) \cong \frac{1}{g_m}$  since  $r_o \gg \frac{1}{g_m}$

## DESIGN NOTE

The equivalent resistance looking into the emitter or source of a transistor is approximately  $1/g_m$ !

Let us further interpret the two terms in Eq. (14.68) by injecting a current into the emitter of the BJT, as in Fig. 14.18. Multiplying  $\mathbf{i}$  by the input resistance gives the voltage that must be developed at the emitter:

$$\mathbf{v}_e = \frac{\alpha_o \mathbf{i}}{g_m} + \frac{\mathbf{i}}{\beta_o + 1} R_{th} \quad (14.71)$$

Current ( $\alpha_o \mathbf{i}$ ) comes out of the collector and must be supported by the emitter-base voltage  $\mathbf{v}_{eb} = \alpha_o \mathbf{i}/g_m$ , represented by the first term in Eq. (14.69). Base current  $\mathbf{i}_b = -\mathbf{i}/(\beta_o + 1)$  creates a voltage drop in resistance  $R_{th}$  and yields the second term. In the FET case, only the first term exists because  $i_g = 0$ .

**EXERCISE:** Drive the emitter node in Fig. 14.17 with a test current source  $i_x$ , and verify the output resistance results in Eq. (14.68).

### 14.3.6 CURRENT GAIN

Terminal current gain  $A_{it}$  is the ratio of the current delivered to the load element to the current being supplied from the Thévenin source. In Fig. 14.19, the current  $i$  plus its amplified replica ( $\beta_o i$ ) are combined in load resistor  $R_L$ , yielding a current gain equal to  $(\beta_o + 1)$ . For the FET,  $r_\pi$  is infinite,  $i$  is zero, and the current gain is infinite. Thus, for the C-C/C-D amplifiers,

$$A_{it}^{CC} = \frac{\mathbf{i}}{\mathbf{i}} = \beta_o + 1 \quad \text{and} \quad A_{it}^{CD} = \infty \quad (14.72)$$

### 14.3.7 C-C/C-D AMPLIFIER SUMMARY

Table 14.5 summarizes the results that have been derived for the common-collector and common-drain amplifiers in Fig. 14.20. As before, the FET results in the table can always be obtained from

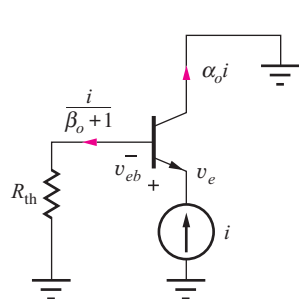


Figure 14.18 Circuit to aid in interpreting Eq. (14.71).

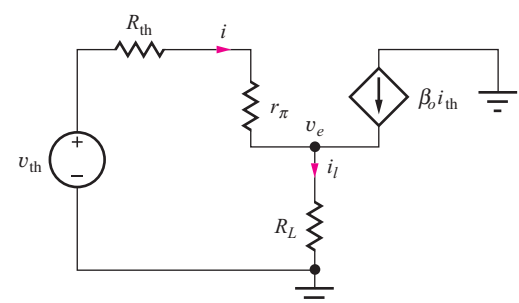
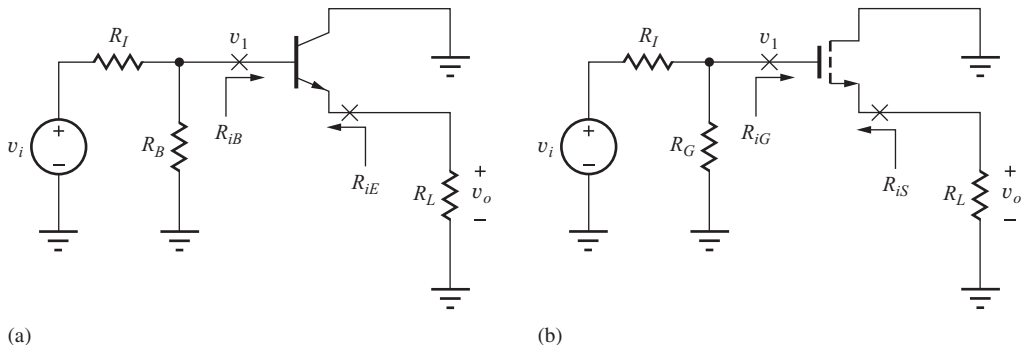


Figure 14.19 Circuit for calculating C-C/C-D terminal current gain.

**TABLE 14.5**  
Common-Collector/Common-Drain Amplifier Design Summary

	COMMON-COLLECTOR (C-C) AMPLIFIER	COMMON-DRAIN (C-D) AMPLIFIER
Terminal voltage gain	$A_{vt}^{CC} = \frac{v_o}{v_i} = +\frac{g_m R_L}{1 + g_m R_L} \cong 1$	$A_{vt}^{CD} = \frac{v_o}{v_i} = +\frac{g_m R_L}{1 + g_m R_L} \cong 1$
Signal source voltage gain	$A_v^{CC} = \frac{v_o}{v_i} = A_{vt}^{CC} \frac{R_B \parallel R_{iB}}{R_I + R_B \parallel R_{iB}}$	$A_v^{CD} = \frac{v_o}{v_i} = A_{vt}^{CD} \frac{R_G}{R_I + R_G}$
Rule-of-thumb estimate for $g_m R_L$	$10(V_{CC} + V_{EE})$	$(V_{DD} + V_{SS})$
Input terminal resistance	$R_{iB} = r_\pi(1 + g_m R_L)$	$R_{iG} = \infty$
Output terminal resistance	$R_{iE} \cong \frac{1}{g_m} + \frac{R_{th}}{\beta_o}$	$R_{iS} = \frac{1}{g_m}$
Input signal range	$0.005(1 + g_m R_L)$ V	$0.2(V_{GS} - V_{TN})(1 + g_m R_L)$
Terminal current gain	$\beta_o + 1$	$\infty$



**Figure 14.20** (a) Common-collector and (b) common-drain amplifiers for use with Table 14.5.

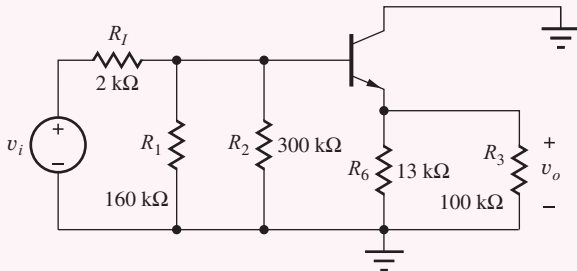
the BJT results by letting  $r_\pi$  and  $\beta_o \rightarrow \infty$ . The similarity between the characteristics of the C-C and C-D amplifiers should be readily apparent. Both amplifiers provide a gain approaching unity, a high input resistance, and a low output resistance. The differences arise because of the finite value of  $r_\pi$  and  $\beta_o$  of the BJT. The FET can more easily achieve very high values of input resistance because of the infinite resistance looking into its gate terminal, whereas the C-C amplifier can more easily reach very low levels of output resistance because of its higher transconductance for a given operating current. Both amplifiers can be designed to handle relatively large input signal levels. The current gain of the FET is inherently infinite, whereas that of the BJT is limited by its finite value of  $\beta_o$ .

#### EXAMPLE 14.4 FOLLOWER CALCULATIONS

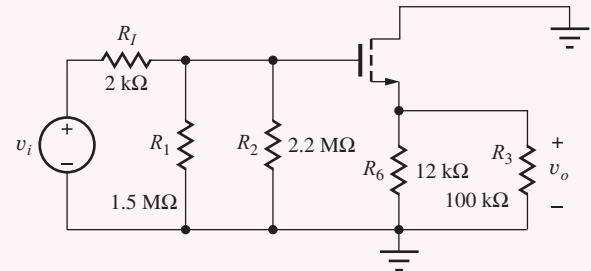
The characteristics of the common-collector and common-drain amplifiers in Fig. 14.4 are calculated using the expressions derived in this section.

**PROBLEM** Calculate the overall gain  $A_v$ , input resistances, output resistances, and signal handling capability of the C-C and C-D amplifiers using the results from Sec. 14.3 and the parameter values from Exs. 14.1 and 14.3.

**SOLUTION** **Known Information and Given Data:** The equivalent circuits with element values are redrawn below. The Q-point and small-signal values appear in the table below from the previous examples.



Common-Collector Amplifier from Fig. 14.4.



Common-Drain Amplifier from Fig. 14.4.

	$I_C$ or $I_D$	$V_{CE}$ or $V_{DS}$	$V_{GS} - V_{TN}$	$g_m$	$r_\pi$	$r_o$	$\mu_f$
BJT	245 $\mu\text{A}$	3.64 V	—	9.80 mS	10.2 kΩ	219 kΩ	2150
FET	241 $\mu\text{A}$	3.81 V	0.982 V	0.491 mS	$\infty$	223 kΩ	110

**Unknowns:** Voltage gains, input and output resistances, and maximum input signal levels for the C-C and C-D amplifiers

**Approach:** Substitute element values from the two circuits into the results in Table 14.5.

**Assumptions:** Use the parameter values tabulated above.

**Analysis:** For the C-C amplifier load resistor  $R_L = R_6 \parallel R_3 = 11.5 \text{ k}\Omega$ , and bias resistor  $R_B = R_1 \parallel R_2 = 104 \text{ k}\Omega$ . The resistances, terminal gain, and input signal level are

$$R_{iB} \cong r_\pi(1 + g_m R_L) = 10.2 \text{ k}\Omega [1 + 9.80 \text{ mS}(11.5 \text{ k}\Omega)] = 1.16 \text{ M}\Omega$$

$$R_{in}^{CC} = R_B \parallel R_{iB} = 104 \text{ k}\Omega \parallel 1.16 \text{ M}\Omega = 95.4 \text{ k}\Omega$$

$$A_{vt}^{CC} \cong \frac{g_m R_L}{1 + g_m R_L} = \frac{9.80 \text{ mS}(11.5 \text{ k}\Omega)}{1 + 9.80 \text{ mS}(11.5 \text{ k}\Omega)} = 0.991$$

$$R_{th} = 2 \text{ k}\Omega \parallel 160 \text{ k}\Omega \parallel 300 \text{ k}\Omega = 0.781 \text{ k}\Omega$$

$$R_{iE} \cong \frac{1}{g_m} + \frac{R_{th}}{\beta_o} = \frac{1}{9.80 \text{ mS}} + \frac{781 \Omega}{100} = 110 \Omega$$

$$R_{out}^{CC} \cong R_6 \parallel R_{iE} = 13 \text{ k}\Omega \parallel 110 \Omega = 109 \Omega$$

$$v_i \leq 0.005 \text{ V} (1 + g_m R_L) \left( \frac{R_I + R_{in}^{CC}}{R_{in}^{CC}} \right)$$

$$v_i \leq 0.005 \text{ V} [1 + 9.80 \text{ mS}(11.5 \text{ k}\Omega)] \frac{2 \text{ k}\Omega + 95.4 \text{ k}\Omega}{95.4 \text{ k}\Omega} = 0.580 \text{ V}$$

Using Eq. (14.61), we find the overall gain to be

$$A_v^{CC} = A_{vt}^{CC} \left[ \frac{R_{in}^{CC}}{R_I + R_{in}^{CC}} \right] = 0.991 \left[ \frac{95.4 \text{ k}\Omega}{2.00 \text{ k}\Omega + 95.4 \text{ k}\Omega} \right] = 0.971$$

For the C-D amplifier, load resistor  $R_L = R_6 \parallel R_3 = 10.7 \text{ k}\Omega$ , and  $R_G = R_1 \parallel R_2 = 892 \text{ k}\Omega$ .

$$A_{vt}^{CD} = \frac{g_m R_L}{1 + g_m R_L} = \frac{0.491 \text{ mS}(10.7 \text{ k}\Omega)}{1 + 0.491 \text{ mS}(10.7 \text{ k}\Omega)} = 0.840$$

and

$$A_v^{CD} = A_{vt}^{CD} \left( \frac{R_G}{R_I + R_G} \right) = 0.840 \left( \frac{892 \text{ k}\Omega}{2 \text{ k}\Omega + 892 \text{ k}\Omega} \right) = 0.838$$

The overall input resistance for the common-drain amplifier is

$$R_{in}^{CD} = R_G \parallel R_{iG} = 892 \text{ k}\Omega \parallel \infty = 892 \text{ k}\Omega$$

The output resistance of the C-D transistor and the source follower are

$$R_{iS} \approx \frac{1}{g_m} = \frac{1}{0.491 \text{ mS}} = 2.04 \text{ k}\Omega \quad R_{out}^{CD} = R_6 \parallel R_{iS} = 12 \text{ k}\Omega \parallel 2.04 \text{ k}\Omega = 1.74 \text{ k}\Omega$$

The input signal limit is

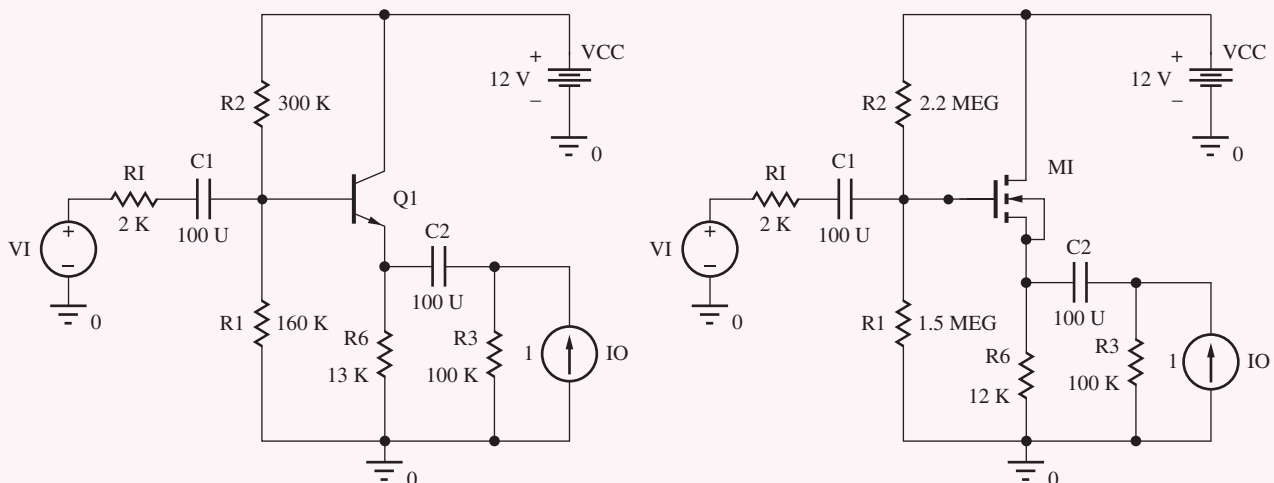
$$v_i \leq 0.2(V_{GS} - V_{TN})(1 + g_m R_L) \left( \frac{R_I + R_{in}^{CD}}{R_{in}^{CD}} \right)$$

$$v_i \leq 0.2(0.982 \text{ V})[1 + 0.491 \text{ mS}(10.7 \text{ k}\Omega)] \frac{2 \text{ k}\Omega + 892 \text{ k}\Omega}{892 \text{ k}\Omega} = 1.23 \text{ V}$$

**Check of Results:** Both voltage gains are approximately +1, as expected for a voltage follower. Both results are in the range specified in Eq. (14.57).

**Discussion:** The C-C amplifier has a gain much closer to 1 because  $g_m R_L$  is much larger than it is for the C-D case. The C-C amplifier will normally have a gain closer to one than will the C-D stage.

 **Computer-Aided Analysis:**<sup>3</sup> We can check the voltage gains using SPICE by performing an operating point analysis followed by an ac analysis with  $v_I$  as the input and  $v_O$  as the output voltage. Make all the capacitor values large, say 100  $\mu\text{F}$ , and sweep the frequency to find the midband range of frequencies (e.g., FSTART = 1 Hz and FSTOP = 100 kHz with 10 frequency points per decade). Analysis of the two circuits yields +0.971 for the gain of the common-collector amplifier and +0.843 for the gain of the common-drain stage. Both agree well with hand calculations. The transistor output resistance  $r_o$  is included in the simulations (VAF = 50 V or LAMBDA = 0.02  $\text{V}^{-1}$ ) and appears to have only a small effect.



The input and resistances for the C-C circuit can be found as  $R_{iB} = VB(Q1)/IB(Q1)$  and  $R_{in}^{CC} = VB(Q1)/I(C1)$ , and those of the C-D circuit are given by  $R_{iG} = VG(M1)/IG(M1)$  and

<sup>3</sup> See the MCD website for help with this circuit.

**TABLE 14.6**  
Follower Comparison—SPICE Results

	COMMON-COLLECTOR	COMMON-DRAIN
$A_v^{CC}, A_v^{CD}$	0.971	0.843
$R_{iB}, R_{iG}$	1.25 MΩ	$\infty$
$R_{in}^{CC}, R_{in}^{CD}$	96.3 kΩ	892 kΩ
$R_{iE}, R_{iS}$	119 Ω	1.90 kΩ
$R_{out}^{CC}, R_{out}^{CD}$	119 Ω	1.64 kΩ
$v_i^{\max}, (\text{THD})$	580 mV (0.033 %)	1.23 mV (0.73 %)

$R_{in}^{CD} = VG(M1)/I(C1)$ . Similarly, the output resistances are given by  $R_{iE} = VE(Q1)/IE(Q1)$ ,  $R_{out}^{CC} = VE(Q1)/I(C2)$ ,  $R_{iS} = VS(M1)/IS(M1)$  and  $R_{out}^{CD} = VS(M1)/I(C2)$ . The results appear in Table 14.6.

The input resistance of the common-drain amplifier is much higher than that of the common-collector stage because the lack of base current in the FET allows much larger resistors to be used for  $R_1$  and  $R_2$ . In contrast, the common-collector output resistance is much smaller than that of the common-drain stage because the transconductance of the BJT is much higher than that of the FET at a given operating current. The input signal capability and harmonic distortion of both stages are increased substantially by the presence of the resistances in the emitter and source of the transistors. The values all agree well with our hand calculations.

**EXERCISE:** How large must  $R_L$  be for the common-drain amplifier to achieve the same value of gain as the common-collector amplifier in Ex. 14.4?

**ANSWER:** 73.1 kΩ

**EXERCISE:** What is the voltage gain for the two amplifiers in Fig. 14.4 if  $R_3$  is removed ( $R_3 \rightarrow \infty$ )?

**ANSWERS:** 0.971, 0.853

**EXERCISE:** Redraw the circuit in Fig. 14.16 including  $r_o$  and show that it can easily be included in the analysis by changing the value of  $R_L$ .

**ANSWER:** Resistor  $r_o$  appears directly in parallel with  $R_L$  in Fig. 14.16; hence we simply replace  $R_L$  with a new value of load resistance in all the equations:  $R'_L = R_L \parallel r_o$

**EXERCISE:** Compare the values of  $g_m R_L$  for the C-C and C-D amplifiers in Ex. 14.4.

**ANSWER:** 113 ≈ 5.25

## 14.4 NONINVERTING AMPLIFIERS—COMMON-BASE AND COMMON-GATE CIRCUITS

The final class of amplifiers to be analyzed consists of the common-base and common-gate amplifiers represented by the two ac equivalent circuits in Fig. 14.21. From our analyses, we will find that the noninverting amplifiers provide a voltage gain and output resistance similar to that of the

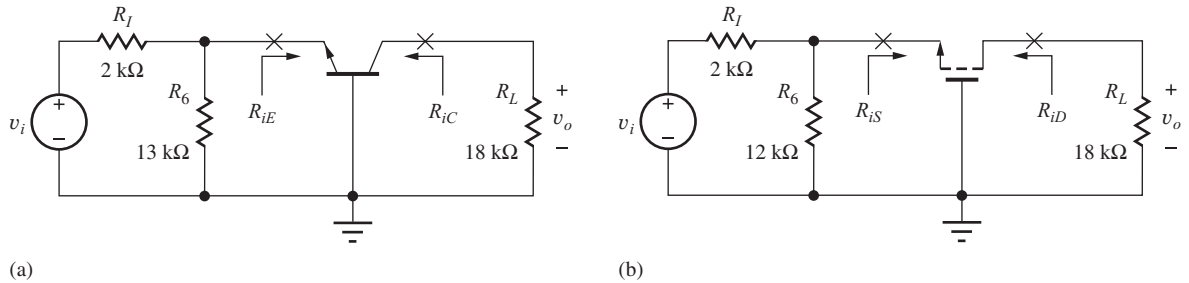


Figure 14.21 ac Equivalent circuits for the (a) C-B and (b) C-G amplifiers.

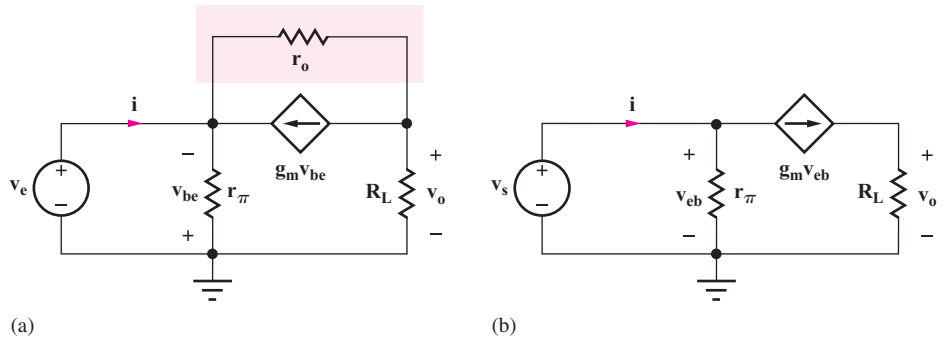


Figure 14.22 (a) Small-signal model for the common-base amplifier. (b) Simplified model neglecting \$r\_o\$ and reversing the direction of the controlled source.

C-E/C-S stages but with much lower input resistance. As in Sec. 14.3, we analyze the BJT circuit first and treat the MOSFET in Fig. 14.21(b) as a special case of Fig. 14.21(a).

#### 14.4.1 TERMINAL VOLTAGE GAIN AND INPUT RESISTANCE

The bipolar transistor is replaced by its small-signal model in Fig. 14.22(a). Because the amplifier has a resistor load, the circuit model is simplified by neglecting \$r\_o\$, as redrawn in Fig. 14.22(b). In addition, the polarities of \$v\_{be}\$ and the dependent current source \$g\_m v\_{be}\$ have both been reversed.

For the common-base circuit, output voltage \$v\_o\$ appears at the collector across resistor \$R\_L\$ and is equal to

$$v_o = +g_m v_{eb} R_L = +g_m R_L v_e \quad (14.73)$$

and the terminal gain for the common-base transistor is

$$A_{vt}^{CB} = \frac{v_o}{v_e} = +g_m R_L \quad (14.74)$$

which is the same as that for the common-emitter stage except for the sign. The input current \$i\$ and input resistance at the emitter are given by

$$i = \frac{v_e}{r_\pi} + g_m v_e \quad \text{and} \quad R_{iE} = \frac{v_e}{i} = \frac{r_\pi}{\beta_o + 1} \cong \frac{1}{g_m} \quad (14.75)$$

assuming \$\beta\_o \gg 1\$.

The corresponding expressions for the common-gate stage (\$r\_\pi \rightarrow \infty\$) are

$$A_{vt}^{CG} = \frac{v_o}{v_e} = +g_m R_L \quad \text{and} \quad R_{iS} = \frac{1}{g_m} \quad (14.76)$$

### Understanding Common-Base and Common-Gate Amplifier Operation

When an input signal  $v_i$  is applied to the emitter of the C-B amplifier, or the source of the C-G amplifier, a current enters the transistor that is set by the transistor's input resistance ( $R_{in} = 1/g_m$ ). This current exits the transistor from the collector or drain terminal and goes through the load resistor to produce output voltage  $v_o$ . The terminal voltage gain is equal to the ratio of the load resistance to the input resistance:

$$i_{in} = \frac{v_i}{R_{in}} = g_m v_i \quad v_o = +\alpha_o i_{in} R_L \cong +i_{in} R_L \quad \text{and} \quad A_{vt}^{ni} = \frac{v_o}{v_i} = +g_m R_L \quad (14.77)$$

However, voltage division between the input resistance and the resistance associated with the signal source can often cause the signal source gain to be substantially less than the terminal gain of the noninverting amplifier.

#### 14.4.2 SIGNAL SOURCE VOLTAGE GAIN

The overall gains for the amplifiers in Fig. 14.21 can now be expressed as

$$A_v^{CB} = \frac{\mathbf{V}_o}{\mathbf{V}_i} = \left( \frac{v_o}{v_e} \right) \left( \frac{v_e}{v_i} \right) = A_{vt}^{CB} \left[ \frac{R_6 \| R_{iE}}{R_I + (R_6 \| R_{iE})} \right] \quad (14.78)$$

and substituting  $R_{iE} = 1/g_m$  yields

$$A_v^{CB} = \frac{g_m R_L}{1 + g_m (R_{th})} \left( \frac{R_6}{R_I + R_6} \right) \quad \text{and} \quad A_v^{CG} = \frac{g_m R_L}{1 + g_m (R_{th})} \left( \frac{R_6}{R_I + R_6} \right) \quad (14.79)$$

where  $R_{th} = R_6 \| R_I$ . If we assume that  $R_6 \gg R_I$ , then the gain expressions in Eq. (14.79) become

$$A_v^{CB,CG} \cong \frac{g_m R_I}{1 + g_m R_I} \quad \text{for} \quad R_6 \gg R_I \quad (14.80)$$

Because of the low input resistance of the common-base and common-gate amplifiers, the voltage gain  $A_v$  from the signal source to the output can be substantially less than the terminal gain. Note that the final expressions in Eq. (14.80) have a similar form to the overall gains for the inverting amplifiers and followers. We will explore this result more fully later in the chapter.

Note that the gain expressions in Eqs. (14.76) and (14.78) are positive, indicating that the output signal is in phase with the input signal. Thus, the C-B and C-G amplifiers are classified as noninverting amplifiers.

#### DESIGN NOTE

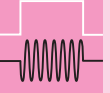
The terminal voltage gain of the noninverting amplifiers is given by

$$A_{vt}^{CB} = A_{vt}^{CG} \cong +g_m R_L$$

#### DESIGN NOTE

An estimate for the overall gain of the noninverting amplifiers is

$$A_{vt}^{CB} = A_{vt}^{CG} \cong +\frac{g_m R_L}{1 + g_m R_{th}} \cong +\frac{R_L}{R_{th}} \quad \text{for} \quad g_m R_{th} \gg 1 \quad \text{and} \quad R_{th} = R_6 \| R_I$$


**DESIGN  
NOTE**

The equivalent resistance  $R$  looking into the emitter or source of a transistor is approximately  $R = 1/g_m$ .

### Important Limits

As for the C-E/C-S amplifiers, two limiting conditions are of particular importance (see Prob. 14.45). The upper bound occurs for  $g_m R_I \ll 1$ , for which Eq. (14.80) reduces to

$$A_v^{CB} \cong +g_m R_L \quad \text{and} \quad A_v^{CG} \cong +g_m R_L \quad (14.81)$$

Equation (14.81) represents the upper bound on the gain of the C-B/C-G amplifiers and is the same as that for the C-E/C-S amplifiers, except the gain is noninverting.

However, if  $g_m R_{th} \gg 1$ , then Eq. (14.81) reduces to

$$A_v^{CB} = A_v^{CG} \cong +\frac{R_L}{R_{th}} \quad (14.82)$$

For this case, the C-B and C-G amplifiers both have a gain that approaches the ratio of the value of the load resistor to that of the Thévenin source resistance ( $R_{th} = R_6 \| R_I$ ) and is independent of the transistor parameters. For resistor loads, the limit in Eq. (14.82) is much less than the amplification factor  $\mu_f$ , so neglecting  $r_o$  is valid.

### 14.4.3 INPUT SIGNAL RANGE

The relationship between  $v_{eb}$  and  $v_i$  in Fig. 14.21(a) is given by

$$v_{eb} = v_i \frac{R_6 \| R_{IE}}{R_I + (R_6 \| R_{IE})} = \frac{v_i}{1 + g_m(R_I \| R_6)} \left( \frac{R_6}{R_I + R_6} \right) \quad \text{and} \quad v_i \cong v_{eb}(1 + g_m R_I) \quad (14.83)$$

for  $R_6 \gg R_I$ .

The small-signal limit requires

$$|v_i| \leq 0.005(1 + g_m R_I) \text{ V} \quad (14.84)$$

For the FET case, replacing  $v_{eb}$  by  $v_{sg}$  yields  $v_i = v_{sg}(1 + g_m R_I)$  and

$$|v_i| \leq 0.2(V_{GS} - V_{TN})(1 + g_m R_I) \quad (14.85)$$

The relative size of  $R_I$  and  $g_m$  will determine the signal-handling limits.

**EXERCISE:** Calculate the maximum values of  $v_i$  for the C-B and C-G amplifiers in Fig. 14.21 based on Eqs. (14.84) and (14.85).

**ANSWERS:** 103 mV; 389 mV

### 14.4.4 RESISTANCE AT THE COLLECTOR AND DRAIN TERMINALS

The resistance at the output terminal of the C-B/C-G transistors can be calculated for the circuit in Fig. 14.23, in which a test source  $v_x$  is applied to the collector terminal. The desired resistance is that looking into the collector with the base grounded and resistor  $R_{th}$  in the emitter. If the circuit is redrawn as shown in Fig. 14.23(b), we should recognize it to be the same as the C-E circuit in Fig. 14.9, repeated in Fig. 14.23(c), except that the equivalent resistance  $R_{th}^{CE}$  in the base is zero, and resistor  $R_E$  has been relabeled  $R_{th}$ .

Thus, the resistance at the output for the C-B device can be found using the results from the common-emitter amplifier, Eq. (14.30), without further detailed calculation, by substituting  $R_{th}^{CE} = 0$

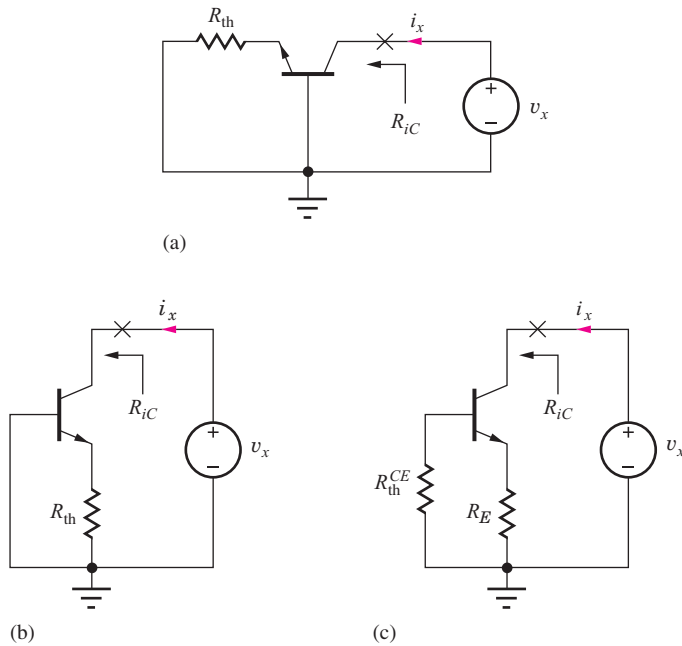


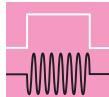
**Figure 14.23** (a) Circuit for calculating the C-B output resistance. (b) Redrawn version of the circuit in (a). (c) Circuit used in common-emitter analysis (see Fig. 14.9).

and replacing \$R\_E\$ with \$R\_{th}\$:

$$R_{iC} = r_o \left( 1 + \frac{\beta_o R_E}{R_{th}^{CE} + r_\pi + R_E} \right) = r_o \left( 1 + \frac{\beta_o R_{th}}{r_\pi + R_{th}} \right) \quad (14.86)$$

Using \$\beta\_o = g\_m r\_\pi\$

$$R_{iC} \cong r_o [1 + g_m (R_{th} \| r_\pi)] \quad \text{and} \quad R_{iD} = r_o (1 + g_m R_{th}) \quad (14.87)$$



## DESIGN NOTE

A quick design estimate for the output resistance of an inverting or noninverting amplifier with an unbypassed resistor \$R\$ in the emitter or source is

$$R_o \cong r_o [1 + g_m (R \| r_\pi)] \cong \mu_f (R \| r_\pi)$$

**EXERCISE:** Calculate the output resistances of the C-B and C-G amplifiers.

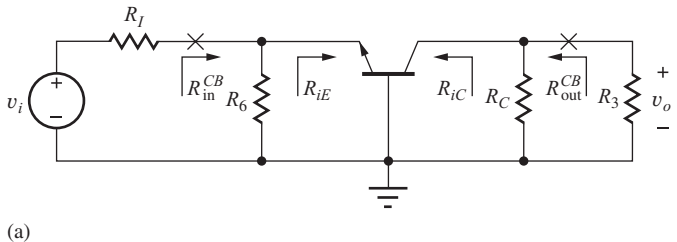
**ANSWERS:** 3.93 M\$\Omega\$; 410 k\$\Omega\$

### 14.4.5 CURRENT GAIN

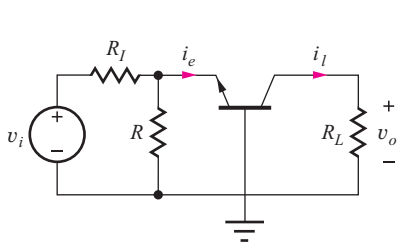
The terminal current gain \$A\_{it}\$ is the ratio of the current through the load resistor to the current being supplied to the emitter. If a current \$i\_e\$ is injected into the emitter of the C-B transistor in Fig. 14.24, then the current \$i\_l = \alpha\_o i\_e\$ comes out of the collector. Thus, the common-base current gain is simply \$\alpha\_o\$.

For the FET, \$\alpha\_o\$ is exactly 1, and we have

$$A_{it}^{CB} = \frac{i_l}{i_e} = +\alpha_o \cong +1 \quad \text{and} \quad A_{it}^{CG} = +1 \quad (14.88)$$



(a)



(b)

**Figure 14.24** Common-base current gain.**Figure 14.25** Midband ac equivalent circuits for the common-base and common gate amplifiers.

#### 14.4.6 OVERALL INPUT AND OUTPUT RESISTANCES FOR THE NONINVERTING AMPLIFIERS

The overall input and output resistances,  $R_{\text{in}}^{CB}$ ,  $R_{\text{in}}^{CG}$ ,  $R_{\text{out}}^{CB}$ , and  $R_{\text{out}}^{CG}$  of the common-base and common-gate amplifiers are defined looking into the input ( $C_1$ ) and output ( $C_2$ ) coupling capacitors in Fig. 14.5, as redrawn in the midband ac models in Fig. 14.25. The overall input resistance of the common-base or common-gate amplifiers equals the parallel combination of resistor  $R_6$  and the resistance looking into the emitter or source terminal of the transistor:

$$R_{\text{in}}^{CB} = R_6 \parallel R_{iE} \cong R_6 \parallel \frac{1}{g_m} \quad \text{and} \quad R_{\text{in}}^{CG} = R_6 \parallel R_{iS} = R_6 \parallel \frac{1}{g_m} \quad (14.89)$$

Similarly, the overall output resistance of the common-base or common-gate amplifiers equals the parallel combination of resistors  $R_C$  or  $R_D$  and the resistance looking into the collector or drain terminal of the transistor:

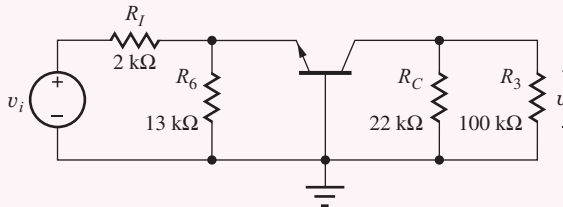
$$\begin{aligned} R_{\text{out}}^{CB} &= R_C \parallel R_{iC} = R_C \parallel r_o [1 + g_m(R_6 \parallel R_I \parallel r_\pi)] \\ \text{and} \quad R_{\text{out}}^{CG} &= R_D \parallel R_{iD} = R_D \parallel r_o [1 + g_m(R_6 \parallel R_1)] \end{aligned} \quad (14.90)$$

#### EXAMPLE 14.5 NONINVERTING AMPLIFIER CHARACTERISTICS

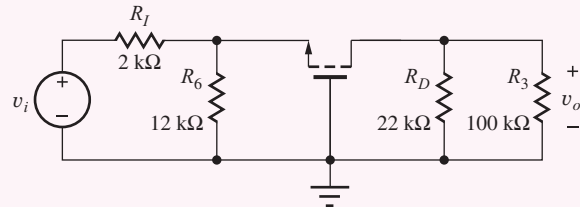
A comparison of the characteristics of the common-base and common-gate amplifiers is provided by this example.

**PROBLEM** Calculate the signal-source voltage gains, input resistances, output resistances, and signal handling capability for the C-B and C-G amplifiers in Fig. 14.5.

**SOLUTION** **Known Information and Given Data:** The equivalent circuit with element values appear below. Q-point and small-signal values appear in the accompanying table.



Common-base amplifier from Fig. 14.5.



Common-gate amplifier from Fig. 14.5.

	$I_C$ or $I_D$	$V_{CE}$ or $V_{DS}$	$V_{GS} - V_{TN}$	$g_m$	$r_\pi$	$r_o$	$\mu_f$
BJT	245 $\mu\text{A}$	3.64 V	—	9.80 mS	10.2 kΩ	219 kΩ	2150
FET	241 $\mu\text{A}$	3.81 V	0.982 V	0.491 mS	$\infty$	223 kΩ	110

**Unknowns:** Voltage gains, input resistances, output resistances, and maximum input signal amplitudes for the common-base and common-gate amplifiers

**Approach:** Verify the value of  $R_L$ , and substitute element values from the two circuits the appropriate equations from Sections 14.4.1–14.4.6.

**Assumptions:** Use the parameter values tabulated above.

**Analysis:** For the C-B amplifier:  $R_I = 2 \text{k}\Omega$ ,  $R_6 = 13 \text{k}\Omega$ ,  $R_L = R_3 \parallel R_C = 18.0 \text{k}\Omega$ . The terminal input resistance and gain are

$$R_{iE} \cong \frac{1}{g_m} = \frac{1}{9.8 \text{ mS}} = 102 \Omega \quad \text{and} \quad A_{vt}^{CB} = +g_m R_L = 9.80 \text{ mS}(18.0 \text{ k}\Omega) = +176$$

and the overall voltage gain is

$$A_v^{CB} = \frac{A_{vt}}{1 + g_m(R_6 \parallel R_I)} \left( \frac{R_6}{R_I + R_6} \right) = \frac{176}{1 + 9.8 \text{ mS}(1.73 \text{ k}\Omega)} \left( \frac{13 \text{ k}\Omega}{2 \text{ k}\Omega + 13 \text{ k}\Omega} \right) = +8.48$$

The input resistance of the common-base amplifier is found using Eq. (14.89)

$$R_{in}^{CB} = R_6 \parallel R_{iE} = 13 \text{ k}\Omega \parallel 102 \Omega = 101 \Omega$$

and the output resistance of the common-base amplifier is calculated using Eq. (14.90)

$$R_{iC} = r_o[1 + g_m(R_6 \parallel R_I \parallel r_\pi)] = 219 \text{ k}\Omega[1 + 9.80 \text{ mS}(13 \text{ k}\Omega \parallel 2 \text{ k}\Omega \parallel 10.2 \text{ k}\Omega)] = 3.40 \text{ M}\Omega$$

$$R_{out}^{CB} = R_C \parallel R_{iC} = 22 \text{ k}\Omega \parallel 3.40 \text{ M}\Omega = 21.9 \text{ k}\Omega$$

The maximum input signal amplitude is computed using Eq. (14.84).

$$\begin{aligned} |v_i| &\leq 0.005V[1 + g_m(R_6 \parallel R_I)] \frac{R_I + R_6}{R_6} \\ |v_i| &= 0.005V[1 + 9.80 \text{ mS}(13 \text{ k}\Omega \parallel 2 \text{ k}\Omega)] \frac{2 \text{ k}\Omega + 13 \text{ k}\Omega}{13 \text{ k}\Omega} = 104 \text{ mV} \end{aligned}$$

For the C-G amplifier:  $R_I = 2 \text{k}\Omega$ ,  $R_6 = 12 \text{k}\Omega$ ,  $R_L = R_3 \parallel R_D = 18.0 \text{k}\Omega$ . We have

$$R_{iS} = \frac{1}{g_m} = \frac{1}{0.491 \text{ mS}} = 2.04 \text{ k}\Omega \quad \text{and} \quad A_{vt}^{CG} = +g_m R_L = 0.491 \text{ mS}(18.0 \text{ k}\Omega) = +8.84$$

and

$$A_v^{CG} = \frac{A_{vt}^{CG}}{1 + g_m(R_6 \parallel R_I)} \left( \frac{R_6}{R_I + R_6} \right) = \frac{8.84}{1 + 0.491 \text{ mS}(1.71 \text{ k}\Omega)} \left( \frac{12 \text{ k}\Omega}{2 \text{ k}\Omega + 12 \text{ k}\Omega} \right) = +4.11$$

The input resistance of the common-gate amplifier is found using Eq. (14.89)

$$R_{in}^{CG} = R_6 \parallel R_{iS} = 12 \text{ k}\Omega \parallel 2.04 \text{ k}\Omega = 1.74 \text{ k}\Omega$$

and the output resistance of the common-gate amplifier is calculated using Eq. (14.90)

$$R_{iD} = r_o[1 + g_m(R_6 \parallel R_I)] = 223 \text{ k}\Omega [1 + 0.491 \text{ mS}(12 \text{ k}\Omega \parallel 2 \text{ k}\Omega)] = 411 \text{ k}\Omega$$

$$R_{\text{out}}^{CG} = R_D \parallel R_{iD} = 22 \text{ k}\Omega \parallel 411 \text{ k}\Omega = 20.9 \text{ k}\Omega$$

The maximum input signal amplitude is computed using Eq. (14.84).

$$|v_i| \leq 0.2(V_{GS} - V_{TN})[1 + g_m(R_6 \parallel R_I)] \frac{R_I + R_6}{R_6}$$

$$|v_i| = 0.2(0.982)[1 + 0.491 \text{ mS}(12 \text{ k}\Omega \parallel 2 \text{ k}\Omega)] \frac{2 \text{ k}\Omega + 12 \text{ k}\Omega}{12 \text{ k}\Omega} = 422 \text{ mV}$$

**Check of Results:** Both values are similar to and do not exceed the design estimate given by

$$A_v^{NI} \cong +\frac{R_L}{R_I} = \frac{18 \text{ k}\Omega}{2 \text{ k}\Omega} = +9.00$$

**Discussion:** Note that the overall gain of the common-base amplifier is much less than its terminal gain because significant signal loss occurs due to the low input resistance of the transistor relative to the source resistance:

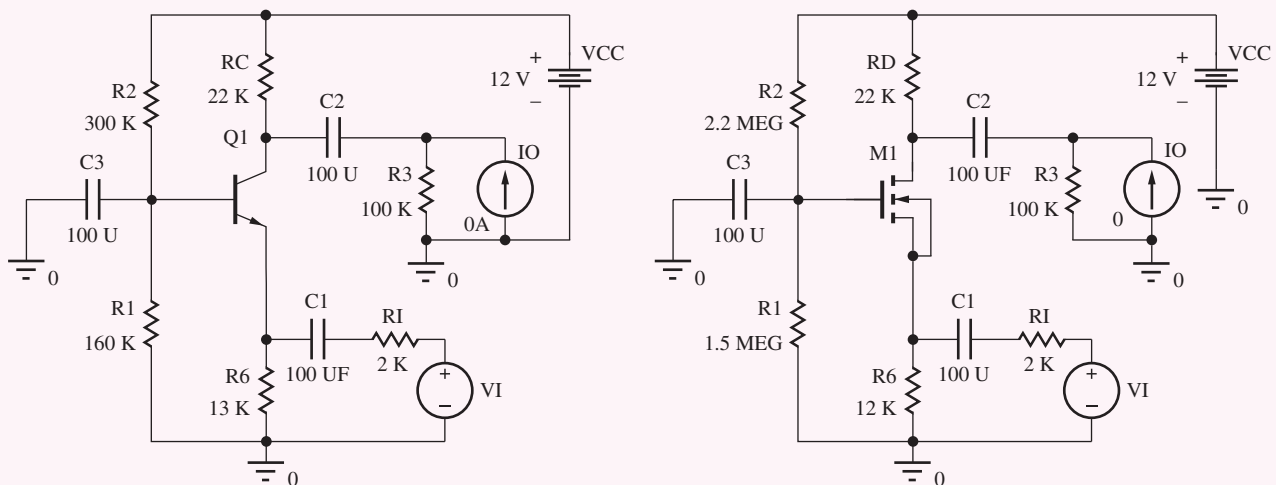
$$A_v^{CB} = A_{vt}^{CB} \left( \frac{R_6 \parallel R_{iE}}{R_I + R_6 \parallel R_{iE}} \right) = 176 \left( \frac{13 \text{ k}\Omega \parallel 102 \text{ }\Omega}{2 \text{ k}\Omega + 13 \text{ k}\Omega \parallel 102 \text{ }\Omega} \right) = 176(0.0482) = +8.48$$

For the common-gate case, the loss factor is less,

$$\begin{aligned} A_v^{CG} &= A_{vt}^{CG} \left( \frac{R_6 \parallel R_{iS}}{R_I + R_6 \parallel R_{iS}} \right) = 8.84 \left( \frac{12 \text{ k}\Omega \parallel 2.04 \text{ k}\Omega}{2.00 \text{ k}\Omega + 12 \text{ k}\Omega \parallel 2.04 \text{ k}\Omega} \right) \\ &= 8.84(0.466) = +4.12 \end{aligned}$$

Once again, we see that the overall C-G gain differs from the simple design estimate by more than that of the C-B stage because of the lower transconductance (and  $g_m R_{\text{th}}$  product) of the FET. The gains are both well below the value of  $\mu_f$ , so neglecting  $r_o$  in Fig. 14.22 is valid.

**WWW Computer-Aided Analysis:**<sup>4</sup> We can check the characteristics of the non-inverting amplifiers using SPICE by performing an operating point analysis followed by an ac analysis with  $v_I$  as



<sup>4</sup> See the MCD website for help with this circuit.

**TABLE 14.7**  
Noninverting Amplifier Comparison—SPICE Results

	COMMON-BASE	COMMON-GATE
$A_v^{CB}, A_v^{CG}$	+8.38	+4.05
$R_{iE}, R_{iS}$	112 $\Omega$	2.08 k $\Omega$
$R_{in}^{CB}, R_{in}^{CG}$	111 $\Omega$	1.77 k $\Omega$
$R_{iC}, R_{iD}$	3.26 M $\Omega$	416 k $\Omega$
$R_{out}^{CB}, R_{out}^{CG}$	21.9 k $\Omega$	20.9 k $\Omega$
$v_i^{\max}, (\text{THD})$	104 mV (0.27 %)	422 mV (2.1 %)

the input and  $v_O$  as the output voltage. Make all the capacitor values large, say 100  $\mu\text{F}$ , and sweep the frequency to find the midband region (e.g., FSTART = 1 Hz and FSTOP = 100 kHz with 10 frequency points per decade). Analysis of the two circuits yields +8.38 for the gain of the common-base amplifier and +4.05 for the gain of the common-gate stage. These values agree closely with our hand calculations. The transistor output resistance  $r_o$  is included in the simulations (VAF = 50 V or LAMBDA = 0.02 V $^{-1}$ ) and appears to have a negligible effect.

The input and resistances for the C-B circuit can be found as  $R_{iE} = VE(Q1)/IE(Q1)$  and  $R_{in}^{CB} = VE(Q1)/I(C1)$ , and those of the C-G circuit are given by  $R_{iS} = VS(M1)/IS(M1)$  and  $R_{in}^{CG} = VS(M1)/I(C1)$ . Similarly, the output resistances are given by  $R_{iC} = VC(Q1)/IC(Q1)$ ,  $R_{out}^{CB} = VC(Q1)/I(C2)$ ,  $R_{iD} = VD(M1)/ID(M1)$ , and  $R_{out}^{CG} = VD(M1)/I(C2)$ . The results appear in Table 14.7.

The input resistance of the common-base amplifier is much lower than that of the common-gate stage because the transconductance of the BJT is much higher than that of the FET at a given operating current.  $R_{iC} \gg R_{iD}$  also because of the larger BJT transconductance, but the overall output resistances are the same since they are controlled by  $R_C$  and  $R_D$ . The input signal capability and harmonic distortion of both stages are increased substantially by the presence of the resistances in the emitter and source of the transistors. The values all agree well with our hand calculations.

**EXERCISE:** Show that Eq. (14.78) can be reduced to Eq. (14.79).

**EXERCISE:** What are the open circuit voltage gains ( $R_3 = \infty$ ) for these two amplifiers?

**ANSWERS:** 10.4; 5.04

**EXERCISE:** Compare the gains of the C-B and C-G amplifiers calculated in Ex. 14.5 to the two limits developed in Eqs. (14.81) and (14.82).

**ANSWERS:**  $8.98 < 10.4 \ll 176$ ;  $4.11 < 8.48 < 10.5$

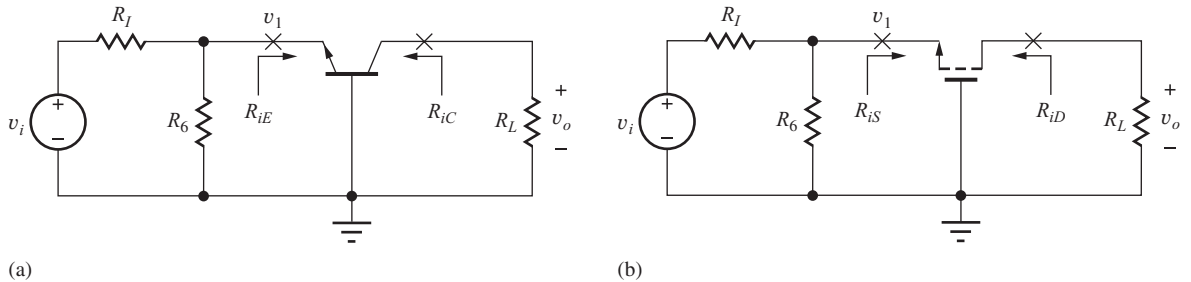
#### 14.4.7 C-B/C-G AMPLIFIER SUMMARY

Table 14.8 summarizes the results derived for the common-base and common-gate amplifiers in Fig. 14.26, and the numeric results for the specific amplifiers in Fig. 14.4 are collected together in Table 14.7. The results show the symmetry between the various characteristics of the common-base and common-gate amplifiers. The voltage gain and current gain are very similar. Numeric differences occur because of differences in the parameter values of the BJT and FET at similar operating points.

Both amplifiers can provide significant voltage gain, low input resistance, and high output resistance. The higher amplification factor of the BJT gives it an advantage in achieving high output

**TABLE 14.8**  
Common-Base/Common-Gate Amplifier Summary

	C-B AMPLIFIER	C-G AMPLIFIER
Terminal voltage gain $A_{vt} = \frac{v_o}{v_i}$	$+g_m R_L$	$+g_m R_L$
Signal-source voltage gain $A_v = \frac{v_o}{v_i}$ $R_{th} = (R_I \parallel R_6)$	$\frac{g_m R_L}{1 + g_m R_{th}} \left( \frac{R_6}{R_I + R_6} \right)$	$\frac{g_m R_L}{1 + g_m R_{th}} \left( \frac{R_6}{R_I + R_6} \right)$
Input terminal resistance	$\frac{1}{g_m}$	$\frac{1}{g_m}$
Output terminal resistance	$r_o(1 + g_m R_{th}) = r_o + \mu_f R_{th}$	$r_o(1 + g_m R_{th}) = r_o + \mu_f R_{th}$
Input signal range	$0.005(1 + g_m R_{th})$	$0.2(V_{GS} - V_{TN})(1 + g_m R_{th})$
Terminal current gain	$\alpha_o \cong +1$	$+1$



**Figure 14.26** Circuits for use with summary Table 14.8. (a) Common-base amplifier, (b) common-gate amplifier.

resistance; the C-B amplifier can more easily reach very low levels of input resistance because of the BJT's higher transconductance for a given operating current. The FET amplifier can inherently handle larger signal levels.

## 14.5 AMPLIFIER PROTOTYPE REVIEW AND COMPARISON

Sections 14.1 to 14.4 compared the three individual classes of BJT and FET circuits: the C-E/C-S, C-C/C-D, and C-B/C-G amplifiers. In this section, we review these results and compare the three BJT and FET amplifier configurations.

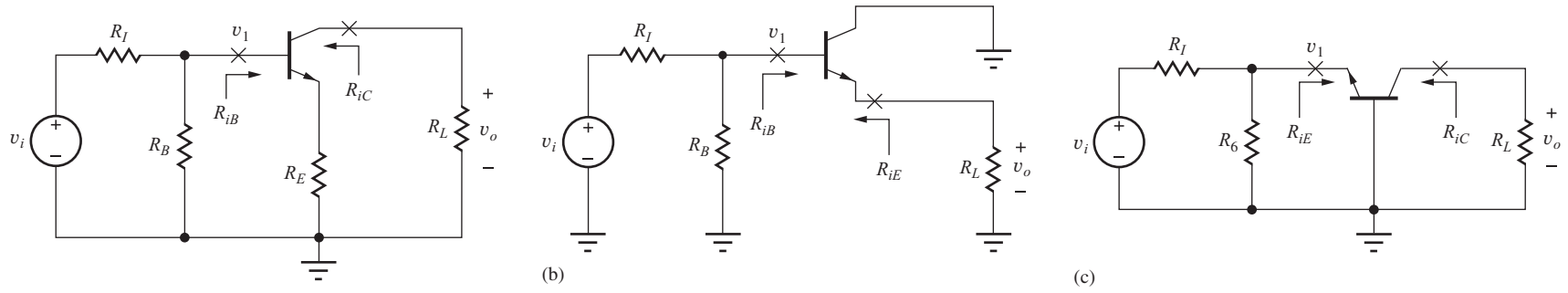
### 14.5.1 THE BJT AMPLIFIERS

Table 14.9 collects the results of analysis of the three BJT amplifiers in Fig. 14.27; Table 14.10 gives approximate results.

A very interesting and important observation can be made from review of Table 14.9. If we assume the voltage loss across the source resistance is small, the signal-source gains of the three amplifiers have exactly the same form:

$$|A_v| \cong \frac{g_m R_L}{1 + g_m R_E} \cong \frac{R_L}{\frac{1}{g_m} + R_E} \quad (14.91)$$

in which  $R_E$  is the external resistance in the emitter of the transistor ( $R_E$ ,  $R_L$ , or  $R_I \parallel R_6$ , respectively). We really only need to commit one formula to memory to get a good estimate of amplifier gain!



**Figure 14.27** The three BJT amplifier configurations: (a) common-emitter amplifier, (b) common-collector amplifier, and (c) common-base amplifier.

**TABLE 14.9**  
Single-Transistor Bipolar Amplifiers

	COMMON-EMITTER AMPLIFIER	COMMON-COLLECTOR AMPLIFIER	COMMON-BASE AMPLIFIER
Terminal voltage gain $A_{vt} = \frac{v_o}{v_i}$	$\cong -\frac{g_m R_L}{1 + g_m R_E}$	$\cong +\frac{g_m R_L}{1 + g_m R_L} \cong +1$	$+g_m R_L$
Signal-source voltage gain $A_v = \frac{v_o}{v_i}$	$-\frac{g_m R_L}{1 + g_m R_E} \left[ \frac{R_B \  R_{iB}}{R_I + (R_B \  R_{iB})} \right]$	$+ \frac{g_m R_L}{1 + g_m R_L} \left[ \frac{R_B \  R_{iB}}{R_I + (R_B \  R_{iB})} \right] \cong +1$	$+ \frac{g_m R_L}{1 + g_m (R_I \  R_4)} \left( \frac{R_6}{R_I + R_6} \right)$
Input terminal resistance	$r_\pi + (\beta_o + 1) R_E$ $\cong r_\pi (1 + g_m R_E)$	$r_\pi + (\beta_o + 1) R_L$ $\cong r_\pi (1 + g_m R_L)$	$\frac{\alpha_o}{g_m} \cong \frac{1}{g_m}$
Output terminal resistance	$r_o (1 + g_m R_E)$	$\frac{\alpha_o}{g_m} + \frac{R_{th}}{\beta_o + 1}$	$r_o [1 + g_m (R_I \  R_4)]$
Input signal range	$\cong 0.005 (1 + g_m R_E)$	$\cong 0.005 (1 + g_m R_L)$	$\cong 0.005 [1 + g_m (R_I \  R_6)]$
Terminal current gain	$-\beta_o$	$\beta_o + 1$	$\alpha_o \cong +1$

**TABLE 14.10**

Simplified Characteristics of Single BJT Amplifiers

	COMMON-EMITTER ( $R_E = 0$ )	COMMON-EMITTER WITH EMITTER RESISTOR $R_E$	COMMON- COLLECTOR	COMMON-BASE
Terminal voltage gain	$-g_m R_L \cong -10V_{CC}$	$-\frac{R_L}{R_E}$	1	$+g_m R_L \cong +10V_{CC}$
$A_{vt} = \frac{v_o}{v_i}$	(high)	(moderate)	(low)	(high)
Input terminal resistance	$r_\pi$ (moderate)	$\beta_o R_E$ (high)	$\beta_o R_L$ (high)	$1/g_m$ (low)
Output terminal resistance	$r_o$ (moderate)	$\mu_f R_E$ (high)	$1/g_m$ (low)	$\mu_f (R_I \parallel R_4)$ (high)
Current gain	$-\beta_o$ (moderate)	$-\beta_o$ (moderate)	$\beta_o + 1$ (moderate)	1 (low)

In addition, the same symmetry exists in the expressions for input signal range:

$$|v_{be}| \leq 0.005(1 + g_m R_E) \text{ V} \quad (14.92)$$

Note as well the similarity in the expressions for the input resistances of the C-E and C-C amplifiers, the input resistance of the C-B amplifier and the output resistance of the C-C amplifier, and the output resistances of the C-E and C-B amplifiers. Carefully review the three amplifier topologies in Fig. 14.27 to fully understand why these symmetries occur.

The second form of Eq. (14.91) deserves further discussion. The magnitude of the terminal gain of all three BJT stages can be expressed as the ratio of total resistance  $R_L$  at the collector to the total resistance  $R_{EQ}$  in the emitter loop!  $R_{EQ}$  is the sum of the external resistance  $R_E$  [i.e.,  $R_E$ ,  $R_L$ , or  $(R_I \parallel R_6)$ , as appropriate] plus the resistance ( $1/g_m$ ) found looking back into the emitter of the transistor itself. This is an extremely important conceptual result.

Table 14.10 is a simplified comparison. The common-emitter amplifier provides moderate-to-high levels of voltage gain, and moderate values of input resistance, output resistance, and current gain. The addition of emitter resistor  $R_E$  to the common-emitter circuit gives added design flexibility and allows a designer to trade reduced voltage gain for increased input resistance, output resistance, and input signal range. The common-collector amplifier provides low voltage gain, high input resistance, low output resistance, and moderate current gain. Finally, the common-base amplifier provides moderate to high voltage gain, low input resistance, high output resistance, and low current gain.

### 14.5.2 THE FET AMPLIFIERS

Tables 14.11 and 14.12 are similar summaries for the three FET amplifiers shown in Fig. 14.28. The signal source voltage gain and signal range of all three amplifiers can again be expressed approximately as

$$|A_v| \cong \frac{g_m R_L}{1 + g_m R} = \frac{R_L}{\frac{1}{g_m} + R} \quad (14.93)$$

and

$$|v_{gs}| \leq 0.2(V_{GS} - V_{TN})(1 + g_m R) \text{ V} \quad (14.94)$$

in which  $R$  is the resistance in the source of the transistor ( $R_S$ ,  $R_L$ , or  $(R_I \parallel R_6)$ , respectively). Note the symmetry between the output resistances of the C-S and C-G amplifiers. Also, the input resistance of the C-G amplifier and output resistance of the C-D amplifier are identical. Review the three amplifier topologies in Fig. 14.28 carefully to fully understand why these symmetries occur. The addition of resistor  $R_S$  to the common-source circuit allows the designer to trade reduced voltage gain for increased output resistance and input signal range.

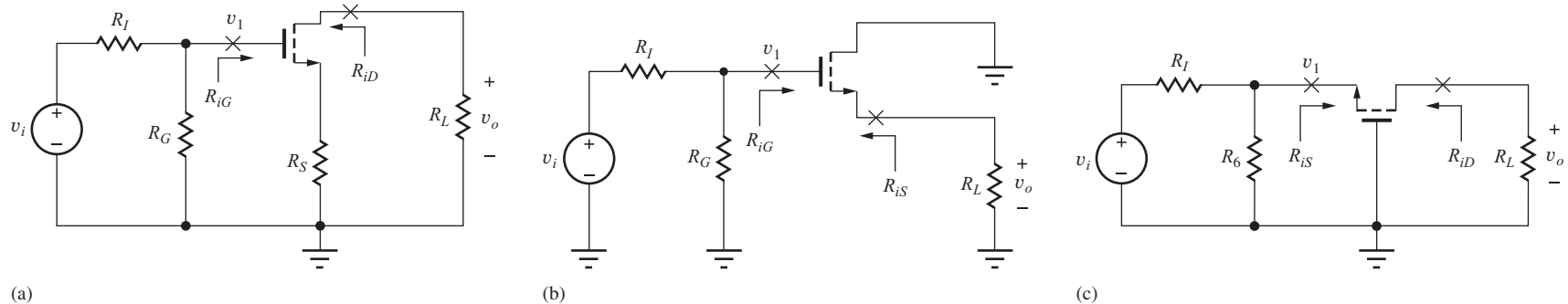


**Figure 14.28** The three FET amplifier configurations: (a) common-source, (b) common-drain, and (c) common-gate.

**TABLE 14.11**

## Single-Transistor FET Amplifiers

	COMMON-SOURCE AMPLIFIER	COMMON-DRAIN AMPLIFIER	COMMON-GATE AMPLIFIER
Terminal voltage gain	$A_{vt} = \frac{v_o}{v_i} = -\frac{g_m R_L}{1 + g_m R_S}$	$+ \frac{g_m R_L}{1 + g_m R_L} \cong +1$	$+g_m R_L$
Signal-source voltage gain	$A_v = \frac{v_o}{v_i} = -\frac{g_m R_L}{1 + g_m R_S} \left( \frac{R_G}{R_I + R_G} \right)$	$+ \frac{g_m R_L}{1 + g_m R_L} \left( \frac{R_G}{R_I + R_G} \right) \cong +1$	$+ \frac{g_m R_L}{1 + g_m (R_I \  R_6)} \left( \frac{R_6}{R_I + R_6} \right)$
Input terminal resistance	$\infty$	$\infty$	$1/g_m$
Output terminal resistance	$r_o(1 + g_m R_S)$	$1/g_m$	$r_o[1 + g_m (R_I \  R_6)]$
Input signal range	$0.2(V_{GS} - V_{TN})(1 + g_m R_S)$	$0.2(V_{GS} - V_{TN})(1 + g_m R_L)$	$0.2(V_{GS} - V_{TN})[1 + g_m (R_I \  R_6)]$
Terminal current gain	$\infty$	$\infty$	$+1$

**TABLE 14.12**

Simplified Characteristics of Single FET Amplifiers

	COMMON-SOURCE ( $R_S = 0$ )	COMMON-SOURCE WITH SOURCE RESISTOR $R_S$	COMMON-DRAIN	COMMON-GATE
Terminal voltage gain	$-g_m R_L \cong -V_{DD}$	$-\frac{R_L}{R_S}$	1	$+g_m R_L \cong +V_{DD}$
$A_{vt} = \frac{v_o}{v_i}$	(moderate)	(moderate)	(low)	(moderate)
Input terminal resistance	$\infty$ (high)	$\infty$ (high)	$\infty$ (high)	$1/g_m$ (low)
Output terminal resistance	$r_o$ (moderate)	$\mu_f R_S$ (high)	$1/g_m$ (low)	$\mu_f (R_L \parallel R_6)$ (high)
Current gain	$\infty$ (high)	$\infty$ (high)	$\infty$ (high)	1 (low)

In a manner similar to the BJT amplifiers, the magnitude of the terminal gain of all three FET stages can be expressed as the ratio of total resistance  $R_L$  at the drain terminal to the total resistance  $R_{SQ}$  in the source loop.  $R_{SQ}$  represents the sum of the external resistance  $R_X$  [i.e.,  $R_S$ ,  $R_L$ , or  $(R_I \parallel R_6)$ , as appropriate] plus the resistance ( $1/g_m$ ) found looking back into the source of the transistor itself. Thus, when properly interpreted, the gain expressions for the single stage BJT and FET amplifier stages can all be considered as identical!

Table 14.12 is a relative comparison of the FET amplifiers. The common-source amplifier provides moderate voltage gain and output resistance but high values of input resistance and current gain. The common-drain amplifier provides low voltage gain and output resistance, and high input resistance and current gain. Finally, the common-gate amplifier provides moderate voltage gain, high output resistance, and low input resistance and current gain. Tables 14.9 to 14.12 are very useful in the initial phase of amplifier design, when the engineer must make a basic choice of amplifier configuration to meet the design specifications.

### DESIGN NOTE

The magnitude of the overall gain of the single-stage amplifiers can all be expressed approximately by

$$|A_v| \cong \frac{g_m R_L}{1 + g_m R_X} = \frac{R_L}{\frac{1}{g_m} + R_X}$$

in which  $R_X$  is the external resistance in the emitter or source loop of the transistor.

Now we have a toolbox full of amplifier configurations that we can use to solve circuit design problems. Design Ex. 14.6 on page 912 demonstrates how to use our understanding to make design choices between the various configurations.

## 14.6 COMMON-SOURCE AMPLIFIERS USING MOS INVERTERS

As originally discussed in Chapter 6, resistor loads are problematic in integrated circuits because they tend to take up a large amount of area relative to the size of MOS transistors. However, we can use a transistor in place of the load resistor in a common-source amplifier as depicted in Fig. 14.29

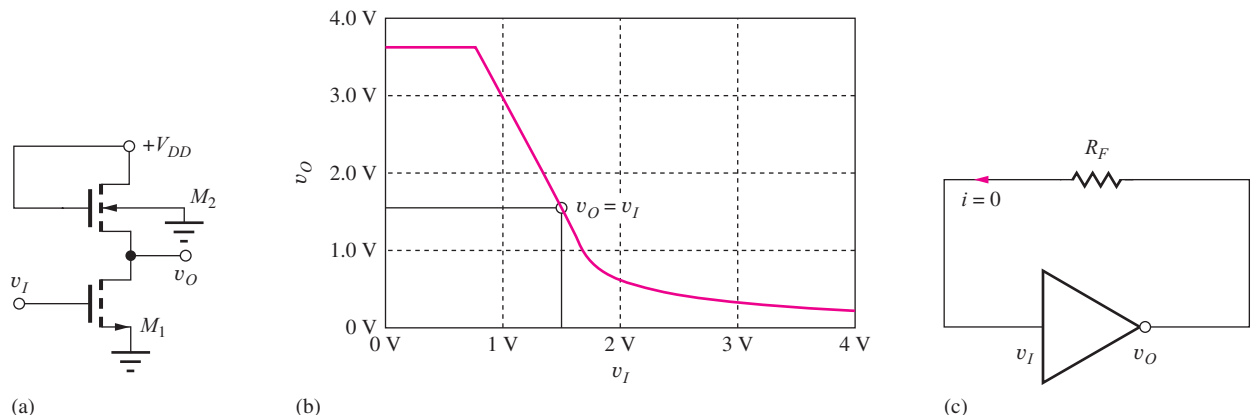


**Figure 14.29** (a) Common-source amplifier with the load resistor replaced with a saturated transistor. (b) Voltage transfer characteristic. (c) Simple bias circuit for high gain operation.

where  $R_L$  is replaced as a transistor operating in the saturation region.<sup>5</sup> This is the same circuit that we encountered in Chapter 6 where it was called the “Saturated Load Inverter.”

Remember from Chapter 10 that the gain is equal to the slope of the amplifier’s voltage transfer characteristic evaluated at the Q-point,  $A_v = dv_O/dv_I|_{Q\text{-pt.}}$ , and the VTC in Fig. 14.29(b) has a region of high gain. In particular, if the circuit can be biased at a Q-point having  $v_O = v_I$ , then the inverter operates as a high-gain amplifier.

It is actually easy to bias the MOS inverter into the high-gain region using negative feedback as in Fig. 14.29(c).<sup>6</sup> Since there is no dc current into the input  $v_I$ ,  $v_I$  and  $v_O$  must be equal, and the circuit operates in its high-gain region.

### 14.6.1 VOLTAGE GAIN ESTIMATE

Let us estimate the gain of the circuit in Fig. 14.29(a) based upon the characteristics of the single-transistor amplifiers studied thus far.  $M_1$  is connected as a common-source transistor, so the gain will be  $A_v = -g_{m1}R_L$  where  $R_L$  is the overall load resistance connected to the drain of  $M_1$ . The load resistance consists of the parallel combination of the output resistance  $r_{o1}$  of  $M_1$  and the resistance  $R_{iS2}$  looking into the source of  $M_2$ :

$$R_L = r_{o1} \parallel R_{iS2} = r_{o1} \parallel \frac{1}{g_{m2}} \cong \frac{1}{g_{m2}} \quad (14.95)$$

Since the transistors must operate at the same drain current, we expect  $r_{o1} \gg 1/g_{m2}$ , and the voltage gain becomes

$$A_v^{CS} \cong -\frac{g_{m1}}{g_{m2}} = \frac{\sqrt{2K_{n1}I_D}}{\sqrt{2K_{n2}I_D}} = \sqrt{\frac{(W/L)_1}{(W/L)_2}} \quad (14.96)$$

The gain of the amplifier with a saturated-load device is equal to the square root of the ratio of the  $(W/L)$  ratios of the input and load transistors. The gain is controlled by the designer’s choice of the size of the transistors and is independent of the other transistor parameters. Unfortunately, even moderate gain requires large differences in the  $W/L$  ratios. For example, a 20 dB gain requires  $(W/L)_1 = 100(W/L)_2$ .

<sup>5</sup> Saturated by connection (see Sec. 6.6).

<sup>6</sup> In Chapter 15, we will see how to eliminate  $R_F$ .

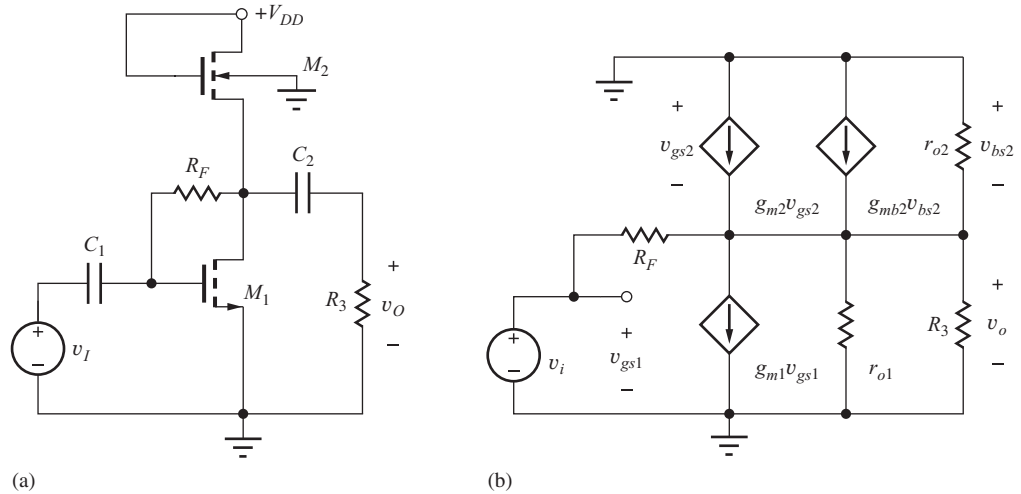


**Figure 14.30** (a) Complete common-source amplifier. (b) Small-signal model.

### 14.6.2 DETAILED ANALYSIS

Now let us explore the C-S amplifier in more detail in order to account for effects that have been neglected in our simplified analysis. The circuit in Fig. 14.30 includes bias resistor \$R\_F\$, coupling capacitors \$C\_1\$ and \$C\_2\$, and external load resistor \$R\_3\$, and the small-signal model includes the back-gate transconductance of transistor \$M\_2\$ (see Sec. 13.8.4). An expression for the gain of the amplifier in Fig. 14.30 is found by writing a nodal equation at the output node:

$$G_F(\mathbf{v}_o - \mathbf{v}_i) + g_{m1}\mathbf{v}_i + \mathbf{v}_o(g_{o1} + g_{o2} + G_F + G_3) - g_{m2}\mathbf{v}_{gs2} - g_{mb2}\mathbf{v}_{bs2} = 0 \quad (14.97)$$

Collecting terms, realizing that both \$v\_{gs2}\$ and \$v\_{bs2}\$ are equal to \$-v\_o\$, and solving for the voltage gain yields

$$A_v^{CS} = \frac{\mathbf{v}_o}{\mathbf{v}_i} = -\frac{(g_{m1} - G_F)}{g_{m2}(1 + \eta) + g_{o1} + g_{o2} + G_F + G_3} \quad (14.98)$$

where \$g\_{mb2} = \eta g\_{m2}\$. This expression can be written in a more recognizable form as

$$A_v^{CS} \cong -g_{m1}R_L \quad \text{where} \quad R_L = R_3 \parallel R_F \parallel r_{o1} \parallel r_{o2} \parallel \frac{1}{g_{m2}(1 + \eta)} \quad (14.99)$$

is the total equivalent resistance on the output node. We already know that \$r\_{o1}\$ and \$r\_{o2}\$ will be much larger than \$1/g\_{m2}\$, and \$R\_F\$ is normally designed to be much larger than \$R\_3\$. In most cases, \$R\_3\$ will also be much greater than \$1/g\_{m2}\$, so the gain reduces to

$$A_v^{CS} \cong -\frac{g_{m1}}{g_{m2}(1 + \eta)} = \frac{1}{1 + \eta} \sqrt{\frac{(W/L)_1}{(W/L)_2}} \quad (14.100)$$

Equation (14.100) is the same as Eq. (14.96) except for the gain degradation caused by the back-gate transconductance. The effective load resistance is still limited by the relatively large conductance of the load transistor.

**EXERCISE:** What is the \$W/L\$ ratio of \$M\_1\$ required to achieve a gain of 26 dB if \$\eta = 0.2\$ and \$(W/L)\_2 = 4/1\$?

**ANSWER:** 2290/1

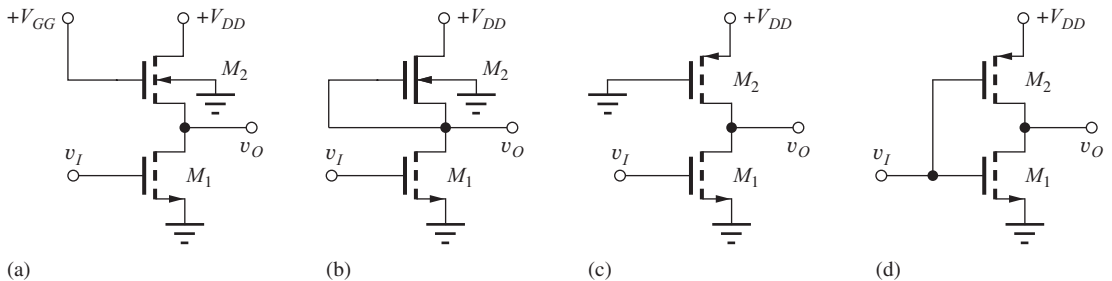


**Figure 14.31** MOS inverting amplifiers. (a) Linear load. (b) Depletion-mode load. (c) Pseudo NMOS. (d) CMOS.

### 14.6.3 ALTERNATIVE LOADS

To improve the gain of the circuit,  $g_{m2}$  needs to be eliminated from the expression for the load resistance, Eq. (14.99). We know from our study of logic gates that there are a number of alternative transistor configurations for the load device as depicted in Fig. 14.31. NMOS transistors can be used as linear loads and depletion-mode loads, whereas PMOS transistors can be employed in psuedo NMOS and CMOS inverters. Any one of these circuits can be substituted for the saturated load inverter in Fig. 14.30.

However, the linear load configuration achieves nothing, since the gate of  $M_2$  is still at ac ground and  $R_{iS2}$  is still determined by  $1/g_{m2}$ . On the other hand, the depletion-mode load yields an improvement. Voltage  $v_{GS}$  is forced to be zero by connection, so the forward transconductance is eliminated and the gain is approximately

$$A_v^{CS} \cong -\frac{g_{m1}}{\eta g_{m2}} \quad (14.101)$$

which improves the gain by a factor of  $(1 + \eta)/\eta$ . For  $\eta = 0.2$ , the gain is improved by a factor of 6. In discrete circuits,  $v_{BS}$  can also be set to zero, and the back-gate transconductance is also eliminated. For this case the gain becomes

$$A_v^{CS} \cong -g_{m1}R_L = -g_{m1}(R_3 \parallel R_F \parallel r_{o1} \parallel r_{o2}) \cong -g_{m1}R_3 \quad (14.102)$$

since we expect  $r_{o1}$  and  $r_{o2}$  to be much larger than  $R_3$ , and  $R_F$  can also be designed to be much larger than  $R_3$ . This configuration has more gain than our original C-S circuit because external load resistor  $R_3$  is normally much larger than drain resistor  $R_D$ .

Circuits in Figure 14.31(c) and (d) employ PMOS transistors and require CMOS technology. For the pseudo NMOS inverter, the load resistance on transistor  $M_1$  is the same as that given in Eq. (14.102), and the gain is also the same. In the CMOS inverter case as depicted in Fig. 14.32, the transistors are connected in parallel: the gates are connected together, the drains are connected together, and the sources are both at ac ground potential. The input is applied to both gates so the gain expression becomes

$$A_v^{CS} \cong -(g_{m1} + g_{m2})R_L = -g_{m1}(R_3 \parallel R_F \parallel r_{o1} \parallel r_{o2}) \cong -(g_{m1} + g_{m2})R_3 \quad (14.103)$$

which can be a factor of two improvement for a symmetrical inverter design ( $K_p = K_n$ ).

Note that if we use a symmetrical CMOS inverter, eliminate  $R_3$ , and make  $R_F$  very large, the gain becomes approximately

$$A_v^{CS} \cong -(g_{m1} + g_{m2})(r_{o1} \parallel r_{o2}) = -2g_{m1}\frac{r_{o1}}{2} \cong -\mu_f \quad (14.104)$$

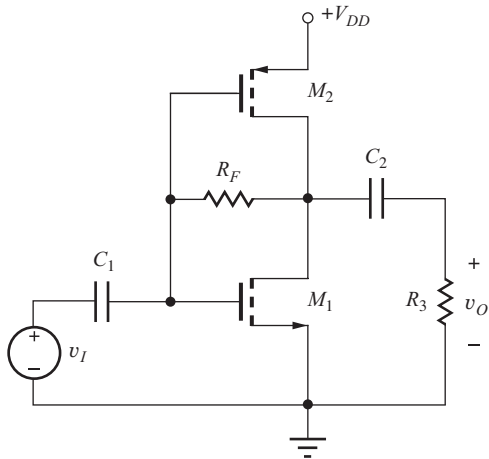


**Figure 14.32** Common-source amplifier employing CMOS inverter.

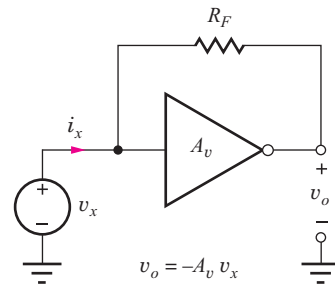


**Figure 14.33** Circuit for determining input resistance.

We have discovered a circuit that achieves a gain equal to the amplification factor of the transistor, and we can't do better than that! Similar techniques will be used to design high-performance amplifiers in the next several chapters.

#### 14.6.4 INPUT AND OUTPUT RESISTANCES

The input resistance of the amplifiers can be found with the assistance of the circuit in Fig. 14.33.  $R_{in}$  is calculated by finding an expression for  $i_x$  in terms of  $v_x$ :

$$\mathbf{i}_x = \frac{\mathbf{v}_x - \mathbf{v}_o}{R_F} = \frac{\mathbf{v}_x - (-A_v \mathbf{v}_x)}{R_F} = \mathbf{v}_x \left( \frac{1 + A_v}{R_F} \right) \quad \text{and} \quad R_{in} = \frac{\mathbf{v}_x}{\mathbf{i}_x} = \frac{R_F}{1 + A_v} \quad (14.105)$$

For high gain, the input resistance is approximately equal to the feedback resistance divided by the amplifier's gain.

If input source  $v_i$  is set to zero in Fig. 14.30(b), we immediately see that the output resistance is given by

$$R_{out} = R_F \parallel r_{o1} \parallel r_{o2} \parallel \frac{1}{g_m 2(1 + \eta)} \quad \text{or} \quad R_{out} = R_F \parallel r_{o1} \parallel r_{o2} \quad (14.106)$$

depending upon the inverter configuration.

**EXERCISE:** Find the Q-point for the amplifier in Fig. 14.30 if  $R_F = 1 \text{ M}\Omega$ ,  $K'_n = 100 \mu\text{A/V}^2$ ,  $V_{TN} = 1 \text{ V}$ ,  $\lambda = 0.02$ ,  $r = 0$ ,  $(W/L)_1 = 8/1$ ,  $(W/L)_2 = 2/1$  and  $V_{DD} = 5 \text{ V}$ .

**ANSWER:**  $V_o = 2.01 \text{ V}$ ,  $I_o = 421 \mu\text{A}$

**EXERCISE:** Find the Q-point for the amplifier in Fig. P14.32 if  $R_F = 560 \text{ k}\Omega$ ,  $K'_n = 100 \mu\text{A/V}^2$ ,  $K'_p = 40 \mu\text{A/V}^2$ ,  $V_{TN} = 0.7 \text{ V}$ ,  $V_{TP} = -0.7 \text{ V}$ ,  $\lambda = 0.02$ ,  $(W/L)_1 = 20/1$ ,  $(W/L)_2 = 50/1$  and  $V_{DD} = 3.3 \text{ V}$ .

**ANSWER:**  $V_o = 1.65 \text{ V}$ ,  $I_o = 932 \mu\text{A}$

## DESIGN SELECTING AN AMPLIFIER CONFIGURATION

### EXAMPLE 14.6

One of the first things we must do to solve a circuit design problem is to decide on the circuit topology to be used. A number of examples are given here.

**PROBLEMS** What is the preferred choice of amplifier configuration for each of these applications?

- A single-transistor amplifier is needed that has a gain of approximately 80 dB and an input resistance of 100 kΩ.
- A single-transistor amplifier is needed that has a gain of 52 dB and an input resistance of 250 kΩ.
- A single-transistor amplifier is needed that has a gain of 30 dB and an input resistance of at least 5 MΩ.
- A single-transistor amplifier is needed that has a gain of approximately 0 dB and an input resistance of 20 MΩ with a load resistor of 10 kΩ.
- A follower is needed that has a gain of at least 0.98 and an input resistance of at least 250 kΩ with a load resistance of 5 kΩ.
- A single-transistor amplifier is needed that has a gain of +10 and an input resistance of 2 kΩ.
- An amplifier is needed with an output resistance of 25 Ω.

**SOLUTION** **Known Information and Given Data:** In each case, we see that a minimum amount of information is provided, typically only a voltage gain and resistance specification.

**Unknowns:** Circuit topologies

**Approach:** Use our estimates of voltage gain, input resistance, and output resistance for the various configurations to make a selection.

**Assumptions:** Typical values of current gain, Early voltage, power supply voltage, and so on will be assumed as necessary:  $\beta_o = 100$ ,  $0.25 \text{ V} \leq V_{GS} - V_{TN} \leq 1 \text{ V}$ ,  $V_T = 0.025 \text{ V}$ ,  $V_A \leq 150 \text{ V}$ .

**Analyses:**

- The required voltage gain is  $A_v = 10^{80/20} = 10,000$ . This value of voltage gain exceeds the intrinsic voltage gain of even the best BJTs:

$$A_v \leq \mu_f = 40V_A = 40(150) = 6000$$

An FET typically has a much lower value of intrinsic gain and is at an even worse disadvantage. Thus, such a large gain requirement cannot be met with a single-transistor amplifier.

- For the second set of specifications, we have  $R_{in} = 250 \text{ k}\Omega$  and  $A_v = 10^{52/20} \cong 400$ . We require both large gain and relatively large input resistance, which point us toward the common-emitter amplifier. For the C-E stage,  $A_v = 10 V_{CC} \rightarrow V_{CC} = 40 \text{ V}$ , which is somewhat large. However, we know that the 10  $V_{CC}$  estimate for the voltage gain is conservative and can easily be off by a factor of 2 or 3, so we can probably get by with a smaller power supply, say 20 V. Achieving the input of resistance requirement requires  $r_\pi$  to exceed 250 kΩ:

$$r_\pi = \frac{\beta_o V_T}{I_C} \geq 250 \text{ k}\Omega \rightarrow I_C \leq \frac{100(0.025 \text{ V})}{2.5 \times 10^5 \text{ }\Omega} = 10 \text{ }\mu\text{A}$$

which is small but acceptable. Achieving the gain specification with an FET would be much more difficult. For example, even with a small gate overdrive,

$$A_v = \frac{V_{DD}}{V_{GS} - V_{TN}} \cong \frac{V_{DD}}{0.25 \text{ V}} \rightarrow V_{DD} = 100 \text{ V}$$

which is unreasonably large for most solid-state designs. Note that the sign of the gain was not specified, so either positive or negative gain would be satisfactory, based on our limited specifications. However, the input resistance of the noninverting (C-B or C-G) amplifiers is low, not high.

- (c) In this case, we require  $R_{in} \geq 5 \text{ M}\Omega$  and  $A_v = 10^{30/20} \cong 31.6$ —large input resistance and moderate gain. These requirements can easily be met by a common-source amplifier:

$$A_v = \frac{V_{DD}}{V_{GS} - V_{TN}} = \frac{15 \text{ V}}{0.5 \text{ V}} = 30$$

The input resistance is set by our choice of gate bias resistors ( $R_1$  and  $R_2$  in Fig. 14.2), and  $5 \text{ M}\Omega$  can be achieved with standard resistor values.

Since the gain is moderate, a C-E stage with emitter resistor could probably achieve the required high input resistance, although the values of the base bias resistor could become a limiting factor. For example, the input resistance and voltage gain could be met approximately with

$$R_{in} \cong \beta_o R_E \geq 5 \text{ M}\Omega \rightarrow R_E \geq \frac{5 \text{ M}\Omega}{100} = 50 \text{ k}\Omega \quad \text{and} \quad |A_v| = \frac{R_L}{R_E} \rightarrow R_L = 1.5 \text{ M}\Omega$$

- (d) Zero-dB gain corresponds to a follower. For an emitter follower,  $R_{in} \cong \beta_o R_L \cong 100(10 \text{ k}\Omega) = 1 \text{ M}\Omega$ , so the BJT will not meet the input resistance requirement. On the other hand, a source follower provides a gain of approximately one and can easily achieve the required input resistance.  
(e) A gain of 0.98 and an input resistance of  $250 \text{ k}\Omega$  should be achievable with either a source follower or an emitter follower. For the MOSFET,

$$A_v = \frac{g_m R_L}{1 + g_m R_L} = 0.98 \quad \text{requires} \quad g_m R_L = \frac{2 I_D R_L}{V_{GS} - V_{TN}} = 49$$

which can be satisfied with  $I_D R_L = 12.3 \text{ V}$  for  $V_{GS} - V_{TN} = 0.5 \text{ V}$ .

The BJT can achieve the required gain with a much lower supply voltage and still meet the input resistance requirement:  $R_{in} \cong \beta_o R_L \cong 100(5 \text{ k}\Omega) = 500 \text{ k}\Omega$ .

$$g_m R_L = \frac{I_C R_L}{V_T} = 49 \rightarrow I_C R_L = 49(0.025 \text{ V}) = 1.23 \text{ V}$$

- (f) A noninverting amplifier with a gain of 10 and an input resistance of  $2 \text{ k}\Omega$  should be achievable with either a common-base or common-gate amplifier with proper choice of operating point. The gain of 10 is easily achieved with either the MOSFET or BJT design estimate:  $A_v = V_{DD}/(V_{GS} - V_{TN})$  or  $A_v = 10V_{CC}$ .  $R_{in} \cong 1/g_m = 2 \text{ k}\Omega$  is within easy reach of either device.  
(g) Twenty-five ohms represents a small value of output resistance. The follower stages are the only choices that provide low output resistances. For the followers,  $R_{out} = 1/g_m$ , and so we need  $g_m = 40 \text{ mS}$ .

For the BJT:  $I_C = g_m V_T = 40 \text{ mS}(25 \text{ mV}) = 1 \text{ mA}$

$$\text{For the MOSFET: } I_D = \frac{g_m(V_{GS} - V_{TN})}{2} = \frac{40 \text{ mS}(0.5 \text{ V})}{2} = 10 \text{ mA}$$

$$K_n = \frac{g_m^2}{2I_D} = \frac{(40 \text{ mS})^2}{2(10 \text{ mA})} = 0.08 \frac{\text{A}}{\text{V}^2} \quad \text{and}$$

$$\frac{W}{L} = \frac{K_n}{K'_n} = \frac{80 \text{ mA/V}^2}{50 \mu\text{A/V}^2} = \frac{1600}{1}$$

The  $25\Omega$  requirement can be met with either device, but the BJT requires an order of magnitude less current. In addition, the MOSFET requires a large  $W/L$  ratio.

**Discussion:** The options developed here represent our first attempts, and there is no guarantee that we will actually be able to fully achieve the desired specifications. After attempting a full design, we may have to change the circuit choice or use more than one transistor in a more complex amplifier configuration.

**EXERCISE:** Suppose the BJT amplifier in part (b) of Design Ex. 14.6 will be designed with symmetric 15-V supplies using a circuit similar to the one in Figure 13.10(a). Choose a collector current.

**ANSWER:** 5  $\mu\text{A}$ , (10  $\mu\text{A}$  does not account for the effect of  $R_B$ )

**EXERCISE:** Estimate the collector current needed for a BJT to achieve the input resistance specification in part (f) of Design Ex. 14.6.

**ANSWER:** 12.5  $\mu\text{A}$

## 14.7 COUPLING AND BYPASS CAPACITOR DESIGN

Up to this point, we have assumed that the impedances of coupling and bypass capacitors are negligible, and have concentrated on understanding the properties of the single transistor building blocks in their “midband” region of operation. However, since the impedance of a capacitor increases with decreasing frequency, the coupling and bypass capacitors generally reduce amplifier gain at low frequencies. In this section, we discover how to pick the values of these capacitors to ensure that our midband assumption is valid. Each of the three classes of amplifiers will be considered in succession. The technique we use is related to the “short-circuit” time constant (SCTC) method that we shall study in greater detail in Chapter 17. In this method, each capacitor is considered separately with all the others replaced by short circuits ( $C \rightarrow \infty$ ).

### 14.7.1 COMMON-EMITTER AND COMMON-SOURCE AMPLIFIERS

Let us start by choosing values for the capacitors for the C-E and C-S amplifiers in Fig. 14.2. For the moment, assume that  $C_3$  is still infinite in value, thus shorting the bottom of  $R_E$  and  $R_S$  to ground, as drawn in Fig. 14.34(a) and (b).

#### Coupling Capacitors $C_1$ and $C_2$

First, consider  $C_1$ . In order to be able to neglect  $C_1$ , we require the magnitude of the impedance of the capacitor (its capacitive reactance) to be much smaller than the equivalent resistance that appears at its terminals. Referring to Fig. 14.34, we see that the resistance looking to the left from capacitor

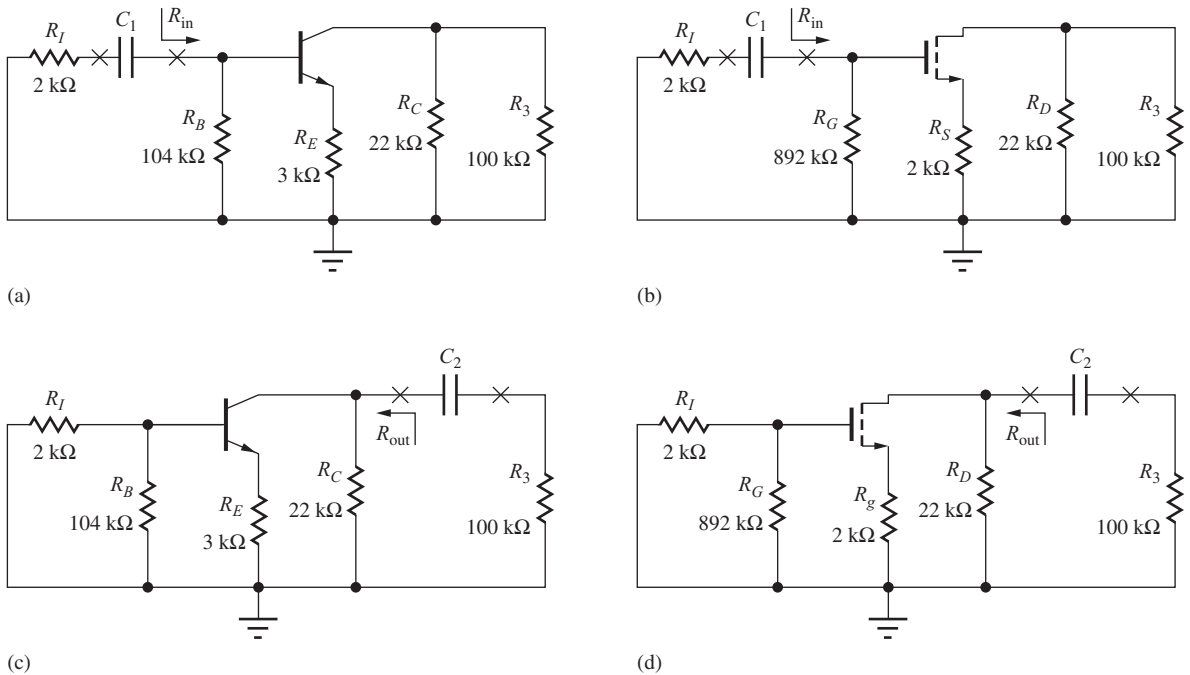


**Figure 14.34** Coupling capacitors in the common-emitter and common-source amplifiers.

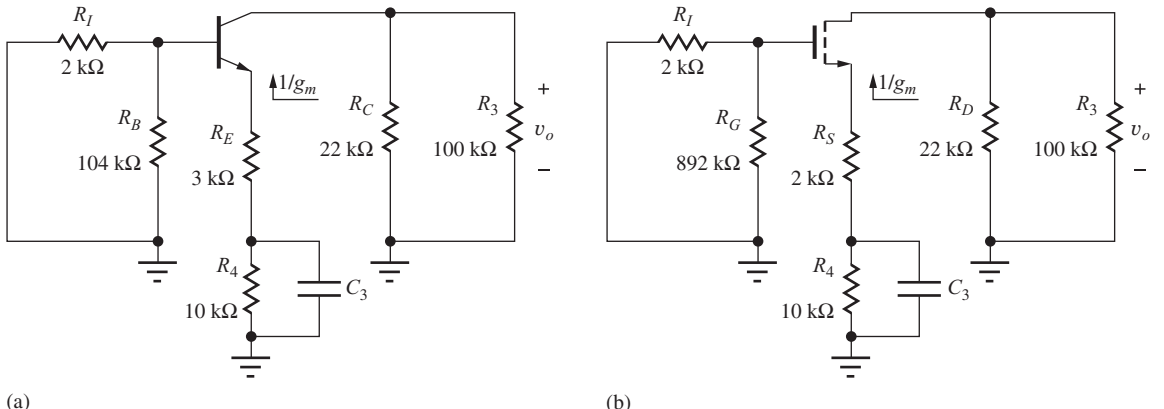


**Figure 14.35** Bypass capacitors in the common-emitter and common-source amplifiers.

$C_1$  (with  $v_i = 0$ ) is  $R_I$ , and that looking to the right is  $R_{in}$ . Thus, design of  $C_1$  requires

$$\frac{1}{\omega C_1} \ll (R_I + R_{in}) \quad \text{or} \quad C_1 \gg \frac{1}{\omega(R_I + R_{in})} \quad (14.107)$$

Frequency  $\omega$  is chosen to be the lowest frequency for which midband operation is required in the given application.

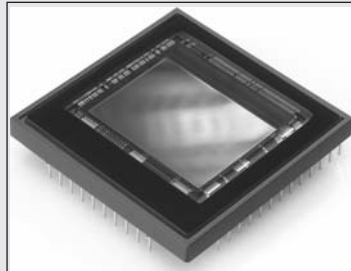
For the common-emitter stage, bias resistor  $R_B$  appears in parallel (shunt) with the input resistance of the transistor, so  $R_{in} = R_B \parallel R_{iB}$ . For the common-source stage, bias resistor  $R_G$  shunts the input resistance of the transistor, and  $R_{in} = R_G \parallel R_{iG} = R_G$ .

A similar analysis applies to  $C_2$ . We require the reactance of the capacitor to be much smaller than the equivalent resistance that appears at its terminals. Referring to Fig. 14.34(b), the resistance

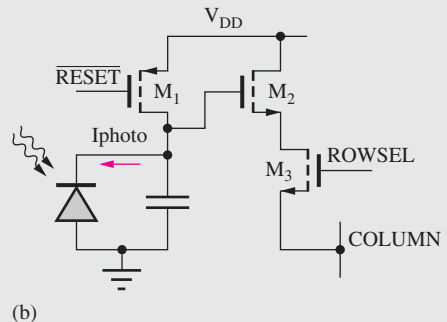


### Revisiting the CMOS Imager Circuitry

In the first Electronics in Action feature in Chapter 4, we introduced the CMOS imager circuit presented on the next page. The chip contains 1.3 million pixels in a  $1280 \times 1024$  imaging array. A typical photodiode based imaging pixel consists of a photo diode with sensing and access circuitry. Let us revisit this sensor circuit in light of what we have learned about single transistor amplifiers.



Dalsa 8 MegaPixel CMOS image sensor.<sup>1</sup>



Typical photo diode pixel architecture.

$M_1$  is a reset switch, and after the  $\overline{\text{RESET}}$  signal is asserted, the storage capacitor is fully charged to  $V_{DD}$ . The reset signal is then removed, and light incident on the photodiode generates a photo current that discharges the capacitor. Different light intensities produce different voltages on the capacitor at the end of the light integration time. Transistor  $M_2$  is a source follower that buffers the photo-diode node. The source follower transfers the signal voltage at the photo-diode node to the output with nearly unity gain, and  $M_2$  does not disturb the voltage at the photo diode output since it has an infinite dc input resistance. The voltage at the source of  $M_2$  is then transferred to the output column via switch  $M_3$ . The source follower provides a low output resistance to drive the capacitance of the output column. The  $W/L$  ratio of switch  $M_3$  must be chosen carefully so it does not significantly degrade the overall output resistance.

<sup>1</sup> The chip pictured above is a DALSA CMOS image sensor and is reprinted here with permission from Dalsa Corporation.

looking to the left from capacitor  $C_2$  is  $R_{\text{out}}$ , and that looking to the right is  $R_3$ . Thus,  $C_2$  must satisfy

$$\frac{1}{\omega C_2} \ll (R_{\text{out}} + R_3) \quad \text{or} \quad C_2 \gg \frac{1}{\omega(R_{\text{out}} + R_3)} \quad (14.108)$$

For the common-emitter stage, collector resistor  $R_C$  appears in parallel with the output resistance of the transistor, and  $R_{\text{out}} = R_C \parallel R_{iC}$ . For the common-source stage, drain resistor  $R_D$  shunts the output resistance of the transistor, so  $R_{\text{out}} = R_D \parallel R_{iD}$ .

#### Bypass Capacitor $C_3$

The formula for  $C_3$  is somewhat different. Figure 14.35 depicts the circuit assuming we can neglect the impedance of capacitors  $C_1$  and  $C_2$ . At the terminals of  $C_3$  in Fig. 14.35(a), the equivalent resistance is equal to  $R_4$  in parallel with the sum  $(R_E + 1/g_m)$ ,<sup>7</sup> the resistance looking up toward the

<sup>7</sup> For the BJT case, we are neglecting the  $R_{th}/(\beta_0 + 1)$  term. Since the additional term will increase the equivalent resistance, its neglect makes Eq. (14.109) a conservative estimate.

emitter of the transistor. Thus, for the C-E and C-S amplifiers,  $C_3$  must satisfy

$$C_3 \gg \frac{1}{\omega \left[ R_4 \left| \left( R_E + \frac{1}{g_m} \right) \right| \right]} \quad \text{or} \quad C_3 \gg \frac{1}{\omega \left[ R_4 \left| \left( R_S + \frac{1}{g_m} \right) \right| \right]} \quad (14.109)$$

In order to satisfy the inequalities in Eqs. (14.107) through (14.109), we will set the capacitor value to be approximately 10 times that calculated in the equations.

## DESIGN CAPACITOR DESIGN FOR THE C-E AND C-S AMPLIFIERS

### EXAMPLE 14.7

In this example, we select capacitor values for the three capacitors in both inverting amplifiers in Figs. 14.2, 14.34, and 14.35.

**PROBLEM** Choose values for the coupling and bypass capacitors for the amplifiers in Fig. 14.2 so that the presence of the capacitors can be neglected at a frequency of 1 kHz (1 kHz represents an arbitrary choice in the audio frequency range).

**SOLUTION** **Known Information and Given Data:** Frequency  $f = 1000$  Hz; for the C-E stage described in Fig. 14.2 and Table 14.4,  $R_{iB} = 310$  k $\Omega$ ,  $R_{iC} = 4.55$  M $\Omega$ ,  $R_I = 2$  k $\Omega$ ,  $R_B = 104$  k $\Omega$ ,  $R_C = 22$  k $\Omega$ ,  $R_E = 3$  k $\Omega$ ,  $R_4 = 10$  k $\Omega$ , and  $R_3 = 100$  k $\Omega$ ; for the C-S stage from Table 14.4,  $R_{iG} = \infty$ ,  $R_{iD} = 442$  k $\Omega$ ,  $R_I = 2$  k $\Omega$ ,  $R_G = 892$  k $\Omega$ ,  $R_D = 22$  k $\Omega$ ,  $R_S = 2$  k $\Omega$ ,  $R_4 = 10$  k $\Omega$ , and  $R_3 = 100$  k $\Omega$

**Unknowns:** Values of capacitors  $C_1$ ,  $C_2$ , and  $C_3$  for the common-emitter and common-source amplifier stages.

**Approach:** Substitute known values in Eq. (14.107) through (14.109). Choose nearest values from the appropriate table in Appendix A.

**Assumptions:** Small-signal operating conditions are valid,  $V_T = 25$  mV.

**Analysis:** For the common-emitter amplifier,

$$R_{\text{in}} = R_B \parallel R_{iB} = 104 \text{ k}\Omega \parallel 310 \text{ k}\Omega = 77.9 \text{ k}\Omega$$

$$R_{\text{out}} = R_C \parallel R_{iC} = 22 \text{ k}\Omega \parallel 4.55 \text{ M}\Omega = 21.9 \text{ k}\Omega$$

$$C_1 \gg \frac{1}{\omega(R_I + R_{\text{in}})} = \frac{1}{2000\pi(2 \text{ k}\Omega + 77.9 \text{ k}\Omega)} = 1.99 \text{ nF} \rightarrow C_1 = 0.02 \mu\text{F} \quad (20 \text{ nF})^8$$

$$C_2 \gg \frac{1}{\omega(R_{\text{out}} + R_3)} = \frac{1}{2000\pi(21.9 \text{ k}\Omega + 100 \text{ k}\Omega)} = 1.31 \text{ nF} \rightarrow C_2 = 0.015 \mu\text{F} \quad (15 \text{ nF})$$

$$\begin{aligned} C_3 &\gg \frac{1}{\omega \left[ R_4 \left| \left( R_E + \frac{1}{g_m} \right) \right| \right]} = \frac{1}{2000\pi \left[ 10 \text{ k}\Omega \left| \left( 3 \text{ k}\Omega + \frac{1}{9.80 \text{ mS}} \right) \right| \right]} \\ &= 67.2 \text{ nF} \rightarrow C_3 = 0.68 \mu\text{F} \end{aligned}$$

For the common-source stage,  $R_{\text{in}} = R_G$  since the input resistance at the gate of the transistor is infinite, and  $R_{\text{out}} = R_D \parallel R_{iD}$

$$C_1 \gg \frac{1}{\omega(R_I + R_{\text{in}})} = \frac{1}{2000\pi(2 \text{ k}\Omega + 892 \text{ k}\Omega)} = 178 \text{ pF} \rightarrow C_1 = 1800 \text{ pF}$$

$$C_2 \gg \frac{1}{\omega(R_{\text{out}} + R_3)} = \frac{1}{2000\pi(210 \text{ k}\Omega + 100 \text{ k}\Omega)} = 1.31 \text{ nF} \rightarrow C_2 = 0.015 \mu\text{F} \quad (15 \text{ nF})$$

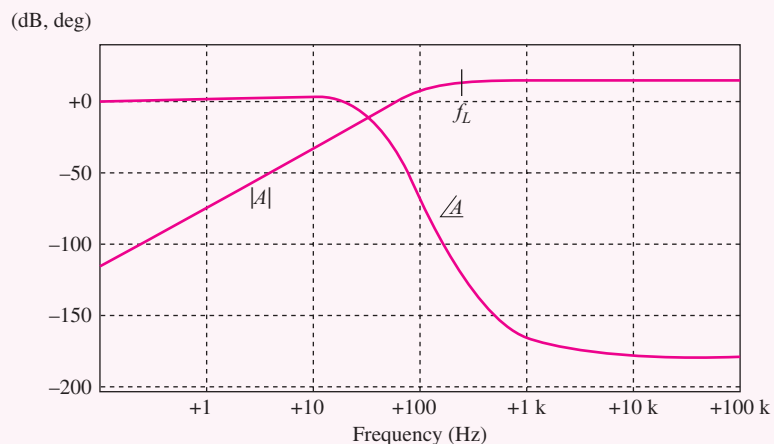
<sup>8</sup> We are using  $C_1 = 10(1.99 \text{ nF})$  to satisfy the inequality.

$$C_3 \gg \frac{1}{\omega \left[ R_4 \parallel \left( R_S + \frac{1}{g_m} \right) \right]} = \frac{1}{2000\pi \left[ 10 \text{ k}\Omega \parallel \left( 2 \text{ k}\Omega + \frac{1}{0.491 \text{ mS}} \right) \right]} \\ = 55.3 \text{ nF} \rightarrow C_3 = 0.56 \mu\text{F}$$

**Check of Results:** A double check of the calculations indicates they are correct. This would be a good place to check the analysis with simulation.

**Discussion:** We have chosen each capacitor to have negligible reactance at the frequency of 1 kHz and would expect the lower cutoff frequency of the amplifier to be well below this frequency. The choice of frequency in this example was arbitrary and depends upon the lowest frequency of interest in the application.

 **Computer-Aided Analysis:** The graph below gives SPICE simulation results for the common-emitter amplifier with the capacitors as designed here. The midband gain is 15.0 dB and the lower cutoff frequency is 195 Hz. Note the two-pole roll-off at low frequencies indicated by the 40-dB/decade slope in the magnitude characteristic. The slope indicates that there are two zeros at dc, which are associated with capacitors  $C_1$  and  $C_2$ . A signal cannot pass through either capacitor at dc, hence the frequency response exhibits a double zero at the origin. We have ended up with an amplifier that has three low frequency poles at approximately 100 Hz ( $1 \text{ kHz}/10$ ), and bandwidth shrinkage (Sec. 12.1.3 and 14.6.4) causes the resulting lower cutoff frequency  $f_L$  to increase to 195 Hz.



Frequency response for the common-emitter amplifier.

**EXERCISE:** Reevaluate the capacitor values for the two amplifiers in Ex. 14.7 if the frequency is 250 Hz and the values of  $R_i$  and  $R_o$  are changed to 1 k $\Omega$  and 82 k $\Omega$ , respectively.

**ANSWERS:** 8.05 nF  $\rightarrow$  0.082  $\mu\text{F}$ , 0.269  $\mu\text{F}$   $\rightarrow$  2.7  $\mu\text{F}$ , 6.13 nF  $\rightarrow$  0.068  $\mu\text{F}$ ; 713 pF  $\rightarrow$  8200 pF, 6.40 nF  $\rightarrow$  0.068  $\mu\text{F}$ , 0.221  $\mu\text{F}$   $\rightarrow$  2.2  $\mu\text{F}$

**EXERCISE:** Use SPICE to simulate the frequency response of the COMMON-SOURCE amplifier and find the midband gain and lower cutoff frequency.

**ANSWERS:** 12.8 dB; 185 Hz

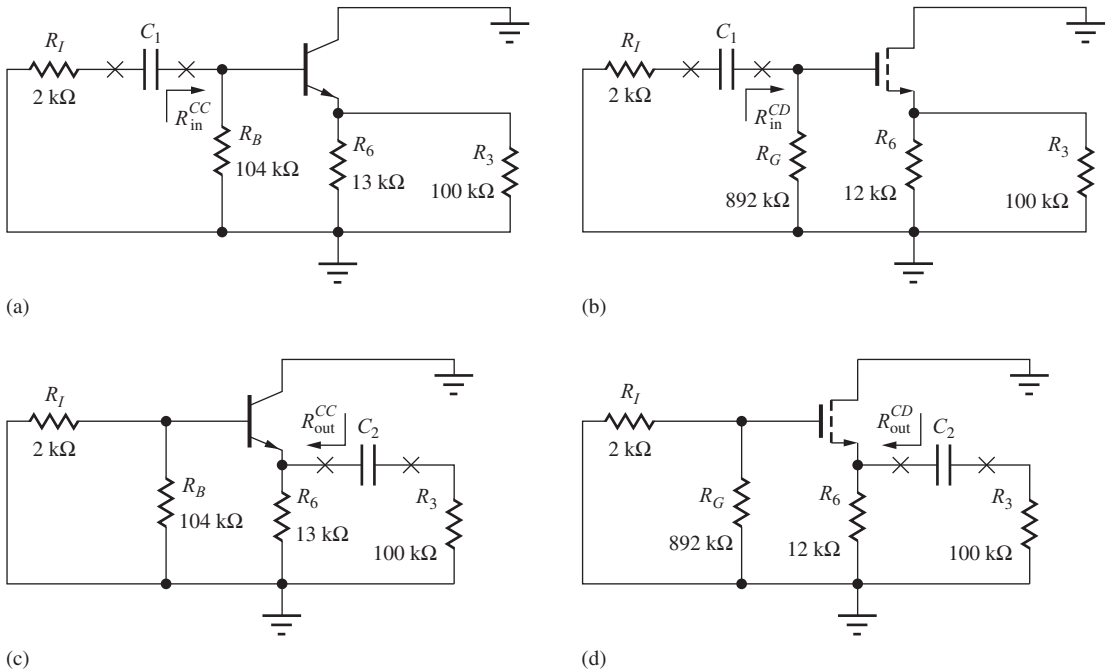


**Figure 14.36** Coupling capacitors in the common-collector and common-drain amplifiers.

### 14.7.2 COMMON-COLLECTOR AND COMMON-DRAIN AMPLIFIERS

The simplified C-C and C-D amplifiers in Fig. 14.4 have only two coupling capacitors. In order to be able to neglect \$C\_1\$, the reactance of the capacitor must be much smaller than the equivalent resistance that appears at its terminals. Referring to Fig. 14.36, we see that the resistance looking to the left from \$C\_1\$ is \$R\_I\$, and that looking to the right is \$R\_{in}\$. Thus, design of \$C\_1\$ is the same as Eq. (14.107):

$$\frac{1}{\omega C_1} \ll (R_I + R_{in}) \quad \text{or} \quad C_1 \gg \frac{1}{\omega(R_I + R_{in})} \quad (14.110)$$

Be sure to note that the values of the input and output resistances will be different in Eq. (14.110) from those in Eq. (14.107)! For the common-collector stage, bias resistor \$R\_B\$ shunts the input resistance of the transistor, so \$R\_{in} = R\_B \parallel R\_{iB}\$. For the common-drain stage, gate bias resistor \$R\_G\$ appears in parallel with the input resistance of the transistor, and \$R\_{in} = R\_G \parallel R\_{iG}\$.

For \$C\_2\$, the resistance looking to the left from capacitor \$C\_2\$ is \$R\_{out}\$, and that looking to the right is \$R\_3\$. Thus, design of \$C\_2\$ requires

$$\frac{1}{\omega C_2} \ll (R_{out} + R_3) \quad \text{or} \quad C_2 \gg \frac{1}{\omega(R_{out} + R_3)} \quad (14.111)$$

where \$R\_{out} = R\_6 \parallel R\_{iE}\$, because resistor \$R\_6\$ appears in parallel with the output resistance of the transistor. Note again that the value of \$R\_{out}\$ in Eq. (14.111) differs from that in Eq. (14.108).

## DESIGN CAPACITOR DESIGN FOR THE C-C AND C-D AMPLIFIERS

### EXAMPLE 14.8

This example selects capacitor values for the followers in Figs. 14.4 and 14.36.

**PROBLEM** Choose values for the coupling and bypass capacitors for the amplifiers in Fig. 14.4 and 14.36 so that the presence of the capacitors can be neglected at a frequency of 2 kHz.

**SOLUTION** **Known Information and Given Data:** Frequency  $f = 2000$  Hz; for the C-C stage from Fig. 14.4 and Table 14.5,  $R_{iB} = 1.17 \text{ M}\Omega$ ,  $R_{iC} = 0.121 \text{ k}\Omega$ ,  $R_6 = 13 \text{ k}\Omega$ ,  $R_I = 2 \text{ k}\Omega$ ,  $R_B = 104 \text{ k}\Omega$ , and  $R_3 = 100 \text{ k}\Omega$ ; for the C-S stage,  $R_{iG} = \infty$ ,  $R_{iS} = 2.04 \text{ k}\Omega$ ,  $R_6 = 12 \text{ k}\Omega$ ,  $R_I = 2 \text{ k}\Omega$ ,  $R_G = 892 \text{ k}\Omega$ , and  $R_3 = 100 \text{ k}\Omega$

**Unknowns:** Values of capacitors  $C_1$  and  $C_3$  for the common-collector and common-drain amplifiers.

**Approach:** Substitute known values in Eqs. (14.110) and (14.111). Choose the nearest values from the capacitor table in Appendix A.

**Assumptions:** Small-signal operating conditions are valid.

**Analysis:** For the common-collector amplifier,

$$R_{\text{in}} = R_B \| R_{iB} = 104 \text{ k}\Omega \| 1.17 \text{ M}\Omega = 95.5 \text{ k}\Omega$$

$$C_1 \gg \frac{1}{\omega(R_I + R_{\text{in}})} = \frac{1}{4000\pi(2 \text{ k}\Omega + 95.5 \text{ k}\Omega)} = 816 \text{ pF} \rightarrow C_1 = 8200 \text{ pF}^9$$

$$R_{\text{out}} = R_6 \| R_{iC} = 13 \text{ k}\Omega \| 121 \Omega = 120 \Omega$$

$$C_2 \gg \frac{1}{\omega(R_{\text{out}} + R_3)} = \frac{1}{4000\pi(120 \Omega + 100 \text{ k}\Omega)} = 795 \text{ pF} \rightarrow C_2 = 8200 \text{ pF}$$

and for the common-drain stage,

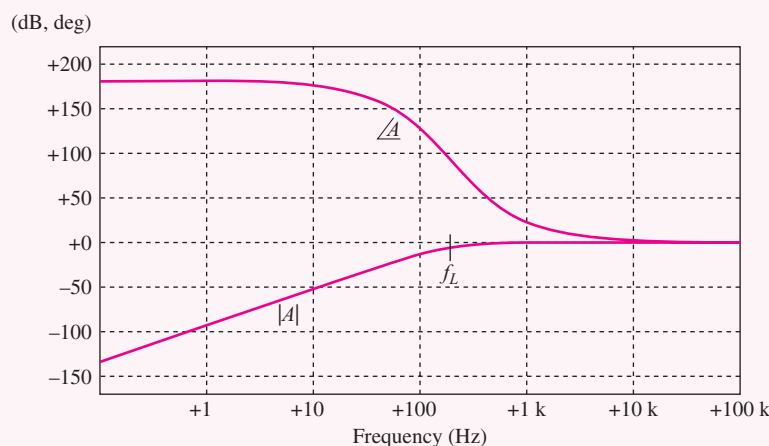
$$R_{\text{in}} = R_G \| R_{iG} = 892 \text{ k}\Omega \| \infty = 892 \text{ k}\Omega$$

$$C_1 \gg \frac{1}{\omega(R_I + R_{\text{in}})} = \frac{1}{4000\pi(2 \text{ k}\Omega + 892 \text{ k}\Omega)} = 89.0 \text{ pF} \rightarrow C_1 = 1000 \text{ pF}$$

$$R_{\text{out}} = R_6 \| R_{iS} = 12 \text{ k}\Omega \| 2.04 \text{ k}\Omega = 1.74 \text{ k}\Omega$$

$$C_2 \gg \frac{1}{\omega(R_{\text{out}} + R_3)} = \frac{1}{4000\pi(1.74 \text{ k}\Omega + 100 \text{ k}\Omega)} = 782 \text{ pF} \rightarrow C_2 = 8200 \text{ pF}$$

**Check of Results:** A double check of the calculations indicates they are correct. This represents a good place to check the analysis with simulation.



Emitter follower frequency response.

<sup>9</sup>  $C_1 = 10(816 \text{ pF})$  is used to satisfy the inequality.

**Discussion:** We have chosen each capacitor to have negligible reactance at the frequency of 2 kHz and would expect the lower cutoff frequency of the amplifier to be well below this frequency. The choice of frequency in this example was arbitrary and depends upon the lowest frequency of interest in the application.

www **Computer-Aided Analysis:** The graph on the previous page shows SPICE simulation results for the common-emitter amplifier with the capacitors as designed above. The midband gain is  $-0.262$  dB (0.970) and the lower cutoff frequency is 310 Hz. Note the two-pole roll off at low frequencies indicated by the 40-dB/decade slope in the magnitude characteristic. As in Design Ex. 14.7, a dc signal cannot pass through capacitor  $C_1$  or  $C_3$ , and the amplifier transfer function is characterized by a double zero at the origin.

**EXERCISE:** Reevaluate the capacitor values for the two amplifiers in Ex. 14.8 if the frequency is 250 Hz and the values of  $R_I$  and  $R_3$  are changed to  $1\text{ k}\Omega$  and  $82\text{ k}\Omega$ , respectively?

**ANSWERS:**  $6.79\text{ nF} \rightarrow 0.068\text{ }\mu\text{F}$ ,  $8.16\text{ nF} \rightarrow 0.082\text{ }\mu\text{F}$ ;  $713\text{ pF} \rightarrow 8200\text{ pF}$ ,  $7.98\text{ nF} \rightarrow 0.082\text{ }\mu\text{F}$

**EXERCISE:** Use SPICE to simulate the frequency response of the common-drain amplifier and find the midband gain and lower cutoff frequency.

**ANSWERS:**  $-1.54\text{ dB}$ ;  $293\text{ Hz}$

### 14.7.3 COMMON-BASE AND COMMON-GATE AMPLIFIERS

For the C-B and C-G amplifiers,  $C_3$  is first assumed to be infinite in value, thus shorting the base and gate of the transistors in Fig. 14.5 to ground as redrawn in Fig. 14.37. In order to neglect  $C_1$  the magnitude of the impedance of the capacitor must be much smaller than the equivalent resistance that appears at its terminals. Referring to Fig. 14.37, the resistance looking to the left from the capacitor

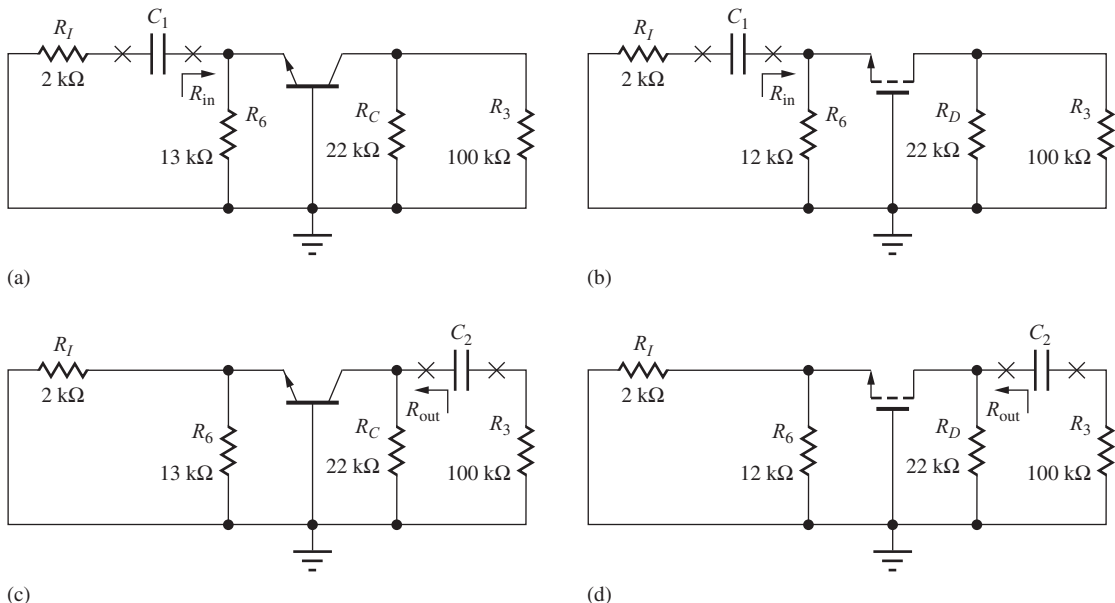
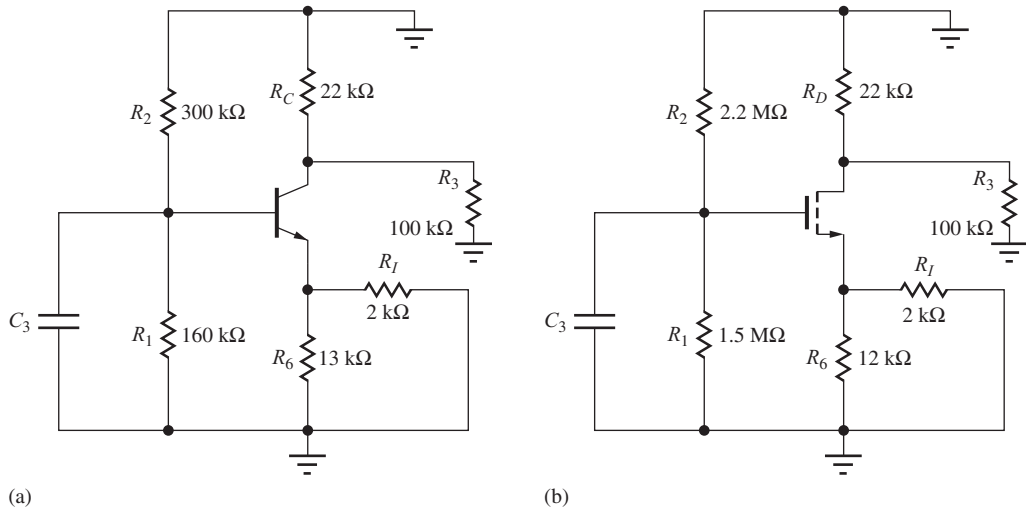


Figure 14.37 Coupling capacitors in the common-base and common-gate amplifiers.



**Figure 14.38** Bypass capacitors in the (a) common-collector and (b) common-drain amplifiers.

is  $R_I$ , and that looking to the right is  $R_{in}$ . Thus, design of  $C_1$  is the same as Eq. (14.107):

$$\frac{1}{\omega C_1} \ll (R_I + R_{in}) \quad \text{or} \quad C_1 \gg \frac{1}{\omega(R_I + R_{in})} \quad (14.112)$$

For the two amplifier stages, resistor  $R_6$  appears in shunt with the input resistance of the transistor, so  $R_{in} = R_6 \parallel R_{iE}$  or  $R_{in} = R_6 \parallel R_{iS}$ .

For  $C_2$ , we see that the resistance looking to the left from capacitor  $C_2$  is  $R_{out}$ , and that looking to the right is  $R_3$ . Thus, design of  $C_2$  requires

$$\frac{1}{\omega C_2} \ll (R_{out} + R_3) \quad \text{or} \quad C_2 \gg \frac{1}{\omega(R_{out} + R_3)} \quad (14.113)$$

For the amplifiers, resistor  $R_C$  or  $R_D$  appears in parallel with the output resistance of the transistor, so  $R_{out} = R_C \parallel R_{iC}$  or  $R_{out} = R_D \parallel R_{iD}$ .

To be an effective bypass capacitor, the reactance of  $C_3$  must be much smaller than the equivalent resistance at the base or gate terminal of the transistors in Fig. 14.5 with the other capacitors assumed to be infinite, as depicted in Fig. 14.38. The resistances at the base and gate nodes are

$$R_{eq}^{CB} = R_1 \parallel R_2 \parallel [r_\pi + (\beta_o + 1)(R_6 \parallel R_I)] \quad \text{and} \quad R_{eq}^{CG} = R_1 \parallel R_2 \quad (14.114)$$

respectively. The corresponding value of  $C_3$  must satisfy

$$C_3 \gg \frac{1}{\omega R_{eq}^{CB,CB}}$$

## DESIGN CAPACITOR DESIGN FOR THE C-B AND C-G AMPLIFIERS

### EXAMPLE 14.9

This example selects capacitor values for the noninverting amplifiers in Figs. 14.5 and 14.37.

**PROBLEM** Choose values for the coupling and bypass capacitors for the amplifiers in Figs. 14.5 and 14.37 so that the presence of the capacitors can be neglected at a frequency of 1 kHz.

**SOLUTION** **Known Information and Given Data:** Frequency  $f = 1000$  Hz; for the C-B stage from Fig. 14.5 and Table 14.6,  $R_{iE} = 102 \Omega$ ,  $R_{iC} = 3.40 \text{ M}\Omega$ ,  $R_I = 2 \text{ k}\Omega$ ,  $R_1 = 160 \text{ k}\Omega$ ,  $R_2 = 300 \text{ k}\Omega$ ,  $R_C = 22 \text{ k}\Omega$ , and  $R_6 = 13 \text{ k}\Omega$ ; for the C-G amplifier,  $R_{iS} = 2.04 \text{ k}\Omega$ ,  $R_{iD} = 411 \text{ k}\Omega$ ,  $R_I = 2 \text{ k}\Omega$ ,  $\Omega$ ,  $R_1 = 1.5 \text{ M}\Omega$ ,  $R_2 = 2.2 \text{ M}\Omega$ ,  $R_6 = 12 \text{ k}\Omega$ , and  $R_D = 22 \text{ k}\Omega$

**Unknowns:** Values of capacitors  $C_1$ ,  $C_2$ , and  $C_3$

**Approach:** Substitute known values in Eqs. (14.112) through (14.114). Choose the nearest values from the capacitor table in Appendix A.

**Assumptions:** Small-signal operating conditions are valid.

**Analysis:** For the common-base amplifier,

$$R_{\text{in}} = R_6 \parallel R_{iE} = 13 \text{ k}\Omega \parallel 102 \Omega = 100 \Omega$$

$$C_1 \gg \frac{1}{\omega(R_I + R_{\text{in}})} = \frac{1}{2000\pi(2 \text{ k}\Omega + 100 \Omega)} = 75.8 \text{ nF} \rightarrow C_1 = 0.82 \mu\text{F}^{10}$$

$$R_{\text{out}} = R_C \parallel R_{iC} = 22 \text{ k}\Omega \parallel 3.40 \text{ M}\Omega = 21.9 \text{ k}\Omega$$

$$C_2 \gg \frac{1}{\omega(R_{\text{out}} + R_3)} = \frac{1}{2000\pi(21.9 \text{ k}\Omega + 100 \text{ k}\Omega)} = 1.31 \text{ nF} \rightarrow C_2 = 0.015 \mu\text{F} \quad (15 \text{ nF})$$

$$C_3 \gg \frac{1}{\omega(R_1 \parallel R_2 \parallel [r_\pi + (\beta_o + 1)(R_6 \parallel R_I)])}$$

$$= \frac{1}{2000\pi(160 \text{ k}\Omega \parallel 300 \text{ k}\Omega \parallel [10.2 \text{ k}\Omega + (101)(13 \text{ k}\Omega \parallel 2 \text{ k}\Omega)])}$$

$$= 2.38 \text{ nF} \rightarrow C_3 = 0.027 \mu\text{F}$$

and for the common-gate stage,

$$R_{\text{in}} = R_6 \parallel R_{iS} = 12 \text{ k}\Omega \parallel 2.04 \Omega = 1.74 \text{ k}\Omega$$

$$C_1 \gg \frac{1}{\omega(R_I + R_{\text{in}})} = \frac{1}{2000\pi(2 \text{ k}\Omega + 1.74 \text{ k}\Omega)} = 42.6 \text{ nF} \rightarrow C_1 = 0.42 \mu\text{F}$$

$$R_{\text{out}} = R_6 \parallel R_{iD} = 22 \text{ k}\Omega \parallel 411 \text{ k}\Omega = 20.9 \text{ k}\Omega$$

$$C_2 \gg \frac{1}{\omega(R_{\text{out}} + R_3)} = \frac{1}{2000\pi(20.9 \text{ k}\Omega + 100 \text{ k}\Omega)} = 1.31 \text{ nF} \rightarrow C_2 = 0.015 \mu\text{F} \quad (15 \text{ nF})$$

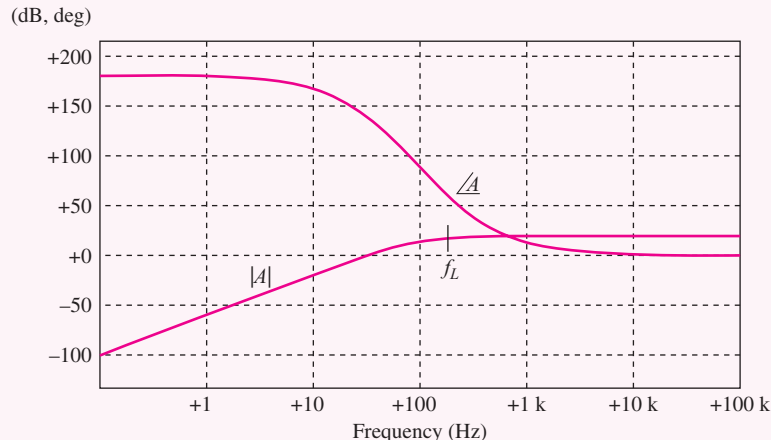
$$C_3 \gg \frac{1}{\omega(R_1 \parallel R_2)} = \frac{1}{2000\pi(1.5 \text{ M}\Omega \parallel 2.2 \text{ M}\Omega)} = 178 \text{ pF} \rightarrow C_3 = 1800 \text{ pF}$$

**Check of Results:** A double check of the calculations indicates they are correct. This is a good place to check the analysis with simulation.

**Discussion:** We have chosen each capacitor to have negligible reactance at the frequency of 1 kHz and expect the lower cutoff frequency of the amplifier to be well below this frequency. The choice of frequency in this example was arbitrary and depends upon the lowest frequency of interest in the application.

 **Computer-Aided Analysis:** The graph below shows SPICE simulation results for the common-base amplifier with the capacitors as just designed. The midband gain is 18.5 dB (8.41) and the lower cutoff frequency is 174 Hz. Note the two-pole roll-off at low frequencies indicated by the 40-dB/decade slope in the magnitude characteristic. Here again, since a dc signal cannot pass through capacitor  $C_1$  or  $C_2$ , the amplifier transfer function exhibits a double zero at the origin.

<sup>10</sup>  $C_1 = 10(75.8 \text{ nF})$  is used to satisfy the inequality.



Common-base amplifier frequency response.

**EXERCISE:** Recalculate the capacitor values for the two amplifiers in Design Ex. 14.9 if the frequency is 250 Hz and the values of  $R_L$  and  $R_3$  are changed to 1 k $\Omega$  and 82 k $\Omega$ , respectively.

**ANSWERS:** 0.579  $\mu\text{F} \rightarrow 6.8 \mu\text{F}$ , 6.13 nF  $\rightarrow 0.068 \mu\text{F}$ , 12.2 nF  $\rightarrow 0.12 \mu\text{F}$ ; 0.232  $\mu\text{F} \rightarrow 2.2 \mu\text{F}$ , 6.19 nF  $\rightarrow 0.068 \mu\text{F}$ , 714 pF  $\rightarrow 8200 \text{ pF}$

**EXERCISE:** Use SPICE to simulate the frequency response of the common-gate amplifier and find the midband gain and lower cutoff frequency.

**ANSWERS:** 12.2 dB, 156 Hz

#### 14.7.4 SETTING LOWER CUTOFF FREQUENCY $f_L$

In the previous sections, we have designed the coupling and bypass capacitors to have a negligible effect on the circuit at some particular frequency in the midband range of the amplifier. An alternative is to choose the capacitor values to set the lower cutoff frequency of the amplifier where we want it to be. Referring back to the high-pass filter analysis in Sec. 10.10.3, we see that the pole associated with the capacitor occurs at the frequency for which the capacitive reactance is equal to the resistance that appears at the capacitor terminals.

##### Multiple Poles and Bandwidth Shrinkage

In the circuits we have considered, there are several poles, and a bandwidth shrinkage occurs at low frequencies in a manner similar to that which was presented in Table 12.2 for high frequencies. A transfer function which exhibits  $n$  identical poles at a low frequency  $\omega_o$  can be written as

$$T(s) = A_{\text{mid}} \frac{s^n}{(s + \omega_o)^n} \quad (14.115)$$

$$|T(j\omega)| = A_{\text{mid}} \frac{\omega^n}{(\sqrt{\omega^2 + \omega_o^2})^n} \quad (14.116)$$

$$|T(j\omega_L)| = \frac{A_{\text{mid}}}{\sqrt{2}} \rightarrow \omega_L = \frac{\omega_o}{\sqrt{2^{1/n} - 1}} \quad \text{or} \quad f_L = \frac{f_o}{\sqrt{2^{1/n} - 1}} \quad (14.117)$$

**TABLE 14.13**

**Bandwidth Shrinkage at Low Frequencies**

<i>n</i>	$f_L/f_0$
1	1
2	1.55
3	1.96
4	2.30
5	2.59

The factor in the denominator of Eq. (14.117) is less than 1, so that the lower cutoff frequency is higher than the frequency corresponding to the individual poles. Table 14.13 gives the relationship between  $\omega_o$  and  $\omega_L$  for various values of *n*.

In Design Exs. 14.7, 14.8, and 14.9, we have effectively located three poles of each amplifier at a frequency of 1/10 of the midband frequency specified in the problem. For three identical poles,  $f_L = 1.96f_0$ . In Design Ex. 14.7, the three poles were placed at a frequency of approximately 100 Hz (1000 Hz/10), which should yield a cutoff of 196 Hz based on the numbers in Table 14.13. The simulation results yielded  $f_L = 195$  Hz. In Design Ex. 14.9, the poles were also placed at a frequency of approximately 100 Hz, which should yield a cutoff of 196 Hz. The simulation results yielded a slightly smaller value of  $f_L$ , 174 Hz.

The situation in Design Ex. 14.8 is slightly different. With capacitor  $C_3$  eliminated from the circuit, the C-C and C-D amplifiers exhibit two poles at low frequencies. In this example, the two poles are at 200 Hz, which should yield a cutoff frequency of 310 Hz, and the simulation results agree with  $f_L = 310$  Hz.

### Setting $f_L$ with a Dominant Pole

It is often easy and preferable to have the pole associated with just one of the capacitors determine the lower cutoff frequency, rather than have  $f_L$  set by the interaction of several poles. In this case, we set  $f_L$  with one of the capacitors, and then choose the other capacitors to have their pole frequencies much below  $f_L$ . This is referred to as a dominant pole design. In Design Exs. 14.7, 14.8, and 14.9, we see that the capacitor associated with the emitter or source portion of the circuit tends to be the largest ( $C_3$  in Fig. 14.35,  $C_2$  in Fig. 14.36, and  $C_1$  in Fig. 14.37) because of the low resistance presented by the emitter or source terminal of the transistor. It is common to use these capacitors to set  $f_L$ , and then increase the value of the other capacitors by a factor of 10 to push their corresponding poles to much lower frequencies.

For the C-E stage in Design Ex. 14.7, we could set  $f_L = 1000$  Hz by choosing  $C_3 = 0.067 \mu\text{F}$  and leaving  $C_1 = 0.02 \mu\text{F}$  and  $C_2 = 0.015 \mu\text{F}$ . In the C-D amplifier in Fig. 14.36(b), using  $C_2 = 780 \text{ pF}$  with  $C_1 = 1000 \text{ pF}$  sets the lower cutoff frequency to 2000 Hz. Finally, for the C-B amplifier in Design Ex. 14.9, choosing  $C_1 = 0.082 \mu\text{F}$ ,  $C_2 = 0.027 \mu\text{F}$ , and  $C_3 = 0.015 \mu\text{F}$  should set the cutoff frequency to approximately 1000 Hz.

**EXERCISE:** Use SPICE to find the values of  $f_L$  for the three designs presented in the preceding paragraph.

**ANSWERS:** C-E: 960 Hz; C-D: 2.04 kHz; C-B: 960 Hz

**EXERCISE:** (a) What value of capacitor  $C_3$  should be used to set  $f_L$  to 1 kHz in the C-S amplifier in Design Ex. 14.7? (b) What value of capacitor  $C_2$  should be used to set  $f_L$  to 2 kHz in the C-C amplifier in Design Ex. 14.8? (c) What value of capacitor  $C_1$  should be used to set  $f_L$  to 1 kHz in the C-G amplifier in Design Ex. 14.9?

**ANSWERS:** (a) 0.056  $\mu\text{F}$ ; (b) 820 pF; (c) 0.042  $\mu\text{F}$

## 14.8 AMPLIFIER DESIGN EXAMPLES

Now that we have become “experts” in the characteristics of single-transistor amplifiers, we will use this knowledge to tackle several amplifier design problems. We should emphasize that no “cookbook” exists for design. Every design is a new, creative experience. Each design has its own unique set of constraints, and there may be more than one way to achieve the desired results. The examples presented here further illustrate the approach to design; they also underscore the interaction between the designer’s choice of Q-point and the small-signal properties of the amplifiers.

## DESIGN A FOLLOWER DESIGN

### EXAMPLE 14.10

In this example, we will design a follower to meet a set of specifications.

**PROBLEM** Design an amplifier with a mid-band input resistance of at least  $20 \text{ M}\Omega$  and a gain of at least 0.95 when driving an external load of at least  $3 \text{ k}\Omega$ . Any capacitors present should not affect the performance of the circuit at frequencies above 50 Hz.

**SOLUTION Known Information and Given Data:**  $A_v \geq 0.95$ ,  $R_{in} \geq 20 \text{ M}\Omega$ ,  $R_{out} \ll 3 \text{ k}\Omega$ .

**Unknowns:** The circuit topology must be chosen, the Q-point must be selected, and the circuit element values must all be determined. The transistor parameters are unknown.

**Approach:** The gain is approximately one, a high input resistance is required, and the relatively small load resistance will require the amplifier to have a low output resistance. All three of these specifications lead us to consider a voltage follower. We must choose between the emitter-follower (C-C) and source-follower (C-D) configurations and then select the circuit values to meet the design specifications.

**Assumptions:** The transistors are operating in the active region. Small-signal operating conditions are satisfied,  $V_T = 25 \text{ mV}$ .

**Analysis:** Reviewing Tables 14.10 and 14.12, we find that the input resistance of the C-D amplifier prototype is infinite, whereas that of the C-C amplifier is limited to  $\beta_o R_L$ . For a load resistance of  $3 \text{ k}\Omega$ , a current gain  $\beta_o$  in excess of 6600 is required to meet the input-resistance specification. This current gain is beyond the range of normal bipolar transistors, so here we rule out the C-C amplifier. (However, be sure to watch for the Darlington circuit in Prob. 15.56.)

Figure 14.39 represents a basic source-follower circuit. In this amplifier, we recognize that  $R_{in}$  is set simply by the value of  $R_G$ , and we can pick  $R_G = 22 \text{ M}\Omega$  ( $\pm 5$  percent) to meet the specification. The 22-M $\Omega$  value ensures that the design specifications are met when the effect of the tolerance is included.

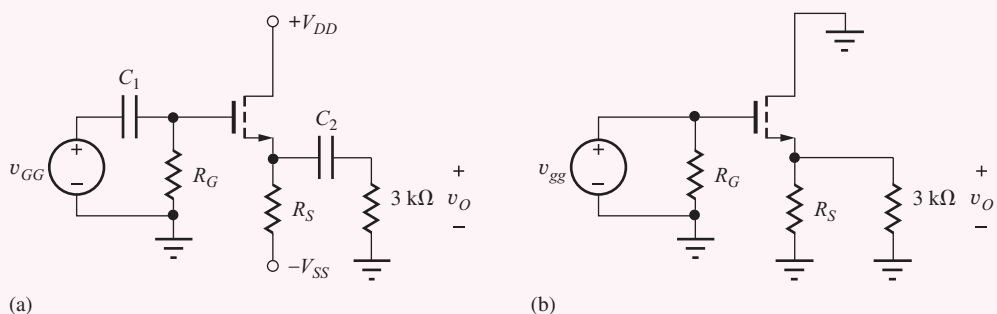


Figure 14.39 (a) Common-drain amplifier and (b) ac equivalent circuit.

The choices of source resistor  $R_S$  and power supply voltages are related to the voltage gain requirement:

$$\frac{g_m R_L}{1 + g_m R_L} \geq 0.95 \quad \text{or} \quad g_m R_L \geq 19 \quad \text{and} \quad R_L = R_S \| 3 \text{ k}\Omega \quad (14.118)$$

The  $g_m R_L$  product can be related to the drain current and device parameter  $K_n$  by using  $g_m \cong \sqrt{2K_n I_D}$ , and from Eq. (14.118),

$$\sqrt{2K_n I_D} R_L \geq 19 \quad \text{or} \quad \sqrt{K_n I_D} \geq \frac{19}{\sqrt{2} R_L} \quad (14.119)$$

**TABLE 14.14**  
Possible Solutions to Eq. (14.120)

$I_D$ (mA)	$K_n$ (mA/V <sup>2</sup> )	$(V_{GS} - V_{TN})$ (V)	$V_{SS}$ (V)
3	10	0.78	$9.8 + V_{TN}$
5	10	1	$16 + V_{TN}$
8	10	1.27	$25.3 + V_{TN}$
5	20	0.71	$16.7 + V_{TN}$

In Fig. 14.39(b), the equivalent load resistor  $R_L = R_S \parallel 3 \text{ k}\Omega \leq 3 \text{ k}\Omega$ . As is often the case in design, one equation—here, Eq. (14.119)—contains more than one unknown. We must make a design decision. Let us choose  $R_L \geq 1.5 \text{ k}\Omega$  (that is,  $R_S \geq 3 \text{ k}\Omega$ ). Substituting this value into Eq. (14.119) yields

$$\sqrt{K_n I_D} \geq \frac{19/\sqrt{2}}{1.5 \text{ k}\Omega} = 8.96 \text{ mA} \quad (14.120)$$

Equation (14.120) indicates that the geometric mean of  $K_n$  and  $I_D$  must be at least 9 mA.

We can now attempt to select an FET and Q-point current. Here again, Eq. (14.120) contains two unknowns. We must make another design decision. Table 14.14 presents some possible solution pairs for Eq. (14.121), as well as their impact on the values of  $(V_{GS} - V_{TN})$  and negative supply voltage  $V_{SS}$  since

$$I_D = \frac{K_n}{2} (V_{GS} - V_{TN})^2 \quad (14.121)$$

and

$$V_{SS} = I_D R_S + V_{GS} \quad (14.122)$$

based on analysis of the dc equivalent circuit in Fig. 14.40 (remember  $I_G = 0$ ). The choice of  $I_D = 5 \text{ mA}$  with  $K_n = 20 \text{ mA/V}^2$  seems to be reasonable, although the power supply voltage might be too large for some applications.

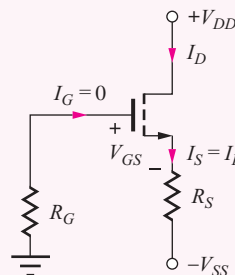


**Figure 14.40** dc Equivalent circuit for the C-D amplifier.

Let us assume we have looked through our device catalogs and found a MOSFET with  $V_{TN} = 1.5 \text{ V}$  and  $K_n = 20 \text{ mA/V}^2$ . Evaluating Eq. (14.121) for this FET gives

$$V_{GS} = V_{TN} + \sqrt{\frac{2I_D}{K_n}} = 1.5 + \sqrt{\frac{2(0.005)}{0.02}} = 2.21 \text{ V} \quad (14.123)$$

Now we are finally in a position to find  $R_S$  using Eq. (14.123).

$$R_S = \frac{V_{SS} - V_{GS}}{I_D} = \frac{V_{SS} - 2.21}{0.005} \quad (14.124)$$

**TABLE 14.15**  
Possible Solutions to Eq. (14.96)

$V_{SS}$	$R_S$
10 V	1.56 k $\Omega$
15 V	2.56 k $\Omega$
20 V	3.56 k $\Omega$
25 V	4.56 k $\Omega$

Values have been selected for  $V_{GS}$  and  $I_D$  but not for  $V_{SS}$ , and Eq. (14.124) is another equation with two unknowns. (The value in Table 14.14 represented only a lower bound.) Table 14.15 presents several possible solution pairs from which to make our design selection. Earlier in the design discussion, we assumed that  $R_S \geq 3 \text{ k}\Omega$ , so one acceptable choice is  $V_{SS} = 20 \text{ V}$  and  $R_S = 3.56 \text{ k}\Omega$ .

Our final design decision is the choice of  $V_{DD}$ , which must be large enough to ensure that the MOSFET operates in the active region under all signal conditions:

$$v_{DS} \geq v_{GS} - V_{TN} \quad (14.125)$$

and

$$v_{DS} = v_D - v_S = V_{DD} + V_{GS} - v_s \quad (14.126)$$

for  $v_S = V_S + v_s$  and  $V_S = -V_{GS}$ . Combining Eqs. (14.125) and (14.126) yields

$$V_{DD} + V_{GS} - v_S \geq V_{GS} - V_{TN} \quad \text{or} \quad V_{DD} \geq v_{gg} - V_{TN} = v_{gg} - 1.5 \text{ V} \quad (14.127)$$

The largest amplitude signal  $v_{gg}$  at the source that satisfies the small-signal requirements is

$$|v_{gg}| \leq 0.2(V_{GS} - V_{TN})(1 + g_m R_L) \frac{g_m R_L}{1 + g_m R_L} \leq 0.2(0.71)(19) = 2.70 \text{ V} \quad (14.128)$$

Thus, if we choose a  $V_{DD}$  of at least 1.2 V, then the MOSFET remains saturated for all signals that satisfy the small-signal criteria.

The final step in this design is to select values for the coupling capacitors. We desire the impedance of the capacitors at frequencies  $\geq 50 \text{ Hz}$  to be negligible with respect to the resistance that appears at their terminals. The resistance looking to the left from  $C_1$  is zero, and that looking to the right is  $R_{in}^{CD}$ , which is  $22 \text{ M}\Omega$ . Therefore,

$$\frac{1}{2\pi(50 \text{ Hz})C_1} \ll 22 \text{ M}\Omega \quad \text{or} \quad C_1 \gg 145 \text{ pF}$$

For  $C_2$ , the resistance looking back toward the source is

$$R_{out} = R_S \left\| \frac{1}{g_m} = 3.6 \text{ k}\Omega \right\| \frac{1}{\sqrt{2K_n I_D}} = 3.6 \text{ k}\Omega \left\| \frac{1}{\sqrt{2(20 \text{ mS})(5 \text{ mA})}} = 69.4 \text{ }\Omega, \right.$$

and the resistance looking toward the right is  $3 \text{ k}\Omega$ . Therefore,

$$\frac{1}{2\pi(50 \text{ Hz})C_2} \ll 3.069 \text{ k}\Omega \quad \text{or} \quad C_2 \gg 1.04 \text{ }\mu\text{F}$$

Let us choose  $C_1 = 1500 \text{ pF}$  and  $C_2 = 10 \text{ }\mu\text{F}$ , which are standard values that exceed the minimum bound by a factor of approximately 10.

The final design appears in Fig. 14.41, in which the nearest 5 percent values have been used for the resistors and  $V_{DD}$  has been chosen to be a common power supply value of +5 V.

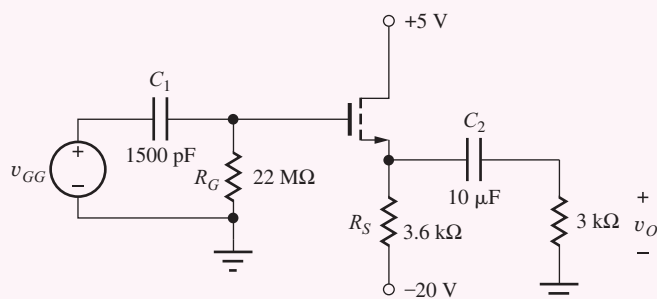
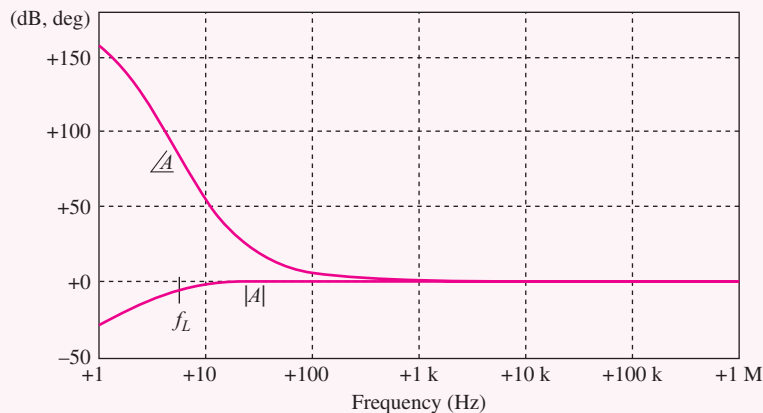


Figure 14.41 Completed source-follower design.

**Check of Results:** To check our design, we should now analyze the circuit and find the actual Q-point, input resistance, and voltage gain. This analysis is left as an exercise. Another approach at this point would be to check the analysis with SPICE.

**Discussion:** In this example, we see that even a problem that appears to be a relatively well specified problem takes considerable effort to achieve a design that meets the requirements and the design required a relatively large value of  $V_{SS}$ . Such is the situation in most real design situations. Most, if not all, real problems will be under-constrained with numerous choices to be made.

**Computer-Aided Analysis:** Simulation of the circuit in SPICE yields these results: Q-point: (4.94 mA, 7.20 V),  $A_v = -0.369$  dB, and  $f_L = 7.8$  Hz. With two poles at 5 Hz, the expected value of  $f_L$  is also 7.8 Hz.



Source follower frequency response.

**EXERCISE:** Find the actual Q-point, input resistance, and voltage gain for the circuit in Fig. 14.41. ( $K_n = 20 \text{ mA/V}^2$ ,  $V_{TN} = 1.5 \text{ V}$ )

**ANSWERS:** (4.94 mA, 7.20 V);  $22 \text{ M}\Omega$ ; +0.959

**EXERCISE:** Find the output resistance of the amplifier in Fig. 14.41. What is the largest value of  $v_{gg}$  that satisfies the small-signal constraints?

**ANSWERS:**  $69.8 \Omega$ ; 3.43 V

**EXERCISE:** Suppose the MOSFET chosen for the circuit in Fig. 14.41 also had  $\lambda = 0.015 \text{ V}^{-1}$ . What are the values of  $r_o$  and the new voltage gain? (Use the Q-point values from Design Ex. 14.10. Does neglecting the output resistance seem a reasonable thing to do?)

**ANSWERS:**  $15.0 \text{ k}\Omega$ , 0.954; yes,  $r_o$  has little effect on the circuit.

**EXERCISE:** An MOS technology has  $K'_n = 50 \mu\text{A/V}^2$ . What is the  $W/L$  ratio required for the NMOS transistor in Design Ex. 14.10?

**ANSWER:** 400/1

**EXERCISE:** (a) Create a Thévenin equivalent circuit for the midband region of the source follower in Fig. 14.41. (b) Use the model to calculate the voltage gain with the  $3\text{-k}\Omega$  load attached to the amplifier.

**ANSWERS:** (a)  $R_{\text{in}} = 22\text{ M}\Omega$ ,  $A = +0.981$ ,  $R_{\text{out}} = 69.4\text{ }\Omega$ ; (b) 0.959

## DESIGN A COMMON-BASE AMPLIFIER

### EXAMPLE 14.11

The requirements of this design problem are even less specific than those in Design Ex. 14.10. A common-base amplifier will be found to be the most appropriate choice to meet the given design specifications.

**PROBLEM** Design an amplifier to match a  $75\text{-}\Omega$  source resistance (for example, a coaxial transmission line) and to provide a voltage gain of 34 dB. Design the capacitors to have negligible impact on the circuit for RF frequencies above 500 kHz.

**SOLUTION** **Known Information and Given Data:** Amplifier input resistance =  $75\ \Omega$ ; voltage gain = 50 (34 dB); capacitors should be negligible at a frequency of 500 kHz; source resistance =  $75\ \Omega$ .

**Unknowns:** Amplifier topology; Q-point; circuit element values; transistor parameters

**Approach:** Use overall specifications to guide choice of circuit topology and transistor type; then choose circuit element values to meet numeric requirements

**Assumptions:** Active region operation;  $V_{EB} = 0.7\text{ V}$ ; Small-signal conditions apply;  $V_T = 25\text{ mV}$ .

**Analysis:** Our first problem is to select a circuit configuration and transistor type. From the various examples in this and previous chapters, we realize that  $A_v = 50$  (34 dB) is a moderate value of gain. At the same time, the required input resistance of  $75\ \Omega$  is relatively low. Looking through our amplifier comparison charts in Tables 14.9 through 14.12, we find that the common-base and common-gate amplifiers most nearly meet these two requirements: good voltage gain and low input resistance. From past examples, we should recognize that it will probably be easier to achieve a gain of 50 with a BJT than with a FET, particularly since the matched input resistance requirement will increase the amplifier terminal gain requirement by a factor of 2! Thus, the common-base amplifier is the choice that seems to most nearly meet the problem specifications.

For simplicity, let us use the dual supply-bias circuit in Fig. 14.42, which requires only two bias resistors. In addition, to get some practice analyzing circuits using *pnp* devices, we have arbitrarily selected a *pnp* transistor. We happen to have a *pnp* transistor available with  $\beta_F = 80$  and  $V_A = 50\text{ V}$  (e.g., a 2N3906—see MCD Web Resources).

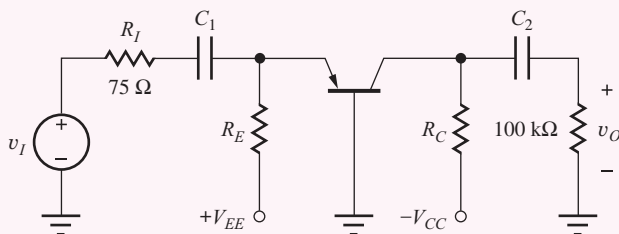


Figure 14.42 Common-base circuit topology.

Next, let us select the power supplies  $V_{CC}$  and  $V_{EE}$ . Remembering our rule-of-thumb from Chapter 13,  $A_v = 10(V_{CC} + V_{EE})$ . The matched input resistance situation causes a factor of two voltage loss between the signal source  $v_i$  and the emitter-base junction. Thus, an overall gain of 50 requires a value of  $g_m R_L = 100$ , and we estimate that a total supply voltage of 10 V is required. Using symmetrical supplies, we have  $V_{CC} = V_{EE} = 5$  V.

Figures 14.43 and 14.44 are the dc and ac equivalent circuits needed to analyze the behavior of the amplifier in Fig. 14.42. Resistor  $R_E$  and the Q-point of the transistor can now be determined from the input resistance requirement. From Fig. 14.44, we recognize that the input resistance of the amplifier is equal to resistor  $R_E$  in parallel with the input resistance at the emitter of the transistor. From Table 14.8,  $R_{iE} = 1/g_m$ :

$$R_{in} = R_E \parallel R_{iE} = R_E \parallel \frac{1}{g_m} \quad (14.129)$$

Expanding Eq. (14.129) and using the expression for  $g_m$  yields

$$R_{in} = \frac{\frac{1}{g_m} R_E}{\frac{1}{g_m} + R_E} = \frac{R_E}{1 + g_m R_E} = \frac{R_E}{1 + 40I_C R_E} \quad (14.130)$$

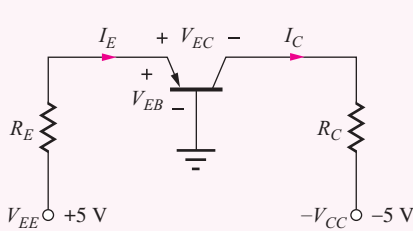


**Figure 14.43** dc Equivalent circuit for common-base amplifier.

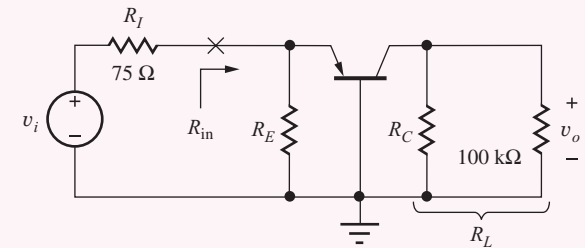


**Figure 14.44** ac Equivalent circuits for the common-base amplifier.

Since  $I_E \cong I_C$ , the  $I_C R_E$  product in Eq. (14.130) represents the dc voltage developed across the resistor  $R_E$ . Here again we see the direct coupling between the small-signal input resistance and the dc Q-point values. From the dc equivalent circuit in Fig. 14.43 and assuming  $V_{EB} = 0.7$  V,

$$I_C R_E \cong I_E R_E = V_{EE} - V_{BE} = 5 - 0.7 = 4.3 \text{ V} \quad (14.131)$$

Combining Eqs. (14.130) and (14.131) with the input resistance specification,

$$75 = \frac{R_E}{1 + 40(4.3)} \quad \text{and} \quad R_E = 13.0 \text{ k}\Omega \quad (14.132)$$

$I_C$  can now be found using Eq. (14.132):

$$I_C \cong I_E = \frac{4.3 \text{ V}}{13 \text{ k}\Omega} = 331 \mu\text{A} \quad (14.133)$$

It is interesting to note that once  $V_{EE}$  was chosen for this circuit,  $R_E$  and  $I_C$  were both indirectly fixed.

The next step in the design is to choose collector resistor  $R_C$ . For the circuit in Fig. 14.44, the gain is

$$A_v^{CB} = g_m R_L \left( \frac{R_{in}}{R_I + R_{in}} \right) \quad (14.134)$$

For our circuit,

$$R_{in} = 75 \Omega \quad g_m = 40I_C = 40(331 \mu A) = 13.2 \text{ mS} \quad (14.135)$$

$$R_L = R_C \parallel 100 \text{ k}\Omega$$

Solving for  $R_L$  in Eq. (14.134) yields

$$50 = (13.2 \text{ mS}) R_L \left( \frac{75}{75 + 75} \right) \quad \text{and} \quad R_L = 7.58 \text{ k}\Omega \quad (14.136)$$

Since  $R_L = R_C \parallel 100 \text{ k}\Omega$ ,  $R_C = 8.20 \text{ k}\Omega$ .

The next step is to finish checking the Q-point of the transistor by calculating  $V_{EC}$ . Using the circuit in Fig. 14.43,

$$V_{EB} = V_{EC} + I_C R_C - 5 \quad (14.137)$$

and solving for  $V_{EC}$  yields

$$V_{EC} = 5 + V_{EB} - I_C R_C = 5 + 0.7 - (331 \mu A)(8.20 \text{ k}\Omega) = 2.99 \text{ V} \quad (14.138)$$

$V_{EC}$  is positive and greater than 0.7 V, so the *pnp* transistor is operating in the active region, as required.

The final step in this design is to select values for the coupling capacitors. We desire the impedance of the capacitors for frequencies of 500 kHz and above to be negligible with respect to the resistance that appears at their terminals. The resistance looking to the left from  $C_1$  is  $75 \Omega$ , and the resistance looking to the right is  $R_{in}$ , which is also  $75 \Omega$ . Therefore,

$$\frac{1}{2\pi(500 \text{ kHz})C_1} \ll 150 \Omega \quad \text{or} \quad C_1 \gg 2.12 \text{ nF}$$

For  $C_2$ , the resistance looking back toward the collector is at most  $8.2 \text{ k}\Omega$ , and the resistance looking toward the right is  $100 \text{ k}\Omega$ . Therefore,

$$\frac{1}{2\pi(500 \text{ kHz})C_2} \ll 108 \text{ k}\Omega \quad \text{or} \quad C_2 \gg 2.95 \text{ pF}$$

Let us choose  $C_1 = 0.022 \mu F$  and  $C_2 = 33 \text{ pF}$ , which are standard values that are larger than the calculated values by a factor of at least 10.

The completed design is shown in Fig. 14.45, in which the nearest 5 percent values have been used for the resistors. This amplifier provides a gain of approximately 50 and an input resistance of approximately  $75 \Omega$ .

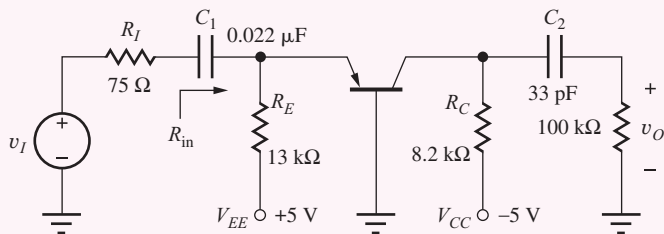


Figure 14.45 Final design for amplifier with  $R_{in} = 75 \Omega$  and  $A_v = 50$ .

One serious limitation of this amplifier design is its signal-handling ability. Only 5 mV can appear across the emitter-base junction, which sets a limit on the signal  $v_i$ :

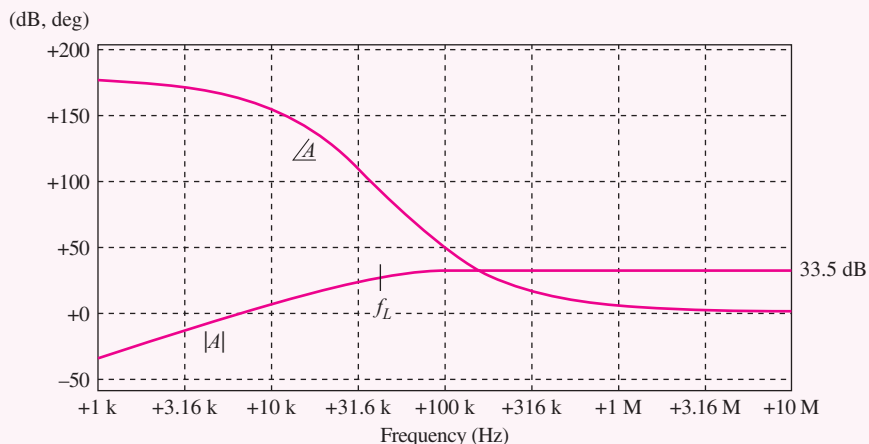
$$v_{eb} = v_i \frac{R_{in}}{R_I + R_{in}} = v_i \frac{75 \Omega}{75 \Omega + 75 \Omega} = \frac{v_i}{2} \quad (14.139)$$

Thus, for small-signal operation to be valid, the magnitude of the input signal  $v_i$  must not exceed 10 mV.

**Check of Results:** At this point, an excellent way to check the design is to simulate the circuit in SPICE, which yields a Q-point of (323  $\mu$ A, 3.09 V). The frequency response results appear in the figure here.

**Discussion:** In this design, we were lucky that we remembered to account for the factor of 2 loss in Eq. (14.139) due to the matched resistance condition at the input. Otherwise, our initial choice of power supplies might not have been sufficient to meet the gain specification, and a second design iteration could have been required. The signal handling capability of this stage is small. If an FET were used in place of the bipolar transistor, a much higher input range could be achieved.

**Computer-Aided Analysis:** The frequency response generated by SPICE with  $v_I$  as the input appears below. The simulation parameters are FSTART = 1000 Hz and FSTOP = 10 MHz with 10 frequency points per decade. The midband voltage gain is found to be 33.5 dB, and  $f_L = 72$  kHz.



Common-base amplifier frequency response.

**EXERCISE:** Draw the *npn* version of the circuit in Fig. 14.45. Use the same circuit element values but change polarities as needed.

**EXERCISE:** What are the actual values of input resistance and gain for the amplifier in Fig. 14.45?

**ANSWERS:** 73.4  $\Omega$ , +50.4

**EXERCISE:** What is the largest sinusoidal signal voltage that can appear at the output of the amplifier in Fig. 14.45? What is the largest output signal consistent with the requirements for small-signal operation?

**ANSWERS:**  $(2.90 \text{ V} - V_{EB}) \cong 2.20 \text{ V}$ , 0.490 V

**EXERCISE:** Suppose that both  $V_{EE}$  and  $V_{CC}$  were changed to 7.5 V. What are the new values of  $I_C$ ,  $V_{EC}$ ,  $R_E$ , and  $R_C$  required to meet the same specifications?

**ANSWERS:** 327  $\mu$ A, 4.10 V, 20.8 k $\Omega$ , 8.27 k $\Omega$

**EXERCISE:** Suppose the resistors and power supplies in the circuit in Fig. 14.45 all have 5 percent tolerances. Will the BJT remain in the active region in the worst-case situation? Repeat for tolerances of 10 percent. Do the values of current gain  $\beta_F$  or  $V_A$  have any significant effect on the design? Discuss.

**ANSWERS:** Yes; yes; no, not unless they become very small.

**EXERCISE:** (a) Create a Thévenin equivalent circuit for the midband region of the common-base amplifier in Fig. 14.45. (b) Use the model to calculate the voltage gain with the 100-k $\Omega$  load attached to the amplifier.

**ANSWERS:** (a)  $v_{th} = 54.1 v_i$ ,  $R_{th} = 8200 \Omega$ ; (b) +49.8

### 14.8.1 MONTE CARLO EVALUATION OF THE COMMON-BASE AMPLIFIER DESIGN

Before going on to the next design example, we carry out a statistical evaluation of the common-base design to see if it is a viable design for the mass production of large numbers of amplifiers. We use a spreadsheet analysis here, although we could easily evaluate the same equation set using a simple computer program written in any high-level language or using the Monte Carlo option in some circuit simulation programs.

To perform a Monte Carlo analysis of the circuit in Fig. 14.45, we assign random values to  $V_{CC}$ ,  $V_{EE}$ ,  $R_C$ ,  $R_E$ , and  $\beta_F$ ; we then use these values to determine  $I_C$  and  $V_{EC}$ ,  $R_{in}$ , and  $A_v$ . Referring back to Eq. (1.45) in Chapter 1, we write each parameter in the form

$$P = P_{nom}(1 + 2\varepsilon(\text{RAND}() - 0.5)) \quad (14.140)$$

where  $P_{nom}$  = nominal value of parameter

$\varepsilon$  = parameter tolerance

$\text{RAND}()$  = random-number generator in spreadsheet

For the design in Fig. 14.45, we assume that the resistors and power supplies have 5 percent tolerances and the current gain has a  $\pm 25$  percent tolerance. As mentioned in Chapter 1 and Ex. 5.13, it is important that each variable invoke a separate evaluation of the random-number generator so that the random values are independent of each other. The random-element values are then used to characterize the Q-point,  $R_{in}$ , and  $A_v$ . The expressions for the Monte Carlo analysis are presented in a logical sequence for evaluation in Eqs. (14.141):

1.  $V_{CC} = 5(1 + 0.1(\text{RAND}() - 0.5))$
2.  $V_{EE} = 5(1 + 0.1(\text{RAND}() - 0.5))$
3.  $R_E = 13,000(1 + 0.1(\text{RAND}() - 0.5))$
4.  $R_C = 8200(1 + 0.1(\text{RAND}() - 0.5))$
5.  $\beta_F = 80(1 + 0.5(\text{RAND}() - 0.5))$
6.  $I_C = \frac{V_{EE} - 0.7}{R_E}$
7.  $V_{EC} = 0.7 + V_{CC} - I_C R_C$
8.  $g_m = 40I_C$
9.  $R_{in} = R_E \parallel \frac{\alpha_o}{g_m}$
10.  $A_v = g_m R_L \frac{R_{in}}{R_I + R_{in}}$  where  $R_L = R_C \parallel 100 \text{ k}\Omega$

Table 14.16 summarizes the results of a 1000-case analysis. The transistor is always in the active region. The mean collector current of 331  $\mu\text{A}$  corresponds closely to the nominal value for the standard 5 percent resistors that were selected for the final circuit. The mean values of  $R_{in}$  and  $A_v$  are 74.3  $\Omega$  and 49.9, respectively, and are also quite close to the design value. The  $3\sigma$  limit

**TABLE 14.16**

Monte Carlo Analysis of the Common-Base Amplifier Design

CASE #	V <sub>CC</sub> (1)	V <sub>EE</sub> (2)	R <sub>E</sub> (3)	R <sub>C</sub> (4)	$\beta_F$ (5)	I <sub>C</sub> (6)	V <sub>EC</sub> (7)	g <sub>m</sub> (8)	R <sub>in</sub> (9)	A <sub>v</sub> (10)
1	4.932	5.090	13602	8461	96.02	3.23E-04	2.902	1.29E-02	76.2	50.8
2	4.951	5.209	12844	8208	93.01	3.51E-04	2.769	1.40E-02	70.1	51.4
3	4.844	4.759	13418	8440	98.33	3.03E-04	2.990	1.21E-02	81.3	49.0
4	4.787	5.162	13193	8294	72.82	3.38E-04	2.682	1.35E-02	72.5	50.9
5	5.073	5.181	12358	8542	79.30	3.63E-04	2.676	1.45E-02	67.7	54.2
:										
996	4.863	5.058	12453	8134	68.56	3.50E-04	2.716	1.40E-02	70.0	50.8
997	5.157	5.016	12945	8225	98.03	3.33E-04	3.115	1.33E-02	73.8	50.3
998	4.932	5.183	12458	8211	78.17	3.60E-04	2.677	1.44E-02	68.2	52.0
999	5.034	4.940	13444	7969	76.71	3.15E-04	3.221	1.26E-02	77.8	47.4
1000	5.119	5.002	12948	7892	95.25	3.32E-04	3.196	1.33E-02	74.0	48.3
Mean	5.006	4.997	12992	8205	79.95	3.31E-04	2.990	1.32E-02	74.29	49.88
std. dev.	0.143	0.146	381	239	11.27	1.44E-05	0.199	5.75E-04	3.22	1.74
min.	4.750	4.751	12351	7792	60.04	2.97E-04	2.409	1.19E-02	66.85	45.36
max.	5.248	5.250	13650	8609	99.98	3.67E-04	3.613	1.47E-02	82.54	54.63

(X) = equation number in Equation Set (14.141).

corresponds to only slightly more than 10 percent deviation from the nominal design specification, and even the worst observed cases of  $R_{in}$  yield acceptable values of SWR (standing wave ratio) on the transmission line that the amplifier was designed to match. Overall, we should be able to mass produce this design and have few problems meeting the specifications.

## DESIGN A COMMON-SOURCE AMPLIFIER

### EXAMPLE 14.12

Let us now try to meet the requirements of the previous design using a C-E/C-S design.

**PROBLEM** Design an amplifier to match a  $75\Omega$  source resistance (for example, a coaxial transmission line) and to provide a voltage gain of 34 dB. Design the capacitors to have negligible impact on the circuit for frequencies above 500 kHz.

**SOLUTION** **Known Information and Given Data:** Amplifier input resistance =  $75\Omega$ ; voltage gain = 50 (34 dB); frequency of application of amplifier is 500 kHz and above; source resistance =  $75\Omega$

**Unknowns:** Amplifier topology; Q-point; circuit element values; transistor parameters

**Approach:** Use overall specifications to guide choice of circuit topology and transistor type; then choose circuit element values to meet numeric requirements. Although the input resistance of the C-E and C-S amplifiers is usually considered in the moderate to high range, we can always limit it by reducing the size of the resistors in the bias network. For example, consider the common-source amplifier in Fig. 14.46. If the gate-bias resistor  $R_G$  is reduced to  $75\Omega$ , then the input resistance of the amplifier will also be  $75\Omega$ . (This design technique is sometimes referred to as **swamping** of the impedance level.) A BJT could also be used, but a depletion-mode MOSFET<sup>11</sup> has been chosen because it offers the potential of a higher signal-handling capability and simple bias circuit design.

**Assumptions:** The transistor is in the active region. Small-signal conditions apply.

<sup>11</sup> This would also be a good place to use a JFET.

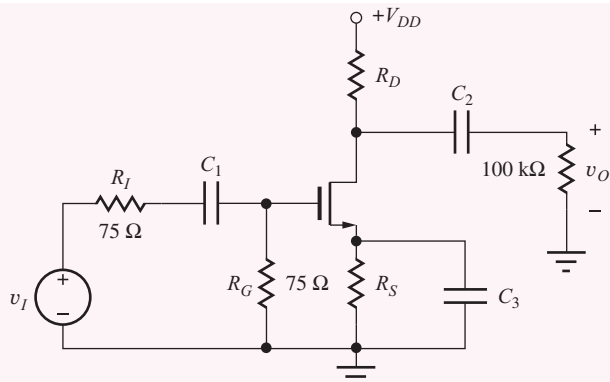


Figure 14.46 Common-source amplifier.

**Analysis:** If resistor  $R_S$  is bypassed, this amplifier yields the full gain  $-g_m R_L$ , but the matched input causes a loss of input signal by a factor of 2:

$$v_{gs} = v_i \frac{R_G}{R_I + R_G} = v_i \frac{75 \Omega}{75 \Omega + 75 \Omega} = \frac{v_i}{2} \quad (14.142)$$

Thus, the prototype amplifier must deliver a gain of 100 for the overall amplifier to have a gain of 50. (This was also the case for the C-B amplifier designed in Design Ex. 14.11.) Referring back to Table 14.11 on page 906, we find that our design guide for the voltage gain of the common-source amplifier is

$$A_v = \frac{V_{DD}}{V_{GS} - V_{TN}} \quad (14.143)$$

**TABLE 14.17 Possibilities for  $A_v = 100$**

$V_{DD}$	$V_{GS} - V_{TN}$
20 V	0.2 V
25 V	0.25 V
30 V	0.3 V

Here again we have a single constraint equation with two variables; Table 14.17 presents some possible design choices. Let us choose the 20 V/0.2 V option.

Because  $V_{GS} - V_{TN}$  must be small in order to achieve high gain, a MOSFET with a large  $K_n$  or  $K_p$  must be chosen if  $I_D$  is to be a reasonable current. Let us assume that we have found an *n*-channel depletion-mode MOSFET with  $K_n = 10 \text{ mS/V}$  and  $V_{TN} = -2 \text{ V}$ . With these parameters, the MOSFET drain current will be

$$I_D = \frac{K_n}{2} (V_{GS} - V_{TN})^2 = \frac{0.01}{2} (0.2)^2 = 0.200 \text{ mA} \quad (14.144)$$

With reference to the dc equivalent circuit in Fig 14.47(a), we can now calculate the value of  $R_S$ . Because the gate current is zero for the FET, the voltage developed across  $R_S$  equals  $-V_{GS}$ :

$$R_S = \frac{-V_{GS}}{I_D} = \frac{-(V_{TN} + 0.2 \text{ V})}{0.200 \text{ mA}} = \frac{1.8 \text{ V}}{0.200 \text{ mA}} = 9.00 \text{ k}\Omega \quad (14.145)$$

The gain of the amplifier is

$$A_v = \frac{v_{gs}}{v_i} (-g_m R_L) = -\frac{g_m R_L}{2} \quad \text{where} \quad R_L = R_D \parallel 100 \text{ k}\Omega \quad (14.146)$$

Setting Eq. (14.87) equal to 50 and solving for  $R_L$  yields

$$R_L = \frac{2A_v}{g_m} = \frac{A_v(V_{GS} - V_{TN})}{I_D} = \frac{50(0.2 \text{ V})}{0.2 \text{ mA}} = 50 \text{ k}\Omega \quad (14.147)$$

For  $R_L = 50 \text{ k}\Omega$ ,  $R_D$  must be 100 kΩ.

Now we have encountered a problem. A drain current of 0.2 mA in  $R_D = 100 \text{ k}\Omega$  requires a voltage drop equal to the total power supply voltage of 20 V. Thus, the power supply voltage must be increased. For active region operation,  $V_{DS} \geq V_{GS} - V_{TN}$ , where

$$V_{DS} = V_{DD} - I_D R_D - I_D R_S \quad (14.148)$$

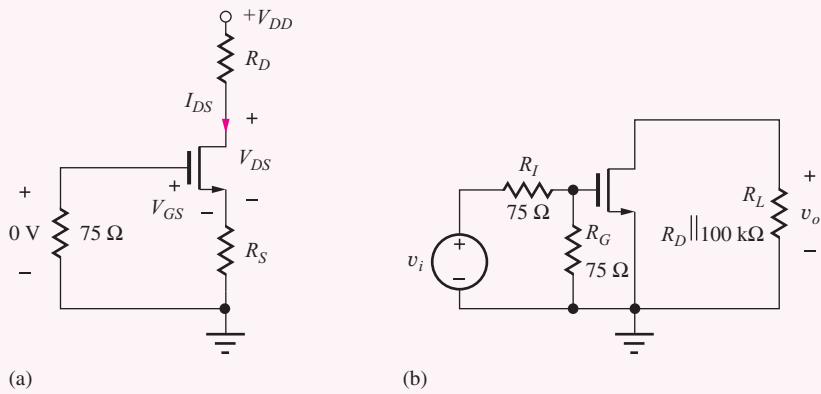


**Figure 14.47** (a) dc and (b) ac equivalent circuits for the common-source amplifier.

Therefore,

$$V_{DD} - 20 - 1.8 \geq (-1.8) - (-2) \quad \text{or} \quad V_{DD} \geq 22 \text{ V} \quad (14.149)$$

is sufficient to ensure pinch-off operation. Let us choose  $V_{DD} = 25 \text{ V}$  to provide additional design margin and room for additional signal voltage swing at the drain.

The final step in this design is to select values for the coupling capacitors. We desire the impedance of the capacitors for frequencies of 500 kHz and above to be negligible with respect to the resistance that appears at their terminals. The resistance looking to the left from  $C_1$  is  $75 \Omega$ , and the input resistance looking to the right is also  $75 \Omega$ . Therefore,

$$\frac{1}{2\pi(500 \text{ kHz})C_1} \ll 150 \Omega \quad \text{or} \quad C_1 \gg 2.12 \text{ nF}$$

For  $C_3$ , the resistance looking back toward the source is  $9.1 \text{ k}\Omega$  in parallel with  $(1/g_m)$  looking into the source of the transistor:

$$R_{eq} = 9.1 \text{ k}\Omega \left\| \frac{1}{g_m} \right\| = 9.1 \text{ k}\Omega \left\| \frac{1}{2 \text{ mS}} \right\| = 474 \Omega$$

Therefore,

$$\frac{1}{2\pi(500 \text{ kHz})C_3} \ll 474 \Omega \quad \text{or} \quad C_3 \gg 644 \text{ pF}$$

For  $C_2$ , the resistance looking back toward the drain is  $100 \text{ k}\Omega$ , and the resistance looking toward the right is also  $100 \text{ k}\Omega$ . Therefore,

$$\frac{1}{2\pi(500 \text{ kHz})C_2} \ll 200 \text{ k}\Omega \quad \text{or} \quad C_2 \gg 1.59 \text{ pF}$$

Let us choose  $C_1 = 0.022 \mu\text{F}$ ,  $C_3 = 0.0068 \mu\text{F}$ , and  $C_2 = 20 \text{ pF}$ , which are standard values that are larger than the calculated values by a factor of approximately 10. The circuit corresponding to the final amplifier design is in Fig. 14.48, where standard 5 percent resistor values have once again been selected.

**Check of Results:** At this point, an excellent way to check the design is to simulate the circuit in SPICE, which yields a Q-point of  $(198 \mu\text{A}, 3.41 \text{ V})$  with a gain of  $33.9 \text{ dB}$  and  $f_L = 91.5 \text{ kHz}$ . The frequency response appears on the next page.

**Discussion:** The designs in Design Exs. 14.11 and 14.12 demonstrate that usually more than one, often very different, design approaches can meet the specifications for a given problem. Choosing one design over another depends on many factors. For example, one criterion could be the use of power supply voltages that are already available in the rest of the system. Total power consumption

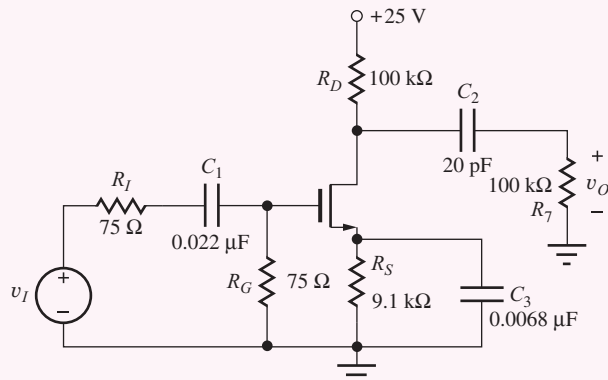
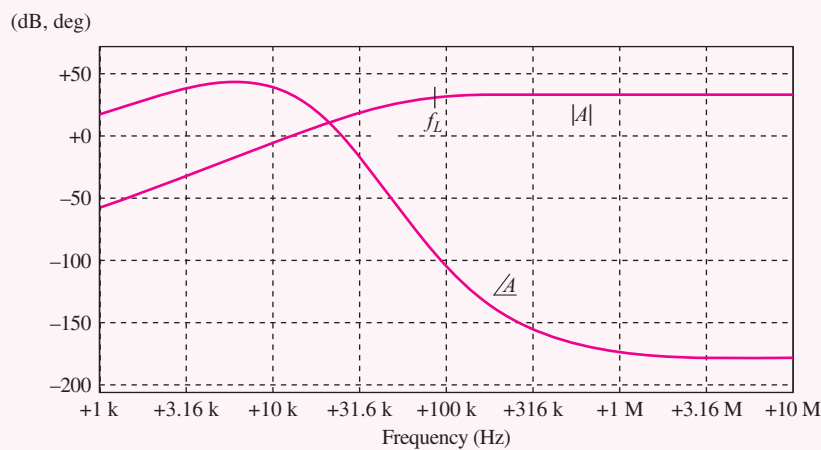


**Figure 14.48** Final common-source amplifier design.

might be an important issue. Our common-base design uses a power of approximately 3.3 mW and uses two power supplies, whereas the common-source design consumes 5 mW from a single 25-V supply. In actuality, the design is somewhat of a struggle using the FET. A large power supply voltage is combined with a FET operating very near cutoff. It may be difficult to find a FET with  $K_n = 10 \text{ mA}$  with  $V_P = -2 \text{ V}$ .

Another important factor could be amplifier cost. The core of the FET amplifier requires three resistors,  $R_D$ ,  $R_G$ , and  $R_S$ ; bypass capacitor  $C_3$ ; and the JFET. The common-base amplifier core requires resistors  $R_E$  and  $R_C$  and the BJT. The cost of the additional parts, plus the expense of inserting them into a printed circuit board (often more expensive than the parts themselves), will probably tilt the economic decision away from the C-S design toward the C-B amplifier. However, the maximum input signal capability of the JFET amplifier,  $|v_i| = 2 \times 0.2(V_{GS} - V_P) = 0.08 \text{ V}$  can be of overriding importance in certain applications. Obviously, the final decision involves many factors.

**Computer-Aided Analysis:** As already noted, the frequency response generated by SPICE with  $v_S$  as the input appears in the graph. The simulation parameters are FSTART = 1000 Hz and FSTOP = 10 MHz with 10 frequency points per decade. The midband voltage gain is 33.9 dB and  $f_L = 91.5 \text{ kHz}$ . Based on Table 14.13, three poles at 50 Hz are expected to produce  $f_L = 97.5 \text{ Hz}$ .



Frequency response of the common-source amplifier.

**EXERCISE:** Verify the results of the SPICE simulation of Design Ex. 14.12. What is the bandwidth predicted using the bandwidth shrinkage factor in Eq. (14.117)?

**ANSWER:** 89 Hz (using the average of the pole frequencies)

**EXERCISE:** Suppose the FET chosen for the circuit in Fig. 14.48 also had  $\lambda = 0.015 \text{ V}^{-1}$ . What are the values of  $r_o$  and the new voltage gain? (Use the Q-point values from the example.) Does neglecting the output resistance seem a reasonable thing to do?

**ANSWERS:** 333 k $\Omega$ , 43.5; No,  $r_o$  is important in this circuit! We will not achieve the desired gain with this FET.

**EXERCISE:** (a) Redesign the circuit using the 25 V/0.25 V case from Table 14.17. Use the same FET device parameters. (b) Verify your design with SPICE.

**ANSWERS:** 5.60 k $\Omega$ , 68 k $\Omega$ ,  $V_{DD} = 25 \text{ V}$ , 0.022  $\mu\text{F}$ , 8200 pF, 20 pF

**EXERCISE:** (a) Create a Thévenin equivalent circuit for the midband region of the common-source amplifier in Fig. 14.48. (b) Use the model to calculate the voltage gain with the 100-k $\Omega$  load attached to the amplifier.

**ANSWERS:** (a)  $v_{th} = 100 v_i$ ,  $R_{th} = 100 \text{ k}\Omega$ ; (b) 50.0

## 14.9 MULTISTAGE ac-COUPLED AMPLIFIERS

In most situations, a single-transistor amplifier cannot meet all the specifications of a given amplifier design. The required voltage gain often exceeds the amplification factor of a single transistor, or the required combination of voltage gain, input resistance, and output resistance cannot be met simultaneously. For example, consider the specifications of a good general purpose operational amplifier having an input resistance exceeding 1 M $\Omega$ , a voltage gain of 100,000, and an output resistance less than a few hundred ohms. It is clear from our investigation of amplifiers in this chapter that these requirements cannot be met with a single-transistor amplifier. A number of stages must be cascaded in order to create an amplifier that can meet all the requirements.

### 14.9.1 A THREE-STAGE ac-COUPLED AMPLIFIER

In this section, we study the three-stage ac-coupled amplifier in Fig. 14.49. Signals are coupled from one stage to the next through the use of coupling capacitors  $C_1$ ,  $C_3$ ,  $C_5$ , and  $C_6$ , whereas the same capacitors provide dc isolation between stages that permits independent design of the bias circuitry of the individual stages.

The function of the various stages can more readily be seen in the midband ac equivalent circuit for this amplifier in Fig. 14.50(a) in which all the capacitors have been replaced with short circuits. MOSFET  $M_1$ , operating in the common-source configuration, provides a high input resistance with modest voltage gain. Bipolar transistor  $Q_2$  in the common-emitter configuration provides a second stage with high voltage gain.  $Q_3$ , an emitter follower, provides a low output resistance and buffers the high-gain stage,  $Q_2$ , from the relatively low load resistance (250  $\Omega$ ). In Fig. 14.50(a), the base bias resistors have been replaced by  $R_{B2} = R_1 \parallel R_2$  and  $R_{B3} = R_3 \parallel R_4$ .

In the amplifier in Fig. 14.49, the input and output of the overall amplifier are ac-coupled through capacitors  $C_1$  and  $C_6$ . Bypass capacitors  $C_2$  and  $C_4$  are used to obtain maximum voltage gain from the two inverting amplifier stages. Interstage coupling capacitors  $C_3$  and  $C_5$  transfer the ac signals between the amplifiers but provide isolation at dc. Thus, the individual Q-points of the transistors are not affected by connecting the stages together. Figure 14.50(b) gives the dc equivalent circuit for the amplifier in which the capacitors have all been removed. The isolation of the three individual transistor amplifier stages is apparent in this figure.

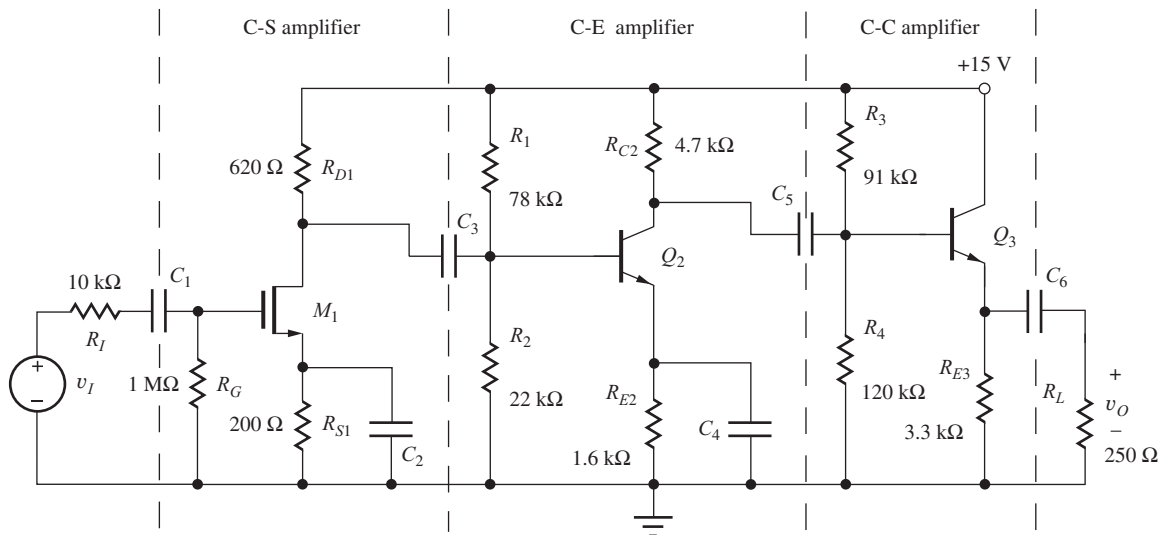


Figure 14.49 Three-stage ac-coupled amplifier.

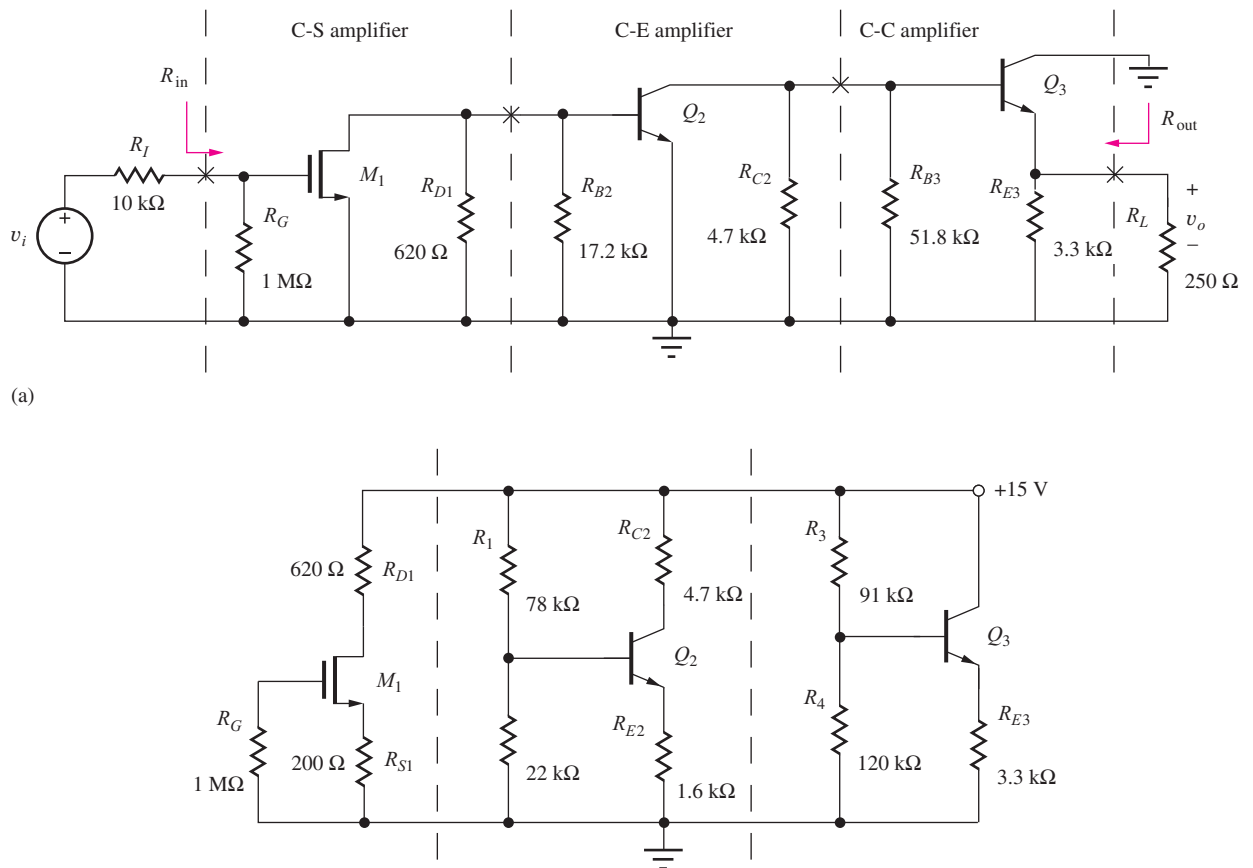


Figure 14.50 (a) Equivalent circuit for ac analysis. (b) dc Equivalent circuit for the three-stage ac-coupled amplifier.

**TABLE 14.18**  
Transistor Parameters for Figs. 14.49–14.54

$M_1$	$K_n = 10 \text{ mA/V}^2$ , $V_{TN} = -2 \text{ V}$ , $\lambda = 0.02 \text{ V}^{-1}$
$Q_2$	$\beta_F = 150$ , $V_A = 80 \text{ V}$ , $V_{BE} = 0.7 \text{ V}$
$Q_3$	$\beta_F = 80$ , $V_A = 60 \text{ V}$ , $V_{BE} = 0.7 \text{ V}$

**TABLE 14.19**  
Q-Points and Small-Signal Parameters for the Transistors in Fig. 14.50

	Q-POINT VALUES	SMALL-SIGNAL PARAMETERS
$M_1$	(5.00 mA, 10.9 V)	$g_{m1} = 10.0 \text{ mS}$ , $r_{o1} = 12.2 \text{ k}\Omega$
$Q_2$	(1.57 mA, 5.09 V)	$g_{m2} = 62.8 \text{ mS}$ , $r_{\pi 2} = 2.39 \text{ k}\Omega$ , $r_{o2} = 54.2 \text{ k}\Omega$
$Q_3$	(1.99 mA, 8.36 V)	$g_{m3} = 79.6 \text{ mS}$ , $r_{\pi 3} = 1.00 \text{ k}\Omega$ , $r_{o3} = 34.4 \text{ k}\Omega$

We want to characterize this amplifier by determining its voltage, input and output resistances, current and power gains, and input signal range using the transistor parameters in Table 14.18. We will also estimate the lower cutoff frequency of the amplifier. First, the Q-points of the three transistors must be found. Each transistor stage in Fig. 14.50 is independently biased, and, for expediency, we assume that the Q-points listed in Table 14.19 have already been found using the dc analysis procedures developed in previous chapters. The details of these dc calculations are left for the next exercise.

**EXERCISE:** Verify the values of the Q-points and small-signal parameters in Table 14.19.

**EXERCISE:** Why can't a single transistor amplifier meet the op amp specifications mentioned in the introduction to this chapter?

### 14.9.2 VOLTAGE GAIN

The ac equivalent circuit for the three-stage amplifier example has been redrawn and is shown in simplified form in Fig. 14.51, in which the three sets of parallel resistors have been combined into the following:  $R_{I1} = 620 \Omega \parallel 17.2 \text{ k}\Omega = 598 \Omega$ ,  $R_{I2} = 4.7 \text{ k}\Omega \parallel 51.8 \text{ k}\Omega = 4.31 \text{ k}\Omega$ , and  $R_{L3} = 3.3 \text{ k}\Omega \parallel 250 \Omega = 232 \Omega$ . The voltage gain of the overall amplifier can be expressed as

$$A_v = \frac{\mathbf{v}_o}{\mathbf{v}_i} = \left( \frac{\mathbf{v}_o}{\mathbf{v}_3} \right) \left( \frac{\mathbf{v}_3}{\mathbf{v}_2} \right) \left( \frac{\mathbf{v}_2}{\mathbf{v}_1} \right) \left( \frac{\mathbf{v}_1}{\mathbf{v}_s} \right) = A_{vt1} A_{vt2} A_{vt3} \left( \frac{\mathbf{v}_1}{\mathbf{v}_i} \right) \quad (14.150)$$

where

$$\frac{\mathbf{v}_1}{\mathbf{v}_i} = \frac{R_{in}}{R_I + R_{in}} = \frac{R_G}{R_I + R_G} \quad (14.151)$$

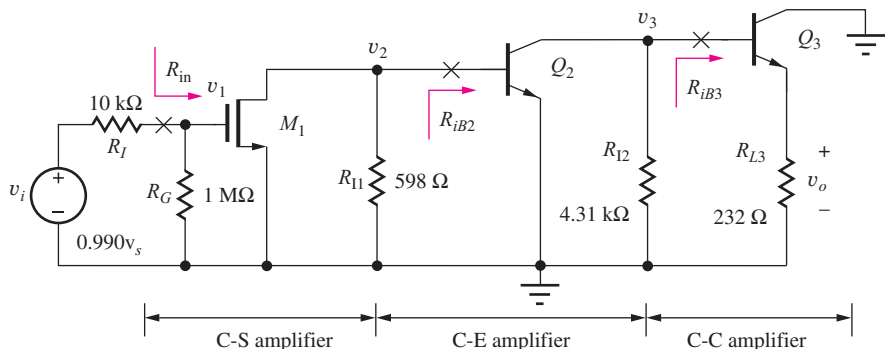
Now it should be more clear why we developed expressions for the terminal gains earlier in this chapter. We see that the overall voltage gain is determined by the product of the individual terminal gains of the three amplifier stages, as well as the signal voltage loss across the source resistance.

We use our knowledge of single-transistor amplifiers, gained in Chapters 13 and 14, to determine expressions for the three voltage gains. The first stage is a common-source amplifier with a terminal gain

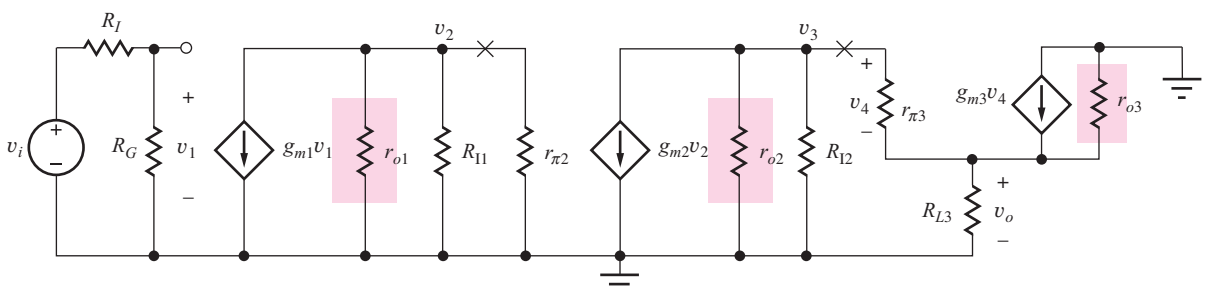
$$A_{vt1} = \frac{\mathbf{v}_2}{\mathbf{v}_1} = -g_{m1} R_{L1} \quad (14.152)$$

in which  $R_{L1}$  represents the total load resistance<sup>12</sup> connected to the drain of  $M_1$ . From the ac circuit in Fig. 14.51(a) and the small-signal version in (b), we can see that  $R_{L1}$  is equal to the parallel

<sup>12</sup> The output resistances  $r_{o1}$ ,  $r_{o2}$ , and  $r_{o3}$  are neglected because each amplifier has an external resistor as a load, and we expect  $|A_v| \ll \mu_f$  for each stage.



(a)



(b)

**Figure 14.51** (a) Simplified ac equivalent circuit for the three-stage amplifier. (b) Small-signal equivalent circuit for the three-stage amplifier. Resistances  $r_{o1}$ ,  $r_{o2}$ , and  $r_{o3}$  are neglected in the calculations.

combination of  $R_{I1}$  and  $R_{IB2}$ , the input resistance at the base of  $Q_2$ . Because  $Q_2$  is a common-emitter stage with zero emitter resistance,  $R_{IB2} = r_{\pi2}$ ,

$$R_{L1} = 598 \Omega \| r_{\pi2} = 598 \Omega \| 2390 \Omega = 478 \Omega \quad (14.153)$$

and the gain of the first stage is

$$A_{vt1} = \frac{v_2}{v_1} = -0.01 \text{ S} \times 478 \Omega = -4.78 \quad (14.154)$$

The terminal gain of the second stage is that of a common-emitter amplifier:

$$A_{vt2} = \frac{v_3}{v_2} = -g_{m2}R_{L2} \quad (14.155)$$

in which  $R_{L2}$  represents the total load resistance connected to the collector of  $Q_2$ . In Fig. 14.51,  $R_{L2}$  is equal to the parallel combination of  $R_{I2}$  and  $R_{IB3}$ , where  $R_{IB3}$  represents the input resistance of  $Q_3$ .  $Q_3$  is an emitter follower with  $R_{IB3} = r_{\pi3}(1 + g_{m3}R_{L3})$ . Thus,  $R_{L2}$  is equal to

$$R_{L2} = R_{I2} \| [r_{\pi3} + (\beta_{o3} + 1)R_{L3}] = 4310 \Omega \| 1000 \Omega [1 + 79.6 \text{ mS}(232 \Omega)] = 3.53 \text{ k}\Omega \quad (14.156)$$

and the gain of the second stage is

$$A_{vt2} = -62.8 \text{ mS} \times 3.53 \text{ k}\Omega = -222 \quad (14.157)$$

Finally, the terminal gain of the emitter follower stage is

$$A_{vt3} = \frac{v_o}{v_3} = \frac{g_{m3}R_{L3}}{1 + g_{m3}R_{L3}} = \frac{(79.6 \text{ mS})(232 \Omega)}{1 + 79.6 \text{ mS}(232) \Omega} = 0.950 \quad (14.158)$$

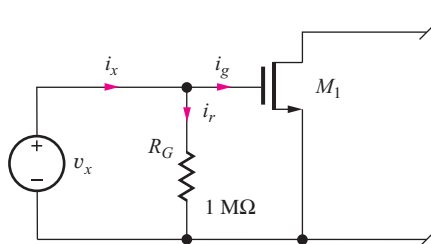


**Figure 14.52** Input resistance of the three-stage amplifier.

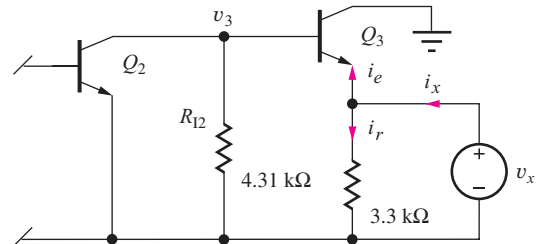


**Figure 14.53** Output resistance of the three-stage amplifier.

Before we can complete the voltage gain calculation in Eq. (14.150), we must find input resistance  $R_{in}$  in order to evaluate the ratio  $v_1/v_i$  given in Eq. (14.151).

### 14.9.3 INPUT RESISTANCE

The input resistance  $R_{in}$  of this amplifier can be determined by referring to Figs. 14.50 through 14.52. Because the current  $i_g$  in Fig. 14.52 is zero, we see that the resistance presented to source  $v_x$  is simply  $R_{in} = R_G = 1 \text{ M}\Omega$ . Note that this result is independent of the circuitry connected to the source or drain of  $M_1$ .

### 14.9.4 SIGNAL SOURCE VOLTAGE GAIN

Substituting the voltage gains and resistance values into Eqs. (14.150) and (14.151) gives the voltage gain for the overall amplifier:

$$A_v = A_{vt1} A_{vt2} A_{vt3} \frac{R_{in}^{CS}}{R_I + R_{in}^{CS}} = (0.95)(-222)(-4.78) \left( \frac{1 \text{ M}\Omega}{10 \text{ k}\Omega + 1 \text{ M}\Omega} \right) = +998 \quad (14.159)$$

We find that the three-stage amplifier circuit realizes a noninverting amplifier with a voltage gain of approximately 60 dB and an input resistance of  $1 \text{ M}\Omega$ . Because of the high input resistance, only a small portion (1 percent) of the input signal is lost across the source resistance.

**EXERCISE:** Recalculate  $A_v$ , including the influence of  $r_{o1}$ ,  $r_{o2}$ , and  $r_{o3}$ .

**ANSWER:** 903 (59.1 dB)

**EXERCISE:** Estimate the gain of the amplifier in Fig. 14.49 using our simple design estimates if  $M_1$  has  $V_{GS} - V_{TN} = 1 \text{ V}$ . What is the origin of the discrepancy?

**ANSWERS:**  $(-15)(-150)(1) = 2250$ ; only 3 V is dropped across  $R_{D1}$ , whereas the estimate assumes  $V_{DD}/2 = 7.5 \text{ V}$ . Taking this difference into account,  $(2250)(3/7.5) = 900$ .

**EXERCISE:** What is the value of  $A_v$  if the interstage resistances  $R_{I1}$  and  $R_{I2}$  could be eliminated (made  $\infty$ )? Would  $r_{o1}$ ,  $r_{o2}$ , and  $r_{o3}$  be required in this case?

**ANSWERS:** 28,200;  $r_{o2}$  would need to be included.

### 14.9.5 OUTPUT RESISTANCE

The output resistance  $R_{out}$  of the amplifier is defined looking back into the amplifier at the position of coupling capacitor  $C_6$ , as indicated in Figs. 14.49 and 14.50. To find  $R_{out}$ , test voltage  $v_x$  is applied to the amplifier output as in Fig. 14.53, and we see that the output resistance of the overall amplifier is determined by the output resistance of the emitter follower in parallel with the  $3300\text{-}\Omega$  resistor.

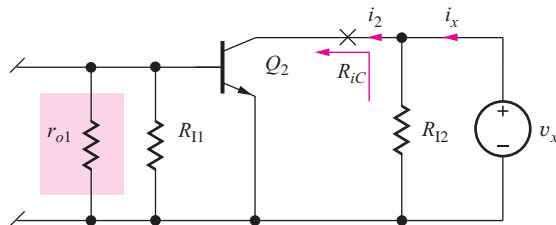


**Figure 14.54** Thévenin equivalent source resistance for stage 3.

Writing this mathematically gives,

$$\mathbf{i}_x = \mathbf{i}_r + \mathbf{i}_e = \frac{\mathbf{v}_x}{3300} + \frac{\mathbf{v}_x}{R_{iE3}} \quad (14.160)$$

Using the results from Table 14.4, we find that the overall output resistance is

$$R_{\text{out}} = \frac{\mathbf{v}_x}{\mathbf{i}_x} = 3300 \parallel R_{iE3} \cong 3300 \left| \left( \frac{1}{g_{m3}} + \frac{R_{\text{th}3}}{\beta_{o3}} \right) \right| \quad (14.161)$$

in which the Thévenin equivalent source resistance of stage 3,  $R_{\text{th}3}$ , must be found.

$R_{\text{th}3}$  can be determined with the aid of Fig. 14.54. The third stage  $Q_3$  is removed, and test voltage  $v_x$  is applied to node  $v_3$ . Current  $i_x$  from the test source  $v_x$  is equal to

$$\mathbf{i}_x = \frac{\mathbf{v}_x}{R_{I2}} + \mathbf{i}_2 = \frac{\mathbf{v}_x}{R_{I2}} + \frac{\mathbf{v}_x}{R_{iC}} \quad \text{or} \quad R_{\text{th}3} = \frac{\mathbf{v}_x}{\mathbf{i}_x} = R_{I2} \parallel R_{iC} = R_{I2} \parallel r_{o2} \quad (14.162)$$

$R_{\text{th}3}$  is equal to the parallel combination of interstage resistance  $R_{I2}$  and the resistance at the collector of  $Q_2$ , which we know is just equal to  $r_{o2}$ :

$$R_{\text{th}3} = 4310 \Omega \parallel 54200 \Omega = 3990 \Omega$$

Evaluating Eq. (14.161) for the output resistance of the overall amplifier yields

$$R_{\text{out}} = 3300 \Omega \left| \left( \frac{1}{0.0796 \text{ S}} + \frac{3990 \Omega}{80} \right) \right| = 62.4 \Omega \quad (14.163)$$

### 14.9.6 CURRENT AND POWER GAIN

The input current delivered to the amplifier from source  $v_i$  in Fig. 14.50 is given by

$$\mathbf{i}_i = \frac{\mathbf{v}_i}{R_I + R_{\text{in}}} = \frac{\mathbf{v}_i}{10^4 + 10^6} = 9.90 \times 10^{-7} \mathbf{v}_i \quad (14.164)$$

and the current delivered to the load from the amplifier is

$$\mathbf{i}_o = \frac{\mathbf{v}_o}{250} = \frac{A_v \mathbf{v}_i}{250} = \frac{998 \mathbf{v}_i}{250} = 3.99 \mathbf{v}_i \quad (14.165)$$

Combining Eqs. (14.164) and (14.165) gives the current gain

$$A_i = \frac{\mathbf{i}_o}{\mathbf{i}_i} = \frac{3.99 \mathbf{v}_i}{9.90 \times 10^{-7} \mathbf{v}_i} = 4.03 \times 10^6 \quad (14.166)$$

Combining Eqs. (14.150) and (14.166) with the power gain expression from Chapter 10 yields a value for overall power gain of the amplifier:

$$A_P = \frac{P_o}{P_s} = \left| \frac{\mathbf{v}_o \mathbf{i}_o}{\mathbf{v}_i \mathbf{i}_i} \right| = |A_v A_i| = 998 \times 4.03 \times 10^6 = 4.02 \times 10^9 \quad (14.167)$$

Because input resistance to the common-source stage is large, only a small input current is required to develop a large output current. Thus, current gain is large. In addition, the voltage gain of the amplifier is significant, and combining a large voltage gain with a large current gain yields a very substantial power gain.

### 14.9.7 INPUT SIGNAL RANGE

Our final step in characterizing this amplifier is to determine the largest input signal that can be applied to the amplifier. In a multistage amplifier, the small-signal assumptions must not be violated anywhere in the amplifier chain. The first stage of the amplifier in Figs. 14.50 and 14.51 is easy to check. Voltage source  $v_1$  appears directly across the gate-source terminals of the MOSFET, and to satisfy the small-signal limit,  $v_1 (= 0.990v_s)$  must satisfy

$$|v_1| \leq 0.2(V_{GS1} - V_{TN}) \quad \text{or} \quad |v_1| \leq \frac{0.2(-1 + 2)}{0.990} = 0.202 \text{ V} \quad (14.168)$$

The first stage limits the input signal to 202 mV.

To satisfy the small-signal requirements, the base-emitter voltage of  $Q_2$  must also be less than 5 mV. In this amplifier,  $v_{be2} = v_2$ , and we have

$$|v_2| = |A_{vt1}v_1| \leq 5 \text{ mV}, \quad |v_1| \leq \frac{5 \text{ mV}}{A_{vt1}} = \frac{0.005}{4.78} = 1.05 \text{ mV} \quad (14.169)$$

and

$$|v_i| \leq \frac{1.05 \text{ mV}}{0.990} = 1.06 \text{ mV}$$

In this design, the small-signal requirements are violated at  $Q_2$  if the amplitude of the input signal  $v_s$  exceeds 1.06 mV.

Finally, using Eq. (14.64) for the emitter-follower output stage (with  $R_{th} = 0$ ),

$$v_{be3} \approx \frac{v_3}{1 + g_m R_{L3}} = \frac{A_{vt1} A_{vt2} v_1}{1 + g_m R_{L3}} = \frac{A_{vt1} A_{vt2} (0.990 v_s)}{1 + g_m R_{L3}} \quad (14.170)$$

and requiring  $|v_{be3}| \leq 5 \text{ mV}$  yields

$$|v_i| \leq \frac{1 + g_m R_{L3}}{A_{vt1} A_{vt2} (0.990)} 0.005 = \frac{1 + 0.0796 \text{ S}(232 \Omega)}{(-4.78)(-222)(0.99)} 0.005 \text{ V} = 92.7 \mu\text{V} \quad (14.171)$$

To satisfy all the small-signal limitations, the maximum amplitude of the input signal to the amplifier must be no greater than the smallest of the three values computed in Eqs. (14.168), (14.169), and (14.171):

$$|v_i| \leq \min(202 \text{ mV}, 1.06 \text{ mV}, 92.7 \mu\text{V}) = 92.7 \mu\text{V} \quad (14.172)$$

In this design, output stage linearity limits the input signal amplitude to less than 93  $\mu\text{V}$ . Note that the maximum output voltage that satisfies the small-signal limit is only

$$|v_o| \leq A_v (92.7 \mu\text{V}) = 998(92.7 \mu\text{V}) = 92.5 \text{ mV} \quad (14.173)$$

### EXAMPLE 14.13 THREE-STAGE AMPLIFIER SIMULATION

Hand analysis of the three-stage amplifier is verified using SPICE simulation.

**PROBLEM** Use SPICE to find the midband voltage gain, input resistance, and output resistance of the amplifier in Fig. 14.49. Confirm the gain with both ac and transient analyses.

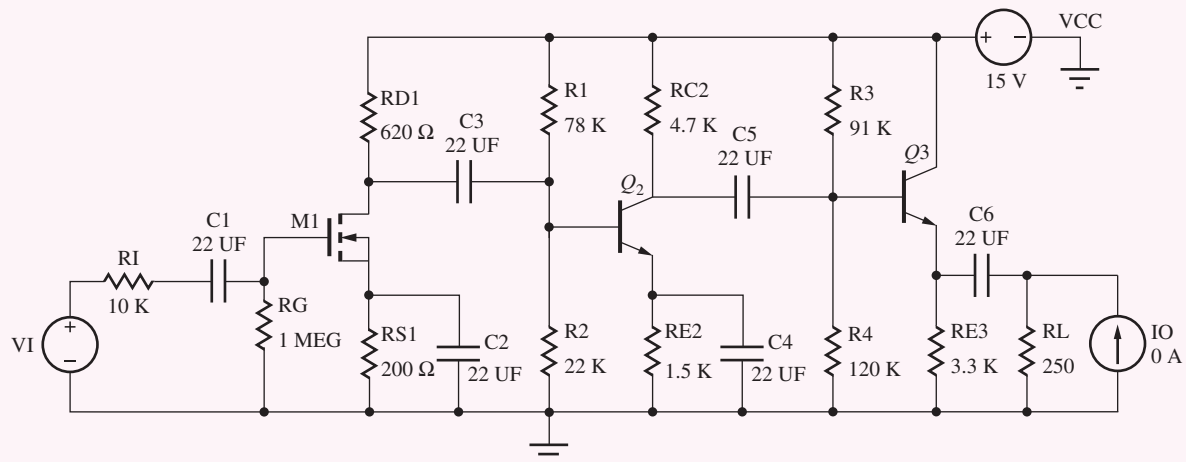
**SOLUTION** **Known Information and Given Data:** The original amplifier circuit appears in Fig. 14.49, and transistor parameters are given in Table 14.18.

**Unknowns:**  $A_v$ ,  $R_{in}$ , and  $R_{out}$

**Approach:** Use SPICE analysis to plot the frequency response and find the midband region. Then choose a midband frequency, and use ac analysis to find the voltage gain, input resistance, and output resistance. Assume large values for the capacitors. Verify the gain with a transient simulation.

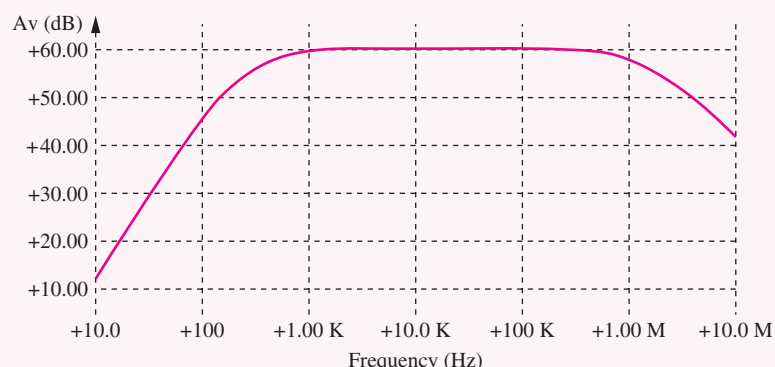
**Assumptions:** The coupling and bypass capacitors are all arbitrarily set to 22  $\mu$ F. Bipolar transistor parameters  $TF = 0.5$  NS and  $CJC = 2$  PF are added to the BJT models to cause the frequency response to roll off at high frequencies. These parameters are discussed in detail in Chapter 17.

**Analysis:** The circuit is created in SPICE using the schematic editor, as shown in the figure.



The MOSFET parameters are set to  $KP = 0.01$  S/V,  $VTO = -2$  V, and  $LAMBDA = 0.02$  V $^{-1}$ . The BJT parameters for  $Q_2$  are set to  $BF = 150$ ,  $VAF = 80$  V,  $TF = 0.5$  NS, and  $CJC = 2$  PF. For  $Q_3$ ,  $BF = 80$ ,  $VAF = 60$  V,  $TF = 0.5$  NS, and  $CJC = 2$  PF. As mentioned,  $TF$  and  $CJC$  are added to create a roll-off in the frequency response at high frequencies and will be discussed further in Chapter 17. Source  $VI$  is used for ac analysis of the voltage gain and input resistance. Source  $IO$  is an ac source used to find the output resistance.

First, we set  $VI = 1\angle 0^\circ$  V and  $IO = 0\angle 0^\circ$  A and perform an ac sweep from 10 Hz to 10 MHz with 20 points per decade in order to find the midband region. We obtain the response shown below.

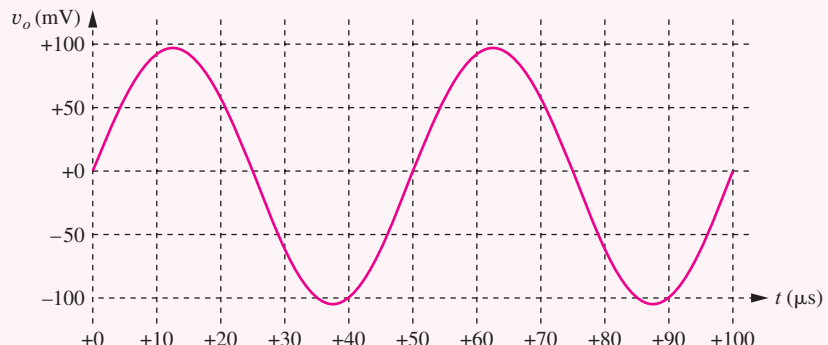


The midband region extends from approximately 500 Hz to 500 kHz. Choosing 20 kHz as a representative midband frequency, we find the gain is 60.1 dB ( $A_v = 1010$ ), and the current in  $VI$  is  $-990$  nA with a phase angle of  $0^\circ$ . The minus sign results from the sign convention in SPICE—positive current enters the positive terminal of an independent source. The input resistance

presented to VI is  $1\text{ V}/990\text{ nA} = 1.01\text{ M}\Omega$ . Subtracting the  $10\text{-k}\Omega$  source resistance yields an amplifier input resistance of  $1\text{ M}\Omega$ . Both the gain and input resistance agree with our hand calculations.

The output resistance is found by setting  $VI = 0\angle 0^\circ\text{ V}$  and  $IO = 1\angle 0^\circ\text{ A}$  and finding the output voltage. The result yields  $R = 45.6\ \Omega$ . Removing the effect of the  $250\text{-}\Omega$  resistor in parallel with the output yields  $R_{out} = 55.7\ \Omega$ . The slight difference is caused by the value of current gain utilized in SPICE:  $\beta_o = BF(1 + VCB/VA) = 80(1 + 7.6\text{ V}/60\text{ V}) = 90.1$ .

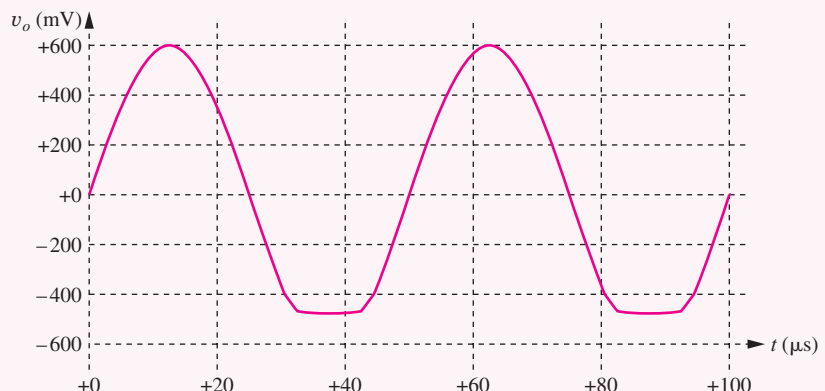
**Check of Results:** As a second check on the gain, we can run a transient simulation at  $f = 20\text{ kHz}$ , which we now know corresponds to a midband frequency. The graph here gives the output with an input amplitude of  $100\ \mu\text{V}$ , Start time = 0, Stop time =  $100\ \text{US}$ , and a time step of  $0.01\ \text{US}$ . The amplitude of the output is approximately  $100\text{ mV}$  corresponding to a gain of 1000.



Simulation with undistorted output and gain of 1000.

**Discussion:** This input value in the transient simulation is just slightly above the small-signal limit that we calculated. The waveform looks like a good sine wave, and the Fourier analysis option in SPICE indicates that the total harmonic distortion in the waveform is less than 0.15 percent.

However, if one uses an input signal larger than about  $650\ \mu\text{V}$  in the transient solution, one discovers a new limitation. An example of the problem appears in the next figure. Because  $Q_3$  is biased at a current of only  $2\text{ mA}$ , the largest output signal that can be developed by the emitter follower is approximately  $2\text{ mA} \times 250\ \Omega$  or  $0.5\text{ V}$ . The output will begin to show substantial distortion before this value is reached. In the figure, the amplitude of input  $v_I$  is  $750\ \mu\text{V}$ . The bottom of the output waveform is “clipped off,” and the total harmonic distortion has increased to 8.2 percent. This output waveform is not desirable.



Distorted output with amplitude exceeding output voltage capability of amplifier.

**TABLE 14.20**  
Three-Stage Amplifier Summary

	HAND ANALYSIS	SPICE RESULTS
Voltage gain	+998	+1010
Input signal range	92.7 $\mu$ V	—
Input resistance	1 M $\Omega$	1 M $\Omega$
Output resistance	60.5 $\Omega$	55.7 $\Omega$
Current gain	$+4.03 \times 10^6$	—
Power gain	$4.02 \times 10^9$	—

**EXERCISE:** Reevaluate Eq. (14.163) using a current gain of 90.1.

**ANSWER:** 55.3  $\Omega$

**EXERCISE:** Find the output waveform, voltage gain, and total harmonic distortion if the amplitude of  $V_I$  is increased to (a) 400  $\mu$ V, (b) 600  $\mu$ V, and (c) 1 mV.

**ANSWERS:** (a) Looks like a sine wave,  $A_v = 826$ , THD = 0.28 percent; (b) looks like a sine wave,  $A_v = 790$ , THD = 2.4 percent; (c) bottom of the waveform is clipped off,  $A_v = 760$ , THD = 18.3 percent. Note that the overall voltage gain is dropping as the signal level increases.

Table 14.20 summarizes the characteristics for the three-stage amplifier in Fig. 14.49. The amplifier provides a noninverting voltage gain of approximately 60 dB, a high input resistance, and a low output resistance. The current and power gains are both quite large. The input signal must be kept below 92.7  $\mu$ V in order to satisfy the small-signal limitations of the transistors.

**EXERCISE:** (a) What would be the voltage gain of the amplifier if  $I_{D1}$  is reduced to 1 mA and  $R_{D1}$  is increased to 3 k $\Omega$  so that  $V_D$  is maintained constant? (b) The FET  $g_m$  decreases by  $\sqrt{5}$ . Why did the gain not increase by a factor of  $\sqrt{5}$ ?

**ANSWERS:** 1150; although  $R_{D1}$  increases by a factor of 5, the total load resistance at the drain of  $M_1$  does not.

#### 14.9.8 ESTIMATING THE LOWER CUTOFF FREQUENCY OF THE MULTISTAGE AMPLIFIER

As discussed in more detail in Chapter 17, the lower cutoff frequency for an amplifier having multiple coupling and bypass capacitors can be estimated from

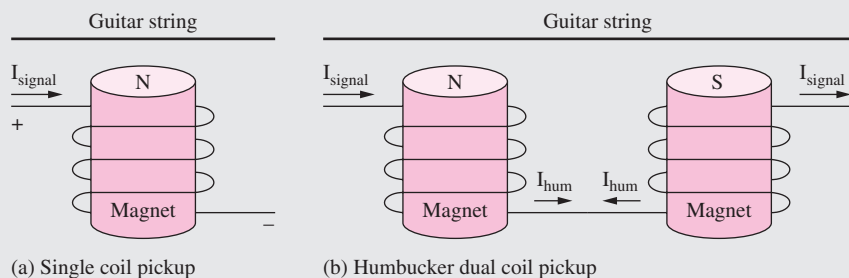
$$\omega_L \cong \sum_{i=1}^n \frac{1}{R_{iS}C_i} \quad (14.174)$$

in which  $R_{iS}$  represents the resistance at the terminals of the  $i$ th capacitor with all the other capacitors replaced by short circuits. The product  $R_{iS}C_i$  represents the short circuit time constant associated with capacitor  $C_i$ . Let us now use this method to estimate the lower cutoff frequency of the three-stage


**ELECTRONICS IN ACTION**

### Humbucker Guitar Pickup

Electric guitar pickups are devices that convert motion of a steel string into electrical signals. They function through an interesting interaction of materials and magnetic fields. A basic schematic of a pickup is shown below. The magnet induces a magnetization (aligning of the magnetic domains) in the steel string. When the string vibrates, this creates a moving magnetic field, which we know from Faraday's law induces a current in the wire coil located beneath the string. The signal from the wire coil is then amplified and sent to the rest of the amplification system. The coil is typically composed of extremely thin wire, with several hundred to over a thousand turns. The choice of magnet, wire material, and number of turns in the coil generates a set of compromises in frequency response and sensitivity. Guitar players often use acoustic feedback to generate a sustained note by placing the guitar near the amplifier speakers. The acoustic energy couples into the guitar, causing the string to vibrate, which generates more signal through the amplifier. Unlike the highly undesirable feedback that we often hear with poorly configured public address systems, a skilled guitarist can use acoustic feedback to create intentionally sustained notes.



Inherent with the use of the single coil pickup is sensitivity to extraneous magnetic fields. In particular, the 60 Hz power moving through most buildings gives rise to magnetic fields at the same frequency. As a result, the guitar pickup coil will generate the desired string vibration signal as well as a 60 Hz signal commonly referred to as hum.

To eliminate hum, one has to make two important observations: First, the polarity of the string vibration signal is a function of both the magnetization polarity of the string and the orientation of the coil relative to the string. Second, the polarity of the undesired hum signal is a function of only the orientation of the coil to the hum-producing external magnetic field.

Making use of these two observations, the humbucker pickup shown above was created. A second pickup coil has been added in series with the first. In the second coil, the orientation of the magnet has been reversed, resulting in the reversing of the string magnetization in the area above the coil. Additionally, the orientation of the second coil with respect to the string has also been reversed. The result is a system where the string vibration signal of the two coils has the same polarity and is additive, while the hum signal, dependent only on the coil orientation, is of opposite sign in the two coils and is cancelled out.

The humbucker coil is an example of excellent sensor design. Recognizing the unique characteristics of the desired versus the undesired signals allowed the designers to implement a sensor that rejects everything but the signal of interest. Rejecting unwanted signals at the sensor is almost always preferred to attempting to reject undesired signals in post-processing after detection and amplification.

For more material refer to the excellent guitar building sites that can be found on the web.

amplifier in Ex. 14.13.

$$C_1: R_{1S} = R_I + R_G = 1.01 \text{ M}\Omega$$

$$C_2: R_{2S} = R_{S1} \| R_{iS1} = R_{S1} \| \frac{1}{g_{m1}} = 200 \Omega \| \frac{1}{0.01S} = 66.7 \Omega$$

$$C_3: R_{3S} = R_{D1} + R_{I1} \| R_{iB2} = R_{D1} + R_{I1} \| r_{\pi2} = 620 \Omega + 17.2 \text{ k}\Omega \| 2.39 \text{ k}\Omega = 2.72 \text{ k}\Omega$$

$$C_4: R_{4S} = R_{E2} \| R_{iE2} = R_{E2} \| \frac{r_{\pi2} + R_{th2}}{\beta_{o2} + 1} = 1.5 \text{ k}\Omega \| \frac{2.39 \text{ k}\Omega + (17.2 \text{ k}\Omega \| 620 \Omega)}{151} = 19.2 \Omega$$

$$C_5: R_{3S} = R_{C2} + R_{I2} \| R_{iB3} = R_{C2} + R_{I2} \| r_{\pi3}(1 + g_{m3}R_{L3}) \\ = 4.7 \text{ k}\Omega + 51.8 \text{ k}\Omega \| 1.0 \text{ k}\Omega [1 + 0.0796S(232 \Omega)] = 18.9 \text{ k}\Omega$$

$$C_6: R_{4S} = R_L + R_{E3} \| R_{iE3} = R_L + R_{E3} \| \frac{r_{\pi3} + R_{th3}}{\beta_{o3} + 1} \\ = 250 \Omega + 3.3 \text{ k}\Omega \| \frac{1.0 \text{ k}\Omega + (51.8 \text{ k}\Omega \| 4.7 \text{ k}\Omega)}{81} = 315 \Omega$$

$$f_L \cong \frac{1}{2\pi} \left[ \frac{1}{1.01 \text{ M}\Omega(22 \mu\text{F})} + \frac{1}{66.7 \Omega(22 \mu\text{F})} + \frac{1}{2.72 \text{ k}\Omega(22 \mu\text{F})} + \frac{1}{19.2 \Omega(22 \mu\text{F})} \right. \\ \left. + \frac{1}{18.9 \text{ k}\Omega(22 \mu\text{F})} + \frac{1}{315 \Omega(22 \mu\text{F})} \right]$$

$$f_L \cong 511 \text{ Hz}$$

The  $f_L = 511 \text{ Hz}$  estimate obtained using the short circuit time constant approach agrees very well with the SPICE simulation results presented in Ex. 14.13.

## SUMMARY

This chapter presented an in-depth investigation of the characteristics of amplifiers implemented using single transistors.

- Of the three available device terminals of the BJT, only the base and emitter are useful as signal input terminals, whereas the collector and emitter are acceptable as output terminals. For the FET, the source and gate are useful as signal input terminals, and the drain and source are acceptable as output terminals. The collector or drain are not used as input terminals, and the base or gate are not used as output terminals.
- There are three basic classifications of amplifiers: inverting amplifiers—the common-emitter and common-source amplifiers; followers—the common-collector and common-drain amplifiers (also known as emitter followers or source followers); and the noninverting amplifiers—common-base and common-gate amplifiers.
- Detailed analyses of these three amplifier classes were performed using the small-signal models for the transistors. These analyses produced expressions for the voltage gain, current gain, input resistance, output resistance, and input signal range, which are summarized in a group of important tables:

Table 14.3 C-E/C-S Amplifier Summary	page 884
Table 14.5 C-C/C-D Amplifier Summary	page 891
Table 14.8 C-B/C-G Amplifier Summary	page 903
Table 14.9 Single-Transistor Bipolar Amplifiers	page 904
Table 14.11 Single-Transistor FET Amplifiers	page 906

The results summarized in these tables form the basic toolkit of the analog circuit designer. A thorough understanding of these results is a prerequisite for design and for the analysis of more complex analog circuits.

- Inverting amplifiers (C-E and C-S amplifiers) can provide significant voltage and current gain, as well as high input and output resistance. If a resistor is included in the emitter or source of the transistor, the voltage gain is reduced but can be made relatively independent of the individual

**TABLE 14.21**  
Relative Comparison of Single-Transistor Amplifiers

	INVERTING AMPLIFIERS (C-E AND C-S)	FOLLOWERS (C-C AND C-D)	NONINVERTING AMPLIFIERS (C-B AND C-G)
Voltage gain	Moderate	Low ( $\leq 1$ )	Moderate
Input resistance	Moderate to high	High	Low
Output resistance	Moderate to high	Low	High
Input signal range	Low to moderate	High	Low to moderate
Current gain	Moderate	Moderate	Low ( $\leq 1$ )

transistor characteristics. This reduction in gain is traded for increases in input resistance, output resistance, and input signal range. Because of its higher transconductance, the BJT more easily achieves higher values of voltage gain than the FET, whereas the infinite input resistance of the FET gives it the advantage in achieving high input resistance amplifiers. The FET also typically has a larger input signal range than the BJT.

- In MOS technology, a transistor can be used to replace the drain bias resistor in the common-source amplifiers, resulting in much more compact circuits suitable for IC realization. The resulting two-transistor amplifier circuits have the same circuit topology as the logic inverters studied in Chapters 6–8. Similar circuits will be encountered in Chapters 14–16.
- Emitter and source followers (C-C and C-D amplifiers) provide a voltage gain of approximately 1, high input resistance, and low output resistance. The followers provide moderate levels of current gain and achieve the highest input signal range. These C-C and C-D amplifiers are the single-transistor equivalents of the voltage-follower operational-amplifier configuration introduced in Chapter 10.
- The noninverting amplifiers (C-B and C-G amplifiers) provide voltage gain, signal range, and output resistances very similar to those of the inverting amplifiers but have relatively low input resistance and a current gain of less than one.
- All the amplifier classes provide at least moderate levels of either voltage gain or current gain (or both) and are therefore capable of providing significant power gain with proper design.
- Table 14.21 presents a relative comparison of these three amplifier classes.
- Design examples were presented for amplifiers using the inverting, noninverting, and follower configurations, and an example using Monte Carlo analysis to evaluate the effects of element tolerances on circuit performance was also given.
- The values of coupling and bypass capacitors can be chosen by setting the reactance of the capacitors to be much smaller than the Thévenin equivalent resistance that appears at the capacitor terminals. The reactance is calculated at the lowest frequency in the midband region of the amplifier's frequency response. The lower cutoff frequency  $f_L$  is determined by the frequency at which the capacitive reactance equals the equivalent resistance at the capacitor terminals. In the amplifiers in this chapter, there are two or three poles that interact to set  $f_L$ , and bandwidth shrinkage moves the cutoff frequency above that set by each individual capacitor acting alone.

## KEY TERMS

- |                                  |                               |
|----------------------------------|-------------------------------|
| Body effect                      | Common-gate (C-G) amplifier   |
| Common-base (C-B) amplifier      | Common-source (C-S) amplifier |
| Common-collector (C-C) amplifier | Emitter follower              |
| Common-emitter (C-E) amplifier   | Input resistance              |
| Common-drain (C-D) amplifier     | Output resistance             |

Signal range  
Source follower  
Swamping

Terminal current gain  
Terminal voltage gain  
Voltage gain

### ADDITIONAL READING

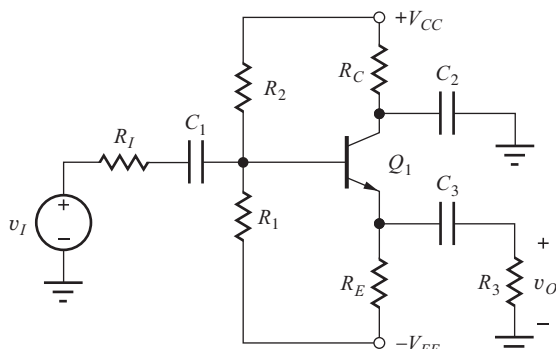
- P. R. Gray, P. J. Hurst, S. H. Lewis, and R. G. Meyer, *Analysis and Design of Analog Integrated Circuits*, 4th ed., John Wiley and Sons, New York: 2001.
- A. S. Sedra and K. C. Smith, *Microelectronic Circuits*, 5th ed., Oxford University Press, New York: 2004.
- M. N. Horenstein, *Microelectronic Circuits and Devices*, 2nd ed., Prentice-Hall, Englewood Cliffs, NJ: 1995.
- C. J. Savant, M. S. Roden, and G. L. Carpenter, *Electronic Design—Circuits and Systems*, 2nd ed., Benjamin/Cummings, Redwood City, CA: 1990.

### PROBLEMS

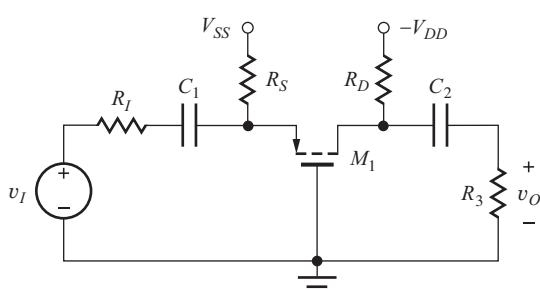
Assume all capacitors and inductors have infinite value unless otherwise indicated.

#### 14.1 Amplifier Classification

- 14.1. Draw the ac equivalent circuits for, and classify (that is, as C-S, C-G, C-D, C-E, C-B, C-C, and not useful), the amplifiers in Figs. P14.1 (a) to (q).

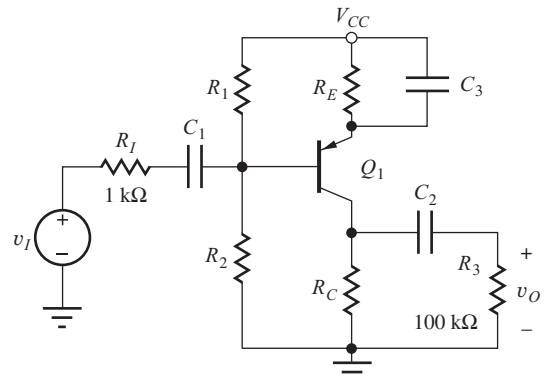


(a)

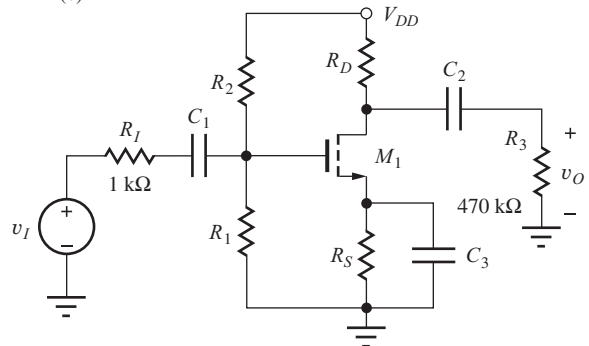


(b)

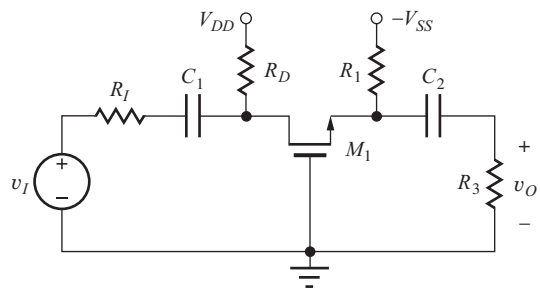
Figure P14.1 (a), (b)



(c)



(d)



(e)

Figure P14.1 (c), (d), (e)

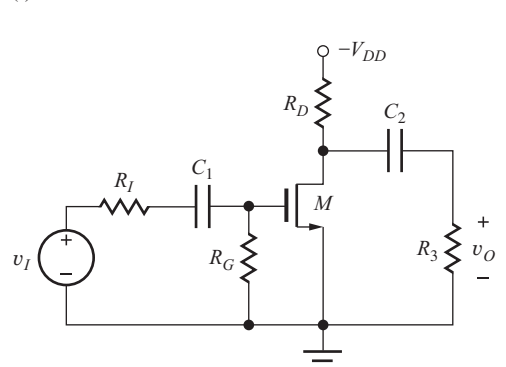
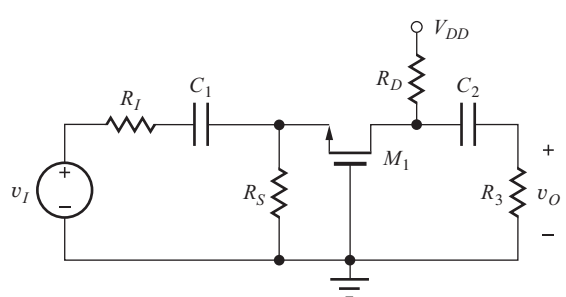
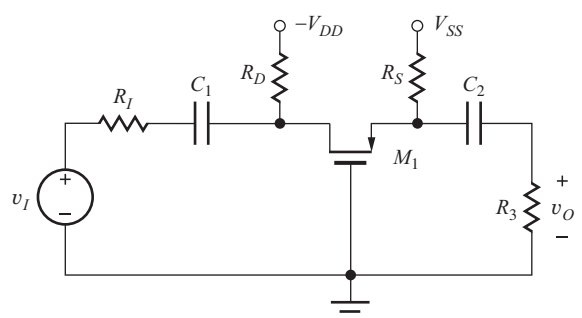
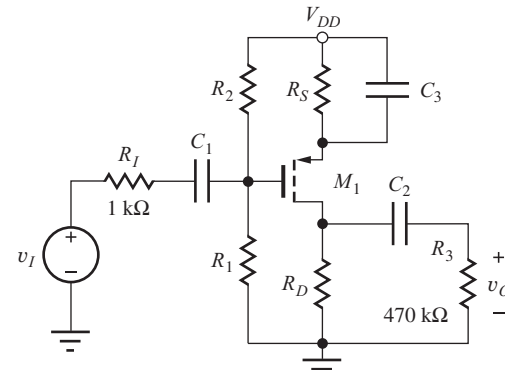
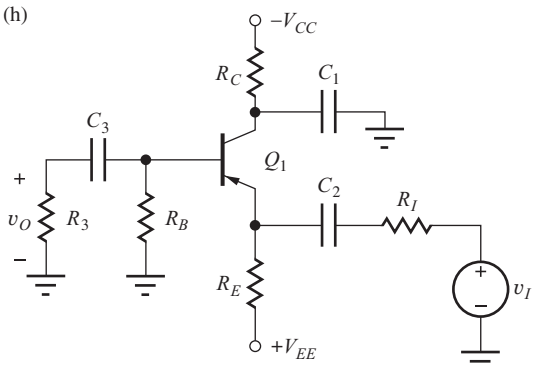
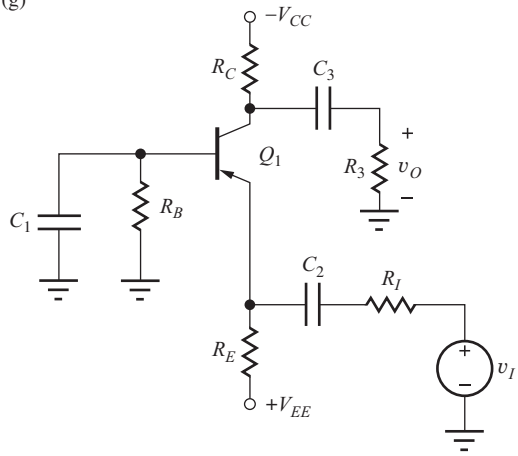
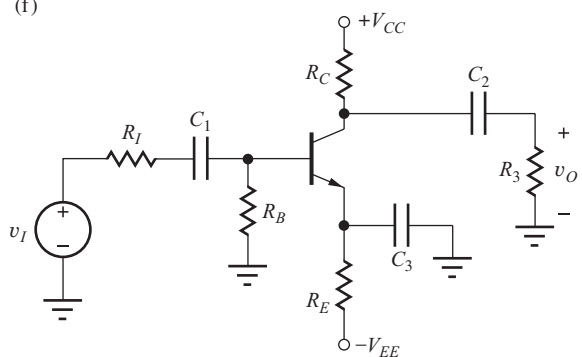
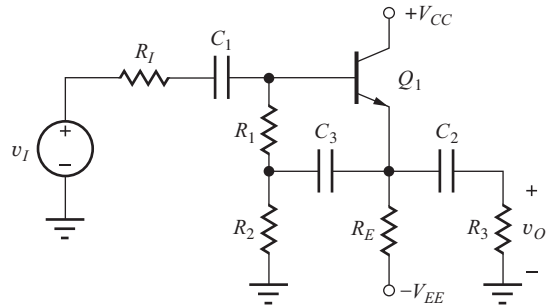
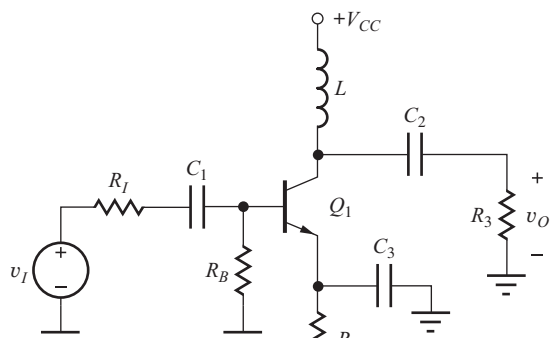
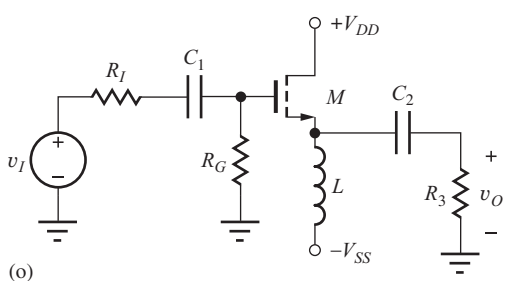


Figure P14.1 (f), (g), (h), (i)

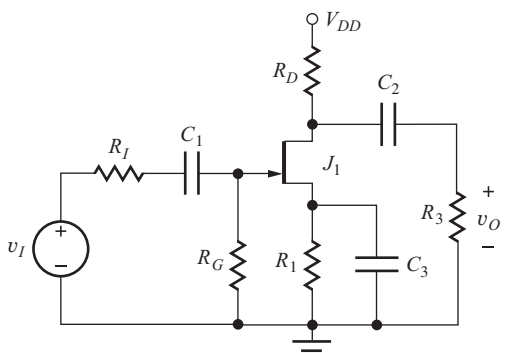
Figure P14.1 (j), (k), (l), (m)



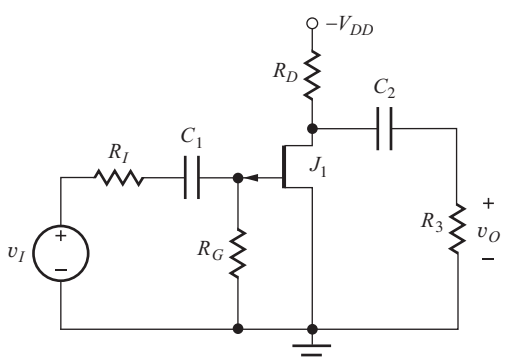
(n)



(o)



(p)



(q)

Figure P14.1 (n), (o), (p), (q)

- 14.2. An *npn* transistor is biased by the circuit in Fig. P14.2. Using the external source and load configurations in the figure, add coupling and bypass capacitors to the circuit to turn the amplifier into a common-emitter amplifier with maximum gain.

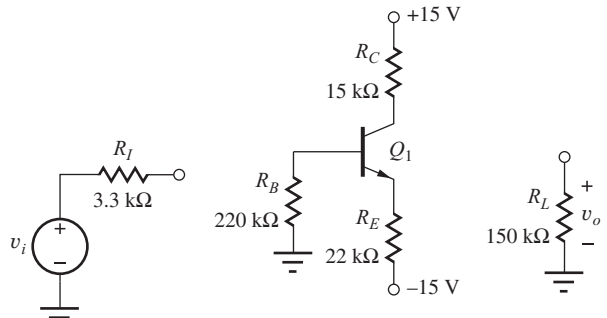


Figure P14.2

- 14.3. (a) Repeat Prob. 14.2 to turn the amplifier into a common-collector amplifier. (b) Redesign the circuit by deleting any unneeded component(s). Draw the new circuit.

- 14.4. (a) Repeat Prob. 14.2 to turn the amplifier into a common-base amplifier. (b) Eliminate  $R_B$  and any other unneeded components and draw the modified circuit.

- 14.5. A *pnp* transistor is biased by the circuit in Fig. P14.5. Using the external source and load configurations in the figure, add coupling and bypass capacitors to the circuit to construct a common-drain amplifier.

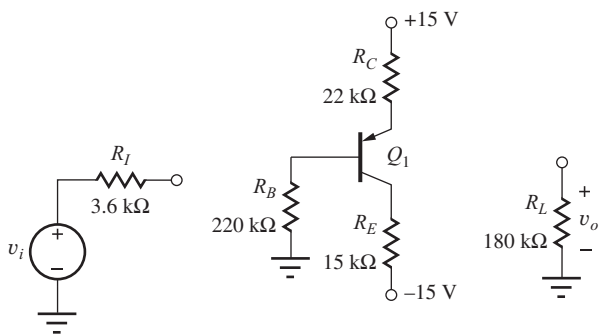


Figure P14.5

- 14.6. Repeat Prob. 14.5 to construct a common-source amplifier with maximum gain.

- 14.7. Repeat Prob. 14.5 to construct a common-base amplifier.

- 14.8. A PMOS transistor is biased by the circuit in Fig. P14.8. Using the external source and load configurations in the figure, add coupling and bypass

capacitors to the circuit to turn the amplifier into a common-gate amplifier.

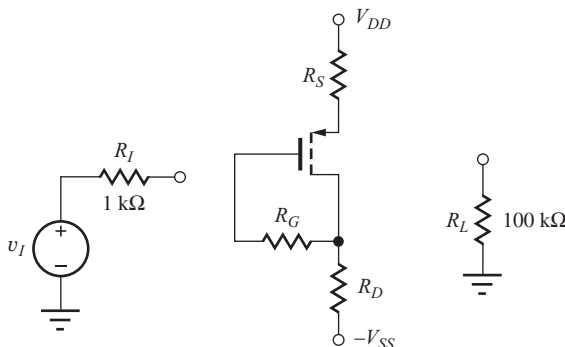


Figure P14.8

- 14.9. Repeat Prob. 14.8 to turn the amplifier into a common-drain amplifier.
- 14.10. Repeat Prob. 14.8 to turn the amplifier into a common-source amplifier with maximum gain.
- 14.11. An NMOS transistor is biased by the circuit in Fig. P14.11. Using the external source and load configurations in the figure, add coupling and bypass capacitors to the circuit to construct a common-source amplifier.

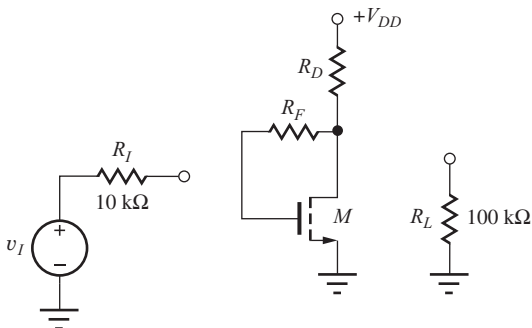


Figure P14.11

- 14.12. Repeat Prob. 14.11 to construct a common-drain amplifier.
- 14.13. Repeat Prob. 14.11 to construct a common-gate amplifier.

## 14.2 Inverting Amplifiers—Common-Emitter and Common-Source Circuits

- 14.14. (a) What are the values of  $A_v$ ,  $R_{in}$ ,  $R_{out}$ , and  $A_i = i_o/i_i$  for the common-emitter stage in Fig. P14.14 if  $g_m = 20 \text{ mS}$ ,  $\beta_o = 75$ ,  $r_o = 100 \text{ k}\Omega$ ,  $R_I = 500 \Omega$ ,  $R_B = 15 \text{ k}\Omega$ ,  $R_L = 12 \text{ k}\Omega$ , and  $R_E = 300 \Omega$ ? (b) What are the values if  $R_E$  is changed to  $620 \Omega$ ?

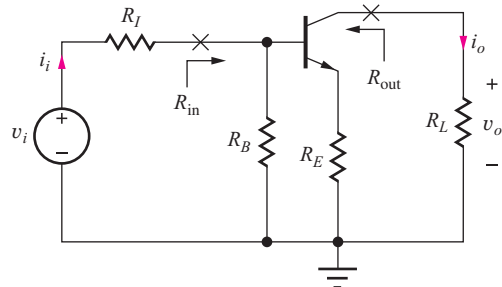


Figure P14.14

- 14.15. (a) What are the values of  $A_v$ ,  $R_{in}$ ,  $R_{out}$ , and  $A_i = i_o/i_i$  for the common-source stage in Fig. P14.15 if  $R_G = 2 \text{ M}\Omega$ ,  $R_I = 75 \text{ k}\Omega$ ,  $R_L = 2 \text{ k}\Omega$ , and  $R_S = 330 \Omega$ ? Assume  $g_m = 5 \text{ mS}$  and  $r_o = 10 \text{ k}\Omega$ . (b) What are the values of  $A_v$ ,  $R_{in}$ ,  $R_{out}$ , and  $A_i$  if  $R_S$  is bypassed by a capacitor?

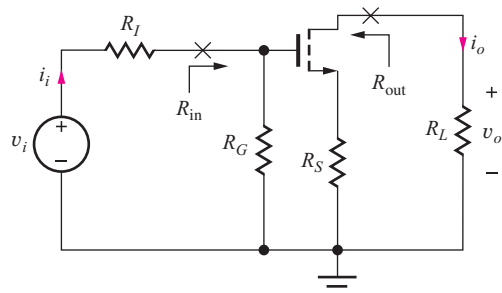


Figure P14.15

- 14.16. (a) Estimate the voltage gain of the inverting amplifier in Fig. P14.16. (b) Place a bypass capacitor in the circuit to change the gain to approximately  $-10$ . (c) Where should the bypass capacitor be placed to change the gain to approximately  $-20$ ? (d) Where should the bypass capacitor be placed to achieve maximum gain? (e) Estimate this gain.

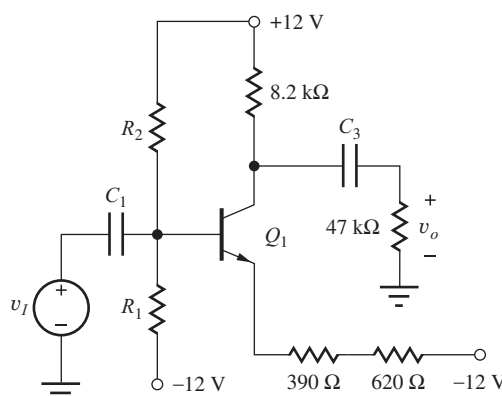


Figure P14.16

- 14.17. What values of  $R_E$  and  $R_L$  are required in the ac equivalent circuit in Fig. P14.17 to achieve  $A_{vt} = -10$  and  $R_{in} = 250 \text{ k}\Omega$ ? Assume  $\beta_o = 75$ .

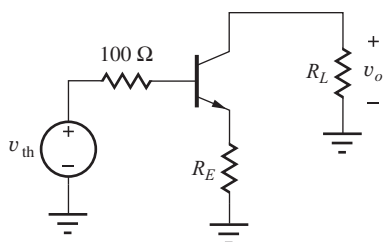


Figure P14.17

- 14.18. Assume that  $R_E = 0$  in Fig. P14.17. What values of  $R_L$  and  $I_C$  are required to achieve  $A_{vt} = 16 \text{ dB}$  and  $R_{in} = 250 \text{ k}\Omega$ ? Assume  $\beta_o = 75$ .
- 14.19. Use nodal analysis to rederive the output resistance of the common-source circuit in Fig. P14.19, as expressed in Table 14.1.

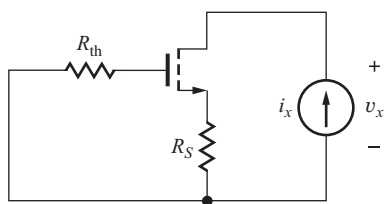


Figure P14.19

- 14.20. What are  $A_v$ ,  $A_i$ ,  $R_{in}$ ,  $R_{out}$ , and the maximum amplitude of the signal source for the amplifier in Fig. P14.1(g) if  $R_I = 500 \Omega$ ,  $R_E = 110 \text{ k}\Omega$ ,  $R_B = 1 \text{ M}\Omega$ ,  $R_3 = 500 \text{ k}\Omega$ ,  $R_C = 42 \text{ k}\Omega$ ,  $V_{CC} = 15 \text{ V}$ ,  $-V_{EE} = -15 \text{ V}$ ? Use  $\beta_F = 100$ .
- 14.21. What are  $A_v$ ,  $A_i$ ,  $R_{in}$ ,  $R_{out}$ , and the maximum amplitude of the signal source for the amplifier in Fig. P14.1(c) if  $R_1 = 20 \text{ k}\Omega$ ,  $R_2 = 62 \text{ k}\Omega$ ,  $R_E = 3.9 \text{ k}\Omega$ ,  $R_C = 8.2 \text{ k}\Omega$ , and  $V_{CC} = 12 \text{ V}$ ? Use  $\beta_F = 75$ . Compare  $A_v$  to our rule-of-thumb estimate and discuss the reasons for any discrepancy.
- 14.22. What are  $A_v$ ,  $A_i$ ,  $R_{in}$ ,  $R_{out}$ , and the maximum amplitude of the signal source for the amplifier in Fig. P14.1(d) if  $R_1 = 500 \text{ k}\Omega$ ,  $R_2 = 1.4 \text{ M}\Omega$ ,  $R_S = 33 \text{ k}\Omega$ ,  $R_D = 82 \text{ k}\Omega$ , and  $V_{DD} = 15 \text{ V}$ ? Use  $K_n = 250 \mu\text{A/V}^2$  and  $V_{TN} = 1.2 \text{ V}$ . Compare  $A_V$  to our rule-of-thumb estimate and discuss the reasons for any discrepancy.
- 14.23. What are  $A_v$ ,  $A_i$ ,  $R_{in}$ ,  $R_{out}$ , and the maximum amplitude of the signal source for the amplifier in Fig. P14.1(j) if  $R_1 = 2.2 \text{ M}\Omega$ ,  $R_2 = 2.2 \text{ M}\Omega$ ,  $R_I = 22 \text{ k}\Omega$ ,  $R_S = 22 \text{ k}\Omega$ ,  $R_D = 18 \text{ k}\Omega$ , and  $V_{DD} = 22 \text{ V}$ ? Use  $K_p = 400 \mu\text{A/V}^2$  and  $V_{TP} = -1.5 \text{ V}$ .

- 14.24. What are  $A_v$ ,  $A_i$ ,  $R_{in}$ ,  $R_{out}$ , and the maximum value of the signal source voltage for the amplifier in Fig. P14.1(m) if  $R_I = 5 \text{ k}\Omega$ ,  $R_G = 10 \text{ M}\Omega$ ,  $R_3 = 36 \text{ k}\Omega$ ,  $R_D = 1.8 \text{ k}\Omega$ , and  $V_{DD} = 16 \text{ V}$ ? Use  $K_n = 0.4 \text{ mS/V}$  and  $V_{TN} = -4 \text{ V}$ .

- 14.25. What are  $A_v$ ,  $A_i$ ,  $R_{in}$ ,  $R_{out}$ , and the maximum value of the signal source voltage for the amplifier in Fig. P14.1(n) if  $R_I = 250 \Omega$ ,  $R_B = 20 \text{ k}\Omega$ ,  $R_3 = 1 \text{ M}\Omega$ ,  $R_E = 7.5 \text{ k}\Omega$ ,  $V_{CC} = 12 \text{ V}$ , and  $V_{EE} = 12 \text{ V}$ ? Use  $\beta_F = 80$  and  $V_A = 100 \text{ V}$ .
- 14.26. What are  $A_v$ ,  $A_i$ ,  $R_{in}$ ,  $R_{out}$ , and the maximum value of the source voltage for the amplifier in Fig. P14.1(p) if  $R_I = 5 \text{ k}\Omega$ ,  $R_1 = 1 \text{ k}\Omega$ ,  $R_G = 10 \text{k}\Omega$ ,  $R_3 = 36 \text{ M}\Omega$ ,  $R_D = 1.8 \text{ k}\Omega$ ,  $V_{DD} = 16 \text{ V}$ ? Use  $I_{DSS} = 10 \text{ mA}$  and  $V_{TN} = -5 \text{ V}$ .

### 14.3 Follower Circuits—Common-Collector and Common-Drain Amplifiers

- 14.27. What are the values of  $A_v$ ,  $R_{in}$ ,  $R_{out}$ , and  $A_i$  for the common-collector stage in Fig. P14.27 if  $R_I = 10 \text{ k}\Omega$ ,  $R_B = 47 \text{ k}\Omega$ ,  $R_L = 1 \text{ k}\Omega$ ,  $\beta_o = 80$ , and  $g_m = 0.5 \text{ S}$ ? ( $A_i = i_o/i_i$ ).

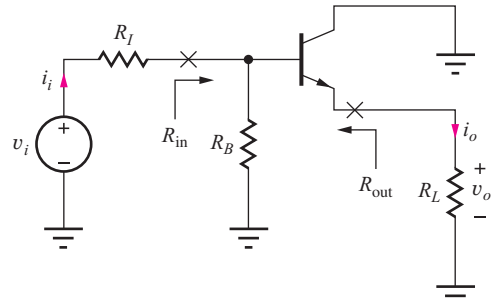


Figure P14.27

- 14.28. What are the values of  $A_v$ ,  $R_{in}$ ,  $R_{out}$ , and  $A_i$  for the common-drain stage in Fig. P14.28 if  $R_G = 2 \text{ M}\Omega$ ,  $R_I = 100 \text{ k}\Omega$ ,  $R_L = 2 \text{ k}\Omega$ , and  $g_m = 8 \text{ mS}$ ? ( $A_i = i_o/i_i$ ).

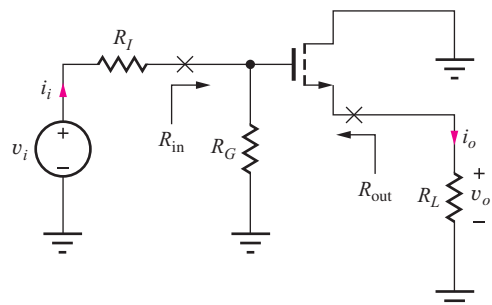


Figure P14.28

- 14.29. What are  $A_v$ ,  $R_{in}$ ,  $R_{out}$ , and maximum input signal amplitude for the amplifier in Fig. P14.1(a) if  $R_I = 500 \Omega$ ,  $R_1 = 100 \text{ k}\Omega$ ,  $R_2 = 100 \text{ k}\Omega$ ,  $R_3 = 24 \text{ k}\Omega$ ,  $R_E = 4.7 \text{ k}\Omega$ ,  $R_C = 2 \text{ k}\Omega$ , and  $V_{CC} = V_{EE} = 12 \text{ V}$ ? Use  $\beta_F = 125$  and  $V_A = 50 \text{ V}$ .

- 14.30. What are  $A_v$ ,  $R_{in}$ ,  $R_{out}$ , and maximum input signal for the amplifier in Fig. P14.1(o) if  $R_I = 10 \text{ k}\Omega$ ,  $R_G = 1 \text{ M}\Omega$ ,  $R_3 = 100 \text{ k}\Omega$ , and  $V_{DD} = V_{SS} = 5 \text{ V}$ ? Use  $K_n = 500 \mu\text{A/V}^2$ ,  $V_{TN} = 1.5 \text{ V}$ , and  $\lambda = 0.02 \text{ V}^{-1}$ .

- 14.31. What are  $A_v$ ,  $R_{in}$ ,  $R_{out}$ , and the maximum input signal amplitude for the amplifier in Fig. P14.1(f) if  $R_I = 500 \Omega$ ,  $R_1 = 500 \text{ k}\Omega$ ,  $R_2 = 500 \text{ k}\Omega$ ,  $R_3 = 500 \text{ k}\Omega$ ,  $R_E = 430 \text{ k}\Omega$ , and  $V_{CC} = V_{EE} = 9 \text{ V}$ ? Use  $\beta_F = 100$  and  $V_A = 60 \text{ V}$ .

- \*14.32. The gate resistor  $R_G$  in Fig. P14.32 is said to be “bootstrapped” by the action of the source follower. (a) Assume that the FET is operating with  $g_m = 3.54 \text{ mS}$  and  $r_o$  can be neglected. Draw the small-signal model and find  $A_v$ ,  $R_{in}$ , and  $R_{out}$  for the amplifier. (b) What would  $R_{in}$  be if  $A_v$  were exactly +1?

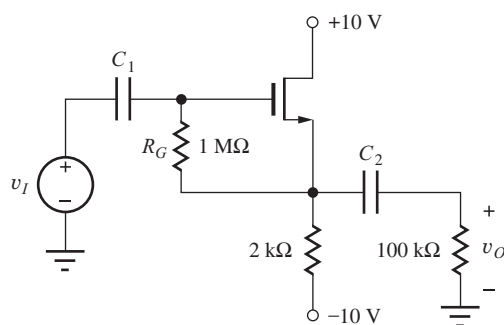


Figure P14.32

- \*14.33. Recast the signal-range formula for the common-collector amplifier in Table 14.4 in terms of the dc voltage developed across the emitter resistor  $R_E$  in Fig. 14.3(a). Assume  $R_3 = \infty$ .

- 14.34. Rework Prob. 14.32(a) by using the formulas for the bipolar transistor by “pretending” that  $R_G$  makes the FET equivalent to a BJT with  $r_\pi = R_G$ .

- \*14.35. The input to a common-collector amplifier is a triangular input signal with a peak-to-peak amplitude of 12 V. (a) What is the minimum gain required of the C-C amplifier to meet the small-signal limit? (b) What is the minimum dc voltage required across the emitter resistor in this amplifier to satisfy the limit in (a)?

- \*14.36. Design the emitter-follower circuit in Fig. P14.36 to meet the small-signal requirements when  $v_o = 3 \sin 2000\pi t \text{ V}$ . Assume  $C_1 = C_2 = \infty$  and  $\beta_F = 50$ .

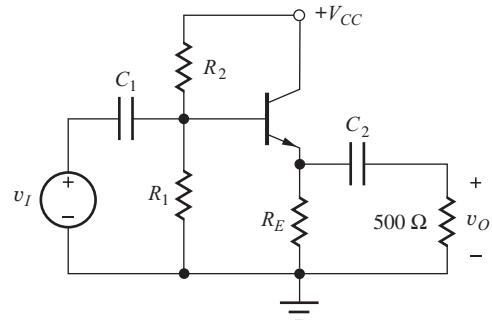


Figure P14.36

#### 14.4 Noninverting Amplifiers—Common-Base and Common-Gate Circuits

- 14.37. What are the values of  $A_v$ ,  $R_{in}$ ,  $R_{out}$ , and  $A_i$  for the common-base stage in Fig. P14.37 operating with  $I_C = 25 \mu\text{A}$ ,  $\beta_o = 100$ ,  $V_A = 60 \text{ V}$ ,  $R_I = 50 \Omega$ ,  $R_4 = 100 \text{ k}\Omega$  and  $R_L = 200 \text{ k}\Omega$ ? (b) What are the values if  $R_I$  is changed to  $2.2 \text{ k}\Omega$ ? ( $A_i = i_o/i_i$ ).

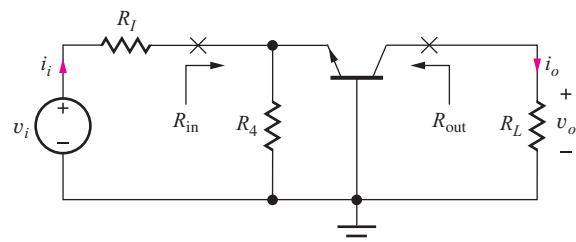


Figure P14.37

- 14.38. What are the values of  $A_v$ ,  $R_{in}$ ,  $R_{out}$ , and  $A_i$  for the common-gate stage in Fig. P14.38 operating with  $g_m = 0.5 \text{ mS}$ ,  $R_I = 50 \Omega$ ,  $R_4 = 3 \text{ k}\Omega$  and  $R_L = 82 \text{ k}\Omega$ ? (b) What are the values if  $R_I$  is changed to  $5 \text{ k}\Omega$ ? ( $A_i = i_o/i_i$ ).

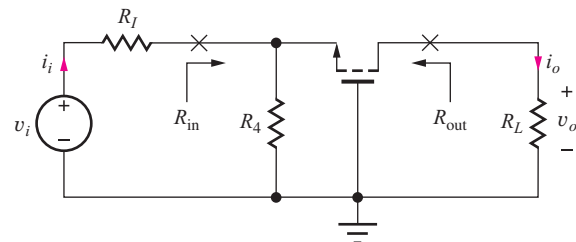


Figure P14.38

- 14.39. Estimate the voltage gain of the amplifier in Fig. P14.39. Explain your answer.

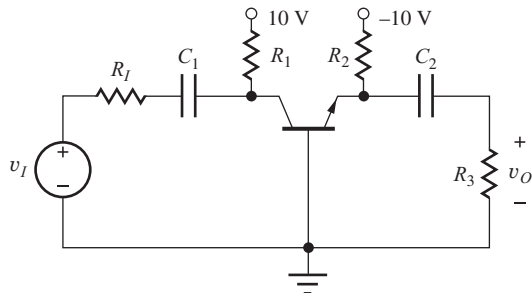


Figure P14.39

- 14.40. What are  $A_v$ ,  $R_{in}$ ,  $R_{out}$ , and the maximum input signal for the amplifier in Fig. P14.1(h) if  $R_I = 5 \text{ k}\Omega$ ,  $R_B = 1 \text{ M}\Omega$ ,  $R_3 = 1 \text{ M}\Omega$ ,  $R_E = 820 \text{ k}\Omega$ ,  $R_C = 390 \text{ k}\Omega$ , and  $V_{EE} = V_{CC} = 9 \text{ V}$ ? Use  $\beta_F = 50$  and  $V_A = 50 \text{ V}$ .

- 14.41. What are  $A_v$ ,  $R_{in}$ ,  $R_{out}$ , and the maximum input signal for the amplifier in Fig. P14.1(h) if  $R_I = 500 \Omega$ ,  $R_B = 100 \text{ k}\Omega$ ,  $R_3 = 100 \text{ k}\Omega$ ,  $R_E = 82 \text{ k}\Omega$ ,  $R_C = 39 \text{ k}\Omega$ , and  $V_{EE} = V_{CC} = 12 \text{ V}$ ? Use  $\beta_F = 50$  and  $V_A = 50 \text{ V}$ .

- 14.42. What are  $A_v$ ,  $R_{in}$ ,  $R_{out}$ , and the maximum input signal for the amplifier in Fig. P14.1(l) if  $R_I = 1 \text{ k}\Omega$ ,  $R_S = 3.9 \text{ k}\Omega$ ,  $R_3 = 51 \text{ k}\Omega$ ,  $R_D = 20 \text{ k}\Omega$ , and  $V_{DD} = 16 \text{ V}$ ? Use  $K_n = 500 \mu\text{A/V}^2$  and  $V_{TN} = -2 \text{ V}$ .

- 14.43. What are  $A_v$ ,  $R_{in}$ ,  $R_{out}$ , and the maximum input signal amplitude for the amplifier in Fig. P14.1(b) if  $R_I = 500 \Omega$ ,  $R_S = 33 \text{ k}\Omega$ ,  $R_3 = 100 \text{ k}\Omega$ ,  $R_D = 24 \text{ k}\Omega$ , and  $V_{DD} = V_{SS} = 10 \text{ V}$ ? Use  $K_p = 200 \mu\text{A/V}^2$  and  $V_{TP} = -1 \text{ V}$ .

- 14.44. What are  $A_v$ ,  $R_{in}$ ,  $R_{out}$ , and the maximum input signal for the amplifier in Fig. P14.1(b) if  $R_I = 250 \Omega$ ,  $R_S = 68 \text{ k}\Omega$ ,  $R_3 = 200 \text{ k}\Omega$ ,  $R_D = 43 \text{ k}\Omega$ , and  $V_{DD} = V_{SS} = 15 \text{ V}$ ? Use  $K_p = 200 \mu\text{A/V}^2$  and  $V_{TP} = -1 \text{ V}$ .

- 14.45. The gain of the common-gate and common-base stages can be written as  $A_v = R_L / [(1/g_m) + R_{th}]$ . When  $R_{th} \ll 1/g_m$ , the circuit is said to be “voltage driven,” and when  $R_{th} \gg 1/g_m$ , the circuit is said to be “current driven.” What are the approximate voltage gain expressions for these two conditions? Discuss the reason for the use of these adjectives to describe the two circuit limits.

- 14.46. (a) What is the input resistance to the common-base stage in Fig. P14.46 if  $I_C = 2 \text{ mA}$  and  $\beta_F = 75$ ? (b) Repeat for  $I_C = 100 \mu\text{A}$  and  $\beta_F = 125$ .

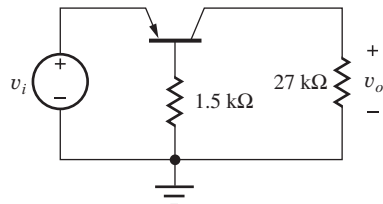


Figure P14.46

- 14.47. (a) What is the input resistance to the common-gate stage in Fig. P14.47 if  $I_D = 1 \text{ mA}$ ,  $K_p = 1.25 \text{ mA/V}^2$ , and  $V_{TP} = 2 \text{ V}$ ? (b) Repeat for  $I_D = 4 \text{ mA}$  and  $V_{TP} = 2.5 \text{ V}$ .

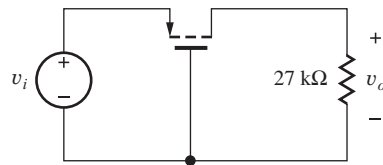


Figure P14.47

- 14.48. (a) Estimate the resistance looking into the collector of the transistor in Fig. P14.48 if  $R_E = 270 \text{ k}\Omega$ ,  $V_A = 50 \text{ V}$ ,  $\beta_F = 100$ , and  $V_{EE} = 15 \text{ V}$ ? (b) What is the minimum value of  $V_{CC}$  required to ensure that  $Q_1$  is operating in the forward-active region? (c) Repeat parts (a) and (b) if  $R_E = 27 \text{ k}\Omega$ .

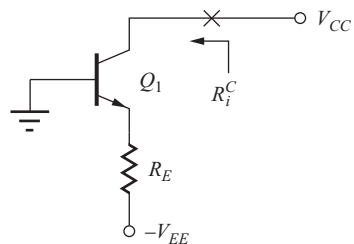


Figure P14.48

- \*14.49. What is the resistance looking into the collector terminal in Fig. P14.49 if  $I_E = 40 \mu\text{A}$ ,  $\beta_o = 125$ ,  $V_A = 60 \text{ V}$ , and  $V_{CC} = 10 \text{ V}$ ? (Hint:  $r_o$  must be considered in this circuit. Otherwise  $R_{out} = \infty$ .)

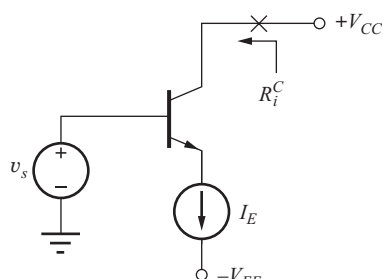


Figure P14.49

## 14.5 Amplifier Prototype Review and Comparison

- 14.50. A single-transistor amplifier is needed that has a gain of 46 dB and an input resistance of  $0.3 \text{ M}\Omega$ . What is the preferred choice of amplifier configuration? Discuss your reasons for making this selection.
- 14.51. A single-transistor amplifier is needed that has a gain of 43 dB and an input resistance of  $350 \Omega$ . What is the preferred choice of amplifier configuration? Discuss your reasons for your selection.
- 14.52. A single-transistor amplifier is needed that has a gain of 58 dB and an input resistance of  $50 \text{ k}\Omega$ . What is the preferred choice of amplifier configuration? Discuss your reasons for making this selection.
- 14.53. A single-transistor amplifier is needed that has a gain of 26 dB and an input resistance of  $10 \text{ M}\Omega$ . What is the preferred choice of amplifier configuration, and why did you make this selection?
- 14.54. A single-transistor amplifier is needed that has a gain of approximately +20 and an input resistance of  $5 \text{ k}\Omega$ . What is the preferred choice of amplifier configuration? Discuss your reasons for making this selection.
- 14.55. A single-transistor amplifier is needed that has a gain of approximately 0 dB and an input resistance of  $20 \text{ M}\Omega$  with a load resistor of  $20 \text{ k}\Omega$ . What is the preferred choice of amplifier configuration, and why did you make this selection?
- 14.56. A single-transistor amplifier is needed that has a gain of  $-100$  and an input resistance of  $5 \Omega$ . What is the preferred choice of amplifier configuration? Discuss your reasons for making this selection.
- 14.57. A single-transistor amplifier is needed that has a gain of approximately 66 dB and an input resistance of  $250 \text{ k}\Omega$ . What is the preferred choice of amplifier configuration, and why did you make this selection?
- 14.58. A follower is needed that has a gain of at least 0.97 and an input resistance of at least  $250 \text{ k}\Omega$  with a load resistance of  $5 \text{ k}\Omega$ . What is the preferred choice of amplifier configuration? Discuss your reasons for making this selection.
- 14.59. A common-collector amplifier is being driven from a source having a resistance of  $250 \Omega$ . Estimate the output resistance of this amplifier if the transistor has  $\beta_o = 150$  and  $V_A = 50 \text{ V}$ .
- 14.60. An inverting amplifier is needed that has an output resistance of at least  $1 \text{ G}\Omega$ . What is the preferred

choice of amplifier configuration? Discuss your reasons for making this selection. Estimate the Q-point current and emitter or source resistance required to achieve this specification.

- \*14.61. Show that the emitter resistor  $R_E$  in Fig. P14.61 can be absorbed into the transistor by redefining the small-signal parameters of the transistor to be

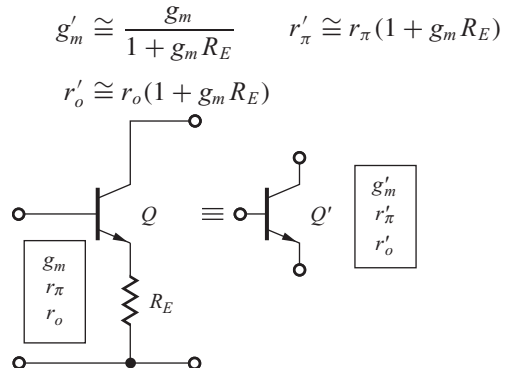


Figure P14.61

What is the expression for the common-emitter small-signal current gain  $\beta'_o$  for the new transistor? What is the expression for the amplification factor  $\mu'_f$  for the new transistor?

- \*14.62. Perform a transient simulation of the behavior of the common-emitter amplifier in Fig. P14.62 for sinusoidal input voltages of  $5 \text{ mV}$ ,  $10 \text{ mV}$ , and  $15 \text{ mV}$  at a frequency of  $1 \text{ kHz}$ . Use the Fourier analysis capability of SPICE to analyze the output waveforms. Compare the amplitudes of the  $2\text{-kHz}$  and  $3\text{-kHz}$  harmonics to the amplitude of the desired signal at  $1 \text{ kHz}$ . Assume  $\beta_F = 100$  and  $V_A = 70 \text{ V}$ .

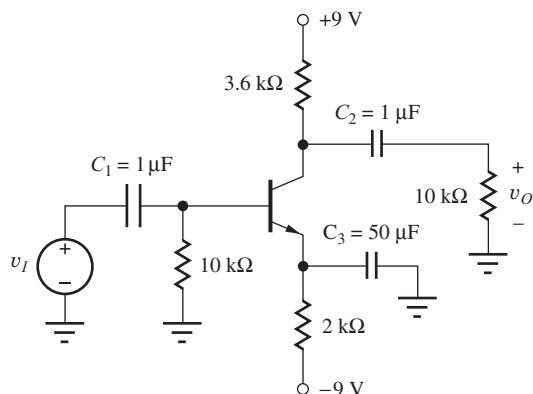


Figure P14.62

- 14.63. In the circuits in Fig. P14.63,  $I_B = 10 \mu\text{A}$ . Use SPICE to determine the output resistances of the

two circuits by sweeping the voltage  $V_{CC}$  from 10 to 20 V. Use  $\beta_F = 60$  and  $V_A = 20$  V. Compare results to hand calculations using the small-signal parameter values from SPICE.

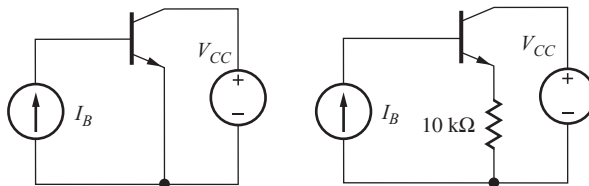


Figure P14.63

- 14.64. (a) What is the Thévenin equivalent representation for the amplifier in Fig. P14.64? (b) What are the values of  $v_{th}$  and  $R_{th}$  if  $R_I = 270 \Omega$ ,  $\beta_o = 100$ ,  $g_m = 2 \text{ mS}$ , and  $r_o = 250 \text{ k}\Omega$ ?

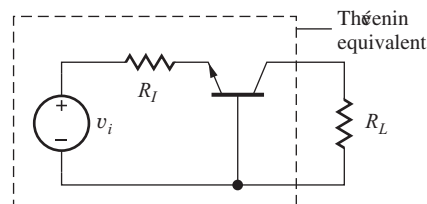


Figure P14.64

- 14.65. (a) What is the Thévenin equivalent representation for the amplifier in Fig. P14.65 if  $R_I = 5 \text{ k}\Omega$ ,  $R_L = 10 \text{ k}\Omega$ ,  $\beta_o = 100$  and  $g_m = 4 \text{ mS}$ ?

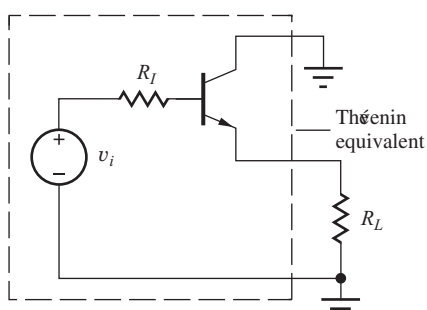


Figure P14.65

- 14.66. (a) What is the Thévenin equivalent representation for the amplifier in Fig. P14.66? (b) What are the values of  $v_{th}$  and  $R_{th}$  if  $R_I = 100 \text{ k}\Omega$ ,  $R_S = 18 \text{ k}\Omega$ ,  $g_m = 500 \mu\text{S}$ , and  $r_o = 250 \text{ k}\Omega$ ?

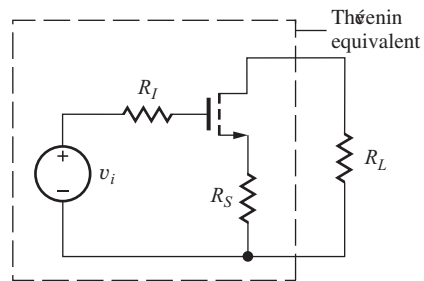


Figure P14.66

Assume the two-port description for Probs. 14.67 through 14.72 is

$$\begin{aligned} i_1 &= G_\pi v_1 + G_r v_2 \\ i_2 &= G_m v_1 + G_o v_2 \end{aligned}$$

- 14.67. (a) An emitter follower is drawn as a two-port in Fig. P14.67. Calculate  $G_m$  and  $G_r$  for this amplifier in terms of the small-signal parameters. Compare the two results. (b) What are the values of  $G_m$  and  $G_r$  if  $R_B = 150 \text{ k}\Omega$ ,  $R_E = 2.4 \text{ k}\Omega$ ,  $\beta_o = 100$ ,  $g_m = 10 \text{ mS}$ , and  $r_o = 250 \text{ k}\Omega$ ?

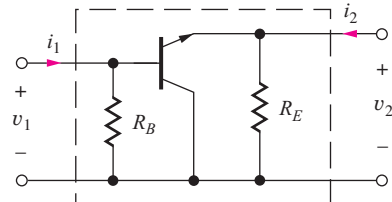


Figure P14.67

- 14.68. (a) A source follower is drawn as a two-port in Fig. P14.68. Calculate  $G_m$  and  $G_r$  for this amplifier in terms of the small-signal parameters. Compare the two results. (b) What are the values of  $G_m$  and  $G_r$  if  $R_G = 1 \text{ M}\Omega$ ,  $R_D = 50 \text{ k}\Omega$ ,  $g_m = 400 \mu\text{S}$ , and  $r_o = 450 \text{ k}\Omega$ ?

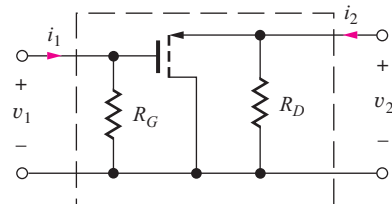


Figure P14.68

- 14.69. (a) A common-base amplifier is drawn as a two-port in Fig. P14.69. Calculate  $G_m$  and  $G_r$  for this

amplifier in terms of the small-signal parameters. Compare the two results. (b) What are the values of  $G_m$  and  $G_r$  if  $R_C = 18 \text{ k}\Omega$ ,  $R_E = 3.9 \text{ k}\Omega$ ,  $\beta_o = 100$ ,  $g_m = 3 \text{ mS}$ , and  $r_o = 800 \text{ k}\Omega$ ?

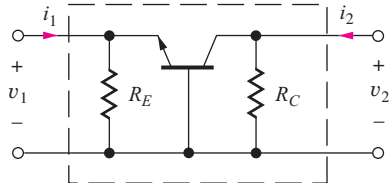


Figure P14.69

- 14.70. (a) A common-gate amplifier is drawn as a two-port in Fig. P14.70. Calculate  $G_m$  and  $G_r$  for this amplifier in terms of the small-signal parameters. Compare the two results. (b) What are the values of  $G_m$  and  $G_r$  if  $R_S = 15 \text{ k}\Omega$ ,  $R_D = 100 \text{ k}\Omega$ ,  $g_m = 500 \mu\text{S}$ , and  $r_o = 500 \text{ k}\Omega$ ?

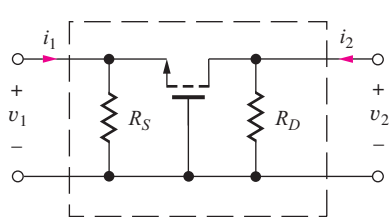


Figure P14.70

- 14.71. (a) A common-emitter amplifier is drawn as a two-port in Fig. P14.71. Calculate  $G_m$  and  $G_r$  for this amplifier in terms of the small-signal parameters. Compare the two results. (b) What are the values of  $G_m$  and  $G_r$  if  $R_B = 180 \text{ k}\Omega$ ,  $R_E = 12 \text{ k}\Omega$ ,  $R_C = 130 \text{ k}\Omega$ ,  $\beta_o = 100$ ,  $g_m = 2 \text{ mS}$ , and  $r_o = 1 \text{ M}\Omega$ ?

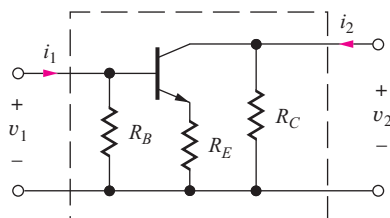


Figure P14.71

- 14.72. (a) A common-source amplifier is drawn as a two-port in Fig. P14.72. Calculate  $G_m$  and  $G_r$  for this amplifier in terms of the small-signal parameters. Compare the two results. (b) What are the values

of  $G_m$  and  $G_r$  if  $R_G = 1.5 \text{ M}\Omega$ ,  $R_S = 12 \text{ k}\Omega$ ,  $R_D = 130 \text{ k}\Omega$ ,  $g_m = 750 \mu\text{S}$ , and  $r_o = 330 \text{ k}\Omega$ ?

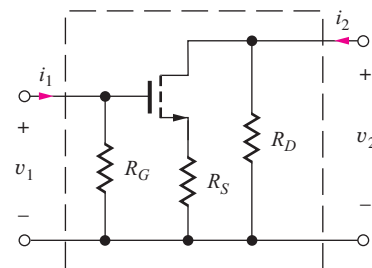


Figure P14.72

- 14.73. Our calculation of the input resistance of the common-gate and common-base amplifiers neglected  $r_o$  in the calculation. Calculate an improved estimate for  $R_{in}$  for the common-gate stage in Fig. P14.73.

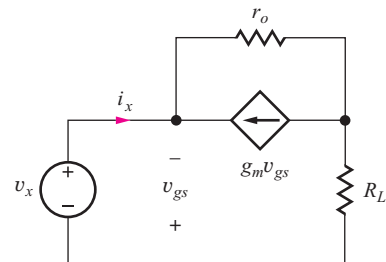


Figure P14.73

- 14.74. The circuit in Fig. P14.74 is called a phase inverter. Calculate the two gains  $A_{v1} = v_{o1}/v_i$  and  $A_{v2} = v_{o2}/v_i$ . What is the largest ac signal that can be developed at output  $v_{o1}$  in this particular circuit? Assume  $\beta_F = 100$ .

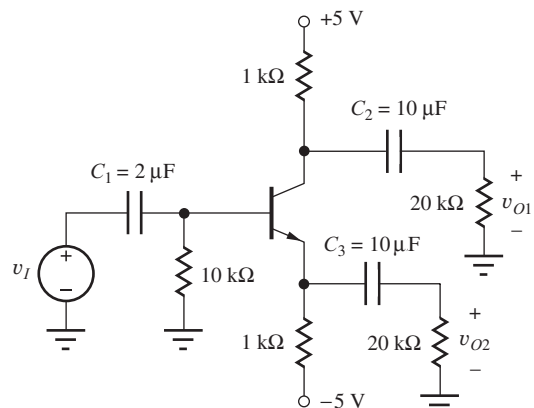


Figure P14.74

- 14.75. (a) Calculate the values of  $A_v$ ,  $R_{in}$ , and  $R_{out}$  for the amplifier in Fig. P14.1(a) if  $R_I = 600 \Omega$ ,  $R_1 = 100 \text{ k}\Omega$ ,  $R_2 = 100 \text{ k}\Omega$ ,  $R_3 = 24 \text{ k}\Omega$ ,  $R_E = 4.7 \text{ k}\Omega$ ,  $R_C = 2 \text{ k}\Omega$ , and  $V_{CC} = V_{EE} = 15 \text{ V}$ . Use  $\beta_F = 125$  and  $V_A = 50 \text{ V}$ . (b) Use SPICE to verify the results of your hand calculations. Assume  $f = 10 \text{ kHz}$  and  $C_1 = 10 \mu\text{F}$ ,  $C_2 = 10 \mu\text{F}$ ,  $C_3 = 47 \mu\text{F}$ .
- 14.76. (a) Calculate the values of  $A_v$ ,  $R_{in}$ , and  $R_{out}$  for the amplifier in Fig. P14.1(g) if  $R_I = 500 \Omega$ ,  $R_E = 68 \text{ k}\Omega$ ,  $R_B = 1 \text{ M}\Omega$ ,  $R_3 = 500 \text{ k}\Omega$ ,  $R_C = 39 \text{ k}\Omega$ ,  $V_{EE} = -10 \text{ V}$ , and  $V_{CC} = 10 \text{ V}$ . Use  $\beta_F = 80$  and  $V_A = 75 \text{ V}$ . (b) Use SPICE to verify the results of your hand calculations. Assume  $f = 4 \text{ kHz}$ ,  $C_1 = C_2 = 2.2 \mu\text{F}$ , and  $C_3 = 47 \mu\text{F}$ .
- 14.77. (a) Calculate the values of  $A_v$ ,  $R_{in}$ , and  $R_{out}$  for the amplifier in Fig. P14.1(c) if  $R_1 = 20 \text{ k}\Omega$ ,  $R_2 = 62 \text{ k}\Omega$ ,  $R_E = 6.8 \text{ k}\Omega$ ,  $R_C = 16 \text{ k}\Omega$ , and  $V_{CC} = 12 \text{ V}$ . Use  $\beta_F = 75$  and  $V_A = 60 \text{ V}$ . (b) Use SPICE to verify the results of your hand calculations. Assume  $f = 5 \text{ kHz}$  and  $C_1 = 2.2 \mu\text{F}$ ,  $C_2 = 10 \mu\text{F}$ ,  $C_3 = 47 \mu\text{F}$ .
- 14.78. (a) Calculate the values of  $A_v$ ,  $R_{in}$ , and  $R_{out}$  for the amplifier in Fig. P14.1(d) if  $R_1 = 500 \text{ k}\Omega$ ,  $R_2 = 1.4 \text{ M}\Omega$ ,  $R_S = 27 \text{ k}\Omega$ ,  $R_D = 75 \text{ k}\Omega$ , and  $V_{DD} = 18 \text{ V}$ . Use  $K_n = 500 \mu\text{A/V}^2$ ,  $\lambda = 0.02 \text{ V}^{-1}$ , and  $V_{TN} = 1 \text{ V}$ . (b) Use SPICE to verify the results of your hand calculations. Assume  $f = 5 \text{ kHz}$  and  $C_1 = 2.2 \mu\text{F}$ ,  $C_2 = 10 \mu\text{F}$ ,  $C_3 = 47 \mu\text{F}$ .
- 14.79. (a) Calculate the values of  $A_v$ ,  $R_{in}$ , and  $R_{out}$  for the amplifier in Fig. P14.1(b) if  $R_I = 500 \Omega$ ,  $R_S = 33 \text{ k}\Omega$ ,  $R_3 = 100 \text{ k}\Omega$ ,  $R_D = 24 \text{ k}\Omega$ , and  $V_{DD} = V_{SS} = 10 \text{ V}$ . Use  $K_p = 250 \mu\text{A/V}^2$ ,  $V_{TP} = -1 \text{ V}$ , and  $\lambda = 0.02 \text{ V}^{-1}$ . (b) Use SPICE to verify the results of your hand calculations. Assume  $f = 50 \text{ kHz}$ ,  $C_1 = 10 \mu\text{F}$ , and  $C_2 = 47 \mu\text{F}$ .
- 14.80. (a) Calculate the values of  $A_v$ ,  $R_{in}$ , and  $R_{out}$  for the amplifier in Fig. P14.1(j) if  $R_I = 2.2 \text{ M}\Omega$ ,  $R_2 = 2.2 \text{ M}\Omega$ ,  $R_S = 110 \text{ k}\Omega$ ,  $R_D = 90 \text{ k}\Omega$ , and  $V_{DD} = 18 \text{ V}$ . Use  $K_p = 400 \mu\text{A/V}^2$ ,  $\lambda = 0.02 \text{ V}^{-1}$ , and  $V_{TP} = -1 \text{ V}$ . (b) Use SPICE to verify the results of your hand calculations. Assume  $f = 7500 \text{ Hz}$  and  $C_1 = 2.2 \mu\text{F}$ ,  $C_2 = 10 \mu\text{F}$ ,  $C_3 = 47 \mu\text{F}$ .
- 14.81. (a) Calculate the values of  $A_v$ ,  $R_{in}$ , and  $R_{out}$  for the amplifier in Fig. P14.1(h) if  $R_I = 500 \Omega$ ,  $R_B = 100 \text{ k}\Omega$ ,  $R_3 = 100 \text{ k}\Omega$ ,  $R_E = 82 \text{ k}\Omega$ ,  $R_C = 39 \text{ k}\Omega$ , and  $V_{EE} = V_{CC} = 12 \text{ V}$ . Use  $\beta_F = 50$  and  $V_A = 50 \text{ V}$ . (b) Use SPICE to verify the results of your hand calculations. Assume  $f = 12 \text{ kHz}$  and  $C_1 = 4.7 \mu\text{F}$ ,  $C_2 = 47 \mu\text{F}$ ,  $C_3 = 10 \mu\text{F}$ .
- 14.82. (a) Calculate the values of  $A_v$ ,  $R_{in}$ , and  $R_{out}$  for the amplifier in Fig. P14.1(l) if  $R_I = 1 \text{ k}\Omega$ ,  $R_3 = 10.0 \text{ k}\Omega$ ,  $R_S = 51 \text{ k}\Omega$ ,  $R_D = 20 \text{ k}\Omega$ , and  $V_{DD} = 15 \text{ V}$ . Use  $K_n = 500 \mu\text{A/V}^2$ ,  $\lambda = 0.02 \text{ V}^{-1}$ , and  $V_{TN} = -2 \text{ V}$ . (b) Use SPICE to verify the results of your hand calculations. Assume  $f = 20 \text{ kHz}$  and  $C_1 = 47 \mu\text{F}$  and  $C_2 = 2.2 \mu\text{F}$ .
- 14.83. (a) Calculate the values of  $A_v$ ,  $R_{in}$ , and  $R_{out}$  for the amplifier in Fig. P14.1(m) if  $R_I = 5 \text{ k}\Omega$ ,  $R_G = 10 \text{ M}\Omega$ ,  $R_3 = 36 \text{ k}\Omega$ ,  $R_D = 1.8 \text{ k}\Omega$ , and  $V_{DD} = 16 \text{ V}$ . Use  $K_n = 10 \text{ mS/V}$ ,  $V_{TN} = -5 \text{ V}$ , and  $\lambda = 0.02 \text{ V}^{-1}$ . (b) Use SPICE to verify the results of your hand calculations. Assume  $f = 3000 \text{ Hz}$  and  $C_1 = 2.2 \mu\text{F}$ ,  $C_2 = 10 \mu\text{F}$ .
- 14.84. (a) Calculate the values of  $A_v$ ,  $R_{in}$ , and  $R_{out}$  for the amplifier in Fig. P14.1(n) if  $R_I = 250 \Omega$ ,  $R_B = 33 \text{ k}\Omega$ ,  $R_3 = 1 \text{ M}\Omega$ ,  $R_E = 7.8 \text{ k}\Omega$ ,  $V_{CC} = 10 \text{ V}$ , and  $V_{EE} = 10 \text{ V}$ . Use  $\beta_F = 80$  and  $V_A = 100 \text{ V}$ . (b) Use SPICE to verify the results of your hand calculations. Assume  $f = 500 \text{ kHz}$  and  $C_1 = 4.7 \mu\text{F}$ ,  $C_2 = 1 \mu\text{F}$ ,  $C_3 = 100 \mu\text{F}$ , and  $L = 1 \text{ H}$ .
- 14.85. (a) Calculate the values of  $A_v$ ,  $R_{in}$ , and  $R_{out}$  for the amplifier in Fig. P14.1(o) if  $R_I = 10 \text{ k}\Omega$ ,  $R_G = 2 \text{ M}\Omega$ ,  $R_3 = 100 \text{ k}\Omega$ , and  $V_{DD} = V_{SS} = 6 \text{ V}$ . Use  $K_n = 400 \mu\text{A/V}^2$ ,  $V_{TN} = 1 \text{ V}$ , and  $\lambda = 0.02 \text{ V}^{-1}$ . (b) Use SPICE to verify the results of your hand calculations. Assume  $f = 1 \text{ MHz}$  and  $C_1 = 2.2 \mu\text{F}$ ,  $C_2 = 4.7 \mu\text{F}$ , and  $L = 100 \text{ mH}$ .
- 14.86. (a) Calculate the values of  $A_v$ ,  $R_{in}$ , and  $R_{out}$  for the amplifier in Fig. P14.1(p) if  $R_I = 10 \text{ k}\Omega$ ,  $R_E = 500 \text{ k}\Omega$ ,  $R_3 = 500 \text{ k}\Omega$ ,  $R_D = 17 \text{ k}\Omega$ , and  $V_{DD} = 9 \text{ V}$ . Use  $I_{DSO} = 1 \text{ mA}$  and  $V_P = -3 \text{ V}$ . (b) Use SPICE to verify the results of your hand calculations. Assume  $f = 10 \text{ kHz}$  and  $C_1 = 10 \mu\text{F}$ ,  $C_2 = 10 \mu\text{F}$ ,  $C_3 = 47 \mu\text{F}$ .

## 14.6 Common-Source Amplifiers Using MOS Inverters

- 14.87. Find the Q-point, voltage gain, input resistance, and output resistance of the amplifier in Fig. P14.87 if  $R_F = 1 \text{ M}\Omega$ ,  $R_3 = 100 \text{ k}\Omega$ ,  $K'_n = 100 \mu\text{A/V}^2$ ,  $V_{TN} = 1 \text{ V}$ ,  $\lambda = 0.02$ ,  $(W/L)_1 = 10/1$ ,  $(W/L)_2 = 2/1$  and  $V_{DD} = 5 \text{ V}$ .

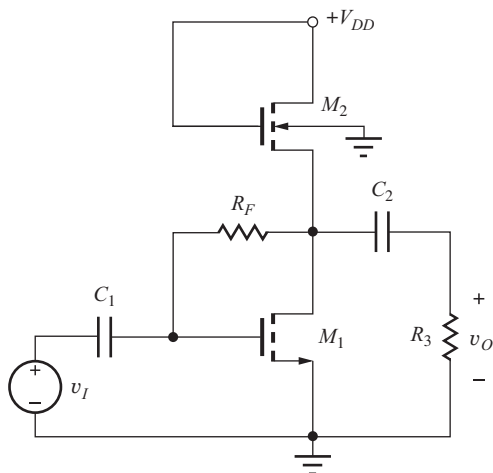


Figure P14.87

- 14.88. Find the Q-point, voltage gain, input resistance, and output resistance of the amplifier in Fig. P14.88 if  $R_F = 560 \text{ k}\Omega$ ,  $R_3 = 100 \text{ k}\Omega$ ,  $K'_n = 100 \mu\text{A}/\text{V}^2$ ,  $K'_p = 40 \mu\text{A}/\text{V}^2$ ,  $V_{TN} = 1 \text{ V}$ ,  $V_{TP} = -1 \text{ V}$ ,  $\lambda = 0.02$ ,  $(W/L)_1 = 40/1$ ,  $(W/L)_2 = 100/1$  and  $V_{DD} = 5 \text{ V}$ .

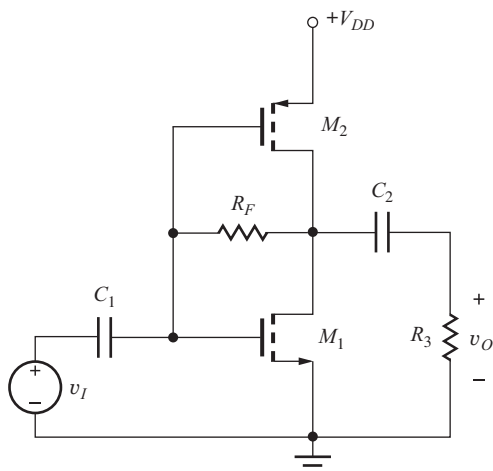


Figure P14.88

- 14.89. (a) Find the Q-point, voltage gain, input resistance, and output resistance of the amplifier in Fig. P14.89 if  $R_1 = 240 \text{ k}\Omega$ ,  $R_2 = 750 \text{ k}\Omega$ ,  $R_3 = 100 \text{ k}\Omega$ ,  $K'_n = 100 \mu\text{A}/\text{V}^2$ ,  $V_{TN} = 1 \text{ V}$ ,  $\lambda = 0.02$ ,  $(W/L)_1 = 4/1$ ,  $(W/L)_2 = 4/1$  and  $V_{DD} = 9 \text{ V}$ .

- 14.90. Redesign the  $W/L$  ratio for  $M_2$  in Prob. 14.89 to achieve a voltage gain of 0.75.

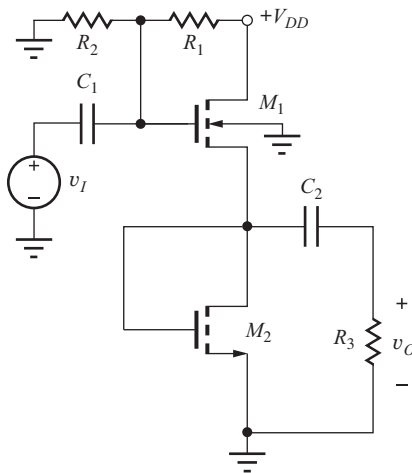


Figure P14.89

#### 14.7 Coupling and Bypass Capacitor Design

- 14.91. (a) The amplifier in Fig. P14.1(d) has  $R_1 = 500 \text{ k}\Omega$ ,  $R_2 = 1.4 \text{ M}\Omega$ ,  $R_S = 27 \text{ k}\Omega$ ,  $R_D = 75 \text{ k}\Omega$ , and  $V_{DD} = 15 \text{ V}$ . Use  $K_n = 400 \mu\text{A}/\text{V}^2$ ,  $V_{TN} = 1 \text{ V}$ , and  $\lambda = 0.02 \text{ V}^{-1}$ . Choose values for  $C_1$ ,  $C_2$ , and  $C_3$  so that they can be neglected at a frequency of 500 Hz. (b) Choose  $C_3$  to set the lower cutoff frequency to 4 kHz assuming  $C_1$  and  $C_2$  remain unchanged.
- 14.92. (a) The amplifier in Fig. P14.1(c) has  $R_1 = 20 \text{ k}\Omega$ ,  $R_2 = 62 \text{ k}\Omega$ ,  $R_C = 8.2 \text{ k}\Omega$ ,  $R_E = 3.9 \text{ k}\Omega$ , and  $V_{CC} = 12 \text{ V}$ . Choose values for  $C_1$ ,  $C_2$ , and  $C_3$  so that they can be neglected at a frequency of 250 Hz. Use  $\beta_F = 75$  and  $V_A = 60 \text{ V}$ . (b) Choose  $C_3$  to set the lower cutoff frequency to 1000 Hz assuming  $C_1$  and  $C_2$  remain unchanged.
- 14.93. Calculate the frequency for which each of the capacitors in Fig. P14.74 can be considered to have a negligible effect on the circuit.
- 14.94. Choose values of  $C_1$  and  $C_2$  in Fig. P14.94 so they will have negligible effect on the circuit at a frequency of 50 kHz. (b) Repeat for a frequency of 100 Hz.

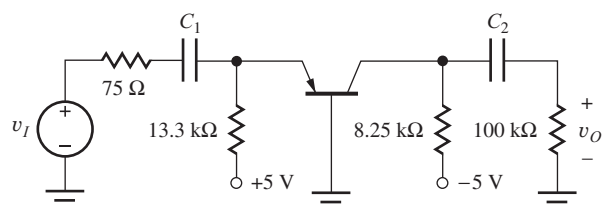


Figure P14.94

- 14.95. The amplifier in Fig. P14.1(a) has  $R_I = 500 \Omega$ ,  $R_1 = 51 \text{ k}\Omega$ ,  $R_2 = 100 \text{ k}\Omega$ ,  $R_3 = 24 \text{ k}\Omega$ ,  $R_E = 4.7 \text{ k}\Omega$ ,  $R_C = 0$ , and  $V_{CC} = V_{EE} = 15 \text{ V}$ . Choose values for  $C_1$ ,  $C_2$ , and  $C_3$  so that they can be neglected at a frequency of 100 Hz. Use  $\beta_F = 100$  and  $V_A = 50 \text{ V}$ .
- 14.96. The amplifier in Fig. P14.1(l) has  $R_I = 1 \text{ k}\Omega$ ,  $R_1 = 3.9 \text{ k}\Omega$ ,  $R_3 = 100 \text{ k}\Omega$ ,  $R_D = 20 \text{ k}\Omega$ , and  $V_{DD} = 15 \text{ V}$ . Choose values for  $C_1$ ,  $C_2$ , and  $C_3$  so that they can be neglected at a frequency of 250 Hz. Use  $K_n = 500 \mu\text{A/V}^2$ ,  $V_{TN} = -2 \text{ V}$ , and  $\lambda = 0.02 \text{ V}^{-1}$ .
- 14.97. (a) Use a dominant-pole approach to set the lower cutoff frequency of the C-S amplifier in Ex. 14.7 to 1000 Hz. Choose values for  $C_1$ ,  $C_2$ , and  $C_3$  based upon the values in the example. (b) Check your design with SPICE.
- 14.98. (a) Use a dominant-pole approach to set the lower cutoff frequency of the C-C amplifier in Ex. 14.8 to 2000 Hz. Choose values for  $C_1$ , and  $C_2$  based upon the values in the example.
- 14.99. Use the dominant-pole approach to set the lower cutoff frequency of the C-G amplifier in Ex. 14.9 to 1000 Hz. Choose values for  $C_1$ ,  $C_2$ , and  $C_3$  based upon the values in the example. (c) Check your two designs with SPICE.
- \*14.106. (a) Calculate worst-case estimates of the gain of the common-base amplifier in Fig. 14.45 if the resistors and power supplies all have 5 percent tolerances. (b) Compare your answers to the Monte Carlo results in Table 14.16.
- \*\*14.107. Use SPICE to perform a 1000-case Monte Carlo analysis of the common-base amplifier in Fig. 14.45 if the resistors and power supplies have 5 percent tolerances. Assume that the current gain  $\beta_F$  and  $V_A$  are uniformly distributed in the intervals [60, 100] and [50, 70], respectively. What are the mean and  $3\sigma$  limits on the voltage gain predicted by these simulations? Compare the  $3\sigma$  values to the worst-case calculations in Prob. 14.106. Compare your answers to the Monte Carlo results in Table 14.16. Use  $C_1 = 47 \mu\text{F}$ ,  $C_2 = 4.7 \mu\text{F}$ , and  $f = 10 \text{ kHz}$ .
- 14.108. A common-gate amplifier is needed with an input resistance of  $10 \Omega$ . Two  $n$ -channel MOSFETs are available: one with  $K_n = 5 \text{ mA/V}^2$  and the other with  $K_n = 500 \text{ mA/V}^2$ . Both are capable of providing the desired value of  $R_{in}$ . Which one would be preferred and why? (Hint: Find the required Q-point current for each transistor.)
- \*\*14.109. The common-base amplifier in Fig. P14.94 is the implementation of the design from Design Ex. 14.11 using the nearest 1 percent resistor values. (a) What are the worst-case values of gain and input resistance if the power supplies have  $\pm 2$  percent tolerances? (b) Use a computer program or spreadsheet to perform a 1000-case Monte Carlo analysis to find the mean and  $3\sigma$  limits on the gain and input resistances. Compare these values to the worst-case estimates from part (a).

## 14.8 Amplifier Design Examples

- 14.100. Repeat the source-follower design in Design Ex. 14.6 for a MOSFET with  $K_n = 30 \text{ mA/V}^2$  and  $V_{TN} = 2.5 \text{ V}$ . Assume  $V_{GS} - V_{TN} = 0.5 \text{ V}$ .
- 14.101. Rework Ex. 14.11 to achieve a  $50\text{-}\Omega$  input resistance.
- 14.102. A common-base amplifier was used in the design problem in Ex. 14.11 to match the  $75\text{-}\Omega$  input resistance. One could conceivably match the input resistance with a common-emitter stage (with  $R_E = 0$ ). What collector current is required to set  $R_{in} = 75 \Omega$  for a BJT with  $\beta_o = 100$ ?
- \*14.103. Redesign the bias network so that the common-base amplifier in Fig. 14.45 can operate from a single  $+10\text{-V}$  supply.
- 14.104. Redesign the amplifier in Fig. 14.45 to operate from symmetrical  $7.5\text{-V}$  power supplies and achieve the same design specifications.
- 14.105.  $(1/g_m)$  is set to  $50 \Omega$  in a common-base design operating at  $27^\circ\text{C}$ . What are the values of  $(1/g_m)$  at  $-40^\circ\text{C}$  and  $+50^\circ\text{C}$ ?
- \*\*14.110. Use SPICE to perform a 1000-case Monte Carlo analysis of the circuit in Fig. P14.94 assuming the resistors have 1 percent tolerances and the power supplies have  $\pm 2$  percent tolerances. Find the mean and  $3\sigma$  limits on the gain and input resistance at a frequency of  $10 \text{ kHz}$ . Assume that the current gain  $\beta_F$  and  $V_A$  are uniformly distributed in the intervals (60, 100) and (50, 70), respectively. Use  $C_1 = 100 \mu\text{F}$ ,  $C_2 = 1 \mu\text{F}$ , and  $f = 10 \text{ kHz}$ .
- 14.111. Suppose that we forgot about the factor of 2 loss in signal that occurs at the input of the common-base stage in Ex. 14.11 and selected  $V_{CC} = V_{EE} = 2.5 \text{ V}$ . Repeat the design to see if the specifications can be met using these power supply values.

- \*\*14.112. (a) Use a spreadsheet or other computer tool to perform a Monte Carlo analysis of the design in Fig. 14.41. The resistors and power supplies have 5 percent tolerances.  $V_{TN}$  is uniformly distributed in the interval [1 V, 2 V], and  $K_n$  is uniformly distributed in the interval [10 mA/V<sup>2</sup>, 30 mA/V<sup>2</sup>]. (b) Use the Monte Carlo option in PSPICE to perform the same analysis at a frequency of 10 kHz for  $C_1 = 4.7 \mu\text{F}$  and  $C_2 = 68 \mu\text{F}$ . Compare the results.

Unless otherwise specified, use  $\beta_F = 100$ ,  $V_A = 70 \text{ V}$ ,  $K_p = K_n = 1 \text{ mA/V}^2$ ,  $V_{TN} = -V_{TP} = 1 \text{ V}$ , and  $\lambda = 0.02 \text{ V}^{-1}$ .

### 14.9 Multistage ac-Coupled Amplifiers

- 14.113. What are the voltage gain, input resistance, and output resistance of the amplifier in Fig. 14.49 if bypass capacitors  $C_2$  and  $C_4$  are removed from the circuit?

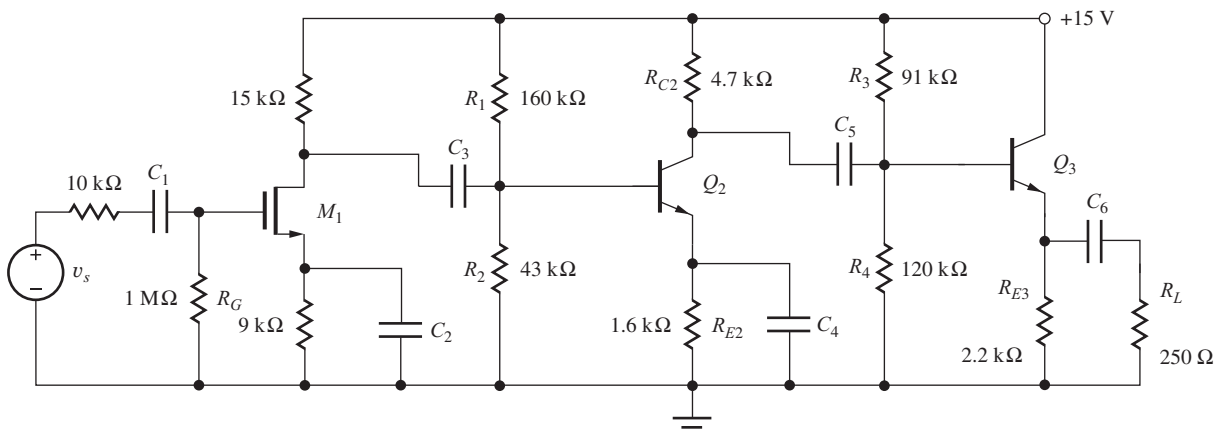


Figure P14.114

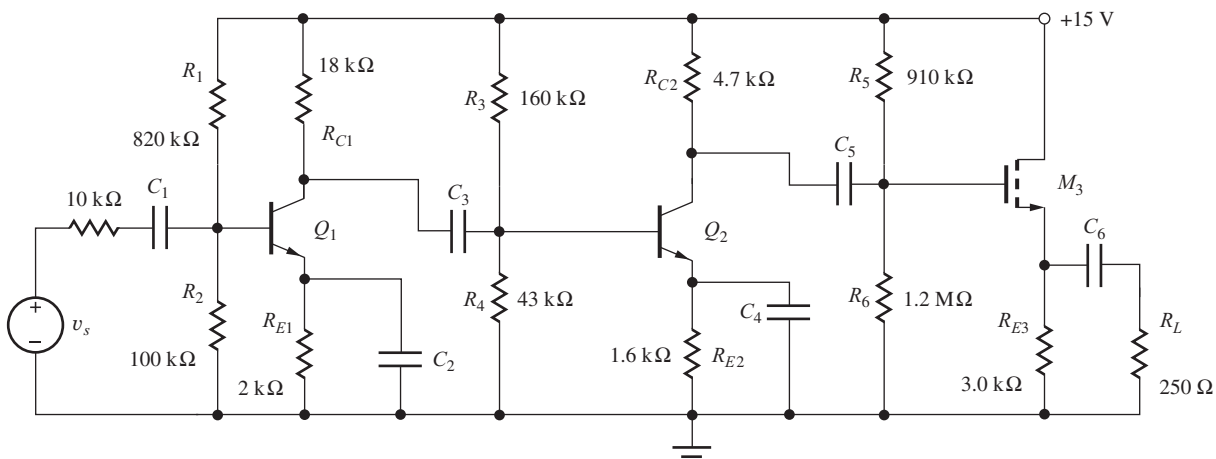


Figure P14.118

- 14.114. Figure P14.114 is an “improved” version of the three-stage amplifier discussed in Sec. 14.9. Find the gain and input signal range for this amplifier. Was the performance actually improved?  
S
- 14.115. Use SPICE to simulate the amplifier in Fig. P14.114 at a frequency of 2 kHz, and determine the voltage gain, input resistance, and output resistance. Assume the capacitors all have a value of  $22 \mu\text{F}$ .  
S
- 14.116. Find the midband voltage gain and input resistance of the amplifier in Fig. P14.114 if capacitors  $C_2$  and  $C_4$  are removed from the circuit.  
S
- 14.117. Use SPICE to determine the gain of the amplifier in Fig. P14.114 if  $C_2$  and  $C_4$  are removed from the circuit. Assume the capacitors all have a value of  $22 \mu\text{F}$ .  
S

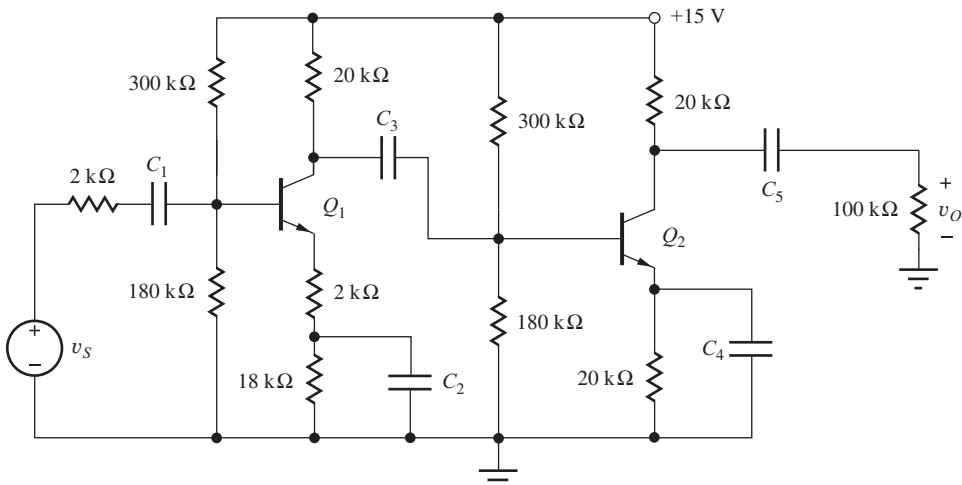


Figure P14.121

- \*14.118. Figure P14.118 shows another “improved” design of the three-stage amplifier discussed in Sec. 14.9. Find the gain and input signal range for this amplifier. Was the performance improved?

- 14.119. Use SPICE to simulate the amplifier in Fig. P14.118 at a frequency of 3 kHz and determine the voltage gain, input resistance, and output resistance. Assume the capacitors all have a value of  $22 \mu\text{F}$ .

- 14.120. What is the gain of the amplifier in Fig. P14.118 if  $C_2$  and  $C_4$  are removed?

- 14.121. What are the midband voltage gain, input resistance, and output resistance of the amplifier in Fig. P14.121?

- 14.122. What are the voltage gain, input resistance, and output resistance of the amplifier in Fig. P14.121 if the bypass capacitors are removed?

- 14.123. Use SPICE to simulate the amplifier in Fig. P14.121 at a frequency of 5 kHz and determine the voltage gain, input resistance, and output resistance. Assume the capacitors all have a value of  $10 \mu\text{F}$ .

- 14.124. Find the midband voltage gain, input resistance, and output resistance of the amplifier in Fig. P14.121 if capacitor  $C_2$  is connected between the emitter of  $Q_1$  and ground?

- 14.125. What are the midband voltage gain, input resistance, and output resistance of the amplifier in Fig. P14.125 if  $K_n = 50 \text{ mA/V}^2$  and  $V_{TN} = -2 \text{ V}$ ?

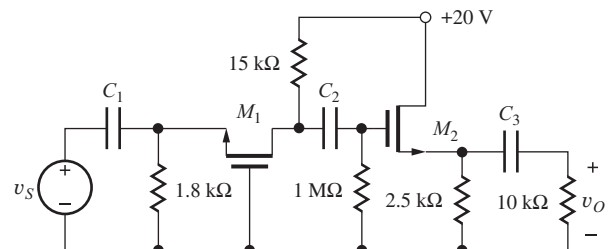


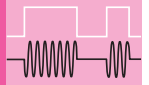
Figure P14.125

### Lower Cutoff Frequency Estimates

- 14.126. Use the short circuit time constant technique to estimate the lower cutoff frequency for the amplifier in Prob. 14.75. Compare your answer to SPICE simulation.
- 14.127. Use the short circuit time constant technique to estimate the lower cutoff frequency for the amplifier in Prob. 14.76. Compare your answer to SPICE simulation.
- 14.128. Use the short circuit time constant technique to estimate the lower cutoff frequency for the amplifier in Prob. 14.77. Compare your answer to SPICE simulation.
- 14.129. Use the short circuit time constant technique to estimate the lower cutoff frequency for the amplifier in Prob. 14.78. Compare your answer to SPICE simulation.
- 14.130. Use the short circuit time constant technique to estimate the lower cutoff frequency for the am-

- plifier in Prob. 14.79. Compare your answer to SPICE1 simulation.
- 14.131. Use the short circuit time constant technique to estimate the lower cutoff frequency for the amplifier in Prob. 14.81. Compare your answer to SPICE simulation.
- 14.132. Use the short circuit time constant technique to estimate the lower cutoff frequency for the amplifier in Prob. 14.82. Compare your answer to SPICE simulation.
- 14.133. Use the short circuit time constant technique to estimate the lower cutoff frequency for the amplifier in Prob. 14.83. Compare your answer to SPICE simulation.
- 14.134. Use the short circuit time constant technique to estimate the lower cutoff frequency for the amplifier in Prob. 14.125. Compare your answer to SPICE simulation. Use  $C_1 = C_2 = C_3 = 1 \mu\text{F}$ .

# CHAPTER 15



## DIFFERENTIAL AMPLIFIERS AND OPERATIONAL AMPLIFIER DESIGN

### CHAPTER OUTLINE

15.1	Differential Amplifiers	969
15.2	Evolution to Basic Operational Amplifiers	991
15.3	Output Stages	1006
15.4	Electronic Current Sources	1016
	Summary	1027
	Key Terms	1028
	References	1029
	Additional Reading	1029
	Problems	1029

### CHAPTER GOALS

In this chapter, we learn to work with dc-coupled amplifiers that contain several interconnected stages, and several important new amplifier concepts are introduced. Overall, we want to achieve these goals:

- Understand analysis and design of dc-coupled multistage amplifiers
- Explore the dc and ac properties of differential amplifiers
- Understand the basic three-stage operational amplifier circuit
- Explore the design of Class-A, Class-B, and Class AB output stages
- Discuss the characteristics and design of electronic current sources
- Learn how to analyze the effects of device and component mismatch on the performance of symmetrical amplifier circuits

In most situations, a single-transistor amplifier cannot meet all the given specifications. The required voltage gain often exceeds the amplification factor of a single transistor, or the combination of voltage gain, input resistance, and output resistance cannot be met simultaneously. For example, consider the specifications of a good general-purpose operational amplifier. Such an amplifier has an input resistance exceeding  $1\text{ M}\Omega$ , a voltage gain of 100,000, and an output resistance of less than  $500\text{ }\Omega$ . It should be clear from our investigation of amplifiers in Chapters 13 and 14 that these requirements cannot all be met simultaneously with

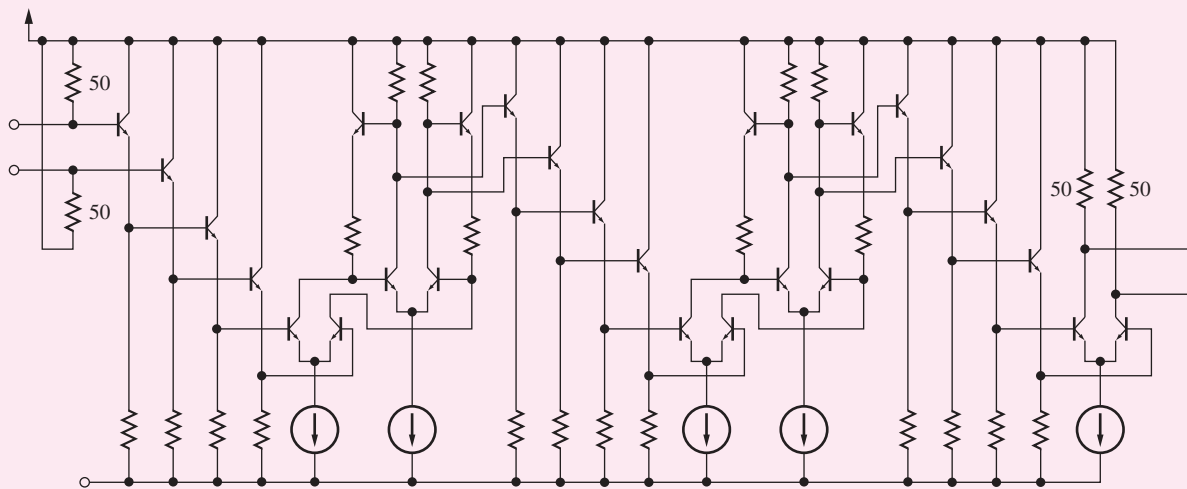
a single-transistor amplifier. A number of stages must be cascaded in order to create an amplifier that can meet all these requirements.

Chapter 15 continues our study of combining single-transistor amplifier stages to achieve higher levels of overall performance. ac-coupled amplifiers discussed in Chapter 14 eliminate dc interactions between the various stages forming the amplifier, thus simplifying bias circuit design. On the other hand, in our work in Chapters 11 and 12, most of the operational amplifier circuits provided amplification of dc signals. To realize amplifiers of this type, coupling capacitors that block dc signal flow through the amplifier must be eliminated, which leads to the concept of direct-coupled or dc-coupled amplifiers that can satisfy the requirement for dc amplification. In the dc-coupled case, the operating point of one stage is dependent on the Q-point of the other stages, making the dc design somewhat more complex.

The most important dc-coupled amplifier is the symmetric two-transistor differential amplifier. Not only is the differential amplifier a key circuit in the design of operational amplifiers, it is also a fundamental building block in all analog IC design. In this chapter, we present the transistor-level implementation of BJT and FET differential amplifiers and explore how the differential-mode and common-mode gains, common-mode rejection ratio, differential-mode and common-mode input resistances, and output resistance of the amplifier are all related to transistor parameters.

Subsequently, a second gain stage and an output stage are added to the differential amplifier, creating the prototype for a basic operational amplifier. The definitions of class-A, class-B, and class-AB amplifiers are introduced, and the basic op amp design is further improved by adding class-B and class-AB output stages. In audio applications, these output stages often use transformer coupling.

Bias for analog circuits is most often provided by current sources. An ideal current source provides a fixed output current, independent of the voltage across the source; that is, the current source has an infinite output resistance. Electronic current sources cannot achieve infinite output resistance, but very high values are possible, and a number of



Schematic of a limiting amplifier in bipolar technology. Y. Baeyens et al., “InP D-HBT IC’s for 40-Gb/s and higher bit rate lightwave transceivers,” *IEEE J. Solid-State Circuits*, vol. 37, no. 9, pp. 1152–1159, September 2002. Copyright © 2002 IEEE. Adapted with permission.

basic current source circuits and techniques for achieving high output resistance are introduced and compared. Anal-

ysis of the various current sources uses the single-stage amplifier results from Chapters 13 and 14.

## 15.1 DIFFERENTIAL AMPLIFIERS

The coupling capacitors that were discussed in Chapter 14 limit the low-frequency response of the amplifiers and prevent their application as dc amplifiers. For an amplifier to provide gain at dc, capacitors in series with the signal path (e.g.,  $C_1$ ,  $C_3$ ,  $C_5$ , and  $C_6$  in Fig. 14.49) must be eliminated. Such an amplifier is called a **dc-coupled** or **direct-coupled amplifier**. Using a direct-coupled design can also eliminate additional resistors that are required to bias the individual stages in an ac-coupled amplifier, thus producing a less expensive amplifier.

The dc-coupled differential amplifier represents one of the most important additions to our “toolkit” of basic building blocks for analog design. Differential amplifiers appear in some form in almost every analog integrated circuit! This circuit forms the heart of operational amplifier design as well as of most dc-coupled analog circuits. Although the differential amplifier contains two transistors in a symmetrical configuration, it is usually thought of as a single-stage amplifier, and our analyses will show that it has characteristics similar to those of common-emitter or common-source amplifiers.

### 15.1.1 BIPOLAR AND MOS DIFFERENTIAL AMPLIFIERS

Figure 15.1 shows bipolar and MOS versions of the differential amplifier. Each circuit has two input terminals,  $v_1$  and  $v_2$ , and the **differential-mode output voltage**  $v_{OD}$  is defined by the voltage difference between the collectors or drains of the two transistors. Ground-referenced outputs can also be taken between either collector or drain— $v_{C1}$ ,  $v_{C2}$ ,  $v_{D1}$ , or  $v_{D2}$ —and ground.

The symmetrical nature of the amplifier provides useful dc and ac properties. We will find that the differential amplifier behaves as either an inverting or noninverting amplifier for differential input signals but tends to reject signals common to both inputs. However, ideal performance is obtained from the differential amplifier only when it is perfectly symmetrical, and the best versions are built using IC technology in which the transistor characteristics can be closely matched. Two transistors are said to be **matched** if they have identical characteristics and parameter values; that is, the parameter sets ( $I_S$ ,  $\beta_{FO}$ ,  $V_A$ ) or ( $K_n$ ,  $V_{TN}$ , and  $\lambda$ ), Q-points, and temperatures of the two transistors are identical.

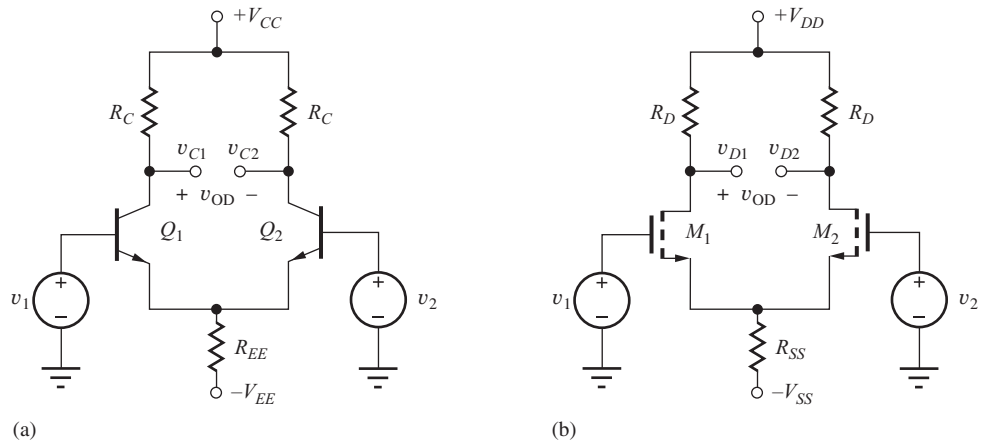


Figure 15.1 (a) Bipolar and (b) MOS differential amplifiers.

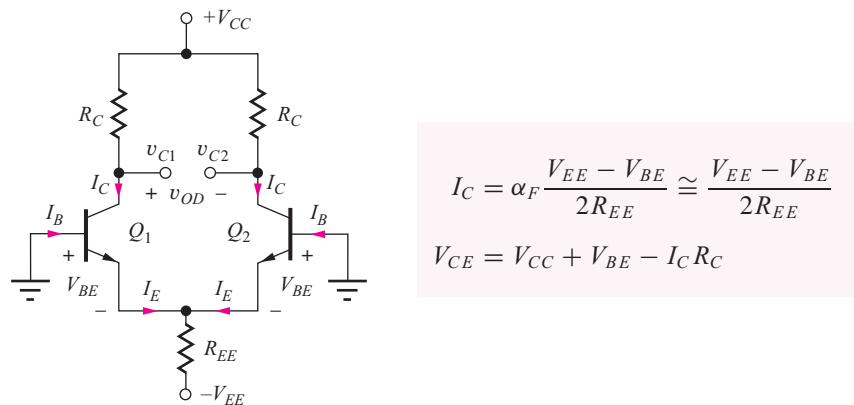


Figure 15.2 Circuit for dc analysis of the bipolar differential amplifier.

### 15.1.2 dc ANALYSIS OF THE BIPOLEAR DIFFERENTIAL AMPLIFIER

We begin our analysis of the differential amplifier by finding the transistor operating points. The quiescent operating points of the transistors in the bipolar differential amplifier can be found by setting both input signal voltages to zero, as in Fig. 15.2. In this circuit, both bases are grounded and the two emitters are connected together. Therefore,  $V_{BE1} = V_{BE2} = V_{BE}$ . If bipolar transistors  $Q_1$  and  $Q_2$  are assumed to be matched, then the symmetry of the circuit also forces  $V_{C1} = V_{C2} = V_C$ , and the terminal currents of the two transistors are identical:  $I_{C1} = I_{C2} = I_C$ ,  $I_{E1} = I_{E2} = I_E$ , and  $I_{B1} = I_{B2} = I_B$ .

The emitter currents can be found by writing a loop equation starting at the base of  $Q_1$ :

$$V_{BE} + 2I_E R_{EE} - V_{EE} = 0 \quad \text{and} \quad I_C = \alpha_F I_E = \alpha_F \frac{V_{EE} - V_{BE}}{2R_{EE}} \quad (15.1)$$

with

$$I_B = I_C / \beta_F$$

The voltages at the two collectors are equal to

$$V_{C1} = V_{C2} = V_{CC} - I_C R_C \quad (15.2)$$

and  $V_{CE1} = V_{CE2} = V_{CC} + V_{BE} - I_C R_C$ . For the symmetrical amplifier, the dc output voltage is zero:

$$V_{OD} = V_{C1} - V_{C2} = 0 \text{ V} \quad (15.3)$$

### EXAMPLE 15.1 DIFFERENTIAL AMPLIFIER Q-POINT ANALYSIS

In this example, we determine the Q-point for an “emitter-coupled pair” of bipolar transistors.

**PROBLEM** Find the Q-points plus  $V_C$  and  $I_B$  for the differential amplifier in Fig. 15.1(a) if  $V_{CC} = V_{EE} = 15 \text{ V}$ ,  $R_{EE} = 75 \text{ k}\Omega$ ,  $R_C = 75 \text{ k}\Omega$ , and  $\beta_F = 100$ .

**SOLUTION** **Known Information and Given Data:** Circuit topology appears in Fig. 15.1(a); symmetrical 15-V power supplies are used to operate the circuit;  $R_C = R_{EE} = 75 \text{ k}\Omega$ ;  $\beta_F = 100$ .

**Unknowns:**  $I_C$ ,  $V_{CE}$ ,  $V_C$ ,  $I_B$  for  $Q_1$  and  $Q_2$

**Approach:** Use the circuit element values and follow the analysis presented in Eqs. (15.1) through (15.3).

**Assumptions:** Active region operation with  $V_{BE} = 0.7 \text{ V}$ ;  $V_A = \infty$

**Analysis:** Using Eqs. (15.1) and (15.2):

$$I_E = \frac{V_{EE} - V_{BE}}{2R_{EE}} = \frac{(15 - 0.7) \text{ V}}{2(75 \times 10^3 \Omega)} = 95.3 \mu\text{A}$$

$$I_C = \alpha_F I_E = \frac{100}{101} I_E = 94.4 \mu\text{A} \quad I_B = \frac{I_C}{\beta_F} = \frac{94.4 \mu\text{A}}{100} = 0.944 \mu\text{A}$$

$$V_C = 15 - I_C R_C = 15 \text{ V} - (9.44 \times 10^{-5} \text{ A})(7.5 \times 10^4 \Omega) = 7.92 \text{ V}$$

$$V_{CE} = V_C - V_E = 7.92 \text{ V} - (-0.7 \text{ V}) = 8.62 \text{ V}$$

Because of the circuit symmetry, both transistors in the differential amplifier are biased at a Q-point of (94.4  $\mu\text{A}$ , 8.62 V) with  $I_B = 0.944 \mu\text{A}$  and  $V_C = 7.92 \text{ V}$ .

**Check of Results:** A double check of results indicates the calculations are correct. Note that when  $R_C$  and  $R_{EE}$  are equal, the voltage drop across  $R_C$  should be approximately one-half of the voltage across  $R_{EE}$ . Our calculations agree with this result. Also,  $V_{CE} > V_{BE}$ , so the assumption of forward-active region operation is correct.

**Discussion:** Note, that for  $V_{EE} \gg V_{BE}$ ,  $I_E$  can be approximated by

$$I_E \cong \frac{V_{EE}}{2R_{EE}} = \frac{15 \text{ V}}{150 \text{ k}\Omega} = 100 \mu\text{A}$$

This estimate represents only a 6 percent error compared to the more accurate calculation.

**Computer-Aided Analysis:** SPICE analysis with  $\text{BF} = 100$  and  $\text{IS} = 5 \times 10^{-16} \text{ A}$  yields a Q-point of (94.6  $\mu\text{A}$ , 8.57 V) with  $V_{BE} = 0.672 \text{ V}$ . The collector voltage and base current values are 7.91 V and 0.946  $\mu\text{A}$ , respectively, all in agreement with our hand calculations. We can also use SPICE to explore the effect of a nonzero Early voltage on the Q-point of the differential amplifier. A second simulation with  $\text{VAF} = 50 \text{ V}$  yields Q-point values of (94.7  $\mu\text{A}$ , 8.56 V). Almost no changes can be observed in the Q-point values! The collector voltage and base current values are now 7.90 V and 0.818  $\mu\text{A}$ , respectively. Since the collector current has not changed,

$V_C$  also has not changed. However, the base current has been reduced by 14 percent. We should wonder why this has occurred. Remember that the current gain of the transistor in our transport model is given by  $\beta_F = \beta_{FO}(1 + V_{CE}/V_A)$ . Also remember that a slightly different form is used in SPICE:

$$\beta_F = \beta_{FO} \left( 1 + \frac{V_{CB}}{V_A} \right) = \beta_{FO} \left( 1 + \frac{V_{CE} - V_{BE}}{V_A} \right) = 100 \left( 1 + \frac{7.90}{50} \right) = 116$$

and there is our discrepancy!

**EXERCISE:** What is the Q-point if  $\beta_F$  is 60 instead of 100?

**ANSWER:** (93.7  $\mu\text{A}$ , 8.67 V)

**EXERCISE:** What are the actual values of  $I_C$  and  $V_{BE}$  for the transistor if the transistor saturation current is 0.5 fA?

**ANSWER:** 0.649 V for  $V_T = 25$  mV; 94.7  $\mu\text{A}$

**EXERCISE:** Draw a *pnp* version of the differential amplifier in Fig. 15.1(a).

**ANSWER:** See Fig. P15.15.

### 15.1.3 TRANSFER CHARACTERISTIC FOR THE BIPOLAR DIFFERENTIAL AMPLIFIER

The differential amplifier provides advantages in terms of signal range and distortion characteristics over that of a single bipolar transistor. We can explore these advantages using results already derived for the current switch in Sec. 9.1.1. The current switch simply represents a digital application of the differential amplifier, and the large-signal transfer characteristic of the differential amplifier is the same as that presented in Eq. (9.5) and repeated here (with  $\alpha_F I_{EE} = 2I_C$ ).

$$\begin{aligned} i_{C1} - i_{C2} &= 2I_C \tanh \left( \frac{v_{BE1} - v_{BE2}}{2V_T} \right) = 2I_C \tanh \left( \frac{v_{id}}{2V_T} \right) \\ G_m &= \frac{d(i_{C1} - i_{C2})}{dv_{id}} = \frac{I_C}{V_T} \operatorname{sech}^2 \left( \frac{v_{id}}{2V_T} \right) = g_m \operatorname{sech}^2 \left( \frac{v_{id}}{2V_T} \right) \end{aligned} \quad (15.4)$$

for the symmetrical differential amplifier with  $v_{BE1} = V_{BE} + \frac{v_{id}}{2}$  and  $v_{BE2} = V_{BE} - \frac{v_{id}}{2}$ .

Expanding the hyperbolic tangent using its Maclaurin series yields

$$I_{C1} - I_{C2} = 2I_C \left[ \left( \frac{v_{id}}{2V_T} \right) - \frac{1}{3} \left( \frac{v_{id}}{2V_T} \right)^3 + \frac{2}{15} \left( \frac{v_{id}}{2V_T} \right)^5 - \frac{17}{315} \left( \frac{v_{id}}{2V_T} \right)^7 + \dots \right] \quad (15.5)$$

First we see that subtraction of the two collector currents eliminates the even order distortion terms in Eq. (15.5). Second, for small-signal operation, we desire the linear term to be dominant. Setting the third-order term to be one-tenth of the linear term requires  $v_{id} \leq 2V_T\sqrt{0.3}$  or  $v_{id} \leq 27$  mV. On the surface, one would expect an increase by a factor of 2 (to 10 mV) since the input signal is shared equally by the two transistors of the differential pair. However, cancellation of the even-order distortion terms further increases the signal-handling capability of the differential pair! This expanded linear region of the transfer function can clearly be seen at the center of the plot of Eq. (15.4) that appears in Fig. 15.3.

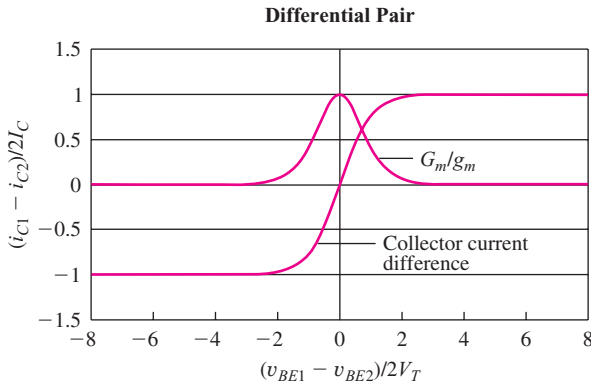


**Figure 15.3** Large-signal transfer characteristic and transconductance for the bipolar differential pair.

The transconductance ( $G_m$ ) of the differential pair defined in Eq. (15.4) as the derivative of the transfer characteristic is also plotted in Fig. 15.3 as a function of the normalized input voltage. The value of  $G_m$  peaks at the transistor  $g_m$  when the pair is balanced with  $i_{C1} = i_{C2}$  and falls to nearly zero for  $|v_{id}| > 6V_T$  (150 mV).

#### 15.1.4 ac ANALYSIS OF THE BIPOLAR DIFFERENTIAL AMPLIFIER

Now that we have the Q-point information we can proceed to use small-signal analysis to characterize the voltage gain and input and output resistances of the differential amplifier. The ac analysis of the differential amplifier can be simplified by breaking input sources  $v_1$  and  $v_2$  into their equivalent **differential-mode input** ( $v_{id}$ ) and **common-mode input** ( $v_{ic}$ ) signal components, shown in Fig. 15.4, and defined by

$$v_{id} = v_1 - v_2 \quad \text{and} \quad v_{ic} = \frac{v_1 + v_2}{2} \quad (15.6)$$

The input voltages can be written in terms of  $v_{ic}$  and  $v_{id}$  as

$$v_1 = v_{ic} + \frac{v_{id}}{2} \quad \text{and} \quad v_2 = v_{ic} - \frac{v_{id}}{2} \quad (15.7)$$

The differential-mode input signal is the difference between inputs  $v_1$  and  $v_2$ , whereas the common-mode input is the signal that is common to both inputs. Circuit analysis is performed using superposition of the differential-mode and common-mode input signal components. This technique was originally used in our study of operational amplifiers in Chapter 11.

The **differential-mode and common-mode output voltages**,  $v_{od}$  and  $v_{oc}$ , are defined in a similar manner:

$$v_{od} = v_{c1} - v_{c2} \quad \text{and} \quad v_{oc} = \frac{v_{c1} + v_{c2}}{2} \quad (15.8)$$

For the general amplifier case, voltages  $v_{od}$  and  $v_{oc}$  are functions of both  $v_{id}$  and  $v_{ic}$  and can be written as

$$\begin{bmatrix} v_{od} \\ v_{oc} \end{bmatrix} = \begin{bmatrix} A_{dd} & A_{cd} \\ A_{dc} & A_{cc} \end{bmatrix} \begin{bmatrix} v_{id} \\ v_{ic} \end{bmatrix} \quad (15.9)$$

in which four gains are defined:

$A_{dd}$  = **differential-mode gain**

$A_{cd}$  = **common-mode (to differential-mode) conversion gain**

$A_{cc}$  = **common-mode gain**

$A_{dc}$  = **differential-mode (to common-mode) conversion gain**

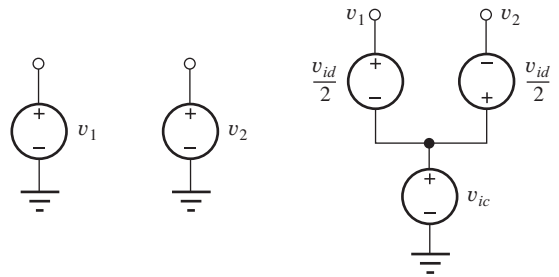


**Figure 15.4** Definition of the differential-mode ( $v_{id}$ ) and common-mode ( $v_{ic}$ ) input voltages.

For an ideal symmetrical amplifier with matched transistors,  $A_{cd}$  and  $A_{dc}$  are zero, and Eq. (15.9) reduces to

$$\begin{bmatrix} v_{od} \\ v_{oc} \end{bmatrix} = \begin{bmatrix} A_{dd} & 0 \\ 0 & A_{cc} \end{bmatrix} \begin{bmatrix} v_{id} \\ v_{ic} \end{bmatrix} \quad (15.10)$$

In this case, a differential-mode input signal produces a purely differential-mode output signal, and a purely common-mode input produces only a common-mode output.

However, when the differential amplifier is not completely balanced because of transistor or other circuit mismatches,  $A_{dc}$  or  $A_{cd}$  are no longer zero. In upcoming discussions, we assume that the transistors are identical unless stated otherwise.

**EXERCISE:** Measurement of a differential amplifier yielded the following sets of values:

$$v_{od} = 2.2 \text{ V and } v_{oc} = 1.002 \text{ V} \quad \text{for } v_1 = 1.01 \text{ V and } v_2 = 0.990 \text{ V}$$

$$v_{od} = 0 \text{ V and } v_{oc} = 5.001 \text{ V} \quad \text{for } v_1 = 4.995 \text{ V and } v_2 = 5.005 \text{ V}$$

What are  $v_{id}$  and  $v_{ic}$  for the two cases? What are the values of  $A_{dd}$ ,  $A_{cd}$ ,  $A_{dc}$ , and  $A_{cc}$  for the amplifier?

**ANSWERS:** 0.02 V, 1.00 V; -0.01 V, 5.00 V; 100, 0.200, 0.100, 1.00

Now we are in a position to fully characterize the signal properties of the differential amplifier. We want to find voltage gains  $A_{dd}$  and  $A_{cc}$ , and the input and output resistances of the amplifier. First we will take a direct nodal analysis approach to the amplifier characterization. The results will subsequently lead us to a simplified analysis method called *half-circuit analysis* that is applicable to symmetric circuits.

### 15.1.5 DIFFERENTIAL-MODE GAIN AND INPUT AND OUTPUT RESISTANCES

Purely differential-mode input signals are applied to the differential amplifier in Fig. 15.5, and the two transistors are replaced with their small-signal models in Fig. 15.6. We will find the gain for both differential and single-ended outputs as well as the input and output resistances. Because the transistors have resistor loads, the output resistances will be neglected in the calculations.

Summing currents at the emitter node in Fig. 15.6:

$$g_\pi v_3 + g_m v_3 + g_m v_4 + g_\pi v_4 = G_{EE} v_e \quad \text{or} \quad (g_m + g_\pi)(v_3 + v_4) = G_{EE} v_e \quad (15.11)$$

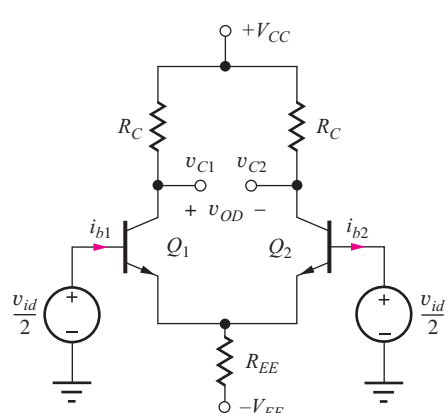


**Figure 15.5** Differential amplifier with a differential-mode input signal.

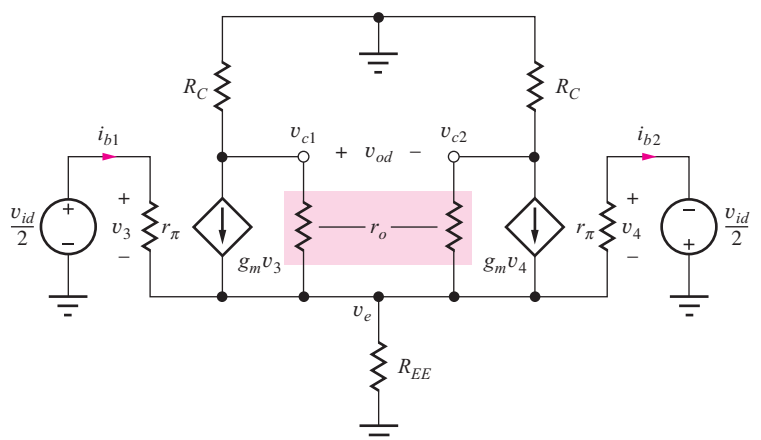


**Figure 15.6** Small-signal model for differential-mode inputs. The output resistances are neglected in the calculations.

These equations have been simplified by representing resistances  $r_\pi$  and  $R_{EE}$  with their equivalent conductances  $g_\pi$  and  $G_{EE}$ . The base-emitter voltages are

$$\mathbf{v}_3 = \frac{\mathbf{v}_{id}}{2} - \mathbf{v}_e \quad \text{and} \quad \mathbf{v}_4 = -\frac{\mathbf{v}_{id}}{2} - \mathbf{v}_e \quad (15.12)$$

giving  $\mathbf{v}_3 + \mathbf{v}_4 = -2\mathbf{v}_e$ . Combining Eq. (15.12) with Eq. (15.11) yields

$$\mathbf{v}_e(G_{EE} + 2g_\pi + 2g_m) = 0 \quad (15.13)$$

which requires  $\mathbf{v}_e = 0$ .

For a purely differential-mode input voltage, the voltage at the emitter node is identically zero. This is an extremely important result. The “virtual ground” at the emitter node causes the differential amplifier to behave as a common-emitter (or common-source) amplifier.

## DESIGN NOTE

The emitter node in the symmetrical differential amplifier represents a **virtual ground** for differential-mode input signals.

Because the voltage at the emitter node is zero, Eq. (15.12) yields

$$\mathbf{v}_3 = \frac{\mathbf{v}_{id}}{2} \quad \text{and} \quad \mathbf{v}_4 = -\frac{\mathbf{v}_{id}}{2} \quad (15.14)$$

and the output signal voltages are

$$\mathbf{v}_{c1} = -g_m R_C \frac{\mathbf{v}_{id}}{2} \quad \mathbf{v}_{c2} = +g_m R_C \frac{\mathbf{v}_{id}}{2} \quad \mathbf{v}_{od} = -g_m R_C \mathbf{v}_{id} \quad (15.15)$$

The differential-mode gain  $A_{dd}$  for a **balanced output**,  $\mathbf{v}_{od} = \mathbf{v}_{c1} - \mathbf{v}_{c2}$ , is

$$A_{dd} = \left. \frac{\mathbf{v}_{od}}{\mathbf{v}_{id}} \right|_{\mathbf{v}_{ic}=0} = -g_m R_C \quad (15.16)$$

If either  $\mathbf{v}_{c1}$  or  $\mathbf{v}_{c2}$  alone is used as the output, referred to as a **single-ended** (or ground-referenced) **output**, then

$$A_{dd1} = \left. \frac{\mathbf{v}_{c1}}{\mathbf{v}_{id}} \right|_{\mathbf{v}_{ic}=0} = -\frac{g_m R_C}{2} \quad \text{or} \quad A_{dd2} = \left. \frac{\mathbf{v}_{c2}}{\mathbf{v}_{id}} \right|_{\mathbf{v}_{ic}=0} = +\frac{g_m R_C}{2} \quad (15.17)$$

depending on which output is selected.

The virtual ground condition at the emitter node causes the amplifier to behave as a single-stage common-emitter amplifier. The balanced differential output provides the full gain of a common-emitter stage, whereas the output at either collector provides a gain equal to one-half that of the C-E stage.

The common-mode output voltage, defined by Eq. (15.8), is zero since  $v_{c2} = -v_{c1}$ , and therefore  $A_{dc}$  is indeed zero, as assumed in Eq. (15.10).

### Differential-Mode Input Resistance

The **differential-mode input resistance**  $R_{id}$  represents the small-signal resistance presented to the full differential-mode input voltage appearing between the two bases of the transistors.  $R_{id}$  is defined as

$$R_{id} = \frac{\mathbf{v}_{id}}{\mathbf{i}_{b1}} = 2r_\pi \quad \text{because} \quad \mathbf{i}_{b1} = \frac{\mathbf{v}_{id}}{r_\pi} \quad (15.18)$$

If  $v_{id}$  is set to zero in Fig. 15.6, then  $g_m v_3$  and  $g_m v_4$  are zero, and the **differential-mode output resistance**  $R_{od}$  is equal to

$$R_{od} = 2(R_C \| r_o) \cong 2R_C \quad (15.19)$$

since node  $v_e$  represents a virtual ground. For single-ended outputs,

$$R_{out} \cong R_C \quad (15.20)$$

## DESIGN NOTE

The differential pair behaves the same as a common-emitter or common-source amplifier for differential-mode input signals.

### 15.1.6 COMMON-MODE GAIN AND INPUT RESISTANCE

Next we evaluate the common-mode characteristics of the differential amplifier and discover that it tends to reject common-mode input signals, a very useful property! Purely common-mode input signals are applied to the differential amplifier in Fig. 15.7. For this case, both sides of the amplifier are completely symmetrical. Thus, the two base currents, the emitter currents, the collector currents, and the two collector voltages must be equal. Using this symmetry as a basis, the output voltage can be developed by writing a loop equation including either base-emitter junction.

For the small-signal model in Fig. 15.8,

$$v_{ic} = i_b r_\pi + v_e = i_b [r_\pi + 2(\beta_o + 1)R_{EE}] \quad \text{and} \quad i_b = \frac{v_{ic}}{r_\pi + 2(\beta_o + 1)R_{EE}} \quad (15.21)$$

The voltage at the emitter is

$$v_e = 2(\beta_o + 1)i_b R_{EE} = \frac{2(\beta_o + 1)R_{EE}}{r_\pi + 2(\beta_o + 1)R_{EE}} v_{ic} \cong v_{ic} \quad (15.22)$$

We recognize that Eq. (15.22) is identical to the gain of an emitter-follower with a resistance of  $2R_{EE}$  in its emitter, and therefore emitter node voltage is approximately equal to the common-mode input signal. (Note that the circuit has been changed to the current-controlled form of the small-signal model.)

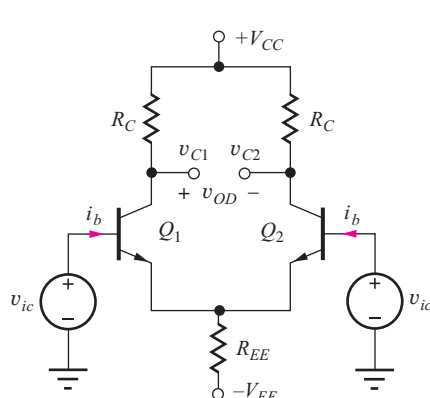


**Figure 15.7** Differential amplifier with purely common-mode input.

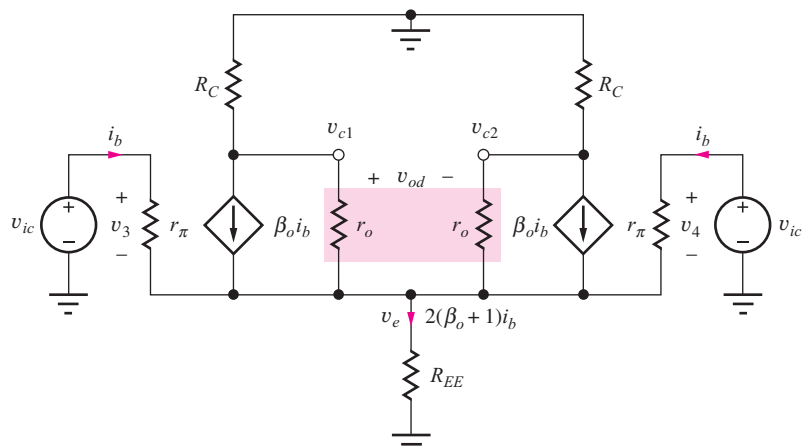


**Figure 15.8** Small-signal model with common-mode input. The output resistances are neglected in the calculations. Note the change to the current-controlled form of the small-signal model.

The output voltage at either collector is given by

$$\mathbf{v}_{c1} = \mathbf{v}_{c2} = -\beta_o \mathbf{i}_B R_C = -\frac{\beta_o R_C}{r_\pi + 2(\beta_o + 1)R_{EE}} \mathbf{v}_{ic} \quad (15.23)$$

The common-mode output voltage  $\mathbf{v}_{oc}$  is defined by Eq. (15.8), and the common-mode gain  $A_{cc}$  is given by

$$A_{cc} = \left. \frac{\mathbf{v}_{oc}}{\mathbf{v}_{ic}} \right|_{v_{id}=0} = -\frac{\beta_o R_C}{r_\pi + 2(\beta_o + 1)R_{EE}} \cong -\frac{R_C}{2R_{EE}} \quad (15.24)$$

for large  $\beta_o$ . Equation (15.24) is identical to the gain of an inverting amplifier with a resistance of  $2R_{EE}$  in its emitter and a collector load resistance  $R_C$ . By multiplying and dividing Eq. (15.24) by collector current  $I_C$ , Eq. (15.24) can be rewritten as

$$A_{cc} = -\frac{I_C R_C}{2I_C R_{EE}} \cong \frac{\frac{V_{CC}}{2}}{2I_C R_{EE}} = \frac{V_{CC}}{2(V_{EE} - V_{BE})} \cong \frac{V_{CC}}{2V_{EE}} \quad (15.25)$$

where it is assumed that  $\alpha_F = \alpha_o$  and  $I_C R_C = V_{CC}/2$ . In Eq. (15.25) we see that the common-mode gain  $A_{cc}$  is determined by the ratio of the two power supplies, and for symmetrical supplies,  $A_{cc} = 0.5$ . Note that the result in Eq. (15.25) only applies to the differential amplifier biased by resistor  $R_{EE}$ . We will shortly improve this result by replacing  $R_{EE}$  with an electronic current source.

Differential output voltage  $\mathbf{v}_{od}$  is identically zero because the voltages at the two collectors are equal:  $\mathbf{v}_{od} = \mathbf{v}_{c1} - \mathbf{v}_{c2} = 0$ . Therefore, the common-mode conversion gain for a differential output is also 0, as assumed in Eq. (15.10):

$$A_{cd} = \left. \frac{\mathbf{v}_{od}}{\mathbf{v}_{ic}} \right|_{v_{id}=0} = 0 \quad (15.26)$$

The result in Eq. (15.24) indicates that the common-mode output voltage and  $A_{cc}$  tend toward zero as  $R_{EE}$  approaches infinity. This is another suspicious result, and it is in fact a direct consequence of neglecting the output resistances in the circuit in Fig. 15.8. If  $r_o$  is included, a small current  $v_{ic}/\beta_o r_o$  results from the finite current gain of the BJT and appears in the collector terminal. A more accurate expression for the common-mode gain is

$$A_{cc} \cong R_C \left( \frac{1}{\beta_o r_o} - \frac{1}{2R_{EE}} \right) \quad (15.27)$$

Now for infinite  $R_{EE}$ , we find that  $A_{cc}$  is limited to  $R_C/\beta_o r_o \cong V_{CC}/2\beta_o V_A$ . It is also interesting to note that the sign difference allows a theoretical cancellation to occur. (See Prob. 15.140.)

### Common-Mode Input Resistance

The **common-mode input resistance** is determined by the total signal current ( $2i_b$ ) being supplied from the common-mode source and can be calculated using Eq. (15.21):

$$R_{ic} = \frac{\mathbf{v}_{ic}}{2\mathbf{i}_b} = \frac{r_\pi + 2(\beta_o + 1)R_{EE}}{2} = \frac{r_\pi}{2} + (\beta_o + 1)R_{EE} \quad (15.28)$$

As mentioned above, equations (15.21), (15.22), (15.23), and the numerator of Eq. (15.28) should be recognized as those of a common-emitter amplifier with a resistor of value  $2R_{EE}$  in the emitter. This observation is discussed in detail shortly.


**DESIGN  
NOTE**

The characteristics of the differential pair with a common-mode input are similar to those of a common-emitter (common-source) amplifier with a large emitter (source) resistor.

### 15.1.7 COMMON-MODE REJECTION RATIO (CMRR)

As defined in Chapter 11, the **common-mode rejection ratio**, or **CMRR**, characterizes the ability of an amplifier to amplify the desired differential-mode input signal and reject the undesired common-mode input signal. For a general differential amplifier stage characterized by Eq. (11.110), CMRR is defined in Eq. (11.111) as

$$\text{CMRR} = \left| \frac{A_{dm}}{A_{cm}} \right| \quad (15.29)$$

where  $A_{dm}$  and  $A_{cm}$  are the overall differential-mode and common-mode gains.<sup>1</sup>

For the differential amplifier, CMRR is dependent on the designer's choice of output voltage. For a differential output  $v_{od}$ , the common-mode gain of the balanced amplifier is zero, and the CMRR is infinite. However, if the output is taken from either collector, we have

$$v_{c1} = v_{oc} + \frac{v_{od}}{2} = A_{cc}v_{ic} + \frac{A_{dd}}{2}v_{id} \quad \text{and} \quad v_{c2} = v_{oc} - \frac{v_{od}}{2} = A_{cc}v_{ic} - \frac{A_{dd}}{2}v_{id} \quad (15.30)$$

using Eqs. (15.8) and (15.10). Based upon Eqs. (15.29) with (15.17) and (15.27), the CMRR is given by

$$\text{CMMR} = \left| \frac{A_{dm}}{A_{cm}} \right| = \left| \frac{\frac{A_{dd}}{2}}{A_{cc}} \right| = \left| \frac{\frac{g_m R_c}{2}}{R_c \left( \frac{1}{\beta_o r_o} - \frac{1}{2R_{EE}} \right)} \right| = \left| \frac{1}{2 \left( \frac{1}{\beta_o \mu_f} - \frac{1}{2g_m R_{EE}} \right)} \right| \quad (15.31)$$

For infinite  $R_{EE}$ ,  $\text{CMMR} \cong \beta_o \mu_f / 2$  and is limited by the  $\beta_o \mu_f$  product of the transistor. On the other hand, if the term containing  $R_{EE}$  is dominant, we find the commonly quoted result:

$$\text{CMRR} \cong g_m R_{EE} \quad (15.32)$$

Let us explore Eq. (15.32) a bit further by writing  $g_m$  in terms of the collector current.

$$\text{CMRR} = 40I_C R_{EE} = 20(2I_E R_{EE}) = 20(V_{EE} - V_{BE}) \cong 20V_{EE} \quad (15.33)$$

For the differential amplifier biased by resistor  $R_{EE}$ , CMRR is limited by the available negative power supply voltage  $V_{EE}$ . Also observe that the differential-mode gain is determined by the positive power supply voltage, that is  $A_{dd} = -20V_{CC}$  based on our design guide from Chapter 13 with  $I_C R_C = V_{CC}/2$ .

**EXERCISE:** Estimate the differential-mode gain, common-mode gain, and CMRR for a differential amplifier with  $V_{EE}$  and  $V_{CC} = 15$  V if the differential output is used and if the output  $v_{c2}$  is used.

**ANSWERS:**  $-300, 0, \infty; +150, -0.5, 49.5$  dB (a poor CMRR)

<sup>1</sup>  $A_{dm}$  and  $A_{cm}$  represent the differential-mode and common-mode gains of a general amplifier such as an op amp, whereas  $A_{dd}$ ,  $A_{cc}$ , and  $A_{cd}$  denote the characteristics of the differential amplifier stage by itself.

### Effects of Mismatches

Although the CMRR for an ideal differential amplifier with differential output is infinite, an actual amplifier will not be perfectly symmetrical because of mismatches in the transistors, and the two conversion gains  $A_{cd}$  and  $A_{dc}$  will not be zero. For this case, many of the errors will be proportional to the result in Eq. (15.32) and will be of the form [1]:

$$\text{CMRR} \propto g_m R_{EE} \left( \frac{\Delta g}{g} \right) \quad (15.34)$$

in which the  $\Delta g/g = 2(g_1 - g_2)/(g_1 + g_2)$  factor represents the fractional mismatch between the small-signal device parameters on the two sides of the differential amplifier (see Probs. 15.21 and 15.23). Therefore, maximizing the  $g_m R_{EE}$  product is equally important to improving the performance of differential amplifiers with differential outputs.

### 15.1.8 ANALYSIS USING DIFFERENTIAL- AND COMMON-MODE HALF-CIRCUITS

We noted that the differential amplifier behaves much as the single-transistor common-emitter amplifier. The analogy can be carried even further using the **half-circuit** method of analysis, in which the symmetry of the differential amplifier is used to simplify the circuit analysis by splitting the circuit into **differential-mode** and **common-mode half-circuits**.

Half-circuits are constructed by first drawing the differential amplifier in a fully symmetric form, as in Fig. 15.9. To achieve full symmetry, the power supplies have been split into two equal value sources in parallel, and the emitter resistor  $R_{EE}$  has been separated into two equal parallel resistors, each of value  $2R_{EE}$ . It is important to recognize from Fig. 15.9 that these modifications have not changed any of the currents or voltages in the circuit.

Once the circuit is drawn in symmetrical form, two basic rules are used to construct the half-circuits: one for differential-mode signal analysis and one for common-mode signal analysis:



#### DESIGN NOTE RULES FOR CONSTRUCTING HALF-CIRCUITS

*Differential-mode signals* Points on the line of symmetry represent virtual grounds and can be connected to ground for ac analysis. (For example, remember that we found that  $v_e = 0$  for differential-mode signals.)

*Common-mode signals* Points on the line of symmetry can be replaced by open circuits. (No current flows through these connections.)

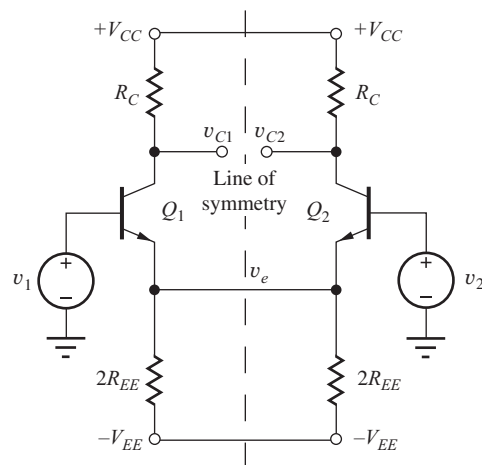


Figure 15.9 Circuit emphasizing symmetry of the differential amplifier.

### Differential-Mode Half Circuits

Applying the first rule to the circuit in Fig. 15.9 for differential-mode signals yields the circuit in Fig. 15.10(a). The two power supply lines and the emitter node all become ac grounds. (Of course, the power supply lines would become ac grounds in any case.) Simplifying the circuit yields the two differential-mode half-circuits in Fig. 15.10(b), each of which represents a common-emitter amplifier stage. The differential-mode behavior of the circuit, as described by Eqs. (15.15) to (15.20), can easily be found by direct analysis of the half-circuits:

$$v_{c1} = -g_m R_C \frac{v_{id}}{2} \quad v_{c2} = +g_m R_C \frac{v_{id}}{2} \quad v_o = v_{c1} - v_{c2} = -g_m R_C v_{id} = -A_{dd} v_{id} \quad (15.35)$$

with

$$R_{id} = \frac{v_{id}}{i_b} = 2r_\pi \quad \text{and} \quad R_{od} = 2(R_C \| r_o) \quad (15.36)$$

### Common-Mode Half-Circuits

If the second rule is applied to the circuit in Fig. 15.9, all points on the line of symmetry become open circuits, and we obtain the circuit in Fig. 15.11. The common-mode half-circuits obtained

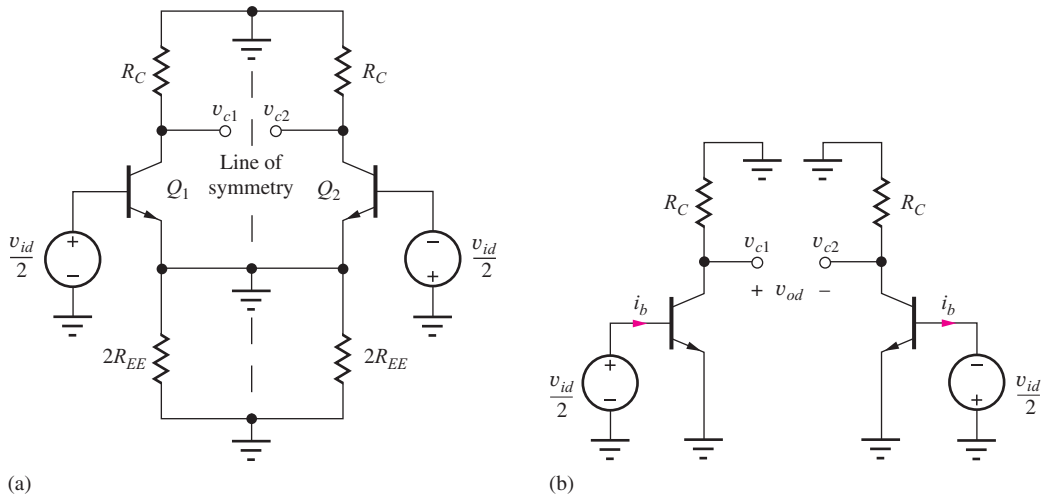


**Figure 15.10** (a) ac Grounds for differential-mode inputs. (b) Differential-mode half-circuits.

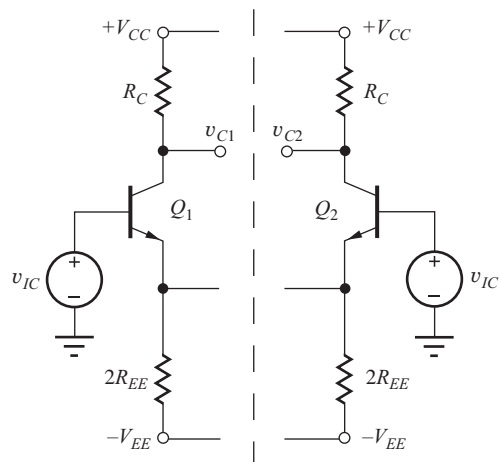


**Figure 15.11** Construction of the common-mode half-circuit.

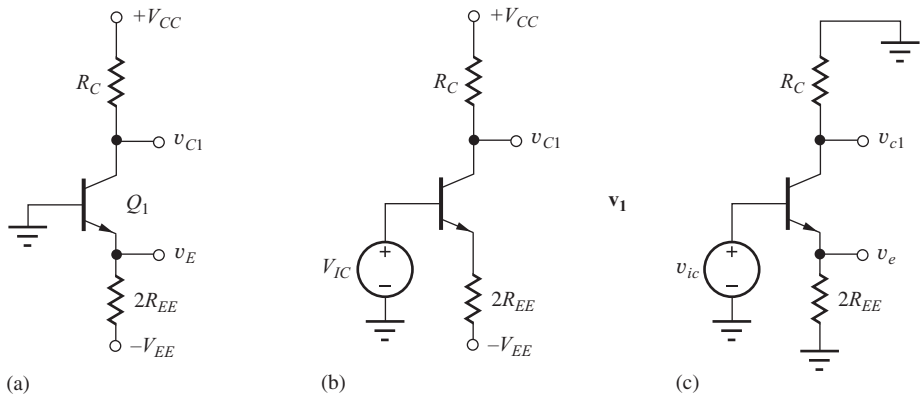


**Figure 15.12** Common-mode half-circuits for (a) Q-point analysis, (b) dc common-mode input, and (c) common-mode signal analysis.

from Fig. 15.11 are redrawn in Fig. 15.12. The dc circuit with  $V_{IC}$  set to zero in Fig. 15.12(a) is used to find the Q-point of the amplifier. The circuit in Fig. 15.12(b) should be used to find the operating point when a dc common-mode input is applied, and the ac circuit of Fig. 15.12(c) is used for common-mode signal analysis.

The common-mode half-circuit in Fig. 15.12(c) simply represents the common-emitter amplifier with an emitter resistor  $2R_{EE}$ , which was studied in great detail in Chapter 14. In addition, Eqs. (15.24), and (15.28) could have been written down directly using the results of our analysis from Chapter 14.

We can see that use of the differential-mode and common-mode half-circuits can greatly simplify the analysis of symmetric circuits. Half-circuit techniques are used shortly to analyze the MOS differential amplifier from Fig. 15.1.

### Common-Mode Input Voltage Range

Common-mode input voltage range is another important consideration in the design of differential amplifiers. The upper limit to the dc common-mode input voltage  $V_{IC}$  in the circuit in Fig. 15.12(b) is set by the requirement that  $Q_1$  remains in the forward-active region of operation. Writing an expression for the collector-base voltage of  $Q_1$ ,

$$V_{CB} = V_{CC} - I_C R_C - V_{IC} \geq 0 \quad \text{or} \quad V_{IC} \leq V_{CC} - I_C R_C \quad (15.37)$$

in which

$$I_C = \alpha_F \frac{V_{IC} - V_{BE} + V_{EE}}{2R_{EE}} \quad (15.38)$$

Solving the preceding two equations for  $V_{IC}$  yields

$$V_{IC} \leq V_{CC} \frac{\frac{R_C}{2R_{EE}} \frac{(V_{EE} - V_{BE})}{V_{CC}}}{1 + \alpha_F \frac{R_C}{2R_{EE}}} \quad (15.39)$$

For symmetrical power supplies,  $V_{EE} \gg V_{BE}$ , and with  $R_C = R_{EE}$ , Eq. (15.39) yields  $V_{IC} \leq V_{CC}/3$ .

Note from Eq. (15.38) that  $I_C$  changes as  $V_{IC}$  changes. The upper limit on  $V_{IC}$  is set by Eq. (15.39) and by the allowable shift in Q-point current as  $V_{IC}$  changes. As  $V_{IC}$  goes negative, the collector current reduces since  $I_C \cong (V_{IC} - V_{BE} + V_{EE})/2R_{EE}$ . The lower bound on  $V_{IC}$  is set by what reduction in bias current is deemed acceptable, and would probably be specified to be symmetrical, that is,  $-V_{CC}/3 \leq V_{IC} \leq V_{CC}/3$ .

**EXERCISE:** Find the positive common-mode input voltage range for the differential amplifier in Fig. 15.7 if  $V_{CC} = V_{EE} = 15$  V and  $R_C = R_{EE}$ .

**ANSWER:**  $\cong 5.30$  V

### 15.1.9 BIASING WITH ELECTRONIC CURRENT SOURCES

From Eqs. (15.1) and (15.2) we see that the Q-point of the differential amplifier is directly dependent on the value of the negative power supply, and from Eq. (15.31) we see that  $R_{EE}$  limits the CMRR. In order to remove these limitations, most differential amplifiers are biased using electronic current sources, which both stabilize the operating point of the amplifier and increase the effective value of  $R_{EE}$ . Electronic current source biasing of both the BJT and MOSFET differential amplifiers is shown in Fig. 15.13. In these circuits, the current source replaces resistor  $R_{EE}$  or  $R_{SS}$ .

The rectangular symbols in Figs. 15.13 and 15.14 denote an electronic current source with a finite output resistance, as shown graphically in the  $i$ - $v$  characteristic in Fig. 15.15. The electronic source has a Q-point current equal to  $I_{SS}$  and an output resistance equal to  $R_{SS}$ .

For hand analysis using the dc equivalent circuit, we will replace the electronic current source with a dc current source of value  $I_{SS}$ . For ac analysis, the ac equivalent circuit is constructed by replacing the source with its output resistance  $R_{SS}$ . These substitutions are depicted symbolically in Fig. 15.14.

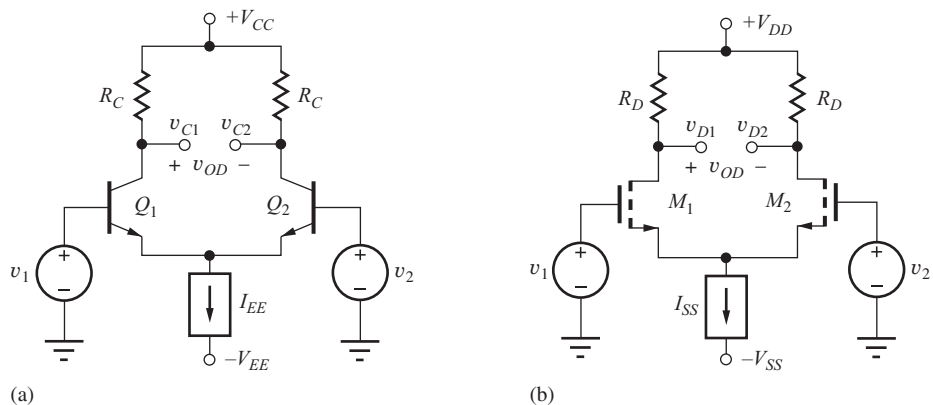


Figure 15.13 Differential amplifiers employing electronic current source bias.

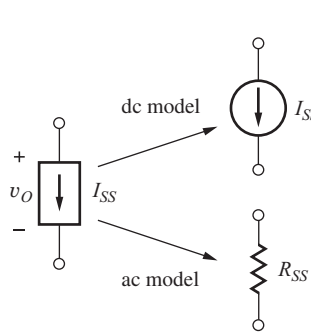


Figure 15.14 Electronic current source and models.

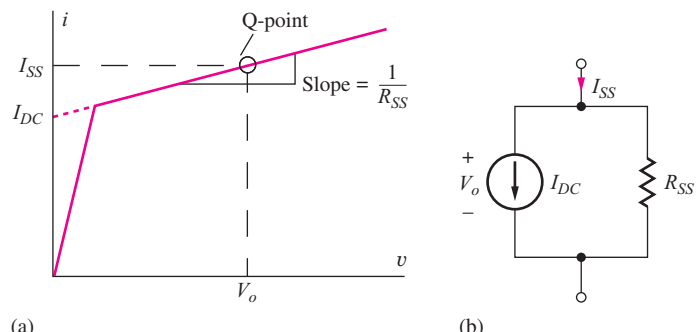


Figure 15.15 (a)  $i$ - $v$  Characteristic for an electronic current source. (b) Proper SPICE representation of the electronic current source.


**DESIGN  
NOTE**

High common-mode rejection in differential amplifiers requires a large value of output resistance  $R_{SS}$  in the current source  $I_{SS}$  used for bias.

### 15.1.10 MODELING THE ELECTRONIC CURRENT SOURCE IN SPICE

Proper modeling of the electronic current source is slightly different in SPICE since the program must create its own dc and ac equivalent circuits. In order for SPICE to properly calculate the dc and ac behavior of a circuit, the network must contain both the dc current source and its output resistance  $R_{SS}$ . In the full circuit model in Fig. 15.15(b), a dc current will exist in the resistance  $R_{SS}$ , and the value of the current source in the SPICE circuit must be set to the value  $I_{DC}$  indicated in Fig. 15.15.  $I_{DC}$  represents the current in the equivalent circuit when voltage  $V_o = 0$  and can be expressed as

$$I_{DC} = I_{SS} - \frac{V_o}{R_{SS}} \quad (15.40)$$

The equivalent circuit to be used in SPICE appears in Fig. 15.15(b). In cases where  $R_{SS}$  is very large,  $I_{DC}$  is approximately equal to  $I_{SS}$ .

**EXERCISE:** Suppose an electronic current source has a current  $I_{SS} = 100 \mu\text{A}$  with an output resistance  $R_{SS} = 750 \text{ k}\Omega$ . (These values are representative of a single transistor current source operating at this current.) If  $V_o = 15 \text{ V}$ , what is the value of  $I_{DC}$ ?

**ANSWER:**  $80 \mu\text{A}$

### 15.1.11 dc ANALYSIS OF THE MOSFET DIFFERENTIAL AMPLIFIER

MOSFETS provide very high input resistance and are often used in differential amplifiers implemented in CMOS and BiFET<sup>2</sup> technologies. In addition to high input resistance, op amps with FET inputs typically have a much higher slew rate than those with bipolar input stages.

The MOS version of the differential amplifier circuit appears in Fig. 15.13(b). We will use the MOSFET differential amplifier as our first direct application of half-circuit analysis. For dc analysis using half-circuits, the amplifier is redrawn in symmetrical form in Fig. 15.16(a). If the connections on the line of symmetry are replaced with open circuits, and the two input voltages are set to zero, we obtain in Fig. 15.16(b) the half-circuit needed for dc analysis.

It is immediately obvious from the dc half-circuit that the current in the source of the NMOS transistor must be equal to one-half of the bias current  $I_{SS}$ :

$$I_S = \frac{I_{SS}}{2} \quad (15.41)$$

The gate-source voltage of the MOSFET can be determined directly from the drain-current expression for the transistor:

$$I_D = \frac{K_n}{2}(V_{GS} - V_{TN})^2 \quad \text{or} \quad V_{GS} = V_{TN} + \sqrt{\frac{2I_D}{K_n}} = V_{TN} + \sqrt{\frac{I_{SS}}{K_n}} \quad (15.42)$$

Note that  $V_S = -V_{GS}$ . The voltages at both MOSFET drains are

$$V_{D1} = V_{D2} = V_{DD} - I_D R_D \quad \text{and} \quad V_O = 0 \quad (15.43)$$

Thus, the drain-source voltages are

$$V_{DS} = V_{DD} - I_D R_D + V_{GS} \quad (15.44)$$

<sup>2</sup> BiFET technologies contain JFETs as well as bipolar transistors.

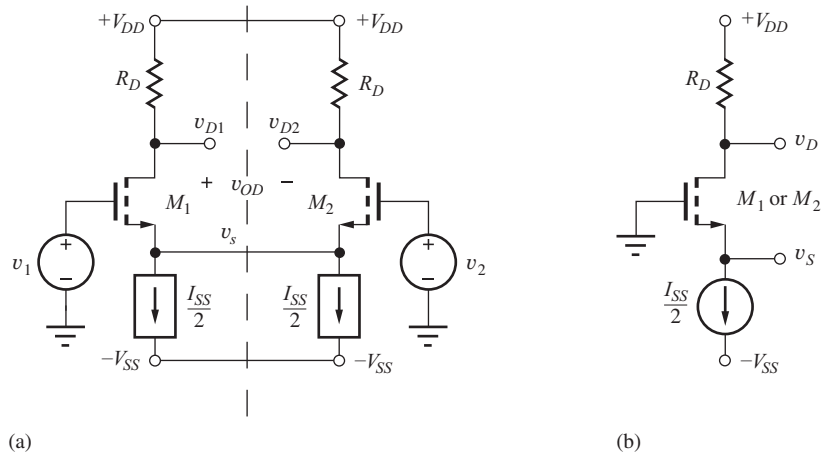


**Figure 15.16** (a) Symmetric circuit representation of the MOS differential amplifier. (b) Half-circuit for dc analysis.

### EXAMPLE 15.2 MOSFET DIFFERENTIAL AMPLIFIER ANALYSIS

A dc Q-point analysis is provided for the MOSFET differential amplifier in this example.

**PROBLEM** Find the Q-points for the MOSFETs in the differential amplifier in Fig. 15.13(b) if  $V_{DD} = V_{SS} = 12$  V,  $I_{SS} = 200$   $\mu$ A,  $R_{SS} = 500$  k $\Omega$ ,  $R_D = 62$  k $\Omega$ ,  $K_n = 5$  mA/V $^2$ ,  $\lambda = 0.0133$  V $^{-1}$ , and  $V_{TN} = 1$  V. What is the maximum  $V_{IC}$  for which  $M_1$  remains in the active region?

**SOLUTION** **Known Information and Given Data:** Circuit topology appears in Fig. 15.13(b); symmetrical 12-V power supplies are used to operate the circuit;  $I_{SS} = 200$   $\mu$ A,  $R_D = 62$  k $\Omega$ ,  $V_{TN} = 1$  V, and  $K_n = 5$  mA/V $^2$

**Unknowns:**  $I_D$ ,  $V_{DS}$ , for  $M_1$  and  $M_2$ , and maximum dc common-mode input voltage  $V_{IC}$

**Approach:** Use the circuit element values and follow the analysis presented in Eq. (15.41) through (15.44).

**Assumptions:** Active region operation; ignore  $\lambda$  and  $R_{SS}$  for hand bias calculations

**Analysis:** Using Eqs. (15.41) through (15.44):

$$I_D = \frac{I_{SS}}{2} = 100 \mu\text{A} \quad V_{GS} = 1 + \sqrt{\frac{200 \mu\text{A}}{5 \text{ mA/V}^2}} = 1.20 \text{ V}$$

$$V_{DS} = 12 \text{ V} - (100 \mu\text{A})(62 \text{ k}\Omega) + 1.2 \text{ V} = 7.00 \text{ V}$$

Thus, both transistors in the differential amplifier are biased at a Q-point of (100  $\mu$ A, 7.00 V). The voltages at the drain and source of the MOSFET are  $V_D = 5.80$  V and  $V_S = -1.20$  V.

Maintenance of pinch-off for  $M_1$  for nonzero  $V_{IC}$  requires

$$V_{GD} = V_{IC} - (V_{DD} - I_D R_D) \leq V_{TN}$$

$$V_{IC} \leq V_{DD} - I_D R_D + V_{TN} = 6.8 \text{ V}$$

**Check of Results:** Checking for pinch-off,  $V_{GS} - V_{TN} = 0.2$  V, and  $V_{DS} \geq 0.2$ . ✓

**Discussion:** Note that the drain currents are set by the current source and will be independent of device characteristics. This is demonstrated next using SPICE.

**Computer-Aided Analysis:** In our SPICE analysis, we can easily include  $\lambda$  and  $R_{SS}$  to see their impact on the Q-points of the transistors. Using Eq. (15.40) and the  $V_{GS} = 1.2$  V as already calculated, the dc current source value for SPICE will be  $200 - 21.6 = 178.4 \mu\text{A}$ . We need to set up  $KP = 0.005 \text{ A/V}^2$ ,  $VTO = 1 \text{ V}$ , and  $LAMBDA = 0.0133 \text{ V}^{-1}$  in the SPICE device models. With these values, the Q-points from a SPICE operating point analysis are virtually the same as our hand calculations ( $100 \mu\text{A}$ ,  $6.99 \text{ V}$ ). Since the drain currents are locked by the current source, including  $\lambda$  causes only a small adjustment to occur in the value of gate-source voltage:  $V_{GS} = 1.198 \text{ V}$ .

**EXERCISE:** Draw a PMOS version of the NMOS differential amplifier in Fig. 15.13(b).

**ANSWER:** See Figs. P15.37 and P15.39.

**EXERCISE:** Replace the MOSFET in Example 15.2 by a four-terminal device with its substrate connected to  $V_{SS} = -12 \text{ V}$ , and find the new Q-point for the transistor. Assume  $V_{TO} = 1 \text{ V}$ ,  $\gamma = 0.75\sqrt{V}$ , and  $2\phi_F = 0.6 \text{ V}$ . What is the new value of  $V_{TN}$ ?

**ANSWERS:** ( $100 \mu\text{A}$ ,  $8.75 \text{ V}$ );  $2.75 \text{ V}$

### 15.1.12 DIFFERENTIAL-MODE INPUT SIGNALS

The differential-mode and common-mode half-circuits for the differential amplifier in Fig. 15.16 are given in Fig. 15.17. In the differential-mode half-circuit, the MOSFET sources represent a virtual ground. In the common-mode circuit, the electronic current source has been modeled by twice its small-signal output resistance  $R_{SS}$ , representing the finite output resistance of the current source.

The differential-mode half-circuit represents a common-source amplifier, and the output voltages are given by

$$v_{d1} = -g_m(R_D \| r_o) \frac{v_{id}}{2} \quad v_{d2} = +g_m(R_D \| r_o) \frac{v_{id}}{2} \quad v_{od} = -g_m(R_D \| r_o)v_{id} \quad (15.45)$$

The differential-mode gain is

$$A_{dd} = \left. \frac{v_{od}}{v_{id}} \right|_{v_{ic}=0} = -g_m(R_D \| r_o) \cong -g_m R_D \quad \text{for } r_o \gg R_D \quad (15.46)$$

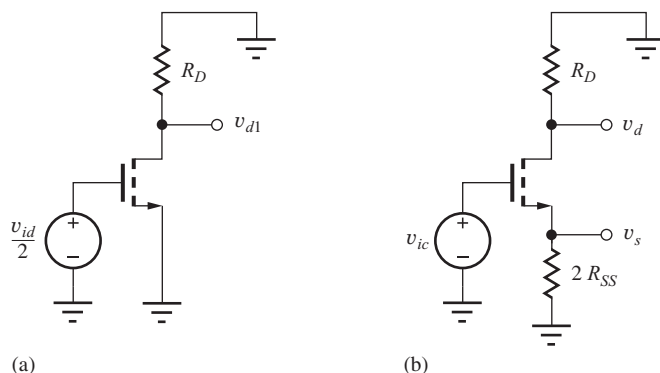


Figure 15.17 (a) Differential-mode and (b) common-mode half-circuits.

whereas taking the single-ended output between either drain and ground provides a gain of one-half  $A_{dd}$ :

$$A_{dd1} = \frac{\mathbf{v}_{d1}}{\mathbf{v}_{id}} \Big|_{\mathbf{v}_{ic}=0} \cong -\frac{g_m R_D}{2} = \frac{A_{dd}}{2} \quad \text{and} \quad A_{dd2} = \frac{\mathbf{v}_{d2}}{\mathbf{v}_{id}} \Big|_{\mathbf{v}_{ic}=0} \cong +\frac{g_m R_D}{2} = -\frac{A_{dd}}{2} \quad (15.47)$$

The differential-mode input and output resistances are infinite and  $2R_D$ , respectively:

$$R_{id} = \infty \quad \text{and} \quad R_{od} = 2(R_D \| r_o) \quad (15.48)$$

The virtual ground at the source node causes the amplifier to again behave as a single-stage inverting amplifier. A differential output provides the full gain of the common-source stage, whereas using the single-ended output at either drain reduces the gain by a factor of 2.

**EXERCISE:** In a manner similar to the analysis of Fig. 15.8, derive the expressions for the differential-mode voltage gains of the MOS differential amplifier directly from the full small-signal model.

### 15.1.13 SMALL-SIGNAL TRANSFER CHARACTERISTIC FOR THE MOS DIFFERENTIAL AMPLIFIER

The MOS differential amplifier also provides improved linear input signal range and distortion characteristics over that of a single transistor. We can explore these advantages using the drain current expression for the MOSFET:

$$I_{D1} - I_{D2} = \frac{K_n}{2} [(v_{GS1} - V_{TN})^2 - (v_{GS2} - V_{TN})^2] \quad (15.49)$$

For the symmetrical differential amplifier with a purely differential-mode input,  $v_{GS1} = V_{GS} + \frac{v_{id}}{2}$ ,  $v_{GS2} = V_{GS} - \frac{v_{id}}{2}$ , and

$$I_{D1} - I_{D2} = K_n(V_{GS} - V_{TN})v_{id} = g_m v_{id} \quad (15.50)$$

The second-order distortion product cancels out, and the output current expression is distortion free! As usual, we should question such a perfect result. In reality, MOSFETs are not perfect square-law devices, and some distortion will exist. There also will be distortion introduced through the voltage dependence of the output impedances of the transistors.

### 15.1.14 COMMON-MODE INPUT SIGNALS

The common-mode half-circuit in Fig. 15.17(b) is that of an inverting amplifier with a source resistor equal to  $2R_{SS}$ . Using the results from Chapter 14,

$$\mathbf{v}_{d1} = \mathbf{v}_{d2} = \frac{-g_m R_D}{1 + 2g_m R_{SS}} \mathbf{v}_{ic} \quad (15.51)$$

and the signal voltage at the source is

$$\mathbf{v}_s = \frac{2g_m R_{SS}}{1 + 2g_m R_{SS}} \mathbf{v}_{ic} \cong \mathbf{v}_{ic} \quad (15.52)$$

The differential output voltage is zero because the voltages are equal at the two drains:

$$\mathbf{v}_{od} = \mathbf{v}_{d1} - \mathbf{v}_{d2} = 0 \quad (15.53)$$

Thus, the common-mode conversion gain for a differential output is zero:

$$A_{cd} = \frac{\mathbf{v}_{od}}{\mathbf{v}_{ic}} = 0 \quad (15.54)$$

The common-mode gain is given by

$$A_{cc} = \frac{V_{oc}}{V_{ic}} = -\frac{g_m R_D}{1 + 2g_m R_{SS}} \cong -\frac{R_D}{2R_{SS}} \quad (15.55)$$

It should be noted, in contrast to the case of the BJT, that Eq. (15.55) is correct even if  $r_o$  is included because of the infinite current gain of the FET.

The common-mode input source is connected directly to the MOSFET gate. Thus, the input current is zero and

$$R_{ic} = \infty \quad (15.56)$$

### Common-Mode Rejection Ratio (CMRR)

For a purely common-mode input signal, the output voltage of the balanced MOS amplifier is zero, and the CMRR is infinite. However, if a single-ended output is taken from either drain,

$$\text{CMRR} = \left| \frac{\frac{A_{dd}}{2}}{A_{cc}} \right| = \left| \frac{-\frac{g_m R_D}{2}}{-\frac{R_D}{2R_{SS}}} \right| = g_m R_{SS} \quad (15.57)$$

For high CMRR, a large value of  $R_{SS}$  is again desired. In Fig. 15.17,  $R_{SS}$  represents the output resistance of the current source in Fig. 15.13, and its value is much greater than resistor  $R_{EE}$ , which is used to bias the amplifier in Fig. 15.1. For this reason, as well as for Q-point stability, most differential amplifiers are biased by a current source, as in Fig. 15.13.

To compare the MOS amplifier more directly to the BJT analysis, however, let us assume for the moment that the MOS amplifier is biased by a resistor of value

$$R_{SS} = \frac{V_{SS} - V_{GS}}{I_{SS}} \quad (15.58)$$

Then Eq. (15.57) can be rewritten in terms of the circuit voltages, as was done for Eq. (15.33):

$$\text{CMRR} = \frac{2I_D R_{SS}}{V_{GS} - V_{TN}} = \frac{I_{SS} R_{SS}}{V_{GS} - V_{TN}} = \frac{(V_{SS} - V_{GS})}{V_{GS} - V_{TN}} \quad (15.59)$$

Using the numbers from the example,

$$\text{CMRR} = \frac{(V_{SS} - V_{GS})}{V_{GS} - V_{TN}} = \frac{(12 - 1.2)}{0.20} = 54 \quad (15.60)$$

— a paltry 35 dB. This is almost 10 dB worse than the result for the BJT amplifier. Because of the low values of CMRR in both the BJT and FET circuits, the use of current sources with much higher effective values of  $R_{SS}$  or  $R_{EE}$  is common in all differential amplifiers.

### 15.1.15 TWO-PORT MODEL FOR DIFFERENTIAL PAIRS

The ac analysis of circuits involving differential amplifiers can often be simplified by using the two-port small-signal model for the differential-pair appearing in Fig. 15.18. The two-port model

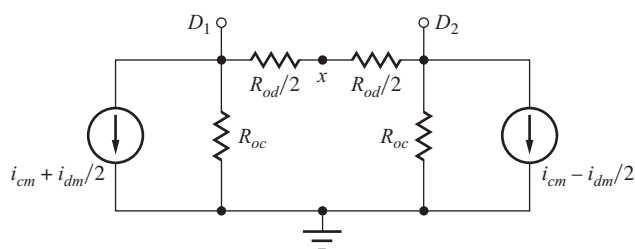


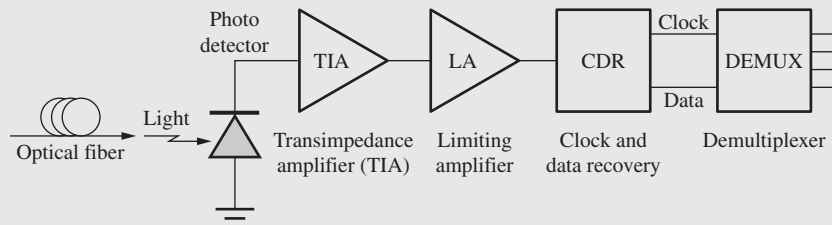
Figure 15.18 Two-port model for the differential pair.



## ELECTRONICS IN ACTION

### *Limiting Amplifiers for Optical Communications*

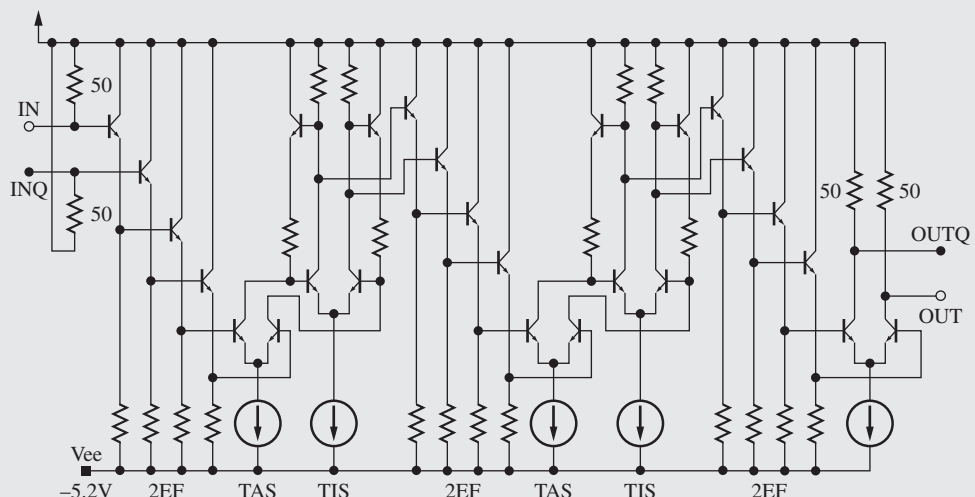
Interface circuits for optical communications were introduced in the Electronics in Action features in both Chapters 9 and 11. Here we discuss the limiting amplifier (LA), another of the important electronic blocks on the receiver side of the fiber optic communication link. The LA amplifies the low level output voltage (e.g., 10 mV) of the transimpedance amplifier up to a level that can drive the clock and data recovery circuits (e.g., 250 mV).



Optical fiber receiver block diagram.

A typical limiting amplifier consists of a wide-band multistage dc-coupled amplifier similar to the one in the circuit schematic here [1–3]. The input signal from the transimpedance amplifier is buffered and level-shifted by two stages of emitter followers (2EF). This is followed by a transadmittance amplifier (TAS) that converts the voltage to a current and then drives a transimpedance amplifier (TIS) that converts the current back to a voltage. This TAS-TIS cascade was developed by Cherry and Hooper [4] and represents an important technique for realizing amplifiers with very wide bandwidth. The output is level-shifted by two more emitter followers and amplified by a second Cherry-and-Hooper stage. A third pair of emitter followers drives a differential amplifier with load resistors chosen to match a transmission line impedance of  $50\ \Omega$ . Note that  $50\text{-}\Omega$  matching is used at the LA input as well.

We see that differential pairs are used throughout the limiting amplifier in the TAS and TIS stages, and in the gain stage at the output. Since these optical-to-electrical interface circuits typically push the state-of-the-art in speed, only *npn* transistors are used in the design.



Schematic of a typical limiting amplifier in bipolar technology. (Copyright 2002 IEEE. Reprinted with permission from [3].) (Note that this is a dc-coupled amplifier.)

Remember that *npn* transistors are inherently faster than *pnp* transistors because of the mobility advantage of electrons over that of holes.

1. H-M. Rein, "Multi-gigabit-per-second silicon bipolar IC's for future optical-fiber transmission systems," *IEEE J. Solid-State Circuits*, vol. 23, no. 3, pp. 664–675, June 1988.
2. R. Reimann and H-M. Rein, "Bipolar high-gain limiting amplifier IC for optical-fiber receivers operating up to 4 Gbits/s," *IEEE J. Solid-State Circuits*, vol. 22, no. 4, pp. 504–510, August 1987.
3. Y. Baeyens et al., "InP D-HBT IC's for 40-Gb/s and higher bit rate lightwave transceivers," *IEEE J. Solid-State Circuits*, vol. 37, no. 9, pp. 1152–1159, September 2002.
4. E. M. Cherry and D. E. Hooper, "The design of wide-band transistor feedback amplifiers," *Proc. Institute of Electrical Engineers*, vol. 110, pp. 375–389, February 1963.

can be substituted directly for the differential pair, or it can be used as a conceptual aid in simplifying circuits. The two current sources represent the signal currents generated by the two transistors in the pair. Resistors  $R_{oc}$  are the common-mode output resistances appearing at each collector or drain,  $D_1$  and  $D_2$ , and  $R_{od}$  is the differential output resistance that appears between the two collectors or drains. (Remember for symmetrical differential-mode circuits, the node "x" will be a virtual ground.) For the pairs in Fig. 15.13, approximate expressions for the elements are

$$\begin{aligned} i_{dm} &= g_m v_{dm} & i_{cm} &= \frac{g_m}{1 + 2g_m R_{EE}} v_{cm} \cong \frac{v_{cm}}{2R_{EE}} \\ R_{od} &= 2r_o & R_{oc} &\cong 2\mu_f R_{EE} \end{aligned} \quad (15.61)$$

Substitute  $R_{SS}$  for  $R_{EE}$  in these expressions for the FET case. We will make use of this two-port in subsequent chapters.

**EXERCISE:** The bipolar differential amplifier in Fig. 15.13(a) is biased by a  $75\text{-}\mu\text{A}$  current source with an output resistance of  $1\text{ M}\Omega$ . If the transistors have Early voltages of  $60\text{ V}$ , estimate values of  $R_{od}$ ,  $R_{oc}$ ,  $i_{dm}$ , and  $i_{cm}$ .

**ANSWERS:**  $3.2\text{ M}\Omega$ ;  $4.8\text{ G}\Omega$ ;  $1.50 \times 10^{-3}v_{dm}$ ;  $5.00 \times 10^{-7}v_{cm}$

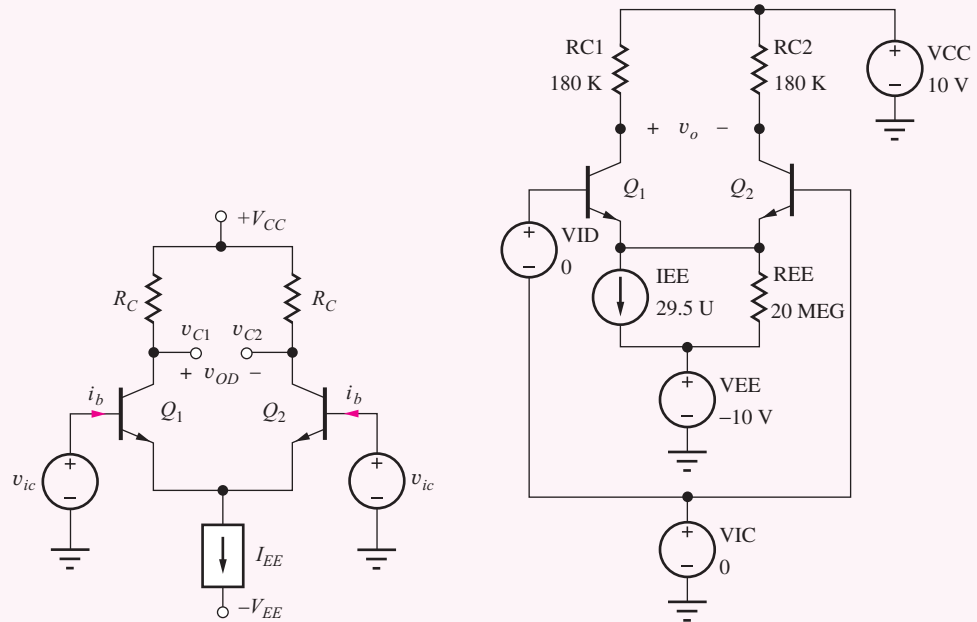
### EXAMPLE 15.3 DIFFERENTIAL AMPLIFIER DESIGN

Design a differential amplifier to meet a given set of specifications.

**PROBLEM** Design a differential amplifier stage with  $A_{dd} = 40\text{ dB}$ ,  $R_{id} \geq 250\text{ k}\Omega$ , and an input common-mode input range of at least  $\pm 5\text{ V}$ . Specify a current source to give CMRR of at least  $80\text{ dB}$  for a single-ended output. MOSFETs are available with  $K'_n = 50\text{ }\mu\text{A/V}^2$ ,  $\lambda = 0.0133\text{ V}^{-1}$ , and  $V_{TN} = 1\text{ V}$ . BJTs are available with  $I_S = 0.5\text{ fA}$ ,  $\beta_F = 100$ , and  $V_A = 75\text{ V}$ .

**SOLUTION** **Known Information and Given Data:** Differential amplifier topologies appear in Fig. 15.13;  $A_{dd} = 40\text{ dB}$ ,  $R_{id} \geq 250\text{ k}\Omega$ , single-ended CMRR  $\geq 80\text{ dB}$ , and  $|V_{IC}| \geq 5\text{ V}$ .

**Unknowns:** Power supply values, Q-points,  $R_C$ , bias source current and output resistance, transistor selection, and maximum dc common-mode input voltage  $V_{IC}$



**Approach:** Use theory developed in Ex. 15.2; choose transistor type and operating current based on \$A\_{dm}\$ and \$R\_{id}\$; choose power supplies based on \$A\_{dm}\$, \$V\_{IC}\$, and small-signal range; choose current source output resistance to achieve desired CMRR.

**Assumptions:** Active region operation; symmetrical power supplies, \$\beta\_o = \beta\_F\$, \$|v\_{id}| \leq 30 \text{ mV}\$.

**Analysis:** 40 dB of gain corresponds to \$A\_{dd} = 100\$. To achieve this gain with a resistively loaded amplifier, use of a BJT is indicated. For \$A\_{dd} = g\_m R\_C = 40 I\_C R\_C\$, a gain of 100 can be achieved with a voltage drop of 2.5 V across the resistor \$R\_C\$.<sup>3</sup> For a bipolar differential amplifier, the input resistance \$R\_{id} = 2r\_\pi\$, so \$r\_\pi = 125 \text{ k}\Omega\$, which requires

$$I_C \leq \frac{\beta_o V_T}{r_\pi} = \frac{100(0.025 \text{ V})}{125 \text{ k}\Omega} = 20 \mu\text{A}$$

based on a current gain of 100. Let us choose \$I\_C = 15 \mu\text{A}\$ to provide some safety margin. Then, \$R\_C = 2.5 \text{ V}/15 \mu\text{A} = 167 \text{ k}\Omega\$. Choose \$R\_C = 180 \text{ k}\Omega\$ as the nearest value from the 5 percent resistor tables in Appendix A. (The larger value will also help compensate for our neglect of \$r\_o\$ in the gain calculation.)

A \$V\_{IC}\$ of 5 V requires the collector voltage of the BJT to be at least 5 V at all times. We do not know the signal level, but we know \$|v\_{id}| \leq 30 \text{ mV}\$ for linearity in the differential pair. Thus, the ac component of the differential output voltage will be no greater than \$100(0.03 \text{ V}) = 3 \text{ V}\$, half of which will appear at each collector. Thus the dc + ac signal across \$R\_C\$ will not exceed 4 V (2.5-V dc + 1.5-V ac), and the positive power supply must satisfy

$$V_{CC} \geq V_{IC} + 4 \text{ V} = 5 + 4 = 9 \text{ V}$$

Choosing \$V\_{CC} = 10 \text{ V}\$ provides a design margin of 1 V. For symmetrical supplies, \$-V\_{EE} = -10 \text{ V}\$. The single-ended CMRR of 80 dB requires

$$R_{EE} \geq \frac{\text{CMRR}}{g_m} = \frac{10^4}{(40/\text{V})(15 \mu\text{A})} = 16.7 \text{ M}\Omega$$

A current source with \$I\_{EE} = 30 \mu\text{A}\$ and \$R\_{EE} \geq 20 \text{ M}\Omega\$ will provide some design margin.

<sup>3</sup> Remember our rule-of-thumb for the FET: \$g\_m R\_D \cong V\_{DD}\$ which would require very large \$V\_{DD}\$.

**Check of Results:** Using the design values,  $A_{dd} = 40(15 \mu\text{A})(180 \text{ k}\Omega) = 108$ . CMRR =  $40(15 \mu\text{A})(20 \text{ M}\Omega) = 12,000$  (81.6 dB), and  $R_{id} = 2(2.5 \text{ V}/15 \mu\text{A}) = 333 \text{ k}\Omega$ . The bias voltages provide  $V_{IC} = 6 \text{ V}$ . Thus the amplifier design should meet the specifications. We will check it further shortly with SPICE.

**Discussion:** Note that the drain currents are set by the current source and will be independent of device characteristics.

**Computer-Aided Analysis:** The SPICE schematic input appears in the figure on the previous page. Zero-value differential- and common-mode sources VID and VIC are for use in transfer function simulations. Requesting the transfer function from VID to output voltage  $v_O$  between the two collectors will produce values for  $A_{dd}$ ,  $R_{id}$ , and  $R_{od}$ . Requesting the transfer function from VIC to either collector node produces values for  $A_{cc}$  and  $R_{ic}$ . In our SPICE analysis, we can easily include the Early voltage (set VAF = 75 V) and  $R_{EE}$  to see their impact on the Q-points of the transistors. Using Eq. (15.40) with  $V_{BE} = (0.025 \text{ V}) \ln(15 \mu\text{A}/0.5 \text{ fA}) \cong 0.6 \text{ V}$ , the dc current source value for SPICE will be  $30 - 0.5 = 29.5 \mu\text{A}$ .

With these values and REE = 20 MEG, the Q-points from a SPICE operating point analysis are virtually the same as our hand calculations ( $14.9 \mu\text{A}$ , 7.33 V). Using two transfer function analyses gives  $A_{dd} = 100$ ,  $R_{id} = 382 \text{ k}\Omega$ ,  $R_{od} = 349 \text{ k}\Omega$ , and  $A_{cc} = 0.00416$ , and we find the CMRR =  $100/0.00416 = 24,000$  or 87.6 dB.

The results of a transient simulation for the output voltage at the right-hand collector are given here for  $v_{id}$  equal to a 30-mV input sine wave at a frequency of 1 kHz and  $V_{IC} = +5 \text{ V}$ . TSTART = 0, TSTOP = 0.002 s, and TSTEP = 0.001 ms (1  $\mu\text{s}$ ). As designed, we see an undistorted 1-kHz sine wave with an amplitude of 1.5 V biased at the Q-point level of 7.3 V.



## 15.2 EVOLUTION TO BASIC OPERATIONAL AMPLIFIERS

One extremely important application of differential amplifiers is at the input stage of operational amplifiers. Differential amplifiers provide the desired differential input and common-mode rejection capabilities, and a ground-referenced signal is available at the output. However, an op amp usually requires higher voltage gain than is available from a single differential amplifier stage, and most op amps use two stages of gain. In addition, a third stage, the output stage, is added to provide low output resistance and high output current capability.

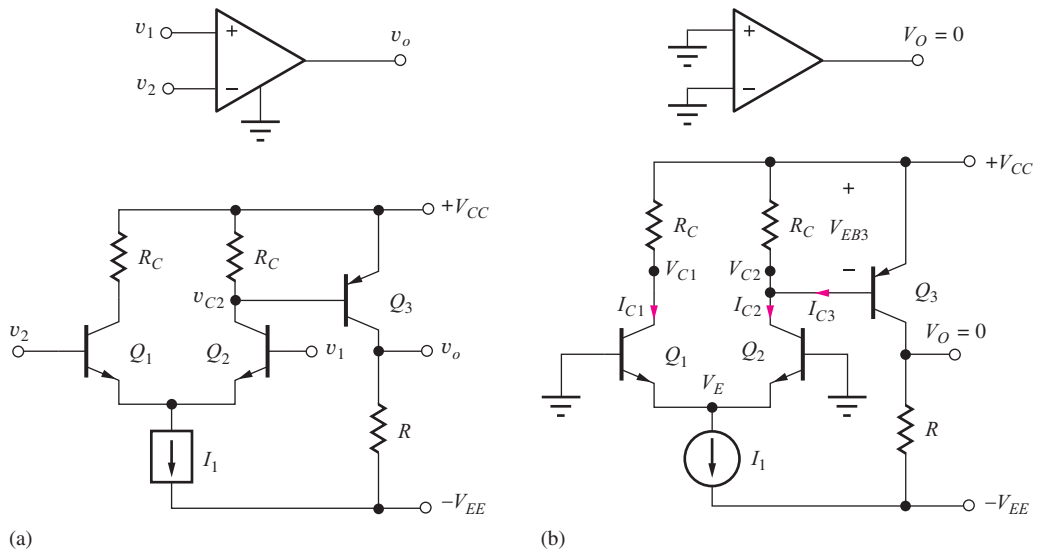


**Figure 15.19** (a) A simple two-stage prototype for an operational amplifier. (b) dc equivalent circuit for the two-stage amplifier.

### 15.2.1 A TWO-STAGE PROTOTYPE FOR AN OPERATIONAL AMPLIFIER

To achieve a higher gain, a *pnp* common-emitter amplifier \$Q\_3\$ has been connected to the output of a differential amplifier, \$Q\_1-Q\_2\$, to form the simple two-stage op amp depicted in Fig. 15.19a. Bias is provided by current source \$I\_1\$. Note the dc coupling between \$Q\_2\$ and \$Q\_3\$. Also note that the positions of inputs \$v\_1\$ and \$v\_2\$ have been reversed to account for the additional phase inversion by \$Q\_3\$.

#### dc Analysis

The dc equivalent circuit for the op amp is shown in Fig. 15.19(b) and will be used to find the Q-points of the three transistors. The emitter currents of \$Q\_1\$ and \$Q\_2\$ are each equal to one-half the bias current \$I\_1\$: \$I\_{E1} = I\_{E2} = I\_1/2\$. The voltage at the collector of \$Q\_1\$ is equal to

$$V_{C1} = V_{CC} - I_{C1}R_C = V_{CC} - \alpha_{F1} \frac{I_1}{2} R_C \quad (15.62)$$

and that at the collector of \$Q\_2\$ is

$$V_{C2} = V_{CC} - (I_{C2} - I_{B3})R_C = V_{CC} - \left( \alpha_{F2} \frac{I_1}{2} - I_{B3} \right) R_C \quad (15.63)$$

If the base current of \$Q\_3\$ can be neglected, and the common-base current gains are approximately 1, then Eqs. (15.62) and (15.63) become

$$V_{C1} \approx V_{C2} \approx V_{CC} - \frac{I_1 R_C}{2} \quad (15.64)$$

and because \$V\_E = -V\_{BE}\$,

$$V_{CE1} \approx V_{CE2} \approx V_{CC} - \frac{I_1 R_C}{2} + V_{BE} \quad (15.65)$$

In this particular circuit, it is important to note that the voltage drop across \$R\_C\$ is constrained to be equal to the emitter-base voltage \$V\_{EB3}\$ of \$Q\_3\$, or approximately 0.7 V.

The value of the collector current of \$Q\_3\$ can be found by remembering that this circuit is going to represent an operational amplifier, and because both inputs in Fig. 15.19 are zero, \$V\_O\$ should also be zero. This is the situation that exists when the circuit is used in any of the negative feedback circuits discussed in Chapters 10–12.

Since  $V_O = 0$ ,  $I_{C3}$  must satisfy

$$I_{C3} = \frac{V_{EE}}{R} \quad \text{and} \quad V_{EC3} = V_{CC} \quad (15.66)$$

We also know that  $V_{EB3}$  and  $I_{C3}$  are intimately related through the transport model relationship,

$$V_{EB3} = V_T \ln \left( 1 + \frac{I_{C3}}{I_{S3}} \right) \quad (15.67)$$

in which  $I_{S3}$  is the saturation current of  $Q_3$ . For the offset voltage of this amplifier to be zero, the value of  $R_C$  must be carefully selected, based on Eqs. (15.66) and (15.68):

$$R_C = \frac{V_T}{\left( \alpha_{F2} \frac{I_1}{2} - \frac{I_{C3}}{\beta_{F3}} \right)} \ln \left( 1 + \frac{I_{C3}}{I_{S3}} \right) \quad (15.68)$$

Otherwise, a small input voltage (the offset voltage) will need to be applied to the op-amp input, to force the output to zero volts.

**EXERCISE:** Find the Q-points for the transistors in the amplifier in Fig. 15.19 if  $V_{CC} = V_{EE} = 15$  V,  $I_1 = 150 \mu\text{A}$ ,  $R_C = 10 \text{ k}\Omega$ ,  $R = 20 \text{ k}\Omega$ , and  $\beta_F = 100$ . What is the value of  $I_{S3}$  if the output voltage is zero?

**ANSWERS:** (74.3  $\mu\text{A}$ , 14.9 V), (74.3  $\mu\text{A}$ , 15.01 V), (750  $\mu\text{A}$ , 15.0 V);  $1.90 \times 10^{-15} \text{ A}$

### dc Bias Sensitivity—A Word of Caution

It should be noted that the circuit in Fig. 15.19 cannot be operated open-loop without some form of feedback to stabilize the operating point of transistor  $Q_3$ , because the collector current of  $Q_3$  is exponentially dependent on the value of its emitter-base voltage. If one attempts to build this circuit, or even simulate it with the default values in SPICE, the output will be found to be saturated at one of the power supply “rails” due to our  $V_{EB} = 0.7$  V approximation. This sensitivity could be reduced by putting a resistance in series with the emitter of  $Q_3$ , at the expense of a loss in voltage gain.



**EXERCISE:** Simulate the circuit in Fig. 15.19 with  $V_{CC} = V_{EE} = 15$  V,  $I_1 = 150 \mu\text{A}$ ,  $R_C = 10 \text{ k}\Omega$ , and  $R = 20 \text{ k}\Omega$  using the default transistor parameters in SPICE. What are the transistor Q-points and output voltage  $v_O$ ?

**ANSWERS:** (74.4  $\mu\text{A}$ , 14.9 V), (74.4  $\mu\text{A}$ , 14.9 V), (164  $\mu\text{A}$ , 26.7 V),  $-11.7$  V — not quite saturated against the negative rail. (The exact values will depend on the default parameters in your version of SPICE.) The problem can be solved by connecting the base of  $Q_1$  to the output. Try the simulation again.

### ac Analysis

The ac equivalent circuit for the two-stage op amp is shown in Fig. 15.20, in which bias source  $I_1$  has been replaced by its equivalent ac resistance  $R_1$ . Analysis of the differential-mode behavior of the op amp can be determined from the simplified equivalent circuit in Fig. 15.21 based on the differential-mode half-circuit for the input stage.

It is important to realize that the overall two-stage amplifier in Fig. 15.20 no longer represents a symmetrical circuit. Thus, half-circuit analysis is not theoretically justified. However, we know that voltage variations at the collector of  $Q_2$  (or at the drain of an FET) do not substantially alter the current in the transistor when it is operating in the forward-active region (or saturation region for the FET). Thus, the emitters of the differential pair will remain approximately a virtual ground. One can also envision a fully symmetrical version of the amplifier with  $Q_3$  and  $R$  replicated on the

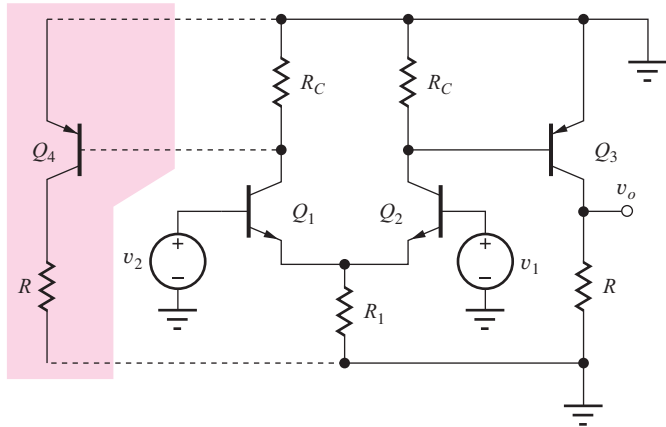


Figure 15.20 ac Equivalent circuit for the two-stage op amp.

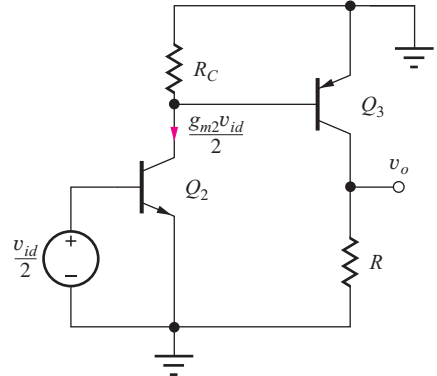


Figure 15.21 Simplified model using differential-mode half-circuit.

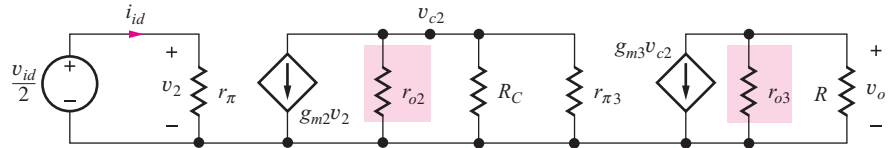


Figure 15.22 Small-signal model for Fig. 15.21.

left-hand side of the circuit with the base of the additional transistor attached to the collector of  $Q_1$ . In fact, special op amps having both differential inputs and differential outputs are built in this manner. Thus, continuing to represent the differential amplifier by its half-circuit is a highly useful engineering approximation.

The small-signal model corresponding to Fig. 15.21 appears in Fig. 15.22. In this analysis, output resistances  $r_{o2}$  and  $r_{o3}$  are neglected because they are in parallel with external resistors  $R_C$  and  $R$ . From Fig. 15.22, the overall differential-mode gain  $A_{dm}$  of this two-stage operational amplifier can be expressed as

$$A_{dm} = \frac{V_o}{V_{id}} = \frac{V_{c2}}{V_{id}} \frac{V_o}{V_{c2}} = A_{vt1} A_{vt2} \quad (15.69)$$

and the terminal gains  $A_{vt1}$  and  $A_{vt2}$  can be found from analysis of the circuit in the figure.

The first stage is a differential amplifier with the output taken from the inverting side,

$$A_{vt1} = \frac{V_{c2}}{V_{id}} = -\frac{g_m}{2} R_{L1} = -\frac{g_m}{2} \frac{R_C r_{\pi 3}}{R_C + r_{\pi 3}} \quad (15.70)$$

in which the load resistance  $R_{L1}$  is equal to the collector resistor  $R_C$  in parallel with the input resistance  $r_{\pi 3}$  of the second stage.

The second stage is also a resistively loaded common-emitter amplifier with gain

$$A_{vt2} = \frac{V_o}{V_{c2}} = -g_m R \quad (15.71)$$

Combining Eqs. (15.69) to (15.71) yields the overall voltage gain for the two-stage amplifier:

$$A_{dm} = A_{vt1} A_{vt2} = \left( -\frac{g_m}{2} \frac{R_C r_{\pi 3}}{R_C + r_{\pi 3}} \right) (-g_m R) = \frac{g_m R_C}{2} \frac{\beta_{o3} R}{R_C + r_{\pi 3}} \quad (15.72)$$

Equation (15.72) appears to contain quite a number of parameters and is difficult to interpret. However, some thought and manipulation will help reduce this expression to its basic design parameters. Multiplying the numerator and denominator of Eq. (15.72) by  $g_m$  and expanding the

transconductances in terms of the collector currents yields

$$A_{dm} = \frac{1}{2} \frac{(40I_{C2}R_C)\beta_{o3}(40I_{C3}R)}{40\frac{I_{C3}}{I_{C2}}I_{C2}R_C + \beta_{o3}} \quad (15.73)$$

If the base current of  $Q_3$  is neglected, then  $I_{C2}R_C = V_{BE3} \cong 0.7$  V, and  $I_{C3}R = V_{EE}$ , as pointed out during the dc analysis. Substituting these results into Eq. (15.73) yields

$$A_{dm} = \frac{1}{2} \frac{(28)\beta_{o3}(40V_{EE})}{28\left(\frac{I_{C3}}{I_{C2}}\right) + \beta_{o3}} = \frac{560V_{EE}}{1 + \frac{28}{\beta_{o3}}\left(\frac{I_{C3}}{I_{C2}}\right)} \quad (15.74)$$

In the final result in Eq. (15.74),  $A_{dm}$  is reduced to its basics. Once the power supply voltage  $V_{EE}$  and transistor  $Q_3$  (that is,  $\beta_{o3}$ ) are selected, the only remaining design parameter is the ratio of the collector currents in the first and second stages. An upper limit on  $I_{C2}$  and  $I_1$  is usually set by the permissible dc bias current,  $I_{B2}$ , at the input of the amplifier, whereas the minimum value of  $I_{C3}$  is determined by the current needed to drive the total load impedance connected to the output node. Generally,  $I_{C3}$  is several times larger than  $I_{C1}$ .

Figure 15.23 is a graph of Eq. (15.74), showing the variation of amplifier gain versus the collector current ratio. Observe that the gain starts to drop rapidly as  $I_{C3}/I_{C2}$  exceeds approximately 5. Such a graph is very useful as an aid in choosing the operating point during the design of the basic two-stage operational amplifier.

### Input and Output Resistances

From the ac model of the amplifier in Figs. 15.21 and 15.22, the differential-mode input resistance of the simple op amp is equal to the input resistance of the differential amplifier given by

$$R_{id} = \frac{V_{id}}{I_{id}} = 2r_{\pi 2} = 2r_{\pi 1} \quad (15.75)$$

and the output resistance is given by

$$R_{out} = R \parallel r_{o3} \cong R \quad (15.76)$$

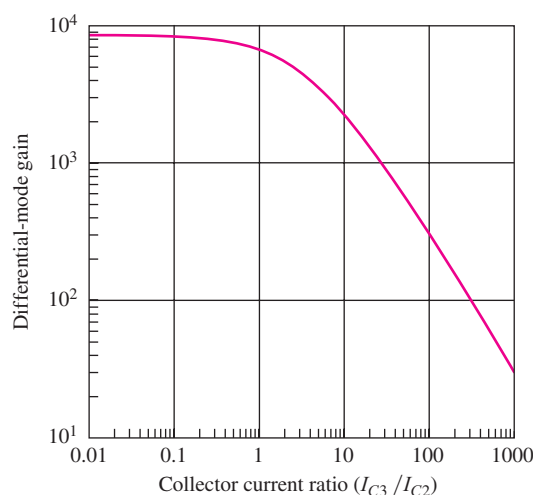


**Figure 15.23** Differential-mode gain versus collector current ratio for  $V_{EE} = 15$  V and  $\beta_{o3} = 100$ .

**EXERCISE:** What is the maximum possible gain of the amplifier described by Eq. (15.74) for  $V_{CC} = V_{EE} = 15$  V,  $\beta_{o1} = 50$ , and  $\beta_{o3} = 100$ ? What is the maximum voltage gain for the amplifier if the input bias current to the amplifier must not exceed 1  $\mu$ A, and  $I_{C3} = 500$   $\mu$ A? Repeat if  $I_{C3} = 5$  mA.

**ANSWERS:** 8400; 2210; 290

**EXERCISE:** What are the input and output resistances for the two amplifier designs in the previous exercise?

**ANSWERS:** 50 k $\Omega$ , 30 k $\Omega$ ; 50 k $\Omega$ , 3 k $\Omega$

**EXERCISE:** What is the maximum possible gain of the amplifier described by Eq. (15.74) if  $V_{CC} = V_{EE} = 1.5$  V?

**ANSWER:** 840

Before proceeding, we need to understand how the coupling and bypass capacitors have been eliminated from the two-stage op amp prototype. The virtual ground at the emitters of the differential amplifier allows the input stage to achieve the full inverting amplifier gain without the need for an emitter bypass capacitor. Use of the *pnp* transistor permits direct coupling between the first and second stages and allows the emitter of the *pnp* to be connected to an ac ground point. In addition, the *pnp* provides the voltage **level shift** required to bring the output back to 0 V. Thus, the need for any bypass or coupling capacitors is entirely eliminated, and  $v_O = 0$  for  $v_1 = 0 = v_2$ .

### CMRR

The common-mode gain and CMRR of the two-stage amplifier can be determined from the ac circuit model with common-mode input that is shown in Fig. 15.24, in which the half-circuit has again been used to represent the differential input stage. If Fig. 15.24 is compared to Fig. 15.21, we see that the circuitry beyond the collector of  $Q_2$  is identical in both figures. The only difference in output voltage is therefore due to the difference in the value of the collector current  $i_{c2}$ . In Fig. 15.24,  $i_{c2}$  is the collector current of a C-E stage with emitter resistor  $2R_1$ :

$$i_{c2} = \frac{\beta_{o2}v_{ic}}{r_{\pi2} + 2(\beta_{o2} + 1)R_1} \cong \frac{g_{m2}v_{ic}}{1 + 2g_{m2}R_1} \quad (15.77)$$

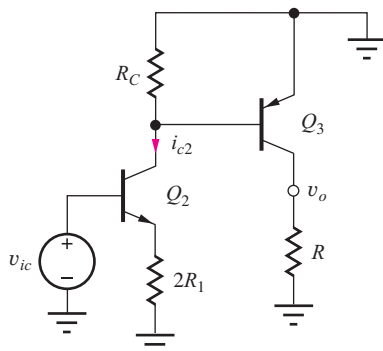


Figure 15.24 ac Equivalent circuit for common-mode inputs.

whereas  $i_{c2}$  in Fig. 15.21 was

$$i_{c2} = \frac{g_{m2}}{2} v_{id} \quad (15.78)$$

Thus, the common-mode gain  $A_{cm}$  of the op amp is found from Eq. (15.72) by replacing the quantity  $g_{m2}/2$  by  $g_{m2}/(1 + 2g_{m2}R_1)$ :

$$A_{cm} = \frac{g_{m2}R_C}{1 + 2g_{m2}R_1} \frac{\beta_{o3}R}{R_C + r_{\pi3}} = \frac{2A_{dm}}{1 + 2g_{m2}R_1} \quad (15.79)$$

From Eq. (15.79), the CMRR of the simple op amp is

$$\text{CMRR} = \left| \frac{A_{dm}}{A_{cm}} \right| = \frac{1 + 2g_{m2}R_1}{2} \cong g_{m2}R_1 \quad (15.80)$$

which is identical to the CMRR of the differential input stage alone.

**EXERCISE:** What is the CMRR of the amplifier in Fig. 15.19 if  $I_1 = 100 \mu\text{A}$  and  $R_1 = 750 \text{ k}\Omega$ ?

**ANSWER:** 63.5 dB

### 15.2.2 IMPROVING THE OP AMP VOLTAGE GAIN

From the previous several exercises, we can see that the prototype op amp has a relatively low overall voltage gain and a higher output resistance than is normally associated with a true operational amplifier. This section explores the use of an additional current source to improve the voltage gain; the next section adds an emitter follower to reduce the output resistance.

Figure 15.23 indicates that the overall amplifier gain decreases rapidly as the quiescent current of the second stage increases. In the exercise, the overall gain is quite low when  $I_{C3} = 5 \text{ mA}$ . One technique that can be used to improve the voltage gain is to replace resistor  $R$  by a second current source, as shown in Fig. 15.25. The modified ac model is in Fig. 15.25(b). The small-signal model is the same as Fig. 15.22 except  $R$  is replaced by output resistance  $R_2$  of current source  $I_2$ . The load on  $Q_3$  is now the output resistance  $R_2$  of the current source in parallel with the output resistance of  $Q_3$  itself. In Sec. 15.7, we shall discover that it is possible to design a current source with  $R_2 \gg r_{o3}$ , and, by neglecting  $R_2$ , the differential-mode gain expression for the overall amplifier becomes

$$A_{dm} = A_{vt1}A_{vt2} = \left( -\frac{g_{m2}}{2} \frac{R_C r_{\pi3}}{R_C + r_{\pi3}} \right) (-g_{m3}r_{o3}) \quad (15.81)$$

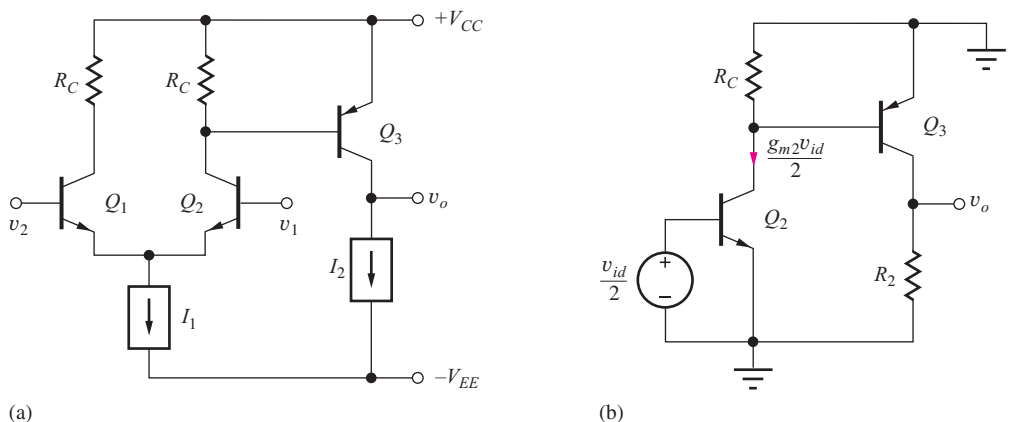


**Figure 15.25** (a) Amplifier with improved voltage gain. (b) Approximate ac differential-mode equivalent for op amp.

We can reduce Eq. (15.81) to

$$A_{dm} = \frac{14\mu_{f3}}{1 + \frac{28}{\beta_{o3}} \left( \frac{I_{C3}}{I_{C2}} \right)} \cong \frac{560V_{A3}}{1 + \frac{28}{\beta_{o3}} \left( \frac{I_{C3}}{I_{C2}} \right)} \quad (15.82)$$

using the same steps that led to Eq. (15.74). This expression is similar to Eq. (15.74) except that power supply voltage  $V_{EE}$  has been replaced by the Early voltage of  $Q_3$ . For low values of the collector current ratio, excellent voltage gains, approaching  $560V_{A3}$ , are possible from this simple two-stage amplifier. Also, note that the amplifier gain is no longer directly dependent on the choice of  $V_{CC}$  and  $V_{EE}$ .

Although adding the current source has improved the voltage gain, it also has degraded the output resistance. The output resistance of the amplifier is now determined by the characteristics of current source  $I_2$  and transistor  $Q_3$ :

$$R_{out} = R_2 \| r_{o3} \cong r_{o3} \quad (15.83)$$

Because of the relatively high output resistance, this amplifier more nearly represents a transconductance amplifier with a current output ( $A_{ic} = i_o/v_{id}$ ) rather than a true low output resistance voltage amplifier.

**EXERCISE:** Start with Eq. (15.81) and show that Eq. (15.82) is correct.

**EXERCISE:** What is the maximum possible voltage gain for the amplifier described by Eq. (15.82) for  $V_{CC} = 15$  V,  $V_{EE} = 15$  V,  $V_{A3} = 75$  V,  $\beta_{o1} = 50$ , and  $\beta_{o3} = 100$ ? What is the voltage gain if the input bias current to the amplifier must not exceed 1  $\mu$ A, and  $I_{C3} = 500$   $\mu$ A? Repeat if  $I_{C3} = 5$  mA.

**ANSWERS:** 42,000; 11,000; 1450

**EXERCISE:** What are the input and output resistances for the last two amplifier designs?

**ANSWERS:** 50 k $\Omega$ , 180 k $\Omega$ ; 50 k $\Omega$ , 18k $\Omega$

### 15.2.3 OUTPUT RESISTANCE REDUCTION

As just mentioned, the two-stage op amp prototype at this point more nearly represents a high-output resistance transconductance amplifier than a voltage amplifier with a low output resistance. A third stage, that maintains the amplifier voltage gain but provides a low output resistance, needs to be added to the amplifier. This sounds like the description of a follower circuit—unity voltage gain, high input resistance, and low output resistance!

An emitter-follower (C-C) stage is added to the prototype amplifier in Fig. 15.26. In this case, the C-C amplifier is biased by a third current source  $I_3$ , and an external load resistance  $R_L$  has been connected to the output of the amplifier. The ac equivalent circuit is drawn in Fig. 15.26(b), in which the output resistances of  $I_2$  and  $I_3$  are assumed to be very large and will be neglected in the analysis. Based on the ac equivalent circuit, the overall gain of the three-stage operational amplifier can be expressed as

$$A_{dm} = \frac{V_2}{V_{id}} \frac{V_3}{V_2} \frac{V_o}{V_3} = A_{vt1} A_{vt2} A_{vt3} \quad (15.84)$$

The gain of the first stage is equal to the gain of the differential input pair (neglecting  $r_{o2}$ ):

$$A_{vt1} = -\frac{g_m 2}{2} (R_C \| r_{\pi3}) \quad (15.85)$$

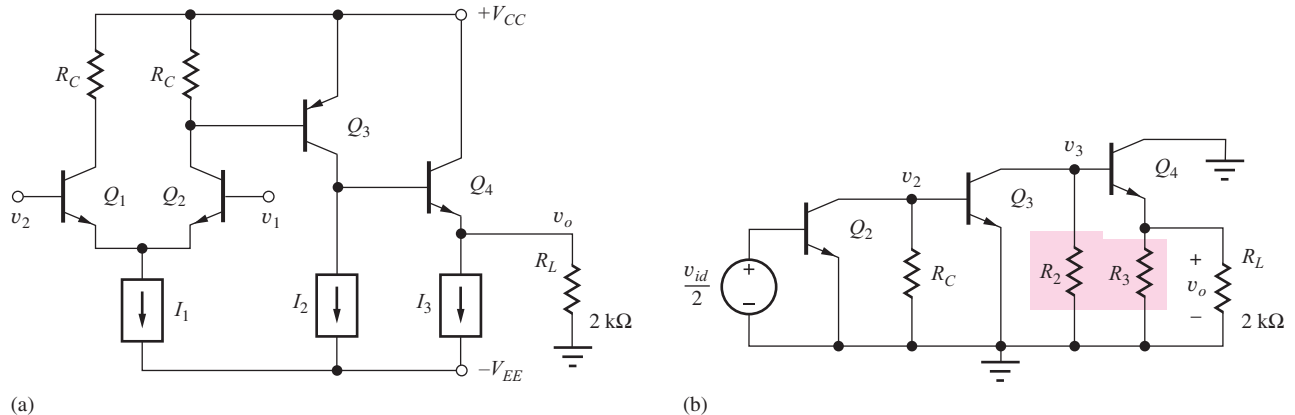


**Figure 15.26** (a) Amplifier with common-collector stage  $Q_4$  added. (b) Simplified ac equivalent circuit for the three-stage op amp.

The second stage is a common-emitter amplifier with a load resistance equal to the output resistance of  $Q_3$  in parallel with the input resistance of emitter follower  $Q_4$ :

$$A_{vt2} = -g_{m3}(r_{o3}\|R_{iB4}) \quad \text{where } R_{iB4} = r_{\pi4}(1 + g_{m4}R_L) \quad (15.86)$$

Finally, the gain of emitter follower  $Q_4$  is (neglecting  $r_{o4}$ ):

$$A_{vt3} = \frac{g_{m4}R_L}{1 + g_{m4}R_L} \cong 1 \quad (15.87)$$

The input resistance is set by the differential pair, and the output resistance of the amplifier is now determined by the resistance looking back into the emitter of  $Q_4$ :

$$R_{id} = 2r_{\pi 2} \quad \text{and} \quad R_{\text{out}} = \frac{1}{g_{m4}} + \frac{R_{\text{th4}}}{\beta_{o4} + 1} \quad (15.88)$$

In this case, there is a relatively large Thévenin equivalent source resistance at the base of  $Q_4$ ,  $R_{th4} \cong r_o3$ , and the overall output resistance is

$$R_{\text{out}} \cong \frac{1}{g_{m4}} + \frac{r_{o3}}{\beta_{o4}} = \frac{1}{g_{m4}} \left[ 1 + \frac{\mu_{f3} I_{C4}}{\beta_{o4} I_{C3}} \right] \quad (15.89)$$

**EXAMPLE 15.4** THREE-STAGE BIPOLAR OP AMP ANALYSIS

Let us now determine the characteristics of a specific implementation of the three-stage op amp implemented with bipolar transistors.

**PROBLEM** Find the differential-mode voltage gain, CMRR, input resistance, and output resistance for the amplifier in Fig. 15.27 if  $V_{CC} = 15$  V,  $V_{EE} = 15$  V,  $V_{A3} = 75$  V,  $\beta_{o1} = \beta_{o2} = \beta_{o3} = \beta_{o4} = 100$ ,  $I_1 = 100 \mu\text{A}$ ,  $I_2 = 500 \mu\text{A}$ ,  $I_3 = 5 \text{ mA}$ ,  $R_1 = 750 \text{ k}\Omega$ , and  $R_L = 2 \text{ k}\Omega$ . Assume  $R_2$  and  $R_3 = \infty$ .

**SOLUTION** **Known Information and Given Data:** Three-stage prototype op amp in Fig. 15.27 with  $V_{CC} = 15 \text{ V}$ ,  $V_{EE} = 15 \text{ V}$ ,  $V_{A3} = 75 \text{ V}$ ,  $\beta_{o1} = \beta_{o2} = \beta_{o3} = \beta_{o4} = 100$ ,  $I_1 = 100 \mu\text{A}$ ,  $I_2 = 500 \mu\text{A}$ ,  $I_3 = 5 \text{ mA}$ ,  $R_1 = 750 \text{ k}\Omega$ , and  $R_L = 2 \text{ k}\Omega$ . Assume  $R_2$  and  $R_3 = \infty$ .

**Unknowns:** Q-point values,  $R_C$ ,  $A_{dm}$ , CMRR,  $R_{id}$ , and  $R_O$

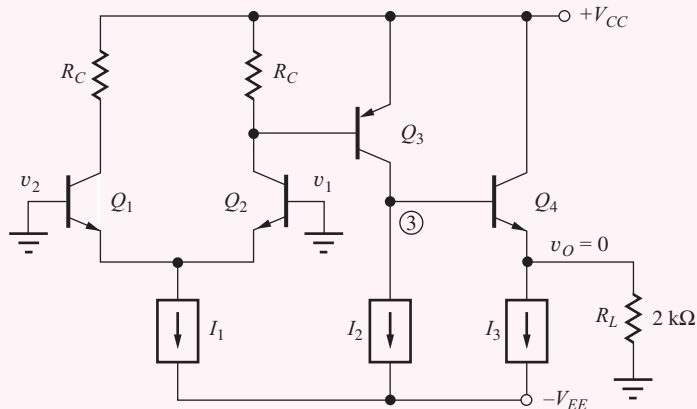


Figure 15.27 Operational amplifier with  $v_1 = 0 = v_2$ .

**Approach:** We need to evaluate the expressions in Eqs. (15.84) through (15.89). First, we must find the Q-point and then use it to calculate the small-signal parameters including  $g_{m2}$ ,  $r_{\pi2}$ ,  $r_{\pi3}$ ,  $g_{m2}$ ,  $r_{\pi3}$ , and  $r_{\pi4}$ . The required Q-point information can be found from Fig. 15.27, in which  $v_1$  and  $v_2$  equal zero.

**Assumptions:** The Q-point is found with  $v_1$  and  $v_2$  set to zero, and output voltage  $v_o$  is also assumed to be zero for this set of input voltages. The transistors are all in the active region with  $V_{BE}$  or  $V_{EB}$  equal to 0.7 V.

**Analysis:** The emitter current in the input stage is one-half the bias current source  $I_1$  and

$$g_{m2} = 40I_{C2} = 40(\alpha_{F2}I_{E2}) = 40(0.99 \times 50 \mu\text{A}) = 1.98 \text{ mS}$$

The collector of the second stage must supply the current  $I_2$  plus the base current of  $Q_4$ :

$$I_{C3} = I_2 + I_{B4} = I_2 + \frac{I_{E4}}{\beta_{F4} + 1}$$

When the output voltage is zero, the current in load resistor  $R_L$  is zero, and the emitter current of  $Q_4$  is equal to the current in source  $I_3$ . Therefore,

$$I_{C3} = I_2 + I_{B4} = I_2 + \frac{I_3}{\beta_{F4} + 1} = 5 \times 10^{-4} \text{ A} + \frac{5 \times 10^{-3} \text{ A}}{101} = 550 \mu\text{A}$$

and

$$g_{m3} = 40I_{C3} = \frac{40}{V}(5.5 \times 10^{-4} \text{ A}) = 2.20 \times 10^{-2} \text{ S}$$

$$r_{\pi3} = \frac{\beta_{o3}}{g_{m3}} = \frac{100}{2.20 \times 10^{-2} \text{ S}} = 4.55 \text{ k}\Omega$$

To find the output resistance of  $Q_3$ ,  $V_{EC3}$  is needed. When properly designed, the dc output voltage of the amplifier will be zero when the input voltages are zero. Hence, the voltage at node 3 is one base-emitter voltage drop above zero, or +0.7 V, and  $V_{EC3} = 15 - 0.7 = 14.3$  V. The output resistance of  $Q_3$  is

$$r_{o3} = \frac{V_{A3} + V_{EC3}}{I_{C3}} = \frac{(75 + 14.3) \text{ V}}{5.50 \times 10^{-4} \text{ A}} = 162 \text{ k}\Omega$$

Remembering that  $I_{E4} = I_3$

$$I_{C4} = \alpha_{F4}I_{E4} = 0.990 \times 5 \text{ mA} = 4.95 \text{ mA}$$

and

$$g_{m4} = 40I_{C4} = 198 \text{ mS} \quad r_{\pi4} = \frac{\beta_{o4}V_T}{I_{C4}} = \frac{100 \times 0.025 \text{ V}}{4.95 \times 10^{-3} \text{ A}} = 505 \text{ }\Omega$$

Finally, the value of  $R_C$  is needed:

$$R_C = \frac{V_{EB3}}{I_{C2} - I_{B3}} = \frac{V_{EB3}}{I_{C2} - \frac{I_{C3}}{\beta_{F3}}} = \frac{0.7 \text{ V}}{\left(49.5 - \frac{550}{100}\right) \times 10^{-6} \text{ A}} = 15.9 \text{ k}\Omega$$

Now, the small-signal characteristics of the amplifier can be evaluated:

$$A_{vt1} = -\frac{g_{m2}(R_C \| r_{\pi3})}{2} = -\frac{1.98 \text{ mS}(15.9 \text{ k}\Omega \| 4.55 \text{ k}\Omega)}{2} = -3.50$$

$$A_{vt2} = -g_{m3}[r_{o3} \| r_{\pi4} + \beta_{o4}R_L] = -22 \text{ mS}(162 \text{ k}\Omega \| 203 \text{ k}\Omega) = -1980!$$

$$A_{vt3} = \frac{g_{m4}R_L}{r_{\pi4}(1 + g_{m4}R_L)} = \frac{0.198 \text{ S}(2 \text{ k}\Omega)}{1 + 0.198 \text{ S}(2 \text{ k}\Omega)} = 0.998 \cong 1$$

$$A_{dm} = A_{vt1}A_{vt2}A_{vt3} = +6920$$

$$R_{id} = 2r_{\pi2} = 2\frac{\beta_{o2}}{g_{m2}} = 2\frac{100}{(40/\text{V})(49.5 \mu\text{A})} = 101 \text{ k}\Omega$$

$$R_O \cong \frac{1}{g_{m4}} + \frac{r_{o3}}{\beta_{o4}} = \frac{1}{(40/\text{V})(4.95 \text{ mA})} + \frac{162 \text{ k}\Omega}{100} = 1.62 \text{ k}\Omega$$

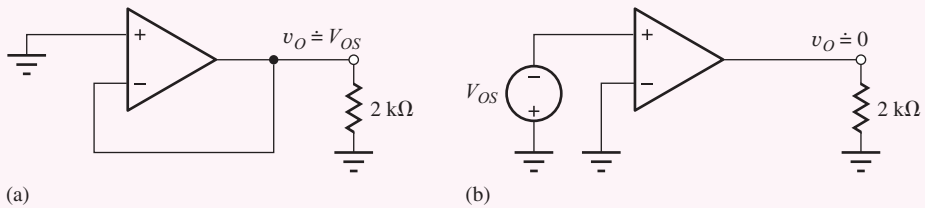
$$\text{CMRR} = g_{m2}R_1 = (40/\text{V})(49.5 \mu\text{A})(750 \text{ k}\Omega) = 1490 \text{ or } 63.5 \text{ dB}$$

**Check of Results:** We can use our rules-of-thumb from Chapter 13 to estimate the voltage gain. The first stage should produce a gain of approximately  $(1/2) \times 40 \times$  the voltage across the load resistor or  $20(0.7) = 14$ . The second stage should produce a gain of approximately  $\mu_f = 40(75) = 3000$ . The product is 42,000. Our detailed calculations give us about 1/6 of this value. Can we account for the discrepancies? We see the gain of the first stage is only 3.5 because  $r_{\pi3}$  is considerably smaller than  $R_C$ , and the gain of the second stage is approximately 2000 because the reflected loading of  $R_L$  is of the same order as  $r_{o3}$ . These two reductions account for the lower overall gain. The emitter follower produces a gain of one, as expected.

**Discussion:** This amplifier achieves a reasonable set of op amp characteristics for a simple circuit:  $A_v = 6920$ ,  $R_{id} = 101 \text{ k}\Omega$ , and  $R_O = 1.62 \text{ k}\Omega$ . Note that the second stage, loaded by current source  $I_2$  and buffered from  $R_L$  by the emitter follower, is achieving a gain that is a substantial fraction of  $Q_3$ 's amplification factor. However, even with the emitter follower, the reflected load resistance  $\beta_{o4}R_L$  is similar to the value of  $r_{o3}$  and is reducing the overall voltage gain by a factor of almost 2. Also, note that the output resistance is dominated by  $r_{o3}$ , present at the base of  $Q_4$ , and not by the reciprocal of  $g_{m4}$ . These last two factors point to a way to increase the performance of the amplifier by replacing  $Q_4$  with an *npn* Darlington stage (See Prob. 15.56).

**Computer-Aided Analysis:** Since this amplifier is dc coupled, a transfer function analysis from an input source to the output node will automatically yield the voltage gain, input resistance, and output resistance. In order to force the output to be nearly zero (the normal operating point), we must determine the offset voltage of the amplifier, and then apply it as a dc input to the amplifier. This is done by first connecting the amplifier as a voltage follower with the input grounded (see the figure below). For this amplifier, the SPICE yields  $V_{OS} = 0.437 \text{ mV}$ . Note that a current of approximately  $20 \mu\text{A}$  will exist in  $R_1$ , the output resistance of current source  $I_1$ . Be sure to choose  $I_1 = 80 \mu\text{A}$  so that the bias currents in  $Q_1$  and  $Q_2$  will each be approximately  $50 \mu\text{A}$ .

Next, the offset voltage is applied to the amplifier input with the feedback connection removed, and a transfer function analysis is requested from source  $V_{OS}$  to the output (Fig. b). The computed values are  $A_{dm} = 8280$ ,  $R_{id} = 105 \text{ k}\Omega$ , and  $R_O = 960 \Omega$ . The values all differ from our hand calculations. Most of the differences can be traced to the higher temperature and hence higher value of  $V_T$  used in the simulations ( $T$  defaults to  $27^\circ\text{C}$  and  $V_T = 25.9 \text{ mV}$ ).  $R_O$  as calculated by SPICE includes the presence of  $R_L$ . Removing the  $2\text{-k}\Omega$  resistor from the SPICE result yields  $R_O = [(1/960) - (1/2000)]^{-1} = 1.85 \text{ k}\Omega$ , which agrees more closely with our hand calculations.



**EXERCISE:** Suppose the output resistances of current sources  $R_2$  and  $R_3$  in the amplifier in Fig. 15.26 are  $150 \text{ k}\Omega$  and  $15 \text{ k}\Omega$ , respectively. (a) Recalculate the gain, input resistance, and output resistance. (b) Compare to SPICE simulation results. (c) What is the power consumption of the amplifier in Ex. 15.4?

**ANSWERS:** 4320,  $101 \text{ k}\Omega$ ,  $776 \Omega$ ; 4480,  $105 \text{ k}\Omega$ ,  $774 \Omega$ ;  $168 \text{ mW}$

**EXERCISE:** Suppose the current gain  $\beta_F$  of all the transistors is 150 instead of 100. Recalculate the gain, input resistance, output resistance, and CMRR of the amplifier in Fig. 15.26.

**ANSWERS:** 11,000;  $152 \text{ k}\Omega$ ;  $1.12 \text{ k}\Omega$ ; 63.4 dB

**EXERCISE:** Suppose the Early voltage of  $Q_3$  in the amplifier in Fig. 15.26 is  $50 \text{ V}$  instead of  $75 \text{ V}$ . Recalculate the gain, input resistance, output resistance, and CMRR.

**ANSWERS:** 5700;  $101 \text{ k}\Omega$ ;  $1.16 \text{ k}\Omega$ ; 63.5 dB

**EXERCISE:** The op amp in Ex. 15.4 is operated as a voltage follower. What are the closed-loop gain, input resistance, and output resistance?

**ANSWERS:**  $+0.99986$ ,  $699 \text{ M}\Omega$ ,  $0.233 \Omega$

#### 15.2.4 A CMOS OPERATIONAL AMPLIFIER PROTOTYPE

Similar circuit design ideas have been used to develop the basic CMOS operational amplifier depicted in Fig. 15.28(a). A differential amplifier, formed by NMOS transistors  $M_1$  and  $M_2$ , is followed by a PMOS common-source stage  $M_3$  and NMOS source follower  $M_4$ . Current sources are again used to bias the differential input and source-follower stages and as a load for  $M_3$ . Referring to the ac equivalent circuit in Fig. 15.28(b), we see that the differential-mode gain is given by the product of the terminal gains of the three stages:

$$A_{dm} = A_{vt1} A_{vt2} A_{vt3} = \left( -\frac{g_{m2}}{2} R_D \right) [-g_{m3}(r_{o3} \| R_2)] \left[ \frac{g_{m4}(R_3 \| R_L)}{1 + g_{m4}(R_3 \| R_L)} \right] \quad (15.90)$$

$$\cong \mu_{f3} \left( \frac{g_{m2}}{2} R_D \right) \left( \frac{g_{m4} R_L}{1 + g_{m4} R_L} \right) \quad (15.91)$$

in which we have assumed that  $R_3 \gg R_L$  and  $R_2 \gg r_{o3}$ .

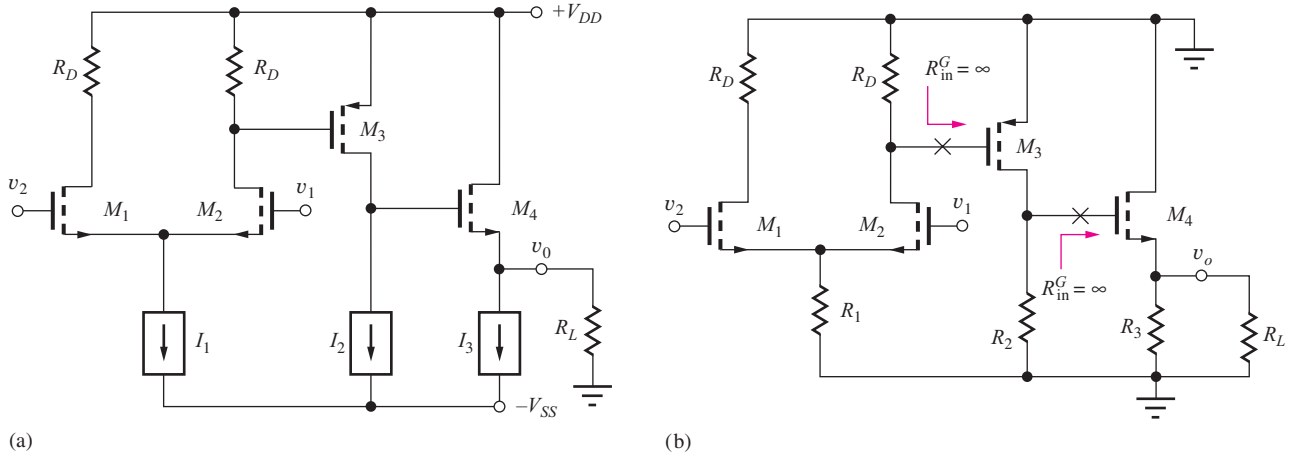


**Figure 15.28** (a) A CMOS operational amplifier prototype. (b) ac Equivalent circuit for the CMOS amplifier, in which the output resistances of current sources \$I\_2\$ and \$I\_3\$ have been neglected.

Equation (15.90) is relatively easy to construct using our single-stage amplifier formulas because the input resistance of each FET is infinite and the gain of one stage is not altered by the presence of the next. The overall differential-mode gain is approximately equal to the product of the voltage gain of the first stage and the amplification factor of the second stage.

Expanding  $g_{m2}$ , realizing that the product  $I_{D2}R_D$  represents the voltage across  $R_D$ , which must equal  $V_{GS3}$ , and assuming that the source follower has a gain of nearly 1 yields

$$A_{dm} \cong A_{v1}A_{v2}(1) = \mu_{f3} \left( \frac{V_{SG3}}{V_{GS2} - V_{TN2}} \right) \quad (15.92)$$

Although Eq. (15.92) is a simple expression, we often prefer to have the gain expressed in terms of the various bias currents, and expanding  $\mu_{f3}$ ,  $V_{GS2}$ , and  $V_{SG3}$  yields

$$A_{dm} = \frac{1}{\lambda_3} \sqrt{\frac{K_{n2}}{I_{D2}} \frac{K_{p3}}{I_{D3}}} \left[ \sqrt{\frac{2I_{D3}}{K_{p3}}} - V_{TP3} \right] \quad (15.93)$$

Because of the Q-point dependence of  $\mu_f$ , there are more degrees of freedom in Eq. (15.93) than in the corresponding expression for the bipolar amplifier, Eq. (15.82). This is particularly true in the case of integrated circuits, in which the values of  $K_n$  and  $K_p$  can be easily changed by modifying the  $W/L$  ratios of the various transistors. However, the benefit of operating both gain stages of the amplifier at low currents is obvious from Eq. (15.93), and picking a transistor with a small value of  $\lambda$  for  $M_3$  is also clearly important.

It is worth noting that because the gate currents of the MOS devices are zero, input-bias current does not place a restriction on  $I_{D1}$ , whereas it does place a practical upper bound on  $I_{C1}$  in the case of the bipolar amplifier. The input and output resistances of the op amp are determined by  $M_1$ ,  $M_2$ , and  $M_4$ . From our knowledge of single-stage amplifiers,

$$R_{id} = \infty \quad R_O = \frac{1}{g_{m4}} \parallel R_3 \quad \text{CMRR} = g_{m2}R_1 \quad (15.94)$$

CMRR is once again determined by the differential input stage, where  $R_1$  is the output resistance of current source  $I_1$ .

**EXERCISE:** For the CMOS amplifier in Fig. 15.28(a),  $\lambda_3 = 0.01 \text{ V}$ ,  $K_{n1} = K_{n4} = 5.0 \text{ mA/V}^2$ ,  $K_{p3} = 2.5 \text{ mA/V}^2$ ,  $I_1 = 200 \mu\text{A}$ ,  $I_2 = 500 \mu\text{A}$ ,  $I_3 = 5 \text{ mA}$ ,  $R_1 = 375 \text{ k}\Omega$ , and  $V_{TP3} = -1 \text{ V}$ . What is the actual gain of the source follower if  $R_L = 2 \text{ k}\Omega$ ? What are the voltage gain, CMRR, input resistance, and output resistance of the amplifier?

**ANSWERS:** 0.934; 2410, 51.5 dB,  $\infty$ ,  $141 \Omega$

**EXERCISE:** What is the quiescent power consumption of this op amp if  $V_{DD} = V_{SS} = 12 \text{ V}$ ?

**ANSWER:** 137 mW

### 15.2.5 BICMOS AMPLIFIERS

A number of integrated circuit processes exist that offer the circuit designer a combination of bipolar and MOS transistors or bipolar transistors and JFETs. These are commonly referred to as BiCMOS and BiFET technologies, respectively. The combination of BJTs and FETs offers the designer the ability to use the best characteristics of both devices to enhance the performance of the circuit. A simple BiCMOS op amp is shown in Fig. 15.29. In this case, a differential pair of PMOS transistors has been used as the input stage to demonstrate another design variation. The PMOS transistors at the input provide high input resistance and can be biased at relatively high input currents, since input current is not an issue. (We will discover later that this increased current improves the slew rate of the amplifier.) The second gain stage utilizes a bipolar transistor, which provides a superior amplification factor compared to the FET. Emitter resistor  $R_E$  increases the voltage across  $R_{D2}$  and hence, the voltage gain of the first stage without reducing the amplification factor of  $Q_1$  (see Section 14.2.7). The follower stage uses another FET in order to maximize second-stage gain while maintaining a reasonable output resistance.

For the circuit shown, SPICE simulation uses  $VTO = -1 \text{ V}$ ,  $KP = 25 \text{ mA/V}^2$ ,  $VAF = 75 \text{ V}$ , and  $BF = 100$ . SPICE is first used to find the offset voltage in the same manner as in Ex. 15.5. The value is found to be  $-11.37 \text{ mV}$ , which is then applied to the input of the open-loop amplifier. A transfer function analysis from  $V_{OS}$  to the output yields infinite input resistance, a voltage gain of 13,200 and an output resistance of  $61.4 \Omega$ .

### 15.2.6 ALL TRANSISTOR IMPLEMENTATIONS

In NMOS and CMOS technology, it is often desirable to eliminate all the resistors wherever possible, and this can be done using the techniques introduced in Section 14.6. For example, we can replace

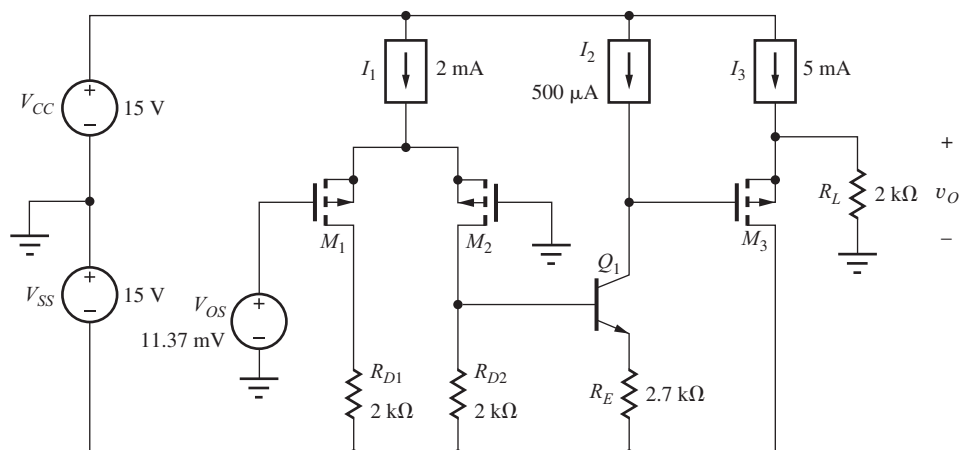
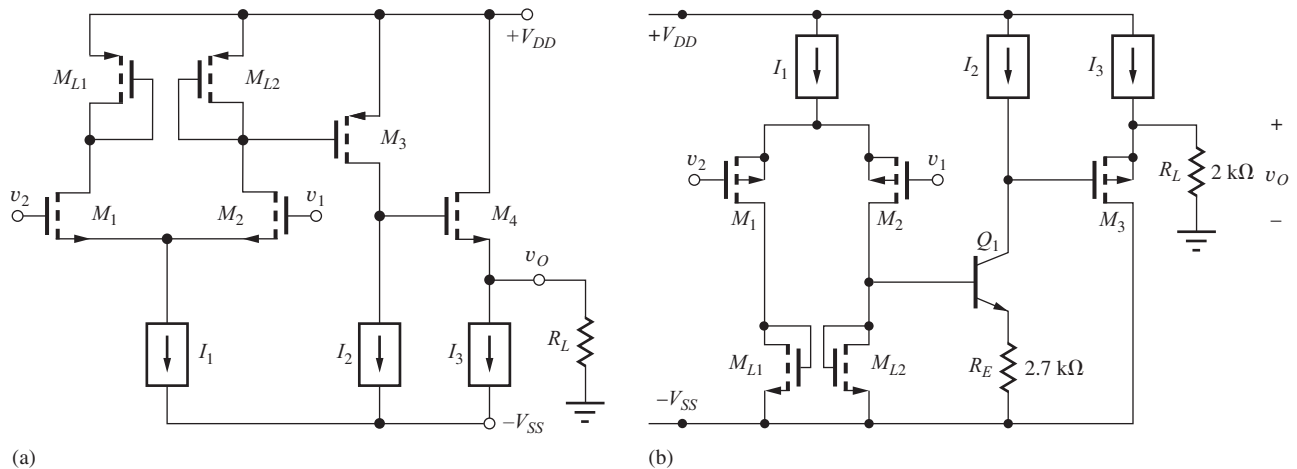


Figure 15.29 Basic BiCMOS op amp.



**Figure 15.30** (a) A version of the CMOS amplifier in Fig. 15.28 with the drain resistors replaced with saturated PMOS transistors. (b) The CMOS amplifier from Fig. 15.29 with the drain resistors replaced with saturated NMOS transistors.

the drain resistors in Fig. 15.28 with either NMOS or PMOS devices connected in saturation. Since the voltage across the transistor will provide the operating bias to  $M_3$ , it makes sense to use PMOS transistors as shown in Fig. 15.30(a) since the devices will then match to each other. The source-gate voltage of  $M_3$  is set by the source-drain voltage of  $M_{L2}$ :  $V_{SG3} = V_{SDL2}$ .

The equivalent small-signal resistance for the “diode-connected” FET is approximately  $R_{eq} = 1/g_m$ , so the differential-mode gain of the input stage becomes  $A_{dd} = -g_{m2}/g_{mL2}$ . The expression for the voltage gain of the input stage is slightly different from that presented in Chapter 14 because the input and load transistors are not the same type.

$$A_{dd} = -\frac{g_{m2}}{g_{mL2}} = -\frac{\sqrt{2K_n I_{D2}}}{\sqrt{2K_p I_{DL2}}} = -\sqrt{\frac{K'_n}{K'_p}} \sqrt{\frac{(W/L)_2}{(W/L)_{L2}}} \quad (15.95)$$

The difference between the transconductance parameters of the NMOS and PMOS transistors improves the gain for this case. Note that the PMOS transistors in Fig. 15.30(a) all have their sources tied to the power supply. The NMOS transistors could all be placed in individual  $p$ -wells in a  $p$ -well process to eliminate the body effect.

A similar technique is used to replace  $R_{D1}$  and  $R_{D2}$  in the BiCMOS amplifier in Fig. 15.30(b). NMOS transistors are used here so their sources can be connected to the negative power supply, and the PMOS transistors could be placed in separate  $p$ -wells if an  $n$ -well CMOS process were utilized. Resistor  $R_E$  is relatively small in value and would probably not be replaced with a transistor. In Chapter 16, we will find an even better way to configure load transistors  $M_{L1}$  and  $M_{L2}$  in both amplifiers in Fig. 15.30.

**EXERCISE:** Write an expression for upper bound on the gain of the amplifier in Fig. 15.30(a).

$$\text{ANSWER: } A_{dm} = \frac{1}{2} \frac{g_{m2}}{g_{mL2}} \mu_{f3} \frac{g_{m4} R_L}{1 + g_{m4} R_L} \leq \frac{1}{2} \frac{g_{m2}}{g_{mL2}} \mu_{f3}$$

**EXERCISE:** The input stage of the amplifier in Fig. 15.30(a) needs  $A_{dd} = 10$  and  $(W/L)_{L2} = 4/1$ . What value of  $(W/L)_2$  is required?

**ANSWER:** 25.3/1

**EXERCISE:** Write an expression for the voltage gain of the input stage in Fig. 15.30(b), ignoring the loading of  $Q_1$ .

**ANSWER:**  $A_{dd} = -\sqrt{\frac{K_p}{K_n}} \sqrt{\frac{(W/L)_2}{(W/L)_L}}$

## 15.3 OUTPUT STAGES

The basic operational amplifier circuits discussed in Sec. 15.2 used followers for the output stages. The final stage of these amplifiers is designed to provide a low-output resistance as well as a relatively high current drive capability. However, because of this last requirement, the output stages of the amplifiers in the previous section consume approximately two-thirds or more of the total power.

Followers are **class-A amplifiers**, defined as circuits in which the transistors conduct during the full  $360^\circ$  of the signal waveform. The class-A amplifier is said to have a **conduction angle**  $\theta_C = 360^\circ$ . Unfortunately, the maximum efficiency of the class-A stage is only 25 percent. Because the output stage must often deliver relatively large powers to the amplifier load, this low efficiency can cause high power dissipation in the amplifier. This section analyzes the efficiency of the class-A amplifier and then introduces the concept of the **class-B push-pull output stage**. The class-B push-pull stage uses two transistors, each of which conducts during only one-half, or  $180^\circ$ , of the signal waveform ( $\theta_C = 180^\circ$ ) and can achieve much higher efficiency than the class-A stage. Characteristics of the class-A and class-B stages can also be combined into a third category, the class-AB amplifier, which forms the output stage of most operational amplifiers.

### 15.3.1 THE SOURCE FOLLOWER – A CLASS-A OUTPUT STAGE

We analyzed the small-signal behavior of follower circuits in detail in Chapter 14 and found that they provide high input resistance, low output resistance, and a voltage gain of approximately 1. The large-signal operation of the emitter follower, biased by an **ideal current source**, was discussed in Chapter 9, so here we focus on the source-follower circuit in Fig. 15.31.

For  $v_I \leq V_{DD} + V_{TN}$ ,  $M_1$  will be operating in the saturation region (be sure to prove this to yourself). The current source forces a constant current  $I_{SS}$  to flow out of the source. Using Kirchhoff's

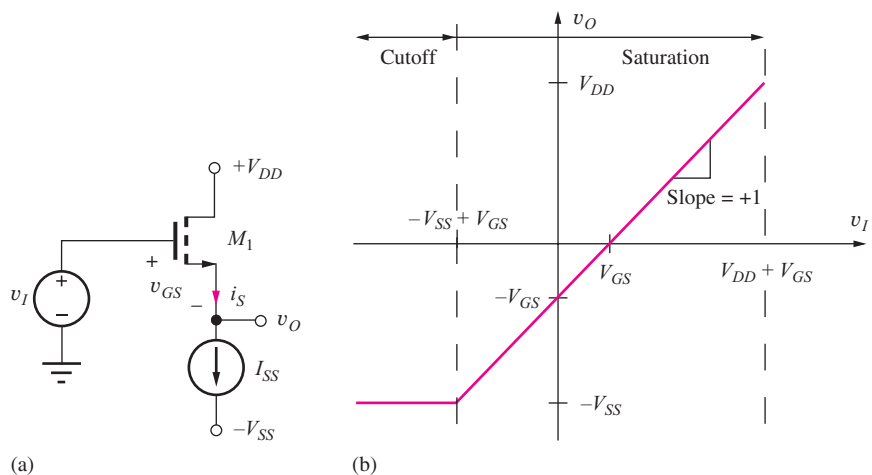


**Figure 15.31** (a) Source-follower circuit. (b) Voltage transfer characteristic for the source follower.

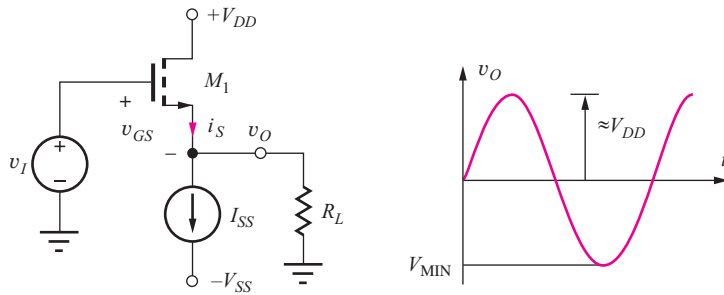


**Figure 15.32** Source follower with external load resistor  $R_L$ .

voltage law,  $v_O = v_I - v_{GS}$ . Since the source current is constant,  $v_{GS}$  is also constant, and  $v_O$  is

$$v_O = v_I - V_{GS} = v_I - \left( V_{TN} + \sqrt{\frac{2I_{SS}}{K_n}} \right) \quad (15.96)$$

The difference between the input and output voltages is fixed. Thus, from a large-signal perspective (as well as from a small-signal perspective), we expect the source follower to provide a gain of approximately 1.

The voltage transfer characteristic for the source follower appears in Fig. 15.31(b). The output voltage at the source follows the input voltage with a slope of +1 and a fixed offset voltage equal to  $V_{GS}$ . For positive inputs,  $M_1$  remains in saturation until  $v_I = V_{DD} + V_{TN}$ . The maximum output voltage is  $v_o = V_{DD}$  for  $v_I = V_{DD} + V_{GS}$ . Note that to actually reach this output, the input voltage must exceed  $V_{DD}$ .

The minimum output voltage is set by the characteristics of the current source. An ideal current source will continue to operate even with  $v_o < -V_{SS}$ , but most electronic current sources require  $v_o \geq -V_{SS}$ . Thus, the minimum possible value of the input voltage is  $v_I = -V_{SS} + V_{GS}$ .

### Source Follower with External Load Resistor

When a load resistor  $R_L$  is connected to the output, as in Fig. 15.32, the output voltage range is restricted by a new limit. The total source current of  $M_1$  is equal to

$$i_S = I_{SS} + \frac{v_O}{R_L} \quad (15.97)$$

and must be greater than zero. In this circuit, current cannot go back into the MOSFET source, so the minimum output voltage occurs at the point at which transistor  $M_1$  cuts off. In this situation,  $i_S = 0$  and  $v_{MIN} = -I_{SS}R_L$ .  $M_1$  cuts off when the input voltage falls to one threshold voltage drop above  $V_{MIN}$ :  $v_I = -I_{SS}R_L + V_{TN}$ .

### 15.3.2 EFFICIENCY OF CLASS-A AMPLIFIERS

Now consider the emitter follower in Fig. 15.32 biased with  $I_{SS} = V_{SS}/R_L$  and using symmetrical power supplies  $V_{DD} = V_{SS}$ . Assuming that  $V_{GS}$  is much less than the amplitude of  $v_I$ , then a sinusoidal output signal can be developed with an amplitude approximately equal to  $V_{DD}$ ,

$$v_O \cong V_{DD} \sin \omega t \quad (15.98)$$

The efficiency  $\zeta$  of the amplifier is defined as the power delivered to the load at the signal frequency  $\omega$ , divided by the average power supplied to the amplifier:

The average power  $P_{av}$  supplied to the source follower is

$$\begin{aligned} P_{av} &= \frac{1}{T} \int_0^T \left[ I_{SS}(V_{DD} + V_{SS}) + \left( \frac{V_{DD} \sin \omega t}{R_L} \right) V_{DD} \right] dt \\ &= I_{SS}(V_{DD} + V_{SS}) = 2I_{SS}V_{DD} \end{aligned} \quad (15.99)$$

where  $T$  is the period of the sine wave. The first term in brackets in Eq. (15.99) is the power dissipation due to the dc current source; the second term results from the ac drain current of the transistor. The last simplification assumes symmetrical power supply voltages. The average of the sine wave current is zero, so the sinusoidal current does not contribute to the value of the integral in Eq. (15.99).

Because the output voltage is a sine wave, the power delivered to the load at the signal frequency is

$$P_{\text{ac}} = \frac{\left(\frac{V_{DD}}{\sqrt{2}}\right)^2}{R_L} = \frac{V_{DD}^2}{2R_L} \quad (15.100)$$

Combining Eqs. (15.99) and (15.100) yields

$$\zeta = \frac{P_{\text{ac}}}{P_{\text{av}}} = \frac{\frac{V_{DD}^2}{2R_L}}{2I_{SS}V_{DD}} = \frac{1}{4} \quad \text{or} \quad 25\% \quad (15.101)$$

because  $I_{SS}R_L = V_{SS} = V_{DD}$ . Thus a follower, operating as a class-A amplifier, can achieve an efficiency of only 25 percent, at most, for sinusoidal signals (see Probs. 15.105 to 15.106 and 15.108). Equation (15.101) indicates that the low efficiency is caused by the Q-point current  $I_{SS}$  that flows continuously between the two power supplies.

### 15.3.3 CLASS-B PUSH-PULL OUTPUT STAGE

**Class-B amplifiers** improve the efficiency by operating the transistors at zero Q-point current, eliminating the quiescent power dissipation. A **complementary push-pull (class-B) output stage** using CMOS transistors is shown in Fig. 15.33, and the voltage and current waveforms for the composite output stage appear in Fig. 15.34. NMOS transistor  $M_1$  operates as a source follower for positive input signals, and PMOS transistor  $M_2$  operates as a source follower for negative inputs.

Consider the sinusoidal input in Fig. 15.34, for example. As the input voltage  $v_I$  swings positive,  $M_1$  turns on supplying current to the load, and the output follows the input on the positive swing.

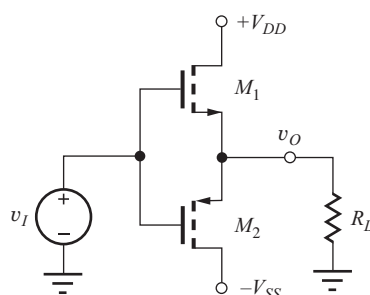


**Figure 15.33** Complementary MOS class-B amplifier.

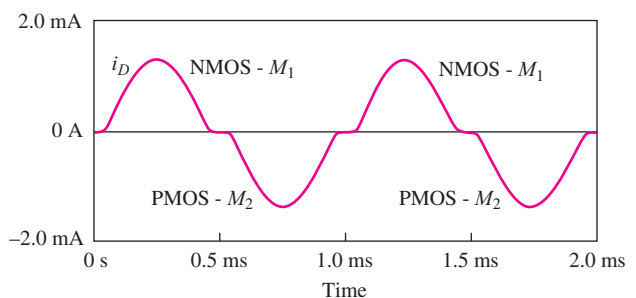
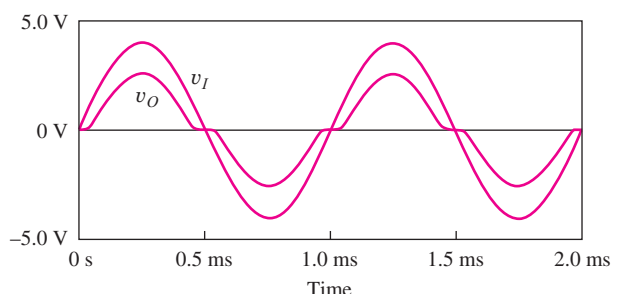


**Figure 15.34** Cross-over distortion and drain currents in the class-B amplifier.

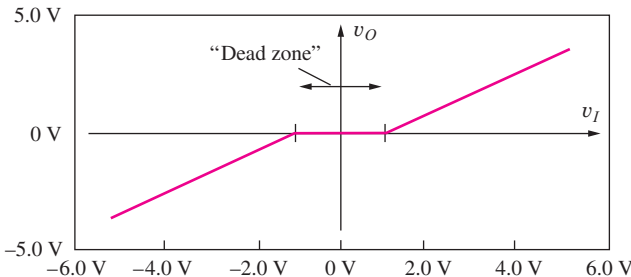


**Figure 15.35** SPICE simulation of the voltage transfer characteristic for the complementary class-B amplifier.

When the input becomes negative,  $M_2$  turns on sinking current from the load, and the output follows the input on the negative swing.

Each transistor conducts current for approximately  $180^\circ$  of the signal waveform, as shown in Fig. 15.34. Because the *n*- and *p*-channel gate-source voltages are equal in Fig. 15.33, only one of the two transistors can be on at a time. Also, the Q-point current for  $v_O = 0$  is zero, and the efficiency can be high.

However, although the efficiency is high, a distortion problem occurs in the class-B stage. Because  $V_{GS1}$  must exceed threshold voltage  $V_{TN}$  to turn on  $M_1$ , and  $V_{GS2}$  must be less than  $V_{TP}$  to turn on  $M_2$ , a “dead zone” appears in the push-pull class-B voltage transfer characteristic, shown in Fig. 15.35. Neither transistor is conducting for

$$V_{TP} \leq v_{GS} \leq V_{TN} \quad (-1 \text{ V} \leq v_{GS} \leq 1 \text{ V} \text{ in Fig. 15.35}) \quad (15.102)$$

This **dead zone**, or **cross-over region**, causes distortion of the output waveform, as shown in the simulation results in Fig. 15.34. As the sinusoidal input waveform crosses through zero, the output voltage waveform becomes distorted. The waveform distortion in Fig. 15.34 is called **cross-over distortion**.

### Class-B Efficiency

Simulation results for the currents in the two transistors are also included in Fig. 15.34. If cross-over distortion is neglected, then the current in each transistor can be approximated by a half-wave rectified sinusoid with an amplitude of approximately  $V_{DD}/R_L$ . Assuming  $V_{DD} = V_{SS}$ , the average power dissipated from each power supply is

$$P_{av} = \frac{1}{T} \int_0^{T/2} V_{DD} \frac{V_{DD}}{R_L} \sin \frac{2\pi}{T} t dt = \frac{V_{DD}^2}{\pi R_L} \quad (15.103)$$

The total ac power delivered to the load is still given by Eq. (15.100), and  $\zeta$  for the class-B output stage is

$$\zeta = \frac{\frac{V_{DD}^2}{2R_L}}{\frac{2V_{DD}^2}{\pi R_L}} = \frac{\pi}{4} \cong 0.785 \quad (15.104)$$

By eliminating the quiescent bias current, the class-B amplifier can achieve an efficiency of 78.5 percent!

In closed-loop feedback amplifier applications such as those introduced in Chapters 10–12, the effects of cross-over distortion are reduced by the loop gain  $A\beta$ . However, an even better solution is to eliminate the cross-over region by operating the output stage with a small nonzero quiescent current. Such an amplifier is termed a class-AB amplifier.

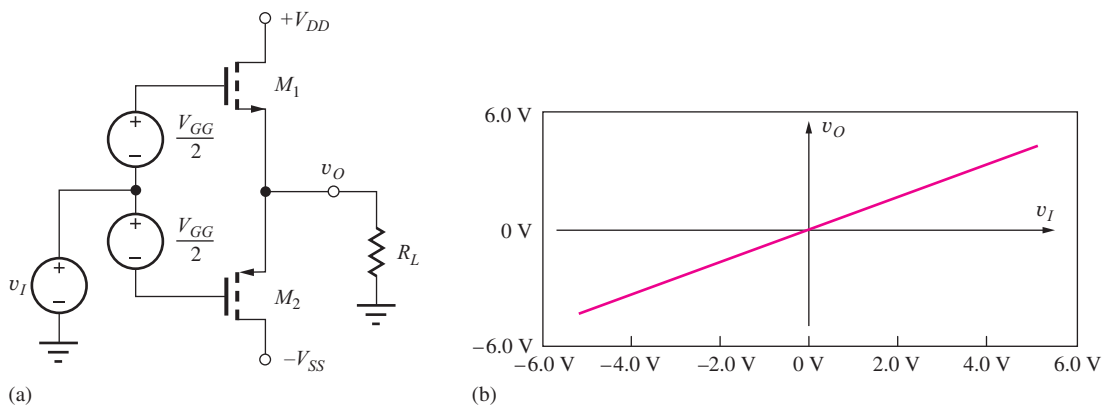
### 15.3.4 CLASS-AB AMPLIFIERS

The benefits of the class-B amplifier can be maintained, and cross-over distortion can be minimized by biasing the transistors into conduction, but at a relatively low quiescent current level. The basic technique is shown in Fig. 15.36. A bias voltage  $V_{GG}$  is used to establish a small quiescent current in both output transistors. This current is chosen to be much smaller than the peak ac current that will be delivered to the load. In Fig. 15.36, the bias source is split into two symmetrical parts so that  $v_O = 0$  for  $v_I = 0$ .

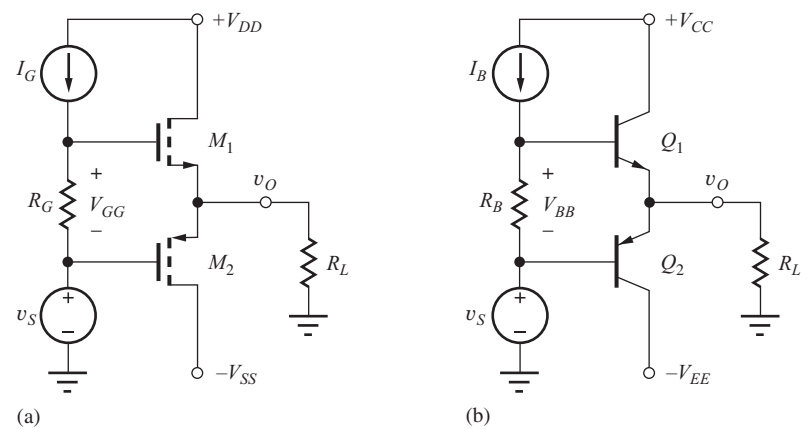
Because both transistors are conducting for  $v_I = 0$ , the cross-over distortion can be eliminated, but the additional power dissipation can be kept small enough that the efficiency is not substantially degraded. The amplifier in Fig. 15.36 is classified as a **class-AB amplifier**. Each transistor conducts for more than the  $180^\circ$  of the class-B amplifier but less than the full  $360^\circ$  of the class-A amplifier.

Figure 15.36(b) shows the results of circuit simulation of the voltage transfer characteristic of the class-AB output stage with a quiescent bias current of approximately  $60 \mu\text{A}$ . The distorted cross-over region has been eliminated, even for this small quiescent bias current.

Figure 15.37(a) shows one method for generating the needed bias voltage that is consistent with the CMOS operational amplifier circuit of Fig. 15.28. Bias current  $I_G$  develops the required bias voltage for the output stage across resistor  $R_G$ . If we assume that  $K_p = K_n$  and  $V_{TN} = -V_{TP}$  for the MOSFETs, and  $v_O = 0$ , then the bias voltage splits equally between the gate-source terminals



**Figure 15.36** (a) Complementary output stage biased for class-AB operation. (b) SPICE simulation of voltage transfer characteristic for class-AB stage with  $I_D \cong 60 \mu\text{A}$ .



**Figure 15.37** (a) Method for biasing the MOS class-AB amplifier. (b) Bipolar class-AB amplifier.

of the two transistors. The drain currents of the two transistors are both

$$I_D = \frac{K_n}{2} \left( \frac{V_{GG}}{2} - V_{TN} \right)^2 \quad (15.105)$$

The bipolar version of the class-AB push-pull output stage employs complementary *npn* and *pnp* transistors, as shown in Fig. 15.28(b). The principle of operation of the bipolar circuit is the same as that for the MOS case. Transistors  $Q_1$  and  $Q_2$  operate as emitter followers for the positive and negative excursions of the output signal, respectively. Current source  $I_B$  develops a bias voltage  $V_{BB}$  across resistor  $R_B$ , which is shared between the base-emitter junctions of the two BJTs.

For class-AB operation, voltage  $V_{BB}$  is designed to be approximately  $2V_{BE} \approx 1.1$  V, so both transistors are conducting a small collector current. If we assume the saturation currents of the two transistors are equal, then the bias voltage  $V_{BB}$  splits equally between the base-emitter junctions of the two transistors, and the two collector currents are

$$I_C = I_S \exp \left( \frac{I_B R_B}{2V_T} \right) \quad (15.106)$$

Each transistor is biased into conduction at a low level to eliminate cross-over distortion.

A simplified small-signal model for the class-AB stage is a single follower transistor with a current gain equal to the average of the gains of  $Q_1$  and  $Q_2$  or with a transconductance parameter equal to the average of the values for  $M_1$  and  $M_2$ .

A class-B version of the bipolar push-pull output stage is obtained by setting  $V_{BB}$  to zero. For this case, the output stage exhibits cross-over distortion for an input voltage range of approximately  $2V_{BE}$ .

**EXERCISE:** Find the bias current in the transistors in Fig. 15.37(a) for  $v_o = 0$  if  $K_n = K_p = 25$  mA/V<sup>2</sup>,  $V_{TN} = 1$  V, and  $V_{TP} = -1$  V,  $I_G = 500$   $\mu$ A, and  $R_G = 4.4$  k $\Omega$ .

**ANSWER:** 125  $\mu$ A

**EXERCISE:** Find the bias current in the transistors in Fig. 15.37(b) for  $v_o = 0$  if  $I_S = 10$  fA,  $I_B = 500$   $\mu$ A, and  $R_B = 2.4$  k $\Omega$ .

**ANSWER:** 265  $\mu$ A

### 15.3.5 CLASS-AB OUTPUT STAGES FOR OPERATIONAL AMPLIFIERS

In Figs. 15.38(a) and (b), the follower output stages of the prototype CMOS and bipolar op amps have been replaced with complementary class-AB output stages. Current source  $I_2$ , which originally provided a high impedance load to transistors  $Q_3$  and  $M_3$ , is also used to develop the dc bias voltage necessary for class-AB operation. The signal current is supplied by transistor  $M_3$  or  $Q_3$ , respectively. The total quiescent power dissipation is greatly reduced in both these amplifiers.

### 15.3.6 SHORT-CIRCUIT PROTECTION

If the output of a follower circuit is accidentally shorted to ground, the transistor can be destroyed due to high current and high power dissipation, or, through direct destruction of the base-emitter junction of the BJT. To make op amps as “robust” as possible, circuitry is often added to the output stage to provide protection from short circuits.

In Fig. 15.39, transistor  $Q_2$  has been added to protect emitter follower  $Q_1$ . Under normal operating conditions, the voltage developed across  $R$  is less than 0.7 V, transistor  $Q_2$  is cut off,

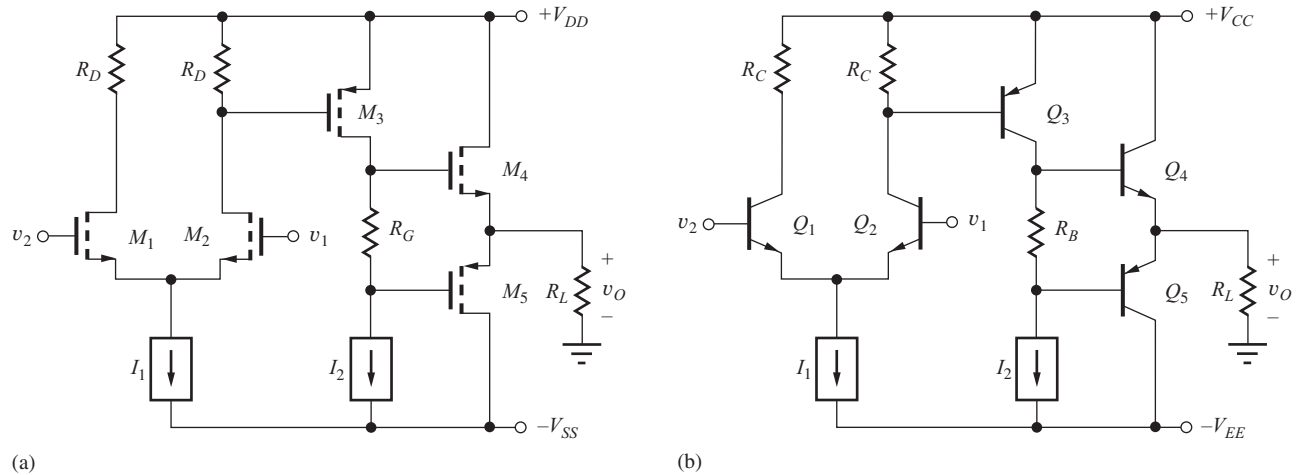


**Figure 15.38** Class-AB output stages added to the (a) CMOS and (b) bipolar operational amplifiers.

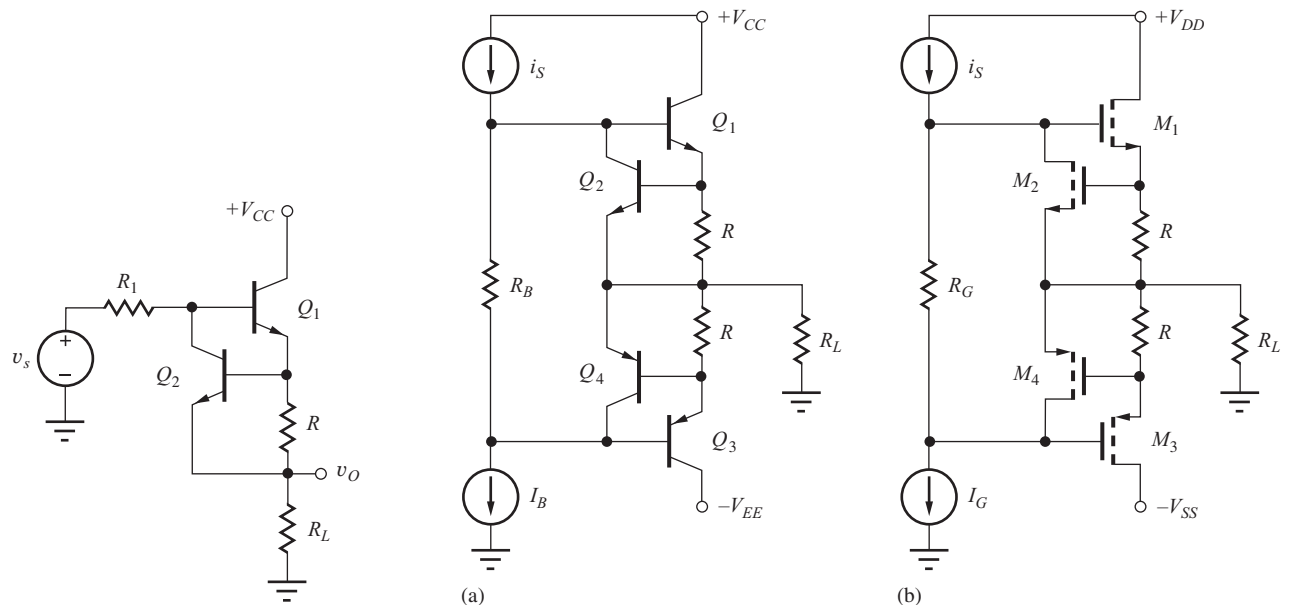


**Figure 15.39** Short-circuit protection for an emitter follower.

**Figure 15.40** Short-circuit protection for complementary output stages. (\$i\_S = I\_B\$ or \$I\_G\$ at the Q-point.)

and \$Q\_1\$ functions as a normal follower. However, if emitter current \$I\_{E1}\$ exceeds a value of

$$I_{E1} = \frac{V_{BE2}}{R} = \frac{0.7 \text{ V}}{R} \quad (15.107)$$

then transistor \$Q\_2\$ turns on and shunts any additional current from \$R\_1\$ down through the collector of \$Q\_2\$ and away from the base of \$Q\_1\$. Thus, the output current is limited to approximately the value in Eq. (15.107). For example, \$R = 25 \Omega\$ will limit the maximum output current to 28 mA. Because \$R\$ is directly in series with the output, however, the output resistance of the follower is increased by the value of \$R\$.

Figure 15.40(a) depicts the complementary bipolar output stage including **short-circuit protection**. \$pnp\$ transistor \$Q\_4\$ is used to limit the base current of \$Q\_3\$ in a manner identical to that of

$Q_2$  and  $Q_1$ . Similar **current-limiting circuits** can be applied to FET output stages, as shown in Fig. 15.40(b). Here, transistor  $M_2$  steals the current needed to develop gate drive for  $M_1$ , and the output current is limited to

$$I_{S1} \cong \frac{V_{GS2}}{R} = \frac{V_{TN2} + \sqrt{\frac{2I_G}{K_{n2}}}}{R} \quad (15.108)$$

Transistor  $M_4$  provides similar protection to  $M_3$ .

### 15.3.7 TRANSFORMER COUPLING

Designing amplifiers to deliver power to low impedance loads can be difficult. For example, loudspeakers typically have only an 8- or 16- $\Omega$  impedance. To achieve good voltage gain and efficiency in this situation, the output resistance of the amplifier needs to be quite low. One approach would be to use a feedback amplifier to achieve a low output resistance, as discussed in Chapter 12. An alternate approach to the problem is to use **transformer coupling**.

In Fig. 15.41, a follower circuit is coupled to load resistance  $R_L$  through an ideal transformer with a turns ratio of  $n:1$ . In this circuit, coupling capacitor  $C$  is required to block the dc path through the primary of the transformer. (See Prob. 15.115 for an alternate approach.)

As defined in network theory, the terminal voltages and currents of the ideal transformer are related by

$$\mathbf{v}_1 = n\mathbf{v}_2 \quad \mathbf{i}_2 = n\mathbf{i}_1 \quad \frac{\mathbf{v}_1}{\mathbf{i}_1} = n^2 \frac{\mathbf{v}_2}{\mathbf{i}_2} \quad \text{or} \quad Z_1 = n^2 Z_L \quad (15.109)$$

The transformer provides an impedance transformation by the factor  $n^2$ . Based on these equations, the transformer and load resistor can be represented by the ac equivalent circuit in Fig. 15.41(b), in which the resistor has been moved to the primary side of the transformer and the secondary is now an open circuit. The effective resistance that the transistor must drive and the voltage at the transformer output are

$$R_{EQ} = n^2 R_L \quad \text{and} \quad \mathbf{v}_o = \frac{\mathbf{v}_1}{n} \quad (15.110)$$

Transformer coupling can reduce the problems associated with driving very low impedance loads. However, the transformer obviously restricts operation to frequencies above dc.

Figure 15.42 is a second example of the use of a transformer, in which an inverting amplifier stage is coupled to the load  $R_L$  through the ideal transformer. The dc and ac equivalent circuits appear in Figs. 15.42(b) and (c), respectively. At dc, the transformer represents a short circuit, the

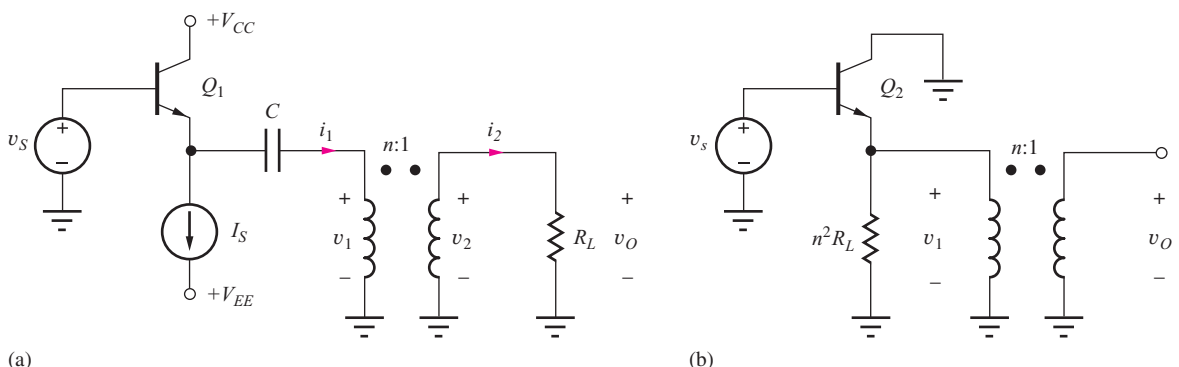
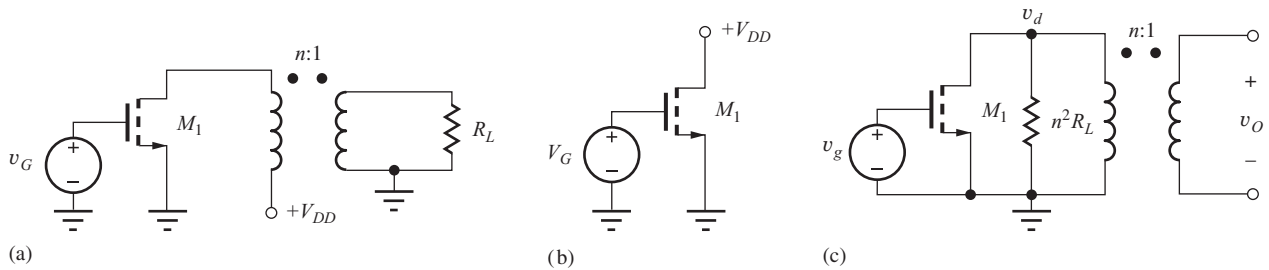
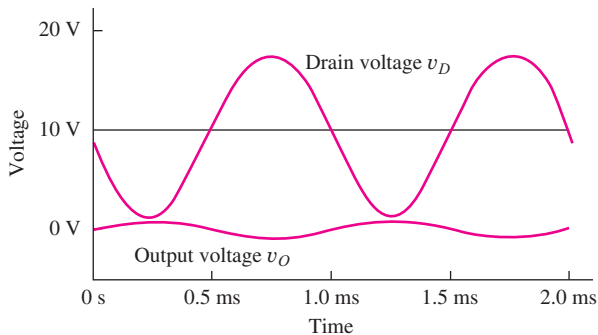


Figure 15.41 (a) Follower circuit using transformer coupling. (b) ac Equivalent circuit representation for the follower.



**Figure 15.42** (a) Transformer-coupled inverting amplifier. (b) dc Equivalent circuit. (c) ac Equivalent circuit.



**Figure 15.43** SPICE simulation of the transformer-coupled inverting amplifier stage for  $n = 10$  with  $V_{DD} = 10$  V.

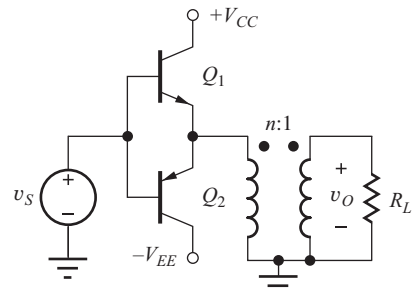


**Figure 15.44** Transformer-coupled class-B output stage.

full dc power supply voltage appears across the transistor, and the quiescent operating current of the transistor is supplied through the primary of the transformer. At the signal frequency, a load resistance equal to  $n^2 R_L$  is presented to the transistor.

Results of simulation of the circuit in Fig. 15.42 are in Fig. 15.43 for the case  $R_L = 8 \Omega$ ,  $V_{DD} = 10$  V, and  $n = 10$ . The behavior of this circuit is different from most that we have studied. The quiescent voltage at the drain of the MOSFET is equal to the full power supply voltage  $V_{DD}$ . The presence of the inductance of the transformer permits the signal voltage to swing symmetrically above and below  $V_{DD}$ , and the peak-to-peak amplitude of the signal at the drain can approach  $2V_{DD}$ .

Figure 15.44 is a final circuit example, which shows a transformer-coupled class-B output stage. Because the quiescent operating currents in  $Q_1$  and  $Q_2$  are zero, the emitters may be connected directly to the primary of the transformer.

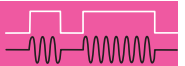
#### EXERCISE: Find the small-signal voltage gains

$$A_{v1} = \frac{v_d}{v_g} \quad \text{and} \quad A_{vo} = \frac{v_o}{v_g}$$

for the circuit in Fig. 15.42 if  $V_{TN} = 1$  V,  $K_n = 50$  mA/V<sup>2</sup>,  $V_G = 2$  V,  $V_{DD} = 10$  V,  $R_L = 8 \Omega$ , and  $n = 10$ . What are the largest values of  $v_g$ ,  $v_d$ , and  $v_o$  that satisfy the small-signal limitations?

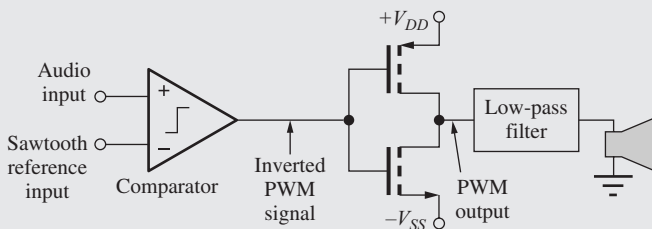
**ANSWERS:**  $-40, -4; 0.2$  V,  $8$  V,  $0.8$  V

## ELECTRONICS IN ACTION



### Class-D Audio Amplifiers

As mentioned in the main body of the text, the efficiency of class-A, -B, and -AB amplifiers is limited to less than 80 percent. To achieve higher efficiencies, a number of forms of switching amplifiers have been developed for use in portable and other low-power electronic applications. One of these is the class-D amplifier shown here, in which the output is a pulse-width modulated (PWM) signal that switches rapidly between the positive and negative power supplies. High efficiency is achieved by using CMOS transistors as switches. In a manner similar to a CMOS inverter, the goal is to have only one transistor on at a given time.

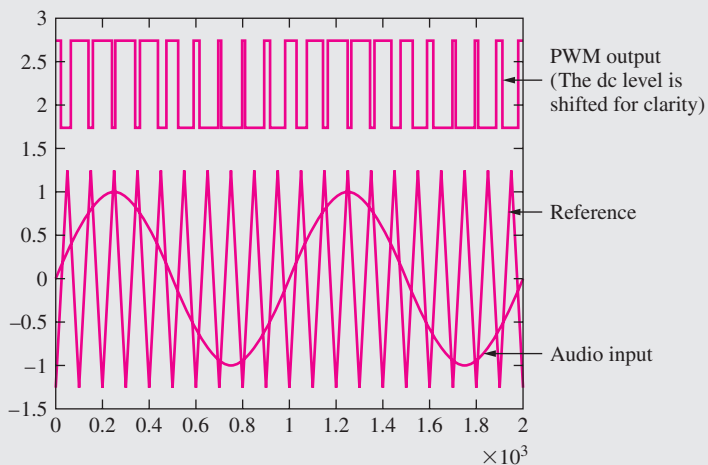


(a)

Conceptual implementation of a class-D audio amplifier.

A basic PWM signal can be generated by comparing the audio input signal to a sawtooth reference waveform. Referring to the sample waveforms, we see that the PWM output is switched high to  $V_{DD}$  when the audio input exceeds the reference waveform, and the output is switched to  $-V_{SS}$  when the reference input exceeds the analog input. In the waveform illustration, the sawtooth reference input is operating at a frequency that is 10 times that of the sinusoidal input. For an audio signal with a bandwidth of 20 Hz to 20 kHz, the reference frequency may range from 250 kHz to more than 1 MHz. Before being fed to the speaker, the PWM signal is passed through a low-pass filter to remove the unwanted high frequency content.

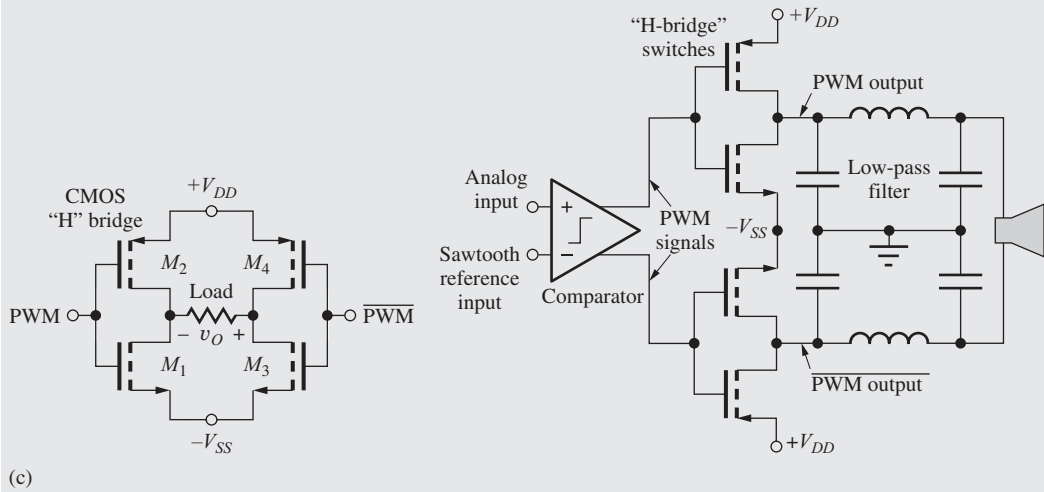
In order to achieve higher power levels with a given supply voltage, the load is often driven in a differential fashion using a complementary “H-bridge.” In the CMOS version shown here, output voltage  $v_O$  equals  $(V_{DD} + V_{SS})$  when input  $V$  is high, and  $v_O$  equals  $-(V_{DD} + V_{SS})$



(b)

Illustration of PWM waveforms.

when input  $V$  is low. Thus, the total signal swing across the load is twice the sum of the power supply span, and the power that can be delivered to the load is four times that achieved without the H-bridge. A class-D amplifier using the H-bridge appears in the final figure in which the speaker is driven by the low-pass filtered output of the CMOS H-bridge.



Class-D amplifier using an H-bridge to drive the speaker.

## 15.4 ELECTRONIC CURRENT SOURCES

The dc current source is clearly a fundamental and highly useful circuit component. In Sec. 15.3 we found that multiple current sources could be used to provide bias to the BJT and MOS op amp prototypes as well as to improve their performance. This section first explores the basic circuits used to realize electronic versions of ideal current sources and then explores current source design in more depth by looking at techniques specifically applicable to the design of integrated circuits.

In Fig. 15.45, the current-voltage characteristics of an ideal current source are compared with those of resistor and transistor current sources of Fig. 15.46. Current  $I_O$  through the ideal source is

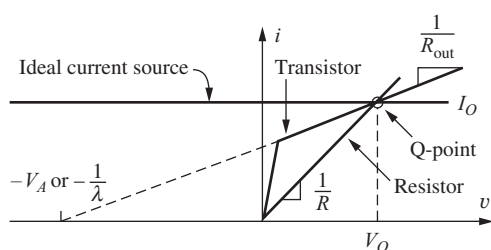


Figure 15.45  $i$ - $v$  Characteristics of basic electronic current sources.

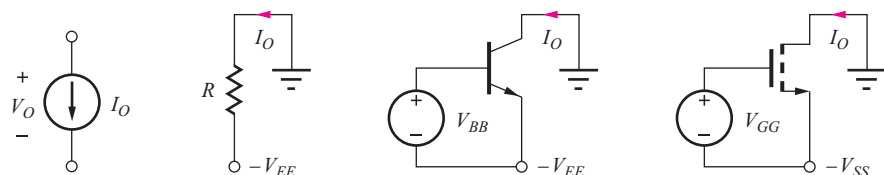


Figure 15.46 Ideal, resistor, BJT, and MOS current sources.

independent of the voltage appearing across the source, and the output resistance of the ideal source is infinite, as indicated by the zero slope of the current source  $i$ - $v$  characteristic.

For the ideal source, the voltage across the source can be positive or negative, and the current remains the same. However, **electronic current sources** must be implemented with resistors and transistors, and their operation is usually restricted to only one quadrant of the total  $i$ - $v$  space. In addition, electronic sources have a finite output resistance, as indicated by the nonzero slope of the  $i$ - $v$  characteristic. We will find that the output resistance of the transistor is much greater than a resistor for an equivalent Q-point.

In normal use, the circuit elements in Fig. 15.45 will actually be *sinking* current from the rest of the network, and some authors prefer to call these elements **current sinks**. In this book, we use the generic term *current source* to refer to both sinks and sources.

### 15.4.1 SINGLE-TRANSISTOR CURRENT SOURCES

The simplest forms of electronic current sources are shown in Fig. 15.46. A resistor is often used to establish bias currents in many circuits — differential amplifiers, for example — but it represents our poorest approximation to an ideal current source. Individual transistor implementations of current sources generally operate in only one quadrant because the transistors must be biased in the forward-active or pinch-off regions in order to maintain high impedance operation. However, the transistor source can realize very high values of output resistance.

For simplicity, the transistors in Fig. 15.46 are biased into conduction by sources  $V_{BB}$  and  $V_{GG}$ . In these circuits, we assume that the collector-emitter and drain-source voltages are large enough to ensure operation in the forward-active or pinch-off (active) regions, as appropriate for each device.

### 15.4.2 FIGURE OF MERIT FOR CURRENT SOURCES

Resistor  $R$  in Fig. 15.46 will be used as a reference for comparing current sources. The resistor provides an output current and output resistance of

$$I_O = \frac{V_{EE}}{R} \quad \text{and} \quad R_{\text{out}} = R \quad (15.111)$$

The product of the dc current  $I_O$  and output resistance  $R_{\text{out}}$  is the effective voltage  $V_{CS}$  across the current source, and we will use it as a **figure of merit (FOM)** for comparing various current sources:

$$V_{CS} = I_O R_{\text{out}} \quad (15.112)$$

For a given Q-point current,  $V_{CS}$  represents the equivalent voltage that will be needed across a resistor for it to achieve the same output resistance as the given current source. The larger the value of  $V_{CS}$ , the higher the output resistance of the source. For the resistor itself,  $V_{CS}$  is simply equal to the power supply voltage  $V_{EE}$ .

If ac models are drawn for each source in Fig. 15.46, the base, emitter, gate, and source of each transistor will be connected to ground, and each transistor will be considered operating in either the common-source or common-emitter configuration. The output resistance therefore will be equal to  $r_o$  in all cases, and the figures of merit for these sources will be

$$\begin{aligned} \text{BJT: } V_{CS} &= I_O R_{\text{out}} = I_C r_o = I_C \frac{V_A + V_{CE}}{I_C} = V_A + V_{CE} \cong V_A \\ \text{FET: } V_{CS} &= I_O R_{\text{out}} = I_D r_o = I_D \frac{\frac{1}{\lambda} + V_{DS}}{I_D} = \frac{1}{\lambda} + V_{DS} \cong \frac{1}{\lambda} \end{aligned} \quad (15.113)$$

$V_{CS}$  for the C-E/C-S transistor current sources is approximately equal to either the Early voltage  $V_A$  or  $1/\lambda$ . We can expect that both these values generally will be at least several times the available power supply voltage. Therefore, any of the single transistor sources will provide an output resistance that is greater than that of a resistor.

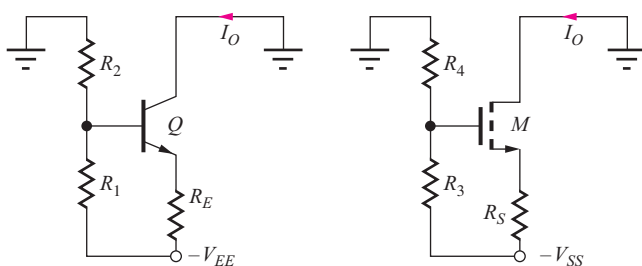


Figure 15.47 High-output resistance current sources.

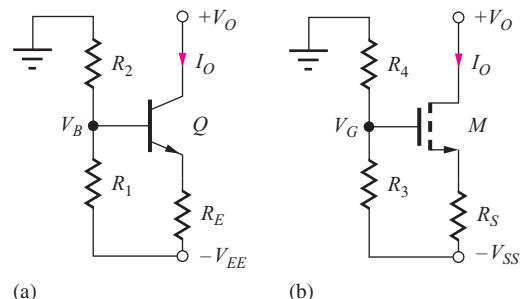


Figure 15.48 (a) npn and (b) NMOS current source circuits.

**TABLE 15.1**Comparison of the Basic Current Sources  $\beta_o = 100$ ,  $V_A = 1/\lambda = 50$  V,  $\mu_{fET} = 100$ 

TYPE OF SOURCE	$R_{out}$	$V_{CS}$	TYPICAL VALUES
Resistor	$R$	$V_{EE}$	15 V
Single transistor	$r_o$	$V_A$ or $\frac{1}{\lambda}$	50–100 V
BJT with emitter resistor $R_E$	$\beta_o r_o$	$\cong \beta_o V_A$	5000 V
FET with source resistor $R_S$ ( $V_{SS} = 15$ V)	$\mu_f R_S$	$\cong \mu_f \frac{V_{SS}}{3}$	500 V or more

### 15.4.3 HIGHER OUTPUT RESISTANCE SOURCES

From our study of single-stage amplifiers in Chapters 13 and 14, we know that placing a resistor in series with the emitter or source of the transistor, as in Fig. 15.47, increases the output resistance. Referring back to Eq. (13.66), we find that the output resistances for the circuits in Fig. 15.47 are

$$\text{BJT: } R_{out} = r_o \left[ 1 + \frac{\beta_o R_E}{R_1 \| R_2 + r_\pi + R_E} \right] \leq (\beta_o + 1)r_o \quad (15.114)$$

and

$$\text{FET: } R_{out} = r_o(1 + g_m R_S) \cong \mu_f R_S \quad (15.115)$$

The figures of merit are

$$\text{BJT: } V_{CS} \cong \beta_o(V_A + V_{CE}) \cong \beta_o V_A \quad \text{and} \quad \text{FET: } V_{CS} \cong \mu_f \frac{V_{SS}}{3} \quad (15.116)$$

where it has been assumed that  $I_o R_S \cong V_{SS}/3$ . Based on these figures of merit, the output resistance of the current sources in Fig. 15.47 can be expected to reach very high values, particularly at low current levels.<sup>4</sup> Table 15.1 compares  $V_{CS}$  for the various sources for typical device parameter values.

### 15.4.4 CURRENT SOURCE DESIGN EXAMPLES

This section provides examples of the design of current sources using the three-resistor bias circuits in Fig. 15.48. The computer (via a spreadsheet) is used to help explore the design space. The current source requirements are provided in the following design specifications.

<sup>4</sup> Because of its importance in analog circuit design, the  $\beta_o V_A$  product is often used as a basic figure of merit for the bipolar transistor.

### Design Specifications

Design a current source using the circuits in Fig. 15.48 with a nominal output current of 200  $\mu\text{A}$  and an output resistance greater than 10 M $\Omega$  using a single -15-V power supply. The source must also meet the following additional constraints.

Output voltage (compliance) range should be as large as possible while meeting the output resistance specification.

The total current used by the source should be less than 250  $\mu\text{A}$ .

Bipolar transistors are available with  $(\beta_o, V_A)$  of (80, 100 V) or (150, 75 V). FETs are available with  $\lambda = 0.01 \text{ V}^{-1}$ ;  $K_n$  can be chosen as necessary.

When used in an actual application, the collector and drain of the current sources in Fig. 15.48 will be connected to some other point in the overall circuit, as indicated by the voltage  $+V_O$  in the figure. For the current source to provide a high output resistance, the BJT must remain in the active region, with the collector-base junction reverse-biased ( $V_O \geq V_B$ ), or the FET must remain in pinchoff ( $V_O \geq V_G - V_{TN}$ ).

Specifications include the requirement that the output voltage range be as large as possible. Thus, the design goal is to achieve  $I_O = 200 \mu\text{A}$  and  $R_{\text{out}} \geq 10 \text{ M}\Omega$  with as low a voltage as possible at  $V_B$  or  $V_G$ . A range of designs is explored to see just how low a voltage can be used at  $V_B$  or  $V_G$  and still meet the  $I_O$  and  $R_{\text{out}}$  requirements. Investigating this design space is most easily done with the aid of the computer.

## DESIGN EXAMPLE 15.5

### DESIGN OF A BIPOLAR TRANSISTOR CURRENT SOURCE

Here we design a current source to meet a given set of design specifications using a bipolar transistor and the three resistor bias circuit. Example 15.6 explores the NMOS current source design.

**PROBLEM** Design a current source using the circuit in Fig. 15.49(a) with a nominal output current of 200  $\mu\text{A}$  and an output resistance greater than 10 M $\Omega$  using a single -15-V power supply. The source must also meet the following additional constraints.

Output voltage (compliance) range should be as large as possible while meeting the output resistance specification.

The total current used by the source should be less than 250  $\mu\text{A}$ .

Bipolar transistors are available with  $(\beta_o, V_A)$  of (80, 100 V) or (150, 75 V).

**SOLUTION** **Known Information and Given Data:** Current source circuit in Fig. 15.48(a);  $I_O = 200 \mu\text{A}$ ;  $V_{EE} = 15 \text{ V}$ ;  $I_{EE} < 250 \mu\text{A}$ ;  $R_{\text{out}} > 10 \text{ M}\Omega$ ;  $V_B$  as low as possible; BJTs are available with  $(\beta_o, V_A)$  of (80, 100 V) and (150, 75 V)

**Unknowns:** Values of resistors  $R_1$ ,  $R_2$ , and  $R_E$

**Approach:** Set up equations for analysis; using a computer program or spreadsheet, search for a set of bias conditions that satisfy the requirements; choose nearest resistor values from 1 percent resistor table in Appendix A.

**Assumptions:** Active region and small-signal operating conditions apply;  $V_{BE} = 0.7 \text{ V}$ ;  $V_T = 0.025 \text{ V}$ ; choose  $V_O = 0 \text{ V}$  as a representative value for the output voltage.

**Analysis:** We start the design of the bipolar version of the current source with the expression for the output resistance of the source. Because we will use a computer to help in the design, we use the most complete expression for the output resistance:

$$R_{\text{out}} = r_o \left[ 1 + \frac{\beta_o R_E}{R_E + r_\pi + R_1 \| R_2} \right] \leq \beta_o r_o \quad (15.117)$$

The figure of merit for this source is

$$V_{CS} = I_o R_{\text{out}} \leq \beta_o V_A \quad (15.118)$$

and the design specifications require

$$\beta_o V_A = I_o R_{\text{out}} \geq (200 \mu\text{A})(10 \text{ M}\Omega) = 2000 \text{ V} \quad (15.119)$$

Although both the specified transistors easily meet the requirement of Eq. (15.119), the denominator of Eq. (15.118) can substantially reduce the output resistance below that predicted by the  $\beta_o r_o$  limit. Thus, it will be judicious to select the transistor with the higher  $\beta_o V_A$  product—that is, (150, 75 V).

Having made this decision, the equations relating the dc Q-point design to the output resistance of the source can be developed. In Fig. 15.49, the three-resistor bias circuit is simplified using a  $-V_{EE}$  referenced Thévenin transformation, for which

$$V_{BB} = 15 \frac{R_1}{R_1 + R_2} = 15 \frac{R_{BB}}{R_2} \quad \text{with} \quad R_{BB} = \frac{R_1 R_2}{R_1 + R_2} \quad (15.120)$$

The Q-point can be calculated using

$$I_B = \frac{V_{BB} - V_{BE}}{R_{BB} + (\beta_F + 1)R_E} \quad I_O = I_C = \beta_F I_B$$

and

$$(15.121)$$

$$V_{CE} = V_O + V_{EE} - (V_{BB} - I_B R_{BB} - V_{BE})$$

The small-signal parameters required for evaluating Eq. (15.117) are given by their usual formulas:

$$r_o = \frac{V_A + V_{CE}}{I_C} \quad \text{and} \quad r_\pi = \frac{\beta_o V_T}{I_C} \quad (15.122)$$

From Eq. (15.117), we can see that  $R_{BB} = (R_1 \| R_2)$  should be made as small as possible in order to achieve maximum output resistance. From the design specifications, the complete current

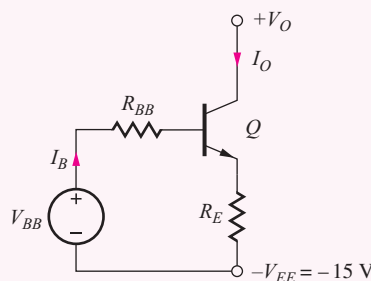


Figure 15.49 Equivalent circuit for the current source.

source must use no more than 250  $\mu\text{A}$ . Because the output current is 200  $\mu\text{A}$ , a maximum current of 50  $\mu\text{A}$  can be used by the base bias network. The bias network current should be a factor of 5 to 10 times larger than the base current of the transistor which is 1.33  $\mu\text{A}$  for the transistor with a current gain of 150. Thus, a bias network current of 20  $\mu\text{A}$  is more than enough. However, in this case, we will trade increased operating current for a higher output resistance by picking a bias network current of 40  $\mu\text{A}$ , which sets the sum of  $R_1$  and  $R_2$  to be (neglecting base current)

$$R_1 + R_2 \cong \frac{15 \text{ V}}{40 \mu\text{A}} = 375 \text{ k}\Omega \quad (15.123)$$

Equations (15.117) to (15.123) provide the information necessary to explore the design space with the aid of a computer. These equations have been rearranged in order of evaluation in Eq. (15.124), with  $V_{BB}$  selected as the primary design variable.

Once  $V_{BB}$  is selected,  $R_1$  and  $R_2$  can be calculated. Then  $R_E$  and the Q-point can be determined, the small-signal parameters evaluated, and the output resistance determined from Eq. (15.114).

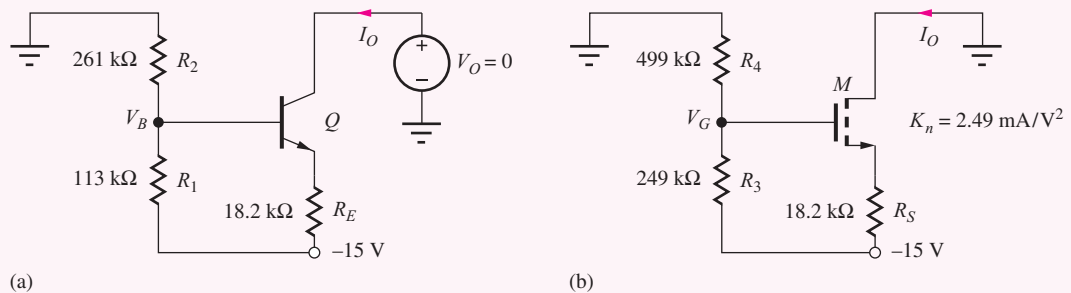
$$\begin{aligned} I_B &= \frac{I_o}{\beta_F} \\ R_1 &= (R_1 + R_2) \frac{V_{BB}}{15} = 375 \text{ k}\Omega \left( \frac{V_{BB}}{15} \right) \\ R_2 &= (R_1 + R_2) - R_1 = 375 \text{ k}\Omega - R_1 \\ R_{BB} &= R_1 \parallel R_2 \\ R_E &= \alpha_F \left[ \frac{V_{BB} - V_{BE} - I_B R_{BB}}{I_o} \right] \\ V_{CE} &= V_{EE} - (V_{BB} - I_B R_{BB} - V_{BE}) \\ r_o &= \frac{V_A + V_{CE}}{I_o} \quad r_\pi = \frac{\beta_o V_T}{I_o} \\ R_{\text{out}} &= r_o \left[ 1 + \frac{\beta_o R_E}{R_{BB} + r_\pi + R_E} \right] \end{aligned} \quad (15.124)$$

Table 15.2 presents the results of using a spreadsheet to assist in evaluating these equations for a range of  $V_{BB}$ . The smallest value of  $V_{BB}$  for which the output resistance exceeds 10 M $\Omega$  with some safety margin is 4.5 V. Note that this value of output resistance is achieved as

$$R_{\text{out}} = 432 \text{ k}\Omega \left[ 1 + \frac{150(18.4 \text{ k}\Omega)}{(78.8 + 18.8 + 18.4) \text{ k}\Omega} \right] = 10.7 \text{ M}\Omega \quad (15.125)$$

**TABLE 15.2**  
Spreadsheet Results for Current Source Design

$V_{BB}$	$R_1$	$R_2$	$R_{BB}$	$R_E$	$r_o$	$R_{\text{out}}$
1.0	2.50E + 04	3.50E + 05	2.33E + 04	1.34E + 03	4.49E + 05	2.52E + 06
2.0	5.00E + 04	3.25E + 05	4.33E + 04	6.17E + 03	4.44E + 05	6.46E + 06
3.0	7.50E + 04	3.00E + 05	6.00E + 04	1.10E + 04	4.39E + 05	8.52E + 06
3.5	8.75E + 04	2.88E + 05	6.71E + 04	1.35E + 04	4.36E + 05	9.31E + 06
4.0	1.00E + 05	2.75E + 05	7.33E + 04	1.59E + 04	4.34E + 05	1.00E + 07
<b>4.5</b>	<b>1.13E + 05</b>	<b>2.63E + 05</b>	<b>7.88E + 04</b>	<b>1.84E + 04</b>	<b>4.32E + 05</b>	<b>1.07E + 07</b>
5.0	1.25E + 05	2.50E + 05	8.33E + 04	2.08E + 04	4.29E + 05	1.13E + 07
5.5	1.38E + 05	2.38E + 05	8.71E + 04	2.33E + 04	4.27E + 05	1.20E + 07
6.0	1.50E + 05	2.25E + 05	9.00E + 04	2.57E + 04	4.24E + 05	1.26E + 07



**Figure 15.50** Final current source designs with  $I_O = 200 \mu\text{A}$  and  $R_{\text{out}} \geq 10 \text{ M}\Omega$ .

**Check of Results:** Analysis of the circuit with the 1 percent resistor values in Fig. 15.50 yields  $I_O = 203 \mu\text{A}$ ,  $R_{\text{out}} = 10.4 \text{ M}\Omega$ , and the supply current is  $244 \mu\text{A}$ .

**Discussion:** For this design, the denominator in Eq. (15.125) reduces the output resistance by a factor of 6.3 below the  $\beta_o r_o$  limit. So, it was a wise decision to choose the transistor with the largest  $\beta_o V_A$  product. The final design appears in Fig. 15.50 using the nearest values from the 1 percent table in Appendix A.

**Computer-Aided Analysis:** Now we can check our hand design using SPICE with  $\text{BF} = 150$ ,  $\text{VAF} = 75 \text{ V}$ , and  $\text{IS} = 0.5 \text{ fA}$ . ( $\text{IS}$  is selected to give  $V_{\text{BE}} \cong 0.7 \text{ V}$  for a collector current of  $200 \mu\text{A}$ .) In the circuit shown here, zero-value source  $V_O$  is added to directly measure the output current  $I_O$  as well as to provide a source that can be used to find  $R_{\text{out}}$  with a SPICE transfer function analysis. The results are  $R_{\text{out}} = 11.4 \text{ M}\Omega$  with  $I_O = 205 \mu\text{A}$  and  $I_{EE} = 245 \mu\text{A}$ , which meet all the design specifications. This could also be a good point to do a Monte Carlo analysis to explore the influence of tolerances on the design.

**EXERCISE:** What is the output resistance of the bipolar current source if the base were bypassed to ground with a capacitor?

**ANSWER:**  $32.5 \text{ M}\Omega$

**EXERCISE:** The current source is to be implemented using the nearest 5 percent resistor values. What are the best values? Are resistors with a  $1/4\text{-W}$  power dissipation rating adequate for use in this circuit? What are the actual output current and output resistance of your current source, based on these 5 percent resistor values?

**ANSWERS:**  $110 \text{ k}\Omega$ ,  $270 \text{ k}\Omega$ ,  $18 \text{ k}\Omega$ ; yes;  $195 \mu\text{A}$ ,  $10.6 \text{ M}\Omega$

**EXERCISE:** Rework Design Ex. 15.5 using a bias network current of  $20 \mu\text{A}$ . What are the new values of  $V_{BB}$ ,  $R_1$ ,  $R_2$ ,  $R_E$ , and  $R_{\text{out}}$ ?

**ANSWERS:**  $9 \text{ V}$ ;  $450 \text{ k}\Omega$ ;  $300 \text{ k}\Omega$ ;  $40.0 \text{ k}\Omega$ ;  $10.7 \text{ M}\Omega$

## DESIGN EXAMPLE 15.6 DESIGN OF A MOSFET CURRENT SOURCE

Now we design a current source to meet the same set of design specifications as in Ex. 15.5 but with a MOSFET replacing the BJT.

**PROBLEM** Design a current source using the circuit in Fig. 15.51(b) with a nominal output current of 200  $\mu\text{A}$  and an output resistance greater than 10  $\text{M}\Omega$  using a single  $-15\text{-V}$  power supply. The source must also meet the following additional constraints.

Output voltage (compliance) range should be as large as possible while meeting the output resistance specification.

The total current used by the source should be less than 250  $\mu\text{A}$ .

MOS transistors are available with  $\lambda = 0.01 \text{ V}^{-1}$ .  $K_n$  can be chosen as required.

**SOLUTION** **Known Information and Given Data:** Current source circuit in Fig. 15.51;  $I_O = 200 \mu\text{A}$ ;  $V_{SS} = 15 \text{ V}$ ;  $I_{SS} < 250 \mu\text{A}$ ;  $R_{\text{out}} > 10 \text{ M}\Omega$ ;  $V_{GG}$  as low as possible; MOS transistors are available with  $\lambda = 0.01 \text{ V}^{-1}$ .  $K_n$  can be chosen as required.

**Unknowns:** Values of resistors  $R_3$ ,  $R_4$ , and  $R_S$

**Approach:** Use  $R_S = R_E$  and  $V_S = V_E$  from the bipolar design in the previous example so the two designs can be easily compared. Find the amplification factor and value of  $K_n$  required to meet the output resistance requirement. Find  $V_{GS}$  and  $V_{GG}$ , and then choose  $R_3$  and  $R_4$  from the 1 percent resistor table in Appendix A.

**Assumptions:** Active region and small-signal operating conditions apply;  $V_{TN} = 1 \text{ V}$ ; choose  $V_O = 0 \text{ V}$  as a representative value for the output voltage.

**Analysis:** We begin the design of the MOSFET current source by writing the expression for the transistor's output resistance. Because of the infinite current gain of the MOSFET, the expression for the output resistance of the current source is much less complex than that of the BJT source and is given by

$$R_{\text{out}} = r_o(1 + g_m R_S) \cong \mu_f R_S$$

If values of  $R_S$  and  $V_S$  are selected that are the same as those of the BJT source, 18  $\text{k}\Omega$  and  $-11.4 \text{ V}$ , respectively, then the MOSFET must have an amplification factor of

$$\mu_f \geq \frac{10 \text{ M}\Omega}{18 \text{ k}\Omega} = 556 \gg 1$$

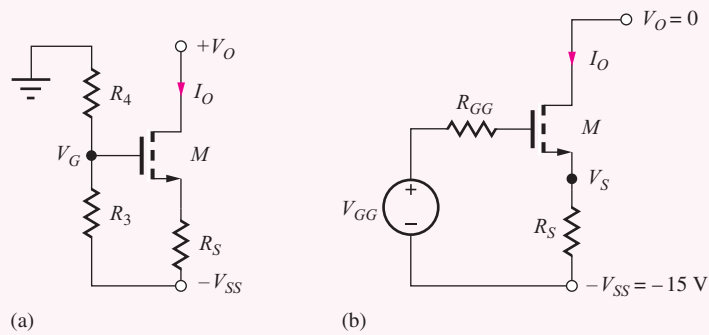


Figure 15.51 (a) MOSFET current source. (b) Equivalent circuit.

The amplification factor of the MOSFET is given by

$$\mu_f = \frac{1}{\lambda} \sqrt{\frac{2K_n}{I_D}} (1 + \lambda V_{DS})$$

and solving for  $K_n$  yields

$$K_n = \frac{I_D}{2} \left( \frac{\lambda \mu_f}{1 + \lambda V_{DS}} \right)^2 = 100 \mu\text{A} \left( \frac{\frac{0.01}{\text{V}}(556)}{1 + \frac{0.01}{\text{V}}(11.5 \text{ V})} \right)^2 = 2.49 \frac{\text{mA}}{\text{V}^2}$$

This value of  $K_n$  is achievable using either discrete components or integrated circuits.

In Fig. 15.51, the required gate voltage  $V_{GG}$  is

$$V_{GG} = I_D R_S + V_{GS} = 3.60 + V_{TN} + \sqrt{\frac{2I_D}{K_n}} \\ = 3.60 \text{ V} + 1 \text{ V} + \sqrt{\frac{2(0.2 \text{ mA})}{\frac{2.49 \text{ mA}}{\text{V}^2}}} = 5.00 \text{ V}$$

If the current in the bias resistors is limited to 10 percent of the drain current, then

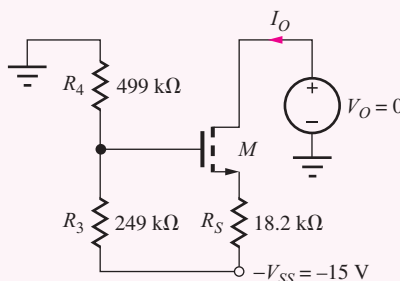
$$R_3 + R_4 = \frac{15 \text{ V}}{20 \mu\text{A}} = 750 \text{ k}\Omega \quad \text{and} \quad R_3 = \frac{5.00 \text{ V}}{15 \text{ V}} 750 \text{ k}\Omega = 250 \text{ k}\Omega$$

The nearest 1 percent values from Appendix A are  $R_3 = 249 \text{ k}\Omega$  and  $R_4 = 499 \text{ k}\Omega$  with  $R_S = 18.2 \text{ k}\Omega$ . The final design appears in Fig. 15.50.

**Check of Results:** A recheck of the math indicates that our calculations are correct. SPICE can now be used to verify our design and the results appear below.

**Discussion:** For the MOS source, we can use a larger set of gate bias resistors, since the output resistance of the current source does not depend on  $R_{GG}$ .

**Computer-Aided Analysis:** Now we can check our hand design using SPICE with  $\text{VTO} = 1 \text{ V}$ ,  $\text{KP} = 2.49 \text{ mA/V}^2$ , and  $\text{LAMBDA} = 0.01 \text{ V}^{-1}$ . In the circuit shown here, zero-value source  $V_O$  is added to directly measure the output current  $I_O$  and to provide a source that can be used to find  $R_{out}$  with a SPICE Transfer Function analysis. The results using the 1 percent resistor values are  $R_{out} = 11.3 \text{ M}\Omega$  with  $I_O = 198 \mu\text{A}$  and  $I_{SS} = 219 \mu\text{A}$ , which meet all the design specifications. This could be a good point to do a Monte Carlo analysis to explore the influence of tolerances on the design. Also, more complex SPICE models can be used to double check the design.

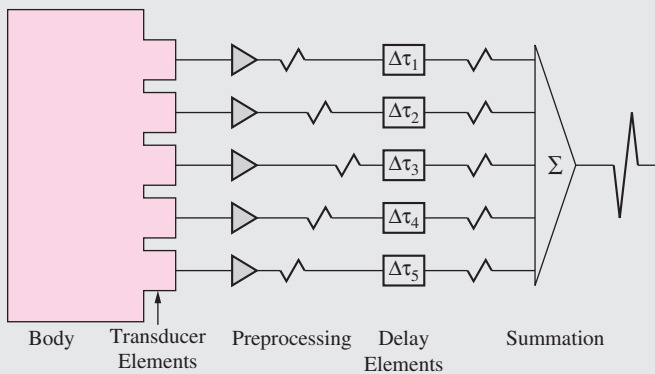


## ELECTRONICS IN ACTION

### Medical Ultrasound Imaging

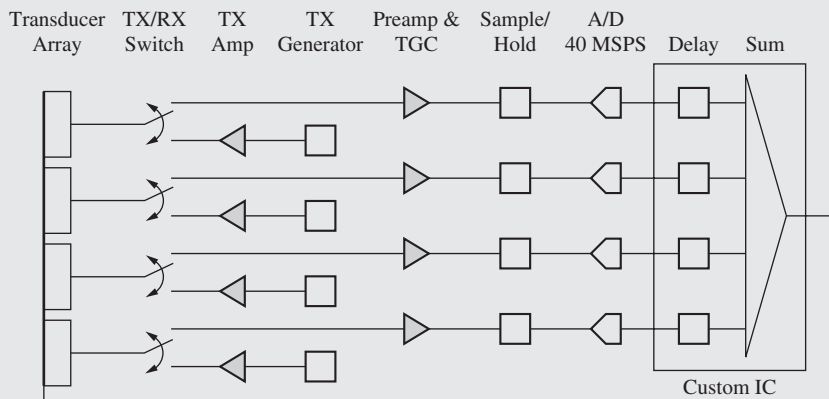
Medical ultrasound imaging systems are widely used in clinical applications for many diagnostic procedures such as characterization of tumors, measurement of cardiac function, and monitoring of prenatal development. Ultrasound systems work by sending 1 to 20 MHz acoustic pulses into the body and then measuring the acoustic echo. Different types of tissue absorb different amounts of acoustic energy, so the acoustic return varies with tissue type and characteristic. In order to measure tissue properties at specific points within the body, a phased array technique is used to focus the transmit and receive pulses. For example, a simplified view of the receive process is depicted below. The acoustic propagation time of the reflected wave varies with the distance from a particular transducer element to the focus point, resulting in a set of received waves separated in time. By introducing the appropriate delays to the received waves, they can then be summed. Random noise will average out, but the signal of interest adds coherently. The transmit process is also focused by time-varying the pulses driven onto each of the transducer elements.

A more detailed look at the electronics of an ultrasound system is shown in the accompanying figures. Because of the lossy nature of the transducers and body tissue, the received



(a)

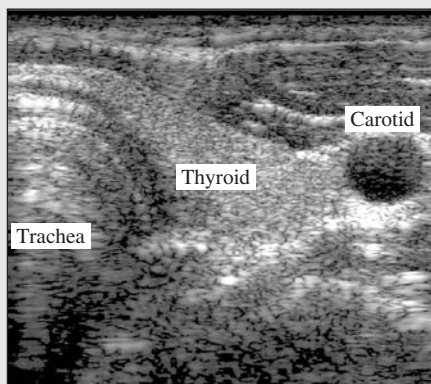
Simplified view of ultrasound receive focusing.



(b)

Block diagram of typical commercial ultrasound system transmit/receive electronics.

ultrasound signal is extremely small, often on the order of microvolts. As a consequence, the analog preamp must be a very low noise, multistage amplifier. Total gain is about 100 dB. With such a high gain, it is important that the amplifier be either ac coupled or have some form of offset-correction. For example, if the amplifier has an input offset of 5 mV, a gain of 100 dB would yield an output that is clipped. Another interesting aspect of ultrasound preamplifiers is the need for time gain control (TGC). As an ultrasound signal propagates through the body, it is heavily attenuated. The longer a signal propagates, the more it attenuates. This is compensated with a circuit that continuously varies the gain of the amplifier over a 60–80 dB range during the few microseconds required to receive an ultrasonic waveform.



(c)

Ultrasound image of trachea, thyroid, and carotid artery.\*

After the preamp, the signal is sampled and then digitized. In a typical 128-channel system with 40 MSample/sec 10-bit ADCs, the total data rate is 6.4 gigabytes/sec! This vast data pipeline is processed by several custom ASICs which digitally perform the real-time delay and summing operations, correcting for many non-idealities not described here.

Modern medical systems, such as the one shown here, are tremendous opportunities for innovative circuit design. As medical knowledge increases, it is increasingly important to accurately measure physiological responses and interactions to properly apply and utilize new understanding.

---

\* Ultrasound image appears courtesy of William F. Walker, University of Virginia.

**EXERCISE:** What is the minimum drain voltage for which MOSFET  $M$  in the figure above remains saturated?

**ANSWER:**  $-9.96\text{ V}$

**EXERCISE:** What  $W/L$  ratio is required for the preceding FET if  $K'_n = 25\text{ }\mu\text{A/V}^2$ ?

**ANSWER:**  $99.6/1$

**EXERCISE:** What is the minimum collector voltage for which the BJT in Fig. 15.50(a) remains in the forward-active region?

**ANSWER:** –10.8 V

**EXERCISE:** The MOS current source is to be implemented using the nearest 5 percent resistor values. What are the best values? Are resistors with a 1/4-W power dissipation rating adequate for use in this circuit? What are the actual output current and output resistance of your current source based on these 5 percent resistor values?

**ANSWERS:** 510 k $\Omega$ , 240 k $\Omega$ , 18 k $\Omega$ ; yes; 189  $\mu$ A, 10.3 M $\Omega$

## SUMMARY

In most situations, the single-stage amplifiers discussed in Chapters 13 and 14 cannot simultaneously meet all the requirements of an application (e.g., high voltage gain, high input resistance, and low output resistance). Therefore, we must combine single-stage amplifiers in various ways to form multistage amplifiers that achieve higher levels of overall performance.

- Both ac- and dc-coupling (also called direct-coupling) methods are used in multistage amplifiers depending on the application. ac coupling allows the Q-point design of each stage to be done independently of the other stages, and bypass capacitors can be utilized to eliminate bias elements from the ac equivalent circuit of the amplifier. However, dc coupling can eliminate circuit elements, including both coupling capacitors and bias resistors, and can represent a more economical approach to design. In addition, direct coupling achieves a low-pass amplifier that provides high gain at dc, and dc-coupling is utilized in most op amp designs.
- The most important dc-coupled amplifier is the symmetric two-transistor differential amplifier. Not only is the differential amplifier a key circuit in the design of operational amplifiers, but it is also a fundamental building block of all analog circuit design. In this chapter, we studied BJT and MOS differential amplifiers in detail. Differential-mode gain, common-mode gain, common-mode rejection ratio (CMRR), and differential- and common-mode input and output resistances of the amplifier are all directly related to transistor parameters and, hence, Q-point design.
- Either a balanced or a single-ended output is available from the differential amplifier. The balanced output provides a voltage gain that is twice that of the single-ended output, and the CMRR of the balanced output is inherently much higher (infinity for the ideal case). A two-port model can be used to model the small-signal characteristics at the output of the differential pairs.
- One of the most important applications of differential amplifiers is to form the input stage of the operational amplifier. By adding a second gain stage plus an output stage to the differential amplifier, a basic op amp is created. The performance of differential and operational amplifiers can be greatly enhanced by the use of electronic current sources. Op amp designs usually require a number of current sources, and, for economy of design, these multiple sources are often generated from a single-bias voltage.
- An ideal current source provides a constant output current, independent of the voltage across the source; that is, the current source has an infinite output resistance. Although electronic current sources cannot achieve infinite output resistance, very high values are possible, and there are a number of basic current source circuits and techniques for achieving high output resistance.
- For a current source, the product of the source current and output resistance represents a figure of merit,  $V_{CS}$ , that can be used to compare current sources. A single-transistor current source can be

built using the bipolar transistor in which  $V_{CS}$  can approach the  $\beta_o V_A$  product of the BJT. For a very good bipolar transistor, this product can reach 10,000 V. For the FET case,  $V_{CS}$  can approach a significant fraction of  $\mu_f V_{SS}$ , in which  $V_{SS}$  represents the power supply voltage. Values well in excess of 1000 V are achievable with the FET source.

- The electronic current source can be modeled in SPICE as a dc current source in parallel with a resistor equal to the output resistance of the source. For greatest accuracy, the value of the dc source should be adjusted to account for any dc current existing in the output resistance.
- Class-A, Class-B, and Class-AB amplifiers are defined in terms of their conduction angles: 360° for Class-A, 180° for Class-B, and between 180° and 360° for Class-AB operation. The efficiency of the Class-A amplifier cannot exceed 25 percent for sinusoidal signals, whereas that of the Class-B amplifier has an upper limit of 78.5 percent. However, Class-B amplifiers suffer from cross-over distortion caused by a dead zone in the transfer characteristic.
- The Class-AB amplifier trades a small increase in quiescent power dissipation and a small loss in efficiency for elimination of the cross-over distortion. The efficiency of the Class-AB amplifier can approach that of the Class-B amplifier when the quiescent operating point is properly chosen. The basic op-amp design can be further improved by replacing the Class-A follower output stage with a Class-AB output stage. Class-AB output stages are often used in operational amplifiers and are usually provided with short-circuit protection circuitry.
- Amplifier stages may also employ transformer coupling. The impedance transformation properties of the transformer can be used to simplify the design of circuits that must drive low values of load resistances, such as loudspeakers, headphones, or earbuds.
- Integrated circuit (IC) technology permits the realization of large numbers of virtually identical transistors. Although the absolute parameter tolerances of these devices are relatively poor, device characteristics can actually be matched to within less than 1 percent. The availability of large numbers of such closely matched devices has led to the development of special circuit techniques that depend on the similarity of device characteristics for proper operation. These matched circuit design techniques are used throughout analog circuit design and produce high-performance circuits that require very few resistors.

## KEY TERMS

ac-coupled amplifiers	dc-coupled (direct-coupled) amplifiers
Balanced output	Dead zone
Cascode amplifier	Differential amplifier
Cascode current source	Differential-mode conversion gain
Class-A, class-B, and class-AB amplifiers	Differential-mode gain
Class-B push-pull output stage	Differential-mode half-circuit
Common-mode conversion gain	Differential-mode input resistance
Common-mode gain	Differential-mode output resistance
Common-mode half-circuit	Differential-mode output voltage
Common-mode input resistance	Electronic current source
Common-mode input voltage range	Figure of merit (FOM)
Common-mode rejection ratio (CMRR)	Half-circuit analysis
Complementary push-pull output stage	Ideal current source
Conduction angle	Level shift
Cross-over distortion	Short-circuit protection
Cross-over region	Single-ended output
Current-limiting circuit	Transformer coupling
Current sink	Virtual ground
Darlington circuit	Voltage reference

## REFERENCES

1. R. D. Thornton, et. al., *Multistage Transistor Circuits*, SEEC Volume 5, Wiley, New York: 1965.
2. P. R. Gray, P. J. Hurst, S. H. Lewis, and R. G. Meyer, *Analysis and Design of Analog Integrated Circuits*, 4th ed., John Wiley and Sons, New York: 2001.

## ADDITIONAL READING

- R. C. Jaeger, "A high output resistance current source," *IEEE JSSC*, vol. SC-9, pp. 192–194, August 1974.
- R. C. Jaeger, "Common-mode rejection limitations of differential amplifiers," *IEEE JSSC*, vol. SC-11, pp. 411–417, June 1976.
- R. C. Jaeger, and G. A. Hellwarth. "On the performance of the differential cascode amplifier," *IEEE JSSC*, vol. SC-8, pp. 169–174, April 1973.

## PROBLEMS

Unless otherwise specified, use  $\beta_F = 100$ ,  $V_A = 70 \text{ V}$ ,  $K_p = K_n = 1 \text{ mA/V}^2$ ,  $V_{TN} = -V_{TP} = 1 \text{ V}$ , and  $\lambda = 0.02 \text{ V}^{-1}$ .

### 15.1 Differential Amplifiers

#### BJT Amplifiers

- 15.1. (a) What are the Q-points for the transistors in the amplifier in Fig. P15.1 if  $V_{CC} = 15 \text{ V}$ ,  $V_{EE} = 15 \text{ V}$ ,  $R_{EE} = 270 \text{ k}\Omega$ ,  $R_C = 330 \text{ k}\Omega$ , and  $\beta_F = 100$ ? (b) What are the differential-mode gain, and differential-mode input and output resistances? (c) What are the common-mode gain, CMRR, and common-mode input resistance for a single-ended output?

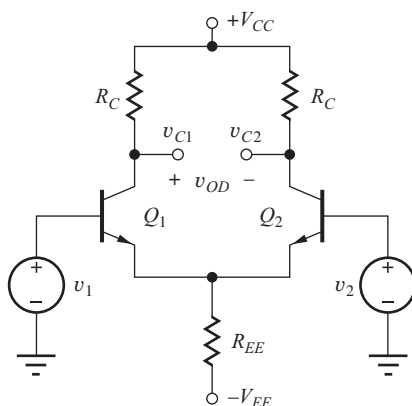


Figure P15.1

- 15.2. (a) What are the Q-points for the transistors in the amplifier in Fig. P15.1 if  $V_{CC} = 1.5 \text{ V}$ ,  $V_{EE} = 1.5 \text{ V}$ ,  $\beta_F = 60$ ,  $R_{EE} = 75 \text{ k}\Omega$ , and  $R_C = 100 \text{ k}\Omega$ ? (b) What are the differential-mode gain, common-mode gain, CMRR, and differential-mode and common-mode input and output resistances?
- 15.3. (a) Use SPICE to simulate the amplifier in Prob. P15.1 at a frequency of 1 kHz, and determine the differential-mode gain, common-mode gain, CMRR, and differential-mode and common-mode input resistances. (b) Apply a 25 mV, 1 kHz sine wave as an input signal, and plot the output signals using SPICE transient analysis. Use the SPICE distortion analysis capability to find the harmonic distortion in the output.
- 15.4. (a) What are the Q-points for the transistors in the amplifier in Fig. P15.1 if  $V_{CC} = 18 \text{ V}$ ,  $V_{EE} = 18 \text{ V}$ ,  $R_{EE} = 47 \text{ k}\Omega$ ,  $R_C = 100 \text{ k}\Omega$ , and  $\beta_F = 100$ ? (b) What are the differential-mode gain, common-mode gain, CMRR, and differential-mode and common-mode input and output resistances?
- \*15.5. (a) Use the common-mode gain to find voltages  $v_{C1}$ ,  $v_{C2}$ , and  $v_{OD}$  for the differential amplifier in Fig. P15.1 if  $V_{CC} = 15 \text{ V}$ ,  $V_{EE} = 15 \text{ V}$ ,  $R_{EE} = 270 \text{ k}\Omega$ ,  $R_C = 390 \text{ k}\Omega$ ,  $v_1 = 5.000 \text{ V}$ , and  $v_2 = 5.000 \text{ V}$ . (b) Find the Q-points of the transistors directly with  $V_{IC}$  applied. Recalculate  $v_{C1}$  and  $v_{C2}$  and compare to the results in part (a). What is the origin of the discrepancy?

- 15.6. Design a differential amplifier to have a differential gain of 58 dB and  $R_{id} = 100 \text{ k}\Omega$  using the topology in Fig. P15.1, with  $V_{CC} = V_{EE} = 9 \text{ V}$  and  $\beta_F = 120$ . (Be sure to check feasibility of the design using our rule-of-thumb estimates from Chapter 13 before you move deeper into the design calculations.)
- 15.7. Design a differential amplifier to have a differential gain of 46 dB and  $R_{id} = 1 \text{ M}\Omega$  using the topology in Fig. P15.1, with  $V_{CC} = V_{EE} = 12 \text{ V}$  and  $\beta_F = 100$ . (Be sure to check feasibility of the design using our rule-of-thumb estimates from Chapter 13 before you move deeper into the design calculations.)
- 15.8. (a) What are the Q-points for the transistors in the amplifier in Fig. P15.8 if  $V_{CC} = 12 \text{ V}$ ,  $V_{EE} = 12 \text{ V}$ ,  $I_{EE} = 400 \mu\text{A}$ ,  $\beta_F = 100$ ,  $R_{EE} = 270 \text{ k}\Omega$ ,  $R_C = 47 \text{ k}\Omega$ ,  $V_A = \infty$ , and  $\beta_F = 100$ ? (b) What are the differential-mode gain, common-mode gain, CMRR, and differential-mode and common-mode input and output resistances? (c) Repeat part (b) for  $V_A = 50 \text{ V}$ .

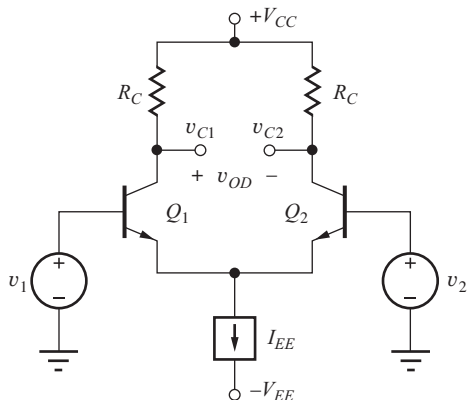


Figure P15.8

- \*15.9. What are the voltages  $v_{C1}$ ,  $v_{C2}$ , and  $v_{OD}$  for the differential amplifier in Fig. P15.8 if  $V_{CC} = 12 \text{ V}$ ,  $V_{EE} = 12 \text{ V}$ ,  $\beta_F = 75$ ,  $I_{EE} = 400 \mu\text{A}$ ,  $R_{EE} = 270 \text{ k}\Omega$ ,  $R_C = 47 \text{ k}\Omega$ ,  $v_1 = 2.005 \text{ V}$ , and  $v_2 = 1.995 \text{ V}$ ? What is the common-mode input range of this amplifier?
- 15.10. What is the value of the current  $I_{EE}$  required to achieve  $R_{id} = 5 \text{ M}\Omega$  in the circuit in Fig. P15.8 if  $\beta_o = 150$ ? What output resistance  $R_{EE}$  is required for  $\text{CMRR} = 100 \text{ dB}$ ?
- 15.11. (a) Use SPICE to simulate the amplifier in Prob. 15.8 at a frequency of 1 kHz, and determine the differential-mode gain, common-mode

gain, CMRR, and differential-mode and common-mode input resistances. Use  $V_A = 60 \text{ V}$ . (b) Apply a 25-mV, 1-kHz sine wave as an input signal and plot the output signal using SPICE transient analysis. Use the SPICE distortion analysis capability to find the harmonic distortion in the output.

- 15.12. For the amplifier in Fig. P15.12,  $V_{CC} = 9 \text{ V}$ ,  $V_{EE} = 9 \text{ V}$ ,  $\beta_F = 100$ ,  $I_{EE} = 20 \mu\text{A}$ , and  $R_C = 910 \text{ k}\Omega$ . (a) What are the output voltages  $v_o$  and  $V_O$  for the amplifier for  $v_s = 0 \text{ V}$  and  $v_s = 2 \text{ mV}$ ? (b) What is the maximum value of  $v_s$ ?

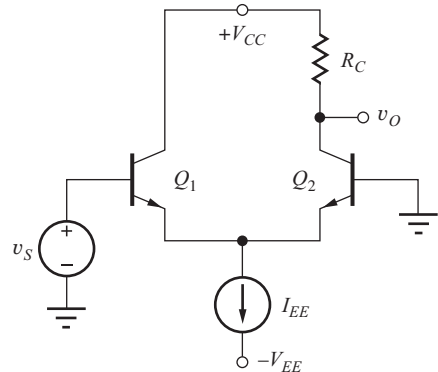


Figure P15.12

- 15.13. For the amplifier in Fig. P15.12,  $V_{CC} = 12 \text{ V}$ ,  $V_{EE} = 12 \text{ V}$ ,  $\beta_F = 120$ ,  $I_{EE} = 200 \mu\text{A}$ , and  $R_C = 100 \text{ k}\Omega$ . (a) What are the output voltages  $V_O$  and  $v_o$  for the amplifier for  $v_s = 0 \text{ V}$  and  $v_s = 1 \text{ mV}$ ? (b) What is the maximum value of  $v_s$ ?
- 15.14. (a) Use SPICE to simulate the amplifier in Prob. 15.13 at a frequency of 1 kHz, and determine the differential-mode gain, common-mode gain, CMRR, and differential-mode and common-mode input resistances. Use  $V_A = 60 \text{ V}$ . (b) Apply a 25-mV, 1-kHz sine wave as an input signal and plot the output signal using SPICE transient analysis. Use the SPICE distortion analysis capability to find the harmonic distortion in the output.
- 15.15. (a) What are the Q-points for the transistors in the amplifier in Fig. P15.15 if  $V_{CC} = 12 \text{ V}$ ,  $V_{EE} = 12 \text{ V}$ ,  $\beta_F = 150$ ,  $R_{EE} = 150 \text{ k}\Omega$ , and  $R_C = 200 \text{ k}\Omega$ ? (b) What are the differential-mode gain, common-mode gain, CMRR, and differential-mode and common-mode input resistances?

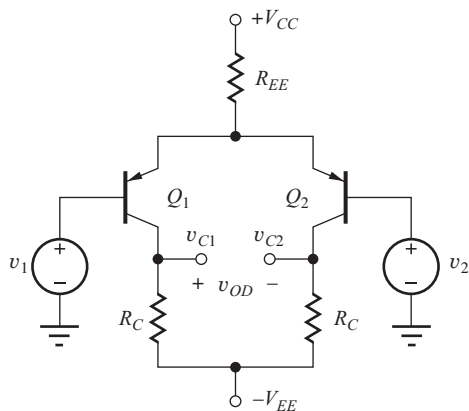


Figure P15.15

- 15.16. What are the voltages  $v_{C1}$ ,  $v_{C2}$ , and  $v_{OD}$  for the differential amplifier in Fig. P15.15 if  $V_{CC} = 10$  V,  $V_{EE} = 10$  V,  $\beta_F = 100$ ,  $R_{EE} = 430$  k $\Omega$ ,  $R_C = 560$  k $\Omega$ ,  $v_1 = 1$  V, and  $v_2 = 0.99$  V?
- 15.17. Use SPICE to simulate the amplifier in Prob. 15.15 at a frequency of 5 kHz, and determine the differential-mode gain, common-mode gain, CMRR, and differential-mode and common-mode input resistances.

- 15.18. (a) What are the Q-points for the transistors in the amplifier in Fig. P15.18 if  $V_{CC} = 3$  V,  $V_{EE} = 3$  V,  $\beta_F = 80$ ,  $I_{EE} = 10 \mu\text{A}$ ,  $R_{EE} = 5 \text{ M}\Omega$ , and  $R_C = 390$  k $\Omega$ ? (b) What are the differential-mode gain, common-mode gain, CMRR, differential-mode and common-mode input resistances, and common-mode input range?

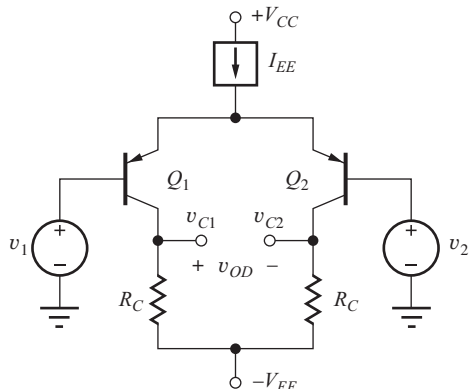


Figure P15.18

- 15.19. What are the voltages  $v_{C1}$ ,  $v_{C2}$ , and  $v_{OD}$  for the differential amplifier in Fig. P15.18 if  $V_{CC} = 18$  V,  $V_{EE} = 18$  V,  $\beta_F = 120$ ,  $I_{EE} = 1 \text{ mA}$ ,  $R_{EE} = 500$  k $\Omega$ ,  $R_C = 15$  k $\Omega$ ,  $v_1 = 0.01$  V, and  $v_2 = 0$  V?

15.20. Use SPICE to simulate the amplifier in Prob. 15.18 at a frequency of 5 kHz, and determine the differential-mode gain, common-mode gain, CMRR, and differential-mode and common-mode input resistances.

- \*15.21. The differential amplifier in Fig. P15.21 has mismatched collector resistors. Calculate  $A_{dd}$ ,  $A_{cd}$ , and the CMRR of the amplifier if the output is the differential output voltage  $v_{od}$ , and  $R = 100$  k $\Omega$ ,  $\Delta R/R = 0.01$ ,  $V_{CC} = V_{EE} = 15$  V,  $R_{EE} = 100$  k $\Omega$ , and  $\beta_F = 100$ .

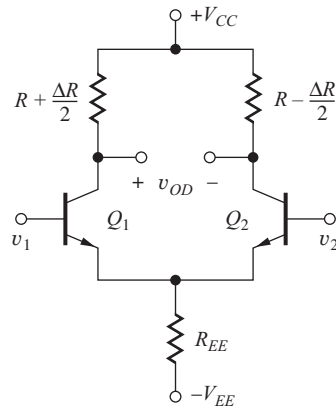


Figure P15.21

- 15.22. Use SPICE to simulate the amplifier in Prob. P15.21 at a frequency of 100 Hz, and determine the differential-mode gain, common-mode gain, and CMRR.
- \*\*15.23. The transistors in the differential amplifier in Fig. P15.23 have mismatched transconductances. Calculate  $A_{dd}$ ,  $A_{cd}$ , and the CMRR of the amplifier if the output is the differential output voltage  $v_{OD}$ , and  $R = 100$  k $\Omega$ ,  $g_m = 3 \text{ mS}$ ,  $\Delta g_m/g_m = 0.01$ ,  $V_{CC} = V_{EE} = 15$  V, and  $R_{EE} = 100$  k $\Omega$ .

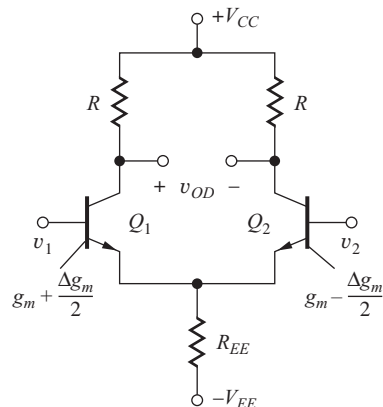


Figure P15.23

### FET Differential Amplifiers

- 15.24. (a) What are the Q-points for the transistors in the amplifier in Fig. P15.24 if  $V_{DD} = 15\text{ V}$ ,  $V_{SS} = 15\text{ V}$ ,  $R_{SS} = 62\text{ k}\Omega$ , and  $R_D = 62\text{ k}\Omega$ ? Assume  $K_n = 400\text{ }\mu\text{A/V}^2$  and  $V_{TN} = 1\text{ V}$ . (b) What are the differential-mode gain, common-mode gain, CMRR, and differential-mode and common-mode input resistances?

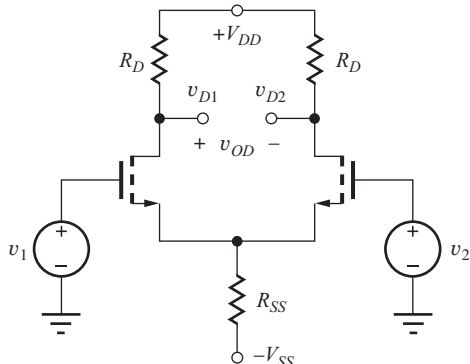


Figure P15.24

- 15.25. (a) What are the Q-points for the transistors in the amplifier in Fig. P15.24 if  $V_{DD} = 12\text{ V}$ ,  $V_{SS} = 12\text{ V}$ ,  $R_{SS} = 220\text{ k}\Omega$ , and  $R_D = 330\text{ k}\Omega$ ? Assume  $K_n = 400\text{ }\mu\text{A/V}^2$  and  $V_{TN} = 1\text{ V}$ . (b) What are the differential-mode gain, common-mode gain, CMRR, and differential-mode and common-mode input resistances?

- 15.26. (a) Use SPICE to simulate the amplifier in Prob. 15.24 at a frequency of 1 kHz, and determine the differential-mode gain, common-mode gain, CMRR, and differential-mode and common-mode input resistances. (b) Apply a 250-mV, 1-kHz sine wave as an input signal and plot the output signals using SPICE transient analysis. Use the SPICE distortion analysis capability to find the harmonic distortion in the output.

- 15.27. Design a differential amplifier to have a differential-mode output resistance of  $5\text{ k}\Omega$  and  $A_{dm} = 20\text{ dB}$ , using the circuit in Fig. P15.24 with  $V_{DD} = V_{SS} = 5\text{ V}$ . Assume  $V_{TN} = 1\text{ V}$  and  $K_n = 25\text{ mA/V}^2$ .

- \*15.28. (a) What are the Q-points for the transistors in the amplifier in Fig. P15.28 if  $V_{DD} = 15\text{ V}$ ,  $V_{SS} = 15\text{ V}$ ,  $R_{SS} = 62\text{ k}\Omega$ , and  $R_D = 62\text{ k}\Omega$ ? Assume  $K_n = 400\text{ }\mu\text{A/V}^2$ ,  $\gamma = 0.75\text{ V}^{0.5}$ ,  $2\phi_F = 0.6\text{ V}$ , and  $V_{TO} = 1\text{ V}$ . (b) What are the differential-mode gain, common-mode gain, CMRR, and differential-mode and common-mode input resistances? (c) What would the Q-points be if  $\gamma = 0$ ?

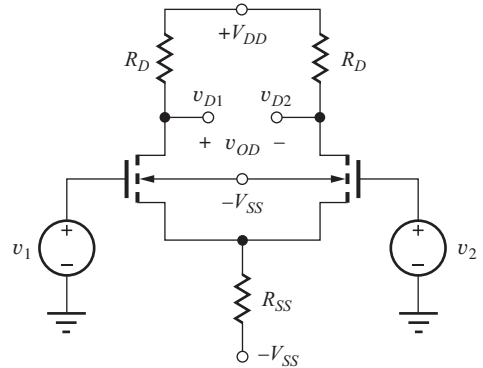


Figure P15.28

- 15.29. (a) Use SPICE to simulate the amplifier in Prob. 15.28 at a frequency of 1 kHz, and determine the differential-mode gain, common-mode gain, CMRR, and differential-mode and common-mode input resistances. (b) Apply a 250-mV, 1-kHz sine wave as an input signal and plot the output signal using SPICE transient analysis. Use the SPICE distortion analysis capability to find the harmonic distortion in the output.

- \*15.30. (a) What are the Q-points for the transistors in the amplifier in Fig. P15.28 if  $V_{DD} = 12\text{ V}$ ,  $V_{SS} = 12\text{ V}$ ,  $R_{SS} = 220\text{ k}\Omega$ , and  $R_D = 330\text{ k}\Omega$ ? Assume  $K_n = 400\text{ }\mu\text{A/V}^2$ ,  $\gamma = 0.75\text{ V}^{0.5}$ ,  $2\phi_F = 0.6\text{ V}$ , and  $V_{TO} = 1\text{ V}$ . (b) What are the differential-mode gain, common-mode gain, CMRR, and differential-mode and common-mode input resistances? (c) What would the Q-points be if  $\gamma = 0$ ?

- 15.31. (a) What are the Q-points for the transistors in the amplifier in Fig. P15.31 if  $V_{DD} = 15\text{ V}$ ,  $V_{SS} = 15\text{ V}$ ,  $I_{SS} = 300\text{ }\mu\text{A}$ ,  $R_{SS} = 160\text{ k}\Omega$ , and  $R_D = 75\text{ k}\Omega$ ? Assume  $K_n = 400\text{ }\mu\text{A/V}^2$  and  $V_{TN} = 1\text{ V}$ .

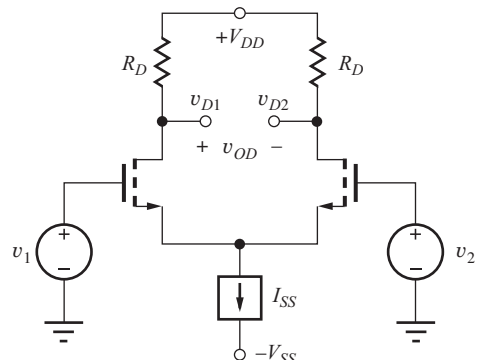


Figure P15.31

(b) What are the differential-mode gain, common-mode gain, CMRR, and differential-mode and common-mode input resistances?

- 15.32. (a) What are the Q-points for the transistors in the amplifier in Fig. P15.31 if  $V_{DD} = 12$  V,  $V_{SS} = 12$  V,  $I_{SS} = 40 \mu\text{A}$ ,  $R_{SS} = 1.25 \text{ M}\Omega$ , and  $R_D = 300 \text{ k}\Omega$ ? Assume  $K_n = 400 \mu\text{A/V}^2$  and  $V_{TN} = 1$  V. (b) What are the differential-mode gain, common-mode gain, CMRR, and differential-mode and common-mode input resistances?

- \*15.33. (a) What are the Q-points for the transistors in the amplifier in Fig. P15.33 if  $V_{DD} = 15$  V,  $V_{SS} = 15$  V,  $I_{SS} = 300 \mu\text{A}$ ,  $R_{SS} = 160 \text{ k}\Omega$ , and  $R_D = 75 \text{ k}\Omega$ ? Assume  $K_n = 400 \mu\text{A/V}^2$ ,  $\gamma = 0.75 \text{ V}^{0.5}$ ,  $2\phi_F = 0.6$  V, and  $V_{TO} = 1$  V. (b) What are the differential-mode gain, common-mode gain, CMRR, and differential-mode and common-mode input resistances?

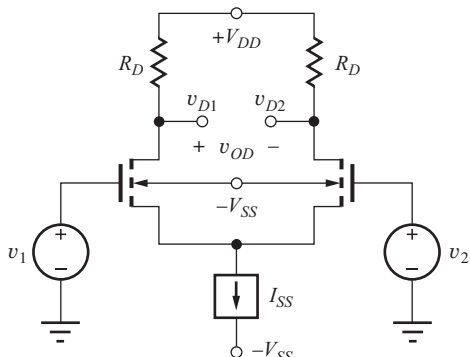


Figure P15.33

- \*15.34. (a) What are the Q-points for the transistors in the amplifier in Fig. P15.33 if  $V_{DD} = 12$  V,  $V_{SS} = 12$  V,  $I_{SS} = 40 \mu\text{A}$ ,  $R_{SS} = 1.25 \text{ M}\Omega$ , and  $R_D = 300 \text{ k}\Omega$ ? Assume  $K_n = 400 \mu\text{A/V}^2$ ,  $\gamma = 0.75 \text{ V}^{0.5}$ ,  $2\phi_F = 0.6$  V, and  $V_{TO} = 1$  V. (b) What are the differential-mode gain, common-mode gain, CMRR, and differential-mode and common-mode input resistances?

- 15.35. Design a differential amplifier to have a differential-mode gain of 30 dB, using the circuit in Fig. P15.31 with  $V_{DD} = V_{SS} = 7.5$  V. The circuit should have the maximum possible common-mode input range. Assume  $V_{TN} = 1$  V and  $K_n = 5 \text{ mA/V}^2$ .

- 15.36. Repeat Prob. 15.35 using the circuit in Fig. P15.33 with  $2\phi_F = 0.6$  V and  $\gamma = 0.75 \text{ V}^{0.5}$ .

- 15.37. (a) What are the Q-points for the transistors in the amplifier in Fig. P15.37 if  $V_{DD} = 16$  V,  $V_{SS} = 16$  V,  $R_{SS} = 56 \text{ k}\Omega$ , and  $R_D = 91 \text{ k}\Omega$ ? Assume  $K_p = 200 \mu\text{A/V}^2$  and  $V_{TP} = -1$  V. (b) What are the differential-mode gain, common-mode gain, CMRR, and differential-mode and common-mode input resistances?

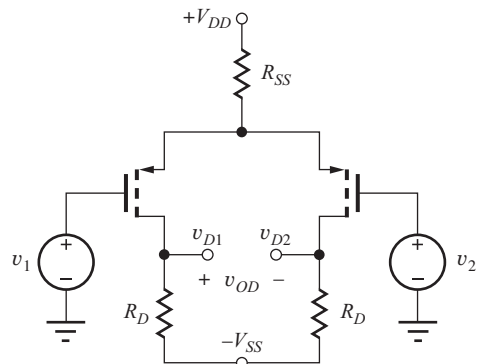


Figure P15.37

- 15.38. Use SPICE to simulate the amplifier in Prob. 15.37 at a frequency of 3 kHz, and determine the differential-mode gain, common-mode gain, CMRR, and differential-mode and common-mode input resistances.

- \*15.39. (a) What are the Q-points for the transistors in the amplifier in Fig. P15.39 if  $V_{DD} = 10$  V,  $V_{SS} = 10$  V,  $I_{SS} = 40 \mu\text{A}$ ,  $R_{SS} = 1.25 \text{ M}\Omega$ , and  $R_D = 300 \text{ k}\Omega$ ? Assume  $K_p = 200 \mu\text{A/V}^2$ ,  $\gamma = 0.6 \text{ V}^{0.5}$ ,  $2\phi_F = 0.6$  V, and  $V_{TO} = -1$  V. (b) What are the differential-mode gain, common-mode gain, CMRR, and differential-mode and common-mode input resistances?

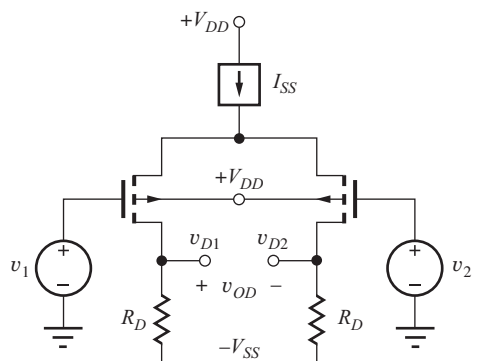


Figure P15.39

- 15.40. For the amplifier in Fig. P15.40,  $V_{DD} = 12$  V,  $V_{SS} = 12$  V,  $I_{SS} = 20 \mu\text{A}$ , and  $R_D = 820 \text{ k}\Omega$ . Assume  $K_p = 1 \text{ mA/V}^2$  and  $V_{TP} = +1$  V. (a) What are the output voltages  $v_O$  for the amplifier for  $v_1 = 0$  V and  $v_1 = 20$  mV? (b) What is the maximum permissible value of  $v_s$ ?

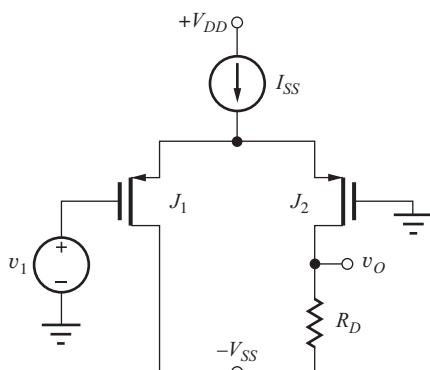


Figure P15.40

- 15.41. For the amplifier in Fig. P15.41,  $V_{DD} = 12$  V,  $V_{SS} = 12$  V,  $I_{SS} = 20 \mu\text{A}$ , and  $R_D = 820 \text{ k}\Omega$ . Assume  $I_{DSS} = 1 \text{ mA}$  and  $V_P = +2$  V. (a) What are the output voltages  $v_O$  for the amplifier for  $v_1 = 0$  V and  $v_1 = 20$  mV? (b) What is the maximum permissible value of  $v_s$ ?

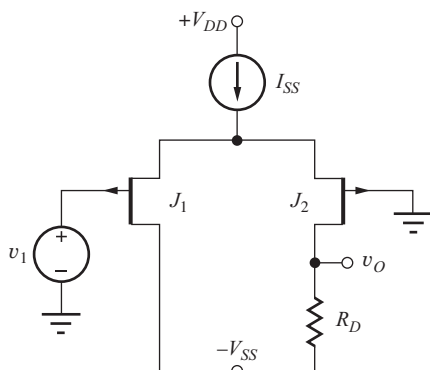


Figure P15.41

- 15.42. Redraw the circuit for the differential amplifier in Prob. P15.41 using *n*-channel JFETs.

### Half-Circuit Analysis

Q-points, differential-mode gain, common-mode gain, and differential-mode input resistance for the amplifier if  $\beta_o = 150$ ,  $V_{CC} = 22$  V,  $V_{EE} = 22$  V,  $R_{EE} = 200 \text{ k}\Omega$ ,  $R_1 = 2 \text{ k}\Omega$ , and  $R_C = 200 \text{ k}\Omega$ .

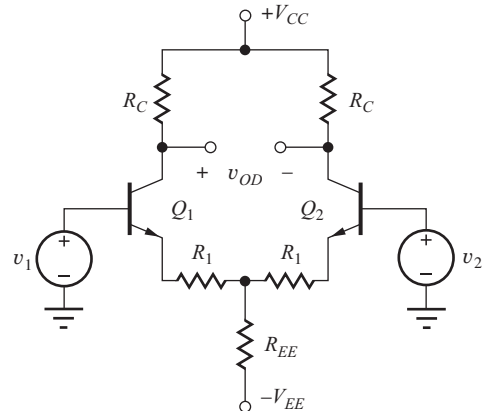


Figure 15.43

- 15.44. Use SPICE to simulate the amplifier in Prob. 15.43 at a frequency of 1 kHz, and determine the differential-mode gain, common-mode gain, and differential-mode input resistances.

- \*15.45. (a) Draw the differential-mode and common-mode half-circuits for the differential amplifier in Fig. P15.45. (b) Use the half-circuits to find the Q-points, differential-mode gain, common-mode gain, and differential-mode input resistance for the amplifier if  $\beta_o = 100$ ,  $V_{CC} = 18$  V,  $V_{EE} = 18$  V,  $I_{EE} = 100 \mu\text{A}$ , and  $R_{EE} = 600 \text{ k}\Omega$ ?

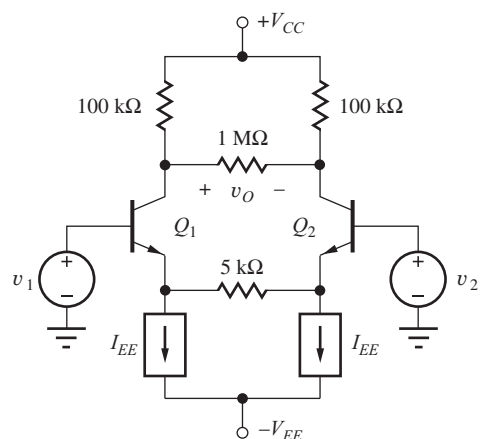


Figure P15.45

- \*15.43. (a) Draw the differential-mode and common-mode half-circuits for the differential amplifier in Fig. P15.43. (b) Use the half-circuits to find the

- 15.46. Use SPICE to simulate the amplifier in Prob. 15.45 at a frequency of 1 kHz, and determine the differential-mode gain, common-mode gain, and differential-mode input resistances.

- \*15.47. (a) Draw the differential-mode and common-mode half-circuits for the differential amplifier in Fig. P15.47. (b) Use the half-circuits to find the Q-points, differential-mode gain, common-mode gain, and differential-mode input resistance for the amplifier if  $V_{CC} = 15$  V,  $V_{EE} = 15$  V,  $I_{EE} = 100 \mu\text{A}$ ,  $R_D = 75 \text{ k}\Omega$ ,  $R_{EE} = 600 \text{ k}\Omega$ ,  $\beta_o = 100$ ,  $K_n = 200 \mu\text{A/V}^2$ , and  $V_{TN} = -4$  V. (c) Show that  $Q_1$  and  $Q_2$  are in the active region.

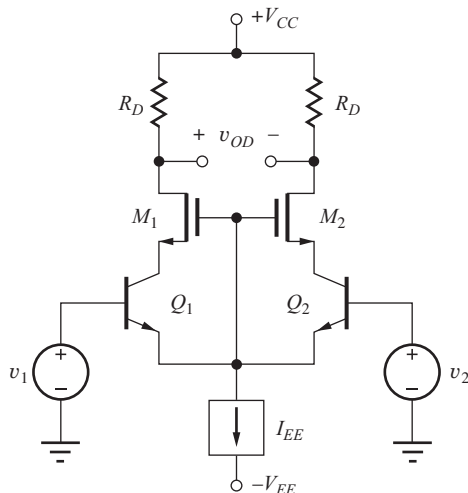


Figure P15.47

- \*\*15.48. (a) Draw the differential-mode and common-mode half-circuits for the differential amplifier in Fig. P15.48. (b) Use the half-circuits to find the Q-points, differential-mode gain, common-mode gain, and differential-mode input resistance for the amplifier if  $K_n = 1000 \mu\text{A/V}^2$ ,  $V_{TN} = 0.75$  V,  $K_p = 500 \mu\text{A/V}^2$ ,  $V_{TP} = -0.75$  V,  $I_1 = 200 \mu\text{A}$ ,  $I_2 = 100 \mu\text{A}$ ,  $V_{DD} = 6$  V,  $V_{SS} = 6$  V, and  $R_D = 30 \text{ k}\Omega$ .

- 15.49. (a) Repeat Prob. 15.48 for  $V_{DD} = 1.5$  V,  $-V_{SS} = -1.5$  V, and  $R_D = 10 \text{ k}\Omega$ . (b) What is the common-mode input range for this amplifier?

- 15.50. (a) Draw the differential-mode and common-mode half-circuits for the differential amplifier in Fig. P15.50. (b) Use the half-circuits to find the Q-points, differential-mode gain, common-mode

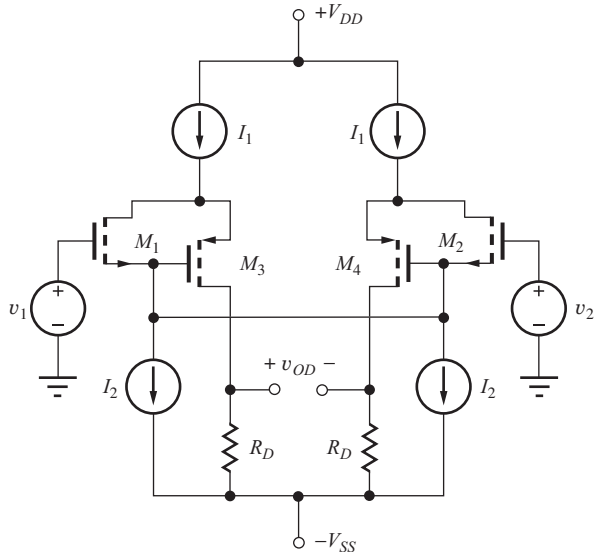


Figure P15.48

gain, and differential-mode input resistance for the amplifier if  $V_{CC} = 15$  V,  $V_{EE} = 15$  V,  $I_{EE} = 100 \mu\text{A}$ ,  $R_D = 75 \text{ k}\Omega$ ,  $R_{EE} = 600 \text{ k}\Omega$ ,  $\beta_o = 100$ ,  $I_{DSS} = 200 \mu\text{A}$ , and  $V_P = -4$  V. (c) Show that  $Q_1$  and  $Q_2$  are in the active region.

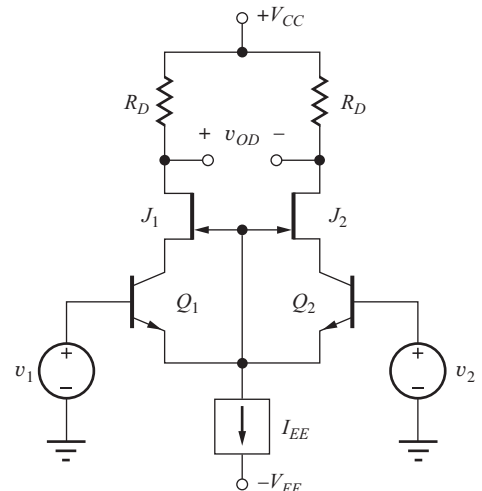


Figure P15.50

## 15.2 Evolution to Basic Operational Amplifiers

- 15.51. (a) What are the Q-points of the transistors in the amplifier in Fig. P15.51 if  $V_{CC} = 15$  V,  $V_{EE} = 15$  V,  $I_1 = 50 \mu\text{A}$ ,  $R = 24 \text{ k}\Omega$ ,  $\beta_o = 100$ , and  $V_A = 60$  V? (b) What are the differential-mode voltage gain and input resistance? (c) What

is the amplifier output resistance? (d) What is the common-mode input resistance? (e) Which terminal is the noninverting input?

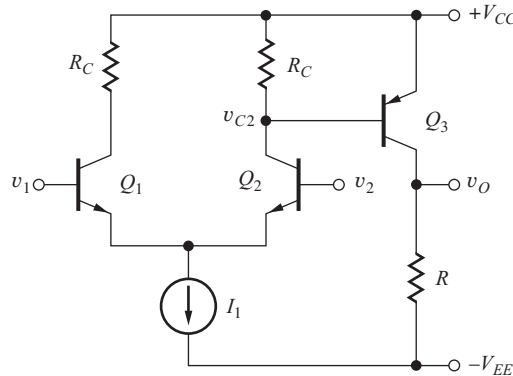


Figure P15.51

- 15.52. What is the common-mode input range for the amplifier in Prob. 15.51 if current source  $I_1$  is replaced with an electronic current source that must have 0.75 V across it to operate properly?
- 15.53. Use SPICE to simulate the amplifier in Prob. 15.51 at a frequency of 1 kHz, and determine the differential-mode gain, CMRR, and differential-mode input resistance and output resistance.
- 15.54. (a) Repeat Prob. 15.51 with  $V_{CC} = V_{EE} = 12$  V. (b) What is the new common-mode range as requested in Prob. 15.52?
- 15.55. Repeat Prob. 15.51 if  $I_1$ ,  $R$ , and  $R_C$  are redesigned to increase the currents by a factor of 5.
- 15.56. The circuit in Fig. P15.56 is called a Darlington connection of two transistors. Assume the emitter is grounded and derive the expressions below.

$$I_{C1} = \beta_{F1} I_B \quad I_{C2} = \beta_{F2} (\beta_{F1} + 1) I_B$$

$$I_C \cong \beta_{F1} \beta_{F2} I_B$$

$$g_{m2} = \beta_{o1} g_{m1} \quad r_{\pi1} = \beta_{o1} r_{\pi2}$$

$$r_{o1} = \beta_{o1} r_{o2}$$

$$\beta_o = \frac{i_c}{i_B} \cong \beta_{o1} \beta_{o2}$$

$$G_m = \frac{i_c}{v_{be}} = \frac{g_{m1}}{2} + \frac{g_{m2}}{2} \cong \frac{g_{m2}}{2}$$

$$R_{iB} = \frac{v_{be}}{i_b} = r_{\pi1} + (\beta_{o1} + 1)r_{\pi2} \cong 2\beta_{o1}r_{\pi2}$$

$$R_{iC} = \frac{v_{ce2}}{i_c} \cong r_{o2} \| 2 \frac{r_{o1}}{\beta_{o2}} \cong \frac{2}{3} r_{o2}$$

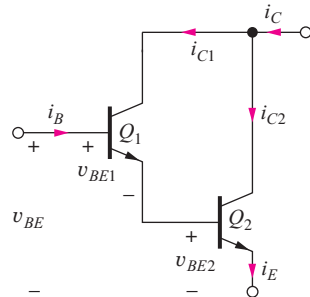


Figure P15.56

- 15.57. Transistor  $Q_3$  in Fig. P15.51 is replaced with a *pnp* Darlington circuit. Draw the new amplifier and repeat Prob. 15.51. (See Figs. P15.56 and P15.88.)
- 15.58. (a) What are the Q-points of the transistors in the amplifier in Fig. P15.58 if  $V_{CC} = 18$  V,  $V_{EE} = 18$  V,  $I_1 = 200 \mu\text{A}$ ,  $R_E = 2.4 \text{ k}\Omega$ ,  $R = 50 \text{ k}\Omega$ ,  $\beta_o = 80$ , and  $V_A = 70$  V? (b) What are the differential-mode voltage gain and input resistance? (c) What is the amplifier output resistance? (d) What is the common-mode input resistance? (e) Which terminal is the noninverting input?

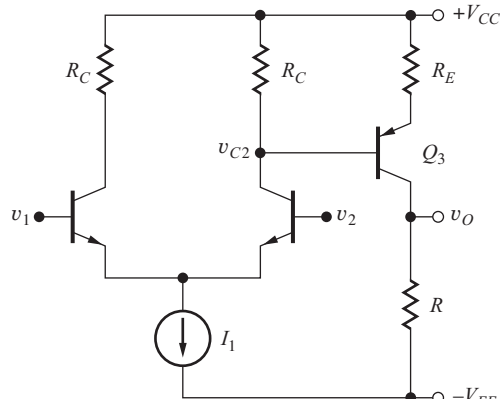


Figure P15.58

- 15.59. What is the common-mode input range for the amplifier in Prob. 15.58 if current source  $I_1$  is replaced with an electronic current source that must have 0.75 V across it to operate properly?
- 15.60. (a) What are the Q-points of the transistors in the amplifier in Fig. P15.58 if  $V_{CC} = 18$  V,  $V_{EE} = 18$  V,  $I_1 = 200 \mu\text{A}$ ,  $R_E = 0$ ,  $R = 50 \text{ k}\Omega$ ,  $\beta_o = 80$ , and  $V_A = 70$  V? (b) What are the differential-mode voltage gain and input resistance? (c) What is the common-mode input resistance?

- \*15.61. Plot a graph of the differential-mode voltage gain of the amplifier in Prob. 15.60 versus the value of  $R_E$ . (The computer might be a useful tool.)

- 15.62. Design an amplifier to have  $R_{out} = 1 \text{ k}\Omega$  and  $A_{dm} = 2000$ , using the circuit in Fig. P15.51. Use  $V_{CC} = V_{EE} = 9 \text{ V}$ , and  $\beta_F = 100$ .

- 15.63. (a) What are the Q-points of the transistors in the amplifier in Fig. P15.63 if  $V_{CC} = 16 \text{ V}$ ,  $V_{EE} = 16 \text{ V}$ ,  $I_1 = 200 \mu\text{A}$ ,  $I_2 = 300 \mu\text{A}$ ,  $R_E = 2.4 \text{ k}\Omega$ ,  $\beta_o = 80$ , and  $V_A = 70 \text{ V}$ ? (b) What are the differential-mode voltage gain, input resistance, and output resistance?

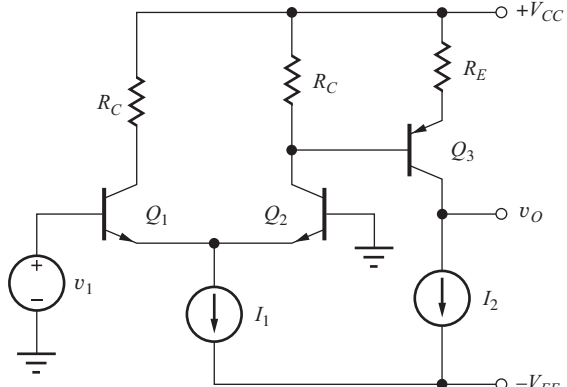


Figure P15.63

- 15.64. Use SPICE to simulate the amplifier in Prob. 15.63 and compare the results to hand calculations.

- 15.65. What are the Q-points of the transistors in the amplifier in Fig. P15.63 if  $V_{CC} = 16 \text{ V}$ ,  $V_{EE} = 16 \text{ V}$ ,  $I_1 = 200 \mu\text{A}$ ,  $I_2 = 300 \mu\text{A}$ ,  $R_E = 0$ ,  $\beta_o = 100$ , and  $V_A = 70 \text{ V}$ ?

- \*15.66. Plot a graph of the differential-mode voltage gain of the amplifier in Prob. P15.63 versus the value of  $R_E$ . (The computer might be a useful tool.)

- 15.67. (a) What are the Q-points of the transistors in the amplifier in Fig. P15.67 if  $V_{CC} = V_{EE} = 18 \text{ V}$ ,  $I_1 = 500 \mu\text{A}$ ,  $R_1 = 2 \text{ M}\Omega$ ,  $I_2 = 500 \mu\text{A}$ , and  $R_2 = 2 \text{ M}\Omega$ ? Use  $\beta_o = 80$ ,  $V_A = 75 \text{ V}$ ,  $K_p = 5 \text{ mA/V}^2$ , and  $V_{TP} = -1 \text{ V}$ . (b) What are the differential-mode voltage gain and input resistance and output resistance of the amplifier? (c) Which terminal is the noninverting input? (d) Which terminal is the inverting input?

- \*15.68. Use SPICE to simulate the amplifier in Prob. 15.67 at a frequency of 1 kHz, and determine the differential-mode gain, CMRR, and differential-mode input resistance and output resistance.

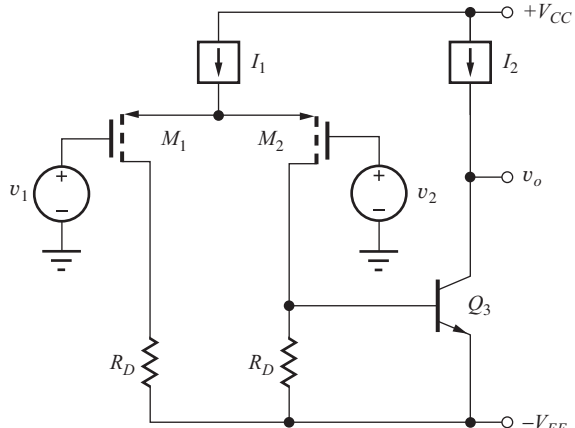


Figure P15.67

- 15.69. What is the voltage gain of the amplifier in Fig. P15.67 if  $V_{CC} = V_{EE} = 5 \text{ V}$ ,  $I_1 = 500 \mu\text{A}$ ,  $R_1 = 20 \text{ M}\Omega$ ,  $I_2 = 100 \mu\text{A}$ ,  $R_2 = 10 \text{ M}\Omega$ ,  $\beta_o = 80$ ,  $V_A = 75 \text{ V}$ ,  $K_p = 5 \text{ mA/V}^2$ , and  $V_{TP} = -1 \text{ V}$ ?

- 15.70. What is the common-mode input voltage range for the amplifier in Prob. 15.69 if current source  $I_1$  must have a 0.75-V drop across it to operate properly?

- 15.71. (a) What are the Q-points of the transistors in the amplifier in Fig. P15.71 if  $I_1 = 500 \mu\text{A}$ ,  $R_1 = 1 \text{ M}\Omega$ ,  $I_2 = 500 \mu\text{A}$ ,  $R_2 = 1 \text{ M}\Omega$ , and  $V_{CC} = V_{EE} = 7.5 \text{ V}$ . Use  $\beta_o = 80$ ,  $V_A = 75 \text{ V}$ ,  $K_p = 5 \text{ mA/V}^2$ , and  $V_{TP} = -1 \text{ V}$ . (b) What are the differential-mode voltage gain and input resistance and output resistance of the amplifier? (See Prob. 15.56.)

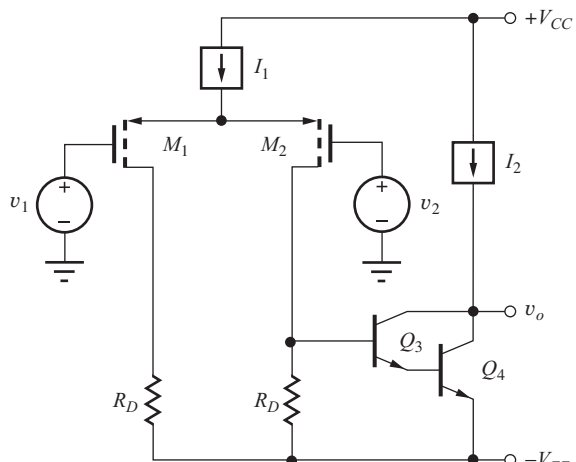


Figure P15.71

- \*15.72. Use SPICE to simulate the amplifier in Prob. 15.71 at a frequency of 1 kHz, and determine the differential-mode gain, CMRR, and differential-mode input resistance and output resistance.

- 15.73. (a) Redraw the op amp circuit in Fig. 15.26(a) with  $Q_4$  replaced by the *npn* Darlington configuration from Prob. 15.56. (b) What are the new values of voltage gain, CMRR, input resistance, and output resistance? Use the circuit element values from Ex. 15.4, and compare your results to those of the example.

- 15.74. Simulate the circuit in Prob. 15.73 using SPICE and compare the results of the two problems.

- 15.75. (a) What are the Q-points of the transistors in the amplifier in Fig. P15.75 if  $V_{CC} = 18$  V,  $V_{EE} = 18$  V,  $I_1 = 100 \mu\text{A}$ ,  $I_2 = 350 \mu\text{A}$ ,  $I_3 = 1 \text{ mA}$ ,  $\beta_F = 100$ , and  $V_A = 50$  V? (b) What are the differential-mode voltage gain and input resistance? (c) What is the amplifier output resistance? (d) What is the common-mode input resistance? (e) Which terminal is the noninverting input?

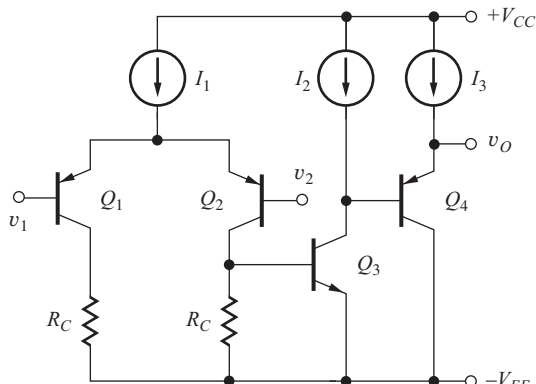


Figure P15.75

- \*15.76. Use SPICE to simulate the amplifier in Prob. 15.75 at a frequency of 1 kHz, and determine the differential-mode gain, CMRR, and differential-mode input resistance and output resistance.

- 15.77. (a) What are the Q-points of the transistors in the amplifier in Fig. P15.77 if  $V_{DD} = 5$  V,  $V_{SS} = 5$  V,  $I_1 = 600 \mu\text{A}$ ,  $I_2 = 500 \mu\text{A}$ ,  $I_3 = 2 \text{ mA}$ ,  $K_n = 5 \text{ mA/V}^2$ ,  $V_{TN} = 0.70$  V,  $\lambda_n = 0.02 \text{ V}^{-1}$ ,  $K_p = 2 \text{ mA/V}^2$ ,  $V_{TP} = -0.70$  V, and  $\lambda_p = 0.015 \text{ V}^{-1}$ ? (b) What are the differential-mode voltage gain and input resistance and output resistance of the amplifier?

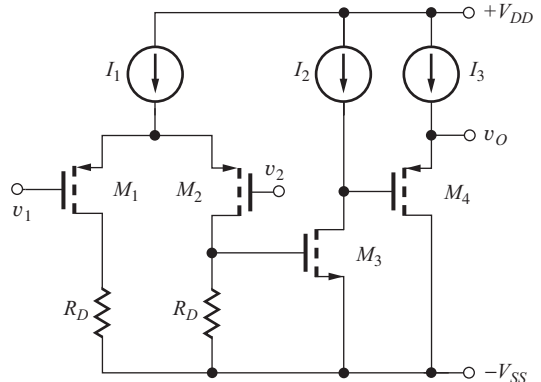


Figure P15.77

- 15.78. Simulate the circuit in Prob. 15.77 using SPICE and compare the results to hand calculations.

- 15.79. Transistor  $M_3$  in Fig. P15.77 is replaced with an *npn* device with  $\beta_o = 150$  and  $V_A = 70$  V. What are the values of the differential-mode voltage gain and input resistance, and the output resistance of the new amplifier? Use the circuit element values from Prob. 15.76.

- 15.80. Simulate the circuit in Prob. 15.79 using SPICE and compare the results with hand calculations.

- 15.81. (a) What are the Q-points of the transistors in the amplifier in Fig. P15.81 if  $V_{DD} = 12$  V,  $V_{SS} = 12$  V,  $I_1 = 500 \mu\text{A}$ ,  $I_2 = 2 \text{ mA}$ ,  $I_3 = 5 \text{ mA}$ ,  $K_n = 5 \text{ mA/V}^2$ ,  $V_{TN} = 0.75$  V,  $\lambda_n = 0.02 \text{ V}^{-1}$ ,  $K_p = 2 \text{ mA/V}^2$ ,  $V_{TP} = -0.75$  V, and  $\lambda_p = 0.015 \text{ V}^{-1}$ ? (b) What are the differential-mode voltage gain and input resistance and output resistance of the amplifier? (c) Use SPICE to simulate the amplifier in Prob. 15.81 at a frequency of 1 kHz, and determine the differential-mode gain, CMRR, and differential-mode input resistance and output resistance.

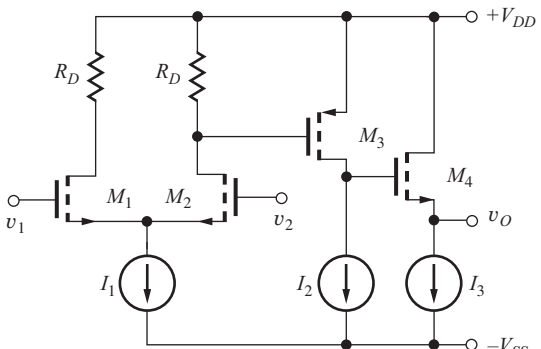


Figure P15.81

- 15.82. (a) What are the Q-points of the transistors in the amplifier in Fig. P15.82 if  $V_{CC} = 5$  V,  $V_{EE} = 5$  V,  $I_1 = 200 \mu\text{A}$ ,  $I_2 = 500 \mu\text{A}$ ,  $I_3 = 2 \text{ mA}$ ,  $R_L = 2 \text{ k}\Omega$ ,  $\beta_o = 100$ ,  $V_A = 50$  V,  $K_n = 5 \text{ mA/V}^2$ , and  $V_{TN} = 0.70$  V? (b) What are the differential-mode voltage gain and input resistance and output resistance of the amplifier? (c) Use SPICE to simulate the amplifier in Fig. P15.82 at a frequency of 2 kHz, and determine the differential-mode gain, CMRR, and differential-mode input resistance and output resistance.

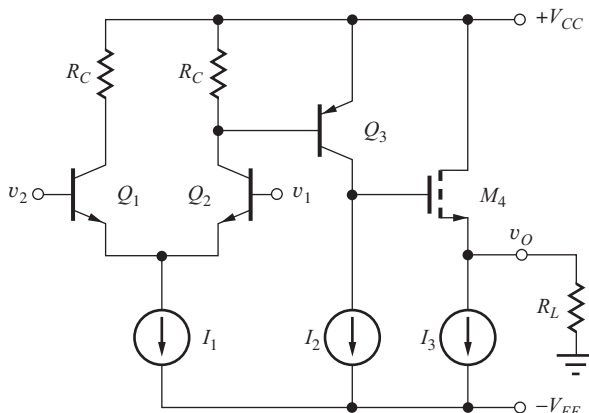


Figure P15.82

- \*15.83. (a) What are the Q-points of the transistors in the amplifier in Fig. P15.83 if  $V_{CC} = 3$  V,  $V_{EE} = 3$  V,  $I_1 = 10 \mu\text{A}$ ,  $I_2 = 50 \mu\text{A}$ ,  $I_3 = 250 \mu\text{A}$ ,  $R_{C1} = 300 \text{ k}\Omega$ ,  $R_{C2} = 78 \text{ k}\Omega$ ,  $R_L = 5 \text{ k}\Omega$ ,  $\beta_{on} = 100$ ,  $V_{AN} = 50$  V,  $\beta_{op} = 50$ , and  $V_{AP} = 70$  V? (b) What are the differential-mode voltage gain and input resistance and output resistance of the amplifier? (c) Which terminal is the noninverting input?

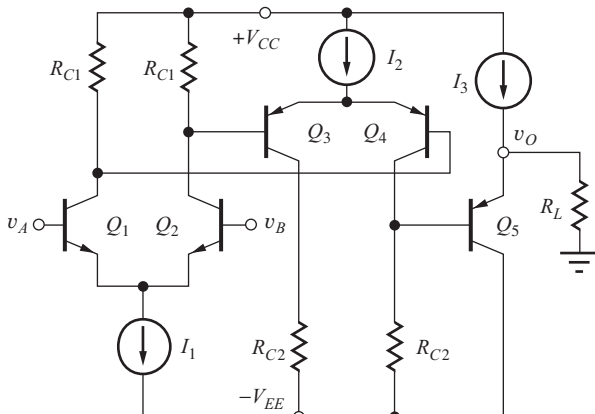


Figure P15.83

Which terminal is the inverting input? (d) What is the gain predicted by our rule-of-thumb estimate? What are the reasons for any discrepancy?

- \*15.84. (a) What are the Q-points of the transistors in the amplifier in Fig. P15.83 if  $V_{CC} = V_{EE} = 16$  V,  $I_1 = 100 \mu\text{A}$ ,  $I_2 = 200 \mu\text{A}$ ,  $I_3 = 750 \mu\text{A}$ ,  $R_{C1} = 120 \text{ k}\Omega$ ,  $R_{C2} = 170 \text{ k}\Omega$ ,  $R_L = 2 \text{ k}\Omega$ ,  $\beta_{on} = 100$ ,  $V_{AN} = 50$  V,  $\beta_{op} = 50$ , and  $V_{AP} = 70$  V? (b) What are the differential-mode voltage gain and input resistance and output resistance of the amplifier? (c) What is the common-mode input range? (d) Estimate the offset voltage of this amplifier.

- 15.85. (a) What are the Q-points of the transistors in the amplifier in Fig. P15.85 if  $V_{CC} = V_{EE} = 15$  V,  $I_1 = 200 \mu\text{A}$ ,  $R = 12 \text{ k}\Omega$ ,  $\beta_F = 100$ , and  $V_A = 70$  V? (b) What are the differential-mode voltage gain and input resistance and output resistance of the amplifier?

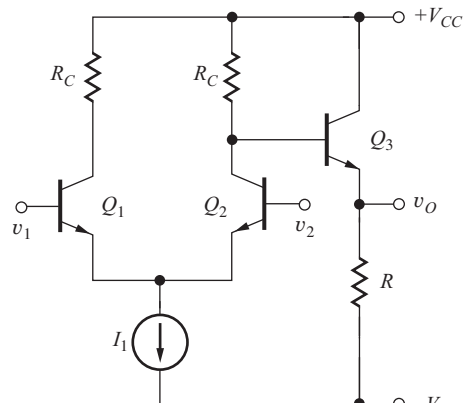


Figure P15.85

- \*15.86. Design an amplifier using the topology in Fig. P15.85 to have an input resistance of  $300 \text{ k}\Omega$  and an output resistance of  $100 \Omega$ . Can these specifications all be met if  $V_{CC} = V_{EE} = 12$  V,  $\beta_{FO} = 100$ , and  $V_A = 60$  V? If so, what are the values of  $I_1$ ,  $R_C$ , and  $R$ , and the voltage gain of the amplifier? If not, what needs to be changed?

- \*15.87. Design an amplifier using the topology in Fig. P15.85 to have an input resistance of  $1 \text{ M}\Omega$  and an output resistance  $\leq 2 \Omega$ . Can these specifications all be met if  $V_{CC} = V_{EE} = 9$  V,  $\beta_{FO} = 100$ , and  $V_A = 60$  V? If so, what are the values of  $I_1$ ,  $R_C$ , and  $R$ , and the voltage gain of the amplifier? If not, what needs to be changed?

- \*\*15.88. (a) What are the Q-points of the transistors in the amplifier in Fig. P15.88 if  $V_{CC} = V_{EE} = 18$  V,

$I_1 = 50 \mu\text{A}$ ,  $I_2 = 500 \mu\text{A}$ ,  $I_3 = 5 \text{ mA}$ ,  $\beta_{on} = 100$ ,  $V_{AN} = 50 \text{ V}$ ,  $\beta_{op} = 50$ , and  $V_{AP} = 70 \text{ V}$ ? (b) What are the differential-mode voltage gain and input resistance and output resistance of the amplifier?

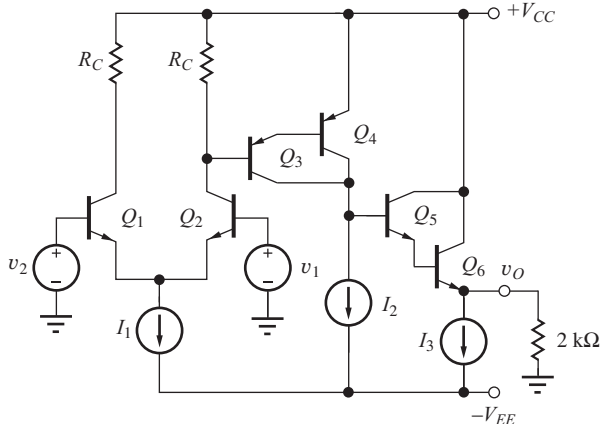


Figure P15.88

- \*\*15.89. (a) What are the Q-points of the transistors in the amplifier in Fig. P15.88 if  $V_{CC} = V_{EE} = 22 \text{ V}$ ,  $I_1 = 50 \mu\text{A}$ ,  $I_2 = 500 \mu\text{A}$ ,  $I_3 = 5 \text{ mA}$ ,  $\beta_{on} = 100$ ,  $V_{AN} = 50 \text{ V}$ ,  $\beta_{op} = 50$ , and  $V_{AP} = 70 \text{ V}$ ? (b) What are the differential-mode voltage gain and input resistance and output resistance of the amplifier?
- 15.90. The drain resistors  $R_D$  in Prob. 15.81 are replaced with PMOS transistors as shown in Fig. 15.30(a). (a) What is the required value of  $K_p$  for these transistors? (b) What is the voltage gain of the new amplifier? (c) What was the original voltage gain?
- 15.91. The drain resistors  $R_D$  in Prob. 15.77 are replaced with NMOS transistors in a manner similar to that in Fig. 15.30(b). (a) What is the required value of  $K_p$  for these transistors? (b) What is the voltage gain of the new amplifier? (c) What was the original voltage gain?
- 15.92. Suppose collector resistors  $R_C$  in Prob. 15.51 are replaced with diode-connected *pnp* transistors that are identical to  $Q_3$ . Assume the dc bias points do not change. (a) What is the voltage gain of the new amplifier? (c) What was the original voltage gain?
- 15.93. The transconductance amplifier in Prob. 15.51 is connected as a voltage follower. What are the closed-loop voltage gain, input resistance, and output resistance of the voltage follower?
- 15.94. Resistor  $R$  in the transconductance amplifier in Prob. 15.51 is replaced with an 1-mA ideal current

source. If the amplifier is connected as a voltage follower, what are the closed-loop voltage gain, input resistance, and output resistance of the voltage follower?

- 15.95. The transconductance amplifier in Prob. 15.63 is connected as a voltage follower. What are the closed-loop voltage gain, input resistance, and output resistance of the voltage follower?
- 15.96. (a) The op amp in Prob. 15.75 is connected as a noninverting amplifier with a gain of 10. What are the closed-loop voltage gain, input resistance, and output resistance of the amplifier? (b) Repeat for connection as a voltage follower.
- 15.97. (a) The op amp in Prob. 15.81 is connected as a noninverting amplifier with a gain of 5. What are the closed-loop voltage gain, input resistance, and output resistance of the amplifier? (b) Repeat for connection as a voltage follower.

### 15.3 Output Stages

- 15.98. What is the quiescent current in the class-AB stage in Fig. P15.98 if  $K_p = K_n = 600 \mu\text{A/V}^2$  and  $V_{TN} = -V_{TP} = 0.75 \text{ V}$ ?
- \*15.99. What is the quiescent current in the class-AB stage in Fig. P15.98 if  $K_p = 400 \mu\text{A/V}^2$ ,  $K_n = 600 \mu\text{A/V}^2$ ,  $V_{TP} = -0.8 \text{ V}$ , and  $V_{TN} = 0.7 \text{ V}$ ?
- 15.100. What is the quiescent current in the class-AB stage in Fig. P15.100 if both transistors have  $I_S = 2 \times 10^{-15} \text{ A}$ ?

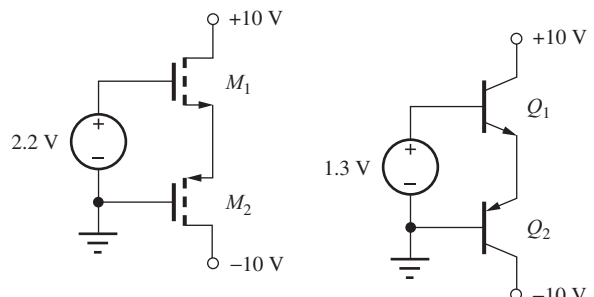


Figure P15.98

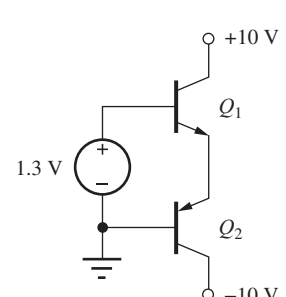


Figure P15.100

- \*15.101. What is the quiescent current in the class-AB stage in Fig. P15.100 if  $I_S = 10^{-15} \text{ A}$  for the *pnp* transistor and  $I_S = 4 \times 10^{-15} \text{ A}$  for the *npn* transistor?
- 15.102. Draw a sketch of the voltage transfer characteristic for the circuit in Fig. P15.102. Label important voltages on the characteristic.

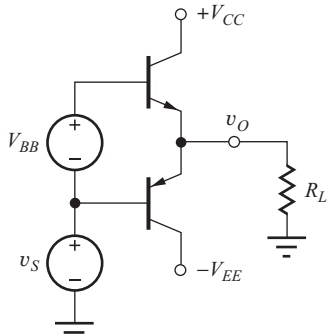


Figure P15.102

- 15.103. Use SPICE to plot the voltage transfer characteristic for the class-AB stage in Fig. P15.102 if  $I_S = 10^{-15}$  A and  $\beta_F = 50$  for the *pnp* transistor,  $I_S = 5 \times 10^{-15}$  A and  $\beta_F = 60$  for the *npn* transistor,  $V_{BB} = 1.3$  V, and  $R_L = 1$  k $\Omega$ . S
- 15.104. What is the quiescent current in the class-AB stage in Fig. P15.104 if  $I_S$  for the *npn* transistor is  $10^{-15}$  A,  $I_S$  for the *pnp* transistor is  $10^{-16}$  A,  $I_B = 250$   $\mu$ A, and  $R_B = 5$  k $\Omega$ ? Assume  $\beta_F = \infty$  and  $v_O = 0$ .

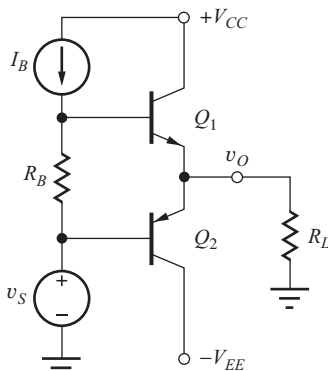


Figure P15.104

- 15.105. What is the quiescent current in the class-AB stage in Fig. P15.105 if  $V_{TN} = 0.75$  V,  $V_{TP} = -0.75$  V,  $K_n = 500$   $\mu$ A/V $^2$ ,  $K_p = 200$   $\mu$ A/V $^2$ ,  $I_G = 500$   $\mu$ A, and  $R_G = 4$  k $\Omega$ ? S
- 15.106. The source-follower in Fig. 15.32 has  $V_{DD} = V_{SS} = 10$  V and  $R_L = 1$  k $\Omega$ . If the amplifier is developing an output voltage of  $5 \sin 2000\pi t$  V, what is the minimum value of  $I_{SS}$ ? What are the maximum and minimum values of source current  $i_S$  that occur during the signal swing? What is the efficiency?
- \*15.107. An ideal complementary class-B output stage is generating a triangular output signal across a

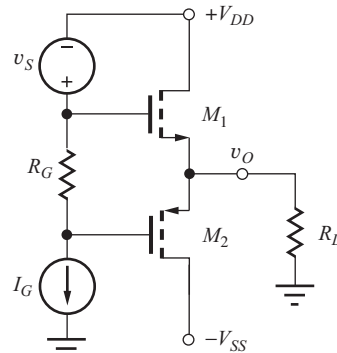


Figure P15.105

100-k $\Omega$  load resistor with a peak value of 10 V from  $\pm 10$ -V supplies. What is the efficiency of the amplifier?

- 15.108. An ideal complementary class-B output stage is generating a square wave output signal across a 5-k $\Omega$  load resistor with a peak value of 5 V from  $\pm 5$ -V supplies. What is the efficiency of the amplifier?

- \*\*15.109. (a) Use the Fourier analysis capability of SPICE to find the amplitude of the first, second, third, fourth, and fifth harmonics of the input signal introduced by the cross-over region of the class-B amplifier in Fig. P15.102 if  $V_{BB} = 0$ ,  $V_{CC} = V_{EE} = 5$  V,  $v_S = 4 \sin 2000\pi t$ , and  $R_L = 2$  k $\Omega$ . (b) Repeat for  $V_{BB} = 1.3$  V. S

### Short-Circuit Protection

- 15.110. What is the current in the  $R_L$  circuit in Fig. 15.39 at the point when current just begins to limit ( $V_{BE2} = 0.7$  V) if  $R = 15$   $\Omega$ ,  $R_1 = 1$  k $\Omega$ , and  $R_L = 250$   $\Omega$ ? For what value of  $v_S$  does the output begin to limit current?
- 15.111. Use SPICE to simulate the circuit in Prob. 15.110, and compare the results to your hand calculations. Discuss the reasons for any discrepancies. S
- 15.112. What would be the Q-point currents in  $M_4$  and  $M_5$  in the amplifier in Fig. 15.38(a) if  $V_{DD} = V_{SS} = 15$  V,  $I_2 = 250$   $\mu$ A,  $R_G = 7$  k $\Omega$ ,  $R_L = 2$  k $\Omega$ , and  $V_{TN} = 0.75$  V,  $V_{TP} = -0.75$  V,  $K_n = 5$  mA/V $^2$ , and  $K_p = 2$  mA/V $^2$ ?
- 15.113. What would be the currents in  $Q_4$  and  $Q_5$  in the amplifier in Fig. 15.38(b) if  $V_{CC} = V_{EE} = 15$  V,  $I_2 = 500$   $\mu$ A,  $R_B = 2.7$  k $\Omega$ ,  $R_L = 2$  k $\Omega$ , and  $Q_3$  is modeled by a voltage of  $V_{CESAT} = 0.2$  V in series with a resistance of 50  $\Omega$  when it is saturated?

### Transformer Coupling

- 15.114. Calculate the output resistance of the follower circuit (as seen at  $R_L$ ) in Fig. 15.41(a) if  $n = 10$  and  $I_S = 10 \text{ mA}$ .
- 15.115. For the circuit in Fig. P15.115,  $v_S = \sin 2000\pi t$ ,  $R_E = 82 \text{ k}\Omega$ ,  $R_B = 200 \text{ k}\Omega$ , and  $V_{CC} = V_{EE} = 9 \text{ V}$ . What value of  $n$  is required to deliver maximum power to  $R_L$  if  $R_L = 10 \Omega$ ? What is the power? Assume  $C_1 = C_2 = \infty$ .

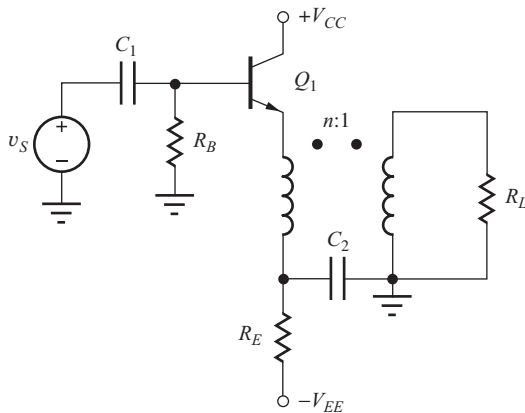
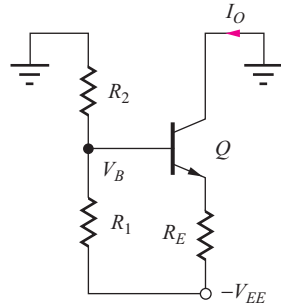


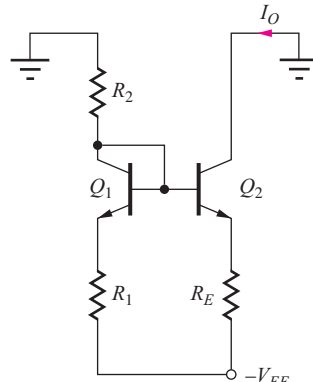
Figure P15.115

### 15.4 Electronic Current Sources

- 15.116. (a) What are the output current and output resistance of the current source in Fig. P15.116(a) if  $V_{EE} = 12 \text{ V}$ ,  $R_1 = 2 \text{ M}\Omega$ ,  $R_2 = 2 \text{ M}\Omega$ ,  $R_E = 270 \text{ k}\Omega$ ,  $\beta_o = 100$ , and  $V_A = 50 \text{ V}$ ? (b) Repeat for the circuit in Fig. P15.116(b).
- 15.117. What are the output current and output resistance of the current source in Prob. 15.116(a) if node  $V_B$  is bypassed to ground with a capacitor?
- 15.118. (a) What are the output current and output resistance of the current source in Fig. P15.116(a) if  $-V_{EE} = -9 \text{ V}$ ,  $R_1 = 270 \text{ k}\Omega$ ,  $R_2 = 470 \text{ k}\Omega$ ,  $R_E = 18 \text{ k}\Omega$ ,  $\beta_o = 150$ , and  $V_A = 75 \text{ V}$ ? (b) Repeat for the circuit in Fig. P15.116(b).
- 15.119. (a) What are the output current and output resistance of the current source in Fig. P15.116(a) if  $-V_{EE} = -5 \text{ V}$ ,  $R_1 = 100 \text{ k}\Omega$ ,  $R_2 = 200 \text{ k}\Omega$ ,  $R_E = 16 \text{ k}\Omega$ ,  $\beta_o = 100$ , and  $V_A = 75 \text{ V}$ ? (b) Repeat for the circuit in Fig. 15.116(b).
- 15.120. Design a current source to provide an output current of 1 mA using the topology of Fig. P15.116(a). The current source should use no more than 1.2 mA and have an output resistance of at least 500 k $\Omega$ . Assume  $V_{EE} = 12 \text{ V}$ . (b) Repeat for Fig. 15.116(b).



(a)



(b)

Figure P15.116

- 15.121. What are the output current and output resistance of the current source in Fig. P15.121 if  $V_O = V_{DD} = 6 \text{ V}$ ,  $R_4 = 200 \text{ k}\Omega$ ,  $R_3 = 100 \text{ k}\Omega$ , and  $R_S = 16 \text{ k}\Omega$ ? Use the device parameters from Prob. 15.121.
- 15.122. What are the output current and output resistance of the current source in Fig. P15.121 if  $V_O = V_{DD} = 10 \text{ V}$ ,  $R_4 = 680 \text{ k}\Omega$ ,  $R_3 = 330 \text{ k}\Omega$ ,  $R_S = 30 \text{ k}\Omega$ ,  $K_n = 500 \mu\text{A/V}^2$ ,  $V_{TN} = 1 \text{ V}$ , and  $\lambda = 0.01 \text{ V}^{-1}$ ?
- 15.123. What are the output current and output resistance of the current source in Fig. P15.121 if  $V_O = V_{DD} = 3 \text{ V}$ ,  $R_4 = 200 \text{ k}\Omega$ ,  $R_3 = 68 \text{ k}\Omega$ , and  $R_S = 56 \text{ k}\Omega$ ? Use the device parameters from Prob. 15.121.
- 15.124. What are the output current and output resistance of the current source in Fig. P15.124 if  $V_{CC} = 10 \text{ V}$ ,  $R_1 = 100 \text{ k}\Omega$ ,  $R_2 = 300 \text{ k}\Omega$ ,  $R_E = 14 \text{ k}\Omega$ ,  $\beta_o = 90$ , and  $V_A = 75 \text{ V}$ ?
- 15.125. What are the output current and output resistance of the current source in Fig. P15.124 if  $V_{CC} = 15 \text{ V}$ ,  $R_1 = 100 \text{ k}\Omega$ ,  $R_2 = 200 \text{ k}\Omega$ ,  $R_E = 47 \text{ k}\Omega$ ,  $\beta_o = 75$ , and  $V_A = 50 \text{ V}$ ?

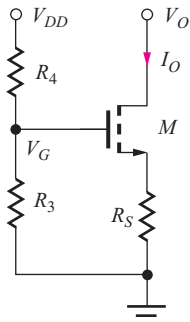


Figure P15.121

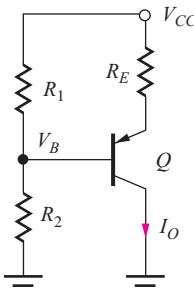


Figure P15.124

- 15.126. What are the output current and output resistance of the current source in Fig. P15.124 if  $V_{CC} = 5$  V,  $R_1 = 10$  k $\Omega$ ,  $R_2 = 39$  k $\Omega$ ,  $R_E = 1.5$  k $\Omega$ ,  $\beta_o = 75$ , and  $V_A = 60$  V?
- 15.127. What are the output current and output resistance of the current source in Fig. P15.127 if  $V_{DD} = 9$  V,  $R_4 = 2$  M $\Omega$ ,  $R_3 = 1$  M $\Omega$ ,  $R_S = 120$  k $\Omega$ ,  $K_p = 750$   $\mu$ A/V $^2$ ,  $V_{TP} = -0.75$  V, and  $\lambda = 0.01$  V $^{-1}$ ?

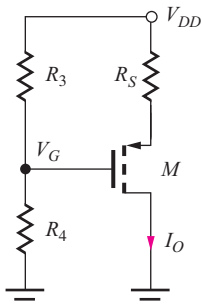
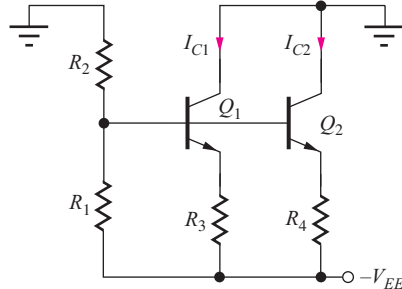


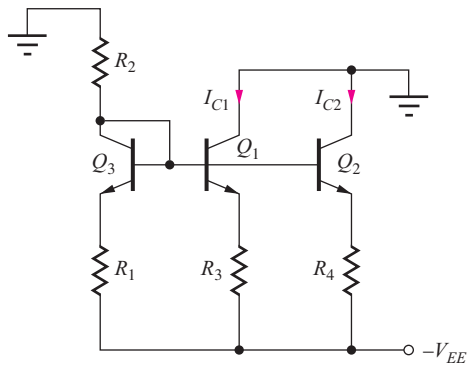
Figure P15.127

- 15.128. What are the output current and output resistance of the current source in Fig. P15.127 if  $V_{DD} = 6$  V,  $R_4 = 200$  k $\Omega$ ,  $R_3 = 100$  k $\Omega$ , and  $R_S = 16$  k $\Omega$ ? Use the device parameters from Prob. 15.127.
- 15.129. What are the output current and output resistance of the current source in Fig. P15.127 if  $V_{DD} = 4$  V,  $R_4 = 200$  k $\Omega$ ,  $R_3 = 62$  k $\Omega$ , and  $R_S = 43$  k $\Omega$ ? Use the device parameters from Prob. 15.127.
- 15.130. Design a current source to provide an output current of 175  $\mu$ A using the topology in Fig. P15.127. The current source should use no more than 200  $\mu$ A and have an output resistance of at least 2.5 M $\Omega$ . Assume  $V_{DD} = 12$  V,  $K_p = 200$   $\mu$ A/V $^2$ ,  $V_{TP} = -0.75$  V, and  $\lambda = 0.02$  V $^{-1}$ .
- 15.131. (a) What are the two output currents and output resistances of the current source in Fig. P15.131(a) if  $V_{EE} = 12$  V,  $\beta_o = 125$ ,  $V_A = 50$  V,  $R_1 = 33$  k $\Omega$ ,

$R_2 = 68$  k $\Omega$ ,  $R_3 = 20$  k $\Omega$ , and  $R_4 = 100$  k $\Omega$ ? (b) Repeat for the circuit in Fig. P15.131(b).



(a)



(b)

Figure P15.131

- 15.132. (a) Use SPICE to simulate the current source array in Prob. 15.131(a) and find the output currents and output resistances of the sources. Use transfer function analysis to find the output resistances. (b) Repeat for Prob. 15.131(b).
- 15.133. What are the two output currents and output resistances of the current sources in Fig. P15.133 if  $V_{DD} = 12$  V,  $K_p = 250$   $\mu$ A/V $^2$ ,  $V_{TP} = -1$  V,  $\lambda = 0.02$  V $^{-1}$ ,  $R_1 = 100$  k $\Omega$ ,  $R_2 = 470$  k $\Omega$ ,  $R_3 = 2$  M $\Omega$ , and  $R_4 = 2$  M $\Omega$ ?

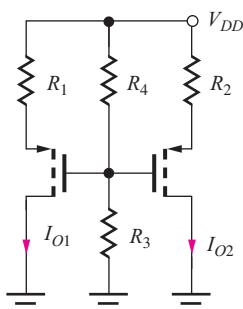


Figure P15.133

- 15.134. Use SPICE to simulate the current source array in Prob. 15.133, and find the output currents and output resistances of the source. Use transfer function analysis to find the output resistances.

- \*15.135. The op amp in Fig. P15.135 is used in an attempt to increase the overall output resistance of the current source circuit. If  $V_{REF} = 5$  V,  $V_{CC} = 0$  V,  $V_{EE} = 15$  V,  $R = 50 \text{ k}\Omega$ ,  $\beta_o = 120$ ,  $V_A = 70$  V, and  $A = 50,000$ , what are the output current  $I_O$  and output resistance of the current source? Did the op amp help increase the output resistance? Explain why or why not.

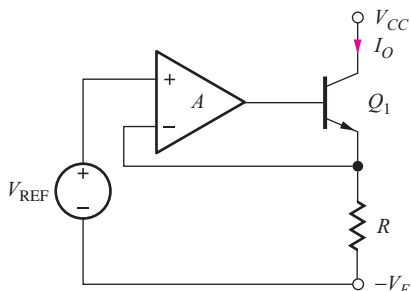


Figure P15.135

- 15.136. The op amp in Fig. P15.136 is used to increase the overall output resistance of current source  $M_1$ . If  $V_{REF} = 5$  V,  $V_{DD} = 0$  V,  $V_{SS} = 15$  V,  $R = 50 \text{ k}\Omega$ ,  $K_n = 800 \mu\text{A}/\text{V}^2$ ,  $V_{TN} = 0.8$  V,  $\lambda = 0.02 \text{ V}^{-1}$ , and  $A = 50,000$ , what are the output current  $I_O$  and output resistance of the current source?

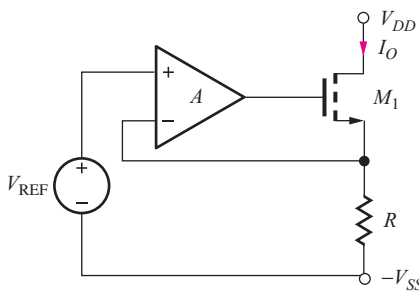
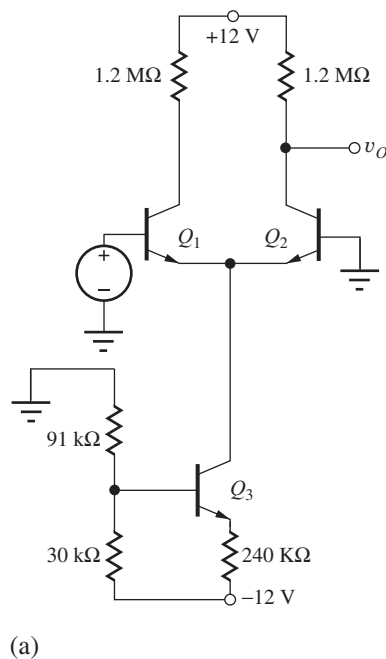
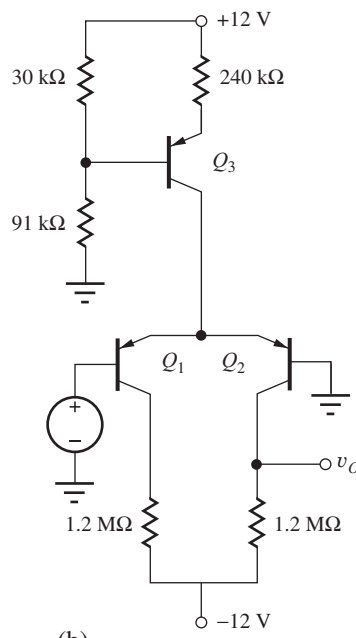


Figure P15.136

- 15.137. (a) What are the Q-points of the transistors in the amplifier in Fig. P15.137(a) if  $\beta_o = 85$  and  $V_A = 70$  V? (b) What are the differential-mode gain and CMRR of the amplifier? (c) Repeat for Fig. P15.137(b).



(a)



(b)

Figure P15.137

- 15.138. (a) What are the Q-points of the transistors in the amplifier in Fig. P15.138 if  $K_n = 400 \mu\text{A}/\text{V}^2$ ,  $V_{TN} = +1$  V,  $\lambda = 0.02 \text{ V}^{-1}$ ,  $R_1 = 51 \text{ k}\Omega$ ,  $R_2 = 100 \text{ k}\Omega$ ,  $R_S = 7.5 \text{ k}\Omega$ , and  $R_D = 36 \text{ k}\Omega$ ? (b) What are the differential-mode gain and CMRR of the amplifier?

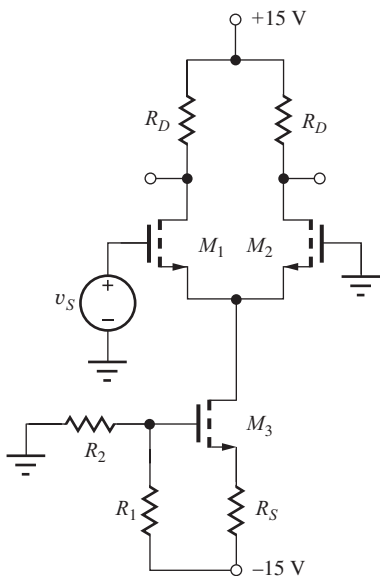
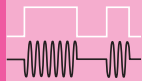


Figure P15.138

- 15.139. The output resistance of the MOS current source in Fig. P15.138 is given by  $R_{\text{out}} = \mu_f R_S$ . How much voltage must be developed across  $R_S$  to achieve an output resistance of  $5 \text{ M}\Omega$  at a current of  $100 \mu\text{A}$  if  $K_n = 500 \mu\text{A/V}^2$  and  $\lambda = 0.02 \text{ V}^{-1}$ ?
- 15.140. (a) A current source with  $R_{\text{out}} = \beta_o r_o$  is used to bias a standard bipolar differential amplifier. What is an expression for the CMRR of this amplifier for single-ended outputs?
- \*\*15.141. Use PSPICE to perform a Monte Carlo analysis of the circuits in Fig. 15.50. Assume 5 percent resistors and a 5 percent power-supply tolerance. Find the nominal and  $3\sigma$  limits on  $I_O$  and  $R_{\text{out}}$ .

# CHAPTER 16



## ANALOG INTEGRATED CIRCUIT DESIGN TECHNIQUES

### CHAPTER OUTLINE

16.1	Circuit Element Matching	1047
16.2	Current Mirrors	1049
16.3	High-Output-Resistance Current Mirrors	1063
16.4	Reference Current Generation	1072
16.5	Supply-Independent Biasing	1073
16.6	The Bandgap Reference	1077
16.7	The Current Mirror as an Active Load	1081
16.8	Active Loads in Operational Amplifiers	1092
16.9	The $\mu$ A741 Operational Amplifier	1097
16.10	The Gilbert Analog Multiplier	1110
	Summary	1112
	Key Terms	1113
	References	1114
	Problems	1114

### CHAPTER GOALS

In Chapter 16 we concentrate on understanding integrated circuit design techniques that are based upon the characteristics of closely matched devices and look at a number of key building blocks of operational amplifiers and other ICs. Our goals are to:

- Understand bipolar and MOS current mirror operation and mirror ratio errors
- Explore high output resistance current sources including cascode and Wilson current source circuits
- Learn to design current sources for use in both discrete and integrated circuits
- Add reference current circuit techniques to our kit of circuit building blocks. These circuits produce currents that exhibit a substantial degree of independence from power supply voltage including the  $V_{BE}$ -based reference and the Widlar current source.
- Investigate the operation and design of bandgap reference circuits, one of the most important techniques for providing an accurate reference voltage that is independent of power supply voltages and temperature

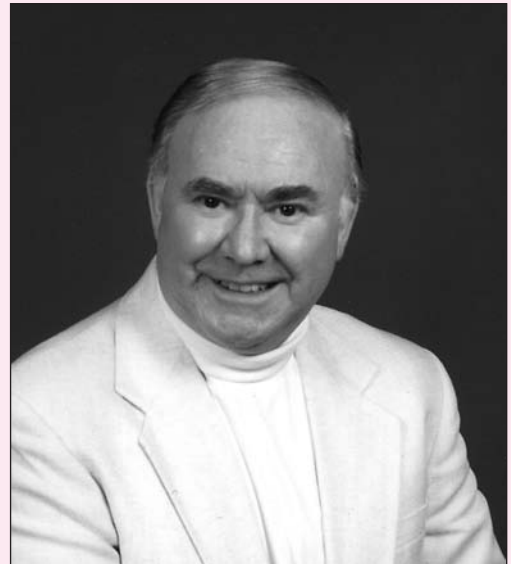
- Use current mirrors as active loads in differential amplifiers to increase the voltage gain of single-stage amplifiers to the amplification factor  $\mu_f$
- Learn how to include the effects of device mismatch in the calculation of amplifier performance measures such as CMRR
- Analyze the design of the classic  $\mu$ A741 operational amplifier
- Understand the techniques used to realize four-quadrant analog multipliers with large input signal range
- Continue to increase our understanding of SPICE simulation techniques

In Chapter 16, we explore several extremely clever and exciting circuits designed by two of the legends of integrated circuit design, Robert Widlar and Barrie Gilbert. Widlar designed the  $\mu$ A702 op amp and later developed the LM101 operational amplifier and many of the circuits that led to the design of the classic  $\mu$ A741 op amp. Widlar was also responsible for the  $\mu$ A723 voltage regulator and the bandgap reference. Gilbert invented a four-quadrant analog multiplier circuit referred to today as the Gilbert multiplier. The  $\mu$ A741 circuit techniques spawned a broad range of follow-on designs that are still in use today. The bandgap reference forms the heart of most precision voltage references and voltage regulator circuits, and is also used as a temperature sensor in digital thermometry. Circuits related to the analog multiplier are used in RF mixers (the Gilbert mixer) and phase detectors in phase-locked loops.

Integrated circuit (IC) technology allows the realization of large numbers of virtually identical transistors. Although the absolute parameter tolerances of these devices are relatively poor, device characteristics can be matched to within 1 percent or better. The ability to build devices with nearly identical characteristics has led to the development of special circuit techniques that take advantage of the tight matching of the device characteristics.



(a)



(b)

Legends of analog design. (a) Robert J. Widlar. (b) Barrie Gilbert  
*(a) Courtesy of National Semiconductor. (b) Courtesy of Analog Devices*

Chapter 16 begins by exploring the use of matched transistors in the design of current sources, called **current mirrors**, in both MOS and bipolar technology. The cascode and Wilson current sources are subsequently added to our repertoire of high-output-resistance current source circuits. Circuit techniques that can be used to achieve **power-supply-independent biasing** are also introduced.

We will also study the bandgap reference circuit which uses the well defined behavior of the pn junction to produce a precise output voltage that is highly independent of power supply voltage and temperature. The bandgap circuit is widely used in voltage references and voltage regulators.

The current mirror is often used to bias analog circuits and to replace load resistors in differential and operational amplifiers. This active-load circuit can substantially enhance the voltage gain capability of many amplifiers, and a number of MOS and bipolar circuit examples are presented. The chapter then discusses circuit techniques used in IC operational amplifiers, including the classic  $\mu$ A741 amplifier. This design provides a robust, high-performance, general-purpose operational amplifier with breakdown-voltage protection of the input stage and short-circuit protection of the output stage. The final section looks at the precision four-quadrant analog multiplier design of Gilbert.

## 16.1 CIRCUIT ELEMENT MATCHING

Integrated circuit (IC) technology allows the realization of large numbers of virtually identical transistors. Although the absolute parameter tolerances of these devices are relatively poor, device characteristics can be matched to within 1 percent or better. The ability to build devices with nearly identical characteristics has led to the development of special circuit techniques that take advantage of the tight matching of device characteristics. Transistors are said to be **matched** when they have identical sets of device parameters:  $(I_S, \beta_{FO}, V_A)$  for the BJT,  $(V_{TN}, K', \lambda)$  for the MOSFET, or  $(I_{DSS}, V_P, \lambda)$  for the JFET. The planar geometry of the devices can easily be changed in integrated designs, and so the emitter area  $A_E$  of the BJT and the  $W/L$  ratio of the MOSFET become important

**TABLE 16.1**  
IC Tolerances and Matching [1]

	ABSOLUTE TOLERANCE, %	MISMATCH, %
Diffused resistors	30	$\leq 2$
Ion-implanted resistors	5	$\leq 1$
$V_{BE}$	10	$\leq 1$
$I_S, \beta_F, V_A$	30	$\leq 1$
$V_{TN}, V_{TP}$	15	$\leq 1$
$K', \lambda$	30	$\leq 1$

circuit design parameters. (Remember from our study of MOS digital circuits in Part II that  $W/L$  represents a fundamental circuit design parameter.)

In integrated circuits, absolute parameter values may vary widely from fabrication process run to process run, with  $\pm 25$  to 30 percent tolerances not uncommon (see Table 16.1). However, the matching between nearby circuit elements on a given IC chip is typically within a fraction of a percent. Thus, IC design techniques have been invented that rely heavily on **matched device** characteristics and resistor ratios rather than absolute parameter values. The circuits described in this chapter depend, for proper operation, on the tight device matching that can be realized through IC fabrication processes, and many will not operate correctly if built with poorly mismatched discrete components. However, many of these circuits can be used in discrete circuit design if integrated transistor arrays are used in the implementation.

Figure 16.1 shows one example of the use of four matched transistors to improve the performance of the differential amplifier that we studied in the previous chapter. The four devices are cross-connected to further improve the overall parameter matching and temperature tracking of the circuit. In Section 16.2, we explore the use of matched bipolar and MOS transistors in the design of IC current sources called **current mirrors**.

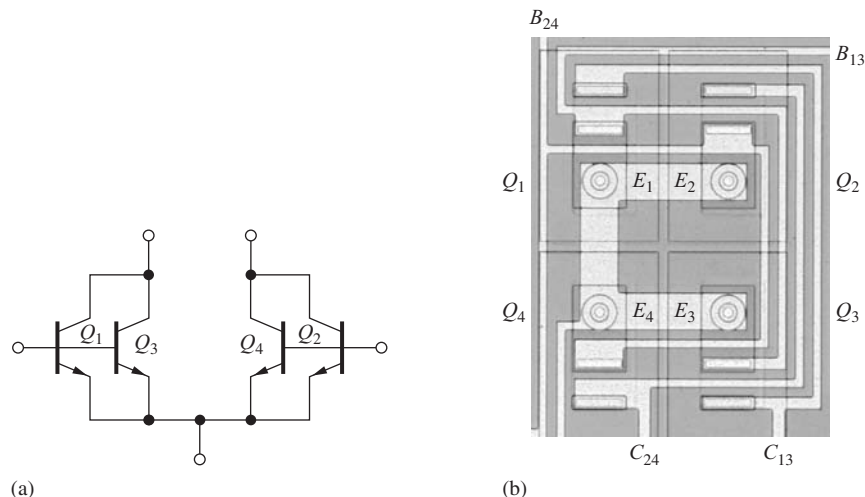


**Figure 16.1** (a) Differential amplifier formed with a cross-connected quad of identical transistors. (b) Layout of the cross-coupled transistor quad in Fig. 16.1(a). Round emitters are used to improve device matching.

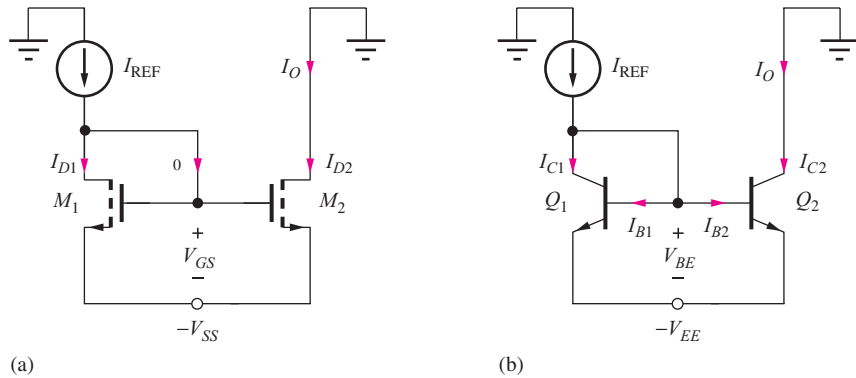


Figure 16.2 (a) MOS and (b) BJT current mirror circuits.

**EXERCISE:** An IC resistor has a nominal value of  $10 \text{ k}\Omega$  and a tolerance of  $\pm 30$  percent. A particular process run has produced resistors with an average value 20 percent higher than the nominal value, and the resistors are found to be matched within 2 percent. What range of resistor values will occur in this process run?

**ANSWER:**  $11.88 \text{ k}\Omega \leq R \leq 12.12 \text{ k}\Omega$

## 16.2 CURRENT MIRRORS

**Current mirror** biasing is an extremely important technique in integrated circuit design. Not only is it heavily used in analog applications, it also appears routinely in digital circuit design as well. Figure 16.2 shows the circuits for basic MOS and bipolar current mirrors. In Fig. 16.2(a), MOSFETs  $M_1$  and  $M_2$  are assumed to have identical characteristics ( $V_{TN}$ ,  $K'_n$ ,  $\lambda$ ) and  $W/L$  ratios; in Fig. 16.2(b), the characteristics of  $Q_1$  and  $Q_2$  are assumed to be identical ( $I_S$ ,  $\beta_{FO}$ ,  $V_A$ ). In both circuits, a **reference current**  $I_{\text{REF}}$  provides operating bias to the mirror, and the output current is represented by current  $I_O$ . These basic circuits are designed to have  $I_O = I_{\text{REF}}$ ; that is, the output current mirrors the reference current—hence, the name “current mirror.” Note that the current mirror circuits do not utilize resistors that were required by the current sources studied in Chapter 15, a characteristic desired for integrated circuit realization.

### 16.2.1 dc ANALYSIS OF THE MOS TRANSISTOR CURRENT MIRROR

In the MOS current mirror in Fig. 16.2(a), reference current  $I_{\text{REF}}$  goes through “diode-connected” transistor  $M_1$ , establishing gate-source voltage  $V_{GS}$ .  $V_{GS}$  is applied to transistor  $M_2$ , developing an identical drain current  $I_{D2} = I_{\text{REF}}$ . Detailed analysis of the current mirror operation follows in the paragraphs below.

Because the gate currents are zero for the MOSFETs, reference current  $I_{\text{REF}}$  must flow into the drain of  $M_1$ , which is forced to operate in saturation (pinch-off) by the circuit connection because  $V_{DS1} = V_{GS1} = V_{GS}$ .  $V_{GS}$  must equal the value required for  $I_{D1} = I_{\text{REF}}$ . Assuming matched devices:<sup>1</sup>

$$I_{\text{REF}} = \frac{K_n}{2}(V_{GS1} - V_{TN})^2(1 + \lambda V_{DS1}) \quad \text{or} \quad V_{GS1} = V_{TN} + \sqrt{\frac{2I_{\text{REF}}}{K_n(1 + \lambda V_{DS1})}} \quad (16.1)$$

<sup>1</sup> Matching between elements in the current mirror is very important; this is a case in which the  $(1 + \lambda V_{DS})$  term is included in the dc, as well as ac, calculations.

Current  $I_O$  is equal to the drain current of  $M_2$ :

$$I_O = I_{D2} = \frac{K_n}{2}(V_{GS2} - V_{TN})^2(1 + \lambda V_{DS2}) \quad (16.2)$$

However, the circuit connection forces  $V_{GS2} = V_{GS1}$ , and  $V_{DS1} = V_{GS1}$ . Substituting Eq. (16.1) into Eq. (16.2) yields

$$I_O = I_{\text{REF}} \frac{(1 + \lambda V_{DS2})}{(1 + \lambda V_{DS1})} \cong I_{\text{REF}} \quad (16.3)$$

For equal values of  $V_{DS}$ , the output current is identical to the reference current (that is, the output mirrors the reference current). Unfortunately, in most circuit applications,  $V_{DS2} \neq V_{DS1}$ , and there is a slight mismatch between the output current and the reference current, as demonstrated in Ex. 16.1.

For convenience, we define the ratio of  $I_O$  to  $I_{\text{REF}}$  to be the **mirror ratio** MR given by

$$\text{MR} = \frac{I_O}{I_{\text{REF}}} = \frac{(1 + \lambda V_{DS2})}{(1 + \lambda V_{DS1})} \quad (16.4)$$

### EXAMPLE 16.1 OUTPUT CURRENT OF THE MOS CURRENT MIRROR

In this example, we find the output current for the standard current mirror configuration.

**PROBLEM** Calculate the output current  $I_O$  for the MOS current mirror in Fig. 16.2(a) if  $V_{SS} = 10$  V,  $K_n = 250 \mu\text{A}/\text{V}^2$ ,  $V_{TN} = 1$  V,  $\lambda = 0.0133 \text{ V}^{-1}$ , and  $I_{\text{REF}} = 150 \mu\text{A}$ .

**SOLUTION** **Known Information and Given Data:** Current mirror circuit in Fig. 16.2(a);  $V_{SS} = 10$  V; transistor parameters are given as  $K_n = 250 \mu\text{A}/\text{V}^2$ ,  $V_{TN} = 1$  V,  $\lambda = 0.0133 \text{ V}^{-1}$ , and  $I_{\text{REF}} = 150 \mu\text{A}$

**Unknowns:** Output current  $I_O$

**Approach:** Find  $V_{GS1}$  and  $V_{DS2}$  and then evaluate Eq. (16.3) to give the output current.

**Assumptions:** Transistors are identical and operating in the active region of operation.

**Analysis:** We need to evaluate Eq. (16.3) and must find the value of  $V_{GS1}$  using Eq. (16.1). Since  $V_{DS1} = V_{GS1}$ , we can write

$$V_{DS1} = V_{TN} + \sqrt{\frac{2I_{\text{REF}}}{K_n}} = 1 + \sqrt{\frac{2(150 \mu\text{A})}{250 \frac{\mu\text{A}}{\text{V}^2}}} = 2.10 \text{ V}$$

in which we have neglected the  $(1 + \lambda V_{DS1})$  term to simplify the dc bias calculation. Substituting this value and  $V_{DS2} = 10$  V in Eq. (16.3):

$$I_O = (150 \mu\text{A}) \frac{[1 + 0.0133(10)]}{[1 + 0.0133(2.10)]} = 165 \mu\text{A}$$

The ideal output current would be  $150 \mu\text{A}$ , whereas the actual currents are mismatched by approximately 10 percent.

**Check of Results:** A double check shows the calculations to be correct.  $M_1$  is saturated by connection, and  $M_2$  will also be active as long as its drain-source voltage exceeds  $(V_{GS1} - V_{TN})$ , which is easily met in Fig. 16.2(a) since  $V_{DS2} = 10$  V.

**Discussion:** We could attempt to improve the precision of our answer slightly by including the  $(1 + \lambda V_{DS1})$  term in the evaluation of  $V_{GS1}$ . The solution then requires an iterative analysis that barely changes the value of  $I_O$ .

**Computer-Aided Analysis:** We can check our analysis directly with SPICE by setting the MOS transistor parameters to  $K_P = 250 \mu\text{A/V}^2$ ,  $V_{TO} = 1 \text{ V}$ ,  $\text{LEVEL} = 1$ , and  $\text{LAMBDA} = 0$ . SPICE yields an output current of  $150 \mu\text{A}$  with  $V_{GS} = 2.095 \text{ V}$ . With nonzero  $\lambda$ ,  $\text{LAMBDA} = 0.0133 \text{ V}^{-1}$ , SPICE yields  $I_O = 165 \mu\text{A}$  with  $V_{GS} = 2.081 \text{ V}$ . The values are in agreement with our hand calculations.

**EXERCISE:** Suppose we include the  $(1 + \lambda V_{DS1})$  term in the evaluation of  $V_{GS1}$ . Show that the equation to be solved is

$$V_{DS1} = V_{TN} + \sqrt{\frac{2I_{REF}}{K_n(1 + \lambda V_{DS1})}}$$

Find the new value of  $V_{DS1}$  using the numbers in Ex. 16.1. What is the new value of  $I_O$ ?

**ANSWERS:**  $2.08 \text{ V}$ ;  $165 \mu\text{A}$

**EXERCISE:** Based on the numbers in Ex. 16.1, what is the minimum value of the drain voltage required to keep  $M_2$  saturated in Fig. 16.2(a)?

**ANSWER:**  $-8.9 \text{ V}$

### 16.2.2 CHANGING THE MOS MIRROR RATIO

The power of the current mirror is greatly increased if the mirror ratio can be changed from unity. For the MOS current mirror, the ratio can easily be modified by changing the  $W/L$  ratios of the two transistors forming the mirror. In Fig. 16.3, for example, remembering that  $K_n = K'_n(W/L)$  for the MOSFET, the  $K_n$  values of the two transistors are given by

$$K_{n1} = K'_n \left(\frac{W}{L}\right)_1 \quad \text{and} \quad K_{n2} = K'_n \left(\frac{W}{L}\right)_2 \quad (16.5)$$

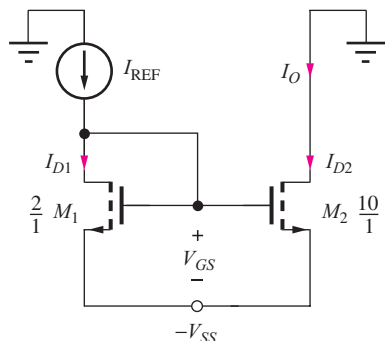


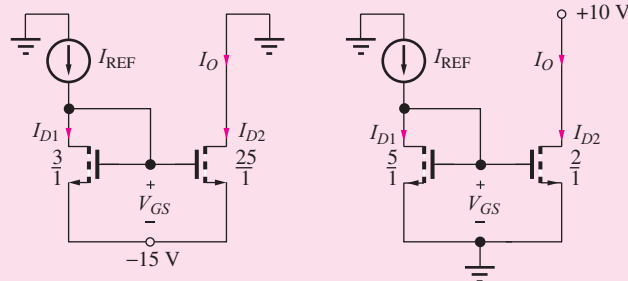
Figure 16.3 MOS current mirror with unequal ( $W/L$ ) ratios.

Substituting these two different values of  $K_n$  in Eqs. (16.1) and (16.2) yields the mirror ratio given by

$$\text{MR} = \frac{\left(\frac{W}{L}\right)_2 (1 + \lambda V_{DS2})}{\left(\frac{W}{L}\right)_1 (1 + \lambda V_{DS1})} \quad (16.6)$$

In the ideal case ( $\lambda = 0$ ) or for  $V_{DS2} = V_{DS1}$ , the mirror ratio is set by the ratio of the  $W/L$  values of the two transistors. For the particular values in Fig. 16.3, this design value of the mirror ratio would be 5, and the output current would be  $I_O = 5I_{\text{REF}}$ . However, the differences in  $V_{DS}$  will again create an error in the mirror ratio.

**EXERCISE:** (a) Calculate the mirror ratio for the MOS current mirrors in the figure here for  $\lambda = 0$ .  
(b) For  $\lambda = 0.02 \text{ V}^{-1}$  if  $V_{TN} = 1 \text{ V}$ ,  $K'_n = 25 \mu\text{A/V}^2$ , and  $I_{\text{REF}} = 50 \mu\text{A}$ .



**ANSWERS:** 8.33, 0.400; 10.4, 0.462

### 16.2.3 dc ANALYSIS OF THE BIPOLAR TRANSISTOR CURRENT MIRROR

The operation of the bipolar current mirror in Fig. 16.2(b) is similar to that of the MOS circuit. Reference current  $I_{\text{REF}}$  goes through diode-connected transistor  $Q_1$ , establishing base-emitter voltage  $V_{BE}$ .  $V_{BE}$  also biases transistor  $Q_2$ , developing an almost identical collector current at its output:  $I_{C2} \cong I_{\text{REF}}$ . Detailed analysis of the current mirror operation follows in the paragraphs below.

Analysis of the BJT current mirror in Fig. 16.2(b) is similar to that of the FET. Applying KCL at the collector of “diode-connected” transistor  $Q_1$  yields

$$I_{\text{REF}} = I_{C1} + I_{B1} + I_{B2} \quad \text{and} \quad I_O = I_{C2} \quad (16.7)$$

The currents needed to relate  $I_O$  to  $I_{\text{REF}}$  can be found using the transport model, noting that the circuit connection forces the two transistors to have the same base-emitter voltage  $V_{BE}$ :

$$\begin{aligned} I_{C1} &= I_S \exp\left(\frac{V_{BE}}{V_T}\right) \left(1 + \frac{V_{CE1}}{V_A}\right) & I_{C2} &= I_S \exp\left(\frac{V_{BE}}{V_T}\right) \left(1 + \frac{V_{CE2}}{V_A}\right) \\ \beta_{F1} &= \beta_{FO} \left(1 + \frac{V_{CE1}}{V_A}\right) & \beta_{F2} &= \beta_{FO} \left(1 + \frac{V_{CE2}}{V_A}\right) \\ I_{B1} &= \frac{I_S}{\beta_{FO}} \exp\left(\frac{V_{BE}}{V_T}\right) & I_{B2} &= \frac{I_S}{\beta_{FO}} \exp\left(\frac{V_{BE}}{V_T}\right) \end{aligned} \quad (16.8)$$

Substituting Eq. (16.8) into Eq. (16.7) and solving for  $I_O = I_{C2}$  yields

$$I_O = I_{\text{REF}} \frac{\left(1 + \frac{V_{CE2}}{V_A}\right)}{\left(1 + \frac{V_{CE1}}{V_A} + \frac{2}{\beta_{FO}}\right)} = I_{\text{REF}} \frac{\left(1 + \frac{V_{CE2}}{V_A}\right)}{\left(1 + \frac{V_{BE}}{V_A} + \frac{2}{\beta_{FO}}\right)} \quad (16.9)$$

If the Early voltage were infinite, Eq. (16.9) would give a mirror ratio of

$$\text{MR} = \frac{I_O}{I_{\text{REF}}} = \frac{1}{1 + \frac{2}{\beta_{FO}}} \quad (16.10)$$

and the output current would mirror the reference current, except for a small error due to the finite current gain of the BJT. For example, if  $\beta_{FO} = 100$ , the currents would match within 2 percent. As for the FET case, however, the collector-emitter voltage mismatch in Eq. (16.9) is generally more significant than the **current gain defect** term, as indicated in Ex. 16.2.

## EXAMPLE 16.2 MIRROR RATIO CALCULATIONS

Compare the mirror ratios for MOS and BJT current mirrors operating with similar bias conditions and output resistances ( $V_A = 1/\lambda$ ).

**PROBLEM** Calculate the mirror ratio for the MOS and BJT current mirrors in Fig. 16.2 for  $V_{GS} = 2$  V,  $V_{DS2} = 10$  V =  $V_{CE2}$ ,  $\lambda = 0.02$  V<sup>-1</sup>,  $V_A = 50$  V, and  $\beta_{FO} = 100$ . Assume  $M_1 = M_2$  and  $Q_1 = Q_2$ .

**SOLUTION** **Known Information and Given Data:** Current mirror circuits in Fig. 16.2 with  $M_2 = M_1$  and  $Q_2 = Q_1$ ;  $V_{SS} = 10$  V; operating voltages:  $V_{GS} = 2$  V,  $V_{DS2} = V_{CE2} = 10$  V and  $V_{BE} = 0.7$  V; transistor parameters:  $\lambda = 0.02$  V<sup>-1</sup>,  $V_A = 50$  V, and  $\beta_{FO} = 100$

**Unknowns:** Mirror ratio MR for each current mirror

**Approach:** Use Eqs. (16.6) and (16.9) to determine the mirror ratios.

**Assumptions:** BJTs and MOSFETs are in the active region of operation, respectively. Assume  $V_{BE} = 0.7$  V for the BJTs and the MOSFETs are enhancement-mode devices.

**Analysis:** For the MOS current mirror,

$$\text{MR} = \frac{(1 + \lambda V_{DS2})}{(1 + \lambda V_{DS1})} = \frac{\left[1 + \frac{0.02}{V}(10 \text{ V})\right]}{\left[1 + \frac{0.02}{V}(2 \text{ V})\right]} = 1.15$$

and for the BJT case

$$\text{MR} = \frac{\left(1 + \frac{V_{CE2}}{V_A}\right)}{\left(1 + \frac{2}{\beta_{FO}} + \frac{V_{CE1}}{V_A}\right)} = \frac{\left(1 + \frac{10 \text{ V}}{50 \text{ V}}\right)}{\left(1 + \frac{2}{100} + \frac{0.7 \text{ V}}{50 \text{ V}}\right)} = 1.16$$

**Check of Results:** A double check shows our calculations to be correct.  $M_1$  is forced to be active by connection.  $M_2$  has  $V_{DS2} > V_{GS2}$  and will be pinched-off for  $V_{TN} > 0$  (enhancement-mode transistor).  $Q_1$  has  $V_{CE} = V_{BE}$ , so it is forced to be in the active region.  $Q_2$  has  $V_{CE2} > V_{BE2}$  and is also in the active region. The assumed regions of operation are valid.

**Discussion:** The FET and BJT mismatches are very similar—15 percent and 16 percent, respectively. The current gain error is a small contributor to the overall error in the BJT mirror ratio.

**Computer-Aided Analysis:** We can easily perform an analysis of the current mirrors using SPICE, which will be done shortly as part of Ex. 16.3.

**EXERCISE:** What is the actual value of  $V_{BE}$  in the bipolar current mirror in Ex. 16.2 if  $I_S = 0.1 \text{ fA}$  and  $I_{REF} = 100 \mu\text{A}$ ? What is the minimum value of the collector voltage required to maintain  $Q_2$  in the active region in Fig. 16.2(b)?

**ANSWERS:** 0.691 V;  $-V_{EE} + 0.691$  V

#### 16.2.4 ALTERING THE BJT CURRENT MIRROR RATIO

In bipolar IC technology, the designer is free to modify the emitter area of the transistors, just as the  $W/L$  ratio can be chosen in MOS design. To alter the BJT mirror ratio, we use the fact that the saturation current of the bipolar transistor is proportional to its emitter area  $A_E$  and can be written as

$$I_S = I_{SO} \frac{A_E}{A} \quad (16.11)$$

$I_{SO}$  represents the saturation current of a bipolar transistor with one unit of emitter area:  $A_E = 1 \times A$ . The actual dimensions associated with  $A$  are technology-dependent.

By changing the relative sizes of the emitters (**emitter area scaling**) of the BJTs in the current mirror, the IC designer can modify the mirror ratio. For the modified mirror in Fig. 16.4,

$$I_{C1} = I_{SO} \frac{A_{E1}}{A} \exp\left(\frac{V_{BE}}{V_T}\right) \left(1 + \frac{V_{CE1}}{V_A}\right) \quad I_{C2} = I_{SO} \frac{A_{E2}}{A} \exp\left(\frac{V_{BE}}{V_T}\right) \left(1 + \frac{V_{CE2}}{V_A}\right) \quad (16.12)$$

$$I_{B1} = \frac{I_{SO}}{\beta_{FO}} \frac{A_{E1}}{A} \exp\left(\frac{V_{BE}}{V_T}\right) \quad I_{B2} = \frac{I_{SO}}{\beta_{FO}} \frac{A_{E2}}{A} \exp\left(\frac{V_{BE}}{V_T}\right)$$

Substituting these equations in Eq. (16.7) and then solving for  $I_O$  yields

$$I_O = n I_{\text{REF}} \frac{1 + \frac{V_{CE2}}{V_A}}{1 + \frac{V_{BE}}{V_A} + \frac{1+n}{\beta_{FO}}} \quad \text{where} \quad n = \frac{A_{E2}}{A_{E1}} \quad (16.13)$$

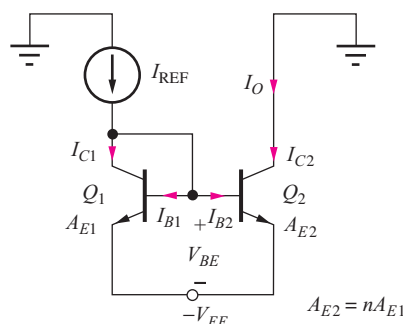


**Figure 16.4** BJT current mirror with unequal emitter area.

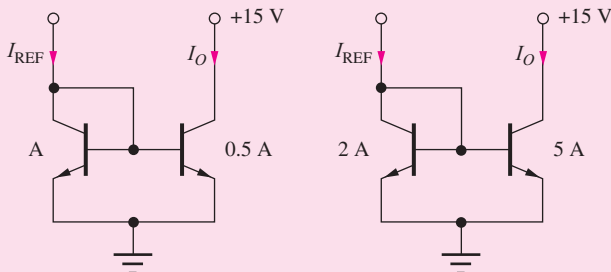
In the ideal case of infinite current gain and identical collector-emitter voltages, the mirror ratio would be determined only by the ratio of the two emitter areas:  $MR = n$ .

However, for finite current gain,

$$MR = \frac{n}{1 + \frac{1+n}{\beta_{FO}}} \quad \text{where} \quad n = \frac{A_{E2}}{A_{E1}} \quad (16.14)$$

For example, suppose  $A_{E2}/A_{E1} = 10$  and  $\beta_{FO} = 100$ ; then the mirror ratio would be 9.01. A relatively large error (10 percent) is occurring even though the effect of collector-emitter voltage mismatch has been ignored. For high mirror ratios, the current gain error term can become quite important because the total number of units of base current increases directly with the mirror ratio.

**EXERCISE:** (a) Calculate the ideal mirror ratio for the BJT current mirrors in the figure below if  $V_A = \infty$  and  $\beta_{FO} = \infty$ . (b) If  $V_A = \infty$  and  $\beta_{FO} = 75$ . (c) If  $V_A = 60$  V,  $\beta_{FO} = 75$ , and  $V_{BE} = 0.7$  V.



**ANSWERS:** 0.500, 2.50; 0.490, 2.39; 0.606, 2.95

### 16.2.5 MULTIPLE CURRENT SOURCES

Analog circuits often require a number of different current sources to bias the various stages of the design. A single reference transistor,  $M_1$  or  $Q_1$ , can be used to generate multiple output currents using the circuits in Fig. 16.5. In Fig. 16.5(a), the unusual connection of the gate terminals through the MOSFETs is being used as a “short-hand” method to indicate that all the gates are connected together. Circuit operation is similar to that of the basic current mirror. The reference current enters the “diode-connected” transistor — here, MOSFET  $M_1$  — establishing gate-source voltage  $V_{GS}$ , that is then used to bias transistors  $M_2$  through  $M_5$ , each having a different  $W/L$  ratio. Because there is no current gain defect in MOS technology, a large number of output transistors can be driven from one reference transistor.

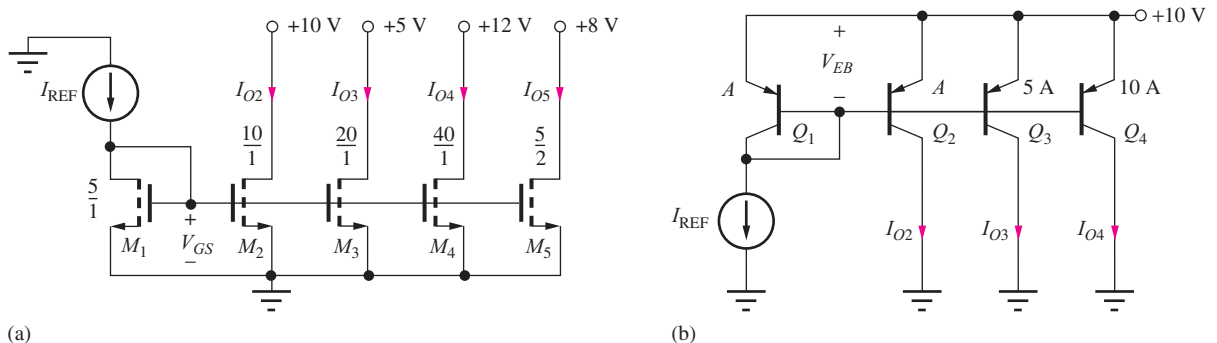


**Figure 16.5** (a) Multiple MOS current sources generated from one reference voltage. (b) Multiple bipolar sources biased by one reference device.

**EXERCISE:** What are the four output currents in the circuit in Fig. 16.5(a) if  $I_{REF} = 100 \mu A$  and  $\lambda = 0$  for all the FETs?

**ANSWERS:** 200  $\mu A$ ; 400  $\mu A$ ; 800  $\mu A$ ; 50.0  $\mu A$

**EXERCISE:** Recalculate the four output currents in the circuit in Fig. 16.5(a) if  $\lambda = 0.02$  for all the FETs. Assume  $V_{GS} = 2 V$ .

**ANSWERS:** 231  $\mu A$ ; 423  $\mu A$ ; 954  $\mu A$ ; 55.8  $\mu A$

The situation is very similar in the *pnp* bipolar mirror in Fig. 16.5(b). Here again, the base terminals of the BJTs are extended through the transistors to simplify the drawing. In this circuit, reference current  $I_{REF}$  is supplied by diode-connected BJT  $Q_1$  to establish the emitter-base reference voltage  $V_{EB}$ .  $V_{EB}$  is then used to bias transistors  $Q_2$  to  $Q_4$ , each having a different emitter area relative to that of the reference transistor. Because the total base current increases with the addition of each output transistor, the base current error term gets worse as more transistors are added, which limits the number of outputs that can be used with the basic bipolar current mirror. The buffered current mirror in Sec. 16.2.6 was invented to solve this problem.

An expression for the output current from a given collector can be derived following the steps that led to Eq. (16.13):

$$I_{Oi} = n_i I_{REF} \frac{1 + \frac{V_{ECi}}{V_A}}{1 + \frac{V_{EB}}{V_A} + \frac{\sum_{i=2}^m n_i}{\beta_{FO}}} \quad \text{where} \quad n_i = \frac{A_{Ei}}{A_{E1}} \quad (16.15)$$

**EXERCISE:** (a) What are the three output currents in the circuit in Fig. 16.5(b) if  $I_{REF} = 10 \mu A$ ,  $\beta_{FO} = 50$ , and  $V_A = \infty$  for all the BJTs? (b) Repeat for  $V_A = 50 V$  and  $V_{EB} = 0.7 V$ . Use Eq. (16.15).

**ANSWERS:** 7.46  $\mu A$ , 37.3  $\mu A$ , 74.6  $\mu A$ ; 8.86  $\mu A$ , 44.3  $\mu A$ , 88.6  $\mu A$

## 16.2.6 BUFFERED CURRENT MIRROR

The current gain defect in the bipolar current mirror can become substantial when a large mirror ratio is used or if many source currents are generated from one reference transistor. However, this error can be reduced greatly by using the circuit in Fig. 16.6, called a **buffered current mirror**. The current gain of transistor  $Q_3$  is used to reduce the base current that is subtracted from the reference

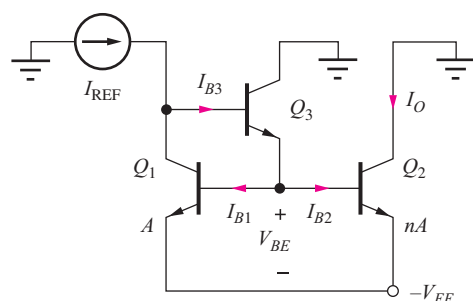


Figure 16.6 Buffered current mirror.

current. Applying KCL at the collector of transistor  $Q_1$ , and assuming that  $V_A = \infty$  for simplicity,  $I_{C1}$  is expressed as

$$I_{C1} = I_{\text{REF}} - I_{B3} = I_{\text{REF}} - \frac{(1+n) \frac{I_{C1}}{\beta_{FO1}}}{\beta_{FO3} + 1} \quad (16.16)$$

and solving for the collector current yields

$$I_O = n I_{C1} = n I_{\text{REF}} \frac{1}{1 + \frac{(1+n)}{\beta_{FO1}(\beta_{FO3} + 1)}} \quad (16.17)$$

The current gain error term in the denominator has been reduced by a factor of  $(\beta_{FO3} + 1)$  from the error in Eq. (16.13).

**EXERCISE:** What is the mirror ratio and the percent error for the buffered current mirror in Fig. 16.6 if  $\beta_{FO} = 50$ ,  $n = 10$ , and  $V_A = \infty$  for all the BJTs? (b) What is that value of  $V_{CE2}$  required to balance the mirror if  $\beta_{FO} = \infty$ ?

**ANSWERS:** 9.96, 0.430 percent; 1.4 V

### 16.2.7 OUTPUT RESISTANCE OF THE CURRENT MIRRORS

Now that we have found the dc output current of the current mirror, we will focus on the second important parameter that characterizes the electronic current source—the output resistance. The output resistance of the basic current mirror can be found by referring to the ac model of Fig. 16.7. Diode-connected bipolar transistor  $Q_1$  represents a simple two-terminal device, and its small-signal model is easily found using nodal analysis of Fig. 16.8:

$$\mathbf{i} = g_\pi \mathbf{v} + g_m \mathbf{v} + g_o \mathbf{v} = (g_m + g_\pi + g_o) \mathbf{v} \quad (16.18)$$

By factoring out  $g_m$ , an approximate result for the diode conductance is

$$\frac{\mathbf{i}}{\mathbf{v}} = g_m \left[ 1 + \frac{1}{\beta_o} + \frac{1}{\mu_f} \right] \cong g_m \quad \text{and} \quad R \cong \frac{1}{g_m} \quad (16.19)$$

for  $\beta_o$  and  $\mu_f \gg 1$ . The small-signal model for the diode-connected BJT is simply a resistor of value  $1/g_m$ . Note that this result is the same as the small-signal resistance  $r_d$  of an actual diode that was developed in Sec. 13.4.

Using this diode model simplifies the ac model for the current mirror to that shown in Fig. 16.9. This circuit should be recognized as a common-emitter transistor with a Thévenin equivalent resistance  $R_{\text{th}} = 1/g_m$  connected to its base; the output resistance just equals the output resistance  $r_{o2}$  of transistor  $Q_2$ .

The equation describing the small-signal model for the two-terminal “diode-connected” MOSFET is similar to that in Eq. (16.19) except that the current gain is infinite. Therefore, the two-terminal MOSFET is also represented by a resistor of value  $1/g_m$ , as in Fig. 16.10; the output resistance of the MOS current mirror is equal to  $r_{o2}$  of MOSFET  $M_2$ .

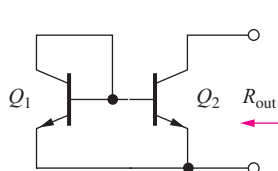


**Figure 16.7** ac Model for the output resistance of the bipolar current mirror.

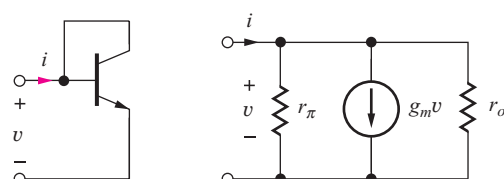


**Figure 16.8** Model for “diode-connected” transistor.

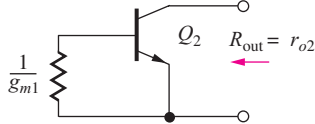


**Figure 16.9** Simplified small-signal model for the bipolar current mirror.

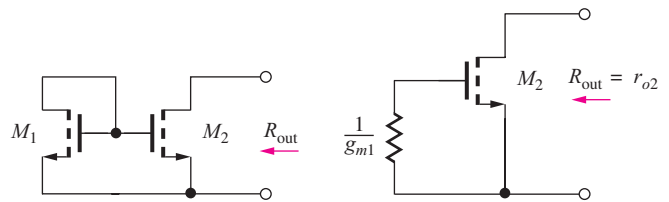


**Figure 16.10** Output resistance of the MOS current mirror.

Thus, the output resistance and figure of merit  $V_{CS}$  (see Section 15.4.2) for the basic current mirror circuits are determined by output transistors  $Q_2$  and  $M_2$ :

$$R_{\text{out}} = r_{o2} \quad \text{and} \quad V_{CS} \cong V_{A2} \quad \text{or} \quad \frac{1}{\lambda_2} \quad (16.20)$$

**EXERCISE:** What are the output resistances of sources  $I_{O2}$  and  $I_{O3}$  in Fig. 16.5(a) for  $I_{\text{REF}} = 100 \mu\text{A}$  and Fig. 16.5(b) for  $I_{\text{REF}} = 10 \mu\text{A}$  if  $V_A = 1/\lambda = 50 \text{ V}$  and  $\beta_F = 100$ ?

**ANSWERS:** 260 kΩ, 130 kΩ; 5.94 MΩ, 1.19 MΩ

### 16.2.8 TWO-PORT MODEL FOR THE CURRENT MIRROR

We shall see shortly that the current mirror can be used not only as a dc current source but, in more complex circuits, as a current amplifier and active load. It will be useful to understand the small-signal behavior of the current mirror, redrawn as a two-port in Fig. 16.11.

The small-signal model for the current mirror is in Fig. 16.12, in which diode-connected transistor  $Q_1$  is represented in its simplified form by  $1/g_{m1}$ . From the circuit in Fig. 16.12(a),

$$\begin{aligned} R_{\text{in}} &= \left. \frac{\mathbf{v}_1}{\mathbf{i}_1} \right|_{\mathbf{v}_2=0} = \frac{1}{(g_{m1} + g_{\pi2})} = \frac{1}{g_{m1} \left( 1 + \frac{n}{\beta_{o2}} \right)} \cong \frac{1}{g_{m1}} \\ n &= \left. \frac{\mathbf{i}_2}{\mathbf{i}_1} \right|_{\mathbf{v}_2=0} = \frac{g_{m2}r_{\pi2}}{1 + g_{m1}r_{\pi2}} \cong \frac{g_{m2}}{g_{m1}} = \frac{I_{C2}}{I_{C1}} \\ R_{\text{out}} &= \left. \frac{\mathbf{v}_2}{\mathbf{i}_2} \right|_{\mathbf{i}_1=0} = r_{o2} \end{aligned} \quad (16.21)$$

Figure 16.12(b) shows the final two-port model representation. The bipolar current mirror has an input resistance of  $1/g_{m1}$ , determined by diode  $Q_1$  and an output resistance equal to  $r_{o2}$  of  $Q_2$ . The current gain is determined approximately by the emitter-area ratio  $n = A_{E2}/A_{E1}$ . Be sure to remember to use the correct values of  $I_{C1}$  and  $I_{C2}$  when calculating the values of the small-signal parameters.

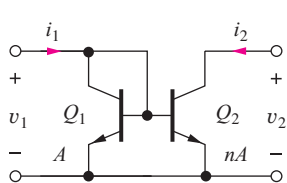


**Figure 16.11** Current mirror as a two-port.

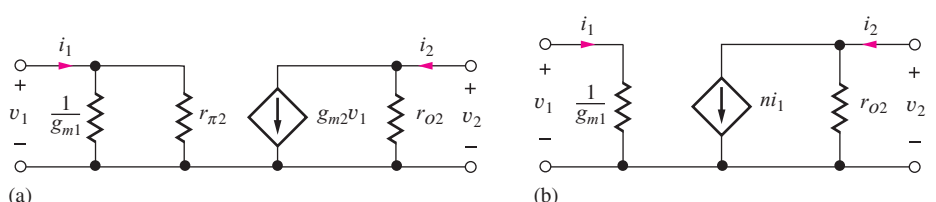


**Figure 16.12** (a) Small-signal model for the current mirror. (b) Simplified small-signal model for the current mirror.

Analysis of the MOS current mirror yields similar results [or by simply setting  $r_{\pi 2} = \infty$  in Eq. (16.21)]:

$$R_{\text{in}} = \frac{1}{g_{m1}} \quad \beta = \frac{g_{m2}}{g_{m1}} \cong \frac{\left(\frac{W}{L}\right)_2}{\left(\frac{W}{L}\right)_1^2} \cong n \quad R_{\text{out}} = r_{o2} \quad (16.22)$$

In this case, the current gain  $n$  is determined by the  $W/L$  ratios of the two FETs rather than by the bipolar emitter-area ratio.

**EXERCISE:** What are the values of  $I_{C1}$  and  $I_{C2}$  and the small-signal parameters for the current mirror in Fig. 16.4 if  $I_{\text{REF}} = 100 \mu\text{A}$ ,  $\beta_{FO} = 50$ ,  $V_A = 50 \text{ V}$ ,  $V_{BE} = 0.7 \text{ V}$ ,  $V_{CE2} = 10 \text{ V}$ , and  $n = 5$ ?

**ANSWERS:**  $89.4 \mu\text{A}$ ;  $529 \mu\text{A}$ ;  $280 \Omega$ ;  $0$ ;  $5.92$ ;  $113 \text{ k}\Omega$

### EXAMPLE 16.3 CALCULATING THE TWO-PORT PARAMETERS OF A CURRENT MIRROR USING SPICE

Transfer function analysis is used to find the two-port parameters of the BJT current mirror.

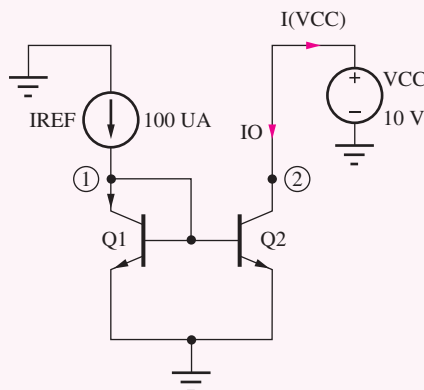
**PROBLEM** Use the transfer function capability of SPICE to find the two-port parameters of the BJT current mirror biased by a reference current of  $100 \mu\text{A}$  and a power supply of  $+10 \text{ V}$ .

**SOLUTION** **Known Information and Given Data:** A current mirror using bipolar transistors;  $I_{\text{REF}} = 100 \mu\text{A}$  and  $V_{CC} = 10 \text{ V}$

**Unknowns:** Output current  $I_O$ ,  $V_{BE}$ ,  $R_{\text{in}}$ ,  $n$ , and  $R_{\text{out}}$  for the current mirror

**Approach:** Construct the circuit using the schematic editor in SPICE. Use the transfer function analysis to find the forward transfer function from  $I_{\text{REF}}$  to  $I(V_{CC})$  and reverse transfer function from  $V_{CC}$  to node 1. The SPICE transfer function analysis automatically calculates three values: the requested transfer function, the resistance at the input source node, and the resistance at the output source node. However, since the output node is connected to  $V_{CC}$ , the output resistance calculated at that node will be zero, and two analyses will be required to find the two-port parameters.

**Assumptions:** Use the current mirror with a single positive supply  $V_{CC}$  biased by current source  $I_{\text{REF}}$ , as shown in the figure here.  $V_A = 50 \text{ V}$ ,  $\beta_{FO} = 100$ , and  $I_S = 0.1 \text{ fA}$ .



**Analysis:** First, we must set the BJT parameters to the desired values: BF = 100, VAF = 50 V, and IS = 0.1 fA. An operating point and two transfer function analyses are used in this example. The first asks for the transfer function from input source  $I_{\text{REF}}$  to output variable  $I(V_{CC})$ . The operating point analysis yields  $V(1) = 0.719$  V and  $I_O = 116 \mu\text{A}$ . The transfer function analysis gives input resistance  $R_{\text{in}} = 259 \Omega$  and current gain  $n = +1.16$ . The second analysis requests the transfer function from voltage source  $V_{CC}$  to node 1. SPICE analysis gives  $R_{\text{out}} = 510 \text{ k}\Omega$ .

**Check of Results:** Based on equation set (16.21) and the operating point results, we expect

$$R_{\text{in}} = 250 \Omega \quad n = +1.16 \quad R_{\text{out}} = 517 \text{ k}\Omega$$

and we see that agreement with theory is very good.

**Discussion:** One should always try to understand and account for the differences between our theory and SPICE. In this example, the input resistance difference can be traced to the use of  $V_T = 25.9$  mV. Be careful not to make a sign error in interpreting the data for  $n$ . A negative sign appears in the SPICE output because of the assumed polarity of  $V_{CC}$  and  $I(V_{CC})$ . Finally, the SPICE model uses  $r_o = (V_A + V_{CB})/I_C = 511 \text{ k}\Omega$ , accounting for the small difference in the values of  $R_{\text{out}}$ .



**EXERCISE:** Use the transfer function capability of SPICE to find the two-port parameters for a MOS current mirror biased by a reference current of 100  $\mu\text{A}$  and a power supply of +10 V. Assume  $K_n = 1 \text{ mA/V}^2$ ,  $V_{TN} = 0.75$  V, and  $\lambda = 0.02/\text{V}$ .

**ANSWERS:**  $I_O = 117 \mu\text{A}$ ,  $V_{GS} = 1.19$  V;  $220 \Omega$ ,  $1.17$ ,  $512 \text{ k}\Omega$

**EXERCISE:** Compare the answers in the previous exercise to hand calculations.

**ANSWERS:**  $I_O = 117 \mu\text{A}$  with  $V_{GS} = 1.20$  V;  $2.24 \text{ k}\Omega$ ,  $1.17$ ,  $513 \text{ k}\Omega$

### 16.2.9 THE WIDLAR CURRENT SOURCE

Resistor  $R$  in the **Widlar**<sup>2</sup> current source circuit shown in the schematic in Fig. 16.13 gives the designer an additional degree of freedom in adjusting the mirror ratio of the current mirror. In this circuit, the difference in the base-emitter voltages of transistors  $Q_1$  and  $Q_2$  appears across resistor  $R$  and determines output current  $I_O$ . Transistor  $Q_3$  buffers the mirror reference transistor in Fig. 16.13(b) to minimize the effect of finite current gain.

An expression for the output current may be determined from the standard expressions for the base-emitter voltage of the two bipolar transistors. In this analysis, we must accurately calculate the individual values of  $V_{BE1}$  and  $V_{BE2}$  because the behavior of the circuit depends on small differences in the values of these two voltages.

Assuming high current gain,

$$V_{BE1} = V_T \ln \left( 1 + \frac{I_{\text{REF}}}{I_{S1}} \right) \cong V_T \ln \frac{I_{\text{REF}}}{I_{S1}} \quad \text{and} \quad V_{BE2} = V_T \ln \left( 1 + \frac{I_O}{I_{S2}} \right) \cong V_T \ln \frac{I_O}{I_{S2}} \quad (16.23)$$

<sup>2</sup> Robert Widlar was a famous IC designer who made many lasting contributions to analog IC design. For examples, see references 3 and 4.

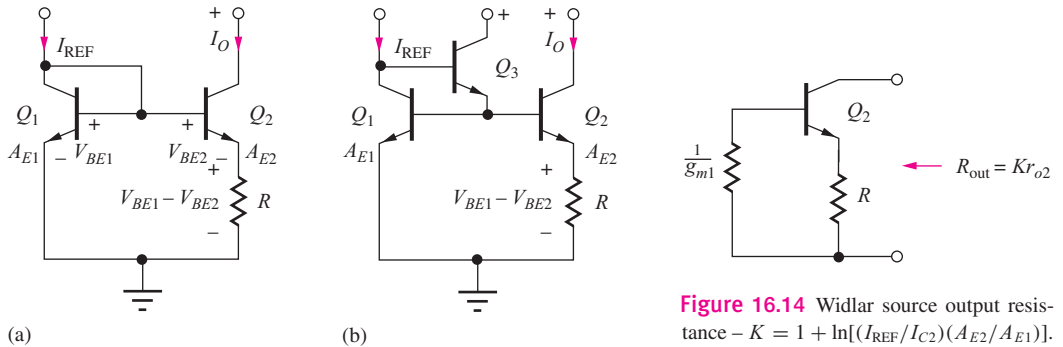


**Figure 16.14** Widlar source output resistance  $-K = 1 + \ln[(I_{\text{REF}}/I_{C2})(A_{E2}/A_{E1})]$ .

**Figure 16.13** (a) Basic Widlar current source and (b) buffered Widlar source.

The current in resistor  $R$  is equal to

$$I_{E2} = \frac{V_{BE1} - V_{BE2}}{R} = \frac{V_T}{R} \ln \left( \frac{I_{\text{REF}} I_{S2}}{I_O I_{S1}} \right) \quad (16.24)$$

If the transistors are matched, then  $I_{S1} = (A_{E1}/A) I_{SO}$  and  $I_{S2} = (A_{E2}/A) I_{SO}$ , and Eq. (16.24) can be rewritten as

$$I_O = \alpha_F I_{E2} \cong \frac{V_T}{R} \ln \left( \frac{I_{\text{REF}} A_{E2}}{I_O A_{E1}} \right) \quad (16.25)$$

If  $I_{\text{REF}}$ ,  $R$ , and the emitter-area ratio are all known, then Eq. (16.25) represents a transcendental equation that must be solved for  $I_O$ . The solution can be obtained by iterative trial and error or utilizing the solver in our calculators.

### Widlar Source Output Resistance

The ac model for the Widlar source in Fig. 16.13(a) represents a common-emitter transistor with resistor  $R$  in its emitter and a small value of  $R_{\text{th}}$  ( $= 1/g_{m1}$ ) from diode  $Q_1$  in its base, as indicated in Fig. 16.14. In normal operation, the voltage developed across resistor  $R$  is usually small ( $\leq 10V_T$ ). By simplifying Eq. (15.114) for this case, we can reduce the output resistance of the source to

$$R_{\text{out}} \cong r_{o2} [1 + g_{m2} R] = r_{o2} \left[ 1 + \frac{I_O R}{V_T} \right] \quad (16.26)$$

in which  $I_O R$  can be found from Eq. (16.25):

$$R_{\text{out}} \cong r_{o2} \left[ 1 + \ln \frac{I_{\text{REF}} A_{E2}}{I_O A_{E1}} \right] = K r_{o2} \quad \text{and} \quad V_{CS} \cong K V_A \quad (16.27)$$

for

$$K = \left[ 1 + \ln \frac{I_{\text{REF}} A_{E2}}{I_O A_{E1}} \right]$$

Using typical values,  $1 < K < 10$ .

**EXERCISE:** What value of  $R$  is required to set  $I_O = 25 \mu\text{A}$  if  $I_{\text{REF}} = 100 \mu\text{A}$  and  $A_{E2}/A_{E1} = 5$ ? What are the values of  $K$  and the output resistance in Eq. (16.27) for this source if  $V_A + V_{CE} = 75 \text{ V}$ ?

**ANSWERS:**  $3000 \Omega$ ;  $12 \text{ M}\Omega$ , 4

**EXERCISE:** Find the output current in the Widlar source if  $I_{\text{REF}} = 100 \mu\text{A}$ ,  $R = 100 \Omega$ , and  $A_{E2} = 10A_{E1}$ . What are the values of  $K$  and the output resistance in Eq. (16.27) for this source if  $V_A + V_{CE} = 75 \text{ V}$ ?

**ANSWERS:** 301  $\mu\text{A}$ ; 551  $\text{k}\Omega$ , 2.20



## ELECTRONICS IN ACTION



### The PTAT Voltage

The voltage developed across resistor  $R$  in Fig. 16.13 represents an extremely useful quantity because it is directly Proportional To Absolute Temperature (referred to as PTAT).  $V_{\text{PTAT}}$  is equal to the difference in the two base-emitter voltages described by Eq. (16.23).

$$V_{\text{PTAT}} = V_{BE1} - V_{BE2} = V_T \ln \left( \frac{I_{C1} A_{E2}}{I_{C2} A_{E1}} \right) = \frac{kT}{q} \ln \left( \frac{I_{C1} A_{E2}}{I_{C2} A_{E1}} \right)$$

and the change of  $V_{\text{PTAT}}$  with temperature is

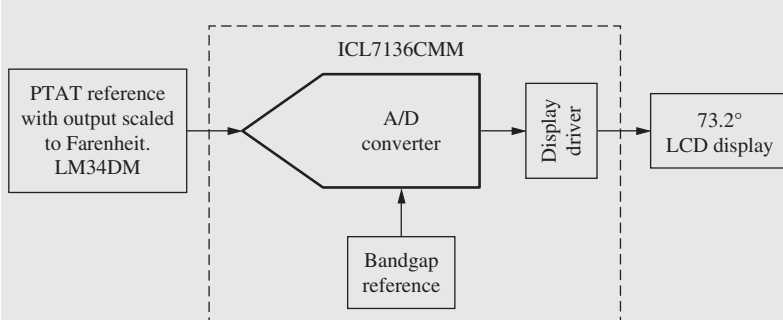
$$\frac{\partial V_{\text{PTAT}}}{\partial T} = +\frac{k}{q} \ln \left( \frac{I_{C1} A_{E2}}{I_{C2} A_{E1}} \right) = +\frac{V_{\text{PTAT}}}{T}$$

For example, suppose  $T = 300 \text{ K}$ ,  $I_{C1} = I_{C2}$  and  $A_{E2} = 10A_{E1}$ . Then  $V_{\text{PTAT}} = 59.6 \text{ mV}$  with a temperature coefficient of slightly less than  $+0.2 \text{ mV/K}$ .

The PTAT voltage developed in the Widlar cell, combined with an analog-to-digital converter, forms the heart of all of today's highly accurate electronic thermometers.

### PTAT Voltage Based Digital Thermometry

The PTAT generator produces a well-defined output voltage that is used in many of today's digital thermometers. One example is shown in the block diagram below that was produced as part of a Senior Design Project at Auburn University. The PTAT output voltage of the LM34DM reference IC is scaled directly to degrees Fahrenheit. This voltage is converted to digital form by the A/D converter in the ICL7136CMM that also contains its own reference generator and circuitry to directly interface with a liquid crystal digital display.



Digital thermometer block diagram.



AU class thermometer.

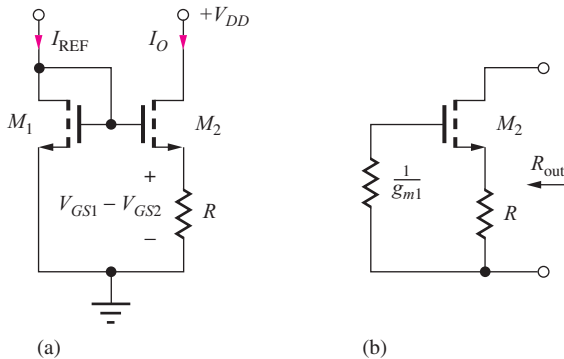


Figure 16.15 (a) MOS Widlar source and (b) small-signal model.

### 16.2.10 THE MOS VERSION OF THE WIDLAR SOURCE

Figure 16.15 is the MOS version of the Widlar source. In this circuit, the difference between the gate-source voltages of transistors \$M\_1\$ and \$M\_2\$ appears across resistor \$R\$, and \$I\_O\$ can be expressed as

$$I_O = \frac{V_{GS1} - V_{GS2}}{R} = \sqrt{\frac{2I_{REF}}{K_{n1}}} - \sqrt{\frac{2I_O}{K_{n2}}} = \frac{1}{R} \sqrt{\frac{2I_{REF}}{K_{n1}}} \left( 1 - \sqrt{\frac{I_O (W/L)_1}{I_{REF} (W/L)_2}} \right) \quad (16.28)$$

If \$I\_O\$ is known, then \$I\_{REF}\$ can be calculated directly from Eq. (16.28). If \$I\_{REF}\$, \$R\$, and the \$W/L\$ ratios are known, then Eq. (16.28) can be written as a quadratic equation in terms of \$\sqrt{I\_O/I\_{REF}}\$:

$$\left( \sqrt{\frac{I_O}{I_{REF}}} \right)^2 + \frac{1}{R} \sqrt{\frac{2}{K_{n1} I_{REF}}} \sqrt{\frac{(W/L)_1}{(W/L)_2}} \left( \sqrt{\frac{I_O}{I_{REF}}} \right) - \frac{1}{R} \sqrt{\frac{2}{K_{n1} I_{REF}}} = 0 \quad (16.29)$$

#### MOS Widlar Source Output Resistance

In Fig. 16.15(b), the small-signal model for the MOS Widlar source is recognized as a common-source stage with resistor \$R\$ in its source. Therefore, from Table 14.9,

$$R_{out} = r_{o2}(1 + g_{m2}R) \cong \mu_{f2}R \quad (16.30)$$

**EXERCISE:** (a) Find the output current in Fig. 16.15(a) if \$I\_{REF} = 200 \mu\text{A}\$, \$R = 2 \text{ k}\Omega\$, and \$K\_{n2} = 10K\_{n1} = 250 \mu\text{A/V}^2\$. (b) What is \$R\_{out}\$ if \$\lambda = 0.02/\text{V}\$ and \$V\_{DS} = 10 \text{ V}\$?

**ANSWERS:** 764 \$\mu\text{A}\$; 176 k\$\Omega\$

## 16.3 HIGH-OUTPUT-RESISTANCE CURRENT MIRRORS

In our introductory discussion of differential amplifiers in Section 15.2, we found that current sources with very high output resistances are needed to achieve good CMRR. The basic current mirrors discussed in the previous sections have a figure of merit \$V\_{CS}\$ equal to \$V\_A\$ or \$1/\lambda\$; that for the Widlar source is typically a few times higher. This section continues our introduction to current mirrors by discussing three additional circuits, the Wilson cascode current sources, which enhance the value of \$V\_{CS}\$ to the order of \$\beta\_o V\_A\$ or \$\mu\_f/\lambda\$, and the regulated cascode source that can achieve an even higher value of \$V\_{CS}\$.

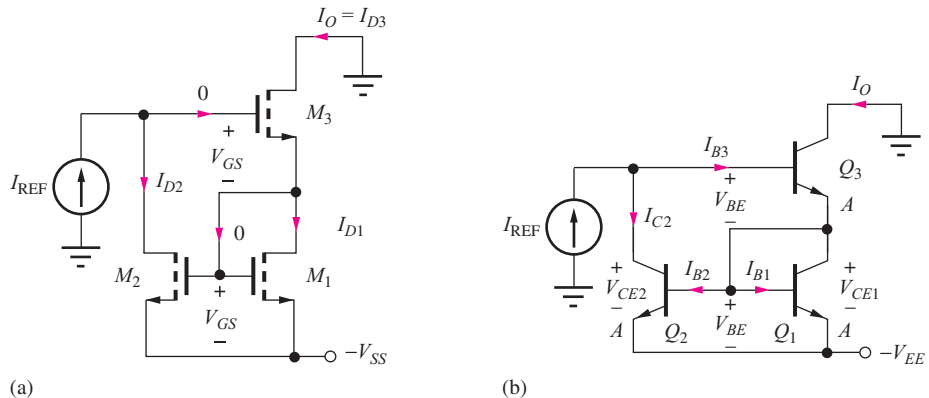


**Figure 16.16** (a) MOS Wilson current source. (b) Original Wilson current source circuit using BJTs.

### 16.3.1 THE WILSON CURRENT SOURCES

The **Wilson current sources** [5] depicted in Fig. 16.16 use the same number of transistors as the buffered current mirror but achieve much higher output resistance; they are often used in applications requiring precisely matched current sources. In the MOS version, the output current is taken from the drain of \$M\_3\$, and \$M\_1\$ and \$M\_2\$ form a current mirror. During circuit operation, the three transistors are all pinched-off and in the active region.

Because the gate current of \$M\_3\$ is zero, \$I\_{D2}\$ must equal reference current \$I\_{REF}\$. If the transistors all have the same \$W/L\$ ratios, then

$$V_{GS3} = V_{GS1} = V_{GS} \quad \text{because } I_{D3} = I_{D1}$$

The current mirror requires

$$I_{D2} = I_{D1} \frac{1 + 2\lambda V_{GS}}{1 + \lambda V_{GS}}$$

and because \$I\_O = I\_{D3}\$ and \$I\_{D3} = I\_{D1}\$, the output current is given by

$$I_O = I_{REF} \frac{1 + \lambda V_{GS}}{1 + 2\lambda V_{GS}} \quad \text{where} \quad V_{GS} \cong V_{TN} + \sqrt{\frac{2I_{REF}}{K_n}} \quad (16.31)$$

For small \$\lambda\$, \$I\_O \cong I\_{REF}\$. For example, if \$\lambda = 0.02/V\$ and \$V\_{GS} = 2\$ V, then \$I\_O\$ and \$I\_{REF}\$ differ by 3.7 percent.

The Wilson source actually appeared first in bipolar form as drawn in Fig. 16.16(b). The circuit operates in a manner similar to the MOS source, except for the loss of current from \$I\_{REF}\$ to the base of \$Q\_3\$ and the current gain error in the mirror formed by \$Q\_1\$ and \$Q\_2\$. Applying KCL at the base of \$Q\_3\$, \$I\_{REF} = I\_{C2} + I\_{B3}\$ in which \$I\_{C2}\$ and \$I\_{B3}\$ are related through the current mirror formed by \$Q\_1\$ and \$Q\_2\$:

$$I_{C2} = \frac{1 + \frac{2V_{BE}}{V_A}}{1 + \frac{V_{BE}}{V_A} + \frac{2}{\beta_{FO}}} I_{E3} = \frac{1 + \frac{2V_{BE}}{V_A}}{1 + \frac{V_{BE}}{V_A} + \frac{2}{\beta_{FO}}} (\beta_{FO} + 1) I_{B3} \quad (16.32)$$

Note in Fig. 16.16(b) that \$V\_{CE1} = V\_{BE}\$ and \$V\_{CE2} = 2V\_{BE}\$.

Solving directly for \$I\_{C3} = \beta\_F I\_{B3}\$ yields a messy expression that is difficult to interpret. However, if we assume the error terms are small, then we can eventually reduce (with considerable effort) the

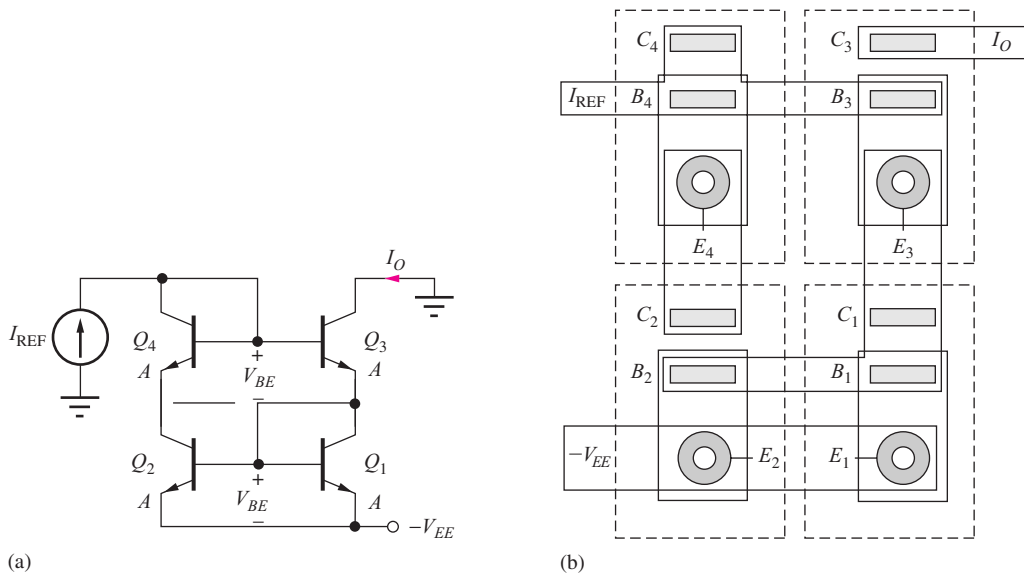


**Figure 16.17** (a) Wilson source using balanced collector-emitter voltages. (b) Layout of Wilson source.

expression to the following approximate result:

$$I_O \cong I_{REF} \frac{1 + \frac{V_{BE}}{V_A}}{1 + \frac{2}{\beta_{FO}(\beta_{FO} + 2)} + \frac{2V_{BE}}{V_A}} \quad (16.33)$$

For \$\beta\_{FO} = 50\$, \$V\_A = 60\$ V, and \$V\_{BE} = 0.7\$ V, the mirror ratio is 0.988. The primary source of error results from the collector-emitter voltage mismatch between transistors \$Q\_1\$ and \$Q\_2\$. The base current error has been reduced to less than 0.1 percent of \$I\_{REF}\$.

The errors due to drain-source voltage mismatch in Fig. 16.16(a), or collector-emitter voltage mismatch in Fig. 16.16(b), may still be too large for use in precision circuits, but this problem can be significantly reduced by adding one more transistor to balance the circuit as in Fig. 16.17. Transistor \$Q\_4\$ reduces the collector-emitter voltage of \$Q\_2\$ by one \$V\_{BE}\$ drop and balances the collector-emitter voltages of \$Q\_1\$ and \$Q\_2\$:

$$V_{CE2} = V_{BE1} + V_{BE3} - V_{BE4} \cong V_{BE}$$

All four transistors are operating at approximately the same value of collector current, and the values of \$V\_{BE}\$ are all the same if the devices are matched with equal emitter areas.

**EXERCISE:** Draw a voltage-balanced version of the MOS Wilson source by adding one additional transistor to the circuit in Fig. 16.16(a).

**ANSWER:** See Fig. P16.42.

### 16.3.2 OUTPUT RESISTANCE OF THE WILSON SOURCE

The primary advantage of the Wilson source over the standard current mirror is its greatly increased output resistance. The small-signal model for the MOS version of the Wilson source is given in Fig. 16.18, in which test current \$i\_x\$ is applied to determine the output resistance.

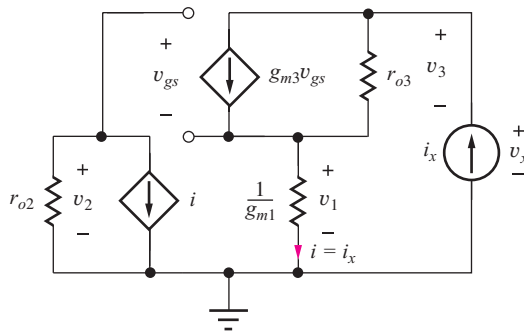


**Figure 16.18** Small-signal model for the MOS version of the Wilson source.

The current mirror formed by transistors  $M_1$  and  $M_2$  is represented by its simplified two-port model assuming  $n = 1$ . Voltage  $v_x$  is determined from

$$v_x = v_3 + v_1 = [i_x - g_{m3}v_{gs}]r_{o3} + v_1 \quad (16.34)$$

where

$$v_{gs} = v_2 - v_1 \quad \text{with} \quad v_1 = \frac{i_x}{g_{m1}} \quad \text{and} \quad v_2 = -\mu_{f2}v_1$$

Combining these equations and recognizing that  $g_{m1} = g_{m2}$  for  $n = 1$  yields

$$R_{\text{out}} = \frac{v_x}{i_x} = r_{o3} \left[ \mu_{f2} + 2 + \frac{1}{\mu_{f2}} \right] \cong \mu_{f2}r_{o3} \quad (16.35)$$

and

$$V_{CS} = I_{D3}\mu_{f2} \frac{1 + \lambda_3 V_{DS3}}{\lambda_3 I_{D3}} \cong \frac{\mu_{f2}}{\lambda_3} \quad (16.36)$$

Analysis of the bipolar source is somewhat more complex because of the finite current gain of the BJT and yields the following result:

$$R_{\text{out}} \cong \frac{\beta_o r_o}{2} \quad \text{and} \quad V_{CS} \cong \frac{\beta_o V_A}{2} \quad (16.37)$$

Derivation of this equation is left for Prob. 16.39.

**EXERCISE:** Calculate  $R_{\text{out}}$  for the Wilson source in Fig. 16.16(b) if  $\beta_F = 150$ ,  $V_A = 50$  V,  $V_{EE} = 15$  V, and  $I_O = I_{\text{REF}} = 50$   $\mu$ A. What is the output resistance of a standard current mirror operating at the same current?

**ANSWER:** 96.6  $\text{M}\Omega$  versus 1.30  $\text{M}\Omega$

**EXERCISE:** Use SPICE to find the output current and output resistance of the Wilson source in the previous exercise.

**ANSWERS:**  $I_O = 49.5$   $\mu$ A;  $118$   $\text{M}\Omega$

### 16.3.3 CASCODE CURRENT SOURCES

In this section, we learn that the output resistance of the cascode connection (C-E/C-B cascade) of two transistors is very high, approaching  $\mu_{f2}r_o$  for the FET case and  $\beta_o r_o / 2$  for the BJT circuit. Figure 16.19 shows the implementation of the MOS and BJT **cascode current sources** using current mirrors.

In the MOS circuit,  $I_{D1} = I_{D3} = I_{\text{REF}}$ . The current mirror formed by  $M_1$  and  $M_2$  forces the output current to be approximately equal to the reference current because  $I_O = I_{D4} = I_{D2}$ .

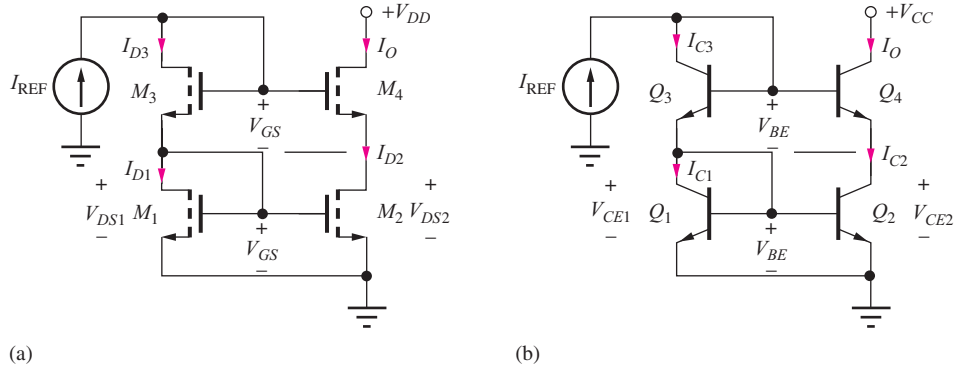


Figure 16.19 (a) MOS and (b) BJT cascode current sources.

Diode-connected transistor \$M\_3\$ provides a dc bias voltage to the gate of \$M\_4\$ and balances \$V\_{DS1}\$ and \$V\_{DS2}\$. If all transistors are matched with the same \$W/L\$ ratios, then the values of \$V\_{GS}\$ are all the same, and \$V\_{DS2}\$ equals \$V\_{DS1}\$:

$$V_{DS2} = V_{GS1} + V_{GS3} - V_{GS4} = V_{GS} \quad \text{and} \quad V_{DS1} = V_{GS}$$

Thus, the \$M\_1\$-\$M\_2\$ current mirror is precisely balanced, and \$I\_O = I\_{\text{REF}}\$.

The BJT source in Fig. 16.19(b) operates in the same manner. For \$\beta\_F = \infty\$, \$I\_{\text{REF}} = I\_{C3} = I\_{C1}\$ on the reference side of the source. \$Q\_1\$ and \$Q\_2\$ form a current mirror, which sets \$I\_O = I\_{C4} = I\_{C2} = I\_{C1} = I\_{\text{REF}}\$. Diode \$Q\_3\$ provides the bias voltage at the base of \$Q\_4\$ needed to keep \$Q\_2\$ in the active region and balances the collector-emitter voltages of the current mirror:

$$V_{CE2} = V_{BE1} + V_{BE3} - V_{BE4} = 2V_{BE} - V_{BE} = V_{BE} = V_{CE1}$$

### 16.3.4 OUTPUT RESISTANCE OF THE CASCODE SOURCES

Figure 16.20 shows the small-signal model for the MOS cascode source; the two-port model has been used for the current mirror formed of transistors \$M\_1\$ and \$M\_2\$. Because current \$i\$ represents the gate current of \$M\_4\$, which is zero, the circuit can be reduced to that on the right in Fig. 16.20, which should be recognized as a common-source stage with resistor \$r\_{o2}\$ in its source. Thus, its output resistance is

$$R_{\text{out}} = r_{o4}(1 + g_{m4}r_{o2}) \cong \mu_{f4}r_{o2} \quad \text{and} \quad V_{CS} \cong \frac{\mu_{f4}}{\lambda_2} \cong \frac{\mu_{f4}}{\lambda_4} \quad (16.38)$$

Analysis of the output resistance of the BJT source in Fig. 16.21 is again more complex because of the finite current gain of the BJT. If the base of \$Q\_4\$ were grounded, then the output resistance would be just equal to that of the cascode stage, \$\beta\_o r\_o\$. However, the base current \$i\_b\$ of \$Q\_4\$ enters the

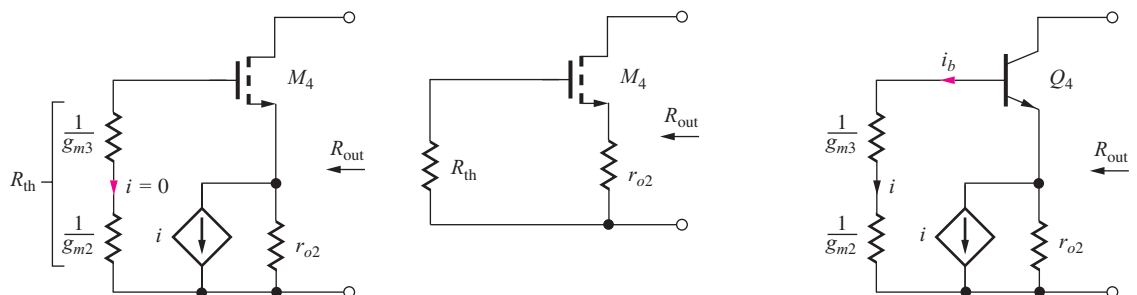


Figure 16.20 Small-signal model for the MOS cascode source.

Figure 16.21 Small-signal model for the BJT cascode source.

current mirror, doubles the output current, and causes the overall output resistance to be reduced by a factor of 2:

$$R_{\text{out}} \cong \frac{\beta_{o4} r_{o4}}{2} \quad \text{and} \quad V_{CS} \cong \frac{\beta_{o4} V_{A4}}{2} \quad (16.39)$$

Detailed calculation of this result is left as Prob. 16.74.

**EXERCISE:** Calculate the output resistance of the MOS cascode current source in Fig. 16.19(a) and compare it to that of a standard current mirror if  $I_O = I_{\text{REF}} = 50 \mu\text{A}$ ,  $V_{DD} = 15 \text{ V}$ ,  $K_n = 250 \mu\text{A/V}^2$ ,  $V_{TN} = 0.8 \text{ V}$ , and  $\lambda = 0.015 \text{ V}^{-1}$ .

**ANSWER:** 379 MΩ versus 1.63 MΩ including all  $\lambda V_{DS}$  terms



**EXERCISE:** Use SPICE to find the output current and output resistance of the cascode current source in the previous exercise.

**ANSWERS:**  $I_O = 50.0 \mu\text{A}$ ; 382 MΩ

**EXERCISE:** Calculate the output resistance of the BJT cascode current source in Fig. 16.19(b) and compare it to that of a standard current mirror if  $I_O = I_{\text{REF}} = 50 \mu\text{A}$ ,  $V_{CC} = 15 \text{ V}$ ,  $\beta_o = 100$ , and  $V_A = 67 \text{ V}$ .

**ANSWER:** 81.3 MΩ versus 1.63 MΩ

### 16.3.5 REGULATED CASCODE CURRENT SOURCE

Another step up in current mirror output resistance can be achieved with the “Regulated Cascode” current source in Fig. 16.22 in which feedback through op amp  $A$  is used to further increase the output resistance. Output current  $I_O$  is set by the basic current mirror formed by  $M_1$  and  $M_2$ . At dc, op amp  $A$  forces the voltage at the source of transistor  $M_2$  to equal  $V_{\text{REF}}$ , whereas variations in the voltage at the source are reduced by the added loop-gain of  $A$ , thereby increasing the output resistance.

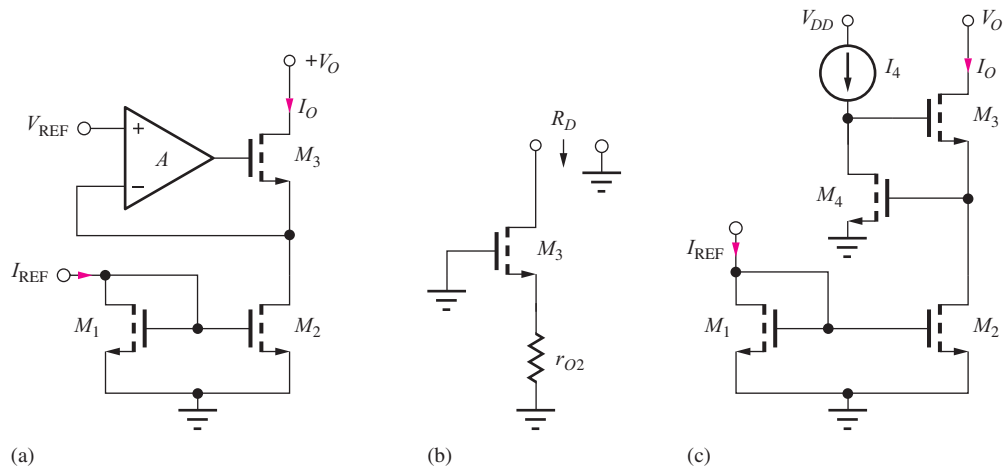


**Figure 16.22** (a) Regulated cascode current source. (b) Small-signal model for  $A = 0$ . (c) Transistor implementation.

We can quickly find the regulated cascode output resistance by applying Blackman's Theorem (see Sec. 11.4.2):

$$R_{\text{out}} = R_D \frac{1 + |T_{SC}|}{1 + |T_{OC}|} \quad (16.40)$$

in which  $R_D$  is the resistance with the feedback loop disabled, and  $T_{OC}$  and  $T_{SC}$  represent the loop-gain with the output terminal open and shorted to ground, respectively. Setting gain  $A$  of the op amp to zero as in Fig. 16.22(b) yields  $R_D = \mu_{f3}r_{o2}$ . With the output terminal open, the drain-source signal current of  $M_2$  will be zero, so  $T_{OC} = 0$ . With the output terminal connected to ac ground,  $T_{SC}$  equals the product of  $A$  and the gain of  $M_3$  acting as a source follower:

$$T_{SC} = A \frac{g_{m3}(r_{o2}\|r_{o3})}{1 + g_{m3}(r_{o2}\|r_{o3})} \cong A \frac{\mu_{f3}/2}{1 + (\mu_{f3}/2)} \cong A \quad \text{and} \quad R_{\text{out}} \cong A\mu_{f3}r_{o2} \quad (16.41)$$

for  $A \gg 1$ . The output resistance is increased by the gain of the amplifier  $A$ .

A common implementation appears in Fig. 16.22(c) where amplifier  $A$  is realized by C-S transistor  $M_4$  with current source load  $I_4$ . In this case  $A = \mu_{f4}$ ,  $R_{\text{out}} = \mu_{f4}\mu_{f3}r_{o2}$  and  $V_{CS} = \mu_f^2/\lambda!$

### 16.3.6 CURRENT MIRROR SUMMARY

Table 16.2 is a summary of the current mirror circuits discussed in this chapter. The cascode and Wilson sources can achieve very high values of  $V_{CS}$  and often find use in the design of differential and operational amplifiers, as well as in many other analog circuits. In the MOS case, it is possible to continue to stack cascode transistors (by adding  $M_5$  and  $M_6$  to the circuit in Fig. 16.19(a)) to further increase the current source output resistance. For instance, a stack of three MOS transistors will give  $R_{\text{out}} = \mu_{f3}\mu_{f2}r_{o1}$ . This does not work in the BJT case because the base current defect is always present in the uppermost transistor. The regulated cascode current source uses additional feedback to increase the output resistance to  $\mu_f^2 r_o$ .

**TABLE 16.2**  
Comparison of the Basic Current Mirrors

TYPE OF SOURCE	$R_{\text{out}}$	$V_{CS}$	TYPICAL VALUES OF $V_{CS}$
Resistor	$R$	$V_{EE}$	15 V
Two-transistor mirror	$r_o$	$V_A$ or $\frac{1}{\lambda}$	75 V
Cascode BJT	$\frac{\beta_o r_o}{2}$	$\frac{\beta_o V_A}{2}$	3750 V
Cascode FET	$\mu_f r_o$	$\frac{\mu_f}{\lambda}$	10,000 V
BJT Wilson	$\frac{\beta_o r_o}{2}$	$\frac{\beta_o V_A}{2}$	3750 V
FET Wilson	$\mu_f r_o$	$\frac{\mu_f}{\lambda}$	10,000 V
Regulated Cascode	$\mu_f^2 r_o$	$\frac{\mu_f^2}{\lambda}$	1,000,000 V

## DESIGN ELECTRONIC CURRENT SOURCE DESIGN

### EXAMPLE 16.4

Design an IC current source to meet a given set of specifications.

**PROBLEM** Design a 1:1 current mirror with a reference current of  $25 \mu\text{A}$  and a mirror ratio error of less than 0.1 percent when the output is operating from a 20-V supply. Devices with these parameters are available:  $\beta_{FO} = 100$ ,  $V_A = 75 \text{ V}$ ,  $I_{SO} = 0.5 \text{ fA}$ ;  $K'_n = 50 \mu\text{A/V}^2$ ,  $V_{TN} = 0.75 \text{ V}$ , and  $\lambda = 0.02/\text{V}$ .

**SOLUTION** **Known Information and Given Data:**  $I_{\text{REF}} = 25 \mu\text{A}$ . A mirror ratio error of less than 0.1 percent requires an output current of  $25 \mu\text{A} \pm 25 \text{ nA}$  when the output voltage is 20 V. Either a bipolar or MOS realization is acceptable.

**Unknowns:** Current source configuration; transistor sizes

**Approach:** The specifications define the required values of  $R_{\text{out}}$  and  $V_{CS}$ . Use this information to choose a circuit topology. Complete the design by choosing device sizes based on the output resistance expressions for the selected circuit topology.

**Assumptions:** Room temperature operation; devices are in the active region of operation.

**Analysis:** The output resistance of the current source must be large enough that 20 V applied across the output does not change (increase) the current by more than 25 nA. Thus, the output resistance must satisfy  $R_{\text{out}} \geq 20 \text{ V}/25 \text{ nA} = 800 \text{ M}\Omega$ . Let us choose  $R_{\text{out}} = 1 \text{ G}\Omega$  to provide some safety margin. The effective current source voltage is then  $V_{CS} = 25 \mu\text{A} (1 \text{ G}\Omega) = 25,000 \text{ V}$ ! From Table 16.2 we see that either a cascode or Wilson source will be required to meet this value of  $V_{CS}$ . In fact, the source must be an MOS version, since our BJTs can at best reach  $V_{CS} = 100(75 \text{ V})/2 = 3750 \text{ V}$ .

The choice between the Wilson and cascode sources is arbitrary at this point. Let us pick the cascode source, which does not involve an internal feedback loop. In order to achieve the small mirror error, a voltage-balanced version is required. Our final circuit choice is therefore the circuit shown in Fig. 16.19(a). Now we must choose the device sizes. In this case, the  $W/L$  ratios are all the same since we require  $\text{MR} = 1$ .

Again referring to Table 16.2, the required amplification factor for the transistor is

$$\mu_f = \lambda V_{CS} = \left( \frac{0.02}{\text{V}} \right) (25,000 \text{ V}) = 500$$

The MOS transistor's amplification factor is given approximately by

$$\mu_f = g_m r_o \cong \sqrt{2K_n I_D} \frac{1}{\lambda I_D}$$

Using  $\mu_f = 500$ ,  $\lambda = 0.02/\text{V}$ , and  $I_D = 25 \mu\text{A}$  gives a value of  $K_n = 1.25 \text{ mS/V}$ . Since  $K_n = K'_n(W/L)$ , we need a  $W/L$  ratio of 25/1 for the given technology. (This  $W/L$  ratio is easy to achieve in integrated circuit form.) In this circuit, all the transistors are operating at the same current, so the  $W/L$  ratios should all be the same size in order to maintain the required voltage balance.

**Check of Results:** Let us check the calculations by directly calculating the output resistance of the source.

$$R_{\text{out}} \cong g_{m4} r_{o4} r_{o2} \quad g_{m4} = \sqrt{2K_n I_D (1 + \lambda V_{DS4})} \quad r_o = \frac{(1/\lambda) + V_{DS}}{I_D}$$

We can either neglect the values of  $V_{DS}$  in these expressions, or we can calculate them. In order to best compare with simulation, let us find  $V_{DS}$  and the corresponding values of  $g_m$  and  $r_o$ .

$$V_{DS2} = V_{GS2} = V_{TN} + \sqrt{\frac{2I_D}{K_n}} = 0.75 + \sqrt{\frac{50 \mu\text{A}}{1.25 \text{ mS}}} = 0.95 \text{ V}$$

$$V_{DS4} = 20 - V_{DS2} = 19.0 \text{ V}$$

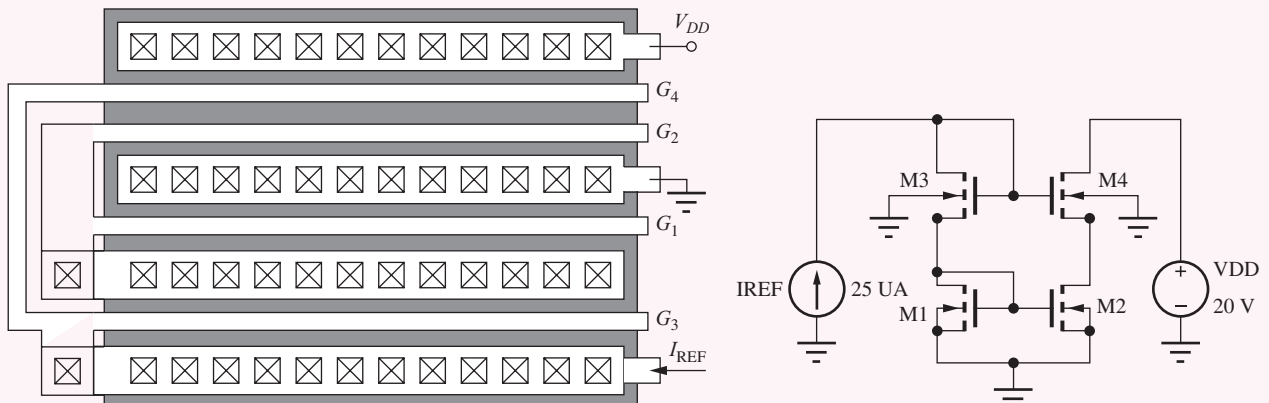
$$g_{m4} = \sqrt{2K_n I_D (1 + \lambda V_{DS4})} = \sqrt{2(1.25 \text{ mA/V}^2)(25 \mu\text{A})[1 + .02(19)]} = 0.294 \text{ mS}$$

$$r_{o2} = \frac{(1/\lambda) + V_{DS2}}{I_D} = \frac{51.0 \text{ V}}{25 \mu\text{A}} = 2.04 \text{ M}\Omega$$

$$r_{o4} = \frac{(1/\lambda) + V_{DS4}}{I_D} = \frac{69.0}{25 \mu\text{A}} = 2.76 \text{ M}\Omega$$

Multiplying the small-signal parameters together produces an output resistance estimate of  $1.65 \text{ G}\Omega$ , which exceeds the design requirement that we originally calculated from the design specifications.

**Discussion:** Note that our ability to set the amplification factor of the MOS transistor was very important in achieving the design goals. In this case  $\mu_{f4} = 811$ . A possible layout for the cascode current source is presented in the figure. The four 25/1 NMOS transistors are stacked vertically.  $G_1$  and  $G_2$  are the gates of the current mirror transistors. Gates  $G_1$  and  $G_3$  are connected directly to their respective drains. The drain of  $M_1$  and the source of  $M_3$  are merged as are those of  $M_2$  and  $M_4$ . However, there are no contacts required to the connection between the drain of  $M_2$  and the source of  $M_4$ .



**Computer-Aided Analysis:** SPICE represents a good way to double check the results. First, we must set the MOS device parameters:  $K_P = 50 \mu\text{A}/\text{V}^2$ ,  $V_{TO} = 0.75 \text{ V}$ ,  $LAMBDA = 0.02/\text{V}$ ,  $W = 25 \mu\text{m}$ , and  $L = 1 \mu\text{m}$ . A dc simulation of the final circuit (shown next) with the given device parameters yields an output current of  $25.014 \mu\text{A}$ . In addition, the voltages at the drains of  $M_1$  and  $M_2$  are  $0.948 \text{ V}$  and  $0.976 \text{ V}$ , respectively, indicating that the voltage balancing is working as desired.

A transfer function analysis from source  $V_{DD}$  to the output node yields an output resistance of  $1.66 \text{ G}\Omega$ , easily meeting the specifications with a satisfactory safety margin. We also have good agreement with the value of  $R_{out}$  that we calculated by hand.

**EXERCISE:** In the SPICE results in Design Ex. 16.4,  $I_O = 25.014 \mu\text{A}$  at  $V_{DD} = 20 \text{ V}$ . If  $R_{out} = 1.66 \text{ G}\Omega$ , what will be the output current at  $V_{DD} = 10 \text{ V}$ ?

**ANSWER:**  $25.008 \mu\text{A}$

**EXERCISE:** What is the minimum value of  $V_{DD}$  for which  $M_4$  remains in the active region of operation?

**ANSWER:**  $1.15 \text{ V}$

**EXERCISE:** Repeat the design in Design Ex. 16.4 for a current source with a mirror ratio of  $2 \pm 0.1$  percent.

**ANSWERS:**  $(W/L)_3 = (W/L)_1 = 25/1$ ;  $(W/L)_4 = (W/L)_2 = 50/1$

## 16.4 REFERENCE CURRENT GENERATION

A **reference current** is required by all the current mirrors that have been discussed. The least complicated method for establishing this reference current is to use resistor  $R$ , as shown in Fig. 16.23(a).

However, the source's output current is directly proportional to the supply voltage  $V_{EE}$ :

$$I_{REF} = \frac{V_{EE} - V_{BE}}{R} \quad (16.42)$$

In MOS technology, the gate-source voltages of MOSFETs can be designed to be large, and several MOS devices can be connected in series between the power supplies to eliminate the need for large-value resistors. An example of this technique is given in Fig. 16.23(b), in which

$$V_{DD} + V_{SS} = V_{SG4} + V_{GS3} + V_{GS1}$$

and the drain currents must satisfy  $I_{D1} = I_{D3} = I_{D4}$ . However, any change in the supply voltages directly alters the values of the gate-source voltages of the three MOS transistors and again changes the reference current. Note that the series device technique is not usable in bipolar technology because of the small fixed voltage ( $\approx 0.7 \text{ V}$ ) developed across each diode, as well as the exponential relationship between voltage and current in the diode.

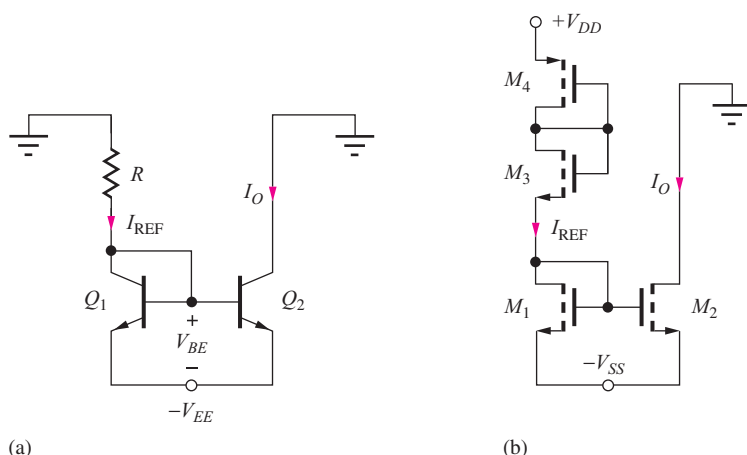


**Figure 16.23** Reference current generation for current mirrors: (a) resistor reference and (b) series-connected MOSFETs.

**EXERCISE:** What is the reference current in Fig. 16.23(a) if  $R = 43 \text{ k}\Omega$  and  $V_{EE} = -5 \text{ V}$ ? (b) If  $V_{EE} = -7.5 \text{ V}$ ?

**ANSWERS:** 100  $\mu\text{A}$ ; 158  $\mu\text{A}$

**EXERCISE:** What is the reference current in Fig. 16.23(b) if  $K_n = K_p = 400 \text{ }\mu\text{A/V}^2$ ,  $V_{TN} = -V_{TP} = 1 \text{ V}$ ,  $V_{DD} = 0$ , and  $V_{SS} = -5 \text{ V}$ ? (b) If  $V_{SS} = -7.5 \text{ V}$ ?

**ANSWERS:** 88.9  $\mu\text{A}$ ; 450  $\mu\text{A}$ . (Note: the variation is worse than in the resistor bias case because of the square-law MOSFET characteristic.)

## 16.5 SUPPLY-INDEPENDENT BIASING

In most cases, a supply voltage dependence of  $I_{\text{REF}}$  is undesirable. For example, we would like to fix the bias points of the devices in general-purpose op amps, even though they must operate from power supply voltages ranging from  $\pm 3 \text{ V}$  to  $\pm 22 \text{ V}$ . In addition, Eq. (16.42) indicates that relatively large values of resistance are required to achieve small operating currents, and these resistors use significant area in integrated circuits, as was discussed in detail in Sec. 6.5.9. Thus, a number of circuit techniques that yield currents relatively independent of the power supply voltages have been invented.

### 16.5.1 A $V_{BE}$ -BASED REFERENCE

One possibility is the  $V_{BE}$ -based reference, shown in Fig. 16.24, in which the output current is determined by the base-emitter voltage of  $Q_1$ . For high current gain, the collector current of  $Q_1$  is equal to the current through resistor  $R_1$ ,

$$I_{C1} = \frac{V_{EE} - V_{BE1} - V_{BE2}}{R_1} \cong \frac{V_{EE} - 1.4 \text{ V}}{R_1} \quad (16.43)$$

and the output current  $I_O$  is approximately equal to the current in  $R_2$ :

$$I_O = \alpha_{F2} I_{E2} = \alpha_{F2} \left( \frac{V_{BE1}}{R_2} + I_{B1} \right) \cong \frac{V_{BE1}}{R_2} \cong \frac{0.7 \text{ V}}{R_2} \quad (16.44)$$

Rewriting  $V_{BE1}$  in terms of  $V_{EE}$ ,

$$I_O \cong \frac{V_T}{R_2} \ln \frac{V_{EE} - 1.4 \text{ V}}{I_{S1} R_1} \quad (16.45)$$

A substantial degree of supply-voltage independence has been achieved because the output current is only logarithmically dependent on changes in the supply voltage  $V_{EE}$ . However, the output current is temperature dependent due to the temperature coefficients of both  $V_{BE}$  and resistor  $R$ .

**EXERCISE:** (a) Calculate  $I_O$  in Fig. 16.24 for  $I_S = 10^{-16} \text{ A}$ ,  $R_1 = 39 \text{ k}\Omega$ ,  $R_2 = 6.8 \text{ k}\Omega$ , and  $V_{EE} = -5 \text{ V}$ . Assume infinite current gains. (b) Repeat for  $V_{EE} = -7.5 \text{ V}$ .

**ANSWERS:** 101  $\mu\text{A}$ ; 103  $\mu\text{A}$

### 16.5.2 THE WIDLAR SOURCE

Actually, we already discussed another source that achieves a similar independence from power supply voltage variations. The expression for the output current of the Widlar source given in Fig. 16.13 and Eq. (16.25) is

$$I_O = \alpha_F I_{E2} \cong \frac{V_T}{R} \ln \left( \frac{I_{\text{REF}}}{I_O} \frac{A_{E2}}{A_{E1}} \right) \quad (16.46)$$

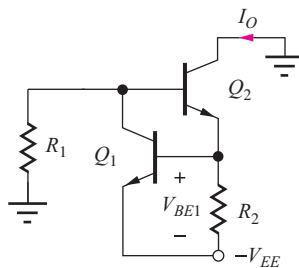
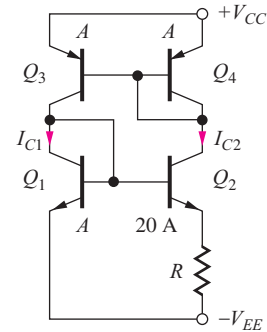
Figure 16.24  $V_{BE}$ -based current source.

Figure 16.25 Power-supply-independent bias circuit using the Widlar source and a current mirror.

Here again, the output current is only logarithmically dependent on the reference current  $I_{REF}$  (which may be proportional to  $V_{CC}$ ).

### 16.5.3 POWER-SUPPLY-INDEPENDENT BIAS CELL

Bias circuits with an even greater degree of power supply voltage independence can be obtained by combining the Widlar source with a standard current mirror, as indicated in the circuit in Fig. 16.25. Assuming high current gain, the *pnp* current mirror forces the currents on the two sides of the reference cell to be equal — that is,  $I_{C1} = I_{C2}$ . In addition, the emitter-area ratio of the Widlar source in Fig. 16.25 is equal to 20.

With these constraints, Eq. (16.46) can be satisfied by an operating point of

$$I_{C2} \cong \frac{V_T}{R} \ln(20) = \frac{0.0749 \text{ V}}{R} \quad (16.47)$$

In this example, a fixed voltage of approximately 75 mV is developed across resistor  $R$ , and this voltage is independent of the power supply voltages. Resistor  $R$  can then be chosen to yield the desired operating current.

Obviously, a wide range of mirror ratios and emitter-area ratios can be used in the design of the circuit in Fig. 16.25. Although the current, once established, is independent of supply voltage, the actual value of  $I_C$  still depends on temperature, as well as the absolute value of  $R$  and varies with run-to-run process variations.

Unfortunately,  $I_{C1} = I_{C2} = 0$  is also a stable operating point for the circuit in Fig. 16.25. **Start-up circuits** must be included in IC realizations of this reference to ensure that the circuit reaches the desired operating point.

**EXERCISE:** Find the output current in the current source in Fig. 16.25 if  $A_{E3} = 10A_{E4}$ ,  $A_{E2} = 10A_{E1}$ , and  $R = 1 \text{ k}\Omega$ .

**ANSWER:** 115  $\mu\text{A}$

**EXERCISE:** What is the minimum power supply voltage for proper operation of the supply-independent bias circuit in Fig. 16.25?

**ANSWER:**  $2V_{BE} \cong 1.4 \text{ V}$

Once the current has been established in the reference cell consisting of  $Q_1-Q_4$  in Fig. 16.25, the base-emitter voltages of  $Q_1$  and  $Q_4$  can be used as reference voltages for other current mirrors, as shown in Fig. 16.26. In this figure, buffered current mirrors have been used in the reference cell to

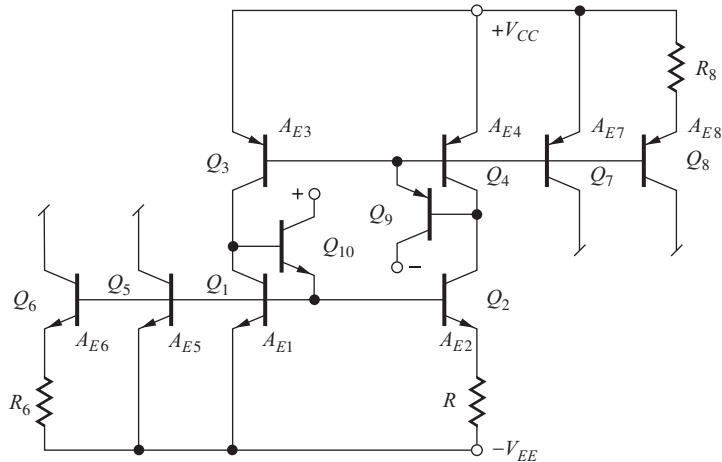


**Figure 16.26** Multiple source currents generated from the supply-independent cell.

minimize errors associated with finite current gains of the *npn* and *pnp* transistors. Output currents are shown generated from basic mirror transistors  $Q_5$  and  $Q_7$  and from Widlar sources,  $Q_6$  and  $Q_8$ .

#### 16.5.4 A SUPPLY-INDEPENDENT MOS REFERENCE CELL

The MOS analog of the circuit in Fig. 16.25 appears in Fig. 16.27. In this circuit, the PMOS current mirror forces a fixed relationship between drain currents  $I_{D3}$  and  $I_{D4}$ . For the particular case in Fig. 16.27,  $I_{D3} = I_{D4}$ , and so  $I_{D1} = I_{D2}$ . Substituting this constraint into Eq. (16.28) yields an equation for the value of  $R$  required to establish a given current  $I_{D2}$ :

$$R = \sqrt{\frac{2}{K_{n1}I_{D2}}} \left( 1 - \sqrt{\frac{(W/L)_1}{(W/L)_2}} \right) \quad (16.48)$$

Based on Eq. (16.48), we see that the MOS source is independent of supply voltage but is a function of the absolute values of  $R$  and  $K'_n$ .

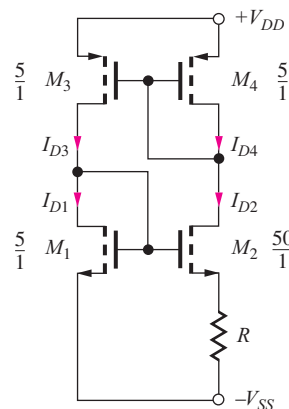


**Figure 16.27** Supply-independent current source using MOS transistors.

**EXERCISE:** What value of  $R$  is required in the current source in Fig. 16.27 if  $I_{D2}$  is to be designed to be  $100 \mu\text{A}$  and  $K'_n = 25 \mu\text{A/V}^2$ ?

**ANSWER:**  $8.65 \text{k}\Omega$

## DESIGN REFERENCE CURRENT DESIGN

### EXAMPLE 16.5

Design a supply-independent current source using bipolar technology.

**PROBLEM** Design a supply-independent current source to provide an output current of  $45 \mu\text{A}$  at  $T = 300 \text{ K}$  using the circuit topology in Fig. 16.25 with symmetrical 5-V power supplies. The circuit should use no more than  $1 \text{k}\Omega$  of resistance or  $60 \mu\text{A}$  of total current. Use SPICE to determine the sensitivity of the design current to power supply voltage variations. Assume that a unit-area BJT has the following parameters:  $\beta_{FO} = 100$ ,  $V_A = 75 \text{ V}$ , and  $I_{SO} = 0.1 \text{ fA}$  for both  $npn$  and  $pnp$  transistors.

**SOLUTION** **Known Information and Given Data:** Circuit topology in Fig. 16.26,  $\beta_{FO} = 100$ ,  $V_A = 75 \text{ V}$ ,  $I_{SO} = 0.1 \text{ fA}$ . Total current  $\leq 60 \mu\text{A}$ .

**Unknowns:**  $R$  and the area ratio between  $Q_1$  and  $Q_2$ ; power supply sensitivity

**Approach:** The current in the circuit is described by Eq. (16.46). Use the maximum resistance values to select the area ratio. Select a current ratio in the sides of the reference to satisfy the total supply current requirement.

**Assumptions:** Transistors operate in the active region.  $I_{C2} = 45 \mu\text{A}$ .

**Analysis:** At  $T = 300 \text{ K}$  and  $V_T = 25.88 \text{ mV}$ , and from Eq. (16.46), we have

$$\ln\left(\frac{I_{C1}}{I_{C2}} \frac{A_{E2}}{A_{E1}}\right) = \frac{I_{C2}R}{V_T} \leq \frac{(45 \mu\text{A})(1 \text{k}\Omega)}{25.88 \text{ mV}} = 1.739 \quad \text{or} \quad \frac{I_{C1}}{I_{C2}} \frac{A_{E2}}{A_{E1}} \leq 5.69$$

In addition, the maximum current specification requires

$$\frac{I_{C2}}{I_{C1}} \geq \frac{45 \mu\text{A}}{15 \mu\text{A}} = \frac{3}{1}$$

Let's choose  $I_{C2} = 5I_{C1}$ . Then  $A_{E2}/A_{E1} \leq 28.45$ . Choosing  $A_{E2}/A_{E1} = 20$ , we obtain

$$R = \frac{25.88 \text{ mV} \ln(4)}{45 \mu\text{A}} = 797 \Omega$$

The final design is  $R = 797 \Omega$ ,  $A_{E1} = A$ ,  $A_{E2} = 20 A$ ,  $A_{E3} = A$ ,  $A_{E4} = 5 A$  with  $35.88 \text{ mV}$  across resistor  $R$ .

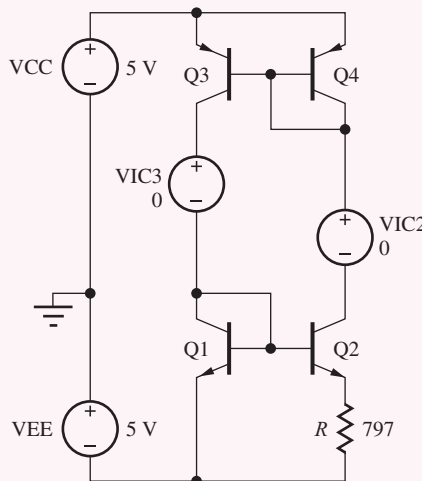
**Check of Results:** Since we need to use SPICE to find the power supply sensitivity, let us use it to also check our design.

**Computer-Aided Analysis:** The circuit shown is drawn using the schematic editor. Zero-valued sources  $V_{IC2}$  and  $V_{IC3}$  function as ammeters to measure the collector currents of transistors  $Q_2$  and  $Q_3$ . First we must remember to set the  $npn$  and  $pnp$  BJT parameters to  $\text{BF} = 100$ ,  $\text{VAF} = 75 \text{ V}$ ,  $\text{IS} = 0.1 \text{ fA}$ , and  $\text{TEMP} = 27 \text{ C}$ . We must also specify  $\text{AREA} = 1$ ,  $\text{AREA} = 20$ ,  $\text{AREA} = 1$  and  $\text{AREA} = 5$  for  $Q_1$  through  $Q_4$ , respectively. SPICE then gives  $I_{C2} = 49.6 \mu\text{A}$  and  $I_{C3} = 10.94 \mu\text{A}$  with  $39.89 \text{ mV}$  across  $R$ . The currents and voltage are slightly higher than predicted, and this is

primarily due to having neglected the mirror ratio error due to the different values of  $V_{EC4}$  and  $V_{EC3}$ . (Try the exercise after this example.) We can correct for this error by modifying the emitter area ratio:

$$A_{E4} = 5 \left( 1 + \frac{V_{EC3} - V_{EC4}}{V_A} \right) = 5 \left( 1 + \frac{9.34 - 0.65}{75} \right) = 5.58$$

SPICE now yields  $I_{C2} = 45.9 \mu\text{A}$ ,  $I_{C3} = 9.08 \mu\text{A}$ , and  $V_{E2} = 36.9 \text{ mV}$ . A transfer function analysis from  $V_{CC}$  to  $V_{IC2}$  gives a total output resistance of  $928 \text{ k}\Omega$  for the current source, and the sensitivity of  $I_{C2}$  to changes in  $V_{CC}$  is  $0.808 \mu\text{A/V}$ .



**Discussion:** The current source meets the specifications.

**EXERCISE:** Explore the errors caused by finite current gain and Early voltage by simulating the circuit with  $BF = 10,000$  and  $VAF = 10,000 \text{ V}$ . What are the new values of  $I_{C2}$ ,  $I_{C3}$ , and the voltage developed across  $R$ ?

**ANSWERS:**  $45.0 \mu\text{A}$ ;  $9.01 \mu\text{A}$ ;  $35.88 \text{ mV}$

**EXERCISE:** What are the new design values if we choose  $A_{E2}/A_{E1} = 25$ ?

**ANSWERS:**  $R = 925 \Omega$ ;  $A_{E1} = A$ ;  $A_{E2} = 25 A$ ;  $A_{E3} = A$ ;  $A_{E4} = 5.57 A$

## 16.6 THE BANDGAP REFERENCE

Precision voltage references need to not only be independent of power supply voltage, but also be independent of temperature. Although the circuits described in Sec. 16.5 can produce reference currents and voltages that are substantially independent of power supply voltage, they all still vary with temperature. Robert Widlar solved this problem with his invention of the elegant bandgap reference circuit, and today, the bandgap reference is the most common technique used to generate a precision voltage. It has supplanted Zener reference diodes in the majority of applications.

Based on his detailed understanding of bipolar transistor characteristics, Widlar realized that the negative temperature coefficient associated with the base-emitter junction could be canceled out

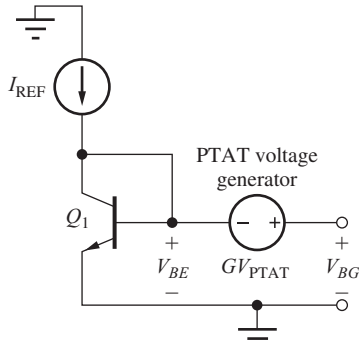


**Figure 16.28** Concept for the bandgap reference.

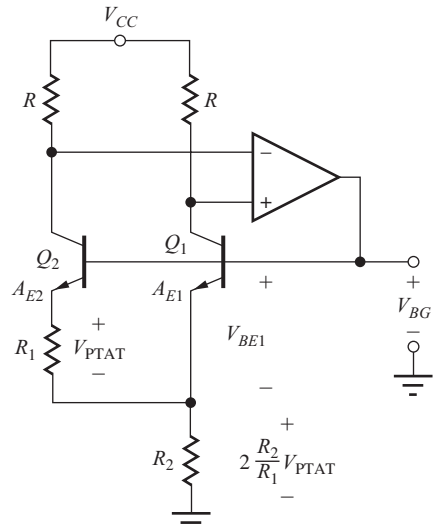


**Figure 16.29** Brokaw version of the bandgap reference.

by the positive temperature dependence of a voltage that is **Proportional to Absolute Temperature** (PTAT) as depicted conceptually in Fig. 16.28. He knew that a PTAT voltage is available from the difference between two base-emitter voltages:

$$V_{\text{PTAT}} = V_{BE1} - V_{BE2} = V_T \ln \left( \frac{I_{C1} A_{E2}}{I_{C2} A_{E1}} \right) = \frac{kT}{q} \ln \left( \frac{I_{C1} A_{E2}}{I_{C2} A_{E1}} \right) \quad (16.49)$$

The output voltage of the circuit in Fig. 16.28 can be written as

$$V_{BG} = V_{BE} + G V_{\text{PTAT}} \quad (16.50)$$

We desire this output voltage to have a zero temperature coefficient:

$$\frac{\partial V_{BG}}{\partial T} = \frac{\partial V_{BE}}{\partial T} + G \frac{\partial V_{\text{PTAT}}}{\partial T} = 0 \quad (16.51)$$

The dependence of  $V_{BE}$  on temperature was developed previously in Eqs. (3.14–3.15) and  $\partial V_{\text{PTAT}}/\partial T = V_{\text{PTAT}}/T$ . Substituting these values into Eq. (16.51) gives

$$\frac{\partial V_{BG}}{\partial T} = \frac{V_{BE} - V_{GO} - 3V_T}{T} + G \frac{V_{\text{PTAT}}}{T} = 0 \quad \text{or} \quad G V_{\text{PTAT}} = V_{GO} + 3V_T - V_{BE} \quad (16.52)$$

where  $V_{GO}$  is the silicon bandgap voltage at 0 K (1.12 V). Substituting this result into Eq. (16.52) reduces the output voltage to

$$V_{BG} = V_{GO} + 3V_T \quad (16.53)$$

The output voltage at which zero temperature coefficient is achieved is slightly above the bandgap voltage of silicon. Hence, this circuit is referred to as a “bandgap reference.” At room temperature, the output voltage is approximately 1.20 V.

A circuit realization of the bandgap reference is shown in Fig. 16.29. This circuit is attributed to another talented designer, Paul Brokaw of Analog Devices [7], and is easier to understand than the original circuit of Widlar. In this case, the output voltage is equal to the sum of the base-emitter voltage of  $Q_1$  plus the voltage across resistor  $R_2$ , which is a scaled replica of the PTAT voltage being developed across resistor  $R_1$ . The scaling factor is controlled by the op amp and resistors  $R$ .

The ideal op amp forces the voltage across the two matched collector resistors to be the same, thereby setting  $I_{C2} = I_{C1}$  and  $I_{E2} = I_{E1}$ . Thus the PTAT voltage is equal to  $V_T \ln(A_{E2}/A_{E1})$ , and the emitter current of  $Q_2$  equals  $V_{\text{PTAT}}/R_1$ . The current in  $R_2$  is twice that in  $R_1$ , since  $I_{E2} = I_{E1}$ .

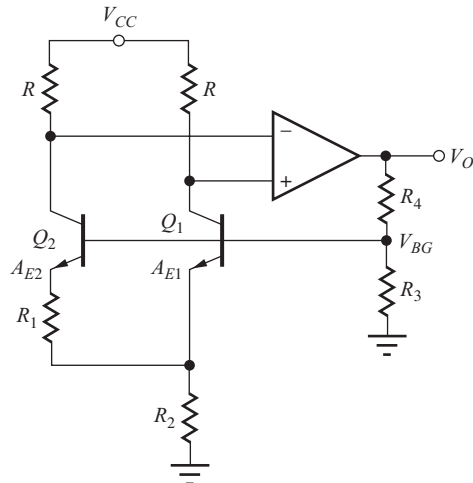


**Figure 16.30** Bandgap reference with  $V_O > V_{BG}$ .

Combining these results yields an expression for the output voltage  $V_{BG}$ :

$$V_{BG} = V_{BE1} + 2 \frac{R_2}{R_1} V_T \ln \frac{A_{E2}}{A_{E1}} \quad (16.54)$$

For this circuit, the gain  $G = 2R_2/R_1$ , and based on Eq. (16.52), the resistor ratio is given by

$$\frac{R_2}{R_1} = -\frac{1}{2} \frac{\frac{\partial V_{BE1}}{\partial T}}{\frac{\partial V_{PTAT}}{\partial T}} = \frac{V_{GO} + 3V_T - V_{BE1}}{2V_{PTAT}} \quad (16.55)$$

Often we want an output voltage that is not equal to 1.2 V, and other voltages are easy to achieve by adding a two-resistor voltage divider to the Brokaw circuit as in Fig. 16.30. In this case the op amp output voltage becomes

$$V_O = \left(1 + \frac{R_4}{R_3}\right) V_{BG} \quad (16.56)$$

which can be scaled up to any desired value (e.g., 2.5 or 5 V).

A word of caution is needed here. In most bandgap reference designs, zero-output voltage is a valid operating point, and some additional circuitry must be added to ensure that the circuit “starts up” and reaches the desired operating point. In many simple circuit cases, SPICE will have considerable difficulty converging to the desired operating point.

## DESIGN BANDGAP REFERENCE DESIGN

### EXAMPLE 16.6

Design of the bandgap reference requires a slightly different sequence of calculations than the analysis in the previous example.

**PROBLEM** Design the bandgap reference in Fig. 16.30 to produce an output voltage of 5.000 V with zero temperature coefficient at a temperature of 47°C. Design for a collector current of 25 μA, and assume  $I_S = 0.5$  fA.

**SOLUTION** **Known Information and Given Data:** The circuit is the Brokaw reference with amplified output given in Fig. 16.30.  $V_O = 5.000$  V with a zero temperature coefficient (TC) at  $T = 320$  K. Collector currents are to be  $25 \mu\text{A}$ , and the transistor saturation current is  $0.5 \text{ fA}$ .

**Unknowns:** Values of resistors  $R$ ,  $R_1$ ,  $R_2$ ,  $R_3$ , and  $R_4$

**Approach:** Find  $V_T$  and  $V_{\text{PTAT}}$ . Then use  $I_C$  to determine  $R_1$ . Use  $I_C$  to find  $V_{BE1}$ . Determine  $R_2$  using Eq. (16.55). Choose  $R_3$  and  $R_4$  to set  $V_O = 5$  V. Choose  $R$  to provide operating voltage to the op amp.

**Assumptions:** BJTs are in the active region of operation.  $\beta_{FO} = \infty$  and  $V_A = \infty$ .  $A_{E2} = 10A_{E1}$  represents a reasonable emitter area ratio. Drop 2 V across  $R$ .

**Analysis:** Because of the precision involved, we will carry four digits in our calculations.

$$V_T = \frac{kT}{q} = \frac{1.380 \times 10^{-23}(320)}{1.602 \times 10^{-19}} = 27.57 \text{ mV}$$

$$V_{\text{PTAT}} = V_T \ln \left( \frac{A_{E2}}{A_{E1}} \right) = V_T \ln(10) = 63.47 \text{ mV}$$

$$R_1 = \frac{V_{\text{PTAT}}}{I_E} = \frac{63.47 \text{ mV}}{25 \mu\text{A}} = 2.539 \text{ k}\Omega$$

$$V_{BE1} = V_T \ln \left( \frac{I_{C1}}{I_{S1}} \right) = (27.57 \text{ mV}) \ln \left( \frac{25 \mu\text{A}}{0.5 \text{ fA}} \right) = 0.6792 \text{ V}$$

$$\frac{R_2}{R_1} = \frac{V_{GO} + 3V_T - V_{BE1}}{2V_{\text{PTAT}}} = \frac{1.12 + 3(0.02757) - 0.6792}{2(0.06347)} = 4.124$$

$$R_2 = 4.124R_1 = 10.47 \text{ k}\Omega$$

$$V_{BG} = V_{BE1} + 2 \frac{R_2}{R_1} V_{\text{PTAT}} = 0.6792 + 2(4.124)(63.47 \text{ mV}) = 1.203 \text{ V}$$

$$\frac{R_4}{R_3} = \frac{V_O}{V_{BG}} - 1 = 3.157$$

We should not waste an excessive amount of current in the output voltage divider, so let us choose  $I_3 = I_4 = 50 \mu\text{A}$ . Also, set the voltage drop across  $R$  to 2 V.

$$R_3 = \frac{V_{BG}}{I_3} = \frac{1.203 \text{ V}}{50 \mu\text{A}} = 24.0 \text{ k}\Omega \quad \text{and} \quad R_4 = \frac{V_O - V_{BG}}{I_3} = \frac{3.797 \text{ V}}{50 \mu\text{A}} = 75.9 \text{ k}\Omega$$

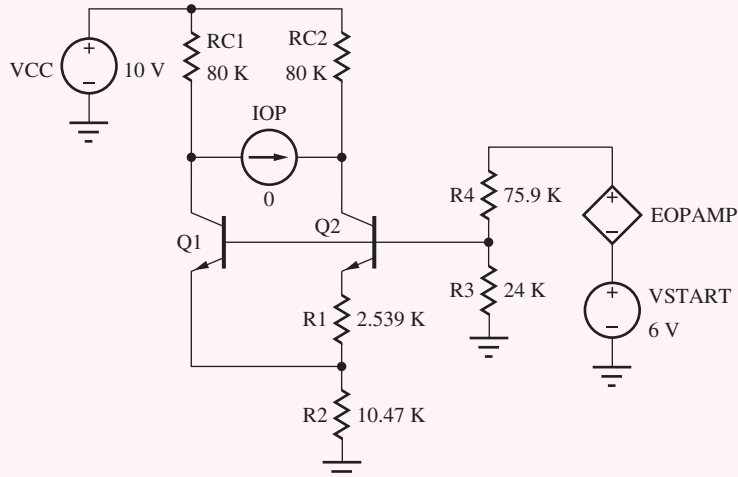
$$R = \frac{2 \text{ V}}{25 \mu\text{A}} = 80 \text{ k}\Omega$$

**Check of Results:**  $V_{BG}$  is approximately 1.20 V so our calculation appears correct. Our analysis showed that the output voltage should also be  $V_{GO} + 3V_T = 1.203$  V, which also checks.

**Discussion:** Note that the voltage drop across the collector resistors must be enough to bring the inputs of the op amp into its common-mode operating range. In this circuit, the drop across the collector resistors is designed to be 2 V.

**Computer-Aided Analysis:** We first set the *n*p*n* parameters to BF = 10,000 and IS = 0.5 fA and let VAF default to infinity. Set AREA = 1 for  $Q_1$ , AREA = 10 for  $Q_2$ , and TEMP = 47°C. In the circuit shown here, the ideal op amp is modeled by EOPAMP whose controlling voltage

appears across zero-value current source IOP. The gain is set to  $10^6$ . Source VSTART may be needed in some versions of SPICE to help the circuit start up. Another help is to sweep VCC from 0 to 10 V. (Remember that  $V_O = 0$  is a valid operating point.) SPICE simulation produces  $V_{BG} = 1.204$  V and  $V_{PTAT} = 63.52$  mV and  $V_O = 5.01$  V. With BF = 100 and VAF = 75 V, the values are  $V_{BG} = 1.201$  V and  $V_{PTAT} = 63.52$  mV and  $V_O = 5.03$  V.



**EXERCISE:** Redesign the reference in Ex. 16.6 using  $A_{E2} = 20A_{E1}$ .

**ANSWER:**  $3.17\text{ k}\Omega$ ,  $10.5\text{ k}\Omega$ ,  $24.0\text{ k}\Omega$ ,  $75.9\text{ k}\Omega$ ,  $80\text{ k}\Omega$

## 16.7 THE CURRENT MIRROR AS AN ACTIVE LOAD

We encountered use of transistors as replacements for the load resistors in amplifiers in Chapters 14 and 15. In this section, we find that one of the most important applications of the current mirror<sup>3</sup> is as a replacement for the load resistors of differential amplifier stages in IC operational amplifiers. This elegant application of the current mirror can greatly improve amplifier voltage gain while maintaining the operating-point balance necessary for good common-mode rejection and low offset voltage. When used in this manner, the current mirror is referred to as an **active load** because the passive load resistors have been replaced with active transistor circuit elements.

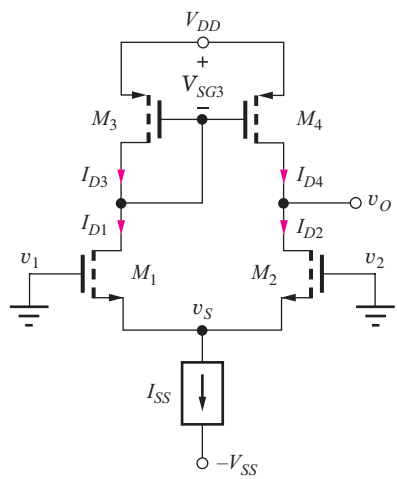
### 16.7.1 CMOS DIFFERENTIAL AMPLIFIER WITH ACTIVE LOAD

Figure 16.31 shows a CMOS differential amplifier with an active load; the load resistors have been replaced by a PMOS current mirror. Let us first study the quiescent operating point of this circuit and then look at its small-signal characteristics.

#### dc Analysis

Assume for the moment that the amplifier is voltage balanced (in fact, it will turn out that it *is* balanced). Then bias current  $I_{SS}$  divides equally between transistors  $M_1$  and  $M_2$ , and  $I_{D1}$  and  $I_{D2}$  are each equal to  $I_{SS}/2$ . Current  $I_{D3}$  must equal  $I_{D1}$  and is mirrored as  $I_{D4}$  at the output of the PMOS

<sup>3</sup> In addition to its role as a current source.



**Figure 16.31** CMOS differential amplifier with PMOS active load.

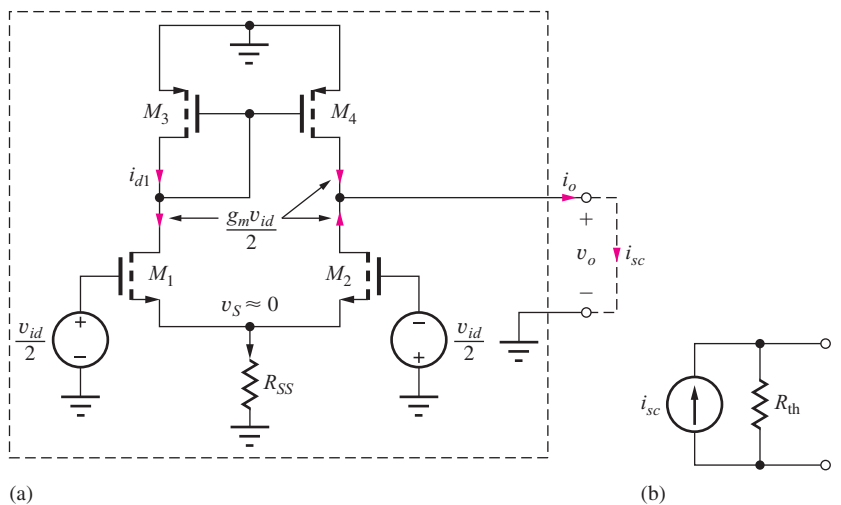


**Figure 16.32** (a) CMOS differential amplifier with differential-mode input. (b) The circuit is a one port and can be represented by its Norton equivalent circuit.

current mirror. Thus,  $I_{D3}$  and  $I_{D4}$  are also equal to  $I_{SS}/2$ , and the current in the drain of  $M_4$  is exactly the current required to satisfy  $M_2$ .

The mirror ratio set by  $M_3$  and  $M_4$  is precisely unity when  $V_{SD4} = V_{SD3}$  and hence  $V_{DS1} = V_{DS2}$ . Thus, the differential amplifier is completely balanced at dc when the quiescent output voltage is

$$V_O = V_{DD} - V_{SD4} = V_{DD} - V_{SG3} = V_{DD} - \left( \sqrt{\frac{I_{SS}}{K_p}} - V_{TP} \right) \quad (16.57)$$

### Q-Points

The drain-source voltages of  $M_1$  and  $M_2$  are

$$V_{DS1} = V_O - V_S = V_{DD} - \left( \sqrt{\frac{I_{SS}}{K_p}} - V_{TP} \right) + \left( V_{TN} + \sqrt{\frac{I_{SS}}{K_n}} \right)$$

or

$$V_{DS1} = V_{DD} + V_{TN} + V_{TP} + \sqrt{\frac{I_{SS}}{K_n}} - \sqrt{\frac{I_{SS}}{K_p}} \cong V_{DD} \quad (16.58)$$

and those of  $M_3$  and  $M_4$  are

$$V_{SD3} = V_{SG3} = \sqrt{\frac{I_{SS}}{K_p}} - V_{TP} \quad (16.59)$$

(Remember that  $V_{TP} < 0$  for  $p$ -channel enhancement-mode devices.)

The drain currents of all the transistors are equal:

$$I_{DS1} = I_{DS2} = I_{SD3} = I_{SD4} = \frac{I_{SS}}{2} \quad (16.60)$$

### Small-Signal Analysis

Now that we have found the operating points of the transistors, we can proceed to analyze the small-signal characteristics of the amplifier, including differential-mode gain, differential-mode input and output resistances, common-mode gain, CMRR, and common-mode input and output resistances.

### Differential-Mode Signal Analysis

Analysis of the ac behavior of the differential amplifier begins with the differential-mode input applied in the ac circuit model in Fig. 16.32. Upon studying the circuit in Fig. 16.32, we realize that

it is a two terminal network and can be represented by its Norton equivalent circuit consisting of the short-circuit output current and Thévenin equivalent output resistance. With the output terminals short circuited, the NMOS differential pair produces equal and opposite currents with amplitude  $g_{m2}v_{id}/2$  at the drains of  $M_1$  and  $M_2$ . Drain current  $i_{d1}$  is supplied by current mirror transistor  $M_3$  and is replicated at the output of  $M_4$ . Thus, the total short circuit output current is

$$\mathbf{i}_o = 2 \frac{g_{m2}v_{id}}{2} = g_{m2}v_{id} \quad (16.61)$$

The current mirror provides a single-ended output but with a transconductance equal to the full value of the C-S amplifier!

The Thévenin equivalent output resistance will be found using the circuit in Fig. 16.33 in which the internal output resistances of  $M_2$  and  $M_4$  are shown next to their respective transistors. In the next sub-section, we will show that  $R_{th}$  is equal to the parallel combination of  $r_{o2}$  and  $r_{o4}$ :

$$R_{th} = r_{o2} \| r_{o4} \quad (16.62)$$

The differential-mode voltage gain of the open-circuited differential amplifier is simply the product of  $i_{sc}$  and  $R_{th}$ :

$$A_{dm} = g_{m2}(r_{o2} \| r_{o4}) = \frac{\mu_f 2}{1 + \frac{r_{o2}}{r_{o4}}} \approx \frac{\mu_f 2}{2} \quad (16.63)$$

Equation (16.63) indicates that the gain of the input stage of the amplifier approaches one-half the intrinsic gain of the transistors forming the differential pair. We are now within a factor of 2 of the theoretical voltage gain limit for the individual transistors.

### Output Resistance of the Differential Amplifier

The origin of the output resistance expression in Eq. (16.63) can be thought of conceptually in the following (although technically incorrect) manner. At node 1 in Fig. 16.33,  $r_{o4}$  is connected directly to ac ground at the positive power supply, whereas  $r_{o2}$  appears connected to virtual ground at the sources of  $M_2$  and  $M_1$ . Thus,  $r_{o2}$  and  $r_{o4}$  are effectively in parallel. Although this argument gives the correct answer, it is not precisely correct. Because the differential amplifier with active load no longer represents a symmetric circuit, the node at the sources of  $M_1$  and  $M_2$  is not truly a virtual ground.

### Exact Analysis

A more precise analysis can be obtained from the circuit in Fig. 16.34. The output resistance  $r_{o4}$  of  $M_4$  is indeed connected directly to ac ground and represents one component of the output resistance.

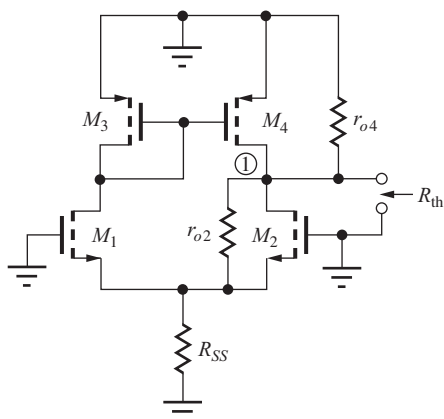


**Figure 16.33** Simple CMOS op amp with active load in the first stage.

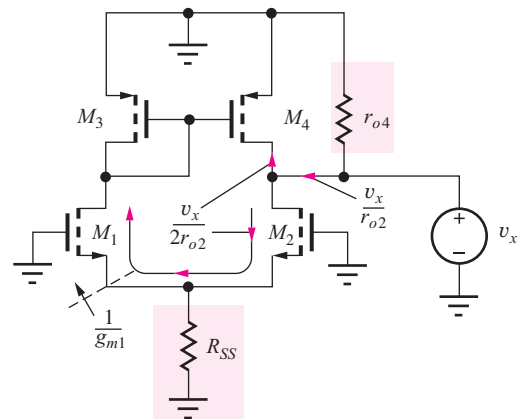


**Figure 16.34** Output resistance component due to  $r_{o2}$ .

However, the current from  $v_x$  due to  $r_{o2}$  is more complicated. The actual behavior can be determined from Fig. 16.34, in which  $R_{SS}$  is assumed to be negligible with respect to  $1/g_{m1}$  ( $R_{SS} \gg 1/g_{m1}$ ).

Transistor  $M_2$  is operating as a common-source transistor with an effective resistance in its source of  $R_S = 1/g_{m1}$ . Based on the results in Table 14.3, the resistance looking into the drain of  $M_2$  is

$$R_{o2} = r_{o2}(1 + g_{m2}R_S) = r_{o2} \left(1 + g_{m2} \frac{1}{g_{m1}}\right) = 2r_{o2} \quad (16.64)$$

Therefore, the drain current of  $M_2$  is equal to  $v_x/2r_{o2}$ . However, the current goes around the differential pair and into the current mirror at  $M_3$ . The current is replicated by the mirror to become the drain current of  $M_4$ . The total current from source  $v_x$  becomes  $2(v_x/2r_{o2}) = v_x/r_{o2}$ .

Combining this current with the current through  $r_{o4}$  yields a total current of

$$i_x^T = \frac{v_x}{r_{o2}} + \frac{v_x}{r_{o4}} \quad \text{and} \quad R_{od} = r_{o2} \parallel r_{o4} \quad (16.65)$$

The equivalent resistance at the output node is, in fact, exactly equal to the parallel combination of the output resistances of  $M_2$  and  $M_4$ .

**EXERCISE:** Find the Q-points of the transistors in Fig. 16.31 if  $I_{SS} = 250 \mu\text{A}$ ,  $K_n = 250 \mu\text{A/V}^2$ ,  $K_p = 200 \mu\text{A/V}^2$ ,  $V_{TN} = -V_{TP} = 0.75 \text{ V}$ , and  $V_{DD} = V_{SS} = 5 \text{ V}$ . What are the transconductance, output resistance, and voltage gain of the amplifier if  $\lambda = 0.0133 \text{ V}^{-1}$ ?

**ANSWERS:** (125  $\mu\text{A}$ , 4.88 V), (125  $\mu\text{A}$ , 1.87 V); 250  $\mu\text{S}$ , 314  $\text{k}\Omega$ , 78.5

### Common-Mode Input Signals

Figure 16.35 is the CMOS differential amplifier with a common-mode input signal. The common-mode input voltage causes a common-mode current  $i_{oc}$  in both sides of the differential pair consisting of  $M_1$  and  $M_2$ . The common-mode current ( $i_{oc}$ ) in  $M_1$  is mirrored at the output of  $M_4$  with a small error since no current can appear in  $r_{o4}$  with the output shorted. In addition, the small voltage difference developed between the drains of  $M_1$  and  $M_2$  causes a current in the differential output resistance ( $2r_{o2}$ ) of the pair that is then doubled by the action of the current mirror.

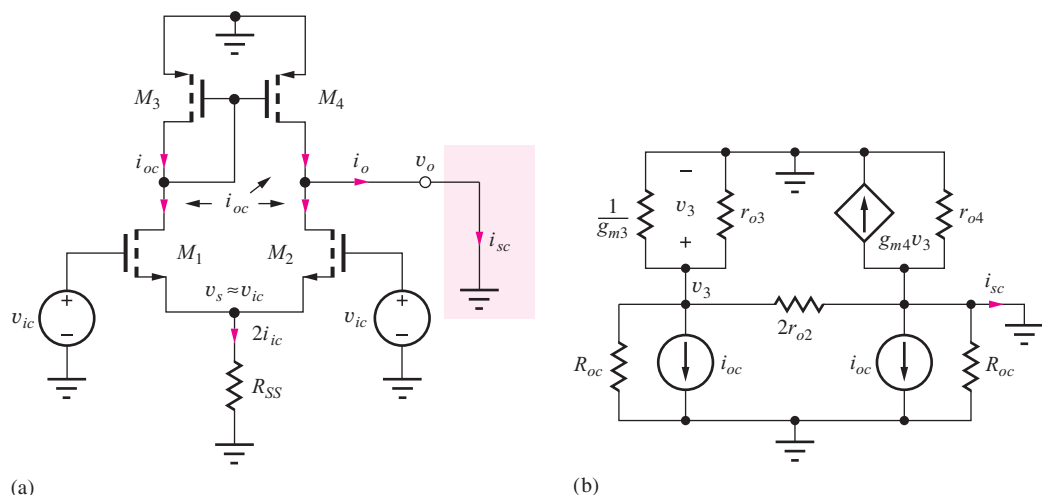


Figure 16.35 (a) CMOS differential amplifier with common-mode input. (b) Small-signal model.

An expression for the short-circuit output current can be found using the small-signal model for the circuit in Fig. 16.35(b). The differential pair with common-mode input is represented by the two-port model from Sec. 15.1.15 with

$$i_{oc} \cong \frac{v_{ic}}{2R_{SS}} \quad R_{od} = 2r_{o2} \quad R_{oc} = 2\mu_f R_{SS} \quad (16.66)$$

With the output short-circuited, we have a one-node problem. Solving for  $v_3$ ,

$$v_3 = \frac{-i_{oc}}{g_{m3} + g_{o3} + \frac{g_{o2}}{2} + G_{oc}} \quad \text{and} \quad i_{sc} = -\left(i_{oc} + g_{m4}v_3 - \frac{g_{o2}}{2}v_3\right) \quad (16.67)$$

which together with Eq. (16.66) yields

$$i_{sc} = -\frac{g_{o3} + g_{o2}}{g_{m3} + g_{o3} + \frac{g_{o2}}{2} + G_{oc}}i_{oc} \cong -\frac{1 + \frac{r_{o3}}{r_{o2}}}{\mu_f r_{o3}} \left(\frac{v_{ic}}{2R_{SS}}\right) \quad (16.68)$$

where it is assumed that  $g_{m4} = g_{m3}$  and  $G_{oc} \ll g_{m3}$ . The Thévenin equivalent output resistance is exactly the same as found in the previous section,  $R_{th} = r_{o2}\|r_{o4}$ . Thus, the common-mode gain is

$$A_{cm} = \frac{i_{sc}R_{th}}{v_{ic}} = -\frac{\left(1 + \frac{r_{o3}}{r_{o2}}\right)}{2\mu_f r_{o3}R_{SS}}(r_{o2}\|r_{o4}) \quad (16.69)$$

where  $\mu_f r_{o3} \gg 1$  has been assumed. The common-mode rejection ratio is

$$\text{CMRR} = \left|\frac{A_{dm}}{A_{cm}}\right| = \frac{2\mu_f r_{o3}R_{SS}}{\left(1 + \frac{r_{o3}}{r_{o2}}\right)} \cong \mu_f r_{o3}R_{SS} \quad \text{for } r_{o3} \cong r_{o2} \quad (16.70)$$

which is improved by a factor of approximately  $\mu_f r_{o3}$  over that of the pair with a resistor load!

**EXERCISE:** Evaluate Eq. (16.70) for  $K_p = K_n = 5 \text{ mA/V}^2$ ,  $\lambda = 0.0167 \text{ V}^{-1}$ ,  $I_{SS} = 200 \mu\text{A}$ , and  $R_{SS} = 10 \text{ M}\Omega$ .

**ANSWER:**  $6.00 \times 10^6$  or 136 dB

In the last exercise, we find that the CMRR predicted by Eq. (16.70) is quite large, whereas typical op amp specs are 80 to 100 dB. We need to look deeper. In reality, this level will not be achieved, but will be limited by mismatches between the devices in the circuit.

### Mismatch Contributions to CMRR

In this section, we explore the techniques used to calculate the effects of device mismatches on CMRR. Figure 16.36 presents the small-signal model for the differential amplifier with mismatches in transistors  $M_1$  and  $M_2$  in which we assume

$$g_{m1} = g_m + \frac{\Delta g_m}{2} \quad g_{m2} = g_m - \frac{\Delta g_m}{2} \quad g_{o1} = g_o + \frac{\Delta g_o}{2} \quad g_{o2} = g_o - \frac{\Delta g_o}{2} \quad (16.71)$$

In this analysis,  $M_3$  and  $M_4$  are still identical. We desire to find the short circuit output current  $i_{sc} = (i_{d1} - i_{d2})$  in which  $i_{d1}$  is replicated by the current mirror. Let us use our knowledge of the gross behavior of the circuit to simplify the analysis. We have  $v_{d2} = 0$ , since we are finding the short-circuit output current, and based on previous common-mode analyses, we expect the signal at  $v_{d1}$  to be small. So let us assume that  $v_{d1} \cong 0$ . With this assumption, and noting that the two gate-source voltages are identical,

$$i_{sc} = i_{d1} - i_{d2} = (g_{m1} - g_{m2})v_{gs} - (g_{o1} - g_{o2})v_s = \Delta g_m v_{gs} - \Delta g_o v_s \quad (16.72)$$

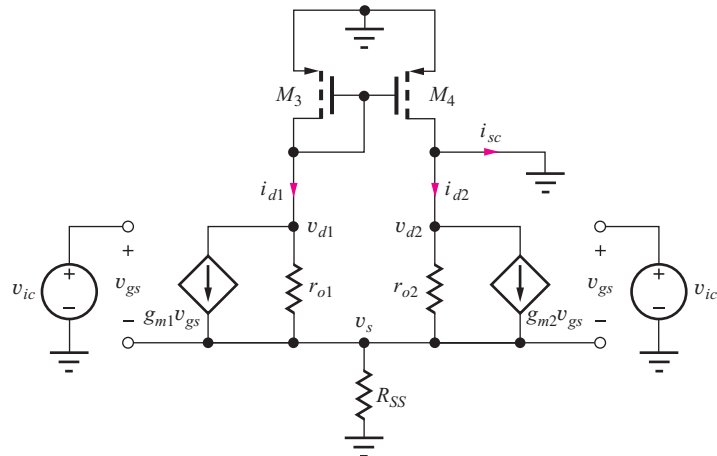


**Figure 16.36** CMOS differential amplifier in which  $M_1$  and  $M_2$  are no longer matched.

To evaluate this expression, we need to find source voltage  $v_s$  and gate-source voltage  $v_{gs}$ . Writing a nodal equation for  $v_s$  with  $v_{gs} = v_{ic} - v_s$ ,  $v_{d1} = 0$  and  $v_{d2} = 0$ , yields

$$\left( g_m + \frac{\Delta g_m}{2} + g_m - \frac{\Delta g_m}{2} \right) (v_{ic} - v_s) = \left( g_o + \frac{\Delta g_o}{2} + g_o - \frac{\Delta g_o}{2} + G_{SS} \right) v_s$$

in which we may be surprised to see all the mismatch terms cancel out! Thus, for common-mode inputs,  $v_s$  and  $v_{gs}$  are not affected by the transistor mismatches.<sup>4</sup>

$$v_s \approx \frac{2g_m R_{SS}}{1 + 2g_m R_{SS}} v_{ic} \approx v_{ic}$$

and

$$v_{gs} \approx \frac{1 + 2g_o R_{SS}}{1 + 2g_m R_{SS}} v_{ic} \approx \left( \frac{1}{2g_m R_{SS}} + \frac{1}{\mu_f} \right) v_{ic} \quad (16.73)$$

The short-circuit output current goes through the Thévenin output resistance  $R_{th} = r_{o2} \| r_{o4}$  to produce the output voltage, and

$$A_{cm} = \frac{i_{sc} R_{th}}{v_{ic}} = \left[ \Delta g_m \left( \frac{1}{2g_m R_{SS}} + \frac{1}{\mu_f} \right) - \Delta g_o \right] (r_{o2} \| r_{o4}) \quad (16.74)$$

The CMRR is then

$$\begin{aligned} \text{CMRR}^{-1} &= \left| \frac{A_{cm}}{A_{dm}} \right| = \left| \frac{A_{cm}}{g_m (r_{o2} \| r_{o4})} \right| \\ &= \left[ \frac{\Delta g_m}{g_m} \left( \frac{1}{2g_m R_{SS}} + \frac{1}{\mu_f} \right) - \frac{\Delta g_o}{g_o} \frac{1}{\mu_f} \right] \end{aligned} \quad (16.75)$$

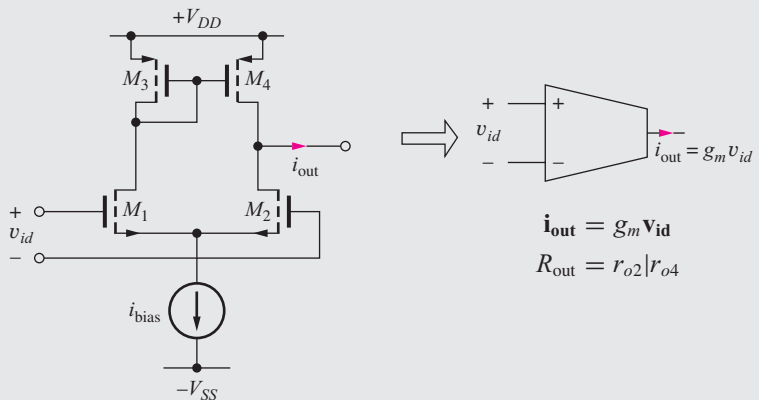
For very large  $R_{SS}$ , we see that CMRR is now limited by the transistor mismatches and value of the intrinsic gain. For example, a 1 percent mismatch with an intrinsic gain of 500 limits the individual terms in Eq. (16.75) to  $2 \times 10^{-5}$ . Since we cannot predict the signs on the  $\Delta g/g$  terms, the expected CMRR is  $2.5 \times 10^4$  or 88 dB. This is much more consistent with observed values of CMRR.

<sup>4</sup> An exact analysis without assuming that  $v_{d1} = 0$  shows that a negligibly small change actually occurs.

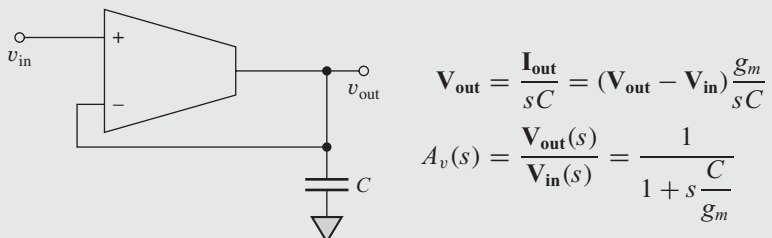


### *G<sub>m</sub>*-C Integrated Filters

The design of integrated circuit filters is complicated by the lack of well-controlled resistive components in most mainstream CMOS processes. One approach to overcome this is the use of  $G_m$ -C filter topologies based on the operational transconductance amplifier (OTA). The OTA is characterized by both a high input and high output impedance. A simple form of an OTA is the CMOS differential amplifier from Fig. 16.31. The high impedance output ( $R_{\text{out}} = r_{o2} \parallel r_{o4}$ ) is a small-signal current given by the product of the differential pair  $g_m$  and the differential input voltage  $v_{id}$ . Typically, commercial OTA designs include additional devices to improve output resistance and voltage swing.



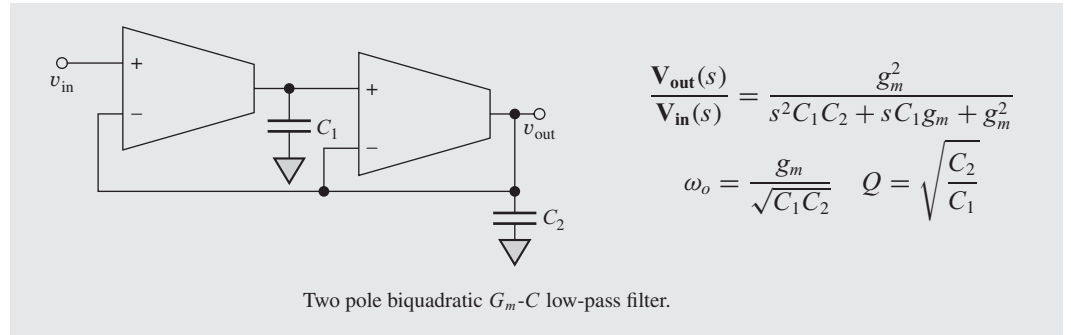
Equivalent schematic symbol for operational transconductance amplifier (OTA).



Single pole  $G_m$ -C low-pass filter.

A simple low-pass filter formed with an OTA and a capacitor is shown above. The transfer characteristic is also included and indicates that the upper cutoff frequency occurs at  $f_H = g_m / 2\pi C$ . One of the more useful characteristics of the  $G_m$ -C filter approach is the ease with which the characteristics can be tuned. Recalling that  $g_m$  is a function of the differential pair current, we see that the cutoff frequency of the filter is easily modified by adjusting the bias current.

A second-order version (a biquad topology) is shown below. This circuit permits the adjustment of cutoff frequency with constant  $Q$ , and still requires no resistors. High-pass, band-pass, and band-reject are also readily derived from this basic form. Because of their compatibility with standard CMOS processes and excellent power efficiency,  $G_m$ -C filters have become prevalent in communication circuits, A/D converter anti-alias filters, noise shaping, and many other applications.



$$\frac{V_{\text{out}}(s)}{V_{\text{in}}(s)} = \frac{g_m^2}{s^2 C_1 C_2 + s C_1 g_m + g_m^2}$$

$$\omega_o = \frac{g_m}{\sqrt{C_1 C_2}} \quad Q = \sqrt{\frac{C_2}{C_1}}$$

### 16.7.2 BIPOLAR DIFFERENTIAL AMPLIFIER WITH ACTIVE LOAD

The bipolar differential amplifier with an active load formed from a *pnp* current mirror is depicted in Fig. 16.37 with  $v_1 = 0 = v_2$ . If we assume that the circuit is balanced with  $\beta_{FO} = \infty$ , then the bias current  $I_{EE}$  divides equally between transistors  $Q_1$  and  $Q_2$ , and  $I_{C1}$  and  $I_{C2}$  are equal to  $I_{EE}/2$ . Current  $I_{C1}$  is supplied by transistor  $Q_3$  and is mirrored as  $I_{C4}$  at the output of *pnp* transistor  $Q_4$ . Thus,  $I_{C3}$  and  $I_{C4}$  are both also equal to  $I_{EE}/2$ , and the dc current in the collector of  $Q_4$  is exactly the current required to satisfy  $Q_2$ .

If  $\beta_{FO}$  is very large, then the current mirror ratio is exactly 1 when  $V_{EC4} = V_{EC3} = V_{EB}$ , and the differential amplifier is completely balanced when the quiescent output voltage is

$$V_O = V_{CC} - V_{EB} \quad (16.76)$$

#### Q-Points

The collector currents of all the transistors are equal:

$$I_{C1} = I_{C2} = I_{C3} = I_{C4} = \frac{I_{EE}}{2} \quad (16.77)$$

The collector-emitter voltages of  $Q_1$  and  $Q_2$  are

$$V_{CE1} = V_{CE2} = V_C - V_E = (V_{CC} - V_{EB}) - (-V_{BE}) \cong V_{CC} \quad (16.78)$$

and for  $Q_3$  and  $Q_4$ ,

$$V_{EC3} = V_{EC4} = V_{EB} \quad (16.79)$$

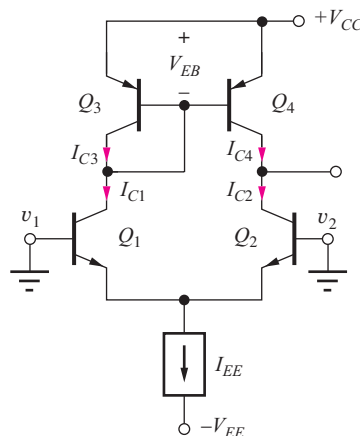


**Figure 16.37** Bipolar differential amplifier with active load.

### Finite Current Gain

The current gain defect in the current mirror upsets the dc balance of the circuit. However, as long as the transistors remain in the forward-active region, the collector current of  $Q_4$  must equal the collector current of  $Q_2$ , and the collector-emitter voltage of  $Q_4$  adjusts itself to make up for the current-gain defect of the current mirror. The required value of  $V_{EC4}$  can be found using the current mirror expression from Eq. (16.9):

$$I_{C4} = I_{C1} \frac{\left[ 1 + \frac{V_{EC4}}{V_A} \right]}{\left[ 1 + \frac{V_{EB}}{V_A} + \frac{2}{\beta_{FO4}} \right]} \quad (16.80)$$

However, because  $I_{C4} = I_{C2}$  and  $I_{C2} = I_{C1}$ , the mirror ratio must be unity, which requires

$$V_{EC4} = V_{EB} + \frac{2V_A}{\beta_{FO4}} \quad (16.81)$$

For  $\beta_{FO3} = 50$ ,  $V_A = 60$  V, and  $V_{EB} = 0.7$  V,  $V_{EC4} = 3.10$  V.

This collector-emitter voltage difference represents a substantial offset at the amplifier output and translates to an equivalent input offset voltage of

$$V_{OS} = \frac{V_{EC4} - V_{EC3}}{A_{dd}} = \frac{V_{EC4} - V_{EB}}{A_{dd}} \quad (16.82)$$

$V_{OS}$  represents the input voltage needed to force the output voltage differential to be zero. For  $A_{dd} = 100$ ,  $V_{OS}$  would be 24.0 mV. To eliminate this error, a buffered current mirror is usually used as the active load, as shown in Fig. 16.38.

It should be noted that Eq. (16.81) actually overestimates the value of  $V_{EC4}$  because the increase in  $V_{EC4}$  decreases  $V_{CE2}$  and thereby reduces  $I_{C2}$ .

**EXERCISE:** Calculate the dc value of  $V_{EC4}$  if the circuit buffered current mirror replaces the active load as in Fig. 16.38. What is  $V_{OS}$  if  $A_{dd} = 100$ ?

**ANSWERS:**  $V_{EC4} = 1.37$  V and  $\Delta V_{EC} = 47$  mV;  $V_{OS} = 0.47$  mV

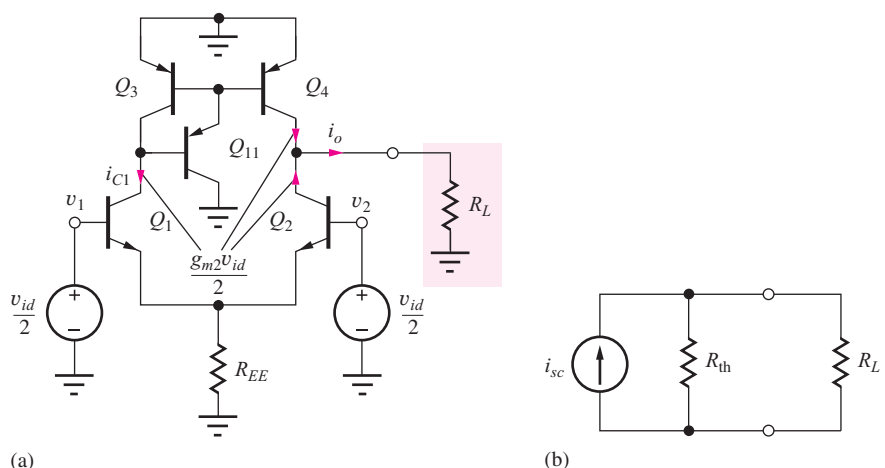
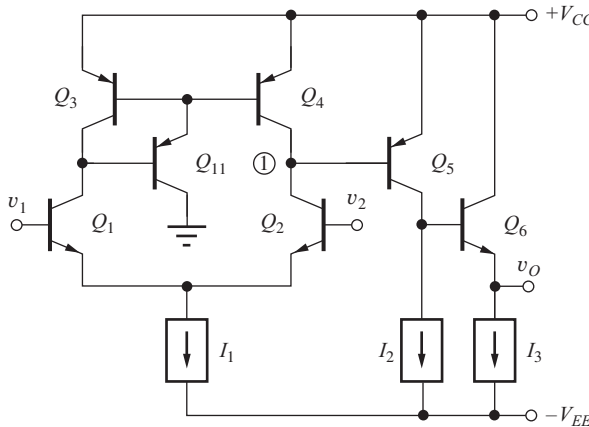


Figure 16.38 (a) BJT differential amplifier with differential-mode input. (b) Equivalent circuit.



**Figure 16.39** Bipolar op amp with active load in first stage.

### Differential-Mode Signal Analysis

Analysis of the ac behavior of the differential amplifier begins with the differential-mode input applied in the ac circuit model in Fig. 16.38. The differential input pair produces equal and opposite currents with amplitude  $g_{m2}v_{id}/2$  at the collectors of  $Q_1$  and  $Q_2$ . Collector current  $i_{c1}$  is supplied by  $Q_3$  and is replicated at the output of  $Q_4$ . Thus, the total short circuit output current is equal to

$$i_{sc} = 2 \frac{g_{m2}v_{id}}{2} = g_{m2}v_{id} \quad (16.83)$$

The output resistance is identical to Eq. (16.65)  $R_{th} = r_{o2} \| r_{o4}$  and

$$A_{dd} = \frac{i_{sc}(R_L \| R_{th})}{v_{dm}} = g_{m2}(R_L \| r_{o2} \| r_{o4}) = -g_{m2}R_L \quad (16.84)$$

The current mirror provides a single-ended output but with a voltage equal to the full gain of the C-E amplifier, just as for the FET case. Here we have included  $R_L$ , which models the loading of the next stage in a multistage amplifier.

The power of the current mirror is again most apparent when additional stages are added, as in the prototype operational amplifier in Fig. 16.39. The resistance at the output of the differential input stage, node 1, is now equivalent to the parallel combination of the output resistances of transistors  $Q_2$  and  $Q_4$  and the input resistance of  $Q_5$  ( $R_L = r_{\pi5}$ ):

$$R_{eq} = r_{o2} \| r_{o4} \| r_{\pi5} \cong r_{\pi5} \quad (16.85)$$

The gain of the differential input stages becomes

$$A_{dm} = g_{m2}R_{eq} \cong g_{m2}r_{\pi5} = \beta_{o5} \frac{I_{C2}}{I_{C5}} \quad (16.86)$$

**EXERCISE:** What is the approximate differential-mode voltage gain of the differential input stage of the amplifier in Fig. 16.39 if  $\beta_{FO} = 150$ ,  $V_A = 75$  V, and  $I_{C5} = 3 I_{C2}$ ?

**ANSWER:** 50

### Common-Mode Input Signals

The circuits in Fig. 16.40 represent the bipolar differential amplifier with current mirror load and a buffered current mirror load. The detailed analysis is quite involved and tedious, particularly for the buffered mirror, so here we will argue the result based on earlier analyses. The common-mode

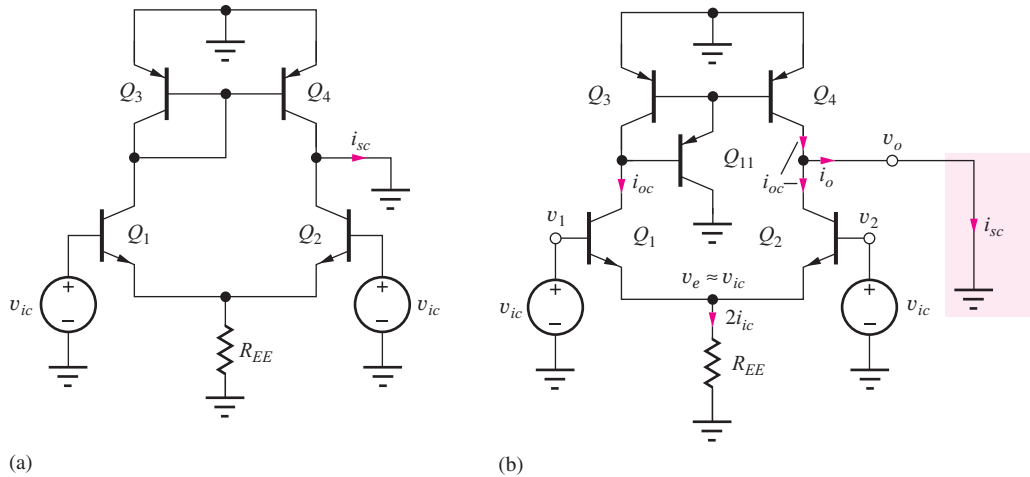


**Figure 16.40** Bipolar differential amplifiers with common-mode input.

current  $i_{oc}$  in  $Q_1$  and  $Q_2$  is found with the help of Eq. (15.27):

$$i_{oc} = \frac{A_{cc}v_{ic}}{R_C} = v_{ic} \left( \frac{1}{2R_{EE}} - \frac{1}{\beta_o r_o} \right) \quad (16.87)$$

The current from  $Q_1$  is mirrored at the output of  $Q_4$  with a mirror error of  $2/\beta_o$ . Thus, the short-circuit output current is

$$i_{sc} = v_{ic} \frac{2}{\beta_o} \left( \frac{1}{\beta_o r_o} - \frac{1}{2R_{EE}} \right) \quad (16.88)$$

In a manner similar to that of the FET pair, the voltage developed at the collector of  $Q_1$ ,  $i_{oc}/gm_3$ , forces a current in the resistance at the output node ( $2r_{o2}$ ), which is doubled by the action of the current mirror:

$$i_{sc} = 2v_{ic} \left( \frac{1}{\beta_{or_o}} - \frac{1}{2R_{EE}} \right) \frac{1}{g_{m3}(2r_{o2})} \cong \frac{v_{ic}}{\mu r_2} \left( \frac{1}{\beta_{or_o}} - \frac{1}{2R_{EE}} \right) \quad (16.89)$$

Since  $\mu_f \gg \beta_o$  for the BJT, the output will be dominated by Eq. (16.88), and the CMRR is

$$\text{CMRR} = \left| \frac{g_{m2} R_{\text{th}}}{i_{sc} R_{\text{th}} / v_{ic}} \right| \cong \left[ \frac{2}{\beta_{o3}} \left( \frac{1}{\beta_{o2} \mu_{f2}} - \frac{1}{2g_{m2} R_{EE}} \right) \right]^{-1} \quad (16.90)$$

**EXERCISE:** Evaluate Eq. (16.90) for  $\beta_E = 100$ ,  $V_A = 75$  V,  $I_{EE} = 200 \mu\text{A}$ , and  $R_{EE} = 10 \text{ M}\Omega$ .

**ANSWER:**  $5.45 \times 10^6$  or 135 dB

The expression in Eq. (16.90) yields a very large CMRR that is almost impossible to achieve. The CMRR predicted for the buffered current mirror is even larger, since the mirror error is approximately  $2/\beta_{o11}\beta_{o3}$ . In both these circuits, however, the CMRR will actually be limited to much smaller levels by small mismatches between the various transistors:

$$\text{CMRR}^{-1} = \left[ \left( \frac{\Delta g_m}{g_m} + \frac{\Delta g_\pi}{g_\pi} \right) \left( \frac{1}{2g_m R_{SS}} + \frac{1}{\mu_f} \right) - \frac{\Delta g_o}{g_o} \frac{1}{\mu_f} \right] \quad (16.91)$$

Equation (16.91) is similar to the results for the FET from Eq. (16.75) with the addition of the  $\Delta g_\pi/g_\pi$  term. In an actual amplifier, the common-mode gain is determined by small imbalances in the bipolar transistors and overall symmetry of the amplifier.

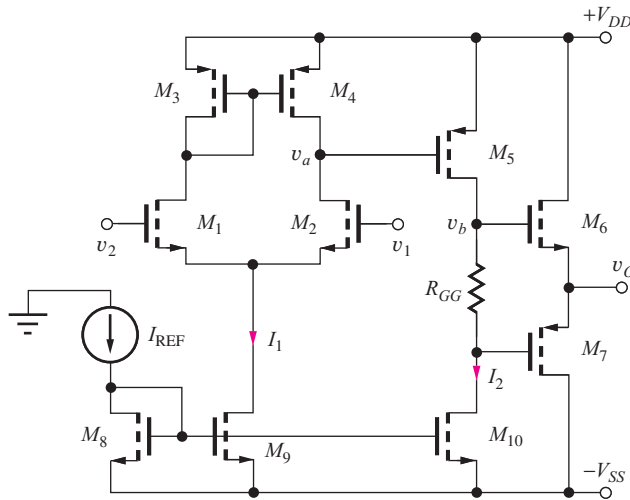


**Figure 16.41** Complete CMOS op amp with current mirror bias.

## 16.8 ACTIVE LOADS IN OPERATIONAL AMPLIFIERS

Let us now explore more fully the use of active loads in MOS and bipolar operational amplifiers. Figure 16.41 shows a complete three-stage MOS operational amplifier. The input stage consists of NMOS differential pair  $M_1$  and  $M_2$  with PMOS current mirror load,  $M_3$  and  $M_4$ , followed by a second common-source gain stage  $M_5$  loaded by current source  $M_{10}$ . The output stage is a class-AB amplifier consisting of transistors  $M_6$  and  $M_7$ . Bias currents  $I_1$  and  $I_2$  for the two gain stages are set by the current mirrors formed by transistors  $M_8$ ,  $M_9$ , and  $M_{10}$ , and class-AB bias for the output stage is set by the voltage developed across resistor  $R_{GG}$ . At most, only two low value resistors are required:  $R_{GG}$  and one for the current mirror reference current.

### 16.8.1 CMOS OP AMP VOLTAGE GAIN

Assuming that the gain of the output stage is approximately 1, then the overall differential-mode gain  $A_{dm}$  of the three-stage operational amplifier is approximately equal to the product of the terminal gains of the first two stages:

$$A_{dm} = \frac{V_o}{V_{id}} = \frac{V_a V_b V_o}{V_{id} V_a V_b} = A_{vt1} A_{vt2}(1) \cong A_{vt1} A_{vt2} \quad (16.92)$$

As discussed earlier, the input stage provides a gain of

$$A_{vt1} = g_m(r_{o2} \| r_{o4}) \cong \frac{\mu_{f2}}{2} \quad (16.93)$$

The terminal gain of the second stage is equal to

$$A_{vt2} = g_m(r_{o5} \|(R_{GG} + r_{o10})) \cong g_m(r_{o5} \| r_{o10}) \cong g_m(r_{o5} \| r_{o5}) = \frac{\mu_{f5}}{2} \quad (16.94)$$

assuming that the output resistances of  $M_5$  and  $M_{10}$  are similar in value and  $R_{GG} \ll r_{o10}$ . Combining the three equations above yields

$$A_{dm} \cong \frac{\mu_{f2}\mu_{f5}}{4} \quad (16.95)$$

The gain approaches one-quarter of the product of the intrinsic gains of the two gain stages.

The factor of 4 in the denominator of Eq. (16.95) can be eliminated by improved design. If a Wilson source is used in the first-stage active load, then the output resistance of the current mirror is much greater than  $r_{o2}$ , and  $A_{vt1}$  becomes equal to  $\mu_{f2}$ . The gain of the second stage can also be increased to the full amplification factor of  $M_5$  if the current source  $M_{10}$  is replaced by a Wilson or

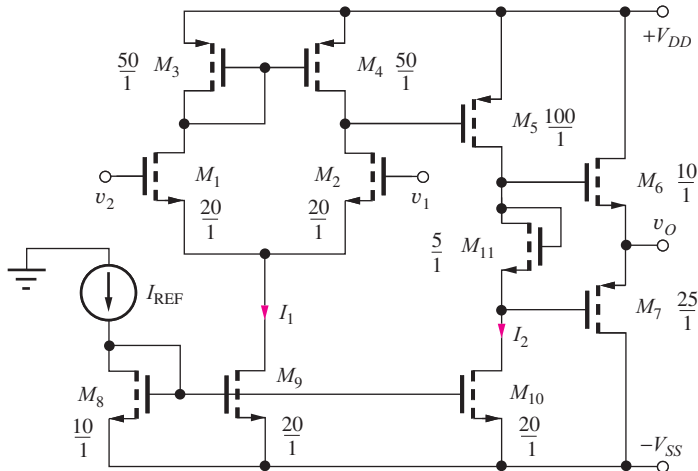


**Figure 16.42** Op amp with current mirror bias of the class-AB output stage.

cascode source. If both these circuit changes are used (see Prob. 16.126), then the gain of the op amp can be increased to

$$A_{dm} \cong \mu_f 2 \mu_f 5 \quad (16.96)$$

This discussion has only scratched the surface of the many techniques available for increasing the gain of the CMOS op amp. Several examples appear in the problems at the end of this chapter; further discussion can be found in the bibliography.

### 16.8.2 dc DESIGN CONSIDERATIONS

When the circuit in Fig. 16.41 is operating in a closed-loop op amp configuration, the drain current of  $M_5$  must be equal to the output current  $I_2$  of current source transistor  $M_{10}$ . For the amplifier to have a minimum offset voltage, the ( $W/L$ ) ratio of  $M_5$  must be carefully selected so the source-gate bias of  $M_5$ ,  $V_{SG5} = V_{SD4} = V_{SG3}$ , is precisely the proper voltage to set  $I_{D5} = I_2$ . Usually the  $W/L$  ratio of  $M_5$  is also adjusted to account for  $V_{DS}$  and  $\lambda$  differences between  $M_5$  and  $M_{10}$ .  $R_{GG}$  and the ( $W/L$ ) ratios of  $M_6$  and  $M_7$  determine the quiescent current in the class-AB output stage.

Even resistor  $R_{GG}$  has been eliminated from the op amp in Fig. 16.42 by using the gate-source voltage of FET  $M_{11}$  to bias the output stage. The current in the class-AB stage is determined by the  $W/L$  ratios of the output transistors and the diode-connected MOSFET  $M_{11}$ .

#### EXAMPLE 16.7 CMOS OP AMP ANALYSIS

Find the small-signal characteristics of a CMOS operational amplifier.

**PROBLEM** Find the voltage gain, input resistance, and output resistance of the amplifier in Fig. 16.42 if  $K'_n = 25 \mu\text{A}/\text{V}^2$ ,  $K'_p = 10 \mu\text{A}/\text{V}^2$ ,  $V_{TN} = 0.75 \text{ V}$ ,  $V_{TP} = -0.75 \text{ V}$ ,  $\lambda = 0.0125 \text{ V}^{-1}$ ,  $V_{DD} = V_{SS} = 5 \text{ V}$ , and  $I_{REF} = 100 \mu\text{A}$ .

**SOLUTION** **Known Information and Given Data:** The schematic for the operational amplifier appears in Fig. 16.42;  $V_{DD} = V_{SS} = 5 \text{ V}$ , and  $I_{REF} = 100 \mu\text{A}$ ; device parameters are given as  $K'_n = 25 \mu\text{A}/\text{V}^2$ ,  $K'_p = 10 \mu\text{A}/\text{V}^2$ ,  $V_{TN} = 0.75 \text{ V}$ ,  $V_{TP} = -0.75 \text{ V}$ ,  $\lambda = 0.0125 \text{ V}^{-1}$ .

**Unknowns:** Q-points,  $A_{dm}$ ,  $R_{id}$ , and  $R_O$

**Approach:** Find the Q-point currents and use the device parameters to evaluate Eq. (16.95) for  $A_{dm}$ . Since we have MOSFETs at the input,  $R_{id} = R_{ic} = \infty$ .  $R_O$  is set by  $M_6$  and  $M_7$ :  $R_O = (1/g_{m6}) \parallel (1/g_{m7})$ .

**Assumptions:** MOSFETs operate in the active region.

**Analysis:** The gain can be estimated using Eq. (16.95).

$$A_{dm} \cong \frac{\mu_{f2}\mu_{f5}}{4} = \frac{1}{4} \left( \frac{1}{\lambda_2} \sqrt{\frac{2K_{n2}}{I_{D2}}} \right) \left( \frac{1}{\lambda_5} \sqrt{\frac{2K_{p5}}{I_{D5}}} \right)$$

For the amplifier in Fig. 16.42,

$$I_{D2} = \frac{I_1}{2} = \frac{2I_{REF}}{2} = 100 \mu\text{A} \quad I_{D5} = I_2 = 2I_{REF} = 200 \mu\text{A}$$

$$K_{n2} = 20K'_n = 500 \frac{\mu\text{A}}{\text{V}^2} \quad K_{p5} = 100K'_p = 1000 \frac{\mu\text{A}}{\text{V}^2}$$

and

$$A_{dm} \cong \frac{\mu_{f2}\mu_{f5}}{4} = \frac{1}{4} \left( \frac{1}{0.0125} \right)^2 \text{V}^2 \sqrt{\frac{2 \left( 500 \frac{\mu\text{A}}{\text{V}^2} \right)}{100 \mu\text{A}}} \sqrt{\frac{2 \left( 1000 \frac{\mu\text{A}}{\text{V}^2} \right)}{200 \mu\text{A}}} = 16,000$$

The input resistance is twice the input resistance of  $M_1$ , which is infinite:  $R_{id} = \infty$ . The output resistance is determined by the parallel combination of the output resistances of  $M_6$  and  $M_7$ , which act as two source followers operating in parallel:

$$R_O = \frac{1}{g_{m6}} \parallel \frac{1}{g_{m7}} = \frac{1}{\sqrt{2K_{n6}I_{D6}}} \parallel \frac{1}{\sqrt{2K_{p7}I_{D7}}}$$

To evaluate this expression, the current in the output stage must be found. The gate-source voltage of  $M_{11}$  is

$$V_{GS11} = V_{TN11} + \sqrt{\frac{2I_{D11}}{K_{n11}}} = 0.75 \text{ V} + \sqrt{\frac{2(200 \mu\text{A})}{125 \left( \frac{\mu\text{A}}{\text{V}^2} \right)}} = 2.54 \text{ V}$$

In this design,  $V_{TP} = -V_{TN}$  and the  $W/L$  ratios of  $M_6$  and  $M_7$  have been chosen so that  $K_{p7} = K_{n6}$ . Because  $I_{D6}$  must equal  $I_{D7}$ ,  $V_{GS6} = V_{SG7}$ . Thus, both  $V_{GS6}$  and  $V_{SG7}$  are equal to one-half  $V_{GS11}$ , and

$$I_{D7} = I_{D6} = \frac{250 \mu\text{A}}{2 \text{V}^2} (1.27 \text{ V} - 0.75 \text{ V})^2 = 33.7 \mu\text{A}$$

The transconductances of  $M_6$  and  $M_7$  are also equal,

$$g_{m7} = g_{m6} = \sqrt{2 \left( 2.50 \times 10^{-4} \frac{\mu\text{A}}{\text{V}^2} \right) (33.7 \times 10^{-6} \mu\text{A})} = 1.30 \times 10^{-4} \text{ S}$$

and the output resistance at the Q-point is  $R_O = 3.85 \text{ k}\Omega$ .

**Check of Results:** A double check of our hand calculations indicates they are correct. Because of the complexity of the circuit, SPICE simulation represents an excellent check of hand calculations. The simulation results appear in the next exercise.

**Discussion:** Simulation of the open-loop characteristics of high-gain amplifiers in SPICE can be difficult. The open-loop gain will amplify the offset voltage of the amplifier and may saturate the output. One approach is to first determine the offset voltage and then to apply a compensating voltage to the amplifier input to bring the output near zero. The steps are outlined next. In very high gain cases, SPICE may still be unable to converge because numerical “noise” during the simulation steps is amplified just as an input voltage. The successive voltage and current injection method discussed previously in Chapter 11 solves this problem.

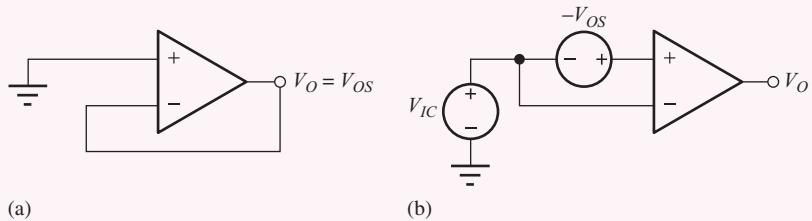


**Figure 16.43** Op amp setups for SPICE simulation. (a) Offset voltage determination. (b) Circuit for open-loop analysis using SPICE transfer functions.

**Computer-Aided Analysis:** After drawing the circuit of Fig. 16.42 with the schematic editor, be sure to set the device parameters to the desired values. For the NMOS devices,  $K_P = 25 \mu\text{A}/\text{V}^2$ ,  $V_{TO} = 0.75 \text{ V}$ , and  $\text{LAMBDA} = 0.0125 \text{ V}^{-1}$ . For the PMOS devices,  $K_P = 10 \mu\text{A}/\text{V}^2$ ,  $V_{TO} = -0.75 \text{ V}$ , and  $\text{LAMBDA} = 0.0125 \text{ V}^{-1}$ .  $W$  and  $L$  must be specified for each individual transistor. For example, use  $W = 5 \mu\text{m}$  and  $L = 1 \mu\text{m}$  for a 5/1 device.

The next step in the simulation is to find the offset voltage by operating the op amp in a voltage-follower configuration for which  $V_O = V_{OS}$ , as in Fig. 16.43(a).  $V_{OS}$  is then applied as a differential input to the amplifier in Fig. 16.43(b) with a common-mode input  $V_{IC} = 0$ . If the value of  $V_{OS}$  is correct, an operating point analysis should yield a value of approximately 0 for  $V_O$ . A transfer function analysis from  $V_{OS}$  to the output will give values of  $A_{dm}$ ,  $R_{id}$ , and  $R_{out}$ . A transfer function analysis from  $V_{IC}$  to the output will give  $A_{cm}$ ,  $R_{ic}$ , and  $R_{out}$ . The SPICE results are given as the answers to the next exercise.



**EXERCISE:** Simulate the amplifier in Fig. 16.42 using SPICE and compare the results to the answers in Ex. 16.7. Which terminal is the noninverting input? What are the offset voltage, common-mode and differential-mode gains, CMRR, common-mode and differential-mode input resistances, and output resistance?

**ANSWERS:**  $v_1; 64.164 \mu\text{V}; 17,800; 0.52; 90.7 \text{ dB}; \infty; \infty; 3.63 \text{ k}\Omega$

### 16.8.3 BIPOLAR OPERATIONAL AMPLIFIERS

Active-load techniques can be applied equally well to bipolar op amps. In fact, most of the techniques discussed thus far were developed first for bipolar amplifiers and later applied to MOS circuits as NMOS and CMOS technologies matured. In the circuit in Fig. 16.44, a differential input stage with active load is formed by transistors  $Q_1$  to  $Q_4$ . The first stage is followed by a high gain C-E amplifier formed of  $Q_5$  and its current source load  $Q_8$ . Load resistance  $R_L$  is driven by the class-AB output stage, consisting of transistors  $Q_6$  and  $Q_7$  biased by current  $I_2$  and diodes  $Q_{11}$  and  $Q_{12}$ . (The diodes will actually be implemented with BJTs, in this case with emitter areas five times those of  $Q_6$  and  $Q_7$ .)

Based on our understanding of multistage amplifiers, the gain of this circuit is approximately  $A_{dm} = A_{vt1}A_{vt2}A_{vt3}$  and

$$A_{dm} \cong [g_{m2}r_{\pi5}][g_{m5}(r_{o5}\parallel r_{o8}\parallel(\beta_{o6}+1)R_L)][1] \cong \frac{g_{m2}}{g_{m5}}g_{m5}r_{\pi5}g_{m5}\frac{r_{o5}}{2} = \frac{I_{C2}}{I_{C5}}\beta_{o5}\frac{\mu_{f5}}{2} \quad (16.97)$$

in which it has been assumed that the input resistance of the class-AB output stage is much larger than the parallel combination of  $r_{o5}$  and  $r_{o8}$ . Note that the upper limit to Eq. (16.97) is set by the  $\beta_o V_A$  product of  $Q_5$ .

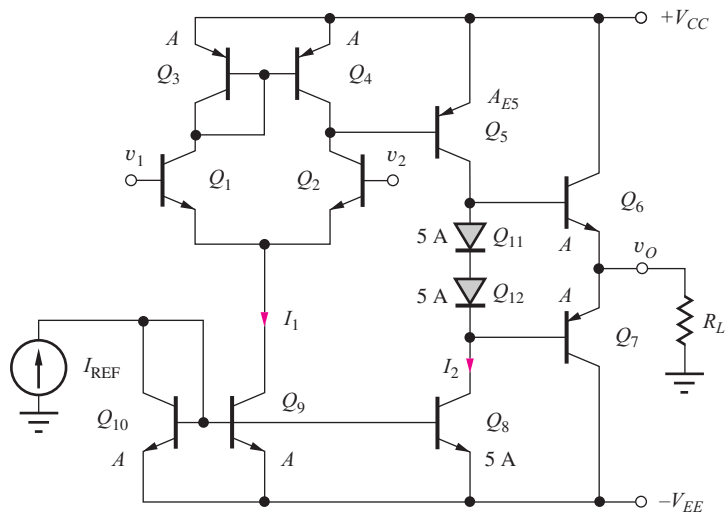


Figure 16.44 Complete bipolar operational amplifier.

**EXERCISE:** Estimate the voltage gain of the amplifier in Fig. 16.44 using Eq. (16.97) if  $I_{\text{REF}} = 100 \mu\text{A}$ ,  $V_{A5} = 60 \text{ V}$ ,  $\beta_{o1} = 150$ ,  $\beta_{o5} = 50$ ,  $R_L = 2 \text{ M}\Omega$ , and  $V_{CC} = V_{EE} = 15 \text{ V}$ . What is the gain of the first stage? The second stage? What should be the emitter area of  $Q_5$ ? What is  $R_{ID}$ ? Which terminal is the inverting input?

**ANSWERS:** 7500; 5; 1500; 10 A; 150 k $\Omega$ ;  $v_1$



**EXERCISE:** Simulate the amplifier in the previous exercise using SPICE and determine the offset voltage, voltage gain, differential-mode input resistance, CMRR, and common-mode input resistance.

**ANSWERS:** 3.28 mV; 8440; 165 k $\Omega$ ; 84.7 dB; 59.1 M $\Omega$

#### 16.8.4 INPUT STAGE BREAKDOWN

Although the bipolar amplifier designs discussed thus far have provided excellent voltage gain, input resistance, and output resistance, the amplifiers all have a significant flaw. The input stage does not offer **overvoltage protection** and can easily be destroyed by the large input voltage differences that can occur, not only under fault conditions but also during unavoidable transients during normal use of the amplifier. For example, the voltage across the input of an op amp can temporarily be equal to the total supply voltage span during slew-rate limited overload recovery.

Consider the worst-case fault condition applied to the differential pair in Fig. 16.45 where one input is connected to the positive power supply voltage and the other is connected to the negative

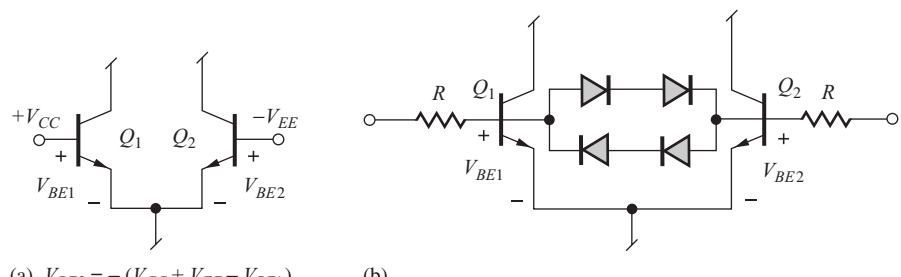


Figure 16.45 (a) Differential input stage voltages under a fault condition. (b) Simple diode input protection circuit.

supply. Under the conditions shown, the base-emitter junction of  $Q_1$  will be forward-biased, and that of  $Q_2$  reverse-biased by a voltage of  $(V_{CC} + V_{EE} - V_{BE1})$ . If  $V_{CC} = V_{EE} = 22$  V, the reverse voltage exceeds 41 V. Because of heavy doping in the emitter, the typical Zener breakdown voltage of the base-emitter junction of an *npn* transistor is only 5 to 7 V. Thus, any voltage exceeding this value by more than one diode drop may destroy at least one of the transistors in the differential input pair.

Early IC op amps required circuit designers to add external diode protection across the input terminals, as shown Fig. 16.45(b). The diodes prevent the differential input voltage from exceeding approximately 1.4 V, but this technique adds extra components and cost to the design. The two resistors limit the current through the diodes. The μA741 described in the next section was the first commercial IC op amp to solve this problem by providing a fully protected input, as well as output, stage.

## 16.9 THE μA741 OPERATIONAL AMPLIFIER

The now classic Fairchild μA741 operational-amplifier design was the first to provide a highly robust amplifier from the application engineer's point of view. The amplifier provides excellent overall characteristics (high gain, input resistance and CMRR, low output resistance, and good frequency response) while providing overvoltage protection for the input stage and short-circuit current limiting of the output stage. The 741 style of amplifier design quickly became the industry standard and spawned many related designs. By studying the 741 design, we will find a number of new amplifier circuit design and bias techniques.

### 16.9.1 OVERALL CIRCUIT OPERATION

Figure 16.46 is a simplified schematic of the μA741 operational amplifier. The three bias sources shown in symbolic form are discussed in more detail following a description of the overall circuit. The op amp has two stages of voltage gain followed by a class-AB output stage. In the first stage, transistors  $Q_1$  to  $Q_4$  form a differential amplifier with a buffered current mirror active load,  $Q_5$  to  $Q_7$ .

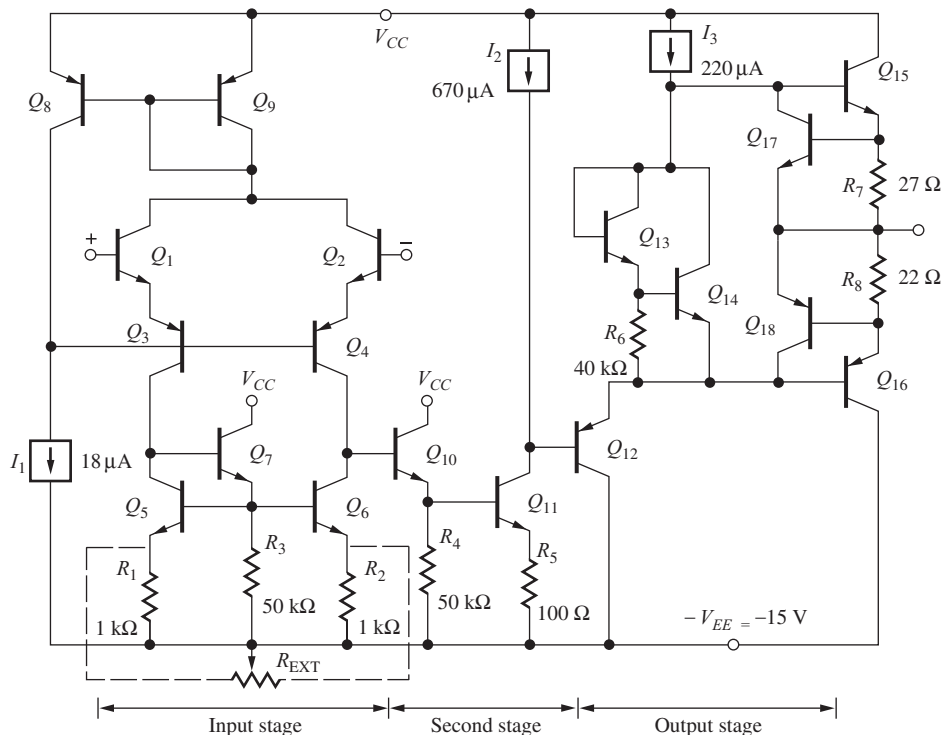


**Figure 16.46** Overall schematic of the classic Fairchild μA741 operational amplifier (the bias network appears in Fig. 16.47).

The second stage consists of emitter follower  $Q_{10}$  driving common-emitter amplifier  $Q_{11}$  with current source  $I_2$  and emitter-follower  $Q_{12}$  as load. Transistors  $Q_{13}$  to  $Q_{18}$  form a short-circuit protected class-AB push-pull output stage that is buffered from the second gain stage by  $Q_{12}$ . Practical operational amplifiers offer an offset voltage adjustment port, which is provided in the 741 through the addition of 1-k $\Omega$  resistors  $R_1$  and  $R_2$  and an external potentiometer  $R_{\text{EXT}}$ .

**EXERCISE:** Reread this section and be sure you understand the function of each individual transistor in Fig. 16.46. Make a table listing the function of each transistor.

### 16.9.2 BIAS CIRCUITRY

The three current sources shown symbolically in Fig. 16.46 are generated by the bias circuitry in Fig. 16.47. The value of the current in the two diode-connected reference transistors  $Q_{20}$  and  $Q_{22}$  is determined by the power supply voltage and resistor  $R_5$ :

$$I_{\text{REF}} = \frac{V_{CC} + V_{EE} - 2V_{BE}}{R_5} = \frac{15 + 15 - 1.4}{39 \text{ k}\Omega} = 0.733 \text{ mA} \quad (16.98)$$

assuming  $\pm 15$ -V supplies. Current  $I_1$  is derived from the Widlar source formed of  $Q_{20}$  and  $Q_{21}$ . The output current for this design is

$$I_1 = \frac{V_T}{5000} \ln \left[ \frac{I_{\text{REF}}}{I_1} \right] \quad (16.99)$$

Using the reference current calculated in Eq. (16.98) and iteratively solving for  $I_1$  in Eq. (16.99) yields  $I_1 = 18.4 \mu\text{A}$ .

The currents in mirror transistors  $Q_{23}$  and  $Q_{24}$  are related to the reference current  $I_{\text{REF}}$  by their emitter areas using Eq. (16.13). Assuming  $V_O = 0$  and  $V_{CC} = 15$  V, and neglecting the voltage drop across  $R_7$  and  $R_8$  in Fig. 16.46,  $V_{EC23} = 15 + 1.4 = 16.4$  V and  $V_{EC24} = 15 - 0.7 = 14.3$  V. Using these values with  $\beta_F = 50$  and  $V_A = 60$  V, the two source currents are

$$I_2 = 0.75(733 \mu\text{A}) \frac{\frac{16.4 \text{ V}}{1 + \frac{60 \text{ V}}{0.7 \text{ V}} + \frac{2}{50}}}{} = 666 \mu\text{A} \quad (16.100)$$

$$I_3 = 0.25(733 \mu\text{A}) \frac{\frac{14.4 \text{ V}}{1 + \frac{60 \text{ V}}{0.7 \text{ V}} + \frac{2}{50}}}{} = 216 \mu\text{A}$$

and the two output resistances are

$$R_2 = \frac{V_{A23} + V_{EC23}}{I_2} = \frac{60 \text{ V} + 16.4 \text{ V}}{0.666 \text{ mA}} = 115 \text{ k}\Omega \quad (16.101)$$

$$R_3 = \frac{V_{A24} + V_{EC24}}{I_3} = \frac{60 \text{ V} + 14.3 \text{ V}}{0.216 \text{ mA}} = 344 \text{ k}\Omega$$

**EXERCISE:** What are the values of  $I_{\text{REF}}$ ,  $I_1$ ,  $I_2$ , and  $I_3$  in the circuit in Fig. 16.47 for  $V_{CC} = V_{EE} = 22$  V?

**ANSWERS:** 1.09 mA, 20.0  $\mu\text{A}$ , 1.08 mA, 351  $\mu\text{A}$

**EXERCISE:** What is the output resistance of the Widlar source in Fig. 16.47 operating at 18.4  $\mu\text{A}$  for  $V_A = 60$  V and  $V_{EE} = 15$  V?

**ANSWER:** 18.8 M $\Omega$

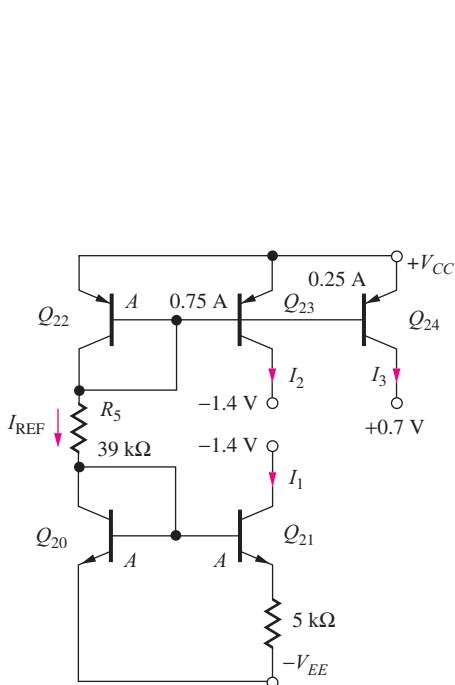


**Figure 16.47** 741 bias circuitry with voltages corresponding to  $V_O = 0$  V.

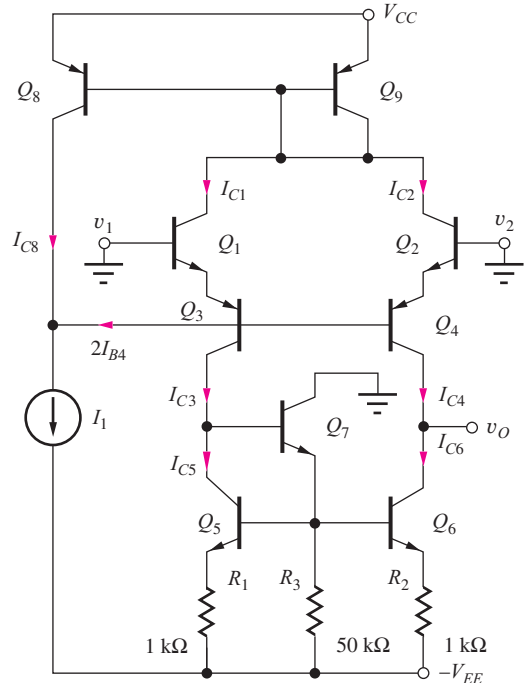


**Figure 16.48** μA741 input stage.

### 16.9.3 dc ANALYSIS OF THE 741 INPUT STAGE

The input stage of the  $\mu$ A741 amplifier is redrawn in the schematic in Fig. 16.48. As noted earlier,  $Q_1$ ,  $Q_2$ ,  $Q_3$ , and  $Q_4$  form a differential input stage with an active load consisting of the buffered current mirror formed by  $Q_5$ ,  $Q_6$ , and  $Q_7$ . In this input stage, there are four base-emitter junctions between inputs  $v_1$  and  $v_2$ , two from the  $npn$  transistors and, more importantly, two from the  $pnp$  transistors. Therefore,  $(v_1 - v_2) = (V_{BE1} + V_{EB3} - V_{EB4} - V_{BE2})$ .

In standard bipolar IC processes, *pnp* transistors are formed from lateral structures in which both junctions exhibit breakdown voltages equal to that of the collector-base junction of the *npn* transistor. This breakdown voltage typically exceeds 50 V. Because most general-purpose op amp specifications limit the power supply voltages to less than  $\pm 22$  V, the emitter-base junctions of  $Q_3$  and  $Q_4$  provide sufficient breakdown voltage to fully protect the input stage of the amplifier, even under a worst-case fault condition, such as that depicted in Fig. 16.45(a).

## Q-Point Analysis

In the 741 input stage in Fig. 16.48, the current mirror formed by transistors  $Q_8$  and  $Q_9$  operates with transistors  $Q_1$  to  $Q_4$  to establish the bias currents for the input stage. Bias current  $I_1$  represents the output of the Widlar source discussed previously ( $18 \mu\text{A}$ ) and must be equal to the collector current of  $Q_8$  plus the base currents of matched transistors  $Q_3$  and  $Q_4$ :

$$I_1 = I_{C8} + I_{B3} + I_{B4} = I_{C8} + 2I_{B4} \quad (16.102)$$

For high current gain, the base currents are small and  $I_{C8} \cong I_1$ .

The collector current of  $Q_8$  mirrors the collector currents of  $Q_1$  and  $Q_2$ , which are summed together in mirror reference transistor  $Q_9$ . Assuming high current gain and ignoring the collector-voltage mismatch between  $Q_7$  and  $Q_8$ ,

$$I_{C8} = I_{C1} + I_{C2} = 2I_{C2} \quad (16.103)$$

Combining Eqs. (16.102) and (16.103) yields the ideal bias relationships for the input stage

$$I_{C1} = I_{C2} \cong \frac{I_1}{2} \quad \text{and} \quad I_{C3} = I_{C4} \cong \frac{I_1}{2} \quad (16.104)$$

because the emitter currents of  $Q_1$  and  $Q_3$  and  $Q_2$  and  $Q_4$  must be equal. The collector current of  $Q_3$  establishes a current equal to  $I_1/2$  in current mirror transistors  $Q_5$  and  $Q_6$ . Thus, transistors  $Q_1$  to  $Q_6$  all operate at a nominal collector current equal to one-half the value of source  $I_1$ .

Now that we understand the basic ideas behind the input stage bias circuit, let us perform a more exact analysis. Expanding Eq. (16.102) using the current mirror expression from Eq. (16.13),

$$I_1 = 2I_{C2} \frac{1 + \frac{V_{EC8}}{V_{A8}}}{1 + \frac{2}{\beta_{FO8}} + \frac{V_{EB8}}{V_{A8}}} + 2I_{B4} \quad (16.105)$$

$I_{C2}$  is related to  $I_{B4}$  through the current gains of  $Q_2$  and  $Q_4$ :

$$I_{C2} = \alpha_{F2} I_{E2} = \alpha_{F2} (\beta_{FO4} + 1) I_{B4} = \frac{\beta_{FO2}}{\beta_{FO2} + 1} (\beta_{FO4} + 1) I_{B4} \quad (16.106)$$

Combining Eqs. (16.105) and (16.106), and solving for  $I_{C2}$  yields

$$I_{C1} = \frac{I_1}{2} \times \left[ \frac{1 + \frac{V_{EC8}}{V_{A8}}}{1 + \frac{2}{\beta_{FO8}} + \frac{V_{EB8}}{V_{A8}}} + \frac{1}{\frac{\beta_{FO2}}{\beta_{FO2} + 1} (\beta_{FO4} + 1)} \right]^{-1} \quad (16.107)$$

which is equal to the ideal value of  $I_1/2$  but reduced by the nonideal current mirror effects from finite current gain and Early voltage.

The emitter current of  $Q_4$  must equal the emitter current of  $Q_2$ , and so the collector current of  $Q_4$  is

$$I_{C4} = \alpha_{F4} I_{E4} = \alpha_{F4} \frac{I_{C2}}{\alpha_{F2}} = \frac{\beta_{FO4}}{\beta_{FO4} + 1} \frac{\beta_{FO2} + 1}{\beta_{FO2}} I_{C2} \quad (16.108)$$

The use of buffer transistor  $Q_7$  essentially eliminates the current gain defect in the current mirror. Note from the full amplifier circuit in Fig. 16.46 that the base current of transistor  $Q_{10}$ , with its 50-kΩ emitter resistor  $R_4$ , is designed to be approximately equal to the base current of  $Q_7$ , and  $V_{CE6} \cong V_{CE5}$  as well. Thus, the current mirror ratio is quite accurate and  $I_{C5} = I_{C6} = I_{C3} \cong I_1/2$ .

If 50-kΩ resistor  $R_3$  were omitted, then the emitter current of  $Q_7$  would be equal only to the sum of the base currents of transistors  $Q_5$  and  $Q_6$  and would be quite small. Because of the Q-point dependence of  $\beta_F$ , the current gain of  $Q_7$  would be poor.  $R_3$  increases the operating current of  $Q_7$  to improve its current gain, as well as to improve the dc balance and transient response of the amplifier. The value of  $R_3$  is chosen to approximately match  $I_{B7}$  to  $I_{B10}$ .

To complete the Q-point analysis, the various collector-emitter voltages must be determined. The collectors of  $Q_1$  and  $Q_2$  are one  $V_{EB}$  below the positive power supply, whereas the emitters are one  $V_{BE}$  below ground potential. Hence,

$$V_{CE1} = V_{CE2} = V_{CC} - V_{EB9} + V_{BE2} \cong V_{CC} \quad (16.109)$$

The collector and emitter of  $Q_3$  are approximately  $2V_{BE}$  above the negative power supply voltage and one  $V_{BE}$  below ground, respectively:

$$V_{EC3} = V_{E3} - V_{C3} = -0.7 \text{ V} - (-V_{EE} + 1.4 \text{ V}) = V_{EE} - 2.1 \text{ V} \quad (16.110)$$

The buffered current mirror effectively minimizes the error due to the finite current gain of the transistors, and  $V_{CE6} = V_{CE5} \cong 2V_{BE} = 1.4$  V, neglecting the small voltage drop (<10 mV) across  $R_1$  and  $R_2$ . Finally, the collector of  $Q_8$  is  $2V_{BE}$  below zero, and the emitter of  $Q_7$  is one  $V_{BE}$  above  $-V_{EE}$ :

$$V_{EC8} = V_{CC} + 1.4 \text{ V} \quad V_{CE7} = V_{EE} - 0.7 \text{ V} \quad (16.111)$$

### EXAMPLE 16.8 μA741 INPUT STAGE BIAS CURRENTS

Find the currents in the 741 input stage.

**PROBLEM** Calculate the bias currents in the 741 input stage if  $I_1 = 18 \mu\text{A}$ ,  $\beta_{FOnpn} = 150$ ,  $V_{Anpn} = 75 \text{ V}$ ,  $\beta_{FOpnp} = 60$ ,  $V_{Apnp} = 60 \text{ V}$ , and  $V_{CC} = V_{EE} = 15 \text{ V}$ .

**SOLUTION** **Known Information and Given Data:** μA741 input stage depicted in Fig. 16.48.  $I_1 = 18 \mu\text{A}$ ,  $\beta_{FOnpn} = 150$ ,  $V_{Anpn} = 75 \text{ V}$ ,  $\beta_{FOpnp} = 60$ ,  $V_{Apnp} = 60 \text{ V}$ , and  $V_{CC} = V_{EE} = 15 \text{ V}$ .

**Unknowns:**  $I_{C1}$ ,  $I_{C2}$ ,  $I_{C3}$ ,  $I_{C4}$ ,  $I_{C5}$ , and  $I_{C6}$

**Approach:** Use given data to evaluate Eqs. (16.107) through (16.111).

**Assumptions:** Transistors are in the active region; use default values of  $I_S$ .

**Analysis:** From Fig. 16.48, we find that the emitter-collector voltage of  $Q_8$  is equal to  $V_{CC} + V_{BE1} + V_{EB3} \cong 16.4 \text{ V}$ . Substituting the known values into Eq. (16.107) gives

$$I_{C1} = I_{C2} = \frac{18 \mu\text{A}}{2} \frac{1}{1 + \frac{16.4 \text{ V}}{\frac{60 \text{ V}}{1 + \frac{2}{50} + \frac{0.7 \text{ V}}{60 \text{ V}}} + \frac{1}{150(60 + 1)}} = 7.32 \mu\text{A}$$

Equation (16.108) yields

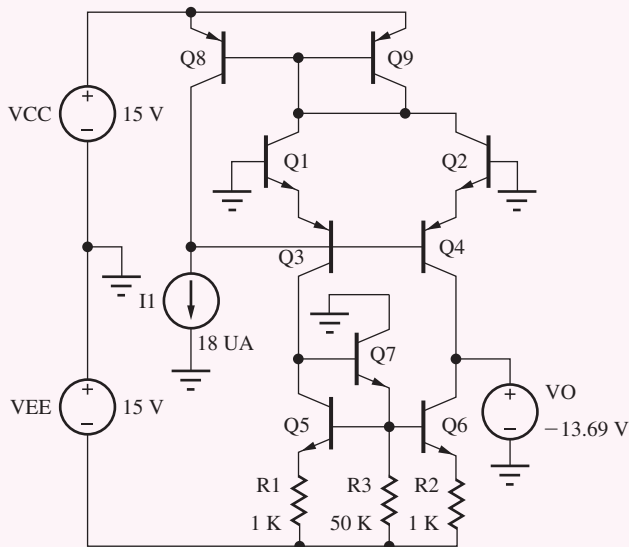
$$I_{C3} = I_{C4} = \alpha_{F4} \frac{I_{C2}}{\alpha_{F2}} = \frac{\beta_{FO4}}{\beta_{FO2} + 1} \left( \frac{\beta_{FO2} + 1}{\beta_{FO2}} \right) I_{C2} = \frac{60}{61} \left( \frac{151}{150} \right) I_{C2} = 7.25 \mu\text{A}$$

$$I_{C5} \cong I_{C3} = 7.25 \mu\text{A} \quad \text{and} \quad I_{C6} = I_{C4} = 7.25 \mu\text{A}$$

**Check of Results:** The basic objective of the bias circuit would be to set all currents to  $18 \mu\text{A}/2$  or  $9 \mu\text{A}$ . Our calculations are close to this value and appear correct.

**Discussion:** The actual bias currents are slightly greater than  $7 \mu\text{A}$ , whereas the ideal value would be  $9 \mu\text{A}$ . The dominant source of error arises from the collector-emitter voltage mismatch of the *pnp* current mirror.

**Computer-Aided Analysis:** We draw the circuit using the schematic editor and set the BJT parameters. For the *npn* devices, BF = 150 and VAF = 75 V. For the *pnp* transistors, BF = 60 and VAF = 60 V. Source  $V_O$  is added to balance the circuit by forcing the output voltage to the same voltage as that which will appear at the collector of  $Q_5$ . Otherwise, the voltage at the collectors of  $Q_4$  and  $Q_6$  will float to a value determined by the difference in overall output resistances of transistors  $Q_4$  and  $Q_6$ . When balance is achieved, the current in source  $V_O$  will be nearly zero. Table 16.3 summarizes the Q-points based on these calculations and Eqs. (16.104) to (16.111) and compares them with the SPICE operating point simulation results.

**TABLE 16.3**Q-points of 741 Input Stage Transistors for  $I_1 = 18 \mu\text{A}$  and  $V_{CC} = V_{EE} = 15 \text{ V}$ 

TRANSISTORS	Q-POINT	SPICE RESULTS
$Q_1$ and $Q_2$	$7.32 \mu\text{A}, 15 \text{ V}$	$7.30 \mu\text{A}, 15.0 \text{ V}$
$Q_3$ and $Q_4$	$7.25 \mu\text{A}, 12.9 \text{ V}$	$7.24 \mu\text{A}, 13.0 \text{ V}$
$Q_5$ and $Q_6$	$7.25 \mu\text{A}, 1.4 \text{ V}$	$7.16 \mu\text{A}, 1.30 \text{ V}$
$Q_7$	$12.2 \mu\text{A}, 14.3 \text{ V}$	$13.1 \mu\text{A}, 14.3 \text{ V}$
$Q_8$	$17.7 \mu\text{A}, 16.4 \text{ V}$	$17.8 \mu\text{A}, 16.3 \text{ V}$
$Q_9$	$14.0 \mu\text{A}, 0.7 \text{ V}$	$14.1 \mu\text{A}, 0.66 \text{ V}$



**EXERCISE:** Remove  $V_O$  and simulate the 741 input stage amplifier. What are the new collector currents? What are the voltages at the collectors of  $Q_5$  and  $Q_6$ ?

**ANSWERS:**  $7.31 \mu\text{A}$ ,  $7.28 \mu\text{A}$ ,  $7.25 \mu\text{A}$ ,  $7.22 \mu\text{A}$ ,  $7.18 \mu\text{A}$ ,  $7.22 \mu\text{A}$ ,  $13.1 \mu\text{A}$ ,  $17.8 \mu\text{A}$ ,  $14.1 \mu\text{A}$ ;  $-13.7 \text{ V}$ ,  $-13.1 \text{ V}$

**EXERCISE:** Suppose buffer transistor  $Q_7$  and resistor  $R_3$  are eliminated from the amplifier in Fig. 16.48 and  $Q_5$  and  $Q_6$  were connected as a standard current mirror. What would be the collector-emitter voltage of  $Q_6$  if  $V_{BE6} = 0.7 \text{ V}$ ,  $\beta_{FO6} = 100$ , and  $V_{A6} = 60 \text{ V}$ ? Use Eq. (16.81).

**ANSWER:**  $1.90 \text{ V}$

#### 16.9.4 ac ANALYSIS OF THE 741 INPUT STAGE

The 741 input stage is redrawn in symmetric form in Fig. 16.49, with its active load temporarily replaced by two resistors. From Fig. 16.49, we see that the collectors of  $Q_1$  and  $Q_2$  as well as the bases of  $Q_3$  and  $Q_4$ , lie on the line of symmetry of the amplifier and represent virtual grounds for differential-mode input signals.

The corresponding differential-mode half-circuit shown in Fig. 16.50 is a common-collector stage followed by a common-base stage, a C-C/C-B cascade. The characteristics of the C-C/C-B cascade can be determined from Fig. 16.50 and our knowledge of single-stage amplifiers.

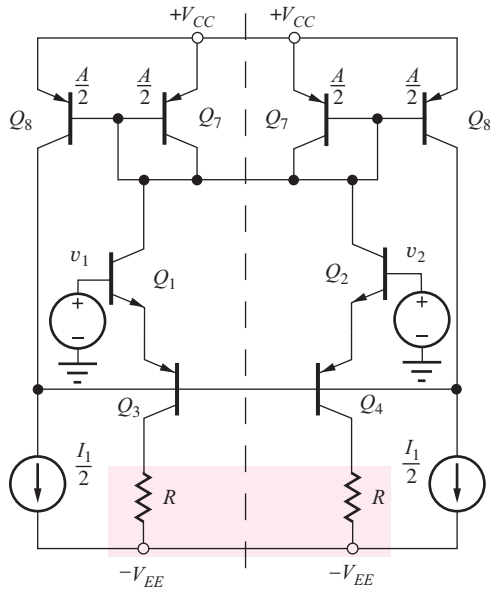


Figure 16.49 Symmetry in the 741 input stage.

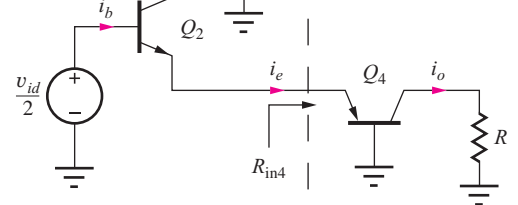


Figure 16.50 Differential-mode half-circuit for the 741 input stage.

The emitter current of  $Q_2$  is equal to its base current  $i_b$  multiplied by  $(\beta_{o2} + 1)$ , and the collector current of  $Q_4$  is  $\alpha_{o4}$  times the emitter current. Thus, the output current can be written as

$$\mathbf{i}_o = \alpha_{o4} \mathbf{i}_e = \alpha_{o4} (\beta_{o2} + 1) \mathbf{i}_b \cong \beta_{o2} \mathbf{i}_b \quad (16.112)$$

The base current is determined by the input resistance to  $Q_2$ :

$$\mathbf{i}_b = \frac{\mathbf{v}_{id}}{r_{\pi2} + (\beta_{o2} + 1) R_{in4}} = \frac{\mathbf{v}_{id}}{r_{\pi2} + (\beta_{o2} + 1) \left( \frac{r_{\pi4}}{\beta_{o4} + 1} \right)} = \frac{\mathbf{v}_{id}}{r_{\pi2} + r_{\pi4}} \cong \frac{\mathbf{v}_{id}}{4r_{\pi2}} \quad (16.113)$$

in which  $R_{in4} = r_{\pi4}/(\beta_{o4} + 1)$  represents the input resistance of the common-base stage. Combining Eqs. (16.112) and (16.113) yields

$$\mathbf{i}_o \cong \beta_{o2} \frac{\mathbf{v}_{id}}{4r_{\pi2}} = \frac{g_{m2}}{4} \mathbf{v}_{id} \quad (16.114)$$

Each side of the C-C/C-B input stage has a transconductance equal to one-half of the transconductance of the standard differential pair. From Eq. (16.113) we can also see that the differential-mode input resistance is twice the value of the corresponding C-E stage:

$$R_{id} = \frac{\mathbf{v}_{id}}{\mathbf{i}_b} = 4r_{\pi2} \quad (16.115)$$

From Fig. 16.51, we can see that the output resistance is equivalent to that of a common-base stage with a resistor of value  $1/g_{m2}$  in its emitter:

$$R_{out4} \cong r_{o4} \left( 1 + g_{m4} R \right) = r_{o4} \left( 1 + g_{m4} \frac{1}{g_{m2}} \right) = 2r_{o4} \quad (16.116)$$

### 16.9.5 VOLTAGE GAIN OF THE COMPLETE AMPLIFIER

We now use the results from the previous section to analyze the overall ac performance of the op amp. We find a Norton equivalent circuit for the input stage and then couple it with a two-port model for the second stage.

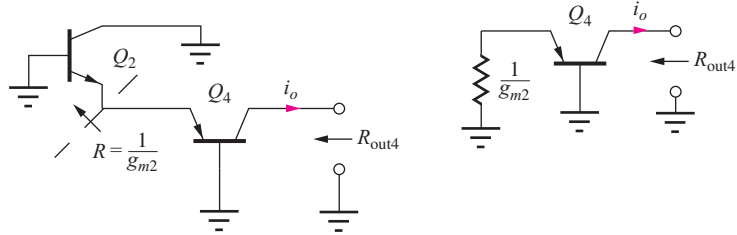


Figure 16.51 Output resistance of C-C/C-B cascade.

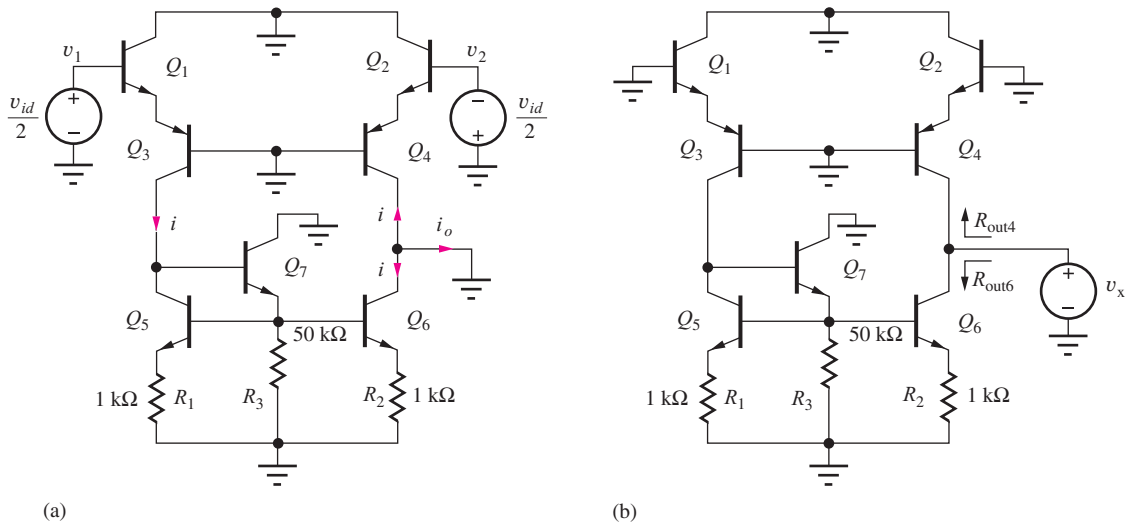


Figure 16.52 Circuits for finding the Norton equivalent of the input stage.

### Norton Equivalent of the Input Stage

Figure 16.52 is the simplified differential-mode ac equivalent circuit for the input stage. We use Figure 16.52(a) to find the short-circuit output current of the first stage. Based on our analysis of Fig. 16.50, the differential-mode input signal establishes equal and opposite currents in the two sides of the differential amplifier where  $i = (g_{m2}/4)v_{id}$ . Current  $i$ , exiting the collector of  $Q_3$ , is mirrored by the buffered current mirror so that a total signal current equal to  $2i$  flows in the output terminal:

$$i_o = -2i = -\frac{g_{m2}v_{id}}{2} = (-20I_{C2})v_{id} = (-1.46 \times 10^{-4} \text{ S})v_{id} \quad (16.117)$$

The Thévenin equivalent resistance at the output is found using the circuit in Fig. 16.52(b) and is equal to

$$R_{th} = R_{out4} \parallel R_{out6} \quad (16.118)$$

Because only a small dc voltage is developed across  $R_2$ , the output resistance of  $Q_6$  can be calculated from

$$R_{out6} \cong r_{o6}[1 + g_{m6}R_2] \cong r_{o6} \left[ 1 + \frac{I_{C6}R_2}{V_T} \right] = r_{o6} \left[ 1 + \frac{0.0073 \text{ V}}{0.025 \text{ V}} \right] = 1.3r_{o6} \quad (16.119)$$

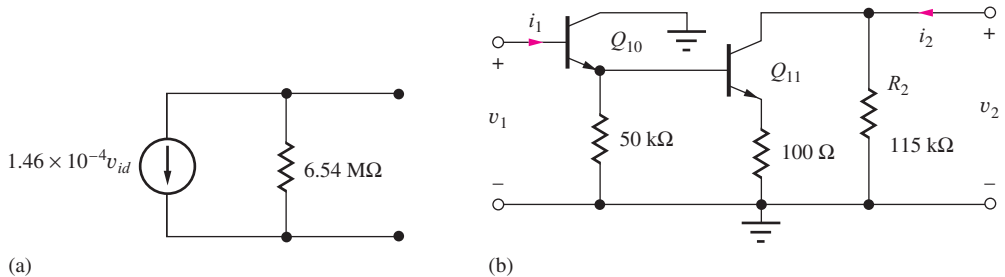


**Figure 16.53** (a) Norton equivalent of the 741 input stage. (b) Two-port representation for the second stage.

The output resistance of  $Q_4$  was already found in Eq. (16.116) to be  $2r_{o4}$ . Using these results,

$$R_{th} = 2r_{o4} \parallel 1.3r_{o6} = 0.79r_{o4} \cong 0.79 \frac{60 \text{ V}}{7.25 \times 10^{-6} \text{ A}} = 6.54 \text{ M}\Omega \quad (16.120)$$

in which  $r_{o4} = r_{o2}$  has been assumed for simplicity with  $V_A + V_{CE} = 60 \text{ V}$ .

The resulting Norton equivalent circuit for the input stage appears in Fig. 16.53(a). Based on the values in this figure, the open-circuit voltage gain of the first stage is  $-955$ . SPICE simulations yield values very similar to those in Fig. 16.53(a):  $(1.40 \times 10^{-4} \text{ S})v_{id}$ ,  $6.95 \text{ M}\Omega$ , and  $A_{dm} = -973$ .

**EXERCISE:** Improve the estimate of  $R_{th}$  using the actual values of  $V_{CE6}$  and  $V_{CE4}$  if  $V_{CC} = V_{EE} = 15 \text{ V}$  and  $V_A = 60 \text{ V}$ . What are the values of  $R_{out4}$  and  $R_{out6}$ ?

**ANSWERS:**  $7.12 \text{ M}\Omega$ ;  $20.2 \text{ M}\Omega$ ,  $11.0 \text{ M}\Omega$

### Model for the Second Stage

Figure 16.53(b) is a two-port representation for the second stage of the amplifier.  $Q_{10}$  is an emitter follower that provides high input resistance and drives a common-emitter amplifier consisting of  $Q_{11}$  and its current source load represented by output resistance  $R_2$ . A  $y$ -parameter model is constructed for this network.

From Fig. 16.46 and the bias current analysis, we can see that the collector current of  $Q_{11}$  is approximately equal to  $I_2$  or  $666 \mu\text{A}$ . Calculating the collector current of  $Q_{10}$  yields

$$I_{C10} \cong I_{E10} = \frac{I_{C11}}{\beta_{F11}} + \frac{V_{B11}}{50 \text{ k}\Omega} = \frac{666 \mu\text{A}}{150} + \frac{0.7 + (0.67 \text{ mA})(0.1 \text{ k}\Omega)}{50 \text{ k}\Omega} = 19.8 \mu\text{A} \quad (16.121)$$

Using these values to find the small-signal parameters with ( $\beta_{on} = 150$ ) gives

$$r_{\pi10} = \frac{\beta_{o10} V_T}{I_{C10}} = \frac{3.75 \text{ V}}{19.8 \mu\text{A}} = 189 \text{ k}\Omega \quad \text{and} \quad r_{\pi11} = \frac{3.75 \text{ V}}{0.666 \text{ mA}} = 5.63 \text{ k}\Omega \quad (16.122)$$

Parameters  $y_{11}$  and  $y_{21}$  are calculated by applying a voltage  $v_1$  to the input port and setting  $v_2 = 0$ , as in Fig. 16.54. The input resistance to  $Q_{11}$  is that of a common-emitter stage with a  $100\text{-}\Omega$  emitter resistor:

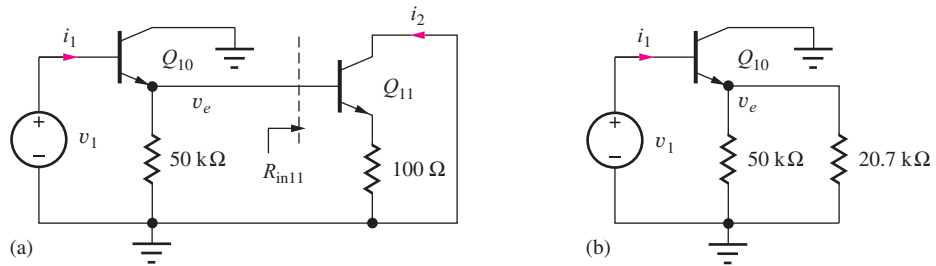
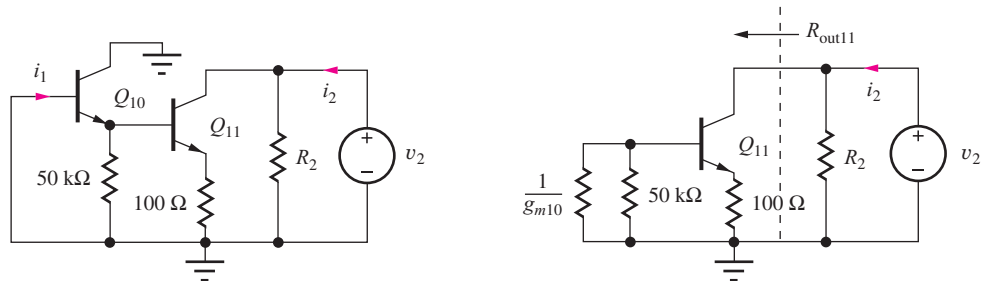
$$R_{in11} = r_{\pi11} + (\beta_{o11} + 1)100 \cong 5630 + (151)100 = 20.7 \text{ k}\Omega \quad (16.123)$$

This value is used to simplify the circuit, as in Fig. 16.54(b), and the input resistance to  $Q_{10}$  is

$$R_{in10} = r_{\pi10} + (\beta_{o10} + 1)(50 \text{ k}\Omega \parallel R_{in11}) = 189 \text{ k}\Omega + (151)(50 \text{ k}\Omega \parallel 20.7 \text{ k}\Omega) = 2.40 \text{ M}\Omega \quad (16.124)$$

The gain of emitter follower  $Q_{10}$  is:

$$v_e = v_1 \frac{(\beta_{o10} + 1)(50 \text{ k}\Omega \parallel R_{in11})}{r_{\pi10} + (\beta_{o10} + 1)(50 \text{ k}\Omega \parallel R_{in11})} = \frac{(151)(50 \text{ k}\Omega \parallel 20.7 \text{ k}\Omega)}{189 \text{ k}\Omega + (151)(50 \text{ k}\Omega \parallel 20.7 \text{ k}\Omega)} = 0.921 v_1 \quad (16.125)$$

Figure 16.54 Network for finding  $y_{11}$  and  $y_{21}$ .Figure 16.55 Network for finding  $y_{12}$  and  $y_{22}$ .

The output current  $\mathbf{i}_2$  in Fig. 16.53(a) is given by

$$\mathbf{i}_2 = \frac{\mathbf{v}_e}{\frac{1}{g_{m11}} + 100 \Omega} = \frac{0.921\mathbf{v}_1}{\frac{40}{V}(0.666 \text{ mA}) + 100 \Omega} = 0.00670\mathbf{v}_1 \quad (16.126)$$

yielding a forward transconductance of

$$G_m = 6.70 \text{ mS} \quad (16.127)$$

Parameters  $y_{12}$  and  $y_{22}$  can be found from the network in Fig. 16.55. We assume that the reverse transconductance  $y_{12}$  is negligible and reserve its calculation for Prob. 16.140. The output conductance can be determined from Fig. 16.55(b).

$$G_o = i_2/v_2 = [R_2 \parallel R_{out11}]^{-1} \quad (16.128)$$

where  $R_2 = 115 \text{ k}\Omega$  was calculated during the analysis of the bias circuit.

Because the voltage drop across the 100-Ω resistor is small, the output resistance of  $Q_{11}$  is approximately

$$\begin{aligned} R_{out11} &= r_{o11}[1 + g_{m11}R_E] = \frac{V_{A11} + V_{CE11}}{I_{C11}} \left[ 1 + \frac{I_{C11}R_E}{V_T} \right] \\ &= \frac{60 \text{ V} + 13.6 \text{ V}}{0.666 \text{ mA}} \left[ 1 + \frac{0.067 \text{ V}}{0.025 \text{ V}} \right] = 407 \text{ k}\Omega \end{aligned} \quad (16.129)$$

and

$$R_o = 115 \text{ k}\Omega \parallel 407 \text{ k}\Omega = 89.1 \text{ k}\Omega \quad (16.130)$$

Figure 16.56 depicts the completed two-port model for the second stage, driven by the Norton equivalent of the input stage. Using this model, the open-circuit voltage gain for the first two stages

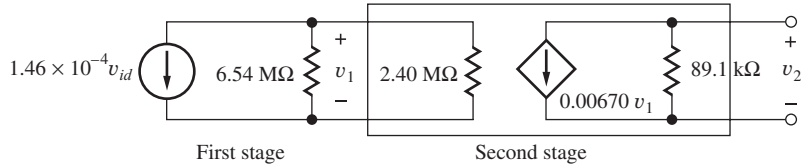


Figure 16.56 Combined model for first and second stages.

of the amplifier is

$$\begin{aligned} v_2 &= -0.00670(89.1 \text{ k}\Omega)v_1 = -597v_1 \\ v_1 &= -1.46 \times 10^{-4}(6.54 \text{ M}\Omega \| 2.40 \text{ M}\Omega)v_{id} = -256v_{id} \\ v_2 &= -597(-256v_{id}) = 153,000v_{id} \end{aligned} \quad (16.131)$$

Note from Eq. (16.130) that the 2.42-MΩ input resistance of  $Q_{10}$  reduces the voltage gain of the first stage by a factor of almost 4.

**EXERCISE:** What is the voltage gain of the input stage if transistor  $Q_{10}$  and its 50-kΩ emitter resistor are omitted so that the output of the first stage is connected directly to the base of  $Q_{11}$ ? Use the small-signal element values already calculated.

**ANSWER:** -3.00

### 16.9.6 THE 741 OUTPUT STAGE

Figure 16.57 shows simplified models for the 741 output stage. Transistor  $Q_{12}$  is the emitter follower that buffers the high impedance node at the output of the second stage and drives the push-pull output stage composed of transistors  $Q_{15}$  and  $Q_{16}$ . Class-AB bias is provided by the sum of the

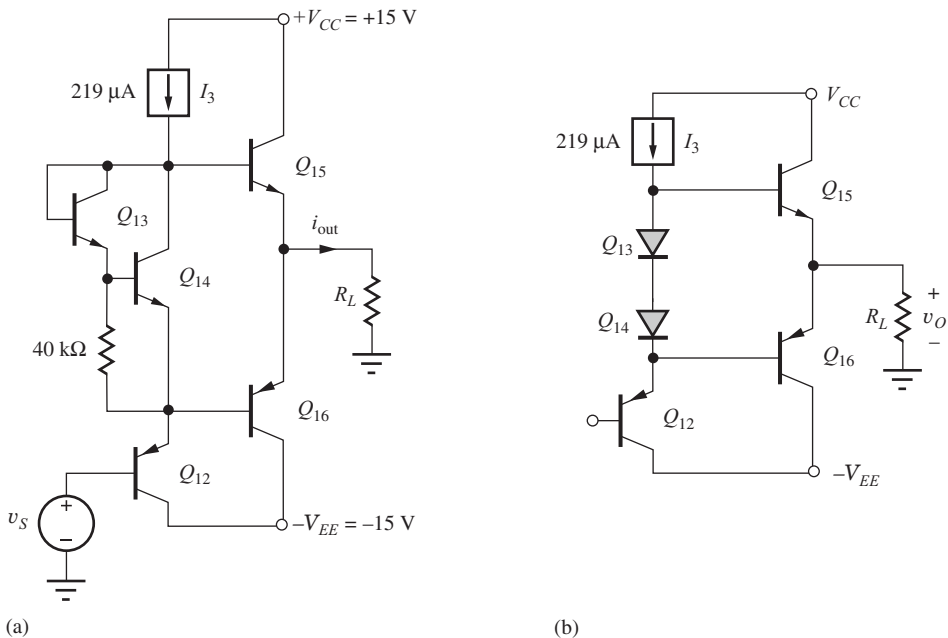


Figure 16.57 (a) 741 output stage without short-circuit protection. (b) Simplified output stage.

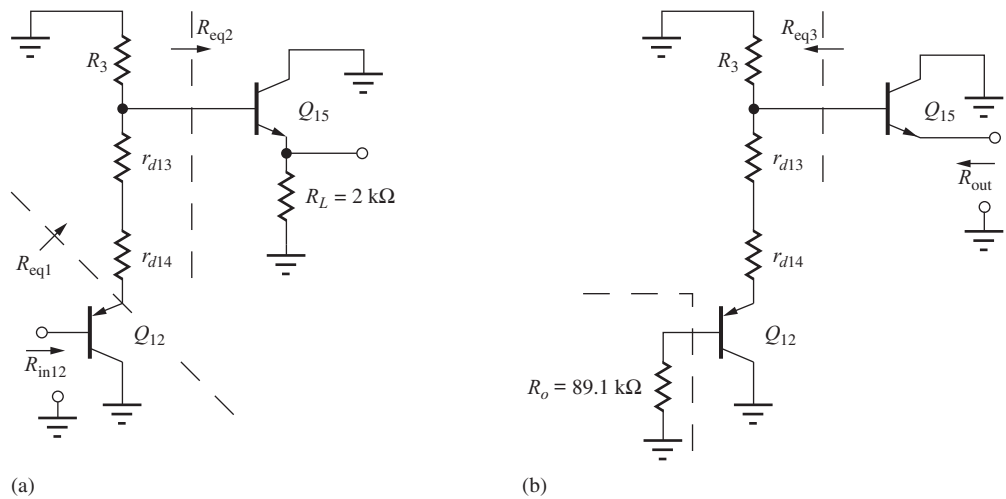


Figure 16.58 Circuits for determining input and output resistance of the output stage.

base-emitter voltages of  $Q_{13}$  and  $Q_{14}$ , represented as diodes in Fig. 16.57(b). The 40-k $\Omega$  resistor is used to increase the value of  $I_{C13}$ . Without this resistor,  $I_{C13}$  would only be equal to the base current of  $Q_{14}$ . The short-circuit protection circuitry in Fig. 16.46 is not shown in Fig. 16.57 in order to simplify the diagram.

The input and output resistances of the class-AB output stage are actually complicated functions of the signal voltage because the operating current in  $Q_{15}$  and  $Q_{16}$  changes greatly as the output voltage changes. However, because only one transistor conducts strongly at any given time in the class-AB stage, separate circuit models can be used for positive and negative output signals. The model for positive signal voltages is shown in Fig. 16.58. (The model for negative signal swings is similar except *npn* transistor  $Q_{15}$  is replaced by *pnp* transistor  $Q_{16}$  connected to the emitter of  $Q_{12}$ .)

Let us first determine the input resistance of transistor  $Q_{12}$ . If  $R_{in12}$  is much larger than the 89-k $\Omega$  output resistance of the two-port in Fig. 16.58, then it does not significantly affect the overall voltage gain of the amplifier. Using single-stage amplifier theory,

$$R_{in12} = r_{\pi12} + (\beta_{o12} + 1)R_{eq1} \quad (16.132)$$

where

$$R_{eq1} = r_{d14} + r_{d13} + R_3 \| R_{eq2} \quad \text{and} \quad R_{eq2} = r_{\pi15} + (\beta_{o15} + 1)R_L \cong (\beta_{o15} + 1)R_L \quad (16.133)$$

The value of  $R_3$  (344 k $\Omega$ ) was calculated in the bias circuit section. For  $I_{C12} = 216 \mu\text{A}$ , and assuming a representative collector current in  $Q_{15}$  of 2 mA,

$$R_{eq2} = r_{\pi15} + (\beta_{o15} + 1)R_L = \frac{3.75 \text{ V}}{2 \text{ mA}} + (151)2 \text{ k}\Omega = 304 \text{ k}\Omega \quad (16.134)$$

Note that the value of  $R_{eq2}$  is dominated by the reflected load resistance  $\beta_{o15}R_L$ . Resistor  $r_{\pi15}$  represents a small part of  $R_{eq2}$ , so knowing the exact value of  $I_{C15}$  is not critical.

$$R_{eq1} = r_{d14} + r_{d13} + R_3 \| R_{eq2} = 2 \frac{0.025 \text{ V}}{0.216 \text{ mA}} + 344 \text{ k}\Omega \| 304 \text{ k}\Omega = 162 \text{ k}\Omega \quad (16.135)$$

and

$$R_{in12} = r_{\pi12} + (\beta_{o12} + 1)R_{eq1} = \frac{0.025 \text{ V}}{0.216 \text{ mA}} + (51)162 \text{ k}\Omega = 8.27 \text{ M}\Omega \quad (16.136)$$

Because  $R_{in12}$  is approximately 100 times the output resistance  $R_o$  of the second stage,  $R_{in12}$  has little effect on the gain of the second stage. Although the value of  $R_{in12}$  changes for different values of load resistance, the overall op amp gain is not affected because the value of  $R_{in12}$  is so much larger than the value of  $R_o$  in Fig. 16.56.

Similar results are obtained for negative signal voltages. The values are slightly different because the current gain of the *pnp* transistor  $Q_{16}$  differs from that of the *npn* transistor  $Q_{15}$ .

### 16.9.7 OUTPUT RESISTANCE

The output resistance of the amplifier for positive output voltages is determined by transistor  $Q_{15}$

$$R_o = \frac{r_{\pi15} + R_{eq3}}{\beta_{o15} + 1} \quad (16.137)$$

in which

$$\begin{aligned} R_{eq3} &= R_3 \left| \left[ r_{d13} + r_{d14} + \frac{r_{\pi12} + R_o}{\beta_{o12} + 1} \right] \right| \\ &= 304 \text{ k}\Omega \left| \left[ 2 \frac{0.025 \text{ V}}{0.219 \text{ mA}} + \frac{5.71 \text{ k}\Omega + 89.1 \text{ k}\Omega}{51} \right] \right| = 2.08 \text{ k}\Omega \end{aligned} \quad (16.138)$$

From Fig. 16.49, we can see that the 27-Ω resistor  $R_7$ , which determines the short-circuit current limit, adds directly to the overall output resistance of the amplifier so that actual op-amp output resistance is

$$R_{out} = R_o + R_7 = \frac{1.88 \text{ k}\Omega + 2.08 \text{ k}\Omega}{151} + 27 \Omega = 53 \Omega \quad (16.139)$$

**EXERCISE:** Repeat the calculation of  $R_{in12}$  and  $R_{out}$  if *pnp* transistor  $Q_{16}$  has a current gain of 50,  $I_{C16} = 2 \text{ mA}$ , and  $I_{C15} = 0$ . Be sure to draw the new equivalent circuit of the output stage for negative output voltages.

**ANSWERS:** 3.94 MΩ ( $\gg 89.1 \text{ k}\Omega$ ), 53 Ω + 22 Ω = 75 Ω

### 16.9.8 SHORT CIRCUIT PROTECTION

For simplicity, the output short-circuit protection circuitry was not shown in Fig. 16.57. Referring back to the complete op amp schematic in Fig. 16.46, we see that **short-circuit protection** is provided by resistors  $R_7$  and  $R_8$  and transistors  $Q_{17}$  and  $Q_{18}$ . The circuit is identical to the one presented in Fig. 15.40(a). Transistors  $Q_{17}$  and  $Q_{18}$  are normally off, but if the current in resistor  $R_7$  becomes too high, then transistor  $Q_{17}$  turns on and steals the base current from  $Q_{15}$ . Likewise, if the current in resistor  $R_8$  becomes too large, then transistor  $Q_{18}$  turns on and removes the base current from  $Q_{16}$ . The positive and negative short-circuit current levels will be limited to approximately  $V_{BE17}/R_7$  and  $-V_{BE18}/R_8$ , respectively. As already mentioned, resistors  $R_7$  and  $R_8$  increase the output resistance of the amplifier since they appear directly in series with the output terminal.

**EXERCISE:** Estimate the positive and negative short-circuit output current in the 741 op amp in Fig. 16.46.

**ANSWERS:** 26 mA; -32 mA

### 16.9.9 SUMMARY OF THE μA741 OPERATIONAL AMPLIFIER CHARACTERISTICS

Table 16.4 is a summary of the characteristics of the μA741 operational amplifier. Column 2 gives our calculated values; column 3 presents values typically found in the actual commercial product.

**TABLE 16.4**  
 **$\mu A741$  Characteristics**

	CALCULATION	TYPICAL VALUES
Voltage gain	153,000	200,000
Input resistance	2.05 M $\Omega$	2 M $\Omega$
Output resistance	53 $\Omega$	75 $\Omega$
Input bias current	49 nA	80 nA
Input offset voltage	—	2 mV

The observed values depend on the exact values of current gain and Early voltage for the *npn* and *pnp* transistors and vary from process run to process run.

## 16.10 THE GILBERT ANALOG MULTIPLIER

In Chapter 10–12 we saw how operational amplifiers could be used to perform scaling, addition, subtraction, integration, and differentiation of electronic signals. However, one of the more difficult operations to realize is accurate multiplication of two analog signals. Barrie Gilbert, another of the “legends” of integrated circuit design, discovered a solution to this problem using the characteristics of the bipolar transistor. The basic multiplier “core” in Fig. 16.59 consists of three differential pairs. The  $Q_1-Q_2$  pair has significant emitter degeneration so that the transconductance of the pair is approximately<sup>5</sup>  $1/R_1$ . Under this assumption, the collector currents of the lower pair can be written as

$$i_{c1} \cong \frac{I_{BB}}{2} + \frac{v_1}{2R_1} \quad i_{c2} \cong \frac{I_{BB}}{2} - \frac{v_1}{2R_1} \quad \text{for } |v_1| \leq I_{BB}R_1 \quad (16.140)$$

The bound on  $v_1$  is determined by the requirement that neither collector current can be negative.

Multiplier output current  $v_o$  is taken from the upper two differential pairs and can be written as

$$v_o = [(i_{c3} + i_{c5}) - (i_{c4} + i_{c6})]R = [(i_{c3} - i_{c4}) + (i_{c5} - i_{c6})]R \quad (16.141)$$

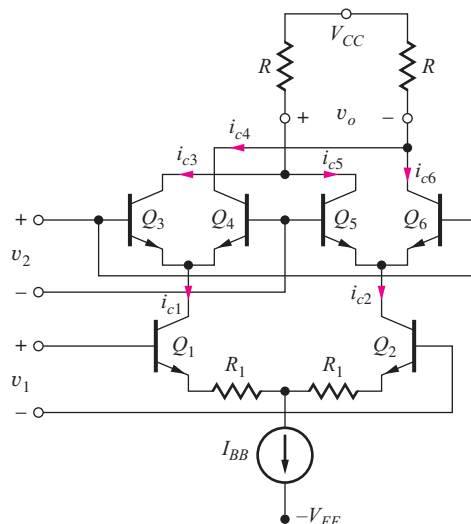


**Figure 16.59** Gilbert multiplier core.

<sup>5</sup> More sophisticated voltage-to-current converters (transconductance amplifiers) can also be used.

Using Eq. (15.4), we can write expressions for the collector current differences in this equation:

$$i_{c3} - i_{c4} = i_{c1} \tanh\left(\frac{v_2}{2V_T}\right) \quad \text{and} \quad i_{c5} - i_{c6} = -i_{c2} \tanh\left(\frac{v_2}{2V_T}\right) \quad (16.142)$$

Using these equations, the output voltage can be reduced to

$$v_o = (i_{c1} - i_{c2})R \tanh\left(\frac{v_2}{2V_T}\right) = v_1 \left(\frac{R}{R_1}\right) \tanh\left(\frac{v_2}{2V_T}\right) \quad (16.143)$$

At this point, one approach to multiplication is to expand the hyperbolic tangent as a series, and then keep only the first term:

$$\tanh(x) = x - \frac{x^3}{3} + \dots \quad \text{and} \quad v_o \cong v_1 \left(\frac{R}{R_1}\right) \left(\frac{v_2}{2V_T}\right) \quad \text{for } \frac{x^3}{3} \ll x \quad (16.144)$$

where  $x = v_2/2V_T$ . However, this approach greatly restricts the input signal range of  $v_2$  to only a few tens of mV [see discussion following Eq. (15.5)].

The key to the full range **Gilbert multiplier** is to use another pair of *pn* junctions to “predistort” the input signal as in Fig. 16.60. Diode connected transistors  $Q_9$  and  $Q_{10}$  are driven by a second transconductance stage formed by  $Q_7$  and  $Q_8$  for which

$$i_{c7} \cong \frac{I_{EE}}{2} + \frac{v_3}{2R_3} \quad i_{c8} \cong \frac{I_{EE}}{2} - \frac{v_3}{2R_3} \quad \text{for } |v_3| \leq I_{EE} R_3 \quad (16.145)$$

to develop voltage  $v_2$ :

$$v_2 = (V_{BB} - v_{BE10}) - (V_{BB} - v_{BE9}) = v_{BE9} - v_{BE10} \quad (16.146)$$

Using the standard expressions for the base-emitter voltages and assuming the two transistors are matched gives

$$v_2 = V_T \ln\left(\frac{\frac{I_{EE}}{2} + \frac{v_3}{2R_3}}{I_S}\right) - V_T \ln\left(\frac{\frac{I_{EE}}{2} - \frac{v_3}{2R_3}}{I_S}\right) = V_T \ln\left(\frac{1 + \frac{v_3}{I_{EE} R_3}}{1 - \frac{v_3}{I_{EE} R_3}}\right) \quad (16.147)$$

Searching our math tables, we might stumble on this identity:

$$\ln\left(\frac{1+x}{1-x}\right) = 2 \tanh^{-1}(x)$$

which can be used to rewrite the expression for  $v_2$  as

$$v_2 = 2V_T \tanh^{-1}\left(\frac{v_3}{I_{EE} R_3}\right) \quad (16.148)$$

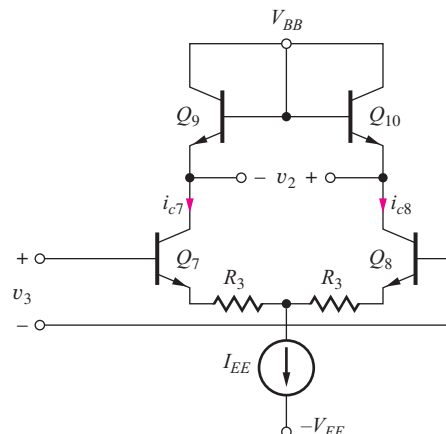


**Figure 16.60** Inverse hyperbolic tangent “predistortion” circuit.

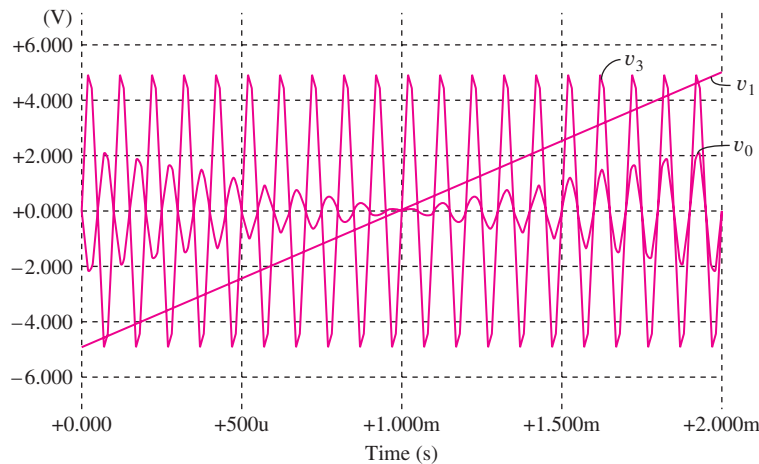


**Figure 16.61** Gilbert multiplier simulation results for  $v_3 = 5 \sin 20000\pi t$  and  $v_1$  ramping between  $-5$  and  $+5$  V with a scale factor of  $0.1$ .

Combining Eq. (16.148) with (16.143) gives the final result for the analog multiplier

$$v_o = \left( \frac{R}{I_{EE} R_1 R_3} \right) v_1 v_3 \quad (16.149)$$

The circuit described by Eq. (16.149) is known as a **four-quadrant multiplier** since both input voltages are permitted to take on both positive and negative values. One common design sets the scaling constant to be  $0.1$  so that the input and output signals can all have a  $10$ -V range.

An example of operation of an analog multiplier appears in Fig. 16.61. Input  $v_3 = 5 \sin 20,000\pi t$  V. Signal  $v_1$  is a ramp starting at  $-5$  V at  $t = 0$  and reaching  $+5$  V at  $t = 2$  ms. The product of the two waveforms appears in the figure. The product is zero and changes sign as  $v_1$  crosses through  $0$  V at  $t = 1$  ms.

**EXERCISE:** What should the scale factor be in Eq. (16.149) if all voltages are to have a  $5$ -V range? A  $1$ -V range?

**ANSWERS:** 0.2; 1.0



**EXERCISE:** Simulate the full Gilbert multiplier with a  $5$ -V,  $1$ -kHz sine wave for  $v_1$  with  $v_3 = 5 \sin 20000\pi t$  V.

## SUMMARY

Integrated circuit (IC) technology permits the realization of large numbers of virtually identical transistors. Although the absolute parameter tolerances of these devices are relatively poor, device characteristics can actually be matched to within less than 1 percent. The availability of large numbers of such closely matched devices has led to the development of special circuit techniques that depend on the similarity of device characteristics for proper operation. These matched circuit design techniques are used throughout analog circuit design and produce high-performance circuits that require very few resistors.

- One of the most important of the IC techniques is the current mirror circuit, in which the output current replicates, or mirrors, the input current. Multiple copies of the replicated current can be generated, and the gain of the current mirror can be controlled by scaling the emitter areas of bipolar transistors or the  $W/L$  ratios of FETs. Errors in the mirror ratio of current mirrors are related directly to the finite output resistance and/or current gain of the transistors through the parameters  $\lambda$ ,  $V_A$ , and  $\beta_F$ .
- In bipolar current mirrors, the finite current gain of the BJT causes an error in the mirror ratio, which the buffered current mirror circuit is designed to minimize. In both FET and BJT circuits, the ideal balance of the current mirror is disturbed by the mismatch in dc voltages between the input and output sections of the mirror. The degree of mismatch is determined by the output resistance of the current sources.
- The figure of merit  $V_{CS}$  for the basic current mirror is approximately equal to  $V_A$  for the BJT or  $1/\lambda$  for the MOS version. However, the value of  $V_{CS}$  can be improved by up to two orders of magnitude through the use of either the cascode or Wilson current sources.
- Current mirrors can also be used to generate currents that are independent of the power supply voltages. The  $V_{BE}$ -based reference and the Widlar reference produce currents that depend only on the logarithm of the supply voltage. By combining a Widlar source with a current mirror, a reference is realized that exhibits first-order independence of the power supply voltages. The only variation is due to the finite output resistance of the current mirror and Widlar source used in the supply-independent cell.
- The Widlar cell produces a PTAT voltage (proportional to absolute temperature) which is used as the basic sensing element in most electronic thermometers and is a key part of the bandgap reference.
- An extremely important application of the current mirror is as a replacement for the load resistors in differential and operational amplifiers. This active-load circuit can substantially enhance the voltage gain capability of most amplifiers while maintaining the operating-point balance necessary for low offset voltage and good common-mode rejection. Amplifiers with active loads can achieve single-stage voltage gains that approach the amplification factor of the transistor. Analysis of the ac behavior of circuits employing current mirrors can often be simplified using a two-port model for the mirror.
- Active current mirror loads are used to enhance the performance of both bipolar and MOS operational amplifiers. The classic μA741 operational amplifier, introduced in the late 1960s, was the first highly robust design combining excellent overall amplifier performance with input-stage breakdown-voltage protection and short-circuit protection of the output stage. Active loads are used to achieve a voltage gain in excess of 100 dB in an amplifier with two stages of gain. This operational amplifier design immediately became the industry standard op amp and spawned many similar designs.
- Four-quadrant multiplication of analog signals can be accurately obtained using the Gilbert multiplier circuit.

## KEY TERMS

Active load	Common-mode input voltage range
Bandgap reference	Common-mode rejection ratio (CMRR)
Buffered current mirror	Complementary push-pull output stage
Cascode current source	Current gain defect
Class-AB amplifiers	Current-limiting circuit
Common-mode gain	Current mirror
Common-mode half-circuit	Differential-mode gain
Common-mode input resistance	Differential-mode half-circuit

Differential-mode input resistance	$\mu\text{A}741$
Differential-mode output resistance	Mirror ratio
Differential-mode output voltage	Oversupply protection
“Diode-connected” transistor	Power-supply-independent biasing
Electronic current source	PTAT voltage
Emitter area scaling	Reference current
Figure of merit (FOM)	Short-circuit protection
Four-quadrant multiplier	Startup circuit
Gilbert multiplier	$V_{BE}$ -based reference
Half-circuit analysis	Voltage reference
Matched (devices)	Widlar current source
Matched transistors	Wilson current source

## REFERENCES

1. R. D. Thornton, et. al., *Multistage Transistor Circuits*, SEEC Volume 5, Wiley, New York: 1965.
2. P. R. Gray, P. J. Hurst, S. H. Lewis, and R. G. Meyer, *Analysis and Design of Analog Integrated Circuits*, 4th ed., John Wiley and Sons, New York: 2001.
3. R. J. Widlar, “Some circuit design techniques for linear integrated circuits,” *IEEE Transactions on Circuit Theory*, vol. CT-12, no. 12, pp. 586–590, December 1965.
4. R. J. Widlar, “Design techniques for monolithic operational amplifiers,” *IEEE Journal of Solid-State Circuits*, vol. SC-4, no. 4, pp. 184–191, August 1969.
5. G. R. Wilson, “A monolithic junction FET-NPN operational amplifier,” *IEEE Journal of Solid-State Circuits*, vol. SC-3, no. 6, pp. 341–348, December 1968.
6. Robert J. Widlar, “New developments in IC voltage regulators,” *IEEE Journal of Solid-State Circuits*, vol. SC-6, no. 1, pp. 2–7, January 1991.
7. A. Paul Brokaw, “A simple three-terminal IC bandgap reference,” *IEEE Journal of Solid-State Circuits*, vol. SC-9, no. 6, pp. 388–393, December 1994.
8. Barrie Gilbert, “The gears of genius,” *IEEE Solid-State Circuits Society News*, vol. 12, no. 4, pp. 10–27, Fall 2007.

## PROBLEMS

### 16.1 Circuit Element Matching

- 16.1. An integrated circuit resistor has a nominal value of  $3.92 \text{ k}\Omega$ . A given process run has produced resistors with a mean value 12 percent higher than the nominal value, and the resistors are found to be matched within 2.5 percent. What are the maximum and minimum resistor values that will occur?
- 16.2. (a) The emitter areas of two bipolar transistors are mismatched by 10 percent. What will be the base-emitter voltage difference between these two transistors when their collector currents are identical? (Assume  $V_A = \infty$ .) (b) Repeat for a 20 percent area mismatch. (c) What degree of matching is required for a base-emitter voltage difference of less than 0.5 mV?
- 16.3. The bipolar transistors in a differential pair are mismatched. (a) What will be the offset voltage if the current gains are mismatched by 5 percent? (b) If the saturation currents are mismatched by 5 percent? (c) If the Early voltages are mismatched by 5 percent? (d) If the collector resistors are mismatched by 5 percent? (Remember, the offset voltage is the input voltage required to force the differential output voltage to be zero.)
- \*16.4. The collector currents of two BJTs are equal when the base-emitter voltages differ by 2 mV. What is the fractional mismatch  $\Delta I_S/I_S$  in the saturation current of the two transistors if  $I_{S1} = I_S + \Delta I_S/2$  and  $I_{S2} = I_S - \Delta I_S/2$ ? Assume that the collector-emitter voltages and Early voltages are matched. If  $\Delta\beta_{FO}/\beta_{FO} = 5$  percent, what are the values of  $I_{B1}$  and  $I_{B2}$  for the transistors at a Q-point of (100  $\mu\text{A}$ , 10 V)? Assume  $\beta_{FO} = 100$  and  $V_A = 50 \text{ V}$ .
- 16.5. What is the worst-case fractional mismatch  $\Delta I_D/I_D$  in drain currents in two MOSFETs if  $K_n = 250 \text{ }\mu\text{A/V}^2 \pm 5$  percent and  $V_{TN} = 1 \text{ V} \pm$

- 25 mV for (a)  $V_{GS} = 2$  V? (b)  $V_{GS} = 4$  V? Assume  $I_{D1} = I_D + \Delta I_D/2$  and  $I_{D2} = I_D - \Delta I_D/2$ .

16.6. The MOS transistors in the differential pair are mismatched. The nominal value of  $(V_{GS} - V_{TN}) = 0.75$  V. (a) What will be the offset voltage if the  $(W/L)$  ratios are mismatched by 5 percent? (b) If the threshold voltages are mismatched by 5 percent? (c) If the values of  $\lambda$  are mismatched by 5 percent? (d) If the drain resistors are mismatched by 5 percent? (Remember, the offset voltage is the input voltage required to force the differential output voltage to be zero.)

16.7. (a) A layout design error causes the  $W/L$  ratios of the two NMOSFETs in a differential amplifier to differ by 10 percent. What will be the gate-source voltage difference between these two transistors when their drain currents are identical if the nominal value of  $(V_{GS} - V_{TN}) = 0.5$  V? (Assume  $V_{TN} = 1$  V,  $\lambda = 0$  and identical values of  $K'_n$ ). (b) What degree of matching is required for a gate-source voltage difference of less than 3 mV? (c) For 1 mV?

16.11. The current sources in Prob. 16.8 could represent the binary weighted currents needed for a 3-bit D/A converter. (a) What are the ideal values of the three output currents (i.e.,  $\lambda = 0$ )? (b) Express the current errors from Prob. 16.8 in terms of LSBs.

\*16.12. What are the output currents and output resistances for the current sources in Fig. P16.12 if  $R = 24$  k $\Omega$ ,  $K'_p = 15$   $\mu\text{A/V}^2$ ,  $V_{TP} = -0.90$  V, and  $\lambda = 0.01$  V $^{-1}$ ?

## 16.2 Current Mirrors

- 16.8. (a) What are the output currents and output resistances for the current sources in Fig. P16.8 if  $I_{REF} = 35 \mu\text{A}$ ,  $K'_n = 25 \mu\text{A/V}^2$ ,  $V_{TN} = 0.75 \text{ V}$  and  $\lambda = 0.01 \text{ V}^{-1}$ ? (b) What are the currents if  $I_{REF}$  is changed to  $50 \mu\text{A}$ ? (c) What would be the values if  $\lambda = 0$ ?

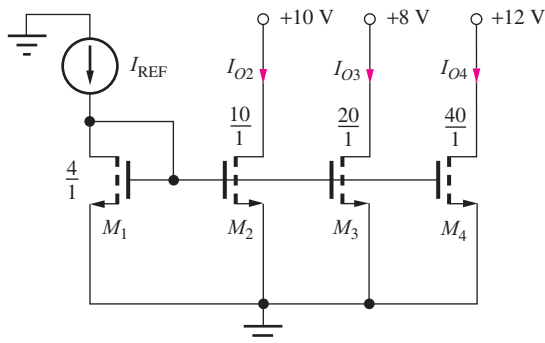


**Figure P16.8**

- 16.9. Simulate the current source array in Fig. P16.8 and compare the results to the hand calculations in Prob. 16.8.

16.10. (a) What are the output currents for the circuit in Prob. 16.8 if the  $W/L$  ratio of  $M_1$  is changed to 2.5/1? (b) If  $I_{REF} = 20 \mu\text{A}$  and  $(W/L)_1 = 5/1$ ?

- 16.11. The current sources in Prob. 16.8 could represent the binary weighted currents needed for a 3-bit D/A converter. (a) What are the ideal values of the three output currents (i.e.,  $\lambda = 0$ )? (b) Express the current errors from Prob. 16.8 in terms of LSBs.

\*16.12. What are the output currents and output resistances for the current sources in Fig. P16.12 if  $R = 24 \text{ k}\Omega$ ,  $K'_p = 15 \mu\text{A/V}^2$ ,  $V_{TP} = -0.90 \text{ V}$ , and  $\lambda = 0.01 \text{ V}^{-1}$ ?

**Figure P16.12**

16.13. Simulate the current source array in Fig. P16.12 and compare the results to the hand calculations in Prob. 16.12.

16.14. (a) What are the output currents for the circuit in Prob. 16.12 if the  $W/L$  ratio of  $M_1$  is changed to  $3.3/1$ ? (b)  $R = 50 \text{ k}\Omega$  and  $(W/L)_1 = 4/1$ ?

16.15. What value of  $R$  is required in Fig. P16.12 to have  $I_{O2} = 55 \mu\text{A}$ ? Use device data from Prob. 16.12.

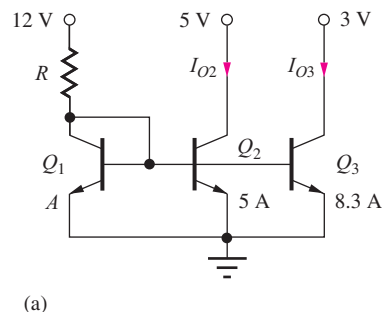
16.16. (a) What are the output currents and output resistances for the current sources in Fig. P16.16(a) if  $R = 68 \text{ k}\Omega$ ,  $\beta_{FO} = 50$ , and  $V_A = 60 \text{ V}$ ? (b) Repeat part (a) if the emitter areas of all the transistors are doubled. (c) Repeat for Fig. P16.16(b).

16.17. Simulate the current source array in Fig. P16.16(a) and compare the results to the hand calculations in Prob. 16.16. (b) Repeat for Fig. P16.16(b).

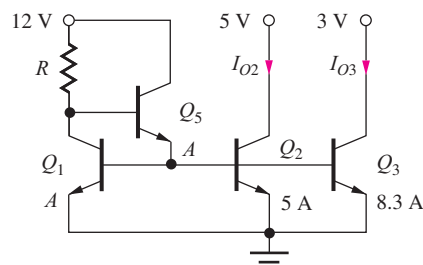
16.18. What value of  $R$  is required in Fig. P16.16(a) to have  $I_{O3} = 180 \mu\text{A}$ ? What is the value of  $I_{O2}$ ? Assume  $\beta_{FO} = 50$  and  $V_A = 60 \text{ V}$ . (b) Repeat for the circuit in Fig. P16.16(b).

16.19. (a) What are the output currents in the circuit in Fig. P16.16(a) if the area of transistor  $Q_1$  is changed to  $2A$ , and  $R = 75 \text{ k}\Omega$ ? Use  $\beta_{FO} = 125$  and  $V_A = 75 \text{ V}$ . (b) Repeat for Fig. P16.16(b).

16.20. (a) What are the output currents in the circuit in Fig. P16.16(a) if  $R = 130 \text{ k}\Omega$ ? Use  $\beta_{FO} = 125$  and  $V_A = 75 \text{ V}$ . (b) What value of  $R$  is required to produce the same output currents in Fig. P16.16(b).



(a)



(b)

Figure P16.16

- 16.21. What are the output currents in the circuit in Fig. P16.16(b) if the area of transistor  $Q_1$  is changed to  $3A$ , and  $R = 91\text{ k}\Omega$ ? Use  $\beta_{FO} = 100$  and  $V_A = 75\text{ V}$ .
- 16.22. (a) What are the output currents in Fig. P16.16(a) if  $R = 100\text{ k}\Omega$ ? (b) What are the output currents if the 5-V supply increases to 6 V? (c) What are the output currents if the 12-V supply decreases to 11 V? (d) Show that the change in  $I_{O2}$  in part (b) is equal to  $g_{o2} \Delta V$ .
- 16.23. What are the output currents and output resistances for the current sources in Fig. P16.23 if  $R = 90\text{ k}\Omega$ ,  $\beta_{FO} = 50$ , and  $V_A = 60\text{ V}$ ?

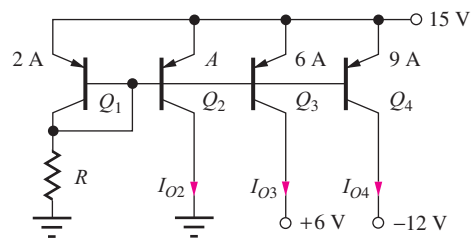


Figure P16.23

- 16.24. What value of  $R$  is required in the circuit in Fig. P16.23 to set  $I_{O3} = 65\text{ }\mu\text{A}$ ? What are the values of  $I_{O2}$  and  $I_{O4}$ ?

\*16.25. Draw a buffered current mirror version of the source in Fig. P16.23 and find the value of  $R$  required to set  $I_{REF} = 25\text{ }\mu\text{A}$  if  $\beta_{FO} = 70$  and  $V_A = 60\text{ V}$ . What are the values of the three output currents? What is the collector current of the additional transistor?

- 16.26. In Fig. P16.26,  $R_2 = 5R_3$ . What value of  $n$  is required to set  $I_{E3}$  to be exactly  $5I_{E2}$ ?

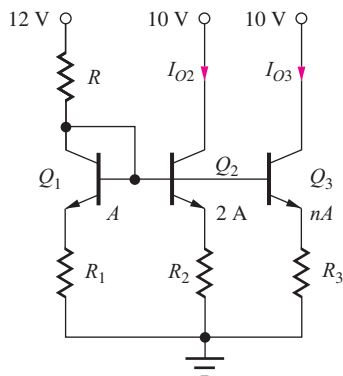


Figure P16.26

\*16.27. What are the output currents and output resistances for the current sources in Fig. P16.26 if  $R = 20\text{ k}\Omega$ ,  $R_1 = 10\text{ k}\Omega$ ,  $R_2 = 5\text{ k}\Omega$ ,  $R_3 = 2.5\text{ k}\Omega$ ,  $n = 4$ ,  $\beta_{FO} = 75$ , and  $V_A = 75\text{ V}$ ?

\*16.28. What values of  $n$  and  $R_3$  would be required in Prob. 16.27 so that  $I_{O2} = 3I_{O3}$ ?

16.29. Repeat Prob. 16.27 if the area of transistor  $Q_1$  is changed to  $0.5\text{ A}$  and  $R_1$  is changed to  $20\text{ k}\Omega$ .

16.30. What are the output current  $I_O$  and output resistance in the circuit in Fig. P16.30 if  $-V_{EE} = -6\text{ V}$ ,  $n = 7.2$ ,  $K_n = 50\text{ }\mu\text{A/V}^2$ ,  $V_{TN} = 0.75\text{ V}$ ,  $I_{REF} = 18\text{ }\mu\text{A}$ ,  $\beta_{FO} = 100$ , and  $V_A = 65\text{ V}$ ?

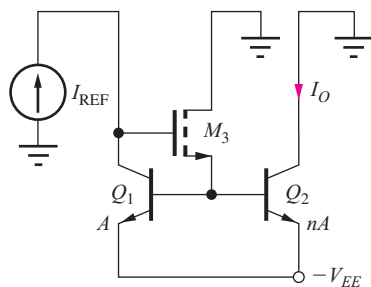


Figure P16.30

- 16.31. Use SPICE to simulate the circuit in Prob. 16.30 and compare the results to hand calculations.

- 16.32. (a) What is the input resistance presented to source  $I_{\text{REF}}$  at the gate of transistor  $M_3$  in Fig. P16.30 if  $n = 1$ ? Use the other parameters from Prob. 16.30. (b) Use transfer function analysis in SPICE to verify your result.

### Widlar Sources

- 16.33. (a) What are the output current and output resistance for the Widlar current source  $I_{O2}$  in Fig. P16.33 if  $R = R_2 = 15 \text{ k}\Omega$  and  $V_A = 60 \text{ V}$ ? (b) For  $I_{O3}$  if  $R_3 = 5 \text{ k}\Omega$  and  $n = 12$ ?

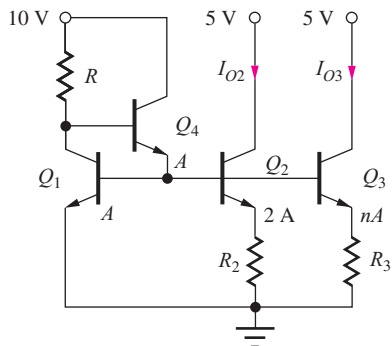


Figure P16.33

- 16.34. What value of  $R$  is required to set  $I_{\text{REF}} = 50 \mu\text{A}$  in Fig. P16.33? If  $I_{\text{REF}} = 50 \mu\text{A}$ , what value of  $R_2$  is needed to set  $I_{O2} = 5 \mu\text{A}$ ? If  $R_3 = 2 \text{ k}\Omega$ , what value of  $n$  is required to set  $I_{O3} = 10 \mu\text{A}$ ?

- 16.35. Simulate the source of Prob. 16.34 and compare the results to hand calculations.

- 16.36. (a) What are the output current and output resistance for the Widlar current source  $I_{O2}$  in Fig. P16.36 if  $R = 50 \text{ k}\Omega$  and  $R_2 = 5 \text{ k}\Omega$ ? Use  $V_A = 70 \text{ V}$  and  $\beta_F = 100$ . (b) For  $I_{O3}$  if  $R_3 = 2.5 \text{ k}\Omega$  and  $n = 20$ ?

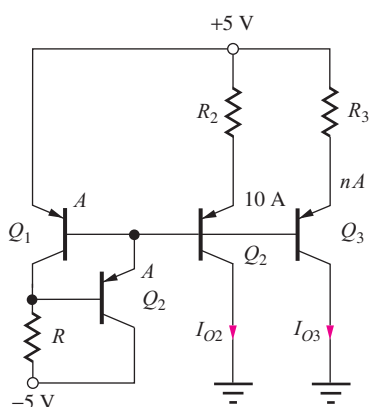


Figure P16.36

- 16.37. What value of  $R$  is required to set  $I_{\text{REF}} = 45 \mu\text{A}$  in Fig. P16.36. If  $I_{\text{REF}} = 45 \mu\text{A}$ , what value of  $R_2$  is needed to set  $I_{O2} = 10 \mu\text{A}$ ? If  $R_3 = 2 \text{ k}\Omega$ , what value of  $n$  is required to set  $I_{O3} = 10 \mu\text{A}$ ?

### 16.3 High-Output-Resistance Current Mirrors

#### Wilson Sources

- 16.38.  $I_{\text{REF}} = 30 \mu\text{A}$ ,  $-V_{EE} = -5 \text{ V}$ ,  $\beta_{FO} = 125$ , and  $V_A = 40 \text{ V}$  in the Wilson source in Fig. P16.38. (a) What are the output current and output resistance for  $n = 1$ ? (b) For  $n = 3$ ? (c) What is the value of  $V_{CS}$  for the current source in (b)? (d) What is the minimum value of  $V_{EE}$ ?

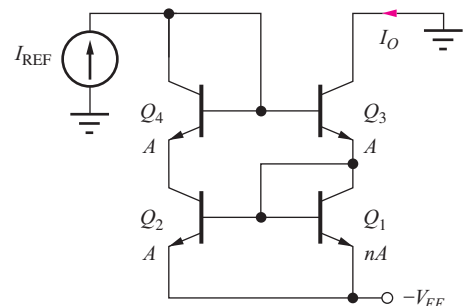


Figure P16.38

- 16.39. Derive an expression for the output resistance of the BJT Wilson source in Fig. P16.38 and show that it can be reduced to Eq. (16.37), use  $n = 1$ . What assumptions were used in this simplification?

- \*16.40. Derive an expression for the output resistance of the Wilson source in Fig. P16.38 as a function of the area ratio  $n$ .

- 16.41. What is the minimum voltage that can be applied to the collector of  $Q_3$  in Fig. P16.38 and have the transistor remain in the active region if  $I_{\text{REF}} = 15 \mu\text{A}$ ,  $n = 5$ ,  $\beta_{FO} = 125$ , and  $I_{SO} = 3 \text{ fA}$ ? Calculate an exact value based on the value of  $I_{SO}$ .

- 16.42.  $R = 40 \text{ k}\Omega$  in the Wilson source in Fig. P16.42. (a) What is the output current if  $(W/L)_1 = 5/1$ ,  $(W/L)_2 = 20/1$ ,  $(W/L)_3 = 20/1$ ,  $K'_n = 25 \mu\text{A}/\text{V}^2$ ,  $V_{TN} = 0.75 \text{ V}$ ,  $\lambda = 0 \text{ V}^{-1}$ , and  $V_{SS} = -5 \text{ V}$ . What value of  $(W/L)_4$  is required to balance the drain voltages of  $M_1$  and  $M_2$ ? (b) What is the output resistance if  $\lambda = 0.015 \text{ V}^{-1}$ ? Use the dc values from part (a). (\*c) Repeat if  $\lambda = 0.015 \text{ V}^{-1}$ . (d) Check your results in (e) with SPICE simulation.

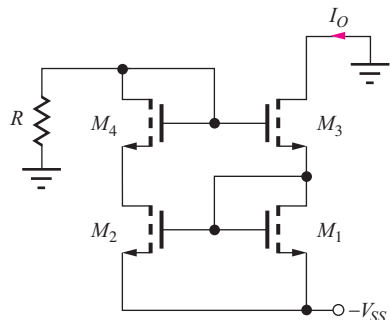


Figure P16.42

- \*16.43. Derive an expression for the output resistance of the Wilson source in Fig. P16.42 as a function of  $(W/L)_1$ ,  $(W/L)_2$ ,  $(W/L)_3$ ,  $(W/L)_4$ , and the reference current  $I_{\text{REF}}$ . Assume  $R = \infty$ .
- 16.44. (a) Derive an expression for the equivalent resistance presented to  $I_{\text{REF}}$  in the Wilson source in Fig. 16.16(a). (b) Derive an expression for the equivalent resistance presented to  $I_{\text{REF}}$  in the Wilson source in Fig. 16.16(b).
- 16.45. What is the minimum voltage required on the drain of  $M_3$  to maintain it in pinch-off in the circuit in Fig. P16.42 if  $I_{\text{REF}} = 125 \mu\text{A}$ ,  $(W/L)_1 = 5/1$ ,  $(W/L)_2 = 20/1$ ,  $(W/L)_3 = 20/1$ ,  $K'_n = 25 \mu\text{A}/\text{V}^2$ ,  $V_{TN} = 0.75 \text{ V}$ ,  $\lambda = 0 \text{ V}^{-1}$ , and  $-V_{SS} = -10 \text{ V}$ ?
- 16.46. In Fig. P16.42,  $(W/L)_3 = 5/1$ ,  $(W/L)_4 = 5/1$ , and  $I_{\text{REF}} = 50 \mu\text{A}$ . What value of  $(W/L)_2$  is required for  $R_{\text{out}} = 300 \text{ M}\Omega$  if  $K'_n = 25 \mu\text{A}/\text{V}^2$ ,  $V_{TN} = 0.75 \text{ V}$ ,  $\lambda = 0.0125 \text{ V}^{-1}$ . Assume  $(W/L)_1 = (W/L)_2$ ,  $R = \infty$ , and  $V_{SS} = 5 \text{ V}$ . Neglect  $V_{DS}$ .
- \*\*16.47. Redraw the equivalent circuit used to calculate the output resistance of the MOS Wilson source in Figs. 16.16(a) and 16.18 including a finite output resistance  $R_{\text{REF}}$  for the reference source. Based on this circuit, how large must  $R_{\text{REF}}$  be to keep from degrading the output resistance of the Wilson source? What type of current source could be used to implement  $I_{\text{REF}}$  to meet this requirement?
- 16.48. Use Blackman's theorem to find the expression for the output resistance of the MOS Wilson source in Fig. 16.16(a).
- 16.49. Find the output resistance of the MOS Wilson source in Prob. 16.42 by applying Blackman's theorem. What are the values of  $R_D$ ,  $T_{OC}$ ,  $T_{SC}$  and  $R_{\text{out}}$ ?
- 16.50. Use Blackman's theorem to find the expression for the output resistance of the BJT Wilson source in Fig. 16.16(b).

- 16.51. Find the output resistance of the BJT Wilson source in Prob. 16.38 by applying Blackman's theorem. What are the values of  $R_D$ ,  $T_{OC}$ ,  $T_{SC}$ , and  $R_{\text{out}}$ ?

### Cascode Current Sources

- 16.52. (a) What are the output current and output resistance for the cascode current source in Fig. P16.52 if  $I_{\text{REF}} = 20 \mu\text{A}$ ,  $V_{DD} = 5 \text{ V}$ ,  $K_n = 75 \mu\text{A}/\text{V}^2$ ,  $V_{TN} = 0.75 \text{ V}$ , and  $\lambda = 0.0125 \text{ V}^{-1}$ . (b) What is the value of  $V_{CS}$  for this current source? (c) What is the minimum value of  $V_{DD}$ ?

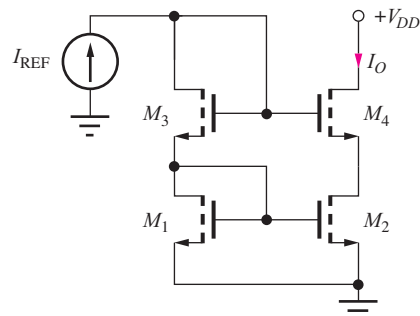


Figure P16.52

- 16.53. Use SPICE to simulate the current source in Prob. 16.52 and compare the results to your calculations.
- 16.54. (a) A layout error causes the  $W/L$  ratio of  $M_2$  to be 5 percent larger than that of  $M_1$  in Prob. 16.52. What is the error in the output current  $I_O$ ? (a) Repeat if  $M_1 = M_2$ , but  $M_4$  is 5 percent larger than that of  $M_3$ .
- 16.55. What is the output resistance of the source in Prob. 16.52 if the body of  $M_4$  is connected to ground and  $V_{TO} = 0.75 \text{ V}$  and  $\gamma = 0.7 \text{ V}^{0.5}$ ? Assume  $\gamma = 0$  for the Q-point calculations.
- 16.56. In Fig. P16.56,  $(W/L)_1 = 5/1$ ,  $(W/L)_2 = 5/1$ ,  $(W/L)_3 = 5/1$ , and  $I_{\text{REF}} = 50 \mu\text{A}$ . What value of  $(W/L)_4$  is required for  $R_{\text{out}} = 250 \text{ M}\Omega$  if  $K'_n = 25 \mu\text{A}/\text{V}^2$ ,  $V_{TN} = 0.75 \text{ V}$ , and  $\lambda = 0.0125 \text{ V}^{-1}$ ?
- 16.57. (a) Repeat Prob. 16.52 for  $I_{\text{REF}} = 25 \mu\text{A}$ . (b) Repeat Prob. 16.52 for  $I_{\text{REF}} = 50 \mu\text{A}$ .
- 16.58. (a) Find the output resistance of the cascode current source in Fig. P16.58. Use the parameters from Prob. 16.52. (b) What is the output resistance for the source in Fig. P16.52?
- 16.59. What is the equivalent resistance presented to  $I_{\text{REF}}$  in the cascode current source in Prob. 16.52?

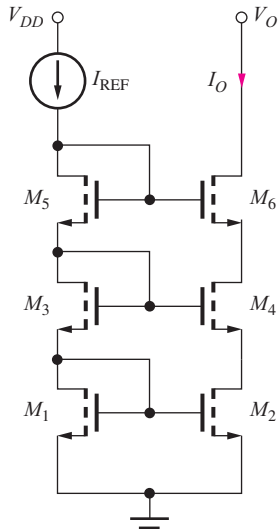


Figure P16.58

- 16.60. (a) What are the output current and output resistance for the cascode current source in Fig. P16.60 if  $I_{REF} = 17.5 \mu\text{A}$ ,  $\beta_{FO} = 110$ , and  $V_A = 50 \text{ V}$ ? (b) What is the value of  $V_{CS}$  for this current source? (c) What is the minimum value of  $V_{CC}$ ?

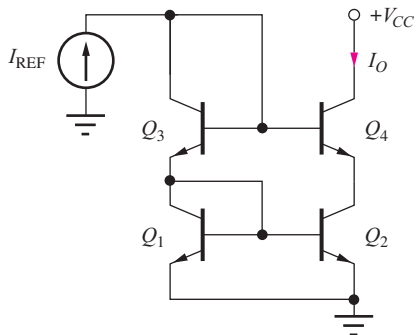


Figure P16.60

- 16.61. Simulate the current source in Prob. 16.60 and compare the results to hand calculations.
- 16.62. What is the equivalent resistance presented to  $I_{REF}$  in the cascode current source in Prob. 16.60?
- 16.63. Repeat Prob. 16.60 if  $I_{REF} = 125 \mu\text{A}$ ,  $\beta_{FO} = 120$  and  $V_A = 60 \text{ V}$ .

### Regulated Cascode

- 16.64. (a) Find the output resistance of the regulated cascode source in Fig. 16.22(c) if  $I_{REF} = I_4 = 25 \mu\text{A}$ ,  $K_n = 100 \mu\text{A/V}^2$ ,  $V_{TN} = 0.75 \text{ V}$  and  $\lambda = 0.015 \text{ V}^{-1}$ . (b) Repeat if  $I_4$  is  $50 \mu\text{A}$ .

16.65 Find the expression for the output resistance of the regulated cascode source in Fig. 16.22(c) if current source  $I_4$  has an output resistance  $R_4$ . How large must  $R_4$  be to not degrade the output resistance of the source?

- 16.66 Repeat Prob. 16.64 if  $I_4$  is supplied by a standard PMOS current mirror whose transistors have  $\lambda = 0.015 \text{ V}^{-1}$ .

### 16.4–16.5 Reference Current Generation and Supply-Independent Biasing

- 16.67. What are the output current and output resistance for the Widlar source in Fig. P16.67 if  $I_{REF} = 80 \mu\text{A}$  and  $R_2 = 500 \Omega$ ? (b) What is the new value of the output current if a layout error causes the area of  $Q_2$  to be 5 percent larger than desired? (c) What are the new values of output current and resistance if the emitter area of  $Q_2$  is reduced to  $14A$ ?

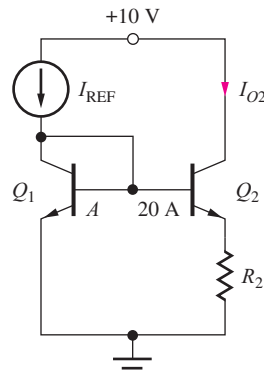


Figure P16.67

- 16.68. What are the output current and output resistance for the Widlar source in Fig. P16.67 if  $I_{REF} = 35 \mu\text{A}$  and  $R_2 = 935 \Omega$ ? (b) What are the new values if the emitter area of  $Q_1$  is increased to  $2A$ ?

- 16.69.  $I_{REF} = 75 \mu\text{A}$  in Fig. P16.67. (a) What value of  $R_2$  is required to set  $I_{O2} = 22 \mu\text{A}$ ? (b) To set  $I_{O2} = 5.7 \mu\text{A}$ ? (c) To set  $I_{O2} = 5.7 \mu\text{A}$  if the area of  $Q_2$  is changed to  $10A$ ?

- 16.70.  $I_{REF} = 62 \mu\text{A}$  in Fig. P16.67. (a) What value of  $R_2$  is required to set  $I_{O2} = 16 \mu\text{A}$  if the area  $Q_1$  is changed to  $2A$ ? (b) If the area of  $Q_2$  is changed to  $10A$ ?

- 16.71. Plot the variation of the output current vs.  $I_{REF}$  for the Widlar source in Fig. P16.67 for  $50 \mu\text{A} \leq I_{REF} \leq 5 \text{ mA}$  if  $R_2 = 4 \text{ k}\Omega$  and  $\beta_{FO} = 100$ .

- 16.72. (a) What is the output current of the  $V_{BE}$ -based reference in Fig. P16.72(a) if  $I_S = 10^{-15} \text{ A}$ ,  $\beta_F = \infty$ ,  $R_1 = 10 \text{ k}\Omega$ ,  $R_2 = 2.2 \text{ k}\Omega$ , and  $V_{EE} = 15 \text{ V}$ ? (b) For  $V_{EE} = 3.3 \text{ V}$ ? (c) What is the output current of the  $V_{BE}$ -based reference in Fig. P16.72(b) if  $R_1 = 10 \text{ k}\Omega$ ,  $R_2 = 10 \text{ k}\Omega$ , and  $V_{CC} = 5 \text{ V}$ ?
- 16.73. (a) Design the reference in Fig. P16.72(a) to produce an output current  $I_O = 30 \mu\text{A}$ . Assume  $-V_{EE} = -3.3 \text{ V}$  and  $I_S = 0.1 \text{ fA}$  and  $\beta_{FO} = 130$  for both transistors. (b) Repeat for the circuit in Fig. P16.72(b) if  $V_{CC} = 3.3 \text{ V}$ .

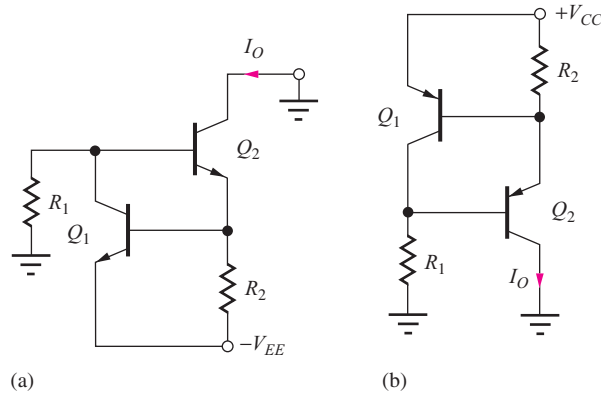


Figure P16.72

- \*16.74. Derive the expression for the output resistance of the cascode current source in Figs. 16.19(b) and 16.21.
- \*16.75. What is the output current of the NMOS reference in Fig. P16.75(a) if  $R_1 = 10 \text{ k}\Omega$ ,  $R_2 = 15 \text{ k}\Omega$ ,  $K_n = 250 \mu\text{A}/\text{V}^2$ ,  $V_{TN} = 0.75 \text{ V}$ ,  $\lambda = 0.017 \text{ V}^{-1}$ , and  $V_{DD} = 10 \text{ V}$ ?

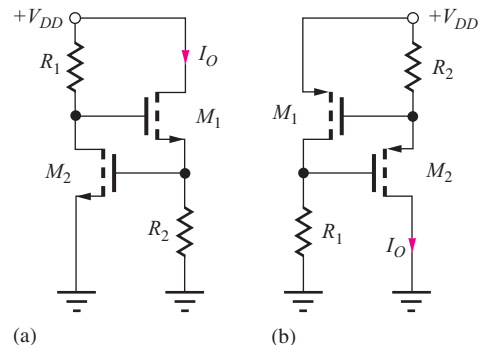


Figure P16.75

- 16.76. Design the reference in Fig. P16.75(a) to produce an output current  $I_O = 75 \mu\text{A}$ . Assume  $V_{DD} = 6 \text{ V}$  and use the transistor parameters from Prob. 16.75.

- \*16.77. What is the output current of the PMOS reference in Fig. P16.75(b) if  $R_1 = 10 \text{ k}\Omega$ ,  $R_2 = 18 \text{ k}\Omega$ ,  $K_p = 100 \mu\text{A}/\text{V}^2$ ,  $V_{TP} = -0.75 \text{ V}$ ,  $\lambda = 0.02 \text{ V}^{-1}$ , and  $V_{DD} = 5 \text{ V}$ ?
- 16.78. Design the reference in Fig. P16.75(b) to produce an output current  $I_O = 115 \mu\text{A}$ . Assume  $V_{DD} = 9 \text{ V}$  and use the transistor parameters from Prob. 16.77.
- 16.79. What are the collector currents in  $Q_1$  and  $Q_2$  in the reference in Fig. P16.79 if  $V_{CC} = V_{EE} = 1.5 \text{ V}$ ,  $n = 18$ , and  $R = 2.2 \text{ k}\Omega$ ? Assume  $\beta_{FO} = \infty$  and  $V_A = \infty$ .

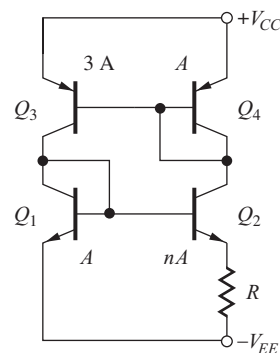


Figure P16.79

- 16.80. Simulate the reference in Prob. 16.79 using SPICE, assuming  $\beta_{FO} = 100$  and  $V_A = 50 \text{ V}$ . Compare the currents to hand calculations and discuss the source of any discrepancies. Use SPICE to determine the sensitivity of the reference currents to power supply voltage changes.
- 16.81. What are the collector currents in the four transistors in Fig. P16.79 if  $V_{CC} = V_{EE} = 3.3 \text{ V}$ ,  $n = 10$ , and  $R = 4 \text{ k}\Omega$ ?
- 16.82. What is the smallest value of  $n$  required for the circuit in Fig. P16.79 to operate properly (i.e.,  $V_{PTAT} > 0$ )?
- 16.83. (a) What value of  $R$  is required to set  $I_{C2} = 28 \mu\text{A}$  in Fig. P16.79 if  $n = 5$  and  $T = 50^\circ\text{C}$ ? (b) For  $n = 10$  and  $T = 0^\circ\text{C}$ ?
- 16.84. What are the drain currents in  $M_1$  and  $M_2$  in the reference in Fig. P16.84 if  $R = 4.2 \text{ k}\Omega$  and  $V_{DD} = V_{SS} = 5 \text{ V}$ ? Use  $K'_n = 25 \mu\text{A}/\text{V}^2$ ,  $V_{TN} = 0.75 \text{ V}$ ,  $K'_p = 10 \mu\text{A}/\text{V}^2$ , and  $V_{TP} = -0.75 \text{ V}$ . Assume  $\gamma = 0$  and  $\lambda = 0$  for both transistor types.
- 16.85. (a) Find the currents in both sides of the reference cell in Fig. P16.84 if  $R = 10 \text{ k}\Omega$  and  $V_{DD} = V_{SS} = 5 \text{ V}$ , using  $K'_n = 25 \mu\text{A}/\text{V}^2$ ,  $V_{TON} = 0.75 \text{ V}$ ,  $K'_p = 10 \mu\text{A}/\text{V}^2$ ,  $V_{TOP} = -0.75 \text{ V}$ ,  $\gamma_n = 0$

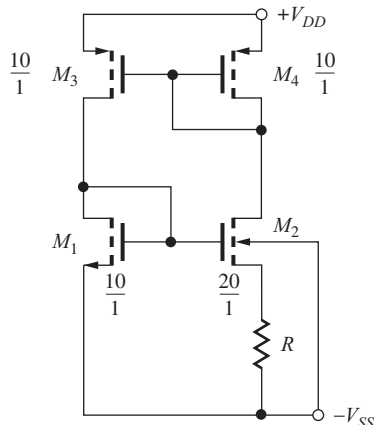


Figure P16.84

and  $\gamma_p = 0$ . Use  $2\phi_F = 0.6$  V and  $\lambda = 0$  for both transistor types. (b) Repeat for  $\gamma_n = 0.5$  V $^{0.5}$  and  $\gamma_p = 0.75$  V $^{0.5}$  and compare the results.

- 16.86. Simulate the references in Prob. 16.85(a) and (b) using SPICE with  $\lambda = 0.017$  V $^{-1}$ . Compare the currents to hand calculations (with  $\gamma = 0$  and  $\lambda = 0$ ) and discuss the source of any discrepancies. Use SPICE to determine the sensitivity of the reference currents to power supply voltage changes.
- 16.87. What are the collector currents in  $Q_1$  to  $Q_8$  in the reference in Fig. P16.87 if  $V_{CC} = 0$  V,  $V_{EE} = 3.3$  V,  $R = 11$  k $\Omega$ ,  $R_6 = 3$  k $\Omega$ ,  $R_8 = 4$  k $\Omega$ , and  $A_{E2} = 5$  A,  $A_{E3} = 2$  A,  $A_{E4} = A$ ,  $A_{E5} = 2.5$  A,  $A_{E6} = A$ ,  $A_{E7} = 5$  A, and  $A_{E8} = 3$  A?

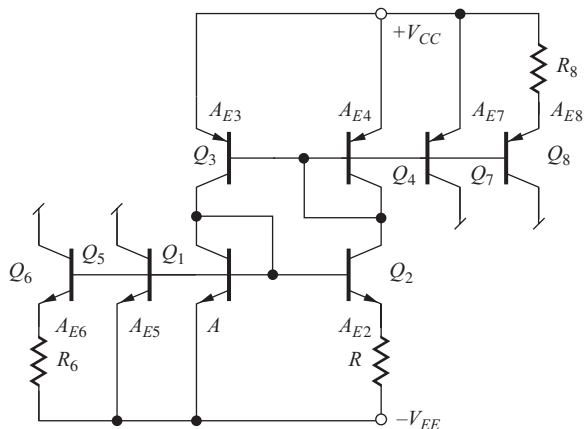


Figure P16.87

- 16.88. Repeat Prob. 16.87 if  $A_{E2} = 10A$  and  $A_{E3} = A$ .
- \*16.89. (a) What are the collector currents in  $Q_1$  to  $Q_7$  in the reference in Fig. P16.89 if  $V_{CC} = 5$  V and

$R = 3900$   $\Omega$ ? Assume  $\beta_F = \infty = V_A$ . (b) Repeat part (a) if the emitter areas of transistors  $Q_5$ ,  $Q_6$ , and  $Q_7$  are all changed to  $2A$ .

- \*16.90. (a) Simulate the reference in Prob. 16.89 using SPICE. Assume  $\beta_{FOn} = 100$ ,  $\beta_{FOp} = 50$ , and both Early voltages = 50 V. Compare the currents to hand calculations and discuss the source of any discrepancies. Use SPICE to determine the sensitivity of the reference currents to power supply voltage changes.

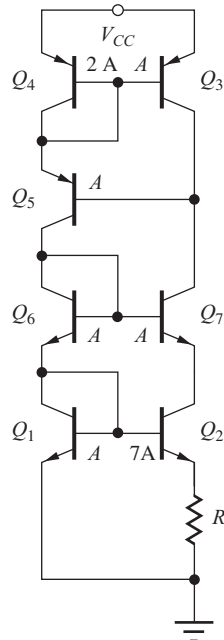


Figure P16.89

- 16.91. Repeat Prob. 16.89 assuming the emitter area of transistor  $Q_3$  is changed to  $2A$ .
- \*16.92. (a) What are the drain currents in  $M_1$  and  $M_2$  in the reference in Fig. P16.92 if  $R = 3600$   $\Omega$ ,  $V_{DD} = 15$  V,  $K'_n = 25$   $\mu\text{A}/\text{V}^2$ ,  $V_{TN} = 0.75$  V,  $K'_p = 10$   $\mu\text{A}/\text{V}^2$ ,  $V_{TP} = -0.75$  V, and  $\lambda = 0$  for both transistor types? (b) Repeat part (a) if the  $W/L$  ratios of transistors  $M_5$ ,  $M_6$ , and  $M_7$  are all increased to  $15/1$ .
- 16.93. Simulate the reference in Prob. 16.92 with SPICE using  $\lambda = 0.017$  V $^{-1}$  for both transistor types. Compare the currents to those in Prob. 16.92 and discuss the source of any discrepancies. Use SPICE to determine the sensitivity of the reference currents to power supply voltage changes.
- 16.94. Repeat Prob. 16.92 assuming the  $W/L$  ratio of transistor  $M_3$  is changed to  $15/1$ .

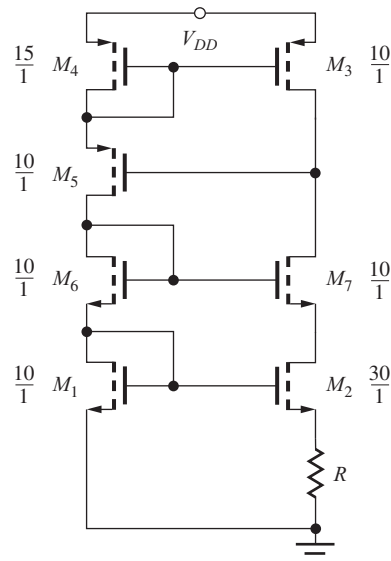


Figure P16.92

## 16.6 The Bandgap Reference

- 16.95. Find  $I_C$ ,  $V_{PTAT}$ ,  $V_{BE}$  and  $V_{BG}$  for the bandgap reference in Fig. 16.29 if  $R = 36 \text{ k}\Omega$ ,  $R_1 = 1 \text{ k}\Omega$  and  $R_2 = 4.16 \text{ k}\Omega$ . Assume  $I_S = 0.2 \text{ fA}$  and  $A_{E2} = 10A_{E1}$ . What temperature corresponds to zero TC?
- 16.96. A layout error caused  $A_{E2} = 9A_{E1}$  in the bandgap reference in Ex. 16.6. What is the new output voltage? What temperature corresponds to zero TC?
- 16.97. Find  $I_C$ ,  $V_{PTAT}$ ,  $V_{BE}$  and  $V_{BG}$  for the bandgap reference in Fig. 16.29 if  $R = 50 \text{ k}\Omega$ ,  $R_1 = 1 \text{ k}\Omega$  and  $R_2 = 4 \text{ k}\Omega$ . Assume  $I_S = 0.1 \text{ fA}$  and  $A_{E2} = 8 A_{E1}$ . What temperature corresponds to zero TC?
- 16.98. (a) Process variations cause the value of the two collector resistors in the circuit in Prob. 16.95 to decrease to  $35 \text{ k}\Omega$ . What is the new value of  $V_{BG}$ ? What temperature corresponds to zero TC?  
(b) Repeat for  $R = 25 \text{ k}\Omega$ .
- 16.99. What are the bandgap reference output voltage and temperature coefficient of the reference in Prob. 16.95 if  $I_S$  changes to  $0.5 \text{ fA}$ ?
- 16.100. What are the bandgap reference output voltage and the temperature coefficient of the reference in Design Ex. 16.6 at  $320 \text{ K}$  if  $I_S$  changes to  $0.3 \text{ fA}$ ?
- 16.101. Process variations cause the values of the two collector resistors in the circuit in Design Ex. 16.6 to be mismatched. If  $R_1 = 82 \text{ k}\Omega$  and  $R_2 = 78 \text{ k}\Omega$ , what is the new value of  $V_{BG}$ ? What temperature corresponds to zero TC?

- 16.102. The bandgap reference in Design Ex. 16.6 was designed to have zero temperature coefficient at  $320 \text{ K}$ . What will be the temperature coefficient at  $280 \text{ K}$ ? At  $320 \text{ K}$ ?
- 16.103. Redesign the bandgap reference in Design Ex. 16.6 to use  $A_{E2} = 8A_{E1}$ .
- 16.104. Redesign the bandgap reference in Design Ex. 16.6 to produce an output voltage of  $7.500 \text{ V}$  with zero TC at  $10^\circ\text{C}$ . Assume  $V_{CC} = 10 \text{ V}$ .

## 16.7 The Current Mirror as an Active Load

- 16.105. What are the values of  $A_{dd}$ ,  $A_{cd}$ , and CMRR for the amplifier in Fig. 16.31 if  $I_{SS} = 200 \mu\text{A}$ ,  $R_{SS} = 25 \text{ M}\Omega$ ,  $K_n = K_p = 500 \mu\text{A/V}^2$ ,  $V_{TN} = 1 \text{ V}$ , and  $V_{TP} = -1 \text{ V}$  and  $\lambda = 0.02 \text{ V}^{-1}$  for both transistors?
- 16.106. Use SPICE to simulate the amplifier in Prob. 16.105 and compare the results to the hand calculations. Use symmetrical 12-V supplies.
- 16.107. What are the values of  $A_{dd}$ ,  $A_{cd}$ , and CMRR for the amplifier in Fig. 16.31 if  $I_{SS} = 1 \text{ mA}$ ,  $R_{SS} = 10 \text{ M}\Omega$ ,  $K_n = K_p = 500 \mu\text{A/V}^2$ ,  $V_{TN} = -V_{TP} = 1 \text{ V}$ , and  $\lambda = 0.015/\text{V}$  for both transistors? What are the minimum power supply voltages if the common-mode input range must be  $\pm 5 \text{ V}$ ? Assume symmetrical supply voltages.
- 16.108. Use SPICE to simulate the amplifier in Prob. 16.107 and compare the results to hand calculations. Use symmetrical 12-V power supplies.
- <sup>\*</sup>16.109. (a) What are  $A_{dd}$  and  $A_{cd}$  for the bipolar differential amplifier in Fig. 16.37 ( $R_L = \infty$ ) if  $\beta_{op} = 70$ ,  $\beta_{on} = 125$ ,  $I_{EE} = 200 \mu\text{A}$ ,  $R_{EE} = 25 \text{ M}\Omega$ , and the Early voltages for both transistors are  $60 \text{ V}$ ? What is the CMRR for  $v_{C1} = v_{C2}$ ? (b) What are the minimum power supply voltages if the common-mode input range must be  $\pm 1.5 \text{ V}$ ? Assume symmetrical supply voltages.
- 16.110. Use SPICE to calculate  $A_{dd}$  and  $A_{cd}$  for the differential amplifier in Prob. 16.109. Compare the results to hand calculations.
- 16.111. (a) Repeat Prob. 16.109 if  $I_{EE}$  is changed to  $50 \mu\text{A}$ ,  $R_{EE} = 100 \text{ M}\Omega$ , and  $V_A = 75 \text{ V}$ . (b) Repeat part (a) for  $V_A = 100 \text{ V}$ .
- 16.112. Use SPICE to simulate the amplifier in Prob. 16.111 and compare the results to hand calculations. Use symmetrical 3-V power supplies.
- <sup>\*</sup>16.113. (a) Find the Q-points of the transistors in the CMOS differential amplifier in Fig. P16.113 if

$V_{DD} = V_{SS} = 10 \text{ V}$ ,  $I_{SS} = 200 \mu\text{A}$ , and  $R_{SS} = 25 \text{ m}\Omega$ . Assume  $K'_n = 25 \mu\text{A/V}^2$ ,  $V_{TN} = 0.75 \text{ V}$ ,  $K'_p = 10 \mu\text{A/V}^2$ ,  $V_{TP} = -0.75 \text{ V}$ , and  $\lambda = 0.017 \text{ V}^{-1}$  for both transistor types. (b) What is the voltage gain  $A_{dd}$  of the amplifier? (c) Compare this result to the gain of the amplifier in Fig. 16.31 if the Q-point and  $W/L$  ratios of  $M_1$  to  $M_4$  are the same.

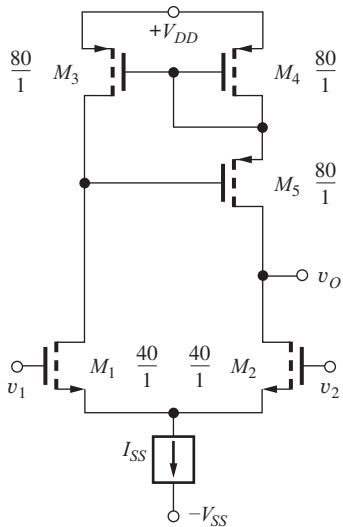


Figure P16.113

- 16.114. Use SPICE to simulate the amplifier in Prob. 16.113(a,b) and compare the results to hand calculations. S
- \*16.115. Find the Q-points of the transistors in the folded-cascode CMOS differential amplifier in Fig. P16.115 if  $V_{DD} = V_{SS} = 5 \text{ V}$ ,  $I_1 = 250 \mu\text{A}$ ,  $I_2 = 250 \mu\text{A}$ , ( $W/L$ ) = 40/1 for all transistors,  $K'_n = 25 \mu\text{A/V}^2$ ,  $V_{TN} = 0.75 \text{ V}$ ,  $K'_p = 10 \mu\text{A/V}^2$ ,  $V_{TP} = -0.75 \text{ V}$ , and  $\lambda = 0.017 \text{ V}^{-1}$  for both transistor types. Draw the differential-mode half-circuit for transistors  $M_1$  to  $M_4$  and show that the circuit is in fact a cascode amplifier. What is the differential-mode voltage gain of the amplifier? S
- 16.116. Use SPICE to simulate the amplifier in Prob. 16.115 and determine its voltage gain, output resistance, and CMRR. Compare to hand calculations. S
- \*16.117. Design a current mirror bias network to supply the three currents needed by the amplifier in Prob. 16.115. Q

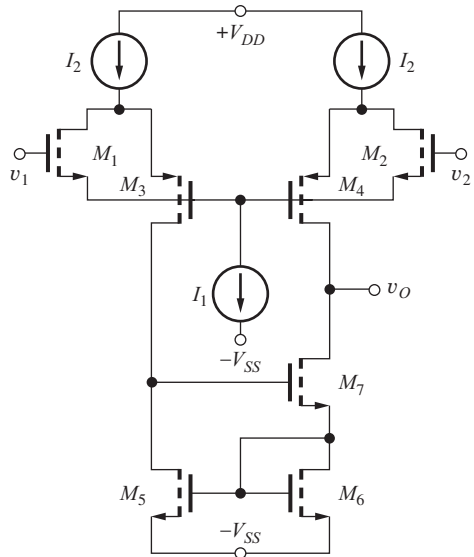


Figure P16.115

### Output Stages

- 16.118. What are the currents in  $Q_3$  and  $Q_4$  in the class-AB output stage in Fig. P16.118 if  $R_1 = 20 \text{ k}\Omega$ ,  $R_2 = 20 \text{ k}\Omega$ , and  $I_{S4} = I_{S3} = I_{S2} = 10^{-14} \text{ A}$ . Assume  $\beta_F = \infty$ .

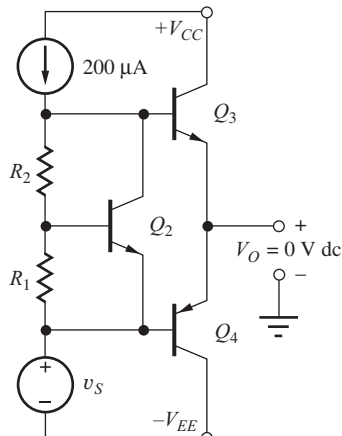


Figure P16.118

- \*16.119. (a) Show that the currents in  $Q_3$  and  $Q_4$  in the class-AB output stage in Fig. P16.119 are equal to  $I_o = I_2 \sqrt{(A_{E3}A_{E4})/(A_{E1}A_{E2})}$ . (b) What are the currents in  $Q_3$  and  $Q_4$  if  $A_{E1} = 3A_{E3}$ ,  $A_{E2} = 3A_{E4}$ ,  $I_2 = 300 \mu\text{A}$ ,  $I_{SO_{pnp}} = 4 \text{ fA}$ , and  $I_{SO_{npn}} = 10 \text{ fA}$ ? Q

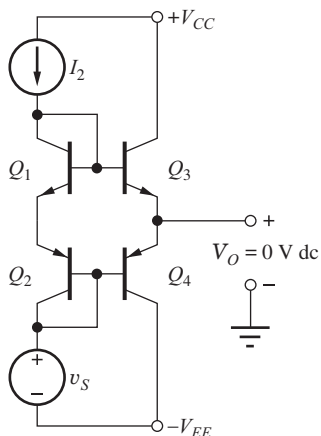


Figure P16.119

## 16.8 Active Loads in Operational Amplifiers

- 16.120. (a) Find the Q-points of the transistors in the CMOS op amp in Fig. 16.42 if  $V_{DD} = V_{SS} = 5$  V,  $I_{REF} = 250 \mu\text{A}$ ,  $K'_n = 25 \mu\text{A/V}^2$ ,  $V_{TN} = 0.75$  V,  $K'_p = 10 \mu\text{A/V}^2$ , and  $V_{TP} = -0.75$  V. (b) What is the voltage gain of the op amp assuming the output stage has unity gain and  $\lambda = 0.017 \text{ V}^{-1}$  for both transistor types? (c) What is the voltage gain if  $I_{REF}$  is changed to 500  $\mu\text{A}$ ?
- 16.121. Based on the example calculations and your knowledge of MOSFET characteristics, what will be the gain of the op amp in Ex. 16.7 if the  $I_{REF}$  is set to (a) 250  $\mu\text{A}$ ? (b) 20  $\mu\text{A}$ ? (Note: These should be short calculations.)
- \*16.122. What is the differential-mode gain of the amplifier in Fig. P16.122 if  $V_{DD} = V_{SS} = 10$  V,  $I_{REF} = 100 \mu\text{A}$ ,  $K'_n = 25 \mu\text{A/V}^2$ ,  $V_{TON} = 0.75$  V,  $K'_p = 10 \mu\text{A/V}^2$ ,  $V_{TOP} = -0.75$  V,  $\gamma_n = 0$ , and  $\gamma_p = 0$ . Use  $\lambda = 0.017 \text{ V}^{-1}$  for both transistor types.
- 16.123. (a) Use SPICE to find the Q-points of the transistors of the amplifier in Prob. 16.122. (b) Repeat with  $2\phi_F = 0.8$  V,  $\gamma_n = 0.60 \text{ V}^{0.5}$ , and  $\gamma_p = 0.75 \text{ V}^{0.5}$ , and compare the results to (a).
- \*16.124. Find the Q-points of the transistors in Fig. P16.122 if  $V_{DD} = V_{SS} = 7.5$  V,  $I_{REF} = 250 \mu\text{A}$ ,  $(W/L)_{12} = 40/1$ ,  $K'_n = 25 \mu\text{A/V}^2$ ,  $V_{TN} = 0.75$  V,  $K'_p = 10 \mu\text{A/V}^2$ , and  $V_{TP} = -0.75$  V. What is the differential-mode voltage gain of the op amp if  $\lambda = 0.017 \text{ V}^{-1}$  for both transistor types?
- \*16.125. (a) Estimate the minimum values of  $V_{DD}$  and  $V_{SS}$  needed for proper operation of the amplifier in Prob. 16.122. Use  $K'_n = 25 \mu\text{A/V}^2$ ,  $V_{TN} =$

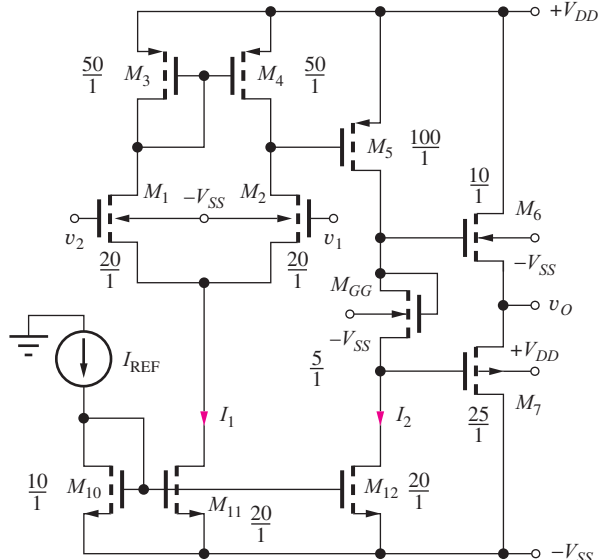


Figure P16.122

0.75 V,  $K'_p = 10 \mu\text{A/V}^2$ , and  $V_{TP} = -0.75$  V.  
(b) What are the minimum values of  $V_{DD}$  and  $V_{SS}$  needed to have at least a  $\pm 5$ -V common-mode input range in the amplifier?

- \*16.126. (a) Find the Q-points of the transistors in Fig. P16.126 if  $V_{DD} = V_{SS} = 10$  V,  $I_{REF} = 250 \mu\text{A}$ ,  $K'_n = 25 \mu\text{A/V}^2$ ,  $V_{TN} = 0.75$  V,

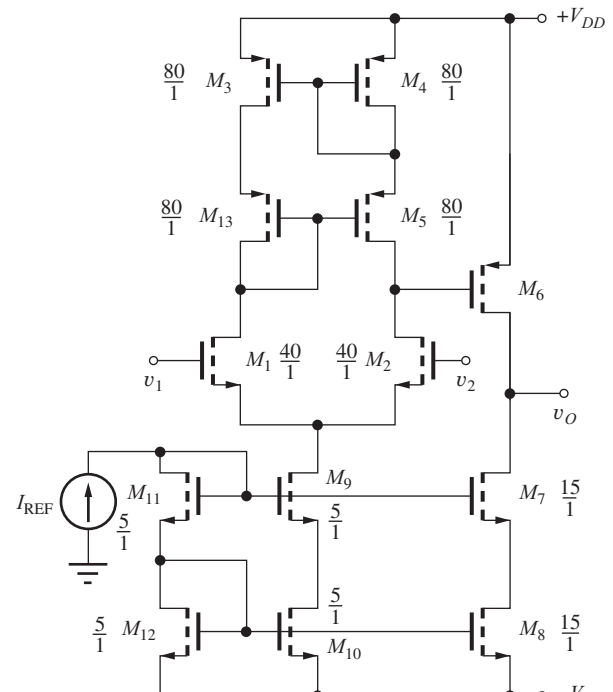


Figure P16.126

$K'_p = 10 \mu\text{A}/\text{V}^2$ , and  $V_{TP} = -0.75 \text{ V}$ . (b) What is the approximate value of the  $W/L$  ratio for  $M_6$  of the CMOS op amp in order for the offset voltage to be zero? What is the differential-mode voltage gain of the op amp if  $\lambda = 0.017 \text{ V}^{-1}$  for both transistor types?

- \*16.127. (a) Simulate the amplifier in Prob. 16.126 and compare its differential-mode voltage gain to the hand calculations in Prob. 16.126. (b) Use SPICE to calculate the offset voltage and CMRR of the amplifier.
- 16.128. Draw the amplifier that represents the mirror image of Fig. 16.42 by interchanging NMOS and PMOS transistors. Choose the  $W/L$  ratios of the NMOS and PMOS transistors so the voltage gain of the new amplifier is the same as the gain of the amplifier in Fig. 16.42. Maintain the operating currents the same and use the device parameter values from Ex. 16.7.
- 16.129. Draw the amplifier that represents the mirror image of Fig. 16.44 by interchanging *npn* and *pnp* transistors. If  $\beta_{on} = 150$ ,  $\beta_{op} = 60$ , and  $V_{AN} = V_{AP} = 60 \text{ V}$ , which of the two amplifiers will have the highest voltage gain? Why?
- \*16.130. What is the approximate emitter area of  $Q_{16}$  needed to achieve zero offset voltage in the amplifier in Fig. P16.130 if  $I_B = 250 \mu\text{A}$  and  $V_{CC} = V_{EE} = 5 \text{ V}$ ? What is the value of

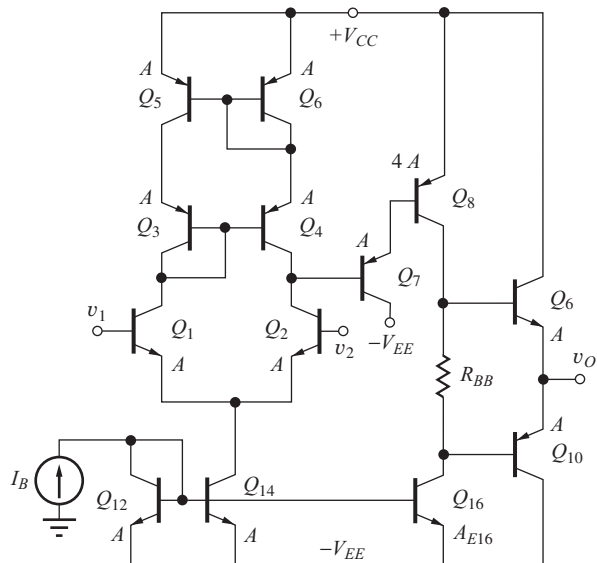


Figure P16.130

$R_{BB}$  needed to set the quiescent current in the output stage to  $75 \mu\text{A}$ ? What are the voltage gain and input resistance of this amplifier? Assume  $\beta_{on} = 150$ ,  $\beta_{op} = 60$ ,  $V_{AN} = V_{AP} = 60 \text{ V}$ , and  $I_{SO_{pn}} = I_{SO_{opn}} = 15 \text{ fA}$ .

- 16.131. Use SPICE to simulate the characteristics of the amplifier in Prob. 16.130. Determine the offset voltage, voltage gain, input resistance, output resistance, and CMRR of the amplifier.
- 16.132. (a) What are the minimum values of  $V_{CC}$  and  $V_{EE}$  needed for proper operation of the amplifier in Fig. P16.130? (b) What are the minimum values of  $V_{CC}$  and  $V_{EE}$  needed to have at least a  $\pm 1\text{-V}$  common-mode input range in the amplifier?

## 16.9 The μA741 Operational Amplifier

- 16.133. (a) What are the three bias currents in the source in Fig. P16.133 if  $R_1 = 100 \text{ k}\Omega$ ,  $R_2 = 4 \text{ k}\Omega$ , and  $V_{CC} = V_{EE} = 3 \text{ V}$ . (b) Repeat for  $V_{CC} = V_{EE} = 22 \text{ V}$ . (c) Why is it important that  $I_1$  in the μA741 be independent of power supply voltage but it does not matter as much for  $I_2$  and  $I_3$ ?

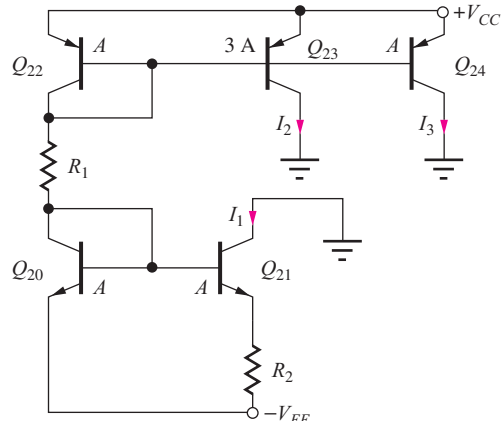


Figure P16.133

- 16.134. Choose the values of  $R_1$  and  $R_2$  in Fig. P16.133 to set  $I_2 = 250 \mu\text{A}$  and  $I_1 = 50 \mu\text{A}$  if  $V_{CC} = V_{EE} = 12 \text{ V}$ . What is  $I_3$ ?
- 16.135. Choose the values of  $R_1$  and  $R_2$  in Fig. P16.133 to set  $I_3 = 300 \mu\text{A}$  and  $I_1 = 75 \mu\text{A}$  if  $V_{CC} = V_{EE} = 15 \text{ V}$ . What is  $I_2$ ?
- \*16.136. (a) Based on the schematic in Fig. 16.46, what are the minimum values of  $V_{CC}$  and  $V_{EE}$  needed for proper operation of μA741 amplifier? (b) What

are the minimum values of  $V_{CC}$  and  $V_{EE}$  needed to have at least a  $\pm 1\text{-V}$  common-mode input range in the amplifier?

- 16.137. What are the values of the elements in the Norton equivalent circuit in Fig. 16.53(a) if  $I_1$  in Fig. 16.46 is increased to  $50\ \mu\text{A}$ ?
- 16.138. Suppose  $Q_{23}$  in Fig. 16.47 is replaced by a cascode current source. (a) What is the new value of output resistance  $R_2$ ? (b) What are the new values of the  $y$ -parameters of Fig. 16.53(b)? (c) What is the new value of  $A_{dm}$  for the op amp?
- 16.139. Draw a schematic for the cascode current source in Prob. 16.138.
- 16.140. Create a small-signal SPICE model for the circuit in Fig. 16.53(b) and verify the values of  $R_{in10}$ ,  $G_m$ , and  $G_o$ . What is the value of  $y_{12}$  for the circuit?
- \*\*16.141. Figure P16.141 represents an op amp input stage that was developed following the introduction of the  $\mu\text{A741}$ . (a) Find the Q-points for all the transistors in the differential amplifier in Fig. P16.141 if  $V_{CC} = V_{EE} = 15\text{ V}$  and  $I_{REF} = 100\ \mu\text{A}$ . (b) Discuss how this bias network operates to establish the Q-points. (c) Label the inverting and noninverting input terminals. (d) What are the transconductance and output resistance of this amplifier? Use  $V_A = 60\text{ V}$ .

the  $\mu\text{A741}$ . Find the Q-points for all the transistors in the differential amplifier in Fig. P16.142 if  $V_{CC} = V_{EE} = 15\text{ V}$  and  $I_{REF} = 100\ \mu\text{A}$ . (b) Discuss how this bias network operates to establish the Q-points. (c) Label the inverting and noninverting input terminals. (d) What are the transconductance and output resistance of this amplifier? Use  $V_A = 60\text{ V}$ .

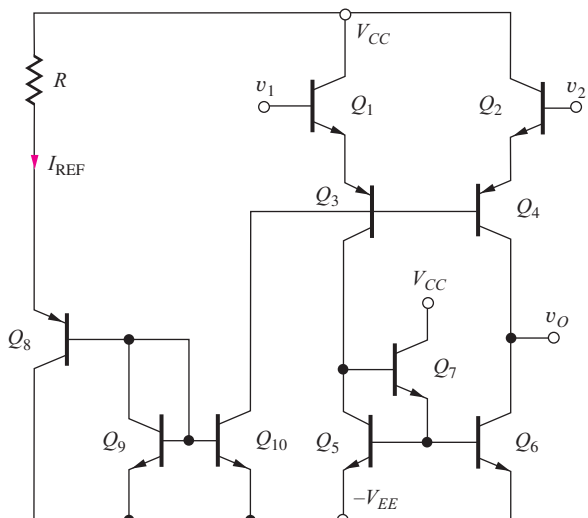


Figure P16.142

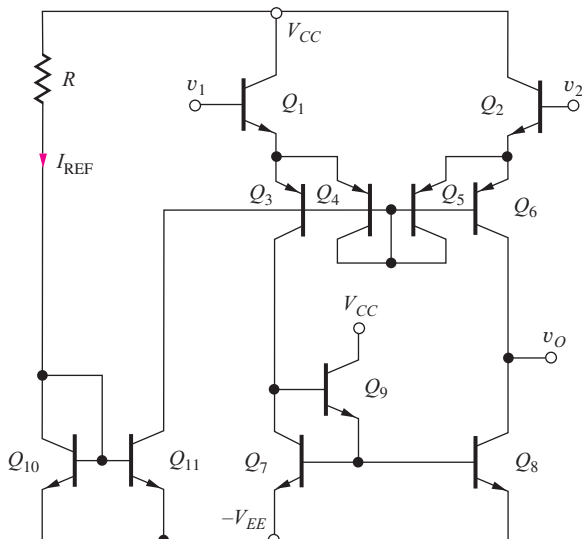


Figure P16.141

- \*\*16.142. Figure P16.142 represents an op amp input stage that was developed following the introduction of

## 16.10 The Gilbert Analog Multiplier

- 16.143. Find the Q-points of the six transistors in Fig. 16.59 if  $V_{CC} = -V_{EE} = 5\text{ V}$ ,  $I_{BB} = 100\ \mu\text{A}$ ,  $R_1 = 10\text{ k}\Omega$ , and  $R = 50\text{ k}\Omega$ . Draw the circuit assuming the bases of  $Q_1$  and  $Q_2$  are biased at a common-mode voltage of  $-2.5\text{ V}$  with  $v_1 = 0$ . Assume the bases of  $Q_3$  through  $Q_6$  are biased at a common-mode voltage of  $0\text{ V}$  with  $v_2 = 0$ .
- 16.144. (a) Find the collector currents of the six transistors in Fig. 16.59 if  $V_{CC} = -V_{EE} = 7.5\text{ V}$ ,  $I_{BB} = 200\ \mu\text{A}$ ,  $R_1 = 10\text{ k}\Omega$ , and  $R = 50\text{ k}\Omega$ . Draw the circuit assuming the bases of  $Q_1$  and  $Q_2$  are biased at a common-mode voltage of  $-3\text{ V}$  with  $v_1 = 0.5\text{ V}$ . Assume the bases of  $Q_3$  through  $Q_6$  are biased at a common-mode voltage of  $0\text{ V}$  with  $v_2 = 0$ . (b) Repeat with  $v_2 = 1\text{ V}$ . (c) Repeat with  $v_2 = -1\text{ V}$ .
- 16.145. Write an expression for the output voltage for the circuit in Fig. 16.59 if  $v_1 = 0.5 \sin 2000\pi t$ , and  $v_2$  is generated by the circuit in Fig. 16.60 with  $v_3 = 0.5 \sin 10,000\pi t$ ? Assume  $V_{CC} = -V_{EE} =$

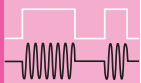
10 V,  $I_{EE} = 500 \mu\text{A}$ ,  $R_1 = R_3 = 2 \text{ k}\Omega$ , and  $R = 10 \text{ k}\Omega$ .

- 16.146. (a) Write expressions for the total collector currents  $i_{C1}$  and  $i_{C2}$  in Fig. 16.59 if  $I_{BB} = 1 \text{ mA}$ ,  $R_1 = 2 \text{ k}\Omega$ , and  $v_1 = 0.4 \sin 5000\pi t \text{ V}$ . Assume the transistors are operating in the active

region. (b) What is the transconductance  $G_m$  of the voltage-to-current converter formed by  $Q_1$  and  $Q_2$ ? [ $G_m = \Delta(i_{C1} - i_{C2})/\Delta v_1$ ]

- 16.147. Use SPICE to plot the VTC for the circuit in Fig. 16.60 with  $V_{BB} = 3 \text{ V}$ ,  $-V_{EE} = -5 \text{ V}$ ,  $I_{EE} = 300 \mu\text{A}$ , and  $R_3 = 3.3 \text{ k}\Omega$ .

# CHAPTER 17



## AMPLIFIER FREQUENCY RESPONSE

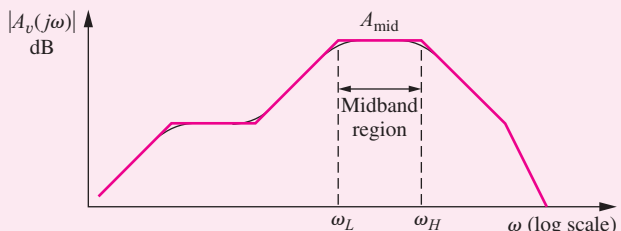
### CHAPTER OUTLINE

- 17.1 Amplifier Frequency Response 1129
- 17.2 Direct Determination of the Low-Frequency Poles and Zeros—The Common-Source Amplifier 1134
- 17.3 Estimation of  $\omega_L$  Using the Short-Circuit Time-Constant Method 1139
- 17.4 Transistor Models at High Frequencies 1148
- 17.5 Base Resistance in the Hybrid-Pi Model 1155
- 17.6 High-Frequency Common-Emitter and Common-Source Amplifier Analysis 1158
- 17.7 Common-Base and Common-Gate Amplifier High-Frequency Response 1175
- 17.8 Common-Collector and Common-Drain Amplifier High-Frequency Response 1177
- 17.9 Single-Stage Amplifier High-Frequency Response Summary 1179
- 17.10 Frequency Response of Multistage Amplifiers 1181
- 17.11 Introduction to Radio Frequency Circuits 1193
- 17.12 Mixers and Balanced Modulators 1205
  - Summary 1213
  - Key Terms 1215
  - Reference 1215
  - Problems 1215

### CHAPTER GOALS

- Review transfer function analysis and determination of cutoff frequencies
- Understand dominant-pole approximations of amplifier transfer functions
- Learn to partition ac circuits into low-frequency and high-frequency equivalent circuits
- Learn the short-circuit time constant approach for estimating lower-cutoff frequency  $f_L$
- Complete development of the small-signal models of both bipolar and MOS transistors with the addition of device capacitances
- Understand the unity-gain bandwidth product limitations of bipolar and field-effect transistors
- Learn the open-circuit time constant technique for estimating upper-cutoff frequency  $f_H$
- Develop expressions for the upper-cutoff frequency of the inverting, noninverting, and follower configurations
- Demonstrate that the gain-bandwidth product limitations of the inverting, noninverting, and follower configurations approach the same upper limit

- Learn to apply the two time-constant approaches to the analysis of the frequency response of multistage amplifiers
- Explore bandwidth limitations of two-transistor circuits including current mirrors, cascode amplifiers, and differential pairs
- Understand the Miller effect
- Develop relationships between op amp unity-gain frequency and amplifier slew rate
- Introduce basic radio frequency (RF) circuits including tuned amplifiers, mixers, and oscillators
- Understand the use of tuned circuits to produce both broad-band (shunt-peaked) and narrow-band RF amplifiers
- Understand the basic concepts of mixing
- Explore single-balanced and double-balanced mixer circuits
- Study application of the Gilbert multiplier as balanced modulator and mixer
- Demonstrate the use of ac analysis in SPICE
- Demonstrate the use of MATLAB® to display frequency response information



Chapters 13 to 16 discussed analysis and design of the midband characteristics of amplifiers. Low-frequency limitations due to coupling and bypass capacitors were also discussed, but the internal capacitances of electronic devices, which limit the response at high frequencies, were neglected. This chapter completes the discussion of basic amplifier design with the introduction of methods used to tailor the frequency response of analog circuits at both low and high frequencies. As part of this discussion, the internal device capacitances of bipolar and field-effect transistors are discussed, and frequency-dependent small-signal models of the transistors are introduced. The unity-gain

bandwidth product of the devices is expressed in terms of the small-signal parameters.

In order to complete our basic circuit-building block toolkit, expressions for the frequency responses of the single-stage inverting, noninverting, and follower configurations are each developed in detail. We show that the bandwidth of high-gain inverting and noninverting stages can be quite limited (although much wider than a typical op-amp stage of equal gain), whereas that of followers is normally very wide. Use of the cascode configuration is shown to significantly improve the frequency response of inverting amplifiers. Narrow-band (high-Q) band-pass amplifiers based on tuned circuits are also discussed.

Transfer functions for multistage amplifiers may have large numbers of poles and zeros, and direct circuit analysis, although theoretically possible, can be complex

and unwieldy. Therefore, approximation techniques—the short-circuit and open-circuit time-constant methods—have been developed to estimate the upper- and lower-cutoff frequencies  $\omega_H$  and  $\omega_L$ .

The Miller effect is introduced, and the relatively low bandwidth associated with inverting amplifiers is shown to be caused by Miller multiplication of the collector-base or gate-drain capacitance of the transistor in the amplifier.

This chapter also provides a brief introduction to radio frequency (RF) circuits including RF amplifiers and mixers. The RF circuit discussion includes both broad-band shunt-peaked and narrow-band (high-Q) tuned amplifiers. The presentation of frequency translation circuits includes single- and double-balanced mixers, including passive and active mixer circuits. High-frequency oscillators are discussed in Chapter 18.

## 17.1 AMPLIFIER FREQUENCY RESPONSE

Figure 17.1 is the Bode plot for the magnitude of the voltage gain of a hypothetical amplifier. Regardless of the number of poles and zeros, the voltage transfer function  $A_v(s)$  can be written as the ratio of two polynomials in  $s$ :

$$A_v(s) = \frac{N(s)}{D(s)} = \frac{a_0 + a_1 s + a_2 s^2 + \cdots + a_m s^m}{b_0 + b_1 s + b_2 s^2 + \cdots + b_n s^n} \quad (17.1)$$

In principle, the numerator and denominator polynomials of Eq. (17.1) can be written in factored form, and the poles and zeros can be separated into two groups. Those associated with the low-frequency response below the midband region of the amplifier can be combined into a function  $F_L(s)$ , and those associated with the high-frequency response above the midband region can be grouped into a function  $F_H(s)$ . Using  $F_L$  and  $F_H$ ,  $A_v(s)$  can be rewritten as

$$A_v(s) = A_{\text{mid}} F_L(s) F_H(s) \quad (17.2)$$

in which  $A_{\text{mid}}$  is the **midband gain**<sup>1</sup> of the amplifier in the region between the **lower- and upper-cutoff frequencies** ( $\omega_L$  and  $\omega_H$ , respectively). For  $A_{\text{mid}}$  to appear explicitly as shown in Eq. (17.2),  $F_H(s)$  and  $F_L(s)$  must be written in the two particular standard forms defined by Eqs. (17.3) and (17.4):

$$F_L(s) = \frac{(s + \omega_{Z1}^L)(s + \omega_{Z2}^L) \cdots (s + \omega_{Zk}^L)}{(s + \omega_{P1}^L)(s + \omega_{P2}^L) \cdots (s + \omega_{Pk}^L)} \quad (17.3)$$

$$F_H(s) = \frac{\left(1 + \frac{s}{\omega_{Z1}^H}\right) \left(1 + \frac{s}{\omega_{Z2}^H}\right) \cdots \left(1 + \frac{s}{\omega_{Zl}^H}\right)}{\left(1 + \frac{s}{\omega_{P1}^H}\right) \left(1 + \frac{s}{\omega_{P2}^H}\right) \cdots \left(1 + \frac{s}{\omega_{Pl}^H}\right)} \quad (17.4)$$

The representation of  $F_H(s)$  is chosen so that its magnitude approaches a value of 1 at frequencies well below the upper-cutoff frequency  $\omega_H$ ,

$$|F_H(j\omega)| \rightarrow 1 \quad \text{for} \quad \omega \ll \omega_{Zi}^H, \omega_{Pi}^H \quad \text{for } i = 1 \dots l \quad (17.5)$$

<sup>1</sup> You may wish to review some of the frequency response definitions in Chapter 10.

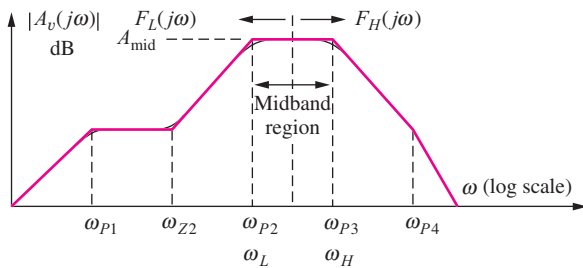


**Figure 17.1** Bode plot for a general amplifier transfer function.

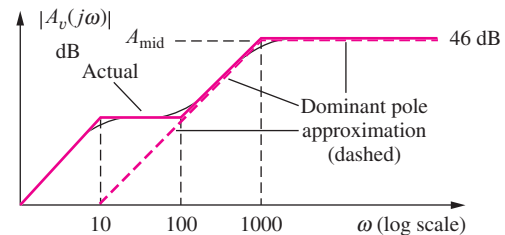


**Figure 17.2** Bode plot for a complete transfer function and its dominant pole approximation.

Thus, at low frequencies, the transfer function  $A_v(s)$  becomes

$$A_L(s) \cong A_{\text{mid}}F_L(s) \quad (17.6)$$

The form of  $F_L(s)$  is chosen so its magnitude approaches a value of 1 at frequencies well above  $\omega_L$ :

$$|F_L(j\omega)| \rightarrow 1 \quad \text{for} \quad \omega \gg \omega_{Zj}^L, \omega_{Pj}^L \quad \text{for } j = 1 \dots k \quad (17.7)$$

Thus, at high frequencies the transfer function  $A_v(s)$  can be approximated by

$$A_H(s) \cong A_{\text{mid}}F_H(s) \quad (17.8)$$

### 17.1.1 LOW-FREQUENCY RESPONSE

In many designs, the zeros of  $F_L(s)$  can be placed at frequencies low enough to not influence the lower-cutoff frequency  $\omega_L$ . In addition, one of the low-frequency poles in Fig. 17.1, say  $\omega_{P2}$ , can be designed to be much larger than the others. For these conditions, the low-frequency portion of the transfer function can be written approximately as

$$F_L(s) \cong \frac{s}{s + \omega_{P2}} \quad (17.9)$$

Pole  $\omega_{P2}$  is referred to as the **dominant low-frequency pole** and the lower-cutoff frequency  $\omega_L$  is approximately

$$\omega_L \cong \omega_{P2} \quad (17.10)$$

The Bode plot in Fig. 17.2 is an example of a transfer function and its dominant pole approximation. The overall transfer function  $A_L(s)$  for this figure has two poles and two zeros.

### 17.1.2 ESTIMATING $\omega_L$ IN THE ABSENCE OF A DOMINANT POLE

If a dominant pole does not exist at low frequencies, then the poles and zeros interact to determine the lower-cutoff frequency, and a more complicated analysis must be used to find  $\omega_L$ . As an example, consider the case of an amplifier having two zeros and two poles at low frequencies:

$$A_L(s) = A_{\text{mid}}F_L(s) = A_{\text{mid}} \frac{(s + \omega_{Z1})(s + \omega_{Z2})}{(s + \omega_{P1})(s + \omega_{P2})} \quad (17.11)$$

For  $s = j\omega$ ,

$$|A_L(j\omega)| = A_{\text{mid}}|F_L(j\omega)| = A_{\text{mid}} \sqrt{\frac{(\omega^2 + \omega_{Z1}^2)(\omega^2 + \omega_{Z2}^2)}{(\omega^2 + \omega_{P1}^2)(\omega^2 + \omega_{P2}^2)}} \quad (17.12)$$

and remembering that  $\omega_L$  is defined as the  $-3$  dB frequency,

$$|A(j\omega_L)| = \frac{A_{\text{mid}}}{\sqrt{2}} \quad \text{and} \quad \frac{1}{\sqrt{2}} = \sqrt{\frac{(\omega_L^2 + \omega_{Z1}^2)(\omega_L^2 + \omega_{Z2}^2)}{(\omega_L^2 + \omega_{P1}^2)(\omega_L^2 + \omega_{P2}^2)}} \quad (17.13)$$

Squaring both sides and expanding Eq. (17.13),

$$\frac{1}{2} = \frac{\omega_L^4 + \omega_L^2(\omega_{Z1}^2 + \omega_{Z2}^2) + \omega_{Z1}^2\omega_{Z2}^2}{\omega_L^4 + \omega_L^2(\omega_{P1}^2 + \omega_{P2}^2) + \omega_{P1}^2\omega_{P2}^2} = \frac{1 + \frac{(\omega_{Z1}^2 + \omega_{Z2}^2)}{\omega_L^2} + \frac{\omega_{Z1}^2\omega_{Z2}^2}{\omega_L^4}}{1 + \frac{(\omega_{P1}^2 + \omega_{P2}^2)}{\omega_L^2} + \frac{\omega_{P1}^2\omega_{P2}^2}{\omega_L^4}} \quad (17.14)$$

If we assume that  $\omega_L$  is larger than all the individual pole and zero frequencies, then the terms involving  $1/\omega_L^4$  can be neglected, and the lower-cutoff frequency can be estimated from

$$\omega_L \approx \sqrt{\omega_{P1}^2 + \omega_{P2}^2 - 2\omega_{Z1}^2 - 2\omega_{Z2}^2} \quad (17.15)$$

For the more general case of  $n$  poles and  $n$  zeros, a similar analysis yields

$$\omega_L \approx \sqrt{\sum_n \omega_{Pn}^2 - 2 \sum_n \omega_{Zn}^2} \quad (17.16)$$

**EXERCISE:** Use Eq. (17.15) to estimate  $f_L$  for the transfer functions

$$A_V(s) = \frac{200s(s+50)}{(s+10)(s+1000)} \quad \text{and} \quad A_V(s) = \frac{100s(s+500)}{(s+100)(s+1000)}$$

**ANSWERS:** 159 Hz, 114 Hz

## EXAMPLE 17.1 ANALYSIS OF A TRANSFER FUNCTION

The midband gain, poles, zeros, and cutoff frequency are identified from a specified transfer function.

**PROBLEM** Find the midband gain,  $F_L(s)$ , and lower-cutoff frequency  $f_L$  for

$$A_L(s) = 2000 \frac{s \left( \frac{s}{100} + 1 \right)}{(0.1s + 1)(s + 1000)}$$

Identify the frequencies corresponding to the poles and zeros. Find a dominant pole approximation for the transfer function, if one exists.

**SOLUTION Known Information and Given Data:** The transfer function is specified.

**Unknowns:**  $A_{\text{mid}}$ ,  $F_L(s)$ ,  $f_L$ , poles, zeros, dominant-pole approximation

**Approach:** Rearrange  $A_L(s)$  into the form of Eqs. (17.6) and (17.3). Identify the pole and zero frequencies. Find the midband region and  $A_{\text{mid}}$ . Since the poles and zeros can all be found, use Eq. (17.16) to find  $f_L$ . If the poles and zeros are widely separated, find the dominant pole representation.

**Assumptions:** None

**Analysis:** To begin, we need to rearrange the transfer function by factoring 0.01 out of the numerator and 0.1 out of the denominator in order to have all the poles and zeros written as in Eq. (17.3):

$$A_L(s) = 200 \frac{s(s+100)}{(s+10)(s+1000)}$$

Now,  $A_L(s) = A_{\text{mid}}F_L(s)$  with  $A_{\text{mid}} = 200$  and

$$F_L(s) = \frac{s(s+100)}{(s+10)(s+1000)}$$

Zeros occur at the values of  $s$  for which the numerator is zero:  $s = 0$  and  $s = -100$  rad/s. Poles occur at the frequencies  $s$  for which the denominator is zero:  $s = -10$  rad/s and  $s = -1000$  rad/s.

Substituting these values in to Eq. (17.16) yields an estimate of  $f_L$ :

$$f_L = \frac{1}{2\pi} \sqrt{10^2 + 1000^2 - 2(0^2 + 100^2)^2} = \frac{990}{2\pi} = 158 \text{ Hz}$$

Note that these are all at low frequencies and are separated from one another by a decade of frequency. Thus, a dominant pole exists at  $\omega = 1000$ , and the lower-cutoff frequency is given approximately by  $f_L \cong 1000/2\pi = 159$  Hz. For frequencies above a few hundred rad/s, the transfer function can be approximated by

$$A_L(s) \cong 200 \frac{s}{s + 1000} \quad \text{for } \omega > 200 \text{ rad/s}$$

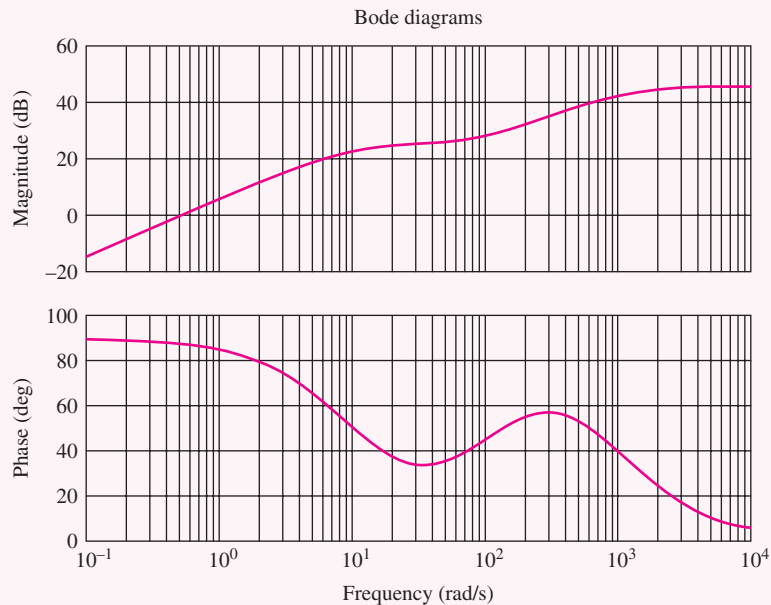
**Check of Results:** The requested unknowns have been found. For  $\omega \gg 1000$ , the transfer original function reaches its largest value and becomes constant — the midband region:

$$A_L(s)|_{s \gg 1000} \cong 200 \frac{s^2}{s^2} = 200$$

Thus,  $A_{\text{mid}} = 200$  or 46 dB. We also see that the value of  $f_L$  predicted by Eq. (17.16) is the same as that of the dominant-pole model, indicating correctness of the dominant-pole approximation.

**Discussion:** Figure 17.2 graphs the original transfer function and its dominant-pole approximation. The midband region is clearly viable for  $\omega > 1000$  rad/s, and the single pole roll-off is valid for frequencies down to approximately 200 rad/s.

**Computer-Aided Analysis:** We can easily visualize the transfer function with the aid of MATLAB®: `bode ([200 20000 0], [1 1010 10000])`. The resulting graph of the magnitude and phase of  $A_L(s)$  appears in the figure. The alternating sequence of zeros and poles is apparent in both the magnitude and phase plots, and the gain approaches 46 dB at high frequencies.



**EXERCISE:** For what range of frequencies does the approximation to  $A_v(s)$  in Ex. 17.1 differ from the actual transfer function by less than 10 percent?

**ANSWER:**  $\omega \geq 205$  rad/s

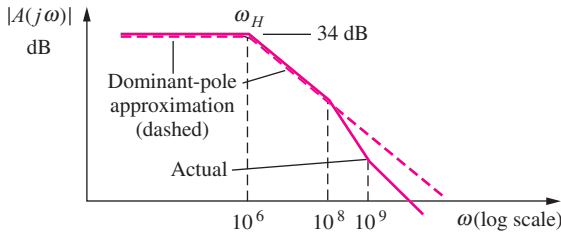


**Figure 17.3** Bode plot for a complete transfer function and its dominant-pole approximation.

### 17.1.3 HIGH-FREQUENCY RESPONSE

In the region above midband,  $A_v(s)$  can be represented by its high-frequency approximation:

$$A_H(s) \cong A_{\text{mid}} F_H(s) \quad (17.17)$$

Many of the zeros of  $F_H(s)$  are often at infinite frequency, or high enough in frequency that they do not influence the value of  $F_H(s)$  near  $\omega_H$ . If, in addition, one of the **pole frequencies** — for example,  $\omega_{P3}$  in Fig. 17.1 — is much smaller than all the others, then a **dominant high-frequency pole** exists in the high-frequency response, and  $F_H(s)$  can be represented by the approximation

$$F_H(s) \cong \frac{1}{1 + \frac{s}{\omega_{P3}}} \quad (17.18)$$

For the case of a dominant pole, the upper-cutoff frequency is given by  $\omega_H \cong \omega_{P3}$ . Figure 17.3 is an example of a Bode plot of a transfer function at high frequencies and its dominant-pole approximation.

**EXERCISE:** The transfer function for the amplifier in Fig. 17.3 is

$$A_H(s) = 50 \frac{\left(1 + \frac{s}{10^9}\right)}{\left(1 + \frac{s}{10^6}\right) \left(1 + \frac{s}{10^8}\right)}$$

What are the locations of the poles and zeros of  $A_H(s)$ ? What are  $A_{\text{mid}}$ ,  $F_H(s)$  for the dominant-pole approximation, and  $f_H$ ?

**ANSWERS:**  $\omega_{Z1} = -10^9 \text{ rad/s}$ ,  $\omega_{P1} = -10^6 \text{ rad/s}$ ,  $\omega_{P2} = -10^8 \text{ rad/s}$ ; 50,  $F_H(s) = \frac{1}{\left(1 + \frac{s}{10^6}\right)}$ ,

159 kHz

### 17.1.4 ESTIMATING $\omega_H$ IN THE ABSENCE OF A DOMINANT POLE

If a dominant pole does not exist at high frequencies, then the poles and zeros interact to determine  $\omega_H$ . An approximate expression for the upper-cutoff frequency can be found from the expression for  $F_H$  in a manner similar to that used to arrive at Eq. (17.16). Consider the case of an amplifier having two zeros and two poles at high frequencies:

$$A_H(s) = A_{\text{mid}} F_H(s) = A_{\text{mid}} \frac{\left(1 + \frac{s}{\omega_{Z1}}\right) \left(1 + \frac{s}{\omega_{Z2}}\right)}{\left(1 + \frac{s}{\omega_{P1}}\right) \left(1 + \frac{s}{\omega_{P2}}\right)} \quad (17.19)$$

and for  $s = j\omega$ ,

$$|A_H(j\omega)| = A_{\text{mid}}|F_H(j\omega)| = A_{\text{mid}} \sqrt{\frac{\left(1 + \frac{\omega^2}{\omega_{Z1}^2}\right) \left(1 + \frac{\omega^2}{\omega_{Z2}^2}\right)}{\left(1 + \frac{\omega^2}{\omega_{P1}^2}\right) \left(1 + \frac{\omega^2}{\omega_{P2}^2}\right)}} \quad (17.20)$$

At the upper-cutoff frequency  $\omega = \omega_H$ ,

$$|A(j\omega_H)| = \frac{A_{\text{mid}}}{\sqrt{2}} \quad \text{and} \quad \frac{1}{\sqrt{2}} = \sqrt{\frac{\left(1 + \frac{\omega_H^2}{\omega_{Z1}^2}\right) \left(1 + \frac{\omega_H^2}{\omega_{Z2}^2}\right)}{\left(1 + \frac{\omega_H^2}{\omega_{P1}^2}\right) \left(1 + \frac{\omega_H^2}{\omega_{P2}^2}\right)}} \quad (17.21)$$

By squaring both sides and expanding Eq. (17.21), and assuming  $\omega_H$  is smaller than all the individual pole and zero frequencies, the upper-cutoff frequency can be found to be

$$\omega_H \approx \frac{1}{\sqrt{\frac{1}{\omega_{P1}^2} + \frac{1}{\omega_{P2}^2} - \frac{2}{\omega_{Z1}^2} - \frac{2}{\omega_{Z2}^2}}} \quad (17.22)$$

The expression for the general case of  $n$  poles and  $n$  zeros can be found in a manner similar to Eq. (17.22), and the resulting approximation for  $\omega_H$  is

$$\omega_H \approx \frac{1}{\sqrt{\sum_n \frac{1}{\omega_{Pn}^2} - 2 \sum_n \frac{1}{\omega_{zn}^2}}} \quad (17.23)$$

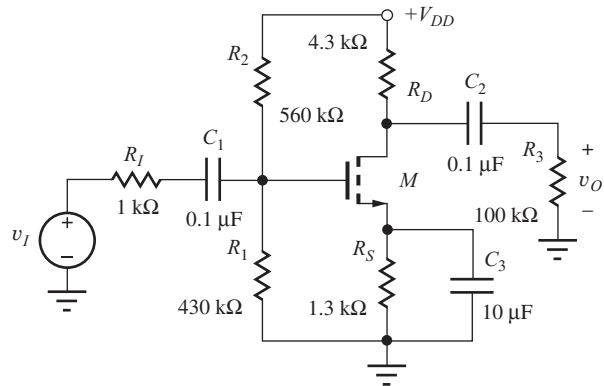
**EXERCISE:** Write the expression for the  $A_H(s)$  below in standard form. What are the pole and zero frequencies? What are  $A_{\text{mid}}$ ,  $F_H(s)$ , and  $f_H$ ?

$$A_H(s) = \frac{2.5 \times 10^7(s + 2 \times 10^5)}{(s + 10^5)(s + 5 \times 10^5)}$$

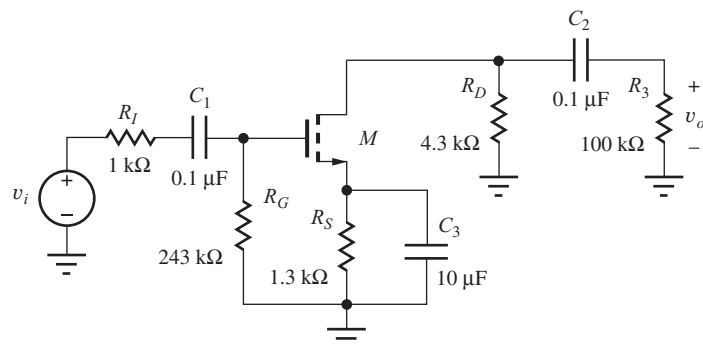
**ANSWERS:**  $A_H(s) = 100 \frac{\left(1 + \frac{s}{2 \times 10^5}\right)}{\left(1 + \frac{s}{10^5}\right) \left(1 + \frac{s}{5 \times 10^5}\right)}$ ;  $-10^5$  rad/s,  $-5 \times 10^5$  rad/s,  $-2 \times 10^5$  rad/s;  $\infty$ , 40 dB, 21.7 kHz

## 17.2 DIRECT DETERMINATION OF THE LOW-FREQUENCY POLES AND ZEROS—THE COMMON-SOURCE AMPLIFIER

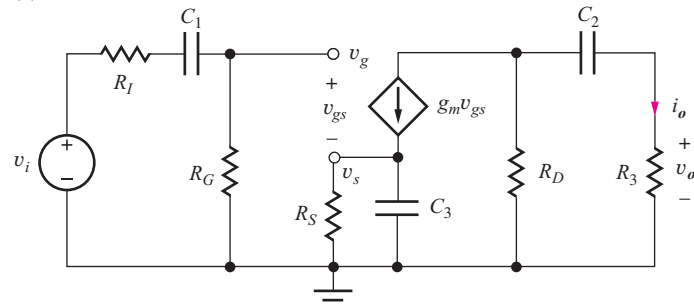
To apply the theory in Sec. 17.1, we need to know the location of all the individual poles and zeros. In principle, the frequency response of an amplifier can always be calculated by direct analysis of the circuit in the frequency domain, so this section begins with an example of this form of analysis for the common-source amplifier. However, as circuit complexity grows, exact analysis by hand rapidly becomes intractable. Although SPICE analysis can always be used to study the characteristics of an amplifier for a given set of parameter values, a more general understanding of the factors that control the cutoff frequencies of the amplifier is needed for design. Because we are most often interested in the position of  $\omega_L$  and  $\omega_H$ , we subsequently develop approximation techniques that can be used to estimate  $\omega_L$  and  $\omega_H$ .



(a)



(b)



(c)

**Figure 17.4** (a) A common-source amplifier, (b) low-frequency ac model, and (c) small-signal model.

The circuit for a common-source amplifier appears in Fig. 17.4(a) along with its ac equivalent circuit in Fig. 17.4(b). At low frequencies below midband, the impedance of the capacitors can no longer be assumed to be negligible, and they must be retained in the ac equivalent circuit. To determine circuit behavior at low frequencies, we replace transistor  $Q_1$  by its low-frequency small-signal model, as in Fig. 17.4(c). Because the stage has an external load resistor,  $r_o$  is neglected in the circuit model.

In the frequency domain, output voltage  $\mathbf{V}_o(s)$  can be found by applying current division at the drain of the transistor:

$$\mathbf{V}_o(s) = \mathbf{I}_o(s)R_3 \quad \text{where} \quad \mathbf{I}_o(s) = -g_m \mathbf{V}_{gs}(s) \frac{R_D}{R_D + \frac{1}{sC_2} + R_3}$$

and

$$\mathbf{V}_o(s) = -g_m \mathbf{V}_{gs}(s) \frac{R_D}{R_D + \frac{1}{sC_2} + R_3} R_3 = -g_m (R_3 \| R_D) \frac{s}{s + \frac{1}{C_2(R_D + R_3)}} \mathbf{V}_{gs}(s) \quad (17.24)$$

Next, we must find  $\mathbf{V}_{gs}(s) = \mathbf{V}_g(s) - \mathbf{V}_s(s)$ . Because the gate terminal in Fig. 17.4(c) represents an open circuit,  $\mathbf{V}_g(s)$  can be determined using voltage division:

$$\mathbf{V}_g(s) = \mathbf{V}_i(s) \frac{R_G}{R_I + \frac{1}{sC_1} + R_G} = \mathbf{V}_i(s) \frac{sC_1 R_G}{sC_1(R_I + R_G) + 1} \quad (17.25)$$

and the voltage at the source of the FET can be found by writing a nodal equation for  $\mathbf{V}_s(s)$ :

$$g_m(\mathbf{V}_g - \mathbf{V}_s) - G_S \mathbf{V}_s - sC_3 \mathbf{V}_s = 0 \quad \text{or} \quad \mathbf{V}_s = \frac{g_m}{sC_3 + g_m + G_S} \mathbf{V}_g \quad (17.26)$$

and

$$\mathbf{V}_{gs}(s) = (\mathbf{V}_g - \mathbf{V}_s) = \mathbf{V}_g \left[ 1 - \frac{g_m}{sC_3 + g_m + G_S} \right] = \frac{sC_3 + G_S}{sC_3 + g_m + G_S} \mathbf{V}_g \quad (17.27)$$

By dividing through by  $C_3$ , Eq. (17.27) can be rewritten as

$$(\mathbf{V}_g - \mathbf{V}_s) = \frac{\frac{1}{s + \frac{1}{C_3 R_S}}}{s + \frac{1}{C_3 \left( \frac{1}{g_m} \| R_S \right)}} \mathbf{V}_g(s) \quad (17.28)$$

Finally, combining Eqs. (17.24), (17.25), and (17.28) yields an overall expression for the voltage transfer function:

$$\begin{aligned} A_v(s) &= \frac{\mathbf{V}_o(s)}{\mathbf{V}_i(s)} = A_{\text{mid}} F_L(s) \\ &= \left[ -g_m (R_3 \| R_D) \frac{R_G}{(R_I + R_G)} \right] \frac{s^2 \left[ s + \frac{1}{C_3 R_S} \right]}{\left[ s + \frac{1}{C_1(R_I + R_G)} \right] \left[ s + \frac{1}{C_3 \left( \frac{1}{g_m} \| R_S \right)} \right] \left[ s + \frac{1}{C_2(R_D + R_3)} \right]} \end{aligned} \quad (17.29)$$

In Eq. (17.29),  $A_v(s)$  has been written in the form that directly exposes the midband gain and  $F_L(s)$ :

$$A_v(s) = A_{\text{mid}} F_L(s) \quad \text{where} \quad A_{\text{mid}} = -g_m (R_D \| R_3) \frac{R_G}{R_G + R_I} \quad (17.30)$$

$A_{\text{mid}}$  should be recognized as the voltage gain of the circuit with the capacitors all replaced by short circuits.

Although the analysis in Eqs. (17.24) to (17.30) may seem rather tedious, we nevertheless obtain a complete description of the frequency response. In this example, the poles and zeros of the transfer function appear in factored form in Eq. (17.29). Unfortunately, this is an artifact of this particular FET circuit and generally will not be the case. The infinite input resistance of the FET and absence of  $r_o$  in the circuit have decoupled the nodal equations for  $v_g$ ,  $v_s$ , and  $v_o$ . In most cases, the mathematical analysis is even more complex. For example, if a bipolar transistor were used in which both  $r_\pi$  and  $r_o$  were included, the analysis would require the simultaneous solution of three equations in three unknowns.

**EXERCISE:** Draw the midband ac equivalent circuit for the amplifier in Fig. 17.2 and derive the expression for  $A_{\text{mid}}$  directly from this circuit.

**ANSWER:** Eq. (17.30)

Let us now explore the origin of the poles and zeros of the voltage transfer function. Eq. (17.29) has three poles and three zeros, *one pole and one zero for each independent capacitor* in the circuit. Two of the zeros are at  $s = 0$  (dc), corresponding to series capacitors  $C_1$  and  $C_2$ , each of which blocks the propagation of dc signals through the amplifier. The third zero occurs at the frequency for which the impedance of the parallel combination of  $R_S$  and  $C_3$  becomes infinite. At this frequency, propagation of signal current through the MOSFET is blocked, and the output voltage must be zero. Thus, the three zero locations are

$$s = 0, 0, -\frac{1}{R_S C_3} \quad (17.31)$$

From the denominator of Eq. (17.29), the three poles are located at frequencies of

$$s = -\frac{1}{(R_I + R_G)C_1}, -\frac{1}{(R_D + R_3)C_2}, -\frac{1}{\left(R_S \parallel \left(\frac{1}{g_m}\right)\right)C_3} \quad (17.32)$$

These pole frequencies are determined by the time constants associated with the three individual capacitors. Because the input resistance of the FET is infinite, the resistance present at the terminals of capacitor  $C_1$  is simply the series combination of  $R_I$  and  $R_G$ , and because the output resistance  $r_o$  of the FET has been neglected, the resistance associated with capacitor  $C_2$  is the series combination of  $R_3$  and  $R_D$ . The effective resistance in parallel with capacitor  $C_3$  is the equivalent resistance present at the source terminal of the FET, which is equal to the parallel combination of resistor  $R_S$  and  $1/g_m$ . Section 17.3 has a more complete interpretation of these resistance expressions.

## DESIGN NOTE

Each independent capacitor (or inductor) contributes one pole and one zero to the circuit transfer function. (Some poles or zeros may be at zero or infinite frequency.)

### EXAMPLE 17.2 DIRECT CALCULATION OF THE POLES AND ZEROS OF THE COMMON-SOURCE AMPLIFIER

Analyze the low-frequency behavior of a common-source amplifier, including the effects of coupling and bypass capacitors.

**PROBLEM** Find the midband gain, poles, zeros, and cutoff frequency for the common-source amplifier in Fig. 17.4. Assume  $g_m = 1.23 \text{ mS}$ . Write a complete expression for the amplifier transfer function. Write a dominant-pole representation for the amplifier transfer function.

**SOLUTION** **Known Information and Given Data:** The circuit with element values appears in Fig. 17.4, and  $g_m = 1.23 \text{ mS}$ . Expressions for  $A_{\text{mid}}$  and the individual poles and zeros are given in Eqs. (17.29) and (17.30).

**Unknowns:**  $A_{\text{mid}}$ , poles, zeros,  $f_L$ , dominant-pole approximation, complete transfer function

**Approach:** Use the circuit element values to find  $A_{\text{mid}}$  and the poles and zeros from Eqs. (17.31) and (17.32). Use the pole and zero values to find  $f_L$  from Eq. (17.15).

**Assumptions:** Small-signal conditions apply; output resistance  $r_o$  can be neglected

**Analysis:** To begin, we will find  $A_{\text{mid}}$ :

$$A_{\text{mid}} = -(1.23 \text{ mS})(4.3 \text{ k}\Omega \parallel 100 \text{ k}\Omega) \frac{243 \text{ k}\Omega}{1.0 \text{ k}\Omega + 243 \text{ k}\Omega} = -5.05 \quad \text{or} \quad 14.1 \text{ dB}$$

From Eq. (17.29), the three zeros are

$$\omega_{Z1} = 0 \quad \omega_{Z2} = 0 \quad \omega_{Z3} = -\frac{1}{(10 \mu\text{F})(1.3 \text{ k}\Omega)} = -76.9 \text{ rad/s}$$

and the three poles are

$$\begin{aligned} \omega_{P1} &= -\frac{1}{(0.1 \mu\text{F})(1 \text{ k}\Omega + 243 \text{ k}\Omega)} = -41.0 \text{ rad/s} \\ \omega_{P2} &= -\frac{1}{(0.1 \mu\text{F})(4.3 \text{ k}\Omega + 100 \text{ k}\Omega)} = -95.9 \text{ rad/s} \\ \omega_{P3} &= -\frac{1}{(10 \mu\text{F}) \left( 1.3 \text{ k}\Omega \parallel \frac{1}{1.23 \text{ mS}} \right)} = -200 \text{ rad/s} \end{aligned}$$

The lower-cutoff frequency is given by

$$f_L = \frac{1}{2\pi} \sqrt{41.0^2 + 95.9^2 + 200^2 - 2(0^2 + 0^2 + 76.9^2)} = \frac{197}{2\pi} = 31.5 \text{ Hz}$$

and the complete transfer function is

$$A_v(s) = -5.05 \frac{s^2(s + 76.9)}{(s + 41.0)(s + 95.9)(s + 200)}$$

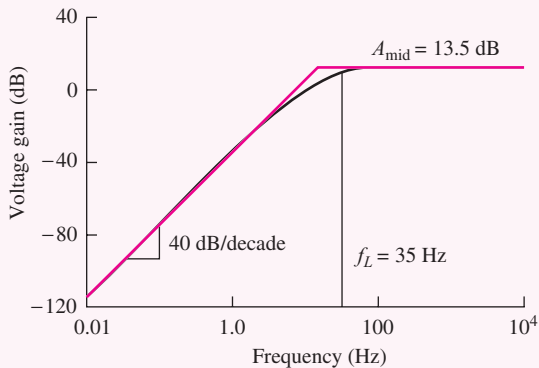
The dominant-pole estimate could be written either using the calculated value of  $f_L$  or the highest pole

$$A_v(s) \cong -5.05 \frac{s}{s + 197} \quad \text{or} \quad A_v(s) \cong -5.05 \frac{s}{s + 200}$$

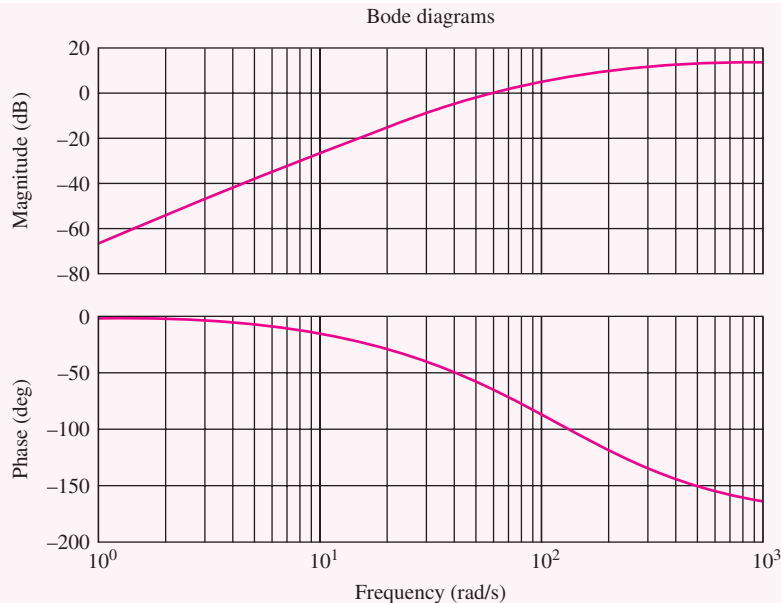
**Check of Results:** A double check of our math indicates the calculations are correct. We see that  $A_{\text{mid}}$  is small, so that neglecting  $r_o$  should be reasonable.

**Discussion:** Although the poles and zeros are not widely spaced, the lower-cutoff frequency is surprisingly close to  $\omega_{P3}$ . This occurs because of an approximate pole-zero cancellation that is taking place between  $\omega_{Z3}$  and  $\omega_{P2}$ .

**Computer-Aided Analysis:** SPICE simulation results for the common-source amplifier appear in the figure here. The simulation used  $V_{DD} = 12 \text{ V}$ , FSTART = 0.01 Hz, and FSTOP = 10 kHz with 10 frequency points per decade. The values of  $A_{\text{mid}}$  and  $f_L$  agree with our hand calculations.



SPICE simulation results for the C-S amplifier in Fig. 17.4 ( $V_{DD} = 12 \text{ V}$ ).



The small discrepancies are related to our neglect of  $r_o$  in the calculations. We can also plot  $A_v(s)$  by multiplying out the numerator and denominator and then using MATLAB®: bode ( $-5.05*[1\ 76.9\ 0\ 0],[1\ 336.9\ 31311.9\ 786380]$ ) or by using the convolution function to multiply the polynomials for us: bode( $-5.05*[1\ 76.9\ 0\ 0],[\text{conv}([1\ 41],\text{conv}([1\ 95.9],[1\ 200]))]$ ).

**EXERCISE:** Find the new values of  $A_{\text{mid}}$ , the poles and zeros, and  $f_L$  if the value of  $C_2$  is reduced to  $2\ \mu\text{F}$ .

**ANSWERS:**  $-5.05; 0; 0; -385\ \text{rad/s}; -41.0\ \text{rad/s}; -95.9\ \text{rad/s}; -1000\ \text{rad/s}; 135\ \text{Hz}$

**EXERCISE:** What value of output resistance  $r_o$  is needed to account for the difference in  $A_{\text{mid}}$  between our hand calculations and the SPICE simulation results?

**ANSWER:**  $57.5\ \text{k}\Omega$

**EXERCISE:** Suppose that the output resistance in the previous exercise appears in parallel with  $R_S$  in the expressions for  $\omega_{P2}$ . What are the new values of  $\omega_{P2}$  and  $f_L$ ?

**ANSWERS:**  $202\ \text{rad/s}, 31.8\ \text{Hz}$

## 17.3 ESTIMATION OF $\omega_L$ USING THE SHORT-CIRCUIT TIME-CONSTANT METHOD

To use Eq. (17.16) or Eq. (17.23), the location of all the poles and zeros of the amplifier must be known. In most cases, however, it is not easy to find the complete transfer function, let alone represent it in factored form. Fortunately, we are most often interested in the values of  $A_{\text{mid}}$ , and the upper- and lower-cutoff frequencies  $\omega_H$  and  $\omega_L$  that define the bandwidth of the amplifier, as indicated in Fig. 17.5. Knowledge of the exact position of all the poles and zeros is not necessary. Two techniques, the **short-circuit time-constant (SCTC) method** and the **open-circuit time-constant (OCTC) method**, have been developed; these produce good estimates of  $\omega_L$  and  $\omega_H$ , respectively, without having to find the complete transfer function.

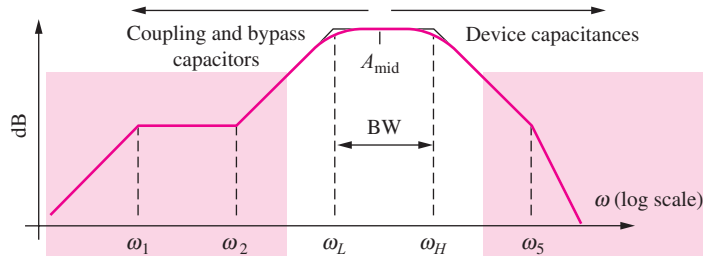


Figure 17.5 Midband region of primary interest in most amplifier transfer functions.

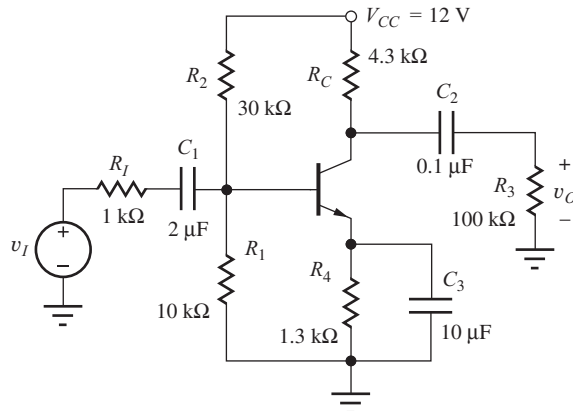


Figure 17.6 Common-emitter amplifier including finite capacitor values.

It can be shown theoretically [1] that the lower-cutoff frequency for a network having  $n$  coupling and bypass capacitors can be estimated from

$$\omega_L \approx \sum_{i=1}^n \frac{1}{R_{iS}C_i} \quad (17.33)$$

in which  $R_{iS}$  represents the resistance at the terminals of the  $i$ th capacitor  $C_i$  with all the other capacitors replaced by short circuits. The product  $R_{iS}C_i$  represents the short-circuit time constant associated with capacitor  $C_i$ . We now use the SCTC method to find  $\omega_L$  for the three classes of single-stage amplifiers.

### 17.3.1 ESTIMATE OF $\omega_L$ FOR THE COMMON-EMITTER AMPLIFIER

We use the C-E amplifier in Fig. 17.6 that includes finite values for the capacitors as a first example of the SCTC method. The presence of  $r_\pi$  in the bipolar model causes direct calculation of the transfer function to be complex; including  $r_o$  leads to even further difficulty. Thus, the circuit is a good example of applying the method of short-circuit time constants to a network.

The ac model for the C-E amplifier in Fig. 17.7 contains three capacitors, and three short-circuit time constants must be determined in order to apply Eq. (17.33). The three analyses rely on the expressions for the midband input and output resistances of the BJT amplifier in Table 14.9.

#### $R_{1S}$

For  $C_1$ ,  $R_{1S}$  is found by replacing  $C_2$  and  $C_3$  by short circuits, yielding the network in Fig. 17.8.  $R_{1S}$  represents the equivalent resistance present at the terminals of capacitor  $C_1$ . Based on Fig. 17.8,

$$R_{1S} = R_I + (R_B \| R_{IB}) = R_I + (R_B \| r_\pi) \quad (17.34)$$

$R_{1S}$  is equal to the source resistance  $R_I$  in series with the parallel combination of the base bias resistor  $R_B$  and the input resistance  $r_\pi$  of the BJT.

The Q-point for this amplifier is found to be (1.66 mA, 2.70 V), and for  $\beta_o = 100$  and  $V_A = 75$  V,

$$r_\pi = 1.51 \text{ k}\Omega \quad \text{and} \quad r_o = 46.8 \text{ k}\Omega$$

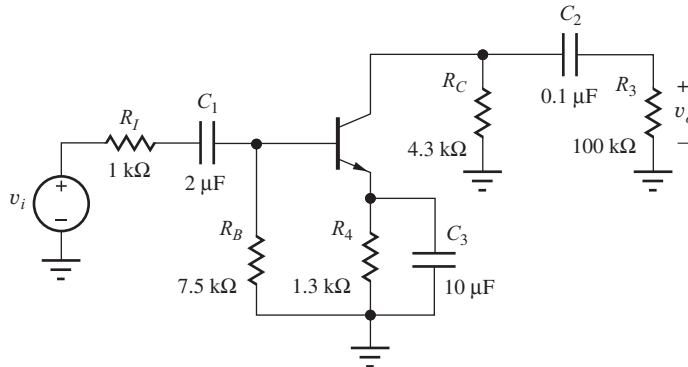
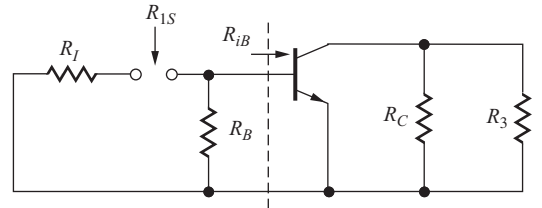
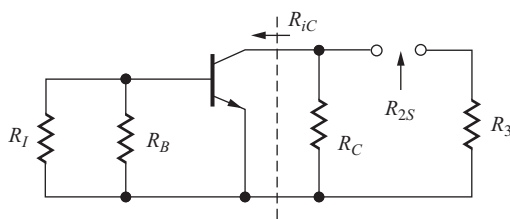
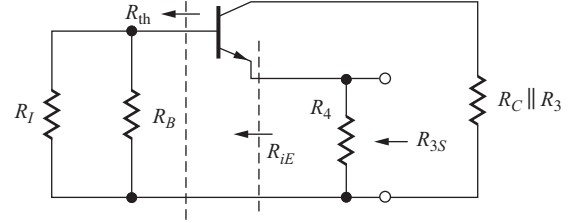


Figure 17.7 ac Model for the C-E amplifier in Fig. 17.6.

Figure 17.8 Circuit for finding  $R_{1S}$ .Figure 17.9 Circuit for finding  $R_{2S}$ .Figure 17.10 Circuit for finding  $R_{3S}$ .

Using these values and those of the other circuit elements,

$$R_{1S} = 1000 \Omega + (7500 \Omega \parallel 1510 \Omega) = 2260 \Omega$$

and

$$\frac{1}{R_{1S}C_1} = \frac{1}{(2.26 \text{ k}\Omega)(2.00 \mu\text{F})} = 222 \text{ rad/s} \quad (17.35)$$

### **R<sub>2S</sub>**

The network used to find  $R_{2S}$  is constructed by shorting capacitors  $C_1$  and  $C_3$ , as in Fig. 17.9. For this network,

$$R_{2S} = R_3 + (R_C \parallel R_{iC}) = R_3 + (R_C \parallel r_o) \cong R_3 + R_C \quad (17.36)$$

$R_{2S}$  represents the combination of load resistance  $R_3$  in series with the parallel combination of collector resistor  $R_C$  and the collector resistance  $r_o$  of the BJT. For the values in this particular circuit,

$$R_{2S} = 100 \text{ k}\Omega + (4.30 \text{ k}\Omega \parallel 46.8 \text{ k}\Omega) = 104 \text{ k}\Omega \quad (17.37)$$

and

$$\frac{1}{R_{2S}C_2} = \frac{1}{(104 \text{ k}\Omega)(0.100 \mu\text{F})} = 96.1 \text{ rad/s} \quad (17.38)$$

### **R<sub>3S</sub>**

Finally, the network used to find  $R_{3S}$  is constructed by shorting capacitors  $C_1$  and  $C_2$ , as in Fig. 17.10, and

$$R_{3S} = R_4 \parallel R_{iE} = R_4 \left| \frac{r_\pi + R_{th}}{\beta_o + 1} \right| \quad \text{where} \quad R_{th} = R_I \parallel R_B \quad (17.39)$$

$R_{2S}$  represents the combination of emitter resistance  $R_4$  in parallel with the equivalent resistance at the emitter terminal of the BJT. For the values in this particular circuit,

$$R_{th} = R_I \parallel R_B = 1000 \Omega \parallel 7500 \Omega = 882 \Omega$$

$$R_{3S} = 1300 \Omega \left| \frac{1510 \Omega + 882 \Omega}{101} \right| = 23.3 \Omega$$

and

$$\frac{1}{R_{3S}C_3} = \frac{1}{(23.3 \Omega)(10 \mu\text{F})} = 4300 \text{ rad/s} \quad (17.40)$$

### The $\omega_L$ Estimate

Using the three time-constant values from Eqs. (17.35), (17.38), and (17.40) yields estimates for  $\omega_L$  and  $f_L$ :

$$\omega_L \cong \sum_{i=1}^3 \frac{1}{R_{iS}C_i} = 222 + 96.1 + 4300 = 4620 \text{ rad/s} \quad (17.41)$$

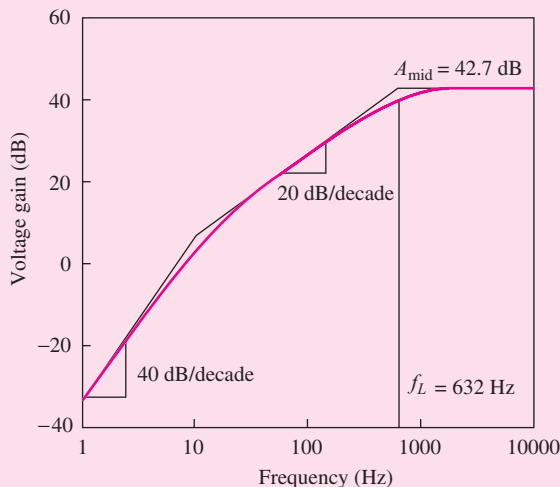
and

$$f_L = \frac{\omega_L}{2\pi} = 735 \text{ Hz}$$

The lower-cutoff frequency of the amplifier is approximately 735 Hz.

Note in this example that the time constant associated with emitter bypass capacitor  $C_3$  is dominant; that is, the value of  $R_{3S}C_3$  is more than an order of magnitude larger than the other two time constants so that  $\omega_L \cong 1/R_{3S}C_3$  ( $f_L \cong 4300/2\pi = 685$  Hz). This is a common situation and represents a practical approach to the design of  $\omega_L$ . Because the resistance presented at the emitter or source of the transistor is low, the time constant associated with an emitter or source bypass capacitor is often dominant and can be used to set  $\omega_L$ . The other two time constants can easily be designed to be much larger.

**EXERCISE:** Simulate the frequency response of the circuit in Fig. 17.6 using SPICE, and find the midband gain and lower-cutoff frequency. Use  $\beta_o = 100$ ,  $I_S = 1 \text{ fA}$ , and  $V_A = 75 \text{ V}$ . What is the Q-point?



**ANSWERS:** 135, 635 Hz, (1.64 mA, 2.79 V)

SPICE simulation results.

**EXERCISE:** Find the short-circuit time constants and  $f_L$  for the common-emitter amplifier in Fig. 17.7 if  $R_B = 75 \text{ k}\Omega$ ,  $R_4 = 13 \text{ k}\Omega$ ,  $R_C = 43 \text{ k}\Omega$ , and  $I_C = 175 \mu\text{A}$ . Assume  $\beta_o = 140$  and  $V_A = 80 \text{ V}$ . The other values remain unchanged.

**ANSWERS:** 33.6 ms; 1.47 ms; 14.3 ms; 124 Hz

## DESIGN EXAMPLE 17.3

### LOWER-CUTOFF FREQUENCY DESIGN IN THE COMMON-EMITTER AMPLIFIER

Choose the coupling and bypass capacitors to set the value of  $f_L$  of the common-emitter to a specified value.

**PROBLEM** Choose  $C_1$ ,  $C_2$ , and  $C_3$  to set  $f_L = 2000$  Hz in the amplifier in Fig. 17.6.

**SOLUTION Known Information and Given Data:** The circuit with resistor values appears in Fig. 17.6 with  $\beta_o = 100$ ,  $r_\pi = 1.51$  k $\Omega$ , and  $r_o = 46.8$  k $\Omega$ . From Eqs. (17.34) through (17.40), we have  $R_{1S} = 2.26$  k $\Omega$ ,  $R_{2S} = 23.3$   $\Omega$ , and  $R_{3S} = 104$  k $\Omega$ .

**Unknowns:**  $C_1$ ,  $C_2$ , and  $C_3$

**Approach:** Because  $R_{3S}$  is much smaller than the other two resistors, its associated time constant can easily be designed to dominate the value of  $\omega_L$  as occurred in Eq. (17.41). Thus, the approach taken here is to use  $C_3$  to set  $f_L$  and to choose  $C_1$  and  $C_2$  so that their contributions are negligible.

**Assumptions:** Small-signal conditions apply.  $V_T = 25.0$  mV.

**Analysis:** Choosing  $C_3$  to set  $f_L$  yields

$$C_3 \cong \frac{1}{R_{3S}\omega_L} = \frac{1}{23.3 \text{ } \Omega(2\pi)(2000 \text{ Hz})} = 3.42 \text{ } \mu\text{F}$$

Let us choose  $C_1$  and  $C_2$  so that their individual time constants are each 100 times larger than that associated with  $C_3$  — that is, each capacitor will contribute a 1 percent error to  $f_L$ .

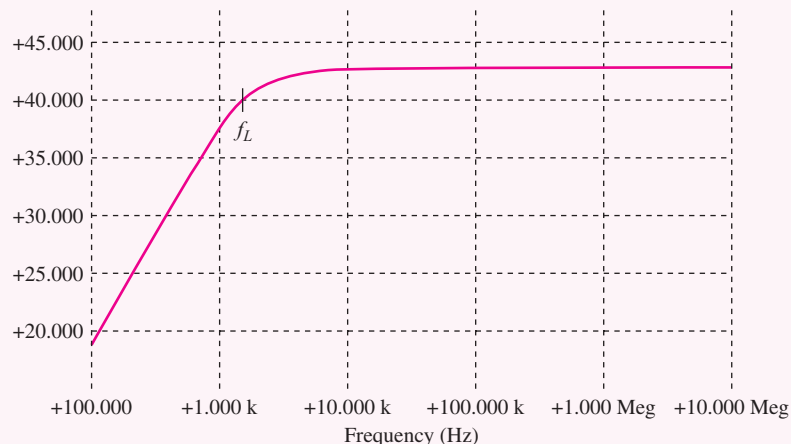
$$C_1 = 100 \frac{R_{3S}C_3}{R_{1S}} = 100 \frac{(23.2 \text{ } \Omega)(3.42 \text{ } \mu\text{F})}{2.26 \text{ k}\Omega} = 3.51 \text{ } \mu\text{F}$$

$$C_2 = 100 \frac{R_{3S}C_3}{R_{2S}} = 100 \frac{(23.2 \text{ } \Omega)(3.42 \text{ } \mu\text{F})}{104 \text{ k}\Omega} = 0.0763 \text{ } \mu\text{F}$$

Picking the nearest values from the capacitor table in Appendix A, we have  $C_1 = 3.9$   $\mu\text{F}$ ,  $C_2 = 0.082$   $\mu\text{F}$ , and  $C_3 = 3.9$   $\mu\text{F}$ .

**Check of Results:** Let us check by calculating the actual values of  $f_L$ .

$$f_L = \frac{1}{2\pi} \left[ \frac{1}{2.26 \text{ k}\Omega(3.9 \text{ } \mu\text{F})} + \frac{1}{104 \text{ k}\Omega(0.082 \text{ } \mu\text{F})} + \frac{1}{23.2 \text{ } \Omega(3.9 \text{ } \mu\text{F})} \right] = 1800 \text{ Hz}$$



**Discussion:** The cutoff frequency is approximately 10 percent lower than the design value because of the use of the  $3.9\text{-}\mu\text{F}$  capacitor and the small contributions from  $C_1$  and  $C_2$ . At additional cost, one could use two capacitors to make up the  $3.5\text{-}\mu\text{F}$  value. However, the tolerances on typical capacitors are relatively large, and one would need to use a precision capacitor (and resistors) if a more accurate value of  $f_L$  is required. (See simulation results on previous page.)

**Computer-Aided Analysis:** The frequency response with the new capacitor values can be simulated using SPICE ac analysis with FSTART = 10 Hz and FSTOP = 10 MHz with 20 frequency points per decade. The transistor parameters were set to  $I_S = 3\text{ fA}$ ,  $B_F = 100$ , and  $V_A = 75\text{ V}$ . SPICE simulation results for the new common-emitter design results yields  $A_{mid} = -138$  and  $f_L = 1610\text{ Hz}$ . The value of  $f_L$  is approximately 10 percent less than our hand calculations. This discrepancy is due to differences in  $V_T$  and the Q-point current.

**EXERCISE:** Estimate the midband gain for the circuit in Fig. 17.6. What is the source of the error between this value and SPICE?

**ANSWER:**  $-157$ ; Neglect of  $r_o$  accounts for most of the difference.

### 17.3.2 ESTIMATE OF $\omega_L$ FOR THE COMMON-SOURCE AMPLIFIER

Equations (17.34), (17.36), and (17.39) can be applied directly to the C-S FET amplifier in Fig. 17.11 by substituting infinity for the values of the transistor's input resistance and current gain. These equations reduce directly to:

$$\begin{aligned} R_{IS} &= R_I + (R_G \parallel R_{iG}) = R_I + R_G \\ R_{2S} &= R_3 + (R_D \parallel R_{iD}) = R_3 + (R_D \parallel r_o) \cong R_3 + R_D \\ R_{3S} &= R_S \parallel R_{iS} = R_S \left\| \frac{1}{g_m} \right. \end{aligned} \quad (17.42)$$

The three expressions in Eq. (17.42) represent the short-circuit resistances associated with the three capacitors in the circuit, as indicated in the ac circuit models in Figs. 17.12(a) to (c). Note that the three time constants are the same as those found by the direct approach that yielded Eq. (17.30).

**EXERCISE:** Find the short-circuit time constants and  $f_L$  for the common-source amplifier in Fig. 17.11 if  $I_D = 1.5\text{ mA}$  and  $V_{GS} - V_{TN} = 0.5\text{ V}$ . Assume  $\lambda = 0.015/\text{V}$ . The other values remain unchanged.

**ANSWERS:** 24.4 ms; 10.4 ms; 1.48 ms; 129 Hz

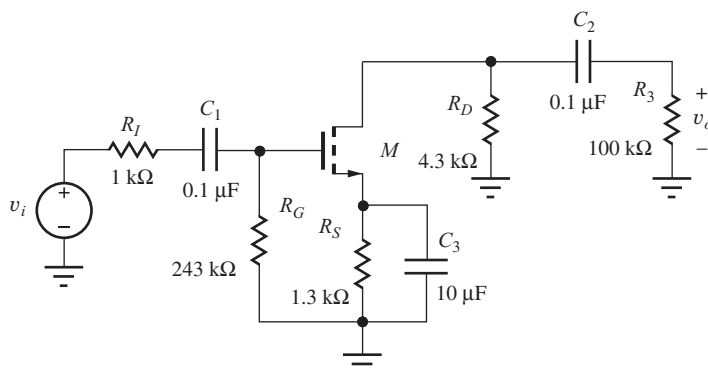
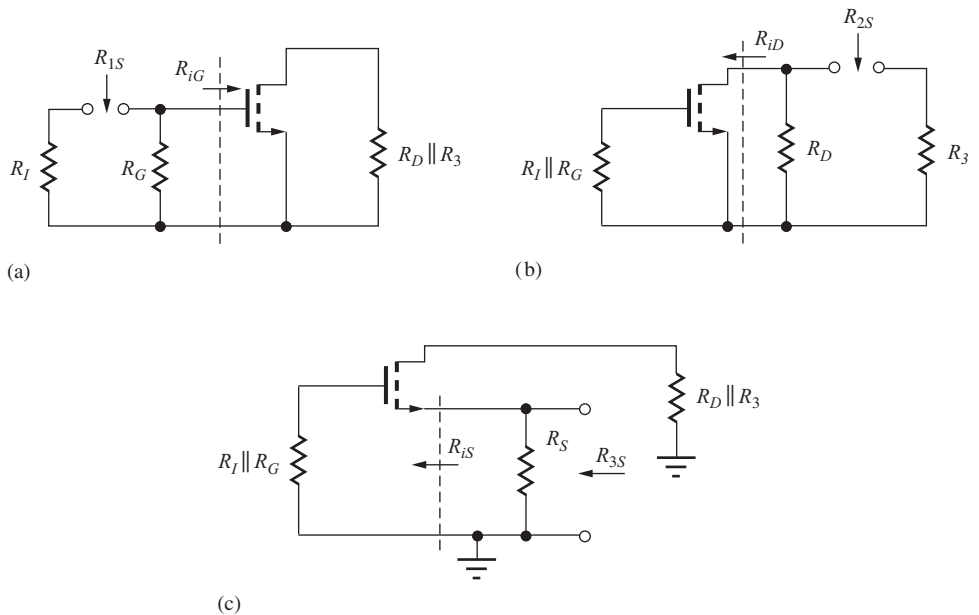
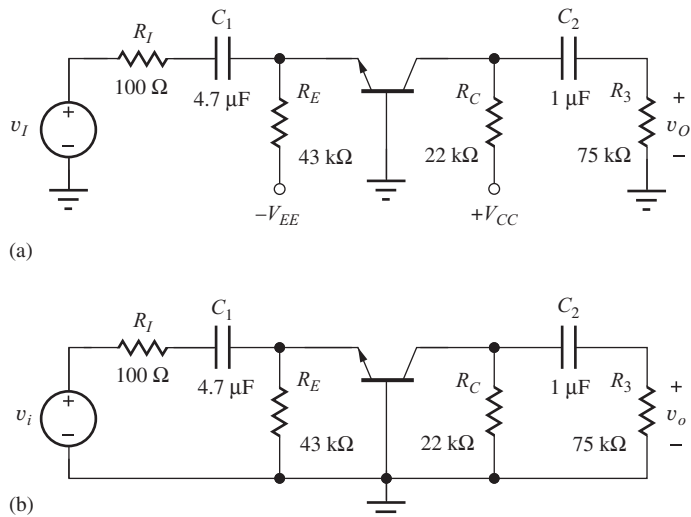


Figure 17.11 ac Model for common-source amplifier.



**Figure 17.12** (a) Resistance  $R_{1S}$  at the terminals of  $C_1$ . (b) Resistance  $R_{2S}$  at the terminals of  $C_2$ . (c) Resistance  $R_{3S}$  at the terminals of  $C_3$ .



**Figure 17.13** (a) Common-base amplifier. (b) Low-frequency ac equivalent circuit.

### 17.3.3 ESTIMATE OF $\omega_L$ FOR THE COMMON-BASE AMPLIFIER

Next, we apply the short-circuit time-constant technique to the common-base amplifier in Fig. 17.13. The results are also directly applicable to the common-gate case if  $\beta_o$  and  $r_\pi$  are set equal to infinity. Figure 17.13(b) is the low-frequency ac equivalent circuit for the common-base amplifier. In this particular circuit, coupling capacitors  $C_1$  and  $C_2$  are the only capacitors present, and expressions for  $R_{1S}$  and  $R_{2S}$  are needed.

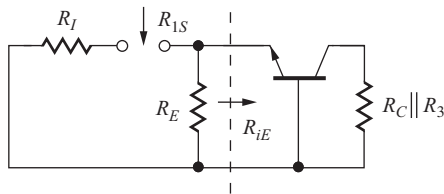
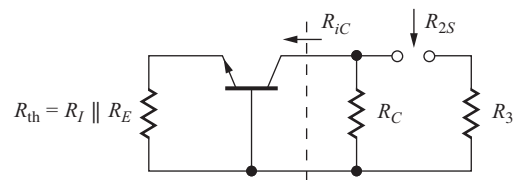
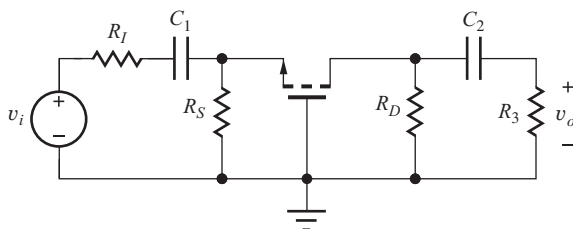
Figure 17.14 Equivalent circuit for determining  $R_{1S}$ .Figure 17.15 Equivalent circuit for determining  $R_{2S}$ .

Figure 17.16 ac Circuit for common-gate amplifier.

 **$R_{1S}$**  $R_{1S}$  is found by shorting capacitor  $C_2$ , as indicated in the circuit in Fig. 17.14. Based on this figure,

$$R_{1S} = R_I + (R_E \parallel R_{iE}) \cong R_I + \left( R_E \left\| \frac{1}{g_m} \right. \right) \quad (17.43)$$

 **$R_{2S}$** Shorting capacitor  $C_1$  yields the circuit in Fig. 17.15, and the expression for  $R_{2S}$  is

$$R_{2S} = R_3 + (R_C \parallel R_{iC}) \cong R_3 + R_C \quad (17.44)$$

because  $R_{iC} \cong r_o(1 + g_m R_{th})$  is large.

**EXERCISE:** Find the short-circuit time constants and  $f_L$  for the common-base amplifier in Fig. 17.13 if  $\beta_0 = 100$ ,  $V_A = 70$  V, and the Q-point is (0.1 mA, 5 V). What is  $A_{mid}$ ?

**ANSWERS:** 1.64 ms, 97.0 ms, 98.7 Hz; 48.6

### 17.3.4 ESTIMATE OF $\omega_L$ FOR THE COMMON-GATE AMPLIFIER

The expressions for  $R_{1S}$  and  $R_{2S}$  for the common-gate amplifier in Fig. 17.16 are virtually identical to those of the common-base stage:

$$R_{1S} = R_I + (R_S \parallel R_{iS}) = R_I + \left( R_S \left\| \frac{1}{g_m} \right. \right) \quad (17.45)$$

$$R_{2S} = R_3 + (R_D \parallel R_{iD}) \cong R_3 + R_D \quad \text{because} \quad R_{iD} \cong \mu_f(R_S \parallel R_I)$$

**EXERCISE:** Draw the circuits used to find  $R_{1S}$  and  $R_{2S}$  for the common-gate amplifier in Fig. 17.16 and verify the results presented in Eq. (17.45).

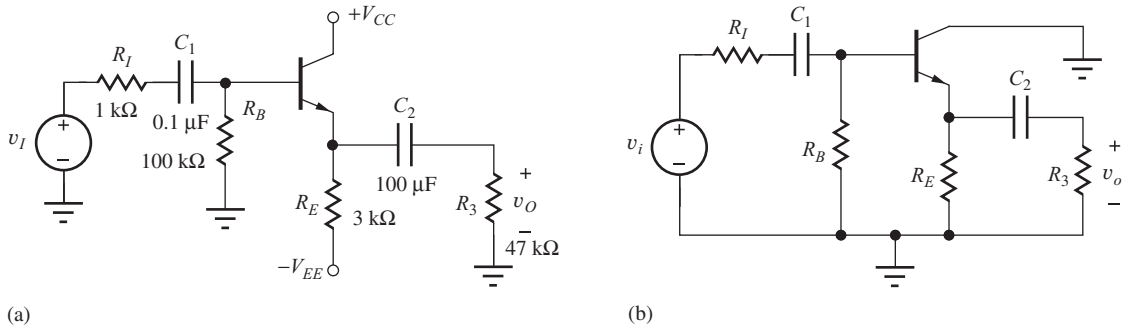


**Figure 17.17** (a) Common-collector amplifier. (b) Low-frequency ac model for the common-collector amplifier.

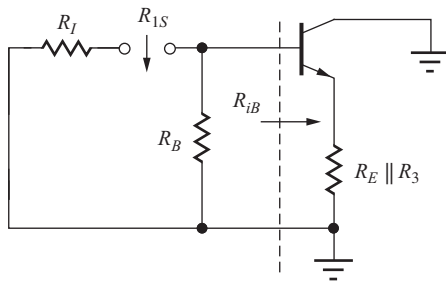


**Figure 17.18** Circuit for finding  $R_{1S}$ .

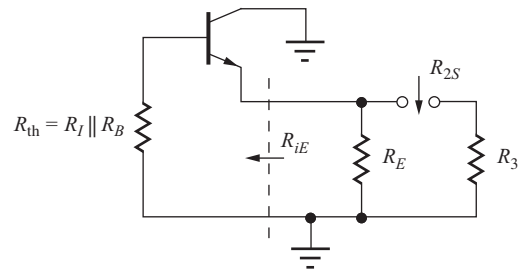


**Figure 17.19** Circuit for finding  $R_{2S}$ .

**EXERCISE:** Find the short-circuit time constants and  $f_L$  for the common-gate amplifier in Fig. 17.16 if  $R_I = 100\text{ }\Omega$ ,  $R_S = 1.3\text{ k}\Omega$ ,  $R_D = 4.3\text{ k}\Omega$ ,  $R_3 = 75\text{ k}\Omega$ ,  $C_1 = 1\text{ }\mu\text{F}$ ,  $C_2 = 0.1\text{ }\mu\text{F}$ ,  $I_D = 1.5\text{ mA}$ , and  $V_{GS} - V_{TN} = 0.5\text{ V}$ . Assume  $\lambda = 0$ .

**ANSWERS:** 0.248 ms; 7.93 ms; 663 Hz

### 17.3.5 ESTIMATE OF $\omega_L$ FOR THE COMMON-COLLECTOR AMPLIFIER

Figures 17.17(a) and (b) are schematics of an emitter follower and its corresponding low-frequency ac model. This circuit has two coupling capacitors,  $C_1$  and  $C_2$ . The circuit for  $R_{1S}$  in Fig. 17.18 is constructed by shorting  $C_2$ , and the expression for  $R_{1S}$  is

$$R_{1S} = R_I + (R_B \parallel R_{iB}) = R_I + (R_B \parallel [r_\pi + (\beta_o + 1)(R_E \parallel R_3)]) \quad (17.46)$$

Similarly, the circuit used to find  $R_{2S}$  is found by shorting capacitor  $C_1$ , as in Fig. 17.19, and

$$R_{2S} = R_3 + (R_E \parallel R_{iE}) = R_3 + \left( R_E \parallel \frac{R_{th} + r_\pi}{\beta_o + 1} \right) \quad (17.47)$$

### 17.3.6 ESTIMATE OF $\omega_L$ FOR THE COMMON-DRAIN AMPLIFIER

The corresponding low-frequency ac model for the common-drain amplifier appears in Fig. 17.20. Taking the limits as  $\beta_o$  and  $r_\pi$  approach infinity, Eqs. (17.46) and (17.47) become

$$R_{1S} = R_I + (R_G \parallel R_{iG}) = R_I + R_G \quad \text{because} \quad R_{iG} = \infty \quad (17.48)$$

and

$$R_{2S} = R_3 + (R_S \parallel R_{iS}) = R_3 + \left( R_S \parallel \frac{1}{g_m} \right)$$

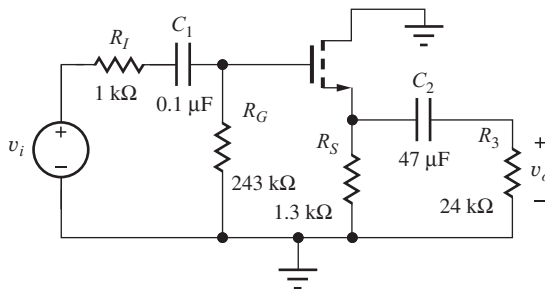


**Figure 17.20** Low-frequency ac equivalent circuit for common-drain amplifier.

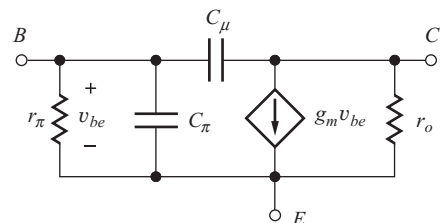


**Figure 17.21** Capacitances in the hybrid-pi model of the BJT.

**EXERCISE:** Find the short-circuit time constants and  $f_L$  for the common-collector amplifier in Fig. 17.17(a) if  $\beta_o = 100$ ,  $V_A = 70$  V, and the Q-point = (1 mA, 5 V). What is  $A_{mid}$ ?

**ANSWERS:** 7.52 ms, 4.70 s, 21.2 Hz; 0.978

**EXERCISE:** Find the short-circuit time constants and  $f_L$  for the common-drain amplifier in Fig. 17.20 if  $g_m = 1$  mS. What is  $A_{mid}$ ?

**ANSWERS:** 24.4 ms, 1.16 ms, 6.66 Hz; 0.550

## 17.4 TRANSISTOR MODELS AT HIGH FREQUENCIES

To explore the upper limits of amplifier frequency response, the high-frequency limitations of the transistors, which we have ignored thus far, must be taken into account. All electronic devices have capacitances between their various terminals, and these capacitances limit the range of frequencies for which the devices can provide useful voltage, current, or power gain. This section develops the description of the frequency-dependent hybrid-pi model for the bipolar transistor, as well as a similar model for the field-effect transistor.

### 17.4.1 FREQUENCY-DEPENDENT HYBRID-PI MODEL FOR THE BIPOLAR TRANSISTOR

In the BJT, capacitances appear between the base-emitter and base-collector terminals of the transistor and are included in the small-signal hybrid-pi model in Fig. 17.21. The capacitance between the base and collector terminals, denoted by  $C_\mu$ , represents the capacitance of the reverse-biased collector-base junction of the bipolar transistor and is related to the Q-point through an expression equivalent to Eq. (3.21), Chapter 3:

$$C_\mu = \frac{C_{\mu o}}{\sqrt{1 + \frac{V_{CB}}{\phi_j}}} \quad (17.49)$$

In Eq. (17.49),  $C_{\mu o}$  represents the total collector-base junction capacitance at zero bias, and  $\phi_j$  is the built-in potential of the collector-base junction, typically 0.6 to 1.0 V.

The internal capacitance between the base and emitter terminals, denoted by  $C_\pi$ , represents the diffusion capacitance associated with the forward-biased base-emitter junction of the transistor.  $C_\pi$  is related to the Q-point through Eq. (5.46) in Sec. 5.8:

$$C_\pi = g_m \tau_F \quad (17.50)$$

in which  $\tau_F$  is the forward transit-time of the bipolar transistor. In Fig. 17.21,  $C_\pi$  appears directly in parallel with  $r_\pi$ . For a given input signal current, the impedance of  $C_\pi$  causes the base-emitter voltage

$v_{be}$  to be reduced as frequency increases, thereby reducing the current in the controlled source at the output of the transistor. At very high frequencies,  $C_\mu$  shorts the base and collector terminals together.

Shunt capacitances such as  $C_\pi$  are always present in electronic devices and circuits. At low frequencies, the impedance of these capacitances is usually very large and so has negligible effect relative to the resistances such as  $r_\pi$ . However, as frequency increases, the impedance of  $C_\pi$  becomes smaller and smaller, and  $v_{be}$  eventually approaches zero. Thus, transistors cannot provide amplification at arbitrarily high frequencies.

### 17.4.2 MODELING $C_\pi$ AND $C_\mu$ IN SPICE

In SPICE, the value of  $C_\pi$  is determined by the forward transit time TF and  $C_\mu$  depends upon the zero-bias value of the collector-junction capacitance CJC, the built-in potential VJC of the collector-base junction, and the grading factor MJC of the collector-base junction. In SPICE,  $C_\pi$  and  $C_\mu$  are referred to as  $C_{BE}$  and  $C_{BC}$ , respectively.

$$C_{BE} = g_m \cdot TF \quad \text{and} \quad C_{BC} = \frac{\text{CJC}}{\left(1 + \frac{\text{VCB}}{\text{VJC}}\right)^{\text{MJC}}} \quad (17.51)$$

VJC defaults to 0.75 V, and MJC defaults to 0.33.

### 17.4.3 UNITY-GAIN FREQUENCY $f_T$

A quantitative description of the behavior of the transistor at high frequencies can be found by calculating the frequency-dependent short-circuit current gain  $\beta(s)$  from the circuit in Fig. 17.22. For a current  $\mathbf{I}_b(s)$  injected into the base, the collector current  $\mathbf{I}_c(s)$  consists of two components:

$$\mathbf{I}_c(s) = g_m \mathbf{V}_{be}(s) - \mathbf{I}_\mu(s) \quad (17.52)$$

Because the voltage at the collector is zero,  $v_{be}$  appears directly across  $C_\mu$  and  $\mathbf{I}_\mu(s) = sC_\mu \mathbf{V}_{be}(s)$ . Therefore,

$$\mathbf{I}_c(s) = (g_m - sC_\mu) \mathbf{V}_{be}(s) \quad (17.53)$$

Because the collector is connected directly to ground,  $C_\pi$  and  $C_\mu$  appear in parallel in this circuit, and the base current flows through the parallel combination of  $r_\pi$  and  $(C_\pi + C_\mu)$  to develop the base-emitter voltage:

$$\mathbf{V}_{be}(s) = \mathbf{I}_b(s) \frac{\frac{1}{r_\pi \frac{s(C_\pi + C_\mu)}{1 + \frac{s(C_\pi + C_\mu)}{r_\pi}}}}{s(C_\pi + C_\mu)r_\pi + 1} = \mathbf{I}_b(s) \frac{r_\pi}{s(C_\pi + C_\mu)r_\pi + 1} \quad (17.54)$$

By combining Eqs. (17.53) and (17.54), we reach an expression for the frequency-dependent current gain:

$$\beta(s) = \frac{\mathbf{I}_c(s)}{\mathbf{I}_b(s)} = \frac{\beta_o \left(1 - \frac{sC_\mu}{g_m}\right)}{s(C_\pi + C_\mu)r_\pi + 1} \quad (17.55)$$

A right-half-plane transmission zero occurs in the current gain at an extremely high frequency,  $\omega_Z = +g_m/C_\mu$ , and can almost always be neglected. Neglecting  $\omega_Z$  results in the following simplified

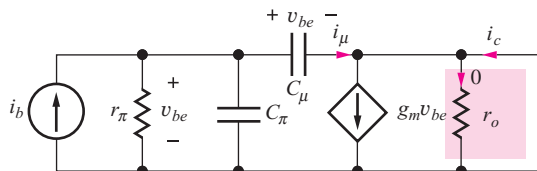
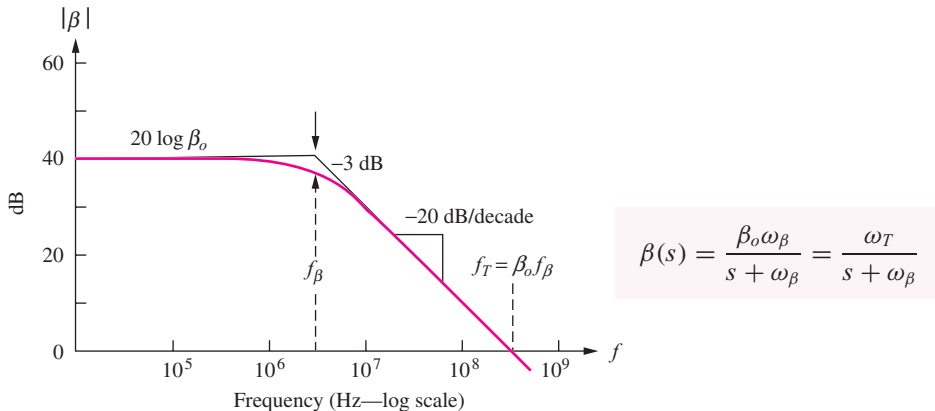


Figure 17.22 Finding the short-circuit current gain  $\beta$  of the BJT.



**Figure 17.23** Common-emitter current gain versus frequency for the BJT.

expression for  $\beta(s)$ :

$$\beta(s) \cong \frac{\beta_o}{s(C_\pi + C_\mu)r_\pi + 1} = \frac{\beta_o}{\frac{s}{\omega_\beta} + 1} \quad (17.56)$$

in which  $\omega_\beta$  represents the **beta-cutoff frequency**, defined by

$$\omega_\beta = \frac{1}{r_\pi(C_\pi + C_\mu)} \quad \text{and} \quad f_\beta = \frac{\omega_\beta}{2\pi} \quad (17.57)$$

Figure 17.23 is a Bode plot for Eq. (17.56). From Eq. (17.56) and this graph, we see that the current gain has the value of  $\beta_o = g_m r_\pi$  at low frequencies and exhibits a single-pole roll-off at frequencies above  $f_\beta$ , decreasing at a rate of 20 dB/decade and crossing through unity gain at  $f = f_T$ . The magnitude of the current gain is 3 dB below its low-frequency value at the beta-cutoff frequency,  $f_\beta$ .

Equation (17.56) can be recast in terms of  $\omega_T = \beta_o \omega_\beta$  as

$$\beta(s) = \frac{\beta_o \omega_\beta}{s + \omega_\beta} = \frac{\omega_T}{s + \omega_\beta} \quad (17.58)$$

where  $\omega_T = 2\pi f_T$ . Parameter  $f_T$  is referred to as the **unity gain-bandwidth product** of the transistor and characterizes one of the fundamental frequency limitations of the transistor. At frequencies above  $f_T$ , the transistor no longer offers any current gain and fails to be useful as an amplifier.

A relationship between the unity gain-bandwidth product and the small-signal parameters can be obtained from Eqs. (17.57) and (17.58):

$$\omega_T = \beta_o \omega_\beta = \frac{\beta_o}{r_\pi(C_\pi + C_\mu)} = \frac{g_m}{C_\pi + C_\mu} \quad (17.59)$$

Note that the transmission zero occurs at a frequency beyond  $\omega_T$ :

$$\omega_Z = \frac{g_m}{C_\mu} > \frac{g_m}{C_\pi + C_\mu} = \omega_T \quad (17.60)$$

To perform numeric calculations, we determine the values of  $f_T$  and  $C_\mu$  from a transistor's specification sheet and then calculate  $C_\pi$  by rearranging Eq. (17.59):

$$C_\pi = \frac{g_m}{\omega_T} - C_\mu \quad (17.61)$$

From Eq. (17.49) we can see that  $C_\mu$  is only a weak function of operating point, but recasting  $g_m$  in Eq. (17.61) demonstrates that  $C_\pi$  is directly proportional to collector current:

$$C_\pi = \frac{40I_C}{\omega_T} - C_\mu \quad (17.62)$$

## EXAMPLE 17.4 BIPOLAR TRANSISTOR MODEL PARAMETERS

Find a set of model parameters for a bipolar transistor from its specification sheet.

**PROBLEM** Find values of  $\beta_o$ ,  $I_S$ ,  $V_A$ ,  $f_T$ ,  $C_\pi$ , and  $C_\mu$  for the CA-3096 *npn* transistors operating at a collector current of 1 mA using the specifications sheets on the MCD website.

**SOLUTION Known Information and Given Data:** CA-3096 specification sheets;  $I_C = 1$  mA

**Unknowns:**  $\beta_o$ ,  $I_S$ ,  $V_A$ ,  $f_T$ ,  $C_\pi$ , and  $C_\mu$

**Approach:** We will use our definitions of, and relationships between, the large-signal and small-signal parameters to find the unknown values.

**Assumptions:**  $T = 25^\circ\text{C}$  and  $V_{CE} = 5$  V, corresponding to the electrical specification sheets; active region operation;  $\beta_o \cong \beta_F$ ; the built-in potential of the collector-base junction is 0.75 V.

**Analysis:** Based on the typical values in the specification sheets, we find  $\beta_F = h_{FE} = 390$ ,  $V_{BE} = 0.69$  V,  $f_T = 280$  MHz, and  $C_{CB} = 0.46$  pF at  $V_{CB} = 3$  V. From the graph of output resistance versus current, we find  $r_o = 80$  k $\Omega$  for  $I_c = 1$  mA. For  $T = 25^\circ\text{C}$ ,  $V_T = 26.0$  mV.

We find the current gain and Early voltage using the values of  $h_{FE}$  and  $r_o$ ,

$$\beta_o \cong h_{FE} = 390 \quad V_A = I_C r_o - V_{CE} = 75 \text{ V}$$

and  $I_S$  is found from  $I_C$ ,  $V_{BE}$ , and  $V_T$ :

$$I_S = \frac{I_C}{\exp\left(\frac{V_{BE}}{V_T}\right)} \frac{1 \text{ mA}}{\exp\left(\frac{0.69 \text{ V}}{26.0 \text{ mV}}\right)} = 2.98 \text{ fA}$$

Capacitance  $C_\mu$  is equal to the collector-base capacitance of the transistor, but it is specified at  $V_{CB} = 3$  V. Using Eq. (17.49), we find  $C_{\mu o}$ , and then calculate  $C_\mu$  for  $V_{CB} = 5 - .69 = 4.31$  V.

$$C_{\mu o} \cong C_{CB} \sqrt{1 + \frac{V_{CB}}{\phi_{jc}}} = 0.46 \text{ pF} \sqrt{1 + \frac{3}{0.75}} = 1.03 \text{ pF}$$

$$C_\mu \cong \frac{C_{\mu o}}{\sqrt{1 + \frac{V_{CB}}{\phi_{jc}}}} = \frac{1.03 \text{ pF}}{\sqrt{1 + \frac{4.31}{0.75}}} = 0.397 \text{ pF}$$

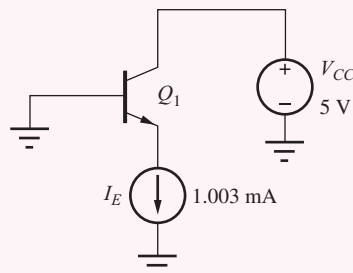
Now we can find  $C_\pi$ :

$$C_\pi = \frac{g_m}{\omega_T} - C_\mu = \frac{1 \text{ mA}}{26.0 \text{ mV}} \frac{1}{2\pi(280 \text{ MHz})} - 0.40 \text{ pF} = 21.5 \text{ pF}$$

**Check of Results:** We have found the required values of  $\beta_o$ ,  $I_S$ ,  $V_A$ ,  $f_T$ ,  $C_\pi$ , and  $C_\mu$ . The calculations appear correct and reasonable. The calculated value of  $C_\mu$  agrees reasonably well with the graph of  $C_{CB}$  versus  $V_{CB}$  in the specification sheets.

**Discussion:** The values in the specification sheets must often be mapped into the parameters that we need, and the data supplied is often incomplete. Some may be presented in tabular form; others must be found from graphs. Note that the current gain peaks at a collector current of approximately 1 mA, whereas  $f_T$  peaks at approximately 4 mA.

**Computer-Aided Analysis:** Let us now attempt to create a SPICE model that has these parameters. We must set  $I_S = 2.98 \text{ fA}$ ,  $B_F = 390$ , and  $V_{AF} = 75 \text{ V}$ . Using Eq. (17.51), we also have  $T_F = 559 \text{ ps}$ ,  $C_{JC} = 1.03 \text{ pF}$ ,  $V_{JC} = 0.75 \text{ V}$ , and  $M_{JC} = 0.5$ . Let us bias the transistor as in the circuit shown here, and request the device parameters as an output following an operating point analysis. The results are  $I_C = 1 \text{ mA}$ ,  $V_{BE} = 0.685 \text{ V}$ ,  $V_{BC} = -5 \text{ V}$ ,  $g_m = 38.7 \text{ mS}$ ,  $\beta_o = g_m/g_\pi = 416$ ,  $r_o = 1/g_o = 79.9 \text{ k}\Omega$ ,  $C_\pi = 21.6 \text{ pF}$ , and  $C_\mu = 0.372 \text{ pF}$ . Our set of device parameters appears to be correct. Note that  $\beta_o = BF(1 + V_{CB}/V_{AF}) = 416$ .



**EXERCISE:** A bipolar transistor has an  $f_T = 500 \text{ MHz}$  and  $C_{\mu o} = 2 \text{ pF}$ . What are the values of  $C_\mu$  and  $C_\pi$  at Q-points of  $(100 \mu\text{A}, 8 \text{ V})$ ,  $(2 \text{ mA}, 5 \text{ V})$ , and  $(50 \text{ mA}, 8 \text{ V})$ ? Assume  $V_{BE} = \phi_{jc} = 0.6 \text{ V}$ .

**ANSWERS:** 0.551 pF, 0.722 pF; 0.700 pF, 24.8 pF; 0.551 pF, 636 pF

#### 17.4.4 HIGH-FREQUENCY MODEL FOR THE FET

To model the FET at high frequencies, gate-drain and gate-source capacitances  $C_{GD}$  and  $C_{GS}$  are added to the small-signal model, as shown in Fig. 17.24. For the MOSFET, these two capacitors represent the gate oxide and overlap capacitances discussed previously in Sec. 4.5. At high frequencies, currents through these two capacitors combine to form a current in the gate terminal, and the signal current  $i_g$  can no longer be assumed to be zero. Thus, even the FET has a finite current gain at high frequencies.

The short-circuit current gain for the FET can be calculated in the same manner as for the BJT, as in Fig. 17.25:

$$\mathbf{I}_d(s) = (g_m - sC_{GD})\mathbf{V}_{gs}(s) = \mathbf{I}_g(s) \frac{(g_m - sC_{GD})}{s(C_{GS} + C_{GD})} \quad (17.63)$$

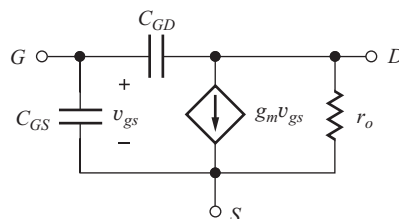


Figure 17.24 Pi model for the FET.

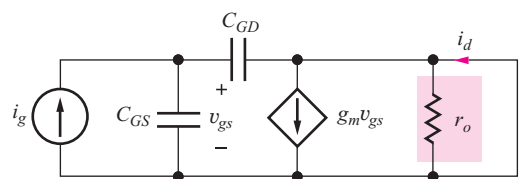


Figure 17.25 Circuit for calculating the short-circuit current gain of the FET.

and

$$\beta(s) = \frac{I_d(s)}{I_g(s)} = \frac{g_m \left( 1 - \frac{sC_{GD}}{g_m} \right)}{s(C_{GS} + C_{GD})} = \frac{\omega_T}{s} \left( 1 - \frac{s}{\omega_T \left( 1 + \frac{C_{GS}}{C_{GD}} \right)} \right) \quad (17.64)$$

At dc, the current gain is infinite but falls at a rate of 20 dB/decade as frequency increases. The unity gain-bandwidth product  $\omega_T$  of the FET is defined in a manner identical to that of the BJT,

$$\omega_T = \frac{g_m}{C_{GS} + C_{GD}} \quad (17.65)$$

and the FET current gain falls below 1 for frequencies in excess of  $\omega_T$ , just as for the case of the bipolar transistor. The transmission zero now occurs at  $\omega_Z = \omega_T(1 + C_{GS}/C_{GD})$ , typically a few times  $\omega_T$ .

### 17.4.5 MODELING $C_{GS}$ AND $C_{GD}$ IN SPICE

As discussed in Sec. 4.5, we remember that the gate-source and gate-drain capacitances in the active region (pinch-off) are expressed as

$$C_{GS} = C'_{OL} W + \frac{2}{3} C''_{ox} WL \quad C_{GD} = C'_{OL} W \quad C''_{ox} = \frac{\varepsilon_{ox}}{T_{ox}} \quad (17.66)$$

The corresponding SPICE parameters are oxide thickness TOX, gate width W, gate length L, gate-source overlap capacitance per unit length CGSO, and gate-drain overlap capacitance per unit length CGDO. Note that SPICE permits definition of different values of overlap capacitance for the source and drain regions of the transistor.

### 17.4.6 CHANNEL LENGTH DEPENDENCE OF $f_T$

The unity-gain bandwidth product of the MOSFET is strongly dependent on the channel length, and this fact represents one of the reasons for continuing to scale the technology to smaller and smaller dimensions. The basic expression for the intrinsic  $f_T$  ( $C'_{OL} = 0$ ) of the MOSFET in terms of technology parameters can be found using Eqs. (17.65) and (17.66). If we remember that  $g_m = K_n(V_{GS} - V_{TN})$ , and assume  $C'_{OL} = 0$ :

$$f_T = \frac{\mu_n C''_{ox} \frac{W}{L} (V_{GS} - V_{TN})}{\frac{2}{3} C''_{ox} WL} = \frac{3 \mu_n (V_{GS} - V_{TN})}{2 L^2} \quad (17.67)$$

The value of  $f_T$  is proportional to transistor mobility and inversely dependent upon the square of the channel length. Thus, an NMOS transistor will have a higher-cutoff frequency than a similar PMOS transistor for a given channel length and bias condition. Reducing the channel length by a factor of 10 results in an increase in  $f_T$  by a factor of 100!

## EXAMPLE 17.5 MOSFET MODEL PARAMETERS

Find a set of model parameters for a MOSFET from its specification sheet.

**PROBLEM** Find values of  $V_{TN}$ ,  $K_P$ ,  $\lambda$ ,  $C_{GS}$ , and  $C_{GD}$  for the NMOS transistors in the ALD-1116 transistor operating at a drain current of 10 mA using the specifications sheets on the MCD website.

**SOLUTION** Known Information and Given Data: ALD-1116 specification sheets;  $I_D = 10$  mA

**Unknowns:**  $V_{TN}$ ,  $K_n$ ,  $\lambda$ ,  $C_{GS}$ , and  $C_{GD}$

**Approach:** We will use our definitions of the relationships between the large-signal and small-signal parameters to find the unknown values.

**Assumptions:**  $T = 25^\circ\text{C}$  and  $V_{DS} = 5 \text{ V}$ , corresponding to the electrical specification sheets; our square-law transistor model applies to the device; the transistor is symmetrical.

**Analysis:** Based on the typical values in the specification sheets, we find  $V_{TN} = 0.7 \text{ V}$  and  $I_D = 4.8 \text{ mA}$  for  $V_{GS} = 5 \text{ V}$ , output conductance  $g_o = 200 \mu\text{S}$  at 10 mA, and  $C_{ISS} = 1 \text{ pF}$ . First, we can find  $\lambda$  using the output conductance value:

$$\lambda = \left( \frac{I_D}{g_o} - V_{DS} \right)^{-1} = \left( \frac{10 \text{ mA}}{0.2 \text{ mS}} - 5 \text{ V} \right)^{-1} = 0.0222 \text{ V}^{-1}$$

Now we can find  $K_n$  using the MOS drain current expression in the active region:

$$K_n = \frac{2I_D}{(V_{GS} - V_{TN})^2(1 + \lambda V_{DS})} = \frac{2(4.8 \text{ mA})}{(5 - 0.7)^2 \left( 1 + \frac{5 \text{ V}}{45 \text{ V}} \right)} = 467 \frac{\mu\text{A}}{\text{V}^2}$$

From these results, we can set SPICE parameters to  $\text{VTO} = 0.7 \text{ V}$ ,  $\text{KP} = 467 \mu\text{A/V}^2$ , and  $\text{LAMBDA} = 0.0222 \text{ V}^{-1}$ .

$C_{ISS}$  is the short-circuit input capacitance of the transistor in the common-source configuration and is equal to the sum of  $C_{GS}$  and  $C_{GD}$ . Unfortunately, the test conditions are not specified, so we cannot be sure if the measurement was in the triode or active region of operation. If we assume active region operation and use Eq. (17.66), then

$$C_{GS} + C_{GD} = \frac{2}{3} C_{ox}'' WL + 2C'_{OL} W = 1 \text{ pF}$$

However, we have no way of directly splitting the 1-pF capacitance between  $C_{GS}$  and  $C_{GD}$ . One approximation is to assume that the oxide capacitance term is approximately dominant. Then  $C_{GS} \cong 1 \text{ pF}$  and  $C_{GD} \cong 0$ . As we shall see shortly, however, neglecting  $C_{GD}$  may cause significant errors in our calculations of the high-frequency response of amplifiers.

**Check of Results:** We have found the required values. The values of  $V_{TN}$  and  $\lambda$  appear reasonable. Let us see if the values of the amplification factor and  $f_T$  are reasonable.

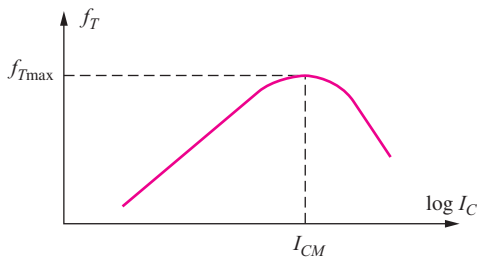
$$g_m = \sqrt{2K_n I_D (1 + \lambda V_{DS})} = \sqrt{2(467 \mu\text{A/V}^2)(10 \text{ mA})(1 + 5/45)} = 3.22 \text{ mS}$$

$$f_T = \frac{1}{2\pi} \frac{g_m}{C_{GS} + C_{GD}} = \frac{1}{2\pi} \frac{3.22 \text{ mS}}{1 \text{ pF}} = 513 \text{ MHz}$$

$$\mu_f = \frac{g_m}{g_o} = \frac{3.22}{0.2 \text{ mS}} = 16.1$$

The value of  $f_T$  is reasonable. The relatively low value of  $\mu_f$  results from the 10-mA drain current condition. Although the value of  $g_m$  is larger than the typical value given in the table, it is reasonably consistent with the graph of the output characteristics:  $g_m = \Delta I_D / \Delta V_{GS} = 4.5 \text{ mA/2 V} = 2.25 \text{ mS}$ .

**Discussion:** The values in the specification sheets must often be mapped into the parameters that we need, and we often find that the data sheet information is incomplete and not necessarily self-consistent. We often must contact the manufacturer for more information. The manufacturer may be able to supply a SPICE model for the device. As a last resort, we can directly measure the parameters for ourselves, or choose another device.

Figure 17.26 Current dependence of  $f_T$ .

**EXERCISE:** What are the values of  $C_{GS}$  and  $C_{GD}$  if  $C_{ISS}$  in Ex. 17.5 had been measured in the triode region?

**ANSWER:** 0.5 pF, 0.5 pF

**EXERCISE:** An NMOSFET has  $f_T = 200$  MHz and  $K_n = 10$  mA/V<sup>2</sup> and is operating at a drain current of 10 mA. Assume that  $C_{GS} = 5C_{GD}$  and find the values of these two capacitors.

**ANSWERS:**  $C_{GS} = 9.38$  pF,  $C_{GD} = 1.88$  pF

### 17.4.7 LIMITATIONS OF THE HIGH-FREQUENCY MODELS

The pi-models of the transistor in Figs. 17.21 and 17.25 are good representations of the characteristics of the transistors for frequencies up to approximately  $0.3f_T$ . Above this frequency, the behavior of the simple pi-models begins to deviate significantly from that of the actual device. In addition, our discussion has tacitly assumed that  $\omega_T$  is constant. However, this is only an approximation. In an actual BJT,  $\omega_T$  depends on operating current, as shown in Fig. 17.26.

For a given BJT, there will be a collector current  $I_{CM}$ , which yields a maximum value of  $f_T = f_{T_{max}}$ . For the FET operating in the saturation region,  $C_{GS}$  and  $C_{GD}$  are independent of Q-point current so that  $\omega_T \propto g_m \propto \sqrt{I_D}$ . In the upcoming discussions, we assume that the specified value of  $f_T$  corresponds to the operating point being used.

**EXERCISE:** As an example of the problem of using a constant value for the transistor  $f_T$ , repeat the calculation of  $C_\pi$  and  $C_\mu$  for a Q-point of (20  $\mu$ A, 8 V) if  $f_T = 500$  MHz,  $C_{\mu o} = 2$  pF, and  $\phi_{jc} = 0.6$  V.

**ANSWERS:** 0.551 pF, -0.296 pF. Impossible —  $C_\pi$  cannot have a negative value.

## 17.5 BASE RESISTANCE IN THE HYBRID-PI MODEL

One final circuit element, the **base resistance**  $r_x$ , completes the basic hybrid-pi description of the bipolar transistor. In the bipolar transistor cross section in Fig. 17.27, base current  $i_b$  enters the transistor through the external base contact and traverses a relatively high resistance region before actually entering the active area of the transistor. Circuit element  $r_x$  models the voltage drop between the base contact and the active region of the transistor and is included between the internal and external base nodes,  $B'$  and  $B$ , respectively, in the circuit model in Fig. 17.28. As discussed in the next section, the base resistance usually can be neglected at low frequencies. However, resistance  $r_x$  can represent an important limitation to the high frequency response of the transistor in low-source resistance applications. The thermal noise of  $r_x$  is also an important limitation in low-noise amplifier design. Typical values of  $r_x$  range from a few ohms to a thousand ohms. In SPICE, BJT base resistance is modeled by parameter RB.

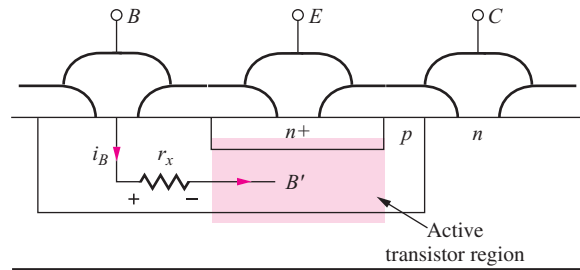
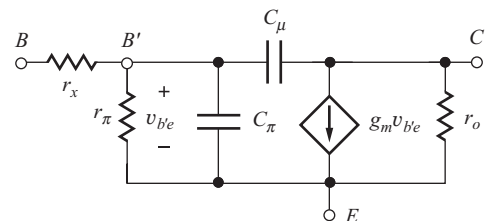
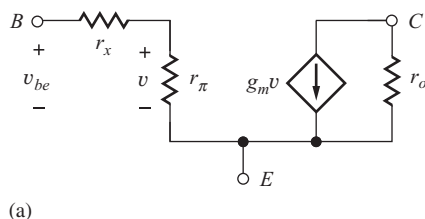
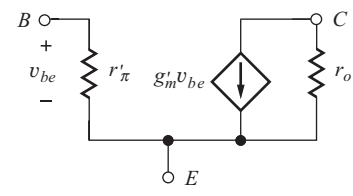


Figure 17.27 Base current flow in the BJT.

Figure 17.28 Completed hybrid-pi model, including the base resistance  $r_x$ .

(a)



(b)

Figure 17.29 (a) Transistor model containing  $r_x$ . (b) Model transformation that “absorbs”  $r_x$ .

### 17.5.1 EFFECT OF BASE RESISTANCE ON MIDBAND AMPLIFIERS

Before considering the high-frequency response of single and multistage amplifiers, we explore the effect of base resistance on the midband gain expressions for single-stage amplifiers. Although the model used in deriving the midband voltage gain expressions in Chapters 13 and 14 did not include the effect of base resistance, the expressions can be easily modified to include  $r_x$ . A simple approach is to use the circuit transformation shown in Fig. 17.29, in which  $r_x$  is absorbed into an equivalent pi model. The current generator in the model in Fig. 17.29(a) is controlled by the voltage developed across  $r_\pi$ , which is related to the total base-emitter voltage through voltage division by

$$\mathbf{v} = \mathbf{v}_{be} \frac{r_\pi}{r_x + r_\pi} \quad (17.68)$$

and the current in the controlled source is

$$\mathbf{i} = g_m \mathbf{v} = g_m \frac{r_\pi}{r_x + r_\pi} \mathbf{v}_{be} = g'_m \mathbf{v}_{be} \quad \text{where} \quad g'_m = \frac{\beta_o}{r_x + r_\pi} \quad (17.69)$$

Equations (17.68) and (17.69) lead to the model in Fig. 17.29(b), in which the base resistance has been absorbed into  $r'_\pi$  and  $g'_m$  of an equivalent transistor  $Q'$  defined by

$$g'_m = g_m \frac{r_\pi}{r_x + r_\pi} = \frac{\beta_o}{r_x + r_\pi} \quad \text{and} \quad r'_\pi = r_x + r_\pi \quad (17.70)$$

Note that current gain is conserved during the transformation:  $\beta'_o = \beta_o$ .

Based on Eq. (17.70), the original expressions from Table 14.9 can be transformed to those in Table 17.1 for the three classes of amplifiers in Fig. 17.30 by simply substituting  $g'_m$  for  $g_m$  and  $r'_\pi$  for  $r_\pi$ . In many cases, particularly at bias points below a few hundred  $\mu\text{A}$ ,  $r_\pi \gg r_x$ , and the expressions in Eq. (17.70) reduce to  $g'_m \cong g_m$  and  $r'_\pi \cong r_\pi$ . The expressions in Table 17.1 then become identical to those in Table 14.9.

**TABLE 17.1**

Single-Stage Bipolar Amplifiers, Including Base Resistance (See Fig. 17.30)

	COMMON-EMITTER AMPLIFIER	COMMON-COLLECTOR AMPLIFIER	COMMON-BASE AMPLIFIER
Terminal voltage gain			
$A_{vt} = \frac{v_o}{v_i}$	$-\frac{\beta_o R_L}{r'_\pi + (\beta_o + 1)R_E}$	$+\frac{\beta_o R_L}{r'_\pi + (\beta_o + 1)R_L}$	$+g'_m R_L$
$r'_\pi = r_x + r_\pi$	$\cong -\frac{g'_m R_L}{1 + g'_m R_E}$	$\cong +\frac{g'_m R_L}{1 + g'_m R_L} \cong +1$	
$g'_m = \frac{\beta_o}{r'_\pi}$			
Signal-source voltage gain			
$A_v = \frac{v_o}{v_i}$	$-\frac{g'_m R_L}{1 + g'_m R_E} \left( \frac{R_B \  R_{iB}}{R_I + R_B \  R_{iB}} \right)$	$+\frac{g'_m R_L}{1 + g'_m R_L} \left( \frac{R_B \  R_{iE}}{R_I + R_B \  R_{iE}} \right) \cong +1$	$+\frac{g'_m R_L}{1 + g'_m (R_I \  R_E)} \left( \frac{R_E}{R_I + R_E} \right)$
Input resistance	$r'_\pi + (\beta_o + 1)R_E$	$r'_\pi + (\beta_o + 1)R_L$	$\frac{1}{g'_m}$
Output resistance	$r_o(1 + g'_m R_E)$	$\frac{1}{g'_m} + \frac{R_{th}}{\beta_o + 1}$	$r_o[1 + g'_m (R_I \  R_E)]$
Input signal range	$\cong 0.005(1 + g'_m R_E)$	$\cong 0.005(1 + g'_m R_L)$	$\cong 0.005[1 + g'_m (R_I \  R_E)]$
Current gain	$-\beta_o$	$\beta_o + 1$	$\alpha_o \cong +1$

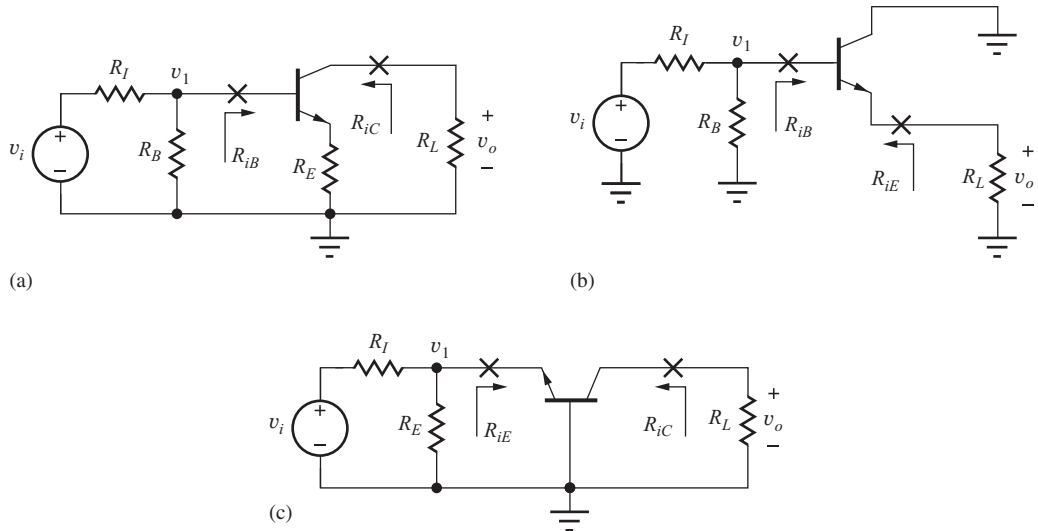


**Figure 17.30** The three BJT amplifier configurations: (a) common-emitter; (b) common-collector; (c) common-base.

**EXERCISE:** Recalculate the midband gain for the circuit in Fig. 17.6, including base resistance  $r_x = 250 \Omega$ . What was the value of  $A_{\text{mid}}$  with  $r_x = 0$ ?

**ANSWER:** -141; -157

## 17.6 HIGH-FREQUENCY COMMON-EMITTER AND COMMON-SOURCE AMPLIFIER ANALYSIS

Now that the complete hybrid-pi model has been described, we can explore the high-frequency limitations of the three basic single-stage amplifiers. For each of the basic stages, we will develop expressions for the high-frequency poles at the input and output of each stage. This approach will allow us to easily extend our analysis to multistage amplifiers.

To begin our analysis, we will first review the high-frequency response of a single pole network as shown in Figure 17.31. An expression for the high-frequency transfer characteristic for the RC circuit can be derived as

$$\frac{V_x}{V_i} = \frac{\frac{R_2}{sC_1}}{R_1 + R_2 \parallel \frac{1}{sC_1}} = \frac{\frac{R_2}{1 + sR_2C_1}}{R_1 + \frac{R_2}{1 + sR_2C_1}} = \frac{R_2}{R_1 + R_2} \frac{1}{1 + s(R_1 \parallel R_2)C_1} \quad (17.71)$$

Substituting  $s = j\omega$  and using  $\omega_p = 1/(R_1 \parallel R_2)C_1$ ,

$$\frac{V_x}{V_i} = \frac{R_2}{R_1 + R_2} \frac{1}{1 + j\frac{\omega}{\omega_p}} = A_{\text{mid}} F_H(s) \quad (17.72)$$

This expression has two parts, the midband gain,  $R_2/(R_2 + R_1)$ , and the high-frequency characteristic,  $1/(1 + j\omega/\omega_p)$ . Notice that the equivalent resistance,  $R_1 \parallel R_2$  is the total equivalent resistance to ground at the output of the example network. If other branch connections are present, the equivalent small-signal resistance of each branch will be added in parallel. Capacitance  $C_1$  is the total equivalent capacitance to small-signal ground at the output. If other capacitors are present they too are simply

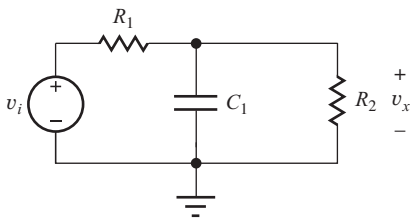


**Figure 17.31** A two-resistor, one-capacitor circuit.

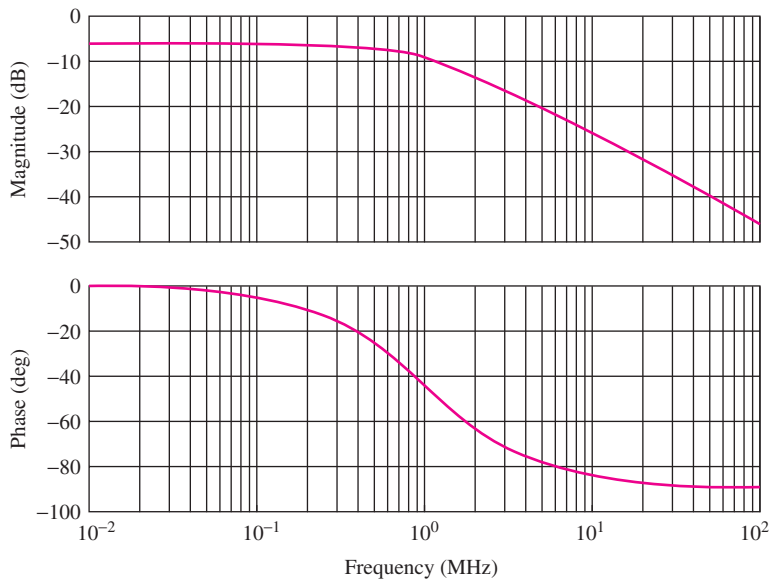


**Figure 17.32** Magnitude and phase of single high-frequency pole with  $R_1 = R_2$  and  $f_p = 1$  MHz.

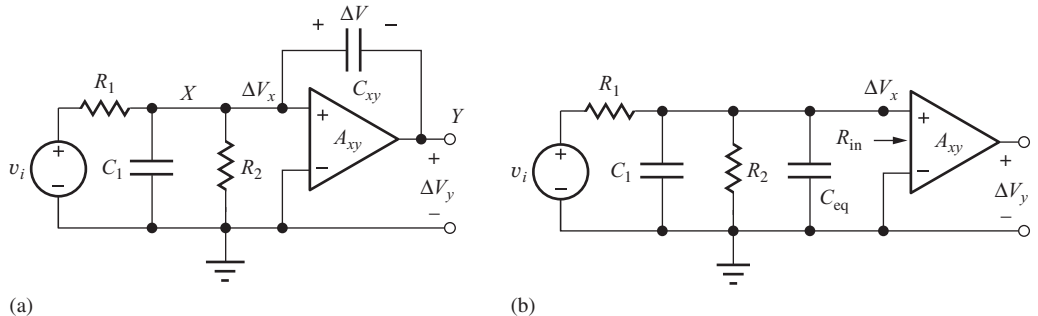


**Figure 17.33** (a) Amplifier with a capacitance coupling its input and output. (b) The amplifier with the input-output capacitance replaced by an equivalent effective capacitance  $C_{eq}$  between the input and small-signal ground.

added to find the total capacitance. The magnitude and phase of this single pole characteristic is shown in Figure 17.32.

### 17.6.1 THE MILLER EFFECT

Figure 17.33(a) shows a typical variation on the simple network of Fig. 17.31. Here a capacitor connected at node  $X$  is connected across an amplifier with a gain  $A_{xy}$  from node  $X$  to node  $Y$ .

We would like to find a method to convert the physical capacitor  $C_{xy}$  across the amplifier to an equivalent capacitance,  $C_{eq}$ , to small-signal ground as shown in Fig. 17.33(b). We observe that a small-signal capacitance can be defined as

$$C = \frac{\Delta Q}{\Delta V} \quad (17.73)$$

where  $\Delta V$  is the voltage change across the capacitor and  $\Delta Q$  is the charge required to develop that voltage change across the capacitor. For the case in Fig. 17.33(a), given a  $\Delta V_x$ , a  $\Delta V_y$  equal to

$A_{xy}\Delta V_x$  will appear at the output. The charge that must be delivered by the driving circuit can be calculated as

$$\Delta Q = C_{xy}(\Delta V_x - \Delta V_y) = C_{xy}(\Delta V_x - A_{xy}\Delta V_x) = C_{xy}\Delta V_x(1 - A_{xy}) \quad (17.74)$$

If we now consider the circuit in Fig. 17.33(b), one terminal of  $C_{eq}$  is connected to small-signal ground, so using our calculation of  $\Delta Q$  from Eq. (17.74),  $C_{eq}$  can be written as

$$C_{eq} = \frac{C_{xy}\Delta V_x(1 - A_{xy})}{\Delta V_x} = C_{xy}(1 - A_{xy}) \quad (17.75)$$

The amplifier gain acts to produce an effective capacitance at its input which is scaled with respect to the physical capacitor by a factor  $(1 - A_{xy})$ . This is known as the **Miller effect**, or **Miller multiplication**, first described by John M. Miller in 1920.<sup>2</sup> Given our new equivalent capacitance,  $C_{eq}$ , based on our previous Eq. (17.70), we can now write an expression for the high-frequency transfer characteristic for the circuit in Fig. 17.33 as

$$\frac{V_x}{V_i} = \frac{R_2 \| R_{in}}{R_1 + R_2 \| R_{in}} \frac{1}{1 + s(R_1 \| R_2 \| R_{in})(C_1 + C_{eq})} \quad (17.76)$$

We see that the pole frequency is determined by a resistance of  $R_1 \| R_2 \| R_{in}$ , and a capacitance of  $C_1 + C_{xy}(1 - A_{xy})$ . As an example, consider the case with a gain =  $-10$  V/V. The input capacitance due to  $C_{xy}$  will be  $(1 - [-10])$  or eleven times larger than the physical capacitance  $C_{xy}$ . To understand this intuitively, consider a  $\Delta V_x$  of 10 mV. With a gain of  $-10$  V/V, the  $\Delta V_y$  will be  $-100$  mV. In other words, as the voltage at the input of the capacitor is increasing, the other terminal is rapidly decreasing in voltage, causing the driving circuit to deliver much more charge than would be expected given the actual value of the capacitor. On the other hand, for a gain of 0.9 V/V, the effective capacitance will be  $(1 - 0.9)$ , or 10 percent of the physical capacitance. For this gain value, the second terminal of the capacitor is approximately “following” the input terminal, leading to a much smaller delivery of charge from the driving circuit. Using the Miller effect allows us to separate capacitively coupled sections of a circuit into simpler RC circuits which are more easily analyzed.

In the following sections, we will generalize this approach to develop the high-frequency response of an amplifier as the product of the midband gain we have developed in previous chapters and a high-frequency transfer characteristic representing the effects of the high-frequency time constant at each node along the signal path.

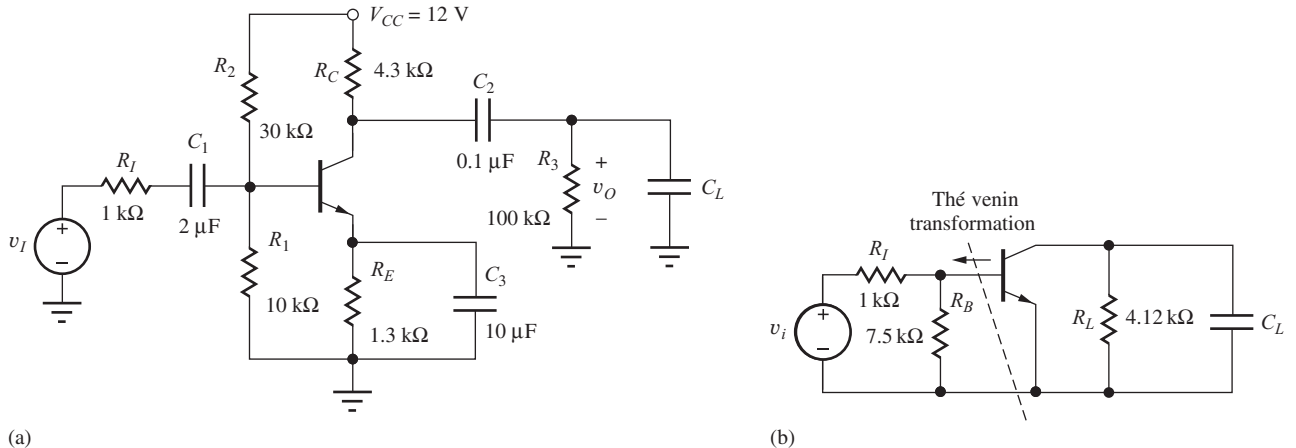
### 17.6.2 COMMON-EMITTER AND COMMON-SOURCE AMPLIFIER HIGH-FREQUENCY RESPONSE

Figure 17.34 is a common-emitter amplifier with low-frequency coupling and bypass capacitors  $C_1$ ,  $C_2$ , and  $C_3$ . In this section, we are concerned with the high-frequency response so we will consider the low-frequency capacitors to be open circuits at dc and short circuits at midband and high-frequencies.  $C_L$  represents the high-frequency load capacitance. We will use a simplified analysis approach similar to that presented in the previous section. We calculate the midband gain and then calculate a time constant at the input and output signal nodes. The Miller effect will be used to calculate an equivalent capacitance at the input.

The ac small-signal equivalent circuit is shown in Figure 17.35(a). The power supplies have been replaced with small-signal ground connections, and the low-frequency coupling and bypass capacitors are replaced with short circuits. The circuit has been further simplified in Fig. 17.35(c). The midband input gain is

$$A_i = \frac{V_b}{V_i} = \frac{R_{in}}{R_I + R_{in}} \cdot \frac{r_\pi}{r_x + r_\pi} = \frac{R_B \| (r_x + r_\pi)}{R_I + R_B \| (r_x + r_\pi)} \cdot \frac{r_\pi}{r_x + r_\pi} \quad (17.77)$$

<sup>2</sup> J. M. Miller, “Dependence of the input impedance of a three-electrode vacuum tube upon the load in the plate circuit,” Scientific Papers of the Bureau of Standards, 15(351):367–385, 1920.



**Figure 17.34** (a) Common-emitter amplifier. (b) High-frequency ac model for amplifier in (a).

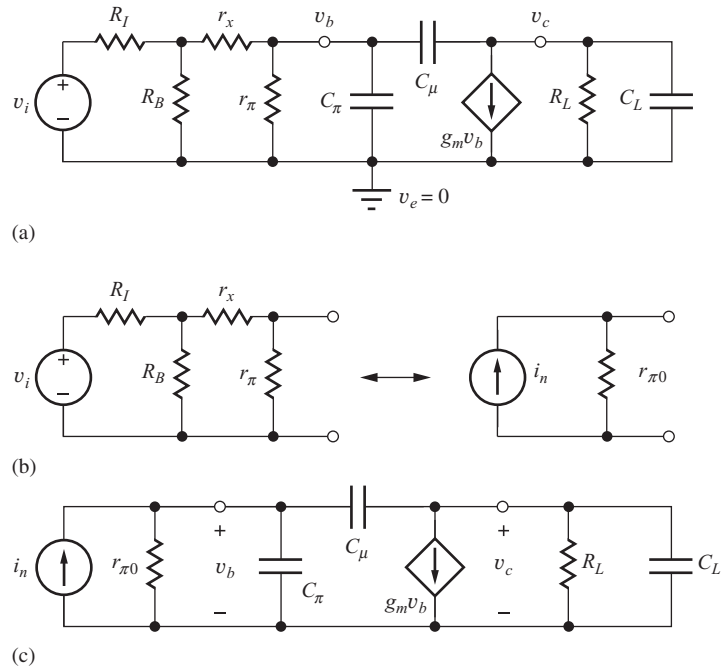


**Figure 17.35** (a) Model for common-emitter stage at high frequencies. (b) Model used to determine the Norton source transformation for the CE amplifier. Resistor  $r_{\pi 0}$  represents the equivalent resistance at the base node. (c) Simplified small-signal model for the high-frequency common-emitter amplifier.

where  $R_{in}$  is the parallel combination of  $R_1$ ,  $R_2$ , and  $(r_x + r_\pi)$ , and  $R_L$  is the parallel combination of  $r_o$ ,  $R_C$ , and  $R_3$ .

The terminal gain of the common-emitter amplifier (the effect of  $r_x$  was included in  $A_i$ ) can be found as

$$A_{vt} = \frac{v_c}{v_b} = -g_m R_L \cong -g_m (R_C \parallel R_3) \quad (17.78)$$

We now use the Miller effect to calculate the input high frequency pole at the base based on the circuit in Fig. 17.35(a).

$$\begin{aligned} C_{eqB} &= C_\mu (1 - A_{bc}) + C_\pi (1 - A_{be}) = C_\mu [1 - (-g_m R_L)] + C_\pi (1 - 0) \\ &= C_\pi + C_\mu (1 + g_m R_L) \end{aligned} \quad (17.79)$$

The equivalent small-signal resistance to ground at base node  $v_b$  is

$$R_{eqB} = r_\pi \parallel (r_x + R_B \parallel R_I) = r_{\pi 0} \quad (17.80)$$

Remember the voltage source  $v_i$  has a small-signal impedance of zero. The resulting time constant at the input is

$$\tau_B = R_{eqB} C_{eqB} \quad (17.81)$$

At the collector output node,  $R_{eqC}$  is found as

$$R_{eqC} = R_L = r_o \parallel R_C \parallel R_3 \cong R_C \parallel R_3 \quad (17.82)$$

We must now determine the equivalent capacitance at the collector,  $C_{eqC}$ . At first glance, we might expect to apply the Miller effect to model the equivalent capacitance at the output due to  $C_\mu$ . However, the transistor does not operate in reverse: applying a signal at the collector does not result in a significant “output” signal at the base node. Therefore, the equivalent capacitance at the output only includes the physical capacitance  $C_\mu$  as well as any additional load capacitance  $C_L$ .

$$C_{eqC} = C_\mu + C_L \quad (17.83)$$

The resulting time constant at the output node is

$$\tau_C = R_{eqC} C_{eqC} \quad (17.84)$$

If the input and output nodes are well isolated, we expect to calculate a separate pole frequency for the input and output time constants. However, in this case the input and output are coupled through  $C_\mu$ . In addition, the input and output impedances are large, so we should expect the two time constants to interact. This interaction gives rise to a dominant pole equal to

$$\omega_{P1} = \frac{1}{r_{\pi 0}[C_\pi + C_\mu(1 + g_m R_L)] + R_L[C_\mu + C_L]} \quad (17.85)$$

We can rewrite this expression in terms of a single resistance and capacitance by scaling the second capacitive term so that when multiplied by the input resistance,  $r_{\pi 0}$ , the resulting time constant is identical to the second term in Eq. (17.85). We will label the resulting capacitance as  $C_T$ .

$$C_T = [C_\pi + C_\mu(1 + g_m R_L)] + \frac{R_L}{r_{\pi 0}}[C_\mu + C_L] \quad (17.86)$$

This substitution allows us to write the dominant pole frequency for the common-emitter as

$$\omega_{P1} = \frac{1}{r_{\pi 0} C_T} = \frac{1}{r_{\pi 0} \left( [C_\pi + C_\mu(1 + g_m R_L)] + \frac{R_L}{r_{\pi 0}}[C_\mu + C_L] \right)} \quad (17.87)$$

### 17.6.3 DIRECT ANALYSIS OF THE COMMON-EMITTER TRANSFER CHARACTERISTIC

At this point, it is desirable to check our simplified analysis approach via a direct analysis of the common-emitter transfer function. Writing and simplifying the nodal equations in the frequency domain for the circuit in Fig. 17.35(c) yields

$$\begin{bmatrix} \mathbf{I}_n(s) \\ 0 \end{bmatrix} = \begin{bmatrix} s(C_\pi + C_\mu) + g_{\pi o} & -sC_\mu \\ -(sC_\mu - g_m) & s(C_\mu + C_L) + g_L \end{bmatrix} \begin{bmatrix} \mathbf{V}_b(s) \\ \mathbf{V}_c(s) \end{bmatrix} \quad (17.88)$$

An expression for the output voltage, node voltage  $\mathbf{V}_c(s)$ , can be found using Cramer's rule:

$$\mathbf{V}_c(s) = \mathbf{I}_n(s) \frac{(sC_\mu - g_m)}{\Delta} \quad (17.89)$$

in which  $\Delta$  represents the determinant of the system of equations given by

$$\Delta = s^2[C_\pi(C_\mu + C_L) + C_\mu C_L] + s[C_\pi g_L + C_\mu(g_m + g_{\pi o} + g_L) + C_L g_{\pi o}] + g_L g_{\pi o} \quad (17.90)$$

From Eqs. (17.89) and (17.90), we see that the high-frequency response is characterized by two poles, one finite zero, and one zero at infinity. The finite zero appears in the right-half of the  $s$ -plane at a frequency

$$\omega_Z = +\frac{g_m}{C_\mu} > \omega_T \quad (17.91)$$

The zero given by Eq. (17.91) can usually be neglected because it appears at a frequency above  $\omega_T$  (for which the model itself is of questionable validity). Unfortunately, the denominator appears in unfactored polynomial form, and the positions of the poles are more difficult to find. However, good estimates for both pole positions can be found using the approximate factorization technique shown below. Note that even though there are three capacitors, the circuit only has two poles. The three capacitors are connected in a “pi” configuration, and only two of the capacitor voltages are independent. Once we know two of the voltages, the third is also defined.

### Approximate Polynomial Factorization

We estimate the pole locations based on a technique for approximate factorization of polynomials. Let us assume that the polynomial has two real roots  $a$  and  $b$ :

$$(s + a)(s + b) = s^2 + (a + b)s + ab = s^2 + A_1s + A_0 \quad (17.92)$$

If we assume that a dominant root exists — that is, that  $a \gg b$  — then the two roots can be estimated directly from coefficients  $A_1$  and  $A_0$  using two approximations:

$$A_1 = a + b \cong a \quad \text{and} \quad \frac{A_0}{A_1} = \frac{ab}{a + b} \cong \frac{ab}{a} = b \quad (17.93)$$

$$\text{so,} \quad a \cong A_1 \quad \text{and} \quad b \cong \frac{A_0}{A_1}$$

Note in Eq. (17.92) that the  $s^2$  term is normalized to unity. Also note that the approximate factorization technique can be extended to polynomials having any number of widely spaced real roots.

#### 17.6.4 POLES OF THE COMMON-EMITTER AMPLIFIER

For the case of the common-emitter amplifier, the smallest root is the most important because it is the one that limits the high-frequency response of the amplifier. From Eq. (17.93) we see that the smaller root is given by the ratio of coefficients  $A_0$  and  $A_1$ , resulting in the following expression for the first pole:

$$\omega_{P1} = \frac{1}{r_{\pi0}C_T} = \frac{1}{r_{\pi0} \left( [C_\pi + C_\mu(1 + g_m R_L)] + \frac{R_L}{r_{\pi0}}[C_\mu + C_L] \right)} \quad (17.94)$$

This result is identical to that of Eq. (17.87). The dominant pole is controlled by the combination of the input and output time constants set by the total equivalent capacitance and resistance at the input and output. Notice that if the driving resistance  $R_I$  is zero,  $r_{\pi0}$  reduces to approximately  $r_x$ , and the bandwidth is primarily limited by  $r_x$ .

There is also a second pole resulting from the normalized version of coefficient  $A_1$ :

$$\omega_{P2} = \frac{C_\pi g_L + C_\mu(g_m + g_{\pi0} + g_L) + C_L g_{\pi0}}{C_\pi(C_\mu + C_L) + C_\mu C_L} \quad (17.95)$$

or

$$\omega_{P2} \cong \frac{g_m}{C_\pi \left( 1 + \frac{C_L}{C_\mu} \right) + C_L} \cong \frac{g_m}{C_\pi + C_L} \quad (17.96)$$

in which the  $C_\mu g_m$  term has been assumed to be the largest term in the numerator, as is most often the case for C-E stages with reasonably high gain. We can interpret the last approximation in Eq. (17.96) in this manner, particularly when  $C_\mu$  is large. At high frequencies, capacitor  $C_\mu$  effectively shorts the collector and base of the transistor together so that  $C_L$  and  $C_\pi$  appear in parallel, and the transistor behaves as a diode with a small-signal resistance of  $1/g_m$ . Recall also that there is a right-half plane zero equal to  $+g_m/C_\mu$ . While the zero is typically quite high in frequency and can be neglected, we will see in Chapter 18 that in FET amplifiers it can be an important aspect of the negative feedback amplifier stability analysis.

### EXAMPLE 17.6 HIGH-FREQUENCY ANALYSIS OF THE COMMON-EMITTER AMPLIFIER

Find the midband gain and upper-cutoff frequency of a common-emitter amplifier.

**PROBLEM** Find the midband gain and upper-cutoff frequency of the common-emitter amplifier in Fig. 17.34 using the  $C_T$  approximation, assuming  $\beta_o = 100$ ,  $f_T = 500$  MHz,  $C_\mu = 0.5$  pF,  $r_x = 250$   $\Omega$ , and a Q-point of (1.60 mA, 3.00 V). Find the additional poles and zeros of the common-emitter amplifier. Assume  $C_L = 0$ ,  $C_1 = C_3 = 3.9$   $\mu\text{F}$ ,  $C_2 = 0.082$   $\mu\text{F}$ .

**SOLUTION** **Known Information and Given Data:** Common-emitter amplifier circuit in Fig. 17.34; Q-point = (1.60 mA, 3.00 V);  $\beta_o = 100$ ,  $f_T = 500$  MHz,  $C_\mu = 0.5$  pF, and  $r_x = 250$   $\Omega$ ; expressions for the gain, poles, and zeros are given in Eqs. (17.77) through (17.96).

**Unknowns:** Values for  $A_{\text{mid}}$ ,  $f_H$ ,  $\omega_{Z1}$ ,  $\omega_{P1}$ , and  $\omega_{P2}$

**Approach:** Find the small-signal parameters for the transistor. Find the unknowns by substituting the given and computed values into the expressions developed in the text.

**Assumptions:** Small-signal operation in the active region;  $V_T = 25.0$  mV;  $C_L = 0$

**Analysis:** The common-emitter stage is characterized by Eqs. (17.77), (17.78), and (17.87).

$$\begin{aligned} A_{\text{mid}} &= A_i A_{vt} & A_i &= \frac{R_{\text{in}}}{R_I + R_{\text{in}}} \left( \frac{r_\pi}{r_x + r_\pi} \right) & A_{vt} &= -g_m R_L \\ \omega_{P1} &= \frac{1}{r_{\pi 0} C_T} & \omega_{P2} &= \frac{g_m}{C_\pi + C_L} & \omega_Z &= \frac{g_m}{C_\mu} \\ r_{\pi 0} &= r_\pi \parallel (R_B \parallel R_I + r_x) & C_T &= C_\pi + C_\mu \left( 1 + g_m R_L + \frac{R_L}{r_{\pi 0}} \right) \end{aligned}$$

The values of the various small-signal parameters must be found:

$$g_m = 40I_C = 40(0.0016) = 64.0 \text{ mS} \quad r_\pi = \frac{\beta_o}{g_m} = \frac{100}{0.064} = 1.56 \text{ k}\Omega$$

$$C_\pi = \frac{g_m}{2\pi f_T} - C_\mu = \frac{0.064}{2\pi(5 \times 10^8)} - 0.5 \times 10^{-12} = 19.9 \text{ pF}$$

$$R_{\text{in}} = 10 \text{ k}\Omega \parallel 30 \text{ k}\Omega \parallel 1.81 \text{ k}\Omega = 1.46 \text{ k}\Omega$$

$$R_L = R_C \parallel R_3 = 4.3 \text{ k}\Omega \parallel 100 \text{ k}\Omega = 4.12 \text{ k}\Omega$$

$$R_{\text{th}} = R_B \parallel R_I = 7.5 \text{ k}\Omega \parallel 1 \text{ k}\Omega = 882 \text{ }\Omega$$

$$r_{\pi o} = r_\pi \parallel (R_{\text{th}} + r_x) = 1.56 \text{ k}\Omega \parallel (882 \text{ }\Omega + 250 \text{ }\Omega) = 656 \text{ }\Omega$$

Substituting these values into the expression for  $C_T$  ( $C_L = 0$ ) yields

$$\begin{aligned} C_T &= C_\pi + C_\mu \left( 1 + g_m R_L + \frac{R_L}{r_{\pi o}} \right) \\ &= 19.9 \text{ pF} + 0.5 \text{ pF} \left[ 1 + 0.064(4120) + \frac{4120}{656} \right] \\ &= 19.9 \text{ pF} + 0.5 \text{ pF}(1 + 264 + 6.28) = 156 \text{ pF} \end{aligned}$$

and

$$\begin{aligned} f_{P1} &= \frac{1}{2\pi r_{\pi o} C_T} = \frac{1}{2\pi(656 \Omega)(156 \text{ pF})} = 1.56 \text{ MHz} \\ \omega_{P2} &\cong \frac{g_m}{C_\pi + C_L} = \frac{0.064}{19.9 \text{ pF}} = 3.22 \times 10^9 \text{ rad/sec} \\ f_{P2} &= \frac{\omega_{P2}}{2\pi} = 512 \text{ MHz} \\ f_z &= \frac{g_m}{2\pi C_\mu} = \frac{0.064}{2\pi(0.5 \text{ pF})} = 20.4 \text{ GHz} \\ A_i &= \frac{1.46 \text{ k}\Omega}{1.00 \text{ k}\Omega + 1.46 \text{ k}\Omega} \left( \frac{1.56 \text{ k}\Omega}{250 \Omega + 1.56 \text{ k}\Omega} \right) = 0.512 \quad A_{vt} = -(0.064S)(4.12 \text{ k}\Omega) = -264 \\ A_{\text{mid}} &= 0.512(-264) = -135 \end{aligned}$$

**Check of Results:** We have found the desired information. By double checking, the calculations appear correct. Let us use the gain-bandwidth product as an additional check:  $|A_{\text{mid}} f_{P1}| = 211 \text{ MHz}$ , which does not exceed  $f_T$ .

**Discussion:** The dominant pole is located at a frequency  $f_{P1} = 1.56 \text{ MHz}$ , whereas  $f_{P2}$  and  $f_z$  are estimated to be at frequencies above  $f_T$  (500 MHz). Thus, the upper-cutoff frequency  $f_H$  for this amplifier is determined solely by  $f_{P1}:f_H \cong 1.56 \text{ MHz}$ . Note that this value of  $f_H$  is less than 1 percent of the transistor  $f_T$  and is consistent with the concept of GBW product. We should expect  $f_H$  to be no more than  $f_T/A_{\text{mid}} = 3.3 \text{ MHz}$  for this amplifier. Note also that  $f_{P1}$  and  $f_{P2}$  are separated by a factor of almost 1000, clearly satisfying the requirement for widely spaced roots that was used in the approximate factorization.

It is important to keep in mind that the most important factor in determining the value of  $C_T$  is the term in which  $C_\mu$  is multiplied by  $g_m R_L$ . To increase the upper-cutoff frequency  $f_H$  of this amplifier, the gain ( $g_m R_L$ ) must be reduced; a direct trade-off must occur between amplifier gain and bandwidth.

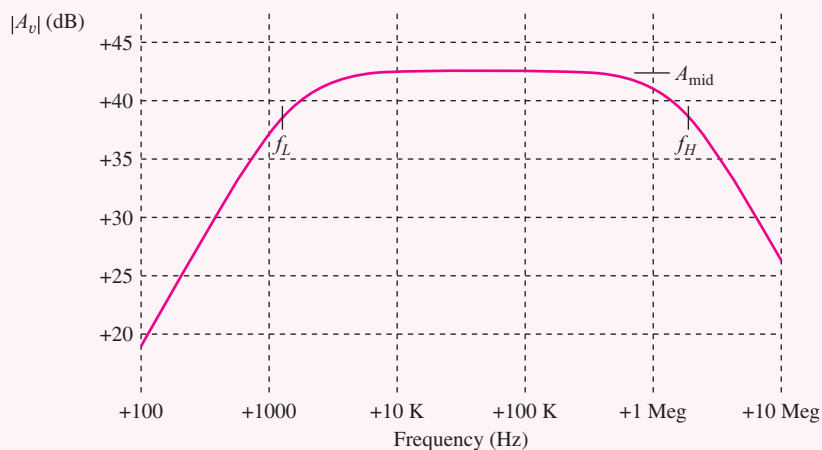
**Computer-Aided Analysis:** SPICE can be used to check our hand analysis, but we must define the device parameters that match our analysis. We set BF = 100 and IS = 5 fA, but let VAF default to infinity. The base resistance  $r_x$  must be added by setting SPICE parameter RB = 250 Ω.  $C_\mu$  is determined in SPICE from the value of the zero-bias collector-junction capacitance CJC and the built-in potential  $\phi_{jc}$ . The Q-point from SPICE gives  $V_{CE} = 2.70 \text{ V}$ , which corresponds to  $V_{BC} = 2.0 \text{ V}$  if  $V_{BE} = 0.7 \text{ V}$ . In SPICE, VJC faults to 0.75 V, and MJC defaults to 0.33 (see Sec. 17.4). Therefore, to achieve  $C_\mu = 0.5 \text{ pF}$ , CJC is specified as

$$\text{CJC} = 0.5 \text{ pF} \left( 1 + \frac{20 \text{ V}}{0.75 \text{ V}} \right)^{0.33} = 0.768 \text{ pF}$$

$C_\pi$  is determined by SPICE forward transit-time parameter TF, as defined by Eqs. (5.46) and (17.50):

$$\text{TF} = \frac{C_\pi}{g_m} = \frac{19.9 \text{ pF}}{64 \text{ mS}} = 0.311 \text{ ns}$$

After adding these values to the transistor model, we perform an ac analysis using FSTART = 100 Hz and FSTOP = 10 MHz with 20 frequency points per decade. The SPICE simulation results in the graph below yield  $A_{\text{mid}} = -135$  (42.6 dB) and  $f_H \cong 1.56$  MHz, which agree closely with our hand calculations. Checking the device parameters in SPICE, we also find  $r_x(\text{RB}) = 250 \Omega$ ,  $C_\pi(\text{CBE}) = 19.9 \text{ pF}$ , and  $C_\mu(\text{CBC}) = 0.499 \text{ pF}$ , as desired.



**EXERCISE:** Use SPICE to recalculate  $f_H$  for  $V_A = 75 \text{ V}$ . For  $V_A = 75 \text{ V}$  and  $r_x = 0$

**ANSWER:** 1.67 MHz; 1.96 MHz

**EXERCISE:** Repeat the calculations in Ex. 17.6 if a load capacitance  $C_L = 3 \text{ pF}$  is added to the circuit.

**ANSWERS:** 1.39 MHz, 445 MHz

**EXERCISE:** Find the midband gain and the frequencies of the poles and zeros of the common-emitter amplifier in Ex. 17.6 if the transistor has  $f_T = 500 \text{ MHz}$ , but  $C_\mu = 1 \text{ pF}$ .

**ANSWERS:** -135, 837 kHz, 525 MHz, 10.2 GHz

### 17.6.5 DOMINANT POLE FOR THE COMMON-SOURCE AMPLIFIER

Analysis of the C-S amplifier in Fig. 17.36 mirrors that of the common-emitter amplifier. The small-signal model is similar to that for the C-E stage, except that both  $r_x$  and  $r_\pi$  are absent from the model. For Fig. 17.36(b),

$$R_{\text{th}} = R_I \| R_G \quad R_L = R_D \| R_3 \quad v_{\text{th}} = v_i \frac{R_G}{R_I + R_G} \quad (17.97)$$

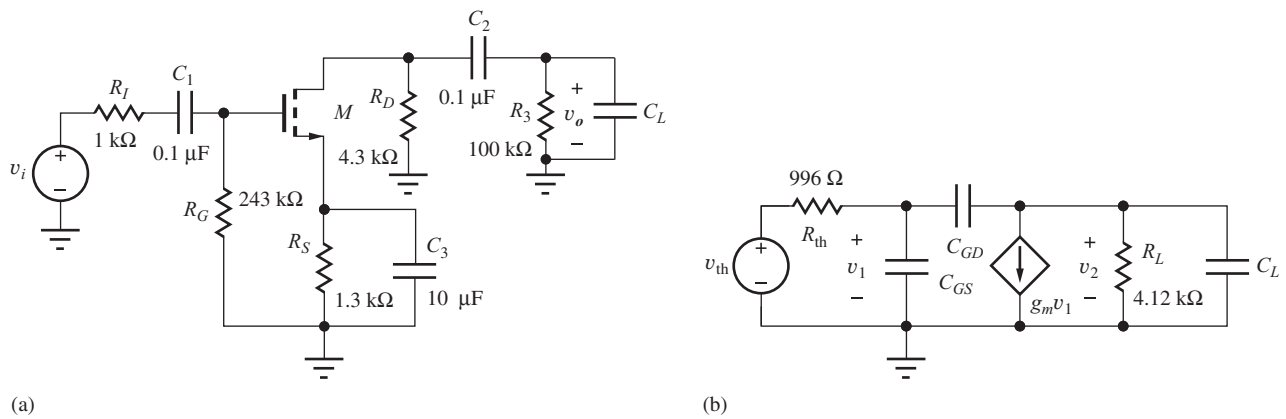


**Figure 17.36** (a) Common-source amplifier. (b) The high-frequency small-signal model.

The expressions for the finite zero and poles of the C-S amplifier can be found by comparing Fig. 17.36(b) to Fig. 17.35:

$$\begin{aligned}\omega_{P1} &= \frac{1}{R_{th}C_T} \quad \text{and} \quad C_T = C_{GS} + C_{GD} \left( 1 + g_m R_L + \frac{R_L}{R_{th}} \right) + C_L \frac{R_L}{R_{th}} \\ \omega_{P2} &= \frac{g_m}{C_{GS} + C_L} \quad \omega_Z = \frac{+g_m}{C_{GD}}\end{aligned}\quad (17.98)$$

**EXERCISE:** What is the upper-cutoff frequency for the amplifier in Fig. 17.36 if \$C\_{GS} = 10\text{ pF}\$, \$C\_{GD} = 2\text{ pF}\$, \$C\_L = 0\text{ pF}\$, and \$g\_m = 1.23\text{ mS}\$? What are the positions of the second pole and the zero? What is the \$f\_T\$ of this transistor?

**ANSWERS:** 5.26 MHz; 19.6 MHz, 97.9 MHz; 16.3 MHz

### 17.6.6 ESTIMATION OF \$\omega\_H\$ USING THE OPEN-CIRCUIT TIME-CONSTANT METHOD

A technique also exists for estimating \$\omega\_H\$ that is similar to the short-circuit time-constant method used to find \$\omega\_L\$. However, the upper-cutoff frequency \$\omega\_H\$ is found by calculating the open-circuit time constants associated with the various device capacitances rather than the short-circuit time constants associated with the coupling and bypass capacitors. At high frequencies, the impedances of the coupling and bypass capacitors are negligibly small, and they effectively represent short circuits. The impedances of the device capacitances have now become small enough that they can no longer be neglected with respect to the internal resistances of the transistors. We will see shortly that the \$C\_T\$ approximation results can also be found using the OCTC method.

Although beyond the scope of this book, it can be shown theoretically<sup>3</sup> that the mathematical estimate for \$\omega\_H\$ for a circuit having \$m\$ capacitors is

$$\omega_H \approx \frac{1}{\sum_{i=1}^m R_{io} C_i} \quad (17.99)$$

<sup>3</sup> See [1]. The OCTC and SCTC methods represent dominant root factorizations similar to Eq. (17.92).

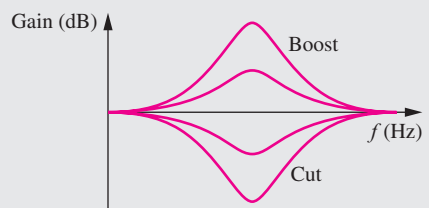

**ELECTRONICS IN ACTION**


### Graphic Equalizer

Graphic equalizers are used in audio applications to fine-tune the frequency response of an audio system. The equalizer is used to compensate for frequency-dependent absorption characteristics of a room, poor quality recordings, or just listener preferences. An example equalizer is shown in the figure below. This is the Ten/Series 2 analog equalizer marketed by Audio Control in 1983 and features total harmonic distortion of only 0.005 percent. The unit sold for \$220 and weighed about 4 pounds. It has a set of slider controls that set boost or cut levels for different frequency bands within the audio frequency range. The term “graphic” is applied to equalizers where the physical position of the controls is representative of the boost or cut levels applied to the different bands.

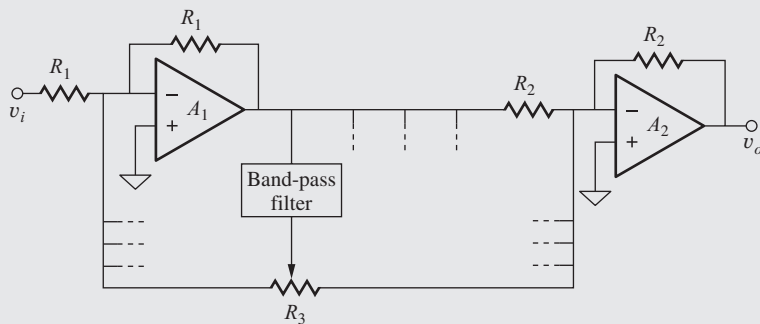


Audio Control/Ten Series 2  
© The McGraw-Hill Companies, Inc./Mark Dierker, photographer



Typical graphic equalizer single band frequency response for different boost/cut settings.

A simplified schematic of a graphic equalizer is shown here. The circuit includes two summing amplifiers and a series of band-pass filters. The band-pass filters provide the frequency band selection. Resistor  $R_3$  divides the output of the filters into two signals. The signal applied to the summing input of  $A_1$  provides band reduction and the signal applied to the summing junction of  $A_2$  provides boost for a particular frequency band.



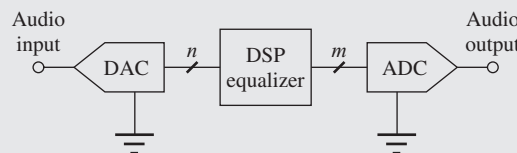
Typical graphic equalizer circuit.<sup>1</sup>

If potentiometer  $R_3$  is set to the center point, the gain and boost signals are balanced, and no net signal is added or subtracted to the output. The slider controls in the picture above correspond to  $R_3$  in the circuit diagram.

Graphic equalizers have been reduced greatly in size since the mid-1970s, and until recently, functioned similarly to the one shown above. However, with the advent of

<sup>1</sup> Dennis A. Bohn, “Constant-Q graphic equalizers.” *J. Audio Eng. Soc.*, vol. 34, no. 9, September 1986.

high-precision, low-cost A/D converters and low-cost high-performance digital signal processing (DSP), graphic equalizers have moved into the digital domain. DSP based equalizers with excellent accuracy and controllability are now available. This new class of equalizer has an A/D converter, followed by DSP circuits, with a digital-to-analog (D/A) converter at the output to move the signal back into the analog domain. The DSP allows the designer to generate complex transfer functions that account for non-idealities such as channel-to-channel interactions. DSP equalizers are commonly found in MP3 music players, for example. As integrated circuit process technology advances, it is always important to reevaluate the appropriate boundaries between analog and digital signal processing.



Graphic equalizer based upon digital signal processing.

in which  $R_{io}$  represents the resistance measured at the terminals of capacitor  $C_i$  with the other capacitors open circuited. Because we already have results for the C-E stages, let us practice by applying the method to the high-frequency model for the C-E amplifier in Fig. 17.35.

Three capacitors,  $C_\pi$ ,  $C_\mu$ , and  $C_L$  are present in Fig. 17.35(c), and  $R_{\pi o}$ ,  $R_{\mu o}$ , and  $R_{L0}$  will be needed to evaluate Eq. (17.99).  $R_{\pi o}$  can easily be determined from the circuit in Fig. 17.37, in which  $C_\mu$  and  $C_L$  are replaced by open circuits, and we see that

$$R_{\pi o} = r_{\pi o} \quad (17.100)$$

$R_{L0}$  is found from Fig. 17.38. There is no current in  $r_{\pi 0}$ , so  $g_m v$  is zero, and

$$R_{L0} = R_L \quad (17.101)$$

$R_{\mu o}$  can be determined from the circuit in Fig. 17.39, in which  $C_\pi$  is replaced by an open circuit. In this case, a bit more work is required. Test source  $i_x$  is applied to the network in Fig. 17.39(b),

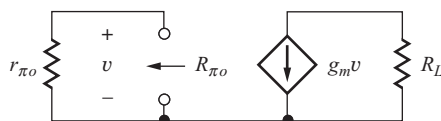


Figure 17.37 Circuit for finding  $R_{\pi o}$ .

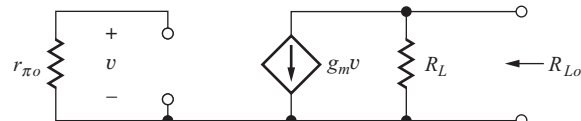


Figure 17.38 Circuit for finding  $R_{\pi o}$ .

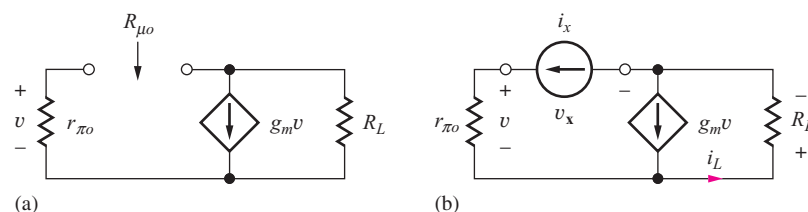


Figure 17.39 (a) Circuit defining  $R_{\mu o}$ . (b) Test source applied.

and  $v_x$  can be found by applying KVL around the outside loop:

$$\mathbf{v}_x = \mathbf{i}_x r_{\pi o} + \mathbf{i}_L R_L = \mathbf{i}_x r_{\pi o} + (\mathbf{i}_x + g_m \mathbf{v}) R_L \quad (17.102)$$

However, voltage  $\mathbf{v}$  is equal to  $\mathbf{i}_x r_{\pi o}$ , and substituting this result into Eq. (17.102) yields

$$R_{\mu o} = \frac{\mathbf{v}_x}{\mathbf{i}_x} = r_{\pi o} + (1 + g_m r_{\pi o}) R_L = r_{\pi o} \left[ 1 + g_m R_L + \frac{R_L}{r_{\pi o}} \right] \quad (17.103)$$

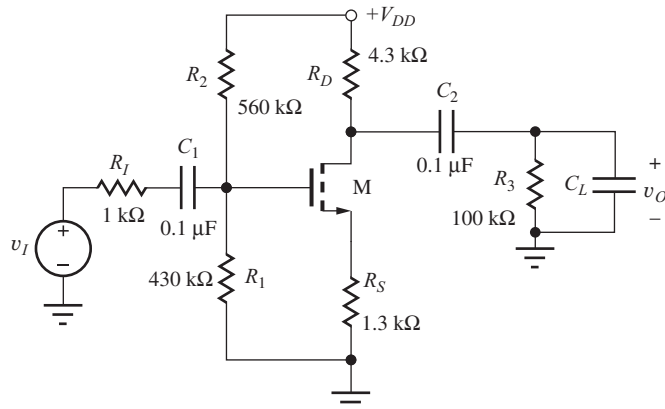
which should look familiar [see Eq. (17.86)]. Substituting Eqs. (17.100), (17.101) and (17.103) into Eq. (17.99) produces the estimate for  $\omega_H$ :

$$\omega_H \cong \frac{1}{R_{\pi o} C_\pi + R_{\mu o} C_\mu} = \frac{1}{r_{\pi o} C_\pi + r_{\pi o} C_\mu \left( 1 + g_m R_L + \frac{R_L}{r_{\pi o}} \right) + R_L C_L} = \frac{1}{r_{\pi o} C_T} \quad (17.104)$$

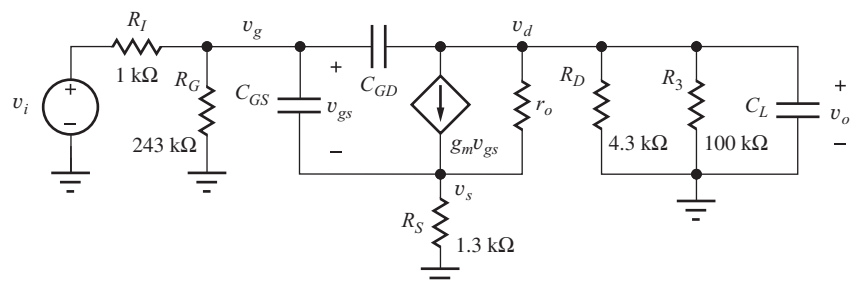
This is exactly the same result achieved from Eqs. (17.94) but with far less effort. (Remember, however, that this method does not produce an estimate for either the second pole or the zeros of the network.)

### 17.6.7 COMMON-SOURCE AMPLIFIER WITH SOURCE DEGENERATION RESISTANCE

Figure 17.40(a) shows a common-source amplifier with unbypassed source resistance  $R_S$  and Fig. 17.40(b) is the small-signal equivalent circuit. We find the input equivalent capacitance and resistance in the same manner as used for the common-emitter circuit. The midband gain is first calculated in two parts as before. The input gain expression is similar to that of the common-emitter



(a)



(b)

**Figure 17.40** (a) Common-source amplifier with unbypassed source resistance. (b) Small-signal high-frequency equivalent circuit.

except that  $r_\pi$  is not included since the impedance looking into the gate is infinite.

$$A_i = \frac{\mathbf{v}_g}{\mathbf{v}_i} = \frac{R_G}{R_I + R_G} = \frac{R_1 \| R_2}{R_I + (R_1 \| R_2)} \quad (17.105)$$

The terminal gain of the common-source amplifier is found as

$$A_{gd} = \frac{v_d}{v_g} = \frac{-g_m R_L}{1 + g_m R_S} = \frac{-g_m (R_{iD} \| R_D \| R_3)}{1 + g_m R_S} \cong \frac{-g_m (R_D \| R_3)}{1 + g_m R_S} \quad (17.106)$$

where

$$R_{iD} = r_o (1 + g_m R_S) \quad (17.107)$$

As seen in Eq. (17.107),  $R_{iD}$  is typically quite large and can be neglected, and  $R_L \cong R_D \| R_3$ . We again use the Miller effect to calculate the input high-frequency time constant.

$$\begin{aligned} C_{eqG} &= C_{GD}(1 - A_{gd}) + C_{GS}(1 - A_{gs}) \\ &= C_{GD} \left( 1 - \frac{[-g_m R_L]}{1 + g_m R_S} \right) + C_{GS} \left( 1 - \frac{g_m R_S}{1 + g_m R_S} \right) \\ &= C_{GD} \left( 1 + \frac{g_m (R_D \| R_3)}{1 + g_m R_S} \right) + \frac{C_{GS}}{1 + g_m R_S} \end{aligned} \quad (17.108)$$

Note that we have used the expression for the gain of the common-drain amplifier to calculate the Miller multiplication of  $C_{GS}$ . Unlike the Miller effect with regard to  $C_{GD}$ , the effective capacitance of  $C_{GS}$  is reduced since  $A_{gs}$  will always be positive and less than 1. The unbypassed source resistance has also had the effect of reducing the effect of  $C_{GD}$  since the gate-to-drain gain has also been reduced by the  $(1 + g_m R_S)$  term. The equivalent small-signal resistance to ground at the gate node is

$$R_{eqG} = R_G \| R_I = R_{th} \quad (17.109)$$

The equivalent capacitance and resistance at the output is similar to that of the common-emitter amplifier.

$$R_{eqD} = R_{iD} \| R_D \| R_3 \cong R_D \| R_3 \quad \text{and} \quad C_{eqD} = C_{GD} + C_L \quad (17.110)$$

Combining these results and using Eq. (17.98), we find the following general form for the poles and right-half plane zero.

$$\omega_{P1} = \frac{1}{R_{th} \left[ \frac{C_{GS}}{1 + g_m R_S} + C_{GD} \left( 1 + \frac{g_m R_L}{1 + g_m R_S} \right) + \frac{R_L}{R_{th}} (C_{GD} + C_L) \right]} \quad (17.111)$$

$$\omega_{P2} = \frac{g_m}{(1 + g_m R_S)(C_{GS} + C_L)} \quad (17.112)$$

$$\omega_z = \frac{+g_m}{(1 + g_m R_S)(C_{GD})} \quad (17.113)$$

Notice the gain bandwidth tradeoff indicated in Equations (17.106) and (17.111). The  $(1 + g_m R_S)$  term decreases gain while increasing the frequency of the dominant pole  $\omega_{P1}$ . In our study of op amps, we found that gain and bandwidth can be traded one for the other and the same relationship generally holds true in transistor circuits. Since the gain and bandwidth are inversely affected by the  $(1 + g_m R_S)$  term, the gain-bandwidth product is held relatively constant, similar to what we found in our study of the gain-bandwidth characteristics of op amp based amplifiers.

The second pole and zero equations are modified to account for the degeneration of the effective  $g_m$  by the source resistance. Notice that although the dominant pole increases in frequency, the frequencies of second pole and zero are decreased. Increasing the gain of the stage increases

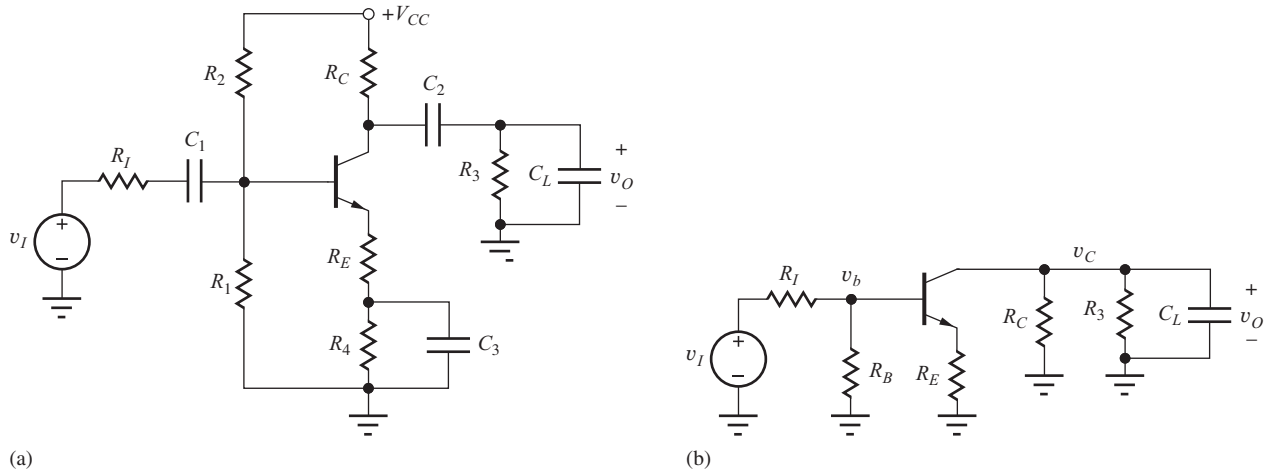


**Figure 17.41** (a) Common-emitter amplifier with unbypassed emitter resistor \$R\_E\$. (b) High-frequency ac equivalent circuit.

the frequency separation between \$\omega\_{P1}\$ and \$\omega\_{P2}\$, resulting in what is often referred to as **pole-splitting**. Decreasing the gain moves the two poles closer in frequency, which can compromise the phase margin of feedback amplifiers.

If the small-signal resistance \$R\_S\$ in the source is reduced to zero, the equations for the common-source poles reduce to the simpler form of the common-source equations found previously. Likewise, if an unbypassed emitter resistance is included in the common-emitter amplifier, the pole equations can be modified in a manner similar to the common-source with source degeneration amplifier above, as discussed in the following section.

### 17.6.8 POLES OF THE COMMON-EMITTER WITH Emitter DEGENERATION RESISTANCE

The equations for the common-emitter with unbypassed source resistance are modified in a manner similar to those of the common-source. In Fig. 17.41 a portion of the emitter resistance \$R\_E\$ is unbypassed, and the input stage gain \$A\_i\$ is modified due to the increased impedance looking into the base.

$$A_i = \frac{v_b}{v_i} = \frac{(R_B \| R_{iB})}{R_I + (R_B \| R_{iB})} \cdot \frac{r_\pi + (\beta_o + 1)R_E}{r_x + r_\pi + (\beta_o + 1)R_E} \cong \frac{R_B \| R_{iB}}{R_I + R_B \| R_{iB}} \quad (17.114)$$

Recall the impedance looking into the base is

$$R_{iB} = r_x + r_\pi + (\beta_o + 1)R_E \quad (17.115)$$

The terminal gain of the common-emitter with unbypassed emitter resistance is found as

$$A_{bc} = \frac{v_c}{v_b} \cong \frac{-g_m(R_C \| R_3)}{1 + g_m R_E} \cong \frac{-g_m R_L}{1 + g_m R_E} \quad (17.116)$$

Including the effect of the emitter degeneration resistance \$R\_E\$, the pole and zero equations are modified as follows:

$$\omega_{P1} = \frac{1}{r_{\pi o} C_T} = \frac{1}{r_{\pi o} \left( \left[ \frac{C_\pi}{1 + g_m R_E} + C_\mu \left( 1 + \frac{g_m R_L}{1 + g_m R_E} \right) \right] + \frac{R_L}{r_{\pi o}} [C_\mu + C_L] \right)} \quad (17.117)$$

$$\text{where } r_{\pi o} = R_{eqB} = (R_{th} + r_x) \parallel [r_\pi + (\beta_o + 1)R_E] \quad \text{with } R_{th} = R_B \| R_I \quad (17.118)$$

$$\omega_{P2} \cong \frac{g_m}{(1 + g_m R_E)(C_\pi + C_L)} \quad (17.119)$$

$$\omega_z = \frac{+g_m}{(1 + g_m R_E)(C_\mu)} \quad (17.120)$$

As with the common-source amplifier, the degeneration resistance causes a decrease in gain and an increase in the dominant pole frequency. The amplifier allows one to directly tradeoff gain and bandwidth, approximately maintaining a constant gain-bandwidth product.

### EXAMPLE 17.7 COMMON-EMITTER AMPLIFIER WITH Emitter DEGENERATION

In this example, we explore the gain-bandwidth trade-off achieved by adding an unbypassed emitter resistor to the common-emitter amplifier from Ex. 17.6.

**PROBLEM** Find the midband gain, upper-cutoff frequency, and gain-bandwidth product for the common-emitter amplifier in Fig. 17.34 if a 300- $\Omega$  portion of the emitter resistor is not bypassed. Assume  $\beta_o = 100$ ,  $f_T = 500$  MHz,  $C_\mu = 0.5$  pF,  $r_x = 250$   $\Omega$ , and the Q-point = (1.6 mA, 3.0 V).

**SOLUTION** **Known Information and Given Data:** Common-emitter amplifier in Fig. 17.34 with a bypass capacitor placed around a 1000- $\Omega$  portion of the emitter resistor;  $\beta_o = 100$ ,  $f_T = 500$  MHz,  $C_\mu = 0.5$  pF,  $r_x = 250$   $\Omega$ ; Q-point: (1.6 mA, 3.0 V).

**Unknowns:**  $A_{\text{mid}}$ ,  $f_H$ , and GBW

**Approach:** Find  $A_{\text{mid}}$  and  $f_H$  using Eqs. (17.114–17.118).  $\text{GBW} = A_{\text{mid}} \times f_H$ .

**Assumptions:**  $V_T = 25.0$  mV; small-signal operation in the active region

**Analysis:** Using the values from the analysis of Fig. 17.34 with  $g_m = 40I_C = 64$  mS:

$$r_\pi = \frac{\beta_o}{g_m} = \frac{100}{0.064} = 1.56 \text{ k}\Omega \quad R_{\text{th}} + r_x = 882 \text{ }\Omega + 250 \text{ }\Omega = 1130 \text{ }\Omega$$

$$R_{iB} = r_x + r_\pi + (\beta_o + 1)R_E = 250 \text{ }\Omega + 1560 \text{ }\Omega + (101)300 \text{ }\Omega = 32.1 \text{ k}\Omega$$

$$r_{\pi0} = R_{iB} \parallel (R_{\text{th}} + r_x) = 1.09 \text{ k}\Omega \quad 1 + g_m R_E = 1 + 0.064(300) = 20.2$$

$$\begin{aligned} \omega_H &\approx \frac{1}{r_{\pi0} \left[ \frac{C_\pi}{1 + g_m R_E} + C_\mu \left( 1 + \frac{g_m R_L}{1 + g_m R_E} + \frac{R_L}{r_{\pi0}} \right) \right]} \\ &\approx \frac{1}{1090 \left[ \frac{19.9 \text{ pF}}{20.2} + 0.5 \text{ pF} \left( 1 + \frac{264}{20.2} + \frac{4120}{1090} \right) \right]} \\ f_H &\approx \frac{1}{2\pi} \frac{1}{1090 \Omega (9.91 \text{ pF})} = 14.7 \text{ MHz} \end{aligned}$$

$$A_i = \frac{R_1 \parallel R_2 \parallel R_{iB}}{R_1 + R_1 \parallel R_2 \parallel R_{iB}} = \frac{10 \text{ k}\Omega \parallel 30 \text{ k}\Omega \parallel 32.1 \text{ k}\Omega}{1 \text{ k}\Omega + 10 \text{ k}\Omega \parallel 30 \text{ k}\Omega \parallel 32.1 \text{ k}\Omega} = 0.859$$

$$A_{bc} = -\frac{g_m R_L}{1 + g_m R_E} = -\frac{0.064(4120 \text{ }\Omega)}{1 + 0.064(300 \text{ }\Omega)} = -13.0 \quad \text{or} \quad 22.3 \text{ dB}$$

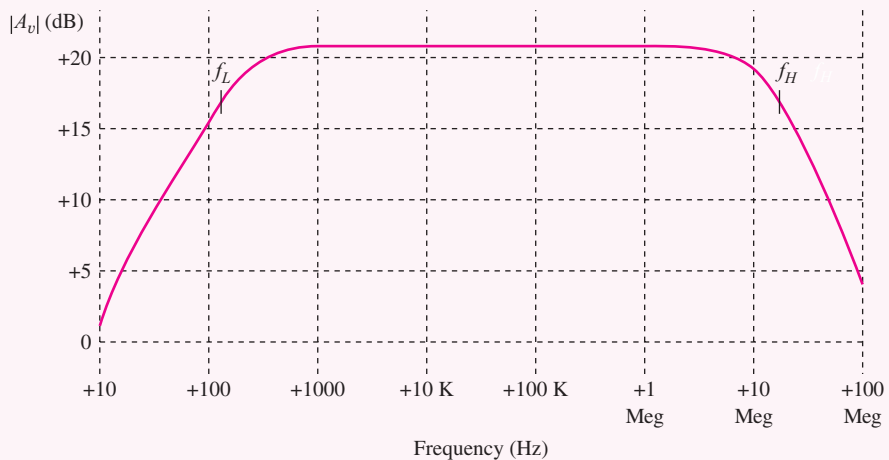
$$A_{\text{mid}} = A_i A_{bc} = 0.859(-13.0) = -11.2 \quad \text{GBW} = 11.2 \times 14.7 \text{ MHz} = 165 \text{ MHz}$$

**Check of Results:** A quick estimate for  $A_{\text{mid}}$  is  $-R_L/R_E = -13.7$ . Our more exact calculation is slightly less than this number, so it appears correct. The GBW product of the amplifier is 165 MHz, which is approximately 1/3 of  $f_T$ , also a reasonable result.

**Discussion:** Remember, the original C-E stage with no emitter resistance had  $A_{\text{mid}} = -153$  and  $f_H = 1.56$  MHz for  $\text{GBW} = 239$  MHz. With  $R_E = 300 \text{ }\Omega$ , the gain has decreased by a factor

of 14, and the bandwidth has increased by a factor of 8.9. The gain-bandwidth trade-off in the expression for  $\omega_H$  is not exact because the effective resistance in the time-constant only increases from  $882 \Omega$  to  $1130 \Omega$ , as well as the  $R_L C_\mu$  term that is not scaled by the  $(1 + g_m R_E)$  factor.

**Computer-Aided Analysis:** SPICE can be used to check our hand analysis, but we must define the device parameters that match our analysis. The base resistance, collector-base capacitance, and forward transit-time were calculated in Ex. 17.6:  $RB = 250 \Omega$ ,  $CJC = 0.768 \text{ pF}$ , and  $TF = 0.311 \text{ ns}$ . After adding these values to the transistor model, we perform an ac analysis using  $FSTART = 10 \text{ Hz}$  and  $FSTOP = 100 \text{ MHz}$  with 20 frequency points per decade. SPICE yields  $A_{\text{mid}} = -11.0$  and  $f_H \cong 15.0 \text{ MHz}$ , which agree well with our hand calculations. Note that the lower-cutoff frequency has changed to 158 Hz. The simulation used  $C_1 = C_2 = 3.9 \mu\text{F}$ ,  $C_3 = 0.082 \mu\text{F}$ .



**EXERCISE:** Use SPICE to recalculate  $f_H$  for  $V_A = 75 \text{ V}$ . For  $V_A = 75 \text{ V}$  and  $r_x = 0$ ?

**ANSWERS:** 14.8 MHz; 17.8 MHz

**EXERCISE:** Use the formulas to recalculate the midband gain,  $f_H$ , and GBW if the un bypassed portion of the emitter resistor is decreased to  $100 \Omega$ ?

**ANSWERS:**  $-29.3$ ;  $6.70 \text{ MHz}$ ;  $196 \text{ MHz}$

## 17.7 COMMON-BASE AND COMMON-GATE AMPLIFIER HIGH-FREQUENCY RESPONSE

We analyze the high-frequency response of the other single-stage amplifiers using the same approach we used in the previous section. At each node along the signal path, we determine an equivalent resistance to small-signal ground and an equivalent capacitance to small-signal ground. The resulting  $RC$  network gives rise to a high-frequency pole. We now apply this approach to the common-base amplifier shown in Figure 17.42(a). The high-frequency ac equivalent circuit is shown in Figure 17.42(b). Base resistance  $r_x$  has been neglected to simplify the analysis, as has output resistance  $r_o$ .

The input gain of the common base circuit is found as

$$A_i = \frac{v_e}{v_i} = \frac{R_{in}}{R_I + R_{in}} = \frac{R_E \parallel R_{iE}}{R_i + R_E \parallel R_{iE}} \quad (17.121)$$

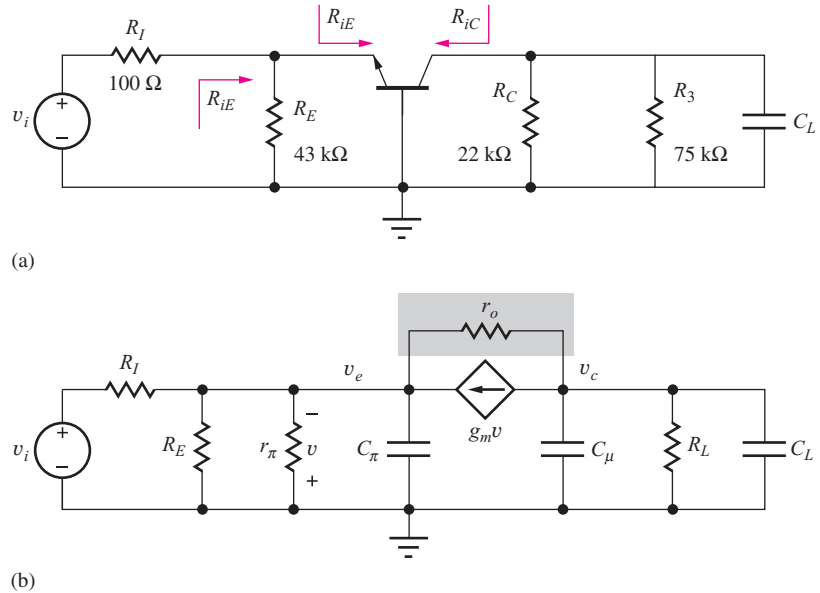


**Figure 17.42** (a) High-frequency ac equivalent circuit for the common-base amplifier. (b) Small-signal model for the common-base amplifier.

where  $R_{iE} = \frac{r_\pi}{\beta_o + 1} \cong \frac{1}{g_m}$ . (To include the effect of  $r_x$ , we can add it to  $r_\pi$ .) Given that  $R_{iE} \cong 1/g_m$  and if  $1/g_m \ll R_E$ , the input gain becomes

$$A_i \cong \frac{1}{1 + g_m R_I} \quad (17.122)$$

The terminal gain of the common-base amplifier is found as

$$A_{ec} = \frac{v_c}{v_e} = g_m (R_{iC} \parallel R_L) \cong +g_m R_L \quad (17.123)$$

where

$$R_{iC} = r_o [1 + g_m (r_\pi \parallel R_{th})] \quad \text{with} \quad R_{th} = R_E \parallel R_I \quad (17.124)$$

The expression for  $R_{iC}$  is the same as Eq. (14.90). Again,  $R_{iC}$  is typically much larger than the other resistances at the collector and can be neglected. The equivalent capacitance at the input is found as

$$C_{eqE} = C_\pi \quad (17.125)$$

An output capacitance associated with a driving stage would be added to  $C_\pi$ . To calculate the equivalent resistance at the emitter node, recall that due to the dependent generator, the resistance looking into the emitter is  $R_{iE} \cong 1/g_m$ . For the circuit in Fig. 17.42,

$$R_{eqE} = \frac{1}{g_m} \parallel R_E \parallel R_I \quad (17.126)$$

At the output, we determine the equivalent capacitance and resistance as

$$C_{eqC} = C_\mu + C_L \quad \text{and} \quad R_{eqC} = R_{iC} \parallel R_L \cong R_L \quad (17.127)$$

Since the input and output are well decoupled, we find the two poles for the common-base amplifier are

$$\omega_{P1} = \frac{1}{\left(\frac{1}{g_m} \| R_E \| R_I\right) C_\pi} \cong \frac{g_m}{C_\pi} \quad (17.128)$$

$$\omega_{P2} = \frac{1}{(R_{out} \| R_L)(C_\mu + C_L)} \cong \frac{1}{R_L(C_\mu + C_L)} \quad (17.129)$$

We should notice that the input pole of this stage has no Miller multiplication terms, and its equivalent resistance is dominated by the typically small  $1/g_m$  term. As a result, the input pole of the common-base amplifier is typically a very high frequency, exceeding  $f_T$ . The bandwidth of the stage is dominated by the load resistance and capacitance, modeled with  $\omega_{P2}$ .

**EXERCISE:** Find the midband gain and  $f_H$  using Eq. (17.129) for the common-base amplifier in Fig. 17.42 if the transistor has  $\beta_o = 100$ ,  $f_T = 500$  MHz,  $r_x = 250$   $\Omega$ ,  $C_\mu = 0.5$  pF, and a Q-point (0.1 mA, 3.5 V). What is the gain-bandwidth product?

**ANSWERS:** +48.2; 18.7 MHz; 903 MHz

Figures 17.43(a) and (b) represent the high-frequency ac and small-signal equivalent circuits for a common-gate amplifier, and the analysis of the common-gate response is analogous to that of the common-base with  $R_4$ ,  $C_{GS}$ , and  $C_{GD}$  replacing  $R_E$ ,  $C_\pi$ , and  $C_\mu$ .

$$\omega_{P1} = \frac{1}{\left(\frac{1}{g_m} \| R_4 \| R_I\right) C_{GS}} \cong \frac{g_m}{C_{GS}} \quad (17.130)$$

$$\omega_{P2} = \frac{1}{[R_{out} \| R_L][C_{GD} + C_L]} \cong \frac{1}{R_L[C_{GD} + C_L]} \quad (17.131)$$

**EXERCISE:** Find the midband gain and  $f_H$  for the common-gate amplifier in Fig. 17.43 if the transistor  $C_{GS} = 10$  pF,  $C_{GD} = 1$  pF,  $g_m = 3$  mS, and  $C_L = 3$  pF. What are the gain-bandwidth product and  $f_T$ ?

**ANSWERS:** +8.98, 9.65 MHz; 86.7 MHz; 43.4 MHz

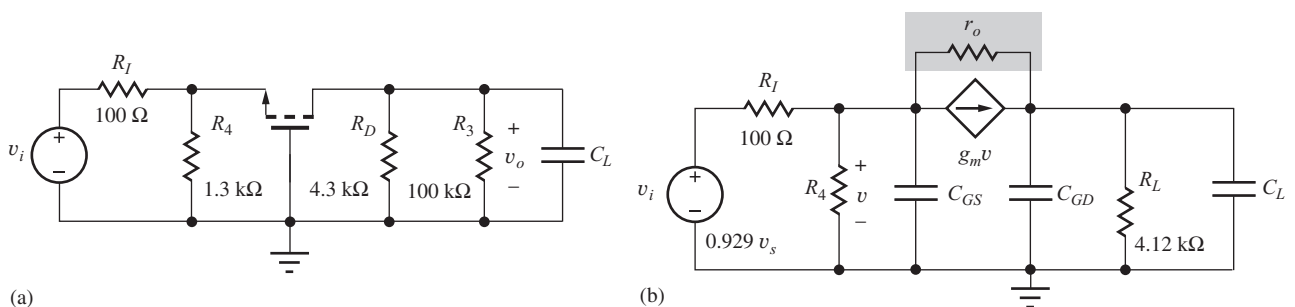


**Figure 17.43** (a) High-frequency ac equivalent circuit for a common-gate amplifier. (b) Corresponding small-signal model.

## 17.8 COMMON-COLLECTOR AND COMMON-DRAIN AMPLIFIER HIGH-FREQUENCY RESPONSE

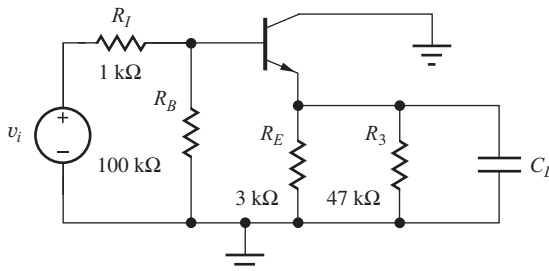
The high-frequency responses of the common-collector and common-drain amplifiers are found in a manner similar to the other single-stage amplifiers. Figure 17.44 illustrates a typical common-collector amplifier and its small-signal equivalents. (Note that  $r_o$  is included in  $R_L$ .)

The midband input gain looks very similar to that of the common-emitter amplifier.

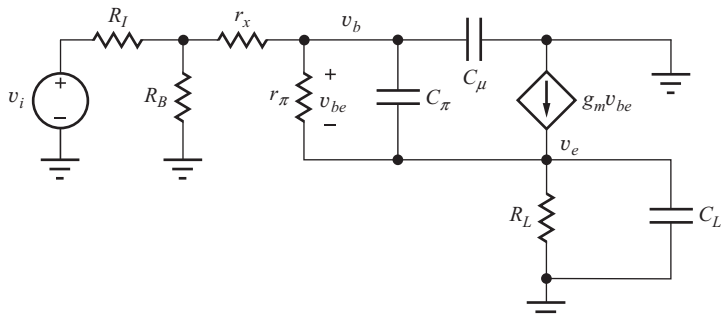
$$A_i = \frac{v_b}{v_i} = \frac{R_{in}}{R_I + R_{in}} = \frac{R_B \| R_{iB}}{R_I + R_B \| R_{iB}} = \frac{R_B \| [r_x + r_\pi + (\beta_o + 1)R_L]}{R_I + R_B \| [r_x + r_\pi + (\beta_o + 1)R_L]} \quad (17.132)$$

The base-to-emitter terminal voltage gain is

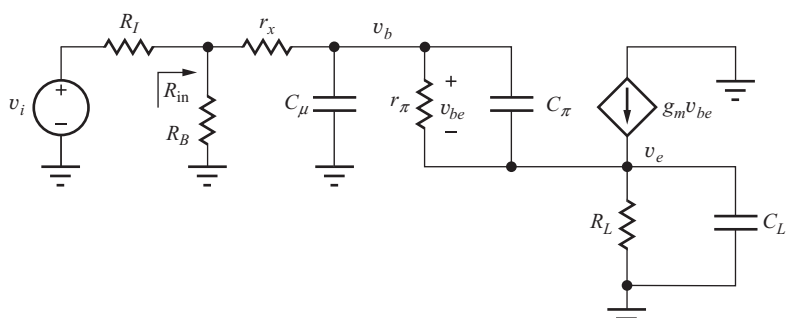
$$A_{be} = \frac{v_e}{v_b} = \frac{g_m R_L}{1 + g_m R_L} \quad (17.133)$$



(a)



(b)



(c)

**Figure 17.44** (a) Common-collector amplifier. (b) Small-signal model for the common-collector amplifier. (c) Simplification of the small-signal circuit for calculation of input and output high-frequency poles. Note  $R_L = R_E \| R_3 \| r_o$ .

**Pole Estimation— $\omega_{P1}$** 

To calculate the high-frequency poles, we first evaluate the equivalent small-signal resistance to ground,  $R_{eqB}$  at node  $v_b$ .

$$R_{eqB} = [(R_I \| R_B) + r_x] \parallel [r_\pi + (\beta_o + 1)R_L] = (R_{th} + r_x) \parallel [r_\pi + (\beta_o + 1)R_L] \quad (17.134)$$

The equivalent capacitance is found using Miller multiplication as

$$C_{eqB} = C_\mu(1 - A_{bc}) + C_\pi(1 - A_{be}) = C_\mu(1 - 0) + C_\pi \left(1 - \frac{g_m R_L}{1 + g_m R_L}\right) = C_\mu + \frac{C_\pi}{1 + g_m R_L} \quad (17.135)$$

Note that  $C_\mu$  really appears directly between the base and ground, so Miller effect does not modify its value. On the other hand, the nearly unity gain between the transistor's base and emitter significantly reduces the effective size of  $C_\pi$ .

**Pole Estimation— $\omega_{P2}$** 

The equivalent small-signal resistance at the emitter can be found as

$$R_{eqE} = R_{iE} \parallel R_L = \left(\frac{r_\pi + R_{th} + r_x}{\beta_o + 1}\right) \parallel R_L \cong \frac{1}{g_m} + \frac{R_{th} + r_x}{\beta_o + 1} \quad (17.136)$$

where  $R_{th} = R_B \| R_I$ . The equivalent capacitance is found as the parallel combination of the load capacitance and the base-to-emitter capacitance.

$$C_{eqE} = C_\pi + C_L \quad (17.137)$$

Because of the low impedance at the output, the input and output time constants are relatively well decoupled, resulting in two poles for the common-collector amplifier.

$$\omega_{P1} = \frac{1}{([R_{th} + r_x] \parallel [r_\pi + (\beta_o + 1)R_L]) \left(C_\mu + \frac{C_\pi}{1 + g_m R_L}\right)} \quad (17.138)$$

$$\omega_{P2} = \frac{1}{[R_{iE} \parallel R_L][C_\pi + C_L]} \cong \frac{1}{\left[\left(\frac{1}{g_m} + \frac{R_{th} + r_x}{\beta_o + 1}\right) \parallel R_L\right][C_\pi + C_L]} \quad (17.139)$$

Notice that the output pole of this stage is dominated by the typically small  $1/g_m$  term. As a result, the output pole of the common-collector amplifier is typically a very high frequency, approaching  $f_T$ . The bandwidth of the stage is dominated by  $\omega_{P1}$ , the pole associated with the input section equivalent resistance and capacitance. We will typically ignore the high-frequency pole at the emitter. Because of the feed-forward high-frequency path through  $C_\pi$ , a common-collector stage also includes a high-frequency zero.

$$\omega_z \cong \frac{g_m}{C_\pi} \quad (17.140)$$

Notice that this zero is in the left-half plane. For low load capacitances,  $\omega_z$  and  $\omega_{P2}$  tend to cancel each other, so we should only include the effects of  $\omega_{P2}$  when we also include  $\omega_z$ .

**EXERCISE:** Find  $A_{mid}$  and  $f_H$  for the common-collector amplifier in Fig. 17.44 if the Q-point is (1.5 mA, 5 V),  $\beta_o = 100$ ,  $r_x = 150 \Omega$ ,  $C_\mu = 0.5 \text{ pF}$ , and  $f_T = 500 \text{ MHz}$ .

**ANSWERS:** 0.980, 229 MHz

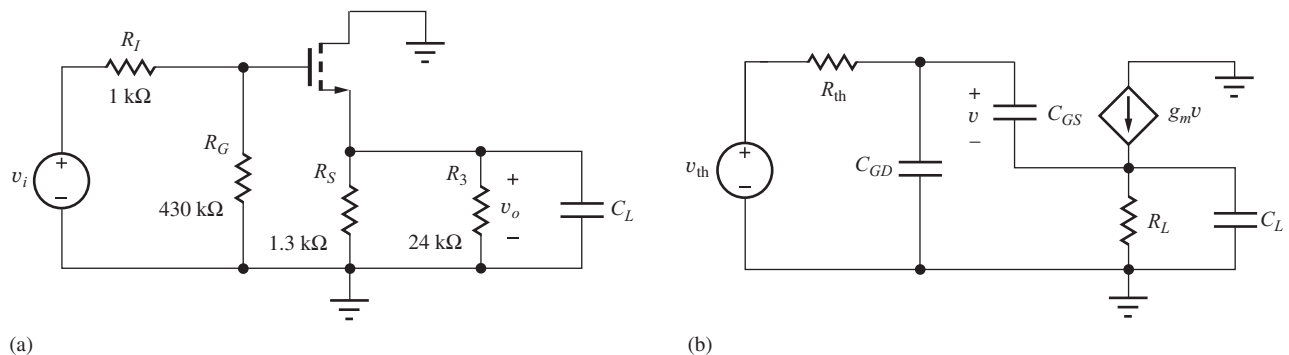


**Figure 17.45** (a) High-frequency ac equivalent circuit for a source follower. (b) Corresponding high-frequency small-signal model. Note  $R_L = R_S \parallel R_3 \parallel r_o$ .

A similar set of equations can be found for the common-drain amplifier of Fig. 17.45, making the appropriate changes for the different characteristics of the FET small-signal model.

$$\omega_{P1} = \frac{1}{R_{th} \left( C_{GD} + \frac{C_{GS}}{1 + g_m R_L} \right)} \quad R_{th} = R_G \parallel R_S \quad (17.141)$$

$$\omega_{P2} = \frac{1}{[R_{th} \parallel R_L][C_{GS} + C_L]} \cong \frac{1}{\left[ \frac{1}{g_m} \parallel R_L \right] [C_{GS} + C_L]} \quad (17.142)$$

$$\omega_z \cong \frac{g_m}{C_{GS}} \quad (17.143)$$

Similar to the common-collector, the common-drain amplifier's high-frequency response is dominated by the input pole,  $f_{p1}$ , due to the small impedance associated with the output pole and zero.

**EXERCISE:** Find  $A_{mid}$  and  $f_H$  for the common-drain amplifier in Fig. 17.45 if  $C_{GS} = 10\text{ pF}$ ,  $C_{GD} = 1\text{ pF}$ , and  $g_m = 3\text{ mS}$ .

**ANSWERS:** 0.785, 51.0 MHz

## 17.9 SINGLE-STAGE AMPLIFIER HIGH-FREQUENCY RESPONSE SUMMARY

Table 17.2 collects the expressions for the dominant poles of the three classes of single-stage amplifiers. The inverting amplifiers provide high voltage gain but with the most limited bandwidth. The noninverting stages offer improved bandwidth with voltage gains similar to those of the inverting amplifiers. Remember, however, that the input resistance of the noninverting amplifiers is relatively low. The followers provide unity gain with very wide bandwidth.

It is also worth noting at this point that both the C-E and C-B (or C-S and C-G) stages have a bandwidth that is always less than that set by the time constant of  $R_L$  and  $(C_\mu + C_L)$  (or  $C_{GD} + C_L$  and  $R_L$ ) at the output node:

$$\omega_H < \frac{1}{R_L(C_\mu + C_L)} \quad \text{or} \quad \omega_H < \frac{1}{R_L(C_{GD} + C_L)}$$

**TABLE 17.2**  
Upper-Cutoff Frequency Estimates for the Single-Stage Amplifiers

	$\omega_H$	
Common-emitter	$\frac{1}{r_{\pi0}C_T} = \frac{1}{r_{\pi0} \left[ C_{\pi} + C_{\mu}(1 + g_m R_L) + (C_u + C_L) \frac{R_L}{r_{\pi0}} \right]}$	$r_{\pi0} = r_{\pi} \  [r_x + (R_I \  R_B)]$
Common-source	$\frac{1}{R_{\text{th}}C_T} = \frac{1}{R_{\text{th}} \left[ C_{GS} + C_{GD}(1 + g_m R_L) + (C_{GD} + C_L) \frac{R_L}{R_{\text{th}}} \right]}$	$R_{\text{th}} = R_I \  R_G$
Common-emitter with emitter resistor $R_E$	$\frac{1}{r_{\pi0} \left[ \frac{C_{\pi}}{1 + g_m R_E} + C_{\mu} \left( 1 + \frac{g_m R_L}{1 + g_m R_E} \right) + (C_u + C_L) \frac{R_L}{r_{\pi0}} \right]}$	$r_{\pi0} = r_{\pi} \  [r_x + (R_I \  R_B)]$
Common-source with source resistor $R_S$	$\frac{1}{R_{\text{th}} \left[ \frac{C_{GS}}{1 + g_m R_S} + C_{GD} \left( 1 + \frac{g_m R_L}{1 + g_m R_S} \right) + (C_{GD} + C_L) \frac{R_L}{R_{\text{th}}} \right]}$	$R_{\text{th}} = R_I \  R_G$
Common-base	$\frac{1}{R_L(C_{\mu} + C_L)}$	
Common-gate	$\frac{1}{R_L(C_{GD} + C_L)}$	
Common-collector	$\frac{1}{[(R_I \  R_B) + r_x] \left( \frac{C_{\pi}}{1 + g_m R_L} + C_{\mu} \right)}$	
Common-drain	$\frac{1}{(R_I \  R_G) \left( \frac{C_{GS}}{1 + g_m R_L} + C_{GD} \right)}$	

### 17.9.1 AMPLIFIER GAIN-BANDWIDTH LIMITATIONS

The importance of the base resistance  $r_x$  (and gate resistance in high-frequency FETs) in ultimately limiting the frequency response of amplifiers should not be overlooked. Consider first the common-emitter amplifiers described by Table 17.2. If the Thévenin equivalent source resistance  $R_I$  were reduced to zero in an attempt to increase the bandwidth, then  $r_{\pi0}$  would not become zero, but would be limited approximately to the value of  $r_x$ . If one assumes that the gain is large and the  $g_m R_L C_{\mu}$  term is dominant in determining  $\omega_H$ , then the gain bandwidth product for the common-emitter stage becomes  $\text{GBW} \leq 1/r_x C_{\mu}$ .

In the common-collector case, the gain is approximately one, and for  $R_I = 0$  and large  $g_m R_L$ , the bandwidth becomes  $1/r_x C_{\mu}$ . Here again we find  $\text{GBW} \leq 1/r_x C_{\mu}$ . If we neglect  $C_{\pi}$  in Fig. 17.44, we can easily see that the bandwidth is set by  $r_x$  and  $C_{\mu}$ , since the input resistance looking into  $r_{\pi}$  will be very large compared to  $r_x$ .

In order to simplify our analysis of the common-base amplifier, we neglected  $r_x$ . If  $r_x$  is included, it can be shown that the gain-bandwidth product is also limited by the  $r_x C_{\mu}$  product in the C-B case as well. However, this limit is seldom reached since  $R_L$  is usually considerably larger than  $r_x$ .

Now we have found two important limits placed upon amplifier gain-bandwidth products by the characteristics of the transistor. The first was the unity-gain frequency for the current gain of the transistor,  $f_T = g_m/(C_{\pi} + C_{\mu})$ . The second is set by  $\text{GBW} \leq 1/r_x C_{\mu}$ . However, in typical amplifier designs, the GBW product will reach less than 60 percent of either of these bounds.

For transistors designed for very high-frequency operation, minimization of the  $r_x C_\mu$  product is one of the main goals guiding the choice of the physical structure and the impurity profiles of the devices. As is often the case in engineering, tradeoffs are involved. The choices that minimize  $r_x$  increase  $C_\mu$ , and vice-versa, and complex device designs are utilized to optimize the  $r_x C_\mu$  (or  $R_{IG} C_{GD}$ ) product.

## 17.10 FREQUENCY RESPONSE OF MULTISTAGE AMPLIFIERS

The open- and short-circuit time-constant methods are not limited to single-transistor amplifiers but are directly applicable to multistage circuits as well; the power of the technique becomes more obvious as circuit complexity grows. This section uses the techniques developed in the previous sections to estimate the frequency response of several important two-stage dc-coupled amplifiers, including the differential amplifier, the cascode stage, and the current mirror. Because these amplifiers are direct-coupled, they have low-pass characteristics and we only need to determine  $f_H$ . Following is an example of analysis of a general three-stage amplifier in which  $f_L$  and  $f_H$  are found.

### 17.10.1 DIFFERENTIAL AMPLIFIER

As pointed out several times, the differential amplifier is a key building block of analog circuits, and hence it is important to understand the frequency response of the differential pair. An important element,  $C_{EE}$ , has been included in the differential amplifier circuit in Fig. 17.46(a).  $C_{EE}$  represents the total capacitance at the emitter node of the differential pair. Analysis of the frequency response of the symmetrical amplifier in Fig. 17.46(a) is greatly simplified through the use of the half-circuits in (b) and (c).

#### Differential-Mode Signals

We recognize the differential-mode half-circuit in Fig. 17.46(b) as being equivalent to the standard common-emitter stage. Thus, the bandwidth for differential-mode signals is determined by the  $r_{\pi o} C_T$  product that was developed in the analysis in Sec. 17.6, and we can expect amplifier gain-bandwidth products equal to a significant fraction of the  $f_T$  of the transistor. Because the emitter node is a virtual ground,  $C_{EE}$  has no effect on differential-mode signals.

#### Common-Mode Frequency Response

The important breakpoints in the Bode plot of the common-mode frequency response depicted in Fig. 17.47 can be determined from analysis of the common-mode half-circuit in Fig. 17.46(c). At very low frequencies, we know that the common-mode gain to either collector is small, given

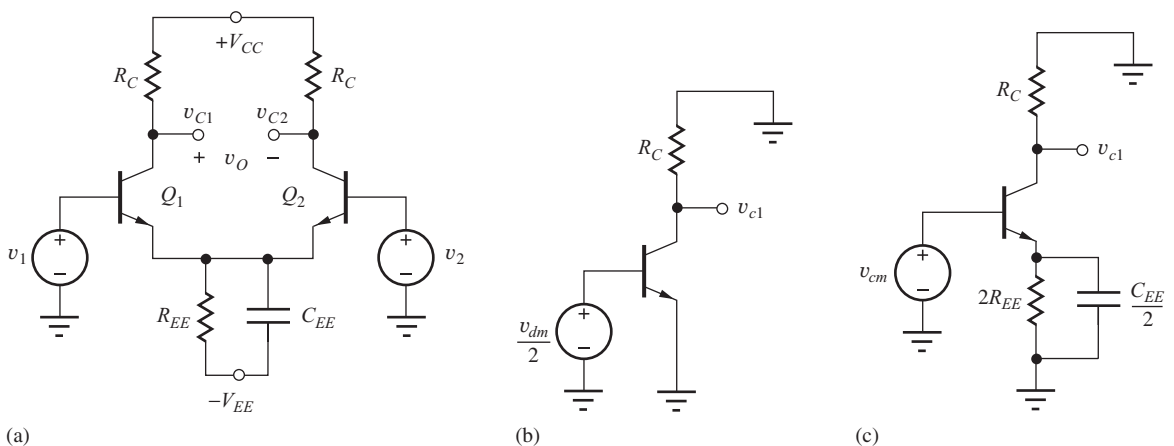


**Figure 17.46** (a) Bipolar differential amplifier, (b) its differential-mode half-circuit, and (c) its common-mode half-circuit.

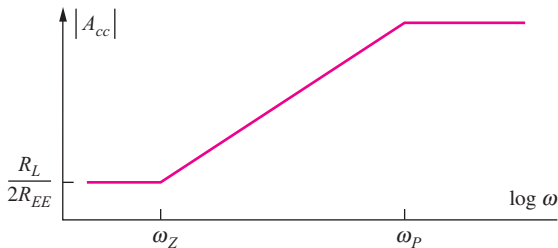


**Figure 17.47** Bode plot for the common-mode gain of the differential pair.

approximately by

$$|A_{cc}(0)| \cong \frac{R_C}{2R_{EE}} \ll 1 \quad (17.144)$$

However, capacitance  $C_{EE}$  in parallel with emitter resistor  $R_{EE}$  introduces a transmission zero in the common-mode frequency response at the frequency for which the impedance of the parallel combination of  $R_{EE}$  and  $C_{EE}$  becomes infinite. This zero is given by

$$s = -\omega_z = -\frac{1}{R_{EE}C_{EE}} \quad (17.145)$$

and typically occurs at relatively low frequencies. Although  $C_{EE}$  may be small, resistance  $R_{EE}$  is normally designed to be large, often the output resistance of a very high impedance current source. The presence of this zero causes the common-mode gain to increase at a rate of +20 dB/decade for frequencies above  $\omega_z$ . The common-mode gain continues to increase until the dominant pole of the pair is reached at relatively high frequencies.

The common-mode half-circuit is equivalent to a common-emitter stage with emitter resistor  $2R_{EE}$ . If we ignore base resistance  $r_x$ , we find that  $C_\pi$  and  $C_{EE}/2$  appear in parallel, and the OCTC method yields

$$\omega_p = -\frac{1}{\left(C_\pi + \frac{C_{EE}}{2}\right)R_{EEO}} \quad (17.146)$$

where  $R_{EEO}$  is the resistance at the terminals of  $C_{EE}/2$ :

$$R_{EEO} = \frac{1}{g_m} \|2R_{EE}\| r_\pi \cong \frac{1}{g_m} \quad (17.147)$$

The resulting pole position and common-mode gain are

$$\omega_p = -\frac{g_m}{C_\pi + \frac{C_{EE}}{2}} \quad \text{and} \quad A_{cc} = -\frac{g_m R_L}{1 + \frac{2C_\pi}{C_{EE}}} \quad (17.148)$$

**EXERCISE:** Find  $f_z$  and  $f_p$  for the common-mode response of the differential amplifier in Fig. 16.45 if  $r_x = 250 \Omega$ ,  $C_\mu = 0.5 \text{ pF}$ ,  $R_{EE} = 25 \text{ M}\Omega$ ,  $C_{EE} = 1 \text{ pF}$ , and  $R_C = 50 \text{ k}\Omega$ .

**ANSWERS:** 6.37 kHz, 6.34 MHz

### 17.10.2 THE COMMON-COLLECTOR/COMMON-BASE CASCADE

Figure 17.48(a) is an unbalanced version of the differential amplifier. This circuit can also be represented as the cascade of a common-collector and common-base amplifier, as in Fig. 17.48(b). The poles of this two-stage amplifier are found by using the results of the previous single-stage amplifier analyses.

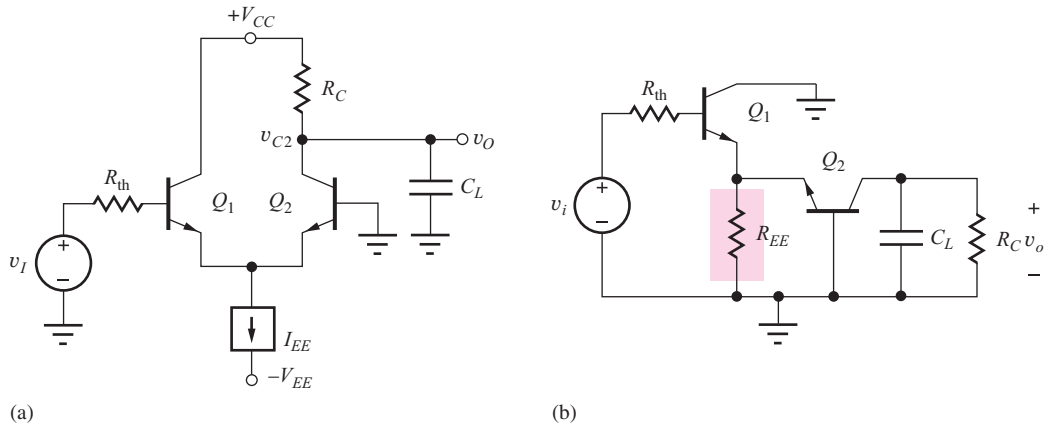


**Figure 17.48** (a) The unbalanced differential amplifier and (b) its representation as a C-C/C-B cascade.

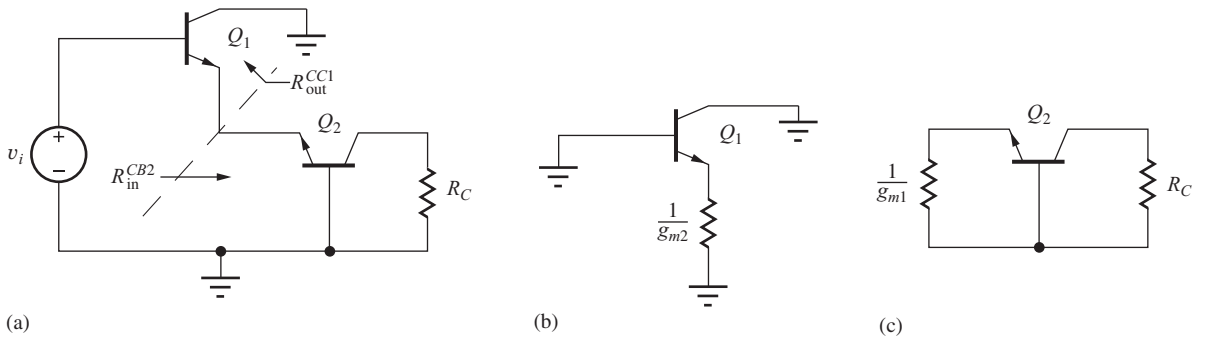


**Figure 17.49** (a) Equivalent circuits for analysis of the poles of (b) \$Q\_1\$ and (c) \$Q\_2\$.

We assume the output resistance \$R\_{EE}\$ of the current source is very large and neglect it in the analysis because the resistances presented at the emitters of \$Q\_1\$ and \$Q\_2\$ in Fig. 17.49 are both small:

$$R_{iE}^{CC1} = \frac{r_{x1} + r_{\pi 1}}{\beta_{o1} + 1} \cong \frac{1}{g_{m1}} \quad \text{and} \quad R_{iE}^{CB2} = \frac{r_{x2} + r_{\pi 2}}{\beta_{o2} + 1} \cong \frac{1}{g_{m2}} \quad (17.149)$$

The high-frequency response of the circuit of Fig. 17.49 is found by utilizing the results of the common-collector and common-base stages. We need to find estimates for the poles at the three nodes in the circuit; the base of \$Q\_1\$, the emitter of \$Q\_1\$, and the collector of \$Q\_2\$.

The pole at the input is that of a common-collector stage with \$R\_L = 1/g\_m\$.

$$\begin{aligned} \omega_{PB1} &= \frac{1}{([R_{th} + r_x] \parallel [r_{\pi 1} + (\beta_{o1} + 1)R_L]) \left( C_{\mu} + \frac{C_{\pi}}{1 + g_m R_L} \right)} \\ &= \frac{1}{([R_{th} + r_{x1}] \parallel [2r_{\pi 1}]) \left( C_{\mu 1} + \frac{C_{\pi 1}}{2} \right)} \end{aligned} \quad (17.150)$$

Notice that if the source impedance is zero, the input pole response is set by \$r\_x\$. The second pole occurs at the emitter of \$Q\_1\$ and \$Q\_2\$ where the capacitance is \$C\_{\pi 1} + C\_{\pi 2}\$, and the resistance is \$1/(g\_{m1} + g\_{m2})\$. The resulting pole frequency is

$$\omega_{PE} = \frac{g_{m1} + g_{m2}}{C_{\pi 1} + C_{\pi 2}} \cong \frac{2g_m}{2C_{\pi}} = \frac{g_m}{C_{\pi}} > \omega_T \quad (17.151)$$

and above the unity-gain frequency of the transistor.

$$\omega_{PC2} \cong \frac{1}{R_C(C_{\mu 2} + C_L)} \quad (17.152)$$

Depending on the impedances in the circuit, both the input and output poles could contribute significantly to the high-frequency response.

**EXERCISE:** Compare the values of midband gain and  $f_H$  for the differential amplifier in Fig. 17.46 and the C-C/C-B cascade in Fig. 17.48 if  $f_T = 500$  MHz,  $C_{\mu} = 0.5$  pF,  $I_{EE} = 200$   $\mu$ A,  $\beta_o = 100$ ,  $r_x = 250$   $\Omega$ , and  $R_C = 50$  k $\Omega$ .

**ANSWERS:** -198, 3.16 MHz, 99.0, 6.27 MHz.

### 17.10.3 HIGH-FREQUENCY RESPONSE OF THE CASCODE AMPLIFIER

The cascade of the common-emitter and common-base stages in Fig. 17.50 is referred to as the **cascode amplifier**. The cascode stage offers a midband gain and input resistance equal to that of the common-emitter amplifier but with a much improved upper-cutoff frequency  $f_H$ , as will be demonstrated by the forthcoming analysis.

The poles of the cascode stage follow directly from the analysis of the common-emitter and common-base stages using the model in Fig. 17.51. At the input to the cascode, we have the pole from our earlier analysis of this stage.

$$\omega_{PB1} = \frac{1}{r_{\pi 0} C_T} = \frac{1}{r_{\pi \phi} \left( [C_{\pi} + C_{\mu}(1 + g_m R_L)] + \frac{R_L}{r_{\pi 0}} [C_{\mu} + C_L] \right)} \quad (17.153)$$

Since the load of the first stage is small ( $1/g_m$ ) we expect the second capacitive term in this expression to be insignificant, allowing us to simplify the expression. The bias current of the two transistors is the same, so the  $g_m$  values of the two transistors are also equal.

$$\omega_{PB1} = \frac{1}{r_{\pi 01} \left( \left[ C_{\pi 1} + C_{\mu 1} \left( 1 + \frac{g_{m1}}{g_{m2}} \right) \right] + \frac{1/g_{m2}}{r_{\pi 01}} [C_{\mu 1} + C_{\pi 2}] \right)} \cong \frac{1}{r_{\pi 01} (C_{\pi 1} + 2C_{\mu 1})} \quad (17.154)$$

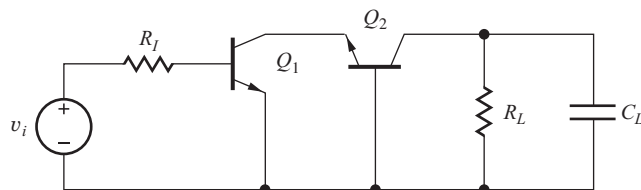


Figure 17.50 ac Model for the direct-coupled cascode amplifier.

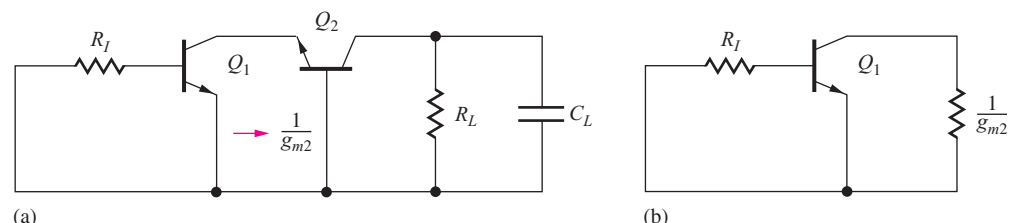


Figure 17.51 (a) Model for determining time constants associated with the two capacitances of  $Q_1$ . (b) Simplified model.

The term due to Miller multiplication of  $C_\mu$  has been reduced from a very large factor (264 in the C-E example in Sec. 17.6) to only 2, and the  $R_L/r_{\pi o}$  term has also been essentially eliminated. These reductions are the primary advantage of the cascode amplifier and can greatly increase the bandwidth of the overall amplifier.

Similar to the previous circuit, the intermediate node impedance is quite low. At high frequencies, roughly equal to  $1/g_{m2}$  (recall the high-frequency shunting of  $Q_1$  due to  $C_\mu$ ). Because of this, we may expect the pole at the intermediate node to be quite high frequency at approximately  $g_{m2}/(C_{\pi 2} + C_{\mu 1})$ .

The output pole is that of a common-base amplifier.

$$\omega_{PC2} \cong \frac{1}{R_L(C_{\mu 2} + C_L)} \quad (17.155)$$

Again, depending on the particular impedances in the circuit, both  $\omega_{PB1}$  and  $\omega_{PC2}$  could be significant in determining the overall high-frequency response.

**EXERCISE:** Find the midband value of  $A_v$  and the poles of the cascode amplifier in Fig. 17.50 assuming  $\beta_o = 100$ ,  $f_T = 500$  MHz,  $C_\mu = 0.5$  pF,  $r_x = 250$   $\Omega$ ,  $R_i = 882$   $\Omega$ ,  $R_L = 4.12$  k $\Omega$ ,  $C_L = 5$  pF, and a Q-point of (1.60 mA, 3.00 V) for  $Q_2$ .

**ANSWERS:** -151, 11.6 MHz, 7.02 MHz

#### 17.10.4 CUTOFF FREQUENCY FOR THE CURRENT MIRROR

As a final example of the analysis of direct-coupled amplifiers, let us find  $\omega_H$  for the current mirror configuration in Fig. 17.52. The small-signal model in Fig. 17.52(b) represents the two-port model developed in Sec. 16.2 with the addition of the gate-source and gate-drain capacitances of  $M_1$  and  $M_2$ . The gate-source capacitances of the two transistors appear in parallel, whereas the gate-drain capacitance of  $M_1$  is shorted out by the circuit connection. The open-circuited load condition at the output represents a worst-case situation for estimating the current mirror bandwidth.

The circuit in Fig. 17.52(b) should be recognized as identical to the simplified model of the C-E stage in Fig. 17.35, and the results of the  $C_T$  approximation are directly applicable to the current mirror circuit with the following substitutions:

$$r_{\pi o} \rightarrow \frac{1}{g_{m1}} \quad R_L \rightarrow r_{o2} \quad C_\pi \rightarrow C_{GS1} + C_{GS2} \quad C_\mu \rightarrow C_{GD2} \quad (17.156)$$

Using the values from Eq. (17.156) in Eq. (17.93),

$$\omega_{P1} \cong \frac{1}{r_{\pi o} C_T} = \frac{1}{\frac{1}{g_{m1}} \left[ C_{GS1} + C_{GS2} + C_{GD2} \left( 1 + g_{m2} r_{o2} + \frac{r_{o2}}{g_{m1}} \right) \right]} \quad (17.157)$$

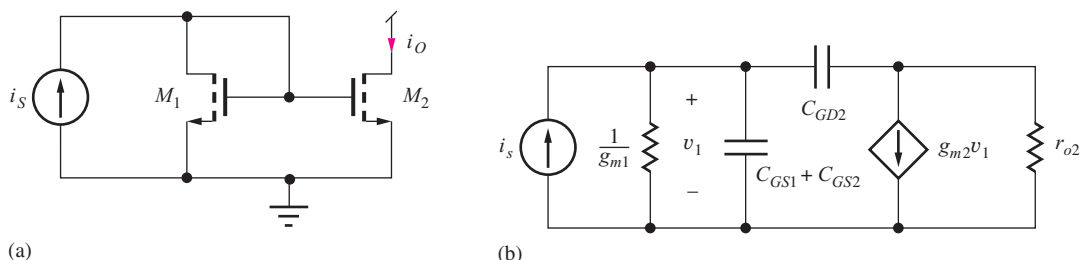


Figure 17.52 (a) MOS current mirror. (b) Small-signal model for the current mirror.

and for matched transistors with equal  $W/L$  ratios,

$$\omega_{P1} \cong \frac{1}{2C_{GS1} + 2C_{GD2}r_{o2}} \cong \frac{1}{2C_{GD2}r_{o2}} \quad (17.158)$$

Equation (17.95) can be used to find an estimate for the second pole

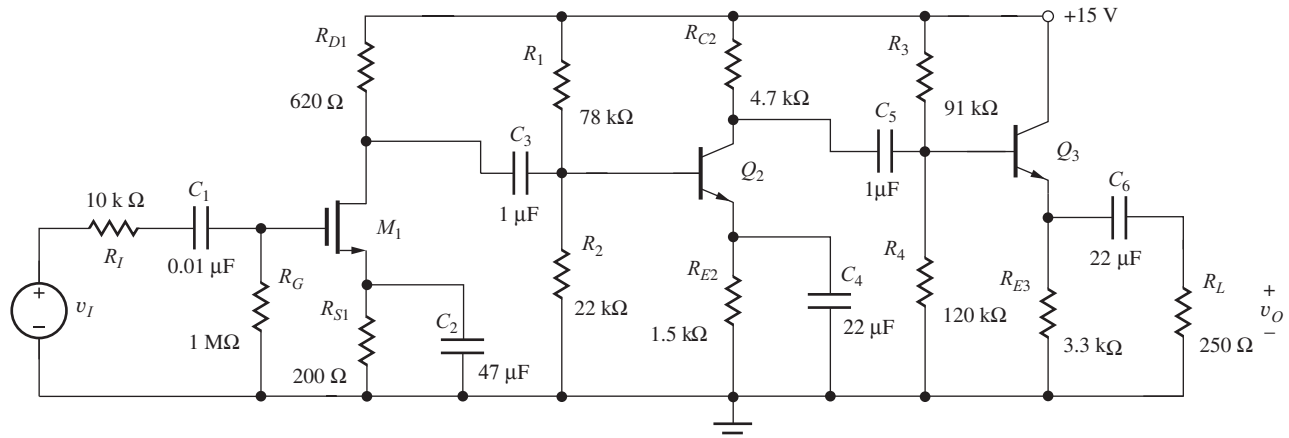
$$\omega_{P2} \cong \frac{g_L C_\pi + 2g_m C_\mu}{C_\pi C_\mu} = \frac{1}{R_L C_\mu} + \frac{2g_m}{C_\pi} > \omega_T \quad (17.159)$$

which is again above  $\omega_T$ .

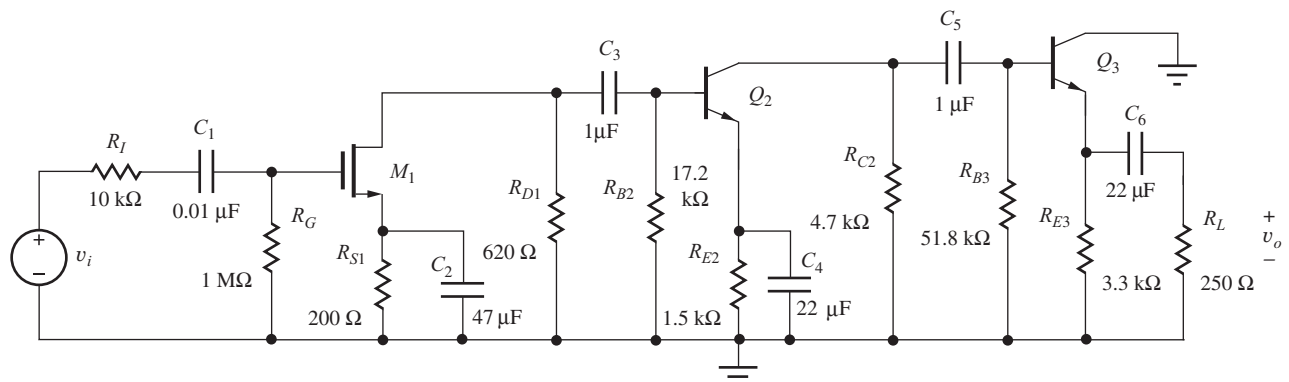
The result in Eq. (17.158) indicates that the bandwidth of the current mirror is controlled by the time constant at the output of the mirror due to the output resistance and gate-drain capacitance of  $M_2$ . Note that the value of Eq. (17.159) is directly proportional to the Q-point current through the dependence of  $r_{o2}$ .

**EXERCISE:** (a) Find the bandwidth of the current mirror in Fig. 17.52 if  $I_1 = 100 \mu\text{A}$ ,  $C_{GD} = 1 \text{ pF}$ , and  $\lambda = 0.02 \text{ V}^{-1}$ . (b) If  $I_1 = 25 \mu\text{A}$ .

**ANSWERS:** 159 kHz; 39.8 kHz



(a)



(b)

Figure 17.53 Three-stage amplifier and ac equivalent circuit.

### 17.10.5 THREE-STAGE AMPLIFIER EXAMPLE

As an example of a more complex analysis, let us estimate the upper- and lower-cutoff frequencies for the multistage amplifier in Fig. 17.53 that was introduced in Chapter 14. We will use the method of short-circuit time constants to estimate the lower-cutoff frequency. In Chapter 18 we will need to know specific pole locations to accurately estimate feedback amplifier stability, so we will illustrate the calculation of high-frequency poles with this multistage example.

#### EXAMPLE 17.8 MULTISTAGE AMPLIFIER FREQUENCY RESPONSE

The time constant methods are used to find the upper- and lower-cutoff frequencies of a multistage amplifier.

**PROBLEM** Use the direct calculation and the short-circuit time constant technique to estimate the upper- and lower-cutoff frequencies of a multistage amplifier.

**SOLUTION** **Known Information and Given Data:** Three-stage amplifier circuit in Fig. 17.53; Q-points and small-signal parameters are given in Tables 14.19 and 17.3.

**Unknowns:**  $f_H$ ,  $f_L$ , and bandwidth

**Approach:** The coupling and bypass capacitors determine the low-frequency response, whereas the device capacitances affect the high-frequency response. At low frequencies, the impedances of the internal device capacitances are very large and can be neglected. The coupling and bypass capacitors remain in the low-frequency ac equivalent circuit in Fig. 17.53(b), and an estimate for  $\omega_L$  is calculated using the SCTC approach. An estimate for the upper-cutoff frequency is calculated based on the calculation of individual high-frequency poles from our single-stage analyses. At high frequencies, the impedances of the coupling and bypass capacitors are negligibly small, and we construct the circuit in Fig. 17.54 by replacing the coupling and bypass capacitors by short circuits.

**TABLE 17.3**  
Transistor Parameters

	$g_m$	$r_\pi$	$r_o$	$\beta_o$	$C_{GS}/C_\pi$	$C_{GD}/C_\mu$	$r_x$
$M_1$	10 mS	$\infty$	12.2 k $\Omega$	$\infty$	5 pF	1 pF	0 $\Omega$
$Q_2$	67.8 mS	2.39 k $\Omega$	54.2 k $\Omega$	150	39 pF	1 pF	250 $\Omega$
$Q_3$	79.6 mS	1.00 k $\Omega$	34.4 k $\Omega$	80	50 pF	1 pF	250 $\Omega$

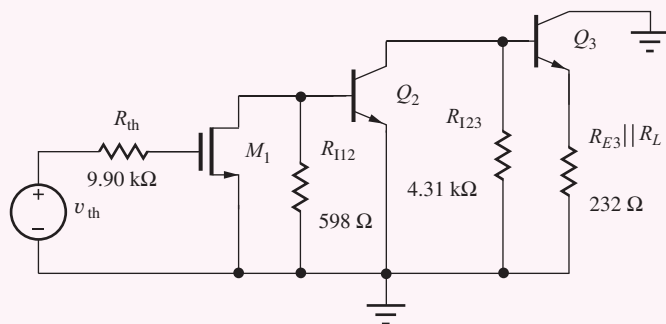


**Figure 17.54** High-frequency ac model for three-stage amplifier in Fig. 17.53.

We develop expressions for the various time constants using our knowledge of input and output resistances of single-stage amplifiers. Finally, the expressions can be evaluated using known values of circuit elements and small-signal parameters.

**Assumptions:** Transistors are in the active region. Small-signal conditions apply.  $V_T = 25 \text{ mV}$ .

**ANALYSIS** (a) **SCTC Estimate for the Lower-Cutoff Frequency  $\omega_L$ :** The circuit in Fig. 17.53(b) has six independent coupling and bypass capacitors; Fig. 17.55 gives the circuits for finding the six short-circuit time constants. The analysis proceeds using the small-signal parameters in Table 17.3.

**$R_{1S}$ :** Because the input resistance to  $M_1$  is infinite in Fig. 17.55(a),  $R_{1S}$  is given by

$$R_{1S} = R_I + R_G \| R_{iG} = 10 \text{ k}\Omega + 1 \text{ M}\Omega \| \infty = 1.01 \text{ M}\Omega \quad (17.160)$$

**$R_{2S}$ :**  $R_{2S}$  represents the resistance present at the source terminal of  $M_1$  in Fig. 17.55(b) and is equal to

$$R_{2S} = R_{S1} \left\| \frac{1}{g_{m1}} = 200 \Omega \right\| \frac{1}{0.01 \text{ S}} = 66.7 \Omega \quad (17.161)$$

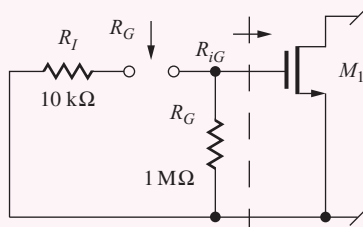
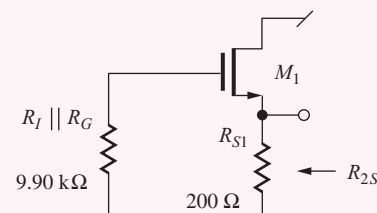
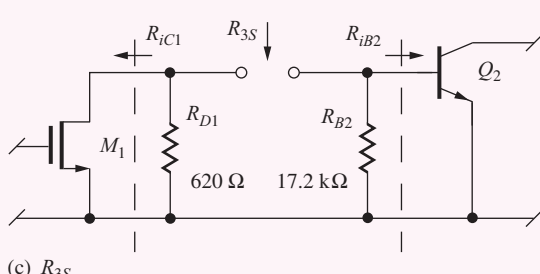
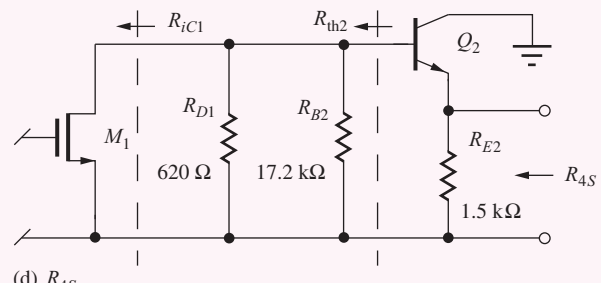
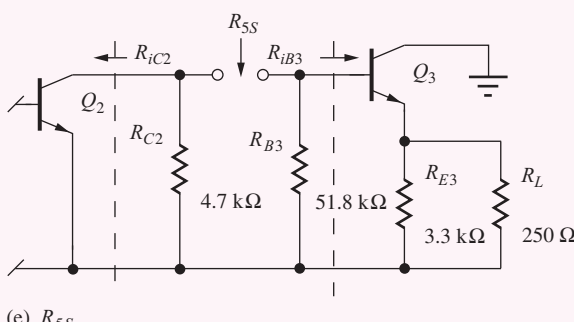
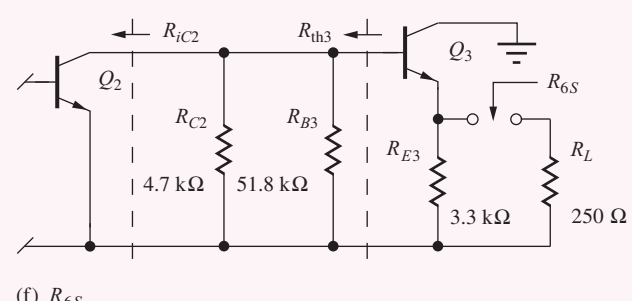
(a)  $R_{1S}$ (b)  $R_{2S}$ (c)  $R_{3S}$ (d)  $R_{4S}$ (e)  $R_{5S}$ (f)  $R_{6S}$ 

Figure 17.55 Subcircuits for finding the short-circuit time constants.

**R<sub>3S</sub>:** Resistance R<sub>3S</sub> is formed from a combination of four elements in Fig. 17.55(c). To the left, the output resistance of M<sub>1</sub> appears in parallel with the 620-Ω resistor R<sub>D1</sub>, and on the right the 17.2-kΩ resistor R<sub>B2</sub> is in parallel with the input resistance of Q<sub>2</sub>:

$$\begin{aligned} R_{3S} &= (R_{D1}\|R_{iC1}) + (R_{B2}\|R_{iB2}) = (R_{D1}\|r_{o1}) + (R_{B2}\|r_{\pi2}) \\ &= (620 \Omega\|12.2 \text{ k}\Omega) + (17.2 \text{ k}\Omega\|2.39 \text{ k}\Omega) = 2.69 \text{ k}\Omega \end{aligned} \quad (17.162)$$

**R<sub>4S</sub>:** R<sub>4S</sub> represents the resistance present at the emitter terminal of Q<sub>2</sub> in Fig. 17.55(d) and is equal to

$$R_{4S} = R_{E2} \left\| \frac{R_{\text{th}2} + r_{\pi2}}{(\beta_{o2} + 1)} \right\| \quad \text{where} \quad R_{\text{th}2} = R_{B2}\|R_{D1}\|R_{iC1} = R_{B2}\|R_{D1}\|r_{o1}$$

$$R_{\text{th}2} = R_{B2}\|R_{D1}\|r_{o1} = 17.2 \text{ k}\Omega\|620 \Omega\|12.2 \text{ k}\Omega = 571 \Omega \quad (17.163)$$

$$R_{4S} = 1500 \Omega \left\| \frac{571 \Omega + 2390 \Omega}{(150 + 1)} \right\| = 19.4 \Omega$$

**R<sub>5S</sub>:** Resistance R<sub>5S</sub> is also formed from a combination of four elements in Fig. 17.55(e). To the left, the output resistance of Q<sub>2</sub> appears in parallel with the 4.7-kΩ resistor R<sub>C2</sub>, and to the right the 51.8-kΩ resistor R<sub>B3</sub> is in parallel with the input resistance of Q<sub>3</sub>:

$$\begin{aligned} R_{5S} &= (R_{C2}\|R_{iC2}) + (R_{B3}\|R_{iB3}) = (R_{C2}\|r_{o2}) + (R_{B3}\|[r_{\pi3} + (\beta_{o3} + 1)(R_{E3}\|R_L)]) \\ &= (4.7 \text{ k}\Omega\|54.2) + 51.8 \text{ k}\Omega\|[1.00 \text{ k}\Omega + (80 + 1)(3.3 \text{ k}\Omega\|250 \Omega)] \\ &= 18.4 \text{ k}\Omega \end{aligned} \quad (17.164)$$

**R<sub>6S</sub>:** Finally, R<sub>6S</sub> is the resistance present at the terminals of C<sub>6</sub> in Fig. 17.55(f):

$$R_{6S} = R_L + \left( R_{E3} \left\| \frac{R_{\text{th}3} + r_{\pi3}}{\beta_{o3} + 1} \right\| \right) \quad \text{where} \quad R_{\text{th}3} = R_{B3}\|R_{C2}\|R_{iC2} = R_{B3}\|R_{C2}\|r_{o2}$$

$$R_{\text{th}3} = 51.8 \text{ k}\Omega\|4.7 \text{ }\Omega\|54.2 \text{ k}\Omega = 3.99 \text{ k}\Omega \quad (17.165)$$

$$R_{6S} = 250 \Omega + \left( 3.3 \text{ k}\Omega \left\| \frac{3.39 \text{ k}\Omega + 1.00 \text{ k}\Omega}{80 + 1} \right\| \right) = 311 \Omega$$

An estimate for ω<sub>L</sub> can now be constructed using Eq. (17.33) and the resistance values calculated in Eqs. (17.160) to (17.165):

$$\begin{aligned} \omega_L &\cong \sum_{i=1}^n \frac{1}{R_{iS}C_i} = \frac{1}{R_{1S}C_1} + \frac{1}{R_{2S}C_2} + \frac{1}{R_{3S}C_3} + \frac{1}{R_{4S}C_4} + \frac{1}{R_{5S}C_5} + \frac{1}{R_{6S}C_6} \\ &\cong \frac{1}{(1.01 \text{ M}\Omega)(0.01 \text{ }\mu\text{F})} + \frac{1}{(66.7 \text{ }\Omega)(47 \text{ }\mu\text{F})} + \frac{1}{(2.69 \text{ k}\Omega)(1 \text{ }\mu\text{F})} \\ &\quad + \frac{1}{(19.4 \text{ }\Omega)(22 \text{ }\mu\text{F})} + \frac{1}{(18.4 \text{ k}\Omega)(1 \text{ }\mu\text{F})} + \frac{1}{(311 \text{ }\Omega)(22 \text{ }\mu\text{F})} \\ &\cong 99.0 + 319 + 372 + 2340 + 54.4 + 146 = 3330 \text{ rad/s} \end{aligned} \quad (17.166)$$

$$f_L = \frac{\omega_L}{2\pi} = 530 \text{ Hz}$$

The estimate of the lower-cutoff frequency is 530 Hz. The dominant contributor is the fourth term, resulting from the time constant associated with emitter-bypass capacitor C<sub>4</sub>. (Remember the design approach used in Design Ex. 17.3.)

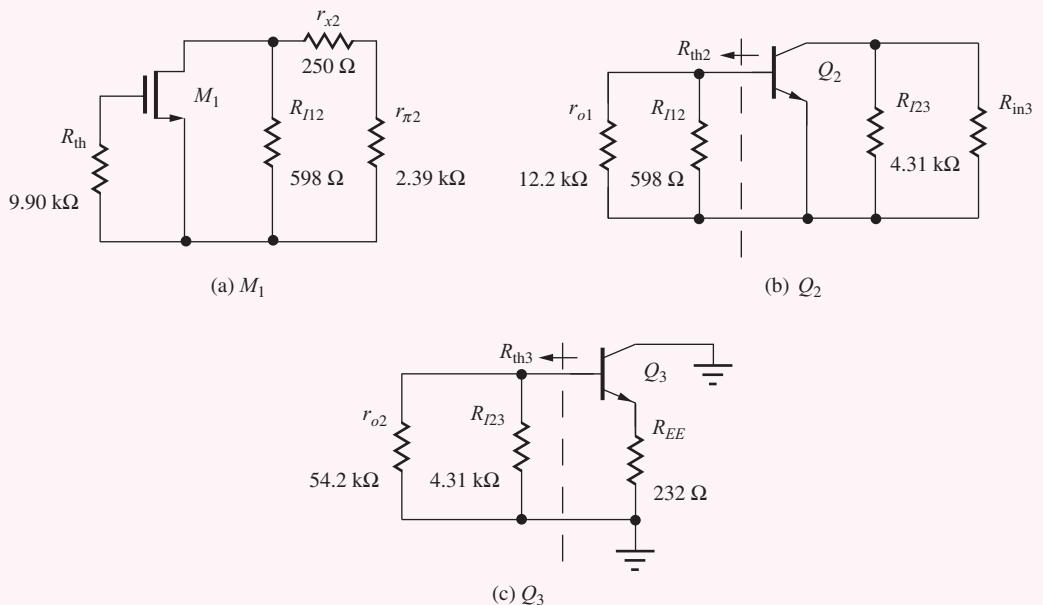


Figure 17.56 Subcircuits for evaluating the OCTC for each transistor.

**(b) Calculation of the Upper-Cutoff Frequency  $f_H$ :** The upper-cutoff frequency can be found by calculating the high-frequency poles at each of the nodes within the high-frequency ac model of the amplifier in Fig. 17.53 and then applying Eq. 17.22. At high frequencies, the impedances of the coupling and bypass capacitors are negligibly small, and we construct the circuit in Fig. 17.54 by replacing the coupling and bypass capacitors with short circuits. The high-frequency poles can be calculated at each node based on our single-stage analyses in Table 17.2.

**High-frequency pole at the gate of  $M_1$ :** From the subcircuit for the transistor in Fig. 17.56(a), we recognize this stage as a common-source stage. Using the  $C_T$  approximation from Table 17.2,

$$f_{p1} = \left( \frac{1}{2\pi} \right) \frac{1}{R_{th1}[C_{GS1} + C_{GD1}(1 + g_{m1}R_{L1}) + \frac{R_{L1}}{R_{th1}}(C_{GD1} + C_{L1})]} \quad (17.167)$$

For this circuit, the unbypassed source resistance is zero, so we use a simpler form of the input pole frequency equation. In Eq. (17.167), the Thévenin source resistance is  $9.9\text{ k}\Omega$ , and the load resistance is the parallel combination of resistances  $R_{I21}$ ,  $(r_{x2} + r_{\pi2})$ , and  $r_{o1}$ :

$$R_{L1} = R_{I12} \| r_{\pi2} + r_x \| r_{o1} = 598\text{ }\Omega \| (2.39\text{ k}\Omega + 250\text{ }\Omega) \| 12.2\text{ k}\Omega = 469\text{ }\Omega \quad (17.168)$$

We use the Miller effect to evaluate  $C_{L1}$ , the capacitance seen looking into the second stage common-emitter amplifier:

$$C_{L1} = C_{\pi2} + C_{\mu2}(1 + g_{m2}R_{L2}) \quad (17.169)$$

From Fig. 17.56(b), we evaluate  $R_{L2}$  as

$$\begin{aligned} R_{L2} &= R_{I23} \| R_{iB3} \| r_{o2} = R_{I23} \| [r_{x3} + r_{\pi3} + (\beta_{o3} + 1)(R_{E3} \| R_L)] \| r_{o2} \\ &= 4.31\text{ k}\Omega \| [250 + 1\text{ k}\Omega + (80 + 1)(3.3\text{ k}\Omega \| 250\text{ }\Omega)] \| 54.2\text{ k}\Omega \\ &= 3.33\text{ k}\Omega \end{aligned} \quad (17.170)$$

Using this result we find  $C_{L1}$  as

$$C_{L1} = 39\text{ pF} + 1\text{ pF}[1 + 67.8\text{ mS}(3.33\text{ k}\Omega)] = 266\text{ pF} \quad (17.171)$$

Combining these results, the pole at the input of  $M_1$  becomes

$$f_{p1} = \left( \frac{1}{2\pi} \right) \frac{1}{(9.9 \text{ k}\Omega)[1 \text{ pF}(1 + 0.01S(469 \Omega)] + 5 \text{ pF} + \frac{469 \Omega}{9.9 \text{ k}\Omega}(1 \text{ pF} + 266 \text{ pF})]} = 689 \text{ kHz} \quad (17.172)$$

**High-frequency pole at the base of  $Q_2$ :** From the subcircuit for the transistor in Fig 17.56(b), we recognize this stage as a common-emitter stage. At first glance we might expect to use the  $C_T$  approximation for the pole at the output of stage 1 and the input of stage 2. However, if we recall the detailed analysis of the common-source and common-emitter stage, we find that the output pole of the common-source stage is described by Eq. (17.95), rewritten here for the common-source case:

$$f_{p2} = \left( \frac{1}{2\pi} \right) \frac{C_{GS1}g_{L1} + C_{GD1}(g_{m1} + g_{th1} + g_{L1}) + C_{L1}g_{th1}}{[C_{GS1}(C_{GD1} + C_{L1}) + C_{GD1}C_{L1}]} \quad (17.173)$$

In this particular case,  $C_{L1}$  is much larger than the other capacitances, so Eq. (17.173) simplifies to

$$f_{p2} \cong \left( \frac{1}{2\pi} \right) \frac{C_{L1}g_{th1}}{[C_{GS1}C_{L1} + C_{GD1}C_{L1}]} \cong \left( \frac{1}{2\pi} \right) \frac{1}{R_{th1}(C_{GS1} + C_{GD1})} \quad (17.174)$$

Substituting for the appropriate parameters, we calculate  $f_{p2}$  as

$$f_{p2} = \left( \frac{1}{2\pi} \right) \frac{1}{(9.9 \text{ k}\Omega)(5 \text{ pF} + 1 \text{ pF})} = 2.68 \text{ MHz} \quad (17.175)$$

**High-frequency pole at the base of  $Q_3$ :** From the subcircuit for the transistor in Fig. 17.56(c), we recognize the third stage as a common-collector stage. Again, due to the pole splitting effect of the common-emitter second stage, we expect that the pole at the base of  $Q_3$  will be set by Eq. (17.95). In this case, due to the small load capacitance and high  $g_{m2}$  of the second stage, the  $g_{m2}C_\mu$  term simplification of Eq. (17.95) will dominate the numerator, and the first form of Eq. (17.95) will hold. However, since  $C_\mu$  is quite small, we cannot simplify Eq. (17.95) to the form that applies when  $C_\mu$  is large. As a consequence, we can expect the pole at the interstage node between  $Q_2$  and  $Q_3$  to be governed by

$$f_{p3} \cong \left( \frac{1}{2\pi} \right) \frac{g_{m2}}{\left[ C_{\pi2} \left( 1 + \frac{C_{L2}}{C_{\mu2}} \right) + C_{L2} \right]} \quad (17.176)$$

The load capacitance of  $Q_2$  is the input capacitance for the common-collector output stage. This is calculated as

$$C_{L2} = C_{\mu3} + \frac{C_{\pi3}}{1 + g_{m3}(R_{E3} \parallel R_L)} = 1 \text{ pF} + \frac{50 \text{ pF}}{1 + 79.6 \text{ mS}(3.3 \text{ k}\Omega \parallel 250 \Omega)} = 3.55 \text{ pF} \quad (17.177)$$

To account for  $r_{x2}$ , we can use  $g_m$  as defined in Eq. (17.70) when evaluating  $f_{p3}$ .

$$f_{p3} \cong \left( \frac{1}{2\pi} \right) \frac{67.8 \text{ mS}[1 \text{ k}\Omega/(1 \text{ k}\Omega + 250 \Omega)]}{\left[ 39 \text{ pF} \left( 1 + \frac{3.55 \text{ pF}}{1 \text{ pF}} \right) + 3.55 \text{ pF} \right]} = 47.7 \text{ MHz} \quad (17.178)$$

There is an additional pole at the emitter of  $Q_3$ , but that will be at a very high frequency due to the relatively low equivalent resistance and capacitance at the output. The midband to high frequency response can now be written as

$$\begin{aligned} A(f) &\cong \frac{A_{mid}}{\left( 1 + j \frac{f}{f_{p1}} \right) \left( 1 + j \frac{f}{f_{p2}} \right) \left( 1 + j \frac{f}{f_{p3}} \right)} \\ &\cong \frac{998 \text{ V/V}}{\left( 1 + j \frac{f}{689 \text{ kHz}} \right) \left( 1 + j \frac{f}{2.68 \text{ MHz}} \right) \left( 1 + j \frac{f}{47.7 \text{ MHz}} \right)} \end{aligned} \quad (17.179)$$

Applying Eq. (17.23), we estimate  $f_H$  as

$$f_H = \frac{1}{\sqrt{\frac{1}{f_{p1}^2} + \frac{1}{f_{p2}^2} + \frac{1}{f_{p3}^2}}} = 667 \text{ kHz} \quad (17.180)$$

**Check of Results:** SPICE is an excellent method to check an analysis of this complexity. After drawing the circuit with the schematic editor, we need to set the MOSFET and BJT parameters. We can set up the device parameters by referring back to Tables 14.18, 14.19, and 17.3. For the depletion-mode MOSFET,  $K_P = 10 \text{ mA/V}^2$ ,  $V_{TO} = -2 \text{ V}$ , and  $\text{LAMDA} = 0.02 \text{ V}^{-1}$ . For this simulation, it is easiest to add external capacitors in parallel with the MOSFET to represent  $C_{GS}$  and  $C_{GD}$ . The values are 5 pF and 1 pF, respectively.

For the BJTs,  $R_B = 250 \Omega$ ,  $B_F = 150$ , and  $V_A F = 80 \text{ V}$ , and we can let  $I_S$  take on its default value of 0.1 fA. The values of  $T_F$  can also be found using the data in Table 17.3:

$$T_{F2} = \frac{C_{\pi 2}}{g_{m2}} = \frac{39 \text{ pF}}{67.8 \text{ mS}} = 0.575 \text{ ns} \quad \text{and} \quad T_{F3} = \frac{50 \text{ pF}}{79.6 \text{ mS}} = 0.628 \text{ ns}$$

The collector-emitter voltages from Table 14.19 are  $V_{CE2} = 5.09 \text{ V}$  and  $V_{CE3} = 8.36 \text{ V}$ . To achieve values of 1 pF for each  $C_\mu$ , we must properly set the values of CJC:

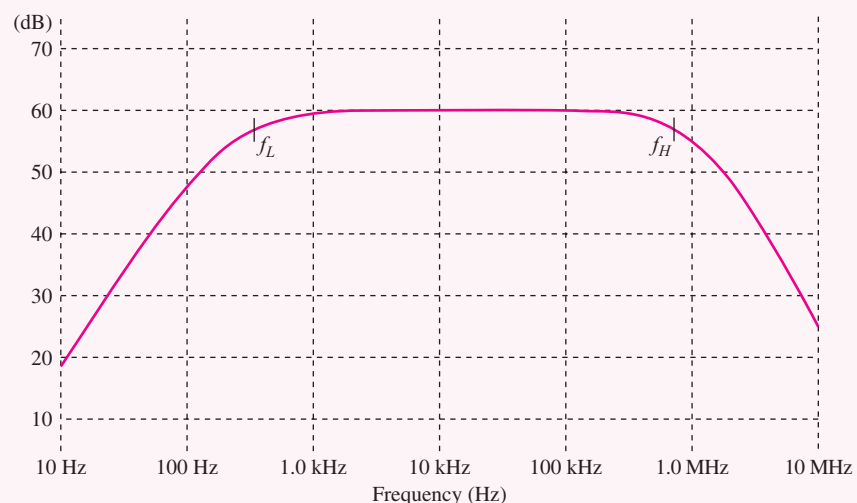
$$\text{CJC2} = (1 \text{ pF}) \left( 1 + \frac{5.09 - 0.7}{0.75} \right)^{0.33} = 1.89 \text{ pF}$$

and

$$\text{CJC3} = (1 \text{ pF}) \left( 1 + \frac{8.36 - 0.7}{0.75} \right)^{0.33} = 2.22 \text{ pF}$$

Once the parameters are set, an ac analysis can be performed with  $\text{FSTART} = 10 \text{ Hz}$ ,  $\text{FSTOP} = 10 \text{ MHz}$ , and 20 points per frequency decade. The resulting Bode magnitude plot appears next. We can also check the device parameters and see that the values of  $C_\pi$  and  $C_\mu$  are approximately correct.

**Discussion:** Note that common-source stage  $M_1$  and common-emitter stage  $Q_2$  are both making contributions to  $f_H$ , whereas follower  $Q_3$  represents a negligible contribution. Based on our calculated results, the midband region of the amplifier extends from  $f_L = 530 \text{ Hz}$  to  $f_H = 667 \text{ kHz}$  for a bandwidth  $\text{BW} = 666 \text{ kHz}$ .



The SPICE results indicate that  $f_L$  and  $f_H$  are approximately 350 Hz and 675 kHz, respectively, and the midband gain is 60 dB. In this amplifier, we see that the SCTC method is overestimating the value of the lower-cutoff frequency. If we look at Eq. (17.166), we see that there is clearly a dominant time constant. If we use only this value, we get much better agreement with the SPICE results:

$$f_L \cong \frac{2340}{2\pi} = 372 \text{ Hz}$$

On the other hand, our estimate of  $f_H$  is in good agreement with simulation. We did have to be quite careful with our calculations to take into account the pole splitting behavior of common-emitter and common-source amplifiers. If we had not taken this into account, the estimate for  $f_H$ , based on dominant-pole calculations for each of the stages, would be less than 550 kHz. Of even more importance for feedback amplifier design, our analysis in this example also accurately characterizes the phase and magnitude response well beyond  $f_H$ .

**EXERCISE:** Calculate the reactance of  $C_{\pi 2}$  at  $f_L$  and compare its value to  $r_{\pi 2}$ . Calculate the reactance of  $C_{\mu 3}$  and compare it to  $R_{B3} \| R_{in3}$  in Fig. 17.55(e).

**ANSWERS:**  $7.7 \text{ M}\Omega \gg 2.39 \text{ k}\Omega$ ;  $300 \text{ M}\Omega \gg 14.3 \text{ k}\Omega$

**EXERCISE:** Calculate the reactance of  $C_1$ ,  $C_2$ , and  $C_3$ , in Fig. 17.53(b) at  $f = f_H$ , and compare the values to the midband resistances in the circuit at the terminals of the capacitors.

**ANSWERS:**  $29.6 \Omega \ll 1.01 \text{ M}\Omega$ ;  $6.29 \text{ m}\Omega \ll 66.7 \Omega$ ;  $296 \text{ m}\Omega \ll 2.69 \text{ k}\Omega$

## 17.11 INTRODUCTION TO RADIO FREQUENCY CIRCUITS

Since its inception, radio frequency (RF) communications has had a pervasive influence on our lives and the way we communicate with each other. There are several important circuits that appear over and over again in RF devices such as our cell phones, radios, televisions, and so on. These include low-noise amplifiers, mixers, and oscillators.

For example, an architecture<sup>4</sup> for a hypothetical transceiver is shown in the block diagram in Fig. 17.57, and it could represent the RF portion of a device for a wireless local area network, or the transceiver for a cellular phone, depending upon the particular frequencies chosen for the design. In the 5-GHz digital radio system depicted here, the signal received from the antenna is amplified by a low-noise amplifier (LNA) and fed to two mixers, one for the in-phase (I) data channel and one for the quadrature (Q) data channel. Two quadrature<sup>5</sup> 5-GHz local oscillators (LOI and LOQ) are used to down-convert the incoming signals to low frequency base-band signals that are then amplified further by variable gain amplifiers and converted to digital form by the ADCs. Data is then recovered by the CMOS digital signal processor (DSP). On the transmit side, data is converted to analog form in the D/A converters and up-converted to the transmitting frequency by additional mixers and local oscillators. The signal level is increased by a power amplifier before being sent to the antenna. The next several sections will look at the basic building blocks of RF transceivers including RF amplifiers and mixers. High-frequency transistor oscillators are discussed in Chapter 18.

<sup>4</sup> Known as a “direct-conversion” architecture.

<sup>5</sup> That is, sine and cosine.

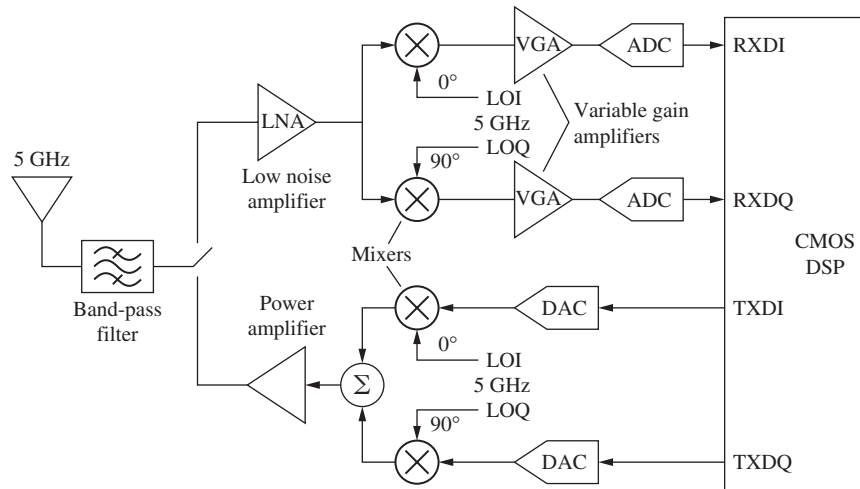


Figure 17.57 Example of an RF transceiver architecture.

### 17.11.1 RADIO FREQUENCY AMPLIFIERS

Sometimes we need a broad-band amplifier with a bandwidth extending from dc, or very low frequencies, well into the radio frequency range. A technique called **shunt peaking** utilizes an inductor to increase the bandwidth of the inverting amplifier with a capacitive load. However, RF amplifiers are more frequently needed with narrow bandwidths in order to select one signal from the large number that may be present (from an antenna, for example). The frequencies of interest are typically well above the unity gain frequency of operational amplifiers so that RC active filters cannot be used. These amplifiers often have high  $Q$ ; that is,  $f_H$  and  $f_L$  are very close together relative to the midband or center frequency of the amplifier. For example, a bandwidth of 20 kHz may be desired at a frequency of 1 MHz for an AM broadcast receiver application ( $Q = 50$ ), or a bandwidth of 200 kHz could be needed at 100 MHz for an FM broadcast receiver ( $Q = 500$ ). These applications often use resonant  $RLC$  circuits to form frequency selective **tuned amplifiers**.

### 17.11.2 THE SHUNT-PEAKED AMPLIFIER

In the shunt-peaked circuit [2], an inductor is added in series with the drain resistor as in Fig. 17.58(b). Inductor  $L$  forms a low  $Q$  resonant circuit with the circuit capacitance and enhances the bandwidth if the value of  $L$  is properly selected. As frequency goes up, the impedance of the inductor increases enhancing the gain.

The gain for the circuit in Fig. 17.58(a) is readily found to be

$$A_v(s) = \frac{V_o(s)}{V_i(s)} = -g_m Z_L = -g_m \frac{R}{1 + s(C_L + C_{GD})R} = -\frac{g_m R}{1 + sCR} \quad \text{for } C = C_L + C_{GD} \quad (17.181)$$

and exhibits a single-pole roll-off with bandwidth  $\omega_H = 1/RC$ , where  $C$  is the total equivalent load capacitance at the output node. Replacing  $R$  by  $(R + sL)$  in Eq. (17.181) yields the gain for the shunt-peaked stage:

$$A_{vsp} = -g_m \frac{R + sL}{1 + sCR + s^2LC} = -g_m R \frac{1 + sL/R}{1 + sRC + s^2LC} \quad (17.182)$$

Here the zero in the numerator tends to increase the gain as frequency goes up. Eventually the two poles in the denominator cause the gain to roll back off. The poles in the denominator can be

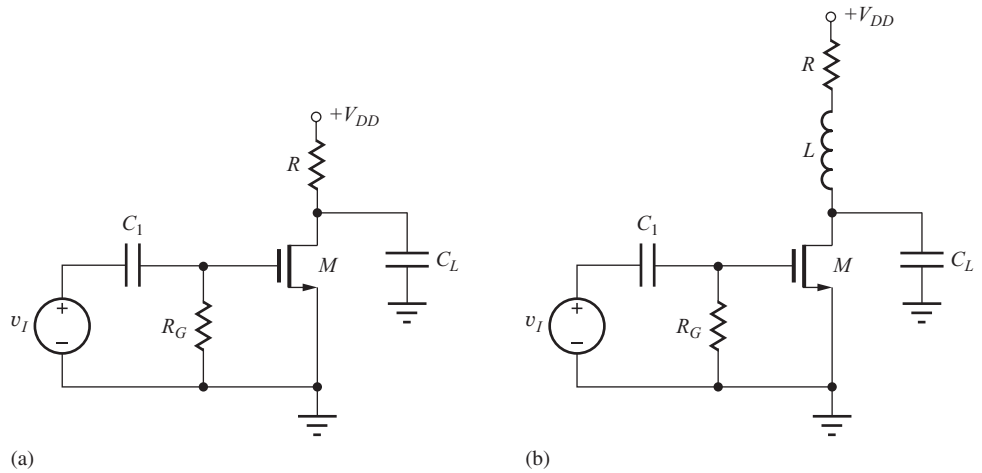
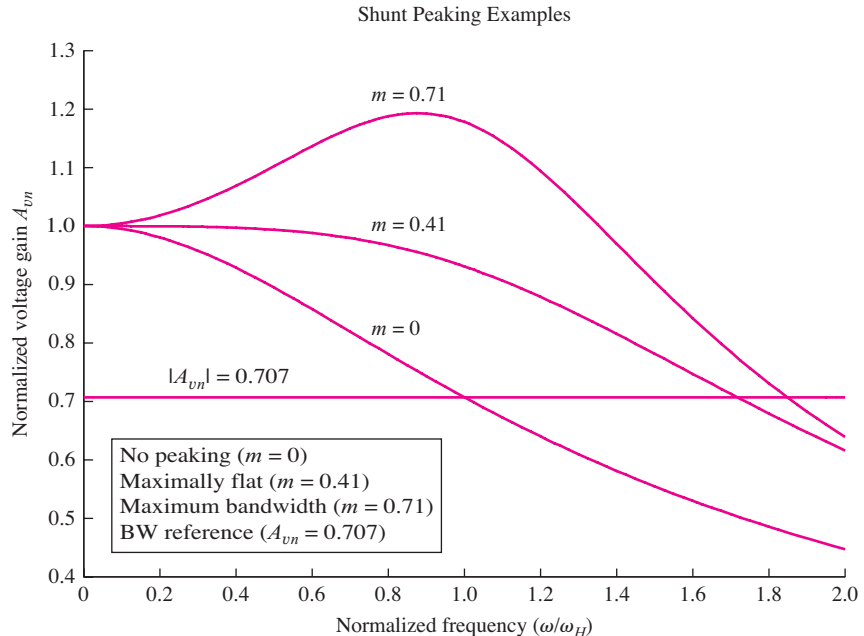


Figure 17.58 (a) Common-source amplifier with capacitive load. (b) Shunt-peaked amplifier.

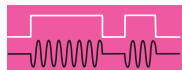
Figure 17.59 Shunt peaking bandwidth for various values of parameter  $m$ .

real or complex depending upon the element values but are often complex to achieve bandwidth extension.

The improvement in bandwidth available through shunt peaking may be explored by normalizing the  $A_{vsp}$  expression. Setting  $\omega_H = 1/RC = 1$  and defining parameter  $m$  as the ratio of the  $L/R$  and  $RC$  time constants [ $m = (L/R)/(RC)$ ], Eq. (17.182) can be rewritten as

$$A_{vn} = \left| \frac{A_{vsp}}{(-g_m R)} \right| = \frac{1 + ms}{1 + s + ms^2} \quad \text{where} \quad L = mR^2C \quad (17.183)$$

Equation (17.183) is plotted in Fig. 17.59 for several values of  $m$ . The  $m = 0$  case corresponds to no shunt peaking, and the bandwidth ( $|A_{vn}| = 0.707$ ) occurs for  $\omega/\omega_H = 1$  as expected. The maximally

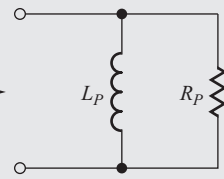
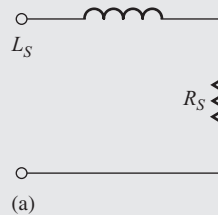


## ELECTRONICS IN ACTION



### RF Network Transformations

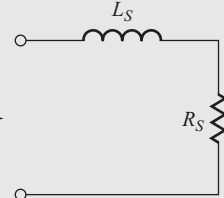
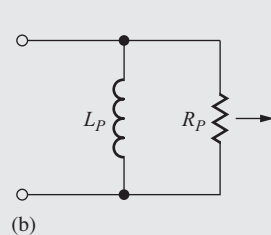
The figure below provides a very useful set of series-to-parallel and parallel-to-series conversions. The impedances or admittances of the networks are equal at the frequency used to calculate the transformation.



$$R_P = R_S(1 + Q_S^2)$$

$$L_P = L_S \left( \frac{1 + Q_S^2}{Q_S^2} \right)$$

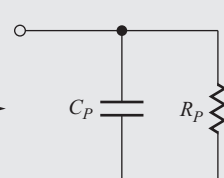
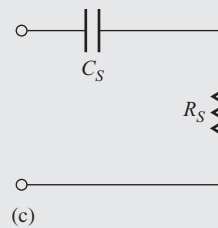
$$Q_S = \frac{\omega L_S}{R_S}$$



$$R_S = \frac{R_P}{1 + Q_P^2}$$

$$L_S = L_P \left( \frac{Q_P^2}{1 + Q_P^2} \right)$$

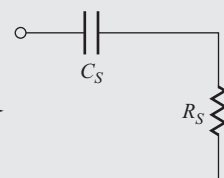
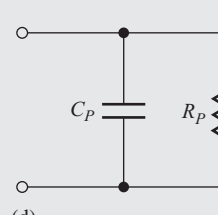
$$Q_P = \frac{R_P}{\omega L_P}$$



$$R_P = R_S(1 + Q_S^2)$$

$$C_P = C_S \left( \frac{Q_S^2}{1 + Q_S^2} \right)$$

$$Q_S = \frac{1}{\omega R_S C_S}$$



$$R_S = \frac{R_P}{1 + Q_P^2}$$

$$C_S = C_P \left( \frac{1 + Q_P^2}{Q_P^2} \right)$$

$$Q_P = \omega R_P C_P$$

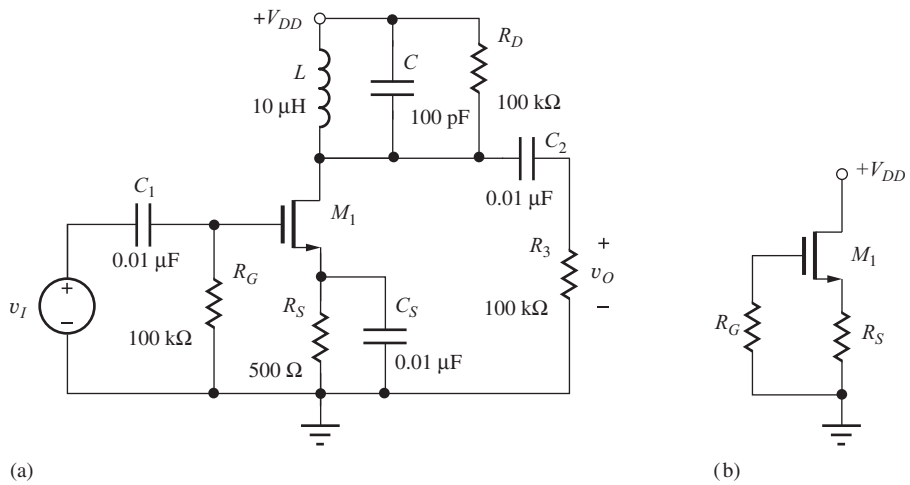
flat, or Butterworth, response occurs for  $m = 0.41$  and improves the bandwidth by a factor of 1.72. A maximum bandwidth of  $1.85\omega_H$  is achieved with  $m = 0.71$ , but significant peaking of the gain can be observed in Fig. 17.59.

In this section we have seen that shunt peaking can significantly improve the bandwidth of wide-band low-pass amplifiers. However, narrow-band (high  $Q$ ) tuned amplifiers are required in many applications, and these circuits are introduced in the next several sections.

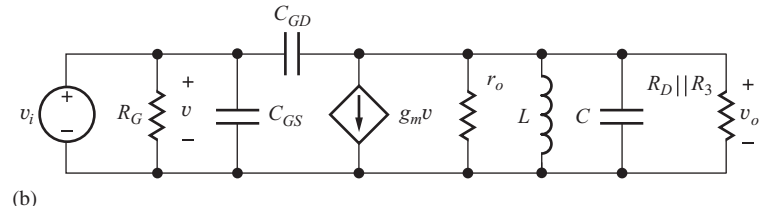
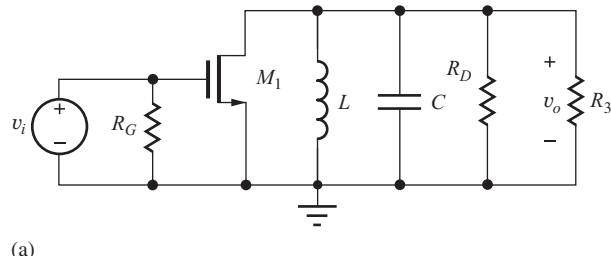
### 17.11.3 SINGLE-TUNED AMPLIFIER

Figure 17.60 is an example of a simple narrow-band tuned amplifier. A depletion-mode MOSFET has been chosen for this example to simplify the biasing, but any type of transistor could be used. The  $RLC$  network in the drain of the amplifier represents the frequency-selective portion of the circuit, and the parallel combination of resistors  $R_D$ ,  $R_3$ , and the output resistance  $r_o$  of the transistor set the  $Q$  and bandwidth of the circuit. Although resistor  $R_D$  is not needed for biasing, it is often included to control the  $Q$  of the circuit.

The operating point of the transistor can be found from analysis of the dc equivalent circuit in Fig. 17.60(b). Bias current is supplied through the inductor, which represents a direct short-circuit connection between the drain and  $V_{DD}$  at dc, and all capacitors  $C_1$ ,  $C_2$ ,  $C_S$ , and  $C$  have been replaced by open circuits. The actual Q-point can easily be found from Fig. 17.60(b) using the methods presented in previous chapters, so this discussion focuses only on the ac behavior of the tuned amplifier using the ac equivalent circuit in Fig. 17.61.



**Figure 17.60** (a) Tuned amplifier using a depletion-mode MOSFET. (b) dc equivalent circuit for the tuned amplifier in (a).



**Figure 17.61** (a) High-frequency ac equivalent circuit and (b) small-signal model for the tuned amplifier in Fig. 17.60.

Writing a single nodal equation at the output node  $v_o$  of the circuit in Fig. 17.61(b) and observing that  $v = v_i$  yields

$$(sC_{GD} - g_m)\mathbf{V}_I(s) = \mathbf{V}_o(s) \left[ g_o + G_D + G_3 + s(C + C_{GD}) + \frac{1}{sL} \right] \quad (17.184)$$

Making the substitution  $G_P = g_o + G_D + G_3$ , and then solving for the voltage transfer function:

$$A_v(s) = \frac{\mathbf{V}_o(s)}{\mathbf{V}_I(s)} = (sC_{GD} - g_m)R_P \frac{\frac{s}{R_P(C + C_{GD})}}{s^2 + \frac{s}{R_P(C + C_{GD})} + \frac{1}{L(C + C_{GD})}} \quad (17.185)$$

If we neglect the right-half-plane zero, then Eq. (17.185) can be rewritten as

$$A_v(s) \cong A_{\text{mid}} \frac{s \frac{\omega_o}{Q}}{s^2 + s \frac{\omega_o}{Q} + \omega_o^2} \quad \text{with} \quad \omega_o = \frac{1}{\sqrt{L(C + C_{GD})}} \quad (17.186)$$

In Eq. (17.186),  $\omega_o$  is the **center frequency** of the amplifier, and the  $Q$  is given by

$$Q = \omega_o R_P (C + C_{GD}) = \frac{R_P}{\omega_o L}$$

The center or midband frequency of the amplifier is equal to the resonant frequency  $\omega_o$  of the  $LC$  network. At the center frequency,  $s = j\omega_o$ , and Eq. (17.186) reduces to

$$A_v(j\omega_o) = A_{\text{mid}} \frac{j\omega_o \frac{\omega_o}{Q}}{(j\omega_o)^2 + j\omega_o \frac{\omega_o}{Q} + \omega_o^2} = A_{\text{mid}} \frac{j\omega_o \frac{\omega_o}{Q}}{-\omega_o^2 + j\omega_o \frac{\omega_o}{Q} + \omega_o^2} = A_{\text{mid}}$$

$$A_{\text{mid}} = -g_m R_P = -g_m (r_o \parallel R_D \parallel R_3) \quad (17.187)$$

For narrow bandwidth circuits — that is, high-Q circuits — the bandwidth is equal to

$$\text{BW} = \frac{\omega_o}{Q} = \frac{1}{R_P(C + C_{GD})} = \frac{\omega_o^2 L}{R_P} \quad (17.188)$$

A narrow bandwidth requires a large value of equivalent parallel resistance  $R_P$ , large capacitance, and/or small inductance. In this circuit, the maximum value of  $R_P = r_o$ . For this case, the  $Q$  is limited by the output resistance of the transistor and thus the choice of operating point of the transistor, and the midband gain  $A_{\text{mid}}$  equals the amplification factor  $\mu_f$ .

An example of the frequency response of a tuned amplifier is presented in the SPICE simulation results in Fig. 17.62 for the amplifier in Fig. 17.60. This particular amplifier design has a center frequency of 4.91 MHz and a  $Q$  of approximately 50.

**EXERCISE:** What is the impedance of the 0.01- $\mu\text{F}$  coupling and bypass capacitors in Fig. 17.60 at a frequency of 5 MHz?

**ANSWERS:**  $-j3.18 \Omega$  (note that  $X_C \ll R_G$  and  $X_C \ll R_3$ )

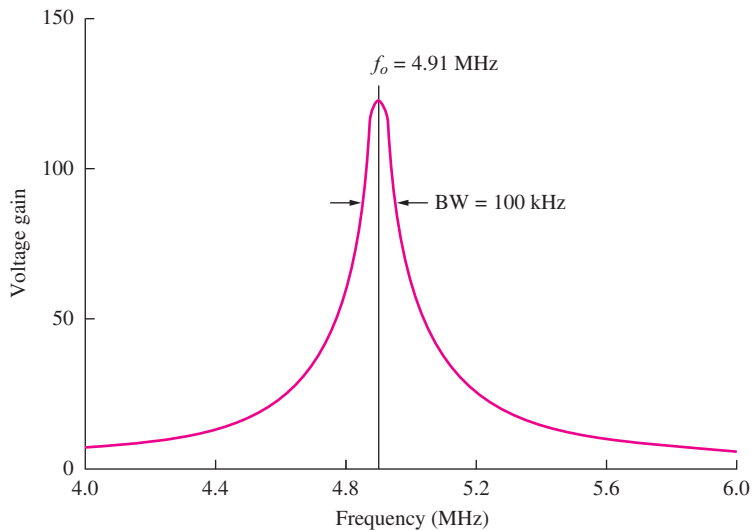


**Figure 17.62** Simulated frequency response for the tuned amplifier in Fig. 17.60 with  $C_{GS} = 50 \text{ pF}$ ,  $C_{GD} = 20 \text{ pF}$ ,  $V_{DD} = 15 \text{ V}$ ,  $K_n = 5 \text{ mA/V}^2$ ,  $V_{TN} = -2 \text{ V}$ , and  $\lambda = 0.02 \text{ V}^{-1}$ .

**EXERCISE:** Find the center frequency, bandwidth, Q, and midband gain for the amplifier in Fig. 17.60 using the parameters in Fig. 17.62, assuming  $I_D = 3.20 \text{ mA}$ .

**ANSWERS:** 4.59 MHz, 94.3 kHz, 49.2, -80.3

**EXERCISE:** What are the new values, of the center frequency and Q if  $V_{DD}$  is reduced to 10 V?

**ANSWER:** 4.59 MHz; 46.4

#### 17.11.4 USE OF A TAPPED INDUCTOR — THE AUTO TRANSFORMER

The impedance of the gate-drain capacitance and output resistance of the transistor,  $C_{GD}$ , and  $r_o$ , can often be small enough in magnitude to degrade the characteristics of the tuned amplifier. The problem can be solved by connecting the transistor to a tap on the inductor instead of across the full inductor, as indicated in Fig. 17.63. In this case, the inductor functions as an auto transformer and changes the effective impedance reflected into the resonant circuit.

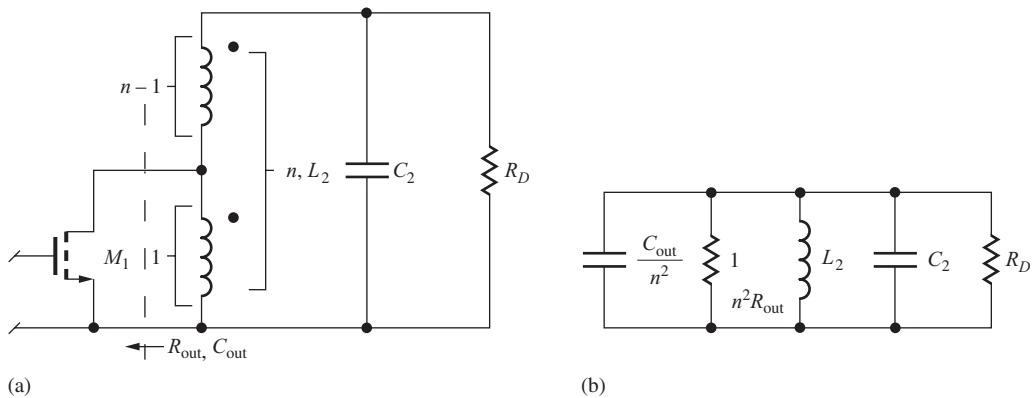


**Figure 17.63** (a) Use of a tapped inductor as an impedance transformer. (b) Transformed equivalent for the tuned circuit elements in Fig. 17.63(a). This circuit can be used to find  $\omega_o$  and  $Q$ .

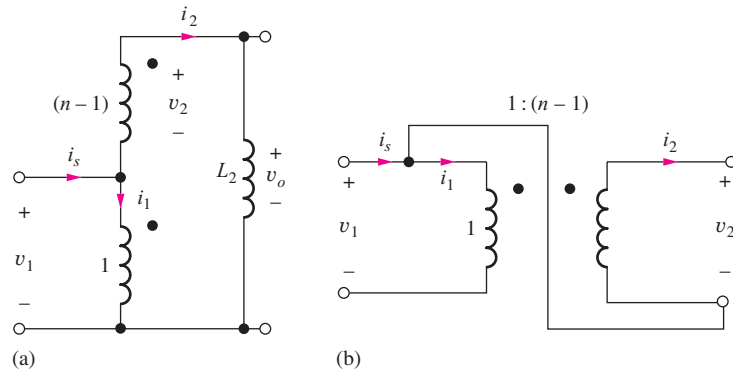


Figure 17.64 (a) Tapped inductor and (b) its representation by an ideal transformer.

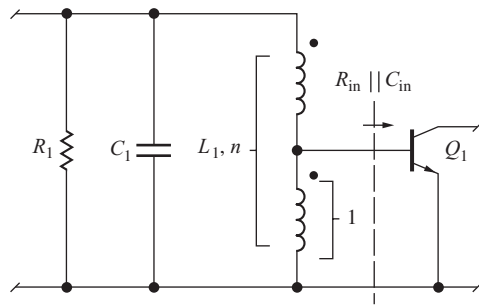
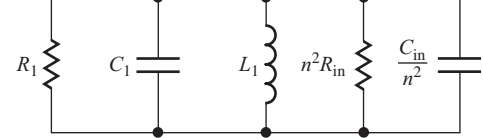
Figure 17.65 Use of an auto transformer at the input of transistor  $Q_1$ .

Figure 17.66 Transformed circuit model for the tuned circuit in Fig. 17.65.

The  $n$ -turn auto transformer can be modeled by its total magnetizing inductance  $L_2$  in parallel with an ideal transformer having a turns ratio of  $(n-1) : 1$ . The ideal transformer has its primary and secondary windings interconnected, as in Fig. 17.64(b). Impedances are transformed by a factor of  $n^2$  by the ideal transformer configuration:

$$\begin{aligned}\mathbf{V}_o(s) &= \mathbf{V}_2(s) + \mathbf{V}_1(s) = (n-1)\mathbf{V}_1(s) + \mathbf{V}_1(s) = n\mathbf{V}_1(s) \\ \mathbf{I}_s(s) &= \mathbf{I}_1(s) + \mathbf{I}_2(s) = (n-1)\mathbf{I}_2(s) + \mathbf{I}_2(s) = n\mathbf{I}_2(s)\end{aligned}\quad (17.189)$$

and

$$\frac{\mathbf{V}_o(s)}{\mathbf{I}_2(s)} = \frac{n\mathbf{V}_1(s)}{\mathbf{I}_s(s)} = n^2 \frac{\mathbf{V}_1(s)}{\mathbf{I}_s(s)} \quad Z_s(s) = n^2 Z_p(s) \quad (17.190)$$

Thus, the impedance  $Z_s(s)$  reflected into the secondary of the transformer is  $n^2$  times larger than the impedance  $Z_p(s)$  connected to the primary.

Using the result in Eq. (17.190), the resonant circuit in Fig. 17.63(a) can be transformed into the circuit representation in Fig. 17.63(b).  $L_2$  represents the total inductance of the transformer. The equivalent output capacitance of the transistor is reduced by the factor of  $n^2$ , and the output resistance is increased by this same factor. Thus, a much higher  $Q$  can be obtained, and the center frequency is not shifted (detuned) significantly by changes in the value of  $C_{GD}$ .

A similar problem often occurs if the tuned circuit is placed at the input of the amplifier rather than the output, as in Fig. 17.65. For the case of the bipolar transistor in particular, the equivalent input impedance of  $Q_1$  represented by  $R_{in}$  and  $C_{in}$  can be quite low due to  $r_\pi$  and the large input capacitance resulting from the Miller effect. The tapped inductor increases the impedance to that in Fig. 17.66, in which  $L_1$  now represents the total inductance of the transformer.

### 17.11.5 MULTIPLE TUNED CIRCUITS – SYNCHRONOUS AND STAGGER TUNING

Multiple  $RLC$  circuits are often needed to tailor the frequency response of tuned amplifiers, as in Fig. 17.67, which has tuned circuits at both the amplifier input and output. The high-frequency ac equivalent circuit for the double-tuned amplifier appears in Fig. 17.67(b). The source resistor is bypassed by capacitor  $C_S$ , and  $C_C$  is a coupling capacitor. The **radio frequency choke (RFC)** is used for biasing and is designed to represent a very high impedance (an open circuit) at the operating frequency of the amplifier.

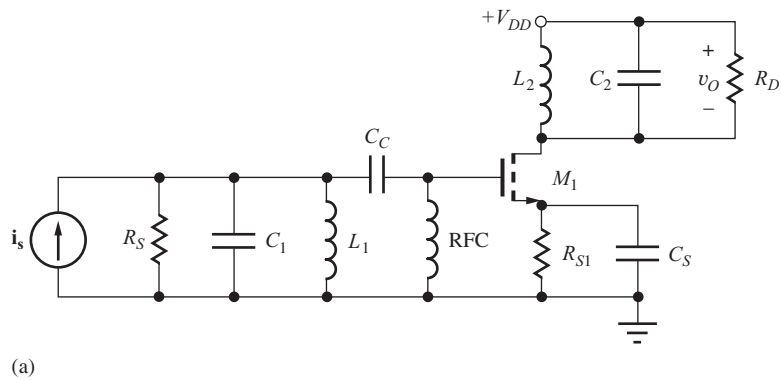
Two tuned circuits can be used to achieve higher  $Q$  than that of a single  $LC$  circuit if both are tuned to the same center frequency (**synchronous tuning**), or a broader band amplifier can be realized if the circuits are tuned to slightly different center frequencies (**stagger tuning**), as shown in Fig. 17.68. For the case of synchronous tuning, the overall bandwidth can be calculated using the bandwidth shrinkage factor that was developed in Chapter 12:

$$BW_n = BW_1 \sqrt{2^{\frac{1}{n}} - 1} \quad (17.191)$$

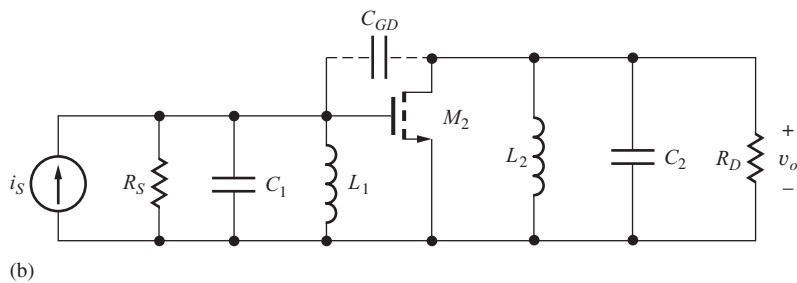
in which  $n$  is the number of synchronous tuned circuits, and  $BW_1$  is the bandwidth for the case of a single tuned circuit.

However, two significant problems can occur in the amplifier in Fig. 17.67, particularly for the case of synchronous tuning. First, alignment of the two tuned circuits is difficult because of interaction between the two tuned circuits due to the Miller multiplication of  $C_{GD}$ . Second, the amplifier can easily become an oscillator due to the coupling of signal energy from the output of the amplifier back to the input through  $C_{GD}$ .

A technique called **neutralization** can be used to solve this feedback problem but is beyond the scope of this discussion. However, two alternative approaches are shown in Fig. 17.69, in which the feedback path is eliminated. In Fig. 17.69(a), a cascode stage is used. Common-base transistor  $Q_2$



(a)



(b)

**Figure 17.67** (a) Amplifier employing two tuned circuits. (b) High-frequency ac model for the amplifier employing two tuned circuits.

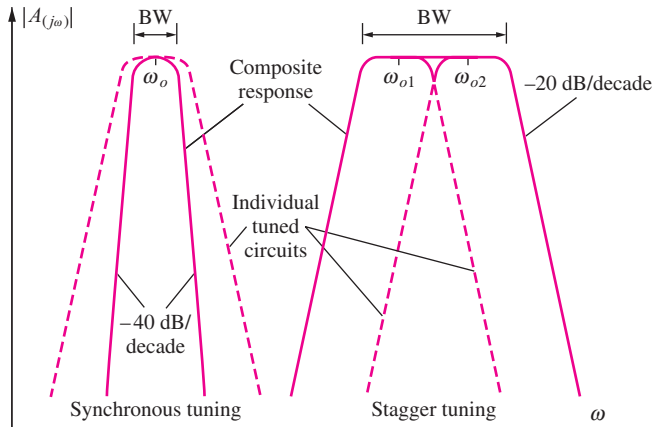


**Figure 17.68** Examples of tuned amplifiers employing synchronous and stagger tuning of two tuned circuits.

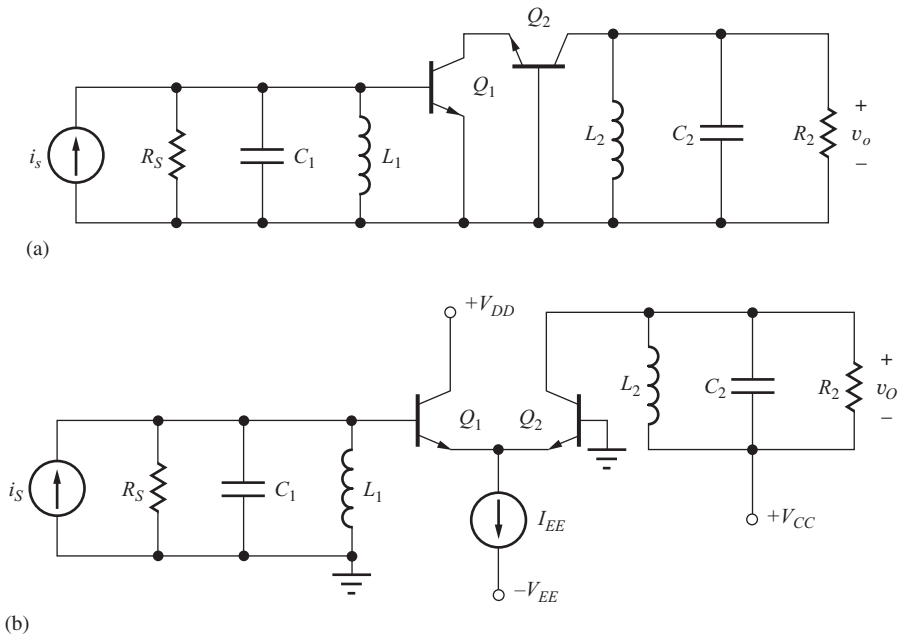


**Figure 17.69** (a) Double-tuned cascode and (b) C-C/C-B cascade circuits that provide inherent isolation between input and output.

effectively eliminates Miller multiplication and provides excellent isolation between the two tuned circuits. In Fig. 17.69(b), the C-C/C-B cascade is used to minimize the coupling between the output and input.

### 17.11.6 COMMON-SOURCE AMPLIFIER WITH INDUCTIVE DEGENERATION

In most RF systems, we desire to match the input resistance of the LNA to the resistance of the antenna, typically 50 or 75  $\Omega$ . In integrated circuits, the clever technique depicted in Fig. 17.70 creates an input match without the use of resistors that would degrade amplifier noise performance. The addition of inductor  $L_S$  in series with the source of transistor  $M_1$  creates a positive real component in  $Z_{in}$ .

Input impedance  $Z_{in}$  can be found using our knowledge of the input resistance of the common-collector and common-drain amplifiers. For the moment, we ignore the gate-drain capacitance of

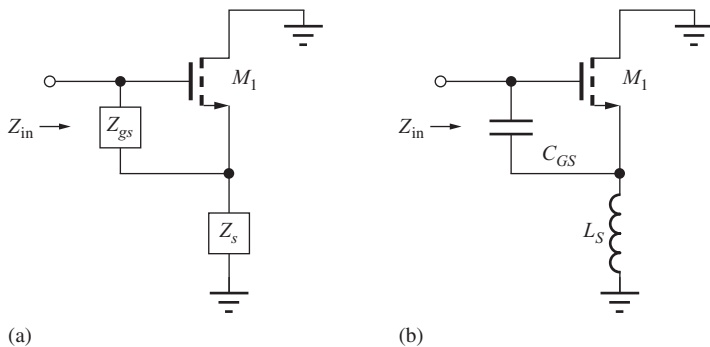


**Figure 17.70** (a) Generalized input impedance circuit. (b) NMOS transistor with inductive source impedance.

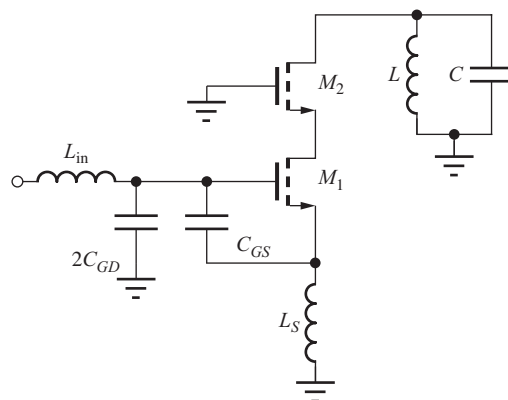


**Figure 17.71** Cascode LNA with inductor  $L_{in}$  added to cancel out the input capacitance part of the input impedance.

the transistor. Based upon our follower analyses, the input impedance of the amplifier is the sum of impedances  $Z_{GS}$  and  $Z_S$  plus an amplified replica of  $Z_S$ :

$$\begin{aligned} Z_{in}(s) &= Z_{GS} + Z_S + (g_m Z_{GS}) Z_S = \frac{1}{s C_{GS}} + s L_S + g_m \frac{L_S}{C_{GS}} \\ Z_{in}(s) &= \frac{1}{s C_{GS}} + s L_S + R_{eq} \quad \text{with} \quad R_{eq} = +g_m \frac{L_S}{C_{GS}} \end{aligned} \quad (17.192)$$

The input impedance is the series combination of the impedances of  $C_{GS}$  and  $L_S$  plus a real input resistance  $R_{eq}$  that can be adjusted to match 50 or 75  $\Omega$  with the proper choice of values for  $L_S$  and the  $W/L$  ratio and  $Q$ -point of the transistor. Normally  $L_S$  and  $C_{GS}$  are not resonant at the desired operating frequency.

In Fig. 17.71, a second inductor  $L_{in}$  is added in series with the input of the amplifier to resonate the input leaving a purely resistive input resistance. A cascode stage is usually utilized to minimize the impact of the gate-drain capacitance that reflects an equivalent capacitance of approximately  $2C_{GD}$  between the gate terminal and ground.

**EXERCISE:** Show that the input resistance can be written as  $R_{eq} = \omega_T L_S$ . What assumption did you make?

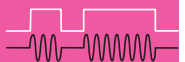
**ANSWER:**  $C_{GS} \gg C_{GD}$

**EXERCISE:** An NMOS transistor has  $\mu_n = 400 \text{ cm}^2/\text{V}\cdot\text{sec}$ ,  $L = 0.5 \mu\text{m}$  and is biased at 0.25 V above threshold. What value of  $L_s$  is required to achieve an input resistance of  $75 \Omega$  in Fig. 17.70(b)?

**ANSWER:** 1.88 nH



## ELECTRONICS IN ACTION

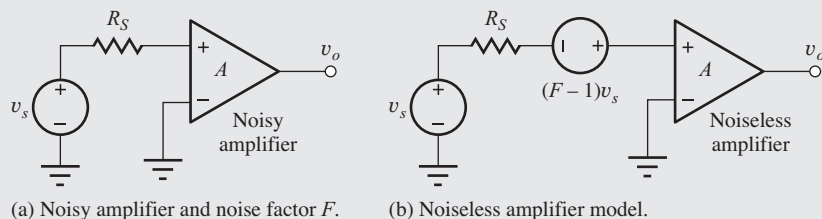


### Noise Factor, Noise Figure, and Minimum Detectable Signal

Resistors and transistors in amplifiers add thermal noise and shot noise to the signal during the amplification process (see the EIA on page 823). **Noise factor  $F$**  of an amplifier (or any electronic system) is a measure of the degradation of the **signal-to-noise ratio (SNR)** by these noisy elements where  $F$  is defined as the ratio of the total noise power at the output of the amplifier to the noise power at the output due to the noise of the source acting alone.  $F$  can also be expressed as the ratio of the SNR at the amplifier input to the SNR ratio at the output.

$$F = \frac{\text{Total noise power at the amplifier output}}{\text{Noise power at the output due to noise of the source}} = \frac{\text{SNR}_{\text{in}}}{\text{SNR}_{\text{out}}}$$

We can model the noise of the amplifier in terms of its noise factor as shown above where the “ $F - 1$ ” noise source is added to model the internal noise of the amplifier. The quantity  $F - 1$  indicates how much additional noise is added by the amplifier. If no noise were added, then  $F$  would be unity, and  $F - 1$  would be zero.



(a) Noisy amplifier and noise factor  $F$ .

(b) Noiseless amplifier model.

If the noise sources at the amplifier input are added up, the result is

$$\overline{v_{\text{tot}}^2} = \overline{v_s^2} + (F - 1)\overline{v_s^2} = F\overline{v_s^2} \quad \text{and} \quad F = \frac{\overline{v_{\text{tot}}^2}}{\overline{v_s^2}}$$

where  $\overline{v_s^2} = 4kT R_S B$  is the thermal noise of the source resistance in bandwidth  $B$ . **Noise figure  $NF$**  is the most often quoted quantity and is simply a conversion of the noise factor to dB:  $NF = 10 \log F$ .

The **minimum detectable signal (MDS)** is defined as the signal with a power equal to the equivalent input noise power of the amplifier. The total noise power available from the noise source in a matched system is

$$S_{\text{mds}} = \frac{\overline{v_{\text{tot}}^2}}{4R_S} = kTB$$

The minimum detectable signal power is most often expressed in dBm ( $10 \log S_{\text{mds}}/10^{-3}$ ), and for  $T = 290 \text{ K}$ ,

$$S_{\text{mds}} = -174 \text{ dBm} + 10 \log B + 10 \log F$$

## 17.12 MIXERS AND BALANCED MODULATORS

In radio frequency applications, we often need to translate signals from one frequency to another. This process includes both mixing and modulation, and generally requires some form of nonlinear multiplication of two signals in order to generate sum and difference frequency components in the output spectrum. **Single-balanced mixers** eliminate one of the two input signals from the output, whereas the outputs of **double-balanced circuits** do not contain spectral components at either of the input frequencies.

### 17.12.1 INTRODUCTION TO MIXER OPERATION

To achieve mixing, we need to multiply two signals together as indicated by the mixer symbol in Fig. 17.72. Suppose we form the product of two sine waves at frequencies  $\omega_1$  and  $\omega_2$  and expand the result using standard trigonometric identities:

$$s_o = s_1 \cdot s_2 = \sin \omega_2 t \cdot \sin \omega_1 t = \frac{\cos(\omega_2 - \omega_1)t - \cos(\omega_2 + \omega_1)t}{2} \quad (17.193)$$

The ideal mixer output contains signal components at frequencies  $\omega_2 - \omega_1$  and  $\omega_2 + \omega_1$ . Usually filters are used to select either the sum or difference output depending upon whether the application employs **up-conversion** ( $\omega_2 + \omega_1$ ) or **down-conversion** ( $\omega_2 - \omega_1$ ).

Figure 17.73 shows an FM receiver application in which a narrow-band VHF signal at 100 MHz is mixed with a **local oscillator** (LO) signal at 89.3 MHz. The narrow-band VHF spectrum is translated to both 10.7 MHz, which is selected by a band-pass filter, and 189.3 MHz, which is rejected by the same filter.

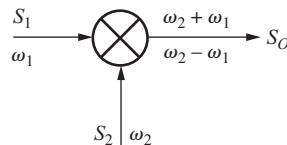


**Figure 17.72** Basic mixer symbol indicating multiplication of signals  $s_1$  and  $s_2$ .

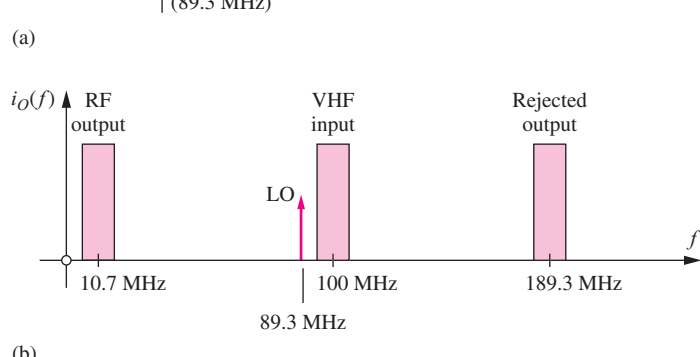
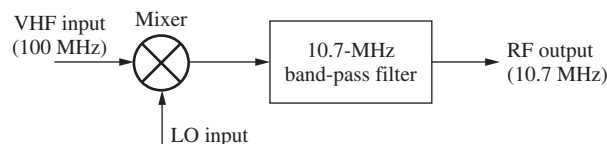


**Figure 17.73** (a) Mixer block diagram and (b) spectrum in FM receiver application.

**EXERCISE:** The LO signal in Fig. 17.73 could also be positioned above the VHF frequency. What would then be the local oscillator frequency and the center frequency of the unwanted output frequency signal?

**ANSWERS:** 110.7 MHz; 210.7 MHz

**EXERCISE:** (a) An FM receiver is to be tuned to receive a station at 104.7 MHz. What must be the local oscillator frequencies to set the output to the 10.7-MHz filter frequency? (b) Repeat for an input frequency of 88.1 MHz.

**ANSWERS:** 94.0 MHz or 115.4 MHz; 77.4 MHz or 98.8 MHz

### Conversion Gain

In the amplifiers covered thus far in this text, gain expressions have generally involved signals at the same frequency. We have assumed that the amplifiers were linear and that the input and output signals were at the same frequency. In fact, a component at any other frequency was considered to be an undesirable distortion product. (Remember the definition of THD, total harmonic distortion.)

In contrast, the mixer is a nonlinear device in which the output signals are at frequencies different from those at the input. A mixer's conversion gain is defined as the ratio of the phasor representation of the output signal to that of the input signal, and the fact that the signals are at two different frequencies is simply ignored. For example, the conversion gain of the mixer described by Eq. 17.193 is 0.5 or  $-6$  dB for either output frequency.

Almost any nonlinear device can be used for mixing. For example, the  $i - v$  characteristics of diodes, bipolar transistors, and field-effect transistors all contain quadratic (and higher) nonlinear terms in their mathematical representations and can therefore generate a wide range of product terms. However, we will focus in the next sections on switching mixers that have relatively high conversion gains (i.e., low conversion losses).

#### 17.12.2 A SINGLE-BALANCED MIXER

There is actually no need for both signals to be sine waves in the mixer in Fig. 17.72. It is very convenient for one of the inputs to be a switching waveform, and the conversion gain is actually higher if a square wave is utilized. In its simplest form, the switching mixer consists of a signal source, a switch, and a load as depicted in Fig. 17.74(a). When the switch is closed, the output is equal to the input signal, and when the switch is open, the output is zero. Thus the output voltage is equal to input voltage  $v_I(t)$  multiplied by the square-wave switching function  $s_S(t)$  in Fig. 17.74(b). If we assume that the input signal is a sine wave and represent the square wave by its Fourier series,

$$v_I(t) = A \sin \omega_1 t \quad \text{and} \quad s_S(t) = \frac{1}{2} + \frac{2}{\pi} \sum_{n \text{ odd}} \frac{1}{n} \sin n\omega_2 t \quad \text{with} \quad \omega_2 = \frac{2\pi}{T} \quad (17.194)$$

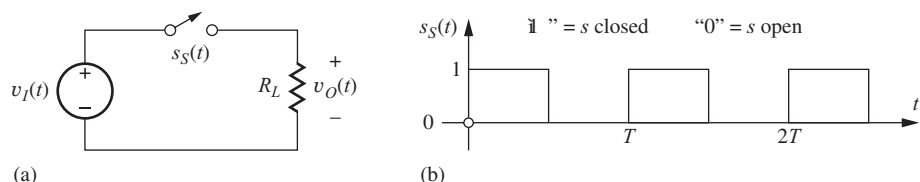


**Figure 17.74** (a) Single-balanced mixer and (b) switching function  $s_S(t)$ .

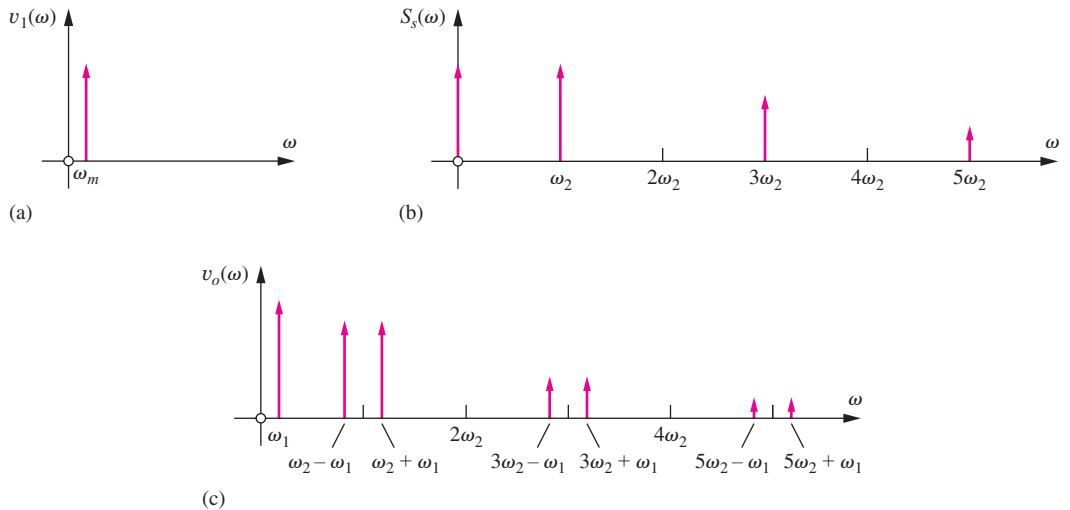


Figure 17.75 Single-balanced mixer spectra. (a) Input 1, (b) input 2, (c) output.

then an expression for the output voltage becomes

$$v_O(t) = v_I \times s_S = \frac{A}{2} \sin \omega_1 t + \frac{2A}{\pi} \sum_{n \text{ odd}} \frac{1}{n} \sin n\omega_2 t \sin \omega_1 t$$

or

$$v_O(t) = \frac{A}{2} \sin \omega_1 t + \frac{A}{\pi} \sum_{n \text{ odd}} \frac{\cos(n\omega_2 - \omega_1)t - \cos(n\omega_2 + \omega_1)t}{n} \quad (17.195)$$

As a result of the mixing operation, the spectrum of the output signal has a component at the original input signal frequency  $\omega_1$ , and copies of the input signal translated by odd multiples of switching frequency  $\omega_2$  as in Fig. 17.75(c). The terms corresponding to  $n = 1$  are the most often utilized since they have the highest conversion gain.

Note that there are no components in the output at harmonics of the switching frequency  $\omega_2$ , whereas there is a component at  $\omega_1$ . This output is said to be single-balanced because only one of the fundamental input frequencies is eliminated from the output; the mixer in Fig. 17.75 is balanced with respect to  $s_S$ .

**EXERCISE:** What is the conversion gain of the single-balanced mixer in Fig. 17.73?

**ANSWER:**  $1/\pi$  or  $-9.94 \text{ dB}$

### 17.12.3 THE DIFFERENTIAL PAIR AS A SINGLE-BALANCED MIXER

One concept for a single-balanced mixer appears in Fig. 17.76(a) with the switch implemented using a differential pair in Fig. 17.76(b). A signal  $v_1$  at frequency  $\omega_1$  is used to vary the current supplied to the emitters of the pair:

$$i_{EE} = I_{EE} + I_1 \sin \omega_1 t \quad (17.196)$$

The second input is driven by a large-signal square wave at frequency  $\omega_2$ , which switches current  $i_{EE}$  back and forth between the two collectors (just as in the ECL gate discussed in Chapter 9), and alternately multiplies the differential output voltage by  $+1$  and  $-1$ . This multiplication can be

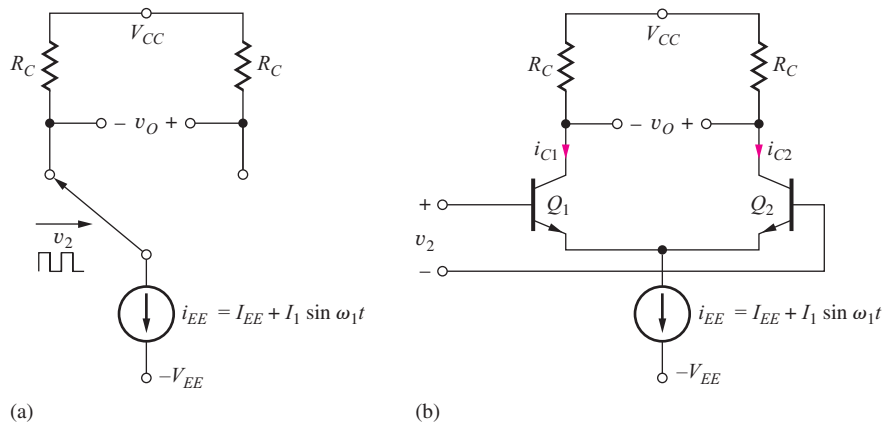


**Figure 17.76** (a) Basic single-balanced mixer. (b) Differential pair implementation.

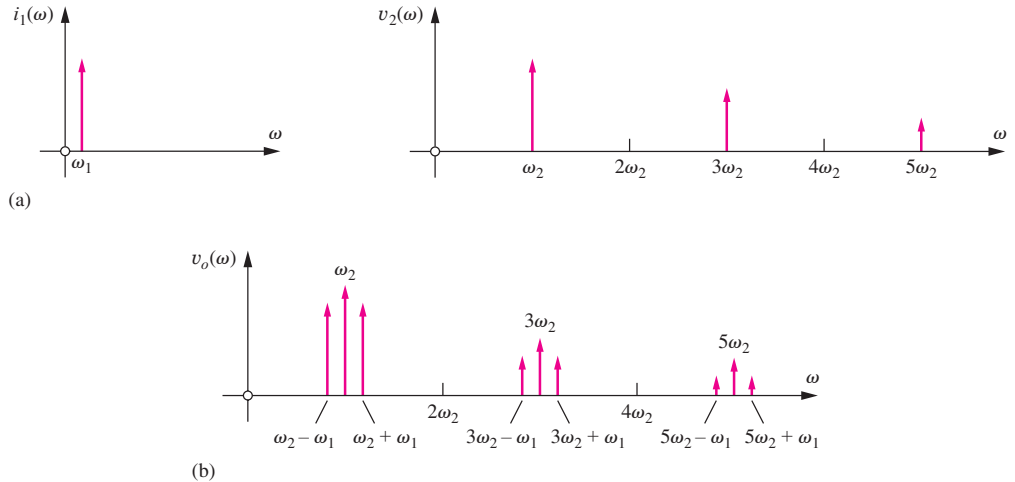


**Figure 17.77** (a) Input and (b) output spectra for the mixer in Fig. 17.76.

represented by a unit amplitude square wave with a Fourier series given by

$$v_2(t) = \sum_{n \text{ odd}} \frac{4}{n\pi} \sin n\omega_2 t \quad (17.197)$$

Using Eqs. (17.196) and (17.197),

$$v_O(t) = [i_{C2}(t) - i_{C1}(t)]R_C = (I_{EE} + I_1 \sin \omega_1 t)R_C \sum_{n \text{ odd}} \frac{4}{n\pi} \sin n\omega_2 t \quad (17.198)$$

$$V_O(t) = \sum_{n \text{ odd}} \frac{4}{n\pi} \left[ I_{EE} R_C \sin n\omega_2 t + \frac{I_1 R_C}{2} \cos(n\omega_2 - \omega_1)t - \frac{I_1 R_C}{2} \cos(n\omega_2 + \omega_1)t \right]$$

The input and output spectra for the differential pair mixer appear in Fig. 17.77. The mixer in Fig. 17.76 is actually balanced relative to the input signal at frequency  $\omega_1$  rather than  $\omega_2$  as was the case in Fig. 17.74.

#### 17.12.4 A DOUBLE-BALANCED MIXER

In many cases, we prefer to eliminate both signals from the output, and the double-balanced mixer solves this problem. If we study Eqs. (17.195) and (17.198), we see that the source of the balance

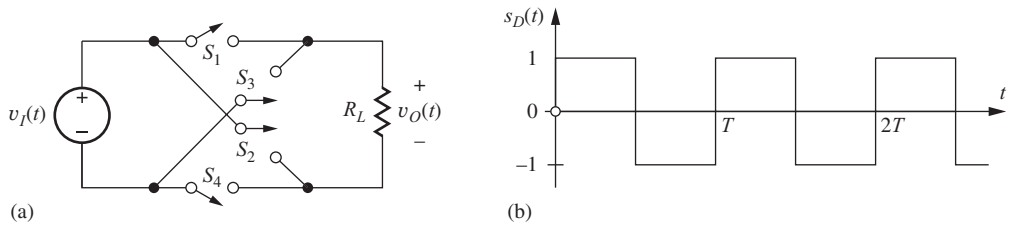
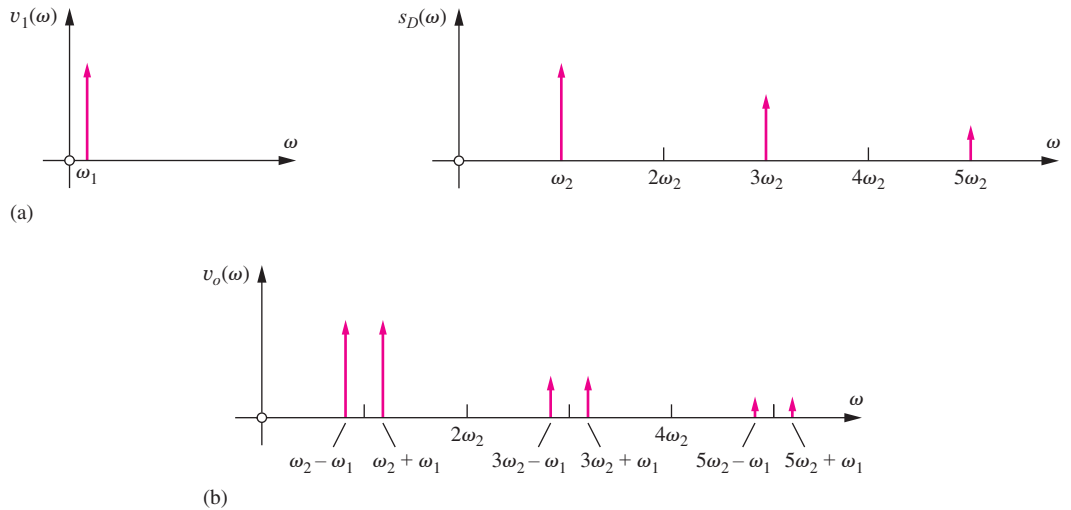
Figure 17.78 (a) Double-balanced mixers and (b) switching waveform  $s_D(t)$ .

Figure 17.79 (a) Input and (b) output spectra for the mixer in Fig. 17.78.

problem is the dc term in the switching waveform, but the dc component can be eliminated by using four switches to modify the switching function as in Fig. 17.78. During the first half of the switching cycle, switches  $S_1$  and  $S_4$  are closed and the input source is connected directly to the output, but during the second half-cycle, switches  $S_2$  and  $S_3$  are closed reversing the polarity of the input signal. Thus the switching waveform alternates between +1 and -1 with zero average value!

The Fourier series for the switching waveform is now

$$s_D(t) = \frac{4}{\pi} \sum_{n \text{ odd}} \frac{1}{n} \sin n\omega_2 t \quad \text{where } \omega_0 = \frac{2\pi}{T} \quad (17.199)$$

and the output signal becomes

$$v_O(t) = \frac{2A}{\pi} \sum_{n \text{ odd}} \frac{\cos(n\omega_2 - \omega_1)t - \cos(n\omega_2 + \omega_1)t}{n} \quad (17.200)$$

Neither of the fundamental components of the input signals appears in the output in Fig. 17.79. Note however that the degree of balance depends upon the symmetry of the square wave, and any asymmetry between the two half cycles will produce a dc term that degrades the rejection of the undesired output signal.

**EXERCISE:** What is the conversion gain for the double-balanced mixer in Fig. 17.78?

**ANSWER:**  $2/\pi$  or  $-3.92 \text{ dB}$

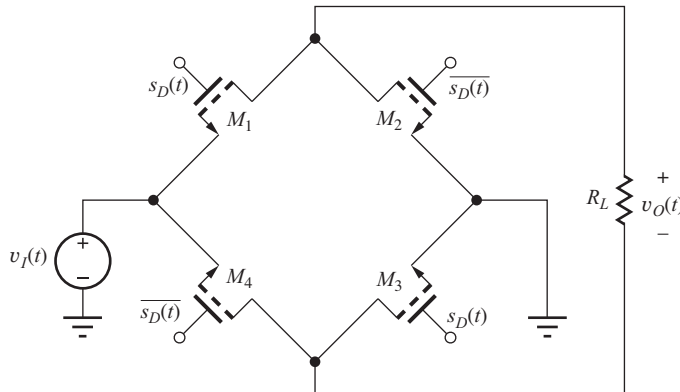


**Figure 17.80** Passive NMOS double-balanced mixers.

### A Passive MOS Double-Balanced Mixer

The circuit in Fig. 17.80 shows an implementation of the double-balanced mixer from Fig. 17.78 using four MOS transistors as switches in which the circuit is redrawn as a bridge. The circuit is considered to be a “passive” mixer because no power is required beyond that supplied from input signal  $v_I$  and the switching signal applied to the gates of the MOSFETs. If the on-resistances of the MOSFETs are designed to be much smaller than load resistor  $R_L$ , then input signal  $v_I$  will appear across  $R_L$  when  $M_1$  and  $M_3$  are turned on, and the negative of  $v_I$  will appear across  $R_L$  when  $M_2$  and  $M_4$  are on. High levels of rejection can be achieved with well-matched transistors in integrated circuit realizations.

SPICE simulation results for the circuit in Fig. 17.79 appear in Fig. 17.81 for a 100 mV, 4 kHz sine wave and a  $\pm 5$  V, 50 kHz switching signal. The output waveform shows the signal polarity reversal that occurs at the switching signal rate and an amplitude loss caused by the on-resistance of the switches. The spectrum shows the mixer products 4 kHz above and below the odd harmonics of 50 kHz, whereas components at 4 kHz and the odd harmonics of 50 kHz are suppressed.

**EXERCISE:** What is the actual conversion gain for the double-balanced mixer in Fig. 17.80?

**ANSWER:**  $0.7 \times 2/\pi$  or  $-7.02$  dB

### 17.12.5 THE GILBERT MULTIPLIER AS A DOUBLE-BALANCED MIXER/MODULATOR

The **Gilbert multiplier** introduced in Chapter 16 can be used directly as a **double-balanced modulator** or **mixer** if transistors  $Q_3-Q_6$  in Fig. 17.82 are driven by the square-wave signal at input  $v_2$  at carrier frequency  $\omega_c$ . The second signal  $v_1$  at modulating frequency  $\omega_m$  is applied to the transconductance stage. (In this case, input  $v_2$  no longer acts as a linear input signal in contrast to the multiplier application in Chapter 16.) For the circuit in Fig. 17.82, we have

$$i_{C1} = I_{BB} + \frac{V_m}{2R_1} \sin \omega_m t \quad \text{and} \quad i_{C2} = I_{BB} - \frac{V_m}{2R_1} \sin \omega_m t \quad (17.201)$$

If we take a differential output, the dc current component cancels out, but the signal current at frequency  $\omega_m$  is switched back and forth by the square-wave input and appears to be multiplied alternately by +1 and -1. Using Eqs. (17.199) and (17.201), the output signal between the collectors can be written as

$$v_O(t) = V_m \frac{R_C}{R_1} \sum_{n \text{ odd}} \frac{4}{n\pi} \sin n\omega_c t \sin \omega_m t \quad (17.202)$$

or

$$v_O(t) = V_m \frac{R_C}{R_1} \sum_{n \text{ odd}} \frac{2}{n\pi} [\cos(n\omega_c - \omega_m)t - \cos(n\omega_c + \omega_m)t]$$

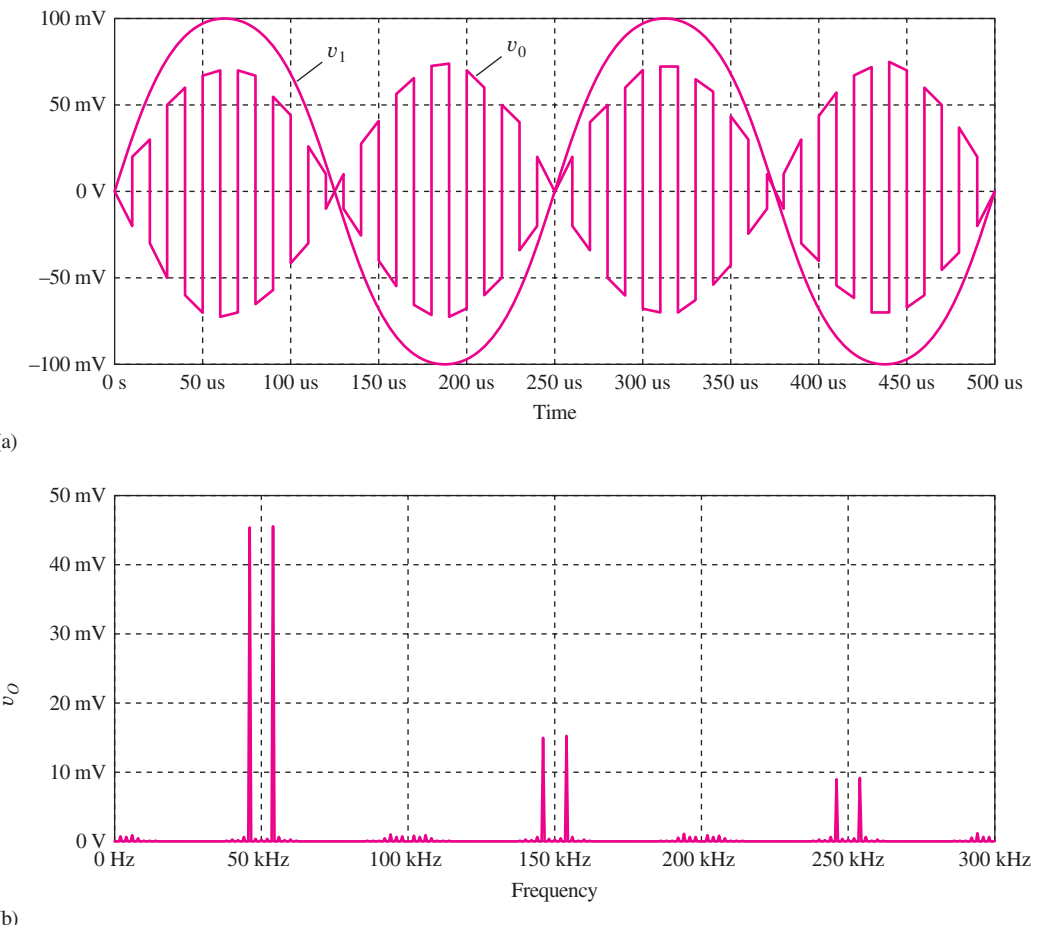


**Figure 17.81** NMOS passive mixer. (a) SPICE output waveform and (b) spectrum.

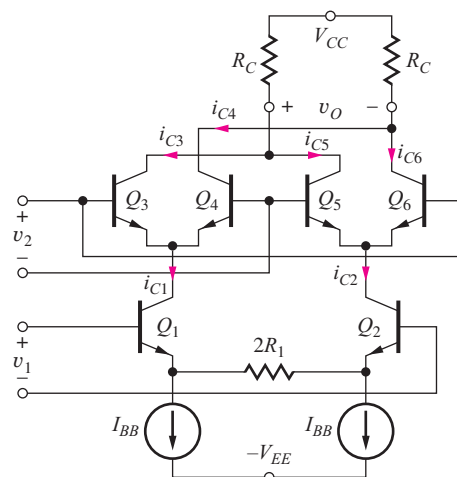


**Figure 17.82** Double-balanced modulator based on the Gilbert multiplier. Signal  $v_2$  is a large-signal square-wave at the carrier frequency  $\omega_c$ , and  $v_1$  is the modulating signal at frequency  $\omega_m$ .

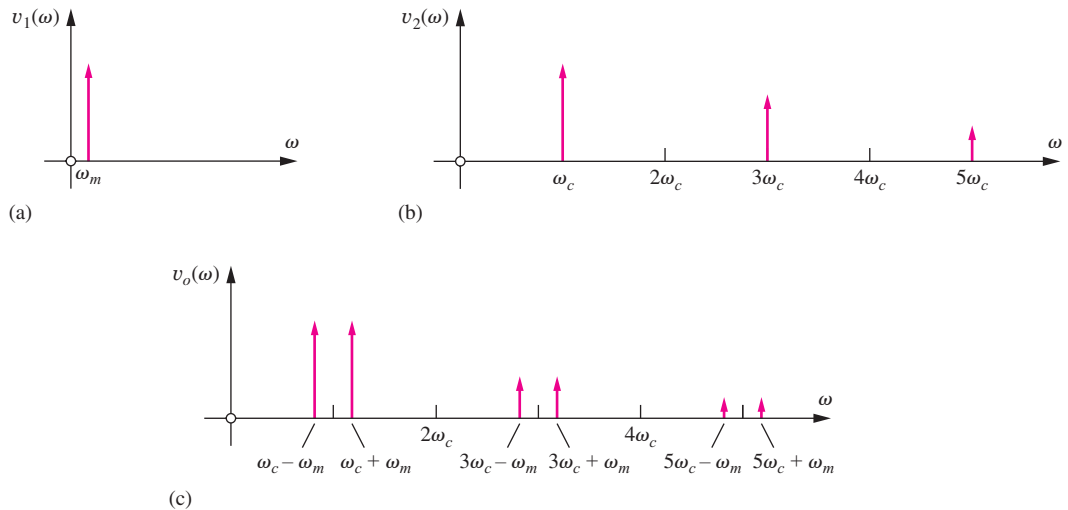


**Figure 17.83** Spectra for double-balanced modulation. (a) Modulation input. (b) Switching input. (c) Output signal.

The output signal has spectral components at frequencies  $\omega_m$  above and below each of the odd harmonics of the carrier frequency  $\omega_c$  as in Fig. 17.83. Note that no signal energy at either the carrier or modulation signal frequencies  $\omega_c$  or  $\omega_m$  appears at the output, and the circuit operates as a double-balanced modulator or mixer. A bandpass filter can be used to select the desired frequencies from the composite spectrum at the output.

In modulator applications, the circuit just described generates a double-sideband suppressed-carrier (DSBSC) output signal. An amplitude-modulated signal (with modulation index  $M$ ,  $0 \leq M \leq 1$ ) can also be generated by adding a dc component to the modulating signal

$$v_1 = V_m(1 + M \sin \omega_m t) \quad (17.203)$$

The dc term unbalances the circuit relative to the carrier frequency thereby injecting a carrier frequency component into the output. (Note the same effect is caused by offset voltages due to mismatches in the transistors.) The output voltage becomes

$$v_O(t) = V_m \frac{R_C}{R_1} \sum_{n \text{ odd}} \frac{4}{n\pi} \left[ \sin n\omega_c t + \frac{M}{2} \cos(n\omega_c - \omega_m)t - \frac{M}{2} \cos(n\omega_c + \omega_m)t \right] \quad (17.204)$$

In this case, the circuit remains balanced with respect to the modulation signal and operates as a single-balanced modulator.

**EXERCISE:** A 20-MHz carrier is modulated with a 10-kHz signal using the double-balanced modulator in Figs. 17.82 and 17.83. What are the frequencies of the spectral components in Fig. 17.83(c)?

**ANSWERS:** 19.99 MHz; 20.01 MHz; 59.99 MHz; 60.01 MHz; 99.99 MHz; 100.01 MHz

**EXERCISE:** The amplitude of the signal at 19.99 MHz in the previous exercise is 3 V. What are the amplitudes of the other components?

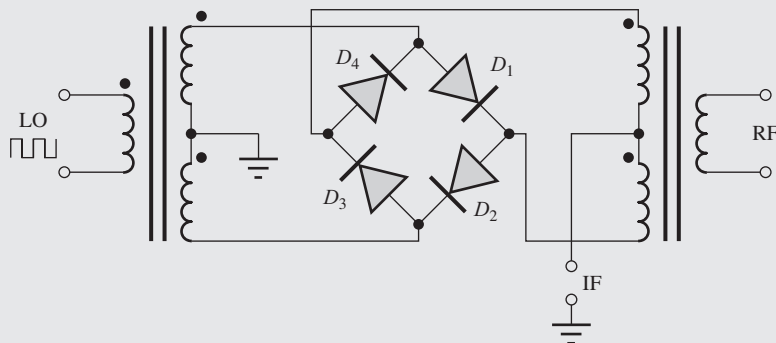
**ANSWERS:** 3 V; 1 V; 1 V; 0.6 V; 0.6 V



## ELECTRONICS IN ACTION

### Passive Diode Mixers

Another popular form of passive double-balanced mixer appears in the figure below. The switches are implemented by a four-diode bridge and are driven by a high-level (10 dBm) local oscillator signal. Both the LO and RF inputs are transformer-coupled to the diode bridge, and the output signal appears at the IF port. Excellent balance can be achieved with well-matched diodes and carefully designed transformers.



An example of such a mixer product produced by Mini-Circuits® appears in the photograph below. Similar mixer products cover a very wide range of frequencies and switching signal levels.



Mini-Circuits ZP-3LH+ Mixer: 0.15–400 MHz, 4.8 dB conversion loss, +10 dBm LO, 50 dB LO-RF isolation, 45 dB LO-IF isolation. Courtesy of Mini-Circuits® ([www.minicircuits.com](http://www.minicircuits.com)).

## SUMMARY

- Amplifier frequency response can be determined by splitting the circuit into two models, one valid at low frequencies where coupling and bypass capacitors are most important, and a second valid at high frequencies in which the internal device capacitances control the frequency-dependent behavior of the circuit.
- Direct analysis of these circuits in the frequency domain, although usually possible for single-transistor amplifiers, becomes impractical for multistage amplifiers. In most cases, however, we are primarily interested in the midband gain and the upper- and lower-cutoff frequencies of the amplifier, and estimates of  $f_H$  and  $f_L$  can be obtained using the open-circuit and short-circuit time-constant methods. More accurate results can be obtained using SPICE circuit simulation.

- The frequency-dependent characteristics of the bipolar transistor are modeled by adding the base-emitter and base-collector capacitors  $C_\pi$  and  $C_\mu$  and base resistance  $r_x$  to the hybrid-pi model. The value of  $C_\pi$  is proportional to collector current  $I_C$ , whereas  $C_\mu$  is weakly dependent on collector-base voltage. The  $r_x C_\mu$  product is an important figure of merit for the frequency limitations of the bipolar transistor.
- The frequency dependence of the FET is modeled by adding gate-source and gate-drain capacitances,  $C_{GS}$  and  $C_{GD}$ , to the pi-model of the FET. The values of  $C_{GS}$  and  $C_{GD}$  are independent of operating point when the FET is operating in the active region.
- Both the BJT and FET have finite current gain at high frequencies, and the unity gain-bandwidth product  $f_T$  for both devices is determined by the device capacitances and the transconductance of the transistor. In the bipolar transistor, the  $\beta$ -cutoff frequency  $f_\beta$  represents the frequency at which the current gain is 3 dB below its low-frequency value.
- In SPICE, the basic high-frequency behavior of the bipolar transistor is modeled using these parameters: forward transit-time TF, zero-bias collector-base junction capacitance CJC, collector junction built-in potential VJC, collector junction grading factor MJC, and base resistance RB.
- In SPICE, the high-frequency behavior of the MOSFET is modeled using the gate-source and gate-drain capacitances determined by the gate-source and gate-drain overlap capacitances CGSO and CGDO, as well as TOX, W, and L.
- If all the poles and zeros of the transfer function can be found from the low- and high-frequency equivalent circuits, then  $f_H$  and  $f_L$  can be accurately estimated using Eqs. (17.16) and (17.23). In many cases, a dominant pole exists in the low- and/or high-frequency responses, and this pole controls  $f_H$  or  $f_L$ . Unfortunately, the complexity of most amplifiers precludes finding the exact locations of all the poles and zeros except through numerical means.
- For design purposes, however, one needs to understand the relationship between the device and circuit parameters and  $f_H$  and  $f_L$ . The short-circuit time constant (SCTC) and open-circuit time constant (OCTC) approaches, as well as Miller effect, provide the needed information and were used to find detailed expressions for  $f_H$  and  $f_L$  for the three classes of single-stage amplifiers, the inverting, noninverting, and follower stages.
- The input impedance of the inverting amplifier is decreased as a result of Miller multiplication, and the expression for the dominant pole of an inverting amplifier can be cast in terms of the Miller effect.
- In contrast, the input impedance of the followers is increased by the Miller effect, and the dominant pole of the follower can also be cast in terms of Miller multiplication.
- It was found that the inverting amplifiers provide high gain but the most limited bandwidth. Non-inverting amplifiers can provide improved bandwidth for a given voltage gain, but it is important to remember that these stages have a much lower input resistance. The follower configurations provide unity gain over a very wide bandwidth. The three basic classes of amplifiers show the direct trade-offs that occur between voltage gain and bandwidth.
- The SCTC approach is used to estimate the value of the lower-cutoff frequency in multistage amplifiers, whereas the Miller effect and equivalent time constant approach is applied to the nodes in the signal path to find the upper cutoff frequency. The frequency responses of the differential pair, cascode amplifier, C-C/C-B cascade stage, and current mirror were all evaluated, as well as an example of calculations for a three-stage amplifier. The frequency response of another multistage amplifier is calculated in Chapter 18.
- Shunt peaking utilizes an inductor to significantly extend the bandwidth of the inverting amplifier.
- Tuned amplifiers employing  $RLC$  circuits can be used to achieve narrow-band amplifiers at radio frequencies. Designs can use either single- or multiple-tuned circuits. If the circuits in a multiple-tuned amplifier are all designed to have the same center frequency, the circuit is referred to as

synchronously tuned. If the tuned circuits are adjusted to different center frequencies, the circuit is referred to as stagger-tuned. Care must be taken to ensure that tuned amplifiers do not become oscillators, and the use of the cascode and C-C/C-B cascade configurations offers improved isolation between multiple-tuned circuits.

- Mixer circuits are widely used in communications electronics to translate the frequency spectrum of a signal. Mixing requires some form of multiplication of two signals, which generates sums and differences of the two input spectra. Single- and double-balanced configurations eliminate one or both of the input signals from the output spectrum. Single-balanced mixers can be designed using differential pairs. Double-balanced mixers often utilize circuits based on passive switching-type mixers employing FETs or diodes.
- Single- and double-balanced modulator circuits are closely related to mixers, and the Gilbert multiplier can be used to generate double-sideband suppressed-carrier (DSBSC) signals as well as amplitude-modulated waveforms.

## KEY TERMS

Amplitude stabilization	Miller multiplication
Base resistance	Mixer Neutralization
Beta-cutoff frequency	Open-circuit time-constant (OCTC) method
Cascode amplifier	Passive mixers
Center frequency	Pole frequencies
Dominant high-frequency pole	Radio frequency choke (RFC)
Dominant low-frequency pole	Short-circuit time-constant (SCTC) method
Dominant pole	Short-peaked amplifier
Double-balanced mixers	Single-balanced mixer
Down-conversion	Stagger tuning
Gilbert mixer	Synchronous tuning
Lower-cutoff frequency	Tuned amplifiers
Midband gain	Unity-gain-bandwidth product
Miller compensation	Up-conversion
Miller effect	Upper-cutoff frequency
Miller integrator	

## REFERENCE

1. P. E. Gray and C. L. Searle, *Electronic Principles*, Wiley, New York: 1969.
2. S. S. Mohan, M. del mar Hershenson, S. P. Boyd and T. H. Lee, "Bandwidth extension in CMOS with optimized on-chip inductors," *IEEE Journal of Solid-State Circuits*, vol. 35, no. 3, pp. 346–355, March 2000.

## PROBLEMS

### 17.1 Amplifier Frequency Response

- 17.1. Find  $A_{\text{mid}}$  and  $F_L(s)$  for this transfer function. Is there a dominant pole? If so, what is the dominant-pole approximation of  $A_v(s)$ ? What is the cutoff frequency  $f_L$  of the dominant-pole approximation? What is the exact cutoff frequency using the complete transfer function?

$$A_v(s) = \frac{50s^2}{(s + 4)(s + 30)}$$

- 17.2. Find  $A_{\text{mid}}$  and  $F_L(s)$  for this transfer function. Is there a dominant pole? If so, what is the dominant-pole approximation of  $A_v(s)$ ? What is the cutoff frequency  $f_L$  of the dominant-pole approximation? What is the exact cutoff frequency using the complete transfer function?

$$A_v(s) = \frac{300s^2}{2s^2 + 1400s + 100,000}$$

- 17.3. Find  $A_{\text{mid}}$  and  $F_L(s)$  for this transfer function. Is there a dominant pole? Use Eq. (17.16) to estimate  $f_L$ . Use the computer to find the exact cutoff frequency  $f_L$ .

$$A_v(s) = -\frac{150s(s+14)}{(s+12)(s+20)}$$

- 17.4. Find  $A_{\text{mid}}$  and  $F_H(s)$  for this transfer function. Is there a dominant pole? If so, what is the dominant-pole approximation of  $A_v(s)$ ? What is the cutoff frequency  $f_H$  of the dominant-pole approximation? What is the exact cutoff frequency using the complete transfer function?

$$A_v(s) = \frac{6 \times 10^{11}}{3s^2 + 3.3 \times 10^5 s + 3 \times 10^9}$$

- 17.5. Find  $A_{\text{mid}}$  and  $F_H(s)$  for this transfer function. Is there a dominant pole? If so, what is the dominant-pole approximation of  $A_v(s)$ ? What is the cutoff frequency  $f_H$  of the dominant-pole approximation? What is the exact cutoff frequency using the complete transfer function?

$$A_v(s) = \frac{(s+3 \times 10^9)}{(s+10^7)\left(1+\frac{s}{5 \times 10^8}\right)}$$

- 17.6. Find  $A_{\text{mid}}$  and  $F_H(s)$  for this transfer function. Is there a dominant pole? Use Eq. (17.16) to estimate  $f_H$ . Use the computer to find the exact cutoff frequency  $f_H$ .

$$A_v(s) = \frac{4 \times 10^9(s+5 \times 10^5)}{(s+1.5 \times 10^5)(s+2 \times 10^6)}$$

- 17.7. Find  $A_{\text{mid}}$ ,  $F_L(s)$ , and  $F_H(s)$  for this transfer function. Is there a dominant pole at low frequencies? At high frequencies? Use Eqs. (17.16) and (17.23) to estimate  $f_L$  and  $f_H$ . Use the computer to find the exact cutoff frequencies and compare to the estimates.

$$A_v(s) = -\frac{4 \times 10^8 s^2}{(s+1)(s+2)(s+1000)(s+2000)}$$

- \*17.8. Find  $A_{\text{mid}}$ ,  $F_L(s)$  and  $F_H(s)$  for this transfer function. Is there a dominant pole at low frequencies? At high frequencies? Use Eqs. (17.16) and (17.23) to estimate  $f_L$  and  $f_H$ . Use the computer to find the exact cutoff frequencies and compare to the estimates.

$$A_v(s) = \frac{2 \times 10^{10} s^2(s+1)(s+200)}{(s+3)(s+5)(s+7)(s+100)^2(s+300)}$$

## 17.2 Direct Determination of the Low-Frequency Poles and Zeros—The Common-Source Amplifier

- 17.9. (a) Draw the low-frequency and midband equivalent circuits for the common-source amplifier in Fig. P17.9 if  $R_I = 5 \text{ k}\Omega$ ,  $R_1 = 430 \text{ k}\Omega$ ,  $R_2 = 560 \text{ k}\Omega$ ,  $R_S = 13 \text{ k}\Omega$ ,  $R_D = 43 \text{ k}\Omega$ , and  $R_3 = 240 \text{ k}\Omega$ . (b) What are the lower-cutoff frequency and midband gain of the amplifier if the Q-point = (0.2 mA, 5 V) and  $V_{GS} - V_{TN} = 1 \text{ V}$ ? (c) What is the value of  $V_{DD}$ ?

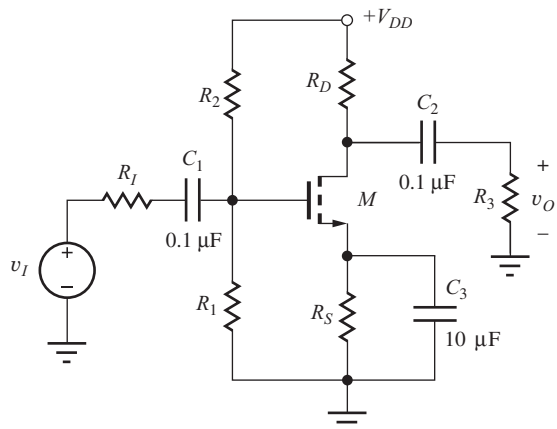


Figure P17.9

- 17.10. (a) Draw the low-frequency and midband equivalent circuits for the common-source amplifier in Fig. P17.9 if  $R_I = 2 \text{ k}\Omega$ ,  $R_1 = 4.3 \text{ M}\Omega$ ,  $R_2 = 5.6 \text{ M}\Omega$ ,  $R_S = 13 \text{ k}\Omega$ ,  $R_D = 43 \text{ k}\Omega$ , and  $R_3 = 430 \text{ k}\Omega$ . (b) What are the lower-cutoff frequency and midband gain of the amplifier if the Q-point = (0.2 mA, 5 V) and  $V_{GS} - V_{TN} = 1 \text{ V}$ ? (c) What is the value of  $V_{DD}$ ?
- 17.11. (a) What is the value of  $C_2$  required to set  $f_L$  to 50 Hz in the circuit in Prob. 17.9? (b) Choose the nearest standard value of capacitance from Appendix A. What is the value of  $f_L$  for this capacitor? (c) Repeat for the circuit in Prob. 17.10.
- 17.12. (a) Draw the low-frequency equivalent circuit for the common-gate amplifier in Fig. P17.12. (b) Write an expression for the transfer function of the amplifier and identify the location of the two low-frequency poles and two low-frequency zeros. Assume  $r_o = \infty$  and  $g_m = 5 \text{ mS}$ . (c) What are the lower-cutoff frequency and midband gain of the amplifier?

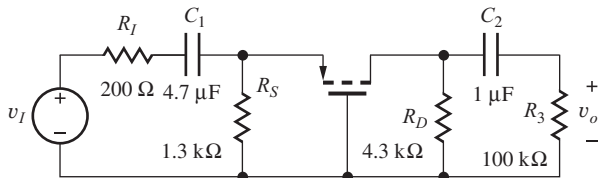


Figure P17.12

- 17.13. (a) What is the value of  $C_1$  required to set  $f_L$  to 2000 Hz in the circuit in Prob. 17.12? (b) Choose the nearest standard value of capacitance from Appendix A. What is the value of  $f_L$  for this capacitor?

- 17.14. (a) Draw the low-frequency ac and midband equivalent circuits for the common-base amplifier in Fig. P17.14 if  $R_I = 75 \Omega$ ,  $R_E = 4.3 \text{ k}\Omega$ ,  $R_C = 2.2 \text{ k}\Omega$ ,  $R_3 = 51 \text{ k}\Omega$ , and  $\beta_o = 100$ . (b) Write an expression for the transfer function of the amplifier and identify the location of the two low-frequency poles and two low-frequency zeros. Assume  $r_o = \infty$  and the Q-point = (1 mA, 5 V). (c) What are the midband gain and lower cutoff frequency of the amplifier? (d) What are the values of  $-V_{EE}$  and  $V_{CC}$ ? (e) What are the lower-cutoff frequency and midband gain of the amplifier if  $R_E = 430 \text{ k}\Omega$ ,  $R_C = 220 \text{ k}\Omega$ ,  $R_3 = 510 \text{ k}\Omega$ , and the Q-point is (10 μA, 5 V)? (f) What are the values of  $-V_{EE}$  and  $V_{CC}$  in part (e)?

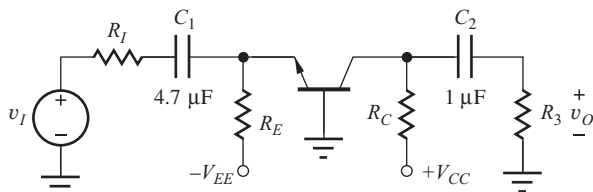


Figure P17.14

- 17.15. (a) What is the value of  $C_1$  required to set  $f_L$  to 500 Hz in the circuit in Prob. 17.14(a)? (b) Choose the nearest standard value of capacitance from Appendix A. What is the value of  $f_L$  for this capacitor? (c) Repeat for the circuit in Prob. 17.14(e).

### 17.3 Estimation of $\omega_L$ Using the Short-Circuit Time-Constant Method

- 17.16. (a) The common-emitter circuit in Fig. 17.6 is redesigned with  $R_1 = 100 \text{ k}\Omega$ ,  $R_2 = 300 \text{ k}\Omega$ ,  $R_E = 15 \text{ k}\Omega$ , and  $R_C = 43 \text{ k}\Omega$ , and the Q-point is (175 μA, 2.3 V). The other values remain the same. Use the SCTC technique to find  $f_L$ . (b) Plot the frequency response of the amplifier with SPICE

and find the value of  $f_L$ . (c) Calculate the Q-point for the transistor.

- 17.17. (a) What is the value of  $C_3$  required to set  $f_L$  to 2500 Hz in the circuit in Fig. 17.6? (b) Choose the nearest standard value of capacitance from Appendix A. What is the actual value of  $f_L$  for this capacitor?

- 17.18. (a) Draw the low-frequency and midband equivalent circuits for the common-emitter amplifier in Fig. P17.18 if  $R_I = 1 \text{ k}\Omega$ ,  $R_1 = 120 \text{ k}\Omega$ ,  $R_2 = 360 \text{ k}\Omega$ ,  $R_E = 13 \text{ k}\Omega$ ,  $R_C = 43 \text{ k}\Omega$ , and  $R_3 = 43 \text{ k}\Omega$ . (b) What are the lower-cutoff frequency and midband gain of the amplifier assuming a Q-point of (0.164 mA, 2.79 V) and  $\beta_o = 100$ ? (c) What is the value of  $V_{CC}$ ?

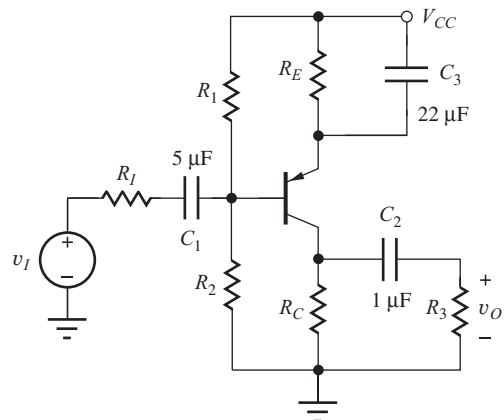


Figure P17.18

- 17.19. Use the SCTC technique to find the lower-cutoff frequency for the common-source amplifier in Fig. 17.11 if  $R_G = 1 \text{ M}\Omega$ ,  $R_3 = 68 \text{ k}\Omega$ ,  $R_D = 22 \text{ k}\Omega$ ,  $R_S = 6.8 \text{ k}\Omega$ , and  $g_m = 1.5 \text{ mS}$ . The other values remain unchanged.

- 17.20. Use the SCTC technique to find the lower-cutoff frequency for the common-source amplifier in Fig. 17.11 if  $R_G = 500 \text{ k}\Omega$ ,  $R_3 = 10 \text{ k}\Omega$ ,  $R_D = 43 \text{ k}\Omega$ ,  $R_S = 10 \text{ k}\Omega$  and  $g_m = 0.75 \text{ mS}$ . The other values remain unchanged.

- 17.21. (a) Draw the low-frequency and midband equivalent circuits for the common-gate amplifier in Fig. P17.21. (b) What are the lower-cutoff frequency and midband gain of the amplifier if the Q-point = (0.1 mA, 8.6 V),  $V_{GS} - V_{TN} = 1 \text{ V}$ ,  $C_1 = 4.3 \mu\text{F}$ ,  $C_2 = 0.1 \mu\text{F}$ , and  $C_3 = 0.1 \mu\text{F}$ ?

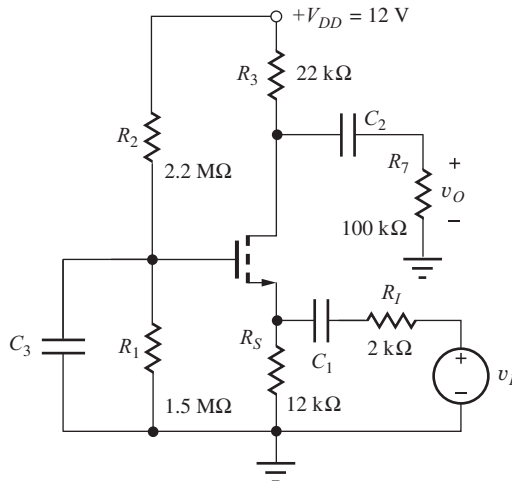


Figure P17.21

- 17.22. (a) Draw the low-frequency and midband equivalent circuits for the emitter follower in Fig. P17.22. (b) What are the lower-cutoff frequency and midband gain of the amplifier if the Q-point is (0.25 mA, 12 V),  $\beta_o = 100$ ,  $C_1 = 4.7 \mu\text{F}$ , and  $C_2 = 12 \mu\text{F}$ ?

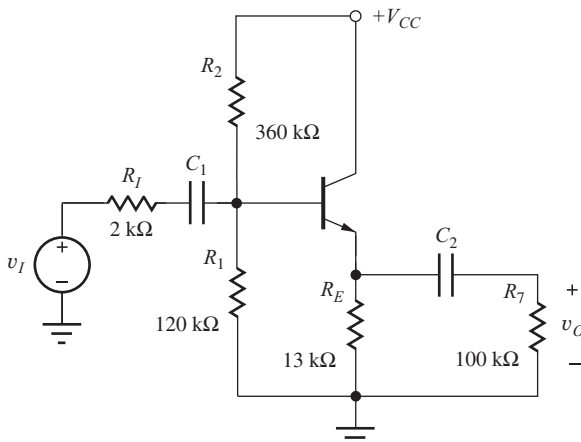


Figure P17.22

- 17.23. (a) Draw the low-frequency and midband equivalent circuits for the source follower in Fig. P17.23. (b) What are the lower-cutoff frequency and midband gain of the amplifier if the transistor is biased at 0.75 V above threshold with a Q-point = (0.1 mA, 8.8 V),  $C_1 = 4.7 \mu\text{F}$ , and  $C_2 = 0.13 \mu\text{F}$ ? (c) What is the value of  $V_{DD}$ ?  
 17.24. Redesign the value of  $C_3$  in the C-S stage in Prob. 17.9 to set  $f_L = 500$  Hz.  
 17.25. Redesign the value of  $C_1$  in the C-G stage in Prob. 17.12 to set  $f_L = 250$  Hz.

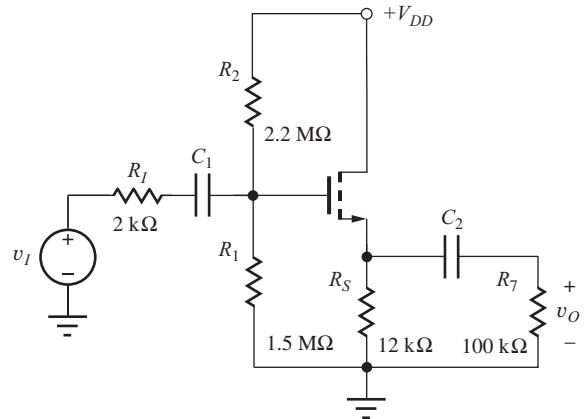


Figure P17.23

- 17.26. Redesign the value of  $C_3$  in the C-E stage in Prob. 17.18 to set  $f_L = 10$  Hz.  
 17.27. Redesign the value of  $C_1$  in the C-G stage in Prob. 17.21 to set  $f_L = 2$  Hz.  
 17.28. Redesign the value of  $C_2$  in the C-C stage in Prob. 17.22 to set  $f_L = 20$  Hz.  
 17.29. Redesign the value of  $C_2$  in the C-D stage in Prob. 17.23 to set  $f_L = 10$  Hz.

#### 17.4 Transistor Models at High Frequencies

- 17.30. A bipolar transistor with  $f_T = 500$  MHz and  $C_{\mu o} = 2 \text{ pF}$  is biased at a Q-point of (2 mA, 5 V). What is the forward-transit time  $\tau_F$  if  $\phi_{jc} = 0.9$  V?  
 17.31. Fill in the missing parameter values for the BJT in the table if  $r_x = 200 \Omega$ .

$I_C$	$f_T$	$C_\pi$	$C_\mu$	$\frac{1}{2\pi r_x C_\mu}$
10 $\mu\text{A}$	50 MHz		0.50 pF	
100 $\mu\text{A}$	300 MHz	0.75 pF		
500 $\mu\text{A}$	1 GHz		0.25 pF	
10 mA		10 pF		1.59 GHz
1 $\mu\text{A}$		1 pF	1 pF	
	5 GHz	1 pF	0.5 pF	

- 17.32. Fill in the missing parameter values for the MOSFET in the table if  $K_n = 2 \text{ mA/V}^2$ .

$I_D$	$f_T$	$C_{GS}$	$C_{GD}$
10 $\mu\text{A}$		1.5 pF	0.5 pF
250 $\mu\text{A}$		1.5 pF	0.5 pF
	250 MHz	1.5 pF	0.5 pF

- 17.33. (a) An *n*-channel MOSFET has a mobility of  $600 \text{ cm}^2/\text{V} \cdot \text{s}$  and a channel length of  $1 \mu\text{m}$ . What is the transistor's  $f_T$  if  $V_{GS} - V_{TN} = 0.25 \text{ V}$ . (b) Repeat for a PMOS device with a mobility of  $250 \text{ cm}^2/\text{V} \cdot \text{s}$ . (c) Repeat for transistors in a new technology with  $L = 0.1 \mu\text{m}$ . (d) Repeat for transistors in a technology with  $L = 25 \text{ nm}$ .

### 17.5 Base Resistance in the Hybrid-Pi Model

- 17.34. (a) What is the midband gain for the common-emitter amplifier in Fig. P17.34 if  $r_x = 500 \Omega$ ,  $I_C = 1 \text{ mA}$ , and  $\beta_o = 110$ ? (b) If  $r_x = 0$ ?

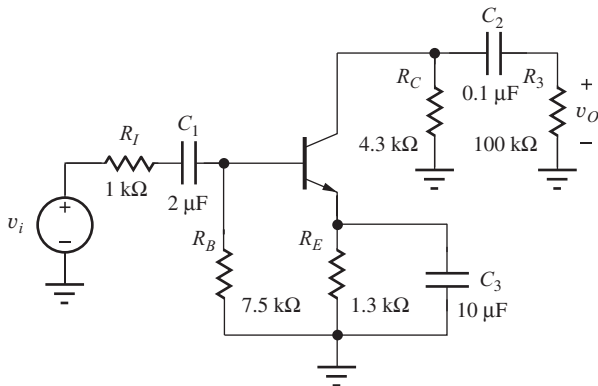


Figure P17.34

- 17.35. (a) What is the midband gain for the common-collector amplifier in Fig. P17.35 if  $r_x = 350 \Omega$ ,  $I_C = 1 \text{ mA}$ , and  $\beta_o = 145$ ? (b) If  $r_x = 0$ ?

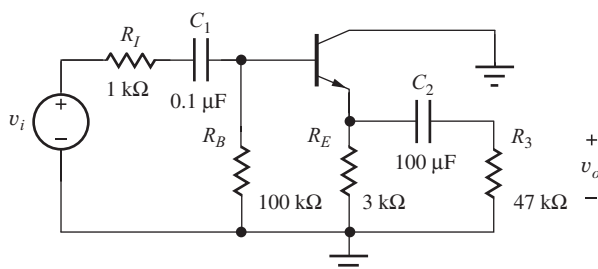


Figure P17.35

- 17.36. (a) What is the midband gain for the common-base amplifier in Fig. P17.36 if  $r_x = 200 \Omega$ ,  $I_C = 0.1 \text{ mA}$ , and  $\beta_o = 115$ ? (b) If  $r_x = 0$ ?

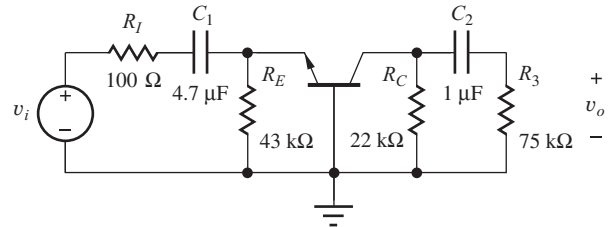


Figure P17.36

### 17.6 High-Frequency Response of the Common-Emitter and Common-Source Amplifiers

#### Factorization

- 17.37. Use dominant root factorization techniques to estimate the roots of these quadratic equations and compare the results to the exact roots: (a)  $s^2 + 5100s + 500,000$ ; (b)  $2s^2 + 700s + 30,000$ ; (c)  $3s^2 + 3300s + 300,000$ ; (d)  $0.5s^2 + 300s + 40,000$ .  
 17.38. (a) Use dominant root factorization techniques to estimate the roots of this equation. (b) Compare the results to the exact roots.

$$s^3 + 1110s^2 + 111,000s + 1,000,000$$

- \*\*17.39. Use Newton's method to help find the roots of this polynomial. (*Hint:* Find the roots one at a time. Once a root is found, factor it out to reduce the order of the polynomial. Use approximate factorization to find starting points for iteration.)

$$\begin{aligned} s^6 &+ 142s^5 + 4757s^4 + 58,230s^3 \\ &+ 256,950s^2 + 398,000s + 300,000 \end{aligned}$$

For Probs. 17.40 to 17.48, use  $f_T = 500 \text{ MHz}$ ,  $r_x = 300 \Omega$ ,  $C_\mu = 0.75 \text{ pF}$ ,  $C_{GS} = C_{GD} = 2.5 \text{ pF}$ .

- 17.40. (a) What are the midband gain and upper-cutoff frequency for the common-emitter amplifier in Prob. 17.34(a) if  $I_C = 1 \text{ mA}$  and  $\beta_o = 100$ ? (b) What is the gain-bandwidth product for this amplifier?  
 17.41. Resistors  $R_1$ ,  $R_2$ ,  $R_E$ , and  $R_C$  in the common-emitter amplifier in Fig. 17.6 are all decreased in value by a factor of 2. (a) Draw the dc equivalent circuit for the amplifier, and find the new Q-point for the transistor. (b) Draw the ac small-signal equivalent circuit for the amplifier, and find the midband gain and upper-cutoff frequency for the amplifier. (c) What is the gain-bandwidth product for this amplifier?

- 17.42. The resistors in the common-emitter amplifier in Fig. 17.6 are all increased in value by a factor of 50. (a) Draw the dc equivalent circuit for the amplifier, and find the new Q-point for the transistor. (b) Draw the ac small-signal equivalent circuit for the amplifier, and find the midband gain and upper-cutoff frequency for the amplifier. (c) What is the gain-bandwidth product for this amplifier?
- 17.43. What are the midband gain and upper-cutoff frequency for the common-source amplifier in Prob. 17.9?
- 17.44. Simulate the frequency response of the amplifier in Prob. 17.9 and determine  $A_{\text{mid}}$ ,  $f_L$ , and  $f_H$ .
- 17.45. In the common-source amplifier in Fig. 17.4, the value of  $R_S$  is changed to 3.9 k $\Omega$  and that of  $R_D$  to 10 k $\Omega$ . For the MOSFET,  $K_n = 500 \mu\text{A}/\text{V}^2$  and  $V_{TN} = 1 \text{ V}$ . (a) Draw the dc equivalent circuit for the amplifier, and find the new Q-point for the transistor if  $V_{DD} = 14 \text{ V}$ . (b) Draw the ac small-signal equivalent circuit for the amplifier, and find the midband gain and upper-cutoff frequency for the amplifier. (c) What is the gain-bandwidth product for this amplifier?
- 17.46. What are the midband gain and upper-cutoff frequency for the common-emitter amplifier in Prob. 17.18? \*\*17.52.
- 17.47. Simulate the frequency response of the amplifier in Prob. 17.18 and determine  $A_{\text{mid}}$ ,  $f_L$ , and  $f_H$ .
- 17.48. The network in Fig. P17.48 models a common emitter stage with a load capacitor in parallel with  $R_L$ . (a) Write the two nodal equations and find the determinant of the system for the network in Fig. P17.48. (b) Use dominant root factorization to find the two poles. (c) There are three capacitors in the network. Why are there only two poles?

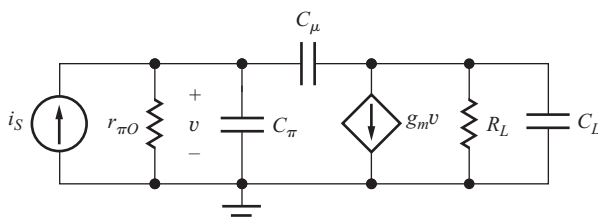


Figure P17.48

### The Miller Effect

- 17.49. (a) What is the total input capacitance in the circuit in Fig. 17.35 if  $C_\pi = 20 \text{ pF}$ ,  $C_\mu = 1 \text{ pF}$ ,

$I_C = 5 \text{ mA}$ , and  $R_L = 1 \text{ k}\Omega$ ? What is the  $f_T$  of this transistor? (b) Repeat for  $I_C = 4 \text{ mA}$  and  $R_L = 2 \text{ k}\Omega$ .

- \*17.50. (a) What is the input capacitance of the circuit in Fig. P17.50 if  $Z$  is a 100-pF capacitor and the amplifier is an op amp with a gain of  $A = -100,000$ ? (\*\*b) What is the input impedance of the circuit in Fig. P17.50 at  $f = 1 \text{ kHz}$  if element  $Z$  is a 100-k $\Omega$  resistor and  $A(s) = -10^6/(s + 10)$ ? (c) At 50 kHz? (d) At 1 MHz?

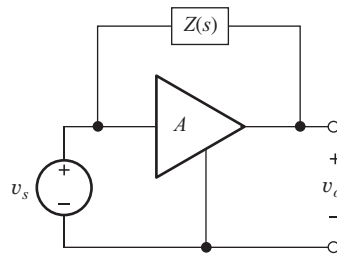


Figure P17.50

- 17.51. What is the input capacitance of the circuit in Fig. P17.50 if the amplifier gain is  $A = +0.992$  and  $Z$  is a 50 pF capacitor?
- 17.52. (a) Find the transfer function of the Miller integrator in Fig. 10.34 if  $A(s) = 10A_o/(s + 10)$ . The transfer function is really that of a low-pass amplifier. What is the cutoff frequency if  $A_o = 10^5$ ? (b) For  $A_o = 10^6$ ? (c) Show that the transfer function approaches that of the ideal integrator if  $A_o \rightarrow \infty$ .
- 17.53. Use Miller multiplication to calculate the impedance presented to  $v_i$  by the circuit in Fig. P17.53 at  $f = 1 \text{ kHz}$  if  $r_x = 250 \Omega$ ,  $r_\pi = 2.5 \text{ k}\Omega$ ,  $g_m = 0.04 \text{ S}$ ,  $R_L = 2.5 \text{ k}\Omega$ ,  $C_\pi = 15 \text{ pF}$ , and  $C_\mu = 1 \text{ pF}$ . (b) At 50 kHz. (c) At 1 MHz. (d) Compare your results to SPICE.

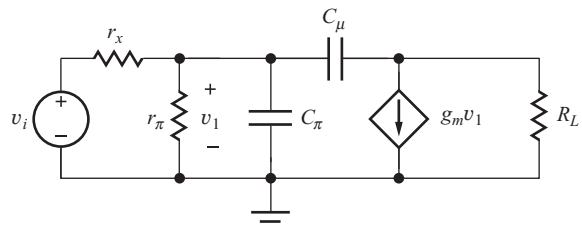


Figure P17.53

- 17.54. Use SPICE to find the midband gain, and upper- and lower-cutoff frequencies of the amplifier in Prob. 17.53.

- 17.55. (a) Estimate the upper-cutoff frequency for the common-emitter amplifier in Prob. 17.34(a) if  $f_T = 500$  MHz and  $C_\mu = 0.75$  pF. (b) Repeat for Prob. 17.34(b).
- 17.56. Resistors  $R_1$ ,  $R_2$ ,  $R_E$ , and  $R_C$  in the common-emitter amplifier in Fig. P17.34 are all increased in value by a factor of 10, and the collector current is reduced to  $100 \mu\text{A}$ . (a) Draw the ac small-signal equivalent circuit for the amplifier, and find the midband gain and upper-cutoff frequency for the amplifier if  $\beta_o = 100$ ,  $r_x = 400 \Omega$ ,  $C_\mu = 0.75$  pF, and  $f_T = 500$  MHz. (b) What is the gain-bandwidth product for this amplifier? Calculate the upper bound on GBW given by the  $r_x C_\mu$  product.
- 17.57. Estimate the upper-cutoff frequency for the common-source amplifier in Prob. 17.9 if  $C_{GS} = 5$  pF and  $C_{GD} = 2$  pF. What is the gain-bandwidth product for this amplifier?

### Estimation of $\omega_H$ for Inverting Amplifiers, Noninverting Amplifiers, and Followers Using the Open-Circuit Time-Constant Method

- 17.58. What are the values of (a)  $A_{\text{mid}}$ ,  $f_L$ , and  $f_H$  for the common-emitter amplifier in Fig. P17.58 if  $C_1 = 1 \mu\text{F}$ ,  $C_2 = 0.1 \mu\text{F}$ ,  $C_3 = 2.2 \mu\text{F}$ ,  $R_3 = 100 \text{ k}\Omega$ ,  $\beta_o = 100$ ,  $f_T = 300$  MHz,  $r_x = 300 \Omega$ ,  $V_{CC} = 12$  V, and  $C_\mu = 0.5$  pF? (b) What is the gain-bandwidth product?

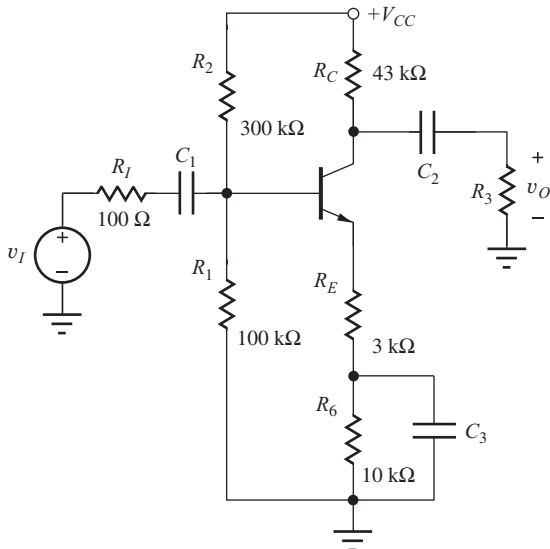


Figure P17.58

- 17.59. (a) Redesign the common-emitter amplifier in Fig. 17.34 to have an upper-cutoff frequency of 5 MHz by changing the value of the collector re-

sistor  $R_C$ . What is the new value of the midband voltage gain? What is the gain-bandwidth product?

- 17.60. (a) Redesign the common-emitter amplifier in Fig. P17.58 to have an upper-cutoff frequency of 7.5 MHz by selecting new values for  $R_E$  and  $R_6$ . Maintain the sum  $R_E + R_6 = 13 \text{ k}\Omega$ . What is the new value of the midband voltage gain? What is the gain-bandwidth product?
- 17.61. Find (a)  $A_{\text{mid}}$ , (b)  $f_L$ , and (c)  $f_H$  for the amplifier in Fig. P17.61 if  $\beta_o = 100$ ,  $f_T = 200$  MHz,  $C_\mu = 1$  pF, and  $r_x = 350 \Omega$ .

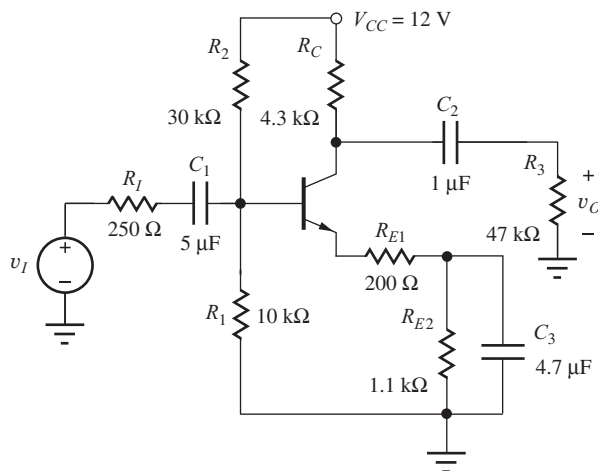


Figure P17.61

- 17.62. Redesign the values of  $R_{E1}$  and  $R_{E2}$  in the amplifier in Prob. 17.61 to achieve  $f_H = 12$  MHz. Do not change the Q-point.
- \*17.63. The network in Fig. P17.63 has two poles. (a) Estimate the lower-pole frequency using the short-circuit time-constant technique if  $C_1 = 1 \mu\text{F}$ ,  $C_2 = 10 \mu\text{F}$ ,  $R_1 = 10 \text{ k}\Omega$ ,  $R_2 = 1 \text{ k}\Omega$ , and  $R_3 = 1 \text{ k}\Omega$ . (b) Estimate the upper-pole frequency. (c) Why do the positions of the poles seem to be backward? (d) Find the system determinant and compare its exact roots to those in (a) and (b).

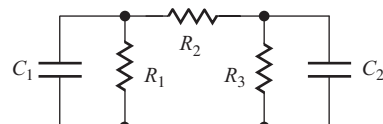


Figure P17.63

For Probs. 17.64–17.76, use  $f_T = 500$  MHz,  $r_x = 300 \Omega$ ,  $C_\mu = 0.60$  pF for the BJT, and  $C_{GS} = 3$  pF and  $C_{GD} = 0.60$  pF for the FET.

## 17.7 High-Frequency Response of Common-Base and Common-Gate Amplifiers

- 17.64. What are the midband gain and upper-cutoff frequency for the common-gate amplifier in Prob. 17.12?
- 17.65. Simulate the frequency response of the amplifier in Prob. 17.12 and determine  $A_{\text{mid}}$ ,  $f_L$ , and  $f_H$ .
- 17.66. What are the midband gain and upper-cutoff frequency for the common-base amplifier in Prob. 17.14(e)?
- 17.67. Simulate the frequency response of the amplifier in Prob. 17.14 with  $V_{CC} = V_{EE} = 5$  V and determine  $A_{\text{mid}}$ ,  $f_L$ , and  $f_H$ .
- 17.68. What are the midband gain and upper-cutoff frequency for the common-base amplifier in Prob. 17.14 if  $V_{CC} = -V_{EE} = 10$  V?
- 17.69. What are the midband gain and upper-cutoff frequency for the amplifier in Prob. 17.21?
- 17.70. What are the midband gain and upper- and lower-cutoff frequencies for the amplifier in Prob. 17.21 if  $V_{DD}$  is increased to 18 V?

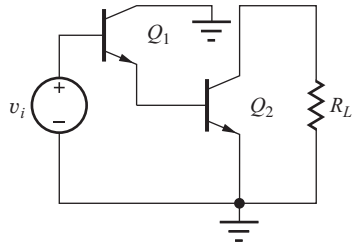
## 17.8 High-Frequency Response of Common-Collector and Common-Drain Amplifiers

- 17.71. What are the midband gain and upper-cutoff frequency for the common-collector amplifier in Fig. P17.22 if  $V_{CC}$  is 10 V?
- 17.72. (a) What are the midband gain and upper-cutoff frequency for the emitter follower in Prob. 17.22? (b) Simulate the frequency response of the amplifier in Prob. 17.22 with  $V_{CC} = 15$  V and determine  $A_{\text{mid}}$ ,  $f_L$ , and  $f_H$ .
- 17.73. (a) What are the midband gain and upper-cutoff frequency for the source follower in Prob. 17.23? (b) Simulate the frequency response of the amplifier in Prob. 17.23 with  $V_{DD} = 10$  V and determine  $A_{\text{mid}}$ ,  $f_L$ , and  $f_H$ .
- 17.74. What are the midband gain and upper-cutoff frequency for the common-drain amplifier in Prob. 17.23 if  $V_{DD}$  is 18 V?
- \*17.75. Derive an expression for the total capacitance looking into the gate of the FET in Fig. 17.45(b). Use the expression to interpret Eq. (17.141).
- \*\*17.76. Derive an expression for the total input capacitance of the BJT in Fig. 17.44(c) looking into node  $v_b$ . Assume  $C_L = 0$ . Use it to interpret Eq. (17.138).

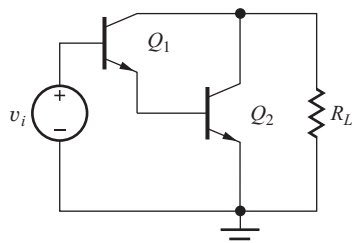
## 17.9 Summary of the High-Frequency Response of Single-Stage Amplifiers

### Gain-Bandwidth Product

- 17.77. A bipolar transistor must be selected for use in a common-base amplifier with a gain of 40 dB and a bandwidth of 40 MHz. What should be the minimum specification for the transistor's  $f_T$ ? What should be the minimum  $r_x C_\mu$  product? (Use a factor of 2 safety margin for each estimate.)
- 17.78. A bipolar transistor must be selected for use in a common-emitter amplifier with a gain of 43 dB and a bandwidth of 6 MHz. What should be the minimum specification for the transistor's  $f_T$ ? What should be the minimum  $r_x C_\mu$  product? (Use a factor of 2 safety margin for each estimate.)
- 17.79. A BJT will be used in a differential amplifier with load resistors of 100 k $\Omega$ . What are the maximum values of  $r_x$  and  $C_\mu$  that can be tolerated if the gain and bandwidth are to be 100 and 1.8 MHz, respectively?
- \*17.80. An FET with  $C_{GS} = 12$  pF and  $C_{GD} = 5$  pF will be used in a common-source amplifier with a source resistance of 100  $\Omega$  and a bandwidth of 25 MHz. Estimate the minimum Q-point current needed to achieve this bandwidth if  $K_n = 25$  mA/V<sup>2</sup> and  $V_{GS} - V_{TN} \geq 0.25$  V.
- 17.81. An FET with  $C_{GS} = 7.5$  pF and  $C_{GD} = 3$  pF will be used in a common-gate amplifier with a source resistance of 100  $\Omega$ ,  $A_{\text{mid}} = 20$ , and a bandwidth of 25 MHz. Estimate the Q-point current needed to achieve these specifications if  $K_n = 20$  mA/V<sup>2</sup> and  $V_{DD} = 15$  V.
- 17.82. What is the upper bound on the bandwidth of the circuit in Fig. P17.14 if  $R_C = 12$  k $\Omega$ ,  $R_3 = 47$  k $\Omega$ , and  $C_\mu = 2$  pF?
- \*\*17.83. (a) Estimate the cutoff frequency of the C-C/C-E cascade in Fig. P17.83(a). (b) Estimate the cutoff frequency of the Darlington stage in Fig. P16.82(b). Assume  $I_{C1} = 0.1$  mA,  $I_{C2} = 1$  mA,  $\beta_o = 100$ ,  $f_T = 300$  MHz,  $C_\mu = 0.5$  pF,  $V_A = 50$  V,  $r_x = 300$   $\Omega$ , and  $R_L = \infty$ . (c) Which configuration offers better bandwidth? (d) Which configuration is used in the second stage in the  $\mu$ A741 amplifier in Chapter 16? Why do you think it was used?
- 17.84. Draw a Bode plot for the common-mode rejection ratio for the differential amplifier in Fig. 17.46 if  $I_C = 100$   $\mu$ A,  $R_{EE} = 10$  M $\Omega$ ,  $R_C = 6$  k $\Omega$ ,  $C_{EE} = 1$  pF,  $\beta_o = 100$ ,  $V_A = 50$  V,  $f_T = 200$  MHz,



(a)



(b)

**Figure P17.83**

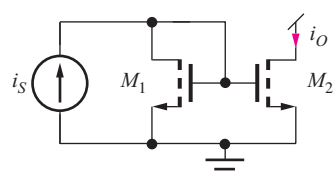
$C_\mu = 0.3 \text{ pF}$ ,  $r_x = 175 \Omega$ , and  $R_L = 100 \text{ k}\Omega$ .  $R_L$  is connected between the collectors of transistors  $Q_1$  and  $Q_2$ .

- 17.85. Use SPICE to plot the graph for Prob. 17.84.



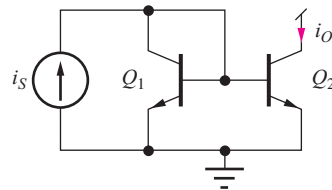
### 17.10 Frequency Response of Multistage Amplifiers

- 17.86. What is the minimum bandwidth of the MOS current mirror in Fig. P17.86 if  $I_S = 200 \mu\text{A}$ ,  $K'_n = 25 \mu\text{A}/\text{V}^2$ ,  $\lambda = 0.02 \text{ V}^{-1}$ ,  $C_{GS1} = 3 \text{ pF}$ ,  $C_{GD1} = 1 \text{ pF}$ ,  $(W/L)_1 = 5/1$ , and  $(W/L)_2 = 25/1$ ?

**Figure P17.86**

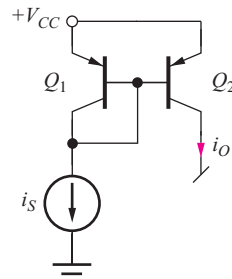
- 17.87. What is the minimum bandwidth of the NMOS current mirror in Fig. P17.86 if  $I_S = 100 \mu\text{A}$ ,  $K'_n = 25 \mu\text{A}/\text{V}^2$ ,  $\lambda = 0.02 \text{ V}^{-1}$ ,  $C_{GS1} = 3 \text{ pF}$ ,  $C_{GD1} = 0.5 \text{ pF}$ , and  $(W/L)_1 = 5/1 = (W/L)_2$ ?

- \*17.88. What is the minimum bandwidth of the bipolar current mirror in Fig. P17.88 if  $I_S = 250 \mu\text{A}$ ,  $\beta_o = 100$ ,  $V_A = 50 \text{ V}$ ,  $f_T = 500 \text{ MHz}$ ,  $C_\mu = 0.3 \text{ pF}$ ,  $r_x = 175 \Omega$ , and  $A_{E2} = 4A_{E1}$ ?

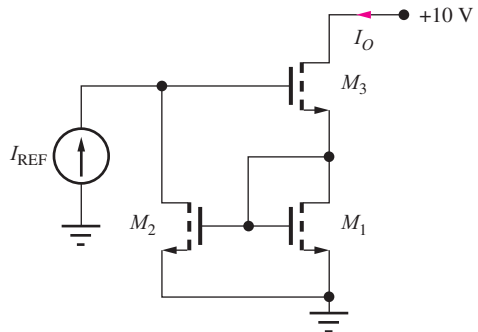
**Figure P17.88**

- 17.89. What is the minimum bandwidth of the *npn* current mirror in Fig. P17.88 if  $I_S = 100 \mu\text{A}$ ,  $\beta_o = 100$ ,  $V_A = 60 \text{ V}$ ,  $f_T = 600 \text{ MHz}$ ,  $C_\mu = 0.5 \text{ pF}$ , and  $A_{E2} = 10 A_{E1}$ ?

- 17.90. What is the minimum bandwidth of the *pnp* current mirror in Fig. P17.90 if  $I_S = 100 \mu\text{A}$ ,  $\beta_o = 50$ ,  $V_A = 60 \text{ V}$ ,  $f_T = 50 \text{ MHz}$ ,  $C_\mu = 2.5 \text{ pF}$ , and  $A_{E2} = A_{E1}$ ?

**Figure P17.90**

- \*\*17.91. Find the minimum bandwidth of the Wilson current mirror in Fig. P17.91 if  $I_{REF} = 250 \mu\text{A}$ ,  $K_n = 250 \mu\text{A}/\text{V}^2$ ,  $V_{TN} = 0.75 \text{ V}$ ,  $\lambda = 0.02 \text{ V}^{-1}$ ,  $C_{GS} = 3 \text{ pF}$ , and  $C_{GD} = 1 \text{ pF}$ .

**Figure P17.91**

- 17.92. (a) The transistors in the differential amplifier in Fig. 17.46 are biased at a collector current of  $15 \mu\text{A}$ , and  $R_C = 430 \text{ k}\Omega$ . The transistors have  $f_T = 75 \text{ MHz}$ ,  $C_\mu = 0.5 \text{ pF}$ , and  $r_x = 500 \Omega$ .

What is the bandwidth of the differential amplifier?

(b) Repeat if the collector current is increased to 50  $\mu\text{A}$  and  $R_C$  is reduced to 140  $\text{k}\Omega$ .

- 17.93. (a) The transistors in the C-C/C-B cascade amplifier in Fig. 17.48 are biased with  $I_{EE} = 200 \mu\text{A}$  and  $R_C = 75 \text{k}\Omega$ . The transistors have  $f_T = 100 \text{ MHz}$ ,  $C_\mu = 1 \text{ pF}$ , and  $r_x = 500 \Omega$ . What is the bandwidth of the amplifier? (b) Repeat if the current source is increased to 2 mA and  $R_C$  is reduced to 7.5  $\text{k}\Omega$ .
- 17.94. (a) The transistors in the cascode amplifier in Fig. 17.50 are biased at a collector current of 100  $\mu\text{A}$  with  $R_L = 75 \text{k}\Omega$ . The transistors have  $f_T = 100 \text{ MHz}$ ,  $C_\mu = 1 \text{ pF}$ , and  $r_x = 500 \Omega$ . What is the bandwidth of the amplifier if  $R_{th} = 0$ ? (b) Repeat if the collector currents are increased to 1 mA and  $R_C$  is reduced to 7.5  $\text{k}\Omega$ .
- 17.95. The bias current in transistor  $Q_3$  in Fig. 17.53(a) is doubled by reducing the value of resistors  $R_3$ ,  $R_4$ , and  $R_{E3}$  by a factor of 2. What are the new values of midband gain, lower-cutoff frequency, and upper-cutoff frequency?
- 17.96. The bias current in transistor  $Q_2$  in Fig. 17.53(a) is reduced by increasing the value of resistors  $R_1$ ,  $R_2$ ,  $R_{C2}$ , and  $R_{E2}$  by a factor of 2. What are the new values of midband gain, lower-cutoff frequency, and upper-cutoff frequency?

## 17.11 Introduction to Radio Frequency Circuits

### Shunt-Peaked Amplifiers

- 17.97. The circuit in Fig. 17.58(a) has  $C_L = 10 \text{ pF}$  and  $R_L = 7.5 \text{k}\Omega$ , and the transistor parameters are  $C_{GS} = 10 \text{ pF}$ ,  $C_{GD} = 4 \text{ pF}$ , and  $g_m = 3 \text{ mS}$ . (a) What is the bandwidth of the amplifier? (b) Find the value of  $L$  required to extend the bandwidth to the maximally flat limit. What is the new bandwidth?
- 17.98. What value of  $L$  is required to increase the bandwidth of the amplifier in Prob. 17.97 by 50 percent?
- 17.99. What is the phase shift at the bandwidth frequency for each of the values of  $m$  in Fig. 17.59?
- 17.100. (a) The transistor in Fig. 17.58(a) is replaced with a bipolar transistor operating at 1 mA. What is the bandwidth of the amplifier if  $C_L = 5 \text{ pF}$  and  $R_L = 10 \text{k}\Omega$ ,  $f_T = 200 \text{ MHz}$  and  $C_\mu = 2 \text{ pF}$ ? (b) Find the value of  $L$  required to extend the bandwidth to the maximally flat limit. What is the new bandwidth?

### Tuned Amplifiers

- 17.101. What are the center frequency,  $Q$ , and midband gain for the amplifier in Fig. P17.101 if the FET has  $C_{GS} = 50 \text{ pF}$ ,  $C_{GD} = 5 \text{ pF}$ ,  $\lambda = 0.0167 \text{ V}^{-1}$ , and it is biased at 2 V above threshold with  $I_D = 10 \text{ mA}$  and  $V_{DS} = 10 \text{ V}$ .

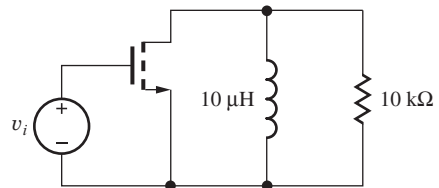


Figure P17.101

- 17.102. (a) What is the value of  $C$  required for  $f_o = 10.7 \text{ MHz}$  in the circuit in Fig. P17.102 if  $I_C = 10 \text{ mA}$ ,  $V_{CE} = 10 \text{ V}$ ,  $\beta_o = 100$ ,  $C_\mu = 2 \text{ pF}$ ,  $f_T = 500 \text{ MHz}$ , and  $V_A = 75 \text{ V}$ ? (b) What is the  $Q$  of the amplifier? (c) Where should a tap be placed on the inductor to achieve a  $Q$  of 100? (d) What is the new value of  $C$  required to achieve  $f_o = 10.7 \text{ MHz}$ ?

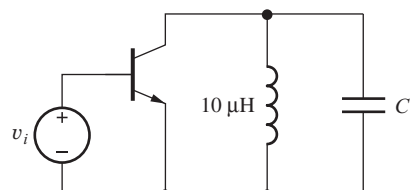


Figure P17.102

- 17.103. (a) Draw the dc and high-frequency ac equivalent circuits for the circuit in Fig. P17.103. (b) What is the resonant frequency of the circuit for  $V_C = 0 \text{ V}$  if the diode is modeled by  $C_{jo} = 20 \text{ pF}$  and  $\phi_j = 0.9 \text{ V}$ ? (c) For  $V_C = 10 \text{ V}$ ?

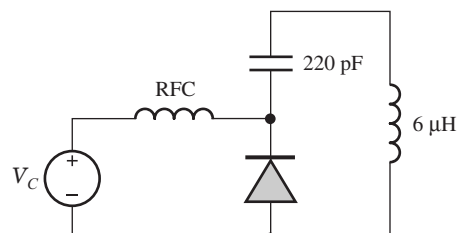


Figure P17.103

- \*17.104. (a) What are the center frequency,  $Q$ , and midband gain for the tuned amplifier in Fig. P17.104 if  $L_1 = 5 \mu\text{H}$ ,  $C_1 = 10 \text{ pF}$ ,  $C_2 = 10 \text{ pF}$ ,  $I_C = 1 \text{ mA}$ ,

- $C_\pi = 5 \text{ pF}$ ,  $C_\mu = 1 \text{ pF}$ ,  $R_L = 5 \text{ k}\Omega$ ,  $r_\pi = 2.5 \text{ k}\Omega$ , and  $r_x = 0 \Omega$ ? (b) What would be the answers if the base terminal of the transistor were connected to the top of the inductor?

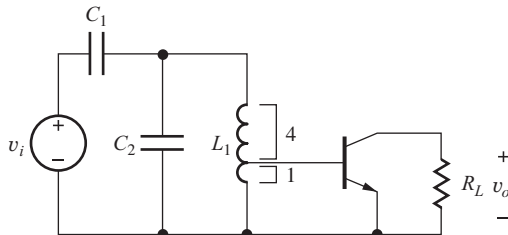
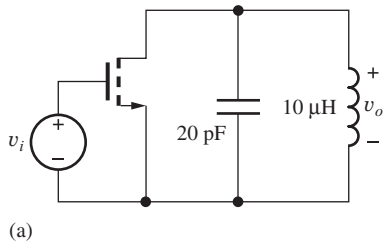
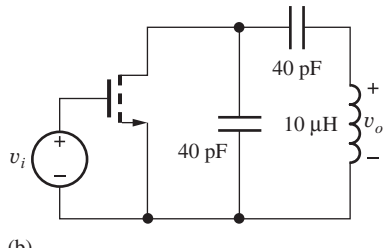


Figure P17.104

- 17.105. (a) What are the midband gain, center frequency, bandwidth, and  $Q$  for the circuit in Fig. P17.105(a) if  $I_D = 20 \text{ mA}$ ,  $\lambda = 0.02 \text{ V}^{-1}$ ,  $C_{GD} = 5 \text{ pF}$ , and  $K_n = 5 \text{ mA/V}^2$ ? (b) Repeat for the circuit in Fig. P17.105(b).



(a)



(b)

Figure P17.105

- \*17.106. Change the two capacitor values in the circuit in Fig. P17.105(a) to give the same center frequency as in Fig. P17.105(b). What are the  $Q$  and midband gain for the new circuit?

- 17.107. (a) Simulate the circuit in Prob. 17.105(a) and compare the results to the hand calculations in Prob. 17.105. (b) Simulate the circuit in Prob. 17.105(b) and compare the results to the hand calculations in Prob. 17.105. (c) Simulate the circuit in Prob. 17.106 and compare the results to the hand calculations in Prob. 17.106.

- 17.108. (a) What is the value of  $C_2$  required to achieve synchronous tuning of the circuit in Fig. P17.108 if  $L_1 = L_2 = 10 \mu\text{H}$ ,  $C_1 = C_3 = 20 \text{ pF}$ ,  $C_{GS} = 20 \text{ pF}$ ,  $C_{GD} = 5 \text{ pF}$ ,  $V_{TN1} = -1 \text{ V}$ ,  $K_{n1} = 10 \text{ mA/V}^2$ ,  $V_{TN2} = -4 \text{ V}$ ,  $K_{n2} = 10 \text{ mA/V}^2$ , and  $R_G = R_D = 100 \text{ k}\Omega$ ? (b) What are the  $Q$ , midband gain, and bandwidth of your design?

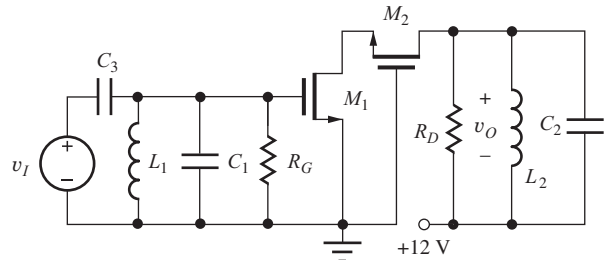


Figure P17.108

- 17.109. Simulate the frequency response of the circuit design in Prob. 17.108 and find the midband gain, center frequency,  $Q$ , and bandwidth of the circuit. Did you achieve synchronous tuning of your design?

- \*\*17.110. (a) What is the value of  $C_2$  required to adjust the resonant frequency of the tuned circuit connected to the drain of  $M_2$  to a frequency 2 percent higher than that connected at the gate of  $M_1$  in Fig. P17.108 if  $L_1 = L_2 = 10 \mu\text{H}$ ,  $C_1 = C_3 = 20 \text{ pF}$ ,  $C_{GS} = 20 \text{ pF}$ ,  $C_{GD} = 5 \text{ pF}$ ,  $V_{TN1} = -1 \text{ V}$ ,  $K_{n1} = 10 \text{ mA/V}^2$ ,  $V_{TN2} = -4 \text{ V}$ ,  $K_{n2} = 10 \text{ mA/V}^2$ , and  $R_G = R_D = 100 \text{ k}\Omega$ ? (b) What are the  $Q$  and bandwidth of your design?

- \*17.111. Simulate the frequency response of the circuit design in Prob. 17.110 and find the midband gain, center frequency,  $Q$  and bandwidth, and the  $Q$  of the circuit. Was the desired stagger tuning achieved?

- \*17.112. (a) Derive an expression for the high frequency input admittance at the base of the common-emitter circuit in Fig. 17.34(b) and show that the input capacitance and input resistance can be represented by the expressions below for  $\omega C_\mu R_L \ll 1$ .

$$C_{in} = C_\pi + C_\mu(1 + g_m R_L)$$

$$R_{in} = r_\pi \left| \frac{R_L}{(1 + g_m R_L)(\omega C_\mu R_L)^2} \right|$$

- (b) A MOSFET has  $C_{GS} = 6 \text{ pF}$ ,  $C_{GD} = 2 \text{ pF}$ ,  $g_m = 5 \text{ mS}$ , and  $R_L = 10 \text{ k}\Omega$ . What are the values of  $C_{in}$  and  $R_{in}$  at a frequency of 5 MHz?

- 17.113. (a) Find the equivalent input capacitance and resistance of the circuit in Fig. 17.70(b) if  $L_S = 10 \text{ nH}$ ,  $C_{GS} = 100 \text{ fF}$  and  $g_m = 1 \text{ mS}$ . (b) Repeat for the circuit in Fig. 17.71 if  $C_{GD} = 20 \text{ fF}$ ,  $L_{in} = 0$  and  $f = 1 \text{ GHz}$ . (You may want to make use of the network transformations in the EIA on page 1195.)
- 17.114. (a) Derive the expressions for the circuit transformation in part (a) of the RF Network Transformation EIA on page 1195 by equating the impedances of the two networks. (b) Repeat for part (c) of the EIA. (c)
- 17.115. (a) Derive the expressions for the circuit transformation in part (b) of the RF Network Transformation EIA on page 1195 by equating the admittances of the two networks. (b) Repeat for part (d) of the EIA.
- 17.116. Derive an expression for the high-frequency input impedance of the bipolar transistor with inductive degeneration  $L_E$  in the emitter. Assume  $r_\pi \gg 1/\omega C_\pi$ .

## 17.12 Mixers and Balanced Modulators

- 17.117. (a) A signal at 900 MHz is mixed with a local oscillator signal at 1.0 GHz. What is the frequency of the VHF output signal? The unwanted output signal? (b) Repeat for a local oscillator signal of 0.8 GHz.
- 17.118. A parallel  $LC$  circuit with a  $Q$  of 75 is used to select the VHF output signal in Prob. 17.117(a). What is the attenuation of the circuit at the unwanted signal frequency?
- 17.119. A parallel  $LC$  circuit with a  $Q$  of 50 is used to select the RF output signal at 10.7 MHz in Fig. 17.82. (a) Draw a possible circuit. (b) What is the attenuation of the circuit at the unwanted signal frequency?
- 17.120. (a) Cell phone signals in the range of 1.8 to 2.0 GHz are mixed with a local oscillator to produce an output signal at 70 MHz. What is the range of local oscillator (LO) frequencies required if the LO is below the cell phone signal frequency? What is the frequency range of the unwanted output signals? (b) Repeat if the local oscillator signal is above the cell phone frequency? (c) Which choice of LO frequency seems most desirable?

## 17.13 Single-Balanced Mixers

- 17.121. (a) Find the conversion gain for the single-balanced mixer in Fig. 17.74 for output frequen-

- cies centered around  $3f_2$ . (b) Repeat for output frequencies centered around  $5f_2$ .
- 17.122. Find the expression similar to Eq. (17.195) for the output voltage for the mixer in Fig. 17.74 if input  $v_1 = A \cos \omega_1 t$ .
- 17.123. Suppose the signal  $s_S(t)$  driving the switch in Fig. 17.74 is not a perfect square wave. Instead, the switch spends 60 percent of the time in the closed position and 40 percent of the time in the open position. What is the amplitude of the output signal at frequency  $f_1$ ?
- 17.124. Suppose that switching signal  $v_2$  in the mixer in Fig. 17.76 is operating at a frequency of  $f_1$ , the same frequency as the signal part of  $i_{EE}$ . What are the amplitudes and frequencies of the first five spectral components of the output voltage if  $I_{EE} = 2.5 \text{ mA}$ ,  $I_1 = 0.5 \text{ mA}$ , and  $R_C = 2 \text{ k}\Omega$ ?
- 17.125. (a) Find the conversion gain for the double-balanced mixer in Fig. 17.78 for output frequencies centered around  $3f_2$ . (b) Repeat for output frequencies centered around  $5f_2$ .
- 17.126. Find the expression similar to Eq. (17.200) for the output voltage for the mixer in Fig. 17.78 if input  $v_1 = A \cos \omega_1 t$ .
- 17.127. Suppose the signal  $s_D(t)$  driving the switch in Fig. 17.78 is not a perfect square wave. Instead, the switch spends 55 percent of the time in the closed position and 45 percent of the time in the open position. What is the amplitude of the output signal at frequency  $f_1$ ?
- 17.128. Use SPICE to simulate the passive mixer in Fig. 17.80 and reproduce the results in Fig. 17.81. Use the default NMOS transistor model with  $W/L = 10/1$  and  $V_{TN} = 0.75 \text{ V}$ .
- 17.129. Suppose an AM signal is generated with the Gilbert balanced modulator with  $M = 1$ . Compare the amplitudes of the carrier and each of the two sideband components.
- 17.130. (a) Write the expression for the output voltage for the Gilbert mixer in Fig. 17.82 for  $I_{BB} = 2 \text{ mA}$ ,  $V_m = 10 \text{ mV}$ ,  $R_C = 5 \text{ k}\Omega$ ,  $2R_1 = 1 \text{ k}\Omega$ ,  $f_c = 90 \text{ MHz}$ , and  $f_m = 10 \text{ MHz}$ . Include the terms for  $n = 1$  and 2. (b) What is the largest value of  $V_1$  that satisfies our small-signal assumption?
- 17.131. What is the conversion gain (for  $n = 1$ ) for the doubly balanced mixer in Fig. 17.82 if  $I_{BB} = 5 \text{ mA}$ ,  $R_C = 1 \text{ k}\Omega$ , and  $2R_1 = 200 \Omega$ . What is the

- largest value of  $V_m$  that satisfies our small-signal assumption?

17.132. The circuit in Fig. P17.132 provides the current  $i_{EE}$  for the mixer in Fig. 17.76(b) where  $v_1 = V_1 \sin \omega_1 t$ . (a) If  $V_1 = 0.25$  V,  $R_C = 6.2$  k $\Omega$ ,  $f_1 = 2000$  Hz, and  $f_2 = 1$  MHz, what are  $I_{EE}$  and  $I_1$ ? (b) What are the amplitudes of the first five spectral components in the output signal? (c) What are the largest values of  $V_1$  and  $I_1$  that satisfy our small-signal assumptions?

\*17.133. Suppose that signal  $v_2$  driving the switch in Fig. 17.76 is not a perfect square wave. Instead, the switch spends 60 percent of the time in the left-hand position and 40 percent of the time in the right-hand position. What is the amplitude of the output signal at frequency  $f_1$ ?

\*17.134. Suppose that signal  $v_2$  driving the switch in Fig. 17.82 is not a perfect square wave. Instead, the switch spends 55 percent of the time in the left-hand position and 45 percent of the time in

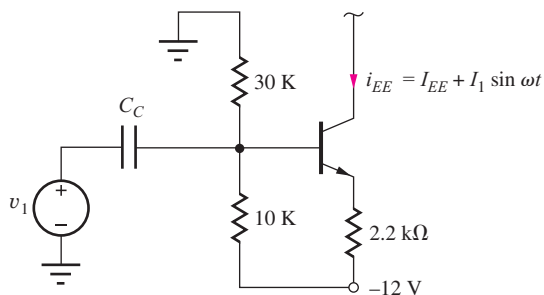
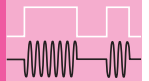


## Figure P17.132

# CHAPTER 18



## TRANSISTOR FEEDBACK AMPLIFIERS AND OSCILLATORS

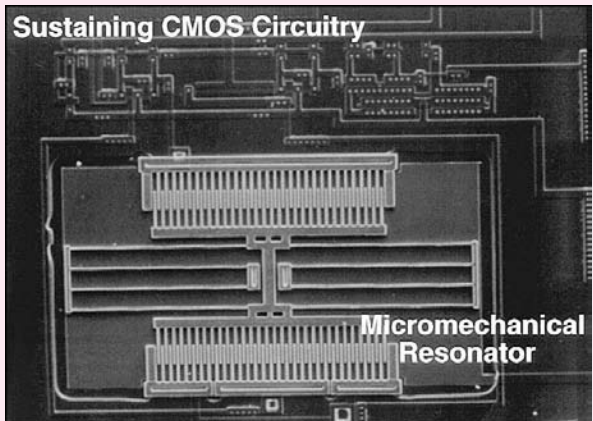
### CHAPTER OUTLINE

- 18.1 Basic Feedback System Review 1229
- 18.2 Feedback Amplifier Analysis at Midband 1232
- 18.3 Feedback Amplifier Circuit Examples 1234
- 18.4 Review of Feedback Amplifier Stability 1254
- 18.5 Single-Pole Operational Amplifier Compensation 1262
- 18.6 High-Frequency Oscillators 1277
- Summary 1287
- Key Terms 1289
- References 1289
- Problems 1289

### CHAPTER GOALS

- Review the concepts of negative and positive feedback
- Review loop transmission feedback analysis techniques
- Review the application of Blackman's theorem to feedback amplifiers
- Understand the topologies and characteristics of the series-shunt, shunt-shunt, shunt-series, and series-series feedback configurations
- Analyze midband characteristics of each feedback configuration with loop transmission theory and Blackman's theorem
- Understand the effects of feedback on frequency response and feedback amplifier stability
- Practice interpreting feedback amplifier stability in terms of Nyquist and Bode plots
- Use SPICE ac and transfer function analyses to characterize feedback amplifiers
- Develop techniques to determine the loop-gain of closed-loop amplifiers using SPICE simulation or measurement
- Learn to design operational amplifier frequency compensation using Miller multiplication
- Develop relationships between op-amp unity gain frequency and slew rate.
- Discuss the Barkhausen criteria for oscillation

- Understand high frequency LC and crystal oscillator circuits
- Explore negative resistance in oscillator circuits
- Present the LCR model of the quartz crystal



An oscillator employing a MEMS<sup>1</sup> frequency selective resonator. Copyright IEEE 1999. Reprinted with permission.

Examples of feedback systems abound in daily life. The thermostat that senses the temperature of a room and turns the air-conditioning system on and off is one example. Another is the remote control that we use to select a channel on the television or set the volume at an acceptable level. The heating and cooling system uses a simple temperature transducer to compare the temperature with a fixed set point. However, we are part of the TV remote control feedback system; we operate the control until our senses tell us that the audio and optical information is what we want.

The theory of negative feedback in electronic systems was first developed by Harold Black of the Bell Telephone System. In 1928, he invented the feedback amplifier to stabilize the gain of early telephone repeaters. Today, some form of feedback is used in virtually every electronic system. This chapter formally reviews the concept of feedback, which is

<sup>1</sup> Micro-Electro-Mechanical System. C. T-C. Nguyen and R. T. Howe, "An integrated micromechanical resonator high-Q oscillator," *IEEE J. Solid-State Circuits*, vol. 34, no. 4, pp. 440–445, April 1999.

an invaluable tool in the design of electronic systems. Valuable insight into the operation of many common electronic circuits can be gained by recasting the circuits as feedback amplifiers.

We already encountered **negative** (or **degenerative**) **feedback** in several forms. The four-resistor bias network uses negative feedback to achieve an operating point that is independent of variations in device characteristics. We also found that a source or emitter resistor can be used in an inverting amplifier to control the gain and bandwidth of the stage. Many of the advantages of negative feedback were actually uncovered during the discussion of operational amplifier circuit design. Generally, feedback can be used to achieve a tradeoff between gain and many of the other properties of amplifiers:

- *Gain stability:* Feedback reduces the sensitivity of gain to variations in the values of transistor parameters and circuit elements.
- *Input and output impedances:* Feedback can increase or decrease the input and output resistances of an amplifier.

- *Bandwidth:* The bandwidth of an amplifier can be extended using feedback.
- *Nonlinear distortion:* Feedback reduces the effects of nonlinear distortion. (For example, feedback can be used to minimize the effects of the dead zone in a class-B amplifier stage.)

Feedback may also be **positive** (or **regenerative**), and we explore the use of positive feedback in sinusoidal **oscillator circuits** in this chapter. We encountered the use of a combination of negative and positive feedback in the discussion of *RC* active filters and multivibrator circuits in Chapter 12. Sinusoidal oscillators use positive feedback to generate signals at specific desired frequencies; they use negative feedback to stabilize the amplitude of the oscillations.

Positive feedback in amplifiers is usually undesirable. Excess phase shift in a feedback amplifier may cause the feedback to become regenerative and cause the feedback amplifier to break into oscillation. Remember that positive feedback was identified in Chapter 17 as a potential source of oscillation problems in tuned amplifiers.

## 18.1 BASIC FEEDBACK SYSTEM REVIEW

Let's review the feedback system introduced in Chapter 11. The diagram in Fig. 18.1 represents a simple feedback amplifier. It consists of an amplifier with transfer function  $A(s)$ , referred to as the **open-loop amplifier**, a **feedback network** with transfer function  $\beta(s)$ , and a summing block indicated by  $\Sigma$ .

### 18.1.1 CLOSED-LOOP GAIN

In Fig. 18.1, the input to the open-loop amplifier  $A$  is provided by the summing block, which actually develops the difference between the input signal  $v_i$  and the feedback signal  $v_f$ :

$$v_d = v_i - v_f \quad (18.1)$$

The output signal is equal to the product of the open-loop amplifier gain and the input signal to the amplifier:

$$v_o = A v_d \quad (18.2)$$

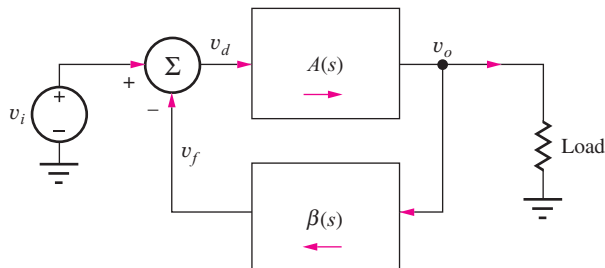


**Figure 18.1** Classic block diagram for a feedback system.

The signal fed back to the input is given by

$$\mathbf{v}_f = \beta \mathbf{v}_o \quad (18.3)$$

Combining these as we did in Chapter 11 results in the core equations which predict the **closed-loop gain** of a negative feedback amplifier:

$$A_v = \frac{\mathbf{v}_o}{\mathbf{v}_i} = \frac{A}{1 + A\beta} = \frac{1}{\beta} \left( \frac{A\beta}{1 + A\beta} \right) = A_v^{\text{ideal}} \frac{T}{1 + T} \quad (18.4)$$

where  $A_v$  is the closed-loop gain,  $A$  is the **open-loop gain** of the amplifier, and the product  $T = A\beta$  is defined as the **loop gain** or **loop transmission**.  $A_v^{\text{ideal}}$  is the **ideal gain** that would be achieved if the amplifier were ideal.  $\beta$  is the feedback factor that describes how much of the sampled output is fed back to the input of the amplifier. As in Chapter 11, we will need to ensure that our feedback is connected as negative feedback to match our basic topology defined in Fig. 18.1 and insure stability. Also, Eq. (18.4) still holds if each of the terms are complex frequency dependent terms instead of simple midband small-signal terms.

### 18.1.2 CLOSED-LOOP IMPEDANCES

Recall from Chapter 11 that we use Blackman's theorem to calculate the resistance (or impedance) looking into an arbitrary pair of terminals in a negative feedback amplifier:

$$R_x = R_x^D \frac{1 + |T_{SC}|}{1 + |T_{OC}|} \quad (18.5)$$

where  $R_x^D$  is the resistance seen with the feedback disabled,  $T_{SC}$  is the loop transmission with a small-signal short across the selected terminal pair, and  $T_{OC}$  is the loop transmission with an open circuit across the selected terminal pair.

### 18.1.3 FEEDBACK EFFECTS

We now turn to an example negative feedback circuit to motivate our analyses. The circuit in Fig. 18.2 is a differential amplifier with current-mirror load. The only difference between this circuit and what we have previously analyzed is the negative feedback connection between the output and the inverting input of the differential pair. As we learned in our analysis of op-amp circuits, negative feedback works to minimize the difference between the inputs. With a direct connection from output to inverting input, the output is made to track the noninverting input, creating a unity-gain amplifier.

To illustrate some of the effects of the feedback, let's explore some simulations of the circuit. We'll use  $BF = 100$ ,  $VAF = 50$  V, and  $IS = 1$  fA for both the *n-p-n* and *p-n-p* models. Simulations show that the midband gain,  $\mathbf{v}_o/\mathbf{v}_i = 0.996$ , so the circuit is indeed a unity-gain amplifier. Without any understanding of feedback, we would expect the input resistance presented to source  $v_i$  is  $2r_\pi + R_i$ , or about  $5.1$  kΩ. If this is the correct value, increasing  $R_i$  to  $5$  kΩ should decrease the gain to about  $0.5$  due to voltage division at the input. However, Table 18.1 shows that the gain decreases less than 4 percent as the source impedance is increased well beyond our apparently erroneous calculation of the input impedance. So, feedback has increased the effective input resistance rather dramatically. Looking at Blackman's theorem, Eq. (18.5), we can see that the  $T_{OC}$  term is zero<sup>2</sup> when the noninverting input is left open-circuited.

On the output side, without the use of Blackman's theorem, we might calculate the output resistance as:<sup>3</sup>

$$R_{\text{out}} = R_{iB2} || R_{iC2} || R_{iC4} \cong 2r_\pi || r_{o2} || r_{o4} \approx 4.2 \text{ k}\Omega \quad (18.6)$$

<sup>2</sup> There is actually a negligibly small value of  $T_{OC}$  because of conduction through  $r_o$ .

<sup>3</sup>  $R_{iB2} = r_{\pi2} + (\beta_{o2} + 1) \frac{r_{\pi1} + R_i}{\beta_{o1} + 1} = r_{\pi2} + r_{\pi1} + R_i \cong R_i + 2r_\pi = 5.1 \text{ k}\Omega$

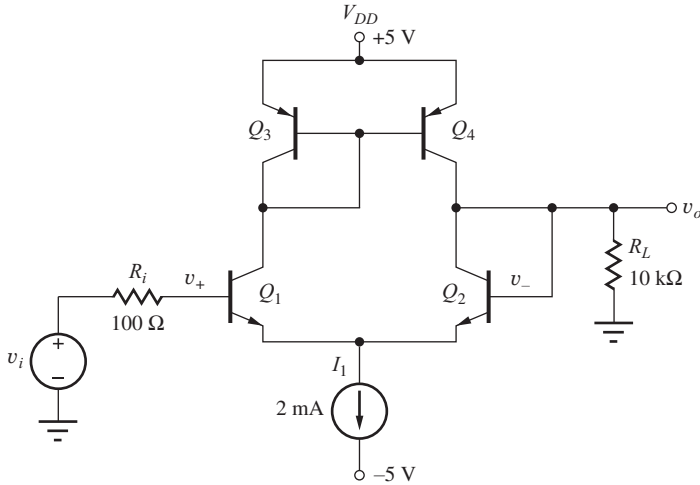


**Figure 18.2** Single-stage differential feedback amplifier. ( $g_m = 0.04 \text{ S}$ ,  $r_\pi = 2.5 \text{ k}\Omega$ ,  $r_o = 55 \text{ k}\Omega$ )

**TABLE 18.1**  
Gain Sensitivity to Source Resistance Variation

$R_I (\text{k}\Omega)$	$V_o / V_I$
0.1	0.996
0.5	0.996
1	0.996
5	0.993
10	0.990
50	0.964

**TABLE 18.2**  
Gain Sensitivity to Load Resistance Variation

$R_L (\text{k}\Omega)$	$V_{\text{OUT}} / V_I$
10	0.996
5	0.994
1	0.974
0.5	0.950

**TABLE 18.3**  
Gain Sensitivity to Parameter Variation

PARAMETER	$V_{\text{OUT}} / V_I$
BF = 100	0.996
BF = 200	0.997
BF = 50	0.996
VAF = 50	0.996
VAF = 100	0.997
VAF = 25	0.996

Note that we neglected the small  $R_i$  in this calculation. Given this result, we expect that the gain will decrease if we reduce the load resistance,  $R_L$ . Table 18.2 shows the results from a series of simulations as the load resistance is changed, but the gain is only reduced by 5 percent when the load resistance has been reduced to  $500\Omega$ . This indicates that the amplifier output resistance must be much less than our estimate of  $4.2 \text{ k}\Omega$ . Here again we find that the negative feedback has significantly changed the circuit characteristics. In this case, the output resistance has been reduced by the feedback.

Another important characteristic of feedback amplifiers is reduced sensitivity to circuit parameter variations. For example, Table 18.3 shows how gain changes with changes in transistor forward current gain and Early voltage. The doubling or halving of these parameters causes less than 0.1 percent change in the simulated closed-loop gain! The results in this section are explained by examination of Eq. (18.4). As long as  $T$  is large,  $T/1 + T$  is nearly 1 and the gain will remain close to its ideal value.

Feedback allows us to create circuits that are robust to changes in device and other parameters. This explains how electronic systems are built with reliable characteristics despite large manufacturing tolerances for many of the parameters of the individual components that are used to build systems. Feedback is essential for reproducible and accurate behavior of amplifiers.

**EXERCISE:** Find the Q-points for the four transistors in the amplifier in Fig. 18.2. What is the Q-point value for the output voltage  $v_o$ ?

**ANSWERS:** (1 mA, 5 V), (1 mA, 0.7 V), (1 mA, 0.7 V), (1 mA, 5 V); 0 V

## 18.2 FEEDBACK AMPLIFIER ANALYSIS AT MIDBAND

Referring to what we learned in Chapter 11, the amplifier in Fig. 18.2 is configured in a series-shunt topology. The feedback connection is directly sampling the output voltage and is therefore shunting the output. The feedback signal is a voltage applied in series (across the differential pair) with the input signal.

### Closed-Loop Gain

We will now calculate the closed-loop gain using our feedback equation with the help of the ac equivalent circuit in Fig. 18.3. First, the ideal feedback factor  $\beta$  is unity, so the ideal gain,  $A_v^{\text{ideal}}$  is 1.0. Loop transmission (loop gain)  $T$  is calculated including the loading effects of the feedback connection to the output. If the signal voltage at the base of  $Q_2$  is  $v_o$ , then the output voltage will be  $(i_{c2} + i_{c4})$  times the resistance at the output node:

$$v_o = (i_{c2} + i_{c4})R_{\text{out}} = - \left( g_{m2} \frac{V_{b2}}{2} + g_{m2} \frac{V_{b2}}{2} \right) (r_{o2} || r_{04} || R_{iB2} || R_L) \quad (18.7)$$

Since the output is connected directly to the base of  $Q_2$ , the loop transmission is

$$T = - \frac{v_o}{V_{b2}} = A\beta = g_{m2}(r_{o2} || r_{04} || R_{iB2} || R_L) = (0.04S)(55 || 55 || 5.1 || 10) \text{ k}\Omega = 120 \quad (18.8)$$

where

$$R_{iB2} = r_{\pi2} + (\beta_{o2} + 1) \frac{r_{\pi1} + R_i}{\beta_{o1} + 1} = r_{\pi2} + r_{\pi1} + R_i \cong R_i + 2r_{\pi} = 5.1 \text{ k}\Omega \quad (18.9)$$

Therefore, the closed-loop gain not including source attenuation is:

$$A_v = (1) \left( \frac{120}{1 + 120} \right) = 0.992 \quad (18.10)$$

Recall that the simulated value of the closed-loop gain is 0.996, quite close to our calculated value.

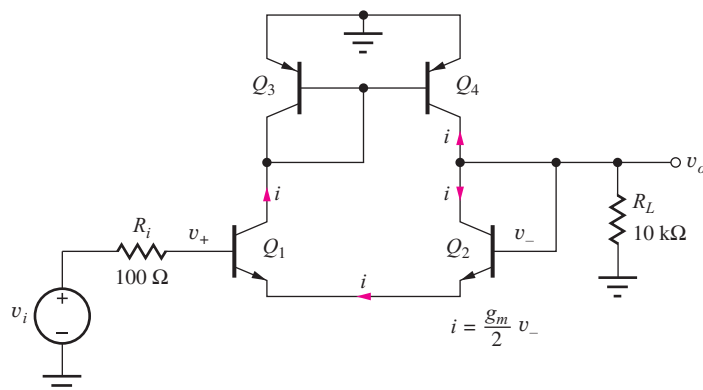


Figure 18.3 ac equivalent circuit with currents for loop-gain calculation.

### Input Resistance

The input resistance can be calculated from Blackman's theorem, and  $T_{SC}$ ,  $T_{OC}$ , and  $R_{in}^D$  must be found in order to evaluate Eq. (18.5). To find  $T_{SC}$ , the input at  $v_i$  is shorted to ground, and we see that  $T_{SC}$  is the same as the loop transmission we calculated for the closed-loop gain. To find  $T_{OC}$ , we open the circuit at the base of  $Q_1$ .  $T_{OC}$  is approximately zero because the amplifier gain (with respect to an input at the base of  $Q_2$ ) is zero with an ac open circuit at the base of  $Q_1$  since no current can go through either  $Q_1$  or  $Q_2$  (neglecting the transistor output resistances). This condition is equivalent to an infinite resistance in series with the equivalent resistance of the differential pair.

Finally we need to find the input resistance with the feedback disabled,  $R_{in}^D$ . If we mentally ignore the presence of the feedback, then the input resistance, including the effects of the equivalent resistance on the base of  $Q_2$ , is  $R_{in}^D = R_i + r_{\pi 1} + r_{\pi 2} + (r_{o4} \| r_{o2} \| R_L) = 12.2 \text{ k}\Omega$ . These values enable the direct calculation of the input resistance from Blackman's theorem:

$$R_{in} = R_{in}^D \frac{1 + |T_{SC}|}{1 + |T_{OC}|} = 12.2 \text{ k}\Omega \left( \frac{1 + 120}{1 + 0} \right) = 1.48 \text{ M}\Omega \quad (18.11)$$

The simulated value of  $R_{in}$  is  $1.43 \text{ M}\Omega$ . Note that although the closed-loop input resistance is increased by feedback, it is directly proportional to the load impedance in this simple feedback configuration, so it is clear that this topology would not work as a buffer to small load resistances. It is important to recognize that we do not actually disconnect the feedback network when we mentally disable the feedback for calculating the open-loop  $R_{in}$ . We still include the loading effects of the elements associated with the feedback connection.

### Output Resistance

Blackman's theorem is also used to calculate the closed-loop output resistance. In this case we need to find the loop transmission with the output open and the output shorted to ground. For this case,  $T_{OC}$  is the loop transmission we calculated earlier when calculating the voltage gain except the effect of  $R_L$  is not included, since we are looking into the amplifier from the load. With this change to Eq. (18.7), we find  $T_{OC} = 171$ .  $T_{SC}$  is zero since the amplifier gain is zero when the output is shorted to small-signal ground. The output impedance with the feedback disabled,  $R_{out}^D$ , is simply the resistance looking into the amplifier output ignoring the effect of feedback and is given by

$$R_{out}^D = R_{iB2} \| r_{o2} \| r_{o4} = \left[ r_{\pi 2} + (\beta_{o2} + 1) \left( \frac{r_{\pi 1} + R_i}{\beta_{o1} + 1} \right) \right] \| r_{o2} \| r_{o4} = (r_{\pi 2} + r_{\pi 1} + R_i) \| r_{o2} \| r_{o4} = 4.30 \text{ k}\Omega \quad (18.12)$$

$R_{out}$  can now be calculated as:

$$R_{out} = R_{out}^D \frac{1 + T_{SC}}{1 + T_{OC}} = 4.30 \text{ k}\Omega \left( \frac{1 + 0}{1 + 171} \right) = 25.0 \text{ }\Omega \quad (18.13)$$

The simulated value of  $R_{out}$  is  $25.6 \text{ }\Omega$ . This is clearly much lower than our earlier estimate and explains why the amplifier gain is so insensitive to the changes in load resistance we simulated in the previous section.

We calculate the overall gain including source attenuation and output loading as:

$$A = \left( \frac{R_{in}}{R_{in} + R_i} \right) A_v = 0.992 \text{ V/V} \quad (18.14)$$

Because the closed-loop input resistance is so large, the input attenuation due to source resistance is small. Notice in the above equations that we included  $R_L$  when calculating closed-loop gain and input resistance. As we can see from the above equations, this amplifier has a high open-loop output resistance and the output load plays a direct role in the gain and input impedance calculations. We therefore need to include  $R_L$  for accurate results. We will see later that amplifiers with low open-loop output resistance or very high loop gain can be analyzed independent of  $R_L$  with minimal impact on accuracy.

**EXERCISE:** For the output resistance calculation, convince yourself that  $T_{SC} = 0$  when the output is short circuited.

**EXERCISE:** For the input resistance calculation, convince yourself that  $T_{OC} = 0$  when the input is open circuited.

**EXERCISE:** Calculate  $T_{OC}$  as required for the output resistance calculation and confirm that its value is 171.

## 18.3 FEEDBACK AMPLIFIER CIRCUIT EXAMPLES

In the following sections we will use this same approach to calculate midband closed-loop gain and the closed-loop input and output impedances of a variety of feedback topologies. The midband analysis can be summarized with the following steps:

### Feedback Analysis Procedure

1. Determine if the feedback output connection is shunt or series. If it is a shunt connection, the network is sensing output voltage. If series, the feedback is sensing the output current.
2. Determine if the feedback input connection is shunt or series. If shunt, current is being fed back to the input, if series, voltage is being fed back to the input.
3. Given the type of feedback connections, the units for the feedback factor,  $\beta$ , are determined, and the type of amplifier can be found from Table 18.4.
4. Calculate feedback factor  $\beta$  for the idealized version of the amplifier. For example, with a series-shunt configuration, the idealized amplifier input impedance is infinite, and the output impedance is assumed to be zero. Ideal gain is then calculated as the reciprocal of the ideal feedback factor.
5. Calculate the loop transmission including the amplifier and feedback network loading effects.
6. Use Eq. (18.4) to calculate the closed-loop gain of the amplifier.
7. Use Blackman's theorem to calculate the amplifier input and output impedances or any other desired impedances in the circuit. The open-circuit and short-circuit loop-gains are calculated including nonideal loading effects.
8. Calculate the overall gain including input and output loading.

We will now use these steps to perform midband analysis of a number of amplifier topologies.

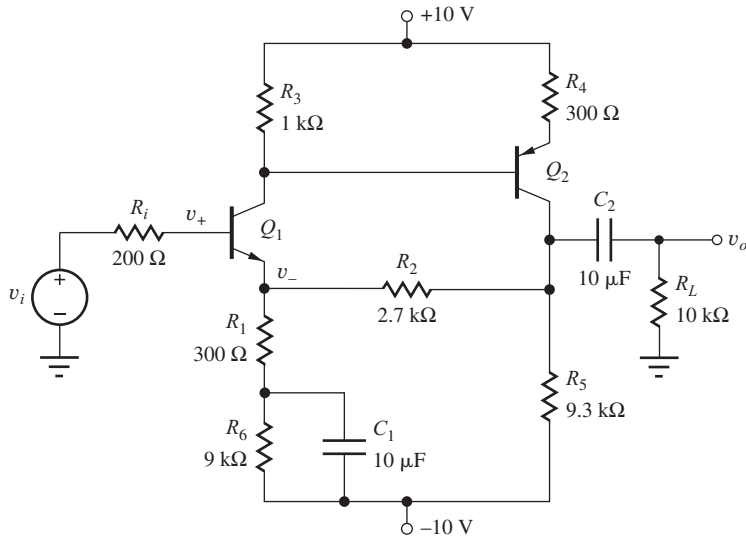
### 18.3.1 SERIES-SHUNT FEEDBACK—VOLTAGE AMPLIFIERS

Figure 18.4 illustrates a two-stage feedback amplifier known as a series-shunt feedback pair. At first glance, the topology may appear a bit confusing. It appears to have two paths from input to output, one through the collector of  $Q_1$  and another through the emitter of  $Q_1$ . While this is true, the dominant forward path is the high gain path through the two common-emitter stages of  $Q_1$  and  $Q_2$ .

**TABLE 18.4**

Determining Amplifier Type Based on Feedback Connections

FEEDBACK CONNECTION	SENSED SIGNAL	FED BACK SIGNAL	FEEDBACK FACTOR, $\beta$	GAIN RATIO	AMPLIFIER GAIN
Series-shunt	Voltage	Voltage	V/V	V/V	Voltage
Shunt-shunt	Voltage	Current	I/V	V/I	Transresistance
Series-series	Current	Voltage	V/I	I/V	Transconductance
Shunt-series	Current	Current	I/I	I/I	Current



**Figure 18.4** Two-stage feedback voltage amplifier—the series-shunt feedback pair.

**Figure 18.5** Ideal small-signal version of amplifier in Fig. 18.4.

Given this, the feedback path is apparently from the output through  $R_2$  back to the emitter of  $Q_1$ . Since the feedback is connected directly to the output, it is a shunt connection and the feedback network is sampling voltage.

The feedback network does not seem to be summing a current into the input network, so it is apparently a series connection at the input. Recall that the small-signal output current at the collector of a transistor is  $g_m v_{be} = g_m(v_b - v_e)$ . So, the transistor is acting as a differential amplifier, generating an output that is proportional to the difference between the small-signal input voltage at the base and the small-signal voltage fed back to the emitter. This leads us to Fig. 18.5, a simplified small-signal equivalent of the series-shunt voltage amplifier in Fig. 18.4. Let's now calculate the midband gain, input, and output impedances in Ex. 18.1.

### EXAMPLE 18.1 TWO-STAGE SERIES-SHUNT VOLTAGE AMPLIFIER

Perform an analysis of a two-stage series-shunt feedback amplifier.

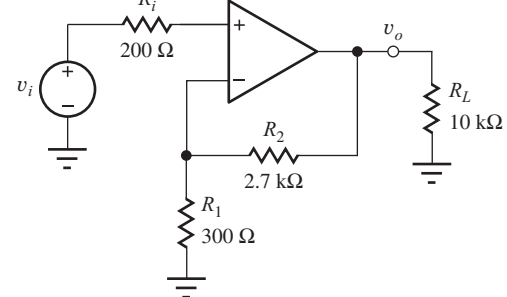
**PROBLEM** The amplifier of Fig. 18.4 has been constructed. Find the small-signal gain and input and output resistances. Assume dc base currents are negligible,  $V_A = \infty$ , and  $\beta_0$  is 100.

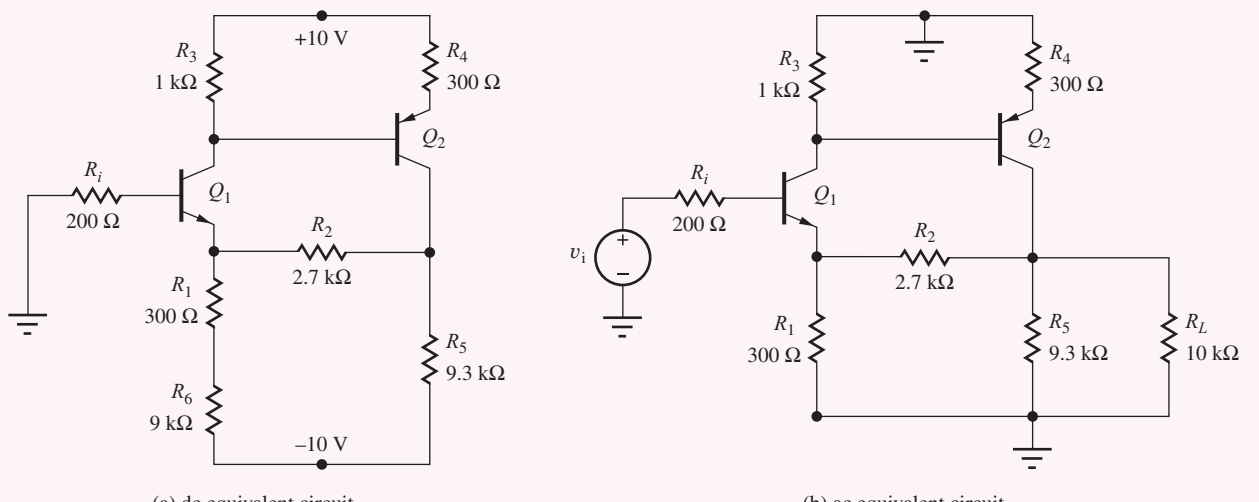
**SOLUTION** **Known Information and Given Data:** The circuit diagram appears in Fig. 18.4 and  $\beta_0 = 100$ . Transistor output resistances are infinite.

**Unknowns:** Ideal gain, open-loop gain, loop transmission, and Blackman terms for the input and output impedances.

**Approach:** Use amplifier gain analysis from previous chapters, feedback analysis procedure, and Blackman's theorem.

**Assumptions:**  $V_{BE} = 0.7$  V,  $V_T = 25$  mV, and small-signal midband conditions apply; dc base currents are negligible and  $r_o$  is infinite.





**Analysis:** First, we must draw the dc equivalent circuit in (a) above and find the dc solution. Neglecting the dc base current,  $V_{B1} = 0$  V, so  $V_{E1} = -0.7$  V. If we assume the dc current through  $R_2$  is negligible,

$$I_{E1} \cong \frac{-0.7 - (-10)}{9.3 \text{ K}} = 1 \text{ mA} \quad V_{C1} = 10 - I_{C1} \cdot R_3 = 9 \text{ V}$$

$$I_{E2} = \frac{10 - (9 - V_{BE2})}{R_4} = 1 \text{ mA} \quad V_{C2} = I_{C2} \cdot R_5 + (-10V) = -0.7 \text{ V}$$

Now our assumption that the dc current in  $R_2$  is zero needs to be checked:

$$I_{R2} = \frac{V_{C2} - V_{E1}}{R_2} = 0$$

Next, we draw the ac equivalent circuit by shorting all the capacitors and placing ac grounds at the two power supplies as in (b) above. The small-signal parameters are:

$$g_{m1} = g_{m2} = 40(0.001) = 0.04 \text{ S}, r_\pi = 100/g_m = 2500 \Omega, r_o = \infty$$

Now we turn to our feedback analysis procedure.

**Step 1:** As discussed above, the feedback network is composed of  $R_2$  and  $R_1$ . The output voltage is directly sampled by  $R_2$ , so it is a shunt connection.

**Step 2:** The signal fed back is the small-signal voltage at the emitter of  $Q_1$ . This is in series with the input voltage at the base of  $Q_1$ , so this is a series feedback connection.

**Step 3:** Since voltage is sampled and voltage is fed back to the input, the feedback factor has units of voltage/voltage and the amplifier is a series-shunt voltage amplifier.

**Step 4:** As is apparent in Fig. 18.5, the amplifier type is a series-shunt configuration, so the ideal feedback factor is just the voltage division across the feedback network,  $\beta = R_1/(R_1 + R_2)$ , and the ideal gain is:

$$A_v^{\text{Ideal}} = \frac{R_2 + R_1}{R_1} = 10$$

**Step 5:** The loop transmission is found by injecting a signal at a point in the circuit and calculating how much signal is returned to that point through the feedback path. Another approach is to calculate the gain around the loop, making sure to include all of the loading effects. We will

start at the emitter of  $Q_1$  and calculate the gain back around the loop to the same point. This requires calculating the common-base gain of  $Q_1$ , the common-emitter gain of  $Q_2$ , and finally the nonideal voltage division at the feedback network.

$$T = [g_{m1}(R_3 \parallel R_{iB2})] \left[ -\frac{g_{m2}}{1 + g_{m2}R_4} ([R_2 + R_1 \parallel R_{iE1}] \parallel R_5 \parallel R_L) \right] \left( \frac{R_{iE1} \parallel R_1}{R_{iE1} \parallel R_1 + R_2} \right)$$

$$R_{iB2} = r_{\pi2} + (\beta_o + 1)R_4 = 32.8 \text{ k}\Omega \quad R_{iE1} = \frac{r_{\pi1} + R_i}{(\beta_{o1} + 1)} = \frac{200 + 2500}{101} \Omega = 26.7 \Omega$$

$$T = 0.04S(970 \Omega) \left[ -\frac{0.04S(1720 \Omega)}{1 + 0.04S(300 \Omega)} \right] \left( \frac{26.7 \Omega}{26.7 \Omega + 2700 \Omega} \right) = -2.01$$

Notice that  $T$  is quite low. As a consequence, the gain error will be large. We also see that  $T$  is negative. Remember we must always check that we have negative feedback when we are building a feedback amplifier.

**Step 6:** The closed-loop gain of the feedback amplifier is calculated according to Eq. (18.4). However, remember that the negative sign on  $T$  is already included in our high-level feedback description in Fig. 18.1, so  $T$  will be positive when we evaluate Eq. (18.4):

$$A_v = A_v^{\text{ideal}} \frac{T}{1 + T} = 10 \frac{-2.01}{1 + -2.01} = 6.68$$

This expression does not include attenuation at the input due to voltage division. We expect this factor to be fairly insignificant since the source impedance is low. The actual value can be calculated after the input impedance is calculated.

**Step 7:** Since the loop transmission is low, the input and output impedances will not be changed much by feedback.

**Input Resistance:** First we calculate the open-loop input resistance looking into the base of  $Q_1$  ignoring the effect of feedback.

$$R_{\text{in}}^D = R_{\text{in}B1} = r_{\pi1} + (\beta_0 + 1)(R_1 \parallel [R_2 + R_5 \parallel R_L \parallel R_{iC2}]) \cong 31.7 \text{ k}\Omega$$

$T_{OC}$  is zero for the input resistance calculation since the gain through  $Q_1$  is reduced to zero if the impedance looking out of the base of  $Q_1$  is infinite (i.e., for an open circuit, zero base current yields zero collector and emitter currents).  $T_{SC}$  is very close to the value calculated above except that the  $R_{iE1}$  term is reduced slightly since the impedance looking out of the base is zero instead of  $200 \Omega$ . With this change,  $T_{SC} = 1.86$  we calculate the closed-loop resistance looking into the input (the base of  $Q_1$ ):

$$R_{\text{in}} = R_{\text{in}}^D \frac{1 + T_{SC}}{1 + T_{OC}} = 31.7 \text{ k}\Omega \left( \frac{1 + 1.86}{1 + 0} \right) = 90.7 \text{ k}\Omega$$

**Output Resistance:** For the output resistance, we mentally disable the feedback and calculate the impedance looking into the output of the amplifier, not including the load resistance.

$$R_{\text{out}}^D = R_{iC2} \parallel R_5 \parallel (R_2 + R_{iE1} \parallel R_1) \cong 2.11 \text{ k}\Omega$$

where  $R_{iC2} = r_{o2}(1 + g_{m2}R_4)$  is negligible.  $T_{SC}$  is now zero since the amplifier gain is zero when the output is shorted to small-signal ground.  $T_{OC}$  is nearly identical to the loop transmission calculated earlier except that  $R_L$  is not included:

$$T_{OC} = [g_{m1}(R_3 \parallel R_{iB2})] \left( -\frac{g_{m2}}{1 + g_{m2}R_4} [(R_2 + R_1 \parallel R_{\text{in}E1}) \parallel R_5] \right) \left( \frac{R_{iE1} \parallel R_1}{R_{iE1} \parallel R_1 + R_2} \right)$$

$$|T_{OC}| = 0.04S(970 \Omega) \left[ \frac{0.04S(2107 \Omega)}{1 + 0.04S(300 \Omega)} \right] \left( \frac{26.7 \Omega}{26.7 \Omega + 2.7 \text{ k}\Omega} \right) = 2.46$$

The output resistance is now calculated with Blackman's theorem.

$$R_{\text{out}} = R_{\text{out}}^D \frac{1 + |T_{SC}|}{1 + |T_{OC}|} = 2.11 \text{ k}\Omega \left( \frac{1 + 0}{1 + 2.46} \right) = 610 \text{ }\Omega$$

**Step 8:** We calculate the overall gain including source attenuation and output loading as:

$$A = \left( \frac{R_{\text{in}}}{R_{\text{in}} + R_i} \right) A_v = \frac{90.7 \text{ k}\Omega}{90.7 \text{ k}\Omega + 200 \text{ }\Omega} 6.68 = 6.67$$

We again see that due to the low ratio of source to input resistance, the overall gain is nearly identical to the amplifier gain. We should also note that we included  $R_L$  directly in the amplifier gain calculations so there is no need to account for signal attenuation from output resistance to load resistance in this equation.

**An Alternate Approach:** This solution uses a slightly different approach to the calculations in which  $R_i$  and  $R_L$  are considered to be part of the amplifier and are included in all the calculations. The closed-loop gain now represents the gain from source  $v_i$  to the output. The input resistance is the total resistance presented to source  $v_i$ , and the output resistance includes the shunting effect of  $R_L$ . The effects of  $R_i$  and  $R_L$  can easily be eliminated at the end of the calculations if desired.

**Closed-Loop Gain:** The loop gain was originally calculated including the effects of  $R_i$  and  $R_L$ , so  $T = -2.01$ , and

$$A_v = A_v^{\text{ideal}} \frac{T}{1 + T} = 10 \frac{2.01}{1 + 2.01} = 6.68$$

The input resistance without feedback now includes  $R_i$ :

$$R_{\text{in}}^D = R_i + R_{iB1} = 31.9 \text{ k}\Omega$$

The loop gain  $T_{OC}$  with  $v_i$  open is zero, and the loop gain with  $v_i$  set to zero is  $T_{SC} = T$ . Thus,

$$R_{\text{in}} = 31.9 \text{ k}\Omega \frac{1 + 2.01}{1 + 0} = 96.0 \text{ k}\Omega$$

The input resistance at the base of  $Q_1$  would then be  $R_{inB1} = R_{\text{in}} - 200 \text{ }\Omega = 95.8 \text{ k}\Omega$ .

The output resistance now includes  $R_L$ :

$$R_{\text{out}}^D = R_L \parallel R_{iC2} \parallel R_5 \parallel (R_2 + R_{iE1} \parallel R_1) \cong 1.74 \text{ k}\Omega$$

The loop gain  $T_{OC}$  with the output open is equal to  $T$ , and the loop gain with a short at the output is zero. Therefore,

$$R_{\text{out}} = 1.74 \text{ k}\Omega \left( \frac{1 + 0}{1 + 2.01} \right) = 578 \text{ }\Omega$$

Removing  $R_L$  from the output resistance yields

$$R'_{\text{out}} = \left[ \frac{1}{R_{\text{out}}} - \frac{1}{R_L} \right]^{-1} = 614 \text{ }\Omega$$

**Discussion:** Our first conclusion from this analysis is that this is not a particularly “good” amplifier design. The loop gain is quite low, so we are not taking advantage of many of the characteristics of negative feedback. In particular, our gain error (reciprocal of  $1 + T$ ) will be high and the input and output impedances are not significantly enhanced by the negative feedback.

On a more general note, from our equations we see that the output load directly impacts the input impedance, so the design is also not well buffered. Increased loop gain would increase the input to output impedance ratio and therefore also improve this characteristic of the amplifier.

**Computer-Aided Analysis:** Simulations of this amplifier with  $BF = 100$ ,  $VAF = 1000$ , and  $IS = 1 \text{ fA}$ , show a gain of 6.52, an input resistance of  $87.0 \text{ k}\Omega$ , and an output impedance of  $644 \Omega$ . These results confirm our hand calculations. The discrepancies are due to the different values of  $T$ ,  $g_m$ , and  $r_\pi$  that are used in SPICE. Note that SPICE transfer function analysis should not be used on this problem because of the presence of bypass and coupling capacitors!

**EXERCISE:** Calculate midband loop gain,  $R_{in}$ ,  $R_{out}$ , and overall gain of the previous circuit if a  $10 \mu\text{F}$  bypass capacitor is placed across  $R_4$ .

**ANSWERS:**  $-19.2$ ,  $596 \text{ k}\Omega$ ,  $85.6 \Omega$ ,  $9.50$ ; SPICE:  $-16.5$ ,  $533 \text{ k}\Omega$ ,  $105 \Omega$ ,  $9.43$

### 18.3.2 DIFFERENTIAL INPUT SERIES-SHUNT VOLTAGE AMPLIFIER

The amplifier in Fig. 18.6 is a more traditional series-shunt voltage amplifier. It is a simple op-amp structure with an FET differential input stage, a common-source gain stage, and a common-drain output buffer stage. The feedback network is composed of  $R_2$  and  $R_1$ . In the following example we will analyze the characteristics of this negative feedback amplifier. Be aware that without additional modification, this amplifier will likely be unstable. Later we will learn how to predict and compensate for feedback instability.

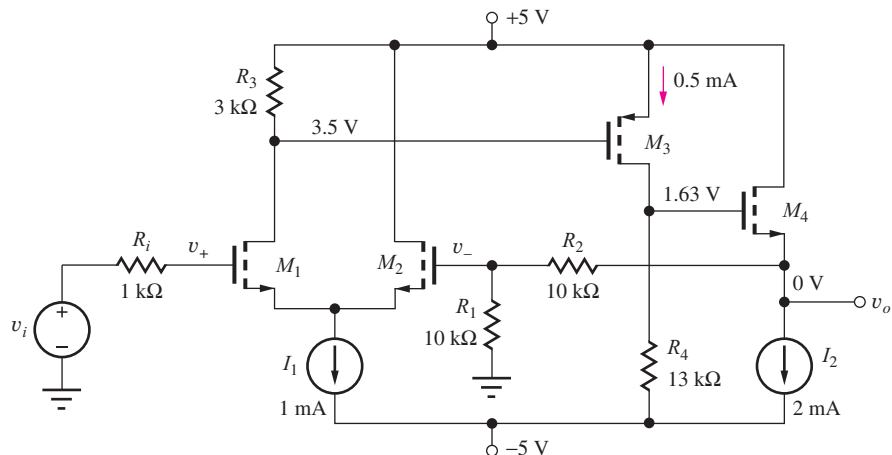


**Figure 18.6** Three-stage MOSFET amplifier with negative feedback. ( $K_n = 10 \text{ mA/V}^2$ ,  $K_p = 4 \text{ mA/V}^2$ ,  $V_{TN} = 1 \text{ V}$ ,  $V_{TP} = -1 \text{ V}$ )

### EXAMPLE 18.2 DIFFERENTIAL INPUT SERIES-SHUNT VOLTAGE AMPLIFIER

Perform an analysis of the three-stage differential input series-shunt feedback amplifier in Fig. 18.6.

**PROBLEM** The amplifier of Fig. 18.6 has been designed. Find the small-signal gain, input resistance, and output resistance.  $K_n = 10 \text{ mA/V}^2$ ,  $K_p = 4 \text{ mA/V}^2$ ,  $V_{TN} = 1 \text{ V}$ ,  $V_{TP} = -1 \text{ V}$ . The dc bias currents and voltages are shown on the schematic.

**SOLUTION** **Known Information and Given Data:** The circuit diagram is presented in Fig. 18.6 with the indicated dc bias values.

**Unknowns:** Ideal gain, open-loop gain, loop transmission, and Blackman terms for the input and output impedances.

**Approach:** Use amplifier gain analysis from previous chapters, feedback analysis procedure, and Blackman's theorem.

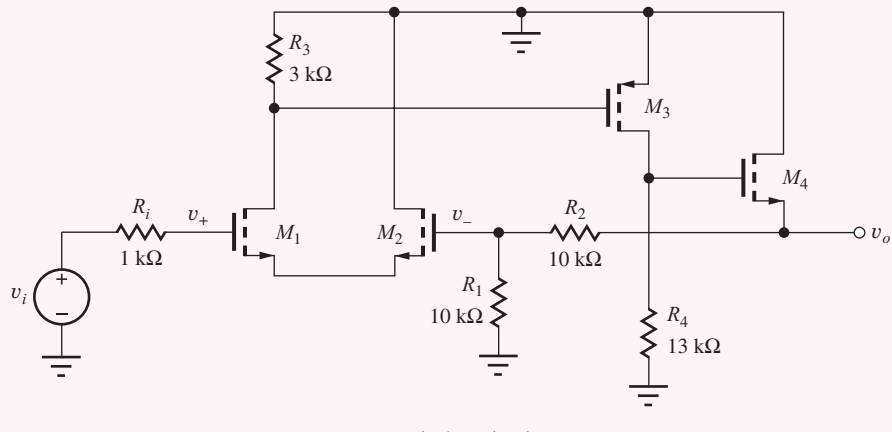
**Assumptions:** Since  $\lambda$  is unspecified, assume transistor output impedances  $r_o$  are infinite; small-signal mid-band conditions apply.  $T = 300$  K.

**Analysis:** Since we have been given a dc bias current solution (0.5 mA, 0.5 mA, 0.5 mA, 20 mA), the small-signal parameters can be directly calculated:

$$g_{m1} = g_{m2} = \sqrt{2K_n I_D} = 3.16 \text{ mS},$$

$$g_{m3} = 2.00 \text{ mS}, g_{m4} = 6.33 \text{ mS}, r_o = \infty$$

Now we turn to our feedback analysis procedure. First we draw the ac equivalent circuit.



ac equivalent circuit

**Step 1:** As discussed above, the feedback network is composed of  $R_2$  and  $R_1$ . The output voltage is directly sampled by  $R_2$ , so it is a shunt connection.

**Step 2:** The signal fed back is the small-signal voltage at the gate of  $M_2$ . This voltage is in series with the input voltage at the gate of  $M_1$  (across the differential pair), so this is a series feedback connection.

**Step 3:** Since voltage is sampled and voltage is fed back to the input, the feedback factor has units of voltage/voltage and the amplifier is a series-shunt voltage amplifier.

**Step 4:** The amplifier type is series-shunt, so the ideal feedback factor is just the voltage division across the feedback network,  $\beta = R_1/(R_1 + R_2)$ . The ideal gain is therefore:

$$A_v^{\text{ideal}} = \frac{1}{\beta} = \frac{R_2 + R_1}{R_1} = +2$$

**Step 5:** We calculate the gain around the loop starting at the gate of  $M_2$  and work our way around the loop back to our starting point. This requires calculating the differential pair gain, the common-source gain, the common-drain gain, and finally the attenuation of the feedback voltage divider. Recall that  $R_{iG}$  and the small-signal resistance of an ideal current source are infinite at midband and  $r_o = \infty$  was assumed for this problem. These conditions simplify our equations considerably.

$$T = \left( +\frac{g_{m2}}{2} R_3 \right) (-g_{m3} R_4) \left[ \frac{g_{m4} (R_2 + R_1)}{1 + g_{m4} (R_2 + R_1)} \right] \left( \frac{R_1}{R_1 + R_2} \right)$$

$$T = (4.74)(-26.0)(.992)(0.5) = -61.1$$

Notice that  $T$  is much larger for this three-stage topology. We also see that  $T$  is again negative, satisfying our requirement for negative feedback.

**Step 6:** The closed-loop gain of the feedback amplifier is calculated according to Eq. (18.4). Remember that the negative sign on  $T$  is already included in our high-level feedback description in Fig. 18.1, so  $T$  will be positive when we evaluate Eq. (18.4):

$$A_v = A_v^{\text{Ideal}} \frac{T}{1+T} = 2 \frac{61.1}{1+61.1} = 1.97$$

Due to the high midband resistance looking into the gate of  $M_1$ , there should be no signal loss at the input due to source resistance.

**Step 7: Input Resistance:** For this topology, input resistance is straight-forward since the open-loop resistance looking into the gate of  $M_1$  is approximately infinite. If we needed to calculate it, we would find that  $T_{OC} = 0$ , and  $T_{SC}$  is equal to the loop transmission we found for the closed-loop gain calculation.

**Output Resistance:** For the output resistance, we mentally disable the feedback and calculate the impedance looking into the output of the amplifier, not including the load resistance.

$$R_{\text{out}}^D = R_{IS4} \| (R_2 + R_1) = (1/g_m4) \| (R_2 + R_1) = 157 \Omega$$

$T_{SC}$  is zero since the amplifier gain is zero when the output is shorted to small-signal ground.  $T_{OC}$  is identical to the loop-gain calculated earlier since there is no  $R_L$  in the problem.

$$T_{OC} = T(\text{loop gain}) = 61.1$$

The output resistance is now calculated with Blackman's theorem.

$$R_{\text{out}} = R_{\text{out}}^D \frac{1 + |T_{SC}|}{1 + |T_{OC}|} = 157 \left( \frac{1 + 0}{1 + 61.1} \right) = 2.53 \Omega$$

**Step 8:** Due to our high input impedance and low output impedance, our overall gain will be approximately equal to the amplifier gain.

**Discussion:** This topology is well suited to high forward gain feedback amplifiers. It can be augmented with active loads and a more efficient output stage to produce a true operational amplifier. As mentioned earlier, feedback stability issues will be addressed later in this chapter.

**Computer-Aided Analysis:** Here we can use a SPICE dc analysis followed by a transfer function analysis from input  $v_i$  to the voltage across  $I_2$ . The results show a gain of 1.98, an extremely high input resistance, and an output impedance of  $2.50 \Omega$ . These results agree well with our hand calculations.

**EXERCISE:** Use Blackman's theorem to calculate the midband resistance between the drain of  $M_1$  and small-signal ground. What are  $R_x^D$ ,  $T_{SC}$ ,  $T_{OC}$ , and  $R_x$ ?

**ANSWERS:**  $3 \text{ k}\Omega$ , 0, 61.1,  $48.3 \Omega$ .

**EXERCISE:** What are the Q-points of the four transistors in the amplifier in Fig. 18.6?

**ANSWERS:** (0.5 mA, 4.50 V), (0.5 mA, 6.00 V), (0.5 mA, 3.50 V), (0.5 mA, 5.00 V)

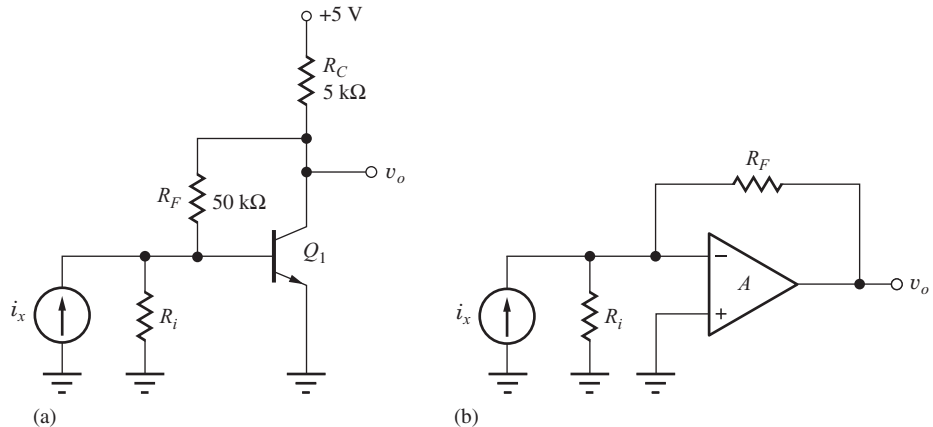


**Figure 18.7** (a) Single-transistor transresistance amplifier. (b) Idealized transresistance amplifier.

### 18.3.3 SHUNT-SHUNT FEEDBACK—TRANSRESISTANCE AMPLIFIERS

Figure 18.7 illustrates a simple single transistor shunt-shunt feedback amplifier. The amplifier itself is considered to be from the base of  $Q_1$  to the collector. Resistor  $R_i$  and current source  $i_x$  represent the Norton equivalent of the signal source. The amplifier converts input current  $i_x$  to a voltage at the output. We will see that the feedback allows the circuit to present a low impedance to the source network to act as an efficient current sink and generate a voltage at the output. The gain is expressed as a voltage/current ratio that leads to the amplifier classification as transresistance. The feedback network is simply  $R_F$ . The output voltage is sampled, and a current is fed back to the input node at the base of  $Q_1$ . The input source also delivers a current to the base of  $Q_1$ , so the input current and the feedback current are summed at the base node.

#### EXAMPLE 18.3 SHUNT-SHUNT FEEDBACK AMPLIFIER ANALYSIS

Use our feedback analysis procedure to understand the operation of a single transistor transresistance amplifier.

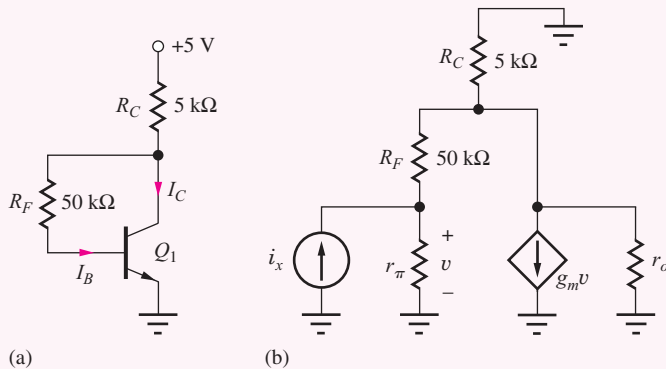
**PROBLEM** Find the small-signal gain, input and output resistance of the amplifier in Fig. 18.7 for the idealized case with  $R_i = \infty$ . Use  $\beta_F = 150$  and  $V_A = 50$  V.

**SOLUTION** **Known Information and Given Data:** The circuit schematic appears in Fig. 18.7; transistor parameters:  $\beta_F = 150$  and  $V_A = 50$  V

**Unknowns:** Ideal gain, open-loop gain, loop transmission, and Blackman terms for the input and output impedances.

**Approach:** Find the dc operating point; use amplifier gain analysis from previous chapters, the feedback analysis procedure, and Blackman's theorem.

**Assumptions:**  $V_{BE} = 0.7$  V,  $V_T = 25$  mV, and small-signal midband conditions apply.

(a) dc equivalent circuit. (b) ac equivalent circuit ( $g_m = 32.0 \text{ mS}$ ,  $r_\pi = 4.69 \text{ k}\Omega$ ,  $r_o = 62.4 \text{ k}\Omega$ ).

**Analysis:** We first find the dc operating point from the dc equivalent circuit. Knowing the relationship between base and collector current ( $I_B = I_C/\beta_F$ ), we can sum the voltage drops with a loop equation,

$$5V = (I_C + I_B)R_C + I_B R_F + V_{BE} \quad \text{or} \quad 5V - V_{BE} = I_C \left( R_C + \frac{R_C}{\beta_F} + \frac{R_F}{\beta_F} \right)$$

Solving for the collector current yields

$$I_C = \frac{5V - V_{BE}}{R_C + \frac{R_C + R_F}{\beta_F}} = 0.801 \text{ mA}$$

and the collector-emitter voltage is

$$V_{CE} = 5V - (I_C + I_B)R_C = I_C \left( 1 + \frac{1}{\beta_F} \right) R_C = 0.968 \text{ V}$$

The corresponding small-signal parameters are

$$g_m = 40(0.801) = 32.0 \text{ mS} \quad r_\pi = \frac{150}{g_m} = 4.69 \text{ k}\Omega \quad r_o \cong \frac{50\text{V}}{0.801 \text{ mA}} = 62.4 \text{ k}\Omega$$

Now we turn to our feedback analysis procedure.

**Step 1:** As discussed above, the feedback network is the resistor  $R_F$ .  $R_F$  directly samples the output voltage, so it is a shunt connection.

**Step 2:** The signal fed back is a current to the base of  $Q_1$  and this current is summed directly with the input current  $i_x$ . This is therefore a shunt feedback connection.

**Step 3:** Since voltage is sampled and current is fed back to the input, the feedback factor has units of current/voltage and the amplifier is a shunt-shunt transresistance amplifier.

**Step 4:** The amplifier type is shunt-shunt, so the ideal feedback factor is just the reciprocal of the resistance of the feedback network. The ideal gain is therefore:

$$A_{tr}^{\text{ideal}} = -\frac{1}{\beta} = -R_F = -50,000 \Omega (\text{V/A})$$

The negative sign accounts for the polarity of the voltage drop across  $R_F$  when  $i_x$  is positive.

**Step 5:** We calculate the gain around the loop starting at the base of  $Q_1$  in the ac equivalent circuit above and work our way around the loop back to our starting point. This requires calculating

the common emitter gain and the attenuation of the feedback network.

$$T = [-g_m(R_C \parallel (R_F + r_\pi) \parallel r_o)] \left( \frac{r_\pi}{r_\pi + R_F} \right)$$

$$T = -0.032S(5\text{ k}\Omega \parallel (50\text{ k}\Omega + 4.69\text{ k}\Omega) \parallel 62.4\text{ k}\Omega) \left( \frac{4.69\text{ k}\Omega}{4.69\text{ k}\Omega + 50\text{ k}\Omega} \right) = -11.7$$

We see that  $T$  is negative satisfying our requirement for negative feedback.

**Step 6:** The closed-loop gain of the feedback amplifier is calculated according to Eq. (18.4). Remember that the negative sign on  $T$  is already included in our high-level feedback description in Fig. 18.1, so  $T$  will be positive when we evaluate Eq. (18.4):

$$A_{tr} = A_{tr}^{\text{Ideal}} \frac{T}{1+T} = -50\text{ k}\Omega \frac{11.7}{1+11.7} = -46.1\text{ k}\Omega$$

The relatively low loop transmission results in a significant reduction of our gain from the ideal value.

**Step 7: Input Resistance:** To calculate input resistance, we start with the open-loop resistance with the feedback disabled (e.g., set  $g_m v = 0$ ).

$$R_{in}^D = r_\pi \parallel (R_F + R_C \parallel r_o) = 4.32\text{ k}\Omega$$

$T_{SC}$  is zero since the signal gain is zero when the base of  $Q_1$  is shorted to ground, whereas  $T_{OC}$  is the same as we calculated for the gain,  $T_{SC} = 11.7$ . Combining these results yields the midband input resistance:

$$R_{in} = R_{in}^D \frac{1 + |T_{SC}|}{1 + |T_{OC}|} = 4.32\text{ k}\Omega \frac{1 + 0}{1 + 11.7} = 340\text{ }\Omega$$

The negative feedback has significantly reduced the input resistance, improving its suitability for sinking input currents.

**Output Resistance:** For the output resistance, we again mentally disable the feedback (by setting  $g_m v = 0$ ) and calculate the impedance looking into the output of the amp.

$$R_{out}^D = R_C \parallel r_o \parallel (R_F + r_\pi) = 4.27\text{ k}\Omega$$

$T_{SC}$  is zero since the amplifier gain is zero when the output is shorted to signal ground.  $T_{OC}$  equals the previously calculated loop-gain,  $T_{OC} = 11.7$ . The output resistance is now calculated with Blackman's theorem.

$$R_{out} = R_{out}^D \frac{1 + |T_{SC}|}{1 + |T_{OC}|} = 4.27\text{ K} \frac{1 + 0}{1 + 11.7} = 336\text{ }\Omega$$

**Step 8:** Since the signal source is an ideal current source and there is no external load in the circuit, the overall transresistance gain is as calculated earlier.

$$A_{tr} = \frac{v_{out}}{i_x} = -46.1\text{ k}\Omega$$

**Discussion:** The transresistance amplifier is widely used for amplification of signals from current-mode detectors such as photodiodes. The low input impedance serves to shunt stray capacitance of the detector to maintain fast response times. We should recognize that the node at the base of  $Q_1$  is equivalent to the virtual ground in op-amp circuits we studied earlier. However, to decrease  $R_{in}$  to levels similar to the op-amp version, the loop gain must be significantly increased.

**Computer-Aided Analysis:** Here we can use a SPICE dc analysis followed by a transfer function analysis from input  $i_x$  to the output voltage. The results yield a transresistance gain of  $-46.0\text{ k}\Omega$ , an input resistance of  $352\text{ }\Omega$ , and an output impedance of  $335\text{ }\Omega$ . These results agree well with our hand calculations.

**EXERCISE:** Repeat the calculations in the example above if  $R_i = 10 \text{ k}\Omega$ . What are the new values of  $T$ ,  $R_{\text{in}}$  and  $R_{\text{out}}$ ?

**ANSWERS:** 8.17, 329  $\Omega$ , 464  $\Omega$

### Impact of Source and Load Resistances

Now that we have looked at the behavior of the basic single-transistor transresistance amplifier, we will look at the impact of including source and load resistances on the performance of the amplifier, as illustrated in Fig. 18.8. Here we use the results of the previous example to create a model for the amplifier.

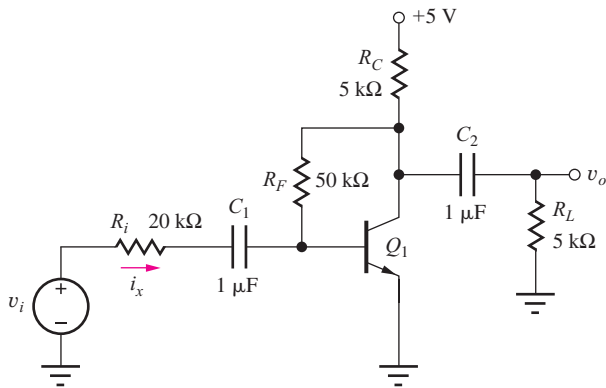


Figure 18.8 Transresistance amplifier with signal source and load resistance.

### EXAMPLE 18.4 SHUNT-SHUNT FEEDBACK WITH NEW SOURCE AND LOAD IMPEDANCES

Understand the interaction of a transresistance amplifier with different source and load impedances. We will also explore the relationship between an inverting voltage amplifier and a transresistance amplifier.

**PROBLEM** Find the small-signal gain of the amplifier in Fig. 18.8. Use  $\beta_F = 150$ ,  $V_A = 50 \text{ V}$ , and the results from Ex. 18.3.

**SOLUTION Known Information and Given Data:** The circuit diagram appears in Fig. 18.8; Transistor parameters are:  $\beta_F = 150$  and  $V_A = 50 \text{ V}$ ; results from Ex. 18.3.

**Unknowns:** Find the gain based on results from the previous exercise.

**Approach:** Include input and output loading effects to adjust previous results to a new source and load impedance. This will be an approximation, so our goal is to understand the validity of the approach.

**Assumptions:**  $V_{BE} = 0.7 \text{ V}$ ,  $V_T = 25 \text{ mV}$ , and small-signal mid-band conditions apply.

**Analysis:** We have previously found the input impedance, output impedance, and transresistance of the circuit in Fig. 18.7.

$$A_{tr} = -46.1 \text{ k}\Omega \quad R_{\text{in}} = 340 \Omega \quad R_{\text{out}} = 336 \Omega$$

Figure 18.9 shows the equivalent circuit we will use to find the gain of the amplifier in Fig. 18.8. The results from Ex. 18.3 are used to generate a model of the transresistance amplifier. The amplifier itself is modeled with an ideal op amp with the calculated input and output resistances pulled out of the amplifier to account for loading effects. Notice that when the circuit is driven with a voltage source, the circuit becomes equivalent to an inverting amplifier.

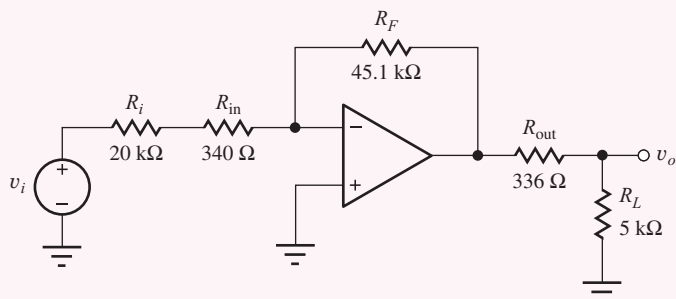


**Figure 18.9** Approximate small-signal equivalent circuit for Fig. 18.8.

We can now calculate  $v_o/v_i$  using our knowledge of the op amp inverting amplifier and voltage division.

$$A_v = \frac{v_o}{v_i} = \left( \frac{-R_F}{R_i + R_{in}} \right) \left( \frac{R_L}{R_{out} + R_L} \right) = \left( \frac{-45.1 \text{ k}\Omega}{20 \text{ k}\Omega + 340 \Omega} \right) \left( \frac{5 \text{ k}\Omega}{336 + 5 \text{ k}\Omega} \right) = -2.08$$

The first portion of the equation is the basic inverting amplifier equation and the second term reflects the voltage division due to the output impedance of the circuit in Fig. 18.9.

**Computer-Aided Analysis:** Simulations of the amplifier produce a small-signal gain of  $-2.09 \text{ V/V}$ . This is quite close to our hand calculation.

**Discussion:** We find that we can use results from an unloaded amplifier to approximate the response for the loaded situation. In this particular case it is quite accurate, but it is less accurate for other combinations of source and load resistance. Predictably, as the source or load impedances approach the input or output resistance the accuracy is compromised. While this is an approximation, it is much more efficient than reevaluating loop transmission for each case and should be one of the tools we apply to design problems.

**EXERCISE:** For the circuit in Fig. 18.8, compare the calculated and simulated gain values for the  $R_i = 2 \text{ k}\Omega$ ,  $R_L = 10 \text{ k}\Omega$ , and  $R_i = 10 \text{ k}\Omega$ ,  $R_L = 2 \text{ k}\Omega$ . Also find the error for the two cases.

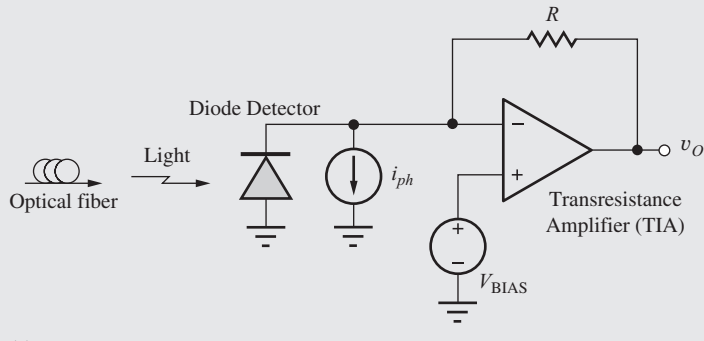
**ANSWERS:** Calculated:  $-18.6$ ,  $-3.73$ ; Simulated:  $-17.9$ ,  $-3.60$ ; Error: 4.2 percent, 3.6 percent

**EXERCISE:** A simulation of the TIA circuit in Fig. (b) in the EIA feature on the next page yields  $A_{tr} = 48.5 \text{ k}\Omega$  and  $R_{out} = 12 \Omega$ . What are the values of  $T$ ,  $g_{m3}$  and  $R_{in}$ ?

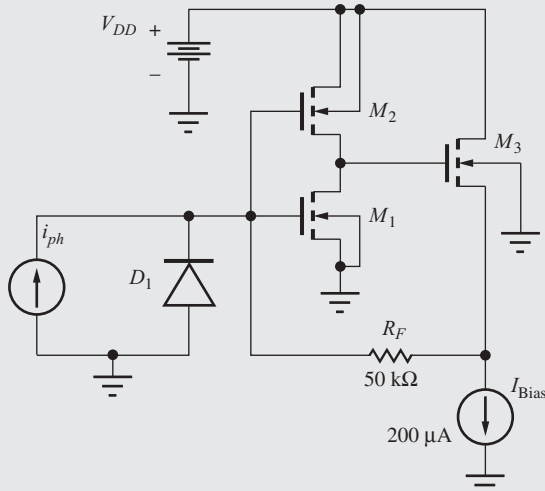
**ANSWERS:** 32.3, 2.50 mS, 1.51 kΩ


**ELECTRONICS IN ACTION**
***A Transresistance Amplifier Implementation***

The application of transresistance amplifiers in optical communications was introduced in Electronics in Action features in Chapters 9 and 10. The transresistance amplifier, Fig. (a), that converts the photodiode current  $i_{ph}$  into an output voltage  $v_o = -i_{ph} R_F$ , is often realized by a shunt-shunt feedback amplifier, and a basic CMOS implementation of such an amplifier appears in Fig. (b).  $M_1$  and  $M_2$  form a high-gain CMOS inverter that is connected to source follower  $M_3$  to achieve a lower output resistance. Current source  $I_{bias}$  and the  $W/L$  ratios of the transistors determine the Q-points of the three devices. Reverse bias for photodiode  $D_1$  is provided by the gate-source voltage of  $M_1$ .



(a)



(b)

The transresistance, input resistance, and output resistance of the shunt-shunt feedback amplifier can be found using the theory just presented in Sec. 18.2:

$$A_{tr} = -R_F \left( \frac{T}{1+T} \right) \quad R_{in} = \left( R_F + \frac{1}{g_{m3}} \right) \left( \frac{T}{1+T} \right) \quad R_{out} = \left( \frac{1}{g_{m3}} \right) \left( \frac{T}{1+T} \right)$$

(The output resistance of the reverse-biased diode has been assumed to be extremely large.)

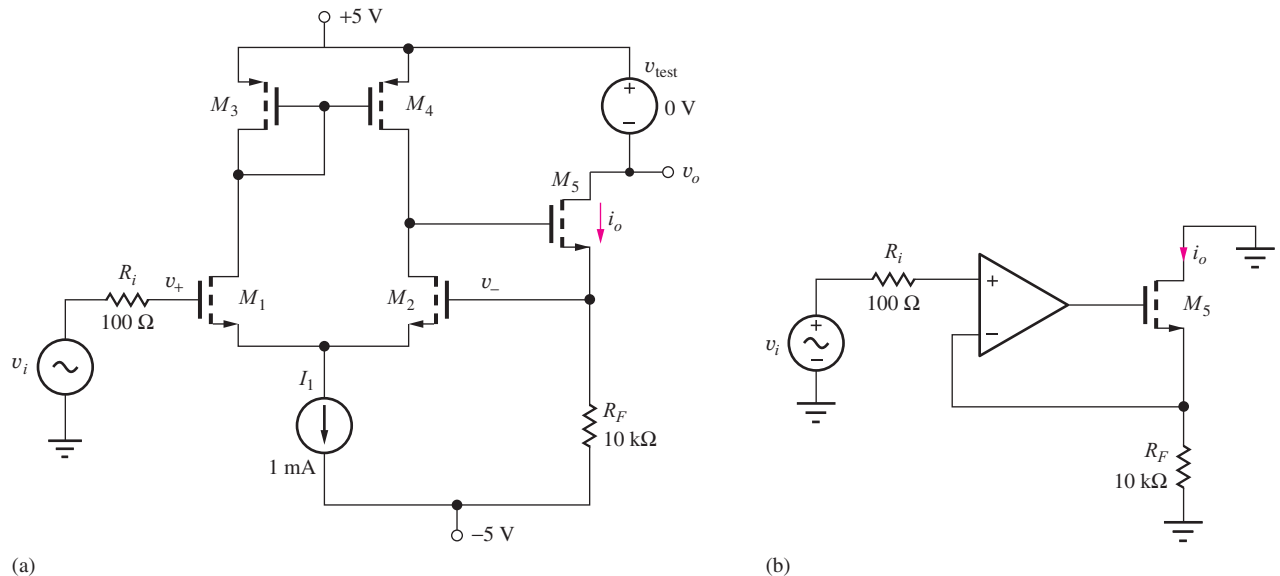


**Figure 18.10** (a) Two-stage transconductance amplifier. (b) Idealized transconductance amplifier.

### 18.3.4 SERIES-SERIES FEEDBACK—TRANSCONDUCTANCE AMPLIFIERS

Transconductance amplifiers have a gain with units of current/voltage. Negative feedback versions have a feedback network that samples the output current and feeds back a voltage in series with the input. A transconductance amplifier can be used to create a high impedance current source or a dynamic voltage-controlled current source, and in other applications where precise control of a current via a voltage signal is required. The circuit in Fig. 18.10 is a two-stage example of a transconductance amplifier. Resistor  $R_F$  senses the  $M_5$  output current and generates a voltage that is summed in series with the input voltage across the input differential pair,  $M_1$  and  $M_2$ . This is a series-series feedback connection.

#### EXAMPLE 18.5 SERIES-SERIES FEEDBACK AMPLIFIER ANALYSIS

Use our feedback analysis procedure to understand the operation of a transconductance amplifier.

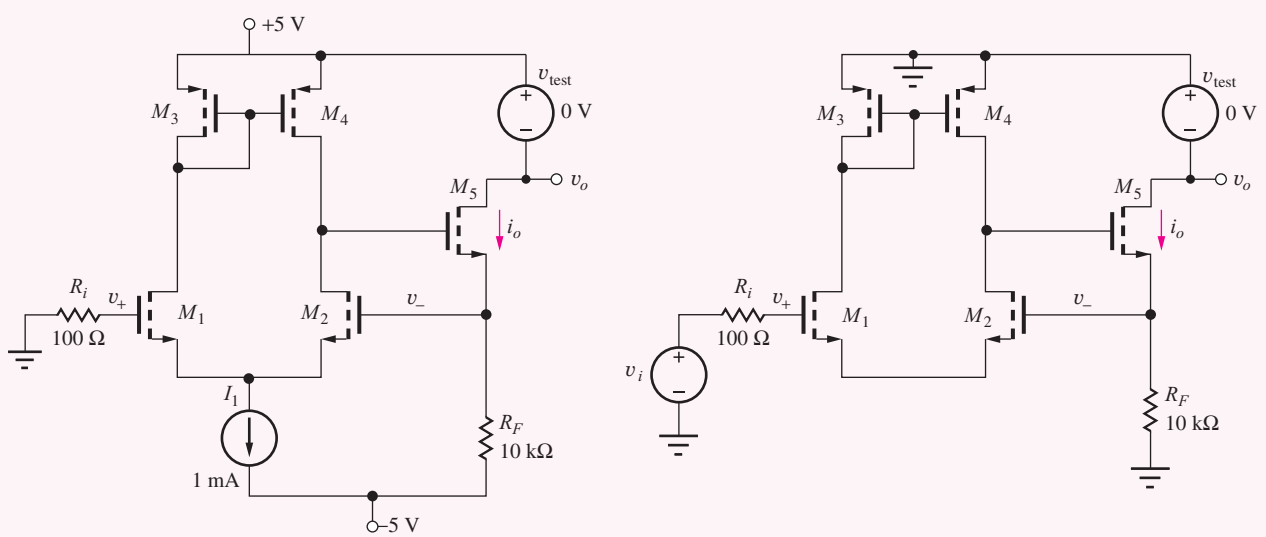
**PROBLEM** Find the small-signal gain, input, and output resistance of the amplifier in Fig. 18.10.  $K_n = 10 \text{ mA/V}^2$ ,  $K_p = 4 \text{ mA/V}^2$ , and  $\lambda = 0.01/\text{V}$ .

**SOLUTION** **Known Information and Given Data:** The circuit diagram appears in Fig. 18.10; transistor parameters:  $K_n = 10 \text{ mA/V}^2$ ,  $K_p = 4 \text{ mA/V}^2$ , and  $\lambda = 0.01/\text{V}$ .  $V_{test}$  is a zero volt source used in simulation to measure the output current,  $i_o$ . In a typical application,  $v_{test}$  would be replaced by some functional circuit which accepts the output current.

**Unknowns:** Ideal gain, open-loop gain, loop transmission, and Blackman terms for the input and output impedances.

**Approach:** Find the dc operating point; use amplifier gain analysis from previous chapters, the feedback analysis procedure, and Blackman's theorem.

**Assumptions:** Small-signal mid-band conditions apply.



(a) dc equivalent circuit.

(b) ac equivalent circuit.

**Analysis:** We first draw the dc equivalent circuit in (a) and find the dc operating point. By inspection we see that  $M_1$ – $M_4$  are all biased at 0.5 mA. Negative feedback works to keep  $v_-$  equal to  $v_+$ , therefore, the  $M_5$  channel current is  $[0 - (-5)]/10\text{ k}\Omega = 0.5\text{ mA}$ .  $V_{\text{test}}$  is a zero volt source for measuring the output current in SPICE. The corresponding small-signal parameters are

$$\begin{aligned} g_{m1} &= g_{m2} = g_{m5} = \sqrt{2K_n I_D} = 3.16\text{ mS} \\ g_{m3} &= g_{m4} = 2.00\text{ mS} \quad r_o \approx \frac{1}{\lambda I_D} = 200\text{ k}\Omega \end{aligned}$$

Now we turn to our feedback analysis procedure.

- Step 1:** As discussed above, the feedback network is the resistor  $R_F$ .  $R_F$  samples the output current, so it is a series connection.
- Step 2:** The signal fed back to the gate of  $M_2$  is the voltage developed across  $R_F$  and summed in series with the input voltage signal. This is therefore a series feedback connection.
- Step 3:** Since current is sampled and voltage is fed back to the input, the feedback factor has units of voltage/current and the amplifier is a series-series transconductance amplifier.
- Step 4:** The amplifier employs series-series feedback that forces  $v_-$  to be equal to  $v_i$ , and the output signal current is then  $i_o = v_i/R_F$ . Thus the ideal feedback factor is just the resistance of the feedback network,  $R_F$ , and the ideal gain is:

$$A_{tc}^{\text{ideal}} = \frac{1}{\beta} = \frac{1}{R_F} = 100\text{ }\mu\text{A/V}$$

- Step 5:** We calculate the gain around the loop in the ac equivalent circuit in (b) starting at the gate of  $M_2$  and work our way around the loop back to our starting point. This requires calculating the differential pair gain and the  $M_5$  common-drain gain.

$$\begin{aligned} T &= -g_{m2}(r_{o2}||r_{o4}) \left( \frac{g_{m5}R_F}{1 + g_{m5}R_F} \right) \\ T &= -3.16\text{ mS}(100\text{ k}\Omega)(0.969) = -306 \end{aligned}$$

We see that  $T$  is negative. Note again that we must always have negative feedback when we are building a feedback amplifier.

**Step 6:** The closed-loop gain of the feedback amplifier is calculated according to Eq. (18.4). Remember that the negative sign on  $T$  is already included in our high-level feedback description in Fig. 18.1, so  $T$  will be positive when we evaluate Eq. (18.4):

$$A_{tc} = A_{tc}^{\text{ideal}} \frac{T}{1+T} = 100 \mu\text{A/V} \frac{306}{1+306} = 99.7 \mu\text{A/V}$$

The high loop transmission results in a low gain error.

**Step 7:** To calculate input resistance looking into the gate of  $M_1$  we start by calculating the open-loop resistance with the feedback disabled.

$$R_{\text{in}}^D = R_{iG1} \approx \infty$$

Clearly, the closed-loop input resistance will be nearly infinite, but we will continue the calculation for completeness.  $T_{OC}$  is zero since the loop gain is zero when the gate of  $M_1$  is open circuited. The infinite impedance looking out of the gate of  $M_1$  prevents a signal from developing across the differential pair. With the gate of  $M_1$  grounded, we see that  $T_{SC}$  is the same as we calculated earlier,  $T_{SC} = -306$ . Combining these results yields the mi-band input resistance:

$$R_{\text{in}} = R_{\text{in}}^D \frac{1 + |T_{SC}|}{1 + |T_{OC}|} = \infty \left( \frac{1 + 0}{1 + 306} \right) = \infty \Omega$$

For the output resistance, we again mentally disable the feedback and calculate the resistance looking into the output of the amp.

$$R_{\text{out}}^D = r_{o5}(1 + g_{m5}R_F) = 6.52 \text{ M}\Omega$$

$T_{OC}$  is zero since the amplifier gain is zero when the drain of  $M_5$  is an open circuit (zero drain and source current in  $M_5$ ). For  $T_{SC}$  the drain of  $M_5$  is connected to ac ground, and  $T_{SC}$  is equal to the previously calculated loop-gain:  $T_{SC} = -306$ . The output resistance is now calculated with Blackman's theorem.

$$R_{\text{out}} = R_{\text{out}}^D \frac{1 + |T_{SC}|}{1 + |T_{OC}|} = 6.52 \text{ M}\Omega \frac{1 + 306}{1 + 0} = 2000 \text{ M}\Omega$$

**Step 8:** Since there is no appreciable signal loss across the low source resistance, the overall transconductance is the value we calculated earlier.

$$\frac{i_o}{v_i} = 99.7 \mu\text{A/V}$$

**Discussion:** The high output impedance of this circuit confirms that a transconductance amplifier can be used to build a nearly ideal current source. Notice that if we took our output at the source of  $M_5$  we have a unity-gain voltage amplifier.

**Computer-Aided Analysis:** SPICE simulation of the amplifier uses a dc analysis and a transfer function analysis from source  $v_i$  to the current through test source  $v_{\text{test}}$ . The TF results show a transconductance gain of  $99.7 \mu\text{A/V}$ , extremely high input resistance, and an output impedance of  $2,250 \text{ M}\Omega$ . These results agree well with our hand calculations.

**EXERCISE:** Calculate the closed-loop gain if a voltage output is taken from the source of  $M_5$ . What are  $A_v^{\text{ideal}}$ ,  $T$ , and  $A_v$ ? What is the closed-loop output resistance? Find  $R_{\text{out}}^D$ ,  $T_{SC}$ ,  $T_{OC}$ , and  $R_{\text{out}}$ .

**ANSWERS:** 1.00 V/V, 306, 0.997 V/V; 307 Ω, 0, -306, 1.00 Ω.

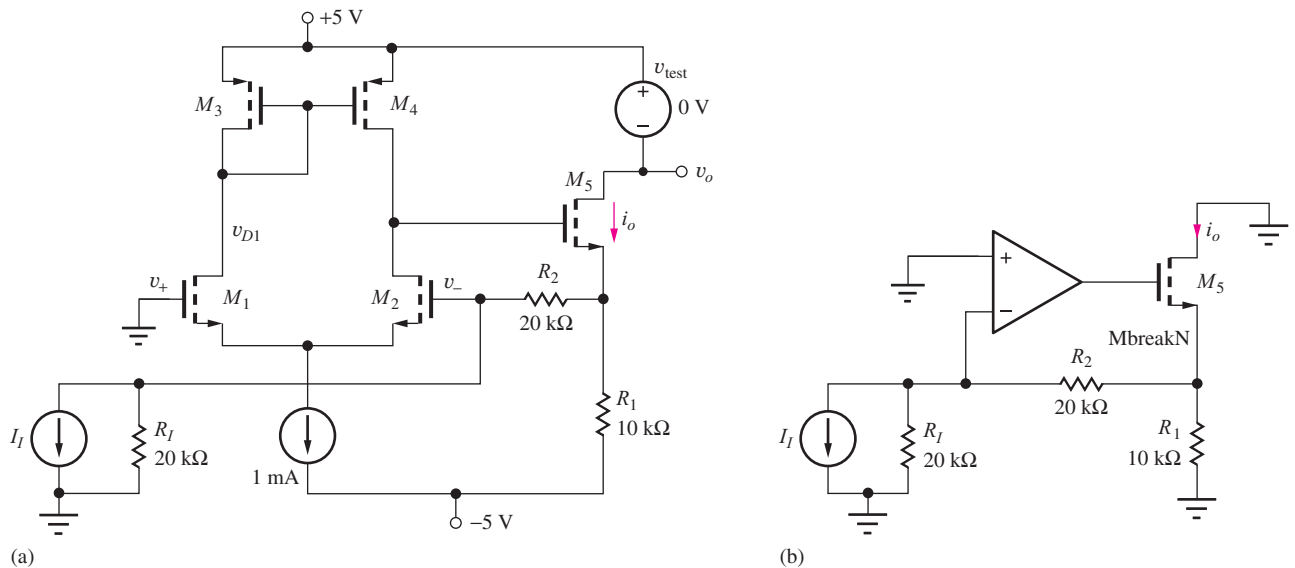


**Figure 18.11** (a) Two-stage shunt-series current amplifier. (b) Idealized current amplifier.

**EXERCISE:** Calculate the midband resistance between the drain node of \$M\_1\$ and small-signal ground in Fig. (b) of Ex. 18.5. What are \$R\_x^D\$, \$T\_{SC}\$, \$T\_{OC}\$, and \$R\_x\$?

**ANSWERS:** \$500\ \Omega\$, \$-153\$, \$-306\$, \$251\ \Omega\$

### 18.3.5 SHUNT-SERIES FEEDBACK—CURRENT AMPLIFIERS

Negative feedback current amplifiers are used to produce a precise scaled current. Such current amplifiers have a feedback network that samples the output current and feeds back a portion of the sampled current to a current summing node at the input. Like the transconductance amplifier, a current amplifier can be used to create a high impedance current source, but one that is controlled by an input current in this topology. The circuit in Fig. 18.11 is a two-stage example of a current amplifier. Feedback resistors \$R\_2\$ and \$R\_1\$ sense the \$M\_5\$ output current and act as a current divider to feed back a portion of the output current to the input summing node. This is a shunt-series feedback connection.

#### EXAMPLE 18.6 SHUNT-SERIES FEEDBACK AMPLIFIER ANALYSIS

Use our feedback analysis procedure to understand the operation of a current amplifier.

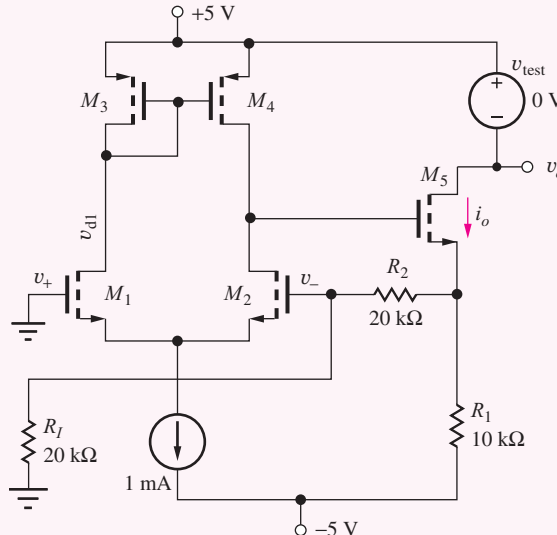
**PROBLEM** Find the small-signal gain, and input and output resistances of the amplifier in Fig. 18.11. \$K\_n = 10\text{ mA/V}^2\$, \$K\_p = 4\text{ mA/V}^2\$, and \$\lambda = 0.01/\text{V}\$.

**SOLUTION** **Known Information and Given Data:** The circuit diagram appears in Fig. 18.11; transistor parameters: \$K\_n = 10\text{ mA/V}^2\$, \$K\_p = 4\text{ mA/V}\$, and \$\lambda = 0.01/\text{V}\$. \$V\_{test}\$ is a zero volt source used in simulation to measure the output current, \$i\_o\$. In a typical application, a functional circuit that accepts the output current will replace \$v\_{test}\$.

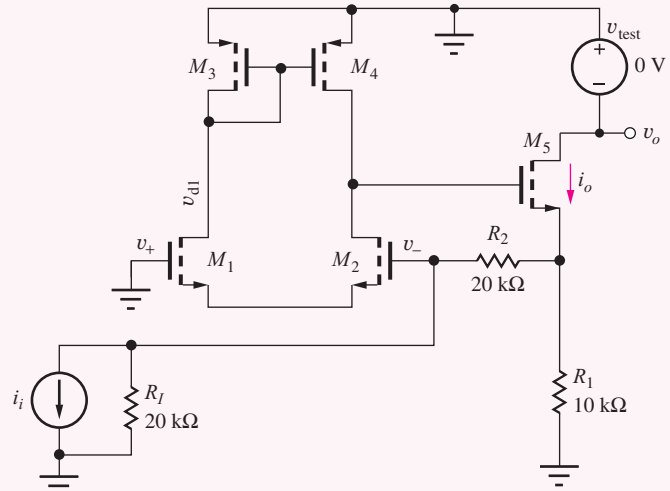
**Unknowns:** Ideal gain, open-loop gain, loop transmission, and Blackman terms for the input and output resistances.

**Approach:** Find the DC operating point; use amplifier gain analyses from previous chapters, the feedback analysis procedure, and Blackman's theorem.

**Assumptions:** Small-signal midband conditions apply.



(a) dc equivalent circuit.



(b) ac equivalent circuit.

**Analysis:** We first draw the dc equivalent circuit in (a) and find the dc operating point. By inspection we see that  $M_1$ – $M_4$  are all biased at 0.5 mA. Negative feedback works to keep  $v_-$  equal to  $v_+$ . So there is no dc current flow through  $R_2$ , and the  $M_5$  channel current is  $[0 - (-5)]/10\text{ k}\Omega = 0.5\text{ mA}$ .  $V_{\text{test}}$  is a zero volt source for measuring current in simulation. The corresponding small-signal parameters are

$$g_{m1} = g_{m2} = g_{m5} = \sqrt{2K_n I_D} = 3.16\text{ mS}$$

$$g_{m3} = g_{m4} = 2.00\text{ mS} \quad r_o \approx \frac{1}{\lambda I_D} = 200\text{ k}\Omega$$

We now use our feedback procedure to analyze the performance of the current amplifier.

- Step 1:** As discussed above, the feedback network is made up of resistors  $R_2$  and  $R_1$ . In the ideal case, the feedback keeps  $v_-$  equal to  $v_+$ , so  $R_2$  and  $R_1$  act as a current divider to feed back a portion of  $i_o$ . Since we are sampling current and not voltage, this is a series connection.
- Step 2:** The signal fed back to the summing node at gate of  $M_2$  is the fraction of output current sampled by the  $R_2$  and  $R_1$  current divider. This is a shunt connection of the feed back signal.
- Step 3:** Since current is sampled and current is fed back to the input, the feedback factor has units of current/current and the amplifier is a shunt-series current amplifier.
- Step 4:** The amplifier type uses shunt-series feedback which forces current  $i_i$  through  $R_2$ . The output current becomes  $i_i$  plus the current through  $R_1$  given by  $i_i R_2/R_1$ . The total current and ideal gain are therefore:

$$\mathbf{i}_o = \mathbf{i}_i \left( 1 + \frac{R_2}{R_1} \right) \quad \text{and} \quad A_c^{\text{ideal}} = \frac{\mathbf{i}_o}{\mathbf{i}_i} = \frac{1}{\beta} = \frac{R_2 + R_1}{R_1} = 3$$

If the sign of the input current is changed we will need to change the sign of our gain. This is often confusing for a number of current amplifier topologies.

**Step 5:** We calculate the loop gain starting at the gate of  $M_2$  in the ac equivalent circuit in (b) and work our way around the loop back to our starting point. This requires calculating the differential pair gain, the  $M_5$  common-drain gain, and the attenuation through  $R_2$  and  $R_I$ .

$$T = -g_{m2}(r_{o2} \parallel r_{o4}) \left( \frac{g_{m5}[R_1 \parallel (R_2 + R_I)]}{1 + g_{m5}[R_1 \parallel (R_2 + R_I)]} \right) \left( \frac{R_I}{R_I + R_2} \right)$$

$$T = -3.16 \text{ mS}(100 \text{ k}\Omega)(0.962)(0.5) = -152$$

We must always check that we have negative feedback and not positive when we are building a feedback amplifier, and we see that  $T$  is negative.

**Step 6:** The closed-loop gain of the feedback amplifier is calculated according to Eq. (18.4). Remember that the negative sign on  $T$  is already included in our high-level feedback description in Fig. 18.1, so  $T$  will be positive when we evaluate Eq. (18.4):

$$A_c = A_c^{\text{ideal}} \frac{T}{1 + T} = 3 \left( \frac{152}{1 + 152} \right) = 2.98$$

High loop transmission results in a low gain error.

**Step 7:** To calculate input resistance looking into the gate of  $M_2$  we start by calculating the open-loop resistance with the feedback disabled.

$$R_{\text{in}}^D = R_{iG2} \left\| \left( R_2 + R_I \right) \left\| \frac{1}{g_{m5}} \right. \right\| = 20.3 \text{ k}\Omega$$

Loop-gain  $T_{SC}$  is found with  $v_-$  shorted to ac ground, so  $T_{SC} = 0$ . With the input open, the loop-gain will be the same as calculated above:  $T_{OC} = -152$ .

$$R_{\text{in}} = R_{\text{in}}^D \frac{1 + |T_{SC}|}{1 + |T_{OC}|} = 20.3 \text{ k}\Omega \left( \frac{1 + 0}{1 + 152} \right) = 133 \Omega$$

For the output resistance, we again mentally disable the feedback and calculate the impedance looking into the output of the amp.

$$R_{\text{out}}^D = r_{o5}(1 + g_{m5}[R_1 \parallel R_2 + R_I]) = 5.26 \text{ M}\Omega$$

$T_{OC}$  is zero since the amplifier gain is zero when the output at the drain of  $M_5$  is open-circuited.  $T_{SC}$  is again equal to the previously calculated loop-gain, so  $T_{SC} = 152$ . The output resistance is now calculated with Blackman's theorem.

$$R_{\text{out}} = R_{\text{out}}^D \frac{1 + |T_{SC}|}{1 + |T_{OC}|} = 5.26 \text{ M}\Omega \left( \frac{1 + 152}{1 + 0} \right) = 805 \text{ M}\Omega$$

**Step 8:** Since we accounted for the source resistance in our earlier gain analysis, our overall gain is:

$$A = A_c = 2.98$$

**Discussion:** The high output impedance of this circuit confirms that like the transconductance case, a current amplifier can be used to build a nearly ideal current source. We also see, that current sampling at the output leads to an output impedance scaled by  $1 + T$ .

**Computer-Aided Analysis:** SPICE transfer function analysis from source  $i_i$  to the current through  $v_{\text{test}}$  yields a current gain of 2.98, extremely high input resistance, and an output impedance of 903 MΩ. These results agree well with our hand calculations, although our output impedance is somewhat low due to our approximate calculation of  $r_o$ .

**EXERCISE:** Calculate the closed-loop gain if a voltage output is taken from the source of  $M_5$  and the input source is replaced with a voltage source in series with a  $20\text{-k}\Omega$  resistance. What are  $A_v^{\text{ideal}}$ ,  $T$ , and  $A_v$ ? What is the closed-loop out resistance? Find  $R_{\text{out}}^D$ ,  $T_{\text{SC}}$ ,  $T_{\text{OC}}$ , and  $R_{\text{out}}$ .

**ANSWERS:**  $-1.00 \text{ V/V}$ ,  $152$ ,  $-0.994 \text{ V/V}$ ;  $304$ ,  $0$ ,  $152$ ,  $1.99 \Omega$ .

## 18.4 REVIEW OF FEEDBACK AMPLIFIER STABILITY

We will now review the negative feedback stability design issues with which we must contend to successfully design and implement feedback amplifiers. We will also discuss our approach to feedback amplifier stability analysis and review some important governing equations.

### 18.4.1 CLOSED-LOOP RESPONSE OF THE UNCOMPENSATED AMPLIFIER

Figure 18.12 is the series-shunt three-stage amplifier that we analyzed at midband frequencies in Ex. 18.2. In our midband analysis of this circuit, we mentioned that this amplifier design wasn't complete since we had not yet addressed stability issues. Figure 18.13 presents simulation results for

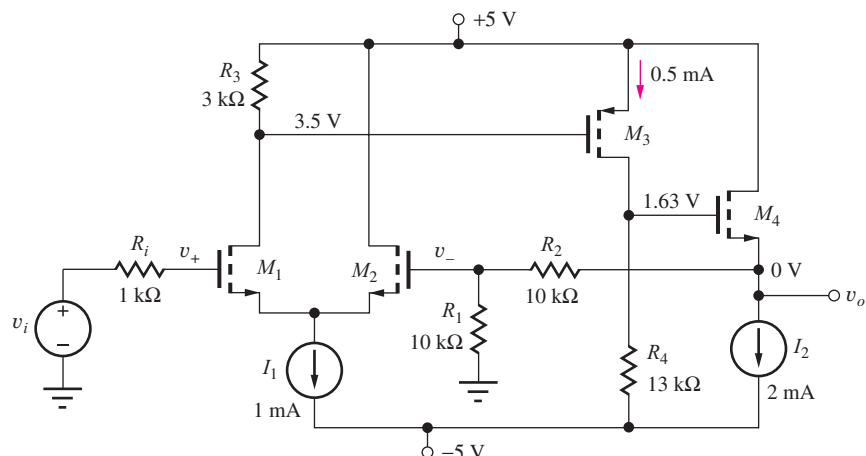


**Figure 18.12** Three-stage MOSFET series-shunt feedback amplifier. ( $K_n = 10 \text{ mA/V}^2$ ,  $K_p = 4 \text{ mA/V}^2$ ,  $V_{TN} = 1 \text{ V}$ ,  $V_{TP} = -1 \text{ V}$ )

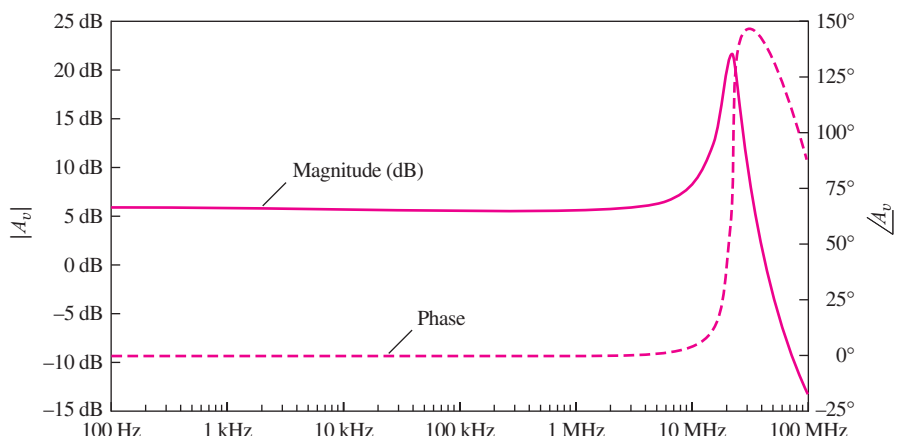


**Figure 18.13** Small-signal gain vs. frequency of the uncompensated three-stage amplifier.

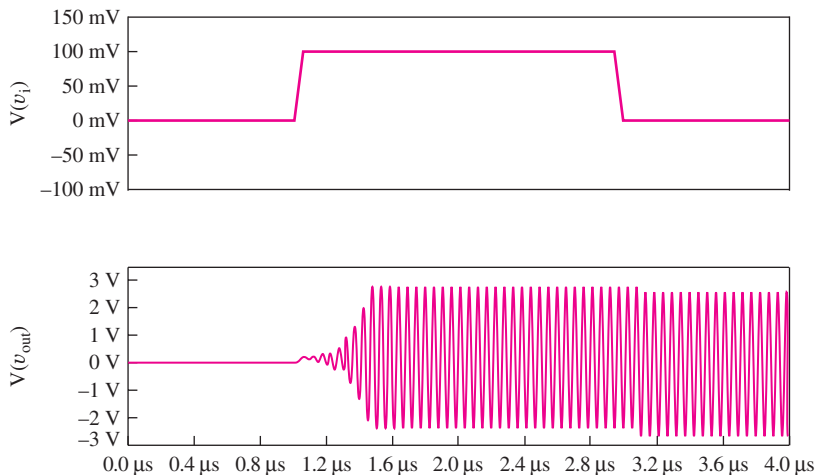


**Figure 18.14** Input and output voltage of the uncompensated amplifier.

the small-signal gain  $v_{\text{out}}/v_i = A_v$  over a wide range of frequencies after capacitances  $C_{GS} = 5 \text{ pF}$  and  $C_{GD} = 1 \text{ pF}$  have been added to each device model in order to extend our analysis to high frequencies. Note the excessive “peaking” of the response near 20 MHz. This is characteristic of a feedback amplifier with poor phase margin. Poor phase margin is typical of an “uncompensated” amplifier, an amplifier whose designer has not yet adjusted the design to address stability issues. A well “compensated” amplifier, an amplifier with good phase margin, will exhibit a smooth roll off from the midband response.

Recall Eq. (18.4), the closed-loop gain feedback equation:

$$A_v = \frac{v_o}{v_i} = A_v^{\text{Ideal}} \frac{T}{1 + T}$$

Loop gain  $T$  has a number of poles and perhaps zeros as well. The plot in Fig. 18.13 expresses the ratio  $T/(1 + T)$ . This ratio results in a complicated relationship between gain and phase for the closed-loop amplifier. We do not have any tools to directly relate the response of this ratio to stability in a way that we can use to improve our design. As we will see shortly, we will instead examine loop gain  $T$  to gain insight into the amplifier stability.

Figure 18.14 is a transient simulation of the amplifier showing its response to a step input. The upper plot shows the input signal and the lower plot is the amplifier output. What is happening here? Recall from Chapter 11 that an amplifier with zero phase margin can oscillate. This occurs when the total phase shift around the loop reaches  $360^\circ$  at some frequency before the magnitude of the loop gain reaches zero db. The loop gain acquires  $180^\circ$  of phase shift from the inverting input to the amplifier, and gathers more phase shift as frequency increases due to poles associated with the parasitic capacitances of the transistors. In a physical circuit there will also be parasitic capacitances and perhaps inductances due to the physical structure and interconnect of the circuit. When the initial input transient reaches the circuit, enough energy has been added to the system to initiate the oscillation. In a real circuit, thermal noise and other signals would initiate the oscillation before the initial transient. Once the oscillation starts, the combination of loop gain and large phase shift around the loop sustains the oscillation. Clearly we will have to modify our design to make this circuit useful as an amplifier.

**EXERCISE:** Estimate the frequency of oscillation in Fig. 18.14.

**ANSWERS:** 17.5 MHz (note that this is near the peak frequency in Fig. 18.13)

**EXERCISE:** What are the values of  $f_T$  for the four transistors in Fig. 18.12 if  $C_{GS} = 5 \text{ pF}$  and  $C_{GD} = 1 \text{ pF}$ ?

**ANSWERS:** 83.8 MHz, 83.8 MHz, 53.1 MHz, 168 MHz

### 18.4.2 PHASE MARGIN

To guide the refinement of our design we must examine the loop gain response phase and magnitude as a function of frequency. Based on equations from Chapter 17, we can find the pole frequencies at each of the nodes in the loop. At the gate of  $M_2$ , the resistance is  $R_1$  in parallel with the resistance looking back through  $R_2$ . The capacitance is  $C_{GD2}$  added to the Miller multiplication applied to  $C_{GS2}$ . Combining these results gives

$$f_{P1} = \frac{1}{2\pi \left[ R_1 \left\| \left( R_2 + \frac{1}{g_{m4}} \right) \right] [C_{GD2} + C_{GS2}(1 - A_{vgs2})]} \quad (1)$$

$$f_{P1} = \frac{1}{2\pi \left[ 10 \text{k}\Omega \left\| \left( 10 \text{k}\Omega + \frac{1}{3.16 \text{ mS}} \right) \right] [1 \text{ pF} + 5 \text{ pF}(1 - 0.5)]} = 8.96 \text{ MHz} \quad (2)$$

At the source of  $M_2$ , the resistance is  $1/g_{m1}$  in parallel with  $1/g_{m2}$  and the capacitance is  $C_{GS1} + C_{GS2}$ :

$$f_{P2} = \frac{1}{2\pi} \left( \frac{g_{m1} + g_{m2}}{C_{GS1} + C_{GS2}} \right) = \frac{1}{2\pi} \frac{g_{m2}}{C_{GS2}} = \frac{1}{2\pi} \frac{3.16 \text{ mS}}{5 \text{ pF}} = 101 \text{ MHz}$$

At the gate of  $M_3$ , we use the  $C_T$  approximation for the dominant pole of the common-source amplifier including the load capacitance from  $M_4$ .

$$f_{P3} = \frac{1}{2\pi} \frac{1}{R_3 [C_{GD1} + C_{GS3} + C_{GD3}(1 - A_{vgd3})] + R_4 [C_{GD3} + C_{GS4}(1 - A_{vgs4}) + C_{GD4}]} \quad (3)$$

$$f_{P3} = \frac{1}{2\pi} \frac{1}{3 \text{k}\Omega [1 \text{ pF} + 5 \text{ pF} + 1 \text{ pF}(1 + 26)] + 13 \text{k}\Omega [1 \text{ pF} + 5 \text{ pF}(1 - 0.992) + 1 \text{ pF}]} = 1.27 \text{ MHz} \quad (4)$$

At the drain of  $M_3$  we have the second pole of the common-source stage:

$$f_{P4} = \frac{1}{2\pi} \left( \frac{g_{m3}}{C_{GS3} + C_{L3}} \right) = \frac{1}{2\pi} \left( \frac{g_{m3}}{C_{GS3} + C_{GD4} + C_{GS4}(1 - A_{vgs4})} \right)$$

$$f_{P4} = \frac{1}{2\pi} \left( \frac{2 \text{ mS}}{5 \text{ pF} + 1 \text{ pF} + 5 \text{ pF}(1 - 0.992)} \right) = 52.7 \text{ MHz}$$

Finally, the pole frequency estimate at the source of  $M_5$  is

$$f_{P5} = \frac{1}{2\pi \left[ \frac{1}{g_{m4}} \parallel (R_1 + R_2) \right] C_{GS4}} = \frac{1}{2\pi \left[ \frac{1}{6.33 \text{ mS}} \parallel 20 \text{k}\Omega \right] 5 \text{ pF}} = 203 \text{ MHz}$$

The lowest frequency pole is found at the gate of  $M_3$  due to the Miller multiplication across  $M_3$ . To generate a single-pole response, the product of the lowest frequency pole and the midband loop gain should be at a lower frequency than the next highest pole frequency. Recall that this product is also  $f_T$ , the 0 dB frequency for a single-pole response. In this amplifier,  $f_{P3} \times T = 1.27 \text{ MHz} \times 61.1 = 77.6 \text{ MHz}$ . If we know  $f_T$ , we can calculate phase margin as

$$\theta_m = 360 - 180(\text{inverting input}) - \tan^{-1} \left( \frac{f_T}{f_{P1}} \right) - \tan^{-1} \left( \frac{f_T}{f_{P2}} \right) - \dots \quad (18.15)$$

However, for this circuit, our estimate of  $f_T$  is higher in frequency than several of the pole frequencies so we can't use Eq. (18.15) because we don't have a good estimate of the actual  $f_T$ . As a result,

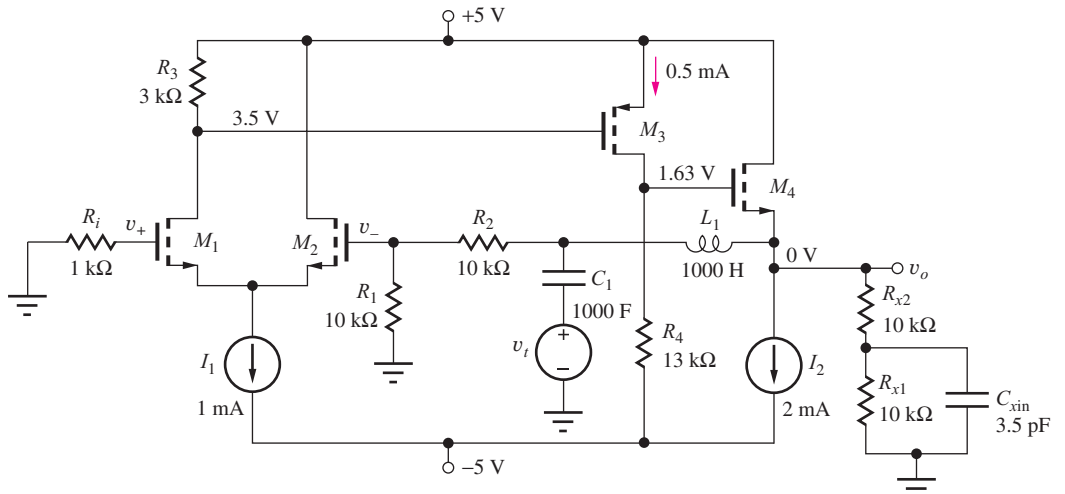


**Figure 18.15** Circuit for simulating small-signal loop gain characteristics.

we expect our phase margin to be zero or worse. For this situation, we can simulate or numerically evaluate the phase margin.

A circuit modification that facilitates the simulation of phase margin is shown in Fig. 18.15. This circuit provides negative feedback at dc but not at midband frequencies and beyond. Inductor  $L_1$  blocks mid and high frequencies to effectively disconnect the feedback loop at those frequencies. Capacitor  $C_1$  blocks dc so that the ac test voltage is only connected into the loop at mid and high frequencies.  $C_1$  and  $L_1$  are set to artificially high values so that the transition from the dc response to midband occurs at very low frequencies. Components  $R_{x1}$ ,  $R_{x2}$ , and  $C_{xin}$  are used to model the output loading due to the feedback network and the inverting input of the amplifier. Note that since the output is nominally biased at 0 V, the resistors will have little impact on the operating point. If the amplifier is not biased at zero volts, a blocking capacitor can be added in series with  $R_{x2}$ . We might ask at this point, why not simply disconnect the feedback network and run our simulation without inserting  $L_1$  and  $C_1$ ? The negative feedback is serving to correct any bias errors and set the proper operating point. When an amplifier has large gain, even small bias errors can lead to large changes in the output dc voltage, and therefore the operating point of the amplifier transistors. Our approach allows us to get the benefits of feedback at dc for operating point stability while still effectively disconnecting the amplifier feedback connection at mid and high frequencies.

Figure 18.16 is the phase and magnitude response of the loop gain  $T$  of our uncompensated amplifier based upon simulation results for the circuit in Fig. 18.15. Phase margin is the difference between 360 degrees and the phase of the loop gain at the frequency for which the loop gain magnitude is 0 dB, that is,  $f_T$ . Recall from Chapter 11 that an ideal single-pole loop gain will have a phase margin of 90 degrees:

$$\theta_m = 90 = 360 - 180 \text{ (inverting input)} - 90 \text{ (max phase shift of single pole)}$$

Unfortunately, our amplifier phase margin is  $-9$  degrees, so the oscillation we saw earlier is not surprising. For stable performance, we desire a phase margin of at least  $45$  degrees, but typically greater than  $60$  degrees.

Now that we have assessed the phase margin, we need to correct the phase margin to make our design usable as an amplifier. The basic approach is to add capacitance to a node in the amplifier to create a dominant pole to force the magnitude response to 0 dB at a lower frequency, thereby reducing the phase shift at 0 dB due to higher frequency poles in the amplifier. Let's assume we would like to move our 0-dB frequency from its present value of about 22 MHz to 2 MHz. If we

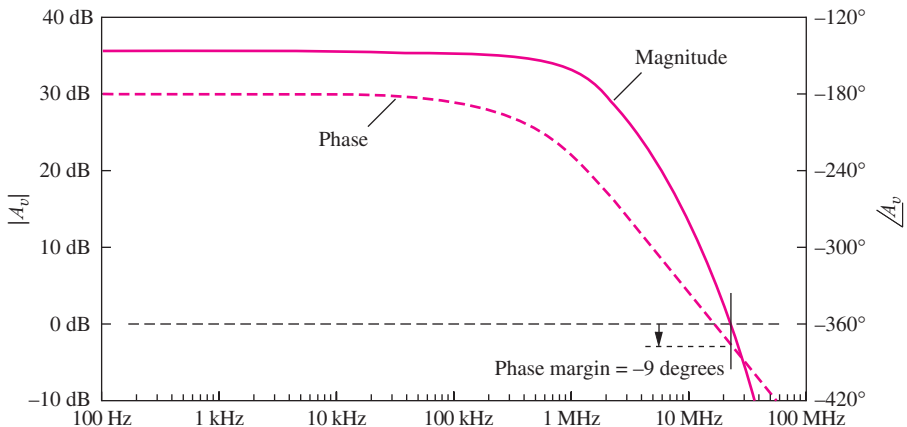


Figure 18.16 Loop transmission magnitude and phase of the three-stage amplifier.

successfully create a dominant pole,  $f_B$ , so that the magnitude response approximates a single-pole response, the 0-dB frequency can be found as:

$$f_T = 2 \text{ MHz} = T f_B = A_0 \beta f_B$$

From Example 18.2 we know that  $T(\text{midband}) = 61.1$ . Therefore, we need to set our dominant pole as

$$f_B = f_T / T = f_T / A_0 \beta = 32.8 \text{ kHz}$$

The equivalent capacitance at the gate of  $M_3$  is dominated by the Miller capacitance due to high gain from the gate to the drain of  $M_3$ . This makes this node a good candidate for setting the dominant pole since the Miller multiplication allows us to use a relatively small physical capacitance to generate a large equivalent capacitance to place the dominant pole at a low frequency. Substituting 32.8 kHz for the pole frequency at the gate of  $M_3$ , we can calculate the expected phase margin with Eq. (18.14):

$$\theta_M = 360 - 180 - \tan^{-1}\left(\frac{2}{8.96}\right) - \tan^{-1}\left(\frac{2}{101}\right) - \tan^{-1}\left(\frac{2}{0.0328}\right) - \tan^{-1}\left(\frac{2}{52.7}\right) - \tan^{-1}\left(\frac{2}{203}\right)$$

$$\theta_M = 360 - 180 - 12.6 - 1.13 - 89.1 - 2.17 - 0.564 = 74.4^\circ$$

This is an acceptable phase margin, so we will continue with the design. To achieve this phase margin we add capacitor  $C_C$  between the gate and drain of  $M_3$ . If we assume the response at that node is dominated by Miller capacitance, our dominant pole frequency can be approximated as

$$f_B = 32.8 \text{ kHz} = \frac{1}{2\pi R_{eq} C_{eq}} = \frac{1}{2\pi(R_3 || R_{iD1})([C_{gd} + C_c][1 - A_{vI3}])} = \frac{1}{2\pi(3 \text{ k}\Omega)([1 \text{ pF} + C_c][27])}$$

Solving for  $C_C$  yields

$$C_C = \frac{1}{2\pi(3 \text{ k}\Omega)(27)(32.8 \text{ kHz})} - 1 \text{ pF} \approx 60 \text{ pF}$$

Adding  $C_C$  to our simulation yields the loop transmission response seen in Fig. 18.17. We find the phase margin by identifying the phase at the frequency for a magnitude response of 0 dB,  $f_T$ , and calculate how far this is from 360 degrees. Note that in the previous loop gain plot the phase axis on the right went from  $-420$  degrees to  $-120$  degrees while this plot goes from  $-150$  to  $180$ . This is an inconsistency in most SPICE circuit simulators. In one case the midband phase shift (due to the inverting input) is  $-180$  while it is  $+180$  in the plot on the next page. For a continuous sine wave these two values are identical. So, in Fig. 18.17, phase margin is measured relative to 0 degrees rather than 360 degrees.

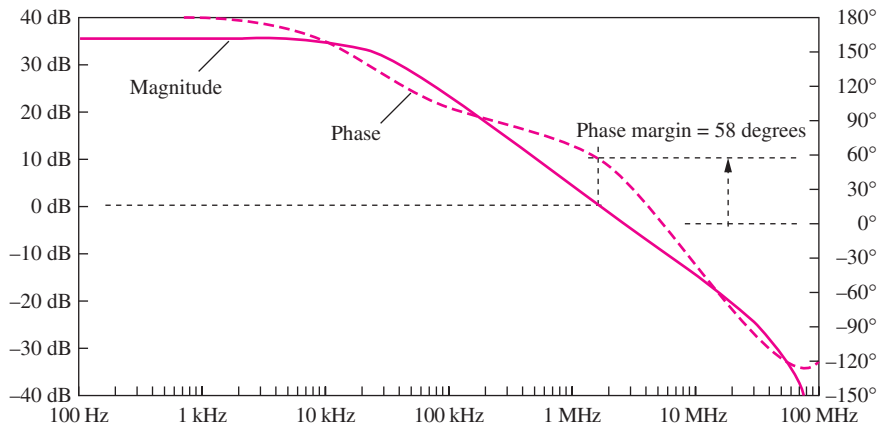


**Figure 18.17** Loop gain response with a compensation capacitance of 60 pF added from gate-to-drain of  $M_3$ .

### 18.4.3 HIGHER ORDER EFFECTS

Rather than the anticipated phase margin of 74 degrees, our simulation yields 58 degrees. This is due to an interesting aspect of the plot in Fig. 18.17 seen between 2 MHz and 20 MHz. The magnitude response is inflecting up, but the phase shift response is falling rapidly. This is surprising since a pole is of the form  $1/(1 + jf/f_p)$  and contributes negative phase shift as frequency increases and a negative inflection in the magnitude response. A zero in the numerator is usually of the form  $(1 + jf/f_z)$  and generates a positive inflection in the magnitude response and in the phase response.

What we see here is known as a right-half plane zero, or a zero that takes the form  $(1 - jf/f_z)$ . We found in the previous chapter that this occurs with common-emitter and common-source amplifier stages. This has a negative phase response and positive magnitude response. As we shall see in more detail later, this is due to a feed-forward path through the large compensation capacitor we added around  $M_3$ . At high frequencies signals can propagate through  $C_C$  instead of through  $M_3$ . Because of the positive inflection of the magnitude and related negative phase shift, a right-half plane zero can dramatically reduce phase margin. In this particular example, the effect is not pronounced (degrading  $\phi_M$  by  $14^\circ$ ), but in many situations it can have a major impact on stability.

The corresponding time domain response is seen in Fig. 18.18. The input pulse is plotted in the top plot and the output is seen in the bottom plot. This response illustrates the relationship between

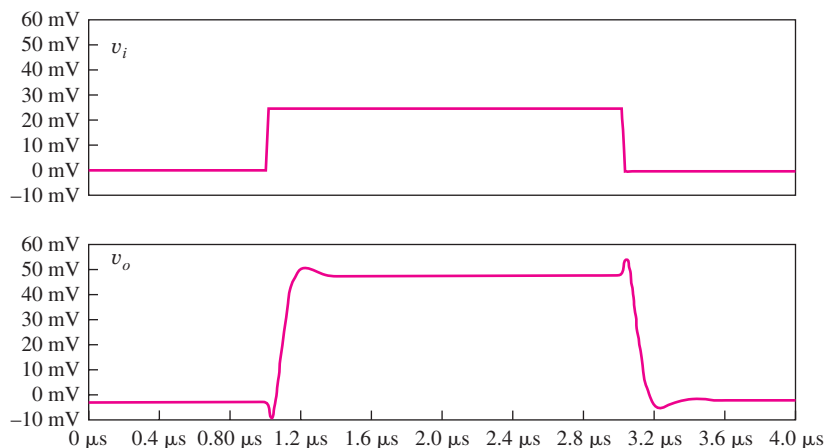


**Figure 18.18** Compensated amplifier step response.

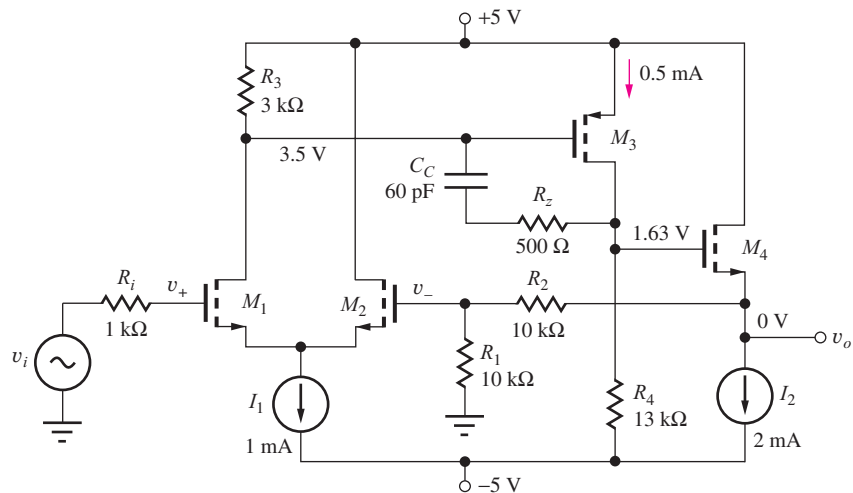


**Figure 18.19** Frequency compensated three-stage feedback amplifier.

overshoot and phase margin presented in Chapter 11. We see overshoot at the top of the rising edge of the output of about 7 percent. From Table 11.5, we expect a phase margin of 62 degrees for an overshoot of 7 percent. This is good agreement with our graphical estimate of 58 degrees when we consider that Table 11.5 was generated for a second-order system and our circuit is higher order. We should also note the small transient at the beginning of each pulse transition. This is also due to the feed-forward signal path through the compensation capacitor. The leading edge of the input signal couples through the compensation capacitance faster than transistor  $M_3$  can respond. (Recall that sharp transitions have significant high frequency content.) After a short delay, the signal path through the transistor catches up and again dominates the output response.

As we will learn in the next section, adding an appropriately valued resistance in series with the compensation capacitor can mitigate the effects of the feed-forward path. The calculation for arriving at the value of  $R_Z$  is discussed in the following sections. Fig. 18.19 shows the complete schematic with the compensation capacitor,  $C_C$ , and the feed-forward cancellation resistor  $R_Z$ .

#### 18.4.4 RESPONSE OF THE COMPENSATED AMPLIFIER

A simulation of the loop gain of the compensated amplifier in Fig. 18.19 is shown in Fig. 18.20. The addition of  $R_Z$  has removed the effects of the right-half plane zero and added an additional 20 degrees

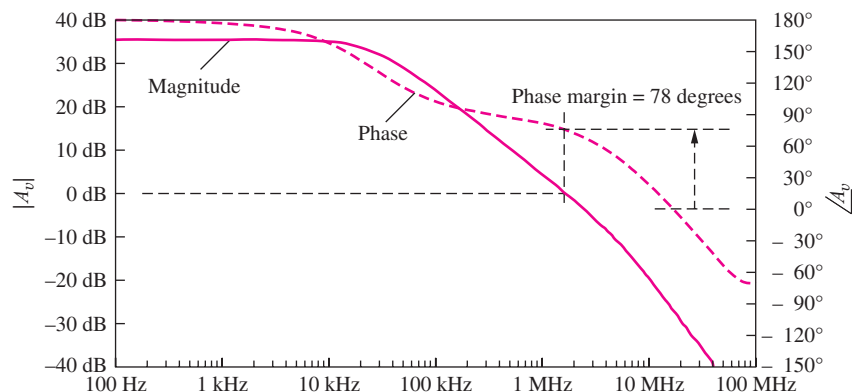


**Figure 18.20** Loop gain characteristic with  $C_C$  and  $R_Z$ .

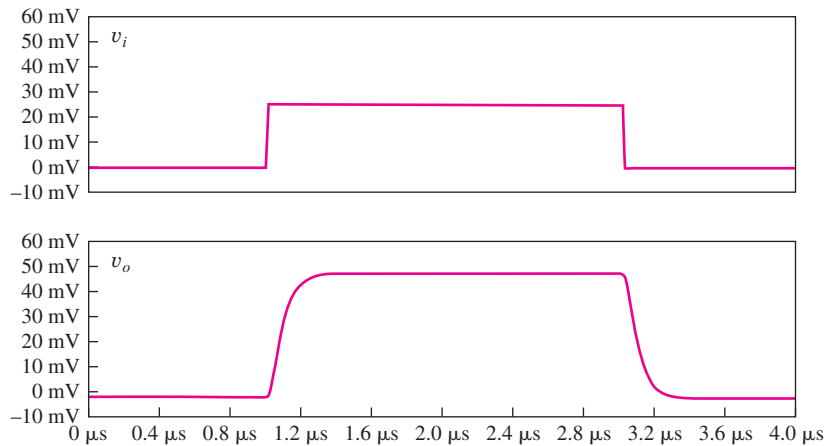


**Figure 18.21** Amplifier transient response with  $C_C$  and  $R_Z$ .

to the phase margin. This is typical of MOSFET feedback amplifiers due to their low  $g_m$  compared to BJT amplifiers. The magnitude response no longer shows the positive inflection at 3 MHz, and the phase shift does not drop as rapidly as it did in Fig. 18.17. This improved phase margin agrees well with our calculated value of  $74.5^\circ$ .

With the improved phase margin we should expect a reduction in the overshoot of our pulse response simulation. According to Table 11.5, a phase margin of 78 degrees should correspond to a pulse response with no overshoot, and this is confirmed in the simulation results in Fig. 18.21 for the fully compensated amplifier. Notice also that the transients at the start of each transition due to the feed-forward path have also been eliminated. The addition of  $R_Z$  increased the high frequency impedance through the feed-forward path, resulting in less feed-forward signal. The extent to which the addition of  $R_Z$  mitigates this issue will vary with the specific conditions of a particular amplifier. Another important characteristic of the final amplifier is an increase in rise and fall time. The edge transitions in Fig. 18.21 are slower than the previous simulation. In some applications, a faster edge transition may be desirable even at the expense of some overshoot.

We started this section by looking at the small-signal closed-loop gain characteristic of our amplifier. Fig. 18.22 shows our new closed-loop gain with the addition of  $C_C$  and  $R_Z$ . Clearly, this response is a more desirable characteristic than the results before compensation. Recall from Chapter 11, that the high-frequency corner,  $f_{-3db}$ , is equal to the loop gain 0 dB frequency,  $f_T$ , for a single-pole response. The frequency compensation changes our design to create a dominant pole

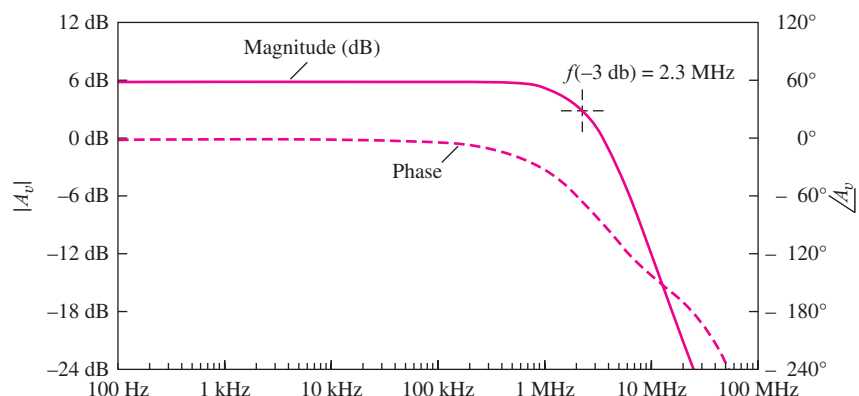


**Figure 18.22** Closed-loop gain characteristic with  $C_C$  and  $R_Z$ .

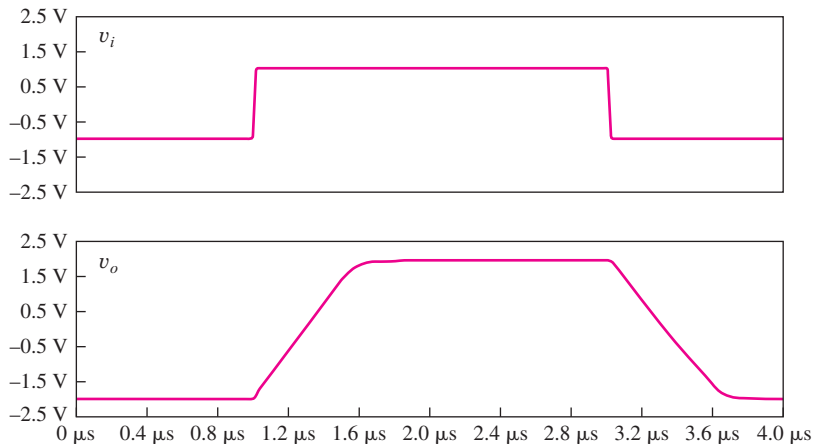


**Figure 18.23** Large-signal response of the compensated amplifier.

and approximate a single-pole response. Our simulation shows that our high-frequency corner is 2.3 MHz, close to the  $f_T$  target of 2 MHz. The two values don't match precisely since we are only approximating a single-pole response.

#### 18.4.5 SMALL-SIGNAL LIMITATIONS

Before we take a more detailed look the analysis of feedback in transistor amplifiers, we need to recognize the small-signal limitations of our analysis to this point. To illustrate the issue, Fig. 18.23 shows a simulation of the amplifier pulse response to a 2-volt pulse instead of the 25-mV pulse we simulated earlier. The rise and fall times of this output pulse are much slower than in the small-signal and are limited by amplifier slew rate. As we will see in a later section, slew rate is usually limited by how much current is available to charge the relatively large compensation capacitor. As we can see in Fig. 18.23, when an amplifier is slewing, the pulse edges deviate from an exponential RC settling characteristic to a linear charging shape. This is a large signal nonideality of a feedback amplifier, and we must be careful to recognize this when simulating or testing small-signal characteristics in the lab. In short, if we are attempting to measure a small-signal parameter and see a characteristic large signal slewing, we must reduce the amplitude of the input signal to ensure that we are operating in the small-signal regime.

In the following sections, we will analyze and design several feedback amplifiers for stable operation. While the example in this section was for an amplifier with a closed-loop gain of 2 and a  $\beta$  of 0.5, we typically design compensation for the worst-case unity-gain situation with gain of 1 and  $\beta$  of 1. Unless stated otherwise, we should assume this as the design goal.

### 18.5 SINGLE-POLE OPERATIONAL AMPLIFIER COMPENSATION

As discussed in the previous section and in Chapter 11, feedback amplifiers use internal frequency compensation to force the amplifier to have a single-pole frequency response. For general-purpose operational amplifiers, we will compensate the amplifiers for stable operation as unity-gain buffers, the worst-case situation for amplifier stability. The voltage transfer functions of these amplifiers can be represented by Eq. (18.16):

$$A_v(s) = \frac{A_o \omega_B}{s + \omega_B} = \frac{\omega_T}{s + \omega_B} \quad (18.16)$$

This form of transfer function can be obtained by connecting a compensation capacitor  $C_C$  around the second gain stage of the basic operational amplifier, as depicted in Fig. 18.24.

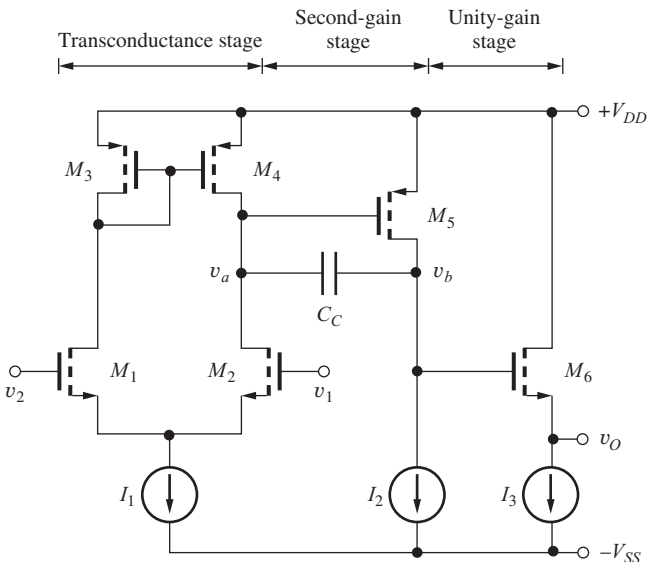
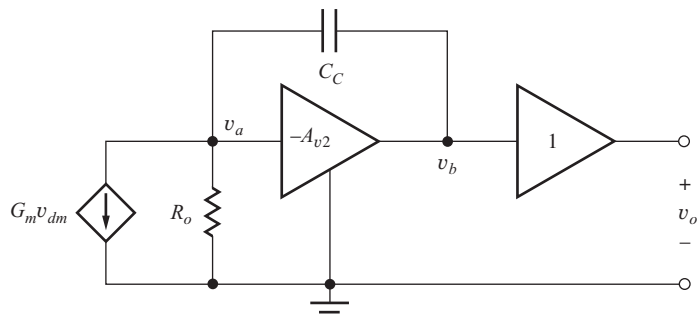


**Figure 18.24** Frequency-compensation technique for single-pole operational amplifiers.

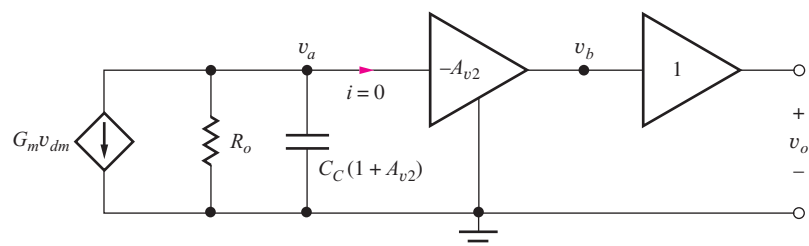
### 18.5.1 THREE-STAGE OP AMP ANALYSIS

Figure 18.25 is a simplified representation for the three-stage op amp. The input stage is modeled by its Norton equivalent circuit, represented by current source  $G_m v_{dm}$  and output resistance  $R_o$ . The second stage provides a voltage gain  $A_{v2} = g_{m5} r_{o5} = \mu_{f5}$ , and the follower output stage is represented as a unity-gain buffer.

The circuit in Fig. 18.25 can be further simplified using the **Miller effect** relations. Feedback capacitor  $C_C$  is multiplied by the factor  $(1 + A_{v2})$  and placed in parallel with the input of the second-stage amplifier, as in Fig. 18.26, and an expression for the output voltage can now be obtained from



**Figure 18.25** Simplified model for three-stage op amp.



**Figure 18.26** Equivalent circuit based on Miller multiplication.

analysis of this figure. The output voltage  $\mathbf{V}_o(s)$  must equal  $\mathbf{V}_b(s)$  because the output buffer has a gain of 1. Also,  $\mathbf{V}_b(s)$  equals  $-A_{v2}\mathbf{V}_a(s)$ .

Writing the nodal equation for  $\mathbf{V}_a(s)$  assuming  $i = 0$ ,

$$-G_m \mathbf{V}_{dm}(s) = \mathbf{V}_a(s)[sC_C(1 + A_{v2}) + G_o] \quad (18.17)$$

and

$$\frac{\mathbf{V}_a(s)}{\mathbf{V}_{dm}(s)} = \frac{-G_m R_o}{s R_o C_C(1 + A_{v2}) + 1} \quad (18.18)$$

Combining these results gives the overall gain of the op amp:

$$A_v(s) = \frac{\mathbf{V}_o(s)}{\mathbf{V}_{dm}(s)} = \frac{\mathbf{V}_b(s)}{\mathbf{V}_{dm}(s)} = \frac{-A_{v2}\mathbf{V}_a(s)}{\mathbf{V}_{dm}(s)} = \frac{G_m R_o A_{v2}}{1 + s R_o C_C(1 + A_{v2})} \quad (18.19)$$

Rewriting Eq. (18.18) in the form of (18.15) yields

$$A_v(s) = \frac{\frac{G_m A_{v2}}{C_C(1 + A_{v2})}}{s + \frac{1}{R_o C_C(1 + A_{v2})}} = \frac{\omega_T}{s + \omega_B} = \frac{A_o \omega_B}{s + \omega_B} \quad (18.20)$$

Figure 18.27 is a Bode plot for this transfer function. At low frequencies the gain is  $A_o = G_m R_o A_{v2}$ , and the gain rolls off at 20 dB/decade above the frequency  $\omega_B$ . Comparing Eq. (18.19) to (18.15),

$$\omega_B = \frac{1}{R_o C_C(1 + A_{v2})} \quad \text{and} \quad \omega_T = \frac{G_m A_{v2}}{C_C(1 + A_{v2})} \quad (18.21)$$

For large  $A_{v2}$ ,

$$\omega_T \approx \frac{G_m}{C_C} \quad (18.22)$$

Equation (18.21) is an extremely useful result. The unity gain frequency of the operational amplifier is set by the designer's choice of the values of the input stage transconductance and **compensation capacitor  $C_C$** .

The single pole of the amplifier is at a relatively low frequency, as determined by the large values of the output resistance of the first stage and the Miller input capacitance of the second stage.

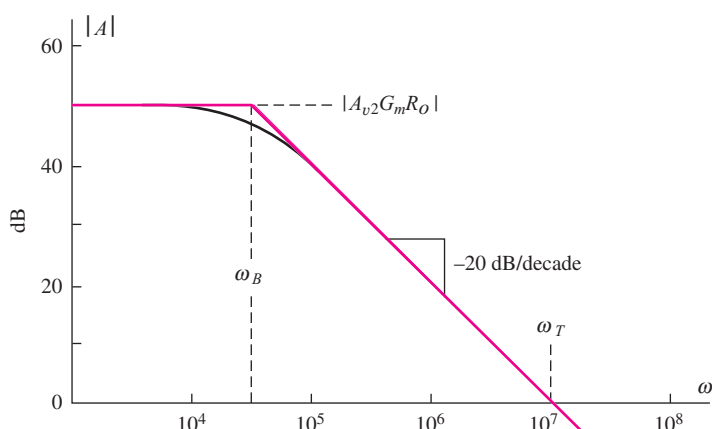


**Figure 18.27** Gain magnitude plot for the ideal single-pole op amp.

**EXERCISE:** What are the approximate values of  $G_m$ ,  $R_o$ ,  $f_T$ , and  $f_B$  for the op amp in Fig. 18.24 if  $K_{n2} = 1 \text{ mA/V}^2$ ,  $K_{p5} = 1 \text{ mA/V}^2$ ,  $C_C = 20 \text{ pF}$ ,  $\lambda = 0.02 \text{ V}^{-1}$ ,  $I_1 = 100 \mu\text{A}$ , and  $I_2 = 500 \mu\text{A}$ ?

**ANSWERS:**  $0.316 \text{ mS}$ ,  $500 \text{ k}\Omega$ ,  $2.52 \text{ MHz}$ ,  $158 \text{ Hz}$

## 18.5.2 TRANSMISSION ZEROS IN FET OP AMPS

Equation (18.21) presents an excellent method for controlling the frequency response of the operational amplifier with two gain stages. Unfortunately, however, we have overlooked a potential problem in the analysis of this amplifier: The simplified Miller approach does not take into account the finite transconductance of the second-stage amplifier.

The source of the problem can be understood by using the complete small-signal model for transistor  $M_5$ , as incorporated in Fig. 18.28. The previous analysis overlooked the zero that is determined by  $g_{m5}$  and the total feedback capacitance between the drain and gate of  $M_5$ . The circuit in Fig. 18.28 should once again look familiar. It is the same topology as the circuit for the simplified C-E amplifier, and we can use the results of the analysis in Eq. (17.94) by making the appropriate symbolic substitutions identified in Eq. (18.22):

$$r_{\pi o} \rightarrow R_o \quad R_L \rightarrow r_{o5} \quad C_\pi \rightarrow C_{GS5} \quad C_\mu \rightarrow C_C + C_{GD5} \quad (18.23)$$

With these transformations, the transfer function becomes

$$A_{vth}(s) = (-g_{m5}r_{o5}) \frac{\left(1 - \frac{s}{\omega_Z}\right)}{\left(1 + \frac{s}{\omega_{P1}}\right)} \quad \text{in which} \quad \omega_Z = \frac{g_{m5}}{C_C + C_{GD5}} = \omega_T \frac{g_{m5}}{g_{m2}}$$

and

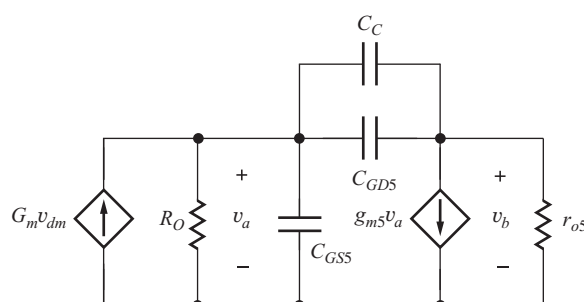
$$\omega_{P1} = \frac{1}{R_o C_T} \quad \text{where} \quad C_T = C_{GS5} + (C_C + C_{GD5}) \left(1 + \mu_{f5} + \frac{r_{o5}}{R_o}\right) \quad (18.24)$$

In the case of many FET amplifier designs,  $\omega_Z$  cannot be neglected because of the relatively low ratio of transconductances between FET  $M_5$  and  $M_2$ . In bipolar designs,  $\omega_Z$  can usually be neglected because of the much higher transconductance that is achieved for a given Q-point current. However,  $\omega_Z$  can also be a problem in common-emitter amplifiers with emitter resistors that reduce the overall transconductance of the amplifier stage.

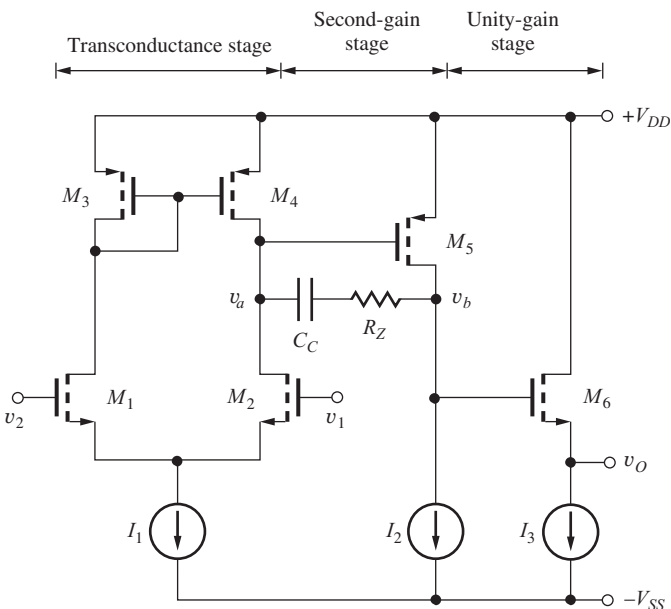
The problem can be overcome in FET amplifiers, however, through the addition of resistor  $R_Z$  in Fig. 18.29, which cancels the zero in Eq. (18.23). If we assume that  $C_C \gg C_{GD}$ , then the location of  $\omega_Z$  in the numerator of Eq. (18.23) becomes

$$\omega_Z = \frac{\left(\frac{1}{g_{m5}}\right) - R_Z}{C_C} \quad (18.25)$$

and the zero can be eliminated by setting  $R_Z = 1/g_{m5}$ .



**Figure 18.28** More complete model for op amp compensation.

Figure 18.29 Zero cancellation using resistor  $R_Z$ .

**EXERCISE:** Find the approximate location of  $f_z$  for the op amp in Fig. 18.29 using the values from the previous exercise. What value of  $R_Z$  is needed to eliminate  $f_z$ ?

**ANSWERS:** 7.96 MHz; 1 k $\Omega$

### 18.5.3 BIPOLAR AMPLIFIER COMPENSATION

The bipolar op amp in Fig. 18.30 is compensated in the same manner as the MOS amplifier. However, because the transconductance of the BJT is generally much higher than that of a FET for a given operating current, the transmission zero occurs at such a high frequency that it does not usually cause a problem. Applying Eq. (18.25) to the circuit in Fig. 18.30 yields an expression for the unity gain frequency of the two-stage bipolar amplifier:

$$\omega_T = \frac{g_{m2}}{C_C} = \frac{40I_{C2}}{C_C} = \frac{20I_1}{C_C} \quad \text{and} \quad \omega_Z = \frac{g_{m5}}{C_C} = \omega_T \left( \frac{I_{C5}}{I_{C2}} \right) \quad (18.26)$$

Because  $I_{C5}$  is 5 to 10 times  $I_{C2}$  in most designs,  $\omega_Z$  is typically at a frequency of 5 to 10 times the unity gain frequency  $\omega_T$ .

The simulated frequency response for the amplifier in Fig. 18.30(a) appears in Fig. 18.30(b) based on the values in the next exercise. The dominant pole, arising from the high resistance at the base of  $Q_5$ , occurs at approximately 565 Hz, and the unity-gain crossover occurs at 10 MHz. A second pole, due to the dominant pole of the *pnp* current mirror, causes the increased roll-off beyond 10 MHz.

**EXERCISE:** Find the approximate locations of  $f_T$ ,  $f_z$ , and  $f_B$  for the bipolar op amp in Fig. 18.30 if  $C_C = 30 \text{ pF}$ ,  $V_A = 50$ ,  $I_1 = 100 \mu\text{A}$ ,  $I_2 = 500 \mu\text{A}$ , and  $I_3 = 5 \text{ mA}$ .

**ANSWERS:** 10.6 MHz, 106 MHz, 565 Hz

### 18.5.4 SLEW RATE OF THE OPERATIONAL AMPLIFIER

Errors caused by slew-rate limiting of the output voltage of the amplifier were discussed in Chapter 11. Slew-rate limiting occurs because there is a limited amount of current available to

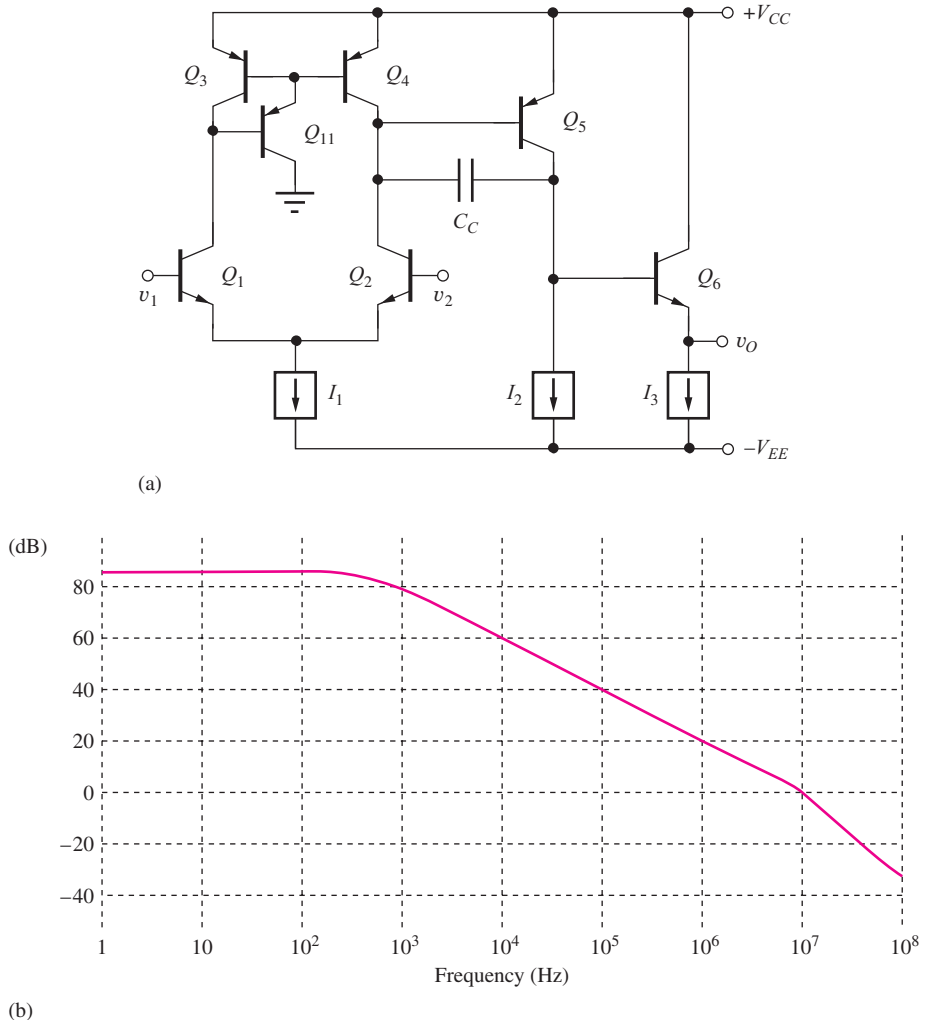


**Figure 18.30** (a) Frequency compensation of a bipolar op amp. (b) Bode plot for amplifier described in exercise.

charge and discharge the internal capacitors of the amplifier. For an internally compensated amplifier, \$C\_C\$ typically determines the **slew rate**. Consider the example of the CMOS amplifier with the large input signal (no longer a small signal) in Fig. 18.31. In this case, the voltages applied to the differential input stage cause current \$I\_1\$ to switch completely to one side of the differential pair, in a manner directly analogous to the current switch discussed in Chapter 9.

Figure 18.32 is a simplified model for the amplifier in this condition. Because of the unity gain output buffer, output voltage \$v\_O\$ follows voltage \$v\_B\$. Current \$I\_1\$ must be supplied through compensation capacitor \$C\_C\$, and the rate of change of the \$v\_B\$, and hence \$v\_O\$, must satisfy

$$I_1 = C_C \frac{d(v_B(t) - v_A(t))}{dt} = C_C \frac{d \left( v_B(t) + \frac{v_B(t)}{A_{v2}} \right)}{dt} \quad (18.27)$$

If \$A\_{v2}\$ is assumed to be very large, then the amplifier will behave in a manner similar to an ideal integrator; that is, node voltage \$v\_A\$ represents a virtual ground, and Eq. (18.26) becomes

$$I_1 \cong C_C \frac{dv_B(t)}{dt} = C_C \frac{dv_O(t)}{dt} \quad (18.28)$$

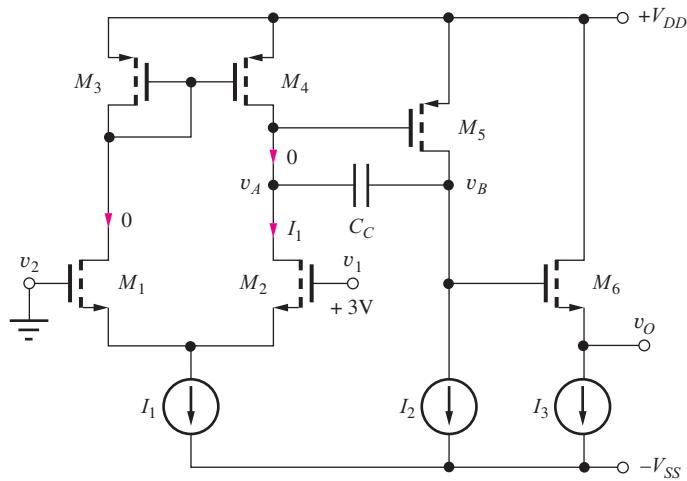


Figure 18.31 Operational amplifier with input stage overload.

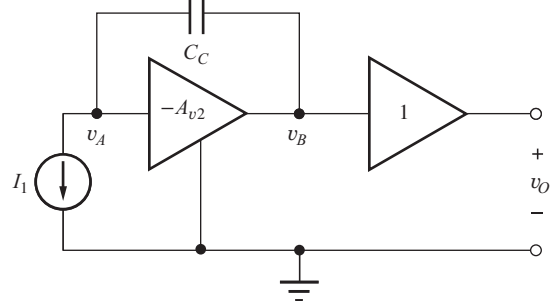


Figure 18.32 Simplified model for three-stage op amp.

The slew rate is the maximum rate of change of the output signal, and

$$\text{SR} = \left. \frac{dv_O(t)}{dt} \right|_{\max} = \frac{I_1}{C_C} \quad (18.29)$$

The slew rate is determined by the total input stage bias current and the value of the compensation capacitor  $C_C$ . (It is seldom pointed out that this derivation tacitly assumes that the output of amplifier  $A_{v2}$  is capable of sourcing or sinking the current  $I_1$ . This requirement will be met as long as the amplifier is designed with  $I_2 \geq I_1$ .)

**EXERCISE:** Show that the slew rate is symmetrical in the CMOS amplifier in Fig. 18.31; that is, what is the current in capacitor  $C_C$  if  $v_1 = 0$  V and  $v_2 = +3$  V?

**ANSWER:**  $I_1$

### 18.5.5 RELATIONSHIPS BETWEEN SLEW RATE AND GAIN-BANDWIDTH PRODUCT

Equation (18.28) can be related directly to the unity gain bandwidth of the amplifier using Eq. (18.21):

$$\text{SR} = \frac{I_1}{C_C} = \frac{I_1}{\left( \frac{G_m}{\omega_T} \right)} = \frac{\omega_T}{\left( \frac{G_m}{I_1} \right)} \quad (18.30)$$

For the simple CMOS amplifier in Fig. 18.24, the input stage transconductance is equal to that of transistors  $M_1$  and  $M_2$ ,

$$\left( \frac{G_m}{I_1} \right) = \frac{1}{I_1} \sqrt{2K_{n2} \frac{I_1}{2}} = \sqrt{\frac{2K_{n2}}{I_1}}$$

and

$$\text{SR} = \omega_T \sqrt{\frac{I_1}{K_{n2}}} \quad (18.31)$$

For a given desired value of  $\omega_T$ , the slew rate increases with the square root of the bias current in the input stage.

For the bipolar amplifier in Fig. 18.30,

$$\left(\frac{G_m}{I_1}\right) = \left(\frac{\frac{40}{2} I_1}{I_1}\right) = 20 \quad \text{and} \quad SR = \frac{\omega_T}{20} \quad (18.32)$$

In this case, the slew rate is related to the choice of unity gain frequency by a fixed factor.

**EXERCISE:** What is the slew rate of the CMOS amplifier in Fig. 18.24 if  $K_{n2} = 1 \text{ mA/V}^2$ ,  $K_{p5} = 1 \text{ mA/V}^2$ ,  $C_C = 20 \text{ pF}$ ,  $\lambda = 0.02 \text{ V}^{-1}$ ,  $I_1 = 100 \mu\text{A}$ , and  $I_2 = 500 \mu\text{A}$ ?

**ANSWER:** 5.00 V/ $\mu$ s

**EXERCISE:** What is the slew rate of the bipolar amplifier in Fig. 18.30 if  $C_C = 20 \text{ pF}$ ,  $I_1 = 100 \mu\text{A}$ , and  $I_2 = 500 \mu\text{A}$ ?

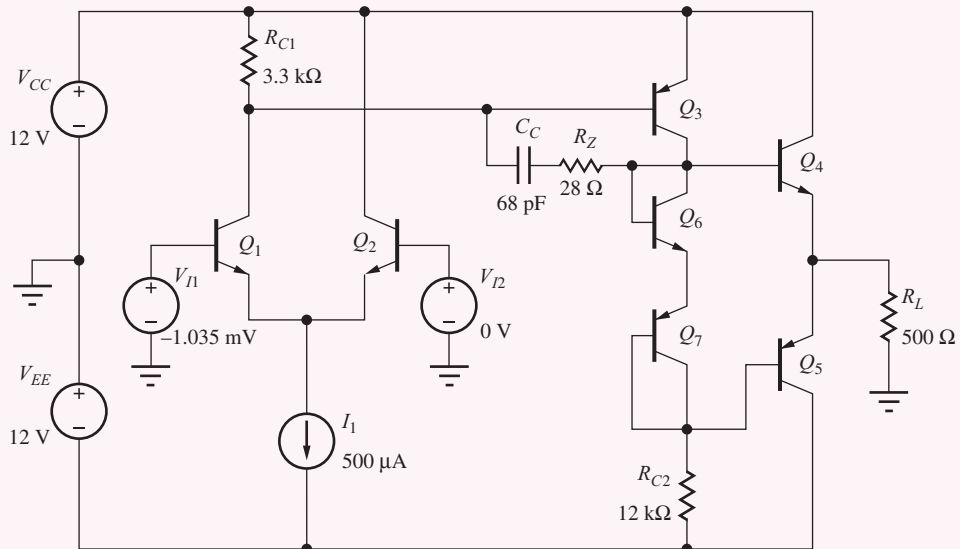
**ANSWER:** 5.00 V/ $\mu$ s

## DESIGN EXAMPLE 18.7 OPERATIONAL AMPLIFIER COMPENSATION

### EXAMPLE 18.7

In this example, we will choose the value of the compensation capacitor in a BJT op amp to give a desired value of phase margin.

**PROBLEM** Design the compensation capacitor in the BJT op amp circuit here to give a phase margin of  $75^\circ$ . Find the open-loop gain, bandwidth, and GBW product for the compensated op amp. For simplicity, assume that the *npn* and *pnp* transistors are described by the same set of SPICE parameters: BF = 100, VAF = 75 V, IS = 0.1 fA, RB = 250  $\Omega$ , TF = 0.75 ns, and CJC = 2 pF.



**SOLUTION** **Known Information and Given Data:** The three-stage op amp circuit appears here and consists of an *npn* differential input stage driving a common-emitter *pnp* gain stage.  $R_{C1} = 3.3 \text{ k}\Omega$  and  $R_{C2} = 12 \text{ k}\Omega$ . The output stage is a complementary *npn-pnp* emitter-follower stage. Transistor parameters are given as BF = 100, VAF = 75 V, IS = 0.1 fA, RB = 250  $\Omega$ , TF = 0.75 ns, and CJC = 2 pF,  $\Phi_M = 75^\circ$ .

**Unknowns:** Value of  $C_C$  for  $75^\circ$  phase margin; the resulting open-loop gain and bandwidth, and unity-gain frequency; positions of the nondominant poles

**Approach:** Find the Q-points of the transistors and the small-signal parameters of the transistors. Assume that the dominant pole of the amplifier is set by compensation capacitor  $C_C$  around the *pnp* common-emitter gain stage. Find the nondominant poles of the amplifier resulting from the differential input stage and the emitter follower. Then choose  $C_C$  to give the unity-gain frequency required to achieve the desired phase margin.

**Assumptions:** The dominant pole of the op amp is set by compensation capacitor  $C_C$  and the *pnp* common-emitter stage;  $R_Z$  is included to remove the zero associated with  $C_C$ ;  $T = 27^\circ\text{C}$ ; the *pnp* and *npn* transistors are identical;  $V_{BE} = V_{EB} = 0.75\text{ V}$ . The quiescent value of  $V_O = 0$ . Neglect all base currents in the Q-point analyses.  $\text{VJC} = 0.75\text{ V}$  and  $\text{MJC} = 0.33$ . Transistors  $Q_4$  and  $Q_5$  operate in parallel. The small-signal resistances of diode-connected transistors  $Q_6$  and  $Q_7$  can be neglected.

**ANALYSIS** **Q-Point:** Bias current  $I_1$  splits equally between  $Q_1$  and  $Q_2$  so that  $I_{C1} = I_{C2} = 250\text{ }\mu\text{A}$ . For  $V_O = 0$ , the voltage across  $R_{C2} = 12 - 0.75 = 11.3\text{ V}$ , and the current in  $Q_3$  is  $I_{C3} = 11.3\text{ V}/12\text{ k}\Omega = 938\text{ }\mu\text{A}$ .  $Q_4$  and  $Q_5$  mirror the currents in  $Q_7$  and  $Q_8$ , so  $I_{C4} = I_{C5} = 938\text{ }\mu\text{A}$ . For  $V_O = 0$ ,  $V_{CE4} = 12\text{ V}$ ,  $V_{EC5} = 12\text{ V}$ , and  $V_{EC3} = 11.3\text{ V}$ . For  $V_I = 0$ ,  $V_{CE2} = 12.8\text{ V}$  and  $V_{CE1} = 12 - 3300(0.25\text{ mA}) + 0.75 = 11.9\text{ V}$ .

**Small-Signal Parameters:** The small-signal parameters are found using these formulas cast in terms of the SPICE parameters:

$$\begin{aligned}\beta_o &= \text{BF} \left( 1 + \frac{V_{CE}}{\text{VAF}} \right) = 100 \left( 1 + \frac{V_{CE}}{75} \right) & g_m &= 40I_C & r_\pi &= \frac{\beta_o}{g_m} \\ r_o &= \frac{\text{VAF} + V_{CE}}{I_C} = \frac{75 + V_{CE}}{I_C} \\ C_\pi &= g_m \text{TF} = g_m(0.75 \times 10^{-9}) & C_\mu &= \frac{\text{CJC}}{\left( 1 + \frac{V_{CB}}{\text{VJC}} \right)^{\text{MJC}}} = \frac{2\text{ pF}}{\left( 1 + \frac{V_{CB}}{0.75} \right)^{0.33}}\end{aligned}$$

	$I_C$ ( $\mu\text{A}$ )	$V_{CE}$ (V)	$\beta_o$	$g_m$ (S)	$r_\pi$ ( $\text{k}\Omega$ )	$r_o$ ( $\text{k}\Omega$ )	$C_\pi$ ( $\text{pF}$ )	$C_\mu$ ( $\text{pF}$ )
$Q_1$	250	11.9	116	0.01	11.6	348	7.50	0.803
$Q_2$	250	12.8	117	0.01	11.7	351	7.50	0.784
$Q_3$	938	11.3	115	0.0375	3.07	92.0	28.1	0.818
$Q_4$	938	12.0	116	0.0375	3.09	92.8	28.1	0.801
$Q_5$	938	12.0	116	0.0375	3.09	92.8	28.1	0.801

**Open Loop-Gain:**  $A_O = A_{vt1}A_{vt2}A_{vt3}$

$$A_{vt1} = \frac{g_{m1}}{2}(2r_{o1} \parallel R_{C1} \parallel r_{\pi3}) = \frac{0.01}{2}(696\text{ k}\Omega \parallel 3.3\text{ k}\Omega \parallel 3.07\text{ k}\Omega) = 7.93$$

$$A_{vt2} = g_{m2} \left[ r_{o3} \parallel R_{C1} \left| \left( \frac{r_{\pi4}}{2} + (\beta_{o4} + 1)R_L \right) \right| \right]$$

$$= 0.0375 \left[ 92.0\text{ k}\Omega \parallel 12\text{ k}\Omega \left| \left( \frac{3.09\text{ k}\Omega}{2} + (117)500\text{ }\Omega \right) \right| \right] = 338$$

$$A_{vt3} = \frac{(\beta_o + 1)R_L}{\frac{r_{\pi4}}{2} + (\beta_o + 1)R_L} = \frac{(117)500}{\frac{3090}{2} + (117)500} = 0.974$$

$$A_O = 2610$$

**Compensation Capacitor Design:** At the unity-gain frequency  $f_T$ , the dominant pole due to  $C_C$  will contribute a phase shift of  $90^\circ$ . The dominant poles of each of the other two stages will determine the phase margin. For a phase margin of  $75^\circ$ , the contributions of the additional poles can only be  $15^\circ$ . We expect these poles to be at frequencies above the op amp unity-gain frequency, typically 50 to 200 MHz.

### Input Stage Pole

We are interested in the transfer function for the loop gain. In the feedback path, the input stage appears as a C-C/C-B cascade. Thus, we will use the equation from Table 17.2 for the pole at the input of a common-collector stage with  $R_{L2} = 1/g_{m1}$ .

$$\begin{aligned} f_{pB2} &= \left(\frac{1}{2\pi}\right) \frac{1}{([R_{th2} + r_{x2}] \parallel [r_{\pi2} + (\beta_o + 1)R_{L2}]) \left(C_{\mu2} + \frac{C_{\pi2}}{1 + g_{m2}R_{L2}}\right)} \\ &= \left(\frac{1}{2\pi}\right) \frac{1}{([R_{th2} + r_{x2}] \parallel 2r_{\pi2}) \left(C_{\mu2} + \frac{C_{\pi2}}{2}\right)} \\ &= \left(\frac{1}{2\pi}\right) \frac{1}{(250 \Omega \parallel 2 \cdot 11.7 \text{ k}\Omega) \left(0.784 \text{ pF} + \frac{7.5 \text{ pF}}{2}\right)} = 142 \text{ MHz} \end{aligned}$$

### Gain Stage Pole

This pole will be dominated by the Miller effect capacitance associated with the compensation capacitance. The actual location of the pole will be calculated based on a desired phase margin.

### Emitter-Follower Pole

The pole at the input to the emitter-follower stage will be affected by the pole-splitting action of the compensation capacitor placed across the gain stage. Assuming the compensation capacitor across the gain stage is much larger than the other capacitances in the circuit, the pole at the input to the follower stage is

$$f_{pB4} \cong \frac{g'_{m3}}{2\pi(C_{\pi3} + C_{L3})}$$

To account for  $r_x$ , we will use  $g'_{m3}$  as defined in Eq. (17.70). The  $C_\pi$  term represents the total equivalent capacitance to small-signal ground at the input to the gain stage, including the output capacitance of the differential pair.  $C_{L3}$  is the capacitance looking into the complementary pair follower stage. Assuming only one of the two devices in the complementary pair is carrying a signal at any instant in time, the complementary pair device is represented by a device with the same  $g_m$ , a current gain equal to the average of the two devices, and TF roughly equal to the average TF. Since  $C_\mu$  is a junction parasitic capacitance, we will see the cumulative capacitance due to the  $C_\mu$  of both devices. Given these conditions, the pole is calculated as

$$f_{pB4} \cong \left(\frac{1}{2\pi}\right) \frac{0.0375 \text{ mS}(3.07 \text{ k}\Omega/3.32 \text{ k}\Omega)}{\left(0.8 \text{ pF} + 28.1 \text{ pF} + 2 \cdot 0.8 \text{ pF} + \frac{28.1 \text{ pF}}{1 + 0.0375 \text{ mS } (500 \Omega)}\right)} = 173 \text{ MHz}$$

In addition to these terms, we should also expect to see a pole equal to approximately  $f_T$ ,  $[1/2\pi(\text{TF} + C_\mu/g_m)]$ , at the emitter junction of the differential pair and at the output node since there is no additional output load capacitance. The  $f_T$  values for  $Q_1$  and  $Q_4$  are 192 MHz and 206 MHz, respectively.

We can now choose the unity-gain frequency,  $f_T$ , of the op amp to give the desired phase margin. At the unity-gain frequency, the primary pole of the op amp will contribute approximately  $90^\circ$  of

phase shift. For a  $75^\circ$  phase margin, the remaining four poles can contribute an additional phase shift of  $15^\circ$ , which allows us to find the required value of  $f_T$ :

$$15^\circ = \tan^{-1} \left( \frac{f_T}{142 \text{ MHz}} \right) + \tan^{-1} \left( \frac{f_T}{173 \text{ MHz}} \right) + \tan^{-1} \left( \frac{f_T}{192 \text{ MHz}} \right) + \tan^{-1} \left( \frac{f_T}{206 \text{ MHz}} \right)$$

Solving for the unity-gain frequency yields  $f_T = 11.5 \text{ MHz}$ .

Using Eq. (18.22) from our op amp analysis,

$$\begin{aligned} (C_C + C_{\mu 3}) &= \frac{G_{m1}}{\omega_T} = \left( \frac{g_{m1}}{2} \right) \left( \frac{1}{2\pi f_T} \right) \\ &= \frac{0.005}{2\pi(11.5 \times 10^6)} = 69 \text{ pF} \end{aligned}$$

since  $C_{\mu 3}$  is approximately in parallel with  $C_C$ . To eliminate the unwanted zero associated with  $C_C$ ,  $R_Z = 1/g_{m3} = 27.5 \Omega$ . Now we can also find the open-loop bandwidth:

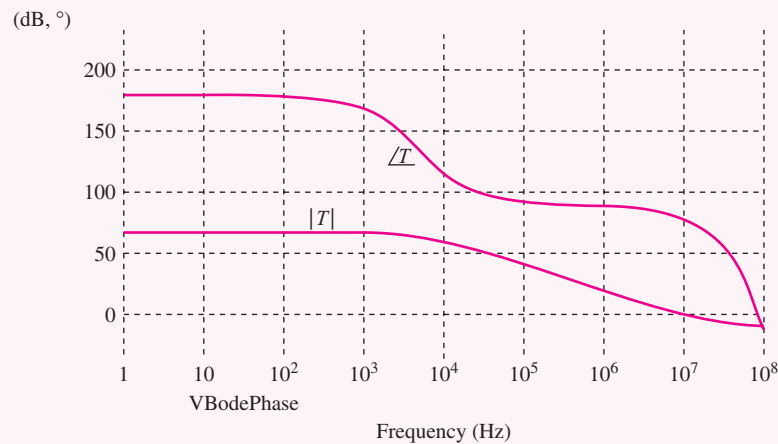
$$f_B = \frac{f_T}{A_o} = \frac{11.5 \text{ MHz}}{2610} = 4.41 \text{ kHz}$$

Thus, our design values are  $A_o = 68.3 \text{ dB}$ ,  $f_T = 11.5 \text{ MHz}$ ,  $f_B = 4.41 \text{ kHz}$ , and  $\Phi_M = 75^\circ$ .

**Check of Results:** We will check our analysis using SPICE as outlined below.

**Computer-Aided Analysis:** In order to simulate the gain with the feedback loop open, we must first find the offset voltage of the amplifier. With the amplifier connected as a voltage follower, the offset voltage was found to be 1.035 mV. The Q-point collector currents for transistors  $Q_1$  through  $Q_7$  are 242  $\mu\text{A}$ , 254  $\mu\text{A}$ , 936  $\mu\text{A}$ , 1.05 mA, 1.05 mA, 917  $\mu\text{A}$ , and 917  $\mu\text{A}$ , respectively.

The offset voltage was then applied to the input of the open-loop amplifier to set the output voltage to zero, and an ac sweep was performed from 1 Hz to 100 MHz with 20 simulation points per decade. The resulting open-loop gain is plotted below. The open-loop gain is 67.2 dB, the open-loop bandwidth is 4.52 kHz, the unity-gain frequency is 10.7 MHz, and the phase margin is  $74^\circ$ . These values all agree well with our design calculations. The phase margin is being affected by a zero that can be seen in the magnitude response above 30 MHz and was not included in our analysis.



**EXERCISE:** Use the technique in Sec. 17.8.3 and Ex. 17.6 to verify the loop-gain plot in Ex. 18.7.

**EXERCISE:** Calculate the unity-gain frequency and phase margin for the amplifier in Ex. 18.7 if  $C_C$  is reduced to 50 pF.

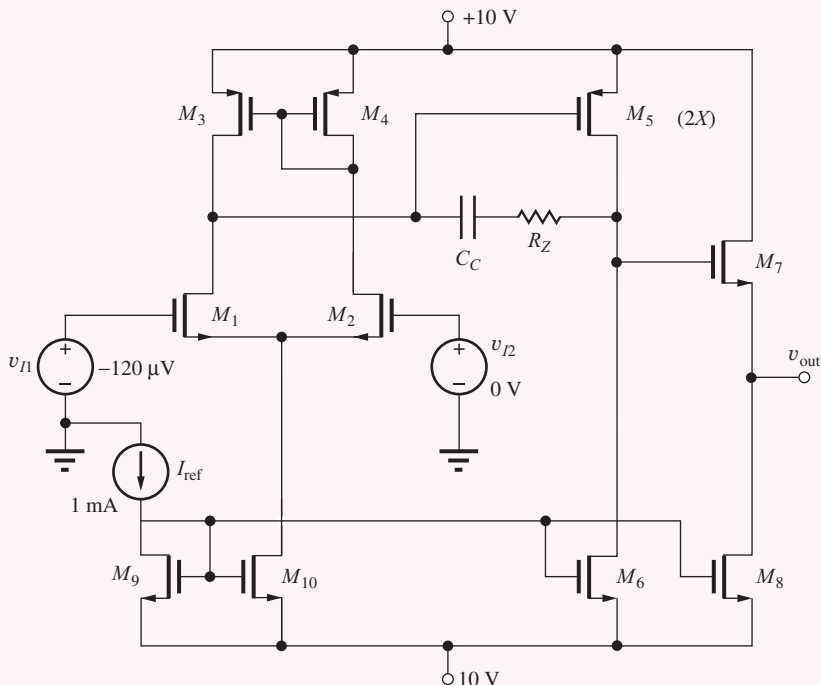
**ANSWER:** 15.9 MHz, 27.6°

## DESIGN EXAMPLE 18.8

### MOSFET OPERATIONAL AMPLIFIER COMPENSATION

In this example, we will choose the value of the compensation capacitor in a FET op amp to produce a desired value of phase margin for use in a unity-gain configuration.

**PROBLEM** Design the compensation capacitor in the FET op-amp circuit here to produce a phase margin of 70°. Find the open-loop gain, bandwidth, and GBW product for the compensated op amp. All of the NMOS FETs have SPICE parameters:  $K_P = 10 \text{ mS/V}$ ,  $V_{TO} = 1 \text{ V}$ ,  $\text{LAMBDA} = 0.01 \text{ V}^{-1}$ . The PMOS FETs have SPICE parameters:  $K_P = 4 \text{ mS/V}$ ,  $V_{TO} = -1 \text{ V}$ ,  $\text{LAMBDA} = 0.01 \text{ V}^{-1}$ .  $C_{GS}$  and  $C_{GD}$  are 5 pF and 1 pF, respectively, and will be added manually to the SPICE schematic. Consider  $M_5$  to be the parallel combination of two PMOS FETs (or a PMOS with twice the  $W/L$  of the other PMOS FETs),  $K_P = 8 \text{ mS/V}$ ,  $C_{GS} = 10 \text{ pF}$ , and  $C_{GD} = 2 \text{ pF}$ .



**SOLUTION Known Information and Given Data:** The three-stage op-amp circuit appears here and consists of an NMOS differential input stage with a PMOS current mirror load. The second stage is a PMOS common-source gain stage. The output stage is an NMOS source-follower stage. Transistor parameters given as  $K_P = 10 \text{ mS/V}$  (NMOS),  $K_P = 4 \text{ mS/V}$  (PMOS),  $V_{TO} = -1 \text{ V}$ ,  $C_{GD} = 1 \text{ pF}$ , and  $C_{GS} = 5 \text{ pF}$ . Device  $M_5$  is twice the width of the other PMOS FETs, so its  $K_P$ ,  $C_{GS}$ , and  $C_{GD}$  are doubled.  $\Phi_M = 70^\circ$ .

**Unknowns:** Value of  $C_C$  for 70° phase margin; the resulting open-loop gain and bandwidth, and unity-gain frequency; positions of the nondominant poles.

**Approach:** Find the Q-points and small-signal parameters of the transistors. We initially assume that the dominant pole of the op amp is set by compensation capacitor  $C_C$  of the PMOS gain stage. Find the nondominant poles at the other nodes of the amplifier and use these to calculate the unity gain frequency required to achieve the desired phase margin.

**Assumptions:** The dominant pole is set by the compensation capacitor  $C_C$  and the C-S stage. We will include the appropriate value of  $R_Z$  to remove the right-half plane zero associated with the C-S gain stage. The circuit is operating at room temperature, and the circuit will be biased to produce a nominal output voltage of 0 volts. We will neglect the finite output impedance effects on device currents when calculating the operating points.

**ANALYSIS** **Q-Point:** The use of current mirror biasing and active loads greatly simplifies the calculation of the device operating currents. Given the reference current of 1 mA, we know that the bias currents for  $M_1-M_4$  will all be 0.5 mA.  $M_6$  and  $M_8$  will nominally sink 1 mA. The  $V_{GS}$  of  $M_5$  is of some interest. Because of the  $\lambda$  term in the FET current equation, we know that for  $I_{D3}$  and  $I_{D4}$  to be matched, they need to have the same  $V_{DS}$ . As a result,  $V_{GS}$  will nominally have the same value as the  $V_{GS}$  of  $M_3$  and  $M_4$ . If  $M_5$  is identical to  $M_4$ , their currents will therefore be approximately equal. However,  $M_6$  is biased to sink twice the current of  $M_4$ , so the output voltage will be saturated near  $V_{SS}$  if  $M_5$  is identical to  $M_4$ . This is why  $M_5$  is specified as having twice the  $W/L$  of  $M_4$ , so it will produce twice the current of  $M_4$ , thus matching the current level of  $M_6$ .

**Small-Signal Parameters:** The small signal parameters are found using the following formulas:

$$r_o \cong \frac{1/\lambda + V_{DS}}{I_D} \quad g_m = \sqrt{2KP \cdot I_D(1 + \lambda V_{DS})}$$

	$I_D$ (mA)	$V_{DS}$ (V)	$g_m$ (mS)	$r_o$ ( $k\Omega$ )	$C_{GD}$ (pF)	$C_{GS}$ (pF)
M1, M2	0.5	9.8	3.46	120	1	5
M3, M4	0.5	1.5	2.03	103	1	5
M5	1	8.6	4.33	58.6	2	10
M6	1	11.4	4.96	61.4	1	5
M7	1	10	4.90	60	1	5
M8	1	10	4.90	60	1	5
M9	1	1.45	4.50	101	1	5
M10	1	8.55	4.66	109	1	5

**Open Loop-Gain:**  $A_o = A_{vt1}A_{vt2}A_{vt3}$

$$A_{vt1} = g_{m1,2}(r_{o1}\|r_{o3}) = 3.46 \text{ mS}(120 \text{ k}\Omega\|103 \text{ k}\Omega) = 192 \text{ V/V}$$

$$A_{vt2} = -g_{m5}(r_{o5}\|r_{o6}) = 4.33 \text{ mS}(58.6 \text{ k}\Omega\|61.4 \text{ k}\Omega) = -130 \text{ V/V}$$

$$A_{vt3} = \frac{g_{m7}R_{S7}}{1 + g_{m7}R_{S7}} = \frac{g_{m7}(r_{o7}\|r_{o8})}{1 + g_{m7}(r_{o7}\|r_{o8})} = \frac{4.90 \text{ mS}(60 \text{ k}\Omega\|60 \text{ k}\Omega)}{1 + 4.90 \text{ mS}(60 \text{ k}\Omega\|60 \text{ k}\Omega)} = 0.993 \text{ V/V}$$

$$A_o = -24,800 \text{ V/V} = 87.9 \text{ dB}$$

**Compensation Capacitor Design:** At  $f_T$ , the loop gain reaches 0 dB and the dominant pole will contribute approximately  $90^\circ$  of phase shift. To achieve a phase margin of  $70^\circ$ , the compensation capacitor is selected to set the unity-gain frequency such that the nondominant poles are contributing a total of  $90 - 70$  or  $20^\circ$  of phase shift (the inverting input contributes another  $180^\circ$ ).

### Input Stage Pole

We are interested in the transfer function for the loop gain, and in the feedback path, the input stage appears as a C-D/C-G cascade. Since we are driving our input with a zero impedance source, the pole at the gate of  $M_2$  has infinite frequency. Since we are designing the op amp to be stable in a unity-gain configuration, we will include the  $M_2$  input capacitance as an additional capacitive load at the output in our calculations to model the capacitive loading seen by the output when the negative feedback is connected.

$$C_{in} = C_{GD} + \frac{C_{GS}}{1 + g_{m2}R_{S2}} = C_{GD} + \frac{C_{GS}}{1 + \frac{g_{m2}}{g_{m1}}} = 1 \text{ pF} + \frac{5 \text{ pF}}{2} = 3.5 \text{ pF}$$

### Differential Pair Source Node Pole

There is a high-frequency pole at the differential pair source node. This pole is found as

$$\begin{aligned} f_{pS1} &\cong \left( \frac{1}{2\pi} \right) \frac{1}{\left( \frac{1}{g_{m1}} \parallel \frac{1}{g_{m2}} \right) (C_{GS1} + C_{GS2} + C_{GD10})} \\ &= \left( \frac{1}{2\pi} \right) \frac{1}{\left( \frac{0.5}{3.46 \text{ mS}} \right) (5 \text{ pF} + 5 \text{ pF} + 1 \text{ pF})} = 100 \text{ MHz} \end{aligned}$$

### Gain Stage Pole

This pole will be dominated by the Miller effect capacitance at the input to the gain stage and associated with the compensation capacitance,  $C_C$ . The actual location of the pole will be calculated based on a desired phase margin.

### Source Follower Input Pole

This pole at the input to the emitter-follower stage will be affected by the pole-splitting action of the compensation capacitor placed across the gain stage. Assuming the compensation capacitor across the gain stage is much larger than the other capacitances in the circuit, the pole at the input to the follower stage is

$$f_{pD5} \cong \frac{g_{m5}}{2\pi(C_{i5} + C_{L5})}$$

As with our bipolar example, the  $C_{GS}$  term above represents the total equivalent capacitance to small-signal ground at the input to the gain stage, including the output capacitance of the differential pair.

$$C_{i5} = C_{GD1} + C_{GD3} + C_{GS5} = (1 + 1 + 10) \text{ pF} = 12 \text{ pF}$$

$C_{L3}$  is the capacitance looking into the C-C output stage plus the capacitance seen looking into the current source.

$$C_{L5} = C_{GD6} + C_{GD7} + \frac{C_{GS7}}{1 + g_{m7}(r_{o7} \parallel r_{o8})} = 1 + 1 + \frac{5}{1 + 4.9 \text{ mS}(30 \text{ k}\Omega)} = 2.03 \text{ pF}$$

Given these results, the pole is calculated as

$$f_{pD5} \cong \left( \frac{1}{2\pi} \right) \frac{4.33 \text{ mS}}{(12 \text{ pF} + 2.03 \text{ pF})} = 49.2 \text{ MHz}$$

### Output Pole

The pole at the output will be set by finding the equivalent resistance and capacitance at the output node. As mentioned earlier, we will include the capacitance at the gate of  $M_2$  to model the loading of the output when the output is fed back to the input.

$$C_{eqS7} = C_{GS7} + C_{GD8} + C_{in} = 5 \text{ pF} + 1 \text{ pF} + 3.5 \text{ pF} = 9.5 \text{ pF}$$

$$R_{eqS7} \cong 1/g_{m7} = 204 \Omega$$

$$f_{pS7} \cong \left( \frac{1}{2\pi} \right) \frac{1}{(204)(9.5 \text{ pF})} = 82.1 \text{ MHz}$$

We can now choose the unity-gain frequency,  $f_T$ , of the op amp to give the desired phase margin. At the unity-gain frequency, the primary pole of the op amp will contribute approximately  $90^\circ$  of phase shift. For a  $70^\circ$  phase margin, the remaining two poles can contribute an additional phase shift of  $20^\circ$ , which allows us to find the required value of  $f_T$ :

$$20^\circ = \tan^{-1} \left( \frac{f_T}{49.2 \text{ MHz}} \right) + \tan^{-1} \left( \frac{f_T}{82.1 \text{ MHz}} \right) + \tan^{-1} \left( \frac{f_T}{100 \text{ MHz}} \right) \rightarrow f_T \cong 8.5 \text{ MHz}$$

Using our single-pole op-amp compensation result from the previous section, we calculate the compensation capacitor as

$$(C_C + C_{GD5}) = \frac{g_{m1}}{2\pi f_T} \rightarrow C_C = \frac{3.46 \text{ mS}}{2\pi(8.5 \text{ MHz})} - 2 \text{ pF} = 63 \text{ pF}$$

To eliminate the unwanted right-half plane zero associated with  $C_C$ ,  $R_Z = 1/g_{m5} = 230 \Omega$ . The open-loop bandwidth is now calculated as a function of the midband gain and the unity-gain frequency.

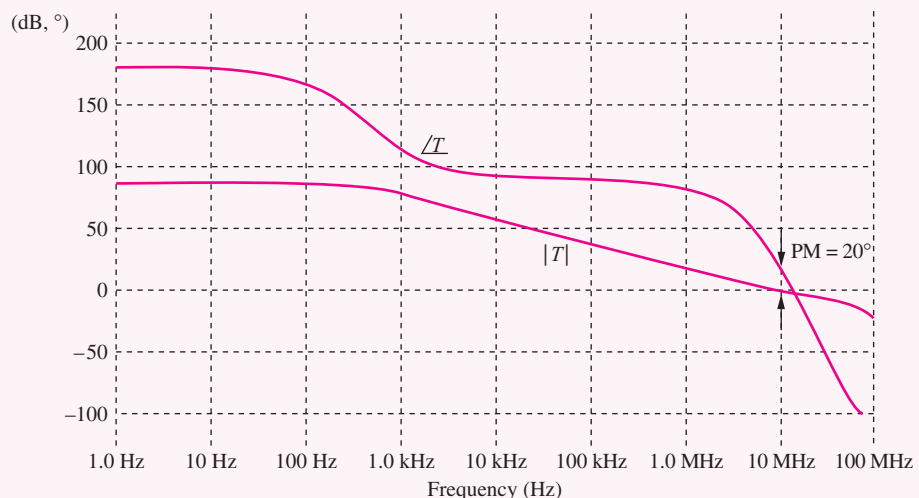
$$f_B = \frac{f_T}{A_O} = \frac{8.5 \text{ MHz}}{24,800} = 343 \text{ Hz}$$

Our final design values are  $A_o = 87.9$  dB,  $f_T = 8.5$  MHz,  $f_B = 343$  Hz, and  $\Phi_M = 70^\circ$ .

**Check of Results:** In this case, results will be verified by SPICE simulation.

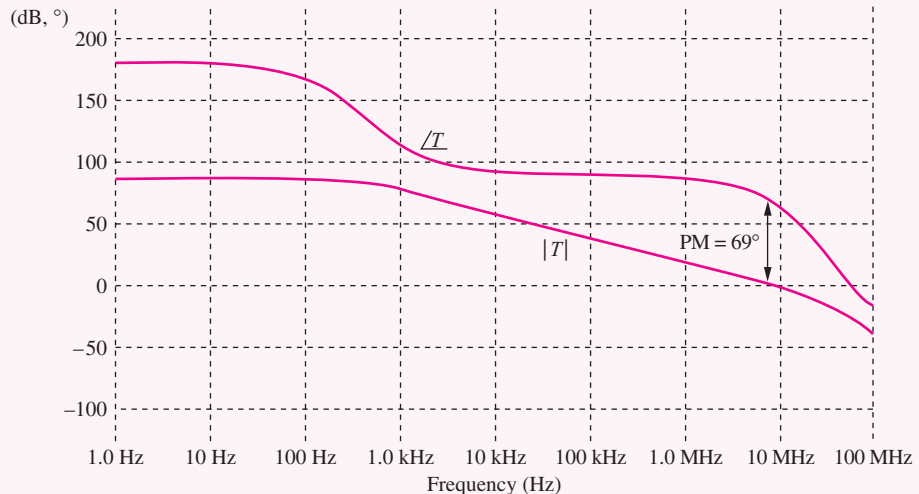
**Simulation:** With such a high gain amplifier, we should expect to have a significant offset at the output when the amplifier is operated in open loop. Any bias error at the input gets multiplied by the gain of the amplifier. As with the previous BJT example, we connect the amplifier in a follower configuration and then apply the opposite offset to the input to cancel the offset and allow us to perform open loop ac simulations while maintaining a 0 V bias at the output.

With the appropriate offset in place, the amplifier is simulated with an ac sweep from 1 Hz to 100 MHz. The first simulation is performed without  $R_Z$  to illustrate the stability problems created by the presence of the RHP zero in FET amplifiers.



Loop gain without  $R_Z$ .

In the first simulation, the unity-gain frequency is 11 MHz but our phase margin is only  $20^\circ$ ! The RHP zero is the worst of all conditions for stability. It simultaneously causes the magnitude response slope to decrease (increasing the 0 dB crossing frequency) while adding negative phase shift. If we resimulate with  $R_Z$  in place, we find the following loop gain response:



Loop gain with  $R_Z$  added to cancel RHP zero.

With the RHP zero cancelled by  $R_Z$ , our simulated result is quite close to the design values. The unity-gain frequency,  $f_T$ , is 8.4 MHz, and our phase margin is  $69^\circ$ . If we desire to increase the phase margin,  $R_Z$  can be increased to move the zero into the left-half plane and introduce some positive phase shift. The open-loop gain,  $A_o$  is 86.5 dB and the open-loop bandwidth,  $f_B$ , is approximately 410 Hz. These values are within the range of expected agreement with our design calculations.

**EXERCISE:** What is the slew rate of the amplifier in Ex. 18.8?

**ANSWER:** 15.4 V/ $\mu$ sec

**EXERCISE:** (a) What value of compensation capacitor is required to achieve a  $60^\circ$  phase margin in the amplifier in Ex. 18.8? (b) Verify your results with SPICE simulation.

**ANSWER:** 31.3 pF

## 18.6 HIGH-FREQUENCY OSCILLATORS

Individual transistors are used in oscillators designed for high-frequency operation, and the frequency-selective feedback network is formed from a high- $Q$   $LC$  network or a quartz crystal resonant element. Two classic forms of  **$LC$  oscillator** are introduced here: The Colpitts oscillator uses capacitive voltage division to adjust the amount of feedback, and the Hartley oscillator employs an inductive voltage divider. Integrated circuit oscillators frequency utilize the negative  $G_m$  cell based upon a differential pair of transistors as presented in this section. Crystal oscillators are discussed in Sec. 18.6.6.

### 18.6.1 THE COLPITTS OSCILLATOR

Figure 18.33 shows the basic **Colpitts oscillator**. A resonant circuit is formed by inductor  $L$  and the series combination of  $C_1$  and  $C_2$ ;  $C_1$ ,  $C_2$ , or  $L$  can be made variable elements in order to adjust the frequency of oscillation. The dc equivalent circuit is shown in Fig. 18.33(b). The gate of the FET is maintained at dc ground through inductor  $L$ , and the Q-point can be determined using standard techniques. In the small-signal model in Fig. 18.33(c), the gate-source capacitance  $C_{GS}$  appears in parallel with  $C_2$ , and the gate-drain capacitance  $C_{GD}$  appears in parallel with the inductor.

This circuit is used to illustrate an alternate approach to finding the conditions for oscillation to those discussed in chapter 12. The algebra in the analysis can be simplified by defining  $G = 1/(R_S \parallel r_o)$  and  $C_3 = C_2 + C_{GS}$ . Writing nodal equations for  $\mathbf{V}_g(s)$  and  $\mathbf{V}_s(s)$  yields

$$\begin{bmatrix} 0 \\ 0 \end{bmatrix} = \begin{bmatrix} \left( s(C_3 + C_{GD}) + \frac{1}{sL} \right) & -sC_3 \\ -(sC_3 + g_m) & (s(C_1 + C_3) + g_m + G) \end{bmatrix} \begin{bmatrix} \mathbf{V}_g(s) \\ \mathbf{V}_s(s) \end{bmatrix} \quad (18.33)$$

The determinant of this system of equations is

$$\Delta = s^2[C_1C_3 + C_{GD}(C_1 + C_3)] + s[(C_3 + C_{GD})G + GC_3] + \frac{(g_m + G)}{sL} + \frac{(C_1 + C_3)}{L} \quad (18.34)$$

Because the oscillator circuit has no external excitation, we must require  $\Delta = 0$  for a nonzero output voltage to exist. For  $s = j\omega$ , the determinant becomes

$$\begin{aligned} \Delta &= \left( \frac{(C_1 + C_3)}{L} - \omega^2[C_1C_3 + C_{GD}(C_1 + C_3)] \right) \\ &\quad + j \left( \omega[(g_m + G)C_{GD} + GC_3] - \frac{(g_m + G)}{\omega L} \right) = 0 \end{aligned} \quad (18.35)$$

after collecting the real and imaginary parts. Setting the real part equal to zero defines the frequency of oscillation  $\omega_o$ ,

$$\omega_o = \frac{1}{\sqrt{L \left( C_{GD} + \frac{C_1C_3}{C_1 + C_3} \right)}} = \frac{1}{\sqrt{LC_{TC}}} \quad \text{where} \quad C_{TC} = C_{GD} + \frac{C_1C_3}{C_1 + C_3} \quad (18.36)$$

and setting the imaginary part equal to zero yields a constraint on the gain of the FET circuit:

$$\omega^2 L \left[ C_{GD} + \frac{G}{(g_m + G)} C_3 \right] = 1 \quad (18.37)$$

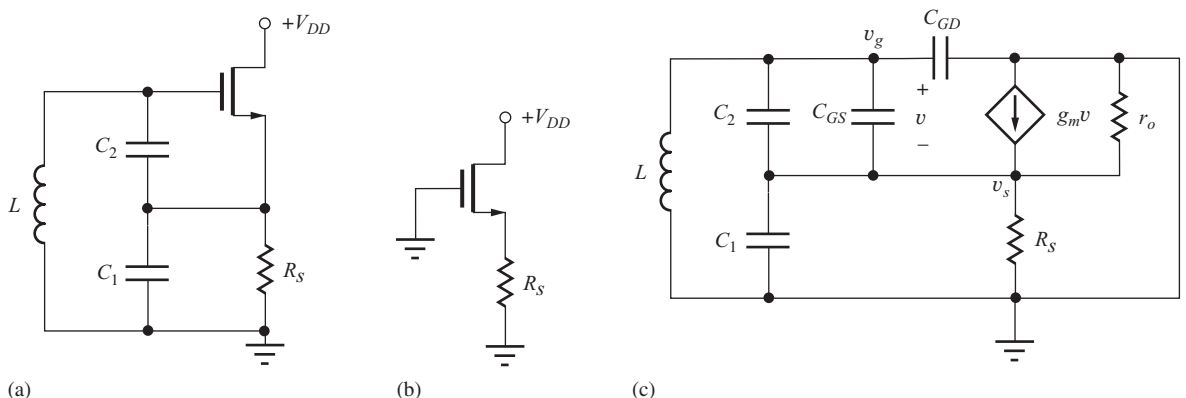


**Figure 18.33** (a) Colpitts oscillator and (b) its dc and (c) small-signal models.

At  $\omega = \omega_o$ , the gain requirement expressed by Eq. (18.37) can be simplified to yield

$$g_m R = \frac{C_3}{C_1} \quad \left( g_m R \geq \frac{C_3}{C_1} \right) \quad (18.38)$$

From Eq. (18.36), we see that the frequency of oscillation is determined by the resonant frequency of the inductor  $L$  and the total capacitance  $C_{TC}$  in parallel with the inductor. The feedback is set by the capacitance ratio and must satisfy the condition in Eq. (18.38). A gain that satisfies the equality places the oscillator poles exactly on the  $j\omega$  axis. However, normally, more gain is used to ensure oscillation, and some form of amplitude stabilization is used.

### 18.6.2 THE HARTLEY OSCILLATOR

Feedback in the **Hartley oscillator** circuit in Fig. 18.34 is set by the ratio of the two inductors  $L_1$  and  $L_2$ . The dc circuit for this case appears in Fig. 18.34(b). The conditions for oscillation can be found in a manner similar to that used for the Colpitts oscillator. For simplicity, the gate-source and gate-drain capacitances have been neglected, and no mutual coupling appears between the inductors. Writing the nodal equations for the small-signal model in Fig. 18.34(c):

$$\begin{bmatrix} 0 \\ 0 \end{bmatrix} = \begin{bmatrix} sC + \frac{1}{sL_2} & -\frac{1}{sL_2} \\ -\left(\frac{1}{sL_2} + g_m\right) & \frac{1}{sL_1} + \frac{1}{sL_2} + g_m + g_o \end{bmatrix} \begin{bmatrix} V_g(s) \\ V_s(s) \end{bmatrix} \quad (18.39)$$

The determinant of this system of equations is

$$\Delta = sC(g_m + g_o) + \frac{g_o}{sL_2} + \frac{1}{s^2 L_1 L_2} + C \left( \frac{1}{L_1} + \frac{1}{L_2} \right) \quad (18.40)$$

For oscillation, we require  $\Delta = 0$ . After collecting the real and imaginary parts for  $s = j\omega$ , the determinant becomes

$$\Delta = \left[ C \left( \frac{1}{L_1} + \frac{1}{L_2} \right) - \frac{1}{\omega^2 L_1 L_2} \right] + j \left( \omega C(g_m + g_o) - \frac{g_o}{\omega L_2} \right) = 0 \quad (18.41)$$

Setting the real part equal to zero again defines the frequency of oscillation  $\omega_o$ ,

$$\omega_o = \frac{1}{\sqrt{C(L_1 + L_2)}} \quad (18.42)$$

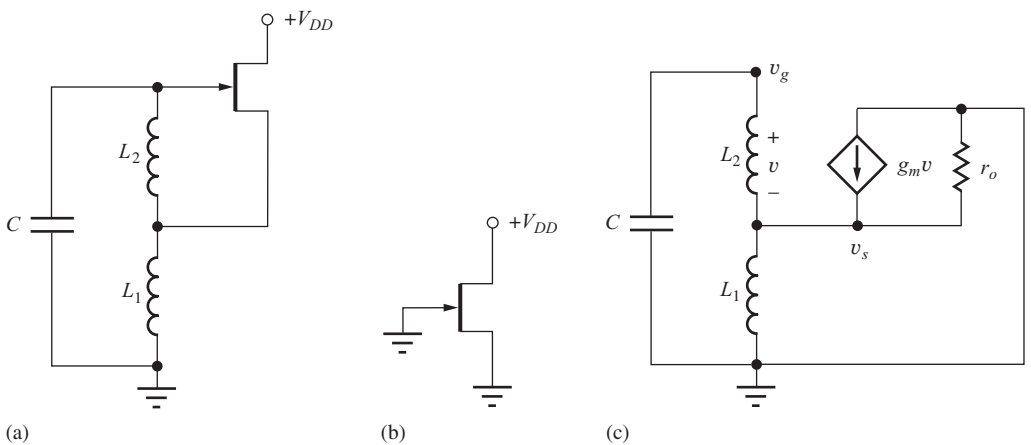


**Figure 18.34** (a) Hartley oscillator using a JFET. (b) DC equivalent circuit. (c) Small-signal model ( $C_{GS}$  and  $C_{GD}$  have been neglected for simplicity).

and setting the imaginary part equal to zero yields a constraint on the amplification factor of the FET:

$$1 + g_m r_o = \frac{1}{\omega C L_2} \quad (18.43)$$

At  $\omega = \omega_o$ , the gain requirement expressed by Eq. (18.42) becomes

$$\mu_f = \frac{L_1}{L_2} \quad \left( \mu_f \geq \frac{L_1}{L_2} \right) \quad (18.44)$$

The frequency of oscillation is set by the resonant frequency of the capacitor and the total inductance,  $L_1 + L_2$ . The feedback is set by the ratio of the two inductors and must satisfy the condition in Eq. (18.44). For poles on the  $j\omega$  axis, the amplification factor must be large enough to satisfy the equality. Generally, more gain is used to ensure oscillation, and some form of amplitude stabilization is used.

### 18.6.3 AMPLITUDE STABILIZATION IN LC OSCILLATORS

The inherently nonlinear characteristics of the transistors are often used to limit oscillation amplitude. In JFET circuits for example, the gate diode can be used to form a peak detector that limits amplitude. In bipolar circuits, rectification by the base-emitter diode often performs the same function. In the Colpitts oscillator in Fig. 18.35, a diode and resistor are added to provide the amplitude-limiting function. The diode and resistor  $R_G$  form a rectifier that establishes a negative dc bias on the gate. The capacitors in the circuit act as the rectifier filter. In practical circuits, the onset of oscillation is accompanied by a slight shift in the Q-point values as the oscillator adjusts its operating point to limit the amplitude.

### 18.6.4 NEGATIVE RESISTANCE IN OSCILLATORS

All oscillators need to have a negative input resistance in the oscillator in order for oscillation to occur. The negative resistance must be of the correct value to at least cancel the resistive losses in the circuit elements including bias resistors, the output resistance of the transistor, and the series resistance of the inductors.

As an example, let us calculate the resistance that appears at the terminals of the inductor in the Colpitts oscillator using the equivalent circuit in Fig. 18.36. We find the input resistance using the same technique that we applied to analysis of the common-source amplifier with inductive source degeneration. Based upon our knowledge of the input resistance of the common-collector and common-drain amplifiers, we have

$$Z_{in}(s) = Z_{gs} (1 + g_m Z_s) + Z_s = \frac{1}{sC_1} \left( 1 + g_m \frac{1}{sC_2} \right) + \frac{1}{sC_2} = \frac{1}{sC_1} + \frac{1}{sC_2} + \frac{g_m}{s^2 C_1 C_2}$$

$$Z_{in}(j\omega) = \frac{1}{j\omega} \left( \frac{1}{C_1} + \frac{1}{C_2} \right) + R_{eq} \quad \text{with} \quad R_{eq} = -\frac{g_m}{\omega^2 C_1 C_2} \quad (18.45)$$

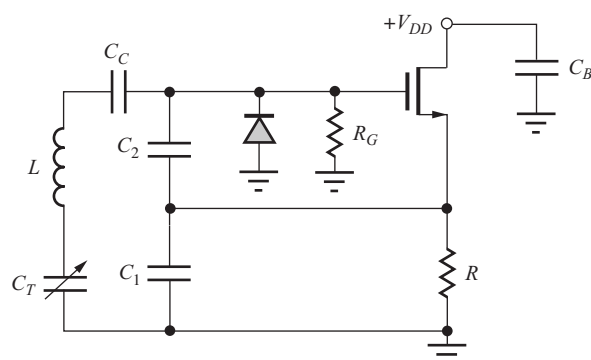


**Figure 18.35** Tunable MOSFET version of the Colpitts oscillator with a diode rectifier for amplitude limiting.

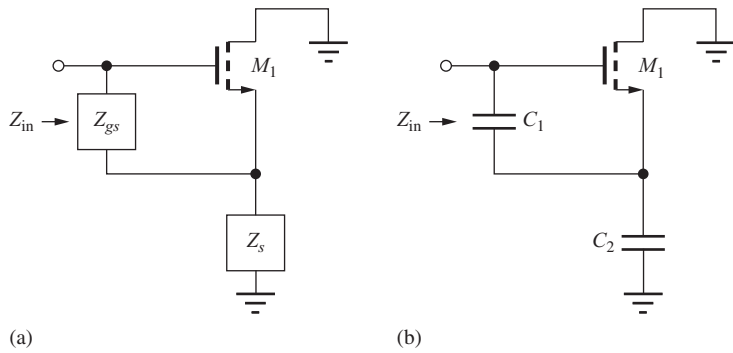


**Figure 18.36** (a) Input impedance of common-drain transistor. (b) ac equivalent circuit at the inductor terminals of the Colpitts oscillator.

The input impedance is the series combination of the impedance of  $C_1$  and  $C_2$  plus a negative real input resistance  $R_{eq}$ .

**EXERCISE:** Show that the Hartley oscillator exhibits a negative input resistance using an analysis similar to that presented above.

**ANSWER:**  $j\omega(L_1 + L_2) - \omega^2 g_m L_1 L_2$

### 18.6.5 NEGATIVE $G_M$ OSCILLATOR

An oscillator that is widely utilized in integrated circuits employs an emitter-coupled pair of transistors biased by current source  $I_{EE}$  as in Fig. 18.37(a). The transistor pair is cross-coupled in a positive feedback configuration that causes a negative resistance to appear between the drains of the transistors. As long as the negative resistance of the cross-coupled transistors is sufficient to overcome the resistive loss in the inductors and output resistances of the transistors, then the circuit will oscillate.

Assuming symmetry, the bias current of each transistor will be  $I_{EE}/2$ . The desired mode of oscillation will be a differential signal appearing between the drains of the two transistors ( $v_{d2} = -v_{d1}$ ), and the frequency of oscillation can be found from the ac equivalent circuit in Fig. 18.37(b).

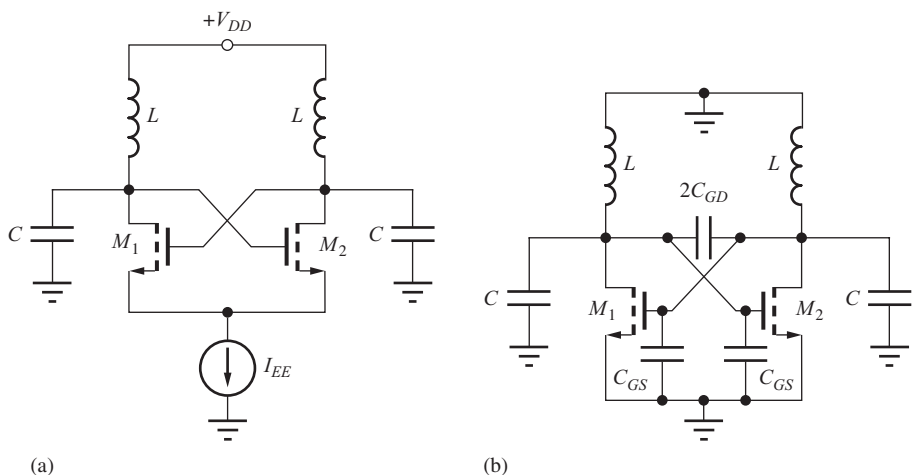


**Figure 18.37** (a) Oscillator employing a negative resistance cell. (b) ac equivalent circuit.

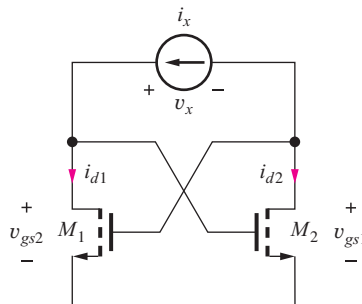


**Figure 18.38** Circuit for finding the resistance of the cross-coupled transistor pair.

The resonant frequency for the circuit is determined by the equivalent capacitance that appears at the terminals of the two inductors:

$$\omega_o = \frac{1}{\sqrt{2L \left( 2C_{GD} + \frac{C + C_{GS}}{2} \right)}} = \frac{1}{\sqrt{LC_{eq}}} \quad \text{with} \quad C_{eq} = C + C_{GS} + 4C_{GD} \quad (18.46)$$

External capacitance  $C$  is usually designed to dominate the device capacitances and is often replaced with a varactor diode for electronic adjustment the oscillator frequency. Note that the current source in Fig. 18.37 presents a high impedance for common-mode signals and prevents common-mode oscillations ( $v_{d2} = v_{d1}$ ) from occurring.

The equivalent input resistance  $R_{in}$  of the negative  $G_m$  cell can be found with the aid of the circuit in Fig. 18.38 in which small-signal test current  $i_x$  is applied, and  $R_{in} = v_x/i_x$ . By applying KVL to the circuit,  $v_x$  is found to equal the difference in the gate-source voltages of transistors  $M_2$  and  $M_1$ , and Kirchoff's current law indicates current  $i_x$  must enter the drain of  $M_1$  and exit the drain of  $M_2$ :

$$v_x = v_{gs2} - v_{gs1} \quad \text{with} \quad i_{d1} = i_x \quad \text{and} \quad i_{d2} = -i_x \quad (18.47)$$

The FET drain current and gate-source voltage are related by  $i_d = g_m v_{gs}$  yielding

$$v_{gs1} = \frac{i_{d1}}{g_m} = +\frac{i_x}{g_m} \quad \text{and} \quad v_{gs2} = \frac{i_{d2}}{g_m} = -\frac{i_x}{g_m} \quad (18.48)$$

We find that the positive feedback loop results in a negative input resistance:

$$v_x = -\frac{i_x}{g_m} - \frac{i_x}{g_m} \quad \text{and} \quad R_{in} = -\frac{2}{g_m} \quad (18.49)$$

Oscillation requires the overall conductance between the drains<sup>4</sup> of the transistors in Fig. 18.39 to be negative:

$$-\frac{g_m}{2} + \frac{g_o + G_P}{2} \leq 0 \quad \text{or} \quad g_m R_P \geq 1 \quad \text{for} \quad r_o \gg R_P \quad (18.50)$$

where  $R_P$  is the equivalent resistance in parallel with the inductor  $R_P = (1 + Q_S^2)R_S \cong Q_S^2 R_S$ . The requirement for oscillation can be written as

$$g_m > \frac{1}{Q_S^2 R_S} \quad \text{for} \quad Q_S = \frac{\omega L}{R_S} \quad (18.51)$$

Equation (18.50) places a lower bound on the transistor transconductance in terms of the inductor characteristics.

**EXERCISE:** Draw a symmetric version of the oscillator in Fig. 18.37(b). Assume that points on the line of symmetry are virtual grounds and demonstrate that the frequency of oscillation is determined by  $L$  and  $C_{eq}$  as defined in Eq. (18.45).

<sup>4</sup> Or any other circuit port.

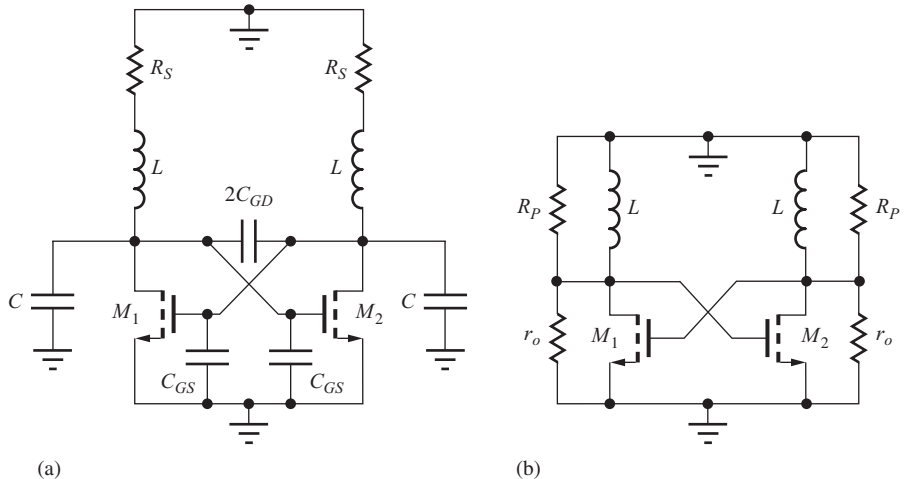


**Figure 18.39** (a) Oscillator with finite Q inductors. (b) Transformed equivalent circuit including output resistance of the transistors with capacitances removed.

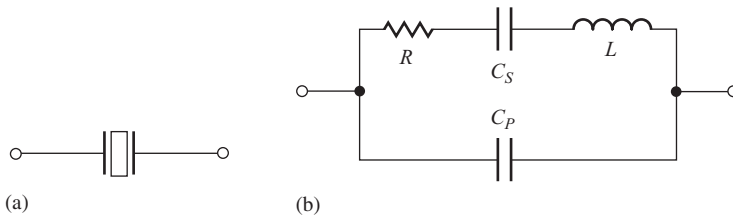


**Figure 18.40** Symbol and electrical equivalent circuit for a quartz crystal.

### 18.6.6 CRYSTAL OSCILLATORS

Oscillators with very high frequency accuracy and stability can be formed using quartz crystals as the frequency-determining element (crystal oscillators). The crystal is a piezoelectric device that vibrates in response to electrical stimulus. Although the frequency of vibration of the crystal is determined by its mechanical properties, the crystal can be modeled electrically by a very high  $Q$  ( $>10,000$ ) resonant circuit, as in Fig. 18.40.

$L$ ,  $C_S$ , and  $R$  characterize the intrinsic series resonance path through the crystal element itself, whereas parallel capacitance  $C_P$  is dominated by the capacitance of the package containing the quartz element. The equivalent impedance of this network exhibits a series resonant frequency  $\omega_S$  at which  $C_S$  resonates with  $L$ , and a parallel resonant frequency  $\omega_P$  that is determined by  $L$  resonating with the series combination of  $C_S$  and  $C_P$ .

The impedance of the crystal versus frequency can easily be calculated using the circuit model in Fig. 18.40:

$$Z_C = \frac{Z_P Z_S}{Z_P + Z_S} = \frac{\frac{1}{sC_P} \left( sL + R + \frac{1}{sC_S} \right)}{\frac{1}{sC_P} + \left( sL + R + \frac{1}{sC_S} \right)} = \frac{1}{sC_P} \left( \frac{s^2 + s \frac{R}{L} + \frac{1}{LC_S}}{s^2 + s \frac{R}{L} + \frac{1}{LC_T}} \right) \quad (18.52)$$

$$\text{where } C_T = \frac{C_S C_P}{C_S + C_P}$$

The figure accompanying Ex. 18.9 is an example of the variation of crystal impedance with frequency. Below  $\omega_S$  and above  $\omega_P$ , the crystal appears capacitive; between  $\omega_S$  and  $\omega_P$ , it exhibits an inductive reactance. As can be observed in the figure, the region between  $\omega_S$  and  $\omega_P$  is quite narrow. If the crystal is used to replace the inductor in the Colpitts oscillator, a well-defined frequency of oscillation will exist. In most crystal oscillators, the crystal operates between the two resonant points and represents an inductive reactance, replacing the inductor in the circuit.

### EXAMPLE 18.9 QUARTZ CRYSTAL EQUIVALENT CIRCUIT

The values of  $L$  and  $C_S$  that represent the crystal have unusual magnitudes because of the extremely high  $Q$  of the crystal.

**PROBLEM** Calculate the equivalent circuit element values for a crystal with  $f_S = 5 \text{ MHz}$ ,  $Q = 20,000$ ,  $R = 50 \Omega$ , and  $C_P = 5 \text{ pF}$ . What is the parallel resonant frequency?

**SOLUTION** **Known Information and Given Data:** The crystal parameters are specified as  $f_S = 5 \text{ MHz}$ ,  $Q = 20,000$ ,  $R = 50 \Omega$ , and  $C_P = 5 \text{ pF}$ .

**Unknowns:**  $L$  and  $C_S$

**Approach:** Use the definitions of  $Q$  and series resonant frequency to find the unknowns.

**Assumptions:** The equivalent circuit in Fig. 18.40 is adequate to model the crystal.

**Analysis:** Using  $Q$ ,  $R$ , and  $f_S$  for a series resonant circuit,

$$L = \frac{RQ}{\omega_S} = \frac{50(20,000)}{2\pi(5 \times 10^6)} = 31.8 \text{ mH} \quad C_S = \frac{1}{\omega_S^2 L} = \frac{1}{(10^7\pi)^2(0.0318)} = 31.8 \text{ fF}$$

Typical values of  $C_P$  fall in the range of 5 to 20 pF. For  $C_P = 5 \text{ pF}$ , the parallel resonant frequency will be

$$f_P = \frac{1}{2\pi\sqrt{L\frac{C_S C_P}{C_S + C_P}}} = \frac{1}{2\pi\sqrt{(31.8 \text{ mH})(31.6 \text{ fF})}} = 5.02 \text{ MHz}$$

whereas

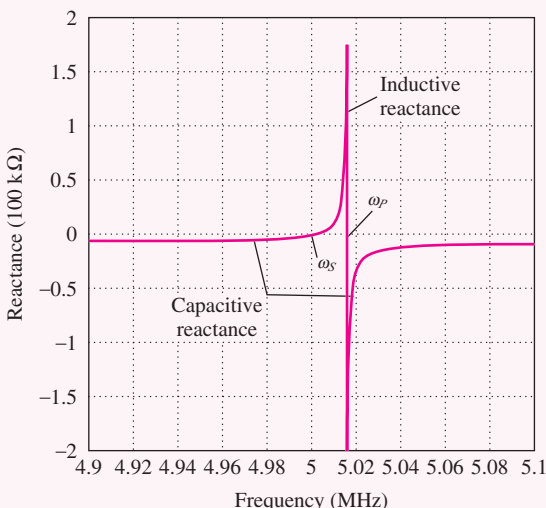
$$f_S = 5.00 \text{ MHz}$$

**Check of Results:** Let us use our values of  $L$  and  $C_S$  to calculate  $f_S$ .

$$f_S = \frac{1}{2\pi\sqrt{31.8 \text{ mH}(31.8 \text{ fF})}} = 5.00 \text{ MHz} \quad \checkmark$$

**Discussion:** Note that the two resonant frequencies differ by only 0.4 percent, and the high  $Q$  of the crystal results in a relatively large effective value for  $L$  and a small value for  $C_S$ .

**Computer-Aided Analysis:** The graph below presents results from a computer calculation of the reactance of the crystal versus frequency using the parameters calculated in Ex. 18.9.



Reactance versus frequency for crystal parameters calculated in the example.

Below the series resonant frequency and above the parallel resonant frequency, the crystal exhibits capacitive reactance. Between  $f_S$  and  $f_P$ , the crystal appears inductive. In many oscillator circuits, the crystal behaves as an inductor and resonates with external capacitance. The oscillator frequency will therefore be between  $f_S$  and  $f_P$ .

**EXERCISE:** Calculate the parallel resonant frequency of the crystal if a 2-pF capacitor is placed in parallel with the crystal. Repeat for a 20-pF capacitor.

**ANSWERS:** 5.016 MHz; 5.008 MHz

Several examples of crystal oscillators are given in Figs. 18.41 to 18.44. Many variations are possible, but most of these oscillators are topological transformations of the Colpitts or Hartley oscillators. For example, the circuit in Fig. 18.41(a) represents a Colpitts oscillator with the source terminal chosen as the ground reference. The same circuit is drawn in a different form in Fig. 18.41(b). Figures 18.42 and 18.43 show Colpitts oscillators using bipolar and JFET devices.

The final crystal oscillator, shown in Fig. 18.44, represents a circuit that is often implemented using a CMOS logic inverter. The circuit forms yet another Colpitts oscillator, similar to Fig. 18.41(b). The inverter is initially biased into the middle of its operating region by feedback resistor  $R_F$  to ensure that the Q-point of the gate is in a region of high gain.

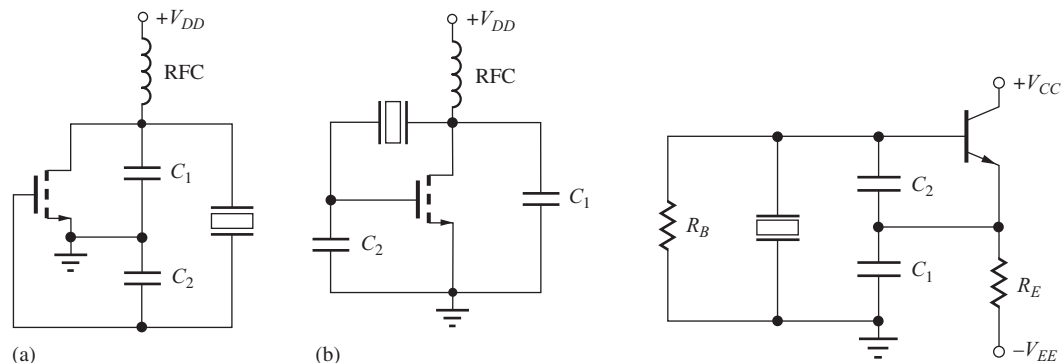


**Figure 18.41** Two forms of the same Colpitts crystal oscillator.

**Figure 18.42** Crystal oscillator using a bipolar transistor.

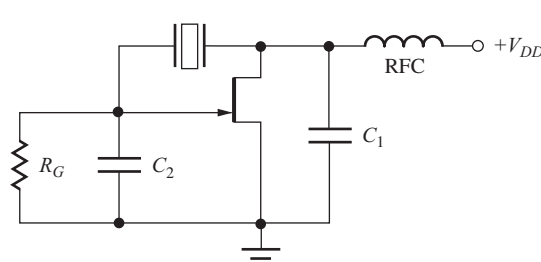


**Figure 18.43** Crystal oscillator using a JFET.

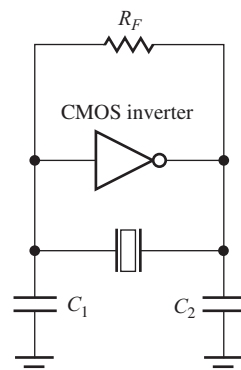


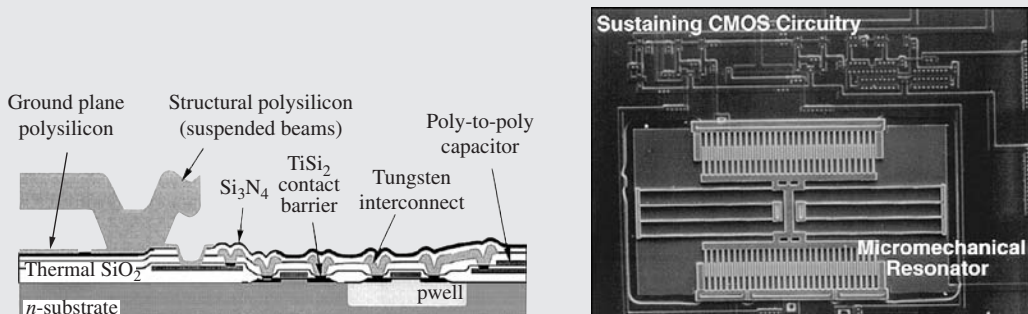
**Figure 18.44** Crystal oscillator using a CMOS inverter as the gain element.



### A MEMS Oscillator

Crystal oscillators have long been a mainstay for creating accurate, stable oscillators for clocks in watches and computer systems. Unlike oscillators based on integrated inductors and capacitors, crystal oscillators have very low equivalent series resistance, leading to low loss and high Q. However, conventional crystal oscillators are relatively bulky and are not easily integrated with CMOS processes. For this reason, researchers have developed microelectromechanical systems (MEMS) based resonant structures that can be integrated directly onto CMOS integrated circuits.

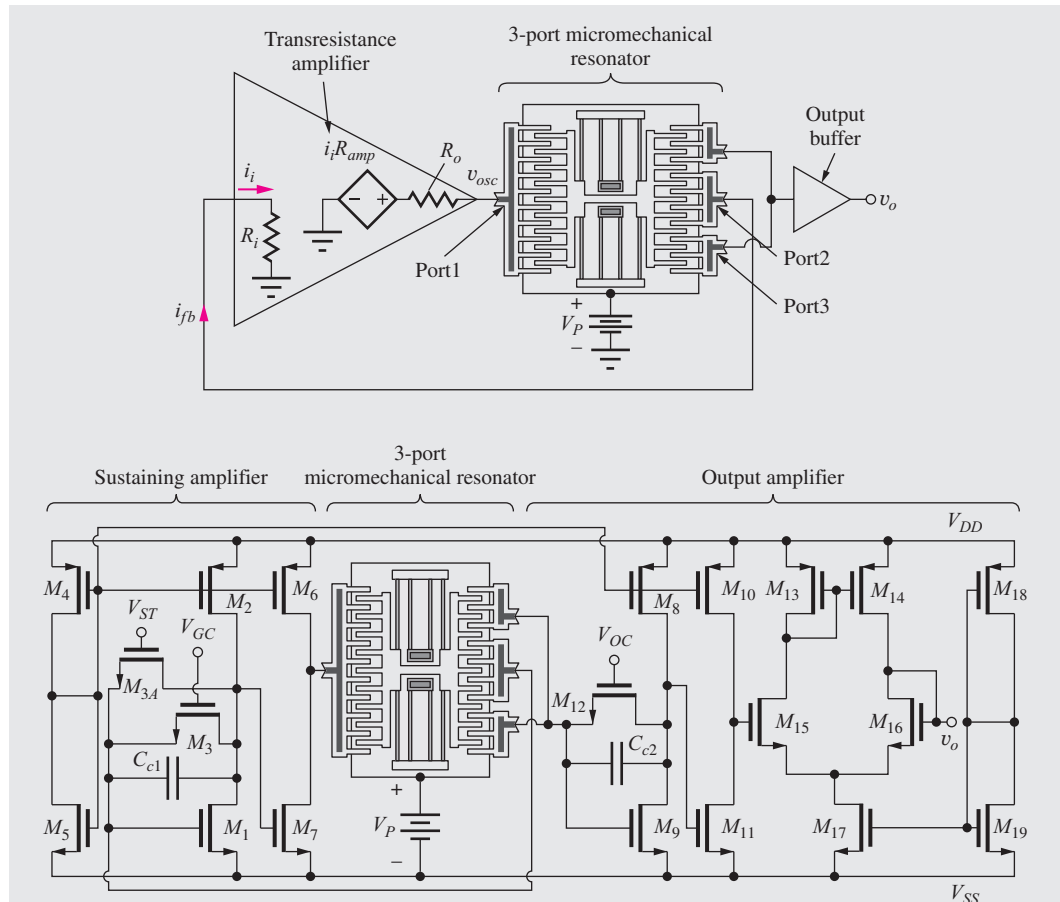
Illustrated below is a MEMS micromechanical resonator published in 1999 by Clark Nguyen and Roger Howe.<sup>1</sup> A photomicrograph of the device is shown below. The structure is an electrostatic comb-drive constructed from polysilicon material. A cross section of the MEMS post processing is also shown. The large polysilicon structure to the left is an example of the structures used to make the resonator structure. The structure makes electrical contact to a metal layer through a thin deposited polysilicon layer. Note that the horizontal beam in the left of the figure is actually suspended above the substrate. The structural polysilicon is deposited over a sacrificial phosphosilicate glass (PSG) that had been previously deposited and patterned. After the structural polysilicon is deposited and patterned, the PSG is chemically etched away, leaving the polysilicon beams suspended above the substrate.



Copyright IEEE 1999. Reprinted with permission from [1].

The physical structure of the comb drive is more clearly seen in the block diagram on the next page. By driving the leftmost finger structure with a voltage, the suspended structure in the middle is pulled to the left. When the voltage is removed, the structure is pulled back to the right by the suspension. When the frequency of the drive voltage approaches the resonant frequency of the structure, sustainable oscillation begins. Similar to a quartz oscillator, the micromechanical resonator has a series RLC and parallel capacitance model. As the center structure oscillates back and forth, a displacement current is generated on the output port comb structure due to the changing capacitance as the comb fingers move in and out. In this design, the displacement current is sensed by a transresistance amplifier which amplifies the signal and drives the input. At the resonant frequency, the Barkhausen criteria is satisfied and the oscillation is sustained.

<sup>1</sup> C. T-C. Nguyen and R. T. Howe, "An integrated CMOS micromechanical resonator high-Q oscillator," *IEEE J. Solid-State Circuits*, vol. 34, no. 4, pp. 440–445, April 1999.



Copyright IEEE 1999. Reprinted with permission from [1].

MEMS based devices are enabling fully integrated mixers, filters, and other resonator based structures. Because the structures are typically made from polysilicon material, they are compatible with conventional CMOS IC processing. The structure shown above has a resonant frequency in the tens of kilohertz, but researchers are exploring other resonator forms with demonstrated resonant frequencies in the hundreds of megahertz. The combination of MEMS and CMOS may soon enable highly efficient single-chip radio frequency transceivers that do not rely on the relatively lossy integrated capacitors and inductors used today.

## SUMMARY

- General feedback amplifiers are separated into four classes depending on the type of feedback utilized at the input and output of the amplifier. Voltage amplifiers employ series-shunt feedback, transresistance amplifiers use shunt-shunt feedback, transconductance amplifiers utilize series-series feedback, and current amplifiers use shunt-series feedback.
- Series feedback places ports in series and increases the overall impedance level at the series-connected port. Shunt feedback is achieved by placing ports in parallel and reduces the overall impedance level at the shunt-connected port.

- The closed-loop gain of a feedback amplifier can be written as

$$A_{cl} = A_{cl}^{\text{Ideal}} \frac{T(s)}{1 + T(s)}$$

where  $A_{cl}^{\text{Ideal}}$  is the ideal closed-loop gain and  $T(s)$  is the frequency dependent loop gain or loop transmission.

- The loop gain  $T(s)$  plays an important role in determining the characteristics of feedback amplifiers. For theoretical calculations, the loop gain can be found by breaking the feedback loop at some arbitrary point and directly calculating the voltage returned around the loop. However, both sides of the loop must be properly terminated before the loop-gain calculation is attempted.
- The resistance  $R_x$  between any pair of terminals in a feedback circuit can be found using Blackman's theorem, originally introduced in Chapter 11,

$$R_x = R_x^D \frac{1 + |T_{SC}|}{1 + |T_{OC}|}$$

where  $R_x^D$  is the resistance at the terminal pair with the feedback loop disabled,  $T_{SC}$  is the loop gain with the terminal pair shorted, and  $T_{OC}$  is the loop gain with the terminal pair open.

- When using SPICE or making experimental measurements, it is often impossible to break the feedback loop. The method of successive voltage and current injection, discussed in Chapter 11, is a powerful technique for determining the loop gain without the need for opening the feedback loop.
- Whenever feedback is applied to an amplifier, stability becomes a concern. In most cases, a negative or degenerative feedback condition is desired. Stability can be determined by studying the characteristics of the loop gain  $T(s) = A(s)\beta(s)$  of the feedback amplifier as a function of frequency, and stability criteria can be evaluated from either Nyquist diagrams or Bode plots.
- In the Nyquist case, stability requires that the plot of  $T(j\omega)$  not enclose the  $T = -1$  point.
- On the Bode plot, the asymptotes of the magnitudes of  $A(j\omega)$  and  $1/\beta(j\omega)$  must not intersect with a rate of closure exceeding 20 dB/decade.
- Phase margin and gain margin, which can be found from either the Nyquist or Bode plot, are important measures of stability.
- Miller multiplication represents a useful method for setting the unity-gain frequency of internally compensated operational amplifiers. This technique is often called Miller compensation. In these op amps, slew rate is directly related to the unity-gain frequency.
- In circuits called oscillators, feedback is actually designed to be positive or regenerative so that an output signal can be produced by the circuit without an input being present. The Barkhausen criteria for oscillation, introduced in chapter 12, state that the phase shift around the feedback loop must be an even multiple of  $360^\circ$  at some frequency, and the loop gain at that frequency must be equal to 1.
- Oscillators use some form of frequency-selective feedback to determine the frequency of oscillation; at high frequencies  $LC$  networks and quartz crystals are used to set the frequency.
- Most  $LC$  oscillators are versions of either the Colpitts or Hartley oscillators. In the Colpitts oscillator, the feedback factor is set by the ratio of two capacitors; in the Hartley case, a pair of inductors determines the feedback. Negative  $G_m$  cells are common in integrated circuit oscillators.
- Crystal oscillators use a quartz crystal to replace the inductor in  $LC$  oscillators. A crystal can be modeled electrically as a very high Q resonant circuit, and when used in an oscillator, the crystal accurately controls the frequency of oscillation.
- In order to oscillate, the circuit must develop a negative resistance to cancel losses in the circuit from bias resistors, transistor output resistances, and loss in the inductors and capacitors that form the resonant circuit.

- For true sinusoidal oscillation, the poles of the oscillator must be located precisely on the  $j\omega$  axis in the  $s$ -plane. Otherwise, distortion occurs. To achieve sinusoidal oscillation, some form of amplitude stabilization is normally required. Such stabilization may result simply from the inherent nonlinear characteristics of the transistors used in the circuit, or from explicitly added gain control circuitry.

## KEY TERMS

Amplitude stabilization	Nyquist plot
Barkhausen criteria for oscillation	Open-loop amplifier
Blackman's theorem	Open-loop gain
Bode plot	Oscillator circuits
Closed-loop gain	Oscillators
Closed-loop input resistance	Phase margin
Closed-loop output resistance	Positive feedback
Colpitts oscillator	Regenerative feedback
Crystal oscillator	Series feedback connection
Current amplifier	Series-series feedback
Degenerative feedback	Series-shunt feedback
Feedback amplifier stability	Shunt feedback connection
Feedback network	Shunt-series feedback
Gain margin (GM)	Shunt-shunt feedback
Hartley oscillator	Sinusoidal oscillator
LC oscillators	Stability
Loop gain	Successive voltage and current injection technique
–1 Point	Transconductance amplifier
Negative feedback	Transresistance amplifier
Negative $G_m$ oscillator	Voltage amplifier
Negative resistance	

## REFERENCES

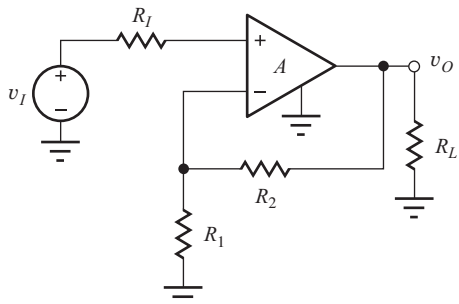
- R. D. Middlebrook, "Measurement of loop gain in feedback systems," *International Journal of Electronics*, vol. 38, no. 4, pp. 485–512, April 1975. Middlebrook credits a 1965 Hewlett-Packard Application Note as the original source of this technique.
- R. C. Jaeger, S. W. Director, and A. J. Brodersen, "Computer-aided characterization of differential amplifiers," *IEEE JSSC*, vol. SC-12, pp. 83–86, February 1977.
- R. B. Blackman, "Effect of feedback on impedance," *Bell System Technical Journal*, vol. 22, no. 3, 1943.
- P. J. Hurst, "A comparison of two approaches to feedback circuit analysis," *IEEE Trans. on Education*, vol. 35, pp. 253–261, August 1992.
- F. Corsi, C. Marzocca, and G. Matarrese, "On impedance evaluation in feedback circuits," *IEEE Trans. on Education*, vol. 45, no. 4, pp. 371–379, November 2002.

## PROBLEMS

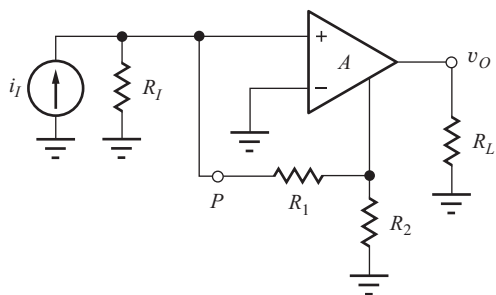
### 18.1 Feedback System Review

- 18.1. The classic feedback amplifier in Fig. 18.1 has  $\beta = 0.2$ . What are the loop gain  $T$ , the closed-loop gain  $A_v$ , and the fractional gain error  $FGE$  (see Sec. 11.1.2) if  $A = 120 \text{ dB}$ ? (b) If  $A = 60 \text{ dB}$ ? (c) If  $A = 15 \text{ dB}$ ?

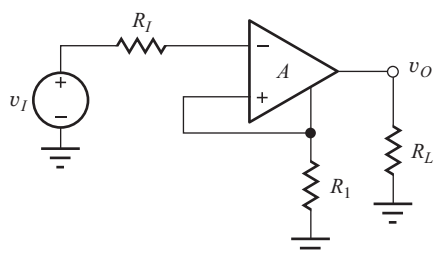
- 18.2. The feedback amplifier in Fig. P18.2(a) has  $R_1 = 1 \text{ k}\Omega$ ,  $R_2 = 47 \text{ k}\Omega$ ,  $R_I = 0$ , and  $R_L = 4.7 \text{ k}\Omega$ . (a) What is  $\beta$ ? (b) If  $A = 80 \text{ dB}$ , what are the loop gain  $T$  and the closed-loop gain  $A_v$ ?



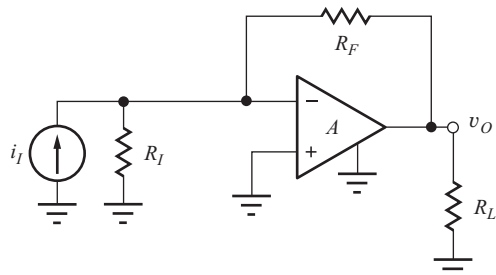
(a)



(b)



(c)

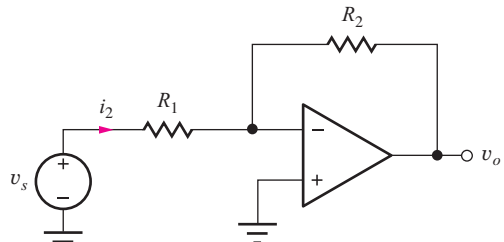


(d)

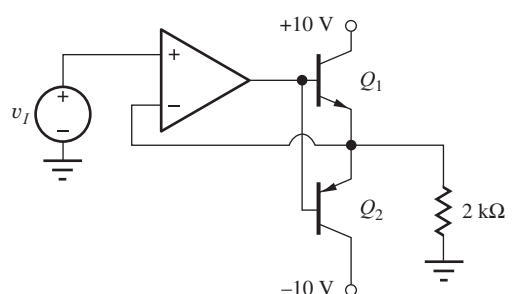
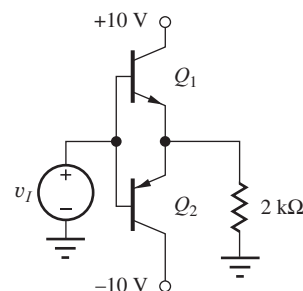
**Figure P18.2** For each amplifier

$$A : A_o = 5000, R_{id} = 25 \text{ k}\Omega, R_o = 500 \Omega.$$

- 18.3. The inverting amplifier in Fig. P18.3 is implemented with an op amp with finite gain  $A = 90 \text{ dB}$ . If  $R_1 = 2 \text{ k}\Omega$  and  $R_2 = 78 \text{ k}\Omega$ , what are  $\beta$ ,  $T$ , and  $A_v$ ?

**Figure P18.3**

- 18.4. An amplifier's closed-loop voltage gain  $A_v$  is described by Eq. (18.4). What is the minimum value of open-loop gain needed if the gain error is to be less than 0.05 percent for a voltage follower ( $A_v \approx 1$  with  $\beta = 1$ )?
- 18.5. An amplifier's closed-loop voltage gain is described by Eq. (18.4). What is the minimum value of open-loop gain needed if the gain error is to be less than 0.1 percent for an ideal gain of 150?
- 18.6. Use SPICE to simulate and compare the transfer characteristics of the two class-B output stages in Fig. P18.6 if the op amp is described by  $A_o = 2500$ ,  $R_{id} = 150 \text{ k}\Omega$ , and  $R_o = 150 \Omega$ . Assume  $V_I = 0$ .

**Figure P18.6**

- 18.7. (a) Calculate the sensitivity of the closed-loop gain  $A_v$  with respect to changes in open-loop gain

$A, S_A^{A_v}$ , using Eq. (18.4) and the definition of sensitivity originally presented in Chapter 12:

$$S_A^{A_v} = \frac{A}{A_v} \frac{\partial A_v}{\partial A}$$

(b) Use this formula to estimate the percentage change in closed-loop gain if the open-loop gain  $A$  changes by 10 percent for an amplifier with  $A = 80$  dB and  $\beta = 0.02$ .

## 18.2 and 18.3 Examples of Feedback Amplifier Analysis

- 18.8. Identify the type of negative feedback that should be used to achieve these design goals: (a) low input resistance and high output resistance, (b) high input resistance and low output resistance, (c) low input resistance and low output resistance, (d) high input resistance and high output resistance.
- 18.9. Identify the type of feedback being used in the four circuits in Fig. P18.2.
- 18.10. Consider the circuits in Fig. P18.2, (a) Which circuits use negative feedback to decrease the input resistance? (b) Which tend to increase the input resistance?
- 18.11. Of the four circuits in Fig. P18.2, (a) Which circuits use negative feedback to increase the output resistance? (b) Which tend to decrease the output resistance?
- 18.12. Given the circuit in Fig. P18.12, use Blackman's theorem to find  $R_x$ . Assume the amplifier inputs and outputs are ideal. For  $A = 400$ ,  $R_1 = 750 \Omega$ ,  $R_2 = 2 \text{ k}\Omega$ , and  $R_3 = 2 \text{ k}\Omega$ , find  $R_x^D$ ,  $T_{SC}$ ,  $T_{OC}$ , and  $R_x$ .

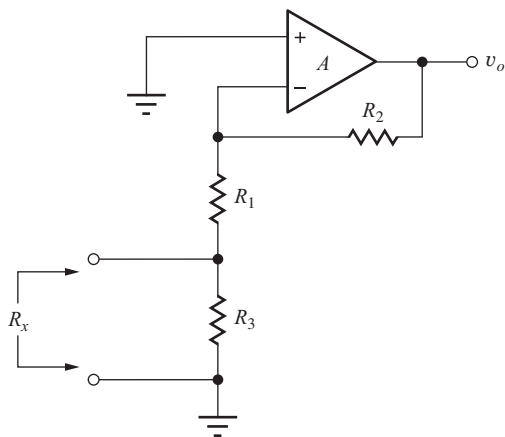
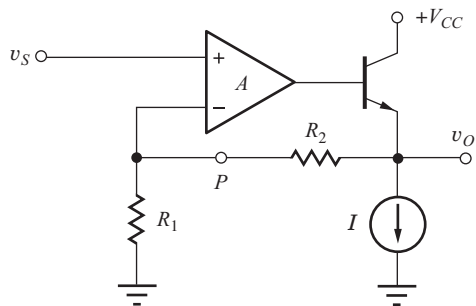


Figure P18.12

- 18.13. Repeat Problem 18.12 with  $A = 200$ ,  $R_1 = 1 \text{ k}\Omega$ ,  $R_2 = 5 \text{ k}\Omega$ , and  $R_3 = 1 \text{ k}\Omega$ .
- 18.14. For the circuit in Fig. 18.2, use Blackman's theorem to find the small-signal resistance,  $R_x$ , looking into the node at the collectors of  $Q_1$  and  $Q_3$ . Find  $R_x^D$ ,  $T_{SC}$ ,  $T_{OC}$ , and  $R_x$ .
- 18.15. For the circuit in Fig. 18.2, use Blackman's theorem to find the small-signal resistance,  $R_x$ , looking into the node at the emitters of  $Q_1$  and  $Q_2$ . Find  $R_x^D$ ,  $T_{SC}$ ,  $T_{OC}$ , and  $R_x$ .
- 18.16. An amplifier has an open-loop gain of 86 dB,  $R_{id} = 50 \text{ k}\Omega$ , and  $R_o = 1200 \Omega$ . The amplifier is used in a feedback amplifier configuration with a resistive feedback network. (a) What is the largest value of input resistance that can be achieved in the feedback amplifier? (b) What is the smallest value of input resistance that can be achieved? (c) What is the largest value of output resistance that can be achieved in the feedback amplifier? (d) What is the smallest value of output resistance that can be achieved?
- 18.17. An amplifier has an open-loop gain of 86 dB,  $R_{id} = 50 \text{ k}\Omega$ , and  $R_o = 1200 \Omega$ . The amplifier is used in a feedback amplifier configuration with a resistive feedback network. (a) What is the largest value of current gain that can be achieved with this feedback amplifier? (b) What is the largest value transconductance that can be achieved with this feedback amplifier?
- 18.18. Find the closed-loop voltage gain, input resistance, and output resistance for the circuit in Fig. P18.2(a). Assume  $R_I = 1 \text{ k}\Omega$ ,  $R_1 = 5.6 \text{ k}\Omega$ ,  $R_2 = 47 \text{ k}\Omega$ , and  $R_L = 5 \text{ k}\Omega$ .
- 18.19. Find the closed-loop voltage gain, input resistance, and output resistance for the circuit in Fig. P18.2(a). Assume  $R_I = 1 \text{ k}\Omega$ ,  $R_1 = 4.3 \text{ k}\Omega$ ,  $R_2 = 51 \text{ k}\Omega$ , and  $R_L = 5.6 \text{ k}\Omega$ .
- 18.20. Find the closed-loop gain, input resistance, and output resistance for the circuit in Fig. P18.20. Assume  $R_1 = 2 \text{ k}\Omega$ ,  $R_2 = 10 \text{ k}\Omega$ ,  $\beta_0 = 150$ ,  $V_A = 75 \text{ V}$ ,  $I = 100 \mu\text{A}$ ,  $V_{CC} = 7.5 \text{ V}$ ,  $A = 40 \text{ dB}$ ,  $R_{id} = 50 \text{ k}\Omega$ , and  $R_o = 500 \Omega$ .
- 18.21. For the circuit in Fig. 18.4, use Blackman's theorem to find the small-signal resistance,  $R_x$ , looking into the node at the emitter of  $Q_2$ . Find  $R_x^D$ ,  $T_{SC}$ ,  $T_{OC}$ , and  $R_x$ .
- 18.22. Rework Ex. 18.1 with a bypass capacitor across  $R$ .



### Figure P18.20

- 18.23. Fig. P18.23 is the circuit of Fig. 18.4 with an emitter-follower stage added to the feedback network. Use feedback analysis to find the small-signal midband gain,  $v_o/v_i$ , the input resistance  $R_{in}$  looking into the base of  $Q_1$ , and the output resistance (without  $R_L$ ),  $R_{out}$ . Assume  $R_i = 100 \Omega$ ,  $R_1 = 200 \Omega$ ,  $R_2 = 2 \text{ k}\Omega$ ,  $R_3 = 2 \text{ k}\Omega$ ,  $R_4 = 300 \Omega$ ,  $R_5 = 8 \text{ k}\Omega$ ,  $R_6 = 14.4 \text{ k}\Omega$ ,  $R_7 = 10 \text{ k}\Omega$ ,  $R_L = 10 \text{ k}\Omega$ ,  $C_1 = 10 \mu\text{F}$ . Do not treat  $Q_1$  and  $Q_3$  as a differential pair, you may assume that  $V_O = V_I$ , neglect dc base currents, and use  $r_o = \infty$ .

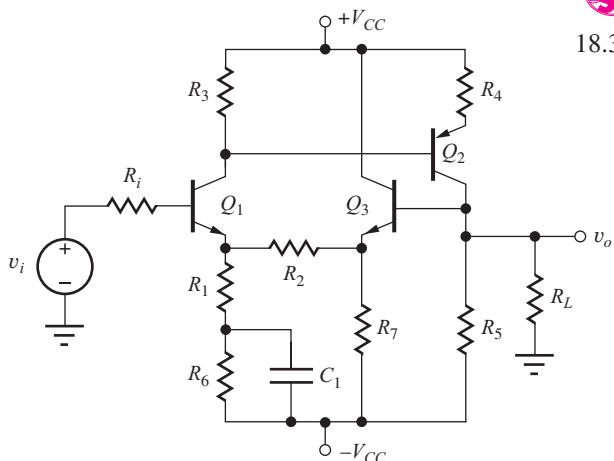


**Figure P18.23**

- 18.24. Simulate the circuit in Prob. 18.23 with SPICE and compare the results to those obtained in Prob. 18.23.

18.25. For the circuit in Prob. 18.23, use Blackman's theorem to find the small-signal resistance looking into the node at the emitter of  $Q_1$ .

18.26. Repeat Ex. 18.2 with  $R_2 = 20 \text{ k}\Omega$ ,  $I_1 = 200 \mu\text{A}$  and  $R_3 = 15 \text{ k}\Omega$ .

18.27. Use Blackman's theorem to find the small-signal impedance looking into the node at the drain of  $M_3$  for the circuit in Prob. 18.26.

- 18.28. Use feedback analysis to find the voltage gain  $v_o/v_{\text{ref}}$ , input resistance, and output resistance for the circuit in Fig. P18.28. Use the results of these calculations to find the transconductance  $A_{tc} = i_o/v_{\text{ref}}$ . Assume  $\beta_0 = 150$ ,  $V_A = 75$  V,  $I = 100 \mu\text{A}$ ,  $V_{\text{REF}} = 0$  V, and  $R = 5 \text{ k}\Omega$ .

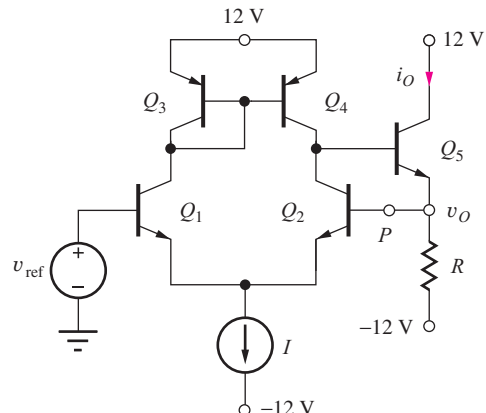


### Figure P18.28

- 18.29. Simulate the circuit in Prob. 18.28 with SPICE and compare the results to those obtained in Prob. 18.28.

18.30. (a) Calculate the sensitivity of the closed-loop output resistance of the series-shunt feedback amplifier with respect to changes in open-loop gain  $A$ :

$$S_A^{R_{\text{out}}} = \frac{A}{R_{\text{out}}} \frac{\partial R_{\text{out}}}{\partial A}$$

- (b) Use this formula to estimate the percentage change in closed-loop output resistance if the open-loop gain  $A$  changes by 5 percent for an amplifier with  $A = 80$  dB and  $\beta = 0.02$ . (c) Calculate the sensitivity of the closed-loop input resistance of the series-shunt feedback amplifier with respect to changes in open-loop gain  $A$ :

$$S_A^{R_{\text{in}}} = \frac{A}{R_{\text{in}}} \frac{\partial R_{\text{in}}}{\partial A}$$

- (c) Use this formula to estimate the percentage change in closed-loop input resistance if the open-loop gain  $A$  changes by 10 percent for an amplifier with  $A = 80 \text{ dB}$  and  $\beta = 0.02$ .

## Transresistance Amplifiers—Shunt-Shunt Feedback

- 18.31. Find the closed-loop transresistance, input resistance, and output resistance for the circuit in Fig. P18.2(d). Assume  $R_I = 100\text{ k}\Omega$ ,  $R_L = 10\text{ k}\Omega$ , and  $R_F = 39\text{ k}\Omega$ .

- 18.32. Find the closed-loop transresistance, input resistance, and output resistance for the circuit in Fig. P18.2(d). Assume  $R_I = 50 \text{ k}\Omega$ ,  $R_L = 10 \text{ k}\Omega$ , and  $R_F = 50 \text{ k}\Omega$ .
- 18.33. The circuit in Fig. P18.33 is a shunt-shunt feedback amplifier. Use feedback analysis to find the midband input resistance, output resistance, and transresistance of the amplifier if  $R_I = 500 \Omega$ ,  $R_E = 2 \text{ k}\Omega$ ,  $\beta_0 = 100$ ,  $V_A = 50 \text{ V}$ ,  $R_L = 5.6 \text{ k}\Omega$ , and  $R_F = 42 \text{ k}\Omega$ , when  $v_i$  and  $R_I$  are replaced by a Norton equivalent circuit. What is the voltage gain for the circuit as drawn?

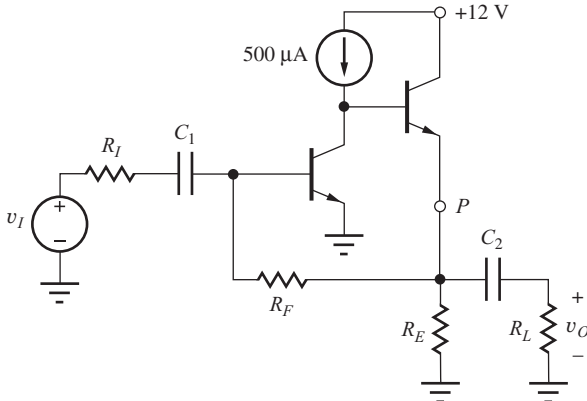


Figure P18.33

- 18.34. Use SPICE to find the midband input resistance, output resistance, and transresistance for the amplifier in Fig. P18.33. Compare the results to those in Prob. 18.24.  $C_1 = 82 \mu\text{F}$ , and  $C_2 = 47 \mu\text{F}$ .
- 18.35. Use feedback analysis to find the midband transresistance, input resistance, and output resistance of the amplifier in Fig. P18.35 if  $g_m = 5 \text{ mS}$  and  $r_o = 50 \text{ k}\Omega$ .
- 18.36. Use SPICE to find the midband input resistance, output resistance, and transresistance for the amplifier in Fig. P18.35. Compare the results to those in Prob. 18.35.

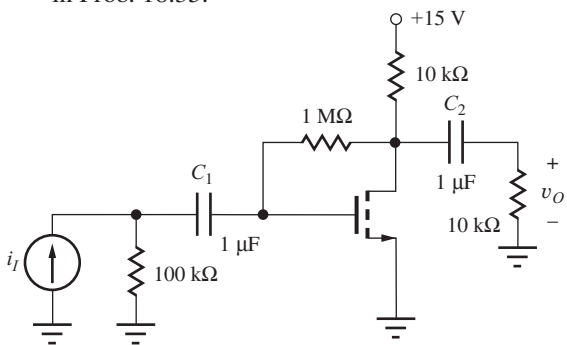


Figure P18.35

### Transconductance Amplifiers—Series-Series Feedback

- 18.37. Find the closed-loop transresistance, input resistance, and output resistance for the circuit in Fig. P18.2(c). Assume  $R_I = 2.4 \text{ k}\Omega$ ,  $R_L = 7.5 \text{ k}\Omega$ , and  $R_1 = 7.5 \text{ k}\Omega$ .
- 18.38. For the circuit in Fig. P18.28 with the output taken as the small-signal current  $i_o$  at the collector of  $Q_5$ , calculate the midband input resistance, output resistance looking into the collector of  $Q_5$ , and transconductance. Assume  $\beta_0 = 150$ ,  $V_A = 75 \text{ V}$ ,  $I = 100 \mu\text{A}$ ,  $V_{\text{REF}} = 0 \text{ V}$ , and  $R = 10 \text{ k}\Omega$ .
- 18.39. Repeat Prob. 18.38 using SPICE to perform the analysis. Compare your results to those found in Prob. 18.38.
- 18.40. For the small-signal equivalent circuit in Fig. P18.40, find expressions for the midband transconductance  $i_o/v_i$ , input resistance, and output resistance looking into the collector of  $Q_3$ . Use  $\beta_0 = 100$ ,  $V_A = 50 \text{ V}$ ,  $g_m = 50 \text{ mS}$ , and  $V_{CC} \ll V_A$ .

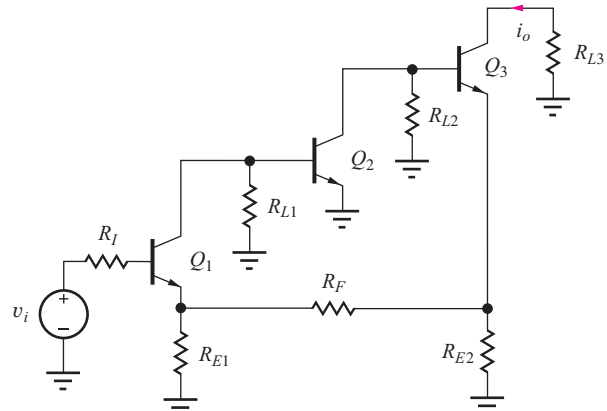


Figure P18.40

- 18.41. Taking the output of the circuit in Prob. 18.20 as the small-signal current flowing into the collector of the output transistor, find the transconductance and the output resistance looking into the output transistor collector.

### Current Amplifiers—Shunt-Series Feedback

- 18.42. Find the closed-loop current gain, input resistance, and output resistance for the circuit in Fig. P18.2(b). Assume  $R_I = 100 \text{ k}\Omega$ ,  $R_L = 7.5 \text{ k}\Omega$ ,  $R_1 = 7.5 \text{ k}\Omega$ , and  $R_2 = 1 \text{ k}\Omega$ .
- 18.43. Find the input resistance, output resistance looking into the drain of  $M_3$ , and current gain  $i_o/i_{\text{ref}}$  for the Wilson current source in Fig. P18.43. Use

the small-signal two-port model in Fig. P18.43(b) for the current mirror. Assume  $g_m = 5 \text{ mS}$  and  $r_o = 50 \text{ k}\Omega$ .

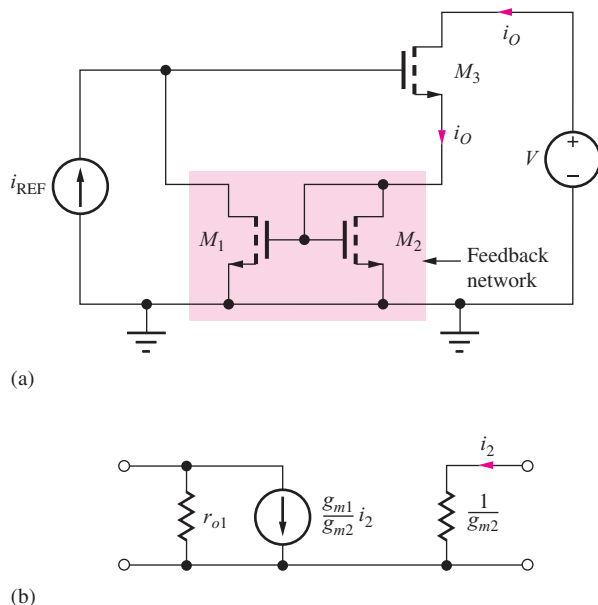


Figure P18.43

- 18.44. Use midband feedback analysis to find the current gain  $i_o/i_{\text{ref}}$ , input resistance, and output resistance of the Wilson BJT current source in Fig. P18.44. Assume all transistors have the same emitter area with  $\beta_0 = 150$ ,  $V_A = 75 \text{ V}$ ,  $g_m = 40 \text{ mS}$ , and  $V_{CC} \ll V_A$ .

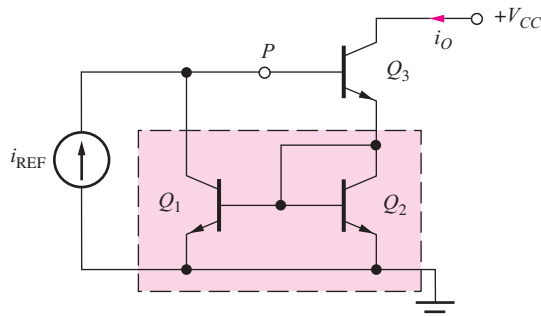


Figure P18.44

- 18.45. Use SPICE to simulate the Wilson BJT current source in Fig. P18.44 to find the output resistance. Use  $I_{\text{REF}} = 200 \mu\text{A}$ ,  $V_{CC} = 6 \text{ V}$ , and  $V_A = 50 \text{ V}$  for current gains of  $10^2$ ,  $10^4$ , and  $10^6$ . Show that  $R_{\text{out}}$  goes from a limit of  $\beta_0 r_o / 2$  to  $\mu_f r_o$ .
- 18.46. Repeat the hand calculation portions Ex. 18.6 with all of the MOSFETs replaced by BJT transistors with  $\beta_0 = 150$  and  $V_A = 75 \text{ V}$ .

- 18.47. Use SPICE to perform the analysis in Prob. 18.46. Compare your results to those from Prob. 18.46.

- 18.48. Use Blackman's theorem to find the output resistance  $R_{\text{out}}$  looking into the drain of  $M_4$ , for the regulated cascode current source in Fig. P18.48. Use  $I_1 = I_2 = 200 \mu\text{A}$ , and  $K_n = 500 \mu\text{A/V}^2$ ,  $V_{TN} = 1 \text{ V}$ ,  $V_{DD} = 10 \text{ V}$ , and  $\lambda = 0.01/\text{V}$ .

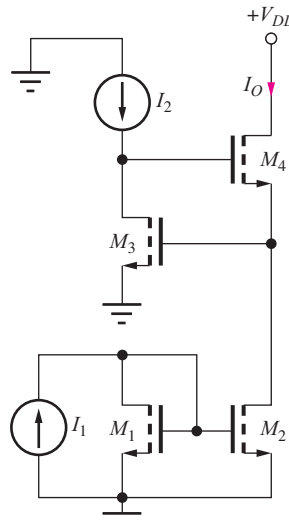


Figure P18.48

- 18.49. Repeat Prob. 18.48 with SPICE and compare your results to hand calculations from 18.48.

- 18.50. Use Blackman's theorem to find the output resistance  $R_{\text{out}}$  for the regulated cascode current source in Fig. P18.48 if the MOSFETs are all replaced with BJTs with  $\beta_F = 100$  and  $V_A = 75 \text{ V}$ . Use the other element values from Prob. 18.48.

- 18.51. Repeat Prob. 18.50 with SPICE and compare your results to hand calculations from 18.50.

- 18.52. Use feedback theory to derive an expression for the input impedance of the “shunt-shunt” feedback amplifier in Fig. P18.52.

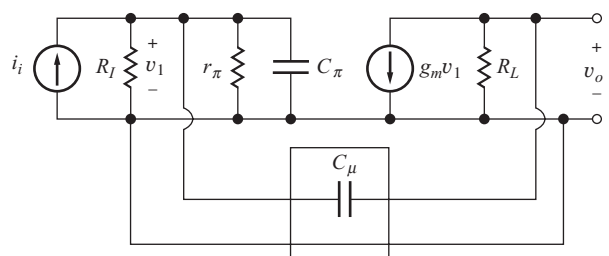


Figure P18.52

### Successive Voltage and Current Injection

- 18.53. Use the successive voltage and current injection technique introduced in Chapter 11 at point *P* with SPICE to calculate the loop gain of the amplifier in Fig. P18.20. Assume  $R_1 = 2 \text{ k}\Omega$ ,  $R_2 = 10 \text{ k}\Omega$ ,  $\beta_F = 150$ ,  $V_A = 75 \text{ V}$ ,  $I = 100 \mu\text{A}$ ,  $V_{CC} = 7.5 \text{ V}$ ,  $A = 40 \text{ dB}$ ,  $R_{id} = 50 \text{ k}\Omega$ , and  $R_o = 500 \Omega$ .
- 18.54. Use the successive voltage and current injection technique introduced in Chapter 11 at point *P* with SPICE to calculate the loop gain of the amplifier in Fig. P18.28. Assume  $\beta_F = 150$ ,  $V_A = 75 \text{ V}$ ,  $I = 100 \mu\text{A}$ ,  $V_{REF} = 0 \text{ V}$ , and  $R = 5 \text{ k}\Omega$ .
- 18.55. Use the successive voltage and current injection technique introduced in Chapter 11 at point *P* with SPICE to calculate the loop gain of Wilson current source in Fig. P18.44. Assume all transistors have the same emitter area with  $\beta_O = 150$ ,  $V_A = 75 \text{ V}$ ,  $g_m = 40 \text{ mS}$ , and  $V_{CC} \ll V_A$ .
- 18.56. Use the successive voltage and current injection technique introduced in Chapter 11 at point *P* with SPICE to calculate the loop gain of the amplifier in Fig. P18.33. Assume all transistors have the same emitter area with  $R_I = 500 \Omega$ ,  $R_E = 2 \text{ k}\Omega$ ,  $\beta_F = 100$ ,  $V_A = 50 \text{ V}$ ,  $R_L = 5.6 \text{ k}\Omega$ , and  $R_F = 42 \text{ k}\Omega$ .

### 18.4 Review of Feedback Amplifier Stability

- 18.57. Work Prob. 11.122.
- 18.58. Work Prob. 11.123.
- 18.59. What is the maximum load capacitance that can be connected to the voltage follower in Fig. P18.59 if the phase margin is to be  $50^\circ$ ? Assume that the op-amp output resistance is  $500 \Omega$ , and  $A(s)$  is given by

$$A(s) = \frac{10^7}{s + 50}$$

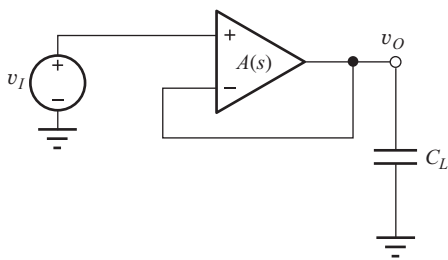


Figure P18.59

- 18.60. Use SPICE to find the phase margin of the shunt-series feedback pair in Ex. 18.1 if the transistors have  $f_T = 250 \text{ MHz}$  and  $C_\mu = 1 \text{ pF}$ .

- 18.61. For the circuit in Fig. P18.61 with the indicated gain characteristic, find  $\beta$ ,  $T$ ,  $A_v$ , and the phase margin if the amplifier inputs and output are ideal. Will the amplifier exhibit overshoot? If so, estimate how much overshoot. Use  $R_2 = R_1 = 5 \text{ k}\Omega$ .

$$A = \frac{500}{(1 + j \frac{f}{10 \text{ kHz}})(1 + j \frac{f}{10 \text{ MHz}})}$$

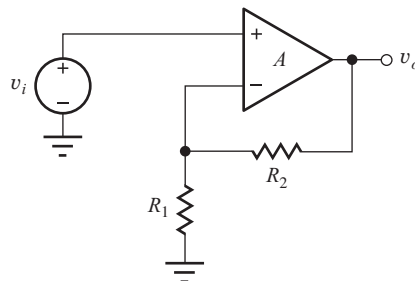


Figure P18.61

- 18.62. Repeat Prob. 18.61 if  $R_2 = 0$ ,  $R_1 = \infty$ , and the voltage gain of the amplifier is given by
- $$A = \frac{20,000}{(1 + j \frac{f}{100 \text{ Hz}})(1 + j \frac{f}{10 \text{ MHz}})}$$
- 18.63. Repeat Prob. 18.61 if  $R_2 = 0$ ,  $R_1 = \infty$ , and the voltage gain of the amplifier is given by
- $$A = \frac{20,000(1 - j \frac{f}{4 \text{ MHz}})}{(1 + j \frac{f}{100 \text{ Hz}})(1 + j \frac{f}{10 \text{ MHz}})}$$
- 18.64. If the amplifier in Prob. 18.61 has an output resistance  $R_o = 100 \Omega$ , what is the maximum load capacitance that can be connected at the output of the amplifier and still maintain a phase margin of  $60^\circ$ ?
- 18.65. If  $R_1 = 5 \text{ k}\Omega$ , what must  $R_2$  in Prob. 18.63 be to improve the phase margin to  $70^\circ$ ? What is the closed-loop gain for this value of  $R_2$ ?

### 18.5 Single-Pole Operational Amplifier Compensation

- 18.66. (a) What are the unity-gain frequency and positive and negative slew rates for the CMOS amplifier in Fig. 18.24 if  $I_1 = 300 \mu\text{A}$ ,  $I_2 = 600 \mu\text{A}$ ,  $K_{n1} = 1 \text{ mA/V}^2$ , and  $C_C = 10 \text{ pF}$ ? (b) If  $I_1 = 400 \mu\text{A}$ ,  $I_2 = 400 \mu\text{A}$ ,  $K_{n1} = 1 \text{ mA/V}^2$ , and  $C_C = 5 \text{ pF}$ ?
- 18.67. Repeat Prob. 18.66 for  $I_1 = 500 \mu\text{A}$ ,  $I_2 = 2 \text{ mA}$ ,  $C_C = 12 \text{ pF}$ .
- 18.68. Simulate the loop transmission frequency response of the CMOS amplifier in Fig. 18.29 for  $R_Z = 0$

and  $R_Z = 1.5 \text{ k}\Omega$ . Compare the values of the unity-gain frequency and phase shift of the amplifier at the unity-gain frequency. Use  $I_1 = 200 \mu\text{A}$ ,  $I_2 = 500 \mu\text{A}$ ,  $I_3 = 2 \text{ mA}$ ,  $(W/L)_1 = 30/1$ ,  $(W/L)_3 = 40/1$ ,  $(W/L)_5 = 80/1$ ,  $(W/L)_6 = 60/1$ , and  $C_C = 10 \text{ pF}$ .  $V_{DD} = V_{SS} = 10 \text{ V}$ . Use CMOS models from Appendix B.

- 18.69. What are the unity-gain frequency and slew rate of the bipolar amplifier in Fig. 18.30 if  $I_1 = 100 \mu\text{A}$ ,  $I_2 = 400 \mu\text{A}$ , and  $C_C = 10 \text{ pF}$ ? (b) If  $I_1 = 300 \mu\text{A}$ ,  $I_2 = 350 \mu\text{A}$ , and  $C_C = 10 \text{ pF}$ ?
- 18.70. Repeat Prob. 18.69(a) for  $I_1 = 400 \mu\text{A}$ ,  $I_2 = 2 \text{ mA}$ , and  $C_C = 12 \text{ pF}$ .
- 18.71. (a) What are the positive and negative slew rates of the amplifier in Fig. P18.71 just after a 1-V step function is applied to input  $v_1$  if  $I_1 = 60 \mu\text{A}$ ,  $I_2 = 350 \mu\text{A}$ ,  $I_3 = 600 \mu\text{A}$ ,  $V_{CC} = V_{EE} = 10 \text{ V}$ , and  $C_C = 7 \text{ pF}$ ? Assume  $v_1$  is grounded. (b) Check your answers with SPICE.

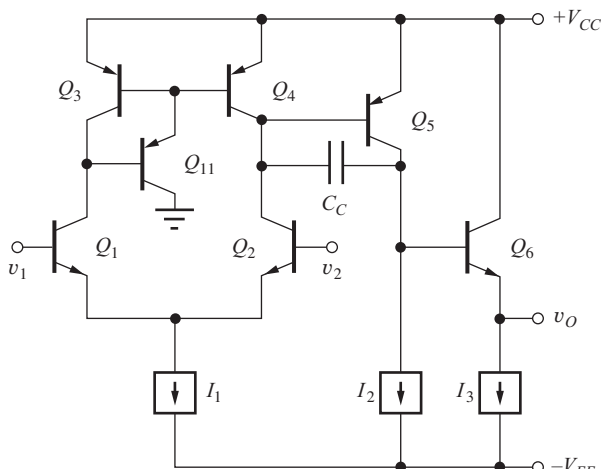


Figure P18.71

- 18.72. Repeat Prob. 18.71 for  $I_1 = 200 \mu\text{A}$ ,  $I_2 = 500 \mu\text{A}$ ,  $I_3 = 1 \text{ mA}$ , and  $C_C = 10 \text{ pF}$ .
- 18.73. (a) Calculate the poles at the base of  $Q_2$ , the base of  $M_5$ , the collector of  $Q_5$ , and the base of  $Q_6$  for the amplifier of Prob. 18.71(a) with  $C_C = 0$ . Use  $f_T = 300 \text{ MHz}$  and  $C_\mu = 1 \text{ pF}$  in addition to the bias parameters in Prob. 18.71. (b) Calculate the gain of the amplifier with  $V_A = 50 \text{ V}$  and  $\beta_o = 100$ . (c) Assuming a unity-gain feedback connection, calculate the phase margin of the amplifier. (d) What value of  $C_C$  is necessary to set the phase margin at  $75^\circ$ ?

- 18.74. Use SPICE to confirm the results from Prob. 18.73. (BF = 100, VAF = 50, TF = 530 PS, CJC = 1 pF) Discuss the reasons for any discrepancy.
- 18.75. For the circuit in Fig. 18.12, find  $R_3$  to set  $I_{D3} = 1 \text{ mA}$  with  $V_{DD} = V_{SS} = 10 \text{ V}$ , and  $I_{D4} = 5 \text{ mA}$ . Calculate a new  $R_4$  to maintain  $V_O = 0 \text{ V}$ . Calculate the poles of the amplifier and calculate  $R_Z$  to cancel the right-half plane zero. Find the unity-gain frequency such that the phase margin is set to  $70^\circ$ . For the phase margin calculation, assume the dominant pole contributes  $90^\circ$  of phase shift at the unity-gain frequency. Calculate the  $C_C$  required to achieve the desired unity-gain frequency and phase margin.
- 18.76. Use SPICE to simulate the results from Prob. 18.75. Discuss the reasons for any discrepancy. Use NMOS: KP = 0.01 A/V<sup>2</sup> and VTO = 1 V, PMOS: KP = 0.004 A/V<sup>2</sup> and VTO = -1 V, LAMBDA = 0.01/V, C<sub>GS</sub> = 5 pF, C<sub>GD</sub> = 1 pF. (You will need to manually add C<sub>GS</sub> and C<sub>GD</sub> into the circuit for this simplified model.)
- 18.77. (a) For the circuit discussed in Sec. 18.4, recalculate the phase margin for a unity-gain feedback connection. (b) Recalculate  $C_C$  to set the phase margin back to the value in the text when the feedback factor  $\beta$  was 0.5.
- 18.78. Use SPICE to simulate the results from Prob. 18.77. Discuss the reasons for any discrepancy. Use NMOS: KP = 0.01 A/V<sup>2</sup> and VTO = 1 V, PMOS: KP = 0.004 A/V<sup>2</sup> and VTO = -1 V, LAMBDA = 0.01/V, C<sub>GS</sub> = 5 pF, C<sub>GD</sub> = 1 pF. (You will need to manually add C<sub>GS</sub> and C<sub>GD</sub> into the circuit for this simplified model.)
- 18.79. Consider the compensation of the circuit in Example 18.1 by creating a dominant pole at the base of  $Q_2$  with a compensation capacitor  $C_C$  from base to collector of  $Q_2$ . For this problem, assume the resistor  $R_4$  is bypassed with a 50  $\mu\text{F}$  capacitor. (a) Calculate the value of  $C_C$  required to set the unity-gain frequency of the circuit to 5 MHz. (b) Calculate the other poles in the loop transmission at the emitter of  $Q_1$  and the collector of  $Q_2$ . (c) Calculate the phase margin of the circuit. Use  $V_A = \infty$ ,  $\beta_F = 100$ ,  $f_T = 300 \text{ MHz}$  and  $C_\mu = 1 \text{ pF}$ .
- 18.80. Use SPICE to confirm the results from Prob. 18.79. (BF = 100, VAF = 50, TF = 530 PS, CJC = 1 pF) Discuss the reasons for any discrepancy.

## 18.6 High Frequency Oscillators

### Colpitts Oscillators

- \*\*18.81. The ac equivalent circuit for a Colpitts oscillator is given in Fig. P18.81. (a) What is the frequency of oscillation if  $g_m = 10 \text{ mS}$ ,  $\beta_o = 100$ ,  $R_E = 1 \text{ k}\Omega$ ,  $L = 5 \mu\text{H}$ ,  $C_1 = 20 \text{ pF}$ ,  $C_2 = 100 \text{ pF}$ ,  $C_4 = 0.01 \mu\text{F}$ , and  $C_3 = \infty$ ? Assume that the capacitances of the transistor can be neglected (see Prob. 18.82). (b) A variable capacitor  $C_3$  is added to the circuit and has a range of 5–50 pF. What range of frequencies of oscillation can be achieved? (c) What is the minimum transconductance needed to ensure oscillation in part (a)? What is the minimum collector current required in the transistor?

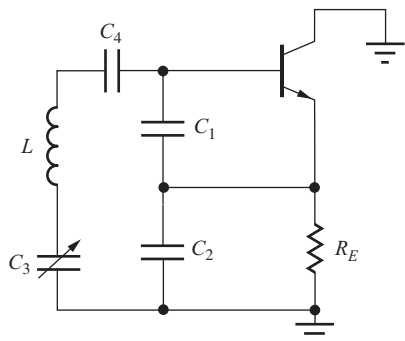


Figure P18.81

- 18.82. The ac equivalent circuit for a Colpitts oscillator is given in Fig. P18.81. (a) What is the frequency of oscillation if  $L = 20 \mu\text{H}$ ,  $C_1 = 20 \text{ pF}$ ,  $C_2 = 100 \text{ pF}$ ,  $C_3 = \infty$ ,  $C_4 = 0.01 \mu\text{F}$ ,  $f_T = 500 \text{ MHz}$ ,  $r_\pi = \infty$ ,  $V_A = 50 \text{ V}$ ,  $r_x = 0$ ,  $R_E = 1 \text{ k}\Omega$ ,  $C_\mu = 3 \text{ pF}$ , and the transistor is operating at a Q-point of (5 mA, 5 V)? (b) What is the frequency of oscillation if the Q-point current is doubled?

- 18.83. Design a Colpitts oscillator for operation at a frequency of 20 MHz using the circuit in Fig. 18.33(a). Assume  $L = 3 \mu\text{H}$ ,  $K_n = 1.25 \text{ mA/V}^2$ , and  $V_{TN} = -4 \text{ V}$ . Ignore the device capacitances.

- 18.84. What is the frequency of oscillation of the MOSFET Colpitts oscillator in Fig. P18.84 if  $L = 10 \mu\text{H}$ ,  $C_1 = 50 \text{ pF}$ ,  $C_2 = 50 \text{ pF}$ ,  $C_3 = 0 \text{ pF}$ ,  $C_{GS} = 10 \text{ pF}$ , and  $C_{GD} = 4 \text{ pF}$ ? What is the minimum amplification factor of the transistor?

- 18.85. Capacitor  $C_3$  is added to the Colpitts oscillator in Prob. 18.84 to allow tuning the oscillator. (a) Assume  $C_3$  can vary from 5 to 50 pF and calculate the

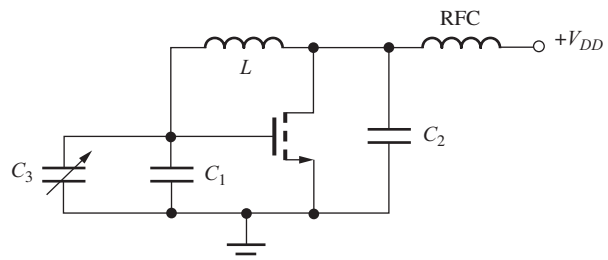


Figure P18.84

frequencies of oscillation for the two adjustment extremes. (b) What is the minimum value of amplification factor needed to ensure oscillation throughout the full tuning range?

- 18.86. A variable-capacitance diode is added to the Colpitts oscillator in Fig. P18.86 to form a voltage tunable oscillator. (a) The parameters of the diode are  $C_{jo} = 20 \text{ pF}$  and  $\phi_j = 0.8 \text{ V}$  [see Eq. (3.21)]. Calculate the frequencies of oscillation for  $V_{TUNE} = 2 \text{ V}$  and 20 V if  $L = 10 \mu\text{H}$ ,  $C_1 = 75 \text{ pF}$ , and  $C_2 = 75 \text{ pF}$ . Assume the RFC has infinite impedance and  $C_C$  has zero impedance. (b) What is the minimum value of voltage gain needed to ensure oscillation throughout the full tuning range?

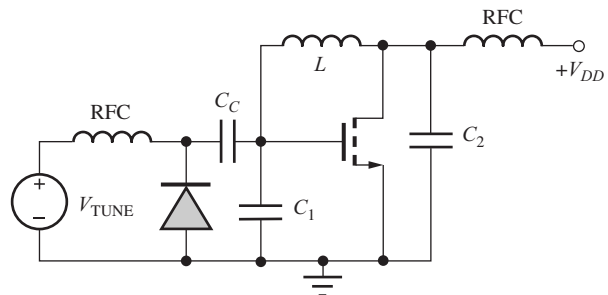


Figure P18.86

- 18.87. (a) Perform a SPICE transient simulation of the Colpitts oscillator in Fig. 18.33 and compare its frequency of oscillation to hand calculations if  $V_{DD} = 10 \text{ V}$ ,  $K_n = 1.25 \text{ mA/V}^2$ ,  $V_{TN} = -4 \text{ V}$ ,  $R_S = 820 \Omega$ ,  $C_2 = 220 \text{ pF}$ ,  $C_1 = 470 \text{ pF}$ , and  $L = 10 \mu\text{H}$ . (b) Repeat if  $C_2 = 470 \text{ pF}$  and  $C_1 = 220 \text{ pF}$ .

- 18.88. Perform a SPICE transient simulation of the Colpitts oscillator in Fig. P18.84 if  $L = 10 \mu\text{H}$ ,  $C_1 = 50 \text{ pF}$ ,  $C_2 = 50 \text{ pF}$ ,  $C_3 = 0 \text{ pF}$ ,  $RFC = 20 \text{ mH}$ ,  $V_{DD} = 12 \text{ V}$ ,  $K_n = 10 \text{ mA/V}^2$ ,  $V_{TN} = 1 \text{ V}$ ,  $C_{GS} = 10 \text{ pF}$ , and  $C_{GD} = 4 \text{ pF}$ . What are the amplitude and frequency of oscillation?

## Hartley Oscillators

- 18.89. What is the frequency of oscillation of the Hartley oscillator in Fig. P18.89 if the diode is replaced by a short circuit and  $L_1 = 10 \mu\text{H}$ ,  $L_2 = 10 \mu\text{H}$ , and  $C = 20 \text{ pF}$ ? Neglect  $C_{GS}$  and  $C_{GD}$ .

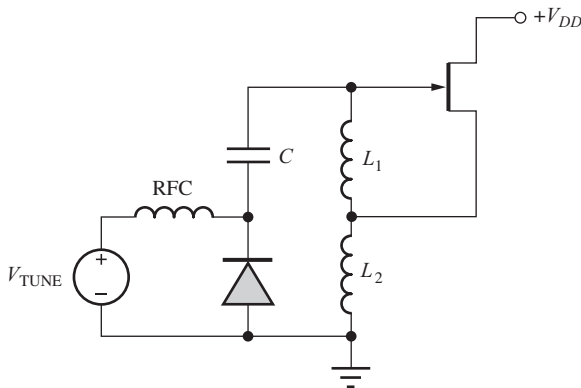


Figure P18.89

- 18.90. A variable-capacitance diode is added to the Hartley oscillator in Prob. 18.89 to form a voltage-tunable oscillator, and the value of  $C$  is changed to 220 pF. (a) If the parameters of the diode are  $C_{jo} = 20 \text{ pF}$  and  $\phi_j = 0.8 \text{ V}$  [see Eq. (3.21)], calculate the frequencies of oscillation for  $V_{TUNE} = 2 \text{ V}$  and 20 V. Assume the RFC has infinite impedance. (b) What is the minimum value of amplification factor of the FET needed to ensure oscillation throughout the full tuning range?

- 18.91 Find the expression for the input impedance in the Hartley oscillator using the circuit in Fig. 18.36 with  $Z_{gs} = L_1$  and  $Z_s = L_2$  and demonstrate that the real part is negative.

## Negative $G_m$ Oscillator

- 18.92. Write nodal equations for the negative  $G_m$  oscillator in Fig. 18.37(b) and directly derive the frequency of oscillation and gain required to sustain oscillation. Assume a differential-mode oscillation.
- 18.93. What are the Q-points of the transistors in the oscillator in Fig. 18.37(a) if  $V_{DD} = 3.3 \text{ V}$ ,  $I_{EE} = 2 \text{ mA}$ ,  $V_{TN} = 0.75 \text{ V}$ , and  $K_n = 2.5 \text{ mA/V}^2$ ?
- 18.94. The oscillator in Fig. 18.37 has  $L = 10 \text{ nH}$  and the transistor has  $C_{GS} = 3 \text{ pF}$  and  $C_{GD} = 0.5 \text{ pF}$ . (a) What value of  $C$  is required to achieve oscillation at 500 MHz? (b) At 1 GHz?

- 18.95. The oscillator in Fig. 18.39 has  $L = 4 \text{ nH}$  with a  $Q$  of 15 at 1 GHz, and the transistor has  $C_{GS} = 1 \text{ pF}$  and  $C_{GD} = 0.25 \text{ pF}$ . (a) What value of  $C$  is required to achieve oscillation at 1 GHz? (b) If the transistor has  $K_n = 2.5 \text{ mA/V}^2$  and  $\lambda = 0$ , what is the minimum value of  $I_{EE}$  required for oscillation? (c) Repeat part (b) for  $\lambda = 0.08$ . (d) \*Estimate the amplitude of the differential output signal from the oscillator.

- 18.96. Draw the ac equivalent circuit for the oscillator in Fig. P18.96 and find an expression for the frequency of oscillation. Include capacitances  $C_{GS}$  and  $C_{GD}$  of the FETs.

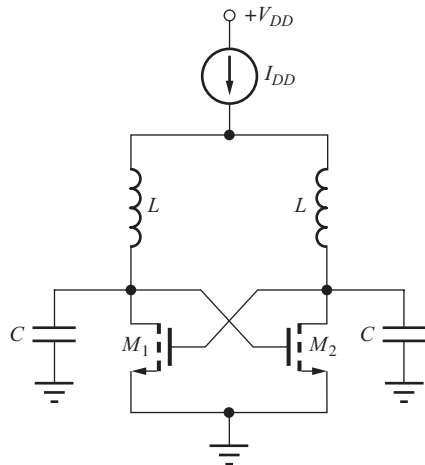


Figure P18.96

## Crystal Oscillators

- 18.97. A crystal has a series resonant frequency of 10 MHz, series resistance of  $40 \Omega$ ,  $Q$  of 25,000, and parallel capacitance of 10 pF. (a) What are the values of  $L$  and  $C_S$  for this crystal? (b) What is the parallel resonant frequency of the crystal? (c) The crystal is placed in an oscillator circuit in parallel with a total capacitance of 22 pF. What is the frequency of oscillation?
- 18.98. The crystal in the oscillator in Fig. P18.98 has  $L = 15 \text{ mH}$ ,  $C_S = 20 \text{ fF}$ , and  $R = 50 \Omega$ . (a) What is the frequency of oscillation if  $R_E = 1 \text{ k}\Omega$ ,  $R_B = 100 \text{ k}\Omega$ ,  $V_{CC} = V_{EE} = 5 \text{ V}$ ,  $C_1 = 100 \text{ pF}$ ,  $C_2 = 470 \text{ pF}$ , and  $C_3 = \infty$ ? Assume the transistor has  $\beta_f = 100$ ,  $V_A = 50 \text{ V}$ , and infinite  $f_T$ . (b) Repeat if  $C_\mu = 5 \text{ pF}$  and  $f_T = 250 \text{ MHz}$ .

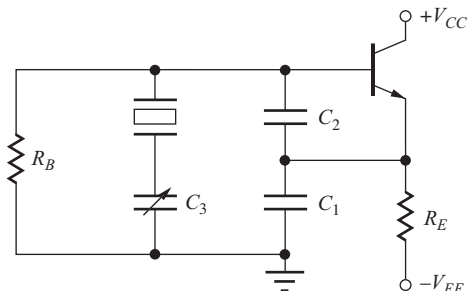
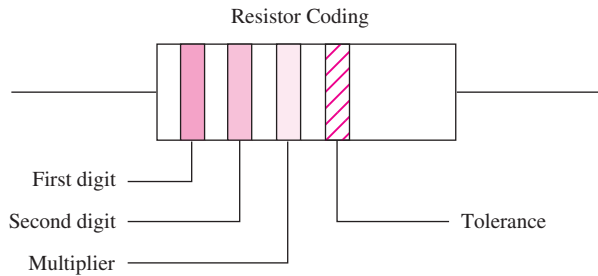


Figure P18.98

- 18.99. A variable capacitor  $C_3$  is placed in series with the crystal in the oscillator in Prob. 18.98(a) to provide a calibration adjustment. Assume  $C_3$  can vary from 1 pF to 35 pF and calculate the frequencies of oscillation for the two adjustment extremes.
- 18.100. Simulate the crystal oscillator in Fig. P18.98 and find the frequency of oscillation if  $R_E = 1 \text{ k}\Omega$ ,  $R_B = 100 \text{ k}\Omega$ ,  $V_{CC} = V_{EE} = 5 \text{ V}$ ,  $C_1 = 100 \text{ pF}$ ,  $C_2 = 470 \text{ pF}$ , and  $C_3 = \infty$ . The crystal has  $L = 15 \text{ mH}$ ,  $C_s = 20 \text{ fF}$ ,  $R = 50 \Omega$ , and  $C_p = 20 \text{ pF}$ . Assume the transistor has  $\beta_F = 100$ ,  $V_A = 50 \text{ V}$ ,  $C_\mu = 5 \text{ pF}$ , and  $\tau_F = 1 \text{ ns}$ .

# APPENDIX A

## Standard Discrete Component Values



### Resistor Color Code

COLOR	DIGIT	MULTIPLIER	TOLERANCE, %
Silver	...	0.01	10
Gold	...	0.1	5
Black	0	1	
Brown	1	10	
Red	2	10 <sup>2</sup>	
Orange	3	10 <sup>3</sup>	
Yellow	4	10 <sup>4</sup>	
Green	5	10 <sup>5</sup>	
Blue	6	10 <sup>6</sup>	
Violet	7	10 <sup>7</sup>	
Gray	8	10 <sup>8</sup>	
White	9	10 <sup>9</sup>	

*Standard resistor values:* All values available with a 5 percent tolerance. Bold values are available with 10 percent tolerance.

OHMS						MEGOHMS		
<b>1.0</b>	<b>5.6</b>	<b>33</b>	<b>180</b>	<b>1000</b>	<b>5600</b>	<b>33000</b>	<b>180000</b>	<b>1.0</b>
1.1	6.2	36	200	1100	6200	36000	200000	1.1
<b>1.2</b>	<b>6.8</b>	<b>39</b>	<b>220</b>	<b>1200</b>	<b>6800</b>	<b>39000</b>	<b>220000</b>	<b>1.2</b>
1.3	7.5	43	240	1300	7500	43000	240000	1.3
<b>1.5</b>	<b>8.2</b>	<b>47</b>	<b>270</b>	<b>1500</b>	<b>8200</b>	<b>47000</b>	<b>270000</b>	<b>1.5</b>
1.6	9.1	51	300	1600	9100	51000	300000	1.6
<b>1.8</b>	<b>10</b>	<b>56</b>	<b>330</b>	<b>1800</b>	<b>10000</b>	<b>56000</b>	<b>330000</b>	<b>1.8</b>
2.0	11	62	360	2000	11000	62000	360000	2.0
<b>2.2</b>	<b>12</b>	<b>68</b>	<b>390</b>	<b>2200</b>	<b>12000</b>	<b>68000</b>	<b>390000</b>	<b>2.2</b>
2.4	13	75	430	2400	13000	75000	430000	2.4
<b>2.7</b>	<b>15</b>	<b>82</b>	<b>470</b>	<b>2700</b>	<b>15000</b>	<b>82000</b>	<b>470000</b>	<b>2.7</b>
3.0	16	91	510	3000	16000	91000	510000	3.0
<b>3.3</b>	<b>18</b>	<b>100</b>	<b>560</b>	<b>3300</b>	<b>18000</b>	<b>100000</b>	<b>560000</b>	<b>3.3</b>
3.6	20	110	620	3600	20000	110000	620000	3.6
<b>3.9</b>	<b>22</b>	<b>120</b>	<b>680</b>	<b>3900</b>	<b>22000</b>	<b>120000</b>	<b>680000</b>	<b>3.9</b>
4.3	24	130	750	4300	24000	130000	750000	4.3
<b>4.7</b>	<b>27</b>	<b>150</b>	<b>820</b>	<b>4700</b>	<b>27000</b>	<b>150000</b>	<b>820000</b>	<b>4.7</b>
5.1	30	160	910	5100	30000	160000	910000	5.1

### PRECISION (1%) RESISTORS

10.0	19.1	36.5	69.8	133	255	487	931	1.78K	3.40K	6.49K	12.4K	23.7K	45.3K	84.5K	158K	294K	549K
10.2	19.6	37.4	71.5	137	261	499	953	1.82K	3.48K	6.65K	12.7K	24.3K	46.4K	86.6K	162K	301K	562K
10.5	20.0	38.3	73.2	140	267	511	976	1.87K	3.57K	6.81K	13.0K	24.9K	47.5K	88.7K	165K	309K	576K
10.7	20.5	39.2	75.0	143	274	523	1.00K	1.91K	3.65K	6.98K	13.3K	25.5K	48.7K	90.9K	169K	316K	590K
11.0	21.0	40.2	76.8	147	280	536	1.02K	1.96K	3.74K	7.15K	13.7K	26.1K	49.9K	93.1K	174K	324K	604K
11.3	21.5	41.2	78.7	150	287	549	1.05K	2.00K	3.83K	7.32K	14.0K	26.7K	51.1K	95.3K	178K	332K	619K
11.5	22.1	42.2	80.6	154	294	562	1.07K	2.05K	3.92K	7.50K	14.3K	27.4K	52.3K	97.6K	182K	340K	634K
11.8	22.6	43.2	82.5	158	301	576	1.10K	2.10K	4.02K	7.68K	14.7K	28.0K	53.6K	100K	187K	348K	649K
12.1	23.2	44.2	84.5	162	309	590	1.13K	2.15K	4.12K	7.87K	15.0K	28.7K	54.9K	102K	191K	357K	665K
12.4	23.7	45.3	86.6	165	316	604	1.15K	2.21K	4.22K	8.06K	15.4K	29.4K	56.2K	105K	196K	365K	681K
12.7	24.3	46.4	88.7	169	324	619	1.18K	2.26K	4.32K	8.25K	15.8K	30.1K	57.6K	107K	200K	374K	698K
13.0	24.9	47.5	90.9	174	332	634	1.21K	2.32K	4.42K	8.45K	16.2K	30.9K	59.0K	110K	205K	383K	715K
13.3	25.5	48.7	93.1	178	340	649	1.24K	2.37K	4.53K	8.66K	16.5K	31.6K	60.4K	113K	210K	392K	732K
13.7	26.1	49.9	95.3	182	348	665	1.27K	2.43K	4.64K	8.87K	16.9K	32.4K	61.9K	115K	215K	402K	750K
14.0	26.7	51.1	97.6	187	357	681	1.30K	2.49K	4.75K	9.09K	17.4K	33.2K	63.4K	118K	221K	412K	768K
14.3	27.4	52.3	100	191	365	698	1.33K	2.55K	4.87K	9.31K	17.8K	34.0K	64.9K	121K	226K	422K	787K
14.7	28.0	53.6	102	196	374	715	1.37K	2.61K	4.99K	9.53K	18.2K	34.8K	66.5K	124K	232K	432K	806K
15.0	28.8	54.9	105	200	383	732	1.40K	2.67K	5.11K	9.76K	18.7K	35.7K	68.1K	127K	237K	442K	825K
15.4	29.4	56.2	107	205	392	750	1.43K	2.74K	5.23K	10.0K	19.1K	36.5K	69.8K	130K	243K	453K	845K
15.8	30.1	57.6	110	210	402	768	1.47K	2.80K	5.36K	10.2K	19.6K	37.4K	71.5K	133K	249K	464K	866K
16.2	30.9	59.0	113	215	412	787	1.50K	2.87K	5.49K	10.5K	20.0K	38.3K	73.2K	137K	255K	475K	887K
16.5	31.6	60.4	115	221	422	806	1.54K	2.94K	5.62K	10.7K	20.5K	39.2K	75.0K	140K	261K	487K	909K
16.9	32.4	61.9	118	226	432	825	1.58K	3.01K	5.76K	11.0K	21.0K	40.2K	76.8K	143K	267K	499K	931K
17.4	33.2	63.4	121	232	443	845	1.62K	3.09K	5.90K	11.3K	21.5K	41.2K	78.7K	147K	274K	511K	953K
17.8	34.0	64.9	124	237	453	866	1.65K	3.16K	6.04K	11.5K	22.1K	42.2K	80.6K	150K	280K	523K	976K
18.2	34.8	66.5	127	243	464	887	1.69K	3.24K	6.19K	11.8K	22.6K	43.2K	82.5K	154K	287K	536K	1.00M
18.7	35.7	68.1	130	249	475	909	1.74K	3.32K	6.34K	12.1K	23.2K	44.2K					

**Standard Capacitor Values (Larger values are also available)**

pF	pF	pF	pF	μF	μF	μF	μF	μF	μF	μF	μF
1	10	100	1000	0.01	0.1	1	10	100	1000	10000	
	12	120	1200	0.012	0.12	1.2	12	120	1200	12000	
1.5	15	150	1500	0.015	0.15	1.5	15	150	1500	15000	
	18	180	1800	0.018	0.18	1.8	18	180	1800		
	20	200	2000	0.020	0.20				2000	20000	
2.2	22	220	2200	0.022	0.22	2.2	22	220	2200	22000	
	27	270	2700	0.027	0.27	2.7	27	270	2700		
3.3	33	330	3300	0.033	0.33	3.3	33	330	3300	33000	
	39	390	3900	0.039	0.39	3.9	39	390	3900		
4.7	47	470	4700	0.047	0.47	4.7	47	470	4700	47000	
5.0	50	500	5000	0.050	0.50					50000	
5.6	56	560	5600	0.056	0.56	5.6	56	560	5600		
6.8	68	680	6800	0.068	0.68	6.8	68	680	6800		
8.2	82	820	8200	0.082	0.82	8.2	82	820	8200		

**Standard Inductor Values**

μH	μH	μH	μH	mH	mH	mH
0.10	1.0	10	100	1.0	10	100
	1.1	11	110			
	1.2	12	120	1.2	12	120
0.15	1.5	15	150	1.5	15	
0.18	1.8	18	180	1.8	18	
	2.0	20	200			
0.22	2.2	22	220	2.2	22	
	2.4	24	240			
0.27	2.7	27	270	2.7	27	
0.33	3.3	33	330	3.3	33	
0.39	3.9	39	390	3.9	39	
	4.3	43	430			
0.47	4.7	47	470	4.7	47	
0.56	5.6	56	560	5.6	56	
	6.2	62	620			
0.68	6.8	68	680	6.8	68	
	7.5	75	750			
0.82	8.2	82	820	8.2	82	
	9.1	91	910			

# APPENDIX B

## Solid-State Device Models and SPICE Simulation Parameters

### B.1 *pn* JUNCTION DIODES

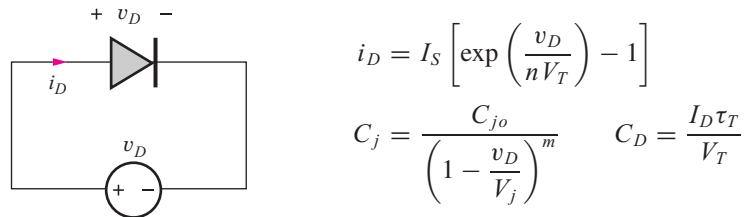


Figure B.1 Diode with applied voltage  $v_D$ .

**TABLE B.1**  
Diode Parameters for Circuit Simulation

PARAMETER	NAME	DEFAULT	TYPICAL VALUE
Saturation current	IS	$1 \times 10^{-14}$ A	$3 \times 10^{-17}$ A
Emission coefficient (ideality factor — $n$ )	N	1	1
Transit time ( $\tau_T$ )	TT	0	0.15 nS
Series resistance	RS	0	$10 \Omega$
Junction capacitance	CJO	0	1.0 pF
Junction potential ( $V_j$ )	VJ	1 V	0.8 V
Grading coefficient ( $m$ )	M	0.5	0.5

### B.2 MOS FIELD-EFFECT TRANSISTORS (MOSFETs)

A summary of the mathematical models for both the NMOS and PMOS transistors follows. The terminal voltages and currents are defined in Fig. B.2.

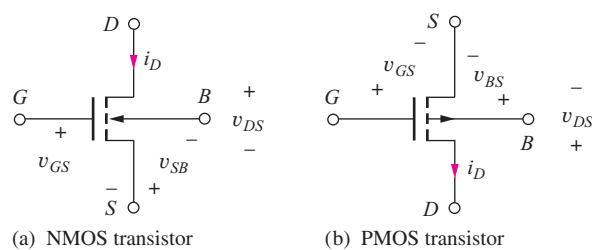


Figure B.2 NMOS and PMOS transistor circuit symbols.

## NMOS TRANSISTOR MODEL SUMMARY

$$K_n = K'_n \frac{W}{L} = \mu_n C''_{\text{ox}} \frac{W}{L}$$

$i_G = 0$  and  $i_B = 0$  for all regions

### Cutoff Region

$$i_D = 0 \quad \text{for } v_{GS} \leq V_{TN}$$

### Triode Region

$$i_D = K_n \left( v_{GS} - V_{TN} - \frac{v_{DS}}{2} \right) v_{DS} \quad \text{for } v_{GS} - V_{TN} \geq v_{DS} \geq 0$$

### Saturation Region

$$i_D = \frac{K_n}{2} (v_{GS} - V_{TN})^2 (1 + \lambda v_{DS}) \quad \text{for } v_{DS} \geq (v_{GS} - V_{TN}) \geq 0$$

### Threshold Voltage

$$V_{TN} = V_{TO} + \gamma (\sqrt{v_{SB} + 2\phi_F} - \sqrt{2\phi_F})$$

## PMOS TRANSISTOR MODEL SUMMARY

$$K_p = K'_p \frac{W}{L} = \mu_p C''_{\text{ox}} \frac{W}{L}$$

$i_G = 0$  and  $i_B = 0$  for all regions

### Cutoff Region

$$i_D = 0 \quad \text{for } v_{GS} \geq V_{TP}$$

### Triode Region

$$i_D = K_p \left( v_{GS} - V_{TP} - \frac{v_{DS}}{2} \right) v_{DS} \quad \text{for } v_{GS} - V_{TP} \leq v_{DS} \leq 0$$

### Saturation Region

$$i_D = \frac{K_p}{2} (v_{GS} - V_{TP})^2 (1 + \lambda |v_{DS}|) \quad \text{for } v_{DS} \leq (v_{GS} - V_{TP}) \leq 0$$

### Threshold Voltage

$$V_{TP} = V_{TO} - \gamma (\sqrt{v_{BS} + 2\phi_F} - \sqrt{2\phi_F})$$

**TABLE B.2**  
Types of MOSFET Transistors

NMOS DEVICE	PMOS DEVICE
Enhancement-mode	$V_{TN} > 0$
Depletion-mode	$V_{TN} \leq 0$

## MOS TRANSISTOR PARAMETERS FOR CIRCUIT SIMULATION

For simulation purposes, use the LEVEL=1 models in SPICE with the following SPICE parameters in your NMOS and PMOS devices:

**TABLE B.3**

Representative MOS Device Parameters for SPICE Simulation (MOSIS 0.5- $\mu\text{m}$   $p$ -well process)

PARAMETER	SYMBOL	NMOS TRANSISTOR	PMOS TRANSISTOR
Threshold voltage	VTO	0.91 V	-0.77 V
Transconductance	KP	50 $\mu\text{A}/\text{V}^2$	20 $\mu\text{A}/\text{V}^2$
Body effect	GAMMA	0.99 $\sqrt{\text{V}}$	0.53 $\sqrt{\text{V}}$
Surface potential	PHI	0.7 V	0.7 V
Channel-length modulation	LAMBDA	0.02 $\text{V}^{-1}$	0.05 $\text{V}^{-1}$
Mobility	UO	615 $\text{cm}^2$	235 $\text{cm}^2/\text{s}$
Channel length	L	0.5 $\mu\text{m}$	0.5 $\mu\text{m}$
Channel width	W	0.5 $\mu\text{m}$	0.5 $\mu\text{m}$
Ohmic drain resistance	RD	0	0
Ohmic source resistance	RS	0	0
Junction saturation current	IS	0	0
Built-in potential	PB	0	0
Gate-drain capacitance per unit width	CGDO	330 $\text{pF}/\text{m}$	315 $\text{pF}/\text{m}$
Gate-source capacitance per unit width	CGSO	330 $\text{pF}/\text{m}$	315 $\text{pF}/\text{m}$
Gate-bulk capacitance per unit length	CGBO	395 $\text{pF}/\text{m}$	415 $\text{pF}/\text{m}$
Junction bottom capacitance per unit area	CJ	$3.9 \times 10^{-4} \text{ F/m}^2$	$2 \times 10^{-4} \text{ F/m}^2$
Grading coefficient	MJ	0.45	0.47
Sidewall capacitance	CJSW	510 $\text{pF}/\text{m}$	180 $\text{pF}/\text{m}$
Sidewall grading coefficient	MJSW	0.36	0.09
Source-drain sheet resistance	RSH	22 $\Omega/\text{square}$	70 $\Omega/\text{square}$
Oxide thickness	TOX	$4.15 \times 10^{-6} \text{ cm}$	$4.15 \times 10^{-6} \text{ cm}$
Junction depth	XJ	0.23 $\mu\text{m}$	0.23 $\mu\text{m}$
Lateral diffusion	LD	0.26 $\mu\text{m}$	0.25 $\mu\text{m}$
Substrate doping	NSUB	$2.1 \times 10^{16}/\text{cm}^3$	$5.9 \times 10^{16}/\text{cm}^3$
Critical field	UCRIT	$9.6 \times 10^5 \text{ V/cm}$	$6 \times 10^5 \text{ V/cm}$
Critical field exponent	UEXP	0.18	0.28
Saturation velocity	VMAX	$7.6 \times 10^7 \text{ cm/s}$	$6.5 \times 10^7 \text{ cm/s}$
Fast surface state density	NFS	$9 \times 10^{11}/\text{cm}^2$	$3 \times 10^{11}/\text{cm}^2$
Surface state density	NSS	$1 \times 10^{10}/\text{cm}^2$	$1 \times 10^{10}/\text{cm}^2$

## B.3 JUNCTION FIELD-EFFECT TRANSISTORS (JFETs)

### CIRCUIT SYMBOLS AND JFET MODEL SUMMARY

Figure B.3 presents the circuit symbols and terminal voltages and currents for *n*-channel and *p*-channel JFETs.

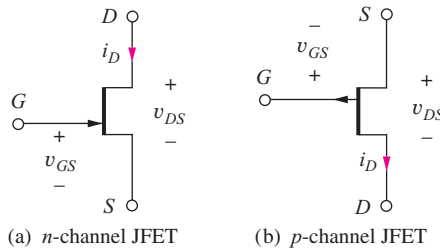


**Figure B.3** *n*-channel and *p*-channel JFET circuit symbols.

### *n*-CHANNEL JFET

$$i_G \cong 0 \quad \text{for } v_{GS} \leq 0; V_P < 0$$

#### Cutoff Region

$$i_D = 0 \quad \text{for } v_{GS} \leq V_P$$

#### Linear Region

$$i_D = \frac{2I_{DSS}}{V_P^2} \left( v_{GS} - V_P - \frac{v_{DS}}{2} \right) v_{DS} \quad \text{for } v_{GS} - V_P \geq v_{DS} \geq 0$$

#### Saturation Region

$$i_D = I_{DSS} \left( 1 - \frac{v_{GS}}{V_P} \right)^2 (1 + \lambda v_{DS}) \quad \text{for } v_{DS} \geq v_{GS} - V_P \geq 0$$

### *p*-CHANNEL JFET

$$i_G \cong 0 \quad \text{for } v_{GS} \geq 0; V_P > 0$$

#### Cutoff Region

$$i_D = 0 \quad \text{for } v_{GS} \geq V_P$$

#### Linear Region

$$i_D = \frac{2I_{DSS}}{V_P^2} \left( v_{SG} - V_P - \frac{v_{DS}}{2} \right) v_{DS} \quad \text{for } v_{GS} - V_P \leq v_{DS} \leq 0$$

#### Saturation Region

$$i_D = I_{DSS} \left( 1 - \frac{v_{GS}}{V_P} \right)^2 (1 + \lambda |v_{DS}|) \quad \text{for } v_{DS} \leq v_{GS} - V_P \leq 0$$

**TABLE B.4**  
JFET Device Parameters for SPICE Simulation (NJF/PJF)

PARAMETER	SYMBOL	NJF DEFAULT	NJF EXAMPLE
Pinch-off voltage ( $V_P$ )	VTO	-2 V	-2 V (+2 V for PJF)
Transconductance parameter	BETA = $\left(\frac{2I_{DSS}}{V_P^2}\right)$	100 $\mu\text{A}/\text{V}^2$	250 $\mu\text{A}/\text{V}^2$
Channel-length modulation	LAMBDA	0 $\text{V}^{-1}$	0.02 $\text{V}^{-1}$
Ohmic drain resistance	RD	0	100 $\Omega$
Ohmic source resistance	RS	0	100 $\Omega$
Zero-bias gate-source capacitance	CGS	0	10 pF
Zero-bias gate-drain capacitance	CGD	0	5 pF
Gate built-in potential	PB	1 V	0.75 V
Gate saturation current	IS	$10^{-14}$ A	$10^{-14}$ A

## B.4 BIPOLAR-JUNCTION TRANSISTORS (BJTs)

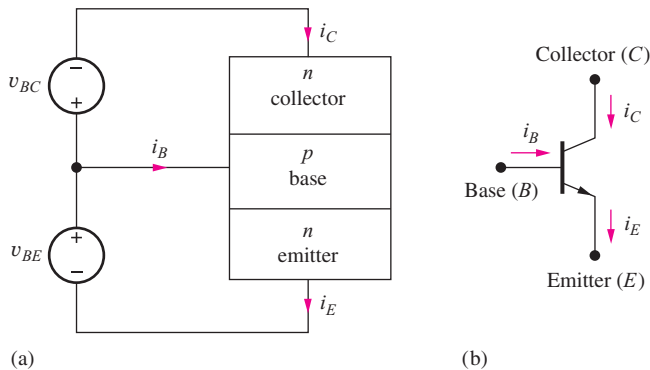


Figure B.4 npn Transistor.

## TRANSPORT MODEL EQUATIONS

$$i_E = I_S \left[ \exp \left( \frac{v_{BE}}{V_T} \right) - \exp \left( \frac{v_{BC}}{V_T} \right) \right] + \frac{I_S}{\beta_F} \left[ \exp \left( \frac{v_{BE}}{V_T} \right) - 1 \right]$$

$$i_C = I_S \left[ \exp \left( \frac{v_{BE}}{V_T} \right) - \exp \left( \frac{v_{BC}}{V_T} \right) \right] - \frac{I_S}{\beta_R} \left[ \exp \left( \frac{v_{BC}}{V_T} \right) - 1 \right]$$

$$i_B = \frac{I_S}{\beta_F} \left[ \exp \left( \frac{v_{BE}}{V_T} \right) - 1 \right] + \frac{I_S}{\beta_R} \left[ \exp \left( \frac{v_{BC}}{V_T} \right) - 1 \right]$$

$$\beta_F = \frac{\alpha_F}{1 - \alpha_F} \quad \text{and} \quad \beta_R = \frac{\alpha_R}{1 - \alpha_R}$$

**TABLE B.5**  
Regions of Operation of the Bipolar Transistor

BASE-EMITTER JUNCTION		BASE-COLLECTOR JUNCTION
FORWARD BIAS	FORWARD BIAS	REVERSE BIAS
	Saturation region (closed switch)	Forward active region (good amplifier)
REVERSE BIAS	Reverse active region (poor amplifier)	Cutoff region (open switch)

### *npn* FORWARD-ACTIVE REGION, INCLUDING EARLY EFFECT

$$i_C = I_S \left[ \exp \left( \frac{v_{BE}}{V_T} \right) \right] \left[ 1 + \frac{v_{CE}}{V_A} \right]$$

$$\beta_F = \beta_{FO} \left[ 1 + \frac{v_{CE}}{V_A} \right]$$

$$i_B = \frac{I_S}{\beta_{FO}} \left[ \exp \left( \frac{v_{BE}}{V_T} \right) \right]$$

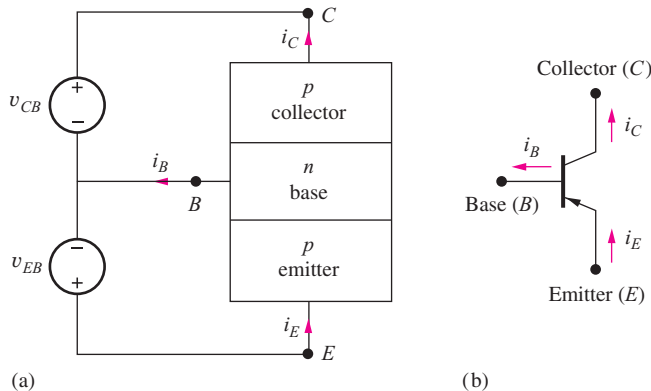


Figure B.5 *pnp* Transistor.

### TRANSPORT MODEL EQUATIONS

$$i_E = I_S \left[ \exp \left( \frac{v_{EB}}{V_T} \right) - \exp \left( \frac{v_{CB}}{V_T} \right) \right] + \frac{I_S}{\beta_F} \left[ \exp \left( \frac{v_{EB}}{V_T} \right) - 1 \right]$$

$$i_C = I_S \left[ \exp \left( \frac{v_{EB}}{V_T} \right) - \exp \left( \frac{v_{CB}}{V_T} \right) \right] - \frac{I_S}{\beta_R} \left[ \exp \left( \frac{v_{CB}}{V_T} \right) - 1 \right]$$

$$i_B = \frac{I_S}{\beta_F} \left[ \exp \left( \frac{v_{EB}}{V_T} \right) - 1 \right] + \frac{I_S}{\beta_R} \left[ \exp \left( \frac{v_{CB}}{V_T} \right) - 1 \right]$$

$$\beta_F = \frac{\alpha_F}{1 - \alpha_F} \quad \text{and} \quad \beta_R = \frac{\alpha_R}{1 - \alpha_R}$$

### *pnp* FORWARD-ACTIVE REGION, INCLUDING EARLY EFFECT

$$i_C = I_S \left[ \exp \left( \frac{v_{EB}}{V_T} \right) \right] \left[ 1 + \frac{v_{EC}}{V_A} \right]$$

$$\beta_F = \beta_{FO} \left[ 1 + \frac{v_{EC}}{V_A} \right]$$

$$i_B = \frac{I_S}{\beta_{FO}} \left[ \exp \left( \frac{v_{EB}}{V_T} \right) \right]$$

**TABLE B.6**Bipolar Device Parameters for Circuit Simulation (*npn/pnp*)

PARAMETER	NAME	DEFAULT	TYPICAL <i>npn</i> VALUES
Saturation current	IS	$10^{-16}$ A	$3 \times 10^{-17}$ A
Forward current gain	BF	100	100
Forward emission coefficient	NF	1	1.03
Forward Early voltage	VAF	$\infty$	75 V
Reverse current gain	BR	1	0.5
Base resistance	RB	0	$100 \Omega$
Collector resistance	RC	0	$10 \Omega$
Emitter resistance	RE	0	$1 \Omega$
Forward transit time	TF	0	0.15 nS
Reverse transit time	TR	0	15 nS
Base-emitter junction capacitance	CJE	0	0.5 pF
Base-emitter junction potential	PHIE	0.75 V	0.8 V
Base-emitter grading coefficient	ME	0.5	0.5
Base-collector junction capacitance	CJC	0	1 pF
Base-collector junction potential	PHIC	0.75 V	0.7 V
Base-collector grading coefficient	MC	0.33	0.33
Collector-substrate junction capacitance	CJS	0	3 pF

# APPENDIX C

## Two-Port Review

The **two-port network** in Fig. C.1a is very useful for modeling the behavior of amplifiers in complex systems. We can use the two-port to provide a relatively simple representation of a much more complicated circuit. Thus, the two-port helps us hide or encapsulate the complexity of the circuit, so we can more easily manage the overall analysis and design. One important limitation must be remembered, however. The two-ports we use are linear network models, and are valid under small-signal conditions that are fully discussed in Chapter 13.

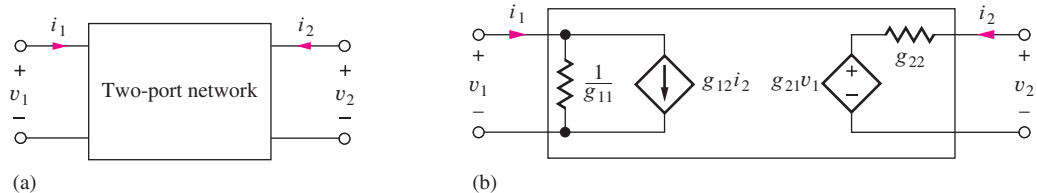


**Figure C.1** (a) Two-port network representation. (b) Two port  $g$ -parameter representation.

From network theory, we know that two-port networks can be represented in terms of **two-port parameters**. Four of these sets are often used as models for amplifiers: the  $g$ -,  $h$ -,  $y$ -, and  $z$ -parameters; the  $s$ - and  $abcd$ -parameters are not required here. Note in these two-port representations that  $(v_1, i_1)$  and  $(v_2, i_2)$  represent the signal components of the voltages and currents at the two ports of the network.

### C.1 THE $g$ -PARAMETERS

The  **$g$ -parameter** description is one of the most commonly used representations for a voltage amplifier:

$$\begin{aligned}\mathbf{i}_1 &= g_{11}\mathbf{v}_1 + g_{12}\mathbf{i}_2 \\ \mathbf{v}_2 &= g_{21}\mathbf{v}_1 + g_{22}\mathbf{i}_2\end{aligned}\tag{C.1}$$

Figure C.1b is a network representation of these equations.

The  $g$ -parameters are determined from a given network using a combination of **open-circuit** ( $i = 0$ ) and **short-circuit** ( $v = 0$ ) **termination** conditions by applying these parameter definitions:

$$\begin{aligned}g_{11} &= \left. \frac{\mathbf{i}_1}{\mathbf{v}_1} \right|_{\mathbf{i}_2=0} = \text{open-circuit input conductance} \\ g_{12} &= \left. \frac{\mathbf{i}_1}{\mathbf{i}_2} \right|_{\mathbf{v}_1=0} = \text{reverse short-circuit current gain} \\ g_{21} &= \left. \frac{\mathbf{v}_2}{\mathbf{v}_1} \right|_{\mathbf{i}_2=0} = \text{forward open-circuit voltage gain} \\ g_{22} &= \left. \frac{\mathbf{v}_2}{\mathbf{i}_2} \right|_{\mathbf{v}_1=0} = \text{short-circuit output resistance}\end{aligned}\tag{C.2}$$

## C.2 THE HYBRID OR $h$ -PARAMETERS

The  **$h$ -parameter** description is also widely used in electronic circuits and is one convenient model for a current amplifier:

$$\begin{aligned}\mathbf{v}_1 &= h_{11}\mathbf{i}_1 + h_{12}\mathbf{v}_2 \\ \mathbf{i}_2 &= h_{21}\mathbf{i}_1 + h_{22}\mathbf{v}_2\end{aligned}\quad (\text{C.3})$$

Figure C.2 is the network representation of these equations.

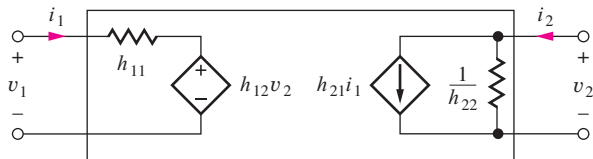


Figure C.2 Two-port  $h$ -parameter representation.

As with the  $g$ -parameters, the  $h$ -parameters are determined from a given network using a combination of open- and short-circuit measurement conditions:

$$\begin{aligned}h_{11} &= \frac{\mathbf{v}_1}{\mathbf{i}_1} \Big|_{\mathbf{v}_2=0} = \text{short-circuit input resistance} \\ h_{12} &= \frac{\mathbf{v}_1}{\mathbf{v}_2} \Big|_{\mathbf{i}_1=0} = \text{reverse open-circuit voltage gain} \\ h_{21} &= \frac{\mathbf{i}_2}{\mathbf{i}_1} \Big|_{\mathbf{v}_2=0} = \text{forward short-circuit current gain} \\ h_{22} &= \frac{\mathbf{i}_2}{\mathbf{v}_2} \Big|_{\mathbf{i}_1=0} = \text{open-circuit output conductance}\end{aligned}\quad (\text{C.4})$$

## C.3 THE ADMITTANCE OR $y$ -PARAMETERS

The admittance, or  **$y$ -parameter**, description is useful in modeling transconductance amplifiers.

$$\begin{aligned}\mathbf{i}_1 &= y_{11}\mathbf{v}_1 + y_{12}\mathbf{v}_2 \\ \mathbf{i}_2 &= y_{21}\mathbf{v}_1 + y_{22}\mathbf{v}_2\end{aligned}\quad (\text{C.5})$$

Figure C.3 is a network representation of these equations.

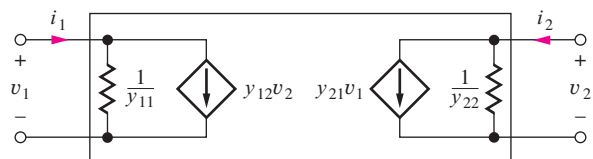


Figure C.3 Two-port  $y$ -parameter representation.

The  $y$ -parameters are often referred to as the short-circuit parameters because they are determined from a given network using only short-circuit terminations:

$$\begin{aligned} y_{11} &= \left. \frac{\mathbf{i}_1}{\mathbf{v}_1} \right|_{\mathbf{v}_2=0} = \text{short-circuit input conductance} \\ y_{12} &= \left. \frac{\mathbf{i}_1}{\mathbf{v}_2} \right|_{\mathbf{v}_1=0} = \text{reverse short-circuit transconductance} \\ y_{21} &= \left. \frac{\mathbf{i}_2}{\mathbf{v}_1} \right|_{\mathbf{v}_2=0} = \text{forward short-circuit transconductance} \\ y_{22} &= \left. \frac{\mathbf{i}_2}{\mathbf{v}_2} \right|_{\mathbf{v}_1=0} = \text{short-circuit output conductance} \end{aligned} \quad (C.6)$$

## C.4 THE IMPEDANCE OR $z$ -PARAMETERS

The impedance, or  **$z$ -parameters**, can also be used for modeling voltage amplifiers.

$$\begin{aligned} \mathbf{v}_1 &= z_{11}\mathbf{i}_1 + z_{12}\mathbf{i}_2 \\ \mathbf{v}_2 &= z_{21}\mathbf{i}_1 + z_{22}\mathbf{i}_2 \end{aligned} \quad (C.7)$$

Figure C.4 is a network representation of Eq. (C.7).

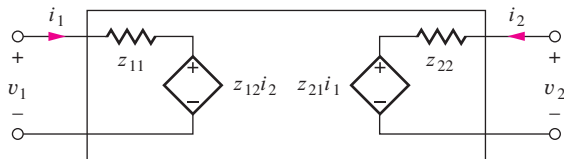


Figure C.4 Two-port  $z$ -parameter representation.

The  $z$ -parameters are determined from a given network using open-circuit measurement conditions and are often referred to as the open-circuit parameters:

$$\begin{aligned} z_{11} &= \left. \frac{\mathbf{v}_1}{\mathbf{i}_1} \right|_{\mathbf{i}_2=0} = \text{open-circuit input resistance} \\ z_{12} &= \left. \frac{\mathbf{v}_1}{\mathbf{i}_2} \right|_{\mathbf{i}_1=0} = \text{reverse open-circuit transresistance} \\ z_{21} &= \left. \frac{\mathbf{v}_2}{\mathbf{i}_1} \right|_{\mathbf{i}_2=0} = \text{forward open-circuit transresistance} \\ z_{22} &= \left. \frac{\mathbf{v}_2}{\mathbf{i}_2} \right|_{\mathbf{i}_1=0} = \text{open-circuit output resistance} \end{aligned} \quad (C.8)$$

# INDEX

## A

$A_{cm}$ , 650  
 $A_{dm}$ , 650  
 $A_P$ , 533  
 $A_v$ , 532–533  
 $A_\beta$ , 604  
ac-coupled amplifier circuit, 794  
ac coupling, 790  
ac equivalent circuit  
    BJT amplifier, 793–794  
    C-C amplifier, 886  
    C-D amplifier, 886  
circuit analysis, 792–796  
MOSFET amplifier, 795–796  
transformer-coupled inverting  
    amplifier, 1014  
    two-stage op amp, 994  
AC voltmeter, 762  
Acceptor energy level ( $E_A$ ), 62  
Acceptor impurities, 52  
Acceptor impurity concentration, 53  
Accumulation, 147  
Accumulation region, 147  
Active filter, 579, 714–728  
Active high-pass filter, 581–582  
Active load, 1081–1091, 1092–1097  
Active low-pass filter, 578–581  
Active pull-up circuit, 500  
Active region, 155  
Active-size mask, 174  
A/D conversion. *See* Analog-to-digital  
    (A/D) conversion  
ADC. *See* Analog-to-digital (A/D)  
    conversion  
Address decoder, 440–444  
Admittance parameters, 1311–1312  
AF, 530  
Agilent Technologies, 713  
Alignment tolerance, 173  
All-pass amplifier, 26  
Allen, Ross, 713  
 $\alpha_F$ , 221  
 $\alpha_R$ , 223  
AM demodulation, 122  
Amorphous materials, 45  
Amplification, 531–534

Amplification factor, 803  
Amplifier, 22–26  
    ac analysis, 792–793  
    band-pass, 575–577  
    BiCMOS, 1004  
    BJT, 788–789, 793–794  
    C-B. *See* C-B/C-G amplifiers  
    C-C. *See* C-C/C-D amplifiers  
    C-D. *See* C-C/C-D amplifiers  
    C-E. *See* C-E amplifier  
    C-G. *See* C-B/C-G amplifiers  
    C-S. *See* C-S amplifier  
    cascaded, 698–711  
    cascode, 1184  
    class-A, 1006–1008  
    class-AB, 1010–1011  
    class-B, 1008–1009  
    clocked sense, 438–440  
    closed-loop, 699  
    compensated, 1260–1262  
    current, 633–637  
    dc analysis, 792  
    dc-coupled, 550, 969  
    difference, 565–567  
    differential. *See* Differential amplifier  
    distortion, 548  
    feedback, 604. *See also*; Feedback  
        amplifier; Transistor feedback  
        amplifier  
    frequency response. *See* Amplifier  
        frequency response  
    high-pass, 572–574  
    ideal op amp. *See* Ideal op amp  
    ideal voltage, 542  
    instrumentation, 711–712  
    inverting. *See* Inverting amplifier  
    limiting, 988–989  
    linear, 531  
    low-pass, 568–572  
    MOSFET, 789–790, 795–796  
    multistage, 939–948  
    noninverting. *See* Noninverting  
        amplifier  
    op amp. *See* Operational amplifier  
        (op amp)  
    open-loop, 601, 699, 1229  
    OTA, 1087  
    power dissipation, 839–840  
RF, 1194  
selecting a configuration,  
    912–914  
sense, 434–440  
series-series feedback, 629–633  
series-shunt feedback, 617–622  
shunt-peaked, 1194–1196  
shunt-series feedback, 633–637  
shunt-shunt feedback, 624–628  
signal source, 841–842  
single-transistor. *See* Single-transistor  
    amplifiers  
single-tuned, 1197–1198  
summing amplifier, 563  
terminology, 699, 700  
transconductance, 629–633  
transistor, 787–790  
transresistance, 556–557, 624–628  
tuned, 1194  
uncompensated, 1254–1255  
voltage, 617–622  
Amplifier frequency response, 25–26,  
    1128–1227  
amplifier gain-bandwidth limitations,  
    1180–1181  
balanced modulator, 1205–1212  
base resistance, 1155–1157  
C-B/C-G amplifier high-frequency  
    response, 1174–1176  
C-C/B cascade, 1182–1184  
C-C/C-D amplifier high-frequency  
    response, 1177–1179  
cascode amplifier, 1184  
current mirror, 1185–1186  
differential amplifier, 1181–1182  
high-frequency C-E/C-S amplifier  
    analysis, 1158–1174  
high-frequency response. *See*  
    High-frequency response  
limitations of high-frequency  
    model, 1155  
low-frequency poles and zeros (C-S  
    amplifier), 1134–1139  
low-frequency response, 1130  
Miller effect, 1160  
mixer, 1205–1213  
multistage amplifier frequency  
    response, 1187–1193

Amplifier frequency response—*Cont.*  
 $\omega_H$  (absence of dominant pole), 1133–1134  
 $\omega_H$  (OCTC method), 1167–1170  
 $\omega_L$  (absence of dominant pole), 1130–1131  
 $\omega_L$  (SCTC method), 1139–1147  
RF circuits, 1193–1204  
shunt-peaked amplifier, 1194–1196  
single-tuned amplifier, 1197–1198  
summary/review, 1213–1215  
synchronous/stagger tuning, 1201  
tapped inductor/auto transformer, 1199–1200  
transistor models at high-frequency, 1148–1155  
unity-gain frequency, 1149–1151, 1153  
upper-cutoff frequency/single-stage amplifiers, 1180  
Amplifier gain-bandwidth limitations, 1180–1181  
Amplifier terminology, 699, 700  
Amplitude stabilization, 757–758, 1280  
Analog electronics. *See also* subentries  
amplifier frequency response, 1128–1227  
analog I/C design templates, 1046–1127  
analog systems and ideal op amps, 529–599  
differential amplifiers and op amp design, 968–1045  
nonideal op amps and feedback amplifier stability, 600–696  
op amp applications, 697–785  
single transistor amplifiers, 857–967  
small-signal modeling and linear amplification, 786–856  
transistor feedback amplifiers and oscillators, 1228–1299  
Analog function generators, 767  
Analog integrated circuit design techniques, 1046–1127  
active load in op amps, 1092–1097  
bandgap reference, 1077–1081  
bipolar differential amplifier with active load, 1088–1091  
bipolar op amp, 1095, 1096  
CMOS differential amplifier with active load, 1081–1086  
CMOS op amp, 1092–1095  
current element matching, 1047–1048  
current mirror. *See* Current mirror  
Gilbert multiplier, 1110–1112

input stage breakdown, 1096–1097  
reference current operation, 1072  
741 design. *See* μA741 op amp  
summary/review, 1112–1113  
supply-independent biasing, 1073–1077  
 $V_{BE}$ -based reference, 1073  
Analog signals, 9–10  
Analog systems and ideal op amps, 529–599  
active high-pass filter, 581–582  
active low-pass filter, 578–581  
amplification, 531–534  
band-pass amplifier, 575–577  
Bode plot, 568  
current gain, 533  
decibel scale, 534  
difference amplifier, 565–567  
differential amplifier, 544–547. *See also* Differential amplifier  
differentiator, 586  
distortion, 548  
frequency dependent feedback, 568–586  
high-pass amplifier, 572–574  
ideal differential amplifier, 551  
ideal op amp. *See* Ideal op amp  
integration, 582–583  
inverting amplifier. *See* Inverting amplifier  
low-pass amplifier, 568–572  
mismatched source and load resistance, 541–542  
noninverting amplifier. *See* Noninverting amplifier  
op amp. *See* Operational amplifier (op amp)  
power gain, 533  
summary/review, 586–587  
summing amplifier, 563  
transresistance amplifier, 556–557  
two-port model, 537–538  
unity-gain buffer, 561  
voltage gain, 532–533  
Analog-to-digital (A/D) conversion, 11, 740–754  
block diagram, 741, 743  
counter-ramp converter, 747  
counting ADC, 744  
delta-sigma A/D converter, 750–754  
dual-ramp (dual-slope) ADC, 748–749  
errors, 742–743  
flash converter, 749–750  
fundamentals, 741  
normal-mode rejection, 749

single-ramp (single-slope) ADC, 746–747  
successive approximation converter, 744–746  
transfer characteristics, 742  
Analog-to-digital converter errors, 742–743  
AND gate, 295  
AND gate symbol, 296  
AND-OR-INVERT (AOI), 296, 329, 394, 505  
Anode, 75  
AOI, 296, 329, 394, 505  
Applications. *See* Electronics in action; Operational amplifier applications  
Approximate polynomial factorization, 1163  
Array personalization, 445  
Associative law, 296  
Astable multivibrator, 765–766  
AU digital thermometer, 1062  
Audio frequency (AF), 530  
Audion, 529  
Auto transformer, 1199–1200  
Avalanche breakdown, 91, 92  
Average propagation delay, 294

## B

Back-gate transconductance parameter, 819  
Bag phone, 8  
Balanced modulator, 1205–1212  
Balanced output, 975  
Band-pass amplifier, 25, 575–577  
Band-pass filter, 720–721  
Band-reject amplifier, 25  
Bandgap energy, 47  
Bandgap reference, 1077–1081  
Bandwidth, 1229  
Bandwidth (BW), 570  
Bandwidth shrinkage factor, 705  
Bardeen, John, 3–5, 217  
Barkhausen criteria, 754  
Base, 218  
Base-collector capacitance, 253  
Base current, 219  
Base-emitter capacitance, 253  
Base resistance, 1155–1157  
Base transit time, 247–249  
Base-width modulation, 251  
Battery chargers, 128  
Baumgartner, Dick, 713

- Bell Laboratories, 4, 217  
 $\beta$ , 604  
 $\beta_F$ , 221  
 $\beta_{FOR}$ , 243  
 $\beta_R$ , 222  
 Beta-cutoff frequency, 250, 1150  
 BFSK, 722  
 Bias  
   BJT, 265–266  
   constant gate-source voltage, 178–180  
   dc, 176, 256  
   depletion-mode MOSFET, 198–200  
   electronic current source/differential amplifier, 982  
   forward, 86, 93  
   four-resistor, 182–184, 188, 258–266  
   input-bias current, 645–646  
   JFET, 198–200  
   μA741 op amp, 1098, 1101–1103  
   NMOS transistor, 176–187  
   reverse, 85, 89–92, 92–93, 104  
   supply-independent biasing,  
     1073–1077  
   tolerances, 266–272  
   two-resistor, 264–265  
   zero, 85  
 Bias point, 96  
 BiCMOS buffer, 509–511  
 BiCMOS logic, 509–513  
 BiCMOS op amp, 1004  
 BiFET processes, 190  
 BiFET technologies, 983  
 Binary digital signals, 9  
 Binary frequency shift keying (BFSK), 722  
 BiNMOS buffer, 511, 512  
 BiNMOS inverter, 511–513  
 Bipolar amplifier compensation, 1266  
 Bipolar differential amplifier, 970, 1181  
 Bipolar differential amplifier with active load, 1088–1091  
 Bipolar junction transistor (BJT), 217–284  
   amplifier, 788–789, 793–794  
   base transit time, 247–249  
   bias, 256–266  
   cutoff region, 231–233  
   diffusion capacitance, 249  
   diodes, 239  
   Early effect/Early voltage, 250–252  
   forward-active region, 233–239  
   four-resistor bias network, 258–266  
   frequency dependence of  
     common-emitter current gain, 250  
   frequency-dependent hybrid-pi model,  
     1148–1149  
   high-performance BJT, 255  
   *i-v* characteristics, 228–230  
   input/output resistance, 838  
   intrinsic voltage gain, 803  
   junction breakdown voltage, 246  
   minority-carrier transport,  
     246–247  
   model parameters, 1151–1152  
   Monte Carlo analysis, 269–272  
   most important part, 218  
   nonideal behavior, 245–252  
   *n-p-n* transistor. *See n-p-n* transistor  
   output characteristics, 228–229  
   parasitic bipolar transistor, 401  
   physical structure, 218–219  
   *p-n-p* transistor. *See p-n-p* transistor  
   regions of operation, 230–231  
   reverse-active region, 240–242  
   saturated BJT, 487–493  
   saturation region, 242–245, 263–264  
   signal injection and extraction,  
     858–859  
   single-transistor amplifiers, 903–905  
   small-signal models, 799–808, 864  
   small-signal parameters, 822, 864  
   SPICE, 253–255, 1307–1309  
   summary/review, 272–273  
   tolerances in bias circuits, 266–272  
   transconductance, 255  
   transfer characteristics, 229–230  
   transport model simplifications,  
     231–242  
   two-resistor biasing, 264–265  
   voltage gain, 838  
   worst-case analysis, 267–269  
 Bipolar logic circuits, 460–526  
 BiCMOS logic, 509–513  
 BiNMOS inverter, 511–513  
 current mode logic, 481–485  
 current source implementation, 469  
 current switch, 461–464  
 ECL gate. *See ECL gate*  
 emitter dotting, 476–477  
 emitter follower, 473–476, 477  
 saturating bipolar inverter, 487–493  
 summary/review, 513–515  
 TTL. *See Transistor-transistor logic (TTL)*  
   wired-OR logic, 477  
 Bipolar op amp, 1095, 1096  
 Bipolar transconductance, 252  
 Bipolar transistor, 5. *See also Bipolar junction transistor (BJT)*  
 Bipolar transistor current sources,  
     1019–1022  
 Bipolar transistor model parameters,  
     1151–1152  
 Bipolar transistor PTAT cell, 240  
 Bistable circuits, 419, 765  
 Bistable multivibrator, 765  
 Bitline (BL), 419  
 Bitline precharge, 431  
 BJT. *See Bipolar junction transistor (BJT)*  
 BJT amplifier, 788–789, 793–794  
 BJT cascode current source, 1067  
 BJT current mirror, 1049, 1052–1055  
 BJT noise model, 824  
 BJT small-signal parameters, 804  
 BJT Wilson current source, 1064  
 BL, 419  
 Black, Harold, 1228  
 BlackBerry, 383  
 Blackman, R. B., 617  
 Blackman's theorem, 617, 635, 1069,  
     1230, 1233, 1234  
 Blalock, Travis, 329, 713  
 Bode plot, 568, 678–680  
 Body effect, 159, 186, 385, 818–819  
 Body-effect parameter, 159  
 Body terminal, 149  
 Boltzmann's constant, 824  
 Boolean algebra, 295–297  
 Boolean identities, 296  
 Brattain, Walter, 3–5, 217  
 Breakdown region, 91, 92  
 Breakdown voltage, 91  
 Breakdown voltage temperature coefficient, 92  
 Brokaw, Paul, 1078  
 Brokaw version (bandgap reference), 1078  
 Buck-gate transconductance, 818  
 Buffered current mirror, 1056–1057  
 Buffered Widlar source, 1061  
 Built-in potential, 77  
 Bulk terminal, 163  
 Butterworth filter, 714  
 BW, 570  
 Bypass capacitor, 790

## C

- $C_{BC}$ , 253  
 $C_{BE}$ , 253  
 $C_D$ , 93  
 $C_{DB}$ , 166  
 $C_{GD}$ , 166  
 $C_{GDO}$ , 166  
 $C_{GS}$ , 166

- $C_{GSO}$ , 166  
 $C_{SB}$ , 166  
C-B/C-G amplifiers, 894–903  
base resistor, 1157, 1158  
capacitor design, 921–924  
current gain, 898, 899  
design example, 930–933  
example, 899–902  
high-frequency response, 1174–1176  
input resistance, 895, 899  
input signal range, 897  
limiting conditions, 897  
Monte Carlo evaluation, 934–935  
 $\omega_L$ , 1145–1146  
operation, 896  
overall input/output resistance, 899  
overview, 858, 863, 951  
resistance at collector and drain terminals, 897–898  
signal source voltage gain, 896  
summary table, 903  
terminal voltage gain, 895  
upper-cutoff frequency, 1180  
C-C/C-B cascade, 1182–1184  
C-C/C-D amplifiers, 886–894  
base resistance, 1157, 1158  
capacitor design, 919–921  
circuit simplification, 862  
current gain, 890  
design example, 926–929  
example, 891–894  
follower operation, 887  
follower signal range, 888  
high-frequency response, 1177–1179  
input resistance, 887–888  
 $\omega_L$ , 1147  
op amp, 998, 999  
output resistance, 889  
overview, 858, 861, 951  
signal source voltage gain, 888  
summary table, 891  
terminal voltage gain, 886  
upper-cutoff frequency, 1180  
C-2C ladder DAC, 740  
C-D amplifier. *See* C-C/C-D amplifiers  
C-E amplifier, 808–814, 860, 864–877  
base resistor, 1157, 1158  
bypassed emitter, 875–876, 877  
capacitor design, 914–918  
design guide, 810–811  
emitter degeneration resistance, 1172–1174  
equivalent transistor representation, 885–886  
high frequency analysis, 1158–1174  
input resistance, 809, 830–831, 866–867  
large emitter resistance, 868  
lower cutoff frequency, 1143–1144  
Monte Carlo analysis, 814  
 $\omega_L$ , 1140–1142  
operation, 868, 869  
output resistance, 812–833, 839, 871  
overview, 838, 877, 884  
poles, 1163–1164  
resistance at collector of bipolar transistor, 869–871  
signal source voltage gain, 810, 867  
small-signal limit, 812, 869  
terminal current gain, 871  
terminal voltage gain, 809, 866  
upper bound, 812  
upper-cutoff frequency, 1180  
voltage gain, 812–814, 872–876  
zero emitter resistance, 867  
C-G amplifier. *See* C-B/C-G amplifiers  
C-S amplifier, 824–833, 860, 877–886  
C-E amplifier, compared, 838, 884, 885  
capacitor design, 914–918  
design example, 935–938  
design guide, 826–827  
dominant pole, 1166–1167  
equivalent transistor representation, 885–886  
high frequency analysis, 1158–1174  
inductive degeneration, 1202–1203  
JFET, 833–837  
MOS inverters, 907–911  
 $\omega_L$ , 1144  
operation, 880  
overview, 838, 884  
poles and zeros, 1134–1139  
signal source voltage gain, 825–826, 879  
small-signal limit, 827, 880–881  
source degeneration resistance, 1170–1172  
terminal voltage gain, 825, 878–879  
upper-cutoff frequency, 1180  
voltage gain, 827–829, 879, 881–883  
zero resistance in the source, 880  
Capacitance  
base-collector, 253  
base-emitter, 253  
bitline, 431  
 $C_{DB}$ , 166  
 $C_{GD}$ , 166  
 $C_{GDO}$ , 166  
 $C_{GS}$ , 166  
 $C_{GSO}$ , 166  
 $C_{SB}$ , 166  
diffusion, 93, 249  
gate, 170  
gate-channel, 166  
JFET, 196  
logic circuits, 337  
Miller, 1258  
MOS device, 337–338  
MOS transistors, 165–167  
pn junction, 92–93  
zero-bias junction, 93  
Capacitance per unit length, 166  
Capacitor, 790  
bypass, 790  
C-B/C-G amplifiers, 921–924  
C-C/C-D amplifiers, 919–921  
C-E/C-S amplifiers, 914–918  
cell, 430  
compensation, 1264  
coupling, 790  
dc blocking, 790  
lower-cutoff frequency, 924–925  
MOS, 146–148  
standard values, 1302  
Cascade current sources, 1066–1069  
Cascaded amplifier, 698–711  
Cascode amplifier, 1184  
Cathode, 75  
CCCS, 13  
CCD camera, 63  
CCVS, 13  
Cell capacitor, 430  
Cell phone chargers, 128  
Cellular phone evolution, 8  
Center frequency, 1198  
Center-tapped transformer, 123  
Channel length, 149  
Channel length dependence, 1153  
Channel-length modulation, 157–158  
Channel-length modulation parameter, 158  
Channel region, 149  
Channel width, 149  
Charge-coupled device (CCD) camera, 63  
Charge neutrality, 53  
Charge sharing, 431  
Charge transfer, 433  
Chemical vapor deposition (CVD), 64  
Clamping diodes, 506  
Class-A amplifier, 1006–1008  
Class-AB amplifier, 1010–1011  
Class-B amplifier, 1008–1009  
Class-B push-pull output stage, 1008  
Class-D audio amplifier, 1015–1016

- Classic feedback systems, 601–602  
 Clocked CMOS sense amplifier, 438–440  
 Closed-loop amplifier, 699  
 Closed-loop feedback amplifier two-port model, 698  
 Closed-loop gain  
     feedback amplifier, 602, 617  
     feedback amplifier analysis at midband, 1232  
     negative feedback amplifier, 1230  
     series-series feedback amplifier, 630  
     series-shunt feedback amplifier, 618  
     shunt-series feedback amplifier, 634  
     shunt-shunt feedback amplifier, 625  
 CML, 461. *See Current mode logic (CML)*  
 CML D-latch, 484  
 CML logic gates, 481–482  
 CML power reduction, 484–485  
 CMOS camera on a chip, 164  
 CMOS differential amplifier with active load, 1081–1086  
 CMOS imager circuitry, 915  
 CMOS inverter. *See CMOS logic design*  
 CMOS logic design, 367–415  
     cascade buffer, 397–399  
     cascaded inverters, 379–380  
     CMOS inverter technology, 368–370  
     CMOS latchup, 401–402  
     CMOS NOR/NAND gates, 384–388  
     CMOS reference inverter, 376,  
         377, 378  
     CMOS transistor parameters, 369  
     CMOS transmission gate, 400–401  
     CMOS voltage transfer characteristics, 371–373  
     complex logic gates, 388–392  
     dynamic behavior of CMOS inverter, 375–380  
     dynamic domino CMOS logic, 395–397  
     fall time, 377  
     minimum size gate design, 393–395  
     noise margin, 373–375  
     PDP, 382  
     performance scaling, 377  
     power dissipation, 380–381  
     propagation delay estimate, 375–376  
     rise time, 377  
     static characteristics of CMOS inverter, 370–375  
     summary/review, 404–405  
     symmetrical CMOS inverter, 371–373  
 CMOS logic gate structure, 384  
 CMOS navigation chip prototype for optical mouse, 713  
 CMOS op amp, 1092–1095  
 CMOS op amp analysis, 1093–1095  
 CMOS op amp prototype, 1002–1004  
 CMRR. *See Common-mode rejection ratio (CMRR)*  
 Collector, 218  
 Collector current, 219  
 Colpitts crystal oscillator, 1285  
 Colpitts oscillator, 1278–1279  
 Column address decoder, 418  
 Common-base amplifier. *See C-B/C-G amplifiers*  
 Common-base current gain, 899  
 Common-base output characteristics, 229  
 Common-collector amplifier.  
     *See C-C/C-D amplifiers*  
 Common-collector/common-base cascade, 1182–1184  
 Common-drain amplifier. *See C-C/C-D amplifiers*  
 Common-emitter amplifier. *See C-E amplifier*  
 Common-emitter/common-base current gain comparison, 220  
 Common-emitter output characteristics, 228  
 Common-emitter transfer characteristics, 229  
 Common-gate amplifier. *See C-B/C-G amplifiers*  
 Common-mode conversion gain, 973  
 Common-mode error calculation, 651–652  
 Common-mode gain, 650, 973  
 Common-mode half-circuit, 980–981  
 Common-mode input resistance, 656, 977  
 Common-mode input voltage, 650  
 Common-mode input voltage range, 981  
 Common-mode rejection ratio (CMRR)  
     alternate interpretation, 657  
     CMOS differential amplifier with active load, 1085–1086  
     dB, 651  
     defined, 651  
     differential amplifier, 978–979, 987  
     importance, 651–652  
     offset voltage/bias current, 658–659  
     two-stage amplifier, 996–997  
     voltage-follower gain error, 654  
 Common-source amplifier. *See C-S amplifier*  
 Commutative law, 296  
 Comparator, 763  
 Compensated amplifier, 1260–1262  
 Compensated amplifier step response, 1259  
 Compensated semiconductor, 62  
 Compensation capacitor, 1264  
 Complementary MOS class-B amplifier, 1008  
 Complementary MOS logic design.  
     *See CMOS logic design*  
 Complementary push-pull output stage, 1008  
 Complements, 296  
 Complex CMOS gate with bridging transistor, 391–392  
 Complex CMOS logic gate design, 388–390  
 Complex NMOS logic design, 328–333  
 Component values, 1300–1302  
 Computer software. *See MATLAB; SPICE*  
 Conduction angle, 116, 1006  
 Conduction band, 61  
 Conduction interval, 116  
 Conductivity, 48  
 Constant electric field scaling, 170  
 Constant gate-source voltage bias, 178–180  
 Constant voltage drop (CVD) model, 104–105  
 Contact opening mask, 174  
 Continuous-time integrator, 729  
 Controlled sources, 12–13  
 Conversion gain, 1206  
 Conversion time, 744  
 Correlated double sampling, 164  
 Counter-ramp converter, 747  
 Counting ADC, 744  
 Coupling capacitor, 790  
 Covalent bond model, 45–48  
 Cramer's rule, 1162  
 Critical frequency, 573  
 Critically damped, 675  
 Cross-coupled inverter, 419  
 Cross-coupled transistor quad, 1048  
 Cross-over distortion, 1009  
 Cross-over region, 1009  
 Crystal oscillator, 1283–1285  
 Current amplifier, 633–637  
 Current-controlled current source (CCCS), 13  
 Current-controlled current source model, 804  
 Current-controlled voltage source (CCVS), 13  
 Current divider restrictions, 16  
 Current division, 16  
 Current element matching, 1047–1048  
 Current gain, 533, 890, 898, 899

Current gain defect, 1053  
 Current-limiting circuit, 1013  
 Current mirror, 1049–1071  
     active load, as, 1081–1091  
     BJT, 1049, 1052–1055  
     buffered, 1056–1057  
     cascade current sources, 1066–1069  
     cutoff frequency, 1185–1186  
     design example, 1070–1071  
     high-output-resistance, 1063–1069  
     mirror ratio, 1051–1055  
     MOS, 1049–1052  
     MOS Widlar source, 1063  
     multiple current sources, 1055–1056  
     other current sources, contrasted, 1049  
     output current, 1050–1051  
     output resistance, 1057–1058  
     regulated cascade current source,  
     1068–1069  
     summary table, 1069  
     two-port model, 1058–1060  
     Widlar current source,  
     1060–1061, 1063  
     Wilson current sources, 1064–1066  
 Current mode logic (CML), 461, 481–485  
     CML logic gates, 481–482  
     CML logic levels, 482  
     CML power reduction, 484–485  
     higher-level CML, 483  
     NMOS CML, 485  
      $V_{EE}$  supply voltage, 482  
 Current sink, 1017  
 Current sources. *See* Electronic current sources  
 Current switch, 461–464  
 Current switch circuit, 461  
 Current-to-voltage converter, 556  
 Cut-in voltage, 81  
 Cutoff frequency, 171  
 Cutoff region, 160, 162, 230, 231–233  
 CVD, 64  
 CVD model, 104–105

## D

D/A conversion. *See* Digital-to-analog converter (D/A) conversion  
 D/A converter errors, 734–736  
 D-FF, 450–451  
 D latch, 450  
 DAC. *See* Digital-to-analog (D/A) conversion  
 DAC circuits, 564–565

DALSA CMOS image sensor, 915  
 Damping coefficient, 674–675, 677  
 Darlington connection, 245  
 dB, 534  
 dc bias, 176, 256  
 dc blocking capacitor, 790  
 dc-coupled amplifier, 550  
 dc-coupled differential amplifier, 969  
 dc equivalent circuit  
     BJT amplifier, 793–794  
     circuit analysis, 792–796  
     MOSFET amplifier, 795–796  
     transformer-coupled inverting amplifier, 1014  
 dc reference voltage, 733  
 DDS, 759, 767–768  
 Dead zone, 1009  
 Decibel (dB), 534  
 Decibel scale, 534  
 DeForest, Lee, 529  
 Degenerative feedback, 1229  
 Delta-sigma A/D converter,  
     750–754  
 Demodulation, 531  
 DeMorgan’s theorem, 296  
 Dennard, Robert H., 416  
 Dependent sources, 12–13  
 Depletion, 148  
 Depletion layer, 76  
 Depletion-layer width, 78  
 Depletion-mode device, 150  
 Depletion-mode MOSFET, 158, 159,  
     198–200  
 Depletion region, 76, 148  
 Design example. *See also* Design note  
     active low-pass filter design, 579–581  
     bandgap reference design, 1079–1081  
     bipolar transistor current source,  
     1019–1022  
     bipolar transistor saturation voltage,  
     489–490  
     C-B amplifier, 930–933  
     C-S amplifier, 935–938  
     capacitor design/C-B and C-G  
     amplifiers, 922–924  
     capacitor design/C-C and C-D  
     amplifiers, 919–921  
     capacitor design/C-E and C-S  
     amplifiers, 917–918  
     cascade amplifier design, 706–708  
     cascade buffer design, 398–399  
     complex CMOS gate with bridging  
     transistor, 391–392  
     complex CMOS logic gate design,  
     388–390  
 current mirror, 1070–1071  
 ECL gate design, 469–471  
 electronic current source design,  
     1070–1071  
 emitter follower design, 475–476  
 follower design, 926–929  
 four-resistor bias design, 261–262  
 frequency response/multistage amplifier, 709–711  
 inverter with resistive load, 300–301  
 inverter with saturated load device,  
     310–312  
 inverting amplifier design, 555–556  
 inverting amplifier with output current limits, 648–649  
 low-pass filter design, 716–717  
 lower cutoff frequency/C-E amplifier,  
     1143–1144  
 MOSFET current source, 1023–1024  
 MOSFET op amp compensation,  
     1273–1277  
 NMOS inverter with depletion-mode load, 317–318  
 open-loop gain design, 608–610  
 operational amplifier compensation,  
     1269–1272  
 propagation delay design for inverter,  
     347–349  
 rectifier design, 126–127  
 reference current design, 1076–1077  
 reference inverter design, 378  
 selecting an amplifier configuration,  
     912–914  
 Tow-Thomás filter design, 724–726  
 transistor sizing/complex logic gates,  
     331–333  
 Design note. *See also* Design example  
     ac equivalent circuit, 792  
     bipolar transconductance, 252  
     bipolar transistor, 859  
     C-E amplifier, 868, 869  
     C-S amplifier, 880, 881  
     cascaded amplifier, 700  
     current divider restrictions, 16  
     differential amplifier, 975, 976,  
     978, 983  
     differential pair, 976, 978  
     diode, 83, 87, 89  
     equivalent resistance/emitter or source  
     of transistor, 890, 897  
     feedback system design, 676  
     FET, 860  
     forward-active region, 234  
     four-resistor bias network, 185,  
     260, 262

- gate voltage divider design, 185  
 half-circuit, 979  
 ideal inverting amplifier, 555  
 ideal op amp, assumptions, 552  
 ideal transresistance amplifier, 557  
 maximum fractional gain error, 603  
 MOS device symmetry, 165  
 NMOS transistor, 162  
 noninverting amplifiers, 896  
 op amp circuit/feedback network, 716  
 output resistance/unbypassed resistor, 898  
 output resistance/voltage gain, 805, 811  
 overall gain/single-stage amplifiers, 907  
 PMOS transistor, 162  
 poles/zeros, 1137  
 practical doping levels, 54  
 RC network, 339  
 reverse-active region characteristics, 242  
 saturation by connection, 178  
 single transistor voltage followers, 887  
 60 mV per decade, 87  
 small-signal conductance of diode, 799  
 small-signal limit of bipolar transistor, 806  
 static logic inverter design, 310  
 thermal voltage, 60  
 transfer function analysis in SPICE, 541  
 transit time, 252  
 $V_L$ , 299  
 virtual ground in op amp circuits, 25  
 voltage divider restrictions, 16  
 voltage gain/amplifier factor, 814, 877  
 voltage gain/C-E amplifier, 811  
 voltage gain/C-S amplifier, 827  
 voltage gain/intrinsic voltage gain, 803  
 worst-case design, 29  
 Design rules, 172  
 Diamond lattice unit cell, 46  
 Difference amplifier, 565–567  
 Differential amplifier, 544–547, 549–551, 969–991  
 ac analysis, 973–974  
 bipolar, 969, 970–971, 972–974  
 bipolar amplifier with active load, 1088–1091  
 CMOS amplifier with active load, 1081–1086  
 CMRR, 978–979, 987  
 common-mode frequency response, 1181–1182  
 common-mode gain and input resistance, 976–977  
 common-mode input signals, 986–987  
 common-mode input voltage range, 981  
 cross-connected quad of identical transistors, 1048  
 dc analysis, 970–971, 983  
 design considerations, 989–991  
 design note, 975, 976, 978, 983  
 differential-mode gain and input and output resistances, 974–986  
 differential-mode input signals, 985–986  
 differential-mode signals, 1181  
 direct-coupled design, 969  
 electronic current sources, 982, 983  
 half-circuit analysis, 979–981  
 ideal, 551  
 MOS, 969, 970, 983, 986  
 MOSFET differential amplifier analysis, 984–985  
 Q-point analysis, 971–972  
 signal amplification, 546–547  
 small-signal transfer characteristics, 986  
 summary/review, 1027–1028  
 transconductance, 973  
 transfer characteristics, 972–973  
 two-port model, 987, 989  
 voltage gain, 545–546, 550–551  
 VTC, 545, 546  
 Differential input series-shunt amplifier, 1239–1241  
 Differential linearity error, 735  
 Differential-mode conversion gain, 973  
 Differential-mode gain, 650, 973  
 Differential-mode half-circuit, 980  
 Differential-mode input resistance, 656, 975  
 Differential-mode input voltage, 651  
 Differential-mode output resistance, 976  
 Differential-mode output voltage, 969  
 Differential pair as single-balanced mixer, 1207–1208  
 Differential subtractor, 566  
 Differentiator, 586  
 Diffusion, 64  
 Diffusion capacitance, 93, 249  
 Diffusion coefficients, 60  
 Diffusion current, 59–60  
 Digital electronics, 285–526  
 bipolar circuits. *See* Bipolar circuits  
 Boolean algebra, 295–297  
 capacitances in logic circuits, 337–338  
 CMOS logic design. *See* CMOS logic design  
 complex NMOS logic design, 328–333  
 dynamic behavior in MOS logic gates, 337–349  
 fall time, 293  
 ideal logic gates, 289  
 logic gate design goals, 292–293  
 logic voltage levels, 291  
 MOS memory and storage circuits. *See* MOS memory and storage circuits  
 NMOS inverter delays, 344–346  
 NMOS inverter with depletion-mode load, 316–318  
 NMOS inverter with linear load device, 315  
 NMOS logic design. *See* NMOS logic design  
 NMOS NAND/NOR gates, 324–328  
 NMOS saturated load inverter, 307–315  
 noise margin, 291–292. *See also* Noise margin  
 PDP, 294  
 PMOS inverter, 349–351  
 PMOS logic, 349–352  
 power dissipation, 333–336  
 power scaling in MOS logic gates, 335–336  
 propagation delay, 294  
 pseudo NMOS inverter, 319–323, 343–344  
 ring oscillator/intrinsic gate delay, 346, 347  
 rise time, 293  
 scaling based on reference circuit simulation, 346  
 summary/review, 352–354  
 transistor alternatives to load resistor, 306–324  
 unloaded inverter delay, 347  
 Digital multimeter (DMM), 652  
 Digital signals, 9  
 Digital thermometer, 88  
 Digital thermometer block diagram, 1062  
 Digital-to-analog (D/A) conversion, 10–11, 733–740  
 C-2C ladder DAC, 740  
 errors, 734–736  
 fundamentals, 733–734  
 inherently monotonic DAC, 739  
 inverted R-2R ladder, 738–739  
 R-2R ladder, 737–738  
 switched-capacitor D/A converter, 740  
 transfer characteristics, 734

Digital-to-analog (D/A)  
 conversion —*Cont.*  
 weighted-capacitor DAC, 740  
 weighted-resistor DAC, 737  
 Digital-to-analog converter (DAC)  
 circuits, 564–565  
 Diode, 5  
 Diode circuit, 99  
 Diode circuit analysis, 96–106  
 CVD model, 104–105  
 ideal diode model, 102–104  
 load-line analysis, 96–98  
 mathematical modeling, 98–100  
 model comparison, 105–106  
 Diode circuit symbol, 75  
 Diode conductance, 798  
 Diode-connected transistor, 239,  
 1055, 1057  
 Diode/diode circuits. *See* Solid-state  
 diodes and diode circuits  
 Diode electric field/space-charge region  
 extents, 79  
 Diode equation, 82  
 Diode input protection circuit, 1096  
 Diode layout, 95–96  
 Diode resistance, 798  
 Diode space charge region width, 78  
 Diode switching behavior, 129  
 Diode temperature coefficient, 89  
 Diode-transistor logic (DTL), 287  
 Diode voltage/current calculations, 83–84  
 DIP, 500  
 Direct-conversion architecture, 1193n  
 Direct-coupled amplifier, 969  
 Direct digital synthesis (DDS), 759,  
 767–768  
 Discrete operational amplifiers, 544  
 Distortion  
 amplifier, 548  
 cross-over, 1009  
 feedback, and, 641–642  
 guitar, 842–843  
 nonlinear, 1229  
 Distributive law, 296  
 DMM, 652  
 Dominant high-frequency pole, 1133  
 Dominant low-frequency pole, 1130  
 Dominant root factorization, 1167n  
 Domino CMOS, 394, 442  
 Donor energy level, 62  
 Donor impurities, 52  
 Donor impurity concentration, 53  
 Doped semiconductor  
 defined, 51  
 electron/hole concentration, 52–55

energy band model, 62  
 equation, 69  
 mobility/resistivity, 55–58  
 Doping, 51  
 Doping levels, 54  
 Double-balanced mixer, 1208–1212  
 Double-balanced mixer/modulator,  
 1210–1212  
 Double-tuned cascode, 1202  
 Down-conversion, 1205  
 Drain, 149  
 Drain-bulk capacitance, 166  
 Drain current, 169  
 DRAM, 417  
 Drift, 49  
 Drift current, 48–49  
 Drift current density, 48  
 Droop, 753  
 DSP based equalizer, 1169  
 DTL, 287  
 Dual-in-line package (DIP), 500  
 Dual-ramp ADC, 583–585  
 Dual-ramp (dual-slope) ADC, 748–749  
 Dynamic behavior in MOS logic gates,  
 337–349  
 Dynamic logic, 394  
 Dynamic memory cells, 428–434  
 Dynamic power dissipation, 334–335, 381  
 Dynamic RAM (DRAM), 417

## E

$E_D$ , 62  
 $E_G$ , 47  
 Early, James, 251  
 Early effect, 251, 252  
 Early voltage, 251  
 Ebers-Moll model, 224  
 ECL, 287  
 ECL gate, 464–467  
 design example, 469–471  
 emitter dotting/wired-OR logic,  
 476–477  
 gate delay, 479–480  
 input current, 466  
 noise margin, 467–468  
 OR-NOR gate, 471–472  
 overview, 466–467  
 PDP, 480–481  
 power dissipation, 477–478  
 TTL, compared, 508–509  
 ECL OR-NOR gate, 471–472  
 EEROM, 447

8 MegaPixel CMOS image sensor, 915  
 Einstein's relationship, 60  
 Electric guitar distortion circuits, 842–843  
 Electric guitar pickups, 949  
 Electrical conductivity, 50  
 Electrical resistivity, 48  
 Electrically erasable read-only memory  
 (EEROM), 447  
 Electron concentration, 52, 54–55  
 Electron diffusivity, 60  
 Electron-hole pair, 46  
 Electron-hole pair generation, 62  
 Electron mobility, 49  
 Electronic current source design,  
 1070–1071  
 Electronic current sources, 1016–1024  
 basic current sources, compared, 1018  
 bias/differential amplifiers, 982  
 bipolar transistor current sources,  
 1019–1022  
 current mirror. *See* Current mirror  
 figure of merit, 1017  
 higher-output resistance sources, 1018  
*i-v* characteristics, 1016  
 MOSFET current source, 1023–1024  
 single-transistor current sources, 1017  
 SPICE, 983  
 Electronics  
 analog. *See* Analog electronics  
 digital. *See* Digital electronics  
 historical overview, 5–8  
 milestones, 3  
 real-life examples. *See* Electronics  
 in action  
 solid-state. *See* Solid-state electronics  
 Electronics in action  
 AC voltmeter, 762  
 AM demodulation, 122  
 AOI gate in standard cell library, 394  
 band-pass filters in BFSK  
 reception, 722  
 bipolar transistor PTAT cell, 240  
 CCD camera, 63  
 cellular phone evolution, 8  
 class-D audio amplifier, 1015–1016  
 CMOS camera on a chip, 164  
 CMOS imager circuitry, 915  
 CMOS navigation chip prototype  
 for optical mouse, 713  
 DAC circuits, 564–565  
 DDS, 767–768  
 dual-ramp ADC, 583–585  
 electric guitar distortion circuits,  
 842–843  
 fiber optic receiver, 557, 629

- flash memory, 448–449  
 FM stereo receiver, 25  
 FPGA, 428–429  
 function generators, 767  
 $G_m$ -C integrated filters, 1087–1088  
 graphic equalizer, 1168–1169  
 handheld technologies, 383  
 humbucker guitar pickup, 949  
 lab-on-a-chip, 66  
 laptop computer touchpad, 543  
 limiting amplifier for optical communications, 988–989  
 medical ultrasound imaging, 1025–1026  
 MEMS-based computer projector, 350–351  
 MEMS oscillator, 1286–1287  
 minimum detectable signal (MDS), 1204  
 NCO, 759  
 noise, 823–824  
 noise factor/noise figure, 1204  
 noise margin, 420–421  
 offset voltage, bias current, CMRR measurement, 658–659  
 optical communications, 486–487  
 optical isolators, 245  
 passive diode mixers, 1213  
 player characteristics, 20–21, 536  
 power cubes/cell phone chargers, 128  
 PTAT voltage, 1062  
 PTAT voltage and electronic thermometry, 88  
 RF network transformation, 1195  
 S/H circuits, 752–753  
 silicon art, 329  
 SOI, 403–404  
 solar power for the home, 132  
 STI, 403  
 thermal inkjet printers, 175  
 three-terminal IC voltage regulators, 623–624  
 transresistance amplifier implementation, 1247  
 Emitter, 218  
 Emitter area scaling, 1054  
 Emitter-coupled logic (ECL), 287  
 Emitter-coupled logic gate. *See* ECL gate  
 Emitter-coupled pair, 461  
 Emitter current, 219  
 Emitter degeneration resistance, 1172–1174  
 Emitter dotting, 476–477  
 Emitter follower, 473–476, 477, 887.  
*See also* C-C/C-D amplifiers
- Energy band model, 61–63  
 Engelbart, Douglas, 543  
 Enhancement-mode device, 150  
 Enhancement-mode PMOS transistor, 161  
 Epitaxial growth, 64  
 EPROM, 447  
 Equation. *See also* Summary tables  
     BJT, 220n, 223, 254–255  
     current, 69  
     density of free electrons, 69  
     diode, 82  
     doped semiconductors, 69  
     full-wave rectifier, 124  
     n-type material, 69  
     p-type material, 69  
 Equilibrium electron density, 246  
 Erasable programmable read-only memory (EPROM), 447  
 Etching, 64  
 Euler path, 395  
 Evaluation phase, 394  
 Evaporation, 64  
 Evolution of basic op amps, 991–1005  
 Extrinsic material, 62
- F**
- F*, 306  
 $f_M$ , 669  
 $f_T$ , 250, 1149–1151, 1153  
 Fall time, 293  
 Fan in, 293  
 Fan out, 293, 498–499, 504  
 Faraday's law, 949  
 Feedback  
     how used, 601, 1229  
     negative, 601, 1229  
     positive, 601, 763–770, 1229  
     series, 609  
     shunt, 609  
 Feedback amplifier, 604, 615–637. *See also* Transistor feedback amplifier  
     closed-loop gain analysis, 617  
     design note, 676  
     overview, 615–616  
     resistance calculations, 617  
     series-series feedback, 629–633  
     series-shunt feedback, 617–622  
     shunt-series feedback, 633–637  
     shunt-shunt feedback, 624–628  
     stability, 671–682
- Feedback amplifier stability, 1254–1262.  
*See also* Nonideal op amps and feedback amplifier stability
- Feedback circuit, 182  
 Feedback factor, 604  
 Feedback network, 24, 553, 601, 1229  
 FET. *See* Field-effect transistor (FET)  
 FGE, 602  
 Fiber optic receiver, 557, 629  
 Field-effect transistor (FET), 145–216.  
*See also* MOSFET  
     accumulation region, 147  
     capacitance, 165–167  
     circuit symbols, 163–165  
     depletion region, 148  
     fabrication/layout rules, 172–176  
     high-frequency model, 1152–1153  
     inversion region, 148  
     JFET. *See* Junction field-effect transistor (JFET)  
     MOS capacitor, 146–148  
     NMOS transistor. *See* NMOS transistor  
     PMOS transistor. *See* PMOS transistor  
     Q-point, 153, 176, 177  
     scaling. *See* MOS transistor scaling  
     signal injection and extraction, 859–860  
     single-transistor amplifiers, 905–907  
     small-signal models, 815–821  
     SPICE, 167–169  
     summary/review, 200–202
- Field programmable gate array (FPGA), 428–429  
 Field programmable logic array (FPGA), 329  
 50 percent point, 294  
 Figure of merit (FOM), 1017  
 Filter, 26  
     active, 579, 714–728  
     band-pass, 720–721  
     Butterworth, 715  
     frequency scaling, 728  
      $G_m$ -C, 1087–1088  
     high-pass, 581–582, 718–719  
     low-pass, 578–581, 714–717  
     magnitude scaling, 727  
     sensitivity, 726–727  
     switched-capacitor, 732  
     Tow-Thomas, 722–726
- Filter capacitor, 114  
 Finite input resistance, 610–614  
 Finite open-loop gain, 603–605  
 Firmware, 444  
 Five-input CMOS NAND gate, 387  
 Five-terminal op amp, 670

Flash converter, 749–750  
 Flash memory, 447, 448–449  
 Flip-flop  
   D-FF, 450–451  
   RS-FF, 449, 450  
 FM stereo receiver, 25, 531  
 Follower circuits. *See* C-C/C-D amplifiers  
 FOM, 1017  
 Forced beta, 243  
 Forward-active region, 230, 231, 233–239  
 Forward bias, 86, 93  
 Forward common-base current gain, 221  
 Forward common-emitter current  
   gain, 221  
 Forward transit time, 247, 493  
 Forward-transport current, 220  
 Fossum, Eric, 164  
 Four-quadrant multiplier, 1112  
 Four-resistor bias network, 258–266  
 Four-resistor biasing, 182–184, 188–190  
 Four-transistor (4-T) cell, 433–434  
 Fourier analysis, 21, 532  
 Fourier series, 21, 1208, 1209  
 Fowler-Nordheim tunneling, 448  
 FPGA, 329, 428–429  
 Fractional gain error (FGE), 602  
 Frequency compensated three-stage  
   feedback amplifier, 1260  
 Frequency dependence of  
   common-emitter current gain, 250  
 Frequency dependent feedback, 568–586  
 Frequency-dependent hybrid-pi model,  
   1148–1149  
 Frequency response, 659–671. *See also*  
   Amplifier frequency response  
   cascaded amplifier, 703–711  
   feedback, 666–667  
   inverting amplifier, 664–666  
   macro model, 669  
   noninverting amplifier, 661–664, 665  
   single-pole, 659  
 Frequency scaling, 728  
 Frequency spectrum, 21  
 Full-power bandwidth, 669  
 Full-scale current, 733  
 Full-scale voltage, 733  
 Full swing BiNMOS inverting  
   buffer, 512  
 Full-wave bridge rectification, 125  
 Full-wave rectifier circuit, 123–124  
 Full-wave rectifier equations, 124  
 Function generators, 767  
 Fundamental frequency, 21  
 Fundamental radian frequency, 21

**G**

$g_d$ , 798  
 $g$ -parameters, 537–541, 1310  
 Gain  
   closed-loop, 1230, 1232. *See also*  
     Closed-loop gain  
   common mode, 973, 977  
   common-mode, 650  
   conversion, 1206  
   current, 533  
   decibels, 534  
   differential amplifier, 973  
   differential-mode, 650, 973  
   forward common-base current, 221  
   forward common-emitter current, 221  
   high-pass filter, 718–719  
   ideal, 602, 1230  
   intrinsic voltage, 803  
   loop, 602, 604, 1230  
   midband, 575, 1129  
   open-loop, 551, 602, 1230  
   power, 533  
   reverse common-base current, 223  
   small-signal current, 802  
   voltage. *See* Voltage gain  
 Gain-bandwidth product, 1268  
 Gain-bandwidth product (GBW),  
   570, 660  
 Gain error, 602, 735  
 Gain error analysis, 605–606  
 Gain margin, 677  
 Gain stability, 1229  
 Gate, 146  
 Gate capacitance, 169  
 Gate-channel capacitance, 166  
 Gate delay, 479–480  
 Gate-drain capacitance, 166  
 Gate-drain overlap capacitance, 166  
 Gate mask, 174  
 Gate-source capacitance, 166  
 Gate-source overlap capacitance, 166  
 Gate voltage divider design, 185  
 GBW, 570, 660  
 GE, 602, 735  
 General-purpose operational amplifier,  
   670–671  
 Generalized input impedance  
   circuit, 1203  
 Generalized inverting-amplifier  
   configuration, 568, 578  
 Geophysical Services Inc., 217  
 Germanium bipolar transistor, 3  
 Giant Stellar Nursery, 63

Giga-scale integration (GSI), 8  
 Gilbert, Barrie, 1046, 1047, 1110  
 Gilbert mixer, 1046  
 Gilbert multiplier, 1110–1112, 1210  
 $G_m$ -C integrated filters, 1087–1088  
 Graphic equalizer, 1168–1169  
 Ground-referenced outputs, 975  
 Ground rules, 172  
 Grove, Andy, 42, 43, 288  
 GSI, 8  
 Guitar, 842–843, 949  
 Gummel-Poon model, 224

**H**

H-bridge, 1015, 1016  
 $h$ -parameters, 1311  
 Half-circuit analysis, 979–981  
 Half-wave rectifier circuit, 113–122  
   diode current, 118–119  
   diode power dissipation, 120–121  
   negative output voltage, 121  
   PIV rating, 120  
   RC load, 115–116  
   rectifier filter capacitor, 114–115  
   resistor load, 113–114  
   ripple voltage/conduction interval,  
 116–117  
   surge current, 120  
 Handheld technologies, 383  
 Hard clipping circuit, 842, 843  
 Harmonic frequencies, 21  
 Hartley oscillator, 1279–1280  
 High-frequency C-E/C-S amplifier  
   analysis, 1158–1174  
 High-frequency oscillator, 1277–1285.  
   *See also* Oscillator  
 High-frequency response, 1133  
   C-B/C-G amplifiers, 1174–1176  
   C-C/C-D amplifiers, 1177–1179  
   limitations, 1155  
   summary, 1179–1181  
   transistor models, 1148–1155  
 High logic level at the gate output, 289  
 High-output-resistance current mirrors,  
   1063–1069  
 High-pass amplifier, 25, 572–574  
 High-pass filter, 581–582, 718–719  
 High-pass filter symbol, 718  
 High-performance bipolar transistors, 255  
 High-performance trench-isolated  
   integrated circuit, 256  
 High-power TTL, 505

- Higher-level CML, 483  
 Higher-output resistance sources, 1018  
 Historical overview, 5–8  
 Hitline capacitance, 431  
 Hoff, Ted, 287  
 Hole, 48  
 Hole concentration, 52, 54–55  
 Hole density, 48  
 Hole diffusivity, 60  
 Hole mobility, 49  
 Hot electrons, 448  
 Howe, Roger, 1286  
 Hum, 949  
 Humbucker guitar pickup, 949  
 Hybrid parameters, 1311  
 Hybrid-pi model, 801–802, 805, 1155  
 Hybrid-pi small-signal model, 801  
 Hyper-abrupt profiles, 93  
 Hysteresis, 764
- I**
- $i_B$ , 219  
 $i_C$ , 219  
 $i_E$ , 219  
 $i_F$ , 220  
 $I_{FS}$ , 733  
 $I_{OS}$ , 645  
 $I_{REF}$ , 1049  
 $I_S$ , 220  
 IC, 5  
 IC fabrication, 64–66  
 IC inverters, 307–324, 353  
 IC technology. *See* Analog integrated circuit design techniques  
 IC voltage regulators, 623  
 Ideal 3-bit ADC, 741  
 Ideal current source, 1006  
 Ideal differential amplifier, 551  
 Ideal diode, 102  
 Ideal diode model, 102–104  
 Ideal gain, 602, 1230  
 Ideal inverting amplifier  
 closed-loop voltage gain, 555  
 input resistance, 554, 555  
 noninverting amplifier, compared, 562  
 output resistance, 554, 555  
 Ideal logic gates, 289  
 Ideal noninverting amplifier  
 closed-loop voltage gain, 560  
 input resistance, 560  
 inverting amplifier, compared, 562  
 output resistance, 560
- Ideal op amp, 23  
 analysis of circuits, 552–567  
 assumptions, 551–552  
 properties, 552  
 Ideal series-series feedback amplifier, 630  
 Ideal shunt-series feedback amplifier, 634  
 Ideal transresistance amplifier, 557  
 Ideal voltage amplifier, 542  
 Idealized current amplifier, 1251  
 Idealized transconductance amplifier, 1248  
 Idealized transresistance amplifier, 1242  
 Idempotency, 296  
 Identity operation, 296  
 IEEE standard MOS transistor circuit symbols, 163  
 IF, 531  
 IKF, 255  
 IKR, 255  
 Impact-ionization process, 91  
 Impedance level transformation, 535–536  
 Impedance parameters, 1312  
 Impurities, 51–52  
 Impurity doping, 51  
 Inductive degeneration, 1202–1203  
 Infinite gain filter, 720  
 Inherently monotonic DAC, 739  
 Inkjet printers, 175  
 Input-bias current, 645–646  
 Input clamping diodes, 506  
 Input high-logic-level, 290  
 Input low-logic-level, 290  
 Input-offset voltage, 643  
 Input resistance, 24  
 bipolar transistor, 822  
 C-B/C-G amplifiers, 895, 899  
 C-C/C-D amplifiers, 887–888  
 C-E amplifier, 809, 830–831, 866–867  
 C-S amplifier, 831, 881  
 C-S amplifier using MOS inverters, 911  
 closed-loop amplifier, 699  
 common-mode, 656, 977  
 current gain, 533  
 differential-mode, 656, 975  
 feedback amplifier analysis, 1233  
 finite, 610–614  
 hybrid-pi model, 801  
 ideal inverting amplifier, 554, 555  
 ideal noninverting amplifier, 560  
 inverting amplifier, 613–614  
 JFET, 822  
 MOSFET, 822  
 multistage amplifier, 943
- noninverting amplifier, 611–613  
 open-loop amplifier, 699  
 series-series feedback amplifier, 630–631  
 series-shunt feedback amplifier, 618–619  
 shunt-series feedback amplifier, 635  
 shunt-shunt feedback amplifier, 625  
 two-stage op amp, 995  
 Input stage breakdown, 1096–1097  
 Instrumentation amplifier, 711–712  
 Integral linearity error, 735  
 Integrated circuit fabrication, 64–66  
 Integrated circuit (IC), 5  
 Integrated circuit miniaturization, 5  
 Integrated circuit technology. *See* Analog integrated circuit design techniques  
 Integration, 582–583  
 Intermediate frequency (IF), 531  
 Internal diode current, 79  
 Intrinsic carrier concentration, 47  
 Intrinsic carrier density, 46  
 Intrinsic material, 47  
 Intrinsic voltage gain, 803, 817, 822  
 Inverse-active region, 231  
 Inverse common-base current gain, 223  
 Inverse common-emitter current gain, 222  
 Inverse hyperbolic tangent predistortion circuit, 1111  
 Inversion layer, 148  
 Inversion region, 148  
 Inverted R-2R ladder, 738–739  
 Inverter  
 BiNMOS, 511–513  
 CMOS. *See* CMOS logic design  
 cross-coupled, 419  
 IC, 307–324, 353  
 NMOS, 298, 300–301, 307–324  
 saturated load, 307–315  
 saturating bipolar, 487–493  
 Inverter logic symbol, 289  
 Inverter symbol, 296  
 Inverting amplifier, 24, 553–556  
 C-E amplifier. *See* C-E amplifier  
 C-S amplifier. *See* C-S amplifier  
 defined, 546  
 design example, 555–556  
 finite open-loop gain, 604–605  
 frequency response, 664–666  
 ideal. *See* Ideal inverting amplifier  
 input resistance, 613–614  
 n-stage cascades, 707  
 noninverting amplifier, compared, 562  
 operation of, 554  
 output current limits, 648–649

Inverting amplifier—*Cont.*  
 summary table, 614, 615  
 transformer-coupled, 1014  
 voltage gain, 553  
 Inverting amplifier circuit, 553, 554, 604  
 Inverting input, 549  
 Ion implantation, 64, 158  
 iPhone, 8  
 iPod, 20, 536

**J**

*j*, 48  
 JFET. *See* Junction field-effect transistor (JFET)  
 Johnson noise, 823  
 Junction breakdown voltage, 246  
 Junction field-effect transistor (JFET),  
 190–200  
 bias, 191, 198–200  
 C-S amplifiers, 833–837  
 capacitance, 196  
 circuit symbols, 195  
 drain-source bias, 191–192  
 input/output resistance, 838  
*n*-channel JFET, 190, 193–195, 196  
*p*-channel JFET, 195, 196  
 small-signal model, 820–821  
 small-signal parameters, 822  
 SPICE, 197, 1306, 1307  
 voltage gain, 838  
 Junction potential, 77  
 Just active region, 231

**K**

KBQ, 255  
 KCL, 15  
 Kilby, Jack St. Clair, 5, 42  
 Kilby integrated circuit, 42  
 Kirchhoff's current law (KCL), 15  
 Kirchhoff's voltage law (KVL), 15  
 Knee current parameters, 255  
 Kodak KAF-1401E CCD image sensor, 63  
 KVL, 15

**L**

LA, 988–989  
 Lab-on-a-chip, 66

Laptop computer touchpad, 543  
 Large-scale integration (LSI), 8  
 Latch, 419  
 Latchup, 401–402  
*LC* oscillator, 1277, 1280  
 Least significant bit (LSB), 10,  
 564, 734  
 LED, 132–133  
 Level shift, 996  
 Level shifters, 465  
 Light-emitting diode (LED), 132–133  
 Lillienfeld patent, 146  
 Limiting amplifier (LA), 988–989  
 Line regulation, 112  
 Linear amplification. *See* Small-signal  
 modeling and linear amplification  
 Linear amplifier, 257, 531  
 Linear load inverter design, 315  
 Linear load inverter VTC, 315  
 Linear region, 150n, 152, 153  
 Linearity error, 735, 736  
 Little Ghost Nebula, 63  
 LO, 1205  
 Load line, 96  
 Load-line analysis, 96–98, 109, 181  
 Load-line visualization, 300, 491  
 Load regulation, 112  
 Load resistor problems, 305–306  
 Local oscillator, 530–531  
 Local oscillator (LO), 1205  
 Logic expression simplification, 297  
 Logic gate design goals, 292–293  
 Logic inverter, 257  
 Logic voltage levels, 291  
 Loop gain, 602, 604, 638–641, 1230  
 Loop transmission, 602, 604, 1230  
 Low-frequency poles and zeros (C-S  
 amplifier), 1134–1139  
 Low-frequency response, 1130  
 Low logic level at the gate output, 289  
 Low-pass amplifier, 25, 26, 568–572  
 Low-pass filter, 578–581, 714–727  
 Low-pass filter symbol, 569, 714  
 Low-power Schottky TTL, 507  
 Low-power TTL, 505  
 Lower –3-dB frequency, 573  
 Lower-cutoff frequency. *See also*  $\omega_L$   
 amplifier frequency response, 1129  
 C-E amplifier, 1143–1144  
 capacitor, 924–925  
 high-pass amplifier, 572  
 multistage amplifier, 948  
 Lower half-power point, 573  
 LSB, 10, 564, 734  
 LSI, 8

**M**

*M*<sub>S</sub>, 298  
 Maclaurin's series, 798, 972  
 Macro model, 669, 670, 709–711  
 Magellan optical navigation chip, 713  
 Magnitude, 568  
 Magnitude scaling, 727  
 Majority carrier, 53  
 Masks, 64, 173, 174  
 Master-slave D flip-flop, 450–451  
 Match transistors, 1047  
 Matched device, 1048  
 Matched transistor, 969  
 Mathematic modeling  
 diode, 82, 98–100  
 NMOS transistor, 155–156  
 static behavior of current switch, 462  
 temperature coefficients, 32  
 tolerances, 26–27  
 Mathematical model summary. *See*  
 Summary tables  
 MATLAB. *See also* SPICE  
 Bode plot, 679, 680  
 diode, 100–101  
 Nyquist plot, 672, 678  
 poles and zeros/C-S amplifier, 1139  
 rand, 29  
 transfer function, 1132  
 Maximally flat magnitude, 714  
 MDS, 1204  
 Medical ultrasound imaging, 1025–1026  
 Medium-scale integration (MSI), 8  
 MegaPixel CMOS active-pixel image  
 sensor, 164  
 Memory. *See* MOS memory and storage  
 circuits  
 MEMS-based computer projector,  
 350–351  
 MEMS frequency selective  
 resonator, 1228  
 MEMS oscillator, 1286–1287  
 Merged transistor structure, 505  
 Mesh analysis, 15  
 Metal mask, 174  
 Metal-oxide-semiconductor field-effect  
 transistor. *See* MOSFET  
 Metal-semiconductor Schottky diode, 95  
 Metallurgical junction, 76  
 MI-MV13 image sensor, 164  
 Micro-mirror pixel structure, 350  
 Microelectromechanical systems (MEMS)  
 devices, 350  
 Micron Technology, 164

- Midband, 575  
 Midband gain, 575, 1129  
 Milestones, 3  
 Miller, John M., 1160  
 Miller capacitance, 1258  
 Miller compensation, 1288  
 Miller effect, 1160, 1263  
 Miller multiplication, 1160, 1263, 1288  
 Mini-Circuits ZP-3LH+ Mixer, 1213  
 Minimum detectable signal (MDS), 1204  
 Minimum feature size, 7, 173, 306  
 Minority carrier, 53  
 Minority-carrier transport, 246–247  
 Mirror ratio (MR), 1050–1055  
 Missing code, 742, 743  
 Mixed signal designs, 530  
 Mixer, 1205–1213  
 Mixing, 531  
 Mobility, 49, 55  
 Monostable multivibrator, 766–770  
 Monostable multivibrator waveforms, 769  
 Monotonicity, 735  
 Monte Carlo analysis, 29–32
  - BJT, 269–272
  - C-B amplifier, 934–935
  - C-E amplifier, 814
  - cascade amplifier, 709
  - SPICE, 272
 Moore, Gordon, 42, 43, 288  
 MOS capacitor, 146–148  
 MOS cascode source, 1067  
 MOS current mirror, 1049–1052, 1185  
 MOS device capacitances, 337  
 MOS differential amplifier, 970  
 MOS logic gates, 297. *See also* Digital electronics  
 MOS memory and storage circuits, 416–459
  - address decoder, 440–444
  - clocked CMOS sense amplifier, 438–440
  - dynamic memory cells, 428–434
  - flip-flop, 447–451
  - 4-T cell, 433–434
  - 1-T cell, 430–433
  - RAM, 417–419
  - read operation, 422–424, 431–433
  - ROM, 444–447
  - sense amplifier, 434–440
  - 6-T cell, 422–427
  - static memory cells, 419–428
  - summary/review, 451–452
  - write operation, 426–428
 MOS transistor layout, 173–176  
 MOS transistor scaling, 169
  - circuit and power densities, 170
  - cutoff frequency, 171
  - drain current, 169
  - gate capacitance, 169
  - high field limitations, 171
  - PDP, 170
  - subthreshold conduction, 172
 MOS Widlar source, 1063  
 MOS Wilson current source, 1064  
 MOSFET, 146. *See also* Field-effect transistor (FET)
  - body effect, 818–819
  - four-resistor bias circuits, 859
  - input/output resistance, 838
  - intrinsic voltage gain, 817
  - small-signal model, 815–817, 864
  - small-signal parameters, 817, 822, 864
  - SPICE, 1303
  - voltage gain, 838
 MOSFET amplifier, 789–790, 795–796  
 MOSFET circuit symbols, 163–165  
 MOSFET common-source amplifier, 789  
 MOSFET current source, 1023–1024  
 MOSFET differential amplifier analysis, 984–985  
 MOSFET model parameters, 1153–1154  
 MOSFET noise model, 824  
 MOSFET op amp compensation, 1273–1277  
 Most significant bit (MSB), 11, 564, 734  
 MR, 1050–1055  
 MSB, 11, 564, 734  
 MSI, 8  
 Multiple-diode circuits, 106–108  
 Multiple tuned circuits, 1201  
 Multistage ac-coupled amplifiers, 939–948
  - current and power gain, 944
  - input signal range, 945
  - lower cutoff frequency, 948
  - output resistance, 943–944
  - signal source voltage gain, 941–943
  - three-stage amplifier, 939–941, 945–948
  - voltage gain, 941–943
 Multistage amplifier cascade, 703  
 Multistage amplifier frequency response, 1187–1193  
 Multivibrator, 765–770  
 $\mu$ , 49  
 $\mu$ A709 amplifier, 544  
 $\mu$ A709 operational amplifier die photograph, 697  
 $\mu$ A741 die photograph, 600, 787  
 $\mu$ A741 op amp, 1097–1110
  - bias circuitry, 1098, 1101–1103
  - input stage, 1099–1107
  - output resistance, 1109
  - output stage, 1107–1109
  - overall circuit operation, 1097–1098
  - Q-point analysis, 1099–1101
  - short-circuit protection, 1109
  - summary table, 1110
  - voltage gain, 1103–1107
- ## N
- $n_{bo}$ , 246  
 $n_i$ , 46  
*n*-bit weighted-resistor DAC, 737  
*n*-channel JFET, 1306  
*n*-channel MOS. *See* NMOS transistor  
*n*-type material, 53  
 NAND decoder, 440–442  
 NAND gate
  - BiCMOS, 513
  - CMOS, 387–388
  - NMOS, 326
  - NMOS depletion-mode technology, 327–328
  - PMOS, 352
  - truth table, 295
  - TTL, 505, 506
 NAND gate symbol, 296  
 NAND RS flip-flop, 450  
 Narrow-band (high-Q) tuned amplifier, 1129  
 NCO, 759  
 Negative feedback, 553, 601, 1229  
 Negative  $G_M$  oscillator, 1281–1282  
 –1 point, 671  
 Network of inverters, 298  
 Neutralization, 1201  
 NGC604, 63  
 NGC2359, 63  
 NGC6369, 63  
 Nguyen, Clark, 1286  
 90 percent point, 293  
 $NM_H$ , 291, 292  
 $NM_L$ , 291, 292  
 NMOS CML, 485  
 NMOS depletion-mode device parameters, 308  
 NMOS enhancement-mode device parameters, 308  
 NMOS inverter delays, 344–346  
 NMOS inverter with depletion-mode load, 316–318

- NMOS inverter with linear load  
device, 315
- NMOS inverter with resistive load, 298, 300–301
- NMOS logic, 297
- NMOS logic design, 297–306  
load-line visualization, 300  
load resistor design, 300  
load resistor problems, 305–306
- NMOS inverter with resistive load, 298, 300–301  
noise margin, 303, 304–305  
on-resistance, 302  
 $V_{IH}/V_{OL}$ , 304  
 $V_{IL}/V_{OH}$ , 303  
 $W/L$  ratio, 299
- NMOS NAND decoder circuit, 441
- NMOS NAND/NOR gates, 324–328
- NMOS passive mixer, 1211
- NMOS saturated load inverter, 307–315
- NMOS static NOR address decoder, 441
- NMOS transistor, 148–160  
bias, 176–187  
body effect, 159  
channel-length modulation, 157–158  
circuit symbols, 163  
depletion-mode MOSFET, 158, 159  
mathematical model/saturation region, 155–156  
on-resistance, 153–154  
qualitative  $i$ - $v$  behavior, 149–150  
saturation of  $i$ - $v$  characteristics, 154–155  
substrate sensitivity, 159  
summary page, 1304  
summary table, 160  
transconductance, 157  
transfer characteristics, 158  
triode region characteristics, 150–153
- Nodal analysis, 15
- Noise, 823–824
- Noise factor, 1204
- Noise figure, 1204
- Noise margin, 291–292  
CMOS logic design, 373–375  
ECL gate, 467–468
- NMOS inverter with depletion-mode load, 317
- NMOS logic design, 303
- pseudo NMOS inverter, 321–323
- real-life example, 420–421
- resistive load inverter, 304–305
- saturated load inverter, 314–315
- TTL inverter, 503–504
- TTL prototype, 496–498
- Noise margin in the high state, 291
- Noise margin in the low state, 291
- Nokia analog phone, 8
- Nominal value, 27
- Nonideal op amps and feedback amplifier stability, 600–683  
classic feedback systems, 601–602  
closed-loop gain analysis, 602
- CMRR. *See* Common-mode rejection ratio (CMRR)
- current amplifier, 633–637  
distortion reduction/feedback, 641–642
- feedback amplifier. *See* Feedback amplifier
- finite input resistance, 610–614
- finite open-loop gain, 603–605
- frequency response. *See* Frequency response
- gain error, 602
- input-bias current, 645–646
- input-offset voltage, 643
- loop gain/successive voltage and current inspection, 638–641
- nonzero output resistance, 606–609
- Nyquist plot, 671–672
- offset current, 645–646
- offset voltage, 643–644
- output voltage and current limits, 647–649
- phase margin. *See* Phase margin
- PSRR, 657
- review/summary, 682–684
- transconductance amplifier, 629–633
- transresistance amplifier, 624–628
- voltage amplifier, 617–622
- Nonideality factor, 82
- Noninverting amplifier, 558–560  
defined, 546  
finite open-loop gain, 603–604  
frequency response, 661–664, 665  
ideal. *See* Ideal noninverting amplifier
- input resistance, 611–613
- inverting amplifier, compared, 562
- $n$ -stage cascades, 707
- overall gain, 896
- single-transistor amplifiers. *See* C-B/C-G amplifiers
- summary table, 614, 615
- terminal voltage gain, 896
- Noninverting amplifier input resistance, 611–613
- Noninverting input, 549
- Noninverting SC integrator, 730–731
- Nonlinear distortion, 1229
- Nonmonotonic converter, 736, 743
- Nonsaturating precision-rectifier circuit, 761
- Nonzero output resistance, 606–609
- NOR decoder, 440, 441
- NOR gate  
BiCMOS, 513  
CMOS, 384–387  
NMOS, 325  
NMOS depletion-mode technology, 327–328  
PMOS, 352  
truth table, 295
- NOR gate symbol, 296
- NOR RS flip-flop, 449
- Normal-active region, 231
- Normal common-base current gain, 221
- Normal common-emitter current gain, 221
- Normal-mode rejection, 585, 749
- Norton circuit transformation, 15
- Norton equivalent circuit, 16–20
- Norton’s theorem, 538
- NOT, 295
- Notational conventions, 12
- Noyce, Robert, 42, 288
- npn* transistor, 1307  
circuit symbol, 220  
common-base output characteristics, 229  
common-emitter output characteristics, 228  
cutoff region, 232
- forward characteristics, 220–222
- reverse characteristics, 222–223
- small-signal model, 807
- SPICE model, 253
- transport model, 219–225
- transport model equivalent circuit, 227
- Null elements, 296
- Numeric precision, 34
- Numerically controlled oscillator (NCO), 759
- Nyquist plot, 671–672

**O**

- OCTC method, 1139, 1167
- Offset current, 645–646, 734
- Offset error, 742
- Offset voltage, 643–644, 734
- $\omega_H$ . *See also* Upper-cutoff frequency  
absence of dominant pole, 1133–1134
- OCTC method, 1167–1170

- $\omega_L$ . *See also* Lower-cutoff frequency  
absence of dominant pole,  
1130–1131  
SCTC method, 1139–1147
- On-resistance  
CMOS NOR gate, 385  
FET, 153–154  
NMOS logic design, 302
- 1-bit DAC, 751  
–1 point, 671  
1 shot, 766  
1-T cell, 430–433  
1-T DRAM cell, 416  
One-transistor cell, 430–433  
One-transistor dynamic RAM cell, 416
- Op amp. *See* Operational amplifier  
(op amp)
- Op amp compensation, 1273–1277  
Op amp output resistance, 608–609  
Op amp transfer function, 660–661
- Open-circuit input conductance, 537
- Open-circuit termination, 537
- Open-circuit time-constant (OCTC)  
method, 1139, 1167
- Open-circuit voltage gain, 537, 551
- Open-loop amplifier, 699, 1229
- Open-loop gain, 551, 602, 1230
- Open-loop gain design, 608–610
- Operational amplifier (op amp), 23–24  
active load, 1092–1097  
all transistor implementations,  
1004–1005  
analysis of circuits, 603–615  
applications. *See* Operational amplifier  
applications  
BiCMOS amplifier, 1004  
bipolar op amp, 1095, 1096  
class-AB output stages, 1011  
CMOS op amp prototype, 1002–1004  
compensation, 1262–1277  
evolution of basic op amps, 991–1005  
general purpose, 670–671  
ideal. *See* Ideal op amp  
input stage breakdown, 1096–1097  
macro model, 670  
nonideal. *See* Nonideal op amps and  
feedback amplifier stability  
origin of name, 544  
output resistance reduction, 998–999  
slew rate, 1266–1269  
three-stage bipolar op amp analysis,  
999–1002  
transfer function, 660–661  
two-stage prototype, 992–997  
voltage gain, 997–998
- Operational amplifier applications,  
697–785
- A/D conversion. *See* Analog-to-digital  
(A/D) conversion
- active filter, 714–728
- amplitude stabilization, 757–758
- astable multivibrator, 765–766
- band-pass filter, 720–721
- cascaded amplifier, 698–711
- comparator, 763
- counting converter, 744
- D/A conversion. *See* Digital-to-analog  
converter (D/A) conversion
- delta-sigma converter, 750–754
- flash converter, 749–750
- frequency scaling, 728
- high-pass filter, 718–719
- instrumentation amplifier, 711–712
- inverted R-2R ladder, 738–739
- low-pass filter, 714–727
- magnitude scaling, 727
- monostable multivibrator, 766–770
- nonlinear circuit applications, 760–761
- nonsaturating precision-rectifier  
circuit, 761
- normal-mode rejection, 749
- oscillator. *See* Oscillator
- positive feedback, 763–770
- precision half-wave rectifier, 760
- R-2R ladder, 737–738
- review/summary, 770–772
- SC circuits, 728–733
- Schmitt trigger, 763–765
- sensitivity, 726–727
- successive approximation converter,  
744–746
- Tow-Thomas biquad, 722–726
- Operational amplifier compensation,  
1269–1272
- Operational-amplifier monostable-  
multivibrator circuit, 769
- Operational transconductance amplifier  
(OTA), 1087
- Operton die plot, 367
- Optical communications, 486–487,  
988–989
- Optical fiber receiver block diagram, 988
- Optical isolators, 245
- Optical mice, 713
- Optical navigation chip photo and block  
diagram, 713
- OR gate, 295
- OR gate symbol, 296
- Oscillator, 754–758, 1288–1289  
amplitude stabilization, 757–758, 1280
- Barkhausen criteria, 754
- Colpitts, 1278–1279
- crystal, 1283–1285
- Hartley, 1279–1280
- high-frequency, 1277–1285
- LC, 1277, 1280
- local, 530–531, 1205
- MEMS, 1286–1287
- negative  $G_M$ , 1281–1282
- negative resistance, 1280
- phase-shift, 756–757
- RC network, 755–758
- ring, 346, 347
- Wien-bridge, 755–756
- OTA, 1087
- Output characteristics, 153, 219, 228
- Output resistance  
bipolar transistor, 802  
C-B/C-G amplifiers, 899  
C-C/C-D amplifiers, 889  
C-E amplifier, 832–833, 871  
C-S amplifier, 833, 881  
C-S amplifier using MOS inverter, 911  
cascode source, 1067–1068  
closed-loop amplifier, 699
- CMOS differential amplifier with  
active load, 1053
- current mirror, 1057–1058
- differential-mode, 976
- feedback amplifier analysis, 1233
- hybrid-pi model, 801
- ideal inverting amplifier, 554, 555
- ideal noninverting amplifier, 560
- JFET, 822
- MOSFET, 822
- multistage amplifier, 943–944
- $\mu$ A741 op amp, 1109
- nonzero, 606–609
- op amp, 608–609
- open-loop amplifier, 699
- reduction of, in op amp, 998–999
- series-series feedback amplifier, 631
- series-shunt feedback amplifier,  
619–620
- shunt-series feedback amplifier, 635
- shunt-shunt feedback amplifier,  
625–626
- two-stage op amp, 995
- voltage gain, 805, 811, 839
- Widlar source, 1061, 1063
- Wilson source, 1065–1066
- Output resistance reduction, 998–999
- Output stages, 1006–1014  
class-A amplifier, 1006–1008  
class-AB amplifier, 1010–1011

- Output stages—*Cont.*  
 class-B amplifier, 1008–1009  
 short-circuit protection, 1011–1013  
 summary/review, 1028  
 transformer coupling, 1013–1014
- Over damped, 674  
 Overshoot, 675–676, 677  
 Overvoltage protection, 1096  
 Oxidation, 64  
 Oxide permittivity, 151  
 Oxide thickness, 148, 151
- P**
- p*-channel JFET, 1306  
*p*-channel MOS. *See* PMOS transistor  
*p*-type material, 54  
 Parallel (flash) converter, 749–750  
 Parasitic bipolar transistor, 401  
 Pass transistor, 623  
 Pass transistor column decoder, 442–444  
 Pass-transistor logic, 442, 444  
 Passive diode mixers, 1213  
 Passive MOS double-balanced mixer, 1210  
 PDP  
   CMOS inverter, 382  
   ECL gate, 480–481  
   logic gates, 294  
   MOS transistor scaling, 170  
   TTL inverter, 503  
 Peak detector, 114  
 Peak-inverse-voltage (PIV), 120  
 Pentium 4 Processor, 288  
 Periodic signal, 22  
 Periodic table, 45  
 Phase angle, 568  
 Phase margin  
   example, 681–682  
   feedback amplifier stability, 1256–1258  
   overshoot/damping coefficient, 677  
   second-order systems, 673–674  
   step response, 674–676  
   unity gain frequency, 676  
 Phase-shift oscillator, 756–757  
 Phasor, 16  
 Phasor representation, 532, 550  
 Photo diode, 129–130  
 Photo diode pixel architecture, 915  
 Photodetector circuit, 130, 131  
 Photolithography, 64  
 Photoresist, 64
- Piecewise linear model, 102, 109  
 Pinch-off locus, 156  
 Pinch-off point, 155  
 Pinch-off region, 155  
 Pinch-off voltage, 156  
 Pioneer SG-9500 graphic equalizer, 1168  
 PIV rating, 120  
 Planck's constant, 130  
 Player characteristics, 20–21, 536  
 PMOS inverter, 349–351  
 PMOS logic, 297, 349–352  
 PMOS transistor, 161–163  
   bias, 188–190  
   circuit symbols, 163  
   small-signal model, 819–820  
   summary page, 1304  
   summary table, 162  
*pn* junction capacitance, 92–93  
*pn* junction diode, 75–80, 1303  
*pn* product, 48  
*pnp* transistor, 225–227, 1308  
   circuit symbol, 225  
   common-base output  
     characteristics, 229  
   common-emitter output  
     characteristics, 228  
   small-signal model, 807  
   SPICE model, 255  
   transport model equivalent circuit, 227  
 Pole frequency, 1133  
 Pole-splitting, 1172  
 Polycrystalline material, 45  
 Polysilicon, 64  
 Polysilicon-gate mask, 173  
 Positive feedback, 601, 763–770, 1229  
 Power cubes, 128  
 Power cubes/cell phone chargers, 128  
 Power-delay product. *See* PDP  
 Power dissipation  
   amplifier, 839–840  
   CMOS inverter, 380–381  
   dynamic, 334–335, 381  
   ECL gate, 477–478  
   NMOS inverters, 333–336  
   power scaling in MOS logic gates, 335–336  
   static, 333–334, 380–381  
 Power electronics, 14  
 Power gain, 533  
 Power scaling in MOS logic gates, 335–336  
 Power-supply-independent bias cell, 1074  
 Power-supply-independent biasing, 1073–1077  
 Power supply rejection ratio (PSRR), 657
- Precharge phase, 394, 437  
 Precharge transistor, 434  
 Precharged sense amplifier, 435–436  
 Precision (1%) resistors, 1301  
 Precision half-wave rectifier, 760  
 Precision voltage, 1077  
 Problem description, 13  
 Problem-solving approach, 13–14  
 Programmable read-only memory (PROM), 447  
 PROM, 447  
 Propagation delay, 294, 375  
 Propagation delay-high-to-low transition ( $\tau_{PLH}$ ), 294  
 Propagation delay-low-to-high transition ( $\tau_{PLH}$ ), 294  
 Propagation delay design for inverter, 347–349  
 Pseudo NMOS inverter, 319–323, 343–344  
 Pseudo NMOS logic gate, 343  
 Pseudo NMOS noise margins, 421  
 PSRR, 657  
 PTAT voltage, 1062, 1078  
 PTAT voltage and electronic thermometry, 88  
 PTAT voltage based digital thermometry, 1062  
 Pulse-width modulated (PWM) signal, 1015  
 PWM signal, 1015
- Q**
- Q-point, 96  
 amplifier characteristics, 787  
 bipolar differential amplifier with active load, 1088  
 bipolar transistor, 256, 257  
 BJT amplifier, 788  
 capacitor, 790, 791  
 CMOS differential amplifier with active load, 1082  
 differential amplifier, 971–972  
 FET, 153, 839  
 four-resistor bias circuit, 260  
 load line analysis, 181  
 MOSFET, 176, 177  
 MOSFET amplifier, 789  
 μA741 op amp, 1099–1101  
 Quad-phase converter, 585, 749  
 Quadruple two-input NAND gates, 505  
 Quantization error, 11, 741

Quartz crystal equivalent circuit, 1284–1285  
Quiescent operating point. *See* Q-point

## R

$r_d$ , 798  
 $R_{ic}$ , 656  
 $R_{id}$ , 656, 975  
 $R_{od}$ , 976  
 $R_{th}$ , 18  
R-2R ladder, 565, 737–738  
Radio frequency amplifier, 1194  
Radio frequency choke (RFC), 1201  
Radio frequency circuits, 1193–1204  
Radio frequency (RF), 537  
Radio spectrum, 530n  
RAM, 417–419  
RAND(), 29  
Random-access memory (RAM), 417–419  
Random numbers, 29  
Ratioed logic, 302  
 $RC$  high-pass filter, 574  
 $RC$  low-pass filter, 571–572  
RC network, 339  
RC oscillator, 755–758  
Read-only memory (ROM), 444–447  
Read-only storage (ROS), 417  
Read operation, 419, 422–424, 431–433  
Real-world examples. *See* Electronics in action  
Reasonable numbers, 14  
Rectifier circuit  
    defined, 113  
    full-wave, 123–124  
    half-wave. *See* Half-wave rectifier circuit  
    rectifier compressions, 126  
    rectifier design, 126–127  
Reference current, 1049, 1072  
Reference current design, 1076–1077  
Reference current operation, 1072  
Reference inverter, 376–378  
Reference inverter designs, 324  
Reference voltage, 289, 461  
Refresh operation, 430  
Regenerative feedback, 601, 1229  
Regulated cascade current source, 1068–1069  
Repartitioned ECL gate, 479  
Resistive voltage divider, 15  
Resistivity, 44, 50, 51, 55  
Resistor coding, 1300

Resistor color coding, 1300  
Resistor load, 298  
Resistor load inverter, 298  
Resistor-transistor logic (RTL), 287  
Resolution of the converter, 10, 734  
Reverse-active region, 230, 231, 240–242  
Reverse bias, 85, 89–93, 104  
Reverse breakdown, 92  
Reverse common-base current gain, 223  
Reverse common-emitter current gain, 222  
Reverse saturation small current, 81  
Reverse transit time, 493  
RF, 537  
RF amplifier, 1194  
RF circuits, 1193–1204  
RF network transformation, 1195  
RF transceiver architecture, 1194  
RFC, 1201  
 $\rho$ , 44  
Right-half plane zero, 1259  
Ring oscillator, 346, 347  
Ripple voltage, 116  
Rise time, 293  
ROM, 444–447  
ROS, 417  
Row address decoder, 418  
RS-FF, 449, 450  
RS flip-flop, 449, 450  
RTL, 287

## S

Sample-and-hold (S/H) circuits, 746, 752–753  
Satellite radio receiver, 530n, 531  
Saturated drift velocity, 49  
Saturated load inverter, 307–315  
Saturating bipolar inverter, 487–493  
Saturation by connection, 178  
Saturation current, 81  
Saturation region, 155, 160, 162, 230, 242–245, 263–264  
Saturation velocity, 171  
Saturation voltage, 156, 242, 243–244  
SC circuits, 728–733  
Scaled inverters, 377  
Scaling, 170, 335–336, 377, 727–728, 1054. *See also* MOS transistor scaling  
Scaling based on reference circuit simulation, 346  
Schmitt trigger, 763–765  
Schottky barrier diode, 93–94, 507  
Schottky-clamped TTL, 506–508  
Schottky TTL NAND gate, 508  
SCR, 76  
SCTC method, 1139, 1187  
Semiconductor  
    compensated, 62  
    compound, 44  
    doped. *See* Doped semiconductor  
    elemental, 44  
    impurities, 51–52  
    materials, 45  
    mobility, 49  
    resistivity, 44  
Semiconductor materials, 45  
Sense amplifier, 434–440  
Sensitivity, 726–727  
Series feedback, 609, 615  
Series-series feedback, 615, 629–633  
Series-series feedback amplifier, 629–633, 1248–1250  
Series-shunt feedback, 615, 617–622  
Series-shunt feedback amplifier, 617–622, 1234–1241  
Settling time, 676  
741 design. *See* μA741 op amp  
7400 series TTL inverter, 500–504  
7404 hex inverter, 500  
SG-9500 classic analog equalizer, 1168  
S/H circuits, 746, 752–753  
Shallow trench isolation (STI), 403  
Shift register, 447  
Shockley, William, 3–5, 4, 217  
Short-circuit current gain, 537  
Short-circuit output resistance, 537  
Short-circuit protection, 1011–1013, 1109  
Short-circuit termination, 537  
Short-circuit time-constant (SCTC)  
    method, 1139, 1187  
Shot noise, 823  
Shunt feedback, 609, 615  
Shunt-peaked amplifier, 1194–1196  
Shunt peaking, 1194  
Shunt-series feedback, 615, 633–637  
Shunt-series feedback amplifier, 633–637, 1251–1253  
Shunt-shunt feedback, 615, 624–628  
Shunt-shunt feedback amplifier, 624–628, 1242–1247  
Shunt-shunt feedback with new source and load impedances, 1245–1246  
Signal injection and extraction, 858–860  
Signal source voltage gain  
    C-B/C-G amplifiers, 896  
    C-C/C-D amplifiers, 888  
    multistage amplifier, 943

- Signal-to-noise ratio (SNR), 1204  
 Silicon art, 329  
 Silicon crystal lattice structure, 46  
 Silicon dioxide, 64, 146  
 Silicon-germanium BiCMOS, 509  
 Silicon nitride, 64  
 Silicon-on-insulator (SOI), 403–404  
 Silicon-on-sapphire, 403  
 Silicon wafer-to-wafer bonding, 404  
 SIMOX, 403  
 Simple rectangular resistor, 305  
 Simplified band-pass filter circuit, 720  
 Simplified hybrid pi model, 805  
 Single-balanced mixer, 1206–1208  
 Single channel technology, 288  
 Single-crystal material, 45  
 Single-ended output, 975  
 Single-pole frequency response, 659  
 Single pole  $G_m$ -C low-pass filter, 1087  
 Single-pole op amp compensation, 1262–1277  
 Single-ramp (single-slope) ADC, 746–747  
 Single shot, 766  
 Single-stage differential feedback amplifier, 1231  
 Single-transistor amplifiers, 857–967  
     amplifiers, compared, 858, 951  
     BJT amplifiers, 903–905  
     capacitor design. *See* Capacitor design examples, 925–938  
     FET amplifiers, 905–907  
     follower circuits. *See* C-C/C-D amplifiers  
     inverting amplifiers. *See* C-E amplifier; C-S amplifier  
     multistaged ac-coupled amplifier. *See* Multistaged ac-coupled amplifier configuration  
     noninverting amplifiers. *See* C-B/C-G amplifiers  
     selecting an amplifier configuration, 912–914  
     signal injection and extraction, 858–860  
     summary/review, 950–951  
     summary tables, 884, 891, 903, 904, 906, 951  
 Single-transistor current sources, 1017  
 Single-transistor transresistance amplifier, 1242  
 Single-tuned amplifier, 1197–1198  
 6-T cell, 422–427  
 Six-transistor (6-T) SRAM cell, 422–427  
 60 mV per decade, 87  
 Slew rate, 668, 1266–1269  
 Small-scale integration (SSI), 8  
 Small signal, 796  
 Small-signal common-emitter current gain, 801  
 Small-signal conductance, 798  
 Small-signal current gain, 802  
 Small signal for the BJT, 806  
 Small-signal modeling and linear amplification, 786–856  
     BJT, 799–808  
     BJT amplifier, 788–789, 793–794  
     C-E amplifier. *See* C-E amplifier  
     C-S amplifier. *See* C-S amplifier circuit analysis, 792–796  
     coupling/bypass capacitor, 790–791  
     diode, 796–799  
     FET, 815–821  
     hybrid-pi model, 801–802, 805  
     JFET, 820–821  
     MOSFET amplifier, 789–790, 795–796  
     PMOS transistor, 819–820  
     power dissipation, 839–840  
     signal range, 840–841  
     summary/review, 843–844  
     transistor as amplifier, 787–790  
 SNR, 1204  
 Soft clipping circuit, 842  
 Software packages. *See* MATLAB; SPICE  
 SOI, 403–404  
 Solar cells, 131–132  
 Solar power for the home, 132  
 Solid-state diodes and diode circuits, 74–144  
     analysis of diodes in breakdown region, 109–112  
     design notes, 83, 87, 89  
     diode circuit analysis. *See* Diode circuit analysis  
     diode equation, 82  
     diode layout, 95–96  
     diode temperature coefficient, 89  
     dynamic switching behavior, 129–130  
     forward bias, 86, 93  
     full-wave bridge rectification, 125  
     full-wave rectifier circuit, 123–124  
     half-wave rectifier circuit, 113–122  
     *i-v* characteristics, 80–81  
     internal diode current, 79  
     LED, 132–133  
     mathematical modeling, 82, 98–100  
     multiple-diode circuits, 106–108  
     photo diode/photodetector, 130–131  
     pn junction capacitance, 92–93  
     pn junction diode, 75–80  
     rectifier circuit. *See* Rectifier circuit  
     reverse bias, 85, 89–92, 92–93, 104  
     saturation current in real diodes, 90  
     Schottky barrier diode, 93–94  
     solar cells, 131–132  
     SPICE, 94–95  
     summary/review, 133–134  
     zero bias, 85  
 Solid-state electronic materials, 44–45  
 Solid-state electronics, 42–73  
     compensated semiconductor, 62  
     covalent bond model, 45–48  
     diffusion current, 59–60  
     doped semiconductor. *See* Doped semiconductor  
     drift current, 48–49  
     electron/hole concentrations, 52–55  
     energy band model, 61–63  
     equations, 69  
     impurities in semiconductors, 51–52  
     integrated circuit fabrication, 64–66  
     materials, 44–45  
     mobility, 49  
     mobility/resistivity, 55–58  
     n-type material, 53  
     p-type material, 54  
     resistivity of intrinsic silicon, 50, 51  
     summary/review, 67–68  
     total current, 60–61  
 Sony, 4, 218  
 SOS, 403  
 Source, 149  
 Source-bulk capacitance, 166  
 Source degeneration resistance, 1170–1172  
 Source follower, 887. *See also* C-C/C-D amplifiers  
 Source-follower circuit, 1006  
 Source resistance, 533  
 Space charge region (SCR), 76  
 SPICE, 1303–1309. *See also* MATLAB ac analysis vs. transient analysis, 807–808  
 AM demodulation, 122, 123  
 amplifier VTC, 547  
 analysis of transistor operating in saturation, 264  
 bandgap reference design, 1080–1081  
 bias (JFET/depletion-mode MOSFET), 200  
 BiCMOS buffer, 510  
 bipolar technology, 253–255  
 bipolar transistor current source, 1022  
 bipolar transistor model parameters, 1152  
 bipolar transistor saturation voltage, 490

- BJT, 1307–1309  
 BJT base resistance, 1155  
 C-B amplifier, 901, 902, 933  
 C-C amplifier, 893, 894  
 C-D amplifier, 893, 894  
 C-E amplifier, 791, 813–814, 873–874,  
   876, 877  
 C-E amplifier with emitter  
   degeneration, 1174  
 C-G amplifier, 901, 902  
 C-S amplifier, 828–829, 837,  
   883, 938  
 capacitor design/C-B and C-G  
   amplifiers, 923, 924  
 capacitor design/C-C and C-D  
   amplifiers, 921  
 capacitor design/C-E and C-S  
   amplifiers, 918  
 cascade amplifier design, 708  
 cascade buffer design, 399  
 cascaded amplifier calculations, 702  
 $C_{GS}/C_{GD}$ , 1153  
 CMOS op amp analysis, 1095  
 CMRR, 659  
 $C_\pi/C_{BC}$ , 1149  
 difference amplifier analysis, 567  
 differential amplifier design, 991  
 differential amplifier Q-point analysis,  
   971–972  
 differential input series-shunt voltage  
   amplifier, 1241  
 diode parameters, 94–95  
 diode switching behavior, 129  
 dynamic performance of inverter with  
   resistor load, 342  
 electronic current source, 983  
 follower design, 929  
 four-resistor bias design, 262  
 four-resistor biasing, 184  
 frequency response of multistage  
   amplifier, 709–711  
 $g$ -parameters, 540  
 half-wave rectifier circuit, 119  
 high-frequency analysis of C-E  
   amplifier, 1165–1166  
 inverter with resistive load, 301  
 inverter with saturated load device, 312  
 inverting amplifier design, 555–556  
 JFET, 1306, 1307  
 JFET modeling, 197  
 latchup, 402  
 logic level analysis/saturated load  
   inverter, 314  
 loop gain and resistance ratio  
   calculation, 639–641  
 lower-cutoff frequency/C-E  
   amplifier, 1144  
 Monte Carlo analysis, 272  
 MOS current mirror, 1051  
 MOS transistor parameters for circuit  
   simulation, 1305  
 MOSFET, 167–169, 1303  
 MOSFET current source, 1024  
 MOSFET differential amplifier  
   analysis, 985  
 MOSFET op amp compensation,  
   1276–1277  
 multiple diode circuit, 108  
 NMOS inverter with depletion-mode  
   load, 316, 318  
 NMOS inverter with saturated  
   load, 310  
 NMOS passive mixer, 1211  
 NMOS transistor model  
   summary, 1304  
 noninverting amplifier analysis, 559  
 noninverting amplifier input  
   resistance, 612  
 op amp macro model, 670  
 phase margin analysis, 681–682  
 PMOS transistor model  
   summary, 1304  
 $pn$  junction diode, 1303  
 poles and zeros/C-S amplifier,  
   1138–1139  
 precharge operation, 434  
 propagation delay design for  
   inverter, 349  
 pseudo MOS inverter, 321  
 pseudo NMOS inverter, 344  
 read operation, 424  
 reference current design, 1076–1077  
 reference inverter design, 378  
 reverse-active region, 242  
 saturation voltage calculation, 244  
 series-series feedback amplifier  
   analysis, 633, 1250  
 shunt-series feedback amplifier  
   analysis, 637, 1253  
 shunt-shunt feedback amplifier  
   analysis, 628, 1244  
 temperature coefficients, 33  
 three-stage amplifier, 945–948  
 three-stage bipolar op amp analysis,  
   1001–1002  
 Tow-Thomas filter design,  
   725–726  
 transfer function analysis, 541  
 transformer-coupled inverting  
   amplifier, 1014  
 transistor sizing/complex logic  
   gates, 332  
 TTL gate, 497  
 TTL inverter propagation delay, 503  
 TTL inverter VTC, 504  
 two-port parameters of current mirror,  
   1059–1060  
 two-resistor biasing, 265  
 two-stage series-shunt voltage  
   amplifier, 1239  
 voltage follower gain error, 655  
 voltage gain (differential amplifier),  
   550–551  
 write operation, 427  
 Sputtering, 64  
 SR, 668  
 SRAM, 417  
 SSI, 8  
 Stagger tuning, 1201  
 Standard 7400 series TTL inverter,  
   500–504  
 Standard capacitor values, 1302  
 Standard cell library, 394  
 Standard discrete component values,  
   1300–1302  
 Standard inductor values, 1302  
 Standard resistor values, 1300  
 Start-up circuit, 1074  
 Statement of the problem, 13  
 Static logic inverter design, 310  
 Static memory cells, 419–428  
 Static power dissipation, 333–334, 380  
 Static RAM (SRAM), 417  
 Stereo receiver, 531  
 STI, 403  
 Storage circuits. *See* MOS memory and  
   storage circuits  
 Storage time, 130, 492  
 Storage time constant, 492  
 Stored based charge, 492  
 Stray-insensitive circuits, 731  
 Substrate sensitivity, 159  
 Substrate terminal, 149  
 Subthreshold conduction, 172  
 Subthreshold region, 172  
 Successive approximation converter,  
   744–746  
 Successive voltage and current injection,  
   638–641  
 Sum-of-products logic function, 296,  
   329, 505  
 Summary tables  
   C-B/C-G amplifiers, 903  
   C-C/C-D amplifiers, 891  
   C-E/C-S amplifiers, 838, 884

Summary tables—*Cont.*

current mirrors, 1069  
 diode circuit analysis, 105  
 ideal inverting/noninverting amplifier, 561  
 inverter characteristics, 324  
 inverting/noninverting amplifier, 615  
 inverting/noninverting frequency response, 665  
 $\mu$ A741 characteristics, 1110  
 NMOS inverter time delays, 344, 345  
 NMOS transistor, 160  
 PMOS transistor, 162  
 single-transistor amplifiers, 951  
 single-transistor bipolar amplifiers, 904  
 single-transistor FET amplifiers, 906  
 small-signal parameter comparison, 822  
 upper-cutoff frequency/single-stage amplifiers, 1180  
 Summing amplifier, 563  
 Summing junction, 563  
 Super-beta transistors, 223n  
 Superdiode, 760  
 Superposition, 723  
 Superposition errors, 564, 737  
 Superposition principle, 22  
 Supply-independent biasing, 1073–1077  
 Supply-independent MOS reference cell, 1075  
 Surface potential parameter, 159  
 Surge current, 120  
 Swamping, 935  
 Switched-capacitor D/A converter, 740  
 Switched-capacitor filter, 732  
 Switched-capacitor integrator, 728–729  
 Switched capacitor integrator and reference switch, 753  
 Switched-capacitor (SC) circuits, 728–733  
 Switching transistor, 298  
 Symmetrical reference inverter design, 377  
 Synchronous tuning, 1201

**T**

$t_f$ , 293  
 $t_r$ , 293, 338  
 $t_s$ , 492  
 $T_T$ , 744  
 T-model, 801n  
 Taper factor, 397

Tapped inductor, 1199–1200  
 TAS-TIS cascade, 988  
 $\tau_P$ , 294, 375  
 $\tau_{PLH}$ , 338  
 TCR, 32  
 TCR analysis, 33  
 Teal, Gordon, 217  
 Temperature coefficient of resistance (TCR), 32  
 Temperature coefficients, 32–33  
 10 percent point, 293  
 Terminal current gain, 871  
 Terminal voltage gain  
     C-B/C-G amplifiers, 895  
     C-C/C-D amplifiers, 886  
     C-E amplifier, 809, 866  
     C-S amplifier, 825, 878–879  
     noninverting amplifier, 896  
 Texas Instruments (TI), 4, 217  
 TGC, 1026  
 THD, 548  
 Thermal equilibrium, 48  
 Thermal inkjet printers, 175  
 Thermal noise, 823  
 Thermal voltage, 60, 78  
 Thévenin circuit transformation, 15  
 Thévenin equivalent circuit, 16–19, 258  
 Thévenin equivalent resistance, 18  
 Thors Helmet, 63  
 3-bit domino CMOS NAND address decoder, 443  
 3-bit flash ADC, 750  
 Three-input CML OR gate, 484  
 Three-input CMOS NOR gate, 386  
 Three-input ECL NOR gate, 472  
 Three-input ECL-OR-NOR gate, 472  
 Three-stage amplifier, 698, 939–941, 945–948  
 Three-stage amplifier cascade, 698  
 Three-stage bipolar op amp analysis, 999–1002  
 Three-stage MOSFET shunt-series feedback amplifier, 1254  
 Three-stage op amp analysis, 1263–1264  
 Three-terminal IC voltage regulators, 623–624  
 Three-terminal op amp, 670  
 Threshold voltage, 148  
 TI, 4, 217  
 TIA, 557, 629  
 Time gain control (TGC), 1026  
 Time-varying binary digital signal, 9  
 Timeline, 6  
 Tokyo Tsushin Kogyo, 218  
 Tolerances, 26  
 Tolerances in bias circuits, 266–272  
 Total current, 60–61  
 Total harmonic distortion (THD), 548  
 Tow-Thomas biquad, 722–726  
 Transconductance, 157, 255  
     back-gate, 818  
     bipolar transistor, 822  
     differential pair, 973  
     graphical interpretation, 802  
     hybrid-pi model, 801  
     JFET, 822  
     MOSFET, 816, 822  
 Transconductance amplifier, 629–633  
 Transconductance parameters, 152  
 Transfer characteristics, 158, 228  
 Transfer function, 568, 1131  
 Transfer function analysis, 541  
 Transformer-coupled class-B output stage, 1014  
 Transformer-coupled inverting amplifier, 1014  
 Transformer coupling, 1013–1014  
 Transformer-driven half-wave rectifier, 114  
 Transimpedance amplifier (TIA), 557, 629  
 Transistor  
     alternative to load resistor, 306–324  
     amplifier, as, 787–790  
     BJT. *See* Bipolar junction transistor (BJT)  
     CMOS inverter, 369  
     CMOS NAND gate, 387  
     CMOS NOR gate, 385  
     complex logic gates, 331–333  
     diode-connected, 239, 1055, 1057  
     FET. *See* Field-effect transistor (FET)  
     JFET. *See* Junction field-effect transistor (JFET)  
     matched, 969, 1047  
     NMOS. *See* NMOS transistor  
     npn. *See* npn transistor  
     origin of name, 5n  
     pass, 623  
     PMOS. *See* PMOS transistor  
     pnp. *See* pnp transistor  
     precharge, 434  
     super-beta, 223n  
 Transistor feedback amplifier, 1228–1299.  
*See also* Feedback amplifier  
 bipolar amplifier compensation, 1266  
 block diagram of feedback system, 1229  
 closed-loop gain, 1229–1230  
 closed-loop impedances, 1230

closed loop response of uncompensated amplifier, 1254–1255  
 compensated amplifier, 1260–1262  
 differential input series-shunt amplifier, 1239–1241  
 feedback amplifier analysis at midband, 1232–1233  
 feedback amplifier stability, 1254–1262  
 feedback amplifiers, compared, 1234  
 feedback analysis procedure, 1234  
 feedback effects, 1230–1231  
 higher order effects, 1259–1260  
 MOSFET op amp compensation, 1273–1277  
 op amp compensation, 1273–1277  
 phase margin, 1256–1258  
 review/summary, 1287–1289  
 series-series feedback amplifier, 1248–1250  
 series-shunt feedback amplifier, 1234–1241  
 shunt-series feedback amplifier, 1251–1253  
 shunt-shunt feedback amplifier, 1242–1247  
 single-pole op amp compensation, 1262–1277  
 slew rate, 1266–1269  
 small-signal limitations, 1262  
 three-stage op amp analysis, 1263–1264  
 transmission zeros in FET op amps, 1265  
 Transistor models at high-frequency, 1148–1155  
 Transistor saturation current, 220  
 Transistor-transistor logic (TTL), 287, 494–509  
     ECL, compared, 508–509  
     fan out, 498–499, 504  
     input clamping diodes, 506  
     logic functions, 504–506  
     multi-emitter input transistor, 505  
     NAND gates, 505, 506  
     noise margin, 496–498, 503–504  
     PDP, 503  
     power consumption, 503  
     propagation delay, 503  
     prototype, 494–499  
     Schottky-clamped transistor, 506–508  
     standard 7400 series TTL inverter, 500–504  
 VTC, 503–504

Transit time, 93, 247–249, 252, 493  
 Transmission gate, 400  
 Transport model, 218  
 Transport model simplifications, 231–242  
 Transresistance amplifier, 556–557, 624–628, 1242–1247  
 Triggering, 766, 769–770  
 Triode, 5  
 Triode region, 152, 160, 162  
 Triple ramp converter, 585, 749  
 Triple three-input NAND gates, 506  
 Truth tables, 295, 296  
 TTL, 287. *See* Transistor-transistor logic (TTL)  
 TTL AOI gate, 506  
 TTL inverter prototype, 493  
 TTL NAND gates, 505, 506  
 TTL three-input NAND gate, 506  
 Tune amplifier, 1194  
 Turn-on voltage, 81  
 TV signal, 22  
 Two-amplifier cascade, 703–704  
 Two-dimensional silicon lattice, 46  
 Two-gate CMOS NAND gate, 387  
 Two-input BiCMOS NOR gate, 513  
 Two-input BiNMOS NOR gate, 513  
 Two-input CMOS NOR gate, 384, 385  
 Two-input ECL OR gate, 472  
 Two-input Exclusive-OR gate, 484  
 Two-input NAND gate, 328  
 Two-input NMOS NAND gate, 326  
 Two-input NMOS NOR gate, 325  
 Two-input NOR gate, 328  
 Two-phase nonoverlapping clock, 728  
 Two pole biquadratics  $Gm-C$  low-pass filter, 1088  
 Two-pole low-pass filter, 714  
 Two port  $g$ -parameter representation, 537, 1310  
 Two-port  $h$ -parameter representation, 1311  
 Two-port model, 537  
     cascaded amplifier, 698–699  
     current mirror, 1058–1059  
     differential pairs, 987, 989  
      $g$ -parameters, 537–541, 1310  
      $h$ -parameters, 1311  
      $nPN$  transistor, 799  
     three-stage cascade amplifier, 699  
      $y$ -parameters, 1311–1312  
      $z$ -parameters, 1312  
 Two-port network, 537  
 Two-port network representation, 537  
 Two-port parameters, 537

Two-port  $y$ -parameter representation, 1311  
 Two-port  $z$ -parameter representation, 1312  
 Two-resistor biasing, 264–265  
 Two resistor, one-capacitor circuit, 1159  
 Two-stage op amp, 992–997  
 Two-stage series-shunt voltage amplifier, 1235  
 Two-stage shunt-series current amplifier, 1251  
 Two-stage transconductance amplifier, 1248  
 Two-terminal circuit, 17  
 256-Mb RAM chip, 418

## U

Ultra-large-scale integration (ULSI), 8  
 Ultrasound, 1025–1026  
 Unbalanced differential amplifier, 1183  
 Uncompensated amplifier, 1254–1255  
 Under damped, 675  
 Uniden bag phone, 8  
 Uniform random number generators, 29  
 Unity gain-bandwidth product, 1150  
 Unity-gain buffer, 561  
 Unity-gain frequency, 250, 570, 659, 676, 1149–1151, 1153  
 Unloaded inverter delay, 347  
 Unstable equilibrium point, 419  
 Up-conversion, 1205  
 Upper-cutoff frequency, 570, 1129, 1180.  
     *See also*  $\omega_H$   
 Upper –3-dB frequency, 570  
 Upper half-power point, 570

## V

$V_{BE}$ -based reference, 1073  
 $V_{BESAT}$ , 497  
 $V_{CESAT}$ , 497  
 $V_{DD}$ , 298n  
 $V_{FS}$ , 733  
 $V_H$ , 289, 291, 308, 319  
 $v_{ic}$ , 650  
 $V_{IH}$ , 290, 291, 304, 467  
 $V_{IL}$ , 290, 291, 303, 467  
 $V_L$ , 289, 291, 299  
 $V_{OH}$ , 291, 303, 467  
 $V_{OL}$ , 291, 304, 467  
 $V_{OS}$ , 643

$V_r$ , 116  
 $V_{REF}$ , 289, 461, 733  
 $v_{sat}$ , 49  
 $V_{SS}$ , 298n  
 $V_T$ , 60, 78  
 $V_{TN}$ , 148  
Vacancy, 48  
Vacuum diode, 5  
Vacuum tube, 5, 7  
VAF, 255  
Valence band, 61  
VAR, 255  
VCCS, 13  
VCVS, 13  
Velocity saturation, 49  
Very high frequency (VHF), 530  
Very-large-scale integration (VLSI), 8  
VHF, 530  
Virtual ground, 24, 25, 554, 975  
Vlach, Dick, 329  
VLSI, 8  
Voltage  
  breakdown, 91  
  common-mode input, 650  
  cut-in, 81  
  dc reference, 733  
  differential-mode output, 969  
  Early, 251  
  full-scale, 733  
  input-offset, 643  
  junction breakdown, 246  
  offset, 643–644, 734  
  pinch-off, 156  
  precision, 1077  
  PTAT, 1078  
  reference, 289  
  ripple, 116  
  saturation, 156, 242, 243–244  
  thermal, 60  
  threshold, 148  
  turn-on, 81

Voltage amplifier, 617–622, 1234–1241  
Voltage-controlled current source  
  model, 804

Voltage-controlled current source  
  (VCCS), 13  
Voltage-controlled voltage source  
  (VCVS), 13  
Voltage divider restrictions, 16  
Voltage division, 15  
Voltage follower, 561  
Voltage follower gain error, 654–655  
Voltage gain  
  amplification, 532–533  
  amplification factor, 814  
  amplifier, 22  
  C-E amplifier, 809, 810, 811, 812–814,  
    872–876  
  C-S amplifier, 825–826, 827–829, 879,  
    881–883  
  closed-loop amplifier, 699  
  CMOS op amp, 1092–1093  
  intrinsic, 803  
  multistage amplifier, 941–943  
  μA741 op amp, 1103–1107  
  op amp, 545–547, 997–998  
  open-loop amplifier, 699  
  output resistance, 805, 811, 839  
  signal source, 810  
  terminal. *See* Terminal voltage gain  
Voltage reference, 1077  
Voltage regulator, 110  
Voltage transfer characteristic (VTC)  
  CMOS, 371–373  
  differential amplifier, 545  
  emitter follower, 474  
  ideal inverter, 289  
  precision rectifier, 760  
  TTL inverter, 503–504  
VTC. *See* Voltage transfer characteristic  
  (VTC)

**W**

Wafer doping, 57–58  
Walker, William F., 1026

Weighted-capacitor DAC, 740  
Weighted-resistor DAC, 574, 737  
White noise, 823  
Widlar, Robert, 1046, 1047, 1077  
Widlar current source, 1060–1061, 1063,  
  1073–1074  
Widlar source output resistance, 1061  
Wien-bridge oscillator, 755–756  
Wilson current sources, 1064–1066  
Wired-OR logic, 477  
WL, 419  
W/L ratio, 297, 299, 316  
( $W/L$ )<sub>P</sub>, 319  
( $W/L$ )<sub>S</sub>, 309, 319  
Wordline (WL), 419  
Wordline drivers, 418  
Worldwide electronics market, 4  
Worst-case analysis, 27–29  
Write operation, 419, 426–428

**Y**

y-parameters, 1311–1312

**Z**

z-parameters, 1312  
Zener breakdown, 91  
Zener diode regulator circuit, 111  
Zener resistance, 111  
Zero bias, 85  
Zero-bias junction capacitance, 93  
Zero-substrate-bias value for  $V_{TN}$ , 159  
Zuras, Dan, 329

### PHYSICAL CONSTANTS

SYMBOL	QUANTITY	VALUE
$N_{AV}$	Avogadro constant	$6.022 \times 10^{26}/\text{kg} \cdot \text{mole}$
$c$	Speed of light in a vacuum	$2.998 \times 10^{10} \text{ cm/s}$
$\epsilon_0$	Permittivity of free space	$8.854 \times 10^{-14} \text{ F/cm}$
$\epsilon_S$	Relative permittivity of silicon	11.7
$\epsilon_{OX}$	Relative permittivity of silicon dioxide	3.9
$E_G$	Bandgap of silicon	1.12 eV
$h$	Planck's constant	$6.625 \times 10^{-34} \text{ J} \cdot \text{s}$ $4.135 \times 10^{-15} \text{ eV} \cdot \text{s}$
$k$	Boltzmann's constant	$1.381 \times 10^{-23} \text{ J/K}$ $8.617 \times 10^{-5} \text{ eV/K}$
$\frac{kT}{q}$	Thermal voltage at 300K	0.0259 V
$m_o$	Electron rest mass	$9.1095 \times 10^{-31} \text{ kg}$
$M_p$	Proton rest mass	$1.6726 \times 10^{-27} \text{ kg}$
$n_i$	Silicon intrinsic carrier density at room temperature	$10^{10}/\text{cm}^3$
$q$	Electronic charge	$1.602 \times 10^{-19} \text{ C}$

### CONVERSION FACTORS

1 angstrom = $10^{-8} \text{ cm}$	$\mu = 10^{-6}$
1 $\mu\text{m} = 10^{-4} \text{ cm}$	$n = 10^{-9}$
1 mil = 25.4 $\mu\text{m}$	$p = 10^{-12}$
1 eV = $1.602 \times 10^{-19} \text{ J}$	$f = 10^{-15}$
	$k = 10^3$
	$M = 10^6$

# Electronics in Action

## CHAPTER 1

- Cellular Phone Evolution 8
- Player Characteristics 20
- Amplifiers in a Familiar Electronic System—  
The FM Stereo Receiver 25

## CHAPTER 2

- CCD Cameras 63
- Lab-on-a-chip 66

## CHAPTER 3

- The PTAT Voltage and Electronic Thermometry 88
- AM Demodulation 122
- Power Cubes and Cell Phone Chargers 128
- Solar Power for the Home 132

## CHAPTER 4

- CMOS Camera on a Chip 164
- Thermal Inkjet Printers 175

## CHAPTER 5

- The Bipolar Transistor PTAT Cell 240
- Optical Isolators 245

## CHAPTER 6

- Silicon Art 329
- MEMS-Based Computer Projector 350

## CHAPTER 7

- CMOS—The Enabler for Handheld  
Technologies 383
- And-Or-Invert Gates in a Standard Cell  
Library 394
- High Performance CMOS Technologies 403

## CHAPTER 8

- A Second Look at Noise Margins 420
- Field Programmable Gate Arrays (FPGAs) 428
- Flash Memory 448

## CHAPTER 9

- Electronics for Optical Communications 486

## CHAPTER 10

- Player Characteristics 536
- Laptop Computer Touchpad 543
- Fiber Optic Receiver 557
- Digital-to-Analog Converter (DAC) Circuits 564

- Dual-Ramp or Dual-Slope Analog-to-Digital  
Converters (ADCs) 583

## CHAPTER 11

- Three-Terminal IC Voltage Regulators 623
- Fiber Optic Receiver 629
- Offset Voltage, Bias Current, and CMRR  
Measurement 658

## CHAPTER 12

- CMOS Navigation Chip Prototype for Optical  
Mice 713
- Band-Pass Filters in BFSK Reception 722
- Sample-and-Hold Circuits 752
- Numerically Controlled Oscillators and Direct Digital  
Synthesis 759
- An AC Voltmeter 762
- Function Generators 767

## CHAPTER 13

- Noise in Electronic Circuits 823
- Electric Guitar Distortion Circuits 842

## CHAPTER 14

- Revisiting the CMOS Imager Circuitry 916
- Humbucker Guitar Pickup 949

## CHAPTER 15

- Limiting Amplifiers for Optical  
Communications 988
- Class-D Audio Amplifiers 1015
- Medical Ultrasound Imaging 1025

## CHAPTER 16

- The PTAT Voltage 1062
- $G_m$ -C Integrated Filters 1087

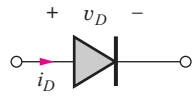
## CHAPTER 17

- Graphic Equalizer 1168
- RF Network Transformations 1195
- Noise Factor, Noise Figure, and Minimum Detectable  
Signal 1204
- Passive Diode Mixers 1213

## CHAPTER 18

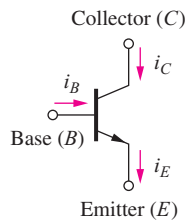
- A Transresistance Amplifier Implementation 1247
- A MEMS Oscillator 1286

## DIODE EQUATIONS



$$i_D = I_S \left[ \exp \left( \frac{v_D}{nV_T} \right) - 1 \right] \quad V_T = \frac{kT}{q} \quad C_j = \frac{C_{j0}A}{\sqrt{1 - \frac{v_D}{\phi_j}}} \quad C_D = \frac{I_D}{V_T} \tau_T$$

## (FORWARD) ACTIVE REGION EQUATIONS – npn TRANSISTOR ( $v_{BE} > 0$ AND $v_{CE} \geq v_{BE}$ )



$$i_C = I_S \exp \left( \frac{v_{BE}}{V_T} \right) \left( 1 + \frac{v_{CE}}{V_A} \right) \quad i_C = \beta_F i_B \quad i_E = (\beta_F + 1)i_B \quad \beta_F = \beta_{FO} \left( 1 + \frac{v_{CE}}{V_A} \right)$$

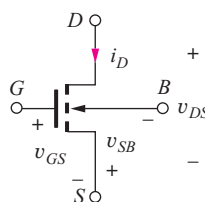
## BJT SMALL-SIGNAL MODEL PARAMETER RELATIONSHIPS ( $\beta_o \cong \beta_F$ )

$$g_m = \frac{I_C}{V_T} \cong 40I_C \quad \beta_o = g_m r_\pi \quad r_o = \frac{V_A + V_{CE}}{I_C} \cong \frac{V_A}{I_C} \quad \mu_f = g_m r_o \quad C_\pi = g_m \tau_F \quad \omega_T = \frac{g_m}{C_\pi + C_\mu}$$

## LARGE SIGNAL MODEL EQUATIONS – NMOS TRANSISTOR

Triode (Linear) Region ( $v_{GS} > V_{TN}$  and  $v_{DS} \leq v_{GS} - V_{TN}$ )

$$i_D = K_n \left( v_{GS} - V_{TN} - \frac{v_{DS}}{2} \right)^2 v_{DS} \quad i_G = 0 \quad i_S = i_D \quad K_n = K'_n \frac{W}{L}$$



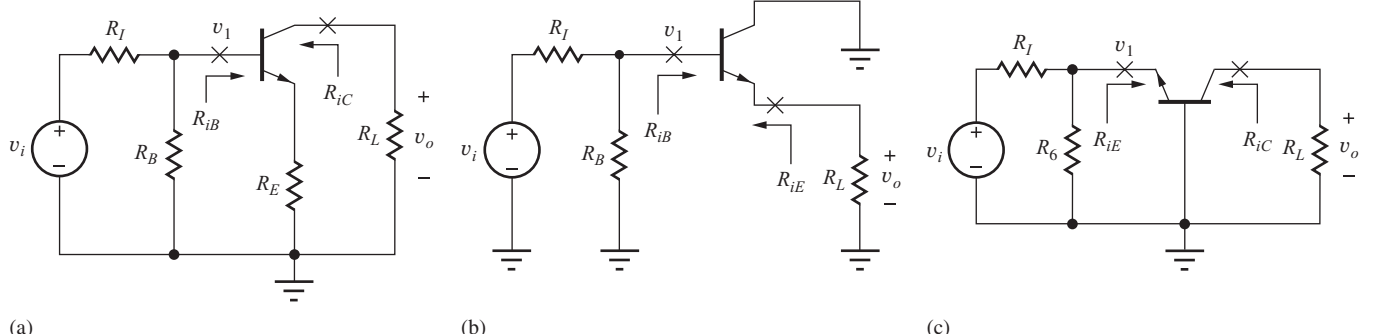
Active (Saturation) Region ( $v_{GS} > V_{TN}$  and  $v_{DS} \geq v_{GS} - V_{TN}$ )

$$i_D = \frac{K_n}{2} (v_{GS} - V_{TN})^2 (1 + \lambda v_{DS}) \quad i_G = 0 \quad i_S = i_D \quad K_n = K'_n \frac{W}{L}$$

$$V_{TN} = V_{TO} + \gamma \left( \sqrt{v_{SB} + 2\phi_f} - \sqrt{2\phi_f} \right)$$

## FET SMALL-SIGNAL MODEL PARAMETER RELATIONSHIPS

$$g_m = \frac{2I_D}{V_{GS} - V_{TN}} \cong \sqrt{2K_n I_D} \quad r_o = \frac{1 + \lambda V_{DS}}{\lambda I_D} \cong \frac{1}{\lambda I_D} \quad \mu_f = g_m r_o \quad \omega_T = \frac{g_m}{C_{GS} + C_{GD}}$$



(a)

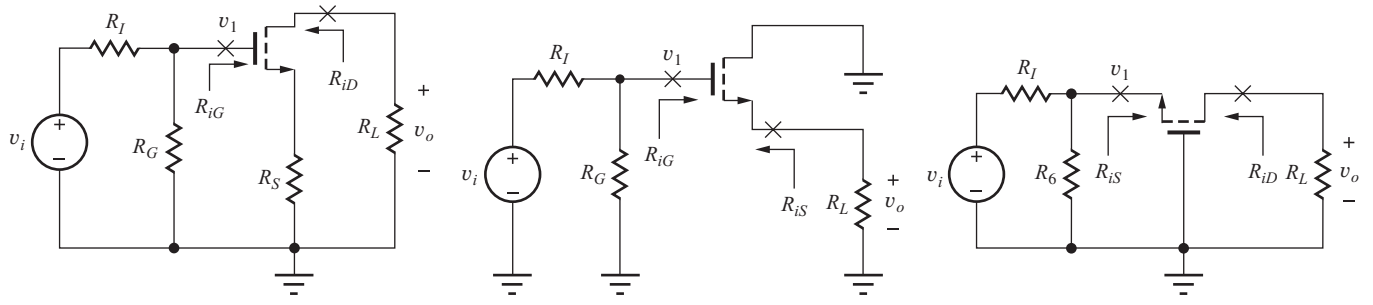
(b)

(c)

The three BJT amplifier configurations: (a) common-emitter amplifier, (b) common-collector amplifier, and (c) common-base amplifier.

#### SINGLE TRANSISTOR BJT AMPLIFIERS—APPROXIMATE EXPRESSIONS

	COMMON-EMITTER AMPLIFIER	COMMON-COLLECTOR AMPLIFIER	COMMON-BASE AMPLIFIER
Terminal voltage gain $A_{vt}$	$\approx -\frac{g_m R_L}{1 + g_m R_E}$	$\approx +\frac{g_m R_L}{1 + g_m R_L} \approx +1$	$+g_m R_L$
Signal-source voltage gain $A_v$	$-\frac{g_m R_L}{1 + g_m R_E} \left[ \frac{R_B \  R_{iB}}{R_I + (R_B \  R_{iB})} \right]$	$+\frac{g_m R_L}{1 + g_m R_L} \left[ \frac{R_B \  R_{iB}}{R_I + (R_B \  R_{iB})} \right] \approx +1$	$+\frac{g_m R_L}{1 + g_m (R_I \  R_6)} \left( \frac{R_6}{R_I + R_6} \right)$
Input terminal resistance	$r_\pi + (\beta_o + 1)R_E$ $\approx r_\pi (1 + g_m R_E)$	$r_\pi + (\beta_o + 1)R_L$ $\approx r_\pi (1 + g_m R_L)$	$\frac{\alpha_o}{g_m} \approx \frac{1}{g_m}$
Output terminal resistance	$r_o (1 + g_m R_E)$	$\frac{\alpha_o}{g_m} + \frac{R_{th}}{\beta_o + 1}$	$r_o [1 + g_m (R_I \  R_6)]$
Input signal range	$\approx 0.005(1 + g_m R_E)$	$\approx 0.005(1 + g_m R_L)$	$\approx 0.005[1 + g_m (R_I \  R_6)]$
Terminal current gain	$-\beta_o$	$\beta_o + 1$	$\alpha_o \approx +1$



(a)

(b)

(c)

The three FET amplifier configurations: (a) common-source, (b) common-drain, and (c) common-gate.

#### SINGLE TRANSISTOR FET AMPLIFIERS—APPROXIMATE EXPRESSIONS

	COMMON-SOURCE AMPLIFIER	COMMON-DRAIN AMPLIFIER	COMMON-GATE AMPLIFIER
Terminal voltage gain $A_{vt}$	$-\frac{g_m R_L}{1 + g_m R_S}$	$+\frac{g_m R_L}{1 + g_m R_L} \approx +1$	$+g_m R_L$
Signal-source voltage gain $A_v$	$-\frac{g_m R_L}{1 + g_m R_S} \left( \frac{R_G}{R_I + R_G} \right)$	$+\frac{g_m R_L}{1 + g_m R_L} \left( \frac{R_G}{R_I + R_G} \right) \approx +1$	$+\frac{g_m R_L}{1 + g_m (R_I \  R_6)} \left( \frac{R_6}{R_I + R_6} \right)$
Input terminal resistance	$\infty$	$\infty$	$1/g_m$
Output terminal resistance	$r_o (1 + g_m R_S)$	$1/g_m$	$r_o [1 + g_m (R_I \  R_6)]$
Input signal range	$0.2(V_{GS} - V_{TN})(1 + g_m R_S)$	$0.2(V_{GS} - V_{TN})(1 + g_m R_L)$	$0.2(V_{GS} - V_{TN})[1 + g_m (R_I \  R_6)]$
Terminal current gain	$\infty$	$\infty$	$+1$